125

PROCEEDINGS OF THE OCEAN DRILLING PROGRAM

INITIAL REPORTS

VOLUME 125
16 FEBRUARY 1989–17 APRIL 1989

NATIONAL SCIENCE FOUNDATION
JOINT OCEANOGRAPHIC INSTITUTIONS, INC.

NS 1.38/2:

pages tightly bound
best copy available

DRILLING LOCATIONS

LEG	LOCATION	REP	SITES
100	Gulf of Mexico	E	625A-625C
101	Bahamas	E	626-636
102	Bermuda Rise	E	418
103	Galicia Margin	E	637-641
104	Norwegian Sea	E	642-644
105	Baffin Bay	E	645-647
106	Mid Atlantic Range	E	648-649
107	Tyrrhenian sea	E	650-656
108	Eastern Tropical Atlantic	E	657-668
109	Mid Atlantic Range	E	669-670, 395, 648
110	Northern Barbados Ridge	E	671-676
111	Costa Rica Rift	G	677-678, 504B
112	Peru Continental Margin	G	679-688
113	Weddel Sea, Antarctica	E	689-697
114	Subantarctica South Atlantic	E	698-704
115	Mascarene Plateau	G	705-716
116	Distal Bengal Fan	G	717-719
117	Oman Margin	G	720-731
118	Southwest Indian Ridge	G	732-735
119	Kerguelen Plateau-Prydz Bay	E	736-746
120	Central Kerguelen Plateau	E	747-751
121	Broken Ridge & Ninetyeast Ridge	G	752-758
122	Exmouth Plateau	G	759-764
123	Argo Abyssal Plain	G	765-766
124	Celebes & Sulu Seas	G	767-771
124E	Philippine Sea	G	772-777
125	Bonin/Mariana Region	G	778-786

Storage:

E East Coast Repository
G Gulf Coast Repository

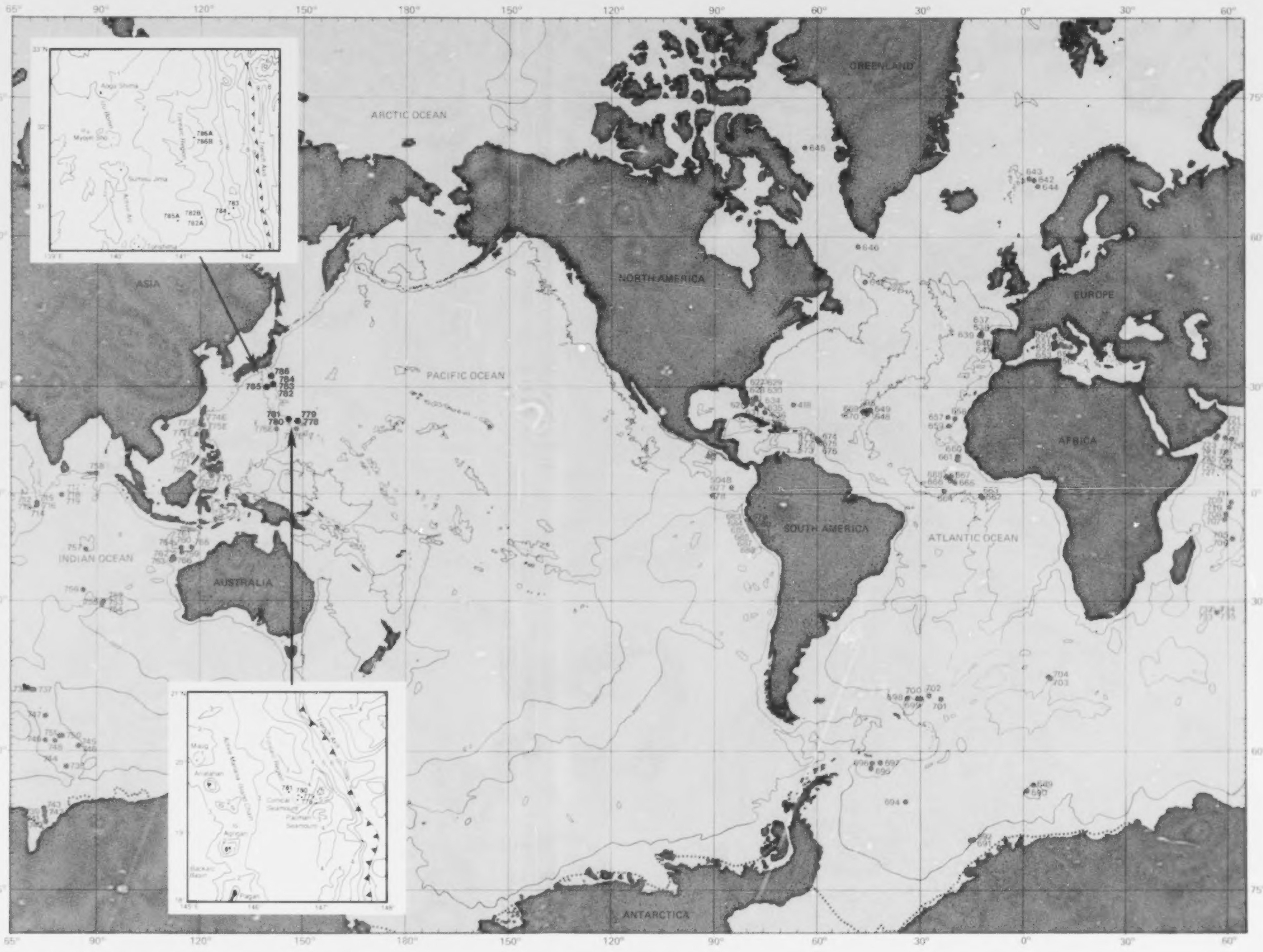
ARCTIC OCEAN
GREENLAND
NORTH AMERICA
EUROPE
ASIA
PACIFIC OCEAN
AFRICA
SOUTH AMERICA
ATLANTIC OCEAN
INDIAN OCEAN
AUSTRALIA
ANTARCTICA
65°
90°
120°
150°
180°
150°
120°
90°
60°
30°
0°
30°
60°
75°
60°
30°
0°
30°
60°
75°
786
784
785
783
782
781
780
779
778
786A
786B
785A
782B
782A
784
783
Aogo Shima
Torishima
Sumisu Jima
Maug
Asuncion
Agrigan
Saipan
Conical Seamount
Pacman Seamount

OCEAN DRILLING PROGRAM

PROCEEDINGS
OF THE
OCEAN DRILLING
PROGRAM

VOLUME 125
INITIAL REPORTS

BONIN/MARIANA REGION

Covering Leg 125 of the cruises of the Drilling Vessel *JOIDES Resolution*,
Apra Harbor, Guam, to Tokyo, Japan, Sites 778–786,
15 February 1989–17 April 1989

Patricia Fryer, Julian A. Pearce, Laura B. Stokking,
Jason Richard Ali, Richard Arculus, Dean L. Ballotti, Margaret M. Burke,
Giuliano Ciampo, Janet A. Haggerty, Roger B. Haston, Dietrich Heling,
Michael A. Hobart, Teruaki Ishii, Lynn E. Johnson, Yves Lagabrielle,
Floyd W. McCoy, Hirokazu Maekawa, Michael S. Marlow, Greg Milner,
Michael J. Mottl, Bramley J. Murton, Stephen P. Phipps, Catherine A. Rigsby,
Kristine L. Saboda, Bjorg Stabell, Sieger van der Laan, Yulin Xu
Shipboard Scientists

Laura B. Stokking
Shipboard Staff Scientist

Prepared by the
OCEAN DRILLING PROGRAM
TEXAS A&M UNIVERSITY

Sondra K. Stewart
Volume Editor

in cooperation with the
NATIONAL SCIENCE FOUNDATION
and
JOINT OCEANOGRAPHIC INSTITUTIONS, INC.

This publication was prepared by the Ocean Drilling Program, Texas A&M University, as an account of work performed under the international Ocean Drilling Program, which is managed by Joint Oceanographic Institutions, Inc., under contract with the National Science Foundation. Funding for the program was provided by the following agencies at the time of this cruise:

Canada/Australia Consortium for the Ocean Drilling Program, Department of Energy, Mines and Resources (Canada) and Department of Primary Industries and Energy (Australia)

Deutsche Forschungsgemeinschaft (Federal Republic of Germany)

European Science Foundation Consortium for Ocean Drilling (Belgium, Denmark, Finland, Iceland, Italy, Greece, the Netherlands, Norway, Spain, Sweden, Switzerland, and Turkey)

Institut Français de Recherche pour l'Exploitation de la Mer (France)

National Science Foundation (United States)

Natural Environment Research Council (United Kingdom)

University of Tokyo, Ocean Research Institute (Japan)

Any opinions, findings, and conclusions or recommendations expressed in this publication are those of the author(s) and do not necessarily reflect the views of the National Science Foundation, the participating agencies, Joint Oceanographic Institutions, Inc., Texas A&M University, or Texas A&M Research Foundation.

It is recommended that reference to the whole or to part of this volume be made in one of the following forms, as appropriate:

Fryer, P., Pearce, J. A., Stokking, L. B., et al. 1990. *Proc. ODP, Init. Repts.*, 125: College Station, TX (Ocean Drilling Program).

Shipboard Scientific Party, 1990. Site 778. *In* Fryer, P., Pearce, J. A., Stokking, L. B., et al., *Proc. ODP, Init. Repts.*, 125: College Station, TX (Ocean Drilling Program), 97–114.

Effective Publication Dates of ODP *Proceedings*

According to the International Code of Zoological Nomenclature, the date of publication of a work and of a contained name or statement affecting nomenclature is the date on which the publication was mailed to subscribers, placed on sale, or when the whole edition is distributed free of charge, mailed to institutions and individuals to whom free copies are distributed. The mailing date, *not the printed date*, is the correct one.

The mailing dates of recent *Proceedings of the Ocean Drilling Program* are as follows:

Volume 122 (*Initial Reports*): January 1990
Volume 123 (*Initial Reports*): May 1990
Volumes 124/124E (*Initial Reports*): May 1990
Volume 110 (*Scientific Results*): May 1990
Volume 111 (*Scientific Results*): December 1989

Distribution

Copies of this publication may be obtained from Publications Distribution Center, Ocean Drilling Program, 1000 Discovery Drive, College Station, Texas 77845-9547. Orders for copies will require advance payment. See current ODP publication list for price and availability of this publication.

Printed July 1990

ISSN 0884-5883
Library of Congress 87-655-674

The paper used in this publication meets the minimum requirements of American National Standard for Information Sciences—Permanence of Paper for Printed Library Materials, ANSI Z39.48–1984 ∞™

Foreword

By the National Science Foundation

The scientists of the Ocean Drilling Program (ODP) have mbarked on what could prove to be one of the most important arth science initiatives of the decade—an initiative rivaling in cope and impact the exploration of the frontiers of outer space. he program explores our planet's last frontier—the Earth's tructure and history as it is revealed beneath the oceans. The cope of the program's scientific goals excites the imagination, hallenges the intellect, and enhances the spirit of cooperation mong peoples in countries around the world.

Between 1872 and 1876, HMS *Challenger* undertook the orld's first major oceanographic expedition. That expedition reatly expanded man's knowledge of the world's oceans and evolutionized our ideas about planet Earth. From 1968 to 1983, nother ship named *Challenger* logged more than 375,000 miles n 96 voyages across every ocean for the Deep Sea Drilling Projct (DSDP), operated by Scripps Institution of Oceanography. Among the project's many remarkable discoveries were the conirmation of seafloor spreading and the establishment of the elative youth of the seafloor, thus verifying the dynamic and hanging nature of the Earth's crust.

Today, the Ocean Drilling Program, which began in 1983, rings new resources to bear on scientific ocean drilling. A new rillship is in operation—the *JOIDES Resolution*—one of the orld's most modern and best equipped drillships with enhanced apability for drilling and coring in polar areas and rough weathr, expanded laboratory space, facilities for more scientists, and major drill-hole logging program. The name of the ship was erived from the international scientific partnership that directs he program—the Joint Oceanographic Institutions for Deep arth Sampling (JOIDES)—and from the flagship of Captain ook's second voyage to the Pacific Ocean in the late 18th cenury. Texas A&M University is responsible for science operations n the program, and Lamont-Doherty Geological Observatory is esponsible for the logging program.

The Ocean Drilling Program truly has international particiation. In 1975, the International Phase of Ocean Drilling bean with member nations—the U.S.A., U.S.S.R., the Federal Reublic of Germany, Japan, the United Kingdom, and France—ll providing funds and scientific guidance for the project. oday, ODP partners include the U.S.A., the Canada/Australia onsortium for the Ocean Drilling Program, France, the Fedral Republic of Germany, Japan, the United Kingdom, and the uropean Science Foundation, which represents Sweden, Finnd, Norway, Iceland, Denmark, Belgium, the Netherlands, Spain, Switzerland, Italy, Greece, and Turkey. The National Science Foundation, with funds contributed by the United States and international partners, supports the scientific operations and planning for the ODP through a contract with Joint Oceanographic Institutions, Inc. (JOI).

The information gained by the program leads to a better understanding of the Earth and its dynamic processes. Drilled sediment cores and logs reveal clues to past climatic history and tie into parallel studies of paleoclimates from glacial ice cores drilled on the continents. Understanding these sediment cores will enable scientists to complete the map of major geologically active regions of the Earth, and to identify processes that lead to dynamic change such as earthquakes, volcanic eruptions, and mountain and continental growth. We are far from being able to predict such changes accurately now; but with the new tools and understanding, the accuracy of such predictions can be improved. This better understanding of the Earth's system(s) will allow us to identify regions of potential mineral and energy resource development, an issue of worldwide human interest. The Ocean Drilling Program is not in itself aimed at finding resources, but the knowledge of the Earth's processes that is gained through such a basic research program will inevitably provide pieces of information required for such resource discovery and exploitation.

The program is fully under way in its aim to further the understanding of the Earth's dynamic systems. People of our planet will benefit directly and indirectly from this research in both their daily living and work activities. This multinational endeavor will perhaps foster other cooperative efforts in science or among societies. The Ocean Drilling Program has distinguished ancestors in the original *Resolution* and *Challenger* expeditions and the Deep Sea Drilling Project. The National Science Foundation is proud to be playing a leading role in this program, and we are looking forward to significant and innovative science for many years to come.

Erich Bloch
Director
National Science Foundation

Washington, D.C.

Foreword

By Joint Oceanographic Institutions, Inc.

This volume presents results from the Ocean Drilling Program (ODP), where scientists use a specially equipped ocean drilling ship to sample and measure the properties of the submerged part of the Earth's crust. These data are then synthesized with other information to yield new insights into earth processes.

These results address the scientific goals of the program, which include providing a global description of geological and geophysical structures and materials, studying in detail areas of major geophysical activity such as mid-ocean ridges and the associated hydrothermal circulations, and studying passive and active continental margins. In addition, the ODP data support the study of sea-level and ocean-circulation changes, the effects of the Earth's orbital variations on climate, and the study of processes and mechanisms of evolution from the biological records in the cores which are recovered from drilling.

The Ocean Drilling Program is a partnership of scientists and governments. Overall scientific policy and management guidance is provided by Joint Oceanographic Institutions for Deep Earth Sampling (JOIDES), which consists of committees and panels made up of representatives of the participating institutions and other scientific and engineering experts. The JOIDES Executive Committee (EXCOM) provides general oversight; the JOIDES Planning Committee (PCOM) is the focal point for all scientific planning for the ODP and is key to the scientific success of the program.

The PCOM has a network of panels and working groups which screen drilling proposals, evaluate instrumentation and measurement techniques, and assess geophysical survey data and other safety and siting information. PCOM uses the recommendations of these panels and committees to select drilling targets, to specify the major scientific objectives of each two-month drilling segment or leg, and to provide the science operator with nominations for co-chief scientists. The science operator, Texas A&M University, in turn is responsible for planning the detailed ship's operations, actual drilling schedules, and final scientific rosters, which are developed in close cooperation with PCOM and the cognizant panels.

Many of the scientific goals can be met only with new technology. Thus the program has identified engineering goals, which include the ability to start a hole and to core on bare rock at mid-ocean ridge sites, to drill in high-temperature and corrosive regions typical of hydrothermal areas, and to core in high latitudes with minimum interference from high seas and sea ice. To meet these needs, the program operates a specially equipped drillship, the *JOIDES Resolution*, which contains laboratories and equipment that are state-of-the-art, and carries a major new logging program.

The ship, registered as SEDCO/BP 471 after her owners and her length in feet (144 meters), is 70 feet (21 meters) wide, and has a displacement of 16,595 long tons. Her derrick towers 200 feet (61 meters) above the waterline, and a computer-controlled dynamic-positioning system stabilizes the ship over a specific location while drilling in water depths up to 27,000 feet (8230 meters). The drilling system collects cores from beneath the seafloor with a derrick and drawworks that can handle 30,000 feet (9144 meters) of drill pipe. More than 12,000 square feet (1115 square meters) of space distributed throughout the ship is devoted to scientific laboratories and equipment. The ship sails with a scientific and technical crew of 50 and a ship's crew of 65.

Logging is a major part of the overall operation. The program provides a full suite of geochemical and geophysical measurements for every hole deeper than 1300 feet (400 meters). For each such hole, there are lowerings of basic oil-industry tools: nuclear, sonic, and electrical. In addition, a borehole televiewer is available for imaging the well-bore wall, a 12-channel logging tool provides accurate velocity and elastic property measurements as well as sonic waveforms for spectral analysis of energy propagation near the well bore, and a vertical seismic profiler records reflectors from below the total depth of the hole.

Texas A&M University serves as science operator for the Ocean Drilling Program. In this capacity, they operate and staff the drillship to collect cores from JOIDES-designated sites from around the world. The science operator also ensures that adequate scientific analyses are performed on the cores by maintaining the shipboard scientific laboratories and by providing logistical and technical support for shipboard scientific teams. Onshore, Texas A&M manages scientific activities after each leg, is curator for the cores, distributes samples, and coordinates the editing and publication of the scientific results. Lamont-Doherty Geological Observatory (LDGO) of Columbia University manages the program's logging operations, which include processing the data and provision of assistance to scientists in data analysis. The ODP Data Bank, a repository for geophysical data, is also managed by LDGO. Core samples from ODP and the previous Deep Sea Drilling Project are stored for future investigation at three sites: ODP Pacific and Indian Ocean cores at Texas A&M University, ODP and DSDP Atlantic and Antarctic cores at Lamont-Doherty Geological Observatory, and DSDP Pacific and Indian Ocean cores at Scripps Institution of Oceanography.

International oversight and coordination are provided by the ODP Council, a governmental consultative body of partner country representatives, chaired by the United States, which periodically reviews the general progress of the program and discusses financial plans and other management issues. Joint Oceanographic Institutions, Inc., a nonprofit consortium of U.S. oceanographic institutions, serves as the National Science Foundation's prime contractor and manages the ODP. JOI is responsible for seeing that the scientific objectives and plans are translated into scientific operations consistent with JOIDES recommendations and budgetary constraints.

Scientific achievements of the ODP already include new data on early seafloor spreading and how continents separate and their margins evolve. We have new insight into glacial cycles and the fluctuations of currents throughout geological time. Technical achievements include the first bare-rock coring, and logging data more accurate and complete than ever before. JOI is pleased to have played a facilitating role in the Ocean Drilling Program.

D. James Baker
President
Joint Oceanographic Institutions, Inc.

Washington, D.C.

OCEAN DRILLING PROGRAM

MEMBER ORGANIZATIONS OF THE JOINT OCEANOGRAPHIC INSTITUTIONS FOR DEEP EARTH SAMPLING (JOIDES):

University of California at San Diego, Scripps Institution of Oceanography

Columbia University, Lamont-Doherty Geological Observatory

University of Hawaii, Hawaii Institute of Geophysics

University of Miami, Rosenstiel School of Marine and Atmospheric Science

Oregon State University, College of Oceanography

University of Rhode Island, Graduate School of Oceanography

Texas A&M University, College of Geosciences

University of Texas at Austin, Institute for Geophysics

University of Washington, College of Ocean and Fishery Sciences

Woods Hole Oceanographic Institution

Canada/Australia Consortium for the Ocean Drilling Program, Department of Energy, Mines and Resources (Canada) and Department of Primary Industries and Energy (Australia)

European Science Foundation Consortium for Ocean Drilling (ECOD), Belgium, Denmark, Finland, Iceland, Italy, Greece, the Netherlands, Norway, Spain, Sweden, Switzerland, and Turkey

Federal Republic of Germany, Bundesanstalt für Geowissenschaften und Rohstoffe

France, Institut Français de Recherche pour l'Exploitation de la Mer

Japan, University of Tokyo, Ocean Research Institute

United Kingdom, Natural Environment Research Council

PRIME CONTRACTOR

Joint Oceanographic Institutions, Inc.
Washington, D.C.

Thomas E. Pyle
Director, Ocean Drilling Programs

OPERATING INSTITUTION

College of Geosciences
Texas A&M University
College Station, Texas

Melvin Friedman, Principal Investigator

OCEAN DRILLING PROGRAM

Philip D. Rabinowitz
Director

Louis E. Garrison
Deputy Director

Richard G. McPherson
Administrator

Audrey W. Meyer, Manager
Science Operations

Barry W. Harding, Manager
Engineering and Drilling Operations

Russell B. Merrill, Curator and Manager
Science Services

Robert E. Olivas, Manager
Technical and Logistics Support

LOGGING OPERATOR

Borehole Research Group
Lamont-Doherty Geological Observatory
Columbia University
Palisades, New York

Roger N. Anderson, Head

PARTICIPANTS ABOARD *JOIDES RESOLUTION* FOR LEG 125*

Patricia Fryer
Co-Chief Scientist
Hawaii Institute of Geophysics
University of Hawaii
2525 Correa Road
Honolulu, Hawaii 96822

Julian A. Pearce
Co-Chief Scientist
Department of Geology
University of Newcastle upon Tyne
Newcastle upon Tyne NE1 7RU
United Kingdom

Laura B. Stokking
ODP Staff Scientist/Paleomagnetist
Ocean Drilling Program
Texas A&M University
1000 Discovery Drive
College Station, Texas 77845-9547

Jason Richard Ali
Paleomagnetist
Department of Oceanography
The University
Southampton SO9 5NH
United Kingdom

Richard Arculus
Petrologist
Department of Geological Sciences
University of Michigan
1006 C. C. Little Bldg.
Ann Arbor, Michigan 48109-1063

Dean L. Ballotti
Physical-Properties Specialist
Rosenstiel School of Marine and Atmospheric Science
University of Miami
4600 Rickenbacker Causeway
Miami, Florida 33149-1098

Margaret M. Burke
Physical-Properties Specialist
Department of Geology
Dalhousie University
Halifax, Nova Scotia B3H 3J5
Canada

Giuliano Ciampo
Paleontologist
Dipartimento Scienze della Terra
Largo
S. Marcellino 10
80138 Napoli
Italy

Janet A. Haggerty
Sedimentologist
Department of Geosciences
University of Tulsa
600 South College Avenue
Tulsa, Oklahoma 74104

Roger B. Haston
Paleontologist
Department of Geological Sciences
University of California, Santa Barbara
Santa Barbara, California 93106

Dietrich Heling
Sedimentologist
Institut für Sedimentforschung
Universität Heidelberg
Postfach 103020
D-6900 Heidelberg 1
Federal Republic of Germany

Michael A. Hobart
LDGO Logging Scientist
Lamont-Doherty Geological Observatory
Columbia University
Palisades, New York 10964

Teruaki Ishii
Petrologist
Centre for Marine Geology
Dalhousie University
Halifax, Nova Scotia B3H 3J5
Canada

Lynn E. Johnson
Petrologist
Hawaii Institute of Geophysics
University of Hawaii
2525 Correa Road
Honolulu, Hawaii 96822

Yves Lagabrielle
Sedimentologist
GIS Océanologie et Géodynamique
6, Avenue Le Gorgeu
29287 Brest Cedex
France

Floyd W. McCoy
Sedimentologist
Lamont-Doherty Geological Observatory
Columbia University
Palisades, New York 10964

Hirokazu Maekawa
Petrologist
Department of Earth Sciences
Faculty of Science
Kobe University
Nada, Kobe 657
Japan

---

*Address at the time of the cruise.

Michael S. Marlow
Logging Scientist
Pacific Arctic Branch of Marine Geology, MS 999
U.S. Geological Survey
345 Middlefield Road
Menlo Park, California 94025

Greg Milner
Paleontologist (foraminifers)
Department of Geology
University of Western Australia
Nedlands, Western Australia 6009
Australia

Michael J. Mottl
Organic Geochemist
Hawaii Institute of Geophysics
University of Hawaii
2525 Correa Road
Honolulu, Hawaii 96822

Bramley J. Murton
Petrologist
Department of Earth Sciences
Open University
Milton Keynes
Buckinghamshire MK7 6AA
United Kingdom

Stephen P. Phipps
Geologist
Department of Geology
University of Pennsylvania
Philadelphia, Pennsylvania 19104-6316

Catherine A. Rigsby
Sedimentologist
Applied Sciences Building
Department of Earth Sciences
University of California, Santa Cruz
Santa Cruz, California 95064

Kristine L. Saboda
Petrologist
Hawaii Institute of Geophysics
University of Hawaii
2525 Correa Road
Honolulu, Hawaii 96822

Bjørg Stabell
Paleontologist (diatoms)
Department of Geology
University of Oslo
Postboks 1047, Blindern
N-0316 Oslo 3
Norway

Sieger van der Laan
Petrologist
Division of Geological and Planetary Sciences 170-25
California Institute of Technology
Pasadena, California 91125

Yulin Xu
Paleontologist (nannofossils)
Department of Geology
Florida State University
Tallahassee, Florida 32306

SEDCO OFFICIALS

Captain Edwin G. Oonk
Master of the Drilling Vessel
Underseas Drilling, Inc.
707 Texas Avenue South
Suite 103D
College Station, Texas 77840-1917

Kenneth D. Horne
Drilling Superintendent
Underseas Drilling, Inc.
707 Texas Avenue South
Suite 103D
College Station, Texas 77840-1917

ODP ENGINEERING AND OPERATIONS PERSONNEL

Thomas Pettigrew	Operations Superintendent

ODP TECHNICAL AND LOGISTICS PERSONNEL

Terri Beehner	Marine Technician, core laboratory
Stacey Cervantes	Photographer
MaryAnn Cusimano	Chemistry Technician
Kenneth du Vall	Marine Technician, underway geophysics
Nicholas Evans	Marine Technician, paleomagnetics laboratory
Jenny Glasser	Marine Technician, underway geophysics and thin-section laboratories
Michiko Hitchcox	Yeoperson
Matt Mefferd	Assistant Laboratory Officer
William M. Meyer	Computer Systems Manager
William G. Mills	Laboratory Officer
Margaret ("Peggy") Myre	Curatorial Representative
Joe Powers	Chemistry Technician
Mike Reitmeyer	Electronics Technician
Mark C. Simpson	Marine Technician, physical-properties laboratory
Don Sims	Marine Technician/X-ray Technician
Barry Weber	Electronics Technician
Charles Williamson	Marine Technician, storekeeper

Ocean Drilling Program Publications Staff

Publications Supervisor
William D. Rose

Chief Editor
Norman J. Stewart

Editors
Eva M. Barbu
Lona Haskins Dearmont
Sondra K. Stewart
William R. Winkler

Chief Production Editor
Jennifer Pattison Hall

Production Editors
Susan Collinsworth
Jaime A. Gracia

Publications Coordinator
Janalisa Braziel Soltis

Assistant Publications Coordinator
Jill Mutschler-Fontenot

Hole Summary Coordinator
Laura Hammond Young

Publications Distribution Specialist
Fabiola Muñoz Byrne

Senior Photographer
John W. Beck

Photographer
Roy T. Davis

Chief Illustrator
Karen O. Benson

Illustrators
Garnet D. Gaither
Larry R. Lewis
Matt Zebrowski
Christine L. Yokley

Compositor
Mary E. Betz

Production Assistants
Gudelia ("Gigi") Delgado
Lisa L. Tirey

TABLE OF CONTENTS

VOLUME 125–INITIAL REPORTS

ACKNOWLEDGMENTS 1

SECTION 1: INTRODUCTION

1. INTRODUCTION 5
Shipboard Scientific Party

2. EXPLANATORY NOTES 15
Shipboard Scientific Party

3. UNDERWAY GEOPHYSICS 41
M. S. Marlow, D. L. Merrill, and Shipboard Scientific Party

4. CONICAL SEAMOUNT: SeaMARC II, *ALVIN* SUBMERSIBLE, AND SEISMIC-REFLECTION STUDIES 69
P. Fryer, K. L. Saboda, L. E. Johnson, M. E. Mackay, G. F. Moore, and P. Stoffers

5. STRUCTURE OF THE OUTER IZU-BONIN FOREARC FROM SEISMIC-REFLECTION PROFILING AND GRAVITY MODELING 81
R. L. Horine, G. F. Moore, and B. Taylor

SECTION 2: SITE REPORTS

6. SITE 778 97
Shipboard Scientific Party

7. SITE 779 115
Shipboard Scientific Party

8. SITE 780 147
Shipboard Scientific Party

9. SITE 781 179
Shipboard Scientific Party

10. SITE 782 197
Shipboard Scientific Party

11. SITE 783 253
Shipboard Scientific Party

12. SITE 784 273
Shipboard Scientific Party

13. SITE 785 307
Shipboard Scientific Party

14. SITE 786 313
Shipboard Scientific Party

SECTION 3: CONCLUSIONS

15. RESULTS OF LEG 125 ... 367
Shipboard Scientific Party

SECTION 4: CORES

Core description forms and core photographs for:

SITE 778 ... 383

SITE 779 ... 433

SITE 780 ... 599

SITE 781 ... 639

SITE 782 ... 669

SITE 783 ... 723

SITE 784 ... 745

SITE 785 ... 813

SITE 786 ... 819

SECTION 5: POLICY

JOIDES ADVISORY GROUPS ... 1087

SAMPLE-DISTRIBUTION POLICY ... 1091

BACK-POCKET MICROFICHE

INITIAL REPORTS, VOLUME 125, CHAPTER 3, TABLE 1. Navigation Data

ACKNOWLEDGMENTS

During Leg 125 of the Ocean Drilling Program, nine sites in the Mariana and Izu-Bonin forearcs were drilled to determine the origin and evolution of the forearc terranes and to investigate the dewatering of the subducted lithosphere. Several sites were located on serpentinite seamounts, material that had never before been drilled. The Scientific Party of Leg 125 expresses its thanks to Captain Ed Oonk, his officers, and his crew for all of their help during Leg 125. We thank Tom Pettigrew, the ODP operations superintendent; Ken Horne, the drilling superintendent; and the SEDCO drilling crew for their patience and enthusiasm, despite the difficult drilling conditions. We thank Bob Olivas, manager of Technical and Logistics Support, for enabling us to leave Guam and to arrive in Tokyo. We are indebted to Bill Mills, the laboratory officer, and the staff of marine technicians for their major contribution to the scientific success of the cruise. Brian Taylor and Greg Moore supplied data crucial to site selection and location. The government of Japan kindly granted us permission to operate in their waters. We are grateful to the editors and illustrators of the Ocean Drilling Program for all their assistance in composing this volume.

SECTION 1: INTRODUCTION

Fryer, P., Pearce, J. A., Stokking, L. B., et al., 1990
Proceedings of the Ocean Drilling Program, Initial Reports, Vol. 125

1. INTRODUCTION[1]

Shipboard Scientific Party[2]

OVERVIEW

The Izu-Bonin-Mariana region is made up of a complex series of arcs and basins that formed since the start of westward subduction of Pacific lithosphere in the Eocene. The principal objective of Leg 125 was to study two important and poorly understood aspects of this system, namely:

1. The origin and evolution of the forearc terranes, to be investigated by drilling a series of holes through the sediments and into the basement of the Mariana and Izu-Bonin forearc basins (Sites 782, 785, and 786) and into and adjacent to serpentinite seamounts from the Mariana mid-forearc region (Sites 778 through 781) and the Izu-Bonin lower-slope terrace (Sites 783 and 784).
2. Dewatering of the subducted lithosphere, to be investigated indirectly from the composition of forearc basin crust and directly from the analyses of fluids, chemical precipitates, and metamorphic rocks from the serpentinite seamounts.

TECTONIC SETTING AND EVOLUTION OF THE IZU-BONIN-MARIANA FOREARC

The present-day tectonic configuration of the Izu-Bonin-Mariana region (Fig. 1) comprises (from east to west): the trench; the forearc terrane; the active Izu-Bonin and Mariana island arcs; the actively spreading Mariana backarc basin or, in the case of the Izu-Bonin region, the incipient rift basins of the Izu-Bonin backarc; the West Mariana Ridge, a remnant arc; the Parece Vela and Shikoku marginal basins; and the Palau-Kyushu Ridge, the westernmost remnant arc. Subduction of Pacific oceanic lithosphere is currently taking place at absolute velocities between 8 and 10 cm/yr to the northwest; the subduction angle is about 12° at shallow depths, steepening in some parts of the Mariana system to nearly vertical below about 100 km.

The evolution of these arc-basin systems is thought to have begun in the early-middle Eocene, when westward subduction of Pacific lithosphere began beneath the Philippine Sea Plate (Uyeda and Ben-Avraham, 1972; Karig, 1975). Development of the system continued through the early Oligocene, forming an intraoceanic volcanic arc on top of a forearc that may have been as much as 200 km wide. In the Mariana area, this arc formed on or near the edge of the West Philippine Basin, whereas in the Izu-Bonin area, it formed on the edge of the Amami-Oki Daito province, a series of island arcs and intervening basins of Santonian to Paleocene age (Karig, 1975).

Middle Oligocene rifting split the arc, and late Oligocene to early Miocene backarc spreading in the Parece Vela and Shikoku basins isolated a remnant arc (the Palau-Kyushu Ridge) from an active Izu-Bonin-Mariana arc (Kobayashi and Nakada, 1979). The initiation of this backarc spreading event was not synchronous along the length of the Oligocene arc. Spreading began at about 31 Ma in what became the central Parece Vela Basin and propagated both north and south, giving the basin its bowed-out shape. A second spreading episode began by 25 Ma in what became the northernmost Shikoku Basin and propagated south (Kobayashi and Nakada, 1979). By 23 Ma the two systems had joined at what is now approximately 25°N, and both basins shared a common spreading axis until spreading ceased at 17 to 15 Ma.

A repetition of this cycle of events began in the late Miocene, when the southern part of the arc split again. Subsequently, 6 to 8 m.y. of spreading in the Mariana backarc basin isolated the active Mariana arc from the West Mariana Ridge remnant arc (Karig et al., 1978; Hussong and Uyeda, 1981). The extent of spreading has been greatest in the center of this backarc basin, causing the active arc to have a marked eastward convexity. Spreading in the Mariana backarc basin may now be propagating to the north, either "unzipping" the Mariana arc from the West Mariana Ridge (Stern et al., 1984) or pivoting about a point north of the volcanic islands (Beal, 1986). The Izu-Bonin arc is still in the early rifting stage of backarc formation, undergoing extension along most of its length (Honza and Tamaki, 1985).

The forearc terrane is made up of an inner trench wall, an outer-arc high, a forearc basin, and a frontal-arc high. In the Izu-Bonin system, the inner trench wall has a 50-km-wide along-strike terrace or ridge. In the Mariana system, the inner trench wall has several reentrants, some of which are adjacent to positions of subducting seamounts and horst blocks associated with partially subducted seamounts. These differences among the forearcs may be attributed in part to differences in arc-basin evolution between the Mariana and Izu-Bonin systems, and in part because seamount chains and aseismic ridges on the subducting plate have collided with only the Mariana forearc and the southernmost Izu-Bonin arc.

In contrast to the Mariana forearc, the Izu-Bonin forearc has experienced only minor deformation since the Eocene, when subduction began (Honza and Tamaki, 1985). This forearc constitutes a broad forearc basin filled with volcaniclastic and hemipelagic sediments that developed behind an outer-arc high, west of the break in slope between the inner trench wall and the forearc basin (Fig. 2A). In the southern part of the Izu-Bonin forearc, this outer-arc high is the Ogasawara Ridge and includes the islands of the Izu-Bonin group (the Ogasawara Islands). Biostratigraphic dating of the strata that lap onto this outer-arc high, both on its subaerial expression on the Ogasawara Islands (Hanzawa, 1947) and offshore, suggests that this high has been a positive topographic feature since its uplift in the early Eocene. North of about 30°N, the outer-arc high is more subdued and is situated at a distance of from 50 to about 100 km from the Izu-Bonin Trench (Fig. 2B). Where imaged by seismic-reflection profiles, the arc has separated from the forearc basin by normal faults with apparent throws of less than 500 km, down-dropped to the west (Horine et al., this volume). Several mature, dendritic submarine canyon systems have developed across the

---

[1] Fryer, P., Pearce, J. A., Stokking, L. B., et al., *Proc. ODP, Init. Repts.*, 125: College Station, TX (Ocean Drilling Program).

[2] Shipboard Scientific Party is as given in the list of participants preceding the contents.

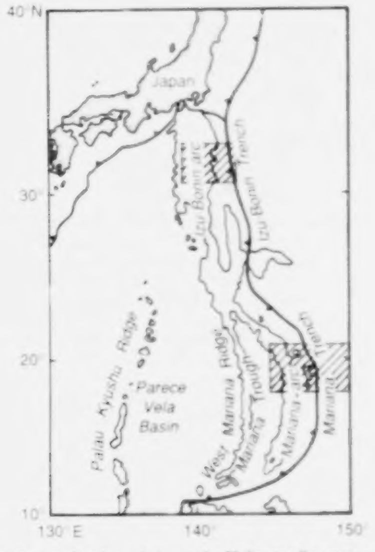

Figure 1. Active plate boundaries in the Philippine Sea region. Barbed lines locate subduction zones. Basins and ridges are outlined by the 4-km bathymetric contour, except for the Izu-Bonin, West Mariana and Mariana arcs, which are outlined by the 3-km contour. Boxes show locations of Figures 2 and 3.

Izu-Bonin forearc basin and the outer-arc high by mass wasting and headward erosion. These canyons have incised as much as 1 km into the 1.5- to 4-km-thick sedimentary section (Taylor and Smoot, 1984). Another feature of the outer forearc appears north of about 30°N. Between the outer-arc high and the Izu-Bonin Trench are a number of serpentinite seamounts, ranging from less than 10 to more than 20 km in diameter and from several hundred to more than 1400 m high (Ishii, 1985). These seamounts are spaced at intervals of 15 to 60 km along a terrace, which is situated less than 50 km from the trench axis on the inner wall of the trench (Fig. 2B).

The Mariana forearc (Fig. 3) has a broadly similar structure, but lacks the lower-slope terrace. This forearc has undergone extensive uplift and subsidence that resulted from both seamount collision and the tensional and rotational fracturing that is associated with adjustments to plate subduction, changes in the configuration of the arc, and variations in the angle of convergence. A broad zone of serpentinite seamounts (up to 2500 m high and 30 km in diameter), 50 to 120 km from the trench axis, has been identified west of the break in slope at the top of the inner trench wall (Fryer et al., 1985a; Fryer and Fryer, 1987). Some of the seamounts in the Mariana forearc appear to be horst blocks. Others have formed by the "diapiric" rise and extrusion of serpentinite. These serpentinite seamounts, and the fault zones with which many of them are associated, may represent pathways whereby fluids that have migrated upward from the subduction zone reach the surface. These fluid pathways contrast with pathways in accretionary forearcs: only very minor, and probably ephemeral, accretionary complexes have been found at the bases of the inner walls of the Izu-Bonin and Mariana trenches.

Scientists of Leg 125 focused on two seamounts: Conical Seamount in the Mariana forearc and Torishima Forearc Seamount in the Izu-Bonin forearc. Conical Seamount, drilled at Sites 778 and 779 (the flank sites) and Site 780 (the summit site) (Fig. 4), lies in the broad zone of forearc seamounts along the Mariana outer-arc high. It is a nearly perfectly circular seamount, 20 km in diameter, that rises 1500 m above the seafloor, a distance of about 80 km from the trench axis. A side-scanning sonar and bathymetry survey showed that flows mantle the surface of the seamount (Hussong and Fryer, 1985). The constitution of these flows was subsequently identified as unconsolidated sedimentary serpentine by submersible exploration, which also discovered evidence for fluid emanations at its summit (Fryer et al., 1987). An additional site (Site 781) was drilled into the forearc just off the flank of the seamount.

The Torishima Forearc Seamount, drilled at Sites 783 and 784 on the outermost part of the Izu-Bonin forearc (Fig. 5), also has yielded serpentinite in dredges (Ishii et al., 1981; Ishii, 1985; Ishii et al., 1985). Several dredges and one core from seamounts along this ridge have yielded serpentinized harzburgite, metamorphosed gabbro, diabase, and basalt, and their sedimentary derivatives (serpentinite breccia, sandstone, and mudstone). Side-scanning sonar and bathymetry surveys of the three seamounts south of 32°N indicate sedimented western slopes, and seismic-reflection profiles along and across the seamounts reveal an acoustically complex basement with thin or no sediment cover (see Horine et al., this volume). Most of the inner trench wall, both above and below the terrace, has been stripped of sediment, presumably by slumping or faulting. However, sediments showing complex unconformities, including turbidite deposits and pelagic sequences, are ponded behind the seamounts, drape their lower flanks, and fill the lows between them (Taylor, 1984). Site 783 is situated on the north flank of a seamount at 31°N, and Site 784 is at its western base.

COMPOSITION OF THE FOREARC BASEMENT

Our knowledge of the basement of the Izu-Bonin and Mariana forearcs comes from three main sources: (1) on-land exposures on Guam, Saipan, and Ogasawara islands; (2) dredges from inner trench walls, seamounts, and large fault scarps; and (3) Sites 458 through 461 of Leg 60 of the Deep Sea Drilling Project (DSDP).

The islands of Guam and Saipan in the Mariana forearc contain exposures of pillow lavas, breccias, and volcanic sediments of middle-late Eocene age known as the Facpi Formation (Tracey et al., 1964; Meijer, 1979; Reagan and Meijer, 1984). This formation is overlain by the late Eocene to Oligocene Alutom Formation, which includes volcanic breccias, clastic and carbonate sediments, and subordinate pillow lavas and is intruded by sills of Oligocene (32 Ma) age, coincident with the rifting of the Palau-Kyushu Ridge. The Alutom Formation is unconformably overlain by the Umatac Formation, comprising middle Miocene limestones, volcanic breccias, and pillow lavas. The magma types present in the lavas range from boninite and island-arc tholeiite series in the Facpi Formation, island-arc tholeiite to calc-alkaline series in the Alutom Formation, and high-potassium, calc-alkaline series in the Umatac Formation (Reagan and Meijer, 1984; Hickey and Frey, 1982; Shiraki et al., 1980).

The Ogasawara Islands are made up of a dominantly Eocene volcanic basement that is overlain by interbedded tuffs and limestones of Eocene-Oligocene age (Kuroda et al., 1988). The volcanic basement is made up mainly of pillow lavas, breccias, hyaloclastites, and dikes belonging to the boninite and island-arc tholeiite series and includes the type locality for boninites on the island of Chichijima.

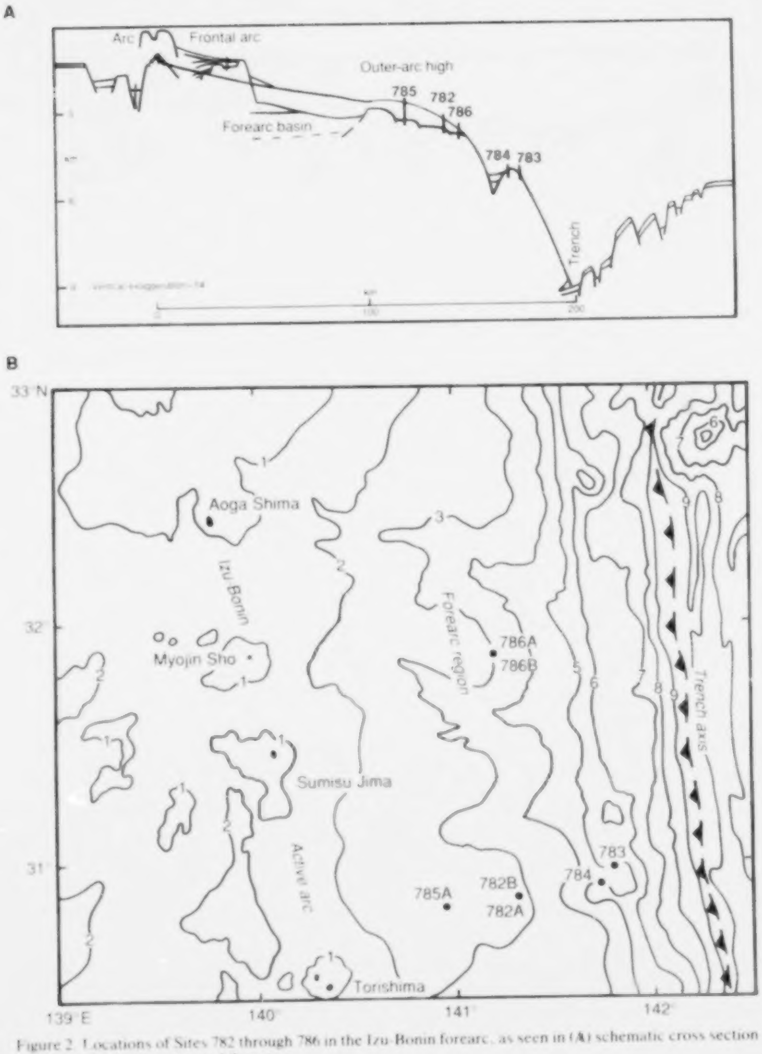
A
Arc
Frontal arc
Outer-arc high
785
782
786
Forearc basin
784
783
Trench
B
33°N
32°
31°
139°E
140°
141°
142°
Aoga Shima
Izu Bonin
Myojin Sho
Sumisu Jima
Active arc
Torishima
Forearc region
786A
786B
785A
782B
782A
784
783
Trench axis
1
2
3
5
6
7
8
9

Figure 2. Locations of Sites 782 through 786 in the Izu-Bonin forearc, as seen in (**A**) schematic cross section and (**B**) plan. Bathymetry in kilometers.

redges from the inner trench walls have recovered a wide
ty of rock types. In the Mariana forearc, Sharaskin et al.
), Beccaluva et al. (1980), Dietrich et al. (1978), Bloomer
), and Bloomer and Hawkins (1983) described serpenti-
l ultramafic rocks from nearly all structural levels of the
trench wall of the Mariana Trench from depths of 1200 to
m. They also described cumulate and isotropic gabbros,
a range of altered to fresh volcanic rocks that included
nites, subalkaline basalts to dacites, and rare alkali ba-
and sedimentary rocks. More detailed dredging and
nersible sampling of Conical Seamount showed that serpentinized ultramafic rocks are the dominant rock type on this seamount (Saboda and Fryer, 1987). Dredge hauls from a fault scarp bounding a deep graben adjacent to Conical Seamount (Sites 778–780) yielded boninites and a variety of basalts of island-arc, mid-ocean ridge basalt (MORB), and alkalic ocean-island affinities (Johnson and Fryer, 1988). The recovery of both MORB and ocean-island basalts from the forearc suggests that relict fragments of pre-Eocene crust (possibly Philippine Sea Plate) and/or accreted fragments of Pacific Plate may also contribute to the forearc crust (Ogawa and Naka, 1984; Bloomer, 1983; Johnson and Fryer, 1988). In the

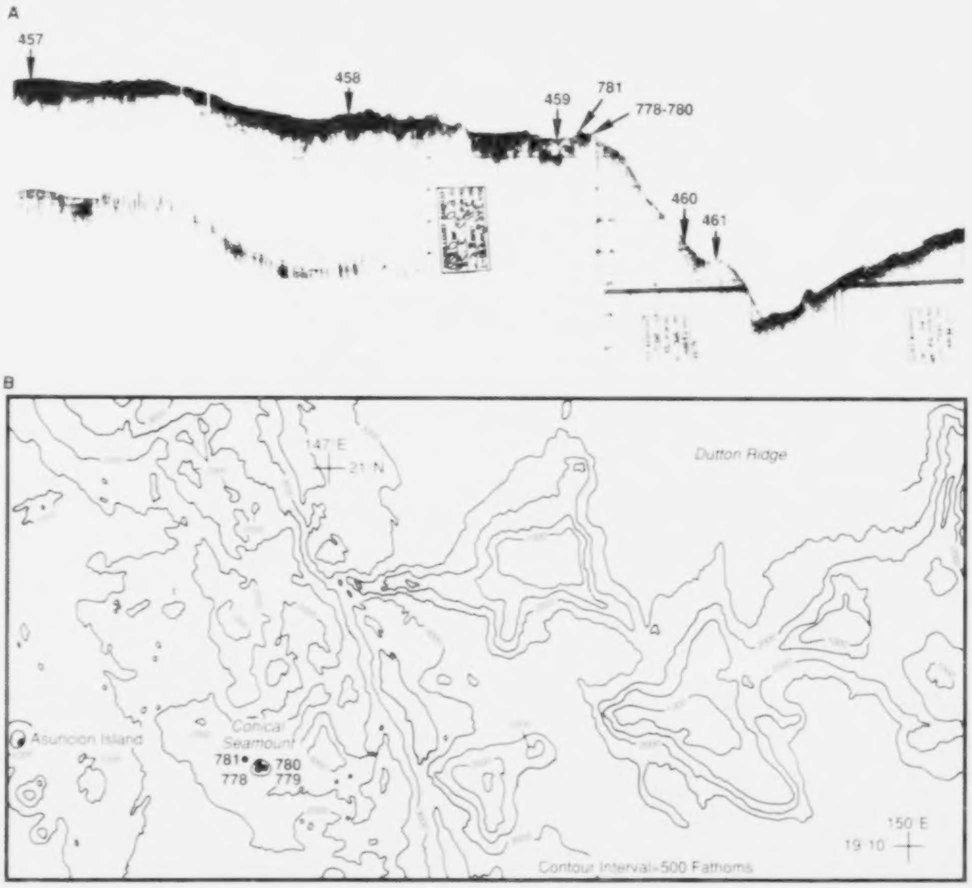

Figure 3. Locations of Sites 778 through 781 in the Mariana forearc, as seen in (**A**) seismic cross section and (**B**) plan. DSDP Leg 60 site locations also are shown.

Izu-Bonin forearc, dredging of seamounts between the Ogasawara Ridge and Izu-Bonin Trench yielded a wide range of rock types, including serpentinized ultramafic rocks, gabbros, diabases, basalts, volcaniclastic rocks, and boninites (Ishii et al., 1981; Ishii, 1985).

At DSDP Leg 60 Sites 458 and 459, on the Mariana outer-arc high east of Guam, Eocene and Oligocene basement rocks also were recovered (Natland and Tarney, 1981). At Site 458, interbedded pillow lavas and massive flows are overlain by lower Oligocene vitric tuffs. The lavas constituted two rock types: high-MgO bronzite andesites of the boninite series and basalts of the island-arc tholeiite series. At Site 459, a series of pillow lavas, massive flows, and possible sills are overlain by middle Eocene claystones. The rock types are basalts and andesites transitional between the boninite and island-arc tholeiite series. Igneous rocks were also recovered at Sites 460 and 461, on the deep inner trench wall of the Mariana Trough, as cobbles of basalts, metabasalts, and metagabbros in conglomerate beneath Eocene sediment or admixed with younger sediment. Fragments of calpionellid limestone of Mesozoic age also were recovered at Site 460 (Azema and Blanchet, 1981), possibly from a subducted seamount accreted to the inner trench wall.

The rocks recovered from the forearc provide us an opportunity for investigations of forearc petrogenesis. Of particular interest are the volcanic rocks of the boninite series, the type locality of which is in the Izu-Bonin Islands, which are predominantly, perhaps uniquely, associated with oceanic terranes and ophiolite complexes that were thought to have formed above subduction zones (e.g., Cameron et al., 1979). Boninite is described petrographically by a phenocryst assemblage dominated by orthopyroxene and/or clinoenstatite, commonly accompanied by olivine; plagioclase is characteristically absent, except in highly fractionated members of the series (e.g., Shiraki et al., 1980). The formation of boninite series rocks appears to require variable degrees of hydrous

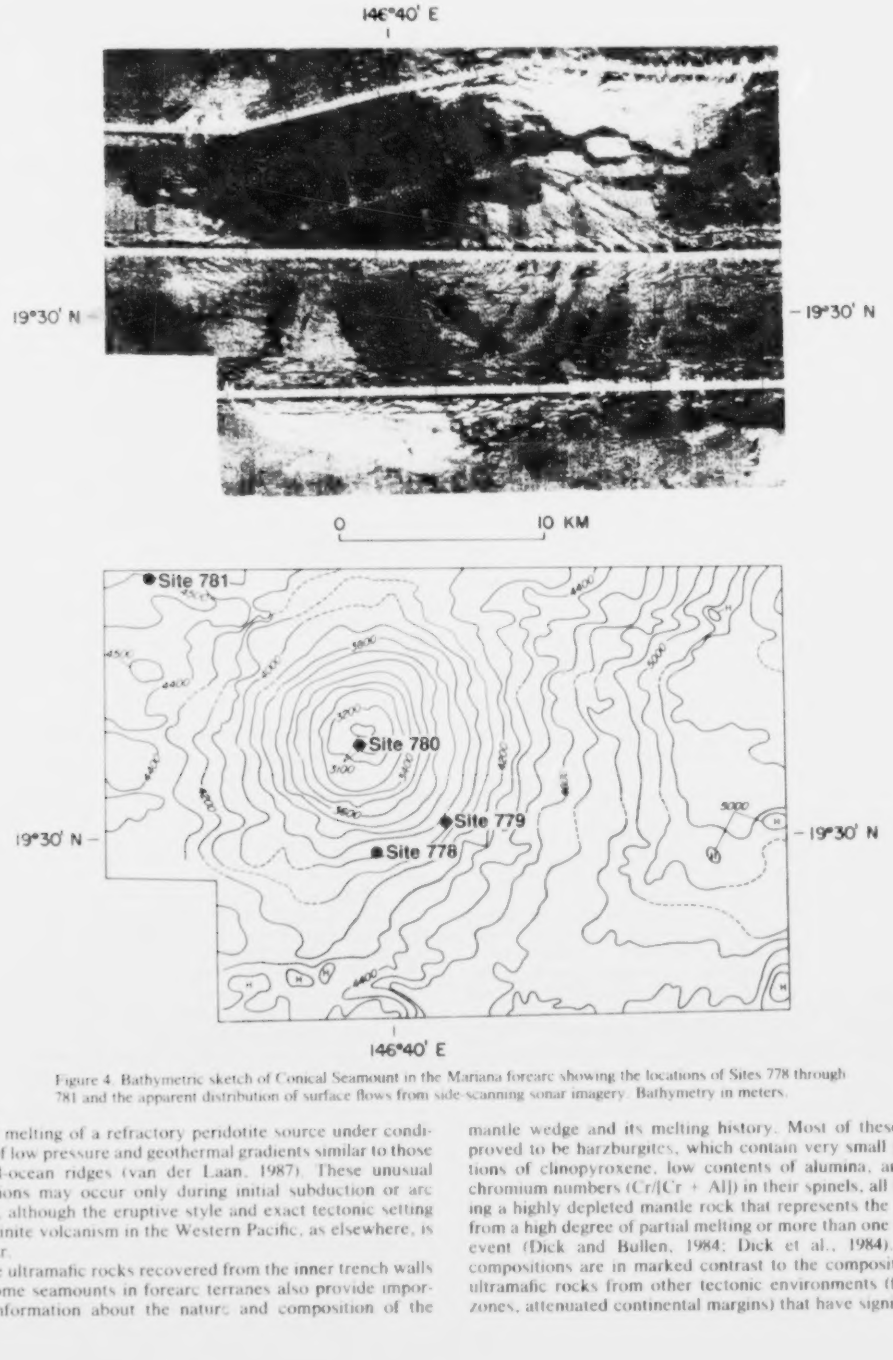

Figure 4. Bathymetric sketch of Conical Seamount in the Mariana forearc showing the locations of Sites 778 through 781 and the apparent distribution of surface flows from side-scanning sonar imagery. Bathymetry in meters.

partial melting of a refractory peridotite source under conditions of low pressure and geothermal gradients similar to those at mid-ocean ridges (van der Laan, 1987). These unusual conditions may occur only during initial subduction or arc rifting, although the eruptive style and exact tectonic setting of boninite volcanism in the Western Pacific, as elsewhere, is unclear.

The ultramafic rocks recovered from the inner trench walls and some seamounts in forearc terranes also provide important information about the nature and composition of the mantle wedge and its melting history. Most of these rocks proved to be harzburgites, which contain very small proportions of clinopyroxene, low contents of alumina, and high chromium numbers (Cr/[Cr + Al]) in their spinels, all indicating a highly depleted mantle rock that represents the residue from a high degree of partial melting or more than one melting event (Dick and Bullen, 1984; Dick et al., 1984). These compositions are in marked contrast to the compositions of ultramafic rocks from other tectonic environments (fracture zones, attenuated continental margins) that have significantly

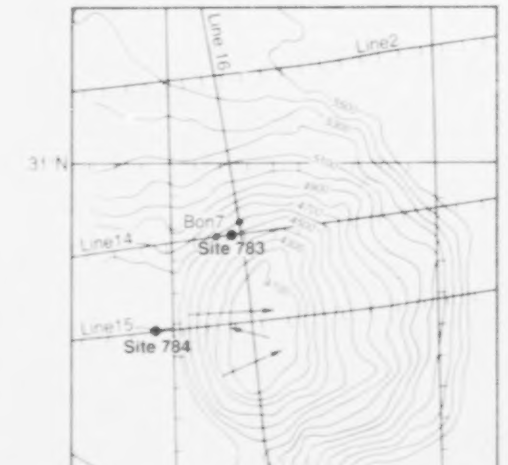

Figure 5. Bathymetric sketch of the Torishima Forearc Seamount drilled at Sites 783 and 784.

more clinopyroxene, more alumina, and more aluminous spinels (Bonatti and Michael, 1989).

Many authors now ascribe a majority of ophiolites to subduction-related settings because of their chemistry and associated sediments. Pearce et al. (1984) proposed the use of the term "supra-subduction zone (SSZ) ophiolites" to describe ophiolites having the geochemical characteristics of island arcs, but the structure of oceanic crust. They proposed that many SSZ ophiolites (including the Troodos Massif of Cyprus and the Semail Nappe of Oman) may have formed by seafloor spreading during the initial stages of subduction prior to the development of any major volcanic arc. The association between ophiolite formation and forearcs has also been noted by marine geologists and petrologists studying the rocks recovered from the inner trench wall, and several authors have used the term "ophiolitic" to describe forearc basement (e.g., Ogawa and Naka, 1984; Bloomer and Hawkins, 1983). The absence of any extant examples, however, has meant that the exact setting, or settings, of formation of SSZ ophiolite complexes are still the subject of debate. Thus, the more comprehensive understanding of forearc basement is needed to establish the precise relationship between ophiolite complexes and forearc terranes.

From the available data, it therefore appears that the present 150- to 220-km-wide Izu-Bonin and Mariana forearcs formed in large part by volcanism during the initial stages of arc development in the Eocene and early Oligocene. Prior to this leg, there has been no evidence for any subsequent volcanic activity within these forearcs. However, basement beneath the thickly sedimented forearc basin between the active volcanic arc and the break in slope of the inner wall of the trench has never been sampled. One of the main objectives of Leg 125 (Sites 782, 785, and 786) was to penetrate basement in the Izu-Bonin forearc basin. The existing evidence also suggests that mobilization of the forearc mantle wedge by serpentinization and diapiric intrusion is an important phenomenon in the region between the outer-arc high and the trench. The study of this process was another major objective of Leg 125 (Sites 778 through 781, 783, and 784).

FOREARC EVOLUTION

Three main alternative hypotheses can be postulated for the origin and evolution of this forearc terrane: (1) the volcanic arc and outer-arc high may have originally been continuous and subsequently separated by forearc spreading; (2) the volcanic arc and outer-arc high may have been built separately, but nearly synchronously, on former Philippine Sea Plate crust; or (3) the terrane may form part of a continuous Eocene arc volcanic province, possibly with overprints of later forearc volcanism.

Each scenario for the development of forearc basement implies a different crustal structure for the forearcs. Multichannel seismic (MCS) surveys of the Izu-Bonin forearc (B. Taylor, pers. comm., 1989) revealed a complicated basement that in many places is seismically stratified and cut by dipping reflectors. These reflection characteristics are unlike those of normal oceanic crustal sections and suggest that the Eocene volcanism may have been accompanied by tectonic activity and/or that it was superimposed on an older arc terrane, such as the Amami Plateau. The Izu-Bonin forearc basin drill sites (Sites 782, 785, and 786) were aimed at investigating the hitherto unstudied forearc basement to constrain some of these models of forearc evolution.

The presence of subduction-related igneous rocks near the trench, together with observations of normal faulting in the forearc and interpretations of outer-arc subsidence, have been cited as evidence for large-scale removal of Mariana forearc material by tectonic erosion since the late Eocene (Hussong and Uyeda, 1981). This analysis was subsequently questioned by Karig and Rankin (1983), who inferred that the Mariana forearc did not undergo significant tectonic subsidence or erosion. Likewise, in the Izu-Bonin forearc, the presence of shallow-water Eocene fossils on the Ogasawara Islands and of a well-developed submarine canyon system and lower-slope terrace elsewhere in the forearc suggest that fairly stable conditions have prevailed since the anomalous Eocene phase of arc-basin development. We hope that data from Leg 125 will enable us to test this hypothesis by providing the information needed to model the uplift-subsidence history across the forearc, using backstripping techniques for cored and logged holes and seismic stratigraphic analyses of interconnecting MCS profiles. Microstructures in the drill cores should also help us to determine the intensity of faulting in space and time across the forearc terrane.

Another fundamental question is whether the volcanic arc and outer-arc high developed by igneous construction or by differential uplift, or whether the upper-slope basin between them was caused by forearc spreading or differential subsidence, or whether flexural loading, either by arc volcanoes or by coupling with the subducting plate, is an important process. Determining the vertical displacement field of the forearc should provide some of the information about forearc flexure and basin development necessary for scientists to evaluate these hypotheses.

The forearc stratigraphy should also record a history of the variations in intensity and chemistry of arc volcanism. Currently, a number of conflicting models exist relating variations in arc volcanism to variations in tectonic processes. Karig (1975) proposed that periods of arc volcanic maxima correlated with periods of marginal basin formation and high subduction rate. Scott and Kroenke (1981) suggested rather that initial periods of backarc spreading are coincident with minimal arc volcanism. Contrary to both hypotheses, Hussong and Uyeda (1981) inferred that arc volcanism has probably been continuous since the Eocene, but that the initiation of backarc spreading by arc rifting produced drastic subsidence of the arc volcanoes, resulting in deep-water eruptions with limited lateral transport of volcanic material. Studies of he tephrachronology, and the frequency and geochemistry of ash and pyroclastic flow deposits in the forearc basin drill cores, will enable scientists to evaluate these various models. Such studies may also enable us to test whether boninitic Beccaluva et al., 1980), alkalic (Stern et al., 1984), and/or rhyodacitic (Gill et al., 1984; Fryer et al., 1985a) volcanism characterizes periods of arc rifting.

Interpretation of the evolution of the forearc terranes must also take into account post-Eocene terrane rotations. Paleomagnetic studies of the rocks recovered from DSDP Legs 31 and 60 in the Izu-Bonin and Mariana forearc suggested that 20° of northward translation has taken place since the Eocene, and paleomagnetic results from subaerial portions of the Izu-Bonin forearc indicate 90° of clockwise rotation since the Eocene (Keating et al., 1983). These data have been used to suggest that the Philippine Sea Plate has rotated like a ball bearing in response to motion between the Pacific and Eurasian plates. The rotation of the Philippine Sea Plate as a whole is further supported by paleomagnetic results from the Palau Islands (Haston et al., 1988), which point to 60° to 70° of clockwise rotation of the Philippine Sea Plate since the mid-Oligocene. Along the Mariana arc, paleomagnetic results from Guam (Larson et al., 1975; Fuller, unpubl. data) and Saipan (Fuller et al., 1980) also indicate clockwise rotations. McCabe and Uyeda (1983) proposed that the clockwise rotations of Guam and Saipan were associated with deformation of the Mariana arc in response to the collision of the Caroline Ridge. Paleomagnetic studies of the Izu-Bonin forearc will further test and refine these models.

ORIGIN AND INTERNAL STRUCTURE OF SERPENTINITE SEAMOUNTS

Drilling into serpentinite at the Mariana and Izu-Bonin forearc Sites 778 through 781 and 783 through 784 provided scientists with an opportunity to address the problems of the nature and origin of serpentinite in nonaccretionary, intraoceanic forearcs and hence provide information about the development of the outer forearc regions of intraoceanic island arcs. Conical Seamount is one of only two Mariana forearc seamounts (the other is a seamount at latitude 14°N) where active protrusion of sedimentary serpentinite is known to be taking place. Conical Seamount therefore provides an *in-situ* locality for studying the formation and emplacement of sedimentary serpentinite seamounts.

Side-scanning sonar and bathymetry surveys (Hussong and Fryer, 1985; Fryer et al., 1987) have not defined the internal structure of the edifice. Two potential "end-member" types of structure exist: a "mushroom" structure in which serpentinite rises up a narrow neck and spreads out near the surface; and a "dome" structure in which the serpentinite rises from a certain depth as a diapiric or tumescent protrusion that is widest at its base and narrows toward the surface. The final shape will then be modified by mass flowage on the surface.

Sedimentary serpentinite deposits of probable forearc origin have been identified in the Great Valley Sequence of California (Phipps, 1984a, 1984b; Lagabrielle, 1987), and around the Mediterranean and Caribbean (e.g., Lockwood, 1971). However, none of these areas has been known to exhibit development of serpentinite protrusion on the scale of that in the Mariana system. Serpentinite protrusion also makes an important contribution to ancient, ophiolitic sequences, although it is not always certain whether these formed during oceanic crustal accretion and/or ocean closure (Lagabrielle et al., 1986; Lagabrielle, 1987).

Serpentinites have been recovered from other present-day oceanic environments, notably transform faults, slow-spreading mid-ocean ridges, and along passive margins. Passive margin serpentinites, thought to have been associated with the tensional tectonics and crustal thinning in the earliest stages of ocean opening, have been identified in a number of localities, such as on Red Sea islands and on the eastern Atlantic margin (e.g., Lagabrielle and Auzende, 1982; Bonatti and Michael, 1989), and were drilled at Site 637 during ODP Leg 103 on the Galicia margin (Shipboard Scientific Party, 1986). Serpentinites have been dredged from a number of large fracture zones in the Atlantic and Indian oceans (e.g., Dick et al., 1984; Kimball et al., 1985) and were recovered as cobbles when drilling at Sites 732 and 734 during ODP Leg 118 on the Southwest Indian Ridge (Robinson et al., 1988). Many serpentinites have been recovered from dredge hauls on the rift valley and rift mountain regions of the slow-spreading Mid-Atlantic Ridge and Mid-Indian Ocean Ridge, not associated with transform faults (Bonatti and Hamlyn, 1981); these were drilled by DSDP during Legs 37 (Shipboard Scientific Party, 1977) and 45 (Shipboard Scientific Party, 1976) and by ODP at Site 670 during Leg 109, at 23°09′N on the mid-Atlantic Ridge (Juteau et al., 1990).

The intrusion of serpentinite in these settings differs in a number of ways from serpentinites that originated above subduction zones. For example, along the Galicia margin where the general shape of the serpentinized mantle resembles the "dome" model, the serpentinite is exposed on a basement ridge similar in some respects to the Izu-Bonin seamount occurrences, not on an isolated, conical-shaped seamount as in the Mariana forearc.

The physical properties of the serpentinite seamounts, and the mechanism, mode of emplacement, and rate of uplift of each, were studied at all of the seamount sites (Sites 778 through 780 and 783 through 784) during Leg 125. Serpentinite protrusions (such as those in the Mariana forearc) may be able to entrain deep-seated fluids during formation and ascent and to lose these fluids during seepage of the serpentine flows onto the surface. There is strong evidence that the flows settled soon after they were erupted, perhaps as a result of the escape of entrained fluids. Once the rising serpentinite has stopped extruding and/or stopped venting fluids, it is likely that the density of the serpentinite will increase. The physical properties of the serpentinite thus may change with depth as well as with age. Documenting such changes and studying the physical properties of the seamount material will allow us to interpret in greater detail the sedimentary serpentinite deposits studied in subaerial exposures.

CHEMICAL FLUXES IN FOREARC TERRANES

An understanding of chemical fluxes at subduction zones is an essential prerequisite for investigating global geochemical mass balances. Currently, however, such fluxes are poorly defined. A major source of information comes from the study of the geochemistry of island-arc basalts, which has provided evidence for cycling of some trace elements, particularly the large-ion-lithophile elements, radiogenic strontium and lead, ^{10}Be, and volatile elements, such as water and chlorine (see the review in Gill, 1981). However, island-arc magmas may not be the sole pathway by which elements are recycled above subduction zones: fluid pathways may also exist within the forearc. Studies of interstitial waters from accretionary convergent plate margins revealed the importance of element transfer by fluid flow in accretionary wedges. These studies include those during

DSDP Legs 66 and 67 (Harrison et al., 1982; Gieskes et al., 1985) and Leg 84 (Hesse et al., 1985) in the Middle America Trench, during ODP Leg 110 on the Barbados Ridge (Shipboard Scientific Party, 1988a), and during ODP Leg 112 at the Peru continental margin (Shipboard Scientific Party, 1988b). The principal characteristics of these forearc fluids are low chlorinities and the presence of hydrocarbons, especially methane, which form gas hydrates, given appropriate temperatures, pressures, and partial pressure of the hydrocarbons.

By contrast, the nature and magnitude of fluid flow within the forearc at nonaccretionary margins still are poorly understood. In the Izu-Bonin-Mariana region, hydration of the crust and upper mantle of the forearc wedge is probably facilitated by the escape of fluids from the subducting Pacific Plate. Large regions beneath the forearc lie within the chlorite, greenschist, and blueschist stability fields (e.g., Sugimura and Uyeda, 1973). Widespread metamorphism of the forearc wedge might explain the apparent capacity of forearc regions to accommodate the potentially large volumes of fluid driven off a descending slab over millions of years of subduction (Fryer and Fryer, 1987).

The Mariana serpentinite seamounts provide access to the products of alteration and metamorphism of a central forearc region that have formed by reaction with components derived from the subducting slab, and through which we can trace the changes in pressure-temperature regimes of the deep forearc. At Conical Seamount (Sites 778–780), fluids are known to be seeping from carbonate and silicate chimneys on the summit of the seamount and are precipitating cements within the uppermost portion of the sedimentary serpentinite flows (Fryer et al., 1987). Drilling at Sites 778 through 780 thus provided scientists an opportunity to sample the escaping fluids and metamorphosed xenoliths within the serpentine flows. At the Torishima Forearc Seamount (Sites 783 and 784), on the seaward part of the forearc, there is no evidence of active fluid exhalation, but study of the serpentine sediments and flows, along with entrained clasts at this locality, may provide an indirect record of the composition and metamorphism of the Izu-Bonin forearc and also provide a limited basis for comparison of the two forearc terranes.

Studies of the composition of fluids actively seeping from chimney structures on Conical Seamount revealed fluids of high pH and high alkalinity that are enriched in CH_4 and H_2S. The presence of these gases is particularly interesting. Because the Mariana forearc has only a small volume of sedimentary substrate (Hussong and Uyeda, 1981) with organic carbon contents typically less than 0.3% (Schorno, 1981), the methane and sulfide in the Mariana vent fluids are unlikely to have formed by the biogenic processes associated with accretionary complexes (Kulm et al., 1986), unless sedimentary underplating is more extensive than hitherto believed. It is probable, therefore, that they were generated during serpentinization reactions. The chemical analyses of these fluids imply that interaction with deep-seated, perhaps subducted, fluids; interaction of seawater with crustal rocks, and interactions of seawater with the surficial serpentinite may all contribute to the composition of these fluids.

Trace-element and stable-isotopic compositions of the carbonate chimney materials and serpentinized matrix from Conical Seamount are consistent with a source of these fluids that is not the same as that in serpentinite and associated carbonates from other environments (Haggerty, 1987; R. Sakai et al., pers. comm., 1989). Compared to fracture zone carbonates thought to have a dominantly seawater origin, for example, Mariana aragonite is depleted in strontium (Mariana samples = 7,000–9,400 ppm; fracture zone aragonite = 9,500–11,600 ppm), enriched in magnesium (Mariana = 750–6,300 ppm, fracture zone, ppm), and has a significantly lighter carbon isotopic signature (Mariana = −1.2 to −21.2 ‰, fracture zone = +0.03 to +1.12 ‰) and heavier oxygen isotopic signature (Mariana = +5.1 to +7.6 ‰, fracture zone = +3.16 to +4.87 ‰). These differences may indicate that serpentinite-related fluids in forearcs contain components from either the forearc mantle or the subducted slab or both (Haggerty, 1987; R. Sakai et al., pers. comm., 1989). By detailed sampling at depth within the serpentinite body and in the neighboring country rock, it should be possible to constrain either the nature of the shallow level reactions influencing the fluid composition or the possible sources of the fluids.

DRILLING OBJECTIVES

The Izu-Bonin and Mariana regions are two of the best-studied intraoceanic arc-trench systems. Yet fundamental questions remain unanswered about their evolution with regard to arc/forearc magmatism and structure, arc/forearc stratigraphy and vertical tectonics, and outer forearc serpentinite diapirism. To address these questions, the Leg 125 objectives were designed as follows:

Mariana Site 781 and Izu-Bonin Sites 782, 785, and 786 were to investigate the following:

1. The vertical tectonic history of the forearc to provide information about (1) forearc flexure and basin development and (2) the extent of tectonic erosion;
2. The stratigraphy of the forearc with its record of (1) sedimentation, depositional environment, and paleoceanography and (2) the variations in intensity and composition of arc volcanism over time;
3. The nature of the igneous basement of the volcanic arc, outermost forearc, and the intervening basin as a source of information for the initial stages of subduction-related volcanism, the origin of boninites, and the formation of the 200-km-wide arc-type forearc crust; and
4. The microstructural deformation and the large-scale rotation and translation of the forearc.

Mariana Sites 778 through 780 and Bonin Sites 783 and 784 were to investigate the following:

1. The timing and mechanism of emplacement of the serpentinite seamounts, including their internal fabric, fracture patterns, and flow structures;
2. The conditions at depth in the outer forearc from the igneous and metamorphic petrology of the lower crust and upper mantle rocks;
3. The chemistry, and hence source, of the associated fluids; and
4. The nature of regional fluid fluxes in forearc regimes and, by implication, the transfer of material from the descending slab into the mantle wedge.

REFERENCES

Azema, J., and Blanchet, R., 1981. The Late Jurassic–Early Cretaceous *Calponella* in reworked pebbles from Deep Sea Drilling Project Site 460, Mariana Transect. In Hussong, D. M., Uyeda, S., et al., *Init. Repts. DSDP*, 60: Washington (U.S. Govt. Printing Office), 575–576.

Beal, K. L., 1986. Backarc spreading in the northern Mariana Trough [M.S. Thesis]. University of Hawaii.

Beccaluva, L., Macciotta, G., Savelli, C., 1980. Geochemistry and K/Ar ages of volcanics dredged in the Philippine Sea. *In* Hayes, D. E. (Ed.), *The Tectonic and Geologic Evolution of Southeast Asian Sea and Islands*. Washington (Am. Geophys. Union), 247–270.

Bloomer, S. H., 1983. Distribution and origin of igneous rocks from the landward slopes of the Mariana Trench. *J. Geophys. Res.*, 88:7411–7428.

Bloomer, S. H., and Hawkins, J. W., 1983. Gabbroic and ultramafic rocks from the Mariana Trench: an island arc ophiolite. *In* Hayes, D. E. (Ed.), *The Tectonic and Geologic Evolution of Southeast Asian Seas and Islands. Part II:* Washington (Am. Geophys. Union), Geophys. Ser. Mono., 27:294–317.

Bonatti, E., and Hamlyn, P. R., 1981. Oceanic ultramafic rocks. *In* Emiliani, C. (Ed.), *The Sea (Vol. 7):* New York (Wiley), 241–283.

Bonatti, E., and Michael, P. J., 1989. Mantle peridotite from continental rifts to ocean basins to subduction zones. *Earth Planet. Sci. Lett.*, 91:297–311.

Cameron, W. E., Nisbet, E. G., and Dietrich, V. J., 1979. Boninites, komatiites and ophiolitic basalts. *Nature*, 280:550–553.

Dick, H.J.B., and Bullen, T., 1984. Chromian spinel as a petrogenetic indicator in abyssal and Alpine-type peridotites and spatially associated lavas. *Contrib. Mineral. Petrol.*, 86:54–76.

Dick, H.J.B., Fisher, R. L., and Bryan, W. B., 1984. Mineralogic variability of the uppermost mantle along mid-ocean ridges. *Earth Planet. Sci. Lett.*, 69:58–106.

Dietrich, V., Emmermann, R., Oberhansli, R., and Puchelt, H., 1978. Geochemistry of basaltic and gabbroic rocks from the West Mariana Basin and the Mariana Trench. *Earth Planet. Sci. Lett.*, 39:127–144.

Fryer, P., Langmuir, C. H., Taylor, B., Zhang, Y., and Hussong, D. M., 1985a. Rifting of the Izu arc, III. Relationships of chemistry to tectonics. *EOS, Trans. Am. Geophys. Union*, 68:1534.

Fryer, P., Ambos, E. L., and Hussong, D. M., 1985b. Origin and emplacement of Mariana forearc seamounts. *Geology*, 13:774–777.

Fryer, P., and Fryer, G. J., 1987. Origins of nonvolcanic seamounts in a forearc environment. *In* Keating, B., Fryer, P., and Batiza, R. (Eds.), Seamounts, Islands, and Atolls: Washington (Am. Geophys. Union), Mono. Ser., 43:61–69.

Fryer, P., Haggerty, J., Tilbrook, B., Sedwick, P., Johnson, L., Saboda, K., Newsom, S., Karig, D., Uyeda, S., and Ishii, T., 1987. Results of *Alvin* studies of Mariana forearc serpentinite diapirism. *EOS, Trans. Am. Geophys. Union*, 68:1534. (Abstract)

Fuller, M., Dunn, J. R., Green, G., Lin, J. L., McCabe, R., Toney, K., and Williams, I., 1980. Paleomagnetism of Truk Islands, Eastern Carolines and of Saipan, Marianas. *In* Hayes, D. E. (Ed.), *The Tectonic and Geologic Evolution of Southeast Asian Seas and Islands:* Washington (Am. Geophys. Union), Geophys. Mono. Ser., 43:235–245.

Gieskes, J. M., Johnston, K., and Boehm, M., 1985. Appendix. Interstitial water studies. *In* von Huene, R., Auboin, J., et al., *Init. Repts. DSDP*, 84: Washington (U.S. Govt. Printing Office), 961–967.

Gill, J. B., 1981. *Orogenic Andesites:* New York-Berlin-Heidelberg (Springer-Verlag).

Gill, J. B., Stock, A. L., and Whelan, P. M., 1984. Volcanism accompanying backarc basin development in the southwest Pacific. *Tectonophysics*, 102:207–224.

Haggerty, J. A., 1987. Petrology and geochemistry of Neogene sedimentary rocks from Mariana forearc seamounts: implications for emplacement of the seamounts. *In* Keating, B., Fryer, P., and Batiza, R. (Eds.), *Seamounts, Islands and Atolls:* Washington (Am. Geophys. Union), Mono. Ser., 43:175–185.

Hanzawa, S., 1947. Eocene foraminifera from Haha-jima. *J. Paleontol.*, 21:254–259.

Harrison, W. E., Hesse, R., and Gieskes, J. M., 1982. Relationship between sedimentary facies and interstitial water chemistry of slope, trench and Cocos Plate sites from the Middle America Trench transect, active margin off Guatemala, Deep Sea Drilling Project Leg 67. *In* Aubouin, J., von Huene, R., et al., *Init. Repts. DSDP*, 67: Washington (U.S. Govt. Printing Office), 603–614.

Haston, R., Fuller, M., and Schmidtke, E., 1988. Paleomagnetic results from Palau, West Caroline Islands: a constraint on Philippine Sea plate motion. *Geology*, 16:654–657.

Hesse, R., Lebel, J., and Gieskes, J. M., 1985. Interstitial water chemistry of gas-hydrate bearing sections on the Middle America Trench slope, Deep Sea Drilling Project Leg 84. *In* von Huene, R., Aubouin, J. et al., *Init. Repts. DSDP*, 84: Washington (U.S. Govt. Printing Office), 727–737.

Hickey, R. L., and Frey, F. A., 1982. Geochemical characteristics of boninite series volcanics: implications of their source. *Geochem. Cosmochim. Acta*, 46:2099–2115.

Honza, E., and Tamaki, K., 1985. Bonin Arc. *In* Nairn, A.E.M., and Uyeda, S. (Eds.), *The Ocean Basins and Margins, Vol. 7, The Pacific Ocean:* New York (Plenum Press), 459–499.

Hussong, D. M., and Uyeda, S., 1981. Tectonic processes and the history of the Mariana Arc: a synthesis of the results of Deep Sea Drilling Project Leg 60. *In* Hussong, D. M., Uyeda, S., et al. (Eds.), *Init. Repts. DSDP*, 60: Washington (U.S. Govt. Printing Office), 909–929.

Hussong, D. M., and Fryer, P., 1985. Fore-Arc tectonics in the northern Mariana Arc. *In* Nasu, N., et al. (Eds.), *Formation of Active Ocean Margins:* Tokyo (Terra Scientific Publ. Co.), 273–290.

Ishii, T., Konishi, K., and Omura, A., 1981. Description of samples. *In* Kobayashi, K. (Ed.), *Preliminary Report of the Hakuho Maru Cruise KH80-3:* Tokyo (Ocean Res. Inst., Univ. of Tokyo), 105–165.

Ishii, T., 1985. Dredged samples from the Ogasawara fore-arc seamount or "Ogasawara Paleoland" fore-arc ophiolite. *In* Nasu, N., et al. (Eds.), *Formation of Active Ocean Margins:* Tokyo (Terra Scientific Publ. Co.), 307–342.

Ishii, T., Kobayashi, K., Shibata, T., Naka, J., Johnson, K., Ikehara, K., Iguchi, M., Konishi, K., Wakita, H., Zhang, F., Nakamura, Y., and Kayane, H., 1985. Description of samples from Ogasawara forearc, Ogasawara Plateau and Mariana Trough during KH84-1 Cruise. *In* Kobayashi, K. (Ed.), *Preliminary Report of the Hakuho Maru Cruise KH84-1:* Tokyo (Ocean Res. Inst., Univ. of Tokyo), 89–167.

Johnson, L. E., and Fryer, P., 1988. Oceanic plate material on the Mariana Forearc. *EOS, Trans. Am. Geophys. Union*, 69:1471.

Juteau, Th., Cannat, M., and Lagabrielle, Y., 1990. Serpentinized peridotites in the upper oceanic crust away from transform zones: a comparison of the results of previous DSDP and ODP legs. *In* Detrick, R., Honnorez, J., Bryan, W. B., Juteau, T., et al., *Proc. ODP, Sci. Results*, 106/109: College Station, TX (Ocean Drilling Program), 303–308.

Karig, D. E., 1975. Basin genesis in the Philippine Sea. *In* Ingle, J. C., Karig, D. E., et al., *Init. Repts. DSDP*, 31: Washington (U.S. Govt. Printing Office), 857–879.

Karig, D. E. Anderson, R. N., and Bibee, L. D., 1978. Characteristics of backarc spreading in the Mariana Trough. *J. Geophys. Res.*, 83:1213–1226.

Karig, D. E., and Ranken, D., 1983. Marine Geology of the forearc region, southern Mariana island arc. *In* Hayes, D. E. (Ed.), *The Tectonic and Geologic Evolution of Southeast Asian Seas and Islands, II:* Washington (Am. Geophys. Union), 266–280.

Keating, B., Kodama, K., and Helsley, C. E., 1983. Paleomagnetic results of the Bonin and Mariana Islands. *In* Shimozuru, D., and Yokoyama, I. (Eds.), *Arc Volcanism, Physics and Tectonics:* Tokyo (Terra Scientific Publ. Co.).

Kimball, K. L., Spear, F. S., and Dick, H.J.B., 1985. High temperature alteration of abyssal ultramafics from the Islas Orcadas Fracture Zone, South Atlantic. *Contrib. Mineral. Petrol.*, 91:307–320.

Kobayashi, K., and Nakada, M., 1979. Magnetic anomalies and tectonic evolution of the Shikoku inter-arc basin. *In* Uyeda, S., et al., (Eds.), *Advances in Earth and Planet. Sci.*, 6:391–402.

Kulm, L. D., et al., 1986. Oregon subduction zone: venting, fauna, and carbonates. *Science*, 231:561–566.

Kuroda, N., Shiraki, K., and Urano, H., 1988. Ferropigeonite quartz dacites from Chichi-jima, Bonin Islands: latest differentiates from boninite-forming magma. *Contrib. Mineral. Petrol.*, 100:129–138.

Lagabrielle, Y., 1987. Les ophiolites: marqueurs dl'histoire tectonique des domaines océaniques. Le cas des Alpes franco-italiennes (Queras-Piemont), comparaison les ophiolites d'Antalya (Turquie) et du Coast Range de Californie [Thèse]. Univ. of Brest.

Lagabrielle, Y., and Auzende, J. M., 1982. Active *in-situ* disaggregation of oceanic crust and mantle on Gorringe Bank: analogy with ophiolitic massifs. *Nature*, 297:490–493.

Lagabrielle, Y., Whitechurch, H., Marcoux, J., Juteau, T., Reuber, I., and Guillocheau, F., 1986. Obduction-related ophiolitic polymict breccias covering the ophiolites of Antalya (S.W. Turkey). *Geology*, 14:734–737.

Larson, E. E., Reynolds, R. L., Ozima, M., Aoki, Y., Kinoshita, H., Zasshu S., Kawai, N., Nakajima, T., Hirooka, K., Merrill, R., and Levi, S., 1975. Paleomagnetism of Miocene volcanic rocks from Guam and the curvature of the southern Mariana island arc. *Geol. Soc. Am. Bull.*, 86:346–350.

Lockwood, J. P., 1971. Sedimentary and gravity-slide emplacement of serpentinite. *Geol. Soc. Am. Bull.*, 82:919–936.

McCabe, R. and Uyeda, S., 1983. Hypothetical model for the bending of the Mariana Arc. *In* Hayes, D. E. (Ed.), *The Tectonic and Geologic Evolution of Southeast Asian Seas and Islands. Part II.* Washington (Am. Geophys. Union) Mono. Ser., 43:281–293.

Meijer, A., 1979. Primitive arc volcanism and a boninite series: Examples from western Pacific Island arcs. *In* Hayes, D. E. (Ed.), *The Tectonic and Geologic Evolution of Southeast Asian Seas and Islands. Part II.* Washington (Am. Geophys. Union), Mono. Ser., 43:269–282.

Natland, J. H., and Tarney, J., 1981. Petrologic evolution of the Mariana arc and backarc basin system—a synthesis of drilling results in the South Philippine Sea. *In* Hussong, D. M., Uyeda, S., et al., *Init. Repts. DSDP*, 60: Washington (U.S. Govt. Printing Office), 877–908.

Ogawa, Y., and Naka, J., 1984. Emplacement of ophiolitic rocks in forearc areas: examples from central Japan and Izu-Mariana-Yap island arc system. *Geol. Soc. (London) Spec. Publ.*, 13:292–304.

Pearce, J. A., Lippard, S. J., and Roberts, S., 1984. Characteristics and tectonic significance of supra-subduction zone ophiolites. *Geol. Soc. (London) Spec. Publ.*, 16:77–94.

Phipps, S. P., 1984a. Mesozoic ophiolitic olistostromes and Cenozoic imbricate thrust faulting in the northern California Coast Ranges: geology of the Mysterious Valley Area, Napa County . Princeton Univ., Princeton, NJ.

________, 1984b. Ophiolitic olistostromes in the basal Great Valley sequence, Napa County, northern California Coast Ranges. *Geol. Soc. Am. Spec. Pap.*, 198:103–125.

Reagan, M. K., and Meijer, 1984. Geology and geochemistry of early sea-volcanic rocks from Guam. *Bull. Geol. Soc. Am.*, 95:701–713.

Robinson, P. T., Von Herzen, R. P., and Adamson, A. C., 1988. *Ocean Drilling Program Leg 118 Preliminary Report.* College Station, TX (Ocean Drilling Program).

Saboda, K., and Fryer, P., 1987. Metamorphism of ultramafic samples from Conical Seamount, Alvin Dives 1987. *EOS, Trans. Am. Geophys. Union*, 68:1534.

Schorno, K. S., 1981. Geochemistry of carbon, International Phase of Ocean Drilling Project 60. *In* Hussong, D. M., and Uyeda, S., et al., *Init. Repts.DSDP*, 60: Washington, D.C. (U.S. Govt. Printing Office), 501–504.

Scott, R. B., and Kroenke, L. W., 1981. Periodicity of remnant arcs and back-arc basins of the South Philippine Sea. *Oceanologica Acta*, 4:193–202.

Sharaskin, A. Ya., Dobretsov, N. L., and Sobolev, N. V., 1980. Marianites: The clinoenstatite bearing pillow lavas associated with the ophiolite assemblage of the Mariana Trench. *In* Panayiotou, A. (Ed.), *Ophiolites: Proc. Int. Ophiolite Symp.(Cyprus)*, 473–479.

Shipboard Scientific Party, 1976. "Challenger" drills on Leg 45. *Geotimes*, 21:20–23.

________, 1977. Introduction and site reports. *In Aumento, F., Melson, W. G.*, et al., *Init. Repts. DSDP*, 37: Washington (U.S. Govt. Printing Office), 15–326.

________, 1986. Introduction, objectives, and principal results: Ocean Drilling Program Leg 103, West Galicia Margin. *In* Boillot, G., Winterer, E. L., Meyer, A. W., et al., *Proc. ODP, Init. Repts.*, 103: College Station, TX (Ocean Drilling Program), 3–17.

________, 1988a. Synthesis of shipboard results: Leg 110 transect of the northern Barbados Ridge. *In* Mascle, A., Moore, J. C., et al., *Proc. ODP, Init. Repts.*, 110: College Station, TX (Ocean Drilling Program), 577–591.

________, 1988b. Introduction, objectives, and principal results, Leg 112, Peru continental margin. *In* Suess, E., von Huene, R., et al., *Proc. ODP, Init. Repts.*, 112: College Station, TX (Ocean Drilling Program), 5–23.

Shiraki, K., Kuroda, N., Urano, H., and Maruyama, S., 1980. Clinoenstatite in boninites from the Bonin Islands, Japan. *Nature*, 285:31–32.

Stern, R. J., Smoot, N. C., and Rubin, M., 1984. Unzipping of the volcano arc, Japan. *Tectonophysics*, 102:153–174.

Sugimura, A., and Uyeda, S., 1973. *Developments in Geotectonics. 3. Island Arcs.* Amsterdam (Elsevier).

Taylor, B., 1984. Morphology of Bonin fore-arc submarine canyons. *Geology*, 12:724–727.

Taylor, B., and Smoot, N. C., 1984. Morphology of Bonin fore-arc submarine canyons. *Geology*, 12:724–727.

Tracey, J. L., Schlanger, S. O., Stark, J. T., Doan, D. B., and May, H. G., 1964. General geology of Guam. *U.S. Geol. Surv. Spec. Pap.*, 403-A:1–104.

Uyeda, S., and Ben-Avraham, Z., 1972. Origin and development of the Philippine Sea. *Nature*, 240:176–178.

Van der Laan, S., 1987. An experimental study of boninite genesis . Univ. of Chicago.

Ms 125A-101

Fryer, P., Pearce, J.A., Stokking, L.B., et al., 1990
Proceedings of the Ocean Drilling Program, Initial Reports, Vol. 125

2. EXPLANATORY NOTES[1]

Shipboard Scientific Party[2]

INTRODUCTION

Standard procedures for both drilling operations and pre- minary shipboard analysis of the material recovered during e Deep Sea Drilling Project (DSDP) and the Ocean Drilling rogram (ODP) have been amended regularly and upgraded nce drilling began in 1968. In this chapter, we have assem- ed information that will help the reader to understand the asis for our preliminary conclusions and also help the inter- sted investigator to select samples for further analysis. This formation concerns only shipboard operations and analyses escribed in the site reports in the *Initial Reports* volume of e Leg 125 *Proceedings of the Ocean Drilling Program*. ethods used by various investigators for shorebased analy- s of Leg 125 data will be described in the individual scientific ontributions published in the *Scientific Results* volume of the roceedings of the Ocean Drilling Program.

Authorship of Site Chapters

The separate sections of each site chapter were written by e following shipboard scientists (authors are listed in alpha- etical order in parentheses, no seniority is implied):

Principal Results: Fryer, Pearce
Background and Scientific Objectives: Fryer, Pearce
Operations: Pettigrew, Stokking
Lithostratigraphy: Haggerty, Heling, McCoy, Rigsby
Biostratigraphy: Ciampo, Milner, Stabell, Xu
Igneous and Metamorphic Petrology: Arculus, Johnson, Ishii, Maekawa, Murton, Saboda, van der Laan
Igneous and Metamorphic Geochemistry: Arculus, Johnson, Ishii, Maekawa, Murton, Saboda, van der Laan
Sediment/Fluid Geochemistry: Mottl
Structural Studies: Lagabrielle, Phipps
Paleomagnetism: Ali, Haston, Stokking
Sediment-Accumulation Rates: Ali, Ciampo, Stabell
Physical Properties: Ballotti, Burke, Marlow
Downhole Measurements: Hobart, Marlow
Summary and Conclusions: Fryer, Pearce, Stokking

Following the text of each site chapter are summary core escriptions ("barrel sheets" and igneous-rock visual core escriptions) and photographs of each core.

Survey Data

Survey data collected prior to Leg 125 and used in the site selection process are discussed in Fryer et al. and Horine et al. (this volume). The underway geophysical data collected aboard *JOIDES Resolution* during Leg 125 are discussed in a separate "Underway Geophysics" chapter (this volume). The underway data include bathymetry, magnetics, and seismic-reflection profiles.

Drilling Characteristics

Water circulation down the hole is open, hence cuttings are lost onto the seafloor and cannot be examined. The only available information about sedimentary stratification in uncored or unrecovered intervals, other than from seismic data or wireline-logging results, is from an examination of the behavior of the drill string as observed and recorded on the drilling platform. Typically, the harder a layer, the slower and more difficult it is to penetrate. A number of other factors, however, determine the rate of penetration, so it is not always possible to relate drilling time directly to the hardness of the layers. Bit weight and revolutions per minute, recorded on the drilling recorder, influence the penetration rate.

Drilling Deformation

When cores are split, many show signs of significant sediment disturbance, including the concave-downward appearance of originally horizontal bands, haphazard mixing of lumps of different lithologies (mainly at the tops of cores), and the near-fluid state of some sediments recovered from tens to hundreds of meters below the seafloor. Core deformation probably occurs during any of several steps in which the core may experience stresses sufficient to alter its physical characteristics: cutting, retrieval (with accompanying changes in pressure and temperature), and core handling on deck.

Shipboard Scientific Procedures

Numbering of Sites, Holes, Cores, Sections, and Samples

ODP drill sites are numbered consecutively from the first site drilled by the *Glomar Challenger* in 1968. A site number refers to one or more holes drilled while the ship was positioned over one acoustic beacon. Multiple holes may be drilled at a single site by pulling the drill pipe above the seafloor (out of the hole), moving the ship some distance from the previous hole, and then drilling another hole.

For all ODP drill sites, a letter suffix distinguishes each hole drilled at the same site. For example, the first hole drilled is assigned the site number modified by the suffix *A*, the second hole takes the site number and suffix *B*, and so forth. Note that this procedure differs slightly from that used by DSDP (Sites 1 through 624), but prevents ambiguity between site- and hole-number designations. It is important, for sampling purposes, to distinguish among holes drilled at a site, because recovered sediments or rocks from different holes usually do not come from equivalent positions in the stratigraphic column.

The cored interval is measured in meters below seafloor (mbsf). The depth interval assigned to an individual core begins with the depth below the seafloor where coring began and extends to the depth where coring ended (see Fig. 1). For example, each coring interval is generally up to 9.5 m long.

---

[1] Fryer, P., Pearce, J. A., Stokking, L. B., et al., 1990. *Proc. ODP, Init. Repts.*, 125: College Station, TX (Ocean Drilling Program).

[2] Shipboard Scientific Party is as given in the list of participants preceding the contents.

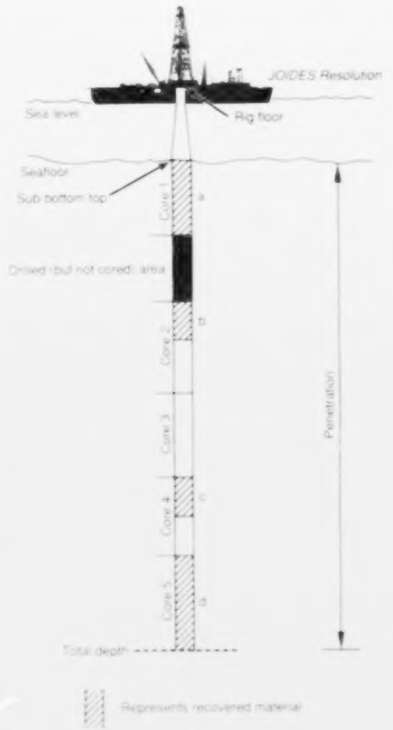
JOIDES Resolution
Sea level
Rig floor
Seafloor
Sub-bottom top
Core 1
a
Drilled (but not cored) area
Core 2
b
Core 3
Core 4
c
Core 5
d
Penetration
Total depth
Represents recovered material

Bottom felt: distance from rig floor to seafloor (number written on the white board)
Total depth: distance from rig floor to the bottom of the hole
Penetration: distance from seafloor to the bottom of the hole
Number of cores: total of all cores recorded, including cores with no recovery
Total length of cored section: distance from sub-bottom top to total depth minus drilled (but not cored) areas in between
Total core recovered: total from adding a, b, c, and d in the diagram
Core recovery (%): equals TOTAL CORE RECOVERED divided by TOTAL LENGTH OF CORED SECTION times 100 (See Fig. 2, "Explanatory notes", *Proc. ODP, Init. Repts.*, Vol. 122)

Figure 1. Coring and depth intervals.

which is the length of a core barrel. Coring intervals may be shorter and may not necessarily be adjacent, if separated by drilled intervals. In soft sediments, the drill string can be "washed ahead" with the core barrel in place, without recovering sediments. This is achieved by pumping water down the pipe at high pressure to wash the sediment out of the way of the bit and up the space between the drill pipe and the wall of the hole. If thin, hard rock layers are present, then it is possible to get "spotty" sampling of these resistant layers within the washed interval, and thus to have a cored interval greater than 9.5 m. When drilling hard rock, a center bit may replace the core barrel if it is necessary to drill without core recovery.

Cores taken from a hole are numbered serially from the top of the hole downward. Core numbers and their associated cored intervals in meters below seafloor usually are unique in a given hole; however, this may not be true if an interval must be cored twice, because of caving of cuttings or other hole problems. Maximum full recovery for a single core is 9.5 m of rock or sediment contained in a plastic liner (6.6-cm internal diameter) plus about 0.2 m (without a plastic liner) in the core catcher (Fig. 2). The core catcher is a device at the bottom of the core barrel that prevents the core from sliding out while the barrel is being retrieved from the hole. In certain situations (e.g., when coring gas-charged sediments that expand while being brought on deck) recovery may exceed the 9.5-m maximum.

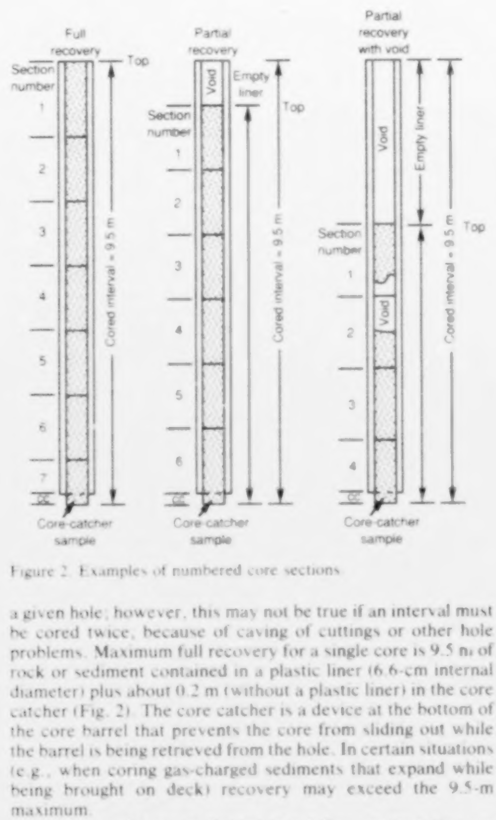
Full recovery
Section number
Top
1
2
3
4
5
6
7
CC
Cored interval = 9.5 m
Core-catcher sample
Partial recovery
Void
Empty liner
Section number
Top
1
2
3
4
5
6
CC
Cored interval = 9.5 m
Core-catcher sample
Partial recovery with void
Void
Empty liner
Section number
Top
1
Void
2
3
4
Cored interval = 9.5 m
Core-catcher sample

Figure 2. Examples of numbered core sections.

A recovered core is divided into 1.5-m sections that are numbered serially from the top (Fig. 2). When full recovery is obtained, the sections are numbered from 1 through 7 (the last section may be shorter than 1.5 m, and, rarely, an unusually long core may require more than seven sections). When less than full recovery is obtained, there will be as many sections as needed to accommodate the length of the core recovered; for example, 4 m of core would be divided into two 1.5-m sections and a 1-m section. If cores are fragmented (recovery less than 100%), sections are numbered serially and intervening sections are noted as void, whether shipboard scientists believe that the fragments were contiguously *in situ* or not. In rare cases, a section less than 1.5 m may be cut to preserve features of interest (e.g., lithological contacts).

By convention, material recovered from the core catcher is placed below the last section when the core is described and labeled core catcher (CC); in sedimentary cores, this material is treated as a separate section. The core catcher is placed at the top of the cored interval in cases where material is recovered only in the core catcher. However, information supplied by the drillers or by other sources may permit more precise interpretation of the correct position of core-catcher material within an incompletely recovered cored interval.

A recovered rock (basalt, gabbro, peridotite, or serpentinite) core is also cut into 1.5-m sections that are numbered serially; however, each piece of rock is then assigned a

ber. Fragments of a single piece are assigned a single
ber, and individual fragments are identified alphabeti-
y. The core-catcher sample is placed at the bottom of the
section and is treated as part of the last section, rather
as a separate section. Scientists completing visual core
criptions describe each lithologic unit, noting core and
ion boundaries only as physical reference points.

When, as is usually the case, the recovered core is shorter
the cored interval, by convention, the top of the core is
ated with the top of the cored interval to achieve consist-
y in handling the analytical data derived from the cores.
nples removed from the cores are designated by the
ance measured in centimeters from the top of the section
he top and bottom of each sample removed from that
ion. In curated hard-rock sections, sturdy plastic spacers
placed between pieces that did not fit together to protect
m from damage in transit and in storage; therefore, the
timeter interval noted for a hard-rock sample has no direct
ationship to the depth of that sample within the cored
erval, but is only a physical reference to the location of the
nple within the curated core.

A full identification number for a sample consists of the
owing information: leg, site, hole, core number, core type,
tion number, piece number (for hard rock), and interval in
timeters measured from the top of section. For example, a
nple identification of "125-778A-10R-1, 10–12 cm" would
interpreted as representing a sample removed from the
erval between 10 and 12 cm below the top of Section 1,
re 10 (R designates that this core was taken with the rotary
e barrel) of Hole 778A during Leg 125.

All ODP core and sample identifiers indicate core type. The
lowing abbreviations are used: R = rotary core barrel
CB); H = hydraulic piston core (HPC; also referred to as
C, or advanced hydraulic piston core); P = pressure core
rel; X = extended core barrel (XCB); B = drill-bit recov-
; C = center-bit recovery; I = *in-situ* water sample; S =
ewall sample; W = wash-core recovery; and M = miscel-
eous material. APC, XCB, and RCB cores were cut during
g 125.

Core Handling

diments

As soon as a core has been retrieved on deck, a sample is
ken from the core catcher and taken to the paleontological
oratory for an initial age assessment. The core is then
iced on the long horizontal rack, and gas samples may be
en by piercing the core liner and withdrawing gas into a
cuum tube. Voids within the core are sought as sites for
s sampling. Some of the gas samples are stored for
orebased study, but others are analyzed immediately as
rt of the shipboard safety and pollution-prevention pro-
am. Next, the core is marked into section lengths, each
ction is labeled, and the core is cut into sections. Intersti-
l-water (IW) and organic geochemistry (OG) samples are
en taken. In addition, some headspace gas samples are
raped from the ends of cut sections on the catwalk and
aled in glass vials for light hydrocarbon analysis. Each
ction is then sealed at the top and bottom by gluing on
lor-coded plastic caps: blue to identify the top of a section
d clear for the bottom. A yellow cap is placed on section
ds from which a whole-round sample has been removed.
e caps are usually attached to the liner by coating the end
the liner and the inside rim of the cap with acetone, and
en the caps are taped to the liners.

These cores then are carried into the laboratory, where the
ctions are again labeled, using an engraver to mark permanently the full designation of the section. The length of the core in each section and the core-catcher sample are measured to the nearest centimeter; this information is logged into the shipboard CORELOG data-base program.

Next, the whole-round sections from APC and XCB cores are run through the multisensor track (MST). This includes the GRAPE (gamma-ray attenuation porosity evaluator) and *P*-wave logger devices, which measure the bulk density, porosity, and sonic velocity, and also includes a meter that determines the volume magnetic susceptibility. After the core has equilibrated to room temperature (approximately 3 hr), thermal conductivities are measured, and the cores are split.

Cores of relatively soft material are split lengthwise into working and archive halves. The softer cores are split with a wire or saw, depending on the degree of induration. Harder cores are split with a band saw or diamond saw. Because cores during Leg 125 were split with wire from the bottom to top, older material may have been transported up the core on the split face of each section. Thus, one should be aware that the very near-surface part of the split core might be contaminated.

The working half is sampled for both shipboard and shore-based laboratory studies. Each extracted sample is logged into the sampling computer data-base program by its location and name of the investigator receiving the sample. Records of all removed samples are kept by the ODP curator. The samples are sealed in plastic vials or bags and labeled. Samples are routinely taken for analyzing shipboard physical properties. These samples are then used to determine calcium carbonate contents (coulometric analysis), and these data are reported in site chapters.

The archive half is described visually. Smear slides are made from samples taken from the archive half and are supplemented by thin sections taken from the working half. Sections from the archive half that do not show evidence of drilling disturbance are measured in the cryogenic magnetometer. The archive half is then photographed with both black-and-white and color film, a core at a time. Close-up photographs (black-and-white) are taken of particular features for illustrations.

Both halves of the core are then placed into labeled plastic tubes, sealed, and transferred to cold-storage space aboard the drilling vessel. At the end of the leg, the cores are transferred from the ship in refrigerated air-freight containers to cold storage at the Gulf Coast Repository at the Ocean Drilling Program, Texas A&M University, College Station, Texas.

Igneous and Metamorphic Rocks

Igneous and metamorphic rock cores are handled differently from sedimentary cores. Once on deck, the core catcher is placed at the bottom of the core liner, and total core recovery is calculated by shunting the rock pieces together and measuring to the nearest centimeter; this information is logged into the shipboard CORELOG data-base program. The core is then cut into 1.5-m-long sections and transferred into the laboratory.

The contents of each section are transferred into 1.5-m-long sections of split core liner, where the bottom of oriented pieces (i.e., pieces that clearly could not have rotated top to bottom about a horizontal axis in the liner) are marked with a red wax pencil. This is to ensure that orientation is not lost during splitting and labeling. The core is then split into archive and working halves. A plastic spacer is used to separate individual pieces, and/or reconstructed groups of pieces, in the core liner. These spacers may represent a substantial interval of no recovery. Each piece is numbered sequentially from the top of each section, beginning with number 1; reconstructed groups of pieces are assigned the same number, but are lettered consecutively. Pieces are labeled on the rounded, not sawn, surfaces. If the piece is oriented, an arrow is added to the label pointing to the top of the section.

The working half is sampled for shipboard laboratory studies. Records of all samples are kept by the curator at ODP. Minicore samples are routinely taken for physical-properties and magnetic studies. Some of these samples are later subdivided for X-ray fluorescence (XRF) analysis and thin-sectioning, so that as many measurements as possible are performed using the same pieces of rock. At least one minicore is taken per lithologic unit when recovery permits, generally from the freshest areas of core. Additional thin sections, X-ray-diffraction (XRD) samples, and XRF samples are selected from areas of particular interest. Samples for shorebased studies are selected in a sampling party held after drilling has ended.

The archive half is described visually, then photographed with both black-and-white and color film, one core at a time. Both halves of the core are then shrink-wrapped in plastic to prevent rock pieces from vibrating out of sequence during transit, placed into labeled plastic tubes, sealed, and transferred to cold-storage space aboard the drilling vessel.

SEDIMENT CORE DESCRIPTION FORMS

Sediments and Sedimentary Rocks

Visual core descriptions, smear slide and thin-section descriptions, $CaCO_3$ concentrations, and biostratigraphic criteria provide the shipboard data for core descriptions in this volume. Core description forms (Fig. 3) summarize these data and also indicate sample locations in the core. This information represents field notes taken on board ship under time constraints. In some cases, changes are made on the basis of post-cruise findings. However, production schedules prohibit modification of the core description forms with subsequent findings; therefore, occasional ambiguities or discrepancies may be present.

Core Designation

Cores are designated using leg, site, hole, core number, and core type as previously discussed (see "Numbering of Sites, Holes, Cores, Sections, and Samples" section, this chapter). In addition, the cored interval is specified in terms of meters below sea level (mbsl) and meters below seafloor (mbsf). On the basis of drill-pipe measurements (dpm), as reported by the SEDCO coring technician and the ODP operations superintendent, depths are corrected for the height above sea level of the dual elevator stool on the rig floor to give true water depth and the correct interval (mbsl).

Age Data

Abundance of microfossils, their preservation, and zone assignment, as determined by shipboard paleontologists, appear on the core-description form under the heading "Biostratigraphic Zone/Fossil Character." The geologic age determined from paleontological and/or paleomagnetic results is shown in the "Time-Rock Unit" column.

Calcareous nannofossils and planktonic foraminifers provided most of the age determinations in the forearc basin sites. Diatom biostratigraphy is critical on the seamount sites located beneath the carbonate compensation depth (CCD). Detailed information about zonations and terms used to report abundance and preservation is presented in the "Biostratigraphy" section (this chapter).

Paleomagnetic, Physical-Properties, and Chemical Data

Columns are provided on the core description form for recording paleomagnetic results, physical-properties values (wet-bulk density, porosity, and compressional-wave velocity) and chemical data (percentage of $CaCO_3$ determined by coulometric analysis, and total organic carbon calculated by difference between total carbon from nitrogen-carbon-sulfur (NCS) analysis and inorganic carbon from coulometric analysis. Additional information about shipboard procedures for collecting these types of data is found in "Paleomagnetism," "Physical Properties," and "Inorganic Geochemistry" sections (this chapter).

Graphic Lithology Column

The lithology of the recovered material is represented on the core description forms by a single symbol or by a group of two or more symbols (Fig. 4) in the column titled "Graphic Lithology." The symbols in a group correspond to end members of sediment constituents, such as clay or nannofossil ooze. For example, sediment composed of 20% nannofossils and 80% clay would be represented by the symbol for nannofossil ooze in 20% of the column and the symbol for clay in the remaining 80% of the column. Where different types of sediment are finely interbedded, symbols given in the column are schematic because the scale of the core description forms does not permit an accurate representation.

Some cores recovered during Leg 125 have intercalations of sedimentary material, as well as serpentine and serpentinite associated with igneous and metamorphic rocks. Intervals described by igneous and metamorphic petrologists are indicated by the symbol "IM" (see "Hard-Rock Core Description Forms" section, this chapter).

Sediment Disturbance

The coring technique, which uses a 25-cm-diameter bit with a 6-cm-diameter core opening, may result in varying degrees of mechanical disturbance of recovered core material. This is illustrated in the "Drilling Disturbance" column on the core description form (using the symbols in Fig. 5). Blank regions indicate a lack of drilling disturbance. Drilling disturbance is recognized for soft and firm sediments using these categories:

1. Slightly deformed: bedding contacts are slightly bent.
2. Moderately deformed: bedding contacts have undergone extreme bowing.
3. Highly deformed: bedding is completely disturbed, sometimes showing symmetrical diapirlike or flow structures.
4. Soupy: intervals are water-saturated and have lost all aspects of original bedding.

The degree of fracturing in indurated sediments and in metamorphic and igneous rocks is described using the following categories:

1. Slightly fractured: core pieces are in place and contain little drilling slurry or breccia.
2. Moderately fragmented: core pieces are in place or partly displaced, but original orientation is preserved or recognizable (drilling slurry may surround fragments).
3. Highly fragmented: pieces are from the interval cored and probably are in the correct stratigraphic sequence (al-

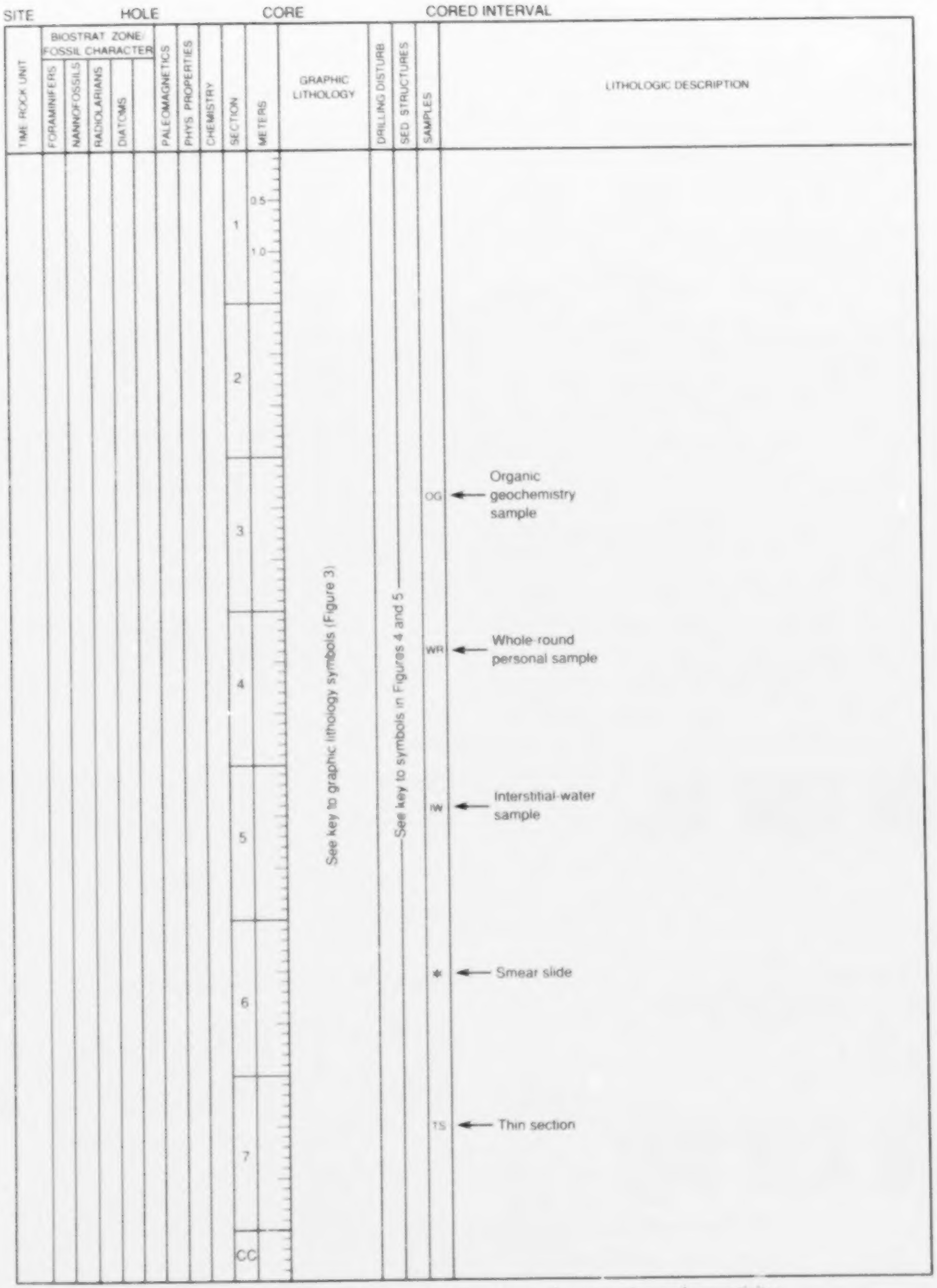
SITE
HOLE
CORE
CORED INTERVAL
TIME ROCK UNIT
BIOSTRAT. ZONE/ FOSSIL CHARACTER
FORAMINIFERS
NANNOFOSSILS
RADIOLARIANS
DIATOMS
PALEOMAGNETICS
PHYS. PROPERTIES
CHEMISTRY
SECTION
METERS
GRAPHIC LITHOLOGY
DRILLING DISTURB.
SED. STRUCTURES
SAMPLES
LITHOLOGIC DESCRIPTION
0.5
1.0
1
2
3
4
5
6
7
CC
See key to graphic lithology symbols (Figure 3)
See key to symbols in Figures 4 and 5
OG
Organic geochemistry sample
WR
Whole-round personal sample
IW
Interstitial-water sample
*
Smear slide
TS
Thin section

Figure 3. Visual core description forms used for sediments, sedimentary rocks, serpentine, and serpentinites.

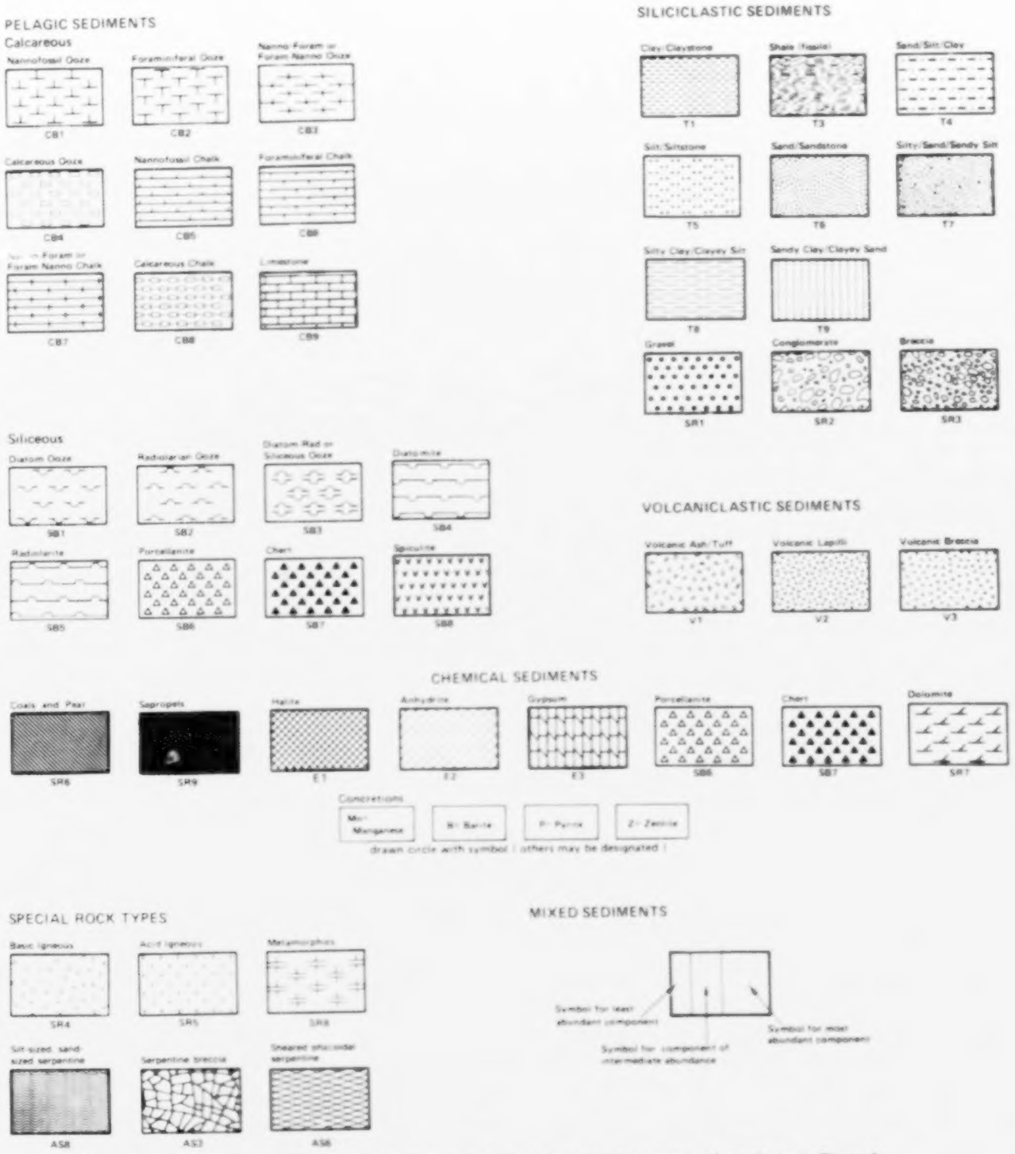
PELAGIC SEDIMENTS
Calcareous
Nannofossil Ooze
CB1
Foraminiferal Ooze
CB2
Nanno-Foram or Foram-Nanno Ooze
CB3
Calcareous Ooze
CB4
Nannofossil Chalk
CB5
Foraminiferal Chalk
CB6
Nanno-Foram or Foram-Nanno Chalk
CB7
Calcareous Chalk
CB8
Limestone
CB9
Siliceous
Diatom Ooze
SB1
Radiolarian Ooze
SB2
Diatom-Rad or Siliceous Ooze
SB3
Diatomite
SB4
Radiolarite
SB5
Porcellanite
SB6
Chert
SB7
Spiculite
SB8
SILICICLASTIC SEDIMENTS
Clay/Claystone
T1
Shale (fissile)
T3
Sand/Silt/Clay
T4
Silt/Siltstone
T5
Sand/Sandstone
T6
Silty/Sand/Sandy Silt
T7
Silty Clay/Clayey Silt
T8
Sandy Clay/Clayey Sand
T9
Gravel
SR1
Conglomerate
SR2
Breccia
SR3
VOLCANICLASTIC SEDIMENTS
Volcanic Ash/Tuff
V1
Volcanic Lapilli
V2
Volcanic Breccia
V3
CHEMICAL SEDIMENTS
Coals and Peat
SR6
Sapropels
SR9
Halite
E1
Anhydrite
E2
Gypsum
E3
Porcellanite
SB6
Chert
SB7
Dolomite
SR7
Concretions
M= Manganese
B= Barite
P= Pyrite
Z= Zeolite
drawn circle with symbol (others may be designated)
SPECIAL ROCK TYPES
Basic Igneous
SR4
Acid Igneous
SR5
Metamorphics
SR8
Silt-sized, sand-sized serpentine
AS8
Serpentine breccia
AS3
Sheared phacoidal serpentine
AS6
MIXED SEDIMENTS
Symbol for least abundant component
Symbol for component of intermediate abundance
Symbol for most abundant component

Figure 4. Key to symbols used in the "Graphic Lithology" column on the visual core description form shown in Figure 3.

Figure

thou
origi
4.
orien
drillin

In
ated
tures
ture'
used
phys
(incl
sedin

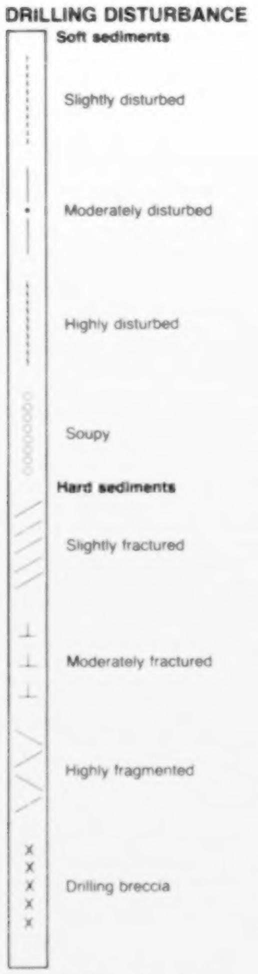
DRILLING DISTURBANCE
Soft sediments
Slightly disturbed
Moderately disturbed
Highly disturbed
Soupy
Hard sediments
Slightly fractured
Moderately fractured
Highly fragmented
Drilling breccia

. Symbols used for drilling disturbance.

they may not represent the entire section), but their orientation is completely lost.

rilling breccia: core pieces have lost their original ion and stratigraphic position and may be mixed with slurry.

Sedimentary and Tectonic Structures

ediment cores, natural structures and structures cre- coring can be difficult to distinguish. Natural struc- bserved are indicated in the "Sedimentary Struc- column of the core description form. The symbols describe the primary structures (both biogenic and l sedimentary structures) and secondary structures ing tectonic structures) are shown in Figure 6. A ntary structure observed frequently in sediments

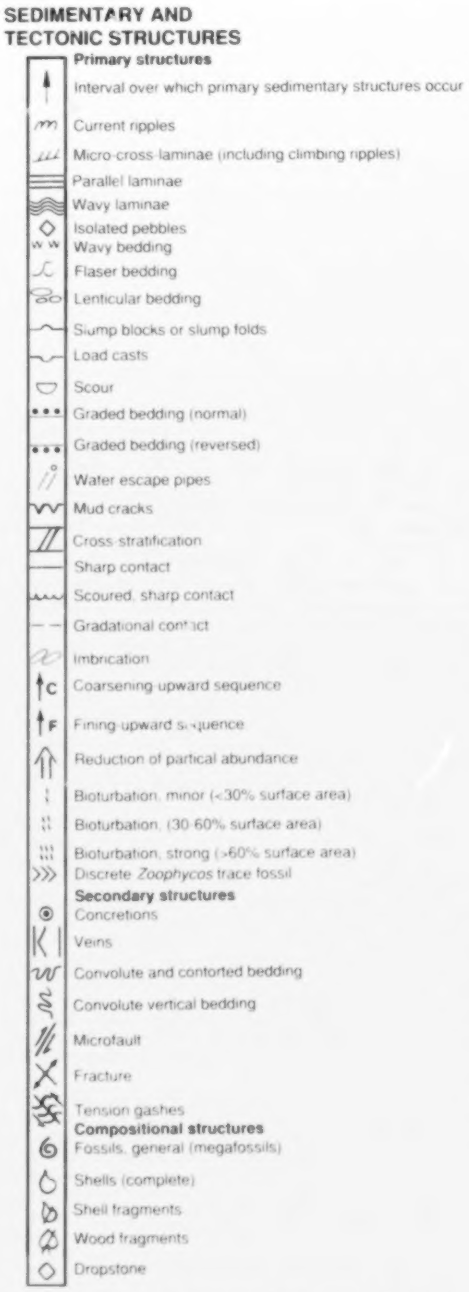
SEDIMENTARY AND TECTONIC STRUCTURES
Primary structures
Interval over which primary sedimentary structures occur
Current ripples
Micro-cross-laminae (including climbing ripples)
Parallel laminae
Wavy laminae
Isolated pebbles
Wavy bedding
Flaser bedding
Lenticular bedding
Slump blocks or slump folds
Load casts
Scour
Graded bedding (normal)
Graded bedding (reversed)
Water escape pipes
Mud cracks
Cross-stratification
Sharp contact
Scoured, sharp contact
Gradational contact
Imbrication
Coarsening-upward sequence
Fining-upward sequence
Reduction of partical abundance
Bioturbation, minor (<30% surface area)
Bioturbation, (30-60% surface area)
Bioturbation, strong (>60% surface area)
Discrete Zoophycos trace fossil
Secondary structures
Concretions
Veins
Convolute and contorted bedding
Convolute vertical bedding
Microfault
Fracture
Tension gashes
Compositional structures
Fossils, general (megafossils)
Shells (complete)
Shell fragments
Wood fragments
Dropstone

Figure 6. Symbols used for sedimentary and tectonic structures.

from Leg 125 is a decreasing concentration upward or downward of particles of approximately equal size. This structure is often observed overlying and underlying beds of vitric ash, where the ash concentration decreases upward within the background sediment. This structure has been interpreted as the result of animal activity that has redistributed ash into the sediment (Bramlette and Bradley, 1942); there is little evidence at Leg 125 sites for bottom-current activity. This structure is termed "fining-upward" or "coarsening-upward" (in deference to existing definitions) or reduction of particle abundance. Convolute vertical bedding is a secondary structure commonly observed in the serpentine units on these seamounts. This structure is commonly associated with foliation, which affects the hardness of clasts within the breccia and is related to post-depositional movement.

Color

Colors of the recovered material (sedimentary, metamorphic, and igneous) are determined by comparison with the Munsell soil-color charts. Colors are determined immediately after the cores have been split because chemical changes may occur when sediments are exposed to the atmosphere; consequently, some colors are ephemeral in deep-sea sediments (Moberly and Klein, 1976). Information on core colors is given in the text of the "Lithologic Description" column on the core description forms.

Samples

The position of samples taken from each core for shipboard analysis is indicated in the "Samples" column on the core description form. The symbol "*" indicates the location of samples used for smear-slide analysis. The symbols "TS," "XRD," and "XRF" indicate the location of samples for shipboard thin sections, XRD analysis, and XRF analysis, respectively. In some cases, an attempt was made to prepare a thin section from material unsuitable for that purpose. Although these sections exist in the thin-section collection at ODP, their poor quality did not permit us to make detailed descriptions. The locations of these samples are indicated by the symbol "X." The symbols "IW," "OG," "PP," and "WR" designate the location of samples for whole-round, interstitial-water geochemistry, frozen organic geochemistry, physical-properties, and personal samples, respectively.

Although not indicated in the "Samples" column, positions of samples for routine physical-properties (porosity [%], wet-bulk density [g/cm^3], and velocity [m/s]) and geochemical (% $CaCO_3$, % organic carbon [OC]) analyses are indicated by a dot and analytical results are presented in the "Physical Properties" column and in the "Chemistry" column. Paleomagnetic results (intervals of normal and reversed polarity) are indicated in the "Paleomagnetics" column. Intervals for which polarity could not be determined are indicated by a question mark.

Shipboard paleontologists generally base their age determinations on core-catcher samples, although additional samples from other parts of the core may be examined when required. Examination of such samples may lead to the recognition of zonal boundaries in the core; these are indicated in the appropriate column. All paleontological sample locations are shown, even if the samples are barren.

Lithologic Description - Text

The lithologic description that appears on each core description form consists of two parts: (1) a heading that lists all the sediment types (see "Classification of Sediment and Sedimentary Rock" section, this chapter) observed in the core, and (2) a more detailed description of these sediments, including data about color, location in the core, significant features, etc. In cases where there are thin beds of minor lithology, a description, including location information, is included in the text, but the beds may be too thin (cm) to appear in the graphic lithology column.

Smear Slide Summary

A table summarizing data from smear slides and thin sections (where available) appears on each core description form. The table includes information about the section and interval from which the sample was taken, whether the sample represents a dominant ("D") or a minor ("M") lithology in the core, and the percentages of sand, silt, and clay, together with all identified components (total 100%). As explained in the following section, these data are used to classify and name the recovered material.

CLASSIFICATION OF SEDIMENT AND SEDIMENTARY ROCK

The sediment classification scheme used during Leg 125 is similar to classification schemes used for previous DSDP and ODP legs. It is descriptive, using composition and texture as the only criteria to define sediment or sedimentary rocks. A primary sediment name is based upon, and named after, a component (or components) that constitutes 60% or more of the sediment. This classification scheme differs from some prior DSDP and ODP sediment classifications in the use of compositional modifiers.

Data for classifying sedimentary material come principally from shipboard visual analyses of smear slides using a petrographic microscope. These are qualitative optical estimates of particle characteristics (mineralogy, biogenic type, grain size, relative particle abundance, etc.) and differ from quantitative analyses of grain size, carbonate content, mineralogy, etc. Smear slide estimates of distinctive major components are accurate to within 5%, but estimates of minor constituents are accurate only to within 10%.

Composition and Texture

The Leg 125 sediment classification is descriptive, rather than genetic, and rock types are classified by their composition and texture. For example, the genetic terms pelagic, hemipelagic, turbidite, debris flow, etc., do not appear in this classification. The term "clay" is used for clay minerals and terrigenous material less than 4 mm in size without regard to origin. Biogenic components of silt or clay size are not described in textural terms. Thus, nannofossils present as silt-sized biogenic grains do not yield the sediment name of "nannofossil silt." Shipboard sedimentologists chose to use this classification (1) to maintain an internal consistency when naming intermediate mixtures of nonbiogenic and/or biogenic components and (2) to provide simple descriptive modifiers that indicate the important components and their abundance in the sediments.

Induration of Sediments

Determination of induration is subjective. For calcareous sediments and sedimentary rocks, three classes of induration or lithification have been recognized (Gealy et al., 1971):

1. Soft: sediment has little strength, is readily deformed under the pressure of a finger or the broad blade of a spatula, and is termed "ooze."

2. Firm: sediment is partially lithified, readily scratched ith a fingernail or the edge of a spatula, and is termed chalk."

3. Hard: sediment is well lithified and cemented, is resistnt or impossible to scratch with a fingernail, and is termed limestone" or "dolomite."

A continuum exists for siliceous biogenic sediments and edimentary rocks between soft siliceous oozes, firm diatonites and radiolarites, and hard porcellanites and cherts. Two ategories of induration have been recognized:

1. Soft: a sediment core may be split with wire cutter and termed "ooze."

2. Hard: a core must be cut by a diamond saw, rather than wire, and is called "porcellanite" or "chert."

Rules for Classification

1. About 60% of a component or group of components e.g., total biogenic silica or biogenic carbonate) determines ne principal name. The following main names are used:

Nonbiogenic: If the total of a nonbiogenic component, xcept serpentine and/or aragonite, is greater than 60%, the nain name is determined by the dominant size(s) as defined in hepard (1954; see Fig. 7), using the size classes defined by Ventworth (1922; see Fig. 8). Materials containing 60% or nore of serpentine or aragonite are discussed in the section on Serpentine and Serpentinite Classification" (this chapter). xamples of nonbiogenic principal names are clay, silt, silty lay, or sand. The terms sand-sized, silt-sized, etc., may be dded to the name as a modifier.

Biogenic: If the total of biogenic components is greater han 60%, the principal name is "ooze," or the appropriate erm denoting sediment induration (see the following).

2. A value of 30% to 60% of a component qualifies for najor modifier status. The following terms are used as major nodifiers:

Nonbiogenic: silty, clayey, sandy, etc., or a specific minral composition (e.g., serpentine).

Biogenic carbonate: nannofossil, foraminifer, or calcareus (should be as specific as possible).

Biogenic silica: diatom, radiolarian, or siliceous biogenic should be as specific as possible).

3. A value of 10% to 30% of a component qualifies for ninor modifier status and is hyphenated with the word "rich" e.g., nannofossil-rich clay, serpentine-rich clay).

4. A value of 5% to 10% of an unusual, important omponent (e.g., serpentine, zeolite, organic carbon, dolonite, thulite) also qualifies for minor modifier status, but is yphenated with the word "bearing" (e.g., zeolite-bearing lay).

5. The most abundant component appears nearest the rincipal name. Major and minor modifiers are listed in order f decreasing abundance to the left of the principal name (e.g., oraminifer-rich nannofossil clay for a sediment containing 0% foraminifers, 30% nannofossils, and 60% clay).

6. Marl is defined as containing 30% to 60% $CaCO_3$, the emainder being mostly clay; thus, an ooze contains greater han 60% $CaCO_3$.

7. For nonbiogenic and calcareous sediments, the suffix "-stone" has been added to the main name if the core is ufficiently indurated that it had to be cut by the diamond saw.

8. For siliceous, indurated sediments, the term "porcellanite" describes a dull, brown to white, porous rock that contains clay, zeolites, or carbonate. Chert is denser and harder than porcellanite. These two siliceous rock types usually can be readily distinguished in hand specimen and are sufficient for shipboard descriptions.

VOLCANICLASTIC SEDIMENTS AND ROCKS

Because of difficulties in distinguishing volcanogenic sedimentation mechanisms (air fall, pyroclastic flow, debris flow, turbidity currents, etc.) in cores, the volcaniclastic classification scheme used during Leg 125 is primarily descriptive. Texture and composition are the only criteria used to define volcaniclastic sediments and rocks; the following scheme has been modified after schemes proposed and discussed by Schmid (1981), Fisher and Schmincke (1984), and others.

Textural terms used are those in common usage and are based upon grain size. For volcanic particles the terms "block," "lapilli," and "ash" are used; for nonvolcanic particles the standard Wentworth (1922) terminology is used (gravel, sand, silt, clay). The terms "breccia" and "conglomerate," denoting angular and rounded clasts, respectively, are applicable to both volcanic and nonvolcanic sediments and rocks. These textural names have been modified with compositional terms on the basis of composition of volcanic grains and clasts. For simplicity three major compositional terms are used: "vitric" for glass particles, "crystal" for mineral particles, and "lithic" for either volcanic or nonvolcanic rock fragments.

Note that this special terminology is applicable only to those sediments and sedimentary rocks where volcaniclastic detritus is present in amounts greater than 60%. Where this detritus occurs in amounts between 60% and 30%, the modifying term "volcanic" is applied. The classification format is given in Table 1.

Rules for Classification

1. Greater than 60% of the sediment or rock consists of volcaniclastic material.

2. A textural term and the state of lithification determine the primary name:

The term "block" is used for a particle size of 64 mm, both nonindurated and indurated sediments are termed "pyroclastic breccia," and the matrix composition is greater than or equal to 60% ash or lapilli.

The term "lapilli" is used for a particle size of 64 to 2 mm, "lapilli tephra" when nonindurated, and "lapilli tuff" when indurated.

The term "ash" refers to a particle size of mm, "vitric/crystal/lithic ash" when nonindurated, and "vitric/crystal/lithic tuff" when indurated.

3. A compositional term forms the major modifier. Multiple modifiers are employed in order of increasing abundance of admixed components, with the modifier nearest the principal term denoting the most abundant admixed component, preceded by modifiers denoting minor components using the terms "-bearing" and "-rich," following the rules previously outlined for sediments and sedimentary rocks. Three compositional terms are used:

"Vitric" refers to a glass particle (bubble-wall, pumiceous, etc.).

"Crystal" refers to a mineral particle (euhedral or anhedral).

"Lithic" refers to a rock fragment (volcanic or nonvolcanic).

SERPENTINE AND SERPENTINITE CLASSIFICATION

Serpentine deposits present a special problem in nomenclature. Textural and compositional criteria for Leg 125 deposits argue for emplacement as cold gravitational flows, either as low- or high-viscosity flows. Thus, these deposits are neither sediment nor igneous rock. Field geologists commonly describe this type of serpentine deposit as a "sedimentary serpentinite" (e.g., Cowan and Mansfield, 1970), but clearly this name is inappropriate for use with Leg 125 material. Use of such terminology could imply tranquil particle-by-particle deposition through the water column of particulate grains of serpentine. Leg 125 scientists therefore have chosen to establish a specific nomenclature and set of criteria applied to data collected from smear slides and the degree of induration of the core.

This classification includes poorly to lithified serpentine-rich materials with clastic, brecciated, or sheared phacoidal textures. Aragonite, chlocite, epidote, zoisite, etc., may be present in addition to serpentine as authigenic, primary or secondary minerals. Aragonite is commonly associated with serpentine in the Leg 125 material, with some occurrences in greater abundance than the serpentine. For material to be classified in this category, it must consist of 60% or more serpentine or nonbiogenic aragonite and contain less than 10% clay and/or biogenic components. If less than 10% clay and/or biogenic components are present, then the material may be primary (the product of igneous, alteration, or tectonic processes) or secondary (sedimentary or detrital) in origin. In situations of potentially equivocal origin, this Leg 125 classification scheme for serpentine deposits is descriptive, rather than genetic.

Rules for Classification

1. If serpentine or aragonite abundance is 60% or more in a nonindurated deposit, then the principal name is "serpentine" or "aragonite," respectively. The principal name is preceded by appropriate textural and compositional modifiers.

2. The textural modifier is classified nearest the principal name; it is based on the dominant sizes, as defined in Shepard (1954; see Fig. 7), and the size classes, as defined by Wentworth (1922; see Fig. 8). Examples are silt-sized serpentine and sand-sized serpentine.

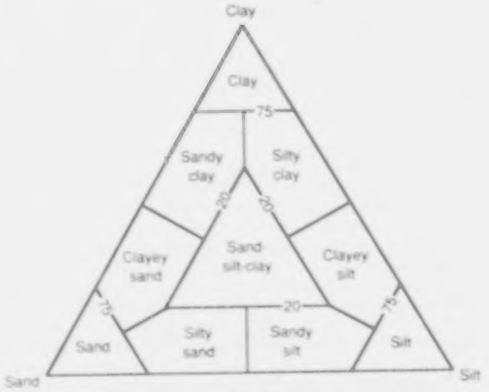

Figure 7. Sediment classification after Shepard (1954), with the sand-, silt-, and clay-sized fractions based on the Wentworth (1922) grain-size scale.

Table 1. Classification of volcaniclastic sediments and rocks.

Clast size	Proportion of volcanic to nonvolcanic clasts 100% —— 60%	—— 30%	—— 0%
Block	Pyroclastic breccia	Vitric volcanic breccia or vitric volcanic conglomerate	Volcanic-rich or volcanic-bearing
Lapilli	Lapilli tephra	Vitric volcanic breccia or vitric volcanic conglomerate	Volcanic-rich or volcanic-bearing
	Lapilli tuff	Vitric volcanic breccia or vitric volcanic conglomerate	Volcanic-rich or volcanic-bearing
Ash	Vitric/crystal and/or lithic ash Vitric/crystal and/or lithic tuff	Vitric volcanic sand/silt/clay Vitric volcanic sandstone, siltstone, claystone	Volcanic-rich or volcanic-bearing Volcanic-rich or volcanic-bearing

3. The compositional modifiers are listed in order of decreasing abundance to the left of the textural modifier and the principal name.

A value of 30% to 60% of a component qualifies for major compositional modifier status. Example: chlorite sand-sized serpentine.

A value of 10% to 30% of a component qualifies for minor compositional modifier status and is hyphenated with the word "rich." Example: zoisite-rich sand-sized serpentine.

A value 5% to 10% of an unusual, important component (e.g., aragonite) qualifies for minor compositional modifier status and is hyphenated with the word "bearing." Example: aragonite-bearing zoisite-rich chlorite silt-sized serpentine.

4. A lithified or indurated form of serpentine is called serpentinite. The preceding definitions apply for textural and compositional modifiers.

5. If large clasts are set in a finer-grained serpentine matrix, then the material is named serpentinite breccia (without tectonic or sedimentary implications) with subsequent modifiers describing the matrix.

6. Sheared phacoidal serpentine is composed of scales or chips of serpentine from 1 mm to larger in size, which may have slickensided surfaces, and whose long axes define an anastomosing foliation. This foliation may enclose angular to subangular blocks of unsheared serpentinite (1 cm or larger in size) or may be associated with horizontal or vertical convolute bedding.

When serpentine is present in amounts of less than 60% or is not associated with nonbiogenic aragonite greater than 60%, the sediment and sedimentary-rock classification scheme previously described is used. The implication is that if more than 10% clay and/or biogenic components are present, then the material is probably deposited as a sediment.

BIOSTRATIGRAPHY

General Remarks

The general correlation between biostratigraphic zones and the record of magnetic polarity reversals, seafloor magnetic anomalies, and an absolute time scale (Figs. 9 to 11) is based upon the scheme given by Berggren et al. (1985). Each

MILLIMETERS		µm	PHI (Ø)	WENTWORTH SIZE CLASS	
			-20		
	4096		-12	Boulder (-8 to -12 Ø)	
	1024		-10		
	256		-8		
	64		-6	Cobble (-6 to -8 Ø)	GRAVEL
	16		-4	Pebble (-2 to -6 Ø)	
	4		-2		
	3.36		-1.75		
	2.83		-1.5	Granule	
	2.38		-1.25		
	2.00		-1.0		
	1.68		-0.75		
	1.41		-0.5	Very coarse sand	
	1.19		-0.25		
	1.00		0.0		
	0.84		0.25		
	0.71		0.5	Coarse sand	
	0.59		0.75		
1/2	0.50	500	1.0		
	0.42	420	1.25		
	0.35	350	1.5	Medium sand	SAND
	0.30	300	1.75		
1/4	0.25	250	2.0		
	0.210	210	2.25		
	0.177	177	2.5	Fine sand	
	0.149	149	2.75		
1/8	0.125	125	3.0		
	0.105	105	3.25		
	0.088	88	3.5	Very fine sand	
	0.074	74	3.75		
1/16	0.0625	63	4.0		
	0.053	53	4.25		
	0.044	44	4.5	Coarse silt	
	0.037	37	4.75		
1/32	0.031	31	5.0		
1/64	0.0156	15.6	6.0	Medium silt	
1/128	0.0078	8	7.0	Fine silt Very fine silt	MUD
1/256	0.0039	3.9	8.0		
	0.0020	2.0	9.0		
	0.00098	0.98	10.0	Clay	
	0.00049	0.49	11.0		
	0.00024	0.24	12.0		
	0.00012	0.12	13.0		
	0.00006	0.06	14.0		

Figure 8. Wentworth (1922) grain-size scale.

microfossil zonation is then fitted into this reversal/anomaly scheme for the Quaternary to middle Eocene. Some minor differences between the scheme of Berggren et al. (1985) and that used for Leg 125 are discussed in the individual sections for each fossil group.

Age assignments are based mainly on core-catcher samples. Additional samples were studied when the core-catcher samples were found barren or restricted to narrow time intervals or when boundaries or unconformities occurred. Sample locations, preservation, and abundance for each fossil group are indicated on the barrel sheets.

Calcareous Nannofossils

The standard calcareous nannoplankton zonation (Martini, 1971; Bukry, 1973; Okada and Bukry, 1980; Backman, Duncan, et al., 1988) is used at all sites to identify the nannoplankton zones. The Pliocene/Pleistocene boundary is defined by the first occurrence of *Gephyrocapsa oceanica*, at the top CN13 Zone of Okada and Bukry (1980). The Miocene/Pliocene boundary is defined by the last occurrence of *Triquetrorhabdulus rugosus* or the last occurrence of *Discoaster quinqueramus* (within CN10a Subzone). The Oligocene/Miocene boundary is defined by the last occurrence of *Sphenolithus ciperoensis* and *Dictyococcites bisectus* (at top of CP19b Subzone or NP25 Zone). The Eocene/Oligocene boundary corresponds to the last appearance of *Discoaster barbadiensis* or *Discoaster saipanensis* (at the top of NP20 Zone or CP15b Subzone).

Nannofossil Abundance and Preservation

Calcareous nannofossils were examined in smear slides prepared from sediment. The abundance of nannofossils is estimated as follows:

A = abundant (10 specimens/field of view).
C = common (1–10 specimens/field of view).
F = few (1 specimen/2–10 fields of view).
R = rare (1 specimen/100 fields of view).

The state of preservation is estimated as follows:

G = good (no or only minor signs of dissolution or overgrowth of placoliths and discoasters).

M = moderate (slight to moderate dissolution of placoliths, discoasters, and others or slight to moderate overgrowth especially on discoasters and other ortholithic forms).

P = poor (severe dissolution in placoliths with abundant broken specimens or heavy overgrowth of discoasters and sphenoliths).

Planktonic Foraminifers

Neogene

The zonation of Blow (1969), as amended by Kennett and Srinivasan (1983), is followed in this volume. This zonation is based on a phylogenetic lineage, using species ranges compiled from Kennett and Srinivasan (1983). The first appearance of *Globorotalia truncatulinoides*, between Zones N21 and N22, marks the Pliocene/Pleistocene boundary. The Miocene/Pliocene boundary, between Zones N18 and N19, is based on the first appearance of *Sphaeroidinella dehiscens*, and the Oligocene/Miocene boundary is equated with the first appearance of *Globoquadrina dehiscens*. The unamended zonation of Blow (1969) for the Neogene was used in this part of the northern Pacific during DSDP Legs 6, 55, 59 and 60.

Paleogene

The tropical zonation of Blow (1969, 1979) is applied to the upper Eocene–Oligocene section, and Berggren's (1977) zonation is used for the Paleocene–middle Eocene.

Methodology

All samples are disaggregated in a hot detergent solution, with Calgon added to clayey samples, and washed over a 63-mm sieve. The following categories describe the frequencies of planktonic foraminifers in each sample, relative to other sand-sized particles:

A = abundant (25% of the residue).
C = common (1–25% of the residue).
F = few (1–5% of the residue).
R = rare (% of the residue).
B = barren (no foraminifers, or rare benthic foraminifers only).

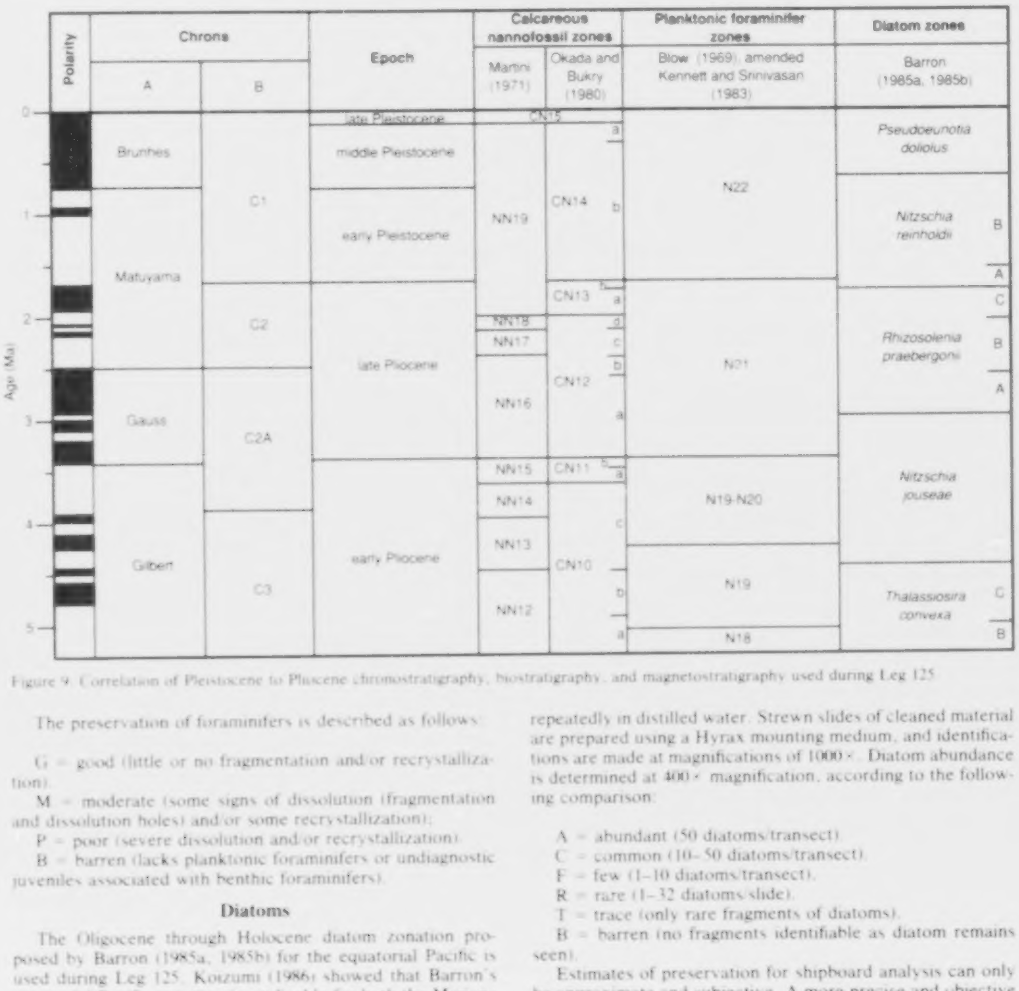

Figure 9. Correlation of Pleistocene to Pliocene chronostratigraphy, biostratigraphy, and magnetostratigraphy used during Leg 125.

The preservation of foraminifers is described as follows:

G = good (little or no fragmentation and/or recrystallization).

M = moderate (some signs of dissolution (fragmentation and dissolution holes) and/or some recrystallization);

P = poor (severe dissolution and/or recrystallization).

B = barren (lacks planktonic foraminifers or undiagnostic juveniles associated with benthic foraminifers).

Diatoms

The Oligocene through Holocene diatom zonation proposed by Barron (1985a, 1985b) for the equatorial Pacific is used during Leg 125. Koizumi (1986) showed that Barron's equatorial Pacific zonation is applicable for both the Mariana and Izu-Bonin areas. This zonation consists of 20 zones and 23 subzones and is based on Burckle's (1972) late Miocene through Quaternary zonation and Barron's (1983) late Oligocene to middle Miocene zonation. Although the chronostratigraphy used during Leg 125 follows Berggren et al. (1985), this time scale does not incorporate a diatom zonation. Therefore, correlations follow those of Barron (1985a, 1985b). Significant contributions to the understanding of the Neogene diatom biostratigraphy from this region include studies by Burckle (1972, 1977, 1978) and Burckle and Trainer (1979), as summarized and modified by Barron (1985a, 1985b).

Shipboard samples are prepared by the following standard procedure: (1) 1 cm^3 of sediment is placed in a 250-mL beaker, (2) 10% HCl is added until the carbonate reaction ceases, (3) the sample is heated in 10% H_2O_2, and then (4) washed repeatedly in distilled water. Strewn slides of cleaned material are prepared using a Hyrax mounting medium, and identifications are made at magnifications of 1000×. Diatom abundance is determined at 400× magnification, according to the following comparison:

A = abundant (50 diatoms/transect).
C = common (10–50 diatoms/transect).
F = few (1–10 diatoms/transect).
R = rare (1–32 diatoms/slide).
T = trace (only rare fragments of diatoms).
B = barren (no fragments identifiable as diatom remains seen).

Estimates of preservation for shipboard analysis can only be approximate and subjective. A more precise and objective classification might be achieved during shorebased laboratory studies.

SEDIMENT/FLUID GEOCHEMISTRY

Sediment Geochemistry

Sediments are analyzed on board ship for inorganic carbon and for total nitrogen, carbon, and sulfur. The organic carbon content of the sediments is then calculated by difference. Inorganic carbon content is determined for all sediment samples taken for physical-properties measurements and for additional samples as necessary, at a frequency of about one per section. Total nitrogen, carbon, and sulfur are determined for a subset of these samples, at a frequency of about one per core. All samples are freeze-dried prior to analysis.

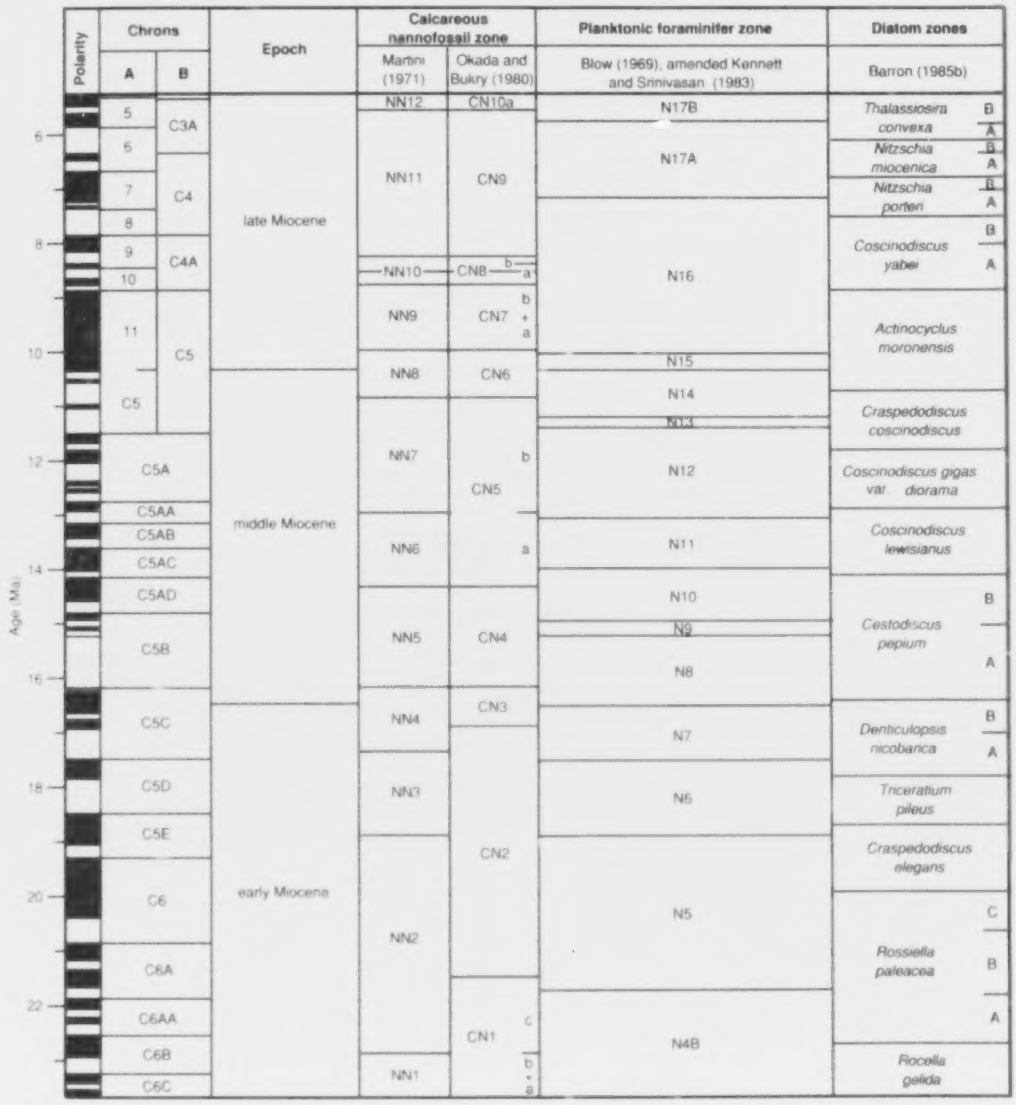
Polarity
Chrons
A
B
Epoch
Calcareous nannofossil zone
Martini (1971)
Okada and Bukry (1980)
Planktonic foraminifer zone
Blow (1969), amended Kennett and Srinivasan (1983)
Diatom zones
Barron (1985b)
Age (Ma)
6
8
10
12
14
16
18
20
22
5
6
7
8
9
10
11
C5
C3A
C4
C4A
C5
C5A
C5AA
C5AB
C5AC
C5AD
C5B
C5C
C5D
C5E
C6
C6A
C6AA
C6B
C6C
late Miocene
middle Miocene
early Miocene
NN12
NN11
NN10
NN9
NN8
NN7
NN6
NN5
NN4
NN3
NN2
NN1
CN10a
CN9
CN8
b
a
CN7
b
+
a
CN6
CN5
b
a
CN4
CN3
CN2
CN1
c
b
+
a
N17B
N17A
N16
N15
N14
N13
N12
N11
N10
N9
N8
N7
N6
N5
N4B
Thalassiosira convexa
B
A
Nitzschia miocenica
B
A
Nitzschia porteri
B
A
Coscinodiscus yabei
B
A
Actinocyclus moronensis
Craspedodiscus coscinodiscus
Coscinodiscus gigas var. diorama
Coscinodiscus lewisianus
Cestodiscus pepium
B
A
Denticulopsis nicobarica
B
A
Triceratium pileus
Craspedodiscus elegans
Rossiella paleacea
C
B
A
Rocella gelida

Figure 10. Correlation of Miocene chronostratigraphy, biostratigraphy, and magnetostratigraphy used during Leg 125.

Total inorganic carbon is determined using a Coulometrics 5011 coulometer equipped with a System 140 carbonate carbon analyzer. Depending on carbonate content, 15 to 70 mg of ground and weighed sediment is reacted in a 2N HCl solution. The liberated CO_2 is titrated in a monoethanolamine solution with a colorimetric indicator, while monitoring the change in light transmittance with a photodetection cell.

Total nitrogen, carbon, and sulfur are determined using an N/C/S analyzer, model NA 1500 from Carlo Erba Instruments. Bulk samples are combusted at 1000°C in an oxygen atmosphere, converting organic and inorganic carbon to CO_2 and sulfur to SO_2. These gases, along with nitrogen, are then separated by gas chromatography and measured using a thermal-conductivity detector.

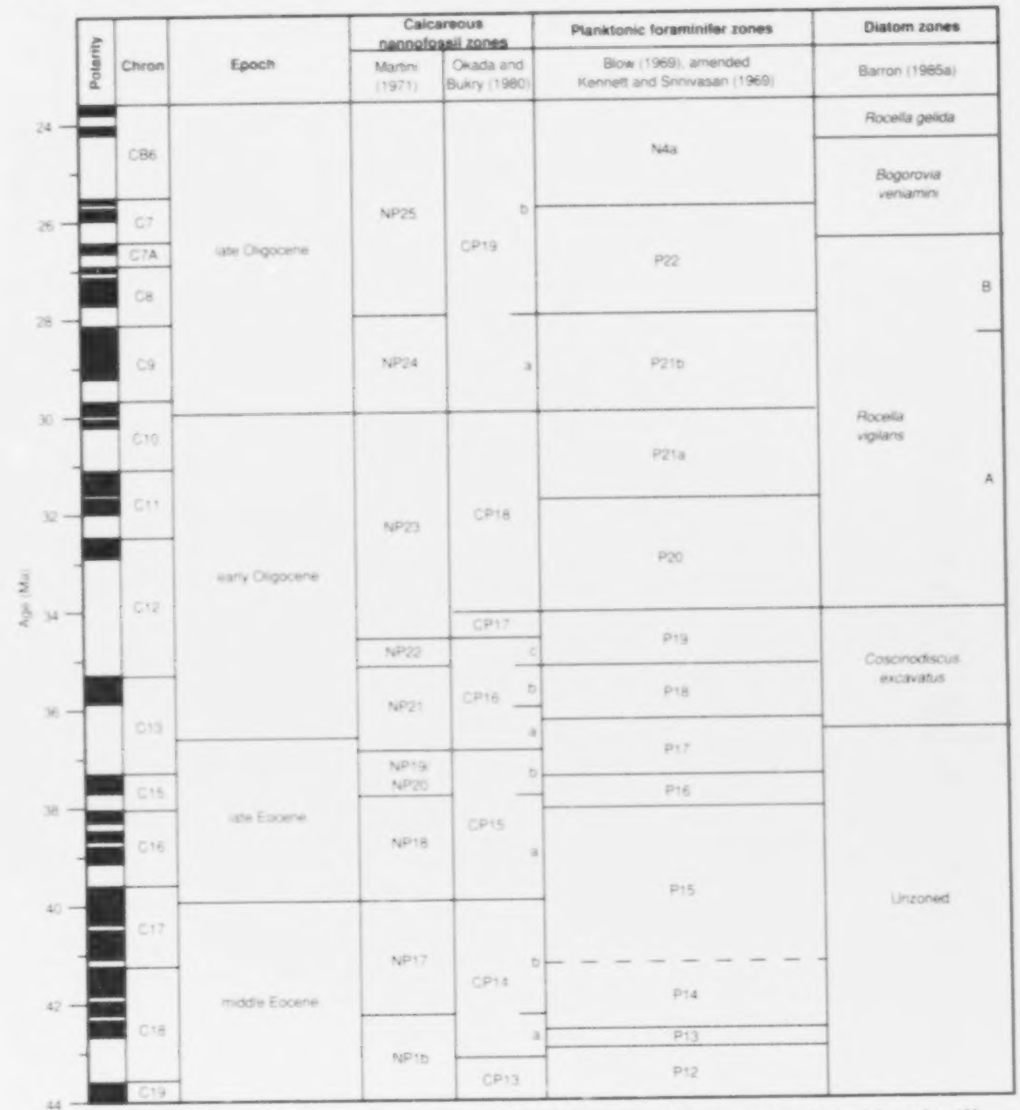

Figure 11. Correlation of Oligocene to late Eocene chronostratigraphy, biostratigraphy, and magnetostratigraphy used during Leg 125.

Fluid Geochemistry

Hydrocarbon Gases

As required by safety considerations, the concentrations of the hydrocarbons methane (C_1), ethane (C_2), and propane (C_3) are monitored in the sediment cores at intervals of about 10 m. Hydrocarbon gases are extracted from bulk sediment using a headspace-sampling technique. As soon as the core arrives on deck, a 5-cm^3 plug of sediment is taken, using a No. 4 cork borer. This sample is placed immediately in a glass vial that is sealed with a septum and metal crimp and then heated to 70°C. The gas driven off is drawn into a syringe and injected into a Hach-Carle AGC Series 100 Model 211 gas chromatograph equipped with a thermal-conductivity detector. Where high concentrations of propane are suspected, a second sample is taken by the same method and analyzed for C_1 through C_6 hydrocarbons using a Hewlett-Packard 5980A natural gas analyzer, a gas chromatograph equipped with Poropak-Q, molecular-sieve, and silicone-oil-coated columns, and a flame ionization detector. After the headspace gas is analyzed, the actual volume of the sediment sample is measured to the nearest 0.5 cm^3 by displacement using water. Details of this method and the complete configuration of both gas chromatographs are given in the "Explanatory Notes" chapter for Leg 112 (Shipboard Scientific Party, 1988).

Also analyzed using the Hach-Carle gas chromatograph are samples of suspected gas pockets in the cores. These samples are taken immediately upon recovery of the core by penetrating the transparent plastic core liner with a hollow stainless-steel punch equipped with a valve and hypodermic needle. The gases are collected through a rubber septum into an evacuated glass tube.

Interstitial Water

During Leg 125, interstitial water was obtained from sediments and unconsolidated serpentine by squeezing and by *in-situ* extraction using the Barnes pore-water sampler.

Whole-round sections of core 5 to 15 cm in length are squeezed. As soon as the core arrives on deck, these samples are cut by slicing the plastic core tube and capping both ends. The samples are then cooled to the appropriate *in-situ* temperature; removed from the core liner; scraped with a stainless-steel spatula to remove the outer, contaminated layer; and placed in a stainless-steel squeezer (Manheim and Sayles, 1974). Both the squeezer and the samples are handled only with plastic gloves to avoid contamination. The squeezer is placed in a Carver hydraulic press and squeezed at pressures of up to 40,000 psi. Interstitial water is collected directly into a 50-mL plastic syringe, from which the various aliquots for analysis are ejected through an on-line 0.45-mm polysulfone filter mounted in a Gelman "acrodisc" disposable filter holder. Squeezed interstitial waters here are designated "IW" samples.

The *in-situ* water sampler-temperature-pressure (WSTP) tool designed by R. Barnes was first used during Leg 110 (Barnes, 1988). This tool collects interstitial water while simultaneously measuring sediment temperature and pore pressure. The tool is lowered on the sand line to the end of the drill string, where it locks into an assembly just above the bit. The hole is flushed with drilling fluid with the bit just off bottom during the descent of the sampler to keep the hole free of fill. After the sampler is latched into place, the bit is lowered into the bottom with the sampling probe projecting about 20 cm through the bit. A timer-operated valve opens, and interstitial water is drawn under negative pressure through two 40-mm stainless-steel filters and one 1-mm polyester filter into the sampler. There it passes through a stainless steel entry tube of 12-mL volume into two sample coils arranged in series and separated by an open ball valve, and then into a steel overflow cylinder of 1200 mL volume that also contains the sample coils and valves. This overflow cylinder generates negative pressure when the sampling valve is opened, as this cylinder is normally filled with air when the tool is sent downhole. For Leg 125, we evacuated this cylinder prior to deployment to prevent oxidation of H_2S in the sampler.

The tubing and coils are initially filled with distilled water, which is displaced into the overflow cylinder on sampling, along with any excess sample and about 1 mL of seawater from the dead volume outside the entry valve. The first of the two sample coils in series is made of stainless steel, has a volume of about 20 mL, and is used for the shipboard analyses. The second is copper, has a volume of 40 to 50 mL, and is typically used for shorebased determination of helium isotopes and dissolved gases. We also analyze the water from the overflow cylinder, as it often is useful for determining major and minor dissolved species. In particular, it sometimes shows higher calcium-to-chlorinity ratios than the undiluted sample from the steel coil, indicating that calcium carbonate has probably precipitated in the latter. The amount of dilution of the overflow aliquot can usually be determined from its chlorinity relative to that of the undiluted sample. The length of time required to fill the Barnes sampler varies with the permeability of the sediment, but typically is about 15 min. Interstitial-water samples collected with the Barnes tool are here designated "BW." When removed from the stainless-steel coil, they are filtered (0.45 mm) like the squeezed samples.

The waters are analyzed immediately when recovered for pH, alkalinity by potentiometric titration, salinity by refractive index, and (when an odor is detected) hydrogen sulfide by colorimetry using methylene blue. Aliquots are refrigerated and analyzed within a few days of collection for calcium, magnesium, and chlorinity by colorimetric titration; sulfate by ion chromatography; silica, ammonium, phosphate, and bromide by colorimetry; and potassium by flame atomic absorption spectrophotometry. All shipboard analyses are performed using standard ODP techniques, as detailed by Gieskes and Peretsman (1986) and described briefly in the "Explanatory Notes" chapter for Leg 112 (Shipboard Scientific Party, 1988). IAPSO standard seawater is the primary standard for determination of calcium, magnesium, and chlorinity and also provides a check on the accuracy of the analyses for alkalinity, potassium, sulfate, and bromide.

PALEOMAGNETISM

Paleomagnetic studies performed on board *JOIDES Resolution* include measurements of the remanent magnetization and magnetic susceptibility of sedimentary, igneous, and metamorphic material. Measurement of remanence is accompanied by alternating field (AF) demagnetization whenever possible in the hope of removing secondary magnetizations.

Instruments

A Molspin spinner magnetometer and a 2-G Enterprises pass-through cryogenic superconducting rock magnetometer are available for measuring remanence. An AF demagnetizer (Model 2G600) capable of alternating fields up to 25 mT is on-line with a cryogenic magnetometer. Both are controlled by a FASTCOM4 multiserial communication board in an IBM PC-AT compatible computer. For measuring the archive half of a core, Leg 125 scientists used a BASIC program (COREMAG), modified by C. Helsley from the SUPERMAG program used during Leg 124E. Up to seven discrete samples (individual samples taken from the working half of the core) can be measured on the cryogenic magnetometer in a single run using the program 7CUBE, modified by C. Helsley during Leg 124E from the SUPRCUBE program. The spinner magnetometer is controlled by a Digital PRO350 computer and is used only to measure discrete samples.

The superconducting quantum interference device (SQUID) sensors in the cryogenic magnetometer measure magnetization over an interval approximately 20 cm long. Each axis has a different response curve. The widths of the sensor regions imply that as much as 150 cm^3 of core contributes to the sensor signals, thereby blurring sharp magnetic transitions. The increased volume of rock within the sensor region permits one to determine accurately the remanence of weakly magnetized samples despite the relatively high background noise caused by the motion of the ship. The SQUID electronics operate at a 1× scale and use the flux-counting mode for most measurements.

Remanent Magnetization Measurements

The maximum AF demagnetizing field allowed for sections from the archive half is 15 mT or the median destructive field, whichever is lower. Discrete samples from the working half of the core also are demagnetized using the Schonstedt GSD-1 AF demagnetizer and thermal demagnetizer, although these samples are then exposed to ambient magnetic fields after demagnetization, but prior to measurement. Therefore, progressive AF and thermal demagnetizations of samples from Leg 125 and their measurement by cryogenic magnetometers will be performed in magnetically shielded laboratories on shore.

Sediments

Remanence measurements of sediments are performed by passing archive-half core sections of the APC cores through the cryogenic magnetometer. Measurements are taken at 10-cm intervals at both natural remanent magnetization (NRM) and the various AF demagnetization levels. These measurements contain the averaging effect of the responses of the three axes because of the broad sensor region in the cryogenic magnetometer; thus, deconvolution will be required to recover the higher frequency changes of magnetization.

Discrete samples are taken from APC, XCB, and RCB sediment cores. The sampling is performed by pressing a plastic box ($6\ cm^3$) into the sediments and removing it. The uphole direction is marked on the box. For more consolidated sediments, a spatula is used to cut the cubes. At least one sample per section is taken in APC, XCB, and RCB cores. The sampling positions in XCB and RCB cores are unevenly controlled, mainly by the distribution of undisturbed portions of the core sections. More than one-third of the discrete samples were measured in the cryogenic magnetometer during Leg 125 after AF demagnetization to 2, 5, 10, and 15 mT.

Igneous and Metamorphic Rocks

To measure the remanence of igneous and metamorphic rocks, minicores of 1-in. diameter are taken where appropriate and measured in the cryogenic magnetometer. The NRM and AF demagnetization steps of archive-half sections containing pieces of core greater than 20 cm are measured in the cryogenic magnetometer at 3-cm intervals.

Magnetic Susceptibility Measurement

Magnetic susceptibilities are measured on all sediment and most igneous and metamorphic cores using a Bartington Instrument magnetic susceptibility meter (model M.S.1) with a M.S.1/CX 80-mm whole-core sensor loop set at 0.47 kHz. The susceptibility meter is on-line with the GRAPE and the *P*-wave logger on the multisensor track. Leg 125 scientists are the first to measure susceptibility with this configuration. The susceptibility of most material encountered during Leg 125 is high, and therefore all measurements are performed in the low-sensitivity mode. As susceptibility is a volume-dependent property, susceptibility data from incomplete cores are rejected.

In addition to characterizing the cored sediments, susceptibility data are used to correlate between holes and sites. Correlation of susceptibility data is performed by observing peak-to-peak spacings and general trends in the susceptibility curve. Absolute individual peak heights are not useful for correlation of susceptibility data.

IGNEOUS AND METAMORPHIC PETROLOGY

Core Curation and Shipboard Sampling

As standard procedure, igneous and metamorphic rocks recovered during coring are examined by petrologists to determine where the core should be split to best preserve unique features and/or to expose important structures. The core is split into archive and working halves using a rock saw equipped with a diamond blade. Care is always taken to ensure that orientation is preserved during splitting and prior to labeling, usually by marking the original base of each piece with red crayon. Each piece is numbered sequentially from the top of each section. Pieces are labeled at the top, uncut surface. Pieces that can be fitted together (reassembled like a jigsaw puzzle) are assigned the same number, but are lettered consecutively (e.g., 1A, 1B, 1C, etc.). Plastic spacers are placed between pieces having different numbers, but not between those having different letters and the same number. The presence of a spacer may represent a substantial interval of no recovery (or may not). If the original unsplit piece is long enough, such that the top and bottom can be distinguished before removal from the core liner (i.e., the piece could not have rotated top to bottom about a horizontal axis in the liner during drilling), an arrow is added to the label pointing to the top of the section. Because pieces are free to turn about a vertical axis during drilling, azimuthal orientation is not possible.

After the core is split, the working half is sampled for measurement of physical and magnetic properties and for XRF, XRD, and thin-section studies. These samples may take the form of minicores and, if appropriate, are stored in seawater prior to measurement. When recovery permits, samples are taken from each lithologic unit. The archive half is described on the visual core description (VCD) form, used for nondestructive physical-properties measurements (such as magnetic susceptibility), and photographed before storage.

Visual Core Descriptions

Igneous VCD forms are used when describing the basement cores (Fig. 12). The left column of the form is a graphic representation of the archive half. A horizontal line across the entire width of the column denotes a plastic spacer glued between rock pieces inside the liner. Oriented pieces are indicated on the form by an upward-pointing arrow to the right of the piece. Shipboard samples and studies are indicated on the VCD in the column headed "Shipboard Studies" using the following notation: XRD = X-ray-diffraction analysis; XRF = X-ray-fluorescence analysis; TS = petrographic thin section; PP = physical-properties analysis. In some cases, we attempted to prepare a thin section from material unsuitable for that purpose. Although these sections exist in the thin-section collection at ODP, their poor quality does not permit us to make a detailed description. These sections are indicated by the symbol "X."

Because igneous and metamorphic rocks are classified mainly on the basis of macroscopic mineralogy and texture, shipboard petrologists follow a checklist of features to ensure consistent and complete descriptions. To this end, VCDs are entered directly into a computerized data base (HARVI). This is advantageous because the HARVI program prompts the describer with a set of questions pertaining to petrologic features, all of which must be diagnosed and entered in the data base. The descriptions on the VCD forms will, to a certain extent, reflect the rigidity of the HARVI program. It is therefore relevant to discuss briefly the organization of the data base. Fine-grained rocks are entered into a data set called HARVI-F, and coarse-grained rocks are entered into the data

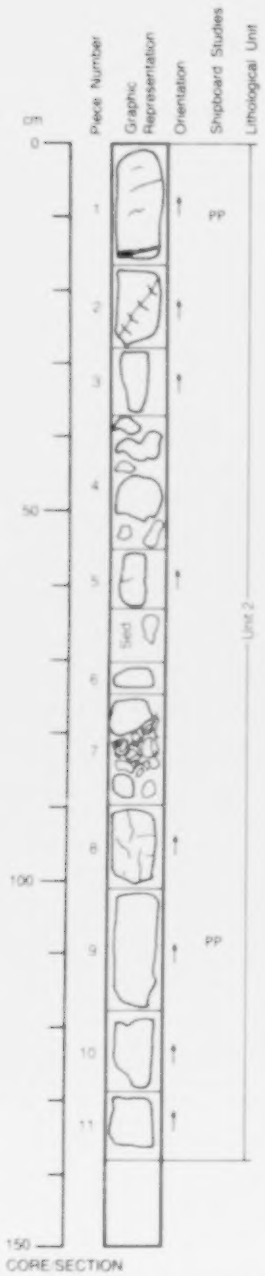

125-779A-35R-1

UNIT 2: TECTONIZED SERPENTINIZED HARZBURGITE

Pieces 1-3

COLOR: Bluish gray (5B 5/1).
LAYERING: Possible alignment of elongate orthopyroxene.
DEFORMATION: Elongate spinels in trains, wavy cleavage on orthopyroxene.
PRIMARY MINERALOGY:
Orthopyroxene - Mode: 15-25%.
Crystal size: 3-5 mm.
Crystal shape: Elongate-ragged.
Crystal orientation: Not visible.
Percent replacement: Variable.

Olivine - Mode: 75-85%.
Crystal size: 3-7 mm.
Crystal shape: Elongate-ragged.
Crystal orientation: Not visible.
Percent replacement: Variable.

Spinel - Mode: Trace.
Crystal size: <2 mm.
Crystal shape: Elongate-ragged.
Crystal orientation: Not visible.
Percent replacement: Variable.
SECONDARY MINERALOGY:
Serpentine.
Total percent: 40-80%.
Texture: N/A.
Vein material: Dark black amorphous serpentine filled vein, <3 mm wide oriented almost parallel to core in Piece 2. This vein has <1 mm wide and 2 cm long white green serpentine veins running perpendicular to it. Piece 1 has white green serpentine vein, <2 mm wide, perpendicular to core.

UNIT 2: SERPENTINIZED HARZBURGITE

Pieces 4-8

COLOR: Dark greenish gray (5B 4/1).
LAYERING: None.
DEFORMATION: Piece 8 appears to be slightly tectonized and exhibits elongation of the pyroxene crystals.
PRIMARY MINERALOGY:
Olivine - Mode: 70-75%.
Crystal size: 1-2 mm.
Crystal shape: Equant-elongate.
Crystal orientation: N/A.
Percent replacement: N/A.

Orthopyroxene - Mode: 25-30%.
Crystal size: 1-3 mm.
Crystal shape: Equant-elongate.
Crystal orientation: N/A.
Percent replacement: N/A.

Spinel - Mode: Trace.
Crystal size: <1 mm.
Crystal shape: Equant.
Crystal orientation: N/A.
Percent replacement: N/A.
SECONDARY MINERALOGY:
Serpentine.
Total percent: 70?
Texture: Serpentinized.
Vein material: <2 mm wide white-pale green serpentine (chrysotile?) veining. Piece 4 is mixed with serpentine sediment.

Figure 12. Visual core description form used for metamorphic and igneous rocks.

set HARVI-C. Each record is checked by the data-base program for consistency, and a hard copy is printed in a format that resembles the final barrel sheets. This copy is pasted directly onto a copy of the barrel sheet.

When describing sequences of fine- to coarse-grained rocks, the core is subdivided into lithologic units on the basis of changes in petrographic and rock-clast types and mineral abundances. For each lithologic unit, section, and rock type, the following information is recorded as appropriate using the HARVI system:

1. Leg, site, hole, core number, core type, and section.
2. Unit number (consecutive downhole), position in the section, number of pieces of the same lithologic type being described, the name of the describer, and rock name.
3. Color of the rock (recorded when the rock piece was dry) using the Munsell (1975) chart, presence of layering and deformation and character thereof. In the case of variably serpentinized ultramafic rocks, particular attention is paid to the presence of deformed cleavage surfaces of relict orthopyroxene ("bastite"), elongate spinel and olivine, and mylonitization and shearing as indicators of deformation.
4. The number of mineral phases and their distribution within the unit. For each mineral phase we note the following: (a) abundance (%), (b) average size in mm, (c) shape, (d) the degree of alteration, and (e) further comments. In the case of heavily serpentinized materials, the original grain size and shape of the primary phases may not be visible or are only estimated.
5. Groundmass texture: glassy, microcrystalline, fine-grained (1 mm), medium-grained (1–5 mm), or coarse-grained (5 mm); relative changes of grain size within the unit (e.g., coarsening from Piece 1 to Piece 5).
6. Presence of alteration and alteration characteristics, including structures imposed during formation of secondary minerals, type of alteration, and abundance of secondary minerals.
7. Vesicles: percentage abundance, distribution, size, shape, and fillings and their relationships (including proportion of vesicles that are filled by alteration minerals).
8. Structure: massive flow, pillow lava, thin flow, breccia, hyaloclastite, etc., and comments.
9. Alteration: fresh (% alteration), slightly (2%–10% alteration), moderately (10–40% alteration), highly (40%–80% alteration), very highly (80%–95% alteration), or completely (95%–100% alteration) altered; type, form, and distribution of alteration.
10. Veins/Fractures: percentage present, width, orientation, and fillings and their relationships. The relationship of the veins and fractures to the alteration is also noted.
11. Comments: notes on the continuity of the unit within the core, and the interrelationship of units are added here, when appropriate.

Basalts are termed aphyric (%), sparsely phyric (1%–2%), moderately phyric (2%–10%), or highly phyric (10%), depending upon the proportion of phenocrysts visible with the hand lens or binocular microscope (approximately 10×). Basalts are further classified by phenocryst type (e.g., a moderately plagioclase-olivine phyric basalt contains 2%–10% phenocrysts, mostly plagioclase, with subordinate olivine).

Serpentinized rocks are classified on the basis of the original phase proportions present in the protolith, using the IUGS classification system (Streckeisen, 1973) for ultramafic rocks. For example, "serpentinized dunite" is a rock with 90% modal olivine originally present that has some specified proportion of serpentinization. Synoptic versions of the Leg 125 igneous/metamorphic VCD forms are published with this volume and are available on microfilm at all three ODP repositories.

Thin-Section Descriptions

Thin-section billets of igneous and metamorphic rocks are examined (1) to confirm the identity of petrographic groups in the cores, (2) to understand better the textures and interrelationships of the mineral phases, (3) to help define unit boundaries indicated by hand-specimen core descriptions, and (4) to define the secondary alteration mineralogy. Percentages of individual mineral phases are estimated and are reported on the detailed thin-section description sheets (Fig. 13). The terminology used for thin-section descriptions is used in the same manner as that for the macroscopic descriptions. In cases where discrepancies arose over the composition and abundance of mineral phases between hand-specimen and thin-section analyses, the thin-section descriptions are preferred.

X-Ray-Diffraction Analyses

A Philips ADP 3520 X-ray diffractometer is used for XRD analysis of mineral phases. Normal instrument conditions employ Cu Ka radiation with a nickel filter, 40 kV, 35 mA, a goniometer scan from 2° to 70° θ, a step size of 0.02°, and a count time of 1 s per step.

Normally, samples are ground using the Spex 8000 Mixer Mill or, when the sample is small, with an agate mortar and pestle. This material is then pressed into the sample holders or smeared on glass plates, which are placed in the sample holders for analysis.

Diffractograms are interpreted with the help of a computerized search and match routine using Joint Committee on Powder Diffraction Standards (JCPDS) powder files.

X-Ray-Fluorescence Analysis

Prior to analysis, samples are crushed in the Spex 8510 Shatterbox using a tungsten carbide barrel. This produces some Ta and massive W contamination of the sample. If post-cruise studies for these elements are envisaged using the shipboard XRF powders, and if time permits, samples are crushed using an agate-lined barrel.

A fully automated wavelength-dispersive ARL8420 XRF (3 kW) system equipped with an Rh target X-ray tube is used to determine the abundance of major oxides and trace elements in whole-rock samples. Analyses of the major oxides are performed using lithium borate glass disks doped with lanthanum as a "heavy absorber" (Norrish and Hutton, 1969). These disks are prepared from a mixture of 500 mg of rock powder, weighed after 2 hr of ignition at about 1030°C, and 6.000 g of dry flux, consisting of 80% lithium tetraborate and 20% La_2O_3. This mixture is then melted at 1150°C in a platinum-gold crucible for about 10 min and poured into a platinum-gold mold using a Claisse Fluxer. The 12:1 flux-to-sample ratio and the use of the lanthanum absorber make matrix effects insignificant over the normal range of igneous rock compositions. Hence, the following linear relationship between X-ray intensity and concentration is valid:

$$C_i = (I_i m_i) b_i$$

where C_i is the concentration of oxide i (wt%), I_i is the net peak X-ray intensity of oxide i, m_i is the slope of the

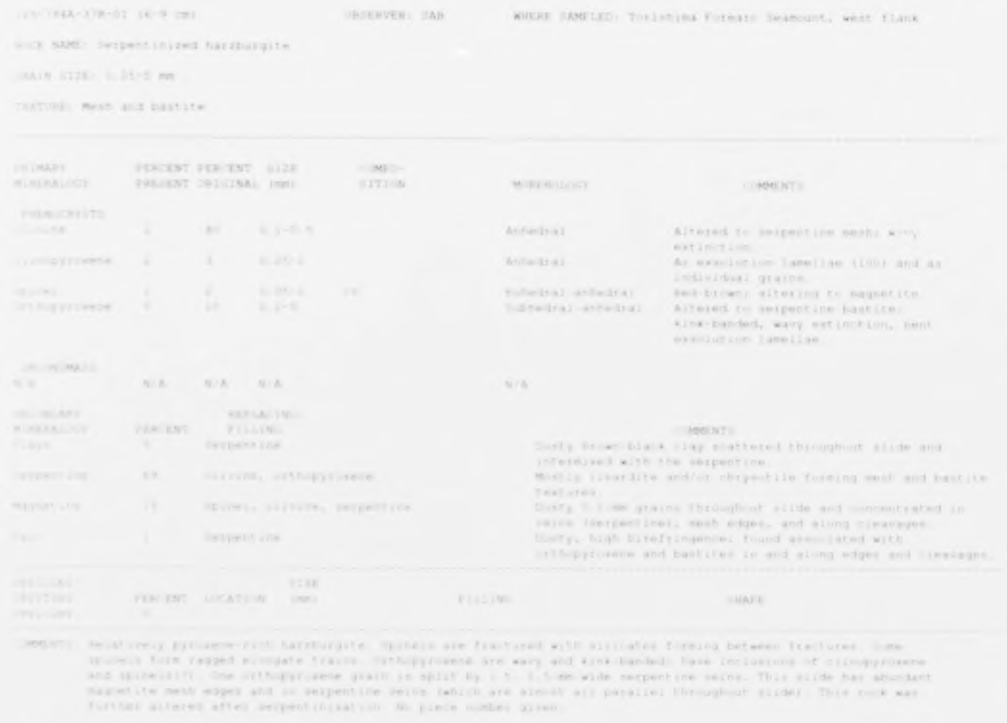

125-784A-37R-01 (6-9 cm)   OBSERVER: SAB   WHERE SAMPLED: Torishima Forearc Seamount, west flank

ROCK NAME: Serpentinized harzburgite

GRAIN SIZE: 0.01-5 mm

TEXTURE: Mesh and bastite

PRIMARY MINERALOGY	PERCENT PRESENT	PERCENT ORIGINAL	SIZE (mm)	COMPO-SITION	MORPHOLOGY	COMMENTS
PHENOCRYSTS						
Olivine	1	80	0.1-0.5		Anhedral	Altered to serpentine mesh; wavy extinction.
Clinopyroxene	2	3	0.05-1		Anhedral	As exsolution lamellae (100) and as individual grains.
Spinel	1	2	0.05-1	Cr	Subhedral-anhedral	Red-brown; altering to magnetite.
Orthopyroxene	9	15	0.2-5		Subhedral-anhedral	Altered to serpentine bastite; kink-banded, wavy extinction, bent exsolution lamellae.
GROUNDMASS						
N/A	N/A	N/A	N/A		N/A	

SECONDARY MINERALOGY	PERCENT	REPLACING/ FILLING	COMMENTS
Clays	5	Serpentine	Dusty brown-black clay scattered throughout slide and intermixed with the serpentine.
Serpentine	69	Olivine, orthopyroxene	Mostly lizardite and/or chrysotile forming mesh and bastite textures.
Magnetite	15	Spinel, olivine, serpentine	Dusty 0.1-mm grains throughout slide and concentrated in veins (serpentine), mesh edges, and along cleavages.
Talc	1	Serpentine	Dusty, high birefringence; found associated with orthopyroxene and bastites in and along edges and cleavages.

VESICLES/ CAVITIES/ OPENINGS	PERCENT	LOCATION	SIZE (mm)	FILLING	SHAPE
	0				

COMMENTS: Relatively pyroxene-rich harzburgite. Spinels are fractured with silicates forming between fractures. Some spinels form ragged elongate traces. Orthopyroxene are wavy and kink-banded; have inclusions of clinopyroxene and spinel(?). One orthopyroxene grain is split by [illegible]-mm-wide serpentine veins. This slide has abundant magnetite mesh edges and in serpentine veins (which are almost all parallel throughout slide). This rock was further altered after serpentinization. No piece number given.

Figure 13. Thin-section description form used for metamorphic and igneous rock.

calibration curve for oxide *i* (wt%/cps), and b_i is the apparent background concentration for oxide *i* (wt%).

The slope m_i is calculated from a calibration curve derived from the measurement of well-analyzed reference rocks (BHVO-1, G-2, AGV-1, PCC-1, JGB-1, JP-1, BR, DR-N, UB-N). The background *bi* is determined either from blanks or is derived by regression analysis from the calibration curves.

Systematic errors resulting from short-term or long-term fluctuations in X-ray tube intensity are corrected by normalizing the measured intensities of the samples to those of a standard that is always run with a set of six samples. To reduce shipboard weighing errors, two glass disks are prepared for each sample. Accurate weighing is difficult on board the moving platform of the *Resolution*, and must be performed with particular care because weighing errors can be a major source of imprecision in the final analysis. Loss on ignition (LOI) values, if required, are determined by drying the sample at 110°C for 8 hr, and then by weighing before and after ignition at 1030°C.

Trace elements are determined by using pressed-powder pellets prepared by pressing (with 7 tons of pressure) a mixture of 5.0 g of dry rock powder (dried at 110°C for 2 hr) and 30 drops of polyvinyl alcohol binder into an aluminum cap. A modified Compton scattering technique, based on the intensity of the Rh Compton peak, is used for matrix absorption corrections (Reynolds, 1967).

An outline of the computation methods is as follows:

1. Input X-ray intensities. Dead-time corrected X-ray intensities are read into the program from an A.R.L. result file.
2. Correct drift. All peak and background intensities are corrected for machine drift by using a one-point correction of the form

$$D_i = S_i/M_i,$$

$$Id_i = I_iD_i,$$

where D_i is the drift factor for element *i* (generally 1.00 ± 0.01), S_i is the peak intensity for element *i* (measured on a synthetic standard, "POOP," at the time of calibration), M_i is the measured peak intensity for element *i* (measured on "POOP" at any time after the calibration), Id_i is the drift-corrected peak or background intensity for element *i*, and I_i is uncorrected peak or background intensity for element *i*.
3. Subtract backgrounds. Peak intensities are corrected for nonlinear backgrounds by measuring a peak-to-average background ratio for each element. This ratio is measured on synthetic and natural blank standards at the time of calibration using the following:

$$BF_i = PK_i/AVBg_i,$$

Table 2. X-ray-fluorescence analytical conditions, Leg 125.

Element	Line	Crystal	Detector[a]	Collimator	Peak (degrees)	Background offset (degrees)	Total count time (s) peak	Total count time (s) background
Major elements								
SiO_2	Kα	PET(002)	FPC	Coarse	109.25	0	40	0
TiO_2	Kα	LIF(200)	FPC	Fine	86.14	0	40	0
Al_2O_3	Kα	PET(002)	FPC	Coarse	145.27	0	100	0
[b]Fe_2O_3	Kα	LiF(200)	FPC	Fine	57.52	0	40	0
MnO	Kα	LiF(200)	KrSC	Fine	62.98	0	40	0
MgO	Kα	TLAP	FPC	Coarse	44.87	±0.80	200	200
CaO	Kα	LiF(200)	FPC	Coarse	113.16	0	40	0
Na_2O	Kα	TLAP	FPC	Coarse	54.71	−1.20	200	200
K_2O	Kα	LiF(200)	FPC	Fine	136.65	0	40	0
P_2O_5	Kα	Ge(111)	FPC	Coarse	140.94	0	100	0
Trace elements								
Rh	K-C	LiF(200)	Scint	Fine	18.59	0	100	0
Nb	Kα	LiF(200)	Scint	Fine	21.37	±0.35	200	200
Zr	Kα	LiF(200)	Scint	Fine	22.53	±0.35	100	100
Y	Kα	LiF(200)	Scint	Fine	23.78	±0.40	100	100
Sr	Kα	LiF(200)	Scint	Fine	25.13	±0.40	100	100
Rb	Kα	LiF(200)	Scint	Fine	26.60	±0.60	100	100
Zn	Kα	LiF(200)	Scint	Fine	41.79	±0.40	60	60
Cu	Kα	LiF(200)	Scint	Fine	45.02	±0.40	60	60
Ni	Kα	LiF(200)	Scint	Coarse	48.67	±0.60	60	60
Cr	Kα	LiF(200)	FPC	Fine	69.35	±0.50	60	60
Fe	Kα	LiF(220)	FPC	Fine	85.37	−0.40+0.70	40	40
V	Kα	LiF(220)	FPC	Fine	122.84	−0.50	60	60
TiO_2	Kα	LiF(200)	FPC	Fine	86.14	±0.50	40	40
[c]Ce	Lα	LiF(220)	FPC	Coarse	127.92	±1.50	100	100
[c]Ba	Lβ	LiF(220)	FPC	Coarse	128.53	±1.50	100	100

Note: All elements analyzed under vacuum on goniometer 1, at generator settings of 60 kV and 50 mA.

[a] FPC = flow proportional counter using P_{10} gas; KrSC = sealed krypton gas counter; Scint = NaI scintillation counter.

[b] Total iron as Fe_2O_3.

[c] Calibrated, but not analyzed for basalts.

where BF_i is the peak to average background ratio for element i, PK_i *is the peak intensity for element* i, and $AVBg_i$ is the average background intensity for element i.

Thus, when measuring unknowns, the true or modified background (MBg_i) is calculated by multiplying the average measured background for element i ($AVBg_i$) by the value of BF_i. This new modified background value is then subtracted from the peak intensity (PK_i) to arrive at the net peak intensity ($NETPK_i$) for element i:

$$MBg_i = AVBg_i \cdot BF_i,$$

$$NETPK_i = PK_i - MBg_i.$$

4. Remove spectral interferences. During calibration, interferences are measured on synthetic pellets containing pure quartz and the interfering element. A ratio of the interference intensity to the net peak intensity of the interfering element is calculated and assumed constant with respect to concentration. When measuring an unknown sample, the net interference ($INTFER_{ij}$) is calculated and removed by the following:

$$INTFER_{ij} = NETPK_i \cdot IR_{ij},$$

$$CNETPK_j = NETPK_j - INTFER_{ij},$$

where $INTFER_{ij}$ is the net interference intensity of element i on element j, and $CNETPK_j$ is the net intensity of element j with the interference element i removed. In the case of mutually interfering elements, an iterative approach to this same calculation is used until all the involved elements converge on their respective corrected values. 5. Measure mass absorption coefficients. To correct for matrix differences between samples, three separate mass absorption coefficients are determined following a modification of the Compton scattering technique of Reynolds (1967). Measured intensities from the Rh K-series Compton, Fe Ka, and Ti Ka lines are compared to the calculated absorption coefficients of rubidium (*ARb*), chromium (*ACr*), and vanadium (*AV*), respectively. From this comparison, three equations can be written to describe the relationship between each coefficient and its respective line. The three equations derived from the Leg 111 calibration are as follows:

$$A_{Rb} = 104/([Rhcps \cdot 0.0698] - 57.79),$$

$$A_{Cr} = A_{Rb}/([Fecps \cdot 1.044 \times 10^{-4}] + 0.081),$$

$$A_V = A_{Cr}/([Ticps \cdot 6.140 \times 10^{-4}] + 0.778)$$

where *Rhcps*, *Fecps*, *Ticps* are the intensities in counts per second of the Rh Compton, Fe Ka, and Ti Ka lines, respectively. Using this method, unknowns can be measured and corrected for matrix differences without calculating the absorption coefficients for each sample.

6. Calculate concentrations. Once all spectral and matrix corrections are calculated, the equation for calculating elemental concentrations is reduced to

$$C_i = (CNETPK_i A_i)/K_i,$$

where C_i is the concentration of element i in parts per million, $CNETPK_i$ is the corrected net peak intensity for element i, A_i is the mass absorption coefficient for element i, and K_i is the calibration factor (ppm/cps) for element i. K_i is analogous to the calibration curve slope (*mi*) for major elements and is determined in the same manner for natural rock (AGV-1, UB-N, G-2, BHVO-1, RGM-1, DRN) and synthetic (com-

sed, spiked quartz powders) standards. Details of the
ytical conditions for each element determined are given in
e 2.

PHYSICAL PROPERTIES

he shipboard physical-properties program provides mea-
ments of the different physical or geotechnical properties
impled materials. The physical properties routinely mea-
d on board *Resolution* are bulk density, grain density,
r content, porosity, compressional-wave velocity, mag-
susceptibility, thermal conductivity, and undrained
r strength. Physical properties assist in the characteriza-
of different lithologic units, allow for verification of
nhole geophysical logging results, and can provide con-
nts on the interpretation of seismic-reflection and other
hysical data. Furthermore, these data may be used to
nate the permeability and degree of consolidation, to
ect sedimentation rates, and to aid in heatflow calcula-
. Depth profiles of geotechnical properties may be used to
nguish lithologic boundaries at drill sites as well as to
elate and establish facies changes between sites.

discussion of physical-property determination with re-
to equipment, methods, errors, correction factors, and
lems related to coring disturbance was presented by
e (1976), who showed that physical properties are influ-
d by drilling and sampling disturbance, as well as by the
ng procedures used in the laboratory. For example, the
r content of a particular sample may be increased by the
ng fluid (seawater) that typically surrounds a disturbed
for many hours prior to removal of the sample from the
for testing.

amples used for determining physical properties were
ted from areas having the least sample disturbance, and
ient samples were tested to permit us to characterize the
r lithologic units. Typically, one sample was taken per
on of core for evaluating index properties; compression-
ve velocity was measured on the same sample or on one
the immediate vicinity. Samples were chosen to be as
sentative as possible of the section as a whole; however,
samples were taken from thinner units having markedly
ent lithologies. Sample selection and relative frequency
nded on the thickness and homogeneity of a particular
ence.

e testing methods employed during Leg 125 are dis-
d in the following text in the order in which they were
rmed on each core. GRAPE, compressional-wave (*P*-
) velocity logging, magnetic susceptibility, and the determi-
n of thermal conductivity of soft sediments were performed
hole-round core samples. Other measurements were con-
d on discrete samples of split cores.

Gamma-Ray Attenuation Porosity Evaluator

e GRAPE technique was described by Boyce (1976).
GRAPE makes a continuous measurement of wet-bulk
ty on whole APC and XCB sections. Generally, piston
and only the first few XCB cores were tested because
PE data are valid only from complete cores. An alumi-
standard was used to calibrate the apparatus and was
zed frequently. The section to be measured was mounted
ontally on the MST, while the core moved through the
rs on a conveyor belt. The attenuation of gamma rays
ng through the liner and core was measured every 1.5 to
n, and the bulk density was calculated from the attenu-
values. GRAPE data were filtered to remove data that
from gas or gaps and end-cap effects before the data
averaged over 0.2- or 0.5-m intervals. All bulk-density
are reported in units of g/cm^3.

P-Wave Logger

The *P*-wave logger (PWL) operates on the MST along with the GRAPE and magnetic susceptibility meter. A transducer produced a short 500-kHz compressional-wave pulse at a repetition rate of 1 kHz. A receiving transducer was positioned so that the two transducers were aligned perpendicular to the core axis. A pair of displacement transducers monitored the separation between the compressional-wave transducers. This compensated for variations in the outside liner diameter without degrading the accuracy of the velocities measured. Measurements were performed at 1.5- to 2.0-cm intervals.

Water was applied to the core liner to improve acoustic contact between the transducers and the liner. As with the GRAPE, only APC and the first few XCB cores were measured because high-quality data can only be obtained from cores that completely fill the liner. The deeper XCB cores and all RCB cores from Leg 125 contained annular voids between the core and the inside of the liner that prevented transmission of the compressional waves between the transducers. Filtering the PWL data removed data resulting from gas, gaps, and end-cap effects. Weak returns with signal strengths below a threshold value of 200 m/s were not recorded. The data were averaged over 0.2- or 0.5-m intervals.

Magnetic Susceptibility

Magnetic susceptibility was measured on the MST. Poor data were recorded for Sites 778 and 779 because of sensor malfunction and improper zeroing of the instrument. Prior to Site 780, the sensor was replaced and functioned well. Like GRAPE and PWL data, magnetic susceptibility data are only valid from full core liners. Erratic values have been observed when liners are only partially filled or contain broken pieces of hard rock. Magnetic susceptibility is dimensionless in the SI system.

Thermal Conductivity

Following MST measurements and prior to measuring thermal conductivity, the whole-round cores were equilibrated to room temperature for 2 to 4 hr. The thermal-conductivity techniques used here have been described by Von Herzen and Maxwell (1959) and Vacquier (1985). All thermal-conductivity data are reported in units of W/mK.

Soft-Sediment Thermal Conductivity

Needle probes connected to a Thermcon-85 unit were inserted into the sediment through holes drilled into the core liner, and the thermal drift was monitored. Probe behavior was monitored by inserting an additional probe into a reference material. Once the temperature became stable, the probes were heated, and the coefficient of thermal conductivity was calculated as a function of the change in resistance in the probe. When the sediment became too stiff to allow for easy insertion of the probe, holes were drilled into the core material. We attempted to insert the probes at locations along each core section that appeared to be the least disturbed. However, an annulus of disturbed sediment and drill fluid that was commonly present along the inside of the liner prevented some visual identification of the more intact segments of the core.

Hard-Rock Thermal Conductivity

Thermal conductivity measurements on well-lithified sediments and rocks were performed on split cores using a needle probe that was partially embedded in a slab of insulating material. The split-core sample was not polished. The flat surface of a selected sample of split core was placed on top of the slab. Dow Corning 3 silicone was used to improve the thermal contact between the slab and the sample. The sample and slab were immersed in a salt-water bath and allowed to equilibrate thermally. The probe was heated, and measurements of changes of resistance in the probe were performed every 9 s for a 9-min interval. Thermal conductivity was determined from the most linear portion of a temperature vs. log-time plot.

Undrained Shear Strength

Undrained shear strength of the sediment (Boyce, 1977; Lee, 1984) was determined using a Wykeham-Farrance motorized vane apparatus. This four-bladed vane has a diameter of 1.28 cm and is 1.28 cm long. It was inserted into the split section perpendicular to the core axis until the top of the blade was covered by about 4 to 6 mm of sediment. The vane was then rotated at a rate of about 90°/min until the sediment failed. The undrained shear strength was calculated from the peak torque obtained at failure. Vane rotation continued for a minimum of 120° to permit determination of remolded shear strength. The peak and remolded "torques" were measured from calibrated plots of torque vs. rotation generated on a Hewlett-Packard 7015B X-Y Recorder. Vane testing ceased when radial cracking or other noncylindrical failure surfaces developed around the vane. During Leg 125, noncylindrical failures were observed in the stiffer sediments that had undrained shear strengths exceeding approximately 50 kPa. All shear strengths are reported in units of kPa.

Compressional-Wave Velocity

Compressional-wave velocities, in addition to those previously described, were measured on samples that were sufficiently stiff to allow for sampling and to provide adequate signal strength. Velocities were calculated from the determination of the traveltime of a 500-kHz compressional wave through a measured thickness of sample, using a Hamilton Frame Velocimeter and Tektronix DC 5010 counter/timer system. Travel distance was measured with an attached variable resistor (LVT) connected to a Tektronix DM 5010 digital multimeter. Parallel-sided samples were cut either with a knife in the softer sediments or with a double-bladed diamond saw in the more brittle or lithified sediments. Samples of igneous and metamorphic rocks were cut with a double-bladed diamond saw or a 2.5-cm rock corer.

The Hamilton Frame velocity transducers were calibrated with lucite and aluminum standards. The variable resistor was calibrated with standard lengths of aluminum cylinders. Zero traveltimes were measured with the two transducers in contact with the signal amplitude adjusted to 2 V on the oscilloscope. Zero times were determined once per core tested. Seawater was used to improve the acoustic contact between the sample and the transducers. Readings of traveltime through samples were taken after the signal amplitude on the oscilloscope had been adjusted to 2 V. When signal strength was insufficient, velocities from the sample were not recorded.

Index Properties

The index properties of wet-bulk density, grain density, porosity, water content, and void ratio were determined on selected samples of sediment and rock. Measuring index properties and compressional-wave velocities from the same samples allowed us to correlate directly among those values that may indicate trends as well as to provide a check for data consistency. Samples were weighed wet using two calibrated Scientech 202 electronic balances interfaced with a PRO350 computer, which compensates for the motion of the ship by taking the average of 200 sample weighings. Dry-sample weight was determined using the same procedure after freeze-drying the sample for at least 12 hr. Dry volumes were measured using a Quantochrome Helium Penta-Pycnometer. The pycnometer was not accurate for wet volumes because of helium absorption by water. Therefore, wet volumes were calculated based on the assumed volume of water extracted from the sample using the following expression:

(wet weight dry weight/density of seawater) + dry volume,

using a value of 1.03 g/cm^3 as the density of seawater.

The following definitions and units were used for the index properties:

1. Porosity (%) = 100 × volume of water/volume of wet sediment.
2. Bulk density (g/cm^3) = weight of wet sediment/volume of wet sediment.
3. Grain density (g/cm^3) = weight of dry sediment/volume of dry sediment.
4. Water content (%) = 100 × weight of water/dry weight of sediment.
5. Void ratio (dimensionless) = volume of water/volume of dry sediment.

Dry-sediment weights and volumes used in the preceding calculations were corrected for salt content (assuming seawater salinity of 35‰) by subtracting the estimated weight and volume of residual salt.

Data Presentation

The physical properties measured for samples during Leg 125 are presented in tables and figures in each site chapter. All index properties and thermal-conductivity data are presented in both the tables and the figures. (Tables of GRAPE and PWL data would be excessively long, however, and thus are not presented.) The GRAPE, PWL, and magnetic susceptibility data were filtered to remove spurious data and to reduce the number of data points. Porosity (j), bulk density (r),and compressional-wave velocity (*Vp*) values are given in the "Physical Properties" column on the barrel sheets for the cores of each site.

DOWNHOLE MEASUREMENTS

Tool Strings

Downhole logging directly determines the physical and chemical properties of formations adjacent to the borehole. Interpretation of these continuous, *in-situ* measurements can provide a stratigraphic, lithologic, geophysical, and mineralogic characterization of the site. After coring is completed at a hole, a tool string is lowered downhole on a seven-conductor cable, and each of several tools in the tool string continuously monitors some property of the adjacent borehole. Of the dozens of different tool strings commonly used in the petroleum industry, two Schlumberger tool strings were used during Leg 125: the seismic stratigraphic and lithoporosity (physical properties) string and the geochemical string. The Lamont-Doherty Geological Observatory (LDGO) borehole televiewer (BHTV) and magnetometer also were run during Leg 125.

The seismic-lithoporosity (physical properties) combination used during Leg 125 is a digital string, normally consisting of the LDGO temperature tool (TLT), the dual induction tool (DIT), the digital sonic tool (SDT), the mechanical caliper device (MCD), and the lithodensity tool (LDT). This tool combination measures compressional-wave velocity and can provide indicators of the two variables that most often control velocity: porosity, as indicated by resistivity, and clay content. This combination can also provide measurements of formation porosity and density and can determine the spectral content of naturally occurring radiation.

The geochemical combination normally consists of the LDGO temperature tool, the compensated neutron tool (CNT), the induced gamma-ray spectrometry tool (GST), the aluminum clay tool (ACT), the natural gamma-ray spectrometry tool (NGT), and the general purpose inclination tool (GPIT). This tool combination can measure the relative concentrations of 11 elements: silicon, calcium, aluminum, iron, sulfur, manganese, hydrogen, chlorine, potassium, thorium, and uranium.

Logs

A brief description of the logging tools run during Leg 125 is provided. The principles and applications of logging tools have been described in detail in Schlumberger (1972), Serra (1984), and Timur and Toksöz (1985).

Temperature Tool

The LDGO temperature tool (TLT) is a self-contained tool that can be attached to any Schlumberger tool string or to the televiewer. Data from two thermistors and a pressure transducer were collected every 0.5 to 5.0 s and stored in a Tattletale computer within the tool. Following the logging run, data are dumped from the Tattletale to the Masscomp computer for analysis. A fast-response thermistor, although not too accurate, is able to detect sudden very small temperature excursions caused by fluid flow from the formation. A slow-response thermistor is very accurate and can be used to estimate heat flow. Data are recorded as a function of time; conversion to depth can be based on the pressure transducer or, preferably, on simultaneous recording by Schlumberger of both depth and time.

Electrical Resistivity

The dual induction tool (DIT) provides three different measurements of electrical resistivity, each with a different depth of investigation. Two induction devices (deep and medium resistivity) send high-frequency alternating currents through transmitter coils, creating magnetic fields that induce secondary (Foucault) currents in the formation. These ground-loop currents produce new inductive signals, proportional to the conductivity of the formation, which are recorded by the receiving coils. Measured conductivities then can be converted to resistivity. A third device (spherically focused resistivity) can measure the current necessary to maintain a constant voltage decrease across a fixed interval. Vertical resolution is approximately 2 m for the medium- and deep- resistivity devices and 1 m for the focused-resistivity device.

Water content and salinity are by far the most important factors controlling the electrical resistivity of rocks. To the first order, resistivity responds to the inverse square root of porosity (Archie, 1942). Other factors influencing resistivity include the concentration of hydrous and metallic minerals, vesicularity, and geometry of interconnected pore space.

Sonic Velocity

The digital sonic (SDT) tool uses two acoustic transmitters and two receivers to measure the time required for sound waves to travel over source-receiver distances of 2.4, 3.0, and 3.6 m. The raw data are expressed as time required for a sound wave to travel through 0.30 m of formation; these traveltimes are then converted to sonic velocities. First arrivals for the individual source-receiver paths can be used to calculate the velocities of the different waves traveling in the formation (compressional, shear, etc.). Only compressional-wave velocity is determined during data acquisition, but waveforms are recorded for post-cruise determination of shear-wave velocities and possibly to improve compressional-wave velocities. The vertical resolution of the tool is 0.30 m. Compressional-wave velocity is dominantly controlled by porosity and lithification; decreases in porosity and increases in lithification cause the velocity to increase.

Mechanical Caliper Device The mechanical caliper device (MCD) can provide a basic two-dimensional caliper log of the borehole by means of a bowspring-mounted measurement system. The hole diameter (HD) log is used to detect washouts or constrictions. Borehole diameter significantly affects many of the other logging measurements, and thus is an important factor in log correction routines.

Lithodensity Tool

The lithodensity tool (LDT) uses a ^{137}Ce gamma-ray source to measure the resulting flux at fixed distances from the source. Under normal operating conditions, attenuation of gamma rays is chiefly caused by Compton scattering (Dewan, 1983). Formation density is extrapolated from this energy flux by assuming that the atomic weight of most rock-forming elements is approximately twice the atomic number. An index of photoelectric effect is also provided. Photoelectric absorption occurs in the energy window below 150 keV and depends on the energy of the incident gamma ray, the atomic cross section, and the nature of the atom. This measurement is almost independent of porosity, thus can be used directly as a matrix lithology indicator. The radioactive source and detector array were placed in a tool that was pressed against the borehole wall by a strong spring. Excessive roughness of the hole may cause some drilling fluid to infiltrate between the skid and the formation. As a consequence, density readings can be artificially low. Approximate corrections can be applied by using caliper data. The vertical resolution is about 0.30 m.

Compensated Neutron Porosity

A radioactive source mounted on the compensated neutron porosity tool (CNT) sonde emits fast neutrons (4 MeV) into the formation, where they are scattered and slowed by collisions with other nuclei. When the neutrons reach a low energy level (0.025 MeV), they are captured and absorbed by atomic nuclei, such as hydrogen, chlorine, silicon, and boron. The scattering cross section is the quantity that describes the rate at which neutrons were slowed. The scattering cross section for hydrogen is about 100 times larger than for any other common element in the crust, so most energy dissipation is caused by collisions with water molecules. Therefore, a change in the number of neutrons detected at a receiver can be related to porosity. In practice, an array of detectors is used to minimize borehole or drilling fluid effects. Because water is present both in pores and as bound water (e.g., clay minerals), porosity measurements made in the presence of hydrous minerals overestimate the true porosity. The vertical resolution of the tool theoretically is about 0.25 m, but low signal-to-noise ratio degrades the potential resolution.

Gamma-Ray Spectrometry Tool

The induced gamma-ray spectrometry tool (GST) consists of a pulsed source of 14-MeV neutrons and a gamma-ray scintillation detector. A surface computer performs spectral analysis of gamma rays resulting from the interactions of neutrons emitted by the source with atomic nuclei in the formation. Characteristic sets of gamma rays from six elements dominate the spectrum: calcium, silicon, iron, chlorine, hydrogen, and sulfur. Processing normalizes the sum of these data, so they do not reflect the actual elemental composition. Therefore, ratios of these elements commonly are used for interpreting the lithology, porosity, and salinity of formation fluid.

Aluminum Clay Tool

Aluminum abundance, as measured by the aluminum clay tool (ACT), is determined by neutron-induced (Californium chemical source) late gamma-ray spectrometry. By placing NaI detectors both above and below the neutron source, contributions from natural gamma-ray activity can be removed. Calibration to elemental weight percent is performed by taking irradiated core samples of known volume and density and measuring their gamma-ray output while placed in a jig attached to the logging tool (typically after logging).

Natural Gamma Ray Tool

The natural gamma-ray tool (NGT) measures the natural radioactivity of the formation. Most gamma rays are emitted by the radioactive isotope ^{40}K and by the radioactive elements of the uranium and thorium series. The gamma-ray radiation originating in the formation near the borehole wall is measured by a scintillation detector mounted inside the sonde. Analysis is achieved by subdividing the entire incident gamma-ray spectrum into five discrete energy windows. The total counts recorded in each window, for a specified depth in the well, are processed at the surface to give the elemental abundances of potassium, uranium, and thorium. Because radioactive elements tend to be most abundant in clay minerals, the gamma-ray curve is commonly used to estimate the clay or shale content. There are rock matrices, however, for which the radioactivity ranges from moderate to extremely high values, as a result of the presence of volcanic ash, potassic feldspar, or other radioactive minerals.

General Purpose Inclination Tool

The general purpose inclination tool (GPIT) contains three accelerometers at right angles to each other and three magnetometers, also at right angles to each other. The device measures the orientation of the tool string within the hole and the orientation (or deviation) of the borehole itself. Several other engineering measurements are also performed.

Borehole Televiewer

The borehole televiewer (BHTV) is an ultrasonic, high-resolution logging tool designed to measure the geometry of the borehole wall, fractures, and lithostratigraphic features. The televiewer contains a rotating acoustic transducer that emits a focused 3° beam pulse at a rate of 1800 times/s. Two transducers allow the BHTV to operate in either low-frequency (400 kHz) or high-frequency (1.4 MHz) mode. The high-frequency transducer is designed to resolve such detailed features as fracture density and fracture aperture. The low-frequency transducer emits a more powerful signal and thus is usually more useful in the large-diameter ODP holes. The orientations of all features are determined by a fluxgate magnetometer that triggers the signal at each crossing of magnetic north, while the tool is pulled uphole at a rate of 2.5 cm/s. A reflectance image of the borehole wall is obtained in real time by windowing the acoustic reflection off the borehole wall and recording this on Polaroid film. The raw output consists of full waveform acoustic seismograms that also are recorded on videotape for later reprocessing. The traveltimes and the degree of acoustic reflectance from these data can then be used to determine a more accurate three-dimensional image of the borehole geometry, as well as to delineate the textural characteristics of the borehole wall.

Quality of Log Data

The quality of log data may be seriously degraded in excessively large sections of the borehole or by rapid changes in the hole diameter. Resistivity and velocity measurements are least sensitive to borehole effects. The nuclear measurements (i.e., density, neutron porosity, and both natural and induced spectral gamma rays) are most seriously impaired because of the large attenuation by the borehole fluid. Corrections can be applied to the original data to reduce the effects of these conditions and, generally, to reduce any departure from the conditions under which the tool was calibrated.

There may be small deviations in depth between different logs. These deviations are caused by either stretching of the cable or heave of the ship during recording. Small errors in correlation can impair the interpretations in zones of frequent changes of lithology. To minimize such errors, a hydraulic heave compensator adjusts for rig motion in real time. Precise correlation between logging depths and depth of features within the cores is not possible in zones where core recovery is low because of the inherent ambiguity of placing the recovered section within the interval cored.

Log Analysis

During logging, incoming data are observed in real time on a monitor oscilloscope and recorded simultaneously on digital tape in either the Schlumberger logging unit or the downhole measurements laboratory. After logging, the Schlumberger tape is read by the Masscomp computer system in the laboratory and reformatted to a file format compatible with the Terralog log-interpretation software package. Rather than being a "black box," Terralog is an interactive system that consists of many log manipulation and plotting options. Thus, log analysis and interpretation vary in duration and procedure for each site. Most log interpretation was conducted aboard ship; logs will be analyzed and interpreted further after the cruise, using a companion system in the Borehole Research Laboratory of Lamont-Doherty Geological Observatory.

Reprocessing of Logs

Raw count rates for six elements (calcium, silicon, iron, sulfur, chlorine, and hydrogen) are obtained in real time by the Schlumberger data acquisition software. These count rates commonly exhibit some inversion interference of chlorine with other elemental count rates, which is manifest as a strong, but spurious, correlation between chlorine and calcium, and weaker correlations with other elements measured by the tool. This interference, which has been attributed to the dominance of the induced gamma-ray spectrum by chlorine, is unavoidable in ODP holes because the minimum pipe diameter is too small to allow for use of a boron sleeve to suppress chlorine counts. Most of the effects of this interference are removed aboard ship by adding to each count-rate log the product of chlorine counts and the slope of a first-degree regression with chlorine.

The shipboard correction is obviated by post-cruise reprocessing, using a Schlumberger Elite 1000 work station and proprietary Schlumberger software. With a revised algorithm, the gamma-ray spectrum at each depth is inverted for titanium, gadolinium, and potassium in addition to the six elements previously listed. Though gadolinium is present in concentrations of only a few parts per million, its neutron-capture cross section is so large that gadolinium can account for 10% to 30% of the total gamma-ray spectrum. Inclusion of these additional elements improves the quality of the overall inversion, particularly by improving the accuracy of calculated abundance of calcium, by converting sources of unaccounted variance to signals. However, the determined potassium concentrations are less accurate than those from the NGT, and the hydrogen concentrations are less accurate than those from the neutron tool.

Aluminum concentrations from the ACT require only one correction, an adjustment for variations in cable speed. Changes in logging speed affect the time lag between neutron irradiation of the formation and recording of the induced gamma-ray spectrum because the number of induced gamma rays decreases rapidly with time. Post-cruise correction will be made on the basis of the cable speed recorded during logging. However, the small amount of ship heave during logging may make this correction less reliable in ODP holes than in land wells.

When both Schlumberger tool strings are run, further reprocessing of geochemical logs is possible. The relative abundances of calcium, silicon, iron, titanium, aluminum, sulfur, potassium, thorium, uranium, and gadolinium are used to calculate a log of predicted photoelectric effect. The difference between this log and the actual log of photoelectric effect can be attributed to the only two major elements not measured directly, magnesium and sodium. Major elements are converted from volume percent to weight percent using logs of total porosity (bound water plus pore water) and density. Major elements are expressed in terms of oxide dry weight percent, based on the assumption that oxygen is 50% of the total dry weight.

If GST data are available, but not enough log types are run to permit complete solution for oxide weight percentage, one further processing step is made. Omitting chlorine and hydrogen, the yields of the other GST elements (calcium, silicon, iron, titanium, sulfur, potassium, and gadolinium) are summed, and each is expressed as a fraction of this total yield. This procedure corrects for variation porosity and count rate. Although the absolute abundance of each element is not determined, downhole variations in relative abundance are indicated.

Sonic logs obtained in real time are not based on full-waveform analysis, but on a threshold-measuring technique that attempts to detect the compressional-wave arrival by a first-break criterion. Sometimes this technique fails and either the threshold is exceeded by noise or the first compressional arrival is below the threshold. This phenomenon, called cycle skipping, creates spurious spikes on the sonic log. During Leg 125, raw traveltimes were reprocessed with an algorithm designed to reject cycle skips (Srivastava, Arthur, et al., 1987). This algorithm was expanded to include calculation of a caliper log, based on Snell's law and the fact that the observed total source-receiver traveltime is a sum of the known refracted-wave traveltime through the formation and unknown traveltime in the borehole. Though the resulting caliper log is sensitive to assumed fluid velocity, it is probably superior to the hole diameter measured by the caliper tool. The caliper tool used at ODP is subject to sticking when formation mud gets into its mechanical parts, resulting in bimodal (fully open or nearly fully closed) readings.

Synthetic Seismograms

Synthetic seismograms are generated from logging data obtained with the long-spaced sonic (LSS) tool. The bulk-density log from the lithodensity tool or a pseudodensity log created from other logs is required in addition to the slowness log. In many cases, a simple constant density log can be used. Experience shows that this often gives surprisingly good results because both velocity and density are usually controlled by the same parameter: porosity. When velocity and density are highly correlated, synthetic seismograms using a constant density log or an actual density log are virtually identical.

The slowness and density logs are used in the program to generate an impedance log (velocity × density), which is convolved with a zero-phase Ricker wavelet. The frequency of this wavelet can be varied, depending on the source generating the original seismic profile. A 30-Hz wavelet is capable of a vertical resolution on the order of 30 m, so reflectors cannot generally be attributed to any small-scale lithologic horizons. The synthetic seismogram is plotted with two-way traveltime on the left scale and depth below seafloor on the right. The plot is scaled to uniform time spacing, not uniform depth spacing.

In-Situ Stress Measurements

The BHTV is used to detect stress directions from borehole breakouts. Stress-induced wellbore breakouts are elongated zones of spalling along cylindrical holes in rocks. They commonly span a few tens of degrees of circumference. In an isotropic, linearly elastic rock subject to differential stresses, breakouts form along the borehole wall as a result of compressive stress concentrations exceeding the strength of the rock. Under these conditions, the breakout orientation will develop in the direction of the least dominant horizontal stress. Research has demonstrated in different areas that stress orientations deduced from breakouts are consistent with other independent indicators (Bell and Gough, 1979; Zoback and Zoback, 1980, in press; Zoback et al., 1988). Differential horizontal stresses that do not cause failure of the borehole wall may cause borehole ellipticity. Ellipticity also can be detected with the BHTV.

REFERENCES

Archie, G. E., 1942. The electrical resistivity log as an aid in determining some reservoir characteristics. *J. Pet. Technol.*, 5:1–8.

Backman, J., Duncan, R. A., et al., 1988. *Proc. ODP, Init. Repts.*, 115: College Station, TX (Ocean Drilling Program).

Barnes, R. O., 1988. ODP *in-situ* fluid sampling and measurement: a new wireline tool. *In* Mascle, A., Moore, J. C., et al., *Proc. ODP, Init. Repts.*, 110: College Station, TX (Ocean Drilling Program), 55–63.

Barron, J. A., 1983. Latest Oligocene through early middle Miocene diatom biostratigraphy of the eastern tropical Pacific. *Mar. Micropaleontol.*, 7:487–515.

————, 1985a. Late Eocene to Holocene diatom biostratigraphy of the equatorial Pacific Ocean, Deep Sea Drilling Project Leg 85. *In* Mayer, L., Theyer, F., et al., *Init. Repts. DSDP*, 85: Washington (U.S. Govt. Printing Office), 413–456.

————, 1985b. Miocene to Holocene planktic diatoms. *In* Bolli, H. M., Saunders, J. B., and Perch-Nielsen, K. (Eds.), *Plankton Stratigraphy*: Cambridge (Cambridge Univ. Press), 763–810.

Bell, J. S., and Gough, D. I., 1979. Northeast-southwest compressive stress in Alberta: evidence from oil wells. *Earth Planet. Sci. Lett.*, 45:475–482.

Berggren, W. A., 1977. Atlas of Paleogene planktonic foraminifera. *In* Ramsey, A.T.S. (Ed.), *Oceanic Micropaleontology* (vol. 1): London (Academic Press), 205–300.

Berggren, W. A., Kent, D. V., Flynn, J. J., and Van Couvering, J. A., 1985. Cenozoic geochronology. *Geol. Soc. Am. Bull.*, 96:1407–1418.

Blow, W. H., 1969. Late Middle Eocene to Recent planktonic foraminiferal biostratigraphy. *In* Renz, H. H., and Brönnimann,

P. (Eds.), *Proc. Int. Conf. Planktonic Microfossils*, Geneva, 1967, 1:199–422.

———, 1979. *The Cainozoic Foraminiferida*. Leiden (E. J. Brill).

Boyce, R. E., 1976. Definitions and laboratory techniques of compressional sound velocity parameters and wet-water content, wet bulk density and porosity parameters by gravimetric and gamma ray attenuation techniques. *In* Schlager, S. O., Jackson, E. D., et al., *Init. Repts. DSDP*, 33: Washington (U.S. Govt. Printing Office), 931–958.

———, 1977. Deep-sea drilling procedures for shear strength measurements of clayey sediment using modified Wykeham Farrance Laboratory Vane Apparatus. *In* Barker, P., Dalziel, I.W.D., et al., *Init. Repts. DSDP*, 36: Washington (U.S. Govt. Printing Office), 1059–1068.

Bramlette, M. N., and Bradley, W. H., 1942. Geology and biology of North Atlantic deep-sea cores between Newfoundland and Ireland. Pt. 1, lithology and geologic interpretations. *U.S. Geol. Surv. Prof. Pap.*, 196(A):1–55.

Bukry, D., 1973. Low-latitude coccolith biostratigraphic zonation. DSDP Leg 15. *In* Edgar, N. T., Saunders, J. B., et al., *Init. Repts. DSDP*, 15: Washington (U.S. Govt. Printing Office), 685–703.

Burckle, L. H., 1972. Late Cenozoic diatom zones from the eastern equatorial Pacific. *Nova Hedwigia*, 39:217–246.

———, 1977. Pliocene and Pleistocene diatom datum levels for the equatorial Pacific. *Quat. Res.*, 7:330–340.

———, 1978. Early Miocene to Pliocene diatom datum levels for the equatorial Pacific. *Proc. 2nd Working Group Mtg., Biostratigraphic Datum-Planes of the Pacific Neogene, IGCP Project 114*, 1:25–44.

Burckle, L. H., and Trainer, J., 1979. Middle and late Pliocene diatom datum levels from the central Pacific. *Micropaleontology*, 25(3):281–293.

Cowan, D. S., and Mansfield, C. F., 1970. Serpentinite flows on Joaquin Ridge, Southern Coast Ranges, California. *Geol. Soc. Am. Bull.*, 81:2615–2628.

Dewan, J. T., 1983. *Essentials of Modern Open Hole Log Interpretation*. Tulsa (Pennwell Books).

Fisher, R. V., and Schmincke, H.-U., 1984. *Pyroclastic Rocks*. New York (Springer-Verlag).

Gealy, E. L., Winterer, E. L., and Moberly, R. M., Jr., 1971. Methods, conventions, and general observations. *In* Winterer, E. L., Riedel, W. R., et al., *Init. Repts. DSDP*, 7, Pt. 1: Washington (U. S. Govt. Printing Office), 9–26.

Gieskes, J. M., and Peretsman, G., 1986. *Water Chemistry Procedures Aboard JOIDES Resolution—Some Comments*. Ocean Drilling Program, Tech. Note 5.

Kennett, J. P., and Srinivasan, M. S., 1983. *Neogene Planktonic Foraminifera: A Phylogenetic Atlas*. Stroudsburg, PA (Hutchinson Ross).

Koizumi, I., 1986. Pliocene and Pleistocene diatom datum levels related with paleoceanography in the northwest Pacific. *Mar. Micropaleontol.*, 10:309–325.

Lee, H. J., 1984. State of the art: laboratory determination of strength of marine soils. *In* Chaney, R. C., and Demars, K. R. (Eds.), *Strength Testing of Marine Sediments: Laboratory and In-Situ Measurements*. ASTM Spec. Tech. Publ., 883:181–250.

Manheim, F. T., and Sayles, F. L., 1974. Composition and origin of interstitial waters of marine sediments based on deep sea drill cores. *In* Goldberg, E. D. (Ed.), *The Sea* (vol. 5): New York (Wiley), 527–568.

Martini, E., 1971. Standard Tertiary and Quaternary calcareous nannoplankton zonation. *In* Farinacci, A. (Ed.), *Proc. 2nd Plankton Conf., Roma 1970*, 2:739–785.

Moberly, R., and Klein, G. de V., 1976. Ephemeral color in deep-sea cores. *J. Sediment. Petrol.*, 46:216–225.

Munsell Soil Color Charts, 1975. Baltimore (Munsell Color).

Norrish, K., and Hutton, J. T., 1969. An accurate X-ray spectrographic method for the analysis of a wide range of geological samples. *Geochim. Cosmochim. Acta*, 33:431–453.

Okada, H., and Bukry, D., 1980. Supplementary modification and introduction of code numbers to the low-latitude coccolith biostratigraphic zonation. *Mar. Micropaleontol.*, 5(3):321–325.

Reynolds, R. C., 1967. Estimations of mass absorption coefficients by Compton scattering: improvements and extensions of the method. *Am. Mineral.*, 48:1133–1143.

Schmid, R., 1981. Descriptive nomenclature and classification of pyroclastic deposits and fragments: recommendations of the IUGS Subcommission on the Systematics of Igneous Rocks. *Geology*, 9:41–43.

Schlumberger Ltd., 1972. *Log Interpretation* (vol. 1): Houston.

Serra, O., 1984. *Fundamentals of Well Log Interpretation*: Amsterdam (Elsevier).

Shepard, F. P., 1954. Nomenclature based on sand-silt-clay ratios. *J. Sediment. Petrol.*, 24:151–158.

Shipboard Scientific Party, 1988. Explanatory Notes: Leg 112. *In* Suess, E., von Huene, R., et al., *Proc. ODP, Init. Repts.*, 112: College Station, TX (Ocean Drilling Program), 25–44.

Srivastava, S., Arthur, M. A., et al., 1987. Site 645. *In* Srivastava, S., Arthur, M. A., et al., *Proc. ODP, Init. Repts.*, 105: College Station, TX (Ocean Drilling Program), 61–418.

Streckeisen, A. L., 1973. Plutonic rocks: classification and nomenclature recommended by the IUGS Subcommission on the Systematics of Igneous Rocks. *Geotimes*, 18–10:26–30.

Timur, A., and Toksöz, M. N., 1985. Downhole geophysical logging. *Annu. Rev. Earth Planet. Sci.*, 14:315–344.

Vacquier, V., 1985. The measurement of thermal conductivity of solids with a transient linear heat source on the plane surface of a poorly conducting body. *Earth Planet. Sci. Lett.*, 74:275–279.

Von Herzen, R. P., and Maxwell, A. E., 1959. The measurement of thermal conductivity of deep-sea sediments by a needle-probe method. *J. Geophys. Res.*, 64:1557–1563.

Wentworth, C. K., 1922. A scale of grade and class terms of clastic sediments. *J. Geol.*, 30:377–390.

Zoback, M. D., and Zoback, M. L., 1980. State of stress in the conterminous United States. *J. Geophys. Res.*, 85:6113–6173.

Zoback, M. L., and Zoback, M. D., in press. Tectonic stress field of the continental United States. *In* Pakiser, L., and Mooney, W. (Eds.), *Geophysical Framework of the Continental United States*. Geol. Soc. Am. Mem.

Zoback, M. D., Zoback, M. L., Mount, V. S., Suppe, J., Eaton, J. P., Healy, J. H., Oppenheimer, D., Reasenberg, P., Jones, L., Raleigh, C. B., Wong, I. G., Scotti, O., and Wentworth, C. K., 1988. New evidence on the state of stress of the San Andreas Fault. *Science*, 238:1105–1111.

Ms 125A-102

Fryer, P., Pearce, J. A., Stokking, L. B., et al., 1990
Proceedings of the Ocean Drilling Program, Initial Reports, Vol. 125

3. UNDERWAY GEOPHYSICS[1]

Michael S. Marlow,[2] Dean L. Merrill,[3] and Shipboard Scientific Party[4]

INTRODUCTION

Underway geophysical data are an important part of the Ocean Drilling Program (ODP) because these data provide the basis for (1) defining the scientific problems to be addressed by drilling, (2) selecting sites, and (3) interpreting the drilling results within a regional structural and stratigraphic context. This chapter describes the acquisition and display of the underway geophysical data collected aboard *JOIDES Resolution* during Leg 125.

SHIPBOARD UNDERWAY GEOPHYSICS

JOIDES Resolution is equipped to acquire, display, and process a variety of geophysical data, including underway navigation, bathymetric, magnetic, single-channel seismic-reflection, and sonobuoy refraction/wide-angle reflection data. Digital logging of most of these data facilitates post-cruise processing. Navigation data, bathymetry, and magnetics data are routinely edited and corrected by the Geological Data Center (GDC) at Scripps Institution of Oceanography under contract to ODP. Merged digital data are produced in MGD77 Exchange Format and, along with microfilm copies of all original analog records, are available from the Data Librarian at ODP headquarters, College Station, Texas, the Site Survey Data Bank at Lamont-Doherty Geological Observatory, and the National Geophysical Data Center, Boulder, Colorado.

The equipment and methods used for the acquisition of underway geophysical data aboard *JOIDES Resolution* are briefly described in the following sections. We then describe and discuss the data collected at each site on Leg 125.

Navigation

Equipment and Methods

Primary navigation data were acquired during Leg 125 by a Magnavox model MX 1107 Transit/Global Positioning System (GPS) satellite navigator, located in the underway geophysics laboratory. Additional navigational equipment is located on the bridge of the vessel, including a Magnavox MX 4400 GPS receiver and a Magnavox MX 702A Transit satellite receiver, as well as Decca and Loran C radio-positioning systems. GPS position fixes were available during two intermittent windows totalling about 10–11 hr each day. Transit satellite fixes were available at various times throughout the day. The satellite receiver automatically calculated dead reckoning (DR) positions between satellite fixes while operating in the Transit mode. All fixes, together with course and speed information, were digitally recorded in a computer file at selected time intervals (typically every 15–30 min during nonseismic transit segments and every 2 min while acquiring seismic data) using a Masscomp 561 supermicrocomputer system. These data were used to produce plots of the ship's position as a function of time. A printout of all of the Transit satellite fixes and GPS and DR fixes at 30-min intervals was also obtained. Fixes collected while on site were averaged to produce the location for that site. Navigation data were compiled by the GDC and used for trackline displays. The navigation data are presented in Table 1 (microfiche, back pocket), and a trackline of the entire cruise is displayed in Figure 1.

Transits between Sites

Underway geophysical data were collected on Leg 125 during transits to and between drill sites. The data collected include (1) 3.5- and 12-kHz precision echo-sounder profiles, (2) total intensity measurements of the Earth's magnetic field, (3) single-channel seismic-reflection profiles (collected through each site), and (4) underway navigation data. The instruments were maintained and operated by ODP marine technicians, in cooperation with the shipboard scientific party and the officers and crew of SEDCO-FOREX, Inc.

Bathymetry: Equipment and Methods

Bathymetric data were acquired using both the 3.5- and 12-kHz systems and displayed using Raytheon model 1807M LSR Line Scan recorders, which were operated generally at a 1-s sweep rate. The 3.5-kHz system used a Raytheon PTR105B transceiver and 12 Raytheon transducers, whereas the 12-kHz system used a Raytheon PTR105B transceiver driving an EDO 323B transducer. Both systems normally operate with CESP-III correlators. Transducers for both systems are mounted in a sonar dome that was recently installed to improve noise conditions at high ship speeds and in rough weather conditions. The 3.5-kHz system provided some information regarding sub-bottom acoustic stratigraphy, generally with penetration of up to 5034, 4100 m. Bathymetric data encompassing the entire cruise are displayed in Figure 2.

Magnetics: Equipment and Methods

Measurements of the total intensity of the Earth's magnetic field were collected along the ship's track by a Geometrics 801 proton-precession magnetometer. The sensor was towed approximately 400 m behind the ship. Measurements were made at 3-s intervals with a sensitivity of about 1 nT. Values were digitally recorded in the header of the seismic-reflection data on the Masscomp computer every 99 s during nonseismic transit periods and once per shot (12-s interval) while acquiring seismic-reflection data. The magnetics data were also displayed in analog form on a strip-chart recorder in real time, with manual entries of the magnetic field intensity logged every 5 min. The magnetics data were processed later by the GDC to remove the regional International Geomagnetic Reference Field and to correct time variations (Fig. 2).

---

[1] Fryer, P., Pearce, J. A., Stokking, L. B., et al., 1990. *Proc. ODP, Init. Repts.*, 125: College Station, TX (Ocean Drilling Program).

[2] Office of Marine Geology, U. S. Geological Survey, 345 Middlefield Road, Menlo Park, CA 94025.

[3] Ocean Drilling Program, Texas A&M University, 1000 Discovery Drive, College Station, TX 77840.

[4] Shipboard Scientific Party is as given in the list of participants preceding the contents.

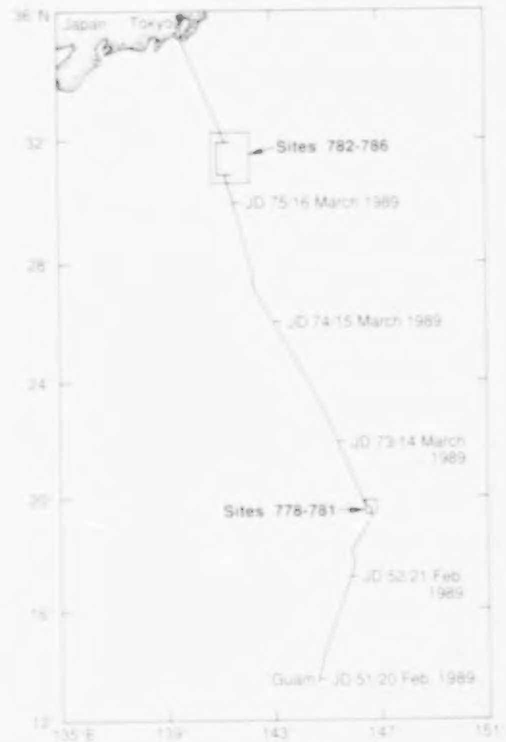

Figure 1. General trackline map of ODP Leg 125, showing site locations generated from GPS and Transit satellite navigation and the course- and speed-change data given in Table 1. Enlarged trackline maps are shown for Sites 778–781 in Figure 3 and for Sites 782–786 in Figure 18.

Seismic-Reflection Profiling: Equipment and Methods

The seismic-reflection data collected across drilling sites during Leg 125 are described in the following site sections. The ship's track along which seismic-reflection data were collected is shown in Figure 1.

Seismic Source

The seismic sources used for underway reflection profiling during Leg 125 consisted of two 80-in.^3 water guns (Seismic Systems, Inc.) fired at approximately 2000-lb pressure. The guns were towed approximately 14 m apart roughly 25 m behind the ship in special towing frames engineered by ODP. The guns were fired every 12 s and were towed at depths between 6 and 13 m, depending on the ship's speed.

Hydrophone Streamer

One 100-m Teledyne hydrophone streamer was towed from the fantail during Leg 125. The streamer was towed approximately 500 m behind the vessel at a depth ranging from 15 to 20 m. The output signals of the 60 active hydrophone elements of the streamer were summed to produce a single seismic signal.

Seismic Data Recording

Real-time analog seismic-reflection data were displayed on the two Raytheon recorders. The seismic signal from the hydrophone streamer was amplified and band pass-filtered at 40 to 150 Hz prior to display.

The seismic-reflection data were also simultaneously recorded in digital format by a Masscomp 561-based acquisition system using the HIGHRES software package. Data were filtered and displayed in real time on a 15-in. Printronix high-resolution graphics printer capable of a resolution of 160 dots per inch. Filtered seismic data were recorded on Cipher tape drives in SEG Y format at a density of 1600 bits per inch.

MARIANA SITES

Sites 778–781 were drilled to investigate Conical Seamount and a prominent reflector within a nearby horst structure. The trackline for these sites is shown in Figure 3.

Sites 778 and 779

Only one geophysical survey (Figs. 4 and 5) of Conical Seamount was run for Sites 778 and 779 because of the extensive SeaMARC II side-scan sonar images of the seamount and the six-channel seismic-reflection data collected during a 1987 site survey. The location for Site 778 was selected on the basis of the Leg 125 shipboard survey and geophysical surveys run during the 1987 survey (see Fryer et al., this volume). Site 778 was located on the flank of the seamount in the middle of a major serpentine flow that was outlined on the side-scan data. Site 779 was located about 3.5 km northeast of Site 778, where the side-scan sonar backscatter was lower and where we hoped there might be greater sediment cover.

Sites 778 and 779 are situated about halfway up the southern flank of Conical Seamount in water depths of 3913.7 and 3947.2 m, respectively (Fig. 6). The geophysical survey of Conical Seamount involved two crossings of the seamount before the beacon was dropped. The seismic-reflection record from the seamount revealed little of the internal structure of the seamount. Only short, discontinuous reflectors are evident in the record, indicating that perhaps thin sediment layers or serpentine flows flank the seamount. Continuous reflectors are absent from the profile of the seamount probably because of its chaotic internal structure related to diapirism and extrusion of flows onto its flanks or because of the lack of power in the seismic system.

Site 780

Site 780 was drilled on the west-southwest side of the summit of Conical Seamount, following a geophysical survey that was started close to Site 779 (Fig. 7). A single-channel seismic-reflection profile across Site 780 (Figs. 8 and 9) shows up to 400 ms (about 400 m at 2 km/s) of stratified layers at the base of the seamount. This stratified section is probably composed of debris flows derived from the seamount. At Site 780, near the crest of the seamount, the reflection record shows a reflector about 100 ms below seafloor (bsf). The reflector may correspond to the sediment and serpentinite layers encountered during drilling. The seamount shows little internal reflectivity, as noted on a previous reflection profile across the seamount (Fig. 6). This lack of reflectivity in the profile probably results from the chaotic internal structure of the seamount or from the lack of power of the seismic system.

Site 781

Two single-channel seismic-reflection profiles were shot across Site 781. The tracklines of the surveys are shown in Figure 10. The surveys outlined a prominent reflector of high relative amplitude about 85 ms bsf of the horst drilled at Site

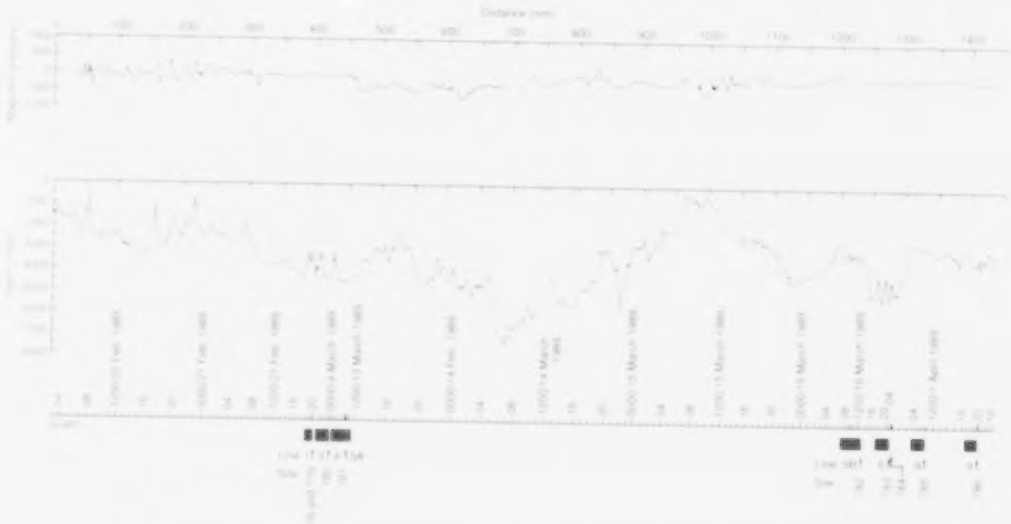

Figure 2. Records of magnetic anomaly and bathymetric profiles obtained during Leg 125. Solid bars indicate the seismic-reflection coverage.

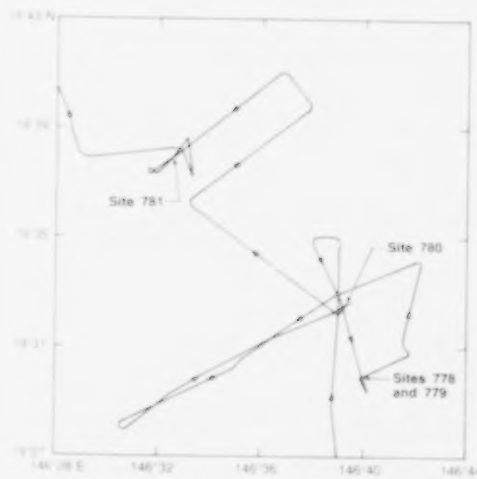
19°43' N
Site 781
Site 780
Sites 778
and 779
146°28' E
146°32'
146°36'
146°40'
146°44'

Figure 3. Enlarged trackline map near Sites 778–781. Trackline maps of individual sites, with locations of seismic-reflection profiles, are shown in Figures 4, 7, and 10.

781. The reflector was thought to be a possible basement horizon (Figs. 11–13), but subsequent drilling showed the reflector to be a basalt layer about 30 m thick. The reflector lies within a horst structure adjacent to a small graben (Fig. 12). The 72-m-thick sedimentary sequence overlying the basalt has an average velocity of 1505 m/s. The layered reflectors beneath the basalt layer are presumably from sedimentary sequences underlying the volcanic section.

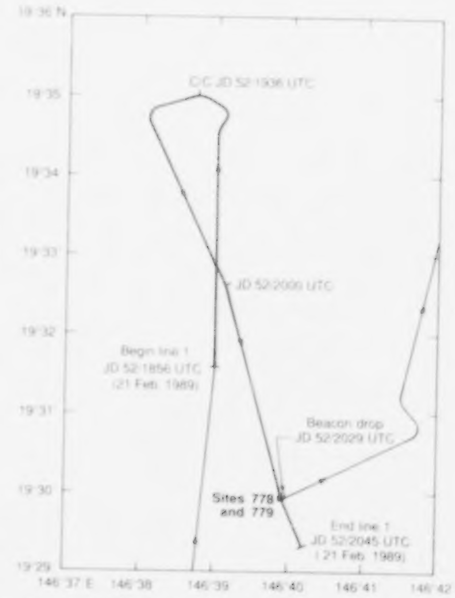
19°36' N
19°35'
19°34'
19°33'
19°32'
19°31'
19°30'
19°29'
C/C JD 52/1936 UTC
JD 52/2000 UTC
Begin line 1
JD 52/1856 UTC
(21 Feb. 1989)
Beacon drop
JD 52/2029 UTC
Sites 778
and 779
End line 1
JD 52/2045 UTC
(21 Feb. 1989)
146°37' E
146°38'
146°39'
146°40'
146°41'
146°42'

Figure 4. Trackline map of Sites 778 and 779, in the southern part of the area investigated during Leg 125, showing the location of the drill sites and geophysical tracklines. Digital seismic-reflection line 125-01 is displayed in Figure 5.

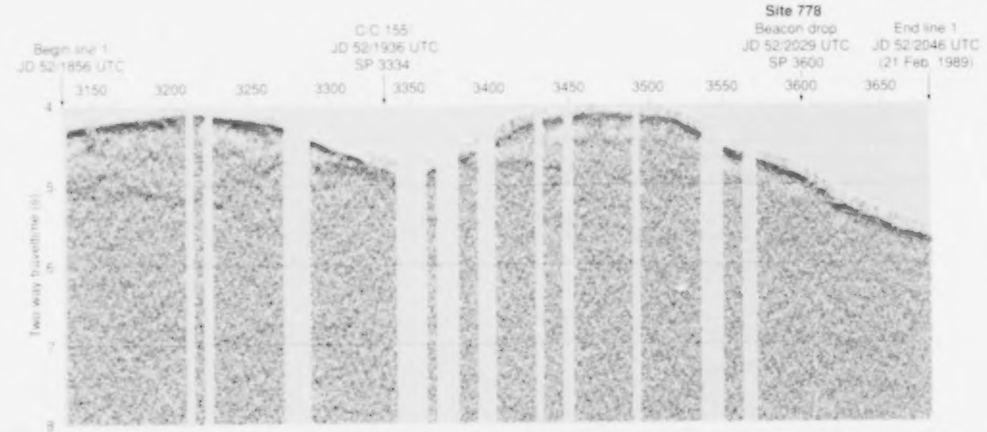

Figure 5. Processed digital seismic data collected from survey line 125-01, en route to Site 778. Automatic gain control (AGC) was applied, and the processing filter parameters were 25-30-70-90 Hz. The trackline navigation is shown in Figure 4.

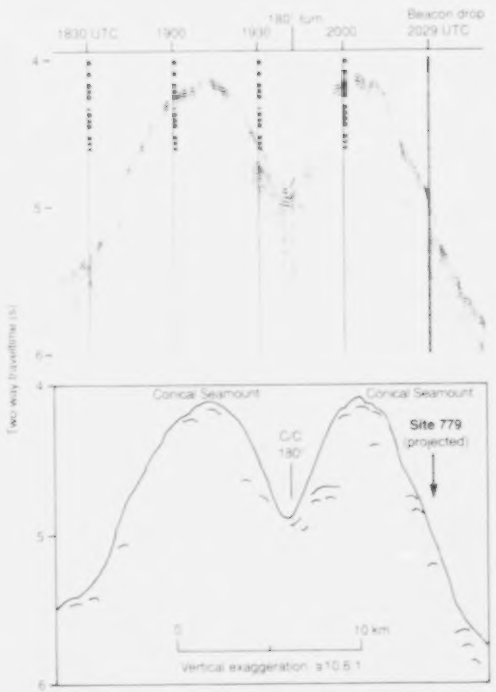

Figure 6. Single-channel seismic-reflection profile across Conical Seamount and an interpretive drawing of the profile. Note the lack of internal reflectors within the seamount. Site 778 is at the arrow marking the projected location for Site 779.

A second prominent reflector of equally high amplitude was recorded beneath a layered sequence that fills a small graben adjacent to the horst block at Site 781 (Figs. 12–14). On these profiles, this second reflector is offset from the basalt layer within the horst at Site 781 by about 100 to 150 ms. One interpretation of the reflector geometry is shown in Figures 12 and 13, where the offset between the reflectors is interpreted as a normal fault separating the graben from the horst.

A different interpretation, however, can be made using the reflection data collected after Site 781 was drilled. The seismic-reflection profile, shown in Figures 15 and 16, reveals irregular and "rubbly-looking" reflectors beneath well-layered, horizontal reflectors from the overlying sedimentary sequences. The irregular reflectors are from the basalt layer drilled at Site 781, and these reflectors can be traced laterally at the same sub-bottom depth to beneath the adjacent graben. Thus, the basalt layer can be interpreted on this profile as extending laterally from the horst into the graben, perhaps originally as a flow or intrusive (sill) structure. The flow or intrusion could have continued horizontally within the horst, but dropped to a deeper level within the graben, as shown in Figures 12 and 13, giving the apparent offset between the two "flow" reflectors on this profile. This interpretation does not require that the two prominent reflectors be separated by a normal fault, as discussed previously.

With the limited seismic-reflection data around Site 781, we cannot determine whether the basalt layers are offset by faulting or if they occupy different levels in the stratigraphy. However, the volcanic layers may be intimately associated with the fault bounding the graben because the volcanic units are limited in lateral extent away from the graben and horst. The 3.5-kHz depth record collected during the post-drilling survey shows several tilted fault blocks within the graben (Fig. 17). An acoustically opaque zone evident at the faulted(?) boundary between the graben and horst could be basaltic material. Thus, the basalt emplacement could be related to activity on the fault separating the horst and graben, and magmas could have used this fault in the forearc to gain access to the surface or near surface at Site 781. Further analysis of magnetic data from the site surveys may help to determine if the sources of the basaltic rocks lie vertically beneath Site 781.

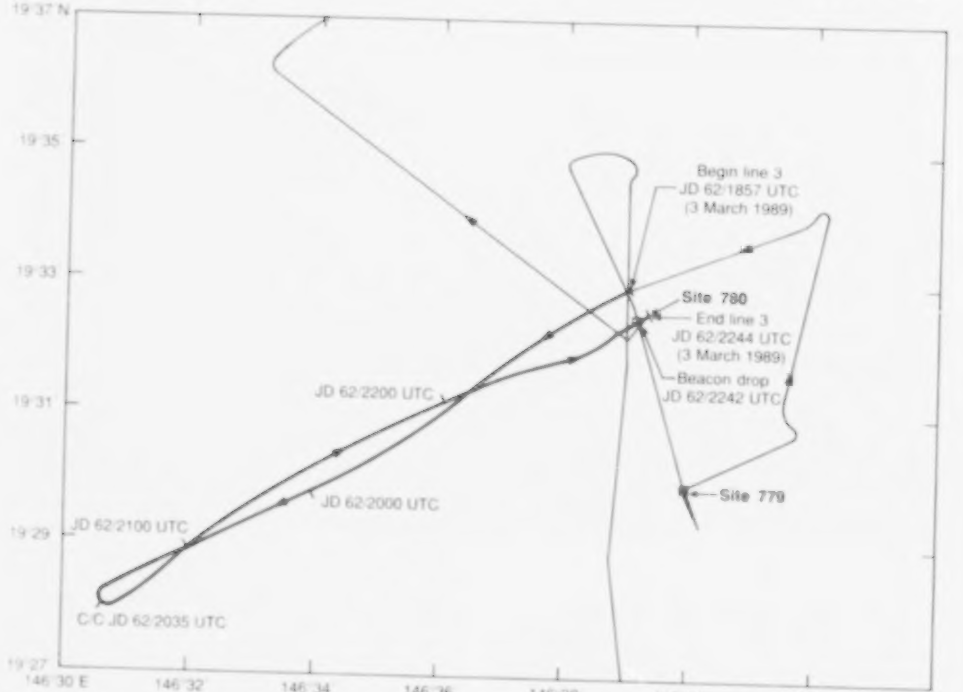

Figure 7. Trackline map of Site 780, in the southern part of the area investigated during Leg 125, showing the location of the drill site and geophysical trackline. Digital seismic-reflection line 125-03 is displayed in Figure 8.

IZU-BONIN SITES

Sites 782–786 were drilled in the Izu-Bonin forearc. A detailed trackline of these sites is shown in Figure 18.

Site 782

Site 782 was drilled in the Izu-Bonin forearc after a geophysical survey was made following the transit from Site 781 (Fig. 19). The single-channel seismic-reflection profile across Site 782 (Fig. 20) shows up to 450 ms (about 400 to 430 m at 1.8 to 1.9 km/s, respectively) of stratified layers overlying a basement reflector labeled *B* on Figure 21. This stratified section is composed mainly of pelagic and hemipelagic sediment and ash layers derived from the ancestral Izu-Bonin Island arc. The oldest sediment overlying the basement reflector is Eocene in age. The basement reflector is basalt, perhaps from the earliest phase of volcanism in the formation of the arc.

Site 783

Site 783 was drilled on the northern flank of Torishima Forearc Seamount on the inner wall of Izu-Bonin Trench in a water depth of 4648.8 m. The geophysical survey of the site involved two crossings of the seamount before the beacon was dropped (Figs. 22 and 23). The seismic-reflection record revealed that the seamount has little internal structure. Only short, discontinuous reflectors are evident in the record, indicating a thin sediment cover over the flanks of the seamount. A break in slope halfway down the eastern flank can be interpreted on the reflection profile as a slump feature (Fig. 24). Continuous reflectors are absent from the seamount probably because of its chaotic internal structure related to faulting and to the possible diapiric intrusion of serpentinite or because of the limited power of the seismic system. The reflection and drilling data also show that the crest of the seamount is not underlain by active serpentinite material, unlike the crest of Conical Seamount.

Site 785

Site 785 was drilled in the Izu-Bonin forearc in a water depth of 2660.8 m. The geophysical survey of the site involved two crossings of the site before drilling commenced (Figs. 25 and 26). The seismic-reflection record from the forearc shows a thick sedimentary sequence more than 1 s (1 km) thick in the east. To the west, basement appears to be truncated by a reverse fault that offsets most of the sedimentary strata and may reach the seafloor along a small swale. Basement was not observed on the west side of this fault, where the forearc is underlain by a thick sedimentary sequence. The reflectors from this sequence are curvilinear and this fact may suggest that channel-filling processes are active adjacent to the fault. Alternatively, the fault structure interpreted in Figure 27 may be the edge of a filled channel. Further processing of the seismic-reflection data may allow better resolution of the fault/channel-fill structures.

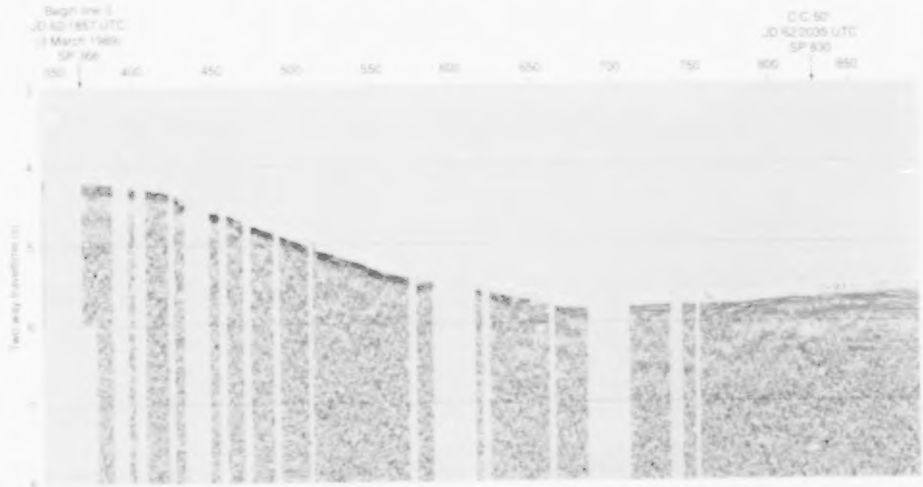

Figure 8. Processed digital seismic data collected from survey line 125-03, en route to Site 780. AGC was applied, and the processing filter parameters were 25-30-70-90 Hz. The trackline navigation is shown in Figure 7.

Site 786

Site 786 was drilled in the Izu-Bonin forearc in a water depth of 3058.1 m. The geophysical survey of the site involved two crossings of the site prior to drilling (Figs. 28–30). The seismic-reflection record shows a thick sedimentary sequence draping volcanic basement. To the west, the section is cut by two high-angle normal faults, which rupture the seafloor and form a series of stepped-down terraces. The faulting and morphology of the area suggest that the forearc is being extensionally deformed.

Site 786 is situated over a basement high that is draped with about 115 m of sediment, as revealed by drilling (Fig. 30). The reflection data suggest that the stratigraphic section recovered at Site 786 is thinner than the adjacent sequences in the surrounding valleys. This relationship indicates that since the beginning of sedimentation the basement knoll at Site 786 may have always been higher than the surrounding country rock.

Ms 125A-103

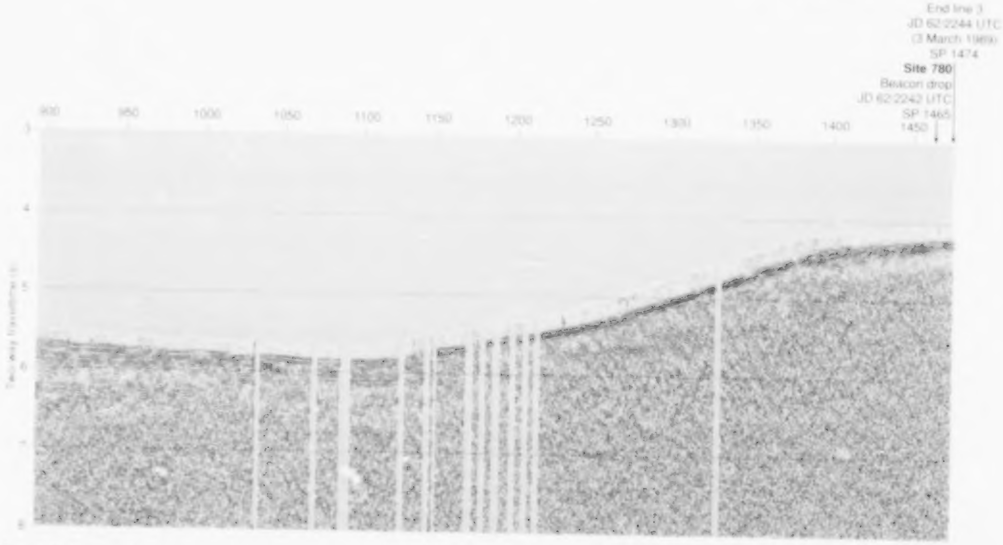

Figure 8 (continued).

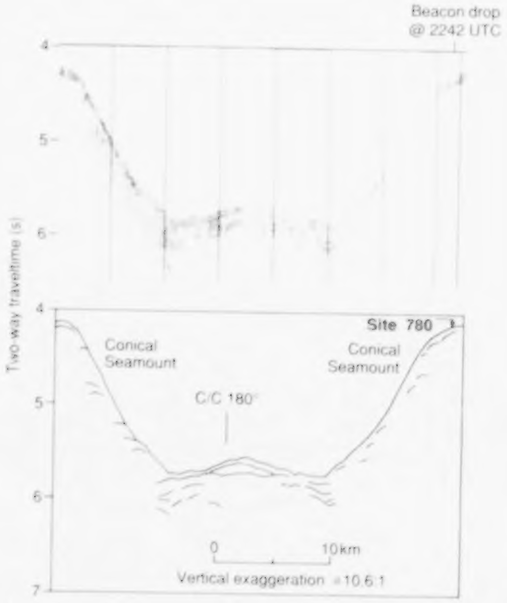
Beacon drop
@ 2242 UTC
4
5
6
Two-way traveltime (s)
4
5
6
7
Site 780
Conical
Seamount
Conical
Seamount
C/C 180°
0
10km
Vertical exaggeration =10.6:1

Figure 9. Single-channel seismic-reflection profile across Conical Seamount and the sediment section at the base of the seamount and an interpretive drawing of the profile.

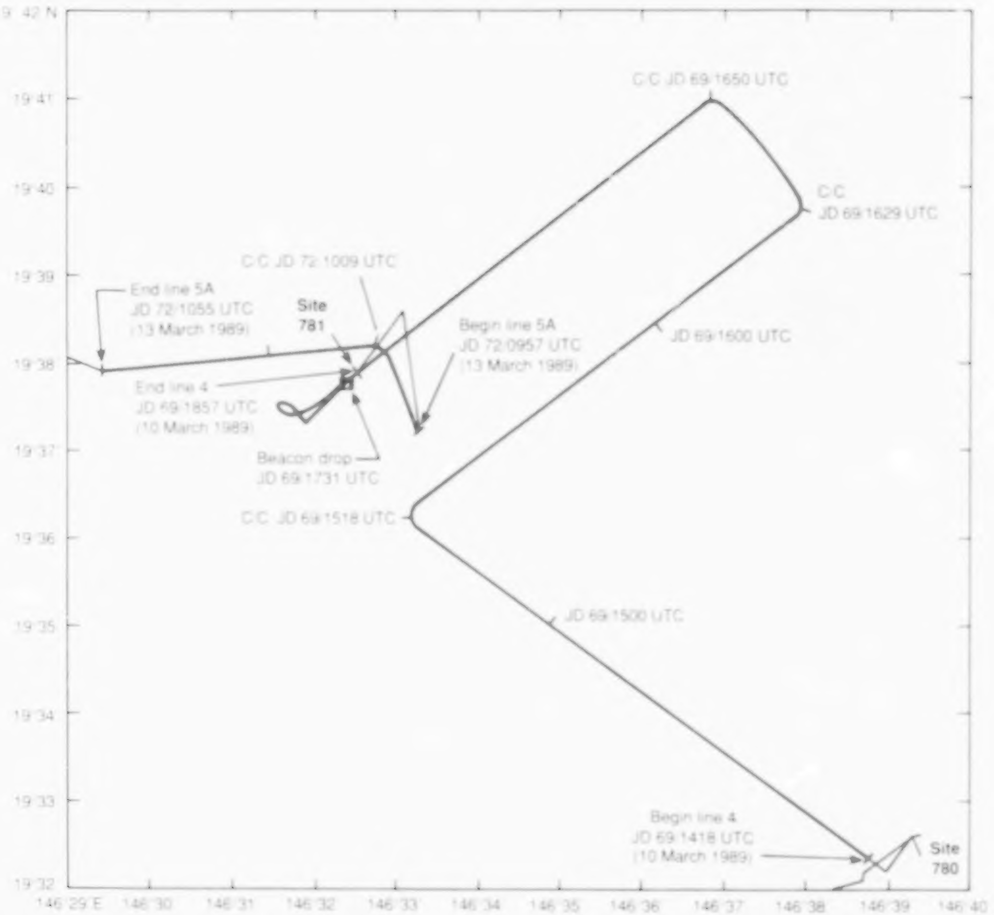
19°42'N
19°41'
19°40'
19°39'
19°38'
19°37'
19°36'
19°35'
19°34'
19°33'
19°32'
146°29'E
146°30'
146°31'
146°32'
146°33'
146°34'
146°35'
146°36'
146°37'
146°38'
146°39'
146°40'
C/C JD 69/1650 UTC
C/C
JD 69/1629 UTC
C/C JD 72/1009 UTC
End line 5A
JD 72/1055 UTC
(13 March 1989)
Site
781
Begin line 5A
JD 72/0957 UTC
(13 March 1989)
JD 69/1600 UTC
End line 4
JD 69/1857 UTC
(10 March 1989)
Beacon drop
JD 69/1731 UTC
C/C JD 69/1518 UTC
JD 69/1500 UTC
Begin line 4
JD 69/1418 UTC
(10 March 1989)
Site
780

Figure 10. Trackline map of Site 781, in the southern part of the area investigated during Leg 125, showing the location of the drill site and geophysical trackline. Digital seismic-reflection lines 125-04 and 125-05A are displayed in Figures 11 and 15, respectively.

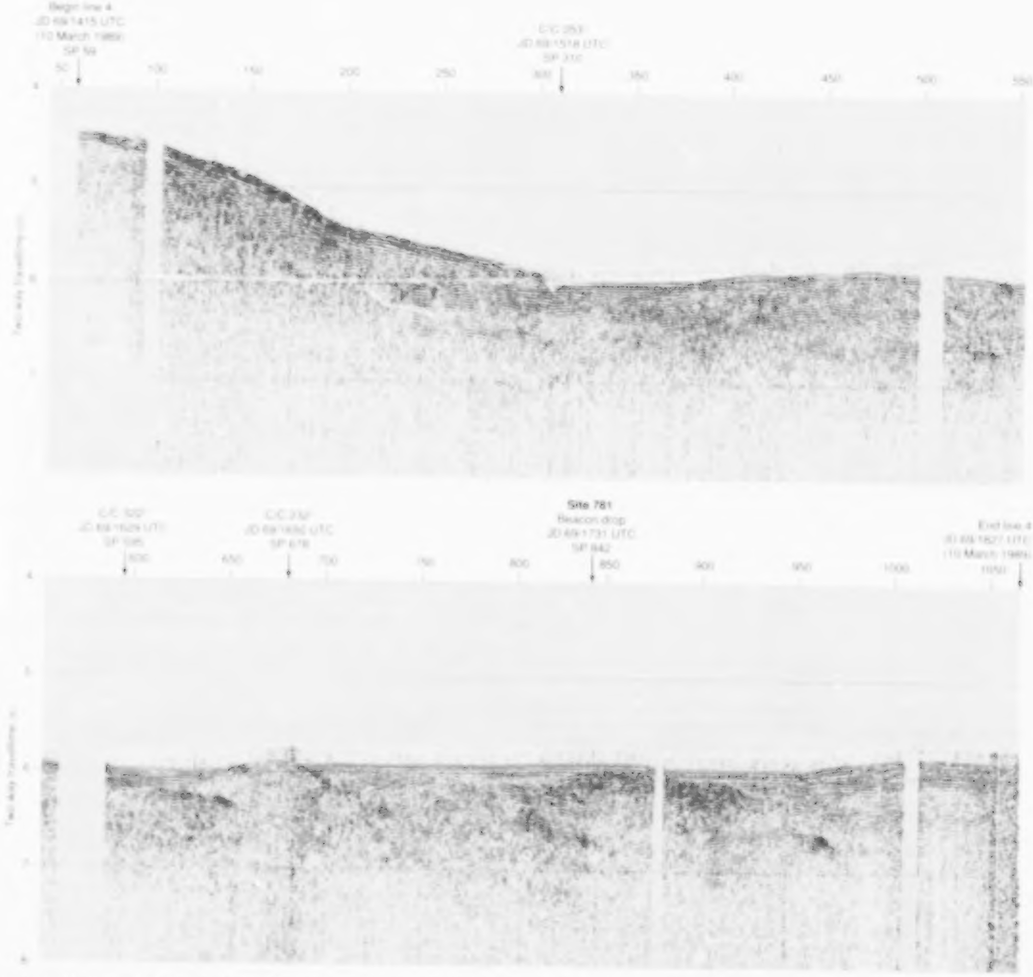

Figure 11. Processed digital seismic data collected from survey line 125-04, en route to Site 781. No AGC was applied, and the processing filter parameters were 25-30-70-90 Hz. The trackline navigation is shown in Figure 10.

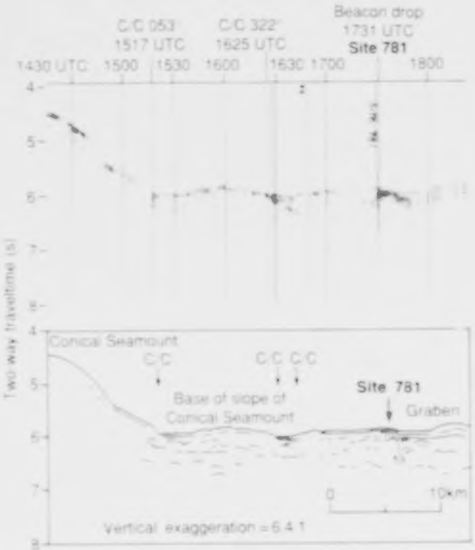

Figure 12. Single-channel seismic-reflection profile (10-s record) across the flank and along the base of Conical Seamount and across Site 781 and an adjacent graben, with an interpretive drawing of the profile. The prominent reflector at about 85 ms two-way traveltime bsf (see Fig. 13 for the detailed reflection profile) corresponds to the top of the basalt layer drilled at Site 781 at 72 mbsf. A similar prominent reflector occurs within the sedimentary sequence filling the adjacent graben. The two reflectors may be part of one volcanic unit that is either separated by faulting, as shown here, or continuous and located at two different depths in the graben and adjacent horst block (see text for discussion).

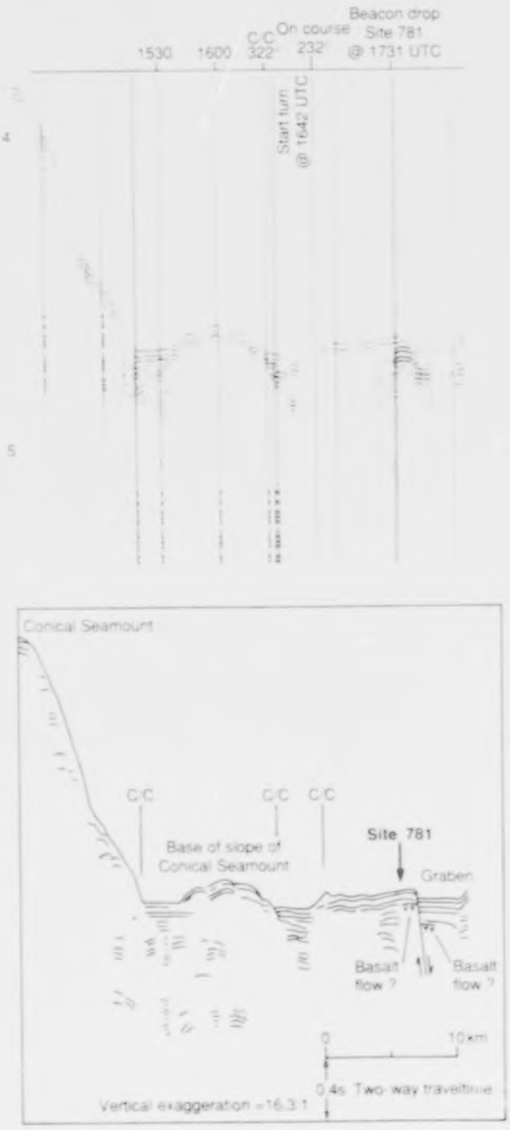

Figure 13. Detailed 4-s record duplicating the seismic-reflection profile shown in Figure 12 and an interpretive drawing of the profile. Note the prominent basaltic reflector at Site 781 and the adjacent reflector in the graben, which is also interpreted as a volcanic layer.

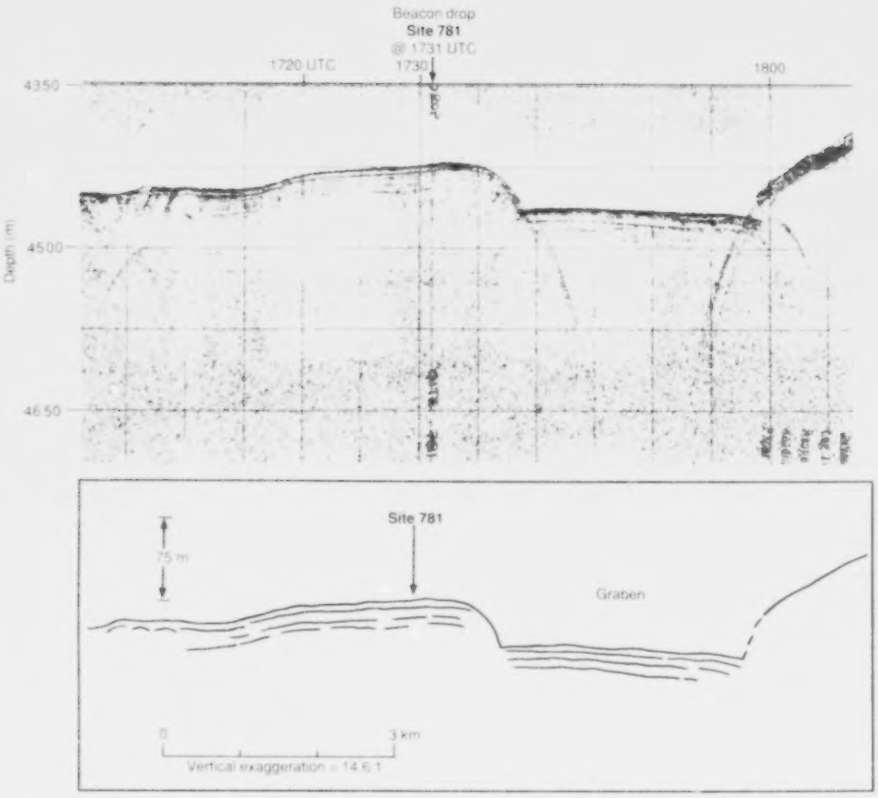

Figure 14. The 3.5-kHz depth record across Site 781 and the adjacent graben and an interpretive drawing of the profile. The graben and adjacent horst are underlain by gently dipping reflectors from sedimentary layers. The strata in the graben are uplifted and thin toward the horst block penetrated at Site 781, suggesting recent tectonic activity.

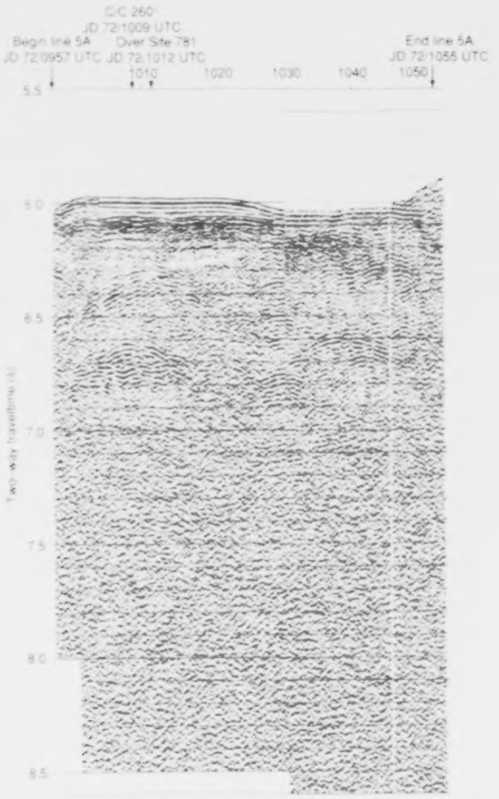

Figure 15. Processed digital seismic data collected from survey line 125-05A, run immediately after leaving Site 781. AGC was applied, and the processing filter parameters were 25–140 Hz with a filter length of 37 Hz. The trackline navigation is shown in Figure 10.

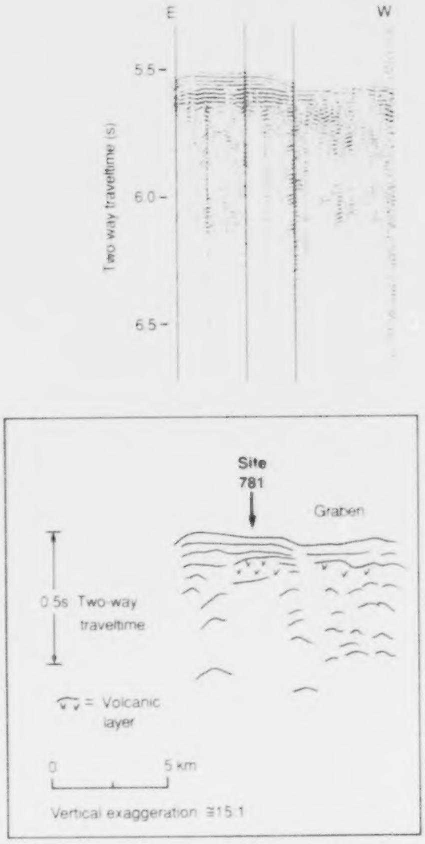
E
W
5.5
6.0
6.5
Two way traveltime (s)
Site 781
Graben
0.5s Two-way traveltime
= Volcanic layer
0
5 km
Vertical exaggeration ≅15:1

Figure 16. Single-channel seismic-reflection profile run east-west across Site 781 after it was drilled and an interpretive drawing of the profile. The profile location is shown in Figure 10. The well-layered, horizontal reflectors are from sedimentary sequences and the irregular, "rubbly-looking" reflectors are from basaltic layers beneath the sedimentary sequences (at least at Site 781). These layers extend laterally and horizontally beneath the graben fill adjacent to Site 781, unlike the basaltic layers shown on the other crossings, which appear to be offset by a normal fault along the graben flank (Figs. 12 and 13; see text for discussion).

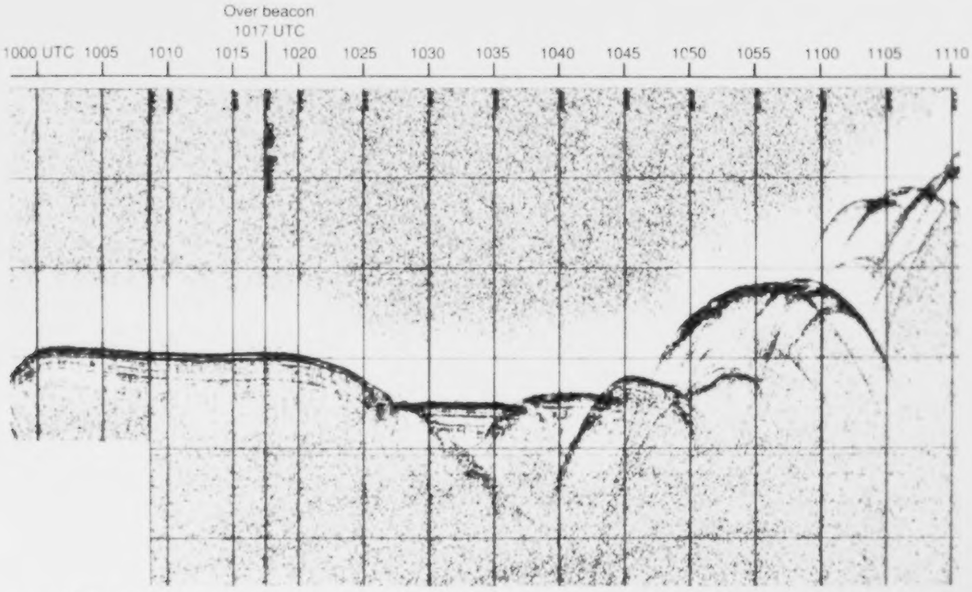

Figure 17. The 3.5-kHz depth record run across Site 781 after drilling and concurrent with the profile shown in Figure 16. The graben adjacent to Site 781 is underlain by a series of stepped blocks, probably offset by faults. The layered reflectors within each block are probably sedimentary layers, and the opaque zone along the east edge of the graben near Site 781 may be volcanic rocks that were not penetrated by the 3.5-kHz sound source. If the opaque zone is underlain by basaltic rocks, then these rocks may be associated with a fault zone flanking the graben.

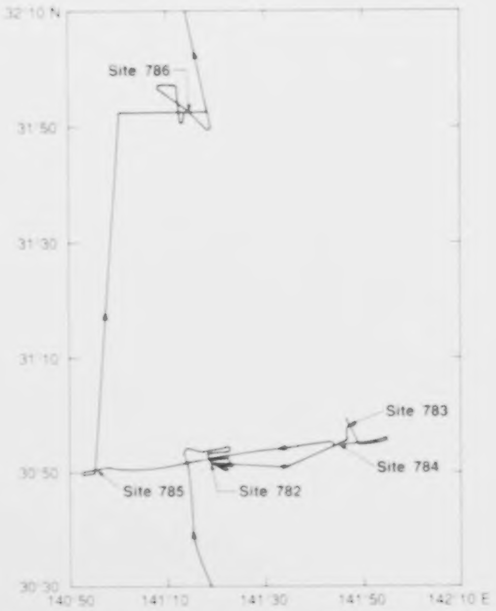
32°10′N
31°50′
31°30′
31°10′
30°50′
30°30′
140°50′
141°10′
141°30′
141°50′
142°10′E
Site 786
Site 783
Site 784
Site 785
Site 782

Figure 18. Enlarged trackline map near Sites 782–786. Trackline maps of individual sites, with locations of seismic-reflection profiles, are shown in Figures 19, 22, 25, and 28.

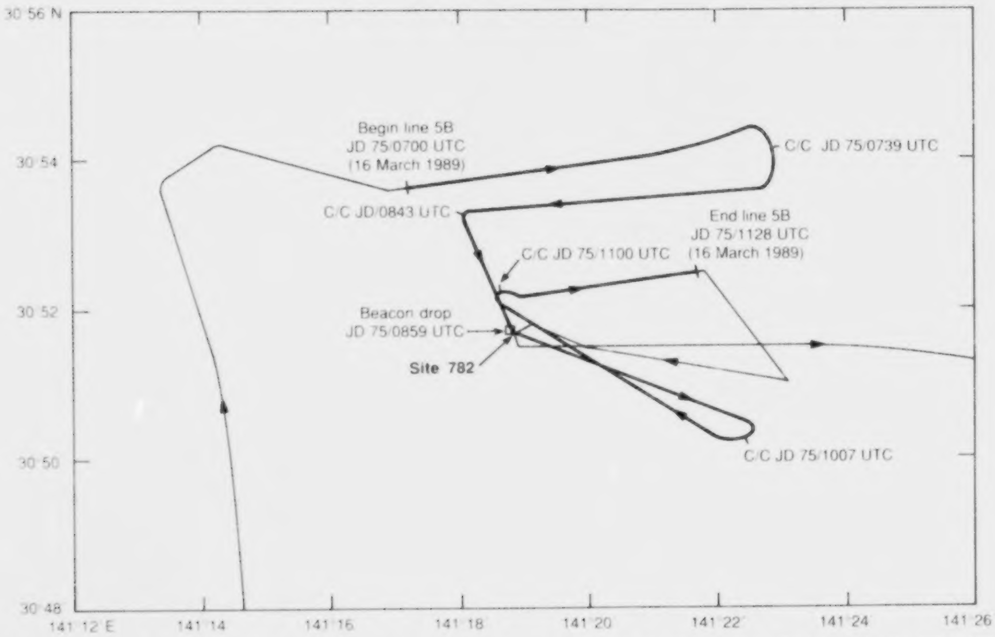
30°56'N
30°54'
30°52'
30°50'
30°48'
141°12'E
141°14'
141°16'
141°18'
141°20'
141°22'
141°24'
141°26'
Begin line 5B
JD 75/0700 UTC
(16 March 1989)
C/C JD 75/0739 UTC
C/C JD/0843 UTC
End line 5B
JD 75/1128 UTC
(16 March 1989)
C/C JD 75/1100 UTC
Beacon drop
JD 75/0859 UTC
Site 782
C/C JD 75/1007 UTC

Figure 19. Trackline map of Site 782, in the northern part of the area investigated during Leg 125, showing the location of the drill site and geophysical trackline. Analog seismic-reflection line 125-05B is displayed in Figure 20.

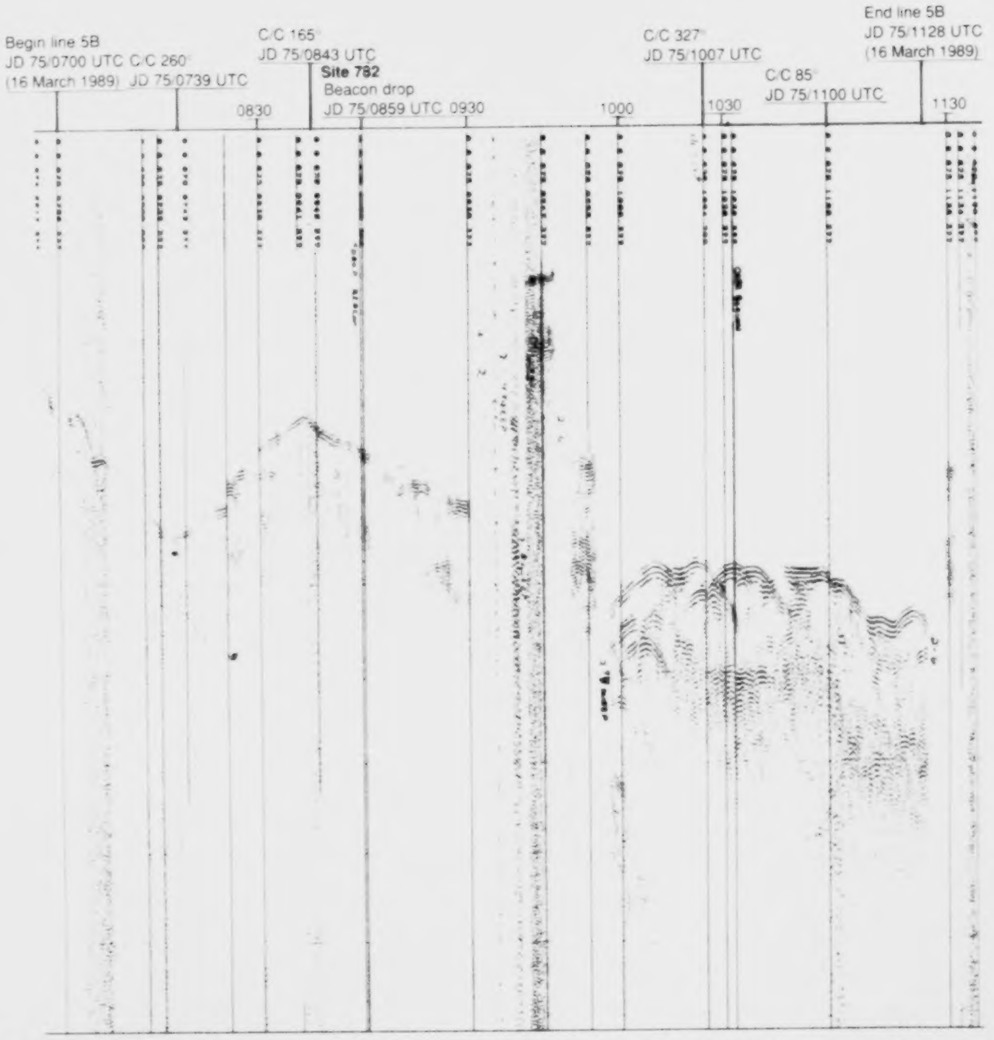

Figure 20. Analog single-channel seismic data collected from survey line 125-05B, en route to Site 782. The trackline navigation is shown in Figure 19.

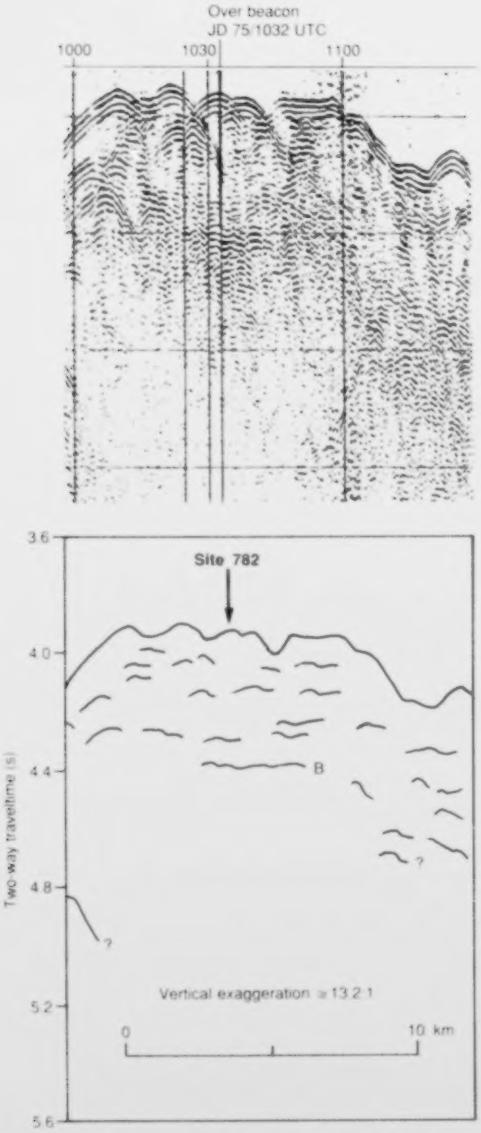

Figure 21. Single-channel seismic-reflection profile across Site 782 in the Izu-Bonin forearc and an interpretive drawing of the profile. The prominent basement reflector is labeled *B*.

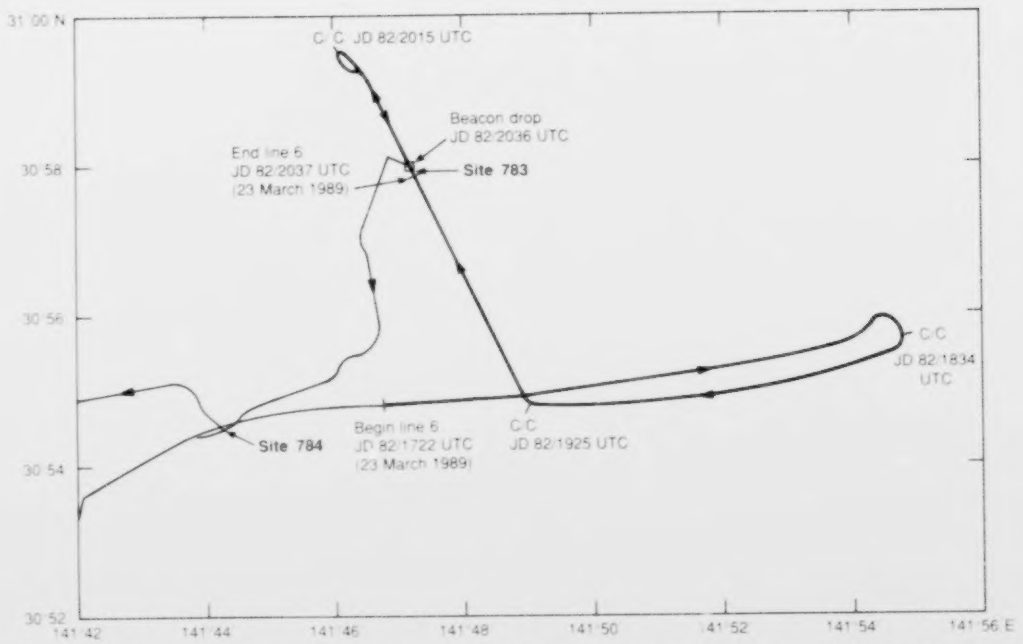
31°00′ N
30°58′
30°56′
30°54′
30°52′
141°42′
141°44′
141°46′
141°48′
141°50′
141°52′
141°54′
141°56′ E
C/C JD 82/2015 UTC
Beacon drop
JD 82/2036 UTC
End line 6
JD 82/2037 UTC
(23 March 1989)
Site 783
C/C
JD 82/1834
UTC
Site 784
Begin line 6
JD 82/1722 UTC
(23 March 1989)
C/C
JD 82/1925 UTC

Figure 22. Trackline map of Sites 783 and 784, in the northern part of the area investigated during Leg 125, showing the location of the drill sites and geophysical trackline. Digital seismic-reflection line 125-06 is displayed in Figure 23.

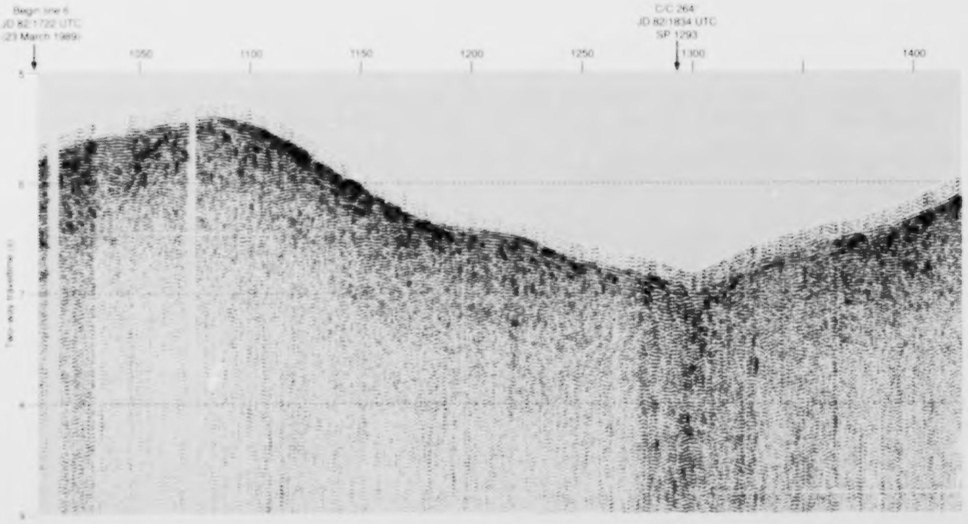

Figure 23. Processed digital seismic data collected from survey line 125-06, en route to Site 783. AGC was applied, and the processing filter parameters were 25-30-70-90 Hz. The trackline navigation is shown in Figure 22.

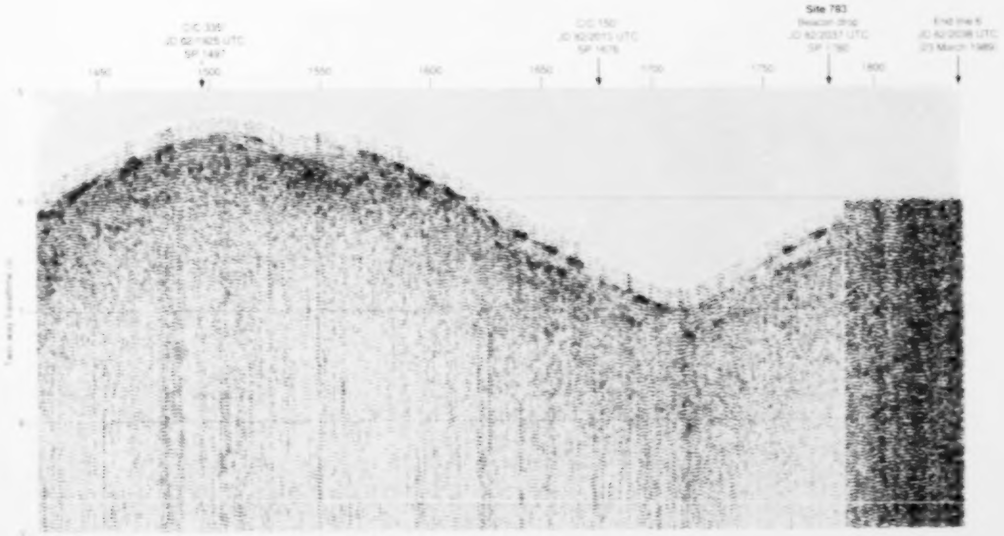

Figure 23 (continued).

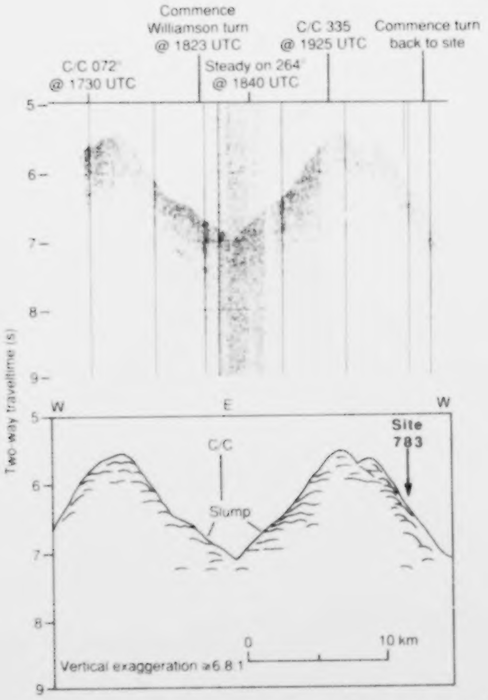

Figure 24. Single-channel seismic-reflection profile across Site 783 of an unnamed seamount in the Izu-Bonin forearc and an interpretive drawing of the profile. The internal structure of the seamount is poorly reflective, and only short, discontinuous reflectors were recorded.

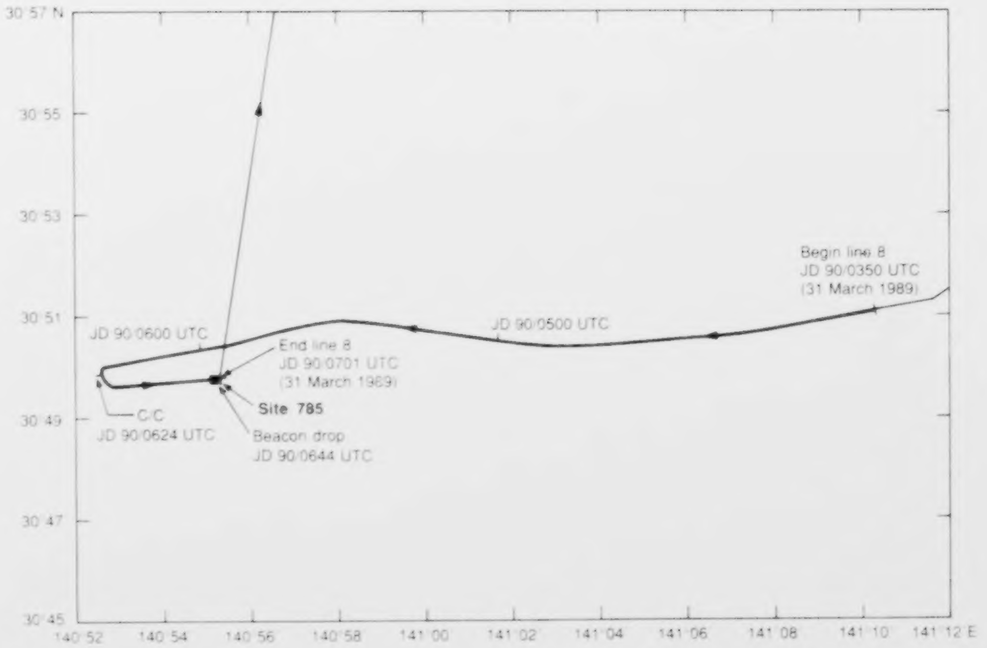
30°57′N
30°55′
30°53′
30°51′
30°49′
30°47′
30°45′
140°52′
140°54′
140°56′
140°58′
141°00′
141°02′
141°04′
141°06′
141°08′
141°10′
141°12′E
Begin line 8
JD 90/0350 UTC
(31 March 1989)
JD 90/0500 UTC
JD 90/0600 UTC
End line 8
JD 90/0701 UTC
(31 March 1969)
Site 785
C/C
JD 90/0624 UTC
Beacon drop
JD 90/0644 UTC

Figure 25. Trackline map of Site 785, in the northern part of the area investigated during Leg 125, showing the location of the drill site and geophysical trackline. Digital seismic-reflection line 125-08 is displayed in Figure 26.

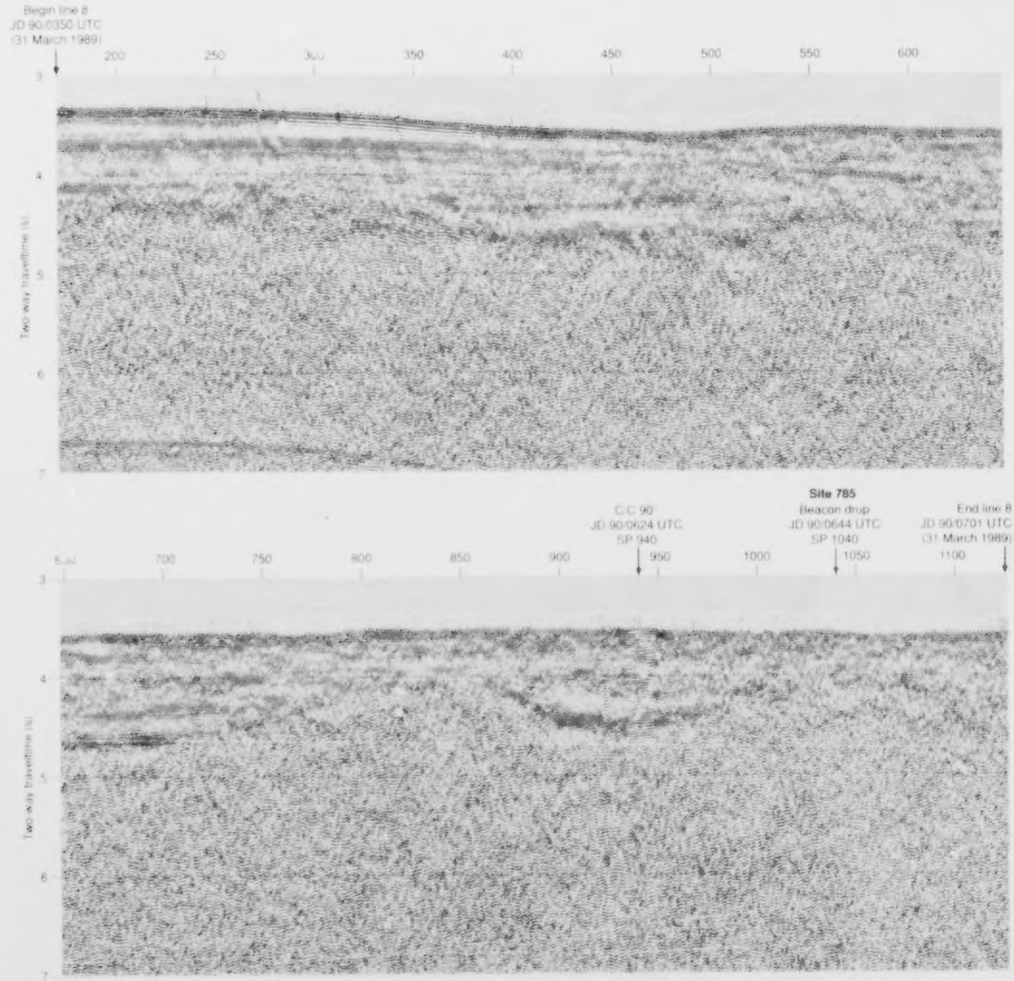

Figure 26. Processed digital seismic data collected from survey line 125-08, en route to Site 785. AGC was applied, and the processing filter parameters were 25-30-70-90 Hz. The trackline navigation is shown in Figure 25.

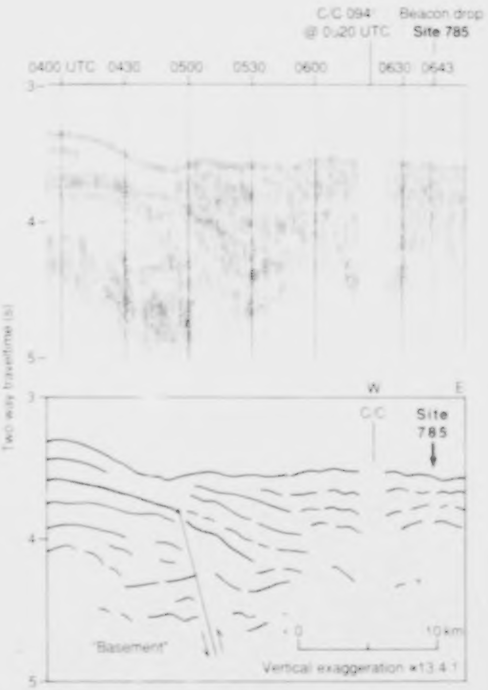
C/C 094°
@ 0620 UTC
Beacon drop
Site 785
0400 UTC
0430
0500
0530
0600
0630
0643
3
4
5
Two-way traveltime (s)
W
E
C/C
Site 785
"Basement"
0
10 km
Vertical exaggeration ≈13.4:1

Figure 27. Single-channel seismic-reflection profile across Site 785 in the Izu-Bonin forearc and an interpretive drawing of the profile. The fault structure shown can be interpreted alternatively as an edge of a channel-fill structure.

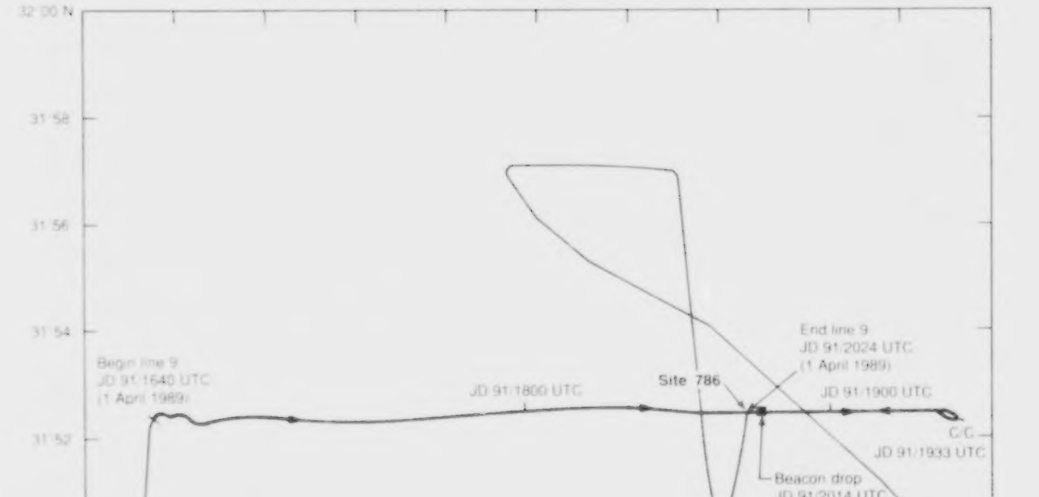
32°00' N
31°58'
31°56'
31°54'
31°52'
31°50'
31°48'
140°59'
141°01'
141°03'
141°05'
141°07'
141°09'
141°11'
141°13'
141°15'
141°17'
141°19' E
Begin line 9
JD 91/1640 UTC
(1 April 1989)
JD 91/1800 UTC
Site 786
End line 9
JD 91/2024 UTC
(1 April 1989)
JD 91/1900 UTC
C/C
JD 91/1933 UTC
Beacon drop
JD 91/2014 UTC

Figure 28. Trackline map of Site 786, in the northern part of the area investigated during Leg 125, showing the location of the drill site and geophysical trackline. Digital seismic-reflection line 125-09 is displayed in Figure 29.

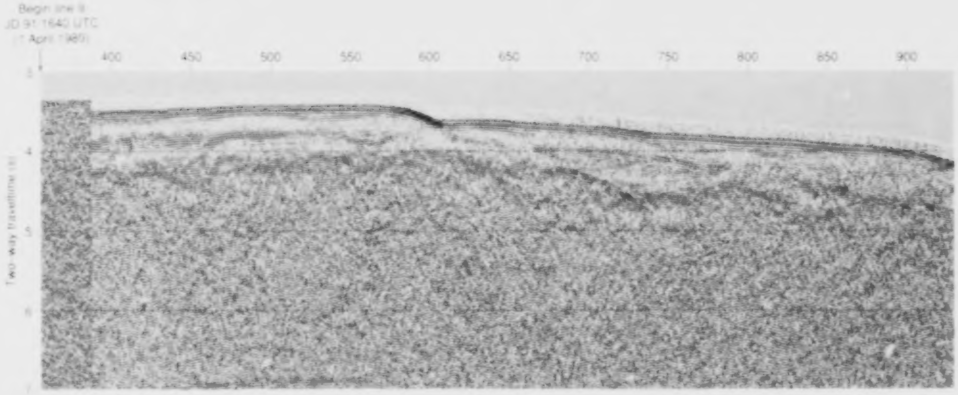

Figure 29. Processed digital seismic data collected from survey line 125-09, en route to Site 786. AGC was applied, and the processing filter parameters were 25-30-70-90 Hz. The trackline navigation is shown in Figure 28.

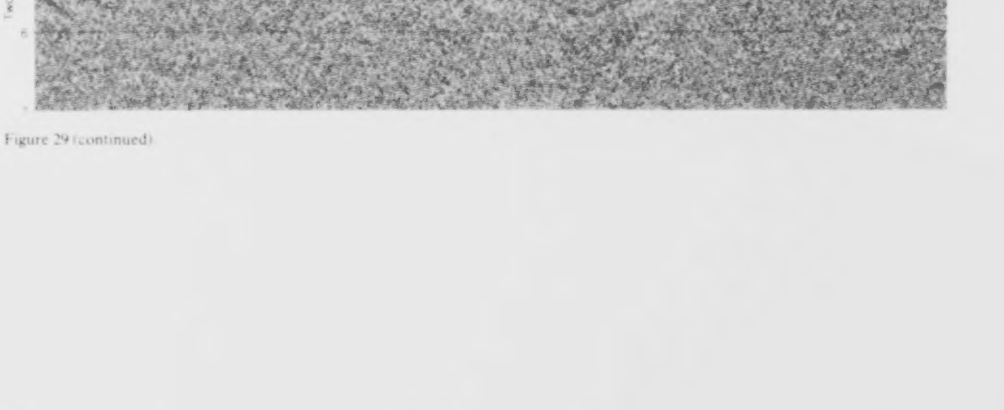

Figure 29 (continued).

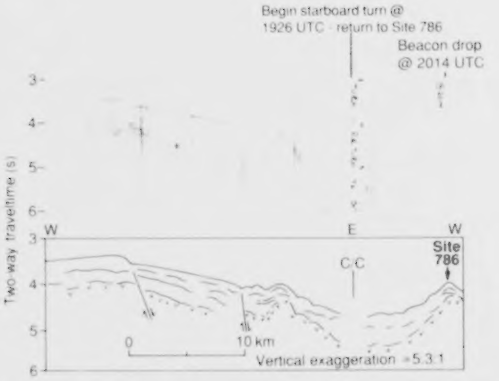
Begin starboard turn @
1926 UTC - return to Site 786
Beacon drop
@ 2014 UTC
Two-way traveltime (s)
3
4
5
6
W
E
W
C/C
Site
786
0
10 km
Vertical exaggeration =5.3:1

Figure 30. Single-channel seismic-reflection profile across Site 786 in the Izu-Bonin forearc and an interpretive drawing of the profile.

Fryer, P., Pearce, J. A., Stokking, L. B., et al., 1990
Proceedings of the Ocean Drilling Program, Initial Reports, Vol. 125

4. CONICAL SEAMOUNT: SeaMARC II, *ALVIN* SUBMERSIBLE, AND SEISMIC-REFLECTION STUDIES[1]

Patricia Fryer,[2] Kristine L. Saboda,[2] Lynn E. Johnson,[2] Mary E. Mackay,[2] Gregory F. Moore,[2]
and Peter Stoffers[3]

ABSTRACT

Conical Seamount, the edifice drilled at Ocean Drilling Program (ODP) Sites 778 through 780, is a large seamount on the outer half of the 200-km-wide Mariana forearc in the western Pacific. It is forming by the protrusion of cold, unconsolidated serpentine mudflows and debris flows and by vertical tectonic activity. Dredging on the flanks of this seamount recovered rocks and serpentine muds that are similar to sedimentary serpentinite deposits found in subaerially exposed convergent margin terranes worldwide. The dredged samples were formed by different mechanisms from those previously proposed for sedimentary serpentinite deposits. The dredged samples from Conical Seamount are primarily serpentinized harzburgite. However, serpentinized dunite, metamorphosed gabbro, and basalts have been retrieved from similar seamounts on the Mariana forearc. SeaMARC II imagery and bathymetry of Conical Seamount revealed sinuous flow forms on the flanks of the seamount. Conical Seamount also has both concentric ridges and radial fractures indicative of tumescence. *Alvin* submersible studies showed these flows to be composed of unconsolidated serpentine muds, containing clasts of serpentinized ultramafic and metamorphosed mafic rocks and authigenic carbonate and silicate minerals. Near the summit of one of the seamounts, chimney structures less than 150 yr old and composed of carbonate and silicate were sampled using *Alvin*. During sampling of a silicate chimney, cold fluids seeped from numerous orifices in the chimney. The fluids associated with the chimney are unique in composition among fluids collected in the oceans and point to a deep source, probably the subducted Pacific lithospheric slab. Small limpets and gastropods and bacterial mats were collected from the chimneys.

Faulting of the forearc region partially controls the distribution of the Mariana forearc serpentinite seamounts. Seismic-reflection profiles show that Conical Seamount is located at the intersection of at least two fault zones. The extent of the exposure of serpentinized ultramafic rocks on the Mariana forearc and the pervasive normal faulting of the region argue for considerable extension. Dredged samples from the 2-km-high wall of a deep graben adjacent to Conical Seamount include a variety of mafic rock types of arc tholeiite, boninite, alkalic basalts, and basalts of mid-ocean ridge (MORB) composition. The presence of MORBs in this part of the forearc suggests either exposure of a fragment of entrapped or accreted oceanic plate or a period of rifting with associated magma generation in the forearc.

The serpentine mud volcanoes and associated egress of fluids generated at great depth in the forearc provide a mechanism for the flux of fluids from the subducted oceanic lithosphere through the outer forearc region. The escape of circulating fluids would alleviate problems of mass balance of constituents derived from subduction in the convergent margin environment. In particular, the disparity between the observed volatile effluent from arc volcanoes and the postulated amount of dehydration of the downgoing slab could be explained by accommodation of large volumes of fluids through metamorphism of the outer forearc region.

INTRODUCTION

Active convergence in the western Pacific over the past 43 m.y. has produced a series of backarc basins and intervening remnant arcs that form the eastern edge of the Philippine Sea Plate (Fig. 1). The Mariana arc-trench system, the easternmost of these western Pacific arcs, is well known as a classic example of an intraoceanic convergence zone. Its evolution has been studied by numerous investigators over nearly two decades (e.g., Karig, 1971; Uyeda and Kanamori, 1979; LaTraille and Hussong, 1980; Fryer and Hussong, 1982; Mrosowski et al., 1982; Hussong and Uyeda, 1982; Bloomer and Hawkins, 1983; Karig and Ranken, 1983; McCabe and Uyeda, 1983; Hsui and Youngquist, 1985; Fryer and Fryer, 1987; Johnson and Fryer, 1988). During the past 5 yr, surveying and sampling of this area resulted in the refinement of models for convergent margin evolution.

Some of the most significant changes in models of arc evolution have been with respect to aspects of the development of the Mariana forearc region. The Mariana forearc comprises a region between the trench axis and the active volcanic arc, approximately 200 km wide and 1500 km long. The eastern half of the region is unusual among western Pacific forearc terranes in that it contains more than 50 large seamounts scattered along its length within 100 km of the trench axis (Fryer et al., 1985; Fryer and Fryer, 1987). The seamounts vary in size from 10 km in diameter and 0.5 km high to 30 km in diameter and 2 km high.

The central forearc (Fig. 2) had been studied previously using several techniques, including U.S. Navy SASS bathymetry surveys (Fryer and Smoot, 1985) and SeaMARC II side-scanning sonar and bathymetry surveys (Hussong and Fryer, 1985; Fryer et al., 1987; Fryer and Fryer, 1987) between 19° to 20°N. The latter survey has facilitated detailed morphologic and structural studies of this part of the Mariana forearc. Following these studies, a series of *Alvin* dives were conducted during 1987 on two serpentinite seamounts near

---

[1] Fryer, P., Pearce, J. A., Stokking, L. B., et al., 1990. *Proc. ODP, Init. Repts.*, 125: College Station, TX (Ocean Drilling Program).

[2] Hawaii Institute of Geophysics, 2525 Correa Road, Honolulu, HI 96822.

[3] Geologisch-Paläontologisches Institut und Museum, Der Universität Kiel, 40 Olshausenstrasse, Kiel 2300, FRG.

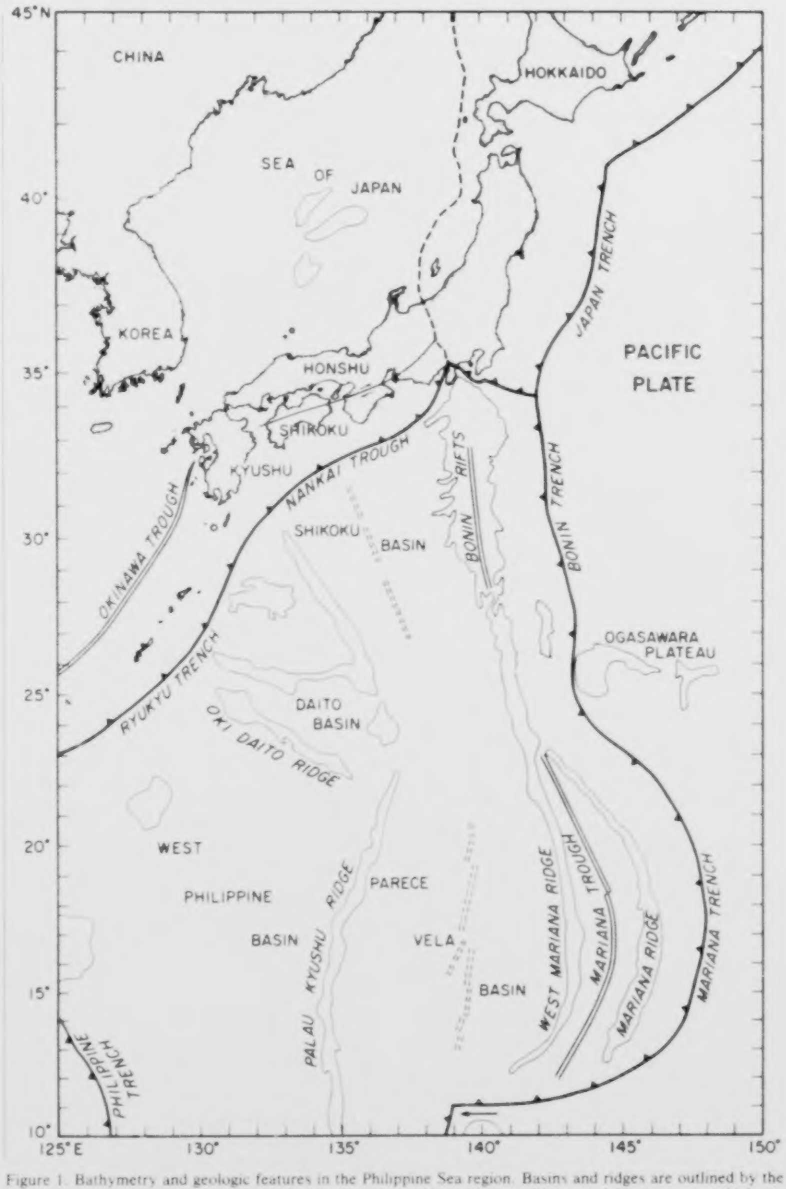
45°N
40°
35°
30°
25°
20°
15°
10°
125°E
130°
135°
140°
145°
150°
CHINA
HOKKAIDO
SEA
OF
JAPAN
KOREA
HONSHU
SHIKOKU
KYUSHU
JAPAN TRENCH
PACIFIC
PLATE
OKINAWA TROUGH
NANKAI TROUGH
BONIN RIFTS
BONIN TRENCH
SHIKOKU
BASIN
OGASAWARA
PLATEAU
RYUKYU TRENCH
DAITO
BASIN
OKI DAITO RIDGE
WEST
PHILIPPINE
BASIN
PALAU KYUSHU RIDGE
PARECE
VELA
BASIN
WEST MARIANA RIDGE
MARIANA TROUGH
MARIANA RIDGE
MARIANA TRENCH
PHILIPPINE
TRENCH

Figure 1. Bathymetry and geologic features in the Philippine Sea region. Basins and ridges are outlined by the 4-km bathymetric contour, except for the Izu-Bonin arc, West Mariana Ridge, and Mariana arc, which are outlined by the 3-km contour. Barbed lines locate subduction zones; medium double lines locate active spreading centers; dashed double lines locat relict spreading centers.

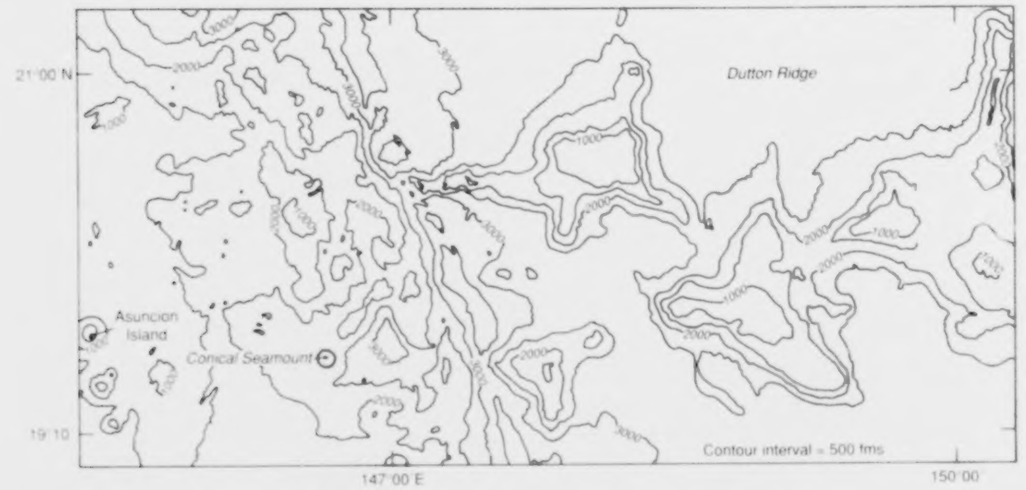

Figure 2. Bathymetry of the central Mariana arc from U.S. Navy SASS data (Fryer and Smoot, 1985).

19°30'N (Fryer et al., 1987). During Leg 125, to prepare for drilling one of these two seamounts (Conical Seamount), a digital single-channel seismic survey of the seamount was conducted using the *Fred H. Moore* in 1987. Subsequently, Conical Seamount was surveyed using a SeaBeam bathymetry system aboard the *Sonne*. These more detailed investigations provided an opportunity for scientists to focus on a number of aspects of the tectonic evolution of the forearc and of Conical Seamount that could not be examined using conventional geophysical survey techniques.

This chapter provides a summary of the regional geology of the outer Mariana forearc and the tectonic evolution of Conical Seamount. In it we present a summary of the principal results of the *Alvin* dive studies, the seismic-reflection studies, and the petrologic and geochemical studies of dredged and *Alvin*-collected samples of that seamount. These data were used in the site selections for drilling at Conical Seamount during Leg 125.

PREVIOUS WORK

Studies of the origin of serpentinite seamounts in the Mariana forearc region have direct application to interpretation of subaerial exposures of serpentinite in former convergent margin terranes. Deposits of "sedimentary" serpentinite similar to the deposits formed on the flanks of the Mariana serpentinite seamounts have been described from numerous locations on land in former convergent margin settings (e.g., Lockwood, 1971; Phipps, 1984; Lagabrielle et al., 1986). The mechanism of emplacement of some of these subaerially exposed deposits has been compared to that of the Mariana seamounts (Carlson, 1984). Seven of the seamounts on the outer half of the Mariana forearc have been sampled and shown to consist in part of serpentinized ultramafic rocks. Many also yielded metagabbros, metabasalts, and metasediments. These results suggested that the seamounts were formed by diapiric intrusion of serpentinized ultramafic rocks into crustal levels within the eastern half of the forearc (Bloomer, 1982; Bloomer and Hawkins, 1983). A diapiric model for the origin of these seamounts implies that the rocks represent materials entrained within the rising serpentinite and thus give us an indication of the nature of the mantle and crust through which they rise and of the metamorphic processes occurring both at depth and within the individual edifices.

From a seamount at about 14°N, we dredged (KK810626-03) a small amount of an aragonite-rich carbonate having a vuggy texture (Haggerty, 1987b). Radiating needles of aragonite around minute tubes in the carbonate and the unusual composition of the carbonate were interpreted initially as evidence of venting fluids that were forming chimneys on the summit of this seamount (Haggerty, 1987a, 1987b).

The best studied of the Mariana seamounts are those near 19°30'N (Fig. 3). Dredging at the summit of these seamounts yielded serpentinized ultramafic materials, metamorphosed mafic rocks, manganese crusts with adhering pelagic sediment, serpentine muds, and some semilithified, vitric siltstones. SeaMARC II side-scanning sonar images and bathymetry of the two seamounts in this region (Fig. 4A) showed flow features of various types on their flanks (Hussong and Fryer, 1985; Fryer et al., 1985; Fryer and Fryer, 1987). The base of Conical Seamount is readily distinguishable from the surrounding seafloor. The lower flanks show concentric, long-wavelength ridges, especially on the southeast side. All flanks of the seamount are mantled with long sinuous flows. The flows extend for a maximum distance of up to 18 km from the summit, and their sinuous morphology indicates that they are composed of nonviscous material. The total area covered by the sinuous flows is approximately 550 km^2. The edifice covers an area of approximately 700 km^2. The flows on Conical Seamount were initially interpreted to be composed of normal forearc sediments mobilized into debris flows by gravitational instability and by infusion of the sediments with fluids venting from a near-surface serpentinite diapir; this implied that Conical Seamount is a large mud volcano (Fryer et al., 1987; Fryer and Fryer, 1987).

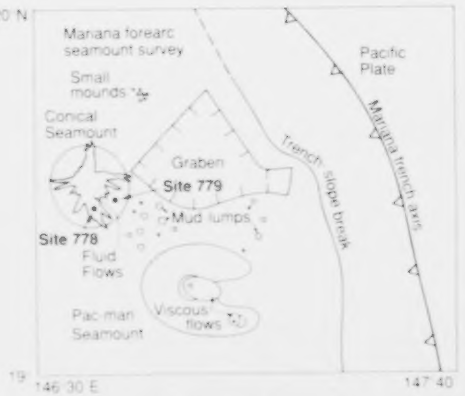

Figure 3. Geologic sketch showing the disposition of seamounts and a large graben in the vicinity of 19°N on the outer Mariana forearc.

ALVIN DIVE STUDIES

The dives at Conical Seamount were designed to characterize and sample the flow features on the flanks of the edifice, to investigate the faults and deformation of the flanks of the seamount, and to study the summit region of the seamount (Fryer et al., 1987). Five dives (1851–1855; Fig. 4B) on the flanks studied the flow composition and morphology, and four dives (1859–1862; Fig. 4B) on the summit area investigated chimney structures and vent morphology.

The results of the dives at Conical Seamount provided us with the first look at an active serpentine mud volcano. The first five dives (1851–1855) were made on the flanks of the seamount to characterize the flows. The flows on Conical Seamount have a variety of surface textures and structures. A relative age discrimination, based on the degree of sediment cover on the flows, on the amount of manganese encrustation of the surface of the flows, and the degree of contortion of the surface of the flows, was applied in an attempt to map regions of recent flow activity.

The presumably youngest flows are light green, have contorted surfaces, and lack a sediment cover. These flows have numerous cobbles and boulders consisting primarily of serpentinized peridotites and dunites, with small amounts of metabasalts and metagabbros scattered over their surfaces (Fig. 5). The older flows have a smoother surface, are covered with sediment and, in places, have ferromanganese and/or carbonate encrustations (Fig. 6). Most of the young flow features are concentrated near the summit area and were best observed in dives 1859 through 1862. The flows apparently originate from near the western side of the two summit knolls, in the vent region of the seamount. Flows also are related to faulting on the flanks of the seamount and may contain remobilized older flow materials.

Normal faults occur on the summit regions and upper flanks of Conical Seamount and expose the interiors of flows. Many of the flow interiors are mottled by patches or streaks of carbonate. The interior of one such flow is shown in Figure 7 (note the lack of rock clasts in the exposure). The paucity of clasts within the fault exposures suggests that some flows consist primarily of serpentine mud. Numerous rock clasts are exposed only on the surface of the younger flow areas, and their absence from the older flow areas suggests that the clasts may sink into the serpentine muds after the flow settles. Too little of the serpentine mud was collected on the *Alvin* dives to permit detailed rheological studies. However, from the push cores we collected we surmise that the rheological properties of the serpentine muds vary considerably over small distances depending on the degree of carbonate precipitation within the muds and on the amount of entrained pore water. The percentage of carbonate in the muds is greatest in the summit areas, near the proposed vents. The distribution of carbonate is probably the result of escape of entrained fluids from the flows as they advance. With removal of the fluids, the degree of precipitation of carbonates decreases.

During dives 1854, 1855, and 1859 through 1862, at depths less than 3200 m, we observed columnar to irregularly shaped, vertical projections of serpentine mud. These structures are veined with and partially cemented by carbonate (Fig. 8), and some are topped with cobbles. The structures vary from a few centimeters to about 1.5 m high. In several cases, the structures provide a pedestal for the growth of chimneys. Escaping fluids probably precipitated carbonate, not only forming chimneys, but also cementing the matrix of the flow below the surface. We suggest that fluids rise from within the serpentinite flow and may be concentrated in one locality or disseminated throughout the flow. Where concentrated, or where impeded from escaping locally by rising beneath cobbles, the precipitating carbonates might form a fortified column. The chimney pedestals probably were exposed as the surrounding serpentinite flow receded, by current erosion, by deflation of the flow as fluid escaped, or by slumping and sliding downslope of uncemented serpentine mud.

Most of the carbonate chimneys, 0.5 to 1.5 m high (Fig. 9), were found in a small field (about 100 m diameter) at a depth of about 3150 m, west of the southern summit knoll, at the end of dive 1854 and near dives 1859 through 1862. The carbonate chimneys are composed of varying proportions of aragonite and calcite. A minor amount of a gel-like substance composed of a previously unknown magnesium silicate was discovered in vugs in the chimneys (Haggerty and Cloutier, 1988). A thin, black ferromanganese encrustation coats parts of the lower part of the chimneys. Many of the chimneys are rough and embayed and thus appear to be corroded. The depth at which these chimneys can be observed is below the local aragonite compensation depth (Li et al., 1969) and thus, the chimneys should undergo rapid dissolution after formation. A sample taken from one of the corroded chimneys contained excess ^{210}Pb, indicating that it is less than 150 yr old (G. McMurtry, pers. comm., 1989). None of these chimneys exhibited signs of active venting.

A second type of chimney, composed of silicate, was also discovered near the summit of Conical Seamount in the same region as the carbonate chimneys (Fig. 10). This type contained only trace amounts of carbonate and did not appear corroded. Most of these chimneys are taller, ranging from 2 to 3.5 m high, and thicker, up to 2 m at the base, than the carbonate chimneys and are uniformly coated with a thin black layer of ferromanganese oxide. The top of one of the larger chimneys has a smooth, white to pale golden-brown surface. The material forming this type of chimney has the same composition as that of the silicate found in vugs within the carbonate chimneys (Haggerty, 1987b).

Scraping the top of the silicate chimney exposed a bright white interior and prompted a diffuse seeping of fluid from several locations on the scraped surface. Scattered small jets of this fluid (less than 10 cm high) escaped from pores in the chimney. Temperatures measured with the *Alvin* low-temperature probe from the interior of the chimney were slightly lower (up to 0.03° ± 0.005°C) than ambient seawater. Samples

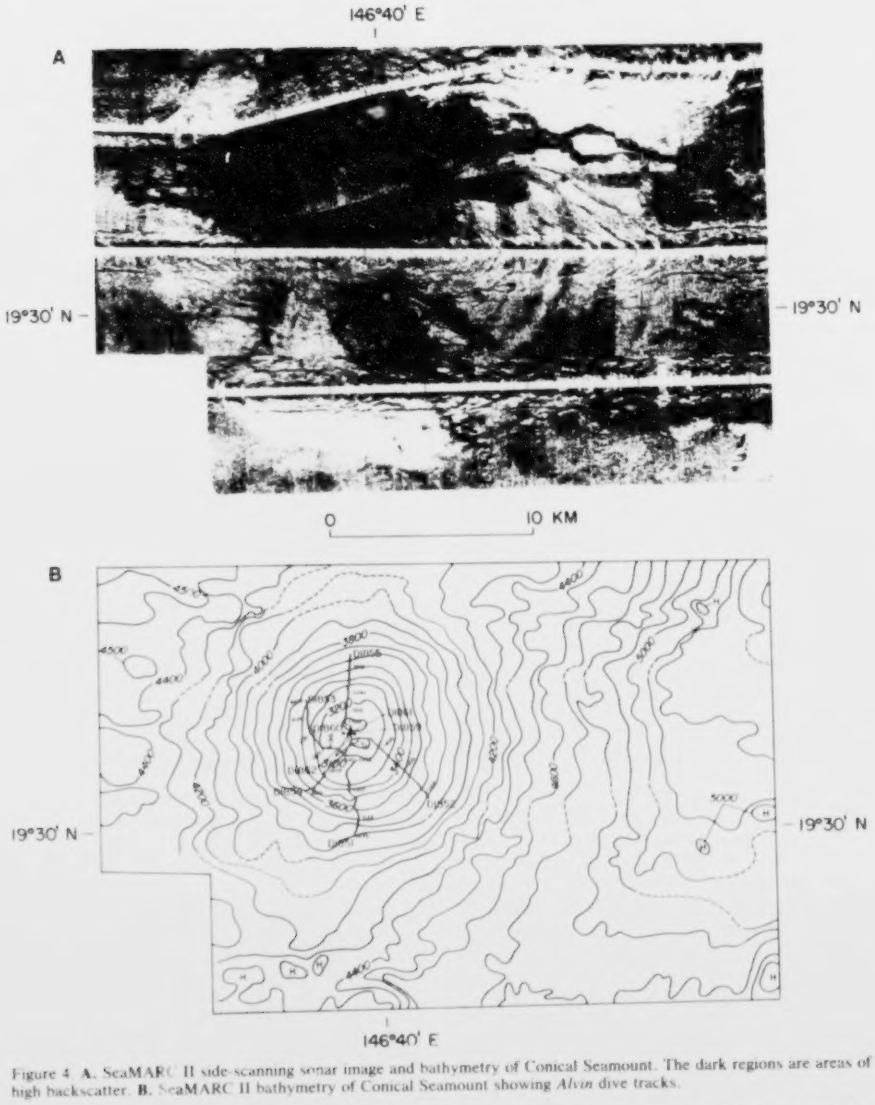

Figure 4. **A.** SeaMARC II side-scanning sonar image and bathymetry of Conical Seamount. The dark regions are areas of high backscatter. **B.** SeaMARC II bathymetry of Conical Seamount showing *Alvin* dive tracks.

of the chimney fluid and of ambient seawater were collected during dives 1860 through 1862. The pH of the vent waters is high (9.28 vs. 7.72 for ambient seawater). Alkalinity is also high (5.53 vs. 2.41 meq/L), and the vent waters are enriched in CH_4 (1000 vs. 2.1 nM), SiO_2 (0.75 vs. 0.12 mM), SO_4^{-2} (30.4 vs. 28.6 mM), and H_2S (2.1 mM vs. not detected in the ambient seawater). Because seawater probably mixed with the fluids during sampling, these enrichments must be considered minima. Detailed results of the chemical analyses of these fluids are reported elsewhere (Fryer et al., 1987). The primary results of the studies of the fluids imply that deep-seated serpentinization processes, interaction of seawater with crustal rocks, and interactions of seawater with the surficial serpentinite may all contribute to the composition of the fluids.

We consider the biogenic sources in the Mariana forearc crust as unlikely for generating the CH_4 and H_2S measured in the chimney vent fluids. The forearc is not accretionary at these latitudes and does not contain a large volume of sedimentary substrate (Hussong and Uyeda, 1982). In addition,

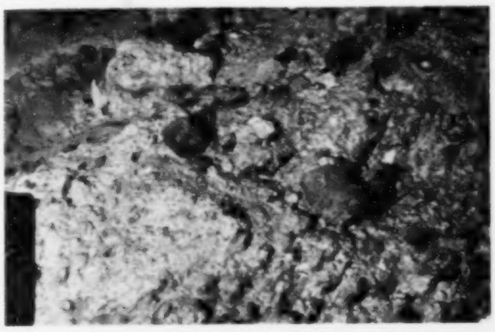

Figure 5. Bottom photograph of an area of unsedimented (presumably recent) serpentine flow showing numerous clasts of metamorphosed rocks presumably entrained in the flow.

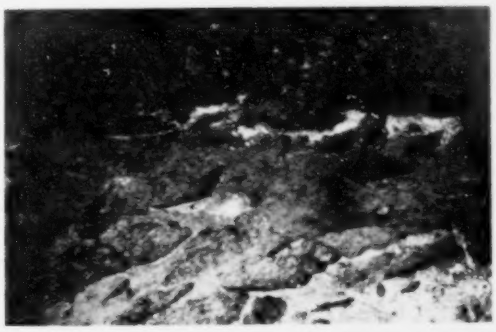

Figure 6. *Alvin* external camera photograph of ferromanganese crust on top of serpentine flow material. Fracturing of the crust is apparent in the photograph.

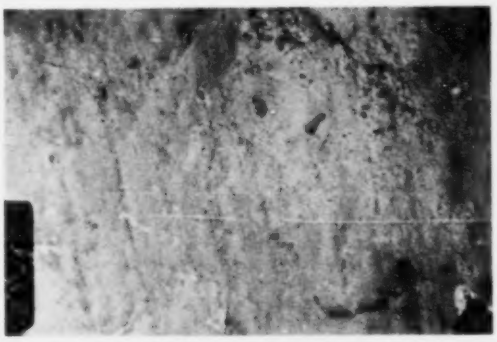

Figure 7. *Alvin* external camera photograph of the interior of a serpentine flow showing a paucity of clasts and apparent carbonate streaking.

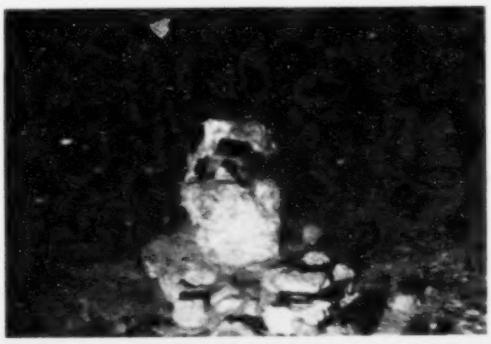

Figure 8. *Alvin* external camera photograph of a pedestal of serpentine cemented by carbonate.

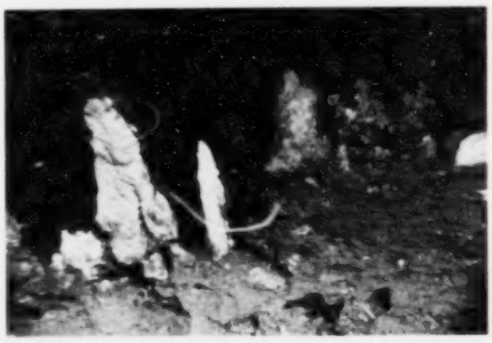

Figure 9. *Alvin* external camera photograph of a carbonate chimney near the summit of Conical Seamount. Note the corroded-appearing surface of the structure.

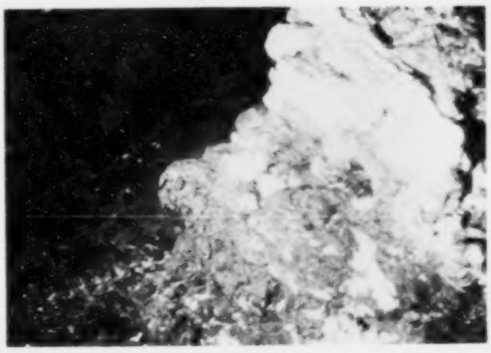

Figure 10. *Alvin* external camera photograph of a silicate chimney near the summit of Conical Seamount.

the small sedimentary substrate present has a low total organic carbon content, 0.06 wt.% (Schorno, 1982). Thus, the organic component in the sediments surrounding these forearc seamounts is insufficient to generate the quantity of methane noted in the vent waters. We suggest that the methane observed in the chimney samples was generated at depth beneath the forearc wedge, possibly derived from sediment on the Pacific Plate.

The carbon and oxygen isotopic compositions of the carbonate chimney precipitates are compatible with a deep source either in the forearc mantle wedge or from the subducted slab or both (Haggerty, 1987b). Mariana aragonite has a significantly lighter carbon isotopic signature, compared with aragonite found in fracture-zone serpentinite (1.2‰ to 21.2‰ for the Mariana samples vs. +0.03‰ to +1.12‰ for fracture-zone aragonite) and a heavier oxygen isotopic signature (Mariana = +5.1‰ to +7.6‰; fracture-zone = +3.16‰ to +4.87‰) (Haggerty, 1987b). Fracture-zone aragonite is precipitated at ocean-floor temperatures from seawater as a consequence of circulation of the seawater through fissures and fractures in the host rock, where the water reacts with ultramafic rocks during serpentinization (Bonatti et al., 1980). In contrast, the composition of the Mariana aragonite precludes a source involving only seawater that has reacted with ultramafic rocks. The fluids forming the Mariana aragonite originate in part by dewatering of the downgoing plate, from juvenile mantle fluids, from deep-seated serpentinization reactions, and from reactions accompanying the emplacement of the serpentinite.

Clasts of metamorphosed ultramafic rocks were recovered from the dives and in dredges from Conical Seamount (Fryer and Fryer, 1987). Preliminary analyses indicate that the clasts are primarily serpentinized harzburgite (Saboda et al., 1987). The harzburgites are 24% to 90% serpentinized and contain 1% to 8% clays, up to 7% carbonate, up to 4% iron oxide, up to 3% chlorite, and up to 1% brucite as secondary phases. Although much of the original mineralogy has been obscured, the modal percentages of the original minerals may be estimated by examination of the serpentine textures, the interrelationships between the various serpentine phases, and the relationships between the serpentine phases and the extant mafic minerals in the rocks. The harzburgite samples are estimated to have contained originally from 62% to 84% olivine, 15% to 35% orthopyroxene, 1% to 2% spinel, and up to 2% clinopyroxene. Metamorphism of the samples indicates low to moderate temperatures and pressures. Although tectonized ultramafic rocks were dredged elsewhere on other serpentinite seamounts of the Mariana forearc (Bloomer and Hawkins, 1983), none of the preliminary studies of the samples from the *Alvin* dives shows tectonized fabrics. We suggest that the harzburgites sampled from the surface of Conical Seamount are primarily upper mantle rocks that were metamorphosed in the forearc as a consequence of the flux of fluids derived from dehydration reactions within the downgoing Pacific Plate. We further suggest that these rocks were plucked from the walls of a deep-seated conduit and entrained within rising pulses of fluid-charged serpentine muds that erupted slowly from the summit of the seamount.

Igneous rocks, collected in dredge hauls on the eastern wall of the graben that lies adjacent to the seamounts, include boninites (high-magnesian andesites) and basalts similar in composition to island-arc tholeiite (IAT), mid-ocean ridge basalt (MORB), ocean island basalt (OIB), and a group of basalts transitional between the alkalic OIB and the tholeiitic IATs and MORBs (Johnson and Fryer, 1988). The samples have been altered, but their provenance can be determined using ratios of trace elements, particularly titanium, zirconium, and vanadium. The petrogenesis of the samples and interpretations of their emplacement in the forearc are presented in Johnson and Fryer (1988). The discovery of MORB in the forearc, particularly at a distance of more than 50 km from the trench axis, requires a modification of the models of forearc evolution. Rocks previously dredged from the inner walls of the Mariana Trench and along scarps in the outer forearc high are of arc composition with the exception of small amounts of OIB found in a few dredges on the inner wall of the trench. The composition of forearc crust thus was suggested to have formed by arc volcanism. The discovery of MORB lavas in the dredges from the graben adjacent to the serpentinite seamounts studied with *Alvin* is the first evidence of such rocks in the forearc of any active interoceanic arc. These lavas support the concept that either exotic fragments of old oceanic plate have been incorporated into the forearc terrane or lavas generated by suprasubduction-zone magmatism make up part of the forearc crustal sequences.

SEISMIC-REFLECTION STUDIES OF CONICAL SEAMOUNT

A site-survey cruise was conducted in 1987 to acquire detailed seismic-reflection data over the prospective drill sites on Conical Seamount (*Fred H. Moore* Cruise 35-11). The navigation for the cruise was restricted to satellite navigation because the Yap station for Loran C had been shut down and the new station in Guam was not yet operating. The signal-to-noise ratio on one of the two Loran C stations for which we could pick up delays was too low to make reasonable calculations of the ship's position. The Global Positioning System was only functional for a few hours each day. The track plot of the survey is shown on the SeaBeam bathymetry (Fig. 11). The sound source was a tuned array of six air guns that totaled 1064 in.^{3}, with a shot interval of approximately 40 m. Reflection returns were received with an analog hydrophone streamer configured with six channels at 16.66-m group intervals and recorded digitally in demultiplexed (SEG D) format on magnetic tape. Field data were sorted into 16.66-m bins, corrected for normal moveout, and stacked (nominal twofold). The stacked traces were mixed (three traces having 1-3-1 weight), deconvolved, filtered (15- to 45-Hz bandpass to 1 s below water bottom; 9- to 35-Hz bandpass to the end of record), and migrated (finite difference) prior to final display. Migration velocities were estimated from previous refraction profiles in the Mariana forearc (LaTraille and Hussong, 1980).

The first seismic-reflection line (Fig. 12) was run east to west across the summit region of Conical Seamount. The reflectors from the sediment in the basin to the east of the seamount extend for several kilometers under the edifice and persist to a sub-bottom depth of about 0.5 s. The lower eastern slopes of the seamount show deformation indicative of folding and/or slumping of the sedimentary layers draping the seamount. Numerous weak reflectors dip inward toward the center of the edifice. These reflectors show the steepest dip on the lower flanks and flatten to become parallel to the seafloor on approach to the summit. The inward-dipping reflectors may indicate subsidence of the edifice as a consequence of loading by subsequent flows or by collapse of the edifice as flows dehydrate after emplacement. At depths shallower than the midflanks of the seamount a semicontinuous reflector can be traced at a subsurface depth that varies from about 0.18 s at the summit to about 0.15 s on the midflank. Because the sub-bottom depth of this reflector varies, we do not believe that it is a processing artifact. This reflector is particularly well-defined on the west flank and on the summit region. On the east flank several reflectors crosscut this reflector. The

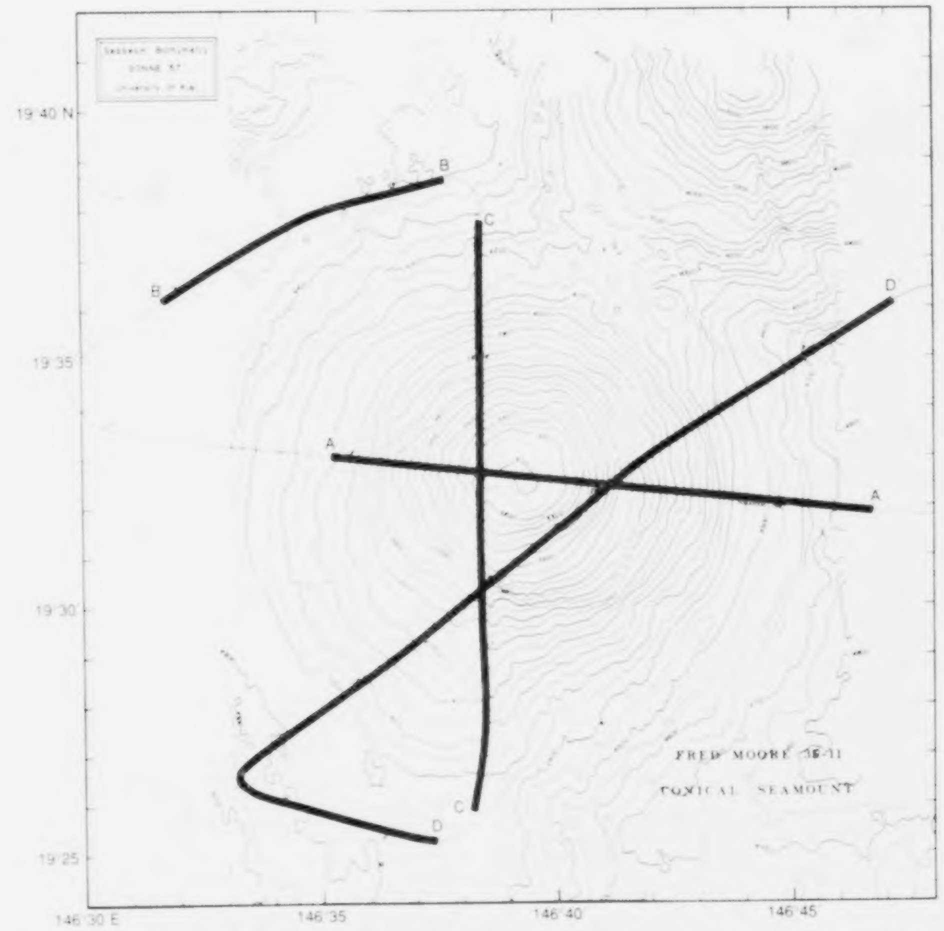

Figure 11. Track plot of the *Fred H. Moore* (FM) Cruise 35-11 seismic-reflection survey of Conical Seamount, superimposed on SeaBeam data from sonne 57. The heavy tracklines show locations of reflection profiles given in Figures 12 through 15.

nature of the reflector remains an enigma that may be resolved by drilling. The central core of the seamount lacks reflectors and is interpreted to be composed of highly unstable, fluid-charged serpentine mud rising through the seamount core. The west side of the seamount shows much better defined reflectors dipping toward the center of the seamount. The sedimentary layers on the west side of the seamount are better defined than those on the east side. Subhorizontal reflectors at a depth of about 6.5 s are apparent beneath the lower west flank. These are interpreted to represent old sedimentary sequences onlapped by serpentine flows.

Seismic-reflection line 2 (Fig. 13) was run from the western to the northern base of the seamount. This line traversed a relatively flat part of the seafloor on the northwest side of the seamount (western end of line 2 in Fig. 13). The region is dominated by thick (1.0 s), flat-lying, sedimentary sequences. At about 1415UTC the profile crosses the southwestern side of a small horst block and graben separated by a throw of about 50 m. A well-defined shallow (100 m below seafloor) reflector occurring near the top of the horst block is interpreted as a sill or buried lava flow. At about 1445UTC on the northeastern side of the horst block an apparent normal fault, down-dropped to the northeast, offsets the reflector. The reflector is deformed (downwarped) beyond 1500Z and terminates at about 1510UTC.

Seismic-reflection line 3 (Fig. 14) was run from north to south across the summit of the seamount. The sedimentary layers on the base of the north flank are severely disturbed, folded, and/or slumped. The midflank portion of the seamount shows a smooth, fairly undisturbed thin drape of sediment. The midflank reflectors are interpreted as relatively recent serpentinite flows seen on the north flank of the seamount on

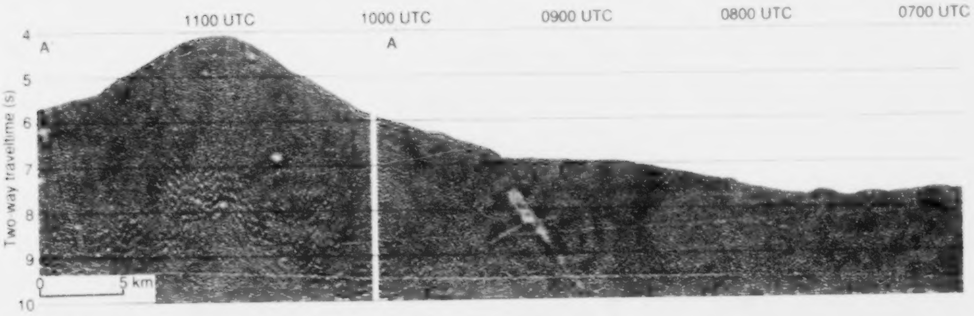

Figure 12. Seismic-reflection line 1, FM35-11.

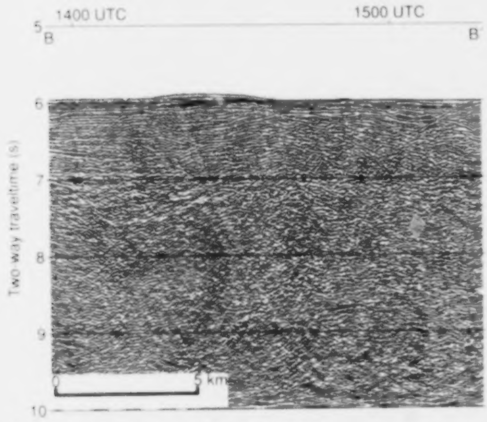

Figure 13. Seismic-reflection line 2, FM35-11.

the SeaMARC II sonar images. Beneath the summit of the seamount, a broad zone of incoherent reflectors is interpreted as unstable, fluid-charged serpentine mud rising through the seamount (also seen on line 1; Fig. 12). In addition, several disturbed regions of serpentinite flows, probably slumps, are apparent on the south flank.

Seismic-reflection line 4 (Fig. 15) was run northeastward across the eastern flank of the seamount. The structures of the seamount are less obvious here than on line 3, which was run across the summit of the seamount. A thin sedimentary reflector can be traced across the entire northeast flank of the seamount. This profile shows numerous down-bowed reflectors, which may be from surfaces of inward dipping horizons that were cut by the oblique profile. Some disturbance of the serpentinite flows is apparent on the southeast face of the seamount, which may result from slumping as seen on *Alvin* dives on that flank.

SUMMARY AND CONCLUSIONS

Several important observations that resulted from the *Alvin* dives and the recent geophysical surveys around Conical Seamount have modified our concepts of convergent margins:

1. Metamorphism (particularly serpentinization) is pervasive in the forearc, and hydration of forearc materials acts as sink for fluids driven off the subducting slab (Fryer and ryer, 1987; Saboda et al., 1987). The extent of metamorhism in the dredge and dive samples is variable, but all of the ltramafic samples recovered are serpentinized to some deree. Prior to these investigations researchers studying the hemical balance of the convergent margins were unable to xplain the apparent inconsistencies between the amount of olatiles released in arc and backarc volcanism and the resumably much greater amount of volatiles driven off the escending slab by dehydration reactions. Fryer and Fryer 987) showed that the fields of stability of metamorphic facies ithin the Mariana forearc are more than adequate to accomodate the fluids driven off the slab.

2. The fluid flux in the convergent margin environment is ntrolled primarily by forearc processes. Fluids, derived at ast in part from the descending slab, are actively venting at vo of the serpentinite seamounts (Fryer et al., 1987; aggerty, 1987b) and in some highly faulted regions near ese seamounts. The seamount vents are capped by chimy structures composed of carbonate (calcite and aragote) and silicate (a new mineral, a Mg-silicate analogous to lophane) (Haggerty, 1987a; Haggerty and Cloutier, 1988). The geochemical and isotopic compositions of the carbonate chimneys differ from normal marine carbonate and distinguish them from carbonates formed in association with serpentinite at fracture zones (Haggerty, 1987b). Recent fluid-inclusion work on the aragonite needles of the *Alvin* chimney samples shows them to contain methane and several varieties of the higher hydrocarbons (Haggerty, 1989). Analyses of the pore waters from push cores and particularly the vent waters collected with *Alvin* also show a high methane content. The source of these fluids and their associated hydrocarbons is interpreted to be the subducted Pacific oceanic plate sediments or sediment underplating the outer forearc.

Active convergent margins can accommodate large quantities of fluids from the subducting slab and thus develop broad regions of lawsonite-albite-chlorite/greenschist/blueschist facies stability fields beneath the entire forearc region (Fryer and Fryer, 1987). Thus, under appropriate tectonic conditions, serpentinite seamounts can be emplaced almost anywhere in a forearc, yet none show development of serpentinite seamounts on the scale of that in the Mariana system. One reason for the paucity of serpentinite seamounts in other forearcs may be that, in contrast with most others, the Mariana forearc shows extensive recent vertical tectonic deformation (Fryer and Fryer, 1987). Numerous sedimentary serpentinite deposits have been described from the Pacific margins and in the Mediterranean and Caribbean

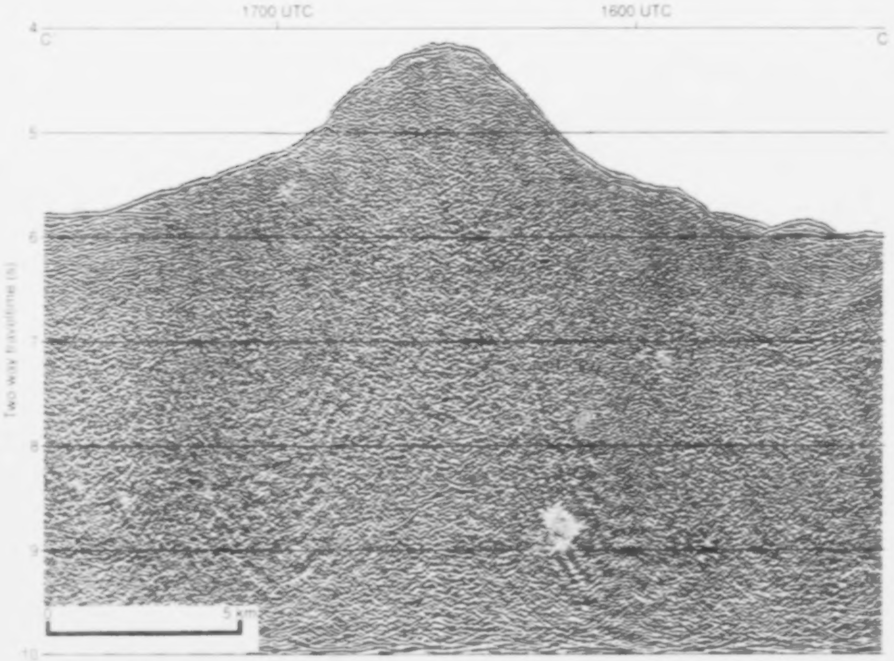

Figure 14. Seismic-reflection line 3, FM35-11.

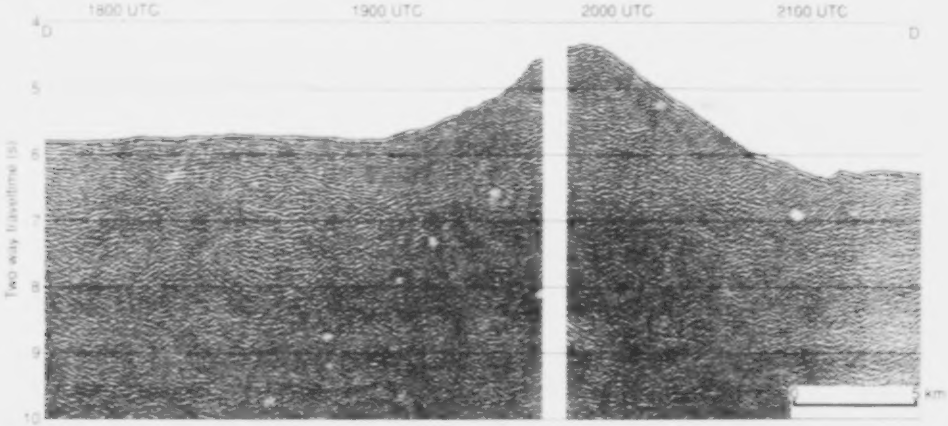

Figure 15. Seismic-reflection line 4, FM35-11.

areas (Lockwood, 1971). Several of these exposures are similar to the deposits forming on Conical and Pacman seamounts. Therefore, we suggest that Conical and Pacman seamounts may represent type localities for the study of *in-situ* formation of many of these sedimentary serpentinite bodies.

The fluid flux through the Mariana forearc must play a critical role in the evolution of the thermal structure of the forearc. The degree of flux channeled by fractures within the outer forearc may be great enough to create major local perturbations of the thermal structure. A better understanding of the distribution of active venting sites will make it possible to develop more accurate models of the thermal structure of the forearc.

3. Several different types of seamounts are present on the Mariana forearc (Fryer et al., 1987). The actively "erupting" serpentinite seamounts, such as Conical Seamount, are one end-member. The uplifted horsts of forearc crust are the other end-member, and between these types are seamounts that exhibit elements of each.

The *Alvin* observations on Conical Seamount imply that nonviscous flow morphologies correlate with active venting and with young, unsedimented serpentinite flows. Conical Seamount is considered to be an active mud volcano and a site at which forearc fluids are escaping. Clasts of serpentinized ultramafic rocks, serpentine muds, and chimney material similar to that obtained from the carbonate chimneys on Conical Seamount were dredged from an unnamed seamount at about 14°N. The chimney materials analyzed by Haggerty (1987a) are in equilibrium with fluids of the same composition as those analyzed from Conical Seamount. The metamorphic grade and composition of the ultramafic clasts and serpentine muds in the dredge hauls from this seamount are similar to those of the clasts and mud from Conical Seamount. Thus, we suggest that the southern seamount may also be an "active" serpentinite seamount. Although similarly metamorphosed ultramafic clasts and serpentine muds have been collected in dredge hauls from several other seamounts (Bloomer and Hawkins, 1983; Saboda et al., 1987), chimney materials have not been retrieved. How many of these or of the other Mariana forearc seamounts might also be "active" is unknown. Desprairies (1982) reported significant amounts of serpentine in the middle Miocene and middle Eocene sedimentary units in Hole 459B, located about 50 km south of Pacman Seamount. If these results indicate formation of serpentinite seamounts nearby, then serpentinite seamounts may have been active for at least the last 40 m.y. in the Mariana system.

4. Complex local as well as regional interrelationships exist between faulting and the distribution of seamounts within the outer forearc. The local structural setting of Conical Seamount is well known (Hussong and Fryer, 1985; Fryer et al., 1987; Newsom and Fryer, 1987; Johnson et al., 1987). Recent seismic-reflection profiles and gravity data (Newsom and Fryer, 1987) show that Conical Seamount was emplaced along local faults.

5. The first documented exposure of MORB lavas in any active forearc was discovered well arcward of the trench axis in the Mariana region during dredging of the scarp of a large graben 80 km east of Conical Seamount (Johnson and Fryer, 1988).

ACKNOWLEDGMENTS

We thank the captains and crews of the *Moana Wave*, *Atlantis II*, and *Fred H. Moore* for their assistance in collecting the data presented here. Particular thanks are extended to the *Alvin* pilots who made the diving such a success and to P. Ganey, whose assistance with the data from the *Fred H. Moore* cruise, both at sea and on shore, was invaluable. We thank an anonymous reviewer who provided a critique of an earlier version of this manuscript and M. Marlow for his helpful suggestions and careful review of the penultimate version.

This work was supported by the National Science Foundation, grant numbers OCE-84-11717, OCE-87-21871, and OCE-8996141, and by a grant from the Joint Oceanographic Institutions United States Science Advisory Committee for collection of the seismic-reflection data during Cruise 35-11 of the *Fred H. Moore*.

REFERENCES

Bloomer, S., 1982. Structure and evolution of the Mariana Trench, petrologic and geochemical studies. Univ. Calif. San Diego.

Bloomer, S. H., and Hawkins, J. W., 1983. Gabbroic and ultramafic rocks from the Mariana Trench: an island arc ophiolite. *In* Hayes, D. E. (Ed.), *The Tectonic and Geologic Evolution of Southeast Asian Seas and Islands, Part 2*. Am. Geophys. Union, Geophys. Monogr. Ser., 27:294–317.

Bonatti, E., Lawrence, J. R., Hamlyn, P. R., and Breger, D., 1980. Aragonite from deep-sea ultramafic rocks. *Geochim. Cosmochim. Acta*, 44:1207–1214.

Carlson, C., 1984. Stratigraphic and structural significance of foliate serpentine breccias, Wilbur Springs. *Soc. Econ. Paleontol. Mineral. Guidebook*, 3:108–112.

Desprairies, A., 1982. Authigenic mineral in volcanogenic sediments cored during Deep Sea Drilling Project Leg 60. *In* Hussong, D. M., Uyeda, S., et al., *Init. Repts. DSDP*, 60: Washington (U.S. Govt. Printing Office), 455–466.

Fryer, P., Ambos, E. L., and Hussong, D. M., 1985. Origin and emplacement of Mariana forearc seamounts. *Geology*, 13:774–777.

Fryer, P., and Fryer, G. J., 1987. Origins of non-volcanic seamounts in a forearc environment. *In* Keating, B. H., Fryer, P., Batiza, R., and Boehlert, G. W. (Eds.), *Seamounts, Islands and Atolls*. Am. Geophys. Union, Geophys. Monogr. Ser., 43:61–72.

Fryer, P., Haggerty, J., Tilbrook, B., Sedwick, P., Johnson, L. E., Saboda, K. L., Newsom, S. Y., Karig, D. E., Uyeda, S., and Ishii, T., 1987. Results of studies of Mariana forearc serpentinite diapirism. *EOS, Trans. Am. Geophys. Union*, 68:1534.

Fryer, P., and Hussong, D. M., 1982. Seafloor spreading in the Mariana Trough: results of Leg 60 drill site selection surveys. *In* Hussong, D. M., Uyeda, S., et al., *Init. Repts. DSDP*, 60: Washington (U.S. Govt. Printing Office), 45–55.

Fryer, P., and Smoot, N. C., 1985. Morphology of ocean plate seamounts in the Mariana and Izu-Bonin subduction zone. *Mar. Geol.*, 64:77–94.

Haggerty, J. A., 1987a. Cold-water, deep-sea chimneys from the Mariana forearc serpentinite seamounts. *EOS, Trans. Am. Geophys. Union*, 68:1534.

________, 1987b. Petrology and geochemistry of Neogene sedimentary rocks from Mariana forearc seamounts. *In* Keating, B. H., Fryer, P., Batiza, R., and Boehlert, G. W. (Eds.), *Seamounts, Islands and Atolls*. Am. Geophys. Union, Geophys. Monogr. Ser., 43:175–186.

________, 1989. Fluid inclusion studies of chimneys associated with serpentinite seamounts in the Mariana forearc. *Biannu. Pan-American Conf.: Res. Fluid Inclusions (Blacksburg, VA), PACROFI II*, 2:29.

Haggerty, J., and Cloutier, M. J., 1988. Biologic and mineralogic studies of deep-sea chimneys venting cold water from Mariana forearc seamounts. *Geol. Soc. Am. Abstracts Programs*, 20:A199. (Abstract)

Hsui, A. T., and Youngquist, S., 1985. A dynamic model of the curvature of the Mariana

Trench. *Nature*, 318:455–457.

Hussong, D. M., and Fryer, P., 1985. Forearc tectonics in the northern Mariana arc. *In* Nasu, N. (Ed.), *Formation of Active Ocean Margins*: Tokyo (Terra Scientific), 273–290.

Hussong, D. M., and Uyeda, S., 1982. Tectonic processes and the history of the Mariana arc: a synthesis of the results of Deep Sea Drilling Leg 60. *In* Hussong, D. M., Uyeda, S., et al., *Init. Repts. DSDP*, 60: Washington (U.S. Govt. Printing Office), 909–929.

Johnson, L. E., and Fryer, P., 1988. Oceanic plate material on the Mariana forearc. *EOS, Trans. Am. Geophys. Union*, 69:1471.

Johnson, L. E., Fryer, P., and Ishii, T., 1987. Mariana forearc basement adjacent to serpentinite diapirs. *EOS, Trans. Am. Geophys. Union*, 68:1534.

Karig, D. E., 1971. Structural history of the Mariana island arc system. *Geol. Soc. Am. Bull.*, 83:323–344.

Karig, D. E., and Ranken, B., 1983. Marine geology of the forearc region, southern Mariana island arc. *In* Hayes, D. E. (Ed.), *The Tectonic and Geologic Evolution of Southeast Asian Seas and Islands, Part 2*. Am. Geophys. Union, Geophys. Monogr. Ser., 27:266–280.

Lagabrielle, Y., Whitechurch, H., Marcoux, J., Juteau, T., Reuben, I., and Guillocheau, F., 1986. Obduction related ophiolitic polymict breccias covering the ophiolites of Antalya (S.W. Turkey). *Geology*, 14:734–737.

LaTraille, S. L., and Hussong, D. M., 1980. Crustal structure across the Mariana island arc. *In* Hayes, D. E. (Ed.), *The Tectonic and Geologic Evolution of Southeast Asian Seas and Islands*. Am. Geophys. Union, Geophys. Monogr. Ser., 23:209–222.

Li, T. L., Takahashi, T., and Broecker, W. S., 1969. Saturation of $CaCO_3$ in oceans. *J. Geophys. Res.*, 75:5507–5525.

Lockwood, J. P., 1971. Sedimentary and gravity slide emplacement of serpentinite. *Geol. Soc. Am. Bull.*, 82:919–936.

McCabe, R., and Uyeda, S., 1983. Hypothetical model for the bending of the Mariana arc. *In* Hayes, D. E. (Ed.), *The Tectonic and Geologic Evolution of Southeast Asian Seas and Islands. Part 2*. Am. Geophys. Union, Geophys. Monogr. Ser., 27:291–293.

Mrosowski, C. L., Hayes, D. E., and Taylor, B., 1982. Multichannel seismic reflection surveys of Leg 60 Sites, Deep Sea Drilling Project. *In* Hussong D. M., Uyeda, S., et al., *Init. Repts. DSDP*, 60: Washington (U.S. Govt. Printing Office), 57–71.

Newsom, S. Y., and Fryer, P., 1987. Three-dimensional gravity modeling of serpentinite seamounts in the Mariana forearc. *EOS, Trans. Am. Geophys. Union*, 68:1534.

Phipps, S. P., 1984. Ophiolitic olistostromes in the basal Great Valley sequences, Napa County, northern California Coast Ranges. *In* Raymond, L. A. (Ed.), *Melanges: Their Nature, Origin, and Significance*. Spec. Pap. Geol. Soc. Am., 198:103–125.

Saboda, K. L., Fryer, P., and Fryer, G., 1987. Preliminary studies of metamorphic rocks collected during *Alvin* studies of Mariana forearc seamounts. *EOS, Trans. Am. Geophys. Union*, 68:1534.

Schorno, K. S., 1982. Geochemistry of carbon, International Phase of Ocean Drilling Project 60. *In* Hussong, D. M., and Uyeda, S., et al., *Init. Repts. DSDP*, 60: Washington (U.S. Govt. Printing Office), 501–504.

Uyeda, S., and Kanamori, H., 1979. Back-arc opening and the mode of subduction. *J. Geophys. Res.*, 84:1049–1061.

Ms 125A-104

Fryer, P., Pearce, J. A., Stokking, L. B., et al., 1990
Proceedings of the Ocean Drilling Program, Initial Reports, Vol. 125

5. STRUCTURE OF THE OUTER IZU-BONIN FOREARC FROM SEISMIC-REFLECTION PROFILING AND GRAVITY MODELING[1]

Robert L. Horine,[2] Gregory F. Moore,[3] and Brian Taylor[3]

ABSTRACT

Geophysical surveys conducted over the trench and lower trench slope of the Izu-Bonin arc have provided new information on the timing and mode of formation of several seamounts in this region. Multichannel seismic data reveal that these seamounts contain a shallow cap (less than 1 km thick) without internal reflections, which dredging and coring results indicate is made of serpentinite. This cap is underlain by a seismically reflective region that may be the original substrate onto which the serpentinite protruded. Sedimentary sequences flanking the seamounts have been uplifted. Gravity data indicate that the forearc near the seamounts is composed of low-density material that extends as deep as the décollement. These seamounts have experienced several periods of deformation, with the seamount at 30°55′N, 141°47′E having undergone very recent, perhaps even current, uplift. A two-stage process is proposed for the formation of these seamounts. The first stage would consist of small serpentinite diapirs breaching the surface to form serpentinite volcanoes. In the second stage, uplift of the seamounts would result from serpentinite intrusions into the volcanoes and a widening zone of serpentinization around the feeder conduits.

INTRODUCTION

As part of a regional investigation conducted prior to Ocean Drilling Program (ODP) Leg 125 drilling, extensive geophysical surveys were made over the Izu-Bonin arc. These surveys include the 96-trace multichannel seismic-reflection (MCS) data collected using the *Fred H. Moore* of the University of Texas Institute for Geophysics. In this chapter, we present and interpret the MCS data as well as model marine gravity data collected in 1979 by the Geological Survey of Japan. Specifically, we examine the internal structures of several seamounts on the inner trench slope and the depositional pattern of the sediment flanking these features to develop a model for the timing and mode of formation of these seamounts.

The Izu-Bonin arc marks an intraoceanic convergent plate boundary where the Pacific Plate is being subducted beneath the Philippine Sea Plate. Many aspects of the subduction process are poorly understood, particularly those concerning coupling between the two plates within the first 150 km of the trench. Two end-member models have been proposed for the mechanical interaction in this region: accretion and tectonic erosion.

Tectonic erosion is a process whereby material is removed from the overriding plate and carried down into the mantle by the subducting slab. This process could result in subsidence of the forearc and will result in landward migration of the trench. Hussong and Uyeda (1982) and Bloomer (1983) proposed that this process was active in the Mariana arc. Tectonic erosion may also be occurring in the Izu-Bonin arc, as suggested by Crawford et al. (1981) and Sakai et al. (in press).

Accretion is essentially the opposite of erosion. During accretion, material from the subducting oceanic crust is scraped off and added to the forearc, resulting in seaward migration of the trench and some uplift of the forearc. In regions with a significant sediment influx, such as the Lesser Antilles (Westbrook and Smith, 1983) or Nankai (Aoki et al., 1982), large accretionary prisms have formed. However, there is little sediment in the Izu-Bonin Trench, so the Izu-Bonin arc has only a small accretionary wedge (Horine et al., 1988).

Accretion and erosion are mechanical interactions. Chemical interactions, such as those produced by dewatering of the subducting slab, are also possible. As the oceanic crust descends into a higher temperature and pressure regime, low-temperature hydrous minerals, such as clays, recrystallize to a more stable phase, such as amphibole, releasing excess water (Sakai et al., in press). The path that this water takes back to the surface, whether along the décollement or directly through the overriding slab, provides information about the mechanical nature of the forearc. The water will follow the path of least resistance, which would be fractures in a brittle forearc or the décollement in a ductile forearc. Chemical reactions between the water and the host rock may also create effects that are detectable at the surface, such as serpentinite diapirism. A series of seamounts on the landward slope of the Mariana Trench appears to be diapirs of this type (Fryer et al., 1984), and similar seamounts occur in the Izu-Bonin arc (Ishii et al., in press; Maekawa et al., in press).

The geophysical surveys over the lower slope of the Izu-Bonin arc were positioned to take advantage of features that facilitate study of the deep structure of the arc. The thin sedimentary cover permits resolution of many structures near the surface. The presence of inferred serpentinite diapirs in the forearc may result from processes deep within the arc.

GEOLOGIC BACKGROUND

The Izu-Bonin arc (Fig. 1) marks the northeast edge of the Philippine Sea. This arc is bounded to the north by Honshu, Japan, and to the south by the Mariana arc. The Izu-Bonin Trench is a roughly linear feature that reaches depths of over 9500 m and strikes approximately 350° (Honza and Tamaki, 1985). The Pacific Plate in this region is moving almost due west, so that the subduction beneath this arc has about 10° of obliquity. The subduction rate is 50 mm/yr at the southern end of the arc and 70 mm/yr at the northern end (Seno et al., 1987). This plate configuration appears to have been stable since the Miocene, when the opening of the Shikoku Basin to the west rotated the arc into its present position (Kodama et al., 1983;

---

[1] Fryer, P., Pearce, J. A., Stokking, L. B., et al., 1990. *Proc. ODP, Init. Repts.*, 125: College Station, TX (Ocean Drilling Program).

[2] Department of Geosciences, University of Tulsa, Tulsa, OK 74104.

[3] Hawaii Institute of Geophysics, 2525 Correa Road, Honolulu, HI 96822.

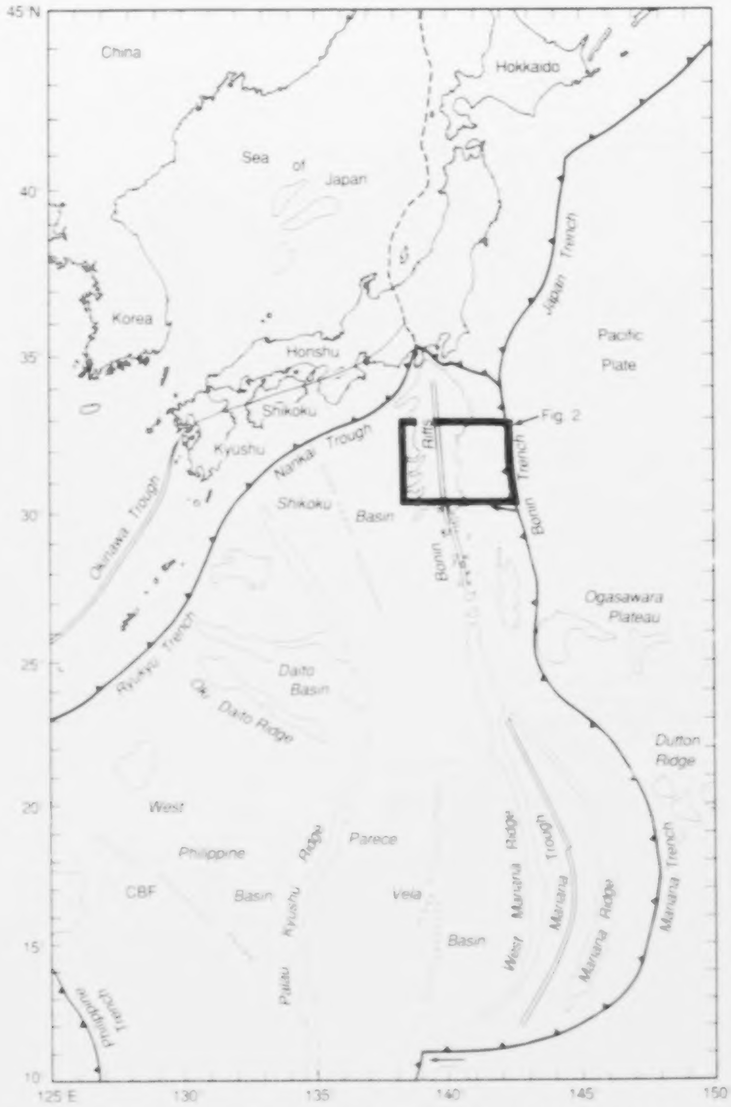
45 N
40
35
30
25
20
15
10
125 E
130
135
140
145
150
China
Hokkaido
Sea of Japan
Korea
Honshu
Shikoku
Kyushu
Japan Trench
Pacific Plate
Fig. 2
Rifts
Nankai Trough
Okinawa Trough
Shikoku Basin
Bonin Trench
Bonin
Ogasawara Plateau
Ryukyu Trench
Daito Basin
Oki Daito Ridge
Dutton Ridge
West Philippine Basin
CBF
Kyushu Palau Ridge
Parece Vela Basin
West Mariana Ridge
Mariana Trough
Mariana Ridge
Mariana Trench
Philippine Trench

Figure 1. Regional map of the western Pacific Ocean showing the location of the survey area (Fig. 2) in the Izu-Bonin arc.

Seno and Maruyama, 1984). A bathymetric map of the survey area (Fig. 2) shows the locations of the seismic lines and gravity profiles discussed in the following sections.

A series of seamounts has formed along the inner trench slope between 20 and 50 km landward of the trench axis. These seamounts rise over 1 km above the surrounding seafloor, and some are up to 20 km in diameter. Small sedimentary basins have formed arcward and between several of these seamounts. Chloritized mafic and serpentinized ultramafic rocks have been dredged from the flanks of several of these features (Ishii et al., in press; Maekawa et al., in press). Similar structures in the Mariana arc to the south are the result of the emplacement and protrusion of serpentinite diapirs (Fryer et al., 1985; Fryer and Fryer, 1987). However, the

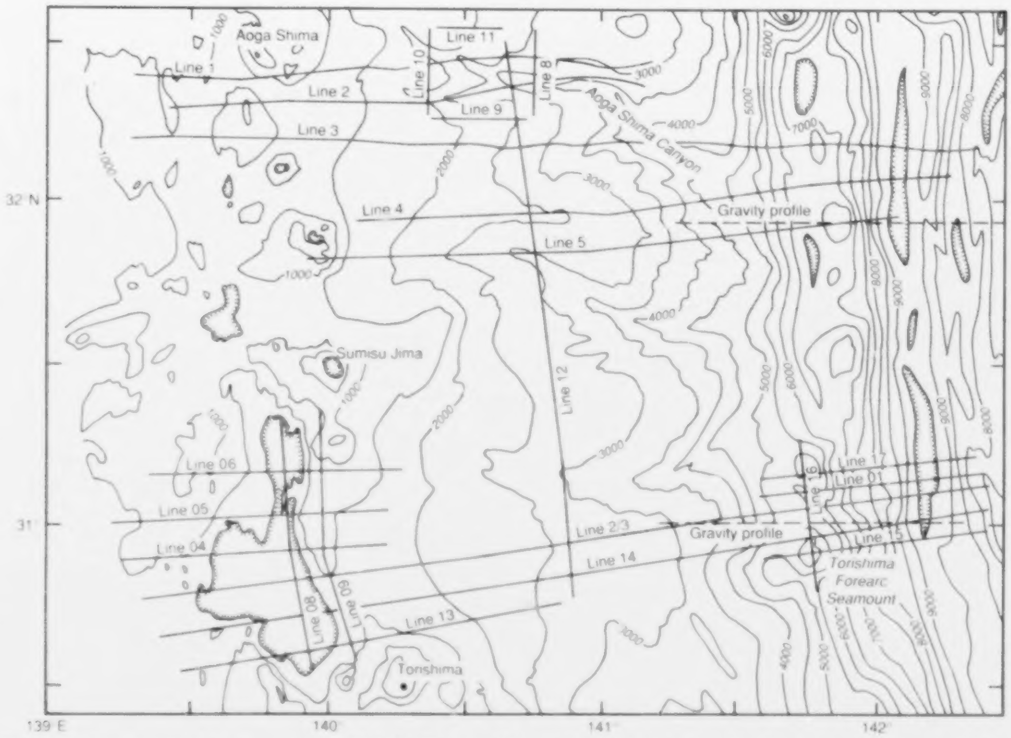
Aoga Shima
Line 1
Line 2
Line 3
Line 4
Line 5
Line 8
Line 9
Line 10
Line 11
Line 12
Line 13
Line 14
Line 15
Line 16
Line 17
Line 2/3
Line 01
Line 04
Line 05
Line 06
Line 08
Line 09
Aoga Shima Canyon
Gravity profile
Gravity profile
Sumisu Jima
Torishima
Torishima Forearc Seamount
1000
2000
3000
4000
5000
6000
7000
8000
9000
32°N
31°
139°E
140°
141°
142°

Figure 2. Bathymetry map of the survey area, modified after Taylor and Smoot (1984), showing the locations of our seismic lines (solid lines) and gravity profiles (dashed lines). The specific area of interest in this paper is east of 141.5°. Contour interval = 500 m.

Mariana forearc is highly fractured, providing conduits for the diapirs, whereas SeaMARC II side-scanning data indicate that the Izu-Bonin forearc is much less fractured. These observations led Fryer and Fryer (1987) to suggest that the entire Izu-Bonin outer forearc has undergone regional serpentinization and uplift and that discrete highs are caused by a locally greater degree of hydration and metamorphism. One of us (B. T.) therefore proposes that these seamounts were formed by localized protrusions of serpentinized material that moved up the décollement between the overriding forearc and the subducted plate. There are thus several possible explanations for these seamounts: simple diapirs, regional serpentinization, and/or deep-seated intrusions. In this chapter, we use seismic data to describe the structures within the seamounts and the shallow sedimentary features within a basin formed between two of the seamounts to illustrate their historical development. We will then examine information provided by gravity data and propose a model for seamount formation.

SEISMIC INTERPRETATION

The acquisition parameters for the seismic data are given in Table 1. The processing sequence in Table 2 is a standard processing sequence, except for the final step, depth conversion. Depth conversion velocity functions were obtained by integrating our stacking and migration velocities with available seismic-refraction velocities from this region (Hotta, 1970; Houtz et al., 1980). These velocities were further refined in the shallow section by comparison with logging velocities at Sites 783 and 784 ("Site 783" and "Site 784" chapters, this volume).

Table 1. Field parameters for the acquisition of seismic-reflection data.

Recording vessel	*Fred H. Moore*
Source	Bolt air-gun array (3065 in.^{3})
Streamer	96 channels
Group interval	33.3 m
Shot interval	30–60 m
Sample rate	2 ms
Recording format	SEG D (demultiplexed)

A detailed bathymetric map of the specific area of interest in this paper, which shows the locations of seismic lines, the position of a gravity profile by the Geologic Survey of Japan, and the location of ODP Sites 783 and 784, is given in Figure 3. There are two seamounts in the center of this region and one to the north. The southernmost seamount has been informally named Torishima Forearc Seamount by Ishii et al. (in press). A small sedimentary basin has formed west of and between the two central seamounts (Fig. 3). Seismic line 14 crosses part of this basin and the flank of a seamount and continues down into the trench axis, as shown in Figure 4.

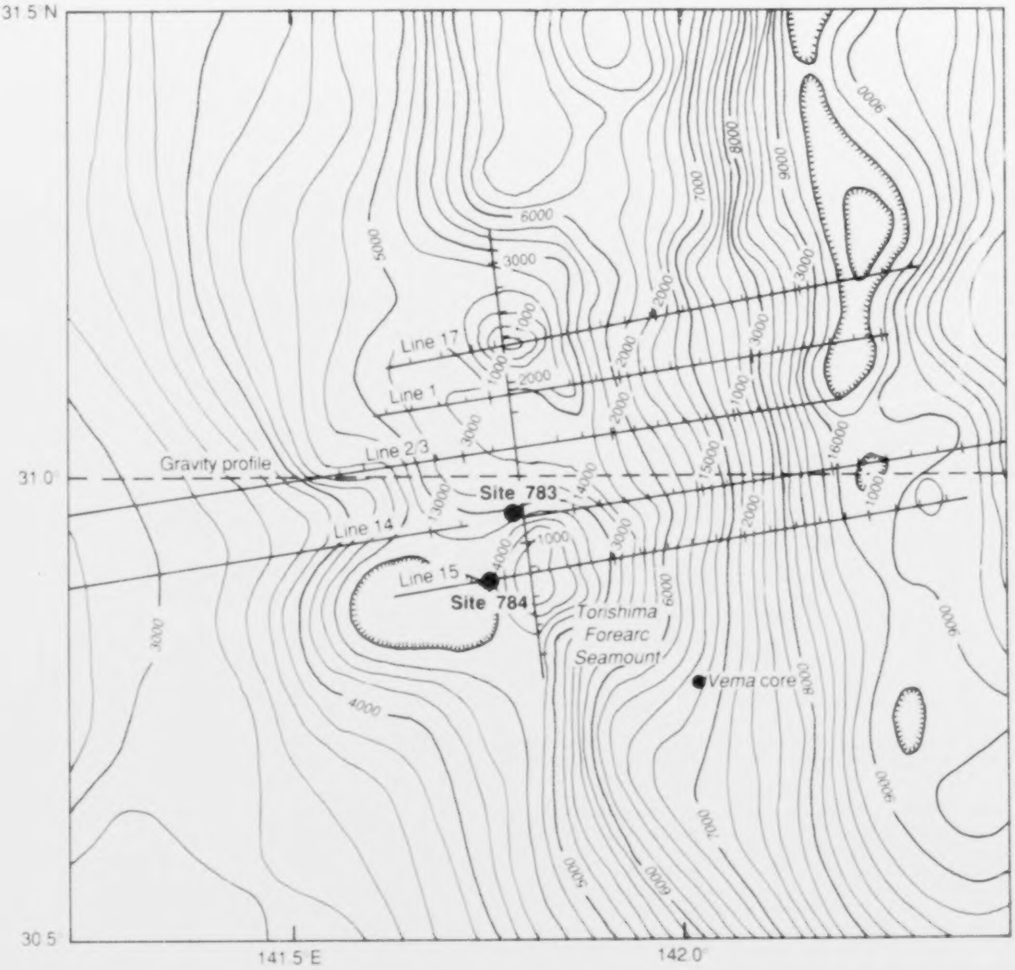

Figure 3. Detailed bathymetric map of the survey area showing the locations of our seismic lines and the gravity profile discussed in the text. Numbers along the lines correspond to the common-depth-point (CDP) numbers on the seismic sections. Bathymetry data from the Geologic Survey of Japan and the U.S. Navy. Contour interval = 200 m.

Note that sediments are scarce outside the basin.

The two central seamounts exhibit internal structures on all the seismic lines. Several internal reflections visible on line 15 (Fig. 5A) over Torishima Forearc Seamount are emphasized in the line drawing of the depth-converted section (Fig. 5B). Features dipping away from the center of the seamount on the time section become subhorizontal on the depth section because of the relatively high velocity (1.6–1.8 km/s) of the seamount material compared to the water velocity. All of these reflectors are fairly weak and discontinuous and exhibit dips ranging from 35° to the east to 20° to the west. However, they also show sufficient continuity on this line, and on the adjoining lines, to suggest that there are regionally significant seismic horizons between 1.2 and 2.5 km below seafloor. Between these deep horizons and the surface is a region containing few coherent reflectors that persists throughout the body of this seamount. Ishii et al. (in press) and Maekawa et al. (in press) dredged sheared serpentinites from the seafloor where this layer crops out, which they interpreted as having formed during the emplacement of a serpentinite diapir.

Figure 6 shows part of seismic line 16, a strike line crossing Torishima Forearc Seamount near its crest. The reflections that are visible within the seamount on line 15 also appear on this line. Although these reflections are more discontinuous than those on line 15, they can be traced to the north, where they are visible on line 14 (Fig. 7). The shallow region above

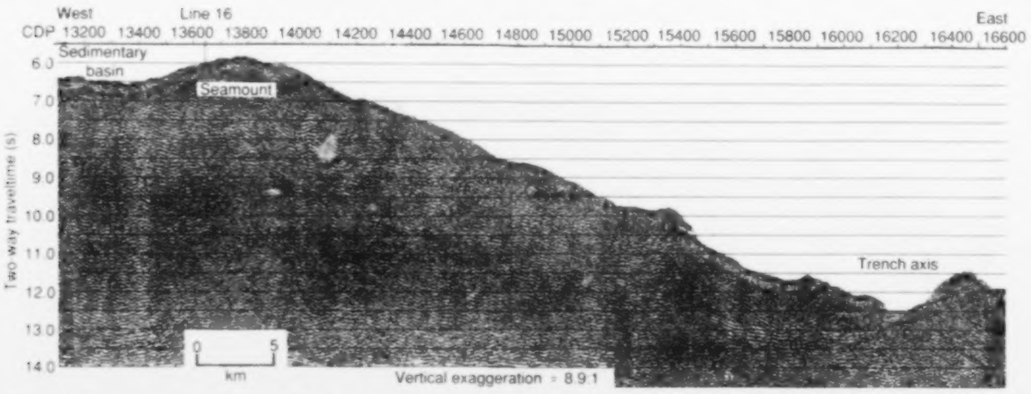

Figure 4. Time section of seismic line 14 from the trench to the seamount, with the location of the sedimentary basin and the seamount.

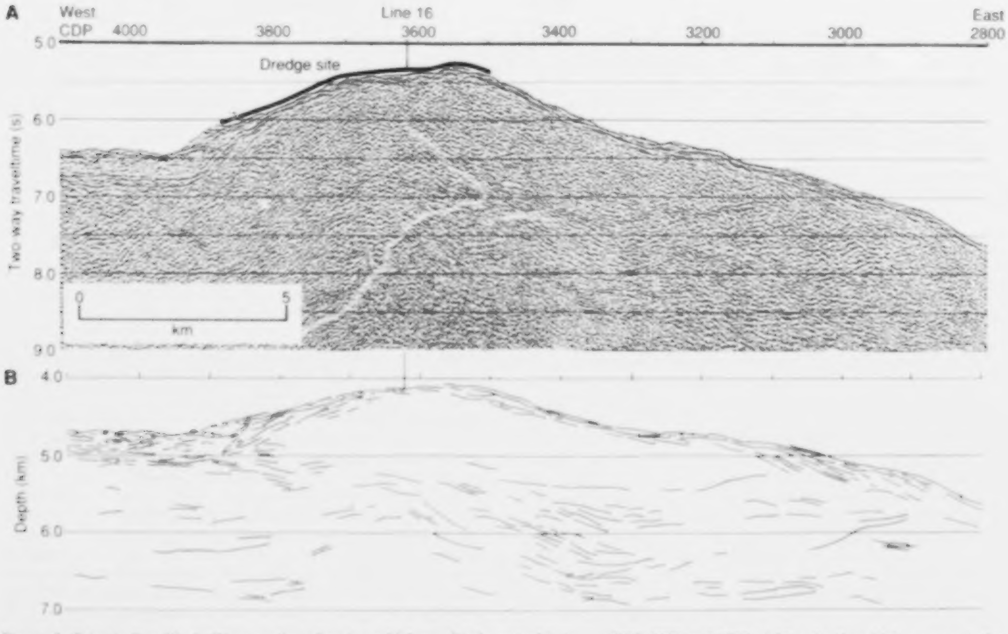

Figure 5. Seismic line 15. **A.** Time section showing a high-amplitude arrival between CDP 3000 and 3200 at 10-s depth, which appears to be sideswipe, uplifted sediments west of CDP 3800 at 6.2 s, and reflections within the seamount at 7.2 s from CDP 3200 to 3500. The dredge location is from Maekawa et al. (in press). **B.** Depth section emphasizing the internal structure of the seamount. The dipping reflectors at 6.0 s below CDP 3200 become subhorizontal on the depth section.

6.5 s between common-depth-points (CDP) 500 and 1100 contains few coherent reflectors and can be traced as far north as line 14.

Site 783 is near the intersection of lines 16 and 14 (Fig. 7). About 150 m of sediment overlies the seamount on the lower north flank, as seen on the depth sections of these lines. A reflector marking the upper limit of the material forming the seamount crops out several kilometers to the east, where serpentinite has been dredged (Maekawa et al., in press). This reflection may be the interface between the sediments and serpentinite forming the seamount, which was confirmed by drilling that encountered serpentine underlying sediments at 120 m below seafloor (mbsf) at Site 783 (see "Site 783" chapter). The shallowest internal reflector is observed on line 14 (Fig. 7) at about 420 mbsf (300 m below the sediment/serpentinite boundary). Based on reflection character, this

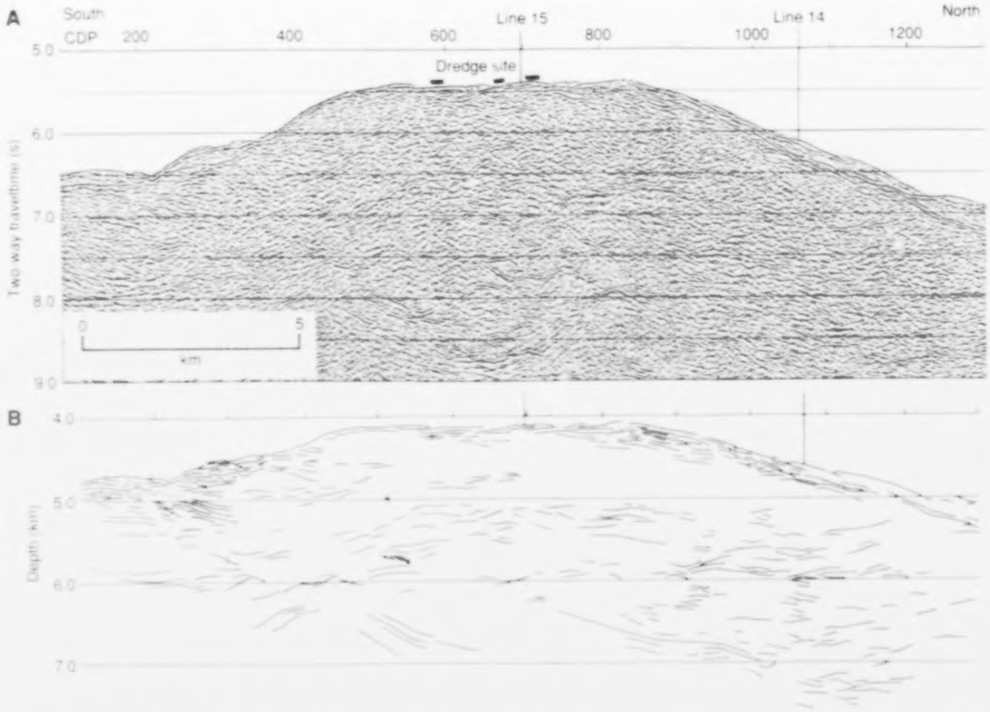

Figure 6. Seismic line 16. **A.** Time section of the part of the line crossing the seamount showing uplifted sediments on the north flank. The three dredge haul locations are from Maekawa et al. (in press). **B.** Depth section showing reflections within the seamount.

Table 2. Processing sequence for the seismic-reflection data.

Edit noisy traces	
Resample to 4 ms	
Sort to 16.67-m common-depth-point (CDP) bins	
Velocity analysis	
Normal moveout	
Mute	
Common-depth-point stack	
Predictive deconvolution	
60-ms prediction distance	
180-ms operator length	
720-ms design window	
Bandpass filter	
Water bottom to 500 ms below water bottom	10-15-50-60 Hz
500 to 1000 ms below water bottom	10-15-40-50 Hz
1000 ms below water bottom to end of record	6-10-35-45 Hz
Finite-difference migration	
Gain	
500 ms automatic gain control	
Depth conversion	

reflector appears to correlate with the reflector marking the base of the sediment farther west. This 420-m reflector may represent the original surface upon which the serpentinite flows forming the seamount were extruded. Unfortunately, drilling was unable to penetrate deep enough to test this interpretation.

Both seamounts are covered by a thin (0–200 m) veneer of sediment (Figs. 5–8). Lines 15 and 17 (Figs. 5 and 8, respectively) indicate that the sediment is commonly thicker on the flanks than on the summit of the seamounts, perhaps as a result of downslope transport. Both seamounts have an irregular surface topography, with maximum dips of 10°–17°. A piston core (*Vema* 21-077, from 30°49′N, 141°59′E, at a water depth of 6790 m; Fig. 3) on the east flank of Torishima Forearc Seamount recovered 4.2 m of gravelly serpentinite sand. This and the discontinuous, hummocky near-surface reflectors suggest that the seamounts themselves may be sediment sources, producing either primary serpentinite flows or secondary slump and debris-flow deposits. The basal sedimentary section at Site 784, drilled on the lower western flank of the southern seamount, contains a mixture of silt-sized serpentine derived from the seamount together with hemipelagic clays (see "Site 784" chapter).

Up to 900 m of strata has accumulated in basins to the west of and between the two seamounts (line 1: CDP 700–1300, 8.3 s; Fig. 9), in contrast to the generally less than 100 m of sediment covering the trench slope to the east and west (line 1: CDP 1800, 8.5 s). Drilling at Sites 783 and 784 (see the site chapters) showed that most of the seamount flank sediment consists of middle Miocene and younger hemipelagic vitric clays. The surrounding basins are probably filled with hemipelagic clays, together with sedimentary serpentinite derived

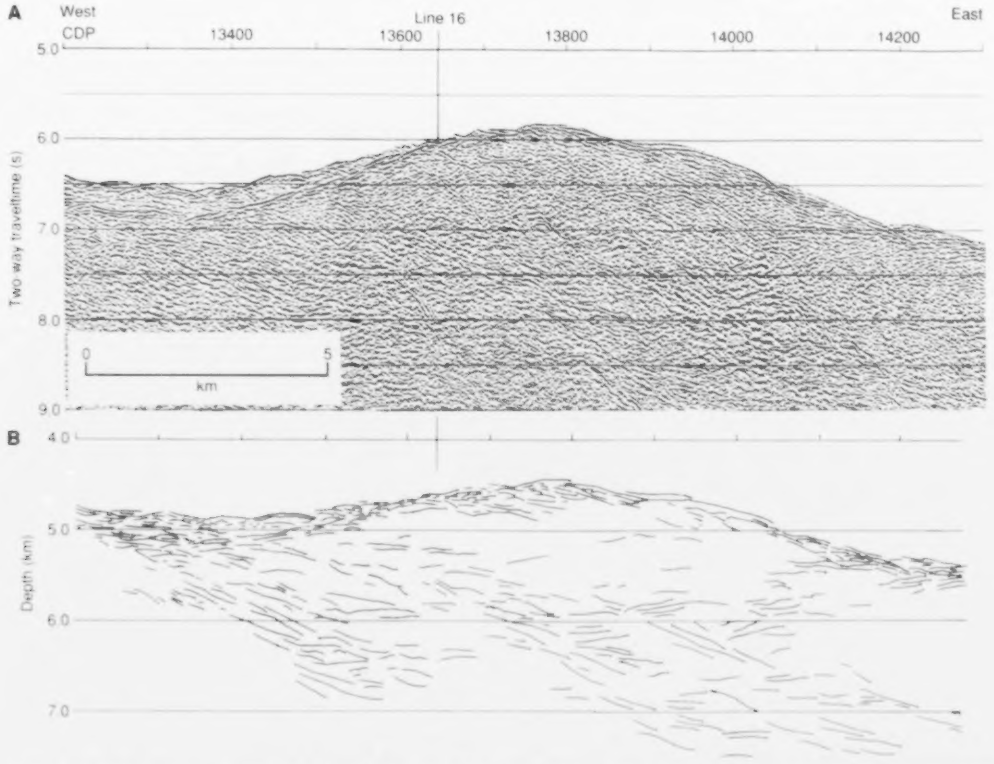

Figure 7. Seismic line 14. **A.** Time section showing disturbed, and possibly slumped, sediments on the west flank of the seamount. The reflector at 7.0 s between CDP 13400 and 13500 appears to be a continuation of the surface marking the bottom of the sediments to the west. **B.** Depth section showing eastward-dipping basement reflections.

from the seamounts, as well as some sediment transported from the volcanic arc to the west. The basins are partially bounded by spurs and ridges trending west-northwest and north-northeast from both seamounts, south-southwest from Torishima Forearc Seamount, and southeast from the northern seamount (see Fig. 3). Seismic line 17 (Fig. 8) along the ridge forming the northern limit of the central basin shows that the strata, which are 500 ms thick on line 1 (Fig. 9), pinch out to the north before reaching this line. The central basin drains to the east through a saddle between the seamounts; the sediment has overtopped the ridge formed by the coalesced spurs from both seamounts (see Fig. 10).

We define four seismic stratigraphic sequences in the basin between the seamounts, based on depositional patterns visible in the seismic data of Figures 9 through 11. Site 783, drilled on the north flank of the southern seamount, penetrated Quaternary to lower Pliocene vitric hemipelagic material above serpentinite basement. This section is the thin basin flank part of sequences 2 through 4. Sequence 1 rests unconformably on truncated, moderately to steeply dipping reflectors within basement (Fig. 11). This sequence is restricted to topographic lows, where it laps onto basement surface irregularities (e.g., line 16: CDP 1620, 8.25 s; Fig. 11). The internal character of sequence 1 is generally chaotic, but in some places exhibits parallel, though dipping, stratification (e.g., line 16: CDP 1600, 8.0 s; Fig. 11). On the flanks of the basin (line 16: CDP 1300–1600 and 1950–2100; Fig. 11), the internal stratification and upper and lower sequence boundaries dip toward the basin axis. We suggest that this sequence consists of serpentinite detritus shed from the adjacent serpentinite seamounts. Serpentinite detritus likely also forms at least a small percentage of the younger sequences.

Sequences 2 through 4 onlap older sequences along the northern side of the basin, onlap basement on the west side of the basin (lines 1 and 2/3; Figs. 9 and 10, respectively), and thin onto the southern flank (Fig. 11). On the east side of the basin, sequences 2 and 3 thin along the spur projecting from the northern seamount (line 1; Fig. 9). Sequence 4 also thins onto the flank of the southern seamount, but onlaps sequence 3 adjacent to the northern seamount. These sequences are thickest within the basin, and all exhibit parallel to hummocky stratification. Sequence 4 is mounded at the west side of the basin on line 1 (CDP 700–900; Fig. 9). Sequences 2, 3, and 4 consist of dominantly hemipelagic sediment underlying the flanks of the seamounts. These sequences should contain significant percentages of hemipelagic sediment, but also represent turbidites generated from slumping of hemipelagic material from the flanks of the seamounts. Detritus carried

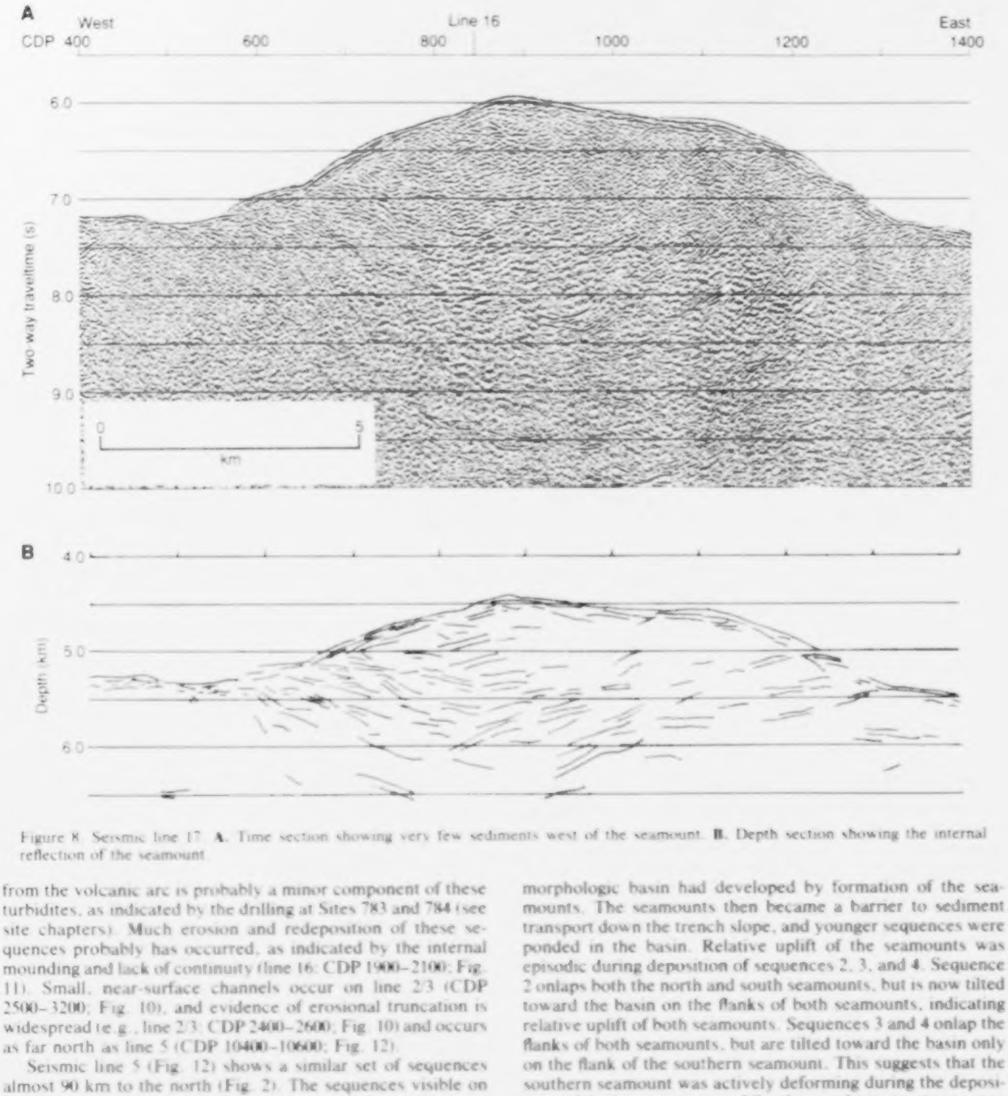

Figure 8. Seismic line 17. **A.** Time section showing very few sediments west of the seamount. **B.** Depth section showing the internal reflection of the seamount.

from the volcanic arc is probably a minor component of these turbidites, as indicated by the drilling at Sites 783 and 784 (see site chapters). Much erosion and redeposition of these sequences probably has occurred, as indicated by the internal mounding and lack of continuity (line 16: CDP 1900–2100; Fig. 11). Small, near-surface channels occur on line 2/3 (CDP 2500–3200; Fig. 10), and evidence of erosional truncation is widespread (e.g., line 2/3: CDP 2400–2600; Fig. 10) and occurs as far north as line 5 (CDP 10400–10600; Fig. 12).

Seismic line 5 (Fig. 12) shows a similar set of sequences almost 90 km to the north (Fig. 2). The sequences visible on this line may not be directly correlative to those discussed previously because they were influenced by sediments transported down Aoga Shima Canyon (Fig. 2). However, these northern sequences do show similar patterns of thinning toward the seamount (CDP 11200, 8.3 s; Fig. 12), suggesting that similar tectonic forces have been acting on this part of the forearc.

The history of seamount diapirism is recorded in the basin fill. Initial formation of the seamounts and protrusion of serpentinite probably took place during the deposition of sequence 1. By the time of deposition of sequence 2, a morphologic basin had developed by formation of the seamounts. The seamounts then became a barrier to sediment transport down the trench slope, and younger sequences were ponded in the basin. Relative uplift of the seamounts was episodic during deposition of sequences 2, 3, and 4. Sequence 2 onlaps both the north and south seamounts, but is now tilted toward the basin on the flanks of both seamounts, indicating relative uplift of both seamounts. Sequences 3 and 4 onlap the flanks of both seamounts, but are tilted toward the basin only on the flank of the southern seamount. This suggests that the southern seamount was actively deforming during the deposition of both sequences, while the northern seamount was quiet. Continuing activity at the southern seamount is indicated by erosional truncation of recent deposits on its flanks (e.g., line 16: CDP 1400–1500; Fig. 11) and a basinward tilting of the seafloor at this same location.

GRAVITY INTERPRETATION

We constructed a two-dimensional model along a gravity profile collected by the Geologic Survey of Japan at 31°N (Figs. 3 and 13). In this model, the seafloor and the structures within 3 km of the seafloor were determined from the seismic-

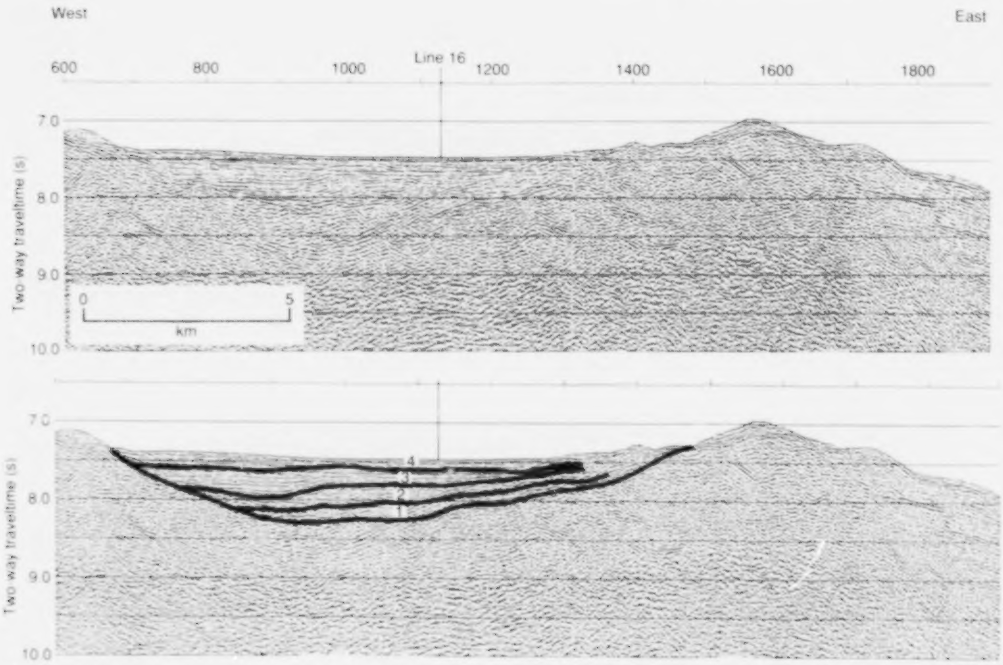

Figure 9. Time section of seismic line 1 showing sediments ponded behind a ridge protruding from the northern seamount. The numbered horizons in the seismic stratigraphic interpretation correspond to sequences 1–4.

reflection data of lines 14 and 2/3 (Figs. 4 and 10). The position of the subducting slab was constrained by refraction data (Hotta, 1970; Houtz et al., 1980) and earthquake seismology (Katsumata and Sykes, 1969; Roeker, 1985), so that the effects of the slab on the regional gravity trend were also incorporated. The crustal thickness beneath the forearc was approximated by refraction data, although there is some uncertainty in this region. Hotta (1970) placed the Moho at a depth of 20 km beneath the seamounts, whereas Houtz et al. (1980) placed it at 16 km just east of the seamounts. The thickness of the oceanic slab was constrained by refraction data and by modeling of the flexure of the subducting plate (Watts et al., 1980). Our initial model produced a reasonable fit to the observed data and provides some information about the deep structure in the vicinity of the basin (Fig. 13). No attempt was made to match the model and data at the western end of the profile, which crosses the eastern edge of the 2- to 4-km-thick forearc sedimentary basin. In the rest of this area, the observed and calculated fields match to within the noise level of the data (about 3 mGal) using only the bathymetry and a thin veneer of sediment filling the forearc basin. This indicates that any structures beaeath the basin must have a low density contrast.

A second gravity profile at 32°N (Fig. 2) was also modeled (Fig. 14A). Seismic-reflection line 5 (Fig. 12) coincides with this profile, which crosses a seamount along the same trend as the seamounts at 31°N. B. T. (unpubl. data) has dredged serpentinized ultramafic and chloritized mafic rocks from this seamount. Figure 12 shows that this seamount is similar to those discussed previously in that it also has internal reflectors, except that this seamount has ponded a larger sedimentary basin behind it. A significant difference between this and the previous gravity model is that the bathymetric expression of the seamount produces a gravity high on the computed curve that is not present in the observed data (Fig. 14A). The difference between the computed and observed values is about 30 mGal. Matching of the observed gravity data required that a body be added to the model with a significantly lower density. A first approximation to such a body is shown in Figure 14B. A density characteristic of serpentinite (Coleman, 1971), 2.46 g/cm^3, was assigned to the seamount and the depth to the bottom of the serpentinized region was increased until a satisfactory fit to the observed data was obtained. The close match between the observed and calculated fields in Figure 14B indicates that beneath this seamount most of the forearc above the décollement is of low density, which suggests that it has undergone extensive serpentinization. In Figure 14A, the wavelength of the computed anomaly is approximately equal to the diameter of the seamount. If this holds true for the southern seamounts, the gravity profile at 31°N (Fig. 13) would have detected only the extreme edges of the anomalies caused by those seamounts. Because the profile at 31°N is off the flanks of the seamounts in this area it need not show any anomaly caused by the seamounts.

DISCUSSION AND CONCLUSIONS

Patterns of onlap and uplift of sediment in the Izu-Bonin outer forearc indicate that two midslope seamounts have been growing episodically during formation of a flanking basin, with Torishima Forearc Seamount experiencing more recent uplift

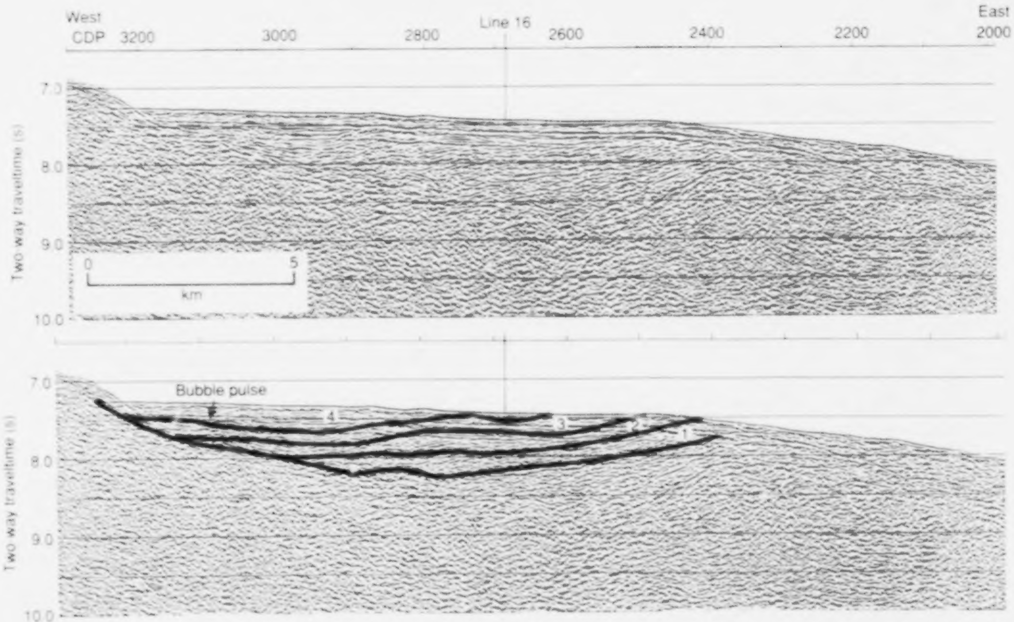

Figure 10. Time section of seismic line 2/3 showing sediments partially ponded behind a basement high. The numbered horizons in the seismic stratigraphic interpretation correspond to sequences 1–4.

(line 16: CDP 1200–1600; Fig. 11). Shallow regions within each seamount exhibit few coherent reflectors, as seen on lines 14, 15, 16, and 17 (Figs. 5–8), and may be composed of serpentinite flows. The deeper and seismically reflective regions beneath the seamount may be the original substrate onto which the serpentinite protruded.

Gravity modeling suggests that the seamounts are made up of low-density material and that the intervening sedimentary basins do not rest on a low-density substrate, so that the low-density (serpentinized?) zones must be limited to the seamounts. One possible model for the evolution of these forearc seamounts involves a two-stage process of emplacement and protrusion of small serpentinite diapirs, followed by uplift as a result of continued intrusion and serpentinization around the original conduits. Mass wasting of the seamounts, as well as primary serpentinite flows, could have deposited sequence 1 in the surrounding forearc basins. This stage ended by middle Miocene time, as evidenced by drilling at Site 784 ("Site 784" chapter).

The second stage in our model of seamount evolution involves intrusion of sills into the serpentinite edifice and serpentinization of the forearc around the original conduits. These processes resulted in the inflation of the seamounts and tilting of strata on their flanks. Serpentinization can increase volume by up to 40% (Thompson, 1960), which is adequate to explain the observed uplift. The serpentinization was centered on the original conduits and did not include the entire forearc, as indicated by the gravity modeling, which shows the low-density material confined to the seamounts. Tilting of the strata of sequences 2 through 4 indicates that this process may still be occurring in the southern seamount.

ACKNOWLEDGMENTS

This work was supported by NSF grant numbers OCE86-14687, OCE87-00826, and OCE89-96141. The authors would like to thank Bryan Tapp, William Underwood, Jamie Austin, and Mike Marlow for their review and critical comments of this paper and Mary MacKay, Todd Jimeson, and Robert Heaton for their help in processing the seismic data. Hawaii Institute of Geophysics contribution no. 2191.

REFERENCES

Aoki, Y., Tamano, T., and Kato, S., 1982. Detailed structure of the Nankai Trough from migration seismic sections. *In* Watkins, J. S., and Drake, C. L. (Eds.), *Continental Margin Geology.* AAPG Mem., 34:309–322.

Bloomer, S. H., 1983. Distribution and origin of igneous rocks from the landward slopes of the Mariana Trench: implications for its structure and evolution. *J. Geophys. Res.*, 88:7411–7428.

Coleman, R. G., 1971. Petrologic and geophysical nature of serpentinites. *Geol. Soc. Am. Bull.*, 82:897–918.

Crawford, A., Beccaluva, L., and Serri, G., 1981. Tectonomagmatic evolution of the Philippine-Mariana region and the origin of boninites. *Earth Planet. Sci. Lett.*, 54:346–356.

Fryer, P., Ambos, E. L., and Hussong, D. M., 1984. Origin and emplacement of serpentine diapirs in the Mariana fore-arc. *EOS, Trans. Am. Geophys. Union*, 65:1104. (Abstract)

________, 1985. Origin and emplacement of Mariana forearc seamounts. *Geology*, 13:744–777.

Fryer, P., and Fryer, G., 1987. Origins of nonvolcanic seamounts in a forearc environment. *In* Keating, B. H., Fryer, P., Batiza, R., and Boehlert, G. W. (Eds.), *Seamounts, Islands, and Atolls.* Am. Geophys. Union, Geophys. Monogr. Ser., 43:50–63.

Honza, E., and Tamaki, K., 1985. The Bonin arc. *In* Nairn, A.E.M., and Uyeda, S. (Eds.), *The Pacific Ocean*: New York (Plenum Press), 459–502.

Horine, R. L., Moore, G. F., Taylor, B. T., and MacKay, M. E., 1988. Structure of the Bonin arc lower slope. *EOS, Trans. Am. Geophys. Union*, 69:1014.

Hotta, H., 1970. A crustal section across the Izu-Ogasawara arc and trench. *J. Phys. Earth*, 18:125–141.

Houtz, R., Windisch, C., and Murauchi, S., 1980. Changes in the crust and upper mantle near the Japan-Bonin Trench. *J. Geophys. Res.*, 85:267

Hussong, D. M., and Uyeda, S., 1982. Tectonic processes and the history of the Mariana arc—a synthesis from the results of DSDP Leg 60. *In* Hussong, D. M., Uyeda, S., et al., *Init. Repts. DSDP*, 60: Washington (U.S. Govt. Printing Office), 909–929.

Ishii, T., Ozawa, H., Maekawa, H., Naha, J., Robinson, P. T., Kobayashi, K., and Uyeda, S., in press. Refractory peridotites from serpentinite diapiric seamounts in the Izu-Ogasawara-Mariana forearc. *Earth Planet. Sci. Lett.*

Katsumata, M., and Sykes, L., 1969. Seismicity and tectonics of the western Pacific: Izu-Mariana-Caroline and Ryukyu-Taiwan regions. *J. Geophys. Res.*, 74:5923.

Kodama, K., Keating, B., and Helsley, C., 1983. Paleomagnetism of the Bonin Islands and its tectonic significance. *Tectonophysics*, 95:25–42.

Maekawa, H., Shozui, M., Ishii, T., and Ozawa, H., in press. Ophiolitic seamounts in the Izu-Ogasawara forearc—evidence of serpentinite diapir. *Earth Planet. Sci. Lett.*

Roeker, S. W., 1985. Velocity structure in the Izu-Bonin seismic zone and the depth of the olivine-spinel phase transition in the slab. *J. Geophys. Res.*, 90:7771–7794.

Sakai, R., Kusakabe, M., Noto, M., and Ishii, T., in press. Origin of waters responsible for serpentinization of the Izu-Ogasawara-Mariana forearc seamounts in view of hydrogen and oxygen isotope ratios. *Earth Planet. Sci. Lett.*

Seno, T., and Maruyama, S., 1984. Paleogeographic reconstruction and origin of the Philippine Sea. *Tectonophysics*, 102:53–84.

Seno, T., Moriyama, T., and Stein, S., 1987. Redetermination of Philippine Sea plate motion. *EOS, Trans. Am. Geophys. Union*, 68:1474. (Abstract)

Taylor, B., and Smoot, N. C., 1984. Morphology of Bonin fore-arc submarine canyons. *Geology*, 12:724–727.

Thompson, R. B., 1960. Serpentinisation accompanied by volume changes. *Pac. Geol.*, 3:167–174.

Watts, A. B., Bodine, J. H., and Ribe, N. M., 1980. Observations of flexure and the geological evolution of the Pacific Ocean basin. *Nature*, 283:532–536.

Westbrook, G. K., and Smith, M. J., 1983. Long décollements and mud volcanoes: evidence from the Barbados Ridge Complex for the role of high pore-fluid pressure in the development of an accretionary complex. *Geology*, 11:279–283.

Ms 125A-105

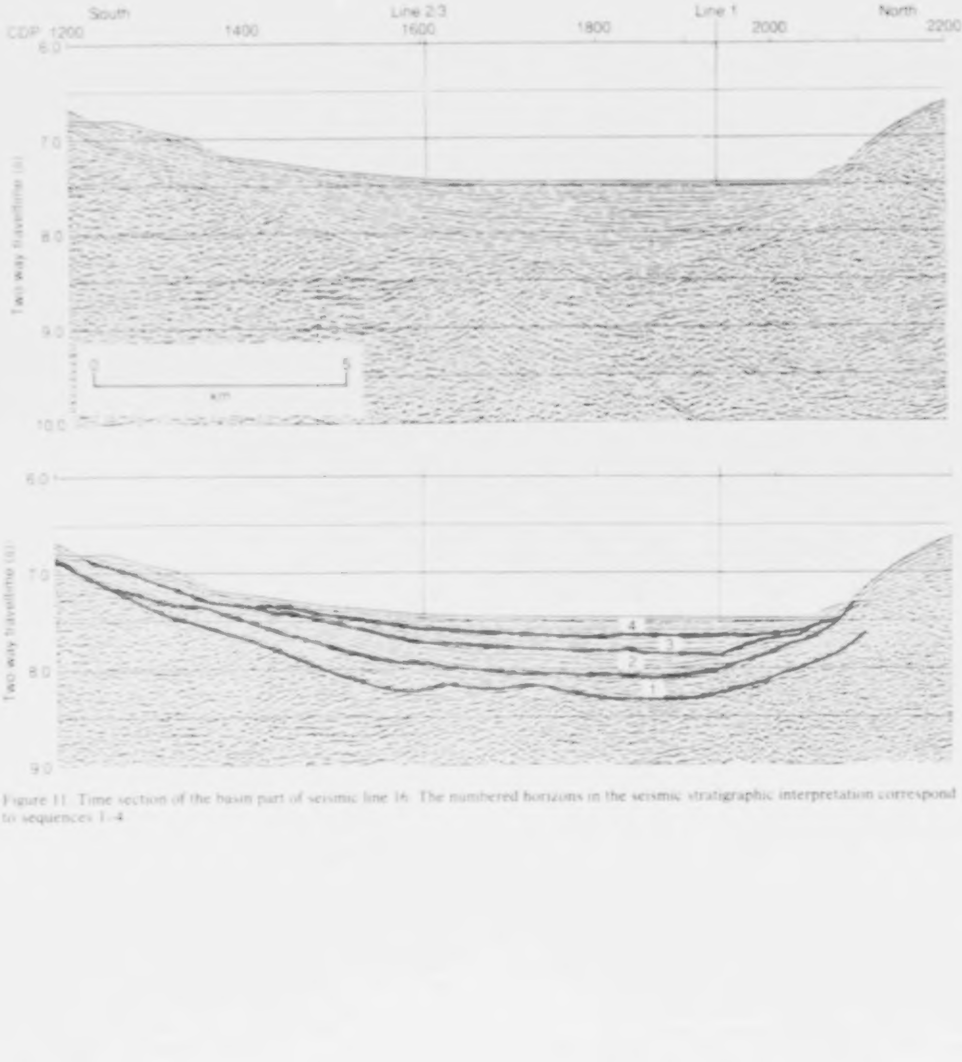

Figure 11. Time section of the basin part of seismic line 16. The numbered horizons in the seismic stratigraphic interpretation correspond to sequences 1–4.

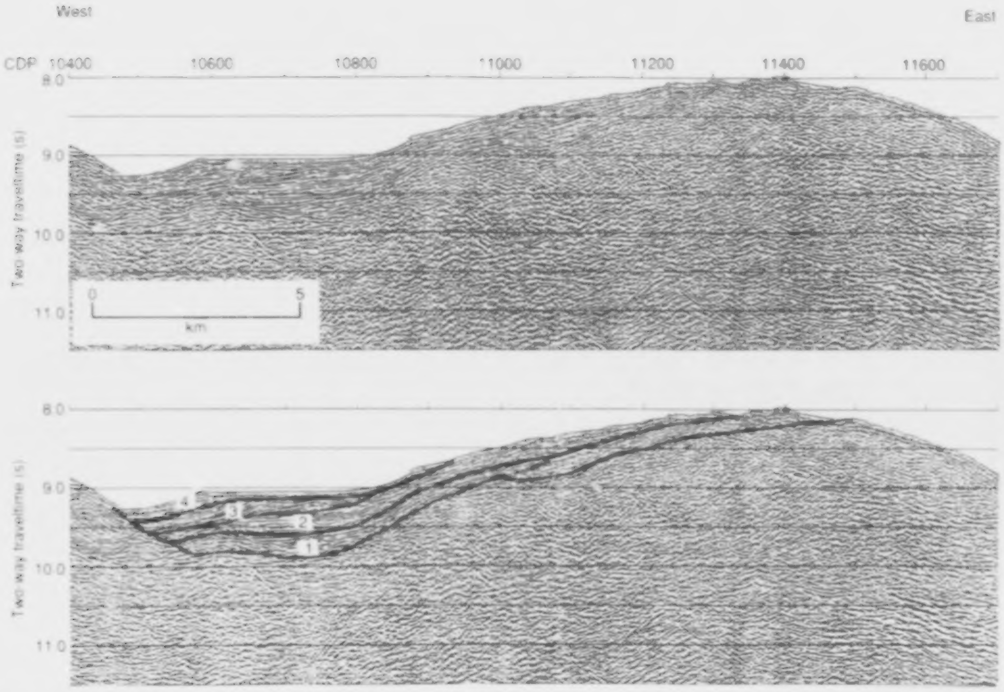

Figure 12. Time section of seismic line 5 at 32°N showing the seamount and sediments deposited in the basin to the west. The numbered horizons in the seismic stratigraphic interpretation correspond to northern area sequences.

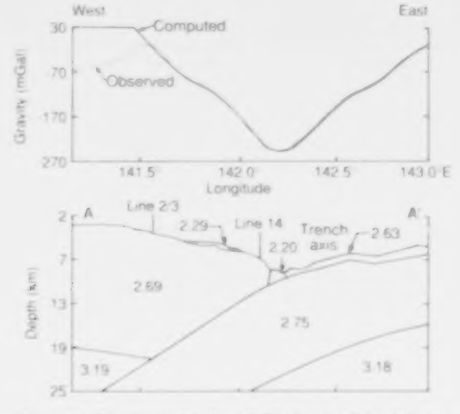

Figure 13. Gravity model along 31°N showing the subducting oceanic plate and trench-fill sediments. The dotted curve is the observed field; the solid curve is the calculated field.

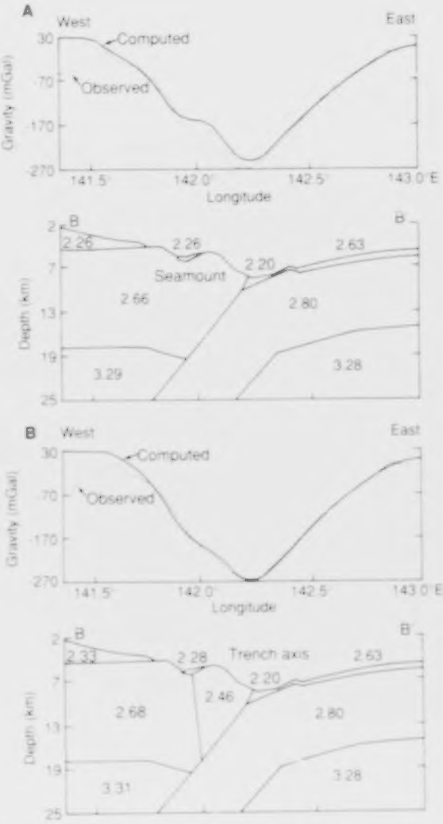

Figure 14. Gravity models along 32°N. The dotted curve is the observed field; the solid curve is the calculated field. **A.** A 30-mGal mismatch between the observed and computed fields in the vicinity of the seamount. **B.** A model with the seamount given a density characteristic of serpentinite has a significantly improved fit at 142°E.

SECTION 2: SITE REPORTS

Fryer, P., Pearce, J. A., Stokking, L. B., et al., 1990
Proceedings of the Ocean Drilling Program, Initial Reports, Vol. 125

6. SITE 778[1]

Shipboard Scientific Party[2]

HOLE 778A

Date occupied: 22 February 1989

Date departed: 24 February 1989

Time on hole: 2 days, 12 hr, 55 min

Position: 19°29.93′N, 146°39.94′E

Bottom felt (rig floor; m; drill-pipe measurement): 3924.4

Distance between rig floor and sea level (m): 10.7

Water depth (drill-pipe measurement from sea level; m): 3913.7

Total depth (rig floor; m): 4032.0

Penetration (m): 107.6

Number of cores: 13

Total length of cored section (m): 107.6

Total core recovered (m): 22.8

Core recovery (%): 21

Oldest sediment cored:
Depth (mbsf): 107.6
Nature: sheared phacoidal serpentine
Earliest age: (?)

Hard rock:
Depth (mbsf): clasts
Nature: serpentinized tectonized harzburgite, dunite, metabasalt
Measured velocity (km/s): 2.1 to 4

Principal results: Site 778 is situated about halfway up the southern flank of Conical Seamount, a 1500-m high, cone-shaped, serpentinite diapiric seamount located on the outer-arc high of the Mariana forearc basin, about 100 km west of the trench axis. Drilling established the presence of phacoidal sheared serpentine beneath a serpentine-rich clay-marl-breccia. Lithologic units are as follows:

1. Unit I (Subunit IA, 0–7.2 mbsf): The subunit contains lower middle Pleistocene-Holocene serpentine-rich sediment and serpentine flows. The uppermost portion has two pebbles (one limestone and one serpentinite) overlying 15 cm of pale blue-gray serpentine clay, then 15 cm of gray-green serpentine clay, 10 cm of red-orange serpentine clay, 1.5 m of pale blue-gray, silt-sized serpentine and 3.57 m of a serpentine-marl breccia.
2. Unit I (Subunit IB, 7.2–29.8 mbsf): The subunit is lower middle Pleistocene to lower Pleistocene and contains a sandy marl and a collection of cobbles and pebbles, including serpentinite, vesicular volcanic rocks, and a foraminifer-bearing, serpentine sandstone.
3. Unit II (29.8–107.6 mbsf): This entire unit is made up of phacoidal, sheared serpentine containing clasts of serpentinized tectonized harzburgite with subordinate metabasalts, metagabbros, serpentinized dunite, and a variety of vein materials.

The serpentine clays provide the strongest evidence that at least part of the seamount originated as serpentine flows. The phacoidal sheared serpentine may have originated as flows, as a mantle diapir, or both.

The primary petrology of the ultramafic rocks (% clinopyroxene predominantly as exsolution lamellae) indicates a depleted mantle source. The metabasalt clasts in Unit II have petrological and geochemical signatures of both mid-ocean ridge basalt and island-arc tholeiite types, and a few exhibit medium-grade metamorphism. One contains blue amphibole, perhaps indicating that this metamorphic grade characterizes the source region of the serpentinite. The material as a whole exhibits a variety of deformation textures that can be interpreted in terms of a combination of primary mantle tectonism, stresses related to intrusion and protrusion (flow emplacement) of the serpentinite diapir materials, and stresses resulting from post-protrusion remobilization.

Analyses of interstitial pore-water samples indicate a 10% decrease in chlorinity downhole (more than 107 m). Seep fluids are thought to have formed in part as a product of dehydration reactions within the subducting Pacific Plate. The decrease in chlorinity with depth in the hole is interpreted as a relative decrease in admixture of seawater with relatively chlorine-poor fluids entrained in the serpentine flow material.

BACKGROUND AND SCIENTIFIC OBJECTIVES

Site 778 is the first of a series of sites (778 through 780) on Conical Seamount, a roughly circular seamount having a basal diameter of about 20 km and a relief of 1500 m that lies on the outer-arc high of the Mariana forearc, at a distance of about 100 km from the trench axis (see "Introduction," this volume, and Fig. 1). The site was chosen to penetrate the flank of the seamount about 5.5 km due south of its summit. *Alvin* dives near this site suggested that the seamount in this area had been mantled by recent flows of unconsolidated serpentine sediments and flows containing serpentinized clasts of mafic and ultramafic rocks (Fryer et al., 1985). SeaMARC II side-scanning sonar imagery (Hussong and Fryer, 1985) further suggested that the site is located within a major serpentine flow (delineated by an area of high sonic backscatter) that mantles much of the southern flank of the seamount (Fig. 2).

The specific objectives for drilling this flank site were to study the following aspects of forearc processes:

1. The internal stratigraphy and the extrusion and deformation history of a typical forearc serpentinite seamount;
2. The mode of emplacement of serpentine flows;
3. The chemical effects of serpentinization on the oceanic lithosphere and its sedimentary cover;
4. The nature, composition, and age of forearc lithosphere; and
5. The dewatering of subducted oceanic lithosphere at a nonaccretionary convergent plate margin.

The first objective was best achieved by a flank site, such as that chosen to penetrate the complete sequence of flows and to reach underlying sediments and basement. The depth of Site 778 is about 500 m above the background seafloor, and the normal sediment thickness in this area is estimated as about 250 m. Thus, drilling calculations were based on a 750-m hole that would penetrate the seamount and the underlying sediment, and perhaps also a short distance into basement if sediment thickness

---

[1] Fryer, P., Pearce, J. A., Stokking, L. B., et al., 1990. *Proc. ODP, Init. Repts.*, 125: College Station, TX (Ocean Drilling Program).

[2] Shipboard Scientific Party is as given in the list of participants preceding the contents.

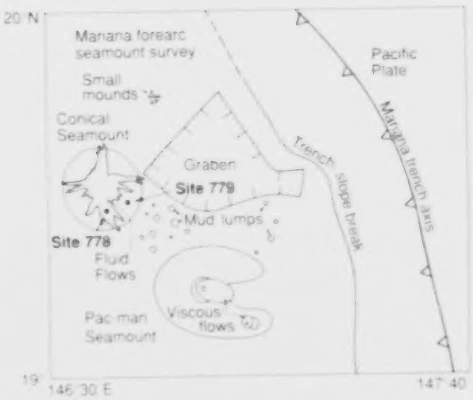

Figure 1. Geological sketch of Mariana forearc geology.

was low or the seamount had uplifted the surrounding seafloor. If successful, the hole would provide data about many unknown aspects of the construction of this serpentinite seamount, including thickness of flow and age of emplacement. The site location, about halfway down the flank, would also favor the second, sedimentary, objective by providing a typical (central) section through at least one serpentine flow within which sedimentary structures could be observed.

The third objective, the study of serpentinization, could be investigated using the mineralogy and composition both of the clasts, veins, and matrix within the serpentine flows, and of the sediments intercalated between and underlying these flows. The compositions of fluids entrained within the serpentine material and sediments should provide additional information about the chemical reactions involved and test whether, as in examples exposed on land, the fluids are of high pH and contain hydrogen and hydrocarbons. These compositions also could be used to investigate the relative roles of subducted water, primary mantle water, and surface seawater in the serpentinization process.

The nature of forearc lithosphere, the fourth objective, could be studied directly from any unserpentinized ultramafic rocks and mafic clasts, and from the basement itself, should it be penetrated. Forearc basement is still poorly characterized. It is dependent on limited information from four previous drill sites (Leg 60), from dredging near Conical Seamount, and from the few on-land examples, such as those on Guam, Saipan, and the Bonin Islands; we still know little about the composition of forearc basement in submarine, sedimented regions. Although the vast majority of basement volcanic samples have proved to exhibit boninitic to depleted island-arc tholeiitic compositions, mid-ocean ridge basalts may also contribute to forearc basements, especially if trapped older crust is present. A further possibility is that clasts may include samples of Pacific oceanic crust that might have been accreted onto the forearc mantle wedge from the Benioff Zone and incorporated into serpentinite diapirs at depth. Pacific crustal fragments should have a composition quite distinct from the forearc crust, but if *in-situ* basement could be penetrated at this site, this distinction should be easier to make. In addition, the study of textures of clasts within the serpentinite should aid in determining both the stress history of the forearc during serpentinization and the emplacement mechanisms of the diapiric body. Information about all these rocks should also aid our understanding of the many ophiolite complexes that have been postulated to have occupied a forearc setting.

Finally, the objective of studying the hydration of the crust and upper mantle of the forearc wedge could be accomplished by drilling into the serpentinite. The hydration of the forearc wedge has been clearly facilitated by the escape of fluids from the subducting Pacific plate, and thermal modeling suggests that large regions beneath the forearc lie within the chlorite, greenschist, and blueschist stability fields (Fryer and Fryer, 1987). The mantle and lower crust of the forearc wedge can thus readily accommodate large volumes of fluids through metamorphic processes. The exact nature of fluid transport is poorly understood, although it can be assumed that, under appropriate tectonic conditions, generation and emplacement of serpentinite diapirs is a major factor in any nonaccretionary forearc. Analyses of hydrous phases could provide evidence for the magnitude of fluid fluxes within the mantle wedge and for the temperatures and compositions of these fluids, while studies of metamorphic assemblages in the clasts should further constrain the pressure/temperature history of metamorphism within the forearc.

OPERATIONS

Guam Port Call

Leg 125 officially began when the first line was passed at 2000 hr UTC (Universal Time Coordinated), 15 February 1989, and the *JOIDES Resolution* (*SEDCO/BP 471*) arrived at Apra Harbor, Guam. The normal operations of crew changes, fueling, and on/off loading of all freight were performed without problems. The ship sailed on schedule, leaving Apra Harbor, Guam at 0200UTC, 20 February.

Guam to Site 778 (MAR-3B)

The 35-hr transit to the Mariana sites was made in calm weather and seas. The *JOIDES Resolution* did not arrive in the vicinity of the Mariana sites during a global positioning system (GPS) window. The location of proposed Site MAR-3A was critical, but could not be determined without GPS. Therefore, proposed Site MAR-3B was drilled first.

Site 778 (Hole 778A)

Site 778 is located on the southern flank of Conical Seamount. Site 778 was established by dropping a recoverable beacon at 2030UTC, 21 February after 5 hr of surveying.

Based on information from *Alvin* photographs and video tapes of Conical Seamount, the hole was spudded with the rotary coring system (RCB) instead of the advanced piston corer/extended-core barrel (APC/XCB). A standard RCB bottom-hole assembly (BHA) with mechanical bit release (MBR) and bit was assembled and run. The mud line was established at 3913.7 m below sea level (bsl) by a punch core at 1445UTC 22 February. The precision depth recorder showed the mud line at 3754.8 m below sea level (bsl); it took 6 hr to find the bottom.

The hole was unstable from the beginning and soon caused problems. After reaching Core 125-778A-4R at 3943.3 mbsl, the hole required cleaning upon each connection. During retrieval of Core 125-778A-13R, the hole caved in and the drillpipe stuck. The drill string was worked with 20,000-lb overpulls before the BHA was freed. During repeated attempts to clean the hole, the drill string stuck again, whereupon the hole was abandoned.

The RCB was used for the entire hole, where we recovered 22.8 m in 13 deployments for a recovery rate of 21% (Table 1). Hole 778A and Site 778 were officially abandoned at 0925UTC, 24 February, when the drill string was pulled clear of the seafloor.

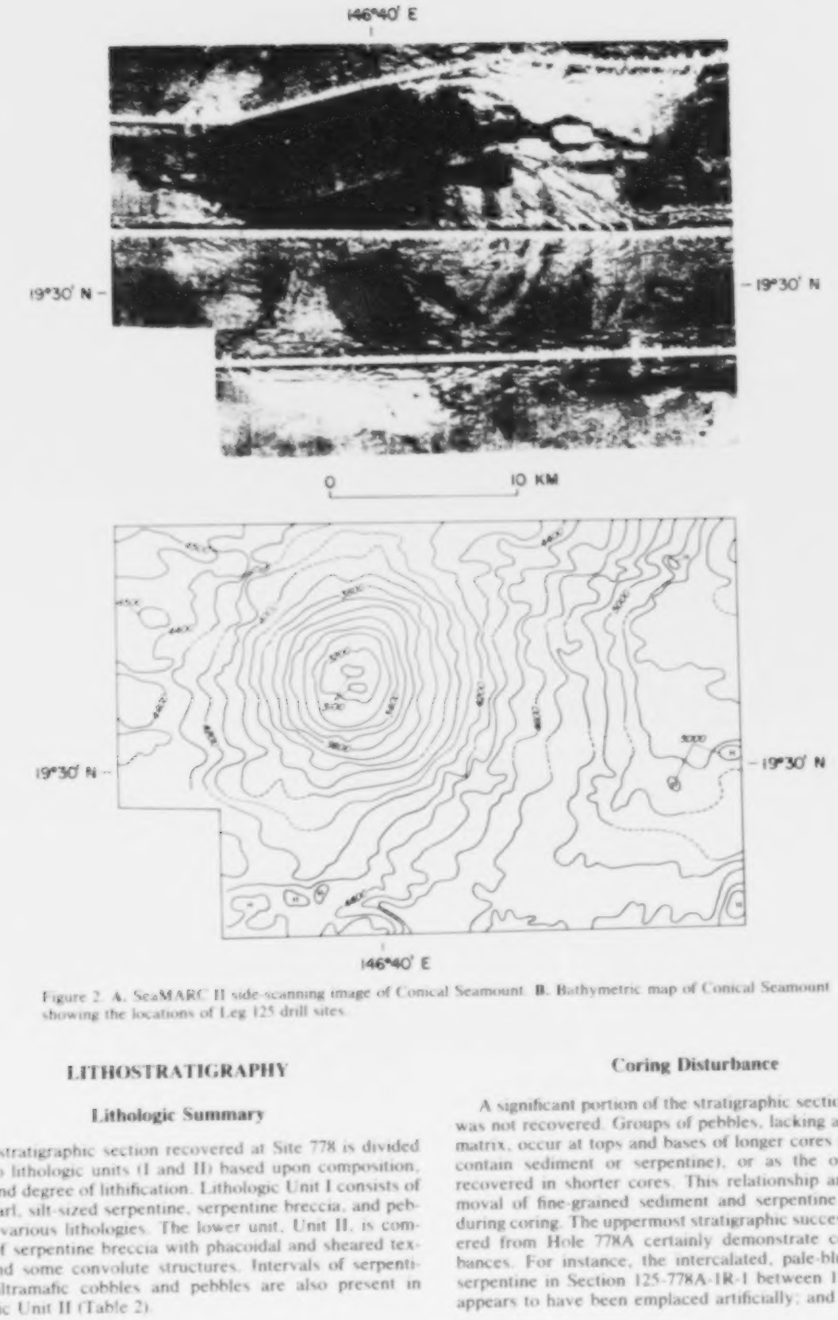

Figure 2. A. SeaMARC II side-scanning image of Conical Seamount. B. Bathymetric map of Conical Seamount showing the locations of Leg 125 drill sites.

LITHOSTRATIGRAPHY

Lithologic Summary

The stratigraphic section recovered at Site 778 is divided into two lithologic units (I and II) based upon composition, color, and degree of lithification. Lithologic Unit I consists of clay, marl, silt-sized serpentine, serpentine breccia, and pebbles of various lithologies. The lower unit, Unit II, is composed of serpentine breccia with phacoidal and sheared textures and some convolute structures. Intervals of serpentinized ultramafic cobbles and pebbles are also present in lithologic Unit II (Table 2).

Coring Disturbance

A significant portion of the stratigraphic section at this site was not recovered. Groups of pebbles, lacking an associated matrix, occur at tops and bases of longer cores (midsections contain sediment or serpentine), or as the only material recovered in shorter cores. This relationship argues for removal of fine-grained sediment and serpentine by washing during coring. The uppermost stratigraphic successions recovered from Hole 778A certainly demonstrate coring disturbances. For instance, the intercalated, pale-blue, silt-sized serpentine in Section 125-778A-1R-1 between 12 and 13 cm appears to have been emplaced artificially; and a serpentine

Table 1. Coring summary for Hole 778A.

Core no.	Date (Feb. 1989)	Time (UTC)	Depth (mbsf)	Length cored (m)	Length recovered (m)	Recovery (%)
1R	22	1540	0.0–6.7	6.7	6.70	100.0
2R	22	1700	6.7–16.2	9.5	1.03	10.8
3R	22	1910	16.2–20.2	4.0	0.18	4.5
4R	22	2200	20.2–29.7	9.5	0.24	2.5
5R	23	0235	29.7–39.2	9.5	0.43	4.5
6R	23	0550	39.2–48.7	9.5	1.70	17.9
7R	23	0810	48.7–58.2	9.5	2.54	26.7
8R	23	1110	58.2–68.2	10.0	1.66	16.6
9R	23	1600	68.2–77.8	9.6	2.16	22.5
10R	23	2012	77.8–82.3	4.5	0.22	4.9
11R	23	2350	82.3–89.8	7.5	1.75	23.3
12R	24	0305	89.8–98.3	8.5	2.40	28.2
13R	24	0700	98.3–107.6	9.3	1.79	19.2
Coring totals				107.6	22.80	21.2

breccia with its sandy silt matrix has been disrupted, resulting in the soupy appearance of the core in Section 125-778A-1R-2 from 37 to 130 cm.

Unit I

Sections 125-778A-1R-1, 0 cm, to 125-778A-5R-1, 10 cm; depth, 0–29.8 mbsf. Age: Holocene(?) to lower Pleistocene(?).

Only Unit I contains sediment with detrital and biogenic components at this site. The serpentine intervals lack biogenic and detrital components but are underlain by sediment of late Pleistocene age, indicating a maximum age of late Pleistocene for the serpentine flow(s) (see "Biostratigraphy" and "Paleomagnetism" sections, this chapter).

Subunit IA

Sections 125-778A-1R-1, 0 cm to 125-778A-2R-1, 50 cm; depth, 0–7.2 mbsf. Age: Holocene(?) to lower/middle Pleistocene.

This subunit extends from the sediment/water interface to a total depth of 7.2 mbsf and primarily consists of serpentine clay, and silt-sized serpentine, with sand- to pebble-sized clasts of serpentinite. The uppermost lithology in the first core has two pebbles (recrystallized limestone and a serpentinized ultramafic rock) atop 15 cm of gray-green (2.5Y 6/2) serpentine clay that has been disturbed by drilling. In addition, the serpentine clay contains opaque minerals (10%), epidote (5%), zoisite (5%), aragonite (10%), nannofossils (5%), and trace amounts of radiolarians and silicoflagellates. Beneath this serpentine clay is a 10-cm-thick sequence of red-orange (5YR 6/8) serpentine clay that has a sharp lower contact. This 10-cm-thick layer of clay has crystalline clay aggregates and lacks biogenic components. The color, composition, and nongradational lower contact of this clay layer may indicate a cool hydrothermal origin or post-depositional alteration by migration of fluids from the underlying serpentine flow. This red-orange clay overlies a 1.5-m layer of pale blue-gray (5B 6/2) silt-sized serpentine that is composed of serpentine (80%), opaque minerals (10%), zoisite (5%), epidote (5%), with trace amounts of chlorite, and thulite. This 1.5-m-thick serpentine layer is interpreted as a serpentine flow that extruded onto the seafloor under cool hydrothermal conditions because (1) it lacks pelagic or detrital components, (2) the color is atypical of pelagic sediments, and (3) biological and sedimentological structures are absent.

Beneath this is a 0.9-m interval of breccia that has been strongly disturbed by drilling. It contains a matrix of sandy clay, perhaps equivalent in lithology to the underlying 4.0-m-thick layer of serpentine breccia with a matrix of sandy silt-sized serpentine. The lithologies of clasts within the breccia are described in the "Igneous and Metamorphic Petrology" section (this chapter). In the breccia, the sandy silt-sized serpentine matrix is light reddish brown (2.5Y 6/4) and composed of serpentine (60%), opaque minerals (15%), aragonite (15%), and epidote (10%). Mixed into the 4.0-m-thick layer, yielding a mottled appearance, is light gray (7.5YR 7/0) and light olive (5Y 5/2) serpentine-chlorite-rich marl (chlorite, 25%; serpentine, 20%; opaque minerals, 15%; micrite, 15%; nannofossils, 10%; aragonite, 10%; clay, 5%; trace amounts of epidote and zoisite) of Pleistocene age. The depositional mechanisms of this layer are not clear. Its similarity to the overlying blue layer (in all but color) may indicate that it is also a flow, in which case the mottling represents entrained

Table 2. Lithologic units recovered at Leg 125 Site 778.

Lithologic unit	Cores	Depth (mbsf)	Dominant lithology	Stratigraphic age
IA	778A-1R-1, 0 cm to 778A-2R-1, 50 cm	0.0 to 7.2	Clay; marl; clayey silt-sized serpentine; serpentine breccia with a matrix of sand- and silt-sized serpentine	Holocene(?) to lower/middle Pleistocene
IB	778A-2R-1, 50 cm to 778A-5R-1, 10 cm	7.2 to 29.8	Sandy marl; volcaniclastic(?) siltstone; foraminifer-bearing serpentine sandstone; various igneous lithologies (see "Igneous and Metamorphic Petrology," this chapter)	lower/middle Pleistocene to lower Pleistocene(?)
II	778A-5R-1, 10 cm to 778A-13R-CC	29.8 to 107.6	Phacoidal sheared serpentine; serpentine breccia with convolute structure; pebbles of various lithologies (see "Igneous and Metamorphic Petrology," this chapter)	(?)

Table 3. X-ray diffraction analysis of samples, Site 778.

Core, sample, interval (cm)	Method of preparation	Identified Minerals												
		An	Cr	T	B	A	G	C	E	Z	Ga	St	Fo	Fa
125-778A-1R-1, 20	pip		x	x	x	x	x	?	?	x				
1R-1, 20	pow		x	x	x		x							x
1R-1, 100	pip		x	x		x			x	x	x			
1R-1, 100	pip		x	x		x	x		?		x	x		
1R-1, 100	pow		x	x	x	x	x				x			
1R-4, 50	pip		x	x	x	x	x						x	
1R-4, 50	pow		x	x	x									
1R-4, 60	pip		x	x	x	x					x		x	
1R-4, 60	pow		x	x	x	x	x						x	x
1R-4, 125	pip		x	x	x		x		?					
1R-4, 125	pow		x	x	x	x								
1R-4, 125	pow		x	x	x		x	x	?					

Note: pip = oriented pipette sample; pow = powder sample; An = antigorite; Fo = forsterite; Cr = chrysotile; Fa = fayalite; T = talc; B = brucite; A = aragonite; G = goethite; C = chlorite; E = enstatite; Z = zoisite; Ga = garnierite; St = stevensite.

pelagic sediment. On the other hand, the mottling may have resulted from coring disturbance. The reddish brown color suggests sufficient seafloor exposure to allow oxidation.

Aragonite in these water depths is unusual - the aragonite compensation depth is approximately at a water depth of 600 m at this site. The delicate, acicular habit of the aragonite crystals (up to 3 mm in length, 0.5 mm in width) in the clay and serpentine imply post-emplacement authigenic growth.

Subunit IB

Sections 125-778A-2R-1, 50 cm, to 125-778A-5R-1, 10 cm; depth, 7.2–29.8 mbsf. Age: lower/middle Pleistocene to lower Pleistocene(?).

This subunit is defined on the basis of an interval of poor recovery, resulting in a collection of cobbles and pebbles, possibly representing drilling breccia. In Section 125-778A-3R-CC (the only section recovered for that core), a sandy marl (clay, 30%; micrite, 25%; nannofossils, 10%; opaque minerals, 10%; zoisite, 10%; epidote, 5%; serpentine, 5%; chlorite, 5%) coated a serpentinized ultramafic pebble. A thin section of a pebble (Sample 125-778A-4R-1, 5–6 cm) revealed a clay matrix containing trace amounts of poorly preserved radiolarians and Neogene planktonic foraminifers among coarser grains of vesicular volcanics and crystals of olivine. The absence of pyroxene and feldspar crystals suggests that the source rock may be dunite. The lowest pebble in this section is a foraminifer-bearing serpentine sandstone of Pleistocene age composed of serpentine (65%), opaque minerals (12%), epidote (10%), chlorite (5%), aragonite (5%), foraminifers (3%), and a trace amount of nannofossils. Biostratigraphic criteria suggest that the vertical succession of sedimentary pebble occurrences may be stratigraphically correct. Igneous lithologies of additional pebbles interspersed in this subunit are described in the "Igneous and Metamorphic Petrology" section (this chapter).

Unit II

Sections 125-778A-5R-1, 10 cm, to 125-778A-13R-CC; depth, 29.8–107.6 mbsf.

This unit is primarily composed of phacoidal sheared serpentine and intervals of serpentine breccia having a convolute structure. A description and discussion of the breccia clast lithologies are given in the "Igneous and Metamorphic Petrology" section (this chapter). The matrix of the breccia is composed of serpentine (50%–80%), opaque minerals (20%–5%), thulite (25%–0%), epidote (20%–0%), chlorite (15%–0%), zoisite (10%–0%), talc (5%–0%), olivine (5%–0%), and trace to 0% of albite. Convolute structures appear in Sections 125-778A-6R-1 at 85 to 150 cm, 125-778A-8R-1 at 60 to 132 cm, 125-778A-9R at 75 to 150 cm, all of Core 125-778-12R, and Section 125-778A-13-1 at 25 to 140 cm. These deformation structures may have been produced by purely tectonic or purely gravitational flow processes (for further discussion see "Structural Studies" section, this chapter).

X-Ray Diffraction Analysis

Mineral identification of five samples from Site 778 was conducted using X-ray diffraction (XRD) on both powder (pow) and oriented pipette (pip) samples. Powder samples were dried, ground manually in an agate mortar, and packed in a sample holder. Pipette samples were prepared from the <4-mm fraction, which was separated by sedimentation in a 20-mL beaker. Preliminary mineral identification is listed in Table 3.

All samples contain both serpentine groups, and it seems that the 2- as well as the 20-Modification of chrysotile is present. Almost all samples contain brucite. Olivine, epidote-zoisite, and aragonite are present. Confirmation of the occurrence of chlorite, goethite, stevensite (a mixed-layered structure of talc/saponite), and garnierite must be left to future shore-based investigations.

BIOSTRATIGRAPHY

Evidence from calcareous nannofossils and planktonic foraminifers indicates that the sedimentary interval overlying the serpentinite ranges in age from early/middle Pleistocene to early Pleistocene. Microfossils were found only in samples from Cores 125-778A-2R and 125-778A-4R. No diatoms were recovered from any of the cores.

Calcareous Nannofossils

A well-preserved, but rare, Quaternary nannofossil assemblage is present in Section 125-778A-2R-1. This core is early/middle Pleistocene (Zone CN14a; Okada and Bukry, 1980) in age, based on the occurrence of *Gephyrocapsa oceanica* and *Pseudoemiliania lacunosa*, together with the lack of *Emiliania huxleyi*.

Moderately preserved Quaternary nannofossils are common in Sample 125-778A-4R-CC. This core has been dated early Pleistocene (Subzone CN14a; Okada and Bukry, 1980) by the co-occurrence of *Gephyrocapsa carribeanica*, *G. oceanica*, and *Calcidiscus macintyrei*. Its absolute age is approximately 1.45 Ma.

Foraminifers

Late Pliocene-Pleistocene foraminiferal assemblages were recovered from Section 125-778A-2R-1, and Samples 125-778A-4R-1, 23–25 cm, and 125-778A-4R-CC. All contain relatively rare, poorly preserved wide-ranging taxa, dominated by *Globigerinoides immaturus* and *G. quadrilobatus* and less common *Orbulina universa*, *Globigerinella aequilateralis*, *Sphaeroidinella dehiscens*, *Globorotalia* (*M.*) *menardii*, *G. tosaensis*, and *G. truncatulinoides*.

A late Pliocene to Pleistocene age (Zone N21-N22) was obtained from planktonic assemblages in Section 125-778A-2R-1 and Sample 125-778A-4R-CC. The presence of *Globorotalia truncatulinoides* in Section 125-778A-2R-1 and Sample 125-778A-4R-CC effectively confines this section (and the sections above) to the Pleistocene (Zone N22), owing to the restriction of *G. truncatulinoides* to Zone N22, as shown by Kennett and Srinivasan (1983). *G. tosaensis* and *G. truncatulinoides* are common components of warm subtropical to tropical water assemblages.

IGNEOUS AND METAMORPHIC PETROLOGY

The following section describes ultramafic, mafic, and other types of clasts that occur both as isolated fragments and as inclusions in a matrix of sheared and deformed, fine-grained serpentine. The characteristics of this matrix are described in the "Structural Studies" section (this chapter). We interpret these clasts as representative of the basement lithologies incorporated during the ascent of the serpentinite. Several different types of clast are present. The majority (80% by volume) are serpentinized ultramafic rocks, mostly of tectonized harzburgite and subordinate dunite protoliths. The remainder are predominantly metabasalts (15%), together with rare metagabbros, talc, and vein minerals. Clast sizes range from about 15 cm to less than 1 mm.

Ultramafic Clasts

Serpentinized Tectonized Harzburgites

These clasts range in color from a deep blackish-green to a light dun. In many samples, veining by serpentine and carbonate leads to small-scale color variations. Although most are massive, some are foliated by the alignment of bastitic orthopyroxene. Chrome spinels are sometimes dumbbell-shaped and occasionally form stringers defining a lineation.

The primary mineralogy has been pervasively altered to serpentine; however, relict orthopyroxene, olivine, clinopyroxene, and apparently fresh chrome spinel are preserved. Serpentinized olivine (about 80–95 modal %) forms a massive mesh-textured fabric having no obvious crystal outlines. Orthopyroxene (bastite; 5–20 modal %; <10 mm in maximum dimension) is typically kink-banded and sometimes elongate. Exsolution lamellae of clinopyroxene along the (100) plane of host orthopyroxene usually have undulose extinction. Relict clinopyroxene (<1 mm in size) is also present in the margins of some orthopyroxene crystals. Preliminary petrographic observations indicate that both olivine and orthopyroxene are highly magnesian. Chrome spinel (<1 mm in size) occurs as disseminated and isolated anhedral grains.

Serpentine dominates the secondary mineralogy and appears mostly to be antigorite or lizardite. Vein serpentine has a fibrous habit, orientated orthogonal to vein walls and is probably chrysotile. Vein carbonate is microcrystalline, whitish-green, and may include subordinate brucite, epidote, and manganese-rich zoisite (thulite). Veins are 0.1 to 1 mm wide and up to 2 cm long.

Serpentinized Dunites

The color of these rocks varies from black to dun, with some local mottling where veined. The primary mineralogy consists of 95% serpentinized olivine, with about 5% orthopyroxene and up to 1% chrome spinel. A mesh texture characterizes these clasts. Bastite pseudomorphs of orthopyroxene are apparently undeformed and are up to 5 mm in size. Spinel is euhedral, <1 mm in size, and forms local bands (up to 10 mm wide) of disseminated grains.

Talc-Serpentine

Two clasts of this type were recovered. The clasts are light greenish-white, have a soapy feel, and are very soft (Mohs' scale hardness of 2). The mineralogy is essentially talc and serpentine, with trace amounts of chrome spinel.

Mafic Clasts

Metabasalt

These clast types are generally dark grayish-green to light gray, ranging in size from a few centimeters (most common) to 10 cm (rare). Most have a subrounded shape, a margin containing patches of shiny black serpentine, and generally a massive internal structure. A minority of samples are cataclastic and contain 1- to 5-mm-wide shear zones; others are brecciated with individual (now recemented) grains 1 to 6 mm in size.

Two variably metamorphosed fine- to medium-grained metabasalts have been identified: plagioclase-clinopyroxene plus orthopyroxene phyric in a glassy groundmass; and orthopyroxene-olivine-chrome spinel-phyric in a glassy groundmass. Several clasts have quench-textures (skeletal and swallow-tailed plagioclase; spinifex pyroxene), but most have a felted texture formed from now-altered plagioclase laths in a more mafic, altered, fine-grained groundmass. Oxide minerals, mainly magnetite, are present in small abundances in some samples.

Many of the metavolcanic clasts are veined by carbonate, chlorite, and epidote. Vein orientations appear to be random. Amygdules composed mostly of chlorite (<0.5 to 1.0 mm) commonly form less than 1% of the rocks.

Metagabbro

Only one example of this type of clast was recovered. In hand specimen the rock is medium- to fine-grained with about 40% plagioclase and 60% mafic phases forming an isotropic texture.

Other Clast Types

This category includes rare, angular fragments of vein-type carbonate, quartz, and amphibolite (<30 cm in diameter). Some of these clasts are partially jacketed with sheared serpentine clay, but most form separate fragments, together with the metabasalt clasts. Both coarsely polycrystalline (0.5–5 mm) and more fine-grained materials are present. A brownish-orange material, apparently a chert fragment, forms an angular (about 2 cm) fragment in one core. One small clast contains fragments of both coarse- and fine-grained amphibolite (possibly from a basic igneous protolith) in a fine-grained, schistose and chloritic matrix. The amphiboles are pale green hornblende rimmed with blue amphibole, possibly crossite or glaucophane. The original nature of this clast is unclear; it may have been a sedimentary or tectonic breccia.

IGNEOUS AND METAMORPHIC GEOCHEMISTRY

Shipboard geochemical analyses of clasts entrained within serpentine at Site 778 were performed for 10 samples of

Table 4. Major-element data for serpentinized, ultramafic rocks from Hole 778A.

Core: Interval (cm):	2R-1 53–56	2R-1 89–92	3R-CC 1–7	7R-2 73–78	7R-CC 7–13	8R-1 36–44	12R-2 43–45	12R-2 73–75	13R-1 15–17	13R-2 8–11
SiO_2	38.17	35.69	40.93	34.14	37.46	34.61	41.52	39.29	37.10	49.99
TiO_2	0.00	0.00	0.00	0.00	0.00	0.00	0.00	0.06	0.00	0.00
Al_2O_3	0.74	0.00	1.09	0.85	0.76	0.68	0.71	1.01	0.47	4.54
Fe_2O_3	6.73	6.77	7.21	8.66	7.86	8.00	8.95	7.64	7.88	6.92
MnO	0.10	0.10	0.10	0.14	0.13	0.16	0.08	0.06	0.11	0.18
MgO	36.59	35.88	36.85	39.32	39.15	39.21	39.61	37.04	39.38	22.65
CaO	0.07	3.52	0.74	0.02	0.03	0.08	0.06	0.07	0.79	8.45
Na_2O	0.09	0.09	0.00	0.09	0.00	0.00	0.00	0.00	0.00	0.51
K_2O	0.01	0.00	0.01	0.01	0.05	0.00	0.00	0.00	0.00	0.02
P_2O_5	0.00	0.01	0.00	0.00	0.00	0.00	0.00	0.00	0.00	0.00
LOI	15.06	15.55	11.49	14.76	13.66	16.06	6.01	11.99	13.49	5.53
NiO	0.29	0.39	0.28	0.39	0.36	0.33	0.36	0.37	0.29	0.07
Cr_2O_3	0.36	0.07	0.37	0.41	0.33	0.37	0.42	0.53	0.27	0.12
Total	98.20	98.08	99.08	98.79	99.79	99.50	97.70	98.00	99.79	98.99

Data (in wt% oxides) are for whole-rock analysis by CXRF. LOI is loss on ignition between 150° and 1030°C.

Table 5. Trace-element data for serpentinized, ultramafic rocks from Hole 778A.

Core: Interval (cm):	2R-1 53–56	2R-1 89–92	3R-CC 1–7	7R-2 73–78	7R-CC 7–13	8R-1 36–44	12R-2 43–45	12R-2 73–75	13R-1 15–17	13R-2 8–11
Nb	tr	tr	tr	tr	tr	tr	tr	tr	tr	tr
Zr	1	2	0	1	1	1	0	1	1	2
Y	0	nd	1	nd	nd	nd	1	nd	0	2
Sr	9	595	5	2	3	8	9	12	3	31
Rb	0	nd	1	nd	1	1	nd	0	0	nd
Zn	52	28	36	39	42	64	42	40	37	38
Cu	3	3	11	2	2	4	8	2	14	9
Ni	2281	3039	2173	3034	2818	2638	2813	2905	2297	571
Cr	2496	501	2523	2786	2261	2510	2866	3603	1875	837
V	46	22	40	38	41	48	48	62	34	75
Ti	0	0	0	0	0	0	0	0	0	0
Ce	tr	tr	nd	tr	nd	nd	tr	nd	12	tr
Ba	tr	nd	tr	nd	nd	10	nd	nd	nd	tr

Data (in ppm) are for whole-rock analysis by XRF, nd = not detected, tr = below detection limits (<2 ppm for Nb; <10 ppm for Ba and Ce).

Table 6. Major-element data for mafic rocks from Hole 778.

Core: Interval (cm):	5R-1 7–10	11R-1 0–3	9R-CC 9–12	11R-1 5–8	13R-1 5–8	13R-1 12–14	13R-CC 4–6
SiO_2	56.03	45.19	46.44	46.07	42.57	40.01	40.78
TiO_2	0.29	2.32	0.91	1.10	1.12	1.09	1.33
Al_2O_3	14.38	6.39	15.52	14.88	12.48	11.98	9.27
Fe_2O_3	8.20	18.21	8.44	12.84	11.97	10.60	10.00
MnO	0.16	0.25	0.17	0.17	0.25	0.23	0.22
MgO	7.57	11.73	7.66	2.52	6.73	16.94	21.81
CaO	3.01	9.27	12.29	9.24	17.38	10.10	6.19
Na_2O	5.15	3.49	0.73	5.08	1.46	0.18	0.87
K_2O	0.16	0.02	3.04	0.79	0.29	0.76	0.01
P_2O_5	0.03	0.23	0.14	0.04	0.07	0.08	0.10
[a]LOI	2.91	1.74	3.78	3.95	4.45	7.30	7.94
TOTAL	97.90	98.93	99.13	98.72	98.80	99.30	98.54

[a]Between 150° and 1030°C. Data (in wt% oxides) are for whole-rock analysis by XRF.

Table 7. Trace-element data for mafic rocks from Hole 778.

Core: Interval (cm):	5R-1 7–10	11R-1 0–3	9R-CC 9–12	11R-1 5–8	13R-1 5–8	13R-1 12–14	13R-CC 4–6
Nb	tr	tr	tr	tr	tr	5	tr
Zr	31	150	50	60		57	78
Y	9	62	21	22	[illegible]	28	28
Sr	51	41	95	62	95	82	44
Rb	3	nd	57	16	6	17	nd
Zn	56	93	71	100	92	95	74
Cu	299	57	35	206	75	51	49
Ni	54	563	44	47	42	41	28
Cr	85	109	117	68	151	170	43
V	215	494	239	357	317	242	281
Ti	1739	13915	5458	6598	6718	6538	7977
Ce	tr	11	nd	nd	16	10	tr
Ba	tr	25	54	46	58	33	14

nd = not detected; tr = below detection levels (<5 ppm for Nb; <10 ppm for Ba and Ce). Data (in ppm) are for whole-rock analysis by XRF.

serpentinized, tectonized harzburgite and for seven samples of metabasalt. Preparation and analytical techniques are given in the "Explanatory Notes" (this volume). These data are given in Tables 4 through 7. Rock descriptions are presented in the "Igneous and Metamorphic Petrology" section (this chapter).

Ultramafic Rocks

The original (pre-serpentinization) composition of these samples, based on modal estimates from thin-section descriptions, is approximately 70% to 95% olivine, 5% to 30% orthopyroxene, and <1% clinopyroxene and spinel. The degree of serpentinization ranges from 50% to 95%.

Major Elements

Overall, the ultramafic rocks analyzed are quite homogeneous in both major and trace element chemistry.

Loss on ignition (LOI) is high in these samples (Table 4), ranging from 5.53 to 16.06 wt%. These values clearly result from serpentinization, although there is no obvious correlation between LOI and observed percentage of serpentinization. LOI only includes volatile loss between 110° and 1030° and thus represents H_2O^+ and CO_2. The upper range of LOI values is similar to that reported from DSDP Leg 82 for serpentinized peridotites recovered from the Middle Atlantic Ridge (12.86–16.07 wt%, Michael and Bonatti, 1985); however, the lower values (5.53 and 6.01) are significantly smaller. Total percentages of major elements are typically 98 to 100 wt% (including Cr_2O_3 and NiO); MgO ranges from 27.30 to 39.61 wt% and SiO_2 ranges from 34.14 to 41.52 wt%. Total iron, calculated as Fe_2O_3, ranges from 6.73 to 8.95 wt%, and Al_2O_3 typically ranges from 0.47 to 1.09 wt%. These are within the range of values reported from serpentinized ultramafic samples recovered during DSDP Leg 82. The abundances of other major elements are predictably low: CaO is typically <0.10 wt%, although two samples reach 0.78 wt% (Table 4); MnO ranges from 0.08 to 0.16 wt% in all samples, and the usual ranges for TiO_2, Na_2O, K_2O, and P_2O_5 are all less than 0.02 wt%. Several samples fall outside the typical ranges of concentrations of major elements and are discussed below; these include Sample 125-778A-2R-1, 89–92 cm, which has low Al_2O_3 (0.09) wt%) and high CaO (3.52 wt%) and Sample 125-778A-13R-2, 8–11 cm, which has high Al_2O_3.

Trace Elements

Concentrations of the compatible elements are predictably high (Fig. 3B). In all except two of the samples, values for nickel range from 2173 to 3039 ppm, whereas chromium is more restricted, ranging from 2260 to 2785 ppm. As expected for residual mantle material, the concentrations of incompatible elements (niobium, zirconium, strontium, and rubidium) are low, ranging from not detected (nd) to 2 ppm (2 ppm is below detection limit for niobium, which therefore should be considered present in trace amounts). Each transition element falls within a fairly restricted range: zinc from 28 to 64 ppm; vanadium from 22 to 62 ppm; and copper from 2 to 14 ppm. Cesium and barium are typically below their detection limits. There are no significant correlations between the concentrations of trace elements and depth.

Of the two samples that do not follow the patterns described above, Sample 125-778A-2R-1, 89–92 cm, has a low concentration of chromium (501 ppm), a high concentration of strontium (595 ppm), and falls at the low end of the ranges for vanadium (22 ppm) and zinc (28 ppm) and the high end of the nickel range (3039 ppm). With the notable exception of strontium, this sample is indistinguishable from the other samples on the basis of the more incompatible elements. High concentrations of strontium may indicate the presence of some unusual phase, such as plagioclase, which is not seen in thin section, or it may suggest that strontium is accommodated in secondary minerals, such as carbonates, which are found within the serpentine veins. The low concentrations of chromium may indicate significant alteration of chromite to magnetite or a low proportion of chromite in the sample. Sample 125-778-12R-2, 8–11 cm, has low values of both chromium (837 ppm) and nickel (571 ppm) and slightly high values of strontium (31 ppm) and vanadium (75 ppm). The precise significance of these valoes is not clear at this stage, although secondary vein materials may be responsible for diluting the abundances of nickel and chromium and enhancing the abundance of strontium.

Mafic Rocks

Several types of mafic rocks are present. The majority of samples analyzed are aphyric and contain microphenocrysts of clinopyroxene (15–25 modal %) and plagioclase (10–30 modal %) in an altered glassy matrix (originally 50–90 modal %). Original glass is now altered, primarily to clays, and samples are heavily veined.

Major Elements

Mafic samples also have high LOI, ranging from 1.74 to 7.30 wt% (Table 6), reflecting extensive metamorphism and alteration. Despite the obvious effects of alteration on the more mobile elements, major element compositions suggest that the samples belong to three groups.

Group 1 contains one sample (125-778A-5X-1, 7–10 cm) with 56.03 wt% Sio_2. This sample also has low iron (Fe_2O_3 8.02 wt%) and moderately high MgO (7.57 wt%). Other chemical characteristics include low TiO_2 (0.28 wt%), high total alkalies (5.18 wt%), and especially high Na_2 Na_2O (5.03 wt%). This sample may be classified as a high-magnesium andesite (boninite) on the basis of major element criteria, although there is no primary petrographic evidence to support this classification.

Group 2 also consists of only a single sample (125-778A-11X-1, 0–3 cm) and is characterized by high abundances of TiO_2 (2.29 wt%), very high Fe_2O_3 (18.21 wt%), high P_2O_5 (0.23 wt%), and high Na_2O (4.89 wt%). In addition, this sample has low abundances of Al_2O_3 (6.31 wt%) and MgO (11.73 wt%), and may be classified as a ferrobasalt.

The remaining four samples fall into a single group, Group 3. All Group 3 samples are of basaltic composition and are characterized by mid-range values of TiO_2 (0.91–1.12 wt%), lower total alkalies (typically 0.94 to 1.73 wt%) and higher LOI (3.78–7.30 wt%). SiO_2 is variable, ranging from 40.01 to 46.44 wt%. Values of CaO typically range from 9.24 to 12.29 wt%, but are unusually high (17.38 wt%) in one sample (125-778A-13X-1, 5–8 cm), probably a result of carbonate veining. Sample 125-778A-13-CC, 4–6 cm, may also be included in Group 3, but this sample has high abundances of MgO (21.81 wt%), probably reflecting serpentine veining and low CaO (6.09 wt%).

Trace Elements

Trace-element compositions are presented in Table 7. The samples making up Group 1 are characterized by lower concentrations of zirconium (31 ppm), yttrium (9 ppm), vanadium (215 ppm), and zinc (56 ppm) than Groups 2 and 3. Group 2 has the highest concentration of zirconium (150 ppm), yttrium (62 ppm), and vanadium (494 ppm) of the three groups, and very high concentrations of nickel (563 ppm). Group 3 has mid-range values of zirconium (50–64 ppm), yttrium (21–28 ppm), and vanadium (242–357 ppm).

The concentration of nickel is almost constant in Group 3 samples and ranges from 41 to 47 ppm. Sample 125-778A-13X-CC, 4–6 cm, exhibits some unusual abundances of trace elements, most notably very low nickel (28 ppm) and chromium (43 ppm), but abundances of vanadium, (281 ppm), zirconium (78 ppm), and yttrium (28 ppm) are typical of Group 3.

The three groups, recognized on the basis of major elements, can also be discriminated on the basis of trace elements. Two examples are given in Figure 3: (A) an yttrium/chromium (Y/Cr) diagram after Pearce and Wanming (1988) and (B) a zirconium/titanium (Zr/Ti) diagram after Pearce and Cann (1973). Group 1, the high-magnesium andesite, falls on the boninite-island arc tholeiite (IAT) boundary of Figure 3A and beyond the lower end of the IAT field in Figure 3B, which overlaps with a boninite field not shown in this diagram. The ferrobasalt of Group 2 plots clearly in the mid-ocean ridge basalt (MORB) field of Figure 3A. Although it falls outside the MORB field toward higher titanium and zirconium in Figure

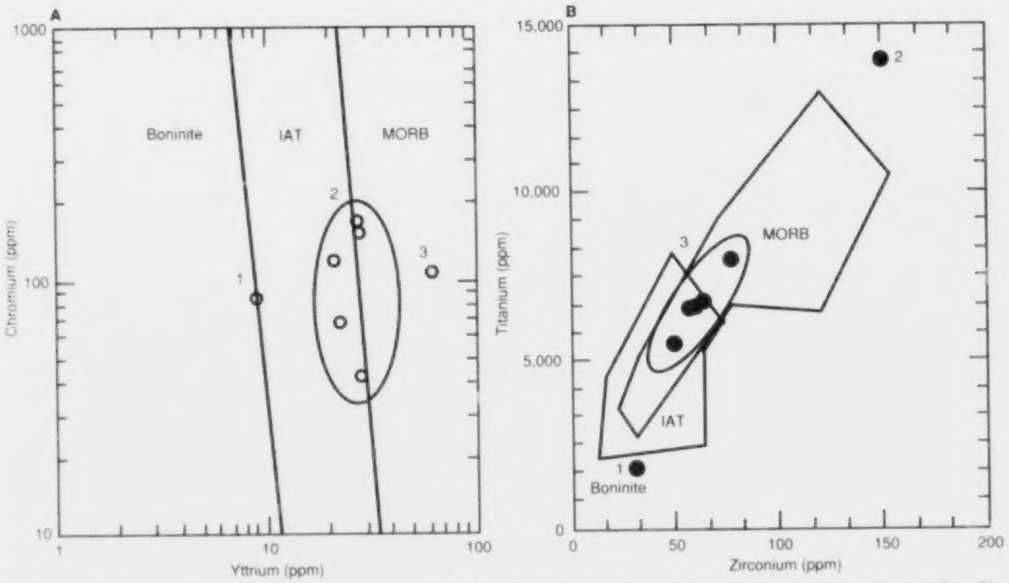

Figure 3. A. Discriminant diagram for tectonic environment of mafic rocks, using log Cr vs. log Y. Samples plotted are mafic clasts from Site 778. Numbers refer to groups defined in the text. Fields are after Pearce and Wanming (1988). B. Discriminant diagram for tectonic environment, using Zr and Ti for mafic basaltic rocks. Samples plotted are mafic clasts from Site 778. Numbers refer to groups defined in the text. Fields are from Pearce and Cann (1973).

3B, the composition of the Group 2 sample is comparable to that of ferrobasalts from propagating rifts in oceanic environments. The Group 3 samples form a coherent group in both discrimination diagrams (Figs. 3A and 3B), plotting near the IAT-MORB boundary in both cases. At this stage we cannot be certain whether these samples are IAT, MORB, or transitional between the two.

We stress that these types of diagrams are not perfectly reliable for determining the tectonic provenance of individual or small groups of samples. Although more data are clearly required to make a confident interpretation of tectonic environment, it is apparent that the mafic clasts may have come from at least three different settings, incorporating magma types of both supra-subduction zone and MORB affinities.

SEDIMENT/FLUID GEOCHEMISTRY

Sediment Geochemistry

Cores from Site 778 were analyzed on board ship for inorganic carbon and for total carbon, nitrogen, and sulfur, using the techniques described in the "Explanatory Notes" (this volume). The organic carbon content was then calculated by difference. These results are presented in Table 8 and in Figure 4. Except for one near-surface interval, the cores are uniformly carbonate-poor, with concentrations ranging from 0.3 to 4.2 wt% $CaCO_3$. The interval that is relatively carbonate-rich lies between 3 and 6 mbsf and contains 13 to 16 wt% $CaCO_3$. The organic carbon content is also uniformly low, ranging from less than 0.01 to 0.29 wt%. Total sulfur ranges from less than 0.10 to 0.18 wt%, and nitrogen from less than 0.05 to 0.10 wt%. At these low levels, nitrogen may be affected by contamination by air inadvertently included with the sample charge.

Fluid Geochemistry

The concentration of hydrocarbon gases measured in 5-cm^3 headspace samples is uniformly low (Table 9). Methane was the only gas detected.

Interstitial waters squeezed from the cores have compositions that differ considerably from that of seawater (Table 10). The pH of the waters from Site 778 varies from 8.5 to 9.1 (Fig. 5). This is about 0.5 to 1 pH unit higher than that measured in interstitial waters from normal deep-sea sediments. The high pH presumably results from reaction with the serpentine mineral assemblage. Alkalinity is uniformly low at one-third to one-half the concentration in seawater. Ammonia increases over nearly the entire sampled interval, but never exceeds 90 mmol/kg. Concentrations of dissolved silica are also low, less than 150 mmol/kg, relative to those in more typical deep-sea sediments and even in ocean bottom water in this area, which contains about 150 mmol/kg. The samples from 84 to 100 mbsf have higher silica concentrations than those from the upper 50 m. Where measured within the upper 6 m of sediment, phosphate is also low (Table 10). Sulfate decreases to about one-half the seawater value over the upper 50 m of the section, then apparently rebounds to a constant value of about 17 mmol/kg between at least 84 and 100 mbsf. Magnesium decreases by more than 99% to very low concentrations; most of this change occurs within the upper 50 m of unconsolidated serpentine (Fig. 6). Calcium and sodium each increase by about 15 mmol/kg over the same interval, thereby accounting for less than one-half of the electrical charge loss associated with the removal of magnesium from solution. Potassium remains constant over the upper 50 m, then decreases by a third over the lower 50 m. Most notably, both salinity and chlorinity decrease nearly linearly with depth, by a total of

Table 8. Total nitrogen, sulfur, and carbon, organic carbon, and carbonate carbon in cores at Site 778.

Core, section, interval (cm)	Depth (mbsf)	Total nitrogen (wt%)	Total sulfur (wt%)	Total carbon (wt%)	Inorganic carbon (wt%)	Organic carbon (wt%)	$CaCO_3$ (wt%)
125-778A-							
1R-1, 77–78	0.77				0.51		4.2
1R-1, 117–118	1.17				0.10		0.8
1R-2, 135–136	2.85				1.72		14.3
1R-3, 115–116	4.15	0.075	0.10	1.51	1.63	0.00	13.6
1R-4, 117–119	5.67				1.87		15.6
1R-5, 15–16	6.15				1.92		16.0
2R-1, 15–16	6.85	0.061	0.11	0.51	0.44	0.07	3.7
2R-1, 45–46	7.15				0.51		4.2
5R-1, 14–16	29.84	nd	0.18	0.30	0.11	0.19	0.9
6R-1, 54–56	39.74	0.12	nd	0.35	0.13	0.22	1.1
6R-1, 57–58	39.77	0.096	0.14	0.46	0.27	0.19	2.3
6R-1, 120–121	40.40				0.16		1.3
6R-1, 125–126	40.45				0.25		2.1
7R-1, 67–69	49.37				0.08		0.7
7R-1, 117–118	49.87	0.088	0.099	0.27	0.12	0.15	1.0
7R-2, 36–37	50.56				0.09		0.7
7R-2, 72–73	50.92				0.11		0.9
8R-1, 83–84	59.03				0.13		1.1
8R-1, 137–139	59.57	0.056	0.12	0.17	0.28	0.00	2.3
9R-1, 87–89	69.07	0.079	0.10	0.24	0.11	0.13	0.9
9R-1, 148–149	69.68				0.15		1.2
9R-2, 30–31	70.00				0.23		1.9
11R-1, 20–21	82.50				0.14		1.2
11R-1, 71–73	83.01	0.073	nd	0.68	0.39	0.29	3.3
11R-1, 106–108	83.36				0.13		1.1
11R-1, 133–134	83.63				0.30		2.5
12R-1, 8–9	89.88	0.076	nd	0.50	0.44	0.06	3.7
12R-1, 45–46	90.25				0.22		1.8
12R-1, 75–76	90.55				0.04		0.3
12R-2, 18–19	91.48				0.11		0.9
12R-2, 42–43	91.72	0.068	0.46	0.39	0.15	0.24	1.3
12R-2, 60–61	91.90				0.10		0.8
13R-1, 50–51	98.80				0.21		1.7
13R-1, 81–83	99.11	nd	nd	0.46	0.25	0.21	2.1
13R-1, 115–116	99.45				0.9		0.8

nd = not detected.

almost 10% at 100 mbsf (Fig. 7). The bromide data are highly scattered and show no obvious trend with depth.

STRUCTURAL STUDIES

The foliated and clastic serpentines recovered at this site are highly disturbed, especially in lithologic Unit II, where the layers are affected by intense plastic deformation (folding) and ductile shearing. This deformation seems to have occurred in the presence of high fluid contents; indeed, the cores shrunk considerably during drying. The tracers of this deformation are convolutions of the layering, asymmetric shapes of poorly consolidated serpentine clasts, development of a foliation, and the presence of shear bands.

Convolutions of the Layering

Small-scale layering within Unit II is most often defined by alternating zones of gravelly serpentine sediments and flows of different colors. These layers show abundant convolutions that develop successively as irregular folds, varying from open to tight (Fig. 8). Because of the folding, the attitude of the layering varies from horizontal to vertical (Fig. 9). Often, two or more fold hinges may face in opposite directions, which increases the chaotic appearance of the deformed material. Opposite-facing folds may be concentrated on both sides of the core, so that the central part of the column shows a vertical layering, as seen, for example, in the bottom of Section 125-778A-9R-1 and in Section 125-778A-6R-1, 115–130 cm (Figs. 8 and 10).

Trains of millimeter-sized serpentinite fragments within the unconsolidated serpentine also outline the deformed layering. As in the previous case, this sedimentary layering is a clear tracer of the plastic deformation.

Shape of Poorly Consolidated Clasts

Some clasts of strongly altered serpentinite exhibit asymmetric shapes characteristic of a ductile, noncoaxial shearing. We noted, however, that the lithified clasts exhibit no deformation, although the matrix foliation around them is disturbed.

Foliation and Cleavage

A clear foliation, either horizontal or oblique, has developed in certain zones, especially around major shear bands that crosscut the cores. The foliation is emphasized both by alignment of stretched millimeter- to centimeter-sized serpentinitic, altered clasts and by discontinuous, sheared laminae. A thin anastomosing cleavage similar to the scaly-clay cleavages (argille scagliose) has also developed, almost parallel to the foliation (Fig. 11). This cleavage is locally emphasized by the development of very pale green laminae (chrysotile-rich laminae?). Further detailed investigations will be required to determine the origin and significance of this cleavage. A preliminary study of the microfabric of the poorly consolidated matrix was conducted using impregnated thin sections. This analysis confirms that the foliation is well defined locally by the preferred orientation of the

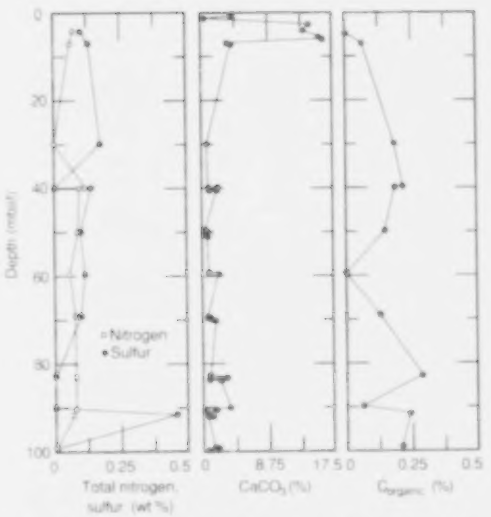

Figure 4. Weight percent of calcium carbonate, total organic carbon, and total nitrogen and sulfur in cores at Site 778.

serpentine flakes. This preferred orientation is visible under crossed nicols, where contiguous portions of the thin sections tend to go to extinction simultaneously. However, on this scale, the deformation is not homogeneous, and a uniform field of deformation cannot be defined. Thus, it would appear that the intensity of deformation has not been sufficient to provide a significant rearrangement of the material.

Hydrogrossular crystals locally form long chainlets and clusters that are located within the foliation planes. Epidote-group minerals (mainly zoisite?) were found within the foliation planes, which indicates that crystallization is pre- to syndeformation. These observations will help constrain models for thermal evolution of the serpentinites.

Decimeter-size folds may affect the foliation, as for example in the bottom of Core 125-778A-9R-1. This observation is confirmed by thin-section analysis that shows tightly folded and sheared serpentine crystals.

Anastomosing foliation planes and curving foliation planes around clasts define shear lenses (phacoids) on all scales (Fig. 12). Lenses may be of millimeter to pluricentimeter scale. In thin section, C-S-type planes also define lenses. However, at this scale, the weakly preferred orientation of the shear planes and lenses does not allow us to define precisely the senses of shear.

Shear Bands

Shear bands affect the sediments at all scales (mm, cm, dm). Decimeter-sized shear bands can be recognized locally throughout Cores 125-778A-5R to -13R. Oblique bands are particularly visible in Section 125-778A-7R-1 at 85 and 120 cm. Small centimeter-to-millimeter shear bands are abundant within all the sections. These bands deform the foliation defined in the previous section.

Table 9. Results of headspace-gas analyses of cores at Site 778.

Core, section, interval (cm)	Depth (mbsf)	Methane	
		(μL/L)[a]	(μM)[b]
125-778A-			
1R-4, 0–5	4.53	8	1
2R-1, 0–5	6.73	21	2
5R-1, 20–25	29.93	20	2
6R-1, 145–150	40.68	37	3
7R-1, 135–140	50.08	452	40
8R-1, 140–145	59.63	33	3
11R-2, 0–5	83.82	12	1
12R-1, 135–145	91.20	29	3

[a] Microliters of gas per liter of wet unconsolidated serpentine.

[b] Micromoles of methane per liter of interstitial water, assuming a porosity of 50%.

Discussion

We list here the different mechanisms that may have been responsible for the development of the observed structures:

1. Drilling disturbances;
2. Syn-emplacement slumps, i.e., deformation during pure gravitational flow;
3. Ball-and-pillow structures (density differences in liquefied sediments);
4. Dewatering of very soft sediments (water-escape structures);
5. Fluid-circulation disturbances ("upwelling" of hydrothermal fluids of deep origin); and
6. Purely tectonic processes within the diapir.

Some of these mechanisms may have acted together. A first approach might be to separate the mechanisms responsible for the creation of foliation from those responsible for its subsequent folding. However, during progressive deformation processes, different structures may appear at different successive stages of the evolution so that earlier structures are deformed by the later ones. In that case, the presence of a folded foliation does not mean that two different successive events took place. Further analyses and discussions will be necessary to propose more detailed hypotheses. However, preliminary microstructural analyses conducted on board the ship allow us to propose that the foliation observed within the serpentine sediments and flows of Site 778 is not related to drilling disturbance; the major argument is that the alignment of syntectonic hydrogarnets parallels this foliation.

Finally, the fabric and microfabric displayed by the soft material drilled at Site 778, and more particularly the fact that the layering attitude is often vertical, might suggest the involvement of tectonic processes with vertical component linked to diapiric processes. However, such features may also be interpreted as the result of gravitational flows involving a thick pile of unconsolidated, fluidized, serpentinous debris covering the diapir flanks. The hydrothermal paragenesis also suggests that water circulation is responsible for a significant amount of the nonpenetrative deformation. The presence of horizontal to gently dipping shear zones indicates that horizontal displacement took place on the flank of the diapir. Such displacements can be related to gravitational instability of the upper part of the diapir.

Table 10. Composition of interstitial waters from Hole 778A cores.

Sample number	Core, section, interval (cm)	Volume (mL)	Squeeze temperature (°C)	Depth (mbsf)	pH	Salinity (R.I., ‰)	Salinity (calcium, ‰)	Chlorinity (mmol/kg)	Alkalinity (meq/kg)	Sulfate (mmol/kg)	Na (mmol/kg)	K (mmol/kg)
Surface seawater (22 February 1989)					8.34	35.4	34.73	539.0	2.410	28.60	461.9	10.12
IW-1	1R-1,145–150	31	2	1.48	9.00	34.5	34.46	542.6	0.985	24.46	475.5	10.22
IW-2	1R-4,145–150	63	2	5.98	8.48	35.5	34.93	547.5	1.185	27.17	469.8	10.21
IW-3	7R-1,140–150	12	4	50.15	8.99	32.3	32.75	532.0	0.827	12.15	488.7	10.09
IW-4	11R-1,140–150	15	3	83.75	8.94	30.8	32.33	510.7	1.339	16.83	486.4	8.60
IW-5	12R-1,140–150	10	5	91.25	9.14	30.0	31.78	502.0	1.339	16.43	477.1	8.47
IW-6	13R-1,140–150	12	6	99.75	8.86	31.2	32.07	508.8	0.783	16.77	484.9	6.71

Note: Values absent from table were not determined.

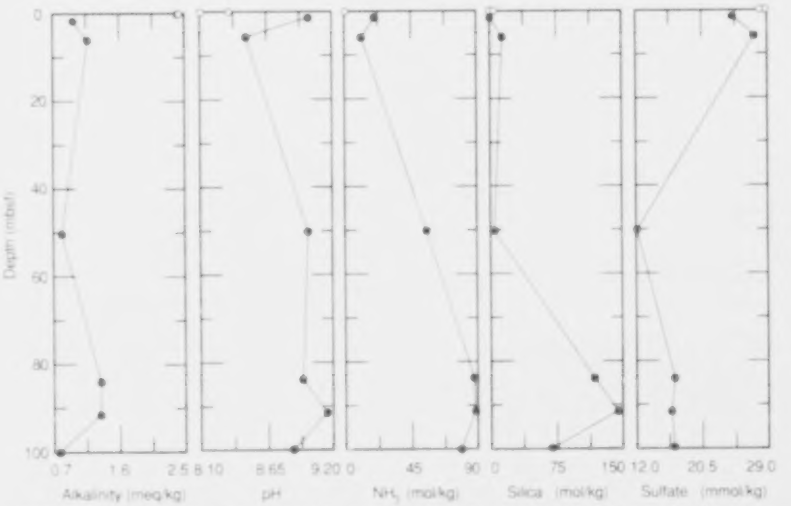

Figure 5. Composition of interstitial waters from cores at Site 778 (closed circles), compared with surface seawater collected 22 February and 4 March 1989 (open circles).

PALEOMAGNETISM

Owing to the extremely poor recovery, the tectonized nature of the rocks, and the limited number of stratigraphic units at Site 778, magnetostratigraphy was nearly impossible. The natural remanent magnetization (NRM) of the archive half of each core was measured using the cryogenic magnetometer. Core 125-778A-2R and Cores 125-778A-4R through 125-778A-11R were demagnetized with the on-line alternating-field (AF) demagnetizer and measured at the 5 and 10 mT levels. Cores 125-778A-1R, -12R, and -13R were demagnetized and measured at the 3, 5, 8, and 10 mT levels.

The only useful magnetostratigraphic information from Site 778 is from Interval 125-778A-1R-1, 50 to 150 cm (0.5–1.5 mbsf). A reversed component of magnetization is evident in this interval (Fig. 13). The top of the serpentine flow must therefore be at least as old as the last reversal at 0.73 Ma (Berggren et al., 1985, and biostratigraphic evidence in "Biostratigraphy" section, this chapter), and very little deposition must have occurred since the time when the flow was deposited.

Within the serpentinite material (lithologic Unit II), some of the more coherent pieces of core exhibited a consistent magnetization. Negative inclinations were measured in Intervals 125-778A-5R-1, 0 to 43 cm (29.7–30.1 mbsf), 125-778A-12R-1, 0 to 150 cm, and 125-778A-12R-2, 0 to 90 cm (89.8–92.2 mbsf). Positive inclinations were measured in the Intervals 125-778A-7R-1, 0 to 140 cm (48.7–50.1 mbsf), and 125-778A-11R-1, 10 to 140 cm (82.4–83.7 mbsf). However, because of the lack of stratigraphic and age control, and the extremely metamorphosed and deformed state of the rocks, it is impossible to place these data into a tectonic or geochronological framework.

The intensities throughout the section were high, ranging from approximately 10 to 100 mA/m. This is not surprising considering that magnetite is a common secondary product of the serpentinization process.

Magnetic susceptibilities were measured with a Bartington Instrument susceptibility meter on the multisensor track, the first time this configuration of the system was tried. However, problems with the program and the instrument prevented acquisition of meaningful data.

PHYSICAL PROPERTIES

Physical properties for Site 778 were measured on both whole-round and discrete samples (Table 11). The multisensor

Table 10 (continued).

Ca (mmol/kg)	Mg (mmol/kg)	Br (mmol/kg)	Si (μmol/kg)	NH_3 (μmol/kg)	PO_4 (μmol/kg)
10.40	52.89	0.83	<5	<5	
10.25	43.16	1.00	<5	20	0.27
8.90	52.59	0.95	15	11	0.16
20.76	8.41	1.07	5	55	
23.90	1.43	0.87	117	87	
24.79	0.55	1.19	143	87	
21.03	4.70	0.97	68	78	

track (MST) and thermal conductivity measurements were performed on whole-round samples, and representative discrete samples were taken from working halves of split cores (Table 12). The compressional-wave velocity logger on the MST did not couple well with the incompletely filled liners, and thus no data were recorded. The gamma-ray attenuation porosity evaluator (GRAPE) was used on all sections. Considerable scatter is apparent in the data, related to incompletely filled liners that introduced artificially large porosity values. Magnetic susceptibility was also measured on the MST; however, the instrument was malfunctioning, and only erratic readings were recorded.

Thermal conductivities from the serpentinites were measured with needle probes, giving values ranging from 0.96 to 2.72 W/mK. The higher values of conductivity are associated with the more water-rich (slurrylike) serpentine sediments and flows.

Measurements of compressional-wave velocity and index properties (wet and dry volumes, wet and dry masses, porosity, and water content) were performed, and values calculated for discrete samples. Hamilton frame velocity measurements were not performed for soft serpentine samples, as these were too mobile to be placed in the apparatus. More compact serpentinites were measured, giving velocities ranging from 2.1 to 4 km/s. Bulk densities and water content, derived from the index properties, were highly variable and dependent upon the water contained in the sections. Porosities were generally in excess of 40%, with values as high as 86%, and water content closely followed these trends. The index properties from Site 778 probably reflect the water entrained in the cores by drilling, rather than the *in-situ* values.

SUMMARY AND CONCLUSIONS

Site 778 (19°29.93′N, 146°39.94′E; water depth, 3913.7 m) is situated about halfway up the southern flank of Conical Seamount, a 1500-m high cone-shaped serpentinite seamount located on the outer-arc high of the Mariana forearc basin, about 100 km west of the trench axis. Site selection was based on a SeaMARC II side-scanning sonar image of the seamount, which indicated recent serpentine flows as areas of high sonar backscatter. The site is located in the center of a major flow.

Hole 778A was spudded at 1445UTC on 22 February 1989 and was RCB-cored to 107.6 mbsf. Episodes of instability of the hole required that the hole be repeatedly washed out, and finally, at 0700UTC on 24 February, prevented further drilling. This lack of stability was attributed to the friable and heterogeneous nature of the serpentine flows (hard clasts of variable size in a soft matrix). Recovery of the cored intervals was low, averaging 21% overall and only 13.7% in Unit II (Fig. 14).

Two lithologic units can be recognized at Site 778: a serpentine-rich clay-marl-breccia (Unit I) and a phacoidal sheared serpentine (Unit II).

Unit I (Subunit IA, 0–7.2 mbsf): The subunit consists of lower/middle Pleistocene-Holocene(?) serpentine-rich sediment and serpentine flows. The uppermost portion has two pebbles (one limestone and one serpentinite) overlying 15 cm of pale blue-gray serpentine clay. Below this is 15 cm of gray-green serpentine clay, 10 cm of red-orange serpentine clay, and 1.5 m of pale blue-gray, silt-sized serpentine (containing 80% serpentine, 10% opaque minerals, 10% epidote-group minerals, and trace amounts of chlorite, glass, and

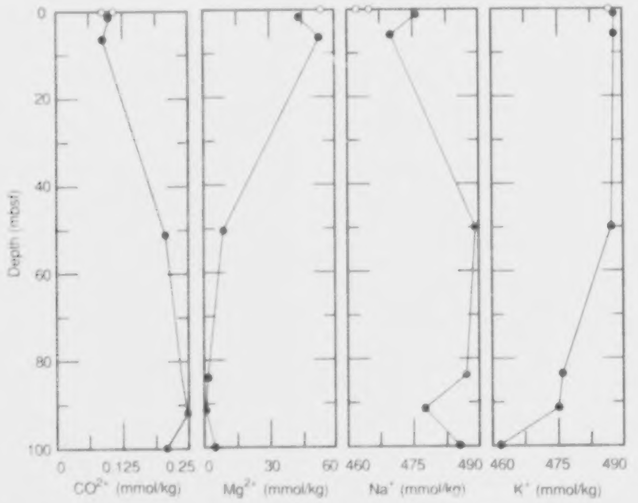

Figure 6. Composition of interstitial waters from cores at Site 778 (closed circles), compared with surface seawater collected 22 February and 4 March 1989 (open circles).

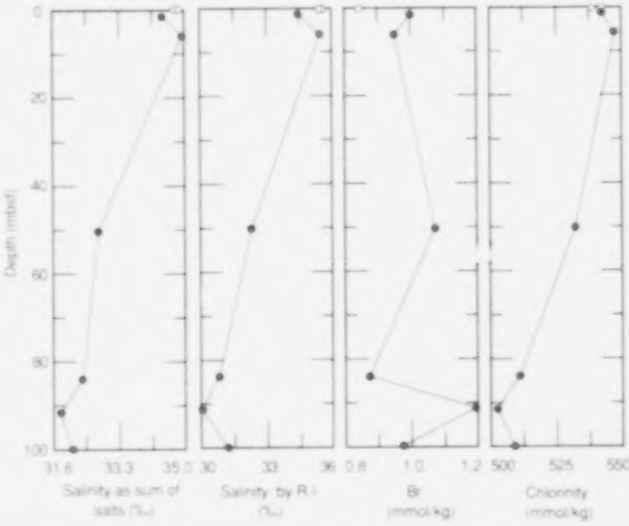

Figure 7. Composition of interstitial waters from cores at Site 778 (closed circles), compared with surface seawater collected 22 Februrary and 4 March 1989 (open circles).

micrite). The bottom of this unit is a breccia that extends to the base of Core 125-778A-1R (an interval of 357 cm) and through the upper 50 cm of Core 125-778A-2R. The upper 0.9 m of the breccia is composed of serpentine and exhibits extensive drilling disturbance; the remainder has a light reddish-brown matrix of sandy- to silt-sized serpentine, occasionally mottled by mixing with a light-gray and light-olive serpentine-chlorite rich marl. The admixture of detrital and serpentine material within this subunit may indicate either drilling disturbance or incorporation of sediment in a remobilized serpentine flow.

Unit I (Subunit IB 7.2–29.8 mbsf): This subunit is lower-middle Pleistocene to lower Pleistocene(?) and contains sandy marl and a collection of cobbles and pebbles, including serpentinite, vesicular volcanic rocks, and a foraminifer-bearing serpentine sandstone.

Unit II (29.8–107.6 mbsf): This entire unit is made up of phacoidal, sheared serpentine. Its matrix is composed of serpentine (50%–80%), opaque minerals (20%–5%), epidote-group minerals, some manganese-rich (thulite) (25%–0%), chlorite (15%–0%), talc (5%–0%), olivine (5%–0%), and albite and micrite (trace–0%). A variety of clasts are present: variably serpentinized tectonized harzburgite (80%); metabasalts (15%); and a variety of other fragments, including metagabbros, serpentinized dunites, and vein materials such as talc, carbonates, and quartz (5%).

The 1.5 m of silt-sized serpentine in Subunit IA has been interpreted as a serpentine flow, rather than a pelagic sediment because of the lack of pelagic or detrital components, the atypical color, and the absence of biological or sedimentological structures. The mottled interval below this layer may also be a flow, but contains both detrital and serpentine materials.

Dating has been based on the magnetostratigraphy and sparse biological components. In the interval from 0.5 to 1.5 mbsf, a reversed component of magnetization gives a minimum age of 0.73 Ma, the age of the last reversal. Biostratigraphic data indicate an early/middle Pleistocene age in Subunit IA at 7 mbsf and an early Pleistocene age in Subunit IB (approximately 1.7 Ma) at 29.5 mbsf. The youngest serpentine flows can thus be dated as Pleistocene. There has been little sediment accumulation since the youngest flow was deposited.

The ultramafic clasts in the cores are of two types: serpentinized, tectonized harzburgite (70%–90% serpentine and estimated protolith composition of 70%–85% olivine, 25%–15% orthopyroxene, with minor quantities of clinopyroxene [mainly as exsolution lamellae in orthopyroxene] and a chromium-rich spinel) and serpentinized dunite. There are several types of variably metamorphosed mafic clasts in the cores. These include metamorphosed volcanics that contain plagioclase-clinopyroxene and/or orthopyroxene phenocrysts or orthopyroxene-olivine-chromium spinel phenocrysts in a glassy groundmass. One metagabbro was observed. A few metabasalts show medium-grade metamorphism (one sample contains blue amphibole rimming green amphibole).

The serpentine flow sequence in lithologic Unit II exhibits a number of structural features, including deformation of primary orthopyroxene, microbrecciation, ductile shearing of clasts, shear zones on all scales (mm, cm and dm) and orientations, a variably developed foliation parallel to shear-plane orientations, and open-to-isoclinal folding of bedding and foliation planes. These features can be interpreted in terms of a combination of primary mantle tectonism, stresses related to intrusion and protrusion (flow emplacement) of the serpentinite diapir materials, and stresses resulting from post-protrusion remobilization.

Analyses of interstitial pore-water samples show a 10% decrease in chlorinity downhole (over 107 m). This observation is consistent with the low (relative to seawater) chlorine content of fluids seeping from chimneys at the summit of the seamount (collected with *Alvin*). These seep fluids are thought to have formed in part as a product of dehydration reactions within the subducting Pacific Plate. The decrease in chlorinity with depth in the hole is inter-

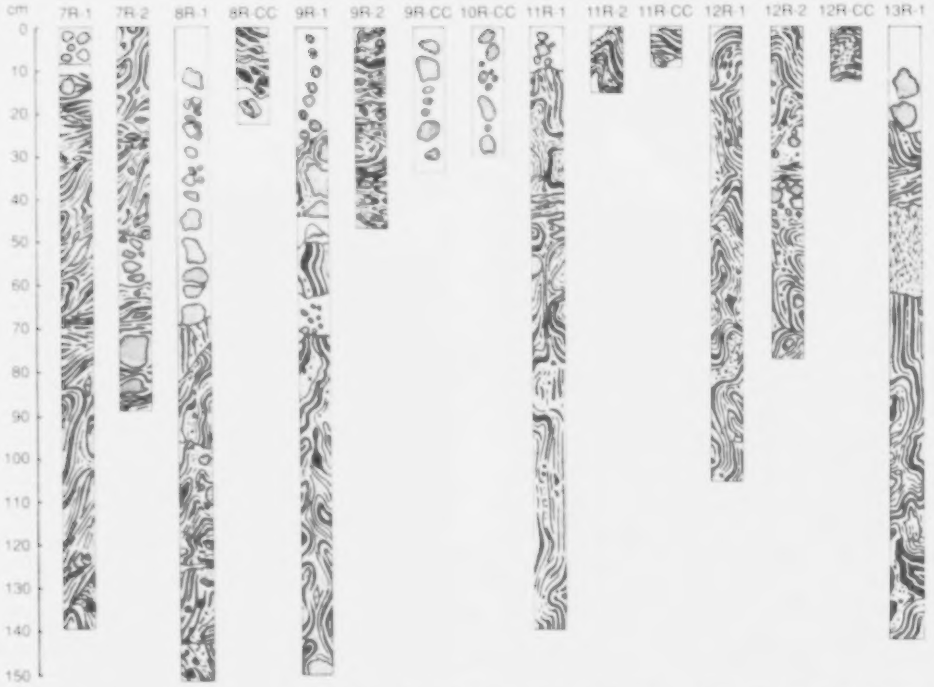

Figure 8. Structural features of Cores 125-778A-7R to 125-778A-13R showing the main outlines of the plastic deformation affecting the layered serpentine microbreccias.

preted as a relative decrease in admixture of seawater with similarly chlorine-poor fluids entrained in the serpentine flow material (a compaction effect?).

The principal results can be summarized as follows:

1. The confirmation that forearc seamounts can be constructed at least in part from serpentine flows emanating from a central diapir;

2. The evidence from clasts that low- to medium-grade metamorphism characterizes the source region of the serpentinite diapirs; and

3. The evidence from water chemistry that dehydration of the subducted lithosphere may have played an important role in the serpentinization of the source region of the serpentinite diapirs.

REFERENCES

Berggren, W. A., Kent, D. V., Flynn, J. J., and Van Couvering, J., 1985. Cenozoic geochronology. *Geol. Soc. Am. Bull.*, 96:1407–1418.

Fryer, P., Ambos, E. L., and Hussong, D. M., 1985. Origin and emplacement of Mariana forearc seamounts. *Geology*, 13:774–777.

Hussong, D. M., and Fryer, P., 1985. Forearc tectonics in the northern Marianas arc. *In* Nasu, N., Kobayashi, K., Uyeda, S., Kushiro, I., and Kagami, H. (Eds.), *Formation of Active Ocean Margins*: Tokyo (Terrapub), Adv. Earth Planet. Sci., 273–290.

Kennett, J. P., and Srinivasan, M. S., 1983. *Neogene Planktonic Foraminifera: A Phylogenetic Atlas*: Stroudsburg, PA (Hutchinson Ross).

Michael, P. J., and Bonatti, E., 1985. Petrology of ultramafic rocks from Sites 556, 558, and 560 in the North Atlantic. *In* Bougault, H., Cande, S. C., et al., *Init. Repts. DSDP*, 82: Washington, (U.S. Govt. Printing Office), 523–528.

Okada, H., and Bukry, D., 1980. Supplementary modification and introduction of code numbers to the low-latitude coccolith biostratigraphic zonation (Bukry, 1973; 1975). *Mar. Micropaleontol.*, 5:321–325.

Pearce, J. A., and Cann, J. R., 1973. Tectonic setting of basic volcanic rocks determined using trace element analysis. *Earth Planet. Sci. Lett.*, 19:290–300.

Pearce, J. A., and Wanming, D., 1988. The ophiolites of the Tibetan Geotraverse, Lhasa to Golmud (1985) and Lhasa to Kathmandu (1986). *Phil. Trans. R. Soc. London*, A327:215–238.

Ms 125A-106

NOTE: All core description forms ("barrel sheets") and core photographs have been printed on coated paper and bound as Section 4, near the back of the book, beginning on page —.

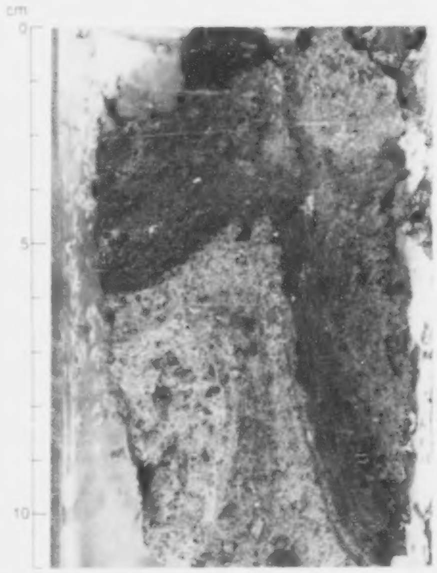

Figure 9. Sample 125-778A-11R-2, 1–11 cm. Fold affecting a layered serpentine microbreccia. Layering varies from horizontal to vertical.

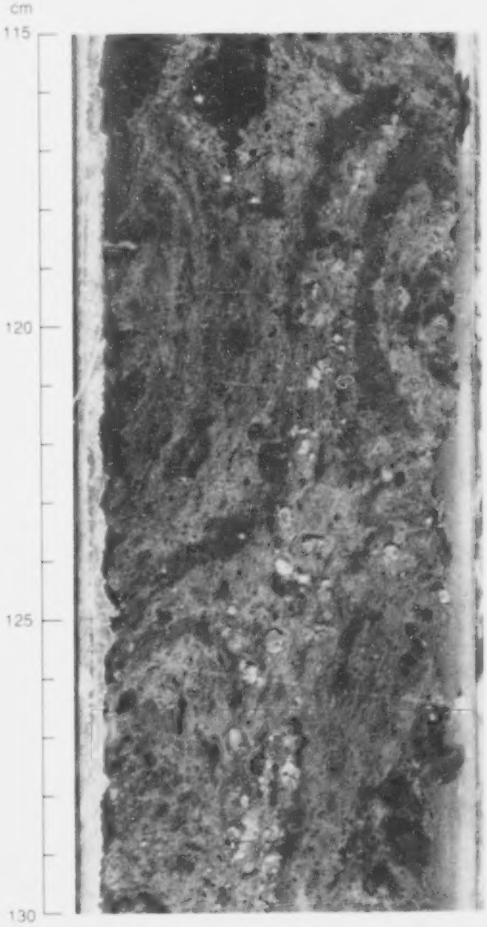

Figure 10. Sample 125-778A-6R-1, 115–130 cm. Folds affecting a layered serpentine microbreccia. In the split plane, the fold hinges are opposite, and the foliation in the central part of the core is vertical. These structures may be drilling disturbances.

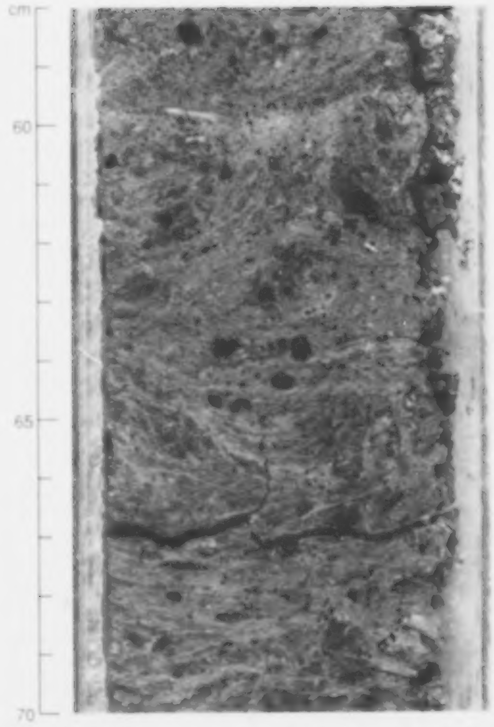

Figure 11. Sample 125-778A-6R-1, 58–70 cm. Foliated layered serpentine microbreccia. Anastomosing cleavage, almost horizontal, defines lenses of different scales. Foliation planes are curved around the coarsest clasts. Poorly consolidated clasts present typical asymmetrical shapes.

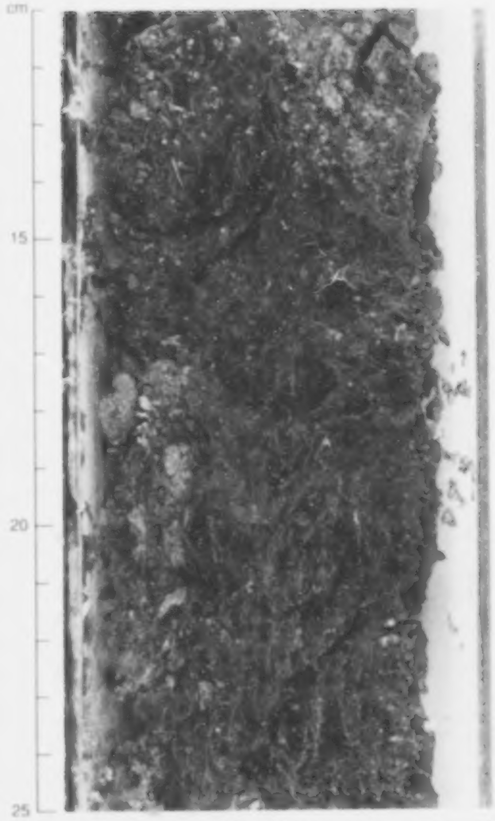

Figure 12. Sample 125-778A-11R-1, 11–25 cm. Sheared phacoidal serpentine. The phacoids are outlined by anastomosing cleavages. The general foliation is vertical.

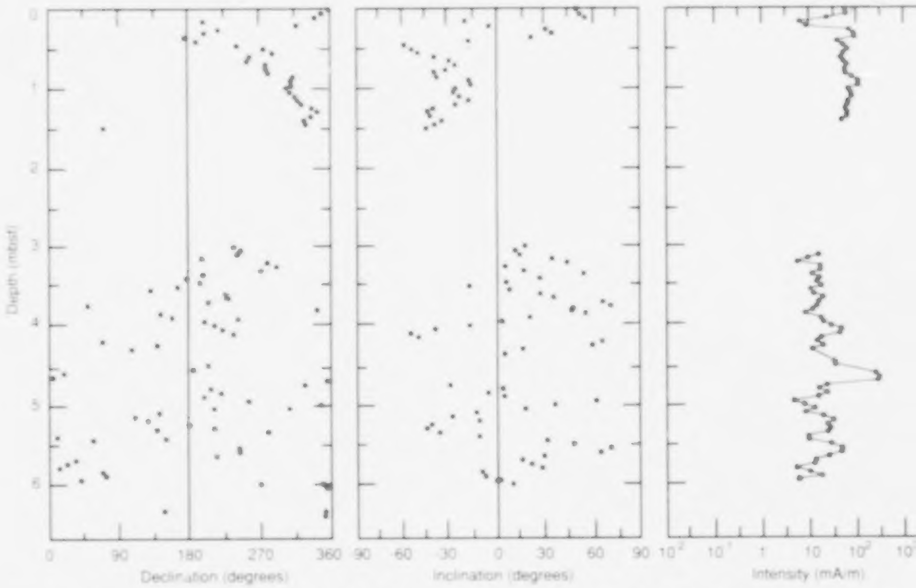

Figure 13. NRM measurement of Core 125-778A-1R. Interval 125-778A-1R-1, 50 to 150 cm (0.5–1.5 mbsf) exhibits a consistently n
inclination, indicating a reversed polarity.

Table 11. Index properties for Hole 778A.

Core, section, interval (cm)	Depth (mbsf)	Bulk density (g/cm^3)	Grain density (g/cm^3)	Porosity (%)	Water content (%)	Void ratio
125-778A-						
1R-4, 117–119	5.67	1.53	2.53	67.0	46.5	0.67
5R-1, 14–16	29.84	2.11	2.6	31.1	15.8	0.31
6R-1, 57–58	39.77	1.81	2.84	56.9	33.3	0.57
7R-1, 67–69	49.37	2.39	3.14	35.6	15.8	0.36
8R-1, 83–84	59.03	2.48	3.13	30.9	13.2	0.31
9R-2, 87–89	70.00	2.07	2.84	43.0	22.1	0.43
11R-1, 71–73	83.01	2.14	2.77	36.6	18.1	0.37
11R-1,106–108	83.36	2.44	3.07	30.6	13.3	0.31
12R-1, 76–78	90.56	2.47	2.99	26.3	11.3	0.26
13R-1, 81–83	99.11	2.70	3.91	42.1	16.3	0.42

Table 12. Physical properties for Hole 778A.

Core, section, interval (cm)	Depth (mbsf)	Thermal conductivity (W/mK)
125-778A-		
1R-1, 50	0.5	1.518
1R-3, 50	3.5	1.219
1R-5, 50	6.5	1.398
8R-1, 132	59.5	1.560
9R-1, 134	69.5	2.725
11R-1, 60	82.9	2.037
13R-1, 73	99.0	1.532

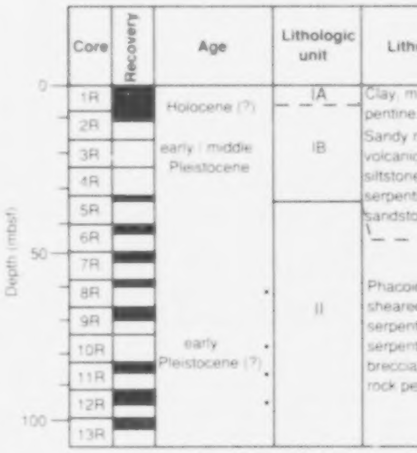
Core
Recovery
Age
Lithologic unit
Litho
Depth (mbsf)
0
50
100
1R
2R
3R
4R
5R
6R
7R
8R
9R
10R
11R
12R
13R
Holocene (?)
early / middle Pleistocene
early Pleistocene (?)
IA
IB
II
Clay, m
pentine
Sandy r
volcanic
siltstone
serpent
sandsto
Phacoid
sheared
serpent
serpent
breccia
rock pe

Figure 14. Core recovery and lithologic summary, Hole 7

Fryer, P., Pearce, J. A., Stokking, L. B., et al., 1990
Proceedings of the Ocean Drilling Program, Initial Reports, Vol. 125

7. SITE 779[1]

Shipboard Scientific Party[2]

HOLE 779A

Date occupied: 25 February 1989

Date departed: 7 days 3 hr 15 min

Position: 19°30.75′N, 146°41.75′E

Bottom felt (rig floor; m, drill-pipe measurement): 3957.9

Distance between rig floor and sea level (m): 10.7

Water depth (drill-pipe measurement from sea level, m): 3947.2

Total depth (rig floor, m): 4275.1

Penetration (m): 317.2

Number of cores: 37

Total length of cored section (m): 319.2

Total core recovered (m): 73.2

Core recovery (%): 22.9

Oldest sediment cored:
Depth (mbsf): 317.2
Nature: serpentine breccia
Earliest age: early Pliocene(?) to late Miocene(?)

Hard rock:
Nature: clasts(?) of serpentinized mafic and ultramafic rocks in a serpentine matrix

HOLE 779B

Date occupied: 28 February 1989

Date departed: 28 February 1989

Time on hole: 1 hr

Position: 19°30.75′N, 146°41.75′E

Bottom felt (rig floor; m, drill-pipe measurement): 3957.9

Distance between rig floor and sea level (m): 10.7

Water depth (drill-pipe measurement from sea level, m): 3947.2

Total depth (rig floor, m): 3966.9

Penetration (m): 9.0

Number of cores: 1

Total length of cored section (m): 9.0

Total core recovered (m): 8.7

Core recovery (%): 96.7

Oldest sediment cored:
Depth (mbsf): 8.7
Nature: silt-sized serpentine, serpentine silt, serpentine-rich silty sand
Earliest age: early Pleistocene

Principal results: Site 779 is situated about halfway up the southeast flank of Conical Seamount, approximately 3.5 km northeast of Site 778. Two holes were drilled: Hole 779A (which reached 317.2 mbsf) and Hole 779B (which was a single 9-m core aimed at recovering the uppermost sediment). Recovery at Hole 779A averaged 22.9%. As at Site 778, our principal aim was to penetrate serpentine flows on the flank of the seamount, to reach the underlying sediments, and if possible, basement in order to study the construction of the seamount, the origin and emplacement of the serpentine flows and serpentinites, and the nature and metamorphic history of forearc lithosphere. Three major lithostratigraphic units were recovered at Site 779:

1. Unit I (0–10.6 mbsf in Hole 779A and 0–9 mbsf in Hole 779B), comprising Holocene (?) to lower Pleistocene unconsolidated sediments and unconsolidated serpentine flows;
2. Unit II, comprising lower Pleistocene to lower Pliocene(?) or upper Miocene(?) sheared serpentine and subdivided into Subunit IIA (10.6–216.2 mbsf) and Subunit IIB (216.2–303.0 mbsf) on the basis of the absence and presence, respectively, of detrital serpentine sediments; and
3. Unit III (303.0–317.2 mbsf), comprising serpentine breccia with convolute layering.

The sheared serpentine is made up of clasts in a soft, serpentinized matrix. Clast lithologies are mostly of two types: (1) serpentinized, tectonized ultramafic rocks and (2) subordinate metabasic rocks. The ultramafic clasts are mostly harzburgite and subordinate dunite, with similar primary mineralogies to Hole 778A. The degree of serpentinization is variable, but shows an overall decrease downhole; serpentine veins are common and show a polystage filling history. Mafic clasts include both metabasalts and metagabbros, with primary mineralogies dominated by plagioclase and clinopyroxene in a glassy matrix (in basalts). Clay minerals, chlorite, pumpellyite, and, rarely, albite and sphene are the common metamorphic minerals. Structural studies show a complex history of deformation with no obvious relationship between the orientation of the clasts and matrix deformation. Gentle flowage under an applied load would explain the observed structures.

The serpentine-rich material in Subunit IIB contains recrystallized carbonate, kerogen(?), and filamentous aggregates of opaque minerals that may be bacterial remnants. The presence of kerogen indicates a primary sedimentary origin for this material, an interpretation supported by the presence of horizontal bedding within the same unit. Hydrocarbons increased dramatically with depth in Hole 779A, with methane, ethane, and propane present in most samples. A maximum of 30% methane was analyzed from one gas pocket sampled through the core liner. Analyses of interstitial pore-water samples at Site 779 show major variations from 0 to 100 mbsf in which pH increases to a maximum of 11.9, alkalinity increases five-fold, calcium decreases by 80%, both salinity and chlorinity decrease by 10%, and magnesium is totally depleted. These results confirm the presence of a fluid other than seawater, possibly from the subducting plate, as proposed for Site 778. The fluids differ sufficiently from those of Site 778 to indicate considerable lateral variation in interstitial water composition within the flank materials of the seamount.

BACKGROUND AND SCIENTIFIC OBJECTIVES

Site 779 is the second of a series of sites (Sites 778 through 780) on Conical Seamount, a roughly circular seamount having a basal diameter of about 20 km and a relief of

---

[1] Fryer, P., Pearce, J. A., Stokking, L. B., 1990. *Proc. ODP, Init. Repts.*, 125: College Station, TX (Ocean Drilling Program).

[2] Shipboard Scientific Party is as given in list of participants preceding the contents.

1500 m, which lies on the outer-arc high of the Mariana forearc at a distance of about 100 km from the trench axis (see "Introduction" chapter, this volume, and Fig. 1). The site was chosen to penetrate the flank of the seamount at about 4000 m in a region devoid of surficial serpentine flows (showing low backscatter on SeaMARC II side-scanning sonar imagery of the seamount) on the southeast flank of the seamount. Site 779 was located about 3.5 km to the east-northeast of the first site on the flank of the seamount. *Alvin* dives near this site suggested that the seamount in this area was mantled by a pelagic sediment cover, and in some places by a thin manganese pavement, overlying exposures of unconsolidated serpentine containing serpentinized clasts of mafic and ultramafic rocks (Fryer et al., 1985; Fryer et al., this volume). Fractures in the manganese pavement that mantles portions of the dive area showed that the region had experienced recent surficial deformation. SeaMARC II side-scanning sonar imagery (Hussong and Fryer, 1985) further suggested that the site is located within a region that has been deformed by local tectonism (Fig. 2). Small relief fractures (mainly concentric to the summit) and a series of long-wavelength (up to 1.5 km) concentric ridges can be seen on the lower flank of the seamount within the area chosen for the site.

The specific objectives of drilling this flank site differ from those of Site 778 only in logistical considerations; we hoped that a more stable hole could be obtained by drilling in a region of potentially thicker sediment cover on the southeast quadrant of the seamount. Thus, our scientific objectives were as follows:

1. To determine the internal stratigraphy and the history of extrusion and deformation of a forearc serpentinite seamount;
2. To investigate the mode of emplacement of serpentine flows;
3. To determine the nature, composition, and age of forearc lithosphere;
4. To study the chemical effects of serpentinization on the forearc lithosphere and its sedimentary cover; and
5. To examine the process of dewatering of subducted oceanic lithosphere at a nonaccretionary convergent plate margin.

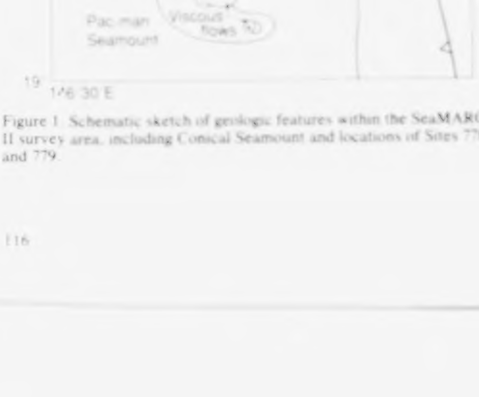

Figure 1. Schematic sketch of geologic features within the SeaMARC II survey area, including Conical Seamount and locations of Sites 778 and 779.

Because of the similarity in objectives between Sites 778 and 779, the same approach was adopted to achieve these objectives at the two sites (see "Background and Objectives" section, Site 778 chapter, this volume).

OPERATIONS

Site 779

Instead of offsetting and drilling another hole, it was proposed that we move around the flank of Conical Seamount to a location that appeared to contain less surface flow material. After obtaining official clearance, the drill string was pulled to 3479.3 m below sea level (bsl), and the ship was moved into the dynamic positioning mode (DP) 1.5 mi northeast to 19°30.75'N, 146°41.75'E. A beacon was dropped at 1400 hr UTC, 24 February, establishing Site 779.

Hole 779A

The drill string was lowered and Hole 779A was spudded at 1700UTC, 24 February. Water depth was established at 3947.2 m below sea level (bsl) by the first core. Hole problems began during the cutting of Core 125-779A-10R at 87.3 mbsf, after which a 20-bbl pill was pumped. Hole problems continued, and after Core 125-779A-11R, a short trip from 53 to 97 mbsf was made to improve the condition of the hole. After penetration to 170 mbsf, and after 51 hr of rotating time, the bit exhibited indications of failure. A free fall funnel (FFF) was dropped so that Hole 779A could be reentered after a round trip for a new bit.

The Colmec television camera was lowered in preparation for reentry. We found the FFF immediately, but owing to several rain squalls in the area, 1.5 hr was required for positioning the vessel before reentry, which we accomplished without incident. The television camera was retrieved and, after 3 hr of hole cleaning, the new bit was back at the previous total depth (TD).

Between taking Cores 125-779A-22R and 125-779A-23R (at a depth of 177.6 mbsf), the bottom of the hole caved in and 8 m of hole was lost. After 4 hr of reaming from 158 mbsf to bottom and pumping high-viscosity mud sweeps, coring resumed. The hole nevertheless required cleaning after each connection. Owing to the high risk to the drill string and logging tools, we did not consider it safe to log Hole 779A. However, we decided to continue coring the hole as long as possible, or until our time at the site expired.

The last 100 m of the hole provided few problems, and drilling continued to the end of our allotted site time. The RCB coring system was used to a TD of 317.2 mbsf, and we recovered 73.2 m of core in 37 deployments for a recovery rate of 23% (Table 1). Hole 779A and Site 779 ended at 1700UTC, 3 March, when the bit was back on deck and the vessel was under way.

Hole 779B

Before making the reentry into Hole 779A, a punch core of mud-line sediments was recovered that established Hole 779B at 2300UTC, 27 February. We retrieved the core barrel with 8.7 m of serpentine sediment for a recovery rate of 97% (Table 1).

LITHOSTRATIGRAPHY

Lithologic Summary

The stratigraphic section recovered at Site 779 has been divided into three lithologic units. Two subunits were assigned to lithologic Unit II, although this division may be artificial because of poor core recovery (having an average of only

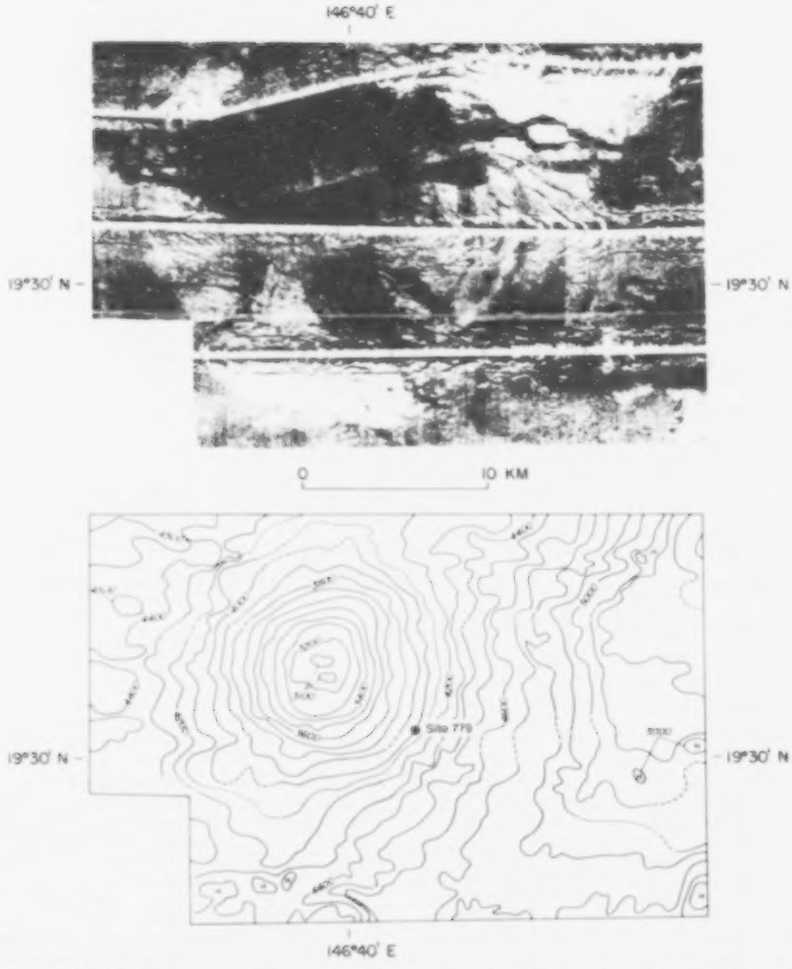

Figure 2. SeaMARC II side-scanning image of Conical Seamount (top), and SeaBeam bathymetric map of Conical Seamount showing Site 779 (bottom); bathymetry in meters.

23%, Table 1) and the possibility that unconsolidated matrix material and sediment were either washed away or created during the coring process. Lithologic Unit I consists of clay, silt-sized serpentine, and serpentine with clasts of serpentinized ultramafic rocks. Lithologic Subunit IIA is composed of blocks of serpentinized harzburgite and dunite, metabasalt, and serpentinite in a serpentine matrix. Lithologic Subunit IIB differs from lithologic Subunit IIA in that it has sediment intervals with distinct primary sedimentary and biologic structures. Lithologic Unit III is composed of serpentine microbreccia that has convolute layering. The units, their subbottom depths, lithologies, and biostratigraphic ages are summarized in Table 2.

Unit I

Hole 779A: Sections 125-779A-1R-1, 0 cm, to 125-779A-2R-5, 68 cm; depth, 0–10.6 mbsf.
Hole 779B: Sections 125-779B-1R-1, 0 cm, to 125-779B-1R-CC; depth, 0–9.0 mbsf.
Age: Holocene(?) to early Pleistocene.

This unit extends from the sediment/water interface to a total depth of 10.6 mbsf and primarily consists of serpentine clay and clayey silt-sized serpentine, with sand- to pebble-sized clasts of serpentinite and other lithic fragments. Of the strata recovered at this site, only Unit I contains sediment with well-preserved biogenic components. Some of the ser-

Table 1. Coring summary, Site 779.

Core no.	Date (1989)	Time (UTC)	Depth (mbsf)	Length cored (m)	Length recovered (m)	Recovery (%)
125-779A-1R	24 Feb.	1815	0–1.1	1.1	1.16	105.0
2R	24 Feb.	1935	1.1–10.6	9.5	6.70	70.5
3R	24 Feb.	2100	10.6–20.1	9.5	0.21	2.2
4R	25 Feb.	0015	20.1–29.6	9.5	0.50	5.3
5R	25 Feb.	0330	29.6–39.1	9.5	3.15	33.1
6R	25 Feb.	0540	39.1–48.5	9.4	0.44	4.7
7R	25 Feb.	0750	48.5–58.5	10.0	0.75	7.5
8R	25 Feb.	0955	58.5–68.1	9.6	0.75	7.8
9R	25 Feb.	1225	68.1–77.7	9.6	1.68	17.5
10R	25 Feb.	1510	77.7–87.3	9.6	1.88	19.6
11R	25 Feb.	1855	87.3–96.9	9.6	0.82	8.5
12R	26 Feb.	0045	96.9–106.6	9.7	0.62	6.4
13R	26 Feb.	0415	106.6–116.2	9.6	2.66	27.7
14R	26 Feb.	0700	116.2–125.9	9.7	2.67	27.5
15R	26 Feb.	0900	125.9–135.5	9.6	1.78	18.5
16R	26 Feb.	1250	135.5–145.2	9.7	2.53	26.1
17R	26 Feb.	1555	145.2–154.9	9.7	3.13	32.2
18R	26 Feb.	1905	154.9–159.4	4.5	3.08	68.4
19R	26 Feb.	2140	159.4–169.1	9.7	2.49	25.7
20R	27 Feb.	0045	169.1–170.1	1.0	0.77	77.0
21R	27 Feb.	0800	168.1–170.1	2.0	1.37	68.5
22R	28 Feb.	1150	170.1–177.6	7.5	3.15	42.0
23R	28 Feb.	1840	177.6–187.2	9.6	1.35	14.0
24R	1 March	0010	187.2–196.8	9.6	0.68	7.1
25R	1 March	0330	196.8–206.5	9.7	1.30	13.4
26R	1 March	0700	206.5–216.2	9.7	2.98	30.7
27R	1 March	0955	216.2–225.8	9.6	0.41	4.3
28R	1 March	1325	225.8–235.5	9.7	2.93	30.2
29R	1 March	1710	235.5–245.0	9.5	2.00	21.0
30R	1 March	2245	245.0–254.7	9.7	3.04	31.3
31R	2 March	0345	254.7–264.4	9.7	3.34	34.4
32R	2 March	0820	264.4–274.0	9.6	3.30	34.4
33R	2 March	1240	274.0–283.7	9.7	1.80	18.5
34R	2 March	1820	283.7–293.3	9.6	1.26	13.1
35R	2 March	200	293.3–303.0	9.7	1.34	13.8
36R	3 March	0245	303.0–312.7	9.7	3.43	35.3
37R	3 March	0610	312.7–317.2	4.5	1.79	39.8
Coring totals				319.2	73.24	22.9
125-779B-1R	27 Feb.	2345	0.0–9.0	9.0	8.70	96.6
	Coring Totals			9.0	8.70	96.6

pentine intervals within this unit lack biogenic and detrital components, but are underlain by sediment containing microfossils that indicate an early Pleistocene age, providing a maximum age for deposition of serpentine (see "Biostratigraphy" and "Paleomagnetism" sections, this chapter). On the basis of similar lithologies and biostratigraphic criteria, this unit correlates with Unit I at Site 778.

Brown (10YR 4/6 and 10YR 3/6) serpentine clay in the first core (Core 125-779A-1R) from Hole 779A is radiolarian-, nannofossil-, and foraminifer-bearing. The top of this core is 45 cm thick, soupy to moderately deformed, and artificially injected at Interval 125-779A-1R-1, 22 to 27 cm, with underlying light yellow (2.5Y 8/4) clayey silt-sized serpentine resulting from deformation. The brown serpentine clay contains clay minerals (40%), serpentine (32%), chlorite (5%), opaque minerals (3%), foraminifers (10%), nannofossils (5%), radiolarians (5%), and trace amounts of amphibole, lithic fragments, diatoms, and sponge spicules. The detrital material in the only core recovered from Hole 779B (100 m east of Hole 779A; see "Operations" section, this chapter) is a dark brown (10YR 3/3) serpentine silt and silty sand with trace amounts of radiolarians, silicoflagellates, nannofossils, and foraminifers. In Core 125-779B-1R, yellow to brownish-yellow (10YR 7/6 to 6/6), silt-sized serpentine is interlayered with soupy and moderately deformed dark-brown serpentine silt. The yellow silt-sized serpentine, found in the first cores from both Holes 779A and 779B, is stiff, very deformed, and lacks biogenic components. This silt-sized serpentine contains authigenic aragonite needles. The composition ranges from 60% to 75% serpentine, 7% to 20% opaque minerals, 0% to 15% aragonite, 5% to 10% zoisite, 0% to 5% clay minerals, 0% to a trace of chlorite, and 0% to a trace of garnet.

Core 125-779A-2R is composed of soupy to moderately deformed, aragonite-rich, sandy, silt-sized multicolored serpentine. In Section 125-779A-2R-1 at 56 to 77 cm, this sandy silt-sized serpentine is gray to very dark gray (2.5YR 5/0 to 3/0) with 70% serpentine, 20% aragonite, 5% opaque minerals, and 5% chlorite. The upper contact with the overlying yellow silt-sized serpentine found in the overlying core (125-779A-1R) was not recovered; there is a void in the core liner from 0 to 56 cm in Section 125-779A-2R-1. The lower contact of the gray sandy silt-sized serpentine is abrupt against a pale brown (10YR 7/4) serpentine with mottling of reddish-yellow (5YR 6/8) and light gray (7.5YR 7/0), sandy, silt-sized serpentine. This mottled lithology extends to the base of the unit. In composition, the light gray serpentine does not differ significantly from underlying mottled serpentine (62% to 75% serpentine, 15% to 20% aragonite, 5% to 10% opaque minerals, trace to 5% amphibole, and 0% to 5% zoisite and chlorite). Scattered black (7.5YR 2/0) and reddish-yellow (5YR 6/8) granule- to pebble-sized clasts of serpentinite or serpentinized ultramafic rocks are found throughout the serpentine of this unit.

Table 2. Lithologic units recovered at Site 779.

Lithologic unit/subunit	Cores	Depth (mbsf)	Dominant lithology	Stratigraphic age
I	125-779A-1R-1, 0 cm to 125-779A-2R-5, 68 cm, 125-779B-1R-1, 0 cm to 125-779B-1R-CC	0.0 to 10.6 0.0 to 9.0	Clay; silt-sized serpentine; lithic fragments in a matrix of sand- and silt-sized serpentine	Holocene(?) to lower Pleistocene
IIA	125-779A-3R-CC to 125-779A-26R-3, 150 cm	10.6 to 216.2	Blocks of serpentinized harzburgite and dunite, metabasalt, and serpentinite in a serpentine matrix	lower Pleistocene(?) to
IIB	125-779A-27R-1, 0 cm to 125-779A-35R-1, 133 cm	216.2 to 303.0	Blocks of gabbro, serpentinized harzburgite and dunite, and metabasalt, in a serpentine matrix with intercalations of detrital, fine-grained serpentine sediments	lower Pliocene(?)/ upper Miocene(?)
III	125-779A-36R-1, 0 cm to 125-779A-37R-CC	303.0 to 317.2	Serpentine breccia with convolute layering	(?)

Gray, sandy, silt-sized serpentine has been interpreted as a serpentine flow that extruded onto the seafloor under cool hydrothermal conditions because (1) the color is atypical of pelagic sediments in this area; (2) pelagic or detrital components are lacking; and (3) biological and sedimentological structures are absent. The gray color of the sandy, silt-sized serpentine may be the result of insufficient exposure to oxidizing conditions. In contrast, the yellowish-brown, pale brown, and reddish-brown of the overlying silt-sized serpentine suggest oxidation during prolonged exposure on the seafloor. On the basis of the second and third criteria, the yellowish-brown and pale brown silt sized serpentines were also interpreted to represent serpentine flows. The reddish-brown and gray mottling in the pale brown silt-sized serpentine may represent mixing of previously oxidized and non-oxidized material (respectively) entrained during the extrusion. Alternatively, the mottling may be the result of drilling disturbance that mixed several layers of different oxidation states.

The yellowish-brown silt-sized serpentine from Core 125-779A-1R was deposited during or after the late middle Pleistocene, because it overlies sediment with nannofossils of this age from the core catcher (see "Biostratigraphy" section, this chapter). Sandy silt- and silt-sized serpentines from Cores 125-779B-1R, and 125-779A-2R were deposited during or after the early Pleistocene on the basis of nannofossils found in Sections 125-779B-1R-CC and 125-779A-2R-5.

Abundant aragonite in these serpentine flows is unusual in waters this deep on the forearc (Haggerty, 1987c). Seawater below a few hundred meters in the present-day Pacific is undersaturated with respect to aragonite (Li et al., 1969; Berner and Honjo, 1981), and the aragonite compensation depth is less than 1000 mbsl in the Pacific, usually as shallow as 400 mbsl (Berger, 1970). The delicate, acicular aragonite crystals (up to 3 mm long and 0.5 mm wide) in the clay and serpentine imply authigenic growth after the serpentine was emplaced. The aragonite needles are not detrital; these needles would have been broken by flow or by transport as detrital particles.

Unit II

Sections 125-779A-3R-CC to 125-779A-35R-1, 133 cm; depth, 10.6–303.0 mbsf.
Age: early Pleistocene(?) to early Pliocene(?)/late Miocene(?).

Lithologic Unit II contains clasts of various igneous and metamorphic rock types (see "Igneous and Metamorphic Petrology" section, this chapter) in a serpentine matrix. This matrix is bluish-gray (5B 5/1) to light gray (N7) downhole to Core 125-779A-11R, with transitions to pale green (5G 6/2) and dark green (5G 3/2). The matrix is clayey silt-sized serpentine composed of 73% to 90% serpentine, 5% to 10% amphibole, 5% to 10% opaque minerals, 0% to 15% zoisite, 0% to 25% thulite, 0% to 5% chlorite, with trace amounts of garnet, epidote, plagioclase, and olivine. The unit is divided into two subunits because sedimentary strata having primary sedimentary structures are intercalated in the lower portion of the unit. The division of the subunits may be artificial because of poor core recovery and the probability that unconsolidated matrix material and sediment were washed away during the coring process.

Subunit IIA: Sections 125-779A-3R-CC to 125-779A-26R-3, 150 cm; depth, 10.6–216.2 mbsf.

The matrix of Subunit IIA is typically highly deformed by drilling, although in some cases primary structural features can be observed. In Cores 125-779A-7R, 125-779A-9R, and 125-779A-10R, the matrix appears to be sheared; in Cores 125-779A-13R, 125-779A-15R, and 125-779A-18R, the matrix has a phacoidal, sheared texture (see "Structural Studies" section, this chapter, for further description and discussion).

Subunit IIB: Sections 125-779A-27R-1, 0 cm, to 125-779A-35R-1, 133 cm; depth, 216.2–303.0 mbsf.

Smear-slide analysis of the sedimentary strata in Cores 125-779A-27R, 125-779A-28R, and 125-779A-32R of Subunit IIB revealed trace amounts of carbonate grains and kerogen(?), and up to 10% filamentous opaque mineral aggregates (tentatively interpreted as remnants of filamentous bacteria). Kerogen is usually interpreted as a detrital particle because it typically is insoluble and does not migrate through the sediment. If kerogen is present in this subunit, then it indicates a primary sedimentary origin, rather than a tectonic or igneous origin, for the subunit.

Faint horizontal bedding and sedimentary structures were also observed in the sediments of Subunit IIB, suggesting a primary sedimentary origin. Clay layers containing filamentous opaque mineral aggregates are horizontal; these separate layers display deformation structures in the serpentine matrix among the blocks of igneous and metamorphic lithologies. These clay layers may represent periods of exposure on the seafloor or hiatuses between episodes of deformation. If the filamentous opaque mineral aggregates represent bacteria that grew at or near the sediment/water interface, then these horizontal beds separate different events of serpentine deposition.

Sparse nannofossils of late Miocene/early Pliocene age were deposited with reworked Oligocene nannofossils in the strata from Core 125-779A-27R (Sample 125-779A-27R-1, 60 cm; see "Biostratigraphy" section, this chapter). The presence of the fossils also confirms the sedimentary origin of the strata in Core 1225-779A-27R. No additional microfossils were found in Unit II. The base of Unit II thus has been interpreted as having been deposited during or prior to the early Pliocene. An early Pleistocene age, determined from sediments in the core-catcher sample of Core 125-779A-2R, limits the youngest time of deposition of Unit II.

Unit III

Sections 125-779A-36R-1, 0 cm, to 125-779A-37R-CC; depth, 303.0–317.2 mbsf.

Unit III is composed of serpentine microbreccia having convolute structures. A description and discussion of the breccia clast lithologies are given in the "Igneous and Metamorphic Petrology" section (this chapter). The light greenish-gray to dark greenish-gray (5G 5/2 to 5G 8/2) matrix of the breccia is composed of serpentine (70%–90%), opaque minerals (4%–10%), chlorite (0%–20%), zoisite (0%–14%), amphibole (0%–5%), micrite (trace to 5%), and 0% to trace amounts of garnet, dolomite, and organic debris. These convolute structures strongly resemble deformation structures produced by tectonic or gravitational flow processes (for further discussion see "Structural Studies" section, this chapter). In Section 125-779A-36R-3, there is a dusky red (5R 3/3) iron oxide staining the matrix and coating pebbles, similar to that observed in the matrix at the base of Subunit IIB at Site 778.

X-Ray Diffraction Analysis

XRD analyses were performed on the less than 4-mm fraction of five selected samples from Site 779 (Table 3). Although we expected to find smectite, none was observed. The sample nearest the sediment surface contained traces of an expandable chlorite. No other expandable clays were observed.

Table 3. X-ray diffraction analyses for selected samples from Site 779.

Sample	Serpentines		Talc	Fayalite
	Chrysotile	Antigorite		
125-779A-2R-3, 39 cm	***	***		
2R-3, 88 cm	***	***	*	
2R-4, 38 cm	***	***	*	
19R-1, 40 cm	***			(*)
125-779B-1R-4, 98 cm	***	***	*	

*** = Major components; * = Minor components.

The less than 4-mm fraction of the clayey silt-sized serpentine is composed entirely of serpentine, probably at least two phases (chrysotile and antigorite). Minor amounts of talc are present in some samples.

BIOSTRATIGRAPHY

Evidence from calcareous nannofossils and planktonic foraminifers indicates that the sedimentary interval overlying the serpentine in Holes 779A and 779B ranges in age from early to middle Pleistocene. A sediment interval in Core 125-779A-27R was dated as early Miocene(?) to late Pliocene(?) on the basis of calcareous nannofossils.

Calcareous Nannofossils

Hole 779A

A moderately preserved, but rare, Pleistocene nannofossil assemblage is present in Samples 125-779A-1R-CC, 125-779A-2R-3, 70 cm, and 125-779A-2R-5, 53 cm. In Sample 125-779A-1R-CC, the nannofossil assemblage is characterized by *Gephyrocapsa oceanica*, *Ceratolithus telesmus*, *C. simplex*, and by the absence of *Emiliania huxleyi*. This assemblage is late middle Pleistocene (CN14b) in age, based on the Okada and Bukry (1980) zonation. Sample 125-779A-2R-3, 70 cm, contained *Pseudoemiliania lacunosa*, *Gephyrocapsa oceanica* and *G. caribbeanica*. Thus, the age could be defined as early to middle Pleistocene (Subzone CN14a). In Sample 125-779A-2R-5, 53 cm, the last occurrence of *Calcidiscus macintyrei*, together with *Pseudoemiliania lacunosa* and *Gephyrocapsa oceanica*, was noted. The highest occurrence of *Calcidiscus macintyrei* is at the base of CN14a; thus, the assemblage was assigned to the early Pleistocene.

Sample 125-779A-27R-1, 60 cm, contains a sparse assemblage. We assume that it is late Miocene/early Pliocene in age, based on the occurrence of *Cricolithus jonesi*, *Reticulofenestra pseudoumbilica*, and *Discoaster variabilis*. Reworked *Dictyococcites bisectus*, *Cyclicargolithus floridanus*, and *C. bisectus* (all latest Oligocene) also are present.

Hole 779B

Moderately to well-preserved, rare-to-few Pleistocene nannofossil assemblages are present in Samples 125-779B-1R-1, 89–91 cm; 125-779B-1R-6, 91–92 cm; and 125-779B-1R-CC. In Sample 125-779B-1R-1, 89–91 cm, the assemblage is characterized by *Pseudoemiliania lacunosa*, *Helicosphaera sellii*, *Gephyrocapsa oceanica*, and *Ceratolithus cristatus*; it is early Pleistocene in age (CN14a) on the basis of Okada and Bukry's (1980) zonation. Sample 125-779B-1R-6, 91–92 cm, shows a comparable association and thereby age. In Sample 125-779B-1R-CC, the last occurrence of *Calcidiscus macintyrei* was found together with the assemblage above, which dates this sample as early Pleistocene (CN14a).

Foraminifers

A sparse, poorly preserved, Quaternary planktonic foraminiferal assemblage was recovered from Sample 125-779A-1R-CC. This sample contained rare specimens of fragmented *Globorotalia (M.) menardii*.

The Pleistocene age (Zone N22) was determined by the sinistral coiling of *G. menardii*, a characteristic of post-Pliocene/Pleistocene boundary forms. Older forms exhibit dominantly dextral coiling. Sample 125-779B-1R-CC was barren.

Diatoms

Moderately preserved diatoms, mainly fragments of the extremely large diatom *Ethmodiscus rex*, were noted in Samples 125-779A-1R-1, at 5, 10, 15, and 20 cm; 125-779A-1R-CC; and 125-779B-1R-CC. Fragments of *E. rex* were common constituents of the diatom assemblage, together with rare *Nitzschia marina* and *Thalassiothrix longissima*. Sample 125-779A-2R-CC was barren of siliceous microfossils. Age-diagnostic taxa (Barron, 1985) were not observed.

IGNEOUS AND METAMORPHIC PETROLOGY

The clasts recovered in this hole comprise about 95% variably serpentinized and tectonized ultramafic and about 5% metamorphosed mafic rocks. Of the ultramafic rocks, about 80% are harzburgite and 20% are dunite. About 60% of the mafic rocks are metabasalts, and the rest are metamicrogabbros. Cores contain maximum continuous recovery of rock through intervals of up to about 150 cm long, enclosed in a sheared and deformed serpentinite matrix that is described in the "Structural Studies" section (this chapter). Contact relationships between the ultramafic and mafic rocks are ambiguous. In some of the mafic units, chilling and/or shearing and annealing along the contacts may have taken place. The intensity of serpentinization appears to decrease downhole.

Ultramafic Rocks

Serpentinized and Tectonized Harzburgites

The harzburgites are massive and vary from light to dark gray (where relatively fresh) to dark gray-green (where serpentinized). The primary mineralogy of these rocks is olivine, orthopyroxene, chromium-spinel, and subordinate clinopyroxene. The modal abundance of orthopyroxene varies from about 10% to 40%, with olivine forming most of the remainder. Clinopyroxene (1–3 modal%) is present as ubiquitous exsolution lamellae in orthopyroxene and as <1-mm blebs and anhedral crystals, typically closely related to orthopyroxene. Chromium-spinel exists in trace amounts to about 2 modal% and contains rare, brightly reflective grains that may be a sulfide mineral or a metallic alloy (rich in platinum-group elements).

The harzburgites have experienced penetrative deformation. Typically, orthopyroxene crystal morphologies range from equant to raggedly elongate; the cleavage surfaces and extinction are wavy; kink-banding is common; and fine clinopyroxene exsolution lamellae are bent. Elongate crystals (<15 mm long) and intracrystalline glide planes characterize some olivine morphologies, but microgranular and granuloblastic (1-mm equant crystals) fabrics, indicative of relatively high-temperature shear, also are present. Chromium-spinel crystals range from equant (<0.2 mm in size) to disrupted dumbbell-type shapes; locally, "trains" or "stringers" of these elongate spinels define a crude lineation parallel to elongate olivine and orthopyroxene. In the orthopyroxene-rich types, rounded olivines sometimes are included in orthopyroxene.

The degree of serpentinization is extremely variable. In some samples, most of the olivine and orthopyroxene has been replaced by mesh-textured serpentine (antigorite-rich) and relict bastite, respectively. In these strongly serpentinized types, all of the chromium-spinel (translucent in shades of deep reddish-brown/green) has been replaced by an opaque oxide mineral, probably magnetite. In some samples, this transformation process is incomplete. These partially altered spinels have original chromium-rich translucent cores, rims of magnetite, and radially arranged halos of microcrystalline chlorite (probably penninite). This type of alteration has also penetrated cracks in the original spinel grains.

Numerous veins of serpentine (up to about 40 mm wide) cut the harzburgites; many of these veins recorded a polystage history of filling. The degree of serpentinization of the harzburgite may be enhanced by the proximity to veins, and many of the breaks in the core may have taken place along veins. The largest veins generally dip at about 60° to 80°, but other conjugate and anastomosing sets with variable dip also are present. Antigorite or lizardite fills most of these veins. Some veins contain chrysotile that has grown both parallel to the original fracture walls and as discontinuous, crosscutting subsets (e.g., Section 125-779A-26R-2; Fig. 3). Subordinate brucite also is present. Shearing dislocated spinel trains in a few samples during the formation of serpentine veins. In some samples, orthopyroxene adjacent to veins has been altered to chlorite. Typically, serpentinization affected olivine the most, orthopyroxene less, and clinopyroxene the least. However, in several samples, serpentinization may have affected orthopyroxene more than olivine.

Serpentinized and Tectonized Dunites

These rocks range from deep greenish-black to black, are generally massive, and sometimes grade to harzburgite over distances of a few millimeters. Possibly, this modal change reflects original cumulus layering. The primary mineralogy consists of 90% to 99% olivine, 1% to 9% orthopyroxene, and up to 1% spinel. Most dunites have been serpentinized extensively, exhibiting mesh texture development and splays of antigorite, and are cut by numerous serpentine-rich veins. Some pieces contain crudely aligned, elongate (<15 mm), and irregularly shaped olivine that tends to form a sheared fabric. Microgranulation of olivine, intracrystalline glide planes (olivine), kink-banding (relict bastite), and elongation of spinel all provide evidence of penetrative tectonism. Deformation of exsolution lamellae of clinopyroxene in orthopyroxene is further evidence of strain in these rocks.

Although a higher proportion of primary orthopyroxene than olivine survived serpentinization, an unusually large amount of relict fresh olivine persists in a few samples, despite transformation of almost all of the orthopyroxene to serpentine. Spinel is completely altered to magnetite in the serpentinized portions. Other secondary minerals include chlorite and brucite.

Metabasalt and Metamicrogabbro

These rock types occur primarily as isolated clasts, but also form more continuous, individual core pieces reaching lengths of about 10 to 20 cm. The intact upper contact of approximately 3 m of mafic-microgabbroic material with serpentinized ultramafic rocks is present in Core 125-779A-31R. These mafic rocks range from greenish-white to dark green; in general, they are aphyric to microphyric and have an original primary mineralogy that consists of subequal proportions of plagioclase and augite. Relict subophitic texture has been preserved in one clast in Core 125-779A-9R. Originally, considerable amounts of glass were present in some of these types (30%–40%), although extensive replacement by chlorite and/or clay minerals has subsequently taken place.

Several samples are brecciated and veined by carbonate and chlorite. Prehnite is also present in "bow-tie" form (with wavy extinction as a vein-filling phase) together with pumpellyite. Pumpellyite is a constituent of the altered matrix in some samples. Sphene and albite also are scattered as metamorphic alteration products. Several zones of in-

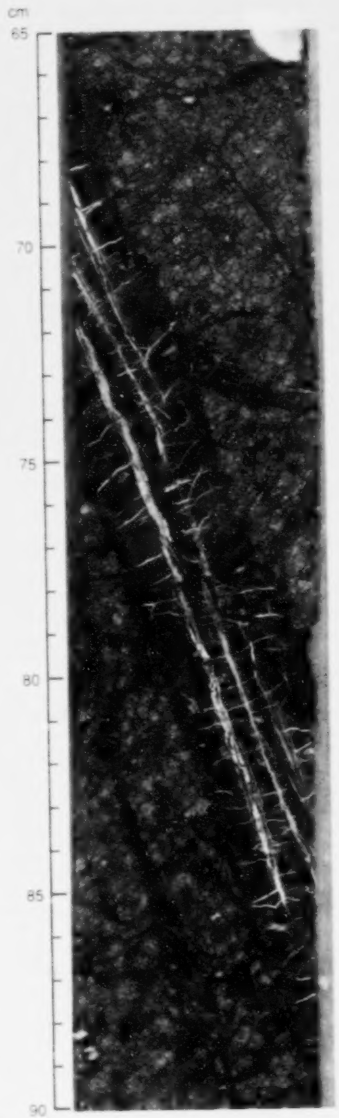

Figure 3. Interval 125-779A-26R-2, 65–90 cm, with a polyphase serpentine vein dipping at 75°, cutting tectonized, serpentinized harzburgite. The white phase is mostly chrysotile.

tense shearing traverse the mafic unit, as illustrated in the "Structural Studies" section (this chapter), and perhaps the contacts of this rock with the surrounding materials have also been sheared. A clear gradation in crystal size is present within this unit from microcrystalline at the margins to 1- to 2-mm relict subophitic in the center, and the unit may represent a sill or dike.

IGNEOUS AND METAMORPHIC GEOCHEMISTRY

Geochemical analyses of clasts entrained within the serpentinite diapir at Site 779 were performed for 32 samples of serpentinized, tectonized ultramafic rocks, for both harzburgites (21 samples) and dunites (11 samples), and for five samples of metamorphosed mafic rocks. The mafic samples range from originally glassy to moderately crystalline (diabase). The diabase comprises a 300-cm-thick zone bounded by glassy margins and is apparently of intrusive origin. Rock descriptions are presented in the "Igneous and Metamorphic Petrology" section (this chapter). Preparation and analytical techniques are given in the "Explanatory Notes" (this volume). The geochemical data are given in Tables 4 through 7.

Ultramafic Samples

Modal estimates of the original (pre-serpentinization) composition of ultramafic samples range from 10% to 25% orthopyroxene and 75% to 85% olivine in the harzburgite samples, and from 1% to 10% orthopyroxene and 90% to 99% olivine in the dunite samples. Both rock types contain 1% clinopyroxene and spinel. All samples are variably serpentinized (25%–100%) and frequently tectonized. All ultramafic samples are remarkably homogeneous chemically (Tables 4 and 5) and standard deviations are small.

Major-Element Chemistry

Loss on ignition (LOI) of these samples ranges from 4.77 to 17.41 and exhibits positive correlation with percentage of serpentinization (Fig. 4). These values also correlate with bulk rock density. (See "Physical Properties" section, this chapter, for details; see "Igneous and Metamorphic Geochemistry" section, Site 778 chapter, and "Explanatory Notes," this volume, for an explanation of LOI.) Although ranges of concentrations of major elements are similar in dunite and harzburgite samples (Table 4), some small distinctions exist. SiO_2 ranges from 29.39 to 40.80 wt% in both harzburgite and dunite samples, and MgO is slightly higher in the dunite samples (38.94 to 43.43 wt%) than in the harzburgite samples (37.34 to 42.69 wt%). Al_2O_3 is slightly lower in the dunites (0.07 to 0.60 wt%) than the harzburgites (0.21 to 0.88 wt%); Fe_2O_3 is also lower in the dunites (5.66 to 8.05 wt%) than in the harzburgites (7.00 to 9.04 wt%). Magnesium number (Mg# = Mg/(Mg + Fe) × 100) is high in all rocks, ranging from 89.84 to 93.65. Na_2O and P_2O_5 are uniformly 0.0 wt%, and K_2O ranges from 0 to 0.3 wt% with one exception: Sample 125-779A-24-1, 36–38 cm, a dunite that contains 4.00 wt% K_2O and high strontium contents. In all rocks, SiO_2 and MgO are inversely correlated with LOI and percentage of serpentinization (Figs. 4A, 4B, and 4C; Table 4). The correlations with LOI are not necessarily significant, however, because of the effect of autocorrelation, whereby the sum of oxides is constrained to about 100%.

Trace-Element Data

Trace-element data are presented in Table 5. Compatible elements are predictably high in both the dunite and harzburgite samples: chromium ranges from 1216 to 2917 ppm, and nickel from 2171 to 2541 ppm, with the exception of a single

Table 4. Tabulated major-element data for serpentinized, ultramafic rocks from Site 779.

	Dunites												Harzburgites			
Hole:	779A	779A	779A	779A	779A	779A	779A	779A	779A	779A	779A		779A	779A	779A	779A
Core:	3R-CC	8R-1	10R-1	14R-1	14R-2	15R-2	16R-1	19R-2	22R-2	24R-1	25R-1	Dunite	4R-1	5R-2	5R-2	6R-1
Interval (cm):	13–15	90–93	40–43	74–77	21–24	24–27	19–23	97–99	18–20	36–38	85–87	Average	27–30	34–37	40–43	18–20
SiO_2	36.74	39.47	38.14	38.30	35.25	35.54	40.80	39.21	39.47	34.50	34.44	37.30	33.64	36.46	35.12	37.57
TiO_2	0.00	0.00	0.00	0.00	0.00	0.00	0.08	0.00	0.00	0.00	0.00	0.00	0.00	0.00	0.00	0.00
Al_2O_3	0.39	0.28	0.63	0.38	0.07	0.07	0.60	0.19	0.4	0.46	0.12	0.30	0.20	0.21	0.21	0.77
Fe_2O_3	7.38	7.63	8.08	7.33	7.14	5.66	8.05	8.15	7.36	7.31	7.02	7.40	7.04	7.71	7.23	7.72
MnO	0.10	0.11	0.12	0.10	0.09	0.08	0.10	0.12	0.10	0.11	0.09	0.10	0.14	0.09	0.10	0.11
MgO	40.31	41.21	41.19	41.71	41.35	42.14	43.43	44.36	40.95	38.94	43.40	41.70	40.13	40.18	39.87	39.61
CaO	0.14	0.15	0.60	0.44	0.10	0.21	0.54	0.25	0.15	0.37	0.20	0.30	0.07	0.22	0.08	0.55
Na_2O	0.00	0.00	0.00	0.00	0.00	0.00	0.00	0.00	0.00	0.00	0.00	0.00	0.00	0.00	0.00	0.30
K_2O	0.02	0.00	0.00	0.01	0.00	0.02	0.01	0.00	0.00	4.00	0.00	0.40	0.00	0.02	0.00	0.01
P_2O_5	0.00	0.00	0.00	0.00	0.00	0.00	0.00	0.00	0.00	0.00	0.00	0.00	0.00	0.00	0.00	0.00
NiO	0.28	0.28	0.30	0.31	0.30	0.45	0.32	0.32	0.27	0.29	0.34	0.32	0.31	0.29	0.28	0.28
Cr_2O_3	0.42	0.39	0.41	0.35	0.21	0.19	0.33	0.22	0.30	0.25	0.32	0.31	0.24	0.19	0.24	0.26
LOI	14.18	9.55	9.28	9.08	14.64	16.71	4.77	6.22	9.26	16.27	12.77	11.20	16.66	14.62	16.35	12.42
Total	99.27	98.39	98.06	97.27	98.64	98.42	98.31	98.50	97.74	101.97	98.05	98.60	96.54	98.83	98.95	98.75
Mg#	91.54	91.45	90.99	91.85	91.98	93.65	91.45	91.51	91.68	91.35	92.45	91.78	91.16	91.88	91.62	91.04
% SERP	80	78	55	70	85	85	17	35	85	93	85	69.8	100	40	93	78

Data (in wt% oxides) are from whole-rock analyses by XRF. LOI is loss on ignition between 150° and 1030°C; % SERP = percentage of serpentinization estimated from thin sections.

Table 5. Tabulated trace-element data for serpentinized, ultramafic rocks from Site 779.

	Dunites												Harzburgites			
Hole:	779A	779A	779A	779A	779A	779A	779A	779A	779A	779A	779A		779A	779A	779A	779A
Core:	3R-CC	8R-1	10R-1	14R-1	14R-2	15R-2	16R-1	19R-2	22R-2	24R-1	25R-1	Dunite	4R-1	5R-2	5R-2	6R-1
Interval (cm):	13–15	90–93	40–43	74–77	21–24	24–27	19–23	97–99	18–20	36–38	85–87	average	27–30	34–37	40–43	18–20
Nb	tr	tr	tr	tr	tr	tr	tr	tr	tr	tr	tr	tr	tr	tr	tr	tr
Zr	1	1	1	0	0	1	1	1	1	1	1	1	1	1	1	1
Y	nd	0	2	1	nd	nd	0	1	1	0	nd	0	nd	1	0	0
Sr	2	2	2	4	0	4	0	nd	1	21	3	4	5	14	6	8
Rb	1	0	nd		0	1		nd	nd	nd	0	0	0	1	nd	0
Zn	31	36	35	34	22	33	37	33	31	46	33	34	44	32	49	35
Cu	1	2	7	nd	1	nd	5	4	2	2	3	2	2	2	4	1
Ni	2238	2208	2396	2446	2398	3527	2512	2520	2163	2667	2486	2424	2290	2203	2171	2302
Cr	2903	2650	2796	2396	1144	1319	2236	1509	2024	1688	2167	2103	1667	1278	1629	1752
V	25	22	42	22	12	11	32	13	29	23	8	22	15	21	19	29
Ce	tr	tr	tr	tr	tr	tr	tr	tr	tr	tr	tr	tr	tr	nd	nd	nd
Ba	tr	13	tr	tr	tr	nd	13	nd	12	tr	nd	tr	tr	20	tr	21

Data (in ppm) are from whole-rock analyses by XRF; nd = not detected (background count was greater than sample count); tr = below the detection limit (<5 ppm for Nb, <10 ppm for Ba and Ce).

dunite (Sample 125-779A-15R-2, 24–27 cm) that contains 3527 ppm nickel and a single harzburgite (Sample 125-779A-22R-1, 58–60 cm) that contains 3914 ppm chromium. Chromium and nickel do not correlate with one another or with the degree of serpentinization. Niobium, zirconium, yttrium, rubidium, and titanium are all present at trace levels or are below detection limits. Values of cesium and barium are typically below detection limits, although four samples have barium values of 16 ppm or greater. Strontium, zirconium, and vanadium are slightly lower in the dunites (Sr = 4 ppm; Zn = 34 ppm; V = 8–42 ppm) than in the harzburgites (Sr = 8 ppm; Zn = 39 ppm; V = 4–50 ppm). A single dunite sample (125-779A-24R-1, 36–38 cm) has a strontium value of 21 ppm. No significant correlation exists between geochemical parameters and depth below the seafloor.

The samples analyzed from Site 779 are similar to those from Site 778 (see "Igneous and Metamorphic Geochemistry" section, Site 778 chapter, this volume), although the concentrations of several elements may be slightly different between

Table 6. Tabulated major-element data for mafic rocks from Site 779.

	Group 1 779A 9R-1 106–108	Group 2 779A 31R-1 119–121	779A 31R-2 103–105	779A 31R-3 32–34	779A 31R-CC 39–41 (cm)
SiO_2	43.45	39.47	38.32	36.88	38.45
TiO_2	2.50	1.41	1.40	1.26	1.48
Al_2O_3	14.92	12.07	14.59	12.19	13.81
Fe_2O_3	12.06	11.04	11.96	10.34	11.66
MnO	0.15	0.21	0.18	0.17	0.18
MgO	7.63	11.43	7.49	6.3	17.57
CaO	7.34	18.24	21.71	21.54	21.09
Na_2O	4.07	0.00	0.00	0.00	0.00
K_2O	0.52	0.00	0.00	0.00	0.00
P_2O_5	0.22	0.09	0.08	0.08	0.09
LOI	5.44	4.47	4.02	9.76	3.96
TOTAL	98.30	98.42	99.74	98.53	98.30
Mg#	53.01	64.85	52.77	52.10	53.66

Data (in wt% oxides) are from whole-rock analyses by XRF. LOI is loss on ignition between 150° and 1030°C.

Table 7. Tabulated trace-element data for mafic rocks from Site 779.

	Group 1 779A 9R-1 106–108	Group 2 779A 31R-1 119–121	779A 31R-2 103–105	779A 31R-3 32–34	779A 31R-CC 39–41 (cm)
Nb	tr	tr	tr	tr	tr
Zr	187	85	82	81	85
Y	48	35	34	34	35
Sr	169	92	49	62	58
Rb	10	nd	nd	nd	nd
Zn	132	94	104	93	99
Cu	51	49	38	56	55
Ni	52	57	72	69	75
Cr	163	130	196	207	219
V	424	345	339	334	337
Ce	23	tr	nd	tr	15
Ba	27	59	32	33	50

Data (in ppm) are from whole-rock analyses by XRF; nd = not detected (background count was greater than sample count); tr = below detection limits (<5 ppm for Nb, <10 ppm for Ba and Ce).

Table 4 (continued).

779A 8R-1 45–48	779A 8R-1 57–60	779A 9R-2 52–54	779A 11R-1 14–18	779A 12R-1 38–42	779A 13R-1 2–5	779A 13R-2 52–54	779A 14R-2 139–141	779A 16R-2 74–77 (cm)	Harzburgites 779A 17R-2 14–17	779A 17R-3 77–80	779A 22R-1 58–60	779A 22R-1 63–65	779A 22R-3 55–57	779A 26R-3 50–52	779A 26R-2 101–103	779A 28R-3 26–28	Harzburgite average
38.35	29.39	35.45	36.49	36.81	32.18	38.62	38.08	38.70	40.20	37.37	29.13	38.61	38.09	39.61	37.09	35.53	36.26
0.00	0.00	0.00	0.00	0.00	0.00	0.00	0.00	0.00	0.00	0.00	0.00	0.00	0.00	0.00	0.00	0.00	0.00
0.49	0.57	0.28	0.41	0.19	0.25	0.66	0.88	0.64	0.37	0.30	0.29	0.17	0.10	0.69	0.63	0.19	0.40
7.69	9.04	7.47	7.00	7.50	8.15	7.77	7.35	7.38	7.36	6.98	9.25	7.47	7.76	8.11	7.08	7.07	7.63
0.11	0.17	0.10	0.10	0.10	0.12	0.11	0.11	0.11	0.10	0.09	0.17	0.11	0.11	0.11	0.10	0.10	0.11
40.00	41.22	41.32	39.14	41.50	40.35	40.03	37.34	39.33	42.69	39.47	41.26	41.84	42.98	40.95	39.50	39.32	40.38
0.53	0.14	0.36	0.50	0.33	0.32	0.79	0.81	0.62	0.35	0.29	0.16	0.23	0.13	0.80	0.58	0.35	0.39
0.00	0.00	0.00	0.00	0.00	0.00	0.00	0.00	0.00	0.00	0.00	0.00	0.00	0.00	0.00	0.00	0.00	0.00
0.01	0.00	0.01	0.01	0.01	0.00	0.00	0.02	0.03	0.01	0.01	0.00	0.01	0.00	0.00	0.00	0.00	0.01
0.00	0.00	0.00	0.00	0.00	0.00	0.00	0.00	0.03	0.00	0.00	0.00	0.00	0.00	0.00	0.00	0.00	0.00
0.29	0.32	0.31	0.28	0.29	0.30	0.29	0.28	0.28	0.32	0.30	0.33	0.30	0.30	0.29	0.28	0.29	0.30
0.37	0.41	0.22	0.24	0.21	0.33	0.27	0.43	0.32	0.28	0.26	0.57	0.42	0.18	0.29	0.24	0.25	0.30
11.01	17.41	14.03	14.83	12.33	16.87	11.28	13.82	11.86	6.81	15.40	16.93	10.01	9.17	8.57	17.32	15.63	13.28
98.19	97.95	99.02	98.48	98.76	98.24	99.27	98.42	98.27	97.98	98.92	97.19	98.44	98.32	98.84	98.30	98.19	98.47
91.16	90.03	91.64	91.72	91.64	90.75	91.08	90.96	91.35	92.00	91.81	89.84	91.73	91.65	90.91	91.70	91.68	91.29
100	100	40	98	78	100	75	50	75	25	35	75	50	60	45	35	100	69.14

Data (in wt% oxides) are from whole-rock analyses by XRF. LOI is loss on ignition between 150° and 1030°C. % SERP = percentage of serpentinization estimated from thin sections.

Table 5 (continued).

779A 8R-1 45–48	779A 8R-1 57–60	779A 9R-2 52–54	779A 11R-1 14–18	779A 12R-1 38–42	779A 13R-1 2–5	779A 13R-2 52–54	779A 14R-2 139–141	779A 16R-2 74–77	Harzburgites 779A 17R-2 14–17	779A 17R-3 77–80	779A 22R-1 58–60	779A 22R-1 63–65	779A 22R-3 55–57	779A 26R-2 50–52	779A 26R-3 101–103	779A 28R-3 26–28	Harzburgite average
tr	tr	tr	tr	tr	tr	tr	tr	tr	tr	tr	tr	tr	tr	tr	tr	tr	tr
1	0	1	1	1	nd	nd	0	0	0	1	1	1	1	1	1	1	1
1	0	0	nd	nd	0	1	0	0	1	nd	0	0	0	1	nd	0	0
11	8	8	20	11	12	1	4	1	1	1	6	1	4	1	21	28	8
0	0	nd	nd	1	0	0	1	1	1	1	nd	0	1	nd	nnd	nd	0
38	63	36	36	51	56	30	39	31	0	32	57	37	32	35	36	37	39
3	3	1	1	2	1	6	10	3	4	3	2	3	3	7	2	1	3
2302	2541	2476	2181	2313	2391	2267	2185	2244	2502	2309	2571	2360	2382	2308	2185	2251	2330
2542	2841	1517	1632	1434	2256	1824	2917	2166	1920	1786	3914	2008	1216	1956	1616	1682	2021
29	41	15	24	20	16	31	50	31	32	21	23	28	8	30	24	4	24
nd	tr	tr	nd	tr	tr	15	tr	tr	tr	tr	tr	nd	tr	nd	tr	nd	tr
tr	nd	nd	tr	14	tr	tr	20	tr	tr	13	nd	tr	tr	tr	tr	17	tr

Data (in ppm) are from whole-rock analyses by XRF; nd = not detected (background count was greater than sample count); tr = below the detection limit (< 5 ppm for Nb; < 10 ppm for Ba and Ce).

the two sites. Values for Al_2O_3 and nickel are slightly less and slightly greater for MgO and CaO in Site 778 samples than in Site 779 samples.

Mafic Samples

Mafic samples fall into two broad categories: metabasalt (Group 1) and metadiabase (or metagabbro, Group 2). Group 1 consists of a single sample that originally contained 40 to 75 modal% glass, 10 to 15 modal% plagioclase, and 10 to 30 modal% clinopyroxene. The original assemblage has now been highly altered to clays and chlorite. The diabase samples (Group 2) are highly altered to prehnite/pumpellyite facies, but may have originally contained 60 to 70 modal% plagioclase and 20 to 40 modal% clinopyroxene.

Major-Element Analysis

One sample (125-779-9R-1, 106–108 cm) was analyzed from the metabasalt clasts (Table 6). SiO_2 (43.45 wt%), MgO (7.63 wt%), Al_2O_3 (14.92 wt%), and most other major oxides are within the normal abundance ranges for mid-ocean ridge basalts (MORBs), although the TiO_2 (2.5 wt%) is moderately high.

Samples in the metadiabase zone (125-779-31R-1, 119–121 cm, to 125-779-31R-CC, 39–41 cm) have mid-range TiO_2 (1.26–1.81 wt%), variable MgO (6.31–11.43 wt%), and low SiO_2 (36.88–39.47 wt%) values (Table 6). Abundances of Al_2O_3 range from 12.19 to 14.59 wt%, and Fe_2O_3 ranges from 10.34 to 11.96 wt%. Values for CaO are high (18.24–21.71 wt%), and neither Na_2O nor K_2O is present. This unusual chemistry may be the result of calcium replacing silicon, potassium, and sodium during prehnite/pumpellyite alteration of the samples.

Trace-Element Analysis

The single Group 1 metabasalt clast has higher incompatible elements (Zr = 187 ppm, Y = 48 ppm, Sr = 169 ppm) and vanadium (424 ppm) than the Group 2 samples, but similar compatible elements (Table 7). Abundances of compatible elements for both groups are similar and restricted in range: nickel ranges from 52 to 75 ppm and chromium from 130 to 218 ppm. The intrusive samples (Group 2) have very uniform, mid-range values for the incompatible elements of zirconium (81–85 ppm), yttrium (34–35 ppm), and strontium (50–92 ppm). Concentrations of vanadium (334–345 ppm) also are uniform, and those of rubidium below detection limits in all samples. This uniformity suggests that this zone of diabase was emplaced as a single flow or intrusion.

The differences in ratios of incompatible elements of these two groups (Fig. 5A) suggest a different source for the Group 1 clast than for the Group 2 samples. The similarity of the major-element chemistry (Table 6) and some of the trace-element chemistry (Table 7 and Fig. 5B) suggests that both groups represent MORB-type sources. The metabasalt clast from Group 1 most resembles the Group 2 clast from Site 778 in its immobile trace-element characteristics, although its Fe_2O_3 content is lower. The Group 2 metadiabase samples resemble the Group 3 clasts from Site 778, classifying as MORBs on the two discriminant diagrams used (Figs. 5A and 5B).

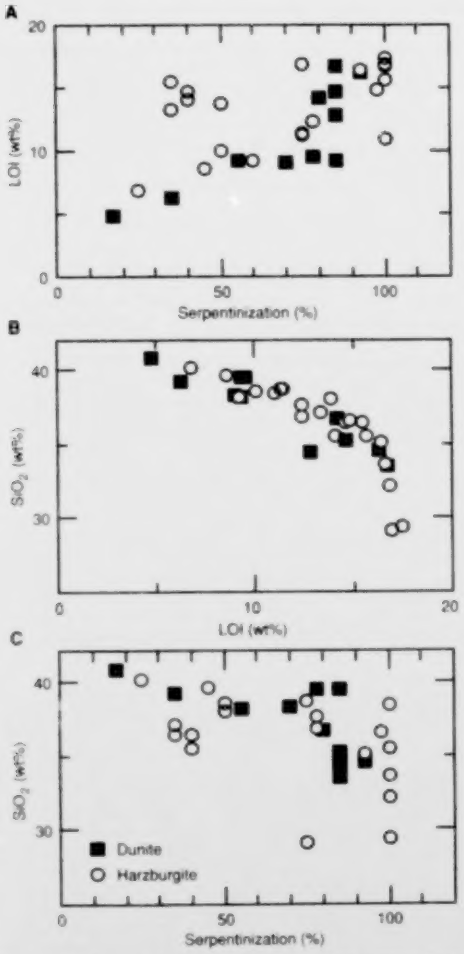

Figure 4. A. Serpentinization (modal%) vs. weight percent loss on ignition (LOI) between 105° and 1030°. B. LOI (modal%) vs. SiO$_2$ (wt%). C. Serpentinization (modal %) vs. SiO$_2$ (wt%). Filled squares represent data from dunite and open circles represent data from harzburgite.

SEDIMENT/FLUID GEOCHEMISTRY

Sediment Geochemistry

Cores from Site 779 were analyzed on board ship for inorganic carbon and for total carbon, nitrogen, and sulfur using the techniques described in the "Explanatory Notes" (this volume). The organic carbon content was then calculated by difference. These results are presented in Table 8 and in Figures 6 and 7. As at Site 778, the cores are uniformly carbonate-poor, except for an interval within the upper 10 m that contains about 15 wt% CaCO$_3$. This interval was less than 6 m thick at Site 778 and at least 8 m thick at Site 779. As at Site 778, the carbonate-rich interval does not extend to the seafloor: samples from about the upper 1 m at both sites have a lower carbonate content. The concentration of organic carbon at Site 779 ranges from 0 to 0.45 wt% and may be slightly higher than that at Site 778. Although sulfur at Site 779 was not detected in most samples, the sulfur content, where detected, is 0.11 wt% and less. Therefore, the sulfur content may be lower than at Site 778. Nitrogen contents are low at both sites, ranging up to 0.15 wt% at Site 779, but are generally lower than 0.1 wt%.

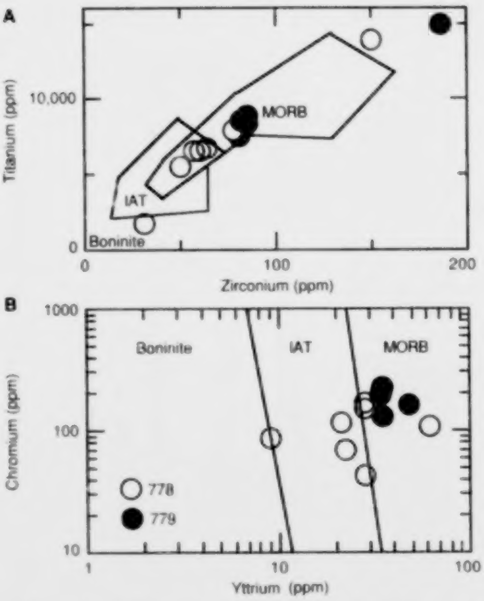

Figure 5. A. Discriminant diagram of tectonic environment for basaltic rocks using zirconium and titanium for mafic basaltic rocks. Data plotted are from mafic samples from Sites 779 and 778. Fields are from Pearce and Cann (1973). B. Discriminant diagram for tectonic environment of mafic rocks using log chromium vs. log yttrium. Data plotted are from mafic samples from Sites 779 and 778. Fields are from Pearce and Wanming (1988). Open circles represent analyses from Site 778; filled circles represent analyses from Site 779. MORB = mid-ocean ridge basalt; IT = island-arc tholeiite.

Fluid Geochemistry

In marked contrast with Site 778, very high concentrations of methane and ethane were measured in the cores at Site 779 (Fig. 8). Propane was also detected in three headspace-gas samples (Table 9) and in three gas pockets sampled directly through the core liner (Table 10). One of the latter samples (from 237 mbsf) contained more than 30 vol.% methane, as well as ethane and propane. A headspace-gas sample from 227 mbsf contained 370 mL of methane per liter of wet unconsolidated serpentine. At the measured porosity of 44% in the cores at this depth, this is equivalent to 38 mM methane in the pore waters, making methane a major dissolved species.

Table 8. Total carbon, organic carbon, and carbonate carbon in cores at Site 779.

Core, section interval (cm)	Depth (mbsf)	Total carbon (%)	Inorganic carbon (%)	Organic carbon (%)	$CaCO_3$ (%)
125-779A-1R-1, 22–23	0.22		0.41		3.4
779A-1R-1, 28–29	0.28		1.17		9.8
779A-1R-1, 55–56	0.55		1.11		9.3
779A-1R-1, 76–77	0.76	2.04	2.07	0.00	17.2
779A-2R-1, 67–68	1.77		0.12		1.0
779A-2R-1, 73–74	1.83		0.14		1.2
779A-2R-1, 94–95	2.04		2.80		23.3
779A-2R-1, 134–135	2.44	2.51	2.06	0.45	17.2
779A-2R-2, 85–86	3.45		1.91		15.9
779A-2R-3, 136–137	5.46		2.01		16.7
779A-2R-4, 86–87	6.46	2.19	2.06	0.13	17.2
779A-2R-5, 36–37	7.46		1.85		15.4
779A-4R-1, 58–59	20.68	0.43	0.13	0.30	1.1
779A-5R-3, 34–35	32.89	0.29	0.12	0.17	1.0
779A-7R-1, 46–47	48.96	0.41	0.05	0.36	0.4
779A-9R-1, 32–35	68.42	0.34	0.03	0.31	0.2
779A-13R-1, 91–92	107.51	0.33	0.06	0.27	0.5
779A-18R-1, 64–67	155.54		0.05		0.4
779A-18R-2, 27–31	156.67	0.31	0.07	0.24	0.6
779A-18R-3, 4–7	157.94		0.07		0.6
779A-27R-1, 57–59	216.77	0.31	0.03	0.28	0.2
779A-28R-2, 58–59	227.05	0.25	0.05	0.20	0.4
779A-28R-2, 87–89	227.34		0.06		0.5
779A-29R-2, 33–35	236.23	0.25	0.07	0.18	0.6
779A-30R-1, 48–49	245.48	0.24	0.05	0.19	0.4
779A-32R-1, 123–125	265.63	0.26	0.04	0.22	0.3
779A-32R-2, 17–19	266.07		0.04		0.3
779A-34R-1, 95–98	284.65		0.05		0.4
779A-36R-1, 46–47	303.46	0.20	0.06	0.14	0.5
779A-36R-1, 106–108	304.06		0.25		2.1
779A-36R-2, 70–71	305.20		0.10		0.8
779A-36R-CC, 9–13	306.38		0.36		3.0
779A-37R-1, 49–50	313.19	0.17	0.03	0.14	0.2
779A-37R-2, 4–5	314.24		0.02		0.2
779A-37R-CC, 4–7	314.42		0.04		0.3
125-779B-1R-1, 0–1	0.00		0.03		0.3
779B-1R-1, 19–21	0.19		0.88		7.3
779B-1R-1, 60–61	0.60		1.54		12.8
779B-1R-1, 96–100	0.98		3.78		31.5
779B-1R-2, 9–10	1.59		1.83		15.2
779B-1R-2, 43–45	1.93		1.44		12.0
779B-1R-2, 108–109	2.58		1.52		12.7
779B-1R-3, 66–68	3.66		1.76		14.7
779B-1R-4, 48–50	4.98		1.85		15.4
779B-1R-5, 91–93	6.91		2.10		17.5
779B-1R-6, 48–50	7.98		1.23		10.2

Except for the upper 10 m, where concentrations are low, and an unsampled interval between 9 and 43 mbsf, methane and ethane concentrations were found to be high throughout the unconsolidated serpentine section. Two large spikes can be seen at 227 and 266 mbsf that are defined by only one or two samples each, but which correspond to the high concentrations of methane, ethane, and propane measured in gas pockets at 237, 275, and 285 mbsf (Table 10). These spikes correspond to maxima in the methane-to-ethane ratio as well (Fig. 8).

Interstitial waters at Site 779 (Table 11) are different from those at Site 778. Moreover, the surficial samples from Hole 779B are different from those from Hole 779A, indicating that there is considerable lateral variation in the composition of interstitial water on Conical Seamount. Results from Sites 778 and 779 are compared in Figures 9, 10, and 11. Interstitial waters from Hole 779A are much more alkaline, with pH rising from 7.5 at 4 mbsf to 11.6 at 108 mbsf (Fig. 9). From 108 to 246 mbsf, pH remains in a narrow range between 11.1 and 11.9. Below 246 mbsf it decreases again to a value of 9.9 at 314 mbsf, near the bottom of the hole. Changes in alkalinity and ammonia (Fig. 9) parallel these changes in pH. Alkalinity rises to a maximum concentration of 15 meq/kg at 246 m and then falls to 2.4 meq/kg near the bottom of the hole. Ammonia reaches a maximum of 152 mmol/kg at 246 mbsf before dropping to less than one-half that value near the bottom of the hole. The concentration of dissolved silica remains below 50 mmol/kg throughout the hole, except for samples from the upper 10 m and the lowermost two samples from 306 and 314 mbsf, which define an abrupt increase to 361 mmol/kg near the bottom of the hole. These silica-rich samples have a lower pH and are relatively poor in alkalinity and ammonia.

The usual mechanism for generating alkalinity and ammonia in the pore waters of deep-sea sediments is reduction of seawater sulfate by bacteria that oxidize buried organic matter. Sulfate does decrease by nearly a third at Site 779, but only to a depth of 108 mbsf (Fig. 9). Below that it increases again to 90% of the seawater value, before decreasing to a second minimum at 285 mbsf. No odor of H_2S was detected in any of the interstitial-water samples from Site 779. However, one would not expect a strong odor at the high pH of these samples, at which H_2S would be dissociated into nearly equal amounts of bisulfide and sulfide ions. (The second ionization constant of H_2S at 25°C is 11.96.) The probable presence of H_2S was detected by formation of a pale yellow to rusty orange to dark brown precipitate in some of the interstitial-water samples when $HgCl_2$ was added. These samples were from 108, 157, 306, and 314 mbsf in Hole 779A. This precipitate did not form in samples from 33 mbsf in Hole 779A or from 1 to 9 mbsf in Holes 779B and 778A. No other samples were tested. As noted above, the organic carbon content of these cores is low. It is highly probable from all these lines of evidence that some sulfate from the interstitial waters has been reduced to sulfide. Whether this reduction was caused by bacterial action or by inorganic processes or by both is not known.

As at Site 778, the concentration of magnesium in the interstitial waters decreases to very low values over the depth interval 0 to 100 mbsf (Fig. 10). The lowermost two samples from Hole 779A show a slight rebound, which may be real or may be an artifact of contamination with seawater during drilling and sample recovery. These are the same two samples that exhibit the large increase in silica noted above; this increase in silica is too large to have been caused by seawater contamination, even by silica-rich ocean bottom water, which contains about 150 mmol/kg silica in this area. Even if the increase in magnesium is entirely the result of seawater contamination, the other dissolved species should have been affected only negligibly, because the small size of the increase limits the amount of seawater contaminant to less than 8% to 12% of the samples.

Calcium also decreases by more than 90% at Site 779, in contrast to Site 778, where it more than doubled (Fig. 10). The decrease in calcium presumably resulted from precipitation of $CaCO_3$ in response to the large increase in alkalinity, an increase that was absent at Site 778. Potassium (Fig. 10) decreases by one-third with depth at both sites. Most of this decrease occurs within 50 m of the bottom of Holes 778A and 779A. Decreases in potassium in the interstitial waters of marine sediments commonly result from alteration of volcanic material at low temperature. The sharp decreases near the bottom of Holes 778A and 779A may indicate that volcanic material is present at these levels in these holes, and possibly also is beneath the serpentinite some distance below the maximum depths drilled. Sodium (Fig. 10) increases with depth at both Site 779 and Site 778, but the size of the increase is much greater at Site 779. Sodium reaches a maximum concentration between 108 and 227 mbsf that is 24% higher

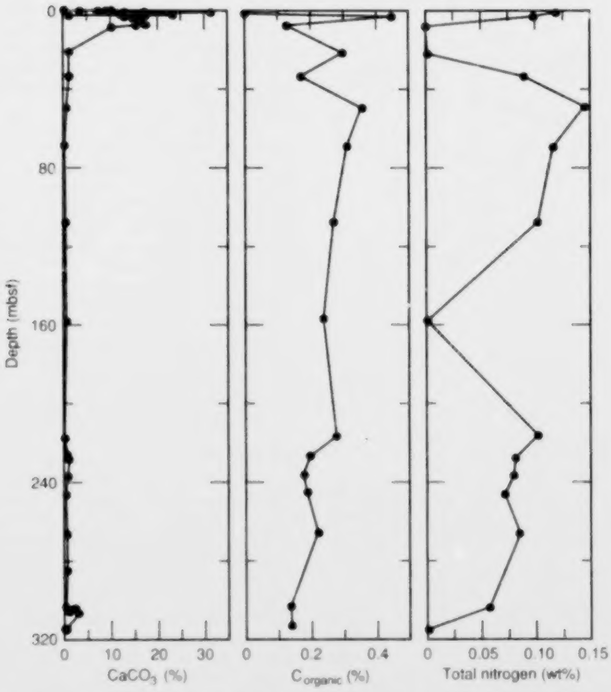

Figure 6. Calcium carbonate, total organic carbon, and total nitrogen (wt%) in cores from Holes 779A and 779B.

than that in seawater, before declining again to a minimum concentration between 274 and 306 mbsf that is still 8% higher than that in seawater. The minimum is defined by the increased sodium in the lowermost two samples, the same two that are also relatively rich in silica, sulfate, and magnesium, and poor in alkalinity, ammonia, potassium, and hydrogen ions.

The depth profiles for salinity, chlorinity, and bromide have somewhat similar shapes to that for sodium, except that salinity and chlorinity exhibit large decreases, rather than increases, relative to their seawater values (Fig. 11). As at Site 778, salinity and chlorinity decrease by about 10% with depth. As is the case for the other dissolved species, the lowermost two samples in Hole 779A reverse the prevailing trend: both salinity and chlorinity increase near the bottom of the hole.

The complexity of the pore-water profiles at Site 779, especially those for sulfate, sodium, salinity, and chlorinity, suggests the possibility of mixing between fluids, with two or more distinct compositions. One of these fluids has a distinctly lower salinity and chlorinity than seawater. Possible origins for this fluid are discussed in the "Sediment/Fluid Geochemistry" section, Site 780 chapter (this volume).

STRUCTURAL STUDIES

At Site 779, structures related to tectonic processes were found in both hard rocks (serpentinized peridotites, metagabbros, and metabasalts) and soft sediments.

Deformation Patterns in Unconsolidated Serpentine and Serpentine Sediments

In the soft sediments recovered between the serpentinized peridotite blocks in lithologic Unit II, plastic folds locally define a nonpenetrative deformation (Fig. 12), and a pervasive, repeated cleavage also is locally present. Anastomosing cleavage planes developing around soft or hard serpentinitic elements define small lenses (phacoids, Fig. 13). A spectacular shear fabric within the soft laminated serpentines exists in Interval 125-779-20R-1, 40 to 60 cm. In this interval, the general foliation is oblique to the core axis (dip angle of 50° to 60°) and is helicoidal. (This foliation is pervasive and thus does not seem to result from drilling disturbance.) An asymmetric sheared fabric is emphasized by both the external shape of the serpentinite blocks and the cleavage developed around them (Fig. 14). In Sections 125-779A-18R-1 and 125-779A-18R-2, the foliation is almost vertical. Vertical, millimeter-scale chrysotile fibers, developed within a vein 3 cm long that opened in the serpentine, define the stretching direction. The vein is deformed along the edge of the core, probably as a result of drilling disturbance (Fig. 15). Abundant, white, discontinuous, distorted laminae found within the serpentine sediments are probably remnants of similar veins that were deformed earlier. On the basis of locally intense flattening and cleavage development, the serpentinous matrix can be interpreted as a probable

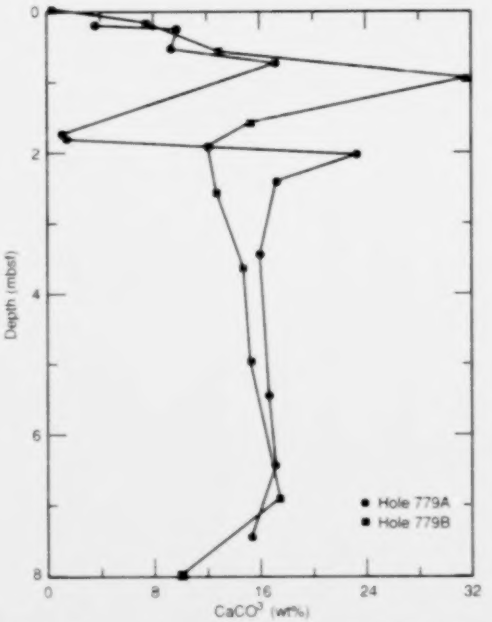

Figure 7. Calcium carbonate (wt%) in cores from Hole 779B and from the upper 8 m of Hole 779A.

fault gouge. Nevertheless, the presence of reworked subangular and unsorted serpentine debris (Interval 125-779A-30R-2, 4 to 10 cm, for example), as well as autochthonous organic matter and nannofossils in Core 125-779A-27R, demonstrate that the material is not purely tectonic in origin. It must be considered a tectonized sedimentary matrix.

Deformation patterns in lithologic Unit III of Site 779 are similar to those described in lithologic Unit II of Hole 778A. The layered serpentine microbreccias exhibit a succession of plastic folds affecting all sections of core. The term "convolute folding" thus can be used to describe the observed disturbances.

Structures and Deformation of Hard Rocks in Lithologic Unit II

Veining

The most visible structural features in the hard rocks in lithologic Subunit IIA are related to veining of the serpentinized harzburgites. Two main types of vein can be distinguished on the basis of color and habit (Fig. 16). Dark veins of antigorite corresponding to a 100% serpentinization of the peridotites have developed as a conjugate system (Fig. 16A). In some cases, the sharp edge of a vein may be observed to crosscut orthopyroxenes. This suggests that these veins do not correspond to a late filling of fractures, but to a progressive serpentinization of the initial ultramafic rocks. Locally, as shown in Figure 17, anastomosing veins define a pervasive grid that outlines elements of rhomboidal shape. These rhomboids are interpreted as the precursors of the major part of the phacoid-shaped elements in the sedimentary matrix. They may have been removed from their parent rock by alteration and softening of the completely serpentinized areas. Significantly, single or adjacent blocks within the cores have parted along the veins. Thus, many of the initial block edges most likely mark the site of early antigorite veins, rather than late shear zones. This implies that the alteration processes that softened the serpentinized peridotites may have initialized along antigorite veins.

The second type of vein consists of white, chrysotile-rich secondary fractures. These result from tensional stresses that opened the rocks. Small offsets of a few millimeters can be observed along the secondary fractures. Three subtypes, which can coexist, were observed (Fig. 16B): (1) veins located in the central part of preexisting antigorite veins parallel to the general trend of the antigorite vein; (2) veins that crosscut the subtype 1 veins and fill successive, centimeter-long tension cracks located within the dark antigorite veins ("Frankenstein" veins); and (3) veins whose distribution is unrelated to the antigorite vein structure.

The distribution of the chrysotile veins is not homogeneous along lithologic Unit II. These veins are present, but not abundant, in Cores 125-779A-3R to 125-779A-13R, are almost absent from Cores 125-779-14R to 125-779A-20R, and become abundant in Cores 125-779A-28R to 125-779A-35R.

Brecciation

Intense cataclasis leading to the development of brecciated shear lenses can be observed in some completely serpentinized samples of Sections 125-779A-30R-2 and 125-779A-31R-1 (Fig. 18). Brecciation post-dated the serpentinization and probably took place at a shallow level. Chrysotile veins crosscut the sheared fabric. Preliminary observations of hand-specimens show that the cleavage planes between the shear lenses are occupied by a light-colored mineral, probably chrysotile, suggesting that this brecciation took place in the chrysotile stability field. Detailed studies will be required to confirm this interpretation. Intense brecciation also affected some of the metagabbros and metabasalts of Core 125-779-31R.

Horizontal Schistosity

Horizontal schistosity developed locally in flattened and sheared pure serpentinites recovered in Sections 125-779A-30R-2 and 125-779A-31R-1. This pervasive schistosity is accompanied by slickensides and, in some places, by the folding of the serpentinites between two shear planes.

Foliation and Ductile-Brittle Shear Zones

Mantle foliation (high-temperature deformation) in the peridotites is not pervasive and develops only locally. It is defined by the alignment of elongated spinels and sheared orthopyroxenes (shearing along cleavages) and by microgranulation of olivines along intracrystalline glide planes. Spinel alignments may be deformed further along serpentine veins, as seen in thin section (Sample 125-779A-16R-1, 16–19 cm).

The tectonic fabrics observed in samples from Cores 125-779A-30R and 125-779A-31R are well defined. Sample 125-779A-30R-2, 34–52 cm, is a lithified tectonic breccia, representing a shear zone 20 cm thick. This zone exhibits a clear foliation defined by the alignment of elongated serpentinite clasts, some of which may have been reduced to millimeter-thick flakes. A weak stretching lineation can be observed on the top surface of the sample. The foliation is crosscut by more brittle conjugate faults. Foliation planes are bent along the fracture plane, indicating a normal sense of shear (Fig. 19). Senses deduced from analysis of other fault planes visible in this sample are consistent with a normal movement, that is, lateral extension of the sample with respect to the vertical axis of the core. The metagabbros recovered in Sections 125-779-31R-2 and 125-779-31R-3 exhibit local, mostly

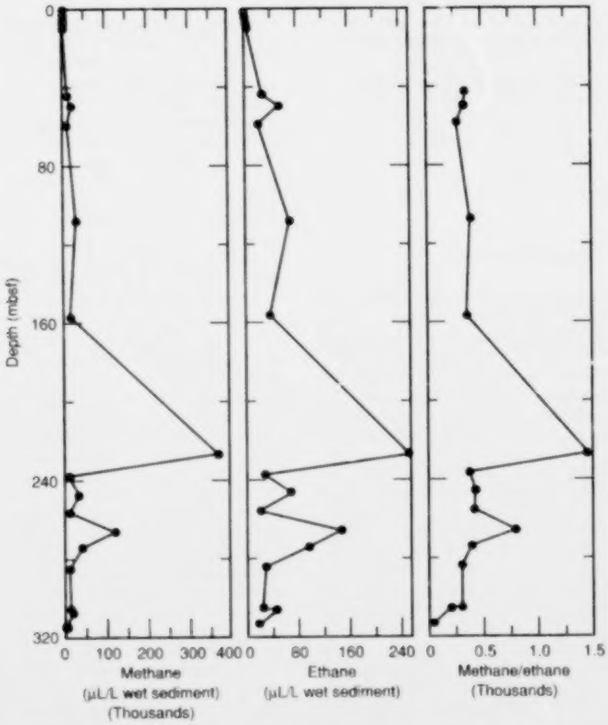

Figure 8. Methane, ethane, and the methane/ethane ratio in cores at Site 779.

horizontal, foliated zones. This early foliation represents probable deep ductile shear zones and is in turn crosscut and deformed by late, more brittle faults, similar to those described above (Fig. 20). In each case, the sense of movement determined by the bending of the foliation along the faults indicates lateral extension with respect to the core axis (Fig. 21).

Discussion

Examination of the orientation of all the veins and fractures affecting the rocks recovered at Site 779 suggests no regular arrangement between the drilled blocks. This supports the idea that lithologic Unit II represents a chaotic formation. Regarding the deformation, Subunit IIB is characterized by the development of an early foliation within the gabbroic blocks and by the presence of brittle-ductile conjugate faults, indicating lateral extension with respect to a vertical drilling axis. Deformation of the unconsolidated serpentine and serpentine sediments between the blocks may have resulted from differential movements between the blocks. This deformation may have coincided either with the rising of the diapiric material or with the lateral flow of the unconsolidated carapace covering the seamount. The presence of fossiliferous sediments within lithologic Subunit IIB, suggesting that lithologic Subunit IIA was emplaced laterally on the seafloor as a gravity nappe, favors the second hypothesis. Deformation within the sediments of lithologic Unit III is important, but might be consistent with gentle flowage under the load of lithologic Unit II.

Table 9. Results of headspace-gas analyses of cores at Site 779.

Core section, interval (cm)	Depth (mbsf)	Methane (µL/L)[a]	Ethane (µL/L)[a]	Propane (µL/L)[a]	Methane (µM)[b]
125-779A-1R-1, 97–100	1.0	4			0.3
779A-5R-3, 80–85	42.9	9,333	27		833
779A-7R-1, 70–75	49.2	18,273	54		1,631
779A-8R-1, 0–5	58.5	5,302	20		473
779A-13R-1, 135–140	108.0	28,274	69		2,523
779A-18R-1, 147–150	156.4	13,050	37		1,164
779A-28R-1, 130–135	227.1	370,202	255	23	33,033
779A-29R-1, 145–150	237.0	10,202	28	9	910
779A-30R-1, 110–115	246.1	30,128	70		2,688
779A-31R-1, 145–150	256.2	8,508	20		759
779A-32R-2, 10–15	266.0	118,320	149	11	10,558
779A-33R-1, 37–42	274.4	36,906	95		3,293
779A-34R-1, 101–105	284.7	8,236	27		735
779A-36R-2, 130–135	305.8	3,938	23		619
779A-36R-3, 45–50	306.5	9,554	45		852
779A-37R-1, 126–130	314.0	751	16		67
125-779B-1R-1, 135–140	1.4	8			0.0
779B-1R-3, 135–140	4.4	12			1.0
779B-1R-5, 135–140	7.4	6			0.6
779B-1R-6, 95–100	8.5	7			0.6

[a] Microliters of gas per liter of wet unconsolidated serpentine.

[b] Micromoles of methane per liter of interstitial water, assuming a porosity of 50%. Where values are absent, the gas was not detected.

Table 10. Composition of gas pockets in cores from Site 779, sampled through the core liner into an evacuated glass tube.

Core, section, interval (cm)		Depth (mbsf)	Methane (ppmv)	Ethane (ppmv)	Propane (ppmv)
125-779A-2R-5,	38	7.48	10.9	0.8	nd
29R-2,	30	237.30	309,584	647.3	54.3
33R-1,	61	274.61	101,296	74.8	6.3
34R-1,101-105		284.73	154,405	203.8	15.5

nd = not detected.

PALEOMAGNETISM

Much of the sediment recovered from Hole 779A was disturbed during drilling. Lithologic Unit I is now a water-saturated slurry unsuitable for paleomagnetic work. Natural remanent magnetizations (NRM) of the material were measured to obtain a general idea of its magnetic properties. The archive halves of core sections were measured using the cryogenic magnetometer. NRM intensities vary, typically between 5 and 100 mA/m, but there is no apparent trend in these values downhole.

Material from Hole 779B proved much more useful for magnetostratigraphic studies, although the hole consisted of only a single core (an 8.7-m-thick interval of sediment). Whole-core NRM measurements were performed for Sections 125-779B-1R-1, 125-779B-2R, 125-779B-3R, 125-779B-5R, and 125-779B-6R. (Section 125-779B-1R-4 was not measured because it would not pass through the cryogenic magnetometer.) NRM intensities vary widely (between 10 and 400 mA/m), and there is a systematic decrease in these values downhole in the upper 2.5 m of the core (Fig. 22). In addition, each section was measured after alternating field (AF) demagnetization to 3, 5, 7, and 10 mT. The magnetostratigraphic results from Core 125-778-1R are presented in Figure 22. All sections carry dominantly reversed polarities, or have magnetizations that "trend" toward reverse at the 10-mT field value. Three short intervals (about 30 cm thick) with possibly normal polarities were also identified in Sections 125-779B-1R-5 and 125-779B-1R-6. The polarity recorded at these levels may be a depositional remanence, but may also represent viscous remanent magnetizations (VRM) from the present-day geomagnetic field that have not been completely demagnetized at the 10-mT step.

Discrete specimens were taken from the working halves of Sections 125-779B-1R-2, 125-779B-1R-3, 125-779B-1R-5, 125-779B-1R-6, and 125-779B-1R-7. For additional analysis, two specimens were taken from Section 125-779B-1R-1, and three specimens from Section 125-779B-1R-4. The specimens were AF demagnetized to 0, 3, 5, 8, 10, and 12 mT using the cryogenic magnetometer. Results from these specimens are summarized in Table 12. Specimens from Sections 125-779B-1R-1, 125-779B-1R-2, 125-779B-1R-3, 125-779B-1R-5 and 125-779B-1R-6 record a polarity similar to that of the adjacent interval in the section from which they were taken (Fig. 22). The three specimens from Section 125-779B-1R-4 are reversed, normal, and reversed downhole, respectively. The single discrete specimen from Section 125-779B-1R-7 is reversely magnetized.

Core 125-779B-1R exhibits a predominantly reversed polarity. Shipboard biostratigraphic studies ("Biostratigraphy" section, this chapter) have identified nannoplankton that have been assigned to the lower part of Okada and Bukry's (1980) Zone CN14a at these levels. This implies that the magnetization in the upper part of Hole 779B is a record of the middle part of the Matuyama Chron (based on magnetostratigraphic and biostratigraphic data presented by Berggren et al., 1985). This interval lies within the lower part of the Pleistocene.

Normal polarity levels within the lower part of the core (Section 125-779B-1R-6) may represent part of the Olduvai Event, or alternatively, could represent a VRM that was not completely demagnetized at the 10-mT step. The poor quality of data at these levels makes accurate correlation difficult.

Combined paleomagnetic and biostratigraphic data did enable us to date accurately the sediments overlying the serpentine "flows" on the southern flank of Conical Seamount. These data imply that the youngest possible age of these "flows" in this area must be earliest Pleistocene.

NRM measurements also were performed for the serpentine and serpentinite material beneath this thin cover of sediments in Hole 779A. Intensities were typically 50 to 250 mA/m. However, owing to the lack of biostratigraphic data and the highly altered and deformed state of the rock, we found it impossible to fit the data into any chronologic framework.

PHYSICAL PROPERTIES

Hole 779A

Physical properties at Site 779 were measured on whole-round core samples as well as discrete samples (Tables 13 to

Table 11. Composition of interstitial waters from cores at Site 779.

Sample number	Core section, interval (cm)	Volume (mL)	Squeeze T T (°C)	Depth (mbsf)	pH	Salinity (R.I., ‰)	Salinity (calc., ‰)	Chlorinity (mmol/kg)	Alkalinity (meq/kg)	Sulfate (mmol/kg)	Sodium (mmol/kg)	Potassium (mmol/kg)
Surface seawater (4 Mar. 1989)					8.10	35.5	34.85	542.6	2.386	27.98	464.8	10.05
IW-1	779A-2R-2, 145–150	18	2	4.08	7.50	36.0	34.81	543.9		27.77	464.3	10.12
IW-2	779A-5R-3, 46–56	30	2	33.11	9.08	33.8	33.68	529.4	1.361	22.46	483.3	10.52
IW-3	779A-13R-1, 140–150	20	6	108.05	11.62	32.2	34.06	523.1	7.482	19.19	545.5	10.56
IW-4	779A-18R-2, 7–17	4	2	156.52	11.76		35.48	525.5	11.677	25.56	575.3	9.89
[a]IW-41	779A-18R-2, 7–17	24	12	156.62	11.10	32.5	34.99	534.1	4.886	22.51	562.1	12.31
IW-5	779A-28R-2, 95–105	9	6	227.47	11.68	32.0	34.39	507.7	11.307	25.52	552.7	9.75
IW-6	779A-30R-1, 140–150	10	6	246.45	11.91	31.7	33.88	495.1	15.102	24.90	544.1	9.32
IW-7	779A-32R-2, 0–10	12	6	265.95	11.27	31.0	32.93	498.0	4.804	23.37	525.8	8.47
IW-8	779A-33R-1, 42–52	19	7	274.47	11.08	31.5	32.59	491.3	4.856	23.79	515.3	8.92
IW-9	779A-34R-1, 111–121	20	7	284.86	11.58	30.0	31.37	480.6	8.228	17.47	503.6	8.23
IW-10	779A-36R-2, 136–150	36	7	305.93	10.32	31.8	33.74	515.5	2.901	24.06	534.8	6.65
IW-11	779A-37R-1, 135–150	28	8	314.18	9.93	32.2	33.75	522.3	2.450	21.33	538.4	6.39
IW-1	779B-1R-1, 145–150	34	2	1.48	8.16	35.4	34.52	537.9	2.364	27.45	463.3	9.39
IW-2	779B-1R-3, 110–115	40	2	4.08	7.92	35.4	34.35	536.0	2.277	27.14	459.8	9.27
IW-3	779B-1R-5, 145–150	42	2	7.48	7.99	35.4	34.83	538.8	2.280	29.25	467.7	9.29
IW-4	779B-1R-6, 105–110	30	2	8.58	7.79	35.3	34.64	539.8	2.282	27.65	464.4	9.09

[a]Material trimmed from the exterior of the core sample prior to squeezing.
Values absent from table were not determined.

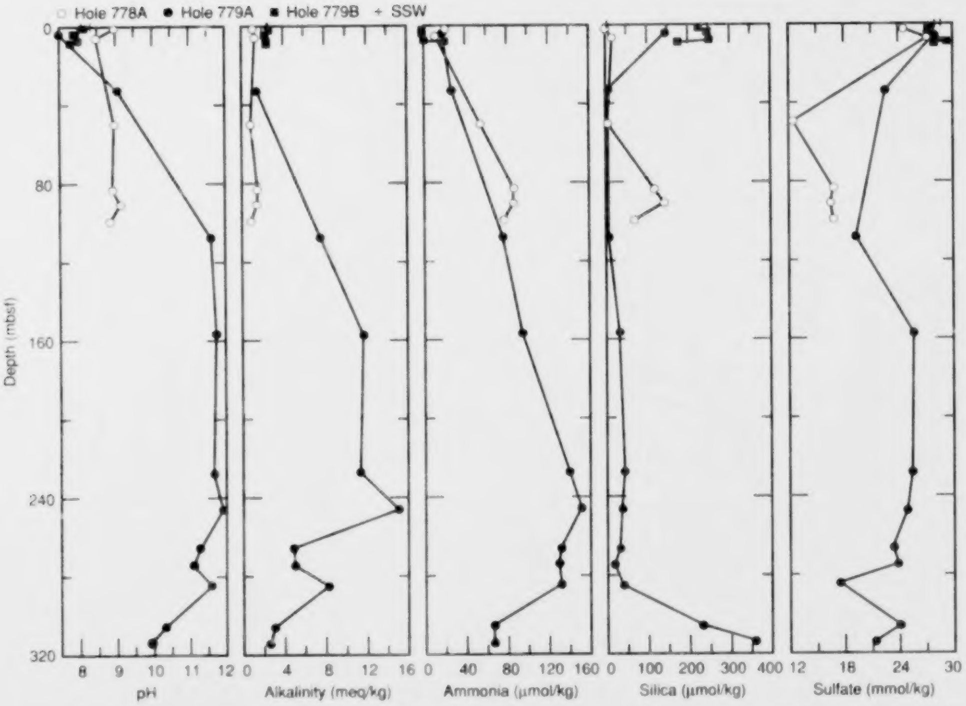

Figure 9. Composition of interstitial waters from cores at Site 779 compared with that at Site 778. SSW = surface seawater collected 22 February and 4 March 1989.

16). The multisensor track (MST) was used for the first 19 cores, but this was later abandoned because core liners were incompletely filled (see "Physical Properties" section, Site 778 chapter). However, the gamma-ray attenuation porosity evaluator (GRAPE) was used on selected whole-round sections and was operated for 2-min intervals to obtain discrete density measurements (results are discussed below). Magnetic susceptibilities were measured only on the first 19 cores run through the MST device; however, the instrument was malfunctioning, and erratic readings were recorded.

Compressional-wave (*P*) velocities were measured on discrete hard-rock samples cut from split-core sections. These velocities range from 3100 to 6850 m/s and are listed in Table 14. Velocities for hard-rock samples were measured along the core (vertically in the A direction) and, in some cases, perpendicular to the vertical (in the B direction, see Table 14). The velocities in both the A and B directions are shown in Figure 23. The average velocities for the hard-rock clasts are 4600 and 5000 m/s in the A and B directions, respectively. Velocities of soft sediment and serpentine samples were not measured because the samples tended to deform in the Hamilton Frame instrument.

Index properties were determined from the hard rocks sampled for velocity measurements. Index properties of soft sediment and serpentine samples also were measured using the same weight and volume determination scheme. The bulk-density measurements of these discrete samples are listed in Table 13. Plots of bulk densities from all specimens are shown in Figure 24.

In addition, bulk densities of hard rocks were measured in selected whole-round sections by the 2-min GRAPE method discussed above. These values range from 1.95 to 3.09 g/cm^3 (Fig. 25) and average 2.55 g/cm^3.

Table 11 (continued).

Calcium (mmol/kg)	Magnesium (mmol/kg)	Bromide (mmol/kg)	Silica (μmol/kg)	Ammonia (μmol/kg)	Phosphate (μmol/kg)
10.17	52.89	0.85	5	<5	
9.76	53.45	0.87	146	18	
9.32	31.62	0.78	5	27	0.27
6.41	0.029	0.85	5	76	
1.55			30	95	
4.55	0.213	1.10	19	45	
3.81	0.002	0.98	41	140	<0.10
3.29	0.005	0.96	35	152	
7.37	0.316	0.92	30	131	
9.69	0.038	0.96	15	129	
5.96	0.322	0.94	37	132	
6.31	6.218	0.78	230	66	<0.10
6.74	4.540	0.79	361	66	<0.10
8.92	52.33	0.73	230	<5	0.82
9.63	52.10	0.98	250	<5	1.15
9.60	51.73	0.88	255	<5	0.93
9.84	52.12	0.90	176	22	0.71

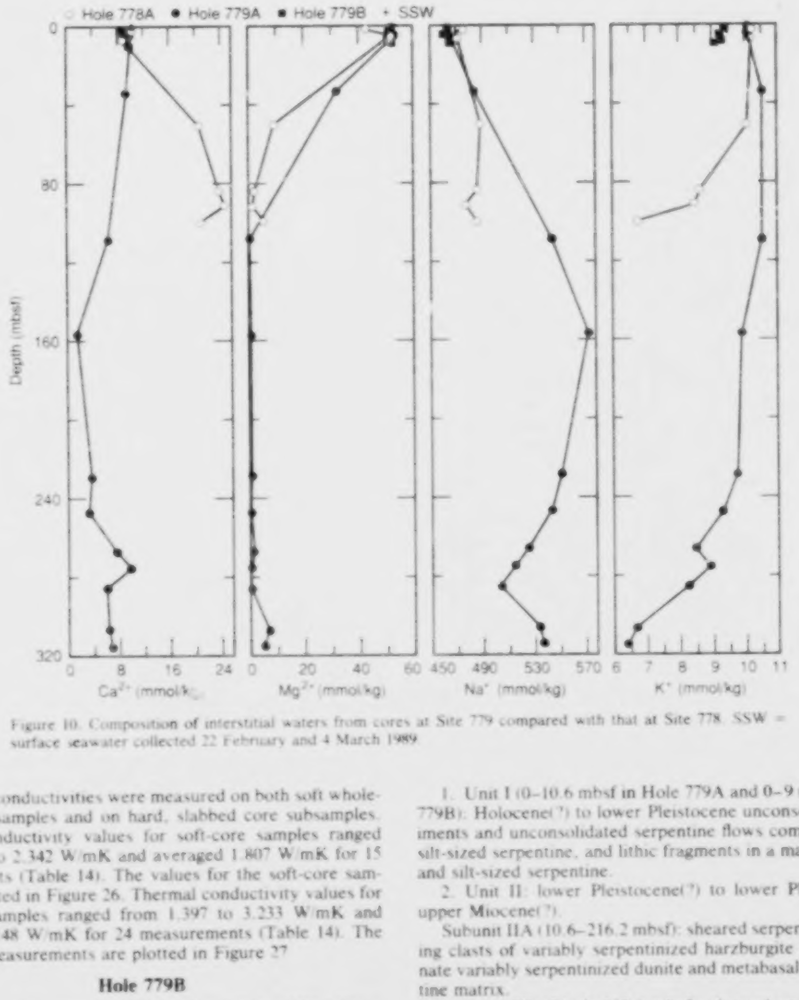

Figure 10. Composition of interstitial waters from cores at Site 779 compared with that at Site 778. SSW = surface seawater collected 22 February and 4 March 1989.

Thermal conductivities were measured on both soft whole-round core samples and on hard, slabbed core subsamples. Thermal conductivity values for soft-core samples ranged from 0.852 to 2.342 W/mK and averaged 1.807 W/mK for 15 measurements (Table 14). The values for the soft-core samples are plotted in Figure 26. Thermal conductivity values for hard-rock samples ranged from 1.397 to 3.233 W/mK and averaged 2.148 W/mK for 24 measurements (Table 14). The hard-rock measurements are plotted in Figure 27.

Hole 779B

Only one core was recovered from Hole 779B. Three bulk-density measurements were performed, which are listed in Table 15. Four conductivity measurements were also run for this core, the results of which are shown in Figure 28. Resistivity and formation-factor values are listed in Table 14.

SUMMARY AND CONCLUSIONS

Site 779 (19°30.75'N, 146°41.75'E; water depth, 3947.2 mbsl) is a second flank site on Conical Seamount situated halfway up the southeast flank, about 3.5 km northeast of Site 778. Two holes were drilled: Hole 779A (which reached 319.2 mbsf) and Hole 779B (which was a single 9-m core aimed at recovering the uppermost sediment). Recovery at Hole 779A averaged 22.9% (Table 1, Fig. 29).

Three major lithologic units were recovered at Site 779:

1. Unit I (0–10.6 mbsf in Hole 779A and 0–9 mbsf in Hole 779B): Holocene(?) to lower Pleistocene unconsolidated sediments and unconsolidated serpentine flows comprising clay, silt-sized serpentine, and lithic fragments in a matrix of sand- and silt-sized serpentine.
2. Unit II: lower Pleistocene(?) to lower Pliocene(?) or upper Miocene(?).

Subunit IIA (10.6–216.2 mbsf): sheared serpentine containing clasts of variably serpentinized harzburgite and subordinate variably serpentinized dunite and metabasalt in a serpentine matrix.

Subunit IIB (216.2–303.0 mbsf): sheared serpentine containing clasts of serpentinized harzburgite with subordinate serpentinized dunite, gabbro and metabasalt in a serpentine matrix with intercalations of detrital serpentine sediments.

3. Unit III (303.0–317.2 mbsf): serpentine microbreccia with convolute layering.

Dating of Hole 779A is based on biostratigraphic data that give Quaternary ages for Unit I (early Pleistocene for its base), and late Miocene(?) to early Pliocene(?) ages for the top of Subunit IIB (this section also contained reworked Oligocene nannofossils). Dating of Hole 779B is based on combined biostratigraphic and magnetostratigraphic evidence: the former gives Pleistocene ages, the latter suggests that the upper part of the hole may record the middle part of the Matuyama Chron (just below the Pliocene/Pleistocene boundary).

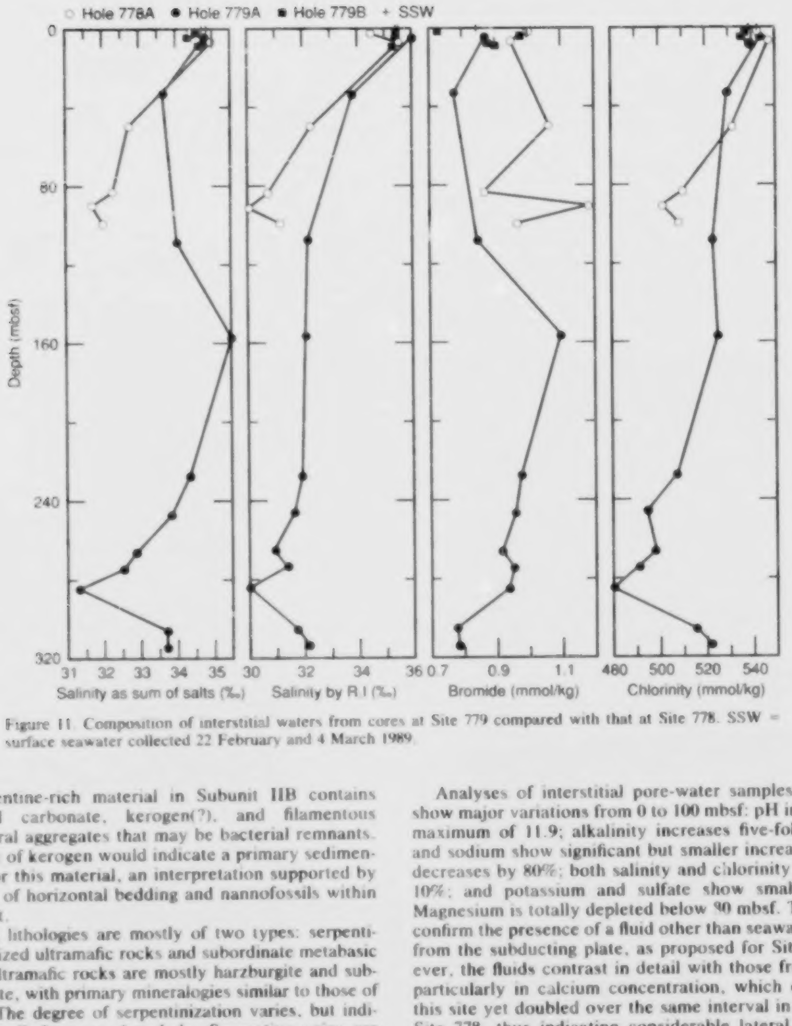

Figure 11. Composition of interstitial waters from cores at Site 779 compared with that at Site 778. SSW = surface seawater collected 22 February and 4 March 1989.

The serpentine-rich material in Subunit IIB contains recrystallized carbonate, kerogen(?), and filamentous opaque mineral aggregates that may be bacterial remnants. The presence of kerogen would indicate a primary sedimentary origin for this material, an interpretation supported by the presence of horizontal bedding and nannofossils within the same unit.

Hard-rock lithologies are mostly of two types: serpentinized, tectonized ultramafic rocks and subordinate metabasic rocks. The ultramafic rocks are mostly harzburgite and subordinate dunite, with primary mineralogies similar to those of Hole 778A. The degree of serpentinization varies, but indicates an overall decrease downhole. Serpentine veins are common and indicate a polystage filling history. Mafic clasts are predominantly metabasalt and metagabbro of primary mineralogy dominated by plagioclase and clinopyroxene and (in basalts) glass; one microgabbro is about 3 m thick in the cored section. Common metamorphic minerals are clay minerals, chlorite, pumpellyite, and rarely, albite and sphene.

Structures indicate a complex history of deformation comparable to that described in Hole 778A. In addition, detailed studies of Subunit IIA have shown that no consistent interrelationships exist between ultramafic clasts, suggesting that this unit at least represents a chaotic formation. The presence and orientations of brittle-ductile conjugate faults in the clasts of Subunit IIB indicate extension about a vertical axis, and the deformation of the matrix is consistent with gentle flowage under an applied load.

Analyses of interstitial pore-water samples at Site 779 show major variations from 0 to 100 mbsf: pH increases to a maximum of 11.9; alkalinity increases five-fold; ammonia and sodium show significant but smaller increases; calcium decreases by 80%; both salinity and chlorinity decrease by 10%; and potassium and sulfate show small decreases. Magnesium is totally depleted below 90 mbsf. These results confirm the presence of a fluid other than seawater, possibly from the subducting plate, as proposed for Site 778. However, the fluids contrast in detail with those from Site 778, particularly in calcium concentration, which decreased at this site yet doubled over the same interval in waters from Site 778, thus indicating considerable lateral variation in interstitial water composition within the flank materials of the seamount. Hydrocarbons increased dramatically with depth in Hole 779A, with methane, ethane, and propane present in most samples. A maximum of 30% methane was analyzed from one gas pocket sampled through the core liner.

The principal results of Site 779 can be summarized as follows:

1. The site provides further evidence for the depleted nature of the mantle wedge beneath Conical Seamount.
2. Flowage of unconsolidated serpentine coupled with sedimentary processes are important in the construction of Conical Seamount.

3. Hydrocarbons are an important component of the fluids associated with the seamount.

4. The serpentinite source region has experienced medium-grade metamorphism.

5. Water derived from the subducted slab might be an important source of fluids involved in the serpentinization of Mariana forearc materials.

REFERENCES

Barron, J. A., 1985. Late Eocene to Holocene diatom biostratigraphy of the equatorial Pacific Ocean, Deep Sea Drilling Project Leg 85. *In* Mayer, L., Theyer, F., et al., *Init. Repts. DSDP*, 85: Washington (U.S. Govt. Printing Office), 413–456.

Berger, W. H., 1970. Planktonic foraminifera: selective solution and the lysocline. *Mar. Geol.*, 8:1–11.

Berggren, W. A., Kent, D. V., Flynn, J. J., and Van Couvering, J., 1985. Cenozoic geochronology. *Geol. Soc. Am. Bull.*, 96:1407–1418.

Berner, R. A., and Honjo, S., 1981. Pelagic sedimentation of aragonite: its geochemical significance. *Science*, 211:940–942.

Fryer, P., Ambos, E. L., and Hussong, D. M., 1985. Origin and emplacement of Mariana forearc seamounts. *Geology*, 13:774–777.

Haggerty, J. A., 1987. Petrology and geochemistry of Neogene sedimentary rocks from Mariana forearc seamounts: implications for emplacement of the seamounts. *In* Keating, B. H., Fryer, P., Batiza, R., and Boehlert, G. W. (Eds.), *Seamounts, Islands, and Atolls*. Geophys. Monogr. Ser. 43: Washington (Am. Geophys. Union), 175–185.

Hussong, D. M., and Fryer, P., 1985. Forearc tectonics in the northern Marianas arc. *In* Nasu, N., Kobayashi, K., Uyeda, S., Kushiro, I., and Kagami, H. (Eds.), *Formation of Active Ocean Margins*: Tokyo (Terrapub), 273–290.

Li, Y.-H., Takahashi, T., and Broecker, W. S., 1969. Degree of saturation of calcium carbonate in the oceans. *J. Geophys. Res.*, 75:5507–5525.

Okada, H., and Bukry, D., 1980. Supplementary modification and introduction of code numbers to the low-latitude coccolith biostratigraphic zonation (Bukry, 1973, 1975). *Marine Micropaleontology*, 5:321–325.

Pearce, J. A., and Cann, J. R., 1973. Tectonic setting of basic volcanic rocks determined using trace element analysis. *Earth Planet. Sci. Lett.*, 19:290–300.

Pearce, J. A., and Wanming, D., 1988. The ophiolites of the Tibetan Geotraverse, Lhasa to Golmud (1985) and Lhasa to Kathmandu (1986). *Phil. Trans. R. Soc. London A.*, 327:215–238.

Ms 125A-108

NOTE: All core description forms ("barrel sheets") and core photographs have been printed on coated paper and bound as Section 4, near the back of the book, beginning on page 383.

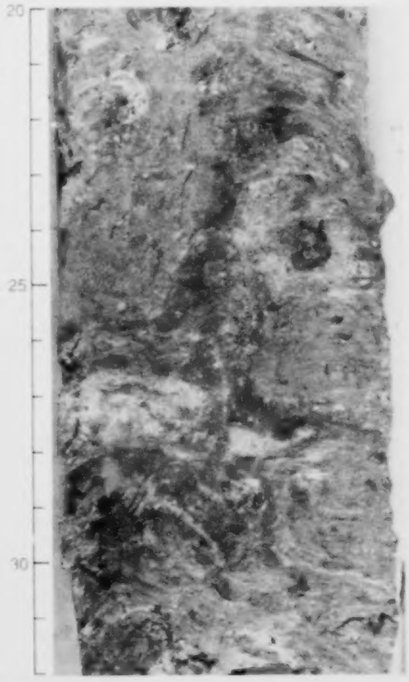

Figure 12. Interval 125-779A-7R-1, 20–32 cm, showing successive convolute folds affecting the serpentine sediments, flows, and microbreccias.

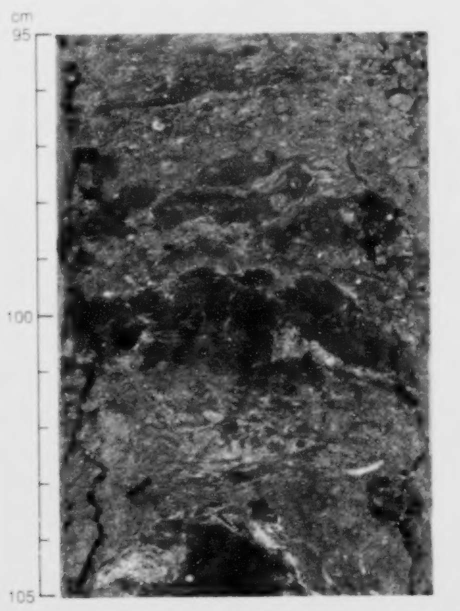

Figure 13. Interval 125-779A-13R-1, 95–105 cm. Primary layering and late foliation and scaly clay cleavage developed within the serpentine siltstones and microbreccias.

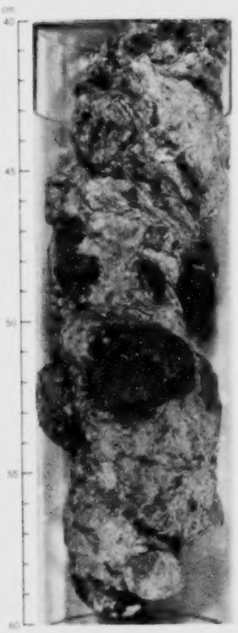
cm
40
45
50
55
60

Figure 14. Interval 125-779A-20R-1, 40–60 cm, showing helicoidal cleavage and asymmetric shape of clasts.

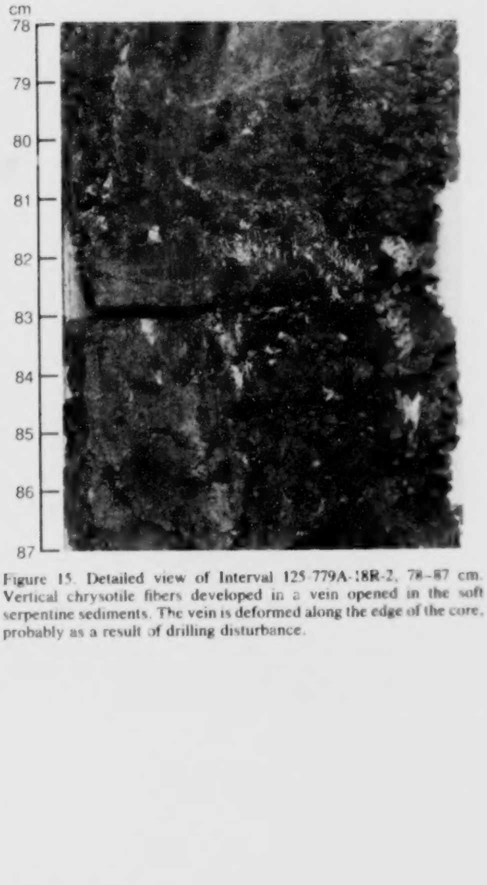
cm
78
79
80
81
82
83
84
85
86
87

Figure 15. Detailed view of Interval 125-779A-18R-2, 78–87 cm. Vertical chrysotile fibers developed in a vein opened in the soft serpentine sediments. The vein is deformed along the edge of the core, probably as a result of drilling disturbance.

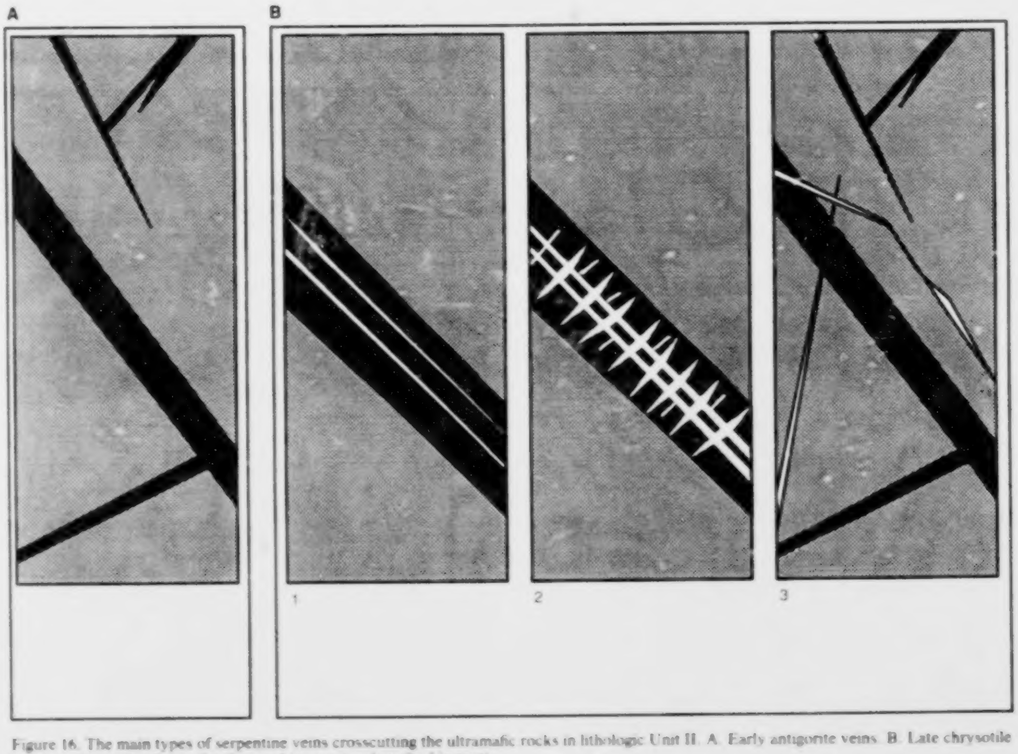

Figure 16. The main types of serpentine veins crosscutting the ultramafic rocks in lithologic Unit II. A. Early antigorite veins. B. Late chrysotile veins (1, 2, and 3 refer to the three subtype veins described in text).

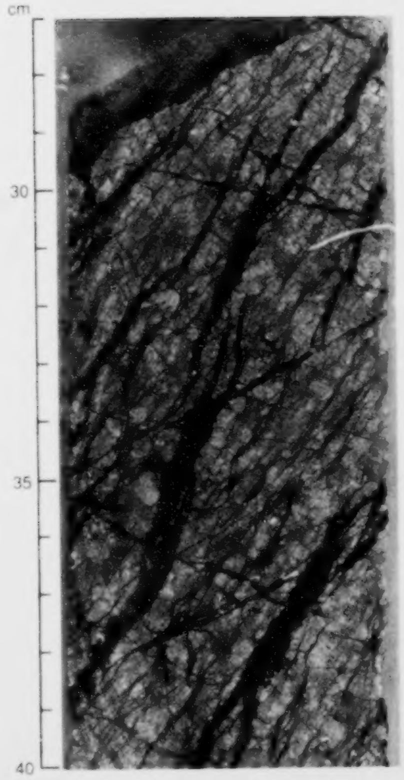

Figure 17. Antigorite veining in Interval 125-779A-17R-2, 27–40 cm. Anastomosing veining defines centimeter-size lenses of serpentinized peridotites. Notice that the uppermost centimeter of the piece corresponds to a major vein.

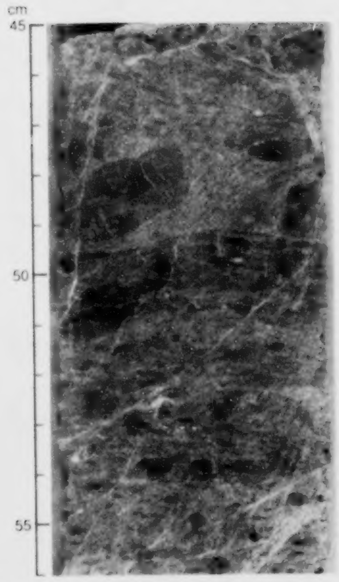

Figure 18. Interval 125-779A-31R-1, 45–56 cm. Cataclasis in a serpentine tectonic breccia.

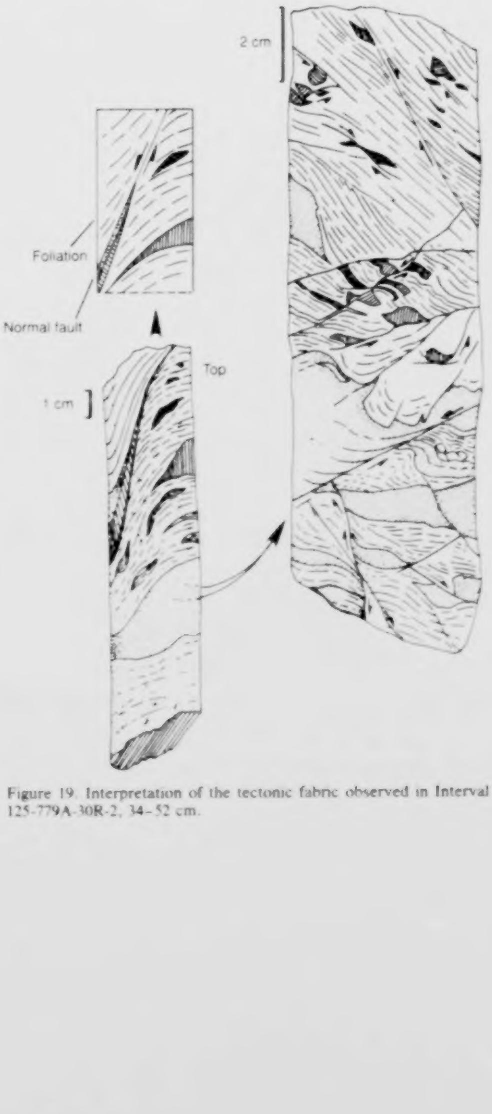
2 cm
Foliation
Normal fault
Top
1 cm

Figure 19. Interpretation of the tectonic fabric observed in Interval 125-779A-30R-2, 34–52 cm.

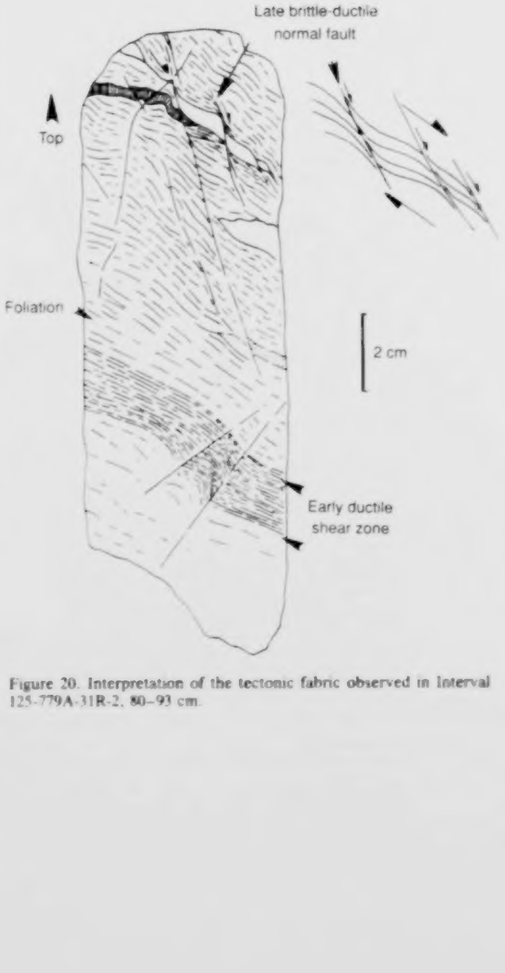
Late brittle-ductile
normal fault
Top
Foliation
2 cm
Early ductile
shear zone

Figure 20. Interpretation of the tectonic fabric observed in Interval 125-779A-31R-2, 80–93 cm.

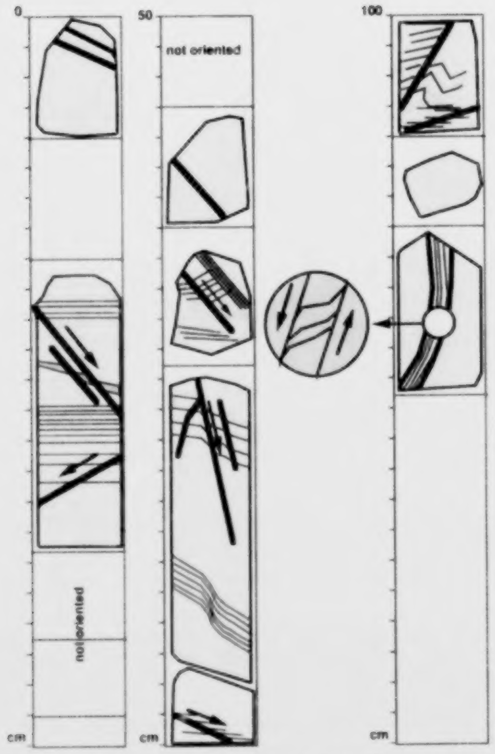
0
50
100
not oriented
not oriented
cm
cm
cm

Figure 21. Summary of the main results related to the tectonic fabric analysis of Section 125-779A-31R-2 (sheared metamicrogabbros). Thick lines represent late brittle faults with a sense of movement indicated. Thin lines parallel the early foliation. The core was split so that the apparent dip of the major faults would correspond to the true dip.

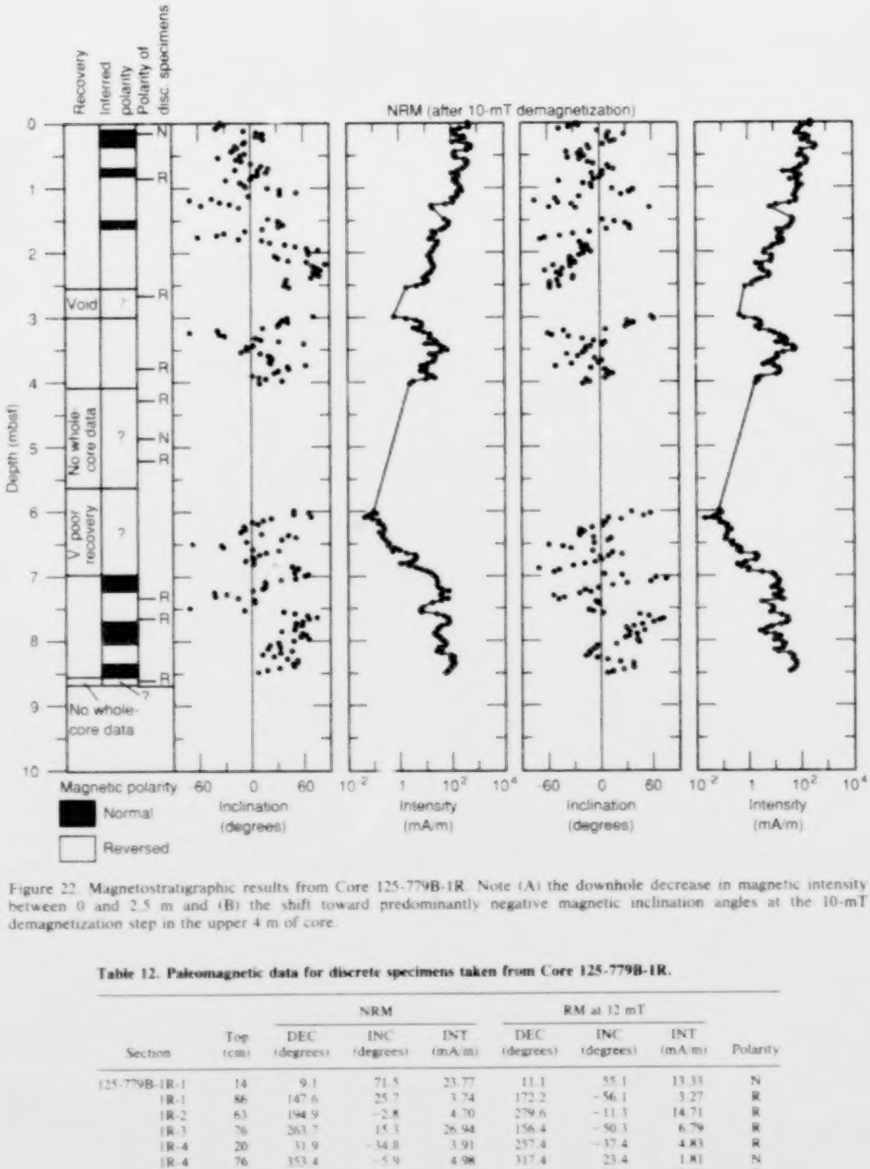

Figure 22. Magnetostratigraphic results from Core 125-779B-1R. Note (A) the downhole decrease in magnetic intensity between 0 and 2.5 m and (B) the shift toward predominantly negative magnetic inclination angles at the 10-mT demagnetization step in the upper 4 m of core.

Table 12. Paleomagnetic data for discrete specimens taken from Core 125-779B-1R.

		NRM			RM at 12 mT			
Section	Top (cm)	DEC (degrees)	INC (degrees)	INT (mA/m)	DEC (degrees)	INC (degrees)	INT (mA/m)	Polarity
125-779B-1R-1	14	9.1	71.5	23.77	11.1	55.1	13.33	N
1R-1	86	147.6	25.7	3.74	172.2	−56.1	3.27	R
1R-2	63	194.9	−2.8	4.70	279.6	−11.3	14.71	R
1R-3	76	263.7	15.3	26.94	156.4	−50.3	6.79	R
1R-4	20	31.9	−34.8	3.91	257.4	−37.4	4.83	R
1R-4	76	353.4	−5.9	4.98	317.4	23.4	1.81	N
1R-4	108	141.0	−17.0	17.80	156.0	−25.6	16.97	R
1R-5	125	84.0	35.6	16.05	141.4	−62.5	5.15	R
1R-6	9	18.4	50.5	4.61	277.3	−20.0	3.24	R
1R-CC	6	353.0	−27.5	387.67	7.5	−18.8	192.12	R

NRM = Natural remanent magnetization, DEC = Declination, INC = Inclination, INT = Intensity of magnetization, RM = remanent magnetization. (Note the rather large increase in intensity for the specimen from Section 125-779B-1R-2). N = normal, R = reversed.

Table 13. Index properties of sediments from Holes 779A and 779B.

Core, section interval (cm)	Depth (mbsf)	Bulk density (g/cm^3)	grain density (g/cm^3)	Porosity (%)	Water content (%)	Void ratio
125-779A-2R-2, 85–86	3.45	1.82	5.69	82.9	48.2	0.83
2R-3, 136–137	5.46	1.67	2.66	60.5	38.5	0.61
2R-4, 86–87	6.46	1.35	2.7	80.6	63.5	0.66
2R-5, 36–37	7.46	1.58	2.66	66.3	44.7	0.66
3R-CC, 17–20	10.77	2.67	2.67	0.3	0.1	0
4R-1, 27–29	20.37	2.29	2.29	0	0	0
4R-1, 58–59	20.68	1.95	2.66	43.6	23.8	0.44
5R-2, 34–37	31.39	2.83	2.83	0	0	0
5R-3, 34–35	32.89	1.88	2.65	47.8	27.1	0.48
6R-1, 18–20	39.38	2.99	3.01	0.9	0.3	0.01
6R-1, 46–47	39.56	1.99	2.62	39.3	20.9	0.39
8R-1, 25–27	58.75	2.39	2.54	9.6	4.3	0.1
8R-1, 45–49	58.95	2.7	2.7	0	0	0
9R-1, 33–35	68.43	1.89	2.35	349	19.6	0.35
9R-2, 52–54	70.05	2.64	2.64	0	0	0
10R-2, 70–73	79.63	2.74	2.74	0.5	0.2	0.01
13R-1, 91–92	107.51	1.86	2.86	54.6	31.2	0.55
14R-1, 76–78	116.96	2.87	2.87	0	0	0
14R-2, 60–62	118.3	2.94	2.94	0.1	0.1	0
16R-3, 48–50	138.98	2.86	2.88	1	0.4	0.01
17R-1, 81–83	146.01	2.99	3	0.3	0.1	0
17R-2, 30–32	147	2.96	2.96	0.1	0	0
17R-3, 30–32	148.42	2.76	2.76	0	0	0
18R-1, 64–67	155.54	1.94	2.64	43.6	23.9	0.44
18R-2, 27–31	156.67	2.17	2.71	32.1	15.8	0.32
18R-3, 13–4	157.94	2.31	2.99	34.6	15.9	0.35
19R-2, 97–99	161.87	3.04	3.04	0	0	0
22R-1, 58–60	170.68	2.65	2.65	0	0	0
22R-1, 63–65	170.73	2.73	2.73	0	0	0
22R-2, 18–20	171.78	2.86	2.86	0.1	0.1	0
22R-3, 55–67	173.65	2.82	2.82	0	0	0
24R-1, 36–38	187.56	2.86	2.86	0	0	0
25R-1, 85–87	197.65	2.65	2.65	0	0	0
26R-2, 50–52	207.94	2.71	2.71	0	0	0
26R-3, 101–103	209.56	2.57	2.58	1.2	0.5	0.01
27R-1, 57–59	216.77	1.9	2.59	44.3	24.8	0.44
28R-2, 58–59	227.05	1.98	2.67	41.8	22.4	0.42
28R-3, 26–28	228.23	2.64	2.64	0	0	0
29R-2, 33–35	236.23	1.86	2.71	50.3	28.7	0.5
30R-1, 48–49	245.48	1.81	2.52	47.2	27.6	0.47
30R-2, 87–89	247.17	2.45	2.63	11.1	4.8	0.11
31R-1, 26–28	254.96	2.47	2.64	10.7	4.6	0.11
31R-CC, 39–41	258.64	3.2	3.2	0	0	0
32R-1, 123–125	265.63	2.01	2.76	43.4	23	0.43
32R-2, 17–19	266.07	2.11	2.61	31.4	15.8	0.31
33R-2, 46–48	274.98	2.92	2.92	0.1	0	0
34R-1, 36–38	284.06	2.59	2.59	0	0	0
35R-1, 13–7	293.37	2.62	2.62	0	0	0
35R-1, 108–109	294.38	2.99	3	0.5	0.2	0.01
36R-1, 46–47	303.46	2.18	2.62	27.4	13.3	0.20
36R-1, 70–71	305.2	2.02	2.82	44.4	23.3	0.44
37R-1, 49–50	313.19	1.96	2.62	41.1	22.2	0.41
37R-2, 13–4	314.24	2.15	2.62	30	14.8	0.3

Table 14. Physical properties of sediments from Holes 779A and 779B.

Core section, interval (cm)	Depth (mbsf)	Thermal conductivity (W/mK)	Resistivity (ohms)	Formation factor	"A" Velocity (km/s)	"B" Velocity (km/s)
125-779A-1R-1, 47-51	0.50	1.004	23.4	2.73		
2R-1, 37	1.47	1.577				
2R-1, 127-131	2.39		21.4	2.50		
2R-3, 37	4.47	1.399				
4R-1, 27-29	20.37				3.10	
5R-2, 32-35	31.37				5.08	
5R-2, 40-43	31.45				6.85	
5R-3, 45	33.00	1.522				
6R-1, 18-20	39.28					4.18
6R-1, 39	39.49	1.876				
7R-1, 93	49.43	2.291				
8R-1, 25-27	58.75					3.64
8R-1, 33	58.83	2.403				
8R-1, 45-49	58.95				4.94	
9R-2, 35	69.88	2.227				
9R-2, 52-54	70.05					3.04
10R-2, 70-73	79.63					5.44
13R-1, 51	107.11	1.930				
13R-1, 74-78	107.36		76.0	8.87		
13R-1, 100-104	107.62		115.0	13.42		
13R-2, 11	108.21	2.062				
13R-2, 92-94	110.00				3.36	3.38
14R-1, 76-78	116.96				3.36	
16R-3, 48-50	138.93				5.27	5.15
17R-1, 81	146.01	2.257				
17R-2, 30	147.00	2.708				
17R-3, 30	148.42	1.889				
17R-4, 20	149.82	2.149				
18R-2, 37-41	156.76	2.298	184.0	21.48		
18R-2, 75-79	157.17		63.0	7.35		
19R-2, 97-99	161.87				5.15	5.27
20R-1, 12	169.22	1.483				
20R-1, 73	169.83	2.180				
22R-1, 58-60	170.68				4.22	3.91
22R-1, 63-65	170.73	3.200			4.56	4.88
22R-2, 18-20	171.78				6.06	6.23
22R-3, 55-57	173.65				4.91	5.86
24R-1, 36-38	187.56				4.23	
25R-1, 81	197.61	2.330				
25-1, 85-87	197.65				5.29	
26R-3, 94	209.49	2.140				
26R-2, 0	207.44	2.000				
26R-2, 50-52	207.94				5.01	
26R-3, 101-103	209.56				4.98	
28R-3, 26-28	228.23					4.31
28R-3, 118	229.15	1.574				
29R-2, 28-32	237.30		37.1	4.35		
29R-2, 147-149	237.35	1.571				3.18
30R-1, 139	238.00	2.022				
30R-2, 84	247.14	2.285				
31R-1, 18	254.88	2.279				
31R-1, 26-28	254.96				3.57	
31R-1, 124	255.94	1.709				
31R-2, 94	257.14	3.233				
31R-2, 101-105	257.23				5.34	4.79
31R-3, 27	257.90	3.014				
31R-CC, 39-41	258.64				4.77	4.88
32R-1, 67-71	265.09		78.3	9.14		
32R-1, 117-121	265.60	2.086	55.2	6.44		
32R-2, 51-55	266.43		82.4	9.62		
32R-2, 81-85	266.73		58.0	6.77		
32R-3, 1	267.41	1.775				
33R-2, 46-48	274.98				4.59	3.85
33R-2, 73	275.25	1.579				
33R-3, 8	275.50	1.397				
34R-1, 32	284.02	1.745				
34R-1, 36-38	284.06				5.12	5.24
35R-1, 13-7	293.30	2.677			5.23	5.67
35R-1, 108-109	294.31	1.937			5.52	5.66
36R-1, 58	303.58	1.749				
36R-1, 43	304.63	2.092				
36R-2, 13-17	304.93		50.6	5.91		
36R-2, 56-60	305.08		60.6	7.07		
36R-2, 76-80	305.28		47.6	5.56		
36R-2, 110-114	305.62		62.3	7.27		
37R-1, 35-39	313.07		44.0	5.14		
37R-1, 100-104	313.70	2.342	106.0	12.37		
37R-2, 10	314.30	2.027				
125-779B-1H-1, 13-7	0.09		22.5	2.63		
1H-1, 60-64	0.62		22.4	2.61		
1H-1, 126-130	1.28		18.5	2.16		
1H-2, 15-19	1.67		19.5	2.28		
1H-2, 83-87	2.35		20.5	2.39		
1H-2, 98-102	2.50		31.4	3.67		

Table 15. Physical properties of sediments from Hole 779B.

Core section, interval (cm)	Depth (mbsf)	Bulk density	Gram density (g/cm^3)	Porosity (%)	Water content (%)	Void ratio
125-779B-1H-2, 43–45	1.93	1.74	2.6	54.5	33.2	0.54
1H-5, 91–93	6.91	1.81	2.79	55.7	32.7	0.56
1H-6, 48–50	7.98	1.55	2.67	68.3	46.9	0.68

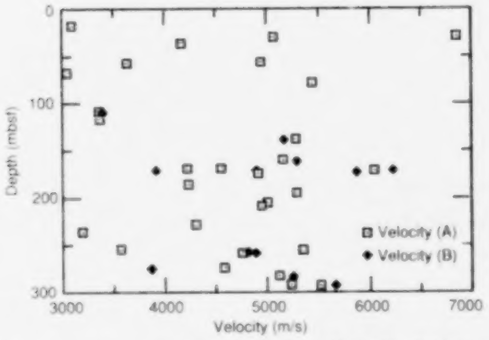

Figure 23. Velocity of subsamples vs. depth in Hole 779A. Velocities measured in the vertical direction along the core are labeled A and velocities measured in the horizontal direction perpendicular to the core are labled B. Note the scatter in the data.

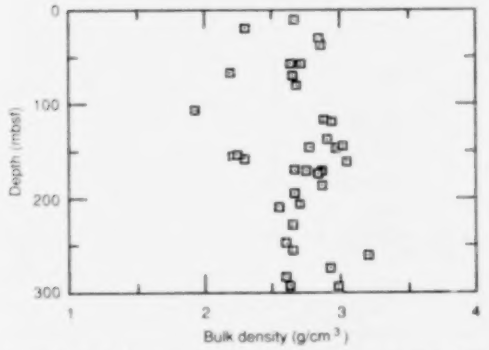

Figure 24. Bulk densities of hard-rock subsamples vs. depth in Hole 779A.

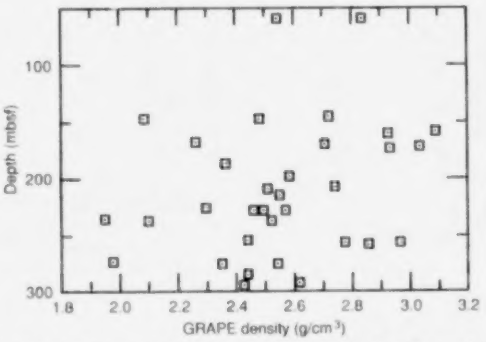

Figure 25. Densities from 2-min GRAPE analysis of whole-round, hard-rock core samples vs. depth in Hole 779A. Note the scatter in the data.

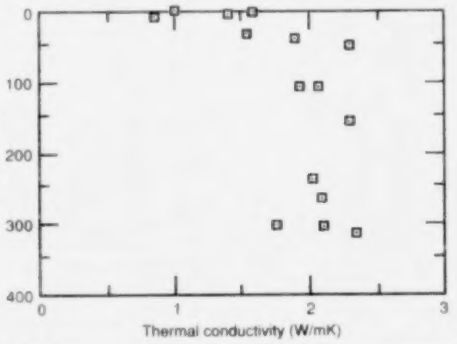

Figure 26. Thermal conductivity of soft, whole-round core samples vs. depth in Hole 779A. Measurements were performed using a needle probe that penetrated the core liner into the core. Conductivity increases slightly in the upper part of the hole and is then nearly constant to the bottom of the hole.

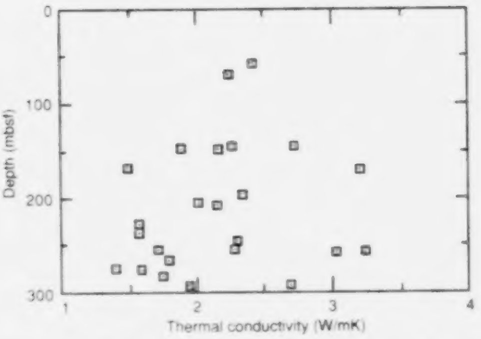

Figure 27. Thermal conductivity of hard-rock subsamples vs. depth in Hole 779A. Note the scatter in the data.

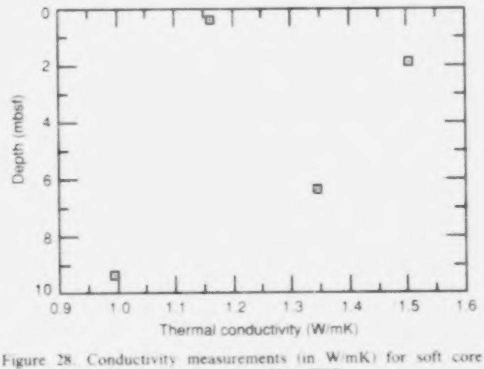

Figure 28. Conductivity measurements (in W/mK) for soft core samples (through the core liner) from Hole 779B.

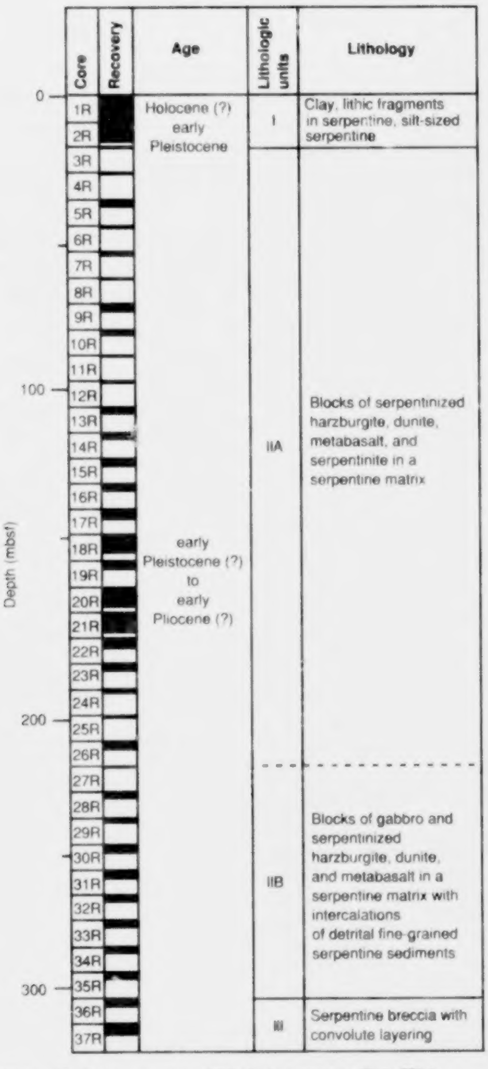

Figure 29. Core recovery and lithologic summary, Hole 779A.

Fryer, P., Pearce, J. A., Stokking, L. B., et al., 1990
Proceedings of the Ocean Drilling Program, Initial Reports, Vol. 125

8. SITE 780[1]

Shipboard Scientific Party[2]

HOLE 780A

Date occupied: 4 March 1989

Date departed: 5 March 1989

Time on hole: 21 hr, 15 min

Position: 19°32.51′N, 146°39.27′E

Bottom felt (rig floor; m, drill-pipe measurement): 3097.0

Distance between rig floor and sea level (m): 11.1

Water depth (drill-pipe measurement from sea level, m): 3086.8

Total depth (rig floor, m): 3101.4

Penetration (m): 3.5

Number of cores: 1

Total length of cored section (m): 3.5

Total core recovered (m): 3.54

Core recovery (%): 101

Oldest sediment cored:
Depth (mbsf): 3.54
Nature: silt-sized serpentine
Earliest age: late Pleistocene

HOLE 780B

Date occupied: 6 March 1989

Date departed: 6 March 1989

Time on hole: 23 hr

Position: 19°32.47′N, 146°39.22′E

Bottom felt (rig floor; m, drill-pipe measurement): 3105.1

Distance between rig floor and sea level (m): 11.1

Water depth (drill-pipe measurement from sea level, m): 3094.0

Total depth (rig floor, m): 3123.3

Penetration (m): 18.2

Number of cores: 2

Total length of cored section (m): 18.2

Total core recovered (m): 10.34

Core recovery (%): 56.6

Oldest sediment cored:
Depth (mbsf): 10.29
Nature: silt-sized serpentine
Earliest age: late Pleistocene

HOLE 780C

Date occupied: 6 March 1989

Date departed: 9 March 1989

Time on hole: 2 days, 23 hr, 30 min

Position: 19°32.53′N, 146°39.21′E

Bottom felt (rig floor; m, drill-pipe measurement): 3094.5

Distance between rig floor and sea level (m): 11.1

Water depth (drill-pipe measurement from sea level, m): 3083.4

Total depth (rig floor, m): 3258.0

Penetration (m): 163.5

Number of cores: 18

Total length of cored section (m): 163.5

Total core recovered (m): 14.4

Core recovery (%): 8.8

Oldest sediment cored:
Depth (mbsf): 33.7
Nature: silt-sized serpentine
Earliest age: middle Pleistocene(?)
Measured velocity (km/s): 1.5–2

Hard rock:
Depth (mbsf): 33.7
Nature: serpentinized ultramafic rocks
Measured velocity (km/s): 5–6

HOLE 780D

Date occupied: 9 March 1989

Date departed: 10 March 1989

Time on hole: 1 day, 19 hr, 15 min

Position: 19°32.55′N, 146°39.20′E

Bottom felt (rig floor; m, drill-pipe measurement): 3100.1

Distance between rig floor and sea level (m): 11.2

Water depth (drill-pipe measurement from sea level, m): 3088.9

Total depth (rig floor, m): 3132.5

Penetration (m): 32.4

Number of cores: 7

Total length of cored section (m): 32.4

Total core recovered (m): 9.09

Core recovery (%): 28

Oldest sediment cored:
Depth (mbsf): 32.4
Nature: sandy silt-sized serpentine
Earliest age: Pleistocene (?)

Principal results: Site 780 is situated on the west-southwest side of the summit of Conical Seamount, about 2 nmi from the flank Sites 778 and 779. Site selection was based on *Alvin* submersible dives that indicated this area was covered with sediment and marked by active venting of fluids and precipitation of material from solution. The principal objectives of this site were to investigate (1) the physical properties and mineralogy of the serpentine flow materials and entrained clasts from the center of the diapir, (2) the composition and source of fluids associated with these materials, and (3) the potential for ore deposition within the seamount. In addition, this site was expected to provide further information about some of the objectives of the flank sites: in particular the nature, composition, and metamorphism of the forearc lithosphere and the construction of the seamount.

---

[1] Fryer, P., Pearce, J. A., Stokking, L. B., et al., 1990. *Proc. ODP, Init. Repts.*, 125: College Station, TX (Ocean Drilling Program).

[2] Shipboard Scientific Party is as given in list of participants preceding the contents.

A total of four holes were drilled: Hole 780A was cored with an APC and recovered only 3.5 m of sediment; Hole 780B was drilled with an RCB to a depth of 18.2 mbsf with 57% recovery; Hole 780C was drilled with an RCB to a depth of 163.5 mbsf with 9% recovery; and Hole 780D was drilled with an XCB to a depth of 32.4 mbsf with 28% recovery. Overall, success in drilling at this site was constrained by the interbedding of hard serpentinized peridotite and very soft, apparently fluid-charged, unconsolidated serpentine.

Two major lithologic units were recovered at Site 780: Unit I (0–3.5 mbsf in Hole 780A; 0–18.2 mbsf in Hole 780B; 0–14.0 mbsf in Hole 780C; and 0–15.4 mbsf in Hole 780D) comprises middle Pleistocene(?) to Holocene(?), sand- and silt-sized serpentine having rare intervals of foraminifer-rich serpentine clay and serpentine-rich silty-clay; and Unit II (14.0–163.5 mbsf in Hole 780C and 15.4–32.4 mbsf in Hole 780D) comprises intervals of serpentinized ultramafic rocks in a matrix of sandy silt- and clayey silt-sized serpentine.

The mineralogy of the clasts and serpentine-rich matrix is similar to that of the materials from the flank sites (Sites 778 and 779), except that the matrix contains delicate aragonite needles indicative of authigenic growth after the serpentine was emplaced. In terms of structure, however, the matrix, though chaotic, typically lacks the foliation and shear fabric seen in the matrix from the flank sites. Therefore, this matrix may be interpreted as upwelling serpentinite, upon which foliation and shear fabric have been imposed by compaction, extension, and pure shear during the downhill creep of serpentinite debris flows. Studies of physical properties give a density range of 1.75 to 2.0 g/cm^3 and compressional-wave velocities of 1.5 to 2 km/s for this serpentine-rich matrix and together with rheological measurements indicate that it is a weak, highly non-ideal, plastic material capable of supporting blocks up to 20 m wide.

Analyses of interstitial pore-water samples at Site 780 revealed marked downhole chemical changes, including an increase in alkalinity from 2.5 to 34 and in pH from about 8 to 12.4, together with major depletions in calcium and magnesium; increases in sulfate, potassium, and ammonia; and decreases in salinity and chlorinity. These changes take place within a few meters of the seafloor, showing that the fluid entrained within the serpentinite may only mix with seawater at shallow levels. The magnitude and direction of these changes also differ in significant ways compared to the flank sites, revealing major variability in fluid chemistry and fluid flow within the seamount.

BACKGROUND AND SCIENTIFIC OBJECTIVES

The summit of Conical Seamount, where Site 780 is located, lies at a depth of about 3100 m (Fig. 1). SeaMARC II side-scanning sonar images of this summit revealed recent flows of unconsolidated sedimentary serpentinite, apparently emanating from and mantling the summit region. Thus, we inferred that the summit region of the seamount might be the site of emanations of recent, diapirically emplaced serpentinite flows (Fryer et al., 1987; Fryer et al., this volume). Results of *Alvin* dive studies of the seamount summit showed that fluids are actively seeping from chimneys and related structures on the west side of the southern summit knoll (Fig. 2). These fluids are precipitating carbonate and silicate compounds that form the chimneys and cement the uppermost portion of the sedimentary serpentinite flows (Fryer et al., 1987). At no other locality on the seamount that was explored with the *Alvin* submersible, or subsequently surveyed with bottom video or still photography (P. Stoffers, pers. comm., 1989), were active seeps or chimney structures observed. The southwestern side of the summit of Conical Seamount therefore provides a locality for studying the active formation of sedimentary serpentinite flows and their associated fluids and mineral deposits.

Drilling at Site 780 was undertaken to enable us to investigate (1) the mechanical properties of the diapiric neck and emplacement mechanism of the diapir, (2) the composition of the associated fluids and entrained metamorphosed xenoliths, (3) the compositional and physical variability of the rising diapiric material, and (4) the potential for ore deposition within serpentinite diapirs. While these immediate objectives are site specific, they apply to the understanding of several larger questions. The most obvious of these are both the relationship of diapirism to the history of development of the forearc region of an intraoceanic arc system and the geochemical mass balance of the subduction process.

The physical properties of the diapir and the mechanism of its emplacement can be studied in greatest detail at Site 780. Here, strong evidence suggests that the rising serpentinite diapir entrains deep-seated fluids as it rises and loses these fluids during protrusion of the serpentine flows onto the surface (Fryer et al., 1987; Haggerty, 1987a, 1987b; Fryer et al., this volume). Strong evidence exists for compaction of these flows soon after they are erupted, perhaps because of the escape of entrained fluids. Once the rising diapir has stopped erupting and/or stopped venting fluids, the density of the serpentinite may increase. It is also possible that the physical properties of the diapir will change with depth as well as with age. Documenting such changes and the study of the physical properties of the diapiric material will permit better interpretation of sedimentary serpentinite deposits in subaerial exposures, such as those of the basal Great Valley sequence in Napa County, California (Phipps, 1984). Studies of the composition of fluids collected with the *Alvin* from an actively seeping chimney structure on Conical Seamount (Fryer et al., this volume) have revealed high pH (9.28 vs. 7.72 for ambient seawater), high alkalinity (5.53 vs. 2.41 meq/L) and enrichment in CH_4 (1000 vs. 2.1 nM), SiO_2 (0.75 vs. 0.12 mM), SO_4 (30.4 vs. 28.6 mM), and H_2S (2.1 nM vs. not detected) (B. Tilbrook, pers. comm., 1988). The CH_4 and H_2S detected in the vent fluids were particularly interesting. Because the Mariana forearc has only a small volume of sedimentary substrate (Hussong and Uyeda, 1981), with organic carbon contents typically less than 0.3% (Schorno, 1981), the methane and sulfide in the Mariana vent fluids are unlikely to have formed by the biogenic processes associated with accretionary complexes (Kulm et al., 1986). Rather, they were probably generated during serpentinization reactions. Overall, the chemical analyses of these fluids imply that deep-seated serpentinization processes, juvenile mantle fluids, interaction of seawater with crustal rocks, and interactions of seawater with the surficial serpentinite may all contribute to the composition of the fluids.

Compositions of trace element and stable isotopes of the carbonate chimney materials from Conical Seamount are also consistent with deposition from serpentinite-related fluids, which contained components from either the forearc mantle or the subducted slab or both (Haggerty, 1987a). Compared with carbonates of the fracture zone thought to have a dominantly seawater origin, for example, Mariana aragonite is depleted in strontium (Mariana samples = 7,000–9,400 ppm; fracture-zone aragonite = 9,500–11,600 ppm), enriched in magnesium (Mariana = 750–6,300 <300 ppm, fracture zone, <300 ppm), and has a significantly lighter carbon isotopic signature (Mariana = −1.2 to −21.2‰, fracture zone = +0.03 to +1.12‰) and heavier oxygen isotopic signature (Mariana = +5.1 to +7.6‰, fracture zone = +3.16 to +4.87‰). These values are consistent with both an origin involving seawater interactions with ultramafic rocks and an origin involving derivation from dewatering of subducted oceanic lithosphere and/or from the

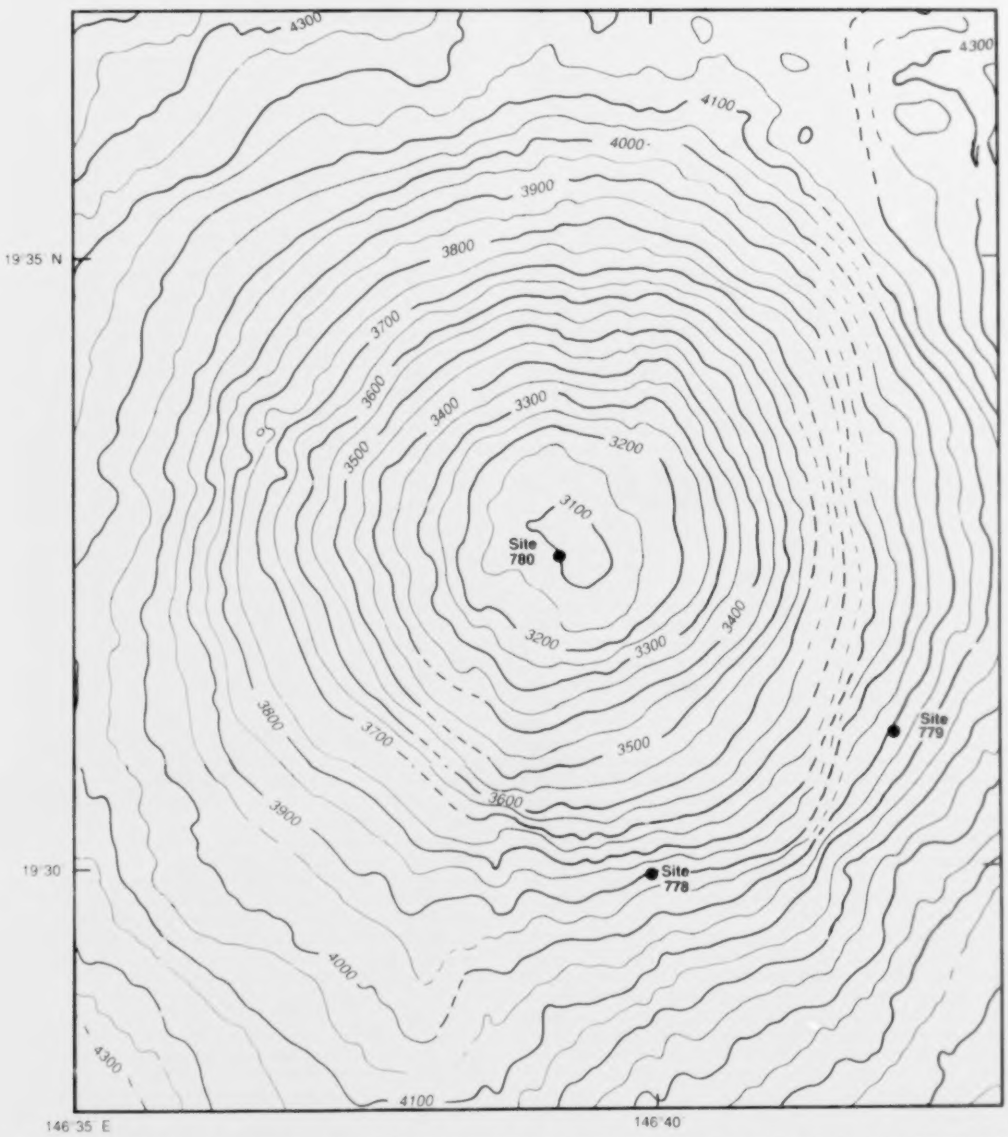
4300
4300
4100
4000
3900
3800
3700
3600
3500
3400
3300
3200
3100
Site 780
3200
3300
3400
3800
3700
3500
3600
3900
Site 779
Site 778
4000
4300
4100
19°35′ N
19°30′
146°35′ E
146°40′

Figure 1. SeaBeam bathymetric contour map (in meters) of the upper flanks of Conical Seamount, showing the positions of Sites 778, 779, and 780.

mantle underlying the forearc. Detailed sampling at depth within the serpentinite body should constrain either the nature of the shallow level reactions influencing the fluid composition or the possible sources of the fluids.

Several sedimentary serpentinite deposits on land have yielded ore-grade deposits of a variety of compounds, notably nickel/iron, mercury, chromium, and native gold. The nature of these deposits depends on the local oxidation-reduction conditions of the rising diapir. By drilling, we hoped to secure samples that would allow us to constrain the small-scale variations in conditions of fluids within the serpentinite.

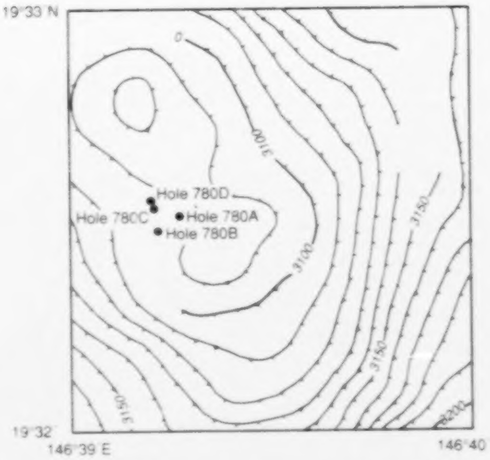

Figure 2. Detailed SeaBeam bathymetry map of the summit of Conical Seamount, showing the positions of Holes 780A through 780D.

Table 1. Coring summary for Site 780.

Core no.	Date (Mar 1989)	Time (UTC)	Depth (mbsf)	Length cored (m)	Length recovered (m)	Recovery (%)
125-780A-1H	4	1845	0–3.5	3.5	3.54	101.0
Coring totals				3.5	3.54	101.0
125-780B-1R	5	0755	0–8.7	8.7	8.75	100.0
2R	5	0915	8.7–18.2	9.5	1.59	16.7
Coring totals				18.2	10.34	56.8
125-780C-1R	6	0450	0–5.5	5.5	5.49	99.8
2R	6	0545	5.5–14.0	8.5	0.56	6.6
3R	6	0830	14.0–23.5	9.5	0.59	6.2
4R	6	0940	23.5–33.0	9.5	0.26	2.7
5R	6	1110	33.0–42.5	9.5	0.67	7.1
6R	6	1330	42.5–52.1	9.6	0.85	8.9
7R	6	1510	52.1–61.5	9.4	0.26	2.8
8R	6	1830	61.5–71.1	9.6	1.15	12.0
9R	6	2030	71.1–80.8	9.7	0.57	5.9
10R	6	2200	80.8–90.5	9.7	0.27	2.8
11R	6	2300	90.5–100.2	9.7	0.07	0.7
12R	7	0300	100.2–106.5	6.3	0.38	6.0
13R	7	0400	106.5–116.0	9.5	0.67	7.1
14R	7	0530	116.0–125.5	9.5	0.09	1.0
15R	7	0630	125.5–135.0	9.5	0.62	6.5
16R	7	0815	135.0–144.6	9.6	0.48	5.0
17R	7	0950	144.6–154.0	9.4	0.06	0.6
18R	7	1515	154.0–163.5	9.5	1.40	14.7
Coring totals				163.5	14.44	8.8
125-780D-1X	8	0800	0–2.5	2.5	2.50	100.0
2X	8	0910	2.5–12.0	9.5	1.51	15.9
3X	8	1015	12.0–15.4	3.4	0.31	9.1
4C	8	1825	15.4–16.9	1.5	0.00	0.0
5X	8	2100	16.9–20.4	3.5	0.16	4.6
6X	9	0030	20.4–27.4	7.0	1.29	18.4
7X	9	0330	27.4–32.4	5.0	3.32	66.4
Coring totals				32.4	9.09	28.1

OPERATIONS

Transit to Site 780 (MAR-3A)

Although Site 780 is located on the summit of Conical Seamount, 2.5 nmi from Site 779, a seismic survey was required to determine its exact location. The survey began during a GPS window at 1715 hr UTC (Universal Time Coordinated), 3 March. Site 780 was established by dropping a beacon at 2245UTC, 3 March.

HOLE 780A

A standard APC/XCB bottom-hole assembly (BHA) was prepared with a soft-formation bit and lockable flapper valve (LFV). The trip in began at 0030UTC, 4 March, when the drill bit was lowered through the drill floor. A small area was targeted for drilling, and the television camera was lowered to scan the seafloor for the best spud site. At 0845UTC, 4 March, Hole 780A was spudded with the APC. The water depth was determined (as 3086.8 mbsl) by observing the drill string tag the seafloor.

Unfortunately, the APC core barrel bent on impact when the first APC was shot. Efforts to retrieve the core barrel proved futile. The drill string was manipulated in an attempt to break off the bent core barrel so that the hole could be continued with the XCB and the pressure core sampler (PCS). During this procedure, the television cable became tangled in the drill string and/or at the moon pool doors, causing the cable to fail in the moon pool area. The vibration-isolated television (VIT) frame with the television camera and 3100 m of cable were lost. The drill string was tripped out slowly in the hope that the fouled cable and bent core barrel would retain the VIT. When the BHA was pulled into the moon pool, however, only the bent core barrel was found. Hole 780A officially ended when the bit was back on deck at 1830UTC, 4 March. The APC was deployed once to a depth of 3.5 mbsf, where we recovered 3.54 m of core for a recovery rate of 101% (Table 1).

HOLE 780B

The vessel was offset 100 m west, and a standard RCB BHA was prepared with a soft-formation bit and mechanical bit release (MBR). Hole 780B was spudded at 0530UTC, 5 March. The first core barrel retrieved had a shattered liner, which required us to respud the hole. Hole 780B was respudded at 0645UTC, 5 March, establishing the mud line at 3094.0 mbsl with the first core.

The sinker-bar assembly was lost during our attempt to retrieve Core 125-780B-3R. Apparently, the bit had followed the slope of a hard serpentinite layer, causing part of the BHA to break off. The drill string was tripped out, and Hole 780B officially ended at 1900UTC, 5 March. Two successful cores were recovered from Hole 780B to a total depth of 18.2 mbsf using the RCB. A total of 10.34 m of core was recovered for a recovery rate of 57% (Table 1).

HOLE 780C

The *Resolution* was offset 50 m north. Another standard RCB BHA was prepared and tripped to the seafloor. Hole 780C was spudded at 1900UTC, 5 March. The mud line was established at 3083.4 mbsl with recovery of the first core. The hard serpentinite present in Hole 780B was encountered at 14 mbsf in Hole 780C and was penetrated after rotation of 1.75 hr. Drilling continued, but with considerable difficulty. At a total depth of 163.5 mbsf, the hole finally collapsed, and 20 m of hole was lost.

The shipboard scientific party hoped to log the hole. Although hole conditions were not favorable, the bit was released and the logging line prepared. The first and second logging runs were aborted because of problems with the cable head. By the time the logging tools reached the open hole, the hole had closed in, curtailing the logging. A temperature profile was the only result of the logging effort.

A total of 18 RCB cores were taken from Hole 780C, recovering 14.44 m of core for a recovery of 9% (Table 1). Hole 780C officially ended with the BHA back on deck at 1830UTC, 8 March.

HOLE 780D

Because of the poor recovery in Hole 780C, the vessel was offset 50 m northwest and, using the new XCB (Leg 124E), Hole 780D was spudded at 0100UTC, 9 March. During retrieval of the first core barrel, at 1100 m below the dual elevator stool (DES), the sand line parted approximately 25 m above the sinker-bar assembly. When finally recovered, the core barrel was empty.

Hole 780D was respudded at 0700UTC, 9 March, and the first core established the mud line at 3088.9 mbsl. A hard serpentinite layer was encountered at 16.9 mbsf, where 7.5 hr of rotation was required to penetrate it. A standard carbide-tooth center bit was used to drill the first meter of the 1.5-m-thick layer. An impregnated diamond cutting shoe was installed on an XCB core barrel and deployed. Penetration rates increased noticeably, and a small core of the serpentinite was recovered.

After penetrating the hard serpentinite layer, the water sampler temperature probe (WSTP) was deployed at a depth of 20.4 mbsf. The water sampler valve failed to open, but temperature data were obtained. The WSTP was deployed again at 27.4 mbsf and at 41.8 mbsf. The second deployment recovered a water sample, but no temperature data. The third deployment resulted in the acquisition of both a water sample and temperature data.

Hole 780D and Site 780 were abandoned at the request of the Co-Chief Scientists and officially ended at 1345UTC, 10 March, when the bit was back on deck. The XCB was deployed six times in Hole 780D, which resulted in 32.4 m cored, and core recovery of 9.1 m for a recovery rate of 28.1% (Table 1). Drilling produced another 10.9 m of penetration to a total depth of 41.8 mbsf.

LITHOSTRATIGRAPHY

Lithologic Summary

At Site 780, four holes were drilled within 163 m of each other into the summit of Conical Seamount. The stratigraphic section at Site 780 has been divided into two lithologic units: lithologic Unit I of sand- and silt-sized serpentine, with intervals of foraminifer-rich serpentine clay and serpentine-rich clayey silt; and lithologic Unit II of serpentinized harzburgite and subordinate serpentinized dunite in a serpentine matrix (for a description of the metamorphosed rocks, see "Igneous and Metamorphic Petrology" section, this chapter). These units, their sub-bottom depths, and biostratigraphic ages are summarized in Table 2.

Unit I

Sections 125-780A-1H-1, 0 cm, to 125-780A-1H-1-CC; depth, 0–3.5 mbsf; Sections 125-780B-1R-1, 0 cm, to 125-780B-2R-CC; depth, 0–18.2 mbsf; Sections 125-780C-1R-1, 0 cm, to 125-780C-2R-CC; depth, 0–14 mbsf; Sections 125-780D-1X-1, 0 cm, to 125-780D-3X-CC; depth 0–15.4 mbsf.

This unit extends from the sediment/water interface to a maximum depth of 18.2 mbsf and is primarily a multicolored sand- and silt-sized serpentine, with sand- to pebble-sized clasts of serpentinite and other lithic types. Filamentous opaque mineral aggregates (interpreted as remnants of bacterial mats) were found in smear slides throughout this unit.

Calcareous nannofossils identified in Sample 125-780C-2R-CC are middle to late Pleistocene in age. The uppermost section of the first core (material associated with the present surface of the seafloor) was not sampled for biostratigraphic dating from the majority of holes on this leg. Therefore, the age of that sediment associated with the top of these holes has been inferred as Holocene. This inference at Site 780 is supported by the biostratigraphic age determined for Sample 125-780D-1X-1, 6 cm, which is of late Pleistocene age on the basis of the nannofossil assemblage. The age of the base of the unit is unknown. A middle to late Pleistocene age was obtained from nannofossil assemblages in Samples 125-780A-1H-CC; 125-780B-1R-3, 11 cm; 125-780C-1R-2, 112 cm; 125-780C-1R-3, 81–83 cm; 125-780C-1R-CC; and 125-780C-2R-CC. Sediments in all remaining core-catcher samples from beneath the above-listed samples from Unit I are barren; the unit can thus be inferred to be at least middle Pleistocene in age and may be older (see "Biostratigraphy" section, this chapter).

Dark green (5B 4/1 to 5G 7/2) and black (7.5YR 2/0), angular to rounded clasts of serpentinite, ranging in size from 1 mm to 5 cm, are scattered throughout the multicolored sand- and silt-sized serpentine in Unit I. Overall, the color of the unit is predominantly bluish gray (5B 4/1 to 7/1). A multicolored appearance results from the presence of light olive gray (5Y 5/2), brown (10YR 5/3), and dark gray (7.5YR 4/0) intervals, mottled with

Table 2. Lithologic units recovered at Site 780, Leg 125.

Lithologic unit/subunit	Cores	Depth (mbsf)	Dominant lithology	Stratigraphic age
I	125-780A-1H-1, 0 cm to 125-780A-1H-CC	0–3.5	Sand-, and silt-sized serpentine with some intervals aragonite-rich;	Holocene(?) to middle Pleistocene(?)
	125-780B-1R-1, 0 cm to 125-780B-2R-CC	0–18.2	rare intervals of foraminifer-rich serpentine clay, and serpentine-rich silty clay.	
	125-780C-1R-1, 0 cm to 125-780C-2R-CC	0–14.0		
	125-780D-1X-1, 0 cm to 125-780D-3X-CC	0–15.4		
II	125-780C-3R-1, 0 cm to 125-780C-18R-CC	14.0–163.5	Intervals of serpentinized harzburgite and dunite in a	(?)
	125-780D-4X-1, 0 cm to 125-780D-7X-CC	15.4–32.4	matrix of sandy silt, and clayey silt-sized serpentine	

dusky blue (5PB 3/2), pale yellow (5Y 8/3), or light green (5G 7/2). The unit has been variably disturbed by drilling, which enhances the mottled appearance. Color variations are not reflected in the composition of the multicolored serpentine, which is 75% to 98% serpentine, 3% to 20% opaque minerals, 0% to 20% aragonite, 0% to 10% zoisite, 2% to 10% chlorite, and up to a trace of amphibole, garnet, and epidote.

Most of the serpentine matrix lacks biogenic and detrital components, but does contain authigenic aragonite needles. An exception is the material recovered in the APC core (Core 125-780A-1H) from Hole 780A, where aragonite crystals are found only in the serpentine clay containing trace amounts of foraminifers, nannofossils, radiolarians, and silicoflagellates (Sample 125-780A-1H-CC). The presence of acicular aragonite crystals is characteristic of the matrix of Unit I, in which the acicular aragonite sometimes forms a mesh that gives a firm or stiff texture to the serpentine. No obvious structures of primary sedimentary origin are present. All structures are indicative of tectonic deformation (see "Structural Studies" section, this chapter).

Unit I also contains some sediments that have an obvious biogenic and detrital component. There are foraminifer-bearing serpentine silts and clays that contain serpentine (68%–76%), opaque minerals (5%–10%), aragonite (5%–6%), foraminifers (10%), nannofossils (1%–2%), spicules (0%–3%), silicoflagellates (1%–2%), diatoms (1%), and radiolarians (0%–1%) (in Samples 125-780B-1R-1, 77 cm; 125-780D-1X-2, 2 cm), as well as serpentine clay that contains clay (20%), serpentine (55%), chlorite (trace), opaque minerals (20%), and zoisite (5%). Where the opaque minerals are abundant in smear slides, they are present as filamentous opaque mineral aggregates that may be a remnant of a bacterial mat (for example, Sample 125-780A-1H-CC). Intercalations of these sediments containing pelagic detritus indicate periods of multiple exposure of serpentine at the seafloor.

Aragonite near the sediment/water interface is unusual at this water depth (Haggerty, 1980), as noted also for Sites 778 and 779, because seawater below a few hundred meters in the present-day Pacific Ocean is undersaturated with respect to aragonite (Li et al., 1969; Berner and Honjo, 1981), and because the aragonite compensation depth is less than 1000 mbsl throughout the Pacific, often as shallow as 400 mbsl (Berger, 1970). The presence of aragonite crystals in the clay and serpentine thus implies authigenic growth after serpentine emplacement and flow.

On the basis of similar lithologies and biostratigraphic criteria, this unit correlates with Unit I at Sites 778 and 779. This assumption may not be valid if the flank site drill holes are through serpentine flows and if the summit holes are through *in-situ* serpentine.

Unit II

Sections 125-780C-3R-1, 0 cm, to 125-780C-18R-CC; depth, 14–163.5 mbsf; Sections 125-780D-4X-1, 0 cm, to 125-780D-7X-CC; depth, 15.4–32.4 mbsf.

Lithologic Unit II contains intervals of serpentinized harzburgite and serpentinized dunite (see "Igneous and Metamorphic Petrology" section, this chapter) in a serpentine matrix. This matrix is bluish gray (5B 5/1) to greenish gray (5BG 5/1 and 6/1) and contains serpentinite clasts ranging from 1 mm to 1 cm in size. The matrix is clayey silt-sized serpentine composed of 70% to 99% serpentine, 1% to 15% opaque minerals, 0% to 10% clay, 0% to 5% zoisite, 0% to trace amounts of thulite, 0% to 5% chlorite, with up to 2% micrite and garnet. The matrix has been highly deformed by drilling.

BIOSTRATIGRAPHY

Calcareous nannofossil and planktonic foraminiferal evidence indicates that the upper portions of the sediments in Holes 780A, 780B, 780C, and 780D range in age from middle to late Pleistocene. A sediment interval in Sample 125-780D-6X-1, 34–40 cm, was dated as Pleistocene; poor preservation of the extracted foraminiferal assemblage did not allow us to refine this age.

Calcareous Nannofossils

Hole 780A

Nannofossils are present in only one sample in Hole 780A (125-780A-1H-CC). This sample contains a common, well-preserved assemblage characterized by the following species: *Emiliania huxleyi*, *Gephyrocapsa oceanica*, *Calcidiscus leptoporus*, *Helicosphaera carteri*, *Oolitothus fragilis*, *Ceratolithus cristatus*, *Ceratolithus telesmus*, *Rhabdosphaera clavigera*, and *Hayaster perplexus*. The absence of *Calcidiscus macintyrei* and *Pseudoemiliania lacunosa* and the presence of *Emiliania huxleyi* confine this sample to the late Pleistocene (Zone CN15).

Hole 780B

A rare, well-preserved coccolith assemblage was found in Sample 125-780B-1R-3, 11 cm. The presence of *Emiliania huxleyi*, *Cricolithus jonesi*, *Gephyrocapsa oceanica*, *G. caribbeanica*, *Helicosphaera wallichii* and *Cerctolithus cristatus* allows the designation of a late Pleistocene age (Zone CN15).

Hole 780C

Moderately to well-preserved, few to common, Pleistocene nannofossil assemblages are present in Samples 125-780C-1R-2, 112 cm; 125-780C-1R-3, 81–83 cm; 125-780C-1R-CC; and 125-780C-2R-CC. These four samples contain similar assemblages that are characterized by *Gephyrocapsa oceanica*, *Calcidiscus leptoporus*, *Umbilicosphaera mirabilis*, *Oolitothus fragilis*, *Umbellosphaera irregularis*, *Scapholithus fossilis* and *Helicosphaera carteri*, but lack *Helicosphaera sellii* and *Calcidiscus macintyrei*. We assigned this assemblage to the middle to late Pleistocene (Zones CN14b to CN15) based on Okada and Bukry (1980) and Backman, Duncan, et al. (1988).

Hole 780D

Only three samples (125-780D-1X-1, 6 cm; 125-780D-2X-CC; and 125-780D-6X-1, 34–40 cm) contain nannofossils. A diverse, well-preserved assemblage in Sample 125-780D-1X-1, 6 cm, includes common *Gephyrocapsa caribbeanica*, *Umbellosphaera irregularis*, *Helicosphaera hyalina*, *Calcidiscus leptoporus* and *Gephyrocapsa oceanica*. This assemblage may be assigned to the late Pleistocene (Zone CN15). In the two other samples (125-780D-2X-CC and 125-780D-6X-1, 34–40 cm), we found a rare, poorly preserved nannofossil assemblage. This assemblage contains *Umbellosphaera irregularis*, *Calcidiscus leptoporus*, *Gephyrocapsa oceanica* and *Helicosphaera* sp. These samples may be assigned to the Pleistocene (Zone CN14 to CN15).

Foraminifers

Pleistocene (Zone N22) planktonic foraminiferal assemblages of moderate preservation were recovered from Samples 125-780A-1H-CC and 125-780C-1R-CC. Both samples contain *Globorotalia truncatulinoides* and are dominated by *Globigerinoides conglobatus*, *G. immaturus* and *Globorotalia menardii*.

Samples 125-780C-1R-3, 81–83 cm, and 125-780D-1X-CC yielded sparse, moderately preserved planktonic foraminiferal assemblages that can be assigned an age of late to early Pliocene to Pleistocene (Zones 19/20 to 22); the absence of diagnostic species precludes a more precise age determination. Both samples contain abundant *G. immaturus* and *G. conglobatus*. We did not find any foraminifers in Hole 780B.

In all samples examined, we noted a conspicuous lack of benthic foraminifers. This absence (of both calcareous and agglutinated forms) may be a result of adverse sediment conditions.

Diatoms

Rare, moderately preserved diatoms (mostly as fragments) were observed in Samples 125-780A-1H-CC and 125-780C-2R-CC only. We were unable to determine an age on the basis of the observed diatoms.

Radiolarians were observed in the above samples and in Sample 125-780B-1R-CC.

IGNEOUS AND METAMORPHIC PETROLOGY

The hard rocks recovered at Site 780 are variably serpentinized and tectonized ultramafic rocks, together with three sedimentary clasts. Of the ultramafic rocks, about 90% are harzburgite and 10% are dunite. Two of the sedimentary clasts are weak red (5R 5/2) siltstone with carbonate veins, and one is greenish white (5Y 8/1) carbonate. The ultramafic clasts reach a maximum recovered thickness of about 1.2 m (Section 125-780C-18R-1) and are enclosed in a sheared and deformed serpentinite matrix that is described in the "Structural Studies" section (this chapter). Contacts between the ultramafic and sedimentary rocks are ambiguous.

Ultramafic Rocks

Serpentinized and Tectonized Harzburgites

The harzburgites are massive and vary from gray (10Y 5/1), where relatively fresh, to bluish gray (5B 4/1), where serpentinized (e.g., Interval 125-780C-18R-1, 36–45 cm, and 25–36 cm, respectively; Fig. 3). The primary mineralogy of these rocks is olivine (75%–90%), orthopyroxene (10%–25%), chromium-spinel (trace to 2%), and clinopyroxene (trace to 2%). Clinopyroxene is present as blebs and anhedral crystals (<1 mm), typically closely related to orthopyroxene, and as exsolution lamellae (on [100]) in orthopyroxene.

The harzburgites display penetrative deformation. Typically, orthopyroxene crystals are 1 to 4 mm in size and have morphologies that range from equant to asymmetric-elongate; cleavage surfaces and extinction are wavy, kink-banding is common, and fine clinopyroxene exsolution lamellae on (100) are bent. Elongate crystals (<5 mm long) and kink-banding (sometimes showing fine lamellae) characterize some of the olivine morphologies. Microgranular (<0.5 mm equant crystals) fabrics indicative of recrystallization under relatively high temperature are also present. Chromium-spinel crystals range from equant (0.5 mm in size) to elongated shapes (up to 2 mm long). Some of the elongate spinels define a lineation parallel to the elongate olivine and orthopyroxene (see "Structural Studies" section, this chapter).

The degree of serpentinization is extremely variable (50%–100%), with the olivine and orthopyroxene replaced by mesh-textured serpentine (chrysotile-rich) and bastite, respectively. In these strongly serpentinized types, most of the chromium-spinel (translucent, shades of red) is fresh. Antigorite and brucite may also be present. The harzburgites are cut by numerous veins of serpentine. Many of these veins show a polystage history of filling. Typically, serpentinization affects

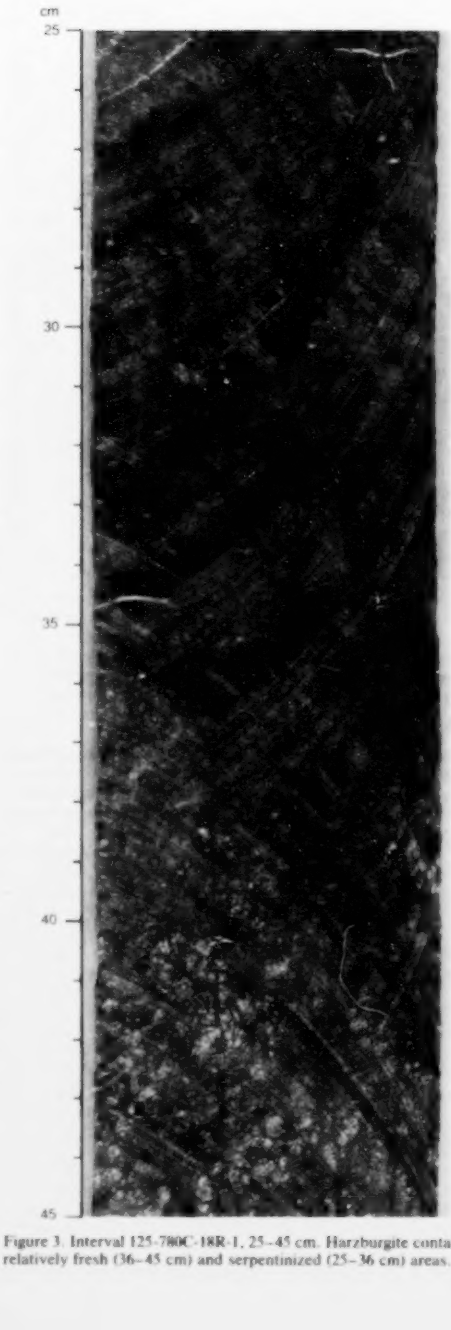

Figure 3. Interval 125-780C-18R-1, 25–45 cm. Harzburgite containing relatively fresh (36–45 cm) and serpentinized (25–36 cm) areas.

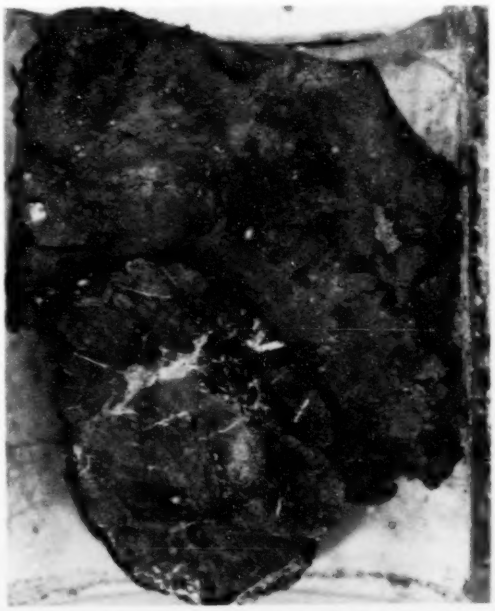

Figure 4. Interval 125-780B-1R-CC, 0–10 cm. Altered clay-rich (brecciated?) siltstone with white carbonate veins, contacting soft sediments.

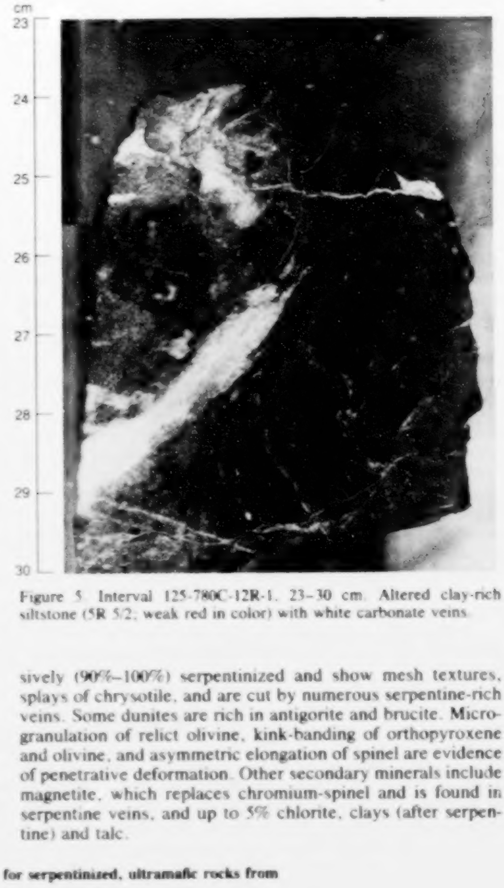

Figure 5. Interval 125-780C-12R-1, 23–30 cm. Altered clay-rich siltstone (5R 5/2; weak red in color) with white carbonate veins.

olivine the most, orthopyroxene less, and clinopyroxene and chromium-spinel the least in this site. Subhedral primary clinopyroxenes (<0.5 mm long) were observed in some samples.

Serpentinized and Tectonized Dunites

These rocks are greenish dark gray (5Y 2.5/1), are generally massive, and sometimes grade to harzburgite. The primary mineralogy consists of olivine (90%–99%), orthopyroxene (1%–9%), and spinel (trace to 1%). Most dunites are extensively (90%–100%) serpentinized and show mesh textures, splays of chrysotile, and are cut by numerous serpentine-rich veins. Some dunites are rich in antigorite and brucite. Microgranulation of relict olivine, kink-banding of orthopyroxene and olivine, and asymmetric elongation of spinel are evidence of penetrative deformation. Other secondary minerals include magnetite, which replaces chromium-spinel and is found in serpentine veins, and up to 5% chlorite, clays (after serpentine) and talc.

Table 3. Tabulated major-element data for serpentinized, ultramafic rocks from Site 789.

	Harzburgites						Dunite
Hole:	780C	780C	780C	780C	780C		780C
Core:	6R-1	10R-1	16R-1	18R-1	18R-1	Average	8R-1
Interval (cm):	61–62	13–16	53–59	54–57	58–61	harzburgites	98–101
SiO_2	40.70	36.42	37.76	38.56	38.85	38.86	38.43
TiO_2	0.00	0.00	0.00	0.00	0.00	0.00	0.00
Al_2O_3	0.47	0.60	0.54	0.63	0.66	0.58	0.65
Fe_2O_3	7.91	7.45	7.44	7.80	7.81	7.68	7.84
MnO	0.11	0.11	0.11	0.11	0.11	0.11	0.11
MgO	42.94	39.04	39.97	39.13	38.87	39.99	39.78
CaO	0.60	0.79	0.69	0.86	0.89	0.77	0.50
Na_2O	0.00	0.00	0.00	0.00	0.00	0.00	0.00
K_2O	0.00	0.02	0.01	0.00	0.00	0.01	0.01
P_2O_5	0.00	0.00	0.03	0.00	0.00	0.01	0.00
NiO	0.29	0.28	0.29	0.29	0.28	0.29	0.29
Cr_2O	30.24	0.31	0.31	0.28	0.34	0.30	0.34
LOI	5.28	12.31	12.06	11.13	11.12	10.38	11.90
Total	98.55	99.31	98.60	98.78	98.92	98.83	99.84
Mg#	91.49	91.21	91.41	90.86	90.79	91.16	90.95
% SERP	65	65	70	75	75	70	55

Data (in wt%) are from whole-rock analyses by XRF. LOI = loss on ignition between 150°C and 1030°C; % SERP = percentage of serpentinization as estimated from thin sections.

Sedimentary Rocks

Of the two sedimentary clasts, one is included in the soft sediments (Interval 125-780B-1R-CC, 0–10 cm; Fig. 4) and the other is isolated (Interval 125-780C-12R-1, 23–30 cm ; Fig. 5). Both clasts may be altered clay-rich siltstones, and include microfossils (foraminifers and radiolarians) and white carbonate veins (Figs. 4 and 5). The greenish white clast in Figure 5 is a calcite fragment (about 5 cm) that also includes microfossils (radiolarians).

IGNEOUS AND METAMORPHIC GEOCHEMISTRY

Six of the ultramafic clasts (five harzburgite, one dunite) from Site 780 were selected for shipboard geochemical analysis. Rock descriptions can be found in the "Igneous and Metamorphic Petrology" section (this chapter) and preparation and analytical techniques in the "Explanatory Notes" (this volume). Geochemical data are listed in Tables 3 and 4.

Ultramafic Samples

Modal estimates of the original (pre-serpentinization) composition of ultramafic rocks range from 5% to 25% orthopyroxene, 75% to 95% olivine, and <1% clinopyroxene and spinel. All samples are variably serpentinized (55%–75%) and most are tectonized. The compositions of the ultramafic rocks are remarkably similar (Tables 3 and 4) and deviate little from average harzburgite values.

Chemistry of Major Elements

Loss on ignition (LOI) of these samples ranges from 5.28 to 12.31 wt% and, unlike data from Sites 778 and 779, does not correlate with percentage of serpentinization. (See "Igneous and Metamorphic Geochemistry" sections, Sites 778 and 779, and "Explanatory Notes," this volume, for an explanation of LOI.) Concentrations of oxides of major elements (Table 3) are similar in the single dunite sample (125-780C-8R-1, 98–101 cm) and the harzburgites. SiO_2 ranges from 37.76 to 40.70 wt%, and MgO ranges from 39.13 to 42.94 wt%. Several poorly constrained trends can be seen in co-variation plots of the data (Figs. 6A and 6B), but we cannot be certain that these trends are real and not an artifact of a small data set (six samples). Both SiO_2 and MgO are inversely correlated with LOI. Al_2O_3 ranges from 0.47 to 0.65 wt%, and Fe_2O_3 ranges from 7.44 to 7.91 wt%. The magnesium number (Mg# = Mg/(Mg+Fe) × 100) is high, ranging from 90.86 to 91.49. Values of Na_2O, K_2O, and P_2O_5 are low in all samples; K_2O and P_2O_5 values reach 0.02 and 0.03 wt% respectively; and Na_2O values are below the detection limit (<0.01 wt%).

Table 4. Tabulated trace-element data for serpentinized, ultramafic rocks from Site 780.

Hole Core Interval (cm)	780C 6R-1 61–62	780C 10R-1 13–16	780C 16R-1 53–59	780C 18R-1 54–57	780C 18R-1 58–61	Average harzburgites	780C 8R-1 98–101
Nb	tr	tr	tr	tr	tr	tr	tr
Zr	0	1	1	1	1	1	1
Y	nd	0	0	1	1	0	0
Sr	3	9	11	nd	0	5	6
Rb	0	1	1	nd	0	0	0
Zn	33	35	45	33	33	36	32
Cu	3	2	8	10	12	7	1
Ni	2319	2188	2264	2318	2307	2259	2280
Cr	1620	2103	2126	1907	2303	2012	2295
V	25	24	30	25	33	27	41
Ce	nd	nd	tr	nd	tr	tr	nd
Ba	tr	tr	tr	nd	tr	13	

Data (in ppm) are from whole-rock analyses by XRF. nd = not detected (background count was greater than sample count). tr = below the detection limit (<5 ppm for Nb, <10 ppm for Ba and Ce).

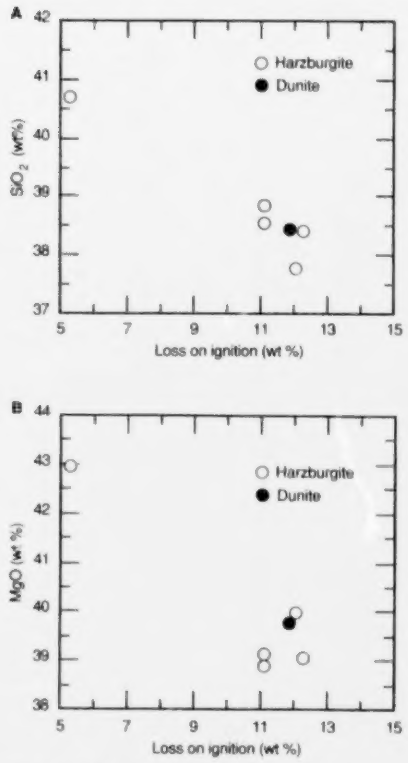

Figure 6. A. Weight percent loss on ignition (LOI) vs. weight percent SiO_2. Data are from Site 780. B. Weight percent loss on ignition (LOI) vs. weight percent MgO. Filled squares represent dunite, and open circles represent harzburgite.

Trace-Element Data

Trace-element data are presented in Table 4. Compatible elements are predictably high in all samples; chromium ranges from 1620 to 2303 ppm, and nickel ranges from 2188 to 2319 ppm. Average concentrations of nickel (harzburgite: 2261 ppm; dunite: 2280 ppm) are slightly lower in samples from Site 780 than for samples from Sites 778 (harzburgite: 2644 ppm) and 779 (harzburgite: 2320 ppm; dunite: 2486 ppm). Chromium and nickel do not correlate with one another or with the degree of serpentinization. Niobium, zirconium, yttrium, rubidium, and titanium are all present at trace levels or arebelow detection limits. Cesium and barium values typically are below detection limits, although two samples have barium concentrations of greater than 13 ppm. Strontium reaches a maximum of 11 ppm, and vanadium values range from 23 to 41 ppm. Strontium and vanadium concentrations are similar to those in Sites 778 and 779. Zinc values range from 32 to 35 ppm, with a single high concentration of 45 ppm (Sample

Table 5. Total carbon, organic carbon, and carbonate carbon in cores at Site 780.

Core, section, interval (cm)	Depth (mbsf)	Total carbon (%)	Inorganic carbon (%)	Organic carbon (%)	$CaCO_3$ (%)
780A-1H-1, 5–6	0.05		0.10		0.8
780A-1H-1, 19–20	0.19		0.12		1.0
780A-1H-1, 39–41	0.39		0.14		1.2
780A-1H-1, 58–60	0.58		0.11		0.9
780A-1H-1, 132–133	1.32		0.05		0.4
780A-1H-2, 68–70	2.18	0.32	0.07	0.25	0.6
780A-1H-CC, 23–25	3.13		0.10		0.8
780B-1R-1, 99–101	0.99		2.40		20.0
780B-1R-2, 39–41	1.89		0.94		7.8
780B-1R-2, 90–91	2.40		1.03		8.6
780B-1R-3, 30–31	3.30	1.32	1.18	0.14	9.8
780B-1R-4, 49–50	4.99		0.75		6.2
780B-1R-6, 99–100	8.49	0.61	0.43	0.18	3.6
780C-1R-1, 0–1	0.00	2.98	2.42	0.56	20.2
780C-1R-1, 30–31	0.30		1.10		9.2
780C-1R-1, 72–74	0.72		0.61		5.1
780C-1R-2, 27–29	1.31		0.88		7.3
780C-1R-2, 64–66	1.68		0.45		3.7
780C-1R-2, 99–100	2.03	2.53	1.97	0.56	16.4
780C-1R-2, 124–125	2.28		2.03		16.9
780C-1R-2, 126–127	2.30		1.49		12.4
780C-1R-3, 16–17	2.70		0.51		4.3
780C-1R-3, 89–91	3.43	0.41	0.26	0.15	2.2
780C-1R-4, 74–75	4.78	0.44	0.14	0.30	1.2
780C-1R-4, 76–78	4.80		0.24		2.0
780C-2R-1, 30–32	5.80	0.37	0.12	0.25	1.0
780C-4R-1, 13–15	23.63	0.46	0.17	0.29	1.4
780C-5R-1, 41–43	33.41	0.33	0.09	0.24	0.7
780C-7R-1, 10–12	52.20	0.25	0.08	0.17	0.7
780C-15R-1, 23–25	125.73	0.31	0.09	0.22	0.7
780C-15R-CC, 12–14	126.08		0.07		0.6
780D-1X-1, 20–22	0.20	3.78	3.77	0.01	31.4
780D-1X-2, 1–2	0.46		0.87		7.3
780D-1X-2, 52–54	0.97	0.59	0.41	0.18	3.4
780D-1X-2, 95–96	1.40		0.13		1.1
780D-1X-3, 45–47	1.96		0.11		0.9
780D-1X-CC, 11–13	2.40		1.14		9.5
780D-2X-1, 30–32	2.80		0.06		0.5
780D-2X-2, 3–5	3.03	0.39	0.09	0.30	0.7
780D-2X-CC, 4–6	3.82		0.09		0.7
780D-3X-1, 13–15	12.13	0.39	0.07	0.32	0.6
780D-6X-1, 62–64	21.02	0.40	0.09	0.31	0.7
780D-6X-2, 41–43	21.59		0.17		1.4
780D-7X-1, 43–45	27.83	0.33	0.08	0.25	0.7
780D-7X-5, 45–47	28.53	0.31	0.07	0.24	0.6
780D-7X-6, 13–15	29.71		0.07		0.6
780D-7X-CC, 20–22	30.69		0.11		0.9

125-780C-16R-1, 53–59 cm). Zinc averages 36 ppm for harzburgite and 32 ppm for dunite in samples from Site 780, which is slightly lower than the average concentrations for Sites 778 (harzburgite = 42 ppm) and 779 (harzburgite = 39 ppm; dunite = 34 ppm). No significant correlation exists between geochemical parameters and depth below the seafloor.

Samples analyzed from Site 780 are therefore quite similar to those from Sites 778 and 779 (see "Igneous and Metamorphic Geochemistry" sections, "Site 778" and "Site 779" chapters, this volume). The few differences between the chemistry of the three sites are noted above, but could be attributed to the smaller data sets for Sites 778 (10 samples) and 780 (six samples) relative to 779 (32 samples).

SEDIMENT/FLUID GEOCHEMISTRY

Sediment Geochemistry

Cores from Site 780 were analyzed on board the ship for inorganic carbon and for total carbon, nitrogen, and sulfur using the techniques described in the "Explanatory Notes" (this volume). The organic carbon content was then calculated by difference. These results are presented in Table 5 and in Figures 7 and 8. Most of the unconsolidated serpentine section at Site 780 is poor in carbonate, containing less than 1 wt% $CaCO_3$. The carbonate-rich layer (up to 8 m thick) that first appeared from 1 to 3 mbsf at Sites 778 and 779 is present at Site 780 as well, although it is more variable here. At the other two sites, this layer contained about 15 wt% $CaCO_3$, whereas at Site 780, it contains 7 to 31 wt%. In Holes 780C and 780D, there are two layers rather than one, separated by 1 to 2 m of unconsolidated serpentine having a lower carbonate content of 1 to 7 wt%. In Holes 780B, 780C, and 780D, this carbonate-rich layer appears to extend all the way to the seafloor, whereas it is absent in Hole 780A, at least below 0.4 mbsf (Fig. 8). Hole 780A, which was drilled with the hydraulic piston corer, penetrated only 3.5 m, but definitely recovered surficial sediments. From the distribution of this layer at the three sites, it is possible that the upper 1 m to a few meters of serpentine was not recovered in Holes 780B, 780C, and 780D, and that Hole 780A did not penetrate far enough to encounter it. The carbonate enrichment in this layer is in the form of aragonite needles distributed throughout the unconsolidated serpentine. Given the occurrence of this layer at or near the seafloor, it is possible that this carbonate enrichment represents a reaction front, in which Ca^{2+} from the overlying

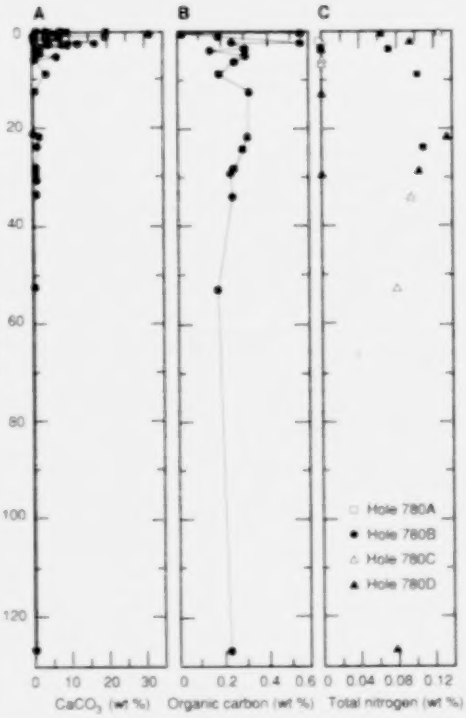

Figure 7. Weight percent of calcium carbonate (A), total organic carbon (B), and total nitrogen (C) in sediments from Holes 780A, 780B, 780C, and 780D.

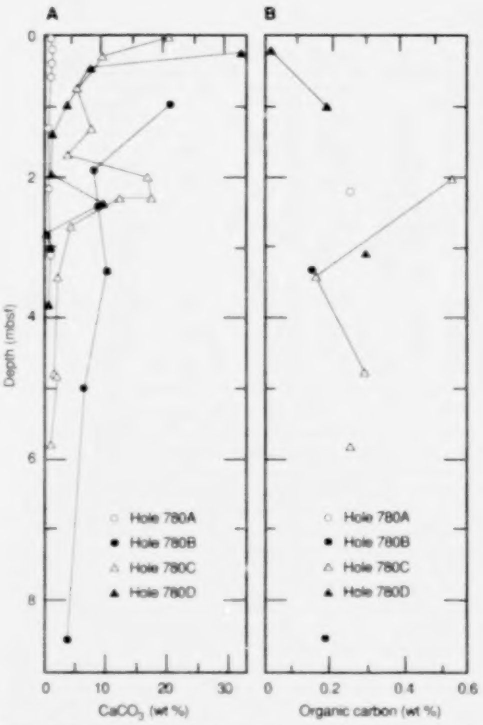

Figure 8. Weight percent of calcium carbonate (A) and total organic carbon (B) in sediments from the upper 9 m at Site 780.

seawater reacts with carbonate ions in the interstitial waters to precipitate authigenic aragonite.

The organic carbon content of the cores at Site 780 (Figs. 7 and 8) varies from 0.01 to 0.56 wt%, in the range of that at Site 779 but higher than that at Site 778. Sulfur ranges up to 0.14 wt%, but was generally not detectable, making Site 780 comparable with Site 779, but sulfur-poor compared with Site 778. Nitrogen ranges up to 0.13 wt%, which is in the same range as values at Sites 778 and 779.

Fluid Geochemistry

Concentrations of methane, ethane, and propane at Site 780 (Tables 6 and 7 and Fig. 9) are as high as those encountered within the upper 156 m of sediment at Site 779 (Fig. 9), and much higher than those at Site 778. Concentrations of these hydrocarbons are very high even in the surficial layer at Site 780; one sample from 1.44 mbsf in Hole 780A yielded 15 mL of methane, 0.1 mL of ethane, and 10 mL of propane per liter of wet unconsolidated serpentine. At the measured porosity of 51% at this depth, this is equivalent to 1.4 mM methane in the interstitial waters. The upper 3 m of serpentine at Site 779 contains low concentrations of hydrocarbons, but we do not know how shallow the high concentrations extend there because the interval between 3 and 43 mbsf could not be sampled. At Site 780, the high concentrations appear to persist to the maximum depth sampled of 126 mbsf, but no samples

Table 6. Results of headspace-gas analyses of cores at Site 780.

Core, section interval (cm)	Depth (mbsf)	Methane (μL/L)[a]	Ethane (μL/L)[a]	Propane (μL/L)[a]	Methane (μM)[b]
125-780A-1H-1, 142–145	1.44	15,229	102	10	1,359
[c]780A-1H-1, 142–145	1.44	12,679	104		1,131
780B-1R-6, 101–106	8.54	18			1.6
780B-2R-1, 145–150	10.18	2,251	50		201
780C-1R-3, 135–140	4.38	9			0.8
780C-4R-1, 20–25	23.73	8,638	41		771
780C-5R-1, 43–48	33.46	31,188	107		2,783
780C-15R-1, 33–38	125.86	22,882	83		2,042
[c]780D-1X-1, 142–145	1.44	177			16
780D-6X-1, 65–68	21.07	13,294	44	4	1,186
780D-7X-5, 125–130	34.68	2,485	11		222

[a] Microliters of gas per liter of wet unconsolidated serpentine.

[b] Micromoles of methane per liter of interstitial water, assuming a porosity of 50%.

[c] Measured using Hewlett-Packard gas chromatograph; all others used Carle.

Note: Where values are absent, gas was not detected.

Table 7. Composition of gas pockets in cores from Site 780, sampled through the core liner into an evacuated glass tube.

Core, section, interval (cm)	Depth (mbsf)	Methane (ppmv)	Ethane (ppmv)	Propane (ppmv)
125-780C-18R-1, 25–25	125.75	2809.5	8.3	nd
780D-7X-5, 58–58	33.98	7491.9	28.7	3.0

nd = not detected.

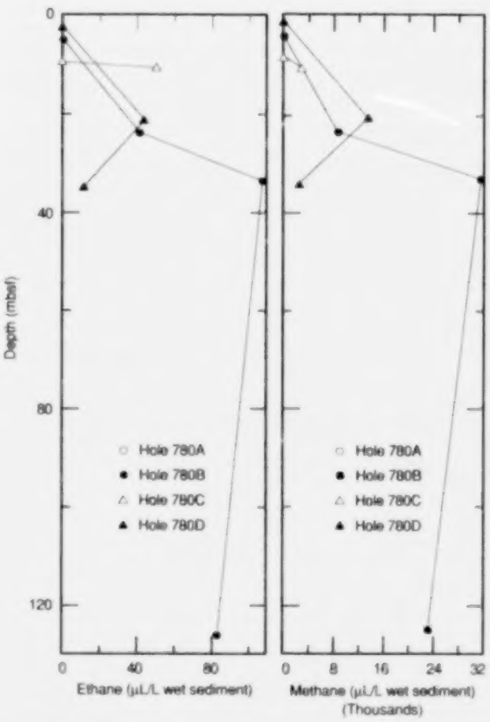

Figure 9. Methane and ethane in cores at Site 780.

Table 8. Composition of interstitial waters from cores at Site 780.

Sample #	Core, section interval (cm)	Volume (mL)	Squeeze T (°C)	Depth (mbsf)	pH	Salinity (R.I., %)	Salinity (calc., %)	Chlorinity (mmol/kg)	Alkalinity (meq/kg)	Sufate (mmol/kg)	Sodium (mmol/kg)	Potassium (mmol/kg)	Calcium (mmol/kg)
Surface seawater (4 March 1989)					8.10	35.5	34.85	542.6	2.386	27.98	464.8	10.05	10.17
IW-1	780A-1H-1, 45–55	16	3	0.50	11.37	26.8	29.07	399.0	10.865	32.41	459.6	14.22	0.44
IW-2	780A-1H-1, 95–105	9	3	1.00	11.43	26.5	29.64	393.2	15.042	36.20	464.8	15.21	0.34
IW-3	780A-1H-1, 145–150	33	2	1.48	12.02	25.5	27.21	338.3	18.362	39.80	420.3	14.88	0.54
IW-4	780A-1H-2, 57–67	12	3	2.12	11.87	24.8	27.17	339.3	19.270	38.59	419.4	15.06	0.63
IW-5	780A-1H-2, 129–139	10	3	2.84	11.74	26.0	27.56	351.8	16.051	38.05	427.7	15.07	0.59
IW-1	780B-1R-6, 106–116	41	2	8.61	19.09	33.2	33.49	517.6	1.275	26.93	462.8	13.70	7.59
IW-1	780C-1R-3, 140–150	53	3	4.45	8.93	35.0	34.43	534.0	1.797	28.58	463.7	10.19	8.14
IW-2	780C-5R-1, 48–58	32	2	33.53	12.49	23.0	26.09	270.8	45.833	43.52	389.1	13.68	0.47
IW-3	780C-15R-1, 38–48	48	5	129.93	12.38	25.1	28.06	315.2	35.636	45.03	422.7	15.49	1.31
IW-1	780D-1X-2, 96–106	50	1	2.51	9.52	30.8	31.96	484.6	1.766	27.31	469.3	11.27	4.76
IW-2	780D-1X-3, 68–78	44	1	2.73	11.86	25.0	27.55	364.7	15.778	33.11	433.6	12.51	0.27
IW-3	780D-2X-1, 40–50	35	2	2.95	12.35	22.7	25.96	284.4	33.791	44.33	392.0	12.53	1.13
IW-4	780D-6X-1, 68–78	25	3	21.13	12.42	22.8	26.59	285.3	40.655	44.27	398.8	12.96	1.36
[a]BW-5	780D-7X-1, 0–1	18	*in situ*	27.41	12.60	22.2	25.82	234.1	62.872	46.84	377.3	12.35	0.46
IW-6	780D-7X-5, 135–150	58	5	34.83	11.72	25.6	27.71	369.5	9.139	36.37	427.1	12.81	5.68
[a]BW-7	780D-8X-1, 0–1	2.6	*in situ*	32.41	8.42		16.97	249.5	2.553	23.05	166.6	7.61	7.43

[a]BW = Barnes *in-situ* sample. BW-7 consisted of 2.6 mL taken from the partially flushed copper coil. The fully flushed steel coil was saved for shore-based gas analyses. Values absent from table were not determined.

were obtained between 35 and 126 mbsf because of poor recovery.

Interstitial waters were collected at Site 780 using the Barnes *in-situ* water sampler, as well as by squeezing of unconsolidated serpentine samples. Operation of the Barnes tool is detailed in the "Explanatory Notes" (this volume). Two samples were recovered with this tool, both from Hole 780D. The first sample consisted of 18 mL of undiluted interstitial water in the steel coil that was analyzed on board the ship, and about 12 mL in a 45-mL copper coil that was crimp-sealed for shore-based determination of gases and their isotopes. The temperature measured downhole in the serpentine while this sample was being collected did not stabilize. The second sample consisted of a total of only 23 mL and was accompanied by a valid temperature measurement of 3.5°C, 2.0°C above the ambient temperature of ocean bottomwater at Site 780. Because of the small volume of interstitial water recovered, the steel coil was saved for shore-based analysis, and 2.6 mL were crimped off in the 20-mL copper coil on recovery and analyzed on board the ship. The copper coil was initially filled with distilled water, which was only partially flushed by interstitial water during sampling because of the small volume recovered. The 2.6-mL sample proved to be highly anomalous, having much lower pH, alkalinity, ammonia, sulfate, sodium, potassium, salinity, and chlorinity, and higher calcium, and especially magnesium, than the other samples from Hole 780D (Table 8). Because this sample was recovered from the copper coil, in which it had presumably mixed heavily with distilled water, data from this sample are highly questionable and thus were not plotted in Figures 10, 11, and 12.

The compositions of surface seawater and of interstitial waters from Holes 780A, 780B, 780C, and 780D are plotted in Figures 10, 11, and 12. Interstitial waters from all four Sites on and near Conical Seamount are plotted in the "Sediment/Fluid Geochemistry" section, Site 781 (this volume).

As in the case of the hydrocarbon gases, the dissolved ions in the interstitial waters of unconsolidated serpentine at Site 780 (Table 8) show extremely large concentration gradients near the seafloor. The pH of these waters increases to 11.4 at 0.5 mbsf and to 12.0 at 1.5 mbsf in Hole 780A, and to 12.4 at 3.0 mbsf in Hole 780D (Fig. 10). The highest pH measured at the site was 12.6, for a water collected with the Barnes *in-situ* sampler from a depth of 27 mbsf in Hole 780D. The highest pH for a squeezed sample was 12.4, at 21 mbsf in the same hole. These pH values are even higher than those at Site 779 and are undoubtedly higher than or comparable to the highest pH values ever measured in interstitial waters of marine sediments. Not all of the near-surface samples have such high values of pH, however; two samples from 4.5 mbsf in Hole 780C and 8.6 mbsf in Hole 780B have a pH of about 9. This indicates that these extremely high gradients are not ubiquitous at the site, but may be patchy in their distribution. After increasing abruptly to about 12.4 in the upper few meters of serpentine, the pH persists at this value to the greatest depth sampled, 130 mbsf in Hole 780C. The single exception is a sample from 35 mbsf in Hole 780D that has a pH of 11.7. This sample has anomalous concentrations of most species, as will be shown later in this section.

The alkalinity of the interstitial waters displays a similar pattern to that of pH, increasing rapidly in the surficial serpentine to high values that persist to the maximum depth sampled (Fig. 10). As in the case of pH, the steepest near-surface gradients are found in Hole 780A, where alkalinity increases eight-fold over the seawater value within the upper 2 m, and Hole 780D, where it increases 14-fold over the upper 3 m. The highest alkalinity measured, 62.9 meq/kg, is that of the *in-situ* sample with the highest pH, from 27 mbsf in Hole 780D. These alkalinities are much higher than those found at Sites 778 and 779. Once again, some near-surface values are much lower than others, indicating that the very high near-surface gradients are localized. The same three samples from the upper 9 m with a much lower pH than the others also have much lower alkalinities, even lower than in seawater, that range from 1.3 to 1.8 meq/kg. The deepest sample from Hole 780D (at 35 mbsf) has a lower alkalinity and pH than other samples from similar depths.

The profiles of ammonia concentration with depth at Site 780 (Fig. 10) are similar to those for pH and alkalinity. The highest concentration reached is 268 μmol/kg, which is higher than that at Sites 778 and 779 and about three times higher than values at similar depths at Site 779. Concentrations of silica are low, although not as low as those in the same depth interval at Site 779. Except for three samples from Hole 780D, all values are less than or equal to 35 μmol/kg.

The profiles of sulfate with depth are similar to those for pH, alkalinity, and ammonia. However, their most remark-

Table 8 (continued).

Magnesium (mmol/kg)	Bromide (mmol/kg)	Silica (μmol/kg)	Ammonia (μmol/kg)	Phosphate (μmol/kg)	Hydrogen Sulfide (μmol/kg)
52.89	0.85	5	<5		
0.008	0.64	20	119		
0.017	0.67	21	104		
0.003	0.64	12	171	0.71	
0.003	0.71	19	137		
0.011	0.64	19	118		
40.499	0.69	24	21	<0.10	
51.39	0.78	35	13	0.27	
0.004	0.56	34	237	0.71	
0.005	0.50	32	264	0.16	
25.422	0.65	<5	43	<0.10	
0.021	0.41	24	141	0.16	2000
0.002	0.48	62	205	0.27	<250
0.003	0.48	48	224	0.27	<250
0.002	0.46	89	268		
0.026	0.53	14	139	<0.10	<250
54.560	0.77	12	20		

able feature is the large increase in concentration relative to seawater shown by all but three of the samples, the same three from less than 9 mbsf that have lower pH, alkalinity, and ammonia than the others. As in the case of these other species, the increases in sulfate occur within 0.5 to 3 m of the seafloor, producing large gradients in the near-surface unconsolidated serpentine. Except for the deepest sample from 35 mbsf in Hole 780D, the high sulfate concentration persists with depth at a value of 43 to 47 mmol/kg, fully two-thirds higher than the concentration in seawater. The sulfate concentration increases at Site 779 as well, between 100 and 160 mbsf, but this increase is relative to a decrease at shallower levels, so that none of the values exceed the concentration in seawater. The increases relative to seawater at Site 780 are highly unusual and require either a large source of sulfate or a large sink for H_2O.

High concentrations of H_2S were encountered at Site 780, in spite of the increase in dissolved sulfate (Table 7). As was the case for Site 779, there was no odor of H_2S in the interstitial water samples, presumably because of their high pH. The presence of H_2S was detected by the formation of a white to pale yellow to rusty orange to dark brown precipitate that formed in all of the samples from Site 780 when mercuric chloride was added. Only small amounts of precipitate formed in the uppermost samples from Holes 780B, 780C, and 780D, from 8.6, 4.5, and 2.5 mbsf, respectively. This precipitate was especially heavy and dark in the samples from 1.5 mbsf in Hole 780A, 34 mbsf in Hole 780C, and 2.73 mbsf in Hole 780D. The concentration of H_2S was measured colorimetrically in the latter sample and was found to be about 2 mmol/kg. Three deeper samples from Hole 780D were also analyzed and were found to contain less than 250 μmol/kg.

The concentration of magnesium in the interstitial waters at Site 780 is extremely low, except for the three samples from the upper 9 m in Holes 780B, 780C, and 780D (Fig. 11). Most values were so low that they could not be determined by the titration method; all values less than 0.5 mmol/kg in Table 8 were determined by flame atomic absorption spectrometry (FAAS). Magnesium decreases with depth to very low concentrations at Sites 778 and 779 as well, but this decrease occurs over the much larger depth interval of about 100 m. In Hole 780A, magnesium decreases to 8 μmol/kg within 0.5 m of the seafloor. It decreases almost as abruptly in Hole 780D, to 2 μmol/kg at only 3 mbsf. The sample from 35 mbsf in Hole 780D that has anomalously low pH, alkalinity, ammonia, silica, and sulfate has the same low concentration of magnesium as the other samples from depths greater than 9 mbsf. Thus, these anomalous values cannot be attributed to contamination by seawater during drilling and recovery of the core, because such contamination would have raised the concentration of magnesium in the sample.

The concentration of dissolved calcium also decreases abruptly with depth at Site 780, to 0.44 mmol/kg at 0.5 mbsf in Hole 780A and to 0.27 mmol/kg at 3 mbsf in Hole 780D (Fig. 11). These calcium concentrations are sufficiently low to make one suspect the titration results. For this reason, all values for calcium in Table 8 of less than 1 mmol/kg were determined by FAAS. The latter results were found to agree within 0.5 mmol/kg with the titration results. The low concentrations of calcium persist with depth at Site 780, except for the single anomalous sample from 35 mbsf in Hole 780D, in which calcium values rebound to about one-half the value of seawater. Calcium also decreases with depth at Site 779, although not as abruptly or to such low levels. It reaches a minimum of 1.6 mmol/kg between 108 and 227 mbsf, then increases again to the bottom of Hole 779A, but never reaches or exceeds the concentration in seawater. At Site 778, calcium increases with depth and exceeds the seawater value at all depths.

The profile of the concentration of sodium with depth closely resembles that for calcium in both shape and direction of change (Fig. 11). The near-surface gradients again are very steep, giving a maximum depletion of 19%. The direction of change at Site 780 is the opposite of that at Sites 778 and 779, where sodium increases with depth by up to 24%. The contrast in direction of change among the sites is true for potassium as well: whereas potassium values decreased with depth by one-third at both Sites 778 and 779, they increase by more than 50% at Site 780 (Fig. 11). The near-surface gradients again are steep, especially for Hole 780A.

The profiles of concentration with depth for salinity, chlorinity, and bromide (Fig. 12) all resemble those of sodium and calcium (Fig. 11). The decreases relative to seawater are large and occur abruptly in the near-surface serpentine material. Salinity decreases by as much as 26%, and chlorinity decreases by up to 57%. Chlorinity decreases by 28% at 0.5 mbsf in Hole 780A and by 38% at 1.5 mbsf. In Hole 780D, chlorinity and bromide each decrease by 48% and salinity by 25% at a depth of only 3 mbsf.

Interpretation of Results from Sites 778, 779, and 780

The interstitial waters collected from serpentine-rich sediments and serpentine flows at Sites 778, 779, and 780 on Conical Seamount are highly unusual compared with waters from more typical deep-sea sediments, such as those sampled just off the seamount at Site 781. These differences are illustrated in the "Sediment/Fluid Geochemistry" section (Site 781, this volume), where the interstitial water compositions from all four sites are plotted together (Figs. 8, 9, and 10).

The most remarkable feature of the interstitial waters from Conical Seamount is a decrease in chlorinity and salinity relative to the values in seawater and in most deep-sea interstitial waters. This decrease is much larger at the summit Site 780, but also occurs at the flank Sites 778 and 779. Equally remarkable is the extreme abruptness of this decrease with depth in the summit holes, especially 780A and 780D. The decrease in chlorinity and salinity is accompanied by other remarkable changes, leading to a pH as high as 12.6, alkalinity

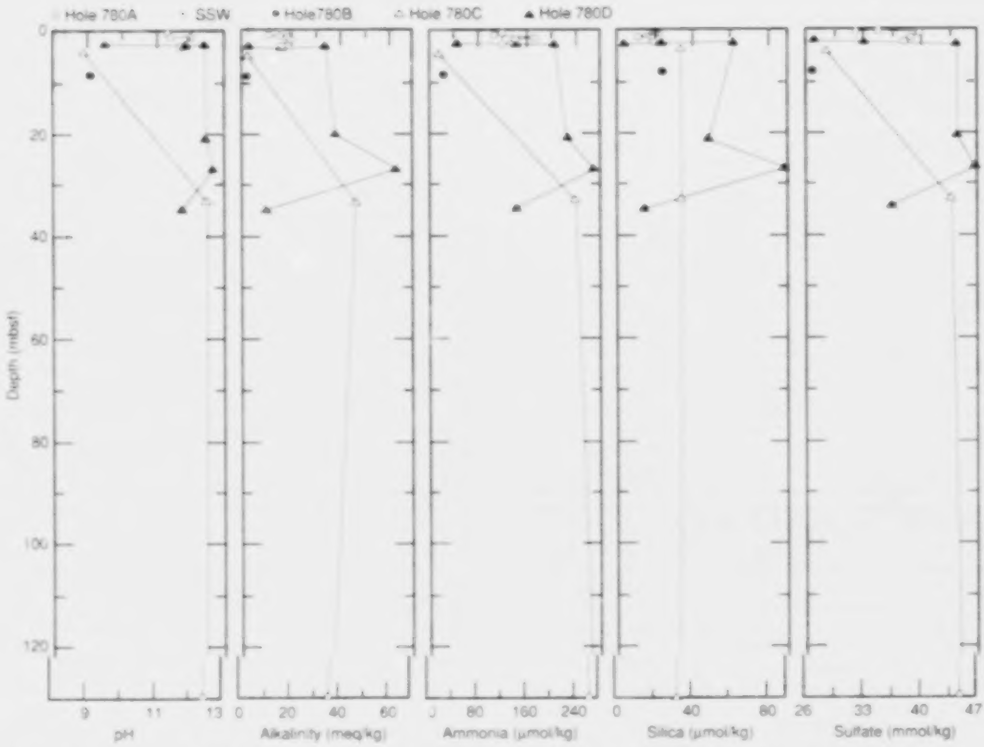

Figure 10. Composition of interstitial waters from cores at Site 780. SSW = surface seawater collected 22 February and 4 March 1989.

up to 26 times that of seawater, methane up to 38 mM, H_2S up to 2 mmol/kg, elevated ammonia, and very low concentrations of magnesium and silica. Sulfate, calcium, sodium, potassium, and alkalinity all change in one direction at the summit and in the other at one or both of the flank sites. Sulfate decreases with depth on the flanks, but increases by two-thirds at the summit. Calcium more than doubles at flank Site 778, but decreases at Site 779 and at the summit. Concentrations of sodium increase on the flanks, but decrease strongly at the summit, whereas potassium values decrease on the flanks and increase at the summit.

The central question regarding these interstitial waters is the cause of the decreases in chlorinity and salinity relative to seawater. Two possibilities exist: (1) the fluids originate mainly as seawater, and chloride is taken up by the solid phases during alteration in greater proportion than water; and (2) the fluids do not originate mainly as seawater, but contain a large component of less-saline water with a much lower chloride concentration than seawater. This less-saline water may have been produced by a number of processes, including membrane filtration through clays, decomposition of hydrocarbon gas hydrates, and dehydration of hydrous minerals.

Seawater-Rock Interaction and Chloride Uptake

Chloride uptake into solid phases during serpentinization has been reported, although the conditions under which this phenomenon can occur and the nature of the chlorine-rich phases are unclear. Janecky and Seyfried (1986) performed experiments reacting seawater and magnesium-free and magnesium- and sulfate-free seawater with peridotites at 200° and 300°C and a pressure of 500 bars. They found that dissolved chloride behaved conservatively when seawater was the reactant solution, but that significant chloride was taken up into partially serpentinized harzburgite when the starting solution lacked magnesium. The distinctive feature of the final solutions in the magnesium-free-seawater experiments was their high pH, which reached 11.5 in the longest experiment. This experiment was performed at a water/rock mass ratio of 10 and ran for 714 days. The loss of chloride from solution was 27 mmol/kg, indicating that the altered harzburgite must have contained about 10,000 ppm, or 1 wt%, chloride that it had picked up from solution during the experiment. Janecky and Seyfried (1986) were unable to determine in what solid phase or phases this chloride resided. They considered several possibilities: (1) a magnesium-iron-chloride mineral like iowaite, which has been reported from serpentinites

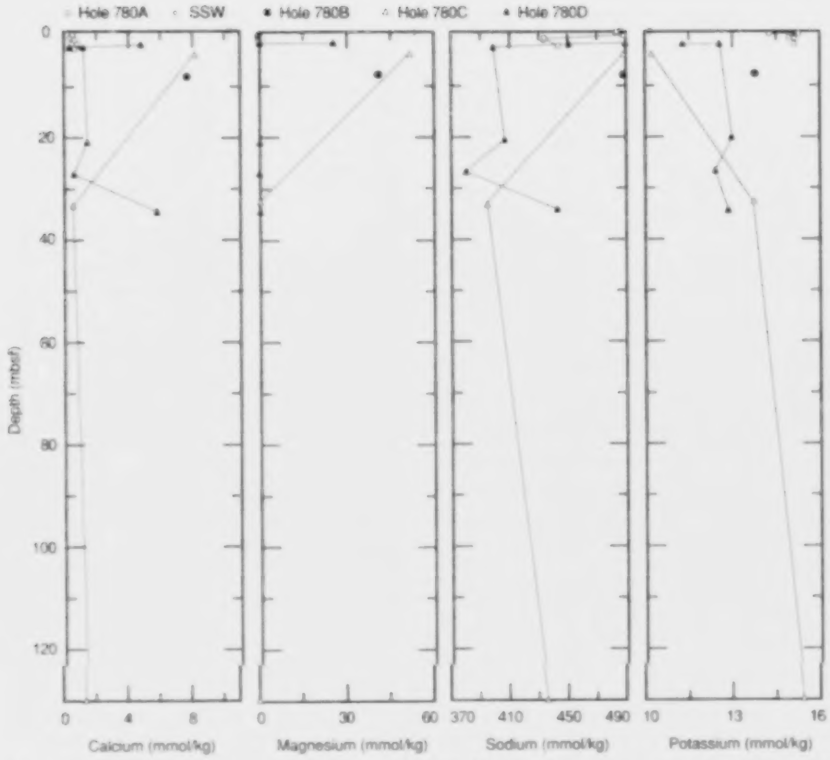

Figure 11. Composition of interstitial waters from cores at Site 780. SSW = surface seawater collected 22 February and 4 March 1989.

(Kohls and Rodda, 1967); (2) an iron-hydroxide-chloride phase, such as was suggested to occur in serpentinites by Rucklidge (1972) and Rucklidge and Patterson (1977); (3) a magnesium-hydroxide-chloride phase, $Mg_2(OH)_3Cl$, produced during experimental serpentinization at 500°C and 1000 bars by Poty et al. (1972); (4) newly formed, poorly crystallized serpentines that might retain chloride in their structure, as suggested by Miura et al. (1981); and (5) poorly crystallized brucite. Given that the chloride decrease in the longest experiment was balanced nearly mole for mole by a decrease in sodium, the latter two possibilities may be most likely. That this sodium did not appear in analyses of the altered rock from the experiment is puzzling and clouds any interpretation of the experimental data.

The large decreases in chlorinity in the interstitial waters at Site 780 are balanced only one-quarter to one-third by decreased sodium. When the nearly complete removal of magnesium and calcium from solution is included as well, only three-quarters of the charge loss can be accounted for. The other one-quarter is balanced about equally by the large gains in sulfate and alkalinity. Relative to seawater, the increase in sulfate is proportionally about equal to that in potassium. If the gains in sulfate and potassium are caused mainly by loss of water from seawater to the serpentinized rocks, and the rocks gain on average about 12 wt% water, then each gram of seawater would have reacted with and hydrated 2 to 3 g of fresh rock. If the rock also took up chloride under these conditions, it would have to gain about 4300 ppm or 0.43 wt% chloride, to account for the chloride decrease observed in the interstitial waters at Site 780. This is well within the range of uptake that apparently occurred in the experiments of Janecky and Seyfried (1986).

There are two main problems with this hypothesis for the chlorinity decrease at Site 780. The first is that the concentration of bromide decreases along with chlorinity (Fig. 12). For most samples, the decrease in bromide is nearly, but not quite, as large as that of chlorinity. If the decrease in chlorinity is mainly the result of uptake of chloride into the altered rocks, then these rocks must be taking up bromide as well.

The second problem is that local reaction between rock and interstitial water probably cannot maintain the very large chemical gradients present in the upper few meters of serpentine sediment and flows at Site 780. To maintain these gradients, the process that lowers the chlorinity must be more rapid than diffusion of chloride from the overlying oceans into the interstitial waters of the near-surface serpentine materials. Otherwise, diffusion would lessen the gradients or erase them altogether. The near-surface lithology in which the gradients were measured consists mainly of the serpentine minerals; the only primary, unaltered phases that may be present are traces of opaque minerals and scattered amphibole. If these serpentine sediments and flows are capable of taking up chloride at

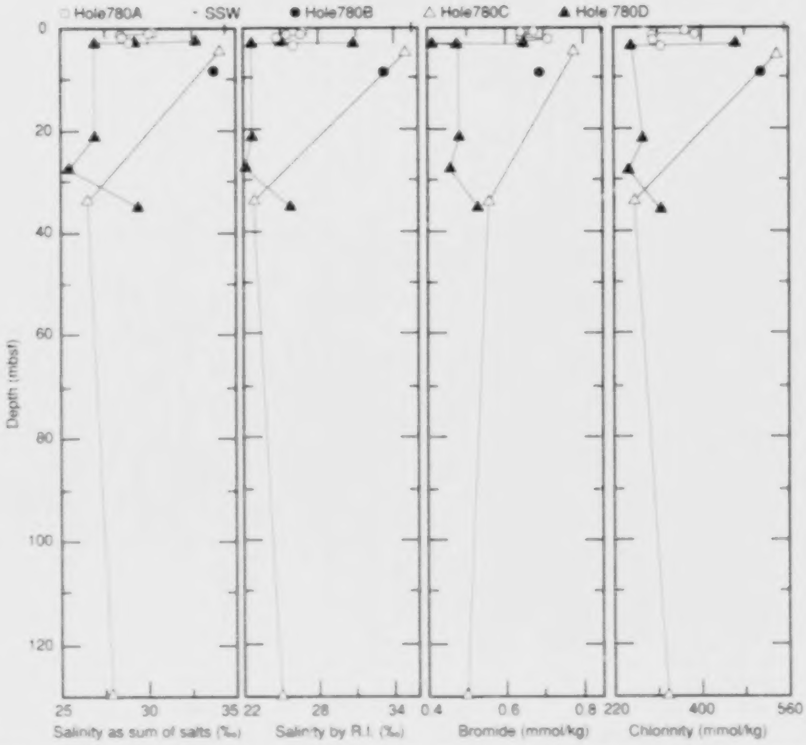

Figure 12. Composition of interstitial waters from cores at Site 780. SSW = surface seawater collected 22 February and 4 March 1989.

all, they should already have become saturated with it; it is highly unlikely that they are actively taking up chloride at the present time because they are already almost completely altered. If a water-rock reaction accompanied by chloride uptake is lowering the chlorinity of interstitial waters within Conical Seamount, this reaction must be occurring deeper in the system, below the maximum depth drilled. The less-saline water would then have to flow upward at Site 780 to maintain the high chlorinity gradients in the near-surface sediments.

The hypothesis of upflow at Site 780 is consistent with observations made from the manned submersible, *Alvin*, of chimneys constructed of calcite, aragonite, and poorly crystallized magnesium-silicates on the summit of Conical Seamount that were apparently precipitated from debouching fluids (Fryer et al., 1987; Haggerty, 1987c, 1989). The flow path and velocity of these solutions and the amount of fresh peridotite they may encounter on their way are not known at present. Whether the conditions encountered would allow uptake of sufficient chloride and bromide to produce the chloride-poor interstitial waters is also not known. However, one can be almost certain that these low-salinity interstitial waters do not originate by reaction within the depth range from which they were sampled, but have been transported there from elsewhere.

In addition to low chlorinity and salinity, the interstitial waters at Site 780 are characterized by high concentrations of methane, alkalinity, and ammonia. If our estimate of one-third to one-half for the seawater/rock mass ratio (based on the increases in sulfate and potassium) is accurate and relevant, then there would be adequate amounts of organic and carbonate carbon and nitrogen in the rocks (Table 5) to account for the observed concentrations of methane, alkalinity, and ammonia, respectively. Whether the rocks have actually supplied these species to the solutions is a question for further study. If the low-salinity fluids have in fact been transported into the sampled region from elsewhere, as concluded above, then the sampled unconsolidated serpentine is not necessarily the source of these species.

Evidence from Drilling in Other Subduction Zones

Low-chlorinity interstitial waters have been sampled from drill holes in other subduction zones, including the Japan Trench, the Middle America Trench off Guatemala and Mexico, the Barbados accretionary prism, and the Peru continental margin.

In the Japan Trench, at Sites 438 and 439 drilled during Deep Sea Drilling Project (DSDP) Leg 57, the chlorinity of the interstitial waters decreases with depth to half the value in seawater at 900 to 1100 mbsf. Moore and Gieskes (1980) suggested that this low-chlorinity water originated from a fossil aquifer.

In the Middle America Trench off Guatemala, the chlorinity of the interstitial waters is lower than that of seawater by up to 54% at 337 mbsf at Site 570 and at 395 mbsf at Site 497. Chlorinity also is lower by 6% to 41% at Sites 490, 491, and 492, drilled during DSDP Leg 66 off Mexico (Gieskes et al., 1985), Site 496, drilled during DSDP Leg 67 off Guatemala (Harrison et al., 1982), and Sites 565 and 568 drilled during DSDP Leg 84 off Guatemala (Hesse et al., 1985). The decrease in chlorinity at all these sites in the Middle America Trench has been attributed to the presence of hydrocarbon gas hydrates in the sediments. These hydrates decompose to methane and water during core recovery as a result of decompression and warming.

On the Northern Barbados Ridge, drilled during ODP Leg 110, chlorinity is lower than that in seawater by up to 28% at Site 674, but by less than 12% at all other sites drilled there. This decrease was tentatively attributed to an ultrafiltration process, in which clay minerals act as semipermeable membranes, selectively passing water but restricting the motions of ionic species (Shipboard Scientific Party, 1988a). Possible contributions from dehydration of smectites and melting of hydrocarbon gas hydrates were also considered. All of these processes were postulated to occur deeper than the maximum depth drilled; the freshwater produced is thought to move upward along faults and other permeable pathways, and especially along the shallowly inclined décollement surface.

On the Peru continental margin, chlorinity increases greatly with depth at five sites drilled during ODP Leg 112 and decreases at the other five. At Site 679, these decreases are up to 38% relative to seawater, but are less than 18% at the other four sites. Several processes may have contributed to these decreases in chlorinity, including decomposition of hydrocarbon gas hydrates, membrane filtration, dewatering of clays and opal, and the possible presence of fossil freshwater. Several chlorinity maxima and minima at Sites 682, 683, 685, and 688 clearly result from formation and decomposition, respectively, of gas hydrates at corresponding depths in the drill holes. As in the case of the Barbados accretionary prism, however, the larger scale decrease with depth suggests that the major source of freshwaters lies below the maximum depth drilled. These freshwaters are thought to have risen upward along permeable channels consisting of unconformities, coarse-grained sedimentary units, and conjugate and intersecting fracture zones (Shipboard Scientific Party, 1988b).

Possible Sources of Low-Chlorinity Water at the Conical Seamount Site

The 57% decrease in chlorinity at 27 mbsf in Hole 780D is larger than any observed in sediment interstitial waters above subduction zones elsewhere. It is also found at much shallower depths below the seafloor. As noted above, the strong chlorinity gradients within the upper few meters beneath the seafloor at Site 780 strongly suggest that interstitial water is flowing upward at this site.

The concentrations of methane at Site 780 may be high enough to stabilize methane hydrates under *in-situ* conditions, either within the sampled interval or at greater depths. These hydrates could supply freshwater on decomposition, either during core recovery if they lie within the sampled interval, or continuously if they are present at greater depths, at or near the bases of their stability fields. The profiles of chlorinity and methane with depth support the latter, deeper location rather than the former, as does the fact that no hydrocarbon gas hydrates were recovered on Conical Seamount. On the other hand, we note that methane concentrations were up to 12 times higher at Site 779 than at Site 780, yet the chlorinity decrease at Site 779 was much smaller, only 9% lower than seawater, compared with 57% lower at Site 780. Unless methane and water derived from melting gas hydrates are somehow separated from each other within the upper few hundred meters of Conical Seamount, this discrepancy suggests that decomposition of gas hydrates is probably not the dominant source of freshwater on Conical Seamount.

Because of the low abundance of clay minerals in the rocks and sediments recovered from Conical Seamount, membrane filtration through clay minerals is an equally unlikely mechanism for generating freshwater. If this process is important, it would have to be taking place at greater depths than those drilled.

Dehydration of hydrous minerals at depth beneath Conical Seamount thus is the most likely mechanism for generating freshwater. The chemistry of the interstitial waters sampled at Sites 778, 779, and 780, especially the high pH strongly suggests that the drilled interval is undergoing serpentinization at the present time. Thus, any dehydration of previously formed hydrous minerals would have to be taking place well below the maximum depth drilled.

Evidence for Mixing of Fluids from Several Sources

If the low-salinity fluids on Conical Seamount were not formed mainly by uptake of chloride into rocks during serpentinization, they must derive in part from some other, presumably deeper, source such as dewatering of the subducted lithospheric slab. From the composition of the interstitial waters at Site 780, we can infer that such waters should be rich in H_2O, CO_2, methane, ammonia, H_2S, and possibly also oxidized sulfur.

In addition to the general trends of an increase or decrease with depth relative to seawater, many of the dissolved species in the interstitial waters at Sites 778, 779, and 780 show more complex profiles that include maxima and minima. In particular, the lowermost one or two samples in Holes 778A, 779A, and 780D exhibit significant changes from the general trends. Interstitial waters from closely spaced holes at Sites 779 and 780 also show large differences in composition within a few meters beneath the seafloor.

Both types of variation might be caused by mixing of fluids of different composition from different sources in a complex plumbing system within Conical Seamount. At least two types of fluids are probably present in this setting: a low-salinity fluid that is ascending from depth, and locally derived seawater that has reacted with rocks and sediments in the vicinity of the seamount. We might also postulate that the latter fluid is of two types, one that has reacted mainly with mafic rocks and sediments and another that has reacted mainly with ultramafic rocks. The solutions ascending through the summit and exiting at Site 780 should be richer in the low-salinity fluid from depth, while the solutions sampled at the flank Sites 778 and 779 should be richer in the locally derived and reacted fluids. The deep fluid should have a high pH and be rich in methane, ethane, propane, alkalinity, ammonia, H_2S, sulfate, and potassium, and poor in silica, magnesium, calcium, chloride, and bromide. The fluid produced by local reaction of seawater with ultramafic rocks should have a high pH and be poor in silica and magnesium. The fluid produced by local reaction of seawater with mafic rocks and sediments should have a lower pH and be rich in silica, calcium, and sodium, and poor in alkalinity, sulfate, magnesium, and potassium. In this model, Site 778 should have the largest mafic-and-sediment component of the two flank sites, which would explain the relatively low pH, alkalinity, and sulfate, and the higher concentrations of silica and calcium at this site. Site 779, with its complex profiles, especially of sulfate, calcium, and sodium, should exhibit the effects of mixing among all three fluids at various depths. A model with three separate fluids may be required to explain the maxima and minima in sulfate, calcium, and chlorinity in Hole 779A that generally do not correlate with one another. Additional modeling, including more chemical and mineralogical data for the solid phases, will be required to refine these interpretations.

STRUCTURAL STUDIES

Introduction

Structures in the materials recovered from Site 780 include (1) relict high-temperature, ductile to brittle fabrics in the unserpentinized regions of ultramafic rocks; (2) symmetric and asymmetric serpentinization fabrics in some ultramafic rocks; (3) post-serpentinization deformation textures within serpentinite clasts; and (4) deformation within the serpentine matrix. In this section, we discuss these in turn and then briefly describe the results and structural implications of rheologic measurements of the serpentine matrix.

High-Temperature Structures in Unserpentinized Ultramafic Rocks

Relict minerals and textures are locally preserved in incompletely serpentinized rocks from Holes 780C and 780D. Some blocks are as little as 50% serpentinized, and the less-serpentinized areas of these blocks contain as little as 30% of serpentine minerals. High-temperature deformation fabrics that developed in the peridotite before serpentinization are preserved in these areas. The fabrics include undulatory extinction, common in both olivine and orthopyroxene, as well as some kink-banding of orthopyroxene and twinning of olivine. In Sample 125-780C-16R-1, 53–59 cm, some of the rock is essentially unstrained, while a shear band marked by necked and pulled-apart olivine can be observed only a centimeter away.

These textures are typical of mantle deformation. In some samples, deformation is distributed throughout the rock and probably occurred at relatively high temperatures and/or low strain rates. In others (e.g., Interval 125-780C-16R-1, 53–59 cm), the deformation is concentrated in relatively narrow shear bands; it is more brittle and appears to have taken place at relatively low temperatures and/or high strain rates.

Serpentinization Textures

Partly to completely serpentinized ultramafic blocks were recovered from both Holes 780C and 780D. Thin sections of these blocks reveal a wide range of textures that appear to reflect serpentinization under isotropic and anisotropic stress conditions, as well as in different temperature (and pressure?) regimes. Serpentinization fabrics observed in the rocks recovered from Holes 780C and 780D include mesh, felted-lath, and bladed-sheaf textures. In addition, late serpentine veins crosscut previously formed serpentinization textures.

Mesh Textures

The cores of many incompletely serpentinized rocks exhibit anastomosing or weblike patterns of dark veins that separate islands of lighter gray rock. These webs of veins may exhibit a crude orthorhombic geometry, one of the ingredients of a "mesh" texture. Locally, bastite grains (serpentine pseudomorphs after orthopyroxene) straddle the boundary between dark veins and the adjoining lighter areas. Examination of these veins in thin section reveals that they are regions where the rock has been completely serpentinized, while the adjoining gray areas preserve relict mineralogy. We refer to these veins as *serpentinization veins*. Serpentinization veins appear to bound many blocks.

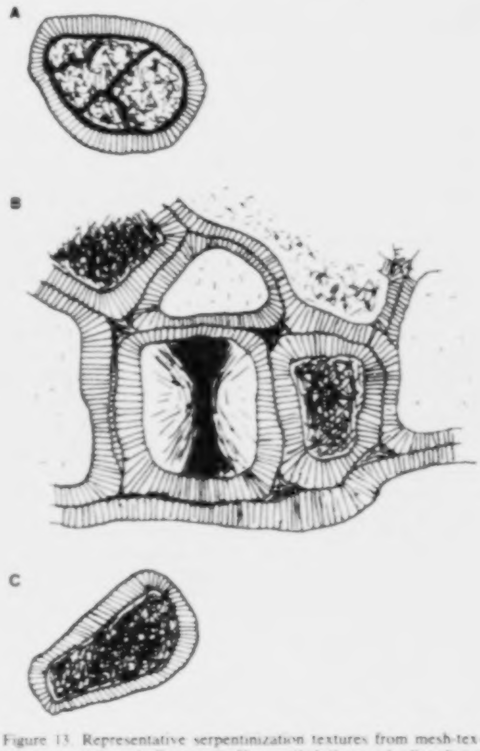

Figure 13. Representative serpentinization textures from mesh-texture serpentinites: A. Symmetric fibrous "halo" around relict olivine grain. B. Serpentine tablet with "hourglass" texture, surrounded by fiber halo. C. Asymmetric fiber halo.

In the less-serpentinized areas between the veins, orthopyroxene is commonly partially serpentinized along cleavage planes, and small olivine grains are separated by a mesh or web of serpentine veins (Fig. 13A). Groups of these small grains have parallel optical orientations, demonstrating that they are actually subgrain remnants of large olivine grains. A serpentine halo, typically consisting of fibrous serpentine minerals, surrounds each subgrain. These haloes adjoin and form the microscopic vein network. Where the haloes abut, a median line or zone is typically present; this may itself be filled with fibrous serpentine, or with magnetite grains. In some instances, stringers of opaque minerals (probably magnetite) line the centers of large veins of fibrous serpentine that surround relict subgrains with the same optical orientation. These magnetite stringers outline crude polygons.

In completely serpentinized rocks, and in serpentinization veins in incompletely serpentinized rocks, orthopyroxene has been completely altered to bastite, while relict olivine subgrains have been altered to tablets of serpentine, probably mostly lizardite. These tablets commonly exhibit "hourglass" texture, in which subgrains reach optical extinction in triangular quadrants with apexes at the center of the subgrains and bases along their edges (Fig. 13B). Like their olivine-subgrain predecessors, these tablets are rimmed by haloes of fibrous serpentine. Opaque stringers similar to those in less-serpentinized areas are also common.

In many rocks (for example, Sample 125-780C-8R-1, 98–101 cm), the fibers in serpentine haloes extend radially outward from each relict olivine subgrain or serpentine tablet to the middle of the vein, and are symmetrical about the subgrain and perpendicular to its surface. In these rocks, the polygons outlined by the magnetite stringers are typically equant. In other rocks, however (for example, Sample 125-780D-7X-5, 94–96 cm), the fibers exhibit preferred orientation and are oblique to the olivine subgrain boundary and to the middle of the vein (Fig. 13C). In these rocks, the magnetite polygons may exhibit distinct elongation and preferred orientation.

Felted-Lath Textures

Thin sections of two rocks (Samples 125-780C-10R-6, 36–37 cm, and 125-780D-2X-1, 7–8 cm) reveal "felted-lath" textures, in which laths of serpentine minerals are felted together to form a fine-grained, interlocking mass. Under crossed polarizers, this fabric appears to have a strong preferred orientation, with two sets of laths at approximately 90° to each other. However, the thin section looks the same in all orientations as the stage is rotated. In reality, the fabric is virtually isotropic, and displays only a weak preferred orientation.

Bladed-Sheaf Texture

In one thin section (Sample 125-780D-7X-1, 25–26 cm), antigorite is present as patches or sheaves of parallel blades. The blades within each patch have nearly the same optical orientation, but the rock is a mass of different patches, each with its own orientation. In the one example studied, this fabric does not appear to have a preferred orientation.

In most of the lizardite-chrysotile serpentinites recovered from Site 780, the serpentine fiber haloes that developed around olivine subgrains are symmetrical and isotropic, both in serpentinization veins and in less-serpentinized areas between the veins. Moreover, the magnetite polygons that presumably mimic the shapes of old olivine grains are not elongate and do not exhibit preferred orientation. These symmetrical textures probably indicate that the rocks were serpentinized under approximately isotropic stress conditions. Likewise, the felted-lath and bladed-sheath textures that developed in some of the rocks appear to be isotropic and probably also recrystallized under low deviatoric stresses. In one specimen (Sample 125-780D-7X-5, 94–96 cm), however, fiber haloes and magnetite polygons appear to have weak asymmetry, suggesting that this rock was recrystallized under anisotropic stress conditions.

In one of the samples exhibiting felted-lath texture, (Sample 125-780D-2X-1, 7–8 cm), the fabric is developed in the serpentine matrix of a metaclastic rock that itself contains many detrital serpentine grains, in addition to rare brown hornblende, plagioclase, and carbonate clasts. The matrix of this detrital rock clearly recrystallized after its deposition.

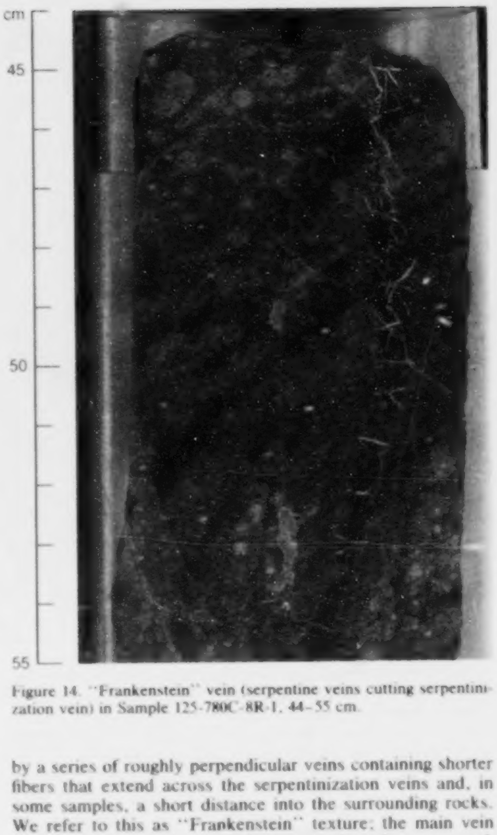

Figure 14. "Frankenstein" vein (serpentine veins cutting serpentinization vein) in Sample 125-780C-8R-1, 44–55 cm.

Serpentine Veins

Many serpentinized ultramafic blocks from Site 780 contain veins of serpentine minerals that crosscut earlier serpentinization fabrics. Typically, these veins are filled with white to light green, fibrous serpentine that has grown perpendicular to the vein boundaries. We refer to these as *serpentine veins*. Many of these macroscopic fiber veins are found approximately in the centers of major, earlier serpentinization veins. In some cases, these cross-fiber veins have been intersected by a series of roughly perpendicular veins containing shorter fibers that extend across the serpentinization veins and, in some samples, a short distance into the surrounding rocks. We refer to this as "Frankenstein" texture; the main vein represents the incision and the cross-veins, the sutures. A good example is Sample 125-780C-8R-1, 44–55 cm, pictured in Figure 14.

The presence of serpentinization veins along block boundaries suggests that these veins are weak and have formed preferred zones of brittle failure along which large bodies of massive serpentinite fragment into smaller blocks.

The serpentine fiber veins in the samples are clearly extensional features in which new serpentine minerals have been deposited, rather than replacement veins. The common presence of these veins in the centers of earlier serpentinization veins is another indication that these serpentinization veins were zones of relative weakening and embrittlement of the rock. They also indicate that a common stress mechanism causes major serpentinization veins to fail in extension. The presence of "Frankenstein" veins indicates that the stress mechanism may be the expansion of the adjoining, less-serpentinized rock as it continues to serpentinize and expand. This expansion should exert tractions on the serpentinization vein, both along and across its length. Because the serpentinization vein cannot expand further, it experiences brittle failure in extension and the opening cracks fill with serpentine cross-fibers, resulting in the "Frankenstein" textures (Fig. 15).

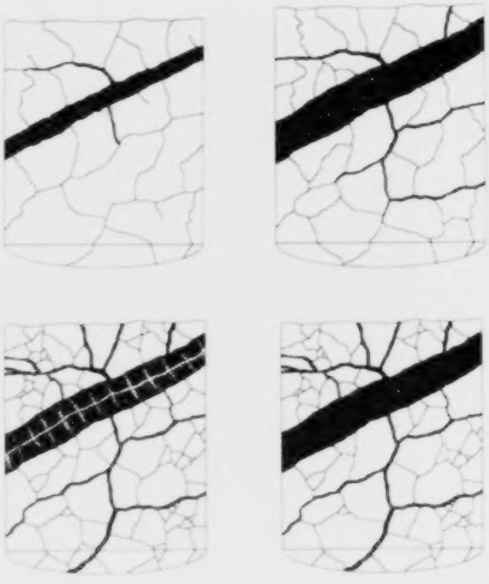

Figure 15. Stages in the growth of a "Frankenstein" vein.

Post-Serpentinization Deformation

Slight deformation after serpentinization is evinced by the kinking of fibers in veins and by irregular undulatory extinction in serpentine mesh structure. Typically, fibers appear to have been shortened parallel to their length, as well as to have undergone simple shear; oblique extensional fabrics (brittle "normal faults" or ductile shear bands) were not observed. Otherwise, little pattern is visible in these deformational features.

Deformation Textures in Serpentine Matrix

A striking feature of the serpentine matrix recovered from Site 780, especially in comparison with matrix from Sites 778 and 779, is the virtual absence of sheared foliation fabrics. In contrast, apparently detrital textures (clasts scattered in matrix and subhorizontal lamination) are common in the upper parts of the cores (Fig. 16). Matrix recovery was generally poor in the lower parts of the holes, but the approximately 3 m of matrix recovered from a depth of 30 m at the bottom of Hole 780D shows clast-in-matrix textures with no shear foliation; faint subhorizontal boundaries between muds of lightly different color can also be seen.

We interpret these undeformed fabrics as primary textures of the upwelling serpentinite and of the pools of serpentinous material formed on top of the seamount. We think that the foliated, sheared, and convoluted fabrics at Sites 778 and 779 were superimposed on the structureless unconsolidated serpentine when it became unstable and began to flow down the slopes of the seamount.

Rheology of Serpentine Sediments and Flows

We conducted extensive tests of the stress-strain behavior of serpentine sediments and flows from Hole 780D using a Wykeham Farrance torsion-vane (torvane) apparatus. These

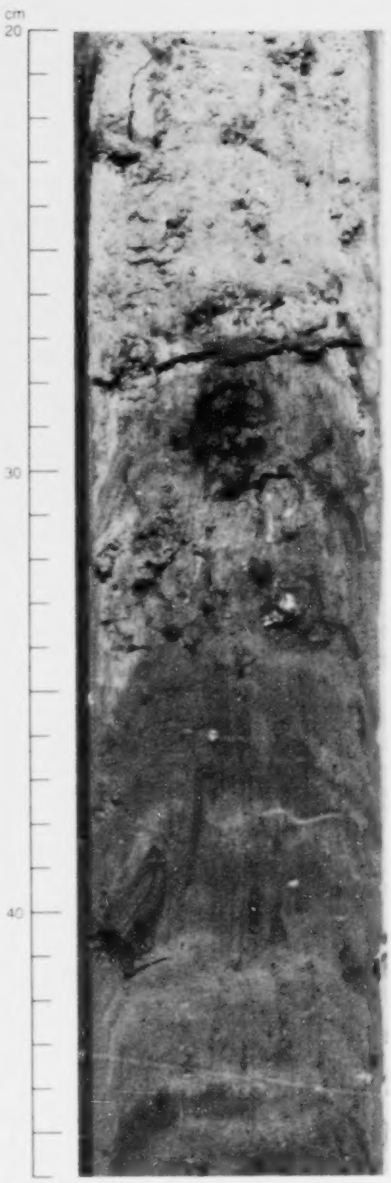

Figure 16. Clast-in-matrix textures and subhorizontal lamination in Sample 125-780D-1X-3, 20–46 cm.

Table 9. Ultimate strengths of serpentine sediments and flows recovered from Hole 780D.

Core, section, interval (cm)	Depth (mbsf)	Stress (kPa)
125-780D-1X-3, 48	1.91	14.5
125-780D-2X-2, 14	3.07	7.1
125-780D-2X-2, 27	3.07	7.3
125-780D-2X-CC, 16	3.87	16.4
125-780D-2X-CC, 23	3.89	18.1
125-780D-2X-CC, 31	3.90	20.1
125-780D-3X-1, 12	12.07	37.5
125-780D-6X-1, 71	21.00	9.1
125-780D-6X-2, 26	21.39	2.7
125-780D-6X-2, 41	21.52	5.2
125-780D-6X-2, 52	21.63	3.8
125-780D-6X-2, 65	21.64	4.0
125-780D-7X-1, 8	27.55	7.1
125-780D-7X-1, 30	27.63	7.5
125-780D-7X-1, 40	27.80	11.7
125-780D-7X-1, 46	27.86	26.9
125-780D-7X-1, 64	27.97	24.6
125-780D-7X-1, 73	28.01	18.6
125-780D-7X-1, 128	27.45	10.0
125-780D-7X-5, 51	28.52	3.0
125-780D-7X-5, 75	28.76	2.2
125-780D-7X-5, 125	29.27	1.3
125-780D-7X-6, 95	30.46	4.2
125-780D-7X-CC, 32	30.74	8.2

tests reveal that the serpentine materials are highly non-ideal and plastic, with ultimate strengths ranging from 1.3 to 38 kPa and averaging 11.6 kPa (see Table 9). For comparison, more "normal" oceanic muds recovered from Site 781 were somewhat stronger, having ultimate strengths ranging from 8.1 to 116.1 kPa. In only two cases did the samples actually fail; most serpentine merely continued to deform at a constant rate at maximum (ultimate) strength. Although we were unable to determine yield strength directly, our observations of the behavior of these materials as they were tested led us to think that their yield strengths are vanishingly low. Representative stress-strain curves for these materials are given in Figure 17.

These rheologic measurements suggest several important conclusions about the mechanics of the formation of Conical Seamount. First, modeling based on the ultimate strengths of the materials suggests that they might carry blocks of serpentinized peridotite (density approximately 2.6–2.7 g/cm^3) as large as 20 m upward against the force of gravity. Second, their low yield strengths suggest that unless the material continues to well upward from within the feeder of the seamount, the blocks will fall back downward into the feeder. Finally, their low strengths suggest that the seamount is rheologically more like a mud volcano than a salt diapir (salt has an ultimate strength of approximately 10^4 to 10^5 kPa). This in turn suggests that the serpentine feeder may be relatively narrow with respect to the width of the edifice.

PALEOMAGNETISM

Magnetostratigraphy was impossible at Site 780 because of the lack of coherent lithologic units, the poor recovery, and the tectonized nature of the rocks. The natural remanent magnetization (NRM) of the archive half of each core was measured and demagnetized with the cryogenic magnetometer and the on-line AF demagnetizer at the 0-, 5-, and 10-mT levels. Several discrete samples (125-780C-1R-1, 95–97 cm; 125-780C-1R-2, 137–139 cm; 125-780C-1R-3, 95–97 cm; 125-780C-1R-4, 61–63 cm) were progressively demagnetized and measured at the 0-, 3-, 5-, 8-, 10-, 12-, and 15-mT levels.

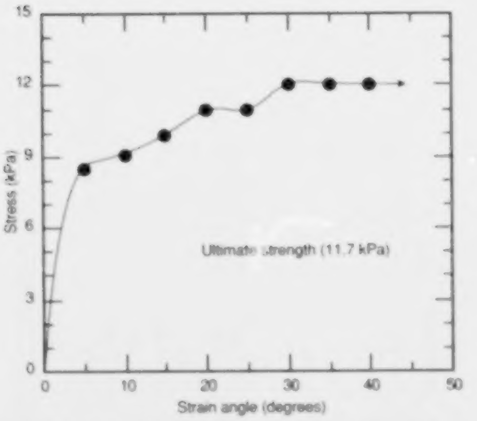

Figure 17. Representative stress-strain curves for serpentine matrix recovered from Hole 780D.

The rocks from Holes 780A, 780B, and 780D display scattered magnetic directions, making the determination of a magnetic polarity for any of the cores impossible. The magnetic intensities of these rocks vary between 10 and 1000 mA/m. In Hole 780C, the magnetic inclination in Core 125-780C-1R moved from steeply positive to predominantly negative at the 10-mT demagnetization level, suggesting a reversed polarity at the top of this hole (Figs. 18A and 18B). However, all of the discrete samples taken from Core 125-780C-1R show a positive inclination after demagnetization to 15 mT (Table 10). Contradictory data make it impossible to define a magnetostratigraphy for Core 125-780C-1R.

Magnetic susceptibilities were measured on the multisensor track. Many of the cores from Hole 780C were not measured because recovery was poor and the rocks in the cores were broken and disturbed by drilling. In Holes 780B, 780C, and 780D, the magnetic susceptibility ranged between $2\pi \times 10^{-3}$ to $10\pi \times 10^{-3}$ SI, with most of the measurements in the uppermost part of this range. In Hole 780A, Core 125-780A-1H shows a generally higher overall susceptibility than the rocks from the other holes in Site 780. The values in this core range from $8\pi \times 10^{-3}$ to $12\pi \times 10^{-3}$ SI. The magnetic susceptibility data display a regular scalloping pattern that has a wavelength of about 40 cm (Fig. 19), an interesting, but at this point inexplicable, observation. However, owing to the poor recovery and lack of coherent units, no systematic downhole changes in susceptibility were observed.

PHYSICAL PROPERTIES

Physical Properties Procedure

Physical and index properties measured at Site 780 are listed in Tables 11 and 12. Shear strength and sonic velocities were determined where possible. Some of the serpentine sediments and flows were too weak to measure shear strength accurately. Shear strengths were obtained for Hole 780D and are reported in the "Structural Studies" section (this chapter). Sonic velocities were determined using the Hamilton Frame apparatus on the hard clasts that were distributed through the serpentine material in Hole 780C. Velocities are reported in

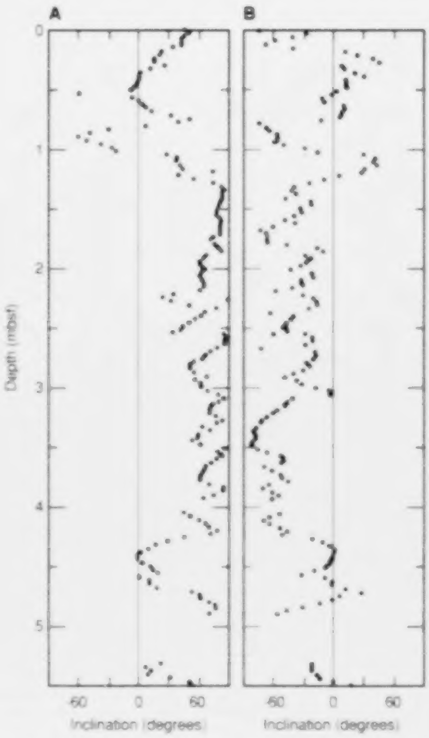

Figure 18. A. NRM inclination data (in degrees) from Core 125-780C-1R at 0 mT. B. Inclination data (in degrees) from Core 125-780C-1R after 10-mT demagnetization.

the "A" direction, parallel to the core axis, and in the "B" direction, normal to the core axis.

Hole 780A

Hole 780A was cored to only 3.5 mbsf. Table 11 lists the index properties, and Table 12 lists the thermal conductivities of material from this core. The average bulk density is 1.83 g/cm³, and the average grain density is 2.64 g/cm³. The GRAPE provided accurate values of bulk density in this hole (Fig. 20). The high bulk-density value of these sediments reflects the density of serpentine, 2.5 to 2.65 g/cm³, and the water content, about 30%.

Hole 780B

Hole 780B was cored to 18.2 mbsf, with 0.34 m recovered. Table 11 lists the index properties, and Table 12 presents thermal conductivities of material from this core. The average bulk density is 1.73 g/cm³, and average grain density is 2.63 g/cm³.

Hole 780C

Hole 780C, cored to 163.5 mbsf, is the deepest hole at this site. The poor recovery (only 8.8%), probably caused by alteration of weak serpentine sediments and flows and clasts of hard rock, leaves large gaps in the record of physical properties of materials from this hole. Tables 11 and 12 list the index properties, thermal conductivities, and sonic velocities of materials from this hole.

Table 10. Paleomagnetic data for discrete specimens taken from Core 125-780C-1R.

Section, interval (cm)	Declination (degrees)	Inclination (degrees)	Intensity (mA/m)	Polarity
	Natural remanent magnetization			
1R-1, 95	352.7	-12.1	356.0	
1R-2, 137	171.1	84.5	83.0	
1R-3, 95	326.8	-25.2	230.0	
1R-4, 61	251.1	70.6	69.0	
1R-CC, 11	303.5	89.7	71.7	
	Remanent magnetization after demagnetization to 15 mT			
1R-1, 95	74.6	56.1	6.04	N
1R-2, 137	122.2	60.1	4.18	N
1R-3, 95	235.8	76.8	6.06	N
1R-4, 61	175.3	50.6	3.52	N
1R-CC, 11	184.3	26.2	4.37	N

Note the large decrease in intensity for all specimens. The median destructive field value for these specimens averages less than 2 mT.

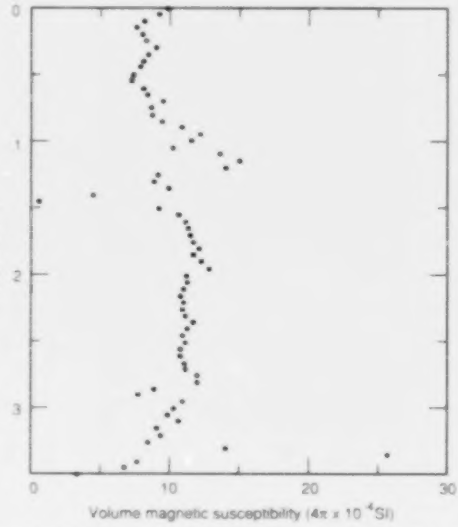

Figure 19. Volume magnetic susceptibility for upper portion of Core 125-780C-1R. Notice the scallop pattern, which has a wavelength of about 40 cm.

Figures 21 and 22 illustrate the index properties of materials from Hole 780C. The average bulk density of the matrix material is 1.77 g/cm³, and the average grain density is 2.65 g/cm³. The average bulk density of the clasts is 2.76 g/cm³, and the average grain density is 2.77 g/cm³. From Figures 21 through 22, one can see that no significant correlation exists between the index properties and depth. The distinction between the matrix and the clasts is clearly seen in Figures 21 and 22.

Figure 23 illustrates the variation of thermal conductivity with depth and shows no significant pattern. However, the thermal conductivity of the clasts is uniformly greater than that of the matrix material.

Table 11. Index properties for Holes 780A, 780B, 780C, and 780D.

Core-section, interval (cm)	Depth (mbsf)	Bulk density (g/cm^3)	Grain density (g/cm^3)	Porosity (%)	Water content (%)	Void ratio
125-780A-1H-1, 39–41	0.39	1.79	2.64	52.6	31.3	0.53
1H-1, 58–60	0.58	1.80	2.56	49.5	29.3	0.49
1H-2, 68–70	2.18	1.91	2.74	48.5	27.1	0.48
1H-CC, 23–25	3.13	1.82	2.63	50.6	29.60	0.51
125-780B-1R-1, 99–101	0.99	1.72	2.63	57.2	35.4	0.57
1R-2, 39–41	1.89	1.75	2.67	55.9	33.8	0.56
1R-3, 30–31	3.30	1.70	2.68	59.3	37.0	0.59
1R-4, 49–50	4.99	1.75	2.56	53.0	32.1	0.53
1R-6, 99–100	8.49	1.75	2.63	55.4	33.7	0.55
125-780C-1R-1, 72–74	0.72	1.64	2.68	62.86	40.61	0.63
1R-2, 64–66	1.68	1.63	2.64	62.72	40.81	0.63
1R-3, 89–91	3.43	1.65	2.57	59.63	38.34	0.60
1R-4, 76–78	4.80	1.71	2.69	58.75	36.41	0.59
2R-1, 30–32	5.80	1.71	2.63	57.36	35.58	0.57
3R-1, 56–59	14.56	3.06	3.06	00.18	00.06	0.00
4R-1, 13–15	23.63	1.75	2.62	54.60	33.11	0.55
5R-1, 41–43	33.41	1.83	2.66	51.14	29.76	0.51
6R-1, 61–62	43.11	2.70	2.70	00.07	00.03	0.00
7R-1, 13–15	52.20	2.05	2.66	37.58	19.49	0.38
8R-1, 98–101	62.48	2.67	2.67	00.18	00.07	0.00
9R-1, 34–37	71.44	2.78	2.80	00.95	00.36	0.01
10R-1, 13–16	80.93	2.74	2.75	00.42	00.16	0.00
12R-1, 17–20	100.37	2.64	2.65	00.59	00.24	0.01
13R-1, 40–43	106.90	2.92	2.92	00.11	00.04	0.00
15R-1, 23–25	125.73	1.81	2.64	51.85	30.48	0.62
15R-CC, 13–14	126.08	1.96	2.67	43.48	23.62	0.43
16R-1, 53–59	135.53	2.66	2.68	01.27	00.51	0.01
18R-1, 107–111	155.07	2.71	2.72	00.53	00.21	0.01
125-780D-1X-1, 20–22	0.20	1.65	2.75	63.8	41.0	0.64
1X-2, 52–54	0.97	1.69	2.58	57.7	36.4	0.58
1X-3, 45–47	1.96	1.83	2.72	53.1	30.9	0.53
1X-CC, 11–13	2.40	1.69	2.65	59.5	37.5	0.59
2X-1, 30–32	2.80	1.85	2.62	48.7	28.0	0.49
2X-2, 3–5	3.03	1.67	2.79	64.0	40.8	0.64
2X-CC, 4–6	3.82	1.71	2.68	58.8	36.6	0.59
3X-1, 13–15	12.13	1.47	2.11	60.2	43.7	0.60
5X-1, 9–11	16.99	2.55	2.57	1.1	0.5	0.01
6X-1, 62–64	21.02	1.67	2.64	60.4	38.5	0.60
6X-2, 41–43	21.59	1.64	2.88	66.7	43.1	0.67
7X-1, 43–45	27.83	1.95	2.83	48.7	26.5	0.49
7X-5, 45–47	28.53	1.68	2.66	60.4	38.3	0.60
7X-6, 13–15	29.71	1.69	2.67	59.7	37.4	0.60
7X-CC, 20–22	30.69	1.72	3.08	66.1	40.8	0.66

Figure 24 is a plot of the "A" and "B" velocities vs. depth. These velocities fall between 5000 and 6000 m/s and exhibit no correlation with depth.

Hole 780D

Hole 780D was cored to a depth of 32.4 mbsf, with 9.09 m recovered. Tables 11 and 12 list the index properties and thermal conductivities of the material from this core. The average bulk density is 1.71 g/cm^3, and the average grain density is 2.66 g/cm^3. Figures 25 and 26 present plots of bulk and grain densities vs. depth. With the exception of a few points, these properties do not vary systematically with depth. Figure 27 is a plot of thermal conductivity vs. depth and indicates a large amount of scatter.

LOGGING

Downhole temperatures were measured and logging was conducted at Site 780. We attempted to log Hole 780C and downhole temperatures were measured at Hole 780D using the Barnes-Uyeda tool. The logging data have been converted from mbrf (meters below rig floor) to mbsf. The Kelly bushing on the ship's rig floor was the reference point at 10.6 m above sea level, while the mud line is located 3083.4 mbsl (meters below sea level).

Logging

We decided to try to log Hole 780C, despite its shallow depth and drilling problems, because of the high scientific interest in this hole and the poor core recovery. The poor hole conditions were revealed when several large overpulls were necessary while the hole was being conditioned for logging, including a 300,000-lb overpull at 234 mbsf. At that same depth, a 260,000-lb overpull was necessary after the bit was dropped at the bottom of the hole.

Once the bit had been dropped, we set the end of the pipe at 56 mbsf. The first logging string consisted of the following tools (listed from the bottom of the string upward): the Lamont-Doherty temperature logging tool (TLT), the Schlumberger phasor induction tool (DIT), the Schlumberger lithodensity tool (HLDT), and the Schlumberger sonic tool (SOT) (see the "Explanatory Notes," this volume, for more details of the tools). The tool string was run down to about 14 mbsf and held there. This served as a reference point for the TLT and allowed us to check the performance of the Schlumberger tools. We resumed lowering after 10 min and proceeded until the tool string touched down at 58 mbsf, just beyond the end of the drill string. The only tool that was outside the drill string at that point was the TLT. Various attempts were made to

Table 12. Physical properties for Holes 780A, 780B, 780C, and 780D.

Core-section, interval (cm)	Depth (mbsf)	Thermal conductivity (W/mK)	Resistivity (ohms)	Formation factor	"A" velocity (km/s)	"B" velocity (km/s)	Ultimate stress (kPa)
125-780A-1H-1, 13–5	0.07		48.0	5.60			
1H-1, 25–25	0.25	1.683					
1H-1, 71–75	0.73		72.0	8.40			
1H-1, 113–117	1.15		53.0	6.19			
1H-2, 25–25	1.75	1.791					
1H-CC, 23–25	3.13	1.901					
125-780B-1R-1, 54–54	0.54	1.161					
1R-2, 39–41	1.89	1.468					
1R-3, 73–73	3.73	1.342					
1R-4, 78–78	5.28	1.579					
1R-6, 41–41	7.91	1.352					
125-780C-1R-1, 72–74	0.72	0.821	22.0	2.57			
1R-2, 36–40	1.68		21.8	2.54			
1R-2, 64–66	1.88	1.434					
1R-2, 103–107	2.55		13.0	1.52			
1R-3, 89–91	3.43	1.254					
1R-3, 127–131	4.29		24.9	2.91			
1R-4, 106–108	5.10	1.350					
2R-1, 19–21	5.69	1.510					
3R-1, 21–33	14.21	2.271					
3R-1, 56–59	14.56				4.25	5.05	
4R-1, 13–15	23.63	1.411					
6R-1, 61–62	43.11	2.273			5.79	5.51	
8R-1, 98–101	62.48	2.648			5.65	5.82	
9R-1, 34–37	71.44	2.626			5.71	5.56	
10R-1, 13–16	80.93				5.18	5.43	
12R-1, 17–20	100.37	2.945			5.26	5.26	
13R-1, 40–43	106.90	3.457			6.21	6.19	
15R-1, 23–25	125.73	1.481					
16R-1, 53–59	135.53	2.293			5.3	5.54	
18R-1, 107–111	155.07	2.624			5.66	5.56	
125-780D-1X-1, 20–22	0.20	1.224					
1X-2, 26–26	0.71	1.244					
1X-3, 26–26	1.77	1.294					
1X-3, 48–48	1.91						14.5
1X-CC, 11–13	2.40	1.372					
2X-1, 30–32	2.80	1.270					
2X-2, 3–5	3.03	1.418					
2X-2, 14–14	3.07						7.1
2X-2, 27–27	3.20						7.3
2X-CC, 4–6	3.82	1.442					
2X-CC, 16–16	3.87						16.4
2X-CC, 23–23	3.94						18.1
2X-CC, 31–31	4.02						20.1
3X-1, 13–15	12.13	1.474					37.5
5X-1, 9–11	16.99	1.911					
6X-1, 44–46	20.84	1.201					
6X-1, 71–71	21.00						9.1
6X-2, 21–23	21.39	0.670					2.7
6X-2, 41–41	21.52						5.2
6X-2, 52–52	21.63						3.8
6X-2, 65–65	21.64						4.0
7X-1, 8–8							7.1
7X-1, 19–23	27.61	38.1		4.45			7.5
7X-1, 43–45	27.83	1.536					11.7
7X-1, 46–46							26.9
7X-1, 50–54	27.92		61.0	7.12			61.0
7X-1, 73–73	28.01						18.6
7X-1, 128–128	28.23						10.0
7X-5, 45–47	28.53	1.092					3.0
7X-5, 75–75	28.76						2.2
7X-5, 125–125	29.27						1.3
7X-6, 77–79	30.35	0.428					
7X-6, 95–95	30.46						4.2
7X-CC, 20–22	30.69	1.139					
7X-CC, 32–32	30.74						8.2

punch the tool through the hole obstruction by raising the tool string, then lowering it quickly, and by moving the drill string. We were unable to push through the obstruction even after trying for 1 hr and therefore decided to retrieve the tools. We felt that the hole had collapsed below the drill string and that attempts to clear it would not be successful, so we terminated the logging run.

The only useful data from this logging run were from the TLT. Quite unexpectedly, the temperature increased dramatically from a seafloor value of 1.52 to 13.5°C by 58 mbsf. Data from the fast-response thermistor are shown in Figure 28, and data from the more accurate slow-response thermistor are shown in Figure 29. Individual data points have been plotted together in Figure 30 for comparison. The differences between

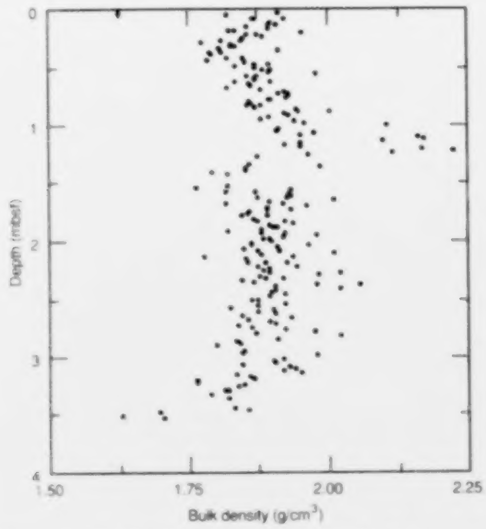

Figure 20. GRAPE-determined bulk density for Hole 780A.

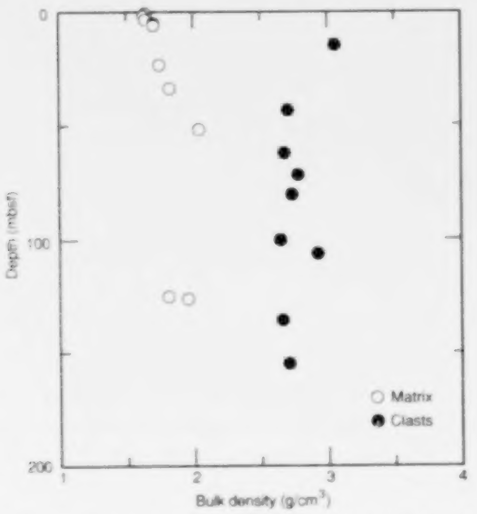

Figure 21. Depth vs. bulk density for Hole 780C. Data plotted as solid circles derive from clasts, and those plotted as open circles derive from the matrix.

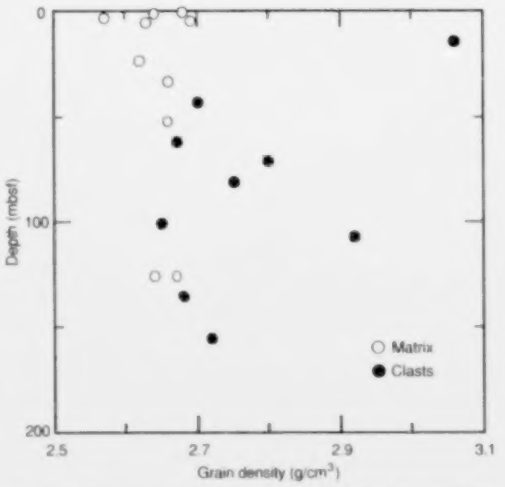

Figure 22. Depth vs. grain density for Hole 780C. Data plotted as solid circles derive from clasts, and those plotted as open circles derive from the matrix.

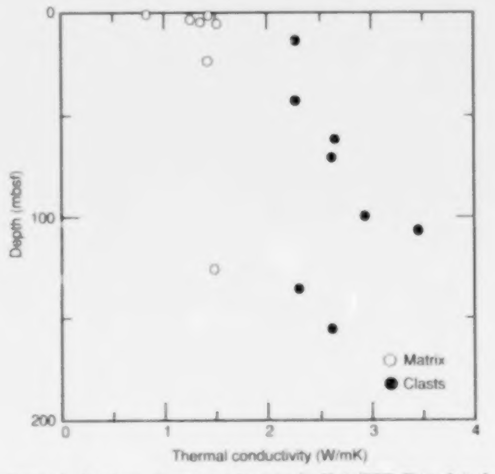

Figure 23. Depth vs. thermal conductivity for Hole 780C. Data plotted as solid circles derive from clasts, and those plotted as open circles derive from the matrix.

the fast- and slow-response thermistors later in the record result from a coating of mud on the slow-response thermistor. A plot of the data over a shorter time interval is shown in Figure 31. The temperature starts to rise at about 1530 s, as the tool travels below the seafloor. Temperatures then increase at a fairly constant rate until about 1580 s, when temperatures again increase at a much faster rate until the peak temperature is reached at about 1630 s. The reason for the change in the rate of the increase in temperature is not readily apparent. The TLT also has a pressure sensor, enabling us determine its depth in the hole. Pressure data are plotted vs. time in Figure 32. There is a large amount of short-term variability in these data because they represent information gained from lowering the logging string, when the wireline heave compensator is not in use. A smoothed version of these pressure data is shown in Figure 33. One can see that although there is a slight change in the rate of descent of the

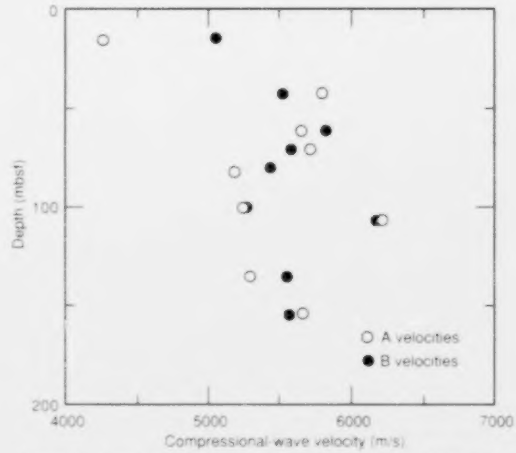

Figure 24. Depth vs. compressional-wave velocity for Hole 780C. Data plotted as solid circles represent *B* velocities, perpendicular to the core hole, and those plotted as open circles represent *A* velocities, parallel to the core hole.

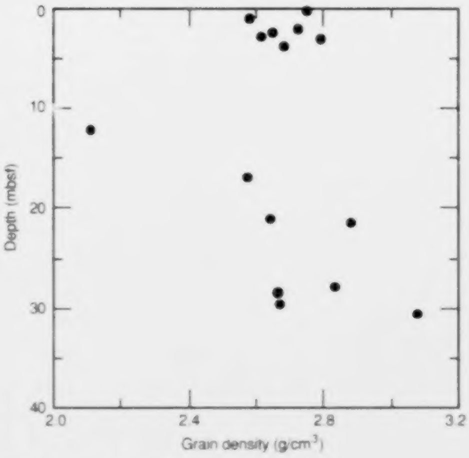

Figure 26. Depth vs. grain density for Hole 780D.

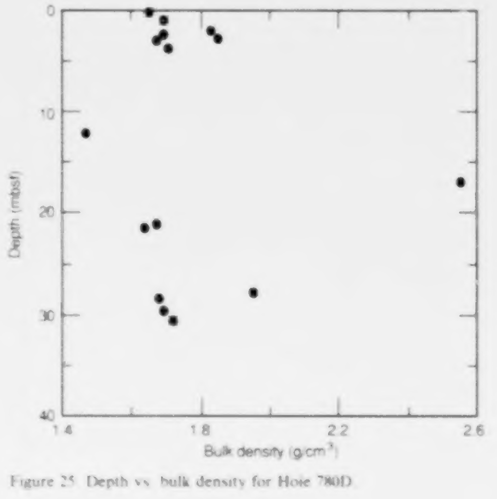

Figure 25. Depth vs. bulk density for Hole 780D.

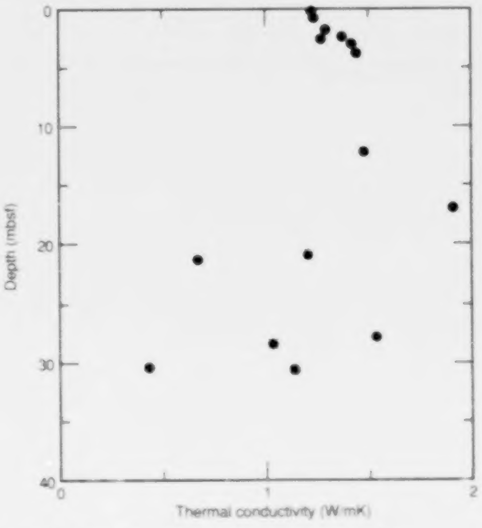

Figure 27. Depth vs. thermal conductivity for Hole 780D.

tool as it is being run into the drill pipe, it is not so dramatic a change as that of the temperature. Interpretation of these temperature results is discussed further below in comparison with results from the Barnes-Uyeda temperature tool.

Temperature Tool

The Barnes-Uyeda water sampler and temperature tool was used for three measurements in Hole 780D. Two temperature measurements were obtained, one during Run 06X at 20.4 mbsf and another during Run 08X at 41.8 mbsf. The temperature record from Run 06X is shown in Figure 34. This temperature record is somewhat noisy. The tool was seated at about 59 min into the run, and there is a usable decay curve from then until about 75 min. A simplified correction for the decay of the frictional heating from emplacement is shown in Figure 35. After the first few minutes of emplacement, the decay curve is proportional to 1/time. A linear least-squares regression on the data, extrapolated to 1/time = 0, is a good estimate of the equilibrium sediment temperature. Run 06X gave an estimated temperature of 2.41°C, with an r^2 value of 0.975. This temperature value might be somewhat high, given the extra frictional heating that occurred before the probe was firmly seated in the bottom of the hole (Fig. 34). The temper-

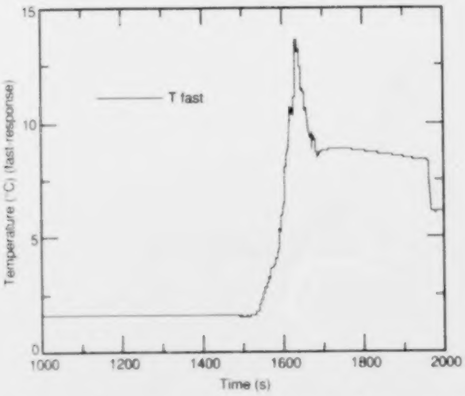

Figure 28. Temperature (°C) measured with the fast-response thermistor of the temperature logging tool (TLT) vs. time.

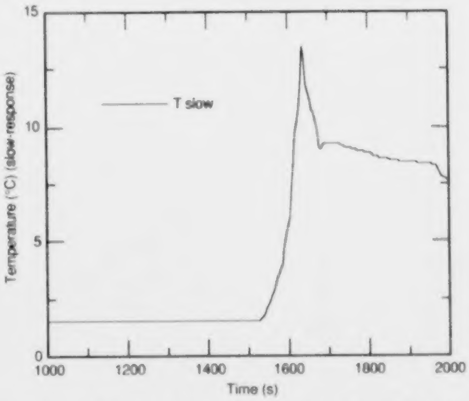

Figure 29. A plot similar to that in Figure 28, using the more precise slow-response thermistor.

ature record from Run 08X is shown in Figure 36. This decay curve is much cleaner for this run from the time the probe was seated in the bottom at 63 min, until pullout at 80 min. The corresponding equilibrium reduction plot, Figure 37, shows a much better fit than the one for Run 06X. The estimated equilibrium temperature is 3.10°C, with an r^2 value of 0.998.

The temperature data must be combined with the thermal conductivity data to determine the heat flow at this site. The thermal conductivity data are discussed in the "Physical Properties" section (this chapter). We combined all the thermal conductivity data for Site 780 (Holes 780A through 780D) in Figure 38. The most useful way to analyze the

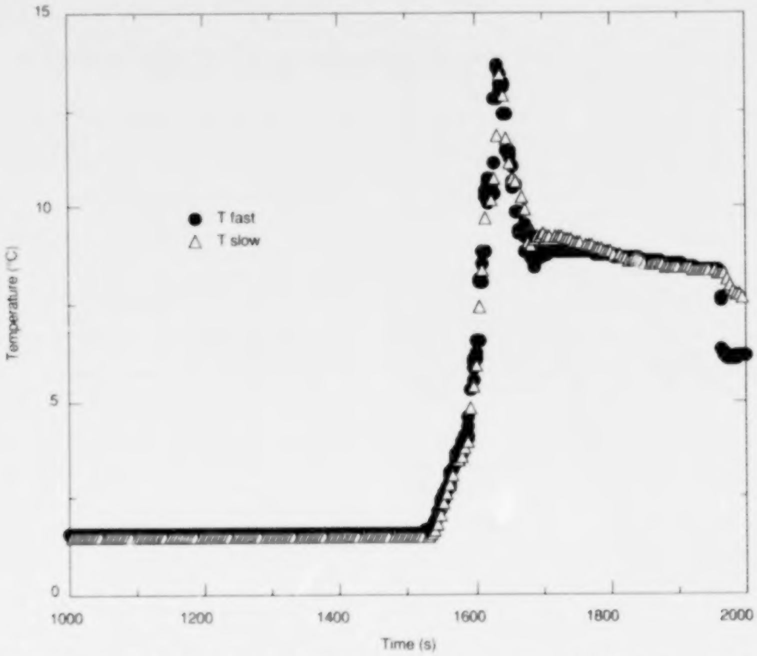

Figure 30. A comparison plot of the two thermistors vs. time. The differences after 1680 s are caused by a coating of mud on the slow-response thermistor.

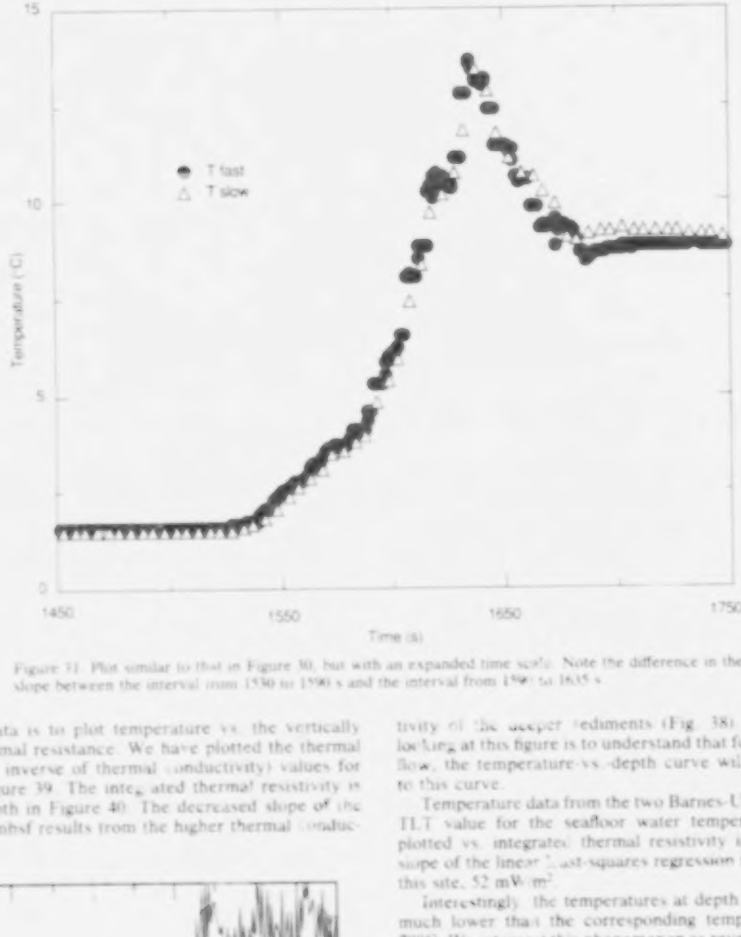

Figure 31. Plot similar to that in Figure 30, but with an expanded time scale. Note the difference in the slope between the interval from 1530 to 1590 s and the interval from 1590 to 1635 s.

temperature data is to plot temperature vs. the vertically integrated thermal resistance. We have plotted the thermal resistivity (the inverse of thermal conductivity) values for Site 780 in Figure 39. The integrated thermal resistivity is plotted vs. depth in Figure 40. The decreased slope of the line below 50 mbsf results from the higher thermal conductivity of the deeper sediments (Fig. 38). A good way of looking at this figure is to understand that for a constant heat flow, the temperature-vs.-depth curve will be proportional to this curve.

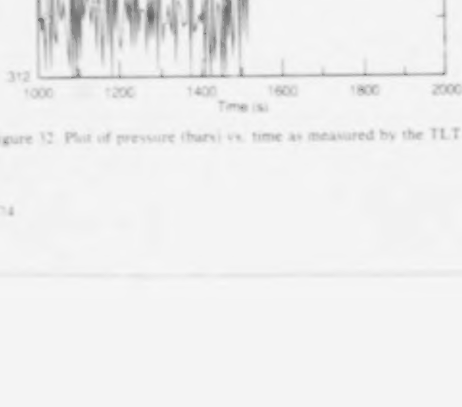

Figure 32. Plot of pressure (bars) vs. time as measured by the TLT.

Temperature data from the two Barnes-Uyeda runs and the TLT value for the seafloor water temperature have been plotted vs. integrated thermal resistivity in Figure 41. The slope of the linear least-squares regression is the heat flow at this site, 52 mW/m².

Interestingly, the temperatures at depth in Hole 780D are much lower than the corresponding temperatures in Hole 780C. We interpret this phenomenon as revealing that temperatures in Hole 780C do not necessarily represent equilibrium conductive heat flow. Sediment/fluid geochemical results from Site 780 indicate that pore fluids must be moving upward within the sediments (see "Sediment/Fluid Geochemistry" section, this chapter). We speculate that the drillhole provided a conduit that allowed higher temperature fluids to escape. The high overpulls at 234 mbsf, about 130 mbsf, may represent a zone of higher fluid flow rates and higher fluid overpressures, which were forcing the formation into the hole at that depth.

SUMMARY AND CONCLUSIONS

Site 780 is situated on the west-southwest side of the summit of Conical Seamount at a depth of 3100 m, in an area shown by *Alvin* submersible dives to be sediment covered and marked by active venting of fluids and precipitation of material from solution. Four holes were drilled at this site: Hole 780A, which was APC-cored to 3.5 mbsf; Hole 780B, which

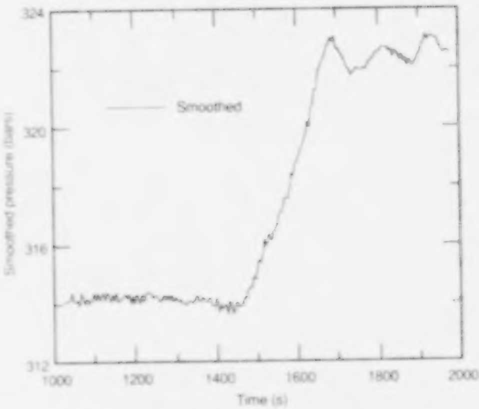

Figure 33. Plot similar to that in Figure 32, but with the pressure signal smoothed. Note that there is no dramatic change in slope at 1590 s, as there was in the temperature data.

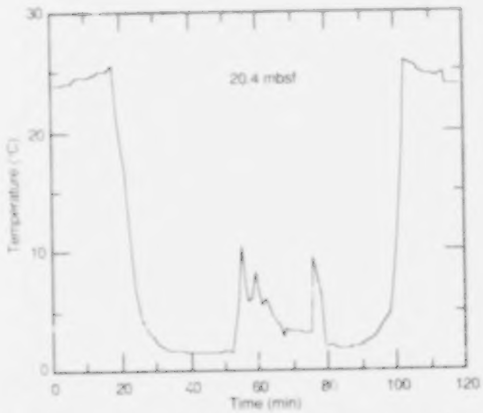

Figure 34. Temperature vs. time for the first Barnes-Uyeda temperature tool Run 06X at 20.4 mbsf. The probe was held stationary near the seafloor between 40 and 50 min into the run. It was firmly seated in the sediment between 59 and 76 min.

was RCB-cored to 18.2 mbsf; Hole 780C, which was RCB-cored to 163.5 mbsf; and Hole 780D, which was XCB-cored to 32.4 mbsf (Fig. 42). Recovery rates were low because of the interbedding of hard serpentinized peridotite and very soft unconsolidated serpentine.

Two major lithostratigraphic units were recovered at Site 780, as follows:

1. Unit I (0–3.5 mbsf in Hole 780A; 0–18.2 mbsf in Hole 780B; 0–14.0 mbsf in Hole 780C; and 0–15.4 mbsf in Hole 780D) comprises middle Pleistocene(?) to Holocene(?) sand- and silt-sized serpentine, with rare intervals of foraminifer-rich serpentine clay and serpentine-rich silty-clay; and

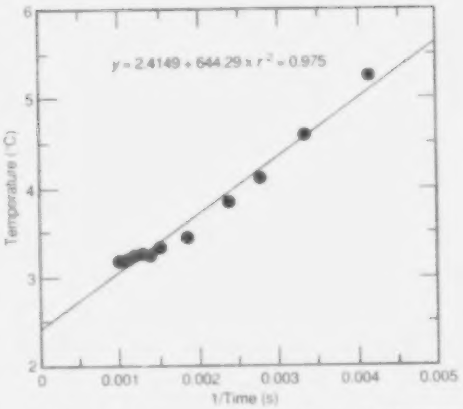

Figure 35. Reduced-temperature fit of the first Barnes-Uyeda temperature run. The intercept value at 1/time = 0 is the equilibrium temperature of the sediment.

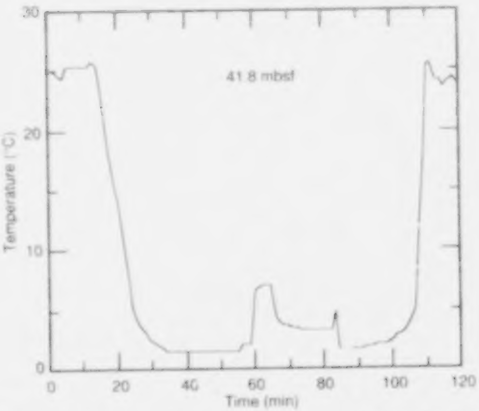

Figure 36. Plot of temperature vs. time for the second Barnes-Uyeda temperature tool Run 08X at 41.8 mbsf. The probe was firmly seated in the sediment between 63 and 81 min. There was less disturbance while the probe was in the sediment than occurred during the first run.

2. Unit II (14.0–163.5 mbsf in Hole 780C and 15.4–32.4 mbsf in Hole 780D) comprises intervals of serpentinized ultramafic rocks in a matrix of sandy silt- and clayey silt-sized serpentine.

The sediments in Unit I contain 65% to 75% serpentine, with minor amounts of opaque minerals, aragonite, and foraminifers and with trace amounts of zoisite, chlorite, nannofossils, spicules, silicoflagellates, diatoms, and radiolarians. Dating at Site 780 is based on the ages of calcareous nannofossils and planktonic foraminifers, which are middle to late Pleistocene in the upper portions of Holes 780A, 780B, 780C and 780D. The presence of delicate aragonite needles implies authigenic growth after the serpentine was emplaced. The

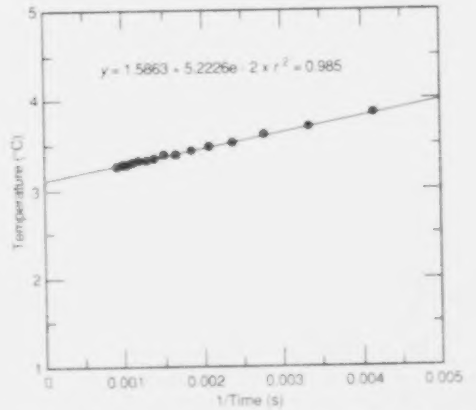

Figure 37. The corresponding reduced temperature fit for the second Barnes-Uyeda run. Notice the improved quality of the fit.

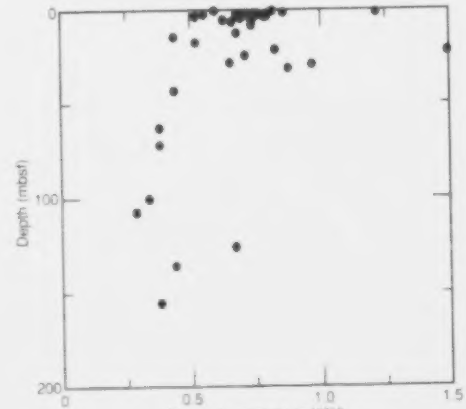

Figure 39. Plot similar to that in Figure 38, except that the value is thermal resistivity (mK/W), the inverse of thermal conductivity.

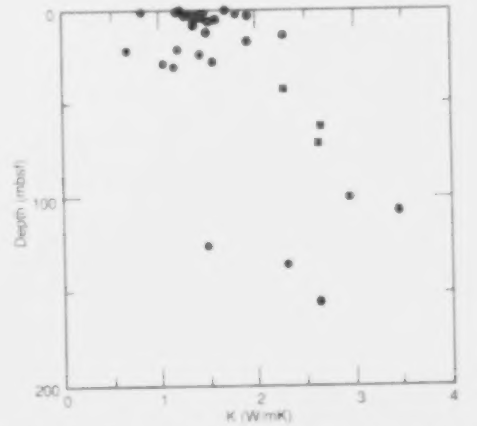

Figure 38. The combined thermal conductivity results (W/mK) for Holes 780A through 780D plotted vs. depth.

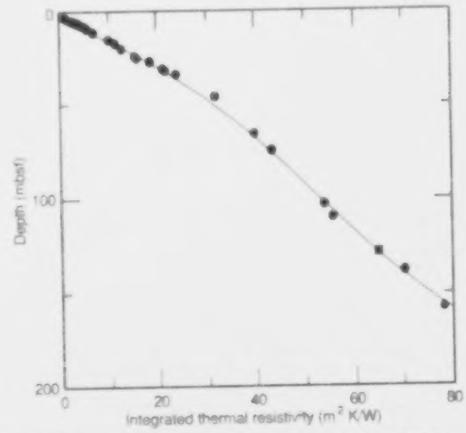

Figure 40. Integrated thermal resistivity, the depth integral of thermal resistivity (m^2K/W), plotted vs. depth.

matrix in Unit II contains 70% to 99% serpentine, with minor to trace amounts of opaque minerals, clay minerals, zoisite, chlorite, micrite, and garnet.

Hard-rock lithologies constitute serpentinized, tectonized ultramafic rocks, and subordinate serpentinized dunites having similar primary mineralogies to the ultramafic rocks from Sites 778 and 779. Serpentine veins are common and show a polystage filling history. The muddy matrix recovered from Site 780 typically lacks the foliation and shear fabric of the matrix from the flank sites; thus, this matrix may be interpreted as the primary fabric of the upwelling serpentinite, upon which foliation and shear fabric have been imposed by compaction, extension, and pure shear during the downhill creep of serpentinite debris flows.

Logging in Hole 780C showed that temperatures increased steadily from seawater values (1.5°C) near the surface to 13.5°C at 60 mbsf; the WSTP in Hole 780D gave the lower value of 3.15°C at 41 mbsf, and an estimated heat flow of 52 mW/m^2. Studies of physical properties give a density range of 1.75 to 2.0 g/cm^3 and compressional-wave velocities of 1.5 to 2 km/s for the serpentine-rich matrix in Unit II. Rheological measurements indicate that this matrix is a weak, highly non-ideal, plastic material capable of supporting blocks up to 20 m wide, and it is compatible with models for diapiric injection of the serpentinite.

Analyses of interstitial pore-water samples at Site 780 revealed marked downhole chemical changes. Holes 780A and 780D show the greatest variation: salinity decreases by 25%, chlorinity by 20%, calcium by 90%; magnesium is totally depleted, sulfate nearly doubles, alkalinity increases from 2.5 to 34, pH increases from about 8 to 12.4, potassium increases significantly, and ammonia increases dramatically. These changes take place within a few meters of the seafloor,

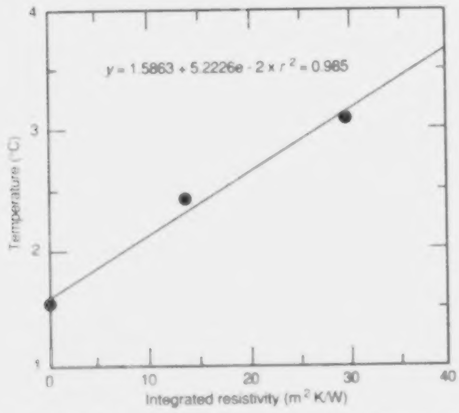

Figure 41. Plot of temperature vs. integrated thermal resistivity. The slope of the best-fitting linear regression is the heat flow value of 52 mW/m^2.

showing that the fluid entrained within the serpentinite may mix only with seawater at very shallow levels. The magnitude and direction of these changes also differs in significant ways when compared to the flank sites.

The principal results of Site 780 can be summarized as follows:

1. High pH, high alkalinity, very low magnesian fluids may exist within a few meters of the seafloor at the summit of Conical Seamount, indicating that mixing of entrained fluids and seawater need not take place at depth.
2. Rheological studies support a model for the origin of the seamount by diapiric intrusion of variably serpentinized clasts supported by a low-density, plastic matrix.
3. Absence of deformation in the serpentine matrix at the summit contrasts with the strongly sheared matrix at the flanks and suggests that much of the deformation of the serpentine matrix at the flank sites was the result of surface or near-surface flow following diapiric intrusion.

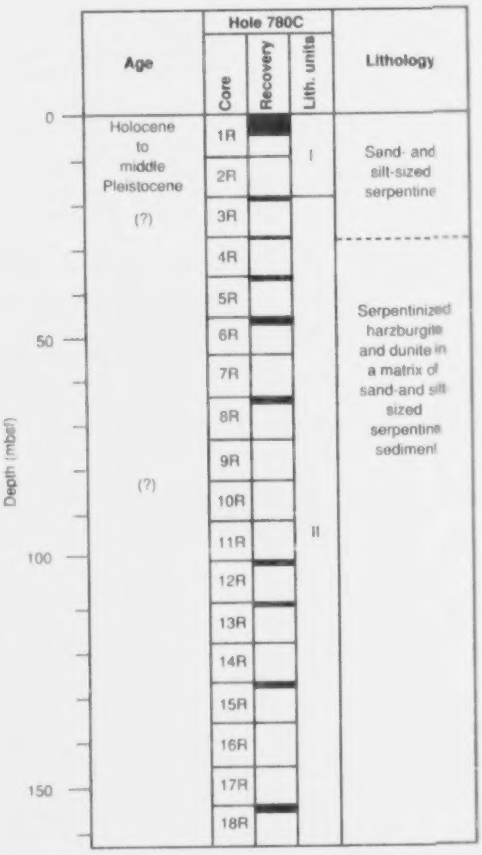
Hole 780C
Age
Core
Recovery
Lith. units
Lithology
Depth (mbsf)
0
50
100
150
Holocene to middle Pleistocene
(?)
(?)
1R
2R
3R
4R
5R
6R
7R
8R
9R
10R
11R
12R
13R
14R
15R
16R
17R
18R
I
II
Sand- and silt-sized serpentine
Serpentinized harzburgite and dunite in a matrix of sand-and silt sized serpentine sediment

Figure 42. Summary of lithology and core recovery, Hole 780C.

REFERENCES

Backman, J., Duncan, R. A., et al., 1988. Explanatory Notes. *Proc. ODP, Init. Repts.*, 115: College Station, TX (Ocean Drilling Program), 17–42.

Berger, W. H., 1970. Planktonic foraminifera: selective solution and the lysocline. *Mar. Geol.*, 8:1–11.

Berner, R. A., and Honjo, S., 1981. Pelagic sedimentation of aragonite: its geochemical significance. *Science*, 211:940–942.

Fryer, P., et al., 1987. Results of *Alvin* studies of Mariana forearc serpentinite diapirism. *EOS, Trans. Am. Geophys. Union*, 68:1534.

Gieskes, J. M., Johnston, K., and Boehm, M., 1985. Interstitial water studies, Leg 66. *In* von Huene, R., Aubouin, J., et al., *Init. Repts. DSDP*, 84: Washington (U.S. Govt. Printing Office), 961–967.

Haggerty, J. A., 1987a. Petrology and geochemistry of Neogene sedimentary rocks from Mariana forearc seamounts: implications for emplacement of the seamounts. *In* Keating, B., Fryer, P., Batiza, R., and Bohlert, G. (Eds.), *Seamounts, Islands and Atolls*. Washington (Am. Geophys. Union) Monogr. Ser., 43:175–185.

———, 1987b. Geochemistry of carbonate and silicate chimney structures from Conical Seamount collected during *Alvin* dive studies. *EOS, Trans. Am. Geophys. Union*, 68:1534.

———, 1987c. Cold-water, deep-sea chimneys from the Mariana forearc serpentinite seamounts (Abst.). *EOS, Trans. Am. Geophys. Union*, 68:1534.

———, 1989. Fluid inclusion studies of chimneys associated with serpentinite seamounts in the Mariana forearc (Abst.). *PACROFI II*, 2:29.

Harrison, W. E., Hesse, R., and Gieskes, J. M., 1982. Relationship between sedimentary facies and interstitial water chemistry of slope, trench, and Cocos plate sites from the Middle America Trench transect, active margin off Guatemala, Deep Sea Drilling Project Leg 67. *In* Aubouin, J., von Huene, R., et al., *Init. Repts. DSDP*, 67: Washington (U.S. Govt. Printing Office), 603–613.

Hesse, R., Lebel, J., and Gieskes, J. M., 1985. Interstitial water chemistry of gas-hydrate-bearing sections on the Middle America Trench slope, Deep Sea Drilling Project Leg 84. *In* von Huene, R., Aubouin, J., et al., *Init. Repts. DSDP*, 84: Washington (U.S. Govt. Printing Office), 727–737.

Hussong, D. M., and Uyeda, S., 1981. Tectonic processes and the history of the Mariana arc: A synthesis of the results of Deep Sea Drilling Project Leg 60. *In* Hussong, D. M., Uyeda, S., et al., *Init. Repts DSDP*, *60*: Washington (U.S. Govt. Printing Office), 909–929.

Janecky, D. R., and Seyfried, W. E., Jr., 1986. Hydrothermal serpentinization of peridotite within the oceanic crust: experimental investigations of mineralogy and major element chemistry. *Geochim. Cosmochim. Acta*, 50:1357–1378.

Kohls, D. W., and Rodda, J. L., 1967. Iowaite, a new hydrous magnesium hydroxide-ferric oxychloride from the Precambrian of Iowa. *Am. Mineral.*, 52:1261–1271.

Kulm, L. D., Suess, E., Moore, J. C., Carson, B., Lewis, B. T., Ritger, S. D., Kadko, D. C., Thornburg, T. M., Embley, R. W., Rugh, W. D., Massoth, G. J., Langseth, M. G., Cochrane, G. R., and Scamman, R. L., 1986. Oregon subduction zone: venting, fauna, and carbonates. *Science*, 231:561–566.

Li, Y.-H., Takahashi, T., and Broecker, W. S., 1969. Degree of saturation of calcium carbonate in the oceans. *J. Geophys. Res.*, 75:5507–5525.

Miura, Y., Rucklidge, J. C., and Nord, G. L., Jr., 1981. The occurrence of chlorine in serpentine minerals. *Contrib. Mineral. Petrol.*, 76:17–23.

Moore, G. W., and Gieskes, J. M., 1980. Interaction between sediment and interstitial water near the Japan Trench, Leg 57, Deep Sea Drilling Project. *In* Scientific Party, von Huene, R., and Nasu, N., *Init. Repts. DSDP*, 56, 57 (Pt. 2): Washington (U.S. Govt. Printing Office), 1269–1275.

Okada, H., and Bukry, D., 1980. Supplementary modification and introduction of code numbers to the low-latitude coccolith biostratigraphic zonation (Bukry, 1973; 1975). *Mar. Micropaleontol.*, 5:321–325.

Phipps, S. P., 1984. Mesozoic ophiolitic olistrostromes and Cenozoic imbricate thrust faulting in the northern California coast ranges: geology of the Mysterious Valley, Napa County [Ph.D dissert.]. Princeton Univ., Princeton, NJ.

Poty, B., Holland, H. D., and Borcsik, M., 1972. Solution-mineral equilibria in the system $MgO-SiO_2-H_2O-MgCl_2$ at 500°C and 1 kbar. *Geochim. Cosmochim. Acta*, 36:1101–1113.

Rucklidge, J. C., 1972. Chlorine in partially serpentinized dunite. *Econ. Geol.*, 67:38–40.

Rucklidge, J. C., and Patterson, G. C., 1977. The role of chlorine in serpentinization. *Contrib. Mineral. Petrol.*, 65:39–44.

Schorno, K. S., 1981. Geochemistry of carbon, International Phase of Ocean Drilling Project Leg 60. *In* Hussong, D. M., Uyeda, S., et al., *Init. Repts. DSDP*, 60: Washington (U.S. Govt. Printing Office), 501–504.

Shipboard Scientific Party, 1988a. Synthesis of shipboard results: Leg 110 transect of the Northern Barbados Ridge. *In* Mascle, A., Moore, J. C., et al., *Proc. ODP, Init. Repts.*, 110: College Station, TX (Ocean Drilling Program), 577–591.

Shipboard Scientific Party, 1988b. Introduction, objectives, and principal results, Leg 112, Peru continental margin. *In* Suess, E., von Huene, R., et al., *Proc. ODP, Init. Repts.*, 112: College Station, TX (Ocean Drilling Program), 5–23.

Ms 125A-108

NOTE: All core description forms ("barrel sheets") and core photographs have been printed on coated paper and bound as Section 4, near the back of the book, beginning on page 383.

Fryer, P., Pearce, J. A., Stokking, L. B., et al., 1990
Proceedings of the Ocean Drilling Program, Initial Reports, Vol. 125

9. SITE 781[1]

Shipboard Scientific Party[2]

HOLE 781A

Date occupied: 11 March 1989

Date departed: 13 March 1989

Time on hole: 2 days, 15 hr, 30 min

Position: 19°37.91′N, 146°32.56′E

Bottom felt (rig floor; m; drill-pipe measurement): 4431.7

Distance between rig floor and sea level (m): 11.10

Water depth (drill-pipe measurement from sea level: 4420.6

Total depth (rig floor; m): 4681.7

Penetration (m): 250.0

Number of cores: 27

Total length of cored section (m): 247.0

Total core recovered (m): 39.62

Core recovery (%): 16

Oldest sediment cored:
  Depth (mbsf): 250.0
  Nature: vitric silty clay and vitric sandy silt
  Earliest age: late Miocene(?)–early Pliocene(?)
Hard rock:
  Depth (mbsf): 67.3
  Nature: basalt (flow or sill)
  Measured velocity (km/s): 3.9–5.3

Principal results: Site 781 is situated about 7 nmi northwest of the summit of Conical Seamount on the outer-arc high of the Mariana forearc basin, about midway between the active Mariana arc and the trench axis. The principal objectives of this site were to fulfill the unachieved aims of the seamount flank Sites 778 and 779, namely to study the sediments and basement beneath the serpentinite seamount and hence to determine the age range of serpentinite diapirism and to characterize the type of crust into which the serpentinite was intruded. We hoped that a site at the base of the seamount free of serpentine flows, as determined by SeaMARC II side-scanning sonar imagery, would achieve these objectives. Precise site selection was based on six-channel seismic records that showed a strong reflector, possibly basement, at about 60 mbsf, a feature that was confirmed by a short underway geophysical survey.

Hole 781A was drilled with an RCB, penetrating 250 m and recovering 39.6 m of core for a recovery rate of 16%. Most of the poor core recovery was in sediments below the basalt subunit that was encountered between 72.6 and 91.8 mbsf. One lithologic unit having three subunits was defined as follows:

1. Subunit IA (0–72.32 mbsf) comprises late Pliocene(?)–Holocene(?) diatom-radiolarian silty clay that grades downward into vitric silty clay and vitric clayey silt.
2. Subunit IB (72.32–91.80 mbsf) is a vesicular, porphyritic basalt.
3. Subunit IC (91.80–250 mbsf) comprises late Pliocene to early Pliocene vitric silty clay and vitric clayey silt.

These sediments exhibit structures indicative of deposition from gravity-driven mass flows and contain interstitial fluids that exhibit only small chemical deviations from seawater composition downhole. The basalt of Subunit IB, which corresponds to the reflector on the seismic records, is 13 to 25 m thick, is massive, and may be a near-surface sill or a lava flow and thus of Pliocene or later age. This basalt provides the first evidence for such recent magmatic activity in any extant intraoceanic forearc terrane. Its geochemical signature indicates an origin from the mantle wedge above the subduction zone, but we cannot be certain if the source of the magma lies some 100 km to the west, in the region of the active Mariana arc, or whether it represents a hitherto unknown source of magma within the forearc basin itself.

BACKGROUND AND SCIENTIFIC OBJECTIVES

The flank sites on Conical Seamount (Sites 778 and 779) had failed to achieve one of the main objectives of drilling at the seamount, that of penetrating basement material. Basement penetration was deemed necessary to determine the nature of the crustal material underlying Conical Seamount and to assess the extent of interaction of that country rock with fluids from the serpentinite diapir. A site was chosen low on the northwest flank of the seamount (Fig. 1) in an area shown by seismic-reflection profiles to have a strong reflector at a depth of about 100 mbsf (Fig. 2). SeaMARC II images of the region showed that Site 781 was near the base of the seamount (Fig. 3). That base may be defined by the change in sonic backscatter on the side-scanning sonar imagery from the circle of very low (light) backscatter, which also shows concentric ridges or fractures, to the higher backscatter region (darker mottled gray) indicative of normal sedimented seafloor surrounding the seamount.

Studies of the seismic-reflection data collected near this site (see "Underway Geophysics" chapter, this volume) show a series of small fault blocks in the vicinity of Site 781. Gravity data collected over the seamount during several previous surveys indicate the presence of a fracture zone striking northwest-southeast beneath the seamount (Newsom, unpubl. data). We hoped that drilling at Site 781 would also enable us to determine the possible timing of the faulting and also determine whether the tectonism responsible for the faulting was related in any way to the formation of the seamount.

Drilling at Site 781 was undertaken to enable us to investigate (1) the nature of the basement underlying the adjacent seamount, (2) the timing of emplacement of the serpentinite seamount, (3) the effects on the basement materials of diapir-related alteration, and (4) the interaction of seamount-related activity with local sedimentation and/or tectonic processes.

OPERATIONS

Transit to Site 781

Problems with Site 780 prevented deep penetration into the top of Conical Seamount, leaving some of the time allotted for that hole unused. To obtain samples of the sediment and

---

[1] Fryer, P., Pearce, J. A., Stokking, L. B., et al., 1990. *Proc. ODP, Init. Repts.*, 125: College Station, TX (Ocean Drilling Program).

[2] Shipboard Scientific Party is as given in the list of participants preceding the contents.

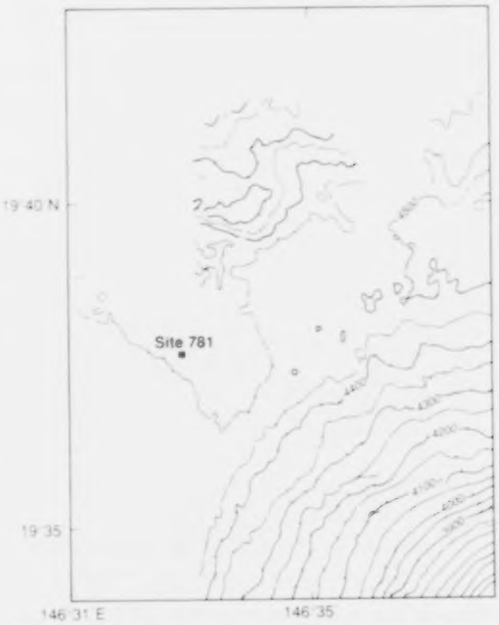

Figure 1. SeaBeam bathymetric contour map of the northwest flank of Conical Seamount (Stoffers, unpubl. data) showing the position of Site 781. Bathymetry in meters.

basement underlying the seamount, a site near the northern base of the seamount was proposed for drilling. Permission to drill to 250 mbsf was received from shorebased operations. The *JOIDES Resolution* was under way at 1345UTC, 10 March, and a seismic survey was conducted to determine the best location for the site. Site 781 was established by the dropping of a beacon at 1730UTC, 10 March.

Hole 781A

The vessel was positioned over a beacon, and the trip in with the drill pipe began at 2000UTC, 10 March. A standard RCB bottom-hole assembly (BHA) with a soft-formation bit was used to spud Hole 781A at 0315UTC, 11 March. The first RCB core retrieved had a recovery of 6.95 m of core to establish the mud line at 4420.6 m below sea level (bsl). No problems with the hole were encountered. A basalt was penetrated from 72.6 to 91.8 mbsf with little difficulty. Very little core was recovered from below the base of the basalt to the final depth of 250 mbsf. Hole 781A was abandoned after reaching the depth restriction at 250 mbsf. A total of 27 RCB coring runs were performed that recovered 39.6 m of core for a recovery rate of 16% (Table 1). Hole 781A and Site 781 officially ended at 0900UTC, 13 March, when the bit was back on deck and the *JOIDES Resolution* departed for the Izu-Bonin sites.

LITHOSTRATIGRAPHY

Lithologic Summary

Poor core recovery, particularly in the lower portion of the hole, limits both lithostratigraphic and biostratigraphic resolution; accordingly, only one lithologic unit has been defined

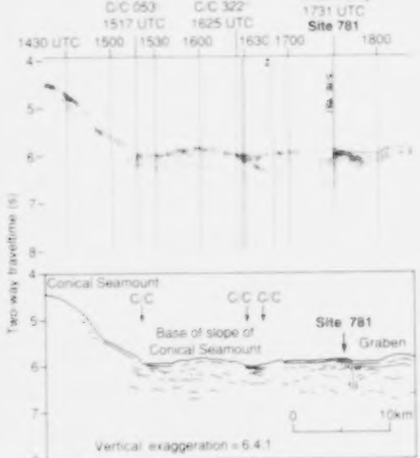

Figure 2. Seismic-reflection profile across Site 781, showing location of the beacon.

for Site 781 (Table 2). Three subunits define two sedimentary sequences (Subunits IA and IC) and one vesicular-porphyritic basalt sequence (Subunit IB).

Unit I

Subunit IA: Cores 125-781A-1R-1, 0 cm, to 125-781A-8R-CC, 7 cm; depth, 0–72.32 mbsf.
Age: Holocene(?) to late Pliocene.

Subunit IA comprises two general lithologies: a brown to dark brown (7.5YR 2/2, 4/2, 4/4) diatom-radiolarian silty clay in the upper portion of the stratigraphic succession near the seafloor, transitional downhole to a gray to dark gray (5Y 5/1–5Y 4/1) vitric silty clay to vitric clayey silt. Diatoms (trace to 25%), radiolarians (trace to 15%), silicoflagellates, and sponge spicules (both trace to 10%) are the biosiliceous components. Calcareous biogenic components are nannofossils (trace to 35%) and foraminifers (trace to 15%); micrite (trace to 25%) in combination with these calcareous components defines calcareous clay and marl as a minor lithology (e.g., Core 125-781A-1R). Vitric particles increase in abundance downsection (trace to 55%) from Core 125-781A-4R to the base of the hole (Core 125-781A-27R). The admixture of vitric particles and microfossils form minor sedimentary lithologies in Subunit IA, such as radiolarian-bearing vitric silty clay, nannofossil silty marl, and biogenic-rich clay. Additional sediment components are opaque minerals (3%–25%), zoisite (3%–15%), serpentine (trace to 13%), feldspar and chlorite (both trace to 15%), lithic fragments (4%–10%), as well as olivine, pyroxene, epidote, and organic debris in amounts less than 5%.

Sedimentary structures indicative of deposition from gravity-driven mass flows suggest that a high proportion of the sediments in this subunit have been displaced. At least 19 turbidite sequences may be defined by basal clastic beds (mainly vitric-rich sands and silts) 0.5 to 40 cm thick (average about 1 cm) that frequently exhibit normal size-grading or cross-beds followed by faint laminae; this combination of sedimentary structures suggests Bouma units "a" through "c." Overlying homogeneous intervals of vitric-bearing clays suggest Bouma "d" units. Basal

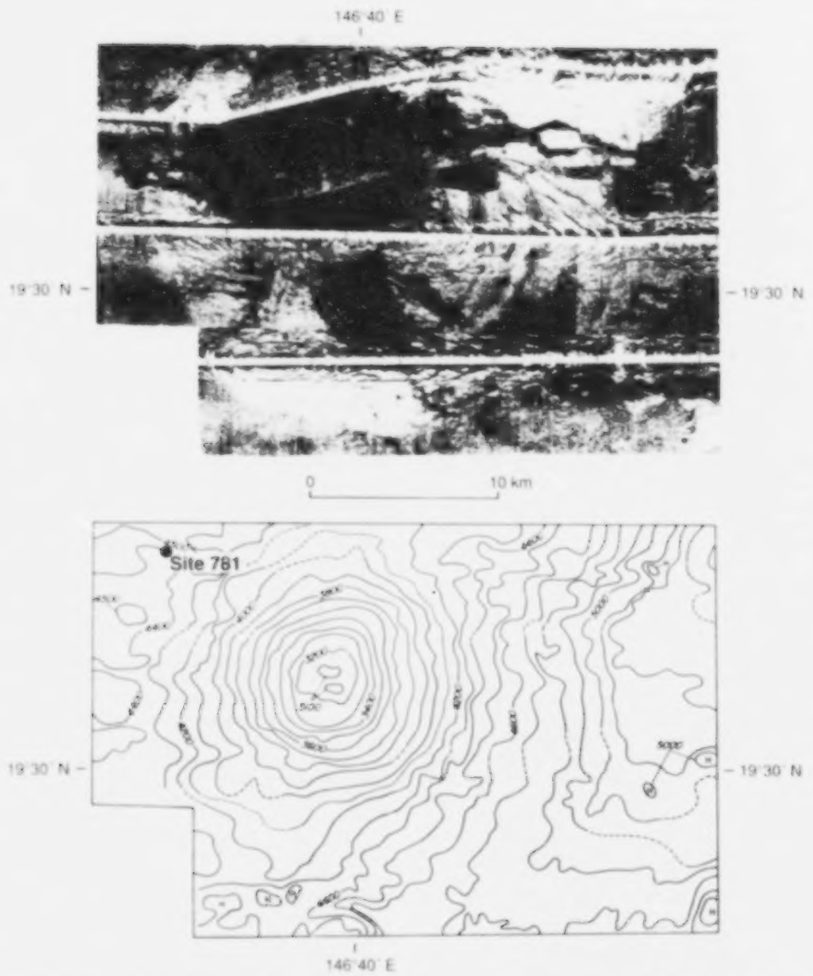

Figure 3. SeaMARC II side-scanning sonar imagery and bathymetry of the region around Site 781. Note the change in backscatter at the base of the seamount. Bathymetry in meters.

contacts are sharp and contain load casts where the basal clastic bed thickness is greater than about 2 cm. Upper contacts of some of these clastic beds have been disrupted by the injection of sands and silts into the overlying clays. Overall thicknesses of turbidite sequences vary between 1 and 180 cm, with an average in the range of 3 to 12 cm.

Subunit IB: Sections 125-781A-8R-CC, 8 cm, to 125-781A-10R-3, 112 cm; depth, 72.32–91.80 mbsf.
Age: late Pliocene.

Subunit IB is defined by a vesicular porphyritic basalt layer (see discussion in "Igneous and Metamorphic Petrology" section, this chapter). The upper sediment/basalt contact occurs in Section 125-781A-8R-CC at 7 cm. The lower basalt/sediment contact was not recovered, and a lower boundary for this subunit has been determined at 91.80 mbsf, between Cores 125-781A-10R and 125-781A-11R, by the decrease in drilling rotation/penetration rates.

Subunit IC: Sections 125-781A-14R-1, 0 cm, to 125-781A-27R-CC, 18 cm; depth, 120.7–250.0 mbsf.
Age: late Pliocene to early Pliocene.

Subunit IC is a sedimentary sequence that is poorly defined because of sparse core recovery. The first core from which sediment was recovered from this subunit is at 120.70 mbsf (Section 125-781A-14R-1), which defines the upper

Table 1. Coring summary for Hole 781A.

Core no.	Date (March 1989)	Time (UTC)	Depth (mbsf)	Length cored (m)	Length recovered (m)	Recovery (%)
1R	11	0420	0–6.9	6.9	6.95	101.0
2R	11	0615	6.9–16.4	9.5	0.00	0.0
3R	11	0745	16.4–25.9	9.5	0.00	0.0
4R	11	0925	25.9–35.4	9.5	0.77	8.1
5R	11	1040	35.4–44.9	9.5	0.20	2.1
6R	11	1220	44.9–54.5	9.6	6.91	72.0
7R	11	1330	54.5–64.5	10.0	4.41	44.1
8R	11	1520	64.5–72.6	8.1	2.85	35.2
9R	11	1950	72.6–82.3	9.7	3.75	38.6
10R	11	2345	82.3–91.8	9.5	2.58	27.1
11R	12	0130	91.8–101.4	9.6	0.00	0.0
12R	12	0300	101.4–111.1	9.7	0.01	0.1
13R	12	0415	111.1–120.7	9.6	0.00	0.0
14R	12	0545	120.7–130.4	9.7	0.06	0.6
15R	12	0700	130.4–140.0	9.6	0.01	0.1
16R	12	0820	140.0–149.6	9.6	0.13	1.4
17R	12	0950	149.6–156.3	6.7	0.00	0.0
18R	12	1150	159.3–168.9	9.6	0.02	0.2
19R	12	1315	168.9–178.6	9.7	0.00	0.0
20R	12	1500	178.6–188.2	9.6	0.00	0.0
21R	12	1630	188.2–197.9	9.7	0.58	6.0
22R	12	1800	197.9–207.6	9.7	0.15	1.5
23R	12	1950	207.6–217.3	9.7	0.02	0.2
24R	12	2100	217.3–226.9	9.6	0.14	1.5
25R	12	2215	226.9–236.5	9.6	0.16	1.7
26R	12	2330	236.5–246.0	9.5	0.54	5.7
27R	13	0145	246.0–250.0	4.0	9.38	234.0
Coring totals				247.0	39.62	16.0

limit of Subunit IC. Thus, a gap of 28.90 m exists between Subunits IB and IC (see Table 2) in which no sediment or rock was recovered, preventing accurate subunit description and boundary definition. However, rapid drilling and penetration rates imply unconsolidated sediment throughout both the subunit and the gap between the subunits. Sediments in Subunit IC are predominantly vitric silty clays and vitric clayey silts, with minor feldspar-rich vitric sands, silts, clays, and all permutations of the latter three textural categories. In addition to volcanic ash (in amounts from 12%–55%) and clays (8%–70%), the minerals and biogenic particles present are feldspar (7%–20%), zoisite and pyroxene (both trace to 10%), opaque minerals (5%–10%), epidote (2%–6%), lithic fragments (predominantly igneous) and serpentine (both trace to 5%), amphibole and olivine (both in trace amounts), micrite (5%–20%), calcareous nannofossils (5%–15%), foraminifers (trace to 5%), and radiolarians (trace). Colors are predominantly gray to dark gray (5Y 5/1 to 5Y 4/1–10YR 4/1), with some dark brown, very dark brown, and black (5YR 3/1, 7.5YR 2/2, 2/0).

Two angular pebbles of basalt were recovered in Core 125-781A-18R; smaller basalt granules are present in minor amounts in Cores 125-781A-16R, 12-781A-21R, 125-781A-24R, and 125-781A-26R. Vitric clay and silt containing basalt granules and clay clasts were recovered in Core 125-781A-27R, the last core at this site. We are still unclear as to whether this entire 9.7-m-long sediment sequence represents *in-situ* material, contaminants accumulated at the bottom of the hole, or both. Information from both drilling operations and sediment analyses implies that at least one-half of this core represents downhole contaminants.

BIOSTRATIGRAPHY

Evidence from calcareous nannofossils in Site 781 cores indicates that the sedimentary interval from Sample 125-781A-1R-1, 2 cm, to Sample 125-781A-7R-CC ranges in age from early to late Pleistocene; that Samples 125-781A-8R-CC, 125-781A-15R-CC, 125-781-16R-CC, 125-781A-18R-CC, and 125-781A-25R-CC are from the late Pliocene; and that the age of the sedimentary interval from Samples 125-781A-26R-CC to 125-781A-27R-CC is early Pliocene, even if mixed assemblages occur that reflect contamination or reworking. Evidence from foraminifers confines Sample 125-781A-21R-CC to late Pliocene and Sample 125-781A-27R-CC to earliest early Pliocene.

Calcareous Nannofossils

Poorly to well-preserved, rare to abundant nannofossil assemblages are present in the sediments overlying the basalt layer in Hole 781A. Samples 125-781A-1R, 2 cm, and 125-781A-1R-CC are late Pleistocene (Zone CN15) in age, on the basis of the occurrence of *Emiliania huxleyi*, *Gephyrocapsa oceanica*, *G. caribbeanica*, *Helicosphaera hyalina*, and *Ceratolithus telesmus*. Samples 125-781A-4R-CC and 125-781A-5R-CC are dated to middle/early Pleistocene (Subzone CN14a) by the occurrence of *Pseudoemiliania lacunosa*. Samples 125-781A-6R-CC, and 125-781A-7R-CC are dated as early Pleistocene (base of Subzone CN14a) from the occurrence of *Helicosphaera sellii* in Sample 125-781A-6R-CC and from the co-occurrence of this species with *Gephyrocapsa oceanica*. A few reworked nannofossils from the Miocene and/or from the Pliocene are also present.

Samples 125-781A-8R-CC and 125-781A-15R-CC contain a rare and poorly preserved nannofossil assemblage with *Pseudoemiliania lacunosa*, *Discoaster surculus*, *D. brouweri*, *D.* aff. *asymmetricus*, *D. pentaradiatus*, *Ceratolithus cristatus*, and *Calcidiscus macintyrei*. These age-diagnostic species together with the lack of *Discoaster tamalis* and *D. variabilis* indicate that the sample is late Pliocene (Subzone CN12b) in age. Reworked *Discoaster* aff. *saipanensis*, *D. deflandrei*, and *Sphenolithus* sp. of Eocene age are also present.

Samples 125-781A-16R-CC to 125-781A-25R-CC contain few or common and poorly preserved nannofossils characterized by the marker species *Pseudoemiliania lacunosa*, *Discoaster asymmetricus*, *D. tamalis*, and *D. variabilis*, which provide an age of late Pliocene (Zone CN12a) for these samples.

Sample 125-781A-26R-CC is latest early Pliocene in age (Zone CN11b) on the basis of the occurrence of *Discoaster tamalis* and *Pseudoemiliania lacunosa* together with *Reticulofenestra pseudoumbilica* and *Sphenolithus abies*.

Table 2. Lithologic units recovered at Site 781.

Lithologic unit/subunit	Cores	Depth (mbsf)	Dominant lithology	Stratigraphic age
IA	125-781A-1R-1, 0 cm to 125-781A-8R-CC, 7 cm	0 to 72.32	Diatom-radiolarian silty clay to vitric silty clay and vitric clayey silt	Holocene(?) to upper Pliocene
IB	135-781A-8R-CC, 8 cm to 125-781A-10R-3, 112 cm	72.32 to 91.80	Vesicular porphyritic basalt	upper Pliocene
IC	125-781A-14R-1, 0 cm to 125-781A-27R-CC, 18 cm	120.70 to 250.00	Vitric silty clay and vitric clayey silt	upper Pliocene to lower Pliocene

Sample 125-781A-27R, CC is characterized by an abundant and moderately preserved nannofossil assemblage. However, several zonal markers covering a range of zones are present. For example, *Amaurolithus delicatus*, *Ceratolithus acutus*, *C. armatus* and *Triquetrorhabdulus rugosus* (zonal markers of the early Pliocene) were found together with *Pseudoemiliania lacunosa*, *Discoaster tamalis*, and *D. asymmetricus* (first occurrence in late early Pliocene). This interval can be interpreted either as reworked, in which case it is late Pliocene in age, or, more probably, as contaminated from coring, which makes it early Pliocene.

Only solution-resistant coccoliths can be found in Sample 125-781A-4R-CC. The assemblage is typical of the Mesolytic Zone (Schneidermann, 1977). This zone lies about 500 m above the carbon compensation depth (CCD). The next sample (125-781A-5R-CC) is high in diversity and contains coccoliths that are not resistant to solution. Moreover, the presence of the genus *Pontosphaera*, an epipelagic taxon, might indicate that Sample 125-781A-5R-CC was deposited at a shallower depth.

Foraminifers

Rare, moderately well-preserved foraminifers useful for age determinations can be found only in Samples 125-781A-21R-CC, 125-781A-27R-4, 58–60 cm, and 125-781A-27R-CC. The remaining samples are either barren or contain sorted assemblages of undiagnostic juveniles. Sample 125-781A-21R-CC contains a sorted, late Pliocene (Zone N21) foraminiferal assemblage that was determined by the presence of *Globorotalia tosaensis*, *Globorotalia ungulata*, and *Globigerinoides extremus*. Both Samples 125-781A-27R-4, 58–60 cm, and 125-781A-27R-CC are latest late Miocene to early Pliocene (Zones N17b to N19/20, Sample 125-781A-27R-4, 58–60 cm; Zones N17b to N19, 125-781A-27R-CC). The foraminiferal assemblage present in Sample 125-781A-27R-4, 58–60 cm, contains the diagnostic species *Sphaeroidinellopsis praedehiscens*. Sample 125-781A-27R-CC contains a foraminiferal assemblage characterized by *Globigerina nepenthes*, *Globigerinoides bulloides*, and *Sphaeroidinellopsis praedehiscens*. An earliest early Pliocene (Zone N19) age is suspected for Sample 125-781A-27R-CC on the basis of the presence of a form similar to *Globorotalia* (*H.*) cf. *margaritidae* (first appearance in Zone N19) that, when combined with the presence of *G. bulloides* and *G. nepenthes* (LAD, Zone N19), confines the sample to Zone N19.

Diatoms

Abundant and moderately preserved fragments of *Ethmodiscus rex* are present in Samples 125-781A-1R-CC and 125-781A-15R-CC. A few other diatom species were found in the same two samples. However, we were unable to determine the age of these samples from their diatom content. Traces of poorly preserved *E. rex* also are present in Samples 125-781A-8R-CC and 125-781A-18R-CC.

IGNEOUS AND METAMORPHIC PETROLOGY

Introduction

A basaltic unit (Subunit I) was penetrated in Hole 781A at 67 to 72.2 mbsf. A total of 6.73 m of basaltic rock was then recovered from the next three cores, followed by 10 cores for a total recovery of 23 cm of sediment. Given that the 10 near-empty cores may or may not have contained basaltic material, the thickness of the basaltic unit can be assumed to lie between 12.7 and 25 m. Although the percentage of recovery (28%–55%) of basalt core leaves the possibility of multiple lava flows in this interval, no obvious internal flow boundaries were found in the core. The basaltic unit is directly overlain in Core 125-781A-8R-CC by sediments of late Pliocene biostratigraphic age (CN12b) that show no evidence of thermal baking. The basal contact was not exposed, but the underlying sediments in Section 125-781A-15R-CC also are of late Pliocene age (see "Biostratigraphy" section, this chapter). The basalt unit is of reversed polarity, contrasting with the overlying sediments, which are of normal polarity (see "Paleomagnetism" section, this chapter). The lateral extent of this unit as seen in seismic profiles (see "Underway Geophysics" chapter, this volume), the monotony of the petrography, and the contrast between fresh glass at the top of the unit and altered glass at the base, all suggest that this is a single lava unit. The presence of schlierenlike structures indicates that it is probably a sill. However, dating may be needed to resolve whether it is a submarine lava flow or a sill.

Petrographic description

The basalt is entirely fresh except for the lowermost meter, where glass has been altered to clay. The top of the basalt is an 8-mm-thick chilled margin of vesicle-free, fresh glass having a somewhat lower abundance of phenocrysts (Fig. 4). The proportion of phenocrysts is constant throughout the basalt, but vesicles increase in abundance from 2% to 10% and in size from 1–5 to 8 mm toward the middle part of the unit. In the lowermost part, the vesicles decrease in size (less than 2 mm), but are relatively abundant (10%). Phenocryst-poor, schlierenlike, centimeter-size structures locally occur in the central part of the basalt unit (Fig. 5). Macroscopic observations, augmented by the study of six thin sections representative of the recovered material, show that phenocrysts of plagioclase, olivine, and augite, and glomerocrysts of plagioclase, clinopyroxene, plagioclase + olivine, and plagioclase + clinopyroxene make up 20% to 30% of the rock. Glomerocrysts containing all three phenocryst phases are rare or absent. Some plagioclase phenocrysts contain glass and some contain opaque inclusions. Typical modal proportions, morphology, and size of phenocrysts are from 20% to 25%

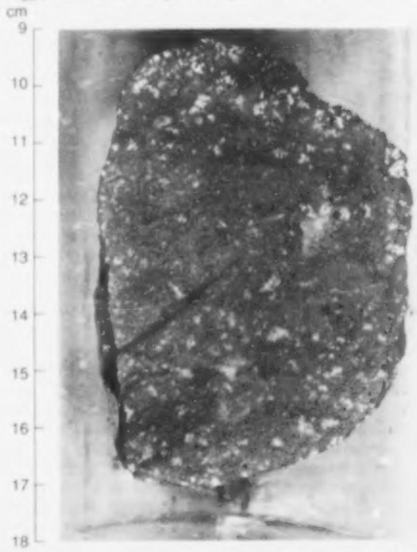

Figure 4. A glassy chilled margin stands out from the rest of a basalt unit by its black color and absence of vesicles (Sample 125-781A-8R-CC, 9–18 cm).

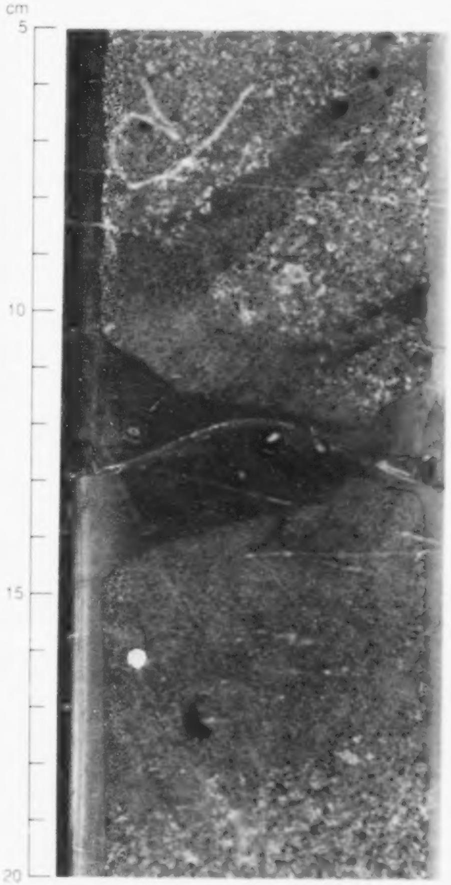

Figure 5. Dark gray structures resembling schlieren from the middle parts of the unit are characterized by the absence of phenocrysts and smaller vesicle size (Sample 125-781A-10R-1, 5–20 cm).

plagioclase (euhedral, less than 3 mm), 1% to 5% olivine (resorbed, round, less than 1 mm), and 1% to 3% clinopyroxene (subhedral to anhedral, 2 mm). Glomerocrysts are commonly smaller than 0.5 mm in size. The groundmass comprises plagioclase (20%–40%), clinopyroxene (10%–25%), olivine (0%–1%), a euhedral opaque phase (possibly magnetite, 5%), and green glass. Proportions of glass vary from up to 80% in the very top to as low as 10% to 15% in the middle of the unit. In the lower parts the glass has been entirely replaced by clay minerals, with the exception of one sample (125-781A-10R-3, 65–67 cm) from the base, which has a low modal proportion (5%) of unaltered glass. Locally, zeolite globules partly fill the vesicles (Fig. 6). The schlierenlike structures are phenocryst-free, have small vesicles (less than 1 mm), and consist of swallowtail and hopper plagioclase (less than 1 mm), feather and radial quench-growth clinopyroxene, and opaque needles in a glassy groundmass.

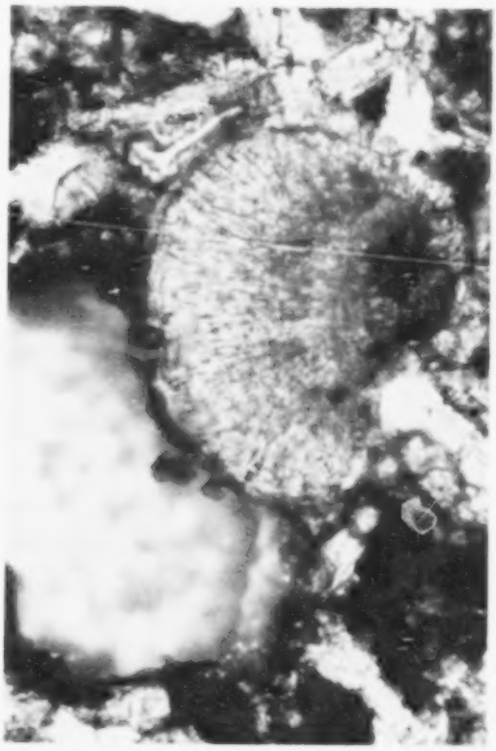

Figure 6. Photomicrograph of a fan-shaped zeolite inclusion in a vesicle (Sample 125-781A-9R-2, 49–51 cm). Field of view is approximately 0.3 mm wide.

IGNEOUS AND METAMORPHIC GEOCHEMISTRY

Drilling in Hole 781 encountered an *in-situ* igneous unit at 67 mbsf. This unit appears to be a single lava flow or sill that is between 12.7 and 25 m thick (28%–55% recovery) and is bound above and below by sediments of late Pliocene age (see "Biostratigraphy" section, this chapter). The unit has a basaltic mineralogy with abundant plagioclase and subordinate clinopyroxene (augite) and olivine phenocrysts in a groundmass dominated by plagioclase, clinopyroxene, olivine, and glass (see "Igneous and Metamorphic Petrology" section, this chapter).

Six samples were analyzed by wavelength spectrometer X-ray fluorescence for abundances of major and trace elements. The samples, originally selected for determining their physical properties, are from Cores 125-781A-8R, 125-781A-9R, and 125-781A-10R. The abundance of each major element was determined from an average of two analyses of a fused glass disk; abundances of trace elements were determined from a pressed powder pellet, using a matrix correction calculated on the basis of the analysis of the fused glass disk (see "Explanatory Notes" chapter, this volume).

Analyses of the major and trace elements are presented in Tables 3 and 4, respectively. Comparison of abundances of trace elements with normal mid-ocean ridge basalt (N-MORB), pre-

Table 3. Abundances of major elements of the six samples taken from the mafic unit in Hole 781A.

Sample no.: Interval (cm):	8R-CC 11-13	9R-1 69-71	9R-2 49-51	10R-1 84-86	10R-2 68-72	10R-3 65-67
SiO_2	48.9	48.42	48.17	48.47	48.66	49.45
TiO_2	0.85	0.86	0.83	0.85	0.84	0.88
Al_2O_3	17.52	17.29	16.98	16.42	17.27	16.97
Fe_2O_3 (Total)	11.86	12.15	11.8	11.87	11.81	12.5
MnO	0.25	0.22	0.24	0.23	0.21	0.24
MgO	4.12	4.3	4.37	4.09	4.38	4.37
CaO	10.96	11.06	10.88	10.52	10.89	10.7
Na_2O	1.77	1.7	1.76	1.79	1.96	1.86
K_2O	0.51	0.41	0.43	0.56	0.38	0.49
P_2O_5	0.06	0.05	0.06	0.06	0.05	0.05
Loss on ignition	0.63	1.28	0.85	1.91	0.74	0.78
Total	98.4	99.01	97.34	98.73	97.94	99.07
Mg#	0.37	0.38	0.39	0.37	0.39	0.38

Note: Elemental analyses (in wt%) were determined on board ship by Don Sims using wavelength-dispersive X-ray fluorescence spectrometry.

sented in Figure 7, was performed with an average of four of the six samples analyzed; the remaining two samples have losses on ignition greater than 1% and thus were excluded on the basis that they may have experienced low-grade alteration.

Major-Element Geochemistry

Little variation in the major elements exists among the samples (Table 3). Silica content varies between 48% and 49%, and magnesium number (i.e., Mg/Mg + Fe) between 0.37 and 0.39, indicating a basaltic composition throughout. The greatest variation is shown by potassium, although this may in part reflect low-grade alteration or mobilization in late-stage magmatic fluids. The low values of potassium and total alkalies suggest that the basalt is a member of the tholeiitic (rather than alkalic or calc-alkaline) rock series. Calcium and aluminium correlate significantly, but vary independently of MgO or SiO_2 (Fig. 8).

Trace-Element Geochemistry

Like the major elements, only minor variations occur in the concentrations of the trace elements (Table 4). These variations may be largely caused by analytical error and minor differences in the proportions of plagioclase phenocrysts. Sample 125-781A-10R-1, 84–86 cm, has the highest concentration of incompatible elements and may be slightly more fractionated than the others. The variation in trace-element abundances relative to N-MORBs is presented here in an N-MORB normalized multi-element diagram (Fig. 7). The compatible trace elements, nickel and chromium, as well as the high-field-strength (HFS) elements, titanium, zirconium, yttrium, and niobium, are depleted relative to N-MORBs. However, the large-ion-lithophile (LIL) elements, strontium, rubidium, potassium, barium, and cerium, a light rare earth element, are enriched with respect to N-MORBs.

Table 4. Abundances of trace elements of the six samples taken from the mafic unit at Hole 781A.

Sample no.: Interval (cm):	8R-CC 11-13	9R-1 69-71	9R-2 49-51	10R-1 84-86	10R-2 68-72	10R-3 65-67
Nb	0.9	0.9	0.6	1.4	1.0	0.9
Zr	48.4	45.9	46.1	51.9	45.7	48.7
Y	23.2	22.3	22.1	23.8	22.2	22.8
Sr	293.6	293.9	295.2	87.7	291.6	292.6
Rb	6.5	6.4	4.0	13.0	2.4	6.8
Zn	98.0	92.0	71.2	94.0	76.9	81.8
Cu	174.5	183.6	71.8	180.9	141.4	195.6
Ni	7.1	9.0	9.9	11.3	11.0	10.4
Cr	10.8	10.7	10.9	8.3	8.9	11.4
V	407.3	428.2	386.5	353.5	408.0	369.9
Ti	5820.0	5700.0	5400.0	5460.0	5520.0	5340.0
Ce	18.3	31.8	15.0	17.12	6.4	23.1
Ba	169.0	142.2	165.3	157.6	280.2	176.6

Note: Elemental analyses (in ppm) were determined on board ship by Don Sims using wavelength-dispersive X-ray fluorescence spectrometry.

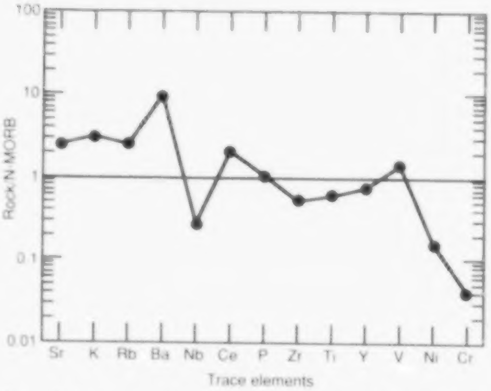

Figure 7. An average of four samples from the mafic unit, normalized to N-MORB, showing relative enrichment in the large-ion-lithophile and light rare earth elements and depletion in the high-field-strength and compatible elements.

Petrogenesis and Eruptive Setting

The petrology of the mafic unit indicates that plagioclase, clinopyroxene, and olivine were the main crystallizing phases (see "Igneous and Metamorphic Petrology" section, this chapter). The co-variation of Al_2O_3 and CaO and the inverse relationship of strontium with the incompatible trace elements may be attributed to either plagioclase fractionation or variation in the proportion of plagioclase phenocrysts. Overall, however, the small variation between samples in the abundances of major and trace elements is consistent with the hypothesis of only a single lava flow or sill that underwent little internal fractionation.

The enrichment of the mafic unit in LIL elements and the depletion in HFS elements, especially niobium, relative to N-MORBs is characteristic of a subduction-related environment of genesis. In such environments the LIL elements are selectively introduced into the mantle wedge during dewatering, and perhaps partial melting, of the subducted oceanic slab. This is supported by the similar abundance of chromium and yttrium in the mafic unit relative to island-arc tholeiites (IAT), compared with MORBs or boninites (Fig. 9). The trace-element data provide evidence of a two-component petrogenetic model for the mafic unit: an addition of LIL elements relative to N-MORBs, indicative of a subduction component, and a lower abundance of HFS elements relative to N-MORBs, indicative of derivation from a depleted or less-fertile source than that for N-MORBs or at a greater degree or partial melting. Therefore, on the basis of shipboard geochemistry, the mafic unit encountered in Hole 781A can be categorized as a basalt of the island-arc-tholeiite series, an interpretation that is consistent with an origin within the mantle wedge above the subducting Pacific Plate.

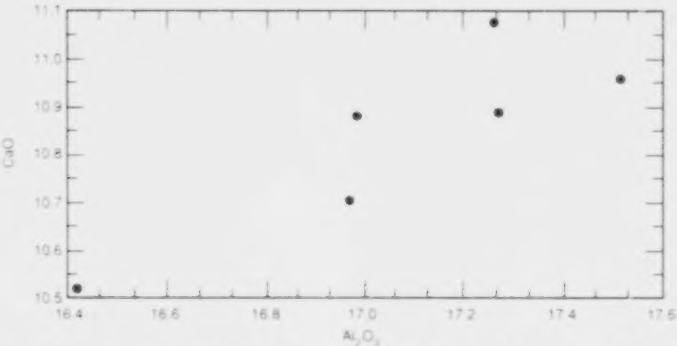

Figure 8. Proportional co-variation of CaO with Al_2O_3 (in wt%) may reflect addition or loss of plagioclase phenocrysts.

SEDIMENT/FLUID GEOCHEMISTRY

Sediment Geochemistry

Cores from Site 781 were analyzed on board ship for inorganic carbon and for total carbon, nitrogen, and sulfur using the techniques described in the "Explanatory Notes" chapter (this volume). The organic carbon content was then calculated by difference. These results are presented in Table 5 and in Figure 10. The sediments at Site 781 are considerably richer in $CaCO_3$ and organic carbon, and poorer in nitrogen and sulfur, than those at Sites 778, 779, and 780 on Conical Seamount. The $CaCO_3$ content varies from 0.2 to 8.6 wt%, with most values between 2 and 5 wt%. The lowest values occur between 49 and 65 mbsf, whereas the highest values are near the bottom of Hole 781A, at 227 and 255 mbsf. The organic carbon content increases from 0.26 wt% near the seafloor to a maximum value of 1.31 wt% at 65 mbsf. Most values fall between 0.6 and 0.8 wt%. Nitrogen was detected in only one sample, at a concentration of 0.12 wt% at 0.73 mbsf. Sulfur was not detected in any of the samples and therefore is uniformly less than 0.06 wt%.

Fluid Geochemistry

The concentration of methane measured for 5-cm^3 sediment headspace samples is uniformly low, usually less than 20 mL/L (Table 6). Methane was the only hydrocarbon detected. These values are even lower than those at Site 778, and they are much lower than those at Sites 779 and 780.

Compared with interstitial waters at Sites 778, 779, and 780, the waters squeezed from sediments at Site 781 (Table 7) are much more like waters from typical deep-sea sediments. The Ph is much lower and in the normal range of 7.5 to 8.5 (Fig. 11). Alkalinity increases slightly from the seawater value

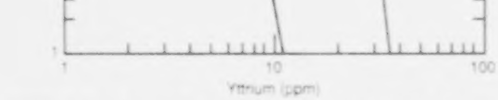

Figure 9. This diagram in chromium/yttrium space (after Pearce and Wanming, 1988) discriminates among environments of formation for boninite, island-arc tholeiite (IAT), and normal mid-ocean ridge basalt (N-MORB). Samples from the mafic unit plot within the field for island-arc tholeiites.

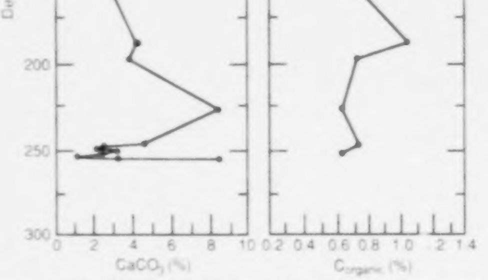

Figure 10. Abundances of calcium carbonate and total organic carbon (in wt%) in sediments from Site 781.

Table 5. Total nitrogen, sulfur, and carbon; organic carbon; and carbonate carbon in sediments of Hole 781A.

Core, section, interval (cm)	Depth (mbsf)	Total N (wt%)	Total sulfur (wt%)	Total carbon (wt%)	Inorganic carbon (wt%)	Organic carbon (wt%)	$CaCO_3$ (wt%)
125-781A-1R-1, 73–75	0.73	0.12	nd	0.86	0.60	0.26	5.0
1R-2, 69–71	1.52				0.21		1.7
1R-3, 19–21	2.52				0.41		3.4
1R-5, 87–89	6.20	nd	nd	0.96	0.44	0.52	3.7
4R-1, 54–56	26.44	nd	nd	0.93	0.30	0.63	2.5
4R-CC, 6–8	26.63				0.58		4.8
6R-1, 64–66	45.54				0.58		4.8
6R-2, 64–66	47.04	nd	nd	1.29	0.45	0.84	3.7
6R-3, 64–66	48.54				0.03		0.2
6R-4, 64–66	50.04				0.03		0.2
6R-5, 15–16	51.05				0.02		0.2
6R-6, 10–12	51.50	nd	nd	0.74	0.02	0.72	0.2
6R-CC, 4–6	51.67				0.02		0.2
7R-1, 38–40	54.88				0.08		0.7
7R-2, 38–40	56.38	nd	nd	0.88	0.02	0.86	0.2
7R-3, 38–40	57.88				0.35		2.9
8R-1, 85–87	65.35	nd	nd	1.34	0.03	1.31	0.2
8R-2, 72–74	66.72				0.27		2.2
16R-CC, 7–9	140.07	nd	nd	0.86	0.27	0.59	2.2
21R-1, 8–10	188.28	nd	nd	1.58	0.52	1.06	4.3
21R-CC, 14–16	188.56				0.51		4.2
22R-CC, 7–9	197.97	nd	nd	1.22	0.47	0.75	3.9
25R-CC, 11–13	227.01	nd	nd	1.68	1.02	0.66	8.5
27R-1, 21–23	246.21				0.56		4.7
27R-2, 21–23	247.71	nd	nd	1.07	0.31	0.76	2.6
27R-3, 21–23	249.21				0.27		2.2
27R-4, 21–23	250.71				0.40		3.3
27R-5, 21–23	252.21	nd	nd	0.96	0.30	0.66	2.5
27R-6, 21–23	253.71				0.15		1.2
27R-7, 3–5	255.03				0.40		3.3
27R-CC, 13–15	255.35				1.03		8.6

nd = not detected.

to 3.1 at 57 mbsf and then decreases to 0.7 at 237 mbsf near the bottom of Hole 781A. Ammonia increases with depth at about the same rate as at Site 778, reaching a maximum value of 197 mmol/kg near the bottom of Hole 781A. Silica is much higher than in waters from Conical Seamount, ranging from 260 to 630 mmol/kg. Sulfate is largely unchanged at the seawater value. Magnesium decreases to about one-half the seawater value with depth, whereas calcium, sodium, and potassium all increase (Fig. 12). Chlorinity and salinity also increase with depth, by less than 2% (Fig. 13).

The slight increase in alkalinity in the upper 60 m of sediment may result from oxidation of organic matter by bacteria that also reduce seawater sulfate. The increase in ammonia may result from the same process. The changes in magnesium, calcium, and sodium may be caused by reaction with volcanic matter in the sediments or in the underlying basement rocks; on the basis of the large changes with depth, the latter reason is more likely. The small increases in chlorinity and salinity with depth were probably caused by the increased salinity of ocean bottomwater during the Pleistocene glaciations (McDuff, 1985).

Table 6. Results of headspace-gas analyses of sediments from Hole 781A.

Core, section, interval (cm)	Depth (mbsf)	Methane (µL/L)[a]	Methane (µM)[b]
125-781A-1R-2, 135–140	2.88	11	0.9
4R-1, 60–62	26.51	19	1.7
6R-4, 135–140	50.7	81	41.2
7R-2, 135–140	57.3	81	51.3
8R-2, 0–3	66.02	11	1.0
22R-CC, 12–15	198.03	12	1.1
24R-CC, 11–14	227.03	12	1.1
26R-1, 29–32	236.81	11	1.0
27R-4, 137–140	251.89	3	0.2

[a] Microliters of gas per liter of wet sediment.
[b] Micromoles of methane per liter of interstitial water, assuming a porosity of 50%.

PALEOMAGNETISM

Magnetic Remanence

Although the recovery from Hole 781A was poor (16%), combined paleomagnetic and biostratigraphic data (see "Biostratigraphy" section, this chapter) have enabled us to construct a tentative magnetostratigraphy for the sediments in the upper 70 m of this hole. The natural remanent magnetization (NRM) of the archive halves of Cores 125-781A-1R, 125-781A-6R to 125-781A-10R, 125-781A-21R, and 125-781A-27R was measured using the cryogenic magnetometer. Intensities decreased systematically downhole from 1000 to 100 mA/m between the top of Section 125-781A-6R-1 and the base of Section 125-781A-1R-2, and also decreased from 600 to 10 mA/m between the top of Section 125-781A-8R-1 and the base of Section 125-781A-8R-CC. A systematic increase in intensity (from about 100 to 1500 mA/m) was observed between the top of Section 125-781A-27R and 35 cm below the top of Section 125-781A-27R-5.

Sections were then alternating-field (AF) demagnetized at 5 and 10 mT and measured between successive steps. Demagnetization typically reduced the intensity by about 20% to 35% of the NRM value. Changes in the declination and inclination were generally between 10° and 20°, making polarity evaluations somewhat difficult. Those intervals within Hole 781A to which we felt confident in assigning a polarity are summarized in Table 8.

Table 7. Composition of interstitial waters from sediments in Hole 781A.

Sample no.	Core, section, interval (cm)	Vol (mL)	Squeeze T (°C)	Depth (mbsf)	pH	Salinity (R.I.,‰)	Salinity (calc.,‰)	Chlorinity (mmol/kg)	Alkalinity (meq/kg)	Sulfate (mmol/kg)	Sodium (mmol/kg)	Potassium (mmol/kg)
Surface seawater (4 March 1989)					8.10	35.5	34.85	542.6	2.386	27.98	464.8	10.05
IW-1	125-781A-1R-2, 140–150	58	3	2.95	7.97	35.2	35.15	548.9	3.266	26.60	469.8	10.42
IW-2	4R-1, 62–67	20	3	26.55	8.00	34.8	35.44	551.3	2.487	27.97	473.1	11.61
IW-3	6R-1, 140–150	35	3	46.35	8.00	35.5	35.75	555.2	2.877	28.34	478.2	10.76
IW-4	6R-4, 140–150	44	3	50.85	8.09	36.5	35.63	556.2	2.904	26.73	478.6	11.81
IW-5	7R-2, 140–150	58	3	57.45	8.34	37.0	35.99	559.1	3.016	28.04	482.7	11.71
IW-6	8R-2, 103–113	60	3	67.08	8.51	35.5	35.60	551.3	2.793	28.77	477.5	11.57
IW-7	21R-CC, 30–36	27	3	197.57	8.34	36.0	36.19	556.2	1.339	29.92	490.1	7.04
IW-8	26R-1, 32–42	19	3	236.87	8.07	36.5	35.84	560.2	0.688	25.77	482.9	5.92

Values absent from table were not determined.

Discrete specimens were taken from the working halves of Cores 125-781A-1R, 125-781A-6R to 125-781A-10R, 125-781A-21R, 125-781A-24R, 125-781A–26R, and 125-781A-27R for additional analysis. These specimens were processed through fields of 0, 5, 10, and 15 mT using the cryogenic magnetometer. Results from these specimens are summarized in Table 9. Data from Cores 125-781A-21R to 125-781A-27R are included, although the relatively disturbed material at these levels (probably resulting from drilling) renders any polarity evaluation suspect.

In most cases, each specimen records a similar polarity to the relevant interval in the archive half of the core. It must be noted, however, that specimens taken from Sections 125-781A-6R-2 and 125-781A-6R-3 are of opposite polarity to the same level within the archive-half of the core (normal polarity instead of reversed). Polarity for these levels should

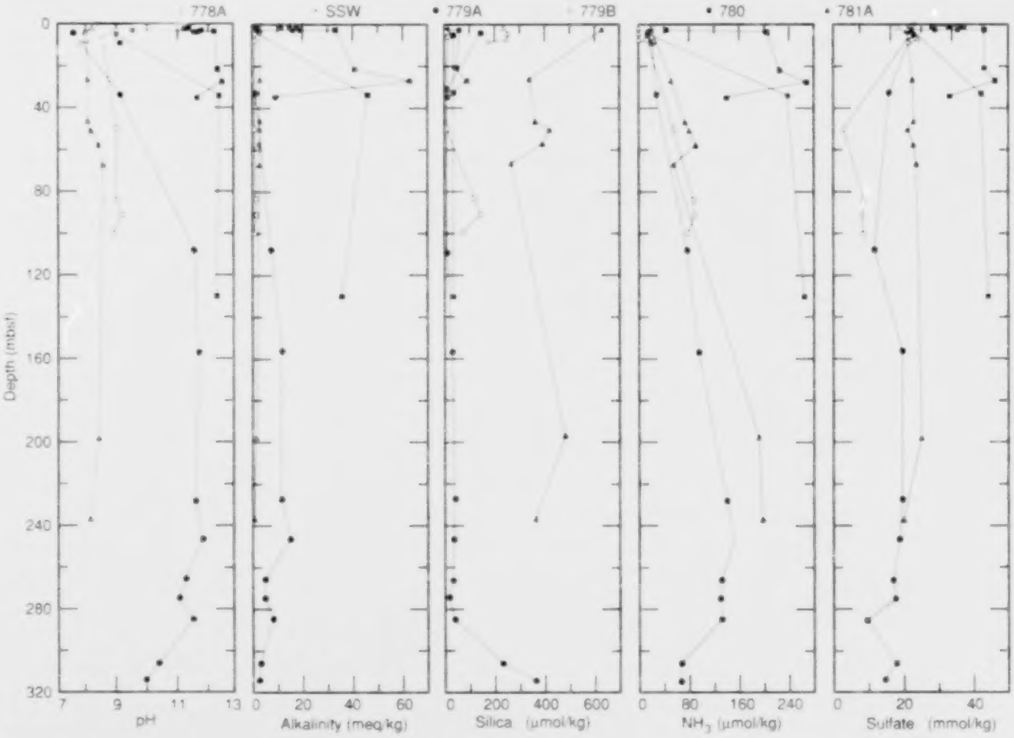

Figure 11. Composition of interstitial waters from sediments at Site 781 compared with those from Site 778, Hole 779A, Hole 779B, Site 780, and surface seawater (SSW) collected 22 February and 4 March 1989.

Table 7 (continued).

Calcium (mmol/kg)	Magnesium (mmol/kg)	Bromide (mmol/kg)	Silica (μmol/kg)	Ammonia (μmol/kg)	Phosphate (μmol/kg)
10.17	52.89	0.85	5	<5	
10.34	52.24	0.80	628	23	
11.04	51.46	0.83	338	51	8.42
12.27	50.62	0.73	361	72	2.91
12.09	48.99	0.89	421	80	0.91
12.60	49.26	0.70	391	90	1.45
11.10	50.21	0.71	264	55	1.02
29.69	30.44	0.77	480	192	0.27
[illegible].63	24.14	0.84	361	197	

be based on whole-core data, but further sampling and shorebased analyses of this interval will be required before this correlation can be established.

Recovery in Cores 125-781A-8R (very base), 125-781A-9R, and 125-781A-10R was about 6.5 m of basalt from either a sill or a flow having an estimated total thickness of between 12.7 and 25 m (see "Igneous and Metamorphic Petrology" section, this chapter). This body is defined as a single subunit (IC) in the "Lithostratigraphy" section (this chapter) and has a reversed polarity. The next datable horizon beneath this subunit is found in Core 125-781A-15R, where sediments have been assigned to Okada and Bukry's (1980) nannoplankton Zone CN12b. Core 125-781A-8R, immediately above the sill, has a normal magnetic polarity and contains nannoplankton that have been assigned to Zone CN12b. According to data presented by Berggren et al. (1985), the nannoplankton Zones CN12a/CN12b are associated with the Gauss Normal Polarity Chron. If this igneous body is a flow, then it must pre-date the sediments immediately overlying it. Its reversed polarity magnetization would then be a record of one of the short reversed events within the Gauss Normal Polarity Chron. Alternatively, if the igneous body is a sill, then it must post-date the normally magnetized sediments in Core 125-781A-8R. In that case, its magnetization could have been acquired anytime during the Matuyama Reversed Polarity Chron (0.73 to 2.47 Ma). This flow vs. sill argument can only be properly re-solved by radiometric dating and detailed petrofabric studies.

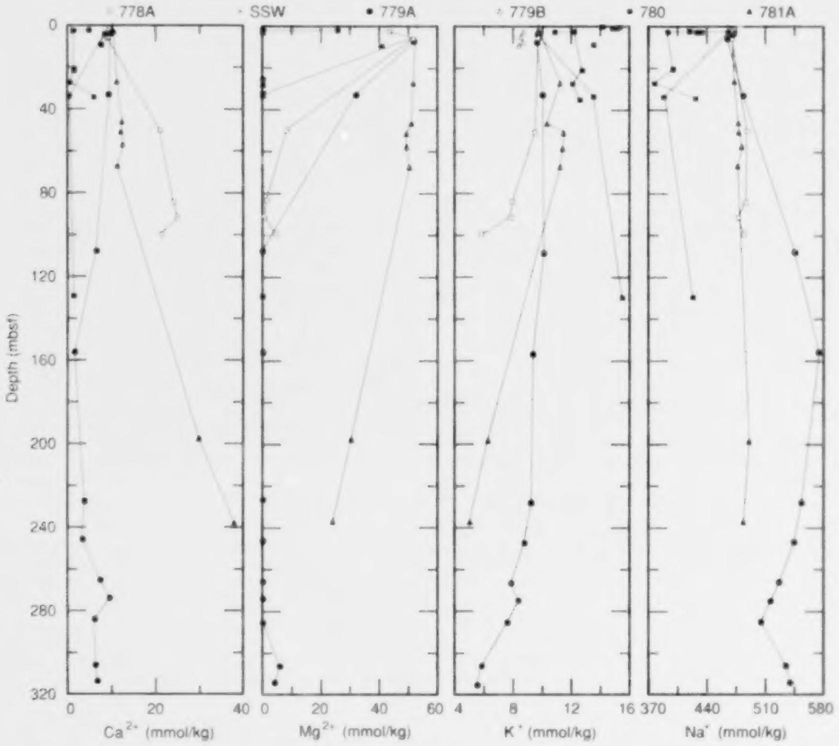

Figure 12. Composition of interstitial waters from sediments at Site 781 compared with those from Site 778, Hole 779A, Hole 779B, Site 780, and surface seawater (SSW) collected 22 February and 4 March 1989.

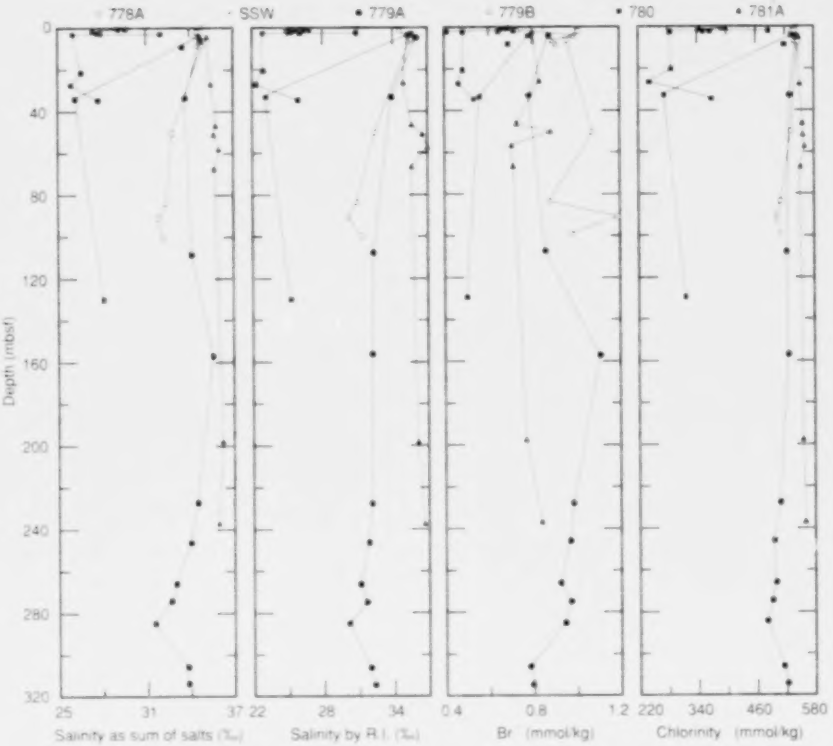

Figure 13. Composition of interstitial waters from sediments at Site 781 compared with those from Site 778, Hole 779A, Hole 779B, Site 780, and surface seawater (SSW) collected 22 February and 4 March 1989.

Magnetic Susceptibility

Whole-core magnetic susceptibilities were measured using the multisensor track. In Cores 125-781A-1R through 125-781A-10R, the susceptibilities range from 0 to 8×10^{-3} SI. There is no marked difference in susceptibility between the igneous body and the overlying sediments. However, a huge increase in susceptibility is observed within Core 125-781A-27R. The value increases from 6×10^{-3} SI at 247 msbf to 40×10^{-3} SI at 254 mbsf (Fig. 14). A similar increase is present in the GRAPE density data (see "Physical Properties" section, this chapter, Fig. 18). Figure 15 is a plot of susceptibility vs.

Table 8. Specific intervals in Hole 781A to which magnetic polarity was assigned.

Core, section, interval	Polarity	Nannofossil zone	Age	Magnetochron
125-781-1R-2, 0–115 cm	N	CN/15	late Pleistocene	Bruhnes
125-781-1R-5, 75–147 cm	N	CN/15	late Pleistocene	Bruhnes
125-781-6R-2, 30 cm to (upper) 125-781-6R-3, 140 cm	R	CN14a	early Pleistocene	Matuyama
125-781-6R-6, 0 cm to (upper) 125-781-6R, CC, 18 cm	R	CN14a	early Pleistocene	Matuyama
125-781-7R-1, 0 cm to (upper) 125-781-7R, CC, 21 cm	R	CN14a	early Pleistocene	Matuyama
125-781-8R-1, 0 cm to 125-781-8R-2, 113 cm	N	CN12b	late Pleistocene	Gauss
125-781-9R-1, 0 cm to 125-781-9R-3, 150 cm	R		(?)	
125-781-10R-1, 0 cm to 125-781-10R-3, 113 cm	R		(?)	

Note: Core 125-781A-15R is the youngest biostratigraphically dated level below 125-781A-10R and has been assigned to CN12b.

Table 9. Paleomagnetic data for discrete specimens taken from Hole 781A.

Section	Top (cm)	NRM			RM at 15mT			Polarity
		DEC	INC	INT	DEC	INC	INT	
125-781A-1R-2	83	59.3	32.9	91.6	57.2	32.6	69.8	N
125-781A-1R-3	36	105.8	6.8	65.2	101.0	3.6	43.9	?
125-781A-1R-4	74	162.8	31.1	107.0	162.0	31.4	74.6	N
125-781A-1R-5	116	157.8	−2.0	120.0	159.0	−4.6	90.6	?
125-781A-6R-1	94	89.7	24.8	33.4	87.9	18.8	22.6	N
125-781A-6R-2	94	232.6	5.0	8.8	87.0	23.6	2.4	N
125-781A-6R-3	94	8.8	39.2	40.6	24.4	33.8	34.2	N
125-781A-6R-4	94	218.8	12.0	6.5	244.5	−6.4	3.3	R
125-781A-6R-5	13	312.3	−17.8	29.3	308.4	−14.8	36.8	R
125-781A-7R-1	50	158.7	−65.0	127.0	161.9	−68.5	129.0	R
125-781A-7R-2	50	20.5	−0.4	30.5	27.2	−13.0	34.5	R
125-781A-7R-3	50	301.7	9.2	58.4	305.1	4.0	55.6	R
125-781A-8R-1	121	1.0	44.5	160.0	1.2	43.9	115.0	N
125-781A-8R-2	32	25.3	37.7	40.8	21.3	31.6	26.3	N
125-781A-9R-1	58	314.5	−25.1	1770.0	309.3	−23.2	1040.0	R
125-781A-9R-2	38	43.1	18.8	1620.0	46.1	2.2	1020.0	R
125-781A-9R-3	44	253.2	19.4	1420.0	262.3	4.0	583.0	R
125-781A-10R-1	23	137.5	−17.6	1740.0	145.7	−11.0	1120.0	R
125-781A-10R-2	105	207.6	−5.4	850.0	201.2	−5.8	209.0	R
125-781A-10R-3	13	85.2	12.0	347.0	88.0	6.4	54.5	R
125-781A-21R-1	16	205.1	18.0	23.6	210.8	14.7	15.1	N
125-781A-21R-C	19	352.4	−26.3	43.5	354.5	−25.6	27.2	R
125-781A-24R-C	26	297.2	−15.0	461.0	298.4	−10.8	275.0	R
125-781A-26R-C	8	73.8	20.4	24.2	65.9	5.5	24.3	R
125-781A-27R-2	120	36.9	11.0	152.0	37.0	−12.9	59.9	R
125-781A-27R-3	38	347.0	32.4	248.0	55.4	24.1	188.0	N
125-781A-27R-4	83	70.2	14.0	417.0	8.2	14.8	183.0	N
125-781A-27R-5	146	147.6	53.5	716.0	148.5	73.0	144.0	N
125-781A-27R-6	58	161.0	51.7	579.0	332.0	73.0	132.0	N
125-781A-27R-7	15	312.6	10.9	118.0	312.6	14.4	91.0	N
125-781A-27R-C	4	135.0	−28.8	803.0	133.8	−16.0	463.0	R

NRM = Natural remanent magnetization; RM = Remanence after demagnetization; DEC = Declination (degrees); INC = Inclination (degrees); INT = Intensity (mA/m); Top = distance from the top of the section. The specimens from Sections 125-781A-21R through 125-781A-27R are from intervals where it was impossible to work out the magnetostratigraphy for the whole-core archive sections.

bulk density for Core 125-781A-27R (between 246 and 256 mbsf). One can see very good correlation of these two parameters, with a correlation coefficient of 0.935. Detailed examination of this core revealed macroscopic pieces of metal (up to 2 mm in diameter), indicating that the correlation between susceptibility and density is almost certainly a result of contamination of the sediment by material from the drilling assembly. This suggests that the core was greatly disturbed by drilling, as contaminants were found in the center of the core, and that the material recovered from between 246 and 256 mbsf contains drill cuttings and does not reflect the stratigraphy at the bottom of Hole 781A.

PHYSICAL PROPERTIES

Thermal conductivity, bulk density, compressional-wave velocities, index properties (bulk and grain densities, porosity, water content, and void ratio), magnetic susceptibility, and shear strength were measured in rocks from Site 781 (Tables 10 and 11). Magnetic-susceptibility data are discussed in the "Paleomagnetism" section (this chapter). Poor recovery from depths of 70 to 220 mbsf prevented most physical properties from being measured in this interval.

Measurements of thermal conductivity for soft rocks from Hole 781A were uniformly low, with no values greater than 1.1 W/mK (Table 11). Thermal conductivity in these samples does not vary with depth in the hole (Fig. 16). Thermal conductivities measured in the basalt are also low (0.556 to 0.885 W/Mk) and, again, no correlations with depth are observed.

Bulk densities were determined from the GRAPE sensor on the multisensor track (MST). The data show considerable scatter, most commonly related to small voids in the sections. However, an increase in average bulk density with increasing depth (Fig. 17) is apparent. GRAPE densities from the lowest intervals of Core 125-781A-27R show a large density increase from 1.8 to 2.0 g/cm^3 (Fig. 18). A similar pattern of increase is seen in magnetic-susceptibility data from the same sections. These patterns may be related to the increased abundance of igneous rock fragments in drill cuttings and iron filings from the drill assembly at the bottom of the hole, and not to geologic processes (see discussion in "Paleomagnetism" section, this chapter).

Index properties measured were the wet weight, dry weight, and dry volume of discrete samples. From these data, wet volume, bulk density, grain density, water content, porosity, and void ratio were calculated. These data are presented in Table 9. Bulk densities of sediment samples ranged from 1.51 to 2.06 g/cm^3, and grain densities had a range of 2.4 to 2.8 g/cm^3. Porosities in the sediment samples ranged from 41% to 74%. The variation of index properties with depth is shown in Figure 19. No significant correlations with depth were observed.

The compressional-wave velocity logger on the MST was successful in obtaining data from many of the sections recovered at Site 781; however, poor coupling of the transducers remained a problem, preventing complete logging of some of these recovered sections. The velocity data show considerable scatter (1400 to 2100 m/s), which probably is related to voids in the cores. Nonetheless, compressional-wave velocities increased with depth (Fig. 20).

Compressional-wave velocities in hard-rock samples were measured on the Hamilton frame apparatus in orthogonal

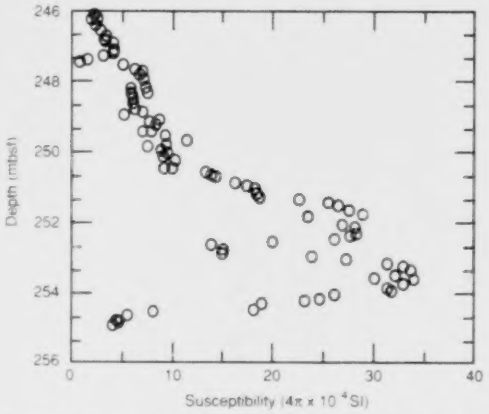

Figure 14. Plot of downhole variations in susceptibility for Core 125-781A-27R.

directions (Table 10). The reported velocities are low for basalts and range from 3906 to 5300 m/s: these values reflect the strong effect of fractures and microcracks on compressional-wave velocities at low confining pressures. The measurement of velocities in two directions allows for an initial assessment of the seismic anisotropy of the rock. Velocities measured along the length of the core range from 4140 to 5270 m/s, and those measured perpendicular to the core axis range from 3960 to 5180 m/s. Therefore, these samples are not seismically anisotropic at low confining pressures.

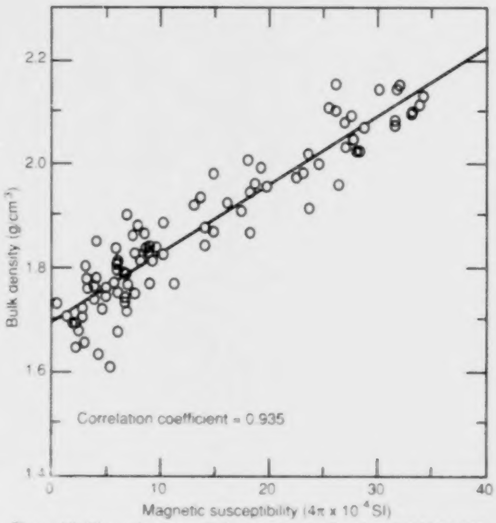

Figure 15. Magnetic susceptibility vs. density for Core 125-781A-27R.

Table 10. Index-property data for Hole 781A.

Core, section, interval (cm)	Depth (mbsf)	Bulk density (g/cm³)	Grain density (g/cm³)	Porosity (%)	Water content (%)	Void ratio
125-781A-1R-1, 73–75	0.73	1.53	2.6	72.9	50.7	0.73
1R-2, 69–71	1.52	1.55	2.5	74.2	51.0	0.74
1R-3, 19–21	3.52	1.58	2.48	64.4	43.4	0.64
1R-5, 87–89	6.2	1.64	2.57	67.5	43.8	0.68
4R-1, 54–56	26.44	1.59	2.6	66.4	44.3	0.66
4R-CC, 13–6	26.63	1.64	2.62	64.9	42.0	0.65
6R-1, 64–66	45.54	1.62	2.43	64.8	42.6	0.65
6R-2, 64–66	47.04	1.65	2.6	65.7	42.2	0.66
6R-3, 64–66	48.54	1.52	2.67	70.9	49.6	0.71
6R-4, 64–66	50.04	1.51	2.79	74.6	52.6	0.75
6R-5, 15–16	51.05	1.51	2.9	72.3	51.0	0.72
6R-CC, 13–4	51.67	1.51	2.67	72.4	50.8	0.72
7R-1, 38–40	54.88	1.65	2.72	65.4	42.1	0.65
7R-2, 38–40	56.38	1.52	2.36	65.0	45.4	0.65
7R-3, 38–40	57.88	1.63	2.62	65.4	42.6	0.65
8R-1, 85–87	65.35	1.51	2.68	71.8	50.6	0.72
8R-2, 72–74	66.72	1.69	2.71	63.6	40.1	0.64
8R-CC, 13–11	67.24	2.65	2.76	6.4	2.5	0.06
9R-1, 69–71	73.29	2.63	2.73	6.0	2.4	0.06
9R-2, 49–51	74.47	2.59	2.75	8.9	3.6	0.09
9R-3, 111–113	76.43	2.60	2.69	2.1	0.8	0.02
10R-1, 84–86	83.14	2.62	2.69	4.0	1.6	0.04
10R-2, 68–70	84.43	2.61	2.71	5.5	2.2	0.05
10R-3, 65–70	85.76	2.62	2.72	6.3	2.6	0.06
16R-CC, 13–7	140.07	1.71	2.72	48.7	30.2	0.49
21R-CC, 14–16	188.56	1.61	2.57	62.7	41.3	0.63
22R-CC, 13–7	197.97	1.55	2.42	63.0	43.3	0.63
25R-CC, 13–11	227.01	1.64	2.54	60.7	39.3	0.61
27R-1, 21–23	246.21	1.67	2.64	60.8	38.7	0.61
27R-2, 21–23	247.71	1.66	2.5	57.4	36.7	0.57
27R-3, 21–23	249.21	1.79	2.62	52.4	31.1	0.52
27R-4, 21–23	250.71	1.79	2.71	55.1	32.7	0.55
27R-5, 21–23	252.21	1.76	2.75	57.8	34.9	0.58
27R-6, 21–23	253.71	2.06	2.78	41.0	21.1	0.41
27R-CC, 13–15	255.35	1.71	2.71	59.8	37.1	0.60

Table 11. Physical-property data for Hole 781A.

Core, section, interval (cm)	Depth (mbsf)	Thermal conductivity (W/mK)	Ultimate strength (kPa)	"A" velocity (km/s)	"B" velocity (km/s)
125-781A-1R-2, 43	1.26	0.824			
1R-2, 91–92	1.81		8.1		
1R-2, 125–126	2.15		12.8		
1R-3, 22	2.55	0.924			
1R-3, 32–33	2.72		7.5		
1R-5, 97	6.3	0.184			
4R-1, 26	26.16	0.946			
4R-CC, 4	26.61	1.008			
6R-1, 89	45.79	0.403			
6R-3, 18–19	48.19		8.7		
6R-3, 89	48.79	0.911			
6R-3, 123–124	49.24		35.9		
6R-4, 78–79	50.29		116.1		
6R-4, 89	50.34	0.935			
6R-4, 118–119	50.75		75.3		
6R-5, 17	51.07	1.023			
6R-5, 20–21	51.1		33.9		
6R-6, 17	51.57	0.934			
7R-1, 68	55.18	0.967			
7R-2, 68	56.68	0.866			
7R-3, 68	58.18	0.929			
8R-1, 79	65.29	0.94			
8R-2, 39	66.39	1.058		4.74	4.72
9R-1, 68	73.28	0.602		4.14	3.96
9R-2, 47	74.45	0.677		4.82	4.84
9R-3, 100	76.32	0.677		4.6	4.4
10R-1, 73	83.03	0.885		5.27	5.18
10R-2, 60	84.35	0.556		5.16	4.9
10R-3, 60	85.71	0.588		5.07	5.1
21R-1, 11	188.31	0.577			
26R-1, 14	236.64	0.997			
27R-1, 60	246.6	0.691			
27R-2, 70	248.2	0.854			
27R-3, 78	249.78	1.063			
27R-4, 72	251.22	1.02			
27R-5, 66	252.66	0.095			
27R-6, 71	254.21	1.054			
27R-7, 10	255.1	0.949			

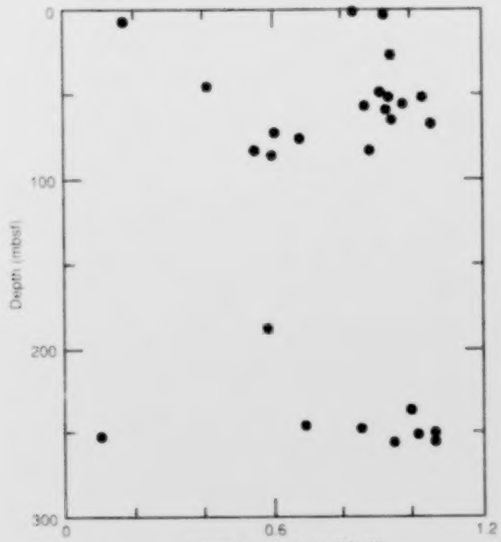

Figure 16. Plot of thermal conductivities vs. depth in Hole 781A. Note complete lack of correlation.

SUMMARY AND CONCLUSIONS

Site 781 lies on the lowermost flank of Conical Seamount about 7 nmi northwest of its summit. This site was chosen on the basis of a strong reflector at about 60 mbsf that was identified during a site survey and confirmed by a short shipboard seismic survey. Drilling at one RCB hole (Hole 781A) penetrated 250 m and recovered 39.6 m of core for a recovery rate of 16% (Fig. 21). Most of the poor core recovery was in sediments below basalt, which was encountered between 72.6 and 91.8 mbsf.

One lithostratigraphic unit having three subunits has been defined at Site 781 as follows:

1. Subunit IA (0–72.32 mbsf) comprises upper Pliocene to Holocene(?) diatom-radiolarian silty-clay grading downward into vitric silty clay and vitric clayey silt.
2. Subunit IB (72.32–91.80 mbsf) is a vesicular, porphyritic basalt.
3. Subunit IC (91.80–250 mbsf) comprises upper Pliocene to lower Pliocene vitric silty clay and vitric clayey silt.

Structures within the sediments in Subunit IA indicate deposition from gravity-driven mass flows. At least 19 turbidite sequences were identified with thicknesses ranging between 1 and 180 cm and with an average of 3 to 12 cm. Subunit IC contains lithologies similar to the lower part of Subunit IA, although poor recovery precludes detailed interpretation. Ages have been assigned on the basis of nannofossil and foraminifer assemblages in both Subunits IA and IC,

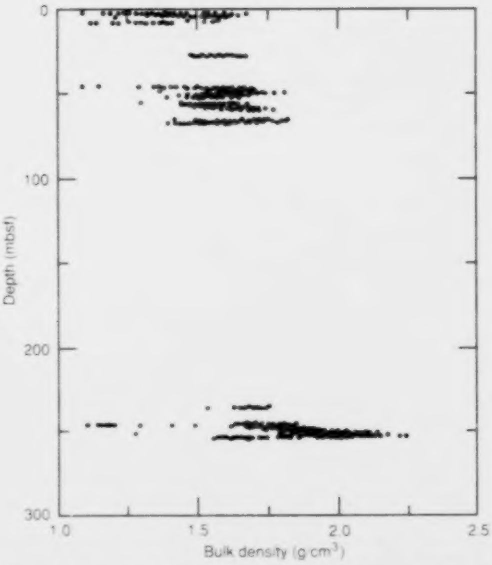

Figure 17. Plot of bulk densities (from the GRAPE sensor) vs. depth in Hole 781A. Bulk densities increase from approximately 1.4 to 2.0 g/cm^3 from the top to the bottom.

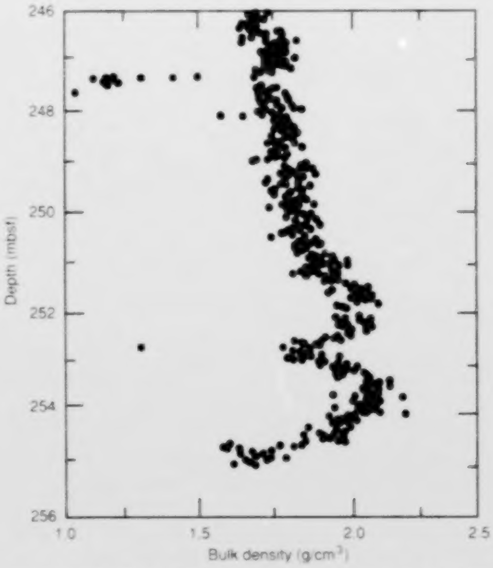

Figure 18. GRAPE bulk densities from the lowermost portion of Core 125-781A-27R (compare to Fig. 15 in "Paleomagnetism" section, this chapter). The increase in density is most probably related to metal filings and drill cuttings.

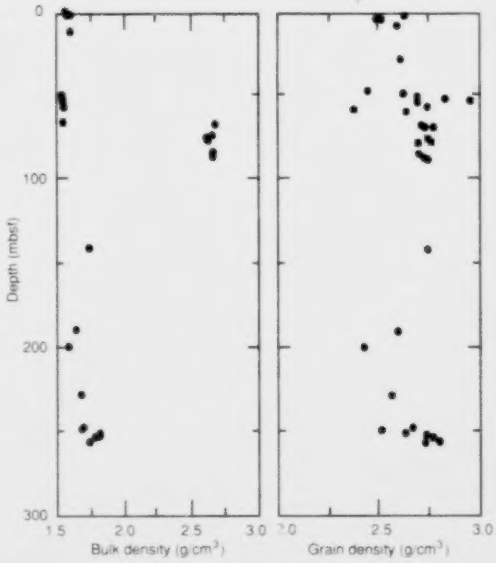

Figure 19. Variation of bulk and grain densities with depth in Hole 781A.

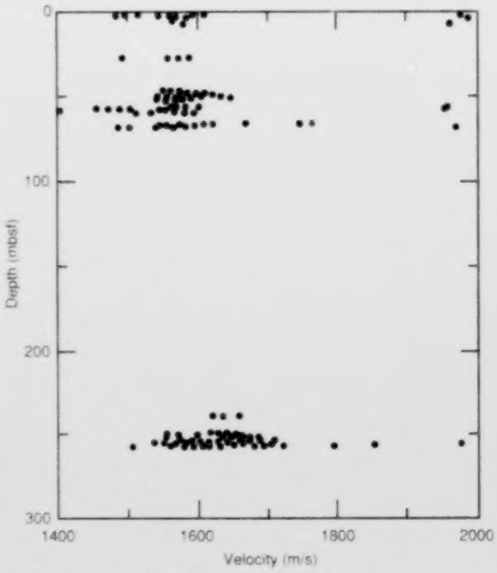

Figure 20. Plot of compressional-wave velocities (from velocity logger) vs. depth in Hole 781A. The increase in velocity is correlative to the increase in bulk density seen by GRAPE values.

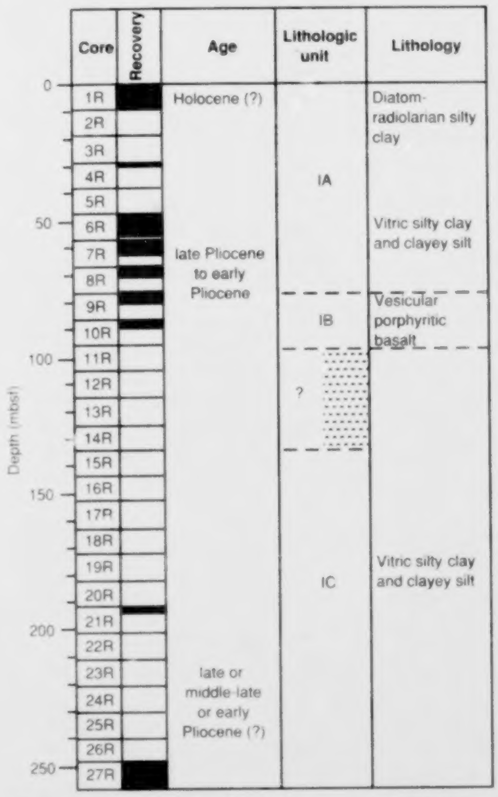
Core
Recovery
Age
Lithologic unit
Lithology
Depth (mbsf)
0
50
100
150
200
250
1R
2R
3R
4R
5R
6R
7R
8R
9R
10R
11R
12R
13R
14R
15R
16R
17R
18R
19R
20R
21R
22R
23R
24R
25R
26R
27R
Holocene (?)
late Pliocene to early Pliocene
late or middle-late or early Pliocene (?)
IA
IB
?
IC
Diatom-radiolarian silty clay
Vitric silty clay and clayey silt
Vesicular porphyritic basalt
Vitric silty clay and clayey silt

Figure 21. Core recovery and lithologic summary, Hole 781A.

although reworking, especially in Subunit IC, caused ambiguity.

Subunit IB, the cause of the reflector on the seismic records, is a 13- to 25-m-thick massive basalt containing up to 30% of phenocrysts and glomerocrysts of plagioclase, olivine, and clinopyroxene in a fine-grained groundmass. This basalt also contains from 2% to 10% of vesicles that increase in abundance and size toward the center of the subunit. The top of the basalt has an 8-mm-thick chilled margin that includes vesicle-free fresh glass. No internal flow boundaries exist in the recovered core. The basalt may be a near-surface sill or a lava flow: its reversed magnetic polarity, which contrasts with the normal polarity of the overlying sediments, is consistent with both possibilities.

Shipboard geochemical analyses of the basalt revealed that it was an island-arc tholeiite characterized by an enrichment in large-ion-lithophile elements relative to high-field-strength elements. This indicates that the magma originated from the mantle wedge above, and hence was modified by fluids from, the subducting lithosphere.

Studies of physical properties revealed high densities and magnetic susceptibilities in the sediments recovered in the final core. However, closer inspection showed that these properties could be explained by the presence of metal filings introduced during drilling of the last core while attempting to dry-drill for improved core recovery.

Unlike interstitial fluids from the summit and mid-flank of Conical Seamount, fluids from Site 781 exhibit only small chemical deviations from seawater composition downhole, which is more typical of a normal pelagic sequence.

In summary, the principal point of interest from Site 781 is the presence of a thick massive basalt of Pliocene or later age, the first evidence for such recent magmatic activity in any extant intraoceanic forearc terrane. The origin, provenance, and precise age of this basalt, when determined, will necessitate some revision of forearc models. The two main options are (1) that this basalt has been intruded laterally over a distance of about 100 km from the zone of active arc magmatism or (2) that it results from a hitherto unknown magmatic source within the forearc itself. A source in the convecting mantle beneath the subducting plate, however, can be considered unlikely on geochemical grounds.

REFERENCES

Berggren, W. A., Kent, D. V., Flynn, J. J., and Van Couvering, J., 1985. Cenozoic geochronology. *Geol. Soc. Am. Bull.*, 96:1407–1418.

McDuff, R. E., 1985. The chemistry of interstitial waters, Deep Sea Drilling Project Leg 86. *In* Heath, G. R., Burckle, L. H., et al., *Init. Repts. DSDP*, 86: Washington (U.S. Govt. Printing Office), 675–687.

Okada, H., and Bukry, D., 1980. Supplementary modification and introduction of code numbers to the low-latitude coccolith biostratigraphic zonation (Bukry, 1973, 1975). *Mar. Micropaleontol.*, 5:321–325.

Pearce, J. A., and Wanming, D., 1988. The ophiolites of the Tibetan Geotraverse, Lhasa to Golmud (1985) and Lhasa to Kathmandu (1986). *Phil. Trans. R. Soc. London*, A327:215–238.

Schneidermann, N., 1977. Selective dissolution of recent coccoliths in the Atlantic Ocean. *In* Ramsay, A.T.S. (Ed.), *Oceanic Micropalaeontology*, 2: London (Academic Press), 1009–1053.

Ms 125A-109

NOTE: All core description forms ("barrel sheets") and core photographs have been printed on coated paper and bound as Section 4, near the back of the book, beginning on page 383.

Fryer, P., Pearce, J. A., Stokking, L. B., et al., 1990
Proceedings of the Ocean Drilling Program, Initial Reports, Vol. 125

10. SITE 782[1]

Shipboard Scientific Party[2]

HOLE 782A

Date occupied: 16 March 1989

Date departed: 21 March 1989

Time on hole: 4 days 13 hr 30 min

Position: 30°51.66'N, 141°18.85'E

Bottom felt (rig floor; m, drillpipe measurement): 2970.0

Distance between rig floor and sea level (m): 11.1

Water depth (drillpipe measurement from sea level, m): 2958.9

Total depth (rig floor, m): 3446.8

Penetration (m): 476.8

Number of cores: 50

Total length of cored section (m): 476.8

Total core recovered (m): 282.0

Core recovery (%): 59.1

Oldest sediment cored:
  Depth (mbsf): 399.5
  Nature: vitric nannofossil chalk
  Earliest age: middle Eocene(?)
  Measured velocity (km/s): 1.5–2.0
Hard rock:
  Depth (mbsf): 399.7
  Nature: andesite

HOLE 782B

Date occupied: 21 March 1989

Date departed: 23 March 1989

Time on hole: 23 hr 30 min

Position: 30°51.60'N, 141°18.34'E

Bottom felt (rig floor; m, drillpipe measurement): 2977.0

Distance between rig floor and sea level (m): 11.1

Water depth (drillpipe measurement from sea level, m): 2965.9

Total depth (rig floor, m): 3438.9

Penetration (m): 468.9

Number of cores: 2

Total length of cored section (m): 468.9

Total core recovered (m): 0.5

Core recovery (%): 1.0

Oldest sediment cored:
  Depth (mbsf): 459.3
  Nature: nannofossil chalk (wash core)
Hard rock:
  Depth (mbsf): 459.3
  Nature: andesite

Principal results: Site 782 lies on the eastern margin of the Izu-Bonin forearc basin, about halfway between the active volcanic arc and the Izu-Bonin trench. Two holes were drilled: Hole 782A, a 476.8-m hole that was cored fully and described; and Hole 782B, a 468.9-m hole, of which only the last 9.5 m was cored and described, but which was used for two logging runs. However, significant penetration of the glassy, siliceous basement rocks proved impossible. A simple subdivision into two lithologic units was made: one sedimentary (Unit I), the other volcanic basement (Unit II). The sedimentary unit, split into Subunits IA through IC, comprises nannofossil marls and nannofossil chalks, with both dispersed volcanic debris and a total of more than 100 ash layers; the volcanogenic component becomes coarser grained and more abundant near the base, with some interbedding of tuffaceous sediment. Stratigraphic age of the sediments is Pleistocene to middle Eocene, with hiatuses between the uppermost Oligocene and middle Miocene, and between the lower Oligocene and upper Oligocene. Sedimentation rates are low in the bottom part of the succession, increasing upward to a maximum of 47 m/m.y. in the late Pliocene. The volcanic basement comprises angular to subrounded clasts (possibly including pillow fragments) of andesite and dacite-rhyolite that are slightly vesicular and typically contain phenocrysts of plagioclase, orthopyroxene, and clinopyroxene in a glassy groundmass. Geochemical data show that these are transitional between the tholeiitic and calc-alkaline volcanic-arc series.

Interstitial fluids in the sediments exhibit typical effects of water-mineral reactions, with potassium and magnesium decreasing steadily with depth, calcium increasing, and silica increasing to a maximum at about 300 mbsf. Ammonia increases to a maximum at about 150 m as a result of bacterial breakdown of organic matter. Most physical properties of the sediments vary systematically downhole: bulk densities increase from 1.6 to 1.95 kg/cm^3, porosities decrease from 70% to 60%, and magnetic susceptibilities and electrical resistivities increase. Logging data show physical and chemical discontinuities at about 300 and 370 m. The latter corresponds to the Oligocene hiatus and is marked by increases in seismic velocity, density, and silica and potassium contents, perhaps reflecting the increased volcanic influx during the Eocene. Magnetic inclination data from Hole 782A cluster around +50° and −50°, indicating little or no translation of the site since the late Eocene. However, declinations are scattered because of core disturbance; thus, no data for the extent of rotation were obtained.

BACKGROUND AND SCIENTIFIC OBJECTIVES

Site 782 is located at 30°51.66'N, 141°18.85'E, at 2958.9 m below sea level (bsl) on the outer half of the Izu-Bonin forearc, about 70 km west of the axis of the Izu-Bonin Trench (Fig. 1). It is the first of a series of sites within the Izu-Bonin forearc region that was drilled during Legs 125 and 126. The purpose of this effort was to study the history of the Izu-Bonin forearc and to compare drilling results in the Izu-Bonin forearc region with those gained in the Mariana forearc region during Leg 60 of the Deep Sea Drilling Project. By drilling at Site 782 we sought to determine the following:

1. The stratigraphy of the forearc and, hence, both the temporal variations in sedimentation, depositional environment, and paleoceanography and the history of intensity and chemistry of arc volcanism;

---

[1] Fryer, P., Pearce, J. A., Stokking, L. B., et al., 1990. *Proc. ODP, Init. Repts.*, 125: College Station, TX (Ocean Drilling Program).

[2] Shipboard Scientific Party is as given in list of participants preceding the contents.

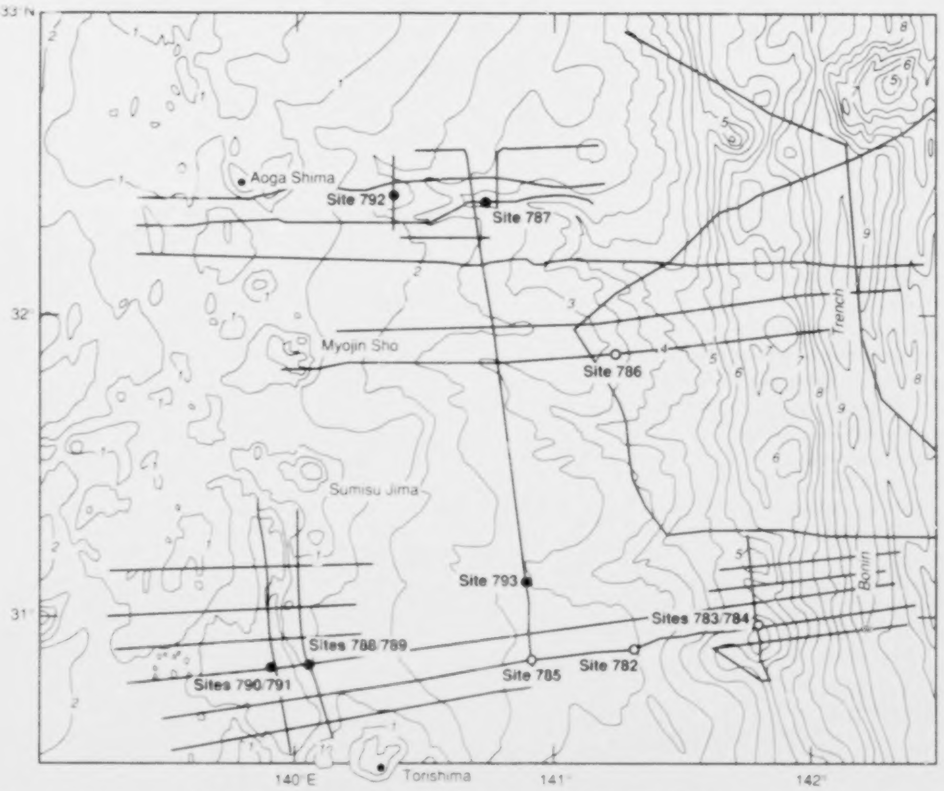

Figure 1. Bathymetry map of the Izu-Bonin forearc and forearc areas from about 30.5°N to 33°N. The locations of sites for Legs 125 and 126 are shown on this map, as are the locations of MCS lines run by B. Taylor. Contour interval is 0.5 km.

2. The uplift/subsidence history of the outer half of the forearc to provide information about forearc flexure and basin development, as well as about the extent of any vertical tectonic activity that may have taken place since formation of the forearc terrane;

3. The nature of igneous basement forming the forearc to answer questions concerning the nature of volcanism in the initial stages of subduction, the origin of boninites, and the formation of the 200-km-wide arc-type forearc crust; and

4. The microstructural deformation and the large-scale rotation and translation of the forearc terrane since the Eocene.

The first of these objectives has been addressed partly through detailed studies of sediments retrieved at Site 782. These sediments contain a record of the history of intensity and composition of arc volcanism, which should help to place constraints on hypotheses regarding the controls over variations in such arc-related phenomena as subduction rates and episodes of backarc spreading.

The complex relationships among tectonic and volcanic phenomena in island arcs, such as changes in subduction rate, periodicity of backarc rifting, pulses of arc volcanism, and variations in sedimentation rates in forearc environments, are difficult to correlate. Several conflicting models suggest possible interrelationships. For instance, Karig (1975) proposed that periods of arc volcanic maxima correlated with periods of marginal basin formation and high subduction rates. By contrast, Scott and Kroenke (1981) suggested that initial periods of backarc spreading are coincident with minimal arc volcanism. Contrary to both, Hussong and Uyeda (1981) inferred that arc volcanism has probably been continuous since the Eocene, but that the initiation of backarc spreading by arc rifting produced drastic subsidence of the arc volcanoes, which resulted in deep-water eruptions with limited lateral transport of volcanic material. Obviously, a unique solution to such complex interrelations as these cannot be determined without integrating the existing geophysical and geochemical studies with the stratigraphic information gained from drilling. Studies of the chronology and geochemistry of tephra deposits in the forearc basin sites should provide constraints for these various models. In addition, such studies will test whether boninitic (Beccaluva et al., 1980), alkalic (Stern et al., 1984), and/or bimodal basalt and rhyodacitic (Gill et al., 1984; Fryer et al., 1985) volcanism characterize particular types of arc tectonic phenomena, such as periods of arc rifting.

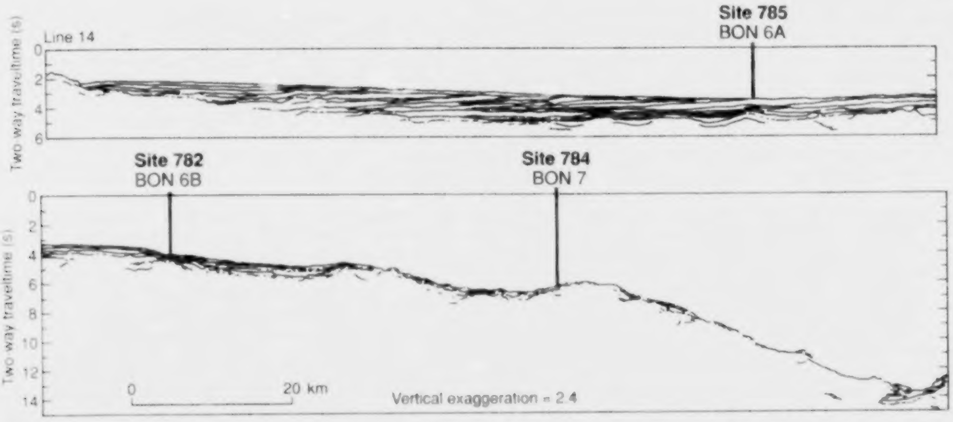

Figure 2. Line drawing of the seismic profile through Site 782.

The second objective can be investigated through a combination of sediment analysis and evaluation of logging results linked to the study of multichannel seismic-reflection data from the forearc. Multichannel seismic (MCS) surveys of the Izu-Bonin forearc revealed a complicated basement that is often seismically stratified and cut by dipping reflectors. These reflection characteristics are unlike those of normal oceanic crustal sections and suggest that Eocene volcanism may have been accompanied or followed by tectonic activity. Alternatively, the Eocene volcanic deposits may have been superimposed on an older terrane stranded in the forearc region (Ogawa and Naka, 1984). The Izu-Bonin forearc basin Site 782 (Fig. 1) was selected in the hope of sampling the hitherto unstudied upper forearc basement to constrain some of the parameters required for modeling forearc evolution. For example, in the Izu-Bonin forearc, the presence of shallow-water Eocene fossils on the Izu-Bonin Islands, and of a well-developed submarine canyon system and lower-slope terrace elsewhere in the forearc (see Fig. 1), suggests that fairly stable conditions have prevailed since the anomalous Eocene phase of arc-basin development. This hypothesis can be tested at Site 782 by determining the uplift-subsidence history and by comparing the results with those from other holes across the forearc, using backstripping techniques on cored/logged holes and seismic stratigraphic analyses of interconnecting MCS profiles (Fig. 2). Microstructures in the drill cores also should help to determine the intensity of faulting in space and time across the forearc terrane.

In addition, several unanswered questions arise regarding a number of other structural aspects of forearc evolution. Were the volcanic arc and forearc regions developed by igneous construction or by differential uplift? Did forearc basins form in response to spreading or to differential subsidence? Was flexural loading by arc volcanoes or by coupling with the subducting plate an important process during construction of the forearc? Determining the forearc vertical displacement history should provide some of the information about forearc flexure and basin development necessary to answer these questions.

The third objective at this site, to answer questions about the nature of volcanism in the initial stages of subduction, can be achieved by evaluating three main alternative hypotheses for the origin and evolution of the Izu-Bonin forearc terrane. The active volcanic arc (Izu arc) and the forearc terrane might have been continuous originally, but may have been separated subsequently by forearc spreading. The volcanic arc and forearc terrane may have been built separately, but nearly synchronously, on former Philippine Sea Plate crust. The terrane might form part of a continuous Eocene arc volcanic province, possibly with overprints of later forearc volcanism. Each scenario of forearc development implies a different crustal structure for the forearc.

Another question is how do the various models for forearc evolution relate to ophiolite formation? Many scientists now ascribe a majority of ophiolites to subduction-related settings because of their chemistry and associated sediments. Pearce et al. (1984) proposed that supra-subduction zone (SSZ) ophiolites (defined as those having the geochemical characteristics of island arcs, but the structure of oceanic crust) formed by seafloor spreading during the initial stages of subduction, prior to the development of any volcanic arc. Boninites, whose type locality is the Izu-Bonin Islands, are a common occurrence in SSZ ophiolites. They may require variable degrees of hydrous partial melting of a refractory source to produce wet magmas. These magmas then rise to shallow depth while maintaining fairly high temperatures to avoid amphibole crystallization. These unusual conditions may prevail only during initial subduction or arc rifting. However, the eruptive style and exact tectonic setting of the Eocene volcanism are unclear.

With the exception of dredge hauls from inner trench walls and large fault scarps (Bloomer, 1983; Bloomer and Hawkins, 1983; Bloomer and Fisher, 1987; Johnson and Fryer, 1988), our direct knowledge of intraoceanic forearc basement is based primarily on data from the Mariana and Tonga frontal arc islands (Guam, Saipan, and 'Eua) and the Izu-Bonin Islands, all of which expose Eocene island-arc tholeiites and boninites (Reagan and Meijer, 1984; Ewart et al., 1977; Shiraki et al., 1980) and from DSDP Leg 60, Sites 458 through 461, which sampled Eocene arc tholeiites and lower Oligocene boninites and arc tholeiites from the Mariana outer-forearc. Only in dredge hauls at one site in the Mariana forearc near Conical Seamount has the deep forearc basement been sampled (Johnson and Fryer, 1988). From the available data, one may assume that the present 150- to 220-km-wide Izu-Bonin-Mariana forearc formed in large part by volcanism in the initial stages of arc development during the Eocene and early Oligocene. Similar volcanism has not taken place since and, to our knowledge, cannot be studied as an active phenomenon anywhere on Earth at present. However, basement beneath the thickly sedimented upper-slope basin between the volcanic arc and the region of the break in slope of the inner trench wall has never been sampled. Thus, drilling at Site 782 should extend our knowledge of forearc basement to this area.

The fourth objective of the site, the study of microstructures and plate rotations, can be addressed through a study of the paleomagnetic properties of the cored materials. Measurements of the paleomagnetic properties of subaerial portions of the Izu-Bonin and Mariana forearcs have shown at least 20° of northward drift and 30° to more than 90° of clockwise rotation since the Eocene (see summary in Keating et al., 1983). How and when these motions took place, and the nature of their relationship to the overall structural evolution of the forearc, are enigmatic. One model suggests that the islands acted as "ball-bearings" between the Pacific and Philippine Sea plates. Karig and Moore (1975), and later Ogawa and Naka (1984), suggested that the islands might be an exotic terrain introduced from the south by oblique motion. However, marine geophysical data indicate a structural continuity of the Izu-Bonin Islands with the outer-arc high (Honza and Tamaki, 1985) and support Keating et al.'s model (1983) that the Izu-Bonin Islands (and therefore the Philippine Sea Plate) were situated near the Equator during the Eocene, roughly perpendicular to their present trend. If true, this hypothesis has major implications for reconstructions of the Philippine Sea and surrounding plates, and the related issues of initial subduction and West Philippine Basin evolution. We hope that studies of the paleomagnetism of the cores will permit testing of this model and its further refinement.

OPERATIONS

Transit from Site 781 to Site 782

The 770-nmi transit from Site 781 to Site 782 was completed in 75 hr, 45 min. Site 782 was established at 0900 Universal Time Coordinated (UTC), 16 March 1989, by dropping a beacon. Because a GPS window did not exist and no good satellite location fixes were obtained during the approach to the site, additional surveying was performed after the beacon drop to ensure that the site location was correct.

Hole 782A

The vessel was positioned over the beacon at 1300UTC, 16 March. A standard APC/XCB bottom-hole assembly (BHA), including a nonmagnetic drill collar, was prepared with a soft-formation bit and lockable flapper valve (LFV). The trip into the hole began at 1330UTC, 16 March, with 45- to 50-kt winds, 15- to 18-ft seas, and 20-ft swells. The topography of the seafloor was such that several echoes were recorded by the precision depth recorder (PDR); therefore, the drill string was tripped in cautiously until weight was taken by the sediments. The first APC core barrel retrieved was completely full and considered a misrun. The BHA was lifted 9.5 m, and another APC core was taken, which produced a water core. The BHA was then lowered 5 m and a third APC core was taken. When retrieved, the core barrel was found to contain 10 m of core. Operations were hampered by inclement weather, and considerable time was required to retrieve the first two core barrels. Therefore, we declared the mud line at 2958.9 mbsl, and Hole 782A was officially spudded at 2200UTC, 16 March. Core orientation began with Core 125-782-5H and continued through Core 125-782-9H. Heat flow was measured after Cores 125-782-4H at 38.3 mbsf and 125-782-7H at 66.8 mbsf.

Approximately 12 hr of coring time was lost during the first 36 hr of drilling at Hole 782A. Rough seas and the heave of the ship caused the latch safety-release pins on the sinker bars to shear during deployment of the APC. During retrieval of the sinker-bar assembly to change shear pins, the core barrels remained in the BHA and were subjected to the heave of the ship, causing core disturbance. After nine cores, the XCB was deployed. The first retrieval of the XCB also resulted in a sheared pin. Finally, with calmer weather and the use of the XCB, coring proceeded without sheared pins.

Excellent recovery was achieved as the hole was advanced to 399.5 mbsf. At that depth, an extensive ash layer was encountered and recovery declined dramatically. A noticeable reduction in the drilling rate occurred at 470 mbsf when drilling in andesite, and the bit became plugged. The core barrel was dropped during recovery and attempts to latch onto it were futile. All circulation was lost, so we decided to trip out of the hole.

The pipe was pulled to 457 mbsf, where it became stuck during removal of a connection. Further attempts to free the drill string failed, and it had to be severed at 1340UTC, 20 March. An explosive charge was used to sever the second joint of drill pipe above the drill collar.

The drill pipe was pulled out of the hole and, with the severed joint back on board at 2230UTC, 20 March, Hole 782A officially ended. The APC had been deployed nine times, with 85.5 m cored and 90 m of recovered core for a recovery rate of 105% (Table 1). The XCB was deployed 41 times, with 391 m cored and 188 m of recovered core for a recovery rate of 48%. The hole was advanced to a final depth of 476.8 mbsf (Table 1).

Hole 782B

Because we had not achieved our basement objective at Site 782, a standard RCB BHA with a mechanical bit release (MBR) and bit was prepared for coring a second hole. The vessel was offset 100 m to the south, and the pipe trip back to the seafloor began at 2230UTC, 20 March. The seafloor was reached at 0700UTC, 21 March, at 2965.9 mbsl. Hole 782B had been drilled to 459.3 mbsf, when problems began in the form of bit plugging and increasing torque. Only one 9.6-m-RCB core was cut, with 0.1 m of recovered core for a recovery rate of 1%. The hole was drilled to 459.3 m and cored 9.6 m to a final depth of 468.9 mbsf.

A wiper trip from 3375.9 to 3424.9 mbsf was made to prepare the hole for logging. The MBR released without any problems, and the hole was filled with KCl mud. The logging equipment was prepared, the BHA was raised to 71 mbsf, and logging began. Two successful logging runs were conducted. The first used the dual induction tool (DIT), the dual lithodensity tool (HLDT), the sonic digital tool (SDT), and the natural gamma-ray spectrometry (NGT) tool; the second run used the induced gamma-ray spectroscopy tool (GST), the general purpose inclination tool (GPIT), the aluminum clay tool (AC), the compensated neutron porosity tool (CNT), and the natural gamma-ray spectrometry tool (NGT). The third run employed the magnetic susceptibility tool, which flooded 100 m below the keel and had to be retrieved, ending the logging program.

The Schlumberger equipment was rigged down, and the pipe trip out of the hole began at 0800UTC, 23 March. Site 782 officially ended at 1345UTC, 23 March, when the BHA was back on deck and the vessel departed for Site 783.

LITHOSTRATIGRAPHY

Introduction

The stratigraphic section recovered at Site 782 is divided into two lithologic units: Unit I (Holocene? to middle Eocene)

Table 1. Coring summaries, Site 782.

Core no.	Date (March 1989)	Time (UTC)	Depth (mbsf)	Length cored (m)	Length recovered (m)	Recovery (%)
125-782A-1H	17	0130	0–9.8	9.8	9.80	100.0
2H	17	0230	9.8–19.3	9.5	9.95	105.0
3H	17	0345	19.3–28.8	9.5	10.0	106.0
4H	17	0445	28.8–38.3	9.5	10.03	105.6
5H	17	0800	38.3–47.8	9.5	10.04	105.7
6H	17	0935	47.8–57.3	9.5	10.01	105.3
7H	17	1315	57.3–66.8	9.5	10.04	105.7
8H	17	1945	66.8–76.3	9.5	10.11	106.4
9H	17	2245	76.3–85.8	9.5	9.93	104.0
10X	18	0105	85.8–95.7	9.9	2.52	25.4
11X	18	0200	95.7–105.3	9.6	4.06	42.3
12X	18	0300	105.3–115.0	9.7	5.07	52.2
13X	18	0345	115.0–124.6	9.6	5.05	52.6
14X	18	0415	124.6–134.3	9.7	6.17	63.6
15X	18	0510	134.3–143.9	9.6	5.07	52.8
16X	18	0550	143.9–153.6	9.7	4.26	43.9
17X	18	0630	153.6–163.2	9.6	7.87	82.0
18X	18	0700	163.2–172.9	9.7	2.78	28.6
19X	18	0745	172.9–182.5	9.6	5.40	56.2
20X	18	0830	182.5–192.1	9.6	0.87	9.1
21X	18	0900	192.1–201.8	9.7	7.16	73.8
22X	18	0945	201.8–211.5	9.7	1.64	16.9
23X	18	1020	211.5–221.0	9.5	9.85	103.0
24X	18	1100	221.0–230.7	9.7	2.68	27.6
25X	18	1140	230.7–240.3	9.6	9.42	98.1
26X	18	1230	240.3–250.0	9.7	9.82	101.0
27X	18	1310	250.0–259.6	9.6	3.94	41.0
28X	18	1350	259.6–269.2	9.6	9.37	97.6
29X	18	1435	269.2–278.8	9.6	9.69	101.0
30X	18	1525	278.8–288.5	9.7	3.35	34.5
31X	18	1700	288.5–294.0	5.5	4.42	80.3
32X	18	2145	294.0–303.5	9.5	8.86	93.2
33X	18	2245	303.5–313.1	9.6	9.82	102.0
34X	18	2345	313.1–322.5	9.4	1.92	20.4
35X	19	0050	322.5–332.1	9.6	9.83	102.0
36X	19	0230	332.1–341.6	9.5	7.92	83.3
37X	19	0400	341.6–351.2	9.6	9.87	103.0
38X	19	0515	351.2–360.9	9.7	0.00	0.0
39X	19	0645	360.9–370.5	9.6	2.64	27.5
40X	19	0800	370.5–380.2	9.7	6.29	64.8
41X	19	0915	380.2–389.8	9.6	9.82	102.0
42X	19	1035	389.8–399.5	9.7	3.45	35.5
43X	19	1200	399.5–409.2	9.7	0.21	2.2
44X	19	1325	409.2–418.8	9.6	0.21	2.2
45X	19	1515	418.8–428.5	9.7	0.40	4.1
46X	19	1655	428.5–438.2	9.7	0.00	0.0
47X	19	1900	438.2–447.9	9.7	0.00	0.0
48X	19	2100	447.9–457.6	9.7	0.00	0.0
49X	19	2305	457.6–467.1	9.5	0.15	1.6
50X	20	0830	467.1–476.8	9.7	0.17	1.8
Coring total				476.8	282.00	59.1
125-782B-1W	22	0100	0–459.3	459.3	0.40	(wash core)
2R	22	0200	459.3–468.9	9.6	0.10	1.0
Coring total				9.6	0.10	1.0
Washing total				459.3	0.40	
Combined total				468.9	0.50	

and Unit II (the andesitic basement rocks, Table 2). Variability within the three subunits of Unit I represents gradational changes in the relative dominance of various sedimentary components. All of the sediment types found at Site 782 are present in each subunit.

Unit I

Cores 125-782A-1H-1, 0 cm, to 125-782A-43X-CC, 16 cm; depth, 0–409.2 mbsf.
Age: Holocene(?) to middle Eocene.

This unit extends from the sediment/water interface to 409.2 mbsf and includes the entire sedimentary sequence overlying andesitic basement. Nannofossil age determinations place the top of this unit as Holocene(?) or late Pleistocene and the base as middle Eocene. The dominant lithology of this unit is nannofossil marl or nannofossil chalk. Ash layers are found throughout Unit I (see Table 3). There are no striking breaks of the lithology, although burrowing, vitric components and induration all increase downsection.

Subunit IA (Cores 125-782A-1H-1 to 125-782A-16X-CC, 9 cm; depth, 0–153.6 mbsf).
Age: Holocene(?) to early Pliocene.

The uppermost part of this subunit is composed of gray (5Y 5/1) to yellow-greenish (5Y 7/1), homogeneous nannofossil marl. Core recovery was more than 100% in the 0- to 100-m interval, probably because of the lithologic homogeneity.

Table 2. Lithologic units recovered at Site 782.

Lithologic unit/subunit	Core section, interval (m)	Depth (mbsf)	Dominant lithology	Stratigraphic age
IA	125-782A-1H-1, 0 to 125-782A-16X-CC, 9	0 to 153.6	Nannofossil marls	Holocene(?) to lower Pliocene
IB	125-782A-17X-1, 0 to 125-782A-35X-5, 145	153.6 to 337.0	Vitric nannofossil marls	upper Miocene to middle Miocene
IC	125-782A-35X-5, 145 to 125-782A-43X-CC, 16	337.0 to 409.2	Nannofossil chalks, vitric nannofossil chalks	upper Oligocene to middle Eocene
II	125-782A-43X-CC, 16 to 125-782A-50X-1, 42	409.2 to 476.8	Andesitic rocks	(?)

Faint horizontal laminations, some graded bedding, and sporadic burrowing were the only sedimentary structures observed.

The section contains volcanic ash layers less than 1 to 8 cm thick, of light and dark colored vitric fragments, often with feldspar, and commonly graded (see Table 3). Inverse grading occurs locally as a result of density segregation during gravitational flow and settling of pumice and smaller vitric/crystal grains. Other characteristic structures of the lower part of Subunit IA include vertical burrows and slumps. Burrows commonly are filled with ash and locally are filled with nannofossil marl. Sedimentary stratigraphy and structures are largely missing in the upper 15 cores because of severe coring disturbance.

In smear slides, the main components present other than calcareous nannofossils, radiolarians, and foraminifers are glass (10%), carbonate grains (7%), opaque minerals (7%), feldspar (5%), with minor pyroxene (2%) and chlorite (1%), and traces of quartz, zoisite/epidote, serpentine, aragonite, and glauconite.

Subunit IB (Cores 125-782A-17X-1, 0 cm, to 125-782A-35X-5, 145 cm; depth,153.6–337.0 mbsf)
Age: late to middle Miocene.

Subunit IB is characterized by extensive bioturbation, by an increase in the amount of volcanic detritus, and by the proportion of alternating light gray (5Y 7/1) and dark gray (5Y 4/1) sequences having thicknesses of 1 dm to several decimeters. Greenish colors are not present; the major lithology remains nannofossil marl (as in Subunit IA); volcanic debris as ash layers and interspersed allochthonous material remains somewhat constant. The increased induration may be the cause of poorer core recovery. Burrows are more common in Subunit IB than in Subunit IA. These burrows are typically horizontal and are rarely larger than about 1 mm, although larger ones are present.

Although rare laminations do occur in the subunit, any primary depositional textures that were present would certainly have been destroyed by this intense bioturbation. Volcanic ash is present, both as separate layers and dispersed and mixed within the nannofossil chalk. The color of the strata depends largely on the relative abundances of the components forming the sediment: large proportions of nannofossils cause lighter colors, whereas abundant glass particles cause darker colors.

In smear slides, components present (other than nannofossils, radiolarians, and foraminifers) are glass (20%), feldspar (8%), opaque minerals (5%), with minor pyroxene (3%), epidote/zoisite, and traces of chlorite, glauconite, amphibole, and zeolite.

Subunit IC (Cores 125-782A-35X-5, 145 cm, to 125-782A-43X-CC, 16 cm; depth, 337.0–409.2 mbsf)
Age: late Oligocene to middle Eocene.

Subunit IC is predominantly vitric nannofossil chalk with frequent intercalations of volcanic ash. Volcanogenic minerals, which include pyroxene (7%), feldspar (5%), glass (approximately 25%) and their alteration products (zeolites, 2-50%; and serpentines, 0–12%), become more abundant with depth. Because of the greater variability of the strata compared with the overlying subunits, the colors of the sediments vary between brownish, grayish, and greenish hues over relatively short intervals.

Breccialike zones and intervals in Intervals 125-782A-39X-1, 21–121 cm, and 125-782A-42X-1, 12–40 cm, may be drilling breccia or primary structures. However, near the base of Subunit IC, pebble-rich sands and gravelly conglomerates are intercalated within the nannofossil chalks and become the dominant lithologies in the bottom of Subunit IC. Serpentine-filled veins and interstitial pore spaces are common in these strata. A thin basaltic layer directly overlies the basaltic basement in Core 125-782A-43X-CC. Core recovery in this interval was less than 50%.

In smear slides, components other than nannofossils, radiolarians, and foraminifers are glass (25%), opaque minerals (8%), pyroxene (7%), feldspar (5%), with minor epidote/zoisite (6%), zeolite (except 50% in one sample), serpentine (except 12% in one sample), amphibole, and traces of quartz.

Unit II

Cores 125-782A-43X-CC, 16 cm, to 125-782A-50X-1, 42 cm; depth, 409.2–476.8 mbsf.

For a description of the rocks recovered from this lithologic unit, see "Igneous and Metamorphic Petrology" section (this chapter).

BIOSTRATIGRAPHY

Evidence from calcareous nannofossils, planktonic foraminifers, and diatoms indicates that the sediments overlying the igneous rock range in age from late Pleistocene to middle Eocene (Fig. 3). Epoch boundary markers are found in Samples 125-782A-4H-CC (Pleistocene), 125-782A-16X-CC (Pliocene), 125-782A-35X-5, 120–121 cm (Miocene), and 125-782A-39X-CC (Oligocene). Hiatuses may exist between the

Table 3. Preliminary compilation of ash layers found in lithologic Unit I at Site 782.

Core, section, interval (cm)	Depth (mbsf)	Volcanic layer
125-782A-1H-1, 90	0.9	1
1H-3, 24	3.24	2
1H-3, 130	4.3	3
2H-4, 86	15.16	4
2H-4, 90	15.2	5
2H-4, 103–104	15.33	6
2H-4, 114	15.44	7
2H-4, 131	15.61	8
2H-5, 107–115	16.87–16.95	9
2H-5, 127–150	17.3	10
2H-6, 0–8	18.1	11
2H-6, 85–86	18.16	12
5H-6, 18–19	45.98	13
6H-3, 21–27	51.01–51.07	14
6H-4, 84–91	53.14–53.21	15
6H-6 55–57	55.85–55.87	16
6H-6, 87–90	56.17–56.20	17
7H-3, 67–69	60.97–60.98	18
7H-3, 106–110	61.36–61.40	19
7H-4, 79–84	62.53–62.64	20
7H-7, 59–61	66.89–66.91	21
8H-4, 94–95	72.24	22
8H-4, 122–123	72.52	23
11X-1, 54–57	96.24–96.27	24
11X-1, 110–117	96.80–96.87	25
11X-2, 37–38	97.57	26
11X-3, 0–1	98.7	27
11X-3, 9.5–10	98.8	28
11X-3, 51–54	99.21–99.24	29
12X-1, 20	105.5	30
12X-1, 28–29	105.58	31
12X-2, 9–10	106.8	32
12X-2, 16–17	106.96	33
12X-CC, 22–23	110.27	34
13X-2, 103–104	117.53	35
13X-3, 51.5–52.5	118.52	36
14X-2, 10–11	126.2	37
14X-2, 82–83	126.52	38
14X-2, 112–116	117.22–127.26	39
14X-2, 140–144	127.50–127.54	40
14X-3, 41–45	128.01–128.05	41
14X-5, 15–18	130.0–130.65	42
15X-2, 105.5–106.5	136.86	43
15X-2, 115	136.95	44
15X-2, 117	136.97	45
15X-3, 8–16	137.38–137.54	46
15X-3, 101–105	138.31–138.35	47
15X-3, 113–115	138.41–138.43	48
15X-4, 13.5–17.0	138.93–138.97	49
16X-3, 96–97	147.86	50
17X-1, 54–55	154.14	51
17X-2, 3–5	155.13–155.15	52
17X-2, 102–103	156.12	53
17X-2, 124–125	156.34	54
17X-3, 121	157.81	55
17X-4, 0–2	158.08–158.12	56
17X-4, 73–74	158.83	57
17X-5, 139–141	160.99–161.01	58
18X-1, 10–16	163.36–163.38	59
19X-1, 147–148	174.37	60
19X-2, 23–27	174.63–174.67	61
19X-3, 104–105	176.94	62
19X-CC, 13–14	178.08	63
20X-CC, 10	183.26	64
21X-1, 51–53	192.61–192.62	65
21X-1, 64–66	192.74–192.76	66
21X-2, 48–51	194.08–194.10	67
21X-2, 82–86.5	194.42–194.46	68
21X-2, 96–97	194.56	69
21X-2, 127–128	194.87	70
21X-3, 0–1	195.1	71
21X-3, 72	195.82	72
21X-5, 42–45	198.52–198.55	73
23X-2, 15–16	213.15	74
23X-3, 23–26	214.73–214.76	75
23X-3, 93–94	215.33	76
23X-4, 107–109	217.07–217.09	77
23X-4, 132–133	217.32	78
23X-5, 40–45	217.90–217.95	79
23X-5, 83–86	218.33–218.36	80
23X-6, 67–68	219.67	81
23X-6, 134–137	220.34–220.37	82
23X-6, 141–144	220.41–220.44	83
24X-1, 44–45	221.44	84
24X-2, 2–3	222.7	85
25X-4, 32–36	235.52–235.56	86
25X-4, 114	236.34	87
26X-1, 138	241.68	88
26X-1, 140	241.7	89
26X-2, 83–85	242.63–242.65	90
28X-1, 98–99	260.58	91
28X-3, 17	262.77	92
29X-3, 9–10	273.1	93
29X-3, 43–46	272.63–272.66	94
29X-3, 90	273.1	95
29X-4, 85–90	274.55–274.67	96
29X-5, 12–15	275.32–272.35	97
29X-6, 19–21	276.89–276.91	98
29X-6, 30–41	277.00–277.11	99
29X-7, 35–37	278.55–278.57	100
30X-2, 9–10	280.39	101
30X-2, 30–31	280.6	102
31X-1, 17	288.63	103
31X-1, 22–24	288.72–288.74	104
32X-2, 41–46	295.91–295.96	105
32X-4, 124	299.74	106
32X-6, 32–35	301.82–301.85	107
33X-3, 82–85	307.82–307.35	108
33X-5, 87–88	310.37	109
33X-7, 27–29.5	312.77–312.80	110
34X-CC, 20–26.5	314.79–314.85	111
37X-5, 85–87	348.45–348.47	112
39X-2, 9	362.49	113
39X-2, 44–45.5	362.88	114
39X-2, 70–71	363.1	115
41X-4, 23–24	384.93	116

These ash layers represent primary ash-fall deposits from a nearby volcanic event. Not listed are additional layers at this site that are interpreted as reworked volcaniclastic debris, presumably deposited by turbidity currents, bottom currents, debris flows, and so forth.

late Oligocene and middle Miocene and between the early Oligocene and late Oligocene.

Calcareous Nannofossils

Pleistocene through middle Eocene nannofossil assemblages are present in Hole 782A.

Pleistocene

Pleistocene nannofossil assemblages are abundant and moderately to well-preserved in Samples 125-782A-1H-1, 20 cm, to 125-782A-4H-CC on the basis of the presence of *Emiliania huxleyi*, *Gephyrocapsa oceanica*, *G. caribbeanica*, *Pseudoemiliania lacunosa*, *Helicosphaera sellii*, and other species. Samples 125-782A-1H-1, 20 cm, to 125-782A-1H-CC, 125-782A-2H-1, 53 cm, and 125-782A-2H-CC to 125-782A-4H-CC define the late Pleistocene (Zone CN15), middle Pleistocene (CN14b subzone), and early Pleistocene (CN14a subzone), respectively.

Gephyrocapsa oceanica is absent in Sample 125-782A-5H-3, 86 cm, whereas *Pseudoemiliania lacunosa*, *Calcidiscus*

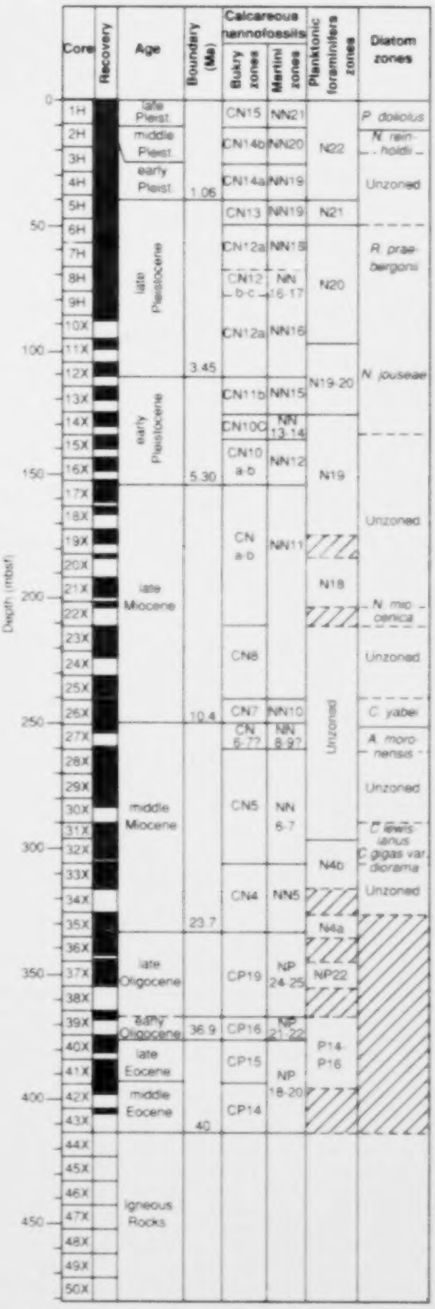
Core
Recovery
Age
Boundary (Ma)
Calcareous nannofossils
Bukry zones
Martini zones
Planktonic foraminifers zones
Diatom zones
Depth (mbsf)
0
50
100
150
200
250
300
350
400
450
1H
2H
3H
4H
5H
6H
7H
8H
9H
10X
11X
12X
13X
14X
15X
16X
17X
18X
19X
20X
21X
22X
23X
24X
25X
26X
27X
28X
29X
30X
31X
32X
33X
34X
35X
36X
37X
38X
39X
40X
41X
42X
43X
44X
45X
46X
47X
48X
49X
50X
late Pleist.
middle Pleist.
early Pleist.
late Pleistocene
early Pleistocene
late Miocene
middle Miocene
late Oligocene
early Oligocene
late Eocene
middle Eocene
Igneous Rocks
1.06
3.45
5.30
10.4
23.7
36.9
40
CN15
CN14b
CN14a
CN13
CN12a
CN12 b-c
CN12a
CN11b
CN10C
CN10 a-b
CN a-b
CN8
CN7
CN 6-7??
CN5
CN4
CP19
CP16
CP15
CP14
NN21
NN20
NN19
NN19
NN18
NN 16-17
NN16
NN15
NN 13-14
NN12
NN11
NN10
NN 8-9?
NN 6-7
NN5
NP 24-25
NP 21-22
NP 18-20
N22
N21
N20
N19-20
N19
N18
Unzoned
N4b
N4a
NP22
P14-P16
P. doliolus
N. reinholdii
Unzoned
R. praebergonii
N. jouseae
Unzoned
N. miocenica
Unzoned
C. yabei
A. moronensis
Unzoned
C. lewisianus
C. gigas var. diorama
Unzoned

Figure 3. Biostratigraphic summary for Site 782.

macintyrei, and *Gephyrocapsa caribbeanica* are common; this sample was assigned to the late Pliocene (CN13a subzone), following Backman, Duncan, et al. (1988). Thus, the Pliocene/Pleistocene boundary is located within Sections 125-782A-5H-1 or 125-782A-5H-2.

Pliocene

Late Pliocene nannofossil assemblages are present from Sample 125-782A-5H-3, 86 cm, to 125-782A-11X-CC. The abundant and moderately to well-preserved assemblages are characterized by marker species of late Pliocene age, *Discoaster asymmetricus*, *D. brouweri*, *D. pentaradiatus*, *D. surculus*, *D. tamalis*, and *Ceratolithus separatus* (CN12a subzone). The last occurrence of *Discoaster brouweri*, together with *D. triradiatus*, is present in Sample 125-782A-6H-CC; the CN12/CN13 boundary thus is present in Core 125-782A-6H.

The last occurrence of *Reticulofenestra pseudoumbilica* (top of Zone CN11), which coincides approximately with the lower Pliocene/upper Pliocene boundary, is present in Sample 125-782A-12X-CC. This moderately preserved assemblage is characterized by *Sphenolithus abies*, *Discoaster asymmetricus*, and *Pseudoemiliania lacunosa*, together with *Discoaster brouweri* and *D. pentaradiatus*. The first occurrence of *Discoaster tamalis* and the last occurrence of *Reticulofenestra pseudoumbilica* and *Sphenolithus* spp. overlap in this sample. This association, together with *Amaurolithus delicatus* and *A. tricorniculatis*, is common to abundant down to Sample 125-782A-16X-CC, where the first occurrence of *Ceratolithus acutus* can be found. In Sample 125-782A-17X-CC, the last occurrence of *Discoaster quinqueramus*, *D. berggreni*, and *Triquetrorhabdulus rugosus*, together with the first occurrence of *Amaurolithus tricorniculatus*, was found. Thus, the Miocene/Pliocene boundary is located within Core 125-782A-17X.

Miocene

Few-to-abundant, moderately preserved late Miocene nannofossil assemblages are present in Samples 125-782A-17X-CC to 125-782A-26X-CC. The top of this assemblage has been defined by the last occurrence of *Discoaster quinqueramus* together with *Triquetrorhabdulus rugosus*; the bottom lies between the first occurrence of *Catinaster coalitus* and the first occurrence of *Catinaster calyculus*, within Zone CN6.

The first occurrence of *Discoaster quinqueramus* in Sample 125-782A-22X-CC defines the Zone CN8/CN9 boundary. We expected *Discoaster berggreni*, *D. surculus*, and *D. neohamatus* to appear before *Discoaster quinqueramus*, indicating drilling disturbances in these cores.

Sample 125-782A-25X-7, 7 cm, contains the first occurrence of *Discoaster pentaradiatus* together with *D. prepentaradiatus*. Sample 125-782A-26X-4, 92–94 cm, is characterized by the last occurrence of *Discoaster hamatus* (although very rare) and *Catinaster coalitus* (marker species for Zone CN7), together with *Catinaster calcylus* and *Discoaster calcaris*. Therefore, the Zone CN7/CN8 boundary has been placed between Samples 125-782A-25X-7, 7 cm, and 125-782A-26X-4, 92–94 cm.

Middle Miocene nannofossil assemblages were found in Samples 125-782A-27X-1, 110 cm, to 125-782A-35X-5, 125 cm, whereas the early Miocene is completely missing. Sample 125-782A-35X-5, 125 cm, is middle Miocene in age (Zone CN4) on the basis of the occurrence of *Sphenolithus heteromorphus*, together with *Calcidiscus macintyrei*, *C. leptoporus*, and *Discoaster variabilis*. The presence of specimens of *Reticulofenestra pseudoumbilica* larger than 7 mm indicates that this sample is located in the upper part of Zone

CN4. Reworked species of Zone CN2 *Discoaster druggi* and *Sphenolithus belemnos* also are present. The top of Zone CN4 can be found in Sample 125-782A-33X-CC, in which the last occurrence of *Spenolithus heteromorphus* was found. The last occurrence of *Cyclocargolithus floridanus* (Sample 125-782A-30X-2, 21 cm) and the first occurrence of *Discoaster kugleri* (Sample 125-782A-29X-CC) indicate the Zone CN5a/CN5b boundary. Drilling disturbances are common in middle Miocene cores.

However, Sample 125-782A-35X-6, 10 cm, belongs to the late Oligocene on the basis of the last appearance of *Dictyococcithes bisectus*. If Zones CN1 to CN4 are partly missing, a hiatus having a duration of more than 7.5 Ma must be present between the middle Miocene and upper Oligocene.

Oligocene

Abundant, moderately to well-preserved nannofossil assemblages are present from Samples 125-782A-35X-6, 10 cm, to 125-782A-39X-CC. The last sample is early Oligocene in age (Zone CP16) on the basis of the occurrence of *Ericsonia formosa* and *Isthmolithus recurvus* and the lack of the Eocene marker *Discoaster saipanensis*. Because of the occurrence of common specimens of *Ericsonia subdisticha*, this may represent Zone CP16a. Samples 125-782A-35X-6, 10 cm, through 125-782A-39X-2, 11 cm, were assigned to the late Oligocene (Zone CP19) on the basis of the occurrence of *Sphenolithus ciperoensis*, *S. distentus*, and *Helicosphaera recta*. A hiatus between early and late Oligocene might be present within Core 125-782A-39X because Zones CP17 and CP18 and Subzone CP16b/c are missing, but this may also result from poor core recovery.

Eocene

The section from Samples 125-782A-40X-CC to 125-782A-43X-CC has been interpreted as late to middle Eocene in age (Zones CP14–CP15) on the basis of the occurrence of *Discoaster bifax*, *Chiasmolithus oamaruensis*, *Discoaster barbadiensis*, *D. saipanensis*, and *Cribrocentrum reticulatum*. Middle Eocene marker species (*Chiasmolithus expansus*, *C. grandis*, and *C. solithus*) were found in Sample 125-782A-41X-4, 16–17 cm, but not in Sample 125-782A-41X-3, 43–44 cm. The CP14/CP15 zonal boundary (middle Eocene/late Eocene boundary) thus is located between these two samples. The assemblages are rare to common in abundance and are poor to moderate in preservation. These samples directly overlie the volcanic basement.

Foraminifers

The Cenozoic planktonic foraminiferal stratigraphy for Hole 782A is summarized in Table 4. The relatively poor preservation and generally low abundance of planktonic foraminifers in the pre-Quaternary cores do not permit one to determine specific ages, thus precluding an accurate biostratigraphic subdivision of Hole 782A. An asterisk (*) is used to denote that the species listed in these columns are the species used to define (based on presence or absence) the age of the sample in question. No ages were determined for samples of poor preservation on the basis of the absence of species.

The planktonic foraminiferal results from Hole 782A place the sedimentary sequence between the Quaternary (Zone P22) and the middle Eocene (Zone P14–low Zone P16). Temperate-to-warm subtropical planktonic foraminiferal forms dominate the whole of the sedimentary sequence, with tropical forms tending to constitute only a small proportion of sample assemblages. The poor preservation, low abundances, and high number of barren samples below the middle-early Pliocene Sample 125-782A-13X-CC correlate with the large amounts of volcaniclastic material present in these samples.

Diatoms

Diatoms are rare to common and poorly to well preserved in Cores 125-782A-1H through 125-782A-34X. Cores 125-782A-35X through 125-782A-43X are barren of diatoms. The diatom assemblage in Hole 782A is characterized by common *Thalassionema nitzschioides* and few *Coscinodiscus* spp., *Nitzschia* spp., *Thalassiosira* spp., and others. Fragments of *Ethmodiscus rex* are present in most samples.

Because of the absence of age-diagnostic species in many samples, large intervals have been left unzoned. However, one may date the sedimentary interval in Hole 782A as ranging from the Quaternary to at least the middle Miocene.

Sample 125-782A-1H-CC was assigned to the *Pseudoeunotia doliolus* Zone by the presence of *P. doliolus* and the absence of *Nitzschia reinholdii*. *N. reinholdii* is present in Sample 125-782A-2H-CC, together with *P. doliolus*; this sample thus was placed in the *N. reinholdii* Zone. Both zones are Quaternary in age.

Samples 125-782A-6H-CC and 125-782A-7H-CC can be assigned a late Pliocene age (*Rhizosolenia praebergonii* Zone) on the basis of the occurrence of *R. praebergonii*. The boundary between the *R. praebergonii* Zone and the *Nitzschia jouseae* Zone was tentatively placed at Sample 125-782A-8H-CC on the basis of the absence of *R. praebergonii* and the occurrence of a fragment that may be *Actinocyclus ellipticus* f. *lanceolatus*.

Samples 125-782A-9H-CC through 125-782A-14X-CC contain *N. jouseae* and are early to late Pliocene in age (*N. jouseae* Zone).

Nitzschia miocenica appears in Sample 125-782A-22X-CC, and *Coscinodiscus yabei* appears in Sample 125-782A-26X-CC; therefore, these samples were assigned to the late Miocene.

Actinocyclus moronensis was found in Sample 125-782A-27X–CC, and *Coscinodiscus lewisianus* is present in Samples 125-782A-31X-CC and 125-782A-32X-CC, where it can be observed with *Coscinodiscus plicatulus* and *Denticulopsis nicobarica*, dating this interval to the middle Miocene (*C. lewisianus*/*C. gigas* var. *diorama* zones).

IGNEOUS AND METAMORPHIC PETROLOGY

Angular to subrounded clasts of moderately to highly phyric, two-pyroxene andesite and dacite were recovered from the bottom of Holes 782A and 782B. These clasts range from about 20 to 50 mm, are gray to greenish-brown and black, contain 60% to 90% glass, and typically are slightly vesicular (less than 10 vol%).

It is possible that some of these clasts are disrupted fragments of pillow lavas. Elongation of the vesicles and some alignment of groundmass felspar laths define a flow texture in a few of the clasts, but other evidence for the original morphology of the materials was not available.

Euhedral, oscillatory-zoned plagioclase up to 5 mm long is the most abundant (less than 25 modal%) phenocryst phase, followed by subequal proportions of about 3 to 5 modal% of euhedral clinopyroxene and pink-green pleochroic orthopyroxene (less than 2–3 mm in size). Euhedral magnetitie (less than 1 mm in size) is a minor (less than 3 modal%) phenocryst type. These phases also form glomerocrystic clusters up to 10 mm wide.

The groundmass of the andesites and dacites is predominantly glass, with numerous quench-textured feldspar laths and minor amounts of dusty iron-titanium oxides. Some chloritic alteration along anastomosing cracks in the glass is present in many of the samples. Fresh, pale brown glass inclusions less than 0.2 mm in diameter are present in the

Table 4. Summary of foraminiferal data for Site 782.

Core, section	Abundance	Preservation	Diagnostic species present*	Diagnostic species absent*	Zone(s)	Age/age range
125-782A-1H-CC	Abundant	Good	*Globorotalia truncatulinoides*	—	N22	Pleistocene
125-782A-2H-CC	Abundant	Good	*Globorotalia truncatulinoides*	—	N22	Pleistocene
125-782A-3H-CC	Abundant	Good	*Globorotalia truncatulinoides*	—	N22	Pleistocene
125-782A-4H-CC	Abundant	Good	*Globorotalia truncatulinoides*	—	N22	Pleistocene
125-782A-5H-CC	Common	Moderate	*Globorotalia tosaensis*	*Globorotalia truncatulinoides*	N21	late Pliocene
125-782A-6H-CC	Abundant	Moderate	*Globorotalia crassaformis*	*Globorotalia truncatulinoides*	upper N19–N21	middle early Pliocene-late Pliocene
125-782A-7H-CC	Common	Moderate	*Globorotalia crassaformis*	*Globorotalia truncatulinoides*	upper N19–N21	middle early Pliocene-late Pliocene
125-782A-8H-CC	Few	Moderate	*Globorotalia crassaformis*	*Globorotalia truncatulinoides*	upper N19–N21	middle early Pliocene-late Pliocene
125-782A-9H-CC	Few	Moderate	*Globorotalia crassaformis*	*Globorotalia truncatulinoides*	upper N19–N21	middle early Pliocene-late Pliocene
125-782A-10X-CC	Few	Moderate	*Globorotalia crassaformis* *Globigerinoides extremus*	*Globorotalia truncatulinoides*	upper N19–N21	middle early Pliocene-late Pliocene
125-782A-11X-CC	Common	Moderate	*Globorotalia crassaformis* *Neogloboquadrina acostaensis*	—	upper N19–N19/20	middle early Pliocene-late early Pliocene
125-782A-12X-CC	Common	Moderate	*Globorotalia crassaformis* *Sphaeroidinellopsis praedehiscens*	—	upper N19–N19/20	middle early Pliocene-late early Pliocene
125-782A-13X-CC	Common	Moderate	*Globorotalia crassaformis* *Globigerinoides bulloideus*	—	upper N19	middle early Pliocene
125-782A-14X-CC	Rare	Moderate	*Globorotalia crassaformis*	*Globorotalia truncatulinoides*	upper N19–N21	early Pliocene-late Pliocene
125-782A-15X-CC	Barren	—	—	—	—	—
125-782A-16X-CC	Barren	—	—	—	—	—
125-782A-17X-CC	Rare	Poor	*Sphaeroidinellopsis seminula* *Orbulina universa*	—	N9–N21	early middle Miocene-late Pliocene
125-782A-18X-CC	Common	Poor	*Globigerina nepenthes* *Globorotalia* (H.) margaritidae	*Globorotalia crassaformis*	lower N19	earliest early Pliocene
125-782A-19X-CC	Barren	—	—	—	—	—
125-782A-20X-CC	Rare	Poor	*Sphaeroidinellopsis seminula* *Globorotalia tumida*	—	N18–N21	late Miocene-late Pliocene
125-782A-21X-CC	Few	Poor	*Globorotalia* cf. *tumida* *Sphaeroidinellopsis kochi*	—	N18–N19	late Miocene-early Pliocene
125-782A-22X-CC	Barren	—	—	—	—	—
125-782A-23X-CC	Rare	Poor	*Sphaeroidinellopsis kochi* *Globigerina nepenthes*	—	N14–N19	late middle Miocene-early Pliocene
125-782A-24X-CC	Rare	Moderate	*Globigerina nepenthes*	—	N14–N19	late middle Miocene-early Pliocene
125-782A-25X-CC	Rare	Moderate	*Orbulina universa*	—	N9–N22	early middle Miocene-recent
125-782A-26X-CC	Rare	Moderate	*Globigerina nepenthes* *Sphaeroidinellopsis kochi*	—	N14–N19	late middle Miocene-early Pliocene
125-782A-27X-CC	Barren	—	—	—	—	—
125-782A-28X-CC	Barren	—	—	—	—	—
125-782A-29X-CC	Barren	—	—	—	—	—
125-782A-30X-CC	Barren	—	—	—	—	—
125-782A-31X-CC	Barren	—	—	—	—	—
125-782A-32X-CC	Rare	Moderate	*Dentaloglobigerina altispira*	—	N4B–N21	early Miocene-late Pliocene
125-782A-33X-CC	Few	Poor	*Globorotalia* (F.) peripheroronda *Globoquadrina dehiscens*	—	N4B–N10	early Miocene-earliest middle Miocene
125-782A-34X-CC	Barren	—	—	—	—	—
125-782A-35X-CC	Few	Poor	*Globorotalia* (J.) *mayeri* *Catapsydrax dissimilis*	—	N4A–N6	latest Oligocene-middle early Miocene
125-782A-36X-CC	Barren	—	—	—	—	—
125-782A-37X-CC	Few	Poor	*Catapsydrax dissimilis* *Globoquadrina venezuelana*	—	P22–N6	late Oligocene-middle early Miocene
125-782A-38X-CC	No Recovery	—	—	—	—	—
125-782A-39X-CC	Few	Poor	*Catapsydrax dissimilis*	—	P13–N6	late middle Eocene-early Miocene
125-782A-40X-CC	Few	Poor	*Catapsydrax dissimilis*	—	P13–N6	late middle Eocene-early Miocene
125-782A-41X-CC	Common	Moderate	*Catapsydrax unicavus* *Globigerinoides* cf. *mexicanus*	—	P14–lower P16	late early Eocene-early late Eocene
125-782A-42X-CC	—	—	—	—	—	—
125-782A-43X-CC	—	—	—	—	—	—

*See text for explanation.

majority of the plagioclase phenocrysts, and these inclusions typically contain one or more shrinkage bubbles. Interstitial fresh glass is also present in the glomerocrystic clusters. Trace amounts of euhedral apatite are present as inclusions in some plagioclase phenocrysts and as a microphenocryst phase in the groundmass. Ilmenite and sulfide minerals are also present in trace quantities in some of the samples.

Note that the phase assemblage characteristic of the basement clasts is also typical of the overlying ashes and glass fragments in the sediments (see "Lithostratigraphy" section, this chapter).

IGNEOUS AND METAMORPHIC GEOCHEMISTRY

Various igneous rocks were encountered in both Holes 782A and 782B. Of these rocks, those that were taken from the core-catcher sample (Core 125-782A-49X-CC) are residues after the hole was washed through and hence may not have been sampled *in situ*. Eight samples were selected for shipboard X-ray fluorescence (see "Explanatory Notes" chapter, this volume). All samples were analyzed for abundance of major elements, but because of their small size, trace-element analysis was conducted on only three of the samples. Abundances of major and trace elements are presented in Table 5.

Major Elements

Two distinct rock types that form high- and low-silica groups were found. Both groups, however, have low potassium, titanium, and magnesium contents. The low-silica group (between 56.50 and 58.42 wt% SiO_2) has moderate-to-low values of magnesium (between 2.70 and 3.12 wt% MgO); the high-silica group (between 66.20 and 72.00 wt% SiO_2) contains virtually no magnesium (between 0 and 0.69 wt% MgO). The variation in titanium is greater for the low-silica group (from 0.64 to 1.13 wt% TiO_2) than for the high-silica group (from 0.34 to 0.43 wt% TiO_2). Potassium ranges from 0.57 to 1.08 wt% and 0.53 to 0.77 wt% K_2O for the high- and low-silica groups, respectively. The rocks are andesites and dacites-rhyolites on the basis of the silica and potassium contents and span the tholeiitic and calc-alkaline fields (Fig. 4). It is possible that the two groups are related by fractional crystallization.

Compared with the lavas recovered from the Mariana forearc at Sites 458 and 459, DSDP Leg 60 (see "Introduction" chapter, this volume), the rocks from Site 782 fall at the lower potassium end of the Leg 60 field. However, these rocks contain considerably less MgO at similar silica values (Fig. 5), and hence probably have a source that is distinct from that of the Leg 60 rocks.

Trace Elements

Two samples from the high-silica group and one sample from the low-silica group were analyzed for their abundance of trace elements. To avoid the possible effects of fractional crystallization on the trace-element ratios, only the most mafic sample (125-782A-49X-CC, 3–5 cm) is presented in a multi-element diagram (Fig. 6) normalized to a normal mid-ocean ridge basalt (N-MORB). Relative to N-MORB, the rock has high abundances of large-ion-lithophile (LIL) elements and low abundances of the high-field-strength (HFS) elements, particularly niobium, zirconium, yttrium, and titanium. The light-to-heavy rare-earth-element ratio, represented by cerium/yttrium (which is similar to cerium/ytterbium), is only slightly higher than N-MORB, implying little if any light rare-earth-element enrichment. These trace-element characteristics thus are consistent with derivation from a parent magma derived from the forearc mantle wedge that was selectively enriched by LIL elements from the downgoing slab.

SEDIMENT/FLUID GEOCHEMISTRY

Sediment Geochemistry

Sediments from Site 782 were analyzed on board ship for inorganic carbon and for total carbon, nitrogen, and sulfur using the techniques described in the "Explanatory Notes"

Table 5. Abundances of major and trace elements for rocks recovered at Site 782.

Core: Interval (cm):	44X-CC, 13–17	45X-1, 30–32	45X-1, 32–35	49X-CC, 58	49X-CC, 3–5	49X-CC, 37–42	782B-2R-1, 16–29	782A-41X-CC, 44–47
(in wt%)								
SiO_2	70.27	66.2	66.92	55.61	55.94	55.63	70.84	72.00
TiO_2	0.37	0.43	0.40	0.64	0.65	0.76	0.38	0.34
Al_2O_3	13.77	15.11	14.23	14.56	14.58	15.1	14.24	13.98
Fe_2O_3 (total)	2.92	4.45	4.05	9.99	10.17	10.42	2.64	2.57
MnO	0.05	0.10	0.10	0.14	0.14	0.16	0.03	0.03
MgO	0.11	0.69	0.68	2.68	2.84	3.08	0.01	0.01
CaO	3.14	3.88	3.37	6.91	6.86	7.37	3.22	2.37
Na_2O	4.56	4.29	3.94	2.35	2.4	2.54	4.45	4.46
K_2O	0.69	0.67	1.08	0.77	0.75	0.53	0.79	0.57
P_2O_5	0.05	0.05	0.07	0.01	0.03	0.05	0.05	0.03
LOI	1.32	0.64	3.49	1.28	3.63	2.18	1.01	1.37
Total	98.52	99.12	100.68	99.49	100.83	99.34	98.21	98.56
Mg#	0.06	0.21	0.22	0.32	0.33	0.34	0.01	0.01
(in ppm)								
Nb			0.9		2.2			0.3
Zr			111		58			115
Y			26		17			27
Sr			202		176			144
Rb			11.1		8.1			3.5
Zn			104		90			69
Cu			11		116			13
Ni			0		8			3
Cr			0		0			0
V			32		459			5
Ti			2820		4320			2220
Ce			20		15			17
Ba			35		30			51

LOI = loss on ignition. (Analyzed on board the *Resolution* by D. Sims using X-ray fluorescence.)

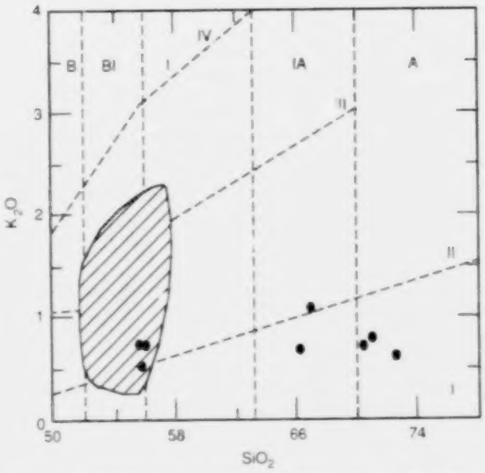

Figure 4. K_2O-SiO_2 igneous-rock classification diagram for destructive and collision margins (after Peccerillo and Taylor, 1976). The vertical boundaries mark the fields for basic (B), intermediate (BI), intermediate (I), intermediate-acid (IA), and acid (A) rocks; boundaries having positive fields mark the slopes for tholeiitic (I), calc-alkaline (II), high-potassium calc-alkaline (III), and shoshonitic (IV) series. Data from Site 782 fall between the tholeitic and calc-alkaline series, but at low abundances of potassium. The field for Mariana forearc basement rocks (recovered during DSDP Leg 60, Sites 458 and 459; after Wood et al., 1981) (hatched area) is also plotted for comparison.

(this volume). The organic carbon content was then calculated by difference. These results are presented in Table 6 and in Figure 7. The $CaCO_3$ content of the sediments varies from 10 to 70 wt%. Abrupt changes were observed at 14, 115, 2[illegible]0, 307, and 330 mbsf. Between these depths, changes are gradual or nonexistent. The organic carbon content is less than [illegible].2 wt%, except for intervals at 0 to 25 and 200 to 300 mbsf, where values approach 0.5 and 0.8 wt%, respectively. Two samples at 119 and 391 mbsf have much higher values of 2.5 and 1.4 wt%, respectively. The profile of nitrogen content with depth resembles that of organic carbon. Values range from less than 0.01 to 0.22 wt%. Sulfur is below the detection limit of 0.06 wt% in all samples.

Fluid Geochemistry

The concentration of methane measured for 5-cm^3 sediment headspace samples is uniformly low, less than 20 μL/L (Table 7). Methane was the only hydrocarbon detected.

Interstitial waters at Site 782 exhibit changes with depth (Table 8) that are typical of many deep-sea sites having moderate rates of sedimentation and organic carbon deposition. Depth profiles show the effects of three main processes: (1) bacterial oxidation of organic matter using various oxidants, including seawater sulfate; (2) precipitation of $CaCO_3$; and (3) alteration of volcanic material in the sediments and basement. Oxidation of organic matter produces bicarbonate alkalinity and ammonia while consuming oxidants in the order oxygen, nitrate, nitrite, MnO_2, FeOOH, sulfate. The enhanced alkalinity causes $CaCO_3$ to precipitate. Alteration of volcanic material by seawater at low temperatures removes magnesium, potassium, and hydroxyl from solution in exchange for calcium and silica from the volcanic sediments and basement rocks. The acidity generated by these reactions consumes bicarbonate alkalinity, as does the precipitation of $CaCO_3$, which is favored in turn by the enhanced concentration of dissolved calcium. The depth profiles for the various dissolved species are determined largely by the relative rates of these competing reactions.

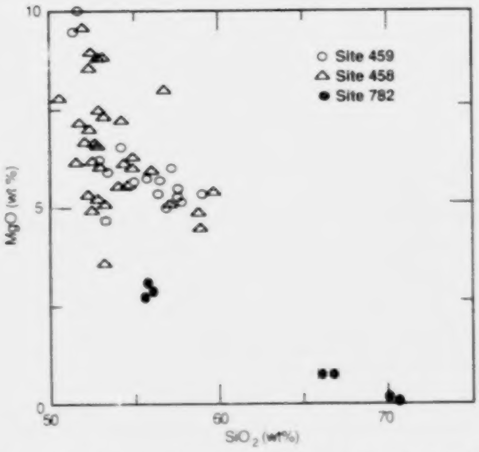

Figure 5. MgO-SiO_2 co-variation diagram separating the andesites and dacites-rhyolites recovered from the basement at Site 782 compared with rocks from Mariana forearc basement recovered during DSDP Leg 60, Sites 458 and 459.

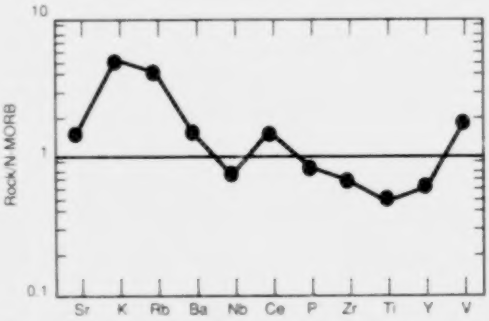

Figure 6. N-MORB normalized patterns for Sample 125-782A-49X-CC, 3–5 cm, the most mafic sample analyzed from Site 782. The high LIL element enrichment and low HFS element abundances are typical of a subduction-related tectonic environment of formation.

At Site 782, oxidation of organic matter causes alkalinity to increase by one-third in the near-surface sediments (Fig. 8). Below that, it decreases steadily toward basement, where it is consumed by reactions involving the removal of mainly magnesium from seawater. The shallow maximum in alkalinity is underlain by a deeper maximum in ammonia, as is typical in deep-sea sediments, where organic matter is being oxidized.

Table 6. Total nitrogen, carbon, organic carbon, and carbonate carbon in sediments at Site 782.

Core, section, interval (cm)	Depth (mbsf)	Total nitrogen (wt%)	Total carbon (wt%)	Inorganic carbon (wt%)	Organic carbon (wt%)	$CaCO_3$ (wt%)
125-782A-1H-1, 76–78	0.76			2.27		18.9
1H-2, 76–78	2.26			2.18		18.2
1H-3, 76–78	3.76	0.11	3.13	2.70	0.43	22.5
1H-4, 76–78	5.26			4.21		35.1
1H-5, 76–78	6.76			1.70		14.2
1H-6, 76–78	8.26			2.06		17.2
1H-7, 29–31	9.29			1.32		11.0
1H-CC, 8–10	9.68			2.98		24.8
2H-1, 74–76	10.54			3.83		31.9
2H-2, 61–63	11.91			4.62		38.5
2H-3, 65–67	13.45	0.08	3.84	3.67	0.17	30.6
2H-4, 61–63	14.91			7.05		58.7
2H-5, 61–63	16.41			5.02		41.8
2H-6, 76–78	18.06			7.16		59.6
2H-7, 30–32	19.10			5.49		45.7
3H-1, 79–81	20.09			4.18		34.8
3H-2, 79–81	21.59			3.32		27.6
3H-2, 79–81	23.09	0.13	4.86	4.56	0.30	38.0
3H-4, 78–90	24.58			2.98		24.8
3H-5, 78–80	26.08			5.32		44.3
3H-6, 78–80	27.58			3.68		30.7
3H-7, 38–40	28.68			7.78		64.8
4H-1, 79–81	29.59			5.73		47.7
4H-2, 79–81	31.09			5.10		42.5
4H-3, 79–81	32.59	0.07	4.57	4.65	0.00	38.7
4H-4, 79–81	34.09			4.58		38.2
4H-5, 79–81	35.59			4.13		34.4
4H-6, 79–81	37.09			6.42		53.5
4H-7, 39–41	38.19			5.30		44.1
5H-1, 78–80	39.08			2.83		23.6
5H-2, 78–80	40.58			5.37		44.7
5H-3, 78–80	42.08	0.10	5.53	5.44	0.09	45.3
5H-4, 78–80	43.58			2.64		22.0
5H-5, 78–80	45.08			5.00		41.7
5H-6, 78–80	46.58			3.41		28.4
5H-7, 36–38	47.66			4.71		39.2
6H-1, 73–75	48.53			2.34		19.5
6H-2, 63–65	49.93			2.75		22.9
6H-3, 97–99	51.77	0.10	2.98	2.83	0.15	23.6
6H-4, 68–70	52.98			2.65		22.1
6H-5, 43–45	54.23			3.12		26.0
6H-6, 53–55	55.83			2.16		18.0
6H-7, 37–39	57.17			4.12		34.3
7H-1, 30–32	57.60			3.68		30.7
7H-2, 30–32	59.10			4.97		41.4
7H-3, 33–35	60.63	0.11	3.19	3.08	0.11	25.7
7H-4, 26–28	62.06			3.40		28.3
7H-5, 79–81	64.09			3.30		27.5
7H-6, 73–75	65.53			1.67		13.9
7H-7, 26–28	66.56			2.76		23.0
8H-1, 74–76	67.54			3.54		29.5
8H-2, 74–76	69.04			4.08		34.0
8H-3, 74–76	70.54	0.12	2.73	2.63	0.10	21.9
8H-4, 74–76	72.04			3.89		32.4
8H-5, 74–76	73.54			4.75		39.6
8H-6, 74–76	75.04			3.28		27.3
8H-7, 35–37	76.15			2.97		24.7
9H-1, 72–74	77.02			1.33		11.1
9H-2, 72–74	78.52			1.44		12.0
9H-3, 78–80	80.08	0.07	1.63	1.47	0.16	12.2
9H-4, 72–74	81.52			4.05		33.7
9H-5, 78–80	83.08			4.02		33.5
9H-6, 78–80	84.58			3.57		29.7
9H-7, 31–33	85.61			3.35		27.9
10X-1, 130–132	87.10			2.29		19.1
10X-2, 36–38	87.66	0.06	2.69	2.58	0.11	21.5
11X-1, 74–76	96.44			2.09		17.4
11X-2, 54–56	97.74			1.21		10.1
11X-3, 69–71	99.39	0.10	3.61	3.39	0.22	28.2
12X-1, 74–76	106.04			3.86		32.2
12X-2, 74–76	107.54			3.25		27.1
12X-3, 67–69	108.97	0.08	4.09	3.92	0.17	32.7
12X-4, 13–15	109.93			3.28		27.3
13X-1, 63–65	115.63			5.38		44.8
13X-2, 80–82	117.30			3.55		29.6

Table 6 (continued).

Core, section, interval (cm)	Depth (mbsf)	Total nitrogen (wt%)	Total carbon (wt%)	Inorganic carbon (wt%)	Organic carbon (wt%)	$CaCO_3$ (wt%)
13X-3, 72–74	118.72	0.14	8.59	6.06	2.53	50.5
13X-4, 22–24	119.72			5.02		41.8
14X-1, 74–76	125.34			5.42		45.1
14X-2, 74–76	126.84			4.10		34.2
14X-3, 74–76	128.34	nd	6.30	6.10	0.20	50.8
14X-4, 74–76	129.84			4.63		38.6
14X-5, 8–10	130.58			3.31		27.6
15X-1, 80–82	135.10			4.14		34.5
15X-2, 73–75	136.53			5.06		42.1
15X-3, 80–82	138.10	nd	4.55	4.35	0.20	36.2
15X-4, 8–10	138.88			2.40		20.0
16X-1, 68–70	144.58			4.12		34.3
16X-2, 55–57	145.95	0.06	2.78	2.74	0.04	22.8
16X-3, 68–70	147.58			4.50		37.5
17X-1, 67–69	154.27			5.57		46.4
17X-2, 75–77	155.85			5.73		47.7
17X-3, 75–77	157.35			7.11		59.2
17X-4, 75–77	158.85			4.00		33.3
17X-5, 39–41	159.99	0.07	5.53	5.40	0.13	45.0
17X-6, 9–11	161.19			5.02		41.8
18X-1, 72–74	163.92			3.61		30.1
18X-2, 47–49	165.17	nd	7.29	7.22	0.07	60.1
18X-CC, 12–14	165.80			7.96		66.3
19X-1, 46–48	173.36			5.47		45.6
19X-2, 46–48	174.86			4.54		37.8
19X-3, 32–34	176.22	nd	4.30	4.17	0.13	34.7
19X-4, 32–34	177.72			2.92		24.3
19X-CC, 20–22	178.15			3.82		31.8
20X-1, 48–50	182.98	0.08	4.99	4.87	0.12	40.6
21X-1, 20–22	192.30	0.07	5.58	5.59	0.00	46.6
21X-1, 95–97	193.05	0.06	1.62	1.55	0.07	12.9
21X-2, 20–22	193.80			6.97		58.1
21X-2, 71–73	194.31			5.57		46.4
21X-3, 34–36	195.44			5.72		47.6
21X-4, 46–48	197.06	0.08	3.97	3.85	0.12	32.1
21X-4, 64–66	197.24	nd	6.89	6.75	0.14	56.2
21X-5, 7–9	198.17	0.07	2.62	2.54	0.08	21.2
21X-5, 61–63	198.71	nd	7.11	7.04	0.07	58.6
22X-1, 72–74	202.52	nd	6.85	6.53	0.32	54.4
22X-CC, 39–41	203.35	nd	5.27	5.04	0.23	42.0
23X-1, 99–101	212.49			4.54		37.8
23X-2, 52–54	213.52	nd	3.90	3.39	0.51	28.2
23X-3, 46–48	214.96	nd	1.77	1.49	0.28	12.4
23X-4, 15–17	216.15			1.87		15.6
23X-5, 68–70	218.18			3.83		31.9
23X-6, 87–89	219.87			2.55		21.2
23X-7, 13–15	220.63			2.78		23.2
24X-1, 72–74	221.72	0.08	1.53	1.35	0.18	11.3
24X-1, 136–138	222.36	0.10	5.14	5.02	0.12	41.8
24X-2, 25–27	222.75			4.68		39.0
24X-2, 87–89	223.37			3.76		31.3
25X-1, 73–74	231.43	0.15	2.69	2.25	0.44	18.7
25X-2, 56–58	232.76	0.23	6.15	5.67	0.48	47.2
25X-3, 64–65	234.34			5.00		41.7
25X-4, 57–58	235.77			1.98		16.5
25X-5, 47–49	237.17			3.57		29.7
25X-6, 74–75	238.94			4.72		39.3
26X-1, 69–71	240.99			5.25		43.7
26X-2, 50–52	242.30			3.68		30.7
26X-3, 60–62	243.90			4.38		36.5
26X-4, 96–98	245.76			4.15		34.6
26X-5, 60–62	246.90			4.80		40.0
26X-6, 60–62	248.40			2.50		20.8
26X-7, 37–39	249.67			6.27		52.2
27X-1, 84–86	250.84			4.62		38.5
27X-2, 73–75	252.23			3.07		25.6
27X-3, 27–29	253.27	0.17	1.80	1.54	0.26	12.8
27X-CC, 13–15	253.81			3.08		25.7
28X-1, 78–80	260.38			3.89		32.4
28X-2, 62–64	261.72			1.66		13.8
28X-3, 65–67	263.25			1.62		13.5
28X-4, 65–67	264.75			2.80		23.3
28X-5, 73–75	266.33			3.49		29.1
28X-6, 56–58	267.66			2.49		20.7
29X-1, 56–58	269.76			3.72		31.0
29X-2, 47–49	271.17			4.61		38.4

Table 6 (continued).

Core, section, interval (cm)	Depth (mbsf)	Total nitrogen (wt%)	Total carbon (wt%)	Inorganic carbon (wt%)	Organic carbon (wt%)	$CaCO_3$ (wt%)
29X-3, 58–60	272.78			2.83		23.6
29X-4, 59–61	274.29			2.55		21.2
29X-5, 50–52	275.70	0.18	4.36	3.64	0.72	30.3
29X-6, 63–65	277.33	0.13	2.50	2.34	0.16	19.5
29X-7, 28–30	278.48			2.38		19.8
30X-1, 74–76	279.54			5.49		45.7
30X-2, 34–36	280.64			1.92		16.0
30X-CC, 22–24	281.67	0.16	4.67	4.22	0.45	35.2
31X-1, 37–39	288.87			5.25		43.7
31X-2, 68–70	289.66			4.03		33.6
31X-3, 54–56	291.02			3.28		27.3
32X-1, 69–71	294.69			2.56		21.3
32X-2, 65–71	296.15			2.43		20.2
32X-3, 65–67	297.65	0.13	4.73	4.03	0.70	33.6
32X-4, 42–44	298.92	0.11	3.56	3.31	0.25	27.6
32X-5, 70–72	300.70			3.73		31.1
32X-6, 58–60	302.08			4.07		33.9
33X-1, 20–23	303.70			4.97		41.4
33X-2, 16–18	305.16			3.15		26.2
33X-3, 63–67	307.13			1.14		9.5
33X-4, 29–31	308.29			3.98		33.2
33X-5, 134–137	310.84			2.60		21.7
33X-6, 37–40	311.37			3.27		27.2
33X-7, 22–25	312.72			3.64		30.3
33X-CC, 25–28	313.21			1.39		11.6
34X-1, 64–66	313.74	0.07	0.43	0.30	0.13	2.5
34X-CC, 33–35	314.92			0.95		7.9
35X-1, 40–42	322.90			4.11		34.2
35X-2, 37–39	324.37	0.06	5.15	5.16	0.00	43.0
35X-3, 41–43	325.91	0.03	1.82	1.80	0.02	15.0
35X-4, 133–135	328.33			4.58		38.2
35X-5, 138–140	329.88			0.63		5.2
35X-6, 60–62	330.60	0.06	8.26	8.26	0.00	68.8
35X-7, 8–10	331.58	0.09	8.66	8.63	0.03	71.9
35X-CC, 3–5	332.00			8.83		73.6
36X-1, 66–68	332.76			7.42		61.8
36X-2, 76–78	334.36	nd	5.56	5.57	0.00	46.4
36X-3, 62–64	335.72	0.08	8.29	8.38	0.00	69.8
36X-4, 50–52	337.10			6.69		55.7
36X-5, 9–11	338.19			7.10		59.1
36X-CC, 28–30	339.74			4.47		37.2
37X-1, 113–115	342.73			5.21		43.4
37X-2, 75–77	343.85			7.78		64.8
37X-3, 36–38	344.96	0.06	5.25	5.09	0.16	42.4
37X-4, 88–90	346.98	0.05	6.78	6.61	0.17	55.1
37X-5, 89–91	348.49			6.11		50.9
37X-6, 119–121	350.29			5.41		45.1
37X-7, 42–44	351.02			2.63		21.9
37X-CC, 29–31	351.35			6.32		52.6
39X-1, 136–138	362.26			6.93		57.7
39X-2, 29–31	362.69			5.74		47.8
40X-1, 142–144	371.92			4.27		35.6
40X-2, 81–83	372.81			5.28		44.0
40X-3, 62–64	374.12	0.11	4.30	4.31	0.00	35.9
40X-4, 82–84	375.82	0.09	2.62	2.44	0.18	20.3
41X-1, 94–96	381.14			2.05		17.1
41X-2, 37–39	382.07			2.58		21.5
41X-3, 44–46	383.64			2.19		18.2
41X-4, 96–98	385.66			2.44		20.3
41X-5, 83–85	387.03			2.18		18.2
41X-6, 41–43	388.11	0.08	4.15	4.02	0.13	33.5
41X-7, 10–12	389.30	nd	9.55	9.58	0.00	79.8
42X-1, 88–90	390.68	nd	10.57	9.14	1.43	76.1
42X-CC, 6–8	392.77	nd	2.06	1.99	0.07	16.6

nd = not detected. Total sulfur was below the detection limit of 0.06 wt% in all samples analyzed for total carbon, nitrogen, and sulfur.

Seawater sulfate decreases by about 10% as a result of these reactions.

Dissolved magnesium decreases with depth, especially as basement is approached (Fig. 9). This decrease is nearly matched by an increase in dissolved calcium, although this increase does not begin until about 120 mbsf. At shallower depths, calcium decreases as a result of $CaCO_3$ precipitation. Like magnesium, potassium decreases steadily with depth as a result of uptake into alteration minerals, mainly in basement. The increase in potassium relative to seawater in the near-surface sediments is probably an artifact of sampling and squeezing. Sodium, chlorinity, bromide, and salinity show relatively little change with depth (Figs. 9 and 10).

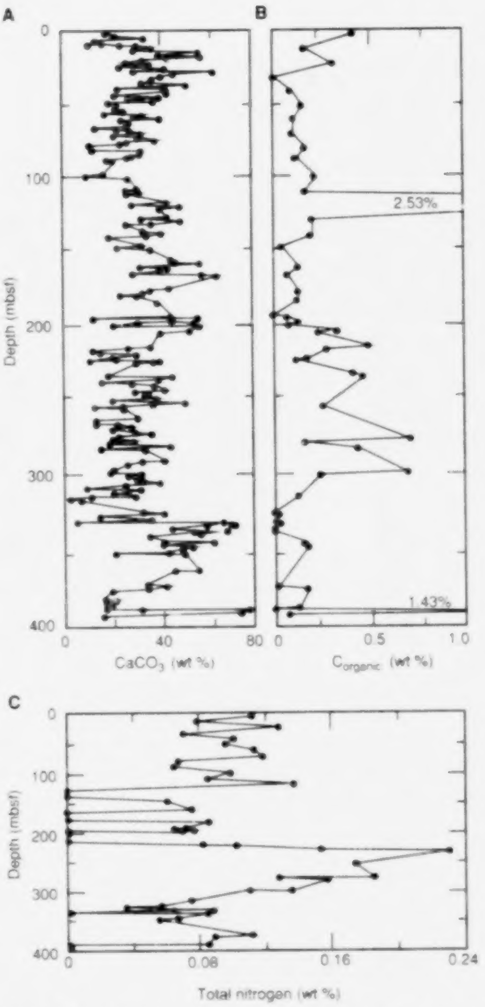

Figure 7. Calcium carbonate (A), total organic carbon (B), and total nitrogen (C) in sediments from Hole 782A.

PALEOMAGNETISM

Magnetic Remanence

Two holes (Holes 782A and 782B) were drilled at Site 782. Hole 782A had an overall core recovery of 59%. We identified many intervals of normal and reversed polarity within the hole. These data, when combined with the biostratigraphic data (see "Biostratigraphy" section, this chapter), enabled us to construct a preliminary magnetostratigraphy for the sediments in the upper 240 m of the hole. Unfortunately, the paleomagnetic data are less reliable below this level because of poor recovery. We hope that more detailed shorebased work will resolve the stratigraphy. Only a small amount (less than 1 m) of fragments of basement rocks unsuitable for paleomagnetic study was recovered in Hole 782B. The natural remanent magnetization (NRM) of the archive half of each core from Hole 782A was measured using the cryogenic magnetometer. Intensities vary widely from 1 to 800 mA/m. Most samples have values between 10 and 100 mA/m. There is no correlation between intensity and sub-bottom depth (Fig. 11). When the cores then were demagnetized at the 10-mT level and remeasured, intensities measured were about 10% to 40% of their initial values. The low latitude of the site can make determination of polarity difficult if the inclinations are very shallow. However, the magnetic directions in many of the cores have steep enough inclinations to allow one to interpret polarity unambiguously. In many cases, the cores record sharp polarity transitions (Fig. 12).

Table 7. Results of headspace-gas analyses of sediments at Site 782.

Core, section, interval (cm)	Depth (mbsf)	Methane (µL/L)[a]	Methane (µM)[b]
125-782A-1H-3, 0–3	3.02	12	1.0
2H-5, 0–3	15.82	11	1.0
3H-4, 140–145	25.23	11	1.0
4H-5, 0–5	34.83	13	1.1
5H-5, 0–5	44.32	12	1.0
6H-5, 0–5	53.82	10	0.9
7H-5, 0–5	63.32	14	1.2
8H-3, 0–3	69.82	16	1.4
9H-3, 0–3	79.32	17	1.5
10X-2, 0–3	87.32	12	1.1
11X-3, 0–3	98.72	12	1.0
12X-3, 0–5	108.33	11	0.9
13X-3, 0–5	118.03	11	0.9
15X-3, 0–5	137.33	11	1.0
16X-3, 0–5	146.93	10	0.9
18X-2, 0–3	164.71	9	0.8
19X-3, 0–3	175.92	10	0.9
23X-5, 0–3	217.52	9	0.8
24X-2, 0–3	222.52	10	0.9
26X-4, 0–3	244.82	9	0.8
29X-5, 0–3	275.22	9	0.8
30X-3, 0–3	281.82	10	0.9
32X-6, 0–3	301.52	12	1.0
35X-4, 0–3	327.02	9	0.8
37X-3, 0–3	344.62	10	0.9
39X-2, 0–3	362.41	11	0.9
41X-5, 0–5	386.22	12	1.0
42X-2, 0–3	391.32	9	0.8

[a] Microliters of methane per liter of wet sediment, assuming a sample volume of 4.2 cm^3 of sediment.

[b] Micromoles of methane per liter of interstitial water, assuming a porosity of 50%.

Many of the cores exhibit signs of drilling disturbance that range from slightly disturbed to disrupted (see the core descriptions and photos). Data from cores described as more than slightly disturbed were rejected for any analysis. However, note that the cores that were recorded as being moderately disturbed display stable magnetic behavior and record changes in magnetic polarity (Fig. 13). This suggests that the disturbance identified in the cores is, in some cases, only a surficial feature.

The magnetostratigraphy for Hole 782A is summarized in Figures 14A and 14B. Also shown are the magnetic polarity scale and the nannofossil zones taken from Berggren et al. (1985). Between 0 and 250 mbsf, the biostratigraphic data allow us to make reliable correlations with the magnetic polarity time scale of Berggren et al. (1985). Below this level, recovery was much poorer, and the biostratigraphic zonations are less precise, making correlations with the observed magnetostratigraphy more difficult. In addition, the sediments between 322 and 332 mbsf were deposited over 10 m.y., making any correlation with the magnetic polarity time scale for this interval impossible.

Past work from drill cores from the Philippine Sea Plate (Bleil, 1982) suggests that the Philippine Sea Plate has moved northward with time. Inclination data from Hole 782A have been separated into 100-m sections, grouped into 10° intervals, and plotted on histograms (Fig. 15). At all depths, the inclinations cluster at about +50° and −50°, suggesting that there has been little or no translation of the site since the late Eocene. However, the distribution of inclinations is dominated by normal polarity, suggesting that many of the rocks are carrying an overprint from the present magnetic field. This is particularly evident in the inclination data between 300 and 400 mbsf. In this interval, one finds more sediments having shallow magnetic inclinations; however, these data would not suggest the large amount of translation, as reported by Bleil (1982). Future shorebased work will better determine paleolatitudes for Hole 782A. Cores 125-782A-5H through 125-782A-9H were oriented using the multishot camera. However, these cores were frequently disturbed by the drilling process, which is reflected by the scatter in declinations. Thus, no rotation data could be obtained.

Magnetic Susceptibility

Whole-core magnetic susceptibilities were measured using the multisensor track (MST). Susceptibilities in the interval from 0 to 240 mbsf range between $6\pi \times 10^{-4}$ SI and $50\pi \times 10^{-4}$ SI and show little scatter. Below this, there is a small, but significant, increase in susceptibility as well as in the amount of dispersion. The increase in susceptibility does not correlate with an increase in the number of ash layers, but rather with an increase in the amount of induration in the sediments. A downhole plot of magnetic susceptibility from Hole 782A is presented in Figure 16.

SEDIMENT ACCUMULATION RATES

Estimates of sedimentation rates for Site 782 are based on calcareous nannofossil zones (Table 9) that were used to construct the age-depth curve shown in Figure 17.

Sedimentation rates in the latest Eocene/earliest Oligocene are extremely low, although only two biostratigraphic events are available for this period. A hiatus between the early and late Oligocene may be present (see "Biostratigraphy" section, this chapter). The estimated rate for the upper Oligocene section is about 4.9 m/m.y. The lower Miocene sequence is characterized by a hiatus. Sedimentation rates for the middle Miocene to late Pliocene sequences are estimated to be about 16.5 m/m.y. Thereafter, sedimentation rates increase to about 47.1 m/m.y. in the upper Pliocene section and are even higher in the Pleistocene.

PHYSICAL PROPERTIES

The high percentage of core recovered from Hole 782A allowed us to measure physical properties for the nearly 400 m of sedimentary section. Unfortunately, poor recovery of basement rocks prevented similar measurements. Physical- and index-property measurements are listed in Tables 10 and 11.

Thermal conductivities in the sedimentary section are clustered at about 1 W/mK (Table 11) and increase slightly and show greater scatter with depth (Fig. 18). This increased scatter may be related to drilling disturbance in the more compacted sediment at deeper levels in the hole. The presence of drilling biscuits supports this hypothesis.

Good quality data were obtained from the gamma-ray attenuation and porosity evaluator (GRAPE), especially for the APC cores (Cores 125-782A-1H through 125-782A-9H). GRAPE bulk densities increase downhole from about 1.6 to 1.95 g/cm^3 (Fig. 19). The amount of scatter increases downhole in a pattern similar to that seen in thermal-conductivity measurements and probably is also related to drilling disturbance. Detailed analyses of GRAPE data show a change in slope of density measurements at 373 mbsf (Fig. 20), which may correspond to changes in downhole measurements of velocity, density, and resistivity (see "Downhole Measurements" section, this chapter). The GRAPE density discontinuity at 373 mbsf is not apparent in the index-property data.

Index-property measurements (bulk and grain densities, porosity, and water content) agree well with GRAPE data (Table 10). Bulk densities derived from measurements of discrete samples show a similar increase with depth to those observed in GRAPE data (Fig. 21). Less scatter was observed in the bulk density of discrete samples than in the GRAPE measurements because the discrete samples were taken from coherent blocks, thus avoiding zones of disturbed core. Grain densities display no depth variability, but instead are nearly constant at 2.8 to 2.9 g/cm^3.

Compressional-wave velocities were determined for the uppermost portion of the core using the *P*-wave logger on the MST. Velocity was constant at 1550 m/s in the APC cores (Fig. 22). These data are in good agreement with values obtained from logging the hole (see "Downhole Measurements" section, this chapter). No velocity information was retrieved from cores in the interval from 70 to 270 mbsf because of poor coupling of the *P*-wave-logger transducers on XCB cores and because we could not measure velocities in poorly consolidated core on the Hamilton frame.

Hamilton-frame velocities were measured for lithified sedimentary rocks recovered from 265 to 390 mbsf (Table 11), both in the "A" direction (propagation direction parallel to the core axis) and in the "B" direction (normal to the axis of the cores). Both "A" and "B" direction velocities increase from about 1680 to 2000 m/s over the measured interval (Fig. 23). The sample velocities are isotropic.

Electrical resistivity was measured for every other section from the cores of Hole 782A (Table 11). Values range from 16 to 41 ohms, averaging about 20 ohms (Fig. 24). Resistivity increases slightly with depth. No measurements were taken below 278 mbsf because of increasing consolidation, which prevented probe insertion.

DOWNHOLE MEASUREMENTS

Logging Operations

During logging at Site 782 we used two logging strings. The first string consisted of the temperature logging tool (TLT), phasor induction tool (DIT), lithodensity tool (HLDT), and the sonic tool (SDT). The second string consisted of the temperature logging tool (TLT), the natural gamma-ray spectrometry tool (NGT), aluminum clay tool (ACT), general purpose instrumentation tool (GPIT), compensated neutron tool (CNT), and the induced gamma-ray spectrometry (GST) tool.

Logging commenced at 1150UTC on 22 March with the deployment of the first string. When this string reached the seafloor, we halted it for 8 min to record a seawater temperature for reference to the logged values. At 1330UTC the string was out of the drillpipe at 105 mbsf. The sonic logs (both

Table 8. Composition of interstitial waters from sediments at Site 782.

Sample no.	Core, section, interval (cm)	Volume (mL)	Squeeze T (°C)	Depth (mbsf)	pH	Salinity (R.I., ‰)	Salinity (calc., ‰)	Chlorinity (mmol/kg)	Alkalinity (meq/kg)	Sulfate (mmol/kg)	Sodium (mmol/kg)	Potassium (mmol/kg)
Surface seawater (17 March 1989)					8.25	35.6	34.654	539.2	2.689	27.78	552.0	10.11
IW-1	782A-1H-3, 145–150	45	3	4.48	7.86	35.4	34.996	545.5	3.279	26.44	468.9	12.11
IW-2	782A-2H-4, 145–150	50	2	15.78	7.71	35.1	35.149	548.4	3.291	26.60	471.3	11.07
IW-3	782A-3H-4, 145–150	51	2	25.28	7.62	35.4	35.259	549.4	3.229	26.93	474.6	10.99
IW-4	782A-4H-4, 145–150	32	2	34.78	7.69	36.0	35.031	546.5	2.829	26.85	470.6	10.74
IW-5	782A-5H-4, 145–150	44	3	44.28	7.75	35.5	35.023	546.5	3.254	26.40	471.0	11.06
IW-6	782A-7H-4, 140–150	52	3	63.25	7.89	35.3	35.233	550.4	3.281	25.86	477.9	11.56
IW-7	782A-11X-2, 145–150	32	4	98.68	7.91	35.1	34.809	546.5	2.987	24.92	470.6	10.55
IW-8	782A-13X-2, 140–150	55	5	117.95	7.83	34.9	34.881	546.5	2.376	25.76	473.4	9.94
IW-9	782A-16X-2, 140–150	63	6	146.85	7.76	35.0	34.767	545.5	2.420	25.21	471.9	9.95
IW-10	782A-19X-2, 140–150	48	6	175.85	7.88	35.0	34.673	544.6	2.271	25.23	470.8	8.73
IW-11	782A-23X-4, 140–150	49	8	217.45	7.82	35.1	34.696	546.5	1.913	24.71	469.0	9.49
IW-12	782A-26X-3, 140–150	51	8	244.75	7.75	35.2	34.733	545.5	2.259	25.08	469.1	9.03
IW-13	782A-29X-4, 140–150	46	8	275.15	7.88	36.1	34.819	547.7	1.754	24.82	471.9	8.98
IW-14	782A-32X-5, 140–150	54	9	301.45	7.65	35.1	34.042	548.7	1.733	26.25	472.9	8.27
IW-15	782A-35X-3, 140–150	50	9	326.95	7.57	35.1	34.877	546.8	2.167	25.28	471.9	7.74
IW-16	782A-39X-1, 140–150	48	10	362.35	7.73	35.2	34.659	543.9	1.426	24.90	469.3	7.54
IW-17	782A-42X-1, 140–150	31	10	391.25	7.82	35.0	34.590	542.9	1.233	24.75	469.3	7.23

short and long) were erratic because of skipped cycle induced by rugose hole conditions. The string touched down at 1414UTC at 453 mbsf; the return logging run began at 1422UTC and reached the pipe at 1534UTC. We completed a short duplicate run in the upper part of the hole and then returned the tool string to the surface at 1607UTC.

The second logging run (using the second, geochemical, string) commenced at 1930UTC and included an 8-min-calibration stop for the TLT near the seafloor. The tool string reached the bottom of the hole (453 mbsf) at 2130UTC. Uphole logging began at 2145UTC and reached the drillpipe at 2356UTC. Logging continued in the drillpipe to 10 m above

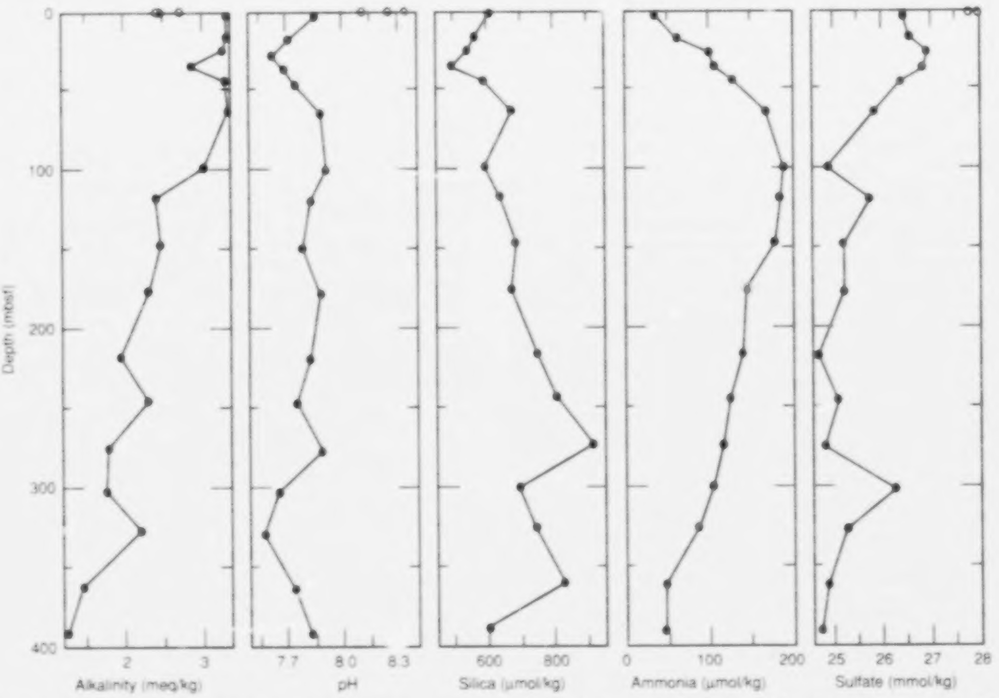

Figure 8. Composition of interstitial waters (alkalinity, pH, silica, sulfate, ammonia) from sediments at Site 782 (solid circles) compared with surface seawater collected 22 February, 4 March, and 17 March 1989 (open circles).

Table 8 (continued).

Calcium (mmol/kg)	Magnesium (mmol/kg)	Bromide (mmol/kg)	Silica (μmol/kg)	Ammonia (μmol/kg)
10.18	52.48	0.81	0	10
9.69	50.62	0.82	610	35
9.62	51.63	0.81	566	61
9.46	51.00	0.92	544	101
9.56	51.30	0.88	493	107
9.27	50.96	0.90	591	128
8.95	49.01	0.86	677	169
9.30	49.76	1.06	595	190
9.26	49.25	0.81	642	185
9.78	48.49	0.90	687	179
10.26	48.64	0.88	673	145
11.17	48.52	0.93	751	138
12.45	47.47	0.91	806	122
13.32	45.82	0.84	917	115
15.07	45.79	0.83	694	102
17.27	42.65	0.86	745	83
20.33	38.81	0.89	827	45
22.31	36.28	0.88	597	42

the seafloor. Two more runs were made in the drillpipe for calibration purposes, one of which required raising the drill string by 2 m. The second pass ended at 0308UTC, 23 March, when the tool string was brought to the surface.

A third logging run (using the magnetic susceptibility tool) then was attempted. The tool failed because of water leakage into the instrument package, and logging at Site 782 was abandoned.

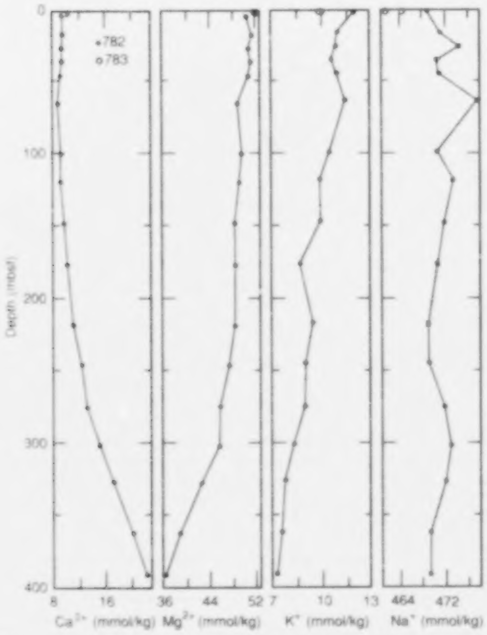

Figure 9. Composition of interstitial waters (calcium, magnesium, potassium, sodium) from sediments at Site 782 (dots) compared with surface seawater collected 22 February, 4 March, and 17 March 1989 (open circles).

Results

Logging results for Hole 782B are presented in Figures 25 through 32. The measurements define four units above basement at Site 782: a first unit from above the end of the drill pipe (about 100 mbsf) to 208 mbsf (Figs. 25–28); a second unit from 208 to 305 mbsf; a third unit from 305 mbsf to 373 mbsf (Figs. 29 and 30); and a fourth unit from 373 mbsf to basement at 409 mbsf (Figs. 31 and 32).

First Unit

The first unit (to 208 mbsf) contains lithologic Subunit IA and the upper part of lithologic Subunit IB. The gamma-ray logs show a broad-scale variation within this unit, with the CGR log varying between 6 and 24 API units (averaging about 14), and the SGR log varying between 14 and 25 API units (averaging about 18). The resistivity log values are about 0.8 to 0.9 ohm-m, with a slow increase with depth. The IDPH log consistently has a slightly higher reading throughout this hole; thus, it may have a slight instrument-calibration error. The caliper log shows that the hole is 0.38 to 0.43 m (15 to 17 in.) in diameter, with scattered washouts to more than 0.48 m (19 in.). This log also indicates scattered small anomalies in hole diameter with an approximate 10-m interval (Fig. 25). These anomalies may be related to washouts that occur when pipe sections are being added, and downward progress of the pipe string is momentarily stopped. Bulk density (as shown in the RHOB curve) is fairly constant at 1.65 to 1.7 g/cm^3. Porosity (PHI) gradually

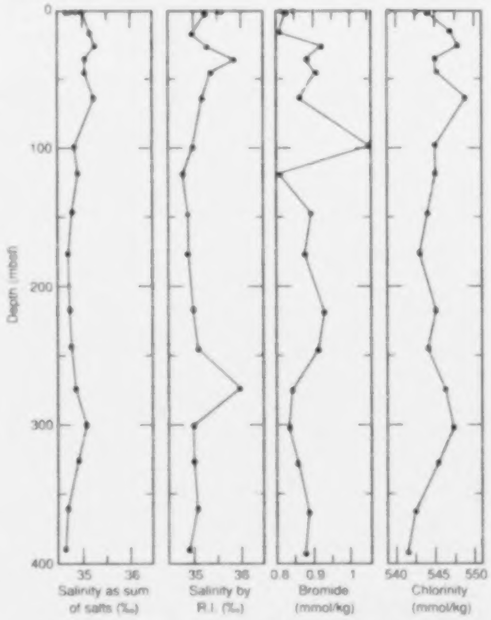

Figure 10. Composition of interstitial waters (salinity, bromide, chlorinity) from sediments at Site 782 (dots) compared with surface seawater collected 22 February, 4 March, and 17 March 1989 (open circles).

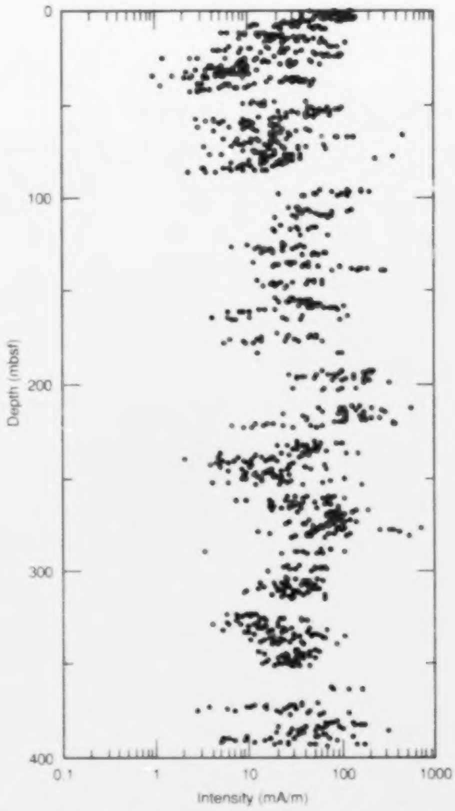

Figure 11. A downhole plot of magnetic intensity for Hole 782A.

decreases with depth to 60% at the base of the unit. The photoelectric effect (PEF) is constant at 2.8 to 3.0. *P*-wave velocity is constant, near 1.65 km/s.

The chemical composition of the unit is variable, despite its uniform appearance and physical properties. SiO_2 content averages about 40%, but varies from 0% to 80%. CaO content averages about 30% and varies from 0% to 50%, generally complementary to SiO_2. Al_2O_3 content is in the range of 15% to 18%, but sometimes reaches 35%. MgO is variable, ranging between 0% and 16%, but is generally found in a layer of about 10%. Elements having lower abundances and less variation include sulfur at 1%, K_2O at 1% to 1.4%, Fe_2O_3 at 1% to 1.5%, and TiO_2 at 0.5% to 1.0%. Trace elements include gadolinium at about 3 ppm (with a few increases to 10 ppm), uranium at about 1 ppm, and thorium at about 1 ppm.

Second Unit

The second unit (208–305 mbsf) is within lithologic Subunit IB. This unit has a gradational boundary with the overlying first unit, but also has an abrupt boundary with the underlying third unit. The gamma-ray logs are more uniform than in the first unit, with CGR values at 20 API units and SGR values at 23 API units. The gamma-ray logs do show two layers of increased values in the bottom few meters of this unit, with values as high as 35 API units in the layer at the very bottom. Resistivity values grade up from 0.8 ohm-m at the upper boundary to 1.0 ohm-m within the unit. Values distinctly increase at the lower boundary. The increasing resistivity with depth reflects increasing consolidation of the sedimentary section. The caliper log shows that the hole is fairly uniform in size (between 0.38 to 0.43 m) in this unit. One washout occurs near the top of the unit and the 10-m-interval anomalies also occur in this unit. Bulk density shows a gradual increase from 1.65 to 1.75 g/cm^3 in the layer just at the bottom of the unit. The photoelectric effect also shows a gradual increase from 2.5 to 3.0 within this unit. Porosity is uniform at 60%, aside from one large increase at 233 mbsf. *P*-wave velocity increases gradually from 1.75 to 1.85 km/s.

The elemental logs show that the dominant composition is SiO_2 at 40%, with a range of from 10% to 70%. Despite the wide range, variability is not as great as in the first unit. CaO is the second most abundant component; it generally varies in a complementary manner to SiO_2. Typically, CaO values are 30%, and the range is from 0% to 45%. The percentage of Al_2O_3 in the second unit is distinctly higher than in the first unit, averaging about 25%. The variability in Al_2O_3 also is

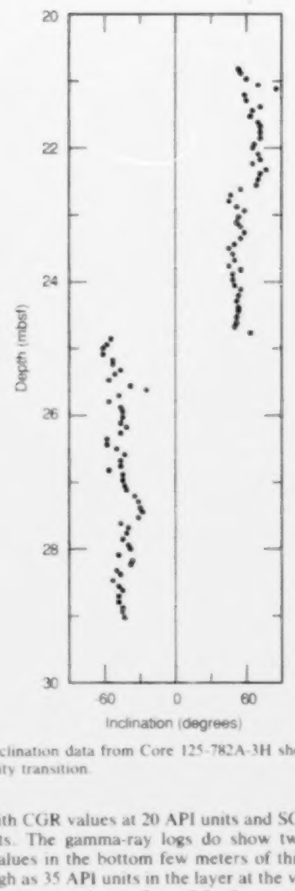

Figure 12. Inclination data from Core 125-782A-3H showing a well-defined polarity transition.

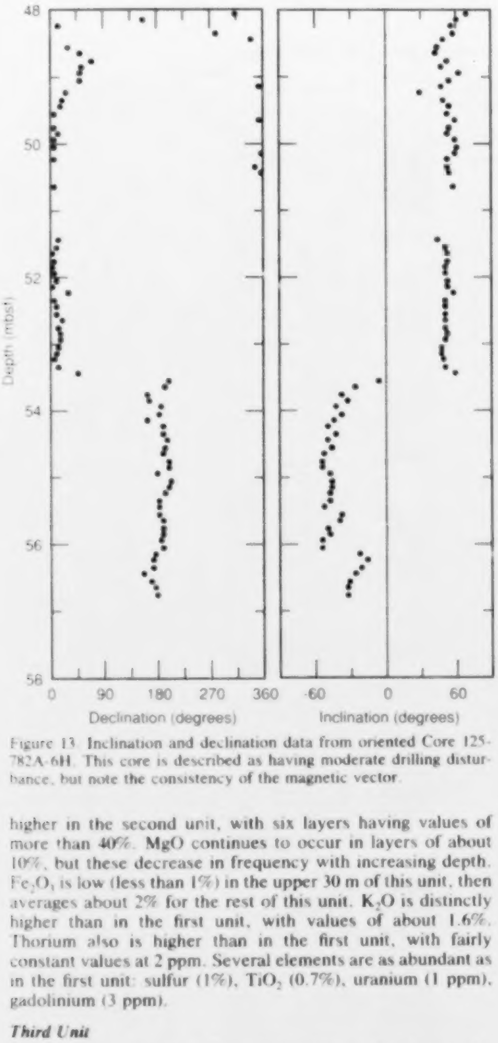

Figure 13. Inclination and declination data from oriented Core 125-782A-6H. This core is described as having moderate drilling disturbance, but note the consistency of the magnetic vector.

higher in the second unit, with six layers having values of more than 40%. MgO continues to occur in layers of about 10%, but these decrease in frequency with increasing depth. Fe_2O_3 is low (less than 1%) in the upper 30 m of this unit, then averages about 2% for the rest of this unit. K_2O is distinctly higher than in the first unit, with values of about 1.6%. Thorium also is higher than in the first unit, with fairly constant values at 2 ppm. Several elements are as abundant as in the first unit: sulfur (1%), TiO_2 (0.7%), uranium (1 ppm), gadolinium (3 ppm).

Third Unit

The third unit extends from 305 to 373 mbsf and spans the transition from lithologic Subunit IB to Subunit IC at 337.0 mbsf. The third unit has distinct differences in composition and physical properties from its neighboring units. The gamma-ray logs abruptly decrease to uniform values of 15 API units for both SGR and CGR. Resistivity values increase abruptly to 1.5 ohm-m at the top of the unit and to 2.0 ohm-m within the unit in two less well-defined steps. The caliper log shows that the hole opens up to a diameter of 0.43 m at the top of the unit, then gradually widens to more than 0.48 m. Bulk density is slightly higher (at 1.75 to 1.8 g/cm^3) than in the second unit. The PEF effect is also slightly higher than in the second unit at 3.0 to 3.2. Porosity values decrease and become more variable, ranging between 40% and 65%. *P*-wave velocities increase from 1.85 to 2.15 km/s. Velocity values exhibit small-scale variability, with some layers having velocities of 2.8 km/s.

The composition of the third unit is also distinct from the overlying second unit. CaO is higher (at 40%–45%) and then slowly decreases down the section. SiO_2 is lower (at 30%–35%) and is somewhat more variable, ranging from 12% to 55%. SiO_2 increases down the section. Abundance of Al_2O_3 is slightly lower than in the second unit (at 18%) and is not as variable as in that unit. The abundance of MgO continues to occur in layers from 0% to 10%. A number of elements have similar values to those in the second unit: Fe_2O_3 (1%–2%), sulfur (1%), TiO_2 (~0.8%), and gadolinium (~4 ppm). The abundances of the radioactive elements are lower in the third unit than in the second: K_2O (slightly lower at 1.4%), thorium (much lower at 1 ppm), and uranium (much lower at 0.6 ppm trending down to 0 ppm at the base of the unit).

Fourth Unit

The fourth unit defined by logging results extends from 373 to 409 mbsf. This unit contains pebble-rich sands and gravelly conglomerates found at the base of lithologic Subunit IC. Physical-property logs show abrupt changes from values of the third unit. Gamma-ray values are about 20 API units for both SGR and CGR. Resistivity values show a sharp increase, which then tails off and ends at 6 to 7 ohm-m. These values decline sharply to 3 ohm-m at 390 mbsf, then gradually rise to 5 ohm-m at the base of the unit. The *P*-wave velocity is variable, but averages 2.4 km/s above 390 mbsf and 2.1 km/s below that depth. The caliper log shows that the hole decreases gradually to 0.43 m diameter at 383 mbsf, after which it opens up again. The diameter then sharply decreases to a uniform value of 0.32 m below 397 mbsf. Bulk densities show an irregular increase from 1.75 to 2.1 g/cm^3, with scattered layers as high as 2.35 g/cm^3. The PEF effect is somewhat less than in the third unit, at 2.5 to 3.0.

Elemental abundances show abrupt changes from the overlying unit. SiO_2 increases down the section from 50% to 70%. CaO shows a dramatic decrease to about 10%. MgO is much higher at 10% to 20% and is present throughout most of the unit. MgO disappears at the base of the section. Al_2O_3 has an increased variability, although the average value is about the same at 20%. Sulfur values are slightly higher at 1.5%; TiO_2 is also slightly higher at 1%. Values of gadolinium are distinctly higher at 6 to 7 ppm. Concentrations of the radioactive elements are higher, with uranium and thorium at about 1 ppm. K_2O increases to 2% and then decreases to 1% down the section.

Basement

The final logging unit is the basement below 409 mbsf (lithologic Unit II). The basement does not stand out from the fourth unit in the same way that the fourth unit is distinct from the third. Gamma-ray values for CGR and SGR increase to 25 API units. Resistivity is constant at 4 to 5 ohm-m to 423 mbsf, where it decreases to 3 ohm-m. Below 433 mbsf, resistivity gradually increases to 9 or 10 ohm-m at the bottom of the hole. The caliper log shows that the hole opens from 0.32 m to 0.48 m, then gradually decreases to 0.28 m. Bulk density is constant near 2.05 g/cm^3. The PEF effect increases to 3.2, then decreases to 2.5 below 423 mbsf. *P*-wave velocity is fairly constant at 2.8 to 3.0 km/s.

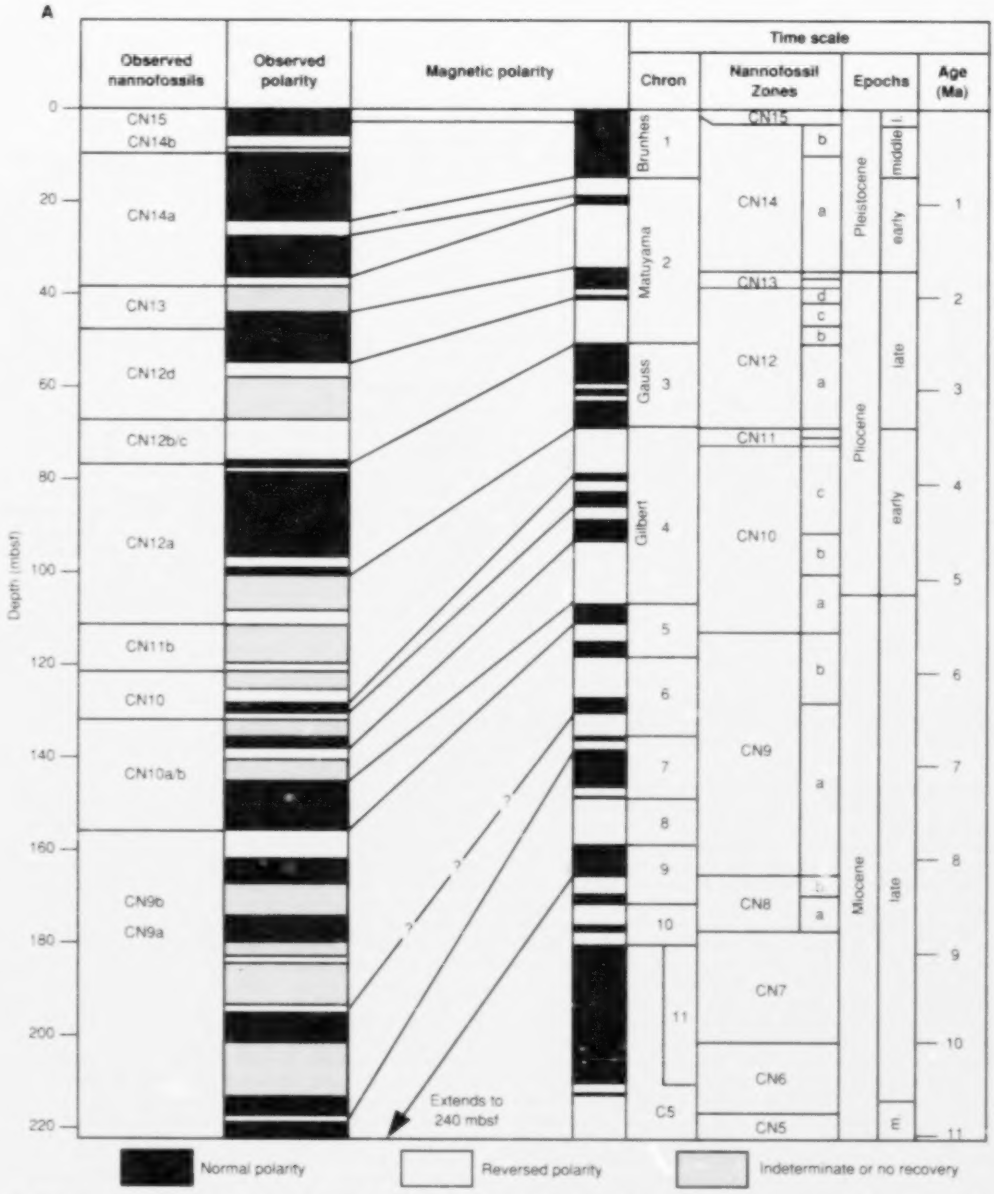

Figure 14. A. Observed magnetostratigraphy of Hole 782A for the interval from 0 to 220 mbsf, correlated with time scale of Berggren et al. (1985). B. Observed magnetostratigraphy of Hole 782A for the interval from 220 to 420 mbsf, correlated with time scale from Berggren et al. (1985).

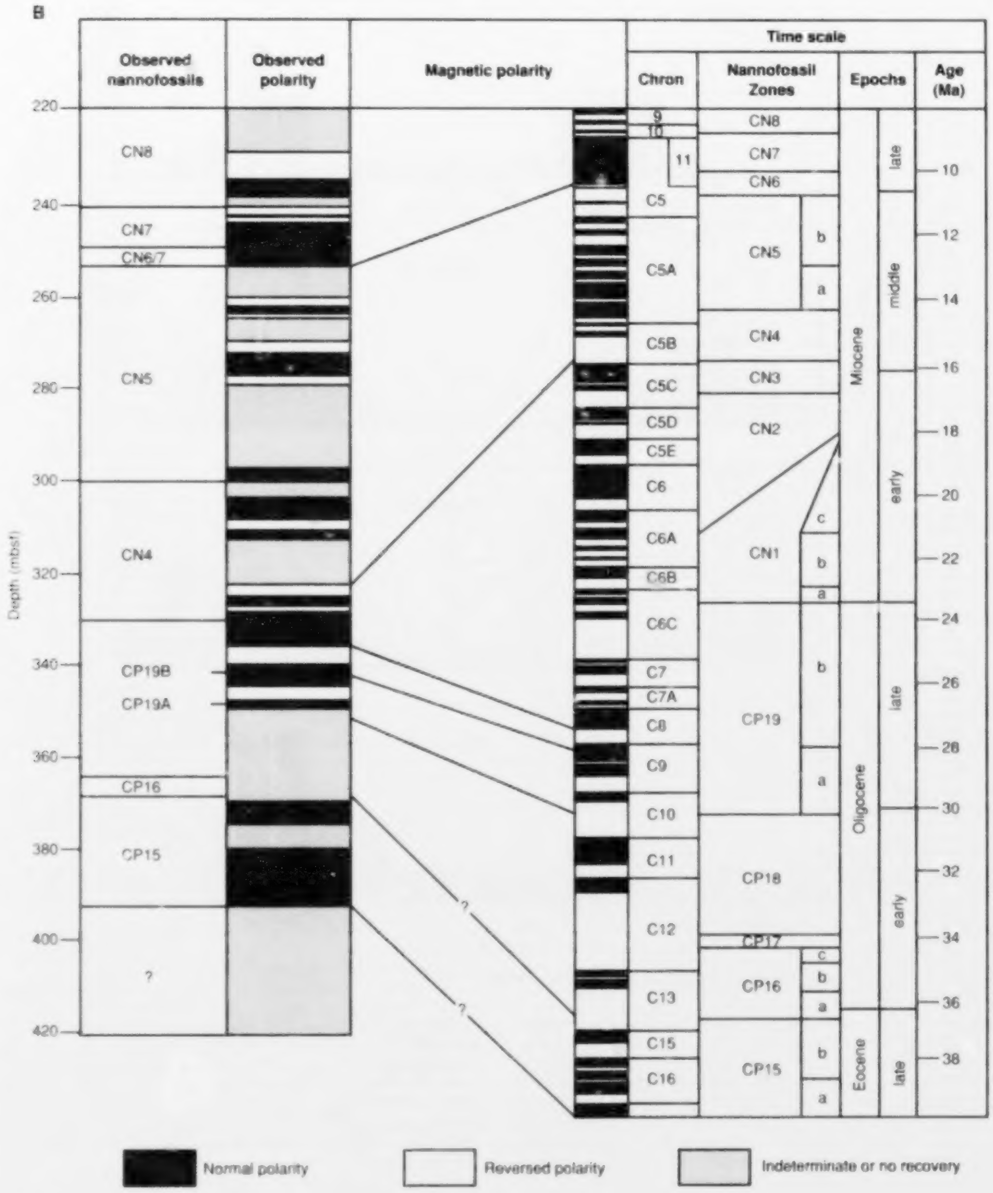

Figure 14 (continued).

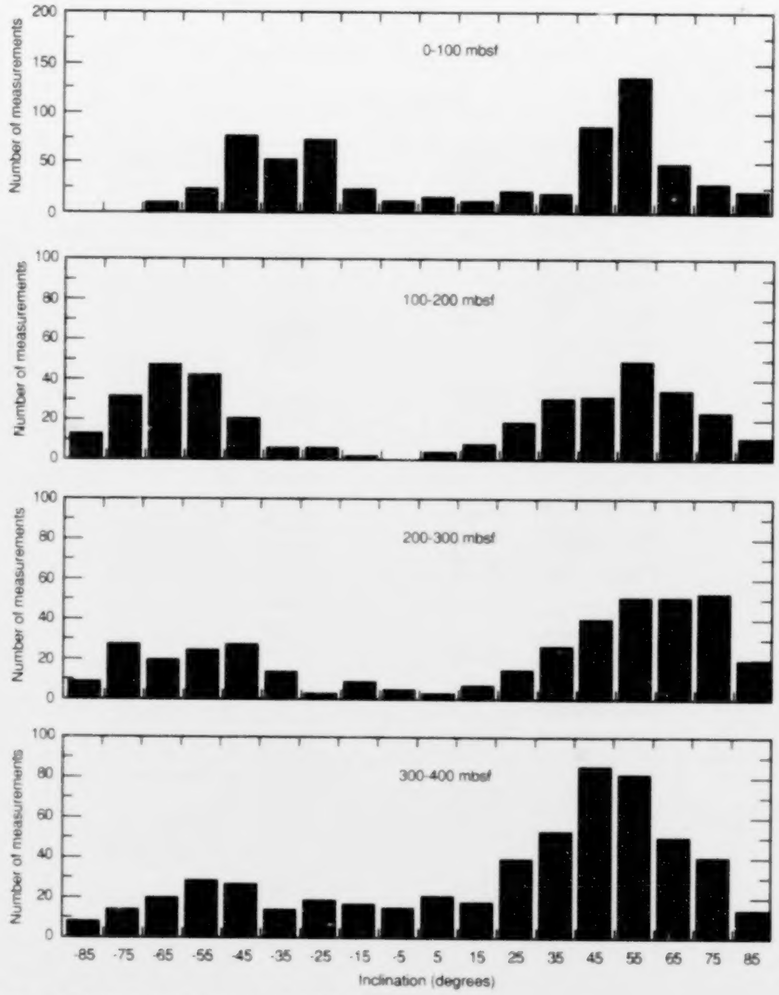

Figure 15. Inclination distribution as a function of depth.

Elemental logs show that SiO_2 is highly variable and ranges between 40% and 70%. CaO is fairly constant at near 10%. Al_2O_3 decreases from 20% down the section, but scattered layers have high values. Abundances of MgO increase from 15% to 20%. Percentages of Fe_2O_3 are higher in the fourth unit, increasing to 4%. Abundance of sulfur is somewhat lower at 1%. TiO_2 is similar at 1%, as is the concentration of gadolinium at 6 ppm. K_2O increases to a uniform 2%, whereas uranium remains steady at 0.7 ppm, and thorium also remains steady at 1 ppm.

Ashes and Magnetic Logs

A three-axis magnetic log is presented in Figure 28, along with an enlarged-scale plot of the vertical component. The logging string is not stabilized in the hole and has no other reference for orientation; thus, these logs primarily show the rotation of the tool during the logging run. In other areas, such as off the Oman margin during Leg 117, the vertical component was correlated successfully with mineralogy (Prell, Niatsuma, et al., 1989). The data here show only an inverse correlation with the *Y* component at Hole 782B, indicating a slightly deviated hole.

More than 100 ash layers were recognized in the cores recovered from Site 782 (see "Lithostratigraphy" section, this chapter). We were unable to correlate any of the logs (including the magnetometer logs; Fig. 28) with the ash layers. The tools in the logging string generally have a resolution of 15 cm or more, whereas the ash layers are generally less than 1 cm

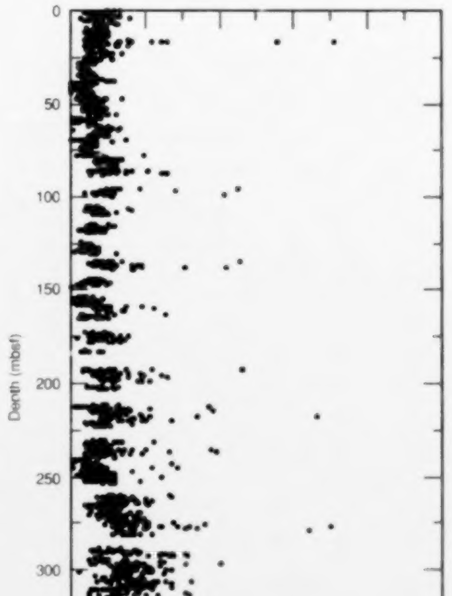

Figure 16. A downhole plot of susceptibility for Hole 782A.

thick. As mentioned previously, the susceptibility tool was deployed but failed to operate.

Heat-Flow Measurements

Two measurements were attempted with the Barnes-Uyeda heat-flow tool at 38.3 and 66.8 mbsf. The results are presented in Figures 33 and 34. Neither run obtained a useful *in-situ* temperature because of excessive motion during logging.

Results from the two TLT runs are shown in Figures 35 and 36. The temperature at the bottom of the hole was about 4.75°C during the first run, but warmed to about 5.75°C during the second run. Engineering data for the hole's drilling and pumping-rate history will be used to construct a time-dependent thermal model for the drill hole. This thermal model will enable us to determine the equilibrium temperature profile for the hole.

Measurements of thermal conductivity (Fig. 37), its inverse thermal resistivity (Fig. 38), and the depth integral of thermal resistivity (Fig. 39) will be used with the temperature profile to determine heat flow at this hole.

Table 9. Biostratigraphic data used to plot the age-depth curve in Figure 17.

Biostratigraphic event		Depth (mbsf)	Age (Ma)
Calcareous nannofossils			
Emiliania huxleyi	FO	9.8	0.26
Pseudoemiliania lacunosa	LO	28.8	0.4
Calcidiscus macintyrei	LO	33.2	1.45
Gephyrocapsa oceanica	FO	38.3	1.66
Discoaster brouweri	LO	57.3	1.98
D. surculus	LO	76.3	2.4
Reticulofenestra pseudoumbilica	LO	115.0	3.4
P. lacunosa	FO	124.6	3.5
Amaurolithus tricorniculatus	LO	134.4	3.6
D. quinqueramus	LO	163.2	5.6
D. neohamatus	LO	221.0	8.3
D. kugleri	LO	251.1	10.8
C. floridanus	LO	280.5	13.0
Sphenolithus heteromorphus	LO	313.1	14.4
D. bisectus	LO	332.1	23.7
S. ciperoensis	FO	363.5	30.1
C. grandis	LO	387.6	39.6
D. bifax	LO	389.8	42.2

For source of age and depth information, see "Biostratigraphy" section, this chapter.

SUMMARY AND CONCLUSIONS

Site 782 (30°51.66′N, 141°18.85′E, 2958.9 mbsl) is located on the eastern margin of the Izu-Bonin forearc basin, about halfway between the active volcanic arc and the Izu-Bonin trench. Two holes were drilled: Hole 782A, a 476.8-m hole that was fully cored and described; and Hole 782B, a 468.9-m hole, of which only the last 9.5 m was cored and described, but that was used for two logging runs (Fig. 40).

Two lithologic units, the first of which is sedimentary and made up of three subunits, the second of which comprises volcanic basement, have been defined at Site 782: Unit I, Subunit IA (0–153.6 mbsf in Hole 782A) is Holocene(?) to lower Pliocene, gray to yellow-greenish, homogeneous, nannofossil marl containing scattered volcanic debris and volcanic ash layers; Unit I, Subunit IB (153.6–337.0 mbsf in Hole 782A) is upper to middle Miocene, light to dark gray, nannofossil marl containing scattered volcanic debris and volcanic ash layers; Unit I, Subunit IC (337.0–409.2 mbsf in Hole 782A) is upper Oligocene to middle Eocene, vitric nannofossil chalks intercalated with tuffaceous sediment and also (aear the base) pebble-rich sands, gravelly conglomerates, and numerous ash layers; Unit II (409.2–476.8 mbsf in Hole 782A and 459.3–468.9 mbsf in Hole 782B) comprises angular to subrounded clasts of intermediate-acid lava.

Sedimentation rates increased from the upper Oligocene section (about 5 m/m.y) through the upper Miocene and lower Pliocene sections (about 16.5 m/m.y.), to the upper Pliocene section (about 47 m/m.y.), with a possible decrease in sedimentation rate in the Pleistocene section. Two possible unconformities were identified in the succession: one between the uppermost Oligocene and middle Miocene sections, the other between the lower Oligocene and upper Oligocene sections. The sediments exhibit common slump structures, burrows, and normal and reverse grading. More than 100 volcanic ash layers were identified in the cored section. Volcanogenic materials in the ash and dispersed within the sediments include primary materials (glass, opaque minerals, feldspar, pyroxenes, and amphibole), together with their alteration products (chlorite, glauconite, zeolite, and epidote group minerals).

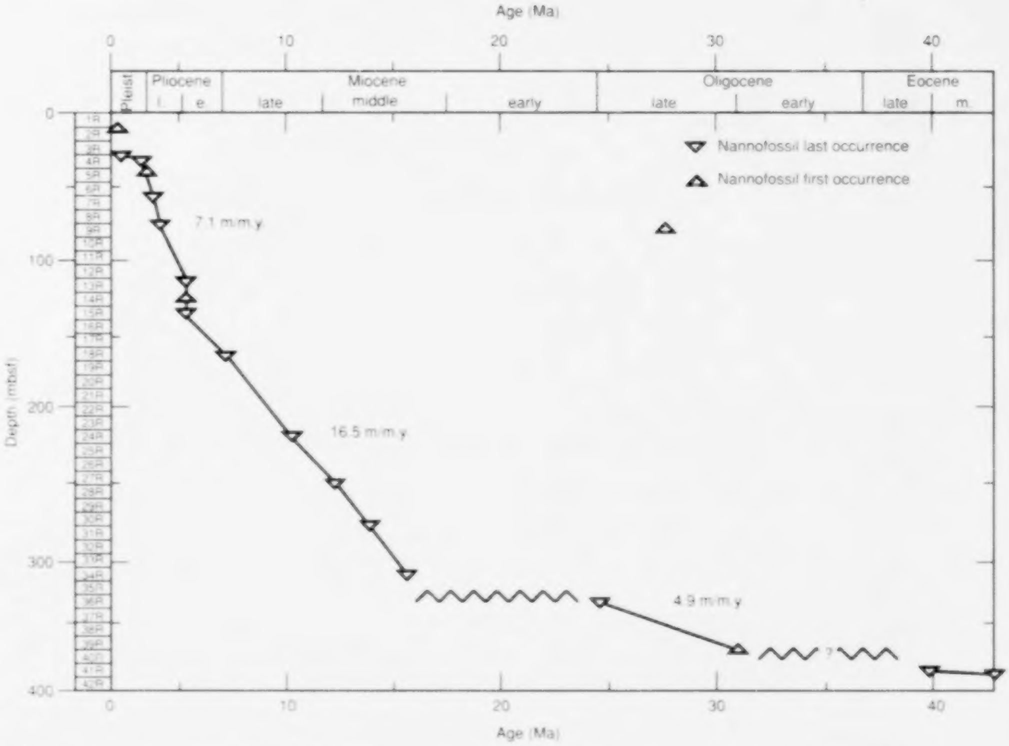

Figure 17. Age and depth curve for Site 782 showing estimated sedimentation rates. Ages determined are described in the text.

The lavas of Unit II typically are slightly vesicular and contain phenocrysts of plagioclase, orthopyroxene, and clinopyroxene in a glassy groundmass. Some may be pillow fragments. Geochemical data show that these phenocrysts fall into two compositional groups, an andesite group and a dacite-rhyolite group, and that they are transitional between the tholeitic and calc-alkaline volcanic-arc series. The andesites have low magnesium contents and thus are distinct from the high-magnesium bronzite andesites of similar age reported from other, more eastern, parts of the Izu-Bonin-Mariana forearc.

Interstitial fluids in lithologic Unit I have seawater pH, sodium, and chlorinity values throughout the section. In response to water-mineral reactions, potassium (from 12 to 7 mmol/kg) and magnesium (from 50 to 36 mmol/kg) decrease steadily with depth, whereas calcium increases from 9 to 22 mmol/kg and silica increases from 600 to a maximum of 900 mmol/kg at about 300 m. Ammonia increases from 35 to a maximum of 190 mmol/kg at about 150 m as a result of bacterial breakdown of organic matter.

Studies of physical properties in Hole 782A reveal thermal conductivities within Unit I of about 1 W/mK and bulk densities that increase downhole within Unit I from 1.6 to 1.95 g/cm^3. Porosities of the sediments decrease downhole from 70% to 60%, with a discontinuity at about 280 mbsf (middle Miocene). Magnetic susceptibilities increase downhole in response to the amount of induration of the sediment. Magnetic inclination data from Hole 782A cluster around +50° and −50°, indicating little or no translation of the site since the late Eocene. However, declinations are scattered because of core disturbance; thus, no data for the extent of rotation could be obtained.

Logging enabled us to divide Hole 782B into three distinct units according to its physical and chemical properties: an upper unit from 0 to about 300 mbsf; a middle unit from about 300 to about 370 mbsf; and a lower unit from about 370 mbsf to the lower limit of logging at about 420 mbsf. The boundary between the upper and middle units is marked by a sudden downhole increase in density and resistivity and may correspond to an increase in sediment compaction or to the Miocene unconformity. The boundary between the middle and lower units is marked by an increase and greater variability in compressional-wave velocity and density, together with an increase in silica and potassium. This boundary may correspond to the Oligocene unconformity.

The principal results of this site are (1) the identification of Eocene basement in this part of the forearc basin, (2) the characterization of the uppermost basement as intermediate-acid submarine volcanic rocks of island-arc tholeiite to calc-alkaline affinities, (3) paleomagnetic evidence that no major translation of the site has occurred since the Eocene, and (4) the recognition that the greatest sedimentation rate is seen in

Table 10. Index properties for Hole 782A.

Core, section, interval (cm)	Depth (mbsf)	Bulk density (g/cm³)	Grain density (g/cm³)	Porosity (%)	Water content (%)	Void ratio
125-782A-1H-1, 76–78	0.76	1.62	2.83	67.5	44.3	0.67
1H-2, 76–78	2.26	1.62	2.68	64.7	42.5	0.65
1H-3, 76–78	3.76	1.63	2.68	64.3	42	0.64
1H-4, 76–78	5.26	1.62	2.69	64.6	42.3	0.65
1H-5, 76–78	6.76	1.54	2.57	66.9	46.1	0.67
1H-6, 76–78	8.26	1.61	2.61	63.4	41.7	0.63
1H-7, 29–31	9.29	1.63	2.7	64.2	41.8	0.64
1H-CC, 13–8	9.68	1.62	2.55	61.5	40.3	0.61
2H-1, 74–76	10.54	1.57	2.48	62.8	42.4	0.63
2H-2, 61–63	11.91	1.54	2.77	70.7	48.6	0.71
2H-3, 65–67	13.45	1.59	2.72	67.1	44.8	0.67
2H-4, 61–63	14.91	1.58	2.61	65.6	44.2	0.66
2H-5, 61–63	16.41	1.64	2.61	61.5	39.7	0.61
2H-6, 76–78	18.06	1.61	2.73	66	43.5	0.66
2H-7, 30–32	19.1	1.69	2.77	62.5	39.3	0.63
3H-1, 79–81	20.09	1.31	2.01	71.4	57.8	0.71
3H-2, 79–81	21.59	1.62	2.62	63.1	41.4	0.63
3H-3, 79–81	23.09	1.57	2.66	67	45.2	0.67
3H-4, 78–80	24.58	1.55	2.63	68	46.7	0.68
3H-5, 78–70	26.08	1.59	2.58	64.6	43.3	0.65
3H-6, 78–80	27.58	1.65	2.63	61.7	39.7	0.62
3H-7, 38–40	28.68	1.61	2.64	64	42.2	0.64
4H-1, 79–81	29.59	1.61	2.75	66.3	43.6	0.66
4H-2, 79–81	31.09	1.57	2.62	66.1	44.6	0.66
4H-3, 79–81	32.59	1.6	2.69	65.8	43.6	0.66
4H-4, 79–81	34.09	1.62	2.7	64.7	42.3	0.65
4H-5, 79–81	35.59	1.6	2.57	63.3	42.1	0.63
4H-6, 79–81	37.09	1.64	2.67	63	40.7	0.63
4H-7, 39–41	38.19	1.59	2.59	64.2	42.9	0.64
5H-1, 74–76	39.04	1.62	2.6	63.1	41.5	0.63
5H-2, 74–76	40.54	1.6	2.59	63.8	42.4	0.64
5H-3, 74–76	42.04	1.6	2.56	63	41.7	0.63
5H-4, 74–76	43.54	1.61	2.66	64.7	42.7	0.65
5H-5, 74–76	45.04	1.62	2.69	65.1	42.8	0.65
5H-6, 74–76	46.54	1.6	2.75	67.1	44.5	0.67
5H-7, 36–38	47.66	1.65	2.39	54.5	35	0.54
6H-1, 73–75	48.53	1.6	2.63	64.7	43	0.65
6H-2, 63–65	49.93	1.62	2.68	64.6	42.4	0.65
6H-3, 97–99	51.77	1.61	2.41	58.2	38.4	0.58
6H-4, 68–70	52.98	1.63	2.58	61.8	40.3	0.62
6H-5, 43–45	54.23	1.48	2.61	71.5	51.2	0.72
6H-5, 53–56	55.83	1.74	2.69	57.4	35	0.57
6H-7, 37–39	57.17	1.59	2.55	63.5	42.4	0.63
7H-1, 30–32	57.6	1.69	2.75	61.9	38.9	0.62
7H-2, 30–32	59.1	1.67	2.73	62.8	39.9	0.63
7H-3, 33–35	60.63	1.63	2.63	62.7	40.8	0.63
7H-4, 26–28	62.06	1.65	2.72	63.7	41	0.64
7H-5, 79–81	64.09	1.68	2.74	62.4	39.5	0.62
7H-6, 73–75	65.53	1.67	2.65	60.6	38.5	0.61
7H-7, 26–28	66.56	1.67	2.6	59.7	38	0.6
8H-1, 74–76	67.54	1.58	2.54	64.1	43.2	0.64
8H-2, 74–76	69.04	1.63	2.66	63.7	41.6	0.64
8H-3, 74–76	70.54	1.59	2.57	64.1	42.9	0.64
8H-4, 74–76	72.04	1.63	2.65	63.1	41.1	0.63
8H-5, 74–76	73.54	1.63	2.66	63.4	41.2	0.63
8H-6, 74–76	75.04	1.55	2.62	67.8	46.5	0.68
8H-7, 35–37	76.15	1.71	2.58	56.3	35	0.56
9H-1, 72–74	77.02	1.64	2.59	61.5	40	0.62
9H-2, 72–74	78.52	1.62	2.65	63.5	41.5	0.63
9H-3, 78–80	80.08	1.61	2.67	65.1	43.1	0.65
9H-4, 72–74	81.52	1.6	2.59	64.2	42.7	0.64
9H-5, 78–80	83.08	1.66	2.66	61.9	39.7	0.62
9H-6, 78–8	84.58	1.67	2.73	62.5	39.7	0.63
9H-7, 31–33	85.61	1.58	2.62	65.9	44.4	0.66
10X-1, 130–132	87.1	1.63	2.76	65.7	42.8	0.66
10X-2, 36–38	87.66	1.54	2.67	69.5	48.1	0.69
11X-1, 74–76	96.44	1.6	2.62	64.3	42.5	0.64
11X-2, 54–56	97.74	1.6	2.74	67	44.5	0.67
11X-3, 69–71	99.39	1.57	2.63	66.3	44.8	0.66
12X-1, 74–76	106.04	1.59	2.75	67.9	45.5	0.68
12X-2, 74–76	107.54	1.61	2.65	64.7	42.7	0.65
12X-3, 67–69	108.97	1.64	2.64	62.4	40.5	0.62
12X-4, 13–15	109.93	1.63	2.69	63.8	41.5	0.64
13X-1, 62–64	115.62	1.59	2.71	67	44.8	0.67
13X-2, 80–82	117.3	1.6	2.59	63.8	42.4	0.64
13X-3, 72–74	118.72	1.61	2.66	64.9	42.9	0.65
13X-4, 22–24	119.72	1.64	2.64	62.6	40.6	0.63
14X-1, 74–76	125.34	1.61	2.62	63.7	41.9	0.64
14X-2, 74–76	126.84	1.58	2.74	68.4	46.1	0.68
14X-4, 74–76	129.84	1.57	2.68	67.6	45.7	0.68
14X-5, 13–8	130.58	1.59	2.76	68	45.5	0.68
15X-1, 73–75	135.03	1.61	2.76	66.8	44	0.67
15X-1, 80–82	135.1	1.66	2.57	59.7	38.3	0.6
15X-3, 80–82	138.1	1.61	2.69	65.4	43.2	0.65
15X-4, 13–8	138.88	1.63	2.64	62.8	40.8	0.63
16X-1, 68–70	144.58	1.67	2.65	60.3	38.4	0.6
16X-2, 55–57	145.95	1.69	2.5	55.1	34.5	0.55

Table 10 (continued).

Core, section, interval (cm)	Depth (mbsf)	Bulk density (g/cm³)	Grain density (g/cm³)	Porosity (%)	Water content (%)	Void ratio
16X-3, 68–70	147.58	1.66	2.71	62.9	40.3	0.63
17X-1, 67–69	154.27	1.7	2.68	59.5	37.1	0.6
17X-2, 75–77	155.85	1.63	2.65	63.2	41.2	0.63
17X-3, 75–77	157.35	1.59	2.69	66.4	44.3	0.66
17X-4, 75–77	158.85	1.68	2.75	62.7	39.7	0.63
17X-5, 39–41	159.99	1.65	2.57	60.1	38.7	0.6
17X-6, 13–9	161.19	1.65	2.69	62.8	40.4	0.63
18X-1, 72–74	163.92	1.64	2.46	57.5	37.3	0.58
18X-2, 47–49	165.17	1.66	2.62	66.3	42.5	0.66
18X-CC, 14–12	165.8	1.72	2.71	59.1	36.5	0.59
19X-1, 46–48	173.36	1.68	2.8	63.4	40	0.63
19X-2, 46–48	174.86	1.65	2.78	64.5	41.4	0.65
19X-3, 32–34	176.22	1.66	2.64	61.3	39.3	0.61
19X-4, 32–34	177.72	1.57	2.39	60.6	41	0.61
19X-CC, 20–22	178.15	1.66	2.87	66.1	42.3	0.66
20X-1, 48–50	182.98	1.6	2.56	63.2	42	0.63
20X-1, 20–22	192.3	1.65	2.65	61.8	39.7	0.62
21X-2, 20–22	193.8	1.66	2.7	62.7	40.2	0.63
21X-3, 34–36	195.44	1.63	2.78	65.9	42.9	0.66
21X-4, 64–66	197.24	1.71	2.77	61.2	38	0.61
21X-5, 61–63	198.71	1.76	2.76	63.6	38.5	0.64
22X-1, 72–74	202.52	1.7	2.59	57.3	35.7	0.57
22X-CC, 39–41	203.35	1.71	2.85	62.8	38.9	0.63
23X-1, 99–101	212.49	1.64	2.71	64	41.4	0.64
23X-2, 52–54	213.52	1.52	2.46	66.2	46.3	0.66
23X-3, 46–48	214.96	1.63	2.66	63.3	41.2	0.63
23X-4, 15–17	216.15	1.6	2.65	64.9	43	0.65
23X-5, 68–70	218.18	1.62	2.47	59.3	38.8	0.59
23X-6, 87–89	219.87	1.67	2.63	60	38	0.6
23X-7, 13–15	220.63	1.97	2.2	91.7	49.5	0.92
24X-1, 72–74	221.72	1.64	2.69	63.3	40.9	0.63
24X-2, 25–27	222.75	1.63	2.6	61.9	40.3	0.62
25X-1, 73–75	231.43	1.59	2.45	68.9	45.9	0.69
25X-2, 56–58	232.76	1.62	2.7	64.7	42.3	0.65
25X-3, 64–66	234.34	1.63	2.62	62.5	40.7	0.62
25X-4, 57–59	235.77	1.62	2.65	64.2	42.2	0.64
25X-5, 47–49	237.17	1.6	2.67	65.6	43.5	0.66
25X-6, 74–76	238.94	1.61	2.66	64.6	42.5	0.65
26X-1, 67–71	240.97	2.06	6.44	81.3	41.9	0.81
26X-2, 50–52	242.3	1.66	2.59	59.8	38.2	0.6
26X-2, 51–53	242.31	1.7	2.71	60.3	37.6	0.6
26X-4, 96–98	245.76	1.71	2.64	58.2	36.2	0.58
26X-5, 60–62	246.9	1.68	2.58	58.3	36.8	0.58
26X-6, 60–62	248.4	1.66	2.74	63.3	40.4	0.63
26X-7, 37–39	249.67	1.64	2.61	61.5	39.8	0.62
27X-1, 84–86	250.84	1.68	2.75	62.5	39.5	0.63
27X-2, 73–75	252.23	1.64	2.57	60.8	39.4	0.61
27X-3, 27–29	253.27	1.65	2.56	59	37.7	0.59
27X-CC, 13–15	253.81	1.6	2.72	66.5	44.1	0.66
28X-1, 78–80	260.38	1.73	2.75	59.4	36.4	0.59
28X-2, 62–64	261.72	1.6	2.58	63.5	42.1	0.64
28X-3, 65–67	263.25	1.58	2.74	67.9	45.7	0.68
28X-4, 65–67	264.75	1.57	2.61	66.2	44.8	0.66
28X-5, 73–75	266.33	1.62	2.79	66.9	43.9	0.67
28X-6, 56–58	267.66	1.67	2.85	65	41.3	0.65
28X-1, 56–58	269.76	1.65	2.64	62.1	40.1	0.62
29X-2, 47–49	271.17	1.63	2.7	64.5	42.1	0.65
29X-3, 58–60	272.78	1.65	2.74	63.8	40.9	0.64
29X-4, 59–60	274.29	1.66	2.72	62.8	40.2	0.63
29X-5, 50–52	275.7	2.1	3.26	52.3	26.5	0.52
29X-6, 63–65	277.33	1.66	2.69	62.6	40.2	0.63
29X-7, 28–30	278.48	1.65	2.71	63.3	40.8	0.63
30X-1, 74–76	279.54	1.81	2.78	56.1	33	0.56
30X-2, 34–36	280.64	1.78	2.75	56.4	33.6	0.56
30X-CC, 22–24	281.67	1.75	2.77	59	35.9	0.59
31X-1, 37–39	288.87	1.8	2.85	58.3	34.5	0.58
31X-2, 54–56	289.52	1.82	2.71	53	30.8	0.53
31X-2, 68–70	289.66	1.8	2.91	59.3	35	0.59
32X-1, 69–70	294.69	1.75	2.6	54.5	33.1	0.55
32X-2, 65–67	296.15	1.91	2.87	52.5	29.2	0.52
32X-3, 65–67	297.65	1.82	3.24	42.5	24.9	0.43
32X-4, 42–44	298.92	1.78	2.78	57.4	34.2	0.57
32X-5, 70–72	300.7	1.83	2.97	59.2	34.4	0.59
32X-6, 58–60	302.08	1.74	2.68	57.2	34.9	0.57
33X-1, 20–23	303.7	1.68	2.6	58.8	37.1	0.59
33X-2, 16–18	305.16	1.74	2.84	53.8	32.9	0.54
33X-3, 63–67	307.13	1.75	2.64	55.8	33.9	0.56
33X-4, 29–31	308.29	1.74	2.75	58.9	36	0.59
33X-5, 134–137	310.84	1.75	2.7	57.4	35	0.57
33X-6, 37–40	311.37	1.75	2.73	58	35.2	0.58
33X-7, 22–25	312.72	1.8	2.88	58.6	34.6	0.59
33X-CC, 25–28	313.21	1.75	2.7	57.4	34.9	0.57
34X-1, 64–66	313.74	1.91	2.64	45.5	25.2	0.45
34X-CC, 33–35	314.92	1.73	2.51	52.8	32.4	0.53
35X-1, 40–42	322.9	1.71	2.59	56.6	35.2	0.57
35X-2, 37–39	324.37	1.72	2.61	56.4	34.8	0.56
35X-3, 41–43	325.91	1.85	2.72	52.2	30	0.52

Table 10 (continued).

Core, section, interval (cm)	Depth (mbsf)	Bulk density (g/cm³)	Grain density (g/cm³)	Porosity (%)	Water content (%)	Void ratio
35X-4, 133–135	328.33	1.83	2.79	55.1	32.1	0.55
35X-5, 138–140	329.88	1.59	2.92	70.6	47.1	0.71
35X-6, 60–62	330.6	1.88	2.73	50.3	28.5	0.5
35X-7, 13–8	331.58	1.84	2.73	52.8	30.5	0.53
35X-CC, 13–3	332	1.92	2.8	50	27.7	0.5
36X-1, 66–68	332.76	1.84	2.8	54.2	31.2	0.54
36X-2, 76–78	334.36	1.83	2.93	58.2	33.7	0.58
36X-3, 62–64	335.72	1.83	2.73	53.3	31	0.53
36X-4, 50–52	337.1	1.76	2.68	56.3	34.1	0.56
36X-5, 13–9	338.19	1.91	2.91	52.3	29	0.52
36X-CC, 28–30	339.74	1.82	2.62	50.7	29.6	0.51
37X-1, 113–115	342.73	1.88	2.83	52.7	29.7	0.53
37X-2, 75–77	343.85	1.86	2.68	50	28.6	0.5
37X-3, 36–37	344.96	1.89	2.91	54.7	30.8	0.55
37X-4, 88–90	346.98	1.88	2.75	51.1	28.9	0.51
37X-5, 89–91	348.49	1.68	2.46	54.8	34.7	0.55
37X-6, 119–121	350.29	1.83	2.78	54.6	31.7	0.55
37X-7, 46–48	351.06	1.68	2.35	51.1	32.3	0.51
37X-CC, 29–31	351.35	1.53	2.19	56.8	39.4	0.57
39X-1, 136–138	362.26	1.84	2.79	54.2	31.3	0.54
39X-2, 29–31	362.69	1.92	3.15	58.1	32.1	0.58
40X-1, 142–144	371.92	1.8	2.98	62.8	37	0.63
40X-2, 81–83	372.81	1.7	2.51	55.1	34.5	0.55
40X-3, 62–64	374.12	1.69	2.77	62.5	39.3	0.62
40X-4, 82–84	375.82	1.72	2.66	57.8	35.7	0.58
41X-1, 94–96	381.14	1.81	2.69	53.3	31.3	0.53
41X-2, 37–39	382.07	1.87	2.81	53	30.1	0.53
41X-3, 44–46	383.64	1.76	2.78	58.7	35.5	0.59
41X-4, 96–98	385.66	1.97	3.25	57.7	31	0.58
41X-6, 41–43	388.11	1.83	2.88	57.2	33.2	0.57
41X-7, 13–10	389.3	1.83	2.57	48	27.8	0.48
42X-1, 88–90	390.68	1.89	2.76	50.4	28.3	0.5
42X-CC, 13–6	392.77	1.92	2.66	45.7	25.3	0.46

the Pliocene and Pleistocene sections and the greatest vitric ash influx in those of the upper Eocene and Oligocene.

REFERENCES

Backman, J., Duncan, R. A., et al., 1988. *Proc. ODP, Init. Repts.*, 115: College Station, TX (Ocean Drilling Program).

Beccaluva, L., Macciotta, G., Savelli, C., et al., 1980. Geochemistry and K/Ar ages of volcanics dredged in the Philippine Sea. *In* Hayes, D. E. (Ed.), *The Tectonic and Geologic Evolution of Southeast Asian Sea and Islands*: Washington (Am. Geophys. Union), 247–270.

Berggren, W. A., Kent, D. V., Flynn, J. J., and Van Couvering, J., 1985. Cenozoic geochronology. *Geol. Soc. Am. Bull.*, 96:1407–1418.

Bleil, U., 1982. Paleomagnetism of Deep Sea Drilling Project Leg 60 sediments and igneous rocks from the Mariana Region. *Init. Repts. DSDP*, 60: Washington (U.S. Govt. Printing Office), 855–873.

Bloomer, S. H., 1983. Distribution and origin of igneous rocks from the landward slopes of the Mariana Trench. *J. Geophys. Res.*, 88:7411–7428.

Bloomer, S. H., and Fisher, R. L., 1987. Petrology and geochemistry of igneous rocks from the Tonga Trench—a non-accreting plate boundary. *J. Geol.*, 95:469–495.

Bloomer, S. H., Hawkins, J. W., 1983. Gabbroic and ultramafic rocks from the Mariana Trench: An island arc ophiolite. *In* Hayes, D.E. (Ed.), *The Tectonic and Geologic Evolution of Southeast Asian Seas and Islands, Part II.* Geophys. Monogr. Ser., 27: Washington (Am. Geophys. Union), 294–317.

Ewart, A., Brothers, R. N., and Manteen, A., 1977. An outline of the geology and geochemistry, and the possible petrogenetic evolution of the volcanic rocks of the Tonga-Kermadec-New Zealand island arc. *J. Volc. Geotherm. Res.*, 2:205–250.

Fryer, P., Langmuir, C. H., Taylor, B., Zhang, Y., and Hussong, D. M., 1985. Rifting of the Izu arc, III, Relationships of chemistry to tectonics. *EOS, Trans. Am. Geophys. Union*, 66:421.

Gill, J. B., Stock, A. L., and Whelan, P. M., 1984. Volcanism accompanying backarc basin development in the southwest Pacific. *Tectonophysics*, 102:207–224.

Honza, E., and Tamaki, K., 1985. Bonin Arc. *In* Nairn, A.E.M., and Uyeda, S. (Eds.), *The Ocean Basins and Margins, Vol. 7, The Pacific Ocean*: New York (Plenum Press), 459–499.

Hussong, D. M., and Uyeda, S., 1981. Tectonic processes and the history of the Mariana Arc: A synthesis of the results of Deep Sea Drilling Project Leg 60. *In* Hussong, D. M., Uyeda, S., et al., *Init. Repts. DSDP*, 60: Washington (U.S. Govt. Printing Office), 909–929.

Johnson, L. E., and Fryer, P., 1988. Oceanic plate material on the Mariana Forearc. *EOS, Trans. Am. Geophys. Union*, 69:1471.

Karig, D. E., 1975. Basin genesis in the Philippine Sea. *In* Ingle, J. C., Karig, D. E., et al., *Init. Repts. DSDP*, 31: Washington (U.S. Govt. Printing Office), 857–879.

Karig, D. E., and Moore, G. F., 1975. Tectonic complexities in the Bonin arc system. *Tectonophysics*, 27:97–118.

Karig, D. E., and Ranken, D., 1983. Marine geology of the forearc region, southern Mariana island arc. *In* Hayes, D. E. (Ed.), *The Tectonic and Geologic Evolution of Southeast Asian Seas and Islands, II*: Washington (Am. Geophys. Union), 266–280.

Keating, B., Kodama, K., Uyeda, S., and Helsley, C. E., 1983. Paleomagnetic results of the Bonin and Mariana Islands. *Advances Earth Planet. Sci. Ser.*, 245–260.

Ogawa, Y., and Naka, J., 1984. Emplacement of ophiolitic rocks in forearc areas: examples from central Japan and Izu-Mariana-Yap island arc system. *Geol. Soc. London, Spec. Publ.*, 13:292–304.

Pearce, J. A., Lippard, S. J., and Roberts, S., 1984. Characteristics and tectonic significance of supra-subduction zone ophiolites. *Geol. Soc. London, Spec. Pub.*, 16:77–94.

Peccerillo, A., and Taylor, S. R., 1976. Geochemistry of Eocene calc-alkaline rocks from the Kastamonu area, northern Turkey. *Contr. Mineral. Petrol.*, 58:63–81.

Prell, W. L., Niatsuma, U., et al., 1989. Site 723. *In* Prell, W. L., Niatsuma, et al., *Proc. ODP, Init. Repts.*, 117: College Station, TX (Ocean Drilling Program), 319–384.

Reagan, M. K., and Meijer, A., 1984. Geology and geochemistry of early arc-volcanic rocks from Guam. *Bull. Geol. Soc. Am.*, 95:701–713.

Scott, R. B., and Kroenke, L. W., 1981. Periodicity of remnant arcs and back-arc basins of the South Philippine Sea. *Oceanologica Acta*, 4:193–202.

Shiraki, K., Kuroda, N., Urano, H., and Maruyama, S., 1980. Clinoenstatite in boninite from the Bonin Islands, Japan. *Nature*, 285:31–32.

Stern, R. J., Smoot, N. C., and Rubin, M., 1984. Unzipping of the volcano arc, Japan. *Tectonophysics*, 102:153–174.

Wood D. A., Marsh, N. J., Tarney J., Joron, J.-L., Fryer, P., and Treul, M., 1981. Geochemistry of igneous rocks recovered from a transect across the Mariana Trough, arc, fore-arc, and trench, Sites 453 through 461, Deep Sea Drilling Project Leg 60. *In* Hussong, D. M., Uyeda, S., et al., *Init. Repts. DSDP*, 60: Washington (U.S. Govt. Printing Office), 611–646.

Ms 125A-110

NOTE: All core description forms ("barrel sheets") and core photographs have been printed on coated paper and bound as Section 4, near the back of the book, beginning on page 383.

Table 11. Physical properties for Hole 782A.

Core, section, interval (cm)	Depth (mbsf)	Thermal conductivity (W/mK)	Resistivity (ohms)	Formation factor	"A" velocity (km/s)	"B" velocity (km/s)
125-782A-1H-1, 75–77	0.75	1.026				
1H-2, 76–78	2.26	1.058				
1H-3, 76–78	3.76	1.05				
1H-4, 76	78	5.26	1.101			
1H-5, 76–78	6.76	1.041				
1H-6, 76–78	8.26	1.043				
1H-7, 29–30	9.29	0.902				
1H-CC, 13–9	9.69	0.973				
2H-1, 76–78	10.56	1.093				
	13.2		19.6	2.29		
2H-3, 76–78	13.56	1.148				
2H-4, -76–78	15.06	1.126				
	16.1		22.4	2.61		
2H-5, 76–78	16.56	1.142				
2H-6, 38–40	17.68	1.414				
	18.3		22.2	2.59		
2H-7, 38–40	19.18	1.121				
	19.4		21.8	2.54		
2H-CC, 13–5	19.7	1.181				
3H-1, 76–78	20.06	1.078				
3H-176–78	20.06	1.07				
3H-2, 76–78	21.56	1.139				
3H-3, 76–78	23.06	1.039				
3H-4, 76–78	24.56	1.061				
3H-5, 76–78	26.06	1.157				
	27.39		23	2.68		
3H-6, 76–78	27.56	1.162				
3H-7, 39–40	28.69	1.125				
3H-CC, 14–12	29.24	1.096				
4H-1, 76–78	29.56	1.088	16.6	1.94		
4H-2, 76–78	31.06	1.124				
4H-3, 76–78	32.56	1.026				
	32.8		20.2	2.36		
4H-4, 55–57	33.85	1.009				
4H-5, 75–77	35.55	1.127	22	2.57		
4H-6, 75–77	37.05	1.223				
4H-7, 40–42	38.2	1.109				
4H-CC, 14–16	38.74	1.059				
5H-1, 78–80	39.08	1.088	20.1	2.35		
5H-2, 78–80	40.58	1.113				
5H-3, 78–80	42.08	1.092	19.7	2.3		
5H-4, 78–80	43.58	1.006				
5H-5, 77–79	45.07	1.099	20.6	2.4		
5H-6, 77–79	46.57	1.088				
	47.41		17.7	2.07		
5H-7, 37–39	47.67	1.106				
5H-CC, 13–11	48.19	1.034				
6H-1, 76–78	48.56	1.108				
	49.6		19.2	2.24		
6H-2, 76–78	50.06	1.41				
6H-3, 76–78	51.56					
	52.4		17.3	2.02		
6H-4, 76–78	53.06	1.068				
6H-5, 77–79	54.57	1.064				
	55.5		19.5	2.28		
6H-6, 77–79	56.07	1.016				
6H-7, 36–38	57.16	1.038				
	57.4		21.3	2.49		
6H-CC, 13–10	57.68	1.034				
7H-1, 75–77	58.05	1.038				
7H-2, 75–77	59.55	1.002				
	60.4		21.7	2.53		
7H-3, 75–77	61.05	1.264				
7H-4, 75–77	62.55	0.999				
	63.4		19.5	2.28		
7H-5, 46–48	63.76	1.096				
7H-6, 46–48	65.26	1.254				
	66.4		22.4	2.61		
7H-7, 46–48	66.76	1.064				
	67.06		21.2	2.47		
8H-1, 65–67	67.45	1.193				
8H-2, 73–75	69.03	1.057				
	70.06		18.4	2.15		
8H-3, 73–75	70.53	0.82				
8H-4, 73–75	72.03	1.108				
8H-5, 73–75	73.53	1.052	23.5	2.74		

Table 11 (continued).

Core, section, interval (cm)	Depth (mbsf)	Thermal conductivity (W/mK)	Resistivity (ohms)	Formation factor	"A" velocity (km/s)	"B" velocity (km/s)
8H-6, 73–75	75.03	1.054				
8H-7, 44–46	76.24	0.953				
	76.49		17.7	2.07		
9H-1, 74–76	77.04	1.031				
	77.26		21.3	2.49		
9H-2, 74–76	78.54	1				
9H-3, 74–76	80.04	1.007				
9H-4, 74–76	81.54					
9H-5, 74–76	83.04	1.115				
9H-6, 74–76	84.54	1.104				
9H-7, 34–36	85.64	1.008				
10X-1, 13–7	85.87	1.073				
9H-CC, 13–10	86.08	0.952				
10X-2, 37–39	87.67	0.978				
10X-CC, 13–7	88.12	0.814				
11X-1, 74–76	96.44	1				
	96.76		19.2	2.24		
11X-2, 51–53	97.71	0.931				
11X-3, 38–40	99.08	1.036				
	99.26		19.7	2.3		
11X-CC, 13–6	99.65	0.955				
12X-1, 74–76	106.04	0.991				
	106.38		23.5	2.74		
12X-2, 74–76	107.54	1.02				
	108.6		18.8	2.19		
12X-3, 74–76	109.04	1.146				
12X-4, 13–10	109.9	1.016				
13X-1, 74–76	115.74	1.103				
	116.18		19.3	2.25		
13X-2, 49–51	116.99	1.042				
13X-3, 74–76	118.74	1.157				
	119		18.3	2.14		
13X-4, 19–21	119.69	1.147				
14X-1, 74–76	125.34	1.112	17.4	2.03		
14X-2, 74–76	126.84	0.992				
	128		22	2.57		
14X-3, 74–76	128.34	1.072				
14X-4, 74–76	129.84	1.052				
15X-1, 74–76	135.04	0.993	19.9	2.32		
15X-2, 74–76	136.54	1.105				
	137.8		20.6	2.4		
15X-4, 13–9	138.89	1.031				
16X-1, 74–76	144.64					
16X-2, 47–49	145.87	1.183				
	146		21.5	2.51		
16X-3, 47–49	147.37	1.102	23.5	2.74		
17X-1, 74–76	154.34	1.123				
	154.8		22.4	2.61		
17X-2, 74–76	155.84	1.103				
17X-3, 74–76	157.34	1.065	20.1	2.35		
17X-4, 74–76	158.84	1.146				
	159.96		29.5	3.44		
17X-5, 74–76	160.34	1.109				
17X-6, 13–7	161.17	1.21				
	163.4		23.2	2.71		
18X-1, 73–75	163.93	1.138				
18X-2, 44–46	165.14	1.135				
18X-CC, 14–16	165.82	1.286				
	173.13		21.9	2.56		
19X-1, 73–75	173.63	1.087				
19X-2, 48–50	174.88	1.106				
	176.13		28.1	3.28		
19X-3, 74–76	176.64	1.071				
19X-4, 28–30	177.68	1.024				
19X-CC, 13–15	178.08	1.095				
20X-1, 30–32	182.8	0.914				
20X-CC, 13–15	183.29	0.926				
	192.25		24.4	2.85		
21X-2, 74–76	194.34	1.147				
	195.2		21.6	2.52		
21X-4, 74–76	197.34	1.293				
	198.2		24.6	2.87		
22X-1, 80–82	202.6	1.228	26.1	3.05		
	211.68		30.8	3.59		
23X-1, 80–82	212.3	1.04				
	214.8		22.5	2.63		

Table 11 (continued).

Core, section, interval (cm)	Depth (mbsf)	Thermal conductivity (W/mK)	Resistivity (ohms)	Formation factor	"A" velocity (km/s)	"B" velocity (km/s)
23X-3, 80–82	215.3	1.064				
	217.6		41.7	4.87		
23X-5, 80–82	218.3	1.014				
	220.6		31.7	3.7		
24X-1, 78–80	221.78	0.814				
	230.8		17.6	2.05		
25X-2, 77–79	232.97	1.228				
	233.86		26	3.03		
25X-4, 77–79	235.97	1.159				
	237.1		31.5	3.68		
25X-6, 77–79	238.97	1.358				
26X-1, 78–80	241.08	0.943				
26X-2, 51–53	242.31				1.67	1.69
	243.9		28.5	3.33		
26X-3, 78–80	244.08	0.995				
26X-5, 78–80	247.08	0.89	27	3.15		
26X-7, 32–34	249.62	1.181				
27X-1, 36–38	250.36	1.106	28.1	3.28		
	251.32		21.3	2.49		
	252.06		23.3	2.72		
27X-3, 44–46	253.44	1.101				
28X-1, 44–46	260.04	1.003	21.9	2.56		
28X-3, 48–50	263.08	1.055				
	263.5		23	2.68		
28X-5, 48–50	266.08	1.05				
	266.62		23	2.68		
29X-1, 48–50	269.68	1.039				
	270.26		27.5	3.21		
29X-3, 48–50	272.68	1.073	36.1	4.21		
29X-4, 118–120	274.88				1.75	1.73
29X-5, 47–49	275.57	1.118	21.3	2.49		
29X-7, 28–30	278.48	1.031	30.5	3.56		
30X-1, 75–77	279.55				1.75	1.73
30X-2, 46–48	280.76	0.56				
31X-1, 37–39	288.87				1.74	1.72
31X-1, 43–45	288.93					
31X-2, 47–49	289.45	0.992				
31X-2, 68–70	289.66				1.72	1.73
31X-3, 54–56	291.02			1.77	1.76	
31X-4, 47–49	292.45					
32X-1, 60–62	294.5	0.809			1.81	1.85
32X-2, 65–67	296.15				1.8	1.84
32X-3, 65–67	297.65				1.69	1.69
32X-4, 42–44	298.92				1.75	1.8
32X-5, 60–62	300.6	1.148			1.74	1.73
32X-6, 58–60	302.08				1.72	1.75
33X-1, 32–34	303.82	1.079			1.76	1.75
33X-2, 16–18	305.16				1.67	1.74
33X-3, 32–34	306.82	1.143				
33X-4, 29–31	308.29				1.67	1.7
33X-5, 32–34	309.82	1.037				
33X-6, 37–40	311.37				1.68	1.72
33X-7, 32–34	312.82	1.127				
33X-CC, 25–28	313.21				1.7	1.7
34X-1, 74–76	313.84	1.017				
34X-CC, 25–27	314.84	0.999				
35X-1, 3–5	322.53				1.62	1.63
35X-1, 40–42	322.9				1.68	
35X-1, 74–76	323.2					
35X-2, 37–39	324.37				1.75	1.73
35X-2, 74–76	324.74	1.072				
35X-3, 48–50	325.98	1.129			1.78	1.78
35X-4, 73–75	327.73	1.2				
35X-4, 133–135	328.33				1.8	1.77
35X-5, 73–75	329.23	1.185				
35X-5, 138–140	329.88				1.74	2.49
35X-6, 73–75	330.73	1.427			2.49	
35X-7, 22–24	331.72	1.435				
36X-1, 72–74	332.82	1.206			1.94	1.86
36X-2, 72–74	334.32	1.236			1.95	
36X-3, 72–74	335.82	1.29			1.88	1.86
36X-4, 50–52	337.1				1.9	1.97
36X-4, 74–76	337.34	1.282				
36X-5, 9–11	338.19				1.97	1.92
36X-5, 58–60	338.68	1.292				
36X-CC, 13–11	339.57	1.27				

Table 11 (continued).

Core, section, interval (cm)	Depth (mbsf)	Thermal conductivity (W/mK)	Resistivity (ohms)	Formation factor	"A" velocity (km/s)	"B" velocity (km/s)
37X-1, 74–76	342.34					
37X-1, 113–115	342.73				1.92	1.91
37X-2, 74–76	343.84	0.913			1.91	1.82
37X-3, 36–38	344.96				2.05	2.09
37X-3, 74–76	345.34	1.304				
37X-4, 74–76	346.84	1.258				
37X-4, 88–90	346.98				1.79	1.75
37X-5, 74–76	348.34	1.118				
37X-6, 74–76	349.84	1.031				
37X-6, 119–121	350.29				2.09	2.19
37X-7, 21–23	350.81	1.124				
39X-1, 70–72	361.6	1.059				
39X-1, 136–138	362.26				2.1	2.01
39X-2, 37–39	362.77	1.087				
39X-CC, 18–20	363.4	1.192				
40X-1, 74–76	371.24	1.187				
40X-2, 74–76	372.74					
40X-3, 54–56	374.04	1.157				
40X-4, 74–76	375.74	1.263				
40X-CC, 14–12	376.62	1.118				
41X-1, 74–76	380.94	1.052				
41X-1, 94–96	381.14				2.23	
41X-2, 74–76	382.44	1.117				
41X-3, 44–46	383.64				2.37	2.29
41X-4, 74–76	385.44					
41X-5, 74–76	386.94	1.05				
41X-6, 41–43	388.11				2	
41X-6, 74–76	388.44	1.243				
41X-7, 15–17	389.35				2.06	2.02
42X-1, 60–62	390.4	1.34				
42X-1, 88–90	390.68				2.07	2.04
42X-2, 61–63	391.91	0.69				
42X-CC, 6–8	392.77				1.84	1.87

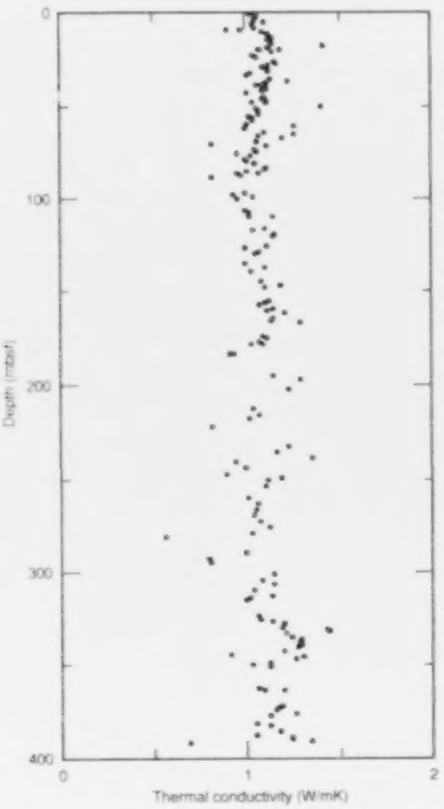

Figure 18. Plot of thermal conductivity vs. depth. Although the data are scattered, conductivities increase with depth.

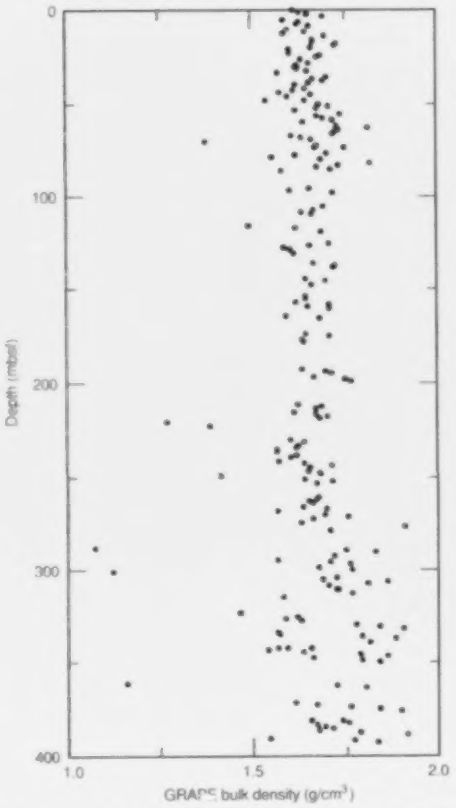

Figure 19. Plot of filtered GRAPE bulk densities vs. depth. The original GRAPE files were edited to reduce the number of data points. Density increases with depth. Increasing scatter in the data with depth probably resulted from drilling disturbance.

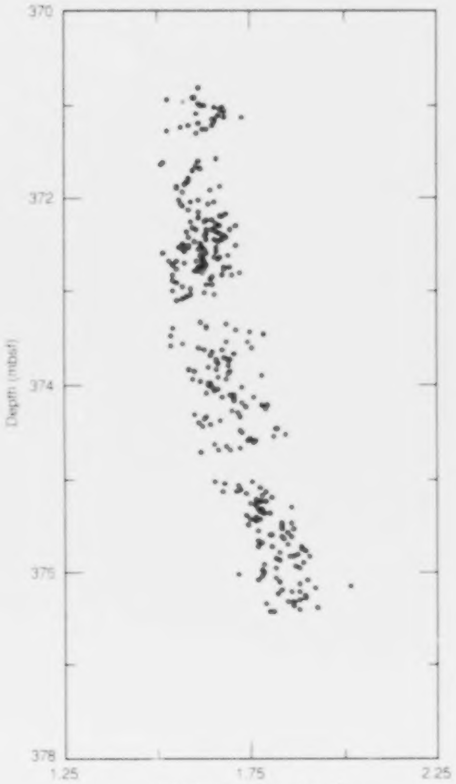

Figure 20. GRAPE bulk density plots for Cores 125-782A-3H, 125-782A-25X, and 125-782-39X through 125-782-40X from Hole 782A. Plots for Cores 125-782A-3H and 125-782A-25X are similar. A significant change in density is apparent at 373 mbsf in these cores.

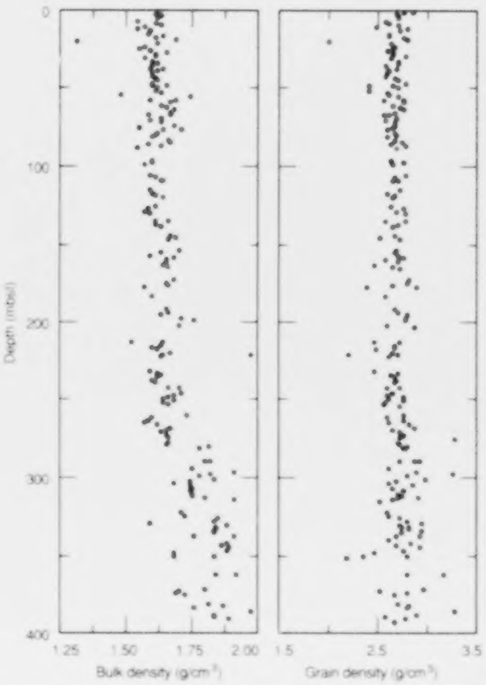

Figure 21. Variation of index properties with depth. Note the similarity of the index bulk-density plot to that from the GRAPE (Fig. 19). Bulk densities show a discontinuity at 280 mbsf, where sediment induration increases.

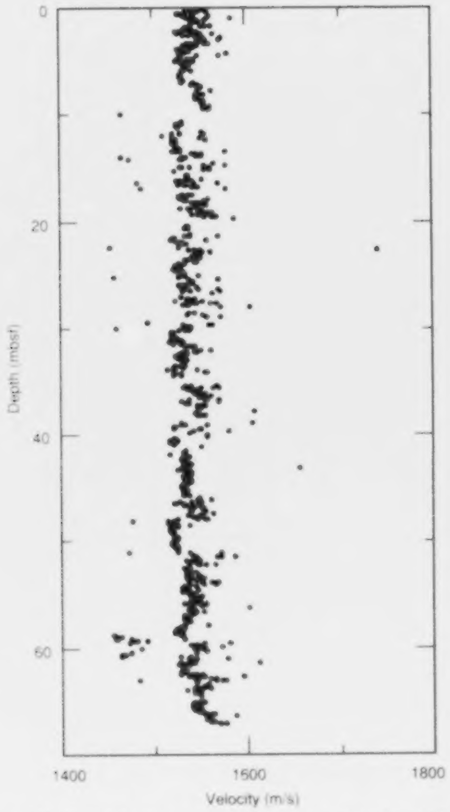

Figure 22. Plot of depth vs. compressional-wave velocities obtained from the *P*-wave logger on the MST for APC cores (125-782A-1H through 125-782A-8H). Velocity is nearly constant over this depth range.

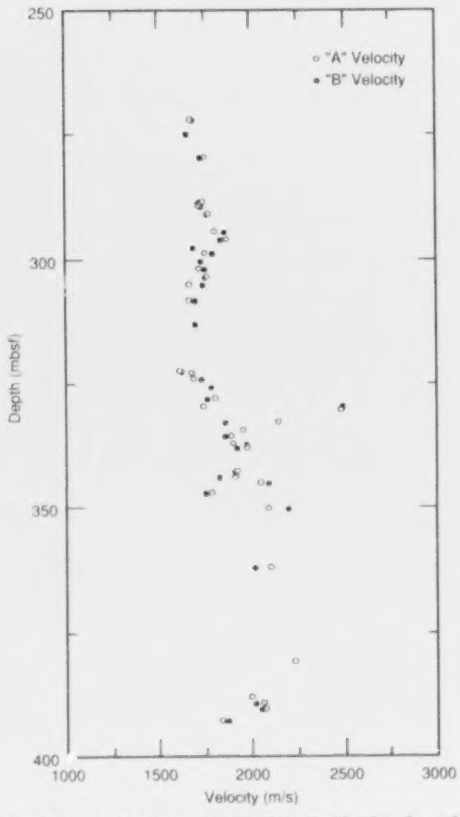

Figure 23. Plot of depth vs. velocities from the Hamilton frame for well-consolidated sediment (depths greater than 278 mbsf). The "A" direction denotes propagation along the core axis, and the "B" direction indicates propagation normal to the core axis. Velocities for "A" and "B" directions are nearly equal, indicating that these sedimentary rocks are isotropic. Velocity increases from 1700 to 2000 m/s over this depth interval.

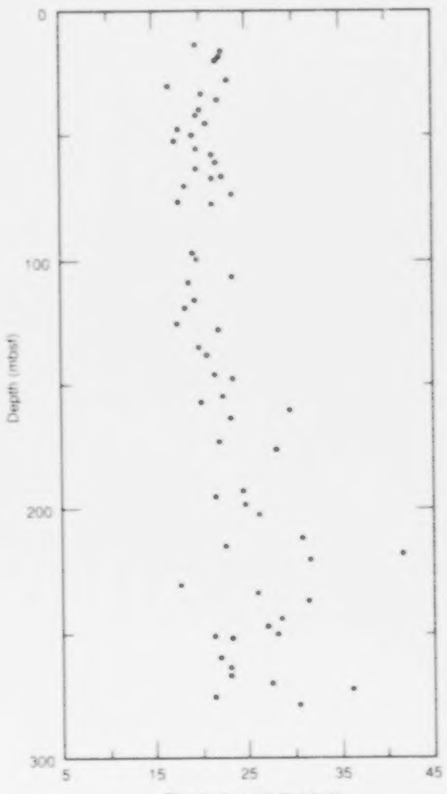

Figure 24. Plot of electrical resistivity vs. depth. Although scattered, these data show higher resistivity with increasing depth.

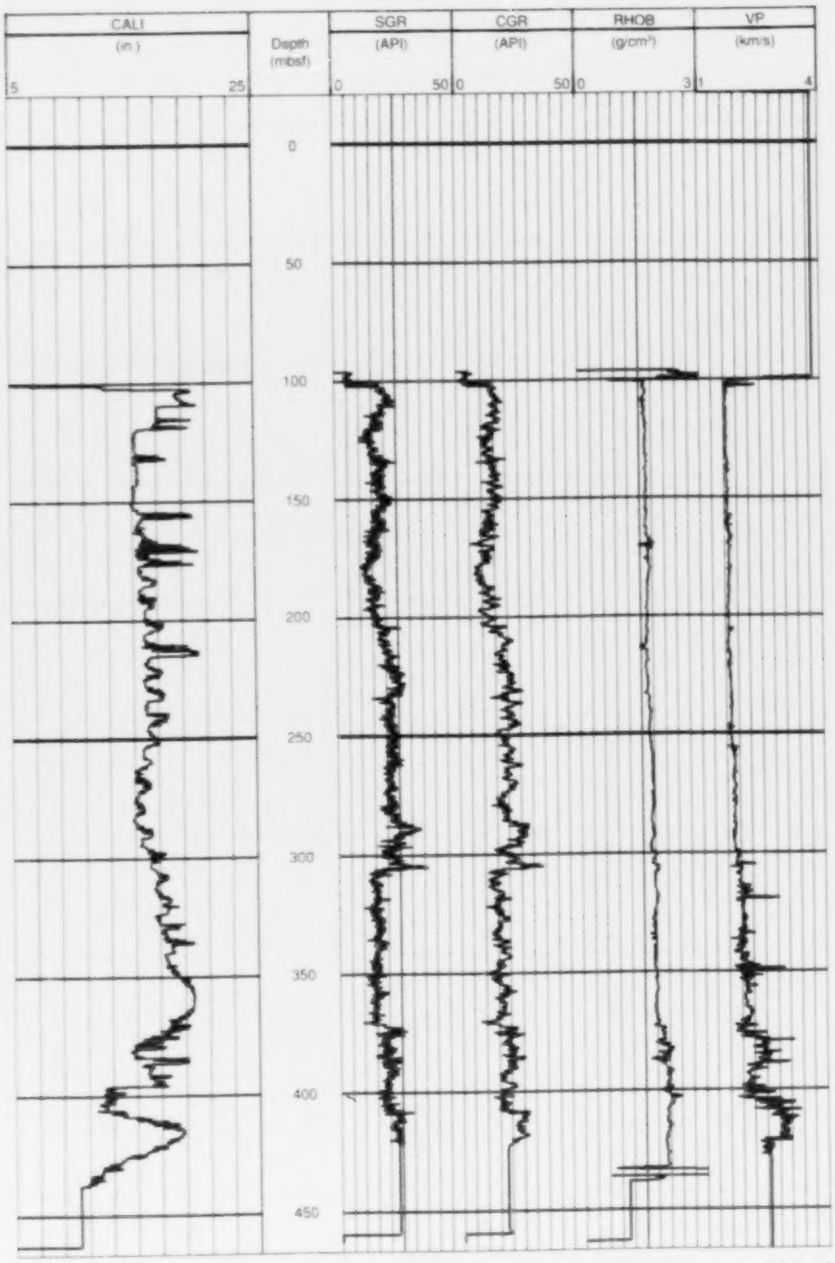

Figure 25. Plot of logs for Hole 782B as a function of depth. Logs shown are caliper (CALI), the gamma ray (SGR and CGR), density (RHOB), and velocity (VP).

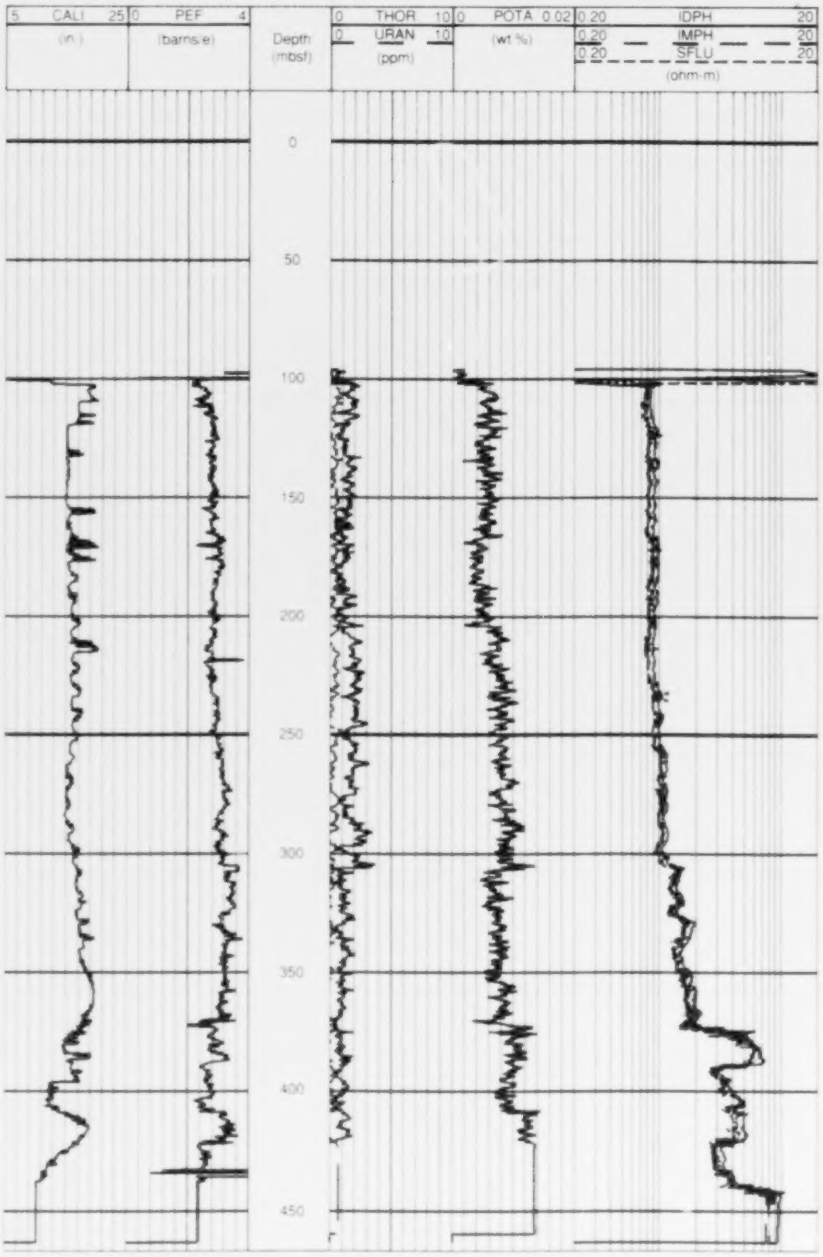

Figure 26. Plot of logs for Hole 782B as a function of depth. Logs shown are caliper (CALI), photoelectric effect (PEF), thorium (THOR), uranium (URAN), potassium (POTA), and resistivity (deep induction: IDPH; medium induction: IMPH; spherically focused: SFLU).

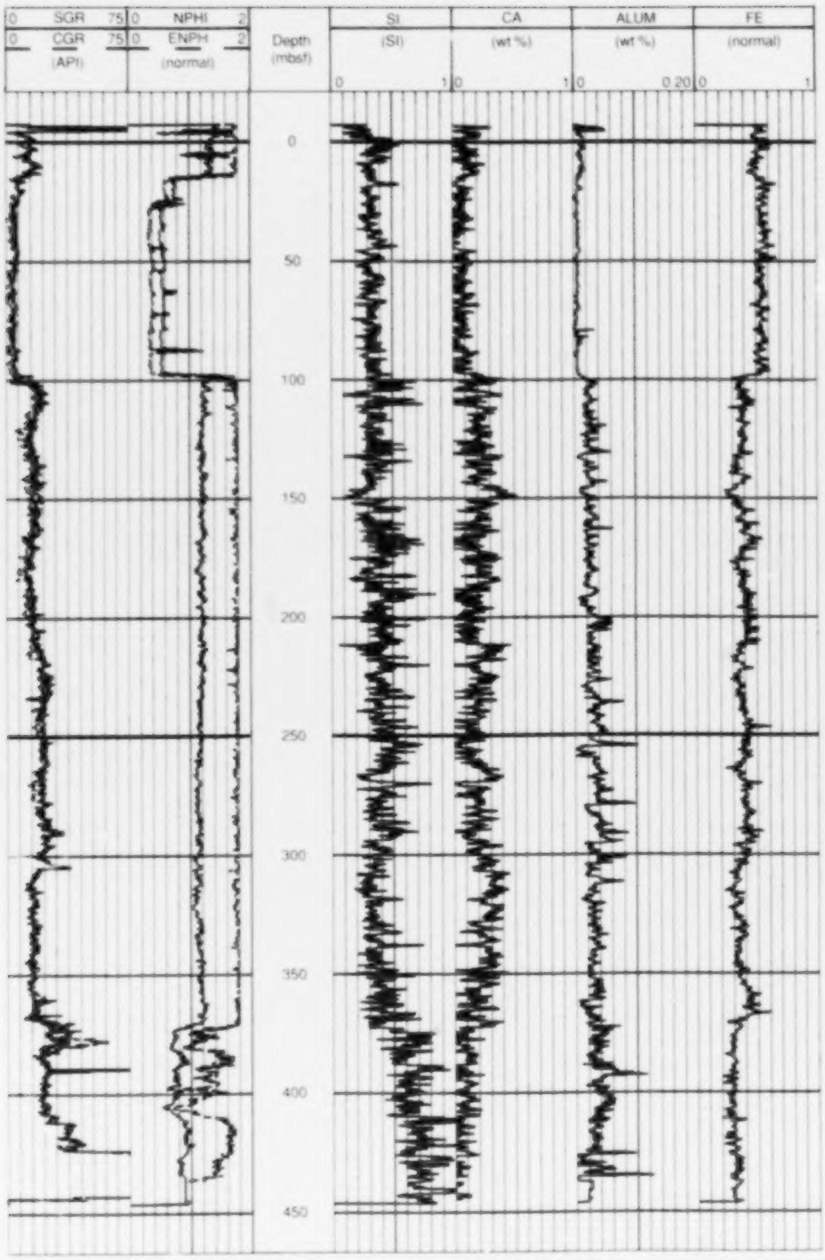

Figure 27. Plot of logs for Hole 782B as a function of depth. Logs shown are gamma ray (SGR and CGR), neutron porosity (NPHI), and epithermal neutron porosity (ENPH) on a relative scale, normalized (see text) silica (SI), normalized calcium (CA), aluminum (ALUM), and normalized iron (FE).

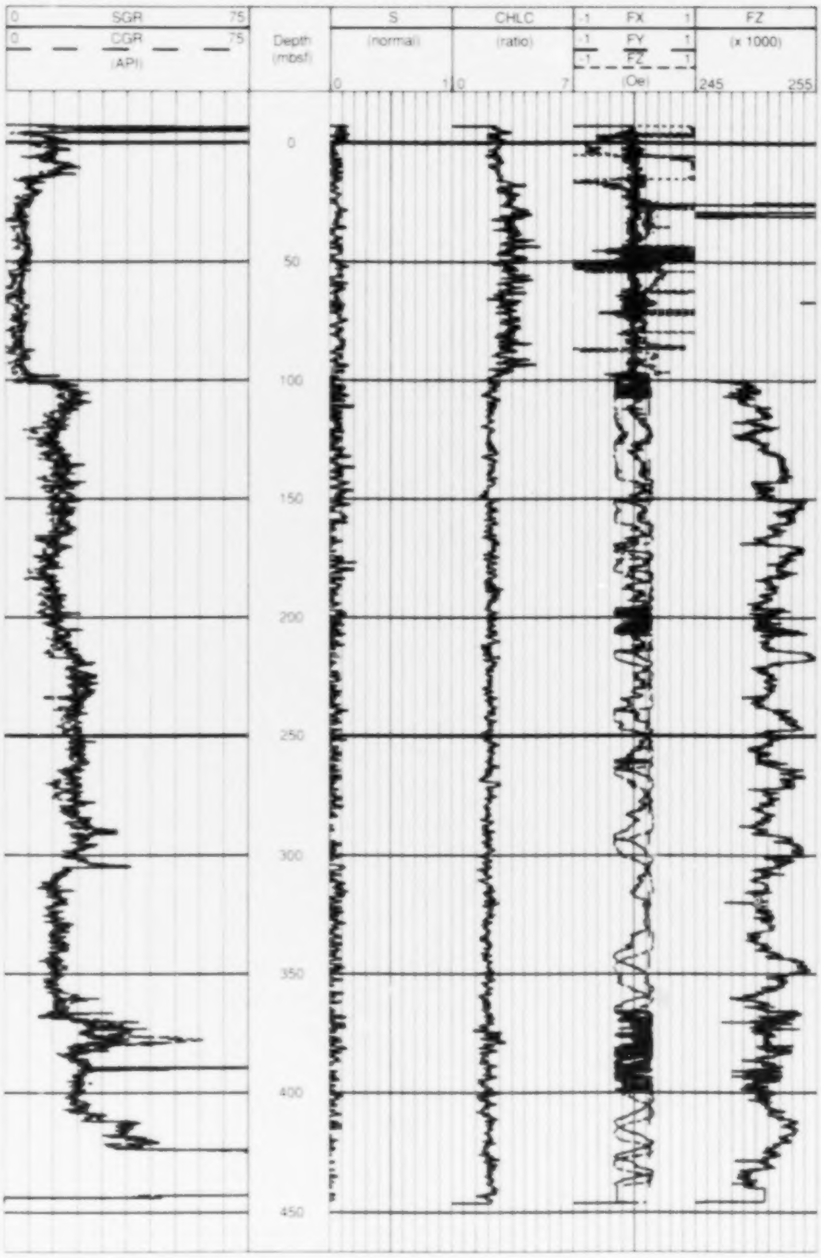

Figure 28. Plot of logs for Hole 782B as a function of depth. Logs shown are gamma ray (SGR and CGR), normalized (see text) sulfur (S), chlorine/hydrogen ratio (CHLC), magnetic field strength (FX, FY, and FZ), and the vertical magnetic field strength × 1000 (FZ10).

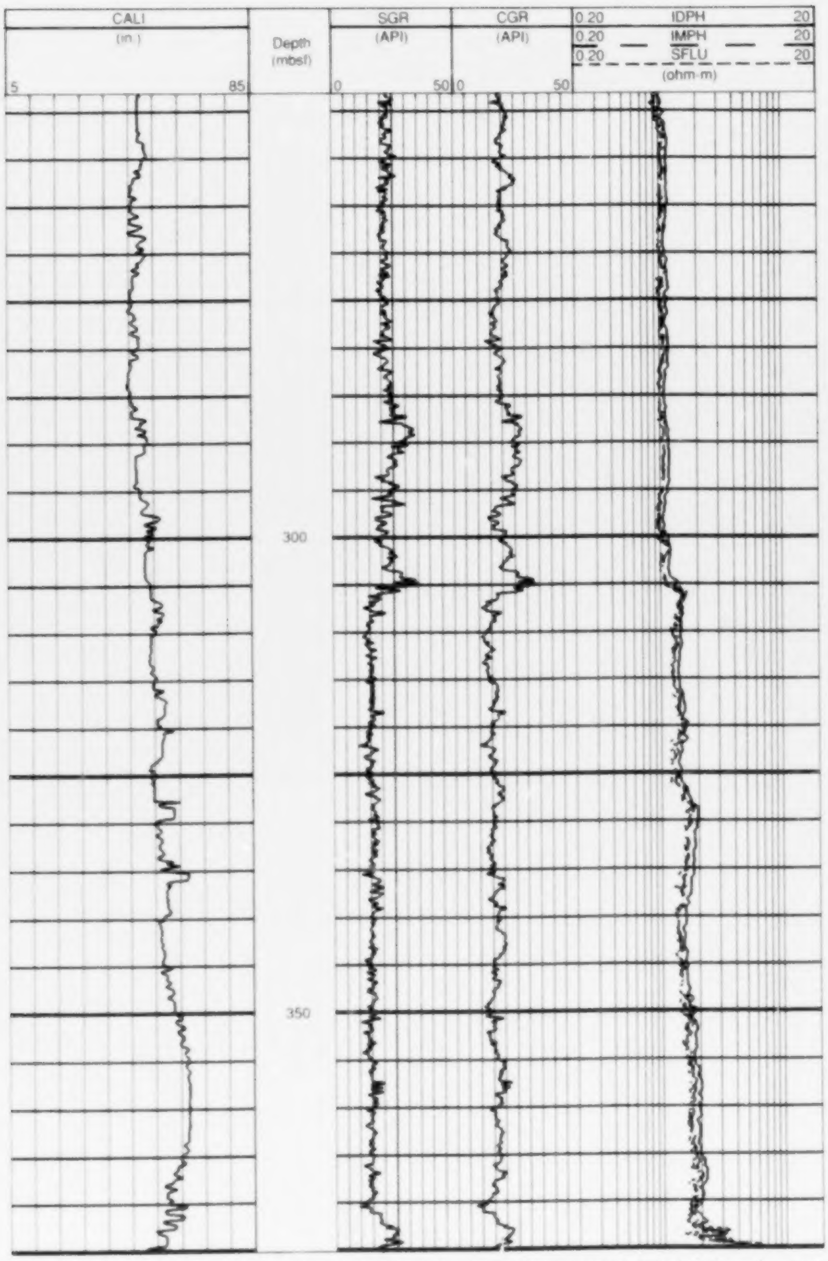

Figure 29. Enlarged plot of logs for second unit (208–305 mbsf) and for the third unit (305–373 mbsf). Logs shown are caliper (CALI), gamma ray (SGR and CGR), and deep (IDPH), medium (IMPH), and spherically focused (SFLU) resistivity.

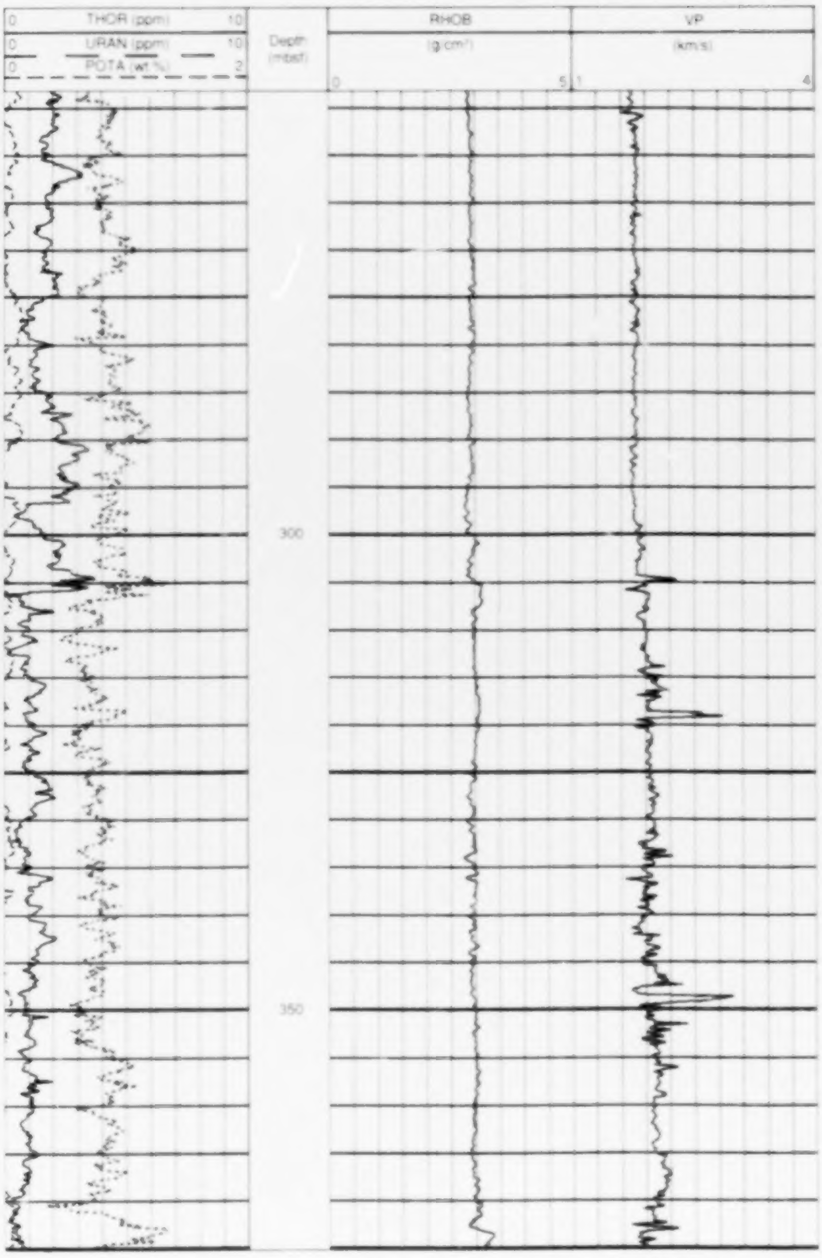

Figure 30. Enlarged plot of logs for the second unit (to 300 mbsf) and for the third unit (305–373 mbsf). Logs shown are thorium (THOR) and uranium (URAN), potassium (POTA), density (RHOB), and sonic velocity (VP).

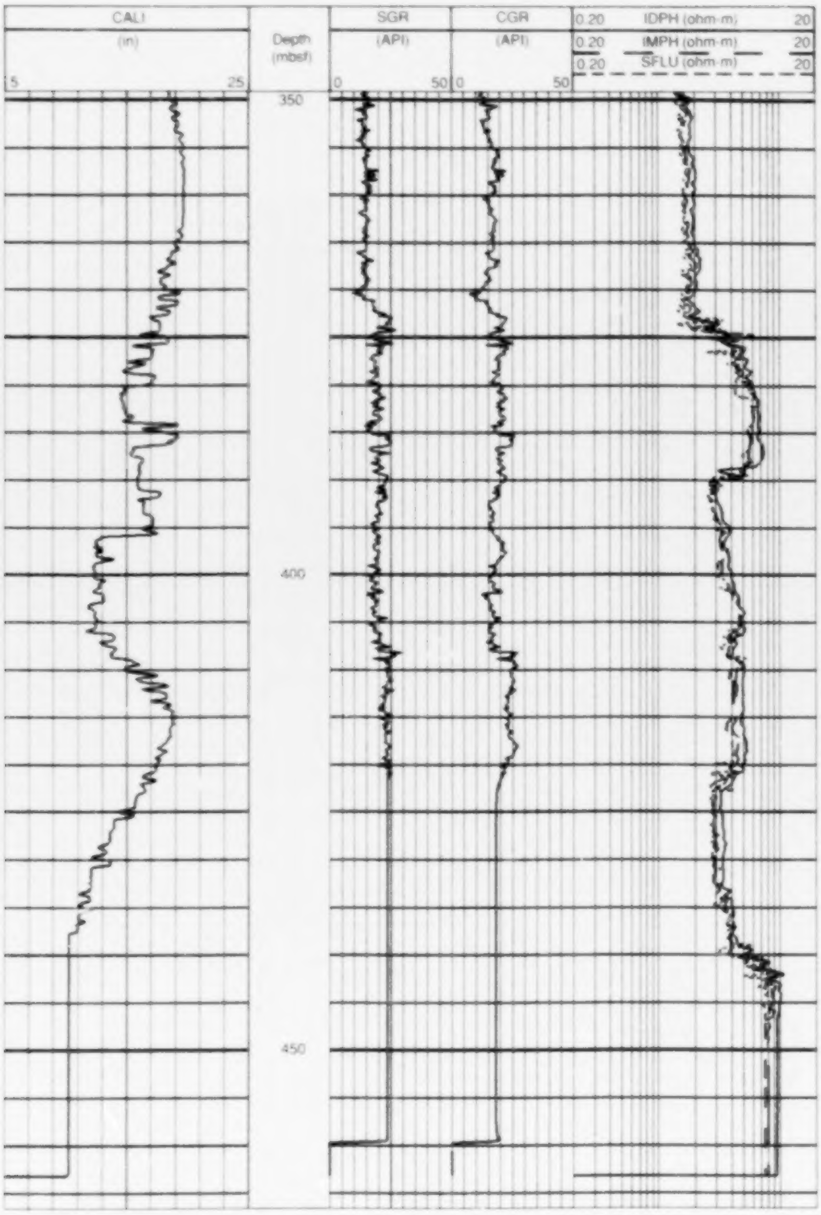

Figure 31. Enlarged plot of logs for the fourth unit (373–409 mbsf) and for basement (409 mbsf to bottom). Logs shown are caliper (CALI), gamma ray (SGR and CGR), and deep (IDPH), medium (IMPH), and spherically focused (SFLU) resistivity.

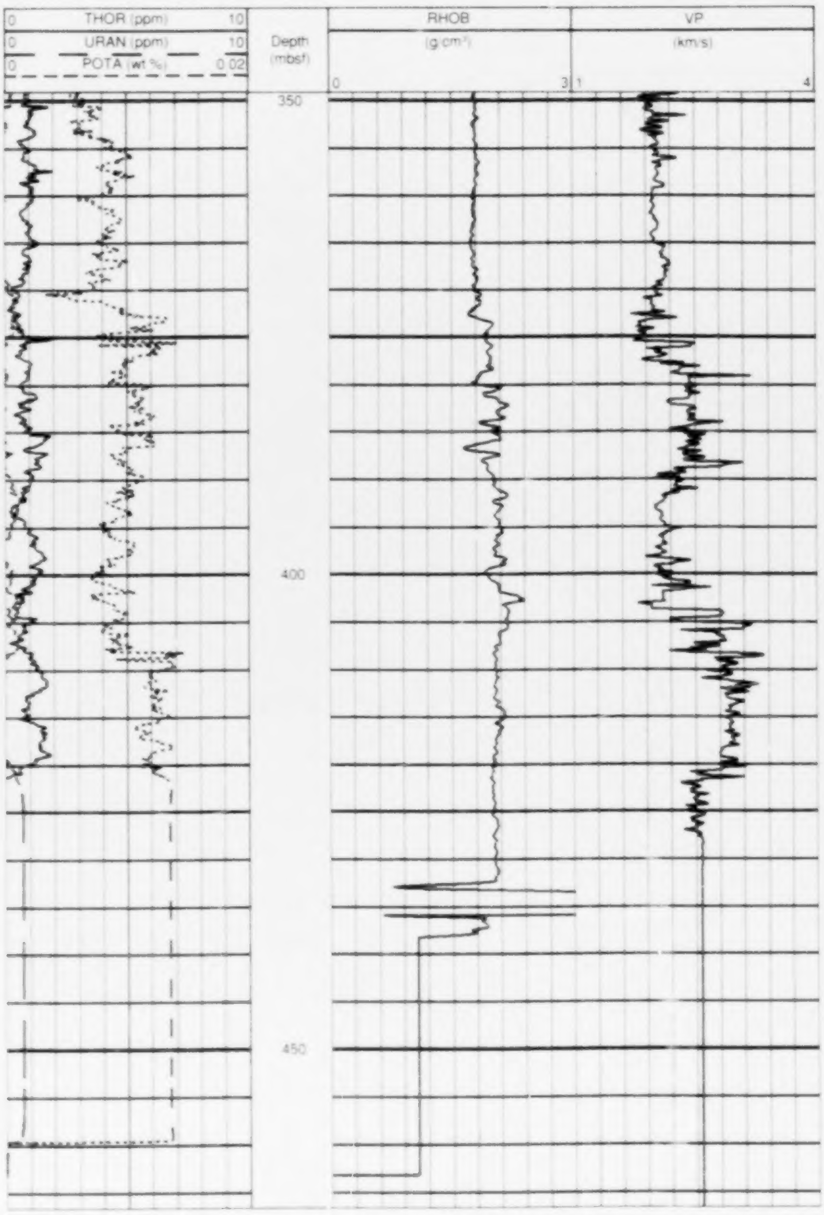

Figure 32. Enlarged plot of logs for the fourth unit (373–409 mbsf) and for basement (409 mbsf to bottom). Logs shown are thorium (THOR), uranium (URAN), potassium (POTA), density (RHOB), and sonic velocity (VP).

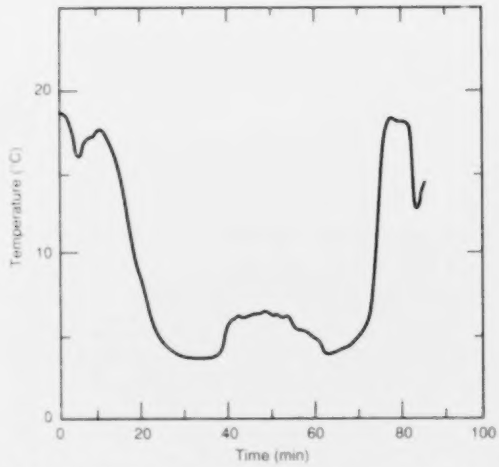

Figure 33. Record of temperature vs. time for Barnes-Uyeda Run 05H at 38.3 mbsf. The irregular temperature record between 40 and 60 min shows that the probe was being moved while it was in the sediment.

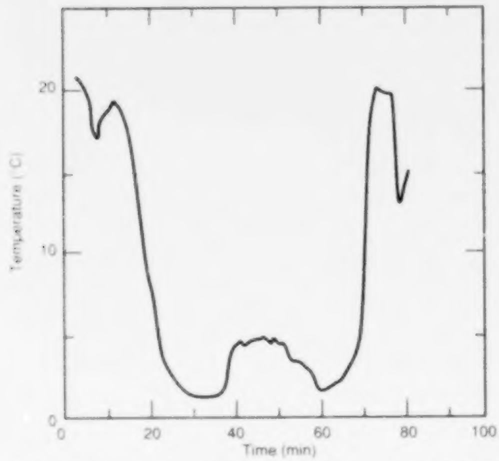

Figure 34. Record of temperature vs. time for Barnes-Uyeda Run 08H at 66.8 mbsf. The irregular temperature record between 50 and 60 min shows that the probe was being moved while it was in the sediment.

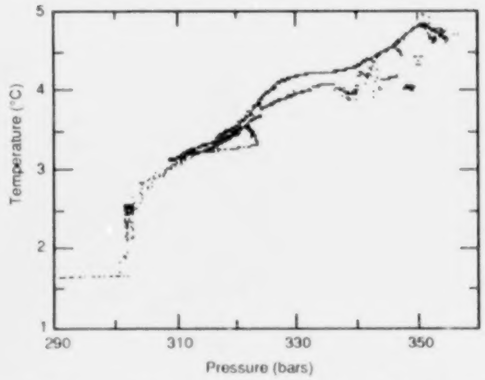

Figure 35. Record of temperature vs. pressure for the first run of the temperature logging tool (TLT). The upper, more solid, line of data is from the slower part of the logging run from the bottom of the hole upward and represents the best data from the run.

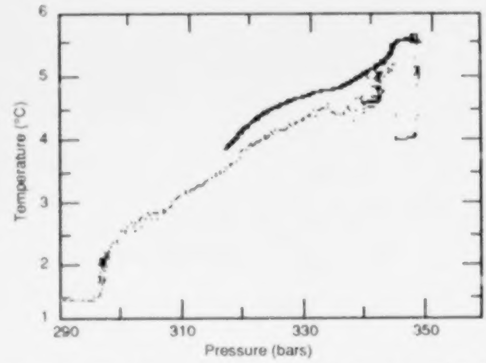

Figure 36. Record of temperature vs. pressure for the second TLT run. The bottom of the hole has warmed by about 1°C relative to the data presented in Figure 38.

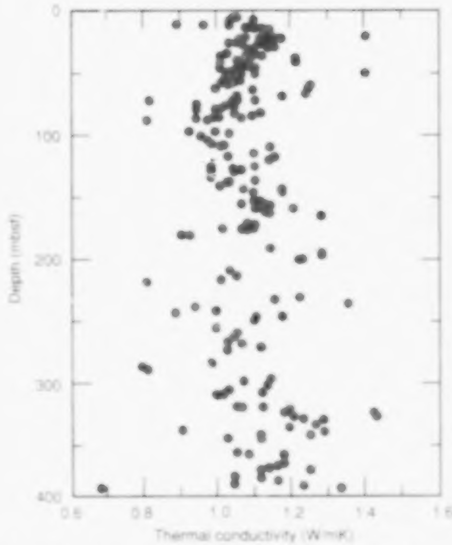

Figure 37. Thermal conductivity vs. depth for Hole 782B. There is little trend with depth.

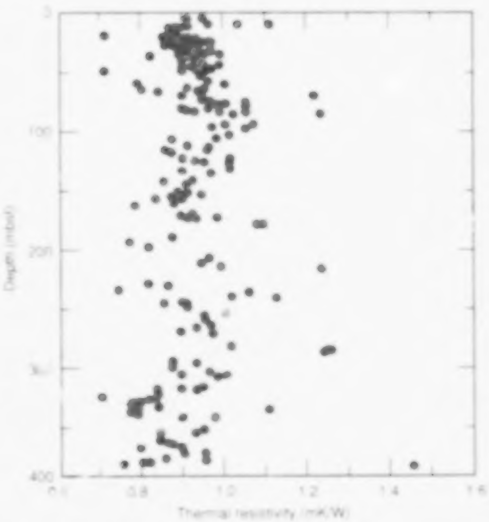

Figure 38. Thermal resistivity (the inverse of thermal conductivity) for Hole 782B.

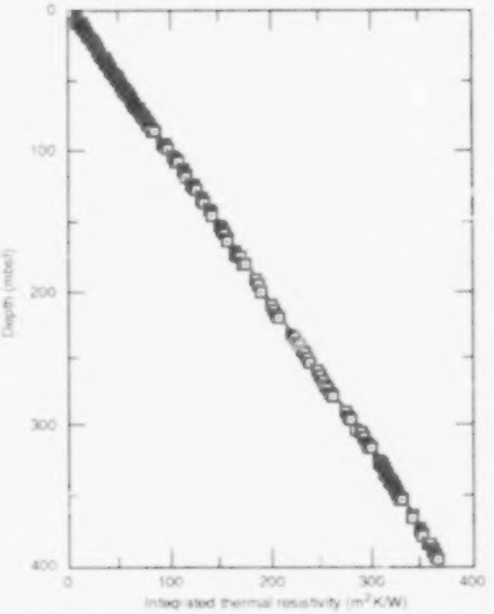

Figure 39. The depth integral of thermal resistivity vs. depth for Hole 782B. This will be combined with a calculated equilibrium temperature profile to determine the heat flow at this site.

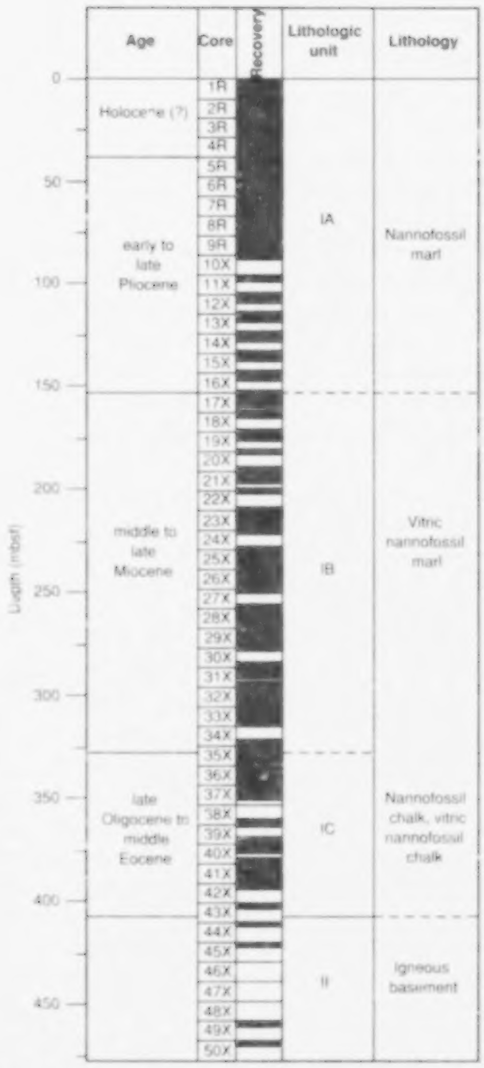

Figure 40. Core recovery and lithologic summary, Hole 782A.

Summary Log for Site 782

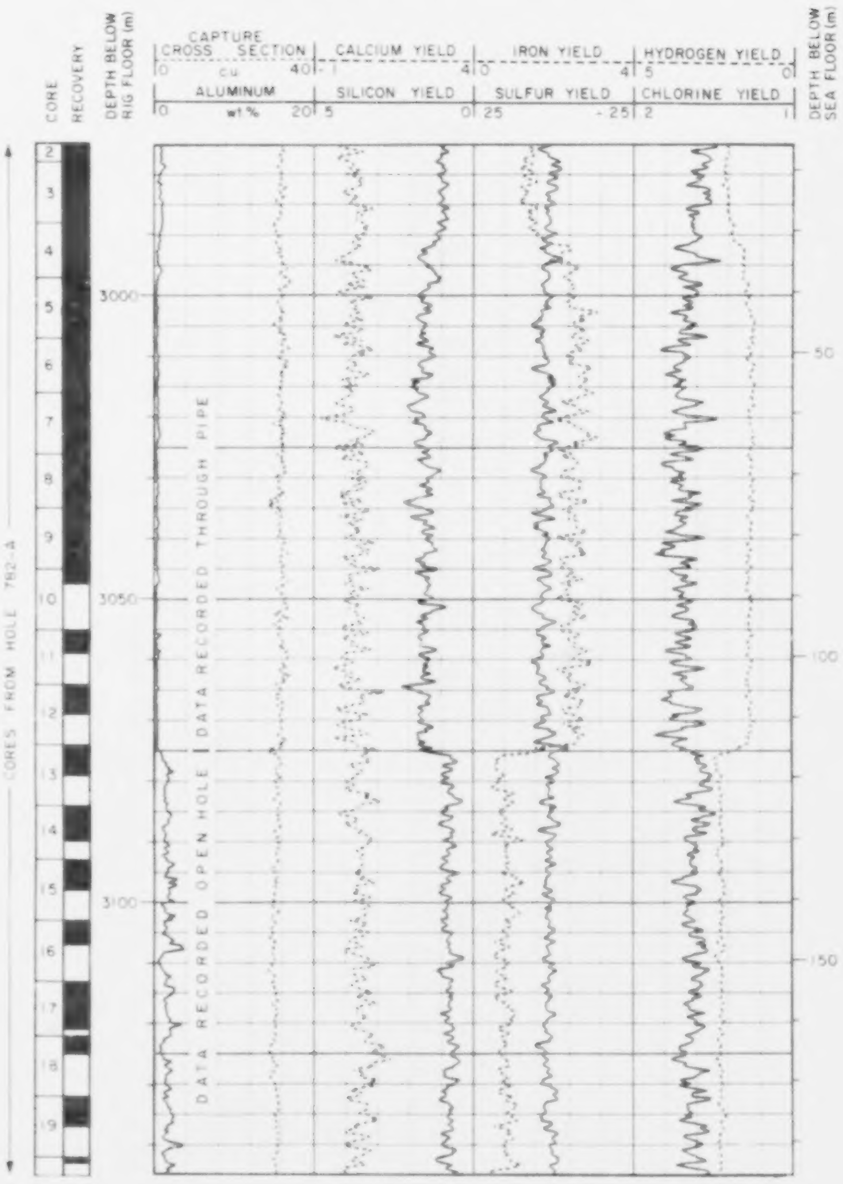

Summary Log for Site 782 (continued)

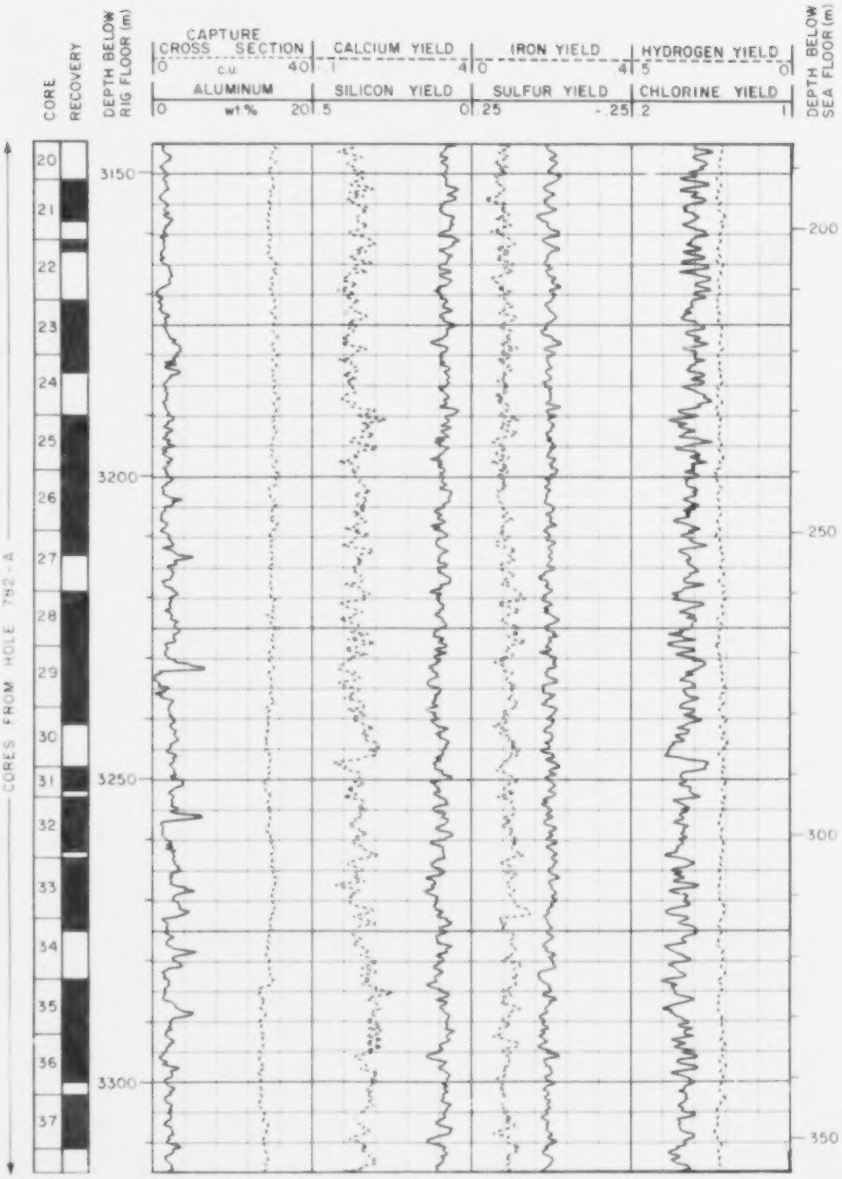

Summary Log for Site 782 (continued)

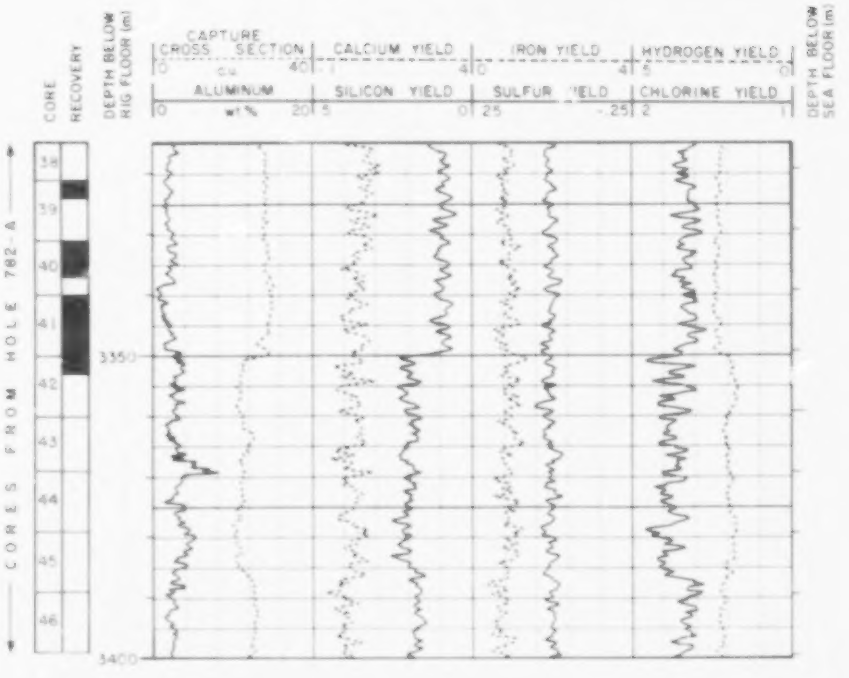

Summary Log for Site 782 (continued)

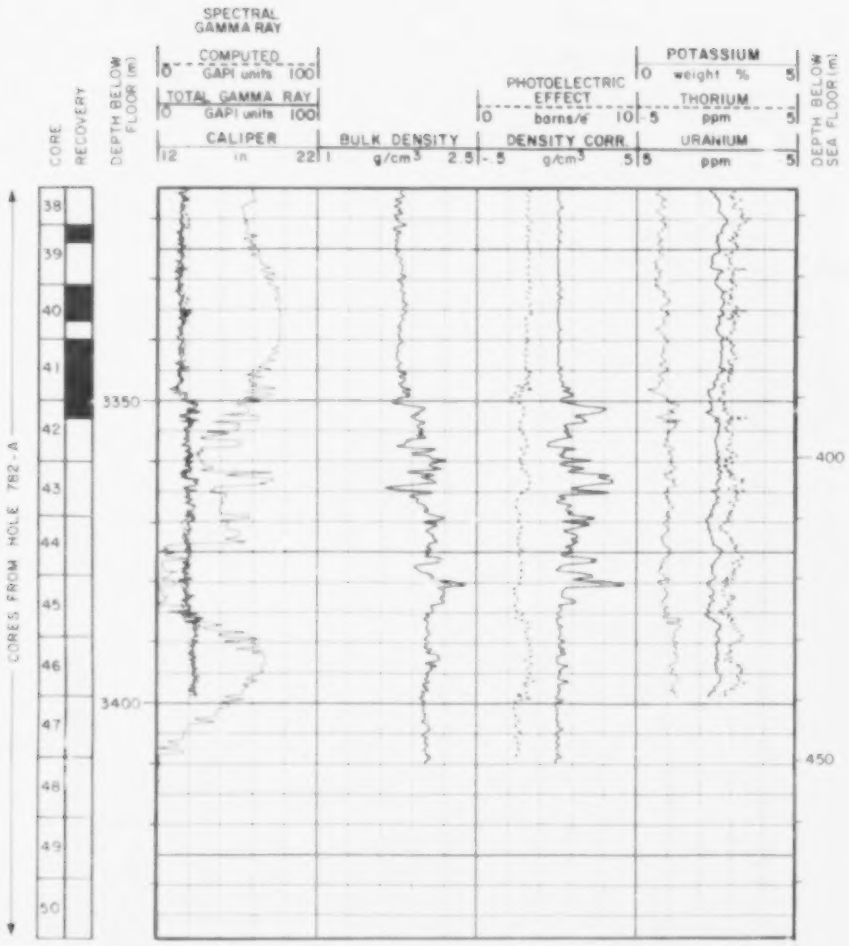

Summary Log for Site 782 (continued)

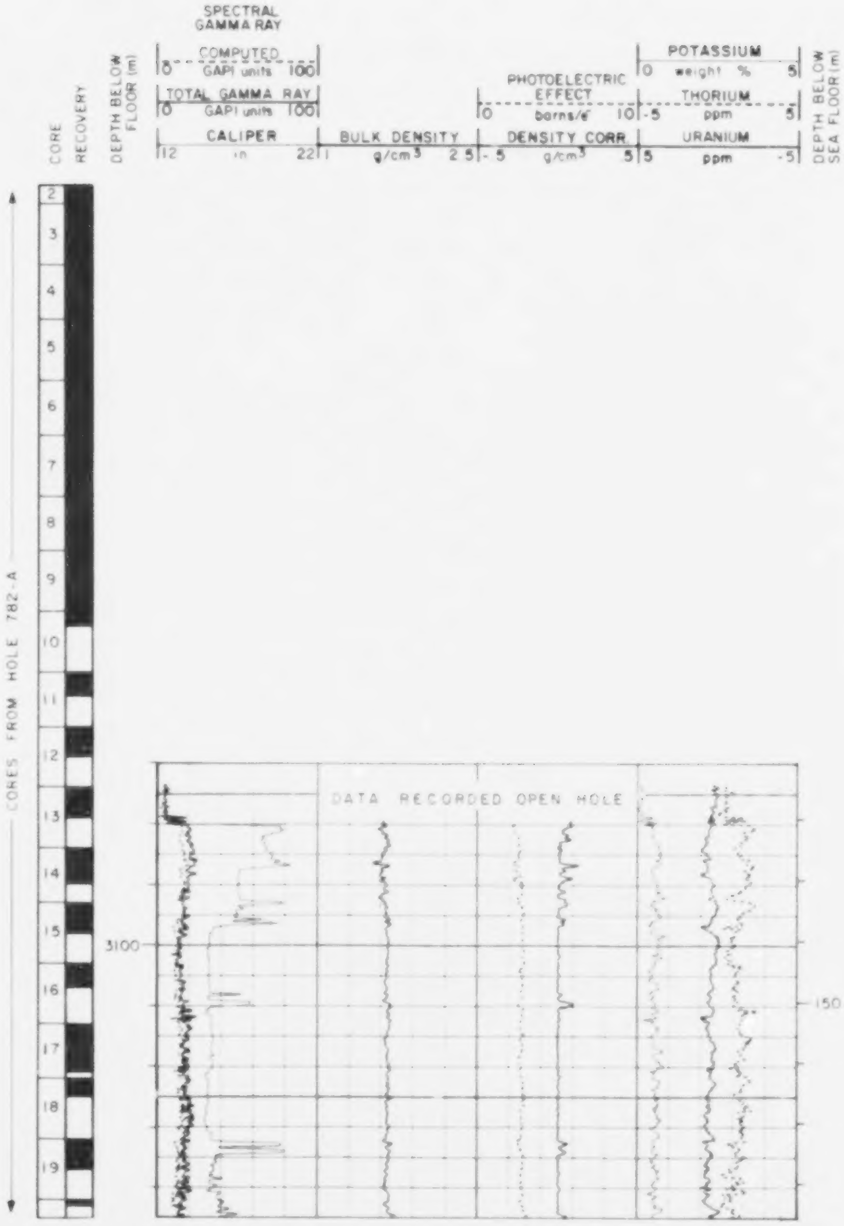

Summary Log for Site 782 (continued)

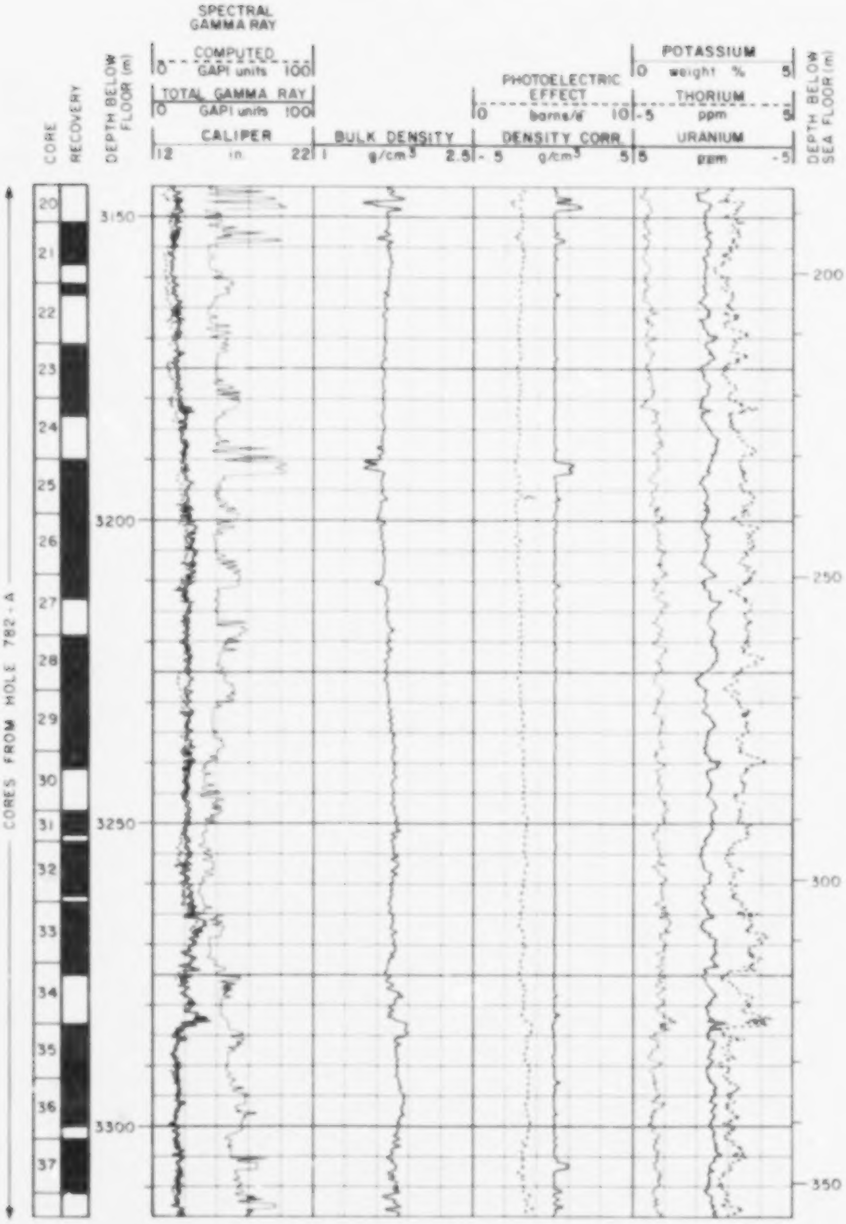

Summary Log for Site 782 (continued)

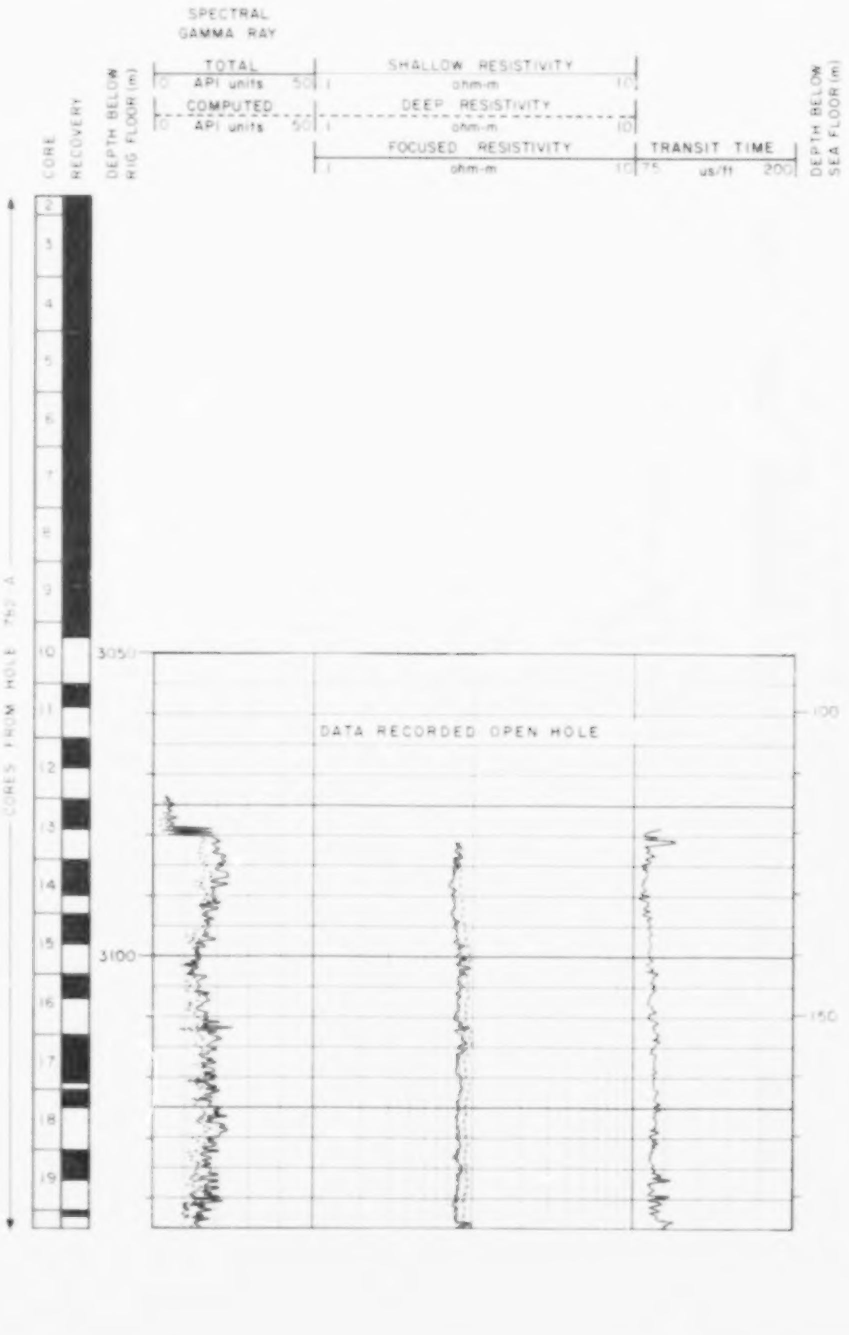

Summary Log for Site 782 (continued)

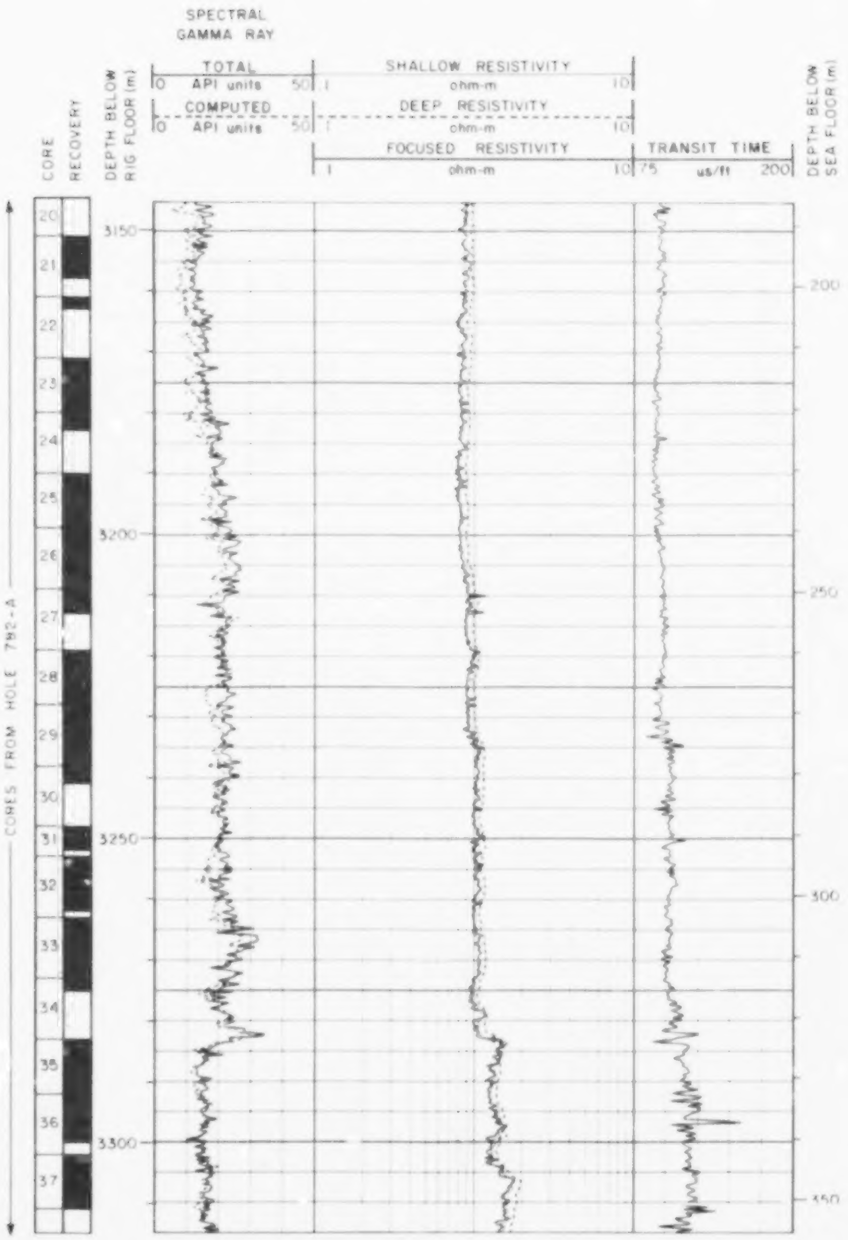

Summary Log for Site 782 (continued)

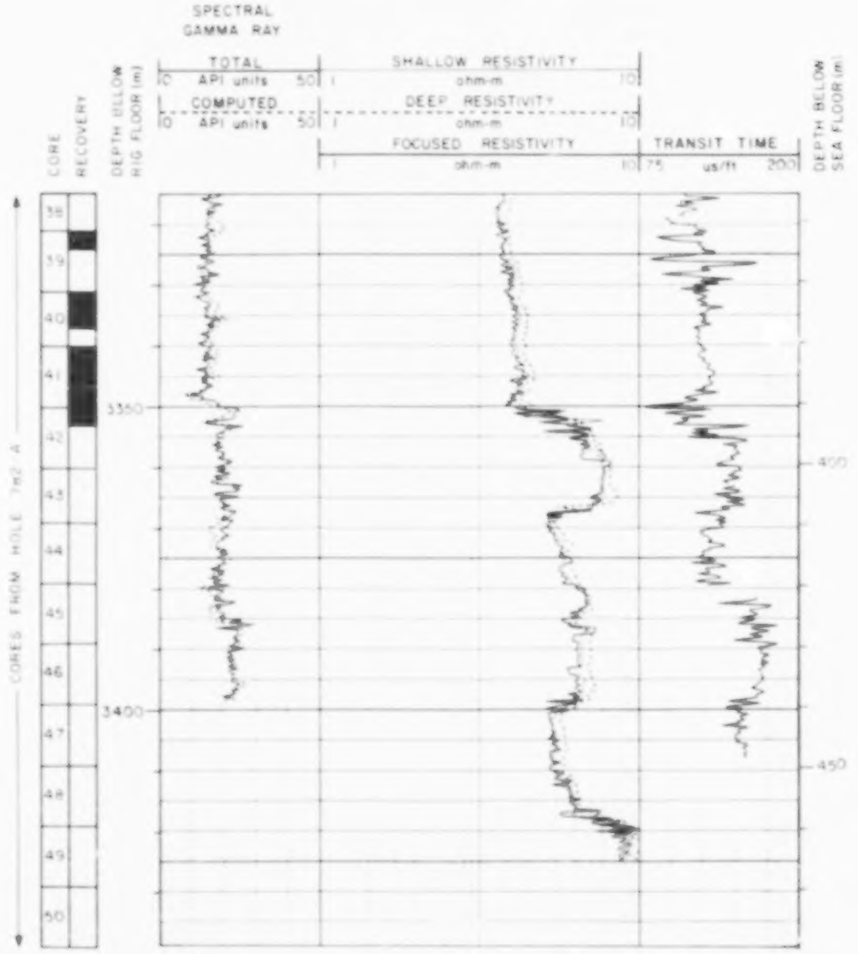

Fryer, P., Pearce, J. A., Stokking, L. B., et al., 1990
Proceedings of the Ocean Drilling Program, Initial Reports, Vol. 125

11. SITE 783[1]

Shipboard Scientific Party[2]

HOLE 783A

Date occupied: 24 March 1989

Date departed: 26 March 1989

Time on hole: 1 day, 5 hr, 45 min

Position: 30°57.86'N, 141°47.27'E

Bottom felt (rig floor; m; drill-pipe measurement): 4660.0

Distance between rig floor and sea level (m): 11.20

Water depth (drill-pipe measurement from sea level; m): 4648.8

Total depth (rig floor; m): 4828.20

Penetration (m): 168.20

Number of cores: 18

Total length of cored section (m): 168.20

Total core recovered (m): 46.95

Core recovery (%): 27.9

Oldest sediment cored:
  Depth (mbsf): 150.27
  Nature: glass-rich silty clay, sheared phacoidal serpentine
  Earliest age: early Pliocene(?)
  Measured velocity (km/s): 1.6
Hard rock:
  Depth (mbsf): 158.60
  Nature: serpentinized ultramafic rock

Principal results: Site 783 is located on the northern, midflank part of a seamount that forms part of a 500-km-long ridge running along the lowermost, inner wall of the Izu-Bonin Trench. The single hole, 783A, attempted at this site was drilled to 168.2 m below seafloor (mbsf) with 27.9% recovery before being abandoned because of high torque. Two lithologic units were defined. Unit I, from 0 to 120.0 mbsf, is middle or lower Pleistocene to lower Pliocene or older, glass-rich, silty clay to claystone. Unit II (120.0–158.6 mbsf) is phacoidal sheared serpentine with clasts of serpentinized harzburgite and metabasalt. The harzburgite has a primary mineralogy of olivine (80–90 modal%) and orthopyroxene (10–15 modal%) with minor clinopyroxene and spinel. Thus, the seamount is confirmed as serpentinite in composition, although the early Pliocene or older age demonstrates that it predates the Mariana serpentinite seamount drilled at Sites 778 through 780.

Shear fabrics and convolute plastic folding indicative of post-emplacement tectonic activity can be seen within the claystones of Unit I and the phacoidal serpentine of Unit II. Studies of physical properties show that the bulk densities increase from 1.47 to 1.59 g/cm^3 in the sediments of Unit I and cluster at about 2.1 g/cm^3 in the serpentine of Unit II. The average compressional-wave velocity in the sediments is 1.9 km/s. Thermal conductivities average about 1 W/mK in sediments and 1.91 W/mK in the serpentine. Heat flow in the sediments is 23 mW/m^2. Interstitial fluids show a sharp chemical discontinuity at the sediment/serpentine boundary with rapid chemical changes thereafter, which include increases in pH, calcium, and sodium, depletions in silica, magnesium, sulfate, and potassium, and little change in chlorinity. The fluid chemistry, therefore, shows that serpentinization is still taking place, but without the low-chlorinity component identified at the Mariana seamount (Sites 778 through 780).

BACKGROUND AND SCIENTIFIC OBJECTIVES

The eastern 50 km of the Izu-Bonin forearc is morphologically, compositionally, and structurally different from the remainder of the forearc. Within 50 km of the trench axis, a ridge runs for more than 500 km along the lowermost, inner wall of the Izu-Bonin Trench, at a latitude of about 30°N (Fig. 1). This ridge is separated from the outer-arc high by a narrow (~10 km wide) sediment trough, which has a series of seamounts along its eastern and western boundaries. Dredges from two of these seamounts, one at 32°N (K. Saboda, pers. comm., 1987) and the other at about 31°N (Kobayashi, 1989), recovered serpentinized ultramafic rocks. The seamount at 31°N, chosen for Ocean Drilling Program (ODP) Site 783, was dredged in 1988 at three locations (Fig. 2), yielding a wide variety of sedimentary, igneous, and metamorphic rocks (Kobavashi, 1989). Most of the samples dredged from the two summit locations are serpentinized ultramafic and mafic rocks, showing slickensides and fractures. Some pumice fragments and sedimentary rocks were also retrieved from the summit and these comprise the bulk of the rocks recovered from the lower west flank of the seamount. A very small amount of serpentine mud adhering to the surfaces of a few of the metamorphosed rocks was recovered.

Several multichannel seismic lines were run across the inner trench wall region, and the structure of the ridge and the seamounts within it are presented in Horine et al. (this volume). The presence of fault planes associated with the seamounts and detected within the ridge suggests that the ridge is still tectonically active. By comparison with Conical Seamount, the seamount at Site 783 is far more complex. The summit region of this seamount is broken by numerous small fault blocks and lacks coherent reflectors ("Underway Geophysics" chapter, this volume). Thus, the seamount is most likely not currently producing serpentine flows, but may be, however, a formerly active serpentinite diapir. The study of the interstitial waters within the sediments (both pelagic and serpentine) at this site is critical to the understanding of the history of this seamount, the flux of subduction-derived fluids through the outer forearc wedge, and the interaction of serpentinite with the associated country rock and overlying sediments.

The history of sedimentation in this part of the forearc has not been studied in detail. The rate of recent sedimentation in this part of the forearc, though expected to be lower than the rate closer to the active arc, is constrained only by seismic profiling. The sequence, if condensed, should provide a comprehensive history of outer-forearc sedimentation as well as a record of the interaction between pelagic sedimentation and influx from seamount serpentinite. In addition, an influx of arc-derived sediment is likely from cross-arc transport via the

---

[1] Fryer, P., Pearce, J. A., Stokking, L. B., et al., 1990. *Proc. ODP, Init. Repts.,* 125: College Station, TX (Ocean Drilling Program).

[2] Shipboard Scientific Party is as given in the list of participants preceding the contents.

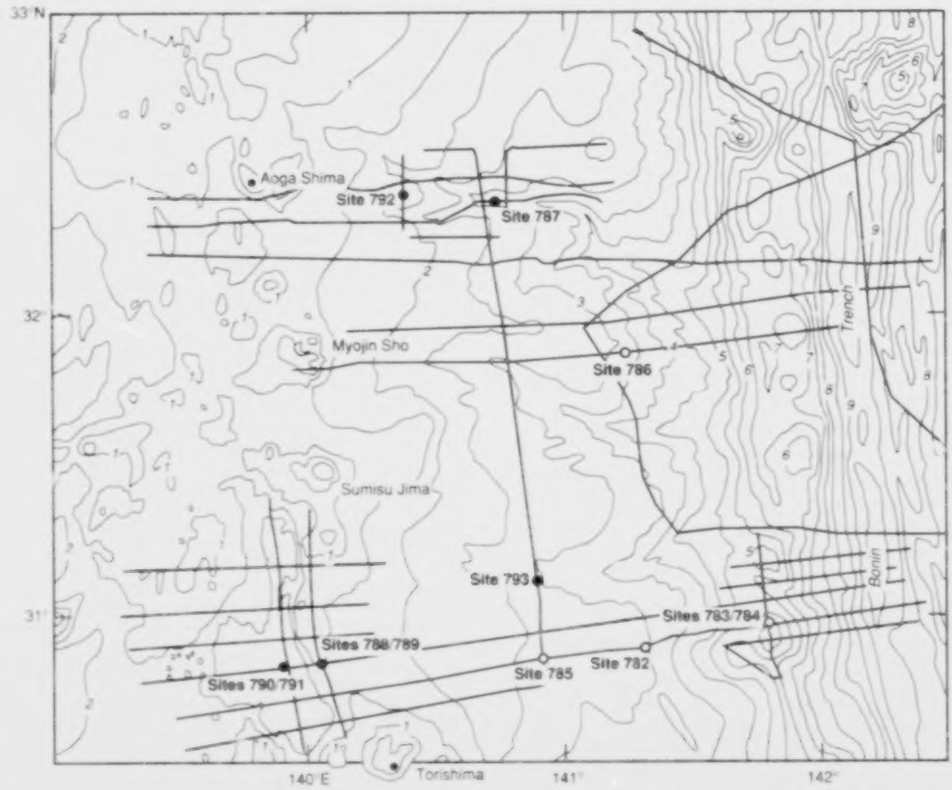

Figure 1. Location of sites in the Izu-Bonin forearc from Legs 125 and 126. Note the north-trending ridge on the inner trench wall. Site 783 was located at proposed Site BON-7. Crosses represent dredge sites on two seamounts of the outer forearc ridge, one at 32°N and the other at Site 783 at 31°N. Bathymetry in kilometers.

large canyon systems of the Izu-Bonin forearc. North of the seamount, a reentrant in the outer forearc ridge forms part of the distal portion of a prominent canyon system that stretches more than halfway across the forearc. Some of the sediment filling this part of the canyon laps onto the seamount. Thus, the nature of sediment transport along this channel can be investigated by drilling into the material on the north flank of the seamount.

The objectives of drilling at this site were as follows: (1) to determine the nature of sediments in the outermost forearc region; (2) to study the sedimentary sequences on the flank of the seamount, and hence to constrain the regional tectonic history of the ridge upon which the seamount is located, the age of the seamount, and the mode of emplacement of the seamount; (3) to study the composition and structure of basement underlying the sedimentary column in order to determine whether the seamount is a block of upfaulted lower crustal material or an older, tectonized analog of Conical Seamount; and (4) to determine the composition of interstitial waters present in the sediments. To achieve these objectives, Site 783 was located at 30°57.86'N, 140°47.27'E, in a water depth of 4648.8 m, on the northern, midflank part of the seamount (Fig. 1). The sediment cover over acoustic basement is approximately 200 m (see "Underway Geophysics" chapter, this volume).

OPERATIONS

Transit from Sites 782 to 783 (Proposed Site BON-7)

After a 26-nmi transit from Site 782, Site 783 was established at 2030UTC, 23 March 1989, by the deployment of a beacon.

Hole 783A

Because the nature of the material on the surface at Site 783 was unclear from the seismic records, a standard rotary core barrel (RCB) bottom-hole assembly with a hydraulic bit release was deployed. The pipe trip began at 2200UTC, 23 March, and Hole 783A was spudded at 0500UTC, 24 March. The first RCB retrieval recovered 9.71 m of core, establishing the mud line at 4648.8 m below sea level (mbsl). Recovery was sporadic in the lithologic units rich in ash, silt, and serpentine. No notable problems occurred until Core 125-783A-18R was being cut, when drill-string torque and circulation pressure

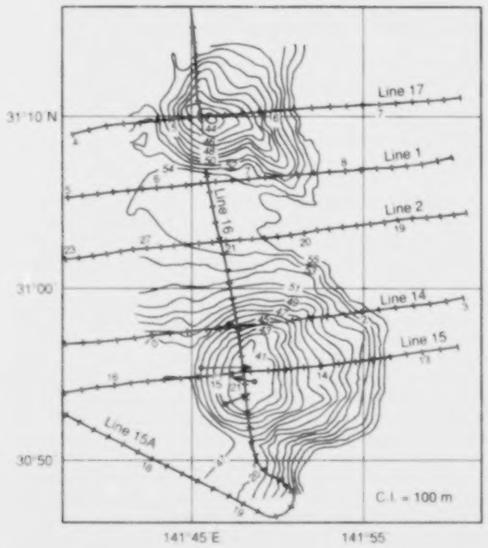

Figure 2. Bathymetry of the inner trench wall seamounts at 31°N. Site 783 is located on the north flank of the southern seamount. Arrows mark the tracks of three dredge hauls made on the seamount in 1988 (Kobayashi, 1989).

increased considerably. A mud pill, circulation of high-viscosity mud, and a wiper trip did not improve hole conditions, so the hole was abandoned.

The RCB was deployed 18 times to a total depth of 168.2 mbsf in Hole 783A, recovering 46.95 m of core for a recovery rate of 27.9% (Table 1). Heat-flow measurements were taken at 42.7 and 90.0 mbsf. Site 783 officially ended at 0215UTC, 26 March, when the drill string was pulled to 4088.8 mbsl and the vessel was under way for Site 784 in dynamic positioning mode.

Table 1. Coring summary for Site 783.

Core no.	Date (March 1989)	Time (UTC)	Depth (mbsf)	Length cored (m)	Length recovered (m)	Recovery (%)
125-783A-						
1R	24	0630	0.0–9.7	9.7	9.71	100.0
2R	24	0800	9.7–16.4	6.7	1.89	28.2
3R	24	0920	16.4–26.0	9.6	0.02	0.2
4R	24	1050	26.0–35.7	9.7	6.72	69.3
5R	24	1210	35.7–42.7	7.0	5.25	75.0
6R	24	1500	42.7–52.4	9.7	0.00	0.0
7R	24	1610	52.4–62.1	9.7	4.70	48.4
8R	24	1720	62.1–71.8	9.7	4.33	44.6
9R	24	1815	71.8–81.3	9.5	0.02	0.2
10R	24	1915	81.3–90.9	9.6	1.87	19.5
11R	24	2230	90.9–100.6	9.7	0.22	2.3
12R	25	0000	100.6–110.2	9.6	0.40	4.2
13R	25	0230	110.2–119.9	9.7	0.11	1.1
14R	25	0500	119.9–129.6	9.7	0.42	4.3
15R	25	0800	129.6–139.2	9.6	4.49	46.8
16R	25	1140	139.2–148.9	9.7	3.87	39.9
17R	25	1500	148.9–158.6	9.7	1.67	17.2
18R	25	1750	158.6–168.2	9.6	1.26	13.1
Coring totals				168.2	46.95	27.9

LITHOSTRATIGRAPHY

The stratigraphic section recovered at Site 783 is divided into two lithologic units: lithologic Unit I, composed primarily of olive brown (2.5Y 4/4) to greenish-gray (5G 4/1) vitric clayey silt and glass-rich silty clay or claystone, and lithologic Unit II, composed of greenish-gray (5GY 6/1 to 5GY 4/1) and bluish-gray (5B 6/1 to 5B 4/1) phacoidal, sheared serpentine with vertical convolute bedding (Table 2).

Lithologic Unit I

Sections 125-783A-1R-1, 0 cm, to 125-783A-14R-1, 12 cm; depth, 120.0 mbsf.
Age: middle or early Pleistocene to early Pliocene(?).

Lithologic Unit I has varying amounts of silt-sized detritus, most of which represents a volcanic influx: glass (7%–58%), feldspar (trace–15%), pyroxene (0%–2%), chlorite (0%–2%), and epidote (0%–7%). A trace to 5% zeolite present in a few cores (Cores 125-783A-1R, 125-783A-3R through 125-783A-5R, 125-783A-7R, 125-783A-11R, and 125-783A-12R) is interpreted as an alteration product of volcanic glass.

The ash layers in Cores 125-783A-1R, 125-783A-4R, 125-783A-5R, and 125-783A-10R of Unit I all have sharp basal contacts, are 1 to 2 cm thick, and are composed of volcanic glass (60%–90%) and feldspar (5%–10%), variable amounts of pyroxene (as much as 15%), opaque minerals (as much as 5%), chlorite (trace amounts), and clays (as much as 15%). In addition to the ash layers are a few layers of vitric sands and silts with large admixtures of clay (30%–60%) that are interpreted as reworked ash.

Pumice, in millimeter- to centimeter-sized clasts, is scattered throughout the unit. The pumice is usually located several centimeters above an ash layer and may be related to the same eruptive event as the underlying ash layer, with the pumice requiring a longer time for gravitational settling through the water column than the smaller vitric fragments.

Lithic fragments, such as marlstone and claystone, were observed in Cores 125-783A-1R, 125-783A-4R, and 125-783A-5R. Thulite, which was commonly observed in association with serpentine at Site 780 (see "Lithostratigraphy" section, "Site 780" chapter, this volume), occurs in Cores 125-783A-4R, 125-783A-5R, and 125-783A-8R. Serpentine was also observed (in Cores 125-783A-5R, 125-783A-7R, 125-783A-8R, 125-783A-10R, 125-783A-12R, and 125-783A-14R) and increases downhole from trace amounts to 10%.

Lithologic Unit I contains a small biogenic contribution: spicules (as much as 10%), radiolarians (as much as 5%), diatoms (as much as 10%), silicoflagellates (rarely present, a trace amount to 1%), nannofossils (rarely present, as much as 15%), and foraminifers (rarely present, 3%–4%). Parts of the unit have sufficient biogenic constituents to be nannofossil-bearing or -rich, or biogenic silica-rich. Calcareous biogenic material is lacking in the lower section of this unit, whereas siliceous biogenic material is present throughout the section. Diatoms are present from the top of the unit down to at least Section 125-783A-10R-CC, and radiolarians occur throughout the section, including the base of Unit I in Core 125-783A-14R.

Nannofossils present in Sample 125-783A-1R-1, 1 cm, from the top of the first core, provide a stratigraphic age of middle or early Pleistocene for the uppermost sediment in Unit I. Section 125-783A-10R-CC, near the base of the unit, has a diatom biostratigraphic age of early Pliocene; the age of the oldest stratum in Unit I is unknown but is at least early Pliocene.

Table 2. Lithologic units recovered at Site 783, Leg 125.

Lithologic unit	Cores	Depth (mbsf)	Dominant lithology	Stratigraphic age
I	783A-1R-1, 0 cm, to 783A-14R-1, 12 cm	0.0–120.0	Vitric clayey silt, glass-rich silty clay/claystone	middle or early Pleistocene to early Pliocene(?)
II	783A-14R-1, 12 cm, to 783A-18R-1, 147 cm	120.0–158.6	Phacoidal sheared serpentine with vertical convolute bedding	?

The change from clay to claystone is typical of burial diagenesis. The clay gradually is compacted, becomes firmer, and eventually is sufficiently lithified in parts of the core so that it becomes necessary to cut the core with a saw to minimize disruption of the sediments. The transition from clay to claystone occurs in Section 125-783A-8R-1. In addition to the burial diagenesis, there is an apparent overprint of tectonic diagenesis beginning in Section 125-783A-8R-2, 130 cm, and continuing into Section 125-783A-8R-3. This is seen as a scaly fabric with slickensided surfaces of claystone and the development of a spongy texture with higher apparent permeability than the overlying claystone (for further discussion see "Structural Studies" section, this chapter). The sediment in this region may have provided a pathway for fluids to escape from the underlying serpentine in lithologic Unit II.

Lithologic Unit II

Sections 125-783A-14R-1, 12 cm, to 125-783A-18R-1, 147 cm; depth, 120.0–158.6 mbsf.
Age: ?

The contact between lithologic Units I and II was not recovered. The immediate interval is represented by serpentine-bearing, feldspar- and glass-rich silty clay underlain by a 1-cm interval of volcanic ash, which is disseminated along the core liner for the next 4 cm (a 4-cm void in the core), followed by a 2-cm-diameter clast of serpentinized ultramafic rock. Lithologic Unit II is composed of phacoidal sheared serpentine that displays convolute bedding and blocks of serpentinized harzburgite; in Core 125-783A-18R the composition is primarily blocks of serpentinized harzburgite with some matrix of phacoidal sheared serpentine.

No fossils or obvious detrital components were found in this unit. The age of these strata is unknown. In the absence of evidence for faulting, it is likely that this unit is in stratigraphic continuity with Unit I, in which case Unit II is probably at least early Pliocene, the oldest diatom biostratigraphic age in the overlying unit.

BIOSTRATIGRAPHY

Calcareous nannofossil and diatom evidence from Site 783 indicates that the sedimentary interval from Samples 125-783A-1R-1, 28 cm, to 125-783A-10R-CC ranges in age from middle to early Pleistocene to the early Pliocene. No ages could be assigned to the remaining sedimentary cores (125-783A-11R to 125-783A-15R).

The sedimentary interval in Hole 783A may have been deposited near the carbonate compensation depth (CCD), as shown by strong dissolution of the calcareous plankton assemblages. Nannofossil evidence suggests that Sample 125-783A-13R-CC was probably reworked.

Calcareous Nannofossils

Samples from Cores 125-783A-1R, 125-783A-3R, 125-783A-4R, and 125-783A-13R contain rare to common, poor to moderately preserved nannofossil assemblages. The poor preservation probably resulted from deposition at or near the CCD. Samples 125-783A-1R-1, 28 cm, 125-783A-3R-CC, and 125-783A-4R-CC can be given a generic middle/early Pleistocene age based upon the presence of rare *Pseudoemiliania lacunosa* and unidentified species of *Gephyrocapsa* sp. A common, moderately preserved assemblage in Sample 125-783A-4R-1, 69 cm, is recognized to have an early Pleistocene age corresponding to the "Small *Gephyrocapsa* Zone" (Gartner, 1977) within Zone CN14a.

A rare, well-preserved late Eocene nannofossil assemblage (Zones CP14b/15) containing *Dictyococcites bisectus*, *Sphenolithus predistentus*, *Discoaster barbadiensis*, and *Cribrocentrum reticulatum*, together with dissolved fragments of coccoliths that appear to be younger in age, is present in Sample 125-783A-13R-CC. The good preservation and rarity of the Eocene nannofossils (usually well-preserved Eocene assemblages are abundant) suggest reworking.

Foraminifers

No samples examined from Site 783 (Samples 125-783A-1R-CC to 125-783A-15R-CC) contained planktonic or benthic foraminifers. This is probably because deposition took place at or below the CCD.

Diatoms

Rare to common, poorly preserved to well-preserved diatom assemblages are present in the sedimentary interval at Hole 783A. In the majority of the samples, however, fragments (of *Thalassionema nitzschioides* and some *Ethmodiscus rex*) dominate. Therefore, it was only possible to date three samples.

Sample 125-783A-1R-CC is characterized by *Pseudoeunotia doliolus* and *Nitzschia reinholdii*. Sample 125-783A-1R-1, 1 cm, also contains *N. reinholdii*, assigning the whole of this core to the lower Pleistocene (*N. reinholdii* Zone).

Sample 125-783A-5R-CC was dated as late Pliocene by the presence of *Rhizosolenia praebergonii* and the absence of *P. doliolus* (*R. praebergonii* Zone).

Nitzschia jouseae is present in Sample 125-783A-10R-CC; therefore, this sample is early Pliocene in age.

IGNEOUS AND METAMORPHIC PETROLOGY

The rocks recovered from Site 783 are serpentinized harzburgite (90%–95%), dunite (5%–10%), and subordinate metabasalt and meta-volcaniclastic rocks. These form clasts of isolated fragments and occur as inclusions in a matrix of highly sheared and pulverized serpentinite. The clasts are 1 to 10 cm in diameter and subangular to subrounded in shape.

Ultramafic Rocks

Serpentinized Harzburgite

The clasts of serpentinized harzburgite are massive and dark bluish gray (5B 4/1) to black (5G 3/2). The primary mineralogy of the harzburgite is olivine (85%–90%), orthopyroxene (10%–15%), clinopyroxene (1%–2%), and chromium-spinel (trace–2%). Olivine is anhedral and 0.5 to 3 mm in size. Orthopyroxene is subhedral to anhedral and 1 to 5 mm in diameter. Clinopyroxene is present as blebs and anhedral crystals (less than 1 mm), closely related to orthopyroxene, and as exsolution lamellae (on [100]) in orthopyroxene. Chromium-spinel is dark red in color, 0.2 to 1 mm in diameter, and exhibits a subhedral to anhedral shape. Wavy extinction and rare kink-banding are recognizable in olivine, orthopyroxene, and clinopyroxene crystals.

One distinctive feature of Sections 125-783A-17R-CC and 125-783A-18R-1 is the presence of 0.5- to 1.5-cm-thick pyroxene-rich lherzolitic bands within the harzburgite (Fig. 3). These contain olivine (60%–75%), orthopyroxene (15%–20%), clinopyroxene (5%–20%), and spinel (trace–2%). Orthopyroxene and olivine are anhedral, 1 to 4 and 1 to 3 mm in diameter, respectively. Clinopyroxene forms subhedral to anhedral crystals (1–2.5 mm) and exsolution lamellae (on [100]) in orthopyroxene. Spinel is subhedral to anhedral and 0.2 to 1 mm in diameter. Spinel is dark brown and probably low in chromium and high in aluminum. The contact between the band and the host rock is obscure.

Olivine and orthopyroxene are variably replaced by serpentine minerals, which appear to be mostly chrysotile and/or lizardite. A mesh texture after olivine is predominant, and undeformed bastite pseudomorphs of orthopyroxene are common. Clinopyroxene is less serpentinized. Anastomosing veins of serpentine can be seen in some clasts. The degree of serpentinization is variable, from 60% to 95%.

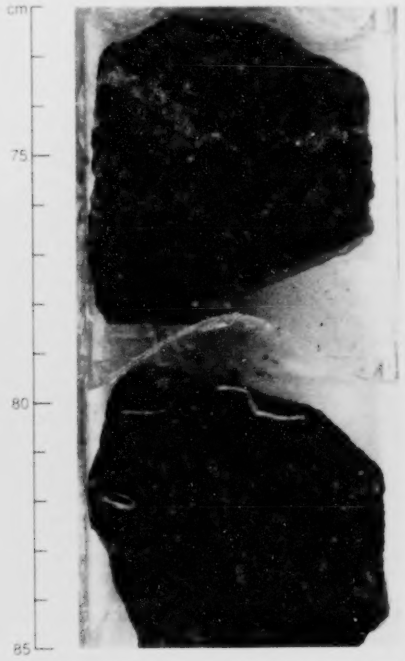

Figure 3. A pyroxene-rich (lherzolitic) band in the upper harzburgite clast in Section 125-783A-18R-1, 72–85 cm.

Serpentinized Dunite

Highly serpentinized (greater than 95% serpentine) dunites are rare. They are massive and black (5G 3/2) in color. The rocks consist of olivine (greater than 95%), orthopyroxene (less than 5%), and chromium-spinel (less than 1%). Serpentinized olivine exhibits a massive mesh-textured fabric, and there are rare, undeformed bastite pseudomorphs of orthopyroxene. Dark reddish chromium-spinel is well preserved.

Metavolcanic Rocks

Metabasalt

Several clasts of metabasalt, 1 to 1.5 cm in diameter, were recovered. Most of the clasts are grayish green (5G 4/2–5G 5/2), and one clast containing abundant limonite is dark reddish brown (5YR 2.5/2). The metabasalts are composed of plagioclase, clinopyroxene, olivine(?), and glass as primary phases and chlorite, albite, sphene, dusty brownish clay, zeolite, and limonite as secondary phases. The primary igneous textures, such as intersertal and aphyric textures, are well preserved, but almost all the primary minerals except clinopyroxene are fully chloritized. All of the clasts are fractured to varying degrees and contain 0.2- to 0.8-mm chlorite veins running throughout. Zeolite fills in vesicles greater than 0.2 mm.

Meta-Volcaniclastic Rock

Only one example of a clast of meta-volcaniclastic rock was recovered. The rock is 5 cm in diameter, light greenish-gray (5G 7/1), and medium- to fine-grained and consists of plagioclase and clinopyroxene as relic minerals and prehnite, aluminum-rich epidote, actinolite, chlorite, sphene, and probably hydrogrossular as secondary minerals. The clast contains abundant subangular to subrounded fragments of plagioclase and clinopyroxene within a fine-grained dusty matrix. The size of the fragments is variable, ranging from less than 0.1 to 1 mm. Most of the clinopyroxene fragments are altered to colorless actinolite, and those of plagioclase to aluminum-rich epidote and prehnite. The textural relationships suggest that prehnite, epidote, and actinolite are an equilibrium assemblage. Later-stage cataclastic deformation has developed along the boundaries of fragments.

IGNEOUS AND METAMORPHIC GEOCHEMISTRY

Five of the ultramafic clasts (harzburgites) from Site 783 were selected for shipboard geochemical analysis. Preparation and analytical techniques are given in the "Explanatory Notes" chapter of this volume. Rock and thin-section descriptions are given in the preceding "Igneous and Metamorphic Petrology" section. The geochemical data are listed in Tables 3 and 4.

Ultramafic Samples

Modal estimates of the original (pre-serpentinization) composition of ultramafic rocks range from 74% to 86% olivine, 12% to 20% orthopyroxene, 1% to 5% clinopyroxene, and less than 2% spinel. The degree of serpentinization of the samples varies from 55% to 92%.

Major-Element Chemistry

Loss on ignition (LOI) of these samples ranges from 12.62 to 15.75 wt% and like that of the samples from Site 779, shows a positive correlation with the degree of serpentinization (Fig. 4). (See "Igneous and Metamorphic Geochemistry" sections of "Site 778" and "Site 779" chapters, this volume, and "Explanatory Notes" for an explanation of LOI.) Concentra-

Table 3. Major-element data for serpentinized harzburgites from Hole 783A.

Core, section: Interval (cm):	16R-CC, 14–17	16R-CC, 19–22	17R-1, 9–12	18R-1, 49–51	18R-1, 96–97
SiO_2	36.41	39.21	35.90	36.01	36.84
TiO_2	0.00	0.00	0.00	0.00	0.00
Al_2O_3	0.41	0.59	0.35	0.47	0.45
Fe_2O_3	7.28	7.37	7.42	7.64	7.87
MnO	0.09	0.11	0.11	0.12	0.11
MgO	40.18	38.19	39.39	39.35	39.91
CaO	0.43	1.66	0.31	0.66	0.63
Na_2O	0.00	0.00	0.00	0.00	0.00
K_2O	0.00	0.00	0.00	0.00	0.00
P_2O_5	0.00	0.00	0.00	0.00	0.00
NiO	0.28	0.25	0.29	0.30	0.29
Cr_2O_3	0.16	0.21	0.18	0.21	0.25
[a]LOI	14.83	12.62	15.75	14.99	13.55
Total	100.07	100.21	99.70	99.75	99.90
Mg#	91.62	91.12	91.32	91.07	90.94
[b]% Serpentinization	70.00	55.00	92.00	60.00	60.00

Note: Data (in wt% oxides) from whole-rock analyses by XRF.

[a] LOI = loss on ignition between 105° and 1030°C.

[b] Estimated from thin sections.

tions of major-element oxides in these rocks are similar to concentrations in the harzburgites from Sites 778, 779, and 780. SiO_2 ranges from 35.90 to 39.21 wt%, MgO from 38.19 to 40.18 wt%, Al_2O_3 from 0.35 to 0.59 wt%, and Fe_2O_3 from 7.28 to 7.87 wt%. Magnesium number is also similar to that in the harzburgites from Sites 778, 779, and 780 and varies from 90.94 to 91.62. The concentrations of Na_2O, K_2O, and P_2O_5 are all below detection limits. The general absence of clinopyroxene crystals and very low concentrations of Al_2O_3 and CaO indicate that the rocks are residues from high degrees of partial melting.

Trace-Element Chemistry

In the trace-element data presented in Table 4, compatible elements are high in all samples, as would be expected. Values of chromium range from 1074 to 1716 ppm, and those of nickel, from 2210 to 2357 ppm, with the exception of low-nickel Sample 125-783A-16-CC (Piece 2, 19–22 cm), which contains 1980 ppm. Average concentrations of nickel in harzburgites from Sites 783 (2215 ppm) and 780 (2261 ppm) are slightly lower than those of the harzburgites from Sites 778 (2644 ppm) and 779 (2320 ppm). Chromium and nickel do not correlate with one another or with the degree of serpentinization.

Table 4. Trace-element data for serpentinized harzburgites from Hole 783A.

Core, section: Interval (cm):	16R-CC, 14–17	16R-CC, 19–22	17R-1, 9–12	18R-1, 49–51	18R-1, 96–97
Nb	tr	tr	tr	tr	tr
Zr	1	0	1	1	1
Y	nd	1	0	1	0
Sr	10	12	9	13	13
Rb	nd	nd	nd	0	nd
Zn	39	31	34	41	38
Cu	0	29	2	2	1
Ni	2210	1980	2267	2357	2260
Cr	1074	1469	1255	1451	1716
V	9	23	21	39	36
Ce	tr	tr	tr	12	tr
Ba	tr	tr	13	tr	15

Note: Data (in ppm) from whole-rock analyses by XRF, nd = none detected, tr = below detection limit (<5 ppm for Nb, <10 ppm for Ba and Ce).

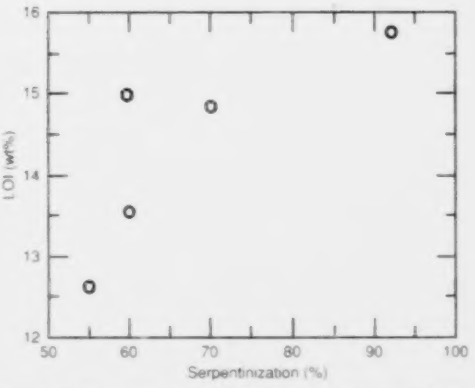

Figure 4. Modal percent of serpentinization vs. weight percent loss on ignition (LOI) of between 105° and 1030°C.

Niobium, zirconium, yttrium, rubidium, and titanium are all present in trace amounts or are below detection limits. Cerium and barium values range from below their detection limits (less than 10 ppm) to 12 and 15 ppm, respectively, although the cerium values at least may result from analytical error. Strontium varies from 9 to 13 ppm, similar to its concentrations in harzburgites from Sites 778, 779, and 780. Zinc ranges from 31 to 41 ppm, with an average concentration of 37 ppm, which is similar to that of the harzburgites from Site 780 (36 ppm) and slightly lower than those of harzburgites from Sites 778 (42 ppm) and 779 (39 ppm). There is no significant correlation between the geochemical parameters and depth.

Sample 125-783A-16R-CC (Piece 2, 19–22 cm) is anomalously rich in copper (29 ppm). It shows the highest concentrations of SiO_2 (39.21 wt%) and Al_2O_3 (0.59 wt%) of all the samples analyzed from this site. It also shows the highest concentration of CaO (1.66 wt%) and lowest nickel (1980 ppm) of all harzburgite samples analyzed from Sites 778 through 780 and 783. Note that this sample contains 5 modal% clinopyroxene (see "Igneous and Metamorphic Petrology" section) and represents the highest concentration of clinopyroxene in any analyzed sample. The petrogenetic implications are not clear, however, as the distribution of clinopyroxene indicates that this mineral was introduced by melt impregnation and was not a genuine residual phase. The hand sample appears to contain a 10-mm anhedral patch of a bronze-colored mineral that may be native copper or a copper sulfide.

In general, the samples analyzed from Site 783 are similar to those from Sites 778, 779, and 780 ("Igneous and Metamorphic Geochemistry" sections of the respective site chapters).

SEDIMENT/FLUID GEOCHEMISTRY

Sediment Geochemistry

Cores from Site 783 were analyzed aboard ship for inorganic carbon and for total carbon, nitrogen, and sulfur using the techniques described in the "Explanatory Notes" (this volume). The organic carbon content was then calculated by difference. These results are presented in Table 5 and Figure 5. The $CaCO_3$ content of the sediments and the phacoidal, sheared serpentine is extremely low, generally less than 1%, except for two intervals of sediment at 0 to 6 and 26 to 30

Table 5. Total nitrogen, carbon, inorganic carbon, organic carbon, and carbonate carbon in sediments and serpentine at Site 783.

Core, section, interval (cm)	Depth (mbsf)	Total nitrogen (wt%)	Total carbon (wt%)	Inorganic carbon (wt%)	Organic carbon (wt%)	$CaCO_3$ (wt%)
125-783A-						
1R-1, 77-79	0.77			7.25		60.4
1R-2, 23-25	1.73			0.15		1.2
1R-3, 76-78	3.76	0.19	2.88	2.47	0.41	20.6
1R-4, 97-99	5.47			0.49		4.1
1R-5, 76-77	6.76			0.03		0.2
1R-6, 74-76	8.24			0.11		0.9
1R-7, 7-9	9.07			0.14		1.2
2R-1, 34-36	10.04			0.02		0.2
2R-2, 15-17	11.35	0.15	0.41	0.04	0.37	0.3
4R-1, 74-76	26.74			0.43		3.6
4R-2, 84-86	28.34			0.80		6.7
4R-3, 67-69	29.67	0.13	2.93	2.59	0.34	21.6
4R-4, 76-78	31.26			0.09		0.7
4R-5, 24-26	32.24			0.47		3.9
4R-CC, 8-10	32.61			0.06		0.5
5R-1, 56-58	36.26			0.09		0.7
5R-2, 62-64	37.82	0.18	0.54	0.04	0.50	0.3
5R-3, 40-42	39.10			0.02		0.2
5R-4, 25-27	40.45			0.03		0.2
5R-CC, 11-13	40.83			0.12		1.0
7R-1, 30-32	52.70			0.04		0.3
7R-2, 50-52	54.40			0.08		0.7
7R-3, 139-141	56.79	0.20	0.61	0.07	0.54	0.6
7R-4, 6-8	56.96			0.03		0.2
8R-1, 37-39	62.47			0.11		0.9
8R-2, 71-73	64.31	0.14	0.35	0.03	0.32	0.2
8R-3, 76-78	65.86			0.05		0.4
10R-1, 33-35	81.63			0.01		0.1
10R-2, 5-7	82.85	0.19	0.48	0.04	0.44	0.3
11R-1, 16-18	91.06	0.07	0.25	0.03	0.22	0.2
12R-1, 7-9	100.67	0.11	0.28	0.02	0.26	0.2
15R-1, 125-127	130.85			0.02		0.2
15R-2, 76-78	131.75	0.06	0.57	0.44	0.13	3.7
15R-3, 76-78	133.25			0.05		0.4
16R-1, 83-85	140.03			0.10		0.8
16R-2, 82-84	141.52	0.09	0.22	0.08	0.14	0.7
16R-CC, 5-7	142.89			0.07		0.6
17R-1, 127-129	150.17	nd	0.31	0.09	0.22	0.7
17R-CC, 10-12	150.50			0.10		0.8
18R-1, 82-84	159.42		0.18	0.05	0.13	0.4

Note: nd = not detected. Total sulfur was below the detection limit of 0.06 wt% in all samples analyzed for total carbon, nitrogen, and sulfur.

mbsf. The near-surface sediment interval contains up to 60 wt% $CaCO_3$, whereas the deeper interval contains up to 22 wt%. The organic carbon content decreases with depth from about 0.5 to 0.1 wt%. The nitrogen content varies with that of organic carbon, decreasing from 0.2 wt% to less than 0.01 wt% with depth. Sulfur is below the detection limit of 0.06 wt% in all samples.

Fluid Geochemistry

The concentration of methane measured for 5-cm^3 headspace samples is uniformly low, less than 20 mL/L (Table 6). A single sample from 31 mbsf may have contained a trace of ethane. Other than this, methane was the only hydrocarbon detected.

The interstitial waters at Site 783 (Table 7 and Fig. 6) contrast markedly with those at Site 782 in response to the presence of serpentine at Site 783 at 120 to 158.6 mbsf. The serpentine consists of a matrix of phacoidal, sheared serpentine containing clasts of serpentinized harzburgite and metabasalt. It underlies 120 m of glass-rich silty clay to claystone. Between the lowest interstitial-water sample from the claystone at 83 mbsf and the highest from the serpentine at 131 mbsf, there are abrupt changes in pH, alkalinity, silica, sulfate, magnesium, calcium, sodium, potassium, and salinity. Only ammonia, chlorinity, and bromide are unaffected by the presence of the serpentine. Between the claystone and the serpentine, pH rises from 8 to almost 10, alkalinity decreases from 2.9 to 1.3 meq/kg, silica decreases from 643 to 2 mmol/kg, and sulfate decreases from 28 to 6 mmol/kg. Magnesium decreases sharply from 50 to less than 1 mmol/kg, potassium decreases from 11 to 9 mmol/kg, calcium increases from 11 to 39 mmol/kg, and sodium increases from 480 to 499 mmol/kg, before decreasing again to 482 mmol/kg. Salinity decreases from 3.58 to 3.32 wt%, and chlorinity increases with depth within the claystone, probably as a result of the increased chlorinity of ocean bottom water during the Pleistocene glaciations (McDuff, 1985). It shows no further change within the serpentine. The decrease in salinity therein results from the decrease in sulfate.

The changes in pore-water composition between the claystone and serpentine almost certainly result from ongoing reactions between seawater-derived solutions and the partially serpentinized peridotite. Some of the changes are similar

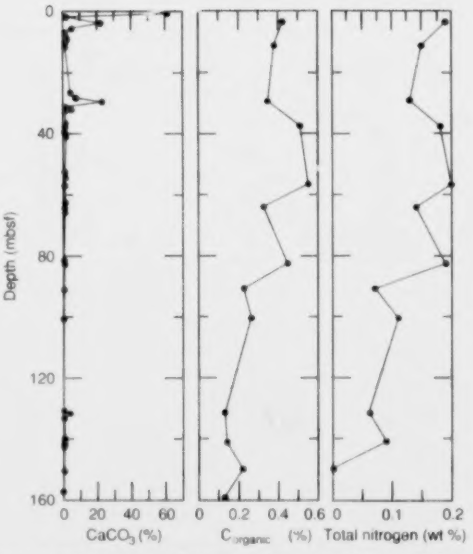

Figure 5. Weight percent of calcium carbonate, total organic carbon, and total nitrogen in sediments and serpentine at Site 783.

Table 6. Results of headspace-gas analyses of cores at Site 783.

Core, section, interval (cm)	Depth (mbsf)	Methane (μL/L)[a]	Methane (μM)[b]
125-783A-			
1R-6, 0-3	7.52	10	0.9
2R-2, 0-3	11.22	9	0.8
4R-4, 0-3	30.52	11	1.0
[c]7R-2, 0-3	53.92	13	1.2
8R-2, 0-3	63.62	15	1.3
10R-2, 137-140	82.69	13	1.2
16R-3, 0-3	142.21	13	1.2
17R-1, 149-150	150.40	15	1.3

[a] Microliters of methane per liter of wet sediment or wet unconsolidated serpentine, assuming a sample volume of 4.2 cm^3 of sediment or serpentine.

[b] Micromoles of methane per liter of interstitial water, assuming a porosity of 50%.

[c] Trace of ethane present.

Table 7. Composition of interstitial waters from cores at Site 783.

Sample number	Core, section, interval (cm)	Depth (mbsf)	Volume (mL)	Squeeze temperature (°C)	pH	Salinity (R.I., ‰)	Salinity (calcium, ‰)	Chlorinity (mmol/kg)	Alkalinity (meq/kg)	Sulfate (mmol/kg)	Sodium (mmol/kg)	Potassium (mmol/kg)
Surface seawater (17 March 1989)					8.25	35.6	34.65	539.2	2.689	27.78	462.0	10.11
IW-1	1R-1, 145–150	1.48	35	2	7.72	35.4	35.00	543.6	3.781	27.31	468.2	10.67
IW-2	1R-2, 145–150	2.98	41	1	7.85	35.4	35.03	544.5	3.212	27.41	468.3	10.87
IW-3	1R-5, 145–150	7.48	36	2	7.95	35.4	35.35	547.5	3.334	28.20	473.1	11.61
IW-4	4R-3, 140–150	30.45	73	2	7.95	35.6	35.61	553.3	3.294	27.77	476.1	11.49
IW-5	7R-1, 140–150	53.85	58	2	8.18	35.9	35.51	552.3	3.768	27.11	474.4	11.56
IW-6	10R-1, 140–150	82.75	35	2	8.01	36.1	35.79	557.2	2.890	27.61	480.5	11.11
IW-7	15R-2, 140–150	131.05	10	6	8.53	33.8	33.99	554.3	1.274	11.54	498.1	9.12
IW-8	16R-1, 135–150	140.63	10	7	9.96	33.0	33.27	549.4	1.377	7.85	489.1	8.46
IW-9	17R-1, 140–150	150.35	9	7	9.49	33.9	33.35	555.2	1.449	6.06	481.8	8.63

to those found in the serpentine sediments and flows at Sites 778, 779, and 780 on Conical Seamount in the Mariana forearc. Interstitial waters from the Conical Seamount sites were interpreted as mixtures of solutions from three sources: (1) seawater that had reacted with ultramafic rocks, (2) seawater that had reacted with mafic rocks and sediments, and (3) low-chlorinity water from a deep source probably associated with dewatering of the subducted lithospheric slab (see "Sediment/Fluid Geochemistry" section, "Site 780" chapter). The deep source of low-chlorinity water predominated at Site 780 on the summit, whereas reacted seawater predominated on the seamount flank at Site 779 and especially Site 778.

Pore waters at Site 783 on the Izu-Bonin seamount resemble the pore waters at the Mariana seamount (Sites 778–780) in their downhole increase in pH and ammonia and their strong downhole depletions in magnesium and silica. Although the concentrations of ammonia, magnesium, and silica are comparable between the two seamounts, the pH is not as high at Site 783 as it is at the Conical Seamount sites, with the exception of Site 778. For other dissolved species, Site 783 resembles Site 779 and especially Site 778 on the flank much more than Site 780 on the summit. Whereas alkalinity increases from the seawater value at Sites 779 and 780, it decreases at Sites 778 and 783. Sulfate likewise increases at Site 780 and decreases slightly and then increases at Site 779, but decreases greatly at Sites 778 and 783. Calcium decreases at Sites 779 and 780, but increases at Sites 778 and 783. Sodium increases at Site 780, but increases at Sites 778, 779, and 783. Potassium increases at Site 780, but decreases at Sites 778, 779, and 783. Chlorinity falls at all three Conical Seamount sites, especially at the summit (Site 780), whereas it increases within the claystone at Site 783 and shows no further change within the serpentine. Methane is abundant at Sites 779 and 780, moderately abundant at Site 778, and nearly absent at Site 783. Ethane and propane are present at Sites 779 and 780, but are absent at Sites 778 and 783.

Comparison of the interstitial waters from serpentinite at Sites 778, 779, 780, and 783 supports interpretation of the Conical Seamount waters as mixtures from three sources, as previously summarized. Because the waters at Site 783 most closely resemble those at Site 778, it is likely that these two sites represent the clearest examples of seawater-harzburgite interaction at low temperature. The associated reactions can be inferred to consume H^+, alkalinity, silica, sulfate, Mg^{2+}, and K^+ and to produce ammonia, Ca^{2+}, and Na^+ while conserving chlorinity. Although a small fraction of low-chlorinity, hydrocarbon-rich water from a deep source is present at Site 778 on Conical Seamount, there is no evidence for such water at Site 783 on the Izu-Bonin seamount.

STRUCTURAL STUDIES

Deformation observed at Site 783 includes (1) shear fabrics developed in poorly lithified muds and in sheared phacoidal serpentine; (2) a possible small fault in poorly lithified material; (3) high-temperature, pre-serpentinization fabrics in peridotites; and (4) lower temperature, post-serpentinization fabrics in serpentinite cobbles. We will discuss these in turn, and then briefly discuss the structural and tectonic significance of the rheological measurements made at this site.

Structures in Pelagic/Volcaniclastic Muds

We observed no tectonic structures within the unlithified sediment that makes up the upper 62 m of material recovered from Hole 783A. The first partially lithified sediment occurs in Section 125-783A-8R-1 (62.1 mbsf). Section 125-783A-8R-3 consists of claystone with several intervals containing weakly developed shear and fracture foliations. From 95 to 107 cm in this section, the foliation consists of at least three sets of shear planes spaced from less than 1 mm to about 3 mm apart. It was possible to measure the orientations of two of these sets; one set is approximately vertical, whereas the other dips approximately 60°. The three sets of shear planes divide the siltstone into angular phacoids, or lozenges, the long axes of which define the macroscopically obvious foliation (Fig. 7). Between 113 and 120 cm is a "columnar" cleavage that consists of vertical fracture planes spaced from less than 1 to perhaps 3 mm apart. This foliation may be related to the presence of the small normal(?) fault described in the following text. Between 120 and 129 cm, the bottom of the section, the siltstone contains a lozenge foliation similar to that described for the interval between 95 and 107 cm, but this lower interval is difficult to study because it is shattered by drilling.

Two small faults cut the partially lithified claystone in the lower part of Section 125-783A-8R-3, one in the upper part of the interval containing the vertical ("columnar") fracture cleavage and one below it (Fig. 7). The upper fault sharply truncates a silty clay or claystone clast, dips about 40°, and flattens downward. Although the nature of the fault is unclear, its sharpness and the lack of anastomosing fault strands, associated gouge or breccia, or drag features suggest that its displacement is quite small, perhaps only a few centimeters.

The abrupt appearance of these brittle strain features (fracture and microfault foliations and small faults) shortly below the first visible lithification suggests that the greater cohesion of the lithified sediment facilitates brittle failure. Thus, diagenetic effects, including overburden pressure, probably determine the interval in which the structures are formed. However, overburden stress is probably not responsible for

Table 7 (continued).

Calcium (mmol/ kg)	Magnesium (mmol/kg)	Bromide (mmol/ kg)	Silica (μmol/ kg)	Ammonia (μmol/kg)
10.18	52.48	0.81	0	10
10.51	51.04	0.89	471	7
10.53	51.18	0.75	503	10
10.69	50.54	0.87	526	103
10.80	51.46	0.85	643	70
11.13	51.06	0.79	654	94
11.39	50.47	0.77	643	120
29.47	6.24	0.84	17	188
34.00	0.45	0.84	2	151
39.21	0.00	0.89	4	125

the foliations or the small faults. The former indicate a greatest principal stress oriented at 15° or more from vertical; the latter indicate horizontal extension that might accompany larger-scale faulting or slumping of adjoining sediment, but would probably not take place at such a small scale during normal compaction in the absence of tectonism. We do not have sufficient data to demonstrate the origin of these structures, but suggest the following: (1) all the structures may be related to large-scale basement faulting (compressional or extensional) in the forearc; (2) the normal(?) faults may have formed during lateral extension allowed by the slumping of material downslope from the hole; and (3) all the structures may have formed in response to stresses exerted by the continuing downhill creep of the underlying serpentine sediments and flows.

Structures in Serpentine Sediments and Flows (Flow Matrix)

The material recovered in Cores 125-783A-15R through 125-783A-18R consists of a matrix of sheared phacoidal serpentine that bears fine-sand- to cobble-sized clasts, largely of serpentinized harzburgite tectonite (Fig. 8). The matrix exhibits a spectacular anastomosing shear foliation defined by deformed color banding (light blue to light blue-green to light green to pale yellow-green) and by the long axes of phacoidal (lens- or pie-shaped) serpentinite fragments. The shear foliation is always parallel to the layering defined by color banding and variations in clast size and concentration. Axial-plane foliations are not observed.

The phacoids are from 1 to 12 cm long and from a few millimeters to a few centimeters across (Fig. 8, 124–127 cm, and Fig. 9). Close inspection shows that much of the material between large phacoids consists of smaller phacoids. The foliation is whorled, contorted, and convolute with foliation streams swirling, branching, and rejoining around the larger clasts. Scattered through the material are smaller, angular to subangular and, less commonly, subrounded, sand- to small-pebble-sized clasts of serpentinite. Although some of these are light green, many are dark green to dark blue-gray; because

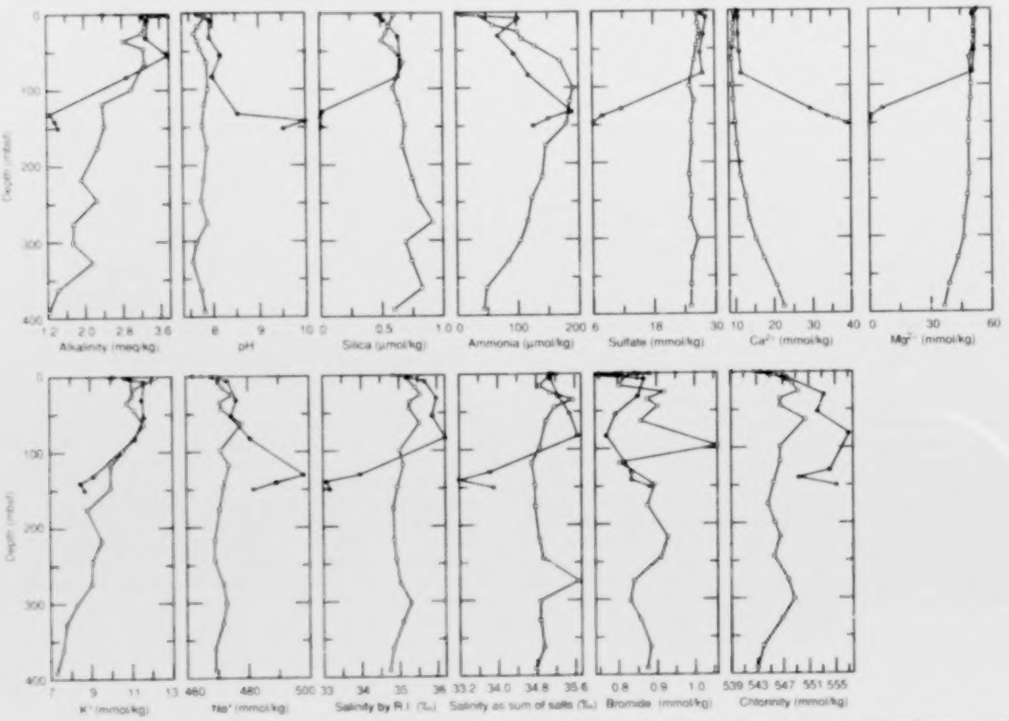

Figure 6. Composition of interstitial waters from sediments at Site 783 (circles) compared with that from Site 782 (squares) and surface seawater collected 22 February and 4 and 17 March 1989 (crosses).

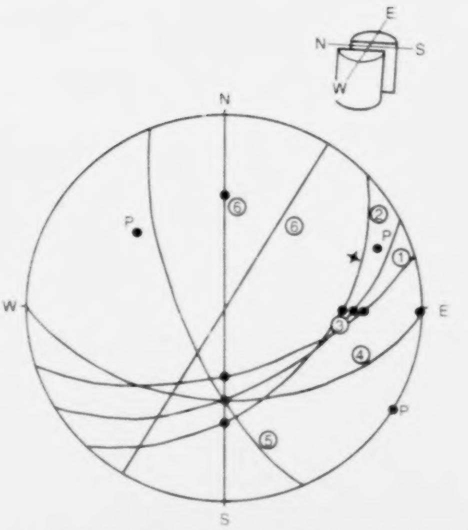

Figure 7. Stereonet showing the orientations of fractures that define shear foliation in Section 125-783A-8R-3, 95–107 cm. 1, 2, and 3 = faults with displacement; 3 is a normal fault. 4, 5, and 6 = cleavage planes. P = pole of plane.

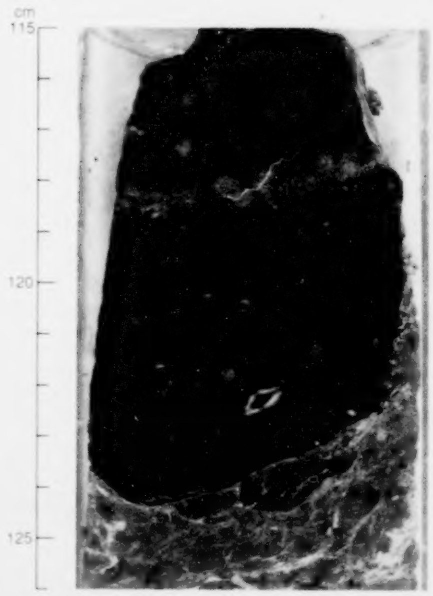

Figure 8. Sheared, phacoidal serpentine matrix enclosing serpentinized harzburgite tectonite clast (Section 125-783A-18R-1, 115–126 cm).

their concentration varies greatly from one layer to the next, they help to define the foliation (Fig. 9).

Phacoids within the matrix typically exhibit pinch-and-swell texture (boudinage) along their long axes and commonly are cut by serpentine veins and/or microfaults at high to moderate angles with respect to their long axes. These microfaults almost universally show a normal sense of movement with respect to the long axes of the phacoids (Fig. 8, 124–127 cm, and Fig. 10, especially between 75 and 77 cm and between 83 and 85 cm). This texture, together with the boudinage and veining, clearly indicates that the phacoidal matrix has undergone major extension (pure shear) parallel to the layering, foliation, and the direction of alignment of the phacoids. This extension was both brittle and ductile, the difference presumably depending on confining stress, strain rate, and the degree of lithification and water content of phacoids and interphacoid matrix.

The phacoids are commonly bounded, and their tapering ends terminated, by shear bands (zones in which the bulk shear is concentrated) within the surrounding finer-grained matrix. Phacoids that lie parallel to the local direction of the matrix foliation are typically lensoid (i.e., their long axes are straight). Phacoids that are oblique to the surrounding foliation are typically sigmoid, with their long axes bent and their ends sheared out parallel to the foliation. Pure and simple shear have thus both played an important part in forming the fabric. Shear bands may extend across the entire core or die out within the matrix. Therefore, the overall geometry of matrix foliation and phacoid alignment outlines the pattern of matrix streamlines, along which extensional flow has occurred.

Although we have not yet measured the orientation of the shear foliation in detail, we observe no strong preferred orientation. Whorled foliation, in which the whorls appear to have long vertical limbs, appears to dominate some parts of the cores. This texture, described elsewhere in this chapter as "vertical convolute lamination," is probably an artifact of the aspect ratios of our core sections, which are 150 cm long and 6.5 cm wide; fabrics parallel to the core will thus appear to dominate the geometry.

We interpret these textures as flow fabrics developed in sheared serpentinite as it continued to hydrate, soften, and flow downhill under the influence of gravity. Although we believe that the original shearing of the serpentinite was tectonic in the sense that it was caused by deep-earth processes, we suggest that these near-surface processes formed much of the present fabric of the rock.

High-Temperature Peridotite Deformation Textures

Clasts larger than 1 cm, mostly of serpentinized harzburgite tectonite, were encountered from Section 125-783A-15R-1, 15 cm, through the bottom of Core 125-783A-18R, but are dominant only in Core 125-783-18R, where they make up about 80% of the material recovered. These clasts preserve some relict mineralogy, but the specimens from which our thin sections were made have been so highly serpentinized that relict textures developed at depth under elevated pressure and temperature could not be observed. Deformation textures observed in similar clasts from Sites 778, 779, and 780 include subgrain bands and deformation lamellae in olivine, kinkbands in orthopyroxene, and undulatory extinction in both.

Serpentinization Textures

The serpentinization textures in clasts are similar to those observed in clasts from Sites 778, 779, and 780 and include serpentinization veins, cross-fiber serpentine veins, and "Frankenstein" veins (see "Structural Studies" sections in "Site 779" and "Site 780" chapters, this volume). A spectac-

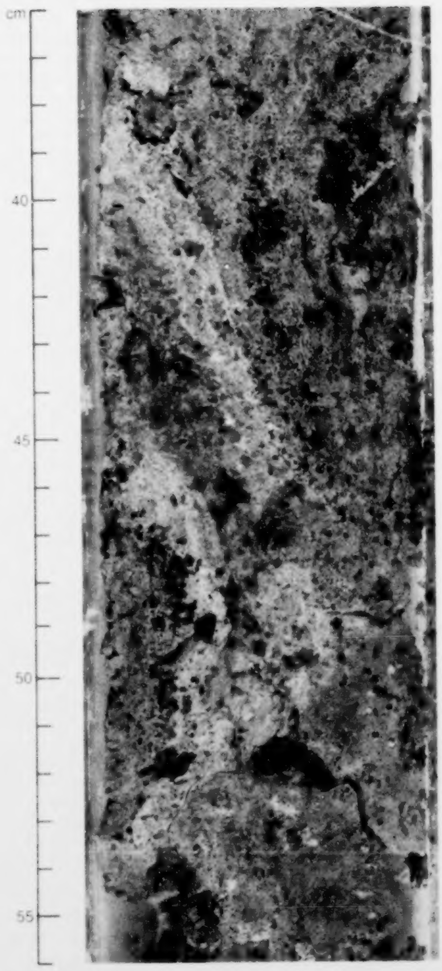

Figure 9. Layering, shear foliation, and phacoids in serpentine sediments and flows (Section 125-783A-15R-2, 36–56 cm).

ular dark serpentinization vein with an unusual light center is shown in the large clast in Figure 8. The upper edge of the larger clast from 116 to 124 cm in Section 125-783A-18R-1 is bounded by a small, poorly developed "Frankenstein" vein. Textures seen in thin section include cross-fiber veins and fiber haloes surrounding relict and pseudomorphed olivine subgrains.

Many fiber haloes in serpentinized harzburgites from Site 783 are asymmetric, in striking contrast to those from Site 780, which are almost all highly symmetric (see Fig. 7). While detailed study will be necessary to confirm and quantify this observation, it probably implies that many of the Site 783 harzburgites were serpentinized in anisotropic stress fields (i.e., under deviatoric stresses).

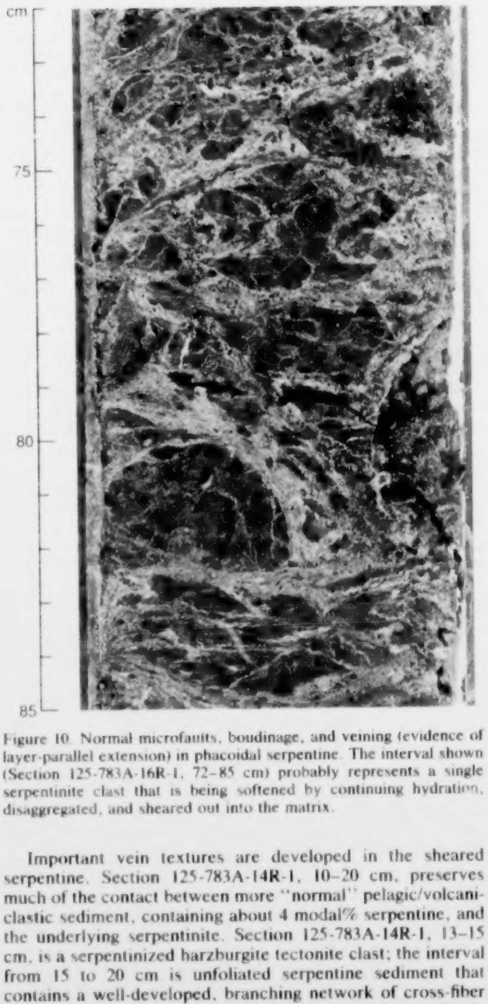

Figure 10. Normal microfaults, boudinage, and veining (evidence of layer-parallel extension) in phacoidal serpentine. The interval shown (Section 125-783A-16R-1, 72–85 cm) probably represents a single serpentinite clast that is being softened by continuing hydration, disaggregated, and sheared out into the matrix.

Important vein textures are developed in the sheared serpentine. Section 125-783A-14R-1, 10–20 cm, preserves much of the contact between more "normal" pelagic/volcaniclastic sediment, containing about 4 modal% serpentine, and the underlying serpentinite. Section 125-783A-14R-1, 13–15 cm, is a serpentinized harzburgite tectonite clast; the interval from 15 to 20 cm is unfoliated serpentine sediment that contains a well-developed, branching network of cross-fiber serpentine veins up to 3 mm across that are clearly growing in the material. This is important because it provides unambiguous evidence that serpentinization is continuing in the disaggregated, unlithified sediment.

Within the sheared phacoidal serpentines below this level, both phacoid and interphacoid material are highly veined with serpentine. Although some veins in phacoids end at the phacoid margin, others pass outward into the matrix. Many of these veins have become deformed by, drawn out into, and incorporated within the matrix. Moreover, in at least two intervals (76–85 and 100–125 cm in Section 125-783A-16R-1) large serpentinite clasts are cut by intricate, anastomosing networks of veins, which pass out into narrow channels of finely phacoidal, serpentine matrix that also cut the clasts (Fig. 10). The clasts were quite soft and water saturated when recovered. We postulate that these intervals preserve in place a late stage of the fragmentation of large clasts by serpentine veins, their continuing hydration and softening, and their shearing and incorporation into the phacoidal matrix.

Inspection under the binocular microscope shows that the matrix consists of slickensided lenses of serpentine that, in turn, consist of smaller scales and lenses; adding water to this material and agitating it gently with a probe causes it to disaggregate completely into submillimeter-sized serpentine fragments, interspersed with which are subangular to subrounded sand-sized grains of serpentine. We suggest that the fragility of the matrix is a consequence of its hydration.

Rheologic Properties of the Materials and Structural and Tectonic Implications

We used a Wykeham-Farrance torsion-vane apparatus to perform stress-strain tests on the unlithified materials recovered from Site 783. The sheared phacoidal, serpentine matrix is weak, with failure strengths that range between 7.3 and 51 kPa and average 23 kPa. These materials are comparable in strength to similar materials recovered from other sites, although they are significantly weaker than the overlying claystones and significantly stronger than the average unfoliated serpentine at Site 780 (Table 8). Moreover, the mode of failure was quite different: at low strains, the stress-strain curves were much more linear, and the strain appeared to be more elastic. Moreover, the material failed in a brittle manner, by cracking, rather than yielding plastically at an ultimate strength (Fig. 11).

We interpret these results as the consequence of the greater dewatering and compaction of these materials than those studied previously on Conical Seamount. This conclusion is compatible with the nature of the material, which is quite different from the pasty, weak, plastic, little-foliated serpentine sediment and flows recovered from the shallow levels of Sites 778 and 779 on the flanks of Conical Seamount. We have interpreted this pasty material as representing young serpentine debris flows that have only begun to dewater. At Site 783, pasty, unfoliated serpentine is restricted to Core 125-783A-14R, at the volcanogenic sediment/serpentine interface, which is likely to be a zone of extensive fluid transfer and is clearly a zone of active serpentinization. The sheared, phacoidal serpentine from Site 783 is also different from the unfoliated serpentine material from Site 780, which we postulate to be a site of active upwelling of water-charged mud. Our interpretation is also compatible with the similarity between the material from Site 783 and that from deep levels at Sites 778 and 779, which we think represent older debris flows that have undergone extensive dewatering. Finally, our interpretation is compatible with the location of the serpentine 60 m below the level at which the volcanogenic sediments may have first lithified.

Table 8. Ultimate strength of serpentine sediments and flows recovered at Site 783.

Core, section	Depth (mbsf)	Stress (kPa)
119-783A-		
1R-1	0.73	13.1
1R-3	3.70	37.1
1R-5	6.68	29.1
2R-1	10.93	17.5
2R-2	11.32	44.4
4R-2	28.16	34.9
4R-4	31.22	41.5
5R-1	36.56	32.8
5R-3	39.56	52.4
7R-1	53.44	29.8
7R-3	56.28	69.2
8R-1	62.97	34.9
15R-1	130.41	16.0
15R-1	130.83	51.0
15R-2	131.87	16.7
15R-3	133.33	35.7
16R-1	139.92	19.7
16R-2	141.92	25.5
16R-3	142.39	26.9
17R-1	149.97	41.5
Sediment		
Average		36.39
Standard deviation		14.88
Maximum		69.20
Minimum		13.10
Serpentine		
Average		29.13
Standard deviation		12.58
Maximum		51.00
Minimum		16.00

The serpentine at Site 783 is blanketed by virtually serpentine-free sediment that is at least as old as early Pliocene. Thus, the stratigraphy, sedimentology, paleontology, and rheology of the materials recovered from Site 783 are all consistent with a scenario in which serpentinite debris-flow processes were once active on Torishima Forearc Seamount but have since ceased, allowing the serpentine and serpentinite to be blanketed with pelagic and volcanogenic sediment. Serpentinization and dewatering have, however, continued until the present.

PALEOMAGNETISM

Magnetic Remanence

The natural remanent magnetization (NRM) of the sediments contained within the archive halves of Cores 125-783A-1R, 125-783A-2R, 125-783A-4R, 125-783A-5R, 125-783A-7R, 125-783A-8R, and 125-783A-10R was measured using the cryogenic magnetometer. Intensities vary typically between 10 and 100 mA/m, but there is no trend in these values downhole. Cores were then demagnetized at 10 mT, which reduced the intensity typically by 10% to 20%. Addi-

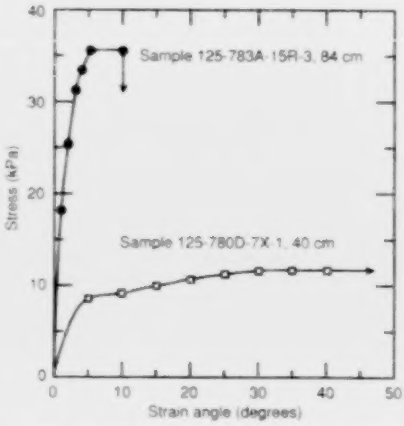

Figure 11. A representative stress-strain test of serpentine sediments and flows from Site 783 (failure strength = 35.7 kPa), compared with material from Site 780 on the summit of Conical Seamount (ultimate strength = 11.7 kPa).

Table 9. Remanence data for the discrete samples taken from Hole 783A.

Core, section, top of interval (cm)	Natural remanent magnetization			Remanent magnetization (10 mT)			Remanent magnetization (20 mT)			Polarity
	Declination (degrees)	Inclination (degrees)	Intensity (mA/m)	Declination (degrees)	Inclination (degrees)	Intensity (mA/m)	Declination (degrees)	Inclination (degrees)	Intensity (mA/m)	
119-783A-										
1R-1, 103	325.4	30.0	77.3	348.0	52.0	47.3	349.5	51.8	36.8	N
1R-2, 33	0.5	15.5	71.4	12.3	23.0	62.5	14.9	28.9	52.1	N
1R-3, 6	343.0	60.2	63.6	351.0	62.1	51.7	351.9	63.1	37.9	N
1R-4, 11	63.0	74.7	101.0	84.4	69.6	69.2	89.0	69.6	49.8	N
1R-5, 86	302.4	62.3	90.7	301.2	63.3	82.4	302.4	65.4	62.1	N
1R-6, 89	344.5	47.8	73.3	344.3	48.0	61.7	345.7	48.8	48.1	N
1R-7, 45	333.0	74.0	7.6	270.3	53.9	7.9	268.1	62.3	6.3	N
2R-1, 52	24.7	−54.2	32.7	5.5	−55.8	37.1	0.7	−56.6	33.1	R
2R-2, 3	252.1	−55.0	44.2	250.2	−51.9	45.8	251.0	−51.4	36.7	R
4R-1, 114	33.0	−48.0	25.7	29.4	−58.3	22.8	36.8	−52.4	17.5	R
4R-2, 113	227.7	28.5	14.6	34.1	19.0	33.4	41.9	6.8	2.6	R
4R-3, 113	220.2	−32.5	23.1	210.9	−33.0	20.3	210.2	−31.2	16.8	R
4R-4, 113	238.6	−79.1	34.5	236.7	−76.1	37.6	238.6	−74.2	28.9	R
4R-5, 40	92.0	−19.0	62.2	93.9	−27.8	57.0	95.7	−25.3	44.2	R
5R-1, 26	171.4	−82.9	47.3	87.9	−51.9	36.6	88.1	−53.1	30.4	R
5R-2, 26	190.9	−75.8	60.5	190.6	−63.8	70.9	190.7	−65.6	60.5	R
5R-3, 26	87.1	−51.7	99.2	89.7	−54.6	110.0	89.6	−51.2	80.7	R
5R-4, 13	262.2	−50.7	67.1	261.3	−53.0	69.5	254.4	−49.9	48.4	R
7R-1, 90	122.7	−67.7	68.9	120.3	−67.5	67.2	119.9	−67.0	53.6	R
7R-2, 90	110.5	−53.6	82.5	108.8	−53.6	77.2	107.9	−52.9	61.5	R
7R-3, 90	182.1	−64.3	84.6	179.5	−63.8	79.1	179.2	−64.4	62.9	R
7R-4, 3	339.0	−46.2	118.0	338.2	−46.6	112.0	338.7	−46.7	87.4	R
8R-1, 120	262.8	53.7	123.0	262.0	53.0	111.0	261.9	54.4	98.3	N
8R-2, 120	86.5	55.3	48.7	92.3	56.7	41.5	92.3	56.4	38.4	N
8R-3, 91	278.8	44.5	41.6	279.6	49.4	37.1	274.1	50.0	31.0	N

Table 10. The polarity of each sediment core from Hole 783A and the corresponding diatom and nannofossil zones.

Core	Polarity	Diatom zone	Nannofossil zone
119-783A-			
1R	N	*N. reinholdii*	CN14a
2R	R		
4R	R		CN14a (lower/middle part)
5R	R	*R. praebergonii*	
7R	R		
8R	N		
10R	?	*N. jouseae*	

tionally, one specimen was removed from the working half of each processed section for a more detailed analysis. The NRM of these specimens was also measured using the cryogenic magnetometer. Intensities vary typically between 50 and 80 mT. Each specimen was then demagnetized at 5, 10, 15, and 20 mT and remeasured between each step. Demagnetization reduced the intensity typically by 25% to 35% at the 20 mT step. The demagnetization data for the discrete specimens are summarized in Table 9. Only small changes in the remanence direction are observed between the 10 and 20 mT steps. This suggests that the 10-mT whole-core data can be used to make reliable polarity evaluations. The polarity of each core is summarized in Table 10. (No polarity transitions were recorded within any of the cores.)

Unfortunately, the biostratigraphic data, obtained almost entirely from core-catcher material (see "Biostratigraphy" section, this chapter), are poor. However, a biostratigraphic zonation, based primarily on diatoms, but also including two horizons dated using nannoplankton biomarkers, allows us to correlate tentatively the polarity sequence with the time scale of Berggren et al. (1985). Barron (1985) correlated the internationally recognized low-latitude diatom zones with the polarity time scale of Ness et al. (1980). At least for the interval from 0 to 4 Ma, the age of each magnetochron boundary in that time scale is not much different from that presented in the time scale of Berggren et al. (1985). For practical purposes, the relative positions of the diatom zones of Barron (1985) can be transferred directly onto the time scale of Berggren et al. (1985). This modified scheme was adopted here.

The magnetostratigraphy of Hole 783A is summarized in Figure 12. We have been able to identify partial records of the Brunhes Normal Polarity Chron (Core 125-783A-1R) and the Matuyama Reverse Polarity Chron (Cores 125-783A-2R through 125-783A-7R). Core 125-783A-8R may record part of the Gauss Normal Polarity Chron.

The pelagic sediment/serpentine sediment contact was identified within Section 125-783A-14R-1. Cores 125-783A-15R through 125-783A-18R were processed in the cryogenic magnetometer at 0 and 10 mT. The serpentine material has an NRM intensity typically between 50 and 200 mA/m. Both Cores 125-783A-16R and 125-783A-17R carry normal polarity magnetizations. However, as the serpentine material is not pelagic sediment, we are unable to fit the magnetic polarity data from these cores into any geochronological framework.

Magnetic Susceptibility

Magnetic susceptibilities were measured on the multisensor track (MST). A downhole plot of these values for Hole 783A is presented in Figure 13. The sediments (between 0 and just past 100 mbsf) have values typically between 3×10^{-4} and 6×10^{-4} SI units, whereas the serpentinite has values typically between 1×10^{-3} to 3×10^{-3} SI units. The high magnetic susceptibility (and NRM intensity) associated with the serpentinite almost certainly results because magnetite is produced during the process of serpentinization. The serpentinite typically contains on the order of 2% by volume of magnetite ("Igneous and Metamorphic Petrology" section, this chapter).

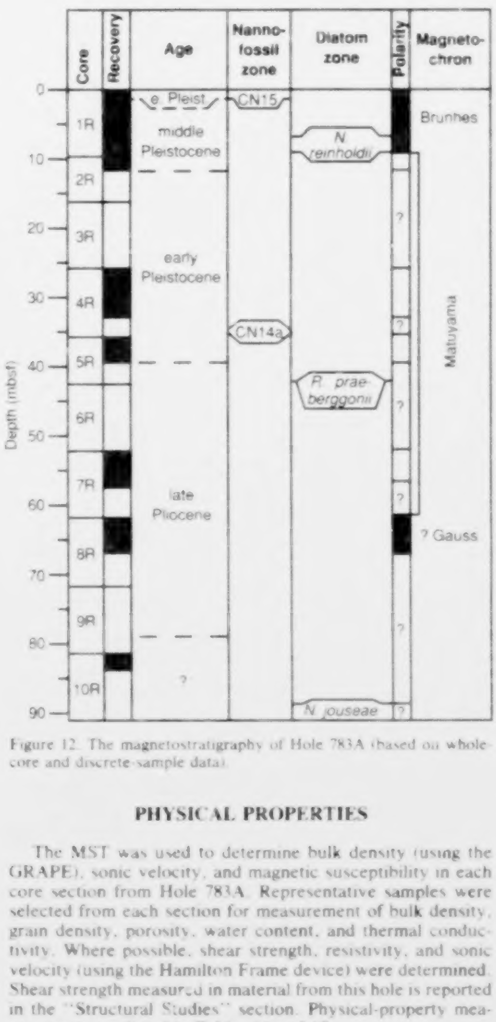

Figure 12. The magnetostratigraphy of Hole 783A (based on whole-core and discrete-sample data).

PHYSICAL PROPERTIES

The MST was used to determine bulk density (using the GRAPE), sonic velocity, and magnetic susceptibility in each core section from Hole 783A. Representative samples were selected from each section for measurement of bulk density, grain density, porosity, water content, and thermal conductivity. Where possible, shear strength, resistivity, and sonic velocity (using the Hamilton Frame device) were determined. Shear strength measured in material from this hole is reported in the "Structural Studies" section. Physical-property measurements are listed in Tables 11 and 12.

A total of 120 m of volcaniclastic and pelagic sediment was cored in Hole 783A. At about 120 mbsf, serpentine sediments and flows with dispersed hard-rock clasts were encountered. The physical properties of the volcaniclastic/pelagic and serpentine material in Hole 783A are distinct (Fig. 14). The separation between the volcaniclastic/pelagic and serpentine material can easily be seen between the two groups on the depth plot of the GRAPE-determined bulk-density data. The discontinuities in data points with depth are gaps in core recovery. The average bulk densities of the volcaniclastic/pelagic and serpentine material are 1.54 ± 0.08 g/cm³ and 2.01 ± 0.19 g/cm³, respectively. The *P*-wave logger, which is mounted on the MST, gave reliable compressional-wave sonic velocities for parts of the core from Hole 783A. Figure 15 illustrates how the velocities vary with depth, the average compressional-wave velocity is 1620 ± 106 m/s and is relatively constant over the depth range shown.

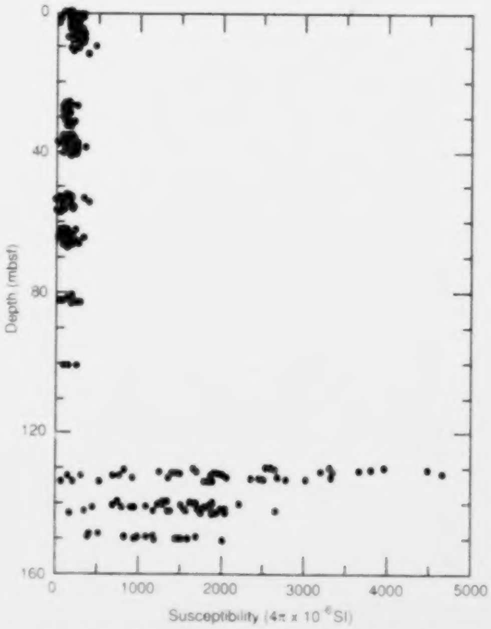

Figure 13. A downhole plot of magnetic susceptibility for Hole 783A.

Table 11 lists the index properties of the discrete samples from Hole 783A. The bulk density of the volcaniclastic and pelagic sediment is relatively constant or decreases slightly to 100 mbsf (Fig. 16). At about 120 mbsf, where the serpentine material was encountered, the bulk density sharply increases. Values of bulk density of the serpentine material cluster around 2.14 ± 0.03 g/cm³ and show no obvious increase with depth. Although the values of grain density are scattered, their average is relatively constant with depth. The average grain densities of the volcaniclastic and pelagic sediment and serpentine material are 2.59 ± 0.13 g/cm³ and 2.71 ± 0.13 g/cm³, respectively.

The average thermal conductivity of sediment is 0.937 ± 0.070 W/mK (Table 11 and Fig. 16). At 120 mbsf, in the serpentine material, the thermal conductivity increases to 1.6 W/mK and rises steadily to 2.1 W/mK at 150 mbsf, resulting in a gradient of 0.029.

Measurements of sonic velocity were obtained from discrete samples of the serpentine material. The A velocities are measured parallel to the surface of the split core and the B velocities are measured perpendicular to the surface of the split core. With the exception of the harzburgite clast at 159 mbsf, the velocities are constant and isotropic with depth, with average A and B velocities of 194 and 196 m/s, respectively.

DOWNHOLE MEASUREMENTS

Two downhole temperature measurements were obtained at Site 783 using the Barnes-Uyeda temperature tool.

Table 11. Index properties for Hole 783A.

Core, section, interval (cm)	Depth (mbsf)	Bulk density (g/cm³)	Grain density (g/cm³)	Porosity (%)	Water content (%)	Void ratio
125-783A-						
1R-1, 77–79	0.77	1.47	2.58	72	52	0.72
1R-2, 23–25	1.73	1.48	2.69	73.2	52.5	0.73
1R-3, 76–78	3.76	1.5	2.73	72.9	51.7	0.73
1R-4, 97–99	5.47	1.46	2.56	72.4	52.8	0.72
1R-5, 76–78	6.76	1.48	2.59	71.3	51	0.71
1R-6, 74–76	8.24	1.49	2.52	69.2	49.2	0.69
1R-7, 7–9	9.07	1.4	2.54	71	53.9	0.71
2R-1, 33–35	10.03	1.42	2.18	66.2	49.4	0.66
2R-2, 15–17	11.35	1.55	2.91	72.6	49.7	0.73
4R-1, 65–67	26.74	1.5	2.59	70	49.5	0.7
4R-2, 84–86	28.34	1.47	2.62	72.4	52.2	0.72
4R-4, 76–79	31.26	1.49	2.63	71.7	51.2	0.72
4R-5, 24–26	32.24	1.52	2.6	69.1	48.3	0.69
4R-CC, 8–10	32.61	1.55	2.54	66	45.3	0.66
5R-1, 56–58	36.26	1.63	2.61	62.5	40.8	0.62
5R-2, 62–64	37.82	1.58	2.65	66.1	44.4	0.66
5R-3, 40–42	39.1	1.53	2.62	68.7	47.6	0.69
5R-4, 25–27	40.45	1.58	2.57	64.6	43.4	0.65
5R-CC, 11–13	40.83	1.54	2.6	68.2	47.1	0.68
7R-1, 30–32	52.7	1.54	2.4	63.3	43.7	0.63
7R-2, 50–52	54.4	1.58	2.64	66.4	44.7	0.66
7R-3, 139–140	56.79	1.58	2.45	61.8	41.6	0.62
7R-4, 6–8	56.96	1.59	2.58	64.4	43.1	0.64
8R-1, 37–39	62.47	1.49	2.42	67.3	48	0.67
8R-2, 71–73	64.31	1.55	2.53	65.5	44.9	0.66
8R-3, 76–78	65.86	1.52	2.41	64.9	45.4	0.65
10R-1, 33–35	81.63	1.5	2.64	70.8	50	0.71
10R-2, 5–7	82.85	1.48	2.68	71.5	51.2	0.72
11R-1, 16–18	91.06	1.62	2.59	62.6	41.1	0.63
12R-1, 7–9	100.67	1.44	2.54	73.2	54.1	0.73
15R-1, 125–127	130.85	2.1	2.67	34.6	17.5	0.35
15R-2, 76–78	131.75	2.15	2.61	29.5	14.6	0.29
15R-3, 76–78	133.25	2.16	2.84	38.1	18.8	0.38
16R-1, 83–85	140.03	2.07	2.57	32.4	16.6	0.32
16R-2, 82–84	141.52	2.11	2.66	34.2	17.2	0.34
16R-CC, 5–7	142.89	2.12	2.68	34.4	17.2	0.34
17R-1, 127–129	150.17	2.23	2.54	20.9	10	0.21
17R-CC, 10–12	150.5	2.17	2.58	26.5	13	0.26
18R-1, 82–84	159.42	2.56	2.57	0.4	0.2	0

The temperature record from Run 06R at 42.7 mbsf is shown in Figure 17A and at an expanded scale in Figure 17B. The probe was firmly seated in the sediment at 51 min into the run and remained relatively undisturbed until 66 min. After the first few minutes of emplacement, the temperature decay curve is proportional to 1/time. A linear least-squares regression on the curve, extrapolated to 1/time = 0, is a good estimate of the equilibrium sediment temperature, 3.29°C (Fig. 18). The correlation coefficient (r^2) has the somewhat low value of 0.527, but the slope of the regression line is negligible, so there should be no significant error.

The temperature record from Run 11R at 90.9 mbsf is shown in Figure 19A and at an expanded scale in Figure 19B. The probe was seated in the sediment from 55 to 66 min into the run, but the minor temperature increases at 59 and 63 min indicate slight disturbances to the probe. The equilibrium temperature of 3.93°C estimated from the decay curve (Fig. 20) has a low r^2 of only 0.334 because of the disturbances.

The temperature data must be combined with the thermal-conductivity data ("Physical Properties" section; Fig. 21) to determine the heat flow at the site. Note that the large increase in thermal conductivity below 120 mbsf takes place below the depth of the temperature measurements from the two runs. The most useful way to analyze the temperature data is to plot temperature vs. the vertically integrated thermal resistivity. Thermal resistivity is simply the inverse of thermal conductivity. In the plot of integrated thermal resistivity vs. depth in Figure 22 the decreased slope of the line below 120 mbsf results from the higher thermal conductivity of the deeper sediment.

The equilibrium temperature and integrated thermal resistivity data are plotted in Figure 23. The slope of the linear least-squares regression is the heat flow at this site, 23 mW/m². The quality of the fit is surprisingly poor.

Several factors might affect these data. The first is instrument performance, but that appears acceptable because the indicated temperature is similar in the bottom water before and after the penetration (Figs. 17 and 19). The second factor is a variation in bottom water temperature with time, but such a change would have to be extremely large, probably over 1°C. The bottom water temperature that we now observe is consistent with temperatures at similar depths in this region from the other temperature runs on this leg and from historic oceanographic data. The third factor is an exothermic chemical reaction in the sediment, but this is unlikely as the sediments were of an unexceptional nature. A fourth factor is slow advection of pore fluids upward through the sediments. If advection is occurring, the total heat flow at this site is higher than the least-squares estimate given here.

SUMMARY AND CONCLUSIONS

Site 783 (30°57.86′N, 141°47.27′E; water depth of 4648.8 m) is located on the northern, midflank part of a seamount that forms part of a 500-km-long ridge running along the lowermost, inner wall of the Izu-Bonin Trench. The single hole, 783A, attempted at this site was drilled to 168.2 mbsf with 27.9% recovery (Fig. 24). Heat-flow measurements were taken at 42.7 and 90 mbsf. Hole 783A was abandoned when the torque and pressure of the drill string suddenly increased.

Two lithologic units were defined as follows:

Unit I (0–120.0 mbsf) is middle or early Pleistocene to early Pliocene (or older) glass-rich silty clay to claystone;

Unit II (120.0–158.6 mbsf) is phacoidal, sheared serpentine with clasts of serpentinized harzburgite.

Dating is based on calcareous nannofossil and diatom biostratigraphy. Microfossil studies also indicate that the upper 100 m was deposited at or near the CCD and that reworking may have been important in places lower in the sequence. Lithologic Unit I as a whole has a small biogenic component, the siliceous biogenic contribution being greater than the calcareous contribution; it also has varying volcanic influx, primarily as glass with lesser amounts of feldspar, pyroxene, and amphibole.

The harzburgites of Unit II consist of olivine (80–90 modal%), orthopyroxene (10–15 modal%) with minor clinopyroxene (as exsolution lamellae in orthopyroxene), and spinel. Other rock types are very rare, although one piece of harzburgite contains a 5- to 15-mm-wide clinopyroxene-rich band and there are several small metabasaltic clasts. The degree of serpentinization is variable, but rarely below 50%.

Deformation observed in the sediments at Site 783 begins with the first partially lithified sediment at 62.1 mbsf and includes shear fabrics and convolute plastic folding within the claystones of Unit I and the phacoidal serpentine of Unit II. High-temperature pre-serpentinization and lower temperature, post-serpentinization fabrics similar to those described from Conical Seamount are found in the ultramafic clasts of Unit II.

Studies of physical properties show that the bulk densities increase from 1.47 to 1.590 g/cm³ in the sediments of Unit I and cluster about 2.1 g/cm³ in the serpentine of Unit II. The average compressional-wave velocity in the sediments is 1.9 km/s. Thermal conductivities average about 1 W/mK in sediments and 1.91 W/mK in the serpentine. Heat flow in the sediments is 23 mW/m².

Table 12. Physical properties for Hole 783A.

Core, section, interval (cm)	Depth (mbsf)	Thermal conductivity (W/mK)	Ultimate strength (kPa)	Resistivity (ohms)	Formation factor	Compressional-wave velocity	
						A direction (km/s)	B direction (km/s)
125-783A-							
1R-1, 76–80	0.75	0.888	13.1	10.8	1.26		
1R-2, 75	2.25	0.863					
1R-3, 76–80	3.75	[illegible]	37.1	11.2	1.31		
1R-4, 75	5.25	[illegible]					
1R-5, 76–80	6.75	0.98	29.1	11.4	1.33		
1R-6, 75	8.25	0.988					
1R-7, 6–10	9.08			11	1.28		
1R-7, 30	9.3	1.039					
2R-1, 30–34	10.02			12.5	1.46		
2R-1, 75	10.45	0.99					
2R-1, 123–125	10.93		17.5				
2R-2, 16–20	11.32	1.006	44.4	13.9	1.62		
2R-CC, 8	11.54	0.991					
4R-1, 60–64	26.62			16.3	1.9		
4R-1, 75	26.75	0.919					
4R-2, 75	28.25	0.925	34.9				
4R-3, 75	29.75	0.976					
4R-3, 86–90	29.88			15.4	1.8		
4R-4, 75	31.25	0.914	41.5				
4R-5, 20–24	32.26	0.994		15.4	1.8		
4R-CC, 7	32.6	0.989					
5R-1, 10–14	35.82			23	2.68		
5R-1, 75	36.45	0.955	32.8				
5R-2, 75	37.95	0.931					
5R-3, 10–14	38.82			18.5	2.16		
5R-3, 75	39.45	0.897	52.4				
5R-4, 24	40.44	0.912					
7R-1, 10–14	52.[illegible]			35.1	4.1		
7R-1, 60	53	0.998	29.8				
7R-2, 60	54.5	0.998					
7R-3, 10–14	55.52			20.1	2.35		
7R-3, 60	56	0.959					
7R-3, 88–90	56.28		69.2				
8R-1, 10–14	62.22			13.5	1.58		
8R-1, 67	62.77	1.004					
8R-1, 87–89	62.97		34.9				
8R-2, 67	64.27	0.906					
8R-3, 10–14	65.22			18.1	2.11		
8R-3, 67	65.77	0.833					
10R-1, 30–34	81.62			16.5	1.93		
10R-1, 58	81.88	0.9					
10R-2, 21	83.01	0.847					
11R-1, 12	91.02	0.682					
12R-1, 19	100.79	0.965					
14R-1, 15	120.05	1.624					
14R-CC, 8	120.22	0.638					
15R-1, 64–66	130.26			37	4.32		
15R-1, 75–81	130.35	1.123	16				
15R-1, 125–127	130.85		51			1.88	1.92
15R-2, 54–56	131.66			91	10.62		
15R-2, 74–76	131.74	1.839	16.7			2.06	1.97
15R-3, 40–42	133.02			43	5.02		
15R-3, 74–76	133.24	1.961	35.7				1.98
15R-3, 87–91	133.49			100	11.67		
15R-CC, 4	134.03	1.606					
16R-1, 16–20	139.38			98	11.44		
16R-1, 75	139.95	1.94	19.7				
16R-1, 83–85	140.03					1.98	
16R-2, 80	141.5	1.827				1.86	
16R-2, 122–124	141.92		25.5				
16R-3, 19–21	142.39		26.9				
16R-3, 30	142.5	1.348					
16R-3, 48–52	142.7			68.2	7.96		
16R-CC, 5–7	142.89					1.9	
16R-CC, 21	143.05	1.93					
17R-1, 30–34	149.22			45.7	5.33		
17R-1, 69	149.59	2.092					
17R-1, 107–109	149.97		41.5				
18R-1, 80	159.4	2.322				5.62	5.76

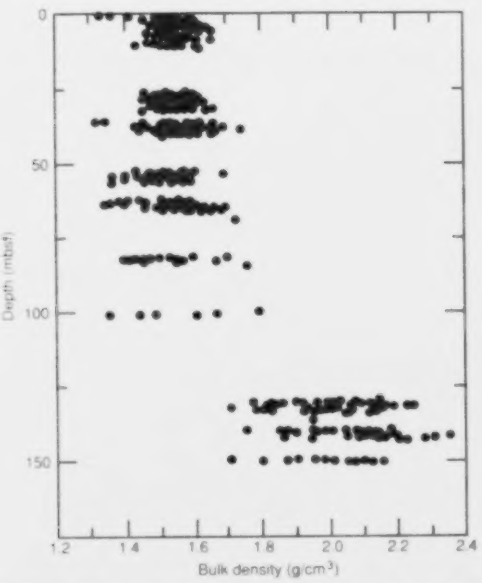

Figure 14. Bulk density (determined by the GRAPE) vs. depth for Hole 783A.

Interstitial-fluid compositions show only small variations with depth in the sediment, a sharp discontinuity at the claystone/serpentine boundary, and rapid chemical changes thereafter. Important variations with depth in the serpentine include an increase in pH from about 8 at the claystone/serpentine boundary to 9.5 to 10 at the bottom of the hole, a decrease in alkalinity (from about 3 to 1.3 meq/kg), depletions in silica (from 43 to 2 mmol/kg), magnesium (from 50 to mmol/kg), and sulfate (from 28 to 6 mmol/kg), increases in calcium (from 11 to 39 mmol/kg) and sodium (from 480 to 499 mmol/kg), decreases in potassium (from 11 to 9 mmol/kg) and salinity (from 3.59 to 3.32 wt%), and little change in ammonia, chlorinity, and bromide. Significant differences from the values measured at Conical Seamount are that calcium was depleted at Conical Seamount (by carbonate precipitation) and chlorinity decreased (possibly by mixing with deeper, fresher water).

The principal results of this site are (1) the confirmation that this seamount is made up, at least in part, of serpentinite; (2) the biostratigraphic evidence that the serpentine sediment is at least early Pliocene in age and hence older than Conical Seamount in the Mariana forearc; (3) the structural evidence for deformation within the overlying sediments as well as within the serpentinite; and (4) the evidence from fluid chemistry that serpentinization is still taking place, but without the low-chlorinity component identified at Conical Seamount (Sites 778–780).

REFERENCES

Barron, J. A. 1985. Miocene to Holocene planktic diatoms. *In* Bolli, H., Saunders, J. B., and Perch-Nielsen, K. (Eds.), *Plankton Stratigraphy*: Cambridge (Cambridge Univ. Press), 763–810.

Berggren, W. A., Kent, D. V., Flynn, J. J., and Van Couvering, J., 1985. Cenozoic geochronology. *Geol. Soc. Am. Bull.*, 96:1407–1418.

Gartner, S., 1977. Calcareous nannofossil biostratigraphy and revised zonation of the Pleistocene. *Mar. Micropaleontol.*, 2:1–25.

Kobayashi, K. (Ed.), 1989. *Preliminary Report of the Hakuho Maru Cruise KH-87-3, July-August 13, 1988, Izu-Ogasawara (Bonin), East Mariana Basin and Yap Trench (WESTPAC, ODP Site Survey)*: Tokyo (Ocean Research Institute, Univ. of Tokyo).

McDuff, R. E., 1985. The chemistry of interstitial waters, Deep Sea Drilling Project Leg 86. *In* Heath, G. R., Burckle, L. H., et al., *Init. Repts. DSDP*, 86: Washington (U.S. Govt. Printing Office), 675–687.

Ness, G., Levi, S., and Crouch, R., 1980. Marine magnetic anomaly time scales for the Cenozoic and Late Cretaceous: A précis, critique and synthesis. *Rev. Geophys. Space Phys.*, 18:753–770.

Ms 125A-111

NOTE: All core description forms ("barrel sheets") and core photographs have been printed on coated paper and bound as Section 4, near the back of the book, beginning on page 383.

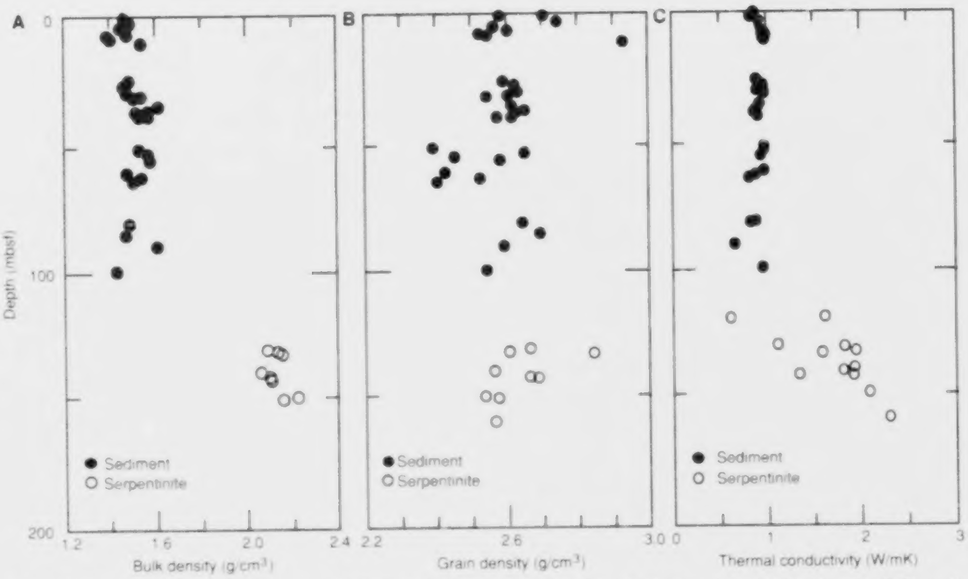

Figure 15. Physical and index properties vs. depth for Hole 783A. **A.** Bulk density (from discrete samples). **B.** Grain density. **C.** Thermal conductivity.

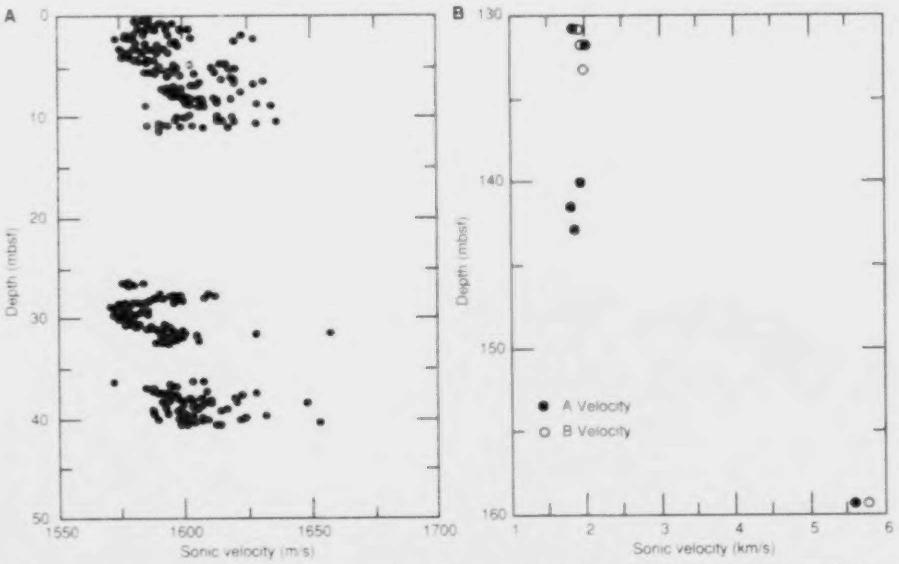

Figure 16. Sonic velocity vs. depth for Hole 783A. **A.** Velocity determined by the *P*-wave logger. **B.** Velocity determined from discrete samples. "A" velocities are parallel to core; "B" velocities are perpendicular to core.

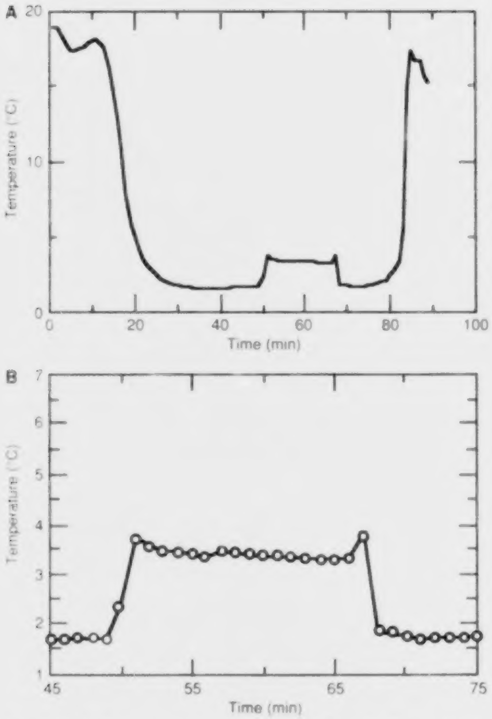

Figure 17. **A.** Temperature vs. time for Run 06R of the Barnes-Uyeda temperature tool at 42.7 mbsf in Hole 783A. **B.** An expanded plot showing the data when the tool was in the seafloor.

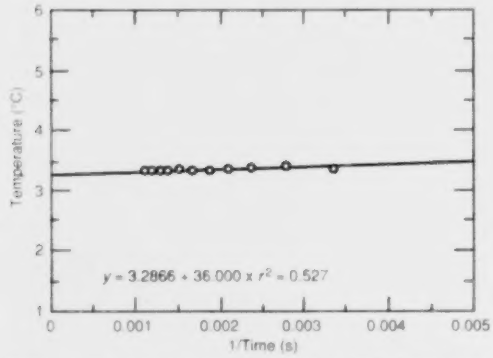

Figure 18. The reduced temperature fit of the first Barnes-Uyeda temperature run. The intercept value at 1/time = 0 is the equilibrium temperature of the sediment.

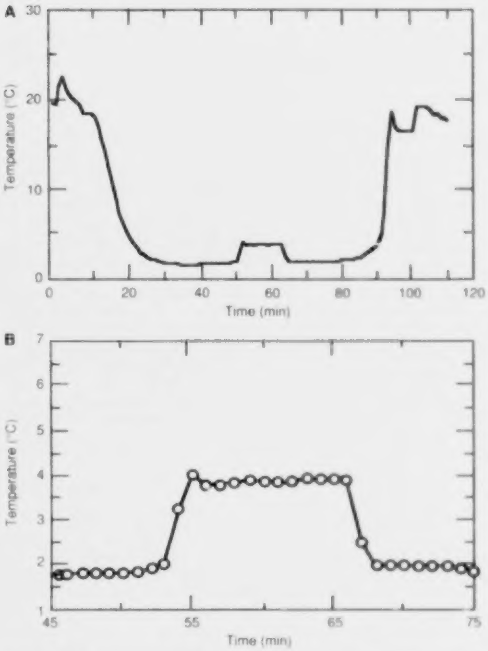

Figure 19. **A.** Temperature vs. time for Run 11R of the Barnes-Uyeda temperature tool at 90.9 mbsf in Hole 783A. **B.** An expanded plot showing the data when the tool was in the seafloor.

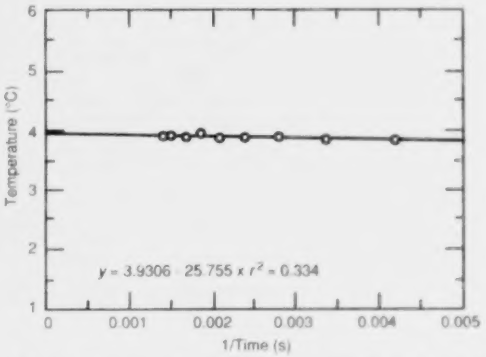

Figure 20. The corresponding reduced temperature fit for the second Barnes-Uyeda run.

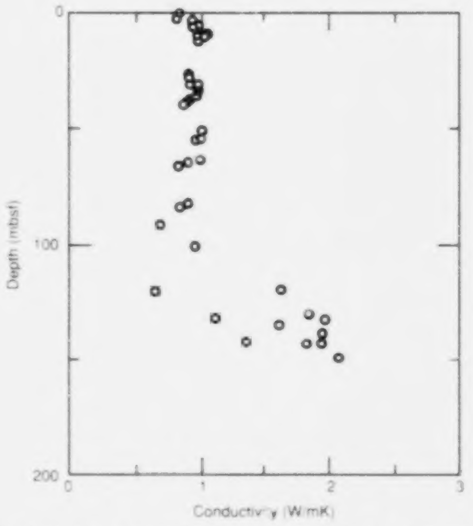

Figure 21. Plot of thermal-conductivity results vs. depth for Hole 783A.

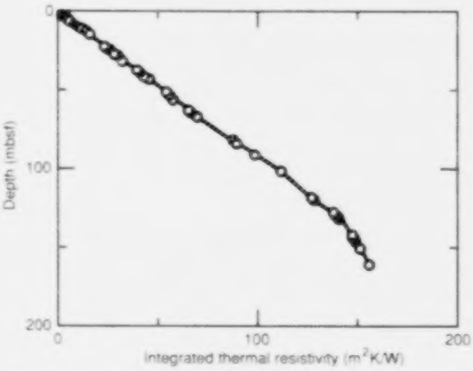

Figure 22. Plot of integrated thermal resistivity vs. depth for Hole 783A.

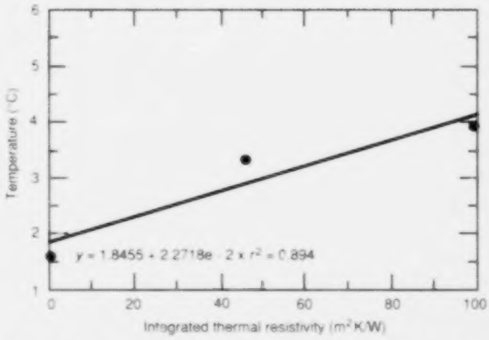

Figure 23. Temperature vs. integrated thermal resistivity for Hole 783A. The slope of the best-fitting linear regression is a heat-flow value of 23 mW/m². See text for discussion of possible explanations for the poor fit.

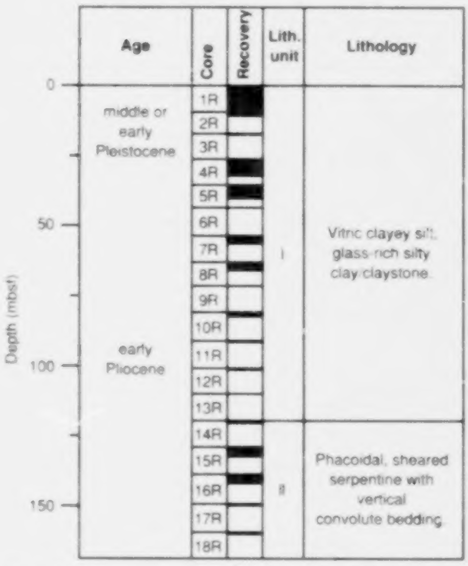
Age
Core
Recovery
Lith. unit
Lithology
0
50
100
150
Depth (mbsf)
middle or early Pleistocene
early Pliocene
1R
2R
3R
4R
5R
6R
7R
8R
9R
10R
11R
12R
13R
14R
15R
16R
17R
18R
I
II
Vitric clayey silt, glass-rich silty clay/claystone
Phacoidal, sheared serpentine with vertical convolute bedding

Figure 24. Core recovery and lithologic summary, Hole 783A.

Fryer, P., Pearce, J. A., Stokking, L. B., et al., 1990
Proceedings of the Ocean Drilling Program, Initial Reports, Vol. 125

12. SITE 784[1]

Shipboard Scientific Party[2]

HOLE 784A

Date occupied: 26 March 1989

Date departed: 30 March 1989

Time on hole: 4 days, 8 hr, 30 min

Position: 30°54.49'N, 141°44.27'E

Bottom felt (rig floor; m; drill-pipe measurement): 4912.1

Distance between rig floor and sea level (m): 11.30

Water depth (drill-pipe measurement from sea level; m): 4900.8

Total depth (rig floor; m): 5337.40

Penetration (m): 425.30

Number of cores: 45

Total length of cored section (m): 425.30

Total core recovered (m): 218.28

Core recovery (%): 51.3

Oldest sediment cored:
Depth (mbsf): 425.3
Nature: sheared, phacoidal serpentine
Age: (?)

Hard rock:
Nature: clasts of metavolcanic, meta-volcaniclastic, or serpentinized ultramafic rocks

Principal results: Site 784 is located approximately 7 km southwest of Site 783 on the lowermost, western flank of the same seamount on the inner wall of the Izu-Bonin Trench. The one hole drilled (Hole 784A) penetrated 425.3 m with a recovery of 51.3%. The stratigraphic section is divided into two lithologic units. The upper 321 m of sedimentary Unit I is of late Pleistocene to middle Miocene age or older and is subdivided into a vitric clayey silt, glass-rich silty clay/claystone (Subunit IA), a vitric claystone (Subunit IB), and a mixed claystone and silt-sized serpentine mud (Subunit IC). The lower 104 m is a phacoidal sheared serpentine microbreccia (Unit II).

Sediments from Subunits IA and IB are typically laminated and contain abundant graded beds, which are structures indicative of current activity during sediment deposition. They contain a high volcanogenic component and numerous ash layers, but a small carbonate/microfossil component, because of deposition at or below the carbonate compensation depth (CCD). Subunit IC shows a clear interfingering of background pelagic sediments, derived from the volcanic areas to the west, and silt-sized serpentine from the topographic high to the east.

Most structures in the Unit I claystones are extensional and include sets of *en echelon* tension veinlets and microfaults, some of which are clearly associated with water-escape pipes. Unit II contains pebbly serpentines with convolute lamination, sheared and relatively unsheared, pebbly, silt-sized serpentines without convolute lamination, and serpentine microbreccias. The ultramafic clasts are of variably serpentinized, tectonized harzburgite, subordinate dunites, and a few metabasalts. The middle Miocene or older age provides further evidence that the seamount is an older feature than that drilled in the Mariana forearc.

Analyses of interstitial waters indicate a steady change in composition with depth within the claystone, followed by an abrupt change in behavior at the claystone/serpentine boundary. Below this boundary, the most abrupt changes are in pH, which increases to 9.6 in the serpentine, and silica, which decreases to less than 10 μmol/kg. Of the other species, alkalinity, sulfate, magnesium, and sodium all decrease, calcium increases, and chlorinity, bromide, and salinity show no major changes. These data provide evidence for ongoing serpentinization at the Torishima Forearc Seamont. Studies of physical properties show that the average bulk densities are 1.57 g/cm^3 in the sediments of Unit I and 2.19 g/cm^3 in the serpentine of Unit II. The average compressional-wave velocities in the sediments and serpentines are 1.66 and 3.08 km/s, respectively. Thermal conductivities average about 0.9 W/mK in the sediments and 1.74 W/mK in the serpentine. Preliminary interpretation of paleomagnetic data from sediments between 0 and 160 m below seafloor (mbsf) indicates that because the inclinations of most samples lie between +15° and 15°, there may have been significant translation between the middle Miocene and the Pliocene.

BACKGROUND AND SCIENTIFIC OBJECTIVES

The choice of site was based on seismic data collected during the survey of the seamount prior to occupation of Site 783 (see "Underway Geophysics" chapter, this volume), which indicated that an eastward-dipping fault plane underlies the west flank of the seamount. Site 784 was located over the fault trace at 30°54.49'N, 140°44.27'E, at a water depth of 4900.8 m (Fig. 1). This position is approximately 7 km south-southwest of Site 783. Site 784 was a second attempt to penetrate the seamount on the inner wall of the Izu-Bonin Trench in order to (1) determine the nature of the pelagic sediments in the outermost forearc region, (2) investigate the regional tectonic history of the ridge upon which the seamount is located, (3) establish the age and mode of emplacement of the seamount through a study of the possible interlayered pelagic sediments and serpentine flows, (4) study the structure and composition of the basement of the seamount, and (5) determine the composition of the interstitial waters in the sediments and in serpentinites that might be encountered in the hole. A further objective specific to Site 784 was to recover interfingered pelagic sediments and serpentine flows that might help constrain the age of emplacement of the seamount or at least indicate the age of movement on faults associated with its uplift.

The seamount drilled at this site was dredged in 1988 in three locations (Fig. 1), yielding a wide variety of sedimentary and igneous/metamorphic rocks (Kobayashi, 1989). Most of the samples dredged from the western flank near Site 784 were sedimentary rocks, although some pumice fragments and a few serpentinized rocks were retrieved.

OPERATIONS

Transit to Site 784 (Proposed Site BON-7)

Because the basement objective had not been reached at Site 783, a hole was attempted on the lowermost western flank of the seamount, approximately 4 nmi from Site 783. Site 784 was established at 0630UTC, 26 March 1989, by the deployment of a beacon.

---

[1] Fryer, P., Pearce, J. A., Stokking, L. B., et al., 1990. *Proc. ODP, Init. Repts.*, 125: College Station, TX (Ocean Drilling Program).

[2] Shipboard Scientific Party is as given in the list of participants preceding the contents.

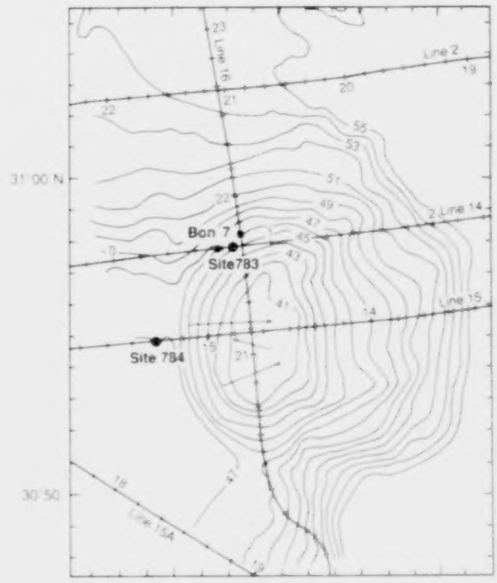

Figure 1. Bathymetry of the seamount at 31°N on the inner wall of the Izu-Bonin Trench. Arrows indicate the direction of the dredges taken on this seamount in 1988 (Kobayashi, 1989). Contour interval = 100 m.

Hole 784A

The trip back to the seafloor began at 0700UTC, and Hole 784A was spudded at 0830UTC, 26 March. From the first rotary core barrel (RCB) core we recovered 1.4 m of core and established the mud line at 4900.8 m below sea level (mbsl).

During preparations for logging, the bit failed to release several times. A core barrel was run in the hole to check for bit release, but became stuck at 21 mbsf. After retrieval of the core barrel, the drill string was tripped out of the hole. Five joints of drill string had bent, six stands above the bottom-hole assembly (BHA).

The RCB was deployed 45 times to a final depth of 425.3 mbsf, during which time we recovered 218.3 m of core for a recovery rate of 51.3% (Table 1). Site 784 officially ended at 0900UTC, 31 March, when the BHA was back on board and the vessel was under way for Site 785 (proposed Site BON-6A).

Table 1. Coring summary for Site 784.

Core no.	Date (March 1989)	Time (UTC)	Depth (mbsf)	Length cored (m)	Length recovered (m)	Recovery (%)
125-784A-						
1R	26	1010	0.0–1.4	1.4	1.40	100.0
2R	26	1210	1.4–10.9	9.5	0.20	2.1
3R	26	1345	10.9–20.4	9.5	5.13	54.0
4R	26	1455	20.4–29.9	9.5	5.43	57.1
5R	26	1820	29.9–39.5	9.6	0.00	0.0
6R	26	1930	39.5–49.1	9.6	8.48	88.3
7R	26	2130	49.1–58.8	9.7	4.30	44.3
8R	26	2215	58.8–68.5	9.7	7.94	81.8
9R	26	2330	68.5–78.1	9.6	6.93	72.2
10R	27	0045	78.1–87.8	9.7	5.86	60.4
11R	27	0200	87.8–97.4	9.6	0.20	2.1
12R	27	0300	97.4–107.1	9.7	2.62	27.0
13R	27	0530	107.1–116.7	9.6	0.78	8.1
14R	27	0700	116.7–126.4	9.7	7.18	74.0
15R	27	0800	126.4–136.0	9.6	9.85	102.0
16R	27	0910	136.0–145.6	9.6	9.82	102.0
17R	27	1200	145.6–155.3	9.7	7.52	77.5
18R	27	1300	155.3–165.0	9.7	9.85	101.0
19R	27	1425	165.0–174.7	9.7	3.29	33.9
20R	27	1525	174.7–184.4	9.7	7.68	79.2
21R	27	1640	184.4–194.0	9.6	8.36	87.1
22R	27	1800	194.0–203.6	9.6	8.67	90.3
23R	27	1915	203.6–213.2	9.6	3.86	40.2
24R	27	2025	213.2–222.9	9.7	9.51	98.0
25R	27	2145	222.9–232.5	9.6	1.19	12.4
26R	27	2300	232.5–242.1	9.6	4.23	44.0
27R	28	0015	242.1–251.8	9.7	7.66	78.9
28R	28	0130	251.8–261.4	9.6	3.60	37.5
29R	28	0245	261.4–271.1	9.7	9.82	101.0
30R	28	0345	271.1–280.8	9.7	6.85	70.6
31R	28	0445	280.8–290.4	9.6	4.43	46.1
32R	28	0545	290.4–300.0	9.6	9.64	100.0
33R	28	0700	300.0–309.7	9.7	5.42	55.9
34R	28	0800	309.7–319.3	9.6	3.31	34.5
35R	28	1145	319.3–329.0	9.7	2.59	26.7
36R	28	1500	329.0–338.7	9.7	1.22	12.6
37R	28	1900	338.7–348.3	9.6	2.26	23.5
38R	28	2330	348.3–357.9	9.6	2.66	27.7
39R	29	0600	357.9–367.5	9.6	2.81	29.3
40R	29	1020	367.5–377.3	9.8	2.76	28.1
41R	29	1320	377.3–386.9	9.6	2.57	26.8
42R	29	1720	386.9–396.6	9.7	2.44	25.1
43R	29	2330	396.6–406.3	9.7	3.90	40.2
44R	30	0400	406.3–415.6	9.3	0.97	10.4
45R	30	0800	415.6–425.3	9.7	3.09	31.8
Coring totals				425.3	218.28	51.3

LITHOSTRATIGRAPHY

The stratigraphic section recovered at Site 784 is divided into two lithologic units (Table 2). Lithologic Unit I consists of ash layers, feldspar- and glass-rich clayey silt, glass-rich silty clay/claystone, vitric claystone, claystone, and silt-sized serpentine and is divided into three subunits. Lithologic Unit II is composed of a serpentine microbreccia that is phacoidal and sheared and also exhibits vertical, convolute bedding.

Table 2. Lithologic units recovered at Site 784.

Lithologic unit	Cores	Depth (mbsf)	Dominant lithology	Stratigraphic age
IA	784A-1R-1, 0 cm, to 784A-14R-CC	0.0–126.4	Feldspar- and glass-rich clayey silt, glass-rich silty clay/claystone	upper Pleistocene to lower Pliocene(?)
IB	784A-15R-1, 0 cm, to 784A-33R-2, 120 cm	126.4–302.7	Vitric claystone	lower Pliocene(?) to middle Miocene
IC	784A-33R-2, 120 cm, to 784A-35R-2, 34 cm	302.7–321.1	Claystone and silt-sized serpentine	?
II	784A-35R-2, 34 cm, to 784A-45R-CC	321.1–425.3	Sheared, phacoidal serpentine microbreccia with vertical convolute bedding	?

Table 3. Volcanic ash layers at Site 784.

Core, section, interval (cm)	Depth of top of section (mbsf)	True depth (mbsf)	Volcanic ash layer
125-784A-			
2R-1, 0–3	1.4	1.40–1.43	1
2R-1, 5–6	1.4	1.45–1.46	2
2R-1, 12–16	1.4	1.52–1.56	3
3R-3, 50–52	13.9	14.40–14.42	4
3R-3, 119–120	13.9	15.09–15.20	5
4R-2, 55–57	21.9	22.65–22.67	6
4R-3, 1–2	23.4	23.41–23.42	7
6R-1, 34	39.5	39.84	8
6R-2, 65–68	41	41.65–41.68	9
6R-2, 72–73	41	41.72–41.73	10
6R-3, 70	42.5	43.2	11
6R-3, 91–94	42.5	43.41–43.44	12
6R-4, 58	44	44.58	13
6R-5, 71–72	45.5	46.21–46.22	14
6R-5, 97–98	45.5	46.47–46.48	15
6R-6, 73.5–74.0	47	47.735–47.740	16
7R-1, 34–37	49.1	49.44–49.47	17
7R-2, 31–35	50.6	50.91–50.95	18
7R-2, 70–74	50.6	51.30–51.34	19
7R-3, 27–31	52.1	52.37–52.41	20
7R-3, 68–76	52.1	52.78–52.86	21
8R-1, 28–30	58.8	59.08–59.1	22
8R-1, 55–56	58.8	59.35–59.36	23
8R-2, 70–71	60.3	61.0–61.01	24
8R-3, 10–17	61.8	61.90–61.97	25
8R-3, 91	61.8	62.71	26
8R-4, 30–33	63.3	63.60–63.63	27
8R-4, 90–91	63.3	64.20–64.21	28
8R-4, 120–121	63.3	64.50–64.51	29
8R-5, 36–37	64.8	65.16–65.17	30
8R-5, 59–62	64.8	65.39–65.42	31
8R-5, 126–127	64.8	66.06–66.07	32
8R-5, 139.5–140.5	64.8	66.195–66.205	33
9R-1, 20–24	68.5	68.70–68.74	34
9R-1, 26.5–28.5	68.5	68.765–68.785	35
9R-1, 68–70	68.5	69.18–69.20	36
10R-3, 28–30	81.1	81.38–81.40	37
12R-2, 63–65	98.9	99.53–99.55	38
14R-2, 0–21	118.2	118.20–118.41	39
15R-1, 67–69	126.4	127.07–127.09	40
15R-2, 36–38	127.9	128.26–128.28	41
15R-2, 39	127.9	128.29	42
15R-2, 48–50	127.9	128.38–128.40	43
15R-2, 62–63	127.9	128.52–128.53	44
15R-2, 63–66	127.9	128.53–128.56	45
15R-4, 56–60	130.9	131.46–131.50	46
15R-5, 5–20	132.4	132.45–132.60	47
15R-5, 86–96	132.4	133.26–133.36	48
15R-6, 128–136	133.9	135.18–135.26	49
16R-2, 53–68	137.5	138.03–138.18	50
16R-3, 33	139	139.33	51
16R-3, 98–106	139	139.98–140.06	52
16R-4, 44–46	140	140.44–140.46	53
16R-4, 103–104	140	141.03–141.04	54
17R-2, 102–114	147.1	148.12–148.24	55
17R-3, 80–81	148.6	149.40–149.41	56
17R-3, 118–123	148.6	149.78–149.83	57
17R-3, 143–150	148.6	150.03–150.10	58
17R-4, 38–39	150.1	150.48–150.49	59
17R-4, 112–115	150.1	151.22–151.25	60
17R-4, 139–140	150.1	151.49–151.50	61
17R-5, 59–62	151.6	152.19–152.22	62
18R-2, 32–33	156.8	157.12–157.13	63
18R-2, 100–101	156.8	157.8–157.81	64
20R-1, 18–19	174.7	174.88–174.89	65
20R-1, 31–32	174.7	175.01–175.02	66
20R-1, 95–96	174.7	175.65–175.66	67
20R-1, 110	174.7	175.8	68
20R-1, 126–127	174.7	175.96–175.97	69
20R-1, 142–144	174.7	176.12–176.14	70
20R-2, 9–10	176.2	176.29–176.30	71
20R-2, 16–17	176.2	176.36–176.37	72
20R-2, 40–41	176.2	176.60–176.61	73
20R-3, 65–70	177.7	178.35–178.40	74
20R-4, 13–17	179.2	179.33–179.37	75
21R-3, 68	187.4	188.08	76
21R-3, 77–80	187.4	188.17–188.20	77
21R-3, 139–140	187.4	188.79–188.80	78
21R-4, 78–84	188.9	189.68–189.74	79
22R-3, 88–95	197	197.88–197.95	80
24R-3, 121-123	216.2	217.41–217.43	81
24R-4, 47–50	217.7	218.17–218.20	82
27R-5, 31–35	248.1	248.41–248.45	83
28R-1, 94–96	251.8	252.74–252.76	84
29R-6, 78–80	268.9	269.68–269.70	85
31R-2, 8–11	282.3	282.38–282.41	86

Unit I

Sections 125-784A-1R-1, 0.0 cm, to 125-784A-35R-2, 34 cm; depth, 0.0–321.1 mbsf.
Age: late Pleistocene to ?

Unit I extends from the sediment/water interface to 321.1 mbsf. The gradational transition from Subunit IA to Subunit IB is based on color change, volcanic input, and extent of bioturbation. The upper part of lithologic Unit I (Subunits IA and IB) is composed primarily of claystone with varying amounts of volcanic glass and ash layers. The general trend of the volcanic input increases downhole, as can be seen in the detailed listing of ash layers in Table 3. Lithologic Subunit IC is distinct from the upper part of lithologic Unit I; this subunit contains nearly glass-free claystone with interbedded silt-sized serpentine.

Subunit IA

Sections 125-784A-1R-1, 0.0 cm, to 125-784A-14R-CC; depth, 0.0–126.4 mbsf.
Age: late Pleistocene to early Pliocene(?).

Lithologic Subunit IA contains ash layers, but is composed predominantly of light and dark gray (2.5Y 6/0 and 2.5Y 4/0), feldspar- and glass-rich clayey silt and glass-rich, silty clay/claystone scattered with brown (10YR 5/3), subangular to subrounded pumice fragments, 0.5 to 4 cm in diameter. Intervals of dark greenish gray (10Y 5/2), vitric silty clay that begin to appear in the light gray sediment of Core 125-784A-6R predominate by the top of lithologic Subunit IB. Lithologic Subunit IA has varying amounts of silt-sized detritus within the claystone, usually representing a volcanic influx. The main components of this detritus are glass (21%–53%), feldspar (8%–22%), pyroxene (0%–7%), epidote (0%–3%), amphibole (0%–2%), and chlorite (rarely present, and only in trace amounts). A trace to 10% of zeolite present in Cores 125-784A-2R through 125-784A-4R and 125-784A-6R through 125-784A-9R is interpreted as an alteration product of volcanic glass. Cores 125-784A-2R through 125-784A-4R, in the uppermost part of this subunit, contain some sand-sized quartz, which on the basis of grain size can be interpreted as terrigenous detritus, rather than an aeolian contribution. Serpentine (less than 10%) was observed in Cores 125-784A-3R, 125-784A-4R, 125-784A-6R, 125-784A-8R, 125-784A-12R, and 125-784A-14R.

The majority of the ash layers in Subunit IA are black (N 4/0 to N 2/0) graded beds with sharp basal contacts, except where drilling disturbance is severe. The different colors of the ash result from a slight variation in the feldspar and opaque mineral contribution to the sediment. The ash from this subunit is composed of volcanic glass (64%–[illegible]%) and feldspar (3%–20%), sporadic amounts of pyroxene (as much as 10%), opaque minerals (as much as 10%), chlorite (trace amounts), and clays (as much as 20%). There are also a few layers of vitric sands and silts with large admixtures of clay (30%–40%) that are interpreted as reworked ash.

In addition to the ash beds with normal grading, the prevalent sedimentary structures in Subunit IA are laminations. Intervals with laminations are present downhole from Core 125-784A-8R, and the number of intervals increases with depth to the base of this subunit, indicating current activity during deposition of the sediment. At the base of this subunit, in Section 125-784A-14R-CC, is a 4.5-cm-thick graded bed with a 0.5-cm-thick base of very pale brown (10YR 8/3) rhodochrosite (confirmed by X-ray diffraction) silt.

The only tectonic structures observed in Subunit IA are *en echelon* tension gashes in Section 125-784A-6R-5, 50–60 cm. For detailed discussion of this feature, see "Structural Studies" section (this chapter).

Biologic sedimentary structures are rare throughout Subunit IA. The background sediment of the subunit contains only a small biogenic contribution of radiolarians (as much as 10%), diatoms (as much as 10%), spicules (as much as 5%), silicoflagellates (rarely present, at trace amounts to 10%), and nannofossils (found only in Core 125-784A-8R as 2% of a reworked ash deposit). Nannofossils are not typically preserved in this environment beneath the CCD unless they were rapidly deposited from shallower depths and rapidly buried in the redeposited ash layer.

Diatoms were used to determine the biostratigraphic age of Subunit IA. Sample 125-784A-1R-1, 10–20 cm, near the top of the first core, provides a stratigraphic age of late Pleistocene for the uppermost sediment in Unit I. Section 125-784A-12R-CC, near the base of the unit, has a diatom biostratigraphic age of early Pliocene; the age of the oldest strata in Subunit IA is not well constrained, but is at least early Pliocene.

Subunit IB

Sections 125-784A-15R-1, 0.0 cm, to 125-784A-33R-2, 120 cm; depth, 126.4–302.7 mbsf.
Age: early Pliocene(?) to middle Miocene.

Lithologic Subunit IB also contains ash layers, but is composed predominantly of dark gray (5GY 4/1), glass-rich silty claystone. This sediment is sufficiently indurated from burial diagenesis to be classified as a claystone. Subunit IB has varying amounts of silt-sized detritus, probably representing a volcanic influx. Glass (15%–52%) is always present; other minerals observed are feldspar (as much as 15%), pyroxene (as much as 3%), chlorite (as much as 1%), and amphibole (as much as trace amounts). Zeolites were found only in Cores 125-784A-16R and 125-784A-17R, and quartz is present in this subunit in Cores 125-784A-20R through 125-784A-22R and 125-784A-24R in amounts less than 2%.

The ash layers of Subunit IB have sharp basal contacts and are composed of volcanic glass (68%–98%) and feldspar (2%–17%), sporadic amounts of pyroxene (as much as 7%), opaque minerals (as much as 10%), chlorite (as much as 1%), and clays (as much as 15%). Some of the ash layers contain both clinopyroxene and orthopyroxene.

Serpentine was also observed in some of the vitric claystones from Cores 125-784A-16R, 125-784A-23R, 125-784A-24R, 125-784A-32R, and 125-784A-33R, in amounts of less than 5%. An exception is in Section 125-784A-16R-6, 51–56 cm, where the core is cut by a series of greenish gray (5G 4/2) veins(?) composed of 20% serpentine, 10% opaque minerals, 70% clays, and trace amounts of feldspar and pyroxene.

Sedimentary structures in this subunit include abundant graded beds, parallel laminations, inclined laminations, micro-cross laminations (Samples 125-784A-15R-2, 36–38 cm, 125-784A-15R-2, 48–50 cm, and 125-784A-16R-3, 33–34 cm), a complete Bouma sequence (Section 125-784A-18R-1, 96–125 cm), and wavy laminations (Section 125-784A-23R-3, 40–46 cm). These structures indicate current activity during deposition of the sediment. Extensive bioturbation is also a characteristic feature of this subunit.

Other physical structures observed in this subunit are synsedimentary microfaults (Sections 125-784A-18R-2, 100–112 cm, 125-784A-19R-1, 60–68 cm, 125-784A-19R-1, 75–77 cm, 125-784A-27R-5, 12–24 cm, and 125-784A-32R-5, 12–18 cm), water-escape structures (Section 125-784A-32R-3, 0–60 cm), and tension gashes (Sections 125-784A-32R-4, 125-784A-32R-5, and 125-784A-33R-1, 28–32 cm). For a detailed discussion of these features, see the "Structural Studies" section (this chapter).

Subunit IB contains a small siliceous biogenic contribution composed of spicules (as much as 10%), radiolarians (as much as 10%), diatoms (as much as 5%), and silicoflagellates (rarely present, in trace amounts). Calcareous biogenic components are only present in Core 125-784A-31R as a trace amount of foraminifers and 5% nannofossils.

The stratigraphic age of this subunit is not well constrained. A diatom biostratigraphic age of late Miocene was obtained from core-catcher Samples 125-784A-21R and 125-784A-22R, and a middle Miocene age from core-catcher Samples 125-784A-26R, 125-784A-27R, and 125-784A-31R. Using this information and the constraint imposed by the age determination for the base of the overlying subunit, Subunit IB must be early Pliocene to at least middle Miocene.

Subunit IC

Sections 125-784A-33R-2, 120 cm, to 125-784A-35R-2, 34 cm; depth, 302.7–321.1 mbsf.

Lithologic Subunit IC is composed of intercalated grayish brown to olive brown (2.5Y 5/2 to 2.5Y 4/4) claystone and dark blue gray (5B 4/1) silt-sized serpentine. The claystone is devoid of any sedimentary structures in Core 125-784A-32R, with the exception of irregular, pale green (5G 6/2) areas (millimeter to centimeter size), some of which surround small white (2.5Y 8/0) preexisting(?) millimeter-sized clasts, and of irregular horizontal zones composed of pale green vitric-bearing claystone. The background claystone is composed of clay (90%–100%), serpentine (trace–2%), feldspar (1%–3%), glass (1%–7%), and a trace of pyroxene and amphibole. The silt-sized serpentine is typically interlayered with the claystone, with the exception of a different structure in the serpentine interval from 91 to 136 cm in Section 125-784A-35R-1. From 91 to 121 cm is a serpentine breccia composed of a dark gray (N 4/0), 5 × 6 cm rounded clast with a faint phacoidal texture and dark greenish gray (5BG 4/1), millimeter-sized angular grains. The matrix is silt-sized serpentine with layers of the following colors: bluish gray (5B 5/1) at 91–117 cm, yellowish brown (10YR 5/6) at 117–118 cm, and greenish gray (5GY 6/1) at 118–121. From 121 to 136 cm in Section 125-784A-35R-1, rounded bluish gray (5B 5/1), angular greenish gray (5GY 6/1), and rounded yellowish brown (10YR 5/6) millimeter-sized clasts are scattered through a finer-scale variegated (same matrix colors as noted for the interval from 91 to 121 cm) matrix with a sigmoidal pattern. Subunit IC contains no biogenic contribution and no stratigraphic age has therefore been determined.

The change from clay to claystone from Subunit IA to Subunit IB is typical of burial diagenesis. Lithologic Subunit IA differs from Subunit IB in color and the degree of bioturbation and probably correlates with lithologic Unit I at Site 783 on the northern flank of the seamount because the ages, lithologies, and thicknesses at the two sites are similar. Subunit IB at Site 784 may correlate with lithologic Subunit IB at Site 782 in the forearc basin because of the similarity in age and ash content, but the lithologies differ. The sediment in Subunit IB at this site has a depleted carbonate contribution because of its proximity to the CCD. The *in-situ* pelagic sediments and the silt-sized serpentine that has flowed down from the adjacent topographic high interfinger at Site 784 in Subunit IC, the lowermost part of Unit I.

Unit II

Sections 125-784A-35R-2, 34 cm, to 125-784A-45R-CC; depth, 321.1–425.3 mbsf.

The contact between lithologic Units I and II is represented by an abrupt change to grayish green (5G 5/2) and bluish gray (5B 5/1) sheared, phacoidal serpentine microbreccia withvertical, convolute bedding. A microbreccia containing blocks of serpentinized harzburgite in a matrix of sheared, phacoidal serpentine first occurs in Core 125-784A-36R and continues throughout the remainder of the unit. In the lowermost part of Unit II is a silt-sized serpentine (bearing apatite in Core 125-784A-44R) associated with the sheared, phacoidal serpentine microbreccia and the blocks of harzburgite.

The presence of Pleistocene nannofossils and siderite (rhodochrosite?) siltstone indicates downhole contamination at the tops of Cores 125-784A-36R through 125-784A-39R and 125-784A-43R. No fossils were found within the serpentine microbreccia; the age of these strata is, therefore, unknown.

Lithologic Unit II is probably either locally derived from the adjacent topographic high or represents the underlying "acoustic basement" at this site. This unit correlates with lithologic Unit II at Site 783 on the northern flank of the seamount.

BIOSTRATIGRAPHY

Evidence from calcareous nannofossils and diatoms in the cores from Site 784 shows that the sedimentary interval from Samples 125-784A-1R-1, 10–20 cm, to 125-784A-31R-CC ranges in age from late Pleistocene to middle Miocene. No ages could be assigned to the remaining sedimentary section in Cores 125-784A-32R to 125-784A-42R.

The strong dissolution of the calcareous plankton assemblages from Site 784 suggests that deposition of the sedimentary interval probably took place at or below the CCD.

The biostratigraphic results of Site 784 are summarized in Figure 2.

Calcareous Nannofossils

Rare, poorly preserved calcareous nannofossil assemblages were found in Samples 125-784A-2R-CC, 125-784A-6R-CC, and 125-784A-8R-3, 15 cm. The presence of *Gephyrocapsa oceanica*, *Gephyrocapsa caribbeanica*, and *Pseudoemiliania lacunosa* confines Samples 125-784A-2R-CC and 125-784A-6R-CC to the middle/early Pleistocene (Zone CN14a). Sample 125-784A-8R-3, 15 cm, contains a late Pliocene (Zone CN12) assemblage of *Discoaster brouweri*, *P. lacunosa*, *Calcidiscus macintyrei*, and *Helicosphaera sellii*. The low abundance and poor preservation are probably the result of deposition at or below the CCD, as shown by the strong etching of the remaining nannofossil assemblages.

Foraminifers

Except for Sample 125-784A-2R-CC, in which a single specimen of *Globigerina* sp. was found, all of the samples examined, from Samples 125-784A-1R-1, 10–20 cm, to 125-784A-42R-CC, are barren of planktonic and benthic foraminifers. This is again most likely the result of deposition below the CCD.

Diatoms

Diatoms are poorly to well preserved and are sparse to abundant in Hole 784A. It was possible to date the sedimentary interval as ranging from late Pleistocene to at least middle Miocene. The interval below Core 125-784A-31R-CC is devoid of diatoms.

Sample 125-784A-1R-1, 10–20 cm, is assigned to the late Pleistocene *Pseudoeunotia doliolus* Zone by the appearance of *P. doliolus* and the absence of *Nitzschia reinholdii*.

Nitzschia reinholdii is present in Sample 125-784A-2R-CC; this sample is, therefore, early Pleistocene (*N. reinholdii* Zone).

No zonal markers were found in Samples 125-784A-3R-CC through 125-784A-6R-CC. The Pliocene/Pleistocene boundary can be assumed to be in this interval, as *Rhizosolenia praebergonii* is present in Samples 125-784A-7R-CC and 125-784A-8R-CC, which assigns these samples to the late Pliocene *R. praebergonii* Zone. Both samples have abundant and well-preserved assemblages.

The early Pliocene marker *Nitzschia jouseae* is present in Samples 125-784A-10R-CC and 125-784-12R-CC.

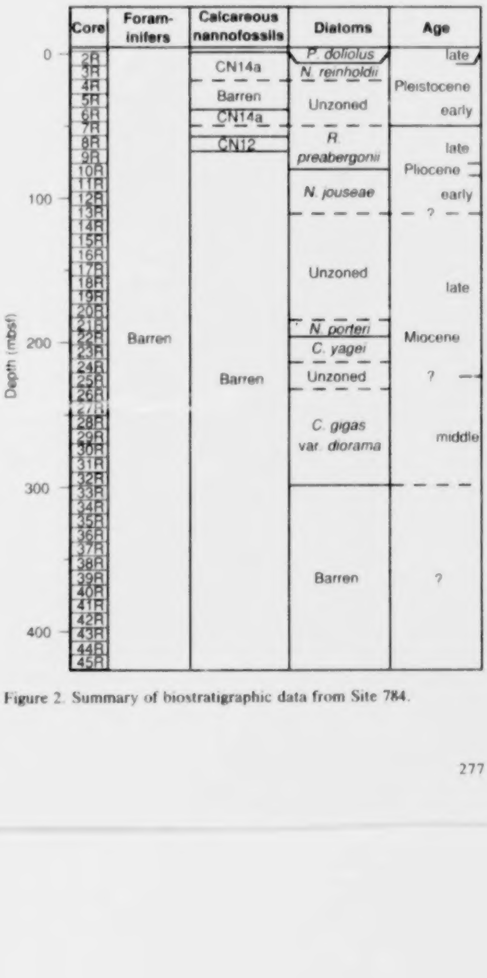

Figure 2. Summary of biostratigraphic data from Site 784.

Samples 125-784A-13R-CC through 125-784A-20R-CC have only traces or rare abundances of diatoms in which no zonal markers were found.

Thalassiosira burckliana is present in Sample 125-784A-21R-CC and *Coscinodiscus yabei* was recorded in Sample 125-784A-22R-CC, which assigns these samples to the late Miocene. Both samples have common and moderately preserved assemblages.

Samples below 125-784A-22R-CC have only traces of diatoms. *Actinocyclus ingens* is present in Samples 125-784A-26R-CC through 125-784A-31R-CC, dating this interval as middle Miocene (*Coscinodiscus gigas* var. *diorama* Zone or older).

IGNEOUS AND METAMORPHIC PETROLOGY

The igneous and metamorphic rocks recovered at Site 784 are variably serpentinized and tectonized ultramafic rocks (harzburgite 80%–90%, dunite 10%–20%) together with weakly metamorphosed volcanic (metabasalt and meta-volcaniclastic) rocks. The ultramafic clasts reach a maximum recovered thickness of about 1.5 m (Section 125-784A-43R-2) and are enclosed in a highly sheared and pulverized serpentine matrix (Fig. 3) that is described in the "Structural Studies" section (this chapter). Contact relationships between the ultramafic and sedimentary rocks are ambiguous. The volcanic clasts are 1 to 5 cm in diameter and show a subangular to subrounded shape. They form clasts of isolated fragments and inclusions in the serpentine matrix.

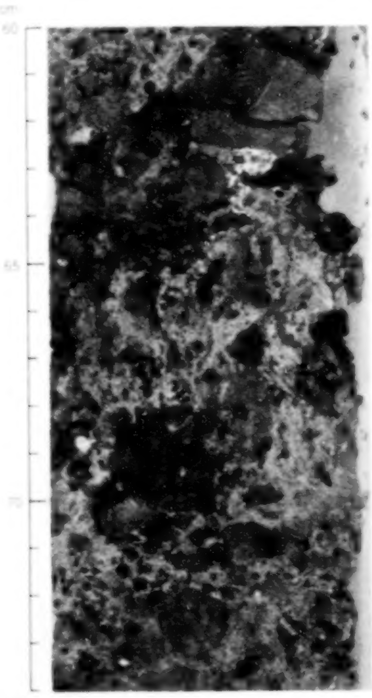

Figure 3. Ultramafic clasts enclosed in a highly sheared and pulverized serpentine matrix (Section 125-784A-43R-2, 60–74 cm).

Ultramafic Rocks

Serpentinized and Weakly Tectonized Harzburgites

The harzburgites are massive and vary from dark greenish-gray (5BG 4/1), where relatively fresh, to black (7.5YR 2/0), where serpentinized (e.g., Sections 125-784A-38R-2, 85–94 cm, and 125-784A-36R-1, 94–107 cm; Figs. 4 and 5, respectively). The primary mineralogy of these rocks is olivine (65%–90%), orthopyroxene (10%–30%), clinopyroxene (trace–4%), and chromium-spinel (trace–2%). Clinopyroxene is present as blebs and anhedral crystals (<2 mm), typically closely related to orthopyroxene, and as exsolution lamellae (on 100) in orthopyroxene.

The harzburgites display weak deformation. Typically, orthopyroxene crystals are 1 to 5 mm in size and have morphologies that range from equant to asymmetric-elongate; the cleavage surfaces and extinction are wavy, kink-banding is not rare, and fine clinopyroxene exsolution lamellae on (100) are bent. Olivine crystals are 1 to 5 mm in size and have an anhedral shape. Kink-banding characterizes some olivine morphologies. Chromium-spinel crystals are subhedral to anhedral (0.05–1.5 mm in size) and dark red to reddish brown in thin section. Some of the elongate spinels define a lineation parallel to the elongate olivine and orthopyroxene (see "Structural Studies" section, this chapter).

The degree of serpentinization is extremely variable (60%–100%), with the olivine and orthopyroxene replaced by mesh-textured serpentine and bastite (which appear to be mostly chrysotile and/or lizardite), respectively. In the strongly serpentinized types, most of the chromium-spinel (translucent, shades of red) is replaced by magnetite (opaque). The harzburgites are cut by numerous veins of serpentine. Many of these veins show a polystage history of filling (Fig. 5). Typically, serpentinization has affected olivine the most, orthopyroxene less, and clinopyroxene and chromium-spinel the least at this site. Subhedral primary clinopyroxenes (<2 mm in length) were observed in some samples.

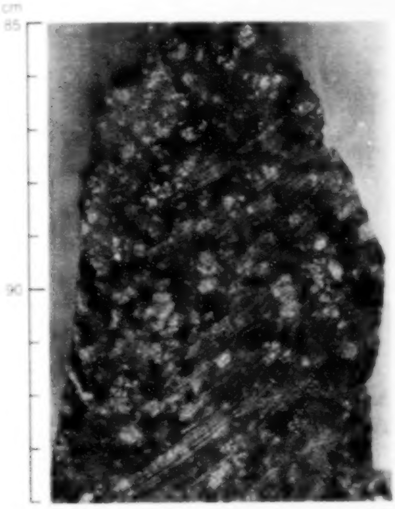

Figure 4. Relatively pyroxene-rich fresh harzburgite (Section 125-784A-38R-2, 85–94 cm).

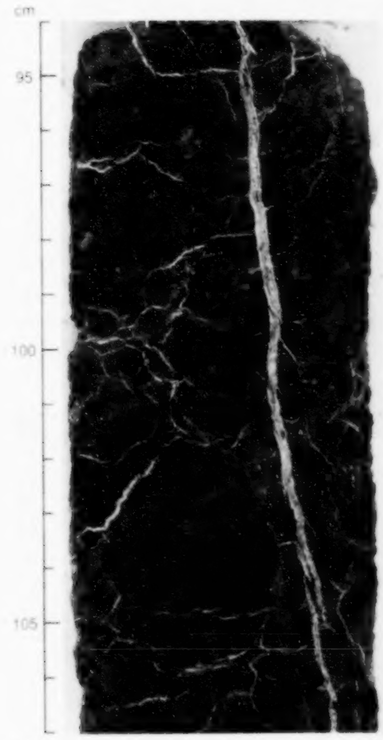

Figure 5. Intensively serpentinized harzburgite cut by numerous veins of serpentine (Section 125-784A-36R-1, 94–107 cm).

Serpentinized and Weakly Tectonized Dunites

The dunites are dark bluish gray (5B 4/1) to black (N 4/) and generally massive; some grade to harzburgite. The primary mineralogy consists of olivine (>95%), orthopyroxene (<5%), and spinel (trace–1%). Most of the dunites are extensively (99%–100%) serpentinized, show mesh textures and splays of chrysotile (and/or lizardite), and are cut by numerous serpentine-rich veins (Fig. 6). Asymmetric elongation of spinel is evidence of deformation. Other secondary minerals include magnetite (replacing chromium-spinel and in serpentine veins) and up to 10% clays (replacing serpentine).

Metavolcanic Rocks

Metabasalt

The several clasts of metabasalt that were recovered are 1 to 5 cm in diameter. Most are grayish green (5G 4/2–5G 5/2), and those containing abundant limonite are dark reddish brown (5YR 2.5/2). The metabasalts are composed of plagioclase, clinopyroxene, magnetite(?), and glass as primary phases and chlorite, sphene, dusty brownish clay, carbonate, pale green actinolite, and limonite as secondary phases. The primary igneous textures, such as intersertal and aphyric textures, are well preserved, but almost all primary minerals, except clinopyroxene and some plagioclase grains, are completely altered.

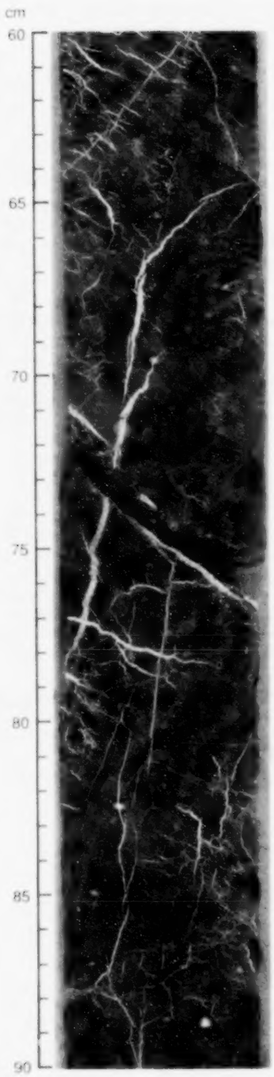

Figure 6. Intensively serpentinized dunite cut by numerous veins of serpentine (Section 125-784A-40R-2, 60–90 cm).

Meta-Volcaniclastic Rock

Only one meta-volcaniclastic rock clast was recovered. The rock is 5 cm in diameter, light greenish gray (5G 7/1), and medium- to fine-grained and consists of clinopyroxene as a relic mineral and prehnite, dusty brownish clay, carbonate, actinolite, and chlorite as secondary minerals. The rock contains abundant subangular to subrounded fragments of clinopyroxene within a fine-grained chlorite and clay matrix.

Most fragments of clinopyroxene have been altered to colorless actinolite. Calcite and chlorite veins (0.01–0.1 mm wide) run throughout the rock.

IGNEOUS AND METAMORPHIC GEOCHEMISTRY

Shipboard geochemical analyses of clasts enclosed in a highly sheared and pulverized serpentine matrix at Site 784 were performed for seven samples of serpentinized harzburgites, three samples of serpentinized dunites, and two matrix samples. Preparation and analytical techniques are given in the "Explanatory Notes" (this volume). Rock and thin-section descriptions are given in "Igneous and Metamorphic Petrology" section of this chapter. The geochemical data are listed in Tables 4 and 5.

Ultramafic Samples

Modal estimates of the original (pre-serpentinization) composition of ultramafic samples range from 65 to 93 modal% olivine, 10 to 30 modal% orthopyroxene, trace to 4 modal% clinopyroxene, and trace to 2 modal% spinel in the harzburgite samples and from 95 to 99 modal% olivine, <5 modal% orthopyroxene, and trace to 1 modal% spinel in the dunite samples. The degree of serpentinization of the samples varies from 60% to 100% for the harzburgites and from 99% to 100% for the dunites.

Major-Element Chemistry

Loss on ignition (LOI) for these samples ranges from 13.63 to 17.01 wt%, and, as for the samples from Sites 779 and 783, shows a positive correlation with the degree of serpentinization (Fig. 7A). (See "Igneous and Metamorphic Geochemistry" sections in the "Site 778" and "Site 779" chapters, this volume, and "Explanatory Notes" chapter for an explanation of LOI.) Although the ranges of major-element concentrations are similar in the dunite and harzburgite samples, some small differences exist. SiO_2 is slightly higher in the harzburgite samples (35.35–38.92 wt%) than in the dunite samples (33.01–34.17 wt%). Al_2O_3 is also slightly higher in the harzburgites (0.27–0.62 wt%) than in the dunites (0.01–0.20 wt%). Fe_2O_3 ranges from 7.13 to 8.94 wt% and CaO ranges from 0.06 to 0.55 wt% in both. MgO values in dunite samples (39.36–41.33 wt%) are slightly higher than in harzburgite samples (37.93–39.67 wt%). Magnesium number (Mg# = Mg/(Mg + Fe) × 100) is high in all rocks and ranges from 89.71 to 91.67. Na_2O, K_2O, and P_2O_5 were not detected in any of the samples. The general absence of clinopyroxene crystals and very low concentrations of Al_2O_3 and CaO (Fig. 7B) indicate that the rocks are residues from high degrees of partial melting. Concentrations of major-element oxides in ultramafic rocks from Site 784 are similar to those from ultramafic samples from Sites 778 through 780 and 783 (see the "Igneous and Metamorphic Geochemistry" sections in the respective site chapters).

Trace-Element Chemistry

Trace-element data are presented in Table 5. Compatible elements are high in all samples, as expected. Nickel ranges from 1991 to 2819 ppm and chromium from 1115 to 2585 ppm, with the exception of a single low value of 444 ppm in Sample 125-784A-40R-2, 41–43 cm. Chromium and nickel do not correlate with one another or with the degree of serpentinization. Niobium, zirconium, yttrium, rubidium, and titanium are all present in trace amounts or are below detection limits, with the exception of Sample 125-784A-45R-1, 98–100 cm, which contained a high value of 18 ppm for zirconium. Cerium and barium values range from below the detection limit (<10 ppm) to trace amounts and 12 ppm, respectively, although these values may result from analyt-

Table 4. Major-element data for serpentinized ultramafic rocks and matrix samples from Hole 784A.

Core, section Interval (cm)	36R-1, 107–109	37R-1, 6–9	38R-1, 66–68	38R-2, 92–95	42R-1, 5–8	45R-1, 98–100	45R-2, 41–44	Average harzburgite	40R-2, 41–43	41R-2, 98–100	42R-1, 39–41	Average dunite	38R-2, 29–31	40R-1, 84–87	Average matrix
SiO_2	36.23	36.97	35.35	38.92	37.57	37.58	37.76	37.20	33.32	34.17	33.01	33.50	36.98	36.18	36.58
TiO_2	0.00	0.00	0.00	0.00	0.00	0.00	0.00	0.00	0.00	0.00	0.00	0.00	0.00	0.00	0.00
Al_2O_3	0.27	0.51	0.29	0.62	0.52	0.34	0.35	0.41	0.01	0.15	0.20	0.12	0.34	0.17	0.26
Fe_2O_3	7.44	7.54	7.21	7.13	7.49	7.24	7.14	7.31	7.92	8.94	8.90	8.59	6.62	7.17	6.90
MnO	0.12	0.16	0.13	0.13	0.11	0.11	0.11	0.12	0.11	0.12	0.13	0.12	0.08	0.09	0.09
MgO	38.45	38.30	39.15	37.93	39.28	39.63	39.67	38.97	41.33	39.36	40.31	40.33	39.86	40.55	40.21
CaO	0.06	0.41	0.07	0.58	0.55	0.46	0.54	0.38	0.14	0.14	0.14	0.14	0.08	0.17	0.13
Na_2O	0.00	0.00	0.00	0.00	0.00	0.00	0.00	0.00	0.00	0.00	0.00	0.00	0.00	0.00	0.00
K_2O	0.00	0.00	0.00	0.00	0.00	0.00	0.00	0.00	0.00	0.00	0.00	0.00	0.00	0.00	0.00
P_2O_5	0.00	0.00	0.00	0.00	0.00	0.00	0.00	0.00	0.00	0.00	0.00	0.00	0.00	0.00	0.00
NiO	0.28	0.29	0.27	0.25	0.30	0.29	0.29	0.28	0.33	0.34	0.36	0.34	0.24	0.30	0.27
Cr_2O_3	0.16	0.29	0.21	0.38	0.30	0.19	0.20	0.25	0.06	0.26	0.27	0.20	0.22	0.17	0.20
^{a}LOI	16.29	15.29	17.01	13.66	13.97	13.63	13.66	14.76	16.38	15.46	16.34	16.06	15.40	14.95	15.18
Total	99.70	99.76	99.69	99.60	100.09	99.47	99.54	99.69	99.60	98.94	99.66	99.40	99.82	99.75	99.79
Mg#	91.18	90.96	91.50	91.33	91.22	91.56	91.67	91.35	91.18	89.71	89.97	90.29	92.26	91.80	92.03
^{b}% Serpentinization	80	70	93	75	80	80	65	77.57	93	85	90	89.33			0.00

Note: Data (in wt% oxides) from whole-rock analyses by XRF.

^{a} Between 105° and 1030°C.

^{b} Estimated from thin sections.

Table 5. Trace-element data for serpentinized ultramafic rocks and matrix samples from Hole 784A.

Core, section Interval (cm)	36R-1, 107–109	37R-1, 6–9	38R-1, 66–68	38R-2, 92–95	42R-1, 5–8	45R-1, 98–100	45R-2, 44–44	Average harzburgite	40R-2, 41–43	41R-2, 98–100	42R-1, 39–41	Average dunite	38R-2, 29–31	40R-1, 84–87	Average matrix
Nb	tr	tr	tr	tr	tr	tr	tr	tr	tr	tr	tr	tr	tr	tr	tr
Zr	0	1	0	1	1	18	1	1	1	1	1	1	1	1	1
Y	nd	0	0	0	1	nd	0	0	nd	nd	0	0	1	0	1
Sr	2	3	3	4	5	5	5	4	3	3	3	3	4	4	4
Rb	0	0	0	0	0	nd	nd	0	0	0	nd	0	1	0	1
Zn	37	43	39	30	31	30	30	34	34	52	33	40	20	25	23
Cu	3	3	2	4	1	4	1	2	1	3	1	2	2	2	2
Ni	2214	2258	2139	1991	2327	2249	2259	2205	2534	2640	2819	2664	1897	2342	2120
Cr	1115	2012	1428	2585	2045	1310	1339	1691	444	1765	1871	1360	1539	1164	1352
V	19	45	23	29	36	32	36	31	7	4	19	10	20	12	16
TiO_2	0	0	0	0	0	0	0	0	0	0	0	0	0	0	0
Ce	nd	nd	nd	nd	nd	tr	tr	nd	tr	nd	tr	tr	tr	tr	tr
Ba	tr	11	12	tr	12	nd	nd	tr	nd	tr	11	tr	tr	tr	tr

Note: Data (in ppm) from whole-rock analyses by XRF; nd = not detected; tr = below detection limit (<2 ppm for Nb, <10 ppm for Ba and Ce).

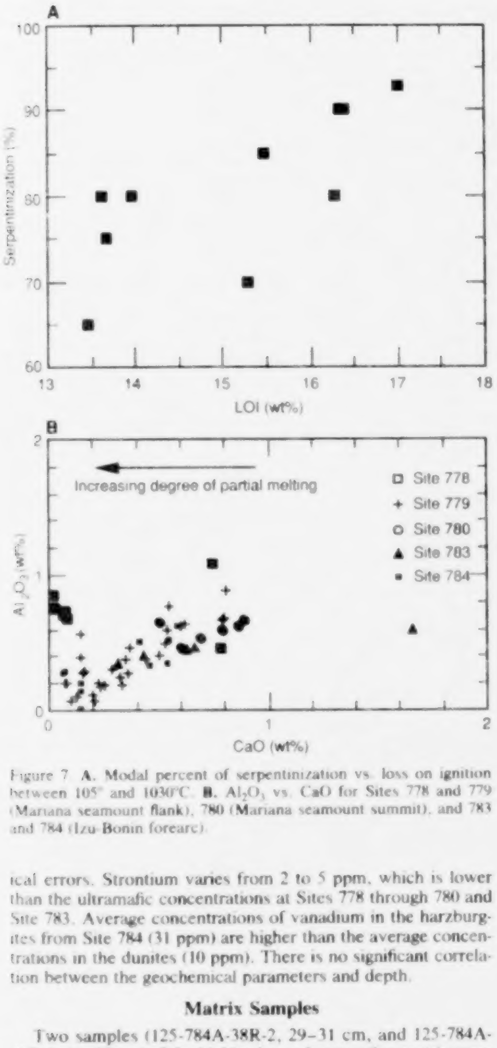

Figure 7. **A.** Modal percent of serpentinization vs. loss on ignition between 105° and 1030°C. **B.** Al_2O_3 vs. CaO for Sites 778 and 779 (Mariana seamount flank), 780 (Mariana seamount summit), and 783 and 784 (Izu-Bonin forearc).

ical errors. Strontium varies from 2 to 5 ppm, which is lower than the ultramafic concentrations at Sites 778 through 780 and Site 783. Average concentrations of vanadium in the harzburgites from Site 784 (31 ppm) are higher than the average concentrations in the dunites (10 ppm). There is no significant correlation between the geochemical parameters and depth.

Matrix Samples

Two samples (125-784A-38R-2, 29–31 cm, and 125-784A-40R-1, 84–87 cm) of the highly sheared serpentine matrix were analyzed by X-ray fluorescence (XRF). The bulk chemistry of these two samples is remarkably similar and deviates little from the average ultramafic values. The average weight percent values for SiO_2, Al_2O_3, Fe_2O_3, MgO, and CaO are 36.58, 0.26, 6.90, 40.21, and 0.13, respectively (Table 4). The values of chromium (1352 ppm) and nickel (2120 ppm) also fall within typical ranges for ultramafic rocks.

SEDIMENT/FLUID GEOCHEMISTRY

Sediment Geochemistry

Cores from Site 784 were analyzed on board the ship for inorganic carbon and for total carbon, nitrogen, and sulfur, using the techniques described in the "Explanatory Notes" (this volume). The organic carbon content was then calculated by difference. Results are presented in Table 6 and Figure 8.

The $CaCO_3$ content of the sediments, serpentine, and phacoidal sheared serpentine microbreccia is low, generally less than 0.3 wt%. Of 147 samples, only five have more than 1% $CaCO_3$; these are from about 1, 13, 269, and 321 mbsf. The sample from 321 mbsf has the highest $CaCO_3$ content, 11 wt%. It is from the uppermost part of the phacoidal sheared serpentine microbreccia of Unit II. In thickness and carbonate content, the $CaCO_3$-rich layer at 321 mbsf at Site 784 is similar to that encountered within a few meters of the seafloor in the serpentine sediments and flows at Sites 778, 779, and 780 on Conical Seamount in the Mariana forearc. Carbonate enrichment at the Conical Seamount sites takes the form of aragonite needles dispersed throughout the serpentine. These needles were tentatively interpreted as precipitates within a reaction front between bicarbonate-rich interstitial waters and calcium-rich ocean bottom water (see "Sediment/Fluid Geochemistry" section, "Site 780" chapter, this volume). The carbonate enrichment at the top of the serpentine unit at Site 784 takes the form of dispersed $CaCO_3$, rather than discrete aragonite needles. However, if needles were originally present, it is likely that they would have recrystallized. It is possible, therefore, that the serpentine at 321 mbsf at Site 784 became enriched in $CaCO_3$ when it was near the seafloor and that the interstitial waters at Site 784 once resembled those sampled from Conical Seamount during Leg 125, at least in having very high carbonate alkalinity. The waters at Site 784 are significantly different from those at Conical Seamount and do not have high alkalinity at the present, as will be shown in the "Fluid Geochemistry" section (this chapter).

The content of organic carbon in the cores at Site 784 nearly always exceeds that of inorganic carbon, varying between 0.2 and 0.7 wt%, except for a carbon-poor interval from 340 mbsf to the bottom of the hole. The nitrogen content varies from less than 0.01 to 0.3 wt% and generally correlates with that of organic carbon. Sulfur was detected in only five samples, from 234, 245, 254, 274, and 378 mbsf, where its concentration varies from 0.17 to 0.29 wt%.

Fluid Geochemistry

As at Sites 782 and 783, the concentration of methane measured on 5-cm^3 headspace samples is generally low, less than 20 μL/L. The sole exception is the deepest sample from Hole 784A, for which a concentration of 32 μL/L was obtained (Table 7). Methane was the only hydrocarbon detected.

Interstitial waters at Site 784 are similar to those at Site 783. The holes drilled at both sites penetrated glass-rich silty clays and claystones, underlain by phacoidal, sheared serpentine containing clasts mainly of harzburgite. The transition between these two units is more gradual at Site 784, where the units are separated by 18 m (303–321 mbsf) of interbedded claystone and silt-sized serpentine. As at Site 783, the composition of the interstitial waters at Site 784 changes abruptly between the claystone and the serpentine units, especially in terms of pH and silica. Values of pH increase to 9.6 in the serpentine and silica decreases to less than 10 μmol/kg (Table 8 and Fig. 9).

The changes in other dissolved species are less abrupt at Site 784 than at Site 783 only because the claystone is much thicker at Site 784, and many of the changes found at the boundary with the serpentine are extensions of changes that are already proceeding with depth in the claystone. This is the case for alkalinity, which has a concentration in waters within the serpentine of about one-half of that in seawater,

Table 6. Total nitrogen, sulfur, carbon, inorganic carbon, organic carbon, and carbonate carbon in cores at Site 784.

Core, section, interval (cm)	Depth (mbsf)	Total nitrogen (wt%)	Total sulfur (wt%)	Total carbon (wt%)	Inorganic carbon (wt%)	Organic carbon (wt%)	$CaCO_3$ (wt%)
125-784A-							
1R-1, 74–76	0.74	0.15	nd	0.53	0.10	0.43	0.8
1R-CC, 22–24	1.16		0.23	1.9			
2R-1, 5–7	1.45	0.12	nd	0.36	0.04	0.32	0.3
3R-1, 74–76	11.64		0.04	0.3			
3R-2, 35–37	12.75	0.09	nd	1.37	1.14	0.23	9.5
3R-3, 67–69	14.57		0.11	0.9			
3R-4, 18–20	15.58		0.01	0.1			
4R-1, 31–33	20.71		0.09	0.7			
4R-2, 31–33	22.21	0.12	nd	0.35	0.01	0.34	0.1
4R-3, 31–33	23.71		0.08	0.7			
4R-4, 31–33	25.21		0.01	0.1			
6R-1, 76–78	40.26		0.01	0.1			
6R-2, 80–82	41.80	0.17	nd	0.56	0.04	0.52	0.3
6R-3, 85–87	43.35		0.03	0.2			
6R-4, 90–92	44.90		0.02	0.2			
6R-5, 91–93	46.41		0.01	0.1			
6R-6, 45–47	47.45		0.06	0.5			
7R-1, 67–69	49.77		0.06	0.5			
7R-2, 65–67	51.25	0.11	nd	0.31	0.02	0.29	0.2
7R-3, 65–67	52.75		0.05	0.4			
8R-1, 69–71	59.49		0.02	0.2			
8R-2, 106–108	61.36	0.18	nd	0.82	0.10	0.72	0.8
8R-3, 52–54	62.32		0.02	0.2			
8R-4, 56–58	63.86		0.02	0.2			
8R-5, 51–53	65.31		0.01	0.1			
9R-1, 85–87	69.35		0.01	0.1			
9R-2, 85–87	70.85	0.12	nd	0.36	0.01	0.35	0.1
9R-3, 77–79	72.27		0.01	0.1			
9R-4, 42–44	73.42		0.01	0.1			
9R-5, 27–29	74.77		0.01	0.1			
10R-1, 49–51	78.59		0.01	0.1			
10R-2, 59–61	80.19	0.14	nd	0.38	0.01	0.37	0.1
10R-3, 103–105	82.13		0.01	0.1			
10R-4, 80–82	83.40		0.01	0.1			
12R-1, 58–60	97.98		0.01	0.1			
12R-2, 44–46	99.34	0.12	nd	0.35	0.01	0.34	0.1
13R-1, 36–38	107.46	0.12	nd	0.38	0.01	0.37	0.1
14R-1, 97–99	117.67		0.09	0.8			
14R-2, 63–65	118.83	nd	nd	0.46	0.01	0.45	0.1
14R-3, 30–32	120.00		0.01	0.1			
14R-4, 30–32	121.50		0.01	0.1			
14R-5, 70–72	123.40		0.01	0.1			
15R-1, 78–80	127.18		0.01	0.1			
15R-2, 56–58	128.46	0.13	nd	0.34	0.01	0.33	0.1
15R-2, 94–96	129.84		0.01	0.1			
15R-4, 96–98	131.86		0.01	0.1			
15R-5, 79–81	133.19		0.03	0.2			
15R-6, 79–81	134.69		0.01	0.1			
15R-7, 39–41	135.79		0.01	0.1			
16R-1, 56–68	136.56		0.01	0.1			
16R-2, 56–58	138.06	0.12	nd	0.31	0.01	0.30	0.1
16R-3, 56–58	139.56		0.01	0.1			
16R-4, 56–58	141.06		0.01	0.1			
16R-5, 56–58	142.56		0.01	0.1			
16R-6, 41–43	143.91		0.01	0.1			
16R-7, 41–43	145.41		0.02	0.2			
17R-1, 86–88	146.46		0.01	0.1			
17R-2, 48–50	147.58	0.11	nd	0.23	0.02	0.21	0.2
17R-3, 51–53	149.11		0.02	0.2			
17R-4 [illegible]–53	150.61		0.02	0.2			
17R-5, 34–36	151.94		0.02	0.2			
18R-1, 90–92	156.20		0.01	0.1			
18R-2, 121–123	158.01	0.12	nd	0.25	0.02	0.23	0.2
18R-3, 105–107	159.35		0.01	0.1			
18R-4, 82–84	160.62		0.01	0.1			
18R-5, 118–120	162.48		0.02	0.2			
18R-6, 86–88	163.66		0.01	0.1			
18R-7, 18–20	164.48		0.01	0.1			
19R-1, 56–58	165.56		0.02	0.2			
19R-2, 36–38	166.86	nd	nd	0.40	0.01	0.39	0.1
20R-1, 104–106	175.74		0.01	0.1			
20R-2, 120–121	177.40	nd	nd	0.32	0.01	0.31	0.1
20R-3, 109–111	178.79		0.01	0.1			
20R-4, 48–49	179.68		0.01	0.1			

Table 6 (continued).

Core, section, interval (cm)	Depth (msbf)	Total nitrogen (wt%)	Total sulfur (wt%)	Total carbon (wt%)	Inorganic carbon (wt%)	Organic carbon (wt%)	$CaCO_3$ (wt%)
20R-5, 56–58	181.26		0.07	0.6			
21R-1, 108–110	185.48		0.01	0.1			
21R-2, 65–67	186.55	nd	nd	0.27	0.01	0.26	0.1
21R-3, 21–23	187.61		0.01	0.1			
21R-4, 106–108	189.96		0.01	0.1			
21R-5, 18–20	190.58		0.01	0.1			
22R-1, 96–98	194.96		0.01	0.1			
22R-2, 96–98	196.46	nd	nd	0.43	0.06	0.37	0.5
22R-3, 124–126	198.24		0.03	0.2			
22R-4, 114–116	199.64		0.01	0.1			
22R-5, 67–69	200.67		0.01	0.1			
22R-6, 66–68	202.16		0.01	0.1			
23R-1, 133–135	204.93		0.01	0.1			
23R-2, 104–106	206.14	0.30	nd	0.69	0.02	0.67	0.2
23R-3, 30–33	206.90		0.01	0.1			
24R-1, 34–36	213.54		0.02	0.2			
24R-2, 41–43	215.11	0.24	nd	0.57	0.02	0.55	0.2
24R-3, 110–112	217.30		0.02	0.2			
24R-4, 127–129	218.97		0.02	0.2			
24R-5, 29–31	219.49		0.02	0.2			
24R-6, 18–20	220.88		0.02	0.2			
25R-1, 59–61	223.49		0.02	0.2			
26R-1, 95–97	233.45		0.02	0.2			
26R-2, 40–42	234.40	0.21	0.29	0.49	0.01	0.48	0.1
27R-1, 117–119	243.27		0.01	0.1			
27R-2, 104–106	244.64	0.16	0.24	0.42	0.02	0.40	0.2
27R-3, 82–84	245.92		0.01	0.1			
27R-4, 53–55	247.13		0.02	0.2			
27R-5, 80–82	248.90		0.03	0.2			
28R-1, 110–112	252.90		0.02	0.2			
28R-2, 86–88	254.16	0.21	0.29	0.50	0.01	0.49	0.1
28R-3, 21–23	255.01		0.09	0.7			
29R-1, 99–101	262.39		0.01	0.1			
29R-2, 107–109	263.97	0.12	nd	0.41	0.02	0.39	0.2
29R-3, 57–59	264.97		0.03	0.2			
29R-4, 49–51	266.39		0.02	0.2			
29R-5, 55–57	267.95		0.04	0.3			
29R-6, 28–30	269.18		0.22	1.8			
29R-7, 39–41	270.79		0.09	0.7			
30R-1, 34–36	271.44		0.01	0.1			
30R-2, 93–95	273.53	0.19	0.27	0.47	0.07	0.40	0.6
30R-3, 82–84	274.92		0.02	0.2			
30R-4, 69–72	276.29		0.02	0.2			
30R-5, 48–50	277.58		0.02	0.2			
31R-1, 31–34	281.11		0.02	0.2			
31R-2, 83–86	283.13	0.26	nd	0.57	0.03	0.54	0.3
31R-3, 81–83	284.61		0.02	0.2			
32R-1, 86–88	291.26		0.02	0.2			
32R-2, 99–101	292.89	0.19	nd	0.44	0.02	0.42	0.2
32R-3, 70–72	294.10		0.03	0.2			
32R-4, 43–45	295.33		0.03	0.2			
32R-5, 24–26	296.64		0.03	0.2			
32R-6, 112–114	299.02		0.03	0.2			
32R-7, 33–35	299.73		0.03	0.2			
33R-1, 33–34	300.33		0.03	0.2			
33R-2, 122–123	302.72	0.15	nd	0.31	0.01	0.30	0.1
33R-3, 35–36	303.35		0.01	0.1			
33R-4, 50–52	305.00		0.01	0.1			
34R-1, 11–13	309.81		0.02	0.2			
34R-2, 31–33	311.51	0.20	nd	0.43	0.01	0.42	0.1
35R-1, 131–133	320.61		0.22	1.8			
35R-2, 22–24	321.02	nd	nd	1.76	1.32	0.44	11.0
36R-1, 33–35	329.33		0.05	0.4			
37R-1, 71–73	339.41		0.05	0.4			
37R-2, 26–28	340.46	nd	nd	0.26	0.05	0.21	0.4
39R-1, 80–82	358.70		0.04	0.3			
39R-2, 83–85	360.23	nd	nd	0.19	0.04	0.15	0.3
40R-1, 94–97	368.44		0.04	0.3			
41R-1, 70–72	378.00	nd	0.17	0.25	0.04	0.21	0.3
42R-1, 80–82	387.70		0.06	0.5			
42R-2, 41–43	388.81	nd	nd	0.20	0.06	0.14	0.5
43R-1, 103–105	397.63		0.07	0.6			
43R-2, 98–100	399.08	0.06	nd	0.18	0.08	0.10	0.7
43R-3, 60–62	400.20		0.08	0.7			

Note: nd = not detected.

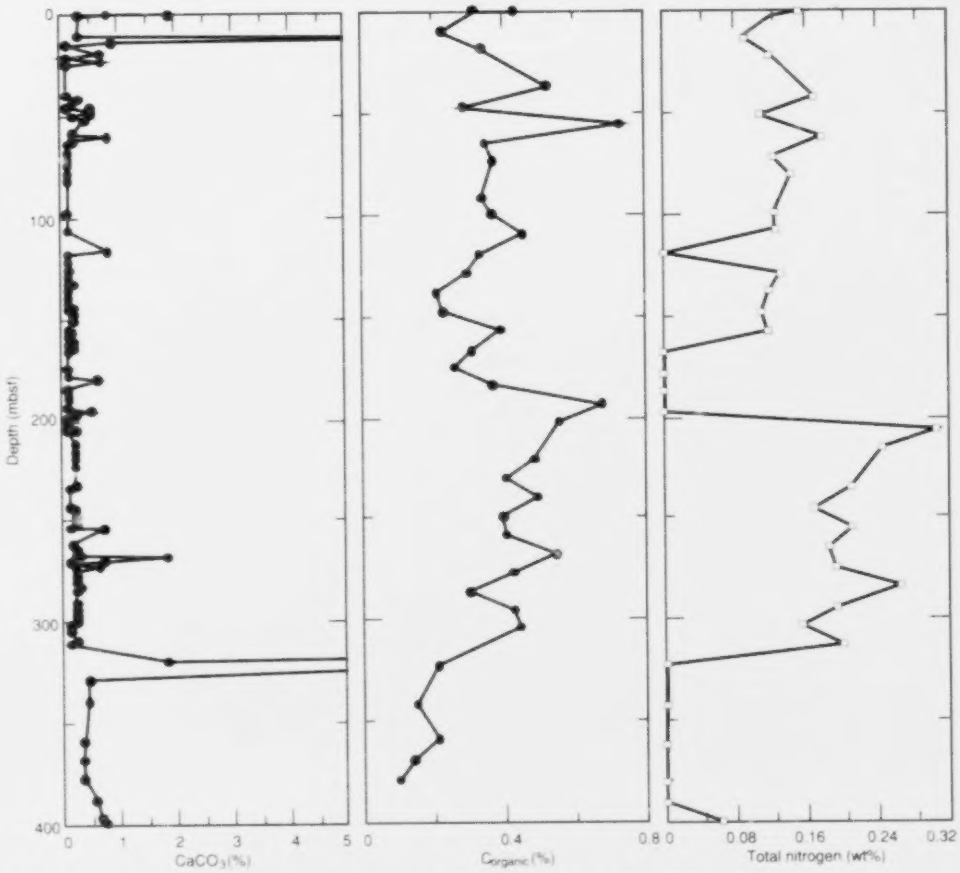

Figure 8. Weight percent of calcium carbonate, total organic carbon, and total nitrogen in sediments at Site 784.

and sulfate, which decreases to 7 mmol/kg with a distinct break in slope at the serpentine boundary (Fig. 9). Also continuing the trend established in the claystone but showing a break in slope at the boundary are calcium, which increases to 57 mmol/kg within the serpentine; magnesium, which decreases to less than 1 mmol/kg; and sodium, which decreases to 452 mmol/kg (Fig. 9). The change in sodium within the serpentine at Site 784 is the opposite of that seen at Site 783, where sodium increases. Ammonia and potassium stabilize at a nearly constant values within the serpentine, after decreasing with depth throughout the lower part of the claystone.

Chlorinity shows no obvious change with depth at Site 784, except for a possible increase within the upper 45 mbsf (Fig. 9). Bromide may increase below 234 mbsf, but the data are so scattered that we cannot be certain of this. As at Site 783, the decrease in salinity with depth results mainly from the decrease in sulfate.

The major difference between the interstitial waters at Site 784 and those at Sites 782 and 783 is the greater effect of bacterial sulfate reduction within the thicker claystone at Site 784. This reduction causes sulfate to decrease markedly with depth within the claystone as well as within the serpentine (Fig. 9). The same bacterial reactions that reduce sulfate and oxidize organic matter cause the largest maxima in alkalinity and ammonia to develop within the upper sediments at Site 784. The waters within the thicker claystone unit at Site 784 also display higher gradients in calcium and magnesium and a greater decrease in potassium than those at Site 783.

As at Site 783, the changes in pore-water composition between the claystone and the serpentine almost certainly result from ongoing reactions between seawater-derived solutions and the partially serpentinized peridotite. The pore waters from Site 784 support the conclusion reached previously ("Sediment/Fluid Geochemistry" section, "Site 783" chapter, this volume) that these reactions consume H^+, silica, sulfate, and magnesium, produce calcium, and conserve chlorinity. The effect of serpentinization reactions on alkalinity, ammonia, and potassium is less evident at Site 784 than at Site 783 because these species already show large changes within

Table 7. Results of headspace-gas analyses of cores at Site 784.

Core, section, interval (cm)	Depth (mbsf)	Methane	
		(μL/L)[a]	(μM)[b]
125-784A-			
2R-1, 19–20	1.60	10	0.9
3R-3, 0–3	13.92	11	0.9
4R-3, 0–3	23.42	11	1.0
6R-5, 0–3	45.52	13	1.2
7R-2, 0–3	50.62	15	1.4
8R-5, 0–3	64.82	15	1.3
9R-2, 0–3	70.02	15	1.3
10R-2, 0–3	79.62	13	1.2
12R-2, 0–3	98.92	14	1.3
14R-3, 0–3	119.72	11	1.0
16R-6, 0–3	143.52	11	0.9
19R-2, 148–150	167.99	12	1.1
20R-4, 0–3	179.21	15	1.3
21R-2, 0–3	185.92	12	1.0
22R-4, 0–3	198.52	11	1.0
23R-2, 0–3	205.11	11	1.0
26R-2, 0–3	234.02	10	0.9
29R-5, 0–3	267.41	10	0.9
32R-6, 0–3	297.91	8	0.7
36R-1, 0–3	329.02	16	1.4
37R-2, 0–3	340.22	13	1.2
39R-2, 112–114	360.53	13	1.2
42R-2, 0–1	388.41	15	1.3
43R-3, 0–1	399.61	32	2.9

[a] Microliters of methane per liter of wet sediment or wet unconsolidated serpentine, assuming a sample volume of 4.2 cm^3 of sediment or serpentine.

[b] Micromoles of methane per liter of interstitial water, assuming a porosity of 50%.

the overlying claystone at Site 784. The effect on sodium is unclear because sodium increases within the serpentine at Site 783, but decreases at Site 784. As at Site 783, the pore waters at Site 784 contain no obvious component of low-chlorinity, hydrocarbon-rich water from a deep source, such as was proposed to explain the composition of pore waters at Conical Seamount in the Mariana forearc (see "Sediment/Fluid Geochemistry" section, "Site 780" chapter, this volume).

STRUCTURAL STUDIES

At Site 784, we observed a wide variety of deformational features within the unlithified and partially lithified sediments of Unit I. Many of these features are closely associated with water-escape structures. Within the underlying serpentine microbreccia of Unit II, we observed pure- and simple-shear and convolute structures. The textures and rheological properties of the serpentine and microbreccia, as well as the structures developed within them, are very similar to those at Site 779 on the flank of Conical Seamount.

Deformation in Unlithified Sediments

Deformation features are rare in the unconsolidated silty clay of Subunit IA. However, between 54 and 60 cm in Section 125-784A-6R-5, we observed a set of *en echelon*, subvertical, sigmoidal veinlets (Fig. 10). This veinlet set exhibits a geometry very similar to that of the *en echelon*, vein-filled, "tension-gash" sets common in well-lithified rocks, especially those in the lower greenschist facies. The veinlets are 3 to 4 cm long and about 1 mm wide. Observation under the binocular microscope shows that the veinlets are zones of greatly increased porosity. We interpret this vein set as having developed when the unlithified sediment was subjected to subhorizontal simple shear and formed sigmoidal zones of extensional or reduced compressional stress into which pore water flowed. This influx of fluid caused the consolidating sediment to disaggregate, increasing its porosity. Similar structures were observed in unlithified sediment on the inner slope of the Middle America Trench during Deep Sea Drilling Project (DSDP) Leg 67 (Cowan, 1982).

Deformation in Partially Lithified Sediments

Deformation of the more consolidated vitric siltstones of Subunit IB includes the following (Fig. 11): (1) subhorizontal to subvertical water-escape structures, along some of which primary sedimentary structures such as ash layers or centimeter-sized burrows have been offset; (2) *en echelon* tension veinlets, some of which have acted as microfaults and are associated with microlithon rotation; (3) *en echelon* sets of microfaults a few centimeters long with offsets of a few millimeters; (4) parallel, gently dipping veinlets, spaced 2 to 5 mm apart and forming sets distributed throughout the entire core over intervals of a few decimeters; (5) small, isolated normal and reverse faults; and (6) ductile shear bands.

Water-escape structures are abundant and generally consist of centimeter- to decimeter-wide pipes or dikes filled with homogeneous light-colored claystone that is distinct from the surrounding darker, burrowed claystones. Sedimentary layering is offset along many of these structures. In a spectacular example within Section 125-784A-28R-2, 42–62 cm (Fig. 12), a subhorizontal ash layer and a burrow were offset about 2 cm along a 5- to 10-mm-wide, subvertical, dikelike water-escape structure. This water-escape structure contains laminae defined by variations in clast content within the filling of the pipe; we interpret these laminae as flow-differentiation bands that formed when fluid escaped. In other instances, water-escape structures terminate along faults. Between 55 and 80 cm in Section 125-784A-32R-2, a 20-cm-long pipe endsabruptly along a low-angle fault. The fault plane may have served as a conduit for water.

Sets of sigmoidal, *en echelon*, tension veinlets, similar to those described previously, are common in the interval between Core 125-784A-22R and Core 125-784A-32R (Fig. 13). Most of the veinlet sets are not associated with faults and thus represent brittle-ductile shear bands. The size of the veinlets (7 to 10 cm long, about 1 mm wide) and their spacing (5 to 10 mm) are remarkably constant within this interval. The veins exhibit generally a simple shape, with a regular curvature and sharp tails. Locally, veins with forked tails were observed. In some sets of tension veinlets, the central part of the set is connected by a second (subsequent?) set of smaller veinlets that have a slightly different orientation. This probably indicates multistage creep along the shear zone. Although the curvature of the sigmoidal veinlets indicates that reverse movements have also taken place, normal movement is much more common, indicating lateral extension with respect to the core axis.

In some cases (e.g., Section 125-784A-22R-4, 130–140 cm), sigmoidal veinlets have served as microfaults. These exhibit the same attitude, size, and shape as the tension veinlets described previously. We postulate that these microfaults are a smaller-scale version of the water-escape dike with offsets described in the preceding text.

In Section 125-784A-27R-5, between 10 and 20 cm, steeply dipping (65° to 70°) sediments are cut by *en echelon* normal microfaults having offsets of a few centimeters. These microfaults are not sigmoidal, and we regard them as a somewhat different phenomenon from those already described.

Numerous parallel, gently dipping veinlets occur in the basal part of Subunit IB, especially in Section 125-784A-32R-4. The veinlets crosscut the core from one edge to the other and are regularly spaced from a few millimeters to 1 cm

Table 8. Composition of interstitial waters from cores at Site 784.

Sample number	Core, section, interval (cm)	Depth (mbsf)	Volume (mL)	Squeeze temperature (°C)	pH	Salinity (R.I., ‰)	Salinity (calcium, ‰)	Chlorinity (mmol/kg)	Alkalinity (meq/kg)	Sulfate (mmol/kg)	Sodium (mmol/kg)	Potassium (mmol/kg)
Surface seawater (17 March 1989)					8.25	35.6	34.65	539.2	2.689	27.28	462.0	10.11
IW-1	3R-2, 140–150	13.85	58	3	7.95	35.8	35.06	546.5	4.257	26.14	469.5	10.22
IW-2	4R-2, 140–150	23.35	58	3	7.84	36.5	35.05	548.4	3.923	25.42	470.1	10.05
IW-3	6R-4, 140–150	45.45	60	3	8.19	36.3	35.32	552.3	4.417	25.07	476.1	9.87
IW-4	8R-4, 140–150	64.75	55	4	8.21	35.0	34.75	549.4	4.260	22.05	470.1	9.52
IW-5	10R-1, 140–150	79.55	45	5	8.17	35.5	34.99	550.4	4.290	23.34	474.6	8.81
IW-6	14R-1, 140–150	118.15	51	5	8.07	35.2	34.73	550.4	4.273	23.08	472.5	8.06
IW-7	16R-5, 140–150	143.45	55	8	8.00	35.5	34.74	549.4	3.447	21.82	472.1	8.01
IW-8	19R-3, 0–10	168.05	48	8	8.17	35.0	34.28	543.6	3.438	20.58	467.0	7.71
IW-9	22R-3, 140–150	198.45	54	8	8.00	34.0	34.55	550.4	3.249	19.61	470.9	6.90
IW-10	26R-1, 140–150	233.95	33	9	7.65	34.3	34.46	550.4	2.227	19.23	471.1	7.14
IW-11	29R-4, 140–150	267.35	35	10	8.07	34.8	34.20	546.4	1.911	17.84	466.3	6.66
IW-12	32R-5, 140–150	297.85	38	10	7.82	34.5	34.03	550.4	1.225	16.38	465.9	5.95
IW-13	34R-3, 0–15	312.78	15	9	7.53	33.8	33.07	540.7	0.517	14.36	450.6	4.61
IW-14	35R-1, 135–150	320.75	30	10	8.16	34.2	33.63	548.4	0.588	14.76	462.2	5.93
IW-15	39R-2, 0–15	359.48	16	11	9.14	35.4	33.37	546.5	1.404	11.48	460.7	5.96
IW-16	40R-1, 135–150	368.93	15	10	9.25	35.5	33.56	553.3	1.362	9.78	455.3	5.31
IW-17	41R-1, 92–107	378.30	22	10	9.61	34.3	33.49	550.4	1.314	10.44	455.0	5.52
IW-18	42R-1, 135–150	388.33	16	10	9.59	34.3	32.94	549.4	0.650	7.00	453.0	5.16
IW-19	43R-2, 135–150	399.53	18	10	9.52	35.0	33.48	552.3	1.625	9.33	452.1	5.48

apart. Otherwise, undeformed burrows exhibit both normal and reverse offsets along the veins within a single set. Because the true orientation of the vein sets is unknown, it is impossible to determine whether these structures represent larger-scale structures similar to the *en echelon* veinlet sets previously described (although with overall subvertical, rather than subhorizontal, movement) or whether they are simply a series of discrete microfaults.

Isolated faults are common throughout Subunit IB. Spectacular examples have been encountered in Sections 125-784A-20R-3, 55–80 cm, (Fig. 14) and 125-784A-32R-2, 80–105 cm. Because the offsets along the fault planes are greater than

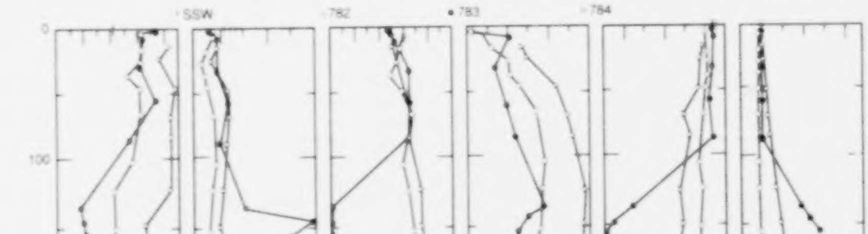

Figure 9. Composition of interstitial waters from sediments at Site 784 compared with that from Sites 782 and 783 and with surface seawater collected 22 February and 4 and 17 March 1989 (crosses).

Table 8 (continued).

Calcium (mmol/kg)	Magnesium (mmol/kg)	Bromide (mmol/kg)	Silica (μmol/kg)	Ammonia (μmol/kg)	Hydrogen Sulfide (μmol/kg)
10.18	52.48	0.81	0	10	
11.72	49.93	0.84	523	134	
12.10	49.40	0.77	557	150	
13.50	46.98	0.85	621	221	
14.29	44.78	0.84	680	246	
15.19	43.80	0.78	658	261	
18.10	40.03	0.80	749	290	
20.23	37.98	0.76	749	288	<3
22.15	34.57	0.81	792	282	
25.22	32.28	0.78	843	250	
26.65	29.74	0.83	972	241	
29.52	27.51	0.93	831	216	
31.79	24.46	0.83	854	172	
34.35	22.99	0.87	224	130	
32.02	23.20	0.89	304	160	
45.19	6.90	0.96	12	142	
54.43	2.36	0.91	6	150	
53.69	2.32	0.86	12	136	
52.87	0.08	0.92	18	161	
56.73	0.77	0.88	2	114	

the cored fault lengths, the true displacement cannot be determined. No offset sedimentary markers were observed; therefore, the sense of movement along the faults also remains unknown.

Sedimentary lamination at Site 784 is subhorizontal in the upper 190 mbsf of the sediments and from about 310 to 320 mbsf in the serpentine. However, from 190 to 275 mbsf

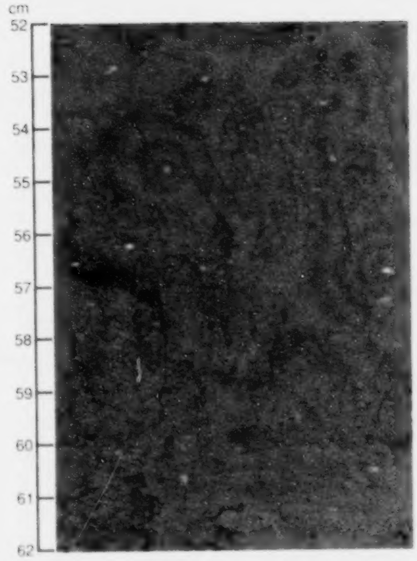

Figure 10. Set of *en echelon* sigmoidal veinlets in unconsolidated sediments (Section 125-784A-6R-5, 52–62 cm).

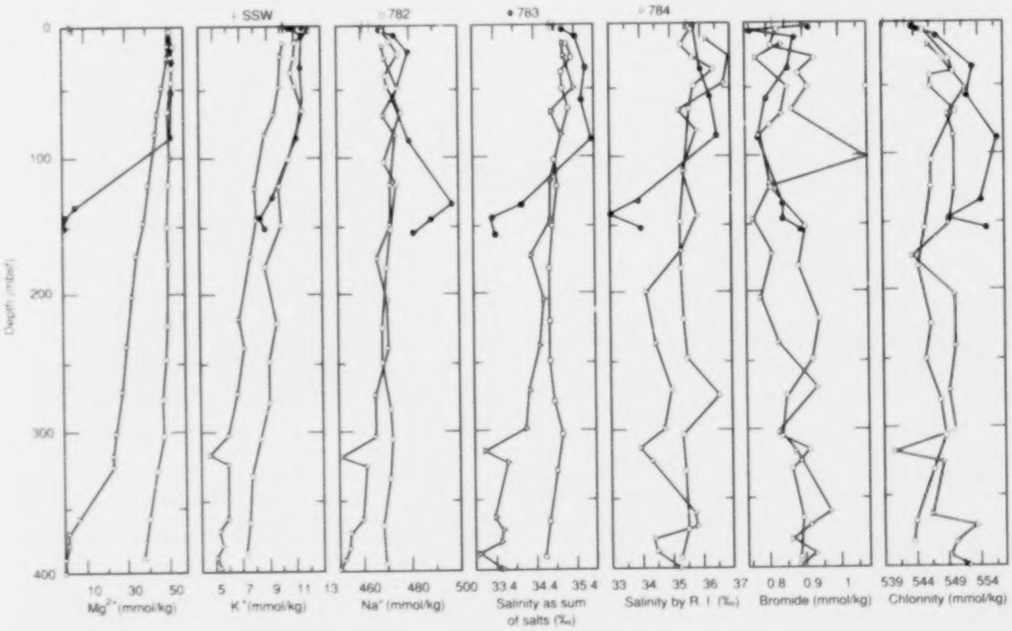

Figure 9 (continued).

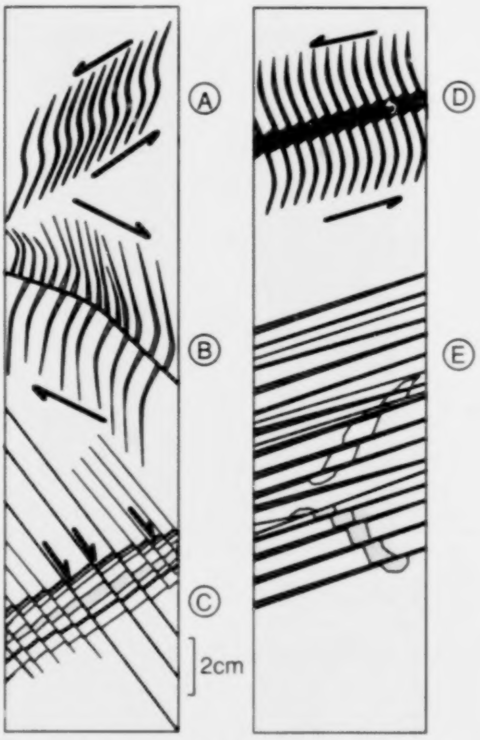

Figure 11. Schematic representation of the main post-depositional tectonic structures in the unconsolidated and partially lithified sediments of Unit I at Site 784. **A.** *En echelon* sigmoidal tension veinlets (no associated discrete fault plane). **B.** *En echelon* tension veinlets crosscut by an associated fault. **C.** Set of microfaults (note lack of microlithon rotation). **D.** *En echelon* tension veinlets with rotated microlithons. **E.** Set of parallel veinlets crosscutting the core.

(Sections 125-784A-21R-4 to 125-784A-30R-4), and possibly as deep as 295 mbsf (Section 125-784A-32R-2), sedimentary laminations dip consistently about 35°. We were unsuccessful in locating exactly the discrete faults that bound this moderately dipping interval. It probably represents a tilted fault block or slump block that was buried by later sedimentation.

A subhorizontal ductile shear zone is present at 112 to 115 cm in Section 125-784A-24R-4 (Fig. 15). In many ways, this shear zone is similar to those observed in crystalline rocks that have undergone high-temperature deformation. The zone contains laminae and burrows that have been transformed into characteristic sigmoidal shapes by ductile deformation. Deformation is confined to a sharply delimited band 3 cm thick. Unlike most high-grade ductile shear zones, however, deformation appears to decrease in the center of the zone and to increase outward toward the boundary surfaces, which are zones of narrowly concentrated shear and may be defined as faults. Sigmoidal laminae bend into these surfaces and are sheared out along them.

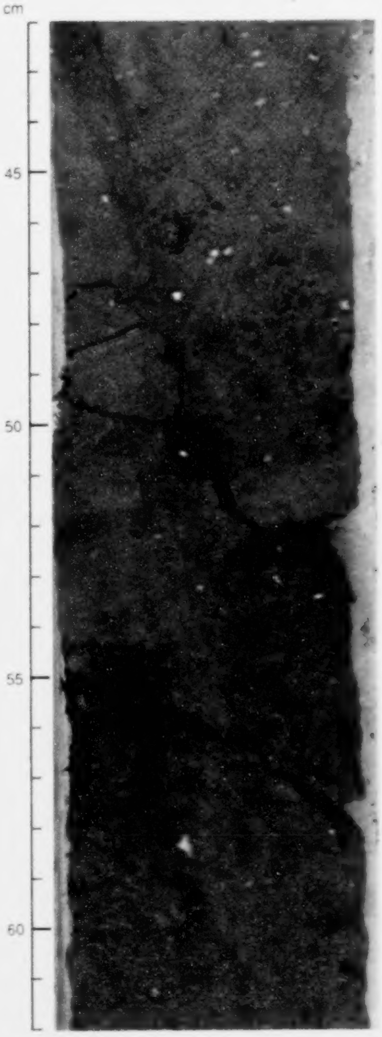

Figure 12. Water-escape dike or pipe offsetting burrows and an ash layer (Section 125-784A-28R-2, 42–62 cm).

Where possible, we performed detailed three-dimensional measurements of the main faults and axial planes of the sets of tension veinlets. The results are plotted on a stereonet (Fig. 16). In this lower-hemisphere stereonet, the vertical axis (plunging at 90° into the net) corresponds to the true vertical (i.e., the long axis of the cores). The north and south directions on the net correspond to the left and right sides of the sawn face of the archive half of the core, and the east and west directions correspond to vectors plunging vertically into the sawn faces of the archive and working halves, respectively.

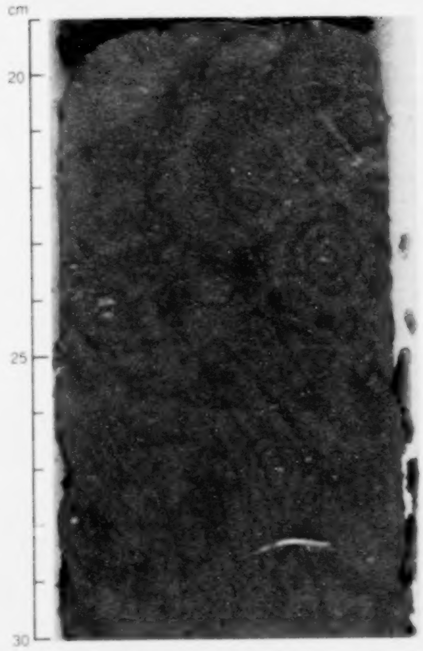

Figure 13. Set of *en echelon* sigmoidal tension veinlets (Section 125-784A-22R-3, 19–30 cm).

Thus, dips plotted on the stereonet represent true dips with respect to horizontal. Almost all faults dip between 30° and 60°, and the majority are in the lower part of this range. Dispersion of the measurements with respect to the vertical axis of the diagram may reflect the rotation of the cores during drilling, but also may indicate variability in the strikes of the fault planes. However, the uniformity of strike in many individual core sections suggests that most faults have about the same orientation.

In conclusion, most of the structures observed in the sediments of Unit I represent extensional processes. The close association of water-escape structures and brittle deformation shows that dewatering, lithification, and tectonism acted contemporaneously. Similar structures were observed at convergent margins on DSDP Legs 56 and 57 near the Japan Trench (Arthur et al., 1980), Leg 67 near the Middle America Trench (Cowan, 1982; Dengo, 1982), and Leg 78A on Barbados Ridge (Cowan et al., 1984).

Deformation in Serpentine Sediments and Microbreccias

Subunit IC and Unit II at Site 784 contain many types of variably sheared clastic serpentine sediments that were recovered at the previous Sites 778, 779, 780, and 783. The serpentine microbreccias exhibit convolute bedding and plastic folding. Phacoidal, sheared serpentine is abundant; most of the phacoids are soft, sheared clasts. Some have asymmetrical shapes, indicating deformation by simple shear. Variously sized blocks of hard, dark green serpentinized harzburgite contain abundant anastomosing asbestos veins and veinlets.

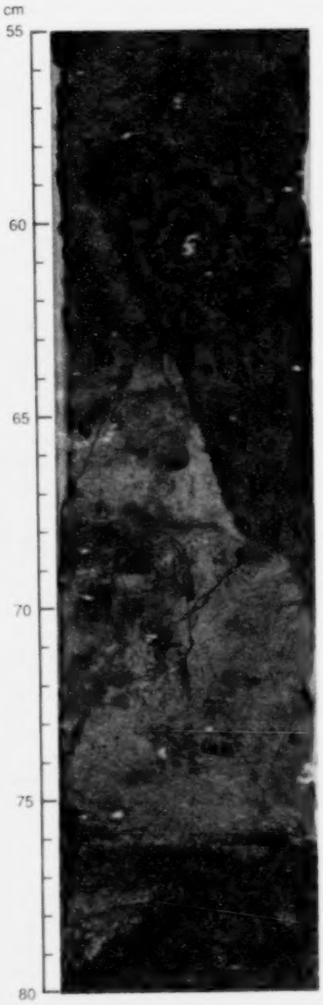

Figure 14. Fault with unknown displacement (Section 125-784A-20R-3, 55–80 cm).

In Subunit IC, the interlayering of poorly sorted, clastic, serpentine sediments bearing coarse, angular fragments with much better sorted, finer-grained, volcanogenic/pelagic sediments (see "Lithostratigraphy" section, this chapter) provides good evidence for interfingering between locally derived serpentinite debris flows and sediment distally derived from arc-related volcanoes. Moreover, these interlayered clastic serpentines, which are as thin as 30 cm, contain weakly to well-developed phacoidal textures, showing that this fabric can be preserved during downslope flow and may even have formed at that time. The individual units of different serpentine types (for instance, convolute zones, relatively unsheared

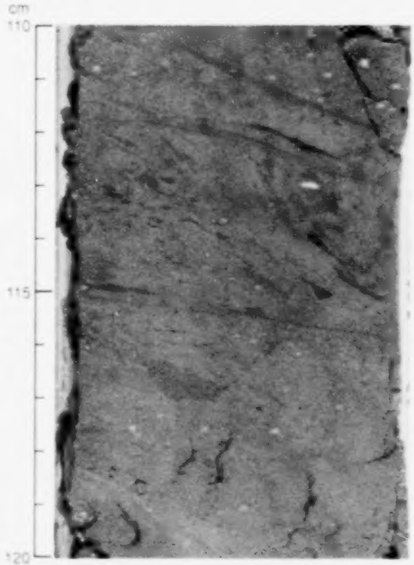

Figure 15. Subhorizontal ductile shear zone (Section 125-784A-24R-4, 110–120 cm).

sediment layers, and block-rich layers) are thinner at Site 784 than at the other sites, possibly because Site 784 (at the foot of the seamount) is relatively far from the probable sources of the serpentinite materials.

Within the cores, we observed intervals of clast-supported, matrix-poor breccias a few tens of centimeters thick. These clast-rich breccias are distinct from the convolute, matrix-rich microbreccias; we think that they may represent talus deposits. *In-situ* serpentinization, hydration, and fragmentation of matrix and clasts are continuing in the serpentinites we studied. As large blocks continue to serpentinize and fragment, they may provide a source for the breccias we describe here.

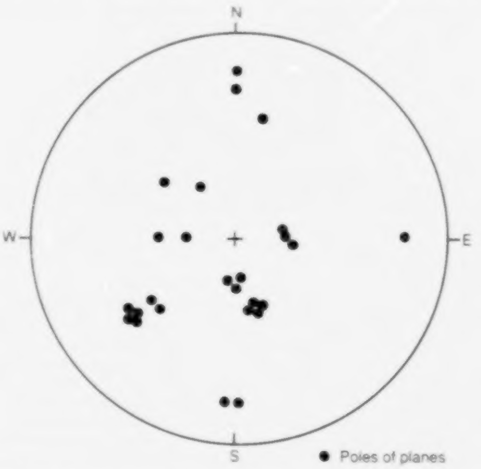

Figure 16. Orientation of main faults in Unit I plotted on a lower hemisphere stereonet. Vertical axis of stereonet = vertical axis of core; points = poles of planes.

Deformation in Serpentinization Fabrics

The general fabric and the microfabric of these rocks are similar to the fabric of the serpentinites at previous sites. Fiber haloes observed in thin sections of Site 784 serpentinites are highly variable and may be either isotropic or anisotropic. Many of them are quite deformed. This suggests that serpentinization occurred under both isotropic and anisotropic stress fields. The orientations of veins and fractures in the biggest blocks drilled at the bottom of the hole in Sections 125-784-45R-1 and 125-784-45R-2 vary from subhorizontal to subvertical. As with the microscopic fiber haloes, development of fiber veins of serpentine is probably associated with volume increase during serpentinization. The presence of veins with a wide range of orientations suggests that expansion was approximately isotropic and, hence, that at least this stage of serpentinization took place under low deviatoric stresses.

Deformation Fabrics in Pre-Serpentinization Peridotites

As with Site 783, the advanced state of serpentinization recorded at Site 784 prevented any systematic observation of high-temperature deformation textures. The few features remaining, like those at Site 783, are compatible with the tectonized nature of the primary peridotites.

Rheology of Sediments and Serpentine Material

Stress-strain tests were performed on the unlithified materials recovered at Site 784 using a Wykeham-Farrance torsion-vane test apparatus. Stress measurements for the samples tested are shown in Table 9, and a typical stress-strain curve is plotted in Figure 17, from which the ultimate and failure strengths can be determined. The serpentine materials tested range in strength from 22.6 to 251.2 kPa and average 79.1 kPa. These values compare with an average of 29.1 kPa and a range of 16.0 to 51.0 kPa at Site 783 and an average of 11.6 kPa and a range of 1.3 to 38.0 kPa at Site 780 on the summit of Conical Seamount. Even excluding the anomalously strong, sheared, phacoidal serpentine at 15 cm in Section 125-784A-40R-2 (failure strength of 251.2 kPa), the average strength of the muds at Site 784 is 54.5 kPa, higher than the maximum strengths at other sites.

We postulate that the strength of these materials is related to their state of dewatering and lithification. This in turn is probably related to their age (older than middle Miocene, which is certainly older than the Site 780 sediments and flows and may be older than those at Site 783) and their depth of burial (340–370 mbsf, compared with 130–150 mbsf at Site 783 and 0–31 mbsf at Site 780). Thus, the strength data from Site 784 are consistent with a model in which serpentine mudflows are dewatering and compacting on the flanks of serpentinite seamounts.

PALEOMAGNETISM

Magnetic Remanence

We have identified many intervals of normal and reversed polarity in Hole 784A. These data, combined with the biostratigraphic data ("Biostratigraphy" section, this chapter), have enabled us tentatively to correlate a magnetostratigraphy

Table 9. Stress measurements of serpentine material recovered at Site 784.

Core, section	Depth (mbsf)	Stress (kPa)
125-784A-		
Sediments		
3R-1	11.81	19.7
3R-3	14.71	43.0
4R-3	24.22	34.9
6R-1	40.40	17.5
6R-3	43.33	29.8
6R-5	46.63	37.9
7R-1	50.08	34.9
7R-3	52.82	18.9
8R-2	60.88	52.4
8R-4	63.94	40.0
9R-2	70.90	32.0
9R-4	73.50	40.0
10R-2	80.20	25.5
10R-4	83.40	24.0
12R-2	99.38	57.5
13R-1	107.46	17.5
14R-2	118.78	54.6
14R-4	121.56	57.5
15R-2	128.75	54.6
15R-4	131.65	72.8
16R-1	137.00	43.0
16R-3	139.82	49.5
16R-5	142.91	57.5
17R-3	149.55	52.4
17R-5	152.60	85.9
Serpentine material		
37R-1	339.35	32.0
37R-1	339.92	22.6
37R-2	340.50	83.0
39R-2	360.35	52.4
40R-1	368.11	35.7
40R-1	368.59	72.1
40R-1	368.65	83.7
40R-2	369.15	251.2

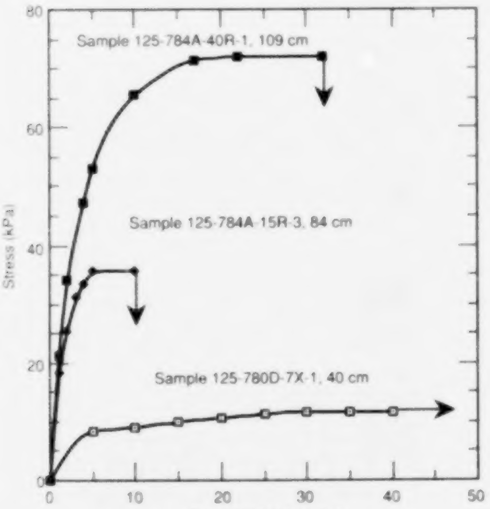

Figure 17. A representative stress-strain test of serpentine material from Site 784 (failure strength = 72.1 kPa), compared with those from Sites 780 (ultimate strength = 11.7 kPa) and 783 (failure strength = 35.7 kPa).

for the sediments in the upper 190-m section of Hole 784A (Fig. 18). However, a precise correlation with the magnetic time scale is impossible because of the lack of biostratigraphic data, the relatively poor magnetic data below 190 mbsf, and structural complications (beds dip at approximately 35° or greater). The natural remanent magnetization (NRM) of the archive half of each core from Hole 784A was measured using the cryogenic magnetometer. Magnetic intensities vary widely, from 1 to 800 mA/m (Fig. 19); most cores have values between 10 and 100 mA/m. At around 310 mbsf (Core 125-784A-34R), magnetic intensities increase, as does the amount of serpentine in the cores. When the cores were then demagnetized at the 10-mT level and remeasured, intensities were about 10% to 50% of their initial values. Some of the cores show signs of significant drilling disturbance. Data from cores described as more than slightly disturbed were rejected from any analysis.

Unfortunately, the biostratigraphic data, which are based almost entirely on the study of material from the core catchers (see "Biostratigraphy" section), are rather poor. A limited diatom zonation allows us to correlate tentatively the polarity sequence with the time scale of Berggren et al. (1985). Barron (1985) correlated the internationally recognized low-latitude diatom zones with the polarity time scale of Ness et al. (1980). At least for the interval from 0 to 11 Ma, the ages of each magnetochron boundary in that time scale are not appreciably different from those presented by Berggren et al. (1985). For practical purposes, the relative positions of the diatom zones of Barron (1985) can be transferred directly onto the time scale of Berggren et al. (1985). This modified scheme has been adopted for the present study. The magnetostratigraphy of the upper 190-m section of Hole 784A is summarized in Figure 18. However, the poor paleomagnetic and biostratigraphic data for Hole 784A make any accurate magnetostatigraphic correlation impossible.

Previous research on drill cores from the Philippine Sea Plate (Bleil, 1982) suggests that the Philippine Sea Plate has moved northward with time. The inclination data from Hole 784A were separated into 80-m sections, grouped into 10° intervals, and plotted on histograms (Fig. 20). The data from the intervals between 0 and 80 mbsf and between 80 and 160 mbsf show good bimodal distributions with peaks at about +50° and 50°. These data suggest little or no translation since the Pliocene. In the interval between 160 and 240 mbsf, there is no good bimodal distribution. Rather, the data are skewed to the positive side, suggesting that some material from this interval was remagnetized in the present field. However, there is a significant amount of data between +15° and 15°, which implies significant translation between the Miocene and Pliocene. Further research will be necessary to determine whether these low inclinations are merely a manifestation of insufficient cleaning of the overprint from the present field. In the interval between 240 and 312 mbsf, the distribution is dominated by positive inclination, with only a small percentage of the measurements showing negative inclination. This suggests that almost all of the rocks below 240 mbsf experienced recent remagnetization, possibly from the serpentization of the underlying rocks or by recent tectonic deformation.

Magnetic Susceptibility

Whole-core magnetic susceptibilities were measured using the multisensor track (MST). A downhole plot of these data for Hole 784A is presented in Figure 21. The sediments between 0 and 310 mbsf have values typically between 0 and 6×10^{-3} SI units. However, at the sediment/serpentine contact, there is a large increase in susceptibility to values between 12×10^{-3} and 48×10^{-3} SI units; this also

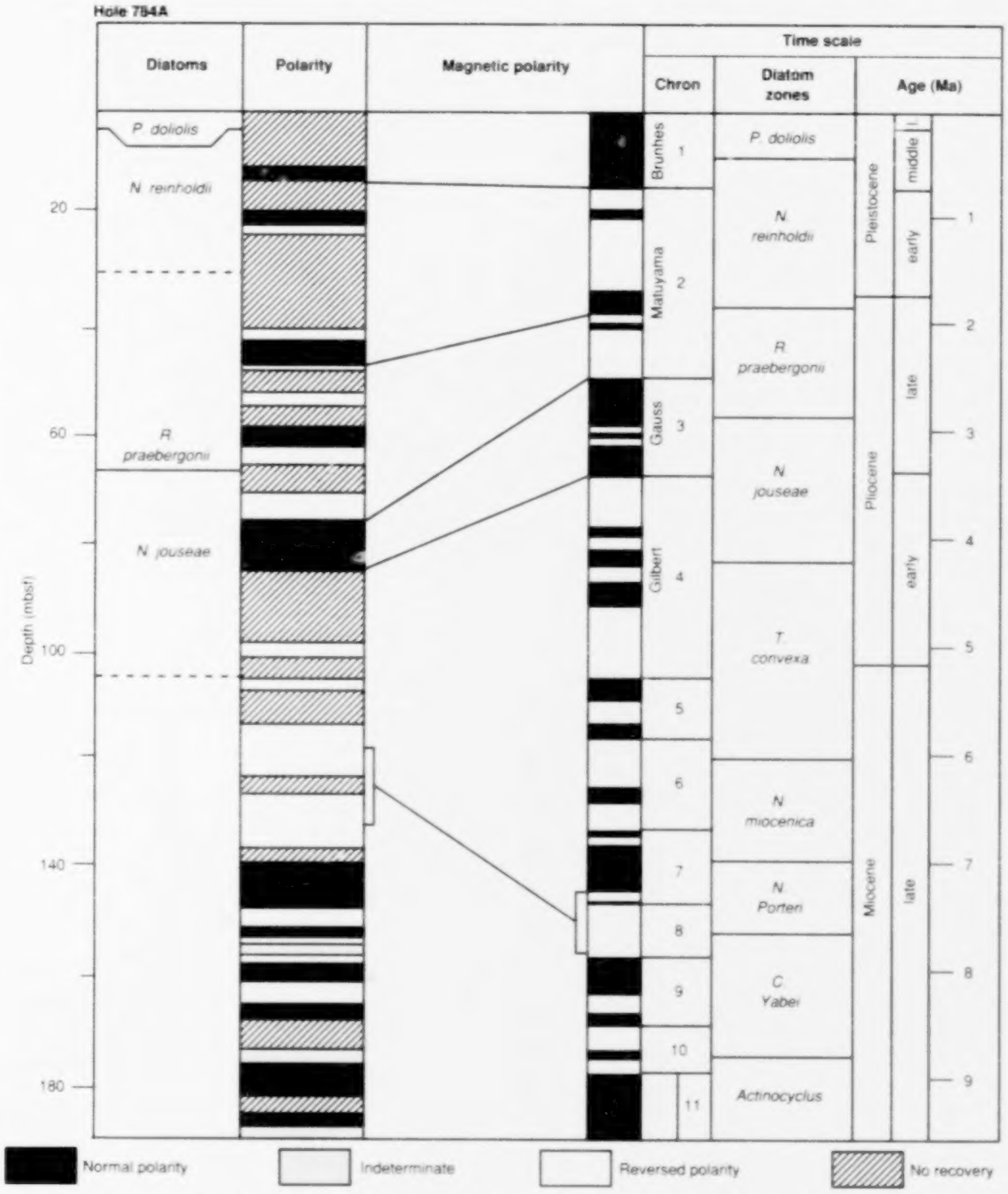

Figure 18. The magnetostratigraphy of Hole 784A for the interval from 0 to 190 mbsf, correlated with the polarity time scale of Berggren et al. (1985) and diatom zones modified from Barron (1985).

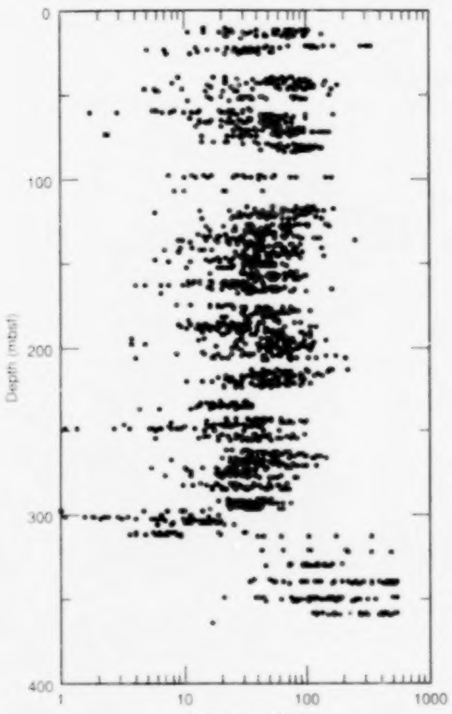

Figure 19. A downhole plot of magnetic intensity for Hole 784A.

correlates with an increase in magnetic intensity. The high magnetic susceptibility (and NRM intensity) associated with the serpentine probably results from the production of magnetite during the serpentinization process.

PHYSICAL PROPERTIES

The MST was used to determine bulk density (using the GRAPE), sonic velocity, and magnetic susceptibility of each core section from Hole 784A. Representative samples were selected from each section for measuring bulk density, grain density, porosity, water content, and thermal conductivity. Where possible, shear strength, resistivity, and sonic velocity (using the Hamilton Frame apparatus) were determined. The physical-properties data for Site 784 are listed in Tables 10 and 11 and plotted vs. depth in Figure 22.

A total of 300 m of volcaniclastic and pelagic sedimentary rocks was cored in Hole 784A. At about 300 mbsf, the serpentine sediment and flows and serpentinite clasts of Unit II were encountered. The physical properties of the volcaniclastic and pelagic sediment are distinct from those of the serpentine and serpentinite in Hole 784A. The average bulk density (as measured by the GRAPE) of the volcaniclastic and pelagic sediment is 1.56 ± 0.11 g/cm^3; that of the serpentine and serpentinite is 1.90 ± 0.23 g/cm^3.

Measurements of discrete samples show that the average bulk densities agree closely with the density values determined by the GRAPE. The average bulk density of the discrete samples of volcaniclastic and pelagic sediment is 1.57 ± 0.09 g/cm^3; that of the serpentine and serpentinite is 2.13 ± 0.37 g/cm^3. Bulk density increases slightly with depth in the sedimentary section and also increases with depth in the serpentine and serpentinite; however, the data are somewhat scattered, which results in a gradient of 0.0032 (Fig. 22). The average grain density, which is constant with depth, is 2.6± 0.17 g/cm^3 in the sediment and 2.70 ± 0.30 g/cm^3 in the serpentine and serpentinite.

The average thermal conductivity of the sediment is 0.914 ± 0.142 W/mK and increases with depth from 0.9 W/mK near the seafloor to 1.0 W/mK at about 310 mbsf (Fig. 22). Between 310 and 400 mbsf, thermal conductivity increases sharply from 1.2 to about 2.0 W/mK, resulting in a gradient of 0.003 in the serpentine and serpentinite.

Strength was measured in sections of sediment that were elastic enough to allow insertion of a shear vane. The sedimentary sections were measured to 150 mbsf, after which the sediment became too brittle to measure. Ultimate strength increases with depth in the sedimentary section from about 20 kPa near the seafloor to 80 kPa at 150 mbsf. Strength was measured in serpentinite from 340 to 370 mbsf. The values of ultimate strength in the serpentinite are scattered and range from 22.0 to 132.0 kPa, with one anomalous data point at 251.0 kPa. The stress-strain relationship of materials from Hole 784A is discussed in more detail in the "Structural Studies" section (this chapter).

The A and B directions of sonic velocity were measured with the Hamilton Frame apparatus (Fig. 22). The A velocity direction is parallel to the surface of the split core and the B velocity direction is perpendicular to the surface of the split core. The A and B velocities in sediment increase with depth from approximately 1600 m/s at 150 mbsf to 1750 m/s at 300 mbsf, resulting in gradients of 0.0016 and 0.0018, respectively. The average of both sonic velocities for sediment is 1670 m/s. However, the velocities from serpentine and serpentinite are widely scattered. The velocity measured in the A direction of serpentine and serpentinite is 1700 to 5700 m/s, and the B direction is from 1700 to 5400 m/s.

DOWNHOLE MEASUREMENTS

Three downhole temperature measurements were obtained at Site 784 using the Barnes-Uyeda temperature tool.

The temperature record from Run 05R at 29.9 mbsf is shown in Figure 23A and at an expanded scale in Figure 23B. The probemoved somewhat after emplacement, but was firmly seated in the sediment at 68 min into the run and remained relatively undisturbed until 80 min. After the first few minutes of emplacement, the temperature decay curve is proportional to 1/time. A linear least-squares regression on the curve, extrapolated to 1/time = 0, is a good estimate of the equilibrium sediment temperature, giving a value of 2.79°C, with a correlation coefficient (r^2) of 0.656 (Fig. 24). This temperature estimate may be somewhat high because of motion just after emplacement.

The temperature record from Run 11R at 107.1 mbsf is shown in Figure 25A and at an expanded scale in Figure 25B. The probe was seated in the sediment from 48 to 63 min into the run and has a clear cooling curve. The equilibrium temperature estimated from the decay curve is 4.62°C (Fig. 26); the r^2 value of 0.973 is high. The final temperature record from Run 17R at 145.6 mbsf is shown in Figure 27A and at an expanded scale in Figure 27B. The probe was in the sediment from 51 to 65 min with very little disturbance. The equilibrium temperature estimated from the decay curve is 5.46°C (Fig.

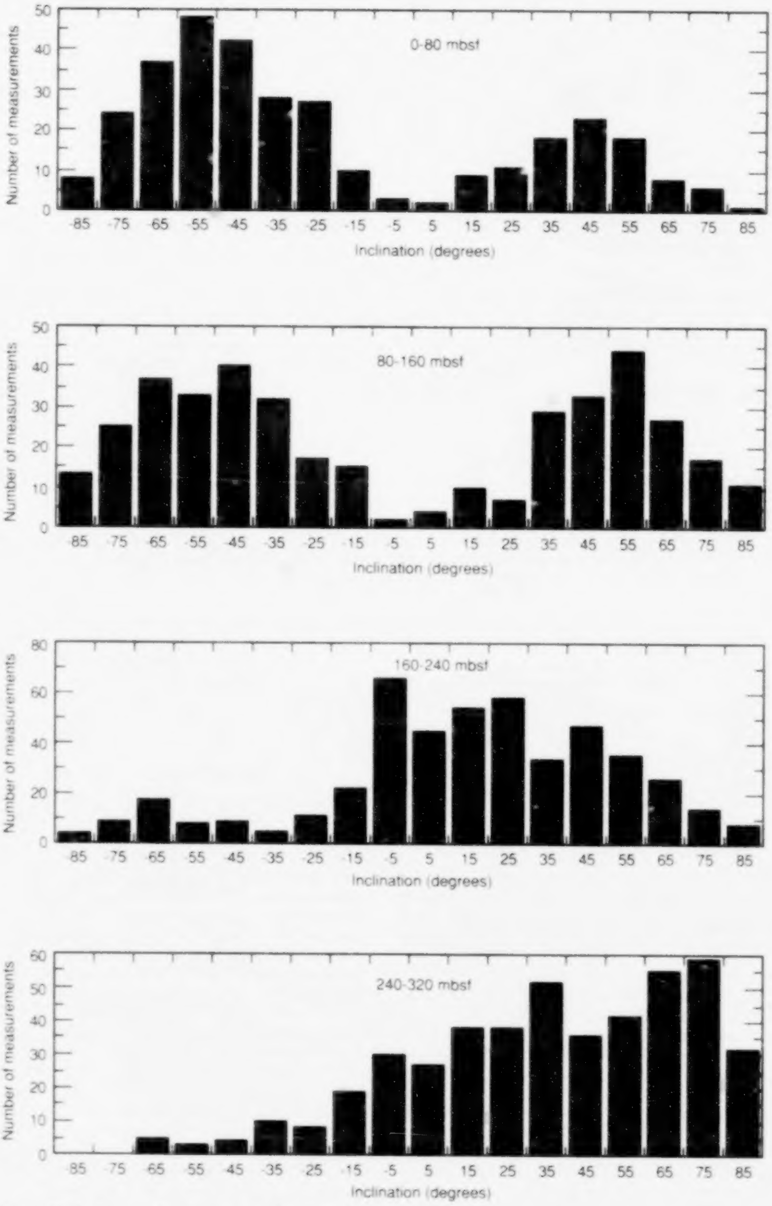

Figure 20. Inclination distribution as a function of depth, Hole 784A.

Table 10 . Index properties from Hole 784A.

Core, section, interval (cm)	Depth (mbsf)	Bulk density (g/cm^3)	Grain density (g/cm^3)	Porosity (%)	Water content (%)	Void ratio
125-784A-						
1R-1, 74–76	0.74	1.53	2.54	66.9	46.4	0.67
1R-CC, 22–24	1.16	1.59	2.63	65.5	43.8	0.66
2R-1, 5–7	1.45	1.51	2.42	66	46.6	0.66
3R-1, 74–76	11.64	1.46	2.48	70.4	51.2	0.7
3R-2, 35–37	12.75	1.51	2.3	62.9	44.3	0.63
3R-3, 67–69	14.57	1.51	2.65	70.8	49.8	0.71
3R-4, 18–20	15.58	1.38	1.98	63.6	49.1	0.64
4R-1, 31–33	20.71	1.44	2.53	73	53.8	0.73
4R-2, 31–33	22.21	1.55	2.81	70.9	48.4	0.71
4R-3, 31–33	23.71	1.47	2.66	73.3	53	0.73
4R-4, 31–33	25.21	1.55	2.55	66.3	45.5	0.66
6R-1, 76–78	40.26	1.49	2.45	68.2	48.7	0.68
6R-2, 80–82	41.8	1.46	2.53	71.5	52	0.72
6R-3, 85–87	43.35	1.42	2.59	75.3	56.2	0.75
6R-4, 90–92	44.9	1.49	2.6	71	50.6	0.71
6R-5, 91–93	46.41	1.57	2.63	66.5	45	0.67
6R-6, 45–47	47.45	1.52	2.61	69.3	48.4	0.69
7R-1, 67–69	49.77	1.54	2.59	67.8	46.8	0.68
7R-2, 65–67	51.25	1.49	2.68	72.3	51.4	0.72
7R-3, 65–67	52.75	1.54	2.87	72.6	50.1	0.73
8R-1, 69–71	59.49	1.46	2.53	71.7	52.3	0.72
8R-2, 106–108	61.36	1.56	2.79	70.1	47.7	0.7
8R-3, 52–54	62.32	1.56	2.61	67	45.7	0.67
8R-4, 56–58	63.86	1.52	2.46	66	46.1	0.66
8R-5, 51–53	65.31	1.54	2.62	67	46.2	0.67
9R-1, 85–87	69.35	1.51	2.56	69	48.5	0.69
9R-2, 85–87	70.85	1.49	2.68	72.7	52	0.73
9R-3, 77–79	72.27	1.52	2.5	66.7	46.5	0.67
9R-4, 42–44	73.42	1.54	2.66	68.8	47.3	0.69
9R-5, 27–29	74.77	1.49	2.74	72.7	51.7	0.73
10R-1, 49–51	78.59	1.55	2.6	67.2	46.1	0.67
10R-2, 59–61	80.19	1.51	2.59	69.6	48.9	0.7
10R-3, 103–105	82.13	1.48	2.59	71.4	51.1	0.71
10R-4, 80–82	83.4	1.49	2.66	72.1	51.4	0.72
12R-1, 58–60	97.98	1.53	2.59	68.1	47.2	0.68
12R-2, 44–46	99.34	1.44	2.59	73.9	54.4	0.74
13R-1, 36–38	107.46	1.52	2.57	68.2	47.6	0.68
14R-1, 97–99	117.67	1.55	2.6	67.4	46.3	0.67
14R-3, 30–32	120	1.47	2.56	71.5	51.5	0.71
14R-4, 30–32	121.5	1.51	3.24	44.5	31.3	0.45
14R-5, 70–72	123.4	1.5	2.52	68.5	48.4	0.68
15R-1, 78–80	127.18	1.45	2.53	72.2	52.8	0.72
15R-2, 56–58	128.46	1.45	2.51	71.8	52.5	0.72
15R-3, 94–96	130.34	1.52	2.49	66.9	46.8	0.67
15R-4, 96–98	131.86	1.45	2.53	72.6	53.3	0.73
15R-5, 79–81	133.19	1.51	2.22	81.2	56.9	0.81
15R-6, 79–81	134.69	1.57	2.69	68.1	46.2	0.68
15R-7, 39–41	135.79	1.53	2.61	68.3	47.3	0.68
16R-1, 56–58	136.56	1.49	2.67	72.4	51.8	0.72
16R-2, 56–58	138.06	1.54	2.42	63.8	44	0.64
16R-3, 56–58	139.56	1.5	2.63	71	50.3	0.71
16R-4, 56–58	141.06	1.52	2.51	67.5	47.3	0.68
16R-5, 56–58	142.56	1.5	2.59	70.1	49.6	0.7
16R-6, 41–43	143.91	1.56	2.54	65	44.2	0.65
16R-7, 41–43	145.41	1.58	2.62	65.9	44.4	0.66
17R-1, 86–88	146.46	1.53	2.66	69.5	48.2	0.7
17R-2, 48–50	147.58	1.53	2.5	66.2	45.9	0.66
17R-3, 51–53	149.11	1.52	2.54	68	47.6	0.68
17R-4, 51–53	150.61	1.51	2.59	69.5	48.8	0.69
17R-5, 34–36	151.94	1.49	2.57	70.4	50.1	0.7
18R-1, 90–92	156.2	1.54	2.5	66.1	45.7	0.66
18R-2, 121–123	158.01	1.58	2.73	67.8	45.5	0.68
18R-3, 105–107	159.35	1.56	2.54	65.4	44.6	0.65
18R-4, 82–84	160.62	1.58	2.5	62.9	42.4	0.63
18R-5, 118–120	162.48	1.47	2.61	72.8	52.7	0.73
18R-6, 18–20	162.98	1.5	2.55	69.2	49	0.69
18R-6, 86–88	163.66	1.53	2.57	68	47.3	0.68
19R-1, 56–58	165.56	1.6	2.5	61.4	40.7	0.61
19R-2, 36–38	166.86	1.67	2.51	56.8	36.1	0.57
20R-1, 104–106	175.74	1.58	2.51	63.1	42.4	0.63
20R-2, 120–121	177.4	1.58	2.88	65.9	44.4	0.66
20R-3, 109–111	178.79	1.59	2.63	65.3	43.7	0.65
20R-4, 48–49	179.68	1.75	2.83	60.1	36.4	0.6
20R-5, 56–58	181.26	1.62	2.71	65.1	42.6	0.65
21R-1, 108–110	185.48	1.42	2.63	52.9	39.5	0.53
21R-2, 65–67	186.55	1.69	2.8	62.9	39.5	0.63
21R-3, 21–23	187.61	1.62	2.7	65.2	42.8	0.65
21R-4, 106–108	189.96	1.73	2.85	61.8	38	0.62
21R-5, 18–20	190.58	1.62	2.89	68.6	45	0.69
22R-1, 96–98	194.96	1.61	2.9	69.2	45.6	0.69
22R-2, 96–98	196.46	1.64	2.91	67.7	43.7	0.68
22R-3, 124–126	198.24	1.58	2.81	69.6	46.8	0.7
22R-4, 114–116	199.64	1.62	2.87	68.4	45	0.68
22R-5, 67–69	200.67	1.65	2.96	68.1	43.8	0.68
22R-6, 66–68	202.16	1.6	2.73	67.2	44.7	0.67
23R-1, 133–135	204.93	1.66	2.74	63.7	40.8	0.64
23R-2, 104–106	206.14	1.51	2.5	68.3	48	0.68
23R-3, 30–32	206.9	1.63	2.78	66	43	0.66
24R-1, 34–36	213.54	1.56	2.76	69.9	47.7	0.7
24R-2, 41–43	215.11	1.5	2.69	72.3	51.3	0.72
24R-3, 110–112	217.3	1.57	2.74	69	46.7	0.69
24R-4, 127–129	218.97	1.49	2.55	70	49.8	0.7
24R-5, 29–31	219.49	1.53	2.69	70.1	48.6	0.7
24R-6, 18–20	220.88	1.58	2.88	70.5	47.3	0.7
25R-1, 59–61	223.49	1.6	2.58	63.6	42.2	0.64
26R-1, 95–97	233.45	1.53	2.79	72.1	50.1	0.72
26R-2, 40–42	234.4	1.56	2.66	68.1	46.5	0.68
27R-1, 117–119	243.27	1.6	2.58	63.3	41.9	0.63
27R-2, 104–106	244.64	1.72	2.85	62.2	38.3	0.62
27R-3, 82–84	245.92	1.79	2.79	57.5	34.2	0.57
27R-4, 53–55	247.13	1.57	2.57	65	43.9	0.65
27R-5, 80–82	248.9	1.61	2.55	63.8	42.2	0.64
28R-1, 110–112	252.9	1.56	2.58	66	44.9	0.66
28R-2, 86–88	254.16	1.68	2.75	62.4	39.3	0.62
28R-3, 21–23	255.01	1.63	2.57	61.1	39.7	0.61
29R-1, 99–101	262.39	1.73	2.79	60.4	37.1	0.6
29R-2, 107–109	263.97	1.74	2.46	56.2	34.2	0.56
29R-3, 57–59	264.97	1.7	2.81	62.7	39.2	0.63
29R-4, 49–51	266.39	1.69	2.82	63.7	40.2	0.64
29R-5, 55–57	267.95	1.64	2.75	64.8	42	0.65
29R-6, 28–30	269.18	1.68	2.95	66.5	42.1	0.67
29R-7, 39–41	270.79	1.74	2.65	56.7	34.7	0.57
30R-1, 34–36	271.44	1.72	2.71	59.1	36.4	0.59
30R-2, 93–95	273.53	1.61	2.53	61.7	40.8	0.62
30R-3, 82–84	274.92	1.71	2.73	60.4	37.6	0.6
30R-4, 69–72	276.29	1.66	2.67	62	39.7	0.62
30R-5, 48–50	277.58	1.72	2.66	57.9	35.8	0.58
31R-1, 31–34	281.11	1.74	2.94	63.2	38.6	0.63
31R-2, 83–86	283.13	1.7	2.64	58.8	36.8	0.59
31R-3, 81–83	284.61	1.72	2.72	59.5	36.8	0.6
32R-1, 86–88	291.26	1.72	2.87	62.8	38.8	0.63
32R-2, 99–101	292.89	1.66	2.84	65.5	41.9	0.66
32R-3, 70–72	294.1	1.69	2.86	64	40.1	0.64
32R-4, 43–45	295.33	1.75	3.1	65.3	39.6	0.65
32R-5, 24–26	296.64	1.67	2.99	67.7	43.1	0.68
32R-6, 112–114	299.02	1.6	2.94	70.7	47	0.71
32R-7, 33–35	299.73	1.54	2.78	70.9	48.8	0.71
33R-1, 33–34	300.33	1.53	2.8	71.9	49.8	0.72
33R-2, 122–123	302.72	1.73	2.74	63.1	38.8	0.63
33R-3, 55–56	303.55	1.85	2.8	53.9	30.9	0.54
33R-4, 50–52	305	1.89	2.54	62.2	34.9	0.62
34R-1, 11–13	309.81	1.91	2.8	50.4	28	0.5
34R-2, 31–33	311.51	1.77	2.63	54.1	32.6	0.54
35R-1, 131–133	320.61	1.98	2.71	43.9	23.6	0.44
35R-2, 22–24	321.02	2.03	2.78	43.4	22.7	0.43
36R-1, 33–35	329.33	1.71	2.57	37.9	23.5	0.38
36R-1, 107–109	330.07	2.39	2.57	11.4	5.1	0.11
37R-1, 71–73	339.41	1.99	2.61	39.4	21	0.39
38R-1, 66–68	348.96	3.55	4.02	15.8	4.7	0.16
38R-2, 29–31	350.09	2.05	2.64	36.8	19.1	0.37
39R-1, 80–82	358.7	2.1	2.66	34.5	17.4	0.34
39R-2, 83–85	360.23	2.09	2.62	33.4	17	0.33
40R-1, 94–97	368.44	2.08	2.8	40.9	20.9	0.41
40R-2, 41–43	369.41	2.48	2.51	2.3	1	0.02
41R-1, 70–72	378	1.81	2.51	47.2	27.6	0.47
41R-2, 98–100	379.35	2.09	2.38	21.6	11	0.22
42R-1, 39–41	387.29	2.34	2.58	15.1	6.8	0.15
42R-1, 80–82	387.7	1.93	2.64	44.1	24.2	0.44
42R-2, 41–43	388.81	1.94	2.67	44.7	24.5	0.45
43R-1, 103–105	397.63	2.01	2.67	40.2	21.2	0.4
43R-2, 98–100	399.08	2.12	2.76	36.9	18.5	0.37
43R-3, 60–62	400.2	2.06	2.79	41.7	21.5	0.42
45R-1, 98–100	416.58	2.68	2.69	0.5	0.2	0
45R-2, 92–94	418.02	2.35	2.51	11	5	0.11

Table 11. Physical properties from Hole 784A.

Core, section, interval (cm)	Depth (mbsf)	Thermal conductivity (W/m·K)	Ultimate strength (kPa)	Resistivity (ohms)	Formation factor	Compressional-wave velocity	
						A direction (km/s)	B direction (km/s)
125-784A-							
1R-1, 76	0.76	0.851					
1R-CC, 22	1.16	0.99					
2R-1, 3–13	1.53	0.968		12.6	1.47		
3R-1, 10–14	11.02			13.9	1.62		
3R-1, 10–14	11.02			13.6	1.59		
3R-1, 33	11.23	0.729					
3R-1, 91–93	11.81		19.7				
3R-2, 33	12.73	0.894					
3R-3, 33	14.23	0.936					
3R-3, 81–83	14.71		43				
3R-4, 33	15.73	0.907					
4R-1, 15–19	20.57			14.9	1.74		
4R-1, 49	20.89	1.011					
4R-2, 49	22.39	0.936					
4R-3, 10–14	23.52			15.2	1.77		
4R-3, 49	23.89	1.01					
4R-3, 82–84	24.22		34.9				
4R-4, 49	25.39	0.963					
6R-1, 30–34	39.82			16.9	1.97		
6R-1, 65	40.15	1.015					
6R-1, 90–91	40.4		17.3				
6R-2, 65	41.65	1.247					
6R-3, 20–24	42.72			17.3	2.02		
6R-3, 65	43.15	0.948					
6R-3, 83–85	43.33		29.8				
6R-4, 65	44.65	0.981					
6R-5, 10–14	45.62			16.5	1.93		
6R-5, 46	45.96	0.899					
6R-5, 113–115	46.63		37.9				
6R-6, 46	47.46	0.857					
7R-1, 74	49.84	0.921					
7R-1, 106–110	50.18		34.9	16.1	1.88		
7R-2, 40–44	51.02			16.6	1.94		
7R-2, 74	51.34	0.852					
7R-3, 60–64	52.72		18.9	15.4	1.8		
7R-3, 74	52.84	1.03					
8R-1, 40–44	59.22			19	2.22		
8R-1, 70	59.5	0.9					
8R-2, 58–60	60.88		52.4				
8R-2, 70	61	0.864					
8R-3, 46–48	62.78			17.4	2.03		
8R-3, 70	62.5	0.971					
8R-4, 64–66	63.94		40				
8R-4, 70	64	0.93					
8R-5, 54–58	65.36			16	1.87		
8R-5, 59–63	65.41			18.5	2.16		
8R-5, 21	65.01	0.784					
8R-6, 21	66.51	0.963					
9R-1, 75	69.25	0.796					
9R-1, 90–94	69.42			16.5	1.93		
9R-2, 75	70.75	0.705					
9R-2, 90–92	70.9		32				
9R-3, 75	72.25	1.021		18.5	2.16		
9R-4, 50–52	73.5		40				
9R-4, 75	73.75	0.951					
9R-5, 20–24	74.72			19.5	2.28		
9R-5, 37	74.87	1.005					
9R-CC, 6	75.33	0.838					
10R-1, 52	78.62	0.931		17.3	2.04		
10R-2, 60–62	80.2		25.5				
10R-2, 75	80.35	0.936					
10R-3, 75	81.85	0.918					
10R-3, 100–104	82.12			17	1.98		
10R-4, 60	83.2	0.915					
10R-4, 80–82	83.4		24				
10R-5, 6–10	83.5			24.5	2.86		
10R-CC, 6	83.86	0.876					
11R-CC, 9	87.89	0.795					
12R-1, 56–60	97.98			17	1.98		
12R-1, 75	98.15	0.921					
12R-1, 104–108	98.46			19	2.22		
12R-2, 41	99.31	0.976	57.5				
13R-1, 29–34	107.39	0.909		18	2.1		
13R-1, 38–42	107.5		17.5	19	2.22		

Table 11 (continued).

Core, section, interval (cm)	Depth (mbsf)	Thermal conductivity (W/mK)	Ultimate strength (kPa)	Resistivity (ohms)	Formation factor	Compressional-wave velocity A direction (km/s)	Compressional-wave velocity B direction (km/s)
13R-1, 38–42	107.5			21	2.45		
13R-1, 42–46	107.54			22	2.57		
14R-1, 80	117.5	0.951					
14R-1, 96–100	117.68			15.5	1.81		
14R-2, 58–60	118.78		54.6				
14R-2, 74	118.94	0.787					
14R-3, 28–32	120			17	1.98		
14R-3, 56	120.26	0.949					
14R-4, 36–38	121.56		57.5				
14R-4, 72	121.92	0.95					
14R-5, 49	123.19	0.969					
14R-5, 64–66	123.26			18.5	2.16		
14R-CC, 10	123.78	0.996					
15R-1, 75	127.15	0.912					
15R-2, 75	128.65	0.979					
15R-2, 85–87	128.75		54.6				
15R-2, 96–100	128.88			18	2.1		
15R-3, 50–54	129.92			15.5	1.81		
15R-3, 75	130.15	0.946					
15R-4, 75–77	131.65	0.858	72.8				
15R-4, 100–104	131.92			19	2.22		
15R-5, 75	133.15	0.947					
15R-6, 75	134.65	0.838					
15R-7, 30	135.7	0.991					
15R-CC, 10	136.11	0.852		24.9	2.91		
16R-1, 75	136.75	0.792					
16R-1, 100–102	137		43				
16R-2, 75	138.25	0.971					
16R-3, 10–14	139.12			19.3	2.25		
16R-3, 75	139.75	0.952	49.5				
16R-4, 75	141.25	0.989					
16R-5, 13–17	142.15			22.6	2.64		
16R-5, 75	142.75	0.801					
16R-5, 91–93	142.91		57.5				
16R-6, 75	144.25	0.995					
16R-7, 10–14	145.12			29.4	3.43		
16R-7, 29	145.29	0.916					
16R-CC, 10	145.7	0.906					
17R-1, 12–16	145.74			24.9	2.91		
17R-1, 75	146.35	0.958					
17R-2, 75	147.85	0.961					
17R-3, 17–21	148.79			23.3	2.72		
17R-3, 75	149.35	0.968					
17R-3, 95–97	149.55		52.4				
17R-4, 75	150.85	0.908					
17R-5, 5–9	151.67			26.9	3.14		
17R-5, 64	152.24	0.875					
17R-5, 100–102	152.6		85.9				
18R-1, 64	155.94	0.938					
18R-1, 90–92	156.2					1.6	1.63
18R-2, 64	157.44	0.985					
18R-3, 64	158.94	0.898					
18R-4, 38	160.18	0.788					
18R-5, 38	161.68	0.998					
18R-6, 38	163.18	0.973					
18R-7, 38	164.68	0.931					
19R-1, 91	165.91	0.952					
19R-2, 36–38	166.86					1.67	1.68
19R-2, 91	167.41	0.924					
20R-1, 54	175.24	0.963					
20R-1, 104–106	175.74					1.6	1.61
20R-2, 54	176.74	0.954					
20R-3, 54	178.24	0.952					
20R-4, 54	179.74	1.062					
20R-5, 44	181.14	0.924					
21R-1, 44	184.84	0.908					
21R-1, 108–110	185.48					1.69	1.68
21R-2, 44	176.34	0					
21R-2, 65–67	186.55					1.7	1.74
21R-2, 88	186.78	0.693					
21R-3, 21–23	187.61					1.62	1.62
21R-3, 44	187.84	1.048					
21R-4, 59	189.49	0.945					
21R-4, 106–108	189.96					1.64	1.63
21R-5, 18–20	190.58					1.57	1.58

Table 11 (continued).

Core, section, interval (cm)	Depth (mbsf)	Thermal conductivity (W/mK)	Ultimate strength (kPa)	Resistivity (ohms)	Formation factor	Compressional-wave velocity A direction (km/s)	Compressional-wave velocity B direction (km/s)
21R-5, 59	190.99	1.039					
21R-6, 59	192.49	0.907					
22R-1, 96–98	194.96					1.58	1.58
22R-2, 59	196.09	0.902					
22R-2, 96–98	196.46					1.58	1.6
22R-3, 80	197.8	1.001					
22R-3, 124–126	198.24					1.57	1.56
22R-4, 80	199.3	0.895					
22R-4, 114–116	199.64					1.57	1.61
22R-5, 67–69	200.67					1.56	1.58
22R-5, 80	200.8	1.027					
22R-6, 66–68	202.16					1.59	1.59
22R-6, 80	202.3	1.026					
23R-1, 54	204.14	1.031					
23R-1, 133–135	204.93					1.62	1.62
23R-2, 54	205.64	0.959					
23R-2, 104–106	206.14					1.58	1.59
23R-3, 54	207.14	0.951					
24R-1, 34–36	213.54					1.58	1.6
24R-1, 81	214.01	0.847					
24R-2, 41–43	215.11					1.57	1.55
24R-2, 81	215.51	0.924					
24R-3, 81	217.01	1.009					
24R-3, 110–112	217.3					1.6	1.6
24R-4, 81	218.51	1.008					
24R-4, 127–129	218.97					1.59	1.58
24R-5, 31	219.51	0.951				1.57	1.56
24R-6, 18–20	220.88					1.58	1.59
24R-6, 31	221.01	0.93					
24R-7, 31	222.51	0.979					
25R-1, 31	223.21	0.774					
25R-1, 59–61	223.49					1.62	1.63
26R-1, 50	233	1.022					
26R-1, 95–97	233.45					1.57	1.59
26R-2, 40–42	234.4					1.58	1.59
26R-2, 68	234.68	0.945					
26R-3, 68	236.18	0.954					
27R-1, 93	243.03	0.955					
27R-1, 117–119	243.27					1.66	1.69
27R-2, 75	244.35	0.966					
27R-2, 104–106	244.64					1.73	1.76
27R-3, 75	245.85	0.965				1.75	1.85
27R-4, 53–55	247.13					1.61	1.64
27R-4, 75	247.35	1.002					
27R-5, 75	248.85	1.003				1.69	1.68
28R-1, 75	252.55	0.355					
28R-1, 110–112	252.9					1.6	1.61
28R-2, 75	254.05	1.002					
28R-2, 86–88	254.16					1.67	1.67
28R-3, 22	255.02	1.018					
28R-3, 99–101	255.8					1.68	1.74
29R-1, 21–23	261.61					1.77	1.88
29R-1, 75	262.15	0.768					
29R-2, 75	263.65	0.979					
29R-2, 107–109	263.97					1.88	1.88
29R-3, 57–59	264.97					1.74	1.74
29R-3, 75	265.15	0.92					
29R-4, 52	266.42	0.545				1.72	1.73
29R-5, 55–57	267.95					1.69	1.7
29R-5, 82	268.22	0.756					
29R-6, 28–30	269.18					1.67	1.67
29R-6, 82	269.72	1.016					
29R-7, 37–39	270.77	1.032				1.75	1.77
30R-1, 34–36	271.44					1.73	1.79
30R-1, 75	271.85	0.746					
30R-2, 75	273.35	0.934					
30R-3, 75	274.85	0.854					
30R-4, 69–75	276.35	0.971				1.78	1.76
30R-5, 41–43	277.49	0.249				1.76	1.83
31R-1, 31–33	281.11					1.84	
31R-1, 70	281.5	0.936					
31R-2, 68	282.98	1.083					
31R-3, 68	284.48	1.005					
31R-3, 81–83	284.61					1.75	
32R-1, 75	291.15	1.06					

Table 11 (continued).

Core, section, interval (cm)	Depth (mbsf)	Thermal conductivity (W/mK)	Ultimate strength (kPa)	Resistivity (ohms)	Formation factor	Compressional-wave velocity	
						A direction (km/s)	B direction (km/s)
32R-1, 86–88	291.26					1.73	1.87
32R-2, 75	292.65	0.954					
32R-3, 75	294.15	0.945				1.79	1.79
32R-4, 43–45	295.33					1.82	1.81
32R-5, 24–26	296.64					1.74	1.76
32R-5, 73	297.13	0.705					
32R-6, 51	298.41	0.954					
32R-7, 32	299.72	0.691					
33R-1, 75	300.75	1.02					
33R-2, 75	302.25	1.405					
33R-3, 75	303.75	1.199					
33R-4, 47	304.97	1.234					
34R-1, 75	310.45	1.426					
34R-2, 75	311.95	1.11					
34R-CC, 6	312.91	1.27					
35R-1, 60	319.9	1.081					
35R-2, 22–24	321.02					1.96	2.33
35R-2, 49	321.29	1.705					
35R-CC, 5	321.78	1.496					
36R-1, 104–107	330.04	1.814				3.45	3.5
36R-1, 116–120	330.18			33.6	3.92		
36R-2, 10–14	330.62			41.1	4.8		
37R-1, 65–67	339.35		32				
37R-1, 99	339.69	0.89					
37R-1, 122–124	339.92		22.6				
37R-2, 27	340.47	2.03	83				
38R-1, 61–66	348.91	1.59				3.63	3.56
38R-2, 29–31	350.09					2.24	1.98
39R-1, 75	358.65	2.458	132.5				
39R-2, 70	360.1	2.983					
39R-2, 95–97	360.35		52.4				
40R-1, 61–64	368.14	2.568	35.7				
40R-1, 94–96	368.44					1.79	
40R-1, 109–111	368.59		72.1				
40R-1, 115–117	368.65		83.7				
40R-2, 15–17	369.15		251.2				
40R-2, 50–52	369.5					4.94	4.84
41R-2, 98–100	379.35					3.81	3.84
42R-1, 39–41	387.29					3.19	3.27
42R-2, 22	388.62	2.35					
43R-1, 96	397.56	1.895				1.74	1.7
43R-2, 47	398.57	2.05					
43R-2, 98–100	399.08					1.84	1.87
43R-3, 33	399.93	1.759					
43R-3, 60–62	400.2					1.74	1.7
45R-1, 83	416.43	1.751					
45R-1, 99–100	416.59					5.66	5.45
45R-2, 60	417.7	2.098					
45R-2, 92–94	418.02					3.82	3.78

28), with a low r^2 of 0.426. The slope of the decay curve is low, thus any errors should be minor.

Thermal-conductivity data are presented in Figure 29 (see "Physical Properties" section, this chapter). Temperatures were measured above the depth where a large increase in thermal conductivity occurs. The integrated thermal resistivity is shown in Figure 30.

The equilibrium temperature and integrated thermal resistivity data are plotted in Figure 31. The slope of the linear least-squares regression at this site gives a heat flow of 24 mW/m^2. The correlation coefficient for the fit is 0.988. The misfit of the data to the regression for the uppermost sediment measurement may be caused by the slight motion of the probe in the sediment, as previously mentioned.

SUMMARY AND CONCLUSIONS

Site 784, at 30°54.49'N, 141°44.27'E, in a water depth of 4900.8 m, is located approximately 7 km southwest of Site 783 on the lowermost, western flank of the same seamount on the inner wall of the Izu-Bonin Trench. The stratigraphic section recovered at Site 784 is divided into the three subunits of lithologic Unit I and a lithologic Unit II (Fig. 32): Subunit IA (0–126.4 mbsf) consists of vitric clayey silt, glass-rich silty clay/claystone of late Pleistocene to early Pliocene(?) age; Subunit IB (126.4–302.7 mbsf) is a vitric claystone of early Pliocene(?) to middle Miocene age; Subunit IC (302.7–321.1 mbsf) consists of claystone and silt-sized serpentine of unknown age; and Unit II (321.1–425.3 mbsf) is a phacoidal, sheared serpentine microbreccia.

Dating is based on calcareous nannofossil and diatom biostratigraphy. Lithologic Subunit IB may correlate with lithologic Subunit IB at Site 782 in the forearc basin on the basis of age and ash content, although there is a depleted carbonate/microfossil component at Site 784 because of sediment deposition at or below the CCD. Sediments from Subunits IA and IB at Site 784 are typically laminated and contain abundant graded beds, structures that are indicative of current activity during sediment deposition. The sediment contains a

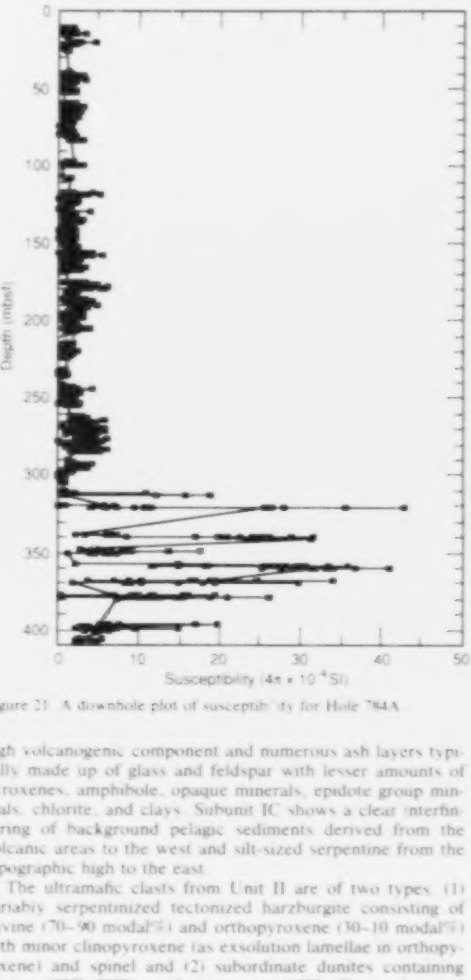

Figure 21. A downhole plot of susceptibility for Hole 784A.

high volcanogenic component and numerous ash layers typically made up of glass and feldspar with lesser amounts of pyroxenes, amphibole, opaque minerals, epidote group minerals, chlorite, and clays. Subunit IC shows a clear interfingering of background pelagic sediments derived from the volcanic areas to the west and silt-sized serpentine from the topographic high to the east.

The ultramafic clasts from Unit II are of two types: (1) variably serpentinized tectonized harzburgite consisting of olivine (70–90 modal%) and orthopyroxene (30–10 modal%) with minor clinopyroxene (as exsolution lamellae in orthopyroxene) and spinel and (2) subordinate dunites containing olivine (90%–99%), orthopyroxene (10%–1%), and spinel (0.5%–2%). About 30 metabasalt clasts were also identified.

Deformation in the claystones of Unit I at Site 784 includes sets of *en echelon* tension veinlets and sets of microfaults, some of which are clearly associated with water-escape pipes. The zone of greatest microfaulting is directly correlated with an interval of increased water content and porosity of the sediments. Most structures are extensional and can be shown to have formed in a nonhydrostatic stress regime. Unit II includes pebbly serpentines with convolute lamination, sheared and relatively unsheared, pebbly silt-sized serpentines without convolute lamination, and serpentine microbreccias. Some of these layers exhibit irregular size grading and many contain larger blocks, mostly of serpentinite.

Analyses of the interstitial waters show a steady change in composition with depth within the claystone, followed by an abrupt change in behavior at the claystone/serpentine boundary. As at Site 783, the most abrupt changes are in pH, which increases to 9.6 in the serpentine, and silica, which decreases to less than 10 μmol/kg. Other species showing a marked change in behavior are alkalinity, which decreases to a value about one-half that of seawater within the serpentine; sulfate, which decreases to 7 mmol/kg; calcium, which increases to 57 mmol/kg; and magnesium, which decreases to very low values. As at Site 783, chlorinity, bromide, and salinity show no major changes, but sodium decreases to 452 μmol/kg, in contrast to its behavior at Site 783. Thus, as at Site 783, there is evidence for ongoing serpentinization at the Torishima Forearc Seamount.

Studies of physical properties show that the average bulk densities are 1.5 g/cm^3 in the sediments of Unit I and 2.2 g/cm^3 in the serpentine of Unit II. The average compressional-wave velocity is 1.66 km/s in the sediments and 3.08 km/s in the serpentine and serpentinites. The thermal conductivity averages about 0.9 W/mK in the sediments and 1.74 W/mK in the serpentine and serpentinite.

Preliminary interpretation of paleomagnetic data from the sediments between 0 and 160 mbsf shows magnetic inclination peaks around −50° and 50°, indicating little translation since the Pliocene. In the interval between 160 and 240 mbsf, there is no good bimodal distribution and a significant number of data points lie between −15° and 15°, which suggests that a significant translation may have occurred between the middle Miocene and the Pliocene. No inclination data were obtained below 240 mbsf, but magnetic susceptibilities did increase markedly at the claystone/serpentine boundary, perhaps because the serpentine contains a high proportion of secondary magnetite.

The principal results of this site are (1) the confirmation that the western lower flank of the seamount is also made up of serpentine-rich sediments and serpentinite, (2) further biostratigraphic evidence that the serpentine sediment is at least middle Miocene and hence that the seamount is considerably older than Conical Seamount in the Mariana forearc, (3) the structural evidence for extensional deformation within the more compacted sediments overlying serpentine-rich sediments and serpentinite, (4) possible paleomagnetic evidence for significant translation of the site between middle Miocene and Pliocene, and (5) the evidence that serpentinization is still taking place, despite the lack of evidence for active protrusion.

REFERENCES

Arthur, M. A., Carson, B., and von Huene, R., 1980. Initial tectonic deformation of hemipelagic sediment at the leading edge of the Japan convergent margin. *In* Langseth, M., Okada, H., et al., *Init. Repts. DSDP*, 56, 57 (Pt. 1): Washington (U.S. Govt. Printing Office), 569–613.

Barron, J. A., 1985. Miocene to Holocene planktonic diatoms. *In* Bolli, H., Saunders, J. B., and Perch-Nielsen, K. (Eds.), *Plankton Stratigraphy*: Cambridge (Cambridge Univ. Press), 763–810.

Berggren, W. A., Kent, D. V., Flynn, J. J., and Van Couvering, J., 1985. Cenozoic geochronology. *Geol. Soc. Am. Bull.*, 96:1407–1418.

Bleil, U., 1982. Paleomagnetism of Deep Sea Drilling Project Leg 60 sediments and igneous rocks from the Mariana region. *In* Hussong, D. M., Uyeda, S., et al., *Init. Repts. DSDP*, 60: Washington (U.S. Govt. Printing Office), 855–873.

Cowan, D. S., 1982. Origin of "vein structure" in slope sediments on the inner slope of the Middle America Trench off Guatemala. *In* Aubouin, J., von Huene, R., et al., *Init. Repts. DSDP*, 67: Washington (U.S. Govt. Printing Office), 645–650.

Cowan, D. S., Moore, J. C., Roeske, S. M., Lundberg, N., and Lucas, S. E., 1984. Structural features at the deformation front of the Barbados Ridge complex, Deep Sea Drilling Project Leg 78A. *In* Biju-Duval, B., Moore, J. C., et al., *Init. Repts. DSDP*, 78A: Washington (U.S. Govt. Printing Office), 535–548.

Dengo, C. A., 1982. A structural analysis of cores from the Leg 67 transect across the Middle America Trench–offshore Guatemala. *In* Aubouin, J., von Huene, R., et al., *Init. Repts. DSDP*, 67: Washington (U.S. Govt. Printing Office), 651–666.

Kobayashi, K. (Ed.), 1989. *Preliminary Report of the Hakuho Maru Cruise KH-87-3, July-August 13, 1988, Izu-Ogasawara (Bonin), East Mariana Basin and Yap Trench (WESTPAC, ODP Site Survey).* Tokyo (Ocean Research Institute, Univ. of Tokyo).

Ness, G., Levi, S., and Crouch, R., 1980. Marine magnetic anomaly time scales for the Cenozoic and Late Cretaceous: A précis, critique and synthesis. *Rev. Geophys. Space Phys.*, 198:753–770.

Ms 125A-112

NOTE: All core description forms ("barrel sheets") and core photographs have been printed on coated paper and bound as Section 4, near the back of the book, beginning on page 383.

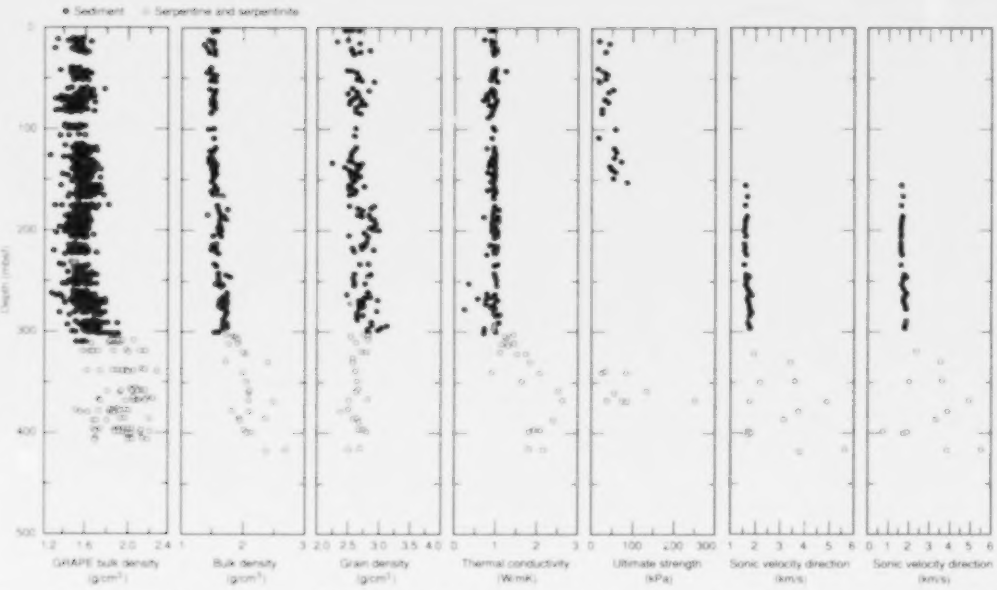

Figure 22. Bulk density (determined by the GRAPE and from discrete samples), grain density, thermal conductivity, ultimate strength, and A (parallel to the split-core surface) and B (perpendicular to the split-core surface) directions of sonic velocity.

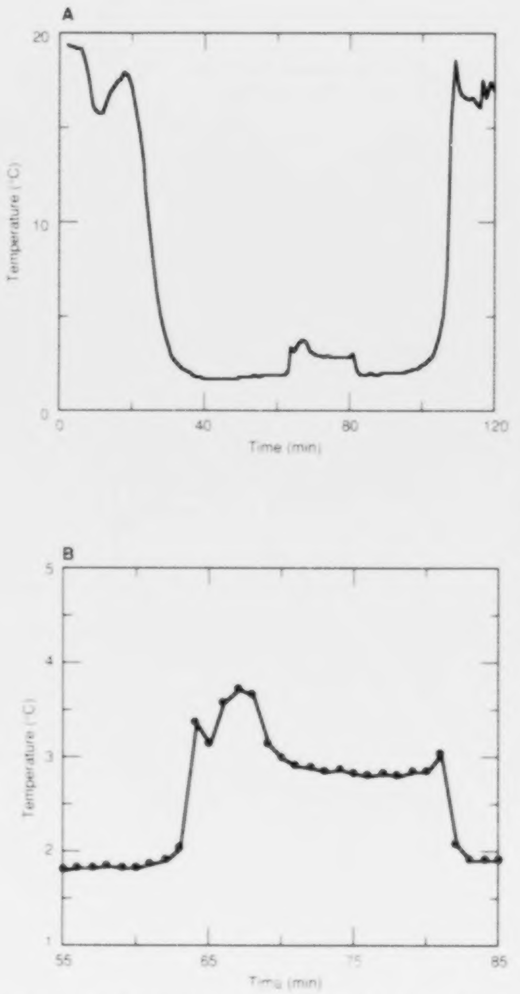

Figure 23. **A.** Temperature vs. time for Run 05R of the Barnes-Uyeda tool at 29.9 mbsf in Hole 784A. **B.** An expanded plot showing the data when the tool was in the seafloor. Note the disturbance of the probe from 65 to 67 min.

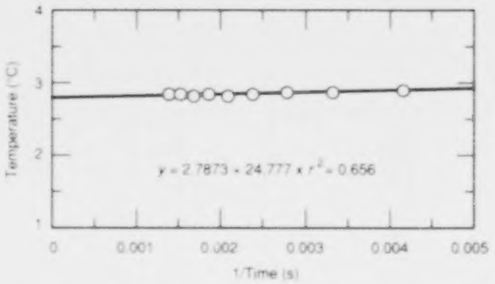

Figure 24. The reduced temperature fit of the first Barnes-Uyeda temperature run using data from the later portion of the run. The intercept value at 1/time = 0 is the equilibrium temperature of the sediment.

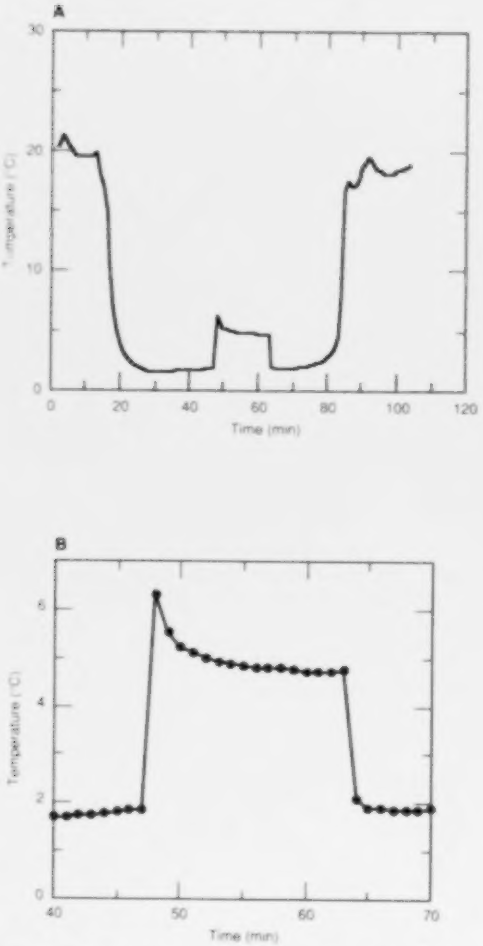

Figure 25. **A.** Temperature vs. time for Run 11R of the Barnes-Uyeda temperature tool at 107.1 mbsf in Hole 784A. **B.** An expanded plot showing the data when the tool was in the seafloor.

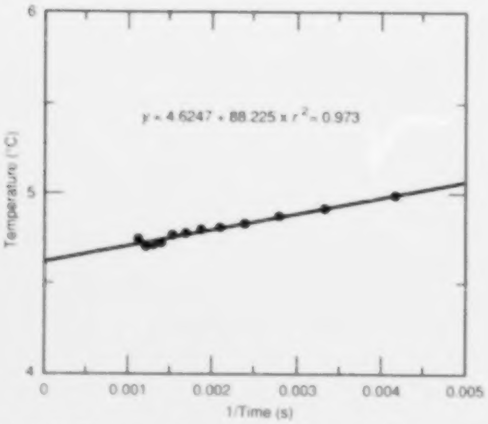

Figure 26. The corresponding reduced temperature fit for the second Barnes-Uyeda temperature run.

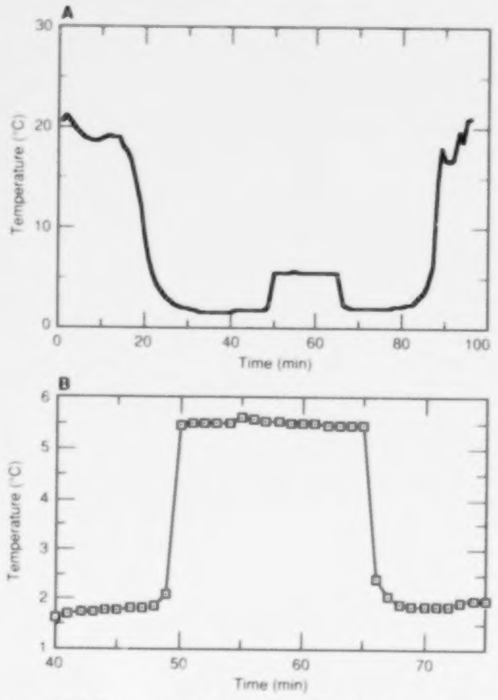

Figure 27. **A.** Temperature vs. time for Run 17R of the Barnes-Uyeda temperature tool at 145.6 mbsf in Hole 784A. **B.** An expanded plot showing the data when the tool was in the seafloor.

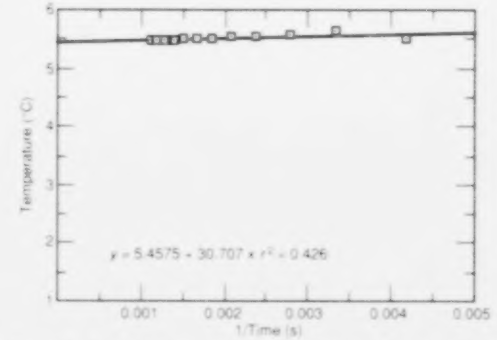

Figure 28. The corresponding reduced temperature fit for the third Barnes-Uyeda temperature run.

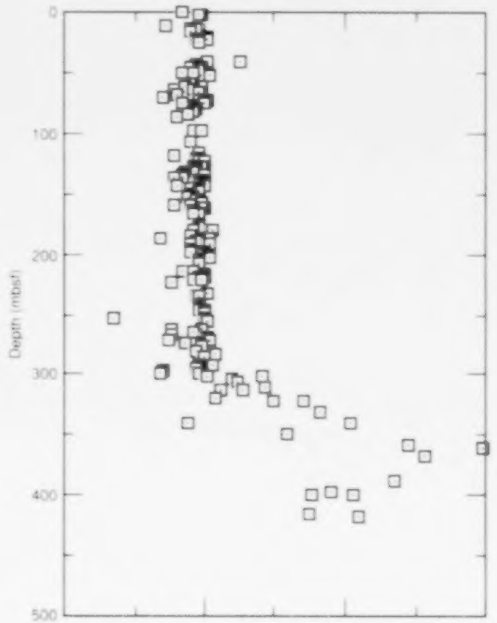

Figure 29. Thermal-conductivity results plotted vs. depth for Hole 784A.

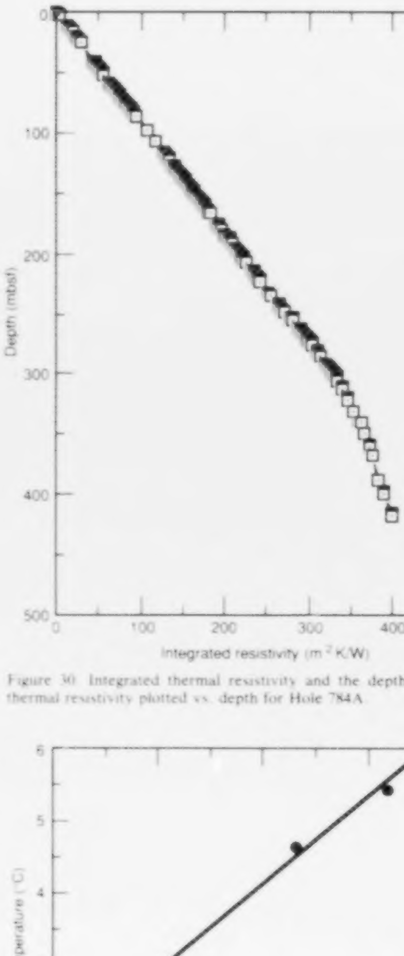

Figure 30. Integrated thermal resistivity and the depth
thermal resistivity plotted vs. depth for Hole 784A.

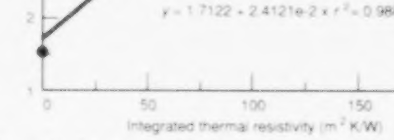

Figure 31. Temperature vs. integrated thermal resistivi
784A. The slope of the best-fitting linear regression is
value of 24 mW/m².

integral of

ty for Hole
a heat-flow

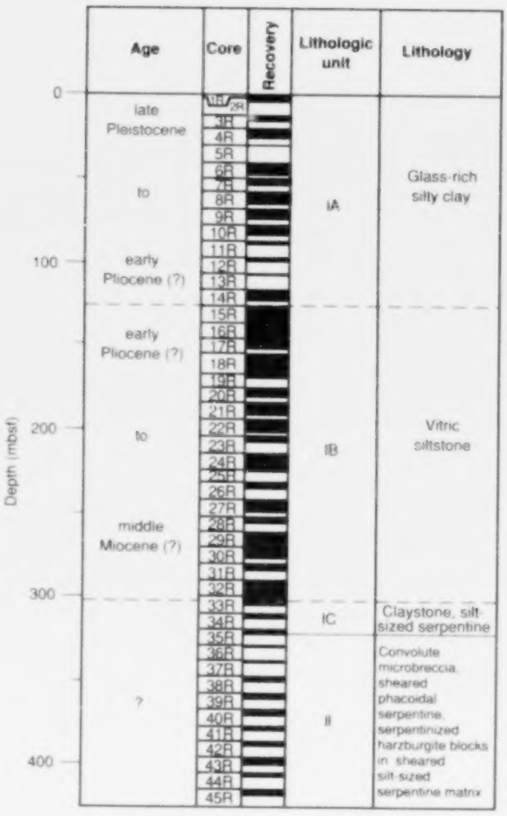

Age
Core
Recovery
Lithologic unit
Lithology
Depth (mbsf)
0
100
200
300
400
late Pleistocene
to
early Pliocene (?)
early Pliocene (?)
to
middle Miocene (?)
?
1R
2R
3R
4R
5R
6R
7R
8R
9R
10R
11R
12R
13R
14R
15R
16R
17R
18R
19R
20R
21R
22R
23R
24R
25R
26R
27R
28R
29R
30R
31R
32R
33R
34R
35R
36R
37R
38R
39R
40R
41R
42R
43R
44R
45R
IA
IB
IC
II
Glass-rich silty clay
Vitric siltstone
Claystone, silt-sized serpentine
Convolute microbreccia, sheared phacoidal serpentine, serpentinized harzburgite blocks in sheared silt-sized serpentine matrix

Figure 32. Core recovery and lithologic summary, Hole 784A.

Fryer, P., Pearce, J. A., Stokking, L. B., et al., 1990
Proceedings of the Ocean Drilling Program, Initial Reports, Vol. 125

13. SITE 785[1]

Shipboard Scientific Party[2]

HOLE 785A

Date occupied: 31 March 1989

Date departed: 1 April 1989

Time on hole: 1 day, 3 hr, 45 min

Position: 30°49.47′N, 140°55.17′E

Bottom felt (rig floor; m; drill-pipe measurement): 2672.0

Distance between rig floor and sea level (m): 11.20

Water depth (drill-pipe measurement from sea level; m): 2660.8

Total depth (rig floor; m): 2776.70

Penetration (m): 104.70

Number of cores: 11

Total length of cored section (m): 104.70

Total core recovered (m): 18.42

Core recovery (%): 17.6

Oldest sediment cored:
Depth (mbsf): 57.61
Nature: nannofossil ooze, pumice
Earliest age: early Pleistocene

Principal results: Site 785 is located in the center of the Izu-Bonin forearc basin about 40 nmi east-northeast of the active volcano Torishima. The objectives of this site were to study (1) the uplift and subsidence history of the forearc basin at this locality, (2) the temporal record of sedimentation, depositional environment, paleoceanography, and intensity and nature of arc volcanism, (3) the nature and age of the igneous basement of the forearc basin, and (4) the microstructural deformation and the large-scale rotation and translation of the forearc. A thick near-surface layer of pumice and ash encountered in Hole 785A produced high torque on the drill string and caused the hole to collapse after drilling to a depth of 104.7 m below seafloor (mbsf) with a recovery of 17.6%.

The single lithologic unit at Site 785, Unit I, is of late to early Pleistocene age and consists of 2 m of light brown pumice-bearing nannofossil ooze overlying a pumice bed. The ooze is dominated by calcareous nannofossils with smaller amounts of foraminifers, micrite, radiolarians, diatoms, sponge spicules, clay, quartz, and vitric fragments. The pumice bed contains fragments of light gray to gray, porphyritic dacite-rhyolite pumice, 1 mm to 6 cm in diameter, in a poorly sorted matrix of mainly vitric particles. The average bulk density of the pumice is 1.3 g/cm^3. The principal result from this site is the evidence for a major Pleistocene pumice bed in this part of the Izu-Bonin forearc basin.

BACKGROUND AND SCIENTIFIC OBJECTIVES

Site 785 is located at 30°49.47′N, 140°55.17′E, in a water depth of 2660.8 m on the outer half of the Izu-Bonin forearc, about 120 km west of the axis of the Izu-Bonin Trench (Fig. 1). The objectives of drilling at this site are similar to those of Site 782 in the study of the following:

1. The stratigraphy of the forearc and hence both the temporal variations in sedimentation, depositional environment, and paleoceanography and the history of intensity and chemistry of arc volcanism;
2. The uplift/subsidence history of the central part of the forearc to provide information about forearc flexure and basin development as well as on the extent of any vertical tectonic activity that may have taken place since formation of the forearc terrane;
3. The nature of igneous basement forming the central basin of the forearc, to answer questions concerning the nature of volcanism in the initial stages of subduction, the origin of boninites, and the formation of the 200-km-wide arc-type forearc crust; and
4. The microstructural deformation and the large-scale rotation and translation of the forearc terrane since the Eocene.

As at Site 782, the first of these objectives can be addressed partly through detailed studies of the sediments recovered at Site 785. These sediments contain a record of the history of intensity and composition of arc volcanism, which might help to place some constraints on hypotheses regarding the controls over variations in such subduction processes as convergence rates and episodicity of backarc spreading.

The second objective can be investigated through a combination of sediment analysis and evaluation of logging results linked to the study of digital seismic-reflection data from the forearc. Multichannel seismic (MCS) surveys of the Izu-Bonin forearc have revealed a complicated basement that is commonly seismically stratified and cut by dipping reflectors. Like Site 782, Site 785 was selected in the hope of sampling the hitherto unstudied upper forearc basement to constrain some of the parameters required for modeling forearc evolution. Several lines of evidence suggest that fairly stable conditions have prevailed since the anomalous Eocene phase of arc-basin development (see "Background and Objectives" section, "Site 782" chapter, this volume). Comparing the results of drilling at Site 785 with those from other holes across the forearc and using backstripping techniques for cored/logged holes as well as analyses of the seismic stratigraphies of interconnecting MCS profiles will provide constraints on models for forearc evolution. Microstructures in the drill cores should also help in determining the intensity of faulting in space and time across the forearc terrane.

The third objective of this site, to determine the nature of volcanism in the initial stages of subduction, can be achieved through the evaluation of several hypotheses for the origin and evolution of the Izu-Bonin forearc terrane over the past 40 m.y. One of the most intriguing aspects of this evaluation will be to provide information about how the various models for forearc evolution relate to the formation of supra-subduction

---

[1] Fryer, P., Pearce, J. A., Stokking, L. B., et al., 1990. *Proc. ODP, Init. Repts.*, 125: College Station, TX (Ocean Drilling Program).

[2] Shipboard Scientific Party is as given in the list of participants preceding the contents.

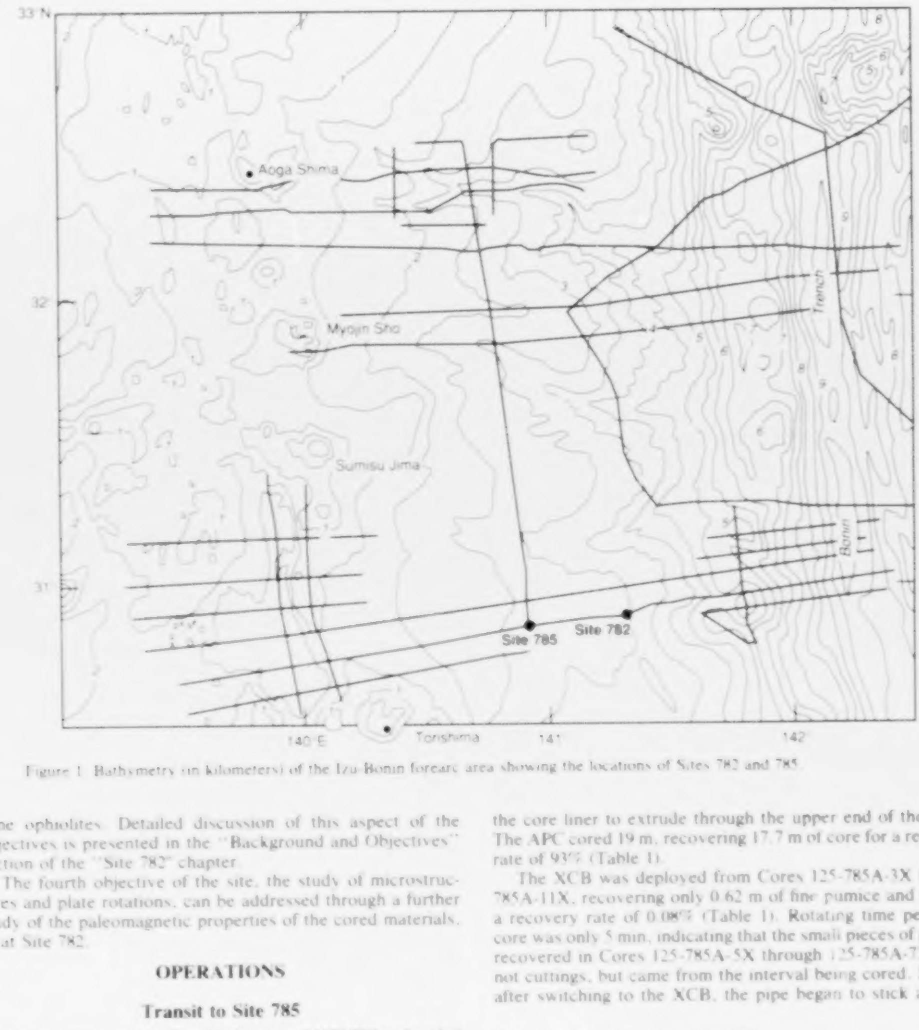

Figure 1. Bathymetry (in kilometers) of the Izu-Bonin forearc area showing the locations of Sites 782 and 785.

zone ophiolites. Detailed discussion of this aspect of the objectives is presented in the "Background and Objectives" section of the "Site 782" chapter.

The fourth objective of the site, the study of microstructures and plate rotations, can be addressed through a further study of the paleomagnetic properties of the cored materials, as at Site 782.

OPERATIONS

Transit to Site 785

The 44-nmi transit to Site 785 began at 0100UTC and ended at 0645UTC, 31 March 1989. Site 785 was established by the deployment of a beacon.

Hole 785A

A standard advanced hydraulic piston corer/extended core barrel (APC/XCB) bottom-hole assembly (BHA) with a lockable flapper valve, nonmagnetic drill collar, and bit was prepared and run in the hole. A center bit was lowered and a jet-in test performed. Only 32 m was penetrated in 90 min. The BHA was then pulled clear of the seafloor, and the center bit was retrieved.

An APC core barrel was deployed, and Hole 785A was spudded at 1800UTC, 1 April. The first core barrel established the mud line at 2660.8 m below sea level (mbsl). The second APC core recovered 8.2 m of fine pumice, which had sufficient frictional drag upon entering the core barrel to cause 1 m of the core liner to extrude through the upper end of the APC. The APC cored 19 m, recovering 17.7 m of core for a recovery rate of 93% (Table 1).

The XCB was deployed from Cores 125-785A-3X to 125-785A-11X, recovering only 0.62 m of fine pumice and ash for a recovery rate of 0.08% (Table 1). Rotating time per XCB core was only 5 min, indicating that the small pieces of pumice recovered in Cores 125-785A-5X through 125-785A-7X were not cuttings, but came from the interval being cored. Shortly after switching to the XCB, the pipe began to stick and the

Table 1. Coring summary for Site 785.

Core no.	Date (April 1989)	Time (UTC)	Depth (mbsf)	Length cored (m)	Length recovered (m)	Recovery (%)
125-785A-						
1H	1	1815	0.0–9.5	9.5	9.52	100.0
2H	1	1845	9.5–19.0	9.5	8.25	86.8
3X	1	2130	19.0–28.5	9.5	0.00	0.0
4X	1	2230	28.5–38.3	9.8	0.00	0.0
5X	1	2330	38.3–47.8	9.5	0.33	3.5
6X	2	0130	47.8–57.3	9.5	0.01	0.1
7X	2	0130	57.3–66.8	9.5	0.31	3.3
8X	2	0230	66.8–76.2	9.4	0.00	0.0
9X	2	0315	76.2–85.7	9.5	0.00	0.0
10X	2	0400	85.7–95.2	9.5	0.00	0.0
11X	2	0445	95.2–104.7	9.5	0.00	0.0
Coring totals				104.7	18.42	17.6

hole began to fill in. Mud was circulated, but did not relieve the hole problems.

The BHA had been risked whene we were trying to pass it through the layer of pumice and ash. If the layer had been penetrated, an attempt at setting the reentry cone and casing would have been justified. Further drilling, however, would probably result in loss of the BHA. In addition, the reentry cone and casing could not be jetted-in deeply enough to pass through the layer of pumice and ash. Even if it were possible to set a reentry cone and 16-in. casing, the hole was not sufficiently stable to allow us to set a string of 113/4-in. casing. The hole therefore was abandoned.

Site 785 officially ended at 1030UTC, 1 April, when the bit was back on board and the vessel was under way for Site 786 (proposed Site BON-6C). A total of 104.7 m was cored in 11 coring runs, recovering 18.4 m of core with 17.6% recovery (Table 1).

LITHOSTRATIGRAPHY

Only one lithologic unit is described for the stratigraphic succession recovered at Site 785 (Table 2). Poor core recovery and unstable drillhole conditions were caused by a thick (greater than 102 m) pumice sequence that terminated drilling at 104.7 mbsf.

Unit I

Sections 125-785A-1H-1 to 125-785A-11X-CC; depth, 0.0–104.7 mbsf.
Age: Pleistocene

Approximately 2 m of light brownish-gray to gray (2.5Y 6/2 to 7.5YR 6/0) nannofossil ooze overlying the pumice layer was recovered in Sections 125-785A-1H-1 and 125-785A-1H-2. The ooze forms the uppermost sediment at Site 785 and contains nannofossils (51%–79%), foraminifers (5%–8%), micrite (3%–10%), radiolarians (2%–3%), diatoms (3%), sponge spicules (1%), clay (5%–20%), quartz (2%–3%), and vitric fragments (2%–3%). Mottling and burrows occur throughout the 2-m-thick sequence with the exception of one bed of normally size-graded silty glass-rich nannofossil ooze, suggesting a pelagic turbidite, and eight thin (each about 5 mm thick) grayish olive green (5GY 3/2) laminae below the graded bed. Small (between 1 mm and 2 cm in diameter) pumice fragments are scattered within the ooze.

Pumice fills the interval from Sections 125-785A-1H-3 through 125-785A-2H-CC and Cores 125-785A-5X and 125-785A-7X; subsequent cores had no recovery. On the presumption that all coring was done within the same pumice bed, 102.75 m is inferred as a minimum thickness for the pumice layer. In general, the pumice fragments are light gray to gray (7.5YR 7/0 to 7.5YR 6/0), subangular to rounded, 1 mm to 6 cm in diameter (i.e., the approximate diameter of the core barrel), and in a poorly sorted mixture that includes black (10YR 2/1) granules and coarse-sand-size vitric particles; it remains unclear how much of these shape and size characteristics is the result of abrasion and breakage during drilling.

BIOSTRATIGRAPHY

Evidence from calcareous nannofossils, planktonic foraminifers, and diatoms indicates that the sediments retrieved from Site 785 are Pleistocene in age. Nannofossil evidence shows that the late/middle to early Pleistocene boundary lies between Samples 125-785A-1H-2, 0 cm, and 125-785A-2H-CC.

Calcareous Nannofossils

All samples examined from Hole 785A contain abundant well-preserved Quaternary nannofossil assemblages. Samples 125-785A-1H-1, 145–150 cm, and 125-785A-1H-2, 0 cm, contain late/middle Pleistocene assemblages (Zones CN14b/CN15) characterized by *Gephyrocapsa oceanica*, *Gephyrocapsa caribbeanica*,and *Helicosphaera hyalina*. Samples 125-785A-2H-CC, 125-785A-5X-CC, 125-785A-6X-CC, and 125-785A-7X-CC are early Pleistocene in age (Zone CN14a) with assemblages characterized by *Pseudoemiliania lacunosa*, *G. oceanica*, *G. caribbeanica*, *Calcidiscus macintyrei*, and *Helicosphaera sellii*.

Foraminifers

Abundant, well-preserved, Quaternary foraminiferal assemblages were found in all samples examined from Hole 785A. Samples 125-785A-1H-1, 145–150 cm, and 125-785A-1H-2, 0 cm, contain Pleistocene (Zone N22) assemblages characterized by *Globorotalia truncatulinoides*. Samples 125-785-2H-CC, 125-785A-5X-CC, 125-785A-6X-CC, and 125-785A-7X-CC are early Pleistocene (lower Zone N22), based on the co-occurrence of *G. truncatulinoides* and *Globorotalia tosaensis* (Samples 125-785-2H-CC, 125-785A-5X-CC, and 125-785A-7X-CC) and *G. truncatulinoides* and *Neogloboquadrina humerosa* (Sample 125-785A-6X-CC).

Common, well-preserved specimens closely resembling *Pulleniatina praecursor* were found in all of the samples examined. This may be evidence for a reworking event (though preservation and abundance seem too high) or that the range for *P. praecursor* in the northwest Pacific actually extends into the early Pleistocene.

Diatoms

The diatom assemblages at Site 785 are Pleistocene in age, and they vary from few to common in abundance and are poorly to moderately preserved.

Sample 125-785A-2H-CC is the first sample with zonal markers and is assigned to the late/middle Pleistocene *Pseudoeunotia doliolus* Zone by the presence of *P. doliolus* and the absence of *Nitzschia reinholdii*. Both *P. doliolus* and *N. reinholdii* are present in Sample 125-785A-5X-CC; this sample therefore belongs to the early Pleistocene *N. reinholdii* Zone. Samples 125-785A-6X-CC and 125-785A-7X-CC contain no diatoms.

Table 2. Lithologic units recovered at Site 785, Leg 125.

Lithologic unit	Cores	Depth (mbsf)	Dominant lithology	Stratigraphic age
I	785A-1H-1, 0 cm, to 785A-11X-CC	0.0–104.7	Nannofossil ooze, pumice	Pleistocene

Table 3. Total nitrogen, carbon, inorganic carbon, organic carbon and carbonate carbon in sediments at Site 785.

Core, section, interval (cm)	Depth (mbsf)	Total nitrogen (wt%)	Total carbon (wt%)	Inorganic carbon (wt%)	Organic carbon (wt%)	$CaCO_3$ (wt%)
125-785A-						
1H-1, 71–73	0.71			4.51		37.6
1H-2, 12–14	1.62	0.24	4.02	3.59	0.43	29.9
1H-3, 34–36	3.34			0.06		0.5
1H-4, 23–25	4.73			0.06		0.5
1H-5, 98–100	6.98			0.05		0.4
2H-1, 72–74	10.22			0.07		0.6
2H-2, 70–72	11.70	0.11	0.43	0.20	0.23	1.7
2H-3, 70–72	13.20			0.07		0.6
2H-4, 99–101	14.99			0.07		0.6
2H-5, 29–31	15.79			0.01		0.1
2H-6, 34–36	17.34			0.12		1.0

Note: Total sulfur was below the detection limit of 0.06 wt% in all samples analyzed for total carbon, nitrogen, and sulfur.

Table 4. Results of headspace-gas analyses of sediment at Site 785.

Core, section, interval (cm)	Depth (mbsf)	Methane	
		(µL/L)[a]	(µM)[b]
125-785A-			
1H-2, 0–1	1.51	11	0.9

[a] Microliters of methane per liter of wet sediment, assuming a sample volume of 4.2 cm³ of sediment.

[b] Micromoles of methane per liter of interstitial water, assuming a porosity of 50%.

SEDIMENT/FLUID GEOCHEMISTRY

Sediment Geochemistry

Sediments from Site 785 were analyzed aboard ship for inorganic carbon and for total carbon, nitrogen, and sulfur using the techniques described in the "Explanatory Notes" chapter (this volume). The organic carbon content was then calculated by difference. The results are presented in Table 3 and Figure 2. Except for two samples from 0.71 and 1.62 mbsf, the $CaCO_3$ content of the sediments is less than 2%, and generally less than 1%. The two uppermost samples (125-785A-1H-1, 71–73 cm, and 125-785A-1H-2, 12–14 cm) have about 38 and 30 wt% $CaCO_3$, respectively. The only two samples analyzed for total carbon, nitrogen, and sulfur, from 1.62 and 11.70 mbsf, contain about 0.4 and 0.2 wt% organic carbon, respectively, and half these concentrations of nitrogen. Sulfur was not detected and therefore is less than about 0.6 wt%.

Fluid Geochemistry

The single sediment sample (1.51 mbsf) analyzed for light hydrocarbons was found to contain only 11 mL/L (Table 4).

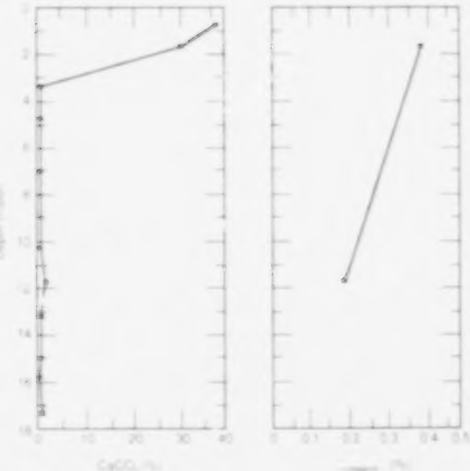

Figure 2. Calcium carbonate and total organic carbon (in wt%) in sediments at Site 785.

Only one sample of interstitial water was obtained at Site 785, from 1.48 mbsf (Table 5). Its composition is very similar to that of seawater, except for a slight increase in alkalinity, ammonia, silica, and potassium and a slight decrease in sulfate and magnesium. These changes are typical of surficial samples from the other sites in this area (Sites 782–784). As at these other sites, the changes indicate that bacteria are oxidizing organic matter and reducing seawater sulfate at Site 785.

Table 5. Composition of interstitial waters from sediment at Site 785.

Sample number	Core, section, interval (cm)	Depth (mbsf)	Vol. (mL)	Squeeze temperature (°C)	pH	Salinity (R.I., ‰)	Salinity (calcium, ‰)	Chlorinity (mmol/kg)	Alkalinity (meq/kg)	Sulfate (mmol/kg)	Na (mmol/kg)
Surface seawater (17 March 1989)					8.25	35.6	34.65	559.2	2.689	27.78	462.0
IW-1	1H-1, 145–150	1.48	51	2	7.93	36.1	34.50	554.7	2.957	25.81	461.8

Table 6. Remanence data for the discrete samples taken from Sections 125-785A-1H-1 and 125A-1H-2.

Core, section, top of interval (cm)	Natural remanent magnetization			Remanent magnetization (10 mT)			Remanent magnetization (20 mT)			
	Declination (degrees)	Inclination (degrees)	Intensity (mA/m)	Declination (degrees)	Inclination (degrees)	Intensity (mA/m)	Declination (degrees)	Inclination (degrees)	Intensity (mA/m)	Polarity
125-785A-										
1H-1, 56	33.3	48.6	50.9	30.8	47.1	41.5	30.4	48.3	30.0	N
1H-1, 133	43.0	48.9	29.0	34.9	48.6	24.3	36.0	47.3	19.0	N
1H-2, 4	15.0	42.9	77.2	20.0	41.0	69.1	15.9	40.0	55.8	N

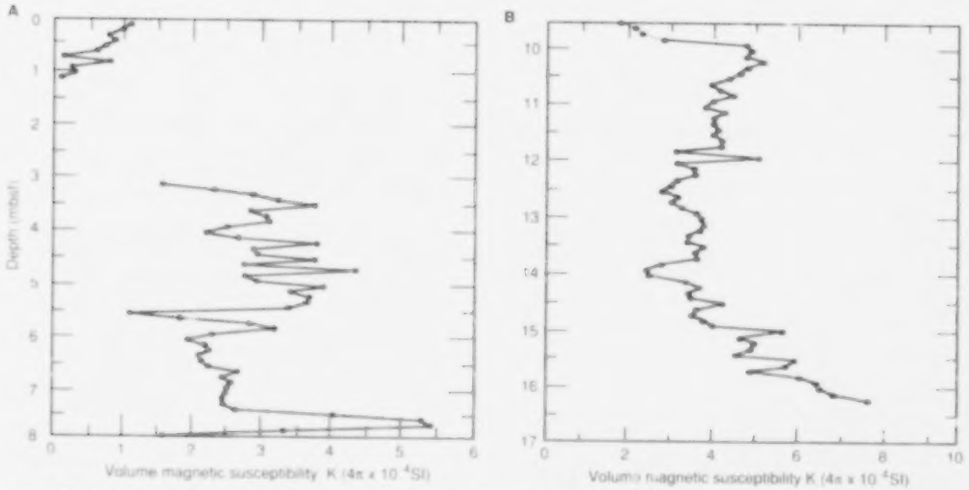

Figure 3. Downhole plots of magnetic susceptibility. A. Core 125-785A-1H. B. Core 125-785A-2H.

PALEOMAGNETISM

Magnetic Remanence

The natural remanent magnetization (NRM) of the archive ore halves of undisturbed nannofossil ooze in Section 125-85A-1H-1 and in the upper 35 cm of Section 125-785A-1H-2 as measured using the cryogenic magnetometer. Intensities ary between 9.5 and 72.4 mA/m. The sections were then emagnetized to 10 mT, which reduced their intensities by 8% 25%. The polarity of the archive halves is normal. The RM intensities of three discrete samples taken from the orking halves of Sections 125-785A-1H-1 and 125-785A-H-2 and measured in the cryogenic magnetometer range from to 77.2 mA/m. These samples were then demagnetized to 5, 15, and 20 mT, which reduced their intensities by 29% to % (Table 6). The discrete samples also carry a normal larity. Nannofossil assemblages from Sections 125-785A-H-1, 145–150 cm, and 125-785A-1H-2, 0 cm, are late/middle eistocene in age (Zones CN14b/CN15), which suggests a correlation of material from this level with the Brunhes Normal Polarity Chron.

The interval from Section 125-785A-1H-3 through Core 125-785A-2H contains pumice and vitric ash. However, the material was too disturbed by drilling to provide reliable polarity information.

Magnetic Susceptibility

Magnetic susceptibilities of whole cores from Site 785 were measured using the multisensor track. Figure 3 plots the variation of susceptibility with depth in the upper two cores from Hole 785A. Values range up to 1×10^{-3} SI units in the nannofossil ooze in the first two sections of Core 125-785A-1H. The magnetic susceptibility of the pumice in Sections 125-785A-1H-3 through 125-785A-1H-6 and in Core 125-785A-2H ranges from 1×10^{-3} to 2×10^{-4} SI units.

PHYSICAL PROPERTIES

The low recovery and the nature of the material in Hole 785A precluded measurement of most physical properties for this hole. We could not measure compressional-wave velocity, electrical resistivity, or shear strength in any of the cores. However, the index properties, bulk and grain density, porosity, water content and void ratio were measured (Table 7).

The bulk density of sediment from Hole 785A averages about 1.6 g/cm^3, and pumice averages about 1.3 g/cm^3 (Table

Table 5 (continued).

K (mmol/kg)	Ca (mmol/kg)	Mg (mmol/kg)	Si (µmol/kg)	NH$_3$ (µmol/kg)
10.11	10.18	52.48	0	0
11.05	10.10	50.62	135	23

Table 7. Index properties for Hole 785A.

Core, section, interval (cm)	Depth (mbsf)	Bulk density (g/cm^3)	Grain density (g/cm^3)	Porosity (%)	Water content (%)	Void ratio
125-785A-						
1H-1, 71-73	0.71	1.59	2.5	62.6	42	0.63
1H-2, 12-14	1.62	1.54	2.55	66.8	46.1	0.67
1H-3, 34-36	3.34	1.38	2.01	65.6	50.6	0.66
1H-4, 23-25	4.73	1.34	2.22	74.6	59.4	0.75
1H-5, 98-100	6.98	1.28	2.11	76.6	63.6	0.77
1H-6, 8-10	7.58	1.31	2.21	76.4	61.8	0.76
2H-1, 72-74	10.22	1.42	2.05	63.4	47.5	0.63
2H-2, 70-72	11.7	1.48	2.01	54.8	39.4	0.55
2H-3, 70-72	13.2	1.49	2.13	58.7	41.9	0.59
2H-4, 99-101	14.99	1.66	2.25	48.2	30.8	0.48
2H-5, 29-31	15.79	1.77	2.38	48.6	29.2	0.49
2H-6, 34-36	17.34	1.61	2.33	54.6	35.7	0.55

7). The grain density of sediment is 2.5 g/cm^3 and that of pumice is 2.0 g/cm^3.

SUMMARY AND CONCLUSIONS

Site 785 (30°49.47'N, 140°55.17'E, in a water depth of 2660.8) is located in the center of the Izu-Bonin forearc basin about 40 nmi east-northeast of the active volcano Torishima. The single hole drilled at this site penetrated 104.7 m with 17.6% recovery before a thick, near-surface layer of pumice and ash prevented further drilling (Fig. 4). The stratigraphic section recovered at Hole 785A was assigned to one lithologic unit. Unit I is of early to late Pleistocene age and consists of 2 m of light brown pumice-bearing nannofossil ooze overlying a pumice bed.

The ooze is made up nannofossils (50%–80%), foraminifers (5%–8%), micrite (3%–10%), radiolarians (2%–3%), diatoms (3%), sponge spicules (1%), clay (5%–20%), quartz (2%–3%), and vitric fragments (2%–3%). Samples have normal magnetic polarity, placing it within the Brunhes Normal Polarity Chron.

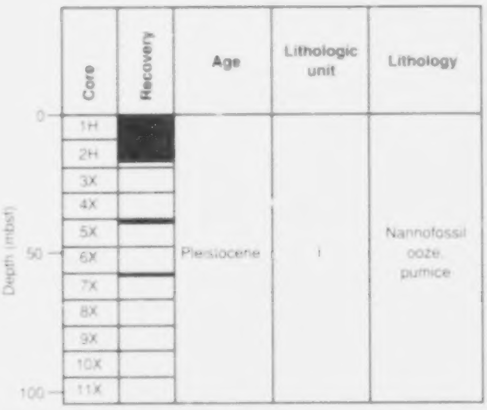

Figure 4. Core recovery and lithologic summary, Hole 785A.

The pumice bed contains light gray to gray pumice fragments, 1 mm to 6 cm in diameter, in a poorly sorted matrix that includes black granules and coarse-sand-sized vitric particles. The pumice and vitric fragments consist of highly vesicular dacitic-rhyolitic glass with phenocrysts of plagioclase feldspar, clinopyroxene, and orthopyroxene. Studies of physical properties show that the average bulk densities are 1.6 g/cm^3 in the sediments and 1.3 g/cm^3 in the pumice; grain densities are 2.5 g/cm^3 in the sediments and 2.0 g/cm^3 in the pumice.

The principal result from this site is the evidence for a major Pleistocene pumice bed in this part of the Izu-Bonin forearc basin.

Ms 125A-113

NOTE: All core description forms ("barrel sheets") and core photographs have been printed on coated paper and bound as Section 4, near the back of the book, beginning on page 383.

Fryer, P., Pearce, J. A., Stokking, L. B., et al., 1990
Proceedings of the Ocean Drilling Program, Initial Reports, Vol. 125

14. SITE 786[1]

Shipboard Scientific Party[2]

HOLE 786A

Date occupied: 2 April 1989

Date departed: 4 April 1989

Time on hole: 2 days, 6 hr, 45 min

Position: 31°52.48'N, 141°13.58'E

Bottom felt (rig floor; m; drill-pipe measurement): 3069.5

Distance between rig floor and sea level (m): 11.40

Water depth (drill-pipe measurement from sea level; m): 3058.1

Total depth (rig floor; m): 3236.00

Penetration (m): 166.50

Number of cores: 19

Total length of cored section (m): 166.50

Total core recovered (m): 84.95

Core recovery (%): 51

Oldest sediment cored:
Depth (mbsf): 115.71
Nature: nannofossil marl
Earliest age: middle Eocene
Hard rock:
Depth (mbsf): 124.90
Nature: metabasalt

HOLE 786B

Date occupied: 4 April 1989

Date departed: 16 April 1989

Time on hole: 12 days, 2 hr, 45 min

Position: 31°52.45'N, 141°13.59'E

Bottom felt (rig floor; m, drill-pipe measurement): 3082.4

Distance between rig floor and sea level (m): 11.40

Water depth (drill-pipe measurement from sea level; m): 3071.0

Total depth (rig floor; m): 3911.00

Penetration (m): 828.60

Number of cores: 72

Total length of cored section (m): 666.10

Total core recovered (m): 190.07

Core recovery (%): 28.5

Oldest sediment cored:
Nature: sedimentary breccias, sandstones, siltstones, and claystones interbedded with igneous rocks
Earliest age: early Eocene
Hard rock:
Depth (mbsf): 162.5
Nature: pillowed and massive flows, breccias, dikes and sills of picrites, high-magnesian basalts, boninites, basalts, andesites, dacites, and rhyolites

Principal results: Site 786 (proposed Site BON-6C) is located in the center of the Izu-Bonin forearc basin about 120 nmi east of the active volcano Myojin Sho.

The stratigraphic section recovered at Site 786 has been assigned to four lithologic units (I through IV). Units I through III are defined only in Hole 786A, in which the sedimentary sequence at the site was recovered. Unit IV is defined in both Holes 786A and 786B. Unit I, from 0 to 83.46 meters below seafloor (mbsf), consists of nannofossil marls and clays and is of early Pleistocene to middle Miocene age. Unit II (83.46–103.25 mbsf) is late Oligocene to middle Eocene age, nannofossil marl and nannofossil-rich clay. Also present is a volcanogenic component containing vitric ash and mineral fragments. Unit III (103.25–124.90 mbsf) is a sequence of volcaniclastic breccia, of middle Eocene age. Unit IV (124.9–166.5 mbsf in Hole 786A and 162.5–826.6 mbsf in Hole 786B) consists of volcaniclastic and sedimentary breccias, vitric siltstones and sandstones, lavas, dikes, and pyroclastic flows.

The rocks in the bottom of Hole 786A and the top of Hole 786B are considered to be the same material. Sedimentation rates were highest in the Pliocene (8.6 m/m.y.) and decreased (to 4.2 m/m.y.) between the latest Miocene and middle Miocene. A hiatus exists between the middle Miocene and the late Oligocene. The igneous basement has mainly massive and brecciated flows, ash flows, and intercalated sediment in an upper part and pillow lavas and dikes or sills below. Rock types include high-magnesian basalts, boninites, basalts, andesites, dacites, and rhyolites. There are several prominent shear zones and hydrothermal breccias within the sequence. Studies of physical properties show that the average bulk densities are 1.65 g/cm^3 in the sediments and 1.8 to 2.1 g/cm^3 in the volcanic sequences; the average grain density of 2.65 g/cm^3 varied little between the sediments and the volcanic rocks. Preliminary interpretation of the paleomagnetic data indicates little translation since the late Miocene.

BACKGROUND AND SCIENTIFIC OBJECTIVES

Site 786 is located on the outer half of the Izu-Bonin forearc, about 120 km east of the active arc volcano of Myojin Sho and about 70 km west of the axis of the Izu-Bonin Trench (Fig. 1). This site was originally designated as a contingency site to augment or fulfill the objectives of Sites 782 and 785. Thus, the objectives of this site are the same as those of Sites 782 and 785, namely to determine the following:

1. The stratigraphy of the forearc and hence the temporal variations in sedimentation, depositional environment, paleoceanography, and intensity and chemistry of the volcanism in the active arc;
2. The uplift/subsidence history of the outer half of the forearc to provide information about forearc flexure and basin development as well as about the extent of any vertical tectonic activity that may have taken place since formation of the forearc terrane;
3. The nature of igneous basement forming the forearc, to answer questions concerning the nature of volcanism in the

---

[1] Fryer, P., Pearce, J. A., Stokking, L. B., et al., 1990. *Proc. ODP, Init. Repts.*, 125: College Station, TX (Ocean Drilling Program).

[2] Shipboard Scientific Party is as given in the list of participants preceding the contents.

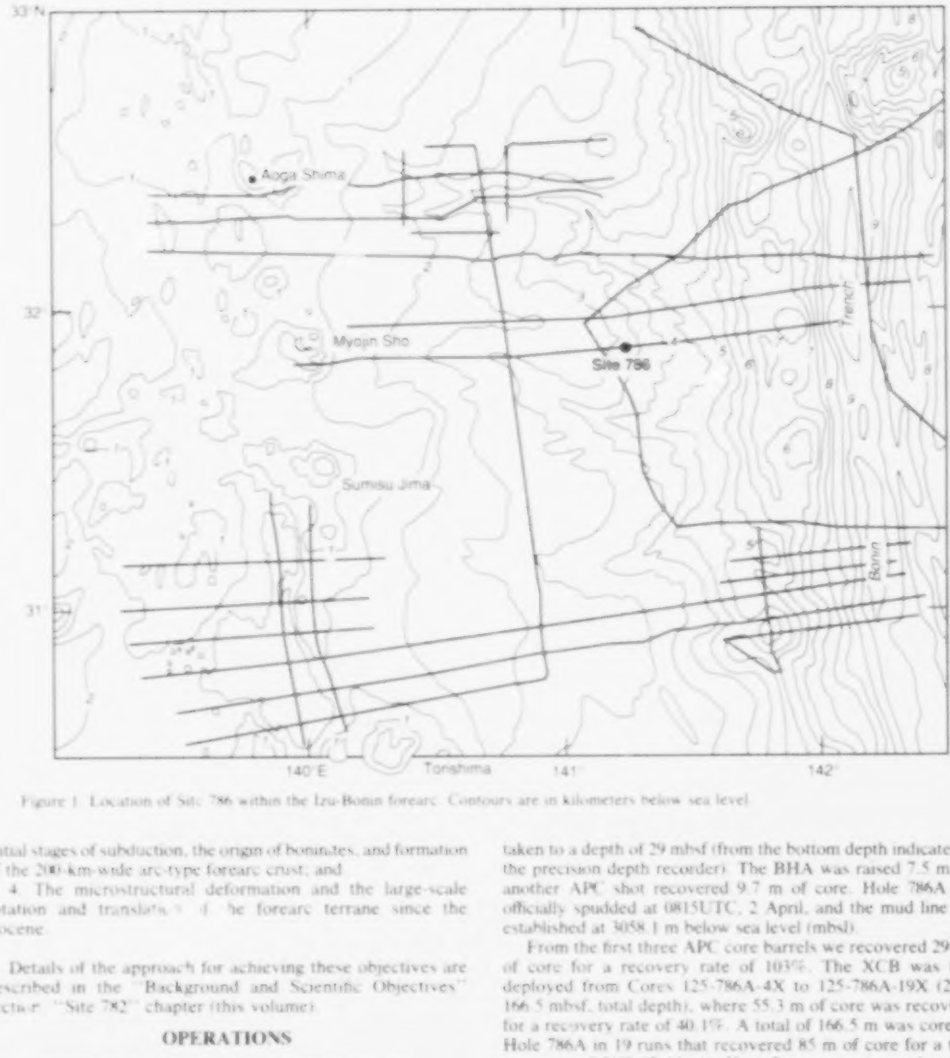

Figure 1. Location of Site 786 within the Izu-Bonin forearc. Contours are in kilometers below sea level.

initial stages of subduction, the origin of boninites, and formation of the 200-km-wide arc-type forearc crust; and

4. The microstructural deformation and the large-scale rotation and translation of the forearc terrane since the Eocene.

Details of the approach for achieving these objectives are described in the "Background and Scientific Objectives" section, "Site 782" chapter (this volume).

OPERATIONS

Transit to Site 786 (proposed Site BON-6C)

Time was available to drill Site 786 (proposed Site BON-6C) because the pumice layer at Site 785 could not be penetrated. The 64-nmi transit to Site 786 was made in 10.5 hr and included a 4.75-hr site survey. A beacon was deployed at 2015UTC, 1 April 1989, to establish Site 786.

Hole 786A

A standard advanced hydraulic piston corer/extended core barrel (APC/XCB) bottom-hole assembly (BHA) with a lockable flapper valve, nonmagnetic drill collar, and soft-formation bit was assembled and deployed. Three APC water cores were taken to a depth of 29 mbsf (from the bottom depth indicated by the precision depth recorder). The BHA was raised 7.5 m and another APC shot recovered 9.7 m of core. Hole 786A was officially spudded at 0815UTC, 2 April, and the mud line was established at 3058.1 m below sea level (mbsl).

From the first three APC core barrels we recovered 29.6 m of core for a recovery rate of 103%. The XCB was then deployed from Cores 125-786A-4X to 125-786A-19X (28.7–166.5 mbsf, total depth), where 55.3 m of core was recovered for a recovery rate of 40.1%. A total of 166.5 m was cored in Hole 786A in 19 runs that recovered 85 m of core for a total recovery of 51% (Table 1). Heat flow was measured at 28.7 and 76.8 mbsf. Upon reaching basement, a round trip was made so that Hole 786B could be drilled into basement using the rotary core barrel (RCB). Hole 786A officially ended at 0300UTC, 4 April, when the bit was back on deck.

Hole 786B

A standard RCB BHA was prepared with a mechanical bit release and a medium-formation bit. The vessel was offset 30 m to the south as the BHA was tripped in. Hole 786B was officially spudded when the seafloor was tagged at a depth of 3071.0 mbsl at 0845UTC, 4 April. The hole was washed to a depth of 162.6 mbsf before coring began.

Table 1. Coring summary for Site 786.

Core no.	Date (April 1989)	Time (UTC)	Depth (mbsf)	Length cored (m)	Length recovered (m)	Recovery (%)
125-786-A-						
1H	2	0830	0.0–9.7	9.7	9.73	100.0
2H	2	0930	9.7–19.2	9.5	9.94	104.0
3H	2	1030	19.2–28.7	9.5	9.98	105.0
4X	2	1150	28.7–38.2	9.5	2.18	22.9
5X	2	1445	38.2–47.6	9.4	5.47	58.2
6X	2	1535	47.6–57.1	9.5	6.70	70.5
7X	2	1700	57.1–67.1	10.0	7.51	75.1
8X	2	1755	67.1–76.8	9.7	1.16	11.9
9X	2	2215	76.8–86.4	9.6	8.61	89.7
10X	2	2300	86.4–96.0	9.6	8.45	88.0
11X	3	0005	96.0–105.7	9.7	8.96	92.4
12X	3	0145	105.7–115.3	9.6	2.27	23.6
13X	3	0430	115.3–124.9	9.6	0.41	4.3
14X	3	0630	124.9–134.6	9.7	0.41	4.2
15X	3	0910	134.6–144.3	9.7	0.25	2.6
16X	3	1140	144.3–154.0	9.7	0.63	6.5
17X	3	1450	154.0–155.0	1.0	0.47	47.0
18X	3	1715	155.0–164.0	9.0	1.36	15.1
19X	3	2035	164.0–166.5	2.5	0.48	19.2
Coring totals				166.5	84.95	51.0
125-786-B-						
1R	4	0030	162.5–169.5	7.0	0.70	10.0
2R	4	0300	169.5–179.2	9.7	0.62	6.4
3R	4	0500	179.2–189.0	9.8	0.87	8.9
4R	4	0600	189.0–198.6	9.6	0.82	8.5
5R	5	0753	198.6–208.2	9.6	1.83	19.0
6R	5	0925	208.2–217.8	9.6	2.70	28.1
7R	5	1030	217.8–227.6	9.8	0.20	2.0
8R	5	1150	227.6–237.1	9.5	0.74	7.8
9R	5	1345	237.1–246.6	9.5	2.16	22.7
10R	5	1530	246.6–256.3	9.7	1.70	17.5
11R	5	1720	256.3–266.0	9.7	1.53	15.8
12R	5	1910	266.0–275.7	9.7	2.21	22.8
13R	5	2130	275.7–285.4	9.7	2.49	25.7
14R	5	2315	285.4–295.0	9.6	0.88	9.2
15R	6	0100	295.0–304.6	9.6	2.55	26.5
16R	6	0300	304.6–314.3	9.7	2.06	21.2
17R	6	0430	314.3–323.9	9.6	0.90	9.4
18R	6	0600	323.9–333.6	9.7	0.86	8.9
19R	6	0800	333.6–343.3	9.7	0.76	7.8
20R	6	0910	343.3–353.0	9.7	0.96	9.9
21R	6	1045	353.0–362.6	9.6	2.10	21.9
22R	6	1210	362.6–372.3	9.7	3.88	40.0
23R	6	1325	372.3–381.9	9.6	0.12	1.3
24R	6	1455	381.9–391.5	9.6	1.81	18.8
25R	6	1700	391.5–401.2	9.7	0.77	7.9
26R	6	1840	401.2–410.8	9.6	1.03	10.7
27R	6	2018	410.8–420.4	9.6	1.85	19.3
28R	6	2215	420.4–430.1	9.7	1.17	12.0
29R	7	0100	430.1–439.7	9.6	0.64	6.7
30R	7	0415	439.7–449.4	9.7	2.95	30.4
31R	7	0730	449.4–459.0	9.6	2.32	24.1
32R	7	0905	459.0–468.7	9.7	1.94	20.0
33R	7	1040	468.7–478.3	9.6	0.95	9.9
34R	7	1515	478.3–488.0	9.7	4.63	47.7
35R	7	1720	488.0–497.7	9.7	4.04	41.6
36R	7	1940	497.7–507.4	9.7	0.85	8.8
37R	8	0000	507.4–517.1	9.7	2.68	27.6
38R	8	0245	517.1–526.8	9.7	1.19	12.2
39R	8	0500	526.8–536.3	9.5	3.00	31.6
40R	8	0800	536.3–545.9	9.6	3.63	37.8
41R	8	0940	545.9–555.6	9.7	4.35	44.8
42R	8	1345	555.6–565.0	9.4	4.40	46.8
43R	8	1650	565.0–574.6	9.6	2.15	22.4
44R	8	2015	574.6–584.3	9.7	1.35	13.9
45R	8	2215	584.3–593.9	9.6	1.25	13.0
46R	9	0100	593.9–603.5	9.6	3.00	31.2
47R	9	0300	603.5–613.2	9.7	1.27	13.1
48R	9	0545	613.2–622.9	9.7	2.57	26.5
49R	9	0745	622.9–632.5	9.6	4.67	48.6
50R	9	0920	632.5–642.2	9.7	1.80	18.5
51R	9	1100	642.2–651.9	9.7	1.38	14.2
52R	9	1300	651.9–661.6	9.7	2.83	29.2
53R	9	1500	661.6–671.2	9.6	1.68	17.5
54R	9	1705	671.2–680.8	9.6	5.54	57.7
55R	9	2030	680.8–690.1	9.3	4.03	43.3
56R	10	0130	690.1–699.8	9.7	7.64	78.7

Table 1 (continued).

Core no.	Date (April 1989)	Time (UTC)	Depth (mbsf)	Length cored (m)	Length recovered (m)	Recovery (%)
125-786-A-						
57R	10	0700	699.8–709.4	9.6	9.53	99.3
58R	10	1035	709.4–714.4	5.0	5.49	110.0
59R	10	1350	714.4–719.0	4.6	4.35	94.5
60R	10	2000	719.0–728.7	9.7	8.32	85.8
61R	10	0130	728.7–738.4	9.7	7.80	80.4
62R	10	0600	738.4–748.0	9.6	3.51	36.5
63R	10	1025	748.0–757.7	9.7	1.63	16.8
64R	10	1310	757.7–767.4	9.7	3.52	36.3
65R	10	1530	767.4–777.1	9.7	2.79	28.7
66R	10	1800	777.1–786.7	9.6	3.26	33.9
67R	11	0030	786.7–796.3	9.6	0.76	7.9
68R	11	0215	796.3–797.3	1.0	0.60	60.0
69R	11	0730	797.3–806.9	9.6	8.13	84.7
70R	11	1145	806.9–815.6	8.7	4.40	50.6
71R	11	1750	815.6–823.6	8.0	4.56	57.0
72R	11	2200	823.6–828.6	5.0	2.42	48.4
Coring totals				66.1	190.07	28.5

The RCB was deployed 72 times, coring 666.1 m and recovering 190.1 m of core for a recovery rate of 28.5%. Total depth was 828.6 mbsf, when coring was halted so that the remainder of the time allotted to Leg 125 could be used for logging.

The BHA was pulled to 3172.6 mbsl, and the logging line was prepared. Six suites of logging tools were used in Hole 786B. The first suite of logging tools, consisting of the dual induction tool (DIT), the digital sonic tool (SDT), and the natural gamma-ray spectrometry tool (NGT), was run from 3520.0 mbsl (the depth of a bridge that the tools could not penetrate) to the top of the hole. The second suite, consisting of the lithodensity tool (LDT), the compensated neutron tool (CNT), and the NGT, was run to 3458.1 mbsl. Another bridge encountered at that depth could not be penetrated by these tools, so the hole was logged from there to the top.

The Schlumberger equipment was rigged down, and the pipe was run in the hole to clear the bridges. The hole was clear from 3516.6 to 3808.6 mbsl, and the BHA was raised to 3519.6 mbsl so that the lower section of the hole could be logged.

The third logging suite, consisting of the DIT, LDT, CNT, and SDT, was deployed to 3892.0 mbsl, and the hole was logged from that point upward to 3535.2 mbsl. The fourth suite, consisting of the induced gamma-ray spectrometry tool (GST), the aluminum clay tool (ACT), and the NGT, was deployed to 3892.0 mbsl, and the hole then was logged to the mud line. The borehole televiewer (BHTV) was deployed for the fifth logging run, but failed downhole. During the sixth logging run, the spare BHTV was deployed, and we logged 80 m of the hole before logging time expired.

The BHTV was pulled out of the hole and the logging equipment was rigged down. The BHA was pulled to the drill floor at 0800UTC, 16 April, officially ending Hole 786B. The BHA was then inspected and secured in the derrick. With the BHA back on deck, the vessel was under way at 1130UTC, 16 April, and the occupation of Site 786 officially ended.

Site 786 to Tokyo

A survey was performed over Site 786 before steaming north to Tokyo. At 1430UTC, 16 April, the seismic gear was retrieved and the transit began. The 252-nmi transit to Tokyo was made in 35.5 hr. The anchor was dropped at 2300UTC, 17 April 1989, officially ending Leg 125.

LITHOSTRATIGRAPHY

A downhole stratigraphy of nannofossil marls, sedimentary breccias interlayered with nannofossil marls, and igneous rocks defines four lithologic units at Holes 786A and 786B (Table 2). Lithologic Units I through III are lower Pleistocene to middle Eocene sediments. Lithologic Unit IV is early Eocene age volcanic basement present in both holes, with drilling-produced chips and pebbles at Hole 786A and the entire stratigraphic section recovered at Hole 786B. Hole 786B is 30 m south of Hole 786A.

Unit I

Sections 125-786A-1H-1, 0 cm, to 125-786A-9X-5, 66 cm; depth, 0.0–83.46 mbsf
Age: early Pleistocene to middle Miocene

Lithologic Unit I is a succession of lower Pleistocene through middle Miocene nannofossil marls and clays with a persistent volcanogenic component. Upper and middle Pleistocene strata are missing, on the basis of an early Pleistocene assemblage of nannofossils in the uppermost sample (125-786A-1H-1, 2 cm). Sediment color varies from very pale brown (10YR 7/3), light brownish gray (2.5Y 6/2), gray (10YR 6/1), and dark grayish brown (2.5Y 4/2) to dark gray (5Y 4/1 and 10YR 4/1). Nannofossils are the dominant biogenic component (present in amounts up to 56%; in one sample up to 70%) forming nannofossil marl (in one sample forming a thin—<1-cm-thick—calcareous ooze), glass-rich nannofossil marl, and nannofossil-rich clay. Foraminifers (trace–30%) and micrite (trace–40%) are also present. Radiolarians (trace–4%), diatoms (trace–3%), and sponge spicules (trace–5%) form the biosiliceous component. Terrigenous detritus is predominantly clay (5%–72%) with some quartz (trace–1%).

Volcaniclastics are ubiquitous as dispersed vitric particles or pumice fragments and in ash layers (Table 3). Locally, concentrations in pelagic sediments are sufficient to define glass-rich nannofossil marls and glass-rich clays, such as in Cores 125-786A-4X and 125-786A-5X. Volcanogenic material is primarily vitric debris (trace–57%) with lesser amounts of pyroxene and feldspar (trace–5%). Pumice is disseminated throughout lithologic Unit I as subrounded to rounded, granule-sized, light brownish gray (2.5Y 6/2) particles. Scattered larger pumice clasts, up to 3 cm in diameter, occurring downhole from about Core 125-786A-3H are brown (7.5YR 5/4), dark gray (5YR 5/1), and white (10YR 8/1). Volcaniclastic layers of predominantly vitric detritus (60%–100%) are common throughout Unit I (see Table 3) and probably represent both pyroclastic air-fall and epiclastic deposits.

Sedimentary structures are rare. A few volcaniclastic layers have normal size grading, and others have poorly defined laminae. A 55-cm-thick layer of feldspar-rich, foraminiferal vitric sand in Section 125-786A-1H-5, 60–115 cm, contains vague laminae. Nonclastic sediment sequences are extensively burrowed; thus, possible sedimentary structures are obliterated. A few synsedimentary normal faults are present, with one prominent example truncating a burrow filled with black (N 4/0) clay (Section 125-786A-2H-7, 28 cm).

Carbonate-cemented pelagic sediment occurs at two levels in Unit I (Sections 125-786A-1H-6, 140 cm, and 125-786A-6X-4, 0–10 cm) as indurated and blocky pieces of black (N 4/0) lithic fragments. A pebble of chlorite-rich, vitric, silty claystone is present in the top 2 cm of Core 125-786A-6X. The lithic fragment is gray (5Y 5/1), with a discoid and rounded shape (3.5 × 3 × 2 cm in size), contains clasts of granule-sized chloritized pumice as well as sand-sized altered igneous rocks, and is cut by numerous chlorite veins. Microfossil assemblages suggest an age of middle Miocene, slightly older than or equivalent to the age of the host sediment (see "Biostratigraphy" section, this chapter).

The basal sediment in lithologic Unit I is a black (10YR 2/1) vitric ash composed of sideromelane and manganese oxide (both in about equal proportions) with trace amounts of calcareous nannofossils. Ferromanganese oxides are present both as disseminated silt-sized particles and as coatings with laminated-botryoidal textures on the edges of blocky sediment clasts. This 10-cm-thick deposit in Section 125-786A-9X, 56–66 cm, represents a hiatus separating middle Miocene and upper Oligocene biozones (see "Biostratigraphy" and "Sediment-Accumulation Rates" sections, this chapter).

Unit II

Sections 125-786A-9X-5, 66 cm, to 125-786A-11X-5, 125 cm; depth, 83.46–103.25 mbsf
Age: late Oligocene to middle Eocene

A distinctive color change to reddish brown (10YR 5/4) nannofossil marls marks the change to lithologic Unit II. Gray

Table 2. Lithologic units recovered at Site 786.

Lithologic unit	Cores	Depth (mbsf)	Dominant lithology	Stratigraphic age
I	786A-1H-1, 0 cm, to 786A-9X-5, 66 cm	0.0–83.46	Nannofossil marl, nannofossil-rich clay, glass-rich clay	lower Pleistocene to middle Miocene
II	786A-9X-5, 66 cm, to 786A-11X-5, 125 cm	83.46–103.25	Nannofossil marl, nannofossil-rich clay	upper Oligocene to upper Eocene
III	786A-11X-5, 125 cm, to 786A-13X-CC, 44 cm	103.25–124.90	Volcaniclastic breccia	middle Eocene
IV	786A-14X-1, 0 cm, to 786A-19X-1, 15 cm	124.90–166.50	Igneous rocks	middle Eocene(?)
	786B-1R-1, 0 cm, to 786B-72R-2, 138 cm	162.50–826.60	Volcaniclastic and sedimentary breccias, lava and pyroclastic flows, vitric siltstone and sandstone	middle Eocene

Table 3. Volcaniclastic layers in lithologic Unit I, Hole 786A.

Core, section, interval (cm)	Depth of top of section (mbsf)	True depth (mbsf)	Volcaniclastic layer
125-786A-			
1H-1, 62–77	0	0.62–0.77	1
1H-2, 3–5	1.5	1.53–1.55	2
1H-2, 5–18	1.5	1.55–1.68	3
1H-4, 12–16	4.5	4.62–4.66	4
1H-4, 23.5–25	4.5	4.735–4.75	5
1H-5, 62–111	6	6.62–7.11	6
1H-6, 77–78	7.5	8.27–8.28	7
1H-7, 5–8	9	9.05–9.08	8
2H-1, 10–14	9.7	9.80–9.94	9
2H-1, 29–30	9.7	9.99–10.0	10
2H-1, 80	9.7	10.5	11
2H-2, 99–113	11.2	12.19–12.33	12
2H-2, 143–146	11.2	12.63–12.66	13
2H-3, 145–146	12.7	14.10–14.14	14
2H-4, 36–40	14.2	14.56–14.60	15
2H-4, 84–85	14.2	15.04–15.05	16
2H-4, 93–96	14.2	15.13–15.16	17
2H-4, 141–145	14.2	15.60–15.65	18
2H-5, 28–30	15.7	15.98–16.00	19
2H-5, 122–125	15.7	16.92–16.95	20
2H-6, 14–17	17.2	17.34–17.37	21
3H-1, 41–44	19.2	19.61–19.64	22
3H-1, 54–58	19.2	19.74–19.78	23
3H-1, 87–90	19.2	20.07–20.10	24
3H-2, 100–103	20.7	21.70–21.73	25
3H-3, 116–120	22.2	23.36–23.40	26
3H-3, 116–120	22.2	23.36–23.40	26
3H-5, 79–80.5	25.2	25.99–26.005	27
3H-6, 102–112	26.7	27.72–27.82	28
3H-CC, 10–17	28.89	28.99–29.06	29
3H-CC, 21	28.89	29.1	30
4X-1, 60–61	28.7	29.30–29.31	31
5X-1, 39–41	38.2	38.59–38.61	32
5X-1, 74–76	38.2	38.94–38.96	33
5X-1, 74–76	38.2	38.94–38.96	33
5X-1, 78–79	38.2	38.98–38.99	34
5X-1, 106–107	38.2	39.26–39.27	35
5X-2, 14–15	39.7	39.84–39.85	36
6X-1, 21–25	47.6	47.81–47.85	37
6X-1, 93–94	47.6	48.53–48.54	38
6X-2, 37–46	49.1	49.91–49.92	39
6X-2, 102–103	49.1	50.12–50.13	40
6X-3, 126.5–128	50.6	51.865–51.88	41
6X-5, 8–9	53.6	53.68–53.69	42
6X-5, 22–27	53.6	53.82–53.87	43
6X-5, 36–40	53.6	53.98–54.0	44
7X-1, 138–140	57.1	58.48–58.50	45
7X-2, 125–127	58.6	59.85–59.87	46
7X-3, 3–4	60.1	60.13–60.14	47
7X-3, 15.5–16	60.1	60.255–60.26	48
7X-5, 9–10	63.1	63.19–63.20	49
7X-5, 14–15	63.1	63.24–63.25	50
7X-5, 18–24	63.1	63.28–63.34	51
7X-5, 64–66	63.1	63.74–63.76	52
7X-6, 27–28	64.29	64.56–64.57	53
9X-1, 43–44	79.8	80.23–80.24	54
9X-1, 85–89	79.8	80.65–80.69	55
9X-1, 128–131	79.8	81.08–81.11	56
9X-4, 23–26	81.3	81.53–81.56	57
9X-5, 56–66	82.8	83.36–83.46	58

and greenish gray colors similar to those of lithologic Unit I (5GY 5/1 and 5Y 5/1) reappear downcore (at Section 125-786A-9X-CC, 14.5 cm) in nannofossil marls and sandy nannofossil oozes. These are followed again (Section 125-786A-10X-4, 70 cm) by nannofossil marls and nannofossil-rich clays, which have the same reddish brown color noted at the top of Unit II. This succession of gray and red nannofossil marls and oozes, which defines lithologic Unit II, spans the upper Oligocene to middle Eocene section. Each color change is in close proximity to an unconformity of minor duration (see "Biostratigraphy" and "Sediment-Accumulation Rates" sections).

Sedimentary components are similar to those noted for Unit I. Biogenic components are dominantly nannofossils (2%–60%), with lesser amounts of foraminifers (2%–10%), micrite (1%–35%), and radiolarians (trace–2%). Clays are present in amounts varying between 10% and 50%, opaque minerals between 3% and 15%, and chlorite and serpentine in trace amounts. Volcanogenic components are usually vitric particles (35%–98%) with feldspar (1%–7%) and pyroxene (1%–10%), disseminated in the sediment as detritus or pumice. Volcaniclastic layers are not present. Pumice colors provide a variegated contrast to the pelagic sediment and range from light gray (10YR 4/1), light brownish gray (2.5Y 6/2), white (10YR 8/1), brown (7.5YR 5/4), dark gray (5YR 5/1), and orange to dark yellowish brown (10YR 5/4) and black (N 4/0).

Extensive mottling reflects bioturbation; no sedimentary structures are present. A fault with apparent normal movement (see "Structural Studies" section, this chapter) in Section 125-786A-11X-4, 100 cm, marks an abrupt sediment color change from light reddish brown and reddish brown (5YR 6/3 and 5YR 5/3) to light yellowish brown (2.5YR 6/4). This continues as the dominant background color for about 0.5 m downhole, and then changes between Sections 125-786A-11X-4 and 125-786A-11X-5 to white (2.5Y 8/2) and light gray (2.5Y 7/2). General sediment types (nannofossil oozes and nannofossil marls) and sedimentary components do not change across the fault. Dispersed throughout the sediment below the fault are rounded clasts, 1 to 3 cm in diameter, of glass-rich silt that have a distinctive bright, light greenish gray color (10Y 6/6).

Unit III

Sections 125-786A-11X-5, 125 cm, to 125-786A-13X-CC, 44 cm; depth, 103.25–124.90 mbsf.
Age: middle Eocene.

Increased clast content and an abrupt color change of the matrix sediment to dark brown (2.5YR 4/2) at Section 125-786A-11X-5, 125 cm, define the volcaniclastic breccia that is the dominant lithology of Unit III in Hole 786A; breccia with this color and clast content was not recovered at Hole 786B. Angular to rounded clasts of vitric ash and dacite are green (5GY 6/4), greenish gray (10Y 6/6), dark greenish gray (5BG 4/1), white (N 8/0), dark yellowish brown (10YR 6/8), grayish brown (10YR 5/2), and black (10YR 2/1). The black color is caused by manganese oxides disseminated within the ash. Clast diameters average about 1 cm, with rare larger clasts reaching 4 cm, such as in a moderately well-sorted breccia in Sections 125-786A-11X-6 and 125-786A-11X-CC. Dacite fragments up to 6 cm in diameter form a poorly sorted breccia in Sections 125-786A-12X-1 and 125-786A-12X-2. Clasts float in a matrix of white (2.5Y 8/2) and light gray (2.5Y 7/2) nannofossil marl.

Sedimentary components in the matrix are predominantly nannofossils (up to 65%, locally forming nannofossil oozes); additional components include foraminifers (1%–10%), micrite (1%–35%), radiolarians (trace–2%), clay (10%–50%), and opaque mineral grains (3%–15%).

No sedimentary structures occur in this unit for interpreting depositional and post-depositional processes.

Unit IV

Sections 125-786A-14X-1, 0 cm, to 125-786A-19X-1, 15 cm; depth, 124.90–166.50 mbsf. Age: middle Eocene(?).
Sections 125-786B-1R-1, 0 cm, to 125-786B-72R-2, 138 cm; depth, 162.50–826.60 mbsf.
Age: middle Eocene.

Hole 786A

Lithologic Unit IV at Hole 786A is a mixture of drilling chips and drilling-produced pebbles of igneous rocks and vein material from these rocks, as well as an assortment of volcaniclastic and sedimentary rocks typical of the clast lithologies in lithologic Unit III. The determination of biostratigraphic age was not attempted because of the uncertain stratigraphic position of the chips and pebbles; however, a middle Eocene age may be assumed for lithologic Unit IV based on the oldest age obtained from similar lithologies in the overlying lithologic unit.

Hole 786B

Sedimentary breccias, sandstones, siltstones, and claystones interbedded within a 666.1-m-thick succession of lava flows, pyroclastic flows, pillow flows, and dikes constitute lithologic Unit IV at Hole 786B. Deposition during the middle to late Eocene is inferred for this unit based upon a limited nannofossil assemblage. Sedimentary rocks form nearly one-half of the stratigraphic sequence if all the volcaniclastic rocks are considered sedimentary. If these rocks are treated as igneous because they may be autobrecciated interflow deposits, then sedimentary rocks represent less than 10% of the stratigraphic succession. In order of abundance, rock types are volcaniclastic breccias, volcaniclastic conglomerates, vitric siltstones, vitric clayey siltstones, and vitric sandstones. The addition of various mineralogic components forms jasper and chlorite siltstones, chlorite vitric sands, chlorite-orthopyroxene-glass-rich sandstones, feldspar-rich vitric silty sandstones and feldspar, and glass-rich silty clays.

The dominant detrital component is volcanogenic, including glass (20%–100%), pyroxene (1%–30%), feldspar (1%–15%), igneous rock fragments (trace–10%), and amphibole (trace–5%). Sideromelane and palagonite are common glass types in interpillow deposits. Pyroxenes (predominantly orthopyroxene) form thick sequences of sand as the matrix within breccias and conglomerates (e.g., in Cores 125-786B-7R to 125-786B-12R). Another detrital component is clay (10%–53%). Clasts in volcaniclastic breccias and conglomerates vary in size from 2 mm (granule size) up to 6 cm (the diameter of the core barrel and thus the limit of megascopic resolution of clasts from flow sedimentary layers), have shapes that are angular to subrounded, and consist of fragments of vitric and lithic volcanic rocks such as pillow rinds.

Minerals of presumed diagenetic origin, perhaps in connection with hydrothermal fluid circulation, include opaque minerals (1%–50%), chlorite (4%–97%), chert and jasper (2%–44%), zeolites (trace–2%), and sepiolite (trace–100%). Pyrite, chlorite, chert, and jasper are found in the lower part of the section (Cores 125-786B-27R to 125-786B-72R for chlorite and 125-786B-61R and 125-786B-62R for chert and jasper). Chlorite sands with vitric and pyroxene grains exhibit cross-bedding and laminae structures (Core 125-786B-27R); it is not clear whether the chlorite here represents a detrital fraction or the post-depositional alteration of detrital vitric grains. Zeolites are found only in the upper part of the middle of the stratigraphic section (Core 125-786B-22R). Section 125-786B-22R-1, 28–42 cm, also includes a spectacular 14-cm-thick sepiolite layer of moderate pink (5R 6/4) to grayish pink (5R 8/2) that may have a hydrothermal origin.

Biogenic components such as nannofossils (trace–5%), radiolarians (trace), and a spicule (trace) are rare. Micrite is present in trace amounts to 4% and may be of either biogenic or authigenic origin.

A marine sedimentary environment is indicated by these biogenic components as well as by small structures interpreted as burrows in Section 125-786B-34R-1. The provenance of clastic particles is assumed to be nearby igneous rocks on the basis of (1) the large size (sand or ash size, gravel or block size) and shapes (usually angular to subangular) of grains and clasts, (2) the high proportion of clasts compared to fine-grained detritus creating poorly sorted deposits, (3) the similarity in lithology between igneous flows/dikes and the volcanogenic detritus, and (4) a predominance of easily abraded, vitric grains. The matrix-supported clast textures of the volcaniclastic breccias and conglomerates suggest either mass-flow or particle-by-particle deposition. Existing criteria are inadequate to differentiate between the two processes in the absence of obvious contacts between these coarse-grained deposits. Sedimentary structures indicative of depositional processes for sandstones and siltstones are scarce, but normal size grading, syndepositional slump structures, cross-bedding, and laminae demonstrate mass-flow and redepositional mechanisms.

Correlation Between Holes 786A and 786B

Lithologic Unit IV is thought to be correlative between Holes 786A and 786B in stratigraphic position and age because (1) of the proximity of the two holes, (2) cores containing this unit were cut at about the same sub-bottom depth, (3) the recovered igneous rocks appear similar in hand specimen and smear slide, and (4) biostratigraphic criteria indicate that both units may be middle Eocene in age. Hole 786B is 30 m south of Hole 786A. The depth of the bottom of Core 125-786A-19X at the base of the hole is 166.50 mbsf; the depth of the top of Core 125-786B-1R is 162.50 mbsf. Rock types from lithologic Unit IV at both sites are dark gray and black, vesicular, olivine- and orthopyroxene-bearing andesites with vesicles commonly filled by a bluish zeolite.

BIOSTRATIGRAPHY

Evidence from calcareous nannofossils, foraminifers, and diatoms assigns an early Pleistocene age to the uppermost sediments in Hole 786A. Nannofossils date the lowermost sediments to the middle Eocene. The sediments interbedded with the lava flows in Hole 786B are assigned an Eocene age based on their nannofossil assemblages. The biostratigraphy from this site is summarized in Figure 2, with the age boundaries based on nannofossil data.

Calcareous Nannofossils

Hole 786A

Pleistocene through middle Eocene nannofossil assemblages from Hole 786A are abundant; their preservation is good to moderate.

The uppermost Sample 125-786A-1H-1, 2 cm, is early Pleistocene (Subzone CN14a) in age on the basis of the co-occurrence of *Pseudoemiliania lacunosa, Calcidiscus macintyrei, Gephyrocapsa oceanica, Gephyrocapsa caribbeanica*, and *Helicosphaera sellii*; thus, upper and middle Pleistocene sediments are missing.

Sample 125-786A-1H-1, 150 cm, is late Pliocene (Subzone CN13b) based on the occurrence of *G. caribbeanica* and the absence of *G. oceanica*. Sample 125-786A-1H-2, 96 cm, has been assigned to Subzone CN12b by the presence of *Discoaster brouweri* and *Discoaster surculus* and the absence of *Discoaster tamalis*. The occurrences of *D. tamalis* together with *Ceratolithus separatus* in Samples 125-786A-1H-4, 92 cm, to 125-786A-2H-CC allow us to assign these sediments to Subzone CN12a (late Pliocene).

Sample 125-786A-3H-CC contains *Reticulofenestra pseudoumbilica, Ceratolithus acutus*, and *Sphenolithus* spp. and is therefore early Pliocene in age (Subzone CN10b).

Samples 125-786A-4X-CC and 125-786A-5X-CC are dated as late Miocene (Zones CN9b and CN9a, respectively) by the occurrence of *Discoaster berggrenii* and *Discoaster quinqueramus* in both and also in the former sample of *Amaurolithus*

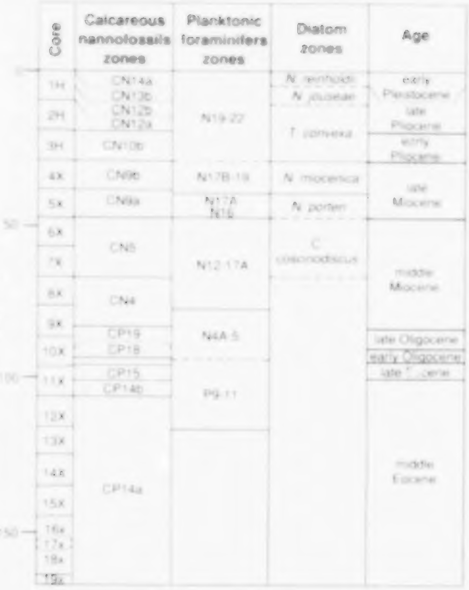

Figure 2. Summary of biostratigraphic data from Hole 786A.

delicatus, *Amaurolithus tricorniculatus*, and *Discoaster blackstockae*. *Discoaster kugleri* and *Discoaster exilis* are present in Samples 125-786A-6X-CC and 125-786A-7X-CC, which are, therefore, middle Miocene in age (Zone CN5). Samples 125-786A-8X-CC to 125-786A-9X-5, 40 cm, are also dated as middle Miocene, but the occurrence of *Sphenolithus heteromorphus*, *D. exilis*, and *C. macintyrei* places these within Zone CN4. The occurrence of specimens of *R. pseudoumbilica* more than 7 mm in size indicates that this is the higher part of Zone CN4. Lower Miocene sediments are missing (Zones CN1 through CN3); a hiatus with a duration of approximately 7.2 m.y. thus is present between the middle Miocene and late Oligocene. A similar hiatus exists between the middle Miocene and the late Oligocene in Hole 782A. The hiatus at Site 786 coincides with a volcanic ash interval at Section 125-786A-9X-5, 56–66 cm.

Abundant, moderately preserved to well-preserved nannofossil assemblages are present from Samples 125-786A-9X-5, 80 cm, to 125-786A-10X-6, 51 cm.

Late Oligocene nannofossil assemblages are found in Samples 125-786A-9X-5, 80 cm, to 125-786A-10X-3, 142 cm; they are characterized by *Dictyococcites bisectus*, *Cyclicargolithus abisectus*, *Helicosphaera recta*, *Sphenolithus ciperoensis*, and *Sphenolithus distentus*, which assigns the assemblages to Zone CP19. Samples 125-786A-10X-4, 42 cm, to 125-786A-10X-5, 95 cm, are dated as early Oligocene (Zone CP18) by the appearance of *Sphenolithus predistentus*. Sample 125-786A-10X-6, 37 cm, is dated by the occurrence of *Ericsonia formosa*, *Reticulofenstra umbilica*, and common *Ericsonia subdisticha* as early Oligocene (Subzone CP16a). A hiatus may occur between Subzones CP18 and CP16a.

Sample 125-786A-10X-CC is near the Oligocene/Eocene boundary. The assemblage contains species usually found in the late Eocene, but the CP15 marker species *Discoaster saipanensis* and *Discoaster barbadiensis* are missing. The last occurrence of these marker species is about 0.5 m.y. before the Oligocene/Eocene boundary. Sample 125-786A-10X-CC is, therefore, latest Eocene in age and is assigned to the base of Subzone CP16a.

The presence of *D. barbadiensis*, *D. saipanensis*, *Cribrocentrum reticulatum*, *Chiasmolithus oamaruensis*, and *Isthmolithus recurvus* dates Sample 125-786A-11X-1, 20 cm, to the late Eocene (Subzone CP15b). The *C. reticulatum* extinction approximates the CP15a/15b boundary; therefore, a short hiatus may be within Subzone CP15b. Samples 125-786A-11X-1, 140 cm, to 125-786A-11X-2, 133 cm, are assigned to the late Eocene (Subzone CP15a) by the occurrence of a late Eocene association and the absence of *Chiasmolithus grandis*, but the genus *Chiasmolithus* is usually rare in samples.

Middle Eocene nannofossil assemblages (Subzone CP14b) (based on the appearance of *C. grandis* together with *D. saipanensis*, *D. barbadiensis*, *C. reticulatum*, *S. predistentus*, and *R. umbilica*) occur in the interval from Samples 125-786A-11X-3, 38 cm, to 125-786A-11X-CC. Nannofossil assemblages from Samples 125-786A-12X-2, 35 cm, to 125-786A-19X-CC are assigned to Subzone CP14a by the occurrence of *Chiasmolithus solitus*, *Sphenolithus furcatolithoides*, and *Reticulofenestra dictyoda*, in association in Sample 125-786A-12X-2, 35 cm, with *D. saipanensis*. The absolute age is between 42.2 and 42.8 m.y., according to Berggren et al. (1985a).

Hole 786B

Rare, poorly to moderately preserved calcareous nannofossils are present in sediments interbedded with the lava flows in Hole 786B.

Samples 125-786B-22R-1, 50 cm, 125-786B-27R-2, 28 cm, and 125-786B-40R-1, 35 cm, are middle to late Eocene in age (CP14-15 Zone), based on the presence of the marker species *Discoaster barbadiensis*, *Discoaster saipanensis*, and *Reticulofenestra umbilica* and the species *Cyclicargolithus floridanus* and *Discoaster deflanderi*.

Nannofossil assemblages were also found in Samples 125-786B-40R-1, 35 cm, 125-786B-41R-3, 60 cm, 125-786B-49R-1, 50 cm, 125-786B-51R-2, 10 cm, and 125-786B-56R-CC. The presence of *Ericsonia formosa*, *Dictyococcites bisectus*, and *Cyclicargolithus floridanus* confines these samples to the middle to late Eocene, although no marker species were found.

Early Eocene nannofossil assemblages are present in Samples 125-786B-61R-6, 26 cm, and 125-786B-63R-1, 92 cm, based on the co-occurrence of *D. barbadiensis*, *Discoaster distinctus*, and *Sphenolithus anarrhopus*.

Foraminifers

The Cenozoic planktonic foraminiferal stratigraphy for Hole 786A is summarized in Table 4. The relatively poor preservation and moderate to low abundance of planktonic foraminifers in most of the cores do not allow an accurate biostratigraphic subdivision of Hole 786A. The presence or absence of the species listed was used to define the age of a sample, but no age determinations using the absence of species were attempted for poorly preserved samples.

The planktonic foraminifers from the sedimentary sequence in Hole 786A were deposited between the Quater-

Table 4. Summary of foraminiferal data, Hole 786A.

Core, section, interval (cm)	Abundance	Preservation	Diagnostic species present	Diagnostic species absent	Nannofossil zone	Age
125-786A-						
1H-6, 140-142	Rare	Poor	*Globorotalia crassaformis*		upper N19-22	middle early Pliocene-Pleistocene
1H-6, 142-144	Rare	Poor	*Globorotalia tosaensis*	—	N21-lower N22	late Pliocene-earliest Pleistocene
1H-CC	Common	Moderate	*Globorotalia tosaensis*	*Globorotalia truncatulinoides*	N21	late Pliocene
2H-CC	Rare	Poor	*Globorotalia crassaformis* *Neogloboquadrina pachyderma*	—	upper N19-21	middle early Pliocene-late Pliocene
3H-CC	Rare	Poor	*Globorotalia crassaformis*	—	upper N19-22	middle early Pliocene-Pleistocene
4X-CC	Rare	Moderate	*Globorotalia plesiotumida* *Sphaeroidinellopsis praedehiscens*	—	N17B-lower N19	middle late Miocene-earliest Pliocene
5X-CC	Rare	Poor	*Globorotalia lenguaensis* *Globigerinoides* cf. *kennetti*	—	N16-17A	early late Miocene-middle late Miocene
6X-CC	Rare	Poor	*Orbulina universa* *Sphaeroidinellopsis seminulina*	—	N9-21	early middle Miocene-late Pliocene
7X-CC	Rare	Poor	*Globorotalia* cf. *lenguaensis*	—	N12-17A	middle middle Miocene-middle late Miocene
8X-CC	Rare	Poor	*Globorotalia* cf. *lenguaensis*	—	N12-17A	middle middle Miocene-middle late Miocene
9X-CC	Abundant	Moderate	*Globigerinoides primordius* *Globoquadrina praedehiscens*	—	N4A-5	latest Oligocene-earliest Miocene
10X-6, 71-73	Common	Poor	*Catapsydrax dissimilis* *Pseudohastigerina micra*	—	P13-upper P19	middle Eocene-early Oligocene
10X-CC	Common	Moderate	*Cribrohantkenina inflata* *Hantkenina alabamensis*	—	P16-17	latest Eocene
11X-3, 9-10	Few	Poor	*Cribrohantkenina inflata*	—	P16-17	latest Eocene
11X-CC	Few	Poor	*Morozovella aragonensis* *Acarinina bullbrooki*	—	P9-11	latest early Eocene-early middle Eocene
12X-CC	Rare	Poor	*Morozovella aragonensis* *Acarinina bullbrooki*	—	P9-11	latest early Eocene-early middle Eocene

nary (lower Zone P22) and the latest early Eocene (Zones P16 and P17). Evidence from the sparse planktonic foraminiferal assemblages suggests that hiatuses may have existed in the late early Miocene to middle Miocene and the late early Oligocene. The relatively poor preservation and low abundance of planktonic foraminifers in Samples 125-786A-1H-6, 51-53 cm, to 125-786A-12X-CC correlate with the large amounts of volcaniclastic material in these samples.

Diatoms

Rare to common and poorly to well-preserved diatom assemblages are present in the first seven cores of Hole 786A. The samples below Sample 125-786A-7X-CC contain no diatoms.

The uppermost Sample 125-786A-1H-1, 0 cm, is assigned to the *Nitzschia reinholdii* A Zone (Pliocene/Pleistocene boundary) by the co-occurrence of *N. reinholdii*, *Pseudoeunotia doliolus*, and *Rhizosolenia praebergonii*.

The presence of *Nitzschia jouseae* in Sample 125-786A-1H-CC dates this sample as late Pliocene (top of *N. jouseae* Zone).

Zonal marker species were not found in Samples 125-786A-2H-CC and 125-786A-3H-CC. However, Sample 125-786A-3H-CC is tentatively placed in the early Pliocene *Thalassiosira convexa* Zone by the absence of *N. jouseae*.

Nitzschia miocenica is present in Sample 125-786A-4X-CC and *Nitzschia porteri* was found in Sample 125-786A-5X-CC, dating this interval as late Miocene.

Zonal markers were not found in Sample 125-786A-6X-CC, but Sample 125-786A-7X-CC contains *Denticulopsis punctata* f. *hustedtii*, which allows us to assign this sample to the middle Miocene *Craspedodiscus coscinodiscus* Zone.

IGNEOUS AND METAMORPHIC PETROLOGY

From the two holes drilled at Site 786, taken together, we penetrated and recovered strata from 0 to 828 mbsf. In Hole 786A, sediments were recovered from 0 to 100.5 mbsf (Sections 125-786A-1X to 125-786A-11X-5, 100 cm; "Lithostratigraphy" section, this chapter), and a sedimentary breccia marks the transition to basement dominated by igneous strata of boninitic affinity. Predominantly igneous rocks were recovered in this hole from 124.9 to 166.5 mbsf (Sections 125-786A-11X-5, 100 cm, to 125-786A-19X-CC). Hole 786B is offset 30 m toward the south with respect to the preceding hole, and cores were recovered from 162.5 to 828.6 mbsf (Sections 125-786B-1R to 125-786B-72R-2), stratigraphically below the interval penetrated in Hole 786A. The cores of Hole 786B contain lava flows, breccias dominated by igneous clasts, rare sedimentary intervals, and very low-grade metamorphic lavas crosscut by dikes. Biostratigraphic studies ("Biostratigraphy" section) constrain the age of the top of the basement to middle Eocene, and several sedimentary intercalations within the basement also give middle Eocene ages. The deepest sedimentary intercalation dated is in Core 125-786B-61R; local faults and a lack of biostratigraphic data leave the ages below this depth ambiguous.

The igneous and sedimentary sequence in Holes 786A and 786B has been divided into four major lithologic units. The first three units form a lower Pleistocene–middle Eocene sedimentary sequence ("Lithostratigraphy" section). The fourth major unit, basement, is divided into 30 subunits, and is the subject of this section. Intercalated sedimentary strata in lithologic Unit IV are described in the "Lithostratigraphy" section. Unit divisions and rock names are based on macroscopic criteria as well as on major-element chemical analyses. The distinction between boninite series rocks and andesite was not obvious in hand specimen. A nomenclature presented in the "Igneous and Metamorphic Geochemistry" section (this chapter) was developed using the MgO and SiO_2 contents of the rocks. Rock names based on these compositional criteria are given precedence but have not been rigidly applied throughout. Common rock names synonymous with, and commonly more specific than, our compositional nomenclature are used in the hand specimen and thin-section descriptions when they do not conflict with the chemical data, or when no analysis is available. Within these limits, the rock names used in unit descriptions, from analyses, thin section, and hand specimen, are internally consistent.

The following approach is used in the assignment of lithologic units. Multiple volcanic strata of similar character are assigned to a single unit. If two volcanic units are separated by strata of clear sedimentary affinities, the latter are assigned to a separate unit; breccias adjacent to these sediments are assigned to this same unit.

A summary of the petrographic characteristics of the rock types encountered at Site 786 is given in Table 5. The characteristics of the individual units are discussed in the following. The basement lithostratigraphy is illustrated in Figure 3.

Table 5. Petrology of the rock types at Site 786.

Basalt	
Phenocrysts	Clinopyroxene (3%–5%) + plagioclase (trace–5%) + orthopyroxene (0%–2%)
Groundmass	Glass (60%–70%) + plagioclase (5%–10%) + clinopyroxene (3%–5%) + opaque minerals (trace–1%)
Comments	Hyalo-ophitic; Sample 125-786B-40R-2, 54–56 cm, contains 15%–20% olivine
High-magnesian basalt	
Phenocrysts	Clinopyroxene (5%–8%) + orthopyroxene (4%–7%) + olivine (0%–3%) + spinel (0%–trace)
Groundmass	Glass (50%–70%) + plagioclase (10%–20%) + clinopyroxene (2%–7%) + orthopyroxene (0%–5%) + opaque minerals (0%–2%)
Comments	Spinel occurs as inclusions in olivine phenocrysts; glomerophyric texture (olivine + orthopyroxene + clinopyroxene); orthopyroxene has clinopyroxene (100) exsolution lamellae and a clinopyroxene reaction rim
Picrite	
Phenocrysts	None
Groundmass	Clinopyroxene (25%–30%) + orthopyroxene (1%–2%) + glass (60%–70%) + opaque minerals (trace–1%)
Boninite	
Phenocrysts	Orthopyroxene (2%–7%) + clinopyroxene (1%–5%) + plagioclase (5%–7%)
Groundmass	Glass (70%–80%) + plagioclase (5%–10%) + clinopyroxene (1%–2%) + orthopyroxene (trace–1%) + opaque minerals (0%–trace)
Comments	Orthopyroxene (2V = −80° to −85°, bronzite) has some (100) clinopyroxene exsolution lamellae and a reaction rim of clinopyroxene
Andesite	
Phenocrysts	Plagioclase (10%–20%) + clinopyroxene (2%–6%) + orthopyroxene (0%–2%) + opaque minerals (0%–trace)
Groundmass	Glass (50%–60%) + plagioclase (10%–20%) + opaque minerals (1%–2%)
Comments	Can be further classified as two-pyroxene (clinopyroxene + orthopyroxene) andesites; glomerocrysts are common
Dacite	
Phenocrysts	Plagioclase (5%–15%) + clinopyroxene (2%–8%) + orthopyroxene (trace)
Groundmass	Glass (60%–70%) + plagioclase (10%–20%) + opaque minerals (1%–2%)
Comments	Porphyritic (partly glomerophyric) and hyalophitic
Rhyolite	
Phenocrysts	Plagioclase (2%–3%)
Groundmass	Glass (40%–50%) + plagioclase + quartz + opaque minerals
Comments	Predominantly massive rhyolite without flow texture

Unit 1

Sections 125-786A-11X-5, 100 cm, to 125-786A-19X-CC and 125-786B-1R-1, 0 cm, to 125-786B-5R-2, 25 cm.

The top of the igneous sequence from Sections 125-786A-11X-5, 100 cm, through 125-786A-12X-CC is formed by a breccia made up of clasts of basaltic andesite in a matrix of marl. The clasts contain 5%–20% fresh phenocrysts consisting of two pyroxenes with olivine or plagioclase. Some olivine phenocrysts contain chromium-spinel and have reaction rims of orthopyroxene. Most of the groundmass has been altered to a low-grade metamorphic assemblage, but unaltered patches are locally preserved. Clasts increase in size (from a few millimeters to 6 cm) and abundance with depth.

The poor recovery precludes a comprehensive lithologic study of the remainder of this unit. Cores 125-786A-13X-CC through 125-786A-19X-CC are mainly cuttings and clasts in clay of high-magnesian basalts, boninites, and picrites. Orthopyroxene is the dominant phenocryst in these samples, with subordinate clinopyroxene and olivine and rare plagioclase in a glassy groundmass; these are typical petrographic characteristics of rocks of the boninite series (Meijer, 1980). Unit 1 lithologies continue in the interval from Sections 125-786B-1R through 125-786B-5R-2, 25 cm, as oligomictic breccias containing boninite clasts. These contain mainly phenocrysts of orthopyroxene with subordinate clinopyroxene and plagioclase, although the latter can be locally predominant. Glass in the groundmass of the clasts has been largely devitrified or replaced by clay.

Unit 2

Sections 125-786B-5R-2, 25 cm, to 125-786B-8R-1, 0 cm.

The top of Unit 2 comprises a flow of intermingled andesite and basalt overlying basalt. The basalt contains 5% to 7% phenocrysts, made up of olivine, which is replaced by a carbonate/iron oxide assemblage, and minor clinopyroxene and traces of orthopyroxene and plagioclase. The glassy groundmass is variably altered (10%–50%) to clay. The base of the unit is formed by a relatively fresh andesite.

Unit 3

Sections 125-786B-8R-1, 0 cm, to 125-786B-17R-1, 130 cm.

Unit 3 is formed by oligomictic breccias containing a small number of exotic fragments. The breccias at the top of the unit contain andesite clasts petrographically similar to those of the overlying flow of Unit 2 (Sections 125-786B-8R-1 through 125-786B-11R-1, 90 cm). The andesite contains 8% to 30% phenocrysts of plagioclase and clinopyroxene and minor orthopyroxene in a black glassy groundmass, with plagioclase and minor clinopyroxene. Glass is partly to largely replaced by clays. Alteration rims of clasts appear similar to the sandy matrix of the breccia, indicating *in-situ* brecciation. Exotic fragments of pumice and basalt are present in the lower part of the andesite breccia (Sections 125-786B-10R-1 through 125-786B-11R-1, 90 cm). High-magnesian basalts and boninite, classified on the basis of bulk-rock chemistry, are present in Sections 125-786B-11R-1, 90 cm, through 125-786B-14R-1, 0 cm. Basalt clasts contain phenocrysts of two pyroxenes and plagioclase in a fine-grained to glassy groundmass. Clasts alter to material similar to the matrix of the breccia. Boninite clasts also contain phenocrysts of two pyroxenes and plagioclase, but clinopyroxene is subordinate. Sections 125-786B-14R-1 through 125-786B-17R-1, 115 cm, are made up of andesite-dacite breccias. Microdiorite fragments, possibly represent-

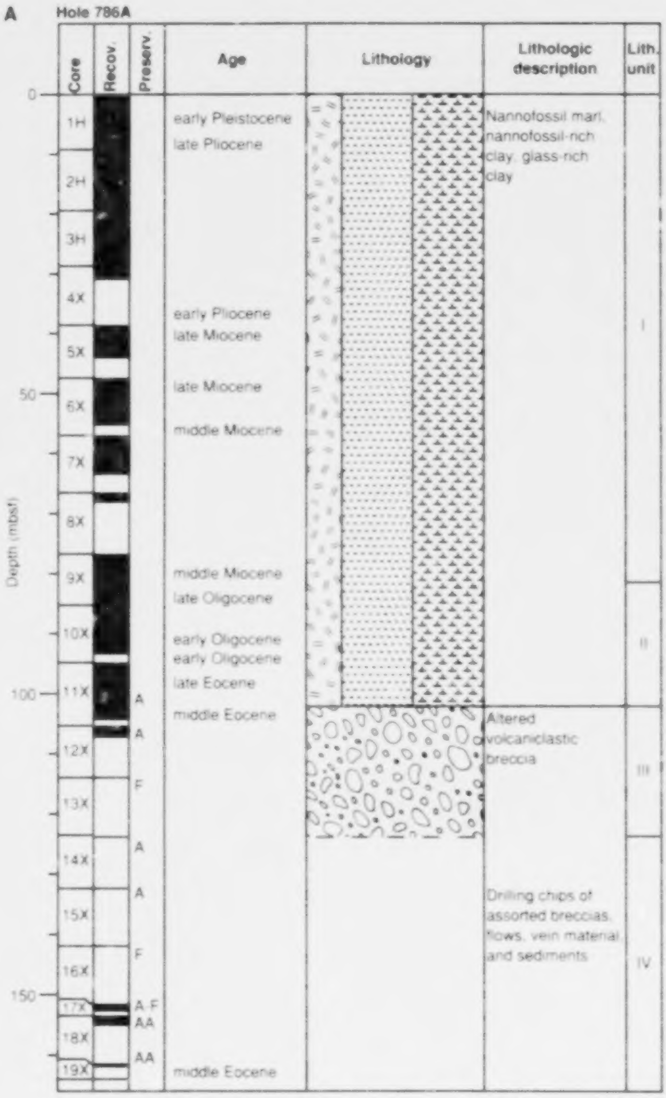

Key for preservation for 7A and 7B

AA= very altered:	groundmass and phenocrysts are pervasively altered, only phenocryst traces remaining.
A = altered:	groundmass and olivines altered, other phenocrysts largely fresh, some fresh glass.
F = fresh:	some alteration of groundmass and phenocrysts, olivine altered.
FF= very fresh:	no signs of alteration, vesicles may contain secondary mineralization.

Figure 3. Lithostratigraphy and core recovery at Site 786. **A.** Hole 786A. **B.** Hole 786B.

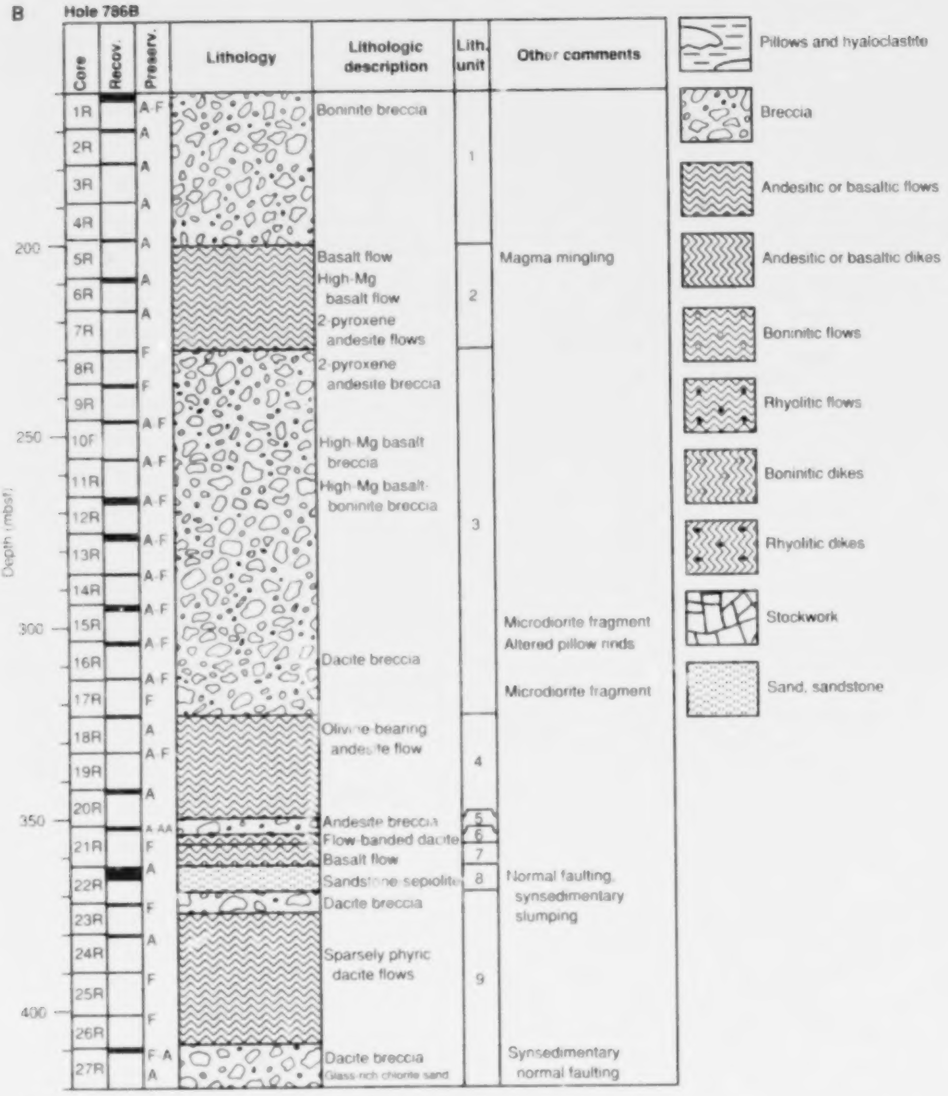
B
Hole 786B
Core
Recov.
Preserv.
Lithology
Lithologic description
Lith. unit
Other comments
Depth (mbsf)
200
250
300
350
400
1R
2R
3R
4R
5R
6R
7R
8R
9R
10R
11R
12R
13R
14R
15R
16R
17R
18R
19R
20R
21R
22R
23R
24R
25R
26R
27R
Boninite breccia
Basalt flow
High-Mg basalt flow
2-pyroxene andesite flows
2-pyroxene andesite breccia
High-Mg basalt breccia
High-Mg basalt-boninite breccia
Dacite breccia
Olivine-bearing andesite flow
Andesite breccia
Flow-banded dacite
Basalt flow
Sandstone-sepiolite
Dacite breccia
Sparsely phyric dacite flows
Dacite breccia
Glass-rich chlorite sand
1
2
3
4
5
6
7
8
9
Magma mingling
Microdiorite fragment
Altered pillow rinds
Microdiorite fragment
Normal faulting, synsedimentary slumping
Synsedimentary normal faulting
Pillows and hyaloclastite
Breccia
Andesitic or basaltic flows
Andesitic or basaltic dikes
Boninitic flows
Rhyolitic flows
Boninitic dikes
Rhyolitic dikes
Stockwork
Sand, sandstone

Figure 3 (continued).

ing cumulates, were recovered in Samples 125-786B-15R-1, 0–3 cm, and 125-786B-17R-1, 0–3 cm. Alteration throughout this unit is highly variable.

Unit 4

Sections 125-786B-18R-1, 0 cm, to 125-786B-21R-1, 0 cm.

Unit 4 consists of two flows of variably altered andesite. The top flow occupies Sections 125-786B-17R-1 through 125-786B-19R-1, and the lower flow, Sections 125-786B-20R-1 through 125-786B-21R-1, 0 cm.

Unit 5

Sections 125-786B-21R-1, 0 cm, to 125-786B-21R-1, 50 cm.

Unit 5 is a brecciated andesite having minor alteration to chlorite and clays and grading downward into highly brecci-

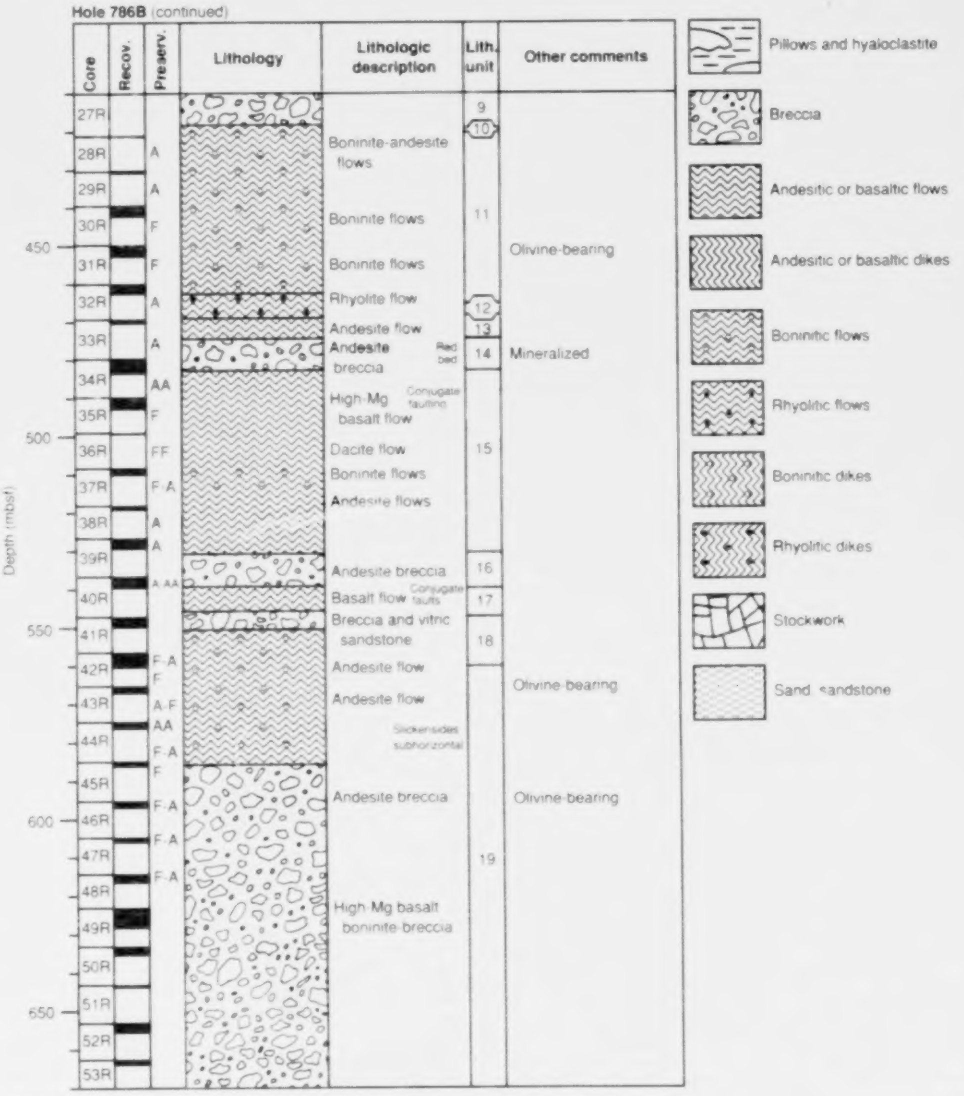
Hole 786B (continued)
Core
Recov.
Preserv.
Lithology
Lithologic description
Lith. unit
Other comments
Depth (mbsf)
450
500
550
600
650
27R
28R
29R
30R
31R
32R
33R
34R
35R
36R
37R
38R
39R
40R
41R
42R
43R
44R
45R
46R
47R
48R
49R
50R
51R
52R
53R
A
A
F
F
A
A
AA
F
FF
F-A
A
A
A-AA
F-A
F
A-F
AA
F-A
F
F-A
F-A
F-A
Boninite-andesite flows
Boninite flows
Boninite flows
Rhyolite flow
Andesite flow
Andesite breccia
Red bed
High-Mg basalt flow
Conjugate faulting
Dacite flow
Boninite flows
Andesite flows
Andesite breccia
Basalt flow
Conjugate faults
Breccia and vitric sandstone
Andesite flow
Andesite flow
Slickensides subhorizontal
Andesite breccia
High-Mg basalt boninite breccia
9
10
11
12
13
14
15
16
17
18
19
Olivine-bearing
Mineralized
Olivine-bearing
Olivine-bearing
Pillows and hyaloclastite
Breccia
Andesitic or basaltic flows
Andesitic or basaltic dikes
Boninitic flows
Rhyolitic flows
Boninitic dikes
Rhyolitic dikes
Stockwork
Sand, sandstone

Figure 3 (continued).

ated and altered andesite. A thin veneer of sediment forms the boundary to the underlying unit.

Unit 6

Sections 125-786B-21R-1, 50 cm, to 125-786B-21R-2, 23 cm.

Unit 6 comprises a flow-banded aphyric dacite. The boundary between Units 6 and 7 is placed at the glassy contact of two cooling units, although the incorporation of Section 125-786B-21R-2, 0–23 cm, into this dacite unit cannot be made with certainty without chemical analyses.

Unit 7

Sections 125-786B-21R-2, 23 cm, to 125-786B-22R-1, 27 cm.

Unit 7 comprises glassy aphyric basalt having minor, variable alteration. The lower contact between basalt and the

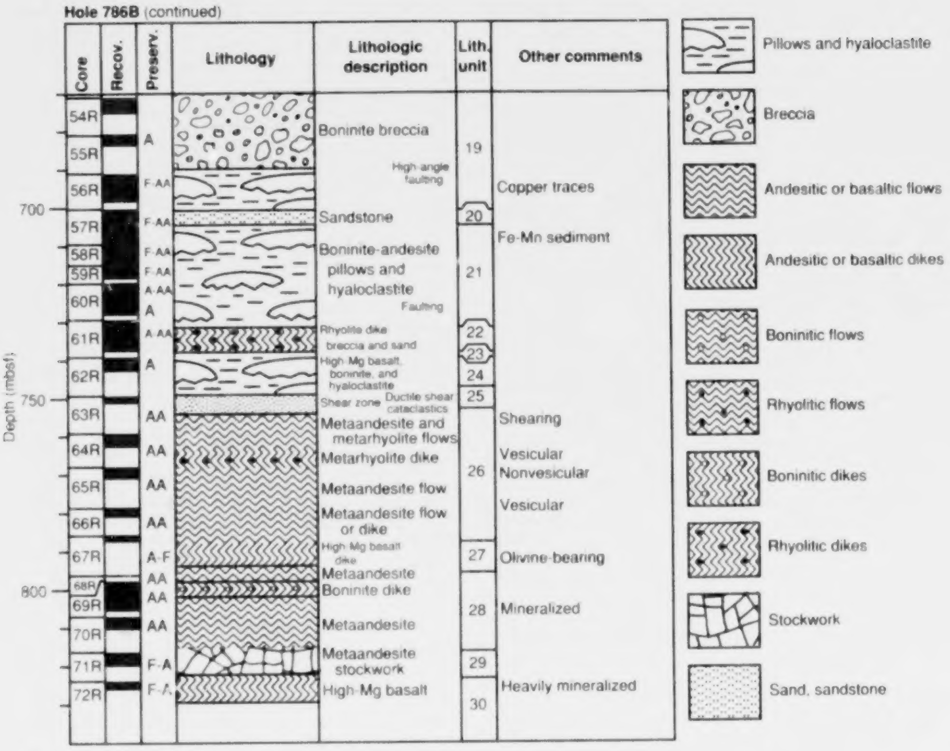
Hole 786B (continued)
Core
Recov.
Preserv.
Lithology
Lithologic description
Lith. unit
Other comments
Depth (mbsf)
700
750
800
54R
55R
56R
57R
58R
59R
60R
61R
62R
63R
64R
65R
66R
67R
68R
69R
70R
71R
72R
A
F-AA
F-AA
F-AA
F-AA
A-AA
A
A-AA
A
AA
AA
AA
AA
A-F
AA
AA
AA
F-A
F-A
Boninite breccia
High-angle faulting
Sandstone
Boninite-andesite pillows and hyaloclastite
Faulting
Rhyolite dike
breccia and sand
High-Mg basalt, boninite, and hyaloclastite
Shear zone
Ductile shear cataclastics
Metaandesite and metarhyolite flows
Metarhyolite dike
Metaandesite flow
Metaandesite flow or dike
High-Mg basalt dike
Metaandesite
Boninite dike
Metaandesite
Metaandesite stockwork
High-Mg basalt
19
20
21
22
23
24
25
26
27
28
29
30
Copper traces
Fe-Mn sediment
Shearing
Vesicular
Nonvesicular
Vesicular
Olivine-bearing
Mineralized
Heavily mineralized
Pillows and hyaloclastite
Breccia
Andesitic or basaltic flows
Andesitic or basaltic dikes
Boninitic flows
Rhyolitic flows
Boninitic dikes
Rhyolitic dikes
Stockwork
Sand, sandstone

Figure 3 (continued).

underlying sediments of Unit 8 is marked by a thin (12 cm) band of sepiolite.

Unit 8

Sections 125-786-22R-1, 27 cm, to 125-786B-22R-3, 124 cm.

Unit 8 consists of vitric siltstones and sandstones intercalated with a polymictic breccia that contains clasts of pumice and volcanic fragments in a matrix of sand and silt.

Unit 9

Sections 125-786B-23R-1, 0 cm, to 125-786B-27R-1, 110 cm.

Unit 9 is made up of dacite flows with a plagioclase, two-pyroxene, rhyolite breccia at the base (below Section 125-786B-26R-1, 115 cm). The dacite has been variably altered into clays, and vesicles are filled with a white zeolite.

Unit 10

Sections 125-786B-27R-1, 110 cm, to 125-786B-27R-2, 0 cm.

Unit 10 is a thin, glass-rich chloritic sandstone, fining upward, with cross-bedding and lamination at the base. It contains a few clasts.

Unit 11

Sections 125-786B-27R-2, 0 cm, to 125-786B-32R-2, 54 cm.

Unit 11 comprises a series of very phyric (30%) boninites. The boninites contain two pyroxenes and plagioclase with olivine increasingly present toward the bottom of the unit. Clinopyroxene and plagioclase are the dominant phenocryst phases. Alteration has been concentrated along veins and fractures that contain carbonate and possible serpentine. In Sections 786B-31R-1 through 125-786B-32R-1, 73 cm, olivine has been altered to hematite and carbonate, and glass has been largely altered to clay.

Unit 12

Sections 125-786B-32R-2, 54 cm, to 125-786B-33R-1, 0 cm.

Unit 12 is a rhyolite flow, variably altered to clays and chlorite.

Unit 13

Sections 125-786B-33R-1, 0 cm, to 125-786B-33R-1, 35 cm.

Unit 13 consists of olivine-bearing, basaltic andesite that exhibits pervasive hematite alteration localized around olivine and also disseminated within the groundmass; carbonate-filled veins are common.

Unit 14

Sections 125-786B-33R-1, 65 cm, to 125-786B-34R-1, 145 cm.

The top of Unit 14 consists of a meta-andesite having pyrite mineralization, underlain by a brecciated, flow-banded andesite. The lower part of the unit (Section 125-786B-34R-1, 53–140 cm) is made up of a feldspar-rich, vitric sandstone and siltstone with graded bedding and a possibly baked upper contact. These sediments in turn overlie brecciated andesite having flow banding and pyrite mineralization. Brecciated zones have experienced pervasive alteration to a low-grade metamorphic assemblage.

Unit 15

Sections 125-786B-34R-1, 145 cm, to 125-786B-39R-2, 0 cm.

The top of Unit 15 (Sections 125-786B-34R-1, 145 cm, through 125-786B-34R-4, 101 cm) has been formed by flow(s) of sparsely phyric basalt with phenocrysts of plagioclase, clinopyroxene, and rare orthopyroxene and olivine. Phenocryst contents are higher toward the lower part of this interval. The basalt groundmass has been pervasively altered to a low-grade mineral assemblage, and traces of pyrite occur throughout. Sparsely phyric dacite flows with plagioclase and clinopyroxene phenocrysts are present in Sections 125-786B-34R-4, 101 cm, through 125-786B-37R-1, 80 cm, and olivine-bearing boninite is present in Sections 125-786B-37R-1, 80 cm, through 125-786B-37R-3, 30 cm. Andesite makes up the lower part of the unit. Dacites and andesites are markedly less altered than the more mafic members of this unit.

Unit 16

Sections 125-786B-39R-2, 0 cm, to 125-786B-40R-1, 75 cm.

Unit 16 comprises a series of andesite breccias. Pyrite is disseminated throughout the unit and concentrated along veins that contain zeolites. The groundmass is slightly to moderately chloritized.

Unit 17

Sections 125-786B-40R-1, 80 cm, to 125-786B-41R-1, 0 cm.

Unit 17 consists of orthopyroxene-olivine-phyric basalt, pervasively altered to chlorite and carbonates and cut by veins filled with chlorite, carbonate, and iron oxide.

Unit 18

Sections 125-786B-41R-1, 0 cm, to 125-786B-42R-2, 0 cm.

The top of Unit 18 is an oligomictic breccia having a matrix component that increases in proportion upward. This overlies a laminated vitric sand, and then a polymictic breccia, also with a matrix component that increases upward and then grades into a vitric sand. Clasts in both breccias are andesites. The base of the unit has been formed by an andesite flow.

Unit 19

Sections 125-786B-42R-2, 0 cm, to 125-786B-57R-1, 0 cm.

Various boninite and andesite breccias and flows make up this unit. The top of Unit 19 is marked by the appearance of rare olivine phenocrysts in the andesite flows. Pervasively altered meta-andesite having a low-grade metamorphic assemblage in Section 125-786B-44R-1 forms the transition to the underlying brecciated, olivine-bearing andesite of Sections 125-786B-44R-2, 10 cm, through 125-786B-50R-1. Breccia clasts in Section 125-786B-51R-1 have the composition of high-magnesian basalts, but the phenocrysts of plagioclase (10%–20%) and two pyroxenes (5%–10% each) suggest a close similarity to the andesites. Breccias continue through Section 125-786B-56R-6 with clasts that appear to be boninitic on the basis of the high proportion of orthopyroxene, in the mode of Section 125-786B-55R-6. The boninite breccia of Sections 125-786B-55R-3 through 125-786B-56R-1 contains a trace of native copper. Chlorite and hematite alteration is pervasive. Veins and fractures are characteristically absent, except in the copper-bearing interval.

Unit 20

Sections 125-786B-57R-1, 0 cm, to 125-786B-57R-1, 104 cm.

A fining-upward sandstone with basal graded bedding and local clasts forms Unit 20.

Unit 21

Sections 125-786B-57R-1, 104 cm, to 125-786B-61R-4, 42 cm.

Unit 21 consists of multiple pillow lavas and hyaloclastites of bronzite-boninite and andesite with red sediments between pillows. White and green zeolite and iron oxide fill veins and vesicles. At the base of the unit, a fault breccia forms the contact with Unit 22.

Unit 22

Sections 125-786B-61R-4, 42 cm, to 125-786B-61R-6, 40 cm, and 125-786B-61R-6, 65 cm, to 125-786B-62R-1, 0 cm.

Unit 22 is a rhyolite flow or (more probably) dike or sill, which is locally oxidized to a dark red color and contains glass altered to chlorite.

Unit 23

Sections 125-786B-61R-6, 40 cm, to 125-786B-62R-1, 0 cm.

Unit 23 is a shear zone consisting of breccia and sandstone.

Unit 24

Sections 125-786B-62R-1, 0 cm, to 125-786B-62R-3, 85 cm.

Unit 24 consists of altered boninite or andesite pillows and hyaloclastites, locally high-magnesian basalt in composition, with red sediment between the pillows. Fine filaments of red ferromanganoan sediment are particularly prominent in the hyaloclastites. Clay and chlorite alteration of glass is pervasive. Zeolite and sparse carbonate fill veins.

Unit 25

Sections 125-786B-62R-3, 85 cm, to 125-786B-63R-2, 44 cm, and 125-786B-63R-2, 78 cm, to 125-786B-63R-2, 92 cm.

Unit 25 consists of cataclastic meta-andesites and sandstone in a shear zone. The andesites are largely altered to a low-grade metamorphic assemblage. Orthopyroxene phenocrysts have been largely altered to a chlorite/carbonate assemblage, but some unaltered cores remain. Clinopyroxene is variably altered.

Unit 26

Sections 125-786B-63R-2, 44 cm, to 125-786B-63R-2, 78 cm, and 125-786B-63R-2, 92 cm, to 125-786B-67R-1, 0 cm.

Metadacite and rhyolite flows of low metamorphic grade form this unit. Orthopyroxene has been replaced by chlorite, carbonate, and iron oxide; clinopyroxene has been variably altered to chlorite, and plagioclase is albitized. Vesicles are filled with zeolite, carbonate, and chlorite and locally contain sulfide minerals.

Unit 27

Sections 125-786B-67R-1, 0 cm, to 125-786B-68R-1, 0 cm.

Dikes of basalt and boninite composition make up Unit 27. The dikes show little evidence of chilled margins and have been locally altered to chlorite and carbonate. Olivine has been completely replaced by a chlorite/carbonate assemblage, and clinopyroxene has been variably chloritized. Veins contain carbonate and sulfide minerals.

Unit 28

Sections 125-786B-68R-1, 0 cm, to 125-786B-71R-1, 0 cm.

Unit 28 consists of meta-two-pyroxene-andesite, probably of boninitic composition, with abundant chlorite and carbonates along fractures and extensive sulfide mineralization. One boninite dike, apparently 30 cm thick, also forms part of this unit.

Unit 29

Sections 125-786B-71R-1, 0 cm, to 125-786B-[illegible]1R-4, 0 cm.

Unit 29 is an argillized, mineralized, andesite stockwork. Andesite has been completely altered to clays, epidote, chlorite, and quartz. Extensive sulfide mineralization is present.

Unit 30

Sections 125-786B-71R-4, 0 cm, to 125-786B-72R-2, 140 cm.

Unit 30 contains fresh, avesicular boninitic glass, possibly intruded as a dike, in a meta-andesite massive flow or dike.

IGNEOUS AND METAMORPHIC GEOCHEMISTRY

Lithologies drilled at Holes 786A and 786B include massive flows, pyroclastic flows and interbedded sediments, massive flows and intrusive sheets, pillow lavas and hyaloclastite flows, and eventually multiple composite intrusive sheets (see "Igneous and Metamorphic Petrology" section, this chapter). Although the metamorphic grade reaches the upper greenschist facies (albite-chlorite-epidote-quartz assemblage) at the base of Hole 786B, most of the extrusive rocks analyzed contain abundant fresh glass. Alteration is therefore thought to have had only a small effect on the concentrations of major elements. A total of 47 samples collected from Site 786 was analyzed on board the ship for abundances of both major and trace elements by XRF spectrometry (see "Explanatory Notes" chapter, this volume). Abundances of major and trace elements are presented in Table 6.

Major-Element Geochemistry

The rock types from Site 786 show a large variation in SiO_2 and MgO (Fig. 4) and hence have been classified on this basis. This classification arbitrarily subdivides the rocks into high- and low-magnesian groups. Although the rock types range from picrites (low SiO_2, >12 wt% MgO) to rhyolites (>70 wt% SiO_2, <2 wt% MgO), the majority of the samples fall into the high-magnesian basalt, boninite, and andesite classification fields. The dispersion on a covariation diagram of magnesium (between 18.5 and 0 wt% MgO) against silica (between 48.5 and 74.5 wt% SiO_2) forms a crescent shape that converges toward both the picrite and the andesite fields. Because the suite of rocks crosses the line of 63 wt% SiO_2 into the dacite and rhyolite fields, the rocks can be inferred to have been derived from parental magmas that were saturated with respect to silica.

Nearly all the rock types at Site 786 contain up to 20 modal% of plagioclase phenocrysts or xenocrysts (see "Igneous and Metamorphic Petrology" section, this chapter). Such large proportions of plagioclase account for the apparent enrichment in aluminum (Fig. 5) and may have been caused by plagioclase accumulation or by a shift in the co-tectic toward plagioclase by an increased water content of the magma. The wide scatter of points on an aluminum-magnesium diagram (Fig. 5) suggests, however, that the modal percentage of plagioclase is independent of the magnesium content of the rock. This scatter may be the result of magma mixing processes (see "Igneous and Metamorphic Petrology" section, this chapter).

Despite the large variations in MgO, SiO_2, and Al_2O_3, all the rocks from Site 786 are characterized by extremely low abundances of these elements and a small range of TiO_2 (from 0.1 to 0.3 wt%). In some rocks, TiO_2 is an order of magnitude less than normal mid-ocean ridge basalt (N-MORB), which has an average TiO_2 content of 1.5 wt%. This suggests that all the rocks may have been derived from a source that was extremely depleted in the incompatible trace elements.

Trace-Element Geochemistry

The characteristically depleted nature of the rocks from Site 786 is reflected by their low abundances of high-field-strength (HFS) elements in general and yttrium and titanium in particular. However, zirconium is variably depleted and the zirconium/yttrium ratio is thus highly variable, ranging from less than 2 to more than 6. The most primitive rocks are also those having the highest abundances of chromium, which ranges from about 220 to 1330 ppm. The accumulation of chromium-rich spinel is probably responsible for abundances of chromium in excess of 1000 ppm; these rocks also have variable amounts of orthopyroxene and olivine phenocrysts (see "Igneous and Metamorphic Petrology" section, this chapter). Two of the factors involved in the petrogenetic history of the rocks are illustrated in the chromium-yttrium diagram in Figure 6. Source effects, either variable depletion or partial melting, generate a subhorizontal array of data points, whereas fractional crystallization produces a subvertical trend. Although large variations in yttrium occur in the primitive rock types, the fractionated rocks exhibit a relatively narrow range of yttrium abundances. The former may be evidence for a range of potential parent magmas related to variable source fertility or variations in partial melting. The latter may be evidence for the generation of the more evolved magmas from a single, homogeneous parental magma. For the majority of primitive rocks at Site 786, the abundance of yttrium is always less than one-half that for N-MORB, which has an average of about 30 ppm yttrium. The HFS-element-depleted nature of the rocks from Site 786 is summarized by N-MORB normalized diagrams for a representative boninite, high-magnesian basalt, and primitive andesite (Figs. 7A–7C). Cerium and phosphorus are near or below their detection limits, and therefore are not included. However, niobium, zirconium, and possibly yttrium may be variably enriched with respect to titanium. The large-ion-lithophile (LIL) elements are enriched in all three representative samples, but their abundances are only slightly higher than those in N-MORB. If the enrichment in LIL elements is derived from

Table 6. Geochemical data, Holes 786A and 786B.

Sample (interval in cm) Rock type[a]	786A-6X-5, 24–27 Andesite	786A-12X-1, 140–142 Basalt	786A-15X-CC, 27–29 High-Mg basalt	786A-16X-CC, 25–28 High-Mg basalt	786A-17X-CC, 4–6 Picrite	786A-19X-CC, 17–20 Picrite	786A-19X-1, 0–30 High-Mg basalt	786B-1R-1, 61–64 Boninite	786B-2R-1, 58–61 Boninite	786B-3R-1, 94–97 Boninite	786B-5R-2, 70–72 Boninite
Major elements (wt%):											
SiO_2	52.27	51.43	52.45	51.00	48.98	47.53	49.96	60.11	60.98	56.66	50.23
TiO_2	0.82	0.29	0.16	0.21	0.13	0.22	0.20	0.14	0.15	0.15	0.28
Al_2O_3	16.12	17.27	12.15	14.62	11.43	10.70	14.22	12.39	12.37	13.09	14.40
Fe_2O_3 (total)	12.23	8.34	7.92	7.81	9.23	8.97	7.67	7.03	6.8	7.38	8.55
MnO	0.20	0.09	0.11	0.10	0.19	0.16	0.10	0.11	0.11	0.11	0.11
MgO	4.10	5.04	12.78	11.53	14.38	18.84	10.82	7.80	7.05	8.54	7.67
CaO	9.65	8.20	5.59	8.06	6.78	5.76	7.93	6.09	6.07	5.31	10.89
Na_2O	1.03	1.83	1.34	1.57	1.74	1.02	1.32	2.05	2.08	1.46	1.57
K_2O	0.34	1.38	0.83	0.32	0.70	0.41	0.50	0.51	0.55	0.80	1.25
P_2O_5	nd	nd	nd	nd	nd	nd	nd	nd	nd	nd	0.01
LOI	0.84	2.92	5.79	2.41	6.16	5.21	4.66	2.19	2.05	3.78	3.40
Total	98.14	96.84	98.99	97.65	99.23	98.98	97.39	98.48	98.10	98.28	97.36
Mg#	0.37	0.51	0.74	0.72	0.73	0.78	0.71	0.66	0.64	0.67	0.61
Trace elements (ppm):											
Nb	0.6	2.4	2.1	0.8	0.8	1.4	—	2.1	1.8	2.2	0.8
Zr	40	46	27	33	22	21	—	44	45	47	34
Y	24	6.1	5.9	9.4	10.9	8.7	—	7.0	2.2	4.6	12.8
Sr	183	165	100	147	93	64	—	174	178	153	147
Rb	6.1	14.1	13.1	2.5	9.5	7.2	—	6.2	7.4	23	6.4
Zn	113	92	63	68	73	71	—	55	53	61	63
Cu	106	40	52	37	160	23	—	67	72	84	63
Ni	18	95	268	190	215	522	—	99	85	103	170
Cr	23	120	615	506	471	1336	—	174	345	385	333
V	428	156	143	226	194	195	—	177	185	200	237
Ti	5520	1680	1320	1680	1140	1620	—	1020	1320	1080	2280
Ce	26	20	5	5	5	nd	—	12	14	9	nd
Ba	27	36	23	8	8	11	—	47	39	21	19

fluids that were driven off from the slab during subduction dewatering, then this component is not as great as might have been expected for West Pacific subduction-related magmas.

SEDIMENT/FLUID GEOCHEMISTRY

Sediment Geochemistry

Sediments from Site 786 were analyzed on board the ship for inorganic carbon and for total carbon, nitrogen, and sulfur using the techniques described in the "Explanatory Notes" chapter (this volume). The organic carbon content was then calculated by difference. These results are presented in Table 7 and in Figure 8. The $CaCO_3$ content of the sediments varies from less than 1 to 40 wt%, except for a single sample from 102.50 mbsf that contains 67.2 wt%. The organic carbon content decreases from 0.41 wt% near the seafloor to less than 0.05 wt% at about 100 mbsf. The single deep sample, from 154.27 mbsf, contains 0.21 wt%. Nitrogen concentrations generally decrease with organic carbon content and with depth, from 0.22 wt% near the seafloor to less than 0.01 wt% at 14 mbsf.

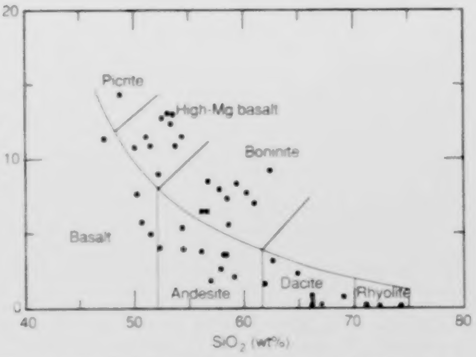

Figure 4. Rock classification based on variation in MgO with SiO_2. The arbitrary separation between high- and low-MgO groups is used to provide a consistent framework of classification.

Fluid Geochemistry

The sediments at Site 786 have uniformly lower concentrations of methane than any of the other eight sites investigated during Leg 125. The concentrations, as measured for 5-cm^3 sediment headspace samples, vary from 8 to 11 μL/L (Table 8). Methane was the only hydrocarbon detected.

Four interstitial-water samples were obtained from 5.98 to 81.25 mbsf in Hole 786A (Table 9). These samples are compared with those from Sites 782 through 785 and with surface seawater in Figure 9. At Site 786, pH varies from 7.6 to 7.9, within the normal range of 7.5 to 8.5 for interstitial waters from deep-sea sediments. Alkalinity and ammonia reach maximum concentrations that are smaller and occur at shallower

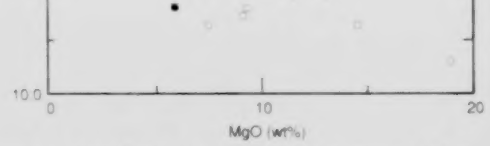

Figure 5. Rocks from Site 786 exhibit a wide variation in MgO vs. Al_2O_3, which may represent variations in the modal% of plagioclase phenocrysts or xenocrysts in the rocks, but not all plagioclase-phyric types have high Al_2O_3. Solid symbols = rocks with plagioclase greater than 10 modal%.

Table 6 (continued).

786B-6R-2, 126–130 High-Mg basalt	786B-8R-1, 45–47 Andesite	786B-9R-1, 10–15 Andesite	786B-11R-1, 122–126 High-Mg basalt	786B-12R-2, 14–16 High-Mg basalt	786B-12R-2, 120–124 Boninite	786B-15R-1, 137–141 Dacite	786B-19R-1, 91–94 Andesite	786B-21R-1, 26–29 Andesite	786B-21R-1, 129–131 Dacite	786B-21R-2, 72–76 Basalt	786B-22R-3, 61–64 Dacite
51.45	54.17	56.06	53.66	54.26	59.24	61.83	58.13	56.85	66.91	50.62	66.14
0.20	0.23	0.24	0.14	0.16	0.12	0.25	0.21	0.27	0.19	0.15	0.17
14.12	17.40	17.07	12.89	13.70	12.78	14.93	16.25	16.95	12.62	11.80	12.13
8.57	7.76	7.43	7.62	8.28	7.11	6.74	7.49	7.30	3.49	8.14	3.29
0.17	0.12	0.11	0.14	0.15	0.12	0.09	0.12	0.10	0.07	0.14	0.06
10.92	3.96	3.83	10.18	11.54	8.38	1.61	3.57	1.85	0.31	5.76	0.11
9.32	7.60	7.52	6.50	7.17	6.77	5.40	7.14	6.56	2.30	13.33	1.90
1.13	2.37	2.07	1.19	1.28	1.56	2.86	2.40	2.80	2.90	1.19	3.56
0.25	0.65	0.57	0.42	0.31	0.64	0.72	0.71	0.85	2.05	0.39	2.30
nd	nd	nd	nd	nd	0.03	nd	nd	0.04	nd	nd	0.02
1.80	2.71	1.97	2.80	2.16	1.53	2.48	2.34	2.91	6.50	5.75	2.97
98.06	97.34	98.88	97.64	98.51	97.99	98.99	97.96	96.88	97.80	97.27	97.06
0.60	0.47	0.47	0.71	0.73	0.67	0.29	0.45	0.29	0.13	0.55	0.05
1.1	0.9	1.6	1.7	1.8	2.1	1.5	1.9	0.9	2.0	1.2	1.5
33	51	53	49	41	37	57	48	58	76	29	76
10.7	16.1	15.4	5.5	5.6	6.5	10	8.7	21	11.6	8.3	13.6
136	227	226	170	125	166	217	214	236	148	150	162
2.9	8.5	6.6	5.8	4.0	6.3	7.2	7.7	11.1	36	7.8	41
68	75	72	71	76	53	65	72	86	49	50	51
69	66	101	40	30	74	91	78	62	68	40	26
223	41	40	159	164	116	9	13	18	6	180	1
561	6	8	471	485	425	6	15	5	0	609	nd
232	236	239	174	153	187	239	226	21	24	185	54
2250	1980	1920	1500	1500	1200	1800	1860	2100	1300	1300	1120
15	8	16	16	3	13	15	13	12	15	13	10
9	17	40	17	25	37	35	31	27	52	20	58

depths than at the other sites, and alkalinity decreases more quickly with depth below its maximum at about 6 mbsf. These changes are consistent with a minimal amount of bacterial sulfate reduction, as indicated by the slight decrease in sulfate with depth. The steep decrease in alkalinity is accompanied by a decrease in silica with depth below 25 mbsf. Like alkalinity, magnesium, potassium, and calcium change more rapidly with depth at Site 786 than at the other sites (Fig. 9). These changes in alkalinity, silica, magnesium, potassium, and calcium probably result from reactions between interstitial water and volcanic material within and below the sediments.

Chlorinity increases by about 2% with depth at Site 786 (Fig. 9), as it does at the other sites. This increase probably results from the increased chlorinity of ocean bottom water during the Pleistocene glaciations, as proposed by McDuff (1985).

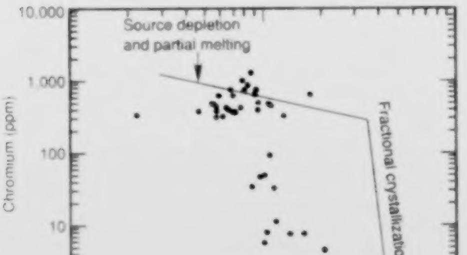

Figure 6. Chromium-yttrium co-variation diagram for volcanic rocks from Site 786. The relatively large variation in yttrium at high chromium indicates a range of primitive liquid compositions that reflects variable source characteristics. The vertical array of data points is a function of crystal fractionation.

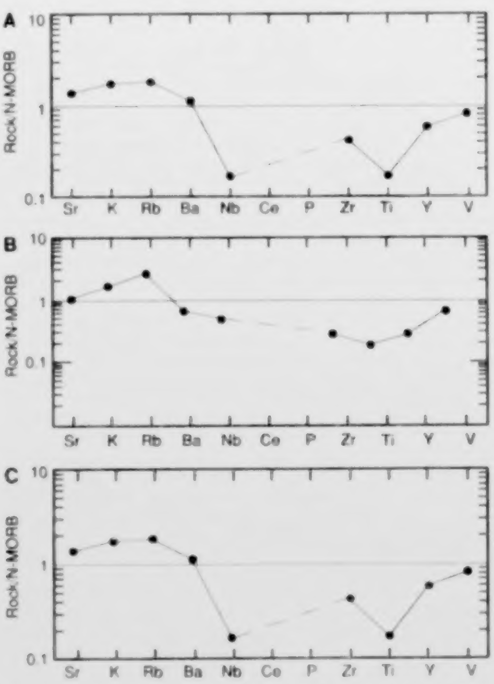

Figure 7. Multi-element N-MORB-normalized diagrams. A. Representative high-Mg basalt (Sample 125-786B-5R-2, 70–72 cm). B. Representative primitive andesite (Sample 125-786B-40R-2, 54–57 cm). C. Representative boninite (Sample 125-786B-11R-1, 122–126 cm).

Table 6 (continued).

Sample (interval in cm) Rock type[a]	786B-24R-1, 9-12 Dacite	786B-26R-1, 68-70 Dacite	786B-30R-1, 29-31 Boninite	786B-30R-1, 119-121 Boninite	786B-31R-2, 84-86 Boninite	786B-32R-2, 86-88 Rhyolite	786B-34R-1, 45-47 High-Mg basalt	786B-35R-1, 73-76 Dacite	786B-35R-2, 122-126 Dacite	786B-37R-1, 95-98 Boninite	786B-37R-3, 45-49 Andesite	786B-38R-1, 6-8 Andesite
Major elements (wt%):												
SiO_2	56.15	56.24	56.03	58.52	57.71	71.04	52.13	62.48	64.80	56.51	57.75	58.98
TiO_2	0.26	0.26	0.09	0.14	0.10	0.23	0.14	0.20	0.23	0.20	0.20	0.21
Al_2O_3	14.85	14.59	12.20	12.94	13.09	12.85	11.61	14.86	14.72	14.80	14.75	15.93
Fe_2O_3 (total)	5.18	4.74	6.98	6.39	6.47	1.85	7.46	5.74	5.39	7.23	8.05	7.01
MnO	0.07	0.06	0.09	0.09	0.10	0.02	0.12	0.04	0.04	0.08	0.10	0.09
MgO	0.89	0.55	6.52	5.63	8.02	nd	9.00	1.25	2.36	6.53	2.65	2.09
CaO	4.46	3.81	9.83	8.07	8.11	2.88	11.05	5.49	5.00	7.77	5.05	6.68
Na_2O	3.41	3.59	1.71	2.07	1.57	5.35	1.42	3.02	2.93	1.46	2.14	2.05
K_2O	0.82	1.14	0.87	0.070	0.51	1.35	0.58	0.52	0.69	0.47	1.45	1.03
P_2O_5	0.02	nd	nd	nd	nd	nd	nd	nd	nd	nd	nd	nd
LOI	0.44	0.31	4.25	3.40	1.67	1.15	3.44	1.72	1.23	2.29	5.39	2.94
Total	96.52	96.76	98.04	97.44	97.36	96.72	98.34	97.28	97.27	97.62	97.50	97.00
Mg#	0.25	0.17	0.62	0.60	0.68	nd	0.66	0.49	0.43	0.61	0.36	0.34
Trace elements (ppm):												
Nb	1.4	1.8	1.6	1.6	1.6	1.8	1.4	1.6	1.6	1.6	1.4	1.7
Zr	70	75	31	42	34	74	29	56	59	38	44	49
Y	13.7	11.8	5.7	7.6	5.7	12.4	8.8	10.1	9.3	9.3	9.1	9.2
Sr	208	495	195	178	211	173	141	213	201	186	293	229
Rb	7.3	16.1	23	15.8	10.2	43	15.3	7.7	11.4	13.4	29	13.9
Zn	45	40	51	51	63	39	55	46	48	68	61	62
Cu	54	22	29	13	20	26	61	54	33	20	94	86
Ni	7	2	126	127	131	2	277	26	24	149	14	12
Cr	8	10	311	444	381	nd	789	50	47	397	nd	nd
V	185	119	132	142	184	40	180	152	134	187	224	259
Ti	1920	1860	960	1280	1120	1680	1320	1680	1620	1620	1620	1740
Ce	7	10	13	10	11	6	7	0	14	nd	12	13
Ba	64	73	43	45	32	77	11	59	53	34	108	54

STRUCTURAL STUDIES

Normal faults have been observed within the soft sediments of Hole 786A in Sections 125-786A-1H-6, 125-786A-2H-4, and 125-786A-2H-7. In Sections 125-786A-2H-4 and 125-786A-2H-7, the faults cut graded ash layers. In Section 125-786A-2H-7, one of the offset parts of the ash layer is missing. Although the total amount of displacement along the fault cannot be determined, it is at least greater than 25 cm. The faults can be related to local disaggregation processes during normal dewatering of the sediments. They may also indicate regional slope instability, as is probably the case for the set of faults visible in Section 125-786A-1H-6, which may represent a major tectonic feature. The site is near a major fault that has a vertical displacement of a few hundred meters and is evident in seismic sections. A fault crosscuts a volcanic pebble in Section 125-786A-11X-4 at 100 cm. This fault also represents the upper limit of the sediments that contain volcanic pebbles and must therefore be regarded as a major break in the sequence recovered from this hole.

Detailed descriptions and genetic interpretations of all the structural post-depositional features encountered in the volcanic sequence, the volcaniclastic breccias and sandstones, and the interbedded pelagic sediments of Hole 786B are too complex to be presented here. We summarize the most important features as follows:

Core 125-786B-21R: Welded tuffs having a vertical foliation that probably results from flow banding. The attitude of banding may be primary or may indicate post-depositional tectonic tilting.

Core 125-786B-22R: The following observations document a major shear zone:

1. Analysis of relationships of C-S planes in a strongly sheared and flattened pink sepiolite layer in Section 125-786B-22R-1 suggests a normal sense of shear.
2. Primary bedding in sedimentary rocks in Section 125-786B-22R-1 has high-angle (60°–70°) dips. Numerous synsedimentary faults and slump structures in the sediments indicate that syn- to post-depositional tectonic activity and related slope instability had taken place before the major tilting.
3. Welded tuffs in Section 125-786B-22R-2 commonly exhibit vertically oriented flow-banding and syn-consolidation extensional microfaulting. This last observation is consistent with the hypothesis of emplacement along a preexisting slope.

Core 125-786B-27R: Extensional syn-depositional faults and related cross-lamination are in the graded, coarse, green volcanic sandstones in Section 125-786B-27R-1, 50–70 cm.

Core 125-786B-34R: Numerous fractures and calcite-filled veins are visible in Sections 125-786B-34R-2 and 125-786B-34R-3. Dips vary from 45° to 80°. Generally, no displacement took place along the fractures. The veins show multiple orientations.

Core 125-786B-40R: Two fault planes dipping 55° and 65° with slickensided surfaces are observed at 30 cm in Section 125-786B-40R-2. The sense of movement is normal along one fault but is reversed along the other. At 95 cm in the same section, a fault surface dips at 62°, although clear evidence of displacement is not present.

Core 125-786B-41R: Section 125-786B-41R-3 contains welded tuffs with flow lamination and depositional layering dipping at 40° to 50°. "Hot" deformation criteria, such as plastic folding of glass laminae are common.

Core 125-786B-43R: In Section 125-786B-43R-1 a strong, subhorizontal striation is visible along a plane dipping at 70°. This is the only indicator of strike-slip movement observed at Site 786.

Core 125-786B-56R: Three fault surfaces occur in Section 125-786B-56R-4 between 30 and 80 cm. They show striation rakes on a slickensided surface indicating normal and reverse movements. Fault dips range from 65° to 75°.

Cores 125-786B-58R and 125-786B-59R: Detailed analysis of vesicle distribution within the glassy rims of the boninitic pillow lavas of these two sections suggests a general tilting (40°–50°?) of this volcanic pile (see "Igneous and Metamorphic Petrology" section, this chapter).

Core 125-786B-61R: This core is characterized by tectonic discontinuities within the sequence of andesitic rocks. Faults, fault breccias and cataclastic rocks, powdered rocks from fault gouges, faint pressure-dissolution cleavages, locally abundant veining, and additional high-angle dips of flow banding and flow contacts (up to 60°) are in Sections 125-786B-61R-4 to 125-786B-61R-6. In Section 125-786B-61R-4, steps on a fault plane dipping at 65° indicate normal movement.

Table 6 (continued).

86B-40R-2, 54–57 Basalt	786B-49R-4, 32–37 Andesite	786B-51R-1, 51–55 High-Mg basalt	786B-61R-5, 56–58 Rhyolite	786B-61R-5, 81–84 Rhyolite	786B-62R-3, 40–42 High-Mg basalt	786B-63R-2, 72–74 Rhyolite	786B-65R-1, 17–19 Andesite	786B-66R-1, 88–90 Dacite	786B-67R-1, 63–65 High-Mg basalt	786B-69R-1, 65–67 Boninite	786B-70R-1, 68–73 Boninite
47.23	58.34	53.25	72.30	71.02	53.47	74.29	54.31	68.95	53.00	62.35	58.44
0.22	0.23	0.15	0.24	0.26	0.14	0.17	0.35	0.18	0.16	0.16	0.15
12.06	15.03	12.74	13.12	12.59	12.05	12.41	17.03	13.41	12.46	11.75	11.43
8.05	7.10	8.49	3.26	3.36	8.44	1.92	7.37	4.07	7.54	6.78	6.11
0.14	0.13	0.17	0.05	0.04	0.13	0.01	0.08	0.06	0.14	0.09	0.13
11.60	3.62	12.36	nd	nd	13.04	nd	5.41	0.82	13.08	9.23	7.40
11.90	7.29	7.78	2.49	1.77	5.27	0.45	6.51	2.26	6.70	3.98	4.95
0.89	2.04	1.17	3.35	3.85	2.18	2.51	2.06	2.22	1.28	2.05	2.27
0.26	0.73	0.26	1.11	1.14	0.67	4.98	0.40	3.12	0.21	0.06	0.20
nd	nd	0.08	nd	nd	nd	nd	nd	nd	nd	nd	nd
5.46	2.89	2.01	1.84	1.43	4.33	0.27	3.23	2.36	2.56	4.31	4.66
97.60	97.39	98.43	96.94	95.52	99.20	97.01	93.59	95.10	94.57	97.41	96.74
0.71	0.47	0.72	nd	nd	0.73	nd	0.58	0.26	0.75	0.70	0.68
1.6	1.4	0.5	1.4	2.1	2.2	2.4	1.4	1.7	1.2	2.1	1.6
27	45	37	77	82	34	78	44	74	28	44	45
8.9	10.8	17.4	14.1	14.1	7.8	12.7	11.5	11.2	6.9	8	9.2
146	195	166	121	122	110	47	163	101	137	143	147
5.6	10.1	3.7	18.1	14.6	6.5	51	3.1	34	2.5	0	1.5
57	58	70	45	52	63	41	65	96	58	75	77
27	89	41	56	18	60	63	60	50	56	177	70
374	39	195	3	6	306	1	22	9	296	212	202
650	93	659	0	0	1032	0	11	33	626	748	764
193	245	220	35	41	166	22	267	31	202	156	148
1500	1800	1560	1680	1800	1200	1440	2400	1440	1380	1260	1320
2	9	20	13	11	5	15	10	19	3	10	9
10	6	22	91	93	46	505	46	332	34	39	52

Note: nd = not detected.
ᵃ Classified according to Figure 4.

Core 125-786P-63R: Section 125-786B-63R-1 contains cataclastic and sheared andesites. Ductile shearing in the interval between 30 and 70 cm is indicated by progressive bending and stretching of andesite breccias. At 66 and 85 cm, a weak, anastomosing, strongly dipping foliation can be seen within the sheared breccias. C-S-like relationships between the cleavage planes are consistent with a normal sense of shear. Both chloritized and primary magmatic minerals are deformed within the shear zone. Slickensided fragments from a fault gouge were recovered from between 95 and 113 cm in this section, and the last sample from this section is a cataclastic andesite having a strongly dipping foliation defined both by pervasive veining and by alignment of broken fragments.

Core 125-786B-69R: The seven sections of this core are characterized by the presence of anastomosing veins and fractures related to hydrothermal brecciation and mineralization. Abundant veins filled with pyrite, quartz, and carbonate dip from 0° to 80° and define a conjugate fracture set. Despite local shearing near vein intersections, no displacement along veins was observed. Fracturing is associated with pods filled with calcite and pyrite. The size and frequency of the pods increase downhole. This fractured zone may represent the upper part or an upper extension of the andesitic stockwork encountered in Core 125-786B-71R.

Core 125-786B-71R: This core contains pervasively fractured volcanic rocks and argillitized and mineralized cataclastites. Pyrite is found in association with quartz and carbonates in anastomosing veins a few centimeters wide. In Section 125-786B-71R-1 the rocks have fractured along variably oriented planes without noticeable displacement. Such features characterize hydraulic fracturing, which is controlled by fluid overpressure. These rocks represent an andesitic stockwork, commonly encountered in arc environments. Sections 125-786B-71R-2 and 125-786B-71R-3 contain intensively argillitized and mineralized fault zones and breccias. The breccias are composed of angular clasts of strongly hydrothermally altered andesites of various colors, ranging from light green to white. The breccias may represent the result of fluid movement along major fractures during the hydrothermal processes or may be fault breccias. At this time, these cataclastic features at Site 786 cannot be related to a particular structural setting or tectonic processes such as normal, reverse, or transcurrent faulting. Two intervals, probably of fault gouge, at 100 and 130 cm in Section 125-786A-71R-2, contain small pieces of slickensided meta-andesite mixed with drill mud.

PALEOMAGNETISM

Magnetic Remanence

Two holes were drilled at Site 786. At Hole 786A, APC/XCB coring penetrated to 166.5 mbsf. There was good recovery of the sediments overlying the volcanic rocks, and many intervals of normal and reversed polarity were identified. No sediments were recovered in Hole 786B. The broken and discontinuous nature of the volcanic rocks in this hole made any magnetostratigraphy impossible.

The natural remanent magnetization of the archive half of each core from Hole 786A was measured using the cryogenic magnetometer. Magnetic intensities range from 1 to 300 mA/m (Fig. 10). Most cores have values of between 10 and 100 mA/m. Intensity does not change systematically downhole. When the cores were demagnetized at the 10-mT level and remeasured, intensities were reduced to about 10% to 30% of their initial values. Discrete samples were also taken from all of the cores in Hole 786A. These samples were measured at levels of 0, 5, 10, and 15 mT. In general, the polarities obtained from these samples agree with the whole-core data (Table 10). Data from whole cores and discrete samples in combination with biostratigraphic data ("Biostratigraphy" section, this chapter) enabled us to construct a tentative magnetostratigraphy for the sediments in Hole 786A (Fig. 11). Only data from the first 55 m of the hole are shown in Figure 11; below this point, correlations are impossible because of poor recovery and sparse biostratigraphic data. The correlations shown are uncertain because of the sparse biostratigraphic data and probable incomplete cleaning of spurious magnetization.

Past research on drill cores from the Philippine Sea Plate (Bleil, 1982) suggests that the Philippine Sea Plate has moved northward with time. Inclination data from Hole 786A were separated into 25-m sections, grouped into 10° intervals, and plotted on histograms (Fig. 12). The data from the intervals between 0 and 25 mbsf and between 25 and 50 mbsf show good bimodal distributions with peaks around +45° and −45°, which suggests that there has been little or no translation since the late Miocene. In the intervals below this, the data are scattered and not bimodally distributed. However, there are

Table 7. Total nitrogen, carbon, inorganic carbon, organic carbon, and carbonate carbon in sediments at Site 786.

Core, section, interval (cm)	Depth (mbsf)	Total nitrogen (wt%)	Total carbon (wt%)	Inorganic carbon (wt%)	Organic carbon (wt%)	$CaCO_3$ (wt%)
125-786A-						
1H-1, 84-86	0.84			4.28		35.7
1H-2, 72-74	2.22	0.22	3.22	2.81	0.41	23.4
1H-3, 76-78	3.76			2.29		19.1
1H-4, 71-73	5.21			2.70		22.5
1H-5, 90-92	6.90			0.27		2.2
1H-6, 51-53	8.01			2.10		17.5
1H-7, 21-23	9.21			1.21		10.1
2H-1, 67-69	10.37			2.92		24.3
2H-2, 73-75	11.93			1.29		10.8
2H-3, 78-80	13.48	0.23	3.05	2.64	0.41	22.0
2H-4, 65-67	14.85			1.72		14.3
2H-5, 73-75	16.43			2.32		19.3
2H-6, 88-90	18.08			3.53		29.4
2H-7, 22-24	18.92			4.45		37.1
3H-1, 75-77	19.95			2.68		22.3
3H-2, 64-66	21.34	0.19	3.58	3.40	0.18	28.3
3H-3, 76-78	22.96			2.51		20.9
3H-4, 75-77	24.45			3.67		30.6
3H-5, 62-64	25.82			2.91		24.2
3H-6, 58-60	27.28			0.08		0.7
3H-7, 44-46	28.64			3.72		31.0
4X-1, 32-34	29.02			3.81		31.7
4X-2, 5-7	30.25	0.22	3.25	2.88	0.37	24.0
4X-CC, 15-17	30.61			3.02		25.2
5X-1, 54-56	38.74			2.49		20.7
5X-2, 54-56	40.24	0.15	3.01	2.93	0.08	24.4
5X-3, 101-103	42.21			2.08		17.3
5X-4, 37-39	43.07			0.35		2.9
6X-1, 59-61	48.19			1.28		10.7
6X-2, 59-61	49.69	0.17	1.61	1.33	0.28	11.1
6X-3, 59-61	51.19			0.50		4.2
6X-4, 59-61	52.69			1.44		12.0
6X-5, 16-18	53.76			0.02		0.2
7X-1, 33-35	57.43			2.34		19.5
7X-2, 33-35	58.93	0.12	1.24	1.04	0.20	8.7
7X-3, 33-35	60.43			1.78		14.8
7X-4, 33-35	61.93			1.64		13.7
7X-5, 33-35	63.43			0.95		7.9
7X-CC, 4-6	64.33			1.28		10.7
8X-1, 48-50	67.58			0.86		7.2
9X-1, 83-85	77.63			0.12		1.0
9X-2, 97-99	79.27	0.12	3.05	2.92	0.13	24.3
9X-3, 93-95	80.73			2.96		24.7
9X-4, 80-82	82.10			2.72		22.7
9X-5, 59-61	83.39	0.14	0.42	0.09	0.33	0.7
9X-5, 98-100	83.78			2.99		24.9
9X-6, 25-27	84.55			4.00		33.3
10X-1, 89-90	87.29			2.12		17.7
10X-2, 82-84	88.72	0.18	2.87	2.76	0.11	23.0
10X-3, 72-74	90.12			3.38		28.2
10X-4, 82-84	91.72			3.57		29.7
10X-5, 82-84	93.22			4.52		37.7
10X-6, 25-27	94.15			2.63		21.9
11X-1, 80-82	96.80			4.72		39.3
11X-2, 83-85	98.33	0.11	4.04	4.04	0.00	33.7
11X-3, 78-80	99.78			2.94		24.5
11X-4, 84-86	101.34			3.81		31.7
11X-5, 50-52	102.50			8.07		67.2
12X-1, 42-44	106.12	0.09	3.27	3.38	0.00	28.2
17X-CC, 27-29	154.27	nd	0.34	0.13	0.21	1.1

Note: nd = not detected. Total sulfur was below the detection limit of 0.06 wt% in all samples analyzed for total carbon, nitrogen, and sulfur.

many more data points between +15° and −15°, which suggests that these rocks may have acquired their magnetization at a lower latitude than their present position. Additional research will be necessary to determine more accurately the translational history for these rocks.

Magnetic Susceptibility

Whole-core magnetic susceptibilities were measured using the multisensor track (MST). A downhole plot of these data is presented in Figure 13. The sediments typically have values between 0 and 19 × 10^{-3} SI units. There are identifiable peaks downhole, but these peaks do not correlate with any major changes in the physical properties of the rocks (see "Physical Properties" section, this chapter).

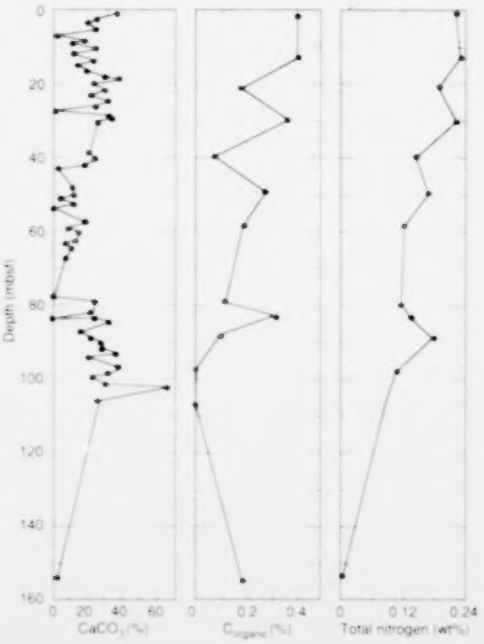

Figure 8. Weight percent of calcium carbonate, total organic carbon, and total nitrogen in sediments at Hole 786A.

SEDIMENT-ACCUMULATION RATES

Estimates of the sediment-accumulation rate for Hole 786A are based on calcareous nannofossils (Table 11), which are used to construct the age vs. depth curve shown in Figure 14.

Sedimentation rates for the middle Eocene through Oligocene are estimated to vary between 1.4 and 0.8 m/m.y. with two possible hiatuses. The hiatuses ("Biostratigraphy" section) are thought to have occurred in the late Eocene and in the early Oligocene. A major hiatus occurred in the early Miocene (7.2 m.y.; "Biostratigraphy" section, this chapter). In the middle and earliest late Miocene, sedimentation rates increased to 4.2 m/m.y., followed by a further increase to 8.6

Table 8. Results of headspace-gas analyses of cores at Site 786.

Core, section, interval (cm)	Depth (mbsf)	Methane (μL/L)[a]	(μM)[b]
125-786A-			
1H-5, 0-5	6.03	9	0.8
2H-3, 0-3	12.72	8	0.7
3H-5, 0-3	25.22	10	0.9
5X-3, 0-3	41.22	10	0.9
6X-4, 0-1	52.11	11	0.9
7X-3, 0-1	60.11	11	0.9
9X-3, 0-1	79.81	10	0.9
12X-2, 0-1	107.21	10	0.9

[a] Microliters of methane per liter of wet sediment, assuming a sample volume of 4.2 cm^3 of sediment.

[b] Micromoles of methane per liter of interstitial water, assuming a porosity of 50%.

Table 9. Composition of interstitial waters from cores at Site 786.

Sample number Core, section, interval (cm)	Depth (mbsf)	Volume (mL)	Squeeze temperature (°C)	Squeeze pressure (psi)	pH	Salinity (R.I., ‰)	(calcium, ‰)	Chlorinity (mmol/kg)	Alkalinity (meq/kg)	Sulfate (mmol/kg)	Sodium (mmol/kg)	Potassium (mmol/kg)
Surface seawater (17 March 1989)					8.25	35.6	34.65	539.2	2.689	27.78	462.0	10.11
1W-1 1H-4, 145–150	5.98	55	3	35,000	7.73	35.4	34.81	541.9	2.921	27.02	464.2	10.05
1W-2 3H-4, 145–150	25.18	85	2	40,000	7.82	35.5	34.85	550.7	1.140	23.81	466.7	9.78
1W-3 6X-3, 140–150	52.05	43	3	36,000	7.61	35.1	35.00	551.7	1.366	24.34	466.0	7.84
1W-4 9X-3, 140–150	81.25	37	4	36,000	7.86	35.1	35.00	552.6	1.209	24.03	468.4	7.92

m/m.y. through the Pliocene. Middle and upper Pleistocene sediments are missing from the succession.

PHYSICAL PROPERTIES

The excellent recovery in Holes 786A and 786B allowed us to make a highly detailed reconstruction of the physical properties of the lithologic sequence at this site. Thermal conductivity, GRAPE bulk densities, index properties (bulk and grain densities, porosity, water content, and void ratio), and electrical resistivity were measured in the sedimentary sections encountered in Hole 786A. The preponderance of voids in the cores precluded the use of the *P*-wave logger for these holes. Thermal conductivity, GRAPE bulk density (on discrete samples), index properties, and compressional-wave velocities of discrete samples were measured for the igneous rocks recovered from Hole 786B. The physical-property measurements are listed in Tables 12 through 14 and plotted in Figures 15 through 19.

Hole 786A

Thermal-conductivity measurements in the sedimentary rocks are scattered about 1 W/mK and show little variation with depth (Table 13 and Fig. 15). Extremely low values (0.127 and 0.171 W/mK) were recorded in cores from the base of the hole, where the probe did not couple well with the sedimentary cores.

Wet-bulk densities measured by the GRAPE sensor on the MST show little variation with depth throughout the sedimentary section (Fig. 16). Densities of sedimentary cores cluster at 1.6 to 1.7 g/cm^3 for the uppermost 100 mbsf. Poor recovery in the interval from 110 to 140 mbsf prevented measurement of GRAPE densities. Rocks from the deepest part of the hole show considerable scatter in bulk density, which may well be related to the brecciated nature of the rocks.

Index properties were measured on discrete samples throughout the hole (Table 12). Bulk densities of sedimentary cores determined from discrete sample measurements are similar to those measured by the GRAPE sensor, and the values are grouped about 1.6 to 1.7 g/cm^3 and show no significant depth variation (Fig. 16). The bulk densities of samples of igneous rock from the base of the hole are higher (1.8 to 2.1 g/cm^3). Grain density also shows little variation with depth in both sediments and igneous rocks and ranges from 2.6 to 2.7 g/cm^3 for both sediment and hard-rock samples.

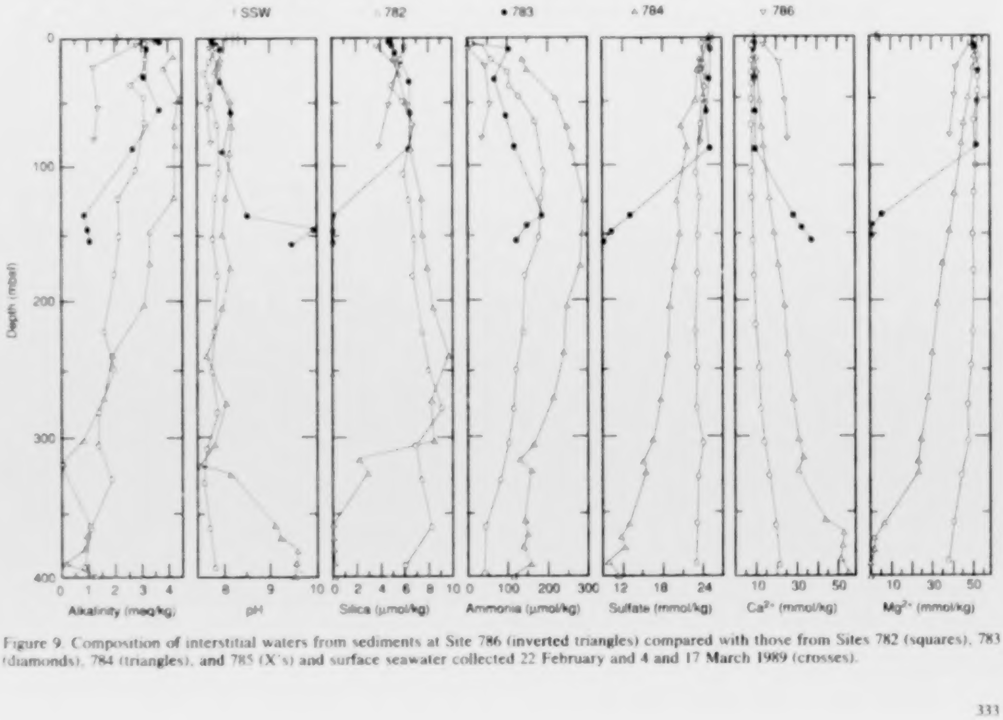

Figure 9. Composition of interstitial waters from sediments at Site 786 (inverted triangles) compared with those from Sites 782 (squares), 783 (diamonds), 784 (triangles), and 785 (X's) and surface seawater collected 22 February and 4 and 17 March 1989 (crosses).

Table 9 (continued).

Calcium (mmol/kg)	Magnesium (mmol/kg)	Bromide (mmol/kg)	Silica (µmol/kg)	Ammonia (µmol/kg)
10.18	52.48	0.830	0	0
14.08	48.24	0.850	385	<12
20.69	40.77	0.866	540	41
24.44	39.06	0.899	467	59
25.00	37.79	0.915	374	37

Where possible, electrical resistivities were measured for every second section of sedimentary material (Table 13). Resistivity may increase with depth, but the data are scattered (Fig. 17).

Hole 786B

Thermal conductivity was measured once per section using the half-slab technique (Table 14). Conductivities ranged from 1.0 to 1.8 W/mK from 150 to 750 mbsf (Fig. 18), but the data show considerable scatter. Below 750 mbsf, the rocks display generally higher thermal-conductivity values (up to 2.5 W/mK). This increase in thermal conductivity corresponds to the boundary between breccias and dikes (see "Igneous and Metamorphic Petrology" section, this chapter).

Discrete measurements of GRAPE density were performed on whole-round core sections, generally twice per section. Density increases with depth from 2.1 to 2.5 g/cm^3 over the 800 m cored (Fig. 18). These data are in good agreement with logging results (see "Downhole Measurements" section, this chapter). Rocks from higher levels in the hole show more scatter than those from deeper levels. The decreased scatter in the data is probably caused by increasing regularity downhole of the core diameter, which allowed us to collect data of higher quality. Index properties do not correlate well with GRAPE and downhole measurements (Fig. 19). Neither bulk density nor grain density shows significant downhole variation. Bulk densities increase from 2.3 to 2.5 g/cm^3, but exhibit a large degree of scatter, probably related to sampling of nonrepresentative rocks. Low bulk densities are recorded for samples from shear zones, where the rocks have significantly higher water contents (see Table 12). Grain densities are nearly constant at 2.7 g/cm^3.

Compressional-wave velocities were measured in two directions in each index-property sample. The A velocity is measured parallel to the split surface of the core, and the B velocity is measured perpendicular to the split surface. The samples measured generally show little seismic anisotropy (Table 14). Velocities range from 3000 to nearly 6000 m/s in each direction, and do not have coherent downhole trends (Fig. 19). The large velocity range is caused by the fractures and microcracks in the samples, which significantly lower compressional-wave velocities.

DOWNHOLE MEASUREMENTS

Hole 786B was logged in five different runs. The first log string consisted of the dual induction tool (DIT), the digital sonic tool (SDT), the natural gamma-ray spectrometry tool (NGT), and the temperature logging tool (TLT) and was run from 449 mbsf up to the end of the drill string. The second string—consisting of the lithodensity tool (LDT), the compensated neutron tool (CNT), NGT, and TLT—was run from a depth of 387 mbsf up to the end of the drill string. These tools were then combined into the Quad string (consisting of the

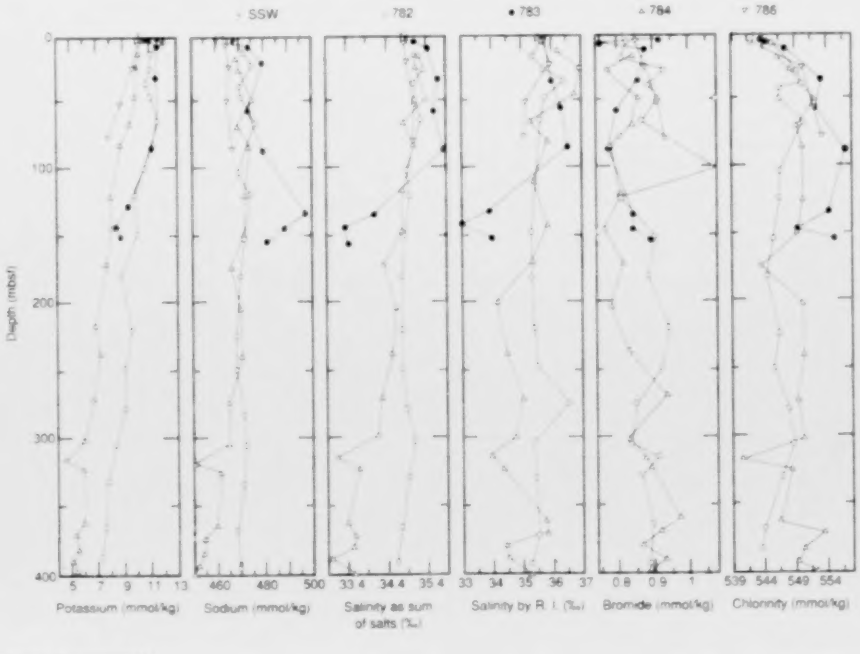

Figure 9 (continued).

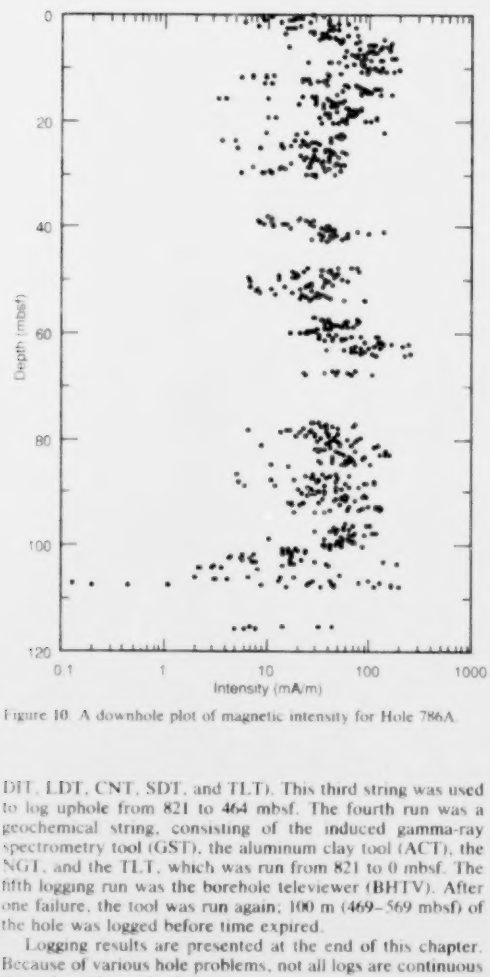

Figure 10. A downhole plot of magnetic intensity for Hole 786A.

DIT, LDT, CNT, SDT, and TLT). This third string was used to log uphole from 821 to 464 mbsf. The fourth run was a geochemical string, consisting of the induced gamma-ray spectrometry tool (GST), the aluminum clay tool (ACT), the NGT, and the TLT, which was run from 821 to 0 mbsf. The fifth logging run was the borehole televiewer (BHTV). After one failure, the tool was run again; 100 m (469–569 mbsf) of the hole was logged before time expired.

Logging results are presented at the end of this chapter. Because of various hole problems, not all logs are continuous throughout the entire hole.

Both lithologic Units I and II, with low percentages of SiO_2 and those of $CaCO_3$ of approximately 5% to 20%, are difficult to distinguish in the logging data. Lithologic Unit III is clearly differentiated from Unit II by the much higher MgO content (~10%), slight decrease in SiO_2, and sharp decrease in $CaCO_3$ in Unit III. The sediment/basement interface at 162.5 mbsf is much less distinct. The only logs that show a significant change at this depth are the bulk density log, which increases to 2.3 g/cm^3, and the porosity log, which decreases to 30%.

Based on the petrology, basement at Hole 786B has been divided into 30 units, some of which are heterogeneous in chemical composition. This large number of units precludes a detailed, unit-by-unit description of the logs here. A more detailed analysis of these logs will appear in the Leg 125 *Scientific Results* volume. In general, the MgO, SiO_2 (upon detailed examination), Al_2O_3, and perhaps sulfur logs are the most useful for distinguishing lithology.

The gamma-ray logs (CGR and SGR) show little variation downhole and average about 20 API units. Certain units stand out with slight variations that are a few API units higher or lower. The most striking feature observed in the gamma-ray logs is an increase of 55 to 70 API units between 752 and 783 mbsf, which is basement Unit 26 (metadacite and rhyolite flows). One dike within the unit has much lower gamma-ray values.

The resistivity logs show a certain amount of variation from unit to unit that is largely controlled by the amount of fracturing and brecciation. Resistivity is about 10 ohm-m in the upper part of the hole and slowly increases to 20 ohm-m at the bottom. Certain intervals, such as from 308 to 358 mbsf, have lower values of 3 to 7 ohm-m. Local variability also changes throughout the hole, with the interval from 468 to 593 mbsf and the zone below 733 mbsf showing increased local variability.

The caliper log shows that the hole is somewhat rugose in the upper part (down to 336 mbsf) with diameters of 0.36 to 0.41 m. The hole is narrower and smoother (from 0.30 m down to 0.25 m) in the lower part of the hole, at 478 mbsf. Data from the interval from 336 to 478 mbsf are unusable.

Bulk density ranges from 2.1 to 2.2 g/cm^3 at the top of the logged interval and 2.4 g/cm^3 at the bottom. Density generally increases with depth, but individual units may show increases or decreases about the trend. Variability can also be enhanced locally, especially at unit boundaries.

Porosity is about 50% at the top of the logged interval and decreases to about 30% at the bottom of the hole. The porosity abruptly decreases between 735 and 740 mbsf, with one small area of increased porosity in an interval with remarkable correspondence to Units 22 (rhyolite dike/sill), 23 (shear zone), and 24 (altered boninite-andesite pillows). The porosity abruptly decreases again at 752 mbsf, in Unit 26 (see the preceding discussion of gamma-ray logs).

The photoelectric effect is 2.9 barns/e at the top of the logged section and 3.2 barns/e at the bottom of the section.

Thorium is low and variable throughout most of the hole and ranges between 0.3 and 1 ppm. Thorium gradually increases to 2 ppm in the interval from 728 to 778 mbsf. Values decrease below that depth.

Uranium values are also low and variable throughout the hole, generally in the range of 0.25 to 0.5 ppm. Values up to 2.0 ppm occur in the interval from 533 to 538 mbsf, which is part of Unit 16, an andesitic breccia.

Potassium values vary somewhat in most of the hole, ranging from 0.5% to 1.0%. The major exception is within Unit 26 between 752 and 783 mbsf, where values range between 2.5% and 4.0%.

A discussion of the elemental logs of MgO, SiO_2, Al_2O_3, sulfur, CaO, and Fe_2O_3 will be presented in the Leg 125 *Scientific Results* volume.

Borehole Televiewer

The ultrasonic borehole televiewer (BHTV) was used to log the interval from approximately 469 to 569 mbsf. Both the high-frequency (1.4 MHz) and low-frequency (400 mHz) transducers were used in logging. The low-frequency transducers gave the best data. Preliminary analysis of the BHTV data indicates breakouts along the N10°E–S10°W direction, which shows the direction of minimum compressive stress. The direction of maximum compressive stress is at right angles to this and is aligned roughly along the orientation of the motion of the Pacific Plate.

SUMMARY AND CONCLUSIONS

Site 786 (proposed Site BON-6C) is located in the center of the Izu-Bonin forearc basin about 120 nmi east of the active volcano Myojin Sho. The objectives of this site were to study (1) the uplift and subsidence history of the forearc basin at this

Table 10. Remanence data for the discrete samples taken from Hole 786A.

Core, section, top of interval (cm)	Natural remanent magnetization			Remanent magnetization (15 mT)			
	Inclination (degrees)	Declination (degrees)	Intensity (mA/m)	Inclination (degrees)	Declination (degrees)	Intensity (mA/m)	Polarity
125-786A-							
1H-1, 142	−46.1	184.3	49.2	−12.4	175.8	7	N?
1H-2, 144	35.2	339.7	176.6	−4.2	163.3	16.2	R
1H-3, 140	56	29.6	21.5	−35.9	178.7	22.6	R
1H-4, 136	40.6	350.8	48.3	−32.7	179	58.3	R
1H-5, 145	32.7	10.8	74.8	−28.3	170.9	35.7	R
1H-6, 112	−0.2	157.1	51	−28.6	181	96.7	R
1H-7, 27	0.5	167.5	18	42.9	103.9	21.9	N
2H-1, 70	47.9	186.5	113.2	51.7	191.1	99.6	N
2H-2, 78	−35.6	27.4	115.6	−44.4	7.1	71.9	R
2H-3, 69	47.8	193	28.6	55.6	180.1	20.5	N
2H-4, 73	57.1	189.3	37.1	58.1	197.9	28.5	N
2H-5, 76	53.9	176.5	73.9	52	175.1	51.7	N
2H-6, 70	33.8	359.9	5.6	37.6	359	4.3	N
2H-7, 33	21.3	340	0.4	14.4	344	0.1	?
3H-1, 70	32.3	53.3	28.9	49.3	26	35.7	N
3H-2, 70	31.7	356.9	156.5	38.7	30.3	86.3	N
3H-3, 70	60.1	65.4	29.3	51.8	23.7	26.1	N
3H-4, 70	50.6	25.1	17.8	35.7	26.2	14.6	N
3H-5, 70	43.7	31.6	21.4	38.2	13.5	13.5	N
3H-6, 70	40	25.2	8.2	40.7	32.1	8.8	N
3H-7, 38	−4.1	227	0.1	−27.7	223.3	0.03	R
4X-1, 69	47.4	5.1	58.3	53.3	5.3	51.3	N
5X-1, 66	40.8	27.9	24.2	48.4	26.7	19.8	N
5X-2, 66	30.1	337.1	28.2	51	328.9	22.5	N
5X-3, 66	−15	242.89	16.3	30.5	220.7	5.2	N
5X-4, 50	10.7	161.9	37.6	61.2	166.6	34	N
6X-1, 87	42.2	185.1	63.2	48.5	182.6	40.2	N
6X-2, 68	37.8	236.2	35.3	39	251.6	34.6	N
6X-3, 68	42	214.6	55.6	42.7	221	39	N
6X-4, 67	3.6	69.1	23.8	−3.5	52.2	20.2	R
7X-1, 59	−33.3	175.7	14.8	53.7	156.8	8.9	N
7X-2, 59	−11.9	181.7	17.2	11.8	158.2	6.5	N
7X-3, 59	−12.5	165	40.4	2.1	152.2	26.9	?
7X-4, 59	−45.8	339.7	62.5	25.4	17.4	39.4	N
7X-5, 59	−38.9	32.4	73.1	−23.7	30.1	14.6	R
8X-1, 55	38.2	193.2	44.8	39.6	211.4	25.9	N
9X-1, 69	15.1	295.4	135	30.3	131.6	12.3	N
9X-1, 69	15.1	295.4	135	30.3	131.6	12.3	N
9X-2, 88	9	1	32	2.5	92.2	16.5	?
9X-3, 30	−38.6	88.6	22.9	−30.7	70.7	13.1	R
9X-4, 85	−8	308	6.5	54.7	219	7.2	N
9X-5, 46	3.2	312.4	43.7	−32.3	88.3	5.5	R
9X-6, 36	−7.5	325.3	28.5	45.7	273	8.7	N
10X-1, 80	38.2	337.2	89.6	50.5	9.2	32.5	N
10X-2, 77	12.7	227.7	207.7	60.8	323.9	16.8	N
10X-3, 63	−22	10.2	176.3	44.9	9.4	21.4	N
10X-4, 89	−2	220.5	222.7	−1	135.8	7.8	?
10X-5, 89	−9	346.4	9.1	7.2	165.3	4.5	?
10X-6, 17	16.2	1.8	32.1	48.5	11.9	9.1	N
11X-1, 43	22.6	353.6	245	47.3	336.3	6	N
11X-2, 96	−2.9	133.2	92.6	55.8	166.6	9.2	N
11X-3, 47	17.4	128.7	14.9	38.4	120.2	7.2	N
11X-4, 92	31.2	163.1	4.1	24	102	5.6	N
11X-5, 90	31.8	266.1	5.5	43.4	255.8	3.2	N

N = normal; R = reversed.

locality; (2) the temporal record of sedimentation, depositional environment, paleoceanography, and the intensity and nature of arc volcanism; (3) the nature and age of the igneous basement to the forearc basin; and (4) the regional stress field of the forearc, microstructural deformation, and large-scale rotation and translation of the forearc. Site selection was based on multichannel seismic records and a short shipboard seismic survey; the site chosen was 5 nmi east of the intersection of line 5 (0510UTC) of *Fred H. Moore* 3505 survey and *Conrad* line 38 (1125UTC). Occupation of the site began at 2015UTC, 1 April, and ended at 0800UTC on 16 April 1989.

Hole 786A (31°52.48′N, 141°13.58′E) was spudded with the APC in a water depth of 3058.1 m at 0815UTC on 2 April. Recovery of 103% was achieved for the 28.7 m drilled before changing to the XCB and drilling an additional 137.8 m with 40.1% recovery, for a total of 166.5 m drilled with 51.0% recovery. Hole 786B (31°52.45′N, 141°13.59′E), in a water depth of 3071.0 m, was washed through 162.5 m of the sedimentary column before recovery of igneous basement began at 162.5 mbsf. Drilling continued to a total depth of 828.6 m using the bionic bit M84F, which showed no signs of failure after 118.4 hr of use when drilling was stopped to begin logging.

Four suites of logging tools were run in Hole 786B. The first suite, consisting of the DIT, SDT, and NGT, was run from 3520.0 mbsl up to the end of the drill string. The second suite, consisting of the LDT, CNT, and NGT, was run from a depth of 3458.1 mbsl up to the end of the drill string. The third logging suite, consisting of the DIT, LDT, CNT, and

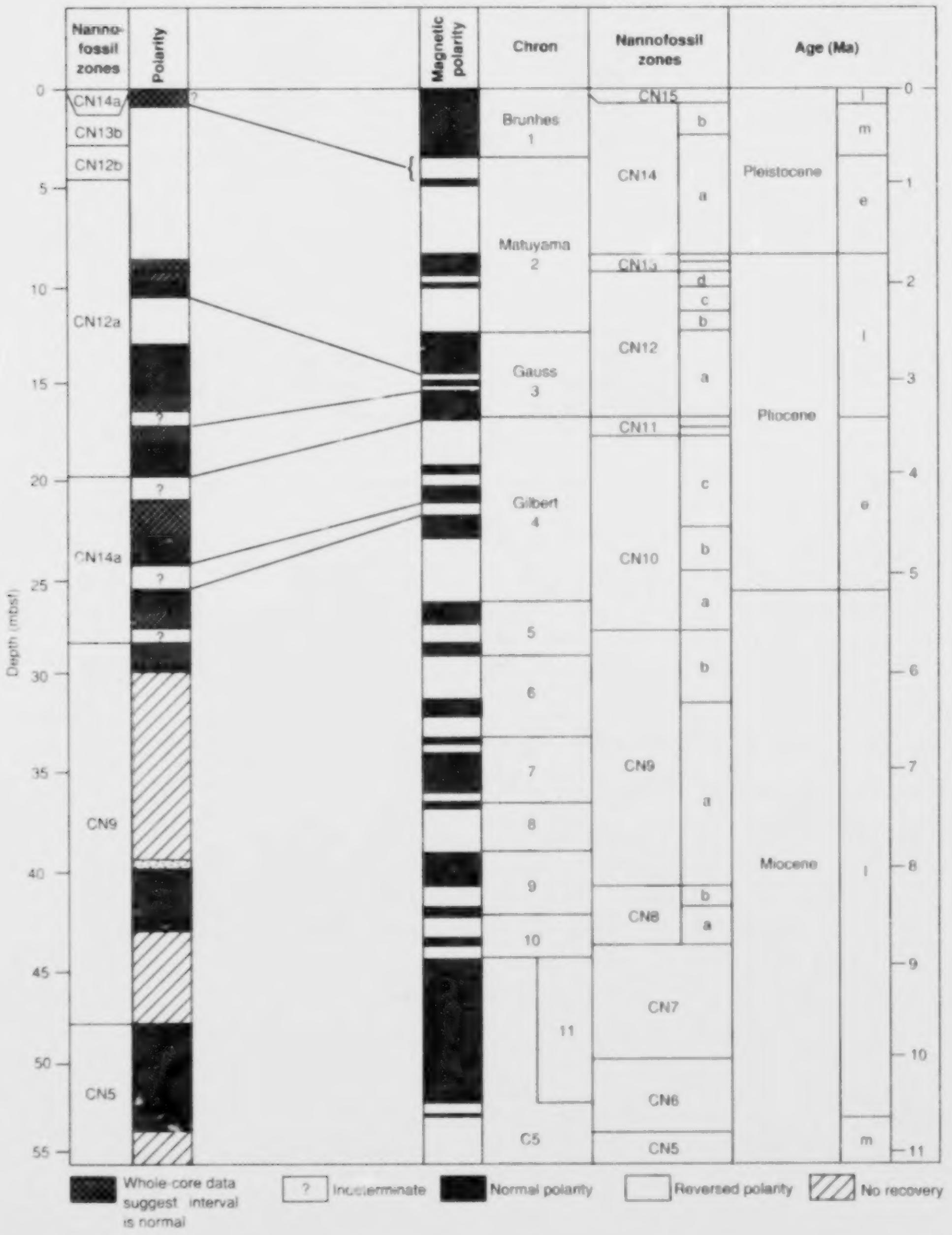

Figure 11. The magnetostratigraphy of Hole 786A for the interval from 0 to 55 mbsf correlated with the polarity time scale of Berggren et al. (1985b).

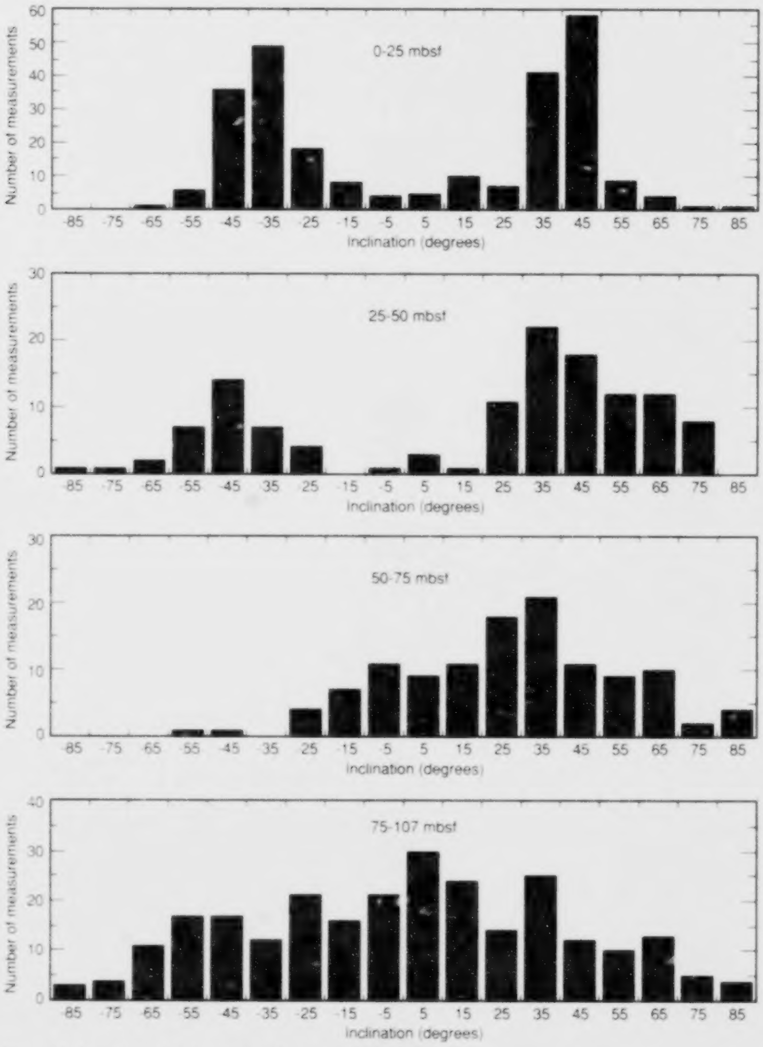

Figure 12. Inclination distribution as a function of depth, Hole 786A.

SDT, was used to log the hole from 3892 up to 3535.2 mbsl. The fourth suite, consisting of the GST, ACT, and NGT, was run from a depth of 3892.0 mbsl to the mud line. The BHTV was deployed for the fifth logging run and logged 80 m of Hole 786B after one failure before logging time expired.

The stratigraphic section recovered at Site 786 is assigned to lithologic Units I through IV (Fig. 3). Units I through III are defined only in Hole 786A, in which the sedimentary sequence was recovered at Site 786. Unit IV is defined in both holes. Unit I (0–83.46 mbsf) comprises 83.46 m of nannofossil marls and clays and is of early Pleistocene to middle Miocene age. It is made up predominantly of nannofossils (up to 70%), with lesser amounts of micrite (trace–40%), foraminifers (trace–30%), clay (5%–7%), sponge spicules (trace–5%), radiolarians (trace–4%), diatoms (trace–3%), and quartz (trace–2%).

Unit II (83.46–103.25 mbsf) is an upper Oligocene to middle Eocene nannofossil marl and nannofossil-rich clay. The unit consists of nannofossils (2%–60%), with lesser amounts of foraminifers (2%–10%), micrite (1%–35%), and radiolarians (trace–2%). Unit II also contains clays (10%–50%) and opaque minerals (3%–15%) with traces of chlorite

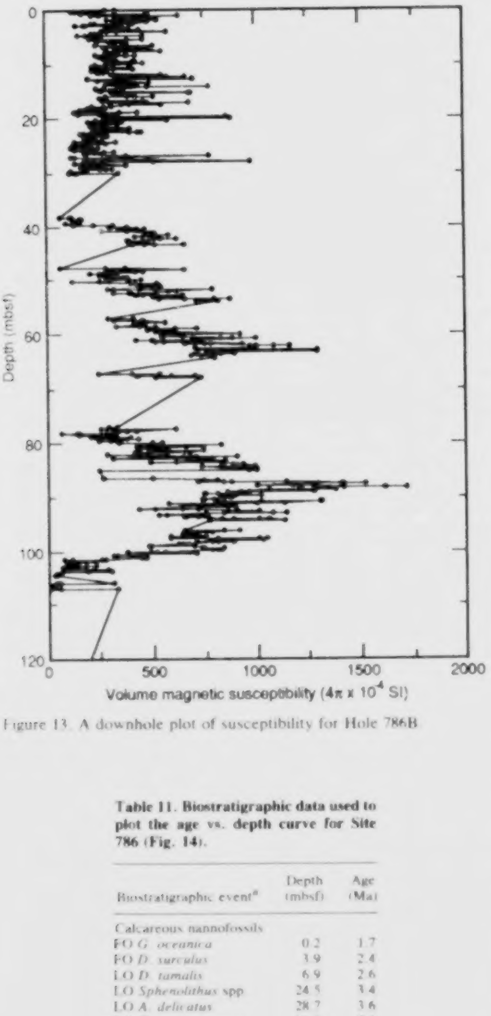

Figure 13. A downhole plot of susceptibility for Hole 786B.

Table 11. Biostratigraphic data used to plot the age vs. depth curve for Site 786 (Fig. 14).

Biostratigraphic event[a]	Depth (mbsf)	Age (Ma)
Calcareous nannofossils		
FO *G. oceanica*	0.2	1.7
FO *D. surculus*	3.9	2.4
LO *D. tamalis*	6.9	2.6
LO *Sphenolithus* spp.	24.5	3.4
LO *A. delicatus*	28.7	3.6
LO *D. quinqueramus*	31.8	5.6
FO *A. delicatus*	41.4	6.5
FO *D. quinqueramus*	47.6	8.3
FO *D. hamatus*	49.5	10.0
LO *D. kugleri*	57.1	10.8
LO *S. heteromorphus*	68.9	14.4
LO *D. bisectus*	85.1	23.7
FO *S. ciperoensis*	92.3	30.1
FO *S. distentus*	94.8	34.1
LO *E. formosa*	95.7	35.1
FO *I. recurvus*	97.7	37.8
LO *C. grandis*	102.9	39.6
FO *S. predistentus*	105.7	42.2
FO *D. saipanensis*	107.5	42.8

[a] FO = first occurrence, LO = last occurrence.

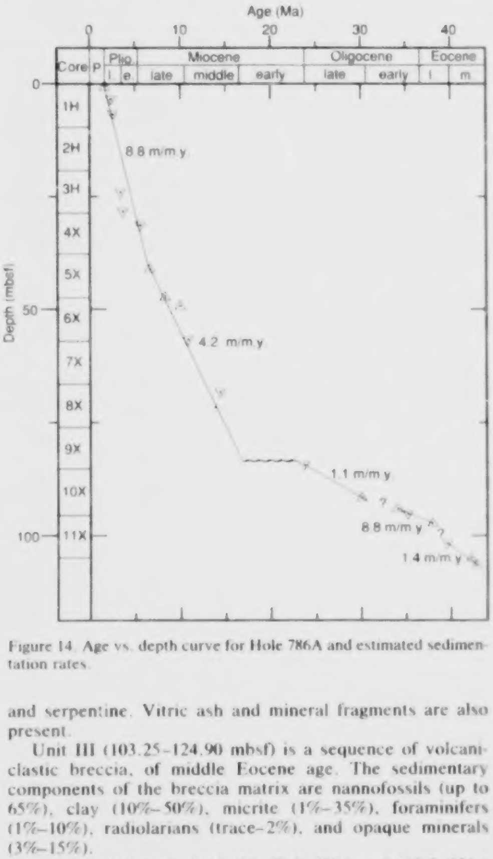

Figure 14. Age vs. depth curve for Hole 786A and estimated sedimentation rates.

and serpentine. Vitric ash and mineral fragments are also present.

Unit III (103.25–124.90 mbsf) is a sequence of volcaniclastic breccia, of middle Eocene age. The sedimentary components of the breccia matrix are nannofossils (up to 65%), clay (10%–50%), micrite (1%–35%), foraminifers (1%–10%), radiolarians (trace–2%), and opaque minerals (3%–15%).

Unit IV (124.9–166.5 mbsf in Hole 786A and 162.5–826.6 mbsf in Hole 786B) consists of volcaniclastic and sedimentary breccias, vitric siltstones and sandstones, lavas, dikes, and pyroclastic flows. Vitric fragments, glass (20%–100%), pyroxene (1%–30%), feldspar (1%–15%), lithic fragments (trace–10%), and amphibole (trace–5%) dominate the detrital component of the sediments; clays (10%–53%) are also present.

Dating is based on calcareous nannofossil, foraminifer, and diatom biostratigraphy. The rocks in the bottom of Hole 786A and the top of Hole 786B are considered to be the same material. Sedimentation rates are highest for the Pliocene (8.6 m/m.y.) and drop (to 4.2 m/m.y.) between the latest Miocene and middle Miocene. A hiatus exists between the middle Miocene and the late Oligocene.

The igneous basement (Fig. 3) consists mainly of massive and brecciated flows, ash flows, and intercalated sediment in its upper part, and pillow lavas and dikes or sills in its lower part. Rock types include high-magnesian basalts, boninites, basalts, andesites, dacites, and rhyolites. There are several prominent shear zones and hydrothermal breccias within the sequence.

Studies of physical properties show that average bulk densities are 1.65 g/cm^3 in the sediments and 1.8–2.1 g/cm^3 in the

the volcanic sequences; the average grain density of 2.65 g/cm^3 varied little between the sediments and the volcanic rocks.

Preliminary interpretation of the paleomagnetic data shows many intervals of normal and reversed polarity. The two intervals between 0 and 50 mbsf show good bimodal distributions with peaks around +45° and −45°, which indicates little translation since the late Miocene. Between 160 and 240 mbsf there is no bimodal distribution, although the many more data points between +15° and −15° suggest translation from a lower latitude.

The principal achievement at this site is the deep penetration of an Eocene volcanic edifice, which will provide (1) a record of the construction and structure of the forearc volcanic basement and (2) the basis for the understanding of early arc magmatism in general and boninite petrogenesis in particular.

REFERENCES

Berggren, W. A., Kent, D. V., and Flynn, J. J., 1985a. Jurassic to Paleogene: part 2. Paleogene geochronology and chronostratigraphy. *In* Snelling, N. J. (Ed.), *The Chronology of the Geological Record.* Geol. Soc. London Mem., 10:141–198.

Berggren, W. A., Kent, D. V., Flynn, J. J., and Van Couvering, J., 1985b. Cenozoic geochronology. *Geol. Soc. Am. Bull.*, 96:1407–1418.

Bleil, U., 1982. Paleomagnetism of Deep Sea Drilling Project Leg 60 sediments and igneous rocks from the Mariana region. *In* Hussong, D. M., Uyeda, S., et al., *Init. Repts. DSDP*, 60: Washington (U.S. Govt. Printing Office), 855–873.

McDuff, R. E., 1985. The chemistry of interstitial waters, Deep Sea Drilling Project Leg 86. *In* Heath, G. R., Burckle, L. H., et al., *Init. Repts. DSDP*, 86: Washington (U.S. Govt. Printing Office), 675–687. Meijer, A., 1980. Primitive arc volcanism and a boninite series: examples from western Pacific island arcs. *In* Hayes, D. E. (Ed.), *The Tectonic and Geologic Evolution of Southeast Asian Seas and Islands, Part I.* Am. Geophys. Union Geophys. Monogr. Ser., 23:269–282.

Ms 125A-114

NOTE: All core description forms ("barrel sheets") and core photographs have been printed on coated paper and bound as Section, near the back of the book, beginning on page 383.

Table 12. Index properties for Holes 786A and 786B.

Core, section, interval (cm)	Depth (mbsf)	Bulk density (g/cm^3)	Grain density (g/cm^3)	Porosity (%)	Water content (%)	Void ratio
125-786A-						
1H-1, 84–86	0.84	1.65	2.43	56.2	36.2	0.56
1H-2, 72–74	2.22	1.73	2.76	59.8	36.7	0.6
1H-3, 76–78	3.76	1.62	2.53	61.3	40.3	0.61
1H-4, 71–73	5.21	1.65	2.66	62.3	40.1	0.62
1H-5, 90–92	6.9	1.51	2.52	67.8	47.6	0.68
1H-6, 51–53	8.01	1.41	2.72	56.7	42.8	0.57
1H-7, 21–23	9.21	1.64	2.54	59.9	38.8	0.6
2H-1, 67–69	10.37	1.59	2.64	65.6	43.9	0.66
2H-2, 73–75	11.93	1.65	2.64	62.3	40.2	0.62
2H-3, 78–80	13.48	1.66	2.76	64.3	41.2	0.64
2H-4, 65–67	14.85	1.63	2.71	64.6	42.1	0.65
2H-5, 73–75	16.43	1.6	2.6	63.9	42.3	0.64
2H-6, 88–90	18.08	1.6	2.64	65	43.2	0.65
2H-7, 22–24	18.92	1.63	2.72	65.7	42.8	0.66
3H-1, 75–77	19.95	1.69	2.71	61.1	38.5	0.61
3H-2, 64–66	21.34	1.66	2.73	63.1	40.3	0.63
3H-3, 76–78	22.96	1.74	2.73	53.4	32.5	0.53
3H-4, 75–77	24.45	1.64	2.66	63	40.8	0.63
3H-5, 62–64	25.82	1.63	2.67	63.7	41.6	0.64
3H-6, 58–60	27.28	1.61	2.62	64	42.3	0.64
3H-7, 44–46	28.64	1.6	2.73	66.9	44.4	0.67
4X-2, 5–7	30.25	1.56	2.71	58.6	46.5	0.69
4X-CC, 15–17	30.61	1.59	2.58	64.4	43.1	0.64
5X-1, 54–56	38.74	1.55	2.73	68.6	46.9	0.69
5X-3, 101–103	42.21	1.66	2.82	64.9	41.5	0.65
5X-4, 37–39	43.07	1.69	2.8	63.3	39.8	0.63
5X-4, 59–61	43.29	1.73	2.98	64.6	39.7	0.65
6X-1, 59–61	48.19	1.7	2.72	60.8	38.1	0.61
6X-2, 59–61	49.69	1.62	2.63	63.5	41.7	0.63
6X-3, 59–61	51.19	1.65	2.76	64.6	41.7	0.65
6X-5, 16–18	53.76	1.63	2.61	62.4	40.6	0.62
7X-1, 33–35	57.43	1.77	2.82	59.1	35.6	0.59
7X-2, 33–35	58.93	1.7	2.83	62.9	39.3	0.63
7X-3, 33–35	60.43	2.15	2.85	77.1	38.2	0.77
7X-4, 33–35	61.93	1.79	2.76	56.7	33.7	0.57
7X-5, 33–35	63.43	1.84	2.82	54.8	31.6	0.55
7X-CC, 4–6	64.33	1.79	2.7	54.9	32.6	0.55
8X-1, 48–50	67.58	1.74	2.71	57.6	35.1	0.58
8X-CC, 6–8	68.18	1.75	2.75	58.2	35.3	0.58
9X-1, 83–85	77.63	1.55	2.69	69	47.3	0.69
9X-2, 97–99	79.27	1.6	2.79	68.1	45.3	0.68
9X-3, 93–95	80.73	1.57	2.66	66.8	45	0.67
9X-4, 80–82	82.1	1.5	2.65	71.1	50.3	0.71
9X-5, 98–100	83.78	1.79	2.98	61.2	36.3	0.61
9X-6, 25–27	84.55	1.79	2.77	56.7	33.7	0.57
10X-1, 88–90	87.28	1.85	2.88	55.8	32	0.56
10X-2, 82–84	88.72	1.67	2.52	57.4	36.5	0.57
10X-3, 72–74	90.12	1.71	2.69	58.9	36.5	0.59
10X-5, 82–84	93.22	1.58	2.51	63.4	42.7	0.63
10X-6, 25–27	94.15	1.79	2.71	54.9	32.5	0.55
11X-1, 80–82	96.8	1.78	2.79	57.9	34.7	0.58
11X-2, 83–85	98.33	1.74	2.78	59.8	36.5	0.6
11X-3, 78–80	99.78	1.38	2.74	79.6	61.1	0.8
11X-4, 84–86	101.34	1.58	2.61	65.3	43.9	0.65
11X-5, 50–52	102.5	1.64	2.81	65.8	42.5	0.66
11X-6, 63–65	104.13	1.92	2.94	53.3	29.5	0.53
12X-1, 42–44	106.12	1.62	2.66	64	41.9	0.64
14X-1, 16–18	125.06	2.05	2.77	41.4	21.4	0.41
15X-CC, 9–11	134.69	1.85	2.66	50.2	28.8	0.5
16X-1, 9–11	144.39	1.54	2.09	52.3	36.1	0.52
16X-CC, 19–21	144.69	2.1	2.86	41.7	21.1	0.42
17X-CC, 27–29	154.27	1.96	2.72	44.9	24.3	0.45
18X-1, 65–67	155.65	2.03	2.73	41.4	21.6	0.41
125-786B-						
1R-1, 61–64	163.11	2.44	2.63	11.4	5	0.11
2R-1, 58–60	170.08	2.51	2.61	6	2.5	0.06
3R-1, 94–97	180.14	2.47	2.86	21.7	9.4	0.22
4R-1, 110–112	190.1	2.7	2.72	1.5	0.6	0.02
5R-1, 1–3	198.61	2.27	2.95	34	15.9	0.34
5R-2, 53–55	200.63	2.4	2.55	9.5	4.2	0.1
6R-1, 38–40	208.58	2.33	2.69	21.6	9.8	0.22
6R-2, 43–45	210.13	2.51	2.73	12.7	5.4	0.13
8R-1, 45–47	228.05	2.25	2.73	28.5	13.5	0.29
9R-1, 10–12	237.2	2.45	2.65	12.9	5.6	0.13
9R-2, 128–129	239.84	2.07	3	47.4	24.3	0.47
10R-2, 68–69	248.73	2.46	2.68	13.5	5.8	0.13
11R-1, 22–24	256.52	2.24	2.79	31.7	15	0.32
12R-1, 49–51	266.49	2.24	2.77	30.4	14.4	0.3
12R-1, 49–51	266.49	2.24	2.77	30.4	14.4	0.3
12R-2, 14–16	267.57	2.23	2.57	22.2	10.6	0.22
13R-1, 85–87	276.55	2.46	2.75	16.8	7.2	0.17
13R-2, 70–72	277.83	2.39	2.78	22.1	9.8	0.22
14R-1, 35–37	285.75	2.4	2.69	18	8	0.18
15R-1, 35–37	295.35	2.19	2.65	28.2	13.7	0.28
15R-2, 128–130	297.75	2.11	2.61	32.1	16.2	0.32
16R-1, 78–80	305.38	2.21	2.73	30.7	14.8	0.31
16R-2, 14–16	306.21	2.3	2.47	11.8	5.4	0.12
17R-1, 67–69	314.97	2.33	2.73	24	10.9	0.24
18R-1, 61–63	324.51	2.34	2.6	16.5	7.5	0.17
19R-1, 27–28	333.87	2.36	2.57	14.1	6.4	0.14
20R-1, 71–73	344.01	2.29	2.55	17.1	7.9	0.17
21R-1, 125–127	354.25	2.22	2.43	14.6	7	0.15
21R-2, 86–88	355.3	2.5	2.66	10.2	4.3	0.1
22R-1, 31–33	362.91	1.86	2.52	44.7	25.6	0.45
22R-1, 70–72	363.3	2.05	2.56	33.6	17.4	0.34
22R-2, 62–64	364.71	1.97	2.29	23.7	12.8	0.24
22R-3, 30–32	365.85	1.96	2.12	14.6	7.9	0.15
24R-1, 10–12	382	2.33	2.52	12.5	5.7	0.12
24R-2, 13–15	383.53	2.38	2.54	10.7	4.8	0.11
25R-1, 68–70	392.18	2.41	2.67	14.9	6.6	0.15
26R-1, 65–67	401.85	2.33	2.63	18.7	8.5	0.19
27R-1, 89–91	411.69	2.16	2.73	34.1	16.8	0.34
27R-2, 40–42	412.7	2.25	2.94	36.3	17.2	0.36
28R-1, 98–100	421.38	2.43	2.56	8.6	3.8	0.09
29R-1, 22–24	430.32	2.39	2.77	21.7	9.6	0.22
30R-1, 82–84	440.52	2.48	2.7	13.3	5.7	0.13
30R-2, 70–72	441.9	2.45	2.71	15.6	6.8	0.16
30R-3, 29–31	442.99	2.51	2.61	6	2.5	0.06
31R-1, 106–108	450.46	2.55	2.63	4.7	2	0.05
31R-2, 84–86	451.68	2.64	2.73	5.1	2	0.05
32R-1, 119–121	460.19	2.53	2.62	5.8	2.4	0.06
32R-2, 86–88	461.36	2.34	2.55	13.7	6.2	0.14
33R-1, 18–20	468.88	2.55	2.62	4.2	1.7	0.04
34R-1, 128–130	479.58	2.14	2.3	12.7	6.3	0.13
34R-2, 73–75	480.53	2.6	2.71	6.5	2.6	0.06
34R-3, 45–47	481.65	2.49	2.64	9.3	4	0.09
34R-4, 90–91	483.6	2.55	2.7	9	3.7	0.09
35R-1, 126–128	489.26	2.36	2.46	6.7	3	0.07
35R-2, 41–43	489.91	2.19	2.46	18.9	9.2	0.19
35R-3, 60–62	491.6	2.15	2.28	10.9	5.4	0.11
35R-4, 35–37	492.85	2.04	2.24	16.9	8.8	0.17
36R-1, 63–65	498.33	2.1	2.27	14.1	7.1	0.14
37R-1, 69–71	508.09	2.4	2.68	17.3	7.6	0.17
37R-2, 82–84	509.63	2.44	2.52	5.7	2.5	0.06
37R-3, 14–16	510.45	2.53	2.65	6.9	2.9	0.07
38R-1, 79–81	517.89	2.4	2.48	5.8	2.6	0.06
39R-1, 48–50	527.28	2.3	2.34	17.7	8.2	0.18
39R-2, 65–67	528.95	2.33	2.36	17.3	7.9	0.17
39R-3, 27–29	530.03	2.43	2.62	11.9	5.2	0.12
40R-1, 102–104	537.32	2.59	1.82	89.3	36.6	0.89
40R-2, 46–48	538.03	2.71	2.78	3.9	1.5	0.04
40R-3, 61–63	539.35	2.7	2.78	4.8	1.9	0.05
40R-4, 25–27	540.49	2.53	2.68	9.9	4.1	0.1
41R-1, 61–63	546.51	2.39	2.86	25.7	11.4	0.26
41R-2, 17–19	547.42	2.33	2.66	20	9.1	0.2
41R-3, 9–11	548.84	2.08	2.93	45.1	23.1	0.45
41R-4, 23–25	550.48	2.47	2.71	14.5	6.2	0.14
42R-1, 67–69	556.27	2.55	2.75	11.8	4.9	0.12
42R-2, 67–69	557.77	2.56	2.65	5.6	2.3	0.06
43R-3, 124–126	559.78	2.48	2.59	7.4	3.2	0.07
42R-4, 13–15	560.17	2.61	2.73	7.2	2.9	0.07
43R-1, 30–32	565.3	2.42	2.58	10.2	4.5	0.1
43R-2, 32–34	566.62	2.34	2.61	16.9	7.7	0.17
44R-1, 30–32	574.9	2.68	2.77	5.5	2.2	0.05
45R-1, 53–55	584.83	2.39	2.69	17.8	7.9	0.18
46R-1, 59–61	594.49	2.58	2.88	16.4	6.7	0.16
46R-2, 59–71	596.09	2.41	2.72	18.5	8.1	0.18
47R-1, 101–103	604.51	2.44	2.75	18.2	7.9	0.18
48R-1, 73–75	613.93	2.28	2.65	23.1	10.8	0.23
48R-2, 50–52	615.09	2.43	2.8	20.8	9.1	0.21
49R-1, 32–34	623.22	2.45	2.57	8.1	3.5	0.08

Table 12 (continued).

Core, section, interval (cm)	Depth (mbsf)	Bulk density (g/cm^3)	Grain density (g/cm^3)	Porosity (%)	Water content (%)	Void ratio
49R-1, 82–84	623.72	2.64	2.76	62.8	25.3	0.63
49R-3, 62–64	625.88	2.33	2.67	20.8	9.5	0.21
49R-4, 50–52	627.18	2.39	2.7	18.7	8.3	0.19
50R-1, 24–26	632.74	2.4	2.95	28.9	12.8	0.29
50R-2, 31–33	634.31	2.53	2.81	16.1	6.8	0.16
51R-1, 49–51	642.69	2.47	2.75	16.4	7.1	0.16
51R-2, 6–8	643.76	2.43	2.71	17.6	7.7	0.18
52R-1, 81–83	652.71	2.44	2.97	29	12.6	0.29
52R-2, 143–145	654.83	2.48	2.61	8	3.4	0.08
53R-1, 48–50	662.08	2.69	2.93	12.8	5.1	0.13
53R-2, 55–57	663.65	2.71	2.89	9.7	3.8	0.1
54R-1, 107–109	672.27	2.37	2.76	22.7	10.2	0.23
54R-2, 85–87	673.49	2.58	2.66	5.9	2.4	0.06
54R-3, 65–67	674.79	2.42	2.67	15.7	6.9	0.16
54R-4, 59–61	676.23	2.53	2.74	12.2	5.1	0.12
54R-5, 44–46	677.26	2.64	2.73	5.3	2.2	0.05
55R-1, 49–51	681.29	2.56	2.65	5.5	2.3	0.06
55R-2, 85–87	683.04	2.45	2.66	13	5.6	0.13
55R-3, 90–92	684.53	2.32	2.44	8.9	4.1	0.09
56R-1, 124–126	691.34	2.31	2.48	11.8	5.4	0.12
56R-2, 107–109	692.67	1.93	1.15	94	51.7	0.94
56R-3, 58–60	693.56	2.26	2.49	15.6	7.3	0.16
56R-4, 65–67	695.06	1.99	2.69	42.6	22.8	0.43
56R-5, 79–81	696.7	2.19	2.36	12.8	6.2	0.13
57R-1, 110–112	700.9	2.36	2.63	16.7	7.5	0.17
57R-2, 89–91	702.1	2.34	2.96	32	14.5	0.32
57R-3, 65–67	703.14	2.53	2.95	21.9	9.2	0.22
57R-4, 66–68	704.6	2.67	3.07	19.7	7.8	0.2
57R-5, 50–52	705.75	2.36	2.63	17	7.6	0.17
57R-6, 86–88	707.42	2.19	2.83	35.6	17.3	0.36
57R-7, 70–72	708.76	2.18	2.49	21.1	10.3	0.21
58R-1, 77–79	710.17	2.3	2.49	13.4	6.2	0.13
58R-2, 127–129	712.17	2.3	2.53	16.1	7.4	0.16
58R-3, 83–85	713.05	2.47	2.88	22.3	9.6	0.22
58R-4, 19–21	713.84	2.24	2.45	14.7	6.9	0.15
59R-1, 68–70	715.08	2.36	2.54	11.9	5.3	0.12
59R-2, 86–88	716.5	2.31	2.53	14.2	6.5	0.14
59R-3, 127–129	718.37	2.29	2.5	15.6	7.2	0.16
59R-4, 35–37	718.93	2.35	2.53	12	5.4	0.12
60R-1, 72–74	719.72	2.37	2.58	13.7	6.1	0.14
60R-2, 115–117	721.45	2.53	2.62	5.5	2.3	0.05
60R-3, 94–96	722.69	2.43	2.53	6.3	2.7	0.06
60R-4, 106–108	724.31	2.32	2.42	7.1	3.3	0.07
60R-5, 49–51	725.16	2.41	2.52	7	3.1	0.07
60R-6, 47–49	726.48	2.31	2.42	7.6	3.5	0.08
61R-1, 74–76	729.44	2.34	2.51	10.5	4.8	0.1
61R-2, 29–31	730.49	2.38	2.59	12.4	5.5	0.12
61R-3, 10–12	731.8	2.35	2.56	14	6.3	0.14
61R-4, 82–84	733.83	2.45	2.57	7.6	3.3	0.08
61R-5, 56–58	735.07	2.48	2.62	8.8	3.8	0.09
61R-6, 53–55	736.26	1.95	2.56	40.2	21.9	0.4
62R-1, 34–36	738.74	2.56	2.65	5.6	2.3	0.06
62R-2, 42–44	740.19	2.39	2.58	12.3	5.5	0.12
62R-3, 107–109	742.12	2.42	2.76	19.7	8.7	0.2
63R-1, 83–85	748.83	2.46	2.11	45.8	19.8	0.46
63R-2, 74–76	750.24	2.5	2.7	10.9	4.6	0.11
64R-1, 136–138	759.06	2.48	2.61	8.7	3.7	0.09
64R-2, 90–92	760.04	2.35	2.5	10.4	4.7	0.1
64R-3, 56–58	761.16	2.52	2.6	5.1	2.2	0.05
65R-1, 17–19	767.57	2.66	2.73	4.3	1.7	0.04
65R-2, 37–39	769.27	2.2	2.58	25.1	12.1	0.25
65R-3, 52–54	770.89	2.22	2.37	11.2	5.4	0.11
66R-1, 88–90	777.98	2.31	2.5	13.3	6.1	0.13
66R-2, 80–82	779.34	2.48	2.56	5.2	2.2	0.05
66R-3, 34–36	780.3	2.41	2.53	8.2	3.6	0.08
67R-1, 35–37	787.05	2.44	2.55	7.1	3.1	0.07
68R-1, 9–11	796.39	2.45	2.54	6	2.6	0.06
69R-1, 78–80	798.08	2.55	2.61	4.1	1.7	0.04
69R-2, 24–26	798.93	2.34	2.66	19.7	9	0.2
69R-3, 130–132	801.1	2.37	2.56	12.4	5.5	0.12
69R-4, 51–53	801.81	2.46	2.69	14.3	6.2	0.14
69R-5, 63–65	803.09	2.48	2.59	7.3	3.1	0.07
69R-6, 75–77	804.66	2.37	2.62	15.8	7.1	0.16
69R-7, 30–33	805.63	2.43	2.54	8.9	3.9	0.09
70R-1, 5–7	806.95	2.45	2.56	7.3	3.1	0.07
70R-2, 5–7	808.45	2.45	2.58	8.3	3.6	0.08
70R-3, 117–119	811	2.48	2.69	12.6	5.4	0.13
70R-4, 49–51	811.68	2.46	2.72	15.6	6.8	0.16
71R-1, 115–117	816.75	2.23	2.5	18.8	8.9	0.19
71R-2, 106–108	818.16	2.33	2.58	17.4	8	0.17
71R-3, 107–109	819.59	2.21	2.54	21.5	10.3	0.22
71R-4, 71–73	820.65	2.53	2.64	7	2.9	0.07
71R-5, 16–18	821.6	2.51	2.59	4.9	2.1	0.05
72R-1, 87–89	824.47	2.55	2.62	4.4	1.8	0.04
72R-2, 80–82	825.9	2.32	2.5	12.3	5.6	0.12

Table 13. Physical properties for Hole 786A.

Core, section, interval (cm)	Depth (mbsf)	Thermal conductivity (W/mK)	Resistivity (ohms)	Formation factor
125-786A-				
1H-1, 75	0.75	1.004		
1H-2, 75	2.25	1.079		
1H-3, 75	3.75	0.971		
1H-4, 75	5.25	0.965		
1H-5, 75	6.75	0.778		
1H-6, 75	8.25	0.999		
1H-CC, 10	9.63	0.77		
2H-1, 75	10.45	0.959		
2H-2, 75	11.95	0.934		
2H-3, 75	13.45	0.894		
2H-4, 75	14.95	0.914		
2H-5, 75	16.45	0.97		
2H-6, 75	17.95	1.01		
2H-7, 27	18.97	1.035		
2H-CC, 22	19.5	1.028		
3H-1, 75	19.95	1.026		
3H-2, 75	21.45	0.991		
3H-4, 75	24.45	1.042		
3H-5, 75	25.95	1.036		
3H-6, 75	27.45	1.069		
3H-7, 34	28.54	0.935		
3H-CC, 8	28.97	0.933		
5X-1, 68	29.38	1.019		
4X-2, 19	30.39	0.954		
4X-CC, 22	30.68	1.006		
5X-1	38.4		23.3	2.72
5X-1, 69	38.89	1.057		
5X-2, 69	40.39	0.997		
5X-2	41.3		27.9	3.26
6X-1	47.9		23.5	2.74
6X-1, 50	48.1	0.708		
6X-2, 50	49.6	0.962		
6X-3	0.8		25.9	3.02
6X-3, 50	51.1	1.037		
6X-4, 40	52.5	0.873		
7X-1	57.13		38.1	4.45
7X-1, 65	57.75	1.039		
7X-3	60.2		24.5	2.86
7X-3, 65	60.75	1.066		
7X-5	63.35		27.7	3.23
7X-5, 65	63.75	1.099		
8X-1	67.25		34.1	3.98
8X-1, 65	67.75	0.994		
9X-1, 65	77.45	0.715		
9X-1	77.8		17.5	2.04
9X-3, 65	80.45	0.915		
9X-3	82.26		24	2.8
9X-5	83.1		18.5	2.16
9X-5, 65	83.45	0.987		
9X-5	83.6		40	4.67
10X-1	86.7		51.5	6.01
10X-1, 75	87.15	0.947		
10X-3, 75	90.15	0.921		
10X-3	90.26		42.5	4.96
10X-4, 75	91.65	0.997		
10X-5, 75	93.15	0.838		
10X-5	93.2		28	3.27
10X-6, 29	94.19	1.019		
11X-1, 75	96.75	1.037		
11X-1, 75	98.25	0.93		
11X-3, 75	99.75	0.834		
11X-5, 75	102.75	1.017		
11X-6, 56	104.06	0.854		
12X-1, 63	106.33	1.001		
12X-2, 20	107.4	0.944		
12X-CC, 24	107.82	0.127		
15X-CC, 10	134.7	0.822		
16X-CC, 35	144.85	0.171		

Table 14. Physical properties for Hole 786B.

Core, section, interval (cm)	Depth (mbsf)	Thermal conductivity (W/mK)	Compressional-wave velocity	
			A direction (km/s)	B direction (km/s)
125-786B-				
1R-1, 60–62	163.1	1.17	5.27	5.01
2R-1, 56–58	170.06	1.643	5.59	5.34
3R-1, 89–91	180.09	1.194	3.77	
4R-1, 52–54	189.52	1.194		
4R-1, 110–112	190.1		5.64	5.82
5R-1, 1–3	198.61		3.25	3.33
5R-2, 53–55	200.63		4.4	4.5
6R-1, 38–40	208.58		3.64	3.45
6R-2, 43–45	210.13		3.96	3.96
8R-1, 45–47	228.05		3.84	3.44
9R-1, 10–12	237.2		4.32	4.34
10R-1, 110–112	247.7		3.78	3.63
10R-2, 16–18	248.21	1.353		
11R-1, 22–24	256.52		3.68	3.58
11R-1, 60–62	256.9	1.215		
12R-1, 46–48	266.46	1.359	3.32	3.36
12R-2, 14–16	267.57		3.75	3.62
13R-1, 82–84	276.52	1.081	5.25	4.79
12R-2, 66–68	277.79	1.243	4.65	4.34
14R-1, 31–33	285.71	1.04	5.28	5.26
15R-1, 33–35	295.33	0.776	4.09	3.77
15R-2, 126–128	297.73	0.975	3.17	3.14
16R-1, 75–77	305.35	1.101	3.74	3.76
16R-2, 12–14	306.19	1.235	4.2	4.03
17R-1, 64–66	314.94	1.472	3.24	3.61
18R-1, 61–63	324.51		4.45	4.19
19R-1, 10–12	333.7	1.04		
20R-1, 77–79	344.07	1.042	4.2	4.21
21R-1, 97–99	353.97	1.28	4.11	4.05
12R-1, 125–127	354.25		4.56	3.74
22R-2, 62–64	364.71		3.72	3.97
22R-2, 107–109	365.16	0.957		
22R-3, 30–32	365.85		3.75	3.74
22R-3, 46–48	366.01	0.949		
24R-1, 10–12	382		4.19	4.44
24R-2, 11–13	383.51	1.728	4.94	4.66
25R-1, 63–65	392.13	1.529	3.98	4.17
26R-1, 61–63	401.81	3.928	3.7	3.99
27R-1, 86–88	411.66	0.916	3.23	3.28
27R-2, 37–39	412.67	1.176		
28R-1, 96–98	421.36	1.692	4.48	4.5
29R-1, 17–18	430.27	1.162	3.59	3.51
30R-2, 65–67	441.85	1.375		
30R-1, 75–77	440.45	1.412	3.73	3.91
30R-2, 70–72	441.9		4.11	4.16
30R-3, 21–23	442.91	1.468	4.48	4.43
31R-1, 102–104	450.42	1.345	4.43	4.37
31R-2, 78–80	451.62	1.619	4.5	4.51
32R-1, 119–120	460.19		4.39	4.42
34R-1, 64–66	478.94	1.671		
34R-2, 80–82	480.6	1.574		
34R-3, 108–110	482.28	1.761		
34R-4, 78–80	483.48	1.69		
35R-1, 115–117	489.15	1.505		
35R-2, 24–26	489.74	2.332		
35R-2, 41–43	489.91		3.67	3.67
35R-3, 57–59	491.57	1.619	3.86	3.58
35R-4, 31–33	492.81	1.732	3.75	3.75
36R-1, 60–62	498.3	1.716	3.67	3.73
37R-1, 67–69	508.07	1.403	3.96	3.7
37R-2, 82–84	509.63		4.33	4.27
37R-3, 11–13	510.42	1.533	4.21	4.27
38R-1, 74–76	517.84	1.072	4.87	4.96
39R-1, 44–46	527.24	1.263	3.99	4.02
39R-2, 64–66	528.94	1.018	4.04	4.1
39R-3, 25–27	530.01	1.192	4.69	4.43
40R-1, 98–100	537.28	1.332		
40R-1, 120–124	537.5		4.06	4.1
40R-2, 41–43	537.98	1.34		
40R-2, 46–48	538.03		4.25	4.34
40R-3, 54–56	539.28	0.924	4.73	4.73
40R-4, 25–27	540.49		4.03	3.97

Table 14 (continued).

Core, section, interval (cm)	Depth (mbsf)	Thermal conductivity (W/mK)	Compressional-wave velocity	
			A direction (km/s)	B direction (km/s)
41R-1, 61–63	546.51		4.06	4.02
41R-2, 17–19	547.42		4.05	3.89
41R-2, 122–124	548.47	1.194		
41R-3, 9–11	548.84		2.66	2.7
41R-4, 23–25	550.48		4.54	4.53
42R-1, 15–17	555.75	0.816		
42R-1, 67–69	556.27		5.06	5.03
42R-2, 67–69	557.77		4.56	4.44
42R-3, 90–92	559.44	1.824		
42R-3, 124–126	559.78		4.37	4.5
42R-4, 13–15	560.17		4.33	4.47
43R-1, 30–32	565.3		4.05	
43R-1, 38–40	565.38	1.911		
43R-2, 34–36	566.64	1.57	3.6	3.6
44R-1, 30–32	574.9		4.46	4.35
45R-1, 53–55	584.83		4.34	4.27
46R-1, 56–58	594.46	0.853	4.43	4.42
46R-2, 65–67	596.05	1.2	4.81	4.12
47R-1, 98–100	604.48	1.046	4.47	4.62
48R-1, 67–69	613.87	1.182	3.65	3.64
48R-2, 45–47	615.04	1.135	3.76	3.72
49R-1, 32–34	623.22	1.19	3.46	3.44
49R-2, 77–79	624.72	1.042	4.81	4.71
49R-3, 60–62	625.86	1.168	3.74	3.87
49R-4, 50–52	627.18		4.57	4.51
50R-1, 24–26	632.74		4.14	4.03
50R-2, 31–33	634.31		4.38	4.47
51R-1, 49–51	642.69		4.43	4.54
51R-1, 59–61	642.79	1.235		
51R-2, 6–8	643.76		4.27	4.19
52R-1, 81–83	652.71		3.94	3.87
52R-2, 140–145	654.83		4.85	4.88
53R-1, 128–130	662.88	1.257		
54R-1, 75–77	671.95	2.248		
54R-1, 107–109	672.27		3.9	3.81
54R-2, 64–66	673.28	1.164		
54R-2, 85–87	673.49		5.11	5.28
54R-3, 60–62	674.74	1.131	3.91	3.82
54R-4, 55–57	676.19	1.343	4.6	4.61
54R-5, 44–46	677.26		5.18	5.35
55R-1, 45–47	681.25	1.379	5.15	5.27
55R-2, 85–87	683.06		4.29	4.25
55R-3, 87–89	684.5	1.332	4.08	3.99
56R-1, 114–116	691.24	1.399		
56R-1, 124–126	691.34		4.16	4.32
56R-2, 100–102	692.6	1.373		
56R-2, 107–109	692.67		3.56	3.62
56R-3, 56–58	693.54	1.458	3.79	3.65
56R-4, 60–62	695.01	1.145	2.75	2.72
56R-5, 73–75	696.64	1.178	3.93	3.84
57R-1, 1–3	699.81	1.198		
57R-1, 12–14	699.92		3.1	3.19
57R-1, 107–109	700.87	1.273	3.14	3.2
57R-2, 83–85	702.04	1.261	4.06	3.92
57R-3, 57–59	703.06	1.316		
57R-4, 59–61	704.53	1.223		
57R-4, 65–67	704.59		3.52	
57R-5, 51–53	705.76	1.106	3.7	3.63
57R-6, 53–55	707.09	1.093		
57R-6, 86–88	707.42		3.24	3.34
57R-7, 85–87	708.91	1.204		
58R-1, 77–79	710.17		4.08	4.1
58R-1, 107–109	710.47	1.125		
58R-2, 53–55	711.43	1.15		
58R-2, 127–129	712.17		3.94	3.75
58R-3, 47–49	712.69	1.278		
58R-3, 83–85	713.05		3.14	
58R-4, 19–21	713.84		3.56	3.58
58R-4, 89–91	714.54	1.432		
59R-1, 68–70	715.08		4.5	4.24
79R-1, 92–94	715.32	1.249		
59R-2, 93–95	716.57	1.353	3.65	3.84
59R-3, 34–36	717.44	1.328		
59R-4, 35–37	718.93		4.24	4.12

Table 14 (continued).

Core, section, interval (cm)	Depth (mbsf)	Thermal conductivity (W/mK)	Compressional-wave velocity	
			A direction (km/s)	B direction (km/s)
60R-1, 44–46	719.44	1.213		
60R-1, 72–74	719.72		4.03	3.89
60R-2, 37–39	720.67	1.143		
60R-2, 115–117	721.45		5.3	5.27
60R-3, 69–71	722.44	1.292		
60R-3, 94–96	722.69		4.93	4.71
60R-4, 91–93	724.16	1.316		
60R-4, 106–108	724.31		4.39	4.44
60R-5, 35–37	725.02	1.399		
60R-5, 49–51	725.16		4.43	4.44
60R-6, 47–49	526.48		4.33	4.33
60R-6, 130–132	727.31	1.334		
61R-1, 68–70	729.38	1.304	4.2	4.4
61R-2, 26–28	730.46	1.542	3.95	4.11
61R-3, 1–3	731.71	2.053	3.45	3.5
61R-4, 71–73	733.72	2.051		
61R-4, 82–84	733.83		4.41	4.53
61R-5, 54–56	735.05	1.85	4.41	4.45
61R-6, 53–55	736.26		2.56	
62R-1, 31–33	738.71	1.858	4.47	4.51
62R-2, 31–33	740.08	1.757	3.74	3.66
62R-3, 104–106	742.09	1.332	3.5	3.45
63R-1, 20–22	748.2	1.253		
62R-1, 83–85	748.83		4.38	4.49
63R-2, 70–72	750.2	1.763	4.66	4.73
64R-1, 126–128	758.96	2.423		
64R-1, 145–147	759.97		4.84	4.84
64R-2, 93–95	760.07	2.265	4.65	4.68
64R-3, 56–58	761.16		4.71	4.77
65R-1, 5–7	767.45	1.759		
65R-1, 17–19	767.57		4.71	4.7
65R-2, 37–39	769.27		4.12	4.1
65R-2, 68–70	769.58	2.151		
65R-3, 52–54	770.89		4.11	4.09
65R-3, 38–40	770.75	2.147		
66R-1, 88–90	777.98		4.01	3.99
66R-1, 95–97	778.05	2.177		
66R-2, 70–72	779.24	2.408		
66R-2, 80–82	779.34		4.78	4.7
66R-3, 34–36	780.3		4.39	4.45
66R-3, 43–45	780.39	2.358		
67R-1, 33–35	787.03	2.252	4.17	4.09
68R-1, 1–3	796.31	1.862	4.99	4.93
69R-1, 69–71	797.99	1.613		
69R-1, 78–80	798.08		3.99	3.93
69R-2, 22–24	798.91	1.676	3.34	3.43
69R-3, 25–27	800.05	1.97		
69R-3, 130–132	801.01		3.86	3.69
69R-4, 35–37	801.65	2.07		
69R-4, 51–53	801.81		4.2	3.51
69R-5, 52–54	802.98	2.173		
69R-5, 63–65	803.09		4.24	4.17
69R-6, 71–73	804.62	1.574	4.18	4.2
69R-7, 33–35	805.66	1.613		
70R-2, 64–66	809.04	1.787		
70R-3, 60–62	810.43	1.708		
70R-4, 23–25	811.42	2.198		
71R-1, 103–105	816.63	2.198		
71R-2, 106–108	818.16		3.4	3.49
71R-2, 126–128	818.36	2.415		
71R-3, 107–109	819.59		3.21	3.25
71R-3, 130–132	819.82	2.177		
71R-4, 43–45	820.37	2.212		
71R-4, 71–73	820.65		4.53	4.44
71R-5, 10–12	821.54		4.83	4.75
72R-1, 80–82	824.4	2.236	4.78	4.75
72R-2, 76–78	825.86	1.761	3.72	3.62

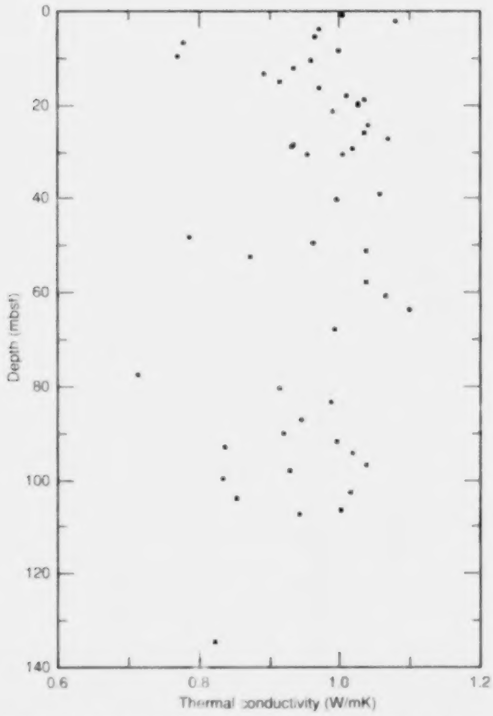

Figure 15. Thermal conductivity vs. depth for Hole 786A (the large degree of scatter in the data from the base of the hole is probably caused by measurement of irregularly shaped hard rocks).

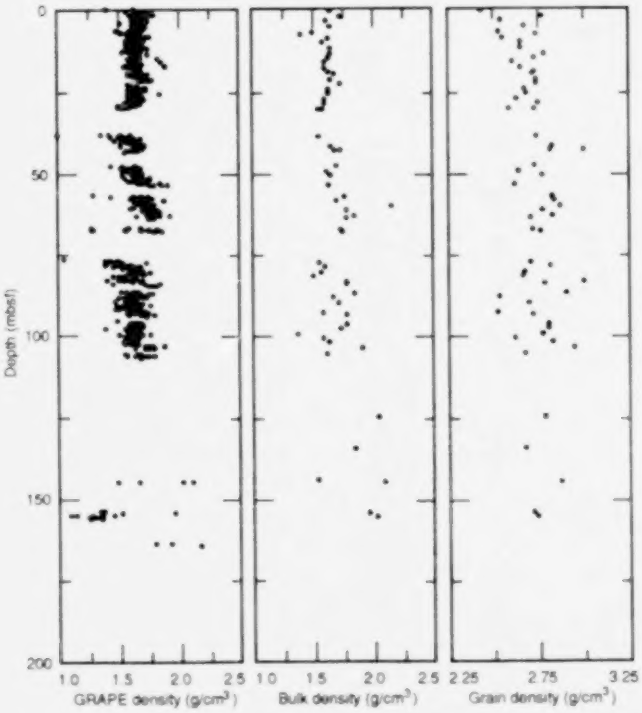

Figure 16. Bulk density (determined by GRAPE), bulk densisty (determined by discrete samples), and grain density vs. depth for Hole 786A.

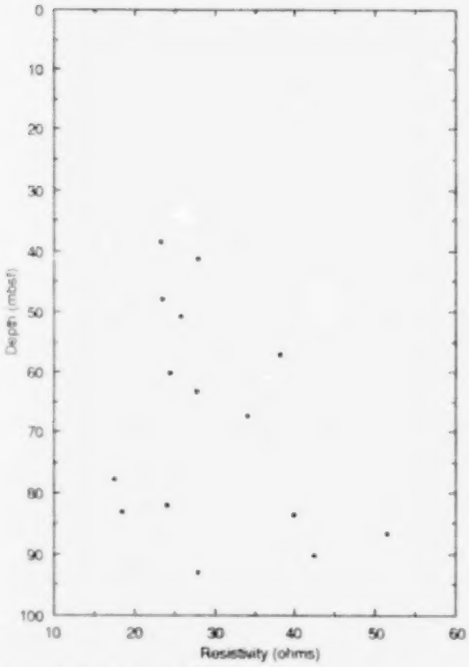

Figure 17. Resistivity vs. depth for Hole 786A.

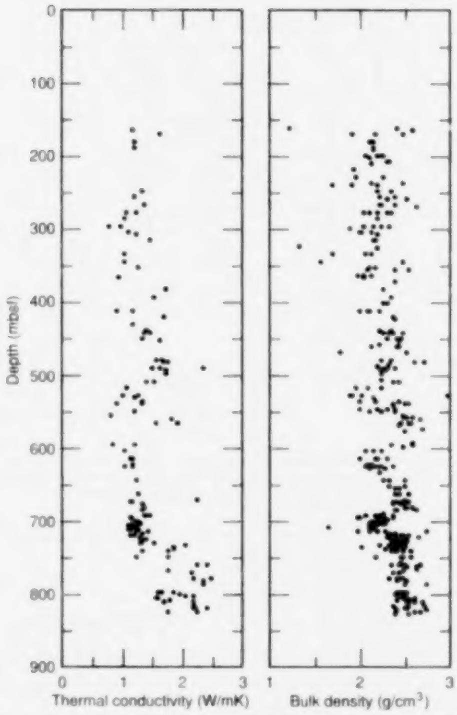

Figure 18. Thermal conductivity and bulk density (determined by 2-min GRAPE counts) vs. depth for hard rocks from Hole 786B.

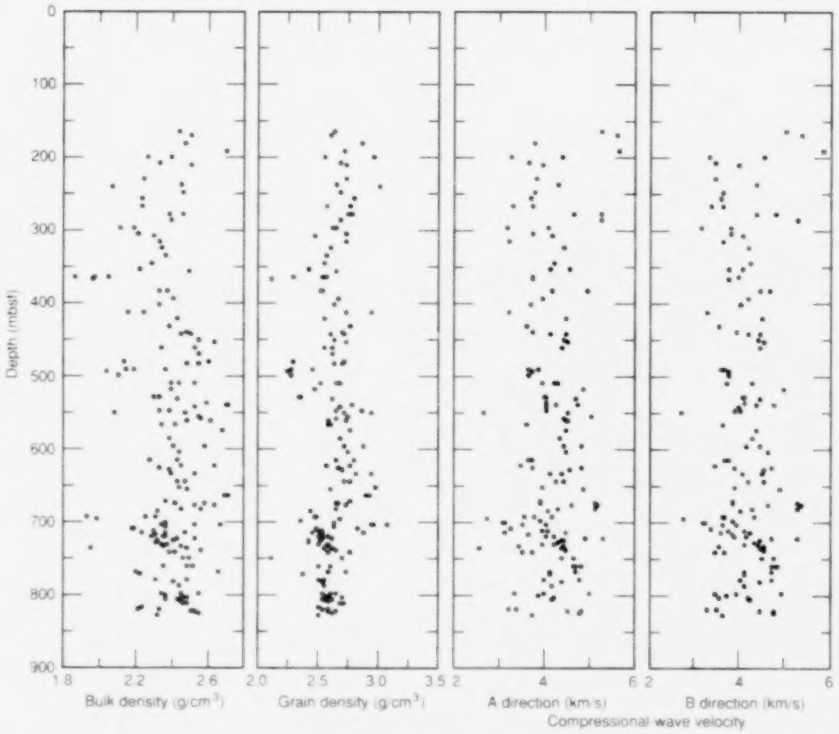

Figure 19. Bulk density, grain density, and compressional-wave velocities measured on the Hamilton Frame apparatus vs. depth for Hole 786B. The velocities in the orthogonal directions are nearly equivalent and show a high degree of scatter, which is related to microcrack effects.

Summary Log for Site 786

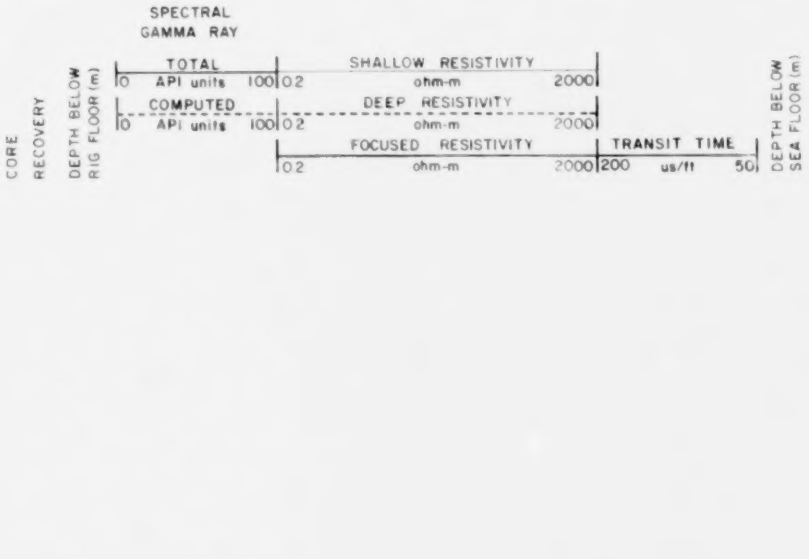

Summary Log for Site 786 (continued)

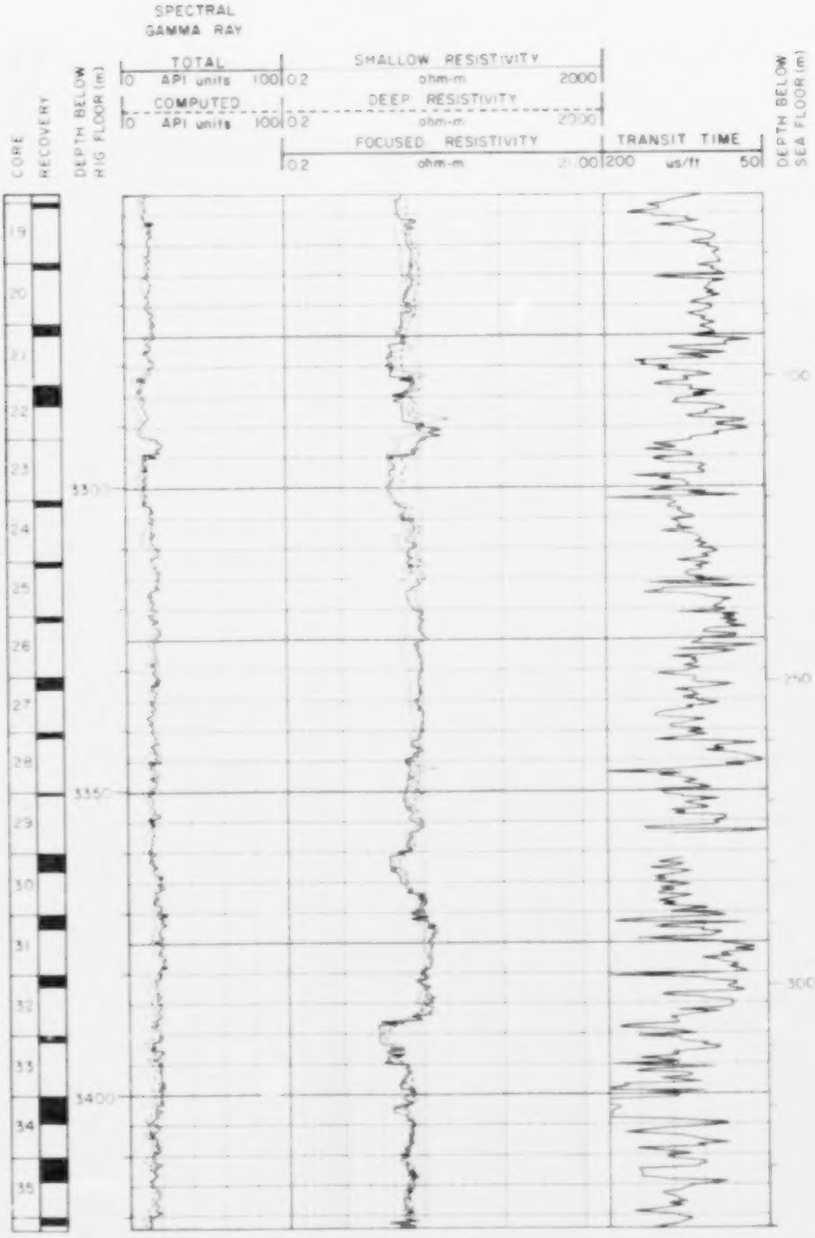

Summary Log for Site 786 (continued)

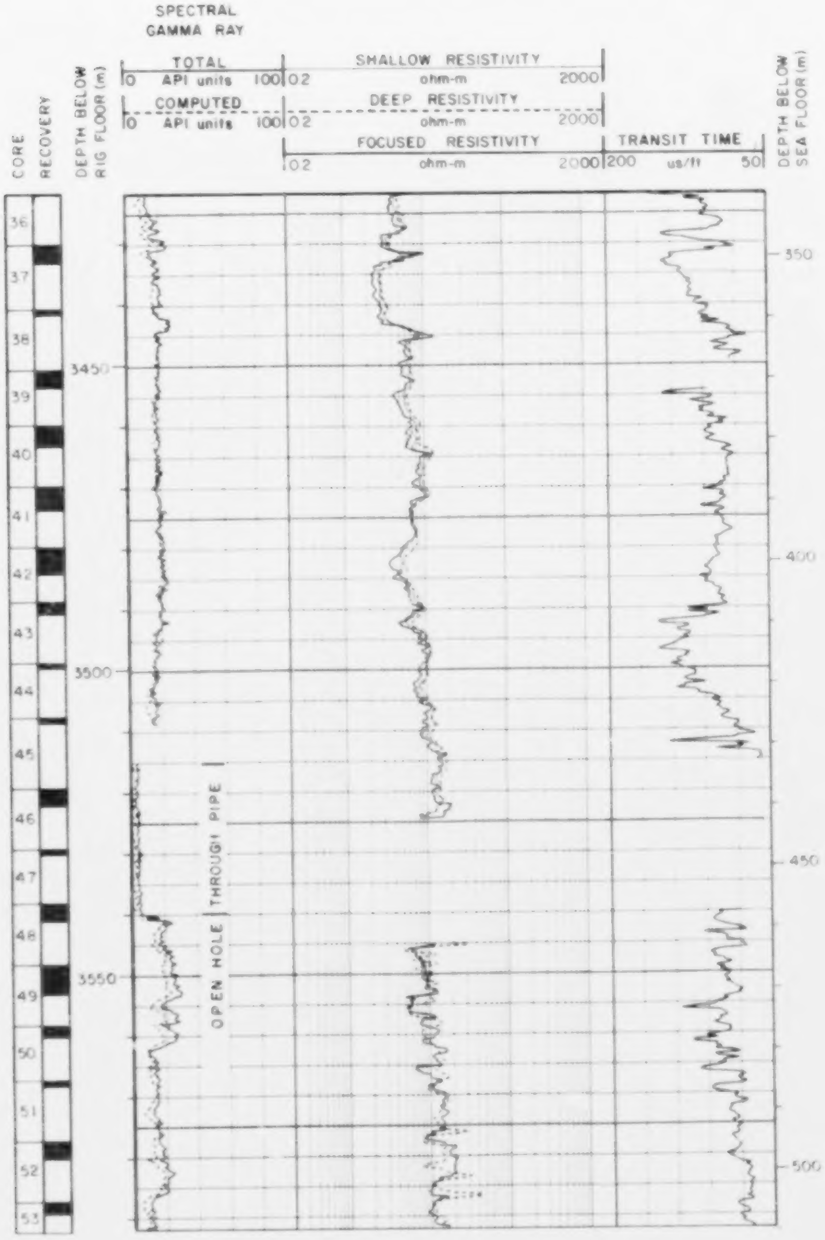

Summary Log for Site 786 (continued)

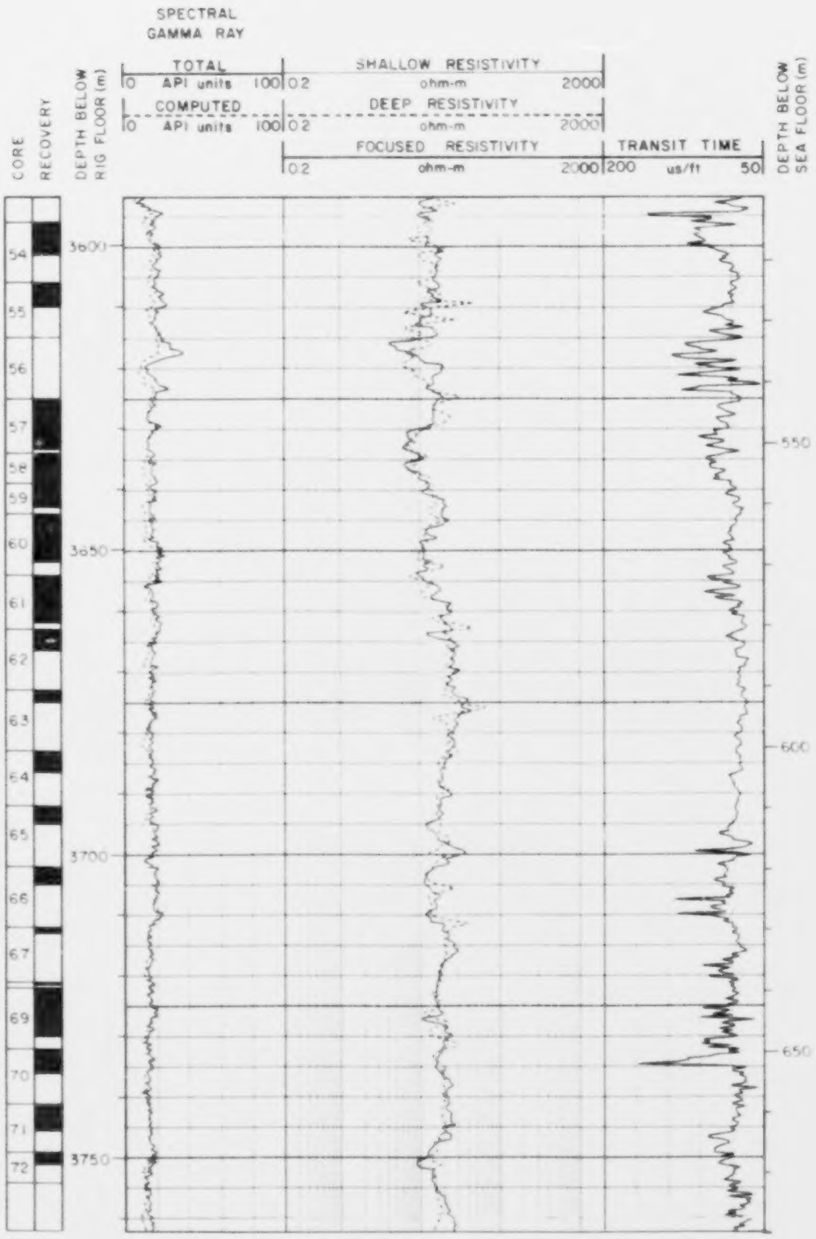

Summary Log for Site 786 (continued)

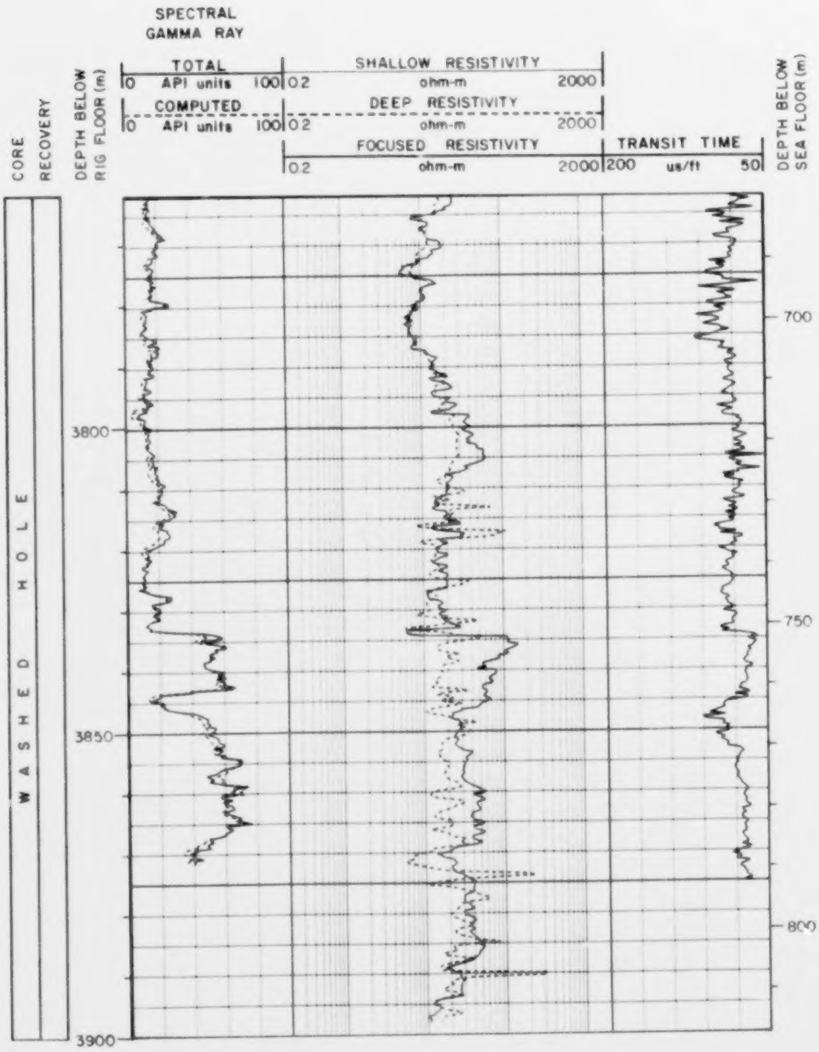

Summary Log for Site 786 (continued)

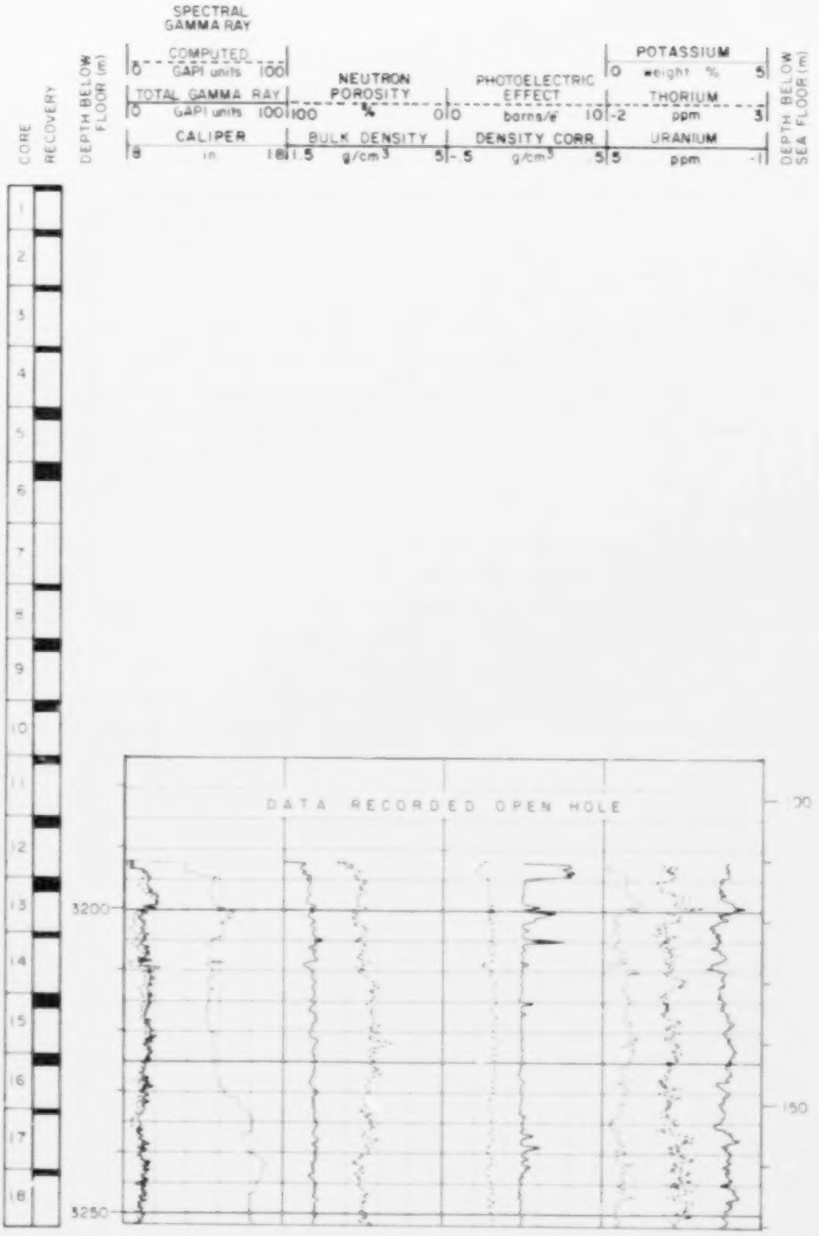

Summary Log for Site 786 (continued)

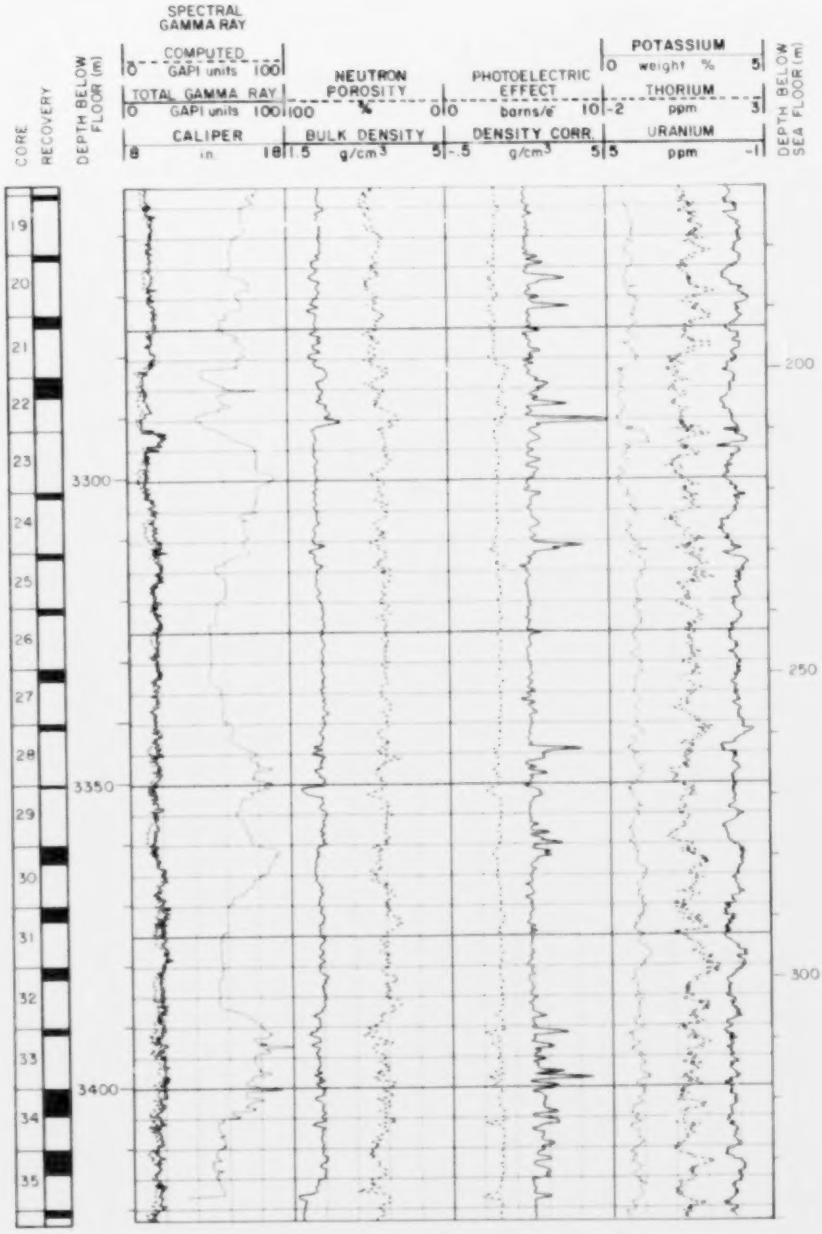

Summary Log for Site 786 (continued)

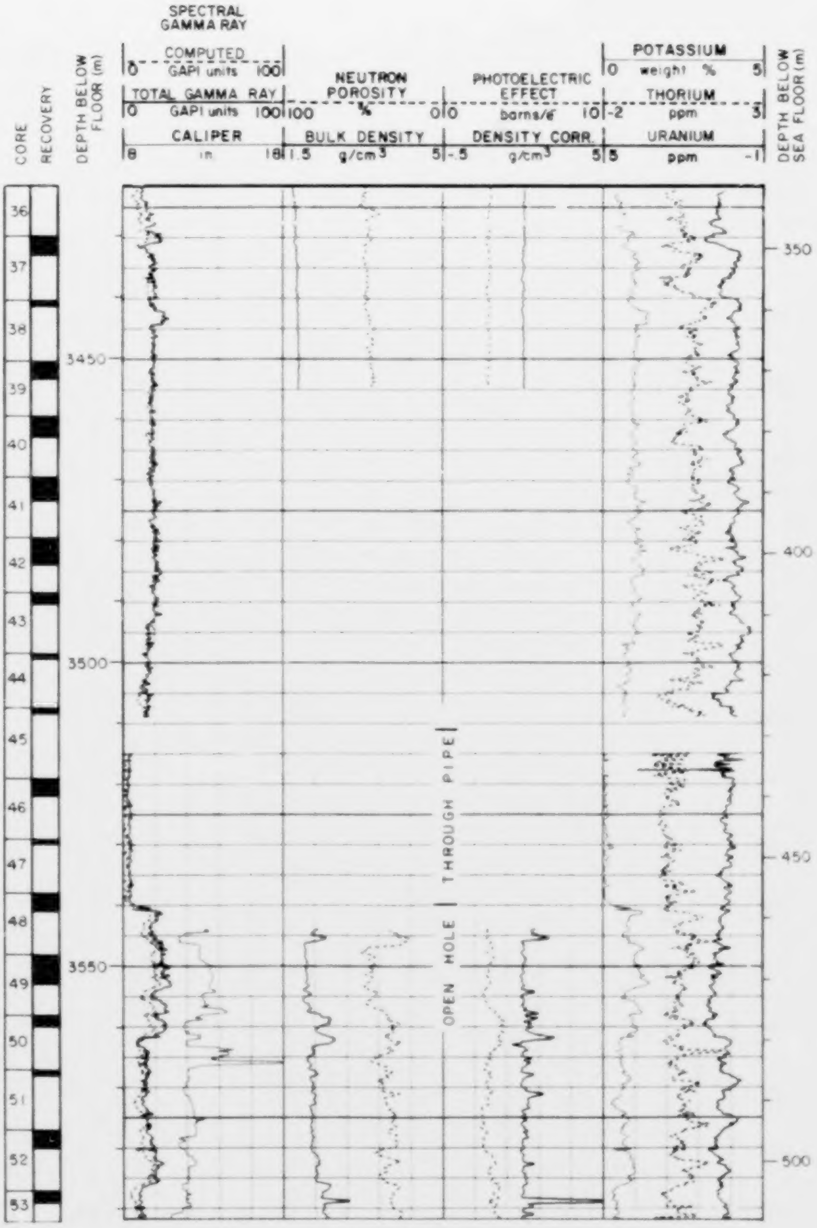

Summary Log for Site 786 (continued)

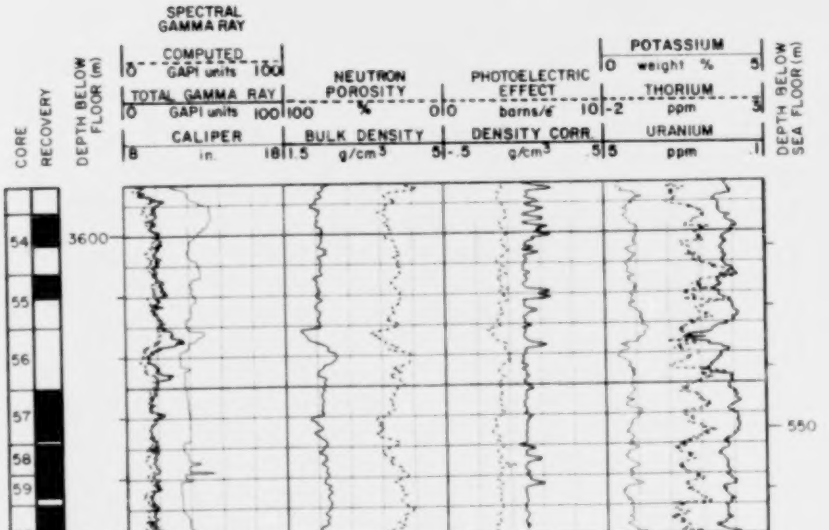

Summary Log for Site 786 (continued)

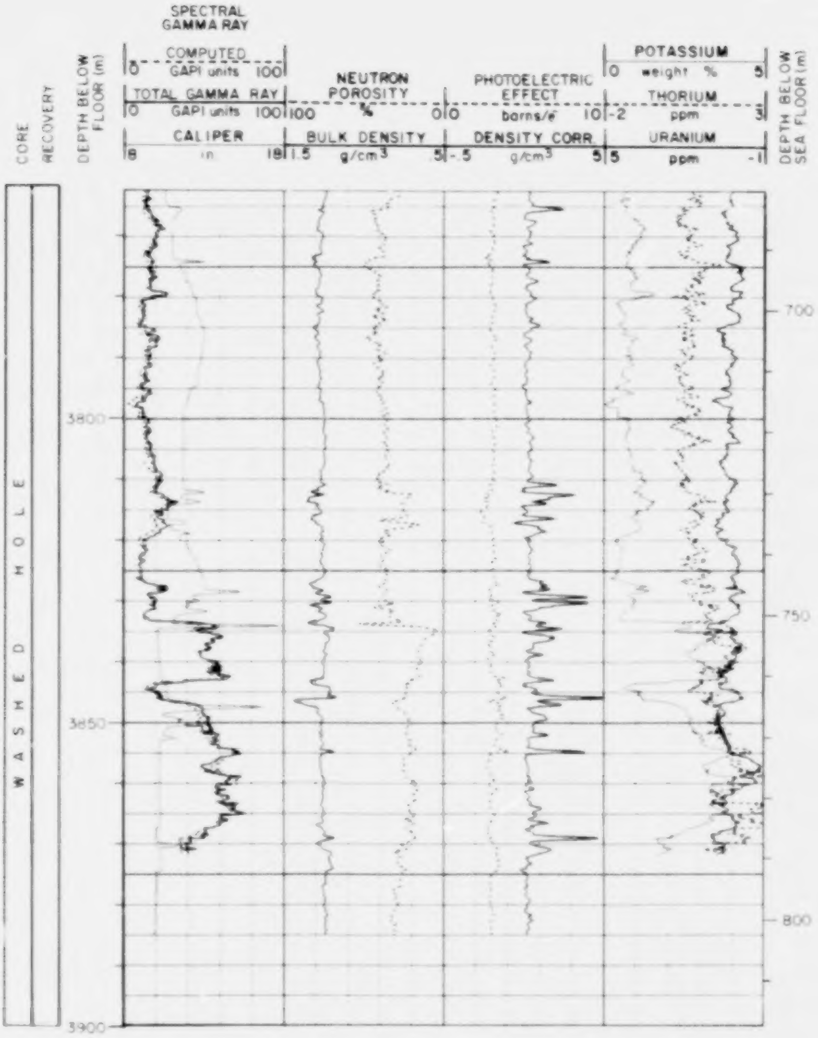

Summary Log for Site 786 (continued)

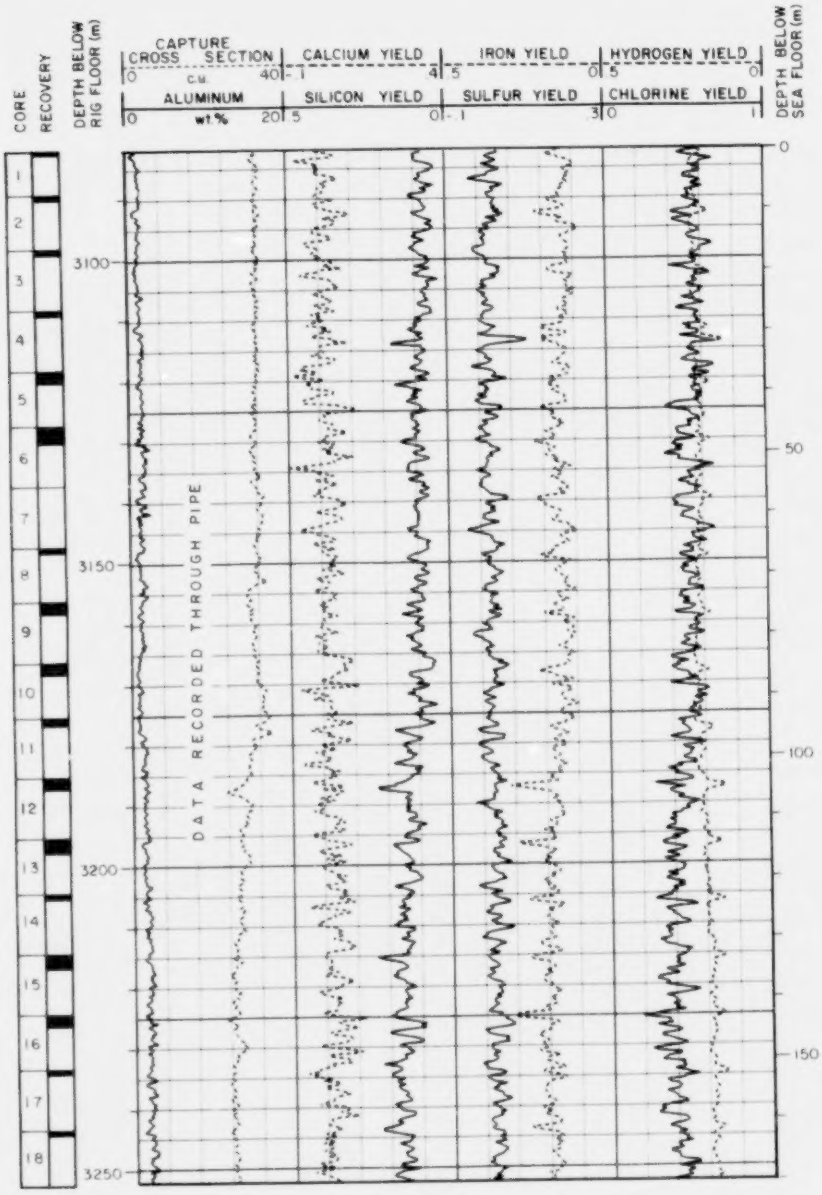

Summary Log for Site 786 (continued)

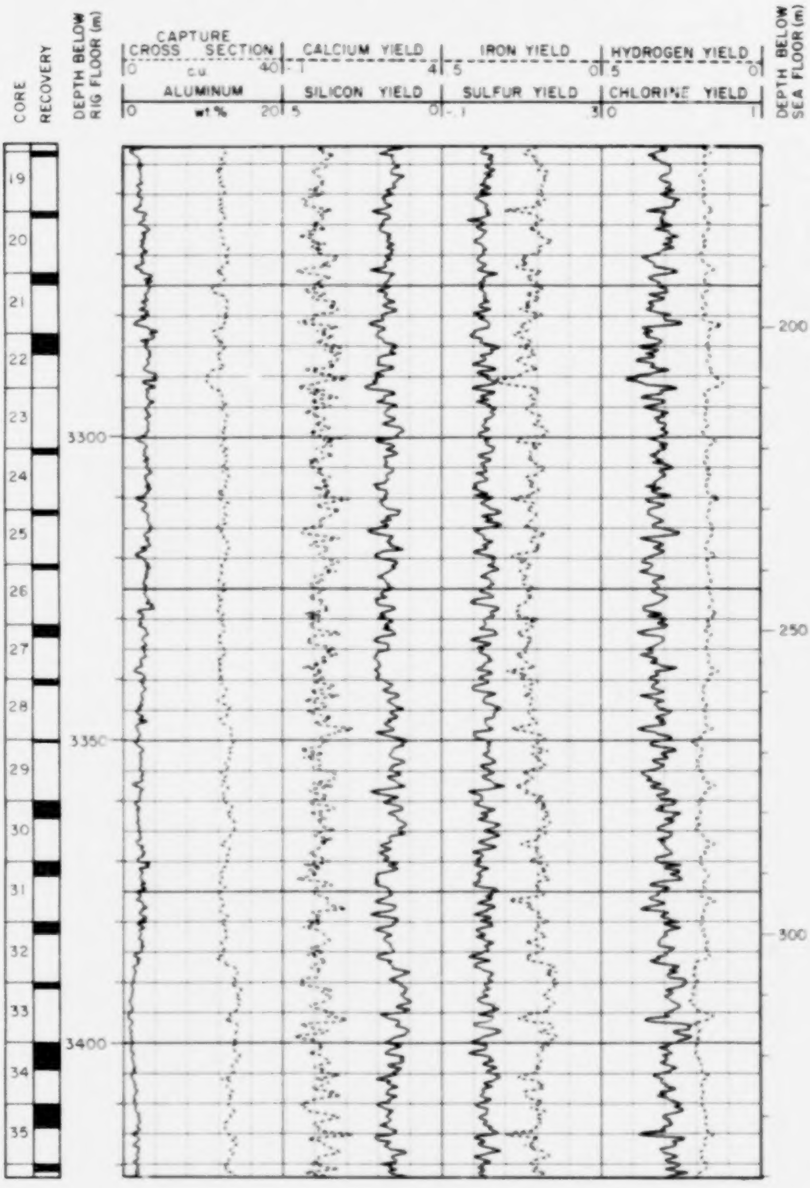

Summary Log for Site 786 (continued)

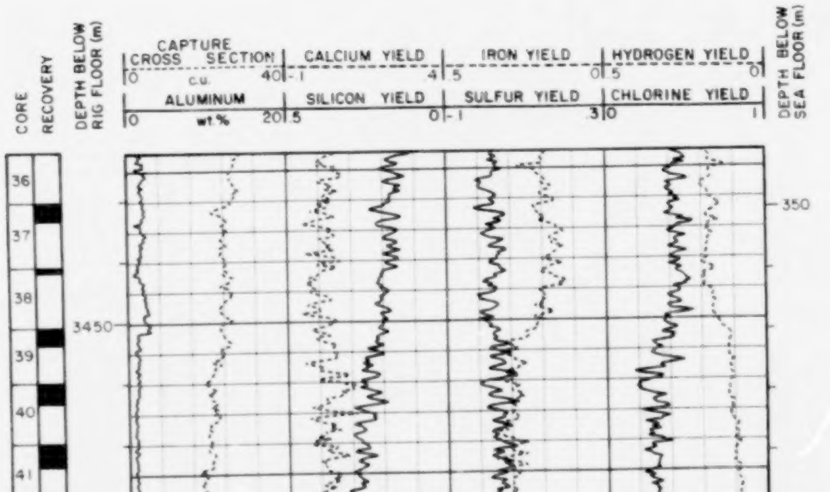

Summary Log for Site 786 (continued)

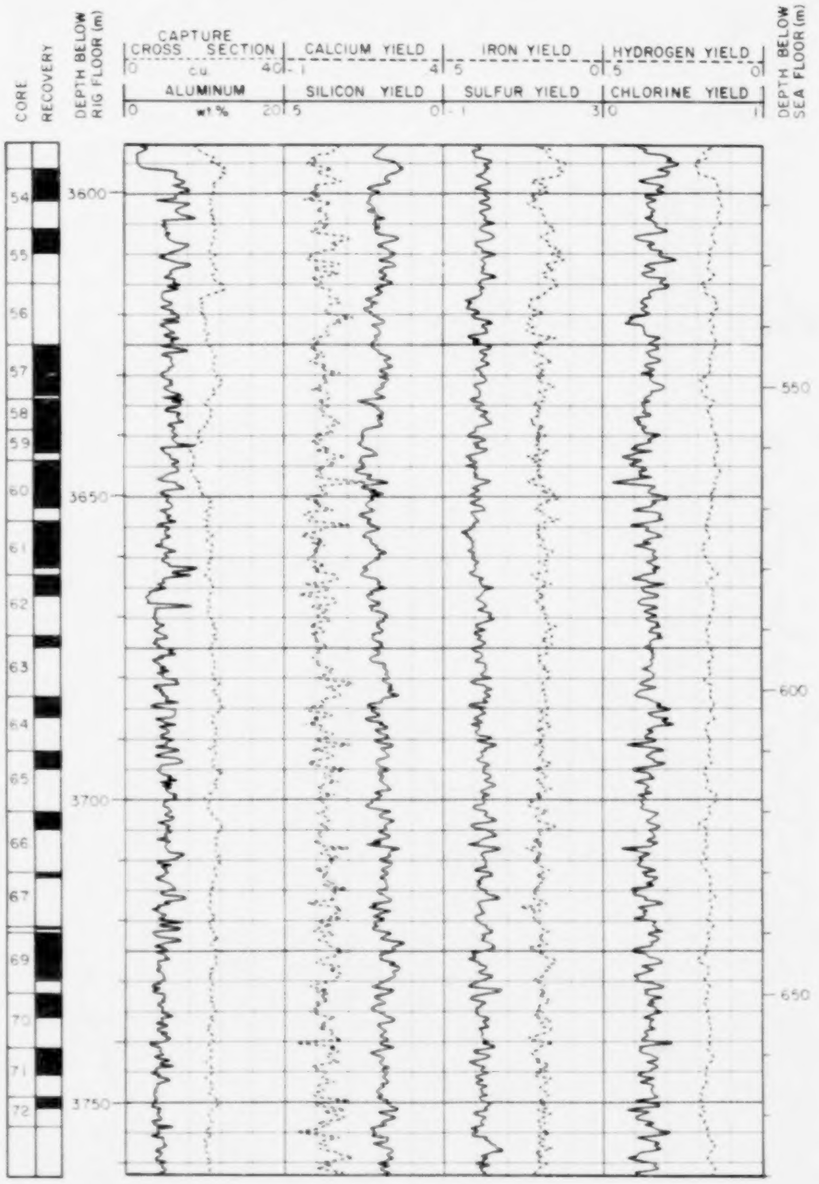

Summary Log for Site 786 (continued)

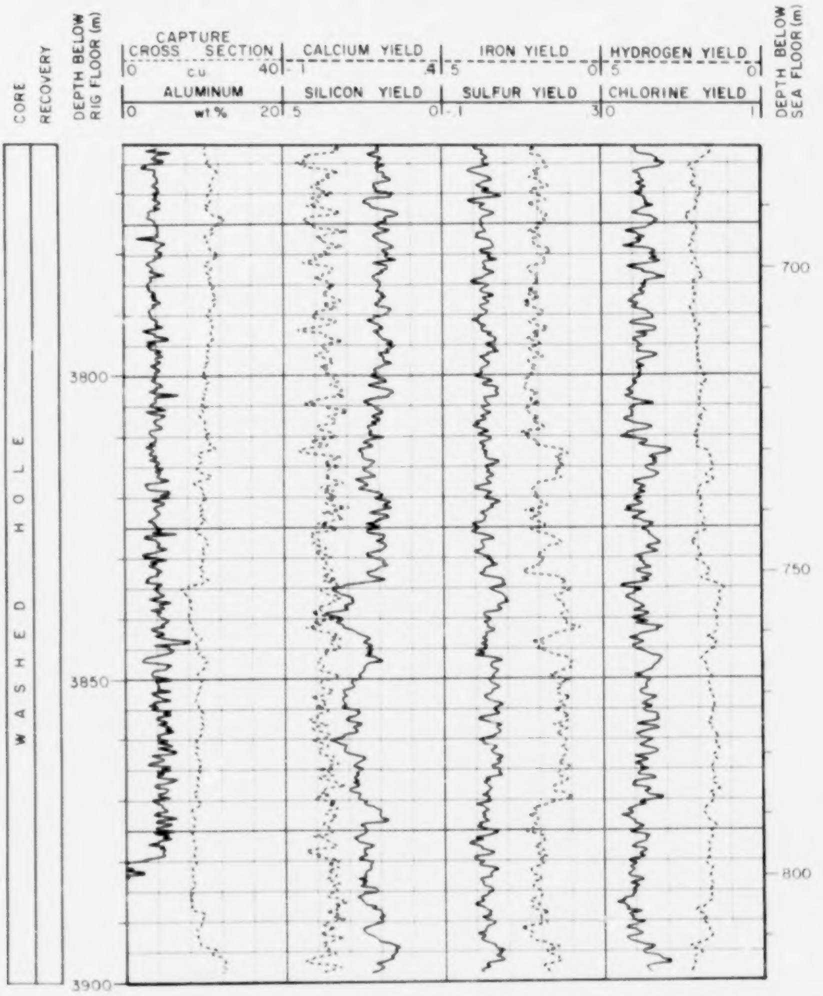

SECTION 3: CONCLUSIONS

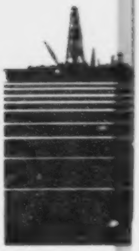

Fryer, P., Pearce, J. A., Stokking, L. B., et al., 1990
Proceedings of the Ocean Drilling Program, Initial Reports, Vol. 125

15. SUMMARY OF RESULTS FROM LEG 125[1]

Shipboard Scientific Party[2]

ABSTRACT

During Leg 125, nine sites were drilled in the Mariana and Izu-Bonin forearcs to determine the origin and evolution of the forearc terranes and to investigate the dewatering of the subducted lithosphere. Six sites were located on or adjacent to serpentinite seamounts between the outer-arc high and the trench, four (Sites 778–781) at Conical Seamount in the Mariana forearc and two (Sites 783 and 784) on the Torishima Forearc Seamount in the Izu-Bonin forearc. The remaining sites (Sites 782, 785, and 786) were located along the eastern edge of the Izu-Bonin forearc basin. The principal scientific achievements of the leg are (1) the recovery of the first evidence for Pliocene or younger magmatic activity in an extant, intraoceanic forearc terrane; (2) the first deep penetration of the Eocene basement of the outer-arc high to recover over 650 m of boninite flows and hyaloclastite, andesite-dacite flows, breccias, sills, and dikes; (3) the confirmation that some forearc serpentinite seamounts can form at least in part by flows of clast-bearing serpentinite sediments and flows from a central conduit as do mud volcanoes; (4) the discovery of mafic clasts within the serpentinite, which have both island-arc tholeiite and normal mid-ocean ridge basalt affinities and are metamorphosed in the greenschist and prehnite-pumpellyite facies; (5) the confirmation of high-pH, low-chlorinity fluids of probable deep subduction-related origin at shallow levels within the summit of the seamounts; (6) the recovery of hydrocarbon-rich gases of probable subduction-related origin within the Mariana serpentinite seamount, and (7) the identification of numerous ash layers within the forearc basin sediments that indicate peaks of volcanic activity in the Eocene-Oligocene and from the late Miocene to the Holocene.

REGIONAL SETTING

The Izu-Bonin-Mariana region (Fig. 1) is made up of a complex series of arcs and basins formed since the start of westward subduction of Pacific lithosphere during the Eocene. Subduction of Pacific oceanic lithosphere is currently taking place at absolute velocities between 8 and 10 cm per year to the northwest; the subduction angle is about 12° at shallow depths, steepening in some places to nearly vertical below about 100 km.

The evolution of these arc and basin systems is thought to have begun in the early to middle Eocene, when westward subduction of Pacific lithosphere began beneath the western part of the Philippine Sea Plate (Ben-Avraham and Uyeda, 1983; Karig, 1975; Ogawa and Naka, 1984). Development of the system continued through the early Oligocene with the formation of an intraoceanic volcanic arc. Rifting in the middle Oligocene split the entire arc system, and the southern part of the arc split again in the late Miocene.

The Mariana and Izu-Bonin forearcs differ in terms of both their tectonic evolution and plate-convergence characteristics. The northern half of the Izu-Bonin forearc has experienced relatively little deformation since subduction began (Honza and Tamaki, 1985) and is made up of a broad forearc basin filled with volcaniclastic and hemipelagic sediments that developed behind an outer-arc high (Fig. 2). The structure of the Mariana forearc is similar (Fig. 3), but the forearc has undergone extensive vertical uplift and subsidence resulting from seamount collision and from tensional and rotational fracturing associated with adjustments to plate subduction and to changes in the configuration of the arc (Fryer et al., 1985b). The serpentinite seamounts occurring in a broad zone along the trench-slope break (outer-arc high) of the Mariana system are suggested to have formed by some type of diapirism (Bloomer, 1983; Fryer et al., 1985a; Fryer and Fryer, 1987). In the Izu-Bonin forearc, chloritized mafic and serpentinized ultramafic rocks have also been dredged from a chain of local highs located less than 50 km from the trench axis along a lower-slope terrace (Ishii, 1985).

The modern 150- to 220-km-wide Izu-Bonin and Mariana forearcs may have formed by volcanism during arc development in the Eocene and early Oligocene. The origin and evolution of the forearc basement may have progressed in accordance with one of the following scenarios, each of which implies a different crustal structure:

1. The frontal arc and outer-arc high may have been continuous originally and subsequently separated by forearc spreading.
2. The frontal arc and outer-arc high may have been built separately but nearly synchronously on former Philippine Sea Plate crust.
3. The terrane may form part of a continuous Eocene arc volcanic province, possibly with overprints of later forearc volcanism.

The forearc stratigraphy records a history of the variations in intensity and chemistry of arc volcanism, which allows the correlation of these variations with such parameters as subduction rate and backarc spreading. Studies of the tephrachronology, and the frequency and geochemistry of ash and pyroclastic flow deposits in the forearc basin drill cores, will enable the various models of arc volcanism to be evaluated.

DRILLING OBJECTIVES

The principal objective of Leg 125 was to study two important and poorly understood aspects of the Izu-Bonin and Mariana forearc terranes:

---

[1] Fryer, P., Pearce, J. A., Stokking, L. B., et al., 1990. *Proc. ODP, Init. Repts.*, 125: College Station, TX (Ocean Drilling Program).

[2] Shipboard Scientific Party is as given in the list of participants preceding the contents.

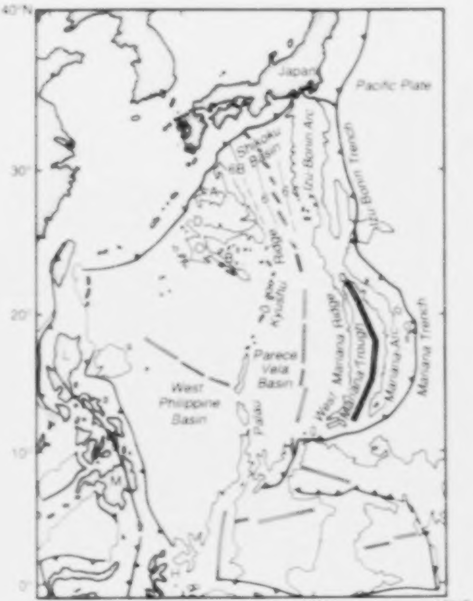

Figure 1. Active plate boundaries and relict spreading centers in the Philippine Sea region. Barbed lines locate subduction zones, medium double lines locate active spreading centers, and thin double lines locate relict spreading centers. Basins and ridges are outlined by the 4-km bathymetric contour, except for the Izu-Bonin arc, West Mariana Ridge, and Mariana arc, which are outlined by the 3-km contour. Magnetic anomalies 6 and 6B are shown by single thin lines in the Shikoku Basin. A = Amami Plateau; B = Daito Basin; D = Daito Ridge; H = Halmahera; L = Luzon; M = Mindanao; O = Oki-Daito Ridge.

1. The origin and evolution of the forearc terranes, investigated by drilling a series of holes through the sediments and into the basement of the Mariana and Izu-Bonin forearc basins (Sites 782, 785, and 786) and into serpentinite seamounts from the Mariana mid-forearc region (Sites 778–781) and Izu-Bonin lower-slope terrace (Sites 783 and 784) (Table 1 and Fig. 4).

2. Dewatering of the subducted lithosphere, investigated indirectly from the composition of forearc basin crust and directly from analyses of fluids, chemical precipitates, and metamorphic rocks from the serpentinite seamounts. The results of these studies were to be compared with those of reference sites drilled on the Pacific Plate near the Mariana and Izu-Bonin trenches.

DRILLING RESULTS

Site 778

Site 778 (19°29.93′N, 146°39.93′E, water depth, 3913.7 m) is situated about halfway up the southern flank of Conical Seamount, a 1500-m-high cone-shaped serpentinite seamount on the outer-arc high of the Mariana forearc basin, about 100 km west of the trench axis. The site is located in the center of a major serpentine flow.

Two lithostratigraphic units are recognized at Site 778 (Fig. 5):

Subunit IA (0–7.2 m below seafloor, or mbsf) of Unit I contains lower to middle Pleistocene to Holocene(?) serpentine-rich sediment and serpentine flows overlying serpentine clay, silt-sized serpentine, and a serpentine-marl breccia.

Subunit IB (7.2–29.8 mbsf) consists of lower to lower to middle Pleistocene sandy marl containing cobbles and pebbles of serpentinite, vesicular volcanic rocks, and a foraminifer-bearing serpentine sandstone.

Unit II (29.8–107.6 mbsf) is made up of phacoidal sheared serpentine. The matrix is composed of serpentine, opaque minerals, epidote-group minerals, chlorite, talc, and olivine. A variety of clasts is present: variably serpentinized tectonized harzburgite (80%), metabasalts (15%), and other fragments including metagabbros, serpentinized dunites, and vein materials such as talc, carbonates, and quartz (5%).

The serpentine flow sequence in Unit II exhibits several structural features, including deformation of primary orthopyroxene, microbrecciation, ductile shearing of clasts, shear zones on all scales, a variably developed foliation parallel to shear-plane orientations, and open-to-isoclinal folding of bedding and foliation planes. These features may represent a combination of primary mantle tectonism, stresses related to intrusion and protrusion (flow emplacement) of the serpentinite diapir materials, and stresses resulting from post-protrusion remobilization.

The original mineralogy of the harzburgite clasts in Unit II was typically 70%–85% olivine, 15%–25% orthopyroxene with 1%–2% clinopyroxene (mainly as exsolution lamellae in orthopyroxene), and spinel.

Analyses of interstitial pore-water samples show a 10% decrease in chlorinity downhole. This decrease is interpreted

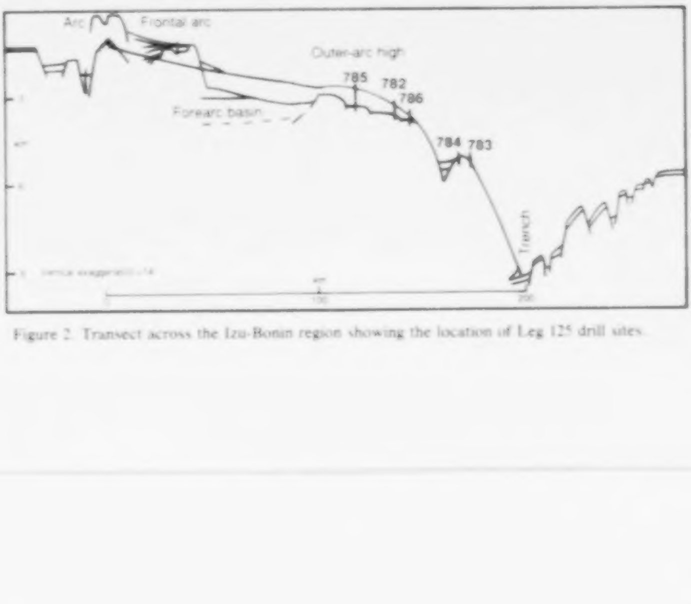

Figure 2. Transect across the Izu-Bonin region showing the location of Leg 125 drill sites.

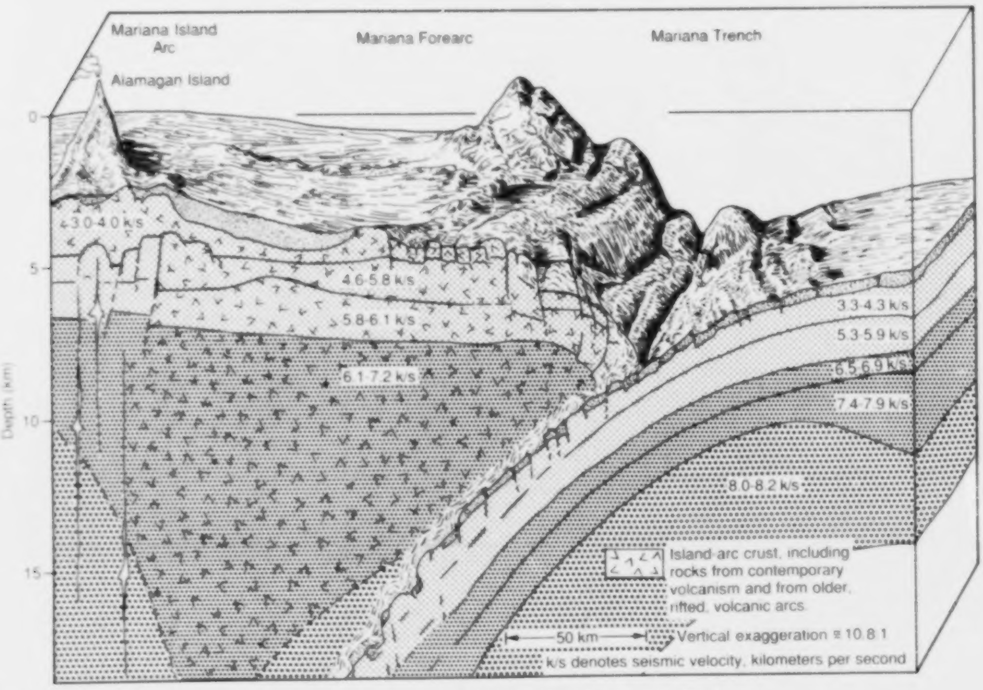
Mariana Island Arc
Alamagan Island
Mariana Forearc
Mariana Trench
0
5
10
15
Depth (km)
4.3.0-4.0 k/s
4.6-5.8 k/s
5.8-6.1 k/s
6.1-7.2 k/s
3.3-4.3 k/s
5.3-5.9 k/s
6.5-6.9 k/s
7.4-7.9 k/s
8.0-8.2 k/s
Island-arc crust, including rocks from contemporary volcanism and from older, rifted, volcanic arcs
50 km
Vertical exaggeration ≅ 10.8:1
k/s denotes seismic velocity, kilometers per second

Figure 3. Block diagram representing the Mariana forearc region (after Hussong, Uyeda, et al., 1982).

as a relative decrease in the admixture of seawater with similarly chlorine-poor fluids entrained in the serpentine flow material.

The principal conclusions of Site 778 investigations are as follows:

1. Forearc seamounts can be constructed, at least in part, from serpentine flows emanating from a central conduit.

2. Low- to medium-grade metamorphism characterizes the source region of the serpentinite seamounts.

3. Dehydration of the subducted lithosphere may have played an important role in the serpentinization of the source region of the serpentinite seamounts.

4. The primary mantle material in the seamount is predominantly highly depleted, tectonized harzburgite with subordinate dunite.

Site 779

Site 779 (19°30.75′N, 146°41.75′E; water depth, 3947.2 m), the second site on the flanks of Conical Seamount, is situated

Table 1. Leg 125 site summary.

Hole	Latitude (N)	Longitude (E)	Water depth[a] (m)	Number of cores	Length cored (m)	Length recovered (m)	Recovery (%)	Total penetration (m)
778A	19°29.93′	146°39.93′	3913.7	13	107.6	22.8	21.2	107.6
779A	19°30.75′	146°41.75′	3947.2	37	319.2	73.2	23.1	317.2
779B	19°30.75′	146°41.75′	3947.2	1	9.0	8.7	96.7	9.0
780A	19°32.51′	146°39.27′	3086.8	1	3.5	3.5	100.0	3.5
780B	19°32.47′	146°39.22′	3094.0	2	18.2	10.3	56.6	27.7
780C	19°32.53′	146°39.21′	3083.4	18	163.5	14.4	8.8	163.5
780D	19°32.55′	146°39.20′	3088.9	7	32.4	9.1	28.1	41.8
781A	19°37.91′	146°32.56′	4420.6	27	250.0	39.6	15.8	250.0
782A	30°51.66′	141°18.85′	2958.6	50	476.8	278.3	58.4	476.8
782B	30°51.60′	141°18.84′	2965.9	1	9.6	0.1	1.0	468.9
783A	30°57.86′	141°47.27′	4648.8	18	168.2	47.0	27.9	168.2
784A	30°54.49′	141°44.27′	4900.8	45	425.3	218.3	51.3	425.3
785A	30°49.47′	140°55.17′	2660.8	11	104.7	18.4	17.6	104.7
786A	31°52.48′	141°13.58′	3058.1	19	166.5	85.0	51.1	166.5
786B	31°52.45′	141°13.59′	3071.0	72	666.0	190.1	28.5	828.5

[a] Below mean sea level, corrected from drill-pipe measurements from the rig floor.

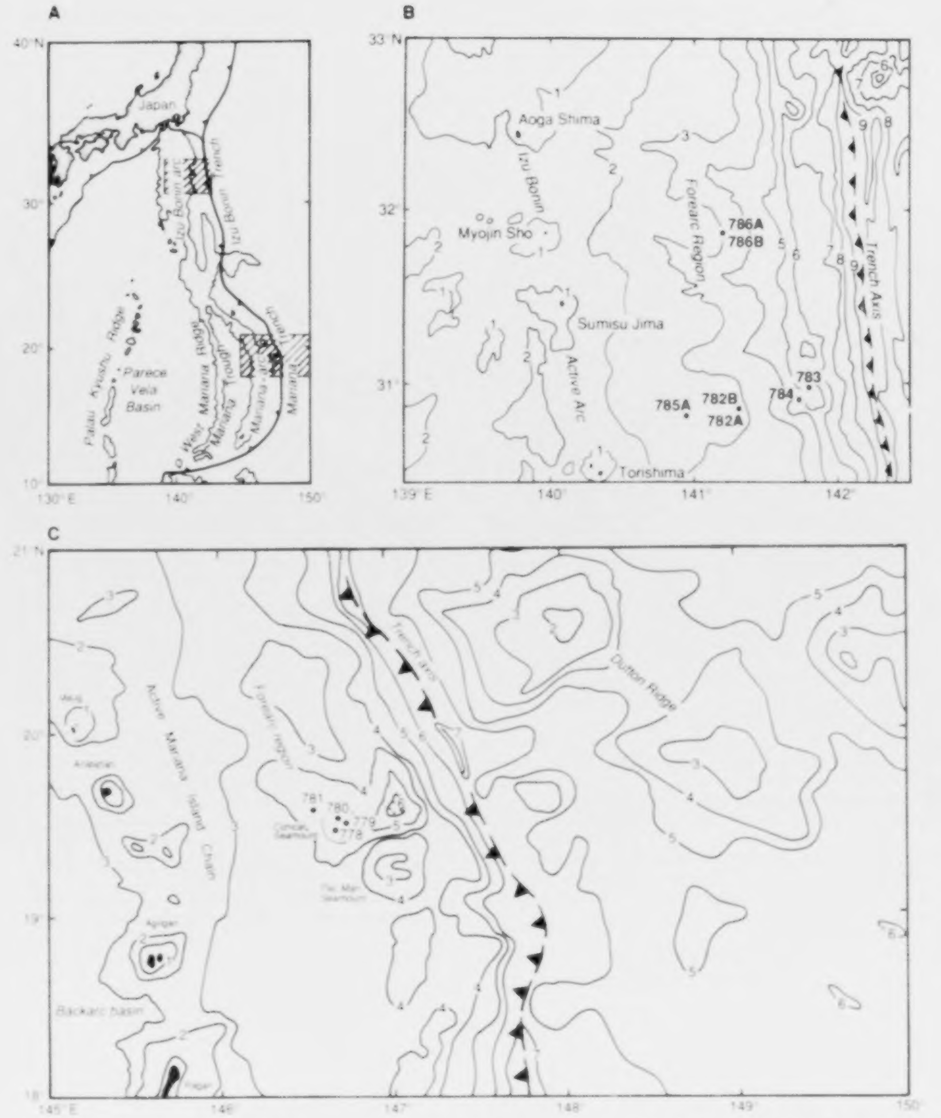
A
40°N
30°
20°
10°
130°E
140°
150°
Japan
Izu Bonin Arc
Izu Bonin Trench
Palau Kyushu Ridge
Parece Vela Basin
West Mariana Ridge
Mariana Trough
Mariana Arc
Mariana Trench
B
33°N
32°
31°
139°E
140°
141°
142°
Aoga Shima
Izu Bonin
Myojin Sho
Sumisu Jima
Active Arc
Torishima
Forearc Region
Trench Axis
786A
786B
785A
782B
782A
784
783
C
21°N
20°
19°
18°
145°E
146°
147°
148°
149°
150°
Active Mariana Island Chain
Forearc region
Trench axis
Dutton Ridge
Backarc basin
Anatahan
Agrigan
781
780
779
778
Conical Seamount
Pac Man Seamount

Figure 4. Location maps for Leg 125. Contour interval = 1 km. **A.** The regional setting of the Izu-Bonin and Mariana forearcs. **B.** Izu-Bonin drill Sites 782 through 786. **C.** Mariana drill Sites 778 through 781.

halfway up the southeast flank, about 3.5 km northeast of Site 778.

Three lithostratigraphic units were recovered at Site 779 (Fig. 5):

Unit I (0–10.6 mbsf in Hole 779A and 0–9 mbsf in Hole 779B) consists of lower Pleistocene to Holocene(?) unconsolidated sediments and flows consisting of clay, silt-sized serpentine, and lithic fragments in a matrix of sand- and silt-sized serpentine.

Subunit IIA (10.6–216.2 mbsf) of Unit II is lower Pleistocene sheared serpentine that contains clasts of variably serpentinized harzburgite and dunite.

Subunit IIB (216.2–303.0 mbsf) is upper Miocene to lower Pleistocene sheared serpentine containing clasts of serpenti-

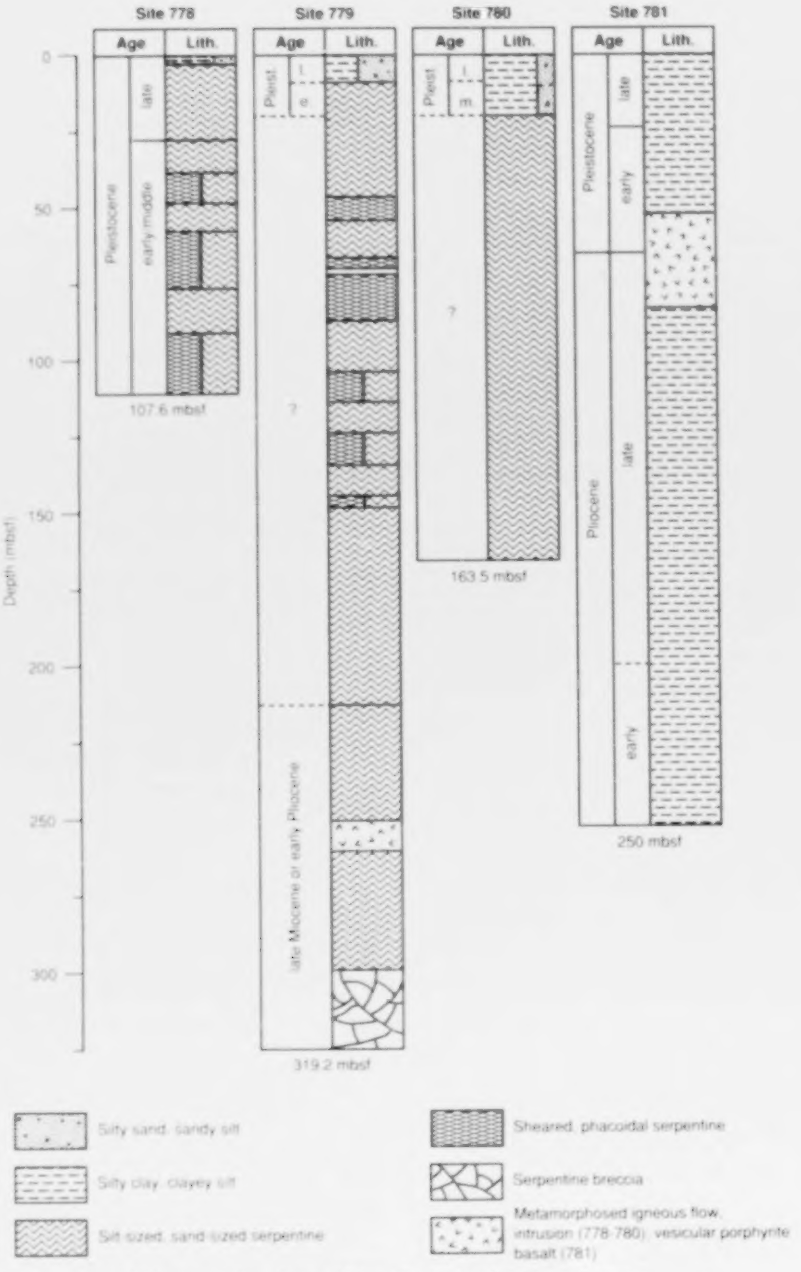
Site 778
Site 779
Site 780
Site 781
Age
Lith.
Depth (mbsf)
0
50
100
150
200
250
300
Pleistocene
late
early-middle
107.6 mbsf
Pleist.
l.
e.
?
late Miocene or early Pliocene
319.2 mbsf
Pleist.
l.
m.
?
163.5 mbsf
Pleistocene
late
early
Pliocene
late
early
250 mbsf
Silty sand, sandy silt
Silty clay, clayey silt
Silt-sized, sand-sized serpentine
Sheared, phacoidal serpentine
Serpentine breccia
Metamorphosed igneous flow, intrusion (778-780); vesicular porphyritic basalt (781)

Figure 5. Summary of lithostratigraphic columns of Sites 778 through 781 at Conical Seamount.

nized harzburgite and dunite, as well as gabbro and metabasalt, with intercalations of detrital serpentine sediments.

Unit III (303.0–317.2 mbsf) is a serpentine breccia exhibiting convolute layering.

The serpentine-rich material in Subunit IIB contains recrystallized carbonate minerals, kerogen, and lithified filamentous chains of opaque minerals that may be bacterial remnants. The presence of kerogen indicates a primary sedimentary origin for this material, an interpretation supported by the presence of horizontal bedding and nannofossils within the same unit.

Ultramafic rocks are mostly harzburgite and subordinate dunite, which have primary mineral assemblages similar to those at Hole 778A. The degree of serpentinization varies, but decreases downhole; serpentine veins are common and show a polystage filling history. Mafic clasts are predominantly metabasalt and metagabbro. Common metamorphic minerals are clays, chlorite, pumpellyite, and rare albite and sphene.

Structures in the serpentinite are similar to those of Hole 778A and thus indicate a similar history. The deformation of the matrix is consistent with gentle flowage under an applied load. The average density of the serpentine matrix is 2.01 g/cm^3. The density of the ultramafic clasts decreases with increasing degree of serpentinization and averages 2.55 g/cm^3.

The composition of the interstitial pore-water samples at Site 779 varies from 0 to 100 mbsf: pH increases to a maximum of 11.9; alkalinity increases five-fold; ammonia and sodium show significant but smaller increases; calcium decreases by 80%; salinity and chlorinity both decrease by 10%; and potassium and sulfate show small decreases. Magnesium is totally depleted below 80 mbsf. These results confirm the presence of a fluid other than seawater, possibly from the subducting plate, as proposed for Site 778. Hydrocarbons increase dramatically with depth in Hole 779A, with methane (up to 30% in one gas pocket), ethane, and propane present in most samples.

The principal conclusions from the studies at Site 779 can be summarized as follows:

1. Site 779 provides further evidence for the depleted nature of the mantle wedge beneath Conical Seamount.

2. The construction of Conical Seamount resulted from the flow of unconsolidated serpentine coupled with sedimentary processes.

3. Hydrocarbons are a significant component of the fluids associated with the seamount.

4. The source region of the serpentinite seamount has experienced medium-grade metamorphism.

5. Water derived from the subducted slab may be an important source of fluids involved in the serpentinization of Mariana forearc materials.

Site 780

Site 780 (proposed Site MAR-3A; 19°32.5'N, 146°39.2'E; water depth 3090 m) is situated on the west-southwest side of the summit of Conical Seamount, in an area shown by *Alvin* submersible dives to be sediment-covered and marked by active venting of fluids and precipitation of material from solution.

Two lithostratigraphic units were recovered at Site 780 (Fig. 5):

Unit I (0–3.5 mbsf in Hole 780A, 0–18.2 mbsf in Hole 780B, 0–14.0 mbsf in Hole 780C, and 0–15.4 mbsf in Hole 780D) comprises middle Pleistocene(?) to Holocene(?) sand- and silt-sized serpentine with rare intervals of foraminifer-rich serpentine clay and serpentine-rich silty clay.

Unit II (14.0–163.5 mbsf in Hole 780C and 15.4–32.4 mbsf in Hole 780D) comprises intervals of serpentinized ultramafic rocks in a matrix of sandy silt-sized serpentine sediment.

The sediments in Unit I contain 65%–75% serpentine with minor amounts of opaque minerals, aragonite, and foraminifers. The presence of delicate aragonite needles implies authigenic growth after the serpentine was emplaced. The matrix in Unit II contains 70%–99% serpentine with minor to trace amounts of opaque minerals, clay, zoisite, chlorite, micrite, and garnet.

Serpentinized, tectonized ultramafic rocks and subordinate serpentinized dunites at Site 780 have primary mineral assemblages similar to those from Sites 778 and 779. Serpentine veins are common. The muddy matrix recovered from Site 780 lacks the foliation and shear fabric of the matrix from the flank sites; therefore, the matrix may be interpreted as the primary fabric of the upwelling serpentine, upon which foliation and shear fabric are imposed by compaction, extension, and pure shear during the downhill creep of serpentine flows.

Logging in Hole 780C showed temperatures increasing steadily from seawater values (1.5°C) near the surface to 13.5°C at 60 mbsf; the water sampler-temperature-pressure tool in Hole 780D measured a lower value, 3.15°C at 41 mbsf, and an estimated heat flow of 52 mW/m^2.

The density of the serpentine matrix in Unit II ranges from 1.75 to 2.0 g/cm^3. Rheological measurements indicate that this matrix is a weak, highly nonideal plastic material capable of supporting blocks up to 20 m across and compatible with models for diapiric injection of the serpentinite.

The composition of the interstitial pore-water samples changes significantly downhole: salinity decreases by 25%, chlorinity by 20%, calcium by 90%, magnesium is totally depleted, sulfate nearly doubles, alkalinity increases from 2.5 to 34, pH increases from about 8 to 12.4, potassium increases significantly, and ammonia increases from 0 to 210 mmol/kg. These changes take place within a few meters of the seafloor, showing that the fluid entrained within the serpentinite may mix with seawater only at very shallow levels. The magnitude and direction of these changes also differ from those at the flank sites.

The principal conclusions from the studies at Site 780 can be summarized as follows:

1. Fluids characterized by high pH, high alkalinity, and very low magnesium can exist within a few meters of the seafloor at the summit of Conical Seamount, indicating that mixing between entrained fluids and seawater need not take place at depth.

2. Rheological studies support a model for the origin of the seamount by the diapiric rise of variably serpentinized clasts supported by a low-density, plastic matrix.

Site 781

Site 781 (proposed Site MAR-3C; 19°37.91'N, 146°32.56'E; water depth 4420.6 m) lies on the lowermost flank of Conical Seamount about 7 nmi northwest of its summit.

One lithostratigraphic unit, divided into three subunits, was defined (Fig. 5):

Subunit IA (0–72.32 mbsf) consists of upper Pliocene(?) to Holocene(?) diatom-radiolarian silty clay that grades downward into vitric silty clay and vitric clayey silt.

Subunit IB (72.32–91.80 mbsf) is a massive basalt containing up to 30% phenocrysts and glomerocrysts of plagioclase, olivine, and clinopyroxene in a fine-grained groundmass. The basalt contains 2%–10% vesicles, which increase in abundance and size toward the center of the subunit.

Subunit IC (91.80–250 mbsf) is a lower to upper Pliocene vitric silty clay and vitric clayey silt.

Structures within the sediments of Subunit IA indicate deposition from gravity-driven mass flows. At least 19 turbidite sequences were identified, with thicknesses ranging between 1 and 180 cm and averaging 3–12 cm.

The principal point of interest at Site 781 is the presence of a thick, massive basalt of Pliocene or later age, the first evidence for such recent magmatic activity in any extant intraoceanic forearc terrane. The basalt of Subunit IB is an island-arc tholeiite characterized by enrichment in large-ion-lithophile elements relative to high-field-strength elements. This indicates that the magma originated from the mantle wedge above, and hence was modified by fluids from, the subducting lithosphere. The basalt produced a strong reflector at 60 mbsf in the site survey and in a brief shipboard seismic survey and may be a near-surface sill or a lava flow.

Site 782

Site 782 (proposed Site BON-6B; 30°51.6′N, 141°18.8′E, water depth, 2959 m) is located on the eastern margin of the Izu-Bonin forearc basin, about halfway between the active volcanic arc and the trench.

Two lithostratigraphic units were defined at Site 782 (Fig. 6):

Subunit IA (0–153.6 mbsf in Hole 782A) of Unit I is lower Pliocene to Holocene(?) gray to yellow-greenish, homogeneous nannofossil marl containing scattered volcanic debris and volcanic ash layers.

Subunit IB (153.6–337.0 mbsf in Hole 782A) is middle to upper Miocene light to dark gray, vitric nannofossil marl containing scattered volcanic debris and volcanic ash layers.

Subunit IC (337.0–409.2 mbsf in Hole 782A) is middle Eocene to upper Oligocene vitric nannofossil chalk intercalated with tuffaceous sediment and pebble-rich sands, gravelly conglomerates, and ash layers.

Unit II (409.2–476.8 mbsf in Hole 782A and 459.3–468.9 mbsf in Hole 782B) consists of angular to subrounded clasts of intermediate-acid lava.

Sedimentation rates increased from the late Oligocene (5 m/m.y.) and middle Miocene (47 m/m.y.), through the early Pliocene (16.5 m/m.y.), to the late Pliocene and even higher in the Pleistocene. Two unconformities were identified in the succession: one between upper Oligocene and middle Miocene sediments, the other between lower Oligocene and upper Oligocene sediments. More than 100 volcanic ash layers were identified.

The lavas of Unit II are slightly vesicular and contain phenocrysts of plagioclase, orthopyroxene, and clinopyroxene in a glassy groundmass. The rocks fall into two compositional groups, an andesite group and a dacite-rhyolite group, and are transitional between the tholeiitic and calc-alkaline volcanic-arc rock series.

Logging enabled us to divide the section penetrated by Hole 782B into three distinct units according to physical and chemical properties: an upper unit from 0 to ~300 mbsf, a middle unit from about ~300 to ~370 mbsf, and a lower unit from ~370 mbsf to the lower limit of logging at ~420 mbsf. The boundary between the upper and middle units is marked by a sudden downhole increase in density and resistivity and may correspond to an increase in sediment compaction. The boundary between the middle and lower units is marked by an increase and greater variability in compressional-wave velocity and density, together with an increase in silica and potassium. This boundary may correspond to the Eocene/Oligocene unconformity.

Preliminary measurements of magnetic inclinations from Hole 782A cluster around +50° and −50°, indicating little or no translation of the site since the late Eocene.

The principal conclusions drawn from studies of Site 782 are these:

1. Basement in this part of the forearc basin is Eocene.
2. The uppermost basement consists of intermediate-acid submarine volcanic rocks of island-arc tholeiite to calc-alkaline affinities.
3. Preliminary paleomagnetic data indicate little or no translation of the site since the late Eocene.

Site 783

Site 783 (proposed Site BON-7; 30°57.86′N, 141°47.27′E; 4648.8 m) is located on the northern, midflank part of a seamount that forms part of a 500-km-long ridge running along the lowermost, inner wall of the Izu-Bonin Trench.

Two lithostratigraphic units were defined at Site 783 (Fig. 6):

Unit I (0–120.0 mbsf) is lower Pliocene to middle or lower Pleistocene or older glass-rich silty clay to claystone.

Unit II (120.0–158.6 mbsf) is phacoidal, sheared serpentine that contains clasts of serpentinized harzburgite.

Deformation observed in the sediments at Site 783 includes shear fabrics and convolute plastic folding within the claystones of Unit I and the phacoidal serpentine of Unit II. High-temperature preserpentinization and lower temperature post-serpentinization fabrics similar to those described from Conical Seamount are found in the ultramafic clasts of Unit II. Densities increase from 1.47 to 1.59 g/cm^3 in the sediments of Unit I and cluster at about 2.10 g/cm^3 in the serpentine of Unit II. Thermal conductivities average ~1 W/mK in sediments and 1.9 W/mK in the serpentine. Heat flow in the sediments is 23 mW/m^2.

Interstitial-fluid compositions vary only slightly with depth in the sediments of Unit I, with a sharp discontinuity at the claystone/serpentine boundary and rapid chemical changes thereafter. The pH of the fluid increases from about 8 at the claystone/serpentine boundary to 9.5–10 at the bottom of the hole, and alkalinity, silica, magnesium, potassium, salinity, and sulfate decrease. Both calcium and chlorinity increase with depth.

The principal conclusions from investigations at Site 783 are these:

1. The seamount is made up, at least in part, of serpentinite.
2. The serpentinite is at least early Pliocene in age and, hence, older than Conical Seamount in the Mariana forearc.
3. There is structural evidence for deformation within the overlying sediments as well as within the serpentinite.
4. Serpentinization is still taking place, but without the low-chlorinity component identified at Conical Seamount.

Site 784

Site 784 (30°54.49′N, 141°44.27′E; water depth, 4900.8 m) is located approximately 7 km southwest of Site 783 on the lowermost, western flank of the same seamount on the inner wall of the Izu-Bonin Trench.

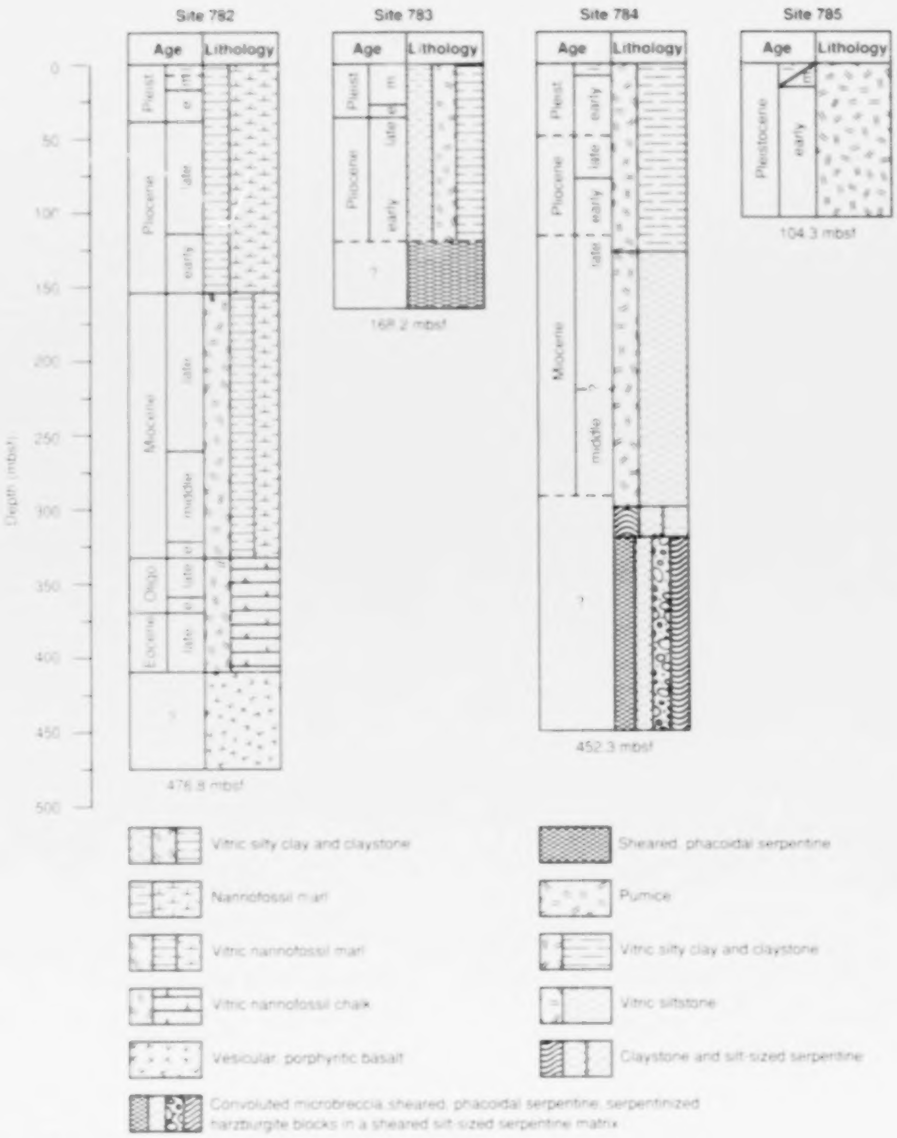
Site 782
Site 783
Site 784
Site 785
Age
Lithology
Depth (mbsf)
0
50
100
150
200
250
300
350
400
450
500
Pleist.
Pliocene
Miocene
Oligo.
Eocene
Pleistocene
early
late
middle
m
e
?
476.8 mbsf
168.2 mbsf
452.3 mbsf
104.3 mbsf
Vitric silty clay and claystone
Nannofossil marl
Vitric nannofossil marl
Vitric nannofossil chalk
Vesicular, porphyritic basalt
Convoluted microbreccia, sheared, phacoidal serpentine, serpentinized harzburgite blocks in a sheared silt-sized serpentine matrix
Sheared, phacoidal serpentine
Pumice
Vitric silty clay and claystone
Vitric siltstone
Claystone and silt-sized serpentine

Figure 6. Summary of lithostratigraphic columns of Sites 782 through 785.

The stratigraphic section recovered at Site 784 is divided into two lithostratigraphic units (Fig. 6):

Subunit IA (0–126.4 mbsf) of Unit I is lower Pliocene(?) to upper Pleistocene vitric silty clay and claystone.

Subunit IB (126.4–302.7 mbsf) is middle Miocene to lower Pliocene (?) vitric claystone.

Subunit IC (302.7–321.1 mbsf) contains claystone and silt-sized serpentine of unknown age.

Unit II (321.1–425.3 mbsf) includes pebbly serpentines with convolute lamination, sheared and relatively unsheared pebbly silt-sized serpentines without convolute lamination, and serpentine microbreccias.

Lithostratigraphic Subunit IB may correlate with Subunit IB at Site 782 in the forearc basin on the basis of age and ash content. Sediments from Subunits IA and IB are laminated and contain abundant graded beds, structures that are indicative of current activity during sediment deposition. The sediment contains an abundant volcanogenic component and numerous ash layers. Subunit IC shows a clear interfingering of background pelagic sediments derived from the volcanic areas to the west and silt-sized serpentine from the topographic high to the east.

The ultramafic clasts from Unit II are of two types: variably serpentinized tectonized harzburgite and subordinate dunites. About 30 metabasalt clasts were also identified.

Deformation in the claystones of Unit I at Site 784 includes sets of en echelon tension veinlets and sets of microfaults, some of which are clearly associated with water-escape pipes. The zone of greatest microfaulting correlates directly with an interval of increased water content and porosity of the sediments. Most structures are extensional and can be shown to have formed in a nonhydrostatic stress regime.

The composition of the interstitial waters varies with depth in the serpentinite, as at Site 783. Silica decreases, and pH increases to 9.6. Alkalinity falls to a value about half that of seawater, sulfate and magnesium decrease, calcium increases, and chlorinity, bromide, and salinity show no major changes. The concentration of sodium decreases with depth, although it increases at Site 783. As at Site 783, therefore, there is evidence for ongoing serpentinization at the Izu-Bonin Seamount.

Average bulk densities are 1.6 g/cm^3 in the sediments of Unit I and 2.2 g/cm^3 in the serpentine of Unit II. Thermal conductivities average about 0.9 W/mK in the sediments and 1.74 W/mK in the serpentine.

Preliminary interpretation of the paleomagnetic data indicates little translation since the Pliocene, although translation may have been significant between the middle Miocene and Pliocene.

The principal conclusions from studies of Site 784 are these:

1. The western lower flank of the seamount is made up of serpentine sediments and serpentinite.

2. The serpentinite is at least middle Miocene in age and hence the seamount is considerably older than Conical Seamount.

3. Structural evidence indicates that deformation within the more compacted sediments overlying the serpentinite was extensional.

4. Preliminary paleomagnetic evidence suggests significant translation of the site between the middle Miocene and the Pliocene.

5. Serpentinization is still taking place despite the lack of evidence for active protrusion.

Site 785

Site 785 (30°49.47'N, 140°55.17'E; water depth, 2660.8 m) is located in the center of the Izu-Bonin forearc basin about 40 nmi east-northeast of the active volcano Torishima.

One lithostratigraphic unit was recovered at Site 785 (Fig. 6):

Unit I (0–104.7 mbsf) consists of lower to upper Pleistocene pumice-bearing nannofossil ooze overlying a bed of porphyritic dacite-rhyolite pumice fragments, 1 mm to 6 cm in diameter.

The principal conclusion from this site is evidence for a major Pleistocene pumice bed in this part of the Izu-Bonin forearc basin.

Site 786

Site 786 (31°52.5'N, 141°13.6'E; water depth, 3062 m) is located in the center of the Izu-Bonin forearc basin about 120 nmi east of the active volcano Myojin Sho.

The stratigraphic section recovered at Site 786 is assigned to four lithostratigraphic units (Fig. 7). Units I through III are defined only in Hole 786A (Fig. 7A), which recovered the sedimentary sequences at the site. Unit IV is defined in both Holes 786A and 786B (Fig. 7B).

Unit I (0–83.46 mbsf) consists of a succession of middle Miocene to lower Pleistocene nannofossil marls and clays.

Unit II (83.46–103.25 mbsf) contains upper Oligocene to middle Eocene nannofossil marl and nannofossil-rich clay, as well as a volcaniclastic sequence containing vitric ash and mineral fragments.

Unit III (103.25–124.90 mbsf) is a sequence of middle Eocene volcaniclastic breccias.

Unit IV (124.9–166.5 mbsf in Hole 786A and 162.5–826.6 mbsf in Hole 786B) includes massive and brecciated flows, ash flows, and intercalated vitric siltstones and sandstones in the upper part of the unit and pillow lavas and dikes or sills in the lower part. Igneous rock types include high-magnesian basalts, boninites, basalts, andesites, dacites, and rhyolites. Secondary minerals include hydrothermal deposits of pyrite and native copper.

Sedimentation rates were highest in the Pliocene (8.6 m/m.y.) and lower (4.2 m/m.y.) between the latest and middle Miocene. A hiatus exists between the middle Miocene and the late Oligocene; below this point, evidence indicates that the rate was very low (0.8–1.4 m/m.y.).

Hole 786B penetrated more than 650 m into the massive, brecciated, and pillowed lavas and dikes of an Eocene volcano, providing information on the tectonic and volcanic activity that marked the initiation of subduction from the deepest hole yet into a submarine volcanic edifice. A simplified stratigraphic column is shown in Figure 7B. The upper part contains primarily welded ash flows and massive and brecciated lavas with interbedded clastic sediments. One of these sedimentary units is reddened and contains hydrated aluminum oxide, indicating a subaerial to shallow-water environment. At deeper levels, pillowed and massive lavas dominate, initially cut by a small number of intrusive dikes and sills. The hole ends at 828.6 mbsf in dikes and sills with minor lava screens. The rock types range from basalt to rhyolite in terms of silica content, but about half the rocks belong to the boninitic series that is thought to characterize the early stages of subduction. Shear zones are common throughout the sequence, and there is abundant evidence of hydrothermal activity, including pyrite-rich breccias and one zone containing native copper. Microfossil determinations from sediments intercalated within the lavas show that the

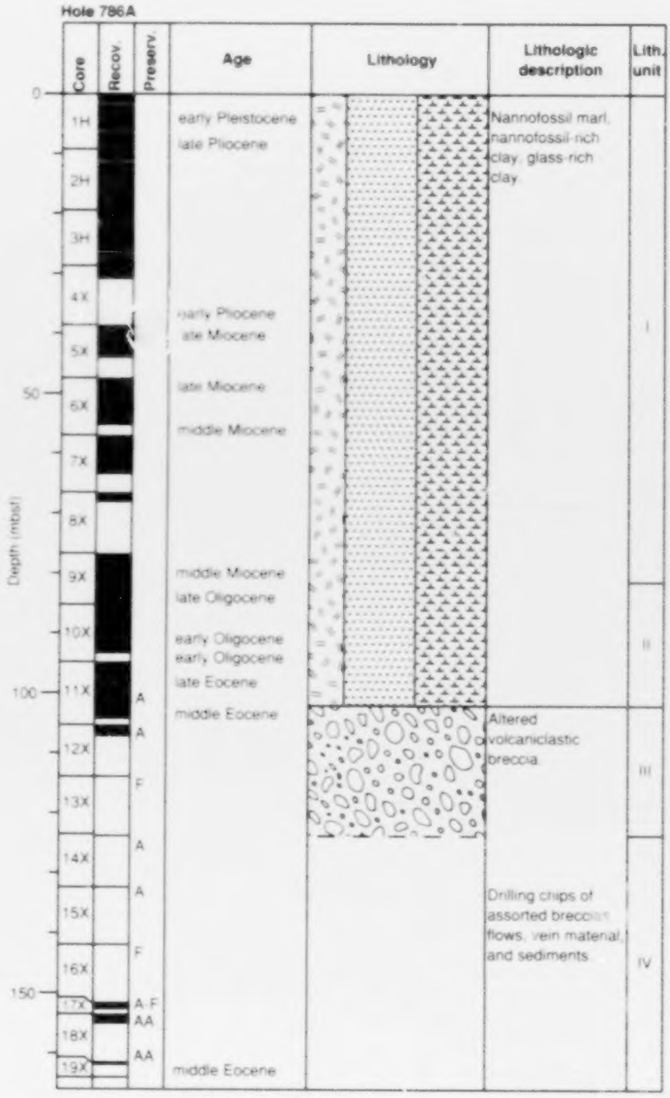
Hole 786A
Core
Recov.
Preserv.
Age
Lithology
Lithologic description
Lith. unit
Depth (mbsf)
0
50
100
150
1H
2H
3H
4X
5X
6X
7X
8X
9X
10X
11X
12X
13X
14X
15X
16X
17X
18X
19X
A
A
F
A
A
F
A-F
AA
AA
early Pleistocene
late Pliocene
early Pliocene
late Miocene
late Miocene
middle Miocene
middle Miocene
late Oligocene
early Oligocene
early Oligocene
late Eocene
middle Eocene
middle Eocene
Nannofossil marl, nannofossil-rich clay, glass-rich clay
Altered volcaniclastic breccia
Drilling chips of assorted breccias, flows, vein material, and sediments
I
II
III
IV

Key for preservation for 7A and 7B

AA= very altered: groundmass and phenocrysts are pervasively altered, only phenocryst traces remaining.
A = altered: groundmass and olivines altered, other phenocrysts largely fresh, some fresh glass.
F = fresh: some alteration of groundmass and phenocrysts, olivine altered.

FF= very fresh: no signs of alteration, vesicles may contain secondary mineralization.

Figure 7. Summary of lithostratigraphic columns of (A) Hole 786A and (B) Hole 786B.

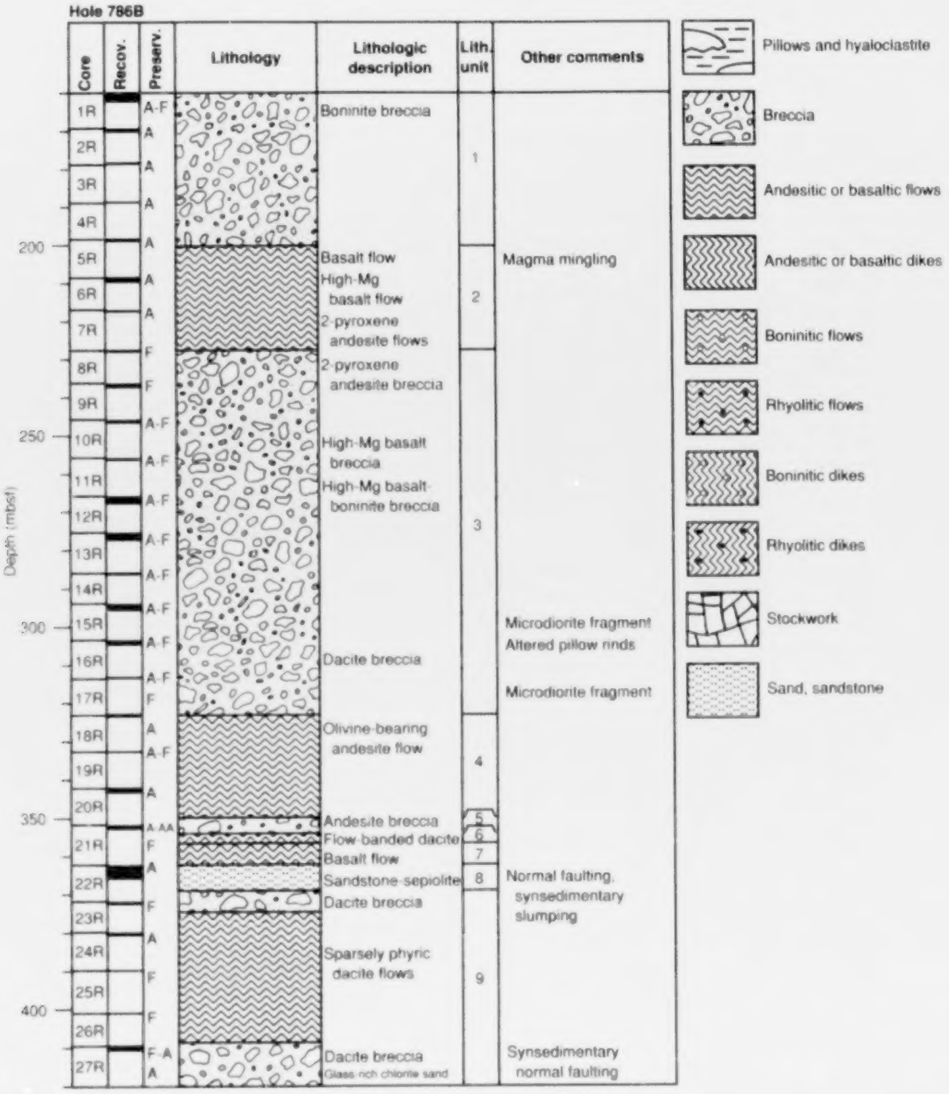
Hole 786B
Core
Recov.
Preserv.
Lithology
Lithologic description
Lith. unit
Other comments
Depth (mbsf)
200
250
300
350
400
1R
2R
3R
4R
5R
6R
7R
8R
9R
10R
11R
12R
13R
14R
15R
16R
17R
18R
19R
20R
21R
22R
23R
24R
25R
26R
27R
A-F
A
F
A-AA
F-A
Boninite breccia
Basalt flow
High-Mg basalt flow
2-pyroxene andesite flows
2-pyroxene andesite breccia
High-Mg basalt breccia
High-Mg basalt-boninite breccia
Dacite breccia
Olivine-bearing andesite flow
Andesite breccia
Flow-banded dacite
Basalt flow
Sandstone-sepiolite
Dacite breccia
Sparsely phyric dacite flows
Dacite breccia
Glass-rich chlorite sand
1
2
3
4
5
6
7
8
9
Magma mingling
Microdiorite fragment
Altered pillow rinds
Microdiorite fragment
Normal faulting, synsedimentary slumping
Synsedimentary normal faulting
Pillows and hyaloclastite
Breccia
Andesitic or basaltic flows
Andesitic or basaltic dikes
Boninitic flows
Rhyolitic flows
Boninitic dikes
Rhyolitic dikes
Stockwork
Sand, sandstone

Figure 7 (continued).

sequence is middle Eocene (~42 Ma), similar in age to other parts of the outer-arc high.

Average bulk densities are 1.65 g/cm^3 in the sediments and 1.8 to 22.1 g/cm^3 in the volcanic sequences. Preliminary paleomagnetic data indicate little translation of the site since the late Miocene. The four suites of logging tools run in Hole 786B consisted of the dual induction tool, the digital sonic tool, the natural gamma-ray spectrometry tool, the lithodensity tool, the compensated neutron tool, the induced gamma-ray spectrometry tool, the aluminum clay tool, and the borehole televiewer.

The principal conclusions from investigations of Site 786 are these:

1. The penetration of over 650 m of Eocene volcanic crust shows that the basement in this region of the Izu-Bonin forearc consists of boninite flows and hyaloclastite and andesite flows, breccias, and dikes.

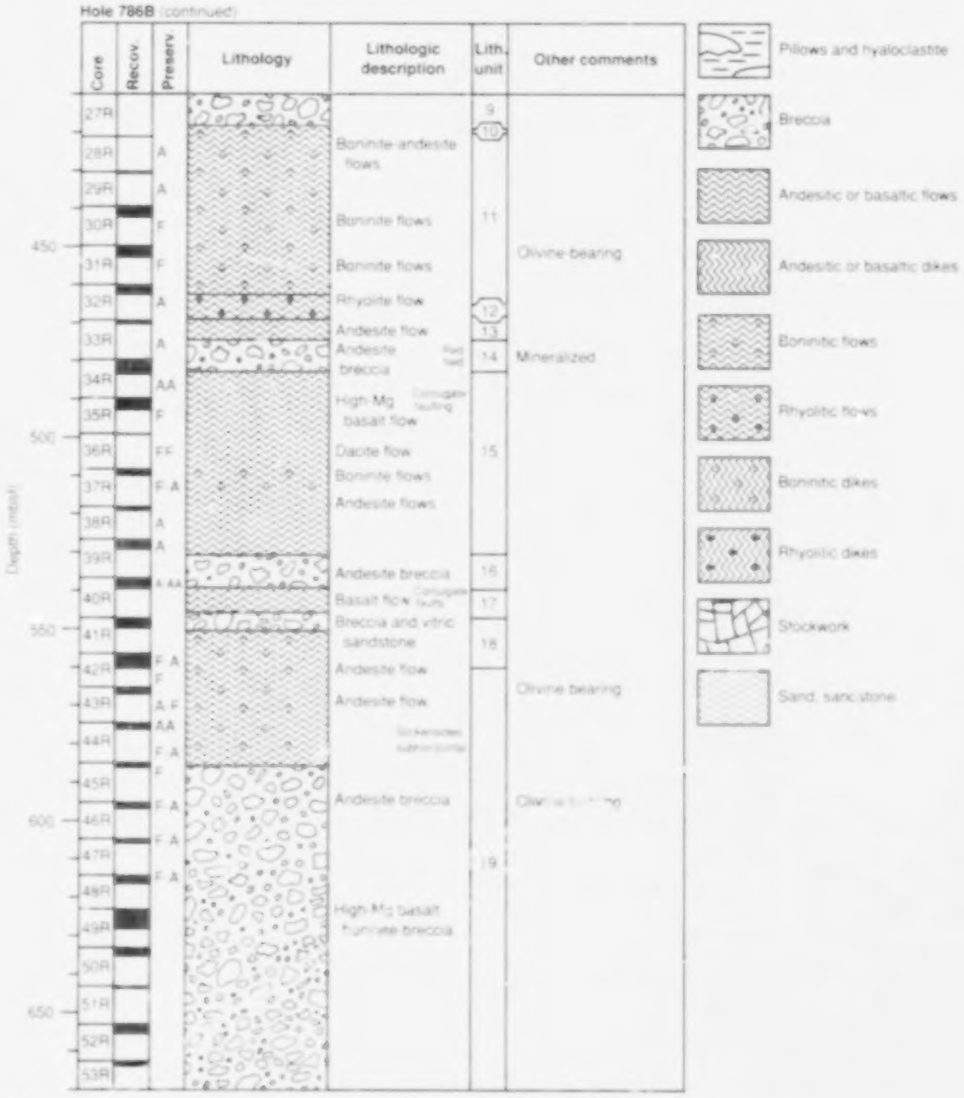
Hole 786B (continued)
Core
Recov.
Preserv.
Lithology
Lithologic description
Lith. unit
Other comments
Depth (mbsf)
450
500
550
600
650
27R
28R
29R
30R
31R
32R
33R
34R
35R
36R
37R
38R
39R
40R
41R
42R
43R
44R
45R
46R
47R
48R
49R
50R
51R
52R
53R
Boninite-andesite flows
Boninite flows
Boninite flows
Rhyolite flow
Andesite flow
Andesite breccia
High-Mg basalt flow
Conjugate faulting
Dacite flow
Boninite flows
Andesite flows
Andesite breccia
Basalt flow
Conjugate faults
Breccia and vitric sandstone
Andesite flow
Andesite flow
Andesite breccia
High-Mg basalt boninite breccia
9
10
11
12
13
14
15
16
17
18
19
Olivine-bearing
Mineralized
Olivine bearing
Pillows and hyaloclastite
Breccia
Andesitic or basaltic flows
Andesitic or basaltic dikes
Boninitic flows
Rhyolitic flows
Boninitic dikes
Rhyolitic dikes
Stockwork
Sand, sandstone

Figure 7 (continued).

2. Rocks recovered from the volcanic basement show extensive evidence of hydraulic fracturing and precipitation of sulfide and other minerals from hydrothermal fluids.

3. Preliminary paleomagnetic evidence indicates little translation of the site since the late Miocene.

4. Sedimentation rates were highest during the Pliocene, decreased between the latest Miocene and middle Miocene, and were quite low (from evidence below a hiatus) from the middle Miocene to the late Oligocene.

The most significant achievement at Site 786 was the deep penetration of an Eocene volcanic edifice that provided (1) a record of the construction and structure of the forearc volcanic basement and (2) a basis for the understanding of early arc magmatism in general and boninite petrogenesis in particular.

SUMMARY

Leg 125 drilled nine sites to answer fundamental questions about the magmatic, tectonic, and sedimentary evolution of

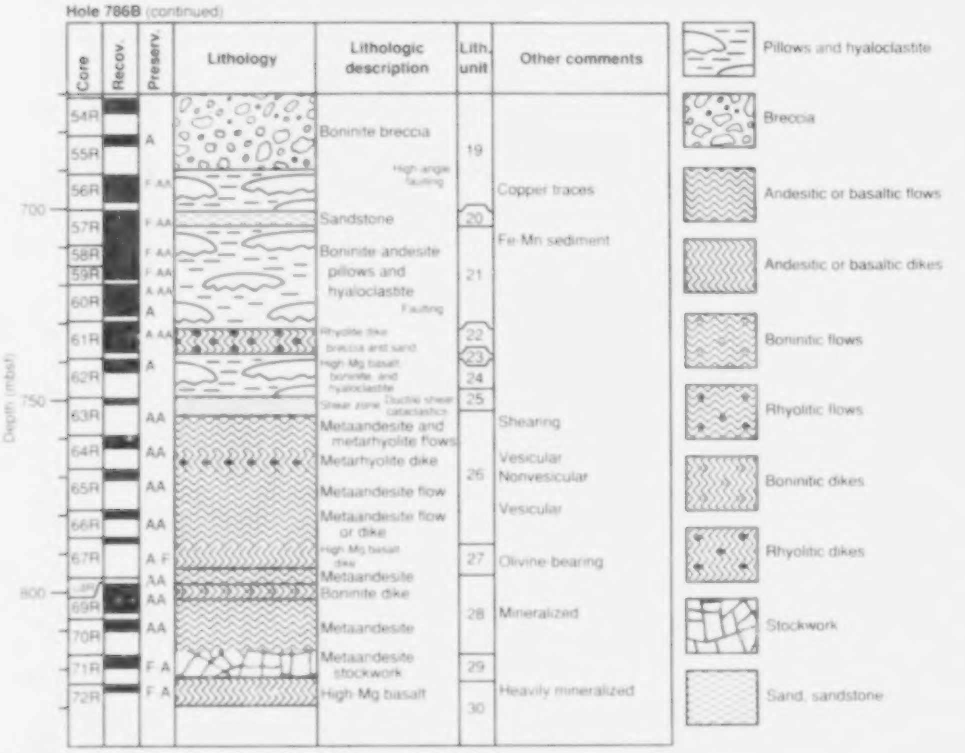
Hole 786B (continued)
Core
Recov.
Preserv.
Lithology
Lithologic description
Lith. unit
Other comments
Depth (mbsf)
700
750
800
54R
55R
56R
57R
58R
59R
60R
61R
62R
63R
64R
65R
66R
67R
68R
69R
70R
71R
72R
A
F-AA
A-AA
AA
A-F
F-A
Boninite breccia
High-angle faulting
Sandstone
Boninite andesite pillows and hyaloclastite
Faulting
Rhyolite dike
breccia and sand
High-Mg basalt, boninite, and hyaloclastite
Shear zone
Ductile shear cataclastics
Metaandesite and metarhyolite flows
Metarhyolite dike
Metaandesite flow
Metaandesite flow or dike
High-Mg basalt dike
Metaandesite
Boninite dike
Metaandesite
Metaandesite stockwork
High-Mg basalt
19
20
21
22
23
24
25
26
27
28
29
30
Copper traces
Fe-Mn sediment
Shearing
Vesicular
Nonvesicular
Vesicular
Olivine-bearing
Mineralized
Heavily mineralized
Pillows and hyaloclastite
Breccia
Andesitic or basaltic flows
Andesitic or basaltic dikes
Boninitic flows
Rhyolitic flows
Boninitic dikes
Rhyolitic dikes
Stockwork
Sand, sandstone

Figure 7 (continued).

the Mariana and Izu-Bonin forearcs and the flux of subduction-derived fluids through the forearc mantle wedge. The principal results and conclusions from drilling in the Mariana and Izu-Bonin forearcs include the following:

1. A Pliocene or younger basalt flow or sill penetrated at Site 781 is the first evidence for such recent magmatic activity in any extant intraoceanic forearc terrane.

2. The uppermost basement recovered in Site 782 consists of Eocene intermediate-acid submarine volcanic rocks of island-arc tholeiite to calc-alkaline affinities.

3. The deep penetration of Eocene volcanic crust at Site 786 provided (1) a record of the construction and structure of the forearc volcanic basement and (2) a basis for the understanding of early arc magmatism in general and boninite petrogenesis in particular. The basement in that part of the Izu-Bonin forearc consists of boninite flows and hyaloclastite and andesite flows, breccias, and dikes.

4. The identification of numerous ash layers within the forearc basin sediments indicates peaks of volcanic activity during the Eocene-Oligocene and from the late Miocene to the Holocene.

5. The volcanic basement at Site 786 shows extensive evidence of hydraulic fracturing and precipitation of sulfide and other minerals from hydrothermal fluids.

The principal results and conclusions from Sites 783, 784, and 778 through 780 drilled in the Mariana and Izu-Bonin serpentinite seamounts are as follows:

1. The Mariana serpentinite seamount may be constructed from protrusions of serpentinite mantle materials and/or flows of unconsolidated serpentine and entrained ultramafic and rare mafic clasts emanating from a central conduit.

2. Low- to medium-grade metamorphism characterizes the source region of the serpentinite that formed both seamounts.

3. Dehydration of the subducted lithosphere may have played an important role in the serpentinization of the source region of the serpentinite seamounts.

4. Hydrocarbons are a significant component of the fluids associated with the Mariana seamount.

5. The Izu-Bonin seamount is at least middle Miocene in age—hence older than Conical Seamount—and currently inactive in terms of flow generation.

6. Serpentinization is still taking place in the Izu-Bonin Seamount, but without the low-chlorinity component identified at Conical Seamount.

REFERENCES

Ben-Avraham, Z., and Uyeda, S., 1983. Entrapment origin of marginal seas. *In* Hilde, T.W.C., and Uyeda, S. (Eds.), *Geodynamics* *of the Western Pacific-Indonesian Region*. Am. Geophys. Union, Geodynamics Ser., 11:91–104.

Bloomer, S. H., 1983. Distribution and origin of igneous rocks from the landward slopes of the Mariana Trench. *J. Geophys. Res.*, 88:7411–7428.

Fryer, P., Ambos, E. L., and Hussong, D. M., 1985a. Origin and emplacement of Mariana forearc seamounts. *Geology*, 13:774–777.

Fryer, P., Langmuir, C. H., Taylor, B., Zhang, Y., and Hussong, D. M., 1985b. Rifting of the Izu arc. III. Relationships of chemistry to tectonics. *EOS, Trans. Am. Geophys. Union*, 66:421.

Fryer, P., and Fryer, G. J., 1987. Origins of nonvolcanic seamounts in a forearc environment. *In* Keating, B., Fryer, P., and Batiza, R. (Eds.), *Seamounts, Islands, and Atolls*. Am. Geophys. Union, Geophys. Monogr. Ser., 43:61–69.

Honza, E., and Tamaki, K., 1985. Bonin arc. *In* Nairn, A.E.M., and Uyeda, S. (Eds.), *The Ocean Basins and Margins* (vol. 7): New York (Plenum Press), 459–499.

Hussong, D. M., Uyeda, S., et al., 1982. *Init. Repts. DSDP*, 60: Washington (U.S. Govt. Printing Office).

Ishii, T., 1985. Dredged samples from the Ogasawara fore-arc seamount or "Ogasawara Paleoland" fore-arc ophiolite. *In* Nasu, N. (Ed.), *Formation of Active Ocean Margins*: Tokyo (Terra Scientific), 307–342.

Karig, D. E., 1975. Basin genesis in the Philippine Sea. *In* Karig, D. E., Ingle, J. C., Jr., et al., *Init. Repts. DSDP*, 31: Washington (U.S. Govt. Printing Office), 857–879.

Ogawa, Y., and Naka, J., 1984. Emplacement of ophiolitic rocks in forearc areas: examples from central Japan and Izu-Mariana-Yap island arc system. *In* Gass, I. G., Lippard, S. J., and Shelton, A. W. (Eds.), *Ophiolites and Oceanic Lithosphere*. Spec. Publ. Geol. Soc. London, 13:291–302.

Ms 125A-115

SECTION 4: CORES

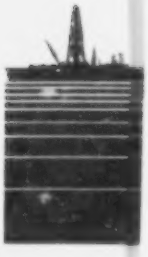

SITE 778 HOLE A CORE 1R CORED INTERVAL 3913.7-3920.4 mbsl; 0.0-6.7 mbsf

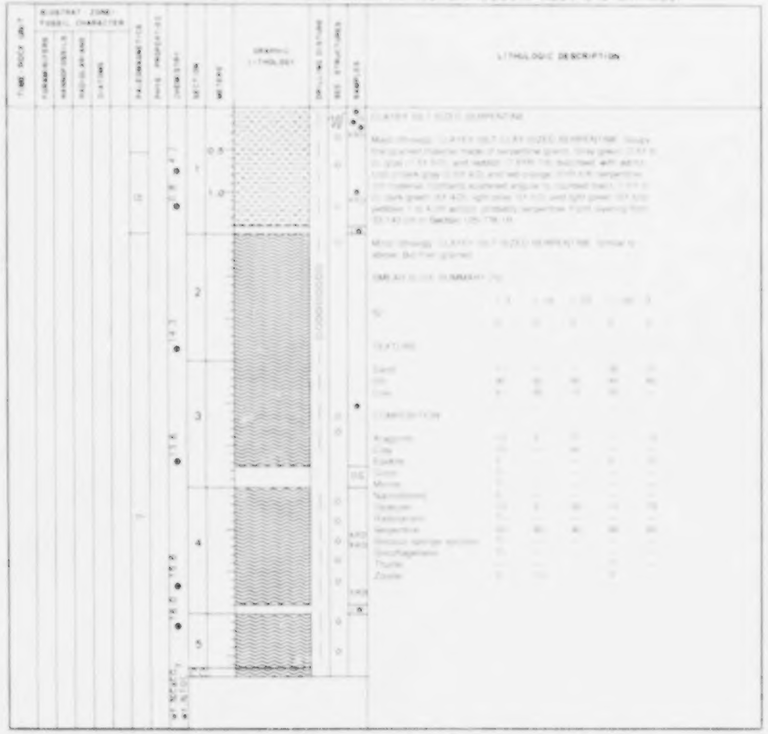
LITHOLOGIC DESCRIPTION
GRAPHIC LITHOLOGY
BIOSTRAT. ZONE/ FOSSIL CHARACTER
1
2
3
4
5
0.5
1.0

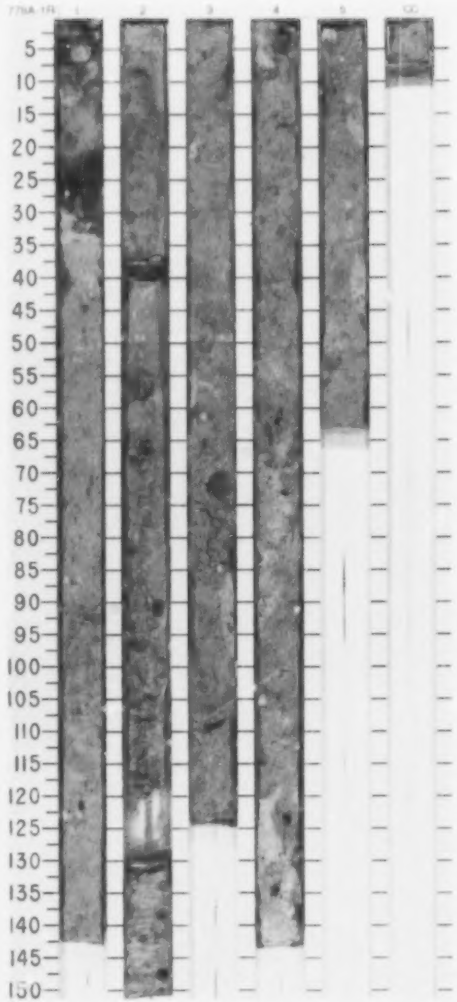
778A-1R
1
2
3
4
5
CC
5
10
15
20
25
30
35
40
45
50
55
60
65
70
75
80
85
90
95
100
105
110
115
120
125
130
135
140
145
150

Information on Core Description Forms, for ALL sites, represents field notes taken aboard ship. Some of this information has been refined in accord with post-cruise findings, but production schedules prohibit definitive correlation of these forms with subsequent findings. Thus, the reader should be alerted to the occasional ambiguity or discrepancy.

SITE 778 HOLE A CORE 2R CORED INTERVAL 3920.4-3929.9 mbsl; 6.7-16.2 mbsf

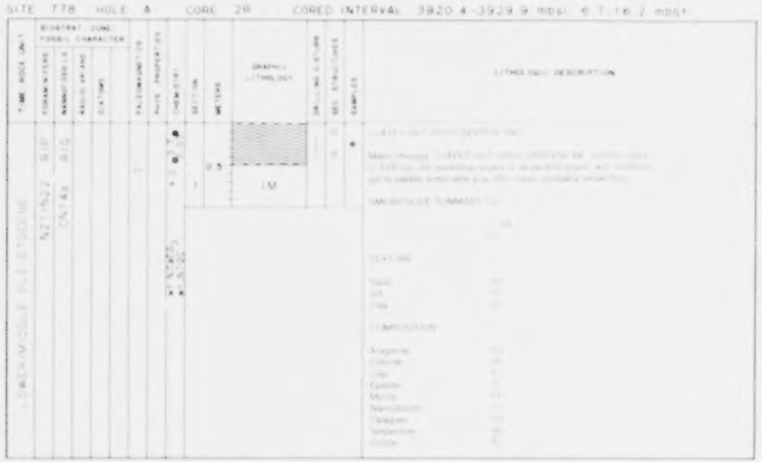
TIME-ROCK UNIT
BIOSTRAT. ZONE/ FOSSIL CHARACTER
FORAMINIFERS
NANNOFOSSILS
RADIOLARIANS
DIATOMS
PALEOMAGNETICS
PHYS. PROPERTIES
CHEMISTRY
SECTION
METERS
GRAPHIC LITHOLOGY
DRILLING DISTURB.
SED. STRUCTURES
SAMPLES
LOWER/MIDDLE PLEISTOCENE
N21/N22 B/P
CN14a B/G
?
1
0.5
1M

LITHOLOGIC DESCRIPTION

[illegible]

Major lithology: [illegible]

SMEAR SLIDE SUMMARY (%):

TEXTURE:

Sand
Silt
Clay

COMPOSITION:

Aragonite
Chlorite
Clay
Epidote
Micrite
Nannofossils
Opaques
Serpentine
Zircon

SITE 778 HOLE A CORE 3R CORED INTERVAL 3929.9-3933.9 mbsl; 16.2-20.2 mbsf

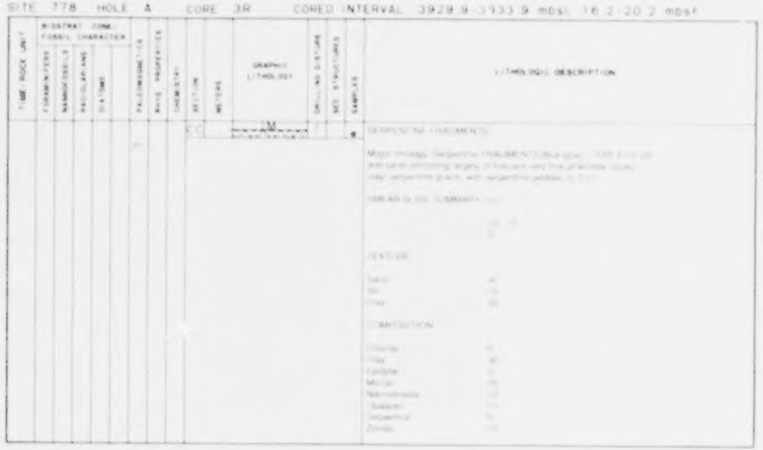
TIME-ROCK UNIT
BIOSTRAT. ZONE/ FOSSIL CHARACTER
FORAMINIFERS
NANNOFOSSILS
RADIOLARIANS
DIATOMS
PALEOMAGNETICS
PHYS. PROPERTIES
CHEMISTRY
SECTION
METERS
GRAPHIC LITHOLOGY
DRILLING DISTURB.
SED. STRUCTURES
SAMPLES
?
CC
1M

LITHOLOGIC DESCRIPTION

SERPENTINE FRAGMENTS

Major lithology: Serpentine FRAGMENTS [illegible]

SMEAR SLIDE SUMMARY (%):

TEXTURE:

Sand
Silt
Clay

COMPOSITION:

Chlorite
Clay
Epidote
Micrite
Nannofossils
Opaques
Serpentine
Zircon

778A-2R 1

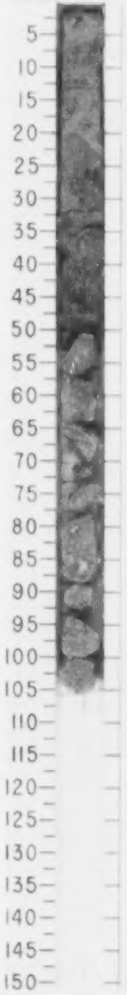
5
10
15
20
25
30
35
40
45
50
55
60
65
70
75
80
85
90
95
100
105
110
115
120
125
130
135
140
145
150

778A-3R CC

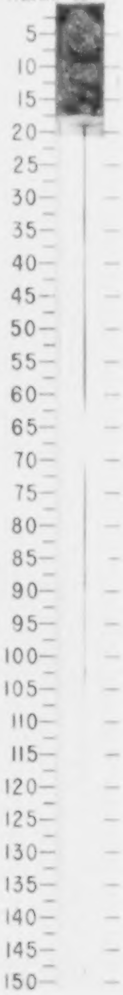
5
10
15
20
25
30
35
40
45
50
55
60
65
70
75
80
85
90
95
100
105
110
115
120
125
130
135
140
145
150

SITE 778 HOLE A CORE 4R CORED INTERVAL 3933.9-3943.4 mbsl; 20.2-29.7 mbsf

TIME-ROCK UNIT	FORAMINIFERS	NANNOFOSSILS	RADIOLARIANS	DIATOMS	PALEOMAGNETICS	PHYS. PROPERTIES	CHEMISTRY	SECTION	METERS	GRAPHIC LITHOLOGY	DRILLING DISTURB.	SED. STRUCTURES	SAMPLES	LITHOLOGIC DESCRIPTION
LOWER PLEISTOCENE	N22 R/M	CN14a C/G		B	?			1					●	FORAMINIFER-BEARING SERPENTINE SANDSTONE Major lithology: FORAMINIFER-BEARING SERPENTINE SANDSTONE. [illegible] SMEAR SLIDE SUMMARY (%): TEXTURE: Sand [illegible] Silt [illegible] Clay [illegible] COMPOSITION: Aragonite [illegible] Epidote [illegible] Foraminifers [illegible] Opaques [illegible] Serpentine [illegible]

SITE 778 HOLE A CORE 5R CORED INTERVAL 3943.4-3952.9 mbsl; 29.7-39.2 mbsf

TIME-ROCK UNIT	FORAMINIFERS	NANNOFOSSILS	RADIOLARIANS	DIATOMS	PALEOMAGNETICS	PHYS. PROPERTIES	CHEMISTRY	SECTION	METERS	GRAPHIC LITHOLOGY	DRILLING DISTURB.	SED. STRUCTURES	SAMPLES	LITHOLOGIC DESCRIPTION
	B	B		B	?		●	1 CC					●	SHEARED PHACOIDAL SERPENTINE Major lithology: SHEARED PHACOIDAL SERPENTINE. [illegible] SMEAR SLIDE SUMMARY (%): TEXTURE: Sand [illegible] Silt [illegible] Clay [illegible] COMPOSITION: Opaques [illegible] Serpentine [illegible] [illegible] [illegible]

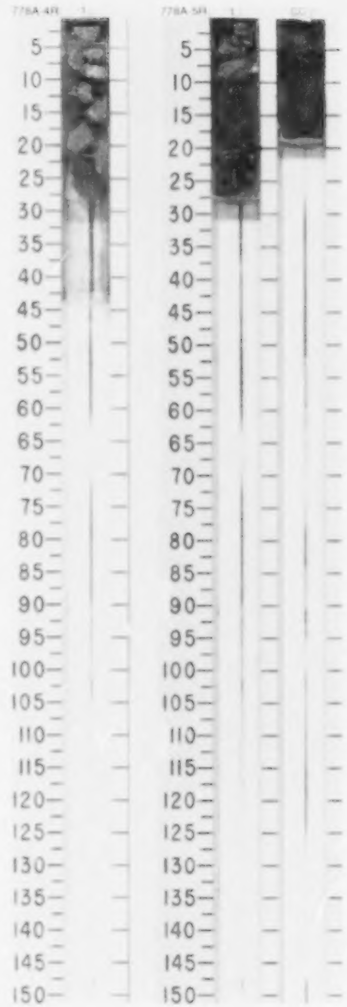

SITE 778 HOLE A CORE 6R CORED INTERVAL 3952.9-3962.4 mbsl; 39.2-48.7 mbsf

TIME-ROCK UNIT	FORAMINIFERS	NANNOFOSSILS	RADIOLARIANS	DIATOMS	PALEOMAGNETICS	PHYS. PROPERTIES	CHEMISTRY	SECTION	METERS	GRAPHIC LITHOLOGY	DRILLING DISTURB.	SED. STRUCTURES	SAMPLES	LITHOLOGIC DESCRIPTION
							●	1	0.5 1.0				● ●	[illegible]

Column group over FORAMINIFERS, NANNOFOSSILS, RADIOLARIANS and DIATOMS: BIOSTRAT. ZONE/ FOSSIL CHARACTER

[illegible]

SMEAR SLIDE SUMMARY (%):

TEXTURE:

Sand [illegible]
Silt [illegible]
Clay [illegible]

COMPOSITION:

Epidote [illegible]
Mica [illegible]
Opaques [illegible]
Serpentine [illegible]
Chlorite [illegible]

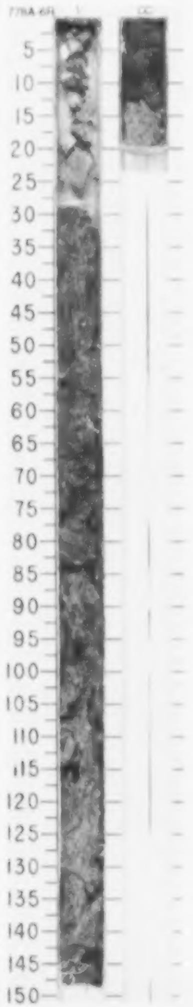

778A-6R
1
CC
5
10
15
20
25
30
35
40
45
50
55
60
65
70
75
80
85
90
95
100
105
110
115
120
125
130
135
140
145
150

SITE 778 HOLE A CORE 7R CORED INTERVAL 3962.4-3971.9 mbsl; 49.7-59.2 mbsf

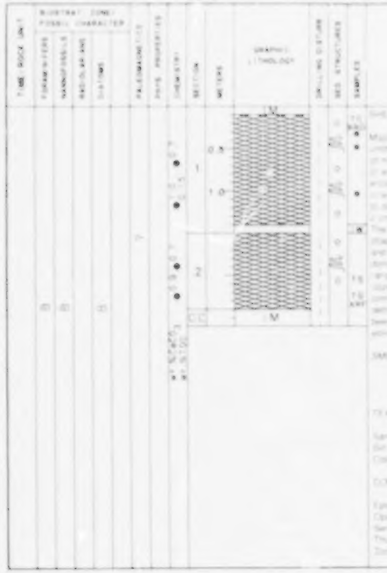
TIME-ROCK UNIT
BIOSTRAT. ZONE/ FOSSIL CHARACTER
FORAMINIFERS
NANNOFOSSILS
RADIOLARIANS
DIATOMS
PALEOMAGNETICS
PHYS. PROPERTIES
CHEMISTRY
SECTION
METERS
GRAPHIC LITHOLOGY
DRILLING DISTURB.
SED. STRUCTURES
SAMPLES
B
B
B
1
2
CC
0.5
1.0
M

LITHOLOGIC DESCRIPTION

SHEARED PHACOIDAL SERPENTINE

Major lithology: SHEARED PHACOIDAL SERPENTINE. [illegible]

SMEAR SLIDE SUMMARY (%):

TEXTURE:

Sand

Silt

Clay

COMPOSITION:

Epidote

Opaques

Serpentine

Thulite

Zoisite

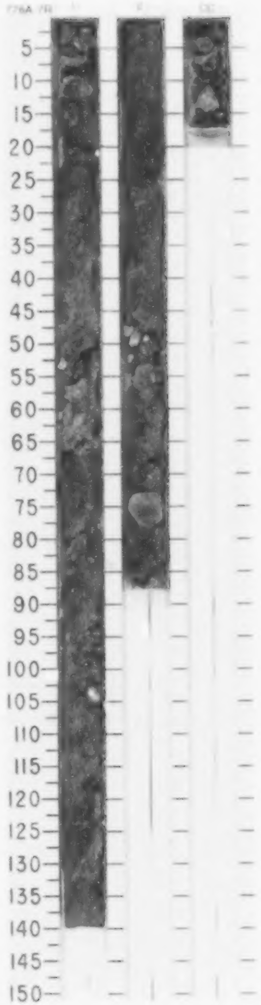
778A-7R
1
2
CC
5
10
15
20
25
30
35
40
45
50
55
60
65
70
75
80
85
90
95
100
105
110
115
120
125
130
135
140
145
150

SITE 778 HOLE A CORE 8R CORED INTERVAL 3971.9-3981.9 mbsl; 58.2-68.2 mbsf

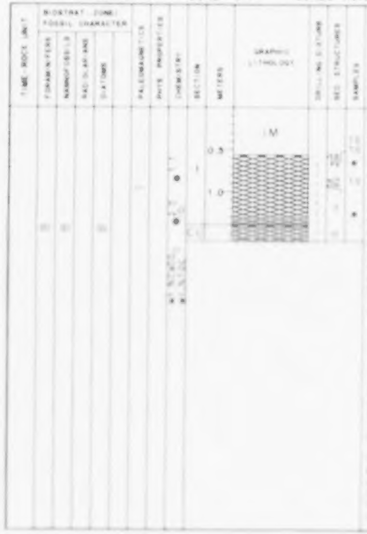
TIME-ROCK UNIT
BIOSTRAT. ZONE/ FOSSIL CHARACTER
FORAMINIFERS
NANNOFOSSILS
RADIOLARIANS
DIATOMS
PALEOMAGNETICS
PHYS. PROPERTIES
CHEMISTRY
SECTION
METERS
GRAPHIC LITHOLOGY
DRILLING DISTURB.
SED. STRUCTURES
SAMPLES
B
B
B
1
CC
0.5
1.0
UM

LITHOLOGIC DESCRIPTION

SHEARED PHACOIDAL SERPENTINE

Major lithology: SHEARED PHACOIDAL SERPENTINE. [illegible]

SMEAR SLIDE SUMMARY (%):

TEXTURE:

Sand

Silt

Clay

COMPOSITION:

[illegible]

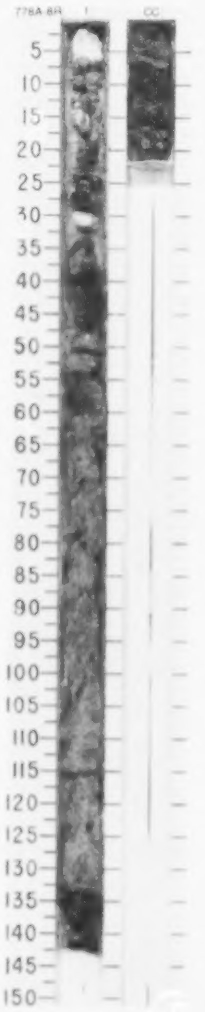
778A-8R
1
CC
5
10
15
20
25
30
35
40
45
50
55
60
65
70
75
80
85
90
95
100
105
110
115
120
125
130
135
140
145
150

SITE 778 HOLE A CORE 9R CORED INTERVAL 3981.9-3991.5 mbsl; 68.2-77.8 mbsf

TIME-ROCK UNIT	FORAMINIFERS	NANNOFOSSILS	RADIOLARIANS	DIATOMS	PALEOMAGNETICS	PHYS. PROPERTIES	CHEMISTRY	SECTION	METERS	GRAPHIC LITHOLOGY	DRILLING DISTURB.	SED. STRUCTURES	SAMPLES	LITHOLOGIC DESCRIPTION
	B	B		B			● ● ●	1 2 CC	0.5 1.0	IM			●	SHEARED PHACOIDAL SERPENTINE

SHEARED PHACOIDAL SERPENTINE

Major lithology: SHEARED PHACOIDAL SERPENTINE. [illegible] plastic mass of sheared, phacoidal serpentine consisting of [illegible] flakes and grains of dark green ([illegible]) to light blue-green ([illegible]) serpentine. This matrix encloses angular clasts as much as [illegible] cm across, probably mostly serpentine. Matrix and clasts less than 1 mm across make up as much as 85% of the core. Color variation at a scale of 1 mm to 2 cm, along with variations in clast density, define a crude layering. The elongate axes of the flakes (phacoids) form an anastomosing foliation that encloses the clasts and is commonly subparallel to layering. Discrete foliation-bearing domains are visible. Some [illegible] of foliation may represent drilling disturbance. Clasts range from equant and crudely rounded to elongate and rhomboid (lozenge-shaped). Softer clasts are drawn out and entrained in the matrix. In the case of rhomboid clasts this commonly forms asymmetric "tails" drawn out into the matrix that define local shear direction and sense.

Minor lithology: MATRIX RICH MATRIX SUPPORTED serpentine BRECCIA, with angular serpentine clasts to [illegible] cm, but as small as 1-3 mm. Clasts are dark gray green ([illegible]) to light yellow green ([illegible]). The matrix is light blue-green ([illegible]). Some clasts appear to have been fragmented and sheared out into the matrix. There are also [illegible] and wisps of dark gray [illegible] material becoming entrained in matrix. Many clasts are elongate, but foliation is weak.

SMEAR SLIDE SUMMARY (%):

TEXTURE:

Sand [illegible]
Silt [illegible]
Clay [illegible]

COMPOSITION:

Epidote [illegible]
Opaques [illegible]
Serpentine [illegible]
Chlorite [illegible]
Zoisite [illegible]

SITE 778 HOLE A CORE 10R CORED INTERVAL 3991.5-3996.0 mbsl; 77.8-82.3 mbsf

TIME-ROCK UNIT	FORAMINIFERS	NANNOFOSSILS	RADIOLARIANS	DIATOMS	PALEOMAGNETICS	PHYS. PROPERTIES	CHEMISTRY	SECTION	METERS	GRAPHIC LITHOLOGY	DRILLING DISTURB.	SED. STRUCTURES	SAMPLES	LITHOLOGIC DESCRIPTION
	B	B		B				CC		IM			[illegible]	All samples described in [illegible] section.

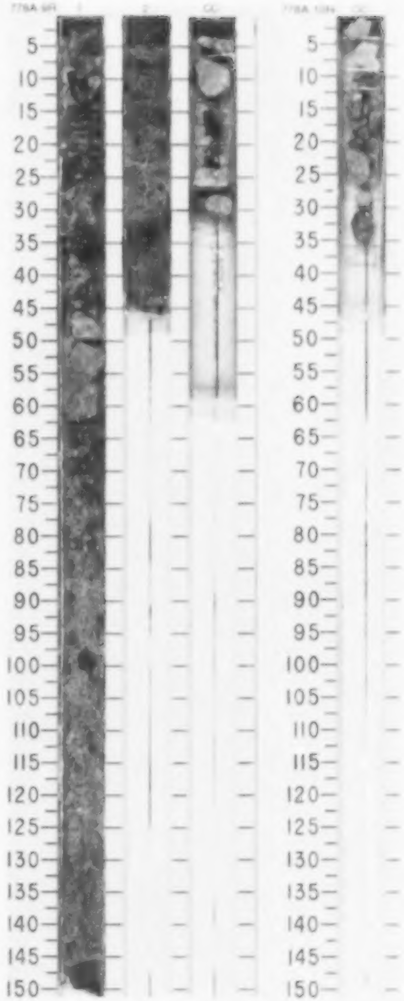

SITE 778 HOLE A CORE 11R CORED INTERVAL 3996.0-4003.5 mbsl; 82.3-89.8 mbsf

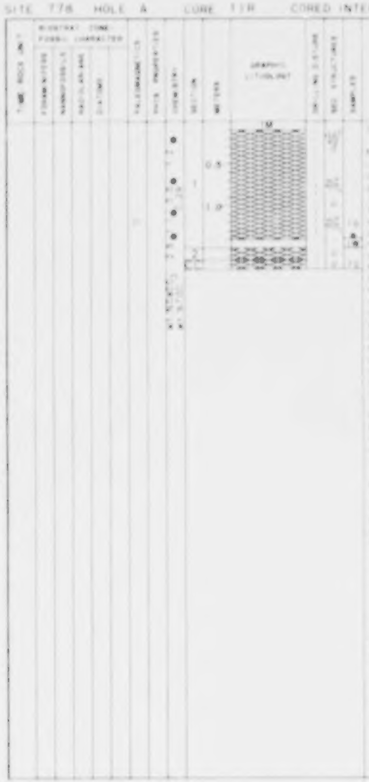
TIME-ROCK UNIT
BIOSTRAT. ZONE/FOSSIL CHARACTER
FORAMINIFERS
NANNOFOSSILS
RADIOLARIANS
DIATOMS
PALEOMAGNETICS
PHYS. PROPERTIES
CHEMISTRY
SECTION
METERS
GRAPHIC LITHOLOGY
DRILLING DISTURB.
SED. STRUCTURES
SAMPLES
0.5
1
1.0
2
CC

LITHOLOGIC DESCRIPTION

SHEARED PHACOIDAL SERPENTINE

Major lithology: SHEARED PHACOIDAL SERPENTINE. [illegible]

[illegible]

Minor lithology: [illegible]

SMEAR SLIDE SUMMARY (%):

TEXTURE:

Sand
Silt
Clay

COMPOSITION:

[illegible]

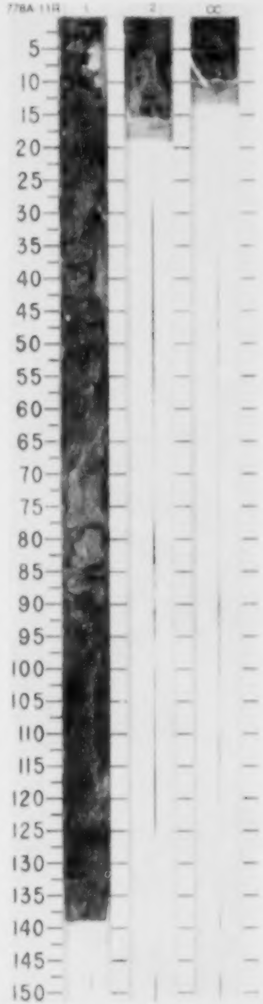
778A 11R
1
2
CC
5
10
15
20
25
30
35
40
45
50
55
60
65
70
75
80
85
90
95
100
105
110
115
120
125
130
135
140
145
150

SITE 778 HOLE A CORE 12R CORED INTERVAL 4003.5-4012.0 mbsl; 89.8-98.3 mbsf

TIME-ROCK UNIT	BIOSTRAT. ZONE/FOSSIL CHARACTER: FORAMINIFERS	NANNOFOSSILS	RADIOLARIANS	DIATOMS	PALEOMAGNETICS	PHYS. PROPERTIES	CHEMISTRY	SECTION	METERS	GRAPHIC LITHOLOGY	DRILLING DISTURB.	SED. STRUCTURES	SAMPLES	LITHOLOGIC DESCRIPTION
								1 2 CC	0.5 1.0				TS XRF	SHEARED PHACOIDAL SERPENTINE

SHEARED PHACOIDAL SERPENTINE

Major lithology: SHEARED PHACOIDAL SERPENTINE. Foliated, unlithified plastic mass of sheared phacoidal serpentine, consisting of mm-sized flakes and grains of green (5G 6/1) and gray blue (?) Munsell matrix serpentine. This matrix encloses serpentine clasts of three different types: equant, dark green (5G 4/1) clasts about a millimeter across; elongate light green ones as much as 5 mm long. Smaller clasts about 1 mm across are most abundant. Most clasts are probably serpentine. Matrix and clasts less than 1 mm across make up as much as 85% of the rock. Color variation at a scale of 1 mm to 3 cm, along with variations in clast density, define a crude layering. Moreover, in this core there are zones of lighter and darker serpentine material 30-50 cm wide. The elongate axes of the serpentine flakes (phacoids) form an anastomosing foliation that encloses the clasts. Discrete foliation domains are visible. Some local folding of foliation may represent drilling disturbance. Clasts range from equant and rounded to elongate and rhomboid (lozenge shaped). Softer clasts are drawn out and entrained in the matrix; in the case of rhomboid clasts this commonly forms asymmetric "tails" drawn out into the matrix that define local shear direction and sense. Between 37 and 41 cm in Section 2 of this core the matrix encloses two large (2-3 cm) and several smaller (1-2 cm) angular, equant to elongate clasts of a jet black material with dull luster that smells strongly of sulfur. Also present are several angular equant clasts 2-3 cm across of what appears to be altered greenstone, and one of serpentine.

Minor lithology: CLAST-SUPPORTED serpentine BRECCIA in core catcher section. Dark green clasts (5G 4/2) from 1/2 mm to 1 cm across, angular and equant (roundness 0.2, sphericity 0.7-0.9), make up 30-40% of the rock and are set in a matrix of light green (5G 7/2) serpentinite. Clast size irregularly coarsens upward. Well-defined planes of shearing occur but are confined to the bottom of the section.

SMEAR SLIDE SUMMARY (%):

	2, 49
	D
TEXTURE:	
Sand	50
Silt	40
Clay	10
COMPOSITION:	
Albite	Tr
Chlorite	[illegible]
Epidote	[illegible]
Opaques	10
Serpentine	75
Talc	[illegible]
Zoisite	Tr

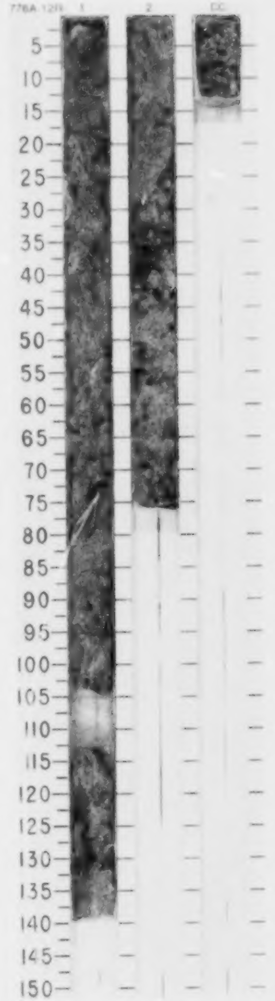

SITE 778 HOLE A CORE 13R CORED INTERVAL 4012.0-4021.3 mbsl; 98.3-107.6 mbsf

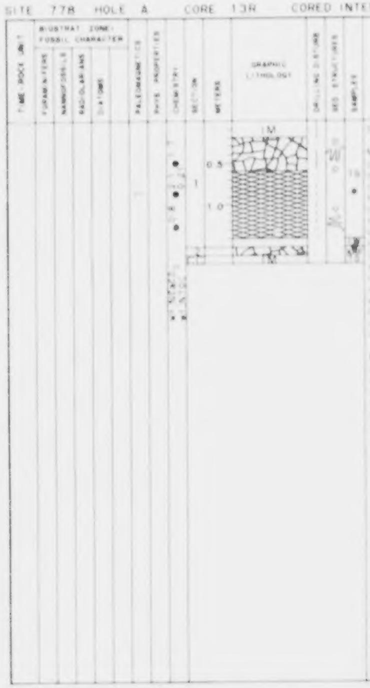
TIME-ROCK UNIT
BIOSTRAT. ZONE/ FOSSIL CHARACTER
FORAMINIFERS
NANNOFOSSILS
RADIOLARIANS
DIATOMS
PALEOMAGNETICS
PHYS. PROPERTIES
CHEMISTRY
SECTION
METERS
GRAPHIC LITHOLOGY
DRILLING DISTURB.
SED. STRUCTURES
SAMPLES
1
0.5
1.0
UM
TS

LITHOLOGIC DESCRIPTION

SHEARED PHACOIDAL SERPENTINE

Major lithology: SHEARED PHACOIDAL SERPENTINE. [illegible]

Minor lithology: SERPENTINE BRECCIA. [illegible]

SMEAR SLIDE SUMMARY (%):

TEXTURE:

Sand
Silt
Clay

COMPOSITION:

Carbonate grains
Chlorite
Epidote
Olivine
Pyroxene
Serpentine
Talc

778A-13R
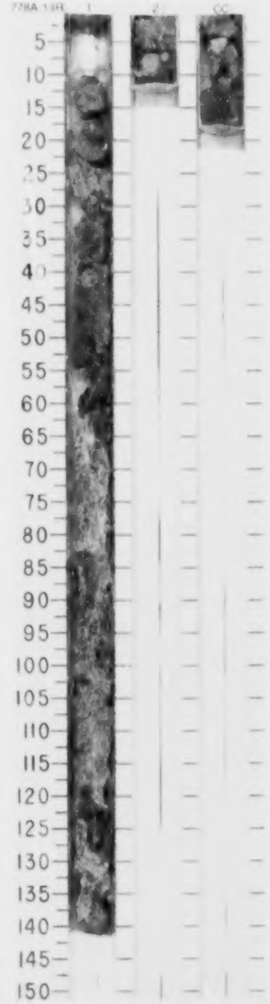
1
2
CC
5
10
15
20
25
30
35
40
45
50
55
60
65
70
75
80
85
90
95
100
105
110
115
120
125
130
135
140
145
150

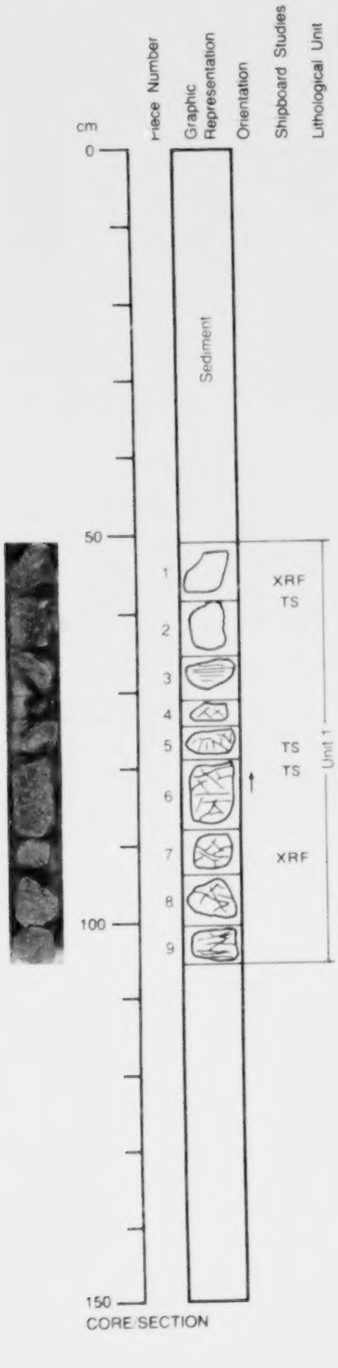

125-778A-2R-1

UNIT 1: SERPENTINIZED TECTONIZED HARZBURGITE

Pieces 1 to 2

COLOR: Dark bluish gray (5B 4/1)
LAYERING: None visible
DEFORMATION: Parallel shears, 1 mm wide, 1 cm apart; wavy cleavage on orthopyroxene
PRIMARY MINERALOGY:
Olivine - Mode: 85%
Crystal size: Not visible
Crystal shape: Not visible
Crystal orientation: Not visible
Percent replacement: 99%

Orthopyroxene - Mode: 15%
Crystal size: <4 mm
Crystal shape: Not visible
Crystal orientation: Not visible
Percent replacement: 70%

Spinel - Mode: <1%
Crystal size: <0.5 mm
Crystal shape: Anhedral
Crystal orientation: Not visible
Percent replacement: Not visible
SECONDARY MINERALOGY:
Serpentine
Total percent: 80-95%
Texture: Anhedral, mesh-textured serpentine replacing olivine; bastite after orthopyroxene
Vein material: Chrysotile, <0.5 mm wide, up to 2 cm long, parallel to and crosscutting shears; chrysotile fibers at high angles to vein walls

UNIT 1: SERPENTINIZED TECTONIZED HARZBURGITE

Pieces 3 to 9

COLOR: Dark gray to gray (2.5Y 7/4 to 7/6)
LAYERING: Not visible
DEFORMATION: Wavy cleavage on orthopyroxene
PRIMARY MINERALOGY:
Olivine - Mode: 80%
Crystal size: <3 mm
Crystal shape: Not visible
Crystal orientation: Not visible
Percent replacement: 90%

Orthopyroxene - Mode: 20%
Crystal size: <5 mm
Crystal shape: Not visible
Crystal orientation: Not visible
Percent replacement: 25%

Spinel - Mode: <0.5%
Crystal size: <0.3 mm
Crystal shape: Equant-elongate
Crystal orientation: Not visible
Percent replacement: 0%
SECONDARY MINERALOGY:
Serpentine and dusty magnetite
Total percent: 80-85%
Texture: Mesh and bastite
Vein material: Serpentine veins (1 to 2 mm wide) randomly oriented; in Pieces 6 to 8 there are thin (<0.3-mm-wide) gray carbonate-filled veins

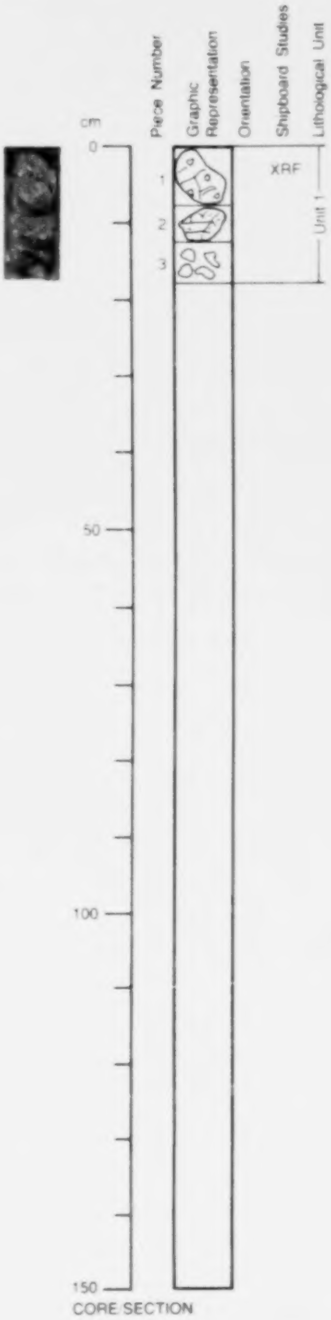

125-778A-3R-CC

UNIT 1: SERPENTINIZED TECTONIZED HARZBURGITE

Piece 1

COLOR: Dark greenish gray to dark gray (10Y 5/1 to 2.5Y 4/0).
LAYERING: None visible.
DEFORMATION: None visible.
PRIMARY MINERALOGY:
Olivine - Mode: 80%.
Crystal size: Not visible.
Crystal shape: Not visible.
Crystal orientation: Not visible.
Percent replacement: 100%.

Orthopyroxene - Mode: 20%.
Crystal size: Not visible.
Crystal shape: Not visible.
Crystal orientation: Not visible.
Percent replacement: 100%.
SECONDARY MINERALOGY:
Serpentine and dusty magnetite.
Total percent: 100%.
Texture: Bastite after orthopyroxene; mesh after olivine.
Vein material: Greenish veins are in top corner of piece (< 0.5-mm wide); black veins with grayish margins (< 0.5 mm wide); veins are anastomosing.

UNIT 1: SERPENTINIZED TECTONIZED HARZBURGITE

Pieces 2 and 3 (multiple fragments)

COLOR: Bluish gray (2.5Y 5/0).
LAYERING: Not visible.
DEFORMATION: Not visible.
PRIMARY MINERALOGY:
Olivine - Mode: 80%.
Crystal size: Not visible.
Crystal shape: Not visible.
Crystal orientation: Not visible.
Percent replacement: 100%.

Orthopyroxene - Mode: 20%.
Crystal size: 1-5 mm.
Crystal shape: Equant.
Crystal orientation: Not visible.
Percent replacement: 100%.

Spinel - Mode: Trace.
Crystal size: 0.1-0.3 mm.
Crystal shape: Anhedral.
Crystal orientation: Disseminated.
Percent replacement: 0%.
SECONDARY MINERALOGY:
Serpentine and dusty magnetite.
Total percent: 100%.
Texture: Bastite and mesh.
Vein material: White and dark gray (2.5Y 4/0) veins, 0.1 - 1 mm wide, cut by dark gray serpentine filled veins which follow the margins and crosscut earlier generation.
ADDITIONAL COMMENTS: One fragment is a foliated and sheared clast of serpentinized dunite (3 cm diameter) with an oxidation halo 1 cm wide (color deep brown red, BM HC/5).

125-778A-4R-1

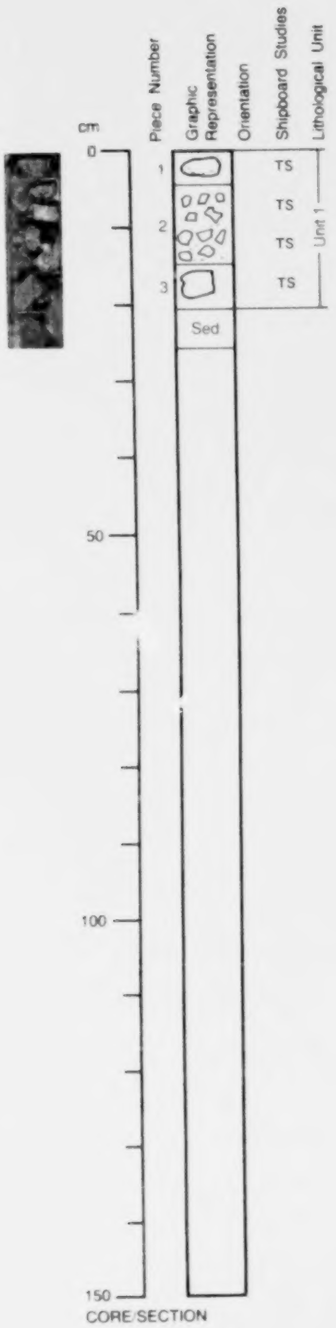
cm
Piece Number
Graphic Representation
Orientation
Shipboard Studies
Lithological Unit
0
1
2
3
TS
TS
TS
TS
Unit 1
Sed
50
100
150
CORE/SECTION

UNIT 1: METABASALT

Pieces 1 to 3 (multiple fragments)

COLOR: Greenish gray (5G 5/2)
LAYERING: Not visible.
DEFORMATION: Cataclastic to mylonitic shears (2 mm wide) parallel to fractures.
PRIMARY MINERALOGY:
Plagioclase microphyric basaltic protolith with extensive glassy groundmass; non-vesicular.
Plagioclase - Mode: 60%.
Crystal size: 0.1-0.5 mm.
Crystal shape: Laths.
Crystal orientation: Felted.
Percent replacement: 100%.

Clinopyroxene - Mode: 3-5%.
Crystal size: 0.05-0.1 mm.
Crystal shape: Equant.
Crystal orientation: Rosettes and clusters.
Percent replacement: 0-10%.

Glass - Mode: 25%.
Crystal size: Not visible.
Crystal shape: Blebs.
Crystal orientation: Not visible.
Percent replacement: 100%.
SECONDARY MINERALOGY:
Predominantly chlorite and clay (smectite?).
Total percent: 35-40%.
Texture: Patchy replacement especially of glass.
Vein material: Pale-green (chlorite and clay) veins (<0.1 mm wide) are randomly oriented.

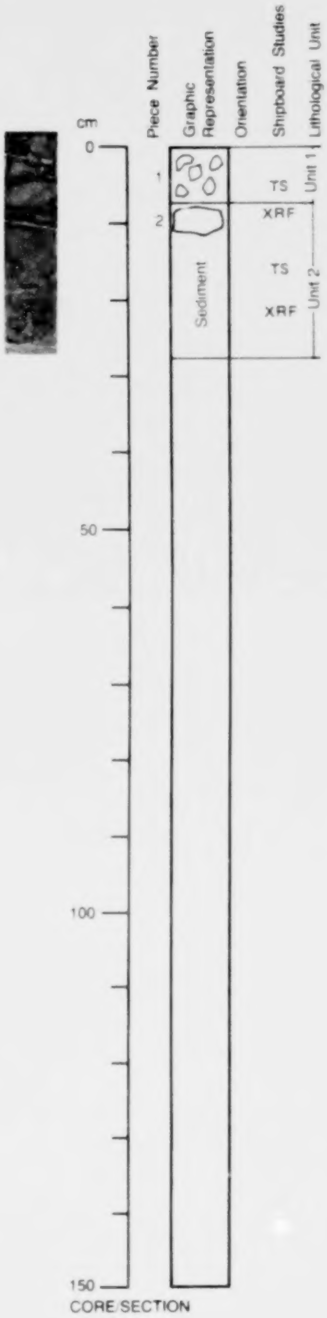
cm
Piece Number
Graphic Representation
Orientation
Shipboard Studies
Lithological Unit
0
50
100
150
1
2
TS
XRF
TS
XRF
Unit 1
Unit 2
Sediment
CORE/SECTION

125-778A-5R-1

UNIT 2: METABASALT

Pieces 1 (multiple fragments) and 2

COLOR: Dark green (5G 3/2)
LAYERING: Not visible
DEFORMATION: Not visible
PRIMARY MINERALOGY:
Fine-grained aphyric basaltic protolith, no vesicles seen; primary sub-ophitic texture preserved.
Plagioclase - Mode: 60%
Crystal size: <0.1 mm
Crystal shape: Subhedral
Crystal orientation: Not visible
Percent replacement: 100%

Clinopyroxene - Mode: 40%
Crystal size: <0.01 mm
Crystal shape: Subhedral
Crystal orientation: Not visible
Percent replacement: 100%
SECONDARY MINERALOGY:
Clay and chlorite
Total percent: 100%
Texture: Very fine-grained
Vein material: Numerous quartzose veins (1-2 mm wide)
ADDITIONAL COMMENTS: One possible phosphorite clast is present, 2 cm in size, white color (10YR 8/2). Piece 2 is a phacoidal clast in sheared serpentine.

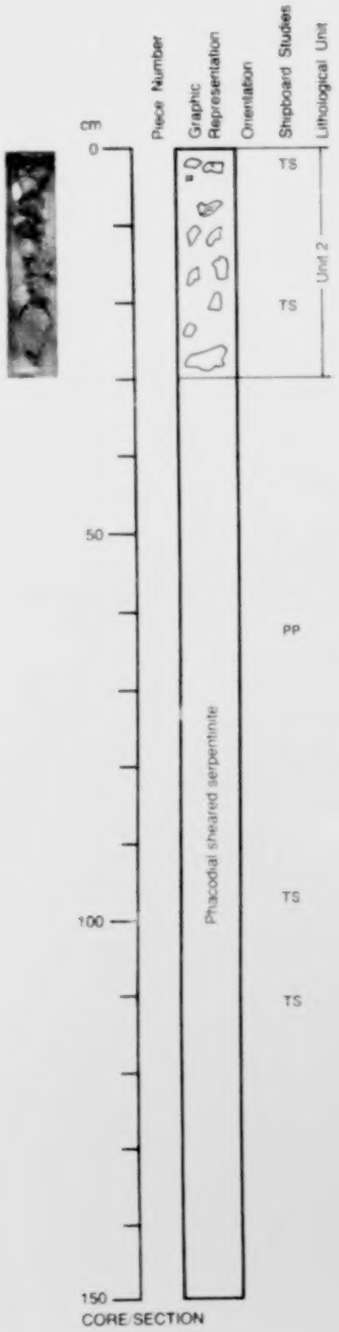
cm
Piece Number
Graphic Representation
Orientation
Shipboard Studies
Lithological Unit
0
50
100
150
TS
Unit 2
TS
PP
TS
TS
Phacoidal sheared serpentinite
CORE/SECTION

125-778A-6R-1

UNIT 2: METABASALT

Piece 1 (multiple fragments)

COLOR: Dark green (5G 3/2)
LAYERING: Not visible
DEFORMATION: Not visible
PRIMARY MINERALOGY:
In thin section, relict igneous groundmass textures appear to be preserved (hence "metabasalt" name for these fragments)
SECONDARY MINERALOGY:
Predominantly amphibole, plagioclase and chlorite
Total percent: 100%
Texture: Fine- to medium-grained
Vein material: Thin <1-mm carbonate, chlorite and albite veins
ADDITIONAL COMMENTS: One piece of red (10R 4/4) massive coarse grained (<0.5 mm) siliceous rock possibly chert with white-gray veins (<1 mm wide)

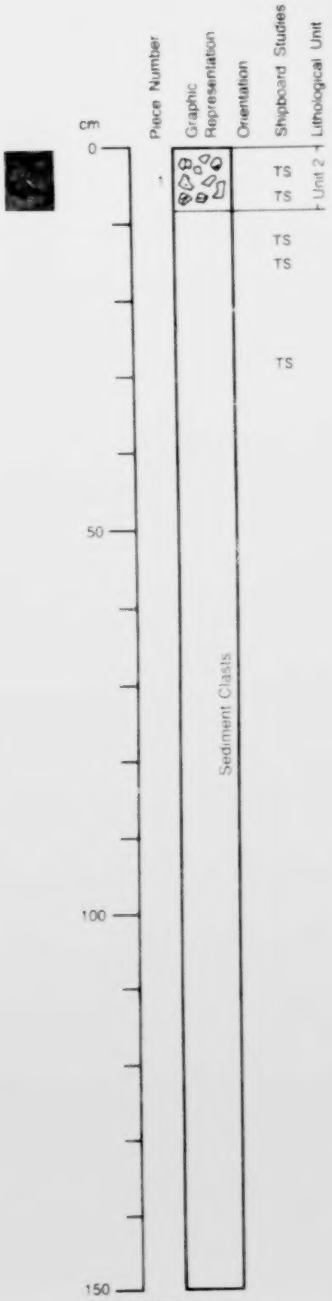

125-778A-7R-1

UNIT 2: SERPENTINIZED TECTONIZED HARZBURGITE

Pieces 1A and 1B

COLOR: Dark blue gray (5B 4/1)
LAYERING: Not visible
DEFORMATION: Weakly foliated
PRIMARY MINERALOGY:
Pieces have a light greenish-white serpentinous and carbonate-rich skin
Olivine - Mode: 70%
Crystal size: Not visible
Crystal shape: Not visible
Crystal orientation: Not visible
Percent replacement: 100%

Orthopyroxene - Mode: 29%
Crystal size: 1-2 mm
Crystal shape: Anhedral elongate
Crystal orientation: Weakly foliated
Percent replacement: 50-100%

Cr-spinel - Mode: 1%
Crystal size: 0.5-1 mm
Crystal shape: Ragged
Crystal orientation: Some stringers
Percent replacement: 0%
SECONDARY MINERALOGY:
Serpentine, dusty magnetite
Total percent: 84-90%
Texture: Bastite and mesh
Vein material: Minor dark green and white veins, throughout
ADDITIONAL COMMENTS: Pieces are slickensided. n.b. Pieces 1C to 1I are described in record 125-778A-7R-01, top = 02

UNIT 2: METABASALT

Pieces 1C to 1I

COLOR: Gray-green (5G 4/2) to 10GY 5/2
LAYERING: Not visible
DEFORMATION: Not visible
PRIMARY MINERALOGY:
Very fine-grained, plagioclase-phyric, glassy, basaltic protolith
Plagioclase - Mode: <3%
Crystal size: 0.5-3 mm
Crystal shape: Lath
Crystal orientation: Not visible
Percent replacement: 0-100%

Spinel - Mode: <1%
Crystal size: 0.1-0.5 mm
Crystal shape: Equant
Crystal orientation: Disseminated
Percent replacement: 0%

Glass - Mode: 5-30%
Crystal size: Not visible
Crystal shape: Not visible
Crystal orientation: Not visible
Percent replacement: 80-100%
SECONDARY MINERALOGY:
Chlorite, epidote and clay
Total percent: 80%
Texture: Very fine-grained
Vein material: Minor calcite veins <1 mm wide

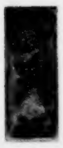

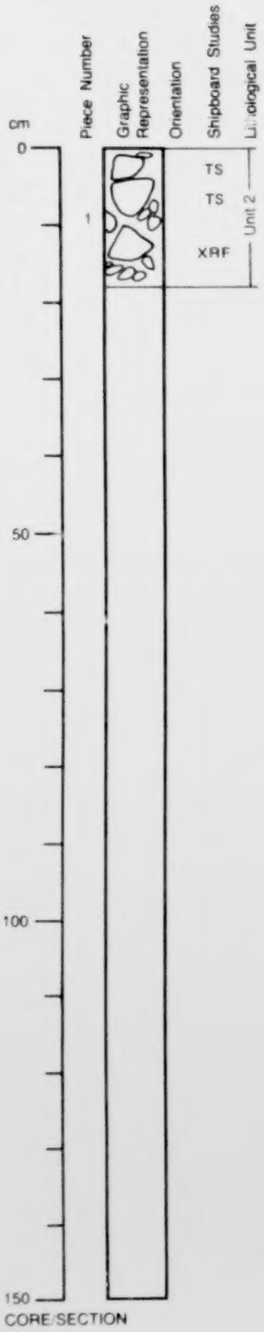
cm
Piece Number
Graphic Representation
Orientation
Shipboard Studies
Lithological Unit
0
50
100
150
1
TS
TS
XRF
Unit 2
CORE/SECTION

125-778A-7R-CC

UNIT 2: SERPENTINIZED TECTONIZED HARZBURGITE

Piece 1 (multiple fragments)

COLOR: Grayish green (5G 4/2).
LAYERING: Not visible.
DEFORMATION: Wavy cleavage and kink-banding on orthopyroxene.
PRIMARY MINERALOGY:
Olivine - Mode: 70-80%.
Crystal size: 0.7-1.5 mm.
Crystal shape: Subhedral.
Crystal orientation: Not visible.
Percent replacement: 99%.

Orthopyroxene - Mode: 20-30%.
Crystal size: 0.3-0.5 mm.
Crystal shape: Anhedral.
Crystal orientation: Not visible.
Percent replacement: 10-20%.

Spinel - Mode: <3%.
Crystal size: <0.5 mm.
Crystal shape: Rounded-elongate.
Crystal orientation: Arranged in trains.
Percent replacement: Not visible.
SECONDARY MINERALOGY:
Serpentine and dusty magnetite.
Total percent: 80-85%.
Texture: Mesh and bastite.
Vein material: White vein (0.1 mm wide), bluish on fracture surfaces.

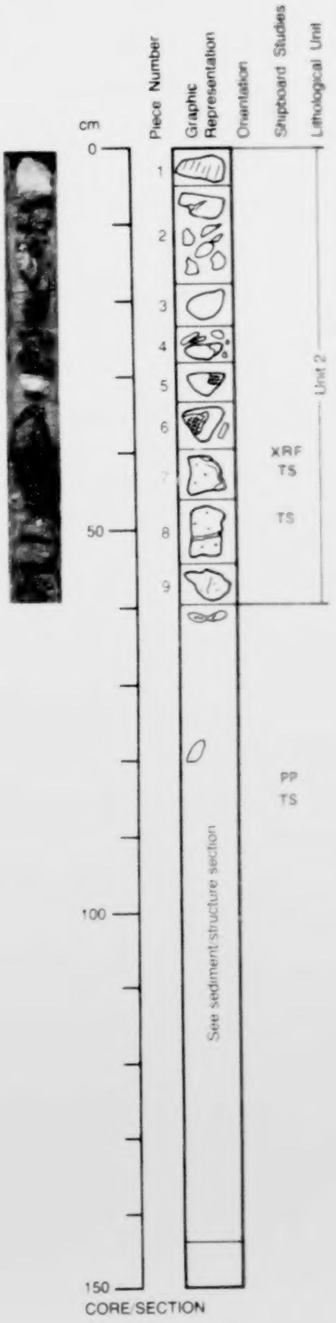
cm
Piece Number
Graphic Representation
Orientation
Shipboard Studies
Lithological Unit
0
50
100
150
1
2
3
4
5
6
7
8
9
XRF
TS
TS
PP
TS
Unit 2
See sediment/structure section
CORE/SECTION

125-778A-8R-1

UNIT 2: TALC-SERPENTINE

Piece 1 and 2

COLOR: Mottled white to gray (1.5YR 8/0 to 6/0)
LAYERING: Crudely banded.
DEFORMATION: Brittle fracture sub-parallel to banding, extensive in Piece 1; slickensides parallel to long axis of Piece 2 and some brittle fracturing within 3 mm of surface of clast.
PRIMARY MINERALOGY: Not visible.
SECONDARY MINERALOGY:
Talc, serpentine, traces of disseminated magnetite.
Total percent: 100%.
Texture: Very fine-grained.
Vein material: N/A.

UNIT 2: SERPENTINITE

Pieces 3, 4 and 6

COLOR: Very dark greenish gray (10Y 3/1) to black (7.5YR 2/0).
LAYERING: Not visible.
DEFORMATION: Some sheared and foliated pieces.
PRIMARY MINERALOGY: Not visible.
SECONDARY MINERALOGY:
Serpentine, talc, disseminated magnetite.
Total percent: 100%.
Texture: Very fine-grained.
Vein material: None present.

UNIT 2: VEIN CALCITE WITH ALTERED LITHIC FRAGMENTS

Piece 5

COLOR: White to light greenish gray (2.5Y 6/2 to 2.5Y 8/0).
LAYERING: Not visible.
DEFORMATION: Not visible.
PRIMARY MINERALOGY:
Aggregates of drusy calcite with lithic fragments consisting of 80% epidote-20% serpentine-trace oxides.
Calcite : Mode: 100%.
Crystal size: <1 mm.
Crystal shape: Equant.
Crystal orientation: Not visible.
Percent replacement: 0%.
SECONDARY MINERALOGY:
Secondary calcite, epidote and serpentine.
Total percent: 100%.
Texture: In lithic fragments only, fine-grained.
Vein material: None.
ADDITIONAL COMMENTS: Irregular contact between vein calcite and lithic fragments.

125-778A-8R-1 (continued)

UNIT 2: SERPENTINIZED TECTONIZED HARZBURGITE

Pieces 7 to 9

COLOR: Dark greenish gray (10Y 5/1).
LAYERING: Not visible.
DEFORMATION: Wavy cleavage on orthopyroxene; elongate spinels in trains and some elongate orthopyroxene parallel to spinel trains.
PRIMARY MINERALOGY:
Olivine - Mode: 80-85%.
Crystal size: 3-5 mm.
Crystal shape: Anhedral.
Crystal orientation: Not visible.
Percent replacement: 90-100%.

Orthopyroxene - Mode: 15-20%.
Crystal size: 2-5 mm.
Crystal shape: Anhedral-elongate.
Crystal orientation: Elongate parallel to spinel trains.
Percent replacement: 80-100%.

Spinel - Mode: <2%.
Crystal size: <1 mm.
Crystal shape: Equant-elongate.
Crystal orientation: Arranged in trains.
Percent replacement: 0%.
SECONDARY MINERALOGY:
Serpentine, dusty black magnetite.
Total percent: 80-99%.
Texture: Mesh and bastite.
Vein material: Some thin veins (<0.3 mm wide) filled with amorphous black serpentine, also minor (<1.0-mm-wide) chrysotile veins.

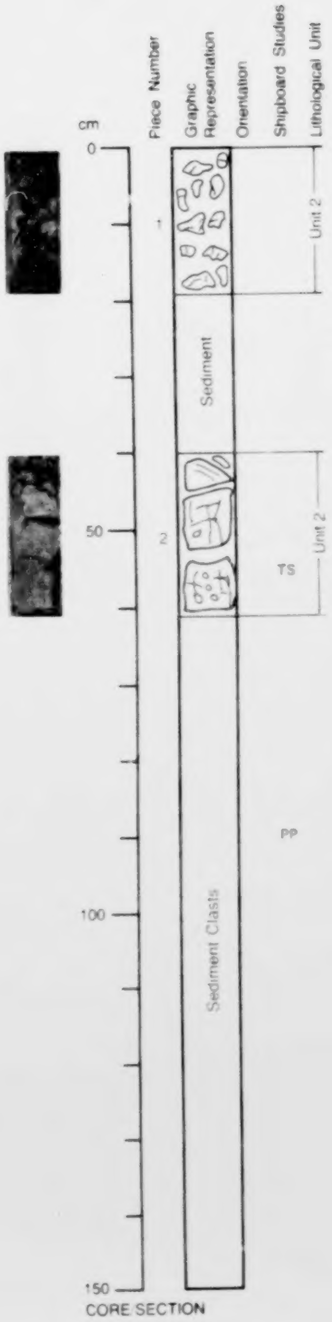
cm
Piece Number
Graphic Representation
Orientation
Shipboard Studies
Lithological Unit
0
50
100
150
1
2
Unit 2
Sediment
Unit 2
TS
PP
Sediment Clasts
CORE SECTION

125-778A-9R-1

UNIT 2: SERPENTINIZED HARZBURGITE/DUNITE

Piece 1 (multiple fragments)

COLOR: Dark green black (10GY 3/2)
LAYERING: Not visible
DEFORMATION: Wavy cleavage on orthopyroxene
PRIMARY MINERALOGY:
Olivine - Mode: 80-90%
Crystal size: Not visible
Crystal shape: Not visible
Crystal orientation: Not visible
Percent replacement: 100%

Orthopyroxene - Mode: 10-20%
Crystal size: 2-3 mm
Crystal shape: Subhedral
Crystal orientation: Not visible
Percent replacement: 100%

Spinel - Mode: Trace
Crystal size: <0.1 mm
Crystal shape: Equant
Crystal orientation: Not visible
Percent replacement: Not visible
SECONDARY MINERALOGY:
Serpentine and dusty magnetite
Total percent: 100%
Texture: Bastite in some patches
Vein material: Serpentine (+ calcite?), <1 mm wide, scattered throughout pieces
ADDITIONAL COMMENTS: Two small fragments (1 - 1.5 cm) have small patches of unidentified dark red (2.5YR 3/4) mineral present

UNIT 2: SERPENTINIZED HARZBURGITE

Piece 2 (multiple fragments)

COLOR: Green gray (5G 4/2)
LAYERING: Not visible
DEFORMATION: Not visible
PRIMARY MINERALOGY:
Olivine - Mode: 70-80%
Crystal size: Not visible
Crystal shape: Not visible
Crystal orientation: Not visible
Percent replacement: 100%

Orthopyroxene - Mode: 20-30%
Crystal size: Not visible
Crystal shape: Not visible
Crystal orientation: Not visible
Percent replacement: 100%
SECONDARY MINERALOGY:
Serpentine
Total percent: 100%
Texture: Bastite present in some areas
Vein material: None

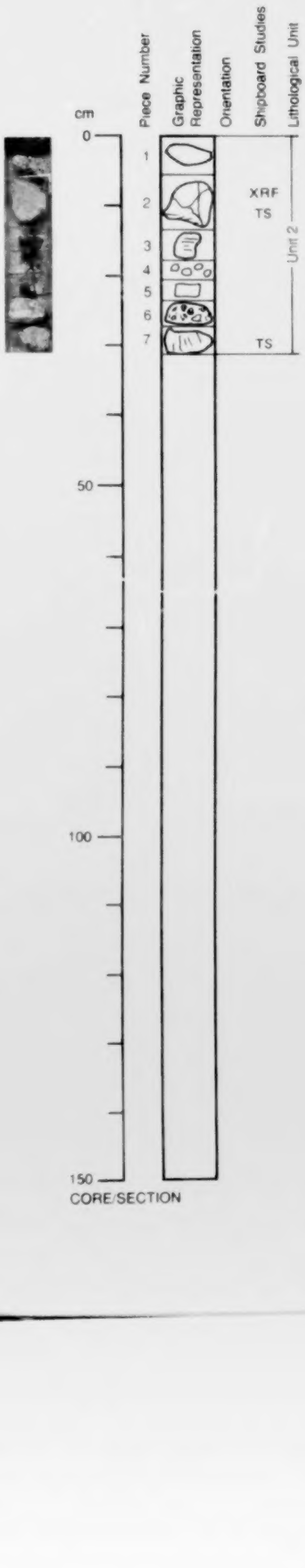
cm
Piece Number
Graphic Representation
Orientation
Shipboard Studies
Lithological Unit
0
1
2
3
4
5
6
7
XRF
TS
TS
Unit 2
50
100
150
CORE/SECTION

125-778A-9R-CC

UNIT 2: METASEDIMENT

Pieces 1 to 7

COLOR: Grayish green (5G 5/2) to dark red (10R 3/6).
LAYERING: Crude layering <2 cm wide.
DEFORMATION: Pinch-and-swell structures, brecciation and recementation.
PRIMARY MINERALOGY: Not visible.
SECONDARY MINERALOGY:
Chlorite, calcite, clay and limonite.
Total percent: 100%.
Texture: Very fine-grained.
Vein material: Thin veins of calcite and chlorite (<0.2 mm wide) scattered throughout pieces; possibly some thin talc veins also.

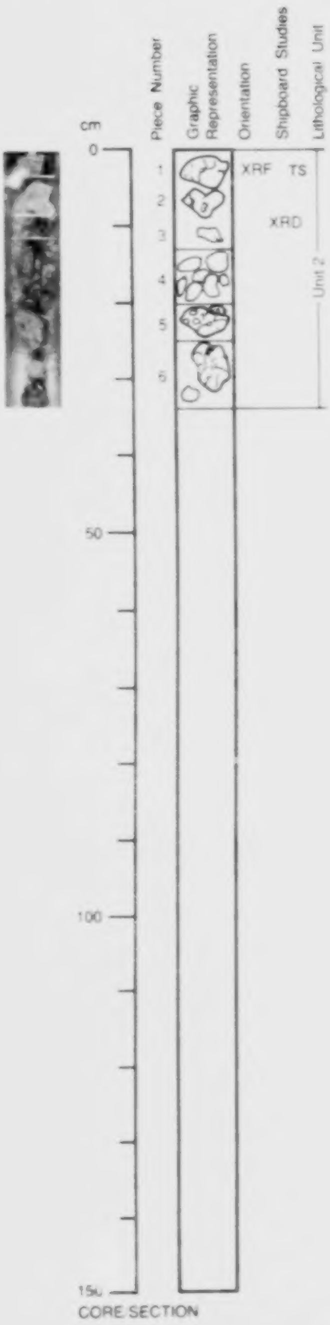
cm
0
50
100
150
Piece Number
Graphic Representation
Orientation
Shipboard Studies
Lithological Unit
1
2
3
4
5
6
XRF
TS
XRD
Unit 2
CORE SECTION

125-778A-10R-CC

UNIT 2: METABASALT

Pieces 1-6

COLOR: Light greenish gray (5G 7/2 to 6/2) to reddish brown (2.5YR 4/4).
LAYERING: Not visible.
DEFORMATION: Slight brecciation.
PRIMARY MINERALOGY:
Plagioclase - Mode: 40-55%.
Crystal size: <0.05 mm.
Crystal shape: Lath.
Crystal orientation: Felted.
Percent replacement: 100%.

Pyroxene - Mode: 45-60%.
Crystal size: <0.05 mm.
Crystal shape: Granular.
Crystal orientation: Not visible.
Percent replacement: Not visible.
SECONDARY MINERALOGY:
Clay and chlorite.
Total percent: 85%.
Texture: Very fine-grained, micro felted texture.
Vein material: Early generation of deformed, black serpentine filled veins; second generation of fracture filling of very light greenish gray to white serpentine and coarsely crystalline drusy calcite.

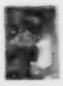

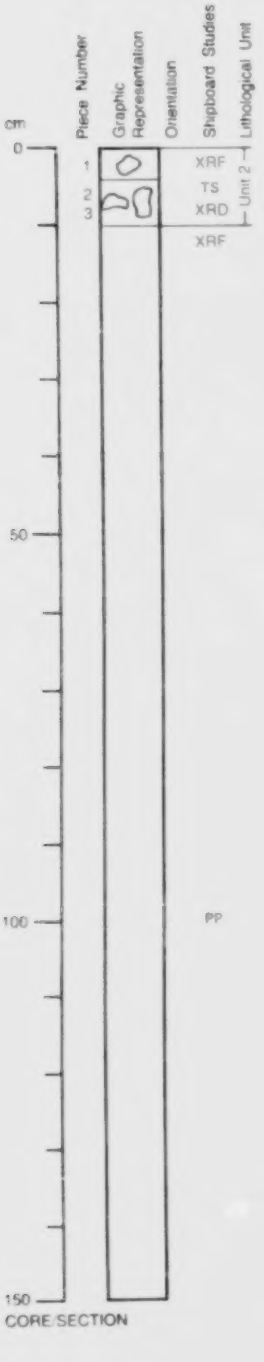
cm
0
50
100
150
Piece Number
Graphic Representation
Orientation
Shipboard Studies
Lithological Unit
1
2
3
XRF
TS
XRD
XRF
PP
Unit 2
CORE/SECTION

125-778A-11R-1

UNIT 2: SERPENTINITE

Piece 1

COLOR: Black (2.5YR 2.5/0) with alteration patches of dark green (10GY 5/2)
LAYERING: Not visible
DEFORMATION: Sheared and folded
PRIMARY MINERALOGY: Not visible
SECONDARY MINERALOGY:
Serpentine
Total percent: 100%
Texture: Very fine-grained
Vein material: 1 - 3% of pieces are filled with veins (1 mm wide) of green serpentine (10GY 7/2), randomly oriented
ADDITIONAL COMMENTS: Rounded clasts 2.5 cm in diameter

UNIT 2: METABRECCIA

Piece 2 (multiple fragments)

COLOR: Pale gray green (10GY 7/2 to 5G 8/2)
LAYERING: Not visible
DEFORMATION: Brecciated and recemented
PRIMARY MINERALOGY:
Brecciated clasts are very fine-grained and may have been basaltic
SECONDARY MINERALOGY:
Clay, chlorite
Total percent: 100%
Texture: Very fine-grained
Vein material: 2 - 4 % of pieces are formed by 1 to 2 mm-wide veins, filled with green (10GY 7/2) material, possibly serpentine; veins are randomly oriented
ADDITIONAL COMMENTS: Phacoidal clasts 3 by 1.5 cm

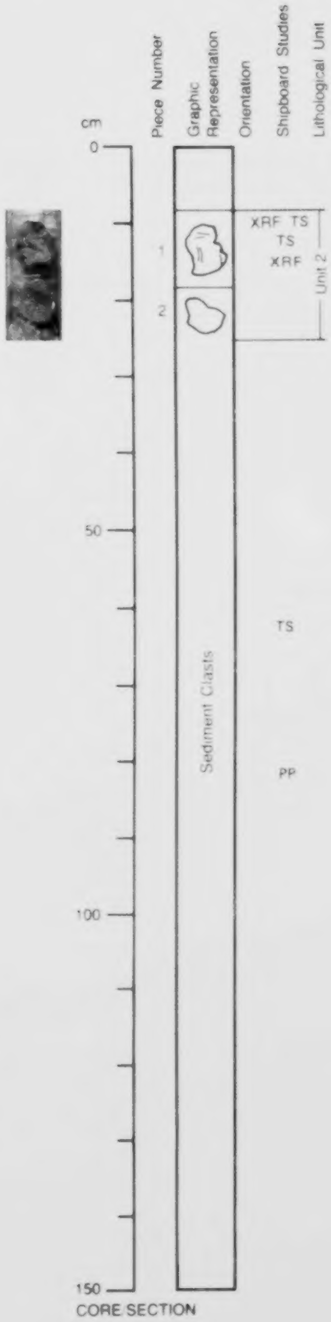
cm
Piece Number
Graphic Representation
Orientation
Shipboard Studies
Lithological Unit
0
50
100
150
1
2
XRF TS
TS
XRF
Unit 2
TS
PP
Sediment Clasts
CORE SECTION

125-778A-13R-1

UNIT 2: METABASALT

Pieces 1 and 2

COLOR: Gray (2.5YR 6/0)
LAYERING: Not visible
DEFORMATION: Heavily veined to brecciated
PRIMARY MINERALOGY:
Fine-grained to glassy groundmass, primary minerals not visible
SECONDARY MINERALOGY:
Clay, chlorite and serpentine with subsidiary carbonate
Total percent: 100%
Texture: Very fine-grained
Vein material: 5-7% of the pieces are formed by two generations of veins: 1st generation 1.5-2 mm wide, filled with blue-green (5G 7/1) mineral oriented sub-perpendicular to long axis of piece; 2nd generation veins form 4-5% of the pieces, filled with white carbonate oriented subparallel to long axis of piece
ADDITIONAL COMMENTS: Phacoidal to subangular pieces 7 by 4 cm to 6 cm wide

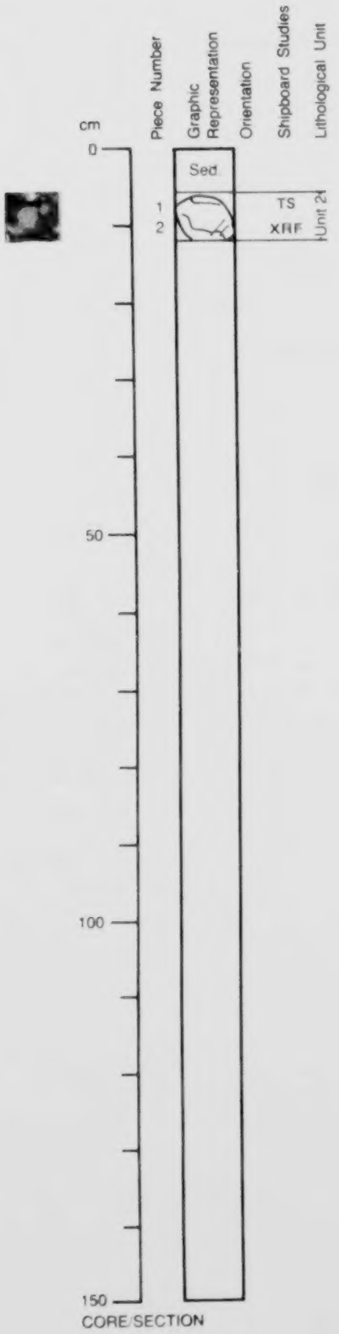
cm
Piece Number
Graphic Representation
Orientation
Shipboard Studies
Lithological Unit
0
Sed
1
2
TS
XRF
Unit 2
50
100
150
CORE/SECTION

125-778A-13R-2

UNIT 2: SERPENTINITE AND METAVOLCANICLASTIC

Pieces 1-2

COLOR: Light brownish gray (2.5Y 6/2) to dusky red (10R 3/3)
LAYERING: Not visible.
DEFORMATION: Some fragments are sheared.
PRIMARY MINERALOGY:
Not visible, very fine grained matrix with minute (<0.5 mm) clasts.
SECONDARY MINERALOGY:
Serpentine, talc, magnetite; there is also hematite staining pervasively penetrating the pieces.
Total percent: 100%.
Texture: Some pieces have a soapy feel, possibly talcose.
Vein material: Randomly oriented (<1 mm wide) filled with serpentine or chlorite.

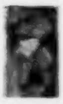

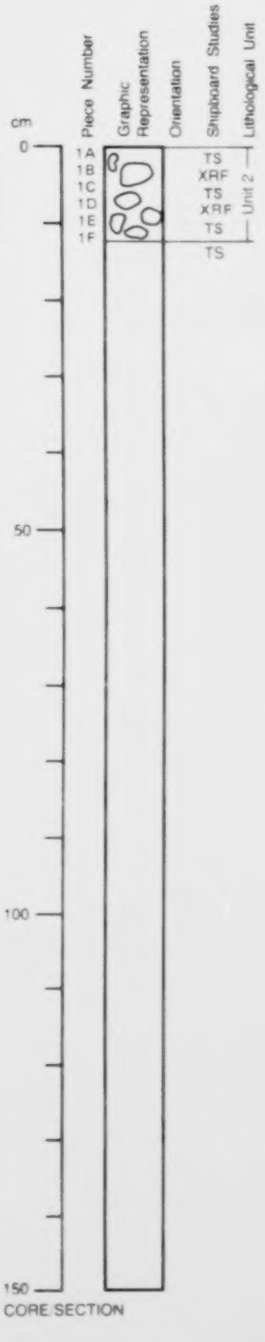
cm
Piece Number
Graphic Representation
Orientation
Shipboard Studies
Lithological Unit
0
1A
1B
1C
1D
1E
1F
TS
XRF
TS
XRF
TS
TS
Unit 2
50
100
150
CORE SECTION

125-778A-13R-CC

UNIT 2: METABASALT

Pieces 1A and 1B

COLOR: Light gray to gray (10YR 6/1 to 5Y 5/1)
LAYERING: Not visible
DEFORMATION: Not visible
PRIMARY MINERALOGY:
Aphyric fine-grained groundmass with felted feldspar fabric
SECONDARY MINERALOGY:
Very fine-grained, probably saussuritized
Total percent: 100%
Texture: Very fine-grained
Vein material: 1% of pieces are cut by 0.1 to 0.5-mm-wide, subparallel to anastomosing veins of carbonate and serpentine or chlorite

UNIT 2: METASEDIMENT BRECCIA

Piece 1C

COLOR: White (2.5Y 8/0 to 5Y 5/3)
LAYERING: Not visible
DEFORMATION: Brecciated
PRIMARY MINERALOGY: Not visible
SECONDARY MINERALOGY:
Serpentine, epidote, oxides
Total percent: 100%
Texture: Coarse-grained; crystal size 1-7 mm
Vein material: None

UNIT 2: AMPHIBOLITE SANDSTONE

Pieces 1D and 1E

COLOR: Gray (5Y 5/1)
LAYERING: Not visible
DEFORMATION: Not visible
PRIMARY MINERALOGY:
Crossite reported in thin-section description
Hornblende - Mode: 10%
Crystal size: <0.5 mm
Crystal shape: Subhedral
Crystal orientation: Not visible
Percent replacement: 0%
SECONDARY MINERALOGY:
Chlorite
Total percent: 90%
Texture: Fine-grained
Vein material: None

125-778A-1R-01 (19-22 cm) OBSERVER: TER WHERE SAMPLED: Conical Seamount, south flank

ROCK NAME: Altered serpentine debris flow

GRAIN SIZE: "Tectonite", but possible soft sediment

TEXTURE: "Melange"-pure shear layer, parallel extension

PRIMARY MINERALOGY	PERCENT PRESENT	PERCENT ORIGINAL	SIZE (mm)	COMPO-SITION	MORPHOLOGY	COMMENTS
PHENOCRYSTS						
Olivine	N/A	90-95	N/A		N/A	Mesh texture.
Spinel	N/A	1	N/A		N/A	
Orthopyroxene	N/A	5-10?	N/A		N/A	Bastite texture.
GROUNDMASS						
N/A	N/A	N/A	N/A		N/A	

SECONDARY MINERALOGY	PERCENT	REPLACING/ FILLING	COMMENTS
Clays	20-30		
Serpentine	70-80		Chrysotile and/or lizardite.
Magnetite	1	Spinel	In vein.

VESICLES/ CAVITIES	PERCENT	LOCATION	SIZE (mm)	FILLING	SHAPE
Vesicles	0				

COMMENTS: Soft "sediment"-unlithified as recovered original textures of serpentinite are preserved in clasts. No piece number given.

125-778A-2R-01 (Piece 2,57-59 cm) OBSERVER: SAB WHERE SAMPLED: Conical Seamount, south flank

ROCK NAME: Serpentinized harzburgite

GRAIN SIZE: 0.5-4 mm

TEXTURE: Mesh and bastite

PRIMARY MINERALOGY	PERCENT PRESENT	PERCENT ORIGINAL	SIZE (mm)	COMPO-SITION	MORPHOLOGY	COMMENTS
PHENOCRYSTS						
Olivine	<0.1	85	Not visible		Anhedral	Altered to serpentine; present as grain in spinel.
Clinopyroxene	.2-.3	.2-.3	0.5		Subhedral/anhedral	Clot and patch, some are twinned.
Spinel	.5-1	.5-1	0.5		Euhedral/anhedral	
Orthopyroxene	5	15	4		Euhedral-subhedral	Altered to serpentine (bastite); has (100) clinopyroxene lamellae.
GROUNDMASS						
N/A	N/A	N/A	N/A		N/A	

SECONDARY MINERALOGY	PERCENT	REPLACING/ FILLING	COMMENTS
Clays	15	Olivine, orthopyroxene, serpentine	As dusty brown clay throughout slide; anastomosed veins (<0.5 mm wide) are common.
Carbonate	<1	Vein	<1-mm-long veins of possible carbonate material.
Serpentine	83	Olivine, orthopyroxene	Lizardite and/or chrysotile after olivine, orthopyroxene.
Magnetite	1	Spinel, olivine	Fine-grained to 0.1 mm after olivine and orthopyroxene.

VESICLES/ CAVITIES	PERCENT	LOCATION	SIZE (mm)	FILLING	SHAPE
Vesicles	0				

COMMENTS: This is a serpentinized harzburgite which may be relatively rich in clinopyroxene and Cr-spinel. Orthopyroxene shows wavy extinction with kink-banding parallel to (100), deformed. Anhedral spinel, not aligned; contains olivine occasionally.

125-778A-19R-01 (Piece 3,70-73 cm) OBSERVER: SAB WHERE SAMPLED: Conical Seamount, south flank

ROCK NAME: Serpentinized harzburgite

GRAIN SIZE: 0.3-4 mm

TEXTURE: Mesh and bastite

PRIMARY MINERALOGY	PERCENT PRESENT	PERCENT ORIGINAL	SIZE (mm)	COMPOSITION	MORPHOLOGY	COMMENTS
PHENOCRYSTS						
Olivine	8	80	4		Anhedral.	Altered to mesh serpentine.
Clinopyroxene	<0.1	<0.1	1.5		Subhedral-anhedral.	As a patch in an orthopyroxene and as exsolution lamellae.
Spinel	0.7	0.7	1.7	Cr-rich	Euhedral-anhedral.	Reddish brown; deformed.
Orthopyroxene	5	15	8		N/A	Has (100) exsolution lamellae of clinopyroxene; wavy extinction, altered to bastite serpentine.
GROUNDMASS						
N/A	N/A	N/A	N/A		N/A	

SECONDARY MINERALOGY	PERCENT	REPLACING/ FILLING	COMMENTS
Clays	1		Dusty tan/orange-red brown clay throughout slide. Anastomosed veins are common (<0.5 mm wide).
Serpentine	75		Lizardite and or chrysotile after olivine, orthopyroxene; flasers of mesh textured, partially serpentinized olivine are aligned and separated by sheared serpentinite and brucite.
Brucite	1		Associated with serpentine.
Magnetite	1		<0.05 mm; altered from spinel(?); associated with serpentine.

VESICLES/ CAVITIES	PERCENT	LOCATION	SIZE (mm)	FILLING	SHAPE
Vesicles	0				

COMMENTS: Freshest sample than 778A-[illegible] ([illegible] cm); spinel is euhedral (some are anhedral) rather than ragged as in [illegible] ([illegible] cm). Considerably more olivine and orthopyroxene. This rock shows two deformation episodes: 1) high-T? ductile, i.e., mantle fabric deforming orthopyroxene, clinopyroxene + spinel; 2) post-serpentinization brittle shearing. Could be called tectonite.

125-778A-2R-01 (Piece 6, 78-81 cm) OBSERVER: SAB WHERE SAMPLED: Conical Seamount, south flank

ROCK NAME: Serpentinized harzburgite (tectonite)

GRAIN SIZE: 0.05-4 mm

TEXTURE: Mesh and bastite

PRIMARY MINERALOGY	PERCENT PRESENT	PERCENT ORIGINAL	SIZE (mm)	COMPO-SITION	MORPHOLOGY	COMMENTS
PHENOCRYSTS						
Olivine	10	80	2	Fo 90	Anhedral	2V=+90; mesh texture serpentine after olivine.
Clinopyroxene	<0.1	<0.1	0.05	Di	Subhedral-anhedral	Clot in shape.
Spinel	0.5	0.5	0.3	Cr	Euhedral-subhedral	Reddish brown.
Orthopyroxene	15	20	4	En	N/A	2V=+ 85; bastite serpentine after orthopyroxene exsolution lamellae of 100 clinopyroxene.
GROUNDMASS						
N/A	N/A	N/A	N/A		N/A	

SECONDARY MINERALOGY	PERCENT	REPLACING/ FILLING	COMMENTS
Clays	20		Dusty brown clay throughout slide; anastomosed veins are common.
Carbonate	<1-1	Veins	Located in interior of veins; short vein segments.
Serpentine	52	Olivine, orthopyroxene	Lizardite and/or chrysotile after orthopyroxene and olivine.
Magnetite	2		Fine-grained to 0.3 mm; located throughout slide [illegible] also concentrated in anastomosing veins.

VESICLES/ CAVITIES	PERCENT	LOCATION	SIZE (mm)	FILLING	SHAPE
Vesicles	0				

COMMENTS: Considerable amount of fresh silicate (olivine, orthopyroxene, clinopyroxene) preserved in this sample.
Cr-spinel is beautifully euhedral (cubes and octahedra); not stretched out, but some grains are "wormy".
Orthopyroxene has wavy extinction.

125-778A-8R-01 (Piece 1,1-2 cm) OBSERVER: SAB WHERE SAMPLED: Conical Seamount, south flank

ROCK NAME: Metabasalt

GRAIN SIZE: 0.03-0.8 mm

TEXTURE: Subophitic, aphyric

PRIMARY MINERALOGY	PERCENT PRESENT	PERCENT ORIGINAL	SIZE (mm)	COMPO-SITION	MORPHOLOGY	COMMENTS
PHENOCRYSTS						
N/A	N/A	N/A	N/A		N/A	
GROUNDMASS						
Plagioclase	5-10	50-60	0.15-0.8		Laths, euhedral	Highly altered (clays, saussuritized)
Clinopyroxene	10-15	15-20	0.1-0.4		Subhedral	Laths and equant crystals intergrown with plagioclase; moderate alteration.
Magnetite/spinel	1-2	1-2	0.03-0.1		Subhedral	Individual euhedral grains to anhedral blebs.
Glass	0	15-20	N/A		N/A	Altered to clays, brown, cloudy.

SECONDARY MINERALOGY	PERCENT	REPLACING/FILLING	COMMENTS
Clays	40-50	Plagioclase	Dusty, brown, pseudomorphs after plagioclase.
Clays	20-25	Glass, matrix, vesicles	1) after glass-dusty brown, amorphous, 2) after matrix and vesicles patches of bright green clays, the patches are up to 10 mm across.
Chlorite	1-2	Glass, clinopyroxene	In groundmass after palagonite, original glass and margins of clinopyroxene grains.

VESICLES/CAVITIES	PERCENT	LOCATION	SIZE (mm)	FILLING	SHAPE	COMMENTS
Vesicles	<1		0.15-0.3	Clays, zeolite	Subround	One or two appear to be gas-rich late fluids.

COMMENTS: Mylonitic, cataclastic smears parallel to fractures, about 2 mm wide with fine-grained (<0.01 mm) mineralogy. Variable texture throughout 1) equigranular (0.1 mm) abundant laths of plagioclase and clinopyroxene intergrowths (subophitic) hollow and swallowtail plagioclase; a few patches of microphenocrysts (0.15 mm, clinopyroxene and plagioclase); One low birefringence straight extinction grain (0.4 mm) (orthopyroxene? chlorite?), high relief of plagioclase. In the more crystalline patches plagioclase:clinopyroxene:groundmass=3:1:3.

125-778A-4R-01 (0-7 cm) OBSERVER: JKB WHERE SAMPLED: Conical Seamount, south flank

ROCK NAME: Tuffaceous mudstone

GRAIN SIZE: <0.4 mm

TEXTURE: Fine-grained, layered

PRIMARY MINERALOGY	PERCENT PRESENT	PERCENT ORIGINAL	SIZE (mm)	COMPO-SITION	MORPHOLOGY	COMMENTS
PHENOCRYSTS						
Olivine	N/A	N/A	N/A		N/A	
Plagioclase	1	N/A	<0.4		N/A	
Clinopyroxene	1	N/A	<0.1		N/A	
Magnetite	1	N/A	<0.1		N/A	
Devitrified glass	30	N/A	N/A		N/A	
GROUNDMASS						
N/A	N/A	N/A	N/A		N/A	

VESICLES/CAVITIES	PERCENT	LOCATION	SIZE (mm)	FILLING	SHAPE
Vesicles	5				

COMMENTS: A lithic fragment of tuffaceous mudstone partly surrounded by serpentine mudstone. No piece number given.

125-778A-4R-01 (Piece 2,5-6 cm) OBSERVER: LAG WHERE SAMPLED: Conical Seamount, south flank

ROCK NAME: Water-lain tuff

GRAIN SIZE: <1 mm

TEXTURE: Fine-grained layered

PRIMARY MINERALOGY	PERCENT PRESENT	PERCENT ORIGINAL	SIZE (mm)	COMPO-SITION	MORPHOLOGY	COMMENTS
PHENOCRYSTS						
Olivine	3	N/A	0.5		Euhedral-subhedral (?)	
Plagioclase	3	N/A	0.2-0.5		Euhedral-subhedral	
Clinopyroxene	3	N/A	0.5-1		Anhedral	
Orthopyroxene	Trace	N/A	N/A		N/A	Thin rind on one clinopyroxene grain.
GROUNDMASS						
Ash	~90	N/A	N/A		N/A	Cryptocrystalline with very small plagioclase needles.

VESICLES/ CAVITIES	PERCENT	LOCATION	SIZE (mm)	FILLING	SHAPE
Vesicles	10	Ubiquitous	0.1	None	Angular

COMMENTS: Clast is in contact with serpentine/carbonate sedimentary material. A number of the pyroxene and plagioclase grains have thin reaction zones in contact with the groundmass. One clast is rounded, pyroxene and plagioclase in glass (light brown) probably altered, but appears isotropic, some other clasts almost entirely glass with clay reactions marginally to groundmass.

125-778A-5R-01 (Piece 1,7-10 cm) OBSERVER: HIR WHERE SAMPLED: Conical Seamount, south flank

ROCK NAME: Metabasalt

GRAIN SIZE: 0.05-0.1 mm

TEXTURE: Aphyric, subophitic

PRIMARY MINERALOGY	PERCENT PRESENT	PERCENT ORIGINAL	SIZE (mm)	COMPO-SITION	MORPHOLOGY	COMMENTS
PHENOCRYSTS						
N/A	N/A	N/A	N/A		N/A	
GROUNDMASS						
Glass	0	10-15	N/A		N/A	Completely altered to clays.
Plagioclase	0	40-55	0.05-0.1		Euhedral-subhedral	Replaced by Ca-poor plagioclase and clays.
Clinopyroxene	5-10	30-35	0.05-0.1		Euhedral-subhedral	Replaced by pale green hornblende.
Spinel	1-2	1-2	<0.01-1		Subhedral	Opaque, black, disseminated.

SECONDARY MINERALOGY	PERCENT	REPLACING/ FILLING	COMMENTS
Chlorite	5-10	Clinopyroxene)	Abnormal interference is typical, associated with clinopyroxene, hornblende.
Albite	2-3	Veins	Numerous, (<0.2 mm wide), twinning.
Sphene	<1		Fine-grained, dusty.
Hornblende	30-35	Clinopyroxene	Pale-green pseudomorphs after clinopyroxene.
Plagioclase	40-55	Plagioclase	Mostly saussuritized; pseudomorphs after plagioclase.

VESICLES/ CAVITIES	PERCENT	LOCATION	SIZE (mm)	FILLING	SHAPE
Vesicles	0				

COMMENTS: Primary subophitic texture is well preserved, but igneous minerals have been fully replaced by metamorphic (alteration) minerals. No foliation or lineation visible. Metamorphism under low P/T greenschist facies (inferred from mineral assemblage). Two different textures: 1) very fine-grained 2) coarse grain showing clastic texture. See inclusions of one mineral within another (igneous texture). Texture boundary may be primary or metamorphic.

125-778A-3R-1 (18-22 cm) OBSERVER: HIR WHERE SAMPLED: Conical Seamount, south flank

ROCK NAME: Debris flow, serpentinous mudstone

GRAIN SIZE: Fine-grained

TEXTURE: Weakly foliate

PRIMARY MINERALOGY	PERCENT PRESENT	PERCENT ORIGINAL	SIZE (mm)	COMPOSITION	MORPHOLOGY	COMMENTS
N/A	N/A	N/A	N/A		N/A	

SECONDARY MINERALOGY	PERCENT	REPLACING/ FILLING	COMMENTS
Clays	10		Dusty brownish clay.
Clays	<2		Slender crystal in serpentinous mudstone, relatively high birefringence.
Serpentine	85-90		
Brucite	2		
Magnetite	2		

VESICLES/ CAVITIES	PERCENT	LOCATION	SIZE (mm)	FILLING	SHAPE
Vesicles	0				

COMMENTS: Foliation defined by micaceous clay minerals is visible. Fragments of brucite crystal are scattered throughout the rock. Where argillaceous materials are predominant, detrital fragments (0.1-0.3 mm) of serpentine are easily distinguished. No piece number given.

125-778A-4R-1 (Piece 1, 0-1 cm) OBSERVER: HIR WHERE SAMPLED: Conical Seamount, south flank

ROCK NAME: Chert

GRAIN SIZE: Fine-grained (<0.1 mm)

TEXTURE: Massive

PRIMARY MINERALOGY	PERCENT PRESENT	PERCENT ORIGINAL	SIZE (mm)	COMPOSITION	MORPHOLOGY	COMMENTS
PHENOCRYSTS						
Quartz	>95	N/A	<0.1		Anhedral	Cryptocrystalline, vein has grains 0.1-2 mm.
GROUNDMASS						
N/A	N/A	N/A	N/A		N/A	

SECONDARY MINERALOGY	PERCENT	REPLACING/ FILLING	COMMENTS
Clays	2-5		Brownish clay throughout slide.
Limonite	2		Distributed throughout slide, fine-grained (<0.01 mm).

VESICLES/ CAVITIES	PERCENT	LOCATION	SIZE (mm)	FILLING	SHAPE
Vesicles	0				

COMMENTS: This rock primarily consists of cryptocrystalline quartz and is fragmented into smaller pieces. Brownish clay partly fills among these fragments. Veins composed of coarse-grained quartz run throughout the rock.

125-778A-6R-01 (Piece 1,20-23 cm) OBSERVER: HIR WHERE SAMPLED: Conical Seamount, south flank

ROCK NAME: Metabasalt

GRAIN SIZE: 0.01 to 1.2 mm

TEXTURE: Blastic, recrystallized, slightly phyric

PRIMARY MINERALOGY	PERCENT PRESENT	PERCENT ORIGINAL	SIZE (mm)	COMPOSITION	MORPHOLOGY	COMMENTS
PHENOCRYSTS						
Plagioclase	<5	5-10	0.05-0.1		Laths	Partially (10-100%) by hornblende.
Clinopyroxene	5-10	20-25	0.5-1.2		Originally euhedral	Equant grains 50-90% replaced by hornblende and chlorite.
Spinel	1-2	1-2	0.01-0.05		Subhedral	Random, disseminated.
GROUNDMASS						
Glass and groundmass	0	60-70	N/A		N/A	Completely altered to clays.
Apatite	<<1	<<1	<0.01		Needles	Within plagioclase and clinopyroxene.

SECONDARY MINERALOGY	PERCENT	REPLACING/ FILLING	COMMENTS
Clays	30-50	Glass	
Carbonate	<1	Vein	Vein filling.
Chlorite	5-10	Clinopyroxene, vein	Vein filling, matrix.
Albite	15-20	Plagioclase, glass	
Hornblende	30-40	Clinopyroxene	Pale green-green, euhedral to anhedral elongate crystals, smaller than original pyroxene random direction of long direction (0.05-0.1 mm).
Prehnite	<1		
Pumpellyite	2	Veins, cavities	Along grain boundaries and as patches.
Hematite	<1		

VESICLES/ CAVITIES	PERCENT	LOCATION	SIZE (mm)	FILLING	SHAPE
Vesicles	<1	Dissemi-nated	0.3-0.4	Chlorite, clays, hornblende	Round

COMMENTS: Metamorphosed under greenschist facies condition, abundant faults, partially fragmented. Mineral identification difficult because of alteration and thickness of section.

125-778A-8R-01 (96-99 cm) OBSERVER: HIR WHERE SAMPLED: Conical Seamount, south flank

ROCK NAME: Serpentinous mudstone, debris flow

GRAIN SIZE: Fine-grained. See close-up photos at 56-70, 115-130.

TEXTURE: Tectonite (soft sediment), melange texture

PRIMARY MINERALOGY	PERCENT PRESENT	PERCENT ORIGINAL	SIZE (mm)	COMPOSITION	MORPHOLOGY	COMMENTS
PHENOCRYSTS						
Spinel	<2	N/A	N/A		N/A	Brown color.
GROUNDMASS						
N/A	N/A	N/A	N/A		N/A	

SECONDARY MINERALOGY	PERCENT	REPLACING/ FILLING	COMMENTS
Clays	10-15		Dusty micaceous mineral, relatively high birefringence, (0.01-0.015).
Serpentine	80-90		Chrysotile and/or lizardite.
Magnetite	<2		

VESICLES/ CAVITIES	PERCENT	LOCATION	SIZE (mm)	FILLING	SHAPE
Vesicles	0				

COMMENTS: Ill-sorted. Clusters of coarse-grained (0.1-0.5 mm) serpentine crystals are scattered in the fine-grained (<0.01 mm) serpentine matrix. These clusters are elongated, and trend parallel to the foliation defined by micaceous clay minerals. Intensely deformed and disturbed serpentine fragments are often visible. Brittle fracture of large aggregates with micro-normal faults Layer-II extension. No piece number given.

[illegible]-778A-4R-01 ([illegible] cm) OBSERVER: TER WHERE SAMPLED: Conical Seamount, south flank

ROCK NAME: Pebbly serpentine mudstone.

GRAIN SIZE: Fine to very coarse (poorly sorted).

TEXTURE: Tectonite, phacoidal.

PRIMARY MINERALOGY	PERCENT PRESENT	PERCENT ORIGINAL	SIZE (mm)	COMPO-SITION	MORPHOLOGY	COMMENTS
PHENOCRYSTS						
Olivine	[illegible]	[illegible]	N/A		N/A	
Clinopyroxene	[illegible]	N/A	N/A		N/A	
Spinel	[illegible]	[illegible]	N/A		N/A	
Orthopyroxene	[illegible]	[illegible]	N/A		N/A	Bastite.
GROUNDMASS						
N/A	N/A	N/A	N/A		N/A	

SECONDARY MINERALOGY	PERCENT	REPLACING/FILLING	COMMENTS
Clays	[illegible]		
Carbonate	[illegible]		
Magnetite	[illegible]		
Serpentine	[illegible]		Chrysotile and/or lizardite.

VESICLES/CAVITIES	PERCENT	LOCATION	SIZE (mm)	FILLING	SHAPE
Vesicles	[illegible]				

COMMENTS: [illegible], phacoidal, some layers show parallel extinction. No piece number given.

[illegible]-778A-7R-01 (Piece 1, [illegible] cm) OBSERVER: [illegible] WHERE SAMPLED: Conical Seamount, south flank

ROCK NAME: Metabasalt metasomatite breccia.

GRAIN SIZE: [illegible]

TEXTURE: Breccia.

PRIMARY MINERALOGY	PERCENT PRESENT	PERCENT ORIGINAL	SIZE (mm)	COMPO-SITION	MORPHOLOGY	COMMENTS
PHENOCRYSTS						
Olivine	[illegible]	[illegible]	[illegible]		Euhedral	Quench textured with Cr-spinel inclusions; sector zoned.
Plagioclase	[illegible]	[illegible]	[illegible]		Subhedral	
Clinopyroxene	[illegible]	[illegible]	[illegible]		Subhedral	Chlorite and clay alteration.
Spinel	[illegible]	[illegible]	[illegible]		Euhedral	Opaque, random distribution.
GROUNDMASS						
Glass Matrix	[illegible]	[illegible]	N/A		N/A	Completely altered to clays, appears to have had original quench texture with plumose structures.

SECONDARY MINERALOGY	PERCENT	REPLACING/FILLING	COMMENTS
Clays	[illegible]	Glass	Pervasive.
Carbonate	[illegible]	[illegible]	Occurs as coating on fragment and veins and splitting quartz veins.
Chlorite	[illegible]	Glass, clinopyroxene	Isolated patches slightly pleochroic.
Quartz	[illegible]	Veins	Equidimensional ([illegible] mm), some veins appear to be filled with zeolite.

VESICLES/CAVITIES	PERCENT	LOCATION	SIZE (mm)	FILLING	SHAPE
Vesicles	[illegible]				

COMMENTS: [illegible]

125-778A-7R-01 (2-3 cm) OBSERVER: RIR WHERE SAMPLED: Conical Seamount, south flank

ROCK NAME: Metabasite

GRAIN SIZE: 0.2-0.4 mm (phenocryst 2-5 mm)

TEXTURE: Intergranular, sparsely phyric

PRIMARY MINERALOGY	PERCENT PRESENT	PERCENT ORIGINAL	SIZE (mm)	COMPOSITION	MORPHOLOGY	COMMENTS
PHENOCRYSTS						
Plagioclase	0	2-3	2-3		Subhedral	Completely altered, original glass inclusions (single grain).
Spinel	<1	<1	0.01-0.1		Euhedral	Skeletal and small equant grains black, opaque.
GROUNDMASS						
Glass	0	25-35	N/A		N/A	Completely altered to clays.
Plagioclase	2-5	40-55	0.1-0.3		Euhedral-subhedral	Saussuritized, clays subophitic, intergrowth with clinopyroxene.
Clinopyroxene	10-20	15-30	0.1-0.4		Subhedral	30-40% altered to chlorite(?).

SECONDARY MINERALOGY	PERCENT	REPLACING/ FILLING	COMMENTS
Clays	25-35	Plagioclase, glass	Gray-brown, throughout slide, after interstitial glass.
Carbonate	<1	Vein	
Chlorite	5-10	Clinopyroxene, plagioclase	May also be after Cx-plagioclase.
Albite	1	Vein	?
Sphene	5	–	
Saussurite	40-50	Plagioclase	Dusty pseudomorphs after plagioclase may be albitic.

VESICLES/ CAVITIES	PERCENT	LOCATION	SIZE (mm)	FILLING	SHAPE
Vesicles	0				

COMMENTS: Minor fault is visible. Plagioclase is intensely altered and saussuritized and may be albitic. Section contains many rock fragments, for example clast with quench crystal. No piece number given.

125-778A-7R-01 (11-14 cm) OBSERVER: SAB WHERE SAMPLED: Conical Seamount, south flank; clast

ROCK NAME: Serpentinized harzburgite

GRAIN SIZE: 0.4-10 mm

TEXTURE: Felted and bastite

PRIMARY MINERALOGY	PERCENT PRESENT	PERCENT ORIGINAL	SIZE (mm)	COMPOSITION	MORPHOLOGY	COMMENTS
PHENOCRYSTS						
Olivine	0	70	Not visible		Not visible	Altered to serpentine.
Spinel	1	1	0.4		Anhedral	Reddish color; partly altered to magnetite.
Orthopyroxene	1	29	5-10		Subhedral	Altered to serpentine; some grains with wavy extinction.
GROUNDMASS						
N/A	N/A	N/A	N/A		N/A	

SECONDARY MINERALOGY	PERCENT	REPLACING/ FILLING	COMMENTS
Serpentine	96	Olivine, orthopyroxene	Mostly antigorite; might be some minor lizardite/chrysotile but difficult to determine.
Magnetite	2	Olivine, orthopyroxene, spinel	<0.05 mm, scattered throughout slide, associated with the serpentine.

VESICLES/ CAVITIES	PERCENT	LOCATION	SIZE (mm)	FILLING	SHAPE
Vesicles	0				

COMMENTS: Heavily serpentinized when compared with samples from higher in core. This slide shows a nice "felted texture" defined by the antigorite blades which have altered from the olivine and orthopyroxene. No piece number given.

[illegible] cm OBSERVER: [illegible] WHERE SAMPLED: Conical Seamount, south flank; clast

ROCK NAME: Serpentinized harzburgite

GRAIN SIZE: [illegible] mm

TEXTURE: Felted [illegible]

PRIMARY MINERALOGY	PERCENT PRESENT	PERCENT ORIGINAL	SIZE (mm)	COMPOSITION	MORPHOLOGY	COMMENTS
PHENOCRYSTS:						
Olivine	0.0	85	Not visible		Not visible	No mesh texture visible; altered to serpentine.
Spinel	<1	1	[illegible]		Anhedral	Red brown; partly altered to magnetite.
Orthopyroxene	<1	15	[illegible]		Subhedral-anhedral	Altered to serpentine (bastite).
GROUNDMASS:						
N.A.	N.A.	N.A.	N.A.		N.A.	

SECONDARY MINERALOGY	PERCENT	REPLACING/FILLING	COMMENTS
Clays	[illegible]		Fine grained and distributed throughout slide. Difficult to tell if it is fine-grained dark clays or fine-grained magnetite.
Serpentine	90	Olivine, orthopyroxene	Mostly antigorite; might be minor lizardite and/or chrysotile, but difficult to determine.
Magnetite	[illegible]		[illegible] mm, scattered throughout slide. Associated with the serpentine; partly altered from spinel.

VESICLES/CAVITIES	PERCENT	LOCATION	SIZE (mm)	FILLING	SHAPE
Vesicles	[illegible]				

COMMENTS: Heavily serpentinized when compared with samples from higher in core. Shows a more "felted texture" defined by the antigorite blades which have formed after olivine and orthopyroxene. No piece number given.

[illegible] cm OBSERVER: [illegible] WHERE SAMPLED: Conical Seamount, south flank; clast

ROCK NAME: Serpentinized harzburgite

GRAIN SIZE: [illegible] mm

TEXTURE: Weakly [illegible]

PRIMARY MINERALOGY	PERCENT PRESENT	PERCENT ORIGINAL	SIZE (mm)	COMPOSITION	MORPHOLOGY	COMMENTS
Olivine	[illegible]	[illegible]	Not visible		Not visible	No mesh visible; altered to serpentine.
Spinel	[illegible]	[illegible]	[illegible]		Anhedral	Chromian spinel.
Orthopyroxene	[illegible]	[illegible]	[illegible]		Subhedral	Minor bastite remnant (altered to serpentine).

SECONDARY MINERALOGY	PERCENT	REPLACING/FILLING	COMMENTS
Clays	[illegible]		Dusty and scattered throughout slide.
Serpentine	[illegible]		Difficult to determine the type of serpentine minerals present, assumed to have altered from olivine/orthopyroxene.

VESICLES/CAVITIES	PERCENT	LOCATION	SIZE (mm)	FILLING	SHAPE
Vesicles					

COMMENTS: Serpentine [illegible] weakly foliated. No piece number given.

125-778A-7R-02 (55-60 cm) OBSERVER: SAB WHERE SAMPLED: Conical Seamount, south flank

ROCK NAME: Serpentinized harzburgite

GRAIN SIZE: 0.05-1 mm

TEXTURE: Mesh and bastite

PRIMARY MINERALOGY	PERCENT PRESENT	PERCENT ORIGINAL	SIZE (mm)	COMPO-SITION	MORPHOLOGY	COMMENTS
PHENOCRYSTS						
Olivine	<0.01	85?	0.1		Subhedral	Only visible as small inclusion in spinel altered to serpentine.
Spinel	<1	~1	0.05-0.1		Subhedral-anhedral	Red color-chromite?; altered to magnetite?
Orthopyroxene	<1	15?	0.5-1		Subhedral-anhedral	Altered to serpentine bastite.
GROUNDMASS						
N/A	N/A	N/A	N/A		N/A	

SECONDARY MINERALOGY	PERCENT	REPLACING/ FILLING	COMMENTS
Clays	15		Located as fine-grained material in veins; rusty brown.
Magnetite	2		0.05 to 0.06 mm plus dusty grains distributed throughout slide; altered from spinel? and as serpentinization by-product.
Serpentine	83		Mostly lizardite and/or chrysotile intermixed throughout slide; chrysotile veins (<1 mm wide) are intermixed with clays.

VESICLES/ CAVITIES	PERCENT	LOCATION	SIZE (mm)	FILLING	SHAPE
Vesicles	0				

COMMENTS: This rock is originally harzburgite. Orthopyroxene bastite is common. Most of spinel were altered to opaque mineral (probably magnetite). Veins of clays and chrysotile are well developed. An unknown mineral of low refractive index and high retardation occurs as a rare vein filling. Olivine is too small to identify exactly, and also resembles diaspore; poor mesh texture is visible in areas. No piece number given.

125-778A-7R-02 (74-75 cm) OBSERVER: SAB WHERE SAMPLED: Conical Seamount, south flank; clast

ROCK NAME: Serpentinized harzburgite

GRAIN SIZE: <1 mm

TEXTURE: Bastitic

PRIMARY MINERALOGY	PERCENT PRESENT	PERCENT ORIGINAL	SIZE (mm)	COMPO-SITION	MORPHOLOGY	COMMENTS
PHENOCRYSTS						
Olivine	0	70-75	Not visible		Not visible	Altered to serpentine completely.
Spinel	<1	1	0.5		Subhedral-anhedral	Altered to magnetite.
Orthopyroxene	0	20-25	0.5-2		Subhedral-anhedral	Altered to serpentine, < or [illegible].
GROUNDMASS						
N/A	N/A	N/A	N/A		N/A	

SECONDARY MINERALOGY	PERCENT	REPLACING/ FILLING	COMMENTS
Clays	<1		Dusty brown clay distributed throughout slide and associated with the serpentine.
[illegible]	<1		Anhedral patches (<0.01 mm) and scattered throughout slide. Associated with serpentine.
Serpentine	92	Olivine, orthopyroxene	Possibly antigorite and chrysotile. No good mesh texture visible but some good bastite and "comb" texture.
Magnetite	2	Olivine, orthopyroxene, spinel	From dusty grains to 0.1-mm anhedral grains. Distributed throughout slide; partly altered from spinel.
Brucite?	5		Found in mm-sized veins and along some cleavages. Associated with serpentine.

VESICLES/ CAVITIES	PERCENT	LOCATION	SIZE (mm)	FILLING	SHAPE
Vesicles	0				

COMMENTS: Bastite texture helps define kinking of orthopyroxene grains, deformation of grains. Pyroxenes appear to be replaced by bladed antigorite crystals as well as fibrous chrysotile. Brucite determination needs further analysis. There are some poor mesh-looking areas that may indicate presence of lizardite(?). No piece number given.

121-778A-[illegible] OBSERVER: JOH WHERE SAMPLED: Conical Seamount, south flank

ROCK NAME: Serpentinized harzburgite

GRAIN SIZE: 0.5-2 mm

TEXTURE: Felted and bastite

PRIMARY MINERALOGY	PERCENT PRESENT	PERCENT ORIGINAL	SIZE (mm)	COMPO-SITION	MORPHOLOGY	COMMENTS
PHENOCRYSTS						
Olivine	[illegible]	[illegible]	Not visible		Not visible	Completely altered to serpentine.
Spinel	[illegible]	[illegible]	[illegible]	[illegible]	Subhedral-anhedral	Red, altered to magnetite, elongate and stretched.
Orthopyroxene	[illegible]	[illegible]	[illegible]		Anhedral	Altered to serpentine bastite texture.
GROUNDMASS						
N/A	N/A	N/A	N/A		N/A	

SECONDARY MINERALOGY	PERCENT	REPLACING / FILLING	COMMENTS
Clays	[illegible]		Dusty brown; may distributed throughout slide; as an alteration of serpentine?
Magnetite	1	Olivine, orthopyroxene, spinel	Dusty, [illegible] mm euhedral grains distributed throughout slide, but appear elongated into clumps which follow serpentine fibers.
Serpentine	[illegible]	Olivine, orthopyroxene	Possibly antigorite and chrysotile; have bladed felted texture, [illegible] bastite; minor "comb" texture.

VESICLES/ CAVITIES	PERCENT	LOCATION	SIZE (mm)	FILLING	SHAPE
Vesicles	[illegible]				

COMMENTS: N.B. Two slides have been made from fragments in this interval. In this slide the spinels are not rimmed by blue-green to yellow pleochroic chlorite. The elongation of the magnetite trains may indicate late-stage serpentinization or possibly tectonism. The slide consists of [illegible] felted blades of serpentine. No piece number given.

121-778A-[illegible] OBSERVER: [illegible] WHERE SAMPLED: Conical Seamount, south flank

ROCK NAME: Serpentinized harzburgite

GRAIN SIZE: 0.5-2 mm

TEXTURE: Felted and bastite

PRIMARY MINERALOGY	PERCENT PRESENT	PERCENT ORIGINAL	SIZE (mm)	COMPO-SITION	MORPHOLOGY	COMMENTS
PHENOCRYSTS						
Olivine	[illegible]	[illegible]	Not visible		Not visible	Completely altered to serpentine and magnetite.
Spinel	[illegible]	[illegible]	[illegible]	[illegible]	Subhedral-anhedral	Red-brown, altered to chlorite and magnetite.
Orthopyroxene	[illegible]	[illegible]	[illegible]		Subhedral-anhedral	Altered to serpentine bastite texture.
GROUNDMASS						
N/A	N/A	N/A	N/A		N/A	

SECONDARY MINERALOGY	PERCENT	REPLACING / FILLING	COMMENTS
Clays	[illegible]		Dusty red-brown, scattered throughout slides as an alteration product of serpentine.
Chlorite	[illegible]		Blue green/yellow pleochroic. Usually found rimming spinel and also in patches throughout slide and along serpentine fibers and blades.
Serpentine	[illegible]	Olivine, orthopyroxene	Possibly antigorite and/or chrysotile; good bastite texture and bladed "comb" textures; some lizardite, but identification difficult.
Magnetite	[illegible]	Olivine, orthopyroxene, spinel	Fine dusty grains to [illegible] mm anhedral grains. Distributed throughout slide.

VESICLES/ CAVITIES	PERCENT	LOCATION	SIZE (mm)	FILLING	SHAPE
[illegible]	[illegible]				

COMMENTS: Spinels are stretched/elongated and strung out in parallel stringers. They are rimmed by chlorite(?). [illegible] bastite [illegible] good "comb" texture in portions of slide. N.B: Two slides have been made from fragments in this interval. One is more orthopyroxene-rich and less serpentinized than the other. No piece number given.

125-778A-8R-01 (Piece 7, 39-40 cm) OBSERVER: JAB WHERE SAMPLED: Conical Seamount, south flank

ROCK NAME: Serpentinized harzburgite

GRAIN SIZE: 0.1-5 mm

TEXTURE: Moderate mesh; sheared

PRIMARY MINERALOGY	PERCENT PRESENT	PERCENT ORIGINAL	SIZE (mm)	COMPO-SITION	MORPHOLOGY	COMMENTS
PHENOCRYSTS						
Olivine	0	75-82	Not visible		Not visible	Completely altered to serpentine.
Clinopyroxene	Trace	1-2	<0.05		Subhedral-anhedral	As exsolution lamellae and some trace patches.
Spinel	2-3	2-3	0.1-0.7	Cr?	Subhedral-anhedral	Red, altered to magnetite and possibly some chlorite.
Orthopyroxene	1-2	15-20	2-5		N/A	Altered to serpentine bastite; exsolution lamellae of clinopyroxene beautifully deformed.
GROUNDMASS						
N/A	N/A	N/A	N/A		N/A	

SECONDARY MINERALOGY	PERCENT	REPLACING/ FILLING	COMMENTS
Clays	5-10		Dusty brown clay distributed throughout the slide.
Chlorite	2-3	Orthopyroxene, serpentine	As anhedral patches mixed in with serpentine.
Sphene	Tr?		Anhedral 0.05 mm grains, high relief, sugary-brown color.
Serpentine	78-87	Olivine, orthopyroxene	Lizardite and/or chrysotile showing mesh-like texture.
Brucite	2		In veins which parallel main fabric; intergrown with serpentine; XRD determination is necessary.
Magnetite	1	Spinel, olivine, orthopyroxene	Dusty to 0.3 mm; distributed along with serpentine.

VESICLES/ CAVITIES	PERCENT	LOCATION	SIZE (mm)	FILLING	SHAPE
Vesicles	0				

COMMENTS: Spinels show anhedral dumbbell shape. They appear somewhat elongate in the direction of the main tectonized fabric. Some spinels show curved fractures in the direction of the fabric. A tectonized fabric runs through slide which is paralleled by brucite and serpentine veins (<0.2 mm wide), elongate trains of spinel + magnetite and elongation of mesh texture. Wavy extinction in bastites.

125-778A-8R-01 (Piece 8, 47-48 cm) OBSERVER: JAB WHERE SAMPLED: Conical Seamount, south flank

ROCK NAME: Serpentinized harzburgite

GRAIN SIZE: 0.1-0.7 mm

TEXTURE: Mesh

PRIMARY MINERALOGY	PERCENT PRESENT	PERCENT ORIGINAL	SIZE (mm)	COMPO-SITION	MORPHOLOGY	COMMENTS
PHENOCRYSTS						
Olivine	0	85	Not visible		Not visible	Completely altered to serpentine mesh.
Spinel	1	1	0.1-0.8	Cr?	Anhedral-elongate	Red-brown, arranged in stringers.
Orthopyroxene	0	14	0.5-0.7		Subhedral-anhedral	Altered to serpentine bastite.
GROUNDMASS						
N/A	N/A	N/A	N/A		N/A	

SECONDARY MINERALOGY	PERCENT	REPLACING/ FILLING	COMMENTS
Clays	5		Dusty brown clay distributed throughout slide but somewhat concentrated in veins and edges of mesh texture.
Chlorite	Trace	Orthopyroxene, serpentine	Dusty to <0.05-mm anhedral patches distributed within serpentine and also present in minor veins(?).
Serpentine	92-93		Lizardite and/or chrysotile forming mesh texture; almost completely replacing the primary mineralogy.
Magnetite	1-2	Spinel, olivine, orthopyroxene	Dusty to 0.1 mm, distributed across the slide.
Brucite	Tr?		Intergrown with serpentine in small (0.1-mm-wide) veins.

VESICLES/ CAVITIES	PERCENT	LOCATION	SIZE (mm)	FILLING	SHAPE
Vesicles	0				

COMMENTS: Bastite shows wavy extinction, clearly deformed; some elongate orthopyroxene is aligned parallel to spinel trains; number of crosscutting veins to this foliation. Spinels are anhedral, elongate, sometimes arranged in short stringers. Small (0.1-mm-wide) veins of serpentine w/wo chlorite, w/wo brucite(?) cutting across slide.

125-778A-[illegible] (81-87 cm) OBSERVER: LAG WHERE SAMPLED: Conical Seamount, south flank; clast

ROCK NAME: Sheared serpentine

GRAIN SIZE: <0.1 mm

TEXTURE: Foliated

PRIMARY MINERALOGY	PERCENT PRESENT	PERCENT ORIGINAL	SIZE (mm)	COMPOSITION	MORPHOLOGY	COMMENTS
PHENOCRYSTS						
Serpentine	95	N/A	N/A		N.R.	Replacing olivine primarily (see clear examples). One grain of orthopyroxene still visible.
[illegible]	N/A	N/A	N/A		N.R.	One grain.
Hydrogrossular	N/A	N/A	[illegible]		N.R.	Euhedral ([illegible] grains). (1st generation).
Hydrogrossular	N/A	N/A	[illegible]		N.R.	Numerous aggregates in the foliation (2nd generation).
GROUNDMASS						
N/A	N/A	N/A	N/A		N.R.	

VESICLES/ CAVITIES/ VEINLETS	PERCENT	LOCATION	SIZE (mm)	FILLING	SHAPE

COMMENTS: Shows well-defined S-C planes, however, there is no true organization perceivable at the scale of this thin-section. Hydrogrossular, clearly follows the foliation, traces of small grains follow folds. No piece number given.

125-778A-[illegible] OBSERVER: TEW WHERE SAMPLED: Conical Seamount, south flank

ROCK NAME: Altered serpentinized harzburgite

GRAIN SIZE: Not given

TEXTURE: Mesh

PRIMARY MINERALOGY	PERCENT PRESENT	PERCENT ORIGINAL	SIZE (mm)	COMPOSITION	MORPHOLOGY	COMMENTS
PHENOCRYSTS						
Olivine	0	85	N.R.		N.R.	Mesh texture in serpentine replacing the olivine.
Clinopyroxene	0	[illegible]	N.R.		N.R.	
Spinel	0	1	N.R.		N.R.	
Orthopyroxene	0	[illegible]	N.R.		N.R.	Bastite texture in serpentine replacing the pyroxene.
GROUNDMASS						
N.R.	N.R.	N.R.	N.R.		N.R.	

SECONDARY MINERALOGY	PERCENT	REPLACING/ FILLING	COMMENT
Clays	10-15		
Serpentine	85-90		Chrysotile and/or lizardite?

VESICLES/ CAVITIES/ VEINLETS	PERCENT	LOCATION	SIZE (mm)	FILLING	SHAPE
Veinlets	[illegible]				

COMMENTS: Texture of pseudomorphs are preserved. No piece number given.

125-778A-4R-02 (11-13 cm) OBSERVER: HIR WHERE SAMPLED: Conical Seamount, south flank

ROCK NAME: Pebbly serpentinous mudstone (debris flow)

GRAIN SIZE: Fine to coarse

TEXTURE: Tectonite

PRIMARY MINERALOGY	PERCENT PRESENT	PERCENT ORIGINAL	SIZE (mm)	COMPO-SITION	MORPHOLOGY	COMMENTS
Spinel	<2	N/A	N/A		N/A	Cr-spinel, dark red.

SECONDARY MINERALOGY	PERCENT	REPLACING/ FILLING	COMMENTS
Clays	20-30		Colorless high birefringence (> 0.03).
Chlorite	Trace		
Serpentine	70-80		
Talc	<2		

VESICLES/ CAVITIES	PERCENT	LOCATION	SIZE (mm)	FILLING	SHAPE
Vesicles	0				

COMMENTS: Slender crystals of micaceous mineral (illite?) are abundant. Ill-sorted. No piece number given.

125-778A-4R-CC (Piece 2, 9-12 cm) OBSERVER: SAR WHERE SAMPLED: Conical Seamount, south flank

ROCK NAME: Metabasalt

GRAIN SIZE: 0.05-0.1 mm

TEXTURE: Intersertal, sparsely phyric

PRIMARY MINERALOGY	PERCENT PRESENT	PERCENT ORIGINAL	SIZE (mm)	COMPO-SITION	MORPHOLOGY	COMMENTS
Glass	0	25-35	N/A		N/A	Completely altered to brown clays.
Plagioclase	0	15-35	0.04-0.1		Subhedral, laths	Completely altered to clays.
Clinopyroxene	20-30	25-35	0.05-0.15		Subhedral, lath-equant	20-60% altered to chlorite and clays, locally recrystallized.
Spinel	<1	<1	0.01-0.1		Euhedral-subhedral	Throughout slide, black, opaque.

SECONDARY MINERALOGY	PERCENT	REPLACING/ FILLING	COMMENTS
Clays	50-60		Brown, throughout rock after glass and pseudomorphs after plagioclase.
Carbonate	<1	Vein	(0.05 to 0.2 mm wide), in-filled by talc.
Chlorite	10	Glass, clinopyroxene	After glass and clinopyroxene, slightly birefringent, throughout.
Pumpellyite	<2	Vein	Pale-green, strong optical dispersion, high refractive index.
Talc	2-4	Veins	Anastamosing veins. Patches, high-birefringent, low-refractive index, throughout rock, no preferred orientation (0.05 to 0.2 mm wide).

VESICLES/ CAVITIES	PERCENT	LOCATION	SIZE (mm)	FILLING	SHAPE
Vesicles	<2	Throughout	0.2-1.7	Chlorite, pumpellyite	Irregular

COMMENTS: Talc veins may be associated with serpentinization of adjoining ultramafic rocks. See filling calcite vein. Veins have no preferred orientation. Large euhedral to subhedral patches may be relict phenocrysts of clinopyroxene(?).

125-778A-9R-CC (Piece 7,28-31 cm) OBSERVER: HIR WHERE SAMPLED: Conical Seamount, south flank

ROCK NAME: Metabasalt

GRAIN SIZE: <0.01-0.1 mm

TEXTURE: Intersertal, aphyric

PRIMARY MINERALOGY	PERCENT PRESENT	PERCENT ORIGINAL	SIZE (mm)	COMPO-SITION	MORPHOLOGY	COMMENTS
Glass	0	40-50	N/A		N/A	
Plagioclase	0	25-35	<0.14		Subhedral	Relict swallowtail, completely altered with clays pseudomorphing.
Clinopyroxene	10-20	15-30	0.04-0.1		Subhedral-anhedral	Patches and radiating splays mostly altered (clays); rarely pseudomorphed associated with limonite.
Spinels	<1	<1	0.01-0.04		Subhedral	Opaque and black to red-brown. Associated with limonite.

SECONDARY MINERALOGY	PERCENT	REPLACING/ FILLING	COMMENTS
Clays	40-60	Glass, plagioclase	Brown, clay occurs throughout slide, poorly defined pseudomorphs after plagioclase. 1-2 %. Green clay occurs as random patches.
Carbonate	<1-1	Cavity	
Zeolites	4	Vein	
Chlorite	<10	Glass, clinopyroxene	As slightly birefringent. Patches throughout slide, poorly defined pseudomorphs after clinopyroxene.
Sphene	2		Dusty.
Pumpellyite	2	Vein	0.02 mm wide.
Limonite	10-20		Along grain boundaries. Veins and patches throughout sample, probably after glass, deep red-brown.

VESICLES/ CAVITIES	PERCENT	LOCATION	SIZE (mm)	FILLING	SHAPE
Vesicles	0				

COMMENTS: Very fine-grained, even textured (smooth) areas intermixed with fine-grained matrix (40/60) may be alteration or brecciation. Contacts are sharp and frequently lined by limonite. Parts appear to be brecciated and exhibit possibly minor recrystallization. Alteration is quite severe and masks most of the original mineralogy and structure.

125-778A-10R-CC (Piece 1,1-3 cm) OBSERVER: SAR WHERE SAMPLED: Conical Seamount, south flank

ROCK NAME: Metabasalt

GRAIN SIZE: 0.04-0.10 mm

TEXTURE: Intersertal; sparsely phyric

PRIMARY MINERALOGY	PERCENT PRESENT	PERCENT ORIGINAL	SIZE (mm)	COMPO-SITION	MORPHOLOGY	COMMENTS
PHENOCRYSTS						
Clinopyroxene	<1	<1	1-2		Euhedral	Single crystal, 10-20% altered.
GROUNDMASS						
Glass	0	15-20	N/A		N/A	Completely altered to clays.
Plagioclase	0	20-40	0.04-0.10		Subhedral, lath	Completely altered to clays, poorly pseudomorphed.
Clinopyroxene	10-20	25-35	0.04-0.10		Subhedral-anhedral	Altered to clays and chlorite.
Spinel, magnetite	<1	<1	0.01-0.04		Subhedral	Rare, opaque throughout rock.

SECONDARY MINERALOGY	PERCENT	REPLACING/ FILLING	COMMENTS
Clays	50-60	Glass	Brown, some pseudomorphs after plagioclase. Also (1-2%) green in vesicles and patches.
Carbonate	2-4	Veins	Calcite, 0.05 mm wide.
Chlorite	5-15	Clinopyroxene, glass?	Light green, slightly pleochroic.
Magnetite	<1	Vesicles/cavity	Minute (<0.01-mm) grains in center of chlorite-filled cavities.

VESICLES/ CAVITIES	PERCENT	LOCATION	SIZE (mm)	FILLING	SHAPE	COMMENTS
Vesicles	<1	Random	0.1-0.25	Chlorite, clay	Round	Scarce.

COMMENTS: Relict swallowtail plagioclase in more crystalline portions of rock. Glassy patches form part of the rock irregularly intermixed with more crystalline patches.

125-778A-11R-01 (Piece 1,4-7 cm) OBSERVER: JOH WHERE SAMPLED: Conical Seamount, south flank

ROCK NAME: Metabasalt

GRAIN SIZE: 1-3 phenocrysts

TEXTURE: Sparsely phyric, glassy (original)

PRIMARY MINERALOGY	PERCENT PRESENT	PERCENT ORIGINAL	SIZE (mm)	COMPO-SITION	MORPHOLOGY	COMMENTS
PHENOCRYSTS						
Plagioclase	<1	1-2	1-3		Lath, subhedral	Single grains, 30-90% altered to clays.
Clinopyroxene	<1	<1	1-2		Euhedral	Twinned and untwinned single grains 10-30% altered to clays with glass (0.1 mm) inclusions now altered.
GROUNDMASS						
Glass	0	50-75	N/A		N/A	Brown and 90-100% altered to clays.
Plagioclase	0	20-25	0.01-0.04		Quench	Swallowtail completely altered.
Clinopyroxene	<1	25-40	0.01-0.06		Subhedral-rounded	50-100% altered to clays.
Olivine	0	<1	0.05-0.1		Euhedral	Pseudomorphed by green clay and/or chlorite.
Spinel	<1	1-2	0.01-0.03		Subhedral	Disseminated through relict glass/matrix.

SECONDARY MINERALOGY	PERCENT	REPLACING/ FILLING	COMMENTS
Clays	85-95	Glass, plagioclase, clinopyroxene	Brown, amorphous throughout rock, 1-2% bright green often as vesicle fill.
Carbonate	1-3	Veins, cavities	Needles and small patches (0.02-0.04 mm) in veins with chlorite.
Chlorite	2-5	Veins, cavities, olivine?	As radiating clusters in cavities and vein walls often intimately associated with calcite.
Quartz	1-2	Veins	Small (0.01-0.04 mm), anhedral low birefringence crystals at veins associated with pumpellyite.
Pumpellyite	>3	Vein	Always coexists with prehnite.
Prehnite	>2	Vein	

VESICLES/ CAVITIES	PERCENT	LOCATION	SIZE (mm)	FILLING	SHAPE	COMMENTS
Vesicles	<1	Random	0.1-1	Chlorite, calcite		Needles of calcite projecting into cavity sometimes intermixed with chlorite.

COMMENTS: This sample is 80-95% altered to clays, some pseudomorphing of original phases (olivine, plagioclase) is present but most of the texture and mineral associations are obscured by clay alteration. Appears to have been originally glassy.

125-778A-11R-01 (Piece 1,119-123 cm) OBSERVER: TER WHERE SAMPLED: Conical Seamount, south flank

ROCK NAME: Pebbly serpentine mudstone

GRAIN SIZE: Fine-coarse

TEXTURE: Tectonite

PRIMARY MINERALOGY	PERCENT PRESENT	PERCENT ORIGINAL	SIZE (mm)	COMPO-SITION	MORPHOLOGY	COMMENTS
N/A	N/A	N/A	N/A		N/A	

SECONDARY MINERALOGY	PERCENT	REPLACING/ FILLING	COMMENTS
Clays	20-30		
Carbonate	1?		
Serpentine	70-80		Chrysotile and/or lizardite; bastite and mesh serpentine pseudomorphs forming clasts.
Magnetite	<1		

VESICLES/ CAVITIES	PERCENT	LOCATION	SIZE (mm)	FILLING	SHAPE
Vesicles	0				

COMMENTS: Sedimentary rock, where original textures of serpentinite are preserved (i.e., bastite). Boudinage and brittle extension of larger grains in matrix. Conjugate fractures cut largest grains, micro-normal faulting also. Piece # not given.

125-778A-11R-CC (7-9 cm) OBSERVER: RIP WHERE SAMPLED: Conical Seamount, south flank

ROCK NAME: Metabasalt

GRAIN SIZE: 0.05-0.3 mm

TEXTURE: Intersertal, microphenocryst-phyric

PRIMARY MINERALOGY	PERCENT PRESENT	PERCENT ORIGINAL	SIZE (mm)	COMPO-SITION	MORPHOLOGY	COMMENTS
Glass	0	20-40	N/A		N/A	Altered to clay.
Plagioclase	0-5	30-40	0.1-0.3		Euhedral; laths	Altered to clays, 70-100%.
Clinopyroxene	0-15	20-30	0.05-0.2		Euhedral, equant	Altered to chlorite and clays 10-60%.
Spinel	<1	<1	0.02-0.05		Euhedral	Sparse, black, opaques.

SECONDARY MINERALOGY	PERCENT	REPLACING FILLING	COMMENTS
Clays	70-80	Glass, plagioclase	Brown, ubiquitous throughout slide obscuring texture and composition of groundmass.
Chlorite	20-40	Clinopyroxene, cavities	Green, with characteristic birefringence and pleochroism.
Limonite	2-10	Glass, veins	Reddish-brown; anastamosing veins throughout slide and along some grain boundaries. Pervasive.
Magnetite	1	Glass, veins	Tiny (0.01 to 0.02 mm), subhedra. Disseminated crystals associated with limonite veins and patches.

VESICLES/ CAVITIES	PERCENT	LOCATION	SIZE (mm)	FILLING	SHAPE
Vesicles	0				

COMMENTS: Despite pervasive clay and limonite, alteration patches of fresh clinopyroxene (0.1-0.15 mm) still remain. No photo # given.

125-778A-20R-CC (43-45 cm) OBSERVER: TAN WHERE SAMPLED: Conical Seamount, south flank; clast

ROCK NAME: Serpentinized harzburgite

GRAIN SIZE: [illegible] mm

TEXTURE: Foliated

PRIMARY MINERALOGY	PERCENT PRESENT	PERCENT ORIGINAL	SIZE (mm)	COMPO-SITION	MORPHOLOGY	COMMENTS
PHENOCRYSTS						
Olivine	0	70-80	Not visible		Not visible	Completely altered to serpentine blades.
Spinel	1	1	0.1-1	Cr?	Subhedral-anhedral	Red, somewhat elongate, altered to magnetite.
Orthopyroxene		20-30	0.5-3		Subhedral-anhedral	Altered to serpentine bastite.
GROUNDMASS						
N/A	N/A	N/A	N/A		N/A	

SECONDARY MINERALOGY	PERCENT	REPLACING FILLING	COMMENTS
Chlorite	<1		As anhedral, fine-grained patches intergrown with serpentine.
Serpentine	80-90	Olivine, orthopyroxene	Mostly antigorite felted blades and chrysotile fibers throughout slide; lizardite may be present in minor amounts.
Magnetite	1-5	Spinel, olivine, orthopyroxene	Dusty, <1 mm, distributed across slide; forms elongate ragged trails which parallel fibers and blades.
Thulite?	1-5	Orthopyroxene	Light pink-dark pink pleochroic, anomalous colors (45 degrees crystal angles, near straight extinction; thulite(?) and/or zoisite(?).

VESICLES/ CAVITIES	PERCENT	LOCATION	SIZE (mm)	FILLING	SHAPE
Vesicles	0				

COMMENTS: Bastite orthopyroxene has kink cleavages and wavy extinction. The serpentine blades and fibers appear to parallel each other throughout slide (45 degrees from long axis of slide); indicates deformation. Appearance of pale pink-dark pink mineral is throughout slide and finely intergrown with serpentine. Identification of this mineral as thulite and/or zoisite is not confirmed. No photo # given.

125-778A-12R-02 (73-75 cm) OBSERVER: SAB WHERE SAMPLED: Conical Seamount, south flank: clast

ROCK NAME: Serpentinized harzburgite

GRAIN SIZE: 0.1-2 mm

TEXTURE: Felted

PRIMARY MINERALOGY	PERCENT PRESENT	PERCENT ORIGINAL	SIZE (mm)	COMPO-SITION	MORPHOLOGY	COMMENTS
PHENOCRYSTS						
Olivine	0	73-78	Not visible		Not visible	Completely altered to serpentine blades.
Spinel	1	2	0.1-0.8		Anhedral-elongate	Appears mainly black and may be all magnetite.
Orthopyroxene	<1	20-25	0.5-2		Subhedral-anhedral	Altered to serpentine bastite & chlorite.
GROUNDMASS						
N/A	N/A	N/A	N/A		N/A	

SECONDARY MINERALOGY	PERCENT	REPLACING/ FILLING	COMMENTS
Chlorite	2-4	Orthopyroxene, serpentine	Fine-grained anhedral patches which are intergrown with the serpentine.
Magnetite	2	Spinel	Dusty, 0.2-mm sized; disseminated throughout slide; trails of fine grains parallel blades and fiber lengths when possible.
Serpentine	93-97	Olivine, orthopyroxene	Mostly antigorite and chrysotile (bladed, felted texture and fibrous bastitic texture).

VESICLES/ CAVITIES	PERCENT	LOCATION	SIZE (mm)	FILLING	SHAPE
Vesicles	0				

COMMENTS: Spinels are elongate and strung out in stringers (as are magnetite grains). Completely altered sample with no primary mineralogy left. Bastite after orthopyroxene shows wavy extinction and bent fiber lengths which indicate deformation. Entire slide consists of bladed felted texture and bastite fiber texture with no apparent orientation of the blades and fiber lengths. No piece # given.

125-778A/13R-01 (Piece 1, 9-12 cm) OBSERVER: RIP WHERE SAMPLED: Conical Seamount, south flank

ROCK NAME: Metabasalt

GRAIN SIZE: <0.01-0.1 mm (matrix)

TEXTURE: Aphyric, microphenocryst phyric

PRIMARY MINERALOGY	PERCENT PRESENT	PERCENT ORIGINAL	SIZE (mm)	COMPO-SITION	MORPHOLOGY	COMMENTS
Matrix/glass	25-50	80-90	N/A		Spherulitic	Radiating clusters of clinopyroxene or devitrified glass.
Plagioclase	2-5	5-10	0.1-0.4		Laths, subhedral	Associated with clinopyroxene altered to clays.
Clinopyroxene	5-10	10-15	0.1-0.3		Subhedral	Dispersed and in association with plagioclase, relatively fresh.
Spinel	<1-1	<1-1	0.05-0.15		Subhedral	Black, disseminated opaques.

SECONDARY MINERALOGY	PERCENT	REPLACING/ FILLING	COMMENTS
Clays	40-60	Glass, plagioclase, vesicles	Brown, amorphous between spherules of recrystallized glass.
Carbonate	1-3	Cavities, veins	As amorphous, high birefringence patches.
Chlorite	1-5	Veins	After glass associated with calcite.
Pumpellyite	<1-2	Veins	

VESICLES/ CAVITIES	PERCENT	LOCATION	SIZE (mm)	FILLING	SHAPE	COMMENTS
Vesicles	<1	Throughout	0.05-0.1	Clays	Round	Green clay.

COMMENTS: Prehnite may be present exhibiting "bow-tie" (or spherulitic) texture after plagioclase.

125-778A-13R-01 (Piece 2,12-14 cm)   OBSERVER: JOM   WHERE SAMPLED: Conical Seamount, south flank

ROCK NAME: Metabasalt

GRAIN SIZE: 0.05-0.15 mm

TEXTURE: Aphyric

PRIMARY MINERALOGY	PERCENT PRESENT	PERCENT ORIGINAL	SIZE (mm)	COMPO-SITION	MORPHOLOGY	COMMENTS
Glass	0	20-40	N/A		N/A	Fully recrystallized, altered to brown clay.
Plagioclase	0	15-20	0.05-0.15		Subhedral	85-100% altered, pseudomorphs.
Clinopyroxene	20-30	30-40	0.05-0.15		Anhedral	20-50% altered to clays. Some intergrowths with plagioclase.
Spinel	<1	2-3	0.01-0.10		Subhedral	Altered (20-70%) to clays.

SECONDARY MINERALOGY	PERCENT	REPLACING/ FILLING	COMMENTS
Clays	60-70	Glass, plagioclase veins	One veins up to 0.4 mm across, may not be clay. After glass and plagioclase - brown amorphous pervasive clay.
Zeolite	~10	Vein	Low refractive index and birefringence.
Chlorite	5-10	Veins	0.1 to 0.5 mm wide, dusty green associated with gray (low birefringence) vein material (clay).
Prehnite/ pumpellyite	<1	Vein	High birefringence, bow-tie structure small (<1-mm wide) vein associated with clay.

VESICLES/ CAVITIES	PERCENT	LOCATION	SIZE (mm)	FILLING	SHAPE
Vesicles	<<1		0.02	Clay, chlorite	Round

COMMENTS: Not all material in veins attributed to clays may be clay - one type of vein, colorless in plane light, gray in crossed nicols may be some other alteration phase.

125-778A-13R-01 (43-47 cm)   OBSERVER: TER   WHERE SAMPLED: Conical Seamount, south flank

ROCK NAME: Serpentine sand

GRAIN SIZE: Sand-sized

TEXTURE: Sedimentary

PRIMARY MINERALOGY	PERCENT PRESENT	PERCENT ORIGINAL	SIZE (mm)	COMPO-SITION	MORPHOLOGY	COMMENTS
N/A	N/A	N/A	N/A		N/A	

SECONDARY MINERALOGY	PERCENT	REPLACING/ FILLING	COMMENTS
Clays	45	Serpentine	
Carbonate	5		
Serpentine	50	Orthopyroxene, olivine	

VESICLES/ CAVITIES	PERCENT	LOCATION	SIZE (mm)	FILLING	SHAPE
Vesicles	0				

COMMENTS: Please observe sedimentologists. No piece # given.

125-778A-13R-02 (7-9 cm) OBSERVER: HIR WHERE SAMPLED: Conical Seamount, south flank

ROCK NAME: Meta-volcaniclastic rock

GRAIN SIZE: 0.3 - 1.0 mm

TEXTURE: Cataclastic texture

PRIMARY MINERALOGY	PERCENT PRESENT	PERCENT ORIGINAL	SIZE (mm)	COMPO-SITION	MORPHOLOGY	COMMENTS
Clinopyroxene	<2	<10	0.5-1		Subhedral	Partly actinolitized.
Hornblende	10	10	0.3-1		Euhedral-subhedral	Mostly actinolitized.

SECONDARY MINERALOGY	PERCENT	REPLACING/ FILLING	COMMENTS
Clays	<5		Brown in color, dusty (illite?).
Chlorite	20		Brownish abnormal interference color. Occurs with actinolite.
Actinolite	70-80		Colorless, mostly acicular.

VESICLES/ CAVITIES	PERCENT	LOCATION	SIZE (mm)	FILLING	SHAPE
Vesicles	0				

COMMENTS: Metamorphosed under greenschist facies condition. Fragmentation occurred during or before the metamorphism. Fine-grained acicular crystals of actinolite occur as a secondary mineral throughout the rock. The protolith is mafic volcaniclastic rock containing fragments of hornblende and clinopyroxene crystal in clay matrix. No piece # given.

125-778A-13R-CC (Piece 1,4-6 cm) OBSERVER: JOH WHERE SAMPLED: Conical Seamount, south flank

ROCK NAME: Metabasalt

GRAIN SIZE: 0.01-0.5 mm, fine-grained

TEXTURE: Aphyric

PRIMARY MINERALOGY	PERCENT PRESENT	PERCENT ORIGINAL	SIZE (mm)	COMPO-SITION	MORPHOLOGY	COMMENTS
Glass	0	45-46	N/A		N/A	Altered to amorphous clays.
Plagioclase	2-5	5-15	0.01-0.1		Laths, quench	80-100% altered by clays. Sometimes in clusters with clinopyroxene.
Clinopyroxene	15-20	20-30	0.05-0.1		Subhedral	10-40% altered.
Spinel	<1	<1	0.01-0.04		Subhedral	Sparse, randomly distributed.

SECONDARY MINERALOGY	PERCENT	REPLACING/ FILLING	COMMENTS
Clays	75-85	Glass, plagioclase	Brown, amorphous sometimes as veins (0.1 to 0.3 mm) and pseudomorphing plagioclase.
Prehnite/ pumpellyite	1-4	Veins	0.1 to 0.4 mm wide, aggregates of low birefringence. Crystals intimately intermixed throughout slide.

VESICLES/ CAVITIES	PERCENT	LOCATION	SIZE (mm)	FILLING	SHAPE
Vesicles	0				

125-778A-13R-CC (Piece 1,6-7 cm) OBSERVER: HIR WHERE SAMPLED: Conical Seamount, south flank

ROCK NAME: Meta-volcaniclastic rock

GRAIN SIZE:

TEXTURE:

PRIMARY MINERALOGY	PERCENT PRESENT	PERCENT ORIGINAL	SIZE (mm)	COMPO-SITION	MORPHOLOGY	COMMENTS
PHENOCRYSTS						
Clinopyroxene	5	>5	0.1-0.2		Anhedral	
GROUNDMASS						
N/A	N/A	N/A	N/A		N/A	

SECONDARY MINERALOGY	PERCENT	REPLACING/FILLING	COMMENTS
Clays	>70		Brown (illite?)
Chlorite	20		
Actinolite	<2		Colorless. Occurs as aggregate of acicular crystals.

VESICLES/CAVITIES	PERCENT	LOCATION	SIZE (mm)	FILLING	SHAPE
Vesicles	0				

COMMENTS: Detrital clinopyroxene grains are visible in highly deformed chaotic matrix. Colorless acicular actinolite occurs along the rim or cleavage trace of relic clinopyroxene.

125-778A-13R-CC (Piece 4,4-10 cm) OBSERVER: HIR WHERE SAMPLED: Conical Seamount, south flank

ROCK NAME: Amphibolite sandstone

GRAIN SIZE: (0.06 - 10.0 mm)

TEXTURE: Matrix-supported sandstone

PRIMARY MINERALOGY	PERCENT PRESENT	PERCENT ORIGINAL	SIZE (mm)	COMPO-SITION	MORPHOLOGY	COMMENTS
Chlorite	45	N/A	N/A		N/A	Very fine-grained grains make up matrix. The clasts are supported by this matrix.
Clays	30	N/A	N/A		N/A	
Serpentine	1	N/A	N/A		N/A	

SECONDARY MINERALOGY	PERCENT	REPLACING/FILLING	COMMENTS
Chlorite	2	Hornblende	Euhedral-anhedral. Replacing hornblende grains throughout slide.
Sphene	Trace	Detrital	Subhedral-euhedral (0.01 to 0.1 mm), clasts.
Hornblende	10	Detrital	0.2-2 mm, subhedral-anhedral. Pale-green to white pleochroism, partly altered to chlorite.
Blue amphibole	Trace	Hornblende, clasts	Greenish-blue to blue in color. Partly replacing a hornblende clast.
Opaques	1		Dusty 0.2-mm grains scattered throughout slide.

VESICLES/CAVITIES	PERCENT	LOCATION	SIZE (mm)	FILLING	SHAPE
Vesicles	0				

COMMENTS: This is sedimentary rock consisting of various-shaped clasts (subrounded-angular) scattered in a matrix of chlorite and clays. Most of clasts are pale-green hornblende. Clasts vary from single crystal fragments to aggregates of multiple crystals (up to 1 cm long). Further analysis on slide is needed. Two thin sections made from this piece.

125-778A-13R-CC (Piece 4,8-10 cm) OBSERVER: HIR WHERE SAMPLED: Conical Seamount, south flank

ROCK NAME: Amphibolite sandstone

GRAIN SIZE: 0.01 mm - 1cm

TEXTURE: Matrix-supported sandstone

PRIMARY MINERALOGY	PERCENT PRESENT	PERCENT ORIGINAL	SIZE (mm)	COMPO- SITION	MORPHOLOGY	COMMENTS
Chlorite	45	N/A	N/A		N/A	Very fine-grained grains make up matrix. The clasts are supported by this matrix.
Clays	30	N/A	N/A		N/A	
Serpentine	1	N/A	N/A		N/A	

SECONDARY MINERALOGY	PERCENT	REPLACING/ FILLING	COMMENTS
Chlorite	2	Hornblende	Euhedral-anhedral; replacing hornblende grains throughout slide.
Sphene	Trace	Detrital	Subhedral-euhedral clasts, (0.01 to 0.1 mm).
Hornblende	10	Detrital	0.2-2 mm; subhedral-anhedral, pale-green to white pleochroic; partly altered to chlorite.
Blue amphibole	Trace	Hornblende, clasts	Greenish-blue to blue in color; partly replacing a hornblende clast.
Opaques	1		Dusty, 0.2-mm grains and scattered throughout slide.

VESICLES/ CAVITIES	PERCENT	LOCATION	SIZE (mm)	FILLING	SHAPE
Vesicles	0				

COMMENTS: This is a sedimentary rock! Various shaped clasts (subrounded-angular) scattered in a matrix of chlorite and clays. Most of clasts consist of pale green hornblende. Further analysis needed on this section in order to fully describe all clasts. Clasts vary from single crystals to aggregates of multiple crystals (up to 1 cm long). Two thin sections made from this piece.

125-778A-13R-CC (8-10 cm) OBSERVER: TEB WHERE SAMPLED: Conical Seamount, south flank

ROCK NAME: Meta-volcaniclastic rock

GRAIN SIZE: Angular fragment (50 mm)

TEXTURE: Melange (pure shear, parallel extinction)

PRIMARY MINERALOGY	PERCENT PRESENT	PERCENT ORIGINAL	SIZE (mm)	COMPO- SITION	MORPHOLOGY	COMMENTS
N/A	N/A	N/A	N/A		N/A	

VESICLES/ CAVITIES	PERCENT	LOCATION	SIZE (mm)	FILLING	SHAPE
Vesicles	0				

COMMENTS: Matrix is highly foliate; foliation defined by elongation and cleavage of sheet silicates (serpentine? now clays) and long axes of elongate clasts. Considerable layer-II extension in foliation direction. Ductile "pinch and swell" in some clasts (esp. serpentine-rich). More brittle fragmentation in hornblende. Pressure shadows bracketing some hornblende. Shadows appear to be largely serpentine + clays. No piece # given.

SITE 779 HOLE A CORE 1R CORED INTERVAL 3947.2-3948.3 mbsl; 0.0-1.1 mbsf

TIME-ROCK UNIT	FORAMINIFERS	NANNOFOSSILS	RADIOLARIANS	DIATOMS	PALEOMAGNETICS	PHYS. PROPERTIES	CHEMISTRY	SECTION	METERS	GRAPHIC LITHOLOGY	DRILLING DISTURB.	SED. STRUCTURES	SAMPLES	LITHOLOGIC DESCRIPTION
MIDDLE PLEISTOCENE	N22	CN14a						1 CC	0.5					[illegible]

[illegible]

[illegible]

SMEAR SLIDE SUMMARY (%):

TEXTURE:

Sand [illegible]
Silt [illegible]
Clay [illegible]

COMPOSITION:

Amphibole [illegible]
Aragonite [illegible]
Chlorite [illegible]
Clay [illegible]
Diatoms [illegible]
Foraminifers [illegible]
Nannofossils [illegible]
Opaques [illegible]
Radiolarians [illegible]
Rock fragments [illegible]
Serpentine [illegible]
Spicules [illegible]
Zeolite [illegible]

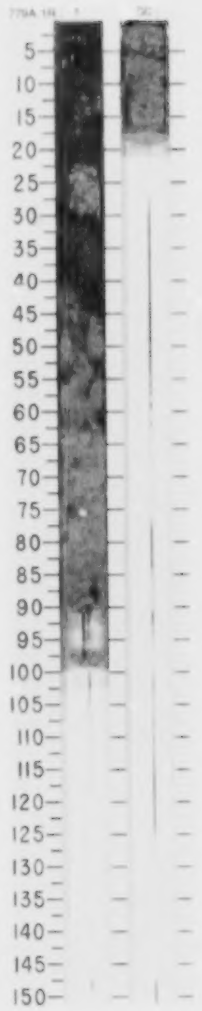
779A-1R
1
CC
5
10
15
20
25
30
35
40
45
50
55
60
65
70
75
80
85
90
95
100
105
110
115
120
125
130
135
140
145
150

SITE 779 HOLE A CORE 2R CORED INTERVAL 3948.5-3957.8 mbsl; 1.1-10.6 mbsf

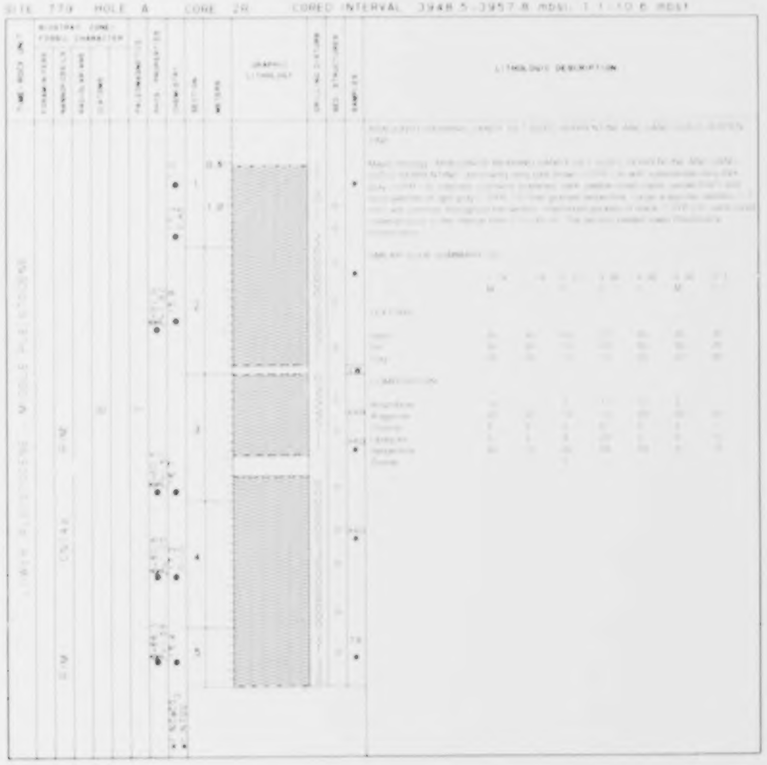
TIME-ROCK UNIT
BIOSTRAT. ZONE/ FOSSIL CHARACTER
FORAMINIFERS
NANNOFOSSILS
RADIOLARIANS
DIATOMS
PALEOMAGNETICS
PHYS. PROPERTIES
CHEMISTRY
SECTION
METERS
GRAPHIC LITHOLOGY
DRILLING DISTURB.
SED. STRUCTURES
SAMPLES
LOWER PLEISTOCENE - MIDDLE PLEISTOCENE
CN14a
0.5
1.0
1
2
3
4
5

LITHOLOGIC DESCRIPTION

[illegible]

SMEAR SLIDE SUMMARY (%):

TEXTURE:

Sand
Silt
Clay

COMPOSITION:

[illegible]

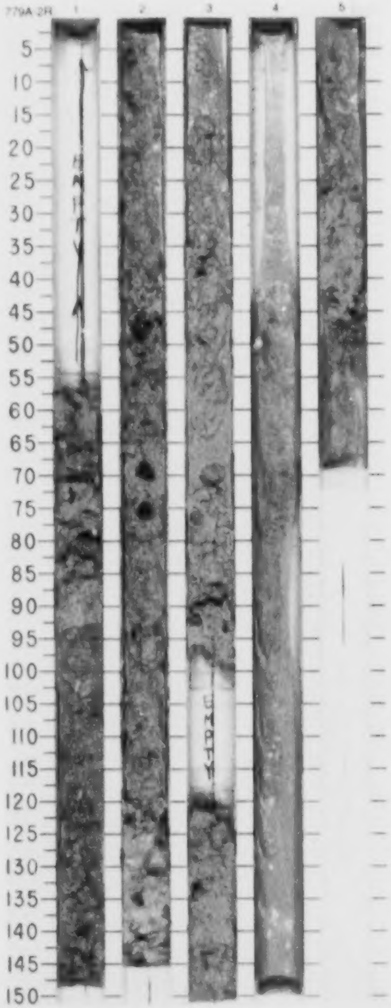
779A-2R
1
2
3
4
5
5
10
15
20
25
30
35
40
45
50
55
60
65
70
75
80
85
90
95
100
105
110
115
120
125
130
135
140
145
150
EMPTY
EMPTY

SITE 779 HOLE A CORE 3R CORED INTERVAL 3957.8-3967.3 mbsl; 10.6-20.1 mbsf

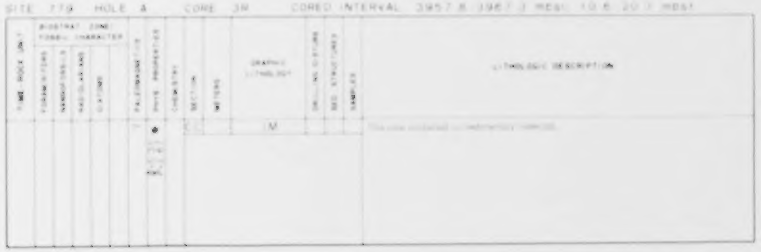
TIME-ROCK UNIT
BIOSTRAT. ZONE/FOSSIL CHARACTER
FORAMINIFERS
NANNOFOSSILS
RADIOLARIANS
DIATOMS
PALEOMAGNETICS
PHYS. PROPERTIES
CHEMISTRY
SECTION
METERS
GRAPHIC LITHOLOGY
DRILLING DISTURB.
SED. STRUCTURES
SAMPLES
CC
M

LITHOLOGIC DESCRIPTION

This core contained no sedimentary material.

SITE 779 HOLE A CORE 4R CORED INTERVAL 3967.3-3976.8 mbsl; 20.1-29.6 mbsf

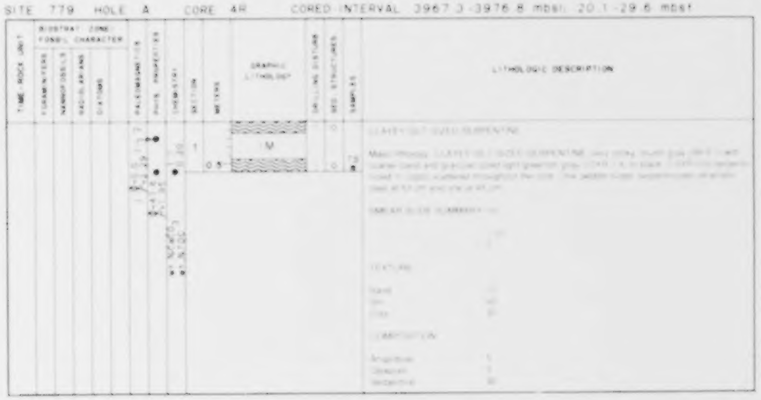
TIME-ROCK UNIT
BIOSTRAT. ZONE/FOSSIL CHARACTER
FORAMINIFERS
NANNOFOSSILS
RADIOLARIANS
DIATOMS
PALEOMAGNETICS
PHYS. PROPERTIES
CHEMISTRY
SECTION
METERS
GRAPHIC LITHOLOGY
DRILLING DISTURB.
SED. STRUCTURES
SAMPLES
1
0.5
M
73

LITHOLOGIC DESCRIPTION

CLAYEY SILT-SIZED SERPENTINE

Major lithology: CLAYEY SILT-SIZED SERPENTINE, [illegible]

SMEAR SLIDE SUMMARY (%):

TEXTURE:

Sand	[illegible]
Silt	[illegible]
Clay	[illegible]

COMPOSITION:

[illegible]	[illegible]
[illegible]	[illegible]
Serpentine	[illegible]

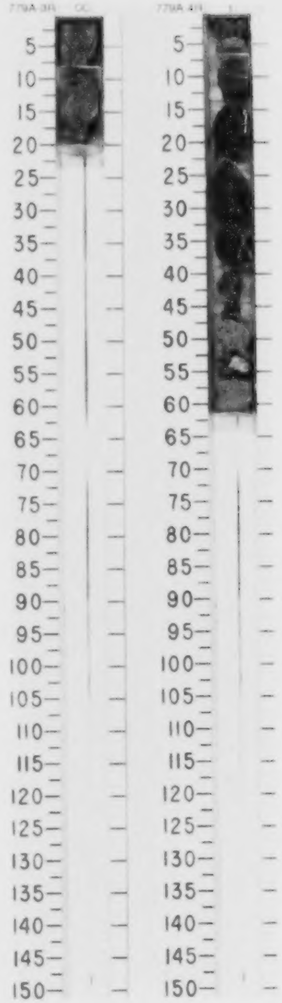
779A-3R, CC
779A-4R, 1
5
10
15
20
25
30
35
40
45
50
55
60
65
70
75
80
85
90
95
100
105
110
115
120
125
130
135
140
145
150

SITE 779 HOLE A CORE 5R CORED INTERVAL 3976.8-3986.3 mbsl; 29.6-39.1 mbsf

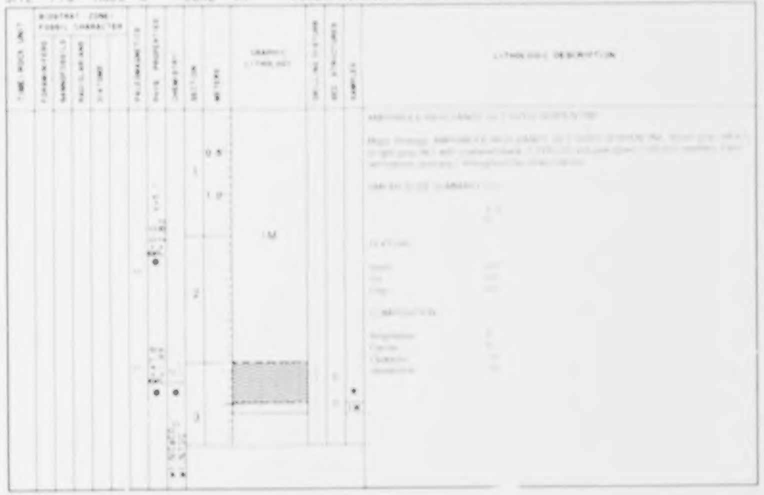
TIME-ROCK UNIT
BIOSTRAT. ZONE/ FOSSIL CHARACTER
FORAMINIFERS
NANNOFOSSILS
RADIOLARIANS
DIATOMS
PALEOMAGNETICS
PHYS. PROPERTIES
CHEMISTRY
SECTION
METERS
GRAPHIC LITHOLOGY
DRILLING DISTURB.
SED. STRUCTURES
SAMPLES
LITHOLOGIC DESCRIPTION
0.5
1
1.0
2
3
1M
TEXTURE:
Sand
Silt
Clay
COMPOSITION:

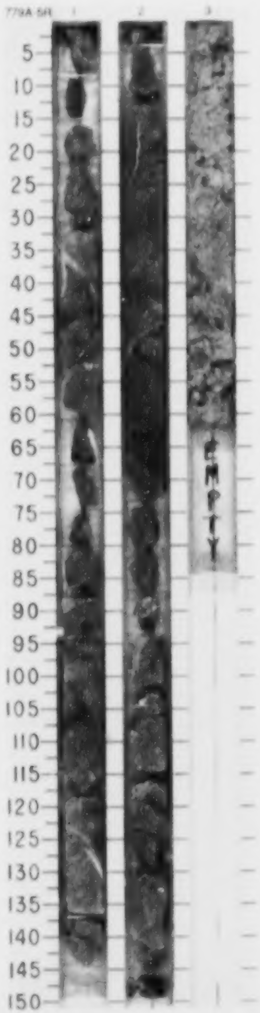
779A-5R
1
2
3
5
10
15
20
25
30
35
40
45
50
55
60
65
70
75
80
85
90
95
100
105
110
115
120
125
130
135
140
145
150
EMPTY

SITE 779 HOLE A CORE 6R CORED INTERVAL 3986.3-3995.7 mbsl; 39.1-48.5 mbsf

TIME-ROCK UNIT	BIOSTRAT. ZONE/FOSSIL CHARACTER: FORAMINIFERS	NANNOFOSSILS	RADIOLARIANS	DIATOMS	PALEOMAGNETICS	PHYS. PROPERTIES	CHEMISTRY	SECTION	METERS	GRAPHIC LITHOLOGY	DRILLING DISTURB.	SED. STRUCTURES	SAMPLES	LITHOLOGIC DESCRIPTION
						● ●		1		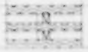			● ●	ZOISITE-BEARING SILT-SIZED SERPENTINE AND [illegible] SERPENTINE Major lithology: ZOISITE-BEARING SILT-SIZED SERPENTINE and [illegible] SERPENTINE [illegible] SMEAR SLIDE SUMMARY (%): TEXTURE: Sand, Silt, Clay COMPOSITION: Chlorite, Epidote, Olivine, Opaques, Serpentine, Talc, Zoisite, [illegible], [illegible]

779A-6R

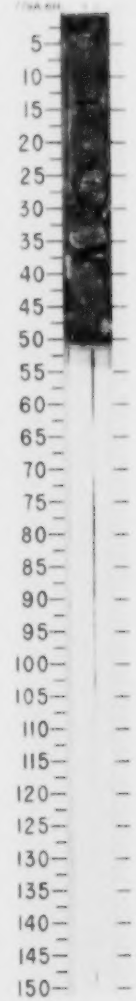
5
10
15
20
25
30
35
40
45
50
55
60
65
70
75
80
85
90
95
100
105
110
115
120
125
130
135
140
145
150

SITE 779 HOLE A CORE 7R CORED INTERVAL 3995.7-4005.7 mbsl; 48.5-58.5 mbsf

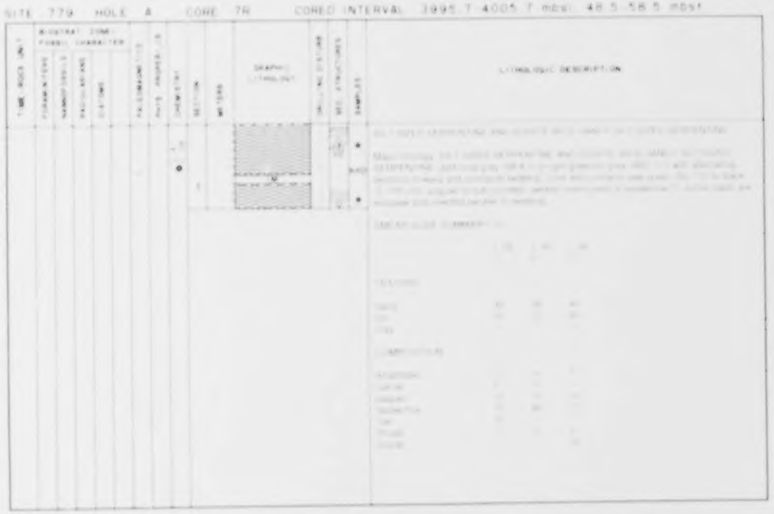
TIME-ROCK UNIT
BIOSTRAT. ZONE/ FOSSIL CHARACTER
FORAMINIFERS
NANNOFOSSILS
RADIOLARIANS
DIATOMS
PALEOMAGNETICS
PHYS. PROPERTIES
CHEMISTRY
SECTION
METERS
GRAPHIC LITHOLOGY
DRILLING DISTURB.
SED. STRUCTURES
SAMPLES
LITHOLOGIC DESCRIPTION
Major lithology:
SMEAR SLIDE SUMMARY (%):
TEXTURE:
COMPOSITION:

SITE 779 HOLE A CORE 8R CORED INTERVAL 4005.7-4015.3 mbsl; 58.5-68.1 mbsf

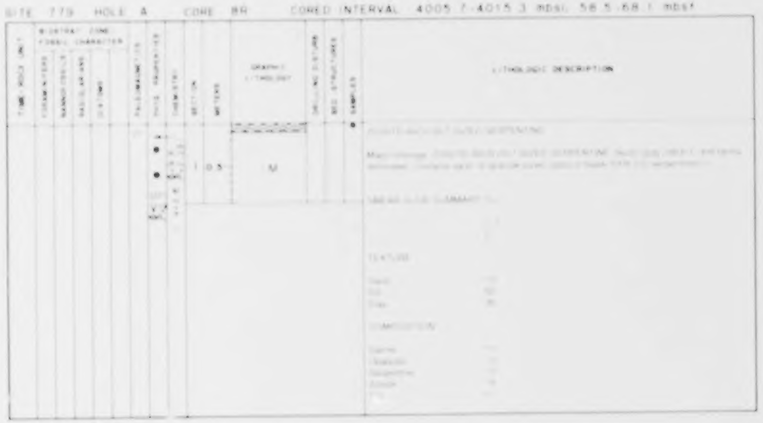
TIME-ROCK UNIT
BIOSTRAT. ZONE/ FOSSIL CHARACTER
FORAMINIFERS
NANNOFOSSILS
RADIOLARIANS
DIATOMS
PALEOMAGNETICS
PHYS. PROPERTIES
CHEMISTRY
SECTION
METERS
GRAPHIC LITHOLOGY
DRILLING DISTURB.
SED. STRUCTURES
SAMPLES
LITHOLOGIC DESCRIPTION
1
0.5
Major lithology:
SMEAR SLIDE SUMMARY (%):
TEXTURE:
COMPOSITION:

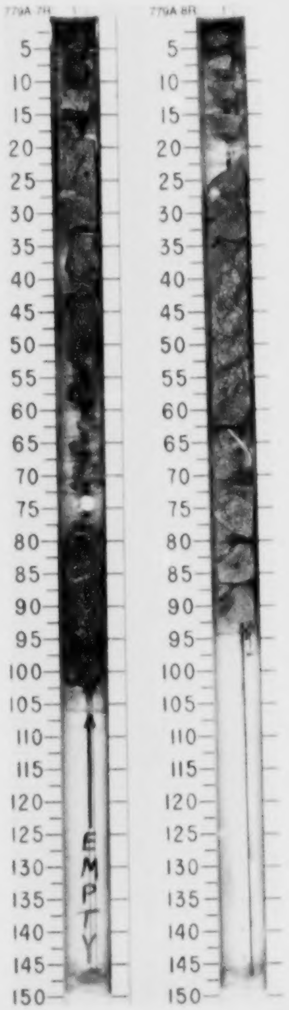
779A 7R
1
779A 8R
1
5
10
15
20
25
30
35
40
45
50
55
60
65
70
75
80
85
90
95
100
105
110
115
120
125
130
135
140
145
150
EMPTY

SITE 779 HOLE A CORE 9R CORED INTERVAL 4015.3-4024.9 mbsl; 68.1-77.7 mbsf

TIME-ROCK UNIT	FORAMINIFERS	NANNOFOSSILS	RADIOLARIANS	DIATOMS	PALEOMAGNETICS	PHYS. PROPERTIES	CHEMISTRY	SECTION	METERS	GRAPHIC LITHOLOGY	DRILLING DISTURB.	SED. STRUCTURES	SAMPLES	LITHOLOGIC DESCRIPTION
						●	●	1	0.5 1.0	M			●	
						●		2		M				

CLAYEY SILT-SIZED SERPENTINE

Major lithology: CLAYEY SILT-SIZED SERPENTINE, gray green (5G 7/1), semi-consolidated, with clasts of altered serpentine(?) and an interval of strongly disturbed bedding at 50 to 60 cm.

SMEAR SLIDE SUMMARY (%):

	[illegible]	[illegible]	[illegible]	[illegible]
TEXTURE:				
Sand	[illegible]	[illegible]	[illegible]	[illegible]
Silt	[illegible]	[illegible]	[illegible]	[illegible]
Clay	[illegible]	[illegible]	[illegible]	[illegible]
COMPOSITION:				
[illegible]	[illegible]	[illegible]	[illegible]	[illegible]
[illegible]		[illegible]		
Chlorite	[illegible]	[illegible]		
Garnet	[illegible]	[illegible]		
Opaques	[illegible]	[illegible]	[illegible]	[illegible]
Serpentine	[illegible]	[illegible]	[illegible]	[illegible]
Talc		[illegible]	[illegible]	[illegible]
[illegible]	[illegible]			

SITE 779 HOLE A CORE 10R CORED INTERVAL 4024.9-4034.5 mbsl; 77.7-87.3 mbsf

TIME-ROCK UNIT	FORAMINIFERS	NANNOFOSSILS	RADIOLARIANS	DIATOMS	PALEOMAGNETICS	PHYS. PROPERTIES	CHEMISTRY	SECTION	METERS	GRAPHIC LITHOLOGY	DRILLING DISTURB.	SED. STRUCTURES	SAMPLES	LITHOLOGIC DESCRIPTION
								1	0.5 1.0	M M				
						●		2		M				

CLAYEY SILT-SIZED SERPENTINE

Major lithology: CLAYEY SILT-SIZED SERPENTINE, dark blue gray (5B 4/1) with pale green (5G 6/2) pebble-sized clasts of sheared serpentine and sand-sized clasts of serpentine(?).

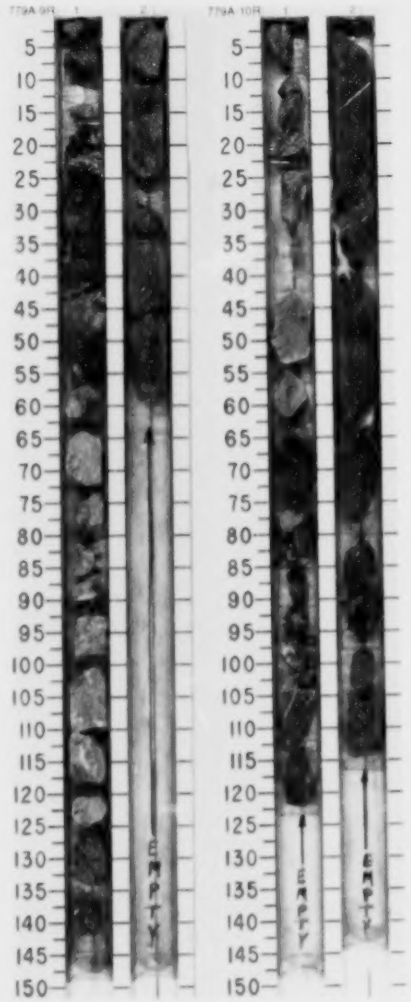
779A 9R
1
2
779A 10R
1
2
5
10
15
20
25
30
35
40
45
50
55
60
65
70
75
80
85
90
95
100
105
110
115
120
125
130
135
140
145
150
EMPTY
EMPTY
EMPTY

SITE 779 HOLE A CORE 11R CORED INTERVAL 4034.5-4044.1 mbsl; 87.3-96.9 mbsf

TIME-ROCK UNIT	BIOSTRAT. ZONE/ FOSSIL CHARACTER: FORAMINIFERS	NANNOFOSSILS	RADIOLARIANS	DIATOMS		PALEOMAGNETICS	PHYS. PROPERTIES	CHEMISTRY	SECTION	METERS	GRAPHIC LITHOLOGY	DRILLING DISTURB.	SED. STRUCTURES	SAMPLES	LITHOLOGIC DESCRIPTION
									1	0.5	M M			●	CLAYEY SILT-SIZED SERPENTINE Major lithology: CLAYEY SILT-SIZED SERPENTINE, [illegible] SMEAR SLIDE SUMMARY (%): TEXTURE: Sand [illegible] Silt [illegible] Clay [illegible] COMPOSITION: Chlorite [illegible] Serpentine [illegible] [illegible] [illegible]

SITE 779 HOLE A CORE 12R CORED INTERVAL 4044.1-4053.8 mbsl; 96.9-106.6 mbsf

TIME-ROCK UNIT	BIOSTRAT. ZONE/ FOSSIL CHARACTER: FORAMINIFERS	NANNOFOSSILS	RADIOLARIANS	DIATOMS		PALEOMAGNETICS	PHYS. PROPERTIES	CHEMISTRY	SECTION	METERS	GRAPHIC LITHOLOGY	DRILLING DISTURB.	SED. STRUCTURES	SAMPLES	LITHOLOGIC DESCRIPTION
									1	0.5	M				[illegible]

779A 11R 1

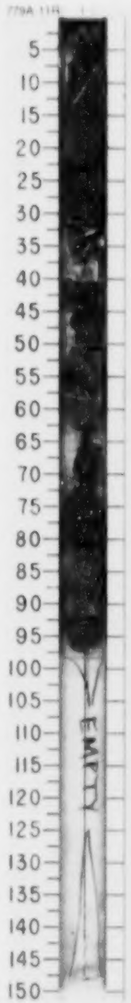
5
10
15
20
25
30
35
40
45
50
55
60
65
70
75
80
85
90
95
100
105
110
115
120
125
130
135
140
145
150
EMPTY

779A 12R 1

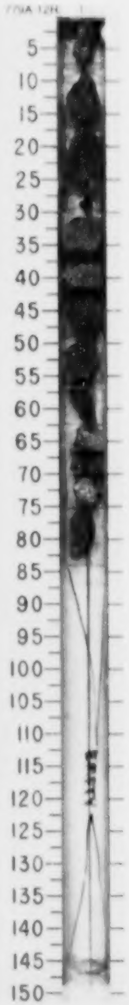
5
10
15
20
25
30
35
40
45
50
55
60
65
70
75
80
85
90
95
100
105
110
115
120
125
130
135
140
145
150
EMPTY

SITE 779 HOLE A CORE 13R CORED INTERVAL 4053.8-4063.4 mbsl; 106.6-116.2 mbsf

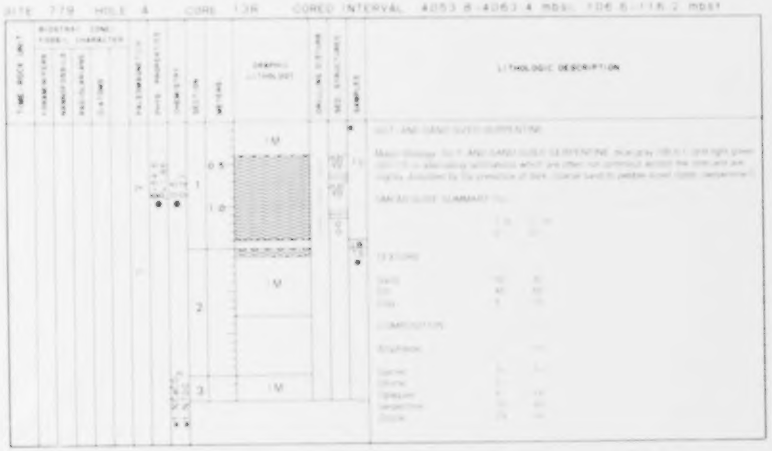
TIME-ROCK UNIT
BIOSTRAT. ZONE/ FOSSIL CHARACTER
FORAMINIFERS
NANNOFOSSILS
RADIOLARIANS
DIATOMS
PALEOMAGNETICS
PHYS. PROPERTIES
CHEMISTRY
SECTION
METERS
GRAPHIC LITHOLOGY
DRILLING DISTURB.
SED. STRUCTURES
SAMPLES
LITHOLOGIC DESCRIPTION
0.5
1.0
1
2
3
M

SILT- AND SAND-SIZED SERPENTINE

Major lithology: SILT- AND SAND-SIZED SERPENTINE, blue-gray (5B 6/1) and light green (5G 7/2) in alternating laminations which are often not continuous across the core and are slightly disturbed by the presence of dark, coarse sand to pebble sized clasts (serpentinite?).

SMEAR SLIDE SUMMARY (%):

	[illegible]	[illegible]
TEXTURE:		
Sand	[illegible]	[illegible]
Silt	[illegible]	[illegible]
Clay	[illegible]	[illegible]
COMPOSITION:		
Accessory	[illegible]	[illegible]
Garnet	[illegible]	[illegible]
Olivine	[illegible]	
Opaques	[illegible]	[illegible]
Serpentine	[illegible]	[illegible]
Zoisite	[illegible]	[illegible]

SITE 779 HOLE A CORE 14R CORED INTERVAL 4063.4-4073.1 mbsl; 116.2-125.9 mbsf

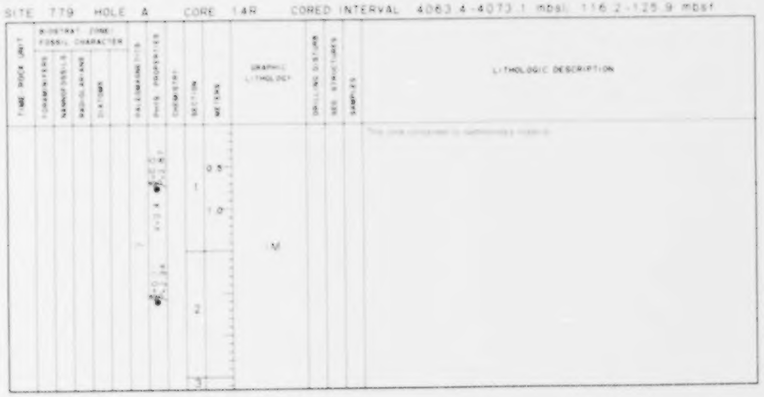
TIME-ROCK UNIT
BIOSTRAT. ZONE/ FOSSIL CHARACTER
FORAMINIFERS
NANNOFOSSILS
RADIOLARIANS
DIATOMS
PALEOMAGNETICS
PHYS. PROPERTIES
CHEMISTRY
SECTION
METERS
GRAPHIC LITHOLOGY
DRILLING DISTURB.
SED. STRUCTURES
SAMPLES
LITHOLOGIC DESCRIPTION
0.5
1.0
1
2
3
M

This core consisted of serpentinized material.

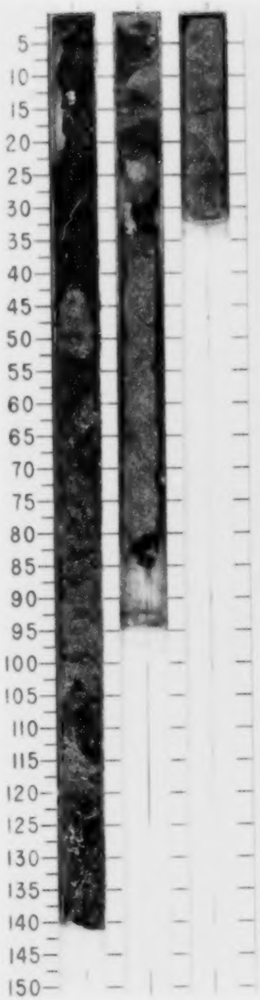
1
2
3
5
10
15
20
25
30
35
40
45
50
55
60
65
70
75
80
85
90
95
100
105
110
115
120
125
130
135
140
145
150

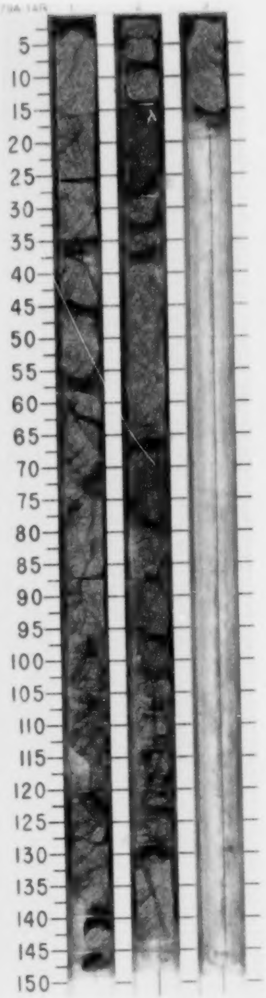
779A-14R
1
2
3
5
10
15
20
25
30
35
40
45
50
55
60
65
70
75
80
85
90
95
100
105
110
115
120
125
130
135
140
145
150

SITE 779 HOLE A CORE 15R CORED INTERVAL 4073.1-4082.7 mbsl; 125.9-135.5 mbsf

TIME-ROCK UNIT	BIOSTRAT. ZONE/FOSSIL CHARACTER: FORAMINIFERS	NANNOFOSSILS	RADIOLARIANS	DIATOMS	PALEOMAGNETICS	PHYS. PROPERTIES	CHEMISTRY	SECTION	METERS	GRAPHIC LITHOLOGY	DRILLING DISTURB.	SED. STRUCTURES	SAMPLES	LITHOLOGIC DESCRIPTION
								1	0.5 1.0	M				[illegible]
								2						

SITE 779 HOLE A CORE 16R CORED INTERVAL 4082.7-4092.4 mbsl; 135.5-145.2 mbsf

TIME-ROCK UNIT	BIOSTRAT. ZONE/FOSSIL CHARACTER: FORAMINIFERS	NANNOFOSSILS	RADIOLARIANS	DIATOMS	PALEOMAGNETICS	PHYS. PROPERTIES	CHEMISTRY	SECTION	METERS	GRAPHIC LITHOLOGY	DRILLING DISTURB.	SED. STRUCTURES	SAMPLES	LITHOLOGIC DESCRIPTION
								1	0.5 1.0	M				[illegible]
								2						
						●		3						

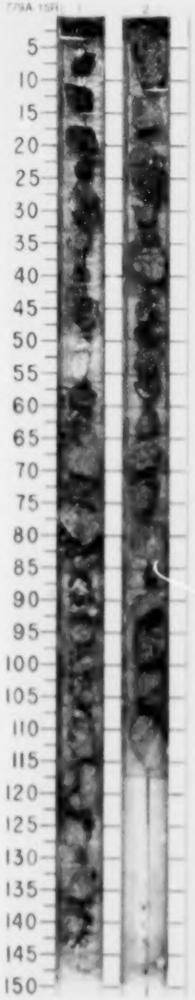
779A-15R
1
2
5
10
15
20
25
30
35
40
45
50
55
60
65
70
75
80
85
90
95
100
105
110
115
120
125
130
135
140
145
150

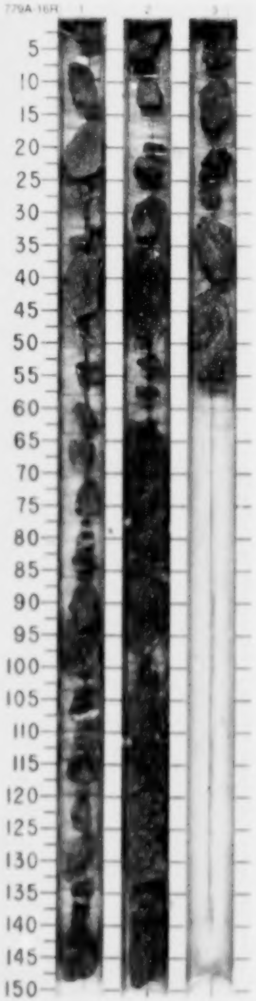
779A-16R
1
2
3
5
10
15
20
25
30
35
40
45
50
55
60
65
70
75
80
85
90
95
100
105
110
115
120
125
130
135
140
145
150

SITE 779 HOLE A CORE 17R CORED INTERVAL 4092.4-4102.1 mbsl; 145.2-154.9 mbsf

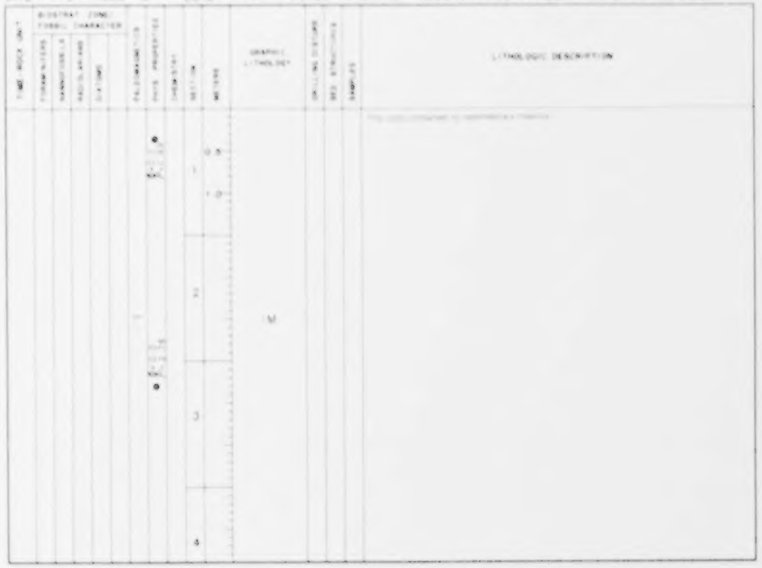
TIME-ROCK UNIT
BIOSTRAT. ZONE/ FOSSIL CHARACTER
FORAMINIFERS
NANNOFOSSILS
RADIOLARIANS
DIATOMS
PALEOMAGNETICS
PHYS. PROPERTIES
CHEMISTRY
SECTION
METERS
GRAPHIC LITHOLOGY
DRILLING DISTURB.
SED. STRUCTURES
SAMPLES
LITHOLOGIC DESCRIPTION
0.5
1.0
1
2
3
4
M

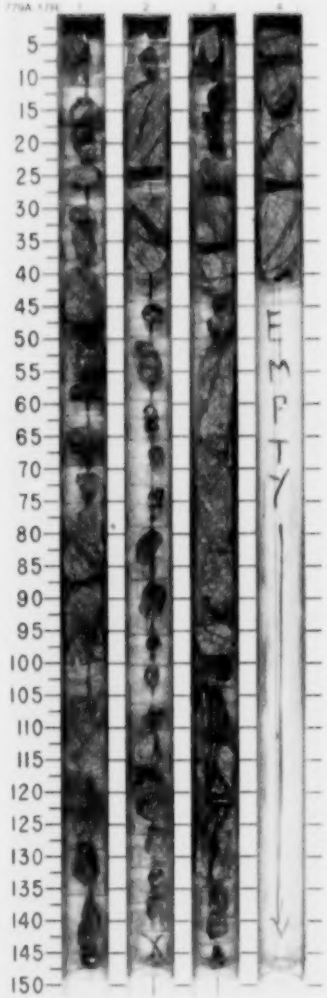
779A-17R
1
2
3
4
5
10
15
20
25
30
35
40
45
50
55
60
65
70
75
80
85
90
95
100
105
110
115
120
125
130
135
140
145
150
EMPTY

SITE 779 HOLE A CORE 18R CORED INTERVAL 4102.1-4106.3 mbsl; 154.9-159.1 mbsf

TIME-ROCK UNIT	BIOSTRAT. ZONE/ FOSSIL CHARACTER: FORAMINIFERS	NANNOFOSSILS	RADIOLARIANS	DIATOMS	PALEOMAGNETICS	PHYS. PROPERTIES	CHEMISTRY	SECTION	METERS	GRAPHIC LITHOLOGY	DRILLING DISTURB.	SED. STRUCTURES	SAMPLES	LITHOLOGIC DESCRIPTION
						●	●	1	0.5 1.0	IM			●	PHACOIDAL SHEARED SERPENTINE Major lithology: PHACOIDAL SHEARED SERPENTINE, dark green [illegible]
						●	●	2					● ●	SMEAR SLIDE SUMMARY (%): TEXTURE: Sand Silt Clay
						●	●	3		IM			●	COMPOSITION: Amphibole Opaques Serpentine Talc [illegible]

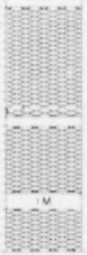

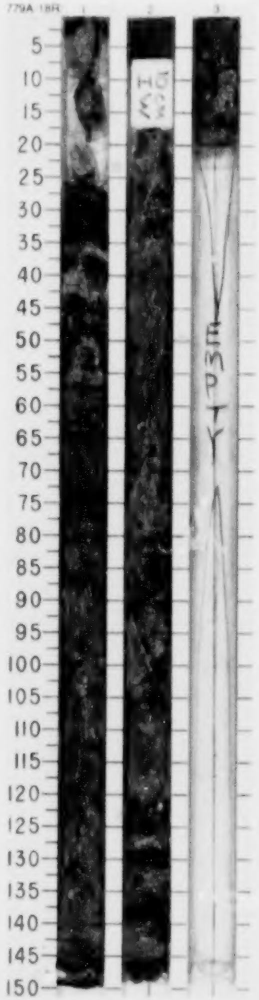
779A-18R
1
2
3
10cm
IW
EMPTY
5
10
15
20
25
30
35
40
45
50
55
60
65
70
75
80
85
90
95
100
105
110
115
120
125
130
135
140
145
150

SITE 779 HOLE A CORE 19R CORED INTERVAL 4106.3-4116.3 mbsl; 159.1-169.1 mbsf

TIME-ROCK UNIT	FORAMINIFERS	NANNOFOSSILS	RADIOLARIANS	DIATOMS	PALEOMAGNETICS	PHYS. PROPERTIES	CHEMISTRY	SECTION	METERS	GRAPHIC LITHOLOGY	DRILLING DISTURB.	SED. STRUCTURES	SAMPLES	LITHOLOGIC DESCRIPTION
					?	●		1 2 3	0.5 1.0	M M			● XRD ●	PHACOIDAL SHEARED SERPENTINE Major lithology: PHACOIDAL SHEARED SERPENTINE, dark green [illegible] with white [illegible] zone at the top and small light green [illegible] grains scattered throughout. Upper zone is rather late stage serpentine [illegible]. Small grains are only [illegible].

SMEAR SLIDE SUMMARY (%):

	1, 90 D	1, 97 D
TEXTURE:		
Sand	5	20
Silt	85	60
Clay	10	20
COMPOSITION:		
Amphibole	Tr	—
Opaques	5	5
Serpentine	90	90
Talc	—	Tr
Thulite	—	Tr
Zoisite	5	5

SITE 779 HOLE A CORE 20R CORED INTERVAL 4116.3-4117.3 mbsl; 169.1-170.1 mbsf

TIME-ROCK UNIT	FORAMINIFERS	NANNOFOSSILS	RADIOLARIANS	DIATOMS	PALEOMAGNETICS	PHYS. PROPERTIES	CHEMISTRY	SECTION	METERS	GRAPHIC LITHOLOGY	DRILLING DISTURB.	SED. STRUCTURES	SAMPLES	LITHOLOGIC DESCRIPTION
					?			1	0.5 1.0	M M			● ●	PHACOIDAL SHEARED SERPENTINE Major lithology: PHACOIDAL SHEARED SERPENTINE, light greenish gray (10Y 7/2). Pebbles of serpentinized ultramafic rock in sand-sized, zoisite and thulite-bearing matrix material. Core exhibits a sheared, phacoidal texture with veins and foliation anastomosing around dark green (5G 3/2) pebbles. Some flattening and brittle pinch and swell (normal faulting) is present.

SMEAR SLIDE SUMMARY (%):

	1, 88 D	1, 92 D
TEXTURE:		
Sand	60	70
Silt	30	20
Clay	10	10
COMPOSITION:		
Opaques	10	15
Serpentine	55	85
Thulite	25	—
Zoisite	10	—

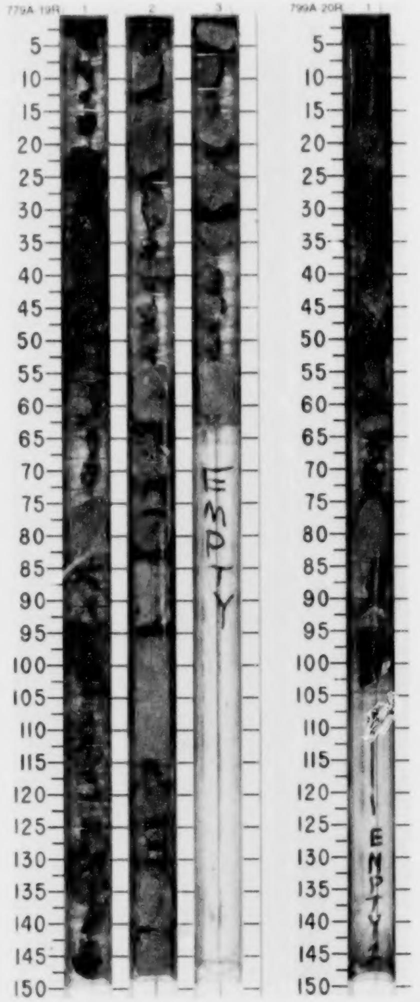

SITE 779 HOLE A CORE 21M CORED INTERVAL 4115.3-4117.3 mbsl; 168.1-170.1 mbsf

LITHOLOGIC DESCRIPTION

SECTION	METERS	GRAPHIC LITHOLOGY
1	0.5 1.0	CUTTINGS

SITE 779 HOLE A CORE 22R CORED INTERVAL 4117.3-4124.8 mbsl; 170.1-177.6 mbsf

LITHOLOGIC DESCRIPTION

SECTION	METERS	GRAPHIC LITHOLOGY
1	0.5 1.0	M
2		
3		CUTTINGS M

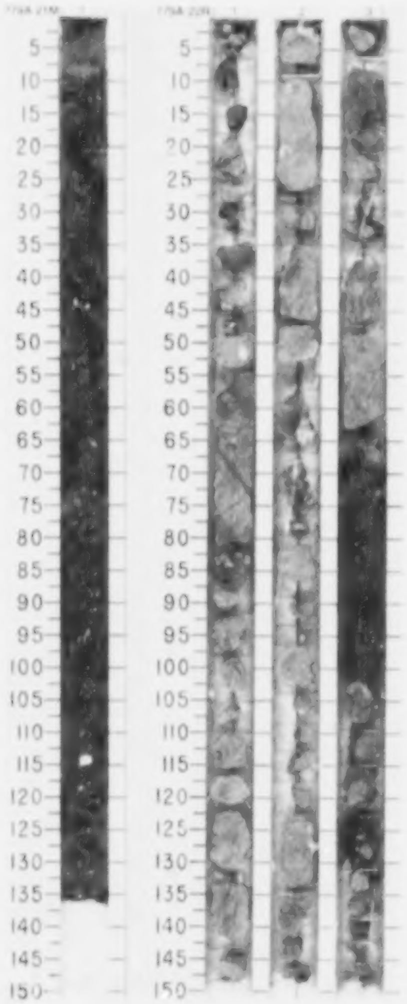
779A-21M
1
779A-22R
1
2
3
5
10
15
20
25
30
35
40
45
50
55
60
65
70
75
80
85
90
95
100
105
110
115
120
125
130
135
140
145
150

SITE 779 HOLE A CORE 23R CORED INTERVAL 4124.8-4134.4 mbsl; 177.6-187.2 mbsf

TIME-ROCK UNIT	BIOSTRAT. ZONE/FOSSIL CHARACTER: FORAMINIFERS	NANNOFOSSILS	RADIOLARIANS	DIATOMS	PALEOMAGNETICS	PHYS. PROPERTIES	CHEMISTRY	SECTION	METERS	GRAPHIC LITHOLOGY	DRILLING DISTURB.	SED. STRUCTURES	SAMPLES	LITHOLOGIC DESCRIPTION
								1	0.5 1.0	CUTTINGS M				[illegible]

SITE 779 HOLE A CORE 24R CORED INTERVAL 4134.4-4144.0 mbsl; 187.2-196.8 mbsf

TIME-ROCK UNIT	BIOSTRAT. ZONE/FOSSIL CHARACTER: FORAMINIFERS	NANNOFOSSILS	RADIOLARIANS	DIATOMS	PALEOMAGNETICS	PHYS. PROPERTIES	CHEMISTRY	SECTION	METERS	GRAPHIC LITHOLOGY	DRILLING DISTURB.	SED. STRUCTURES	SAMPLES	LITHOLOGIC DESCRIPTION
						● [illegible]	[illegible]	1	0.5 1.0	M				[illegible]

SITE 779 HOLE A CORE 25R CORED INTERVAL 4144.0-4153.7 mbsl; 196.8-206.5 mbsf

TIME-ROCK UNIT	BIOSTRAT. ZONE/FOSSIL CHARACTER: FORAMINIFERS	NANNOFOSSILS	RADIOLARIANS	DIATOMS	PALEOMAGNETICS	PHYS. PROPERTIES	CHEMISTRY	SECTION	METERS	GRAPHIC LITHOLOGY	DRILLING DISTURB.	SED. STRUCTURES	SAMPLES	LITHOLOGIC DESCRIPTION
						[illegible] ●		1	0.5 1.0	M				[illegible]
								2		M				

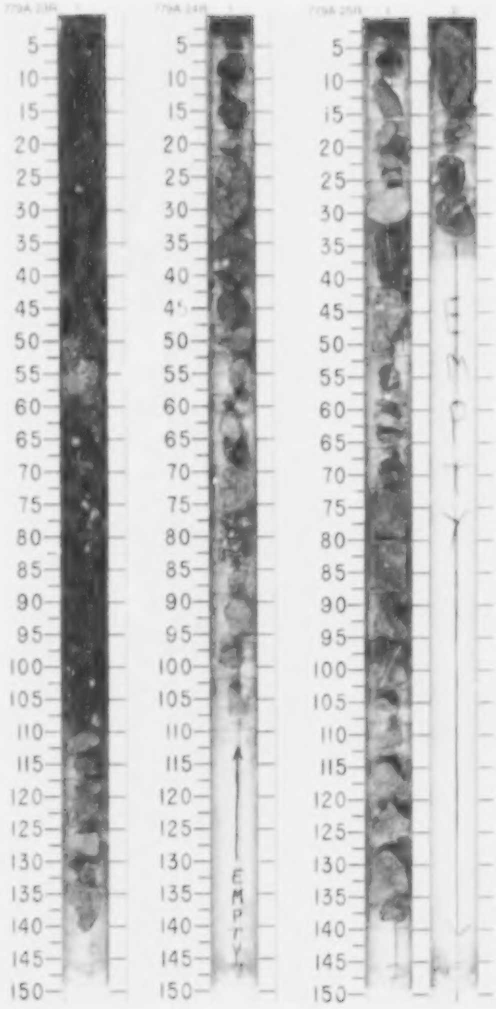

779A-23R 1
779A-24R 1
779A-25R 1 2
EMPTY
5
10
15
20
25
30
35
40
45
50
55
60
65
70
75
80
85
90
95
100
105
110
115
120
125
130
135
140
145
150

SITE 779 HOLE A CORE 26R CORED INTERVAL 4153.7-4163.4 mbsl; 208.5-216.2 mbsf

SITE 779 HOLE A CORE 27R CORED INTERVAL 4163.4-4173.0 mbsl; 216.2-225.8 mbsf

LITHOLOGIC DESCRIPTION
GRAPHIC LITHOLOGY
UPPER MIOCENE to LOWER MIOCENE

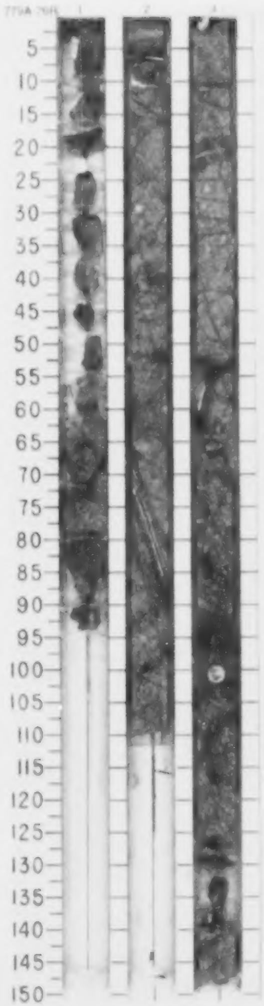
779A-26R
1
2
3
5
10
15
20
25
30
35
40
45
50
55
60
65
70
75
80
85
90
95
100
105
110
115
120
125
130
135
140
145
150

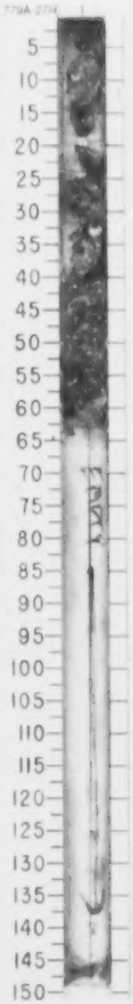
779A-27R
1
EMPTY

SITE 779 HOLE A CORE 28R CORED INTERVAL 4173.0-4182.7 mbsl; 225.8-235.5 mbsf

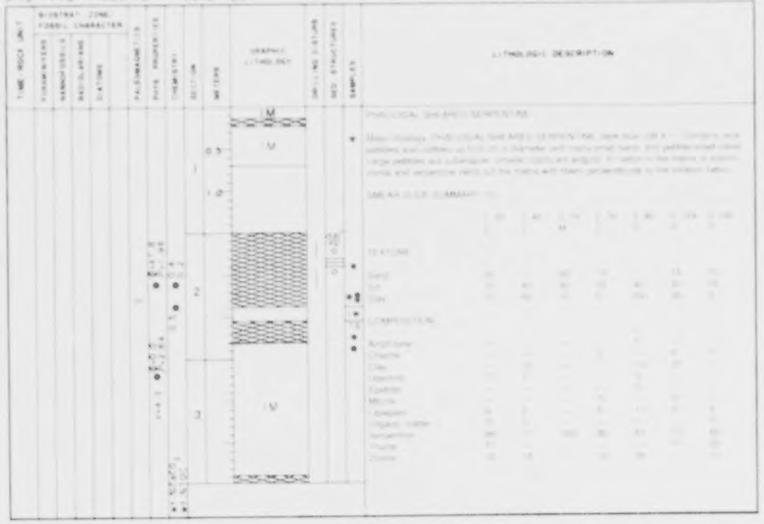
TIME-ROCK UNIT
BIOSTRAT. ZONE/ FOSSIL CHARACTER
FORAMINIFERS
NANNOFOSSILS
RADIOLARIANS
DIATOMS
PALEOMAGNETICS
PHYS. PROPERTIES
CHEMISTRY
SECTION
METERS
GRAPHIC LITHOLOGY
DRILLING DISTURB.
SED. STRUCTURES
SAMPLES
LITHOLOGIC DESCRIPTION
1
2
3
0.5
1.0
M

PHACOIDAL SHEARED SERPENTINE

Major lithology: PHACOIDAL SHEARED SERPENTINE, [illegible]

SMEAR SLIDE SUMMARY (%):

TEXTURE:

Sand

Silt

Clay

COMPOSITION:

[illegible]

SITE 779 HOLE A CORE 29R CORED INTERVAL 4182.7-4192.2 mbsl; 235.5-245.0 mbsf

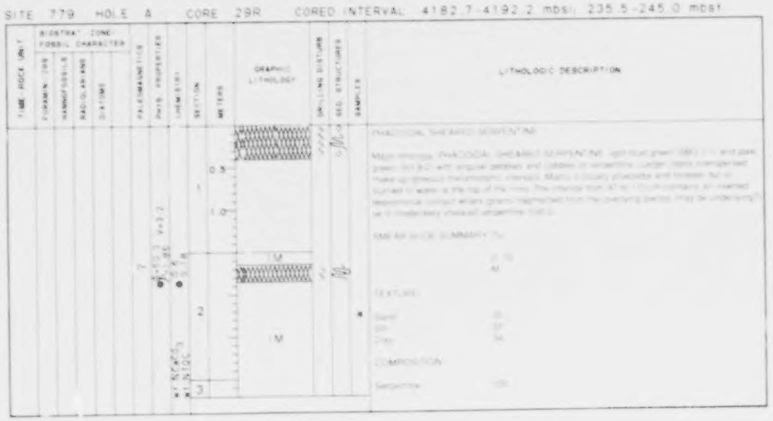
TIME-ROCK UNIT
BIOSTRAT. ZONE/ FOSSIL CHARACTER
FORAMINIFERS
NANNOFOSSILS
RADIOLARIANS
DIATOMS
PALEOMAGNETICS
PHYS. PROPERTIES
CHEMISTRY
SECTION
METERS
GRAPHIC LITHOLOGY
DRILLING DISTURB.
SED. STRUCTURES
SAMPLES
LITHOLOGIC DESCRIPTION
1
2
3
0.5
1.0
M

PHACOIDAL SHEARED SERPENTINE

Major lithology: PHACOIDAL SHEARED SERPENTINE, [illegible]

SMEAR SLIDE SUMMARY (%):

M

TEXTURE:

Sand

Silt

Clay

COMPOSITION:

Serpentine

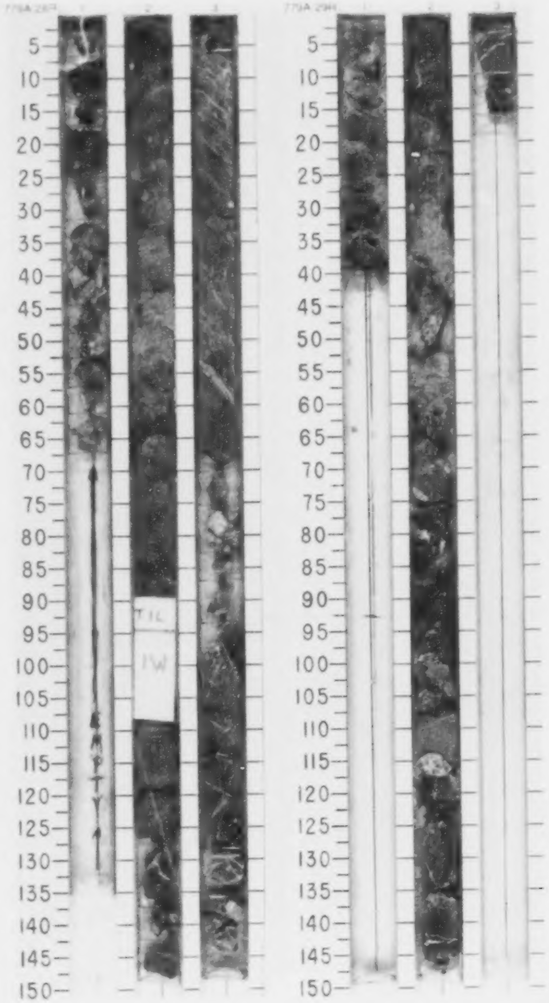
779A-28R
1
2
3
779A-29R
1
2
3
5
10
15
20
25
30
35
40
45
50
55
60
65
70
75
80
85
90
95
100
105
110
115
120
125
130
135
140
145
150
TIL
IW

SITE 779 HOLE A CORE 30R CORED INTERVAL

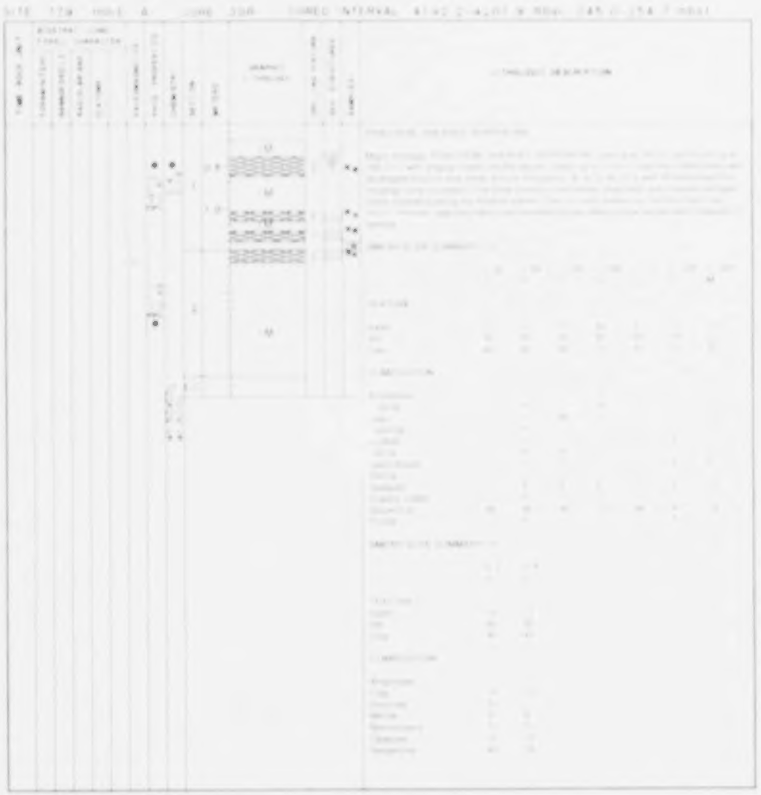
TIME-ROCK UNIT
BIOSTRAT. ZONE / FOSSIL CHARACTER
FORAMINIFERS
NANNOFOSSILS
RADIOLARIANS
DIATOMS
PALEOMAGNETICS
PHYS. PROPERTIES
CHEMISTRY
SECTION
METERS
GRAPHIC LITHOLOGY
DRILLING DISTURB.
SED. STRUCTURES
SAMPLES
LITHOLOGIC DESCRIPTION
SMEAR SLIDE SUMMARY (%)
TEXTURE
COMPOSITION
SMEAR SLIDE SUMMARY (%)
TEXTURE
COMPOSITION

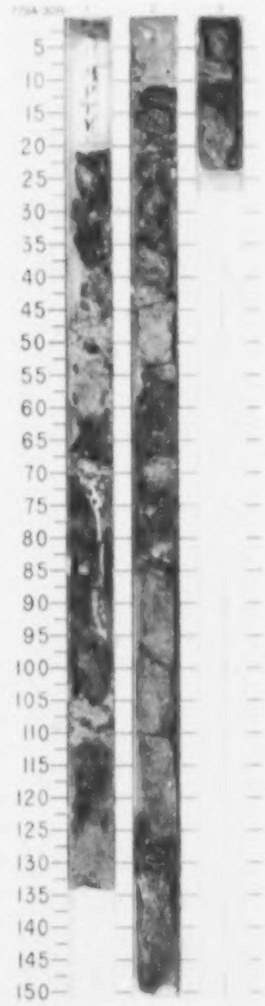
779A-30R
1
2
3
5
10
15
20
25
30
35
40
45
50
55
60
65
70
75
80
85
90
95
100
105
110
115
120
125
130
135
140
145
150

SITE 779 HOLE A CORE 31R CORED INTERVAL 4201.9-4211.6 mbsl; 254.7-264.4 mbsf

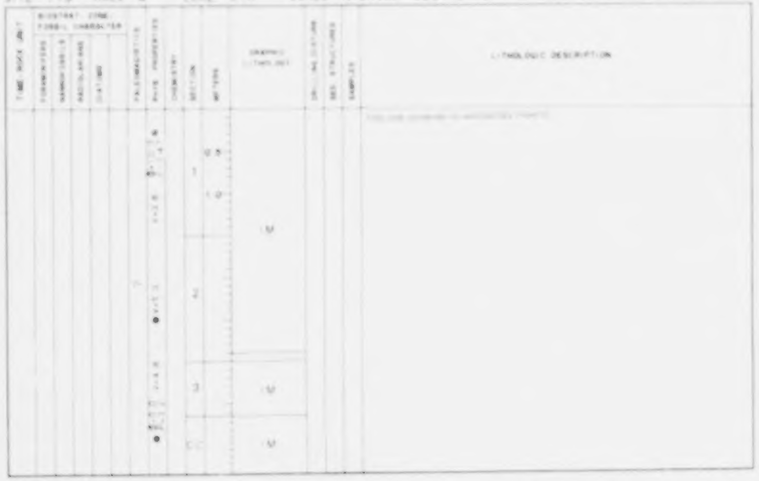
TIME-ROCK UNIT
BIOSTRAT. ZONE/FOSSIL CHARACTER
FORAMINIFERS
NANNOFOSSILS
RADIOLARIANS
DIATOMS
PALEOMAGNETICS
PHYS. PROPERTIES
CHEMISTRY
SECTION
METERS
GRAPHIC LITHOLOGY
DRILLING DISTURB.
SED. STRUCTURES
SAMPLES
LITHOLOGIC DESCRIPTION
0.5
1
1.0
2
3
CC
M
?

SITE 779 HOLE A CORE 32R CORED INTERVAL 4211.6-4221.2 mbsl; 264.4-274.0 mbsf

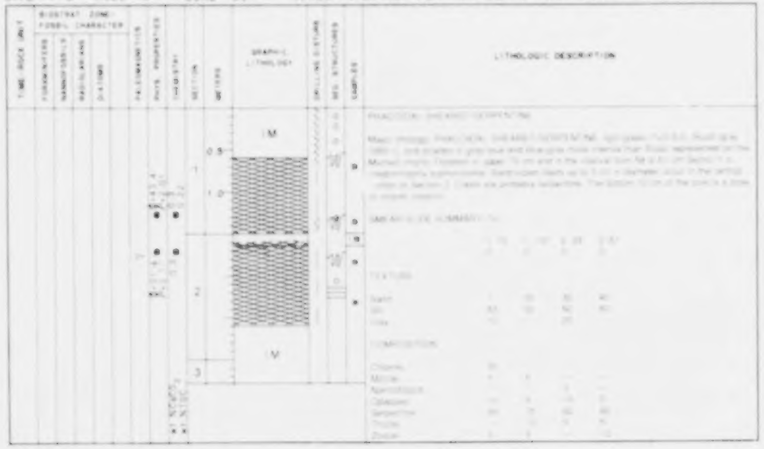
TIME-ROCK UNIT
BIOSTRAT. ZONE/FOSSIL CHARACTER
FORAMINIFERS
NANNOFOSSILS
RADIOLARIANS
DIATOMS
PALEOMAGNETICS
PHYS. PROPERTIES
CHEMISTRY
SECTION
METERS
GRAPHIC LITHOLOGY
DRILLING DISTURB.
SED. STRUCTURES
SAMPLES
LITHOLOGIC DESCRIPTION
0.5
1
1.0
2
3
M
?

PHACOIDAL SHEARED SERPENTINE

SMEAR SLIDE SUMMARY (%):

TEXTURE:

Sand

Silt

Clay

COMPOSITION:

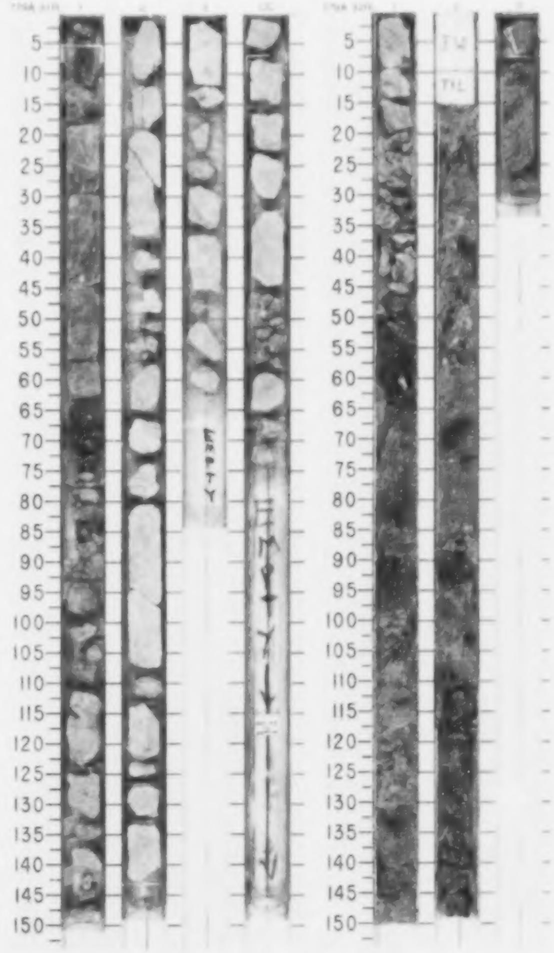
779A-31R
779A-32R
5
10
15
20
25
30
35
40
45
50
55
60
65
70
75
80
85
90
95
100
105
110
115
120
125
130
135
140
145
150

SITE 779 HOLE A CORE 33R CORED INTERVAL 4221.2-4230.9 mbsl; 274.0-283.7 mbsf

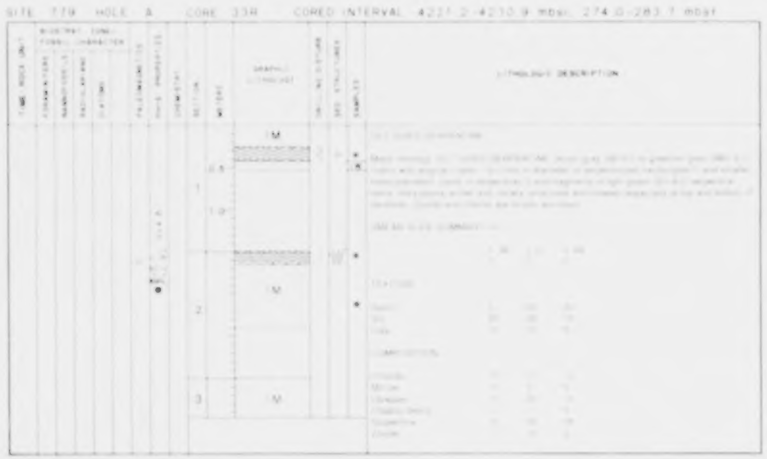
TIME-ROCK UNIT
BIOSTRAT. ZONE/ FOSSIL CHARACTER
FORAMINIFERS
NANNOFOSSILS
RADIOLARIANS
DIATOMS
PALEOMAGNETICS
PHYS. PROPERTIES
CHEMISTRY
SECTION
METERS
GRAPHIC LITHOLOGY
DRILLING DISTURB.
SED. STRUCTURES
SAMPLES
LITHOLOGIC DESCRIPTION
0.5
1.0
1
2
3
M

[illegible]

SITE 779 HOLE A CORE 34R CORED INTERVAL 4230.9-4240.5 mbsl; 283.7-293.3 mbsf

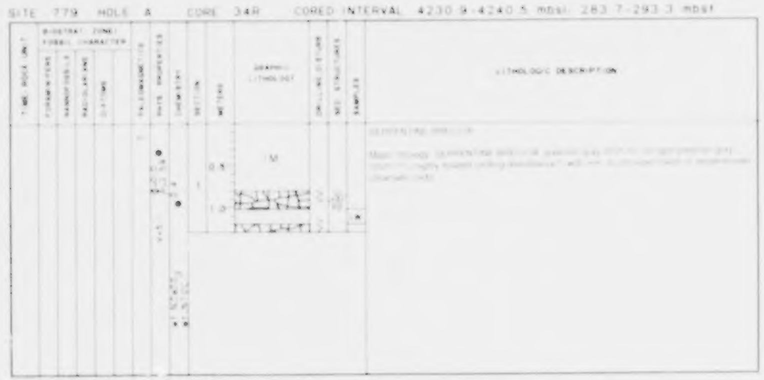
TIME-ROCK UNIT
BIOSTRAT. ZONE/ FOSSIL CHARACTER
FORAMINIFERS
NANNOFOSSILS
RADIOLARIANS
DIATOMS
PALEOMAGNETICS
PHYS. PROPERTIES
CHEMISTRY
SECTION
METERS
GRAPHIC LITHOLOGY
DRILLING DISTURB.
SED. STRUCTURES
SAMPLES
LITHOLOGIC DESCRIPTION
0.5
1.0
1
M

[illegible]

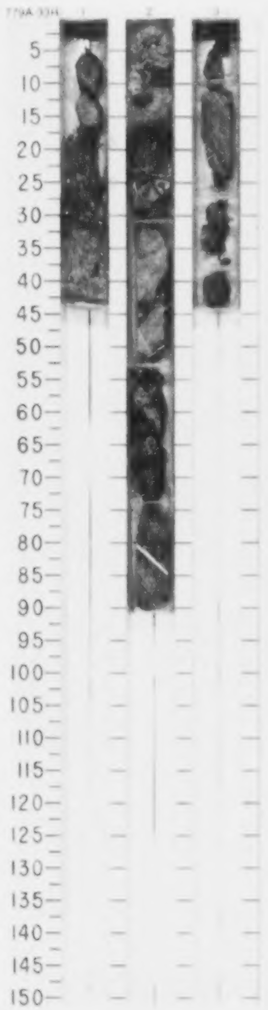
779A-33R
1
2
3
5
10
15
20
25
30
35
40
45
50
55
60
65
70
75
80
85
90
95
100
105
110
115
120
125
130
135
140
145
150

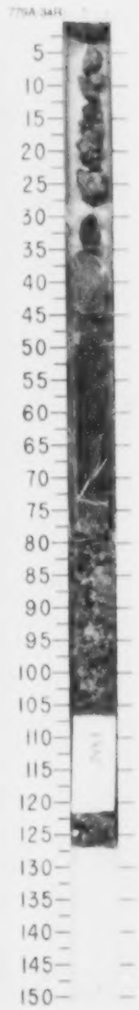
779A-34R
1
5
10
15
20
25
30
35
40
45
50
55
60
65
70
75
80
85
90
95
100
105
110
115
120
125
130
135
140
145
150

SITE 779 HOLE A CORE 35R CORED INTERVAL 4240.5-4250.2 mbsl; 293.3-303.0 mbsf

TIME-ROCK UNIT
BIOSTRAT. ZONE/FOSSIL CHARACTER
FORAMINIFERS
NANNOFOSSILS
RADIOLARIANS
DIATOMS
PALEOMAGNETICS
PHYS. PROPERTIES
CHEMISTRY
SECTION
METERS
GRAPHIC LITHOLOGY
DRILLING DISTURB.
SED. STRUCTURES
SAMPLES
LITHOLOGIC DESCRIPTION
SMEAR SLIDE SUMMARY (%):
TEXTURE:
Sand
Silt
Clay
COMPOSITION:

SITE 779 HOLE A CORE 36R CORED INTERVAL 4250.2-4259.9 mbsl; 303.0-312.7 mbsf

TIME-ROCK UNIT
BIOSTRAT. ZONE/FOSSIL CHARACTER
FORAMINIFERS
NANNOFOSSILS
RADIOLARIANS
DIATOMS
PALEOMAGNETICS
PHYS. PROPERTIES
CHEMISTRY
SECTION
METERS
GRAPHIC LITHOLOGY
DRILLING DISTURB.
SED. STRUCTURES
SAMPLES
LITHOLOGIC DESCRIPTION
SMEAR SLIDE SUMMARY (%):
TEXTURE:
Sand
Silt
Clay
COMPOSITION:
Amphibole
Barite
Chlorite
Dolomite
Garnet
Micrite
Opaques
Organic debris
Serpentine
Zoisite

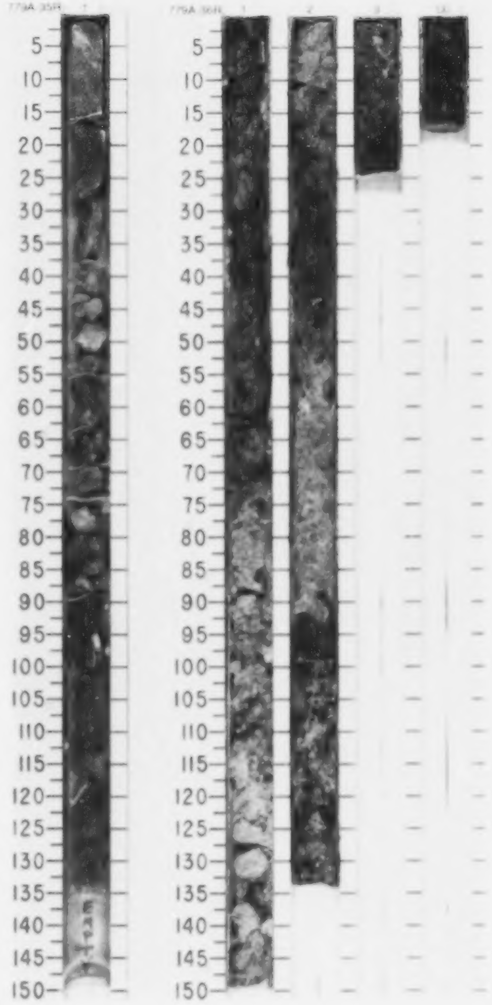
779A-35R
1
779A-36R
1
2
3
CC
5
10
15
20
25
30
35
40
45
50
55
60
65
70
75
80
85
90
95
100
105
110
115
120
125
130
135
140
145
150

SITE 779 HOLE A CORE 37R CORED INTERVAL 4259.9-4264.4 mbsl; 312.7-317.2 mbsf

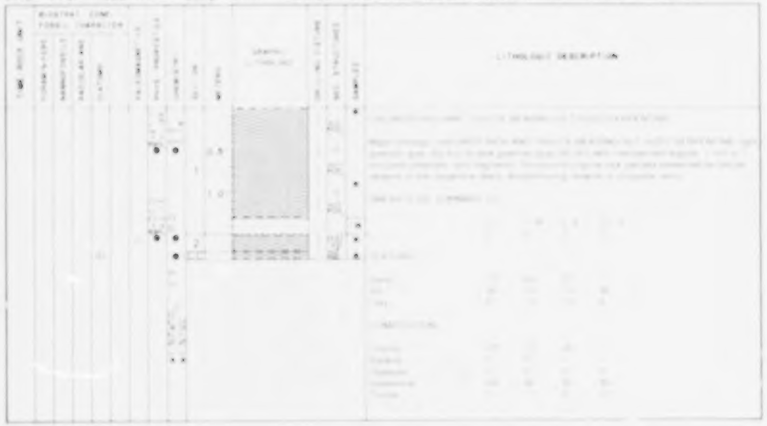
TIME-ROCK UNIT
BIOSTRAT. ZONE/FOSSIL CHARACTER
FORAMINIFERS
NANNOFOSSILS
RADIOLARIANS
DIATOMS
PALEOMAGNETICS
PHYS. PROPERTIES
CHEMISTRY
SECTION
METERS
GRAPHIC LITHOLOGY
DRILLING DISTURB.
SED. STRUCTURES
SAMPLES
1
2
CC

LITHOLOGIC DESCRIPTION

[illegible]

[illegible]

SMEAR SLIDE SUMMARY (%):

TEXTURE:

COMPOSITION:

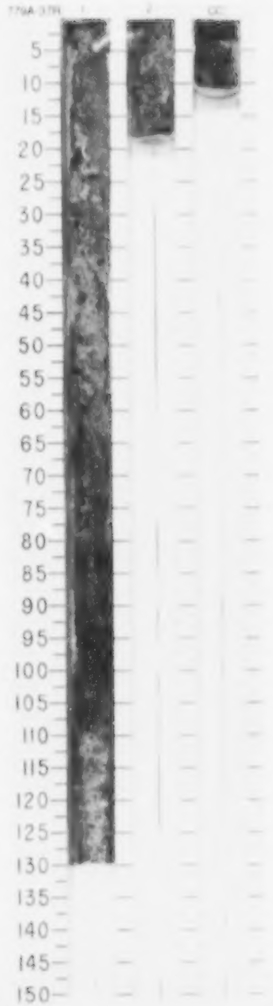
779A-37R
1
2
CC
5
10
15
20
25
30
35
40
45
50
55
60
65
70
75
80
85
90
95
100
105
110
115
120
125
130
135
140
145
150

SITE 779 HOLE B CORE 1R CORED INTERVAL 3947.2-3956.2 mbsl; 0-9.0 mbsf

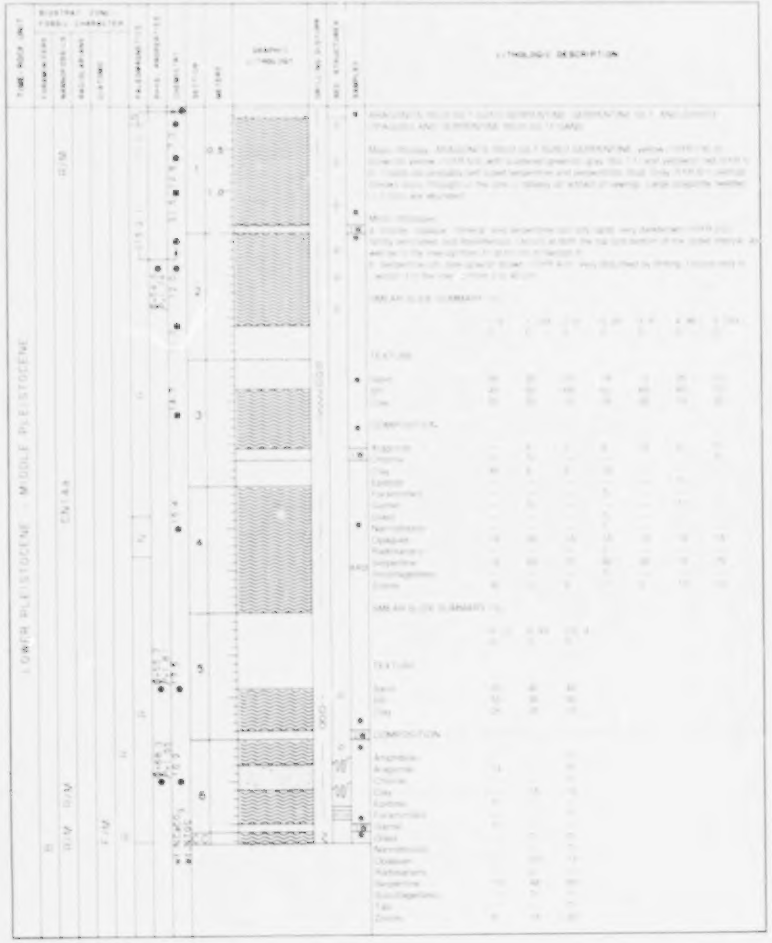
TIME-ROCK UNIT
BIOSTRAT. ZONE/FOSSIL CHARACTER
FORAMINIFERS
NANNOFOSSILS
RADIOLARIANS
DIATOMS
PALEOMAGNETICS
PHYS. PROPERTIES
CHEMISTRY
SECTION
METERS
GRAPHIC LITHOLOGY
DRILLING DISTURB.
SED. STRUCTURES
SAMPLES
LITHOLOGIC DESCRIPTION
LOWER PLEISTOCENE - MIDDLE PLEISTOCENE
CN14a
0.5
1.0
1
2
3
4
5
6
CC
SMEAR SLIDE SUMMARY (%):
TEXTURE:
Sand
Silt
Clay
COMPOSITION:

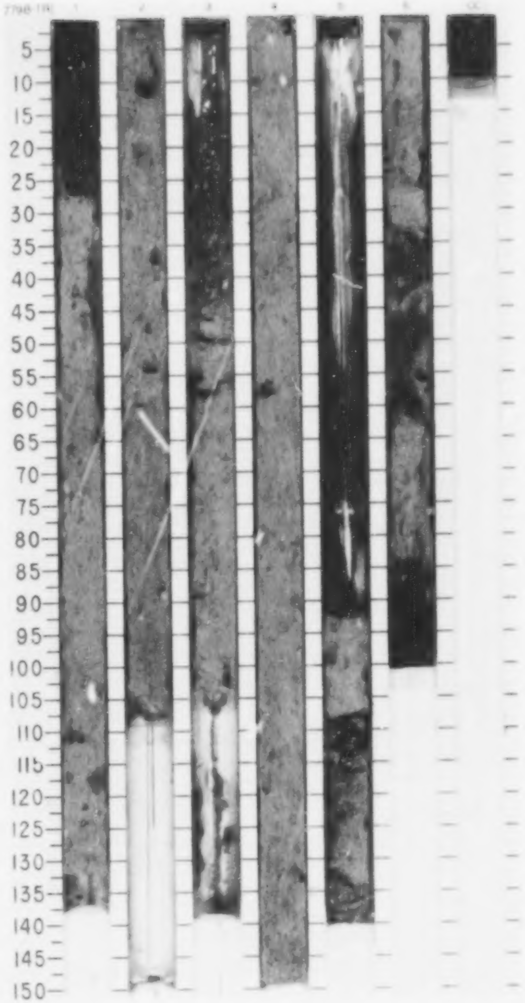
779B-1R
1
2
3
4
5
6
CC
5
10
15
20
25
30
35
40
45
50
55
60
65
70
75
80
85
90
95
100
105
110
115
120
125
130
135
140
145
150

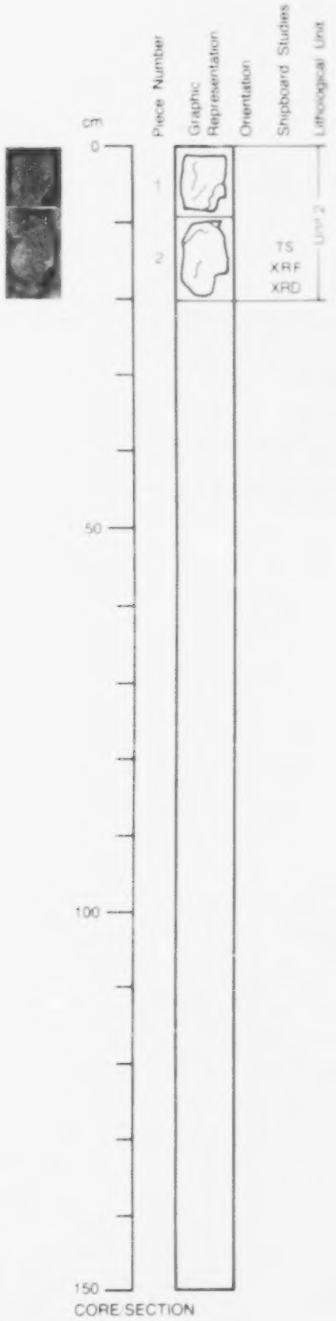
cm
Piece Number
Graphic Representation
Orientation
Shipboard Studies
Lithological Unit
0
50
100
150
1
2
TS
XRF
XRD
Unit 2
CORE/SECTION

125-779A-3R-CC

UNIT 2: SERPENTINIZED HARZBURGITE

Pieces 1-2

COLOR: Gray black (5B 4/1)
LAYERING: None
DEFORMATION: None
PRIMARY MINERALOGY:
Olivine - Mode: 90-95%
Crystal size: Not visible
Crystal shape: Not visible
Crystal orientation: Not visible
Percent replacement: Not visible

Orthopyroxene - Mode: 0-5%
Crystal size: 1-2 mm
Crystal shape: Not visible
Crystal orientation: Not visible
Percent replacement: Not visible
SECONDARY MINERALOGY:
Serpentine, magnetite (dusty grains)
Total percent: 85% ?
Texture: Mesh texture with some bastitic texture
Vein material: Light green (serpentine?) and white (carbonate?) veins (1-3 mm wide) throughout pieces; vein of light serpentine rimmed by darker serpentine and whiter (?) mineral.

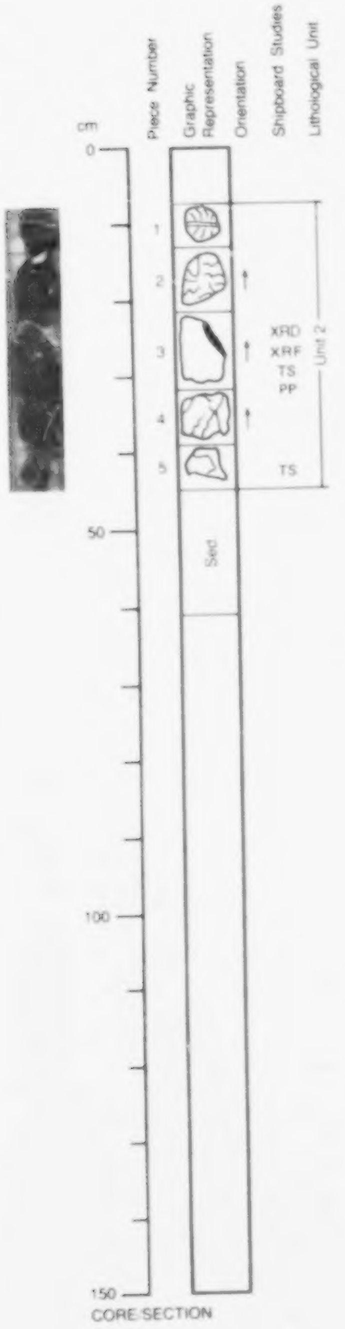

125-779A-4R-1

UNIT 2: SERPENTINIZED HARZBURGITE

Pieces 1 and 5

COLOR: Dark greenish gray (5BG 4/1)
LAYERING: None
DEFORMATION: Abundant fracturing and veining
PRIMARY MINERALOGY:
Olivine : Mode: 70-85%
Crystal size: Not visible
Crystal shape: Not visible
Crystal orientation: Not visible
Percent replacement: 80-100

Orthopyroxene : Mode: 15-30%
Crystal size: Not visible
Crystal shape: Not visible
Crystal orientation: Not visible
Percent replacement: 80-100

Spinel : Mode: Trace
Crystal size: Not visible
Crystal shape: Not visible
Crystal orientation: Not visible
Percent replacement: Not visible
SECONDARY MINERALOGY:
Serpentine:
Total percent: 90-99%
Texture: N/A
Vein material: Oldest: Light greenish gray 5GY7/1 veins (<1 mm wide) crosscut by bluish gray 5B5/1 veins (<2 mm wide); sometimes rimmed by chrysotile fibers perpendicular to vein wall in thick veins (8 mm wide).

UNIT 2: SERPENTINIZED HARZBURGITE

Pieces 2-4

COLOR: Dark greenish gray (5BG4/1).
LAYERING: None
DEFORMATION: Sub-parallel veins and cracks (minor)
PRIMARY MINERALOGY:
Olivine : Mode: 80-90%
Crystal size: Not visible
Crystal shape: Not visible
Crystal orientation: Not visible
Percent replacement: 80-90

Orthopyroxene : Mode: 10-20%
Crystal size: 2-4 mm
Crystal shape: Euhedral-anhedral
Crystal orientation: Not visible
Percent replacement: 90

Spinel : Mode: <2%
Crystal size: <2 mm
Crystal shape: Elongate, ragged
Crystal orientation: Not visible
Percent replacement: Not visible
SECONDARY MINERALOGY:
Serpentine:
Total percent: 90-99%
Texture: Mesh (?) and bastite
Vein material: Few very thin white veins (<0.1 mm wide); occasionally thicker veins (5 mm wide) of light green serpentine (chrysotile?); veins show no specific orientation.

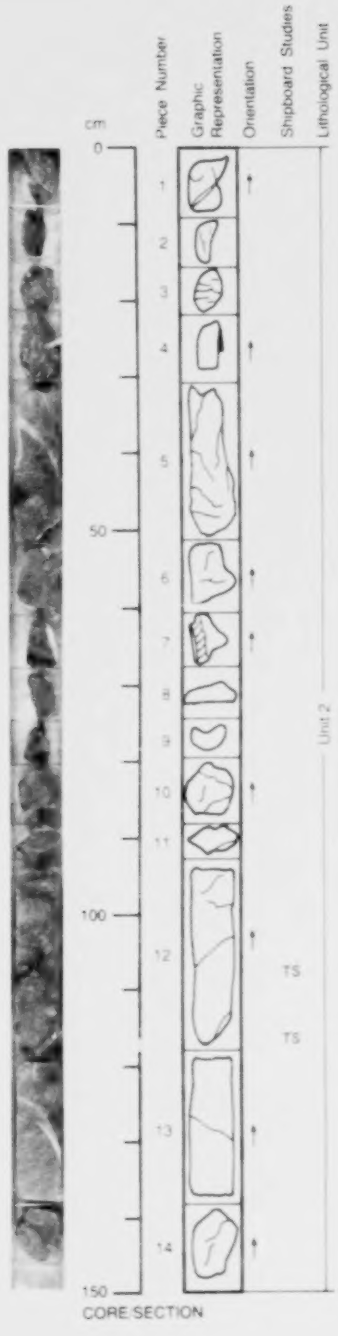

125-779A-5R-1

UNIT 2: SERPENTINIZED HARZBURGITE

Pieces 1-11

COLOR: Dark greenish gray to dark blue gray (5BG 4/1-5B 4/1).
LAYERING: None visible.
DEFORMATION: Minor brecciation in Pieces 1 and 2; abundant small fractures (<0.1 mm wide) in Pieces 3-4.
PRIMARY MINERALOGY:
Olivine - Mode: 70-85%
Crystal size: Not visible
Crystal shape: Not visible
Crystal orientation: Not visible
Percent replacement: 90-100

Orthopyroxene - Mode: 10-30%
Crystal size: Not visible
Crystal shape: Not visible
Crystal orientation: Not visible
Percent replacement: 90-100

Spinel? - Mode: Trace
Crystal size: <1 mm
Crystal shape: Not visible
Crystal orientation: Not visible
Percent replacement: Not visible
SECONDARY MINERALOGY:
Serpentine; dusty black magnetite?
Total percent: 90-99%
Texture: Bastitic in areas?
Vein material: Serpentine (chrysotile?) veins (1-2 mm wide), minor white (carbonate?) veins (0.1-1 mm wide).
ADDITIONAL COMMENTS: Pieces 3-4 have exterior shear rouding. Piece 7 is rimmed by 7-mm thick chrysotile vein. Veins show no specific orientation.

UNIT 2: SERPENTINIZED HARZBURGITE OR DUNITE (?)

Pieces 12-14

COLOR: Dark greenish gray (5BG 4/1).
LAYERING: Some pyroxene-rich layers (5 cm wide).
DEFORMATION: None.
PRIMARY MINERALOGY:
Olivine - Mode: 80-90%
Crystal size: Not visible
Crystal shape: Not visible
Crystal orientation: Not visible
Percent replacement: 90-95

Orthopyroxene - Mode: 5-20?
Crystal size: 1-2 mm
Crystal shape: Euhedral?
Crystal orientation: Not visible
Percent replacement: 50-90

Spinel - Mode: <1%
Crystal size: <1 mm
Crystal shape: Elongate-ragged
Crystal orientation: None visible
Percent replacement: Not visible
SECONDARY MINERALOGY:
Serpentine; dusty black magnetite?
Total percent: 90-99%
Texture: Bastitic after pyroxenes.
Vein material: A few dark green serpentine (0.1-1 mm wide) veins,minor white veins (<0.1 mm wide).

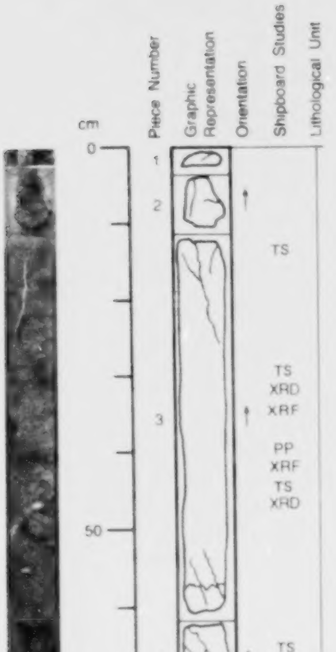

125-779A-5R-2

UNIT 2: SERPENTINIZED HARZBURGITE

Pieces 1-3; 5-13

COLOR: Dark greenish gray (5BG 4/1).
LAYERING: Crude layering defined by pyroxene rich intervals (4-5 cm wide), 6 layers in 1.5 m.
DEFORMATION: minor brecciation in Pieces 1-2, 10-11.
PRIMARY MINERALOGY:
Olivine - Mode: 80-90%
Crystal size: Not visible
Crystal shape: Not visible
Crystal orientation: None visible
Percent replacement: 80-95

Orthopyroxene - Mode: 10-15%
Crystal size: 1-3 mm
Crystal shape: Subhederal
Crystal orientation: None visible
Percent replacement: 50-90

Spinel - Mode: <5%
Crystal size: <2 mm
Crystal shape: Subhedral-euhedral
Crystal orientation: None visible
Percent replacement: Not visible
SECONDARY MINERALOGY:
Serpentine, dusty black magnetite?
Total percent: 95-99%
Texture: Bastitic after pyroxenes and in layers.
Vein material: Locally white veins (<1 mm wide) and light green veins (<1 mm wide) at no specific orientation.

UNIT 2: SERPENTINIZED DUNITE (?)

Piece 4

COLOR: Dark greenish gray (5BG 4/1)
LAYERING: None
DEFORMATION: None visible.
PRIMARY MINERALOGY:
Olivine - Mode: 95-99%
Crystal size: Not visible
Crystal shape: Not visible
Crystal orientation: None visible
Percent replacement: 95-99

Orthopyroxene - Mode: <5%
Crystal size: <1 mm
Crystal shape: Not visible
Crystal orientation: None visible
Percent replacement: 95-99

Spinel - Mode: Trace
Crystal size: <1 mm
Crystal shape: Anhedral-subhedral
Crystal orientation: None visible
Percent replacement: Not visible
SECONDARY MINERALOGY:
Serpentine: dusty magnetite?
Total percent: 95-99%
Texture: Mesh (?) texture in areas.
Vein material: Many small serpentine veins (<1 mm wide) at no specific orientation.

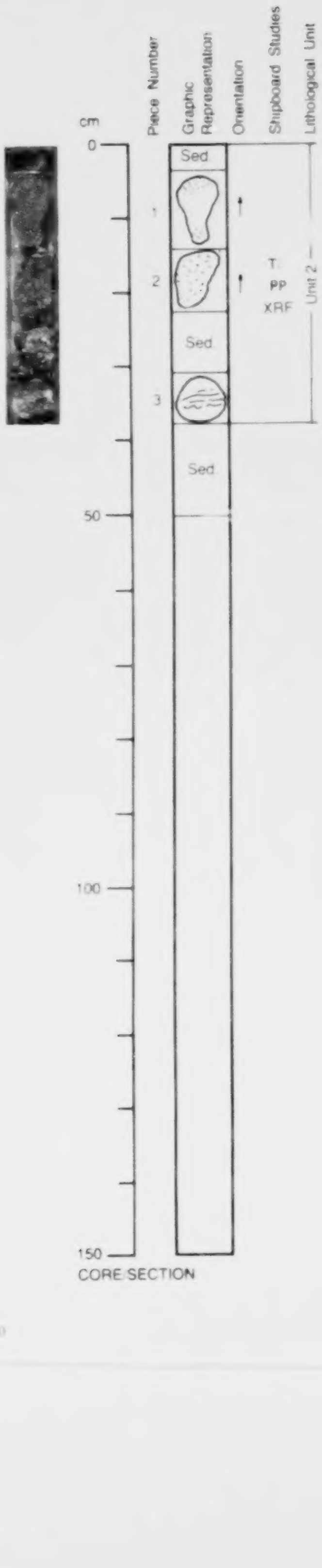

125-779A-6R-1

UNIT 2: SERPENTINIZED HARZBURGITE

Pieces 1-2

COLOR: Dark greenish gray (5BG4/1)
LAYERING: Crude pyroxene layers (5 cm wide). Two layers within 20 cm
DEFORMATION: None
PRIMARY MINERALOGY:
Severely altered: relict orthopyroxene, Cr-spinel
Olivine - Mode: 80-85%
Crystal size: 3-4 mm
Crystal shape: Anhedral
Crystal orientation: None
Percent replacement: 70-80

Orthopyroxene - Mode: 15-20%
Crystal size: 3-4 mm
Crystal shape: Euhedral
Crystal orientation: None
Percent replacement: 50

Clinopyroxene - Mode: <1%
Crystal size: <2 mm
Crystal shape: Euhedral
Crystal orientation: None
Percent replacement: 30-40

Spinel - Mode: <2%
Crystal size: <2 mm
Crystal shape: Euhedral-subhedral
Crystal orientation: None
Percent replacement: 20-30
SECONDARY MINERALOGY:
Serpentine
Total percent: 70-90%
Texture: Bastite after pyroxene (3 mm)
Vein material: minor white veins (<1 mm wide) at no specific orientation

UNIT 2: SERPENTINIZED HARZBURGITE

Piece 3

COLOR: Dark greenish gray (5GB 4/1)
LAYERING: None
DEFORMATION: Severely brecciated
PRIMARY MINERALOGY:
Completely altered. Cr-spinel shows diamond shape
Olivine - Mode: 80-85%
Crystal size: 3-4 mm
Crystal shape: Euhedral
Crystal orientation: None
Percent replacement: 100

Orthopyroxene - Mode: 15-20%
Crystal size: 3-4 mm
Crystal shape: Euhedral
Crystal orientation: None
Percent replacement: 100

Spinel - Mode: <2%
Crystal size: <2 mm
Crystal shape: Euhedral-subhedral
Crystal orientation: None
Percent replacement: 50
Comments: Cr-spinel
SECONDARY MINERALOGY:
Serpentine
Total percent: 100%
Texture: N/A
Vein material: White veins (1 mm wide), partly greenish

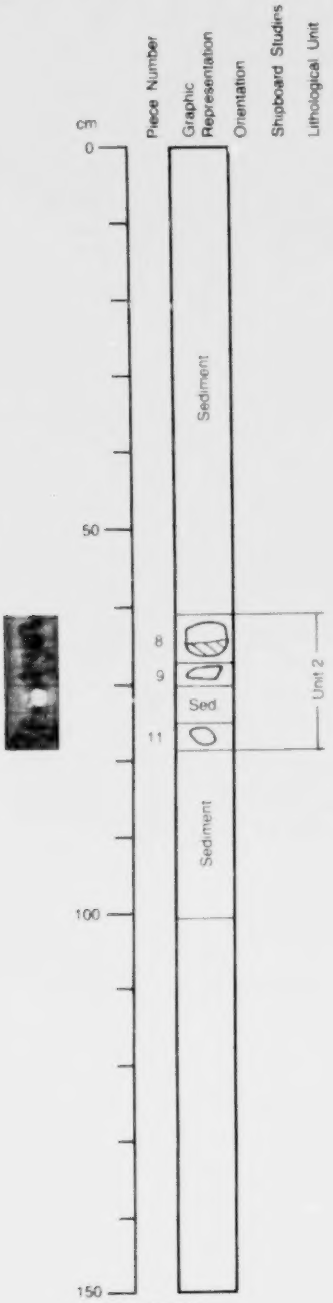
cm
Piece Number
Graphic Representation
Orientation
Shipboard Studies
Lithological Unit
0
50
100
150
Sediment
8
9
Sed
11
Sediment
Unit 2
CORE/SECTION

125-779A-7R-1

UNIT 2: SERPENTINIZED DUNITE (?)

Pieces 8, 9

COLOR: Light gray-green with a hint of gray (5G 5/1)
LAYERING: None
DEFORMATION: Preferred orientation of Cr-spinel grains
PRIMARY MINERALOGY:

- Olivine - Mode: 99%
  - Crystal size: Not visible
  - Crystal shape: Not visible
  - Crystal orientation: Not visible
  - Percent replacement: 100% replaced by serpentine
- Cr-spinel - Mode: <1%
  - Crystal size: 0.5-1 mm
  - Crystal shape: Elongated parallel preferred orientation
  - Crystal orientation: Not visible
  - Percent replacement: Not visible

SECONDARY MINERALOGY:

- Total percent: >99%
- Texture: Micro-mesh texture
- Vein material: Dark serpentine less than 1 mm wide

ADDITIONAL COMMENTS: No orthopyroxene discernible in this small piece

UNIT 2: MAGNESITE

Piece 11

COLOR: White (5YR 8/1)
LAYERING: None
DEFORMATION: None
PRIMARY MINERALOGY:

- This is not an igneous rock sensu stricto rather it is a surface product of serpentinization
- Magnesite Mode 100%
- Crystal size: Polycrystalline
- Crystal shape: Amorphous
- Crystal orientation: None
- Percent replacement: None
- Comments: Mg-carbonate forming a nodule with characteristic colliform surface texture

SECONDARY MINERALOGY: None

- Total percent: 0%
- Texture: None
- Vein material: None

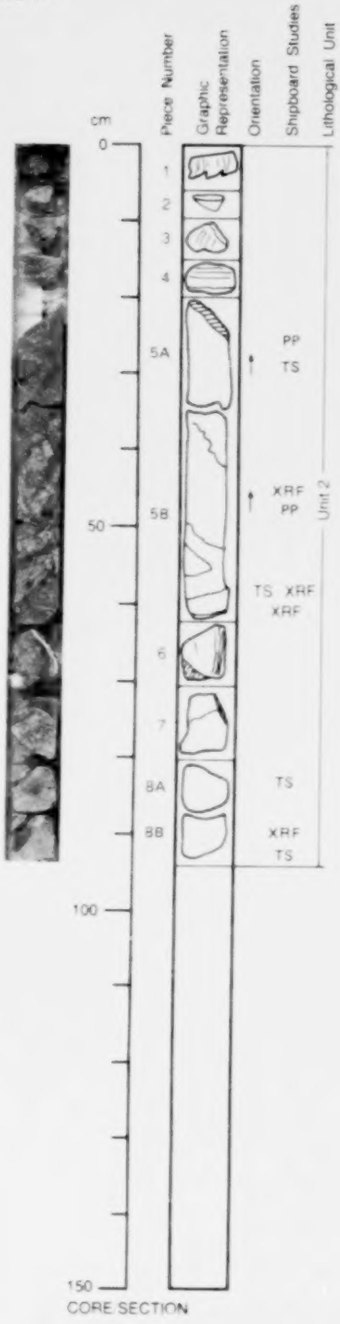

125-779A-8R-1

UNIT 2: SERPENTINIZED HARZBURGITE

Piece 1 Zoisite-rich silt-sized serpentine (See Sedimentary Barrel Sheets)

UNIT 2: SERPENTINIZED HARZBURGITE

Pieces 2, 3

COLOR: Pale blue gray (5B 6/1)
LAYERING: Massive
DEFORMATION: Random cracks
PRIMARY MINERALOGY:
Apparently cumulate texture
Orthopyroxene - Mode: 20%
Crystal size: 5 mm
Crystal shape: Equant
Crystal orientation: Random
Percent replacement: Variable

Olivine - Mode: 80%
Crystal size: 8-10 mm
Crystal shape: Corroded
Crystal orientation: Random
Percent replacement: Variable

Spinel - Mode: Trace
Crystal size: 0.2-0.5 mm
Crystal shape: Euhedral
Crystal orientation: Disseminated
Percent replacement: 10-20
SECONDARY MINERALOGY: Serpentine replacing olivine, chlorite (?) also present
Total percent: 10-70%
Texture: N.A.
Vein material: None
ADDITIONAL COMMENTS:
The cumulate texture of this rock distinguishes it from the ultramafic rocks above and below it.

UNIT 2: SHEARED SERPENTINIZED HARZBURGITE

Piece 4

COLOR: Dark greenish gray (5GY 4/1)
LAYERING: None
DEFORMATION: Top is sheared normal to core axis; top 5 mm microlaminated pale blue serpentine (chrysotile ?), next 1.5 cm consists of sheared serpentine and sheared/nonsheared crosscutting chrysotile veins. Both lamination and shearing normal to core axis, except for one riedel shear.
PRIMARY MINERALOGY:
Seem to be fully replaced by serpentine
Olivine - Mode: 95%
Crystal size: 5-10 mm
Crystal shape: None visible
Crystal orientation: None
Percent replacement: 100

Orthopyroxene - Mode: 0-5%
Crystal size: 5-10 mm
Crystal shape: Equant
Crystal orientation: None
Percent replacement: 100

Spinel - Mode: Trace
Crystal size: 2 mm
Crystal shape: Elongate
Crystal orientation: None
Percent replacement: 100
SECONDARY MINERALOGY:
Serpentine
Total percent: 100%
Texture: None visible
Vein material: 20%, chrysotile filled and other serpentine minerals
ADDITIONAL COMMENTS: This piece is probably the upper sheared contact of underlying Piece 5.

125-779A-8R-1 (continued)

UNIT 2: SERPENTINIZED HARZBURGITE

Pieces 5A, 5B

COLOR: Green blue (5BG 4/2) to pale gray (5B 6/1).
LAYERING: Color layering between massive fine-grained serpentinite with few mineral relics to less serpentinized rock in which primary mineral textures are preserved.
DEFORMATION: Fracturing, both at high and moderate angle to core axis. Shearing in zones at 30 degrees to core axis.
PRIMARY MINERALOGY:
Olivine - Mode: 95%.
Crystal size: 5-8 mm.
Crystal shape: Rounded.
Crystal orientation: Subparallel to 30 degree shears.
Percent replacement: 90-100.

Orthopyroxene - Mode: 0-5%.
Crystal size: 0.2-0.8 mm.
Crystal shape: Elongate to rounded.
Crystal orientation: Not visible.
Percent replacement: 90-100.
Comments: Kink banded.

Spinel - Mode: Trace.
Crystal size: 1 mm.
Crystal shape: Ragged elongate.
Crystal orientation: Not visible.
Percent replacement: 50-60.
Comments: Forms stringers.
SECONDARY MINERALOGY:
100% serpentinized for Piece A, 90% for Piece B.
Total percent: 90-99%.
Texture: N/A.
Vein material: Chrysotile fills some fractures.
ADDITIONAL COMMENTS: It appears that the degree of serpentinization is fracture controlled, with a serpentinization halo proximal to the fracture.

UNIT 2: SERPENTINIZED HARZBURGITE

Piece 6

COLOR: Gray green (5BG 4/1).
LAYERING: Massive.
DEFORMATION: Shearing at 60 degrees to core axis.
PRIMARY MINERALOGY:
Spinel forms stringers at 30 degrees to core axis, other primary minerals are serpentinized.
Olivine - Mode: 90-95%.
Crystal size: Not visible.
Crystal shape: Not visible.
Crystal orientation: Not visible.
Percent replacement: Variable.

Orthopyroxene - Mode: 5-10%.
Crystal size: 0.5-9 mm.
Crystal shape: Equant.
Crystal orientation: Not visible.
Percent replacement: Variable.

Cr-spinel - Mode: <1%.
Crystal size: 0.1-1 mm.
Crystal shape: Equant to ragged elongate.
Crystal orientation: 30 degrees to core axis.
Percent replacement: Variable.
SECONDARY MINERALOGY:
Serpentine replaces the primary minerals.
Total percent: 40-70%.
Texture: N/A.
Vein material: 60 degrees to core axis, up to 8 mm wide, anastomosing, filled with a white translucent mineral.

125-779A-8R-1 (continued)

UNIT 2: SERPENTINIZED HARZBURGITE

Piece 7

COLOR: Green gray (5G 4/1 to 5B 6/1)
LAYERING: Apparent color-banding at 70 degrees to core axis.
DEFORMATION: Fractures at 60 and 70 degrees, conjugate plus relict; olivines appear elongated at 60 degrees to core axis.
PRIMARY MINERALOGY:
Variably serpentinized with some primary olivine textures preserved.
Olivine - Mode: 90-95%
Crystal size: 5-15 mm
Crystal shape: Elongate-rounded
Crystal orientation: Not visible
Percent replacement: Variable

Orthopyroxene - Mode: 5-10%
Crystal size: 5-10 mm
Crystal shape: Equant
Crystal orientation: Not visible
Percent replacement: Variable

Cr-spinel - Mode: Trace
Crystal size: 0.2-2 mm
Crystal shape: Equant to elongate
Crystal orientation: 60 degrees to core axis
Percent replacement: Variable
Comments: Stringers also at 60 degrees to core axis.
SECONDARY MINERALOGY:
Pervasively (80-100%) serpentinized.
Total percent: 40-70%
Texture: N/A
Vein material: Black serpentine, oriented at 30-60 degrees to core axis.
ADDITIONAL COMMENTS: 30-degree set cuts the 60-degree vein set.

UNIT 2: SERPENTINIZED HARZBURGITE

Pieces 8A and B

COLOR: Pale gray green (N 6)
LAYERING: Color banding apparent, possibly caused by serpentinized olivine layer at top of piece.
DEFORMATION: Not visible.
PRIMARY MINERALOGY:
Apparent olivine-rich band with wavy contact with orthopyroxene-rich rock at top of piece.
Olivine - Mode: 90%
Crystal size: 3-8 mm
Crystal shape: Granular
Crystal orientation: Not visible
Percent replacement: 40-50

Orthopyroxene - Mode: <10%
Crystal size: 3-8 mm
Crystal shape: Subhedral-anhedral
Crystal orientation: Not visible
Percent replacement: 40-50

Cr-spinel - Mode: Trace
Crystal size: 0.5-1 mm
Crystal shape: Ragged equant to elongate
Crystal orientation: 30 degrees to core axis
Percent replacement: 10-20
SECONDARY MINERALOGY:
Rock is partially serpentinized.
Total percent: 40-50%
Texture: N/A
Vein material: Some veining along fractures, possibly serpentine.
ADDITIONAL COMMENTS: Rock appears to be orthopyroxene-rich cumulate, with a different general appearance to the overlying tectonized harzburgites.

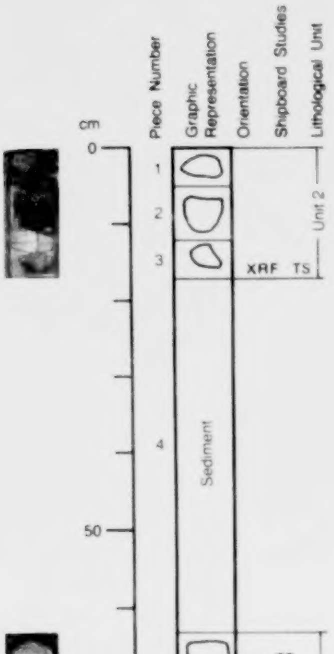

125-779A-9R-1

UNIT 2: SERPENTINIZED HARZBURGITE

Piece 1

COLOR: Greenish gray (5B 5/1).
LAYERING: None.
DEFORMATION: Bent pyroxenes.
PRIMARY MINERALOGY:
This appears to have a cumulate texture.
Olivine - Mode: 90-95%.
Crystal size: Not visible.
Crystal shape: Not visible.
Crystal orientation: Not visible.
Percent replacement: Not visible.

Pyroxene - Mode: <10%.
Crystal size: 5-20 mm.
Crystal shape: Equant.
Crystal orientation: Random.
Percent replacement: None.
Comments: Coarse granular texture probably orthopyroxene.

Spinel - Mode: <1%.
Crystal size: 0.5-1 mm.
Crystal shape: Elongate.
Crystal orientation: Random.
Percent replacement: Not visible.
Comments: Cr spinel probable.
SECONDARY MINERALOGY:
Serpentine.
Total percent: 10-60%.
Texture: N/A.
Vein material: None.

UNIT 2: SERPENTINIZED HARZBURGITE

Piece 2

COLOR: Greenish gray (5B 5/1).
LAYERING: None.
DEFORMATION: None.
PRIMARY MINERALOGY:
Olivine - Mode: 75-85%.
Crystal size: 2-8 mm.
Crystal shape: Subhedral-euhedral.
Crystal orientation: None.
Percent replacement: 80-90.
Comments: Apparently cumulus texture.

Orthopyroxene - Mode: 15-25%.
Crystal size: 2-8 mm.
Crystal shape: Equant, subhedral.
Crystal orientation: Random.
Percent replacement: 40-70.
Comments: Occurs as interstitial grains.

Spinel - Mode: Trace.
Crystal size: 1 mm.
Crystal shape: Equant.
Crystal orientation: Disseminated.
Percent replacement: 10-20.
Comments: Probably Cr-spinel.
SECONDARY MINERALOGY:
Serpentine.
Total percent: 40-70%.
Texture: N/A.
Vein material: Irregular, amorphous looking serpentine filled veins (not chrysotile), 0.5-1.5 mm width, irregular orientation.

125-779A-9R-1 (continued)

UNIT 2: METASEDIMENT (MAFIC)

Piece 3

COLOR: Light greenish gray (5G 6/1 to 7/1)
LAYERING: Massive
DEFORMATION: None
PRIMARY MINERALOGY:
  Primary minerals occur as detrital grains.
  Clinopyroxene : Mode: 20%
  Crystal size: 1-2 mm
  Crystal shape: Subhedral-anhedral
  Crystal orientation: None
  Percent replacement: 30-40

  Spinel : Mode: Trace
  Crystal size: <1 mm
  Crystal shape: Anhedral
  Crystal orientation: None
  Percent replacement: 80-90
SECONDARY MINERALOGY:
  Pale green hornblende occurs along the rim or cleavage trace of detrital clinopyroxene.
  Total percent: 80%
  Texture: Sedimentary textures
  Vein material: None
ADDITIONAL COMMENTS: Matrix is occupied by dusty brownish clay.

UNIT 2: METABASALT

Pieces 5 to 10

COLOR: Gray (7.5YR 6/0)
LAYERING: None
DEFORMATION: Brecciated and recemented, individual clasts range from 0.5 to 70 mm in size.
PRIMARY MINERALOGY:
  Subophitic, fine-grained
  Plagioclase : Mode: 40-50%
  Crystal size: <0.5 mm
  Crystal shape: Lath
  Crystal orientation: Felted
  Percent replacement: 100

  Clinopyroxene : Mode: 25-30%
  Crystal size: <0.5 mm
  Crystal shape: Granular
  Crystal orientation: None
  Percent replacement: 30
SECONDARY MINERALOGY:
  Chlorite, pumpellyite, prehnite, dusty clay occur as secondary minerals.
  Total percent: 70%
  Texture: N/A
  Vein material: 0.5-3 mm wide prehnite-pumpellyite and zeolite veins; thickest oriented subparallel to the core axis.
ADDITIONAL COMMENTS: In-situ brecciation is apparent with dominant fractures oriented at 45 degrees to the core axis.

125-779A-9R-1 (continued)

UNIT 2: SERPENTINIZED HARZBURGITE

Pieces 11, 12

COLOR: Gray (2.5Y 4/0-6/0)
LAYERING: None
DEFORMATION: Tectonized
PRIMARY MINERALOGY:
- Olivine - Mode: 85-90%
  Crystal size: 1-8 mm
  Crystal shape: Equant
  Crystal orientation: None
  Percent replacement: 80-90

- Orthopyroxene - Mode: 10-15%
  Crystal size: 3-5 mm
  Crystal shape: Equant
  Crystal orientation: None
  Percent replacement: 80-90
  Comments: Kink-banded; highly deformed

- Spinel - Mode: <1%
  Crystal size: 0.5 mm
  Crystal shape: Euhedral
  Crystal orientation: None
  Percent replacement: 40-50

SECONDARY MINERALOGY:
Mostly serpentinized.
Total percent: 80-90%
Texture: N/A
Vein material: Crosscutting, <0.1 mm, orthogonal sets apparently filled with serpentine.

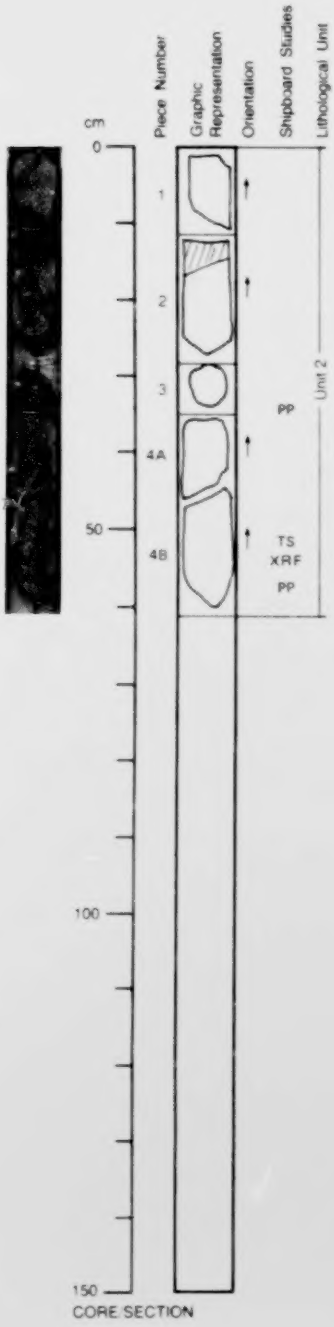

125-779A-9R-2

UNIT 2: SERPENTINIZED HARZBURGITE

Piece 1

COLOR: Light greenish gray (10Y 5/1).
LAYERING: None
DEFORMATION: Orthopyroxene shows wavy deformation
PRIMARY MINERALOGY:
Olivine - Mode: 80-90%.
Crystal size: 3-8 mm.
Crystal shape: Not visible.
Crystal orientation: None.
Percent replacement: 80-90.
Comments: Shows mesh texture.

Orthopyroxene - Mode: 10-20%.
Crystal size: 3-8 mm.
Crystal shape: Equant.
Crystal orientation: None.
Percent replacement: 80-90.

Spinel - Mode: Trace.
Crystal size: 2-4 mm.
Crystal shape: Euhedral to ragged.
Crystal orientation: None.
Percent replacement: 30-40.

SECONDARY MINERALOGY:
Serpentine.
Total percent: 80-90%.
Texture: Mesh texture after olivine.
Vein material: Veins (0.1 mm wide) filled with serpentine; no preferred orientation.

UNIT 2: SERPENTINIZED TECTONIZED HARZBURGITE

Pieces 2 to 4B

COLOR: Gray (10Y 4/1 to 3/1).
LAYERING: Apparent color change.
DEFORMATION: Orthopyroxene shows minor kink banding.
PRIMARY MINERALOGY:
Olivine - Mode: 80-95%.
Crystal size: 1-7 mm.
Crystal shape: Equant, mesh.
Crystal orientation: None.
Percent replacement: Variable.

Orthopyroxene - Mode: 5-8%.
Crystal size: 3-5 mm.
Crystal shape: Equant.
Crystal orientation: None.
Percent replacement: Variable.

Spinel - Mode: <2-3%.
Crystal size: <1 mm.
Crystal shape: Elongate, ragged.
Crystal orientation: None.
Percent replacement: Variable.
SECONDARY MINERALOGY:
Serpentine.
Total percent: 60-80%.
Texture: N/A.
Vein material: First generation parallel to core axis, 1-2 mm wide, with serpentine fill; 2nd set @ 45 degrees to core axis, same fill and mineralogy; 3rd set @ 75 degrees dip with respect to core axis, 5-10 mm wide with two-stage growth of serpentine; 4th set horizontal, 2-5 mm wide, filled with milky green phase.
ADDITIONAL COMMENTS: Major color change possibly because of 100% serpentinization.

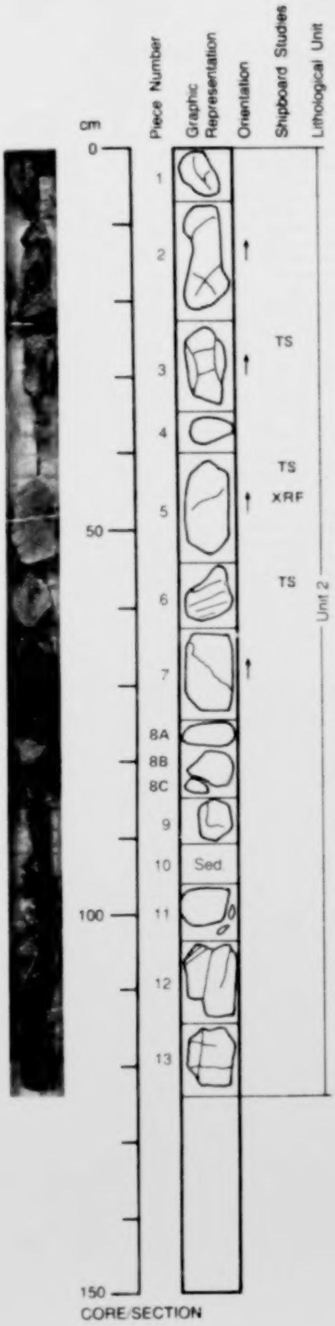

125-779A-10R-1

UNIT 2: SERPENTINIZED TECTONIZED HARZBURGITE

Pieces 1-5

COLOR: Gray blue-green (10Y 5/1 to 4/1).
LAYERING: None.
DEFORMATION: Mylonitization dipping at 70 degrees, elongation of olivine in plane of foliation in a discrete shear zone forming the bottom 8 cm of Piece 5. Other pieces have kink-banded orthopyroxene.
PRIMARY MINERALOGY:
Olivine - Mode: 95%.
Crystal size: Variable <10 mm.
Crystal shape: Equant-elongate.
Crystal orientation: None visible.
Percent replacement: Not visible.
Comments: Variable shape of olivine because of deformation.

Orthopyroxene - Mode: <5%.
Crystal size: 3-5 mm.
Crystal shape: Equant.
Crystal orientation: None visible.
Percent replacement: Not visible.

Spinel - Mode: Trace.
Crystal size: 0.1-0.5 mm.
Crystal shape: Ragged-elongate,disseminated.
Crystal orientation: None visible.
Percent replacement: Not visible.
SECONDARY MINERALOGY:
Serpentine.
Total percent: 80-99%.
Texture: N/A.
Vein material: 1st set sigmoidal and en echelon showing vertical, dextral shear and filled with milky green serpentine, and 2nd generation chrysotile, 2nd set dip 45 degrees. Sets 1 and 2 are mutually orthogonal. Serpentinization is greatest next to veins.
ADDITIONAL COMMENTS: Macro-shape of pieces because of breakage along serpentine veins.

UNIT 2: SERPENTINIZED DUNITE

Piece 6

COLOR: Light gray green (5Y 6/1).
LAYERING: Probably primary cumulate layering dipping at 60 degrees, accentuated by parallel tectonic fabric.
DEFORMATION: Shearing indicates dextral vertical shear.
PRIMARY MINERALOGY:
Olivine - Mode: 90-95%.
Crystal size: Variable, tectonized.
Crystal shape: Ragged.
Crystal orientation: None visible.
Percent replacement: 90-99.

Orthopyroxene - Mode: 5-10%.
Crystal size: 0.5-10 mm.
Crystal shape: Elongate.
Crystal orientation: Aligned, dip 60 degrees.
Percent replacement: 90-99.

Spinel - Mode: Trace.
Crystal size: 0.1 mm.
Crystal shape: Elongate.
Crystal orientation: None visible.
Percent replacement: Not visible.
SECONDARY MINERALOGY:
Serpentine.
Total percent: 80-99%.
Texture: N/A.
Vein material: En echelon veins 0.1-2 mm wide filled with amorphous dark gray serpentine, oriented vertically.
ADDITIONAL COMMENTS: Cumulate rock with shear overprinting primary layering.

125-779A-10R-1 (continued)

UNIT 2: TECTONIZED SERPENTINIZED HARZBURGITE

Pieces 7-9

COLOR: Very dark gray (2.5Y 3/0).
LAYERING: None.
DEFORMATION: Kink-banded pyroxene, elongate spinel.
PRIMARY MINERALOGY:
Olivine - Mode: 95%.
Crystal size: Variable.
Crystal shape: Not visible.
Crystal orientation: None visible.
Percent replacement: 90-99.

Orthopyroxene - Mode: 5%.
Crystal size: 5-8 mm.
Crystal shape: Elongate.
Crystal orientation: None visible.
Percent replacement: 90-99.

Spinel - Mode: <1%.
Crystal size: 0.5-1.5 mm.
Crystal shape: Ragged.
Crystal orientation: None visible.
Percent replacement: Not visible.
SECONDARY MINERALOGY:
Serpentine.
Total percent: 95-99%.
Texture: Bastitic pseudomorphs after orthopyroxene in areas.
Vein material: Two sets, first set (2-5 mm wide) filled with milky green amorphous serpentine. 2nd set dipping subvertically filled with chrysotile and other serpentine mineral showing sub-horizontal dextral shear.

UNIT 2: SERPENTINIZED HARZBURGITE/DUNITE CLAST, IN FOLIATED SERPENTINE MATRIX

Piece 11

COLOR: Dark gray green (2.5Y 3/0 to 4/2).
LAYERING: None.
DEFORMATION: Sheared and foliated matrix.
PRIMARY MINERALOGY:
Heavily serpentinized clast coated with serpentine.
Spinel - Mode: <2%.
Crystal size: 2-3 mm.
Crystal shape: Elongate.
Crystal orientation: None visible.
Percent replacement: Not visible.
SECONDARY MINERALOGY:
Serpentine.
Total percent: 95-99%.
Texture: N/A.
Vein material: N/A.

125-779A-10R-1 (continued)

UNIT 2: TECTONIZED SERPENTINIZED HARZBURGITE

Pieces 12-13

COLOR: Dark green gray (10Y 4/1 to 4/2)
LAYERING: None.
DEFORMATION: Elongate spinel.
PRIMARY MINERALOGY:
Olivine - Mode: 90-95%.
Crystal size: Variable 2-10 mm.
Crystal shape: Deformed.
Crystal orientation: None visible.
Percent replacement: 90-99.

Orthopyroxene - Mode: 5-10%.
Crystal size: 2-5 mm.
Crystal shape: Elongate.
Crystal orientation: None visible.
Percent replacement: 80-90.

Spinel - Mode: <1%.
Crystal size: 0.2-0.5 mm.
Crystal shape: Elongate.
Crystal orientation: Along shear planes.
Percent replacement: Not visible.
SECONDARY MINERALOGY:
Serpentine
Total percent: 90-99%.
Texture: N/A.
Vein material: 1-3 mm, filled with amorphous serpentine sub- vertical, also 1 mm wide, probably chrysotile at no specific orientation.
ADDITIONAL COMMENTS: Primary mineralogy obscured by heavy serpentinization.

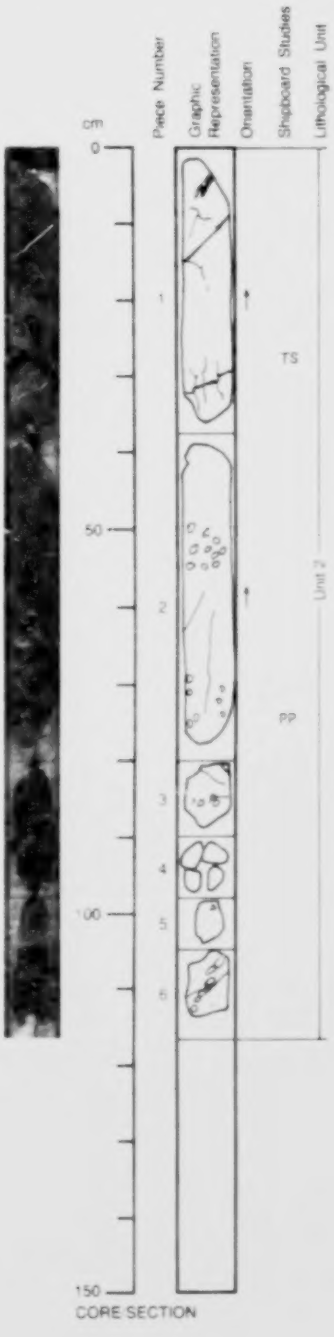

125-779A-10R-2

UNIT 2: TECTONIZED SERPENTINIZED HARZBURGITE

Piece 1

COLOR: Dark greenish gray (5BG4/1)
LAYERING: None
DEFORMATION: Two filled fractures at 30-45 degree dip; offset 0.5 cm; normal fault.
PRIMARY MINERALOGY: Spinel commonly disseminated
Olivine : Mode: 90%
Crystal size: Not visible
Crystal shape: Not visible
Crystal orientation: None visible
Percent replacement: 95

Orthopyroxene : Mode: 9%
Crystal size: 1-3 mm
Crystal shape: Anhedral
Crystal orientation: None visible
Percent replacement: 70?

Spinel : Mode: 1%
Crystal size: <1 mm
Crystal shape: Subhedral-anhedral
Crystal orientation: None visible
Percent replacement: Not visible
SECONDARY MINERALOGY:
Serpentine
Total percent: 80-99%
Texture: Bastitic after pyroxenes
Vein material: Early generation of light greenish serpentine veins (up to 1 cm wide) offset by white and greenish veins along faults; less texture preserved near fault veins.
ADDITIONAL COMMENTS: Orthopyroxene has intercumulus shape.

UNIT 2: SERPENTINIZED HARZBURGITE

Pieces 2-3

COLOR: Dark greenish gray (5BG 4/1)
LAYERING: None; locally pyroxene-rich zones.
DEFORMATION: Some filled fractures (<0.1 mm wide).
PRIMARY MINERALOGY:
Olivine : Mode: 80-85%
Crystal size: Not visible
Crystal shape: Not visible
Crystal orientation: None visible
Percent replacement: 80-90

Orthopyroxene : Mode: 15-20%
Crystal size: 1-3 mm
Crystal shape: Subhedral
Crystal orientation: None visible
Percent replacement: 70-80

Spinel : Mode: Trace
Crystal size: <1 mm
Crystal shape: Subhedral
Crystal orientation: None visible
Percent replacement: Not visible
SECONDARY MINERALOGY:
Severely altered to serpentine
Total percent: 80-99%
Texture: Bastitic after pyroxenes
Vein material: Some greenish white veins (<1 mm), randomly oriented.

125-779A-10R-2 (continued)

UNIT 2: SERPENTINIZED HARZBURGITE

Piece 4

COLOR: Dark greenish gray (5BG 4/1)
LAYERING: None
DEFORMATION: None
PRIMARY MINERALOGY:
Severely altered
Olivine - Mode: 90-95%
Crystal size: Not visible
Crystal shape: Not visible
Crystal orientation: None visible
Percent replacement: 90-99

Orthopyroxene - Mode: 5-10%
Crystal size: Not visible
Crystal shape: Not visible
Crystal orientation: None visible
Percent replacement: 80-90

Spinel - Mode: Trace
Crystal size: Not visible
Crystal shape: Subhedral-anhedral
Crystal orientation: In stringers
Percent replacement: Not visible
SECONDARY MINERALOGY:
Serpentine
Total percent: 90-99%
Texture: Bastitic after orthopyroxenes
Vein material: Few greenish serpentine veins at no specific orientation.

UNIT 2: SERPENTINIZED HARZBURGITE (?)

Piece 5

COLOR: Dark greenish gray (5BG4/1)
LAYERING: None
DEFORMATION: None
PRIMARY MINERALOGY:
Severely altered
Olivine - Mode: 60-80%
Crystal size: Not visible
Crystal shape: Not visible
Crystal orientation: None visible
Percent replacement: 90-99

Orthopyroxene - Mode: 20-40%
Crystal size: Not visible
Crystal shape: Anhedral
Crystal orientation: None visible
Percent replacement: 80-90

Spinel - Mode: Trace
Crystal size: Not visible
Crystal shape: Subhedral-anhedral
Crystal orientation: In stringers
Percent replacement: Not visible
SECONDARY MINERALOGY:
Serpentine
Total percent: 90-99%
Texture: Bastitic after orthopyroxene
Vein material: <1-mm-wide green-white serpentine(?) veins showing no preferred orientation
ADDITIONAL COMMENTS: Intercumulus pyroxene

125-779A-10R-2 (continued)

UNIT 2: SERPENTINIZED HARZBURGITE

Piece 6

COLOR: Dark greenish gray (5BG 4/1)
LAYERING: None; pyroxene-zone at 80 degree dip
DEFORMATION: Parallel vein-filled cracks at 60 degree dip
PRIMARY MINERALOGY:
Severely altered; zone of large pyroxene (<2 cm wide) with kink bands?
Olivine - Mode: 90%
Crystal size: Not visible
Crystal shape: Not visible
Crystal orientation: None visible
Percent replacement: 90-99

Orthopyroxene - Mode: 10%
Crystal size: <4 mm
Crystal shape: Subhedral-anhedral
Crystal orientation: None visible
Percent replacement: Variable

Spinel - Mode: Trace
Crystal size: Not visible
Crystal shape: Subhedral-anhedral
Crystal orientation: In stringers
Percent replacement: Not visible
SECONDARY MINERALOGY:
Serpentine
Total percent: 90-99%
Texture: Bastitic after pyroxenes
Vein material: Minor bluish green-white serpentine veins (<1 mm wide)

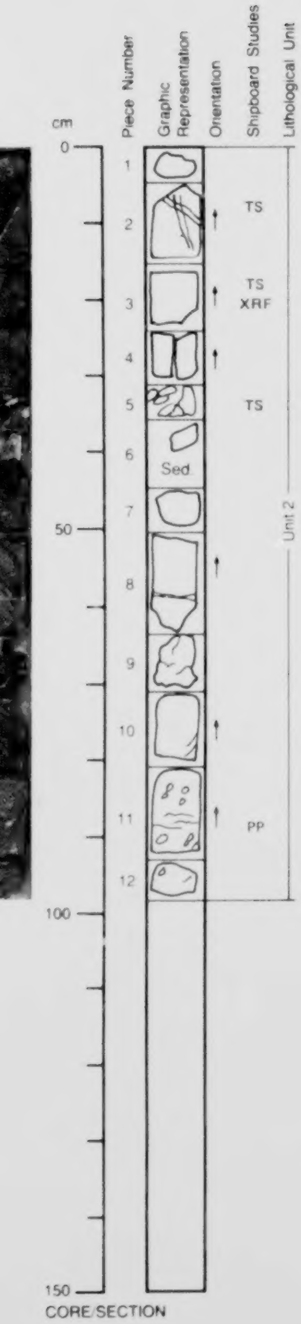

125-779A-11R-1

UNIT 2: SERPENTINIZED HARZBURGITE

Piece 1

COLOR: Dark greenish gray (5BG 4/1) with bluish gray patches
LAYERING: None
DEFORMATION: Fractured
PRIMARY MINERALOGY:
Olivine - Mode: 80-90%
Crystal size: Not visible
Crystal shape: Not visible
Crystal orientation: None visible
Percent replacement: 95-99

Orthopyroxene - Mode: 10-20%
Crystal size: <3 mm
Crystal shape: Anhedral
Crystal orientation: None visible
Percent replacement: Variable

Spinel - Mode: Trace
Crystal size: <1 mm
Crystal shape: Equant
Crystal orientation: None visible
Percent replacement: Not visible
SECONDARY MINERALOGY:
Serpentine
Total percent: 100%
Texture: blue-gray serpentine pseudomorphs after anhedral pyroxenes (<1 cm)
Vein material: Sub-parallel bluish green veins (<2 mm wide)
ADDITIONAL COMMENTS: Intercumulate(?) pyroxene

UNIT 2: SERPENTINIZED HARZBURGITE

Pieces 2-4

COLOR: Dark greenish gray (5BG 4/1)
LAYERING: None
DEFORMATION: None
PRIMARY MINERALOGY:
Olivine - Mode: 80-90%
Crystal size: Not visible
Crystal shape: Anhedral
Crystal orientation: None visible
Percent replacement: 90-99

Orthopyroxene - Mode: 10-15%
Crystal size: <2 mm
Crystal shape: Subhedral
Crystal orientation: None visible
Percent replacement: Variable

Spinel - Mode: Trace
Crystal size: <2 mm
Crystal shape: Subhedral-anhedral
Crystal orientation: Stringers
Percent replacement: Not visible
SECONDARY MINERALOGY:
Serpentine
Total percent: 90-99%
Texture: Bastitic after pyroxenes in areas
Vein material: 1 green serpentine vein (4 mm wide) and few white veins (<0.2 mm wide) at no specific orientation

125-779A-11R-1 (continued)

UNIT 2: SERPENTINIZED DUNITE (?)

Pieces 5-6 (clast)

COLOR: Dark greenish gray (5BG4/1) with bluish white patchy fracture surfaces from vein serpentine.
LAYERING: Sub parallel veins.
DEFORMATION: Vein-filled fractures.
PRIMARY MINERALOGY:
- Olivine - Mode: 90%.
  Crystal size: Not visible.
  Crystal shape: Not visible.
  Crystal orientation: None visible.
  Percent replacement: 90-99.

- Orthopyroxene - Mode: 10%.
  Crystal size: <5 mm.
  Crystal shape: Subhedral-anhedral.
  Crystal orientation: None visible.
  Percent replacement: 90.

- Spinel - Mode: Trace.
  Crystal size: <1 mm.
  Crystal shape: Equant.
  Crystal orientation: None visible.
  Percent replacement: Not visible.

SECONDARY MINERALOGY:
- Serpentine.
  Total percent: 100%.
  Texture: Bastitic pseudomorphs after euhedral pyroxenes in areas.
  Vein material: abundant greenish white veins (up to 2 cm thick) non fibrous serpentine (?) at no specific orientation.

UNIT 2: SERPENTINIZED HARZBURGITE

Pieces 7-10

COLOR: Dark greenish gray (5BG 4/1) with lighter patches.
LAYERING: None.
DEFORMATION: None visible.
PRIMARY MINERALOGY:
- Olivine - Mode: 80-90%.
  Crystal size: Not visible.
  Crystal shape: Not visible.
  Crystal orientation: None visible.
  Percent replacement: 90-99.

- Orthopyroxene - Mode: 10-20%.
  Crystal size: <0.5 mm.
  Crystal shape: Not visible.
  Crystal orientation: None visible.
  Percent replacement: 90-99.

- Spinel - Mode: Trace.
  Crystal size: <1 mm.
  Crystal shape: Rounded.
  Crystal orientation: Stringers.
  Percent replacement: Not visible.

SECONDARY MINERALOGY:
- Serpentine.
  Total percent: 100%.
  Texture: Mesh textured.
  Vein material: Few light greenish white veins (<1 mm).

125-779A-11R-1 (continued)

UNIT 2: SERPENTINIZED DUNITE (?)

Pieces 11-12

COLOR: Dark greenish gray (5BG 4/1) with lighter patches.
LAYERING: None.
DEFORMATION: None visible.
PRIMARY MINERALOGY:
Olivine - Mode: 90-95%.
Crystal size: Not visible.
Crystal shape: Not visible.
Crystal orientation: None visible.
Percent replacement: 90-99.

Orthopyroxene - Mode: 4-8%.
Crystal size: Not visible.
Crystal shape: Not visible.
Crystal orientation: None visible.
Percent replacement: 80-90.

Spinel - Mode: 1-2%.
Crystal size: Not visible.
Crystal shape: Stringers.
Crystal orientation: None visible.
Percent replacement: Not visible.
SECONDARY MINERALOGY:
Serpentine.
Total percent: 99%.
Texture: Bastitic after orthopyroxene in areas and mesh textured after olivine.
Vein material: Minor serpentine veins present.

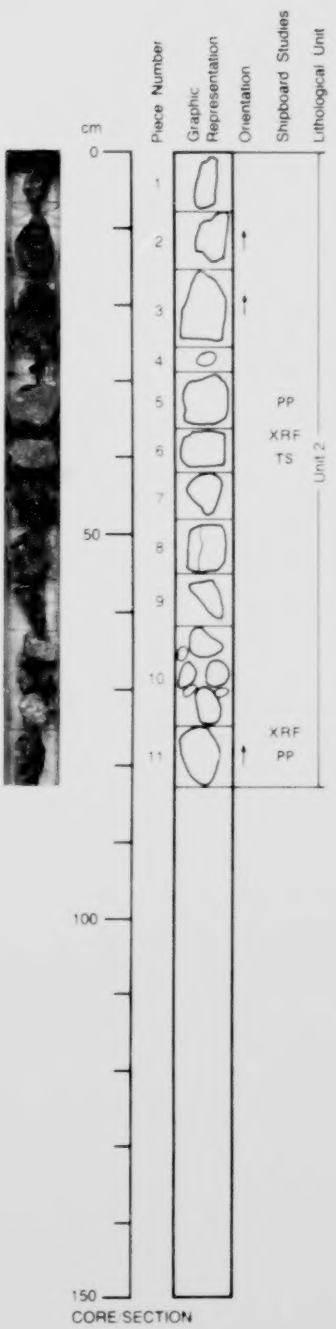

125-779A-12R-1

UNIT 2: SERPENTINIZED TECTONIZED HARZBURGITE

Pieces 1-2

COLOR: Dark greenish gray (5BG 4/1) with lighter patches
LAYERING: None
DEFORMATION: Deformed serpentinized pyroxenes
PRIMARY MINERALOGY:
Olivine : Mode: 90%
Crystal size: Not visible
Crystal shape: Not visible
Crystal orientation: None visible
Percent replacement: 90-99

Orthopyroxene : Mode: 10%
Crystal size: Not visible
Crystal shape: Not visible
Crystal orientation: None visible
Percent replacement: 90-99

Spinel : Mode: Trace
Crystal size: <1 mm
Crystal shape: Equant round
Crystal orientation: None visible
Percent replacement: Not visible
SECONDARY MINERALOGY:
Serpentine
Total percent: 95-99%
Texture: Mesh serpentine and bastitic pseudomorphs after pyroxenes
Vein material: Few light greenish veins (<0.1 mm)

UNIT 2: SERPENTINIZED DUNITE

Piece 3

COLOR: Dark greenish gray (5BG 4/1)
LAYERING: None
DEFORMATION: Sub-parallel vein-filled cracks
PRIMARY MINERALOGY:
Olivine : Mode: >95%
Crystal size: Not visible
Crystal shape: Not visible
Crystal orientation: None visible
Percent replacement: 95-99

Orthopyroxene : Mode: 5%
Crystal size: Not visible
Crystal shape: Equant-elongate
Crystal orientation: None visible
Percent replacement: 95-99
Comments: Intercumulus ?

Spinel : Mode: Trace
Crystal size: <1 mm
Crystal shape: Round
Crystal orientation: None visible
Percent replacement: Not visible
SECONDARY MINERALOGY:
Serpentine
Total percent: 95-99%
Texture: Serpentine mesh-textured after olivine with some bastites after pyroxenes
Vein material: Some white subparallel (<0.2 mm) veins; few green veins

125-779A-12R-1 (continued)

UNIT 2: SERPENTINIZED HARZBURGITE

Piece 4

COLOR: Greenish black (5Y 2.5/1)
LAYERING: None
DEFORMATION: None
PRIMARY MINERALOGY:
Olivine - Mode: 80-90%
Crystal size: Not visible
Crystal shape: Not visible
Crystal orientation: None visible
Percent replacement: 90-99

Orthopyroxene - Mode: 10-20%
Crystal size: <1.5 mm
Crystal shape: Subhedral-anhedral
Crystal orientation: None visible
Percent replacement: 80-90
SECONDARY MINERALOGY:
Serpentine
Total percent: 80-90%
Texture: N/A
Vein material: N/A

UNIT 2: SERPENTINIZED HARZBURGITE

Piece 5

COLOR: Dark greenish gray (5BG 4/1)
LAYERING: Locally pyroxene-rich and olivine-rich pockets
DEFORMATION: None
PRIMARY MINERALOGY:
Olivine - Mode: 50%
Crystal size: Not visible
Crystal shape: Not visible
Crystal orientation: None visible
Percent replacement: 95-99

Orthopyroxene - Mode: 50%
Crystal size: Not visible
Crystal shape: Not visible
Crystal orientation: None visible
Percent replacement: 90

Spinel - Mode: Trace
Crystal size: <1 mm
Crystal shape: Not visible
Crystal orientation: None visible
Percent replacement: Not visible
SECONDARY MINERALOGY:
Serpentine
Total percent: 95-99%
Texture: Slightly developed bastite pseudomorphs after pyroxenes
Vein material: N/A

125-779A-12R-1 (continued)

UNIT 2: SERPENTINITE HARZBURGITE

Piece 6

COLOR: Dark greenish gray (5GB 4/1) with lighter patches.
LAYERING: None.
DEFORMATION: None.
PRIMARY MINERALOGY:
Olivine - Mode: 90%.
Crystal size: Not visible.
Crystal shape: Not visible.
Crystal orientation: None visible.
Percent replacement: 90-99.

Orthopyroxene - Mode: 10%.
Crystal size: Not visible.
Crystal shape: Subhedral-anhedral.
Crystal orientation: None visible.
Percent replacement: 90.
Comments: Intercumulus ?

Spinel - Mode: Trace.
Crystal size: <2 mm.
Crystal shape: Subhedral.
Crystal orientation: None visible.
Percent replacement: Not visible.
SECONDARY MINERALOGY:
Serpentine.
Total percent: 90-99%.
Texture: Bastite pseudomorphs after pyroxenes.
Vein material: N/A.

UNIT 2: SERPENTINIZED HARZBURGITE

Pieces 7-8

COLOR: Dark greenish gray (5BG 4/1).
LAYERING: None.
DEFORMATION: None.
PRIMARY MINERALOGY:
One equant spinel has a metallic inclusion.
Olivine - Mode: 90%.
Crystal size: Not visible.
Crystal shape: Not visible.
Crystal orientation: None visible.
Percent replacement: 95-99.

Orthopyroxene - Mode: 10%.
Crystal size: 1-2 mm.
Crystal shape: Euhedral-anhedral.
Crystal orientation: None visible.
Percent replacement: 90.

Spinel - Mode: Trace.
Crystal size: <1 mm.
Crystal shape: Equant?
Crystal orientation: None visible.
Percent replacement: Not visible.
SECONDARY MINERALOGY:
Serpentine.
Total percent: 95-99%.
Texture: Bastite pseudomorphs after pyroxenes.
Vein material: White (<1 mm) and bluish (<1 mm) veins.

125-779A-12R-1 (continued)

UNIT 2: SERPENTINIZED HARZBURGITE

Piece 10 (multiple fragments)

COLOR: Dark greenish gray (5BG 4/1).
LAYERING: None.
DEFORMATION: Brecciated.
PRIMARY MINERALOGY:
Modal proportions vary in each fragment.
Olivine - Mode: 40-90%.
Crystal size: Not visible.
Crystal shape: Not visible.
Crystal orientation: None visible.
Percent replacement: 90-99.

Orthopyroxene - Mode: 10-60%.
Crystal size: Not visible.
Crystal shape: Not visible.
Crystal orientation: None visible.
Percent replacement: 90.

Spinel - Mode: Trace.
Crystal size: Not visible.
Crystal shape: Not visible.
Crystal orientation: None visible.
Percent replacement: Not visible.
SECONDARY MINERALOGY:
Serpentine.
Total percent: 99%.
Texture: Bastite pseudomorphs after pyroxenes in areas.
Vein material: Abundant light green veins of serpentine (<1 mm wide).

UNIT 2: SERPENTINIZED TECTONIZED HARZBURGITE

Piece 11

COLOR: Dark greenish gray (5BG 4/1) with light patches.
LAYERING: None.
DEFORMATION: Deformed pyroxenes.
PRIMARY MINERALOGY:
Olivine - Mode: 90%.
Crystal size: Not visible.
Crystal shape: Not visible.
Crystal orientation: None visible.
Percent replacement: 90-99.

Orthopyroxene - Mode: 10%.
Crystal size: Not visible.
Crystal shape: Not visible.
Crystal orientation: None visible.
Percent replacement: 90.

Spinel - Mode: Trace.
Crystal size: <1 mm.
Crystal shape: Equant.
Crystal orientation: None visible.
Percent replacement: Not visible.
SECONDARY MINERALOGY:
Serpentine.
Total percent: 95-99%.
Texture: Bastite pseudomorphs after pyroxenes in areas.
Vein material: Very few light greenish serpentine veins.

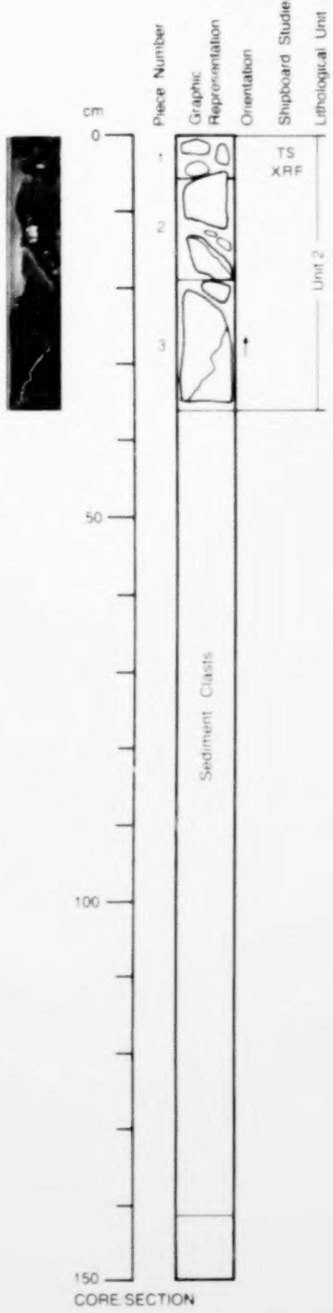
cm
Piece Number
Graphic Representation
Orientation
Shipboard Studies
Lithological Unit
0
1
2
3
TS
XRF
Unit 2
50
Sediment Clasts
100
150
CORE SECTION

125-779A-13R-1

UNIT 2: SERPENTINIZED HARZBURGITE

Pieces 1-3 (multiple fragments)

COLOR: Black (2.5YR 2.5/0)
LAYERING: None
DEFORMATION: None discernible in hand sample
PRIMARY MINERALOGY:
Heavily serpentinized
Olivine - Mode: 80-90%
Crystal size: < 1 visible
Crystal shape: Not visible
Crystal orientation: None
Percent replacement: 100

Orthopyroxene - Mode: >10%
Crystal size: 5 mm?
Crystal shape: Equant
Crystal orientation: None
Percent replacement: 100

Spinel - Mode: 1-2%
Crystal size: 0.5-2 mm
Crystal shape: Euhedral (equant) to elongate
Crystal orientation: None
Percent replacement: Variable
SECONDARY MINERALOGY:
Serpentine
Total percent: 100%
Texture: N/A
Vein material: Numerous, up to 5 mm, filled with pale green serpentine; anastomosing

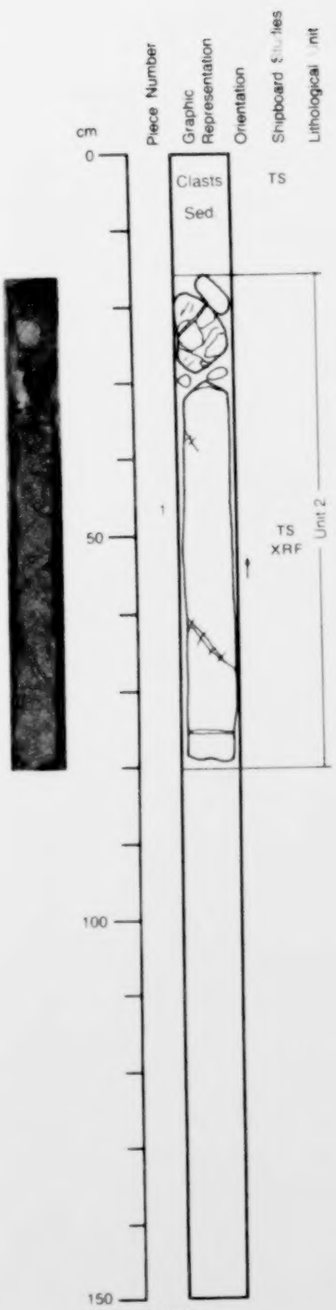
cm
Piece Number
Graphic Representation
Orientation
Shipboard Studies
Lithological Unit
0
50
100
150
CORE/SECTION
Clasts
Sed.
TS
1
TS
XRF
Unit 2

125-779A-13R-2

UNIT 2: SERPENTINIZED TECTONIZED HARZBURGITE

Piece 1

COLOR: Gray (2.5Y 5/0)
LAYERING: None.
DEFORMATION: Orthopyroxenes show wavy cleavage.
PRIMARY MINERALOGY:
Olivine - Mode: 80-85%.
Crystal size: 5-10 mm.
Crystal shape: Equant, ragged.
Crystal orientation: None.
Percent replacement: Variable.

Orthopyroxene - Mode: 10-15%.
Crystal size: 5-8 mm.
Crystal shape: Equant.
Crystal orientation: None.
Percent replacement: Variable.
Spinel - Mode: <1%.
Crystal size: 0.1-3 mm.
Crystal shape: Elongate, ragged.
Crystal orientation: None.
Percent replacement: Variable.
SECONDARY MINERALOGY:
Serpentine.
Total percent: 90-99%.
Texture: N/A.
Vein material: 0.5-2 mm wide veins, dipping at 45 degrees, filled with dark serpentine cross-stitched with second generation of chrysotile ("Frankenstein" texture); second vein set: dipping at 30 degrees, dark serpentine filling.

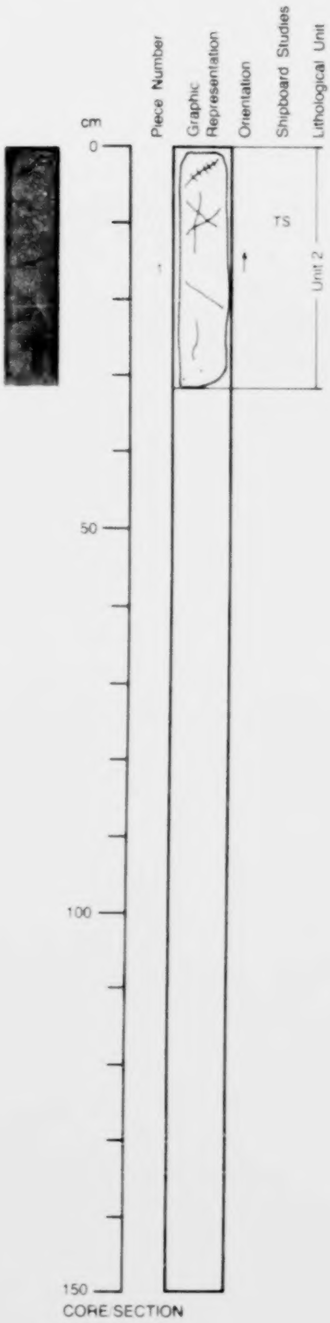
cm
Piece Number
Graphic Representation
Orientation
Shipboard Studies
Lithological Unit
0
50
100
150
1
TS
Unit 2
CORE SECTION

125-779A-13R-3

UNIT 2: TECTONIZED SERPENTINIZED HARZBURGITE

Piece 1

COLOR: Dark gray (2.5YR 4/0)
LAYERING: None
DEFORMATION: Orthopyroxenes show wavy deformation on exposed cleavage surfaces
PRIMARY MINERALOGY:
Primary minerals are variably serpentinized.
Orthopyroxene - Mode: 15-20%
Crystal size: 4-8 mm
Crystal shape: Equant
Crystal orientation: None
Percent replacement: 50-60

Olivine - Mode: 80-85%
Crystal size: 5-10 mm
Crystal shape: Equant to ragged
Crystal orientation: None
Percent replacement: 50-60

Spinel - Mode: >1%
Crystal size: 0.1-2 mm
Crystal shape: Ragged to elongate
Crystal orientation: None
Percent replacement: 10-20
SECONDARY MINERALOGY:
Serpentine
Total percent: 50-60%
Texture: N/A
Vein material: Numerous, conjugate sets, 1-2 mm wide, some are filled with black serpentine, some have "Frankenstein texture" with crosscutting light serpentine; sets dip at 45 degrees to core axis, others subparallel to core axis, order of veining indeterminate.

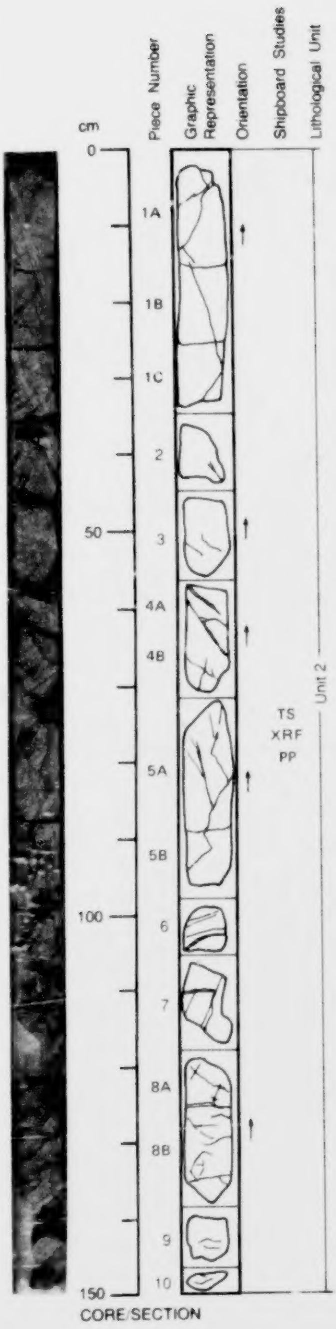
cm
Piece Number
Graphic Representation
Orientation
Shipboard Studies
Lithological Unit
0
50
100
150
1A
1B
1C
2
3
4A
4B
5A
5B
6
7
8A
8B
9
10
TS
XRF
PP
Unit 2
CORE/SECTION

125-779A-14R-1

UNIT 2: SERPENTINIZED TECTONIZED HARZBURGITE

Pieces 1 to 10

COLOR: Gray (N 6/).
LAYERING: Massive, with alteration banding caused by variable serpentinization.
DEFORMATION: Orthopyroxene shows wavy cleavage surfaces.
PRIMARY MINERALOGY:
Olivine - Mode: 80-85%.
Crystal size: 1-5 mm.
Crystal shape: Mesh-like.
Crystal orientation: None.
Percent replacement: 80-90.

Orthopyroxene - Mode: 15-20%.
Crystal size: 1-5 mm.
Crystal shape: Equant.
Crystal orientation: None.
Percent replacement: 80-90.

Spinel - Mode: <1%.
Crystal size: 0.5-1 mm.
Crystal shape: Equant to elongate.
Crystal orientation: Elongate parallel to serp.-filled fract.
Percent replacement: 30-40.
SECONDARY MINERALOGY:
Serpentine.
Total percent: 80-90%.
Texture: N/A.
Vein material: Two conjugate sets, oriented at about 45 degrees to core axis, 0.5-2 mm wide, alteration haloes of serpentine extending into the host; most are filled with black serpentine, minority filled with chrysotile.

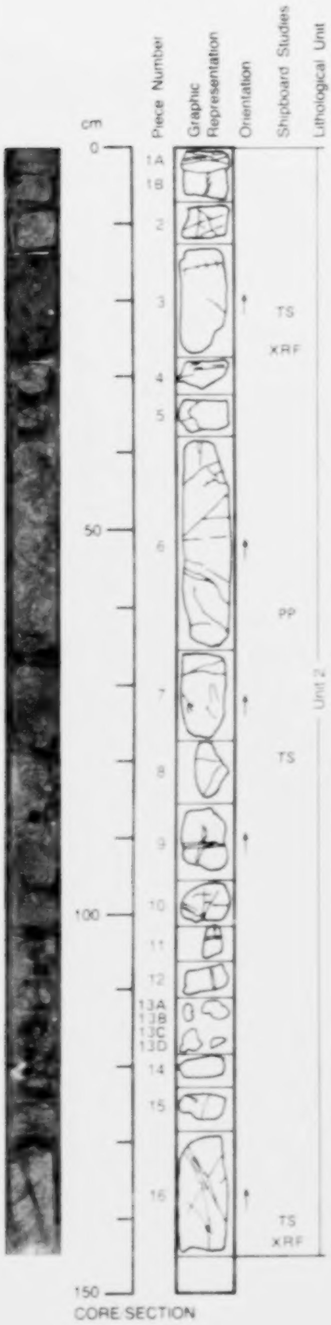

125-779A-14R-2

UNIT 2: SERPENTINIZED TECTONIZED HARZBURGITE

Pieces 1 to 2, 4 to 16

COLOR: Gray (N 6/)
LAYERING: None, but rock exhibits color banding caused by variable serpentinization.
DEFORMATION: Pyroxene shows wavy cleavage surfaces.
PRIMARY MINERALOGY:
Olivine - Mode: 80-90%
Crystal size: 3-5 mm
Crystal shape: Equant
Crystal orientation: None visible
Percent replacement: Variable

Orthopyroxene - Mode: 10-20%
Crystal size: 3-8 mm
Crystal shape: Equant
Crystal orientation: None visible
Percent replacement: Variable

Spinel - Mode: <1%
Crystal size: 0.01-2 mm
Crystal shape: Equant-elongate
Crystal orientation: Parallel to fractures
Percent replacement: Variable
SECONDARY MINERALOGY:
Rock is variably serpentinized; extent more pronounced close to visible fractures.
Total percent: 50-90%
Texture: N/A
Vein material: Numerous, crosscutting, about 45 degrees to core axis and some normal to core axis; some are polyphase-filled with dark and light serpentine.

UNIT 2: SERPENTINIZED TECTONIZED HARZBURGITE

Piece 3

COLOR: Very dark gray (2.5Y 3/0)
LAYERING: None
DEFORMATION: None visible
PRIMARY MINERALOGY:
Appears to be less orthopyroxene than overlying and underlying core pieces.
Olivine - Mode: 80-90%
Crystal size: <4 mm
Crystal shape: Not visible
Crystal orientation: None visible
Percent replacement: 80-90

Orthopyroxene - Mode: 10-20%
Crystal size: 3-7 mm
Crystal shape: Equant
Crystal orientation: None visible
Percent replacement: 80-90

Spinel - Mode: <1%
Crystal size: 0.2-1 mm
Crystal shape: Equant
Crystal orientation: None visible
Percent replacement: Not visible
SECONDARY MINERALOGY:
Serpentine
Total percent: 80-90%
Texture: N/A
Vein material: Perpendicular to core axis, dark serpentine in center of vein; chrysotile outer part and at right angles (Frankenstein- texture) to the main (1.5 mm wide) vein. Other chrysotile veins 0.2 mm wide.

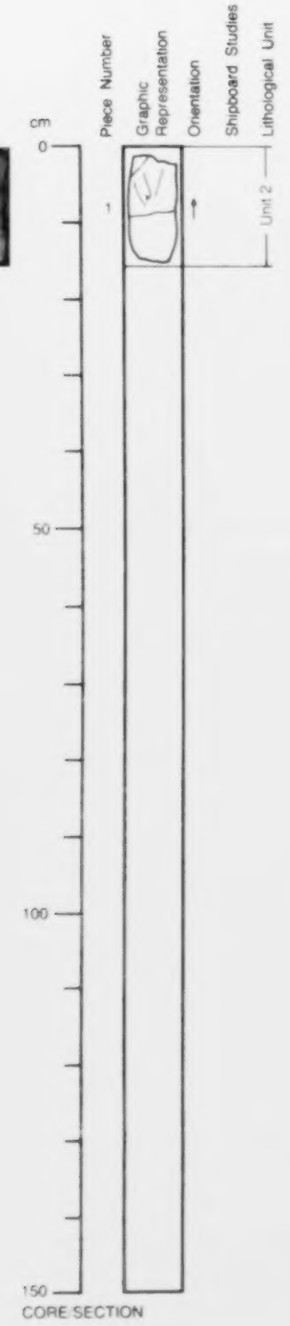
cm
Piece Number
Graphic Representation
Orientation
Shipboard Studies
Lithological Unit
0
1
Unit 2
50
100
150
CORE/SECTION

125-779A-14R-3

UNIT 2: TECTONIZED SERPENTINIZED HARZBURGITE

Piece 1

COLOR: Very dark gray (2.5Y 4/)
LAYERING: None
DEFORMATION: Wavy cleavage surfaces on the orthopyroxene
PRIMARY MINERALOGY:
Olivine - Mode: 65-80%
Crystal size: 1-4 mm
Crystal shape: Not visible
Crystal orientation: None visible
Percent replacement: Not visible

Orthopyroxene - Mode: 20-35%
Crystal size: 2-5 mm
Crystal shape: Not visible
Crystal orientation: None visible
Percent replacement: Not visible

Spinel - Mode: <1%
Crystal size: 0.2-3 mm
Crystal shape: Equant to elongate
Crystal orientation: None visible
Percent replacement: Not visible
SECONDARY MINERALOGY:
Serpentine
Total percent: 50-90%
Texture: N/A
Vein material: Minor veining, filled with dark serpentine

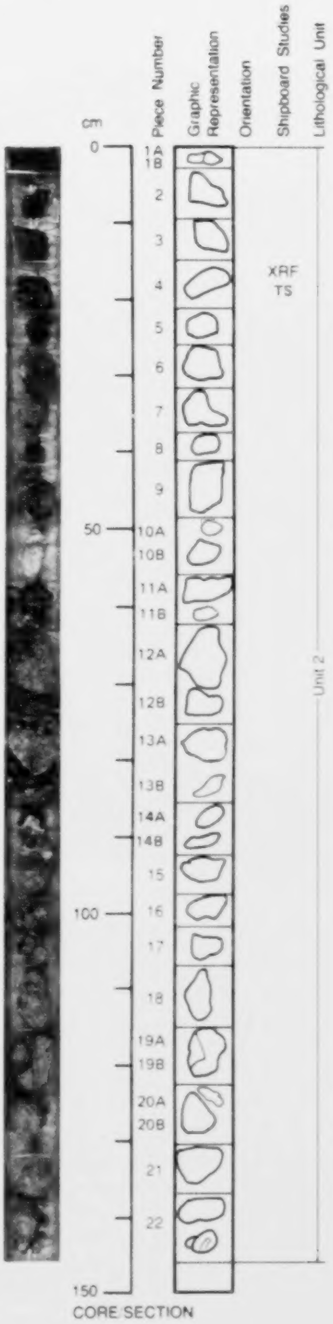

125-779A-15R-1

UNIT 2: SERPENTINIZED HARZBURGITE

Pieces 1-9

COLOR: Gray (2.5YR 5/0)
LAYERING: None
DEFORMATION: None
PRIMARY MINERALOGY:
Olivine - Mode: 70-80%
Crystal size: 2-5 mm
Crystal shape: Equant
Crystal orientation: None visible
Percent replacement: 50

Orthopyroxene - Mode: 20-30%
Crystal size: 0.5-5 mm
Crystal shape: Equant-elongate
Crystal orientation: None visible
Percent replacement: 20-50

Spinel - Mode: <1%
Crystal size: 0.2-1
Crystal shape: Equant
Crystal orientation: None visible
Percent replacement: Not visible
SECONDARY MINERALOGY:
Serpentine
Total percent: 50-60%
Texture: N/A
Vein material: Numerous small (2-mm-wide chrysotile-filled veins)

UNIT 2: SERPENTINIZED HARZBURGITE

Pieces 10A and B, 14A and B (@85cm)

COLOR: White to light gray (7.5YR 8/0-7/0)
LAYERING: None
DEFORMATION: None
PRIMARY MINERALOGY: Pyroxene through a screen of chrysotile coating on clasts
SECONDARY MINERALOGY: Serpentine
ADDITIONAL COMMENTS: Primary bulk of sample obscured

UNIT 2: SERPENTINIZED TECTONIZED HARZBURGITE

Pieces 11-13; 15-22

COLOR: Variable depending on degree of serpentinization, gray (7.5YR 3/0-6/0)
LAYERING: None
DEFORMATION: Pyroxene shows kink banding and stretching
PRIMARY MINERALOGY:
Olivine - Mode: 70-80%
Crystal size: 3-10 mm
Crystal shape: Equant-ragged
Crystal orientation: None visible
Percent replacement: Not visible

Orthopyroxene - Mode: 20-30%
Crystal size: 2-6 mm
Crystal shape: Equant-elongate
Crystal orientation: None visible
Percent replacement: Not visible

Spinel - Mode: <1%
Crystal size: 0.1-3 mm
Crystal shape: Elongate-ragged
Crystal orientation: Some dip at 30 degrees to horizontal
Percent replacement: Not visible
SECONDARY MINERALOGY:
Serpentine
Total percent: 50-80%
Texture: N/A
Vein material: 2 sets: 1st generation 65 degrees, filled with amorphous black serpentine, 1-2 mm wide. 2nd generation: occasionally crosscut 1st set, filled with (1) amorphous black-gray serpentine, (2) laminated fibrous chrysotile (ranges from 1-15 mm wide). Thickest veins show Frankenstein texture.
ADDITIONAL COMMENTS: Some sediment occurs with Piece 13A, half coating the clast, and underlies 13A. Sediment is sheared serpentine, 3 cm thick.

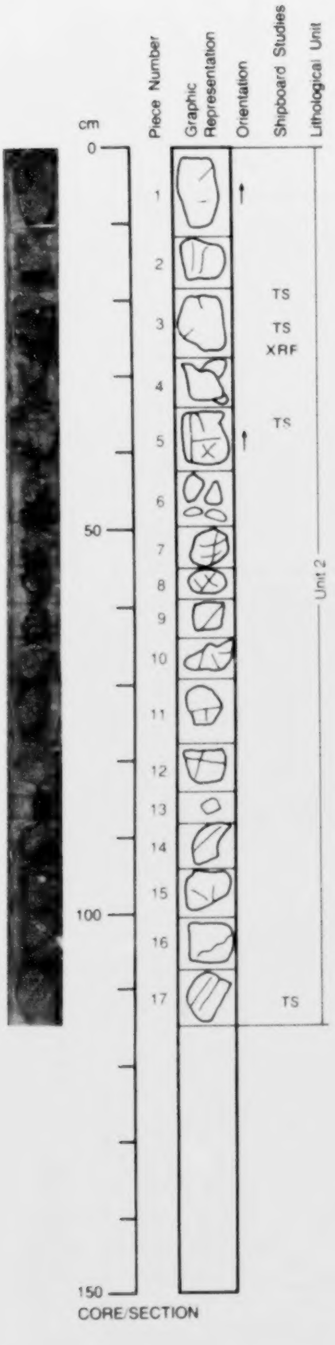

125-779A-15R-2

UNIT 2: SERPENTINIZED TECTONIZED HARZBURGITE

Pieces 1 and 2

COLOR: Dark-gray, blue-gray, mottled (N 6/ to 5B 5/1).
LAYERING: None.
DEFORMATION: Pyroxenes show wavy extinction and minor kink banding; spinel shows dumbbell shape.
PRIMARY MINERALOGY:
Orthopyroxene - Mode: 10-15%
Crystal size: 5-10 mm.
Crystal shape: Elongate.
Crystal orientation: None visible.
Percent replacement: Variable.

Olivine - Mode: 85-90%.
Crystal size: 5-15 mm.
Crystal shape: Ragged.
Crystal orientation: None visible.
Percent replacement: Variable.

Spinel - Mode: Trace.
Crystal size: 0.1-0.5 mm.
Crystal shape: Elongate.
Crystal orientation: None visible.
Percent replacement: Not visible.
Comments: Cr-bearing?
SECONDARY MINERALOGY:
Serpentine.
Total percent: 30-80%.
Texture: N/A.
Vein material: En echelon and sigmoidal sets indicating vertical dextral shear, completely filled with amorphous black serpentine.

UNIT 2: SERPENTINIZED DUNITE

Pieces 3, 4A, 4B, 5

COLOR: Dark greenish-gray (5B 4/1).
LAYERING: None.
DEFORMATION: Spinels are sheared, orthopyroxenes show kink banding and stretching.
PRIMARY MINERALOGY:
Orthopyroxene - Mode: 0-1%.
Crystal size: 0.2-1.5 mm.
Crystal shape: Equant to elongate.
Crystal orientation: None visible.
Percent replacement: Not visible.

Olivine - Mode: 99%.
Crystal size: Not visible.
Crystal shape: Not visible.
Crystal orientation: None visible.
Percent replacement: Not visible.

Spinel - Mode: <1%.
Crystal size: 0.2-0.8.
Crystal shape: Elongate.
Crystal orientation: None visible.
Percent replacement: Not visible.
SECONDARY MINERALOGY:
Serpentine.
Total percent: 50-80%.
Texture: N/A.
Vein material: Two generations: (1)anastomosing, vertical and horizontal, steeply dipping, 1-5 mm wide, two generations of dark amorphous serpentine fill; (2) vertical and horizontal, 0.5-2 mm wide, filled with white and green fibrous chrysotile showing sinistral and vertical shear; veins total up to 2% of rocks.

125-779A-15R-2 (continued)

UNIT 2: SERPENTINIZED TECTONIZED HARZBURGITE

Pieces 6-17

COLOR: Gray to dark greenish gray (N 5/ to 5B 4/1).
LAYERING: Disseminated spinel grains, 25 cm thick and forming 1% to 2% modal volume dipping at 65 degrees (found only in Piece 16).
DEFORMATION: Orthopyroxene shows kink banding and elongation defining a coarse foliation dipping at 50 degrees.
PRIMARY MINERALOGY:
Olivine - Mode: 85-95%
Crystal size: Not visible
Crystal shape: Not visible
Crystal orientation: None visible
Percent replacement: 80-99

Orthopyroxene - Mode: 5-15%
Crystal size: 2-12 mm
Crystal shape: Equant-elongate
Crystal orientation: Defines foliation
Percent replacement: 80-90

Spinel - Mode: <1%
Crystal size: 0.2-1 mm
Crystal shape: Equant-dumbbell
Crystal orientation: Defines foliation
Percent replacement: Not visible
SECONDARY MINERALOGY:
Serpentine
Total percent: 80-99%
Texture: N/A
Vein material: Two generations: first, conjugate sets, 0.2-8 mm wide, steeply dipping, filled with amorphous black serpentine, cut by second generation dipping at 15-25 degrees, filled with white chrysotile and carbonate(?) with occasional "Frankenstein veins" of chrysotile perpendicular to strike of veins.
ADDITIONAL COMMENTS: Orthopyroxene and spinel define primary foliation.

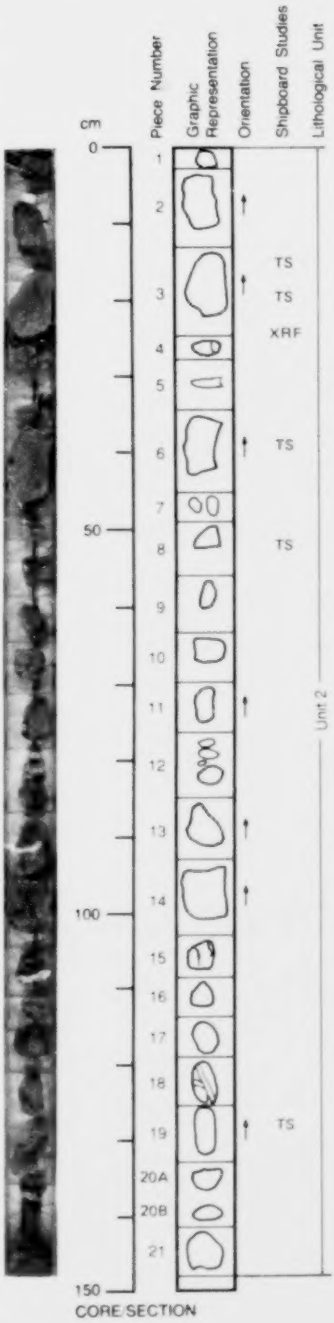
cm
Piece Number
Graphic Representation
Orientation
Shipboard Studies
Lithological Unit
0
50
100
150
1
2
3
4
5
6
7
8
9
10
11
12
13
14
15
16
17
18
19
20A
20B
21
TS
TS
XRF
TS
TS
TS
Unit 2
CORE/SECTION

125-779A-16R-1

UNIT 2: TECTONIZED SERPENTINIZED HARZBURGITE

Pieces 1 to 21

COLOR: Bluish gray (5B 5/1) with altered dark greenish gray zones (5BG 4/1).
LAYERING: None.
DEFORMATION: Fractures, locally low angle, 20 degree normal faulting with a few mm offset in dark veins, kink banded orthopyroxene. Shearing is caused by brecciation.
PRIMARY MINERALOGY:
Orthopyroxene - Mode: 5-15%.
Crystal size: 2-8 mm.
Crystal shape: Elongate, ragged.
Crystal orientation: None visible.
Percent replacement: Variable.

Olivine - Mode: 85-95%.
Crystal size: Not visible.
Crystal shape: Not visible.
Crystal orientation: None visible.
Percent replacement: Variable.

Spinels - Mode: <1%.
Crystal size: 0.1-0.8 mm.
Crystal shape: Flame, ragged.
Crystal orientation: None visible.
Percent replacement: Variable.
SECONDARY MINERALOGY:
Serpentine.
Total percent: 50-70%.
Texture: Strongly deformed serpentine orthopyroxene pseudomorphs, set in a matrix of mesh-textured serpentine replacing olivine.
Vein material: Dark greenish gray altered zones usually contain black-green major veins, black-green veins also occur; occasionally greenish white veins of chrysotile (< 5mm).
Pyroxene may control location of fractures and veins.

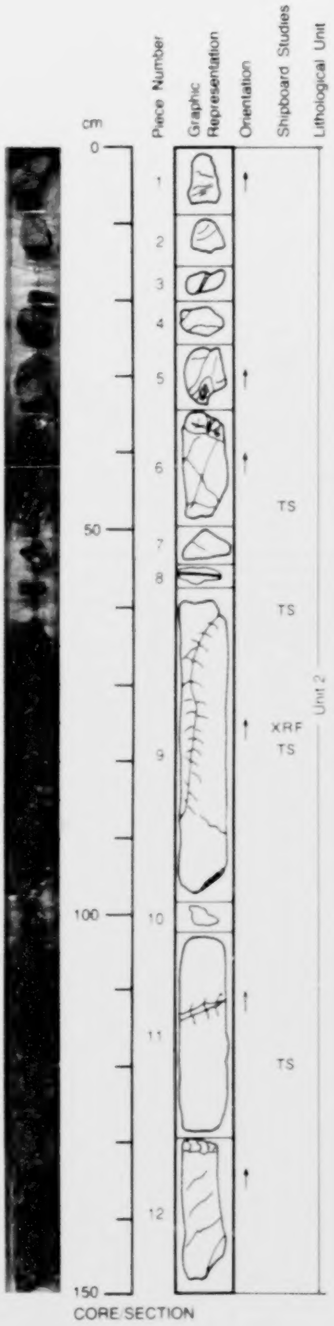

125-779A-16R-2

UNIT 2: TECTONIZED SERPENTINIZED HARZBURGITE

Pieces 1-5

COLOR: Bluish gray (5B 5/1) with altered dark greenish gray zones (5BG 4/1)

LAYERING: None

DEFORMATION: Strongly fractured locally with few mm offset in dark veins

PRIMARY MINERALOGY:

Olivine - Mode: 90%

Crystal size: Not visible

Crystal shape: Not visible

Crystal orientation: None

Percent replacement: 95-99

Orthopyroxene - Mode: 10%

Crystal size: Not visible

Crystal shape: Not visible

Crystal orientation: None

Percent replacement: 95-99

SECONDARY MINERALOGY:

Serpentine and magnetite

Total percent: 95-99%

Texture: Strongly deformed bastite pseudomorphs after orthopyroxene

Vein material: Dark greenish gray altered zones usually contain: black-green major veins, black-green veins also occur without reaction zone, occasionally greenish white veins (<5 mm). Pyroxenes may control location of fractures and veins

ADDITIONAL COMMENTS: Low temperature deformation ??

UNIT 2: SERPENTINIZED TECTONIZED HARZBURGITE

Pieces 6-12

COLOR: Dark greenish gray (5BG 4/1) with lighter patches

LAYERING: None

DEFORMATION: Vein-filled fractures with perpendicular chrysotile-filled tension cracks (Frankenstein veins)

PRIMARY MINERALOGY:

Olivine - Mode: 50%

Crystal size: Not visible

Crystal shape: Mesh?

Crystal orientation: None

Percent replacement: 95-99

Orthopyroxene - Mode: 50%

Crystal size: <2 cm?

Crystal shape: Round?

Crystal orientation: None

Percent replacement: 95-99

SECONDARY MINERALOGY:

Serpentine

Total percent: 100%

Texture: Bastite pseudomorphs after rounded pyroxene

Vein material: Early generation of dark veins crosscut by white tension veins

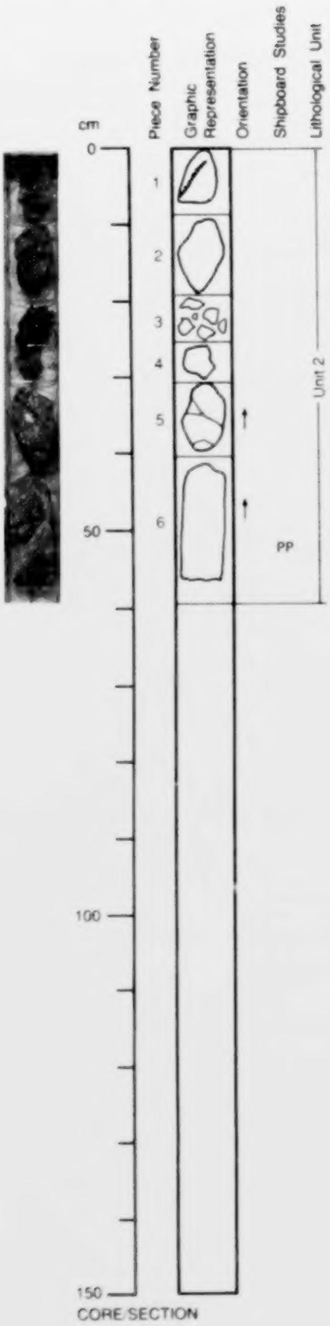
cm
Piece Number
Graphic Representation
Orientation
Shipboard Studies
Lithological Unit
0
50
100
150
1
2
3
4
5
6
PP
Unit 2
CORE/SECTION

125-779A-16R-3

UNIT 2: SERPENTINIZED TECTONIZED HARZBURGITE

Pieces 1-6

COLOR: Dark greenish gray (5BG 4/1) with lighter patches.
LAYERING: None.
DEFORMATION: Vein-filled fractures with perpendicular chrysotile filled tension crack (Frankenstein).
PRIMARY MINERALOGY:
- Olivine - Mode: 50%.
- Crystal size: Not visible.
- Crystal shape: Not visible.
- Crystal orientation: None.
- Percent replacement: 95-99.

- Orthopyroxene - Mode: 50%.
- Crystal size: <2 cm?
- Crystal shape: Round?
- Crystal orientation: None.
- Percent replacement: 95-99.

SECONDARY MINERALOGY:
- Serpentine.
- Total percent: 100%.
- Texture: Bastite pseudomorphs after rounded deformed orthopyroxene.
- Vein material: Early generation of dark green veins crosscut by white tension veins.

ADDITIONAL COMMENTS: Probably cumulate origin.

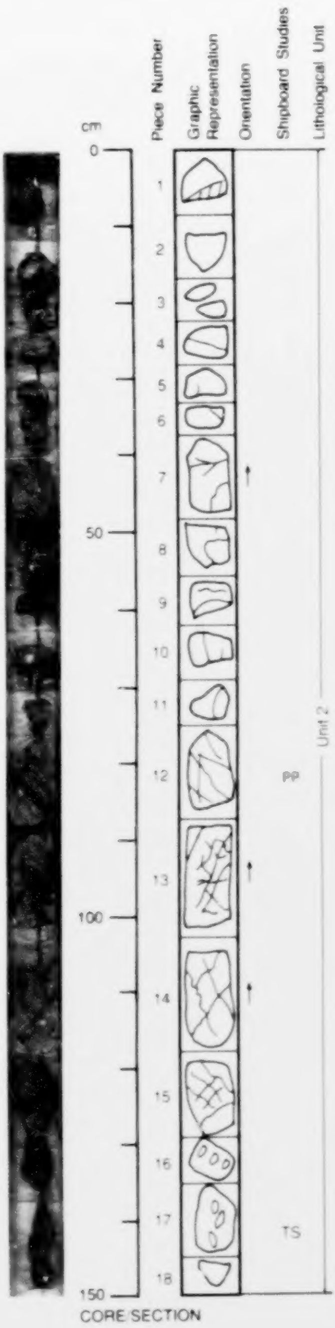

125-779A-17R-1

UNIT 2: SERPENTINIZED TECTONIZED HARZBURGITE

Pieces 1 to 2

COLOR: Bluish gray, variable (5B 5/1) to very dark gray (5Y 3/1)
LAYERING: Not visible
DEFORMATION: Rare wavy cleavage surface in orthopyroxene
PRIMARY MINERALOGY:
Olivine - Mode: 80-90%
Crystal size: 5-8 mm
Crystal shape: Ragged
Crystal orientation: Not visible
Percent replacement: Not visible

Orthopyroxene - Mode: 10-20%
Crystal size: 3-5 mm
Crystal shape: Equant
Crystal orientation: Not visible
Percent replacement: Not visible

Spinel - Mode: <0.3%
Crystal size: 0.1-1 mm
Crystal shape: Dumbbell-elongate
Crystal orientation: Not visible
Percent replacement: Not visible
SECONDARY MINERALOGY:
Serpentine
Total percent: 70-90%
Texture: N/A
Vein material: Numerous veins (0.1-0.5 mm wide) filled with dark serpentine; minor (<0.2 mm) filled with white serpentine

UNIT 2: SERPENTINE-TALC

Pieces 3A and B

COLOR: Mottled gray-green to green gray (4G 4/1 to 5G 7/1)
LAYERING: Not visible
DEFORMATION: Not visible
PRIMARY MINERALOGY: Not visible
SECONDARY MINERALOGY:
Serpentine and talc forming a phacoidal clast
Total percent: 100%
Texture: Massive, fine grained
Vein material: Not visible

UNIT 2: SERPENTINIZED HARZBURGITE

Pieces 4, 5 and 6

COLOR: Blue gray (5B 5/1)
LAYERING: Not visible
DEFORMATION: Pyroxene elongate, ragged, with wavy cleavage
PRIMARY MINERALOGY:
Olivine - Mode: 90-95%
Crystal size: 10-15 mm
Crystal shape: Equant
Crystal orientation: Not visible
Percent replacement: Not visible

Orthopyroxene - Mode: 5-10%
Crystal size: 5-10 mm
Crystal shape: Equant-elongate
Crystal orientation: Not visible
Percent replacement: Not visible

Spinel - Mode: Trace
Crystal size: <0.1 mm
Crystal shape: Dusty
Crystal orientation: Not visible
Percent replacement: Not visible
SECONDARY MINERALOGY:
Serpentine
Total percent: 70-90%
Texture: N/A
Vein material: 1-2 mm wide, filled with black amorphous serpentine, white chrysotile and a white laminated amorphous phase

125-779A-17R-1 (continued)

UNIT 2: SERPENTINIZED DUNITE

Pieces 7 and 8

COLOR: Mottled pale to dark gray (N 5/ to N 4/).
LAYERING: Not visible.
DEFORMATION: Not visible.
PRIMARY MINERALOGY:
Olivine - Mode: 99%.
Crystal size: Not visible.
Crystal shape: Not visible.
Crystal orientation: Not visible.
Percent replacement: Not visible.

Cr-spinel - Mode: 1%.
Crystal size: 0.5-1.5 mm.
Crystal shape: Equant.
Crystal orientation: Disseminated.
Percent replacement: Not visible.
Comments: Some have a white halo.
SECONDARY MINERALOGY:
Serpentine.
Total percent: 100%.
Texture: Mesh-textured, massive.
Vein material: Rock is mottled because of serpentinization halos around veins of several types. Two generations at least of (1) 0.5 to 1.5-mm-wide, amorphous black serpentine sub-vertical, crosscut by (2) conjugate subhorizontal, white amorphous phase.
ADDITIONAL COMMENTS: First dunite sampled downward in the core for a considerable interval.

UNIT 2: SERPENTINIZED DUNITE

Piece 9

COLOR: Dark gray (N 4/).
LAYERING: Caused by sheared veining of upper 10 mm of surface.
DEFORMATION: Sheared.
PRIMARY MINERALOGY:
Olivine - Mode: 99%.
Crystal size: Not visible.
Crystal shape: Not visible.
Crystal orientation: Not visible.
Percent replacement: Not visible.

Spinel - Mode: 1%.
Crystal size: 0.5 mm.
Crystal shape: Rounded-equant.
Crystal orientation: Not visible.
Percent replacement: Not visible.
SECONDARY MINERALOGY:
Serpentine replaces all of the primary minerals.
Total percent: 100%.
Texture: N/A.
Vein material: 40% of the rock is made of veins. Two generations: (1) dark blue-green amorphous serpentine in upper 1 cm, apparently subhorizontal; (2) anastomosing chrysotile.
ADDITIONAL COMMENTS: Spinels have white halos (probably of chlorite).

125-779A-17R-1 (continued)

UNIT 2: SERPENTINIZED DUNITE

Piece 10

COLOR: Pale to dark gray (N 5/ to N 4/)
LAYERING: None visible
DEFORMATION: Elongate spinels
PRIMARY MINERALOGY:
Olivine - Mode: >99%
Crystal size: Not visible
Crystal shape: Not visible
Crystal orientation: Not visible
Percent replacement: Not visible

Spinel - Mode: <1%
Crystal size: 0.5-1 mm
Crystal shape: Elongate to equant
Crystal orientation: Not visible
Percent replacement: Not visible
SECONDARY MINERALOGY:
Serpentine
Total percent: 100%
Texture: N/A
Vein material: Predominantly vertical, anastomosing, 0.1-8 mm wide, filled with massive dark green, laminated serpentine phase.

UNIT 2: SERPENTINIZED HARZBURGITIC DUNITE

Pieces 11 to 14

COLOR: Pale gray to dark gray (N 6/ to 5B 4/1)
LAYERING: Olivine layering (in Piece 14)
DEFORMATION: Bent orthopyroxene cleavage
PRIMARY MINERALOGY:
Olivine - Mode: 95-99%
Crystal size: 5-15 mm
Crystal shape: Elongate
Crystal orientation: Subhorizontal
Percent replacement: Not visible
Comments: Oval shaped and cleaved.

Orthopyroxene - Mode: <5%
Crystal size: 0.5-0.8 mm
Crystal shape: Equant-elongate
Crystal orientation: Not visible
Percent replacement: Not visible

Cr-spinel - Mode: <1%
Crystal size: 0.2-0.5 mm
Crystal shape: Ovoid
Crystal orientation: Not visible
Percent replacement: Not visible
SECONDARY MINERALOGY:
Serpentine
Total percent: 85-95%
Texture: N/A
Vein material: Primary conjugate set dipping steeply, 0.5-6 mm wide, filled with laminar black amorphous-looking serpentine, making up 5-10% of rock. Crosscut by 45 degree, 0.2-mm-wide amorphous white-filled veins.

125-779A-17R-1 (continued)

UNIT 2: SERPENTINIZED MYLONITIZED DUNITE

Pieces 16 to 18

COLOR: Dark blue gray (5B 4/1).
LAYERING: Not visible.
DEFORMATION: Mylonitized, serpentinized olivine has pervasive sheared fabric.
PRIMARY MINERALOGY:
  Olivine - Mode: 99%.
  Crystal size: Not visible.
  Crystal shape: Ovoid-stretched.
  Crystal orientation: Long axes steeply dipping.
  Percent replacement: Not visible.

  Cr-spinel - Mode: <1%.
  Crystal size: <0.1 mm.
  Crystal shape: Ellipsoidal.
  Crystal orientation: Length parallel to schistosity.
  Percent replacement: Not visible.
SECONDARY MINERALOGY:
  Olivine appears to have completely recrystallized to produce mylonitic fabric.
  Total percent: 30-50%.
  Texture: N/A.
  Vein material: White chrysotile veins subparallel to fabric, 0.5 mm wide.
ADDITIONAL COMMENTS: First mylonitized rock observed downhole.

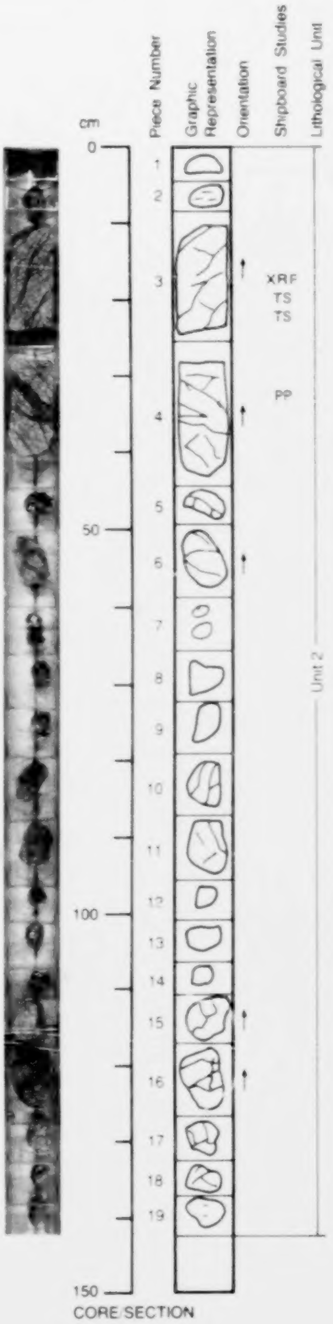
cm
0
50
100
150
Piece Number
Graphic Representation
Orientation
Shipboard Studies
Lithological Unit
1
2
3
4
5
6
7
8
9
10
11
12
13
14
15
16
17
18
19
XRF
TS
TS
PP
Unit 2
CORE/SECTION

125-779A-17R-2

UNIT 2: SERPENTINIZED DUNITE

Piece 1

COLOR: Dark gray (N 4)
LAYERING: Not visible
DEFORMATION: Not visible
PRIMARY MINERALOGY:
Olivine : Mode: 99%
Crystal size: Not visible
Crystal shape: Not visible
Crystal orientation: Not visible
Percent replacement: Not visible

Spinel : Mode: 1%
Crystal size: 0.1-0.2 mm
Crystal shape: Elongate-dumbbell
Crystal orientation: Not visible
Percent replacement: Not visible
SECONDARY MINERALOGY:
Extensively serpentinized
Total percent: 70-90%
Texture: N/A
Vein material: Two generations: (1) dark gray-green serpentine, 1-2 mm wide, cut by (2) chrysotile-filled veins

UNIT 2: SERPENTINIZED HARZBURGITE

Piece 2

COLOR: Blue gray (5B 5/1)
LAYERING: Not visible
DEFORMATION: Not visible
PRIMARY MINERALOGY:
Olivine : Mode: 70%
Crystal size: 5-9 mm
Crystal shape: Not visible
Crystal orientation: Not visible
Percent replacement: Variable

Orthopyroxene : Mode: 25-30%
Crystal size: 3-5 mm
Crystal shape: Equant
Crystal orientation: Not visible
Percent replacement: Variable

Spinel : Mode: Trace
Crystal size: 1.5 mm
Crystal shape: Equant
Crystal orientation: Not visible
Percent replacement: Not visible
SECONDARY MINERALOGY:
Variable serpentinization
Total percent: 25-75%
Texture: N/A
Vein material: Chrysotile veins, 0.3 mm wide

125-779A-17R-2 (continued)

UNIT 2: TECTONIZED SERPENTINIZED HARZBURGITE

Pieces 3 to 5

COLOR: Bluish gray (5B 5/1) to dark gray (N 4/)
LAYERING: Not visible
DEFORMATION: Orthopyroxene shows wavy cleavage
PRIMARY MINERALOGY:
Olivine - Mode: 60-80%
Crystal size: 5-10 mm
Crystal shape: Ragged
Crystal orientation: Not visible
Percent replacement: Variable

Orthopyroxene - Mode: 20-40%
Crystal size: 1-3 mm
Crystal shape: Equant
Crystal orientation: Not visible
Percent replacement: Variable

Spinel - Mode: Trace
Crystal size: 0.2-1 mm
Crystal shape: Equant
Crystal orientation: Not visible
Percent replacement: Not visible
SECONDARY MINERALOGY:
Serpentine
Total percent: 20-35%
Texture: N/A
Vein material: Multiple and numerous: (1) amorphous black serpentinite, 2 conjugate sets @ 45 degrees, 1-12 mm wide; (2) chrysotile parallel and normal to dark veins, 1 mm wide

UNIT 2: SERPENTINIZED TECTONIZED HARZBURGITE

Pieces 6 and 7

COLOR: Bluish gray (5B 5/1)
LAYERING: Not visible
DEFORMATION: Not visible
PRIMARY MINERALOGY:
Olivine - Mode: 90-95%
Crystal size: 5-10 mm
Crystal shape: Not visible
Crystal orientation: Not visible
Percent replacement: Variable

Orthopyroxene - Mode: 5-10%
Crystal size: 2-6 mm
Crystal shape: Not visible
Crystal orientation: Not visible
Percent replacement: Variable

Spinel - Mode: <1%
Crystal size: 0.3-1 mm
Crystal shape: Elongate
Crystal orientation: Not visible
Percent replacement: Not visible
SECONDARY MINERALOGY:
Variable serpentinization
Total percent: 35-65%
Texture: N/A
Vein material: Two generations: (1) dark amorphous serpentinite, 0.5-2 mm wide; (2) chrysotile following original vein paths; two veins also appear to be superimposed forming a sheared pale-green vein

125-779A-17R-2 (continued)

UNIT 2: SERPENTINIZED TECTONIZED HARZBURGITE

Pieces 8-19

COLOR: Dark greenish gray (5BG 4/1).
LAYERING: Not visible.
DEFORMATION: Pyroxenes are kinked and folded; elongated spinels.
PRIMARY MINERALOGY:
Orthopyroxene - Mode: 10-20%
Crystal size: 5-7 mm.
Crystal shape: Equant.
Crystal orientation: Not visible.
Percent replacement: Not visible.

Olivine - Mode: 80-90%
Crystal size: 5-10 mm.
Crystal shape: Equant.
Crystal orientation: Not visible.
Percent replacement: Not visible.

Spinel - Mode: <1%.
Crystal size: 0.1-2 mm.
Crystal shape: Elongate.
Crystal orientation: Not visible.
Percent replacement: Not visible.
SECONDARY MINERALOGY:
Variably serpentinized with respect to major veins.
Total percent: 25-50%.
Texture: N/A.
Vein material: Numerous, two generations (at least); primary dark green-black amorphous serpentine, up to 6 mm wide, cut by second generation chrysotile, 0.2 mm wide.

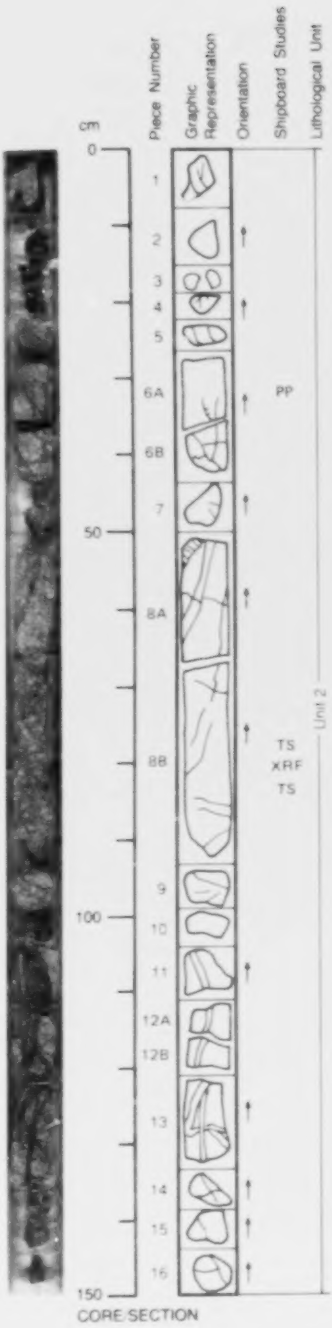
cm
Piece Number
Graphic Representation
Orientation
Shipboard Studies
Lithological Unit
0
50
100
150
1
2
3
4
5
6A
6B
7
8A
8B
9
10
11
12A
12B
13
14
15
16
PP
TS
XRF
TS
Unit 2
CORE/SECTION

125-779A-17R-3

UNIT 2: TECTONIZED SERPENTINIZED HARZBURGITE WITH DUNITE LAYER

Pieces 1 to 16

COLOR: Variable from blue-gray to green-gray (5B 4/1 to N 5/) with subordinate (5BG 4/1).
LAYERING: 6-cm-thick massive dunite band, rich in disseminated Cr spinel (<1%), transitional into harzburgite over 2 cm; layering dips at 65-70 degrees parallel to dumbbell spinel.
DEFORMATION: Wavy cleavage on orthopyroxene, stretched spinel.
PRIMARY MINERALOGY:
Olivine - Mode: 99-80%
Crystal size: 5-8 mm
Crystal shape: Equant-ragged
Crystal orientation: Not visible
Percent replacement: Not visible

Orthopyroxene - Mode: 0-20%
Crystal size: 2-5 mm
Crystal shape: Equant
Crystal orientation: Not visible
Percent replacement: Not visible

Cr-spinel - Mode: Trace
Crystal size: <3 mm
Crystal shape: Dumbbell
Crystal orientation: Not visible
Percent replacement: Not visible
SECONDARY MINERALOGY:
Serpentine
Total percent: 25-60%
Texture: N/A
Vein material: Multiple: (1) anastomosing set, thickest of which are vertical; (2) subordinate conjugate set, steeply dipping; both filled with amorphous black serpentine; (2) vertical, laminar filled with milky green amorphous serpentine (2-8 mm wide); (3) 0.5 mm subhorizontal chrysotile.
ADDITIONAL COMMENTS: Dunite layer has a primary contact with the harzburgite.

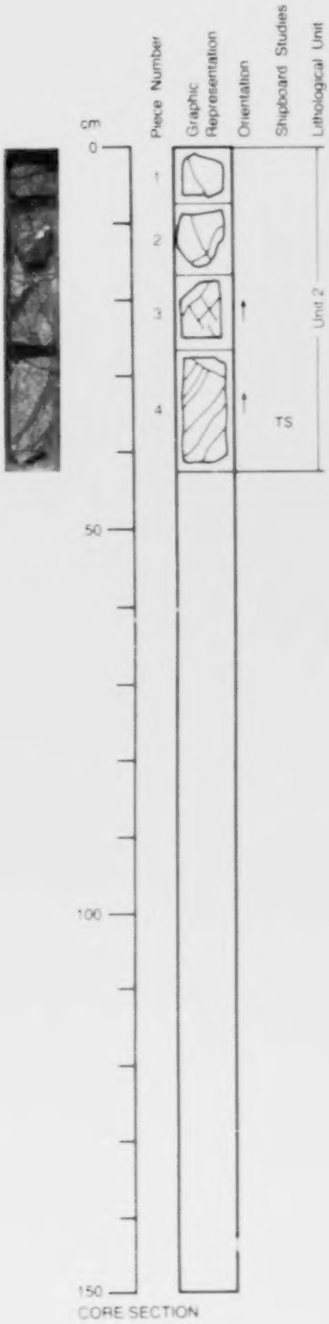
cm
0
50
100
150
Piece Number
Graphic Representation
Orientation
Shipboard Studies
Lithological Unit
1
2
3
4
TS
Unit 2
CORE SECTION

125-779A-17R-4

UNIT 2: SERPENTINIZED TECTONIZED HARZBURGITE

Pieces 1 to 4

COLOR: Gray to dark gray (N 5/ to N 4/).
LAYERING: Not visible.
DEFORMATION: Wavy cleavage on orthopyroxene; elongated, dumbbell-shaped spinel.
PRIMARY MINERALOGY:
Olivine : Mode: 75-95%.
Crystal size: 5-12 mm.
Crystal shape: Ragged.
Crystal orientation: Not visible.
Percent replacement: Not visible.

Orthopyroxene : Mode: 25-30%.
Crystal size: 3-7 mm.
Crystal shape: Equant.
Crystal orientation: Not visible.
Percent replacement: Not visible.

Spinel : Mode: <2%.
Crystal size: <3 mm.
Crystal shape: Elongate-dumbbell.
Crystal orientation: Not visible.
Percent replacement: Not visible.
SECONDARY MINERALOGY:
Serpentine.
Total percent: 70-80%.
Texture: Mess texture.
Vein material: (1) Conjugate set dipping at 45 degrees, <10 mm wide, filled with amorphous dark-green serpentine; (2) thin (<0.2 mm) variable orientation, filled with chrysotile.

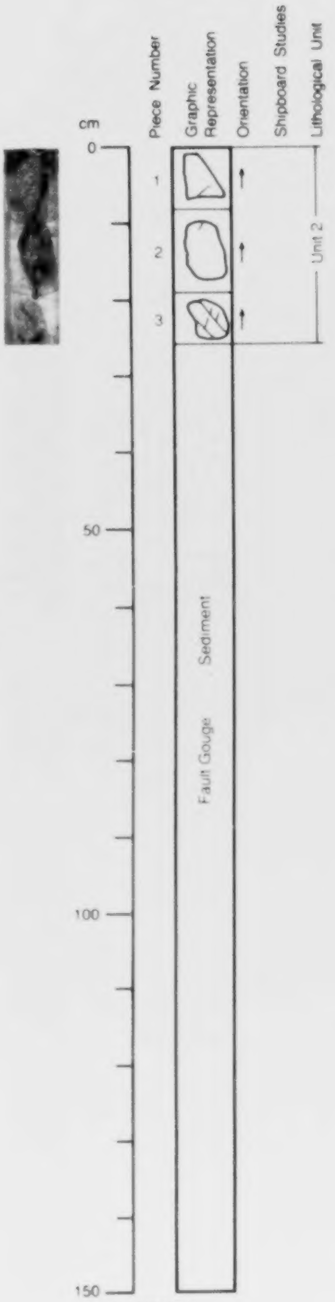
cm
Piece Number
Graphic Representation
Orientation
Shipboard Studies
Lithological Unit
0
1
2
3
Unit 2
50
100
150
Fault Gouge
Sediment
CORE/SECTION

125-779A-18R-1

UNIT 2: SERPENTINIZED TECTONIZED HARZBURGITE

Pieces 1 to 3

COLOR: Greenish gray, mottled to pale greenish gray (5B 5/1)
LAYERING: Not visible
DEFORMATION: Wavy orthopyroxene cleavage
PRIMARY MINERALOGY:
Olivine - Mode: 70-80%
Crystal size: 8-12 mm
Crystal shape: Rounded
Crystal orientation: Not visible
Percent replacement: Not visible

Orthopyroxene - Mode: 20-30%
Crystal size: 5-15 mm
Crystal shape: Elongated
Crystal orientation: Generally subvertical
Percent replacement: Not visible

Cr-spinel - Mode: Trace
Crystal size: 0-2 mm
Crystal shape: Equant to elongate
Crystal orientation: Not visible
Percent replacement: Not visible
SECONDARY MINERALOGY:
Serpentine
Total percent: 35-75%
Texture: N/A
Vein material: <3 mm wide veins, anastomosing, subvertical, filled with amorphous dark serpentine

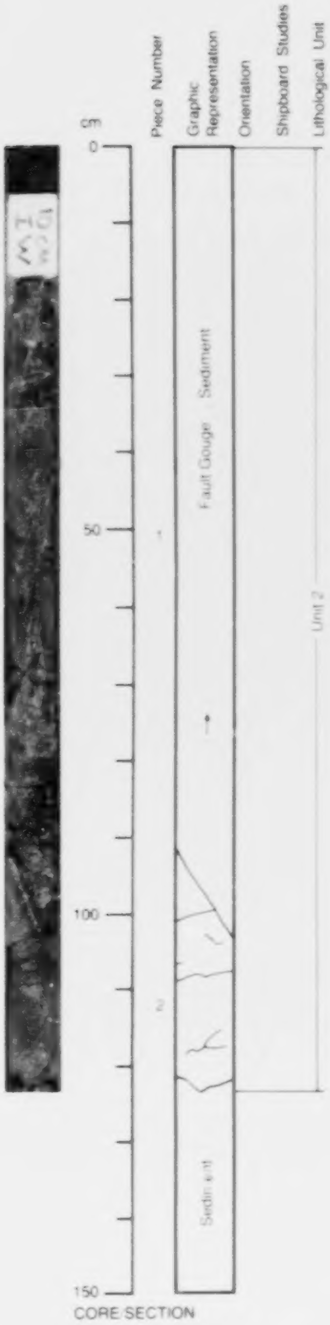
cm
0
50
100
150
Piece Number
Graphic Representation
Orientation
Shipboard Studies
Lithological Unit
1
2
Fault Gouge
Sediment
Sediment
Unit 2
CORE/SECTION

125-779A-18R-2

UNIT 2: SERPENTINIZED TECTONIZED HARZBURGITIC DUNITE

Piece 2

COLOR: Dark gray (N 4)
LAYERING: Not visible
DEFORMATION: Orthopyroxene shows wavy cleavage, possibly aligned parallel to 70 degrees, dipping contact with overlying fault gouge.
PRIMARY MINERALOGY:
Olivine : Mode: 90-95%
Crystal size: Not visible
Crystal shape: Not visible
Crystal orientation: Not visible
Percent replacement: Not visible

Orthopyroxene : Mode: 5-10%
Crystal size: 3-10 mm
Crystal shape: Elongate
Crystal orientation: Not visible
Percent replacement: Not visible

Spinel : Mode: Trace
Crystal size: 0.2-2 mm
Crystal shape: Equant, elongate
Crystal orientation: Not visible
Percent replacement: Not visible
SECONDARY MINERALOGY:
Serpentine
Total percent: 35-75%
Texture: N/A
Vein material: <0.1 mm, dark green serpentine-filled, and white serpentine-filled, but relatively minor compared with many other blocks higher in the hole.
ADDITIONAL COMMENTS: Contact between clast and overlying softer, serpentinous material dips at 70 degrees.

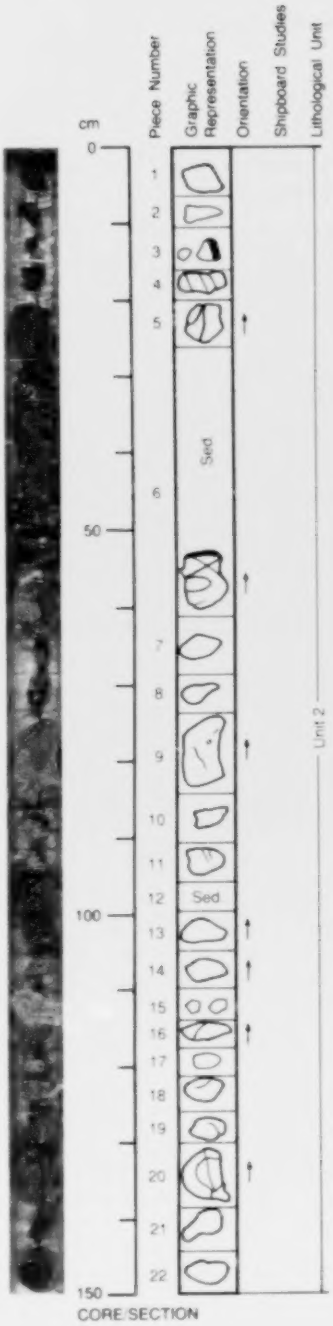

125-779A-19R-1

UNIT 2: SERPENTINIZED DUNITE

Pieces 1, 3-5, and 11

COLOR: Dark green-gray to dark black gray (5 BG 4/1 to 5B 4/1)
LAYERING: Not visible
DEFORMATION: Appears slightly sheared
PRIMARY MINERALOGY:
Olivine - Mode: 95%
Crystal size: Not visible
Crystal shape: Not visible
Crystal orientation: Not visible
Percent replacement: Not visible

Orthopyroxene - Mode: 5%
Crystal size: Not visible
Crystal shape: Not visible
Crystal orientation: Not visible
Percent replacement: Not visible

Spinel? - Mode: Trace
Crystal size: Not visible (<1 mm?)
Crystal shape: Equant
Crystal orientation: Not visible
Percent replacement: Not visible
SECONDARY MINERALOGY:
Serpentine
Total percent: 90-99%
Texture: N/A
Vein material: Small 0.2-mm serpentine (chrysotile?) veins; small (0.2 mm) white-green veins appear in some samples
ADDITIONAL COMMENTS: Piece 5 appears slightly tectonized

UNIT 2: SERPENTINIZED HARZBURGITE

Piece 2

COLOR: Green-gray to black gray (5BG 4/1 to 5B 4/1)
LAYERING: Not visible
DEFORMATION: Not visible
PRIMARY MINERALOGY:
Olivine - Mode: 75-85%
Crystal size: Not visible
Crystal shape: Not visible
Crystal orientation: Not visible
Percent replacement: Not visible

Orthopyroxene - Mode: 15-25%
Crystal size: Not visible
Crystal shape: Not visible
Crystal orientation: Not visible
Percent replacement: Not visible
SECONDARY MINERALOGY:
Serpentine
Total percent: 95-99%
Texture: Bastitic in some areas
Vein material: Small, 0.1-mm-wide, pale green serpentine(?) veins

UNIT 2: SERPENTINIZED DUNITE

Pieces 13 and 22

COLOR: Dark greenish gray (5BG 4/1)
LAYERING: Not visible
DEFORMATION: Not visible
PRIMARY MINERALOGY:
Olivine - Mode: 90-95%
Crystal size: Not visible
Crystal shape: Not visible
Crystal orientation: Not visible
Percent replacement: Not visible

Orthopyroxene - Mode: 5-10%
Crystal size: Not visible
Crystal shape: Not visible
Crystal orientation: Not visible
Percent replacement: Not visible

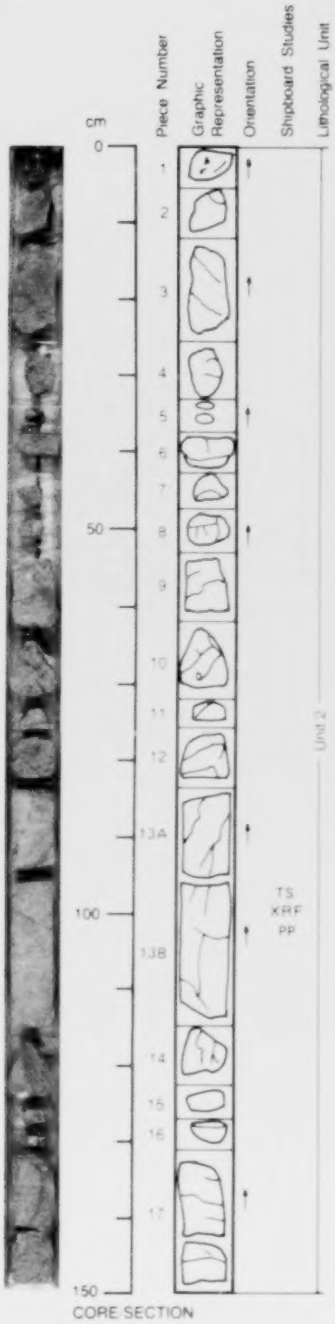

125-779A-19R-1 (continued)

SECONDARY MINERALOGY:
Serpentine
Total percent: 95-99%
Texture: N/A
Vein material: Dark black, 0.1-mm-wide, serpentine(?) veining
ADDITIONAL COMMENTS: Small, 1 cm patches of light mineral within pieces

UNIT 2: SERPENTINIZED HARZBURGITE

Pieces 6-10 and 14-21

COLOR: Dark greenish gray to dark gray (5BG 4/1 to N)
LAYERING: Not visible
DEFORMATION: Appears slightly sheared; fractures and veining are abundant
PRIMARY MINERALOGY:
Olivine - Mode: 75-80%
Crystal size: Not visible
Crystal shape: Not visible
Crystal orientation: Not visible
Percent replacement: Not visible

Orthopyroxene - Mode: 20-25%
Crystal size: 1-2 mm
Crystal shape: Equant-elongate
Crystal orientation: Not visible
Percent replacement: Not visible

Spinel? - Mode: Trace
Crystal size: <1 mm?
Crystal shape: Equant
Crystal orientation: Not visible
Percent replacement: Not visible
SECONDARY MINERALOGY:
Serpentine: Piece 9 has a rind (1-2 cm) of dark green mineral (composition?) on edge of sample.
Total percent: 90-99%
Texture: Bastitic texture in some samples
Vein material: Abundant veins 0.1-0.3 mm wide of dark black, serpentine(?); also very few 0.1-0.2 mm wide veins of white-green mineral (chrysotile?)

125-779A-19R-2

UNIT 2: SERPENTINIZED HARZBURGITE

Piece 1

COLOR: Dark green gray (5BG/1)
LAYERING: Not visible
DEFORMATION: Slightly deformed
PRIMARY MINERALOGY:
Olivine - Mode: 80%
Crystal size: Not visible
Crystal shape: Not visible
Crystal orientation: Not visible
Percent replacement: Not visible

Orthopyroxene - Mode: 20%
Crystal size: 1-2 mm?
Crystal shape: Subhedral
Crystal orientation: Not visible
Percent replacement: Not visible

Spinel? - Mode: Trace
Crystal size: Not visible
Crystal shape: Not visible
Crystal orientation: Not visible
Percent replacement: Not visible
SECONDARY MINERALOGY:
Serpentine
Total percent: 95-99%
Texture: Serpentine pseudomorphic after olivine, possibly originally cumulate? Vein material: 0.5 mm pale, green-black serpentine vein 2 cm long.

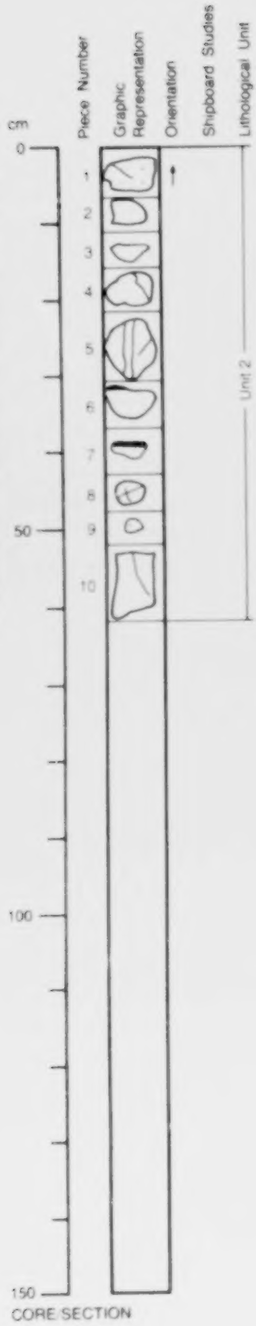
cm
Piece Number
Graphic Representation
Orientation
Shipboard Studies
Lithological Unit
0
50
100
150
1
2
3
4
5
6
7
8
9
10
Unit 2
CORE/SECTION

125-779A-19R-3

UNIT 2: SERPENTINIZED HARZBURGITE

Pieces 1-10

COLOR: Bluish gray (5B 5/1).
LAYERING: Not visible
DEFORMATION: Not visible
PRIMARY MINERALOGY:
Olivine - Mode: 20%
Crystal size: Not visible
Crystal shape: Not visible
Crystal orientation: Not visible
Percent replacement: Not visible

Orthopyroxene - Mode: 80%
Crystal size: 1-2 mm
Crystal shape: Subhedral
Crystal orientation: Not visible
Percent replacement: Not visible

Spinel? - Mode: Trace
Crystal size: <1 mm?
Crystal shape: Equant
Crystal orientation: Not visible
Percent replacement: Not visible
SECONDARY MINERALOGY:
Serpentine pseudomorphs after orthopyroxene and olivine; secondary magnetite(?) is visible in areas.
Total percent: 95-99%
Texture: Bastitic
Vein material: Laminar, filled with milky-green amorphous serpentine, 2-4 mm wide.

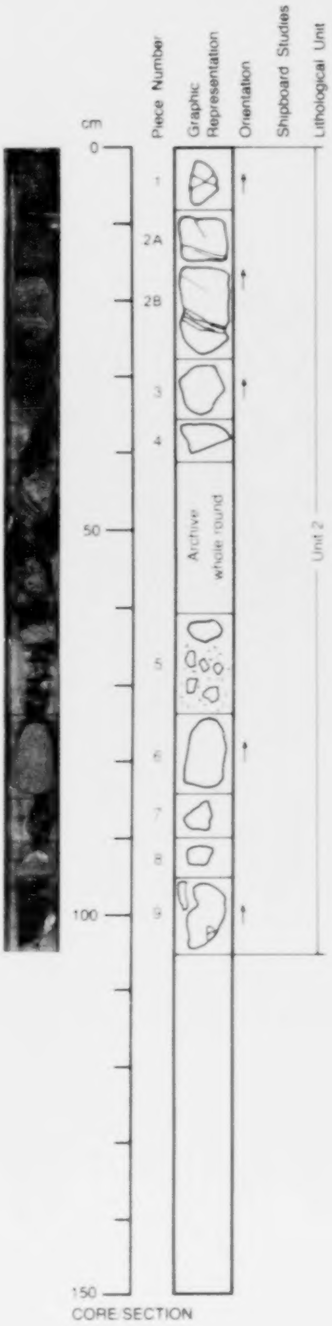

125-779A-20R-1

UNIT 2: SERPENTINIZED HARZBURGITE

Pieces 1, 2, 7

COLOR: Dark black gray (5B 4/1)
LAYERING: crude layering defined by pyroxene-rich zone, 8 cm wide, in Piece 2
DEFORMATION: None visible
PRIMARY MINERALOGY:
Olivine - Mode: 70-80%
Crystal size: Not visible
Crystal shape: Not visible
Crystal orientation: Not visible
Percent replacement: Not visible

Orthopyroxene - Mode: 20-30%
Crystal size: 1-4 mm
Crystal shape: Not visible
Crystal orientation: Not visible
Percent replacement: Not visible

Spinel ? - Mode: Trace
Crystal size: Not visible
Crystal shape: Not visible
Crystal orientation: Not visible
Percent replacement: Not visible
SECONDARY MINERALOGY:
Serpentinized 90-99%. Piece 2 appears to represent a serpentinization halo.
Total percent: 90-99%
Texture: Bastitic texture in the pyroxene-rich areas and mesh(?) texture in the pyroxene-poor areas.
Vein material: veins (0.1-0.3 mm) of dark, black vitreous serpentine(?) occur in these pieces. Veins in Piece 1 occur as conjugate sets.

UNIT 2: SERPENTINIZED DUNITE(?)

Pieces 3 and 4

COLOR: Dark greenish gray (5BG 4/1)
LAYERING: None
DEFORMATION: Appears slightly sheared
PRIMARY MINERALOGY:
Olivine - Mode: 90-95%
Crystal size: Not visible
Crystal shape: Not visible
Crystal orientation: Not visible
Percent replacement: Not visible

Orthopyroxene - Mode: 5-10%
Crystal size: Not visible
Crystal shape: Not visible
Crystal orientation: Not visible
Percent replacement: Not visible
SECONDARY MINERALOGY:
Serpentine and possibly magnetite
Total percent: 95-99%
Texture: Possible mesh-like texture which appears slightly sheared
Vein material: Small 0.1-mm, pale milky-green serpentine(?) veins

125-779A-20R-1 (continued)

UNIT 2: SERPENTINIZED HARZBURGITE

Pieces 5, 6 and 8

COLOR: Bluish gray (5B 5/1).
LAYERING: None.
DEFORMATION: Piece 5 is sheared and brecciated.
PRIMARY MINERALOGY:
Olivine - Mode: 60-70%.
Crystal size: Not visible.
Crystal shape: Not visible.
Crystal orientation: Not visible.
Percent replacement: Not visible.

Orthopyroxene - Mode: 30-40%.
Crystal size: 1-2 mm.
Crystal shape: Not visible.
Crystal orientation: Not visible.
Percent replacement: Not visible.
SECONDARY MINERALOGY:
Serpentine
Total percent: 90%.
Texture: Bastitic in areas.
Vein material: Small, 0.1-mm, veins parallel to the long axis of the larger sample.

UNIT 2: SERPENTINIZED DUNITE(?)

Piece 9

COLOR: Dark black gray (5B 4/1).
LAYERING: None.
DEFORMATION: Some areas appear slightly sheared.
PRIMARY MINERALOGY:
Olivine - Mode: 80-85%.
Crystal size: Not visible.
Crystal shape: Not visible.
Crystal orientation: Not visible.
Percent replacement: Not visible.

Orthopyroxene - Mode: 15-20%.
Crystal size: 1-2 mm?
Crystal shape: Slightly elongated.
Crystal orientation: Not visible.
Percent replacement: Not visible.
SECONDARY MINERALOGY:
Serpentine
Total percent: 90%.
Texture: Serpentine alteration of olivine.
Vein material: 0.1-mm pale-green serpentine veining; edge and exterior of rock has chrysotile(?) coating, 0.2 mm thick.

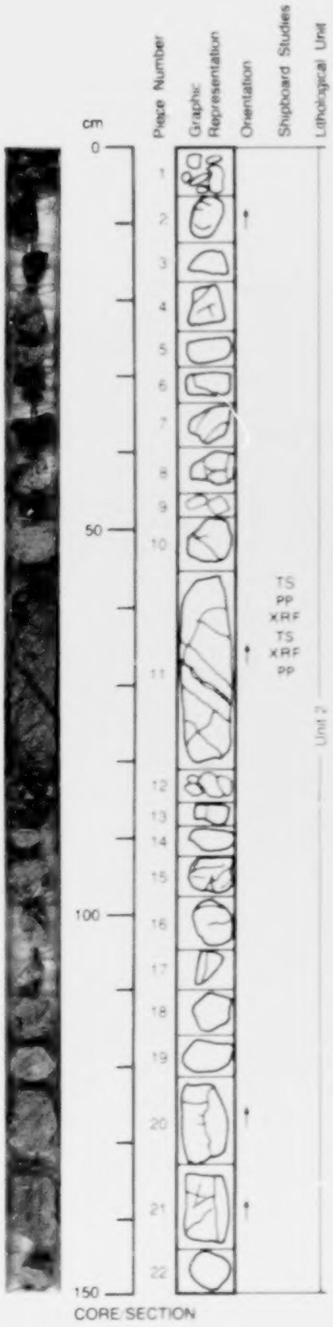

125-779A-22R-1

UNIT 2: FRAGMENTS OF SERPENTINIZED HARZBURGITE, OLIVINE PYROXENITE(?)

Piece 1

COLOR: Dark greenish gray (5BG 4/1) to greenish gray (5BG 5/1)
LAYERING: Not visible
DEFORMATION: Wavy cleavage of orthopyroxene
PRIMARY MINERALOGY:
Fragments show variable degrees of serpentinization
Olivine : Mode: 70-95%
Crystal size: 3-8 mm
Crystal shape: Not visible
Crystal orientation: Not visible
Percent replacement: Not visible

Orthopyroxene : Mode: 5-30%
Crystal size: 3-5 mm
Crystal shape: Equant
Crystal orientation: Not visible
Percent replacement: Not visible

Spinel : Mode: Trace <2%
Crystal size: 0.1-0.3 mm
Crystal shape: Ragged
Crystal orientation: Not visible
Percent replacement: Not visible
SECONDARY MINERALOGY:
Serpentine
Total percent: 40-80%
Texture: N/A
Vein material: Veins of greenish-white serpentine, 0.2 mm wide cutting pyroxenite(?)
ADDITIONAL COMMENTS: Piece 1 consists of 6 separate fragments

UNIT 2: SERPENTINIZED TECTONIZED HARZBURGITE

Pieces 2-4

COLOR: Greenish gray to dark greenish gray (5B 5/1 to 5BG 4/1)
LAYERING: Not visible
DEFORMATION: Wavy cleavage on orthopyroxene, elongate spinels in trains
PRIMARY MINERALOGY:
Olivine : Mode: 70-95%
Crystal size: 5-8 mm
Crystal shape: Not visible
Crystal orientation: Not visible
Percent replacement: Not visible

Orthopyroxene : Mode: 5-30%
Crystal size: 3-5 mm
Crystal shape: Equant
Crystal orientation: Not visible
Percent replacement: Not visible

Spinel : Mode: Trace <2%
Crystal size: 0.1-3 mm
Crystal shape: Equant to elongate dumbbell
Crystal orientation: Not visible
Percent replacement: Not visible
SECONDARY MINERALOGY:
Variable amounts of serpentine
Total percent: 50-80%
Texture: N/A
Vein material: At least two types: (1) dark amorphous black green serpentine 1-2 mm in width, (2) linear green-white, 2 mm wide, chrysotile filled

125-779A-22R-1 (continued)

UNIT 2: SERPENTINIZED HARZBURGITE

Piece 5

COLOR: Bluish gray (5B 5/1).
LAYERING: Orthopyroxene appears to form layers, possibly tectonic.
DEFORMATION: Wavy cleavage of orthopyroxene.
PRIMARY MINERALOGY:
Orthopyroxene - Mode: 70-90%.
Crystal size: 2-4 mm.
Crystal shape: Equant-ragged.
Crystal orientation: Not visible.
Percent replacement: Not visible.

Olivine - Mode: 10-30%.
Crystal size: 3-5 mm.
Crystal shape: Not visible.
Crystal orientation: Not visible.
Percent replacement: Not visible.

Spinel - Mode: Trace.
Crystal size: <1 mm.
Crystal shape: Equant.
Crystal orientation: Not visible.
Percent replacement: Not visible.
SECONDARY MINERALOGY:
Serpentine.
Total percent: 80-95%.
Texture: N/A.
Vein material: 1 mm wide, filled with dark serpentine.

UNIT 2: SERPENTINIZED TECTONIZED DUNITE GRADING TO HARZBURGITE

Pieces 6 and 7

COLOR: Black (2.5Y 2/0) to dark bluish gray (5B 4/1).
LAYERING: Not visible.
DEFORMATION: Olivine intensively kink banded.
PRIMARY MINERALOGY:
Olivine - Mode: 85-99%.
Crystal size: 5-10 mm.
Crystal shape: Ragged.
Crystal orientation: Not visible.
Percent replacement: Not visible.

Orthopyroxene - Mode: Trace-15%.
Crystal size: 3-5 mm.
Crystal shape: Equant.
Crystal orientation: Not visible.
Percent replacement: Not visible.

Spinel - Mode: <1%.
Crystal size: <2 mm.
Crystal shape: Equant.
Crystal orientation: Not visible.
Percent replacement: Not visible.
SECONDARY MINERALOGY:
Serpentine.
Total percent: 80-95%.
Texture: N/A.
Vein material: 0.1-0.3 mm wide, filled with both dark serpentine and white chrysotile.
ADDITIONAL COMMENTS: Serpentinization is extensive.

125-779A-22R-1 (continued)

UNIT 2: SERPENTINIZED TECTONIZED PYROXENITE GRADING TO DUNITE (8 AND ONE FRAGMENT OF PIECE 9)

Pieces 8-10

COLOR: Bluish gray (5B 5/1) to black (2.5Y 2/0)
LAYERING: Apparent in gradation from pyroxenite to dunite
DEFORMATION: Undulose cleavage on orthopyroxene
PRIMARY MINERALOGY:
Orthopyroxene - Mode: 50-5%
Crystal size: 3-5 mm
Crystal shape: Equant
Crystal orientation: Not visible
Percent replacement: Not visible

Olivine - Mode: 95-50%
Crystal size: 8-15 mm
Crystal shape: Equant
Crystal orientation: Not visible
Percent replacement: Not visible

Spinel - Mode: Trace-<1%
Crystal size: <2 mm
Crystal shape: Equant
Crystal orientation: Not visible
Percent replacement: Not visible
SECONDARY MINERALOGY:
Serpentine
Total percent: 60-85%
Texture: N/A
Vein material: Top of Piece 8 has laminar banded vein sub-horizontal (5-8 mm wide), filled with dark-green and white amorphous serpentine. This vein is cut by a vertical vein wedging downwards from 5-0 mm over 3 cm distance, and filled with same as above.
ADDITIONAL COMMENTS: Note gradation from pyroxenite to dunite in one piece; variable serpentinization.

UNIT 2: TECTONIZED SERPENTINIZED HARZBURGITE

Piece 11

COLOR: Mottled and variable from gray (N 6/) to dark gray (N 4/)
LAYERING: Not visible
DEFORMATION: Strong orthopyroxene foliation parallel to orthopyroxene elongation and dipping at 45 degrees.
PRIMARY MINERALOGY:
Olivine - Mode: 85-90%
Crystal size: Not visible
Crystal shape: Not visible
Crystal orientation: Not visible
Percent replacement: Not visible

Orthopyroxene - Mode: 15-10%
Crystal size: 8-15 mm
Crystal shape: Elongate
Crystal orientation: Not visible
Percent replacement: Not visible

Spinel - Mode: <1%
Crystal size: 0.5-1 mm
Crystal shape: Elongate-dumbbell
Crystal orientation: Not visible
Percent replacement: Not visible
SECONDARY MINERALOGY:
Serpentine
Total percent: 70-80%
Texture: Variable serpentinization in vicinity of veins.
Vein material: multiple: (1) dip @ 45 degrees, anastomosing, 0.1-10 mm wide, filled with amorphous dark serpentine; (2) conjugate: 1st set, dipping at 45 degrees, generally linear, 0.5-5 mm wide, filled with amorphous black to massive blue-gray material.
ADDITIONAL COMMENTS: Primary vein set dominates serpentinization zones and is parallel to orthopyroxene foliation.

125-779A-22R-1 (continued)

UNIT 2: SERPENTINIZED TECTONIZED HARZBURGITE

Pieces 12, 14, and 16-22

COLOR: Bluish gray (5B 5/1)
LAYERING: Crude layering apparent, results from orthopyroxene alignment.
DEFORMATION: Orthopyroxene has wavy cleavage surfaces.
PRIMARY MINERALOGY:
Orthopyroxene - Mode: 50-90%.
Crystal size: 3-8 mm.
Crystal shape: Equant.
Crystal orientation: Not visible.
Percent replacement: Not visible.

Olivine - Mode: 50-10%.
Crystal size: 3-5 mm.
Crystal shape: Equant.
Crystal orientation: Not visible.
Percent replacement: Not visible.

Spinel - Mode: <1%.
Crystal size: <1 mm.
Crystal shape: Equant.
Crystal orientation: Arranged in stringers.
Percent replacement: Not visible.
SECONDARY MINERALOGY:
Serpentine.
Total percent: 60-85%.
Texture: Variable serpentinization.
Vein material: <2 mm wide veins, some subvertical, others dipping at 45 degrees, filled with dark amorphous and light green-white serpentine.

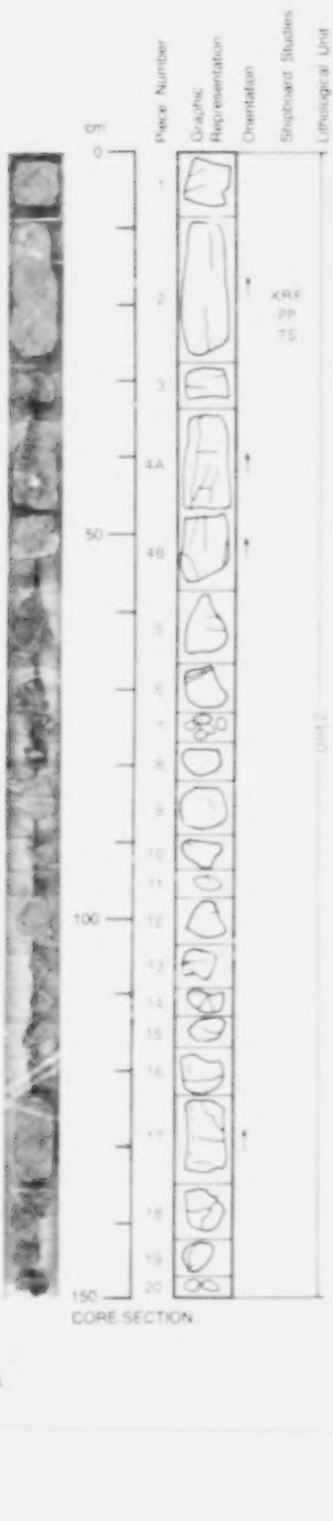
cm
0
50
100
150
Piece Number
Graphic Representation
Orientation
Shipboard Studies
Lithological Unit
1
2
3
4A
4B
5
6
7
8
9
10
11
12
13
14
15
16
17
18
19
20
XRF
PP
TS
Unit 2
CORE SECTION

125-779A-22R-2

UNIT 2: SERPENTINIZED TECTONIZED HARZBURGITE

Pieces 1, 15 and 16

COLOR: Bluish gray (5B 5/1).
LAYERING: Not visible.
DEFORMATION: Wavy cleavage and bent exsolution lamellae in orthopyroxene.
PRIMARY MINERALOGY:
Orthopyroxene - Mode: 50-75%
Crystal size: 3-8 mm.
Crystal shape: Equant ragged.
Crystal orientation: Not visible.
Percent replacement: Not visible.

Olivine - Mode: 30-50%
Crystal size: 3-8 mm.
Crystal shape: Equant.
Crystal orientation: Not visible.
Percent replacement: Not visible.

Spinel - Mode: <1%
Crystal size: 0.1-1 mm.
Crystal shape: Euhedral.
Crystal orientation: Not visible.
Percent replacement: Not visible.
SECONDARY MINERALOGY:
Serpentine
Total percent: 70-80%.
Texture: Variable serpentinization.
Vein material: <1 mm wide, filled with greenish white serpentine.

125-779A-22R-2 (continued)

UNIT 2: TECTONIZED SERPENTINIZED HARZBURGITE

Pieces 2-4,9,10,12-14,17,18,20

COLOR: Gray to dark gray (N 6/ to N 5/).
LAYERING: Strong layering defined by olivine and orthopyroxene.
DEFORMATION: Wavy cleavage on orthopyroxene.
PRIMARY MINERALOGY:
Olivine - Mode: 50-80%.
Crystal size: 8-20 mm.
Crystal shape: Elongate-ragged.
Crystal orientation: Not visible.
Percent replacement: Not visible.

Orthopyroxene - Mode: 20-50%.
Crystal size: 5-10 mm.
Crystal shape: Elongate-equant.
Crystal orientation: Not visible.
Percent replacement: Not visible.

Spinel - Mode: Trace.
Crystal size: 0.5-1.5 mm.
Crystal shape: Equant-elongate-dumbbell.
Crystal orientation: Not visible.
Percent replacement: Not visible.
SECONDARY MINERALOGY:
Serpentine.
Total percent: 70-80%.
Texture: N/A.
Vein material: 2 sets: (1) sub-horizontal and vertical, 0.5-3 mm, amorphous gray-black serpentine fill; (2) horizontal and 65 degrees dip, 1-5 mm, filled with laminar milky green amorphous serpentine and chrysotile.
ADDITIONAL COMMENTS: Piece 2 has layering of olivine and orthopyroxene. It may be primarily magmatic or tectonic transposition; dips at 45 degrees.

UNIT 2: TECTONIZED SERPENTINIZED DUNITE

Pieces 5-8, 11 and 19

COLOR: Dark bluish gray (5B 4/1).
LAYERING: Olivine appears to be strongly stretched in some pieces, defining an apparent layering.
DEFORMATION: Elongated olivines.
PRIMARY MINERALOGY:
Olivine - Mode: 95-99%.
Crystal size: 5-12 mm.
Crystal shape: Elongate-ragged.
Crystal orientation: Not visible.
Percent replacement: Not visible.

Orthopyroxene - Mode: 5-Trace.
Crystal size: 5-8 mm.
Crystal shape: Equant.
Crystal orientation: Not visible.
Percent replacement: Not visible.

Spinel - Mode: <1%.
Crystal size: <2 mm.
Crystal shape: Equant.
Crystal orientation: Not visible.
Percent replacement: Not visible.
SECONDARY MINERALOGY:
Serpentine.
Total percent: 70-85%.
Texture: Variable serpentinization.
Vein material: <5 mm wide, filled with milky white and pale green serpentine.

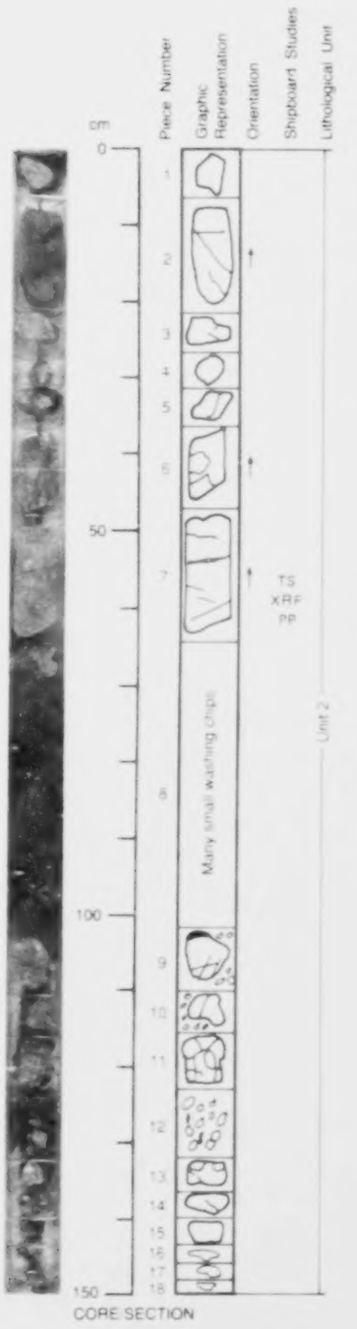
cm
Piece Number
Graphic Representation
Orientation
Shipboard Studies
Lithological Unit
0
50
100
150
1
2
3
4
5
6
7
8
9
10
11
12
13
14
15
16
17
18
Many small washing chips
TS
XRF
PP
Unit 2
CORE SECTION

125-779A-22R-3

UNIT 2: TECTONIZED SERPENTINIZED HARZBURGITE

Pieces 1, 3-8, 10, 11, 15, 16-18

COLOR: Bluish gray (5B 5/1)
LAYERING: Not visible
DEFORMATION: Wavy cleavage on orthopyroxene
PRIMARY MINERALOGY:
Olivine - Mode: 80-90%
Crystal size: 1-3 mm
Crystal shape: Elongate-ragged
Crystal orientation: Not visible
Percent replacement: Not visible

Orthopyroxene - Mode: 10-20%
Crystal size: 1-10 mm
Crystal shape: Elongate-equant
Crystal orientation: Not visible
Percent replacement: Not visible

Spinel - Mode: Trace
Crystal size: 0.1-2 mm
Crystal shape: Equant-elongate-dumbbell
Crystal orientation: Not visible
Percent replacement: Not visible
SECONDARY MINERALOGY:
Serpentine
Total percent: 65-85%
Texture: Variable serpentinization
Vein material: <3 mm wide, filled with milky white, pale green and dark green serpentine

UNIT 2: TECTONIZED SERPENTINIZED DUNITE

Pieces 2, 9, 12-14

COLOR: Dark blue gray (5B 4/1)
LAYERING: Not visible
DEFORMATION: Wavy cleavage is observed in some orthopyroxene
PRIMARY MINERALOGY:
Olivine - Mode: 90-98%
Crystal size: 1-4 mm
Crystal shape: Elongate-ragged
Crystal orientation: Not visible
Percent replacement: Not visible

Orthopyroxene - Mode: 2-10%
Crystal size: 1-10 mm
Crystal shape: Elongate-equant
Crystal orientation: Not visible
Percent replacement: Not visible

Spinel - Mode: 1-2%
Crystal size: 0.1-3 mm
Crystal shape: Equant-elongate-dumbbell
Crystal orientation: Not visible
Percent replacement: Not visible
SECONDARY MINERALOGY:
Serpentine
Total percent: 65-85%
Texture: Variable serpentinized
Vein material: <2 mm wide, filled with milky white and dark green serpentine

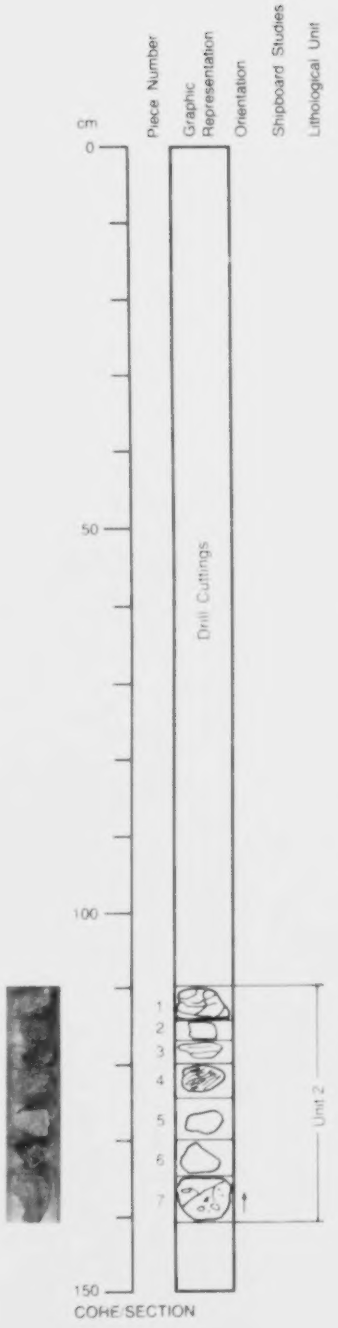

125-779A-23R-1

UNIT 2: TECTONIZED SERPENTINIZED DUNITE

Pieces 2 and 3

COLOR: Dark blue gray (5BG 5/1)
LAYERING: Not visible
DEFORMATION: Wavy cleavage in some pyroxenes.
PRIMARY MINERALOGY:
Olivine - Mode: 90-95%
Crystal size: 1-3 mm
Crystal shape: Elongate-ragged
Crystal orientation: Not visible
Percent replacement: Not visible

Orthopyroxene - Mode: 5-10%
Crystal size: 2-7 mm
Crystal shape: Equant-elongate
Crystal orientation: Not visible
Percent replacement: Not visible

Spinel? - Mode: Trace
Crystal size: 0.1-0.3 mm
Crystal shape: Equant-elongate
Crystal orientation: Not visible
Percent replacement: Not visible
SECONDARY MINERALOGY:
Serpentine
Total percent: 90-95%
Texture: Not visible
Vein material: <2 mm wide filled with milky white and green serpentine.

UNIT 2: SERPENTINIZED HARZBURGITE

Pieces 1, 4-7

COLOR: Greenish gray (5BG 5/1)
LAYERING: Not visible
DEFORMATION: Some pyroxenes appear to have wavy cleavages.
PRIMARY MINERALOGY:
Olivine - Mode: 80%
Crystal size: Not visible
Crystal shape: Not visible
Crystal orientation: Not visible
Percent replacement: Not visible

Orthopyroxene - Mode: 20%
Crystal size: 1-3 mm
Crystal shape: Not visible
Crystal orientation: Not visible
Percent replacement: Not visible

Spinel - Mode: Trace
Crystal size: <1 mm?
Crystal shape: Elongate
Crystal orientation: Not visible
Percent replacement: Not visible
SECONDARY MINERALOGY:
Serpentine
Total percent: 90%
Texture: N/A
Vein material: <2 mm wide, filled with milky white, pale green and dark green serpentine.
ADDITIONAL COMMENTS: Piece 4 shows anastomosing and dark green serpentine veins.

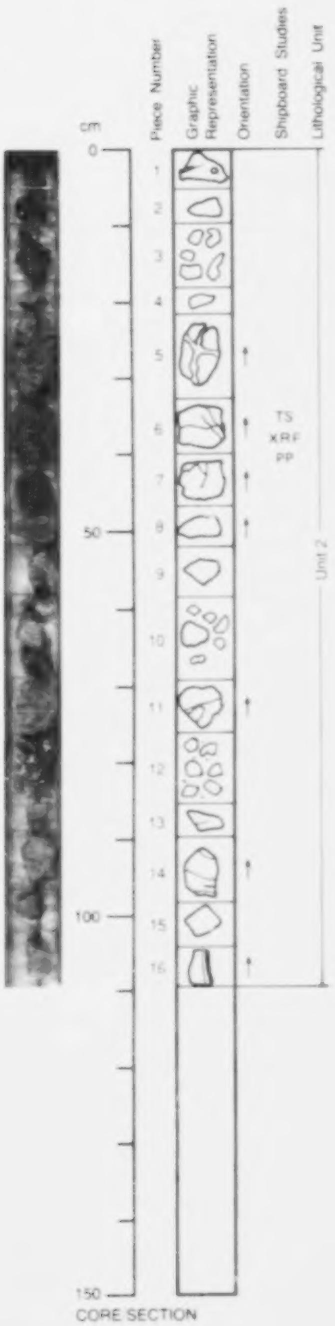

125-779A-24R-1

UNIT 2: SERPENTINIZED DUNITE

Pieces 1, 2, 3, 6, 7

COLOR: Dark bluish gray (5B 4/1)
LAYERING: None
DEFORMATION: Appears slightly sheared (tectonized?)
PRIMARY MINERALOGY:
Olivine - Mode: 80-90%
Crystal size: Not visible
Crystal shape: Not visible
Crystal orientation: Not visible
Percent replacement: 100%

Orthopyroxene - Mode: 10-15%
Crystal size: 1-3 mm
Crystal shape: Equant-elongate
Crystal orientation: Not visible
Percent replacement: 100%

Spinel? - Mode: Trace
Crystal size: 0.5-1.0 mm
Crystal shape: Equant-elongate
Crystal orientation: Not visible
Percent replacement: 0%
SECONDARY MINERALOGY:
Serpentine
Total percent: 100%
Texture: Serpentinized mesh texture is visible
Vein material: <2 mm wide black and pale milky green serpentine veining

UNIT 2: SERPENTINIZED TECTONIZED HARZBURGITE

Pieces 4, 5, 8, 9, 11, 13-16

COLOR: Bluish gray to dark bluish gray (5B 6/1 to 5B 4/1)
LAYERING: None
DEFORMATION: Some pyroxenes show wavy extinction
PRIMARY MINERALOGY:
Olivine - Mode: 80%
Crystal size: Not visible
Crystal shape: Not visible
Crystal orientation: Not visible
Percent replacement: 90%

Orthopyroxene - Mode: 15%
Crystal size: 1-2 mm
Crystal shape: Equant-elongate
Crystal orientation: Not visible
Percent replacement: 50%

Spinel? - Mode: Trace-5%
Crystal size: <0.5 mm
Crystal shape: Equant-elongate
Crystal orientation: N/A
Percent replacement: 0%
SECONDARY MINERALOGY:
Total percent: 70%
Texture: Serpentine; bastitic in areas
Vein material: Pale green and milky white serpentine veining, <2 mm wide; black serpentine veining <2 mm wide
ADDITIONAL COMMENTS: Pieces 11 and 13 have serpentinization halos 2-3 cm wide

125-779A-24R-1(continued)

UNIT 2: FRAGMENTS OF SERPENTINIZED HARZBURGITES AND DUNITES

Pieces 10 and 12

COLOR: Dark bluish gray-dark greenish gray (5B 4/1- 5G 4/1).
LAYERING: None.
DEFORMATION: None visible.
PRIMARY MINERALOGY:
Olivine - Mode: 75-95%.
Crystal size: 2-6 mm.
Crystal shape: Equant.
Crystal orientation: Not visible.
Percent replacement: 80-90%.

Orthopyroxene - Mode: 5-25%.
Crystal size: 2-5 mm.
Crystal shape: Elongate.
Crystal orientation: Not visible.
Percent replacement: 70-80%.

Spinel - Mode: Trace.
Crystal size: <0.5 mm.
Crystal shape: Ragged.
Crystal orientation: Not visible.
Percent replacement: 0%.
SECONDARY MINERALOGY:
Serpentine.
Total percent: 80-90%.
Texture: Mesh and bastite.
Vein material: Two types of veins: 1) black serpentine 2) pale white green serpentine <2 mm wide.

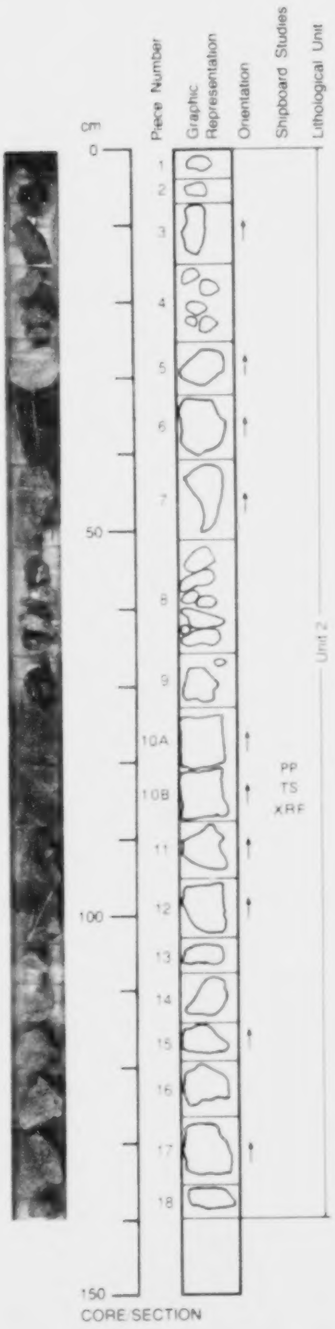
cm
0
50
100
150
Piece Number
Graphic Representation
Orientation
Shipboard Studies
Lithological Unit
1
2
3
4
5
6
7
8
9
10A
10B
11
12
13
14
15
16
17
18
PP
TS
XRF
Unit 2
CORE/SECTION

125-779A-25R-1

UNIT 2: SERPENTINIZED TECTONIZED HARZBURGITE

Pieces 1-2

COLOR: Dark gray (N4/)
LAYERING: Not visible
DEFORMATION: Wavy cleavage on orthopyroxene
PRIMARY MINERALOGY:
Olivine - Mode: 90%
Crystal size: Not visible
Crystal shape: Not visible
Crystal orientation: Not visible
Percent replacement: 100%

Orthopyroxene - Mode: 10%
Crystal size: 2-5 mm
Crystal shape: Equant
Crystal orientation: Not visible
Percent replacement: 100%

Spinel - Mode: <1%
Crystal size: 0.1-1 mm
Crystal shape: Ragged
Crystal orientation: Not visible
Percent replacement: 0%
SECONDARY MINERALOGY:
Serpentine
Total percent: 99%
Texture: Bastite and mesh
Vein material: Chrysotile veins (<4 mm) and fine dark serpentine veins

125-779A-25R-1 (continued)

UNIT 2: SERPENTINIZED TECTONIZED HARZBURGITE

Pieces 3 and 6

COLOR: Dark greenish gray (5B 4/1).
LAYERING: Not visible.
DEFORMATION: Elongated ragged spinel, distorted orthopyroxene, some elongated.
PRIMARY MINERALOGY:
Olivine - Mode: 90%.
Crystal size: Not visible.
Crystal shape: Not visible.
Crystal orientation: Not visible.
Percent replacement: 90%.

Orthopyroxene - Mode: 10%.
Crystal size: 5-12 mm.
Crystal shape: Equant to elongate.
Crystal orientation: Random.
Percent replacement: 90%.

Cr spinel - Mode: Trace.
Crystal size: <1 mm.
Crystal shape: Equant to ragged.
Crystal orientation: Random.
Percent replacement: 0%.
SECONDARY MINERALOGY:
Serpentine.
Total percent: 90-99%.
Texture: Micro-mesh texture after olivine with bastite after orthopyroxene.
Vein material: One subhorizontal white vein (<0.5 mm) cut by vertical white vein (1 mm thick).

UNIT 2: SERPENTINIZED TECTONIZED HARZBURGITE

Pieces 4 and 5

COLOR: Bluish gray (5B 5/1).
LAYERING: Not visible.
DEFORMATION: Shear fabric dipping at 60 degrees.
PRIMARY MINERALOGY:
Orthopyroxene - Mode: 50%.
Crystal size: 3-4 mm.
Crystal shape: Elongated.
Crystal orientation: 60-70 degrees.
Percent replacement: 20%.

Olivine - Mode: 5-10%.
Crystal size: 8-10 mm.
Crystal shape: Elongate.
Crystal orientation: Parallel to orthopyroxene.
Percent replacement: 20%.

Cr spinel - Mode: Trace.
Crystal size: <1 mm.
Crystal shape: Rounded-equant.
Crystal orientation: Random.
Percent replacement: 0%.
SECONDARY MINERALOGY:
Serpentine.
Total percent: 20%.
Texture: Serpentinization along orthopyroxene cleavage planes.
Vein material: None.
ADDITIONAL COMMENTS: Comparatively orthopyroxene-rich pieces; fabric possibly relict cumulate origin now accentuated by deformation.

125-779A-25R-1 (continued)

UNIT 2: SERPENTINIZED TECTONIZED DUNITE

Pieces 7 to 15

COLOR: Dark gray (N4)
LAYERING: Not visible
DEFORMATION: Some unfilled fractures
PRIMARY MINERALOGY:
Olivine : Mode: >95%
Crystal size: 8-15 mm
Crystal shape: Elongated
Crystal orientation: Not visible
Percent replacement: 60%

Orthopyroxene : Mode: 5%
Crystal size: 3-5 mm
Crystal shape: Elongated
Crystal orientation: Not visible
Percent replacement: 100%

Spinel : Mode: Trace
Crystal size: <1 mm
Crystal shape: Elongated
Crystal orientation: Not visible
Percent replacement: 0%
SECONDARY MINERALOGY:
Serpentine
Total percent: 10-70%
Texture: Variably deformed mesh texture after olivine
Vein material: Black veins surrounded by alteration zones (<1 mm wide), crosscut by white laminated veins at 60 degrees dip (2 mm wide)

UNIT 2: SERPENTINIZED TECTONIZED HARZBURGITE

Pieces 16 to 18

COLOR: Dark gray (N4)
LAYERING: Orthopyroxene rich layer dipping at 50 degrees.
DEFORMATION: Wavy cleavage on orthopyroxene
PRIMARY MINERALOGY:
Olivine : Mode: 90%
Crystal size: 8-12 mm
Crystal shape: Rounded
Crystal orientation: Not visible
Percent replacement: 60%

Orthopyroxene : Mode: 10%
Crystal size: 5-1.5 mm
Crystal shape: Rounded
Crystal orientation: Not visible
Percent replacement: 30%

Spinel : Mode: Trace
Crystal size: <2 mm
Crystal shape: Equant
Crystal orientation: Not visible
Percent replacement: 0%
SECONDARY MINERALOGY:
Serpentine
Total percent: 30-60%
Texture: Mesh texture after olivine and bastite after orthopyroxene
Vein material: Set of black horizontal and vertical veins (<2 mm wide) cut by white veins.
ADDITIONAL COMMENTS: Bulk of pieces broken by orthogonal set of serpentine-filled fractures

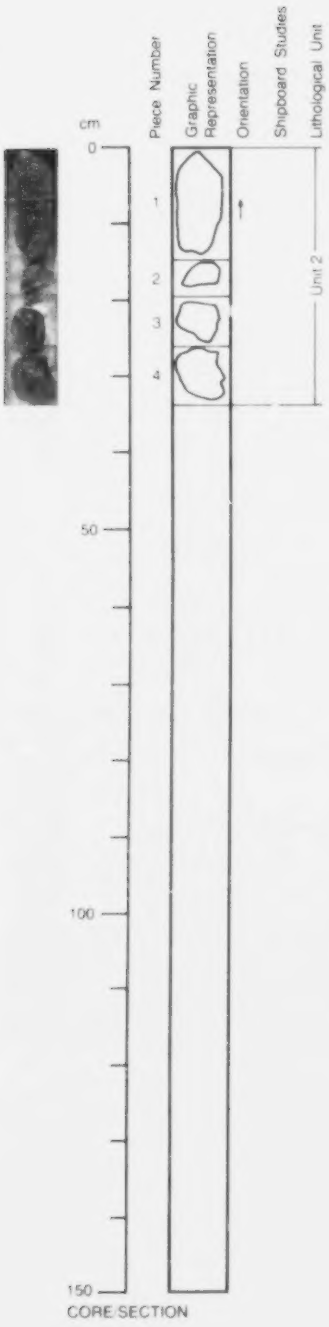

125-779A-25R-2

UNIT 2: SERPENTINIZED TECTONIZED HARZBURGITE

Piece 1

COLOR: Dark bluish gray (5B 4/1).
LAYERING: Not visible.
DEFORMATION: Elongated ragged spinel; some elongated and deformed orthopyroxene.
PRIMARY MINERALOGY:
Olivine - Mode: 85%.
Crystal size: <10 mm.
Crystal shape: Not visible.
Crystal orientation: Not visible.
Percent replacement: 80%.

Orthopyroxene - Mode: 15%.
Crystal size: <10 mm.
Crystal shape: Equant-elongate.
Crystal orientation: Not visible.
Percent replacement: 50%.

Spinel - Mode: 1%.
Crystal size: <2 mm.
Crystal shape: Elongate-ragged.
Crystal orientation: Not visible.
Percent replacement: 0%.
SECONDARY MINERALOGY:
Serpentine.
Total percent: 70%.
Texture: Mesh and bastite.
Vein material: Dark green vein (8 mm wide) cuts across the core.

UNIT 2: SERPENTINIZED DUNITE

Pieces 2, 3 and 4

COLOR: Grayish green (5G 4/2).
LAYERING: Not visible.
DEFORMATION: Brittle fracture and elongation of Cr-spinel.
PRIMARY MINERALOGY:
Olivine - Mode: 95%.
Crystal size: Not visible.
Crystal shape: Not visible.
Crystal orientation: Not visible.
Percent replacement: Variable.

Orthopyroxene - Mode: <5%.
Crystal size: <5 mm.
Crystal shape: Elongated.
Crystal orientation: Random.
Percent replacement: Variable.

Cr-spinel - Mode: <1%.
Crystal size: <2 mm.
Crystal shape: Ragged.
Crystal orientation: Disseminated.
Percent replacement: 0%.
SECONDARY MINERALOGY:
Serpentine.
Total percent: 50-70%.
Texture: Micro-mesh texture after olivine, bastite after orthopyroxene.
Vein material: 1st generation of anastomosing veins, 2-15 mm wide, of black serpentine with alteration halos 15 mm wide; dipping at 60-65 degrees.

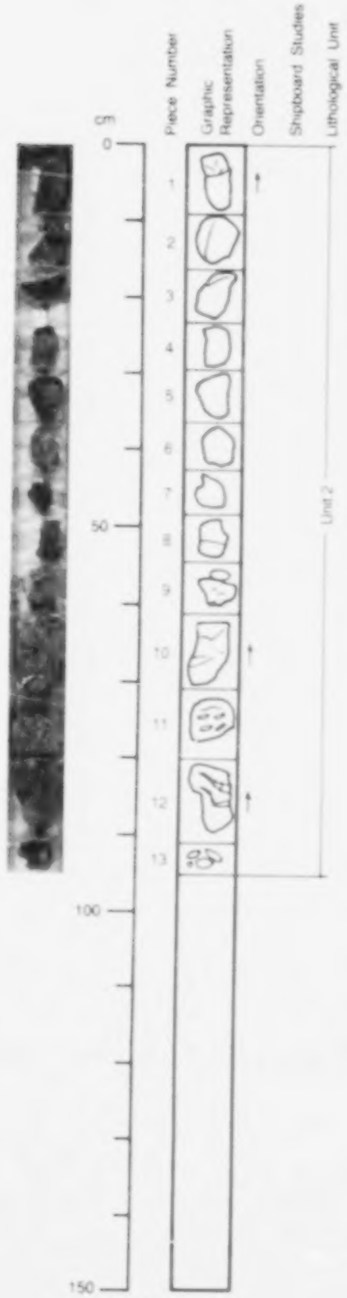

125-779A-26R-1

UNIT 2: SERPENTINIZED TECTONIZED HARZBURGITE

Pieces 1, 2, 3, 5, 6, 8, 10

COLOR: Bluish gray (5B 5/1)
LAYERING: Not visible
DEFORMATION: Wavy cleavage surfaces on orthopyroxene
PRIMARY MINERALOGY:
Orthopyroxene - Mode: 5-10%
Crystal size: 3-5 mm
Crystal shape: Equant
Crystal orientation: Not visible
Percent replacement: Variable

Olivine - Mode: 90-95%
Crystal size: 5-10 mm
Crystal shape: Ragged
Crystal orientation: Not visible
Percent replacement: Variable

Spinel - Mode: Trace
Crystal size: <0.1 mm
Crystal shape: Equant
Crystal orientation: Not visible
Percent replacement: 0%
SECONDARY MINERALOGY:
Serpentine
Total percent: 40-50%
Texture: Mesh after olivine and bastite after orthopyroxene
Vein material: <5 mm wide, anastomosing, filled with dark gray, black amorphous serpentine
ADDITIONAL COMMENTS: In Piece 1, there appears to be an apparent downhole gradation from harzburgite to dunite

UNIT 2: SERPENTINIZED TECTONIZED DUNITE

Pieces 4, 7, 9, 11, 12, 13

COLOR: Mottled, variable from dark greenish to bluish gray (5BG 4/1 to 5B 6/1)
LAYERING: Not visible
DEFORMATION: Apparent cataclastic appearance in some pieces resulting from extensive alteration of olivine, dipping at 30 degrees
PRIMARY MINERALOGY:
Olivine - Mode: 95-99%
Crystal size: 3-12 mm
Crystal shape: Ragged and elongate to equant
Crystal orientation: N.A.
Percent replacement: Variable

Spinel - Mode: <1%
Crystal size: <2 mm
Crystal shape: Equant to elongate
Crystal orientation: Arranged in ragged trains
Percent replacement: 0%
SECONDARY MINERALOGY:
Serpentine
Total percent: 90%
Texture: Mesh after olivine
Vein material: Multiple: (1) <5 mm wide, irregular, filled with dark green-black amorphous serpentine; (2) "Frankenstein texture", chrysotile filled (<1 mm wide)

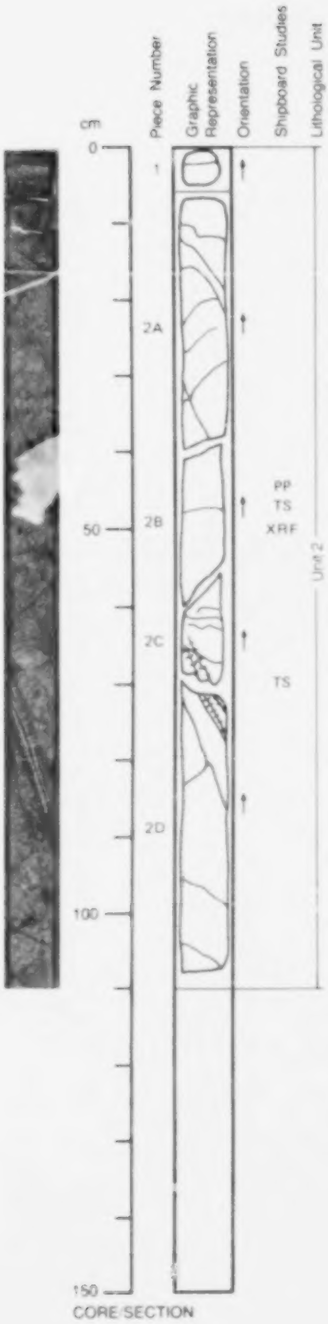
cm
0
50
100
150
Piece Number
Graphic Representation
Orientation
Shipboard Studies
Lithological Unit
1
2A
2B
2C
2D
PP
TS
XRF
TS
Unit 2
CORE/SECTION

125-779A-26R-2

UNIT 2: SERPENTINIZED TECTONIZED HARZBURGITE

Pieces 1 and 2

COLOR: Bluish gray to dark bluish gray (5B 5/1 to 5B 4/1) with grayish green (5G 4/2) veins.
LAYERING: Not visible.
DEFORMATION: Orthopyroxene has wavy cleavage; some cataclasis with sense of horizontal shear in Piece 1.
PRIMARY MINERALOGY:
Olivine - Mode: 80-90%.
Crystal size: 5-8 mm.
Crystal shape: Equant-ragged.
Crystal orientation: Not visible.
Percent replacement: 25-30%.

Orthopyroxene - Mode: 10-20%.
Crystal size: 1-5 mm-5mm.
Crystal shape: Equant.
Crystal orientation: Not visible.
Percent replacement: 0%.

Spinel - Mode: <1.5%.
Crystal size: <1 mm.
Crystal shape: Subhedral.
Crystal orientation: Disseminated.
Percent replacement: 0%.
SECONDARY MINERALOGY:
Serpentine.
Total percent: 30%.
Texture: Protomesh after olivine and bastite after orthopyroxene.
Vein material: Polyphase veins dipping at 75 degrees, filled with several generations of dark green black serpentine, 30 mm wide; later generation of pale green amorphous serpentine 2-3 mm wide, followed by chrysotile veins (<1-2 mm wide); also a conjugate set of dark amorphous serpentine, dipping at 30 degrees.
ADDITIONAL COMMENTS: This is one of the longest complete sections of core so far recovered from 779A; intense serpentinization more pronounced closest to the veins dipping at 70 degrees.

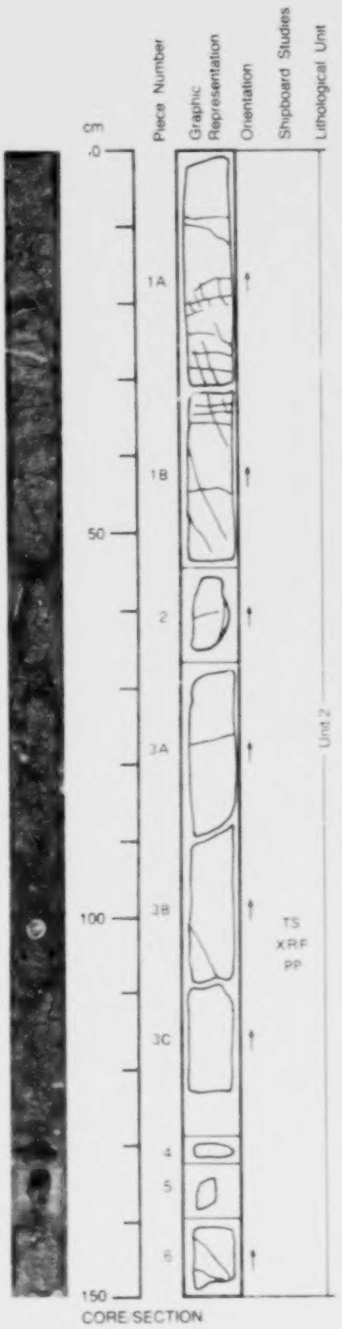
cm
Piece Number
Graphic Representation
Orientation
Shipboard Studies
Lithological Unit
0
50
100
150
1A
1B
2
3A
3B
3C
4
5
6
TS
XRF
PP
Unit 2
CORE SECTION

125-779A-26R-3

UNIT 2: SERPENTINIZED TECTONIZED HARZBURGITE

Pieces 1 to 6

COLOR: Bluish gray to dark bluish gray (5B 5/1 to 5B 4/1) with dark gray green (5G 4/2) veins.
LAYERING: None.
DEFORMATION: Wavy cleavage on orthopyroxene; spinels show weak alignment in trains.
PRIMARY MINERALOGY:
Olivine - Mode: 80-90%.
Crystal size: 5-12 mm.
Crystal shape: Equant-ragged.
Crystal orientation: Not visible.
Percent replacement: 20%.

Orthopyroxene - Mode: 10-20%.
Crystal size: 3-5 mm.
Crystal shape: Equant-elongate.
Crystal orientation: Not visible.
Percent replacement: 10%.

Spinel - Mode: Trace.
Crystal size: <1 mm.
Crystal shape: Equant-dumbbell.
Crystal orientation: Not visible.
Percent replacement: 0%.
SECONDARY MINERALOGY:
Serpentine.
Total percent: 20%.
Texture: Protomesh after olivine and bastite after orthopyroxene.
Vein material: (1) major set, <4 mm wide, dipping @ 70 degrees, filled with dark green/black serpentine, subsequently same fracture cannibalized by chrysotile veining and cross-stitching; (2) another generation, possibly first in sequence of conjugate, <5 mm wide, filled with amorphous dark serpentine.
ADDITIONAL COMMENTS: Serpentinization most intense around the veins dipping at 70 degrees.

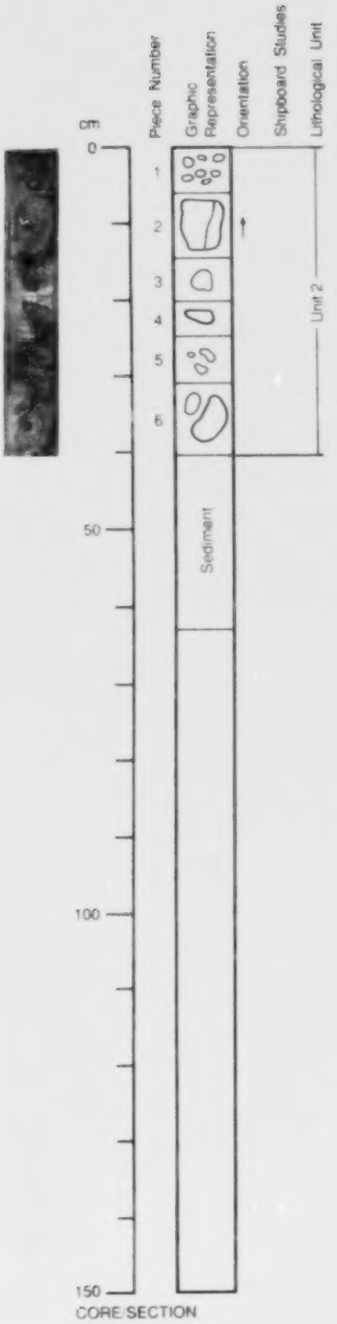
cm
0
50
100
150
CORE/SECTION
Piece Number
Graphic Representation
Orientation
Shipboard Studies
Lithological Unit
1
2
3
4
5
6
Unit 2
Sediment

125-779A-27R-1

UNIT 2: SERPENTINIZED TECTONIZED HARZBURGITE

Pieces 2, 3, 4 and 6

COLOR: Dark bluish gray (5B 4/1).
LAYERING: Not visible.
DEFORMATION: Wavy cleavage on orthopyroxene.
PRIMARY MINERALOGY:
Olivine - Mode: 80-90%.
Crystal size: 3-8 mm.
Crystal shape: Ragged.
Crystal orientation: Not visible.
Percent replacement: Variable.

Orthopyroxene - Mode: 10-20%.
Crystal size: 4-6 mm.
Crystal shape: Equant-elongate.
Crystal orientation: Not visible.
Percent replacement: Variable.

Spinel - Mode: Trace.
Crystal size: <2 mm.
Crystal shape: Elongate.
Crystal orientation: Not visible.
Percent replacement: 0%.
SECONDARY MINERALOGY:
Serpentine.
Total percent: 70%.
Texture: Mesh after olivine and bastite after orthopyroxene.
Vein material: 2 mm wide, dark blue-gray, serpentine-filled.

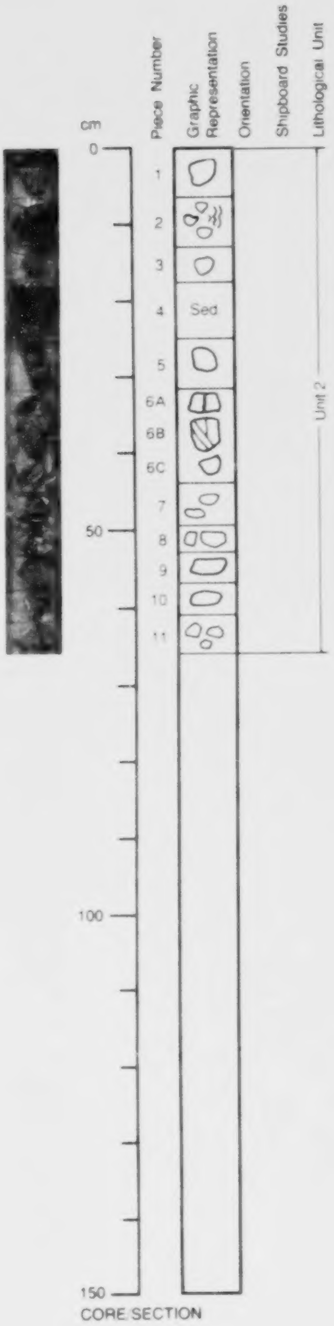
cm
0
50
100
150
CORE/SECTION
Piece Number
Graphic Representation
Orientation
Shipboard Studies
Lithological Unit
1
2
3
4
Sed
5
6A
6B
6C
7
8
9
10
11
Unit 2

125-779A-28R-1

UNIT 2: SERPENTINIZED TECTONIZED HARZBURGITE

Pieces 1 and 3

COLOR: Bluish gray to dark bluish gray (5B 5/1 TO 5B 4/1).
LAYERING: Not visible.
DEFORMATION: Wavy cleavage on orthopyroxene.
PRIMARY MINERALOGY:
Olivine - Mode: 90-95%.
Crystal size: 5-8 mm.
Crystal shape: Ragged.
Crystal orientation: Not visible.
Percent replacement: 80%.

Orthopyroxene - Mode: 5-10%.
Crystal size: 2-4 mm.
Crystal shape: Equant.
Crystal orientation: Not visible.
Percent replacement: 50%.

Spinel - Mode: Trace.
Crystal size: <1 mm.
Crystal shape: Equant.
Crystal orientation: Not visible.
Percent replacement: 0%.
SECONDARY MINERALOGY:
Serpentine.
Total percent: 70%.
Texture: Mesh after olivine and bastite after orthopyroxene.
Vein material: N/A.

UNIT 2: SERPENTINIZED TECTONIZED DUNITE

Pieces 5 to 11

COLOR: Black (5Y 2.5/1).
LAYERING: Not visible.
DEFORMATION: Not visible.
PRIMARY MINERALOGY:
Olivine - Mode: 99%.
Crystal size: Not visible.
Crystal shape: Not visible.
Crystal orientation: Not visible.
Percent replacement: 100%.

Spinel - Mode: 1%.
Crystal size: <2 mm.
Crystal shape: Equant to elongate.
Crystal orientation: Not visible.
Percent replacement: Not visible.
SECONDARY MINERALOGY:
Serpentine.
Total percent: 99%.
Texture: Mesh.
Vein material: <3 mm, overall linear, but irregular on a small scale, with dark green serpentine-filled (plus some chrysotile) veining and cross stitching.

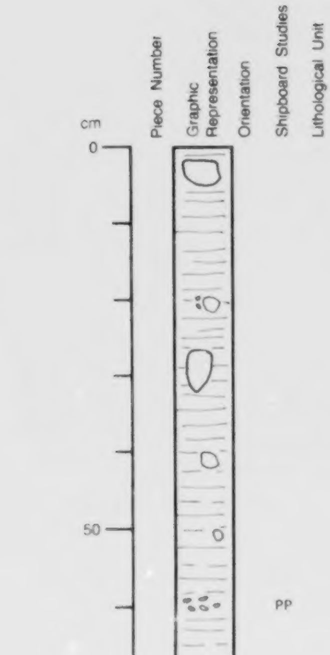
cm
0
50
100
150
Piece Number
Graphic Representation
Orientation
Shipboard Studies
Lithological Unit
Sediment
PP
TIL
IW
Sediment
1
2
3
Unit 2
CORE/SECTION

125-779A-28R-2

UNIT 2: SERPENTINIZED TECTONIZED DUNITE

Pieces 1 to 3

COLOR: Very dark greenish gray (10Y 3/1)
LAYERING: Not visible.
DEFORMATION: Spinels appear to be elongate and arranged in trains.
PRIMARY MINERALOGY:
- Olivine - Mode: 99%.
  - Crystal size: Not visible.
  - Crystal shape: Not visible.
  - Crystal orientation: Not visible.
  - Percent replacement: 100%.

- Spinel - Mode: 1%.
  - Crystal size: <3 mm.
  - Crystal shape: Equant to elongate.
  - Crystal orientation: Not visible.
  - Percent replacement: 0%.

SECONDARY MINERALOGY:
- Serpentine.
  - Total percent: 100%.
  - Texture: Very fine-grained.
  - Vein material: <3-mm wide, green-white, serpentine-filled veins.

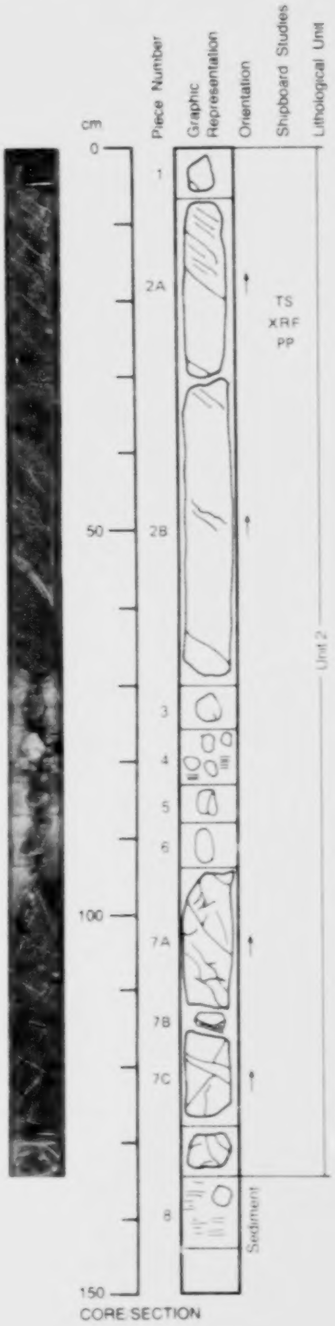

125-779A-28R-3

UNIT 2: SERPENTINIZED TECTONIZED DUNITE

Pieces 1, 3 to 8

COLOR: Very dark greenish gray (10Y 3/1).
LAYERING: Not visible.
DEFORMATION: Possible alignment of elongate spinels.
PRIMARY MINERALOGY:
Olivine - Mode: 99%.
Crystal size: Not visible.
Crystal shape: Not visible.
Crystal orientation: Not visible.
Percent replacement: 100%.

Spinel - Mode: 1%.
Crystal size: <5 mm.
Crystal shape: Elongate.
Crystal orientation: Not visible.
Percent replacement: 0%.
SECONDARY MINERALOGY:
Serpentine.
Total percent: 100%.
Texture: Mesh after olivine.
Vein material: numerous <3-mm linear and en echelon milky-green and white serpentine-filled veins; hint of conjugate set dipping at 70 degrees.

UNIT 2: SERPENTINIZED TECTONIZED HARZBURGITE

Piece 2

COLOR: Dark gray to dark bluish gray (N 4/ to 5B 4/1).
LAYERING: Apparently elongated olivine dipping at 70 degrees.
DEFORMATION: Wavy cleavage on orthopyroxene.
PRIMARY MINERALOGY:
Olivine - Mode: 90-95%.
Crystal size: <15 mm.
Crystal shape: Ragged to elongate.
Crystal orientation: Not visible.
Percent replacement: 100%.

Orthopyroxene - Mode: 5-10%.
Crystal size: 3-5 mm.
Crystal shape: Equant.
Crystal orientation: Not visible.
Percent replacement: 10%.

Spinel - Mode: Trace.
Crystal size: <5 mm.
Crystal shape: Elongate-equant.
Crystal orientation: Not visible.
Percent replacement: 0%.
SECONDARY MINERALOGY:
Serpentine.
Total percent: 80%.
Texture: Mesh after olivine and bastite after orthopyroxene.
Vein material: <2 mm wide, dipping @ 70 degrees, filled with white-green amorphous serpentine.

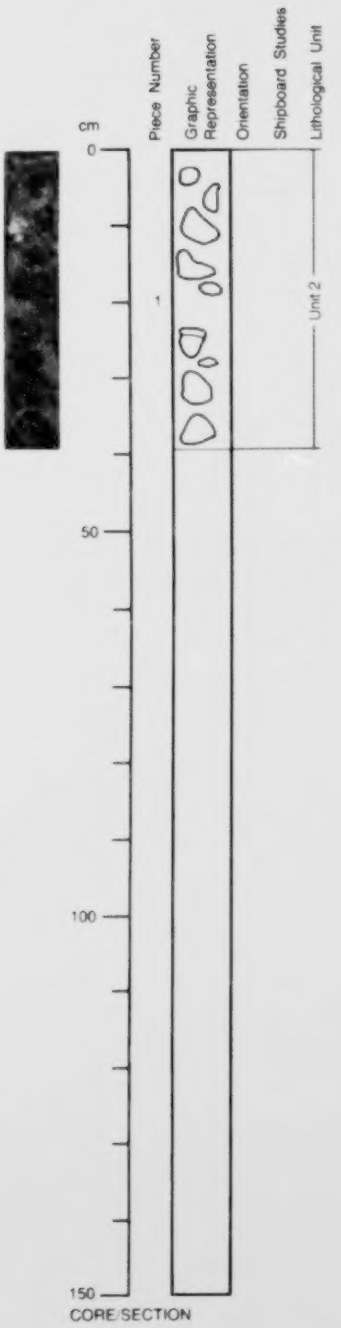
cm
Piece Number
Graphic Representation
Orientation
Shipboard Studies
Lithological Unit
0
50
100
150
1
Unit 2
CORE/SECTION

125-779A-29R-1

UNIT 2: TECTONIZED SERPENTINIZED DUNITE CLASTS

Piece 1

COLOR: Greenish black (10GY3/2)
LAYERING: Not visible
DEFORMATION: Fractured to pulverized
PRIMARY MINERALOGY:
- Olivine - Mode: 95-99%
  - Crystal size: Not visible
  - Crystal shape: Not visible
  - Crystal orientation: None
  - Percent replacement: 95-99

- Spinel - Mode: <1%
  - Crystal size: <1 mm
  - Crystal shape: Not visible
  - Crystal orientation: None
  - Percent replacement: Variable

SECONDARY MINERALOGY:
- Serpentine
  - Total percent: 95-99%
  - Texture: Very fine grained
  - Vein material: White veins (<0.5 mm wide)

ADDITIONAL COMMENTS: Variably fractured clasts in serpentine matrix

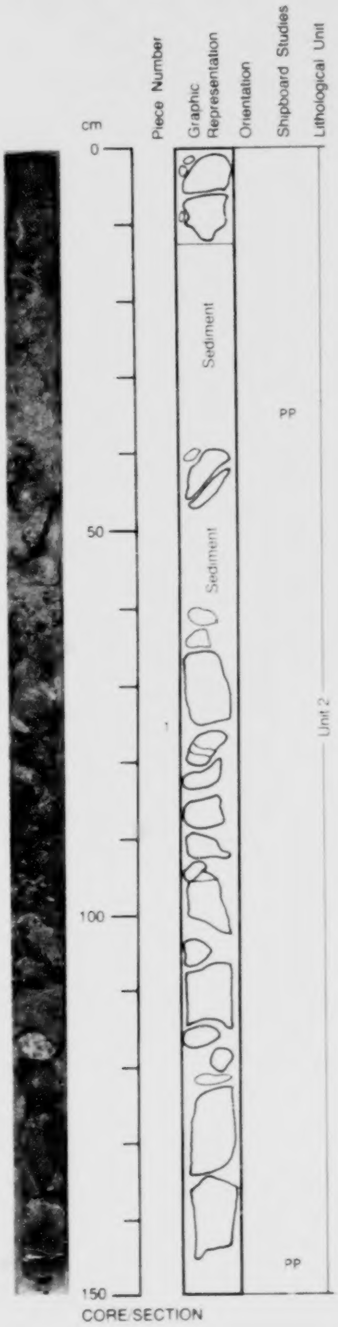
cm
Piece Number
Graphic Representation
Orientation
Shipboard Studies
Lithological Unit
0
50
100
150
Sediment
Sediment
PP
1
Unit 2
PP
CORE/SECTION

125-779A-29R-2

UNIT 2: SERPENTINIZED DUNITE TO HARZBURGITE

Piece 1 (fragments in serp. matrix)

COLOR: Black (10Y3/2)
LAYERING: Not visible
DEFORMATION: Locally strongly fractured after last vein generation
PRIMARY MINERALOGY:
Olivine - Mode: 85-95%
Crystal size: 3-5 mm
Crystal shape: Elongate
Crystal orientation: Not visible
Percent replacement: 99%

Orthopyroxene - Mode: 5-15%
Crystal size: 2-8 mm
Crystal shape: Equant
Crystal orientation: Not visible
Percent replacement: 80%

Cr-spinel - Mode: <1%
Crystal size: <1 mm
Crystal shape: Round to subequant
Crystal orientation: Stringers
Percent replacement: 0%
SECONDARY MINERALOGY:
Serpentine
Total percent: 80-99%
Texture: Mesh serpentine after olivine, some bastite after orthopyroxene
Vein material: White chrysotile veins at 45-70 degrees dip; also commonly with vertical orientation (along core length)
ADDITIONAL COMMENTS: Fragments are mainly olivine, but there are locally orthopyroxene-rich patches.

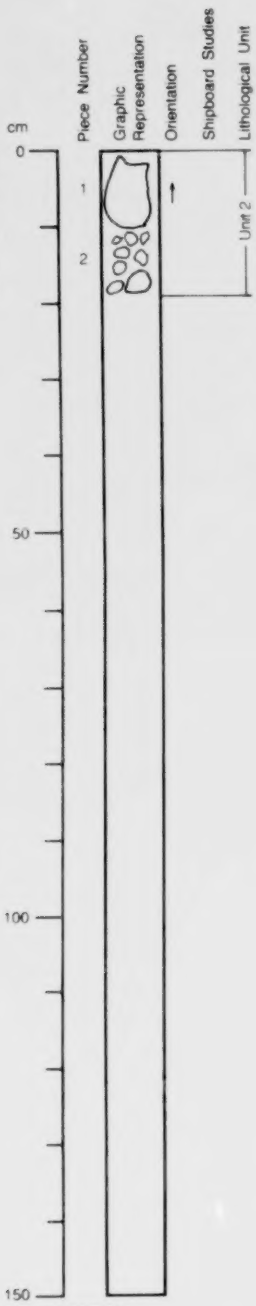
cm
Piece Number
Graphic Representation
Orientation
Shipboard Studies
Lithological Unit
0
1
2
Unit 2
50
100
150
CORE/SECTION

125-779A-29R-3

UNIT 2: SERPENTINIZED HARZBURGITE

Pieces 1 and 2

COLOR: Dark greenish gray (5B4/1).
LAYERING: Not visible.
DEFORMATION: Vein-filled fractures.
PRIMARY MINERALOGY:
- Olivine - Mode: 85-90%.
  Crystal size: 2-3 mm.
  Crystal shape: Not visible.
  Crystal orientation: Not visible.
  Percent replacement: 95%.

- Orthopyroxene - Mode: 15-10%.
  Crystal size: 5 mm.
  Crystal shape: Anhedral.
  Crystal orientation: Not visible.
  Percent replacement: 80%.

- Spinel - Mode: 1%.
  Crystal size: 1 mm.
  Crystal shape: Equant.
  Crystal orientation: Not visible.
  Percent replacement: 0%.

SECONDARY MINERALOGY:
- Serpentine.
  Total percent: 99%.
  Texture: Mesh after olivine, bastite after orthopyroxene.
  Vein material: Steeply dipping white veins of chrysotile (1-8 mm).

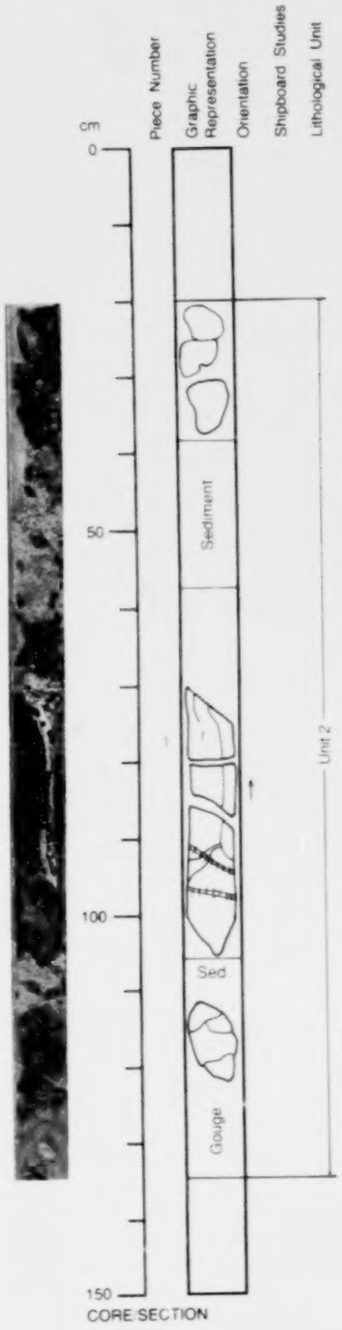
cm
Piece Number
Graphic Representation
Orientation
Shipboard Studies
Lithological Unit
0
50
100
150
Sediment
1
Sed
Gouge
Unit 2
CORE SECTION

125-779A-30R-1

UNIT 2: TECTONIZED SERPENTINIZED HARZBURGITE AND DUNITE

Pieces 1 (multiple fragments)

COLOR: Dark greenish gray (5BG 4/1).
LAYERING: Apparent between pyroxene-rich (harzburgitic) and dunitic layers.
DEFORMATION: Wavy cleavage on orthopyroxene.
PRIMARY MINERALOGY:
Olivine - Mode: 85-99%.
Crystal size: 5-10 mm.
Crystal shape: Ragged.
Crystal orientation: Not visible.
Percent replacement: 60-90%.

Orthopyroxene - Mode: 1-15%.
Crystal size: 3-5 mm.
Crystal shape: Equant-elongate.
Crystal orientation: Not visible.
Percent replacement: 30-50%.

Spinel - Mode: <1%.
Crystal size: <2 mm.
Crystal shape: Equant.
Crystal orientation: Not visible.
Percent replacement: 0%.
SECONDARY MINERALOGY:
Serpentine.
Total percent: 80%.
Texture: Mesh after olivine, bastite after orthopyroxene.
Vein material: Prominent subvertical but wavy <10 mm, filled with light-dark green amorphous serpentine, with a fringe (<1 mm) of chrysotile; another set dips at 30 degrees, filled with dark gray-black serpentine, cross-stitched by chrysotile; other <2-mm conjugate veins of chrysotile at 30 degrees dip.
ADDITIONAL COMMENTS: Major serpentine vein in this rock is one of the largest seen in the core.

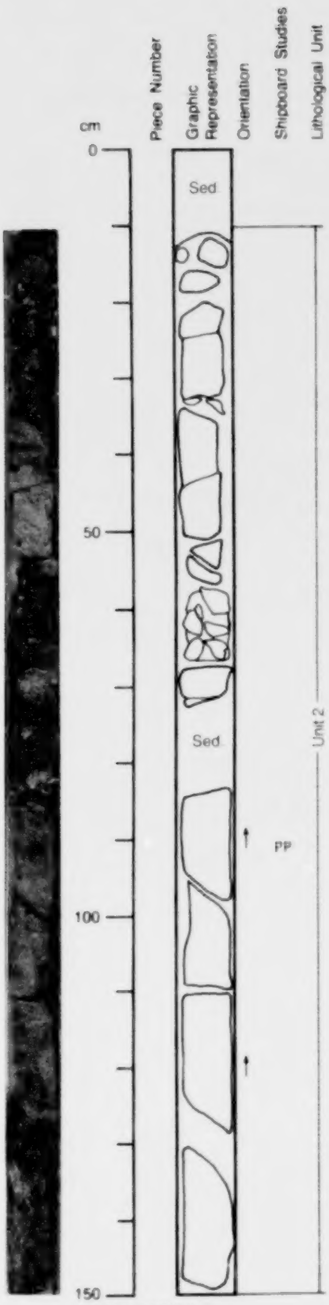
cm
Piece Number
Graphic Representation
Orientation
Shipboard Studies
Lithological Unit
0
50
100
150
Sed
Sed
PP
Unit 2
CORE/SECTION

125-779A-30R-2

UNIT 2: STRONGLY TECTONIZED SERPENTINIZED HARZBURGITE

Pieces multiple clasts in clay

COLOR: Dark green black with light green fractured zones
LAYERING: Not visible
DEFORMATION: Strongly fractured
PRIMARY MINERALOGY:
Olivine - **Mode:** 90%
Crystal size: Not visible
Crystal shape: Not visible
Crystal orientation: Not visible
Percent replacement: 90-99

Orthopyroxene - **Mode:** 10%
Crystal size: Not visible
Crystal shape: Not visible
Crystal orientation: Not visible
Percent replacement: 90-99

Spinel - **Mode:** Trace
Crystal size: Not visible
Crystal shape: Not visible
Crystal orientation: Disseminated
Percent replacement: None
SECONDARY MINERALOGY:
Serpentine
Total percent: 99%
Texture: Cataclasis
Vein material: White veins, (<0.1-3 mm), in all orientations chrysotile
ADDITIONAL COMMENTS: Strongly serpentinized

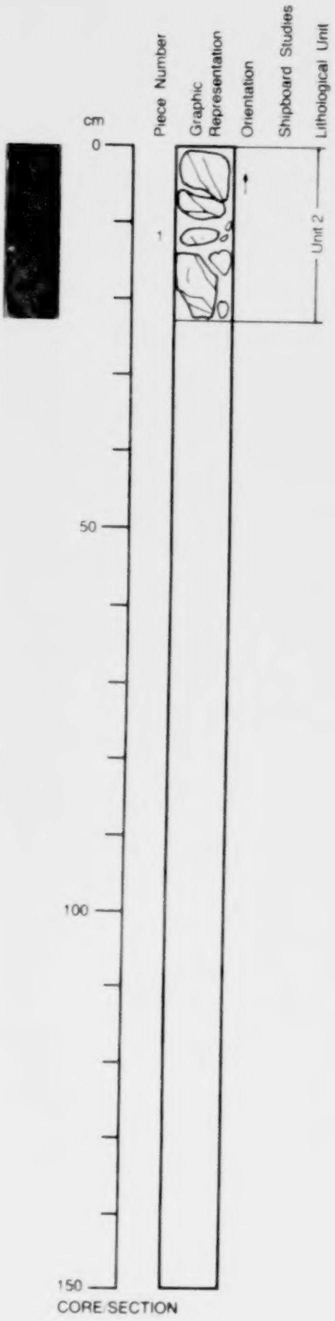
cm
Piece Number
Graphic Representation
Orientation
Shipboard Studies
Lithological Unit
0
1
Unit 2
50
100
150
CORE/SECTION

125-779A-30R-CC

UNIT 2: INTENSIVELY TECTONIZED AND SERPENTINIZED DUNITE

Piece 1

COLOR: Very dark greenish gray (10Y 3/1)
LAYERING: Crudely defined by elongate appearing serpentinized olivine
DEFORMATION: Intensely deformed olivine
PRIMARY MINERALOGY:
  Olivine - Mode: 99%
  Crystal size: <20 mm
  Crystal shape: Elongate-ragged
  Crystal orientation: Not visible
  Percent replacement: Not visible

  Spinel - Mode: Trace
  Crystal size: <1-2 mm
  Crystal shape: Equant-elongate
  Crystal orientation: Not visible
  Percent replacement: Not visible
SECONDARY MINERALOGY:
  Serpentine
  Total percent: 90%
  Texture: N/A
  Vein material: Numerous, <2 mm wide, filled with pale-dark green amorphous serpentine, dipping at 40 degrees, but many others at irregular dips and orientations.

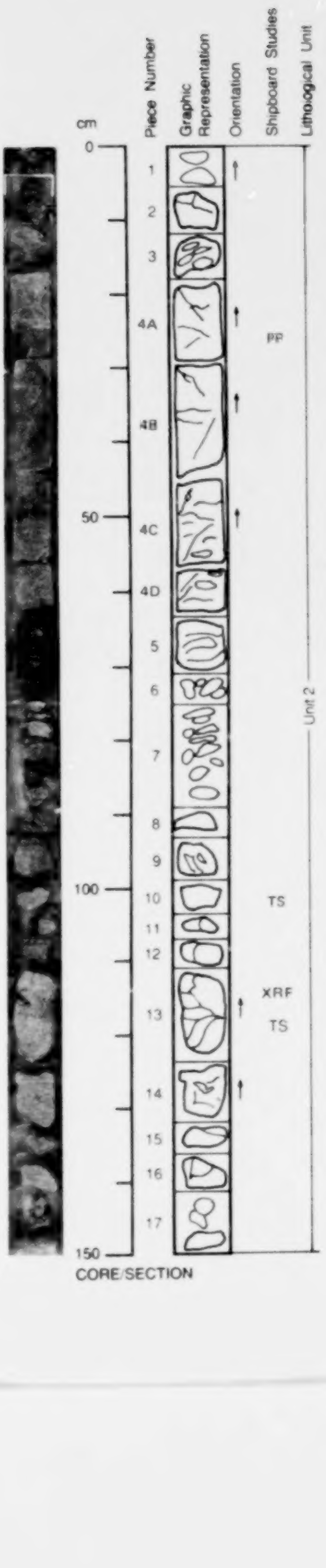

125-779A-31R-1

UNIT 2: TECTONIZED SERPENTINIZED HARZBURGITE

Pieces 1 and 2

COLOR: Dark greenish gray to greenish gray (5BG 4/1 to 5GY 5/1).
LAYERING: Not visible.
DEFORMATION: Wavy appearance to orthopyroxene cleavage.
PRIMARY MINERALOGY:
Olivine - Mode: 90-95%.
Crystal size: 5-12 mm.
Crystal shape: Elongate-ragged.
Crystal orientation: Not visible.
Percent replacement: Variable.

Orthopyroxene - Mode: 5-10%.
Crystal size: 3-5 mm.
Crystal shape: Equant-elongate.
Crystal orientation: Not visible.
Percent replacement: Variable.

Spinel - Mode: Trace.
Crystal size: <1 mm.
Crystal shape: Equant-elongate.
Crystal orientation: Not visible.
Percent replacement: Not visible.
SECONDARY MINERALOGY:
Serpentine.
Total percent: 75-95%.
Texture: Variable serpentinization.
Vein material: <1-mm wide, conjugate sets, dark serpentine filled.

UNIT 2: STRONGLY TECTONIZED AND SERPENTINIZED DUNITE

Pieces 3 to 9

COLOR: Dark greenish gray (5BG 4/1).
LAYERING: Not visible.
DEFORMATION: Cataclastic appearance with micro-shears and elongate serpentinized olivine.
PRIMARY MINERALOGY:
Olivine - Mode: 99%.
Crystal size: <20 mm.
Crystal shape: Elongate, ragged.
Crystal orientation: Along shears.
Percent replacement: Variable.

Spinel - Mode: Trace.
Crystal size: <2 mm.
Crystal shape: Elongate.
Crystal orientation: Not visible.
Percent replacement: Not visible.
SECONDARY MINERALOGY:
Serpentine.
Total percent: 90-95%.
Texture: N/A.
Vein material: Numerous anastomosing, <2 mm wide, filled with amorphous gray-green cataclastic serpentine.
ADDITIONAL COMMENTS: All pieces are strongly serpentinized and deformed; it is possible that some orthopyroxene may exist, but no cleavage is visible.

125-779A-31R-1 (continued)

UNIT 2: METABASALT

Pieces 10 to 17

COLOR: Bluish gray (5B 6/1)
LAYERING: Not visible
DEFORMATION: Brecciated into angular clasts and elongate clasts 10-30 mm in size indurated
PRIMARY MINERALOGY:
Aphyric very fine-grained
Plagioclase - Mode: 10-20%
Crystal size: <1 mm?
Crystal shape: Not visible
Crystal orientation: None
Purcent replacement: 80-90

Clinopyroxene - Mode: 20-40%
Crystal size: <1 mm
Crystal shape: Not visible
Crystal orientation: None
Percent replacement: 80-90

Glass - Mode: 50-60%
Crystal size: Not visible
Crystal shape: None
Crystal orientation: None
Percent replacement: 80-90
SECONDARY MINERALOGY:
Clays: chlorite
Total percent: 90%
Texture: N/A
Vein material: White, non-carbonate
ADDITIONAL COMMENTS: These pieces appear to be the upper chilled margin of a rock unit that becomes coarser-grained downwards in the core, eventually returning to a fine-grained character at the base; whole unit constitutes the majority of Core 31R except for the upper 90 cm.

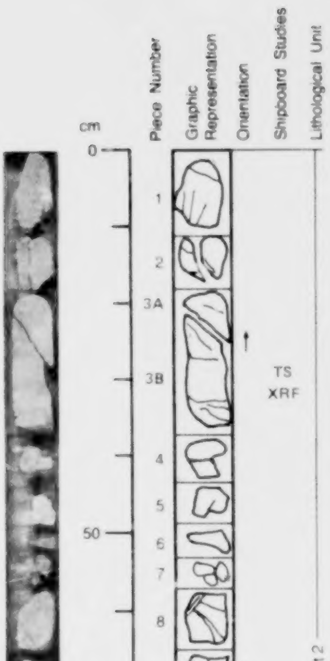
cm
Piece Number
Graphic Representation
Orientation
Shipboard Studies
Lithological Unit
0
1
2
3A
3B
TS
XRF
4
5
50
6
7
8
9
Unit 2
10
11A
100
TS
PP
XRF
11B
12
13
TS
14
15
16
150
CORE/SECTION

125-779A-31R-2

UNIT 2: META-MICROGABBRO

Pieces 1 to 16

COLOR: Greenish gray (5G 6/1).
LAYERING: Massive locally.
DEFORMATION: Shear zones sub-horizontal to dipping at 45 degrees, up to 100 mm wide, showing normal faulting.
PRIMARY MINERALOGY:
Size varies downwards in the section from fine-grained to sizes given below; plagioclase extensively replaced by secondary phases.
Plagioclase - Mode: 30-60%.
Crystal size: <3 mm.
Crystal shape: Euhedral.
Crystal orientation: Not visible.
Percent replacement: Not visible.

Clinopyroxene - Mode: 40-60%.
Crystal size: <6 mm.
Crystal shape: Ophitic.
Crystal orientation: Not visible.
Percent replacement: Not visible.

Oxide - Mode: <2%.
Crystal size: <0.2 mm.
Crystal shape: Anhedral.
Crystal orientation: Not visible.
Percent replacement: Not visible.
SECONDARY MINERALOGY:
Clays, chlorite and other low-temperature phases.
Total percent: 30-70%.
Texture: Massive.
Vein material: <3 mm wide, sub-horizontal to steeply dipping, filled with pale gray-green material.

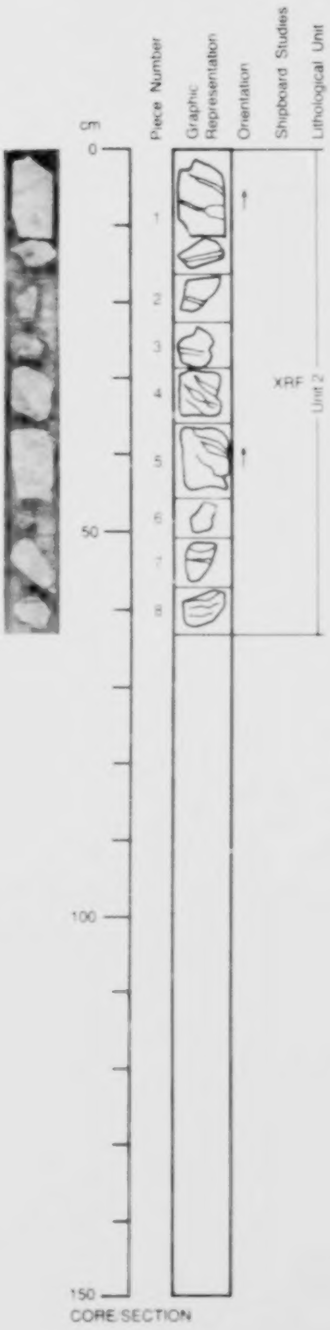
cm
Piece Number
Graphic Representation
Orientation
Shipboard Studies
Lithological Unit
0
50
100
150
1
2
3
4
5
6
7
8
XRF
Unit 2
CORE SECTION

125-779A-31R-3

UNIT 2: META-MICROGABBRO

Pieces 1 to 8

COLOR: Greenish gray (5G 6/1).
LAYERING: Not visible.
DEFORMATION: Shear zones dipping at 45 degrees, <30 mm wide.
PRIMARY MINERALOGY:
  Plagioclase extensively altered.
  Plagioclase - Mode: 30-60%.
  Crystal size: 1-3 mm.
  Crystal shape: Euhedral.
  Crystal orientation: Not visible.
  Percent replacement: Not visible.

  Clinopyroxene - Mode: 40-50%.
  Crystal size: <5 mm.
  Crystal shape: Ophitic.
  Crystal orientation: Not visible.
  Percent replacement: Not visible.

  Oxide - Mode: Trace.
  Crystal size: <0.1 mm.
  Crystal shape: Equant.
  Crystal orientation: Not visible.
  Percent replacement: Not visible.
SECONDARY MINERALOGY:
  Clays; chlorite.
  Total percent: 30-60%.
  Texture: N/A.
  Vein material: <1 mm wide, following shear zones and anastomosing from these; filled with greenish-white material.

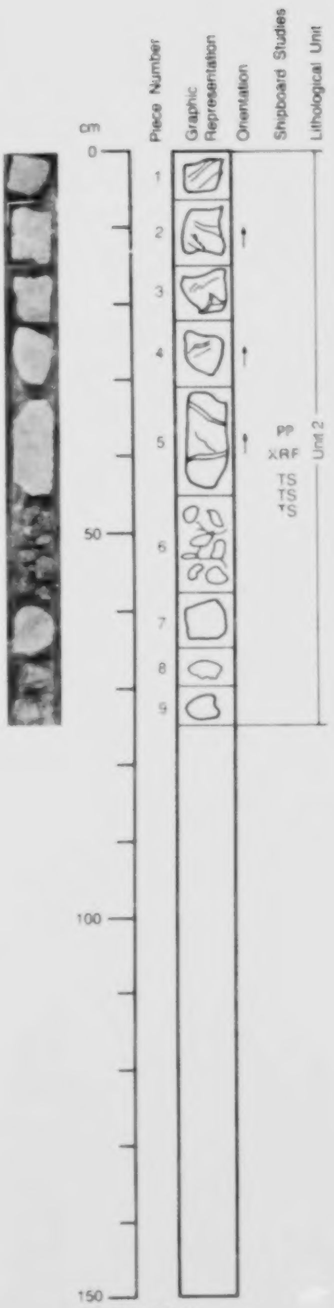
cm
Piece Number
Graphic Representation
Orientation
Shipboard Studies
Lithological Unit
0
50
100
150
1
2
3
4
5
6
7
8
9
PP
XRF
TS
TS
TS
Unit 2
CORE/SECTION

125-779A-31R-CC

UNIT 2: META-MICROGABBRO

Pieces 1-9

COLOR: Greenish gray (5G 6/1)
LAYERING: Not visible
DEFORMATION: Extensive shearing in zones <5 mm wide, subhorizontal and dipping at 40 degrees.
PRIMARY MINERALOGY:
Plagioclase - Mode: 40-60%.
Crystal size: <0.5-4 mm
Crystal shape: Euhedral tabular
Crystal orientation: Not visible
Percent replacement: Extensive

Clinopyroxene - Mode: 40-50%.
Crystal size: 5-8 mm
Crystal shape: Ophitic
Crystal orientation: Not visible
Percent replacement: Not visible

Oxide - Mode: Trace
Crystal size: Equant
Crystal shape: Not visible
Crystal orientation: Not visible
Percent replacement: Not visible
SECONDARY MINERALOGY:
Clays, chlorite, hydrogrossular
Total percent: 40-70%.
Texture: N/A
Vein material: Filling shears, light green and black vein-filling materials.

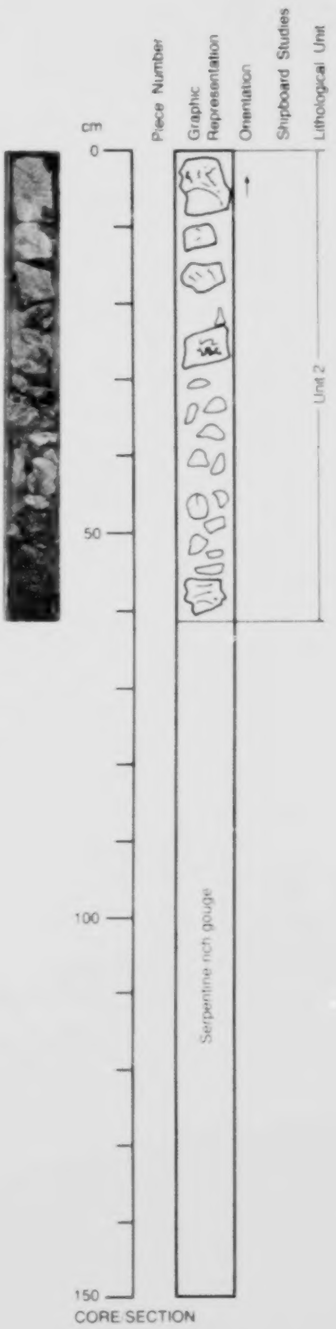
cm
Piece Number
Graphic Representation
Orientation
Shipboard Studies
Lithological Unit
0
50
100
150
Unit 2
Serpentine rich gouge
CORE SECTION

125-779A-32R-1

UNIT 2: TECTONIZED AND BRECCIATED METABASALT AND DUNITE

Pieces multiple pieces

COLOR: Greenish gray (5G 6/1) (brecciated material) to very dark greenish gray (10Y 3/1)
LAYERING: Not visible
DEFORMATION: Strong brecciation present in uppermost pieces, grades into sheared, deformed serpentinous fragments to tectonized dunite
PRIMARY MINERALOGY: Ultramafic fragments (olivine-rich) are fine-grained. Fragments are also extensively altered
SECONDARY MINERALOGY:
Serpentine
Total percent: 100%
Texture: N/A
Vein material: Deep green, serpentinous material infilling between angular brecciated fragments

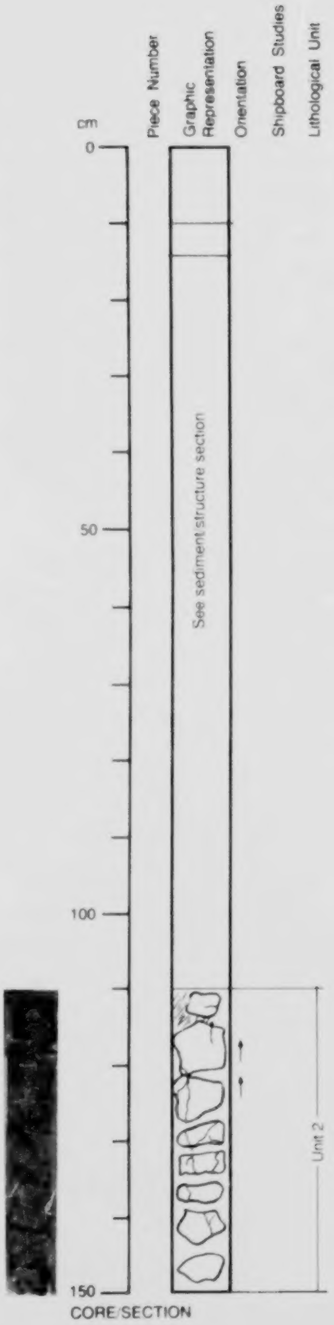
cm
Piece Number
Graphic Representation
Orientation
Shipboard Studies
Lithological Unit
0
50
100
150
See sediment structure section
Unit 2
CORE/SECTION

125-779A-32R-2

UNIT 2: FRAGMENTS OF SERPENTINIZED HARZBURGITE

Pieces multiple fragments

COLOR: Dark greenish gray (5BG 4/1)
LAYERING: Not visible
DEFORMATION: Not visible
PRIMARY MINERALOGY:
Olivine - Mode: 85-95%
Crystal size: Not visible
Crystal shape: Equant-elongate
Crystal orientation: Not visible
Percent replacement: Not visible

Orthopyroxene - Mode: 5-15%
Crystal size: 3-4 mm
Crystal shape: Equant-ragged
Crystal orientation: Not visible
Percent replacement: Not visible

Spinel - Mode: Trace
Crystal size: <2 mm
Crystal shape: Elongate-ragged
Crystal orientation: Not visible
Percent replacement: Not visible
SECONDARY MINERALOGY:
Serpentine
Total percent: 75-85%
Texture: N/A
Vein material: <2 mm, filled with white layered serpentine, paralleling side of core barrel
Also black and green serpentine veins (<2 mm) dipping at various angles to core barrel

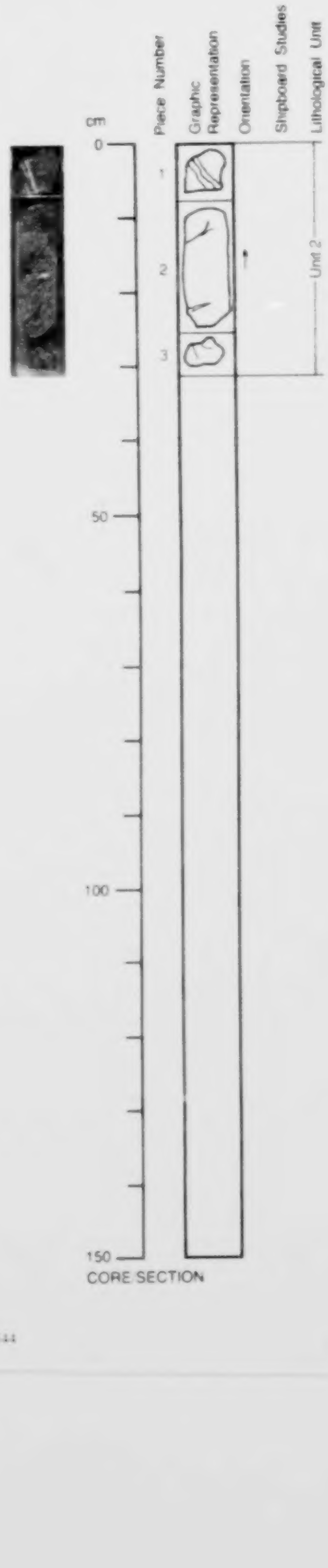
cm
0
50
100
150
CORE SECTION
Piece Number
Graphic Representation
Orientation
Shipboard Studies
Lithological Unit
1
2
3
Unit 2

125-779A-32R-3

UNIT 2: TECTONIZED SERPENTINIZED HARZBURGITE

Pieces 1 to 3

COLOR: Bluish gray to dark bluish gray (5B 5/1 to 5B 4/1)
LAYERING: Not visible
DEFORMATION: Wavy cleavage on orthopyroxene
PRIMARY MINERALOGY:
Olivine - Mode: 85-95%
Crystal size: 5-10 mm
Crystal shape: Ragged
Crystal orientation: Not visible
Percent replacement: Variable

Orthopyroxene - Mode: 5-15%
Crystal size: 3-5 mm
Crystal shape: Elongate-irregular
Crystal orientation: Not visible
Percent replacement: Variable

Spinel - Mode: Trace
Crystal size: <2 mm
Crystal shape: Elongate
Crystal orientation: Not visible
Percent replacement: Not visible
SECONDARY MINERALOGY:
Serpentine
Total percent: 50-80%
Texture: Variable serpentinization
Vein material: Numerous, anastomosing, filled with dark gray, amorphous serpentine <2 mm wide; fibrous, steeply dipping packets, <5 mm wide, composed of light green to white and fibrous (chrysotile) serpentine

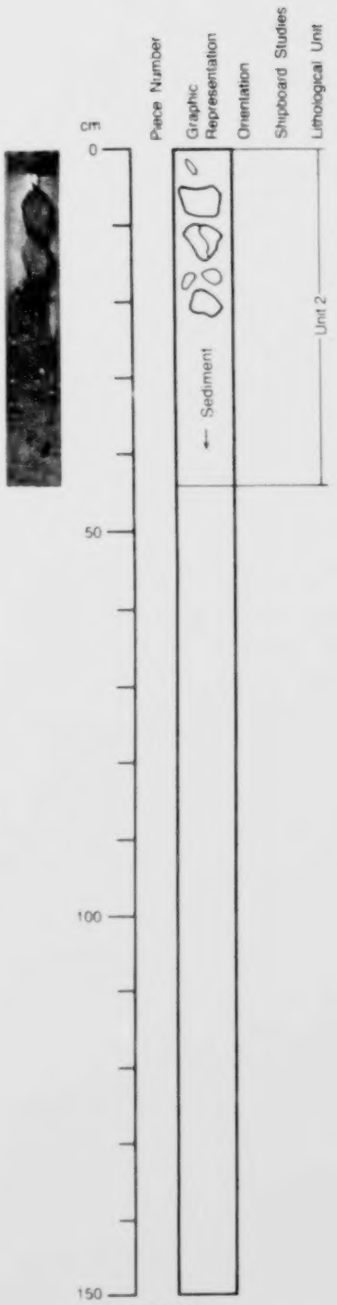
cm
Piece Number
Graphic Representation
Orientation
Shipboard Studies
Lithological Unit
0
50
100
150
Sediment
Unit 2
CORE/SECTION

125-779A-33R-1

UNIT 2: TECTONIZED SERPENTINIZED HARZBURGITE

Pieces 1 (7 fragments)

COLOR: Greenish gray to bluish gray (5BG 5/1 to 5B 5/1)
LAYERING: Not visible
DEFORMATION: Wavy cleavage surface on orthopyroxene; spinels arrayed in crude trains
PRIMARY MINERALOGY:
Olivine - Mode: 85-95%
Crystal size: 5-10 mm
Crystal shape: Irregular
Crystal orientation: Not visible
Percent replacement: Variable

Orthopyroxene - Mode: 5-15%
Crystal size: 2-5 mm
Crystal shape: Elongate
Crystal orientation: Not visible
Percent replacement: Variable

Spinel - Mode: Trace
Crystal size: <2 mm
Crystal shape: Equant-elongate
Crystal orientation: Not visible
Percent replacement: Not visible
SECONDARY MINERALOGY:
Serpentine
Total percent: 70-95%
Texture: N/A
Vein material: <1 mm wide, filled with dark gray-black serpentine

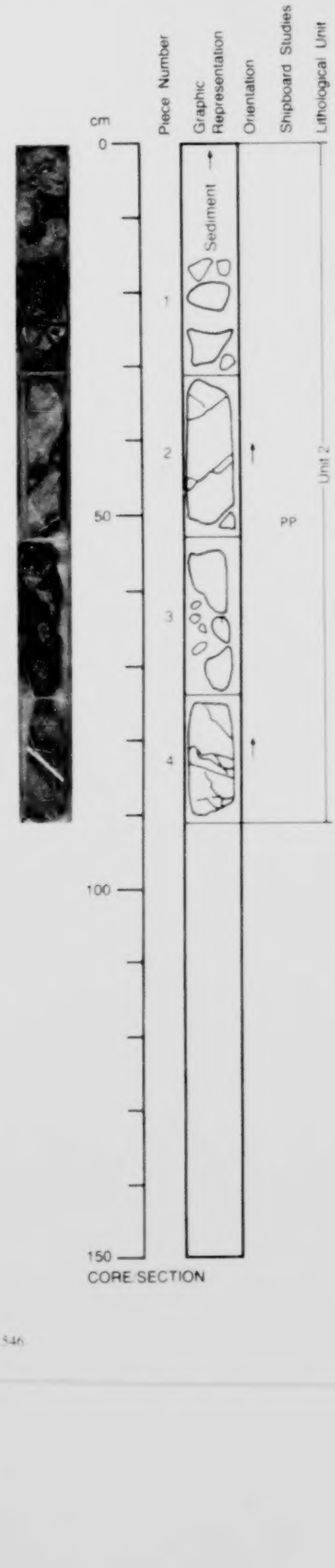

125-779A-33R-2

UNIT 2: TECTONIZED SERPENTINIZED HARZBURGITE

Pieces 1 and 2

COLOR: Bluish gray (5B 5/1)
LAYERING: Possible alignment of elongate pyroxene
DEFORMATION: Wavy cleavage on orthopyroxene; elongate spinels arranged in crude trains
PRIMARY MINERALOGY:
Orthopyroxene - Mode: 40-70%
Crystal size: 3-5 mm
Crystal shape: Ragged elongate
Crystal orientation: Not visible
Percent replacement: Variable

Olivine - Mode: 30-60%
Crystal size: 3-12 mm
Crystal shape: Ragged elongate
Crystal orientation: Not visible
Percent replacement: Variable

Spinel - Mode: Trace
Crystal size: <2 mm
Crystal shape: Ragged elongate
Crystal orientation: Not visible
Percent replacement: Not visible
SECONDARY MINERALOGY:
Serpentine
Total percent: 65-90%
Texture: N/A
Vein material: Dark gray/black amorphous serpentine filled, <3 mm wide, dipping at 50-30 degrees, and thin <1-mm veins filled with green-white serpentinous material

UNIT 2: TECTONIZED SERPENTINIZED HARZBURGITE

Pieces 3 and 4

COLOR: Dark greenish gray (5BG 4/1)
LAYERING: Not visible
DEFORMATION: Elongated olivine is aligned dipping subvertically; spinel trains crudely similarly aligned
PRIMARY MINERALOGY:
Olivine - Mode: 85-95%
Crystal size: 5-12 mm
Crystal shape: Elongate ragged
Crystal orientation: Not visible
Percent replacement: Variable

Orthopyroxene - Mode: 5-15%
Crystal size: 3-4 mm
Crystal shape: Equant ragged
Crystal orientation: Not visible
Percent replacement: Variable

Spinel - Mode: Trace
Crystal size: <2 mm
Crystal shape: Elongate ragged
Crystal orientation: Not visible
Percent replacement: Not visible
SECONDARY MINERALOGY:
Serpentine
Total percent: 65-90%
Texture: N/A
Vein material: <4 mm wide, filled with white layered serpentine, dipping at 45 degrees and, others (<2 mm) more irregular dips but similar fill

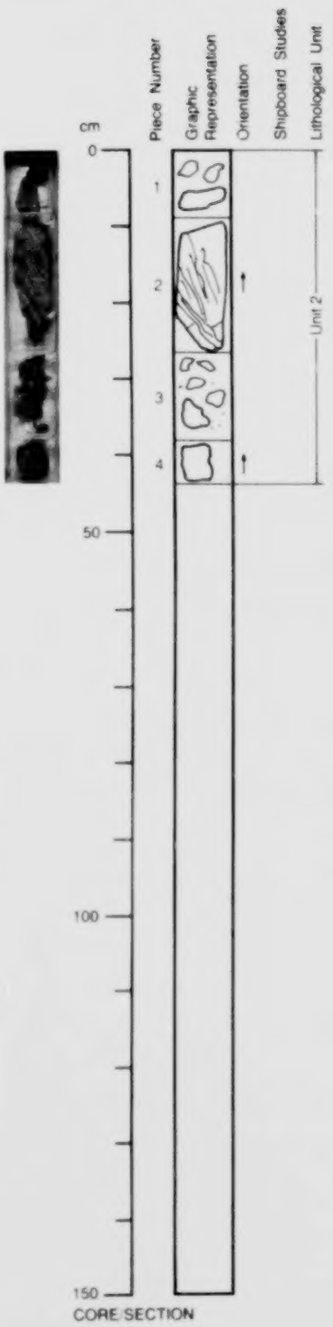

125-779A-33R-3

UNIT 2: SERPENTINIZED HARZBURGITE

Pieces 1, 3, 4

COLOR: Dark greenish gray (5BG 4/1).
LAYERING: possible alignment of elongate pyroxenes.
DEFORMATION: None visible.
PRIMARY MINERALOGY:
Olivine - Mode: 80%.
Crystal size: Not visible.
Crystal shape: Equant.
Crystal orientation: Not visible.
Percent replacement: Not visible.

Orthopyroxene - Mode: 10-20%.
Crystal size: 3-4 mm.
Crystal shape: Equant-elongate.
Crystal orientation: Not visible.
Percent replacement: Not visible.

Spinel - Mode: Trace.
Crystal size: <2 mm.
Crystal shape: Elongate-ragged.
Crystal orientation: Not visible.
Percent replacement: Not visible.
SECONDARY MINERALOGY:
Serpentine.
Total percent: 70-80%.
Texture: N/A.
Vein material: <1 mm wide veins of pale-green serpentine.

UNIT 2: TECTONIZED SERPENTINIZED HARZBURGITE

Piece 2

COLOR: Dark greenish gray (5BG 4/1).
LAYERING: Alignment of elongate pyroxenes.
DEFORMATION: Tectonized, crystals oriented 45 degrees from side of core barrel.
PRIMARY MINERALOGY:
Olivine - Mode: 80%.
Crystal size: Not visible.
Crystal shape: Equant elongate.
Crystal orientation: Not visible.
Percent replacement: Not visible.

Orthopyroxene - Mode: 10-20%.
Crystal size: 3-4 mm.
Crystal shape: Equant elongate.
Crystal orientation: Not visible.
Percent replacement: Not visible.

Spinel - Mode: Trace.
Crystal size: <2 mm.
Crystal shape: Elongate-ragged.
Crystal orientation: Not visible.
Percent replacement: Not visible.
SECONDARY MINERALOGY:
Serpentine.
Total percent: 70-80%.
Texture: N/A.
Vein material: 0.5-cm-wide veins filled with pale-green and dark black serpentine. Veins parallel orientation of tectonized crystals. Also minor (1 mm) white veins. Larger vein has two white-green serpentine veins oriented perpendicular to it.

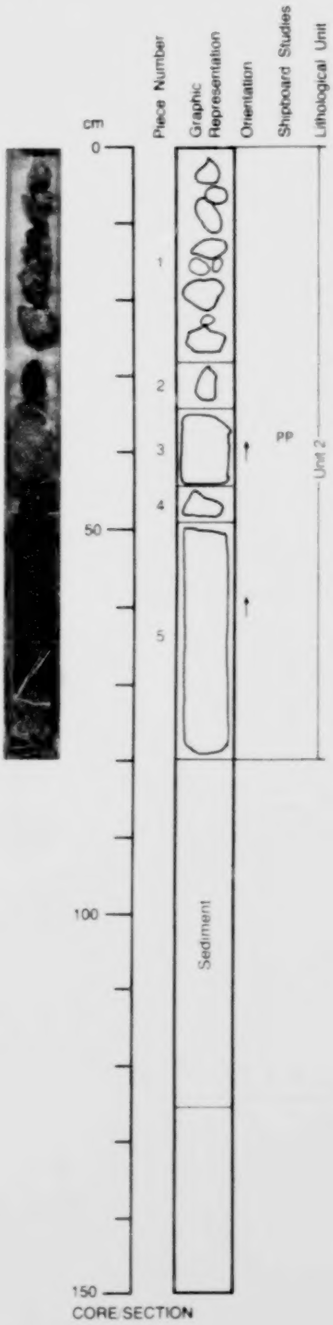

125-779A-34R-1

UNIT 2: SERPENTINIZED HARZBURGITE

Piece 1 (multiple fragments)

COLOR: Dark greenish gray (5B 4/1)
LAYERING: None visible
DEFORMATION: Some fracturing
PRIMARY MINERALOGY:
Strongly altered
Olivine - Mode: 85-90%
Crystal size: Not visible
Crystal shape: Not visible
Crystal orientation: Not visible
Percent replacement: Variable

Orthopyroxene - Mode: 10-15%
Crystal size: 3-6 mm
Crystal shape: Subhedral
Crystal orientation: Not visible
Percent replacement: Variable

Spinel - Mode: Trace
Crystal size: <1 mm
Crystal shape: Equant
Crystal orientation: Not visible
Percent replacement: Not visible
SECONDARY MINERALOGY:
Serpentine
Total percent: 90-99%
Texture: Bastite orthopyroxene
Vein material: Some green serpentine on fragment surfaces.

UNIT 2: SERPENTINIZED HARZBURGITE

Pieces 2-5

COLOR: Dark greenish gray (5B 4/1)
LAYERING: Not visible
DEFORMATION: Some fractures.
PRIMARY MINERALOGY:
Highly altered
Olivine - Mode: 85%
Crystal size: 2-4 mm
Crystal shape: Anhedral to subhedral
Crystal orientation: Not visible
Percent replacement: Variable

Orthopyroxene - Mode: 15%
Crystal size: <8 mm
Crystal shape: Subhedral to anhedral
Crystal orientation: Not visible
Percent replacement: Variable

Spinel - Mode: Trace
Crystal size: 1 mm
Crystal shape: Subhedral-equant
Crystal orientation: Not visible
Percent replacement: Not visible
SECONDARY MINERALOGY:
Serpentine
Total percent: 90-99%
Texture: Bastite orthopyroxene, olivine-mesh
Vein material: White veins (<1.5 mm) all orientations from subhorizontal to vertical

125-779A-35R-1

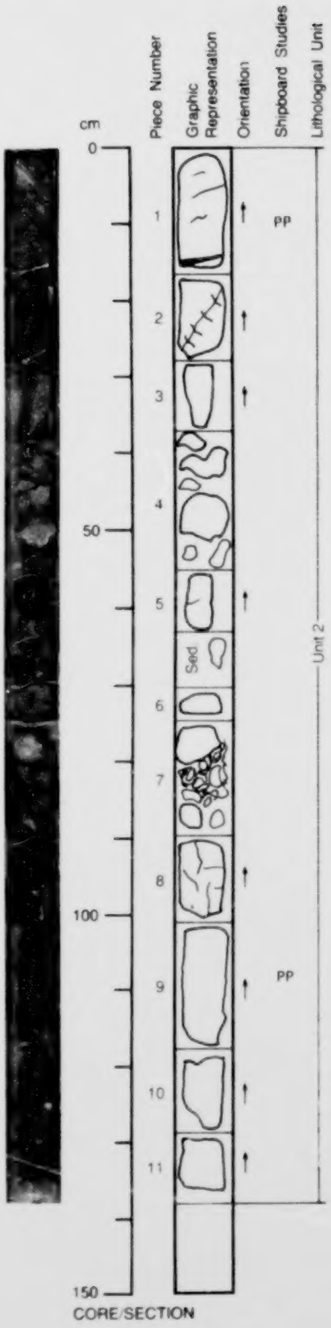

UNIT 2: TECTONIZED SERPENTINIZED HARZBURGITE

Pieces 1-3

COLOR: Bluish gray (5B 5/1)
LAYERING: Possible alignment of elongate orthopyroxene
DEFORMATION: Elongate spinels in trains, wavy cleavage on orthopyroxene
PRIMARY MINERALOGY:
Orthopyroxene - Mode: 15-25%.
Crystal size: 3-5 mm
Crystal shape: Elongate-ragged
Crystal orientation: Not visible
Percent replacement: Variable

Olivine - Mode: 75-85%.
Crystal size: 3-7 mm
Crystal shape: Elongate-ragged
Crystal orientation: Not visible
Percent replacement: Variable

Spinel - Mode: Trace
Crystal size: <2 mm
Crystal shape: Elongate-ragged
Crystal orientation: Not visible
Percent replacement: Variable
SECONDARY MINERALOGY:
Serpentine
Total percent: 40-80%
Texture: N/A
Vein material: Dark black amorphous serpentine-filled vein, <3 mm wide oriented almost parallel to core in Piece 2. This vein has <1-mm-wide and 2-cm-long white-green serpentine veins running perpendicular to it. Piece 1 has white-green serpentine vein, <2 mm wide, perpendicular to core

UNIT 2: SERPENTINIZED HARZBURGITE

Pieces 4-8

COLOR: Dark greenish gray (5B 4/1)
LAYERING: None
DEFORMATION: Piece 8 appears to be slightly tectonized and exhibits elongation of the pyroxene crystals
PRIMARY MINERALOGY:
Olivine - Mode: 70-75%
Crystal size: 1-2 mm
Crystal shape: Equant-elongate
Crystal orientation: N/A
Percent replacement: N/A

Orthopyroxene - Mode: 25-30%
Crystal size: 1-3 mm
Crystal shape: Equant-elongate
Crystal orientation: N/A
Percent replacement: N/A

Spinel - Mode: Trace
Crystal size: <1 mm
Crystal shape: Equant
Crystal orientation: N/A
Percent replacement: N/A
SECONDARY MINERALOGY:
Serpentine
Total percent: 70?
Texture: Serpentinized
Vein material: <2-mm wide white-pale green serpentine (chrysotile?) veining. Piece 4 is mixed with serpentine sediment

UNIT 2: SERPENTINIZED DUNITE (?)

Pieces 9-11

COLOR: Dark blue gray (5B 4/1)
LAYERING: None
DEFORMATION: None visible
PRIMARY MINERALOGY:
Olivine - Mode: 90-95%
Crystal size: 1-3 mm
Crystal shape: Equant
Crystal orientation: Not visible
Percent replacement: Variable

Orthopyroxene - Mode: 5-10%
Crystal size: 1-4 mm
Crystal shape: Equant-elongate
Crystal orientation: Not visible
Percent replacement: Variable

Spinel - Mode: 0-3%
Crystal size: <2 mm
Crystal shape: Equant-ragged
Crystal orientation: Not visible
Percent replacement: Variable
SECONDARY MINERALOGY:
Serpentine
Total percent: 40-90%
Texture: N/A
Vein material: <2 mm wide black/green amorphous serpentine veins

125-779A-28R-CC (Piece 2,13-21 cm) OBSERVER: SAB WHERE SAMPLED: Conical Seamount, southeast flank

ROCK NAME: Serpentinized dunite

GRAIN SIZE: 0.2-4 mm

TEXTURE: Mesh

PRIMARY MINERALOGY	PERCENT PRESENT	PERCENT ORIGINAL	SIZE (mm)	COMPO-SITION	MORPHOLOGY	COMMENTS
PHENOCRYSTS						
Olivine	20	94	1-4		Anhedral	Altered to mesh texture serpentine.
Spinel	0.1	1	0.1-0.5	Cr?	Equant-elongate	Red; altered to magnetite.
Orthopyroxene	1	5	1-3		Subhedral-anhedral	Altered to serpentine bastite and chlorite.
GROUNDMASS						
N/A	N/A	N/A	N/A		N/A	

SECONDARY MINERALOGY	PERCENT	REPLACING/ FILLING	COMMENTS
Chlorite	5-10	Orthopyroxene, serpentine	Bladed prismatic crystals-anhedral equant patches, 0.1-1 mm in size; green blue-brown pleochroism; distributed throughout slide and also associated with orthopyroxene bastite.
Serpentine	70-75	Olivine, orthopyroxene	Mostly lizardite and/or chrysotile distributed throughout slide forming good-poor mesh texture.
Magnetite	1	Spinel	Dusty 0.1-mm grains; some are elongated along bastite cleavages; some spinels have cores of magnetite(?).

VESICLES/ CAVITIES	PERCENT	LOCATION	SIZE (mm)	FILLING	SHAPE
Vesicles	0				

COMMENTS: Spinels are equant elongate and some form short stringers. Chlorite (green-brown) pleochroic present in patches, possibly in part replacing orthopyroxene. Orthopyroxenes are all altered to serpentine, but olivine is still fresh.

125-779A-44R-1 (Piece 3,27-30 cm) OBSERVER: SAB WHERE SAMPLED: Conical Seamount, southeast flank

ROCK NAME: Serpentinized harzburgite

GRAIN SIZE: 0.5-5 mm

TEXTURE: Mesh and bastite

PRIMARY MINERALOGY	PERCENT PRESENT	PERCENT ORIGINAL	SIZE (mm)	COMPO-SITION	MORPHOLOGY	COMMENTS
PHENOCRYSTS						
Olivine	0	79.5	Not visible		Not visible	Altered to mesh serpentine.
Clinopyroxene	Trace	Trace	N/A		Subhedral-anhedral	As exsolution lamellae of clinopyroxene.
Spinel	0.5	0.5	0.5-1		Euhedral-anhedral	Euhedral grains are undeformed.
Orthopyroxene	20	20	0-5		Subhedral-anhedral	Altered to serpentine bastite; some small relic olivine (now serpentinized) included in bastite pseudomorphs of orthopyroxene-a relic poikiloblastic texture.
GROUNDMASS						
N/A	N/A	N/A	N/A		N/A	

SECONDARY MINERALOGY	PERCENT	REPLACING/ FILLING	COMMENTS
Clays	10	Serpentine?	Dusty brown clay distributed throughout slide & associated with the serpentine.
Magnetite	1	Spinel	Altered from spinel; dusty to elongate trails distributed throughout slide.
Serpentine	67	Olivine, orthopyroxene	Lizardite and/or chrysotile mostly; distributed across slide; forms mesh and bastite textures plus possible hourglass texture in a few places.

VESICLES/ CAVITIES	PERCENT	LOCATION	SIZE (mm)	FILLING	SHAPE
Vesicles	0				

COMMENTS: Fresh olivine-orthopyroxene preserved as inclusions inside spinel; some spinel are nicely equant and euhedral. Orthopyroxene is kink-banded and deformed. Some fresh material may still be present in the bastites. The absence of relic poikiloblastic texture indicates an original cumulate protolith.

125-779A-4R-1 (Piece 3,27-30 cm)   OBSERVER: SAB   WHERE SAMPLED: Conical Seamount, southeast flank

ROCK NAME: Serpentinized harzburgite

GRAIN SIZE: 0.3-5 mm

TEXTURE: Mesh and bastite

PRIMARY MINERALOGY	PERCENT PRESENT	PERCENT ORIGINAL	SIZE (mm)	COMPO-SITION	MORPHOLOGY	COMMENTS
PHENOCRYSTS						
Olivine	0	78.5	Not visible		Not visible	Altered to mesh serpentine.
Clinopyroxene	Trace	Trace	N/A		Subhedral-anhedral	As exsolution lamellae of clinopyroxene.
Spinel	1.5	1.5	0.3-1		Euhedral-anhedral	Euhedral grains are undeformed.
Orthopyroxene	<1	20	2-5		Subhedral-anhedral	Altered to serpentine bastite; some small relic olivine (now serpentitized) included in bastite pseudomorphs of orthopyroxene-a relic poikiloblastic texture.
GROUNDMASS						
N/A	N/A	N/A	N/A		N/A	

SECONDARY MINERALOGY	PERCENT	REPLACING/ FILLING	COMMENTS
Clays	10	Serpentine?	Dusty brown clay distributed throughout slide & associated with the serpentine.
Magnetite	1	Spinel	Altered from spinel; dusty to elongate trails distributed throughout slide.
Serpentine	87	Olivine, orthopyroxene	Lizardite and/or chrysotile mostly; distributed across slide; forms mesh and bastite textures plus possible hourglass texture in a few places.

VESICLES/ CAVITIES	PERCENT	LOCATION	SIZE (mm)	FILLING	SHAPE
Vesicles	0				

COMMENTS: Fresh olivine-orthopyroxene preserved as inclusions inside spinel; some spinel are nicely equant and euhedral. Orthopyroxene is kink-banded and deformed. Some fresh material may still be present in the bastites. The absence of relic poikiloblastic texture indicates an original cumulate protolith.

125-779A-4R-1 (Piece 3,41-44 cm)   OBSERVER: SAB   WHERE SAMPLED: Conical Seamount, southeast flank

ROCK NAME: Serpentinized harzburgite

GRAIN SIZE: 0.2-4 mm

TEXTURE: Mesh and bastite

PRIMARY MINERALOGY	PERCENT PRESENT	PERCENT ORIGINAL	SIZE (mm)	COMPO-SITION	MORPHOLOGY	COMMENTS
PHENOCRYSTS						
Olivine	0	83-88	Not visible		Not visible	Completely altered to mesh serpentine; some rounded pseudomorphs found.
Spinel	2	2	0.2-1.5	Cr?	Anhedral-elongate	Red brown, contain some small round olivine grains.
Orthopyroxene	0	10-15	2-4		Subhedral-anhedral	Altered to serpentine bastite.
GROUNDMASS						
N/A	N/A	N/A	N/A		N/A	

SECONDARY MINERALOGY	PERCENT	REPLACING/ FILLING	COMMENTS
Clays	10	Serpentine?	Dusty brown clay distributed across slide and also associated with serpentine in the veins.
Serpentine	88	Olivine, orthopyroxene	Probably lizardite and/or chrysotile forming mesh and bastitic textures; chrysotile is dominant phase in veins (1-4 mm wide) that cut across slide.
Magnetite	<1	Spinel	Dusty 0.1-mm grains; distributed throughout slide and associated with serpentine and spinel.

VESICLES/ CAVITIES	PERCENT	LOCATION	SIZE (mm)	FILLING	SHAPE
Vesicles	0				

COMMENTS: Elongate spinels are arranged in ragged trains - individual serpentine veins (1-4 mm wide) cut across this alignment at a high angle. Bastite is kink-banded and deformed (wavy extinction). Rock appears to have some relic poikilitic textures (i.e., after a protolithic cumulate). Veins are dominant across slide and consist of clays and serpentine.

125-779A-18R-01 (Piece 10A,116-120 cm) OBSERVER: KIR WHERE SAMPLED: Conical Seamount, southeast flank

ROCK NAME: Serpentinized harzburgite

GRAIN SIZE: 1-4 mm

TEXTURE: Mesh and bastite

PRIMARY MINERALOGY	PERCENT PRESENT	PERCENT ORIGINAL	SIZE (mm)	COMPO-SITION	MORPHOLOGY	COMMENTS
PHENOCRYSTS						
Olivine	8-20	76-83	1-4		Anhedral	Altering to serpentine mesh texture
Clinopyroxene	Trace	Trace	<1.50		Anhedral	As anhedral dot in an orthopyroxene grain.
Spinel	1-2	2	1-3	Cr	Euhedral-anhedral	Red; altered to magnetite
Orthopyroxene	1	13-20	1-4		Subhedral-anhedral	Altered to serpentine bastite + chlorite.
GROUNDMASS						
N/A	N/A	N/A	N/A		N/A	

SECONDARY MINERALOGY	PERCENT	REPLACING/ FILLING	COMMENTS
Clays	3	Serpentine	Dusty brown in color and distributed throughout slide, associated with serpentine and also in veins.
Chlorite	[illegible]		Blue-green to brown pleochroism, as anhedral patches throughout slide and along orthopyroxene cleavages and edges.
Serpentine	75-81	Olivine, orthopyroxene	Lizardite and/or chrysotile defining mesh texture; chrysotile veins (2 to 4 mm wide) at various orientations in slide (see comments).
Magnetite	1	Spinel	Dusty, 0.1 mm, sometimes elongate in trains.
Brucite	3+?	Olivine, orthopyroxene	Forms in association with serpentization and appears mostly in second-generation veining.

VESICLES/ CAVITIES	PERCENT	LOCATION	SIZE (mm)	FILLING	SHAPE
Vesicles	0				

COMMENTS: Olivine and orthopyroxene show wavy extinction. Veins show wavy extinction (2-mm-wide) and consist of chrysotile, brucite(?) and clays. Two generations of veins: 1) large (4-mm-wide) veins cut across slide completely, 2) small (1 to 2 mm-wide) and shorter (2-mm) veins cut perpendicular to 1st set; may be "Frankenstein" veins which were observed in hand sample. Spinels are elongate and ragged and are pulled apart across serpentine veins.

125-779A-28R-1 (Piece 12,118-124 cm) OBSERVER: SAK WHERE SAMPLED: Conical Seamount, southeast flank

ROCK NAME: Serpentinized dunite

GRAIN SIZE: 0.5-5 mm

TEXTURE: Mesh and bastite

PRIMARY MINERALOGY	PERCENT PRESENT	PERCENT ORIGINAL	SIZE (mm)	COMPO-SITION	MORPHOLOGY	COMMENTS
PHENOCRYSTS						
Olivine	1?	44	4-5		Anhedral	Altered to mesh serpentine.
Clinopyroxene	<1	[illegible]	<0.2		Subhedral-anhedral	As exsolution lamellae in orthopyroxene
Spinel	0.5	1.0	0.5-1.5	Cr?	Ragged and elongated	Altered to magnetite and possibly chlorite.
Orthopyroxene	0	[illegible]	1-5		N/A	Altered to bastite serpentine and chlorite.
GROUNDMASS						
N/A	N/A	N/A	N/A		N/A	

SECONDARY MINERALOGY	PERCENT	REPLACING/ FILLING	COMMENTS
Chlorite	[illegible]	Orthopyroxene, serpentine	Blue-green-brown pleochroic distributed throughout slide in association with serpentine and orthopyroxene.
Magnetite	[illegible]	Spinel	Located near spinels, in the veins, and grown at rims outlining olivine crystals.
Serpentine	[illegible]	Olivine, orthopyroxene	Lizardite and/or chrysotile; mesh texture is only partly developed in olivine.
Brucite	[illegible]		Small, 0.1-mm-wide veins crossing slide; post-serpentinization; magnetite is concentrated in these veins.

VESICLES/ CAVITIES	PERCENT	LOCATION	SIZE (mm)	FILLING	SHAPE
Vesicles	0				

COMMENTS: Orthopyroxene and olivine have wavy extinction, deformation. Spinels form ragged strings of trains. Orthopyroxene bastite also has been [illegible].

125-779A-5R-02 (Piece 3,14-15 cm) OBSERVER: SAB WHERE SAMPLED: Conical Seamount, southeast flank

ROCK NAME: Altered serpentinized harzburgite

GRAIN SIZE: 0.5-4 mm

TEXTURE: Mesh and bastite (minor)

PRIMARY MINERALOGY	PERCENT PRESENT	PERCENT ORIGINAL	SIZE (mm)	COMPO-SITION	MORPHOLOGY	COMMENTS
PHENOCRYSTS						
Olivine	0	83-89	Not visible		Not visible	Completely altered to serpentine mesh.
Spinel	1-2	1-2	0.5-2	Cr?	Euhedral-subhedral	Red; fractured; altered to magnetite.
Orthopyroxene	0	10-15	1-4		Subhedral-anhedral	Completely altered to serpentine bastite.
GROUNDMASS						
N/A	N/A	N/A	N/A		N/A	

SECONDARY MINERALOGY	PERCENT	REPLACING/ FILLING	COMMENTS
Clays	50-60	Serpentine	Dusty brownish clay distributed throughout slide after serpentine.
Serpentine	38-49	Olivine, orthopyroxene	Lizardite and/or chrysotile after olivine and orthopyroxene, distributed throughout slide, chrysotile veins.
Magnetite	<1	Spinel	Dusty 0.1-mm grains; distributed throughout slide and along veins.

VESICLES/ CAVITIES	PERCENT	LOCATION	SIZE (mm)	FILLING	SHAPE
Vesicles	0				

COMMENTS: This serpentinized rock has been further altered to clays. Numerous veins. Two generations: 1) 0.5 mm wide and consisting of chrysotile, clays, and magnetite; mostly parallel (indicating formation in uniform stress field?); 2) vein set intersecting 1st generation at ~ 40 degree angle. Secondary mesh and bastite textures are obscured by the abundant veining.

125-779A-5R-02 (Piece 3,40-43 cm) OBSERVER: SAB WHERE SAMPLED: Conical Seamount, southeast flank

ROCK NAME: Serpentinized harzburgite

GRAIN SIZE: 0.05-4 mm

TEXTURE: Mesh and bastite

PRIMARY MINERALOGY	PERCENT PRESENT	PERCENT ORIGINAL	SIZE (mm)	COMPO-SITION	MORPHOLOGY	COMMENTS
PHENOCRYSTS						
Olivine	<1	83-88	1-3		Anhedral	Completely altered to serpentine mesh.
Clinopyroxene	<1	<1	0.05-0.1		Anhedral	Small grains surrounded by serpentine.
Spinel	2	2	0.5-2	Cr?	Euhedral-anhedral	Red brown; altered to magnetite; some rimmed by chlorite.
Orthopyroxene	1-2	10-15	1-4		Subhedral-anhedral	Altered to serpentine bastite.
P.G.E.	<0.1	<0.1	<0.05		Euhedral	Very bright reflectance grain disseminated - serpentine groundmass.
GROUNDMASS						
N/A	N/A	N/A	N/A		N/A	

SECONDARY MINERALOGY	PERCENT	REPLACING/ FILLING	COMMENTS
Chlorite	2	Serpentine, spinel	Small fine-grained, anhedral patches intermixed with the serpentine; also appears to be rimming a few spinels.
Serpentine	90-91	Olivine, orthopyroxene	Lizardite and/or chrysotile present, forming characteristic bastite and mesh textures (minor hourglass texture visible).
Magnetite	1		Dusty, 0.1 mm; located throughout mesh edges and also in veins.
Brucite	2	Olivine, orthopyroxene	Yellow birefringence mineral occurring mostly in veins brucite(?).

VESICLES/ CAVITIES	PERCENT	LOCATION	SIZE (mm)	FILLING	SHAPE
Vesicles	0				

COMMENTS: Orthopyroxene is kinked and has wavy extinction. Some spinels have round inclusions of possible olivine or orthopyroxene? Veins (0.05 to 2 mm wide) are abundant. They appear to be two generations which occur almost perpendicular to one another. Veins consist of mostly chrysotile, magnetite, and brucite(?). Brucite determination needs further analysis, but believe the yellow birefringence intergrown with chrysotile vein is brucite. P.G.E. refers to platinum group elements.

125-779A-18R-02 (Piece 4,47-49 cm) OBSERVER: [illegible] WHERE SAMPLED: Conical Seamount, southeast flank

ROCK NAME: Serpentinized dunite

GRAIN SIZE: 0.1-2 mm

TEXTURE: Mesh

PRIMARY MINERALOGY	PERCENT PRESENT	PERCENT ORIGINAL	SIZE (mm)	COMPOSITION	MORPHOLOGY	COMMENTS
PHENOCRYSTS						
Olivine	0	99	Not visible		Not visible	Completely altered to serpentine mesh.
Spinel	1	1	0.1-2	???	Subhedral-anhedral	Red, altered to magnetite, a few round inclusions of olivine are found in some grains.
GROUNDMASS						
N/A	N/A	N/A	N/A		N/A	

SECONDARY MINERALOGY	PERCENT	REPLACING/FILLING	COMMENTS
Magnetite	1-2	Spinel	Dusty, 0.1 mm in size; distributed throughout slide, but appears concentrated in veins and mesh edges.
Serpentine	97-98	Olivine, orthopyroxene	Lizardite and/or chrysotile distributed throughout slide and forming characteristic mesh texture.
Brucite	1	Olivine, orthopyroxene, serpentine	Found in veins which cross slide; associated with magnetite and serpentine.

VESICLES/CAVITIES	PERCENT	LOCATION	SIZE (mm)	FILLING	SHAPE
Vesicles	0				

COMMENTS: Rock is totally serpentinized. Mesh texture is well developed in areas, but is also deformed by tectonic fabric. This fabric is defined by parallel orientation of many small (<0.2mm-wide) serpentine (chrysotile?), magnetite, brucite(?) veins oriented roughly parallel to the long axis of the slide.

125-779A-[illegible] (Piece [illegible] cm) OBSERVER: [illegible] WHERE SAMPLED: Conical Seamount, southeast flank

ROCK NAME: Serpentinized harzburgite (lherzolite)

GRAIN SIZE: [illegible] mm

TEXTURE: Mesh and bastite

PRIMARY MINERALOGY	PERCENT PRESENT	PERCENT ORIGINAL	SIZE (mm)	COMPOSITION	MORPHOLOGY	COMMENTS
PHENOCRYSTS						
Olivine	15-20	75-80	1-3		Anhedral	Altered to serpentine mesh; some neoblastic crystals may be present.
Clinopyroxene	Trace	Trace	[illegible]		Subhedral-anhedral	As exsolution lamellae in orthopyroxene.
Spinel	[illegible]	1	[illegible]	???	Subhedral-anhedral	Red, altered to magnetite and chlorite(?).
Orthopyroxene	[illegible]	15-20	[illegible]		Subhedral-anhedral	Altered to serpentine bastite and chlorite.
GROUNDMASS						
N/A	N/A	N/A	N/A		N/A	

SECONDARY MINERALOGY	PERCENT	REPLACING/FILLING	COMMENTS
Chlorite	[illegible]	Orthopyroxene, spinel, serpentine	Colorless to blue-yellow birefringence, distributed as anhedral patches intermixed with serpentine; also found rimming some spinels, and along orthopyroxene cleavage planes and grain boundaries.
Serpentine	80-85	Olivine, orthopyroxene	Lizardite and/or chrysotile; forms mesh and bastite textures along with minor hourglass textures.
Magnetite	[illegible]	Spinel	Dusty, 0.1 mm; distributed throughout slide, concentrated in edges of mesh, and within veins in elongated trails.

VESICLES/CAVITIES	PERCENT	LOCATION	SIZE (mm)	FILLING	SHAPE
Vesicles	0				

COMMENTS: Olivine and orthopyroxene have wavy extinction; orthopyroxene has kink-banding. Some spinels have inclusions of mineral (olivine?) which has been serpentinized completely. Olivine and orthopyroxene may be fresh enough for microprobing. 2-mm-wide veins cut across slide (45 degrees to long axis). These may define a foliation which is apparent in the sample. This foliation is pervasive throughout the slide.

125-779A-8R-1 (Piece 2,18-20 cm) OBSERVER: SAB WHERE SAMPLED: Conical Seamount, southeast flank

ROCK NAME: Serpentinized harzburgite

GRAIN SIZE: 0.05-4 mm

TEXTURE: Mesh (minor bastite)

PRIMARY MINERALOGY	PERCENT PRESENT	PERCENT ORIGINAL	SIZE (mm)	COMPO-SITION	MORPHOLOGY	COMMENTS
PHENOCRYSTS						
Olivine	15-20	75-82	3-4		Anhedral	Altered to serpentine mesh.
Clinopyroxene	1	1	0.05-1		Euhedral-anhedral	Exsolution lamellae, as inclusions in orthopyroxene and as a primary phase.
Spinel	2	2	0.2-1	Cr?	Euhedral-subhedral	Red; altered to magnetite.
Orthopyroxene	10-15	15-20	1-4		Subhedral-anhedral	Altered to serpentine bastite; has (100) clinopyroxene exsolution lamellae.
GROUNDMASS						
N/A	N/A	N/A	N/A		N/A	

SECONDARY MINERALOGY	PERCENT	REPLACING/ FILLING	COMMENTS
Clays	<1	Serpentine	Dusty brown clay, located mainly in veins, but also after serpentine.
Chlorite	1	Orthopyroxene, serpentine	Blue-green, anhedral, patches intergrown with serpentine, also forming along orthopyroxene cleavage planes.
Serpentine	58-68	Olivine, orthopyroxene	Lizardite and/or chrysotile forming characteristic mesh texture throughout slide plus minor bastite texture.
Magnetite	1	Spinel	Dusty, 0.1 mm, occurs throughout slide, also concentrated in some chrysotile veins.

VESICLES/ CAVITIES	PERCENT	LOCATION	SIZE (mm)	FILLING	SHAPE
Vesicles	0				

COMMENTS: Orthopyroxene and olivine show wavy extinction; orthopyroxene is also kink-banded. Orthopyroxene has inclusions of olivine and clinopyroxenes. Chrysotile veins (0.2 mm wide) are present, some anastomosing. Olivine and orthopyroxene are still relatively fresh, rock appears relatively clinopyroxene-rich.

125-779A-8R-1 (Piece 5A,27-29 cm) OBSERVER: SAB WHERE SAMPLED: Conical Seamount, southeast flank

ROCK NAME: Altered serpentinized harzburgite

GRAIN SIZE: 0.1-5 mm

TEXTURE: Mesh and minor bastite

PRIMARY MINERALOGY	PERCENT PRESENT	PERCENT ORIGINAL	SIZE (mm)	COMPO-SITION	MORPHOLOGY	COMMENTS
PHENOCRYSTS						
Olivine	0	85-88	Not visible		Not visible	Completely altered to serpentine mesh.
Spinel	1-2	2	0.1-2	Cr?	Subhedral-anhedral	Red, altered to magnetite.
Orthopyroxene	0	10-15	1-5		Subhedral-anhedral	Altered to serpentine bastite.
GROUNDMASS						
P.G.E.	<0.1	<0.1	0.02-0.05		Anhedral	

SECONDARY MINERALOGY	PERCENT	REPLACING/ FILLING	COMMENTS
Clays	20	Serpentine	Dusty brown-red clay after serpentine and distributed throughout slide in anastomosed veins.
Serpentine	77	Olivine, orthopyroxene	Lizardite and/or chrysotile distributed throughout slide, further altered to clays.
Magnetite	2	Spinel	

VESICLES/ CAVITIES	PERCENT	LOCATION	SIZE (mm)	FILLING	SHAPE
Vesicles	0				

COMMENTS: Completely serpentinized rock which has been further altered to clays. The spinel still appears relatively fresh. Some orthopyroxene have inclusions of round serpentine pseudomorphs of olivine within themselves. Chrysotile + clay veins (<1.0 mm wide) throughout slide at no particular orientation. P.G.E. refers to platinum group elements.

125-779A-8R-01 (Piece 5B,57-60 cm) OBSERVER: SAB WHERE SAMPLED: Conical Seamount, southeast flank

ROCK NAME: Serpentinised harzburgite

GRAIN SIZE: 0.05-5 mm

TEXTURE: Mesh and bastite

PRIMARY MINERALOGY	PERCENT PRESENT	PERCENT ORIGINAL	SIZE (mm)	COMPO-SITION	MORPHOLOGY	COMMENTS
PHENOCRYSTS						
Olivine	0	78	Not visible		Not visible	Completely altered to serpentine mesh.
Spinel	2	2	0.05-3	Cr?	Anhedral	Red, altered to magnetite, has inclusions (see below).
Orthopyroxene	0	20	3-5		Subhedral-anhedral	Altered to bastite serpentine and chlorite.
GROUNDMASS						
P.G.E.	<<0.1	<<0.1	0.02-0.1		Anhedral	Disseminated, many

SECONDARY MINERALOGY	PERCENT	REPLACING/ FILLING	COMMENTS
Clays	10	Serpentine?	Dusty brown clay distributed throughout slide in anastomosed veins.
Chlorite	1	Orthopyroxene, serpentine	As anhedral, fine-grained patches intermixed with serpentine, and near bastite grains.
Serpentine	57-67	Olivine, orthopyroxene	Lizardite and/or chrysotile distributed throughout slide forming bastite and mesh textures.
Brucite	20-30	Olivine, orthopyroxene	Formed as a by-product of serpentinization and is associated with serpentine.

VESICLES/ CAVITIES	PERCENT	LOCATION	SIZE (mm)	FILLING	SHAPE
Vesicles	0				

COMMENTS: Bastite is deformed (wavy extinction) and former exsolution lamellae are bent. Cr-spinel is anhedral and arranged in ragged trains, subparallel to elongation of bastite. Spinels have apparent inclusions of rounded serpentine and chrysotile pseudomorphs of olivine(?) or orthopyroxene. Minor chrysotile and brucite veins (< 1 mm wide) in slide. P.G.E. refers to platinum group elements.

125-779A-8R-01 (Piece 8A,82-83 cm) OBSERVER: SAB WHERE SAMPLED: Conical Seamount, southeast flank

ROCK NAME: Tectonized serpentinized dunite

GRAIN SIZE: 0.1-0.4 mm

TEXTURE: Felted tectonized texture

PRIMARY MINERALOGY	PERCENT PRESENT	PERCENT ORIGINAL	SIZE (mm)	COMPO-SITION	MORPHOLOGY	COMMENTS
PHENOCRYSTS						
Olivine	45-55	93	0.1-4		Euhedral-anhedral	Altering to serpentine; some are neoblastic.
Clinopyroxene	Trace	Trace	<0.2		Anhedral	As exsolution lamellae.
Spinel	2	2	0.5-2	Cr?	Euhedral-anhedral	Red brown, altered to magnetite?
Orthopyroxene	4	5	1-4		Subhedral-anhedral	Altered to serpentine; deformed crystals.
GROUNDMASS						
P.G.E.	<0.01	<0.01	0.05		Disseminated.	

SECONDARY MINERALOGY	PERCENT	REPLACING/ FILLING	COMMENTS
Serpentine		Olivine, orthopyroxene	Antigorite and/or chrysotile mostly; needles and fibers of crystals are localized, proximal to a vein set and invade the olivine from the vein.
Magnetite	1	Spinel	As dusty 0.1-mm grains; forms ragged trails.

VESICLES/ CAVITIES	PERCENT	LOCATION	SIZE (mm)	FILLING	SHAPE
Vesicles	0				

COMMENTS: Exsolution lamellae, bastitic grains, and primary olivine have wavy extinction. Recrystallized, small olivine grains in shear zone of larger optically continuous olivine grain (not shear fabric) (120 degree triple junction). This slide appears tectonized, but olivine is fresh and big enough for probing. P.G.E. refers to platinum group elements.

125-779A-8R-01 (Piece 8B,90-93 cm) OBSERVER: JOH WHERE SAMPLED: Conical Seamount, southeast flank

ROCK NAME: Tectonized serpentinized dunite

GRAIN SIZE: 0.8-4 mm

TEXTURE: Felted tectonized texture

PRIMARY MINERALOGY	PERCENT PRESENT	PERCENT ORIGINAL	SIZE (mm)	COMPO-SITION	MORPHOLOGY	COMMENTS
PHENOCRYSTS						
Olivine	40-50	96	1-4		Euhedral-anhedral	Altering to serpentine, some are neoblastic.
Spinel	0.5	1	0.8-1	Cr	Euhedral-ragged	Deep red, altered to magnetite.
Orthopyroxene	2	3	1-3		Subhedral-anhedral	Altered to serpentine, deformed crystals.
GROUNDMASS						
P.G.E.	N/A	N/A	N/A		N/A	

SECONDARY MINERALOGY	PERCENT	REPLACING/ FILLING	COMMENTS
Clays	5	Serpentine?	Dusty brownish clay distributed throughout slide.
Serpentine	42-52	Olivine, orthopyroxene	Antigorite blades and chrysotile fibers mainly, but lizardite may also be present.
Magnetite	<1	Spinel?	Dusty 0.1-mm grains along olivine boundaries, sometimes occur as ragged trains.

VESICLES/ CAVITIES	PERCENT	LOCATION	SIZE (mm)	FILLING	SHAPE
Vesicles	0				

COMMENTS: Quite fresh. Olivine grains are large enough and fresh enough for probing. Original texture obscured by serpentine feather-like crystals. Olivine and orthopy: some have wavy extinction, deformation. The whole slide appears tectonized and some olivine grains have been somewhat sheared. A few smaller olivine grains may have been recrystallized. P.G.E. refers to platinum group elements.

125-779A-9R-01 (Piece 3,15-17 cm) OBSERVER: TER WHERE SAMPLED: Conical Seamount, southeast flank

ROCK NAME: Metamorphosed volcanic sandstone

GRAIN SIZE: 0.1 to <1 mm

TEXTURE: Sandstone

PRIMARY MINERALOGY	PERCENT PRESENT	PERCENT ORIGINAL	SIZE (mm)	COMPO-SITION	MORPHOLOGY	COMMENTS
PHENOCRYSTS						
Olivine	Trace	N/A	Not visible		N/A	
Plagioclase	0	1	<1 mm		Not visible	Altered.
Clinopyroxene	2	2	< 1 mm		N/A	Lining.
Spinel	Trace	N/A	N/A		Not visible	
GROUNDMASS						
Glass	N/A	70-80	N/A		Anhedral	Altered. Fills in matrix in volcanic fragment.
Plagioclase	0	20-30	0.1-0.2		Subhedral	Altered.
Clinopyroxene	10-20	10-20	0.1-0.2		Subhedral	Lining.
Opaque	2	2	0.1		Subhedral	

SECONDARY MINERALOGY	PERCENT	REPLACING/ FILLING	COMMENTS
Clays	40-50	Glass matrix	Dusty.
Chlorite	10-15		
Hornblende	20		Pale brown to pale green in color, elongation positive, extinction angle is 5-10 degrees.

VESICLES/ CAVITIES	PERCENT	LOCATION	SIZE (mm)	FILLING	SHAPE
Vesicles	0				

COMMENTS: This rock contains many kinds of lithic and mineral fragments, which are mainly volcanic rocks and their derivatives. All minerals excluding augite are altered. Pale-green hornblende replacing augite is observed. Whether hornblende is metamorphic or igneous is not known.

125-779A-9R-[illegible] (24-26 cm)   OBSERVER: LAI   WHERE SAMPLED: Conical Seamount, southeast flank

ROCK NAME: Silt-sized serpentine

GRAIN SIZE: Silt

TEXTURE: Detrital

PRIMARY MINERALOGY	PERCENT PRESENT	PERCENT ORIGINAL	SIZE (mm)	COMPO-SITION	MORPHOLOGY	COMMENTS
PHENOCRYSTS						
Olivine	0	[illegible]	N/A		N/A	
Spinel	<1	2	N/A		Rounded-angular (detrital)	
Orthopyroxene	0	5	N/A		N/A	Bastite.
GROUNDMASS						
N/A	N/A	N/A	N/A		N/A	All serpentine with very small amounts of blue chlorites.

SECONDARY MINERALOGY	PERCENT	REPLACING/FILLING	COMMENTS
Carbonate	3		"Flowers" of calcite.
Serpentine			Chrysotile and/or lizardite.
Magnetite	1-2		

VESICLES/CAVITIES	PERCENT	LOCATION	SIZE (mm)	FILLING	SHAPE
Vesicles	0				

COMMENTS: Layered serpentine silt-sized detrital mud. Shows layers of brownish agglomerates with bacteria. One layer is folded. A clear fabric axial plane to the fold is outlined by the preferred alignment of serpentine flakes. Detrital grains of serpentine are scattered everywhere. No piece # given.

125-779A-[illegible] (14-16 cm)   OBSERVER: SCA   WHERE SAMPLED: Conical Seamount, southeast flank

ROCK NAME: Serpentinous mudstone.

GRAIN SIZE: Fine-grained

TEXTURE: Foliate serpulite (soft-sediment)

PRIMARY MINERALOGY	PERCENT PRESENT	PERCENT ORIGINAL	SIZE (mm)	COMPO-SITION	MORPHOLOGY	COMMENTS
N/A	N/A	N/A	N/A		N/A	

SECONDARY MINERALOGY	PERCENT	REPLACING/FILLING	COMMENTS
Clays	10-15		
Serpentine	80-90		
Magnetite	<2		

VESICLES/CAVITIES	PERCENT	LOCATION	SIZE (mm)	FILLING	SHAPE
Vesicles	0				

COMMENTS: A 5-mm prismatic fragment had been originally a serpentine vein of tectonized and serpentinized peridotite. It shows rhythmical kinking, which is similar to texture of serpentine vein observed in tectonized peridotite. Foliation is defined by parallel arrangements of serpentine crystal and brownish black cleavage. No piece number given.

125-779A-9R-01 (Piece 5,66-68 cm)   OBSERVER: JOH   WHERE SAMPLED: Conical Seamount, southeast flank

ROCK NAME: Metabasalt

GRAIN SIZE: 0.05-0.15 mm

TEXTURE: Micro-aphyric intersertal

PRIMARY MINERALOGY	PERCENT PRESENT	PERCENT ORIGINAL	SIZE (mm)	COMPO-SITION	MORPHOLOGY	COMMENTS
PHENOCRYSTS						
Plagioclase	0	15-25	0.1-0.15		Laths	100% altered to clays.
Clinopyroxene	20-30	25-35	0.05-0.15		Anhedral	10-25% altered to chlorite.
GROUNDMASS						
Glass	0	50-60	N/A		N/A	Completely altered to brown clays and chlorite.

SECONDARY MINERALOGY	PERCENT	REPLACING/ FILLING	COMMENTS
Clays	50-60	Glass, plagioclase, veins	Brown clays after glass and plagioclase and forming many veins.
Carbonate	<1-1	Cavities	0.5 mm across.
Zeolites	<5	Vein	Low index of refraction, colorless, determination uncertain.
Chlorite	15-20	Veins, glassy matrix, clinopyroxene	Pale-green, minor radiating fabric, but mostly after clinopyroxene and matrix.
Prehnite/ pumpellyite	3-4	Veins	Lime-green in color with radiating habit; the two minerals appear to be intimately intermixed.
Magnetite?	<1	Matrix	Random, anhedral crystals, black, opaque, in matrix, <0.5 mm.

VESICLES/ CAVITIES	PERCENT	LOCATION	SIZE (mm)	FILLING	SHAPE
Vesicles	0				

COMMENTS: Rare radiating intergrowths of plagioclase and clinopyroxene. Crystallization sequence=clinopyroxene-plagioclase.

125-779A-9R-01 (Piece 8,97-99 cm)   OBSERVER: HIR   WHERE SAMPLED: Conical Seamount, southeast flank

ROCK NAME: Metabasalt

GRAIN SIZE: <0.01-0.03 mm

TEXTURE: Aphyric, glassy

PRIMARY MINERALOGY	PERCENT PRESENT	PERCENT ORIGINAL	SIZE (mm)	COMPO-SITION	MORPHOLOGY	COMMENTS
Glass	0	60-70	N/A		N/A	Completely altered/recrystallized.
Plagioclase	5	10-20	0.01-0.03		Subhedral, laths	Random occurrence, occasionally aggregated with clinopyroxene.
Clinopyroxene	10-15	20-40	0.01-0.02		Subhedral	Microphenocrysts within glassy/finely crystalline matrix.

SECONDARY MINERALOGY	PERCENT	REPLACING/ FILLING	COMMENTS
Clays		Glass, plagioclase	Brown, amorphous clays after glass and pseudomorphs after plagioclase.
Chlorite	10-50	Glass, clinopyroxene, veins	Most is in veins with prehnite and pumpellyite, 1-5% replaces clinopyroxene and glass.
Sphene	<2	Matrix	
Prehnite/ pumpellyite	5-15	Veins	Veins up to 1.5 mm wide of intermixed prehnite and pumpellyite apparently in equilibrium, both are green and have wavy extinction.
Magnetite	<1	?	Found as clusters of anhedral crystals (0.01 mm).

VESICLES/ CAVITIES	PERCENT	LOCATION	SIZE (mm)	FILLING	SHAPE
Vesicles	0				

COMMENTS: Original crystallization sequence was plagioclase-clinopyroxene. Difficult to distinguish chlorite from prehnite/pumpellyite. They appear intimately intergrown in veins.

125-779A-9R-01 (Piece 9A,106-108 cm)　OBSERVER: JOB　WHERE SAMPLED: Conical Seamount, southeast flank

ROCK NAME: Metabasalt

GRAIN SIZE: <0.01-0.02

TEXTURE: Aphyric

PRIMARY MINERALOGY	PERCENT PRESENT	PERCENT ORIGINAL	SIZE (mm)	COMPO-SITION	MORPHOLOGY	COMMENTS
Glass/matrix	0	50-60	N/A		N/A	100% altered to clays and chlorite.
Plagioclase	0	10-15	0.01-0.02		Lath, subhedral	85-100% altered (saussuritized) to clays.
Clinopyroxene	<5	25-40	0.01-0.02		Subhedral	10-95% altered to clays.
Spinel	<1	<1	0.01-0.02		Subhedral	Probably alteration products.

SECONDARY MINERALOGY	PERCENT	REPLACING/ FILLING	COMMENTS
Clays	45-60	Glass, matrix, plagioclase	Brown amorphous clays pervasive alteration (illite?).
Chlorite	25-35	Glass, matrix, clinopyroxene	Pale-green, slightly pleochroic, in matrix and may form after clinopyroxene.
Prehnite/pumpellyite	5-10	Vein	Occurs intimately associated in veins, as radiating bundles with wavy extinction and bow-tie structure.
Magnetite	<1	Spinel?	Randomly distributed, but locally altered, anhedral blebs, black opaque.

VESICLES/ CAVITIES	PERCENT	LOCATION	SIZE (mm)	FILLING	SHAPE
Vesicles	0				

COMMENTS: Very fine-grained rock altered to prehnite/pumpellyite facies and showing lower greenschist facies alteration. Prehnite and pumpellyite appear to be in equilibrium with each other.

125-779A-9R-02 (Piece 4B,32-34 cm)　OBSERVER: SAB　WHERE SAMPLED: Conical Seamount, southeast flank

ROCK NAME: Tectonized serpentinized harzburgite

GRAIN SIZE: 0.5-5 mm

TEXTURE: Mesh (and minor bastite)

PRIMARY MINERALOGY	PERCENT PRESENT	PERCENT ORIGINAL	SIZE (mm)	COMPO-SITION	MORPHOLOGY	COMMENTS
PHENOCRYSTS						
Olivine	20-30	83.5+	2-4		Anhedral	Altered to serpentine mesh.
Clinopyroxene	1	1	<0.5		Anhedral	As exsolution lamellae and small patches.
Spinel	1.5	1.5	0.05-1	Cr?	Subhedral-anhedral	Red, altered to magnetite.
Orthopyroxene	10	10-15	1-5		Subhedral-anhedral	Altered to serpentine bastite.
GROUNDMASS						
P.G.E.	<0.1	N/A	N/A		N/A	Found disseminated 0.03 mm grains in veins with magnetite + serpentine.

SECONDARY MINERALOGY	PERCENT	REPLACING/ FILLING	COMMENTS
Clays	2	Serpentine	Dusty brown clay distributed throughout slide and also concentrated in small chrysotile veins.
Chlorite	1		Anhedral patches intergrown with serpentine; also minor (0.1-mm-wide) veins which cut across mesh texture.
Magnetite	1	Spinel	Dusty 0.1-mm sized; analyzed in elongated ragged trails which usually follow chrysotile veining.
Serpentine		Olivine, orthopyroxene	Lizardite and/or chrysotile altered from olivine and orthopyroxene and distributed throughout slide.

VESICLES/ CAVITIES	PERCENT	LOCATION	SIZE (mm)	FILLING	SHAPE
Vesicles	0				

COMMENTS: Olivine and orthopyroxene have wavy extinctions; clinopyroxene exsolution lamellae are bent also. Orthopyroxene has minor olivine and clinopyroxene inclusions. The northwest corner of the slide shows a good example of mesh texture developed by the intersecting of 2 generations of veins: small 0.1-mm-wide chlorite vein (Fe-Mg-rich) cut by second generation chrysotile and magnetite veins <0.05 mm wide. Slide appears tectonized. P.G.E. refers to platinum group elements.

125-779A-10R-01 (Piece 3,26-29 cm) OBSERVER: SAB WHERE SAMPLED: Conical Seamount, southeast flank

ROCK NAME: Serpentinized tectonized dunite(?)

GRAIN SIZE: 0.05-2 mm

TEXTURE: Mesh in areas; tectonized

PRIMARY MINERALOGY	PERCENT PRESENT	PERCENT ORIGINAL	SIZE (mm)	COMPOSITION	MORPHOLOGY	COMMENTS
PHENOCRYSTS						
Olivine	55	94	0.1-2	Fo90	N/A	2V=+85-+90 degrees; altered to serpentine mesh, but mesh texture is poorly developed.
Clinopyroxene	<0.1	<0.1	0.05		Anhedral	Clots besides orthopyroxene.
Spinel	0.5	1	0.05-1	Cr?	Subhedral-anhedral	Red, altered to magnetite and chlorite.
Orthopyroxene	1	5	1-2		Subhedral-anhedral	Altered to serpentine bastite and chlorite.
GROUNDMASS						
PGE sulfide	<0.01	<0.01	0.5		N/A	Disseminated rounded grains.

SECONDARY MINERALOGY	PERCENT	REPLACING/ FILLING	COMMENTS
Chlorite	3	Orthopyroxene, spinel, serpentine	Blue-green to brown pleochroism; forms anhedral patches intermixed with serpentine and also forms along orthopyroxene grains, colorless chlorite rims some spinels.
Serpentine	37	Olivine, orthopyroxene	Lizardite and chrysotile are mainly present. They are mostly concentrated near the central 1-cm-wide chrysotile vein, less serpentinization near the edges of the slide.
Magnetite	3	Spinel	Dusty 0.1-mm grains; distributed throughout slide, also concentrated in veins.
Brucite	Trace	Serpentine	Might be occurring along with serpentine in the veins.

VESICLES/ CAVITIES	PERCENT	LOCATION	SIZE (mm)	FILLING	SHAPE
Vesicles	0				

COMMENTS: Orthopyroxene and primary olivine have wavy extinction; olivine shows mylonitization with recrystallization of neoblastic olivine with 120 degrees triple junction!!! Slide has veins criss-crossing it. A beautiful 1-cm-wide chrysotile vein cuts the slide. This vein is also sheared in some places. This vein also cuts across an earlier generation (5-mm-wide) vein of serpentine which is perpendicular to it. P.G.E. refers to platinum group elements.

125-779A-10R-01 (Piece 5,39-43 cm) OBSERVER: KIR WHERE SAMPLED: Conical Seamount, southeast flank

ROCK NAME: Tectonized serpentinized dunite

GRAIN SIZE: 0.5-7 mm

TEXTURE: Felted, tectonized

PRIMARY MINERALOGY	PERCENT PRESENT	PERCENT ORIGINAL	SIZE (mm)	COMPO-SITION	MORPHOLOGY	COMMENTS
PHENOCRYSTS						
Olivine	40	97	0.5-7		Subhedral-anhedral	Altered to serpentine, neoblasts(?), deformed.
Spinel	0.8	1	0.5-2	Cr?	Anhedral	Red-red brown, some have inclusions of olivine? clinopyroxene?
Orthopyroxene	2	3	2-3		Subhedral-anhedral	Altered to serpentine bastite; deformed crystals.
GROUNDMASS						
P.G.E.	<0.05	N/A	N/A		N/A	May be sulfide. Form disseminated, grains and veins <= 0.05 mm.

SECONDARY MINERALOGY	PERCENT	REPLACING/ FILLING	COMMENTS
Carbonate	1	?	Not calcite; refractive index is higher than calcite; found in association with tectonized portion of slide.
Serpentine	51	Olivine, orthopyroxene	Lizardite, chrysotile, antigorite all present; concentrated mainly on edges of tectonized fresher zone in middle. Antigorite-rich veins (<3 mm wide) cut across lizardite and chrysotile areas and fresher olivine, orthopyroxene areas.
Magnetite	2	Spinel	Dusty 0.1-mm size anhedral grains which forms elongated trails and concentrates mostly in veins.
Brucite	3	Olivine, orthopyroxene	Usually found in completely serpentinized portion on edge of slide.

VESICLES/ CAVITIES	PERCENT	LOCATION	SIZE (mm)	FILLING	SHAPE
Vesicles	0				

COMMENTS: This section contains two different types of rocks. In one portion the olivine and orthopyroxene are fresher and are intensely elongated with wavy extinction and kink-banding. Some olivine appears recrystallized. Portion of slide appears tectonized and somewhat sheared. In the other portion the minerals are completely altered to serpentine (lizardite, antigorite and chrysotile): olivine to antigorite and brucite; orthopyroxene to bastite; Cr-spinel is still fresh-looking. This portion appears to be a serpentinization rind around the fresher minerals. It appears on both sides of the tectonized fresher minerals. Also the serpentinized part may show prograde metamorphism because of the presence of orthopyroxene-lizardite-antigorite. P.G.E. refers to platinum group elements.

125-779A-10R-01 (Piece 6,54-57 cm) OBSERVER: TER WHERE SAMPLED: Conical Seamount, southeast flank

ROCK NAME: Tectonized serpentinized dunite

GRAIN SIZE: 0.1-4 mm

TEXTURE: Tectonized

PRIMARY MINERALOGY	PERCENT PRESENT	PERCENT ORIGINAL	SIZE (mm)	COMPO-SITION	MORPHOLOGY	COMMENTS
PHENOCRYSTS						
Olivine	53	97	1-4		Anhedral	Altered to serpentine (blades and fibers).
Spinel	1.5	1	0.1-2	Cr?	Euhedral-anhedral	Red, altered to magnetite.
Orthopyroxene	2	3	1-2		Subhedral-anhedral	Altered to serpentine.
GROUNDMASS						
P.G.E. ?	<0.1	N/A	N/A		N/A	Disseminated and with magnetite in veins.

SECONDARY MINERALOGY	PERCENT	REPLACING/ FILLING	COMMENTS
Serpentine	42	Olivine, orthopyroxene	Mostly antigorite and chrysotile; serpentine forms mostly elongated fibers across olivine cleavages and fractures.
Brucite	1	Olivine	Associated with serpentine and intermixed with it.
Magnetite	2	Spinel	Fine-grained (0.1 mm); located in veins, altered from spinels.

VESICLES/ CAVITIES	PERCENT	LOCATION	SIZE (mm)	FILLING	SHAPE
Vesicles	0				

COMMENTS: Olivine and orthopyroxene are deformed and show wavy extinctions and kink-banding. Olivine shares in wavy extinction of serpentine (ductilely deformed bent along with serpentine), but also forms subgrains. Most easily visible in some long olivine lamellae, which are segmented, but individual segments have undulatory extinction. Therefore, deformation at high temperature and/or high confining pressure. Minerals also appear slightly elongated; serpentine formation and texture is interesting because of formation along olivine cleavages. P.G.E. refers to platinum group elements.

125-779A-15R-02 (Piece 3,28-31 cm) OBSERVER: TER WHERE SAMPLED: Conical Seamount, southeast flank

ROCK NAME: Serpentinized harzburgite

GRAIN SIZE: 0.05-5 mm

TEXTURE: Bastite (poor)

PRIMARY MINERALOGY	PERCENT PRESENT	PERCENT ORIGINAL	SIZE (mm)	COMPO-SITION	MORPHOLOGY	COMMENTS
PHENOCRYSTS						
Olivine	0	88	Not visible		Not visible	Completely altered to serpentine; mesh texture is very poorly developed.
Spinel	Trace	<1	<0.05		Euhedral-anhedral	Altered to magnetite?
Orthopyroxene	0	12	1-5		Anhedral?	Altered to serpentine bastite.
GROUNDMASS						
N/A	N/A	N/A	N/A		N/A	

SECONDARY MINERALOGY	PERCENT	REPLACING/ FILLING	COMMENTS
Serpentine	98	Olivine, orthopyroxene	Lizardite and chrysotile mainly throughout entire slide. No good mesh texture is visible; minor bastitic texture is visible.
Magnetite	<1	Spinel	Dusty and fine-grained, appears concentrated next to veins.
Brucite?	1?	Olivine, orthopyroxene	Yellow interference color mineral with slightly different relief than serpentine; intermixed with serpentine.

VESICLES/ CAVITIES	PERCENT	LOCATION	SIZE (mm)	FILLING	SHAPE
Vesicles	0				

COMMENTS: Veins (1-3 mm wide) of chrysotile cutting across slide larger vein (3 mm wide) may have post-dated smaller (1 mm wide) veins. These small ones are oriented almost perpendicular to the larger one. Slide is completely serpentinized with no relic mineralogy left.

125-779A-11R-01 (Piece 2,6-9 cm) OBSERVER: VAN WHERE SAMPLED: Conical Seamount, southeast flank

ROCK NAME: Serpentinized harzburgite

GRAIN SIZE: 0.1-3 mm

TEXTURE: Mesh and (minor) bastite

PRIMARY MINERALOGY	PERCENT PRESENT	PERCENT ORIGINAL	SIZE (mm)	COMPO-SITION	MORPHOLOGY	COMMENTS
PHENOCRYSTS						
Olivine	<1	87	0.1-0.3		Anhedral	Altered to serpentine mesh texture but a few relic grains are still visible.
Clinopyroxene	Trace	Trace	0.1-0.2		Anhedral	One anhedral grain visible near larger orthopyroxene.
Spinel	1	1	0.1-1	Cr?	Subhedral-anhedral	Red; appear disseminated.
Orthopyroxene	0	12	0.5-3		N/A	Altered to serpentine bastite; few orthopyroxene (bastite) grains have inclusions of anhedral olivine?
GROUNDMASS						
N/A	N/A	N/A	N/A		N/A	

SECONDARY MINERALOGY	PERCENT	REPLACING/ FILLING	COMMENTS
Serpentine	98	Olivine, orthopyroxene	Lizardite and/or chrysotile form mesh-texture throughout slide. The mesh is cut by a later-stage chrysotile vein (3 mm wide).
Magnetite	<1	Spinel	Dusty grains throughout slide.
Brucite	<1	Olivine, orthopyroxene	Yellow interference color mineral appears in smaller (<0.5 mm wide) veins crosscutting serpentine; XRD is necessary.

VESICLES/ CAVITIES	PERCENT	LOCATION	SIZE (mm)	FILLING	SHAPE
Vesicles	0				

COMMENTS: Orthopyroxene is kinked and has wavy extinction. This slide is completely serpentinized. A larger (3 mm wide) chrysotile vein crosses slide at 45 degrees orientation to the long axis of slide.

125-779A-11R-01 (Piece 3, 14-18 cm) OBSERVER: SAB WHERE SAMPLED: Conical Seamount, southeast flank

ROCK NAME: Serpentinized harzburgite

GRAIN SIZE: 0.05-5 mm

TEXTURE: Mesh (minor bastite)

PRIMARY MINERALOGY	PERCENT PRESENT	PERCENT ORIGINAL	SIZE (mm)	COMPO-SITION	MORPHOLOGY	COMMENTS
PHENOCRYSTS						
Olivine	Tr?	82	Not visible		Not visible	Completely altered to serpentine mesh texture, but small inclusions in orthopyroxene(?) still remain.
Clinopyroxene	1.5	1.5	0.05-0.3		Anhedral	As exsolution lamellae, also as fresh grains.
Spinel	1.5	1.5	0.5-2	Cr?	Subhedral-anhedral	Red; some are elongated.
Orthopyroxene	0	15	1-5		Subhedral-anhedral	Altered to serpentine bastite; has (100) clinopyroxene exsolution lamellae.
GROUNDMASS						
P.G.E. (sulfide)	<0.01	N/A	N/A		N/A	Disseminated, rare with magnetite in serpentine.

SECONDARY MINERALOGY	PERCENT	REPLACING/ FILLING	COMMENTS
Serpentine	97	Olivine, orthopyroxene	Lizardite and/or chrysotile, forming mostly mesh texture with minor bastite texture throughout the slide. The mesh appears undeformed in areas, but somewhat deformed in other areas.
Magnetite	<1	Spinel	Dusty 0.1-mm grains scattered throughout slide.

VESICLES/ CAVITIES	PERCENT	LOCATION	SIZE (mm)	FILLING	SHAPE
Vesicles	0				

COMMENTS: Orthopyroxene has wavy extinction and clinopyroxene exsolution lamellae are bent; some appear slightly elongated. Some spinels and orthopyroxene have inclusions which are now rounded serpentine pseudomorphs after olivine? (or orthopyroxene or clinopyroxene); orthopyroxene also have inclusions of anhedral clinopyroxene which is still very fresh. Completely serpentinized rock but the clinopyroxene is fresh. Clinopyroxene-rich harzburgite. P.G.E. refers to platinum group elements.

125-779A-11R-01 (Piece 5, 34-36 cm) OBSERVER: TER WHERE SAMPLED: Conical Seamount, southeast flank

ROCK NAME: Serpentinized dunite

GRAIN SIZE: <0.1 mm

TEXTURE: Mesh

PRIMARY MINERALOGY	PERCENT PRESENT	PERCENT ORIGINAL	SIZE (mm)	COMPO-SITION	MORPHOLOGY	COMMENTS
PHENOCRYSTS						
Olivine	0	99	Not visible		Not visible	Completely altered to mesh textured serpentine.
Spinel	Trace	1	0.2	Cr	Subhedral-anhedral	Cr=red; 1 small grain present and elongated.
GROUNDMASS						
N/A	N/A	N/A	N/A		N/A	

SECONDARY MINERALOGY	PERCENT	REPLACING/ FILLING	COMMENTS
Serpentine	100	Olivine, orthopyroxene	Lizardite and/or chrysotile forming mesh texture, large chrysotile veins cross slide and cut mesh texture.
Magnetite	Trace	Spinel	Dusty grains in trace amounts across slide.

VESICLES/ CAVITIES	PERCENT	LOCATION	SIZE (mm)	FILLING	SHAPE
Vesicles	0				

COMMENTS: Quality of this thin section is bad. It covers a small area and is too thin, therefore quality of optical determination is low. 1 to 3-mm-wide chrysotile veins run throughout the slide cutting across mesh texture.

125-779A-12R-1 (Piece 6,38-42 cm) OBSERVER: JCM WHERE SAMPLED: Conical Seamount, southeast flank

ROCK NAME: Serpentinized harzburgite

GRAIN SIZE: 0.05-4 mm

TEXTURE: Mesh and bastite

PRIMARY MINERALOGY	PERCENT PRESENT	PERCENT ORIGINAL	SIZE (mm)	COMPO-SITION	MORPHOLOGY	COMMENTS
PHENOCRYSTS						
Olivine	10	86	2-4		Subhedral-anhedral	Altered to serpentine mesh texture.
Clinopyroxene	1	1	0.05		Anhedral	As exsolution lamellae and small anhedral grains.
Spinel	1	1	0.2-0.8	Cr?	Euhedral-anhedral	Red; altered to magnetite and chlorite (see comments).
Orthopyroxene	8	12	0.1-4		Subhedral-anhedral	Altered to serpentine bastite; has exsolution lamellae of clinopyroxene; altered to chlorite.
GROUNDMASS						
N/A	N/A	N/A	N/A		N/A	

SECONDARY MINERALOGY	PERCENT	REPLACING/ FILLING	COMMENTS
Chlorite	2	Serpentine? orthopyroxene, spinel	Blue-green yellow pleochroic anhedral patches distributed throughout serpentine and along orthopyroxene cleavages grain boundaries; some spinels.
Serpentine	78	Olivine, orthopyroxene	Lizardite and/or chrysotile altering from olivine and orthopyroxene, forming mesh and minor bastite texture.
Magnetite	<1	Spinel	A few dusty 0.1-mm grains throughout slide.

VESICLES/ CAVITIES	PERCENT	LOCATION	SIZE (mm)	FILLING	SHAPE
Vesicles	0				

COMMENTS: Orthopyroxene has wavy extinction, kink-banding; inclusions of olivine and clinopyroxene. Olivine has wavy extinction and is altering to textured serpentine. One 0.8-mm euhedral spinel has two different rinds. The first has anomalous brown interference colors (some oxide phase) and surrounds the spinel. This is then further rimmed by anomalous blue interference colors (chlorite and/or serpentine). May be tectonized because mesh is deformed in portions of the slide.

125-779A-13R-01 (Piece 1,2-5 cm) OBSERVER: SAB WHERE SAMPLED: Conical Seamount, southeast flank

ROCK NAME: Serpentinized harzburgite

GRAIN SIZE: 0.05-5 mm

TEXTURE: Mesh (minor bastite)

PRIMARY MINERALOGY	PERCENT PRESENT	PERCENT ORIGINAL	SIZE (mm)	COMPO-SITION	MORPHOLOGY	COMMENTS
PHENOCRYSTS						
Olivine	0	87	Not visible		Not visible	Completely altered to serpentine mesh.
Spinel	<1	1	0.05-1	Cr	Subhedral-anhedral	Red brown, altered to magnetite.
Orthopyroxene	0	12	1-4		Subhedral-anhedral	Altered to serpentine bastite and chlorite.
GROUNDMASS						
P.G.E./sulfide	<0.1	N/A	N/A		N/A	With magnetite, as isolated grains in matrix, <0.1 mm, moderate abundance.

SECONDARY MINERALOGY	PERCENT	REPLACING/ FILLING	COMMENTS
Clays	<1	Serpentine	Dusty light brown clay distributed throughout slide and in mesh texture edges.
Chlorite	2	Orthopyroxene, serpentine	Fine-grained anhedral patches intermixed with serpentine minerals along orthopyroxene cleavages in bastites.
Magnetite	<1	Spinel	Dusty, fine grains distributed throughout slide.
Serpentine	95	Olivine, orthopyroxene	Lizardite and/or chrysotile distributed throughout slide in mesh and bastite textures.

VESICLES/ CAVITIES	PERCENT	LOCATION	SIZE (mm)	FILLING	SHAPE
Vesicles	0				

COMMENTS: Orthopyroxene bastites have wavy extinction. Rock is strongly serpentinized with no relic mineral grains present. Mesh texture is strongly developed in portions of slide. In other portions it is poorly developed. Slide appears slightly tectonized(?) because of the deformation of the mesh in places. P.G.E. refers to platinum group elements.

125-779A-13R-02 (0-3 cm) OBSERVER: HIR WHERE SAMPLED: Conical Seamount, southeast flank

ROCK NAME: Pebbly serpentinous mudstone (debris flow)

GRAIN SIZE: Fine-coarse parallel "melange" fabric

TEXTURE: Tectonite (soft sediment), foliate

PRIMARY MINERALOGY	PERCENT PRESENT	PERCENT ORIGINAL	SIZE (mm)	COMPO-SITION	MORPHOLOGY	COMMENTS
PHENOCRYSTS						
Spinel	<1	N/A	N/A		N/A	Cr-spinel, dark red.
GROUNDMASS						
N/A	N/A	N/A	N/A		N/A	

SECONDARY MINERALOGY	PERCENT	REPLACING/ FILLING	COMMENTS
Clays	20-30		Dusty brownish clay.
Serpentine	70-80		
Magnetite	<2		

VESICLES/ CAVITIES	PERCENT	LOCATION	SIZE (mm)	FILLING	SHAPE
Vesicles	0				

COMMENTS: Spectacular "melange" structure. Ductile boudinage and brittle fracture (former dominant) of large clasts in fine-grained matrix. Strong foliation and layer II shortening. No piece # given.

125-779A-17R-02 (Piece 1,52-54 cm) OBSERVER: SAB WHERE SAMPLED: Conical Seamount, southeast flank

ROCK NAME: Serpentinized harzburgite

GRAIN SIZE: 0.1-5 mm

TEXTURE: Mesh and bastite (developing)

PRIMARY MINERALOGY	PERCENT PRESENT	PERCENT ORIGINAL	SIZE (mm)	COMPO- SITION	MORPHOLOGY	COMMENTS
PHENOCRYSTS						
Olivine	20-25	78-84	0.5-3		Anhedral	Altering to serpentine mesh texture.
Clinopyroxene	<1	<1	0.2-1		Anhedral	As exsolution lamellae; anhedral grains near orthopyroxene.
Spinel	<1	2	0.2-1	Cr?	Subhedral-anhedral	Red; altered to magnetite.
Orthopyroxene	10-15	15-20	1-5		Subhedral-anhedral	Altered to serpentine bastite texture, have inclusions of olivine?
GROUNDMASS						
N/A	N/A	N/A	N/A		N/A	

SECONDARY MINERALOGY	PERCENT	REPLACING/ FILLING	COMMENTS
Chlorite	2	Orthopyroxene, spinel, serpentine	Blue-green to yellow pleochroism (weak), in fine-grained anhedral patches intermixed with serpentine and orthopyroxene also rimming some spinel.
Serpentine	58-64		Lizardite and/or chrysotile forming mesh and bastite textures throughout slide. Some minor bladed antigorite may be present.
Magnetite	2	Spinel	Dusty 0.1mm grains throughout slide; also some form elongated trails with minor chrysotile veins (<0.2 mm). Plus moderate abundance of platinum group elements, some sulfide (< 0.1 mm), disseminated.

VESICLES/ CAVITIES	PERCENT	LOCATION	SIZE (mm)	FILLING	SHAPE
Vesicles	0				

COMMENTS: Orthopyroxene has wavy extinction and clinopyroxene exsolution lamellae are bent. Olivine has wavy extinction. Some anhedral olivine inclusions occur in orthopyroxene crystals. Cleavage of magnetite infilled with silicate. Some portions of slide appear tectonized (? mylonitized) because of disruption of mesh, olivine and orthopyroxene grains into finer grains.

125-779A-13R-03 (Piece 1,9-11 cm) OBSERVER: SAB WHERE SAMPLED: Conical Seamount, southeast flank

ROCK NAME: Serpentinized harzburgite

GRAIN SIZE: 0.2-6 mm

TEXTURE: Cumulative (primary) altering to mesh and bastite

PRIMARY MINERALOGY	PERCENT PRESENT	PERCENT ORIGINAL	SIZE (mm)	COMPO-SITION	MORPHOLOGY	COMMENTS
PHENOCRYSTS						
Olivine	50	86	1-5		Anhedral	Altering to serpentine mesh, highly fractured grains.
Clinopyroxene	Trace	Trace	0.2		Anhedral	Exsolution lamellae of orthopyroxene; small separate grains.
Spinel	1	2	0.3-1	Cr	Subhedral-anhedral	Red; altered to magnetite and chlorite.
Orthopyroxene	5	12	1-6		Subhedral-anhedral	Altering to serpentine bastite.
GROUNDMASS						
P.G.E./sulfide	<1	N/A	N/A		N/A	A few 0.05-0.08 mm disseminated grains.

SECONDARY MINERALOGY	PERCENT	REPLACING/ FILLING	COMMENTS
Chlorite	1	Spinel, Serpentine	Anomalous blue bladed crystals surrounding some spinel and intermixed with serpentine.
Serpentine	42	Olivine, orthopyroxene	Lizardite and/or chrysotile mainly altering from olivine and orthopyroxene. Concentrated along olivine fractures and orthopyroxene cleavages.
Magnetite	1	Spinel	Fine dusty grains (0.3 mm) throughout slide, also in elongated trains in some portions.

VESICLES/ CAVITIES	PERCENT	LOCATION	SIZE (mm)	FILLING	SHAPE
Vesicles	0				

COMMENTS: Orthopyroxene has wavy extinction and clinopyroxene exsolution lamellae are deformed. Olivine has wavy extinction and kink-banding; olivine is still fairly fresh, but is serpentinized to mesh textured serpentine. Slide is still relatively fresh harzburgite. Spinels appear altered to some other oxide phase, then further rimmed by chlorite. P.G.E. refers to platinum group elements.

125-779A-14R-02 (Piece 3,21-24 cm) OBSERVER: SAB WHERE SAMPLED: Conical Seamount, southeast flank

ROCK NAME: Serpentinized dunite

GRAIN SIZE: 0.5-4 mm

TEXTURE: Mesh

PRIMARY MINERALOGY	PERCENT PRESENT	PERCENT ORIGINAL	SIZE (mm)	COMPO-SITION	MORPHOLOGY	COMMENTS
PHENOCRYSTS						
Olivine	20-25	95	0.5-4		Anhedral	Altered to serpentine mesh texture.
Clinopyroxene	<0.1	<0.1	0.5		Anhedral	Formed as small anhedral grains (rare).
Spinel	1	2	0.1-0.5	Cr	Subhedral-anhedral	Red, altered to magnetite.
Orthopyroxene	1	3	0.5-1		Subhedral-anhedral	Altered to serpentine bastite and chlorite.
GROUNDMASS						
N/A	N/A	N/A	N/A		N/A	

SECONDARY MINERALOGY	PERCENT	REPLACING/ FILLING	COMMENTS
Clays	2	Veins	Dusty brown clay concentrated mainly in serpentine vein (1 mm wide) crossing slide.
Chlorite	3	Orthopyroxene, serpentine	Blue green-yellow pleochroic anhedral blades and patches throughout slide and near bastite grains along old orthopyroxene cleavages.
Serpentine	67-72	Olivine, orthopyroxene	Lizardite and/or chrysotile altering from olivine and orthopyroxene, forming mesh and bastite textures. A serpentine vein (0.1 mm wide) crossing slide.
Magnetite	1	Spinel	Dusty 0.1-mm grains; also elongated trails (>0.5 mm long) which are crudely perpendicular to main serpentine vein.

VESICLES/ CAVITIES	PERCENT	LOCATION	SIZE (mm)	FILLING	SHAPE
Vesicles	0				

COMMENTS: Spinels are altered to magnetite, polyphase material present in the oxide grains, gray-yellow reflectivity.

125-779A-14R-01 (Piece 5A,74-77 cm)   OBSERVER: JON   WHERE SAMPLED: Conical Seamount, southeast flank

ROCK NAME: Serpentinized dunite

GRAIN SIZE: 0.2-7 mm

TEXTURE: Cataclastic (going to mesh and bastite)

PRIMARY MINERALOGY	PERCENT PRESENT	PERCENT ORIGINAL	SIZE (mm)	COMPO-SITION	MORPHOLOGY	COMMENTS
PHENOCRYSTS						
Olivine	60	80	0.2-7		Subhedral-anhedral	Altering to serpentine mesh; some may be neoblastic(?).
Clinopyroxene	11	11	0.2		Subhedral-anhedral	As minor exsolution lamellae.
Spinel	1	1	0.5-1	Cr	Subhedral-anhedral	Red brown; altered to magnetite and chlorite(?).
Orthopyroxene	2	8	1-2		Subhedral-anhedral	Altering to serpentine bastite and chlorite.
GROUNDMASS						
N/A	N/A	N/A	N/A		N/A	

SECONDARY MINERALOGY	PERCENT	REPLACING/ FILLING	COMMENTS
Chlorite	2	Orthopyroxene, serpentine	Anomalous brown interference colors (some oxide phase) rims some spinel(s); Blue-green to yellow pleochroic chlorite is intermixed with serpentine and along orthopyroxene cleavages.
Serpentine	18	Olivine, orthopyroxene	Lizardite and/or chrysotile altering from olivine and orthopyroxene and forming mesh and bastite textures; forming along olivine fractures and orthopyroxene cleavages. Chrysotile vein (<1 mm wide) cuts across slide.
Magnetite	1	Spinel	Dusty 0.5mm grains, anhedral elongated trails which are concentrated within serpentine veins.

VESICLES/ CAVITIES	PERCENT	LOCATION	SIZE (mm)	FILLING	SHAPE
Vesicles	0				

COMMENTS: Olivine fractures appear to parallel main serpentine (chrysotile) vein. The serpentine which forms along the olivine fractures also parallels the main vein. This may indicate formation of primary veins with secondary veins at the same time as the olivine fractures. Some olivine grains (<0.2 mm) may be neoblastic(?). Spinels are altered to some other oxide phase, and are rimmed by chlorite.

125-779A-14R-02 (Piece 16,139-141 cm)   OBSERVER: SAB   WHERE SAMPLED: Conical Seamount, southeast flank

ROCK NAME: Serpentinized harzburgite

GRAIN SIZE: 0.01-5 mm

TEXTURE: Cumulate, mesh

PRIMARY MINERALOGY	PERCENT PRESENT	PERCENT ORIGINAL	SIZE (mm)	COMPO- SITION	MORPHOLOGY	COMMENTS
PHENOCRYSTS						
Olivine	40	78-83	0.5-4		N/A	Altering to poor-looking mesh texture serpentine, some olivine may be recrystallized.
Clinopyroxene	<1	<1	0.01		Subhedral-anhedral	As exsolution lamellae; as scattered grains.
Spinel	1	1.5	0.05-1	Cr?	Anhedral	Red
Orthopyroxene	10	15-20	0.5-5		Subhedral-anhedral	Altering to serpentine bastite texture; some orthopyroxene appears recrystallized.
GROUNDMASS						
N/A	N/A	N/A	N/A		N/A	

SECONDARY MINERALOGY	PERCENT	REPLACING/ FILLING	COMMENTS
Chlorite	3	Orthopyroxene, spinel	Blue-green to yellow pleochroism bladed grains, associated with the serpentine bastite and some spinels.
Serpentine	45	Olivine, orthopyroxene	Lizardite and/or chrysotile forming mesh and bastite; chrysotile vein (2 mm wide) crosses slide and cuts earlier serpentine veins (0.5 mm wide) that run 60 degrees to it. Serpentinization is greatest near larger chrysotile vein.
Magnetite	1	Spinel	Dusty 0.1-mm anhedral grains located in veins.

VESICLES/ CAVITIES	PERCENT	LOCATION	SIZE (mm)	FILLING	SHAPE
Vesicles	0				

COMMENTS: Relatively fresh tectonized serpentinized harzburgite. Elongate anhedral spinels arranged in trains; orthopyroxene is kink-banded and exsolved clinopyroxene lamellae are bent; spinel has a reaction halo, altering to some other oxide phase and chlorite surrounding that. Olivine has wavy extinction and appears kinked also. Orthopyroxene has inclusions of anhedral olivine. Some orthopyroxene and olivine may be recrystallized; slide is tectonized.

125-779A-14R-02 (Piece 9, 77-79 cm) OBSERVER: JOH WHERE SAMPLED: Conical Seamount, southeast flank

ROCK NAME: Serpentinized harzburgite

GRAIN SIZE: 0.01-6 mm

TEXTURE: Cumulate (primary) forming mesh

PRIMARY MINERALOGY	PERCENT PRESENT	PERCENT ORIGINAL	SIZE (mm)	COMPO-SITION	MORPHOLOGY	COMMENTS
PHENOCRYSTS						
Olivine	45-50	80-85	1.0-5		Anhedral	Kink-banding, wavy extinction, mesh texture serpentine.
Clinopyroxene	3	3	0.01-0.5		Anhedral	As exsolution lamellae and smaller grains.
Spinel	2	2	0.25-2		Euhedral-anhedral	Red; altering to magnetite.
Orthopyroxene	10-15	15-20	0.5-6		Subhedral-anhedral	Altering to serpentine bastite; wavy extinction and recrystallization.
GROUNDMASS						
N/A	N/A	N/A	N/A		N/A	

SECONDARY MINERALOGY	PERCENT	REPLACING/ FILLING	COMMENTS
Serpentine	30-45	Olivine, orthopyroxene	Lizardite and/or chrysotile forming mostly mesh and bastite textures along olivine fractures and orthopyroxene cleavages.
Magnetite	<1	Spinel	Fine-grained, disseminated, many follow olivine grain boundaries.

VESICLES/ CAVITIES	PERCENT	LOCATION	SIZE (mm)	FILLING	SHAPE
Vesicles	0				

COMMENTS: Relatively fresh harzburgite; highly tectonized. Serpentine alters olivine along the fractures, but appears to leave the orthopyroxene unchanged. Both olivine and orthopyroxene grains exhibit recrystallization; exsolved clinopyroxene lamellae are bent. Orthopyroxene has inclusions of anhedral olivine and possible clinopyroxene(?).

125-779A-13R-03 (Piece 4, 15-17 cm) OBSERVER: SAB WHERE SAMPLED: Conical Seamount, southeast flank

ROCK NAME: Clinopyroxene-rich serpentinized harzburgite

GRAIN SIZE: 0.05-4 mm

TEXTURE: Cumulate, mesh

PRIMARY MINERALOGY	PERCENT PRESENT	PERCENT ORIGINAL	SIZE (mm)	COMPO-SITION	MORPHOLOGY	COMMENTS
PHENOCRYSTS						
Olivine	33	83-85	0.25-3		Anhedral	Altering to mesh serpentine.
Clinopyroxene	3	3	0.2-1.5		Subhedral-anhedral	Primary clinopyroxene grains; also as exsolution lamellae.
Spinel	1	2	0.05-1		Subhedral-anhedral	Red; altering to magnetite.
Orthopyroxene	12	12	0.5-4		Subhedral-anhedral	No good serpentine bastite formed; only minor alteration to serpentine.
GROUNDMASS						
N/A	N/A	N/A	N/A		N/A	

SECONDARY MINERALOGY	PERCENT	REPLACING/ FILLING	COMMENTS
Serpentine	50	Olivine, orthopyroxene	Lizardite and/or chrysotile altering olivine along fractures and forming mesh texture.
Magnetite	1	Spinel	Dusty 0.1-mm grains; some elongated trails are formed.

VESICLES/ CAVITIES	PERCENT	LOCATION	SIZE (mm)	FILLING	SHAPE
Vesicles	0				

COMMENTS: Orthopyroxene has wavy extinction, bent exsolution lamellae but is still relatively fresh and not altered to serpentine. Olivine has wavy extinction and serpentine alteration along fractures forming mesh texture; some olivines may be recrystallized(?). Portions of slide appear fresh and portions appear altered and tectonized.

125-779A-15R-02 (Piece 3,18-20 cm) OBSERVER: TER WHERE SAMPLED: Conical Seamount, southeast flank

ROCK NAME: Serpentinized harzburgite

GRAIN SIZE: 0.01-5 mm

TEXTURE: Mesh

PRIMARY MINERALOGY	PERCENT PRESENT	PERCENT ORIGINAL	SIZE (mm)	COMPO-SITION	MORPHOLOGY	COMMENTS
PHENOCRYSTS						
Olivine	21	87	1-5		Anhedral	Altering to serpentine mesh texture; appears deformed and kinked, wavy extinction.
Clinopyroxene	<1	<1	0.1-1		Subhedral-anhedral	Appears as small patches.
Spinel	1	1	0.01-1	Cr	Subhedral-anhedral	Red brown; altered to magnetite.
Orthopyroxene	7	12	1-3		Anhedral	Altered to serpentine bastite texture; wavy extinction.
GROUNDMASS						
N/A	N/A	N/A	N/A		N/A	

SECONDARY MINERALOGY	PERCENT	REPLACING/ FILLING	COMMENTS
Serpentine	70	Olivine, Orthopyroxene	Lizardite and/or chrysotile forming mesh and bastite textures.
Magnetite	1	Spinel	Dusty 0.1-mm grains, most are concentrated in veins as elongate trails and also in mesh edges.

VESICLES/ CAVITIES	PERCENT	LOCATION	SIZE (mm)	FILLING	SHAPE
Vesicles	0				

COMMENTS: Some spinels are elongated into trails; olivine is kink-banded. Olivine and orthopyroxene have wavy extinction; some orthopyroxene appear to have anhedral olivine inclusions.

125-779A-15R-02 (Piece 3,24-27 cm) OBSERVER: SAH WHERE SAMPLED: Conical Seamount, southeast flank

ROCK NAME: Serpentinized dunite

GRAIN SIZE: 0.1-4 mm

TEXTURE: Mesh texture dominant

PRIMARY MINERALOGY	PERCENT PRESENT	PERCENT ORIGINAL	SIZE (mm)	COMPO-SITION	MORPHOLOGY	COMMENTS
PHENOCRYSTS						
Olivine	10	94-97	1-3		Anhedral	Altered to serpentine mesh texture.
Spinel	0.3	1	0.1-0.5	Cr	Subhedral-anhedral	Red brown; altered to magnetite and chlorite.
Orthopyroxene	0	2-5	1-4		N/A	Altered to serpentine bastite completely.
GROUNDMASS						
N/A	N/A	N/A	N/A		N/A	

SECONDARY MINERALOGY	PERCENT	REPLACING/ FILLING	COMMENTS
Chlorite	<1	Serpentine, spinel	Blue green yellow pleochroic; anhedral patches within serpentine, also rimming some spinel.
Serpentine	82	Olivine, orthopyroxene	Lizardite and/or chrysotile forms mesh texture throughout the slide.
Brucite?	5	Olivine, orthopyroxene	Occurs in veins cutting slide; XRD determination is needed.
Magnetite	2	Spinel	Dusty 0.1-mm grains; occurs concentrated in veins.

VESICLES/ CAVITIES	PERCENT	LOCATION	SIZE (mm)	FILLING	SHAPE
Vesicles	0				

COMMENTS: Veining occurs mostly at 40 degrees angle from the long axis of slide. Veins also serpentine (chrysotile) and brucite, and magnetite assemblage. They are <0.01-0.05 mm wide. Veining seems to be post-serpentinization. Mesh texture appears tectonized in portions of slide. Some spinels are rimmed by yellow-brown interference color mineral (fibers) which may be another oxide phase.

125-779A-15R-02 (Piece 5,37-40 cm) OBSERVER: SAB WHERE SAMPLED: Conical Seamount, southeast flank

ROCK NAME: Serpentinized harzburgite

GRAIN SIZE: 0.5-3 mm

TEXTURE: Cataclastic

PRIMARY MINERALOGY	PERCENT PRESENT	PERCENT ORIGINAL	SIZE (mm)	COMPO-SITION	MORPHOLOGY	COMMENTS
PHENOCRYSTS						
Olivine	40	83	0.5-2		Anhedral	Highly fractured, broken up, and altering to serpentine.
Clinopyroxene	1	1	0.2-0.5		Subhedral/anhedral	As exsolution lamellae, also anhedral grains.
Spinel	1	1	0.5-2	Cr	Subhedral/anhedral	Red brown; altered to magnetite.
Orthopyroxene	10	15	0.5-3		Subhedral/anhedral	Altered to serpentine bastite; wavy extinction.
GROUNDMASS						
N/A	N/A	N/A	N/A		N/A	

SECONDARY MINERALOGY	PERCENT	REPLACING/ FILLING	COMMENTS
Serpentine	45	Olivine, orthopyroxene	Lizardite and/or chrysotile mainly occur in larger veins, cross-cutting the slide almost perpendicular to one another.
Magnetite	3	Spinel	Dusty grains concentrated in veins mostly.

VESICLES/ CAVITIES	PERCENT	LOCATION	SIZE (mm)	FILLING	SHAPE
Vesicles	0				

COMMENTS: Orthopyroxene has wavy extinction, bent clinopyroxene exsolution lamellae; olivine has wavy extinction; most of serpentine in slide is concentrated in a number of cross-cutting veins (0.2-2.5 mm wide). The rest of slide has tectonized (mylonitized) olivine and orthopyroxene grains.

125-779A-15R-02 (Piece 17,110-113 cm) OBSERVER: SAB WHERE SAMPLED: Conical Seamount, southeast flank

ROCK NAME: Serpentinized dunite

GRAIN SIZE: 0.2-7 mm

TEXTURE: Porphyroclastic

PRIMARY MINERALOGY	PERCENT PRESENT	PERCENT ORIGINAL	SIZE (mm)	COMPO-SITION	MORPHOLOGY	COMMENTS
PHENOCRYSTS						
Olivine	54	97	0.2-7		Subhedral-anhedral	Relic grains are anhedral to subhedral and neoblasts are subhedral to euhedral.
Spinel	2	2	0.5-2	Cr	Euhedral-anhedral	Red; altered to magnetite, chlorite.
Orthopyroxene	Trace	Trace	3		Anhedral	No bastite visible; orthopyroxene is severely fractured and tectonized.
GROUNDMASS						
N/A	N/A	N/A	N/A		N/A	

SECONDARY MINERALOGY	PERCENT	REPLACING/ FILLING	COMMENTS
Clays	2	Vein	Pale brown; forming feather-like crystals.
Chlorite	<1	Spinel, serpentine	Pale green to colorless; rims some spinels and in some veins.
Serpentine	40		Mostly lizardite and/or chrysotile occurring in vicinity of major veining. Minor antigorite blades are visible.
Magnetite	2	Spinel	Dusty 0.2-mm elongated trails; concentrated in veins as well as throughout slide.

VESICLES/ CAVITIES	PERCENT	LOCATION	SIZE (mm)	FILLING	SHAPE
Vesicles	0				

COMMENTS: This slide is pervasively tectonized. Recrystallized olivine subgrains occur as an aggregate of fine-grained crystals. A portion of recrystallized olivine grains occur along the cleavages or rim of the olivine crystals (7 mm across). Olivines (relic) have wavy extinction and kink-banding; spinels show alteration to another mineral phase (brown interference, fibers), and then to anomalous blue chlorite(?). Veins may occur as a conjugate set with 70-110 degrees orientation.

125-779A-18R-01 (Piece 3,16-19 cm)   OBSERVER: SAB   WHERE SAMPLED: Conical Seamount, southeast flank

ROCK NAME: Serpentinized harzburgite

GRAIN SIZE: 0.05-10 mm

TEXTURE: Porphyroblastic, felted

PRIMARY MINERALOGY	PERCENT PRESENT	PERCENT ORIGINAL	SIZE (mm)	COMPO-SITION	MORPHOLOGY	COMMENTS
PHENOCRYSTS						
Olivine	55	86	0.1-10		Subhedral-anhedral	Kink-banded, neoblasts; hardly serpentinized, some grains appear elongated.
Spinel	2	2	0.05-2	Cr	Subhedral-anhedral	Red; altered to magnetite; some elongated.
Orthopyroxene	1	12	1-3		Subhedral-anhedral	Altered to serpentine bastite. Some grains appear elongated.
GROUNDMASS						
N/A	N/A	N/A	N/A		N/A	

SECONDARY MINERALOGY	PERCENT	REPLACING/ FILLING	COMMENTS
Chlorite	Tr	Spinel	Colorless; anomalous, blue interference color; located around some spinels mostly.
Serpentine	40	Olivine, orthopyroxene	Appears to be mostly bladed antigorite concentrated in serpentine veins. Might be some lizardite present; chrysotile fibers are present in veins and along olivine cleavages.
Magnetite	2	Spinel	Dusty 0.1-mm elongate; distributed throughout serpentinized portion and in veins.

VESICLES/ CAVITIES	PERCENT	LOCATION	SIZE (mm)	FILLING	SHAPE
Vesicles	0				

COMMENTS: Elongated Cr-spinels arranged in trains; one set crossing a vein shows a well-formed "sinistral" shear. Orthopyroxene shows wavy extinction and exsolved clinopyroxene lamellae are bent. Orthopyroxene and spinels are altered but olivine appears relatively fresh, but still has wavy extinction and kink-bands. Some olivine has recrystallized into neoblastic subgrains. Veins are oriented mostly parallel and are ~40 degrees to long axis of slide (0.2-2 mm wide). Spinels are also altered to a mineral with brownish anomalous interference color (could be another oxide phase), also altered to chlorite(?).

125-779A-16R-01 (Piece 3,19-23 cm) OBSERVER: SAB WHERE SAMPLED: Conical Seamount, southeast flank

ROCK NAME: Dunite

GRAIN SIZE: 0.01-4 mm

TEXTURE: Porphyroclastic-granoblastic

PRIMARY MINERALOGY	PERCENT PRESENT	PERCENT ORIGINAL	SIZE (mm)	COMPO- SITION	MORPHOLOGY	COMMENTS
PHENOCRYSTS						
Olivine	78-81	85	0.1-4		Anhedral	Kink-banded, elongated, wavy extinction, recrystallized neoblasts.
Clinopyroxene	<1	<1	0.01		Subhedral-anhedral	Small patch of crystals in slide.
Spinel	0.5	1.0	0.05-0.5	Cr?	Subhedral-anhedral	Red; some altered to magnetite; elongated trains.
Orthopyroxene	2	7	1-2		Subhedral-anhedral	Altered to serpentine bastite.
GROUNDMASS						
N/A	N/A	N/A	N/A		N/A	

SECONDARY MINERALOGY	PERCENT	REPLACING/ FILLING	COMMENTS
Serpentine	15-20		Mostly antigorite blades forming 0-1 mm wide veins which cross the slide perpendicular to each other. Chrysotile fibers are also present. Lizardite may be present.
Magnetite	1		Dusty 0.1 mm anhedral grains distributed mostly in veins and along cleavages.

VESICLES/ CAVITIES	PERCENT	LOCATION	SIZE (mm)	FILLING	SHAPE
Vesicles	0				

COMMENTS: Relatively fresh tectonized Dunite. There were two slides made from this rock. The other slide (779A 16R-1, 19-19) is described as a serpentinized harzburgite. Orthopyroxene is altered to serpentine while olivine is still very fresh and recrystallized in portions; two vein sets running perpendicular to one another and composed of serpentine and magnetite; rest of slide is recrystallized. Tectonized olivine grains elongated parallel to 2nd generation veins.

125-779A-16R-01 (Piece 6,37-40 cm) OBSERVER: SAB WHERE SAMPLED: Conical Seamount, southeast flank

ROCK NAME: Harzburgite

GRAIN SIZE: 0.01-4 mm

TEXTURE: Cataclastic, granoblastic (minor mesh)

PRIMARY MINERALOGY	PERCENT PRESENT	PERCENT ORIGINAL	SIZE (mm)	COMPO-SITION	MORPHOLOGY	COMMENTS
PHENOCRYSTS						
Olivine	69	83	0.01-4		Anhedral	Kink-banded, wavy extinction, elongated neoblasts; altering to serpentine (poor mesh).
Clinopyroxene	<1	<1	0.01-0.05		Anhedral	Exsolution lamellae in orthopyroxene, small anhedral patches.
Spinel	<1	2	0.05-1	Cr	Anhedral	Red; altered to magnetite.
Orthopyroxene	7	15	0.5-4		Subhedral-anhedral	Altering to serpentine bastite; has (100) lamellae of clinopyroxene, wavy extinction, elongated.
GROUNDMASS						
N/A	N/A	N/A	N/A		N/A	

SECONDARY MINERALOGY	PERCENT	REPLACING/ FILLING	COMMENTS
Serpentine	25	Olivine, orthopyroxene	Looks like bladed antigorite and fibrous chrysotile, but lizardite may also be present. Concentrated mostly in central zone.
Magnetite	2	Spinel	Dusty 0.2-mm anhedral grains concentrated mostly in 4-mm veins.
Talc?	4	Orthopyroxene	Elongation, extinction angle = 0 degree; high interference color; may not be talc rather mylonitized olivine; appears mostly in sheared central zone as fine-grained fibers.

VESICLES/ CAVITIES	PERCENT	LOCATION	SIZE (mm)	FILLING	SHAPE
Vesicles	0				

COMMENTS: Rock is pervasively tectonized. Olivine and orthopyroxene are elongated and deformed (kink-banded and wavy extinction). Orthopyroxene appears to be more extensively altered than olivine; olivine is mostly recrystallized into smaller neoblasts; center of slide appears to be a tectonized or shear zone where most of serpentine is where the primary minerals have been altered, sheared, and practically obliterated. Away from the center zone, the primary minerals are hardly serpentinized, but are elongated, deformed, and recrystallized. Orthopyroxene has small anhedral inclusions of olivine.

125-779A-16R-1 (Piece 4,50-52 cm)   OBSERVER: SAB   WHERE SAMPLED: Conical Seamount, southeast flank

ROCK NAME: Harzburgite

GRAIN SIZE: 0.01-2.4 mm

TEXTURE: Cataclastic, granoblastic (mesh bastite)

PRIMARY MINERALOGY	PERCENT PRESENT	PERCENT ORIGINAL	SIZE (mm)	COMPOSITION	MORPHOLOGY	COMMENTS
PHENOCRYSTS						
Olivine	68	74	0.01-4		Anhedral	Kinked, elongated, wavy extinction, neoblastic in areas, altering to serpentine (plus mesh).
Clinopyroxene	1	1	0.2		Anhedral	Exsolution lamellae, small subhedral-euhedral inclusions in orthopyroxene
Spinel	<1	1	0.1-0.3		Anhedral	Dark red brown, altering to magnetite
Orthopyroxene	7	20	0.2-4		Subhedral-anhedral	Altered to serpentine bastite, elong wavy extinction, recrystallized, associated with talc(?).
GROUNDMASS						
N.A.	N.A.	N.A.	N.A.		N.A.	

SECONDARY MINERALOGY	PERCENT	REPLACING/FILLING	COMMENTS
Clays	Trace	Veins	Dusty brown clay along the edge of olive [illegible] zone.
Serpentine	22	Olivine, orthopyroxene	Could be lizardite and/or chrysotile, with antigorite [illegible] Appear concentrated mostly in and near veins [illegible] cutting olive.
Magnetite	1	Olivine	
Talc	1	Orthopyroxene	[illegible] elongate grains located mostly in veins [illegible] high interference colors, fibrous [illegible] [illegible] associated with alteration of orthopyroxene.

VESICLES/CAVITIES	PERCENT	LOCATION	SIZE (mm)	FILLING	SHAPE
[illegible]	1				

COMMENTS: Rock is severely deformed; olivine and orthopyroxene are deformed (kink banded wavy extinction) and elongated. Orthopyroxene appears to be more extensively altered than olivine. Olivine is recrystallizing into small neoblasts. Orthopyroxene has rounded inclusions of olivine and anhedral to subhedral inclusions of clinopyroxene; orthopyroxene also has been exsolution lamellae, some grains appear recrystallized. Primary crystals are all elongated in same direction which parallel the long direction of olive; some chromite appears rimmed by magnetite. Some of olive has [illegible].

125-779A-16R-2 (Piece 19,127-129 cm)   OBSERVER: SAB   WHERE SAMPLED: Conical Seamount, southeast flank

ROCK NAME: Serpentinized dunite

GRAIN SIZE: 0.01-5 mm

TEXTURE: Granoblastic-cataclastic (felted in areas; bastite also)

PRIMARY MINERALOGY	PERCENT PRESENT	PERCENT ORIGINAL	SIZE (mm)	COMPO-SITION	MORPHOLOGY	COMMENTS
PHENOCRYSTS						
Olivine	10	90	0.01- 5		Anhedral	Kink-banded, wavy extinction, neoblastic; elongated, altering to serpentine (poor mesh).
Clinopyroxene	Trace	Trace	0.01		Subhedral-anhedral	As exsolution lamellae.
Spinel	1	2	0.2-1		Anhedral	Dark red brown; altered to magnetite.
Orthopyroxene	3	8	1-4		Subhedral-anhedral	Altered to serpentine bastite and talc; kinked, wavy extinction, recrystallized.
GROUNDMASS						
N/A	N/A	N/A	N/A		N/A	

SECONDARY MINERALOGY	PERCENT	REPLACING/ FILLING	COMMENTS
Clays	1	Serpentine	Dusty brown clay located on one side of slide, intermixed with the serpentine.
Serpentine	82	Olivine, orthopyroxene	Mostly antigorite and chrysotile; might be lizardite, but difficult to tell. Serpentine is mostly in veins (0.1-0.4 mm) which cut slide and tend to alter minerals closest to veins.
Magnetite	1	Spinel	Dusty 0.1-mm elongated trains; mostly concentrated in serpentine veins (0.1-0.4 mm).
Talc?	2	Orthopyroxene	High birefringence, (+) elongation, fibrous extinction angle ~0 degrees. May or may not be talc, but associated with orthopyroxene alteration.

VESICLES/ CAVITIES	PERCENT	LOCATION	SIZE (mm)	FILLING	SHAPE
Fractures	0				

COMMENTS: Slide appears tectonized. Olivine and orthopyroxene are elongated in a parallel direction that defines a fabric across the slide. Olivine and orthopyroxene are both deformed (kink-banded and wavy extinction) and recrystallized. Serpentine veins appear to have a conjugate set orientation (roughly?). Tectonic elongation tends to follow first-generation serpentine veins. The second-generation serpentine veins cut across elongation fabric and first-generation vein set. One orthopyroxene grain has clinopyroxene lamellae and is altered to serpentine, but clinopyroxene lamellae still extend into serpentine.

125-779A-18R-02 (Piece 6,44-47 cm)   OBSERVER: SAB   WHERE SAMPLED: Conical Seamount, southeast flank

ROCK NAME: Serpentinized harzburgite

GRAIN SIZE: 0.1-3 mm

TEXTURE: Mesh and bastite

PRIMARY MINERALOGY	PERCENT PRESENT	PERCENT ORIGINAL	SIZE (mm)	COMPO-SITION	MORPHOLOGY	COMMENTS
PHENOCRYSTS						
Olivine	18	81	1-3		Anhedral	Wavy extinction altered to serpentine mesh.
Clinopyroxene	5	5	0.1-0.4		Equant-anhedral	Exsolution lamellae, occur at orthopyroxene edges, fresh.
Spinel	1	2	0.2-0.5	Cr	Anhedral	Red; elongated-ragged alters to magnetite, some clinopyroxene inclusions.
Orthopyroxene	5	12	1-3		Subhedral-anhedral	Ragged appearance in some grains, altered to serpentine bastite.
GROUNDMASS						
N/A	N/A	N/A	N/A		N/A	

SECONDARY MINERALOGY	PERCENT	REPLACING/FILLING	COMMENTS
Serpentine	70	Olivine, orthopyroxene	Lizardite and/or chrysotile forming mesh and bastite textures; Chrysotile also concentrated in major vein sets veining slide (0.5-2 mm wide).
Magnetite	1	Spinel	Dusty 0.2-mm grains, ragged trains concentrated serpentine veins.

VESICLES/CAVITIES	PERCENT	LOCATION	SIZE (mm)	FILLING	SHAPE
Vesicles	0				

COMMENTS: Orthopyroxenes are kink-banded and have bent clinopyroxene exsolution lamellae. Spinels sometimes form ragged trails. Multiple vein sets with a crude conjugate set orientation. Possibly even a crude "Frankenstein" texture in an area. Appears that the 1st-generation vein set developed, then 2nd set and 3rd set, but difficult to decipher. Relatively clinopyroxene-rich harzburgite.

125-779A-16R-02 (Piece 9,61-64 cm) OBSERVER: SAB WHERE SAMPLED: Conical Seamount, southeast flank

ROCK NAME: Serpentinized harzburgite

GRAIN SIZE: 0.1-5 mm

TEXTURE: Mesh (minor bastite)

PRIMARY MINERALOGY	PERCENT PRESENT	PERCENT ORIGINAL	SIZE (mm)	COMPO-SITION	MORPHOLOGY	COMMENTS
PHENOCRYSTS						
Olivine	20	85	0.1-3		Anhedral	Altering to serpentine mesh, wavy extinction, neoblastic?
Clinopyroxene	2	2	0.8-2		Subhedral-anhedral	Exsolution lamellae; and near orthopyroxene margins.
Spinel	1	1	0.4-2	Cr	Ragged-anhedral	Red; altered to magnetite.
Orthopyroxene	10	12	0.5-5		N/A	Altering to serpentine bastite and chlorite; have (100) exsolution lamellae.
GROUNDMASS						
N/A	N/A	N/A	N/A		N/A	

SECONDARY MINERALOGY	PERCENT	REPLACING/ FILLING	COMMENTS
Chlorite	1	Orthopyroxene	Blue-green to yellow pleochroism; associated mainly along orthopyroxene cleavages and grains.
Serpentine	65	Olivine, orthopyroxene	Lizardite and/or chrysotile forming mesh and bastite texture; chrysotile also dominates in multiple veins sets (0.2-3 mm wide) crossing slide.
Magnetite	1	Spinel	Dusty 0.1-mm grains; disseminated throughout and in veins mostly.

VESICLES/ CAVITIES	PERCENT	LOCATION	SIZE (mm)	FILLING	SHAPE
Vesicles	5				

COMMENTS: Relatively clinopyroxene-rich harzburgite; orthopyroxene has wavy extinction, and inclusions of clinopyroxene and olivine. Spinels have inclusions of serpentine pseudomorphs of round olivine(?); olivine and orthopyroxene may be slightly recrystallized in areas. Very complicated sets of vein criss crossing slide; may be some "Frankentein" texture. One large vein set (1 cm wide) is cut perpendicular by minor (2 mm wide) veins.

[illegible] OBSERVER: [illegible] WHERE SAMPLED: Conical Seamount, southeast flank

ROCK NAME: Serpentinized harzburgite

GRAIN SIZE: [illegible] mm

TEXTURE: mesh (major part)

PRIMARY MINERALOGY [illegible]

[illegible]

SECONDARY MINERALOGY [illegible]

[illegible]

COMMENTS: [illegible]

[illegible] OBSERVER: [illegible] WHERE SAMPLED: Conical Seamount, southeast flank

ROCK NAME: Serpentinized dunite

GRAIN SIZE: [illegible] mm

TEXTURE: [illegible] and mesh

PRIMARY MINERALOGY [illegible]

[illegible]

SECONDARY MINERALOGY [illegible]

[illegible]

COMMENTS: [illegible]

125-779A-17R-02 (Piece 1,17-21 cm)   OBSERVER: SAB   WHERE SAMPLED: Conical Seamount, southeast flank

ROCK NAME: Harzburgite

GRAIN SIZE: 0.1-5 mm

TEXTURE: [illegible]

PRIMARY MINERALOGY	PERCENT PRESENT	PERCENT ORIGINAL	SIZE mm	COMPO-SITION	MORPHOLOGY	COMMENTS
PHENOCRYSTS						
Olivine	49	73	1-5		Subhedral-anhedral	Kink-banded, wavy extinction, altering to serpentine (pure mesh serpentine)
Clinopyroxene	Trace	Trace	0.25-0.5		Anhedral	No exsolution lamellae
Spinel	[illegible]	2	0.1-1	Cr	Subhedral-anhedral	Red brown; altered to magnetite, elongate.
Orthopyroxene	[illegible]	25	0.5-6		Subhedral-anhedral	Altered to serpentine bastite and chlorite has exsolution lamellae of clinopyroxene.
GROUNDMASS						
N.A.	N.A.	N.A.	N.A.		N.A.	

SECONDARY MINERALOGY	PERCENT	REPLACING-FILLING	COMMENTS
Chlorite	<1	Orthopyroxene	Blue-green to pale-yellow pleochroism. Found mostly along orthopyroxene cleavages and fractures.
Serpentine	[illegible]	Olivine, orthopyroxene	Mostly lizardite and/or chrysotile in wide vein across slide. Serpentinization of primary minerals is greatest in vein and its vicinity.
Magnetite	[illegible]	Spinel	Tiny [illegible] mm grains concentrated mainly in veins.

VESICLES/CAVITIES	PERCENT	LOCATION	SIZE mm	FILLING	SHAPE
Vesicles	0				

COMMENTS: Orthopyroxene is kink-banded, wavy extinction, [illegible] clinopyroxene exsolution lamellae. Olivine is kinked, has wavy extinction, altering to serpentine, but is mainly suffering cataclastic deformation with minor amount of [illegible] rotation. Slide is [illegible]. Have major vein set of serpentine and magnetite [illegible] mm wide crossing slide. The elongation of olivine roughly parallel the veins orientation. Some brighter yellowish phase in [illegible] spinels, developed along cracks (magnetite, [illegible]).

125-779A-17R-02 (Piece 3,21-24 cm) OBSERVER: SAB WHERE SAMPLED: Conical Seamount, southeast flank

ROCK NAME: Harzburgite

GRAIN SIZE: 0.1-4 mm

TEXTURE: Cataclastic-granoblastic

PRIMARY MINERALOGY	PERCENT PRESENT	PERCENT ORIGINAL	SIZE (mm)	COMPO-SITION	MORPHOLOGY	COMMENTS
PHENOCRYSTS						
Olivine	41	74	0.1-1		Anhedral	Kinked, wavy extinction, tectonized with minor neoblasts formation; altering to serpentine.
Clinopyroxene	Trace	Trace	N/A		Anhedral	As exsolution lamellae in orthopyroxene. Minor patches.
Spinel	1	1	0.2-0.3	Cr	Subhedral-anhedral	Altering to magnetite; minor inclusions of olivine(?).
Orthopyroxene	20	25	1-4		Subhedral-anhedral	Wavy extinction, clinopyroxene exsolution lamellae, altered to serpentine bastite(?).
GROUNDMASS						
N/A	N/A	N/A	N/A		N/A	

SECONDARY MINERALOGY	PERCENT	REPLACING/FILLING	COMMENTS
Chlorite	Trace	Orthopyroxene	Blue-green to pale-green pleochroic; associated with orthopyroxene cleavages and fractures mostly.
Serpentine	32	Olivine, orthopyroxene	Mostly lizardite and/or chrysotile; large (0.05-5 mm) serpentine veins cutting slide and altering primary minerals.
Magnetite	6	Spinel	Dusty 0.2-mm grains throughout slide and concentrated along serpentine veins.

VESICLES/CAVITIES	PERCENT	LOCATION	SIZE (mm)	FILLING	SHAPE
Vesicles	0				

COMMENTS: Rock appears tectonized, but is still fairly fresh. Serpentinization occurs in veins and in the vicinity of veins and decreases as move away from veins. The fresher (non-altered) minerals have been deformed cataclastically and some minor neoblasts have formed from both olivine and orthopyroxene. Orthopyroxene has been exsolution lamellae, wavy extinction, slight elongation and minor olivine inclusions. Olivine has wavy extinction and kink-bands, but is still fairly fresh and is elongated.

SITE 779

[illegible]

125-779A-27R-3 (Piece 5B, 80-83 cm)   OBSERVER: SAB   WHERE SAMPLED: Conical Seamount, southeast flank

ROCK NAME: Harzburgite

GRAIN SIZE: 0.01-5 mm

TEXTURE: Granoblastic; cataclastic

PRIMARY MINERALOGY	PERCENT PRESENT	PERCENT ORIGINAL	SIZE (mm)	COMPO-SITION	MORPHOLOGY	COMMENTS
PHENOCRYSTS						
Olivine	83	83	0.05-4		Subhedral-anhedral	Wavy extinction; altered to serpentine mesh, microgranoblastic.
Clinopyroxene	1	1	0.02-0.5		Anhedral	Exsolution lamellae in orthopyroxene; grains near orthopyroxene.
Spinel	1	1	N/A	Cr	Anhedral	Red; altered to magnetite; some are elongate.
Orthopyroxene	15	15	1-5		Subhedral-anhedral	Altered to serpentine bastite and chlorite, deformed wavy extinction.
GROUNDMASS						
N/A	N/A	N/A	N/A		N/A	

SECONDARY MINERALOGY	PERCENT	REPLACING/ FILLING	COMMENTS
Chlorite	Trace	Orthopyroxene	Blue-green to pale-green pleochroic. Forms along cleavages and cracks.
Serpentine	85	Olivine, orthopyroxene	Lizardite and/or chrysotile altering from olivine and orthopyroxene. Forming anastomosing veins throughout slide.
Magnetite	1	Spinel	Dusty 0.2-mm elongate trails concentrated in veins throughout slide.

VESICLES/ CAVITIES	PERCENT	LOCATION	SIZE (mm)	FILLING	SHAPE
Vesicles	0				

COMMENTS: Relatively fresh (unaltered harzburgite). Olivines contain inclusions of primary minerals (olivine) and contain irregular veins of a more yellowish reflective phase. Orthopyroxene grains have wavy extinction and clinopyroxene exsolution lamellae are bent; spinels are elongate, ragged, and may be present in traces. Possible tectonic texture. Some of the fresh olivine is microgranular (0.05 mm).

125-779B-[illegible] (Piece [illegible], [illegible] cm)   OBSERVER: [illegible]   WHERE SAMPLED: Conical Seamount, southeast flank

ROCK NAME: Serpentinized harzburgite

GRAIN SIZE: [illegible] mm

TEXTURE: [illegible] and mesh

PRIMARY MINERALOGY	PERCENT PRESENT	PERCENT ORIGINAL	SIZE (mm)	COMPOSITION	MORPHOLOGY	COMMENTS
PHENOCRYSTS						
Olivine	[illegible]	[illegible]	[illegible]		Subhedral/anhedral	Kinked, wavy extinction, altering to serpentine mesh, also recrystallizing.
Clinopyroxene	Trace	Trace	[illegible]		Subhedral-anhedral	As exsolution lamellae and minor grains in orthopyroxene.
Spinel	[illegible]	[illegible]	[illegible]		Subhedral-anhedral	Red, altered to magnetite.
Orthopyroxene	[illegible]	[illegible]	[illegible]		Subhedral-anhedral	Kinked, wavy extinction, altering to serpentine bastite.
GROUNDMASS						
N/A	N/A	N/A	N/A		N/A	

SECONDARY MINERALOGY	PERCENT	REPLACING/FILLING	COMMENTS
Serpentine	[illegible]	Olivine, orthopyroxene	Lizardite and/or chrysotile occurring throughout slide and forming mesh and minor bastite textures; serpentine veins about [illegible] mm wide throughout [illegible].
Magnetite	[illegible]		Fine-grained, dusty, [illegible]-mm grains occurring mostly in serpentine veins.

VESICLES/CAVITIES	PERCENT	LOCATION	SIZE (mm)	FILLING	SHAPE
Vesicles	0				

COMMENTS: Olivine and orthopyroxene have kink bands, wavy extinction, deformation. Olivine appears more pervasively altered than orthopyroxene because of amount of fractures. Serpentine and magnetite [illegible]. Orthopyroxene doesn't appear to be recrystallizing to any great degree. Orthopyroxene has inclusions of anhedral clinopyroxene. Serpentine veins occur at no specific orientation with a wider zone of serpentinization following the major vein[illegible].

125-779B-[illegible] (Piece [illegible], [illegible] cm)   OBSERVER: [illegible]   WHERE SAMPLED: Conical Seamount, southeast flank

ROCK NAME: Dunite

GRAIN SIZE: [illegible]

TEXTURE: [illegible] and [illegible]

PRIMARY MINERALOGY	PERCENT PRESENT	PERCENT ORIGINAL	SIZE (mm)	COMPOSITION	MORPHOLOGY	COMMENTS
PHENOCRYSTS						
Olivine	[illegible]	99	[illegible]	[illegible]	Subhedral/anhedral	Kink-banded; wavy extinction, altered to serpentine blades and fibers, [illegible].
Spinel	1	1	[illegible]		Subhedral/anhedral	Dark red-brown, altered to magnetite.
GROUNDMASS						
N/A	N/A	N/A	N/A		N/A	

SECONDARY MINERALOGY	PERCENT	REPLACING/FILLING	COMMENTS
Serpentine	[illegible]	Olivine	Mostly antigorite blades and chrysotile fibers forming after olivine. Possible lizardite also.
Magnetite	1	Spinel	Dusty [illegible]-mm anhedral grains which occur in serpentine veins and along cleavages.
[illegible]	1	Olivine, serpentine	Might be disseminated within serpentinized area, but determination is very difficult.

VESICLES/CAVITIES	PERCENT	LOCATION	SIZE (mm)	FILLING	SHAPE
Vesicles	0				

COMMENTS: Serpentine tends to form along concave "shear" fractures. May indicate [illegible] mantle deformation? Rock appears to have deformed and recrystallized, then antigorite formed. This is apparent in the [illegible] which appear to be serpentinized. The antigorite blades don't form in a preferred orientation, but rather form a feather-like, felted texture across olivine.

[illegible] (Piece [illegible], 58-63 cm)   OBSERVER: SAB   WHERE SAMPLED: Conical Seamount, southeast flank

ROCK NAME: Altered serpentinized harzburgite

GRAIN SIZE: 0.01-1 mm

TEXTURE: Mesh and bastite

PRIMARY MINERALOGY	PERCENT PRESENT	PERCENT ORIGINAL	SIZE (mm)	COMPOSITION	MORPHOLOGY	COMMENTS
PHENOCRYSTS						
Olivine	Trace	88	0.01		Subhedral	Altered completely to serpentine mesh texture; located as 1 grain in spinel.
Spinel	1	1	0.5-1		Subhedral/anhedral	Dark brown-red; altered to magnetite.
Orthopyroxene	1	11	1-3		Subhedral-anhedral	Altered to serpentine bastite; bastite appears kinked with wavy extinction.
GROUNDMASS						
N/A	N/A	N/A	N/A		N/A	

SECONDARY MINERALOGY	PERCENT	REPLACING/FILLING	COMMENTS
Clays	25	Serpentine	Dusty, brownish-blue clay scattered throughout the slide.
Serpentine	[illegible]	Olivine, orthopyroxene	Chrysotile and/or lizardite completely replacing primary mineralogy, forming mesh and bastite textures. The serpentine that appears to be altered to clays. Also chrysotile veins <0.5 mm wide throughout slide.
Magnetite	1	Spinel	Dusty 0.2-mm grains throughout slide and along serpentine veins.
Brucite	1	Serpentine	Distributed throughout slide within later chrysotile veins.

VESICLES/CAVITIES	PERCENT	LOCATION	SIZE (mm)	FILLING	SHAPE
Vesicles	0				

COMMENTS: Spinels are subhedral-anhedral and form ragged trains across the slide. Antigorite may be present in later cutting veins (0.5 mm wide) and contains brucite(?) and magnetite.

[illegible] (Piece [illegible], 43-45 cm)   OBSERVER: SAB   WHERE SAMPLED: Conical Seamount, southeast flank

ROCK NAME: Serpentinized harzburgite

GRAIN SIZE: [illegible]-4 mm

TEXTURE: [illegible], mesh and bastite.

PRIMARY MINERALOGY	PERCENT PRESENT	PERCENT ORIGINAL	SIZE (mm)	COMPOSITION	MORPHOLOGY	COMMENTS
PHENOCRYSTS						
Olivine	[illegible]	[illegible]	[illegible]		Anhedral	Altered to serpentine mesh, fractured.
Spinel	<1	1	[illegible]	[illegible]	Subhedral-euhedral	Red-dark brown; altered to magnetite.
Orthopyroxene	[illegible]	[illegible]	[illegible]		Subhedral-anhedral	Altered to serpentine bastite and chlorite; wavy extinction, kink-banded.
GROUNDMASS						
N/A	N/A	N/A	N/A		N/A	

SECONDARY MINERALOGY	PERCENT	REPLACING/FILLING	COMMENTS
Chlorite	1	Orthopyroxene	Blue-green to green pleochroism. Found along orthopyroxene edges, cleavages and fractures.
Serpentine	[illegible]	Olivine, orthopyroxene	Lizardite and/or chrysotile forming mesh and bastite textures. Numerous chrysotile + magnetite veins (0.2 mm wide) cutting across slide.
Magnetite	1	Spinel	Dusty 0.2-mm grains forming elongate trains and located mostly in serpentine veins; some grains are euhedral.
Brucite	<1	Serpentine	Possibly located in center of chrysotile + magnetite veins.

VESICLES/CAVITIES	PERCENT	LOCATION	SIZE (mm)	FILLING	SHAPE
Vesicles	0				

COMMENTS: Relatively coarse-grained, orthopyroxene-rich harzburgite. Orthopyroxene is still relatively fresh and not as altered as olivine. Orthopyroxene has anhedral olivine inclusions and is somewhat elongated. One spinel grain has an olivine inclusion (euhedral). One orthopyroxene grain has an interesting set of inclusions: looks slightly like [illegible] veining within a crystal.

[illegible]

[illegible] (Piece 1B, [illegible]) OBSERVER: SAK WHERE SAMPLED: Conical Seamount, southeast flank

ROCK NAME: Peridotite

GRAIN SIZE: [illegible] mm

TEXTURE: [illegible]

PRIMARY MINERALOGY	PERCENT PRESENT	PERCENT ORIGINAL	SIZE (mm)	COMPOSITION	MORPHOLOGY	COMMENTS
PHENOCRYSTS:						
Olivine	[illegible]	[illegible]	[illegible]		Subhedral; anhedral	Wavy extinction, kink-banded, altering to serpentine; locally recrystallized(?).
Clinopyroxene	[illegible]	[illegible]	N/A		N/A	As exsolution lamellae, inclusions in orthopyroxene, rims orthopyroxene.
Spinel	[illegible]	[illegible]	[illegible]		Anhedral	Red-brown, altering to magnetite.
Orthopyroxene	[illegible]	[illegible]	[illegible]		N/A	Wavy extinction, elongated, clinopyroxene exsolution lamellae, altering to serpentine.
GROUNDMASS:						
N/A	N/A	N/A	N/A		N/A	

SECONDARY MINERALOGY	PERCENT	REPLACING/FILLING	COMMENTS
Serpentine	[illegible]	Olivine, orthopyroxene	Chrysotile and/or lizardite altering olivine and orthopyroxene to mesh and bastite texture, but still too fresh to fully develop these textures.
Magnetite		Spinel	Dusty 0.1-mm grains concentrated in serpentine areas and veins.

VESICLES/CAVITIES	PERCENT	LOCATION	SIZE (mm)	FILLING	SHAPE
[illegible]	[illegible]				

COMMENTS: Relatively fresh serpentinized harzburgite. Some spinels have small euhedral inclusions of olivine; spinels form ragged trails; sometimes olivine and orthopyroxene appear [illegible] and deformed (wavy extinction, elongated, kinks). Olivine is locally recrystallized into microporphyroblasts; orthopyroxene appears to be recrystallized. Orthopyroxene has inclusions of clinopyroxene; clinopyroxene occurs as rims around orthopyroxene.

[illegible] (Piece [illegible]) OBSERVER: SAK WHERE SAMPLED: Conical Seamount, southeast flank

ROCK NAME: Altered serpentinized harzburgite

GRAIN SIZE: [illegible] mm

TEXTURE: Minor mesh and bastite [illegible]

PRIMARY MINERALOGY	PERCENT PRESENT	PERCENT ORIGINAL	SIZE (mm)	COMPOSITION	MORPHOLOGY	COMMENTS
PHENOCRYSTS:						
Olivine	[illegible]	[illegible]	[illegible]		Anhedral	Altering to serpentine mesh, wavy extinction.
Clinopyroxene	Trace	Trace	[illegible]		Subhedral; anhedral	As exsolution lamellae in orthopyroxene.
Spinel	[illegible]	[illegible]	[illegible]		Subhedral; anhedral	Dark brown, altered to magnetite.
Orthopyroxene	[illegible]	[illegible]	[illegible]		Subhedral; anhedral	Altered to serpentine bastite; wavy extinction; bent clinopyroxene lamellae.
GROUNDMASS:						
N/A	N/A	N/A	N/A		N/A	

SECONDARY MINERALOGY	PERCENT	REPLACING/FILLING	COMMENTS
Clays	[illegible]	Serpentine	Dusty brown clay distributed mainly along serpentine veins.
Serpentine		Olivine, orthopyroxene	Chrysotile and/or lizardite forming multiple veins which run in various orientations through slide.
Magnetite	[illegible]	Spinel	Dusty 0.1-mm grains concentrated in vein zone.
Brucite	Trace	Serpentine	May be intermixed with serpentine and magnetite in veins.

VESICLES/CAVITIES	PERCENT	LOCATION	SIZE (mm)	FILLING	SHAPE
Veinlets	[illegible]				

COMMENTS: Slide consists mostly of [illegible]-mm-wide zone of veins (serpentine, magnetite, brucite(?)) which run 45 degrees from long axis of slide. This slide has numerous crosscutting relationships. Has a moderate "Frankenstein" texture. Orthopyroxene and olivine have wavy extinctions; orthopyroxene has bent exsolution lamellae. Spinel grains are arranged in trails perpendicular to main vein zone.

[illegible] WHERE SAMPLED: Conical Seamount, southeast flank

ROCK NAME: Serpentinized harzburgite

GRAIN SIZE: [illegible] mm

TEXTURE: [illegible]

PRIMARY MINERALOGY	PERCENT PRESENT	PERCENT ORIGINAL	SIZE (mm)	COMPOSITION	MORPHOLOGY	COMMENTS
PHENOCRYSTS						
Olivine	[illegible]	[illegible]	[illegible]		[illegible]	[illegible]
Clinopyroxene	1	1	[illegible]		[illegible]	[illegible]
Spinel	[illegible]	[illegible]	[illegible]		[illegible]	[illegible]
Orthopyroxene	[illegible]	[illegible]	[illegible]		[illegible]	[illegible]
GROUNDMASS						
N/A	N/A	N/A	N/A		N/A	

SECONDARY MINERALOGY	PERCENT	REPLACING/FILLING	COMMENTS
Serpentine	[illegible]	Olivine, orthopyroxene	[illegible]
Magnetite	1	Spinel	[illegible]

VESICLES/CAVITIES	NUMBER	LOCATION	SIZE (mm)	FILLING	SHAPE
Vesicles	0				

COMMENTS: [illegible]

[illegible] WHERE SAMPLED: Conical Seamount, southeast flank

ROCK NAME: Altered serpentinized [illegible]

GRAIN SIZE: [illegible] mm

TEXTURE: [illegible]

PRIMARY MINERALOGY	PERCENT PRESENT	PERCENT ORIGINAL	SIZE (mm)	COMPOSITION	MORPHOLOGY	COMMENTS
PHENOCRYSTS						
Olivine	0	[illegible]	[illegible]		[illegible]	[illegible]
Spinel	Trace	Trace	[illegible]		[illegible]	[illegible]
GROUNDMASS						
N/A	N/A	N/A	N/A		N/A	

SECONDARY MINERALOGY	PERCENT	REPLACING/FILLING	COMMENTS
Clays	[illegible]	Serpentine	[illegible]
Serpentine	[illegible]	Olivine	[illegible]
Magnetite	[illegible]	Spinel	[illegible]
[illegible]	[illegible]	Serpentine; [illegible] mm	[illegible]

VESICLES/CAVITIES	NUMBER	LOCATION	SIZE (mm)	FILLING	SHAPE
Vesicles	0				

COMMENTS: [illegible]

125-779A-28R-2 (Piece 2A,24-28 cm)   OBSERVER: SAR   WHERE SAMPLED: Conical Seamount, southeast flank

ROCK NAME: Serpentinized harzburgite

GRAIN SIZE: 0.05-6 mm

TEXTURE: Mesh and bastite

PRIMARY MINERALOGY	PERCENT PRESENT	PERCENT ORIGINAL	SIZE (mm)	COMPO-SITION	MORPHOLOGY	COMMENTS
PHENOCRYSTS						
Olivine	Tr.-0	83.5	0.1		Anhedral	Completely altered to serpentine mesh; two anhedral grains present as inclusions in euhedral spinels.
Spinel	1	1.5	0.05-1	Cr	Euhedral-anhedral	Rims altered to magnetite.
Orthopyroxene	0	15	1-6		Subhedral-anhedral	Completely altered to serpentine bastite.
GROUNDMASS						
N/A	N/A	N/A	N/A		N/A	

SECONDARY MINERALOGY	PERCENT	REPLACING/ FILLING	COMMENTS
Clays	5	Serpentine	Rusty brown clay distributed across slide; also clay with blue-green to yellow pleochroism which is in orthopyroxene bastite grains (may be chlorite?).
Serpentine	95	Olivine, orthopyroxene	Lizardite and/or chrysotile forming mesh and bastite textures; antigorite is present in feather-like blades, but in very minor amounts (<1%).
Magnetite	<1		Dusty grains concentrated in veins and mesh edges.

VESICLES/ CAVITIES	PERCENT	LOCATION	SIZE (mm)	FILLING	SHAPE
Vesicles	0				

COMMENTS: Completely serpentinized harzburgite; spinels are nicely euhedral. One grain has two inclusions of olivine. Orthopyroxene bastites show evidence of primary mineral inclusions which have since been altered to serpentine mesh. Spinels are ringed with other phases forming within the cracks.

[illegible] (Piece [illegible],112-115 cm)   OBSERVER: RCH   WHERE SAMPLED: Conical Seamount, southeast flank

ROCK NAME: Metabasalt

GRAIN SIZE: 0.05-0.25

TEXTURE: Microphyric with glassy margin

PRIMARY MINERALOGY	PERCENT PRESENT	PERCENT ORIGINAL	SIZE (mm)	COMPO-SITION	MORPHOLOGY	COMMENTS
PHENOCRYSTS						
Clinopyroxene	10-15	15-20	0.05-0.25		Subhedral	Some radiating bunches may be quench features. 10-20% alteration to chlorite.
GROUNDMASS						
Glass	0	50-60	N/A		N/A	100% altered to brown amorphous clays.
Plagioclase	0	15-20	0.01-0.2		Lath	Quench textured needles occasionally associated with clinopyroxene. 100% altered to clays.
Opaques	<1	<1	0.01-0.05		Subhedral	Black, disseminated.

SECONDARY MINERALOGY	PERCENT	REPLACING/ FILLING	COMMENTS
Clays		Glass, plagioclase	Brown clay usually as pseudomorphs after plagioclase.
Chlorite	25-30	Glass, clinopyroxene veins	Light-green and weakly birefringent in matrix and after clinopyroxene. Veins: colorless in plane light, but blue-gray in crossed nicols (0.01-1.5 mm).

VESICLES/ CAVITIES	PERCENT	LOCATION	SIZE (mm)	FILLING	SHAPE
Vesicles	0				

COMMENTS: One half of this section is a glassy chilled margin with <5% glass and a few quenched crystals of plagioclase. The other half is microcrystalline. Entire sample is heavily veined with chlorite veins and pervasively altered to clays.

SITE 779

[illegible] OBSERVER: [illegible] WHERE SAMPLED: [illegible]

ROCK NAME: Metabasalt

GRAIN SIZE: [illegible] mm

TEXTURE: Aphyric

PRIMARY MINERALOGY	PERCENT PRESENT	PERCENT ORIGINAL	SIZE (mm)	COMPO-SITION	MORPHOLOGY	COMMENTS
Glass	[illegible]	[illegible]	[illegible]		[illegible]	[illegible] altered to brown clays.
Plagioclase	[illegible]	[illegible]	[illegible]		[illegible]	[illegible]
Clinopyroxene	[illegible]	[illegible]	[illegible]		Anhedral	[illegible]
[illegible]	[illegible]	[illegible]	[illegible]		[illegible]	[illegible]

SECONDARY MINERALOGY	PERCENT	REPLACING/ FILLING	COMMENTS
Clays	[illegible]	[illegible]	[illegible]
[illegible]	[illegible]	[illegible]	[illegible]
[illegible]	[illegible]	[illegible]	[illegible]

VESICLES/ CAVITIES	PERCENT	LOCATION	SIZE (mm)	FILLING	SHAPE	COMMENTS
[illegible]	[illegible]	[illegible]	[illegible]	[illegible]	[illegible]	[illegible]

COMMENTS: [illegible]

[illegible] OBSERVER: [illegible] WHERE SAMPLED: [illegible]

ROCK NAME: [illegible]

GRAIN SIZE: [illegible]

TEXTURE: [illegible]

PRIMARY MINERALOGY	PERCENT PRESENT	PERCENT ORIGINAL	SIZE (mm)	COMPO-SITION	MORPHOLOGY	COMMENTS
[illegible]	[illegible]	[illegible]	[illegible]		[illegible]	[illegible]
[illegible]	[illegible]	[illegible]	[illegible]		[illegible]	[illegible]
[illegible]	[illegible]	[illegible]	[illegible]		[illegible]	[illegible]
[illegible]	[illegible]	[illegible]	[illegible]		[illegible]	[illegible]

SECONDARY MINERALOGY	PERCENT	REPLACING/ FILLING	COMMENTS
[illegible]	[illegible]	[illegible]	[illegible]
[illegible]	[illegible]	[illegible]	[illegible]

VESICLES/ CAVITIES	PERCENT	LOCATION	SIZE (mm)	FILLING	SHAPE
[illegible]	[illegible]	[illegible]	[illegible]	[illegible]	[illegible]

COMMENTS: [illegible]

125-779A-31R-02 (Piece 11,103-105 cm) OBSERVER: NIR WHERE SAMPLED: Conical Seamount, southeast flank

ROCK NAME: Metabasalt

GRAIN SIZE: 0.2-1 mm, medium grained

TEXTURE: Intersertal, microphyric

PRIMARY MINERALOGY	PERCENT PRESENT	PERCENT ORIGINAL	SIZE (mm)	COMPO-SITION	MORPHOLOGY	COMMENTS
PHENOCRYSTS						
Plagioclase	0	10-30	0.3-0.8		Laths	100% pseudomorphed by clays; hydrogrossular
Clinopyroxene	20-25	25-35	0.02-1		Anhedral	20-30% altered to chlorite and clays.
Spinel	<<1	<<1	0.03-0.1		Subhedral	Black, opaque, sparse.
GROUNDMASS						
Glass/matrix	0	40-55	N/A		N/A	100% altered to brown and deep green amorphous clays and hydrogrossular.

SECONDARY MINERALOGY	PERCENT	REPLACING/ FILLING	COMMENTS
Clays	50-60	Glass, matrix, cavities	Brown clays. Pervasive after glass and plagioclase.
Chlorite	15-20	Clinopyroxene, glass, cavities	Pale- to deep-green in plane light, slightly pleochroic.
Hydrogrossular	<10	Glass, plagioclase	Anhedral, fine-grained.
Opaque	1-2	Matrix	Unevenly dispersed, concentrated in chlorite patches, 0.01-0.02 mm, black.

VESICLES/ CAVITIES	PERCENT	LOCATION	SIZE (mm)	FILLING	SHAPE
Cavities	2	Throughout	1-2	Chlorite, clay	Irregular

COMMENT: Occasionally spherulitic intergrowths of plagioclase after clinopyroxene. Sample is extensively and pervasively altered.

125-779A-[illegible]R-02 (Piece 13,119-121 cm) OBSERVER: [illegible] WHERE SAMPLED: Conical Seamount, southeast flank

ROCK NAME: Metabasalt

GRAIN SIZE: 0.5-0.8 mm

TEXTURE: Phyric, intersertal

PRIMARY MINERALOGY	PERCENT PRESENT	PERCENT ORIGINAL	SIZE (mm)	COMPO-SITION	MORPHOLOGY	COMMENTS
PHENOCRYSTS						
Plagioclase	0	5-25	0.02-0.08		Laths, subhedral	100% altered to clays + hydrogrossular.
Clinopyroxene	15-20	20-40	0.03-0.08		Subhedral	20-40 % altered, occasionally associated with plagioclase.
Spinel	<<1	<<1	0.03-0.05		Anhedral	Black, sparse.
GROUNDMASS						
Glass	0	40-55	N/A		N/A	100% altered to clays and hydrogrossular?

SECONDARY MINERALOGY	PERCENT	REPLACING/ FILLING	COMMENTS
Clays	30-35	Glass, veins, plagioclase	Brown amorphous clays pervasive in sample after glass and plagioclase.
Chlorite	15-20	Patches, veins	Clinopyroxene pervasive in matrix; pale-green, slightly pleochroic, usually amorphous, although a few veins show fibrous texture.
Hydrogrossular	8-10	?	Anhedral, fine-grained.

VESICLES/ CAVITIES	PERCENT	LOCATION	SIZE (mm)	FILLING	SHAPE
Cavities	1-2	Throughout	0.1-0.5	Chlorite clay	Mostly round

COMMENTS: Extensive and pervasive alteration. Original texture and mineral relationships have been obscured.

125-779A-31R-CC (Piece 5,39-41 cm) OBSERVER: HIA WHERE SAMPLED: Conical Seamount, southeast flank

ROCK NAME: Metadiabase

GRAIN SIZE: 0.2-2 mm medium-coarse grained

TEXTURE: Ophitic

PRIMARY MINERALOGY	PERCENT PRESENT	PERCENT ORIGINAL	SIZE (mm)	COMPO-SITION	MORPHOLOGY	COMMENTS
PHENOCRYSTS						
Plagioclase	0	20-40	0.24-0.36		Lath, euhedral	100% altered to clays and hydrogrossular.
Clinopyroxene	5-15	20-40	0.8-2.2		Subhedral	60-85% altered to clays, chlorite.
GROUNDMASS						
Glass matrix	0	15-35	N/A		N/A	100% replaced by amorphous brown clays.

SECONDARY MINERALOGY	PERCENT	REPLACING/ FILLING	COMMENTS
Clays	45-55	Glass, plagioclase	Pervasive after glass (matrix) and plagioclase. Few (5%) pseudomorphs after plagioclase.
Chlorite	15-25	Matrix, plagioclase, clinopyroxene	Around clinopyroxene and plagioclase crystals and as patches within matrix.
Hydrogrossular	15-25	Matrix, plagioclase(?)	0.2-0.4 mm, subhedral, dark red, brown, semiopaque.

VESICLES/ CAVITIES	PERCENT	LOCATION	SIZE (mm)	FILLING	SHAPE
Vesicles	0				

COMMENTS: Sample is extensively and pervasively altered to clays, chlorite and hydrogrossular. Alteration masks primary mineral abundance and relationships.

125-779A-[illegible]R-CC (Piece 6,47-[illegible] cm) OBSERVER: HIA WHERE SAMPLED: Conical Seamount, southeast flank

ROCK NAME: Altered pyroclastic rocks, may be tuffaceous

GRAIN SIZE: <0.1 mm

TEXTURE: Clastic, layered

PRIMARY MINERALOGY	PERCENT PRESENT	PERCENT ORIGINAL	SIZE (mm)	COMPO-SITION	MORPHOLOGY	COMMENTS
Clinopyroxene	45-55	25	<0.1		Anhedral	Occurs as feather-like crysts. throughout the rock.
Plagioclase	[illegible]	25	<0.1		Subhedral	Occurs as feather-like crysts. throughout the rock.
Glass	0	40	N/A		N/A	

SECONDARY MINERALOGY	PERCENT	REPLACING/ FILLING	COMMENTS
Clays	45-55	Matrix	Dusty brownish clay.
Chlorite	[illegible]	[illegible]	

VESICLES/ CAVITIES	PERCENT	LOCATION	SIZE (mm)	FILLING	SHAPE
Vesicles	0				

COMMENTS: Hydrogrossular determined by XRD cannot be observed.

125-779A-31R-CC (Piece 6,47-59 cm)   OBSERVER: HIR   WHERE SAMPLED: Conical Seamount, southeast flank

ROCK NAME: Altered basalt

GRAIN SIZE: 0.5-1 mm

TEXTURE: Ophitic

PRIMARY MINERALOGY	PERCENT PRESENT	PERCENT ORIGINAL	SIZE (mm)	COMPOSITION	MORPHOLOGY	COMMENTS
Clinopyroxene	35	35	1		Subhedral	
Plagioclase	0	65	0.5-1		Subhedral	Altered to hydrogrossular and clay.

SECONDARY MINERALOGY	PERCENT	REPLACING/ FILLING	COMMENTS
Clays	10		Brownish dusty clay.
Chlorite	5		Pale-green, anomalous interference color.
Hydrogrossular	50		Birefringence ~0, high reflective index.

VESICLES/ CAVITIES	PERCENT	LOCATION	SIZE (mm)	FILLING	SHAPE
Vesicles	0				

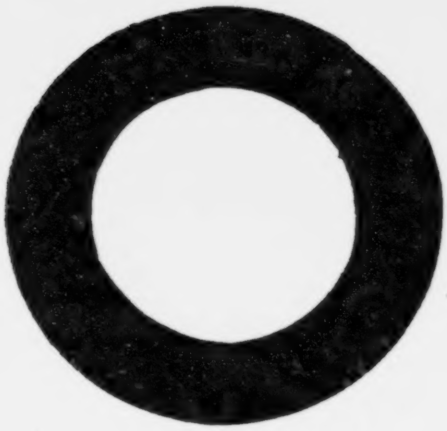

SITE 780 HOLE A CORE 1H CORED INTERVAL 3088.8-3090.3 mbsl; 0.0-1.5 mbsf

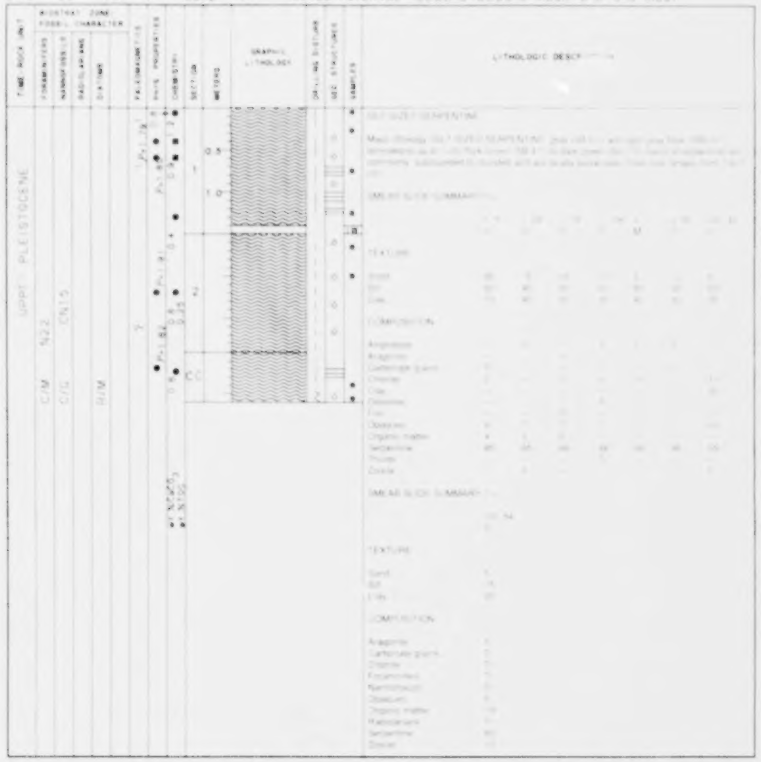
TIME-ROCK UNIT
BIOSTRAT. ZONE/ FOSSIL CHARACTER
FORAMINIFERS
NANNOFOSSILS
RADIOLARIANS
DIATOMS
PALEOMAGNETICS
PHYS. PROPERTIES
CHEMISTRY
SECTION
METERS
GRAPHIC LITHOLOGY
DRILLING DISTURB.
SED. STRUCTURES
SAMPLES
UPPER PLEISTOCENE
C/M N22
C/G CN15
R/M
?
0.5
1.0
1
2
CC

LITHOLOGIC DESCRIPTION

SILT-SIZED SERPENTINE

Major lithology: SILT-SIZED SERPENTINE, [illegible]

SMEAR SLIDE SUMMARY (%):

TEXTURE:

Sand
Silt
Clay

COMPOSITION:

Amphibole
Aragonite
Carbonate grains
Chlorite
Clay
Dolomite
Fish
Opaques
Organic matter
Serpentine
Pyrite
Zeolite

SMEAR SLIDE SUMMARY (%):

TEXTURE:

Sand
Silt
Clay

COMPOSITION:

Aragonite
Carbonate grains
Chlorite
Foraminifers
Nannofossils
Opaques
Organic matter
Radiolarians
Serpentine
Zeolite

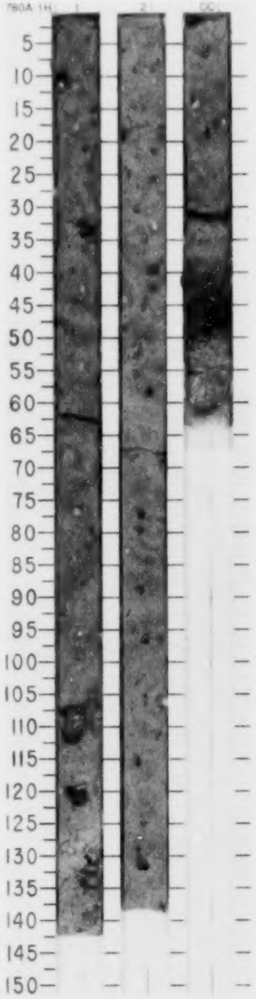
780A-1H
1
2
CC
5
10
15
20
25
30
35
40
45
50
55
60
65
70
75
80
85
90
95
100
105
110
115
120
125
130
135
140
145
150

SITE 780 HOLE B CORE 1R CORED INTERVAL 3094.0-3102.7 mbsl; 0.0-8.7 mbsf

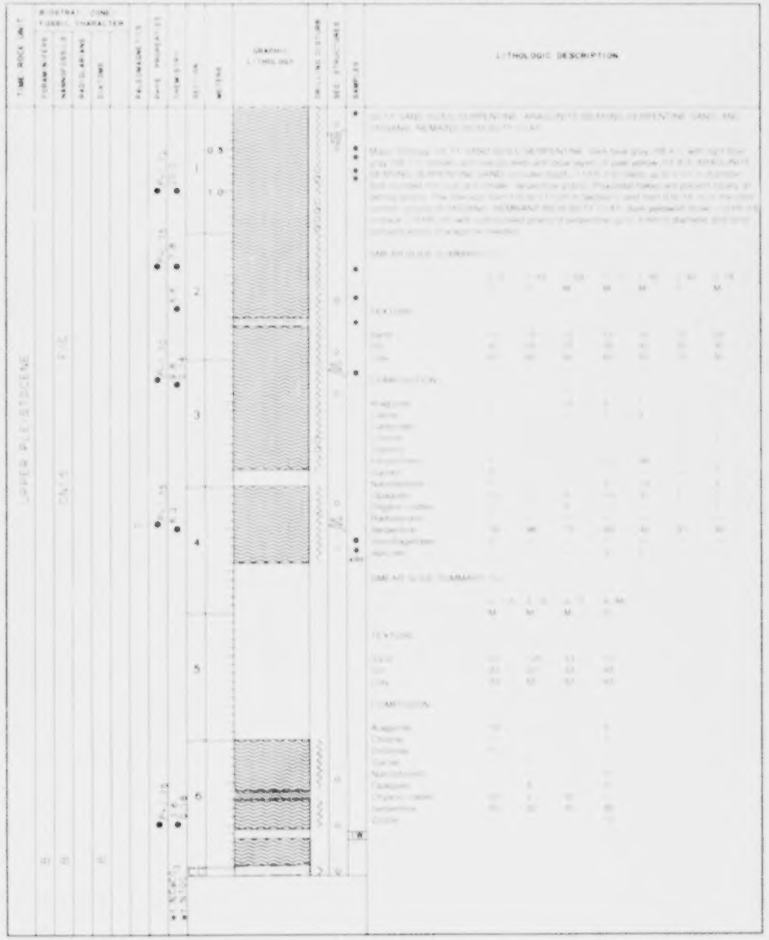
TIME-ROCK UNIT
BIOSTRAT. ZONE/ FOSSIL CHARACTER
FORAMINIFERS
NANNOFOSSILS
RADIOLARIANS
DIATOMS
PALEOMAGNETICS
PHYS. PROPERTIES
CHEMISTRY
SECTION
METERS
GRAPHIC LITHOLOGY
DRILLING DISTURB.
SED. STRUCTURES
SAMPLES
LITHOLOGIC DESCRIPTION
UPPER PLEISTOCENE
1
2
3
4
5
6
0.5
1.0

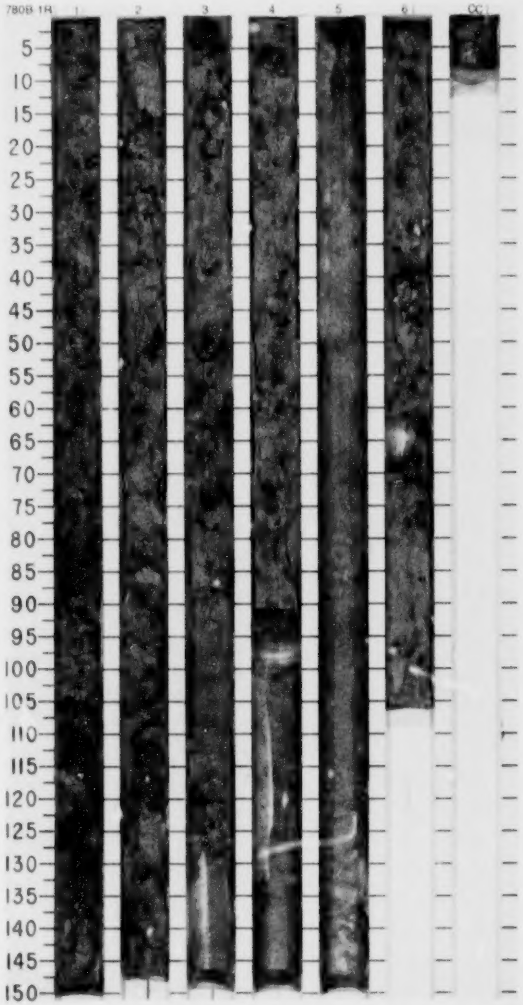
780B-1R
1
2
3
4
5
6
CC
5
10
15
20
25
30
35
40
45
50
55
60
65
70
75
80
85
90
95
100
105
110
115
120
125
130
135
140
145
150

SITE 780 HOLE B CORE 2R CORED INTERVAL 3102.7-3112.2 mbsl; 8.7-18.2 mbsf

TIME-ROCK UNIT	BIOSTRAT. ZONE/ FOSSIL CHARACTER: FORAMINIFERS	NANNOFOSSILS	RADIOLARIANS	DIATOMS	PALEOMAGNETICS	PHYS. PROPERTIES	CHEMISTRY	SECTION	METERS	GRAPHIC LITHOLOGY	DRILLING DISTURB.	SED. STRUCTURES	SAMPLES	LITHOLOGIC DESCRIPTION
	B	B		B	?			1 CC	0.5 1.0				● ●	SILT-SIZED SERPENTINE Major lithology: SILT-SIZED SERPENTINE, medium bluish gray (5B 5/1), [illegible] stratigraphic integrity. One black clast (serpentinized ultramafic?) occurs in the upper portion of the core and fibrous debris (bacterial mats?) are scattered through the middle and lower sections, especially 40 to 67 cm, 92 to 106 cm, and 115 to 150 cm. Sand to granule-sized black clasts (serpentine?) are scattered throughout the core.

SMEAR SLIDE SUMMARY (%):

	1, 30	1, 125
	M	D
TEXTURE:		
Sand	[illegible]	[illegible]
Silt	[illegible]	40
Clay	[illegible]	[illegible]
COMPOSITION:		
Carbonate grains	[illegible]	[illegible]
Epidote	[illegible]	[illegible]
Opaques	[illegible]	[illegible]
Serpentine	[illegible]	[illegible]
Zircon	[illegible]	[illegible]

780B-2R
1
CC
5
10
15
20
25
30
35
40
45
50
55
60
65
70
75
80
85
90
95
100
105
110
115
120
125
130
135
140
145
150

SITE 780 HOLE C CORE 1R CORED INTERVAL 3087.4-3088.9 mbsl; 0.0-5.5 mbsf

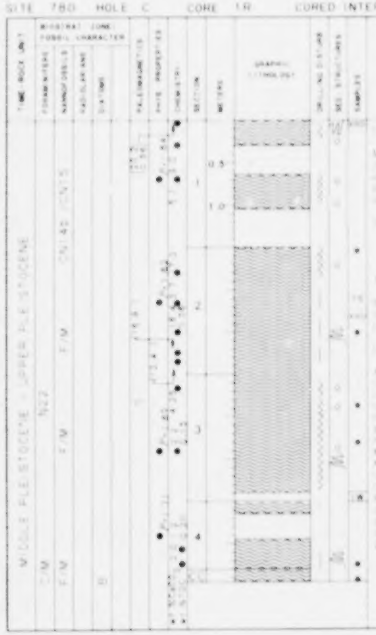

LITHOLOGIC DESCRIPTION

CLAYEY SILT SIZED SERPENTINE

Major lithology: CLAYEY SILT SIZED SERPENTINE, [illegible]

SMEAR SLIDE SUMMARY (%):

TEXTURE:

Sand
Silt
Clay

COMPOSITION:

Aragonite
Carbonate
Chlorite
Clay
Dolomite
Epidote
Foraminifers
Mica
Nannofossils
Opaques
Organic matter
Radiolarians
Serpentine
Silicoflagellates
Sponges
Zircon

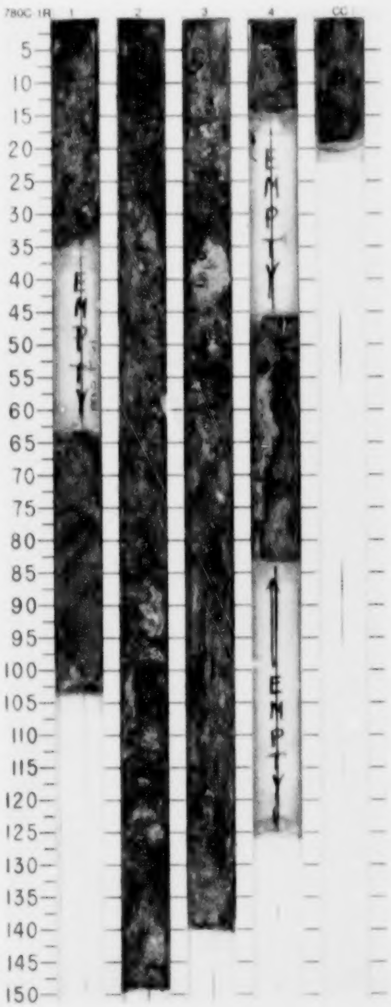
780C-1R
1
2
3
4
CC
EMPTY
EMPTY
EMPTY
5
10
15
20
25
30
35
40
45
50
55
60
65
70
75
80
85
90
95
100
105
110
115
120
125
130
135
140
145
150

SITE 780 HOLE C CORE 2R CORED INTERVAL 3088.9-3097.4 mbsl; 5.5-14.0 mbsf

TIME-ROCK UNIT	FORAMINIFERS	NANNOFOSSILS	RADIOLARIANS	DIATOMS	PALEOMAGNETICS	PHYS. PROPERTIES	CHEMISTRY	SECTION	METERS	GRAPHIC LITHOLOGY	DRILLING DISTURB.	SED. STRUCTURES	SAMPLES
MIDDLE PLEISTOCENE (UPPER PLEISTOCENE)	B	CN14b/CN15 F/M		R/M	?	●	●	1 CC				O	● ● ●

SILTY SAND-SIZED SERPENTINE

Major lithology: SILTY SAND-SIZED SERPENTINE, dark blue gray [illegible]

SMEAR SLIDE SUMMARY (%):

TEXTURE:

Sand

Silt

Clay

COMPOSITION:

Aragonite

Carbonate unspec.

Chlorite

Diatoms

Epidote

Foraminifers

Opaques

Organic matter

Serpentine

SITE 780 HOLE C CORE 3R CORED INTERVAL 3097.4-3106.9 mbsl; 14.0-23.5 mbsf

TIME-ROCK UNIT	FORAMINIFERS	NANNOFOSSILS	RADIOLARIANS	DIATOMS	PALEOMAGNETICS	PHYS. PROPERTIES	CHEMISTRY	SECTION	METERS	GRAPHIC LITHOLOGY	DRILLING DISTURB.	SED. STRUCTURES	SAMPLES	LITHOLOGIC DESCRIPTION
					?	●		1	0.5	M				No sedimentary material was recovered in this core.

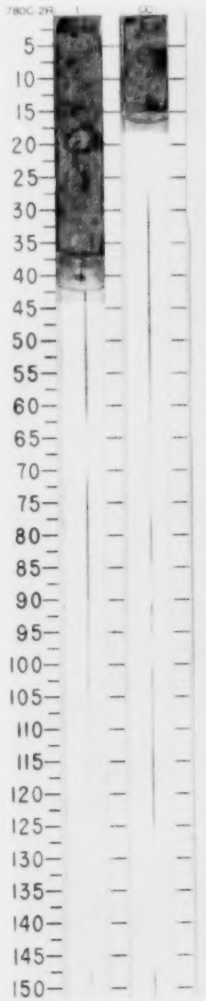

SITE 780 HOLE C CORE 4R CORED INTERVAL 3106.9-3116.4 mbsl; 23.5-33.0 mbsf

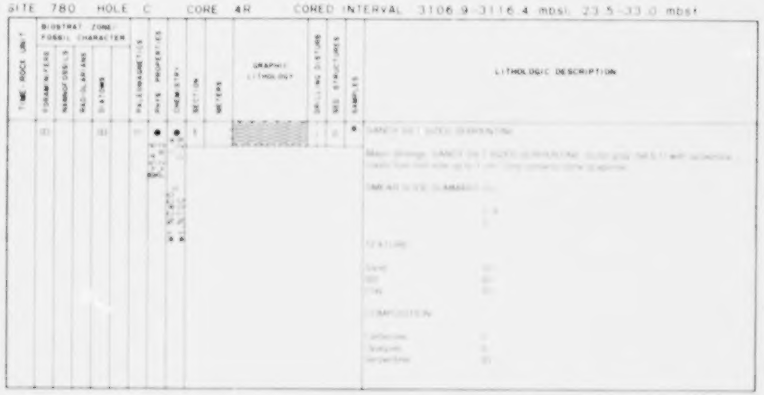
TIME-ROCK UNIT
BIOSTRAT. ZONE/ FOSSIL CHARACTER
FORAMINIFERS
NANNOFOSSILS
RADIOLARIANS
DIATOMS
PALEOMAGNETICS
PHYS. PROPERTIES
CHEMISTRY
SECTION
METERS
GRAPHIC LITHOLOGY
DRILLING DISTURB.
SED. STRUCTURES
SAMPLES
LITHOLOGIC DESCRIPTION
1
SANDY SILT-SIZED SERPENTINE
Major lithology: SANDY SILT-SIZED SERPENTINE
SMEAR SLIDE SUMMARY (%):
TEXTURE:
Sand
Silt
Clay
COMPOSITION:
Serpentine

SITE 780 HOLE C CORE 5R CORED INTERVAL 3116.4-3125.9 mbsl; 33.0-42.5 mbsf

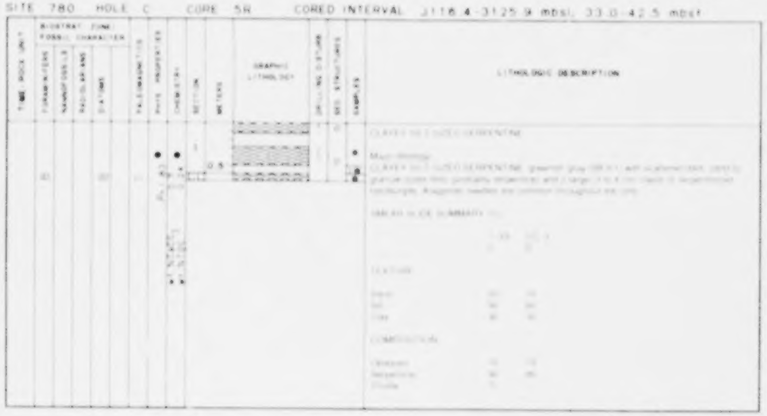
TIME-ROCK UNIT
BIOSTRAT. ZONE/ FOSSIL CHARACTER
FORAMINIFERS
NANNOFOSSILS
RADIOLARIANS
DIATOMS
PALEOMAGNETICS
PHYS. PROPERTIES
CHEMISTRY
SECTION
METERS
GRAPHIC LITHOLOGY
DRILLING DISTURB.
SED. STRUCTURES
SAMPLES
LITHOLOGIC DESCRIPTION
1
0.5
CLAYEY SILT-SIZED SERPENTINE
Major lithology:
CLAYEY SILT-SIZED SERPENTINE
SMEAR SLIDE SUMMARY (%):
TEXTURE:
Sand
Silt
Clay
COMPOSITION:
Opaques
Serpentine

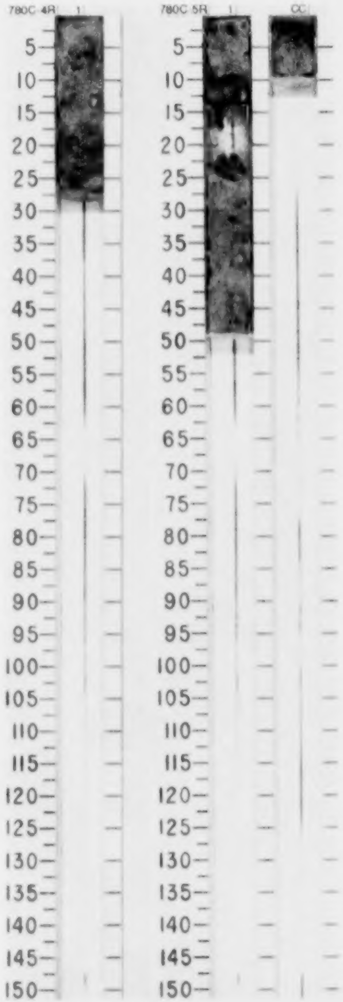
780C-4R 1
780C-5R 1
CC
5
10
15
20
25
30
35
40
45
50
55
60
65
70
75
80
85
90
95
100
105
110
115
120
125
130
135
140
145
150

SITE 780 HOLE C CORE 6R CORED INTERVAL 3125.9-3135.5 mbsl; 42.5-52.1 mbsf

TIME-ROCK UNIT	BIOSTRAT. ZONE/ FOSSIL CHARACTER: FORAMINIFERS	NANNOFOSSILS	RADIOLARIANS	DIATOMS	PALEOMAGNETICS	PHYS. PROPERTIES	CHEMISTRY	SECTION	METERS	GRAPHIC LITHOLOGY	DRILLING DISTURB.	SED. STRUCTURES	SAMPLES
					?		●	1	0.5	M			●

LITHOLOGIC DESCRIPTION

CLAYEY SILT-SIZED SERPENTINE

Major lithology: CLAYEY SILT-SIZE SERPENTINE, greenish gray ([illegible]), with several 1-2 cm clasts of serpentinized ultramafic rocks.

SMEAR SLIDE SUMMARY (%):

TEXTURE:

Sand [illegible]
Silt [illegible]
Clay [illegible]

COMPOSITION:

Opaques [illegible]
Serpentine [illegible]

SITE 780 HOLE C CORE 7R CORED INTERVAL 3135.5-3144.9 mbsl; 52.1-61.5 mbsf

TIME-ROCK UNIT	BIOSTRAT. ZONE/ FOSSIL CHARACTER: FORAMINIFERS	NANNOFOSSILS	RADIOLARIANS	DIATOMS	PALEOMAGNETICS	PHYS. PROPERTIES	CHEMISTRY	SECTION	METERS	GRAPHIC LITHOLOGY	DRILLING DISTURB.	SED. STRUCTURES	SAMPLES
					?	●	●	1					●

LITHOLOGIC DESCRIPTION

CLAYEY SILT-SIZED SERPENTINE

Major lithology: CLAYEY SILT-SIZED SERPENTINE, greenish gray ([illegible]) with approximately [illegible] angular, small pebble-sized serpentine(?) clasts and sand- to granule-sized clasts. Lithics vary from light greenish gray ([illegible]) to dark greenish gray ([illegible]). The basal portion of the core exhibits faint planar laminations (primary?) and the entire core coarsens upward; the size of the lithics progresses from coarse sand size at the base to pebble size at the top.

SMEAR SLIDE SUMMARY (%):

1, 13
D

TEXTURE:

Sand [illegible]
Silt [illegible]
Clay [illegible]

COMPOSITION:

Opaques [illegible]
Serpentine [illegible]

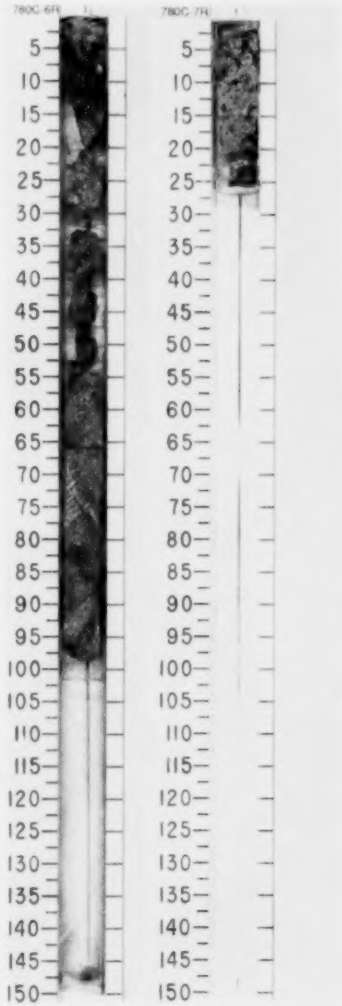

SITE 780 HOLE C CORE 8R CORED INTERVAL 3144.9-3154.5 mbsl; 61.5-71.1 mbsf

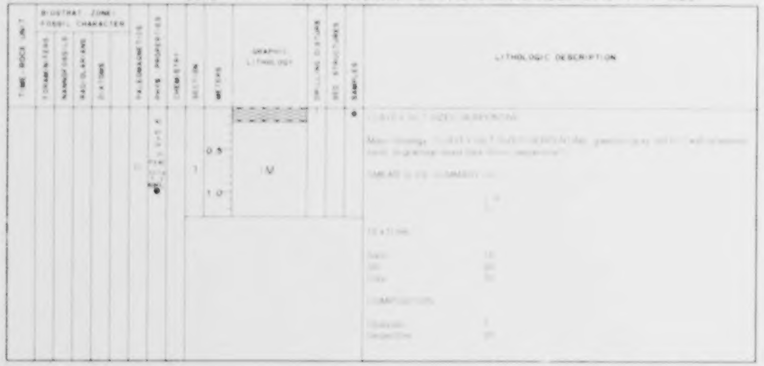

TIME-ROCK UNIT	FORAMINIFERS	NANNOFOSSILS	RADIOLARIANS	DIATOMS	PALEOMAGNETICS	PHYS. PROPERTIES	CHEMISTRY	SECTION	METERS	GRAPHIC LITHOLOGY	DRILLING DISTURB.	SED. STRUCTURES	SAMPLES	LITHOLOGIC DESCRIPTION
						[illegible]		1	0.5 1.0	IV			●	CLAYEY SILT-SIZED SERPENTINE Major lithology: CLAYEY SILT-SIZED SERPENTINE, [illegible] SMEAR SLIDE SUMMARY (%): TEXTURE: Sand [illegible] Silt [illegible] Clay [illegible] COMPOSITION: [illegible] Serpentine [illegible]

SITE 780 HOLE C CORE 9R CORED INTERVAL 3154.5-3164.2 mbsl; 71.1-80.8 mbsf

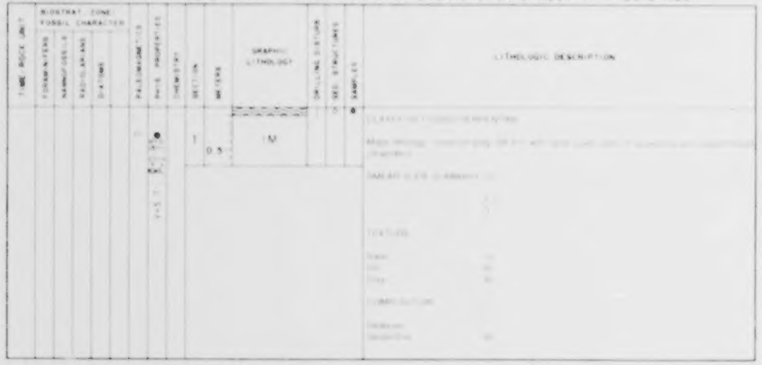

TIME-ROCK UNIT	FORAMINIFERS	NANNOFOSSILS	RADIOLARIANS	DIATOMS	PALEOMAGNETICS	PHYS. PROPERTIES	CHEMISTRY	SECTION	METERS	GRAPHIC LITHOLOGY	DRILLING DISTURB.	SED. STRUCTURES	SAMPLES	LITHOLOGIC DESCRIPTION
						[illegible]		1	0.5	IV			●	CLAYEY SILT-SIZED SERPENTINE Major lithology: [illegible] SMEAR SLIDE SUMMARY (%): TEXTURE: Sand [illegible] Silt [illegible] Clay [illegible] COMPOSITION: [illegible] Serpentine [illegible]

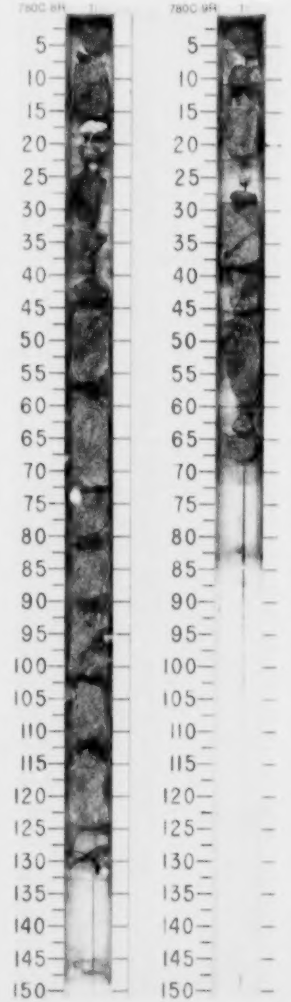
780C 8R
1
780C 9R
1
5
10
15
20
25
30
35
40
45
50
55
60
65
70
75
80
85
90
95
100
105
110
115
120
125
130
135
140
145
150

SITE 780 HOLE C CORE 10R CORED INTERVAL 3164.2-3173.9 mbsl; 80.8-90.5 mbsf

TIME-ROCK UNIT	BIOSTRAT. ZONE/ FOSSIL CHARACTER: FORAMINIFERS	NANNOFOSSILS	RADIOLARIANS	DIATOMS	PALEOMAGNETICS	PHYS. PROPERTIES	CHEMISTRY	SECTION	METERS	GRAPHIC LITHOLOGY	DRILLING DISTURB.	SED. STRUCTURES	SAMPLES	LITHOLOGIC DESCRIPTION
				B	?	● [illegible] V=5.2				M				This core contained no sedimentary material.

SITE 780 HOLE C CORE 11R CORED INTERVAL 3173.9-3183.6 mbsl; 90.5-100.2 mbsf

TIME-ROCK UNIT	BIOSTRAT. ZONE/ FOSSIL CHARACTER: FORAMINIFERS	NANNOFOSSILS	RADIOLARIANS	DIATOMS	PALEOMAGNETICS	PHYS. PROPERTIES	CHEMISTRY	SECTION	METERS	GRAPHIC LITHOLOGY	DRILLING DISTURB.	SED. STRUCTURES	SAMPLES	LITHOLOGIC DESCRIPTION
					?			1		M				This core contained no sedimentary material.

SITE 780 HOLE C CORE 12R CORED INTERVAL 3183.6-3189.9 mbsl; 100.2-106.5 mbsf

TIME-ROCK UNIT	BIOSTRAT. ZONE/ FOSSIL CHARACTER: FORAMINIFERS	NANNOFOSSILS	RADIOLARIANS	DIATOMS	PALEOMAGNETICS	PHYS. PROPERTIES	CHEMISTRY	SECTION	METERS	GRAPHIC LITHOLOGY	DRILLING DISTURB.	SED. STRUCTURES	SAMPLES	LITHOLOGIC DESCRIPTION
					?	● φ=10.6 γ=2.64 V=5.3		1		M			■	SANDY SILT-SIZED SERPENTINE

Major lithology: SANDY SILT-SIZED SERPENTINE, dark greenish gray ([illegible]) with pebble-sized clasts. One clast is pale green (5G 7/2), the other is dark blue gray (5B 4/1). Both clasts are serpentinized ultramafics rock.

SMEAR SLIDE SUMMARY (%):

1, 8
D

TEXTURE:

Sand 40
Silt 40
Clay 20

COMPOSITION:

Chlorite [illegible]
Clay [illegible]
Micrite [illegible]
Opaques [illegible]
Serpentine 75
Zoisite 5

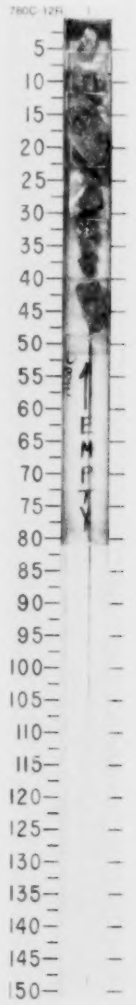

SITE 780 HOLE C CORE 13R CORED INTERVAL 3189.9-3199.4 mbsl; 106.5-116.0 mbsf

TIME-ROCK UNIT	FORAMINIFERS	NANNOFOSSILS	RADIOLARIANS	DIATOMS	PALEOMAGNETICS	PHYS. PROPERTIES	CHEMISTRY	SECTION	METERS	GRAPHIC LITHOLOGY	DRILLING DISTURB.	SED. STRUCTURES	SAMPLES	LITHOLOGIC DESCRIPTION
						●		1	0.5	M			●	[illegible]

SITE 780 HOLE C CORE 14R CORED INTERVAL 3199.4-3208.9 mbsl; 116.0-125.5 mbsf

TIME-ROCK UNIT	FORAMINIFERS	NANNOFOSSILS	RADIOLARIANS	DIATOMS	PALEOMAGNETICS	PHYS. PROPERTIES	CHEMISTRY	SECTION	METERS	GRAPHIC LITHOLOGY	DRILLING DISTURB.	SED. STRUCTURES	SAMPLES	LITHOLOGIC DESCRIPTION
								1		M				[illegible]

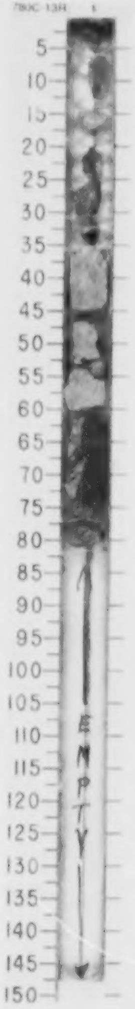
780C-13R 1
5
10
15
20
25
30
35
40
45
50
55
60
65
70
75
80
85
90
95
100
105
110
115
120
125
130
135
140
145
150
EMPTY

SITE 780 HOLE C CORE 15R CORED INTERVAL 3208.9-3218.4 mbsl; 125.5-135.0 mbsf

TIME-ROCK UNIT	FORAMINIFERS	NANNOFOSSILS	RADIOLARIANS	DIATOMS	PALEOMAGNETICS	PHYS. PROPERTIES	CHEMISTRY	SECTION	METERS	GRAPHIC LITHOLOGY	DRILLING DISTURB.	SED. STRUCTURES	SAMPLES	LITHOLOGIC DESCRIPTION
						●	●	1					●	SANDY SILT-SIZED SERPENTINE Major lithology: SANDY SILT-SIZED SERPENTINE, [illegible] SMEAR SLIDE SUMMARY (%): TEXTURE: Sand, Silt, Clay COMPOSITION: [illegible]

SITE 780 HOLE C CORE 16R CORED INTERVAL 3218.4-3228.0 mbsl; 135.0-144.6 mbsf

TIME-ROCK UNIT	FORAMINIFERS	NANNOFOSSILS	RADIOLARIANS	DIATOMS	PALEOMAGNETICS	PHYS. PROPERTIES	CHEMISTRY	SECTION	METERS	GRAPHIC LITHOLOGY	DRILLING DISTURB.	SED. STRUCTURES	SAMPLES	LITHOLOGIC DESCRIPTION
						●		1	0.5	M IM			●	SILT-SIZED SERPENTINE Major lithology: SILT-SIZED SERPENTINE, [illegible] SMEAR SLIDE SUMMARY (%): TEXTURE: Sand, Silt, Clay COMPOSITION: [illegible]

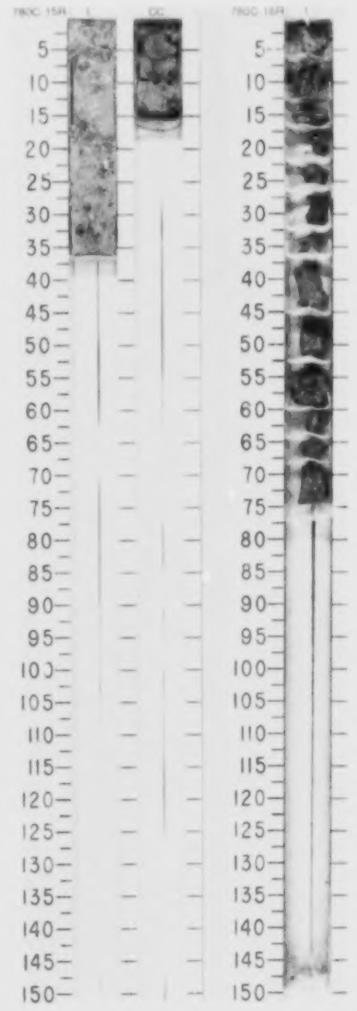
780C-15R 1
CC
780C-16R 1
5
10
15
20
25
30
35
40
45
50
55
60
65
70
75
80
85
90
95
100
105
110
115
120
125
130
135
140
145
150

SITE 780 HOLE C CORE 17R CORED INTERVAL 3228.0-3237.4 mbsl; 144.6-154.0 mbsf

TIME-ROCK UNIT	FORAMINIFERS	NANNOFOSSILS	RADIOLARIANS	DIATOMS	PALEOMAGNETICS	PHYS. PROPERTIES	CHEMISTRY	SECTION	METERS	GRAPHIC LITHOLOGY	DRILLING DISTURB.	SED. STRUCTURES	SAMPLES	LITHOLOGIC DESCRIPTION
								1		M				[illegible]

SITE 780 HOLE C CORE 18R CORED INTERVAL 3237.4-3246.9 mbsl; 154.0-163.5 mbsf

TIME-ROCK UNIT	FORAMINIFERS	NANNOFOSSILS	RADIOLARIANS	DIATOMS	PALEOMAGNETICS	PHYS. PROPERTIES	CHEMISTRY	SECTION	METERS	GRAPHIC LITHOLOGY	DRILLING DISTURB.	SED. STRUCTURES	SAMPLES	LITHOLOGIC DESCRIPTION
				B		[illegible] ●		1	0.5 1.0	M			•	[illegible] [illegible] SMEAR SLIDE SUMMARY TEXTURE: Sand [illegible] Silt [illegible] Clay [illegible] COMPOSITION: [illegible]

780C 18R

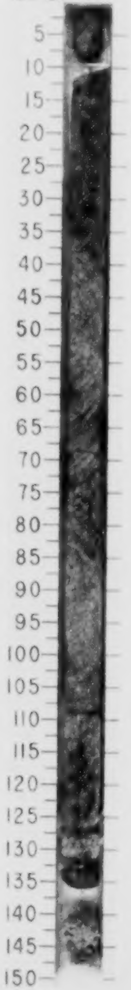
1
5
10
15
20
25
30
35
40
45
50
55
60
65
70
75
80
85
90
95
100
105
110
115
120
125
130
135
140
145
150

SITE 780 HOLE D CORE 1X CORED INTERVAL 3088.9-3091.4 mbsl; 0.0-2.5 mbsf

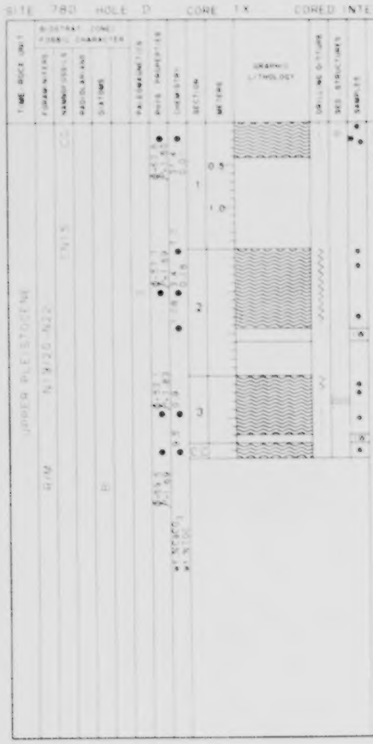
TIME-ROCK UNIT
BIOSTRAT. ZONE/ FOSSIL CHARACTER
FORAMINIFERS
NANNOFOSSILS
RADIOLARIANS
DIATOMS
PALEOMAGNETICS
PHYS. PROPERTIES
CHEMISTRY
SECTION
METERS
GRAPHIC LITHOLOGY
DRILLING DISTURB.
SED. STRUCTURES
SAMPLES
UPPER PLEISTOCENE
N1/9/20-N22
CN15
B/M
B
0.5
1.0
1
2
3
CC

LITHOLOGIC DESCRIPTION

SILT-SIZED SERPENTINE

Major lithology: SILT-SIZED SERPENTINE, light gray (2.5Y 5/0) to dark blue gray (5B 4/1), with scattered angular to subangular black clasts (1 to 3 cm in size). Black sediment occurs in patches and spots rather than forming distinct layers. [illegible] of H.O. Aragonite needles are abundant in Section 1.

SMEAR SLIDE SUMMARY (%):

	[illegible]	[illegible]	[illegible]	[illegible]	[illegible]	[illegible]	[illegible]
	D	D	D	D	M	D	M
TEXTURE:							
Sand	[illegible]	[illegible]	[illegible]	[illegible]	[illegible]	—	[illegible]
Silt	[illegible]	[illegible]	[illegible]	[illegible]	[illegible]	[illegible]	[illegible]
Clay	[illegible]	[illegible]	[illegible]	[illegible]	[illegible]	[illegible]	[illegible]
COMPOSITION:							
Aragonite	[illegible]	[illegible]	[illegible]	[illegible]	[illegible]		—
Clay	—	[illegible]	—	—	—		—
Diatoms				[illegible]	—	—	—
Epidote		[illegible]		—	—		
Foraminifers	[illegible]			[illegible]	[illegible]	—	
Garnet	[illegible]	[illegible]		—	[illegible]		
Nannofossils	[illegible]				—	—	
Opaques	[illegible]	[illegible]	[illegible]	[illegible]	[illegible]	[illegible]	[illegible]
Organic matter	[illegible]				[illegible]	—	—
Radiolarians	[illegible]			—	—	—	—
Serpentine	[illegible]	[illegible]	[illegible]	[illegible]	[illegible]	[illegible]	[illegible]
Silicoflagellates	—			[illegible]	—	—	—

SMEAR SLIDE SUMMARY (%):

	[illegible]	[illegible]	[illegible]
	D	D	M
TEXTURE:			
Sand	[illegible]	[illegible]	[illegible]
Silt	[illegible]	[illegible]	[illegible]
Clay	[illegible]	[illegible]	[illegible]
COMPOSITION:			
Aragonite	[illegible]		[illegible]
Epidote			[illegible]
Opaques		[illegible]	[illegible]
Organic debris		[illegible]	[illegible]
Serpentine	[illegible]	[illegible]	[illegible]

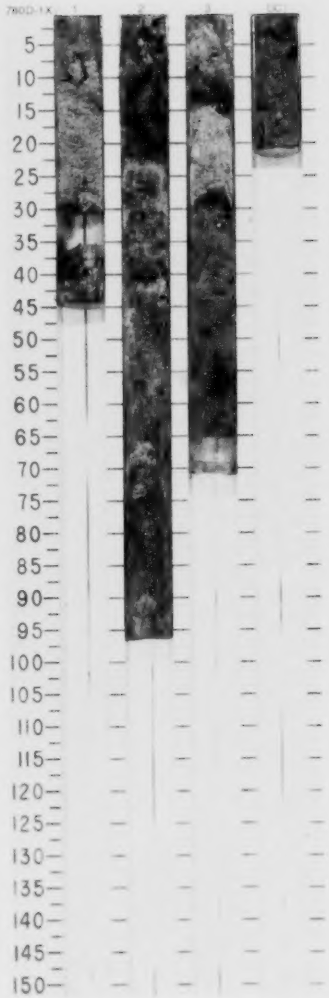
780D-1X
1
2
3
CC
5
10
15
20
25
30
35
40
45
50
55
60
65
70
75
80
85
90
95
100
105
110
115
120
125
130
135
140
145
150

SITE 780 HOLE D CORE 2X CORED INTERVAL 3091.4-3100.9 mbsl; 2.5-12.0 mbsf

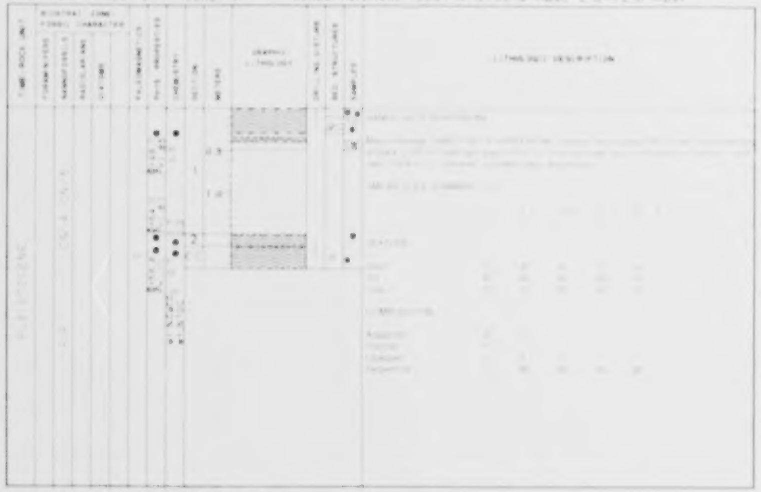
TIME-ROCK UNIT
BIOSTRAT. ZONE/FOSSIL CHARACTER
FORAMINIFERS
NANNOFOSSILS
RADIOLARIANS
DIATOMS
PALEOMAGNETICS
PHYS. PROPERTIES
CHEMISTRY
SECTION
METERS
GRAPHIC LITHOLOGY
DRILLING DISTURB.
SED. STRUCTURES
SAMPLES
LITHOLOGIC DESCRIPTION

SITE 780 HOLE D CORE 3X CORED INTERVAL 3100.9-3104.3 mbsl; 12.0-15.4 mbsf

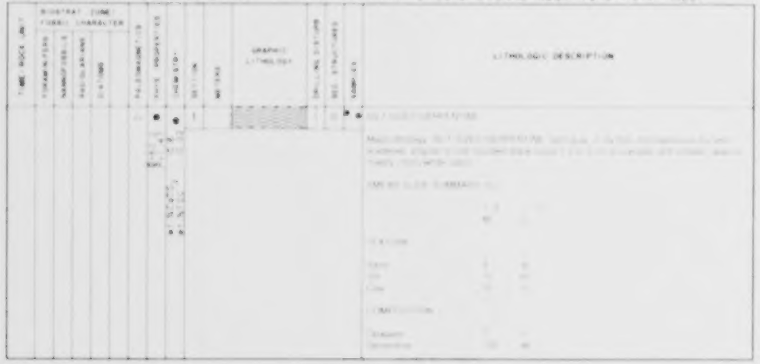
TIME-ROCK UNIT
BIOSTRAT. ZONE/FOSSIL CHARACTER
FORAMINIFERS
NANNOFOSSILS
RADIOLARIANS
DIATOMS
PALEOMAGNETICS
PHYS. PROPERTIES
CHEMISTRY
SECTION
METERS
GRAPHIC LITHOLOGY
DRILLING DISTURB.
SED. STRUCTURES
SAMPLES
LITHOLOGIC DESCRIPTION

780 D 4X NO RECOVERY

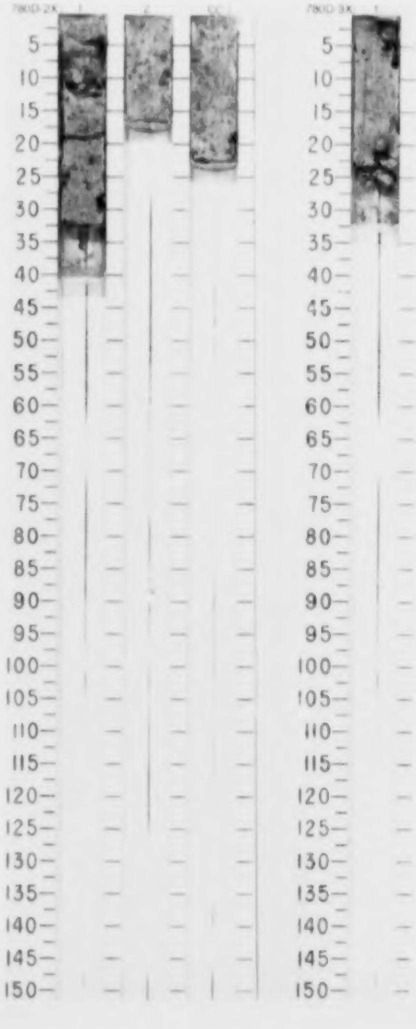
780D-2X
1
2
CC
780D-3X
1
5
10
15
20
25
30
35
40
45
50
55
60
65
70
75
80
85
90
95
100
105
110
115
120
125
130
135
140
145
150

SITE 780 HOLE D CORE 5X CORED INTERVAL 3105.8-3109.3 mbsl; 16.9-20.4 mbsf

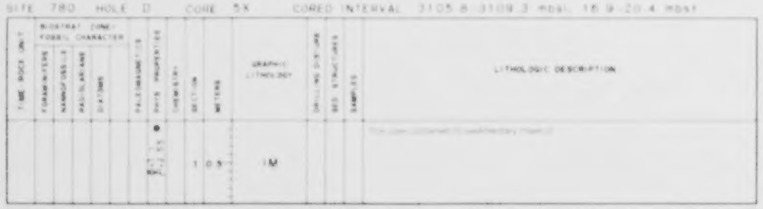
TIME-ROCK UNIT
BIOSTRAT. ZONE/ FOSSIL CHARACTER
FORAMINIFERS
NANNOFOSSILS
RADIOLARIANS
DIATOMS
PALEOMAGNETICS
PHYS. PROPERTIES
CHEMISTRY
SECTION
METERS
GRAPHIC LITHOLOGY
DRILLING DISTURB.
SED. STRUCTURES
SAMPLES
1
0.5
1M

LITHOLOGIC DESCRIPTION

[illegible]

SITE 780 HOLE D CORE 6X CORED INTERVAL 3109.3-3116.3 mbsl; 20.4-27.4 mbsf

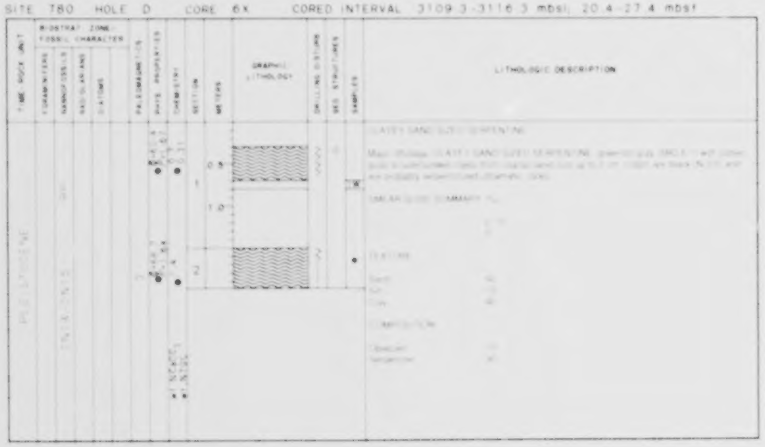
TIME-ROCK UNIT
BIOSTRAT. ZONE/ FOSSIL CHARACTER
FORAMINIFERS
NANNOFOSSILS
RADIOLARIANS
DIATOMS
PALEOMAGNETICS
PHYS. PROPERTIES
CHEMISTRY
SECTION
METERS
GRAPHIC LITHOLOGY
DRILLING DISTURB.
SED. STRUCTURES
SAMPLES
PLEISTOCENE
INDETERMINATE
1
2
0.5
1.0

LITHOLOGIC DESCRIPTION

CLAYEY SAND-SIZED SERPENTINE

Major lithology: CLAYEY SAND-SIZED SERPENTINE, greenish gray [illegible]

SMEAR SLIDE SUMMARY (%):

TEXTURE:

Sand [illegible]
Silt [illegible]
Clay [illegible]

COMPOSITION:

Opaques [illegible]
Serpentine [illegible]

780D-6X
1
2
EMPTY
5
10
15
20
25
30
35
40
45
50
55
60
65
70
75
80
85
90
95
100
105
110
115
120
125
130
135
140
145
150

SITE 780 HOLE D CORE 7X CORED INTERVAL 3116.3-3121.3 mbsl; 27.4-32.1 mbsf

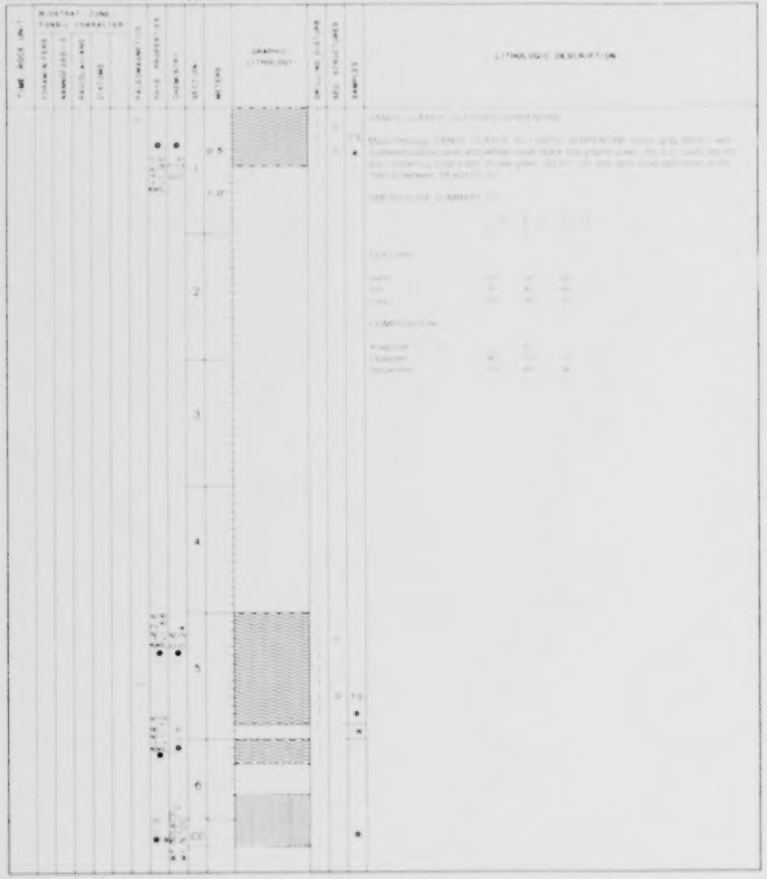
TIME-ROCK UNIT
BIOSTRAT. ZONE/FOSSIL CHARACTER
FORAMINIFERS
NANNOFOSSILS
RADIOLARIANS
DIATOMS
PALEOMAGNETICS
PHYS. PROPERTIES
CHEMISTRY
SECTION
METERS
GRAPHIC LITHOLOGY
DRILLING DISTURB.
SED. STRUCTURES
SAMPLES
LITHOLOGIC DESCRIPTION
0.5
1.0
1
2
3
4
5
6
CC

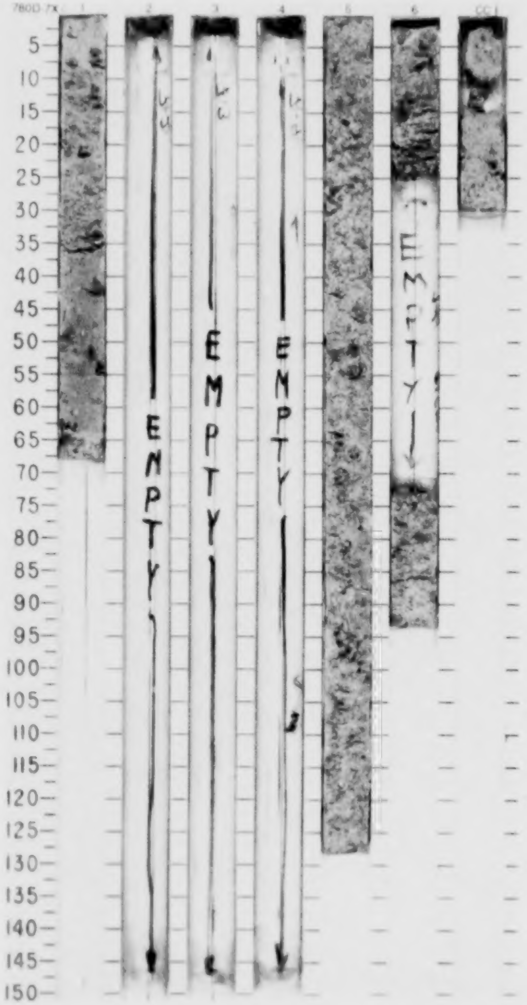
780D-7X
1
2
3
4
5
6
CC
5
10
15
20
25
30
35
40
45
50
55
60
65
70
75
80
85
90
95
100
105
110
115
120
125
130
135
140
145
150
EMPTY
EMPTY
EMPTY
EMPTY

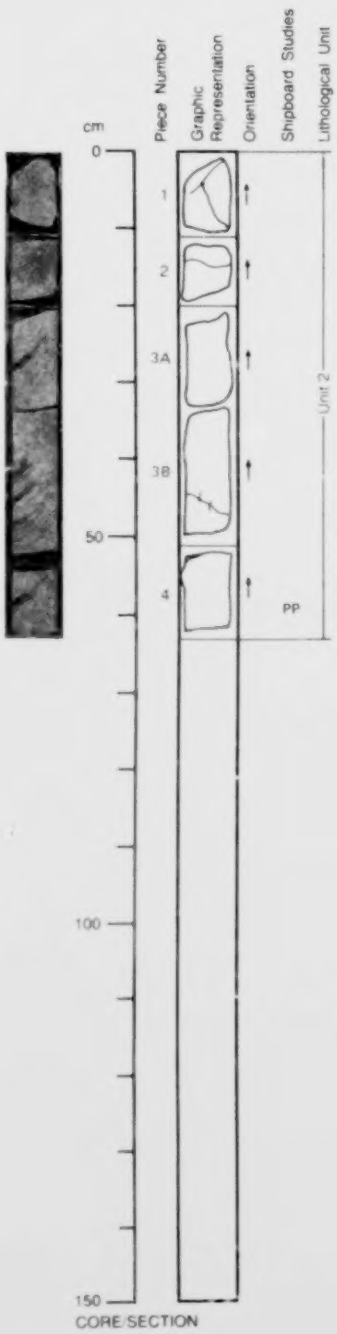
cm
Piece Number
Graphic Representation
Orientation
Shipboard Studies
Lithological Unit
0
1
2
3A
3B
50
4
PP
Unit 2
100
150
CORE/SECTION

125-780C-3R-1

UNIT 2: SERPENTINIZED HARZBURGITE

Pieces 1-4

COLOR: Dark blue gray (5B 4/1)
LAYERING: None
DEFORMATION: None visible
PRIMARY MINERALOGY:
- Olivine - Mode: 75-85%
  Crystal size: Not visible
  Crystal shape: Not visible
  Crystal orientation: None
  Percent replacement: Variable

- Orthopyroxene - Mode: 15-25%
  Crystal size: 2-4 mm
  Crystal shape: Equant-elongate
  Crystal orientation: None
  Percent replacement: Variable

- Spinel - Mode: Trace
  Crystal size: <2 mm
  Crystal shape: Equant
  Crystal orientation: None
  Percent replacement: Variable

SECONDARY MINERALOGY:
- Serpentine
  Total percent: 70%
  Texture: Bastitic in areas
  Vein material: <2-mm-wide black amorphous serpentine veins oriented at various angles to core barrel; pale-green serpentine (<1 mm) veins. Piece 1 has <1-cm-wide green serpentine "rind" on edge of sample

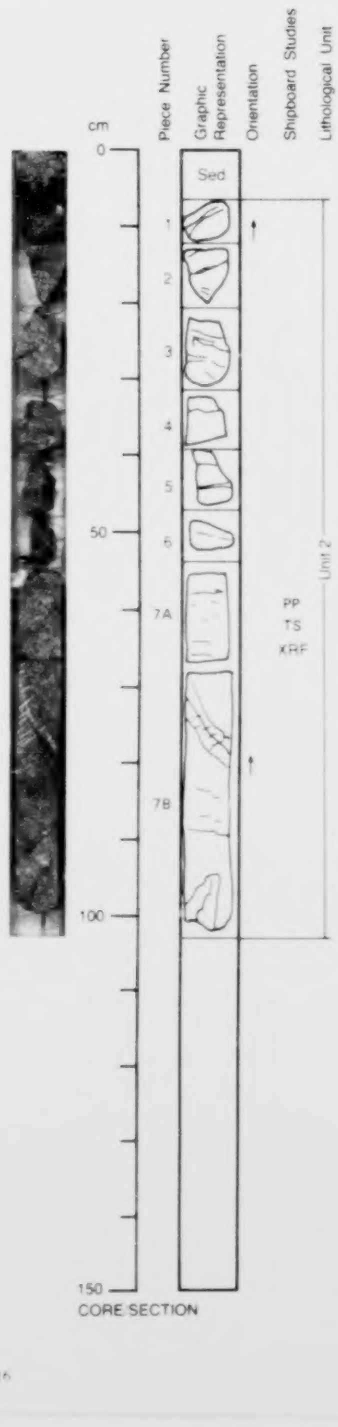
cm
Piece Number
Graphic Representation
Orientation
Shipboard Studies
Lithological Unit
0
50
100
150
Sed
1
2
3
4
5
6
7A
7B
PP
TS
XRF
Unit 2
CORE/SECTION

125-780C-6R-1

UNIT 2: SERPENTINIZED TECTONIZED HARZBURGITE

Pieces 1 to 7

COLOR: Dark greenish gray to dark bluish gray (5G 4/1 to 5B 4/1).
LAYERING: In Piece 3, a crude layering is apparently caused by elongation of olivine.
DEFORMATION: Wavy cleavage on pyroxene; some spinels are elongated; elongate deformed olivine.
PRIMARY MINERALOGY:
Primary silicates are variably serpentinized.
Olivine - Mode: 70-90%.
Crystal size: 5-14 mm.
Crystal shape: Equant to ragged and elongate.
Crystal orientation: None.
Percent replacement: 60-70.

Orthopyroxene - Mode: 10-30%.
Crystal size: 3-8 mm.
Crystal shape: Equant-ragged.
Crystal orientation: None.
Percent replacement: 60-70.

Spinel - Mode: Trace.
Crystal size: <3 mm.
Crystal shape: Equant-elongate.
Crystal orientation: None.
Percent replacement: 60-70.
SECONDARY MINERALOGY:
Intensity of serpentinization is higher closer to the veins.
Total percent: 60-70%.
Texture: N/A.
Vein material: Major polyphase vein cutting Piece 7B, dipping at 60-70 degrees, filled with dark gray-green serpentine and subsequent chrysotile. Latter mineral also forms cross stitching ("Frankenstein") texture along this vein. Total vein width: <30 mm; other pieces of this section have veins <5 mm wide.

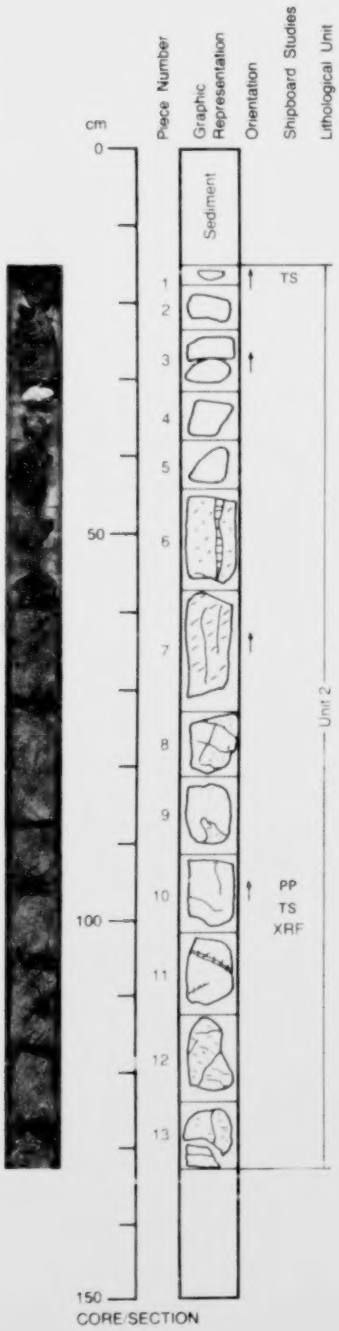
cm
0
50
100
150
CORE/SECTION
Piece Number
Graphic Representation
Orientation
Shipboard Studies
Lithological Unit
Sediment
1
2
3
4
5
6
7
8
9
10
11
12
13
TS
PP
TS
XRF
Unit 2

125-780C-8R-1

UNIT 2: CALCITE WITH SERPENTINE COATING

Piece 1

COLOR: Greenish white (5Y 8/1)
LAYERING: Result from impurities causing green bands that are irregular, 2-5 mm wide, and subparallel
DEFORMATION: None
PRIMARY MINERALOGY:
    Calcite appears drusy
    Calcite - Mode: 95%
    Crystal size: 1-5 mm
    Crystal shape: Equant
    Crystal orientation: None
    Percent replacement: None
SECONDARY MINERALOGY:
    Serpentine
    Total percent: 25?
    Texture: N/A
    Vein material: Possibly serpentinous

UNIT 2: SERPENTINIZED DUNITE

Pieces 2 to 5

COLOR: Greenish dark gray (5Y 2.5/1)
LAYERING: Massive
DEFORMATION: Some mylonitization; elongate spinels
PRIMARY MINERALOGY:
    Primary minerals are extensively serpentinized
    Olivine - Mode: 99%
    Crystal size: Not visible
    Crystal shape: Not visible
    Crystal orientation: None
    Percent replacement: 50-60

    Spinel - Mode: Trace
    Crystal size: Equant-elongate
    Crystal shape: Not visible
    Crystal orientation: None
    Percent replacement: 10-20

    Orthopyroxene - Mode: 1%
    Crystal size: 2-5 mm
    Crystal shape: Equant
    Crystal orientation: None
    Percent replacement: 50-60
SECONDARY MINERALOGY:
    Serpentinite
    Total percent: 50-60%
    Texture: N/A
    Vein material: Two generations: (1) dark amorphous serpentinite, 0.5-1 mm wide; (2) white chrysotile crosscutting first set, 0.25-1.5 mm wide

125-780C-8R-1 (continued)

UNIT 2: SERPENTINIZED TECTONIZED HARZBURGITE

Pieces 6 to 13

COLOR: Greenish gray (5Y 2.5/3)
LAYERING: None
DEFORMATION: Orthopyroxene foliation formed by alignment of elongate orthopyroxene with an apparent dip of 45 degrees; wavy cleavage on orthopyroxene; spinels in stringers.
PRIMARY MINERALOGY:
Primary silicates variably serpentinized.
Olivine - Mode: 70-90%
Crystal size: Not visible
Crystal shape: Not visible
Crystal orientation: None
Percent replacement: Variable

Orthopyroxene - Mode: 10-30%
Crystal size: 3-7 mm
Crystal shape: Elongate
Crystal orientation: None
Percent replacement: Variable

Spinel - Mode: Trace
Crystal size: 0.5-1.0 mm
Crystal shape: Subelongate-equant
Crystal orientation: None
Percent replacement: Variable
SECONDARY MINERALOGY:
Serpentine
Total percent: 70?
Texture: N/A
Vein material: Two generations: subvertical, 0.1-0.5 mm wide, filled with black amorphous serpentine. Cut by white chrysotile veins forming cross-stitched texture as well as individual veins of variable orientation and between 0.1-3 mm wide.
ADDITIONAL COMMENTS: Serpentinization is maximized adjacent to first generation veins where it forms veins up to 8 mm wide.

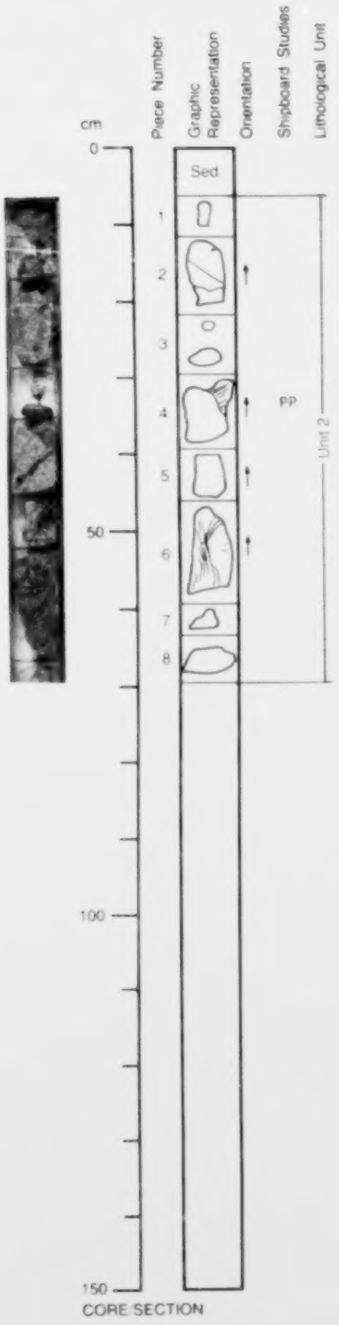
cm
Piece Number
Graphic Representation
Orientation
Shipboard Studies
Lithological Unit
0
50
100
150
Sed.
1
2
3
4
5
6
7
8
PP
Unit 2
CORE/SECTION

125-780C-9R-1

UNIT 2: TECTONIZED SERPENTINIZED HARZBURGITE

Pieces 1 to 8

COLOR: Green olive gray to gray (5Y 5/2 to 2.5Y 4/5)
LAYERING: None
DEFORMATION: Piece 2 appears to have deformed and elongate bastite after pyroxene
PRIMARY MINERALOGY:
Olivine - Mode: 80-90%
Crystal size: Not visible
Crystal shape: Not visible
Crystal orientation: None
Percent replacement: 80-95

Orthopyroxene - Mode: 10-20%
Crystal size: 0.2-6 mm
Crystal shape: Ragged elongate
Crystal orientation: None
Percent replacement: 80-95

Spinel - Mode: Trace
Crystal size: 0.9 mm
Crystal shape: Equant
Crystal orientation: None
Percent replacement: 30-40
SECONDARY MINERALOGY:
Serpentine
Total percent: 80-95%
Texture: N/A
Vein material: Three generations: (1) steeply dipping filled with black amorphous serpentine 8-12 mm wide; (2) amorphous pale gray serpentine apparently at low angle in Piece 2 (1-5 mm wide); (3) small cross-stitched veins of chrysotile in various directions, 0.1 mm wide
ADDITIONAL COMMENTS: Variable serpentinization appears to be controlled by position of veins

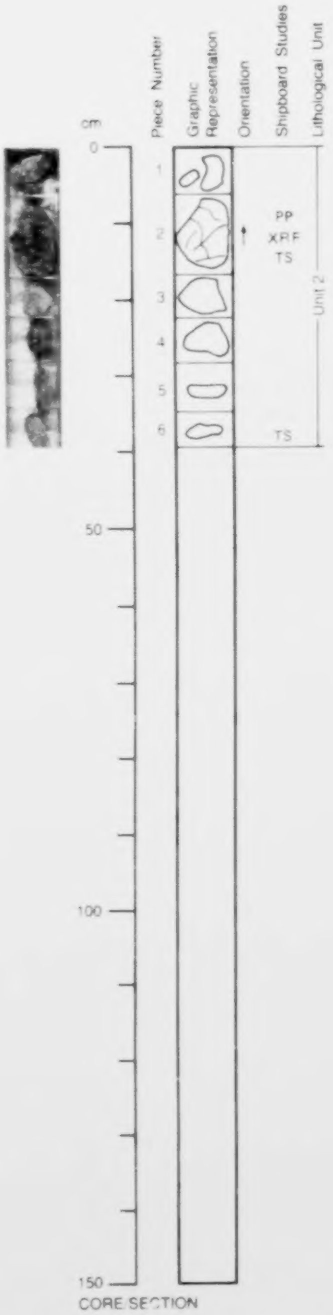

125-780C-10R-1

UNIT 2: SERPENTINIZED DUNITE

Pieces 1, 3, 4

COLOR: Dark greenish gray (5BG 4/1)
LAYERING: None
DEFORMATION: None
PRIMARY MINERALOGY:
Primary silicates variably serpentinized
Olivine - Mode: 90-95%
Crystal size: Not visible
Crystal shape: Not visible
Crystal orientation: None
Percent replacement: 90-95

Orthopyroxene - Mode: <5%
Crystal size: Not visible
Crystal shape: Not visible
Crystal orientation: None
Percent replacement: 90-95

Spinel - Mode: <2%
Crystal size: <2 mm
Crystal shape: Equant
Crystal orientation: None
Percent replacement: 20-40
SECONDARY MINERALOGY:
Serpentine
Total percent: 90-95%
Texture: N/A
Vein material: <1-mm-wide black amorphous serpentine veins; <1-mm-wide white veins also

UNIT 2: SERPENTINIZED HARZBURGITE

Piece 2

COLOR: Dark greenish gray (5G 4/1)
LAYERING: None
DEFORMATION: None
PRIMARY MINERALOGY: Primary silicates variably serpentinized
Olivine - Mode: 70-80%
Crystal size: 1-4 mm
Crystal shape: Equant
Crystal orientation: None
Percent replacement: 70-80

Orthopyroxene - Mode: 20-25%
Crystal size: 1-3 mm
Crystal shape: Equant
Crystal orientation: None
Percent replacement: 70-80

Spinel - Mode: 1-2%
Crystal size: <2 mm
Crystal shape: Equant
Crystal orientation: None
Percent replacement: 10-30
SECONDARY MINERALOGY:
Serpentine
Total percent: 70-80%
Texture: Bastitic pseudomorphs after pyroxenes in areas?
Vein material: Anastomosing black-green serpentine veins at various orientations (<2 mm wide)

125-780C-10R-1 (continued)

UNIT 2: TECTONIZED SERPENTINIZED DUNITE

Pieces 5, 6

COLOR: Dark greenish gray (5B 4/1)
LAYERING: None
DEFORMATION: Appears tectonized; orthopyroxenes are elongated parallel to fabric
PRIMARY MINERALOGY:
Olivine - Mode: 90-95%
Crystal size: Not visible
Crystal shape: Not visible
Crystal orientation: None
Percent replacement: 95-99

Orthopyroxene - Mode: 5-10%
Crystal size: 1-3 mm
Crystal shape: Elongated
Crystal orientation: None
Percent replacement: 95-99

Spinel - Mode: Trace
Crystal size: <2 mm
Crystal shape: Equant - elongated
Crystal orientation: None
Percent replacement: 20-40
SECONDARY MINERALOGY:
Serpentine
Total percent: 95-99%
Texture: N/A
Vein material: <1-mm wide veining
ADDITIONAL COMMENTS: Piece 6 contains an olivine-rich area (1 cm X 1 cm)

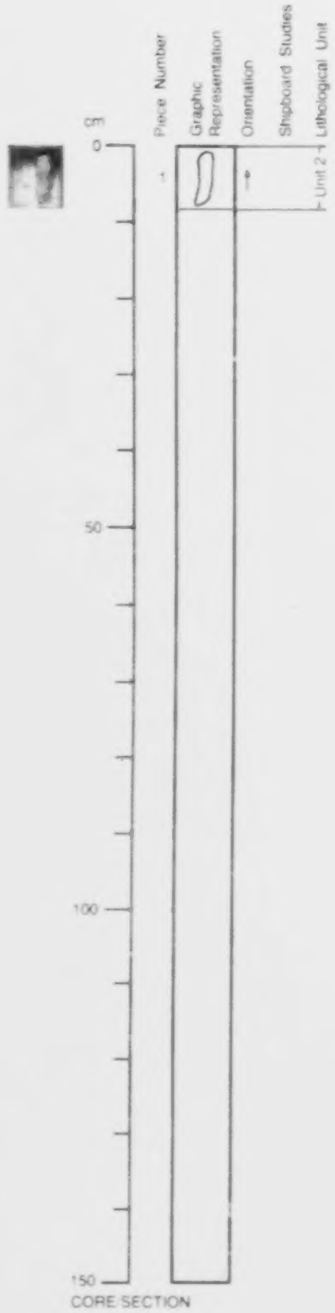
cm
Piece Number
Graphic Representation
Orientation
Shipboard Studies
Lithological Unit
0
1
Unit 2
50
100
150
CORE/SECTION

125-780C-11R-1

UNIT 2: SERPENTINIZED DUNITE

Piece 1

COLOR: Dark greenish gray (5BG 4/1)
LAYERING: None visible
DEFORMATION: None visible
PRIMARY MINERALOGY:
Olivine - Mode: 90-95%
Crystal size: 1-2 mm
Crystal shape: Equant
Crystal orientation: None visible
Percent replacement: Variable

Orthopyroxene - Mode: 5%
Crystal size: <2 mm
Crystal shape: Equant
Crystal orientation: None visible
Percent replacement: Variable

Spinel - Mode: 2%
Crystal size: <2 mm
Crystal shape: Equant
Crystal orientation: None visible
Percent replacement: Not visible
SECONDARY MINERALOGY:
Serpentine
Total percent: 60-70%
Texture: N/A
Vein material: <1-mm-wide black serpentine veins at no specific orientation

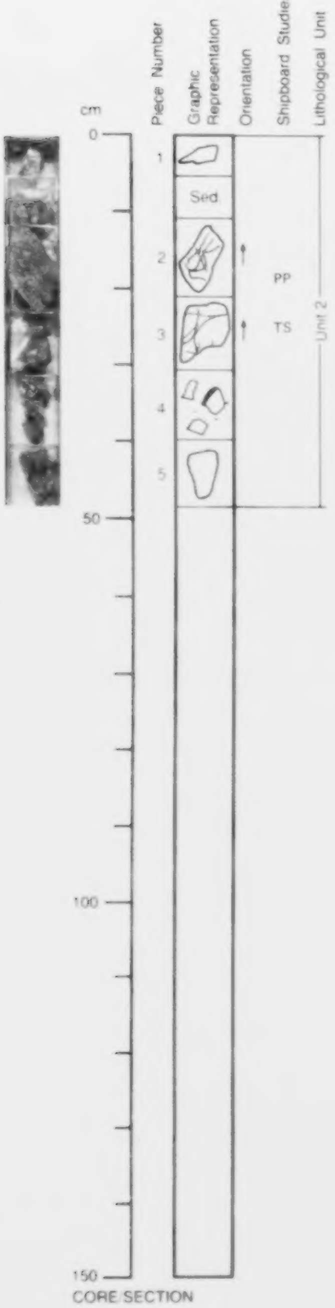

125-780C-12R-1

UNIT 2: SERPENTINIZED DUNITE(?)

Piece 1

COLOR: Dark greenish gray (5BG 4/1)
LAYERING: None visible
DEFORMATION: None visible
PRIMARY MINERALOGY:
Olivine: Mode: 90-95%
Crystal size: Not visible
Crystal shape: Not visible
Crystal orientation: None visible
Percent replacement: Variable

Orthopyroxene: Mode: <5%
Crystal size: Not visible
Crystal shape: Not visible
Crystal orientation: None visible
Percent replacement: Variable

Spinel: Mode: <2%
Crystal size: <2 mm
Crystal shape: Equant
Crystal orientation: None visible
Percent replacement: Variable
SECONDARY MINERALOGY:
Serpentine
Total percent: 90-95%
Texture: N/A
Vein material: <1 mm wide black amorphous serpentine veins at no specific orientation
ADDITIONAL COMMENTS: Similar to 780C-10R-1, Pieces 1, 3, and 4

UNIT 2: SERPENTINIZED HARZBURGITE

Piece 2

COLOR: Dark gray (N 4/)
LAYERING: None
DEFORMATION: Orthopyroxene appears slightly elongated and has possible wavy cleavages
PRIMARY MINERALOGY:
Olivine: Mode: 75-80%
Crystal size: 1-2 mm
Crystal shape: Equant-elongate
Crystal orientation: None visible
Percent replacement: Variable

Orthopyroxene: Mode: 20-25%
Crystal size: 2-3 mm
Crystal shape: Equant ragged
Crystal orientation: None visible
Percent replacement: Variable

Spinel: Mode: <2%
Crystal size: <2 mm
Crystal shape: Equant ragged
Crystal orientation: None visible
Percent replacement: Not visible
SECONDARY MINERALOGY:
Serpentine
Total percent: 60?
Texture: Bastitic pseudomorphs after orthopyroxene in areas but basically appear fresh
Vein material: Anastomosing black serpentine veins <2 mm wide at no specific orientation

125-780C-12R-1 (continued)

UNIT 2: CLAY-RICH SILTSTONE WITH CARBONATE VEINS

Piece 3

COLOR: Weak red (5R 5/2)
LAYERING: Possible layering defined by light red to dark red zones
DEFORMATION: None
PRIMARY MINERALOGY: Hard to discern crystals
SECONDARY MINERALOGY:
Clays (red) 85%, carbonate 5%, quartz 15% (based on thin-section description)
Total percent: 100%
Texture: N/A
Vein material: Calcite (white) veins 1-5 mm wide
ADDITIONAL COMMENTS: Clast appears to be hydrothermally altered. It may be an altered clay-rich siltstone. It contains 15% microfossils (foraminifers) which are silicified.

UNIT 2: SERPENTINIZED HARZBURGITE

Pieces 4A; 4B; 5

COLOR: Dark greenish gray (5BG 4/1)
LAYERING: Not visible
DEFORMATION: None visible
PRIMARY MINERALOGY:
Olivine - Mode: 80%
Crystal size: 1-2 mm
Crystal shape: Equant
Crystal orientation: None visible
Percent replacement: Variable

Orthopyroxene - Mode: 15-20%
Crystal size: 1-3 mm
Crystal shape: Equant-elongated
Crystal orientation: None visible
Percent replacement: Variable

Spinel - Mode: Trace
Crystal size: <1 mm
Crystal shape: Equant
Crystal orientation: None visible
Percent replacement: Not visible
SECONDARY MINERALOGY:
Serpentine
Total percent: 70%
Texture: Bastitic pseudomorphs after orthopyroxene in areas
Vein material: <1-mm wide white veins. Piece 4A has a 6-mm wide pale green amorphous serpentine vein.

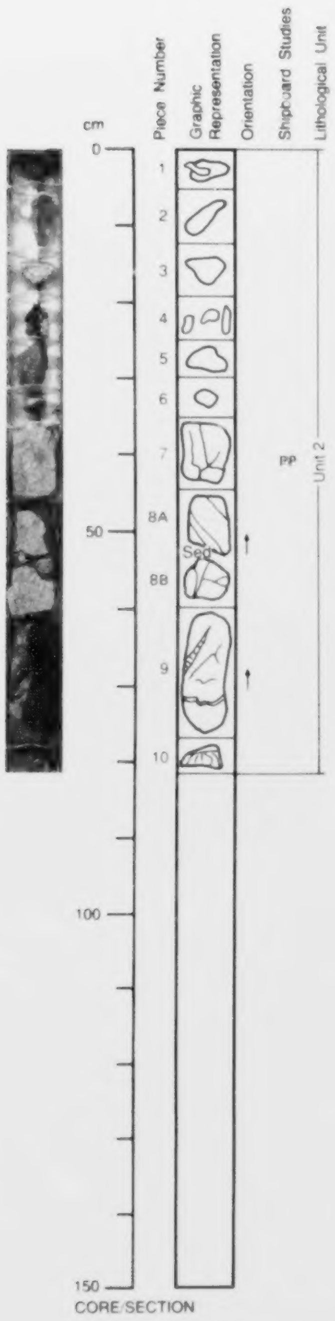

125-780C-13R-1

UNIT 2: SERPENTINIZED DUNITE

Pieces 1; 2; 4; 6

COLOR: Dark greenish gray (5BG 4/1).
LAYERING: None visible.
DEFORMATION: None visible.
PRIMARY MINERALOGY:
Olivine - Mode: 90%.
Crystal size: Not visible.
Crystal shape: Not visible.
Crystal orientation: None visible.
Percent replacement: Variable.

Orthopyroxene - Mode: <10%.
Crystal size: 1-2 mm.
Crystal shape: Not visible.
Crystal orientation: None visible.
Percent replacement: Variable.

Spinel - Mode: Trace.
Crystal size: <1 mm.
Crystal shape: Not visible.
Crystal orientation: Not visible.
Percent replacement: Not visible.
SECONDARY MINERALOGY:
Serpentine.
Total percent: 80-90%.
Texture: N/A.
Vein material: <1-mm pale-green serpentine veins.

UNIT 2: SERPENTINIZED HARZBURGITE

Pieces 7, 8A, 8B

COLOR: Bluish gray (5B 6/1).
LAYERING: None visible.
DEFORMATION: None visible.
PRIMARY MINERALOGY:
Olivine - Mode: 80%.
Crystal size: Not visible.
Crystal shape: Not visible.
Crystal orientation: None visible.
Percent replacement: Variable.

Orthopyroxene - Mode: 20%.
Crystal size: 1-3 mm.
Crystal shape: Equant-elongate.
Crystal orientation: None visible.
Percent replacement: Variable.

Spinel - Mode: Trace.
Crystal size: 1-3 mm.
Crystal shape: Elongate-ragged.
Crystal orientation: None visible.
Percent replacement: Variable.
SECONDARY MINERALOGY:
Serpentine.
Total percent: 75%.
Texture: N/A.
Vein material: <2-mm-wide black amorphous serpentine oriented at various angles.

125-780C-13R-1 (continued)

UNIT 2: SERPENTINIZED HARZBURGITE

Pieces 3; 5; 9; 10

COLOR: Dark greenish gray (5BG 4/1)
LAYERING: None visible
DEFORMATION: None visible
PRIMARY MINERALOGY:
Olivine - Mode: 70%
Crystal size: Not visible
Crystal shape: Not visible
Crystal orientation: None visible
Percent replacement: Variable

Orthopyroxene - Mode: 25-30%
Crystal size: 1-3 mm
Crystal shape: Equant-elongate
Crystal orientation: None visible
Percent replacement: Variable

Spinel - Mode: <5%
Crystal size: <2 mm
Crystal shape: Equant-ragged
Crystal orientation: None visible
Percent replacement: Variable
SECONDARY MINERALOGY:
Serpentine
Total percent: 70%
Texture: Bastitic pseudomorphs after orthopyroxene in areas
Vein material: anastomosing black serpentine veins <2 mm wide; <1-mm-wide pale green-white veins
ADDITIONAL COMMENTS: Piece 9 shows possible serpentinization halo. Piece 10 appears to be part of the halo.

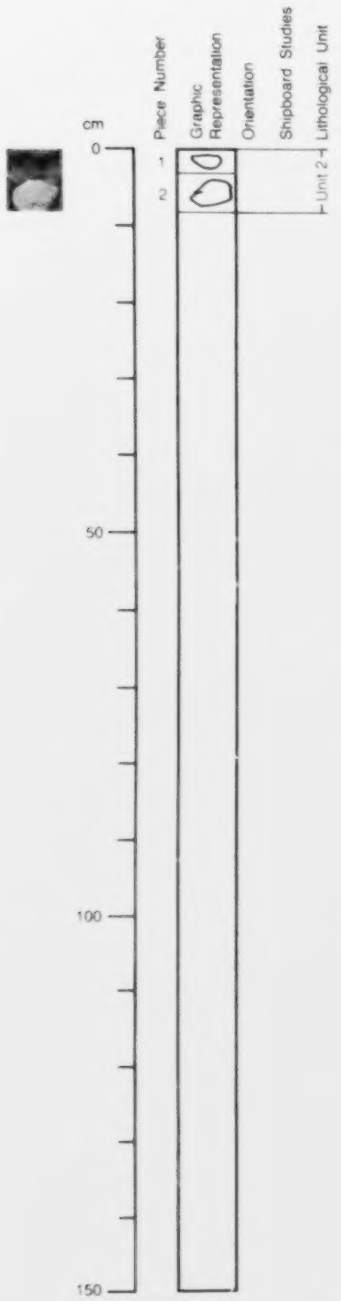
cm
Piece Number
Graphic Representation
Orientation
Shipboard Studies
Lithological Unit
0
1
2
Unit 2
50
100
150
CORE/SECTION

125-780C-14R-1

UNIT 2: TECTONIZED SERPENTINIZED HARZBURGITE

Pieces 1 and 2

COLOR: (Piece 1) grayish green (5G 4/2) to (Piece 20) greenish gray (5BG 5/1)
LAYERING: None
DEFORMATION: Possible lamination/foliation of orthopyroxene
PRIMARY MINERALOGY:

Olivine - Mode: 55-65%
Crystal size: Not visible
Crystal shape: Not visible
Crystal orientation: None visible
Percent replacement: Variable

Orthopyroxene - Mode: 35-45%
Crystal size: 3-5 mm
Crystal shape: Elongate-equant
Crystal orientation: Possible lamination/foliation of grains
Percent replacement: Variable

Spinel - Mode: Trace
Crystal size: <0.1 mm
Crystal shape: Equant
Crystal orientation: None visible
Percent replacement: Variable

SECONDARY MINERALOGY:

Serpentine
Total percent: 50-80%
Texture: N/A
Vein material: N/A

ADDITIONAL COMMENTS: Piece 2 is more completely serpentinized than most (almost talcose?)

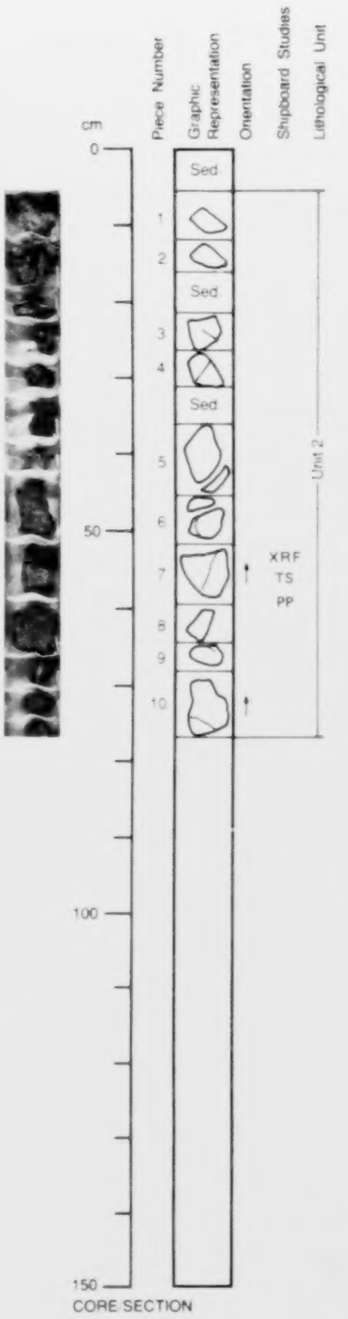
cm
Piece Number
Graphic Representation
Orientation
Shipboard Studies
Lithological Unit
0
Sed
1
2
Sed
3
4
Sed
5
6
50
7
XRF
TS
PP
8
9
10
Unit 2
100
150
CORE SECTION

125-780C-16R-1

UNIT 2: TECTONIZED SERPENTINIZED HARZBURGITE

Pieces 1 to 10

COLOR: Dark bluish gray to bluish gray (5B 4/1 to 5B 5/1)
LAYERING: None
DEFORMATION: Wavy cleavage on orthopyroxene; elongate ragged spinel
PRIMARY MINERALOGY:
Olivine - Mode: 80-90%
Crystal size: 3-10 mm
Crystal shape: Elongate-ragged
Crystal orientation: None visible
Percent replacement: 70-80

Orthopyroxene - Mode: 10-20%
Crystal size: 3-5 mm
Crystal shape: Ragged
Crystal orientation: None visible
Percent replacement: 50-70

Spinel - Mode: <1%
Crystal size: <2 mm
Crystal shape: Equant-elongate
Crystal orientation: None visible
Percent replacement: Not visible
SECONDARY MINERALOGY:
Serpentine
Total percent: 70-80%
Texture: N/A
Vein material: <4 mm wide, filled with gray-green and black amorphous serpentine; small <1-mm chrysotile-filled veins
ADDITIONAL COMMENTS: Pieces 3-6 appear more serpentinized than Pieces 7-10.

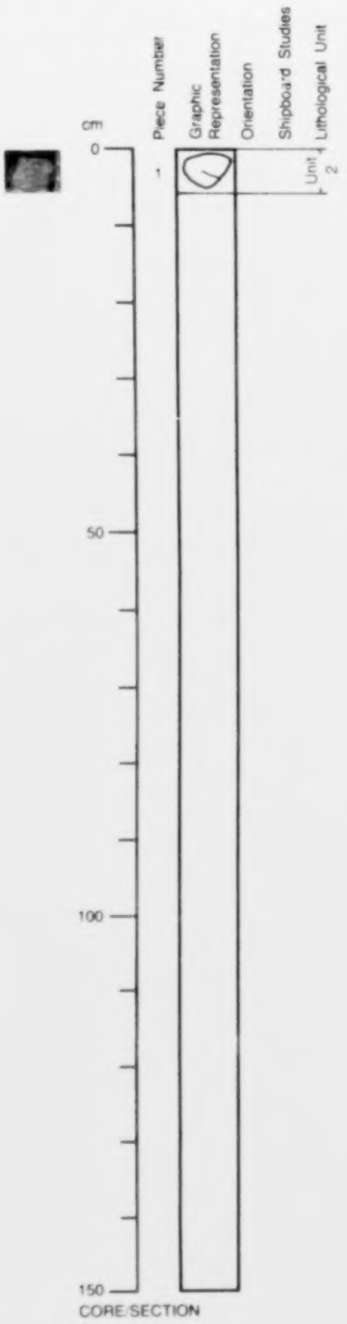
cm
Piece Number
Graphic Representation
Orientation
Shipboard Studies
Lithological Unit
0
1
Unit 2
50
100
150
CORE/SECTION

125-780C-17R-1

UNIT 2: SERPENTINIZED AND STRONGLY FOLIATED HARZBURGITE

Piece 1

COLOR: Bluish gray (5B 5/1)
LAYERING: Strong apparent layering defined by orthopyroxene cleavage and crystal alignment.
DEFORMATION: Strong preferred orientation of silicates; wavy cleavage surface of orthopyroxene; elongate spinels in stringers.
PRIMARY MINERALOGY:
Olivine - Mode: 50-80%
Crystal size: 3-10 mm
Crystal shape: Elongate-ragged
Crystal orientation: None visible
Percent replacement: Variable

Orthopyroxene - Mode: 20-50%
Crystal size: 3-6 mm
Crystal shape: Elongate-equant
Crystal orientation: Defines layering
Percent replacement: Variable

Spinel - Mode: <3%
Crystal size: <4 mm
Crystal shape: Equant-elongate
Crystal orientation: Arranged in stringers
Percent replacement: Not visible
SECONDARY MINERALOGY:
Serpentine
Total percent: 50-80%
Texture: N/A
Vein material: Thin (<0.5 mm), filled with a white serpentinous phase
ADDITIONAL COMMENTS: Relatively orthopyroxene-rich rock with an eye-catching preferred orientation of the orthopyroxene.

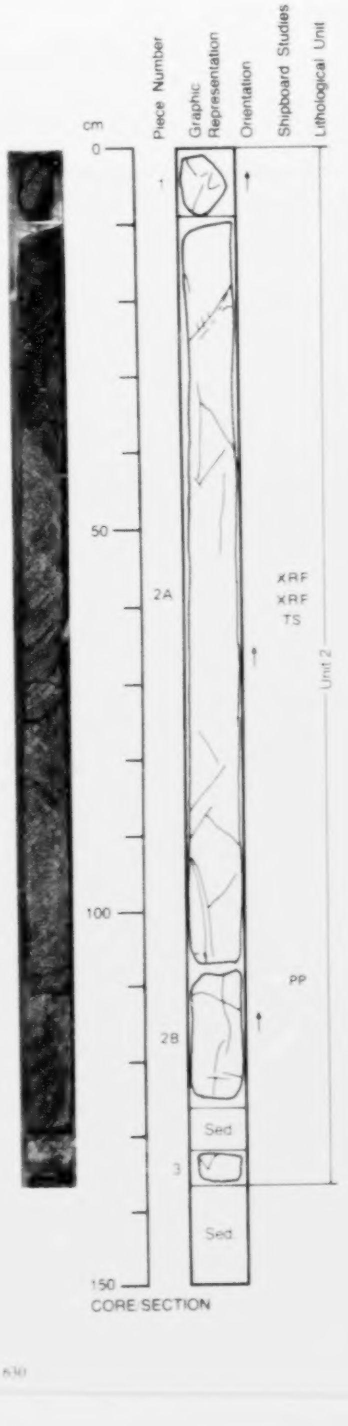
cm
Piece Number
Graphic Representation
Orientation
Shipboard Studies
Lithological Unit
0
50
100
150
1
2A
2B
3
XRF
XRF
TS
PP
Sed
Sed
Unit 2
CORE SECTION

125-780C-18R-1

UNIT 2: SERPENTINIZED TECTONIZED HARZBURGITE

Pieces 1-3

COLOR: Dark greenish gray to dark bluish gray (5G 4/1 to 5B 4/1).
LAYERING: None.
DEFORMATION: Orthopyroxene has wavy cleavage; some elongate spinels.
PRIMARY MINERALOGY:
Olivine - Mode: 80-90%
Crystal size: 4-10 mm.
Crystal shape: Irregular-equant.
Crystal orientation: None visible.
Percent replacement: 70-80.

Orthopyroxene - Mode: 10-20%
Crystal size: 3-6 mm.
Crystal shape: Equant-irregular.
Crystal orientation: None visible.
Percent replacement: 50-70.

Spinel - Mode: <1%
Crystal size: <4 mm.
Crystal shape: Equant-irregular.
Crystal orientation: Some elongation of grains.
Percent replacement: Not visible.
SECONDARY MINERALOGY:
Serpentine
Total percent: 50-80%.
Texture: N/A.
Vein material: At least two generations: (1) linear anastomosing <4 mm wide filled with dark gray-black amorphous serpentine; (2) <1 mm wide, near top of Piece 2A, filled with chrysotile following and cross stitching an earlier vein.
ADDITIONAL COMMENTS: Primary silicates are variably serpentinized with some fresh-looking areas left. Piece 2 is the largest single core piece recovered from Conical Seamount, and shows a gradation in degree of serpentinization from top to the middle.

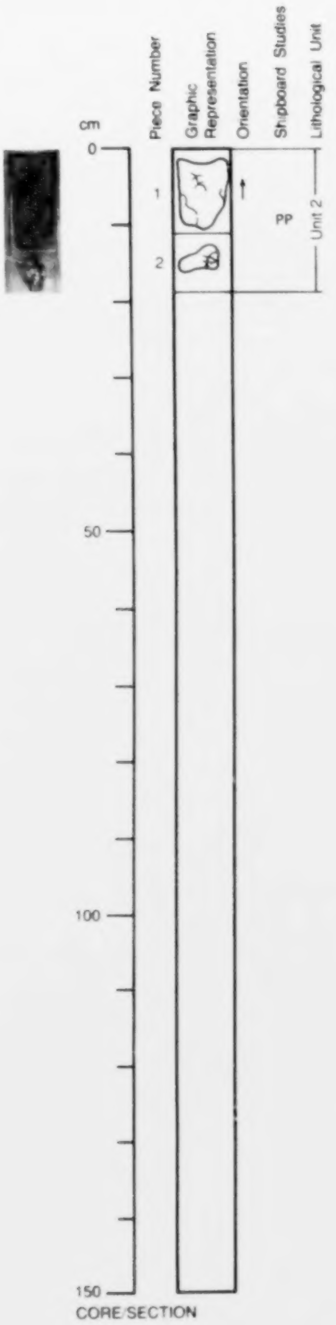
cm
Piece Number
Graphic Representation
Orientation
Shipboard Studies
Lithological Unit
0
1
2
PP
Unit 2
50
100
150
CORE/SECTION

125-780D-5X-1

UNIT 2: SERPENTINIZED HARZBURGITE

Pieces 1 and 2

COLOR: Dark bluish gray (5B 4/1).
LAYERING: None.
DEFORMATION: Some tectonized fabric defined by elongation of pyroxenes and some stringers of spinel.
PRIMARY MINERALOGY:
Olivine - Mode: 70-80%.
Crystal size: <2 mm.
Crystal shape: Not visible.
Crystal orientation: None visible.
Percent replacement: Variable.

Orthopyroxene - Mode: 20-25%.
Crystal size: 1-4 mm.
Crystal shape: Equant-elongate.
Crystal orientation: Defines a fabric.
Percent replacement: Variable.

Spinel - Mode: <5%.
Crystal size: <2 mm.
Crystal shape: Equant-ragged.
Crystal orientation: Some stringers.
Percent replacement: Not visible.
SECONDARY MINERALOGY:
Serpentine.
Total percent: 50-80%.
Texture: Bastitic pseudomorphs after pyroxenes in areas.
Vein material: <1-mm-wide white veins oriented mostly 45 degrees from core barrel. Also these veins are crosscut by smaller (<1-mm-wide and <3-mm-long) veins oriented 90 degrees to main vein, dark black amorphous serpentine veins <1 mm wide.

125-780C-[illegible] (Piece 7A, 61-62 cm) OBSERVER: SAB WHERE SAMPLED: Conical Seamount summit

ROCK NAME: Serpentinized harzburgite

GRAIN SIZE: 0.1-5 mm

TEXTURE: Mesh

PRIMARY MINERALOGY	PERCENT PRESENT	PERCENT ORIGINAL	SIZE (mm)	COMPO-SITION	MORPHOLOGY	COMMENTS
PHENOCRYSTS						
Olivine	2	78	0.1-5		Anhedral	Altered to serpentine mesh; wavy extinction, kinked.
Clinopyroxene	1	1	0.2-0.4		Anhedral	Around orthopyroxene margins usually and lamellae.
Spinel	1	1	0.5-2	Cr	Anhedral	Red, altered to magnetite.
Orthopyroxene	15	20	0.5-3		Subhedral-anhedral	Wavy extinction, kink-banded, altered to serpentine bastite and chlorite(?).
GROUNDMASS						
N/A	N/A	N/A	N/A		N/A	

SECONDARY MINERALOGY	PERCENT	REPLACING/ FILLING	COMMENTS
Chlorite	2	Orthopyroxene	Blue-green to green pleochroism, anhedral patches forming around orthopyroxene cleavages and fractures.
Serpentine	80	Olivine, orthopyroxene	Lizardite and/or chrysotile forming mesh and bastite textures from olivine and orthopyroxene.
Magnetite	1	Spinel	Dusty [illegible]-mm grains concentrated in serpentine vein.

VESICLES/ CAVITIES	PERCENT	LOCATION	SIZE (mm)	FILLING	SHAPE
Vesicles	0				

COMMENTS: Spinels sometimes form ragged trails; spinels have inclusions of orthopyroxene and olivine. Orthopyroxene have wavy extinction, kink-bands, exsolution lamellae of clinopyroxene which are bent; inclusions of olivine(?). Olivine grains are fractured, show wavy extinction, and have kink-banding. Some olivine and orthopyroxene have recrystallized into smaller [illegible](?). Many chrysotile and magnetite veins (1-2 mm wide) parallel each other at 45 degree angle to long axis of slide.

125-780C-[illegible] ([illegible] cm) OBSERVER: [illegible] WHERE SAMPLED: Conical Seamount summit

ROCK NAME: Serpentine sandstone

GRAIN SIZE: Up to 2 mm

TEXTURE: Poorly sorted

PRIMARY MINERALOGY	PERCENT PRESENT	PERCENT ORIGINAL	SIZE (mm)	COMPO-SITION	MORPHOLOGY	COMMENTS
PHENOCRYSTS						
Olivine	[illegible]	[illegible]	N/A		N/A	
Plagioclase	[illegible]	[illegible]	N/A		N/A	
Clinopyroxene	1	1	N/A		N/A	
Spinel	1	1	[illegible]	Cr	N/A	
Orthopyroxene	1	8	2-3		N/A	
GROUNDMASS						
Serpentine	90	N/A	N/A		N/A	Forms very fine-grained unsorted matrix with brucite, serpentine grains are oriented (i.e. by bedding processes?).
Brucite	8	N/A	N/A		N/A	Forms very fine-grained unsorted matrix with serpentine.

VESICLES/ CAVITIES	PERCENT	LOCATION	SIZE (mm)	FILLING	SHAPE
Vesicles	0				

COMMENTS: No piece number given.

125-780C-8R-01 (Piece 1,16-17 cm) OBSERVER: TER WHERE SAMPLED: Conical Seamount summit

ROCK NAME: Carbonate rock

GRAIN SIZE: Fine, <2 mm

TEXTURE:

PRIMARY MINERALOGY	PERCENT PRESENT	PERCENT ORIGINAL	SIZE (mm)	COMPO-SITION	MORPHOLOGY	COMMENTS
PHENOCRYSTS						
Calcite	90	100	fine <2		Subhedral-euhedral	
GROUNDMASS						
N/A	N/A	N/A	N/A		N/A	

SECONDARY MINERALOGY	PERCENT	REPLACING/ FILLING	COMMENTS
Clays (?)	10	Calcite	

VESICLES/ CAVITIES	PERCENT	LOCATION	SIZE (mm)	FILLING	SHAPE
Vesicles	0				

COMMENTS: Carbonate includes microfossils (radiolarians) and a greenish white section (5 cm by 2 cm) that may be part of a calcite vein.

125-780C-8R-01 (Piece 10,98-101 cm) OBSERVER: SAB WHERE SAMPLED: Conical Seamount summit

ROCK NAME: Serpentinized dunite

GRAIN SIZE: 0.1-3 mm

TEXTURE: Mesh (and cataclastic?)

PRIMARY MINERALOGY	PERCENT PRESENT	PERCENT ORIGINAL	SIZE (mm)	COMPO-SITION	MORPHOLOGY	COMMENTS
PHENOCRYSTS						
Olivine	38.5	92	1-2	Fo95	Anhedral	Altered to serpentine mesh; 2V=-85 degrees wavy extinction.
Spinel	0.5	1	0.1-1		Anhedral	Dark brown-red; altered to magnetite.
Orthopyroxene	0	7	1-3		Anhedral	Completely altered to serpentine bastite and chlorite.
GROUNDMASS						
N/A	N/A	N/A	N/A		N/A	

SECONDARY MINERALOGY	PERCENT	REPLACING/ FILLING	COMMENTS
Chlorite	2		Pale-green to yellow pleochroism, located along bastite cleavages and grains.
Serpentine	55	Olivine, orthopyroxene	Lizardite and/or chrysotile forming mesh and bastite textures. Chrysotile and magnetite veins occur.
Magnetite	1	Spinel	Dusty, 0.1-mm grains concentrated mostly along serpentine veins.
Talc	3	Orthopyroxene, serpentine	High birefringence, fibrous, altering from serpentine bastite and olivine mesh throughout slide.

VESICLES/ CAVITIES	PERCENT	LOCATION	SIZE (mm)	FILLING	SHAPE
Vesicles	0				

COMMENTS: Olivine has wavy extinction, elongated and extremely fractured (almost cataclastic looking). Few spinels are rimmed by another phase (anomalous brown interference colors) and then rimmed by chlorite (anomalous deep-blue colors). Multiple vein sets have conjugate set orientation. First generation veins have elongate magnetite trails. Second generation cuts these trails. Orthopyroxene is completely altered although olivine is still present (highly fractured and broken up). Veins are 0.5-3 mm wide.

[illegible] (Piece 2, 13-14 cm) OBSERVER: SAB WHERE SAMPLED: Conical Seamount summit

ROCK NAME: Tectonized serpentinized harzburgite

GRAIN SIZE: 0.1-4 mm

TEXTURE: Porphyroclastic-mesh

PRIMARY MINERALOGY	PERCENT PRESENT	PERCENT ORIGINAL	SIZE (mm)	COMPO-SITION	MORPHOLOGY	COMMENTS
PHENOCRYSTS						
Olivine	15	75	1-5		Elongate-anhedral	Altered to serpentine mesh; wavy extinction.
Clinopyroxene	0.5	1.5	0.2-0.5		Euhedral-anhedral	As exsolution lamellae, as grains in and around orthopyroxene.
Spinel	1.5	1.5	0.1-1	Cr	Ragged-equant	Red brown, altered to magnetite.
Orthopyroxene	10	22	2-8		Elongate-anhedral	Altered to serpentine bastite, wavy extinction, fractures, strained; bent exsolution lamellae.
GROUNDMASS						
N/A	N/A	N/A	N/A		N/A	

SECONDARY MINERALOGY	PERCENT	REPLACING/ FILLING	COMMENTS
Chrysotile(?)	<1	Serpentine	Very pale-green to yellow [illegible] in anastomosing veins across slide.
Serpentine	82	Olivine, orthopyroxene	In veins, fractures, and shears. Mostly after olivine, amorphous microcrystalline aggregate-deformed mesh. Many coarse multi-length fiber veins (probably across fiber) (Chrysotile(?) lizardite and/or chrysotile mainly; probably antigorite(?))
Magnetite	<1	Spinel	Dusty 0.1-mm grains concentrated along serpentine veins.

VESICLES/ CAVITIES	PERCENT	LOCATION	SIZE (mm)	FILLING	SHAPE
Vesicles	0				

COMMENTS: This rock has been tectonized. It has suffered brittle deformation, pervasive but with small total strain. The primary mineralogy has been disintegrated forming a porphyroclastic texture. The serpentine (antigorite?/lizardite) (?) has been sheared and pervasively deformed with serpentine veins now preferentially aligned indicating shearing. Olivines are disintegrated and strained and have serpentine pseudomorphs inclusions. Orthopyroxenes are deformed and have large number of olivine and clinopyroxene inclusions.

125-780D-10R-1 (Piece 6,36-37 cm) OBSERVER: SAB WHERE SAMPLED: Conical Seamount summit

ROCK NAME: Serpentinized dunite

GRAIN SIZE: Fine-grained serpentine

TEXTURE: Felted

PRIMARY MINERALOGY	PERCENT PRESENT	PERCENT ORIGINAL	SIZE (mm)	COMPO-SITION	MORPHOLOGY	COMMENTS
PHENOCRYSTS						
Olivine	0	95	Not visible		Not visible	Completely altered to serpentine blades; trace mesh serpentine visible.
Spinel	0.5	1	0.2-0.5	Cr	Ragged-anhedral	Forms stringers of 3-4 grains.
Orthopyroxene	0.5	3	0.1-0.5		Anhedral	Altered to serpentine bastite; broken grains relict in bastite which is commonly kink-banded.
GROUNDMASS						
N/A	N/A	N/A	N/A		N/A	

SECONDARY MINERALOGY	PERCENT	REPLACING/ FILLING	COMMENTS
Chlorite	0.2	Orthopyroxene	Small patches forming along cleavages in orthopyroxene relics.
Serpentine	98.6	Olivine, orthopyroxene	Antigorite blades are the major phase present and forms a matted felt of splays of grain aggregates. Lizardite and/or chrysotile: May appear in minor amounts (5%).
Magnetite	Tr	Olivine, spinel	Dusty 0.1-mm grains disseminated throughout serpentine.
Brucite(?)	0.2	Serpentine	Intermixed with serpentine but XRD is needed.

VESICLES/ CAVITIES	PERCENT	LOCATION	SIZE (mm)	FILLING	SHAPE
Vesicles	0				

COMMENTS: This rock has suffered an unusual style of serpentinization with no/rare mesh texture preserved, and only a few bastite pseudomorphs. Instead the rock is almost entirely replaced by a felted texture of radiating laths of serpentine with no preferred orientation. All relic textures have been destroyed. Major serpentine phase is probably antigorite. No post-serpentinization deformation visible. Two thin sections made from this interval from the same piece.

125-780D-10R-1 (Piece 6,36-37 cm) OBSERVER: MHS WHERE SAMPLED: Conical Seamount summit

ROCK NAME: Serpentinized dunite

GRAIN SIZE: Fine-grained serpentine

TEXTURE: Felted

PRIMARY MINERALOGY	PERCENT PRESENT	PERCENT ORIGINAL	SIZE (mm)	COMPO-SITION	MORPHOLOGY	COMMENTS
PHENOCRYSTS						
Olivine	0	89.5	Not visible		Not visible	Completely altered to serpentine blades.
Spinel	1.5	1.5	0.1-0.8	Cr	Squat-anhedral	Forms stringers 3-4 grains, altered to magnetite.
Orthopyroxene	0	9	0.5-1		Anhedral	Completely altered to serpentine bastite.
GROUNDMASS						
N/A	N/A	N/A	N/A		N/A	

SECONDARY MINERALOGY	PERCENT	REPLACING/ FILLING	COMMENTS
Serpentine	96.5	Olivine, orthopyroxene	Antigorite felted laths in radiating aggregates throughout slide.
Magnetite	1.5	Olivine, orthopyroxene, spinel	Dusty 0.1-mm grains disseminated throughout.
Brucite	0.5	Serpentine	Distributed throughout slide intermixed with serpentine.

VESICLES/ CAVITIES	PERCENT	LOCATION	SIZE (mm)	FILLING	SHAPE
Vesicles	0				

COMMENTS: Rock is totally replaced by serpentine (antigorite). No post-serpentinization deformation is apparent in the slide. There are two thin sections made from this piece. This slide appears to be more orthopyroxene-rich, but is nonetheless a dunite. It is difficult to tell because of the degree of serpentinization and the fact that not all orthopyroxene forms bastite when being serpentinized! Spinels are altering to two phases-one with anomalous brown colors and one with anomalous blue.

[illegible] OBSERVER: [illegible] WHERE SAMPLED: [illegible]

ROCK NAME: [illegible]

GRAIN SIZE: Extremely fine-grained

TEXTURE: [illegible]

PRIMARY MINERALOGY PERCENT PRESENT PERCENT ORIGINAL SIZE (mm) COMPOSITION MORPHOLOGY COMMENTS

N.A. N.A. N.A. N.A. N.A.

SECONDARY MINERALOGY PERCENT REPLACING/FILLING COMMENTS

[illegible]

VESICLES/CAVITIES PERCENT LOCATION SIZE (mm) FILLING SHAPE

[illegible]

COMMENTS: [illegible]

[illegible] OBSERVER: [illegible] WHERE SAMPLED: [illegible]

ROCK NAME: [illegible]

GRAIN SIZE: [illegible]

TEXTURE: [illegible]

PRIMARY MINERALOGY PERCENT PRESENT PERCENT ORIGINAL SIZE (mm) COMPOSITION MORPHOLOGY COMMENTS

[illegible]

N.A. N.A. N.A. N.A. N.A.

SECONDARY MINERALOGY PERCENT REPLACING/FILLING COMMENTS

[illegible]

VESICLES/CAVITIES PERCENT LOCATION SIZE (mm) FILLING SHAPE

[illegible]

COMMENTS: [illegible]

[illegible] (Piece 2A,60-63 cm) OBSERVER: SAB WHERE SAMPLED: Conical Seamount summit

ROCK NAME: Serpentinized harzburgite

GRAIN SIZE: 0.1-2 mm

TEXTURE: Granular, mesh and bastite

PRIMARY MINERALOGY	PERCENT PRESENT	PERCENT ORIGINAL	SIZE (mm)	COMPOSITION	MORPHOLOGY	COMMENTS
PHENOCRYSTS						
Olivine	13	79.5	0.5-3		Anhedral	Altering to serpentine mesh.
Clinopyroxene	0.5	0.5	0.1-0.8		Anhedral	Grains in and near orthopyroxene crystals.
Spinel	0.5	1	0.1-0.5	Cr	Anhedral	Red; altering to magnetite and chlorite(?).
Orthopyroxene	15	20	1-3		Subhedral-anhedral	Altering to serpentine bastite, wavy extinction, kink-banded.
GROUNDMASS						
N/A	N/A	N/A	N/A		N/A	

SECONDARY MINERALOGY	PERCENT	REPLACING/FILLING	COMMENTS
Clays	<1	Serpentine	Rusty brown clays throughout slide and mainly within serpentine veinlets.
Chlorite	<1	Orthopyroxene	Pale-green to pale yellow pleochroic; along orthopyroxene fractures and cleavages.
Serpentine	67	Olivine; orthopyroxene	Lizardite and/or chrysotile starting to form mesh and bastite textures throughout slide.
Magnetite	1	Olivine; orthopyroxene; spinel	Dusty + some grains concentrated mostly in serpentine veins.
Talc	2	Orthopyroxene	High birefringence, fibrous, altering from orthopyroxene grains throughout slide.

VESICLES/CAVITIES	PERCENT	LOCATION	SIZE (mm)	FILLING	SHAPE
Vesicles	[illegible]				

COMMENTS: Relatively clinopyroxene-rich harzburgite. Olivines are crossed by planes which have anomalous brown and anomalous blue interference colors. Olivine and orthopyroxene show strain because of kink-banding and wavy extinction.

[illegible] (1-3 cm) OBSERVER: MFG WHERE SAMPLED: Conical Seamount summit

ROCK NAME: Metamorphosed serpentine sandstone

GRAIN SIZE: Very fine-grained, 1 mm

TEXTURE: Granular to pebbly sandstone with recrystallized matrix.

PRIMARY MINERALOGY	PERCENT PRESENT	PERCENT ORIGINAL	SIZE (mm)	COMPOSITION	MORPHOLOGY	COMMENTS
Serpentine	75-80	N/A	N/A		N/A	Makes up very fine grained matrix. Carbonate occurs as euhedral and subhedral grains as well as cavity
Calcite	11	N/A	N/A		N/A	
[illegible]	11	N/A	N/A		N/A	
Chlorite	[illegible]	N/A	N/A		N/A	

SECONDARY MINERALOGY	PERCENT	REPLACING/FILLING	COMMENTS
Chlorite	15-20		Located in clasts and in matrix. Pleochroism is very weak pale green (or even absent) with anomalous blue birefringence in this section; some of it may be serpentine(?)
Hornblende	Trace	Detrital	One euhedral grain of brown hornblende.
Plagioclase	Trace	Detrital	One grain of plagioclase.
OPX PSEUDOMORPH		Detrital	Few clasts of serpentine pseudomorphs which may have previously been orthopyroxene; size ranges from 0.5 to 1 mm.
Magnetite		Detrital	0.1-0.5 mm, ragged to dusty clasts.
Spinel	[illegible]	Detrital	0.2-0.5 mm [illegible] spinel, clastic, equant.

VESICLES/CAVITIES	PERCENT	LOCATION	SIZE (mm)	FILLING	SHAPE
Vesicles	[illegible]				

COMMENTS: A fascinating section that needs further analysis. Rock has a carbonate-rich layer/coating on the side of the section. Obviously a reworked sediment with detrital grains of serpentinized ultramafic rock. Some carbonate appears to replace earlier plagioclase. Some anhydrite(?) in clasts. Felted lath texture dominates the matrix and is undisturbed hence formation of this texture post-dates the clastic sedimentary history of sample (including matrix). No piece number given.

[illegible] OBSERVER: [illegible] WHERE SAMPLED: [illegible]

ROCK NAME: [illegible]

GRAIN SIZE: [illegible]

TEXTURE: [illegible]

[illegible]

COMMENTS: [illegible]

[illegible] OBSERVER: [illegible] WHERE SAMPLED: [illegible]

ROCK NAME: [illegible]

GRAIN SIZE: [illegible]

TEXTURE: [illegible]

[illegible]

COMMENTS: [illegible]

SITE 781 HOLE A CORE 1R CORED INTERVAL 4420.6-4427.5 mbsl; 0-6.9 mbsf

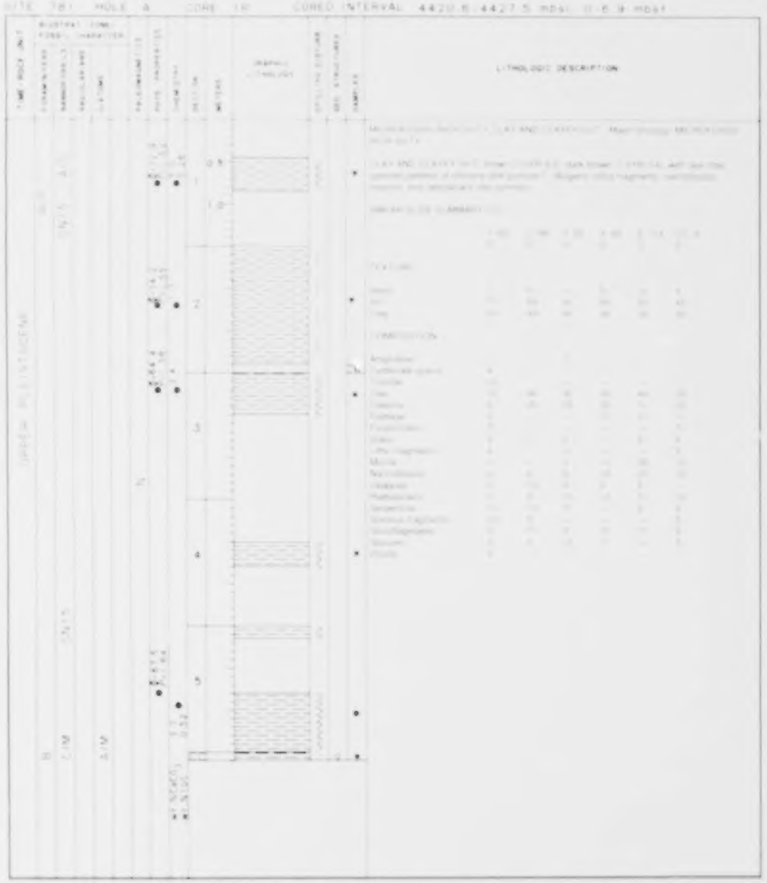
TIME-ROCK UNIT
BIOSTRAT. ZONE/ FOSSIL CHARACTER
FORAMINIFERS
NANNOFOSSILS
RADIOLARIANS
DIATOMS
PALEOMAGNETICS
PHYS. PROPERTIES
CHEMISTRY
SECTION
METERS
GRAPHIC LITHOLOGY
DRILLING DISTURB.
SED. STRUCTURES
SAMPLES
LITHOLOGIC DESCRIPTION
0.5
1.0
1
2
3
4
5
UPPER PLEISTOCENE
SMEAR SLIDE SUMMARY (%):
TEXTURE:
Sand
Silt
Clay
COMPOSITION:

781 A 2R NO RECOVERY

781 H 3R NO RECOVERY

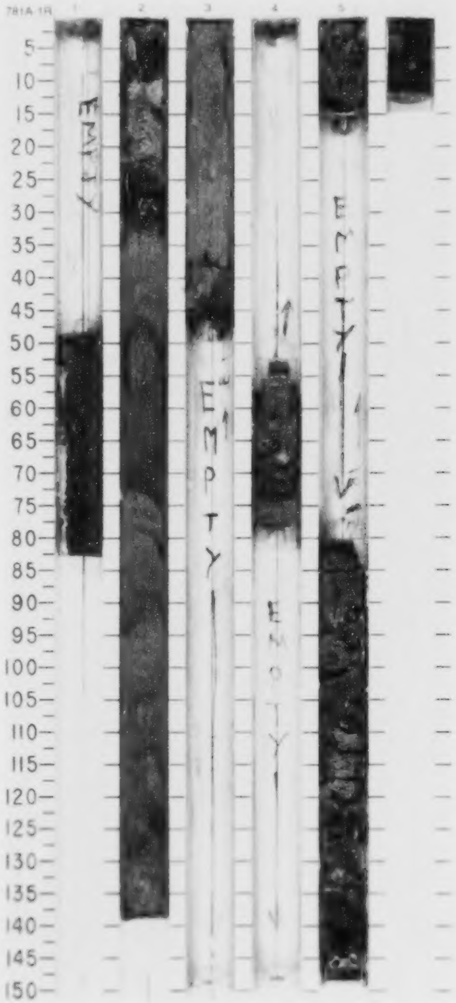
781A-1R
1
2
3
4
5
EMPTY
EMPTY
EMPTY
EMPTY
5
10
15
20
25
30
35
40
45
50
55
60
65
70
75
80
85
90
95
100
105
110
115
120
125
130
135
140
145
150

SITE 761 HOLE A CORE 4R CORED INTERVAL [illegible] mbsl; [illegible] mbsf

GRAPHIC LITHOLOGY

LITHOLOGIC DESCRIPTION

[illegible]

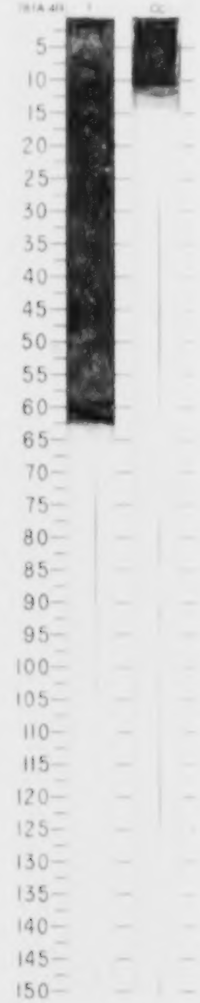
761A-4R
1
CC
5
10
15
20
25
30
35
40
45
50
55
60
65
70
75
80
85
90
95
100
105
110
115
120
125
130
135
140
145
150

SITE 781 HOLE A CORE 5R CORED INTERVAL 4456.0-4465.5 mbsl; 35.4-44.9 mbsf

TIME-ROCK UNIT	BIOSTRAT. ZONE/FOSSIL CHARACTER: FORAMINIFERS	NANNOFOSSILS	RADIOLARIANS	DIATOMS	PALEOMAGNETICS	PHYS. PROPERTIES	CHEMISTRY	SECTION	METERS	GRAPHIC LITHOLOGY	DRILLING DISTURB.	SED. STRUCTURES	SAMPLES	LITHOLOGIC DESCRIPTION
[illegible]	[illegible]	[illegible]		[illegible]		[illegible]			1 CC	[illegible]			● ○	[illegible] Major lithology: [illegible] SMEAR SLIDE SUMMARY (%): TEXTURE: Sand Silt Clay COMPOSITION: [illegible]

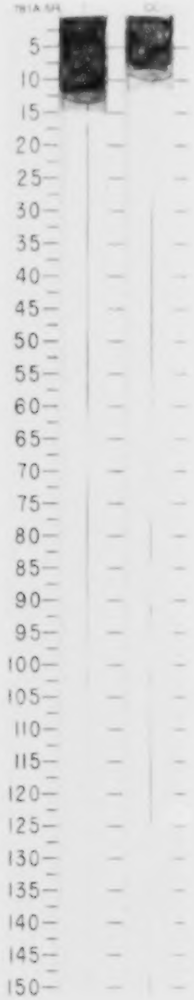
781A-5R
1
CC
5
10
15
20
25
30
35
40
45
50
55
60
65
70
75
80
85
90
95
100
105
110
115
120
125
130
135
140
145
150

SITE 781 HOLE A CORE 6R CORED INTERVAL 4465.5-4475.1 mbsl; 44.9-54.5 mbsf

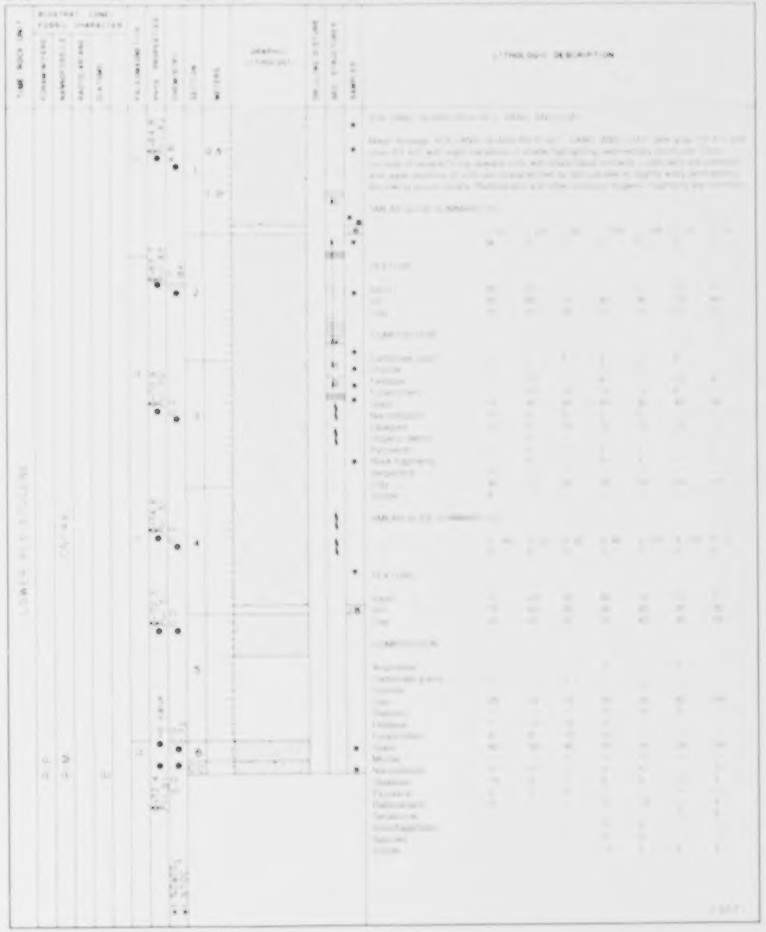

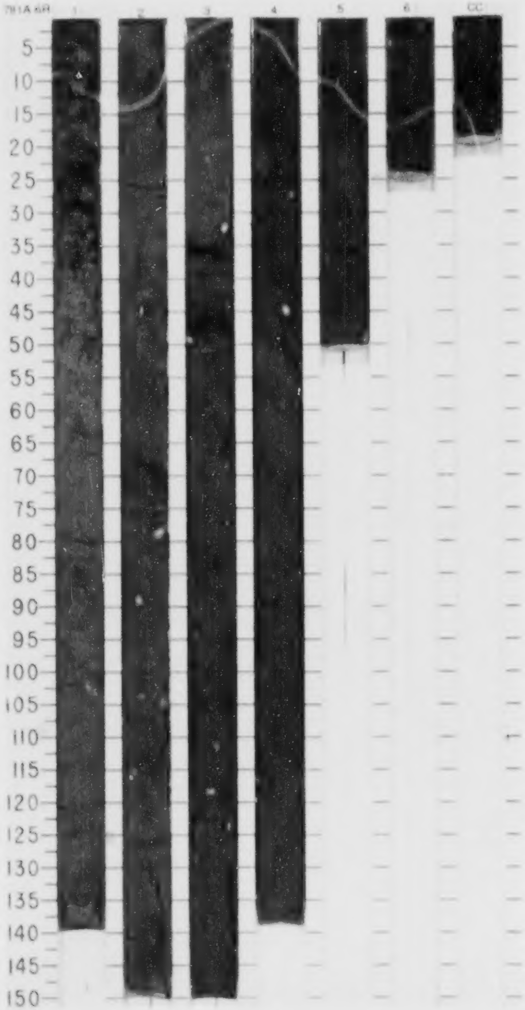
781A-6R
1
2
3
4
5
6
CC
5
10
15
20
25
30
35
40
45
50
55
60
65
70
75
80
85
90
95
100
105
110
115
120
125
130
135
140
145
150

SITE 781 HOLE A CORE 6R CORED INTERVAL 4465.5-4475.1 mbrf; 44.9-54.5 mbsf

TIME-ROCK UNIT	BIOSTRAT. ZONE/ FOSSIL CHARACTER: FORAMINIFERS	NANNOFOSSILS	RADIOLARIANS	DIATOMS	PALEOMAGNETICS	PHYS. PROPERTIES	CHEMISTRY	SECTION	METERS	GRAPHIC LITHOLOGY	DRILLING DISTURB.	SED. STRUCTURES	SAMPLES	LITHOLOGIC DESCRIPTION
								1 2	0.5 1.0					SMEAR SLIDE SUMMARY (%): TEXTURE: Sand [illegible] Silt [illegible] Clay [illegible] COMPOSITION: Quartz [illegible] Clay [illegible] [illegible] Mica [illegible] Accessory minerals [illegible] Opaques [illegible] Radiolarians [illegible] [illegible] [illegible]

SITE 781 HOLE A CORE 7R CORED INTERVAL 4475.1-4485.1 mbsl; 54.5-64.5 mbsf

LITHOLOGIC DESCRIPTION

[illegible] SILT, SAND, AND CLAY

SMEAR SLIDE SUMMARY (%):

TEXTURE:

Sand

Silt

Clay

COMPOSITION:

SMEAR SLIDE SUMMARY (%):

TEXTURE:

COMPOSITION:

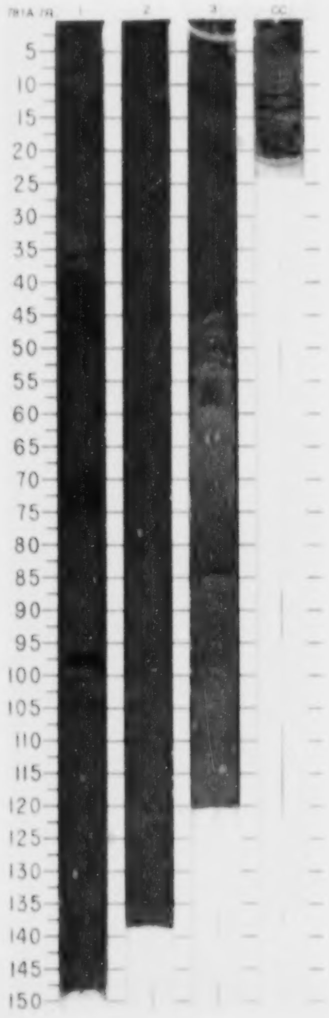
781A-7R
1
2
3
CC
5
10
15
20
25
30
35
40
45
50
55
60
65
70
75
80
85
90
95
100
105
110
115
120
125
130
135
140
145
150

SITE 781 HOLE A CORE 8R CORED INTERVAL 4485.1-4493.2 mbsl; 64.5-72.6 mbsf

TIME-ROCK UNIT	FORAMINIFERS	NANNOFOSSILS	RADIOLARIANS	DIATOMS	PALEOMAGNETICS	PHYS. PROPERTIES	CHEMISTRY	SECTION	METERS	GRAPHIC LITHOLOGY	DRILLING DISTURB.	SED. STRUCTURES	SAMPLES	LITHOLOGIC DESCRIPTION
UPPER PLIOCENE	B	CN12b F/M	R/P		N	[illegible]	[illegible]	1 2 CC	0.5 1.0	M			● ● ● ● ● ●	SILTS AND CLAY-RICH SILT Major lithology: [illegible] SMEAR SLIDE SUMMARY (%): [illegible]

TEXTURE:

Sand

Silt

Clay

COMPOSITION:

Amphibole

Carbonate grains

Chlorite

Clay

Diatoms

Feldspar

Foraminifers

Glass

Nannofossils

Opaques

Pyroxene

Radiolarians

Rock fragments

Spicules

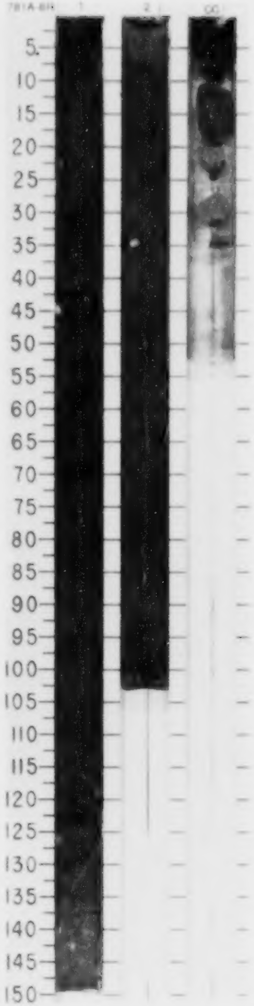
781A-8R
1
2
CC
5
10
15
20
25
30
35
40
45
50
55
60
65
70
75
80
85
90
95
100
105
110
115
120
125
130
135
140
145
150

SITE 781 HOLE A CORE 9R CORED INTERVAL 4493.2-4502.9 mbsl; 72.6-82.3 mbsf

TIME-ROCK UNIT	FORAMINIFERS	NANNOFOSSILS	RADIOLARIANS	DIATOMS	PALEOMAGNETICS	PHYS. PROPERTIES	CHEMISTRY	SECTION	METERS	GRAPHIC LITHOLOGY	DRILLING DISTURB.	SED. STRUCTURES	SAMPLES	LITHOLOGIC DESCRIPTION
						[illegible] ●		1	0.5 1.0	M				
						[illegible] ●		2		M				
						[illegible] ●		3		M				

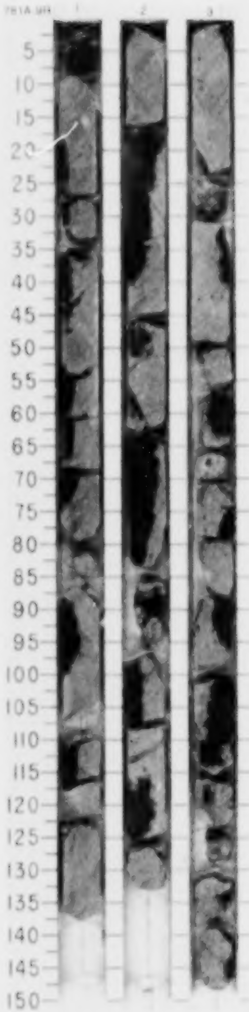
781A-9R
1
2
3
5
10
15
20
25
30
35
40
45
50
55
60
65
70
75
80
85
90
95
100
105
110
115
120
125
130
135
140
145
150

SITE 781 HOLE A CORE 10R CORED INTERVAL 4502.9-4512.4 mbsl; 82.3-91.8 mbsf

TIME-ROCK UNIT
BIOSTRAT. ZONE/FOSSIL CHARACTER
FORAMINIFERS
NANNOFOSSILS
RADIOLARIANS
DIATOMS
PALEOMAGNETICS
PHYS. PROPERTIES
CHEMISTRY
SECTION
METERS
GRAPHIC LITHOLOGY
DRILLING DISTURB.
SED. STRUCTURES
SAMPLES
LITHOLOGIC DESCRIPTION
0.5
1.0
1
2
3
IM
IM
IM

781 A 11R NO RECOVERY

781 A 12R NO RECOVERY

781 A 13R NO RECOVERY

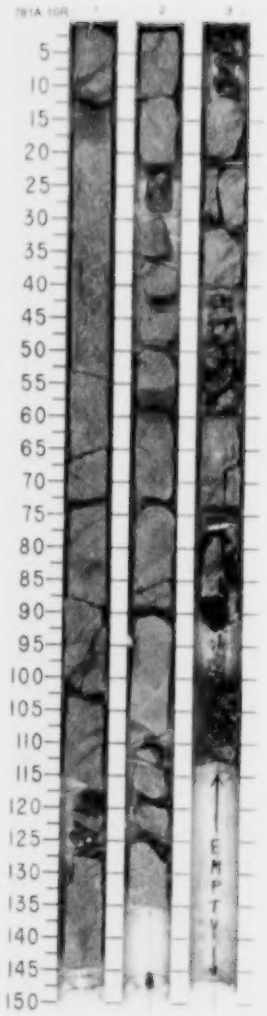
781A 10R
1
2
3
5
10
15
20
25
30
35
40
45
50
55
60
65
70
75
80
85
90
95
100
105
110
115
120
125
130
135
140
145
150
EMPTY

SITE 781 HOLE A CORE 14R CORED INTERVAL 4541.3-4551.0 mbsl; 120.7-130.4 mbsf

TIME-ROCK UNIT	BIOSTRAT. ZONE/FOSSIL CHARACTER: FORAMINIFERS	NANNOFOSSILS	RADIOLARIANS	DIATOMS	PALEOMAGNETICS	PHYS. PROPERTIES	CHEMISTRY	SECTION	METERS	GRAPHIC LITHOLOGY	DRILLING DISTURB.	SED. STRUCTURES	SAMPLES	LITHOLOGIC DESCRIPTION
								CC					●	[illegible] [illegible] SMEAR SLIDE SUMMARY (%): TEXTURE: [illegible] COMPOSITION: [illegible]

SITE 781 HOLE A CORE 15R CORED INTERVAL 4551.0-4560.6 mbsl; 130.4-140.0 mbsf

TIME-ROCK UNIT	BIOSTRAT. ZONE/FOSSIL CHARACTER: FORAMINIFERS	NANNOFOSSILS	RADIOLARIANS	DIATOMS	PALEOMAGNETICS	PHYS. PROPERTIES	CHEMISTRY	SECTION	METERS	GRAPHIC LITHOLOGY	DRILLING DISTURB.	SED. STRUCTURES	SAMPLES	LITHOLOGIC DESCRIPTION
UPPER PLIOCENE		[illegible]						1	0.5 1.0					[illegible]

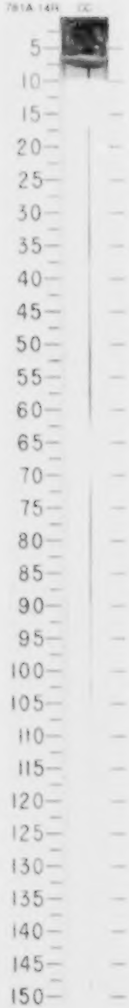
781A-14R
CC
5
10
15
20
25
30
35
40
45
50
55
60
65
70
75
80
85
90
95
100
105
110
115
120
125
130
135
140
145
150

SITE 781 HOLE A CORE 16R CORED INTERVAL 4560.6-4570.2 mbsl; 140.0-149.6 mbsf

TIME-ROCK UNIT	BIOSTRAT. ZONE/ FOSSIL CHARACTER: FORAMINIFERS	NANNOFOSSILS	RADIOLARIANS	DIATOMS	PALEOMAGNETICS	PHYS. PROPERTIES	CHEMISTRY	SECTION	METERS	GRAPHIC LITHOLOGY	DRILLING DISTURB.	SED. STRUCTURES	SAMPLES	LITHOLOGIC DESCRIPTION
UPPER PLIOCENE	C/M	CN12a		B		● [illegible]	● [illegible]	CC					●	VITRIC SILTY CLAY Major lithology: VITRIC SILTY CLAY, dark gray (5Y 4/1). [illegible] SMEAR SLIDE SUMMARY (%): TEXTURE: Sand [illegible] Silt [illegible] Clay [illegible] COMPOSITION: [illegible] Clay [illegible] Feldspar [illegible] Glass [illegible] Micrite [illegible] Nannofossils [illegible] Opaques [illegible] Quartz [illegible]

781 A 17R NO RECOVERY

SITE 781 HOLE A CORE 18R CORED INTERVAL 4576.9-4589.5 mbsl; 159.3-168.9 mbsf

TIME-ROCK UNIT	BIOSTRAT. ZONE/ FOSSIL CHARACTER: FORAMINIFERS	NANNOFOSSILS	RADIOLARIANS	DIATOMS	PALEOMAGNETICS	PHYS. PROPERTIES	CHEMISTRY	SECTION	METERS	GRAPHIC LITHOLOGY	DRILLING DISTURB.	SED. STRUCTURES	SAMPLES	LITHOLOGIC DESCRIPTION
UPPER PLIOCENE	A/M	CN12a		B/P				1 2	0.5 1.0					All samples from the core catcher were given to the Paleontologists.

781 A 19R NO RECOVERY

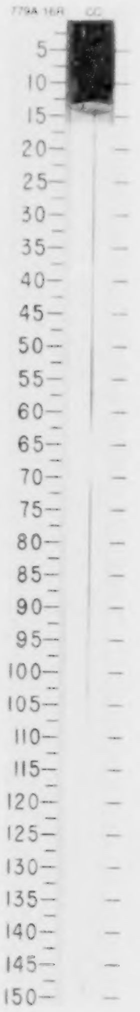

781 A 20R NO RECOVERY

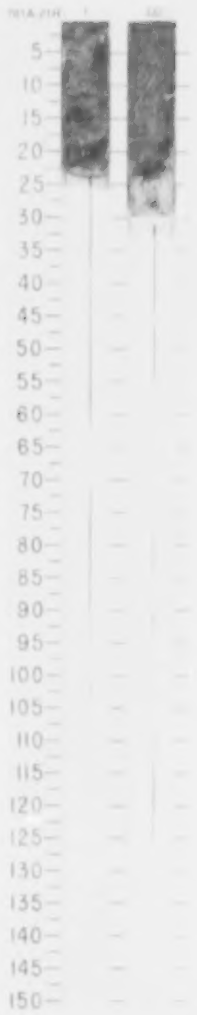
781A-21R
1
CC
5
10
15
20
25
30
35
40
45
50
55
60
65
70
75
80
85
90
95
100
105
110
115
120
125
130
135
140
145
150

SITE 781 HOLE A CORE 22R CORED INTERVAL [illegible] mbsl; [illegible] mbsf

TIME-ROCK UNIT	BIOSTRAT. ZONE / FOSSIL CHARACTER: FORAMINIFERS	NANNOFOSSILS	RADIOLARIANS	DIATOMS	PALEOMAGNETICS	PHYS. PROPERTIES	CHEMISTRY	SECTION	METERS	GRAPHIC LITHOLOGY	DRILLING DISTURB.	SED. STRUCTURES	SAMPLES	LITHOLOGIC DESCRIPTION
[illegible]	[illegible]	[illegible]	[illegible]	[illegible]	[illegible]	[illegible]	[illegible]	[illegible]	[illegible]	[illegible]	[illegible]	[illegible]	[illegible]	[illegible]

SITE 781 HOLE A CORE 23R CORED INTERVAL 4628.2-4637.8 mbsl; 207.6-217.3 mbsf

TIME-ROCK UNIT	BIOSTRAT. ZONE / FOSSIL CHARACTER: FORAMINIFERS	NANNOFOSSILS	RADIOLARIANS	DIATOMS	PALEOMAGNETICS	PHYS. PROPERTIES	CHEMISTRY	SECTION	METERS	GRAPHIC LITHOLOGY	DRILLING DISTURB.	SED. STRUCTURES	SAMPLES	LITHOLOGIC DESCRIPTION
[illegible]	[illegible]	[illegible]	[illegible]	[illegible]	[illegible]	[illegible]	[illegible]	[illegible]	0.5 1.0	[illegible]	[illegible]	[illegible]	[illegible]	[illegible]

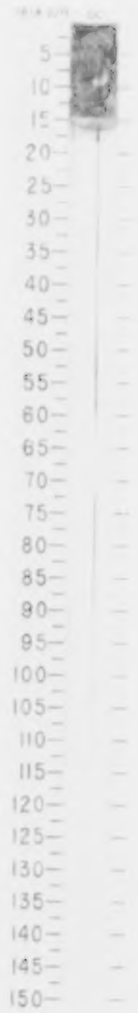
cm
5
10
15
20
25
30
35
40
45
50
55
60
65
70
75
80
85
90
95
100
105
110
115
120
125
130
135
140
145
150

SITE 781 HOLE A CORE 24R CORED INTERVAL [illegible]

TIME-ROCK UNIT	BIOSTRAT. ZONE/FOSSIL CHARACTER: FORAMINIFERS	NANNOFOSSILS	RADIOLARIANS	DIATOMS	PALEOMAGNETICS	PHYS. PROPERTIES	CHEMISTRY	SECTION	METERS	GRAPHIC LITHOLOGY	DRILLING DISTURB.	SED. STRUCTURES	SAMPLES	LITHOLOGIC DESCRIPTION
[illegible]	[illegible]	[illegible]		[illegible]				CC					*	[illegible]

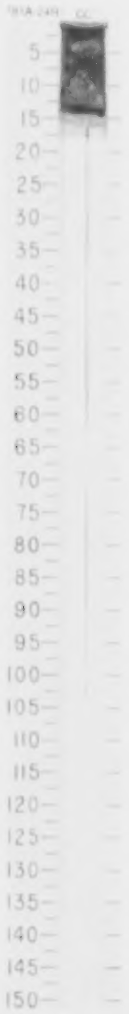
781A-24R
CC
5
10
15
20
25
30
35
40
45
50
55
60
65
70
75
80
85
90
95
100
105
110
115
120
125
130
135
140
145
150

SITE 781 HOLE A CORE 25R CORED INTERVAL [illegible] mbsl; 226.9-236.5 mbsf

TIME-ROCK UNIT	BIOSTRAT. ZONE / FOSSIL CHARACTER: FORAMINIFERS	NANNOFOSSILS	RADIOLARIANS	DIATOMS	PALEOMAGNETICS	PHYS. PROPERTIES	CHEMISTRY	SECTION	METERS	GRAPHIC LITHOLOGY	DRILLING DISTURB.	SED. STRUCTURES	SAMPLES	LITHOLOGIC DESCRIPTION
[illegible]	[illegible]	[illegible]				● [illegible]	● [illegible]						●	[illegible] Major lithology: [illegible] gray [illegible] [illegible] [illegible]: Sand [illegible], Silt [illegible], Clay [illegible] COMPOSITION: [illegible]

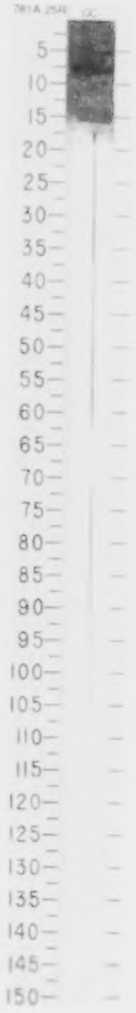
781A-25R
CC
5
10
15
20
25
30
35
40
45
50
55
60
65
70
75
80
85
90
95
100
105
110
115
120
125
130
135
140
145
150

SITE 781 HOLE A CORE 26R CORED INTERVAL [illegible]

GRAPHIC LITHOLOGY

LITHOLOGIC DESCRIPTION

[illegible]

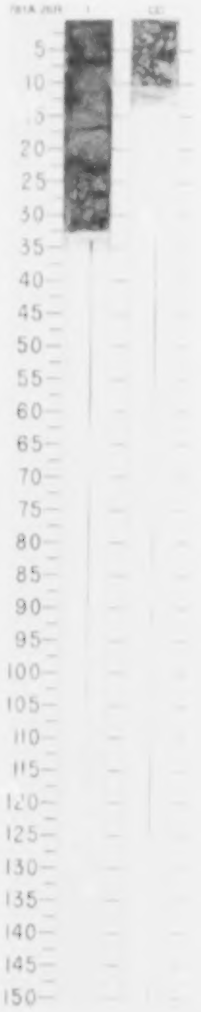
781A-26R
1
CC
5
10
15
20
25
30
35
40
45
50
55
60
65
70
75
80
85
90
95
100
105
110
115
120
125
130
135
140
145
150

SITE 781 HOLE A CORE 27R CORED INTERVAL 4666.0-4675.6 mbsl; 246.0-255.6 mbsf

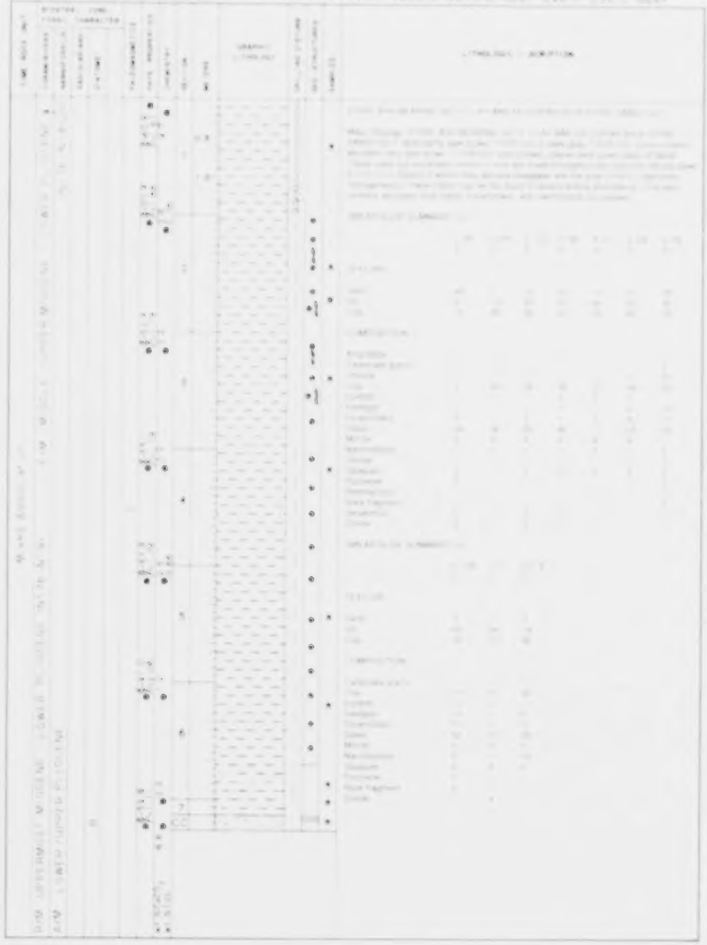
BIOSTRAT. ZONE/ FOSSIL CHARACTER
GRAPHIC LITHOLOGY
LITHOLOGIC DESCRIPTION
UPPERMOST MIOCENE - LOWER PLIOCENE

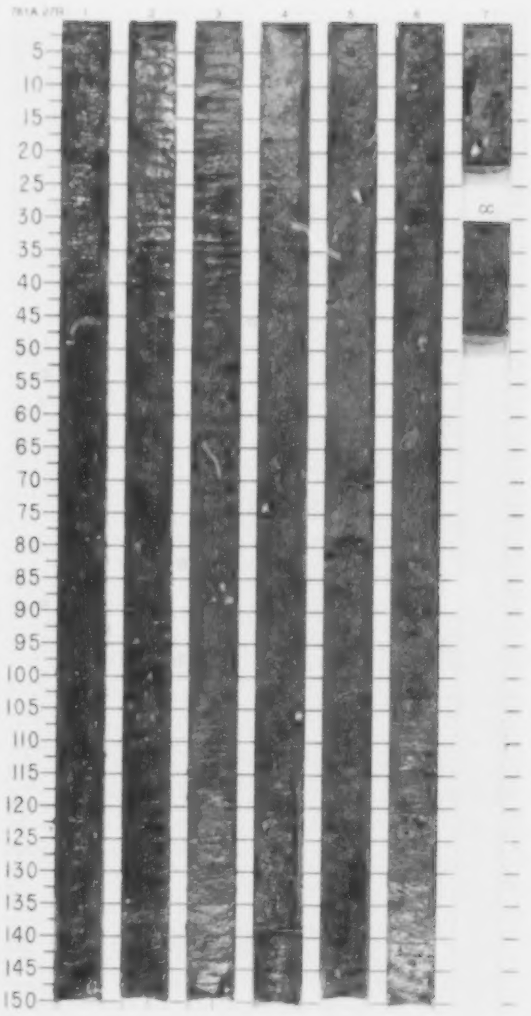
781A 27R
1
2
3
4
5
6
7
CC
5
10
15
20
25
30
35
40
45
50
55
60
65
70
75
80
85
90
95
100
105
110
115
120
125
130
135
140
145
150

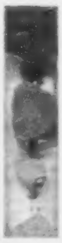

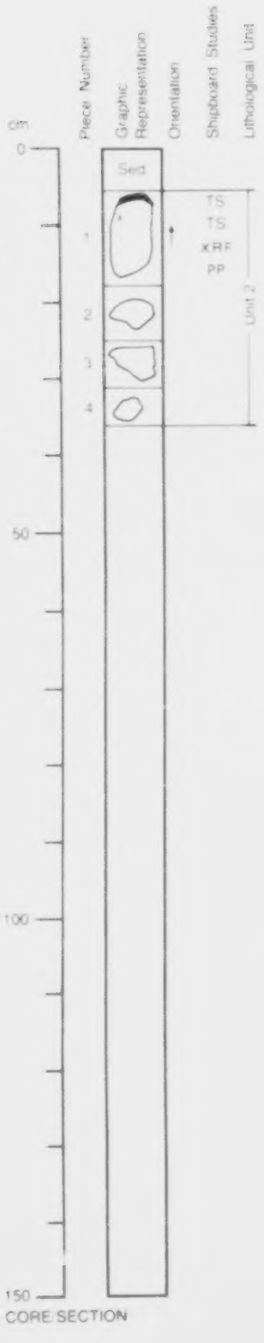
cm
0
50
100
150
CORE SECTION
Piece Number
Graphic Representation
Orientation
Shipboard Studies
Lithological Unit
Sed.
1
2
3
4
TS
TS
XRF
PP
Unit 2

125-781A-8R-CC

UNIT 2: OLIVINE-PLAGIOCLASE PHYRIC BASALT

Pieces 1-4

CONTACTS: Upper surface of Piece 1 (8 mm thick) is chilled glass.
PHENOCRYSTS: Appear to be fresh.
Plagioclase - 15%, 1-3 mm, euhedral-subhedral; occurs in glomerocrystic clots; also with olivine.
Olivine - 5%, <2 mm, euhedral; also occurs in glomerocrystic clots with plagioclase.
Clinopyroxene - trace, <2 mm, deep green; occurs with plagioclase, but may be alteration of plagioclase.
GROUNDMASS: Fine grained to glassy.
VESICLES: <2%, <1.5 mm, round to irregular, distributed throughout rock; some may be arranged in pipe form.
Miaroles: None.
COLOR: 2.5Y 8.0 black.
STRUCTURE: Massive.
ALTERATION: Appears to be fresh.
VEINS/FRACTURES: None obvious.
ADDITIONAL COMMENTS: Appears to be the top surface of a flow unit.

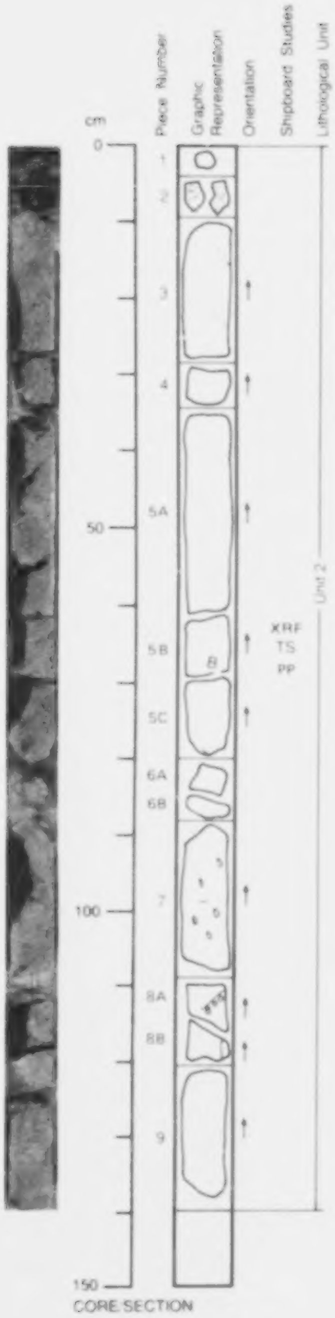
cm
Piece Number
Graphic Representation
Orientation
Shipboard Studies
Lithological Unit
0
50
100
150
1
2
3
4
5A
5B
5C
6A
6B
7
8A
8B
9
B
XRF
TS
PP
Unit 2
CORE/SECTION

125-781A-9R-1

UNIT 2: OLIVINE-PLAGIOCLASE-CLINOPYROXENE PHYRIC BASALT

Pieces 1-9

CONTACTS: None.
PHENOCRYSTS:
Plagioclase - 20-25%, 1-3 mm, euhedral to subhedral, glomerocrystic; also with olivine and pyroxene.
Olivine - 1-2%, 2 mm, euhedral to subhedral, also occurs in glomerocrystic clots with plagioclase and orthopyroxene.
Clinopyroxene - 1%, <1 mm, glomerophyric; also occurs with plagioclase and olivine.
GROUNDMASS: Fine grained to glassy.
VESICLES: 3-5%, 1-5 mm, round, distributed evenly throughout rock. Vesicle size appears to increase from Piece 1 - 9.
Miaroles: None.
COLOR: 7.5YR 4/0 gray.
STRUCTURE: Massive.
ALTERATION: Appears to be relatively fresh.
VEINS/FRACTURES: <3%, 0.8-1.0 cm wide, dip at 35-45 degrees.
ADDITIONAL COMMENTS: Appears to be a part of a sill. Piece 1 is probably near the top of the sill.

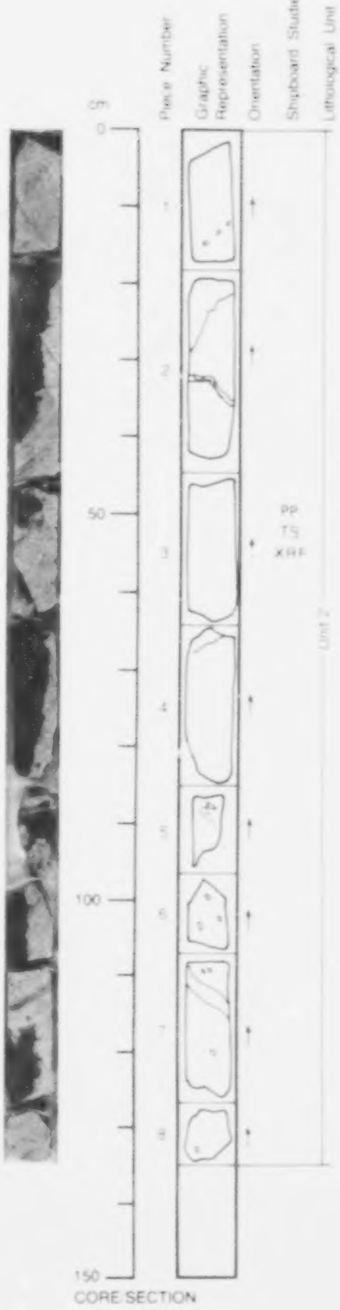
cm
0
50
100
150
CORE/SECTION
Piece Number
Graphic Representation
Orientation
Shipboard Studies
Lithological Unit
1
2
3
4
5
6
7
8
PP
TS
XRF
Unit 2

125-781A-9R-2

UNIT 2: OLIVINE-PLAGIOCLASE-CLINOPYROXENE PHRYIC BASALT

Pieces 1-8

CONTACTS: None.
PHENOCRYSTS:
Plagioclase - 20-25%, 2 mm, euhedral to subhedral, occurs in glomerocrystic clots and with olivine and pyroxene.
Olivine - 1-2%, 2 mm, euhedral to subhedral, also occurs in glomerocrystic clots with plagioclase and clinopyroxene.
Clinopyroxene - 1%, <1 mm, glomerocrystic, also occurs with plagioclase and olivine.
GROUNDMASS: Fine grained to glassy.
VESICLES: 3-5%, 1-3 mm, round, distributed evenly throughout rock.
Miaroles: None.
COLOR: 7.5YR 6/0 gray.
STRUCTURE: Massive.
ALTERATION: Appears to be relatively fresh.
VEINS/FRACTURES: <1%, 0.1-0.8 mm, dip at 35-45 degrees.
ADDITIONAL COMMENTS: Pieces 2, 5, 7 have <1 cm wide darker gray bands, which may have less plagioclase than the surrounding rock.

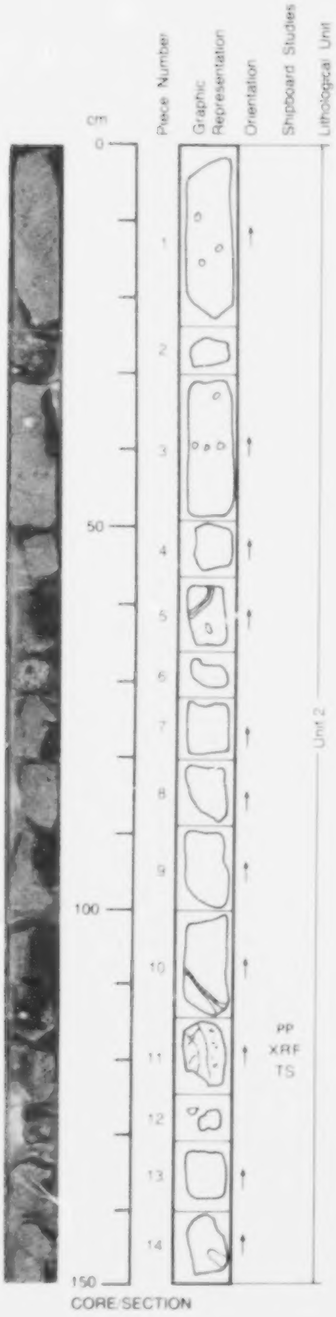
cm
Piece Number
Graphic Representation
Orientation
Shipboard Studies
Lithological Unit
0
50
100
150
1
2
3
4
5
6
7
8
9
10
11
12
13
14
PP
XRF
TS
Unit 2
CORE/SECTION

125-781A-9R-3

UNIT 2: OLIVINE-PLAGIOCLASE-CLINOPYROXENE PHYRIC BASALT

Pieces 1-14

CONTACTS: None.
PHENOCRYSTS:
Plagioclase - 20-25%, 1-3 mm, euhedral-subhedral, glomerocrystic, also with olivine and pyroxene olivine - 1-2%, 2 mm, euhedral-subhedral, also in glomerocrystic clots with plagioclase and orthopyroxene.
Clinopyroxene - 1%, <1 mm, glomerophyric, also with plagioclase and olivine.
GROUNDMASS: Fine-grained to glassy.
VESICLES: 3-5%, 1-4 mm, round, distributed evenly throughout rock.
Miaroles: None.
COLOR: 7.5YR 4/0 gray.
STRUCTURE: Massive.
ALTERATION: Appears to be relatively fresh.
VEINS/FRACTURES: None visible.
ADDITIONAL COMMENTS: Pieces 5, 10, 11, 14 have "bands" (<1 cm-1.5 cm wide) of darker gray material which may reflect a decrease in the abundance of plagioclase. Piece 11 is a contact between a plagioclase-rich, vesicular basalt and a plagioclase-poor, less vesicular basalt. TS and XRF samples were taken from the finer grained portion.

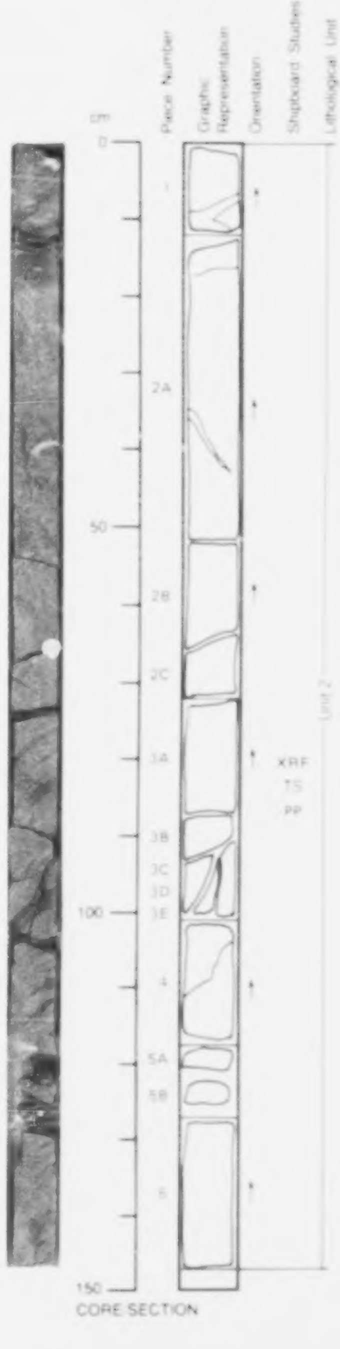
cm
0
50
100
150
CORE SECTION
Piece Number
Graphic Representation
Orientation
Shipboard Studies
Lithological Unit
1
2A
2B
2C
3A
3B
3C
3D
3E
4
5A
5B
6
XRF
TS
PP
Unit 2

125-781A-10R-1

UNIT 2: OLIVINE-PLAGIOCLASE-CLINOPYROXENE PHRYIC BASALT

Pieces 1-6

CONTACTS: None.
PHENOCRYSTS:
Plagioclase - 20-30%, 1-3 mm, euhedral to subhedral, glomerocrystic, also with olivine and pyroxene.
Olivine - 5%, 1-3 mm, euhedral to subhedral, glomerocrystic.
Clinopyroxene - 5-10%, ≤2 mm, euhedral to subhedral, glomerocrystic.
GROUNDMASS: Fine grained to glassy.
VESICLES: 5-10%, 0.3-4 mm, round to subround to irregular, throughout rock.
Miaroles: None.
COLOR: 7.5YR 4/0 gray.
STRUCTURE: Massive.
ALTERATION: Appears to be fresh.
VEINS/FRACTURES: None obvious.
ADDITIONAL COMMENTS: Pieces 1, 2A, 3A(?) all darker gray "bands" (< 5 cm thick?) which may have less plagioclase than the surrounding rock.

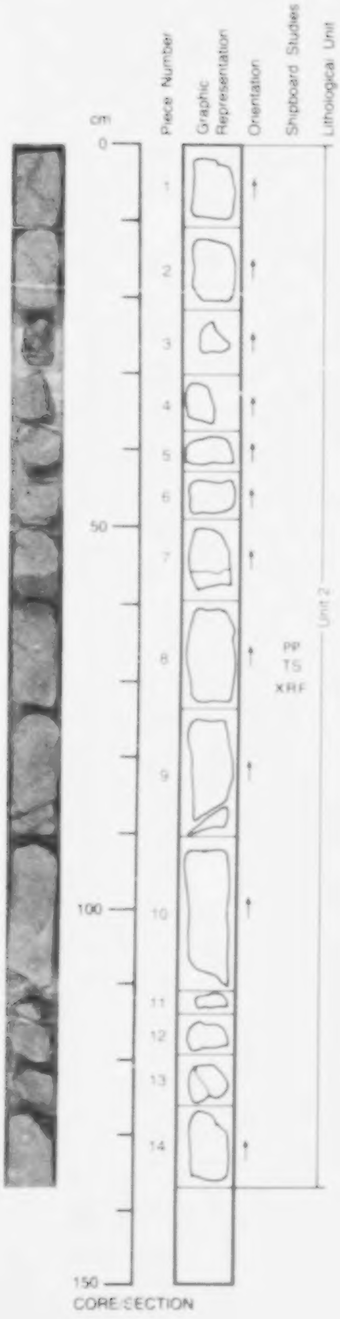
cm
0
50
100
150
Piece Number
Graphic Representation
Orientation
Shipboard Studies
Lithological Unit
1
2
3
4
5
6
7
8
9
10
11
12
13
14
PP
TS
XRF
Unit 2
CORE/SECTION

125-781A-10R-2

UNIT 2: OLIVINE-PLAGIOCLASE-CLINOPYROXENE PHYRIC BASALT

Pieces 1-14

CONTACTS: None

PHENOCRYSTS:

Plagioclase - 20-25%, 1-3 mm, euhedral to subhedral, glomerocrystic, also with olivine and pyroxene.

Olivine - 2-3%, 1-3 mm, euhedral to subhedral, glomerocrystic.

Clinopyroxene - 5-8%, 1-2 mm, euhedral-subhedral, glomerocrystic.

GROUNDMASS: Fine grained to glassy.

VESICLES: 4-5%, 0.2-1 mm wide, round to angular; throughout rock.

Minerals: None.

COLOR: 7.5YR 4/0 gray.

STRUCTURE: Massive.

ALTERATION: Appears to be relatively fresh.

VEINS/FRACTURES: <1%, <1 mm; no visible orientation; <1 mm wide black veining in some samples.

ADDITIONAL COMMENTS: Piece 7 shows contact between plagioclase-rich and plagioclase-poor basalt.

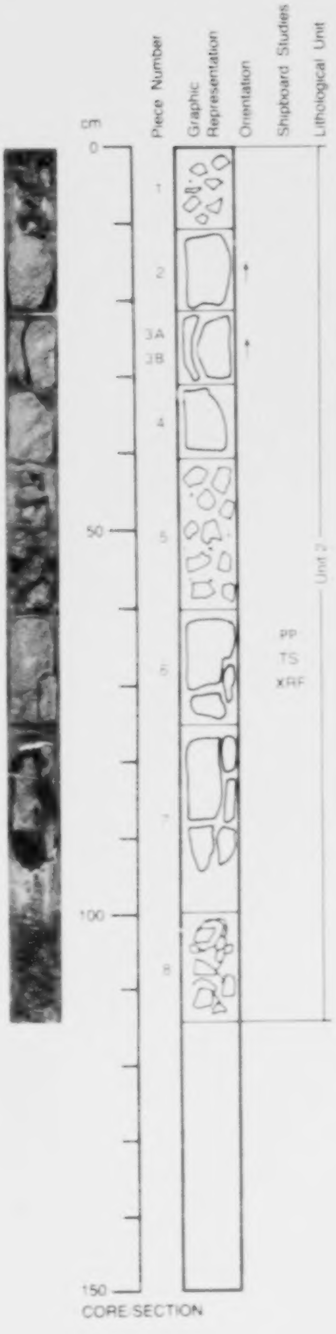
cm
Piece Number
Graphic Representation
Orientation
Shipboard Studies
Lithological Unit
0
50
100
150
1
2
3A
3B
4
5
6
7
8
PP
TS
XRF
Unit 2
CORE/SECTION

125-781A-10R-3

UNIT 2: OLIVINE-PLAGIOCLASE-CLINOPYROXENE PHYRIC BASALT

Pieces 1-8

CONTACTS: None

PHENOCRYSTS:

Plagioclase - 15-25%, 1-3 mm, euhedral to subhedral, glomerocrystic; also with olivine and pyroxene.

Olivine - 2-3%, <2 mm, euhedral to subhedral, glomerocrystic.

Clinopyroxene - 2-4%, 1-3 mm, euhedral-subhedral, glomerocrystic.

GROUNDMASS: Fine-grained to glassy.

VESICLES: 10%, <2 mm, round to angular, distributed evenly throughout rock.

Miaroles: None.

COLOR: 7.5YR 4/0 gray.

STRUCTURE: Massive.

ALTERATION: Appears to be relatively fresh.

VEINS/FRACTURES: Pieces 6 and 7 are fractured; no veining is visible.

ADDITIONAL COMMENTS: Pieces 1, 5, 8 consist of multiple fragments of basalt. Piece 8 also contains some fine-grained altered basaltic(?) rocks which appear to result from drilling disturbance.

125-781A-48R-CC (Piece 1,10-14 cm)   OBSERVER: MUR   WHERE SAMPLED: Northwest of Conical Seamount

ROCK NAME: Andesite-arc tholeiite

GRAIN SIZE: 0.1-3 mm

TEXTURE: Fine-grained, plagioclase phyric

PRIMARY MINERALOGY	PERCENT PRESENT	PERCENT ORIGINAL	SIZE (mm)	COMPO-SITION	MORPHOLOGY	COMMENTS
PHENOCRYSTS						
Plagioclase	35-40	35-40	0.5-3		Euhedral	Often as glomerocrysts, oscillatory zoning common.
Clinopyroxene	8-10	8-10	0.5-1		Subhedral-euhedral	Occurs with plagioclase in glomerocrysts.
Magnetite	0.5-1	0.5-1	0.2-0.5		Euhedral	Euhedral clusters.
GROUNDMASS						
Plagioclase	10	17-23	0.1-0.3		Laths, subhedral	
Clinopyroxene	10	10-8	0.1-0.1		Anhedral-subhedral	
Glass	15-20	15-20	N/A		N/A	Chilled margin with fresh yellow-brown glass plagioclase and clinopyroxene quench crystals.

SECONDARY MINERALOGY	PERCENT	REPLACING/ FILLING	COMMENTS
Clays	5-10	Glass	Abundant glass, quenched plagioclase and rapidly grown plagioclase in groundmass that has abundant (now altered) dark brown glass. Brown amorphous clay throughout matrix and plagioclase.
Clays	15-17	Plagioclase	

VESICLES/ CAVITIES	PERCENT	LOCATION	SIZE (mm)	FILLING	SHAPE
Vesicles	10-15	Throughout	<1-3	No	Irregular

COMMENTS: Two thin sections—one from 11-17 cm is slightly fresher than 10-14 cm.

125-781A-48R-CC (Piece 2,13-16 cm)   OBSERVER: JOR   WHERE SAMPLED: Northwest of Conical Seamount

ROCK NAME: Olivine-clinopyroxene-plagioclase-phyric basalt

GRAIN SIZE: 0.01-4 mm

TEXTURE: Hypocrystalline-intersertal

PRIMARY MINERALOGY	PERCENT PRESENT	PERCENT ORIGINAL	SIZE (mm)	COMPO-SITION	MORPHOLOGY	COMMENTS
PHENOCRYSTS						
Olivine	1-2	1-2	0.3-0.5		Rounded	
Plagioclase	15-20	15-20	0.2-2		Euhedral	Inclusions of opaques and glass fragment as glomerocryst and +/- clinopyroxene and olivine.
Clinopyroxene	4-6	4-6	0.02-1		Anhedral	As glomerocrysts +/- plagioclase infrequent twinning.
GROUNDMASS						
Glass	0	40-50	N/A		N/A	100% altered to dark brown clay.
Plagioclase	4-7	4-7	0.01-0.04		Euhedral	Laths, occasionally quench needles.
Clinopyroxene	20-25	22-25	<0.01-0.02		Anhedral	10-20% alteration to clay.
Opaques	1-3	1-3	<0.01-0.01		Euhedral-subhedral	Randomly distributed and as inclusions.

SECONDARY MINERALOGY	PERCENT	REPLACING/ FILLING	COMMENTS
Clays	40-50	Glass, clinopyroxene	Dark brown, amorphous after glass and dusty gray brown after clinopyroxene.

VESICLES/ CAVITIES	PERCENT	LOCATION	SIZE (mm)	FILLING	SHAPE
Vesicles	15-20	Throughout	0.1-4	None	Irregular

COMMENTS: Glassy margin contains euhedral quench clinopyroxene (lengths <0.01 mm) and plagioclase laths (0.01-0.03 mm, albite-twinned) and phenocrysts of plagioclase and clinopyroxene. Plagioclase grains are usually albite-twinned and typically zoned.

[illegible] OBSERVER: [illegible] WHERE SAMPLED: Northwest of Conical Seamount

ROCK NAME: [illegible]-plagioclase-phyric basalt

GRAIN SIZE: [illegible]

TEXTURE: [illegible]

PRIMARY MINERALOGY | PERCENT PRESENT | PERCENT ORIGINAL | SIZE (mm) | COMPOSITION | MORPHOLOGY | COMMENTS

PHENOCRYSTS
Olivine [illegible] Euhedral
Plagioclase [illegible] Euhedral Inclusions of opaques and glass fragments; as glomerocrysts and +/- clinopyroxene and olivine.
Clinopyroxene [illegible] Anhedral As glomerocrysts +/- plagioclase. Interpenetrant twinning.

GROUNDMASS
Glass [illegible] N/A [illegible] altered to dark brown clay.
Plagioclase [illegible] Euhedral Random; occasionally quench needles.
Clinopyroxene [illegible] Anhedral Little alteration to clay.
Opaques [illegible] Subhedral-anhedral Randomly distributed and as inclusions.

SECONDARY MINERALOGY | PERCENT | REPLACING/FILLING | COMMENTS
Clays [illegible] Glass, clinopyroxene Dark brown, amorphous after glass and dusty gray brown after clinopyroxene.

VESICLES/CAVITIES | PERCENT | LOCATION | SIZE (mm) | FILLING | SHAPE
Vesicles [illegible] None Irregular

COMMENTS: [illegible]

[illegible] OBSERVER: [illegible] WHERE SAMPLED: Northwest of Conical Seamount

ROCK NAME: [illegible]-plagioclase-clinopyroxene-phyric basalt

GRAIN SIZE: [illegible]

TEXTURE: [illegible]

PRIMARY MINERALOGY | PERCENT PRESENT | PERCENT ORIGINAL | SIZE (mm) | COMPOSITION | MORPHOLOGY | COMMENTS

PHENOCRYSTS
Olivine [illegible] Euhedral In glomerocrysts with plagioclase and as phenocrysts.
Plagioclase [illegible] Euhedral In glomerocrysts with minor olivine.
Clinopyroxene [illegible] Augite [illegible] In glomerocrysts; small rounded crystals in core, subhedral larger crystals at [illegible]

GROUNDMASS
Plagioclase [illegible] Subhedral Random in orientation.
Clinopyroxene [illegible] Anhedral-subhedral
Glass [illegible] N/A Greenish- to brown, slightly devitrified.
Opaques [illegible] Subhedral Blocky, random.
Olivine [illegible] Subhedral

SECONDARY MINERALOGY | PERCENT | REPLACING/FILLING | COMMENTS
[illegible] Vesicles [illegible]

VESICLES/CAVITIES | PERCENT | LOCATION | SIZE (mm) | FILLING | SHAPE | COMMENTS
Vesicles [illegible] Throughout [illegible] None Spherical to elongate Very irregular shapes, no preferred orientation.

COMMENTS: Plagioclase is rarely zoned, sometimes with glass and opaque inclusions [illegible] Clinopyroxene [illegible]

125-781A-38R-02 (Piece 3,49-51 cm) OBSERVER: VAN WHERE SAMPLED: Northwest of Conical Seamount

ROCK NAME: Olivine-plagioclase-clinopyroxene phyric basalt

GRAIN SIZE: < 3 mm

TEXTURE: Glomerophyric

PRIMARY MINERALOGY	PERCENT PRESENT	PERCENT ORIGINAL	SIZE (mm)	COMPO-SITION	MORPHOLOGY	COMMENTS
PHENOCRYSTS						
Olivine	1-2	1-2	<1		Round/resorbing	
Plagioclase	25-30	25-30	<3		Euhedral	Glomerocrysts of plagioclase; plagioclase + olivine; plagioclase + clinopyroxene.
Clinopyroxene	1-2	1-2	<1		Anhedral	
GROUNDMASS						
Plagioclase	30	30	<0.2		Euhedral, laths	
Clinopyroxene	20	20	<0.1		Anhedral, rounded	
Glass	10-15	10-15	N/A		N/A	Greenish devitrified.
Opaques	5	5	<0.1		Euhedral-subhedral	Black.
Olivine	<1	<1	<0.01		N/A	

VESICLES/ CAVITIES	PERCENT	LOCATION	SIZE (mm)	FILLING	SHAPE	COMMENTS
Vesicles	25	Random	<1	Glass distributed into cavity	Irregular	Partly filled with glass.

COMMENTS: Clinopyroxene - no zoning. Plagioclase, sometimes zoned; opaque inclusions outlining crystal shape. Surface nucleation of clinopyroxene on plagioclase observed.

125-781A-38R-03 (Piece 11,117-119 cm) OBSERVER: TER WHERE SAMPLED: Northwest of Conical Seamount

ROCK NAME: Olivine-augite-plagioclase phyric basalt

GRAIN SIZE: Chilled margin to 3 mm

TEXTURE: Intergranular, glomerophyric

PRIMARY MINERALOGY	PERCENT PRESENT	PERCENT ORIGINAL	SIZE (mm)	COMPO-SITION	MORPHOLOGY	COMMENTS
PHENOCRYSTS						
Olivine	1-2	1-2	0.5-1		Euhedral	
Plagioclase	10-20	10-20	1-3		Euhedral, laths	Many are zoned, some glomerocrysts with clinopyroxene.
Clinopyroxene	2-4	2-4	1-2		Euhedral-subhedral	2V=45 degrees.
GROUNDMASS						
Glass	40-50	40-50	N/A		N/A	Olive-brown, devitrified.
Plagioclase	20-30	20-30	<0.3		Laths, needles	Random laths to quench needles.
Clinopyroxene	15-25	15-25	<0.1	Augite	Subhedral, plumose	Random crystals, plumose crystals in glassy portion.
Olivine	<1	<1			?	
Opaques	4-7	4-7	0.01-0.3		Euhedral, laths, needles	Random crystals in coarser part of rock, random needles in chilled zone.

VESICLES/ CAVITIES	PERCENT	LOCATION	SIZE (mm)	FILLING	SHAPE	COMMENTS
Vesicles	5-35	Throughout	0.1-1.1	No	Irregular	Variable percent throughout.

COMMENTS: Top of this section is a chilled margin with 50-60% glass and <2% phenocrysts. Quench textured plagioclase, clinopyroxene and opaque grains are present. Texture ranges from intersertal to intergranular and is partly variolitic. Glomerocrysts of plagioclase and clinopyroxene occur.

125-781A-11R-01 (Piece 3A,64-66 cm) OBSERVER: VAN WHERE SAMPLED: Northwest of Conical Seamount

ROCK NAME: Olivine-plagioclase-clinopyroxene phyric basalt

GRAIN SIZE: <1 mm

TEXTURE: Glomeroporphyric intersertal

PRIMARY MINERALOGY	PERCENT PRESENT	PERCENT ORIGINAL	SIZE (mm)	COMPO-SITION	MORPHOLOGY	COMMENTS
PHENOCRYSTS						
Olivine	<1	<1	<1		Round	
Plagioclase	17-20	17-20	0.6-3		Euhedral	Laths occasionally zoned, opaque inclusions, glomerocryst with clinopyroxene.
Clinopyroxene	2-4	2-4	0.3-2		Subhedral-anhedral	Occasionally as glomerocrysts with plagioclase.
GROUNDMASS						
Glass	<7	35-37	N/A		N/A	45-100% altered to brown clay.
Plagioclase	25-30	25-30	0.25-1.13		Euhedral	Laths random orientation.
Clinopyroxene	11-13	11-13	0.02-0.4		Anhedral	Intimate intergrowth, infrequent twinning with plagioclase.
Olivine	<1?	<1?			N/A	
Opaques	5?	5?	0.01-0.1		Subhedral	Black, random, occasionally as inclusions in plagioclase.

SECONDARY MINERALOGY	PERCENT	REPLACING/FILLING	COMMENTS
Clays	25-30	Glass	Brown, amorphous after glass.

VESICLES/CAVITIES	PERCENT	LOCATION	SIZE (mm)	FILLING	SHAPE	COMMENTS
Vesicles	<1-2	Throughout	0.1-1	None	Irregular	Equant to elongate.

125-781A-[illegible] (Piece [illegible] cm) OBSERVER: [illegible] WHERE SAMPLED: Northwest of Conical Seamount

ROCK NAME: Olivine-plagioclase phyric basalt

GRAIN SIZE: <1 mm

TEXTURE: Glomeroporphyritic intersertal

PRIMARY MINERALOGY	PERCENT PRESENT	PERCENT ORIGINAL	SIZE (mm)	COMPO-SITION	MORPHOLOGY	COMMENTS
PHENOCRYSTS						
Olivine	1-2	1-2	[illegible]		Rounded	Glomerocrysts with plagioclase.
Plagioclase	15-20	15-20	[illegible]		Euhedral-subhedral	Glomerocrysts with olivine, occasionally zoned opaque inclusions.
Clinopyroxene	Trace	Trace	[illegible]	Augite	Rounded	
GROUNDMASS						
Plagioclase	25	25	0.1-0.5		Euhedral	Laths, rare hollow (swallow) shapes.
Clinopyroxene	20	20	0.1-0.5		Anhedral	Rare twinning.
Glass	[illegible]	35	N/A		N/A	Altered and devitrified.
Opaques	5	5	0.05-0.1	Magnetite	Euhedral	Black, random distribution.
Olivine	[illegible]	10	N/A		N/A	

SECONDARY MINERALOGY	PERCENT	REPLACING/FILLING	COMMENTS
Clays	10	Glass	Brown amorphous clays.

VESICLES/CAVITIES	PERCENT	LOCATION	SIZE (mm)	FILLING	SHAPE	COMMENTS
Vesicles	<1	Random	1-4	None	Round	Glass extruded into cavities and devitrified.

COMMENTS: Two generations of plagioclase phenocryst growth apparent in glomeroporphyritic crystals.

125-781A-10R-01 (Piece 6,45-47 cm) OBSERVER: VAN WHERE SAMPLED: Northwest of Conical Seamount

ROCK NAME: Olivine-clinopyroxene-plagioclase phyric basalt

GRAIN SIZE: 0.5-3 mm

TEXTURE: Glomerophyric intersertal

PRIMARY MINERALOGY	PERCENT PRESENT	PERCENT ORIGINAL	SIZE (mm)	COMPO-SITION	MORPHOLOGY	COMMENTS
PHENOCRYSTS						
Olivine	1-2	1-2	0.2-1	Fo80-85	Subhedral	2V=+90 degrees.
Plagioclase	25-30	25-30	0.5-1		Euhedral	Albite and Carlsbad twinning, as glomerocryst +/- clinopyroxene, olivine and glass inclusions.
Clinopyroxene	2-4	2-4	0.1-1	Augite	Subhedral	Carlsbad twinning rare.
GROUNDMASS						
Glass	N/A	20-30	N/A		N/A	10-50% altered to clay and chlorite.
Plagioclase	35-40	35-40	0.05-0.15		Euhedral	Laths, albite and Carlsbad twinning.
Clinopyroxene	20-30	20-30	0.01-0.05		N/A	Infrequent Carlsbad twinning.
Olivine?	<1	<1	<0.02		Rounded	
Opaques	N/A	N/A	0.01-0.2		Euhedral-subhedral	Black, disseminated.

SECONDARY MINERALOGY	PERCENT	REPLACING/ FILLING	COMMENTS
Clays	5-10	Glass	Brown, microcrystalline after devitrified glass.
Chlorite	10-15	Glass	Pleochroic, green-brown, radiating, low birefringence.

VESICLES/ CAVITIES	PERCENT	LOCATION	SIZE (mm)	FILLING	SHAPE	COMMENTS
Vesicles	10-15	Throughout	0.2-4	No	Elongate, [illegible]	Some glass extrusions into vesicles.

COMMENTS: Plagioclase phenocrysts have glass (0.01-0.02 mm, now altered) and opaque (0.01-0.02 mm) inclusions. Olivine appears to be out of equilibrium (resorbing).

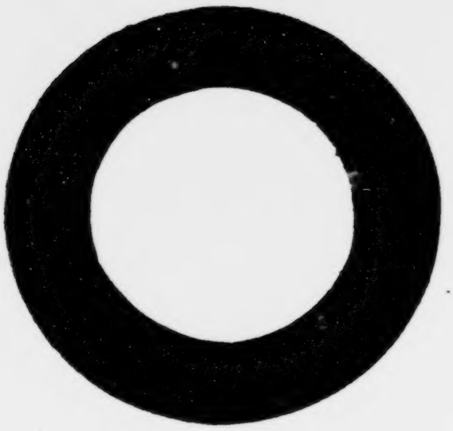

SITE 782 HOLE A CORE 1H CORED INTERVAL 2958.9-2968.7 mbsl; 0.0-9.8 mbsf

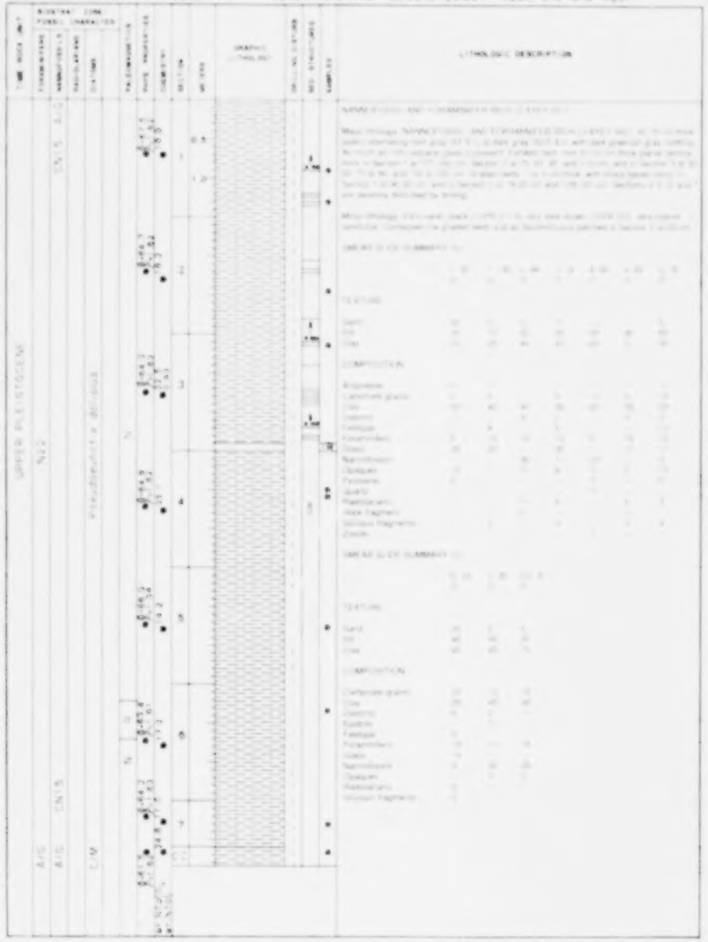
TIME-ROCK UNIT
BIOSTRAT. ZONE/FOSSIL CHARACTER
FORAMINIFERS
NANNOFOSSILS
RADIOLARIANS
DIATOMS
PALEOMAGNETICS
PHYS. PROPERTIES
CHEMISTRY
SECTION
METERS
GRAPHIC LITHOLOGY
DRILLING DISTURB.
SED. STRUCTURES
SAMPLES
LITHOLOGIC DESCRIPTION
UPPER PLEISTOCENE
N22
CN15
A/G
Pseudoeunotia doliolus
C/M
1
2
3
4
5
6
7
CC

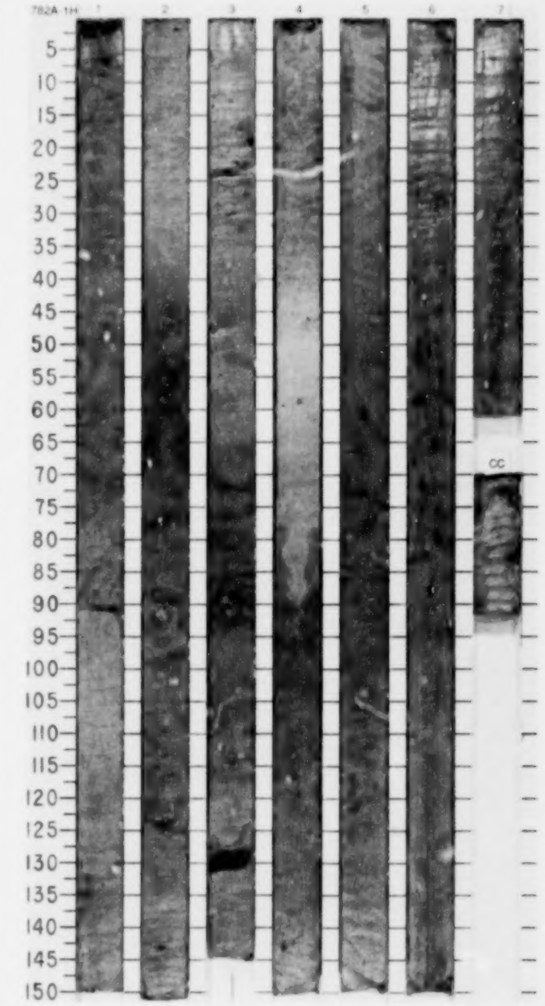
782A-1H
1
2
3
4
5
6
7
CC
5
10
15
20
25
30
35
40
45
50
55
60
65
70
75
80
85
90
95
100
105
110
115
120
125
130
135
140
145
150

SITE 782 HOLE A CORE 2H CORED INTERVAL 2968.7-2978.2 mbsl; 9.8-19.3 mbsf

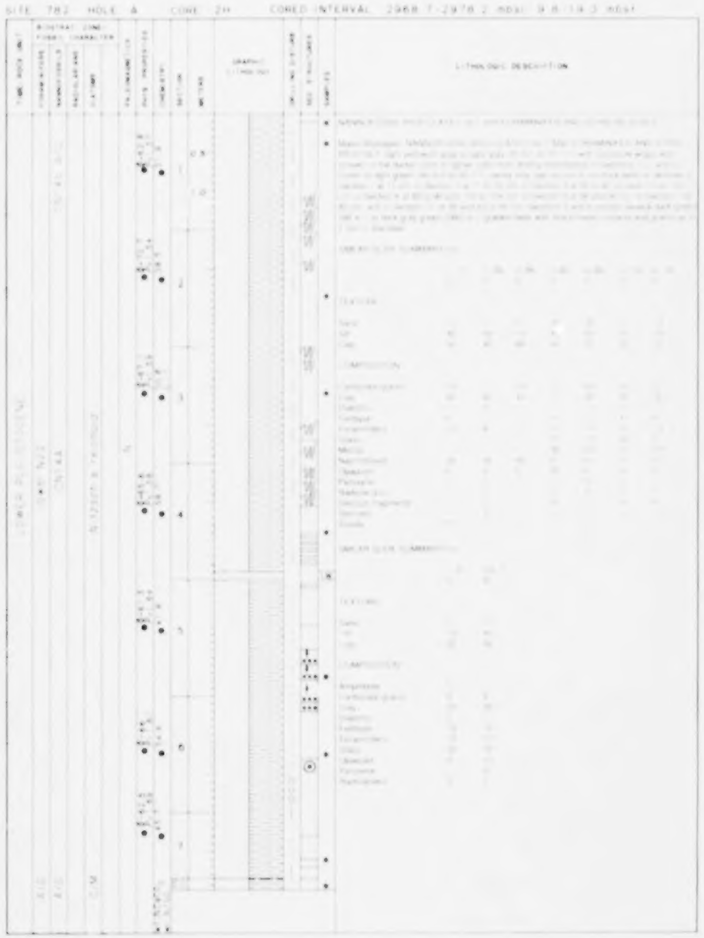
TIME-ROCK UNIT
BIOSTRAT. ZONE/FOSSIL CHARACTER
FORAMINIFERS
NANNOFOSSILS
RADIOLARIANS
DIATOMS
PALEOMAGNETICS
PHYS. PROPERTIES
CHEMISTRY
SECTION
METERS
GRAPHIC LITHOLOGY
DRILLING DISTURB.
SED. STRUCTURES
SAMPLES
LITHOLOGIC DESCRIPTION
1
2
3
4
5
6
7
CC

[illegible]

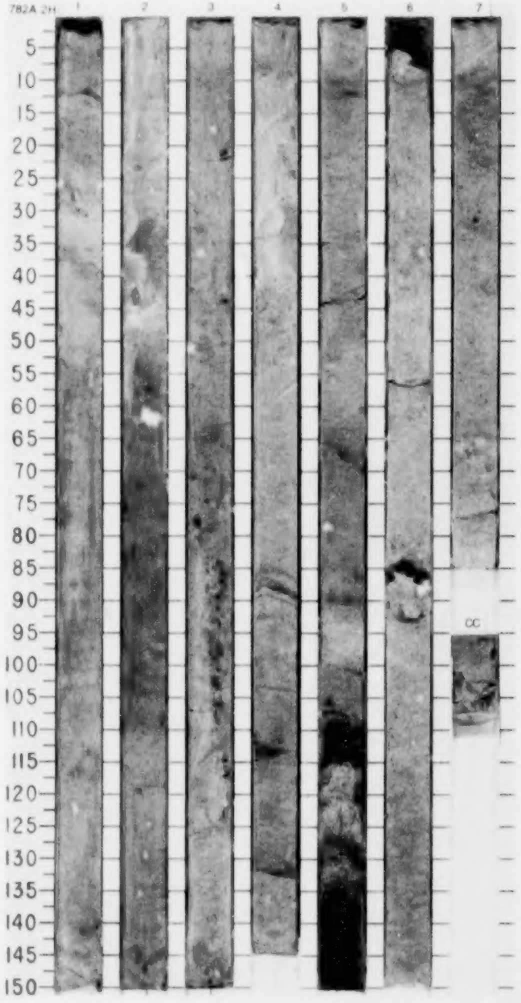
782A 2H
1
2
3
4
5
6
7
CC
5
10
15
20
25
30
35
40
45
50
55
60
65
70
75
80
85
90
95
100
105
110
115
120
125
130
135
140
145
150

SITE 782 HOLE A CORE 3H CORED INTERVAL 2978.2-2987.7 mbsl; 19.3-28.8 mbsf

TIME-ROCK UNIT	FORAMINIFERS	NANNOFOSSILS	RADIOLARIANS	DIATOMS	PALEOMAGNETICS	PHYS. PROPERTIES	CHEMISTRY	SECTION	METERS	GRAPHIC LITHOLOGY	DRILLING DISTURB.	SED. STRUCTURES	SAMPLES	LITHOLOGIC DESCRIPTION
LOWER PLEISTOCENE	N22 A/G	CN14a A/M	F/P		N	[illegible]		1 2 3 4 5 6 7 CC	0.5 1.0					NANNOFOSSIL MARL and GLASS-RICH MARL

Major lithologies: NANNOFOSSIL MARL, gray [illegible]

Minor lithologies: [illegible]

SMEAR SLIDE SUMMARY (%):

TEXTURE:

Sand
Silt
Clay

COMPOSITION:

Carbonate grains
Clay
Diatoms
[illegible]
Feldspar
Foraminifers
Glass
Micrite
Nannofossils
Opaques
Pyroxene
Radiolarians
Zeolite

SMEAR SLIDE SUMMARY (%):

TEXTURE:

Silt
Clay

COMPOSITION:

Carbonate grains
Clay
Diatoms
Foraminifers
Nannofossils

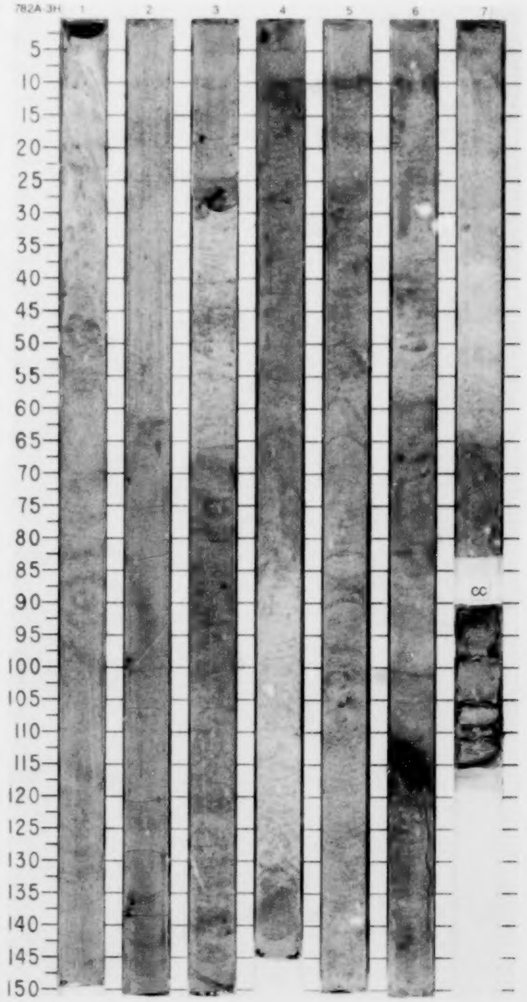
782A-3H
1
2
3
4
5
6
7
CC
5
10
15
20
25
30
35
40
45
50
55
60
65
70
75
80
85
90
95
100
105
110
115
120
125
130
135
140
145
150

SITE 782 HOLE A CORE 4H CORED INTERVAL 2987.7-2997.2 mbsl; 28.8-38.3 mbsf

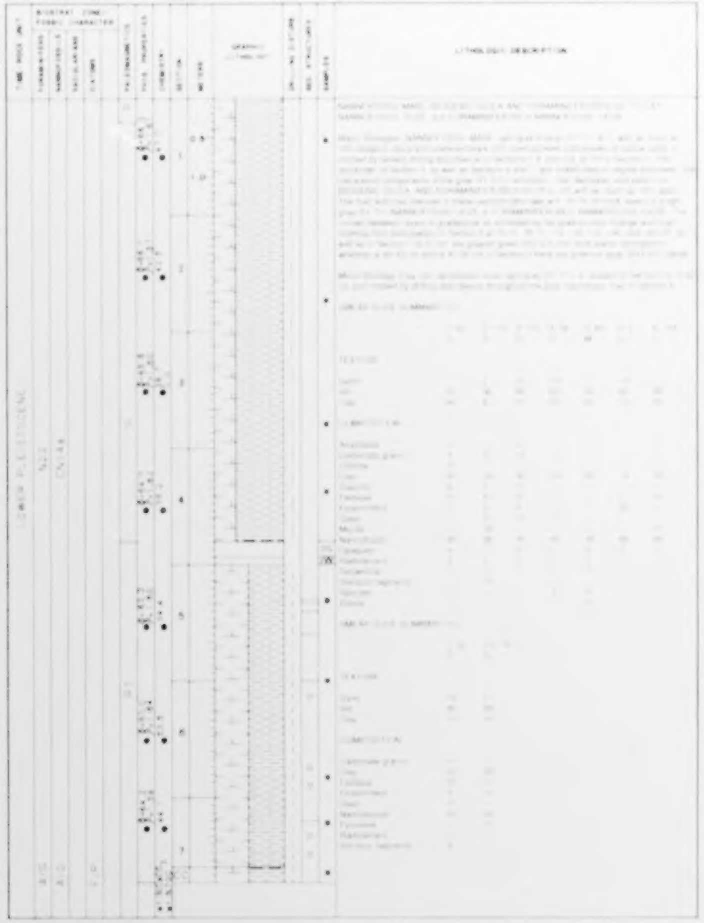
LITHOLOGIC DESCRIPTION
GRAPHIC LITHOLOGY
LOWER PLEISTOCENE

[illegible]

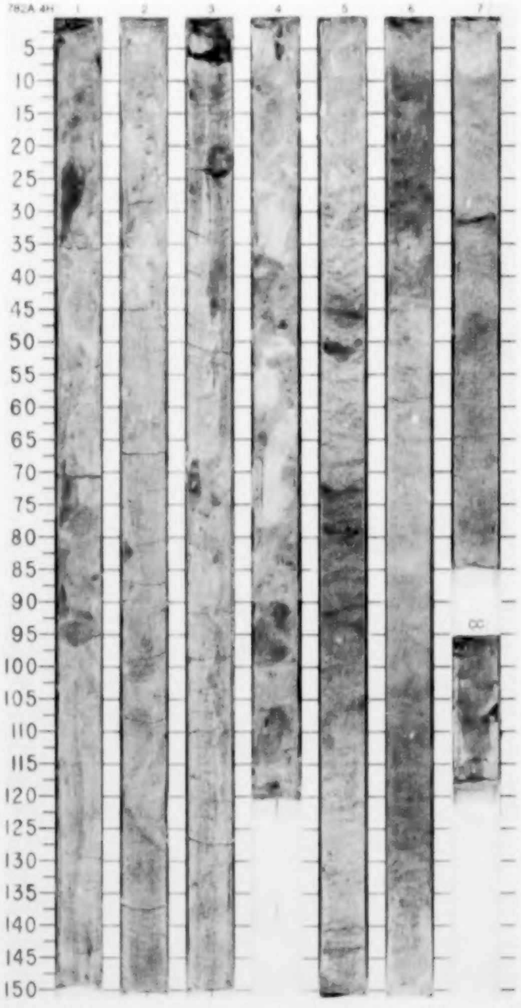
782A 4H
1
2
3
4
5
6
7
CC
5
10
15
20
25
30
35
40
45
50
55
60
65
70
75
80
85
90
95
100
105
110
115
120
125
130
135
140
145
150

SITE 782 HOLE A CORE 5H CORED INTERVAL 2997.2-3006.7 mbsl; 38.3-47.8 mbsf

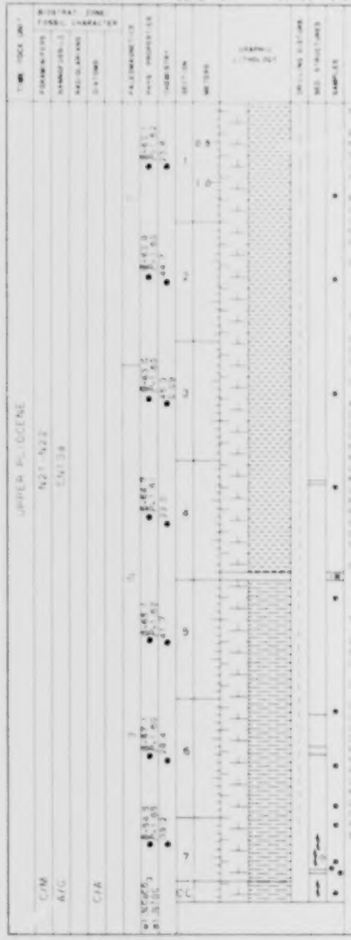
TIME-ROCK UNIT
BIOSTRAT. ZONE/FOSSIL CHARACTER
FORAMINIFERS
NANNOFOSSILS
RADIOLARIANS
DIATOMS
PALEOMAGNETICS
PHYS. PROPERTIES
CHEMISTRY
SECTION
METERS
GRAPHIC LITHOLOGY
DRILLING DISTURB.
SED. STRUCTURES
SAMPLES
UPPER PLIOCENE
N21-N22
CN13a
C/M
A/G
C/A
0.5
1.0
1
2
3
4
5
6
7
CC

LITHOLOGIC DESCRIPTION

NANNOFOSSIL MARL and NANNOFOSSIL OOZE

Major lithologies: NANNOFOSSIL MARL, dark gray (5Y 4/1), alternated with gray (5Y [illegible]) NANNOFOSSIL OOZE [illegible]

Minor lithologies: [illegible]

SMEAR SLIDE SUMMARY (%):

TEXTURE:

Sand
Silt
Clay

COMPOSITION:

Amphibole
Carbonate grains
Clay
Diatoms
Feldspar
Foraminifers
Glass
Nannofossils
Opaques
Pyroxene
Radiolarians
Serpentine
Silicoflagellates
Spicules

SMEAR SLIDE SUMMARY (%):

TEXTURE:

Sand
Silt
Clay

COMPOSITION:

Carbonate grains
Chlorite
Clay
Diatoms
Epidote
Feldspar
Foraminifers
Glass
Nannofossils
Opaques
Pyroxene
Radiolarians
Spicules

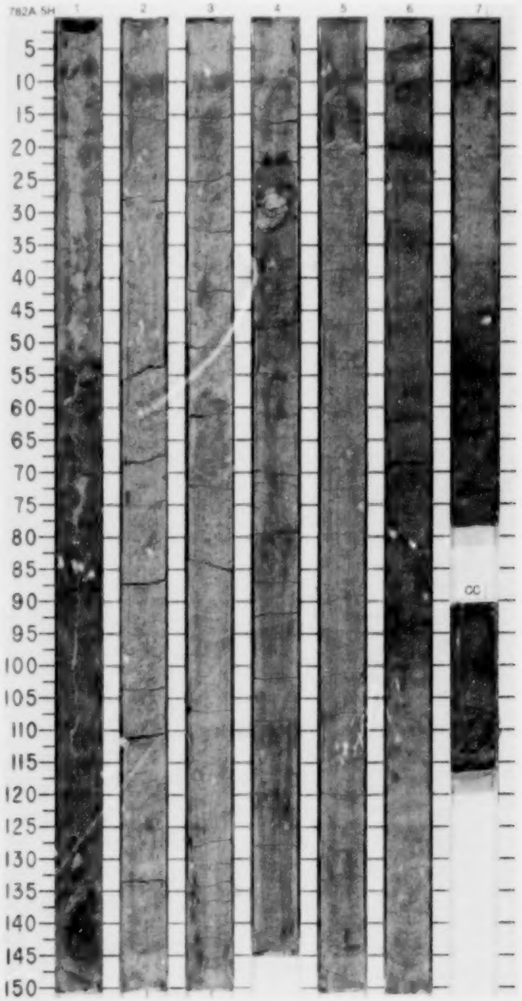
782A 5H
1
2
3
4
5
6
7
CC
5
10
15
20
25
30
35
40
45
50
55
60
65
70
75
80
85
90
95
100
105
110
115
120
125
130
135
140
145
150

SITE 782 HOLE A CORE 6H CORED INTERVAL 3006.7-3016.2 mbsl; 47.8-57.3 mbsf

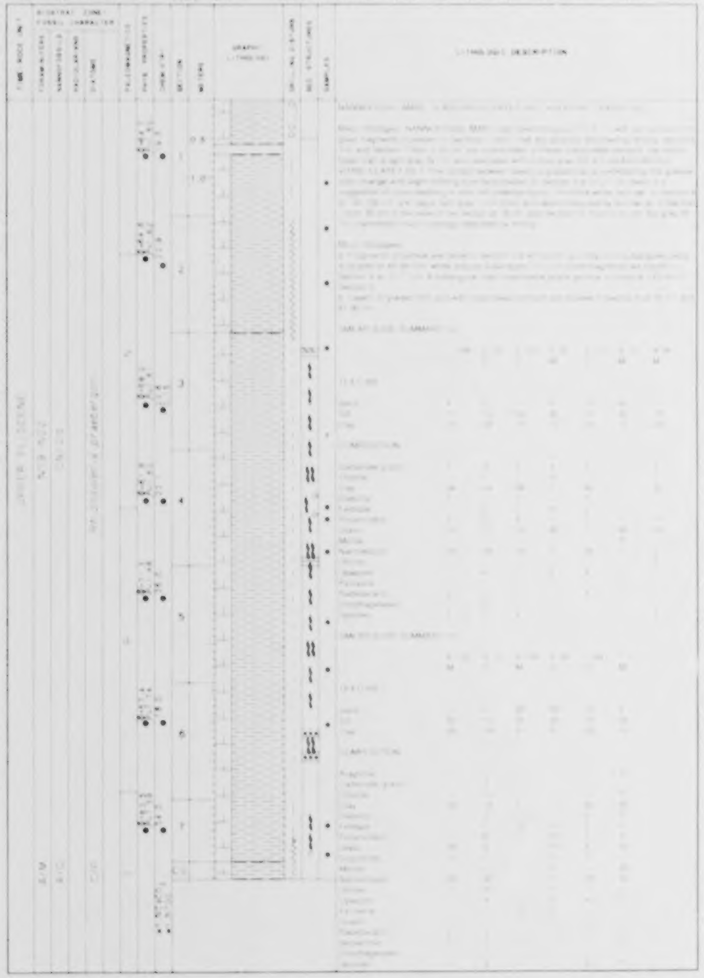

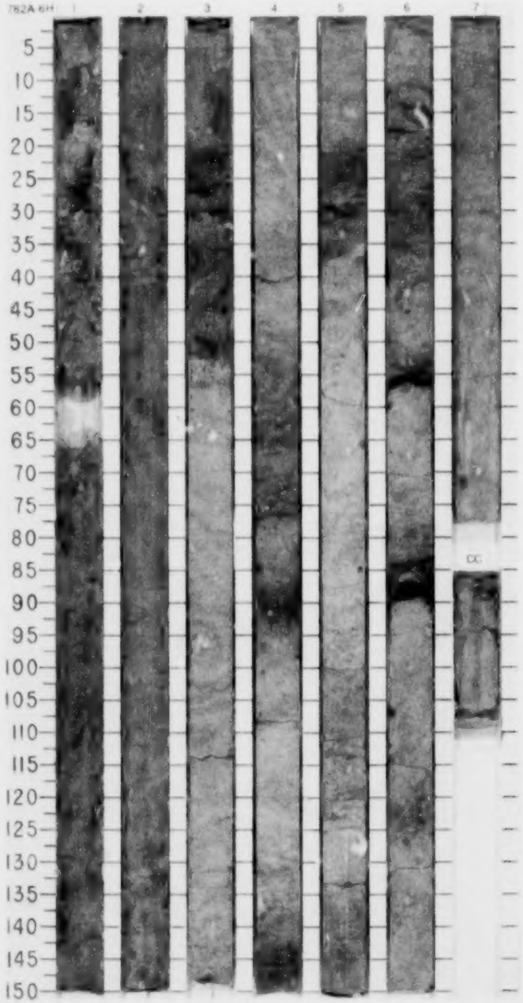
782A-6H
1
2
3
4
5
6
7
CC
5
10
15
20
25
30
35
40
45
50
55
60
65
70
75
80
85
90
95
100
105
110
115
120
125
130
135
140
145
150

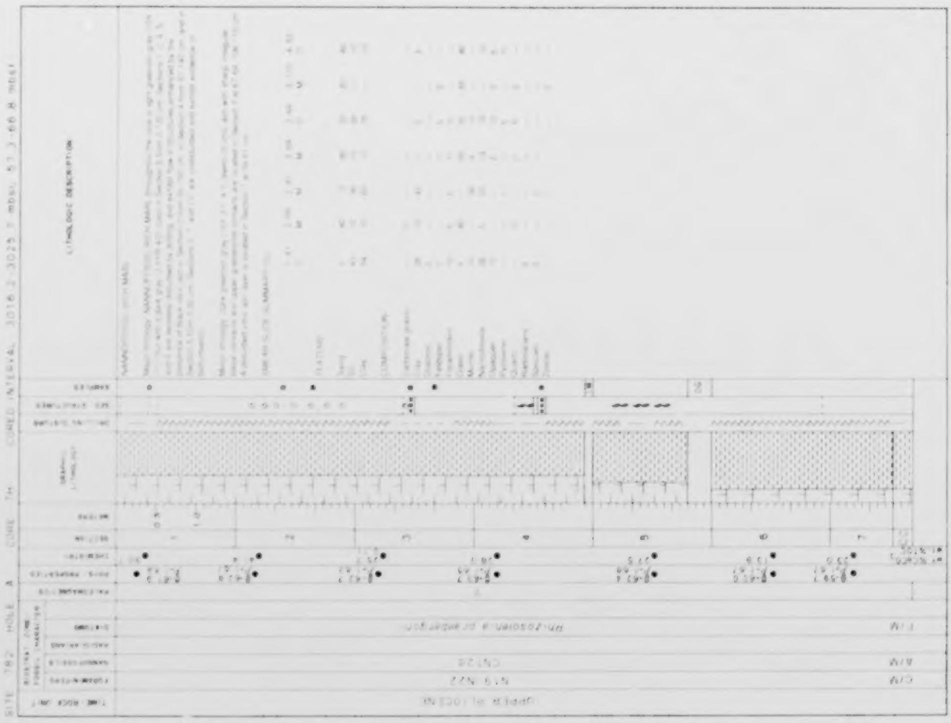
SITE 782 HOLE A CORE 7H CORED INTERVAL 3016.2-3025.7 mbsl; 57.3-66.8 mbsf
TIME-ROCK UNIT
BIOSTRAT. ZONE/FOSSIL CHARACTER
FORAMINIFERS
NANNOFOSSILS
RADIOLARIANS
DIATOMS
PALEOMAGNETICS
PHYS. PROPERTIES
CHEMISTRY
SECTION
METERS
GRAPHIC LITHOLOGY
DRILLING DISTURB.
SED. STRUCTURES
SAMPLES
LITHOLOGIC DESCRIPTION
UPPER PLIOCENE
N19-N22
CN12a
Rhizosolenia praebergonii
C/M
A/M
F/M
1
2
3
4
5
6
7
CC

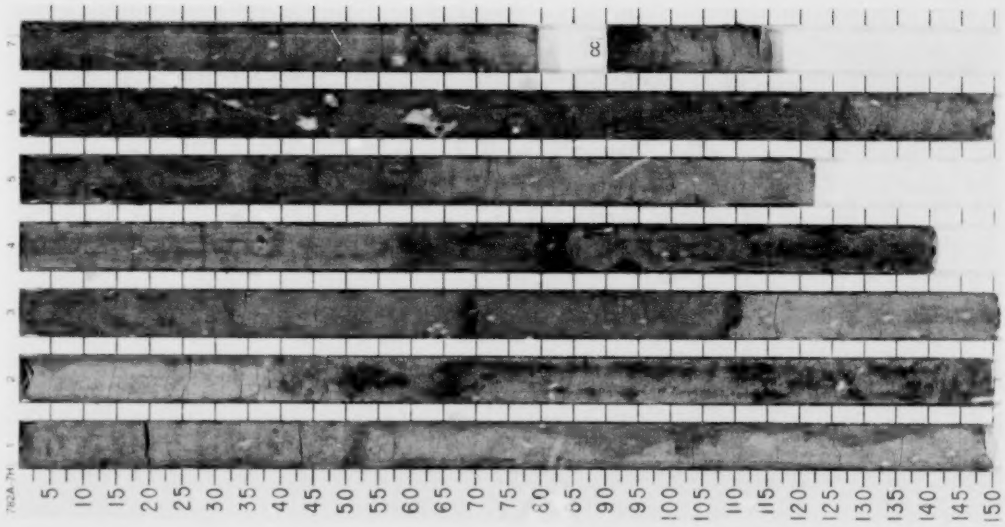
782A-7H
1
2
3
4
5
6
7
5
10
15
20
25
30
35
40
45
50
55
60
65
70
75
80
85
90
95
100
105
110
115
120
125
130
135
140
145
150

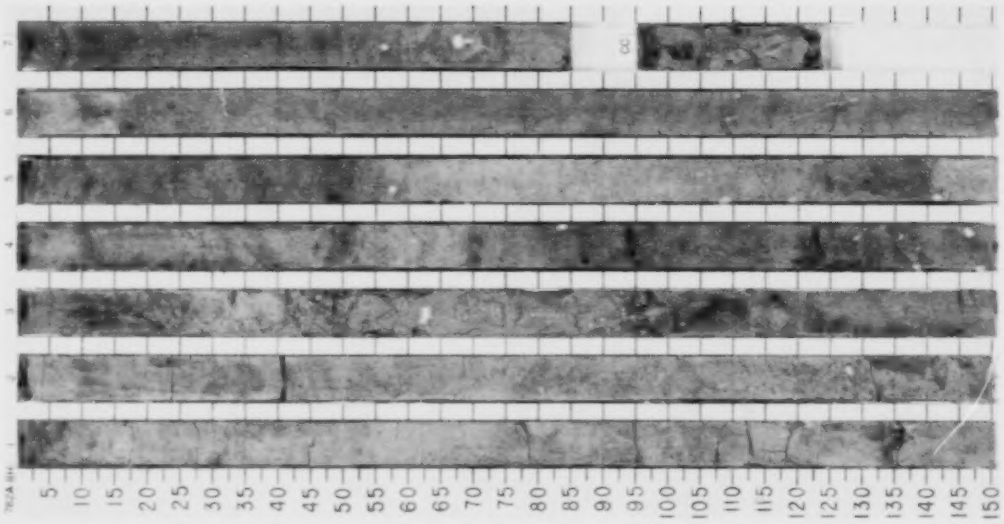
1
2
3
4
5
6
7
CC
782A-8H
5
10
15
20
25
30
35
40
45
50
55
60
65
70
75
80
85
90
95
100
105
110
115
120
125
130
135
140
145
150

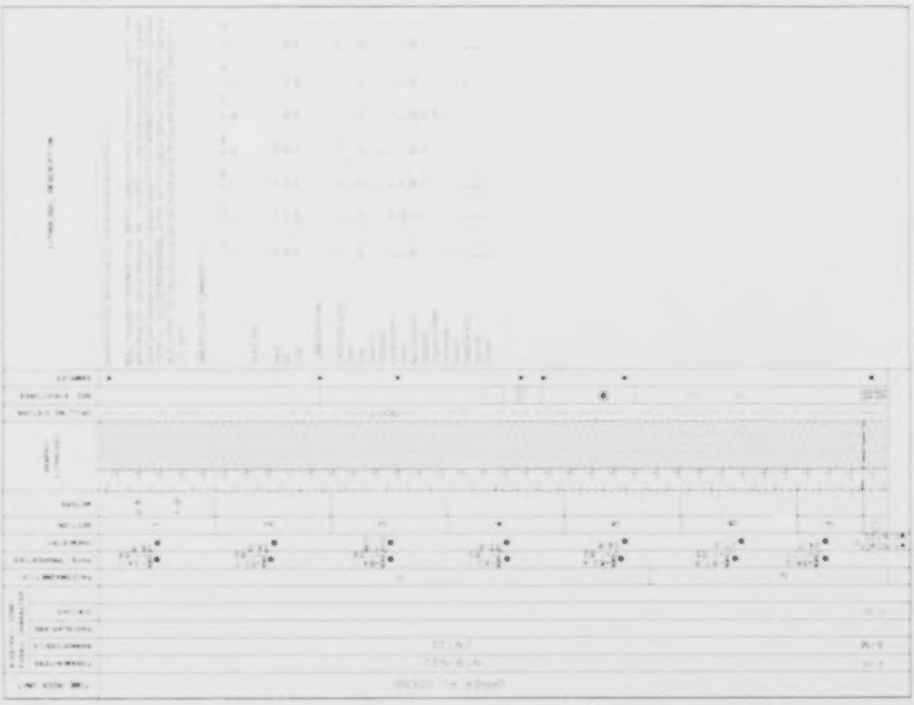

SITE 782 HOLE A CORE 9H CORED INTERVAL 3035.2-3044.7 mbsl; 76.2-85.8 mbsf

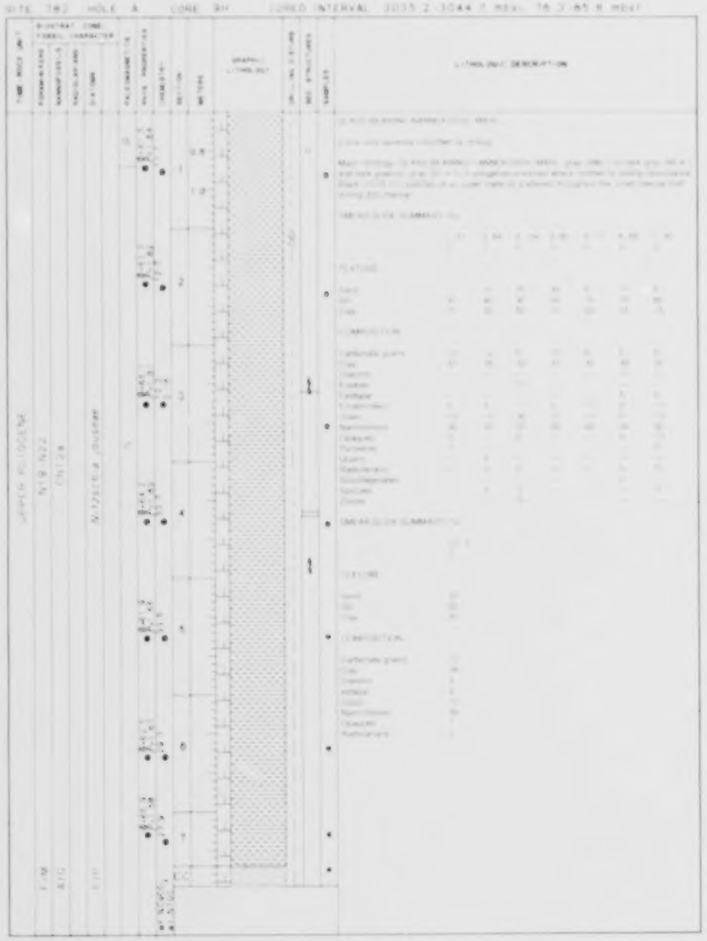
TIME-ROCK UNIT
BIOSTRAT. ZONE/FOSSIL CHARACTER
FORAMINIFERS
NANNOFOSSILS
RADIOLARIANS
DIATOMS
PALEOMAGNETICS
PHYS. PROPERTIES
CHEMISTRY
SECTION
METERS
GRAPHIC LITHOLOGY
DRILLING DISTURB.
SED. STRUCTURES
SAMPLES
LITHOLOGIC DESCRIPTION
UPPER PLIOCENE
N19-N22
CN12a
0.5
1.0
1
2
3
4
5
6
7
CC
SMEAR SLIDE SUMMARY (%):
TEXTURE:
Sand
Silt
Clay
COMPOSITION:
Carbonate grains
Clay
Feldspar
Glass
Nannofossils
Radiolarians
Sponge spicules
SMEAR SLIDE SUMMARY (%):
TEXTURE:
COMPOSITION:

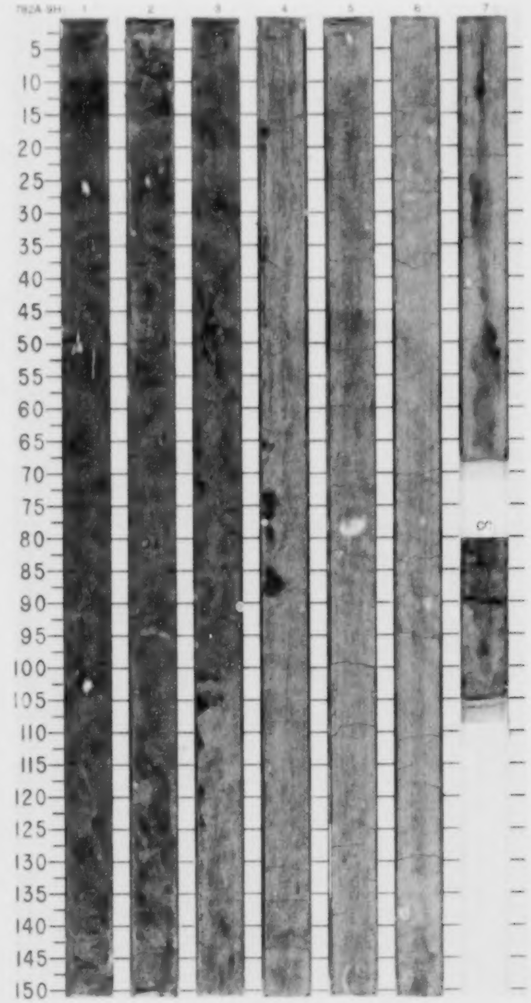
782A-9H
1
2
3
4
5
6
7
5
10
15
20
25
30
35
40
45
50
55
60
65
70
75
80
85
90
95
100
105
110
115
120
125
130
135
140
145
150
CC

SITE 782 HOLE A CORE 10X CORED INTERVAL 3044.7-3054.6 mbsl; 85.8-95.7 mbsf

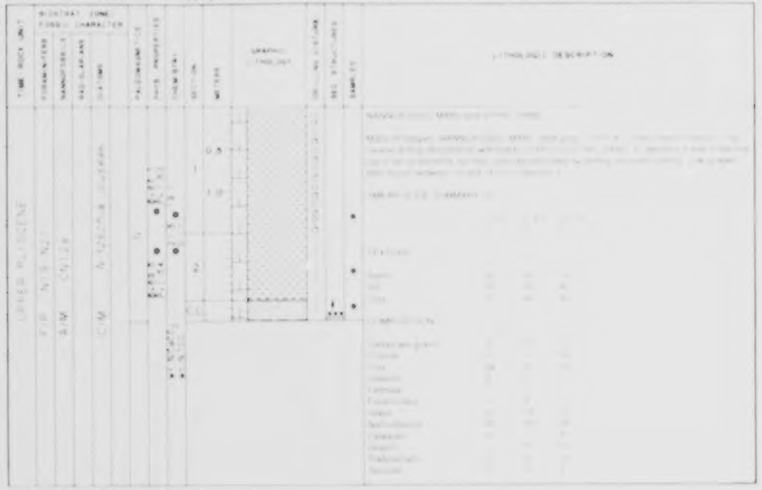
TIME-ROCK UNIT
BIOSTRAT. ZONE / FOSSIL CHARACTER
FORAMINIFERS
NANNOFOSSILS
RADIOLARIANS
DIATOMS
PALEOMAGNETICS
PHYS. PROPERTIES
CHEMISTRY
SECTION
METERS
GRAPHIC LITHOLOGY
DRILLING DISTURB.
SED. STRUCTURES
SAMPLES
UPPER PLIOCENE
F/P N19-N21
A/M CN12a
C/M N. reinholdii
0.5
1.0
1
2
CC

LITHOLOGIC DESCRIPTION

[illegible]

SMEAR SLIDE SUMMARY (%):

TEXTURE:

Sand

Silt

Clay

COMPOSITION:

[illegible]

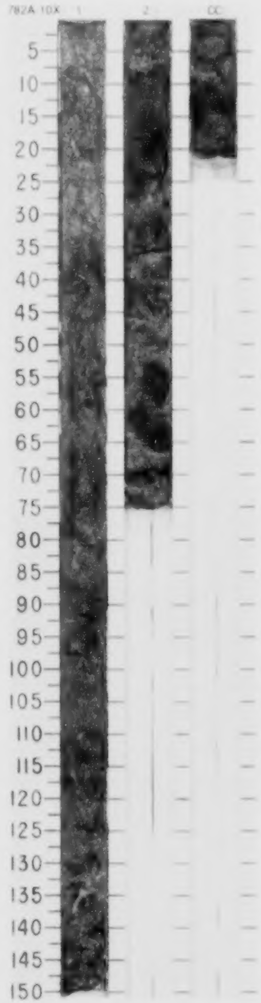
782A-10X 1
2
CC
5
10
15
20
25
30
35
40
45
50
55
60
65
70
75
80
85
90
95
100
105
110
115
120
125
130
135
140
145
150

SITE 782 HOLE A CORE 11X CORED INTERVAL 3054.6-3064.2 mbsl; 95.7-105.3 mbsf

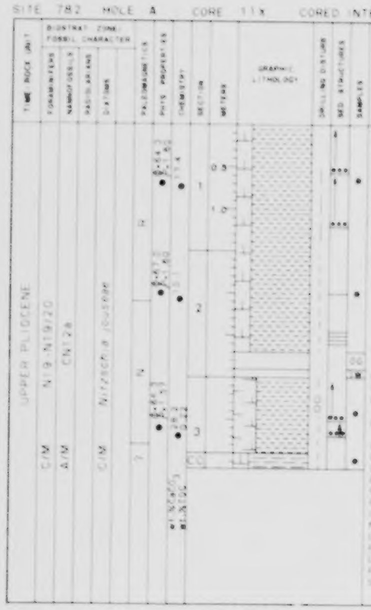
TIME ROCK UNIT
BIOSTRAT. ZONE/ FOSSIL CHARACTER
FORAMINIFERS
NANNOFOSSILS
RADIOLARIANS
DIATOMS
PALEOMAGNETICS
PHYS. PROPERTIES
CHEMISTRY
SECTION
METERS
GRAPHIC LITHOLOGY
DRILLING DISTURB.
SED. STRUCTURES
SAMPLES
UPPER PLIOCENE
C/M N19-N19/20
A/M CN12a
C/M Nitzschia jouseae
R
N
?
1
2
3
CC
0.5
1.0
OG

LITHOLOGIC DESCRIPTION

NANNOFOSSIL MARL and NANNOFOSSIL OOZE

Major lithologies: NANNOFOSSIL MARL and NANNOFOSSIL OOZE, gray (5Y 5/1) to dark gray (5Y 4/1), intervals with five [illegible] cm graded beds in their bases; sharp basal contacts overlain by marl with decreasing amounts of ash, occur at [illegible] cm and [illegible] cm in Section 1 and at [illegible] cm and [illegible] cm in Section 3. The intervals grade from coarse sand at the base to finely laminated fine sand and silt in their central portions to bioturbated silt at the top. Section 1 contains faint grayish green (5G 5/2) to very dark gray (7.5YR 3/0) laminations at 98, 105, 108, 110, 112 and 115 cm. These laminations contain up to 10 percent volcanic glass.

Minor lithology: Black (10YR 2/1) vitric ash occurs as [illegible] patches in Sections 1, 2 and [illegible].

SMEAR SLIDE SUMMARY (%):

	1, 66	2, 90	3, 41	CC, 5
	D	D	D	D
TEXTURE:				
Sand	—	2	5	5
Silt	30	28	20	15
Clay	70	70	75	80
COMPOSITION:				
Carbonate grains	15	—	10	5
Clay	34	30	35	4
Dolomite	—	—	5	—
Epidote	5	—	—	—
Feldspar	—	5	—	5
Foraminifers	2	—	—	4
Glass	—	13	—	3
Nannofossils	30	43	45	80
Opaques	5	—	—	2
Pyroxene	—	—	5	—
Quartz	3	—	—	—
Radiolarians	5	20	—	15
Spicules	1	—	5	—

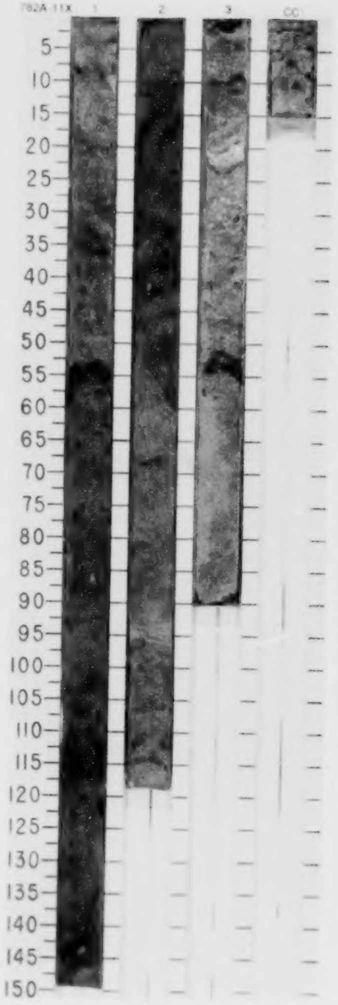
782A-11X
1
2
3
CC
5
10
15
20
25
30
35
40
45
50
55
60
65
70
75
80
85
90
95
100
105
110
115
120
125
130
135
140
145
150

SITE 782 HOLE A CORE 12X CORED INTERVAL 3064.2-3073.9 mbsl; 105.3-115.0 mbsf

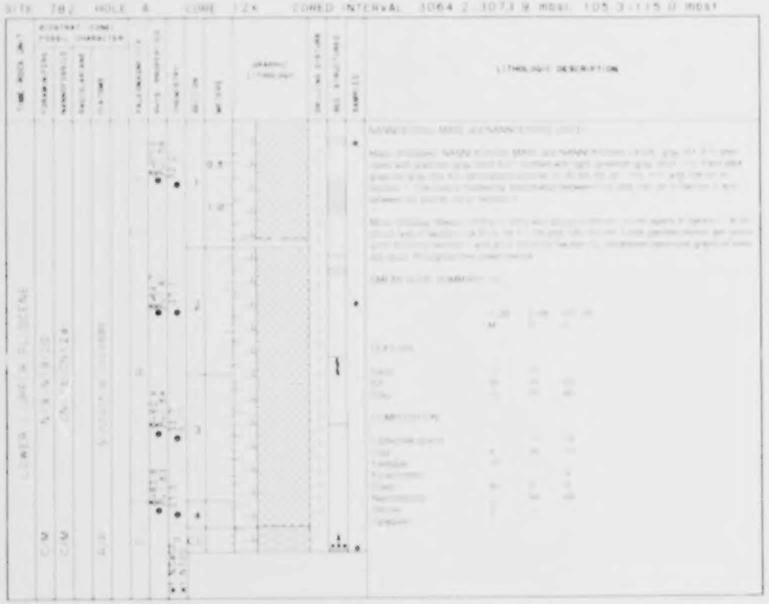
TIME-ROCK UNIT
BIOSTRAT. ZONE/FOSSIL CHARACTER
FORAMINIFERS
NANNOFOSSILS
RADIOLARIANS
DIATOMS
PALEOMAGNETICS
PHYS. PROPERTIES
CHEMISTRY
SECTION
METERS
GRAPHIC LITHOLOGY
DRILLING DISTURB.
SED. STRUCTURES
SAMPLES
LOWER / UPPER PLIOCENE
C/M
C/M
B/B
0.5
1.0
1
2
3
4
CC

LITHOLOGIC DESCRIPTION

[illegible]

SMEAR SLIDE SUMMARY (%):

TEXTURE:

Sand

Silt

Clay

COMPOSITION:

Clay

Feldspar

Glass

Nannofossils

[illegible]

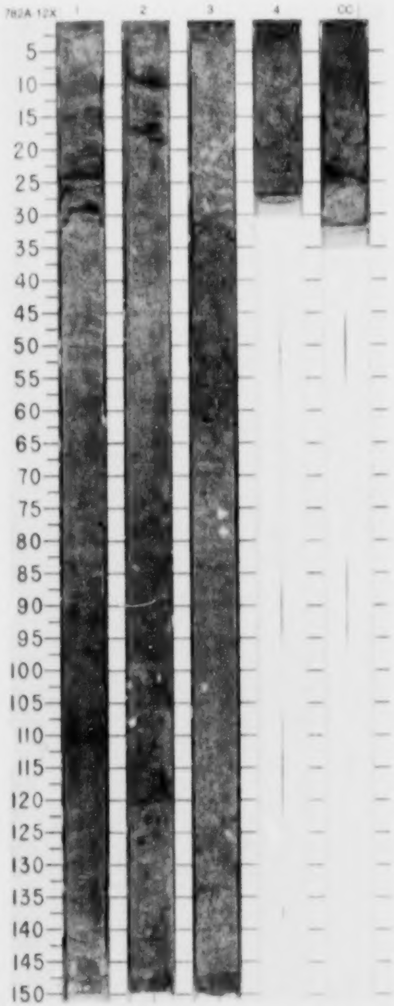
782A 12X
1
2
3
4
CC
5
10
15
20
25
30
35
40
45
50
55
60
65
70
75
80
85
90
95
100
105
110
115
120
125
130
135
140
145
150

SITE 782 HOLE A CORE 13X CORED INTERVAL 3073.9-3083.5 mbsl; 115.0-124.6 mbsf

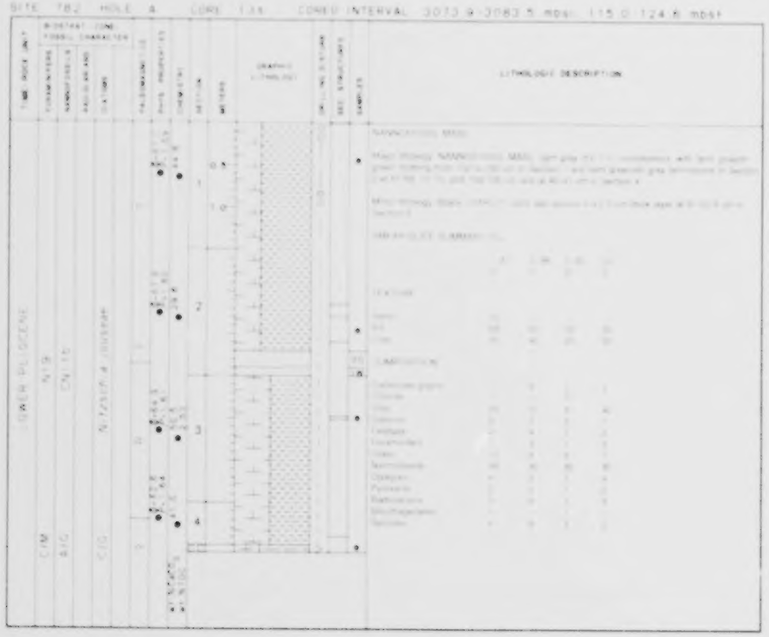
TIME-ROCK UNIT
BIOSTRAT. ZONE/FOSSIL CHARACTER
FORAMINIFERS
NANNOFOSSILS
RADIOLARIANS
DIATOMS
PALEOMAGNETICS
PHYS. PROPERTIES
CHEMISTRY
SECTION
METERS
GRAPHIC LITHOLOGY
DRILLING DISTURB.
SED. STRUCTURES
SAMPLES
LITHOLOGIC DESCRIPTION
LOWER PLIOCENE
N19
C/M
A/G
C/G
1
2
3
4
0.5
1.0
NANNOFOSSIL MARL
TEXTURE:
COMPOSITION:

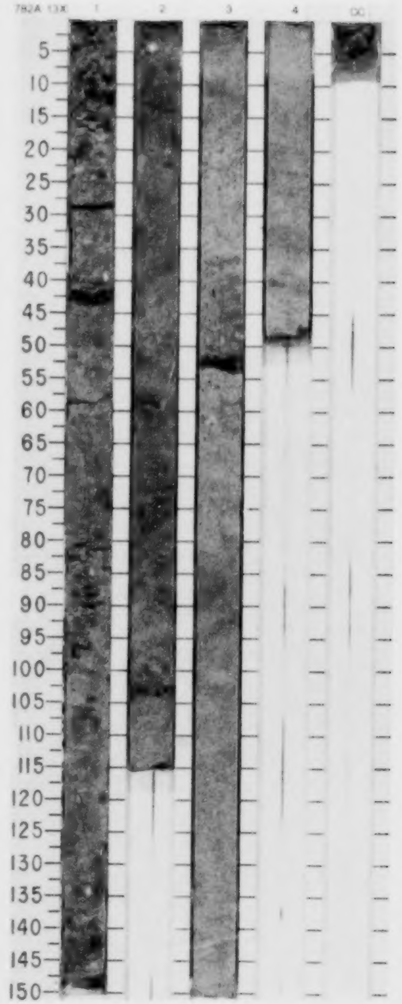
782A-13X
1
2
3
4
CC
5
10
15
20
25
30
35
40
45
50
55
60
65
70
75
80
85
90
95
100
105
110
115
120
125
130
135
140
145
150

SITE 782 HOLE A CORE 14X CORED INTERVAL 3083.5-3093.2 mbsl; 124.6-134.3 mbsf

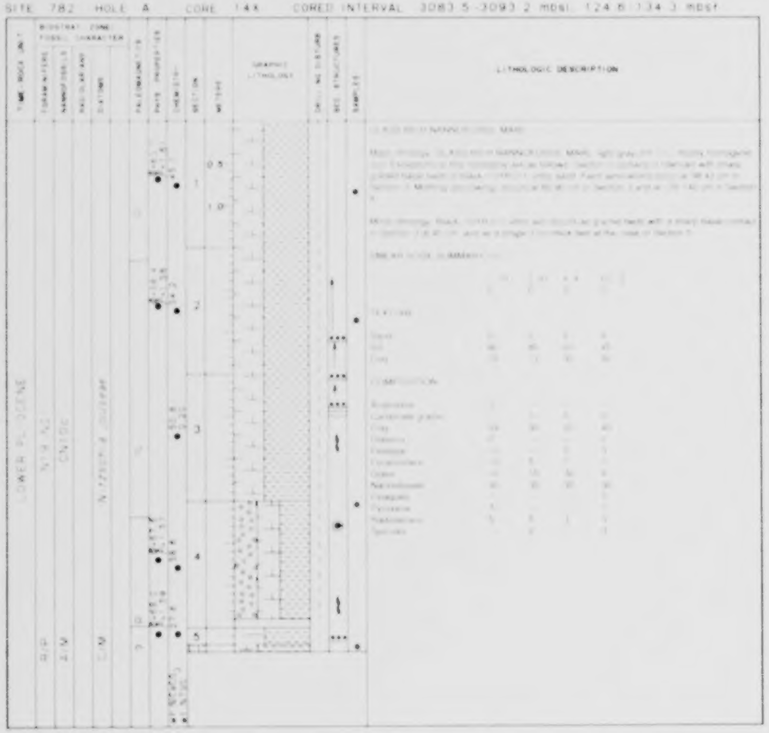
TIME-ROCK UNIT
BIOSTRAT. ZONE/FOSSIL CHARACTER
FORAMINIFERS
NANNOFOSSILS
RADIOLARIANS
DIATOMS
PALEOMAGNETICS
PHYS. PROPERTIES
CHEMISTRY
SECTION
METERS
GRAPHIC LITHOLOGY
DRILLING DISTURB.
SED. STRUCTURES
SAMPLES
LITHOLOGIC DESCRIPTION
LOWER PLIOCENE
N19-N20
CN10c
N. jouseae
B/P
A/M
C/M
0.5
1.0
1
2
3
4
5
CC

[illegible] NANNOFOSSIL MARL

Major lithology: [illegible] NANNOFOSSIL MARL, [illegible]

Minor lithology: [illegible]

SMEAR SLIDE SUMMARY (%):

TEXTURE:

Sand
Silt
Clay

COMPOSITION:

[illegible]

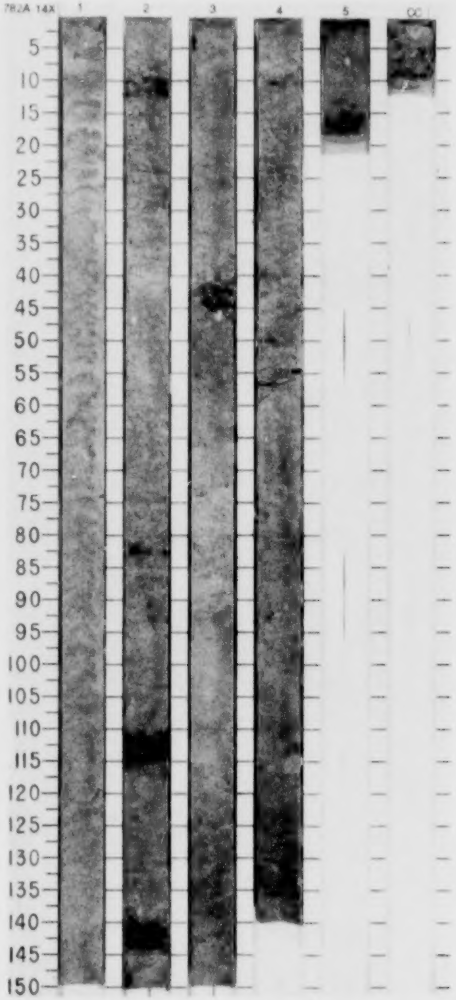
782A 14X
1
2
3
4
5
CC
5
10
15
20
25
30
35
40
45
50
55
60
65
70
75
80
85
90
95
100
105
110
115
120
125
130
135
140
145
150

SITE 782 HOLE A CORE 15X CORED INTERVAL 3093.2-3102.8 mbsl; 134.3-143.9 mbsf

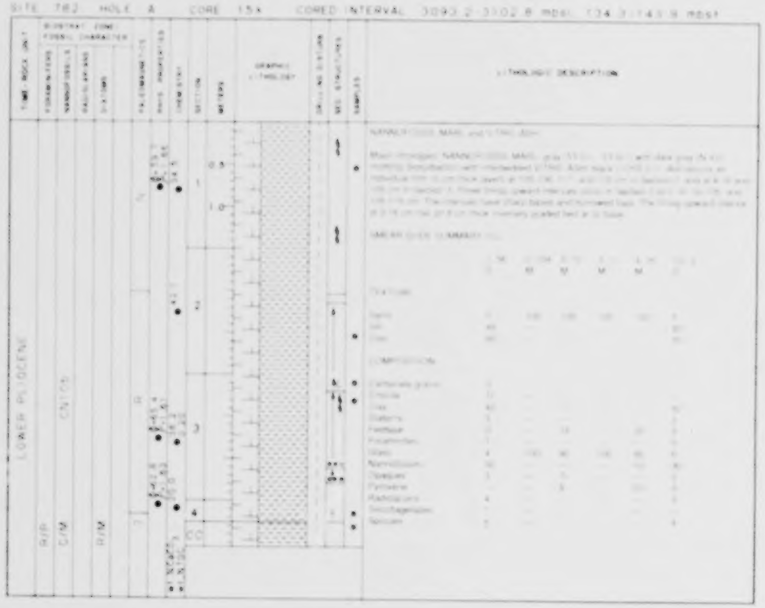
TIME-ROCK UNIT
BIOSTRAT. ZONE/FOSSIL CHARACTER
FORAMINIFERS
NANNOFOSSILS
RADIOLARIANS
DIATOMS
PALEOMAGNETICS
PHYS. PROPERTIES
CHEMISTRY
SECTION
METERS
GRAPHIC LITHOLOGY
DRILLING DISTURB.
SED. STRUCTURES
SAMPLES
LOWER PLIOCENE
R/P
C/M
CN10b
R/M
0.5
1.0
1
2
3
4
CC

LITHOLOGIC DESCRIPTION

NANNOFOSSIL MARL and VITRIC ASH

Major lithologies: NANNOFOSSIL MARL, gray [illegible] with dark gray [illegible] mottling (bioturbation) with interbedded VITRIC ASH [illegible]

SMEAR SLIDE SUMMARY (%):

TEXTURE:

Sand
Silt
Clay

COMPOSITION:

Carbonate grains
Dolomite
Clay
Diatoms
Feldspar
Foraminifers
Glass
Nannofossils
Opaques
Pyroxene
Radiolarians
Silicoflagellates
Spicules

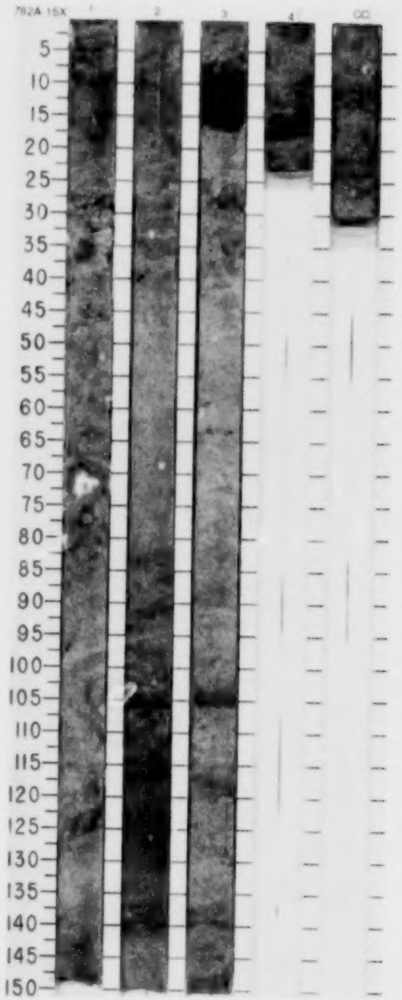
782A 15X
1
2
3
4
CC
5
10
15
20
25
30
35
40
45
50
55
60
65
70
75
80
85
90
95
100
105
110
115
120
125
130
135
140
145
150

SITE 782 HOLE A CORE 16X CORED INTERVAL 3102.8-3112.5 mbsl; 143.9-153.6 mbsf

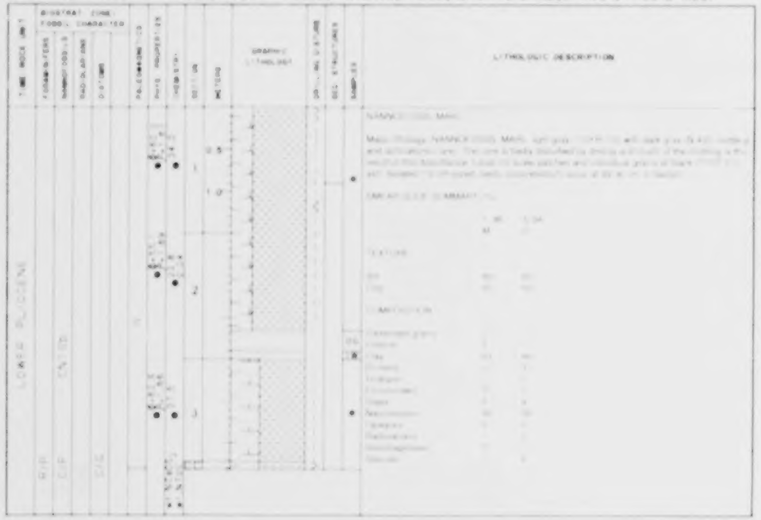
TIME ROCK UNIT
BIOSTRAT. ZONE/FOSSIL CHARACTER
FORAMINIFERS
NANNOFOSSILS
RADIOLARIANS
DIATOMS
PALEOMAGNETICS
PHYS. PROPERTIES
CHEMISTRY
SECTION
METERS
GRAPHIC LITHOLOGY
DRILLING DISTURB.
SED. STRUCTURES
SAMPLES
LITHOLOGIC DESCRIPTION
LOWER PLIOCENE
CN10b
R/P
C/P
0.5
1.0
1
2
3
OG

NANNOFOSSIL MARL

Main lithology: NANNOFOSSIL MARL, light gray [illegible] with dark gray [illegible] mottling and [illegible]. [illegible]

SMEAR SLIDE SUMMARY (%):

[illegible]

TEXTURE:

Silt [illegible]

Clay [illegible]

COMPOSITION:

[illegible]

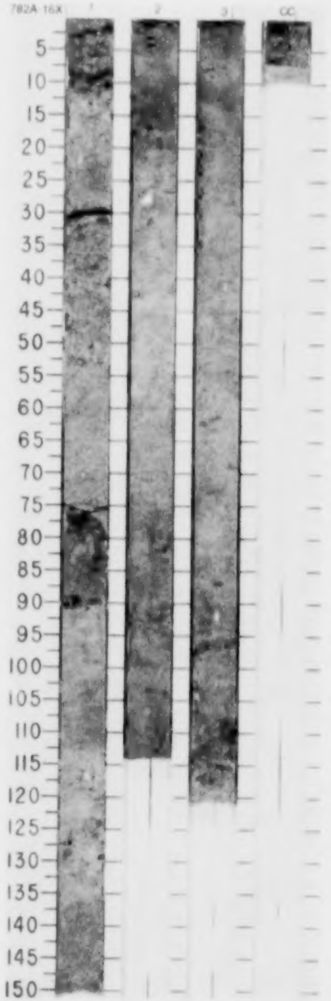
782A 16X
1
2
3
CC
5
10
15
20
25
30
35
40
45
50
55
60
65
70
75
80
85
90
95
100
105
110
115
120
125
130
135
140
145
150

SITE 782 HOLE A CORE 17X CORED INTERVAL 3112.5-3122.1 mbsl; 153.6-163.9 mbsf

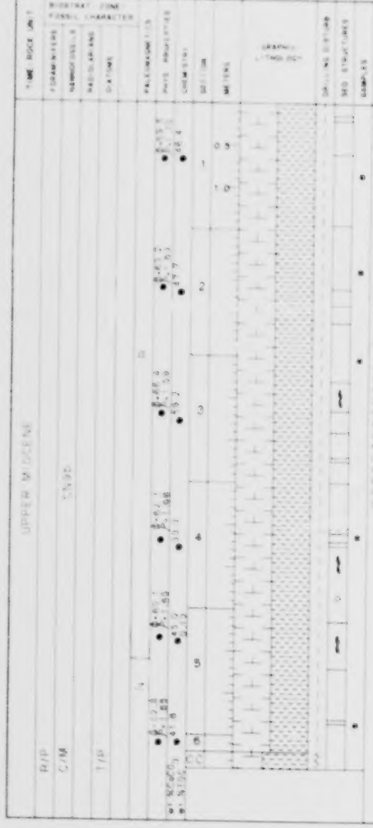
TIME-ROCK UNIT
BIOSTRAT. ZONE/ FOSSIL CHARACTER
FORAMINIFERS
NANNOFOSSILS
RADIOLARIANS
DIATOMS
PALEOMAGNETICS
PHYS. PROPERTIES
CHEMISTRY
SECTION
METERS
GRAPHIC LITHOLOGY
DRILLING DISTURB.
SED. STRUCTURES
SAMPLES
UPPER MIOCENE
CN9b
R/P
C/M
T/P
0.5
1.0
1
2
3
4
5
6
CC

LITHOLOGIC DESCRIPTION

NANNOFOSSIL MARL and NANNOFOSSIL OOZE

Major lithologies: NANNOFOSSIL MARL, dominantly gray (5Y 6/1), interbedded and gradational with NANNOFOSSIL OOZE, dominantly light gray (5Y 7/1). Both color and compositional changes are gradual. Core is locally bioturbated and contains thin dark greenish gray (5GY 4/1) to black (N1) laminations and beds of volcanic glass- and feldspar-rich silt and sand.

SMEAR SLIDE SUMMARY (%):

	1, 8 D	2, 44 [illegible]	3, 7 D	4, 64 D	5, 136 D
TEXTURE:					
Sand	—	[illegible]	[illegible]	[illegible]	[illegible]
Silt	40	[illegible]	40	[illegible]	[illegible]
Clay	60	[illegible]	60	[illegible]	[illegible]
COMPOSITION:					
Amphibole	Tr	—			—
Chlorite	—	—	—		Tr
Clay	[illegible]	[illegible]	[illegible]	[illegible]	[illegible]
Diatoms	—	Tr	—	—	—
Feldspar		[illegible]	[illegible]		[illegible]
Foraminifers	—	[illegible]	—		—
Glass	[illegible]	[illegible]	[illegible]	[illegible]	[illegible]
Nannofossils	[illegible]	[illegible]	[illegible]	[illegible]	[illegible]
Opaques	—	[illegible]	[illegible]	[illegible]	—
Pyroxene	—	—	—	Tr	Tr
Radiolarians	Tr	[illegible]	[illegible]	—	—
Rock fragment		—	—	[illegible]	—
Spicules		—	[illegible]	—	—

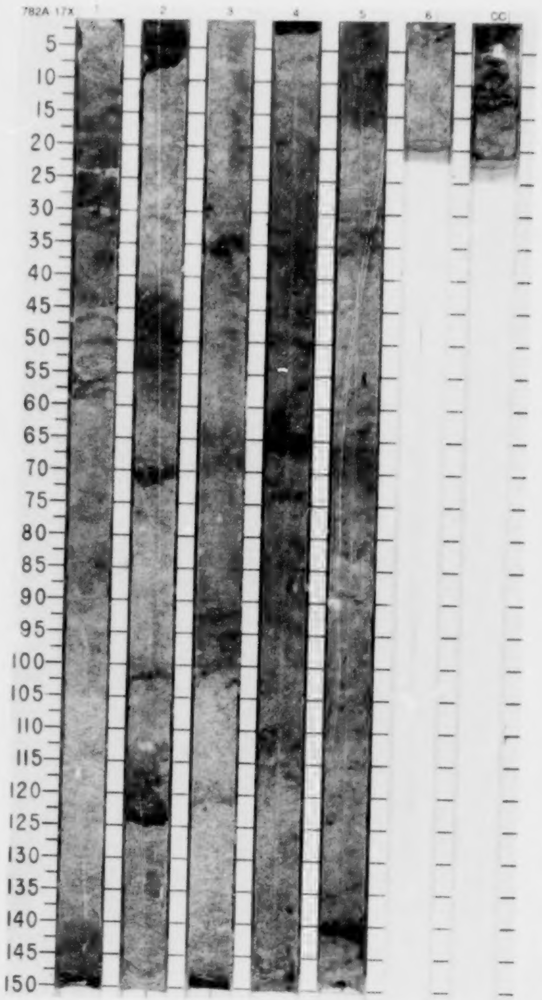
782A 17X
1
2
3
4
5
6
CC
5
10
15
20
25
30
35
40
45
50
55
60
65
70
75
80
85
90
95
100
105
110
115
120
125
130
135
140
145
150

SITE 782 HOLE A CORE 18X CORED INTERVAL 3122.1-3131.8 mbsl; 163.2-172.9 mbsf

TIME-ROCK UNIT
BIOSTRAT. ZONE / FOSSIL CHARACTER
FORAMINIFERS
NANNOFOSSILS
RADIOLARIANS
DIATOMS
PALEOMAGNETICS
PHYS. PROPERTIES
CHEMISTRY
SECTION
METERS
GRAPHIC LITHOLOGY
DRILLING DISTURB.
SED. STRUCTURES
SAMPLES
LITHOLOGIC DESCRIPTION
UPPER MIOCENE / EARLIEST PLIOCENE
N19
CN10
0.5
1.0
1
2

SMEAR SLIDE SUMMARY (%):

TEXTURE:

Sand

Silt

Clay

COMPOSITION:

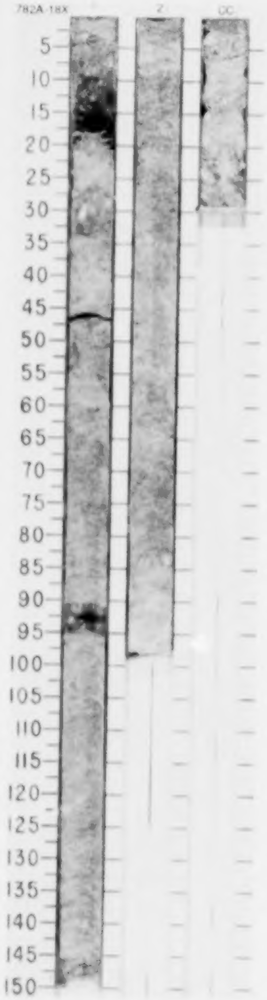
782A-18X
1
2
CC
5
10
15
20
25
30
35
40
45
50
55
60
65
70
75
80
85
90
95
100
105
110
115
120
125
130
135
140
145
150

5
10
15
20
25
30
35
40
45
50
55
60
65
70
75
80
85
90
95
100
105
110
115
120
125
130
135
140
145
150
UPPER MIOCENE

SITE 782 HOLE A CORE 20X CORED INTERVAL 3141.4-3151.0 mbsl; 182.5-192.1 mbsf

TIME-ROCK UNIT	BIOSTRAT. ZONE/ FOSSIL CHARACTER				PALEOMAGNETICS	PHYS. PROPERTIES	CHEMISTRY	SECTION	METERS	GRAPHIC LITHOLOGY	DRILLING DISTURB.	SED. STRUCTURES	SAMPLES	LITHOLOGIC DESCRIPTION
	FORAMINIFERS	NANNOFOSSILS	RADIOLARIANS	DIATOMS										
[illegible]	[illegible]	[illegible]		[illegible]		●	●	1	0.5	[illegible]		[illegible]	● ●	[illegible]

782A-20X
1
CC
5
10
15
20
25
30
35
40
45
50
55
60
65
70
75
80
85
90
95
100
105
110
115
120
125
130
135
140
145
150

SITE 782 HOLE A CORE 21X CORED INTERVAL 3151.0-3160.7 mbsl; 192.1-201.8 mbsf

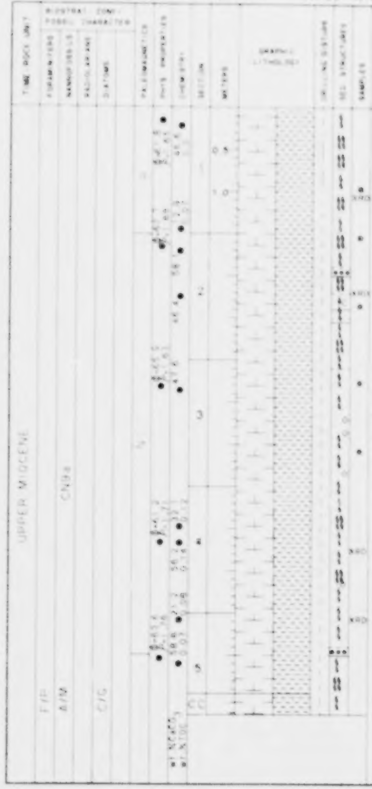
TIME ROCK UNIT
BIOSTRAT. ZONE/ FOSSIL CHARACTER
FORAMINIFERS
NANNOFOSSILS
RADIOLARIANS
DIATOMS
PALEOMAGNETICS
PHYS. PROPERTIES
CHEMISTRY
SECTION
METERS
GRAPHIC LITHOLOGY
DRILLING DISTURB.
SED. STRUCTURES
SAMPLES
UPPER MIOCENE
CN9a
F/P
A/M
C/G
0.5
1.0
1
2
3
4
5
CC
XRD

LITHOLOGIC DESCRIPTION

NANNOFOSSIL MARL

Major lithology: NANNOFOSSIL MARL, gray (5Y 5/1), light gray (5Y 6/1), dark gray (5Y 4/1), and light greenish gray (5GY 6/1), intensely bioturbated. Rare scattered rounded pumice fragments up to 1.5 cm in diameter. Several sharp contacts outlined by concentrations of black [illegible] with [illegible] and by subtle color changes.

SMEAR SLIDE SUMMARY (%):

	[illegible]	[illegible]	[illegible]	[illegible]	[illegible]
TEXTURE:					
Sand	[illegible]	[illegible]	[illegible]	[illegible]	[illegible]
Silt	[illegible]	[illegible]	[illegible]	[illegible]	[illegible]
Clay	[illegible]	[illegible]	[illegible]	[illegible]	[illegible]
COMPOSITION:					
Quartz	[illegible]	[illegible]	[illegible]	[illegible]	[illegible]
Clay	[illegible]	[illegible]	[illegible]	[illegible]	[illegible]
Diatoms	[illegible]	[illegible]	[illegible]	[illegible]	[illegible]
Feldspar	[illegible]	[illegible]	[illegible]	[illegible]	[illegible]
Foraminifers	[illegible]	[illegible]	[illegible]	[illegible]	[illegible]
Glass	[illegible]	[illegible]	[illegible]	[illegible]	[illegible]
Nannofossils	[illegible]	[illegible]	[illegible]	[illegible]	[illegible]
Opaques	[illegible]	[illegible]	[illegible]	[illegible]	[illegible]
Pyroxene	[illegible]	[illegible]	[illegible]	[illegible]	[illegible]
Radiolarians	[illegible]	[illegible]	[illegible]	[illegible]	[illegible]
Silicoflagellates	[illegible]	[illegible]	[illegible]	[illegible]	[illegible]
Spicules	[illegible]	[illegible]	[illegible]	[illegible]	[illegible]

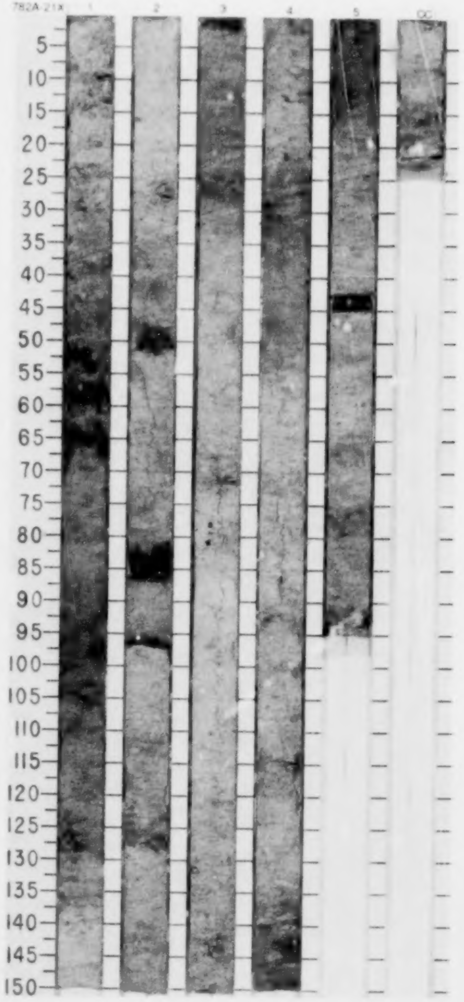
782A-21X
1
2
3
4
5
CC
5
10
15
20
25
30
35
40
45
50
55
60
65
70
75
80
85
90
95
100
105
110
115
120
125
130
135
140
145
150

SITE 782 HOLE A CORE 22X CORED INTERVAL 3160.7-3170.4 mbsl; 201.8-211.5 mbsf

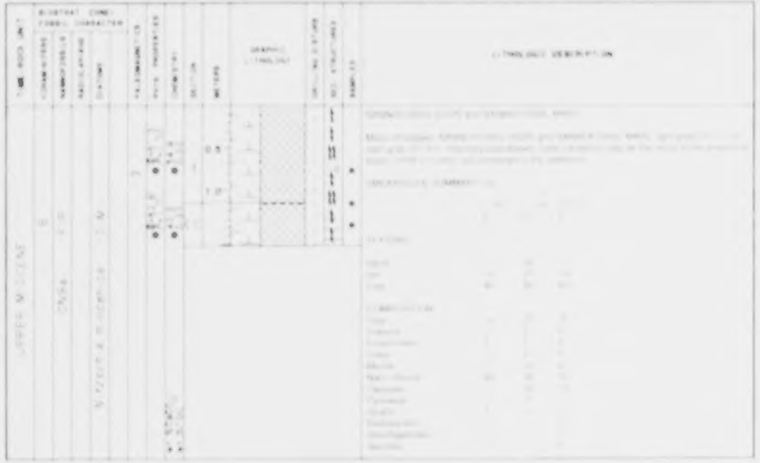
TIME-ROCK UNIT
BIOSTRAT. ZONE/ FOSSIL CHARACTER
FORAMINIFERS
NANNOFOSSILS
RADIOLARIANS
DIATOMS
PALEOMAGNETICS
PHYS. PROPERTIES
CHEMISTRY
SECTION
METERS
GRAPHIC LITHOLOGY
DRILLING DISTURB.
SED. STRUCTURES
SAMPLES
LITHOLOGIC DESCRIPTION
UPPER MIOCENE
CN9A
0.5
1.0

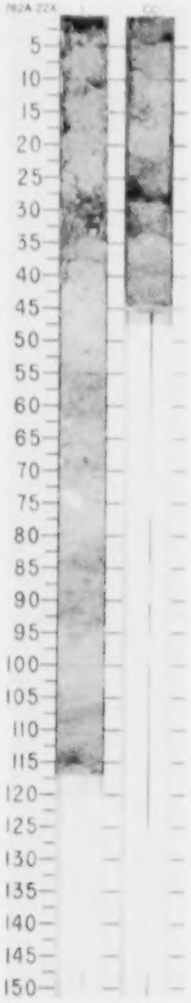
782A-22X
1
CC
5
10
15
20
25
30
35
40
45
50
55
60
65
70
75
80
85
90
95
100
105
110
115
120
125
130
135
140
145
150

SITE 782 HOLE A CORE 23X CORED INTERVAL 3170.4-3179.9 mbsl; 211.5-221.0 mbsf

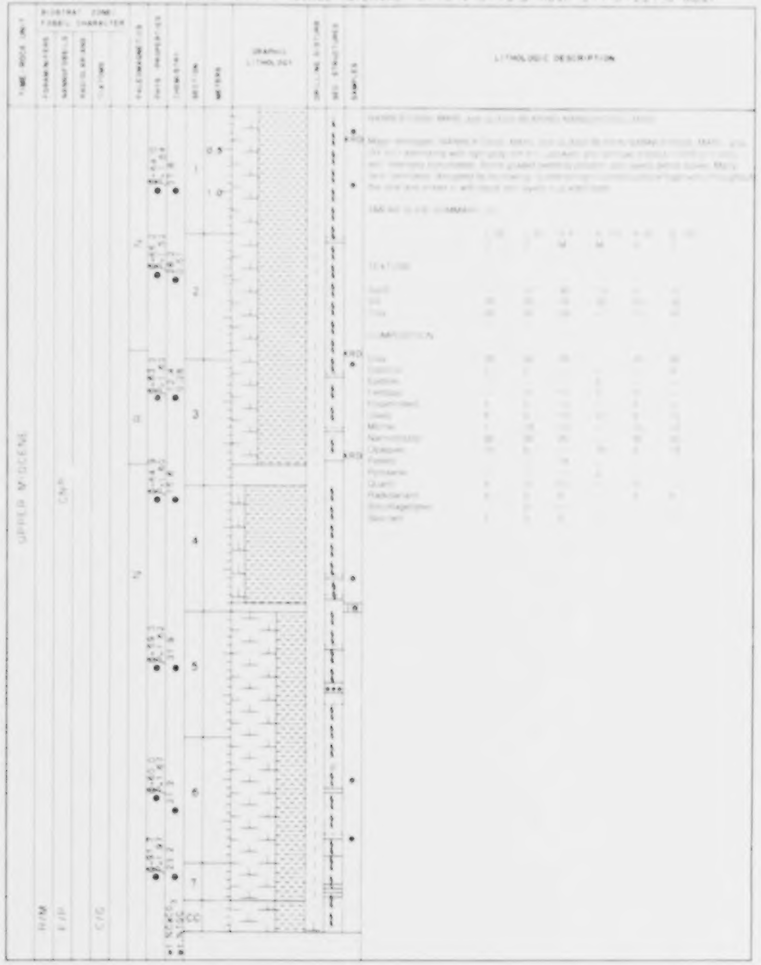
TIME-ROCK UNIT
BIOSTRAT. ZONE/ FOSSIL CHARACTER
FORAMINIFERS
NANNOFOSSILS
RADIOLARIANS
DIATOMS
PALEOMAGNETICS
PHYS. PROPERTIES
CHEMISTRY
SECTION
METERS
GRAPHIC LITHOLOGY
DRILLING DISTURB.
SED. STRUCTURES
SAMPLES
UPPER MIOCENE
CN9
N/M
F/P
C/G
0.5
1.0
1
2
3
4
5
6
7
CC

LITHOLOGIC DESCRIPTION

[illegible]

SMEAR SLIDE SUMMARY (%):

TEXTURE:

Sand
Silt
Clay

COMPOSITION:

Clay
Feldspar
Foraminifers
Glass
Micrite
Nannofossils
Opaques
Pyroxene
Quartz
Radiolarians
Silicoflagellates

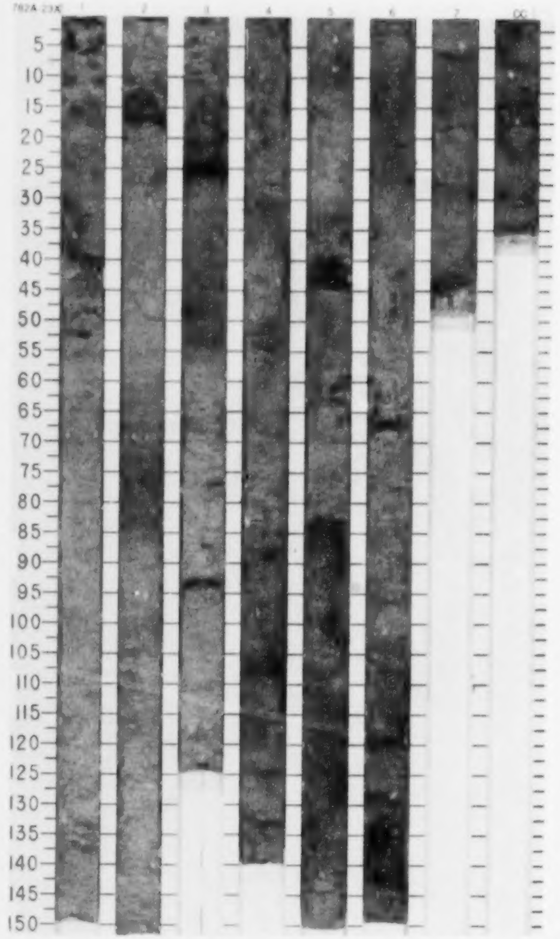
782A-23X
1
2
3
4
5
6
7
CC
5
10
15
20
25
30
35
40
45
50
55
60
65
70
75
80
85
90
95
100
105
110
115
120
125
130
135
140
145
150

SITE 782 HOLE A CORE 24X CORED INTERVAL 3159.9-3169.6 mbsl; 221.0-230.7 mbsf

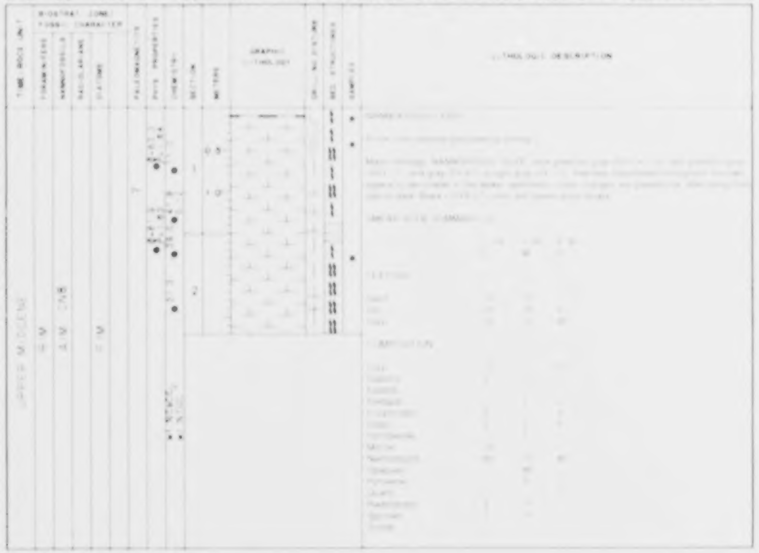
TIME-ROCK UNIT
BIOSTRAT. ZONE/ FOSSIL CHARACTER
FORAMINIFERS
NANNOFOSSILS
RADIOLARIANS
DIATOMS
PALEOMAGNETICS
PHYS. PROPERTIES
CHEMISTRY
SECTION
METERS
GRAPHIC LITHOLOGY
DRILLING DISTURB.
SED. STRUCTURES
SAMPLES
LITHOLOGIC DESCRIPTION
UPPER MIOCENE
F/M
A/V CN8
F/M
?
1
2
0.5
1.0
SMEAR SLIDE SUMMARY (%)
TEXTURE:
Sand
Silt
Clay
COMPOSITION:
Clay
Nannofossils
Radiolarians

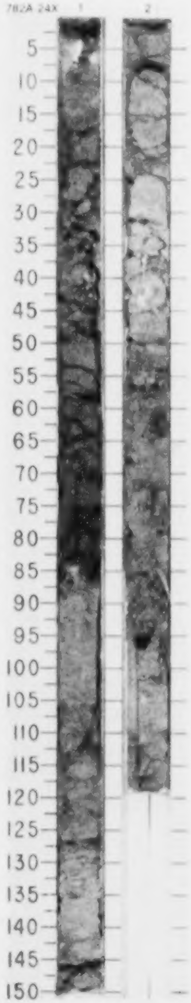
782A-24X
1
2
5
10
15
20
25
30
35
40
45
50
55
60
65
70
75
80
85
90
95
100
105
110
115
120
125
130
135
140
145
150

SITE 782 HOLE A CORE 25X CORED INTERVAL 3189.6-3199.2 mbsl; 230.7-240.3 mbsf

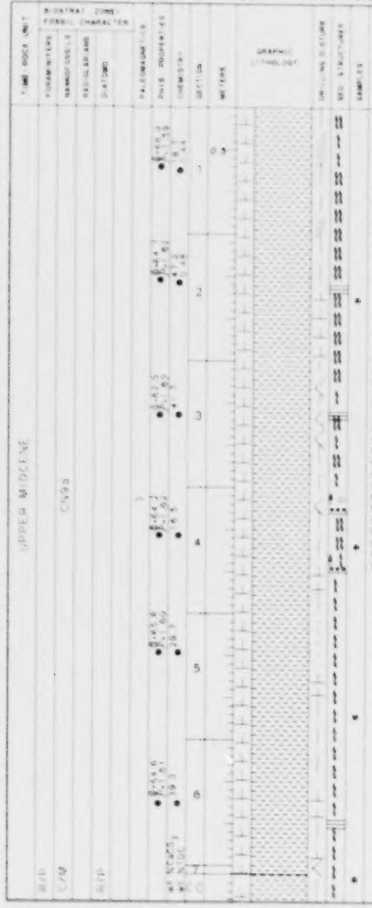
TIME-ROCK UNIT
BIOSTRAT. ZONE/ FOSSIL CHARACTER
FORAMINIFERS
NANNOFOSSILS
RADIOLARIANS
DIATOMS
PALEOMAGNETICS
PHYS. PROPERTIES
CHEMISTRY
SECTION
METERS
GRAPHIC LITHOLOGY
DRILLING DISTURB.
SED. STRUCTURES
SAMPLES
UPPER MIOCENE
CN9a
R/P
C/M
R/P
0.5
1
2
3
4
5
6
7
CC

LITHOLOGIC DESCRIPTION

NANNOFOSSIL MARL and GLASS-RICH NANNOFOSSIL MARL.

Major lithologies: NANNOFOSSIL MARL and GLASS-RICH NANNOFOSSIL MARL, light gray (5Y 7/1), light greenish gray (5Y [illegible]), to dark greenish gray (5Y [illegible]). Color changes are frequent and very gradational. Intensely bioturbated with zones of varying burrow size. In Section 2 large, vertical burrows occur at [illegible] cm, [illegible] cm, and [illegible] cm. Elsewhere small-scale vertical and horizontal burrows are pervasive. Tiny, feathery horizontal burrows are concentrated between [illegible] and [illegible] cm in Section 3. Primary laminations are preserved at [illegible] cm in Section 2, [illegible] cm in Section 3, and [illegible] cm in Section 5. Slight changes in color mark graded bedding with thin, black (10YR [illegible]) vitric ash layers at their bases from 0 to 40 cm and from 90 to 110 cm in Section 4. Ash also occurs as scattered grains throughout the entire cored interval. A drilling breccia or possibly a sedimentary breccia occurs between 30 and 40 cm in Section 3.

SMEAR SLIDE SUMMARY (%):

	[illegible]	[illegible]	[illegible]	[illegible]
	[illegible]	[illegible]	[illegible]	[illegible]
TEXTURE:				
Sand	[illegible]	26	26	12
Silt	[illegible]	[illegible]	[illegible]	[illegible]
Clay	[illegible]	[illegible]	[illegible]	[illegible]
COMPOSITION:				
Clay	[illegible]	[illegible]	[illegible]	[illegible]
Calcite	[illegible]	[illegible]	[illegible]	[illegible]
Epidote	—	—	—	[illegible]
Feldspar	[illegible]	[illegible]	[illegible]	—
Foraminifers	—	[illegible]	—	[illegible]
Glass	14	[illegible]	7	[illegible]
Micrite	16	[illegible]	[illegible]	[illegible]
Nannofossils	[illegible]	[illegible]	[illegible]	[illegible]
Opaques	[illegible]	—	[illegible]	—
Pyroxene	—	—	—	[illegible]
Quartz	[illegible]	[illegible]	[illegible]	—
Radiolarians	[illegible]	[illegible]	[illegible]	[illegible]
Spicules	[illegible]	[illegible]	[illegible]	[illegible]

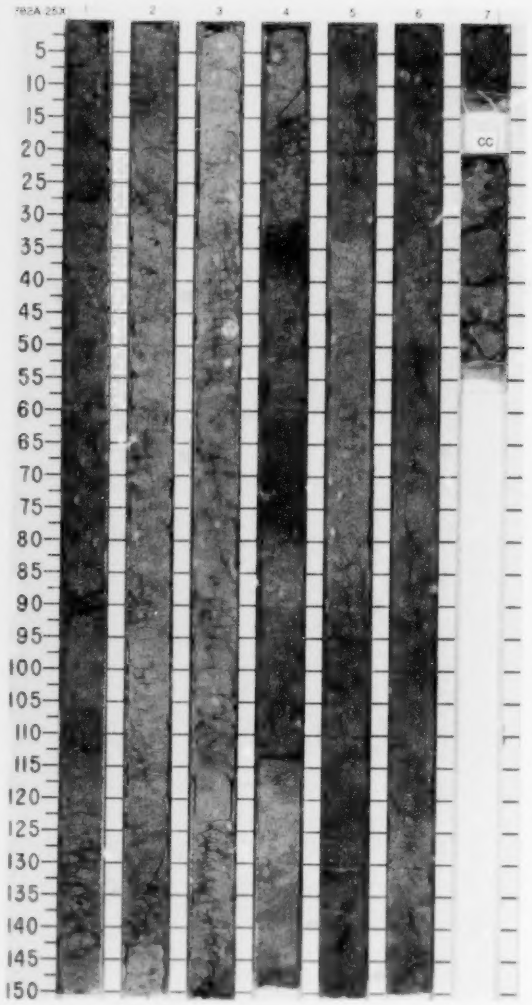
782A 25X
1
2
3
4
5
6
7
CC
5
10
15
20
25
30
35
40
45
50
55
60
65
70
75
80
85
90
95
100
105
110
115
120
125
130
135
140
145
150

SITE 782 HOLE A CORE 26X CORED INTERVAL 3199.2-3208.9 mbsl; 240.3-250.0 mbsf

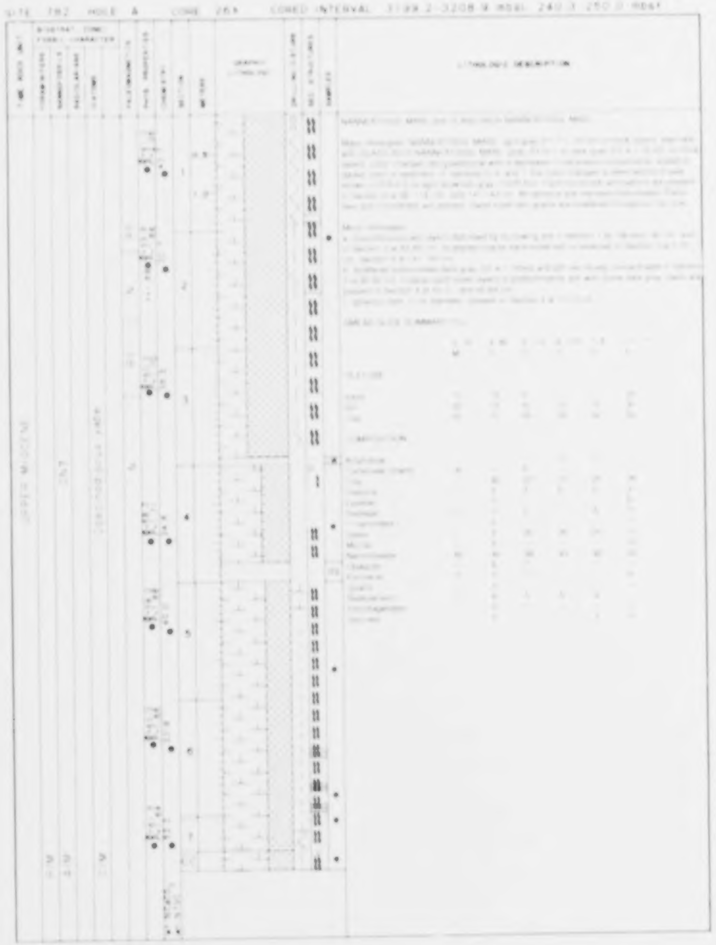
LITHOLOGIC DESCRIPTION
GRAPHIC LITHOLOGY

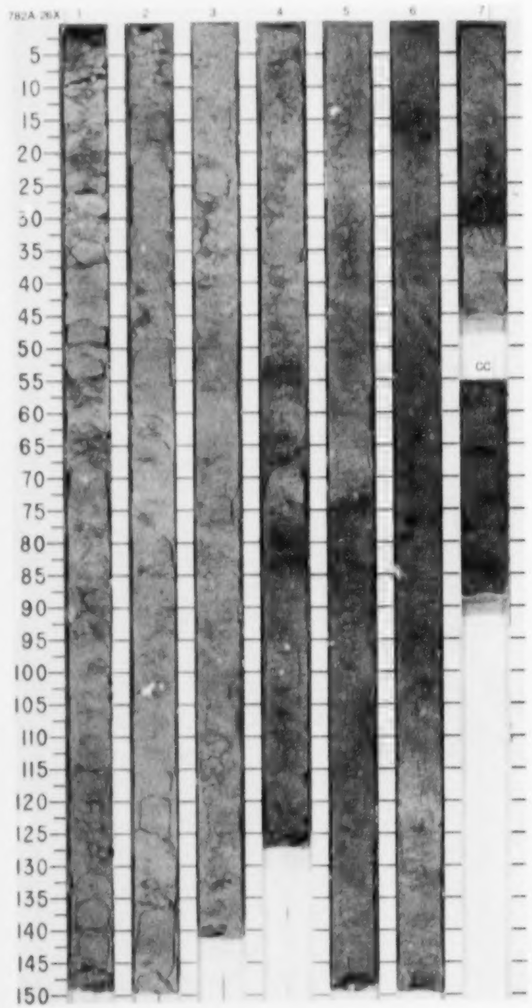
782A-26X
1
2
3
4
5
6
7
CC
5
10
15
20
25
30
35
40
45
50
55
60
65
70
75
80
85
90
95
100
105
110
115
120
125
130
135
140
145
150

SITE 782 HOLE A CORE 27X CORED INTERVAL 3208.9-3218.5 mbsl; 250.0-259.6 mbsf

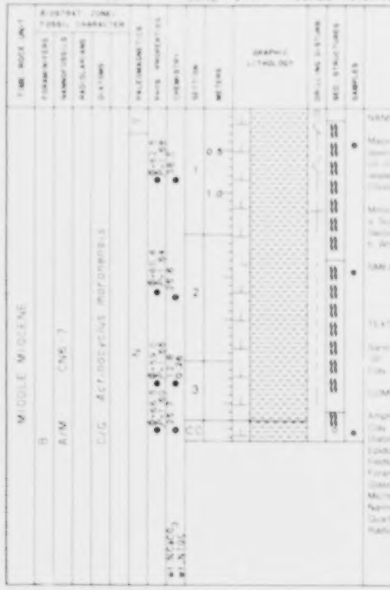
TIME-ROCK UNIT
BIOSTRAT. ZONE/ FOSSIL CHARACTER
FORAMINIFERS
NANNOFOSSILS
RADIOLARIANS
DIATOMS
PALEOMAGNETICS
PHYS. PROPERTIES
CHEMISTRY
SECTION
METERS
GRAPHIC LITHOLOGY
DRILLING DISTURB.
SED. STRUCTURES
SAMPLES
MIDDLE MIOCENE
B
A/M CN5 ?
C/G Actinocyclus moronensis
N
1
2
3
CC
0.5
1.0
%CaCO₃
%TOC

LITHOLOGIC DESCRIPTION

NANNOFOSSIL MARL and GLASS-RICH NANNOFOSSIL MARL

Major lithologies: NANNOFOSSIL MARL, light brownish gray (10YR 6/2), 20-50-cm-thick layers, alternate with GLASS-RICH NANNOFOSSIL MARL, grayish brown (10YR 5/2), 20-40 cm thick layers. Color changes are gradational with a decrease in calcareous components related to darker color of sediment. All sections are intensely bioturbated. Planolites and Chondrites are present. Sand-sized ash grains are scattered throughout the core.

Minor lithologies:
a. Scattered coarse sand-sized ash, brown (10YR 5/3), and white (10YR 8/1), is located in Section 1 at 0-7 cm, Section 2 at 30-32 cm, and Section 3 at 48-52 cm.
b. White clast, 1 cm diameter, present in Section CC at 15 cm.

SMEAR SLIDE SUMMARY (%):

	1, 33 D	2, 47 D	CC, 14 D
TEXTURE:			
Sand	5	15	—
Silt	80	20	60
Clay	15	65	40
COMPOSITION:			
Amphibole	1	—	—
Clay	15	32	12
Diatoms	—	3	5
Epidote	—	Tr	—
Feldspar	5	1	—
Foraminifers	2	2	—
Glass	15	10	25
Micrite	—	12	—
Nannofossils	60	38	60
Quartz	—	Tr	—
Radiolarians	2	2	5

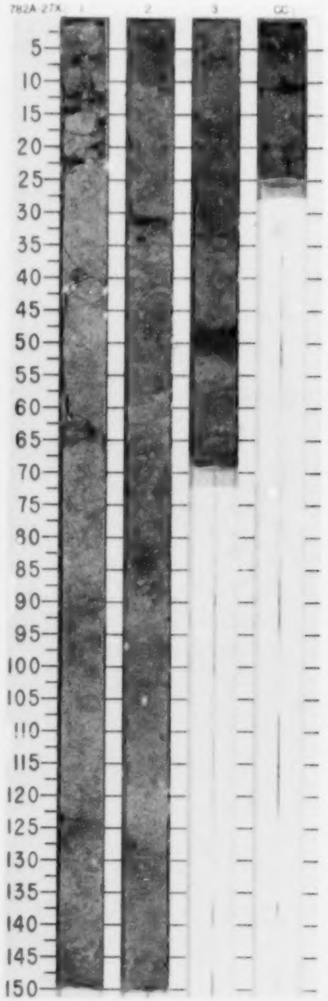
782A-27X
1
2
3
CC
5
10
15
20
25
30
35
40
45
50
55
60
65
70
75
80
85
90
95
100
105
110
115
120
125
130
135
140
145
150

SITE 782 HOLE A CORE 28X CORED INTERVAL 3216.5-3226.1 mbsl; 259.6-269.2 mbsf

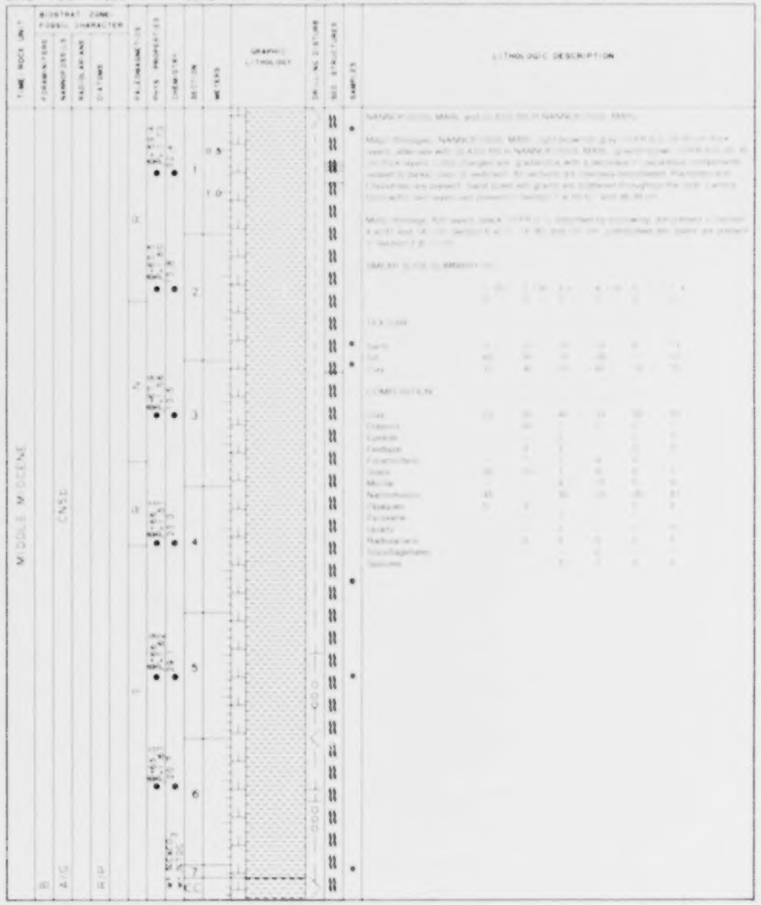
TIME-ROCK UNIT
BIOSTRAT. ZONE/ FOSSIL CHARACTER
FORAMINIFERS
NANNOFOSSILS
RADIOLARIANS
DIATOMS
PALEOMAGNETICS
PHYS. PROPERTIES
CHEMISTRY
SECTION
METERS
GRAPHIC LITHOLOGY
DRILLING DISTURB.
SED. STRUCTURES
SAMPLES
LITHOLOGIC DESCRIPTION
MIDDLE MIOCENE
CN5b
B
A/G
R/P
0.5
1.0
1
2
3
4
5
6
7
CC

NANNOFOSSIL MARL and [illegible] NANNOFOSSIL MARL.

[illegible]

SMEAR SLIDE SUMMARY (%):

TEXTURE:

Sand
Silt
Clay

COMPOSITION:

Clay
Diatoms
Calcite
Feldspar
Foraminifers
Glass
Mica
Nannofossils
Opaques
Pyroxene
Quartz
Radiolarians
Silicoflagellates
Sponges

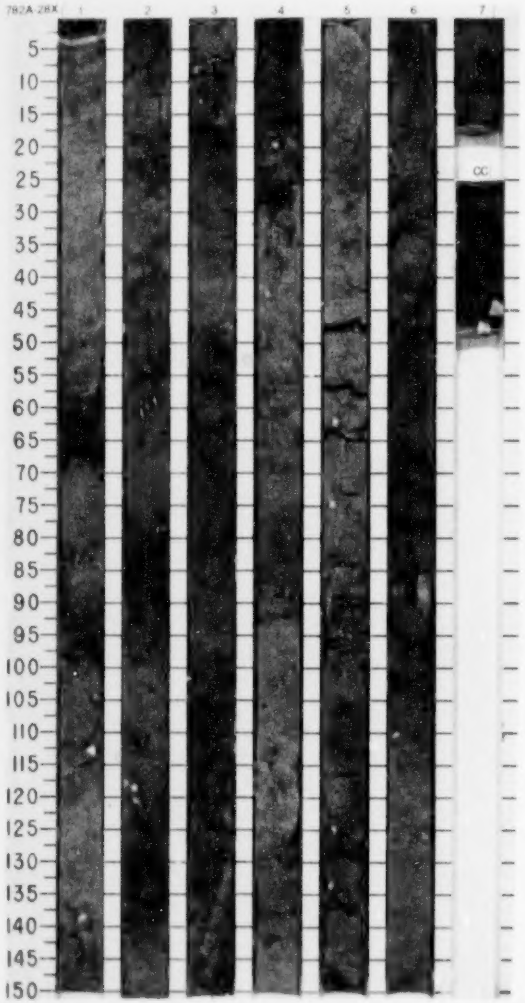
782A-28X
1
2
3
4
5
6
7
CC
5
10
15
20
25
30
35
40
45
50
55
60
65
70
75
80
85
90
95
100
105
110
115
120
125
130
135
140
145
150

SITE 782 HOLE A CORE 29X CORED INTERVAL 3228.1-3237.7 mbsl; 269.2-278.8 mbsf

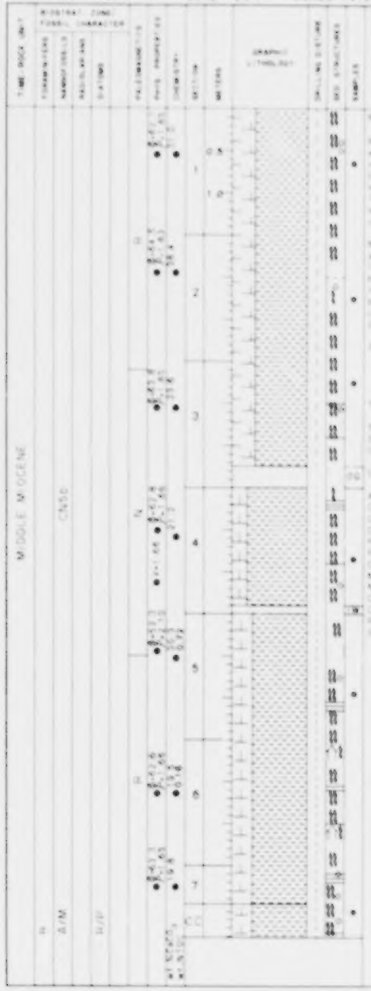
TIME-ROCK UNIT
BIOSTRAT. ZONE/ FOSSIL CHARACTER
FORAMINIFERS
NANNOFOSSILS
RADIOLARIANS
DIATOMS
PALEOMAGNETICS
PHYS. PROPERTIES
CHEMISTRY
SECTION
METERS
GRAPHIC LITHOLOGY
DRILLING DISTURB.
SED. STRUCTURES
SAMPLES
MIDDLE MIOCENE
B
CN5b
A/M
R/P
N
R
1
2
3
4
5
6
7
CC
0.5
1.0

LITHOLOGIC DESCRIPTION

NANNOFOSSIL MARL and GLASS-BEARING NANNOFOSSIL MARL

Major lithologies: NANNOFOSSIL MARL, gray (10YR 6/1), 20-55 cm thick layers, alternates with GLASS-BEARING NANNOFOSSIL MARL, dark gray (10YR 4/1, 3/1), 25-55 cm thick layers. Color changes are gradational with a decrease in calcareous components related to darker color of sediment. All sections are intensely bioturbated. Planolites and Chondrites are scattered throughout the core. Slight increase in local concentration of ash in Section 1 at 130-140 cm. A zone of laminations composed of gray (10YR 5/1) coarse sand and granule sized ash is present in Section 5 at 119-122 cm, and in Section 7 at 7-9 cm. Intervals with an upward decrease in ash are present in Section 6 at 13-19, and 120-125 cm.

Minor lithologies:

a. Ash layer, black (10YR 2/1), has a sharp basal contact in Section 6 at 18-21, 39-41, and 124-126 cm; in Section 7 at 35-37 cm; in Section CC at 39-40 cm, and contains pin-sized brown (10YR 5/3) shell fragments in Section 3 at 43-44 cm. Ash layers disturbed by burrowing are present in Section 4 at 90 cm, and in Section 4 at 40-46 cm.

b. Lithics are present in Section 6 at 44-45 cm (1 cm dia).

c. Dark yellowish brown (10YR 4/4), angular pumice is present in Section 1 at 13-35 cm (1-2 cm size), and 20-25 cm, and in Section CC at 0-20 cm.

SMEAR SLIDE SUMMARY (%):

	1, 55 D	2, 79 D	3, 24 D	4, 84 D	5, 97 D	CC, 10 M
TEXTURE:						
Sand	5	—	5	—	—	5
Silt	5	15	45	60	50	80
Clay	90	85	50	40	50	15
COMPOSITION:						
Amphibole	—	—	T	—	—	Tr
Chlorite	—	—	2	2	—	—
Clay	40	50	30	35	32	20
Diatoms	2	—	T	T	1	60
Feldspar	Tr	Tr	—	3	2	5
Foraminifers	1	1	1	—	—	—
Glass	3	—	5	10	8	Tr
Mica	—	1	—	—	Tr	—
Nannofossils	50	40	47	40	47	—
Opaques	—	5	2	5	5	1
Quartz	Tr	Tr	—	—	—	—
Radiolarians	3	1	8	3	5	1
Spicules	1	1	3	2	2	—

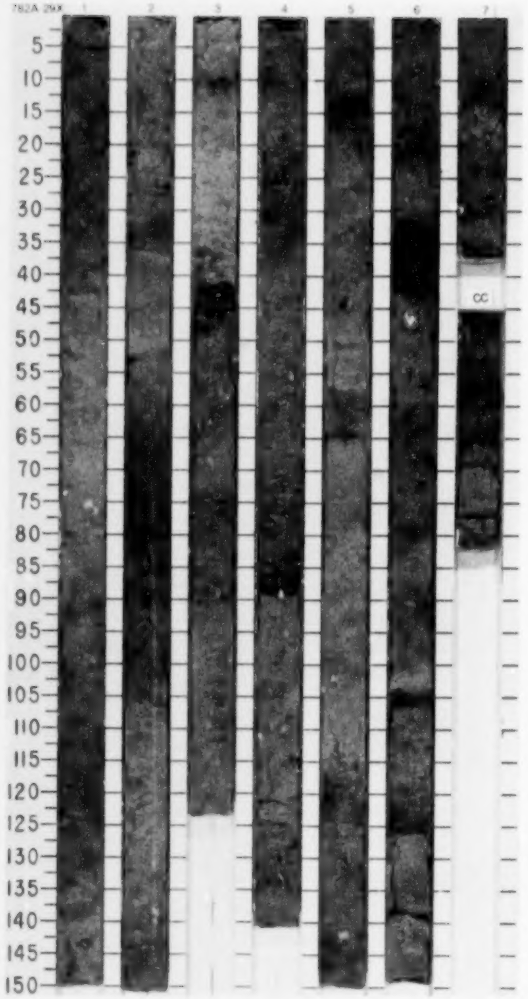
782A 29X
1
2
3
4
5
6
7
CC
5
10
15
20
25
30
35
40
45
50
55
60
65
70
75
80
85
90
95
100
105
110
115
120
125
130
135
140
145
150

SITE 782 HOLE A CORE 30X CORED INTERVAL 3237.7-3247.4 mbsl; 278.8-288.5 mbsf

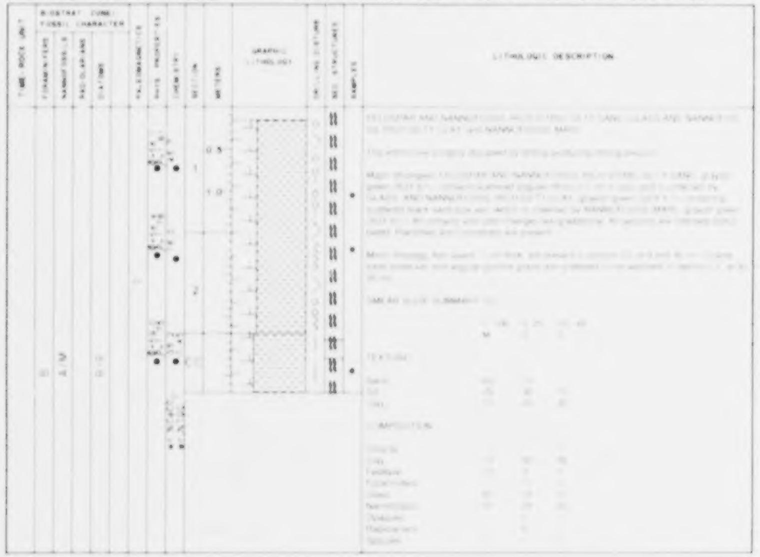
TIME-ROCK UNIT
BIOSTRAT. ZONE/ FOSSIL CHARACTER
FORAMINIFERS
NANNOFOSSILS
RADIOLARIANS
DIATOMS
PALEOMAGNETICS
PHYS. PROPERTIES
CHEMISTRY
SECTION
METERS
GRAPHIC LITHOLOGY
DRILLING DISTURB.
SED. STRUCTURES
SAMPLES
0.5
1.0
1
2
CC
A/M

LITHOLOGIC DESCRIPTION

[illegible]

SMEAR SLIDE SUMMARY (%):

TEXTURE:

Sand
Silt
Clay

COMPOSITION:

Quartz
Clay
Feldspar
Glass
Nannofossils
Diatoms
Radiolarians
Spicules

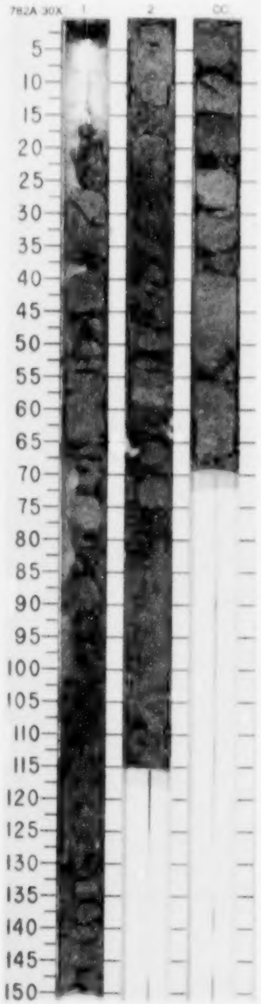
782A 30X
1
2
CC
5
10
15
20
25
30
35
40
45
50
55
60
65
70
75
80
85
90
95
100
105
110
115
120
125
130
135
140
145
150

SITE 782 HOLE A CORE 31X CORED INTERVAL 3247.4-3252.9 mbsl; 288.5-294.0 mbsf

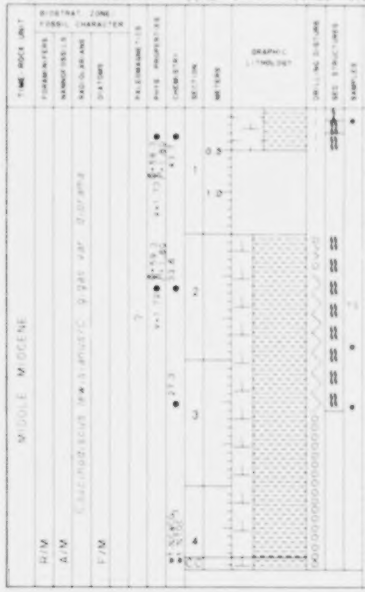
TIME-ROCK UNIT
BIOSTRAT. ZONE/ FOSSIL CHARACTER
FORAMINIFERS
NANNOFOSSILS
RADIOLARIANS
DIATOMS
PALEOMAGNETICS
PHYS. PROPERTIES
CHEMISTRY
SECTION
METERS
GRAPHIC LITHOLOGY
DRILLING DISTURB.
SED. STRUCTURES
SAMPLES
MIDDLE MIOCENE
R/M
A/M
F/M
Coscinodiscus lewisianus/C. gigas var. diorama
?
0.5
1.0
1
2
3
4
CC
TS

LITHOLOGIC DESCRIPTION

NANNOFOSSIL MARLSTONE, NANNOFOSSIL-RICH SILTY CLAYSTONE, and NANNOFOSSIL AND GLASS-RICH SILTY CLAYSTONE

The entire core is highly disturbed by drilling.

Major lithologies: Drilling biscuits of grayish green (5GY 5/1, 5/1) bioturbated NANNOFOSSIL MARLSTONE contain 1-3 cm sized, angular clasts in Section 1 from [illegible] cm, and coarse sand sized clasts throughout the remainder of the section. Section 2 is composed of grayish green (5GY 5/1) bioturbated NANNOFOSSIL-RICH SILTY CLAYSTONE drilling biscuits with slurry intervals near the top of the section. Sand sized ash is evenly dispersed throughout the biscuits. Grayish green (5GY 5/1) bioturbated NANNOFOSSIL AND GLASS-RICH SILTY CLAYSTONE contains sand sized ash and rare 1 cm sized pumice fragments in Section 3 from 0-60 cm. A slurry mixture of coarse to granule black (10YR 2/1) ash and grayish green (5GY 5/1) silty clay is located below 60 cm in Section 3 and continues to the base of the core.

Minor lithology: Ash layers are present in Section 1 at 17 and 20-24 cm.

SMEAR SLIDE SUMMARY (%):

	1, 18	2, 104	3, 18
	D	D	M
TEXTURE:			
Sand	—	5	5
Silt	50	20	30
Clay	50	80	70
COMPOSITION:			
Clay	47	30	40
Diatoms	—	—	—
Feldspar	1	2	5
Foraminifers	3	5	—
Glass	7	8	10
Nannofossils	40	30	15
Opaques	1	1	—
Pyroxene	—	—	—
Radiolarians	—	8	1
Spicules	—	3	—

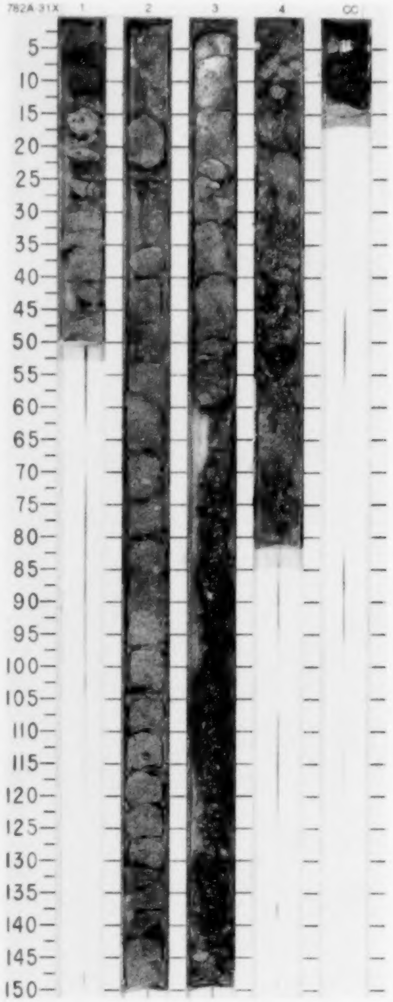
782A-31X
1
2
3
4
CC
5
10
15
20
25
30
35
40
45
50
55
60
65
70
75
80
85
90
95
100
105
110
115
120
125
130
135
140
145
150

SITE 782 HOLE A CORE 32X CORED INTERVAL 3252.9-3262.4 mbsl; 294.0-303.5

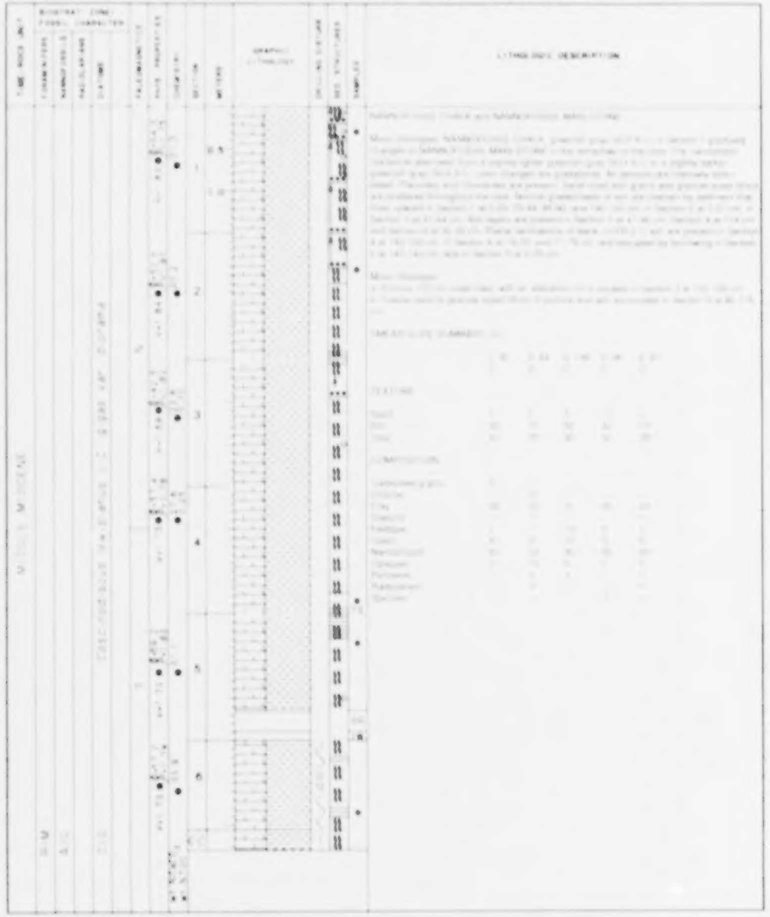
TIME-ROCK UNIT
BIOSTRAT. ZONE/ FOSSIL CHARACTER
FORAMINIFERS
NANNOFOSSILS
RADIOLARIANS
DIATOMS
PALEOMAGNETICS
PHYS. PROPERTIES
CHEMISTRY
SECTION
METERS
GRAPHIC LITHOLOGY
DRILLING DISTURB.
SED. STRUCTURES
SAMPLES
LITHOLOGIC DESCRIPTION
MIDDLE MIOCENE
0.5
1.0
1
2
3
4
5
6
CC

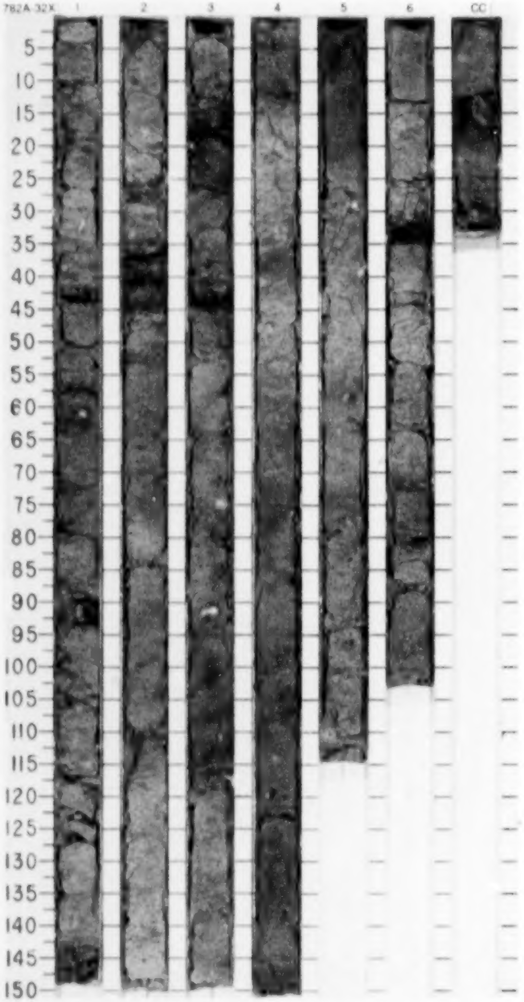
782A-32X
1
2
3
4
5
6
CC
5
10
15
20
25
30
35
40
45
50
55
60
65
70
75
80
85
90
95
100
105
110
115
120
125
130
135
140
145
150

SITE 782 HOLE A CORE 33X CORED INTERVAL 3262.4-3272.0 mbsl; 303.5-313.1 mbsf

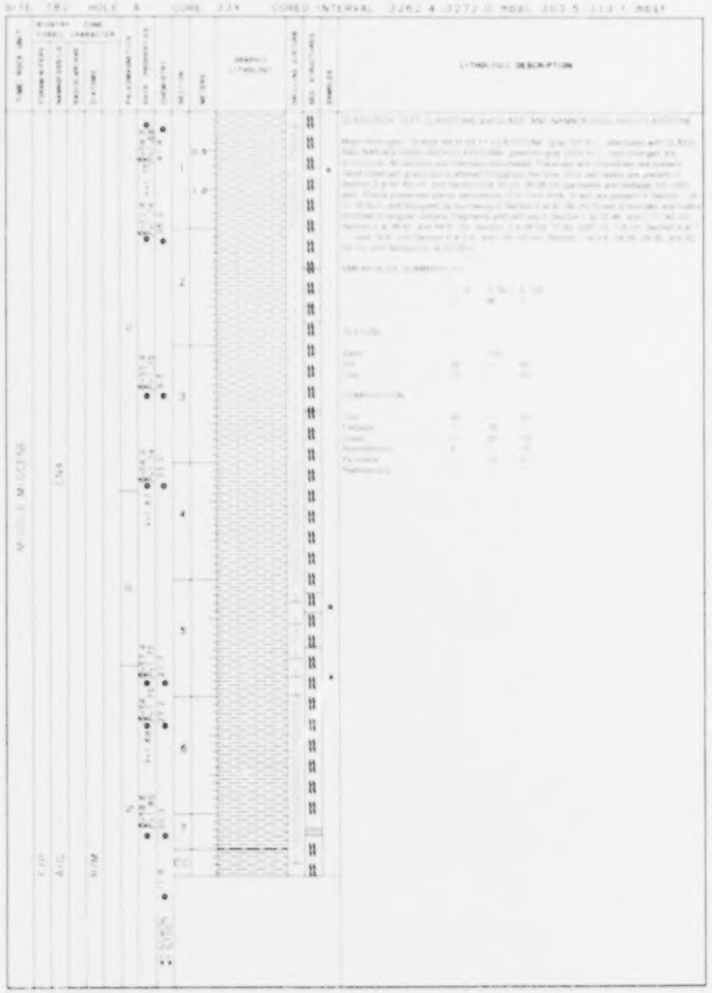
LITHOLOGIC DESCRIPTION
GRAPHIC LITHOLOGY
MIDDLE MIOCENE

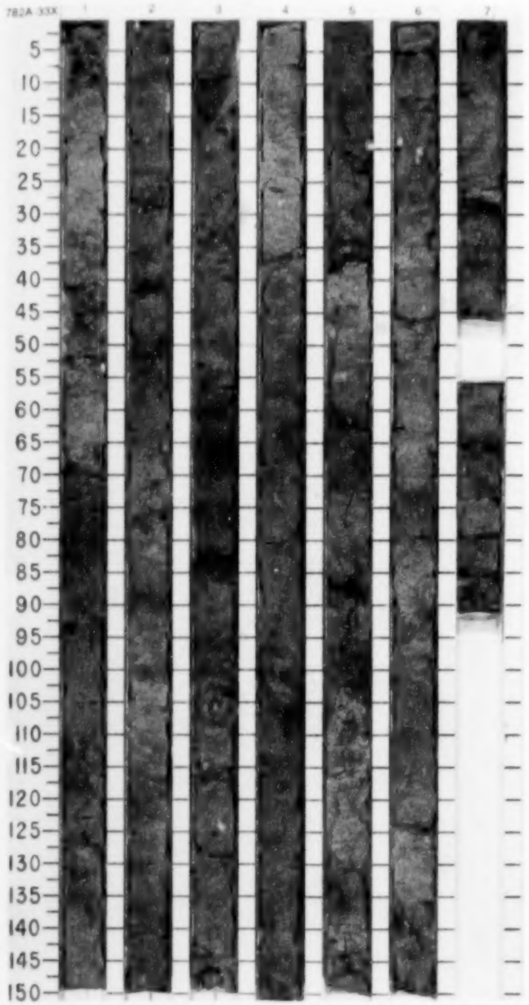
782A-33X
1
2
3
4
5
6
7
5
10
15
20
25
30
35
40
45
50
55
60
65
70
75
80
85
90
95
100
105
110
115
120
125
130
135
140
145
150

SITE 782 HOLE A CORE 34X CORED INTERVAL 3272.0-3281.4 mbsl; 313.1-322.5 mbsf

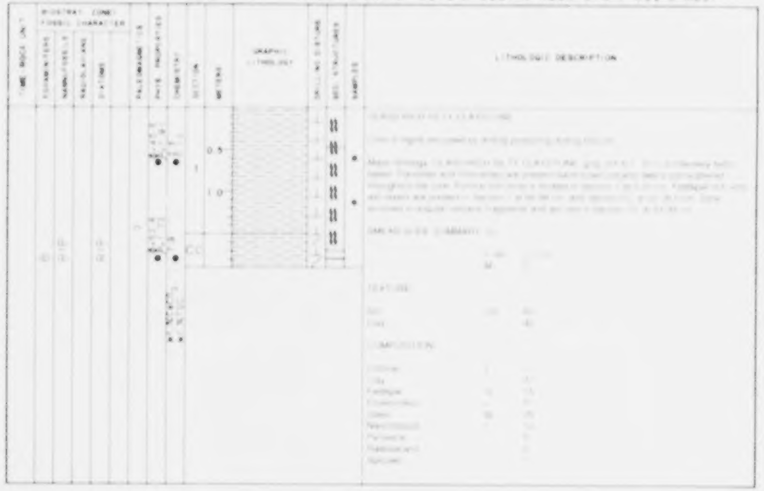

TIME-ROCK UNIT	BIOSTRAT. ZONE / FOSSIL CHARACTER: FORAMINIFERS	NANNOFOSSILS	RADIOLARIANS	DIATOMS	PALEOMAGNETICS	PHYS. PROPERTIES	CHEMISTRY	SECTION	METERS	GRAPHIC LITHOLOGY	DRILLING DISTURB.	SED. STRUCTURES	SAMPLES	LITHOLOGIC DESCRIPTION
						●	●	1	0.5 1.0				● ●	[illegible]
	[illegible]	[illegible]		[illegible]		●	●	CC						

782A 34X
1
CC
5
10
15
20
25
30
35
40
45
50
55
60
65
70
75
80
85
90
95
100
105
110
115
120
125
130
135
140
145
150

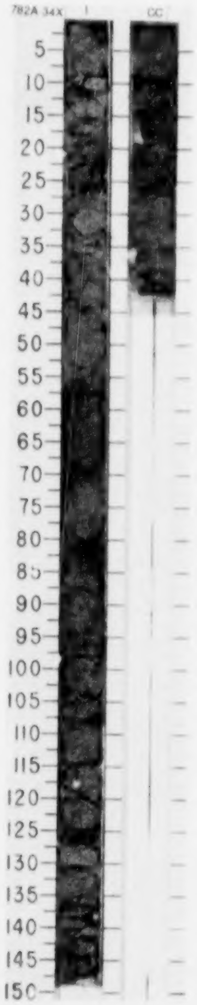

SITE 782 HOLE A CORE 35X CORED INTERVAL 3281.4-3291.0 mbsl; 322.5-332.1 mbsf

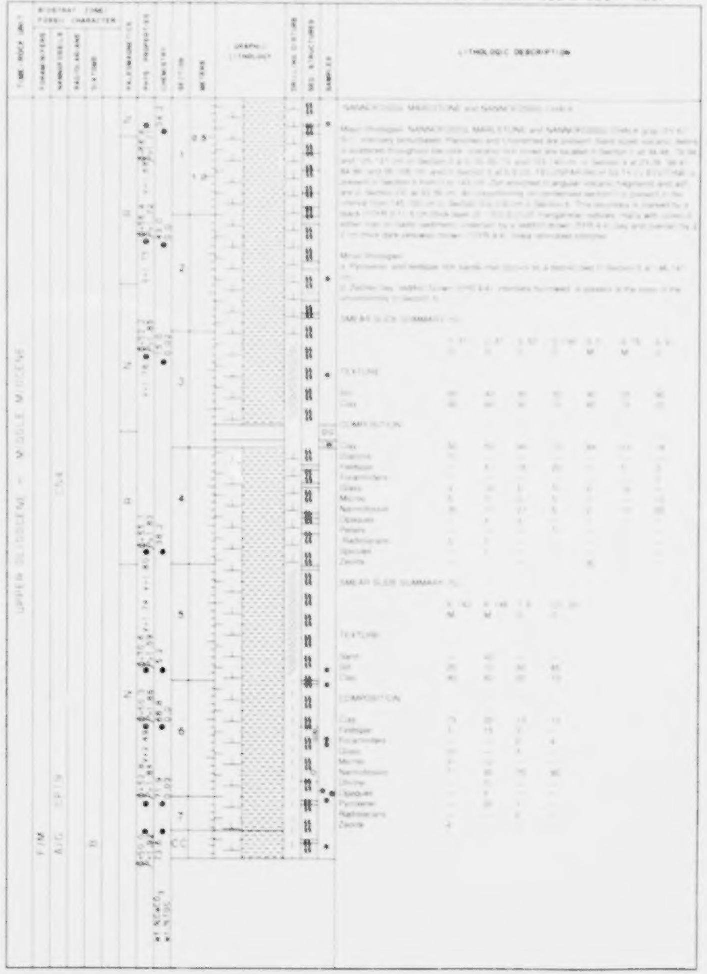
TIME-ROCK UNIT
BIOSTRAT. ZONE/ FOSSIL CHARACTER
FORAMINIFERS
NANNOFOSSILS
RADIOLARIANS
DIATOMS
PALEOMAGNETICS
PHYS. PROPERTIES
CHEMISTRY
SECTION
METERS
GRAPHIC LITHOLOGY
DRILLING DISTURB.
SED. STRUCTURES
SAMPLES
LITHOLOGIC DESCRIPTION
UPPER OLIGOCENE – MIDDLE MIOCENE
CN4
CP19
F/M
A/G
B
N
R
1
2
3
4
5
6
7
CC
0.5
1.0

NANNOFOSSIL MARLSTONE and NANNOFOSSIL CHALK

Major lithologies: NANNOFOSSIL MARLSTONE and NANNOFOSSIL CHALK [illegible]

Minor lithologies:

A. [illegible]

B. [illegible]

SMEAR SLIDE SUMMARY (%):

TEXTURE:

Silt

Clay

COMPOSITION:

Clay

Diatoms

Feldspar

Foraminifers

Glass

Micrite

Nannofossils

Opaques

Pellets

Radiolarians

Spicules

Zeolite

SMEAR SLIDE SUMMARY (%):

TEXTURE:

Sand

Silt

Clay

COMPOSITION:

Clay

Feldspar

Foraminifers

Glass

Micrite

Nannofossils

Olivine

Opaques

Pyroxene

Radiolarians

Zeolite

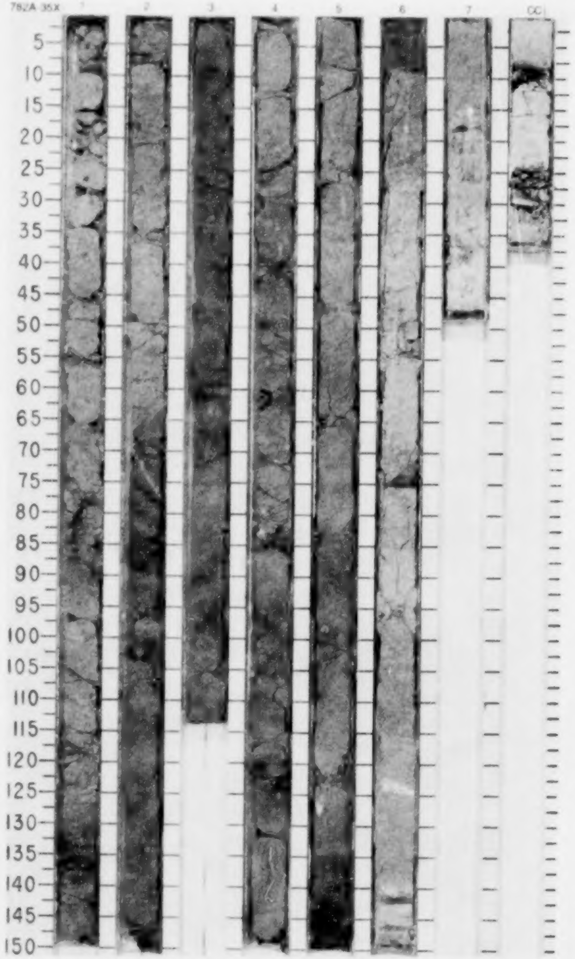
782A-35X
1
2
3
4
5
6
7
CC
5
10
15
20
25
30
35
40
45
50
55
60
65
70
75
80
85
90
95
100
105
110
115
120
125
130
135
140
145
150

SITE 782 HOLE A CORE 36X CORED INTERVAL 3291.0-3300.5 mbsl; 335.1-344.6 mbsf

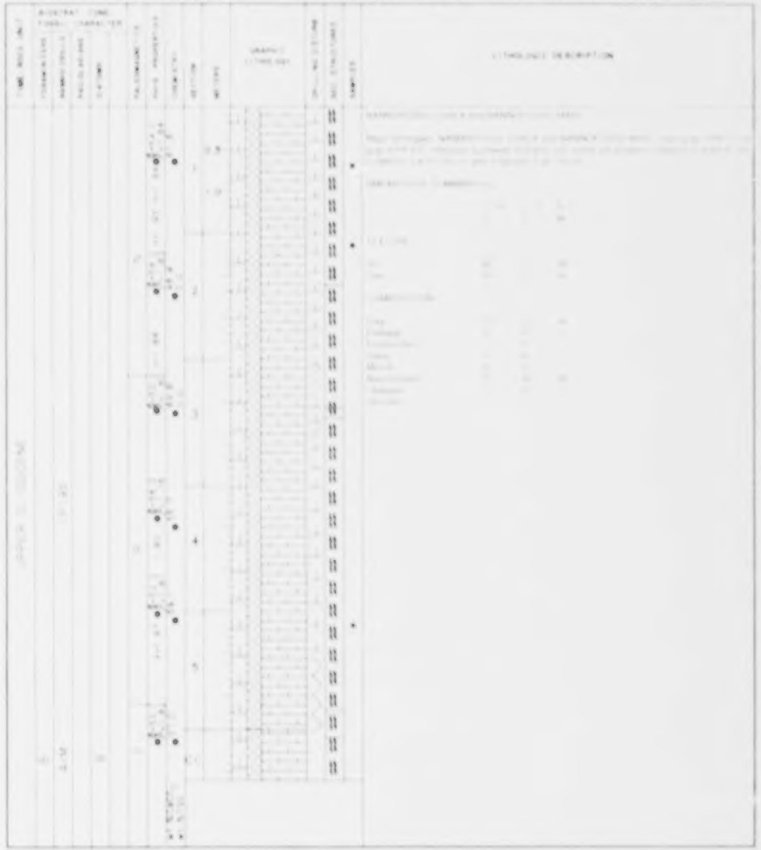
TIME-ROCK UNIT
BIOSTRAT. ZONE/FOSSIL CHARACTER
FORAMINIFERS
NANNOFOSSILS
RADIOLARIANS
DIATOMS
PALEOMAGNETICS
PHYS. PROPERTIES
CHEMISTRY
SECTION
METERS
GRAPHIC LITHOLOGY
DRILLING DISTURB.
SED. STRUCTURES
SAMPLES
LITHOLOGIC DESCRIPTION
1
2
3
4
5
CC

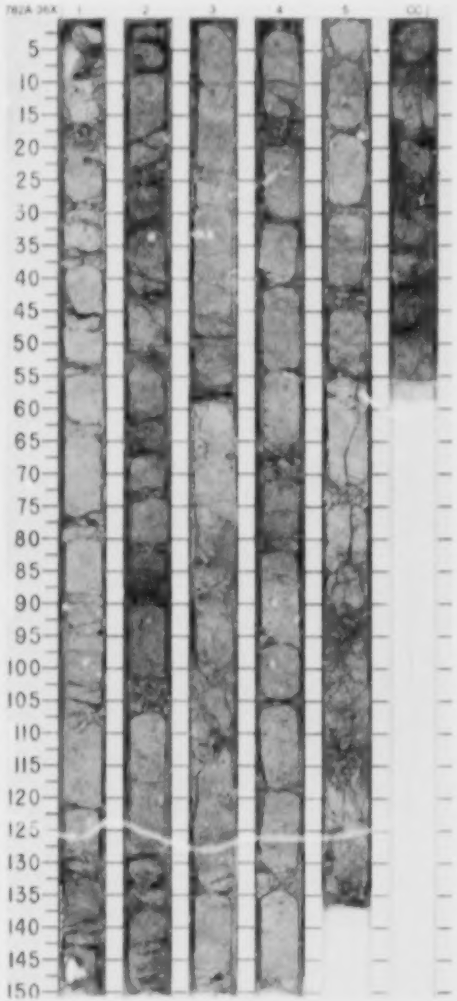
782A-36X
1
2
3
4
5
CC
5
10
15
20
25
30
35
40
45
50
55
60
65
70
75
80
85
90
95
100
105
110
115
120
125
130
135
140
145
150

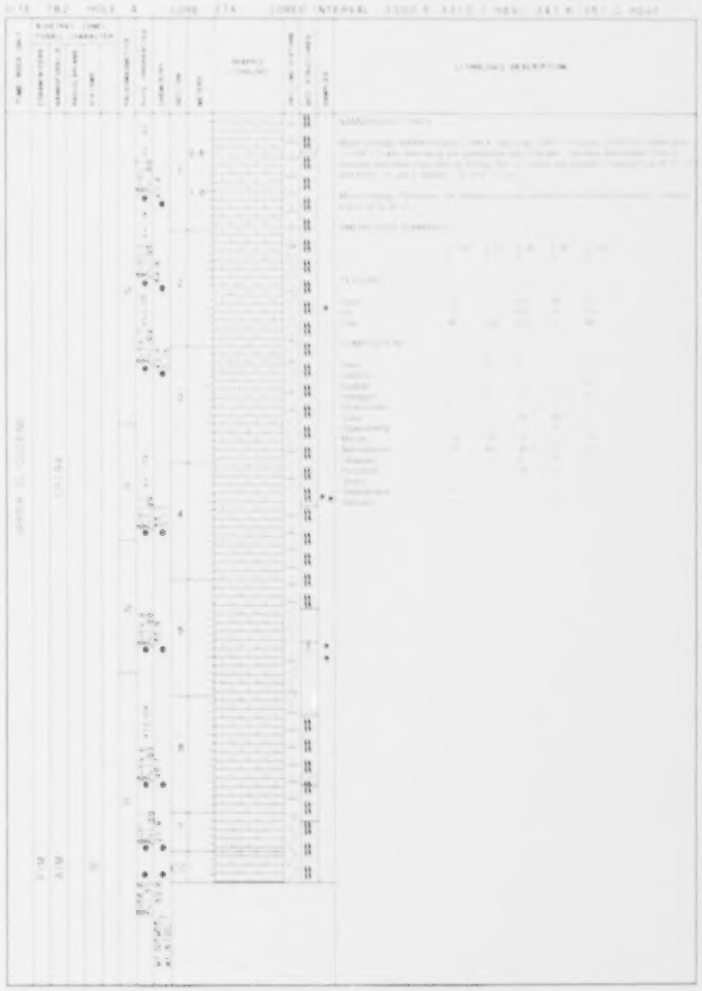
SITE 782 HOLE A CORE 37X CORED INTERVAL
GRAPHIC LITHOLOGY
LITHOLOGIC DESCRIPTION

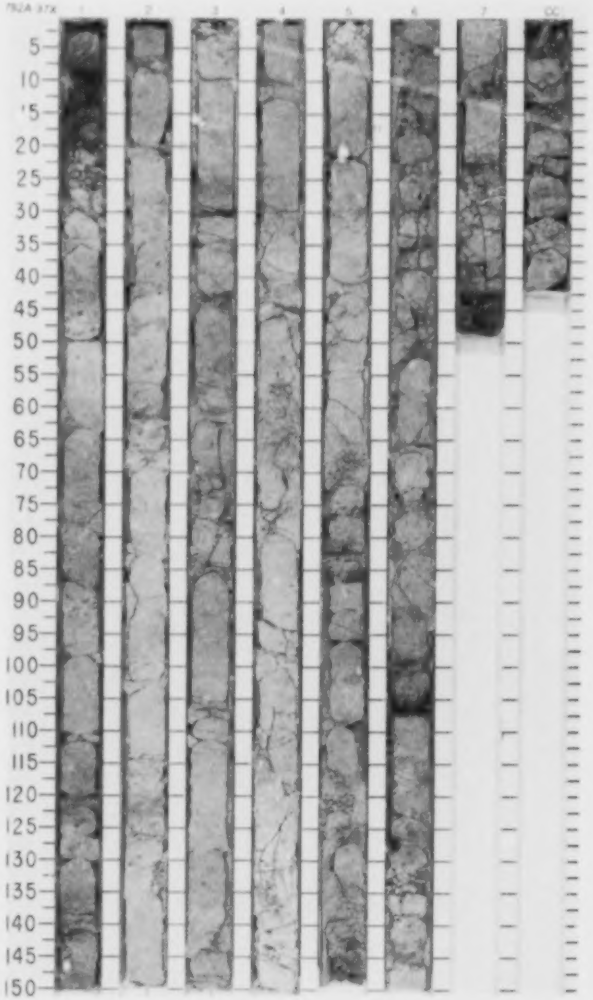
782A-37X
1
2
3
4
5
6
7
CC
5
10
15
20
25
30
35
40
45
50
55
60
65
70
75
80
85
90
95
100
105
110
115
120
125
130
135
140
145
150

782 A 38X NO RECOVERY

SITE 782 HOLE A CORE 39X CORED INTERVAL 3319.8-3329.4 mbsl; 360.9-370.5 mbsf

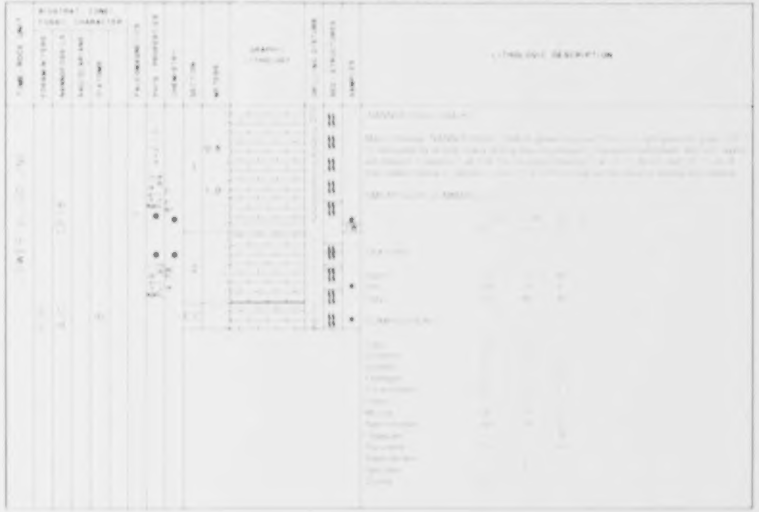
LITHOLOGIC DESCRIPTION
GRAPHIC LITHOLOGY

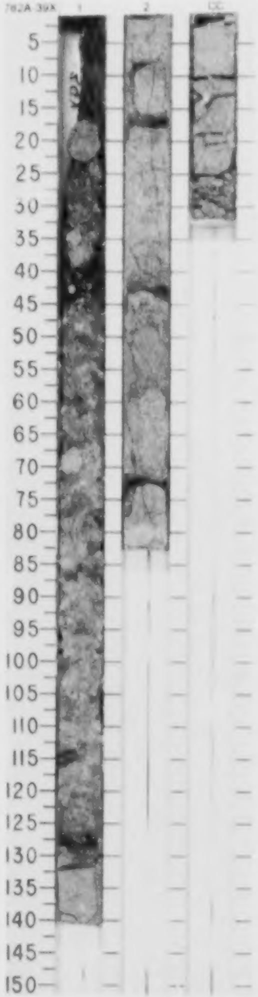
782A 39X
1
2
CC
5
10
15
20
25
30
35
40
45
50
55
60
65
70
75
80
85
90
95
100
105
110
115
120
125
130
135
140
145
150

SITE 782 HOLE A CORE 40X CORED INTERVAL 3329.4-3339.1 mbsl; 370.5-380.2 mbsf

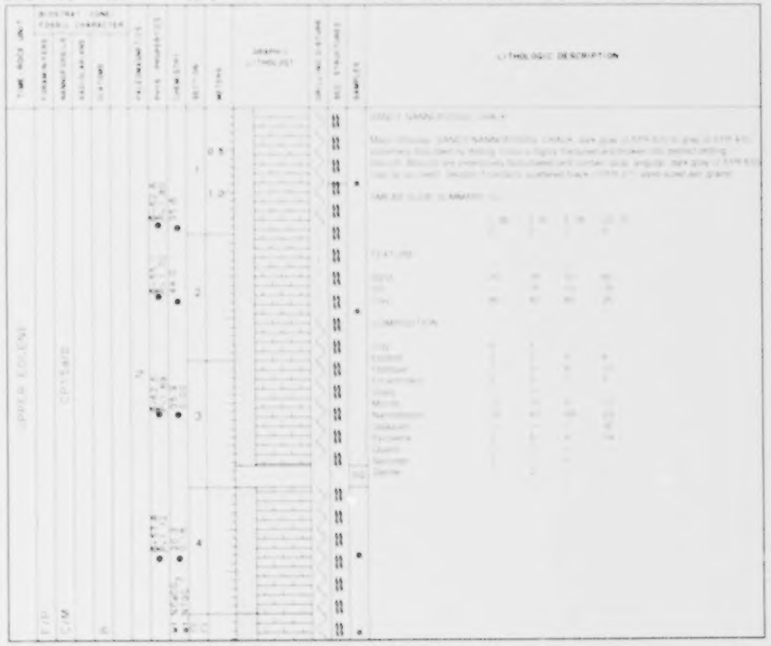

SANDY NANNOFOSSIL CHALK

Major lithology: SANDY NANNOFOSSIL CHALK, dark gray [illegible]

SMEAR SLIDE SUMMARY (%):

TEXTURE:

Sand

Silt

Clay

COMPOSITION:

[illegible]

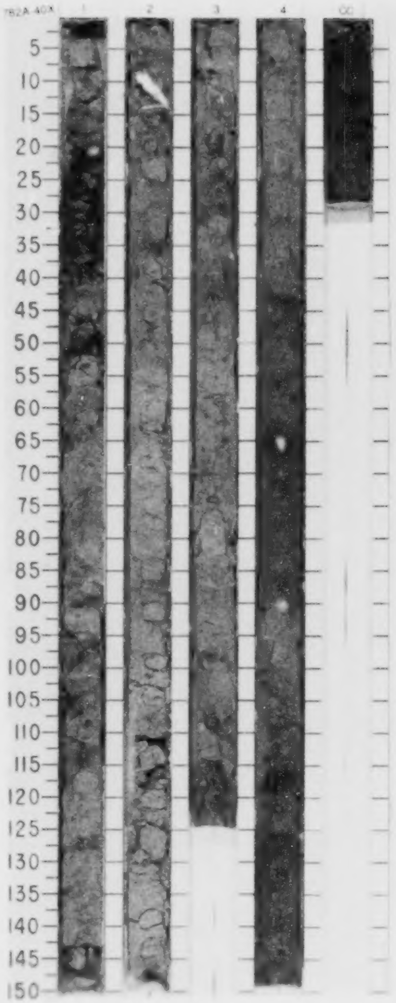
782A-40X
1
2
3
4
CC
5
10
15
20
25
30
35
40
45
50
55
60
65
70
75
80
85
90
95
100
105
110
115
120
125
130
135
140
145
150

SITE 782 HOLE A CORE 41X CORED INTERVAL 3339.1-3348.7 mbsl; 380.2-389.8 mbsf

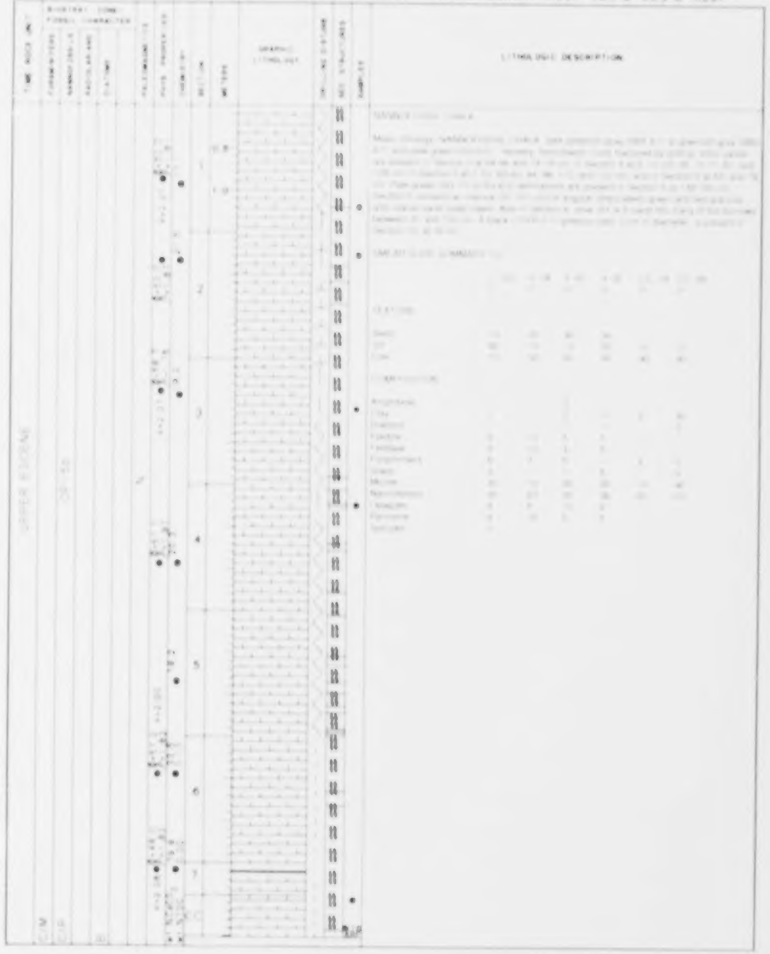
TIME-ROCK UNIT
BIOSTRAT. ZONE/FOSSIL CHARACTER
PALEOMAGNETICS
SECTION
METERS
GRAPHIC LITHOLOGY
SED. STRUCTURES
SAMPLES
LITHOLOGIC DESCRIPTION
SMEAR SLIDE SUMMARY (%)
TEXTURE:
COMPOSITION:
UPPER EOCENE

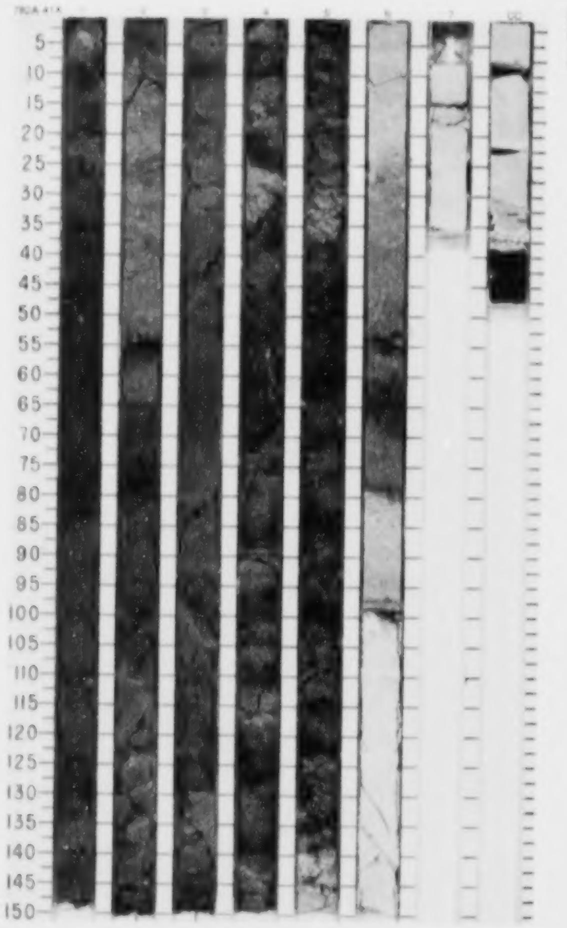
782A-41X
1
2
3
4
5
6
7
CC
5
10
15
20
25
30
35
40
45
50
55
60
65
70
75
80
85
90
95
100
105
110
115
120
125
130
135
140
145
150

SITE 782 HOLE A CORE 42X CORED INTERVAL 3348.7-3358.4 mbsl; 389.8-399.5 mbsf

TIME-ROCK UNIT	FORAMINIFERS	NANNOFOSSILS	RADIOLARIANS	DIATOMS	PALEOMAGNETICS	PHYS. PROPERTIES	CHEMISTRY	SECTION	METERS	GRAPHIC LITHOLOGY	DRILLING DISTURB.	SED. STRUCTURES	SAMPLES
MIDDLE EOCENE	R/M	B		B	N?	●	●	1 2 CC	0.5 1.0				●

LITHOLOGIC DESCRIPTION

NANNOFOSSIL CHALK

Major lithology: NANNOFOSSIL CHALK, dark green [illegible] and [illegible] to very light green [illegible] [illegible]

Minor lithologies:
a. Zeolite-bearing [illegible] in Section 1 [illegible]
b. Clay [illegible] serpentine [illegible] in Section CC.

SMEAR SLIDE SUMMARY (%):

	[illegible]	[illegible]	[illegible]	[illegible]	[illegible]	[illegible]	[illegible]
TEXTURE:							
Sand	20	30	5	5	10	25	—
Silt	50	40	15	45	40	50	20
Clay	30	30	80	50	50	25	80
COMPOSITION:							
Amphibole	[illegible]	[illegible]	[illegible]	[illegible]	[illegible]	[illegible]	[illegible]
Chlorite	[illegible]	[illegible]	[illegible]	[illegible]	[illegible]	[illegible]	[illegible]
Clay	[illegible]	[illegible]	[illegible]	[illegible]	[illegible]	[illegible]	[illegible]
Feldspar	[illegible]	[illegible]	[illegible]	[illegible]	[illegible]	[illegible]	[illegible]
Foraminifers	[illegible]	[illegible]	[illegible]	[illegible]	[illegible]	[illegible]	[illegible]
Glass	[illegible]	[illegible]	[illegible]	[illegible]	[illegible]	[illegible]	[illegible]
Micrite	[illegible]	[illegible]	[illegible]	[illegible]	[illegible]	[illegible]	[illegible]
Nannofossils	[illegible]	[illegible]	[illegible]	[illegible]	[illegible]	[illegible]	[illegible]
Opaques	[illegible]	[illegible]	[illegible]	[illegible]	[illegible]	[illegible]	[illegible]
Pyroxene	[illegible]	[illegible]	[illegible]	[illegible]	[illegible]	[illegible]	[illegible]
Radiolarians	[illegible]	[illegible]	[illegible]	[illegible]	[illegible]	[illegible]	[illegible]
Serpentine	[illegible]	[illegible]	[illegible]	[illegible]	[illegible]	[illegible]	[illegible]
Zeolite	[illegible]	[illegible]	[illegible]	[illegible]	[illegible]	[illegible]	[illegible]
Epidote	[illegible]	[illegible]	[illegible]	[illegible]	[illegible]	[illegible]	[illegible]

SITE 782 HOLE A CORE 43X CORED INTERVAL 3358.4-3368.1 mbsl; 399.5-409.2 mbsf

TIME-ROCK UNIT	FORAMINIFERS	NANNOFOSSILS	RADIOLARIANS	DIATOMS	PALEOMAGNETICS	PHYS. PROPERTIES	CHEMISTRY	SECTION	METERS	GRAPHIC LITHOLOGY	DRILLING DISTURB.	SED. STRUCTURES	SAMPLES
MIDDLE EOCENE	B	CP14 C/M		B				CC					

LITHOLOGIC DESCRIPTION

ANDESITIC SANDSTONE AND CONGLOMERATE

Major lithology: ANDESITIC SANDSTONE AND CONGLOMERATE, predominantly black (10YR 2/1). Immediately overlies andesitic basement rock. Matrix of sand and conglomerate is tuffaceous.

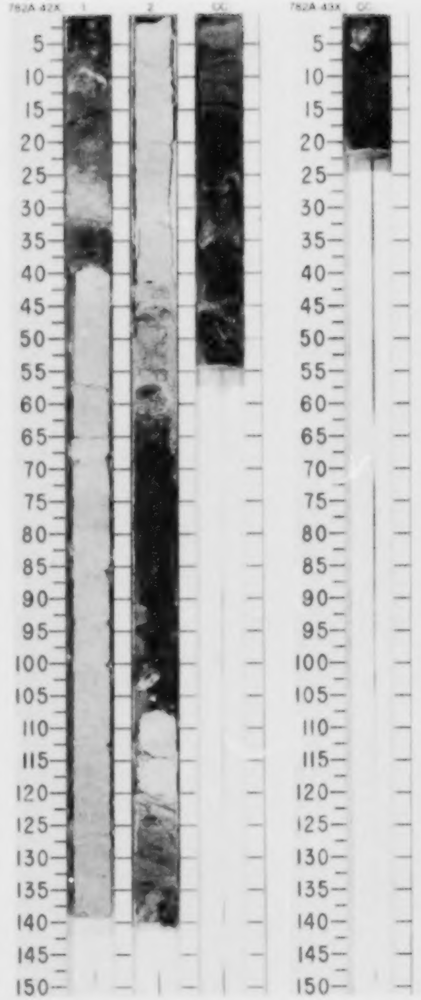

782A 44X NO RECOVERY

782A 45X NO RECOVERY

782A 46X NO RECOVERY

782A 47X NO RECOVERY

782A 48X NO RECOVERY

782A 49X NO RECOVERY

782A 50X NO RECOVERY

SITE 782 HOLE B CORE 1W CORED INTERVAL 2965.9-3428.2 mbsl; 0.0-459.3 mbsf

BIOSTRAT. ZONE/FOSSIL CHARACTER
GRAPHIC LITHOLOGY
LITHOLOGIC DESCRIPTION
NANNOFOSSIL OOZE and NANNOFOSSIL CHALK

782B 2R NO RECOVERY

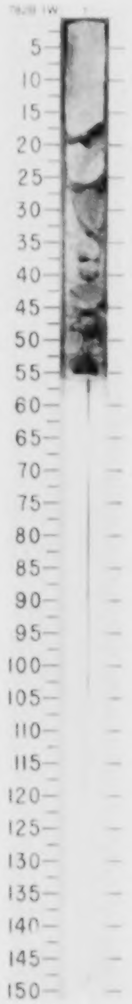
782B 1W
5
10
15
20
25
30
35
40
45
50
55
60
65
70
75
80
85
90
95
100
105
110
115
120
125
130
135
140
145
150

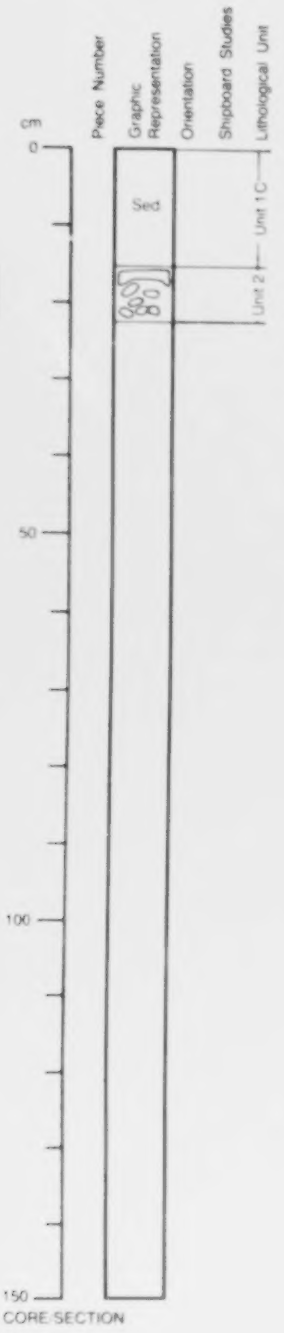
cm
0
50
100
150
Piece Number
Graphic Representation
Orientation
Shipboard Studies
Lithological Unit
Sed
Unit 1C
Unit 2
CORE/SECTION

125-782A-43X-CC

UNIT 2: PLAGIOCLASE-HYPERSTHENE ANDESITE

Pieces multiple fragments

CONTACTS: Not visible
PHENOCRYSTS: Plagioclase and pyroxene in glomerocrysts.
Plagioclase 10%, <2 mm, euhedral, also in glomerocrysts.
Hypersthene - 5%, <1 mm, euhedral, also in glomerocrysts.
Augite - 3%, <2 mm, euhedral, with hypersthene in glomerocrysts.
Magnetite - 1%, <0.5 mm, octahedral shape.
GROUNDMASS: No crystals visible
VESICLES: 2%, <3 mm, may be interconnected, random.
Miaroles: None
COLOR: Gray (2.5Y 5/0)
STRUCTURE: None
ALTERATION: Fresh
VEINS/FRACTURES: Not present

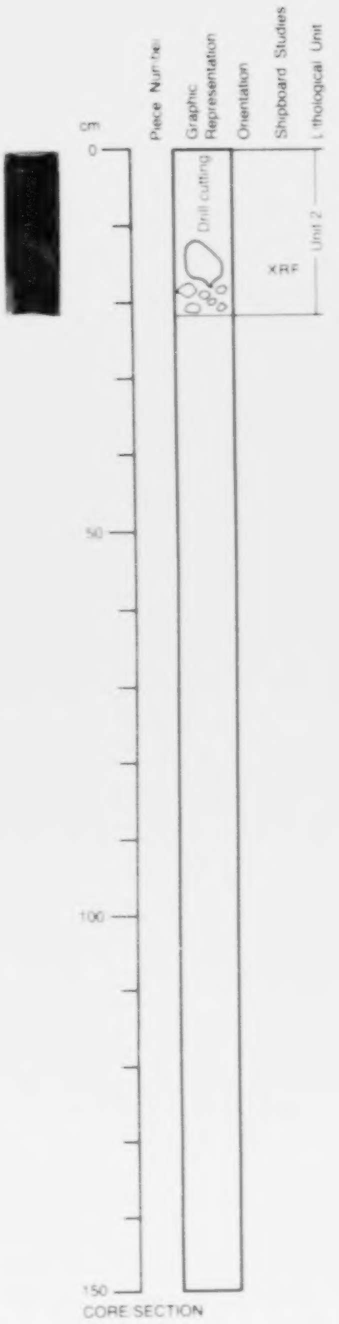
cm
0
50
100
150
Piece Number
Graphic Representation
Orientation
Shipboard Studies
Lithological Unit
Drill cutting
XRF
Unit 2
CORE/SECTION

125-782A-44X-CC

UNIT 2: PLAGIOCLASE-HYPERSTHENE PHYRIC ANDESITE

Pieces cuttings and large fragment

CONTACTS: Not visible.
PHENOCRYSTS: Glomerocrysts are common, especially plagioclase and pyroxene.
  Plagioclase - 10% <2 mm; single phenocrysts and glomerocrysts.
  Hypersthene - 5% <1 mm; pheno- and glomerocrysts; golden green, altering to green bluish zeolite?
  Magnetite - 1% <0.5 mm; octahedral shape.
GROUNDMASS: No crystals visible; very vesiculated.
VESICLES: 5% <3 mm; elongated; perhaps interconnected; locally concentrated.
  Miaroles: None.
COLOR: Greenish black (5G 3/2).
STRUCTURE: None.
ALTERATION: Groundmass is altered.
VEINS/FRACTURES: Not present.

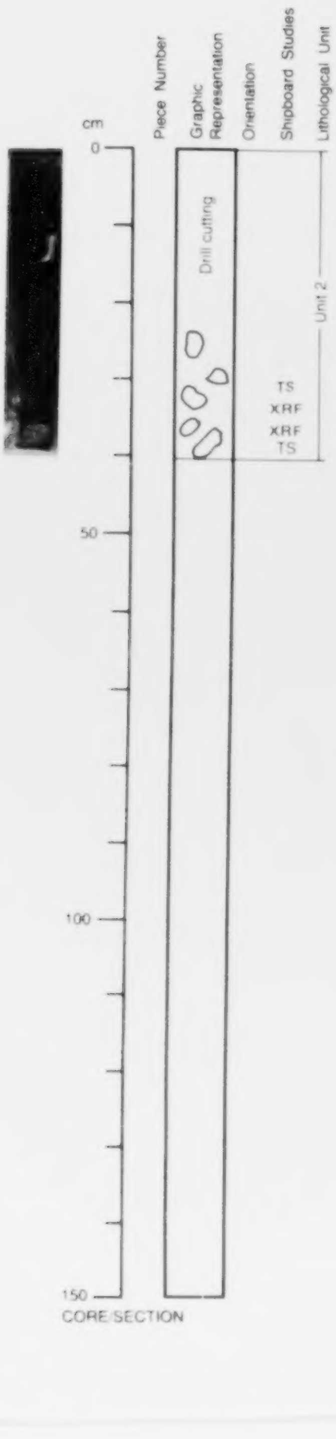
cm
Piece Number
Graphic Representation
Orientation
Shipboard Studies
Lithological Unit
0
50
100
150
Drill cutting
Unit 2
TS
XRF
XRF
TS
CORE/SECTION

125-782A-45X-1

UNIT 2: ANDESITE

Pieces drill cuttings

CONTACTS: Not visible
PHENOCRYSTS: Glomerocrysts.
Plagioclase - 10%, <2 mm, euhedral
Hypersthene - 1%, <1 mm, euhedral
Magnetite - <1%, < 0.5 mm, octahedral
Augite - 5%, <2 mm, euhedral
GROUNDMASS: Approximately 30-40%, no crystals visible.
VESICLES: 1%, <1 mm, irregular, random.
Miaroles: None.
COLOR: Brownish gray (2.5Y 3/2)
STRUCTURE: None
ALTERATION: Pyroxene altered to an unidentified greenish phase.
VEINS/FRACTURES: 1%, 1 mm diameter, none, sugary white material with silky luster.

UNIT 2: PYROXENE PHYRIC DACITE

Pieces various, drill cuttings

CONTACTS: None visible
PHENOCRYSTS:
Plagioclase - 25%, 2-4 mm
Pyroxene - <5%, <2 mm
GROUNDMASS: Approximately 65-70%, no matrix phases visible.
VESICLES: 10%, <3 mm, irregular, random.
Miaroles: None.
COLOR: Brownish gray (2.5Y 3/2)
STRUCTURE: None visible
ALTERATION: Minor (<2.5%) chloritization.
VEINS/FRACTURES: None visible

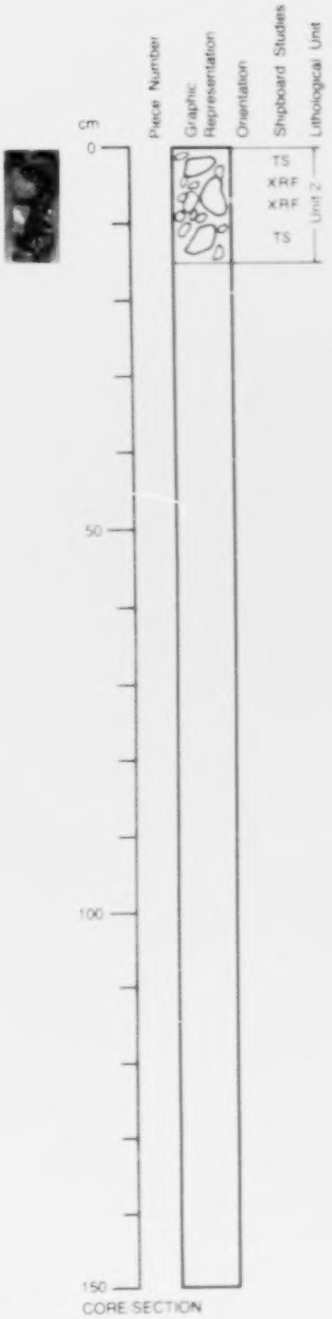
cm
Piece Number
Graphic Representation
Orientation
Shipboard Studies
Lithological Unit
0
50
100
150
TS
XRF
XRF
TS
Unit 2
CORE SECTION

125-782A-49X-CC

UNIT 2: PLAGIOCLASE PHYRIC ANDESITE

Pieces multiple rounded fragments

CONTACTS: Not visible
PHENOCRYSTS:
Plagioclase: 5%, <2 mm, elongate, tabular
Pyroxene: <3%, <1 mm
GROUNDMASS: Approximately 65-75% matrix glass, no crystals visible
VESICLES: 3-5%, 3 to 15 mm, round, random; appear as trains of bubbles (pipe vesicles?)
Miaroles: None present
COLOR: Gray (2.5Y 2/0)
STRUCTURE: None
ALTERATION: Fresh
VEINS/FRACTURES: Not present

UNIT 2: ANDESITE GLASS

Pieces multiple fragments

CONTACTS: Not visible
PHENOCRYSTS:
Plagioclase: 20%, <3 mm, euhedral
Augite: 10%, <2 mm, euhedral
Hypersthene: 10%, <3 mm, euhedral
GROUNDMASS: Glass
VESICLES: 20%, <3 mm in diameter, elongate, interconnected, random, like parallel tubes
COLOR: Black
STRUCTURE: None
ALTERATION: Some alteration of orthopyroxene
VEINS/FRACTURES: None

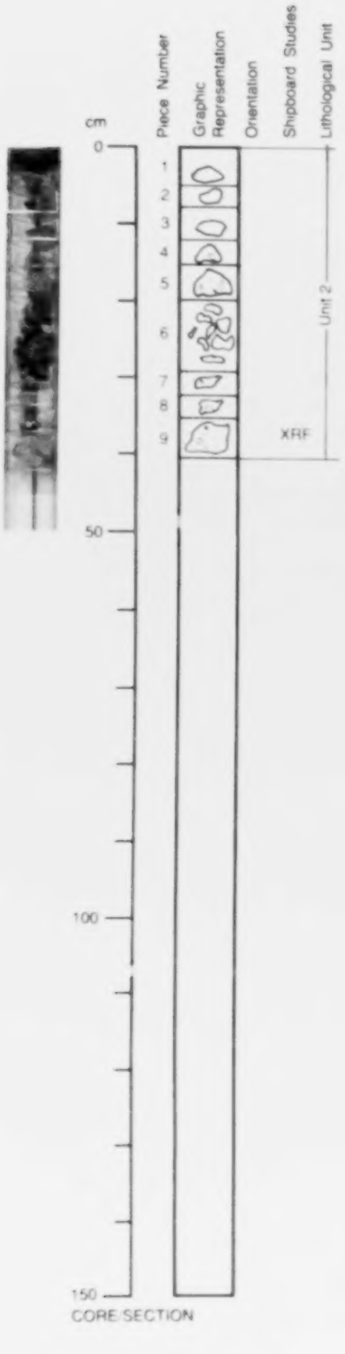
cm
Piece Number
Graphic Representation
Orientation
Shipboard Studies
Lithological Unit
0
50
100
150
1
2
3
4
5
6
7
8
9
XRF
Unit 2
CORE/SECTION

125-782A-50X-1

UNIT 2: PLAGIOCLASE PHYRIC ANDESITE

Pieces multiple rounded fragments

CONTACTS: None visible
PHENOCRYSTS:
Plagioclase - 5%, <2 mm, elongate, tabular
Pyroxene - <3%, <1 mm
GROUNDMASS: Approximately 65-75% matrix glass, no crystals visible
VESICLES: 3-5%, 3 to 5 mm, round, random, appear as trains of bubbles (pipe vesicles?)
Miaroles: None present
COLOR: Gray (2.5Y 2/0)
STRUCTURE: None
ALTERATION: Fresh
VEINS/FRACTURES: Not present

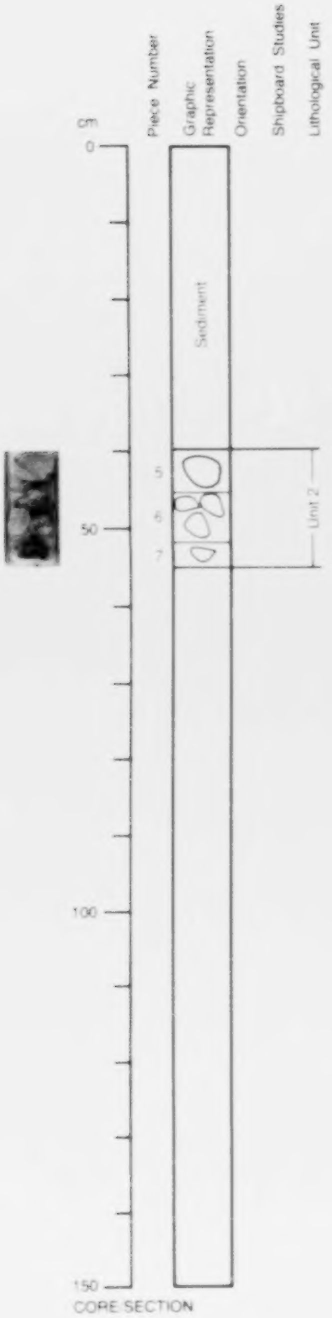
cm
Piece Number
Graphic Representation
Orientation
Shipboard Studies
Lithological Unit
0
50
100
150
Sediment
5
6
7
Unit 2
CORE SECTION

125-782B-1W-1

UNIT 2: ANDESITE

Pieces 5, 6A, B, C

CONTACTS: Not visible
PHENOCRYSTS: Plagioclase and augite in glomerocrysts
Plagioclase - 10-20%, 1-3 mm, euhedral, also in glomerocrysts
Augite - 1-3%, <1 mm, euhedral
Magnetite - <1%, <1 mm, octahedral
GROUNDMASS: No crystals visible
VESICLES: <5%, <2 mm, elongate, irregular, random
COLOR: Light gray to gray (7.5YR 5/0 to 7.5YR 4/0)
STRUCTURE: None
ALTERATION: Not visible
VEINS/FRACTURES: Not present

UNIT 2: GLASSY ANDESITE

Piece 7

CONTACTS: Not visible
PHENOCRYSTS:
Plagioclase - 15%, 1-2 mm, euhedral
GROUNDMASS: Black to golden glass
VESICLES: 30%, up to 1 cm, elongate, parallel, random, collapsed?
COLOR: Black (10YR 2/1)
STRUCTURE: Trachytic plagioclase in glass
ALTERATION: None
VEINS/FRACTURES: Not present

125-782B-2R-1

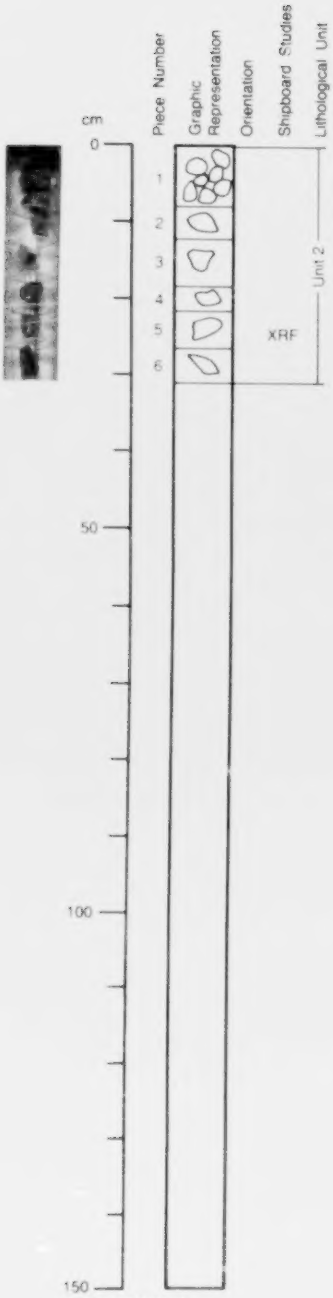
cm
Piece Number
Graphic Representation
Orientation
Shipboard Studies
Lithological Unit
0
50
100
150
1
2
3
4
5
6
XRF
Unit 2
CORE/SECTION

UNIT 2: ANDESITE

Pieces 1-6

CONTACTS: Not visible
PHENOCRYSTS:
Plagioclase 10-15%, 1-3 mm, euhedral
Augite 1%, <2 mm, euhedral
Magnetite trace <0.3 mm, octahedral
GROUNDMASS: No crystals visible
VESICLES: 5%, <3 mm, round, random
Miaroles: With plagioclase
COLOR: Gray (2.5Y 5/0)
STRUCTURE: None
ALTERATION: Not visible
VEINS/FRACTURES: Absent

[illegible] OBSERVER: [illegible] WHERE SAMPLED: [illegible]

ROCK NAME: Andesite

GRAIN SIZE: Fine-grained

TEXTURE: Porphyritic

[illegible]

[illegible]

125-782A-43X-1, 17-24 cm OBSERVER: ABC WHERE SAMPLED: Izu-Bonin outer-arc high

ROCK NAME: Two pyroxene dacite

GRAIN SIZE: 1-4 mm

TEXTURE: Moderately phyric

PRIMARY MINERALOGY	PERCENT PRESENT	PERCENT ORIGINAL	SIZE (mm)	COMPO-SITION	MORPHOLOGY	COMMENTS
PHENOCRYSTS						
Plagioclase	25	25	1-4		Euhedral	Oscillatory zoned; contain fresh brown glass inclusions.
Clinopyroxene	3	3	<2		Tabular, euhedral	Some small crystal enclosed in plagioclase.
Opaque (magnetite)	1	1	<1		Euhedral	
Orthopyroxene	1	1	<2		Tabular, euhedral	Strong pink-brown-green pleochroism; contain glass inclusions.
Apatite	Trace	Trace	<0.1		Euhedral	Enclosed in plagioclase and as microphenocrysts.
GROUNDMASS						
Glass	68	70	N/A		N/A	Contains numerous quench feldspar laths; some chloritic alteration along anastomosing fractures.

SECONDARY MINERALOGY	PERCENT	REPLACING/FILLING	COMMENTS
Clays	1	Glass	Occurs along fractures in glass.
Chlorite	2	Glass	Occurs along fractures.

VESICLES/CAVITIES	PERCENT	LOCATION	SIZE (mm)	FILLING	SHAPE	COMMENTS
Vesicles	15	Random	1	Some chlorite	Irregular	No preferred orientation.

COMMENTS: Glomerocrystic clusters of plagioclase, clinopyroxene and orthopyroxene and magnetite; quench feldspar-free glass is trapped interstitially in these clusters. Magnetite has black reaction rims, otherwise unresolved. Appear to be traces of ilmenite and sulfide (enclosed in magnetite). No piece number given.

125-782A-[illegible], [illegible] cm OBSERVER: [illegible] WHERE SAMPLED: Izu-Bonin outer-arc high

ROCK NAME: Basalt

GRAIN SIZE: Fine-grained

TEXTURE: Quench, microphyric

PRIMARY MINERALOGY	PERCENT PRESENT	PERCENT ORIGINAL	SIZE (mm)	COMPO-SITION	MORPHOLOGY	COMMENTS
PHENOCRYSTS						
Plagioclase	[illegible]	[illegible]	[illegible]		Euhedral, subhedral; laths	Occurs as glomerocrysts.
Clinopyroxene	[illegible]	[illegible]	[illegible]		Euhedral, subhedral; equant	
Opaque	<1	<1	[illegible]		Euhedral	In plagioclase, clinopyroxene glomerocrysts.
GROUNDMASS						
Glass	55-65	45-55	N/A		N/A	Light yellow-brown fresh.
Plagioclase	25-35	25-35	0.02-0.36		Laths, subhedral	Quench (locally aligned), spherulites.
Clinopyroxene	2-3	2-3	0.02-0.14		Subhedral, equant	Elongate, quench.
Opaque	<1	<1	<0.1		Euhedral	Disseminated, as inclusions.

SECONDARY MINERALOGY	PERCENT	REPLACING/FILLING	COMMENTS
Clay	10-15	Glass	Brown amorphous clay disseminated through rock but concentrated more highly at one end.

VESICLES/CAVITIES	PERCENT	LOCATION	SIZE (mm)	FILLING	SHAPE
Vesicles	5-8	Throughout	[illegible]	None	Round-ish

COMMENTS: Opaque microcrystals are concentrated in glassy patches and occur as inclusions in plagioclase and clinopyroxene phenocrysts. Plagioclase matrix crystals locally "flow" around phenocryst. No piece number given.

SITE 782

[illegible]

SITE 783 HOLE A CORE 1R CORED INTERVAL 4848.8-4858.5 mbsl; 0.0-9.7 mbsf

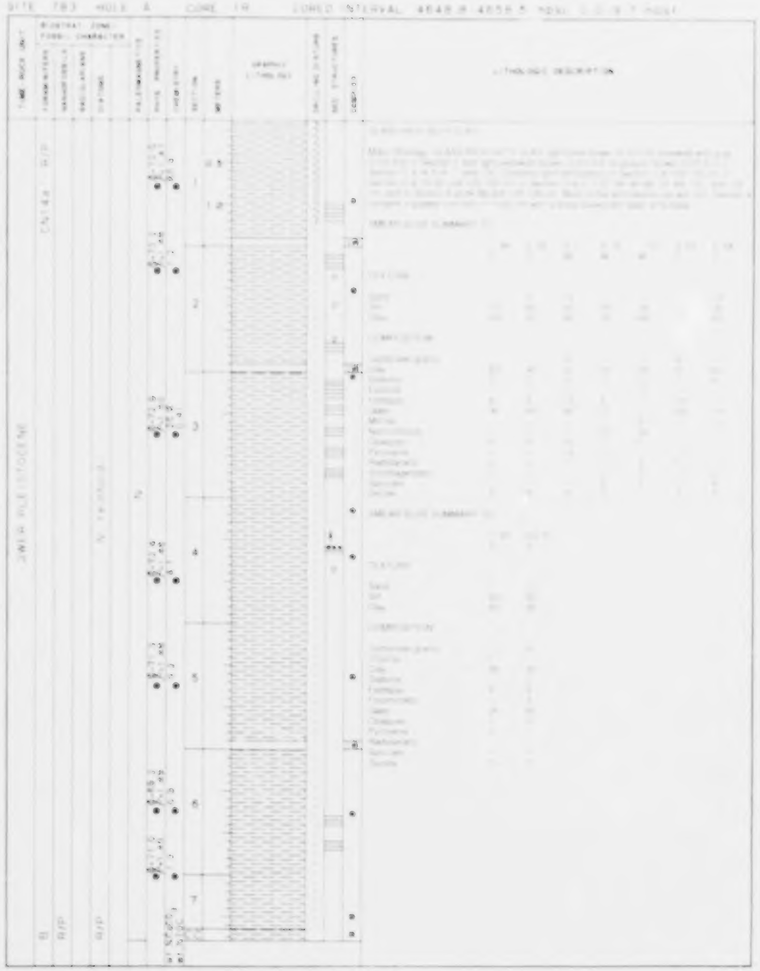
TIME-ROCK UNIT
BIOSTRAT. ZONE/FOSSIL CHARACTER
FORAMINIFERS
NANNOFOSSILS
RADIOLARIANS
DIATOMS
PALEOMAGNETICS
PHYS. PROPERTIES
CHEMISTRY
SECTION
METERS
GRAPHIC LITHOLOGY
DRILLING DISTURB.
SED. STRUCTURES
SAMPLES
LITHOLOGIC DESCRIPTION
UPPER PLEISTOCENE
CN14a
1
2
3
4
5
6
7
CC

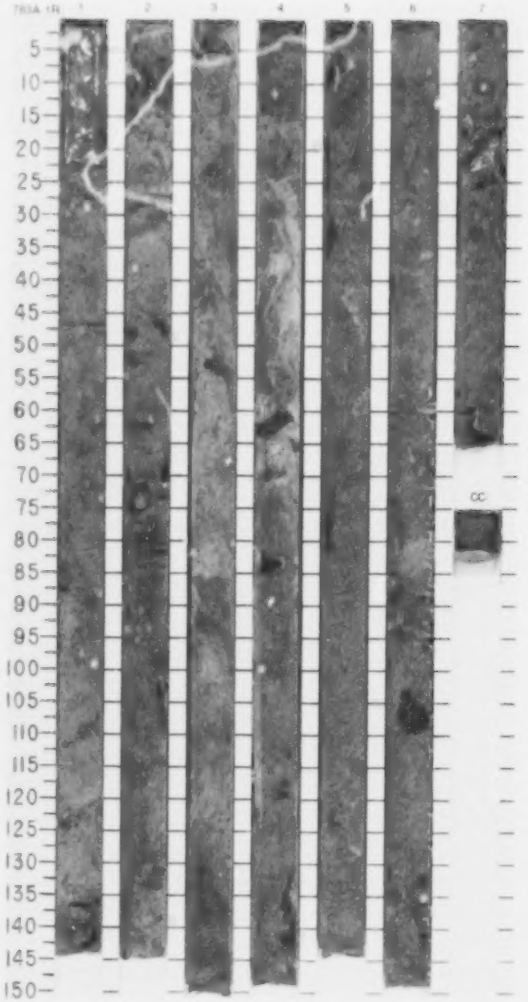
783A-1R
1
2
3
4
5
6
7
CC
5
10
15
20
25
30
35
40
45
50
55
60
65
70
75
80
85
90
95
100
105
110
115
120
125
130
135
140
145
150

SITE 783 HOLE A CORE 2R CORED INTERVAL 4658.5-4665.2 mbsl; 9.7-16.4 mbsf

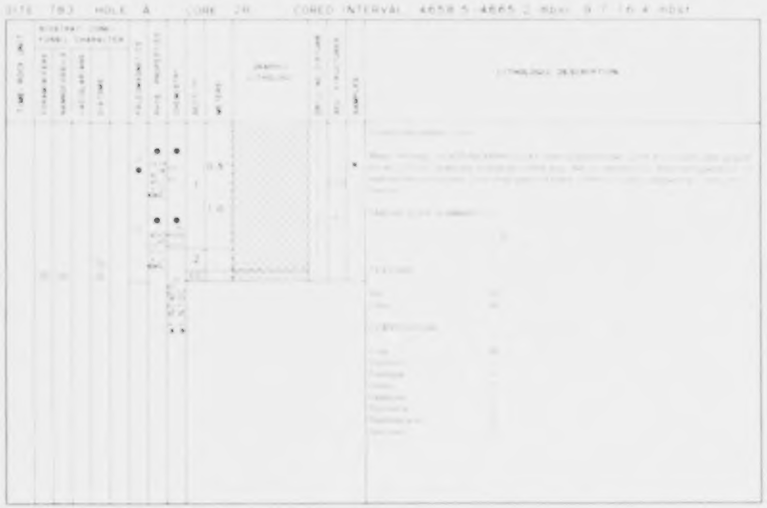
TIME-ROCK UNIT
BIOSTRAT. ZONE/FOSSIL CHARACTER
FORAMINIFERS
NANNOFOSSILS
RADIOLARIANS
DIATOMS
PALEOMAGNETICS
PHYS. PROPERTIES
CHEMISTRY
SECTION
METERS
GRAPHIC LITHOLOGY
DRILLING DISTURB.
SED. STRUCTURES
SAMPLES
0.5
1.0
1
2
CC

LITHOLOGIC DESCRIPTION

[illegible]

[illegible]

SMEAR SLIDE SUMMARY [illegible]

TEXTURE:

[illegible]

COMPOSITION:

[illegible]

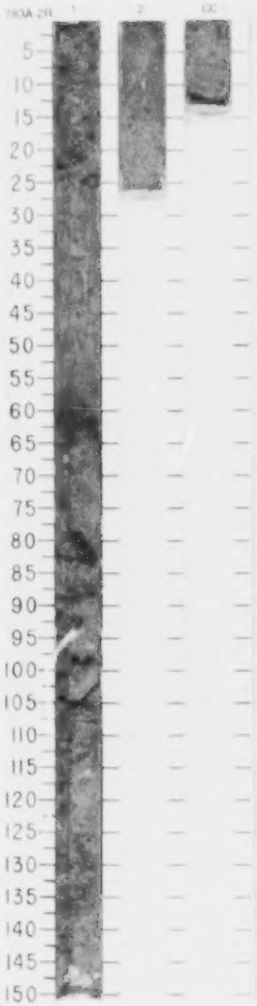
783A-2R
1
2
CC
5
10
15
20
25
30
35
40
45
50
55
60
65
70
75
80
85
90
95
100
105
110
115
120
125
130
135
140
145
150

SITE 783 HOLE A CORE 36 CORED INTERVAL 4665.2-4674.8 mbsl; 16.4-26.0 mbsf

TIME-ROCK UNIT	BIOSTRAT. ZONE/FOSSIL CHARACTER: FORAMINIFERS	NANNOFOSSILS	RADIOLARIANS	DIATOMS	PALEOMAGNETICS	PHYS. PROPERTIES	CHEMISTRY	SECTION	METERS	GRAPHIC LITHOLOGY	DRILLING DISTURB.	SED. STRUCTURES	SAMPLES	LITHOLOGIC DESCRIPTION
LOWER PLEISTOCENE	[illegible]	CN14a		[illegible]				CC					●	[illegible]

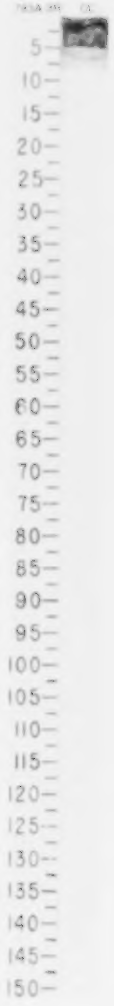
783A-36 CC
5
10
15
20
25
30
35
40
45
50
55
60
65
70
75
80
85
90
95
100
105
110
115
120
125
130
135
140
145
150

SITE 783 HOLE A CORE 4R CORED INTERVAL 4674.6-4684.5 mbsl; 26.0-35.7 mbsf

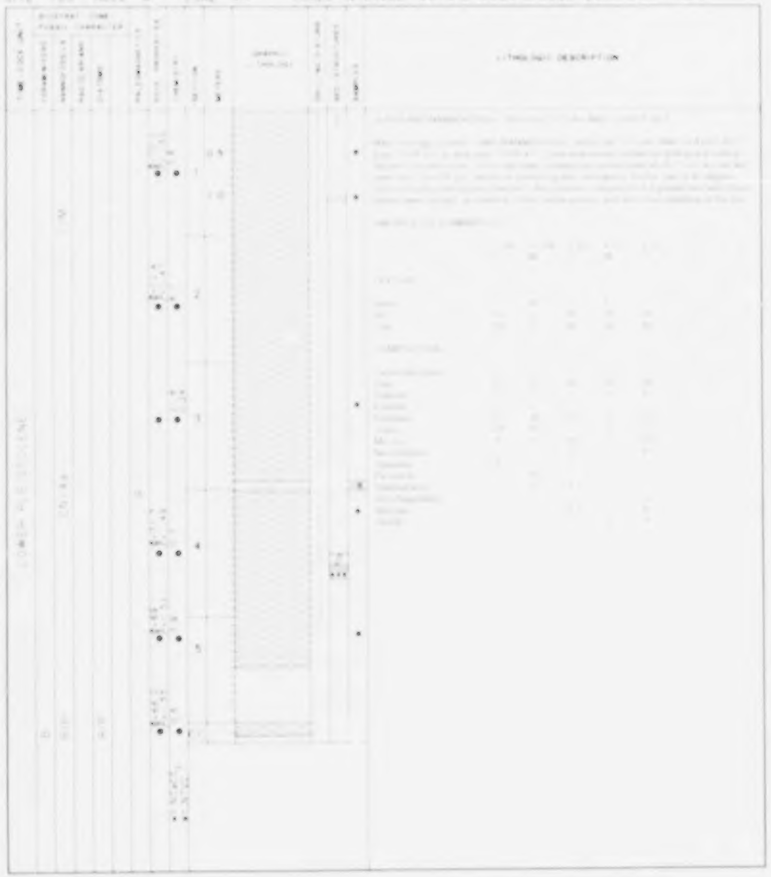
LITHOLOGIC DESCRIPTION
GRAPHIC LITHOLOGY
LOWER PLEISTOCENE

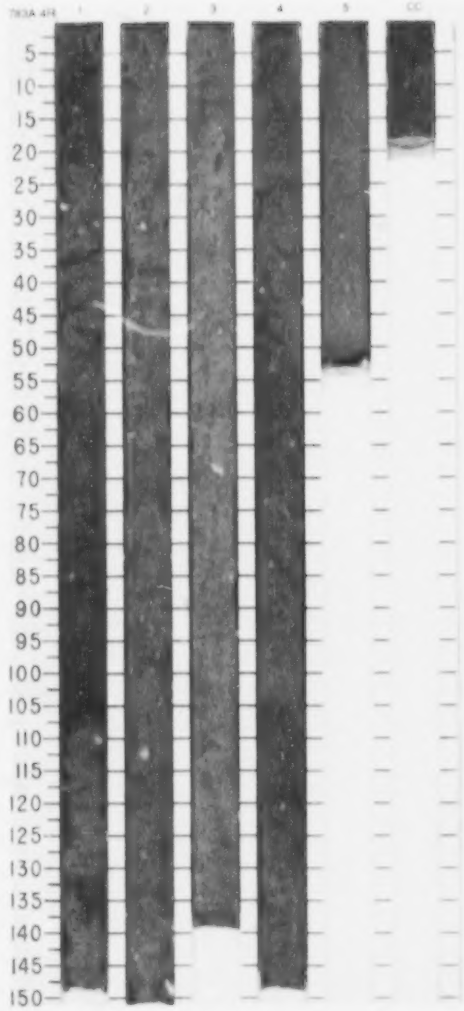
783A-4R
1
2
3
4
5
CC
5
10
15
20
25
30
35
40
45
50
55
60
65
70
75
80
85
90
95
100
105
110
115
120
125
130
135
140
145
150

SITE 783 HOLE A CORE 5R CORED INTERVAL 4884.5-4891.5 mbsl; 35.7-42.7 mbsf

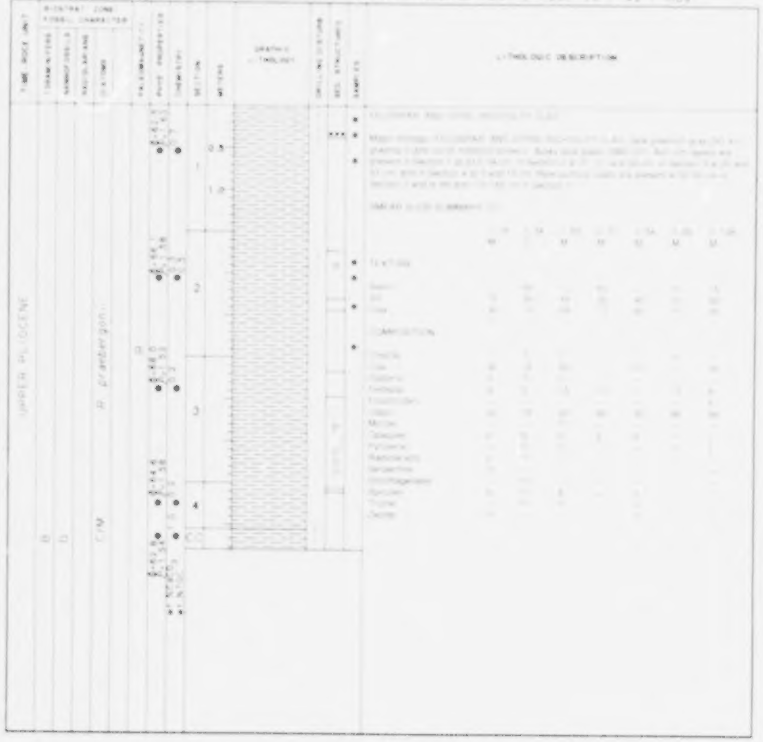
TIME-ROCK UNIT
BIOSTRAT. ZONE/FOSSIL CHARACTER
FORAMINIFERS
NANNOFOSSILS
RADIOLARIANS
DIATOMS
PALEOMAGNETICS
PHYS. PROPERTIES
CHEMISTRY
SECTION
METERS
GRAPHIC LITHOLOGY
DRILLING DISTURB.
SED. STRUCTURES
SAMPLES
LITHOLOGIC DESCRIPTION
UPPER PLIOCENE
R. praebergonii
C/M
0.5
1.0
1
2
3
4
CC
TEXTURE
COMPOSITION

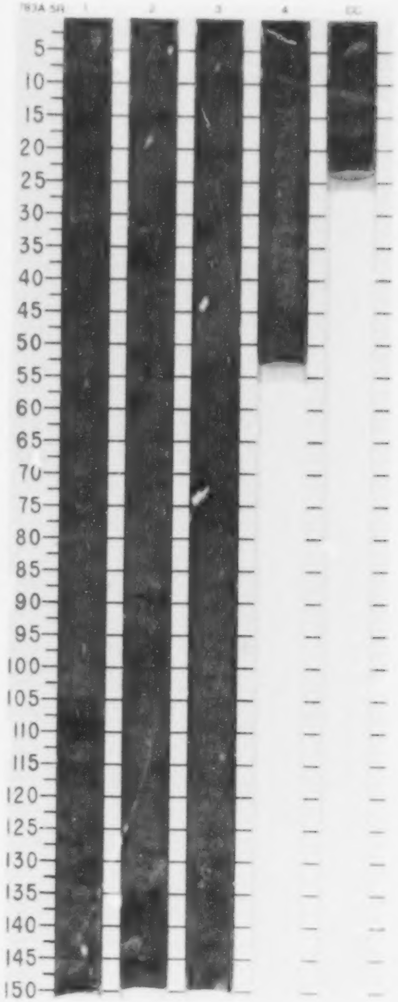
783A 5R
1
2
3
4
CC
5
10
15
20
25
30
35
40
45
50
55
60
65
70
75
80
85
90
95
100
105
110
115
120
125
130
135
140
145
150

783 A 6R NO RECOVERY

SITE 783 HOLE A CORE 7R CORED INTERVAL 4707.2-4710.9 mbsl; 52.4-62.1 mbsf

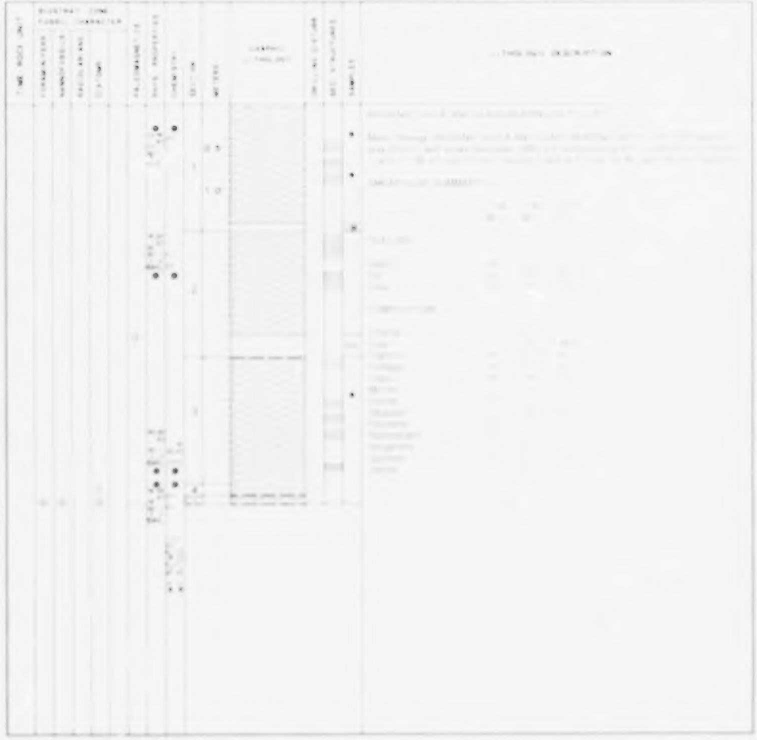

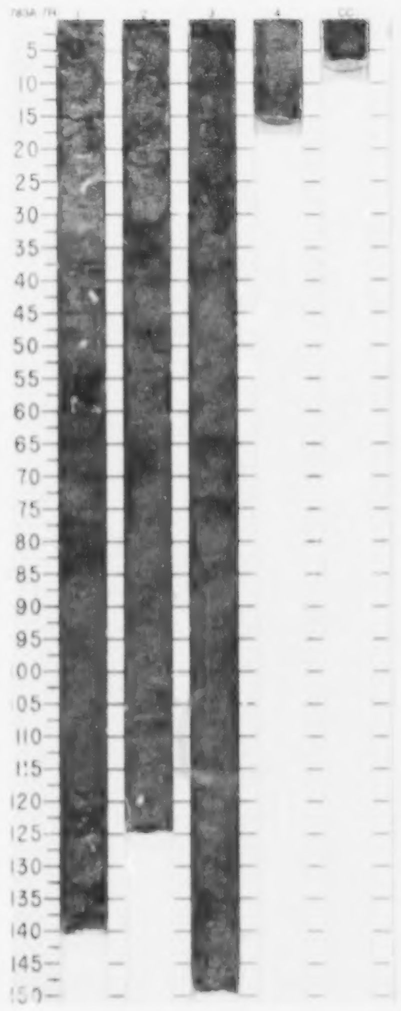
783A-7R
1
2
3
4
CC
5
10
15
20
25
30
35
40
45
50
55
60
65
70
75
80
85
90
95
100
105
110
115
120
125
130
135
140
145
150

SITE 783 HOLE A CORE 8R CORED INTERVAL 4712.9-4720.6 mbsl; 62.7-71.6 mbsf

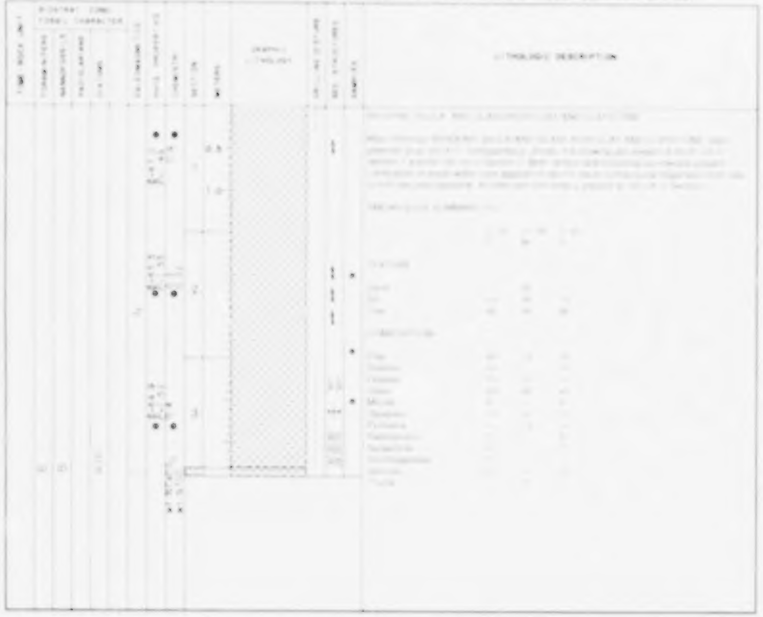
BIOSTRAT. ZONE/ FOSSIL CHARACTER
TIME-ROCK UNIT
FORAMINIFERS
NANNOFOSSILS
RADIOLARIANS
DIATOMS
PALEOMAGNETICS
PHYS. PROPERTIES
CHEMISTRY
SECTION
METERS
GRAPHIC LITHOLOGY
DRILLING DISTURB.
SED. STRUCTURES
SAMPLES
LITHOLOGIC DESCRIPTION
0.5
1.0
1
2
3

SITE 783 HOLE A CORE 9R CORED INTERVAL 4720.6-4730.1 mbsl; 71.6-81.3 mbsf

BIOSTRAT. ZONE/ FOSSIL CHARACTER
TIME-ROCK UNIT
FORAMINIFERS
NANNOFOSSILS
RADIOLARIANS
DIATOMS
PALEOMAGNETICS
PHYS. PROPERTIES
CHEMISTRY
SECTION
METERS
GRAPHIC LITHOLOGY
DRILLING DISTURB.
SED. STRUCTURES
SAMPLES
LITHOLOGIC DESCRIPTION
0.5
1
1.0

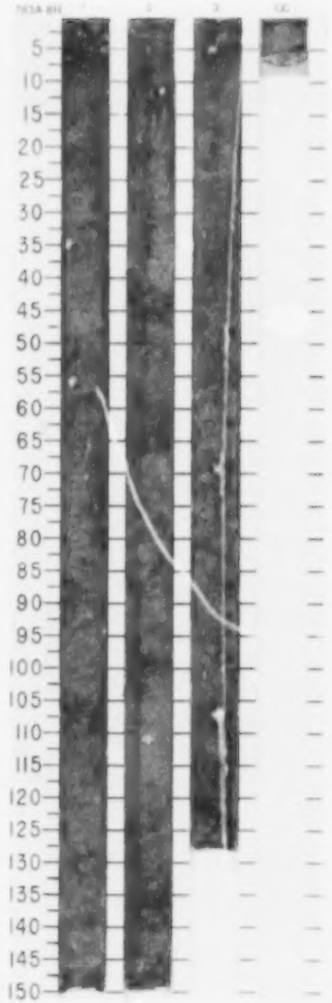
783A-8R
1
2
3
CC
5
10
15
20
25
30
35
40
45
50
55
60
65
70
75
80
85
90
95
100
105
110
115
120
125
130
135
140
145
150

SITE 783 HOLE A CORE 10R CORED INTERVAL 4730.1-4739.7 mbsl; 81.2-90.9 mbsf

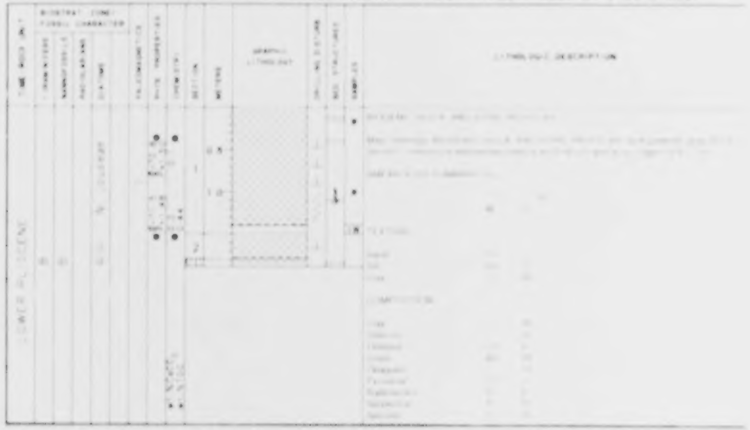
TIME-ROCK UNIT
BIOSTRAT. ZONE/FOSSIL CHARACTER
FORAMINIFERS
NANNOFOSSILS
RADIOLARIANS
DIATOMS
PALEOMAGNETICS
PHYS. PROPERTIES
CHEMISTRY
SECTION
METERS
GRAPHIC LITHOLOGY
DRILLING DISTURB.
SED. STRUCTURES
SAMPLES
LITHOLOGIC DESCRIPTION
LOWER PLIOCENE
0.5
1.0
1
2
TEXTURE:
COMPOSITION:

SITE 783 HOLE A CORE 11R CORED INTERVAL 4739.7-4749.4 mbsl; 90.9-100.6 mbsf

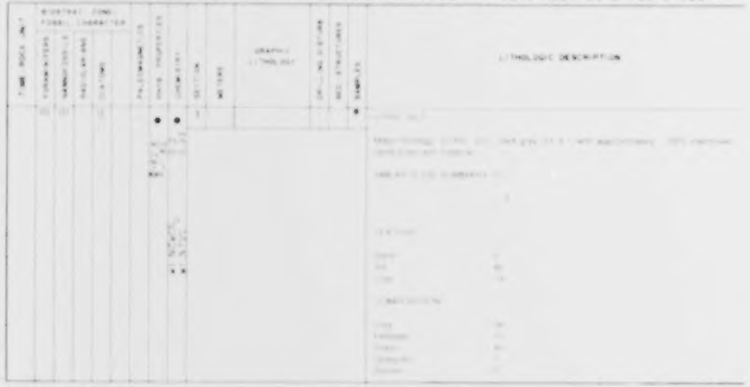
TIME-ROCK UNIT
BIOSTRAT. ZONE/FOSSIL CHARACTER
FORAMINIFERS
NANNOFOSSILS
RADIOLARIANS
DIATOMS
PALEOMAGNETICS
PHYS. PROPERTIES
CHEMISTRY
SECTION
METERS
GRAPHIC LITHOLOGY
DRILLING DISTURB.
SED. STRUCTURES
SAMPLES
LITHOLOGIC DESCRIPTION
1
TEXTURE:
COMPOSITION:

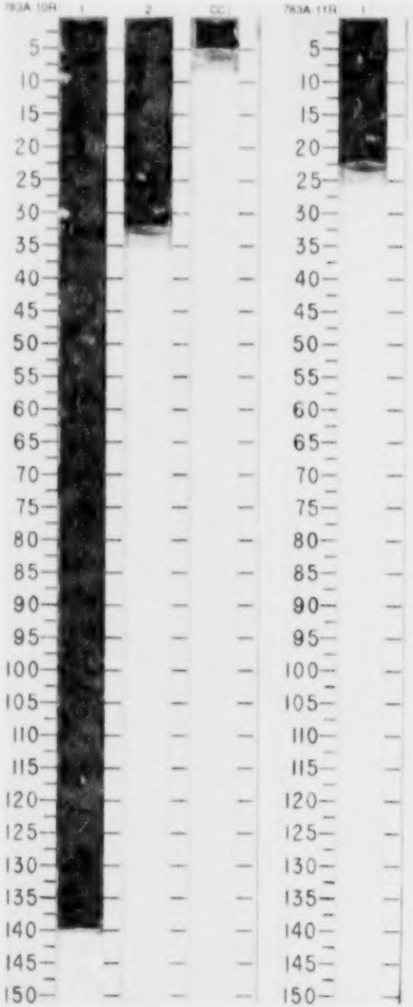
783A-10R
1
2
CC
783A-11R
1
5
10
15
20
25
30
35
40
45
50
55
60
65
70
75
80
85
90
95
100
105
110
115
120
125
130
135
140
145
150

SITE 783 HOLE A CORE 12R CORED INTERVAL 4749.4-4759.0 mbsl; 100.6-110.2 mbsf

TIME-ROCK UNIT	FORAMINIFERS	NANNOFOSSILS	RADIOLARIANS	DIATOMS	PALEOMAGNETICS	PHYS. PROPERTIES	CHEMISTRY	SECTION	METERS	GRAPHIC LITHOLOGY	DRILLING DISTURB.	SED. STRUCTURES	SAMPLES	LITHOLOGIC DESCRIPTION
	B	B		R/P		●	●	1					● ●	CLAY-RICH SILT and FELDSPAR-BEARING VITRIC-RICH SILT

Major lithology: CLAY-RICH SILT and FELDSPAR-BEARING VITRIC-RICH SILT, dark greenish gray (5G 4/1); [illegible] graded interval from 0 to 40 cm in Section 1 [illegible] of small angular pebbles [illegible] supported conglomerate bed [illegible] grading [illegible] into coarse sand [illegible] and then into a sandy silt [illegible] 40 cm). Clasts are dark greenish gray (5G 4/1) to grayish brown (10YR 5/2).

SMEAR SLIDE SUMMARY (%):

TEXTURE:

Sand	—	5
Silt	15	75
Clay	85	20

COMPOSITION:

Clay	85	34
Feldspar	4	15
Glass	10	50
Opaques	1	1
Serpentine	10	—
Zeolite	2	20

SITE 783 HOLE A CORE 13R CORED INTERVAL 4759.0-4768.7 mbsl; 110.2-119.9 mbsf

TIME-ROCK UNIT	FORAMINIFERS	NANNOFOSSILS	RADIOLARIANS	DIATOMS	PALEOMAGNETICS	PHYS. PROPERTIES	CHEMISTRY	SECTION	METERS	GRAPHIC LITHOLOGY	DRILLING DISTURB.	SED. STRUCTURES	SAMPLES	LITHOLOGIC DESCRIPTION
	B	R/P CP14b/CP15		B				CC					●	CONGLOMERATIC FELDSPAR-BEARING VITRIC-RICH SILTSTONE

Major lithology: CONGLOMERATIC FELDSPAR-BEARING VITRIC SILT, dark greenish gray (5G 4/1); [illegible] clasts with mud coatings are present from 0 to 5 cm and one large piece of indurated mud-clast bearing siltstone.

SMEAR SLIDE SUMMARY (%):

CC, 8
D

TEXTURE:

Sand	5
Silt	65
Clay	30

COMPOSITION:

Carbonate grains	2
Clay	62
Feldspar	10
Glass	25
Opaques	1

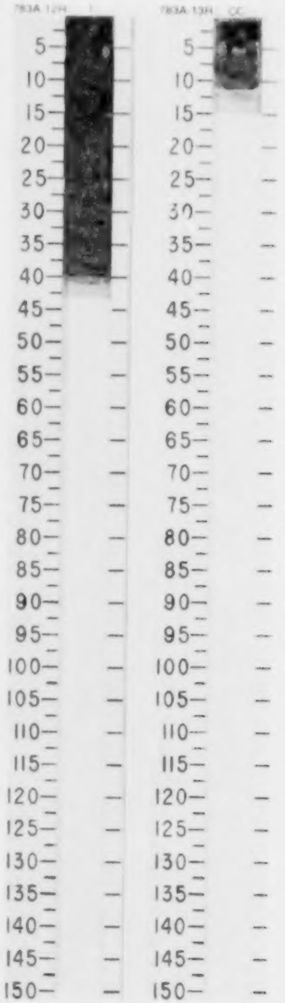

SITE 783 HOLE A CORE 14R CORED INTERVAL 4768.7-4778.4 mbsl; 119.9-129.6 mbsf

TIME-ROCK UNIT	FORAMINIFERS	NANNOFOSSILS	RADIOLARIANS	DIATOMS	PALEOMAGNETICS	PHYS. PROPERTIES	CHEMISTRY	SECTION	METERS	GRAPHIC LITHOLOGY	DRILLING DISTURB.	SED. STRUCTURES	SAMPLES	LITHOLOGIC DESCRIPTION
	B	B						1 CC						[illegible]

[illegible]

SMEAR SLIDE SUMMARY (%):

TEXTURE:

Sand

Silt

Clay

COMPOSITION:

[illegible]

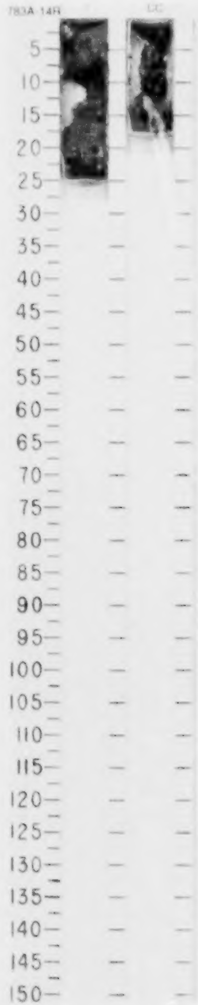
783A-14R
1
CC
5
10
15
20
25
30
35
40
45
50
55
60
65
70
75
80
85
90
95
100
105
110
115
120
125
130
135
140
145
150

SITE 783 HOLE A CORE 15R CORED INTERVAL 4778.4-4788.0 mbsl; 129.6-139.2 mbsf

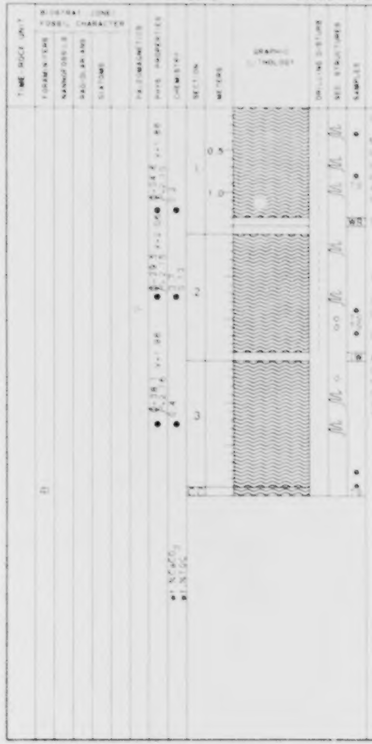
TIME-ROCK UNIT
BIOSTRAT. ZONE/ FOSSIL CHARACTER
FORAMINIFERS
NANNOFOSSILS
RADIOLARIANS
DIATOMS
PALEOMAGNETICS
PHYS. PROPERTIES
CHEMISTRY
SECTION
METERS
GRAPHIC LITHOLOGY
DRILLING DISTURB.
SED. STRUCTURES
SAMPLES
B
1
2
3
0.5
1.0
CC

LITHOLOGIC DESCRIPTION

SILT-SIZED SERPENTINE

Major lithology: SILT-SIZED SERPENTINE, bluish gray (5B 6/1) and dark bluish gray (5B 4/1) to light gray (5Y 7/1), and greenish gray (5G 6/1). Blue material is highly sheared and phacoidal; green is less sheared and less abundant. Angular to subrounded, sand- to small pebble-sized clasts of serpentinite. Chlorite is common in the upper part of Section 1 and aragonite occurs in a brecciated interval from 112-120 cm in Section 2. Red hematite-stained serpentine is present as successive laminations at 135-150 cm in Section 3.

SMEAR SLIDE SUMMARY (%):

	1, 30	1, 90	2, 36	2, 112	3, 111	3, 148
	D	D	M	D	M	M
TEXTURE:						
Silt	100	100	100	100	100	50
Clay	—	—	—	—	—	50
COMPOSITION:						
Aragonite	—	—	—	30	—	—
Chlorite	—	20	10	30	—	—
Hematite	—	—	—	—	—	40
Opaques	4	5	[illegible]	2	—	—
Serpentine	95	80	90	38	100	50
Thulite	—	—	T	T	—	—

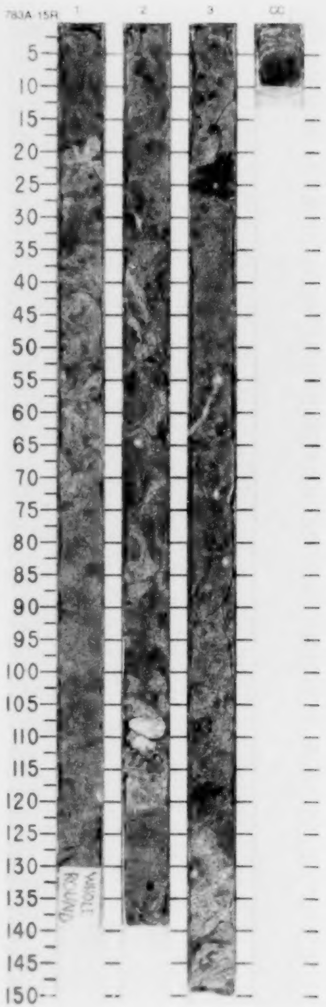
783A 15R
1
2
3
CC
5
10
15
20
25
30
35
40
45
50
55
60
65
70
75
80
85
90
95
100
105
110
115
120
125
130
135
140
145
150
WHOLE ROUND

SITE 783 HOLE A CORE 16R CORED INTERVAL 4788.0-4797.7 mbsl; 139.2-148.9 mbsf

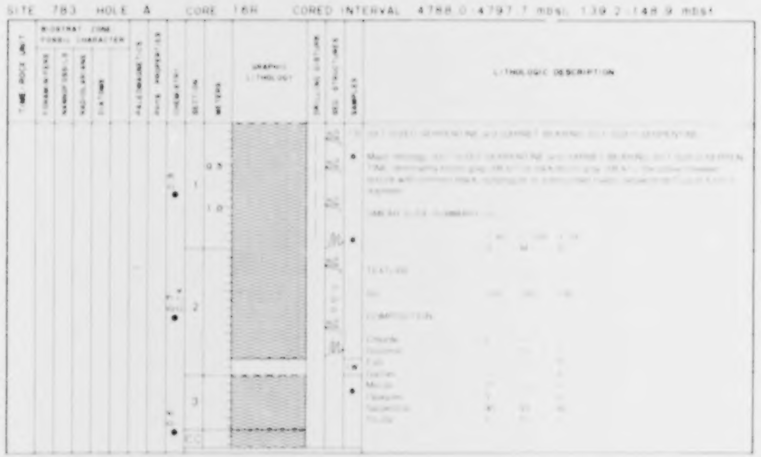
TIME-ROCK UNIT
BIOSTRAT. ZONE/ FOSSIL CHARACTER
FORAMINIFERS
NANNOFOSSILS
RADIOLARIANS
DIATOMS
PALEOMAGNETICS
PHYS. PROPERTIES
CHEMISTRY
SECTION
METERS
GRAPHIC LITHOLOGY
DRILLING DISTURB.
SED. STRUCTURES
SAMPLES
0.5
1.0
1
2
3
CC

LITHOLOGIC DESCRIPTION

[illegible] SERPENTINE and GARNET-BEARING SILT-SIZED SERPENTINE

Major lithology: SILT-SIZED SERPENTINE and GARNET-BEARING SILT-SIZED SERPENTINE, [illegible]

SMEAR SLIDE SUMMARY (%):

TEXTURE:

COMPOSITION:

SITE 783 HOLE A CORE 17R CORED INTERVAL 4797.7-4807.4 mbsl; 148.9-158.6 mbsf

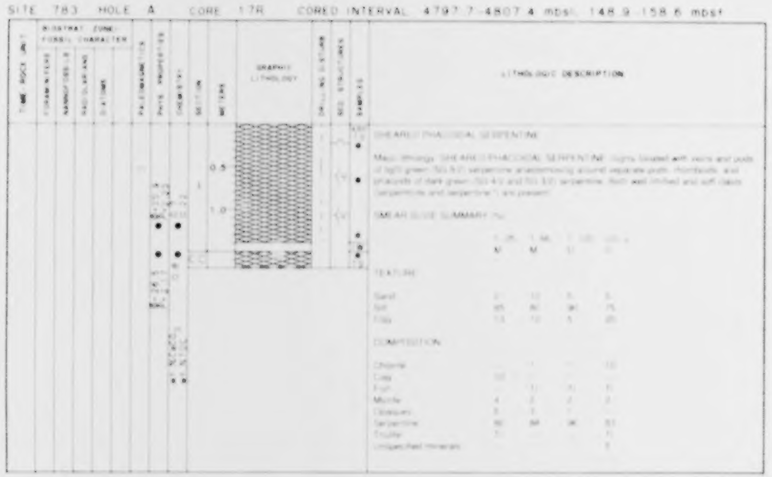
TIME-ROCK UNIT
BIOSTRAT. ZONE/ FOSSIL CHARACTER
FORAMINIFERS
NANNOFOSSILS
RADIOLARIANS
DIATOMS
PALEOMAGNETICS
PHYS. PROPERTIES
CHEMISTRY
SECTION
METERS
GRAPHIC LITHOLOGY
DRILLING DISTURB.
SED. STRUCTURES
SAMPLES
0.5
1.0
1
CC

LITHOLOGIC DESCRIPTION

SHEARED PHACOIDAL SERPENTINE

Major lithology: SHEARED PHACOIDAL SERPENTINE, [illegible] with veins and pods of light green (5G [illegible]) serpentine anastomosing around separate pods, rhomboids, and phacoids of dark green (5G 4/2 and 5G 3/2) serpentine. Both well lithified and soft clasts [illegible] are present.

SMEAR SLIDE SUMMARY (%):

	[illegible]	[illegible]	[illegible]	[illegible]
	M	M	D	D
TEXTURE:				
Sand	[illegible]	[illegible]	5	5
Silt	85	80	90	75
Clay	[illegible]	[illegible]	5	20
COMPOSITION:				
Chlorite	—	[illegible]	—	[illegible]
Clay	[illegible]	—	—	—
[illegible]	—	[illegible]	[illegible]	[illegible]
Micrite	4	2	2	2
Opaques	5	[illegible]	1	—
Serpentine	[illegible]	[illegible]	[illegible]	[illegible]
[illegible]	[illegible]	—	—	[illegible]
Unspecified minerals	—	—	—	[illegible]

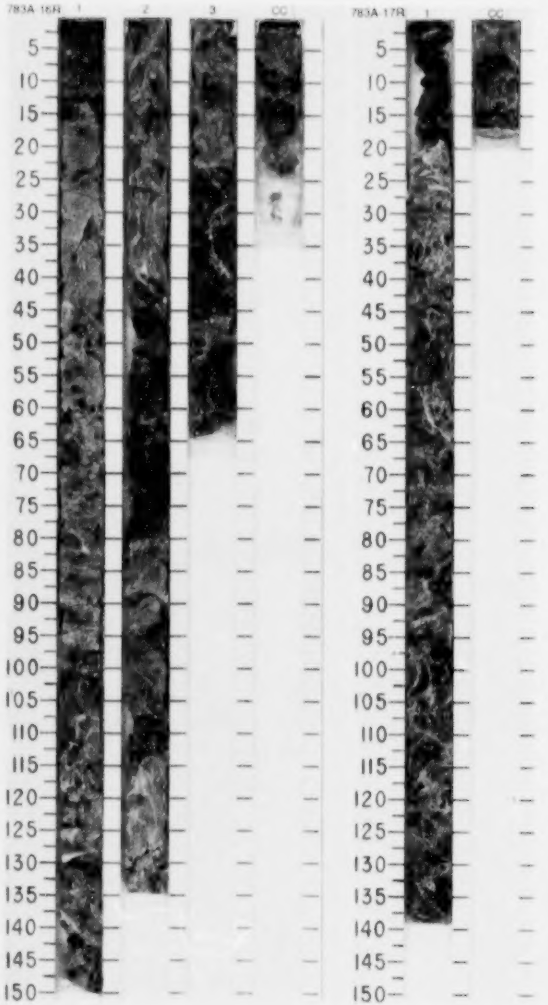
783A-16R 1
2
3
CC
783A-17R 1
CC
5
10
15
20
25
30
35
40
45
50
55
60
65
70
75
80
85
90
95
100
105
110
115
120
125
130
135
140
145
150

SITE 783 HOLE A CORE 18R CORED INTERVAL 4807.4-4817.0 mbsl; 158.6-168.2 mbsf

TIME-ROCK UNIT	FORAMINIFERS	NANNOFOSSILS	RADIOLARIANS	DIATOMS	PALEOMAGNETICS	PHYS. PROPERTIES	CHEMISTRY	SECTION	METERS	GRAPHIC LITHOLOGY	DRILLING DISTURB.	SED. STRUCTURES	SAMPLES	LITHOLOGIC DESCRIPTION
						●	●	1	0.5 1.0	M M			● ●	SHEARED PHACOIDAL SERPENTINE

BIOSTRAT. ZONE/FOSSIL CHARACTER

SHEARED PHACOIDAL SERPENTINE

Major lithology: SHEARED PHACOIDAL SERPENTINE, light blue gray (5B 7/1) to bluish gray (5B 6/1) and dark blue gray (5B 4/1), with interlaced anastomosing very pale yellow (5Y 8/[illegible]) and white streaks in a fine-grained phacoidal texture. Very soft phacoids [illegible] serpentinized ultramafic clasts up to 3.5 cm in diameter are common.

SMEAR SLIDE SUMMARY (%):

	1, 30 D	1, 135 D
TEXTURE:		
Sand	[illegible]	[illegible]
Silt	[illegible]	[illegible]
Clay	[illegible]	[illegible]
COMPOSITION:		
Chlorite	[illegible]	6
Epidote	5	—
Garnet	—	[illegible]
Micrite	1	[illegible]
Opaques	—	4
Serpentine	[illegible]	[illegible]
Thulite	[illegible]	[illegible]
Zoisite	—	5

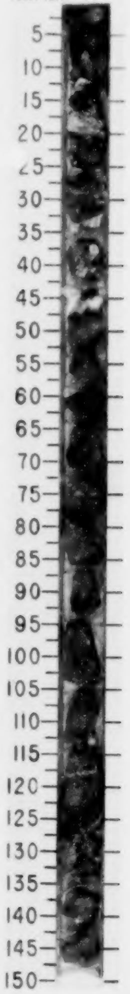

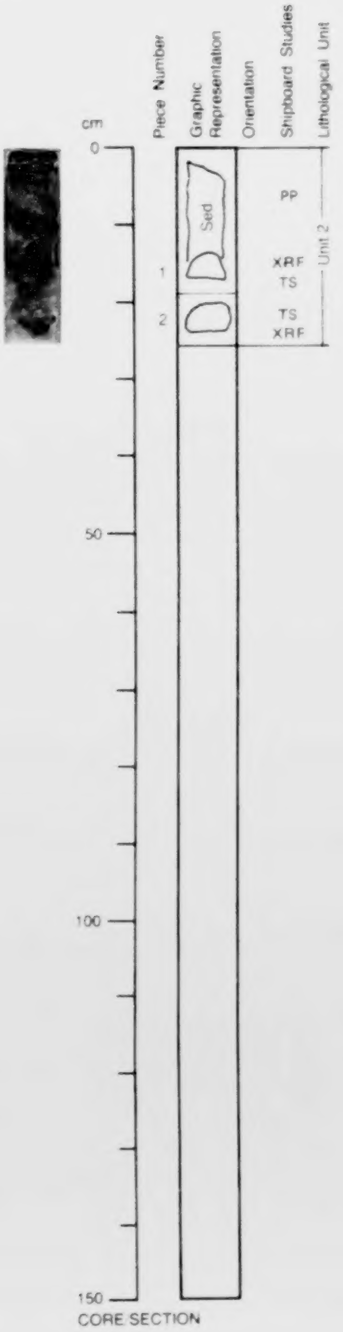
cm
0
50
100
150
CORE SECTION
Piece Number
Graphic Representation
Orientation
Shipboard Studies
Lithological Unit
1
2
Sed
PP
XRF
TS
TS
XRF
Unit 2

125-783A-16R-CC

UNIT 2: SERPENTINIZED HARZBURGITE

Pieces 1, 2

COLOR: Black (5G 3/2)
LAYERING: None
DEFORMATION: None
PRIMARY MINERALOGY: Primary silicates, variably serpentinized
Olivine - Mode: 85-90%
Crystal size: Not visible
Crystal shape: Not visible
Crystal orientation: Not visible
Percent replacement: Variable

Orthopyroxene - Mode: 10-15%
Crystal size: 1-5 mm
Crystal shape: Subhedral
Crystal orientation: Not visible
Percent replacement: Variable

Spinel - Mode: <1%
Crystal size: 0.5 mm
Crystal shape: Euhedral-subhedral
Crystal orientation: Not visible
Percent replacement: 0

Native copper - Mode: Trace
Crystal size: 0.1-0.5 mm
Crystal shape: Anhedral
Crystal orientation: Not visible
Percent replacement: 0
SECONDARY MINERALOGY:
Serpentine
Total percent: 70-80%
Texture: N/A
Vein material: None

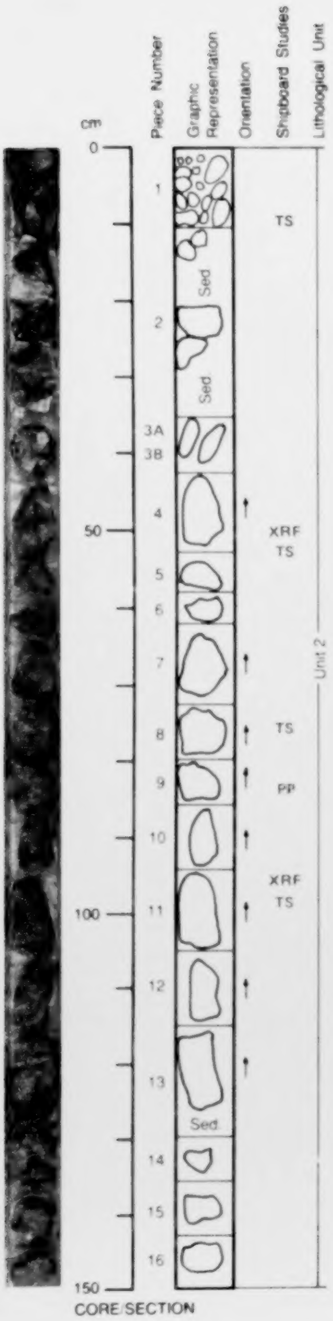
cm
Piece Number
Graphic Representation
Orientation
Shipboard Studies
Lithological Unit
0
50
100
150
1
2
3A
3B
4
5
6
7
8
9
10
11
12
13
14
15
16
Sed.
Sed.
Sed.
TS
XRF
TS
TS
PP
XRF
TS
Unit 2
CORE/SECTION

125-783A-18R-1

UNIT 2: SERPENTINIZED TECTONIZED HARZBURGITE

Pieces 1-16

COLOR: Black (5B 4/1)
LAYERING: Locally bastitic orthopyroxene-rich layers, <1 cm wide
DEFORMATION: Some vein-filled fractures
PRIMARY MINERALOGY: Primary minerals are largely replaced by serpentine
Olivine - Mode: 80-95%
Crystal size: Not visible
Crystal shape: Not visible
Crystal orientation: Not visible
Percent replacement: Variable

Orthopyroxene - Mode: 5-20%
Crystal size: <5 mm
Crystal shape: Raggedy to euhedral
Crystal orientation: Random
Percent replacement: Variable

Spinel - Mode: Trace
Crystal size: < 0.1 mm
Crystal shape: Subhedral to anhedral
Crystal orientation: Random
Percent replacement: None visible
SECONDARY MINERALOGY:
Serpentine
Total percent: 70-90%
Texture: Bastitic pyroxene in olivine mesh groundmass
Vein material: filled with dark green or white serpentine

UNIT 2: METABASALT

Pieces 1, one of multiple fragments

COLOR: Dark reddish brown (5YR 2.5/2)
LAYERING: Massive
DEFORMATION: None
PRIMARY MINERALOGY: No primary mineralogy visible
SECONDARY MINERALOGY: Very fine grained, black dots
Total percent: 100%
Texture: Brecciated and recrystallized?
Vein material: Not visible

125-783A-14R-1 (9-11 cm)   OBSERVER: HIR   WHERE SAMPLED: Torishima Forearc Seamount, north flank

ROCK NAME: Serpentinized harzburgite

GRAIN SIZE: 0.2-2 mm

TEXTURE: Mesh and bastite

PRIMARY MINERALOGY	PERCENT PRESENT	PERCENT ORIGINAL	SIZE (mm)	COMPO-SITION	MORPHOLOGY	COMMENTS
Olivine	1	85-90	1-2		Anhedral	90-95% serpentinized to mesh texture.
Clinopyroxene	Trace	1?	<0.5		Anhedral	Occurs in small patches in and around orthopyroxene.
Spinel	<1	<1	0.2-1		Subhedral-anhedral	Dark red in color, chrome-rich spinel.
Orthopyroxene	1-2	10-15	0.5-1.5		Subhedral	85-90% serpentinized to bastite texture.

SECONDARY MINERALOGY	PERCENT	REPLACING/ FILLING	COMMENTS
Clays	2	Serpentine	Dusty brownish clay scattered throughout slide and intermixed with serpentine.
Chlorite	<1	Orthopyroxene bastite	Pale-green in color. Sometimes recognized in orthopyroxene bastite.
Talc	<1	Orthopyroxene bastite	High birefringence, mainly fills in orthopyroxene bastite.
Chrysotile-lizardite	90-95	Orthopyroxene olivine	Serpentine pseudomorph of olivine, shows typical mesh texture.
Magnetite	<1	Spinel	Very fine-grained, mainly occurs in serpentinite veins.

VESICLES/ CAVITIES	PERCENT	LOCATION	SIZE (mm)	FILLING	SHAPE
Vesicles	0				

COMMENTS: This core is highly serpentinized. No deformation texture is recognized. No piece number given.

125-783A-15R-1 (89-91 cm)   OBSERVER: SAI   WHERE SAMPLED: Torishima Forearc Seamount, north flank

ROCK NAME: Sand-sized serpentine

GRAIN SIZE: Fine to very fine-grained

TEXTURE: Foliated (clastic) mélange

PRIMARY MINERALOGY	PERCENT PRESENT	PERCENT ORIGINAL	SIZE (mm)	COMPO-SITION	MORPHOLOGY	COMMENTS
PHENOCRYSTS						
Olivine	[illegible]	N/A	N/A		N/A	
Orthopyroxene	[illegible]	N/A	N/A		N/A	
GROUNDMASS						
N/A	N/A	N/A	N/A		N/A	

SECONDARY MINERALOGY	PERCENT	REPLACING/ FILLING	COMMENTS
Clays	5	Olivine, orthopyroxene(?)	
Serpentine	90	Olivine, orthopyroxene(?)	
Opaques	<5	Olivine, orthopyroxene(?)	

VESICLES/ CAVITIES	PERCENT	LOCATION	SIZE (mm)	FILLING	SHAPE
Vesicles	0				

COMMENTS: Angular to rounded grains (< 0.5 mm) of serpentine set in a fine-grained serpentine matrix with moderately anastomosing foliation. Minor clay in highly altered areas. Some large grains are rotated and others are fractured and separated by fine-grained matrix. These shear textures probably reflect flowing of the materials. No piece number given.

125-783A-15R-02 (84-86 cm) OBSERVER: HIR WHERE SAMPLED: Torishima Forearc Seamount, north flank

ROCK NAME: Metabasalt

GRAIN SIZE: (0.05-0.2 mm) fine-grained

TEXTURE: Primary intersertal

PRIMARY MINERALOGY	PERCENT PRESENT	PERCENT ORIGINAL	SIZE (mm)	COMPO-SITION	MORPHOLOGY	COMMENTS
Plagioclase	0	40	0.05-0.1		Anhedral-subhedral	Completely altered to chlorite.
Clinopyroxene	20	25	0.05-0.15		Anhedral	Partly altered to chlorite.
Glass	0	35	N/A		N/A	Completely altered to clay and chlorite.

SECONDARY MINERALOGY	PERCENT	REPLACING/ FILLING	COMMENTS
Clays	40	Glass, plagioclase and clinopyroxene	Dusty brownish clay replacing glass.
Zeolites	Trace	Vesicles	Shows very low reflective index and characteristic wavy extinction.
Chlorite	40	Plagioclase/vein	Pale-green in color.
Albite	Trace	Plagioclase	Low reflective index, colorless.

VESICLES/ CAVITIES	PERCENT	LOCATION	SIZE (mm)	FILLING	SHAPE
Vesicles	Trace	Random	<0.2	Chlorite, zeolite	Round

COMMENTS: Plagioclase has been completely chloritized. Chlorite veins (0.2 to 0.8 mm) developed throughout the rock. No piece number given.

125-783A-15R-02 (107-109 cm) OBSERVER: HIR WHERE SAMPLED: Torishima Forearc Seamount, north flank

ROCK NAME: Metavolcaniclastic rock

GRAIN SIZE: 1-2 mm

TEXTURE: Secondary cataclastic

PRIMARY MINERALOGY	PERCENT PRESENT	PERCENT ORIGINAL	SIZE (mm)	COMPO-SITION	MORPHOLOGY	COMMENTS
Clinopyroxene	5	10-15	1-2		Anhedral	Mostly altered to actinolite.

SECONDARY MINERALOGY	PERCENT	REPLACING/ FILLING	COMMENTS
Clays	40-50	Matrix	Dusty brownish clay arbitrarily fills in matrix.
Chlorite	5-10		Shows brownish abnormal interference color; coexists with actinolite plus or minus sphene.
Albite	1-2		Colorless, low refractive index, twinning.
Epidote	1-2		Clinozoisite, tabular shape; bluish, abnormal interference color.
Actinolite	5-10	Clinopyroxene	Occurs as colorless acicular crystal; replacing clinopyroxene.
Sphene	Trace		Fine-grained crystal, high refractive index, coexists with chlorite.
Prehnite	20-30	Clinopyroxene	Shows wavy extinction.

VESICLES/ CAVITIES	PERCENT	LOCATION	SIZE (mm)	FILLING	SHAPE
Vesicles	0				

COMMENTS: Prehnite and actinolite secondarily replaced detrital clinopyroxene fragments. Prehnite also occurs in vein that cuts both detrital fragments and matrix. The stable mineral assemblage of this rock appears to be prehnite and actinolite and chlorite which occurs in Fe-rich rock under prehnite-pumpellyite facies conditions. No piece number given.

125-783A-15R-CC (1-3 cm) OBSERVER: PRI WHERE SAMPLED: Torishima Forearc Seamount, north flank

ROCK NAME: Foliated sand-sized serpentine

GRAIN SIZE: Fine to very fine-grained

TEXTURE: Foliated clastic (melange)

PRIMARY MINERALOGY	PERCENT PRESENT	PERCENT ORIGINAL	SIZE (mm)	COMPO-SITION	MORPHOLOGY	COMMENTS
PHENOCRYSTS						
Olivine	N/A	Most	N/A		N/A	
Orthopyroxene	N/A	Some?	N/A		N/A	
GROUNDMASS						
N/A	N/A	N/A	N/A		N/A	

SECONDARY MINERALOGY	PERCENT	REPLACING/ FILLING	COMMENTS
Clays	10%	Olivine, orthopyroxene(?)	
Chlorite	trace	Olivine, orthopyroxene(?)	
Opaques	10%	Olivine, orthopyroxene(?)	
Serpentine	80%	Olivine, orthopyroxene(?)	

VESICLES/ CAVITIES	PERCENT	LOCATION	SIZE (mm)	FILLING	SHAPE
Vesicles	0				

COMMENTS: Most of section was abraded away during polishing; fragmentary remnants show rounded, lenticular (phacoidal) grains of serpentine and opaque minerals set in a fine-grained foliated matrix that anastomoses around the larger clasts. Probably a serpentinite debris flow. No piece number given.

125-783A-18R-CC (12-14 cm) OBSERVER: SAB WHERE SAMPLED: Torishima Forearc Seamount, north flank

ROCK NAME: Serpentinized dunite

GRAIN SIZE: 0.01-3 mm

TEXTURE: Mesh

PRIMARY MINERALOGY	PERCENT PRESENT	PERCENT ORIGINAL	SIZE (mm)	COMPO-SITION	MORPHOLOGY	COMMENTS
PHENOCRYSTS						
Olivine	[illegible]	97.5	1-3		Anhedral	Completely altered to serpentine, mesh; only present as rounded inclusions within spinel.
Spinel	0.5	1	[illegible]	Cr	Subhedral/anhedral	Red-brown; fractured.
Orthopyroxene	0	1.5	1-3		Anhedral	Completely altered to serpentine bastite.
GROUNDMASS						
N/A	N/A	N/A	N/A		N/A	

SECONDARY MINERALOGY	PERCENT	REPLACING/ FILLING	COMMENTS
Clays	<1	Serpentine	Rusty brown clay intermixed with serpentine at the edge of slide.
Serpentine	98	Olivine, orthopyroxene	Lizardite and/or chrysotile forming mesh texture after olivine.
Magnetite	1	Spinel	Dusty grains arranged in elongated trains along serpentine mesh edges.

VESICLES/ CAVITIES	PERCENT	LOCATION	SIZE (mm)	FILLING	SHAPE
Vesicles	0				

COMMENTS: Completely serpentinized dunite? Spinel grains have serpentine pseudomorphic inclusions. One spinel has inclusion of fresh-looking olivine grain. Mesh texture is well developed throughout slide. In some areas the mesh looks locally deformed, but doesn't look like there has been any post-serpentinization deformation. No piece number given.

125-783A-16R-CC (Piece 1,14-17 cm)   OBSERVER: SAB   WHERE SAMPLED: Torishima Forearc Seamount, north flank

ROCK NAME: Serpentinized harzburgite

GRAIN SIZE: 0.1-5 mm

TEXTURE: Mesh and bastite

PRIMARY MINERALOGY	PERCENT PRESENT	PERCENT ORIGINAL	SIZE (mm)	COMPO-SITION	MORPHOLOGY	COMMENTS
PHENOCRYSTS						
Olivine	17	85	0.5-2		Anhedral	Altered to serpentine mesh; elongated wavy extinction.
Clinopyroxene	1	1	0.2-0.3		Subhedral-anhedral	As exsolution lamellae, as grains in and near orthopyroxene margins.
Spinel	1	1	0.2-2	Cr	Euhedral-anhedral	Red, fractured.
Orthopyroxene	10	13	1-5		Subhedral-anhedral	Altered to serpentine bastite; has clinopyroxene exsolution lamellae, wavy extinction.
GROUNDMASS						
N/A	N/A	N/A	N/A		N/A	

SECONDARY MINERALOGY	PERCENT	REPLACING/ FILLING	COMMENTS
Serpentine	70	Olivine, orthopyroxene	Lizardite and/or chrysotile forming bastite and mesh texture from olivine and orthopyroxene.
Magnetite	1	Spinel	Dusty grains concentrated along serpentine veins and mesh edges.

VESICLES/ CAVITIES	PERCENT	LOCATION	SIZE (mm)	FILLING	SHAPE
Vesicles	0				

COMMENTS: Spinels form crudely elongate trails across slide. Some silicate appears to be forming between fractures in the spinels. Spinels have minor inclusions of rounded olivine(?). Olivine and orthopyroxene appear slightly deformed because of wavy extinction and elongation of grains. Small (0.2-mm-wide) serpentine veins cutting mesh texture. Orthopyroxene has inclusions of clinopyroxene.

125-783A-16R-CC (Piece 2,19-22 cm)   OBSERVER: SAB   WHERE SAMPLED: Torishima Forearc Seamount, north flank

ROCK NAME: Serpentinized clinopyroxene-rich harzburgite

GRAIN SIZE: 0.1-6 mm

TEXTURE: Mesh and bastite

PRIMARY MINERALOGY	PERCENT PRESENT	PERCENT ORIGINAL	SIZE (mm)	COMPO-SITION	MORPHOLOGY	COMMENTS
PHENOCRYSTS						
Olivine	26	74	0.2-1		Anhedral	Altered to serpentine mesh texture.
Clinopyroxene	5	5	0.5-2		Anhedral	As exsolution lamellae and separate grains, fractured.
Spinel	1	1	0.1-2	Cr	Anhedral	Red-brown, fractured, elongate(?).
Orthopyroxene	12	20	0.5-6		Anhedral	Altered to serpentine bastite; deformed crystals, wavy extinction.
GROUNDMASS						
N/A	N/A	N/A	N/A		N/A	

SECONDARY MINERALOGY	PERCENT	REPLACING/ FILLING	COMMENTS
Serpentine	55	Olivine, orthopyroxene	Lizardite and/or chrysotile forming mesh and bastite textures from olivine and orthopyroxene. Minor (<0.2-mm-wide) serpentine veins cutting mesh and bastite textures.
Magnetite	1	Spinel, olivine	Dusty 0.1-mm grains scattered throughout more serpentinized portion of slide. Concentrated along cleavages and veins and mesh texture.

VESICLES/ CAVITIES	PERCENT	LOCATION	SIZE (mm)	FILLING	SHAPE
Vesicles	0				

COMMENTS: Clinopyroxene-rich harzburgite! The clinopyroxene appears freshest in this section. Clinopyroxene is fractured, has wavy extinction, and is distributed throughout slide (not just around orthopyroxene grains). Orthopyroxene grains have small clinopyroxene inclusions. Most of olivine is altered but some orthopyroxene grains are still fresh looking. Spinels are crudely aligned in some elongate trains.

125-783A-17R-01 (Piece 1, 9-12 cm) OBSERVER: SAB WHERE SAMPLED: Torishima Forearc Seamount, north flank

ROCK NAME: Serpentinized harzburgite

GRAIN SIZE: 0.5-5 mm

TEXTURE: Mesh and bastite

PRIMARY MINERALOGY	PERCENT PRESENT	PERCENT ORIGINAL	SIZE (mm)	COMPO-SITION	MORPHOLOGY	COMMENTS
PHENOCRYSTS						
Olivine	1	85	Not visible		Not visible	Altered to serpentine mesh.
Clinopyroxene	1	2	0.1-0.8		Anhedral	As relic grains mostly near orthopyroxenes and spinels.
Spinel	0.5	1	0.1-0.5	(?)	Subhedral-anhedral	Red-brown, fractured; some are elongated(?).
Orthopyroxene	<1	12	0.5-5		Anhedral	Altered to serpentine bastite.
GROUNDMASS						
N/A	N/A	N/A	N/A		N/A	

SECONDARY MINERALOGY	PERCENT	REPLACING/FILLING	COMMENTS
Clays	5	Serpentine	Dusty brown clay intermixed with serpentine throughout slide.
Serpentine	92	Olivine, orthopyroxene	Lizardite and/or chrysotile forming bastite and mesh textures from olivine and orthopyroxene.
Magnetite	2	Spinel; olivine	Dusty 0.2-mm grains throughout slide and concentrated mainly in serpentine veining and bastite "cleavages".

VESICLES/CAVITIES	PERCENT	LOCATION	SIZE (mm)	FILLING	SHAPE
Vesicles	0				

COMMENTS: Spinel has inclusions of round olivines plus serpentine pseudomorphic inclusions. The slide represents a completely altered harzburgite. Relic clinopyroxenes are the only primary grains left (excluding spinels). Minor serpentine and clay veins (0.3 mm wide) cutting mesh and bastite textures. Orthopyroxene bastite appears to have serpentine pseudomorph inclusions with the grain. One portion of slide (appears to represent inner portion of rock) has no clay intermixed with serpentine.

125-783A-17R-01 (11-14 cm) OBSERVER: TER WHERE SAMPLED: Torishima Forearc Seamount, north flank

ROCK NAME: Sedimentary serpentinized harzburgite

GRAIN SIZE: 0.5-4 mm

TEXTURE: Mesh and bastite

PRIMARY MINERALOGY	PERCENT PRESENT	PERCENT ORIGINAL	SIZE (mm)	COMPO-SITION	MORPHOLOGY	COMMENTS
PHENOCRYSTS						
Olivine	0	80-85	N/A		Anhedral	Mesh texture.
Spinel	Trace	1	<0.1		Subhedral	Reddish brown Cr-spinel.
Orthopyroxene	0	10-15	1-4		Anhedral	Bastite; kink-band.
GROUNDMASS						
N/A	N/A	N/A	N/A		N/A	

SECONDARY MINERALOGY	PERCENT	REPLACING/FILLING	COMMENTS
Clays	40	Serpentine	Variably replacing bastite and olivine pseudomorph.
Serpentine	58	Olivine and orthopyroxene	Lizardite and chrysotile.
Magnetite	2	Spinel and in veins	

VESICLES/CAVITIES	PERCENT	LOCATION	SIZE (mm)	FILLING	SHAPE
Vesicles	0				

COMMENTS: Sedimentary serpentine of tectonized harzburgite. Shearing texture is also visible among clasts. No piece number given.

125-783A-18R-01 (Piece 1,0-2 cm)　　OBSERVER: JOH　　WHERE SAMPLED: Torishima Forearc Seamount, north flank

ROCK NAME: Metabasalt

GRAIN SIZE: <0.01 mm

TEXTURE: Aphyric to sparsely phyric

PRIMARY MINERALOGY	PERCENT PRESENT	PERCENT ORIGINAL	SIZE (mm)	COMPO-SITION	MORPHOLOGY	COMMENTS
PHENOCRYSTS						
Olivine	0	1-2?	1.2		Euhedral	100% altered, clays, hematite.
Clinopyroxene	Trace	<1	0.2-0.5		Euhedral	Elongate 98% altered to clays.
GROUNDMASS						
Glass	0	N/A	N/A		N/A	Highly altered to clays with hematite staining.
Plagioclase	0	10-20	0.01-0.05		Laths	Completely altered.
Clinopyroxene	<1	1-2	1-2		Euhedral-subhedral	
Opaques	<1-1	<1-2	0.01-0.03		Euhedral to anhedral	

SECONDARY MINERALOGY	PERCENT	REPLACING/ FILLING	COMMENTS
Clays	50-65	Glass, plagioclase, clinopyroxene	
Chlorite	10-25	Glass	Slightly brown-green.
Hematite	2*-45	Glass	Red to red-brown staining, pervasive and staining.
Iddingsite	1	Olivine	

VESICLES/ CAVITIES	PERCENT	LOCATION	SIZE (mm)	FILLING	SHAPE
Vesicles	3-10	Throughout	0.1-1	Clay	Round to elongate

COMMENTS: Primary mineralogy has been largely obscured by alteration. Trace amounts of plagioclase may have been present but are indistinguishable now.

125-783A-18R-01 (Piece 4,49-51 cm)　　OBSERVER: SAB　　WHERE SAMPLED: Torishima Forearc Seamount, north flank

ROCK NAME: Serpentinized harzburgite

GRAIN SIZE: 0.1-5 mm

TEXTURE: Mesh and bastite

PRIMARY MINERALOGY	PERCENT PRESENT	PERCENT ORIGINAL	SIZE (mm)	COMPO-SITION	MORPHOLOGY	COMMENTS
PHENOCRYSTS						
Olivine	22.5	81.5	0.5-4		Anhedral	Fractured, altering to serpentine mesh; slightly wavy extinction in some grains.
Clinopyroxene	2	2	0.1-0.6		Anhedral	As exsolution lamellae and grains in and near orthopyroxene.
Spinel	1.5	1.5	0.5-3	Cr	Subhedral-anhedral	Fractured, red color.
Orthopyroxene	15	15	1-5		Subhedral-anhedral	Slightly wavy extinction; altering to serpentine bastite; some anhedral clinopyroxene inclusions.
GROUNDMASS						
N/A	N/A	N/A	N/A		N/A	

SECONDARY MINERALOGY	PERCENT	REPLACING/ FILLING	COMMENTS
Clays	2	Serpentine	Dusty brown clay distributed throughout serpentine but mostly concentrated in one-half of slide.
Serpentine	45	Olivine, orthopyroxene	Lizardite and/or chrysotile forming mesh and bastite texture from olivine and orthopyroxene throughout slide.
Magnetite	2	Spinel	Dusty, 0.1-mm grains; arranged in elongated trails within serpentine veins and mesh edges and orthopyroxene cleavages.

VESICLES/ CAVITIES	PERCENT	LOCATION	SIZE (mm)	FILLING	SHAPE
Vesicles	0				

COMMENTS: Harzburgite is relatively clinopyroxene-rich. Olivine and orthopyroxene are altered to serpentine mesh and bastite. The mesh appears undeformed in most of slide. The spinels have minor anhedral inclusions of serpentine pseudomorphs (of orthopyroxene???). Orthopyroxene has some kink-bands in a few grains.

[illegible]

SITE 784 HOLE A CORE 1R CORED INTERVAL 4900.8-4902.2 mbsl; 0.0-1.4 mbsf

TIME-ROCK UNIT	BIOSTRAT. ZONE/ FOSSIL CHARACTER: FORAMINIFERS	NANNOFOSSILS	RADIOLARIANS	DIATOMS	PALEOMAGNETICS	PHYS. PROPERTIES	CHEMISTRY	SECTION	METERS	GRAPHIC LITHOLOGY	DRILLING DISTURB.	SED. STRUCTURES	SAMPLES	LITHOLOGIC DESCRIPTION
UPPER PLEISTOCENE	B	B		R/M R/M B B		● ●	● ●	1	0.5		[illegible]		● ● ●	[illegible]
								CC						

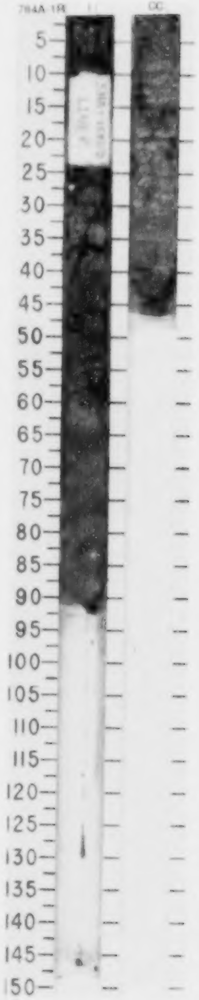
784A-1R
1
CC
5
10
15
20
25
30
35
40
45
50
55
60
65
70
75
80
85
90
95
100
105
110
115
120
125
130
135
140
145
150

SITE 764 HOLE A CORE 2R CORED INTERVAL 4902.2-4911.7 mbsl; 1.4-10.9 mbsf

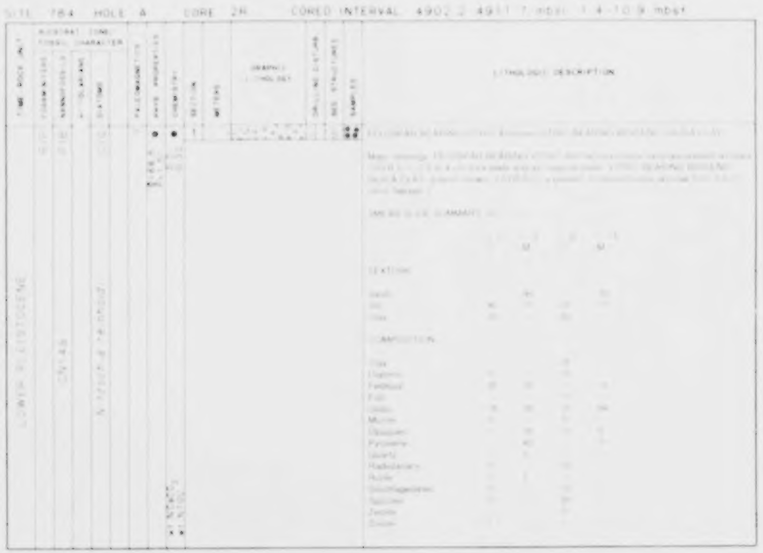
TIME-ROCK UNIT
BIOSTRAT. ZONE/ FOSSIL CHARACTER
FORAMINIFERS
NANNOFOSSILS
RADIOLARIANS
DIATOMS
PALEOMAGNETICS
PHYS. PROPERTIES
CHEMISTRY
SECTION
METERS
GRAPHIC LITHOLOGY
DRILLING DISTURB.
SED. STRUCTURES
SAMPLES
LITHOLOGIC DESCRIPTION
LOWER PLEISTOCENE
CN14a
N. reinholdii Zone
1

SAMPLE SUMMARY

TEXTURE:

Sand
Silt
Clay

COMPOSITION:

Clay
Diatoms
Feldspar
Fish
Glass
Mica
Opaques
Pyroxene
Quartz
Radiolarians
Rutile
Silicoflagellates
Spicules
Zeolite
Zircon

784A 2R

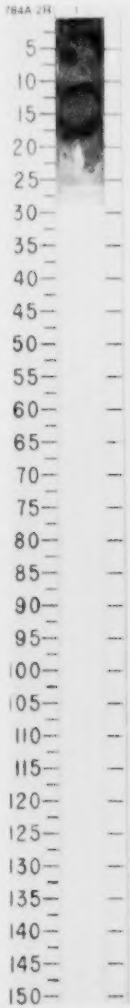
1
5
10
15
20
25
30
35
40
45
50
55
60
65
70
75
80
85
90
95
100
105
110
115
120
125
130
135
140
145
150

SITE 784 HOLE A CORE 3R CORED INTERVAL 4911.7-4921.2 mbsl; 10.9-20.4 mbsf

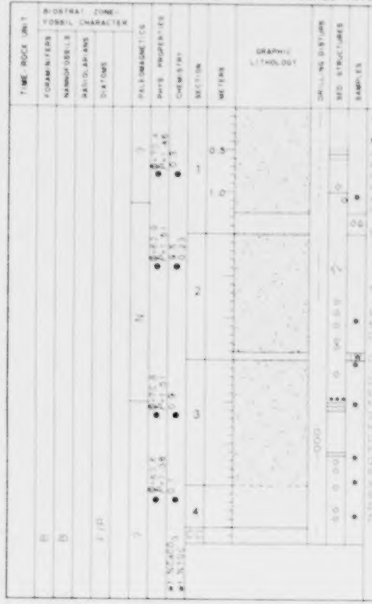
TIME-ROCK UNIT
BIOSTRAT. ZONE/ FOSSIL CHARACTER
FORAMINIFERS
NANNOFOSSILS
RADIOLARIANS
DIATOMS
PALEOMAGNETICS
PHYS. PROPERTIES
CHEMISTRY
SECTION
METERS
GRAPHIC LITHOLOGY
DRILLING DISTURB.
SED. STRUCTURES
SAMPLES
B
B
R/P
?
N
?
0.5
1.0
1
2
3
4
CC

LITHOLOGIC DESCRIPTION

VITRIC SILT and VITRIC SILTY SAND

Major lithology: VITRIC SILT, very dark gray (2.5Y 3/0) to light gray (2.5Y 6/0), mottled by coring and by bioturbation. Inclined and disturbed greenish gray [illegible] laminations, approximately 0.5 cm wide, are present at 45-50 cm in Section 2. Rare, scattered, subrounded to subangular gray (2.5Y 4/0) pumice fragments up to 2 cm in diameter are present in all sections. Thin (1 mm), faint, disturbed laminations are present in Section 1 at 55 cm and in Section 3 at 58 cm. A black (10YR 2/1), 2-cm-thick, graded bed with a sharp basal contact is present at 50-52 cm in Section 3.

SMEAR SLIDE SUMMARY (%):

	1, 108	2, 100	3, 1	3, 51	3, 117	3, 144	4, 38
	M	M	D	M	M	M	M
TEXTURE:							
Sand	50	100	90	80	30	10	10
Silt	40	—	10	20	50	60	80
Clay	10	—	—	—	20	30	10
COMPOSITION:							
Diatoms	—	—	—	—	—	1	—
Epidote	—	—	—	—	1	—	—
Feldspar	10	—	—	10	20	10	10
Glass	60	100	100	60	60	80	60
Hornblende	—	—	—	—	—	1	—
Opaques	30	—	—	10	4	2	—
Pyroxene	—	Tr	—	1	10	—	—
Quartz	—	—	—	—	5	—	2
Radiolarians	—	—	—	—	—	1	4
Serpentine	—	—	—	—	—	—	4
Sponge spicules	—	—	—	—	—	—	5
Zeolite	1	—	—	—	—	5	10
Zircon	—	—	—	5	5	—	—

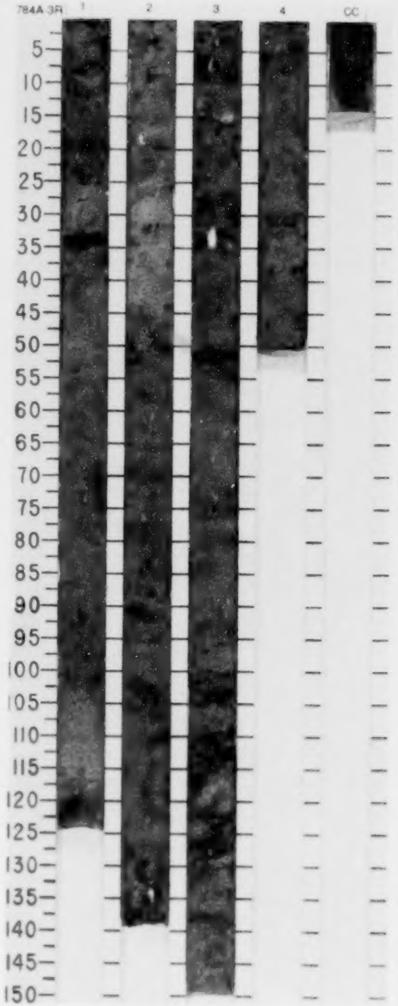
784A-3R
1
2
3
4
CC
5
10
15
20
25
30
35
40
45
50
55
60
65
70
75
80
85
90
95
100
105
110
115
120
125
130
135
140
145
150

SITE 784 HOLE A CORE 4R CORED INTERVAL 4921.2-4930.7 mbsl; 20.4-29.9 mbsf

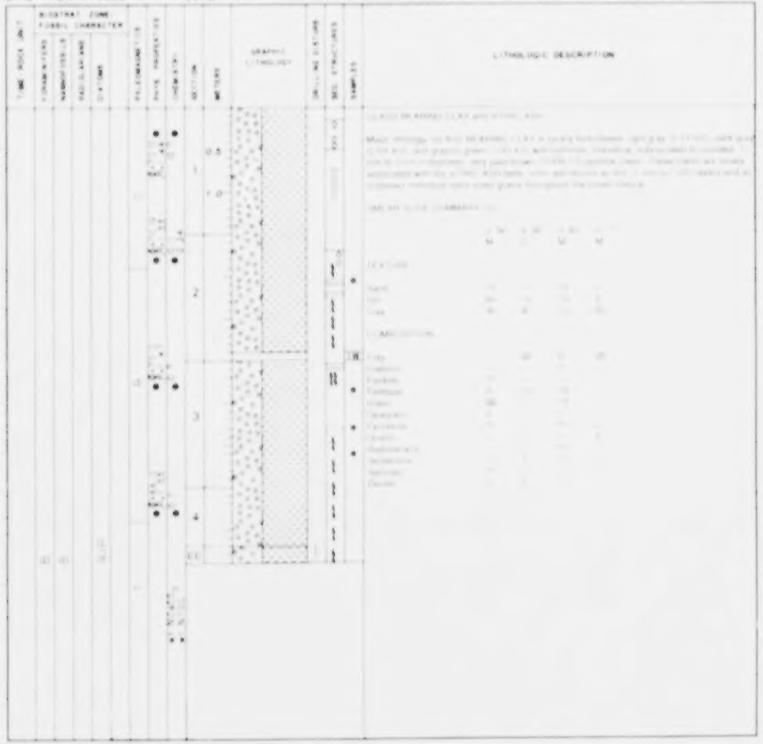
TIME-ROCK UNIT
BIOSTRAT. ZONE/FOSSIL CHARACTER
FORAMINIFERS
NANNOFOSSILS
RADIOLARIANS
DIATOMS
PALEOMAGNETICS
PHYS. PROPERTIES
CHEMISTRY
SECTION
METERS
GRAPHIC LITHOLOGY
DRILLING DISTURB.
SED. STRUCTURES
SAMPLES
LITHOLOGIC DESCRIPTION
0.5
1.0
1
2
3
4
CC
M
M
M

784 A 5R NO RECOVERY

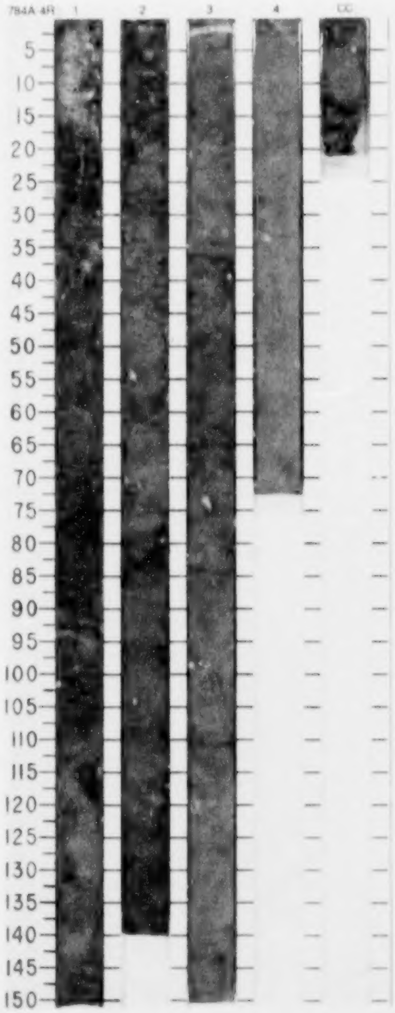
784A 4R
1
2
3
4
CC
5
10
15
20
25
30
35
40
45
50
55
60
65
70
75
80
85
90
95
100
105
110
115
120
125
130
135
140
145
150

SITE 784 HOLE A CORE 6R CORED INTERVAL 4940.3-4949.9 mbsl; 39.5-49.1 mbsf

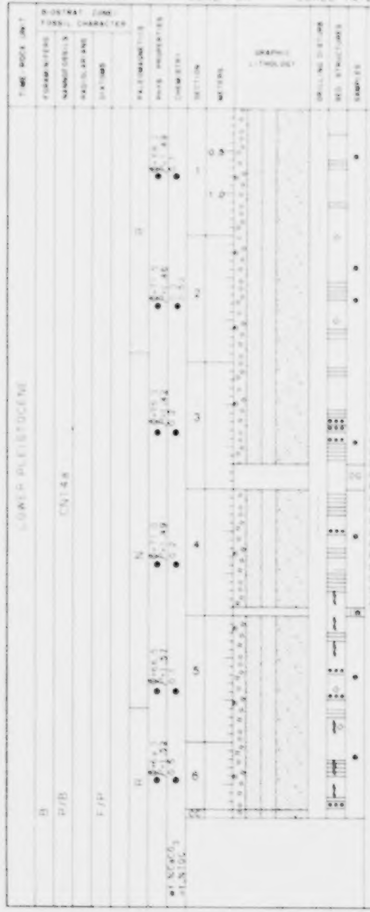
TIME-ROCK UNIT
BIOSTRAT. ZONE/ FOSSIL CHARACTER
FORAMINIFERS
NANNOFOSSILS
RADIOLARIANS
DIATOMS
PALEOMAGNETICS
PHYS. PROPERTIES
CHEMISTRY
SECTION
METERS
GRAPHIC LITHOLOGY
DRILLING DISTURB.
SED. STRUCTURES
SAMPLES
LOWER PLEISTOCENE
CN14a
B
P/B
F/P
R
N
R
0.5
1.0
1
2
3
4
5
6
CC

LITHOLOGIC DESCRIPTION

VITRIC SILTY SAND, VITRIC SAND, FELDSPAR- AND BIOGENIC-RICH VITRIC SILTY SAND, and VITRIC SANDY CLAY

Major lithology: VITRIC SILTY SAND, VITRIC SAND, FELDSPAR- AND BIOGENIC-RICH VITRIC SILTY SAND, and VITRIC SANDY CLAY, predominantly light brownish gray [illegible] with laminae of gray [illegible] and dark gray [illegible]. Laminae are [illegible] and subhorizontal; they are present at [illegible] cm in Section 1, [illegible] cm in Section 2, [illegible] cm in Section 3, [illegible] cm in Section 4, [illegible] cm in Section 5, [illegible] cm in Section 6. Graded beds, commonly [illegible] cm thick and composed of [illegible], are present at [illegible] cm in Section 3, [illegible] cm in Section 4, [illegible] cm in Section 5, and [illegible] cm in Section 6. Clasts of dark gray [illegible] mud are present at [illegible] cm in Section 1, [illegible] cm in Section 2, [illegible] cm in Section 3, [illegible] cm in Section 5, and [illegible] cm in Section CC. Bioturbation is present locally, but is not pervasive in any of the sections.

SMEAR SLIDE SUMMARY (%):

	[illegible]	[illegible]	[illegible]	[illegible]	[illegible]	[illegible]	[illegible]
	M	D	M	M	M	M	M
TEXTURE:							
Sand	[illegible]	45	60	40	80	80	25
Silt	[illegible]	25	35	20	20	5	15
Clay	15	30	5	40	—	15	60
COMPOSITION:							
[illegible]				[illegible]	[illegible]	[illegible]	[illegible]
Clay		[illegible]		[illegible]	[illegible]	[illegible]	[illegible]
Diatoms	[illegible]	[illegible]	[illegible]	[illegible]	[illegible]	[illegible]	[illegible]
Feldspar	[illegible]	[illegible]	[illegible]	[illegible]	[illegible]	[illegible]	[illegible]
Foraminifers	[illegible]	[illegible]		[illegible]	[illegible]	[illegible]	
Garnet	[illegible]	[illegible]	[illegible]	[illegible]	[illegible]	[illegible]	[illegible]
Glass	[illegible]	[illegible]	[illegible]	[illegible]	[illegible]	[illegible]	[illegible]
Glauconite	[illegible]	[illegible]	[illegible]	[illegible]	[illegible]	[illegible]	[illegible]
Opaques	[illegible]	[illegible]	[illegible]	[illegible]	[illegible]	[illegible]	[illegible]
Pyroxene	[illegible]	[illegible]	[illegible]	[illegible]	[illegible]	[illegible]	[illegible]
Radiolarians	[illegible]	[illegible]	[illegible]	[illegible]	[illegible]	[illegible]	[illegible]
Serpentine	[illegible]	[illegible]	[illegible]	[illegible]	[illegible]		
Silicoflagellates	[illegible]	[illegible]		[illegible]		[illegible]	[illegible]
Spicules	[illegible]	[illegible]		[illegible]		[illegible]	[illegible]
Zeolite	[illegible]	[illegible]		[illegible]		[illegible]	[illegible]

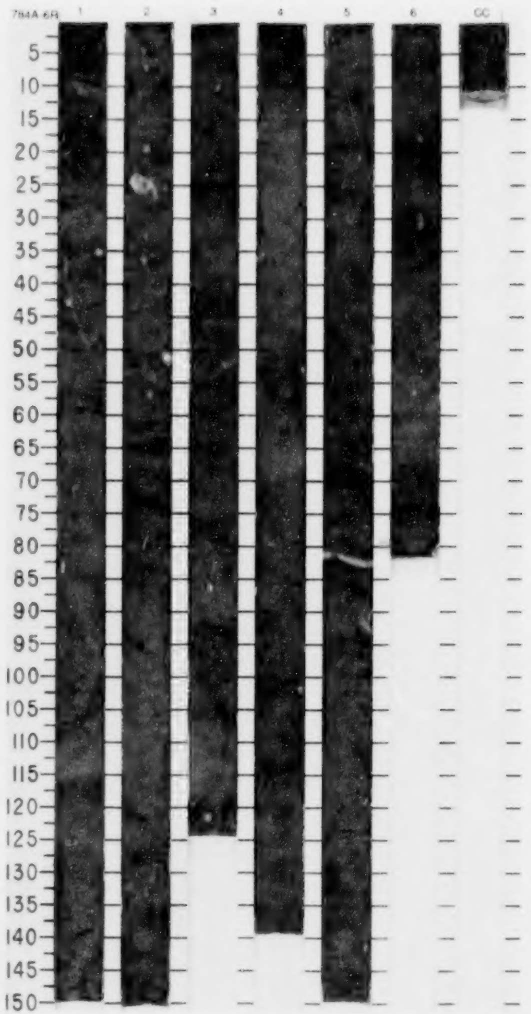
784A 6R
1
2
3
4
5
6
CC
5
10
15
20
25
30
35
40
45
50
55
60
65
70
75
80
85
90
95
100
105
110
115
120
125
130
135
140
145
150

SITE 784 HOLE A CORE 7R CORED INTERVAL 4949.9-4959.6 mbsl; 49.1-58.8 mbsf

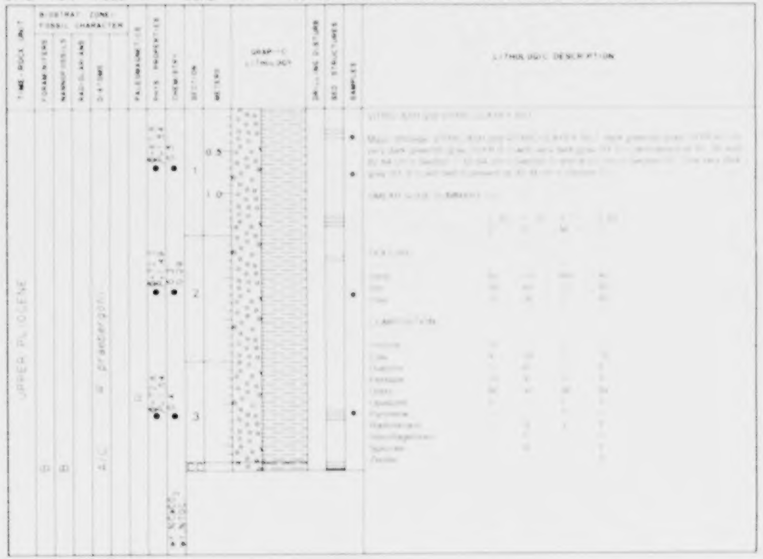
TIME-ROCK UNIT
BIOSTRAT. ZONE/FOSSIL CHARACTER
FORAMINIFERS
NANNOFOSSILS
RADIOLARIANS
DIATOMS
PALEOMAGNETICS
PHYS. PROPERTIES
CHEMISTRY
SECTION
METERS
GRAPHIC LITHOLOGY
DRILLING DISTURB.
SED. STRUCTURES
SAMPLES
LITHOLOGIC DESCRIPTION
UPPER PLIOCENE
R. praebergonii
B
B
A/C
0.5
1.0
1
2
3
CC

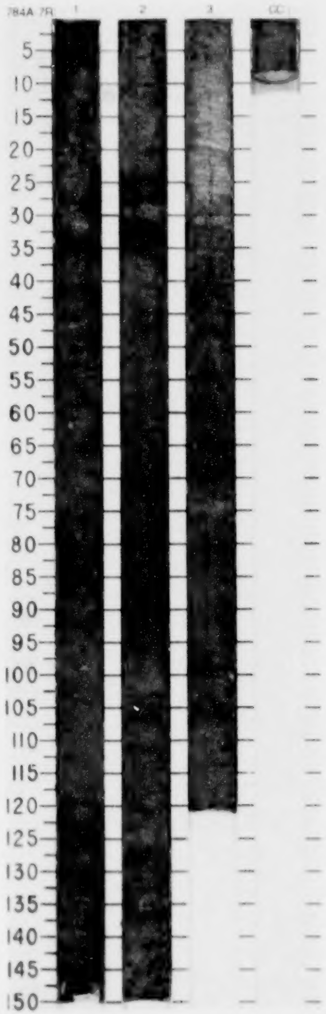
784A 7R
1
2
3
CC
5
10
15
20
25
30
35
40
45
50
55
60
65
70
75
80
85
90
95
100
105
110
115
120
125
130
135
140
145
150

SITE 784 HOLE A CORE 8R CORED INTERVAL 4959.6-4969.3 mbsl; 58.8-68.5 mbsf

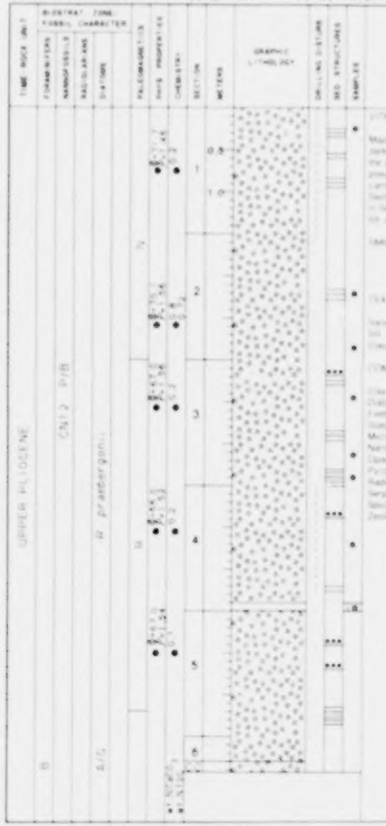

LITHOLOGIC DESCRIPTION

VITRIC ASH

Major lithology: VITRIC ASH, predominantly gray (5Y 5/1) mottled and locally laminated with dark greenish gray (5BG 4/1) and very dark greenish gray (10Y 3/1). Percentage of glass in the ash ranges from 60 to 85. Very dark gray to black (10YR 2/1) beds of glass (all ash) are present at 53-59 cm in Section 1, at 136-138 cm in Section 4, and at 120 cm in Section 5. Laminations are present at 28-29, 34-36, and 37-38 cm in Section 1, at 11 and 78-80 cm in Section 2, at 29, 31, 136, and 140-142 cm in Section 3, and at 120-124, 126, 132, and 141 cm in Section 4. Patches of dark brown (7.5YR 4/2) sand-sized material are present at 43-44, 58-69, and 87-88 cm in Section 3.

SMEAR SLIDE SUMMARY (%):

	1, 20 D	2, 70 D	2, 136 D	3, 44 D	3, 112 M	3, 140 D	4, 39 D
TEXTURE:							
Sand	5	30	10	10	20	10	15
Silt	75	70	70	60	70	80	75
Clay	20	—	20	30	10	10	10
COMPOSITION:							
Clay	20	—	20	[illegible]	[illegible]	6	6
Diatoms	1	—	1	[illegible]	[illegible]	6	—
Feldspar	5	5	[illegible]	[illegible]	[illegible]	5	[illegible]
Glass	[illegible]	85	[illegible]	[illegible]	[illegible]	[illegible]	[illegible]
Micrite	—	—	—	[illegible]	—	—	—
Nannofossils	—	—	—	[illegible]	—	—	—
Opaques	2	5	2				
Pyroxene	—	[illegible]	—		—	—	—
Radiolarians	2	—	2	—	[illegible]	[illegible]	[illegible]
Serpentine	—	—		[illegible]	—	—	—
Spicules	—		1	—	[illegible]	[illegible]	[illegible]
Zeolite	—		[illegible]		—	—	—

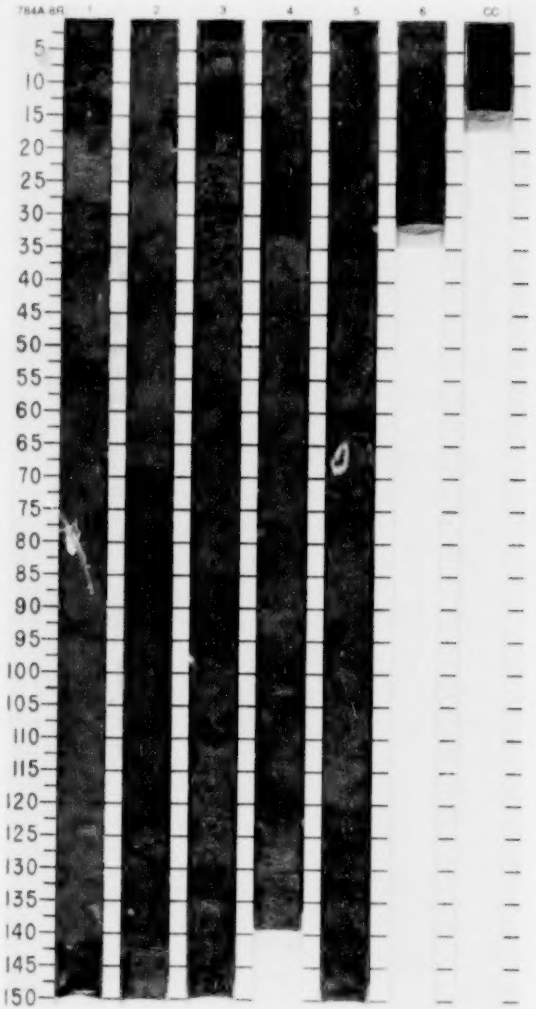

SITE 784 HOLE A CORE 9R CORED INTERVAL 4969.3-4978.9 mbsl; 68.5-78.1 mbsf

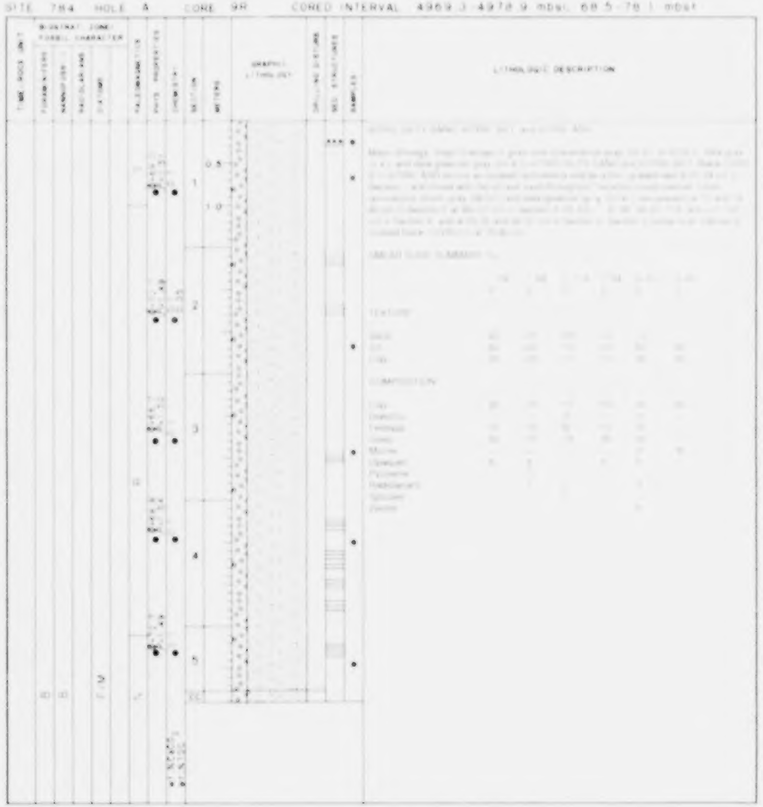
TIME-ROCK UNIT
BIOSTRAT. ZONE/ FOSSIL CHARACTER
FORAMINIFERS
NANNOFOSSILS
RADIOLARIANS
DIATOMS
PALEOMAGNETICS
PHYS. PROPERTIES
CHEMISTRY
SECTION
METERS
GRAPHIC LITHOLOGY
DRILLING DISTURB.
SED. STRUCTURES
SAMPLES
0.5
1.0
1
2
3
4
5
CC

LITHOLOGIC DESCRIPTION

[illegible]

[illegible]

SMEAR SLIDE SUMMARY (%):

TEXTURE:

Sand

Silt

Clay

COMPOSITION:

Clay

Feldspar

Mica

Opaques

Pyroxene

Radiolarians

Spicules

Zeolite

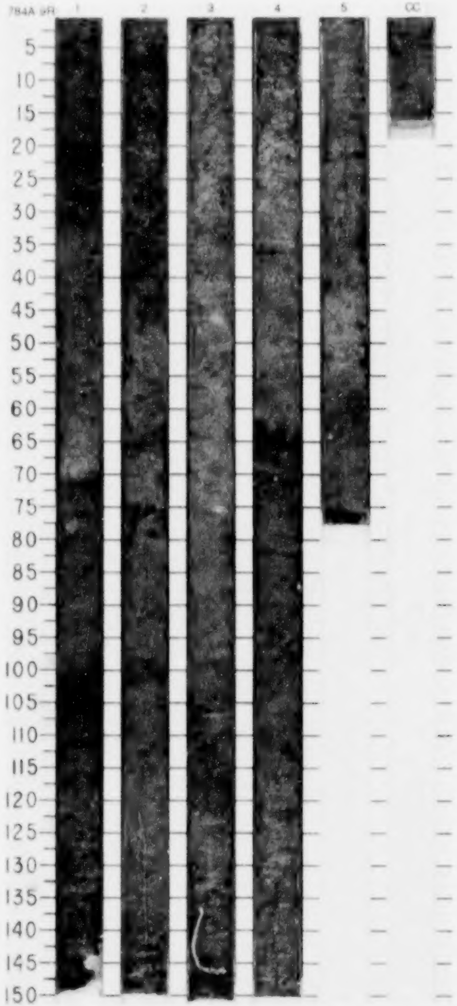
784A 9R
1
2
3
4
5
CC
5
10
15
20
25
30
35
40
45
50
55
60
65
70
75
80
85
90
95
100
105
110
115
120
125
130
135
140
145
150

SITE 784 HOLE A CORE 10R CORED INTERVAL 4978.9-4988.6 mbsl; 78.1-87.8 mbsf

TIME-ROCK UNIT	FORAMINIFERS	NANNOFOSSILS	RADIOLARIANS	DIATOMS	PALEOMAGNETICS	SECTION	LITHOLOGIC DESCRIPTION
LOWER PLIOCENE	B	B		N. jouseae F/P	N ?	1 2 3 4 CC	see below

VITRIC SILT

Major lithology: VITRIC SILT, predominantly gray (5Y 5/1 to 5Y 6/1) to dark gray (5Y 4/1). Dark laminations are present at 14-15 and 85-86 cm in Section 1. A dark brown (7.5YR 4/2) ash layer is present at 29-30 cm in Section 3. Black (10YR 2/1) ash laminations are present at 80-81 cm in Section 2 and at 12-15 and 55-58 cm in Section 4.

SMEAR SLIDE SUMMARY (%):

	1, 20 D	1, 100 M	2, 85 D	3, 39 D	4, 40 D
TEXTURE:					
Sand	5	2	10	20	10
Silt	25	40	70	70	50
Clay	70	58	20	10	40
COMPOSITION:					
Chlorite	—	T	T	—	—
Clay	50	40	40	10	36
Feldspar	7	8	10	10	10
Glass	35	40	30	70	30
Micrite	8	10	8	—	—
Opaques	2	—	10	5	5
Pyroxene	—	—	—	5	—
Radiolarians	—	2	—	—	5
Spicules	3	—	—	—	—

SITE 784 HOLE A CORE 11R CORED INTERVAL 4988.6-4998.2 mbsl; 87.8-97.4 mbsf

TIME-ROCK UNIT	FORAMINIFERS	NANNOFOSSILS	RADIOLARIANS	DIATOMS	PALEOMAGNETICS	SECTION	LITHOLOGIC DESCRIPTION
	B	B		C/M		CC	see below

GLASS-RICH SILTY CLAYSTONE

Major lithology: GLASS-RICH SILTY CLAYSTONE, gray (5Y 5/1), homogeneous. The core contains no sedimentary structures and no evidence of bioturbation.

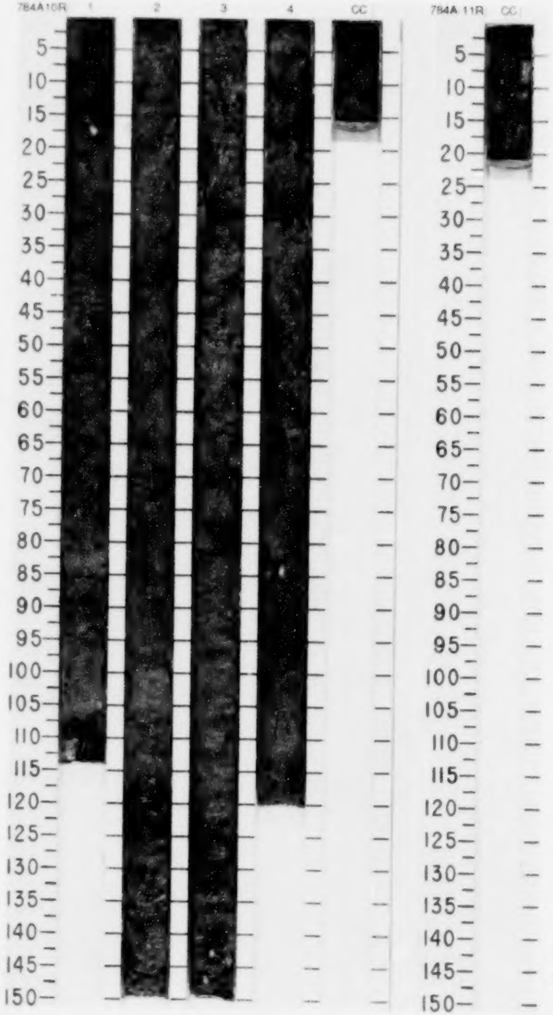

SITE 784 HOLE A CORE 12R CORED INTERVAL 4998.2-5007.9 mbsl; 97.4-107.1 mbsf

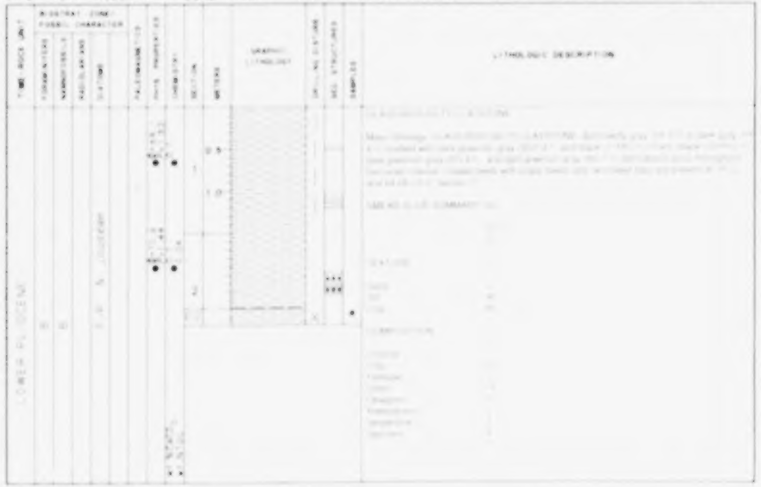
TIME-ROCK UNIT
BIOSTRAT. ZONE/FOSSIL CHARACTER
FORAMINIFERS
NANNOFOSSILS
RADIOLARIANS
DIATOMS
PALEOMAGNETICS
PHYS. PROPERTIES
CHEMISTRY
SECTION
METERS
GRAPHIC LITHOLOGY
DRILLING DISTURB.
SED. STRUCTURES
SAMPLES
LITHOLOGIC DESCRIPTION
LOWER PLIOCENE
0.5
1.0
1
2
TEXTURE
COMPOSITION

SITE 784 HOLE A CORE 13R CORED INTERVAL 5007.9-5017.5 mbsl; 107.1-116.7 mbsf

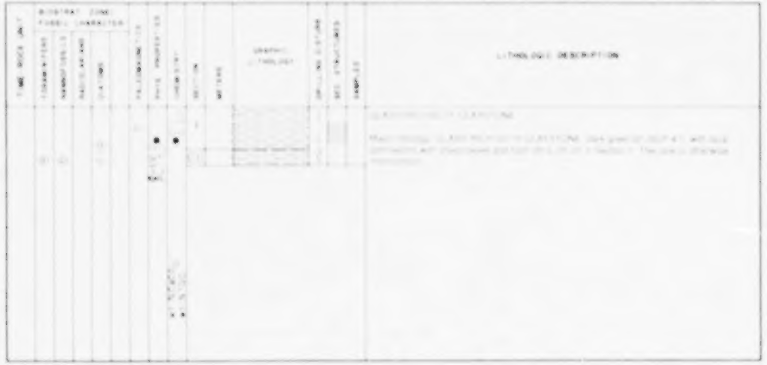
TIME-ROCK UNIT
BIOSTRAT. ZONE/FOSSIL CHARACTER
FORAMINIFERS
NANNOFOSSILS
RADIOLARIANS
DIATOMS
PALEOMAGNETICS
PHYS. PROPERTIES
CHEMISTRY
SECTION
METERS
GRAPHIC LITHOLOGY
DRILLING DISTURB.
SED. STRUCTURES
SAMPLES
LITHOLOGIC DESCRIPTION
1

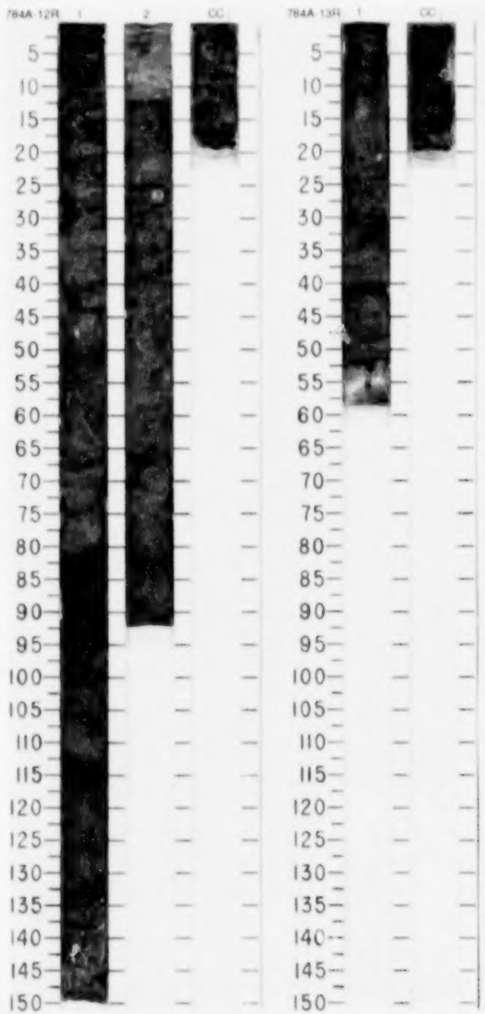
784A-12R
1
2
CC
784A-13R
1
CC
5
10
15
20
25
30
35
40
45
50
55
60
65
70
75
80
85
90
95
100
105
110
115
120
125
130
135
140
145
150

SITE 784 HOLE A CORE 14R CORED INTERVAL 5017.5-5027.2 mbsl; 116.7-126.4 mbsf

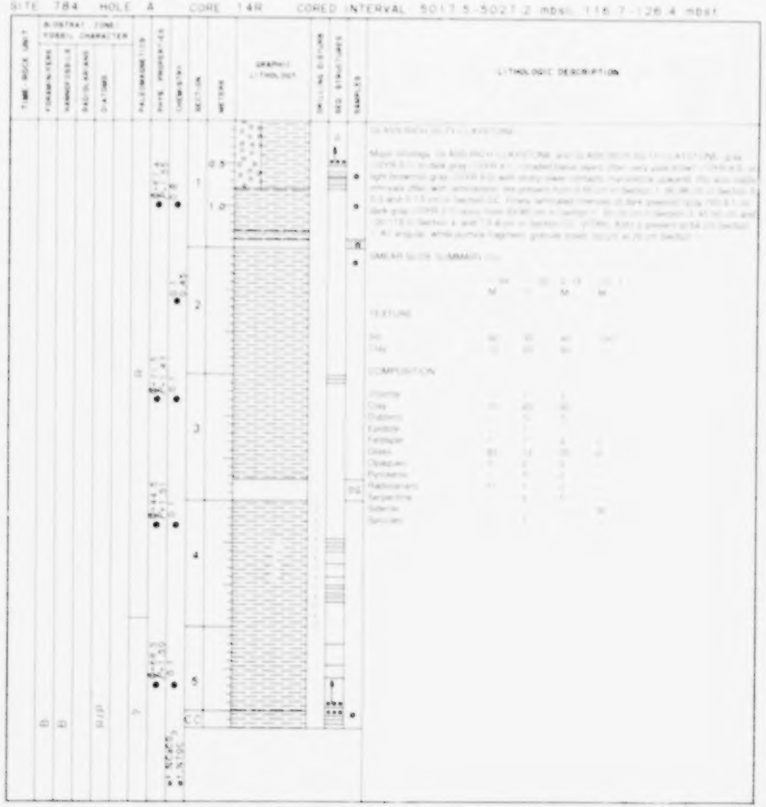
TIME-ROCK UNIT
BIOSTRAT. ZONE/FOSSIL CHARACTER
FORAMINIFERS
NANNOFOSSILS
RADIOLARIANS
DIATOMS
PALEOMAGNETICS
PHYS. PROPERTIES
CHEMISTRY
SECTION
METERS
GRAPHIC LITHOLOGY
DRILLING DISTURB.
SED. STRUCTURES
SAMPLES
B
B
B/B
0.5
1.0
1
2
3
4
5
CC

LITHOLOGIC DESCRIPTION

GLASS-RICH SILTY CLAYSTONE

Major lithology: GLASS-RICH CLAYSTONE and GLASS-RICH SILTY CLAYSTONE, gray (10YR 5/1) to dark gray (10YR 4/1). [illegible] light brownish gray (10YR 6/2) with sharp lower contacts [illegible] Section 1, [illegible] Section 5, [illegible] and [illegible] cm in Section CC. Finely laminated intervals of dark greenish gray [illegible] dark gray (10YR [illegible]) [illegible] Section 4, [illegible] Section 2, [illegible] and [illegible] Section 4, and [illegible] cm in Section CC. [illegible] present at 54 cm Section 1. An angular white pumice fragment [illegible] at 76 cm Section [illegible]

SMEAR SLIDE SUMMARY (%):

	[illegible]	[illegible]	[illegible]	[illegible]
	M	D	M	M
TEXTURE:				
Silt	[illegible]	[illegible]	[illegible]	[illegible]
Clay	[illegible]	[illegible]	[illegible]	[illegible]
COMPOSITION:				
Chlorite	[illegible]	[illegible]	[illegible]	
Clay	[illegible]	[illegible]	[illegible]	
Diatoms	[illegible]	[illegible]	[illegible]	
Epidote	[illegible]	[illegible]		
Feldspar	[illegible]	[illegible]	[illegible]	[illegible]
Glass	[illegible]	[illegible]	[illegible]	[illegible]
Opaques	[illegible]	[illegible]	[illegible]	[illegible]
Pyroxene	[illegible]	[illegible]	[illegible]	[illegible]
Radiolarians	[illegible]	[illegible]	[illegible]	[illegible]
Serpentine	[illegible]	[illegible]	[illegible]	[illegible]
Siderite				[illegible]
Spicules		[illegible]		[illegible]

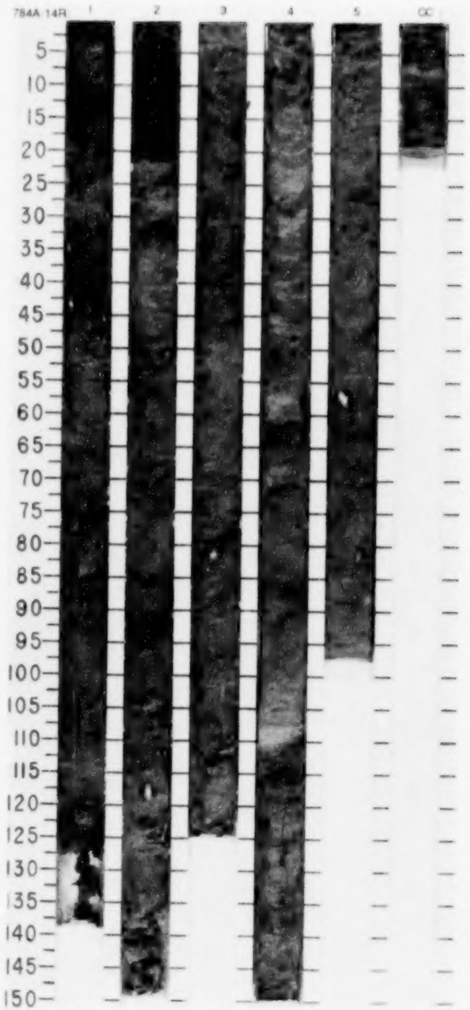
784A-14R
1
2
3
4
5
CC
5
10
15
20
25
30
35
40
45
50
55
60
65
70
75
80
85
90
95
100
105
110
115
120
125
130
135
140
145
150

SITE 784 HOLE A CORE 15R CORED INTERVAL 5027.2-5036.8 mbsl; 126.4-136.0 mbsf

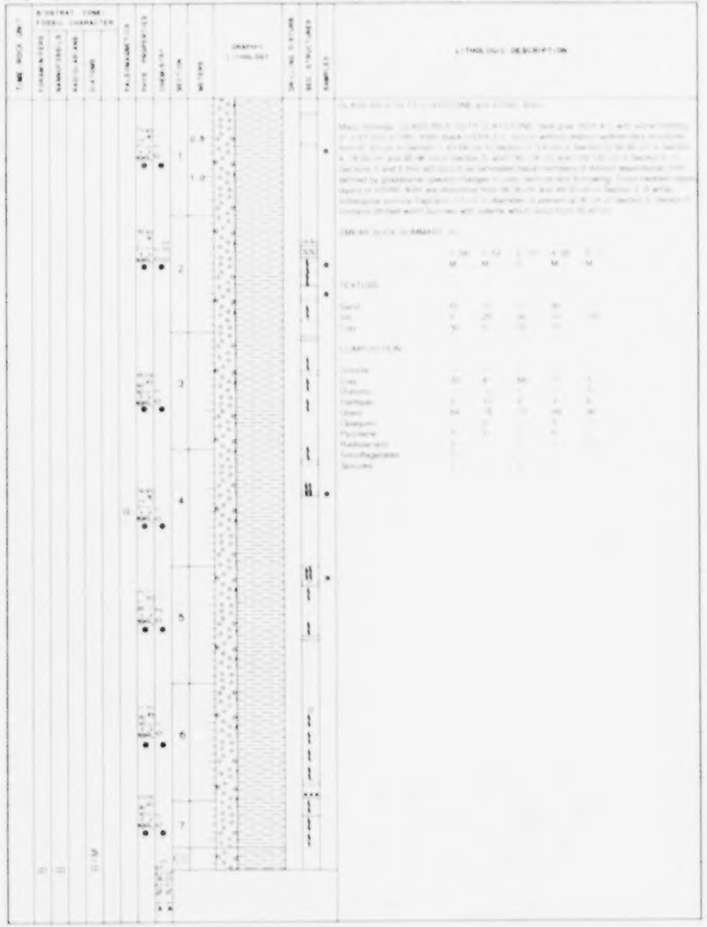
BIOSTRAT. ZONE/ FOSSIL CHARACTER
GRAPHIC LITHOLOGY
LITHOLOGIC DESCRIPTION
SMEAR SLIDE SUMMARY (%):
M
TEXTURE:
Sand
Silt
Clay
COMPOSITION:
Clay
Feldspar
Glass
Opaques
Pyroxene
Radiolarians
Silicoflagellates
Spicules
0.5
1.0
1
2
3
4
5
6
7
CC

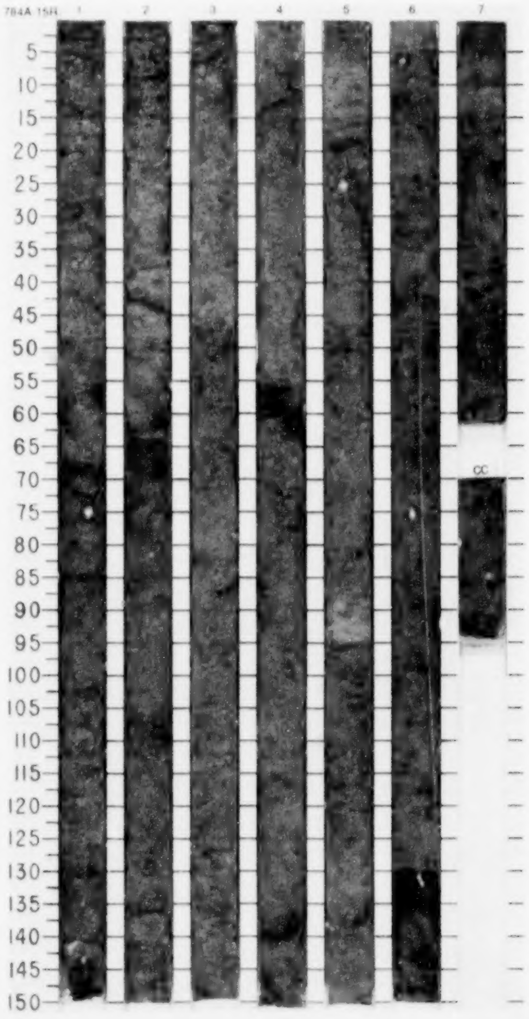
784A 15R
1
2
3
4
5
6
7
CC
5
10
15
20
25
30
35
40
45
50
55
60
65
70
75
80
85
90
95
100
105
110
115
120
125
130
135
140
145
150

SITE 784 HOLE A CORE 16R CORED INTERVAL 5036.8-5046.4 mbsl; 136.0-145.6 mbsf

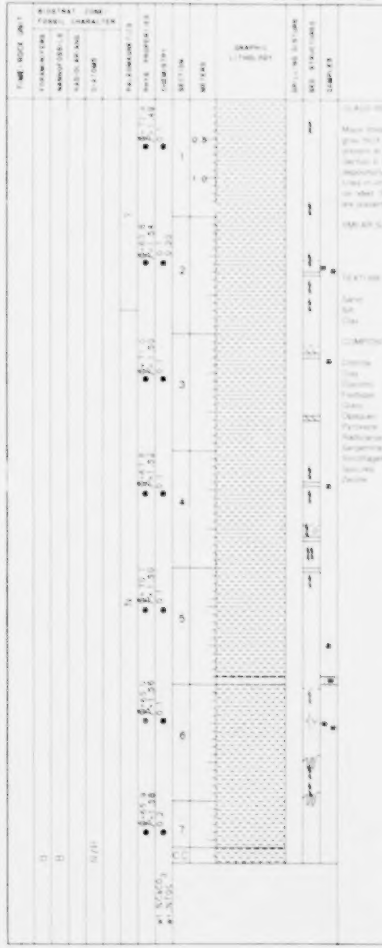
TIME-ROCK UNIT
BIOSTRAT. ZONE / FOSSIL CHARACTER
FORAMINIFERS
NANNOFOSSILS
RADIOLARIANS
DIATOMS
PALEOMAGNETICS
PHYS. PROPERTIES
CHEMISTRY
SECTION
METERS
GRAPHIC LITHOLOGY
DRILLING DISTURB.
SED. STRUCTURES
SAMPLES
1
2
3
4
5
6
7
CC
0.5
1.0
B
B
R/B
N

LITHOLOGIC DESCRIPTION

GLASS-RICH CLAYSTONE

Major lithology: GLASS-RICH CLAYSTONE, FELDSPAR-RICH VITRIC CLAYSTONE, dark gray [illegible] with some intervals of gray [illegible]. [illegible] Section 2 [illegible] Section 4 [illegible] Section 6 [illegible] Section 3 [illegible] Section 4 [illegible] Section 3. A pumice fragment [illegible] Section 4. [illegible] of greenish gray [illegible] serpentine are present between [illegible] in Section 6.

SMEAR SLIDE SUMMARY (%):

	[illegible] D	[illegible] D	[illegible] M	[illegible] M	[illegible] D	[illegible] D	[illegible] M
TEXTURE:							
Sand	—	—	15	—	—	—	—
Silt	30	[illegible]	40	100	20	[illegible]	[illegible]
Clay	70	[illegible]	45	—	80	90	90
COMPOSITION:							
Calcite	[illegible]	[illegible]	[illegible]	[illegible]	[illegible]	[illegible]	[illegible]
Clay	[illegible]	[illegible]	[illegible]	[illegible]	[illegible]	[illegible]	[illegible]
Dolomite	[illegible]	[illegible]	[illegible]	[illegible]	[illegible]	[illegible]	[illegible]
Feldspar	[illegible]	[illegible]	[illegible]	[illegible]	[illegible]	[illegible]	[illegible]
Glass	[illegible]	[illegible]	[illegible]	[illegible]	[illegible]	[illegible]	[illegible]
Opaques	[illegible]	[illegible]	[illegible]	[illegible]	[illegible]	[illegible]	[illegible]
Pyroxene	[illegible]	[illegible]	[illegible]	[illegible]	[illegible]	[illegible]	[illegible]
Radiolarians	[illegible]	[illegible]	[illegible]	[illegible]	[illegible]	[illegible]	[illegible]
Serpentine	[illegible]	[illegible]	[illegible]	[illegible]	[illegible]	[illegible]	[illegible]
Rock fragments	[illegible]	[illegible]	[illegible]	[illegible]	[illegible]	[illegible]	[illegible]
Spicules	[illegible]	[illegible]	[illegible]	[illegible]	[illegible]	[illegible]	[illegible]
Zeolite	[illegible]	[illegible]	[illegible]	[illegible]	[illegible]	[illegible]	[illegible]

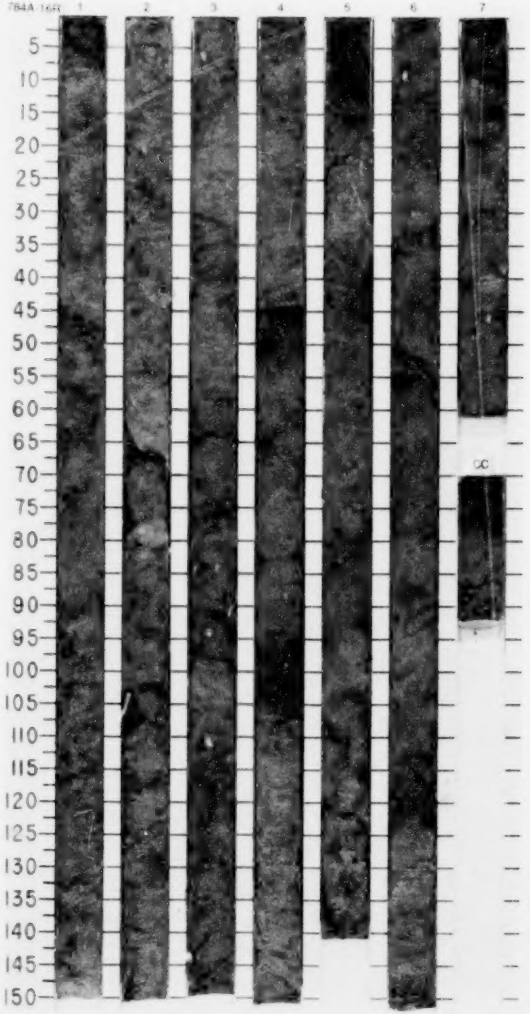
784A 16R
1
2
3
4
5
6
7
CC
5
10
15
20
25
30
35
40
45
50
55
60
65
70
75
80
85
90
95
100
105
110
115
120
125
130
135
140
145
150

SITE 784 HOLE A CORE 17R CORED INTERVAL 5046.4-5056.1 mbsl; 145.6-155.3 mbsf

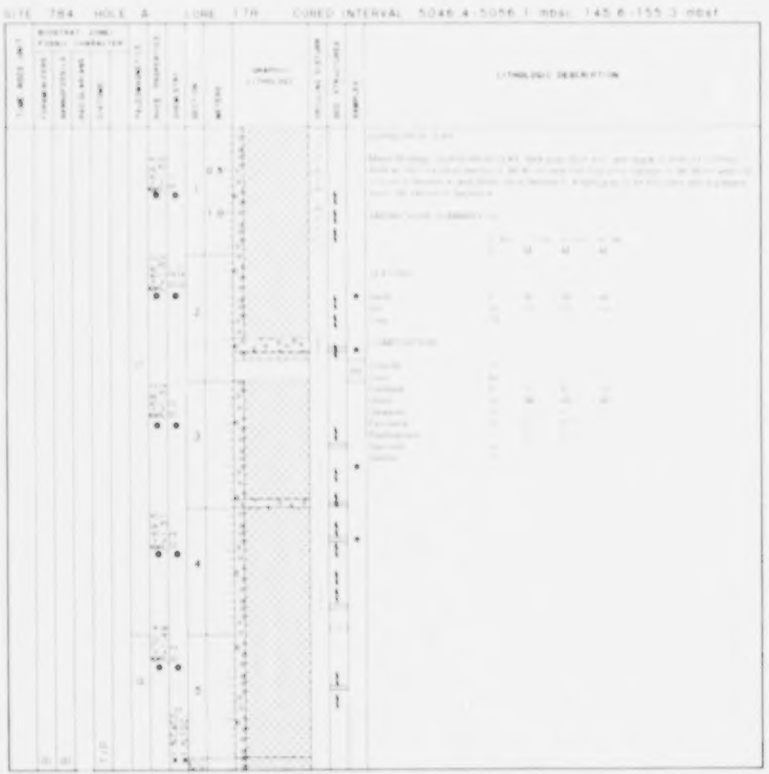
TIME-ROCK UNIT
BIOSTRAT. ZONE/FOSSIL CHARACTER
FORAMINIFERS
NANNOFOSSILS
RADIOLARIANS
DIATOMS
PALEOMAGNETICS
PHYS. PROPERTIES
CHEMISTRY
SECTION
METERS
GRAPHIC LITHOLOGY
DRILLING DISTURB.
SED. STRUCTURES
SAMPLES
LITHOLOGIC DESCRIPTION
1
2
3
4
5
0.5
1.0

[illegible]

SMEAR SLIDE SUMMARY (%):

TEXTURE:

COMPOSITION:

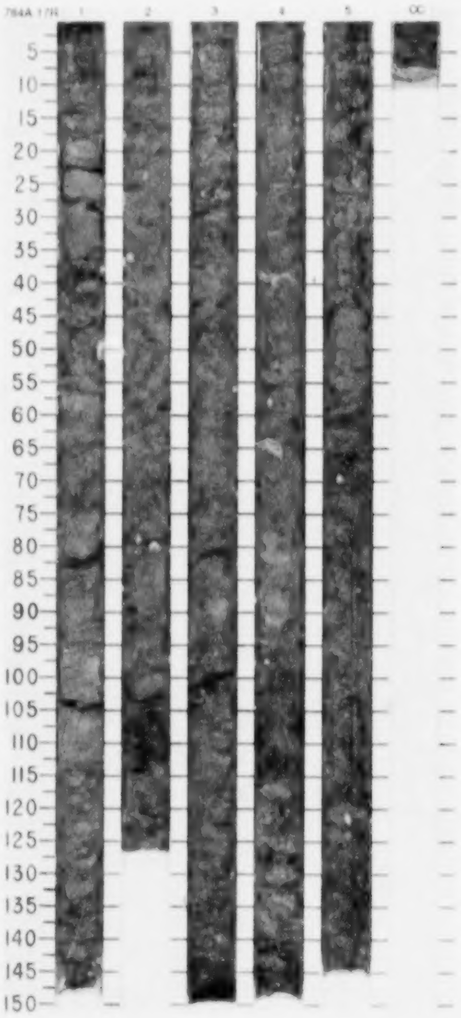
784A-17R
1
2
3
4
5
CC
5
10
15
20
25
30
35
40
45
50
55
60
65
70
75
80
85
90
95
100
105
110
115
120
125
130
135
140
145
150

SITE 784 HOLE A CORE 18R CORED INTERVAL 5056.1-5065.8 mbsl; 155.3-165.0 mbsf

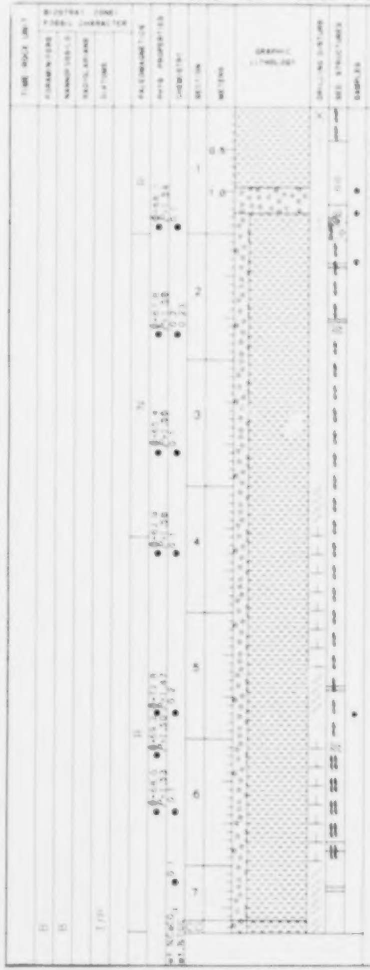
TIME-ROCK UNIT
BIOSTRAT. ZONE/ FOSSIL CHARACTER
FORAMINIFERS
NANNOFOSSILS
RADIOLARIANS
DIATOMS
PALEOMAGNETICS
PHYS. PROPERTIES
CHEMISTRY
SECTION
METERS
GRAPHIC LITHOLOGY
DRILLING DISTURB.
SED. STRUCTURES
SAMPLES
0.5
1.0
1
2
3
4
5
6
7
CC
B
B
T/F

LITHOLOGIC DESCRIPTION

VITRIC SILTY CLAYSTONE

Major lithology: VITRIC SILTY CLAYSTONE, dark greenish gray (5GY 4/1), containing scattered volcaniclastic fragments that are subangular, black (10YR 2/1) in the granule and sand sizes. Intervals of particular concentration of these volcaniclastics occur from [illegible] cm in Section 1, [illegible] cm in Section 2, [illegible] cm in Section 5, [illegible] in Section 6, and [illegible] cm in Section 7. VITRIC ASH, light gray [illegible], forms a turbidite layer extending from [illegible] cm in Section 1. Black (10YR 2/1) VITRIC ASH occurs from [illegible] cm and [illegible] in Section 3; the latter layer is offset by a possible synsedimentary fault that does not cut an overlying lamina at 120 cm.

SMEAR SLIDE SUMMARY (%):

	1, 46	1, 124	3, 32	6, 120
	D	D	D	D
TEXTURE:				
Sand	5	15	10	5
Silt	75	[illegible]	70	70
Clay	20	[illegible]	20	25
COMPOSITION:				
Clay	—	—	—	[illegible]
Diatoms	—	—	—	[illegible]
Feldspar	[illegible]	[illegible]	[illegible]	[illegible]
Glass	[illegible]	[illegible]	[illegible]	[illegible]
Opaques	—	[illegible]	[illegible]	—
Pyroxene	—	—	[illegible]	—
Radiolarians	[illegible]	—	—	[illegible]
Sponges	[illegible]	—	—	—

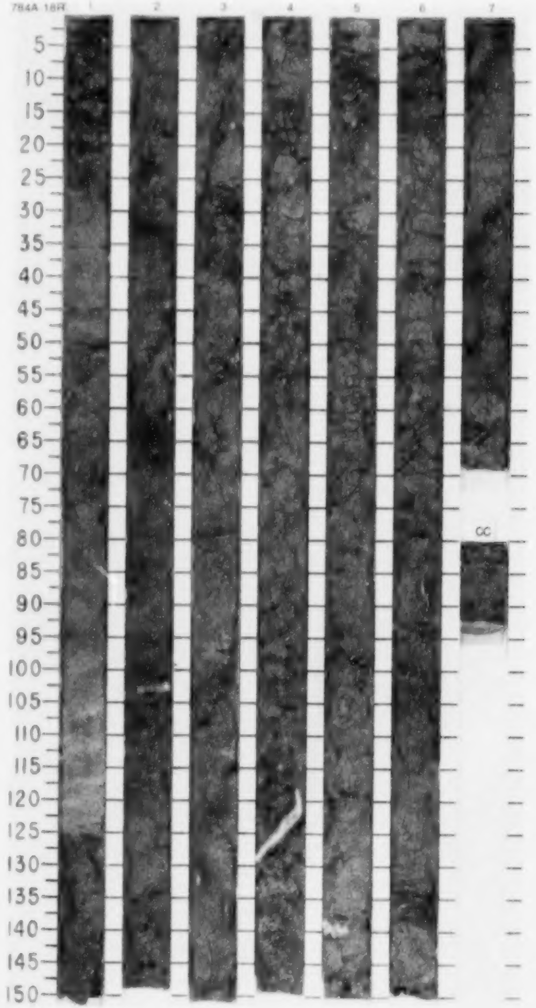
784A 18R
1
2
3
4
5
6
7
CC
5
10
15
20
25
30
35
40
45
50
55
60
65
70
75
80
85
90
95
100
105
110
115
120
125
130
135
140
145
150

SITE 784 HOLE A CORE 19R CORED INTERVAL 5065.8-5075.5 mbsl; 165.0-174.7 mbsf

TIME-ROCK UNIT
BIOSTRAT. ZONE/FOSSIL CHARACTER
FORAMINIFERS
NANNOFOSSILS
RADIOLARIANS
DIATOMS
PALEOMAGNETICS
PHYS. PROPERTIES
CHEMISTRY
SECTION
METERS
GRAPHIC LITHOLOGY
DRILLING DISTURB.
SED. STRUCTURES
SAMPLES
LITHOLOGIC DESCRIPTION
0.5
1.0
1
2

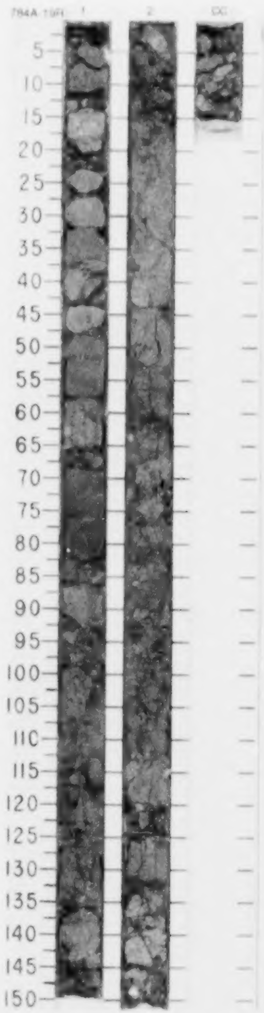
784A-19R 1
2
CC
5
10
15
20
25
30
35
40
45
50
55
60
65
70
75
80
85
90
95
100
105
110
115
120
125
130
135
140
145
150

SITE 784 HOLE A CORE 20R CORED INTERVAL 5075.5-5085.2 mbsl; 174.7-184.4 mbsf

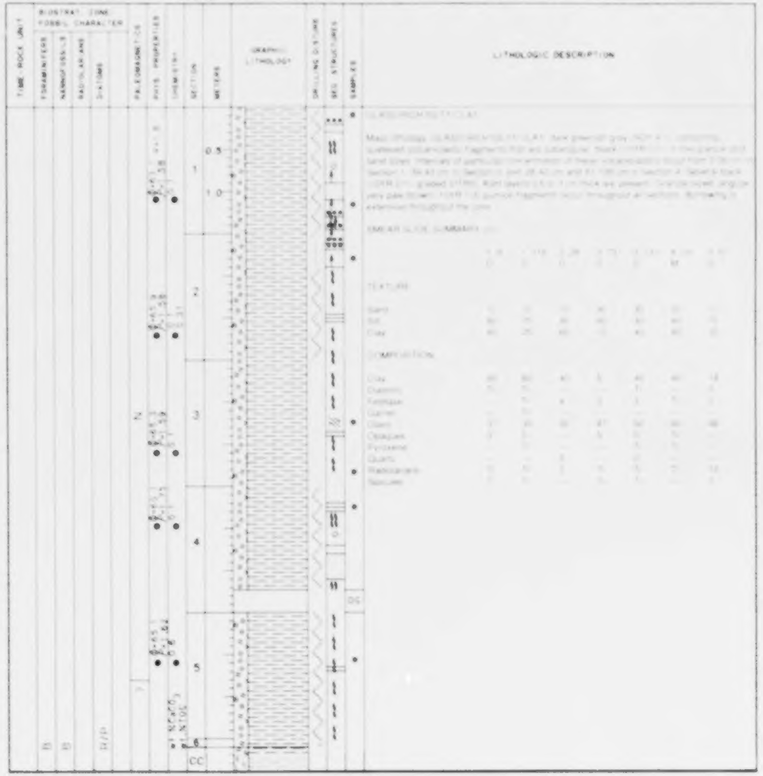
TIME-ROCK UNIT
BIOSTRAT. ZONE/FOSSIL CHARACTER
FORAMINIFERS
NANNOFOSSILS
RADIOLARIANS
DIATOMS
PALEOMAGNETICS
PHYS. PROPERTIES
CHEMISTRY
SECTION
METERS
GRAPHIC LITHOLOGY
DRILLING DISTURB.
SED. STRUCTURES
SAMPLES
LITHOLOGIC DESCRIPTION
B
B
R/P
N
?
0.5
1.0
1
2
3
4
5
6
CC
IW

GLASS-RICH SILTY CLAY

Major lithology: GLASS-RICH SILTY CLAY, dark greenish gray [illegible]

SMEAR SLIDE SUMMARY (%):

TEXTURE:

Sand
Silt
Clay

COMPOSITION:

Clay
Diatoms
Feldspar
Garnet
Glass
Opaques
Pyroxene
Quartz
Radiolarians
Sponge

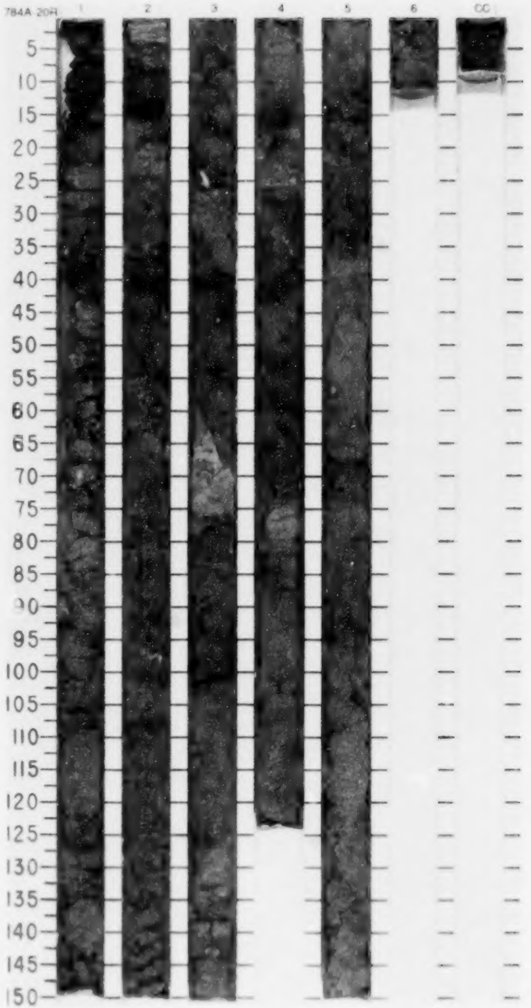
784A 20R
1
2
3
4
5
6
CC
5
10
15
20
25
30
35
40
45
50
55
60
65
70
75
80
85
90
95
100
105
110
115
120
125
130
135
140
145
150

SITE 784 HOLE A CORE 21R CORED INTERVAL 5085.2-5094.8 mbsl; 184.4-194.0 mbsf

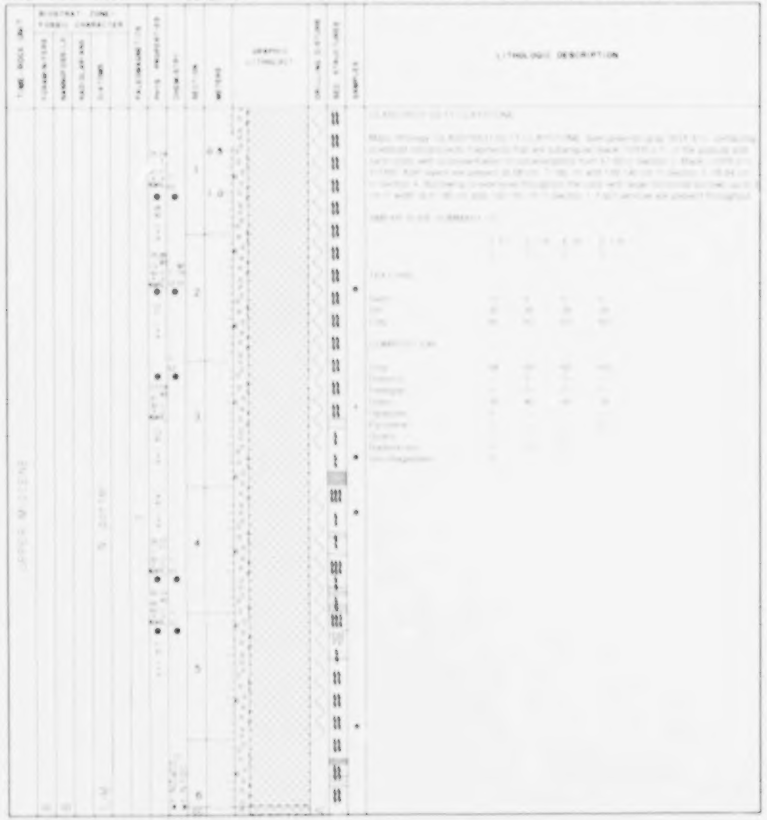
BIOSTRAT. ZONE/ FOSSIL CHARACTER
GRAPHIC LITHOLOGY
LITHOLOGIC DESCRIPTION

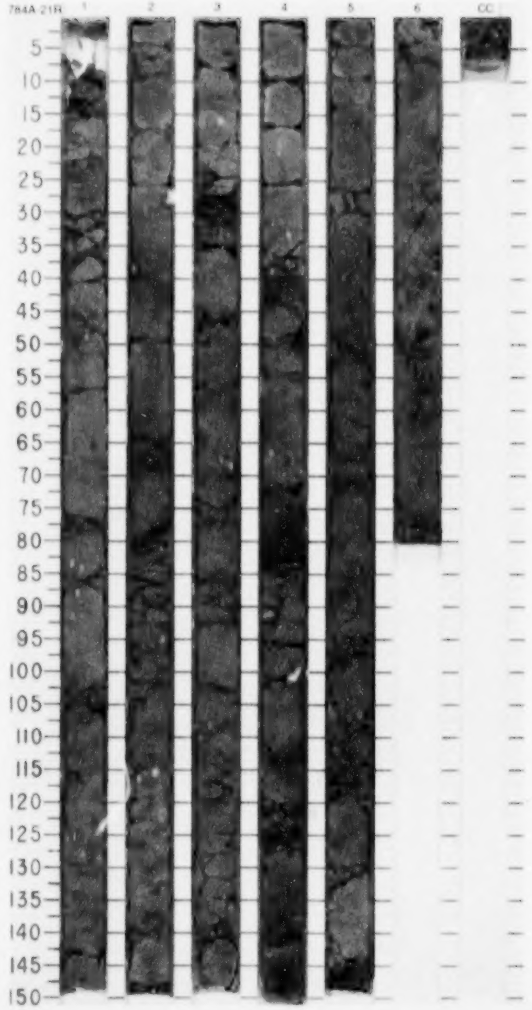
784A 21R
1
2
3
4
5
6
CC
5
10
15
20
25
30
35
40
45
50
55
60
65
70
75
80
85
90
95
100
105
110
115
120
125
130
135
140
145
150

SITE 784 HOLE A CORE 22R CORED INTERVAL 5094.8-5104.4 mbsl; 194.0-203.6 mbsf

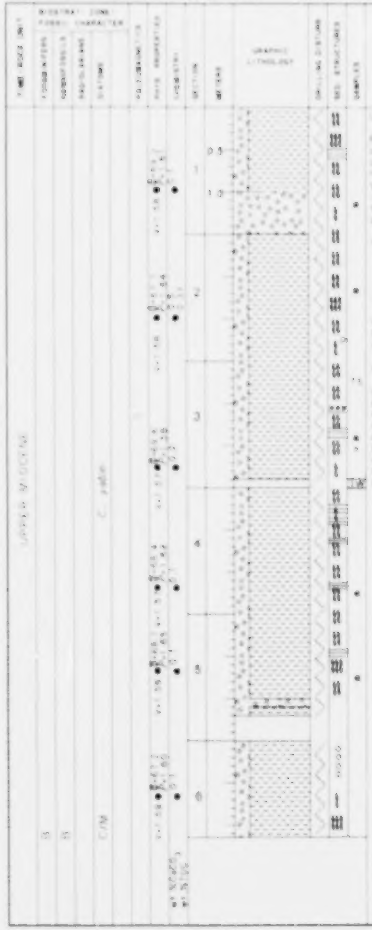
TIME ROCK UNIT
BIOSTRAT. ZONE/ FOSSIL CHARACTER
FORAMINIFERS
NANNOFOSSILS
RADIOLARIANS
DIATOMS
PALEOMAGNETICS
PHYS. PROPERTIES
CHEMISTRY
SECTION
METERS
GRAPHIC LITHOLOGY
DRILLING DISTURB.
SED. STRUCTURES
SAMPLES
UPPER MIOCENE
C/M
B
B
1
2
3
4
5
6
0.5
1.0

LITHOLOGIC DESCRIPTION

GLASS-RICH SILTY CLAYSTONE

Major lithology: GLASS-RICH SILTY CLAYSTONE and GLASS-RICH CLAYEY SILTSTONE, dark greenish gray (5GY 4/1), containing scattered volcaniclastic fragments that are subangular, black (10YR 2/1) in the granule and sand sizes. Concentrations of volcaniclastics occur from 110-150 cm in Section 1 and 95-112 cm in Section 5. A black (10YR 2/1) graded VITRIC ASH layer is present at 66 cm in Section 3. Pumice fragments, very pale brown (10YR 7/3), subangular to subrounded, are scattered from 133-134 cm in Section 2 and throughout Section 6. Extensive burrowing occurs through Section 3. A few laminae are also present, often with approximate dips of about 4?.

SMEAR SLIDE SUMMARY (%):

	1, 140	2, 108	3, 66	4, 107	6, 18
	D	D	D	D	M
TEXTURE:					
Sand	[illegible]	5	5	[illegible]	[illegible]
Silt	[illegible]	[illegible]	[illegible]	15	15
Clay	45	[illegible]	[illegible]	80	80
COMPOSITION:					
Clay	[illegible]	[illegible]	[illegible]	[illegible]	[illegible]
Diatoms	[illegible]	—	—	[illegible]	—
Feldspar	[illegible]	—	[illegible]	—	—
Glass	[illegible]	[illegible]	[illegible]	[illegible]	[illegible]
Opaques	[illegible]	—	[illegible]	—	—
Pyroxene	[illegible]	—	—	—	—
Quartz	[illegible]	—	—	—	—
Radiolarians	[illegible]	[illegible]	—	[illegible]	—
Spicules	[illegible]	—	—	—	—

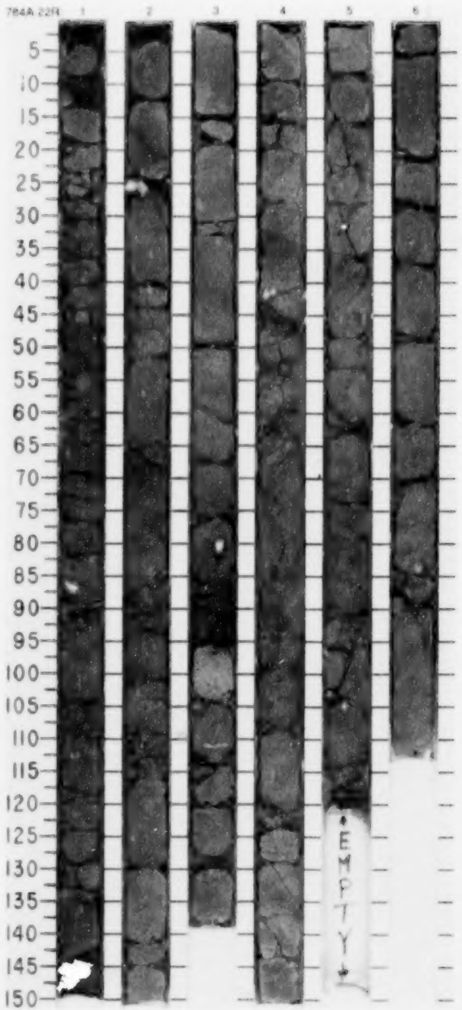
784A 22R
1
2
3
4
5
6
5
10
15
20
25
30
35
40
45
50
55
60
65
70
75
80
85
90
95
100
105
110
115
120
125
130
135
140
145
150
EMPTY

SITE 784 HOLE A CORE 23R CORED INTERVAL 5104.4-5114.0 mbsl; 203.6-213.2 mbsf

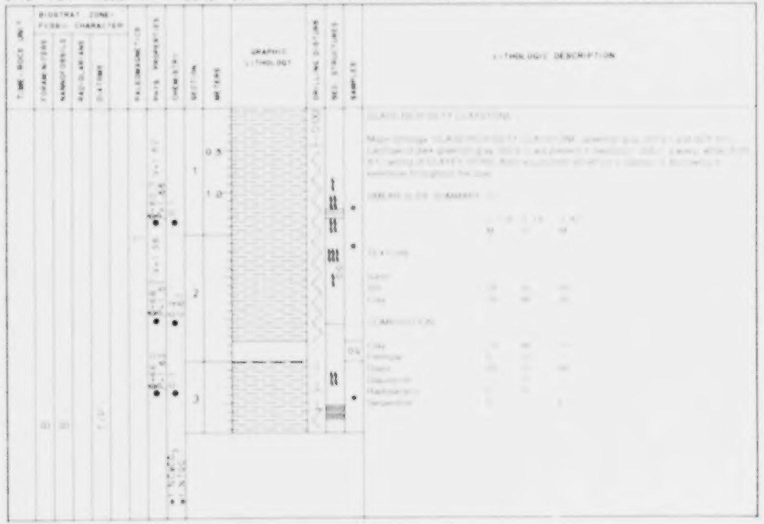
TIME-ROCK UNIT
BIOSTRAT. ZONE/ FOSSIL CHARACTER
FORAMINIFERS
NANNOFOSSILS
RADIOLARIANS
DIATOMS
PALEOMAGNETICS
PHYS. PROPERTIES
CHEMISTRY
SECTION
METERS
GRAPHIC LITHOLOGY
DRILLING DISTURB.
SED. STRUCTURES
SAMPLES
1
2
3
0.5
1.0
B
B
OG

LITHOLOGIC DESCRIPTION

[illegible]

Major lithology: [illegible]

SMEAR SLIDE SUMMARY (%):

TEXTURE:

Sand
Silt
Clay

COMPOSITION:

Clay
Feldspar
Quartz
Glauconite
Radiolarians
Serpentine

784A 23R

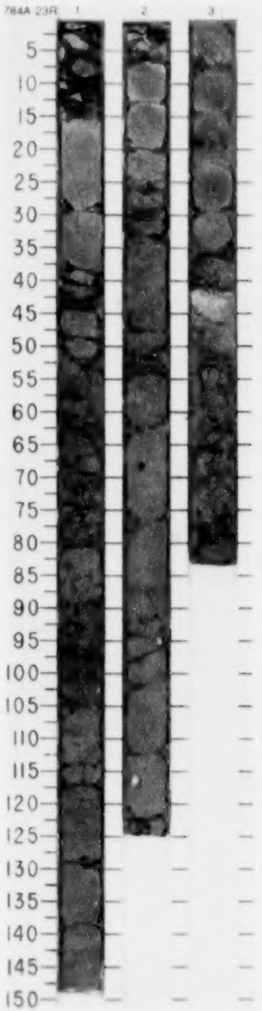
1
2
3
5
10
15
20
25
30
35
40
45
50
55
60
65
70
75
80
85
90
95
100
105
110
115
120
125
130
135
140
145
150

SITE 784 HOLE A CORE 24R CORED INTERVAL 5114.0-5123.7 mbsl; 213.2-222.9 mbsf

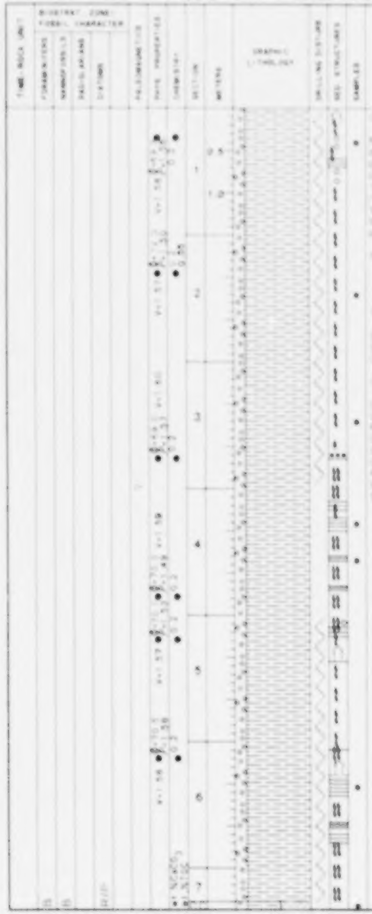

TIME-ROCK UNIT
BIOSTRAT. ZONE/ FOSSIL CHARACTER
FORAMINIFERS
NANNOFOSSILS
RADIOLARIANS
DIATOMS
PALEOMAGNETICS
PHYS. PROPERTIES
CHEMISTRY
SECTION
METERS
GRAPHIC LITHOLOGY
DRILLING DISTURB.
SED. STRUCTURES
SAMPLES
1
2
3
4
5
6
7

LITHOLOGIC DESCRIPTION

GLASS-BEARING CLAYSTONE

[illegible]

SMEAR SLIDE SUMMARY (%):

	[illegible]	[illegible]	[illegible]	[illegible]	[illegible]	[illegible]	[illegible]
TEXTURE:							
Sand	[illegible]	[illegible]	[illegible]	[illegible]	[illegible]	[illegible]	[illegible]
Silt	[illegible]	[illegible]	[illegible]	[illegible]	[illegible]	[illegible]	[illegible]
Clay	[illegible]	[illegible]	[illegible]	[illegible]	[illegible]	[illegible]	[illegible]
COMPOSITION:							
Clay	[illegible]	[illegible]	[illegible]	[illegible]	[illegible]	[illegible]	[illegible]
Opaques	[illegible]	[illegible]	[illegible]	[illegible]	[illegible]	[illegible]	[illegible]
Feldspar	[illegible]	[illegible]	[illegible]	[illegible]	[illegible]	[illegible]	[illegible]
Glass	[illegible]	[illegible]	[illegible]	[illegible]	[illegible]	[illegible]	[illegible]
Glauconite	[illegible]	[illegible]	[illegible]	[illegible]	[illegible]	[illegible]	[illegible]
Quartz	[illegible]	[illegible]	[illegible]	[illegible]	[illegible]	[illegible]	[illegible]
Radiolarians	[illegible]	[illegible]	[illegible]	[illegible]	[illegible]	[illegible]	[illegible]
Serpentine	[illegible]	[illegible]	[illegible]	[illegible]	[illegible]	[illegible]	[illegible]
Spicules	[illegible]	[illegible]	[illegible]	[illegible]	[illegible]	[illegible]	[illegible]

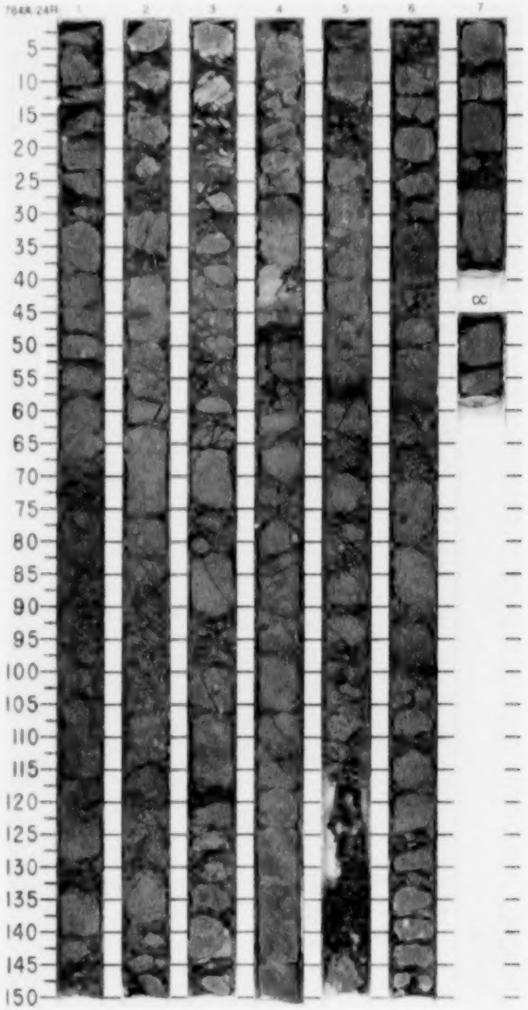

784A-24R
1
2
3
4
5
6
7
CC
5
10
15
20
25
30
35
40
45
50
55
60
65
70
75
80
85
90
95
100
105
110
115
120
125
130
135
140
145
150

SITE 784 HOLE A CORE 25R CORED INTERVAL 5123.7-5133.3 mbsl; 222.9-232.5 mbsf

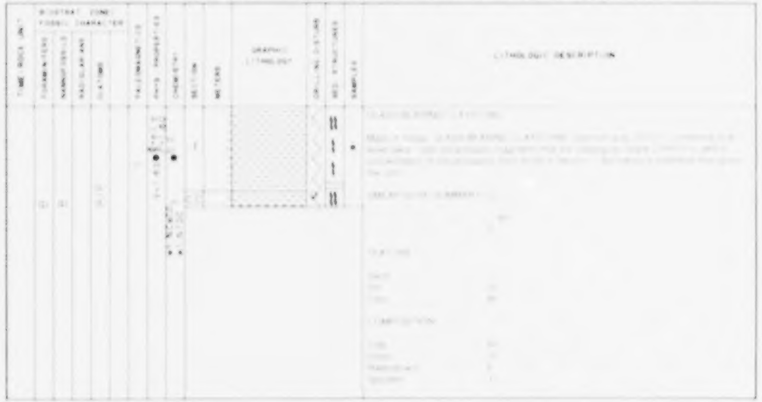
TIME-ROCK UNIT
BIOSTRAT. ZONE/ FOSSIL CHARACTER
FORAMINIFERS
NANNOFOSSILS
RADIOLARIANS
DIATOMS
PALEOMAGNETICS
PHYS. PROPERTIES
CHEMISTRY
SECTION
METERS
GRAPHIC LITHOLOGY
DRILLING DISTURB.
SED. STRUCTURES
SAMPLES
LITHOLOGIC DESCRIPTION
B
B
1
CLAST-BEARING CLAYSTONE
SMEAR SLIDE SUMMARY (%):
TEXTURE:
Sand
Silt
Clay
COMPOSITION:
Clay
Glass
Radiolarians
Spicules

SITE 784 HOLE A CORE 26R CORED INTERVAL 5133.3-5142.9 mbsl; 232.5-242.1 mbsf

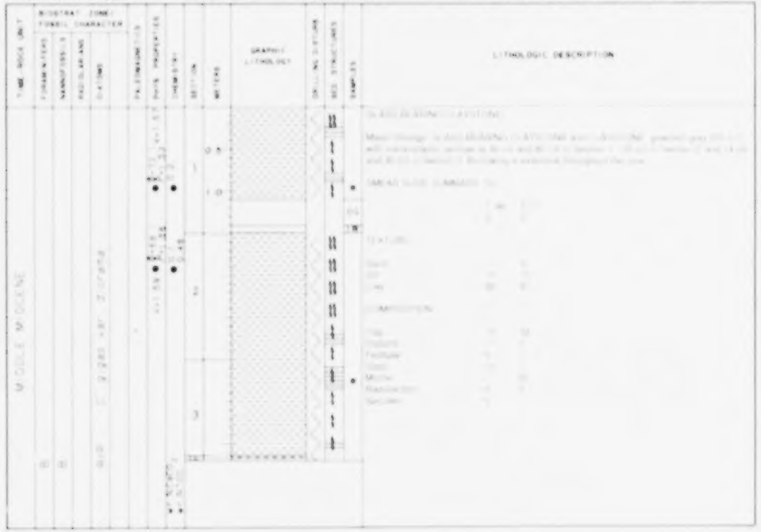
TIME-ROCK UNIT
BIOSTRAT. ZONE/ FOSSIL CHARACTER
FORAMINIFERS
NANNOFOSSILS
RADIOLARIANS
DIATOMS
PALEOMAGNETICS
PHYS. PROPERTIES
CHEMISTRY
SECTION
METERS
GRAPHIC LITHOLOGY
DRILLING DISTURB.
SED. STRUCTURES
SAMPLES
LITHOLOGIC DESCRIPTION
MIDDLE MIOCENE
B
B
1
2
3
0.5
1.0
CC
CLAST-BEARING CLAYSTONE
SMEAR SLIDE SUMMARY (%):
TEXTURE:
Sand
Silt
Clay
COMPOSITION:
Clay
Glass
Radiolarians
Spicules

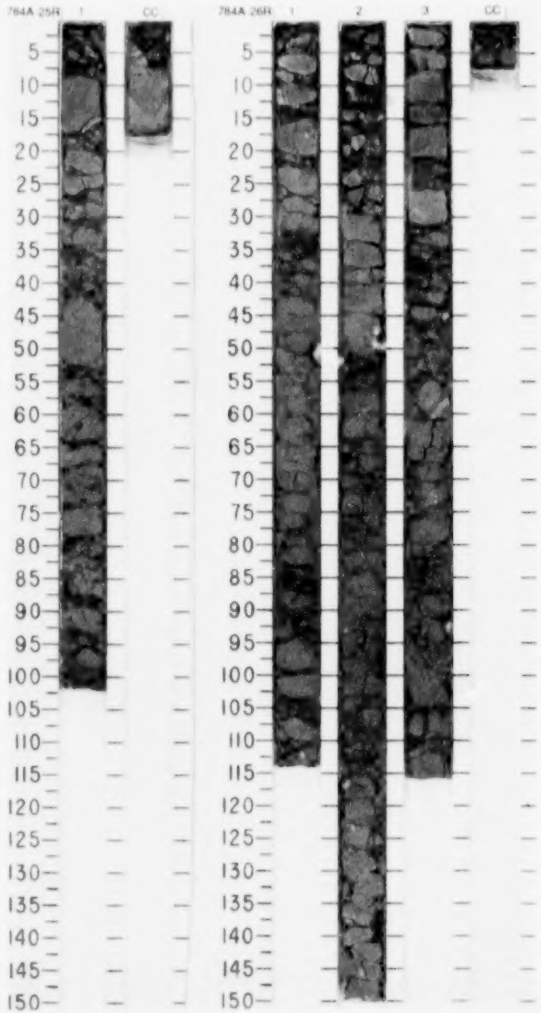
784A 25R
1
CC
784A 26R
1
2
3
CC
5
10
15
20
25
30
35
40
45
50
55
60
65
70
75
80
85
90
95
100
105
110
115
120
125
130
135
140
145
150

SITE 784 HOLE A CORE 27R CORED INTERVAL 5142.9-5152.6 mbsl; 242.1-251.8 mbsf

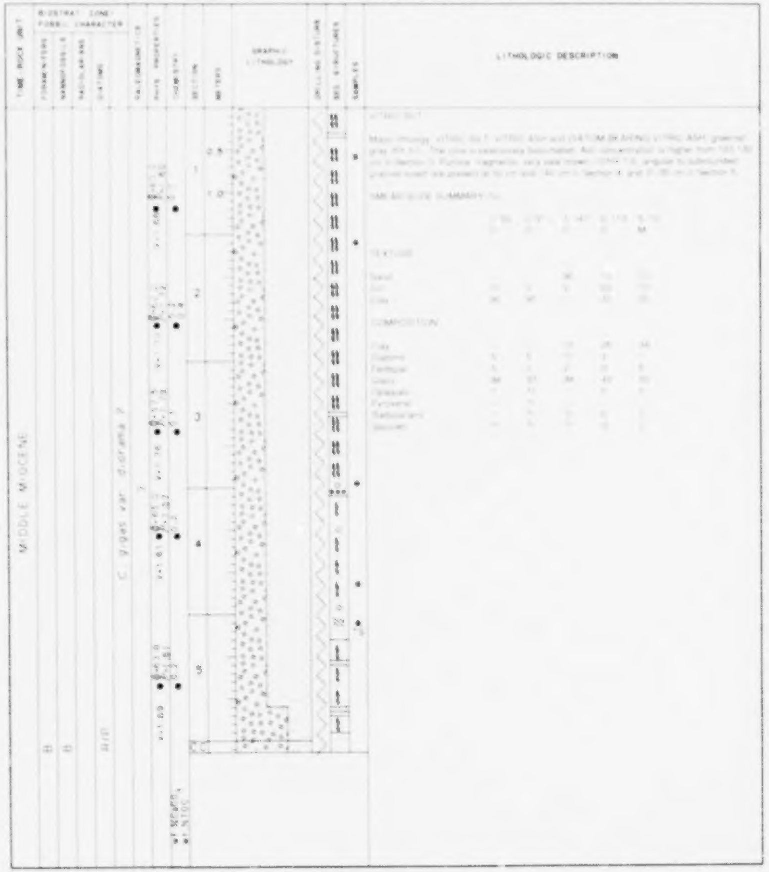
TIME-ROCK UNIT
BIOSTRAT. ZONE/FOSSIL CHARACTER
FORAMINIFERS
NANNOFOSSILS
RADIOLARIANS
DIATOMS
PALEOMAGNETICS
PHYS. PROPERTIES
CHEMISTRY
SECTION
METERS
GRAPHIC LITHOLOGY
DRILLING DISTURB.
SED. STRUCTURES
SAMPLES
LITHOLOGIC DESCRIPTION
MIDDLE MIOCENE
B
B
R/G
C. gigas var. diorama ?
?
0.5
1.0
1
2
3
4
5
CC

VITRIC SILT

Major lithology: VITRIC SILT, VITRIC ASH and DIATOM-BEARING VITRIC ASH, greenish gray [illegible]

SMEAR SLIDE SUMMARY (%):

TEXTURE:

Sand
Silt
Clay

COMPOSITION:

Clay
Diatoms
Feldspar
Glass
Opaques
Pyroxene
Radiolarians
Spicules

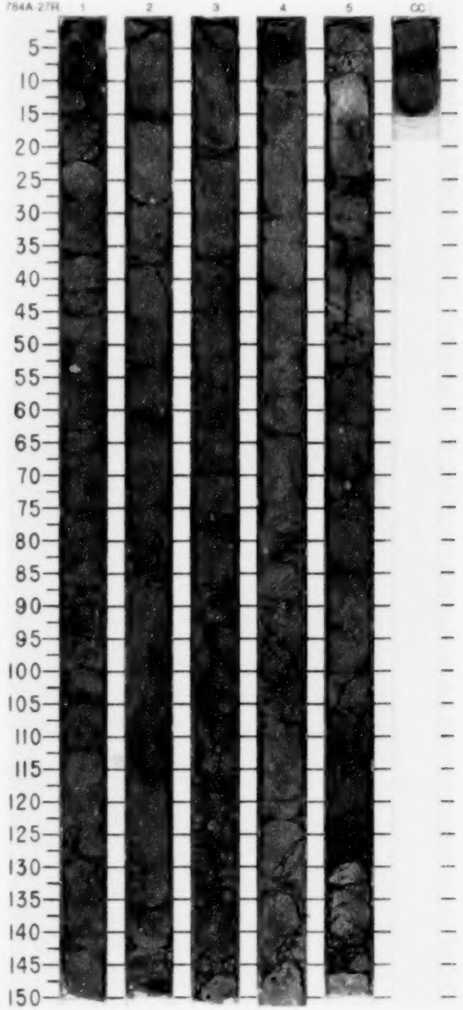
784A-27R
1
2
3
4
5
CC
5
10
15
20
25
30
35
40
45
50
55
60
65
70
75
80
85
90
95
100
105
110
115
120
125
130
135
140
145
150

SITE 784 HOLE A CORE 28R CORED INTERVAL 5152.6-5162.2 mbsl; 251.8-261.4 mbsf

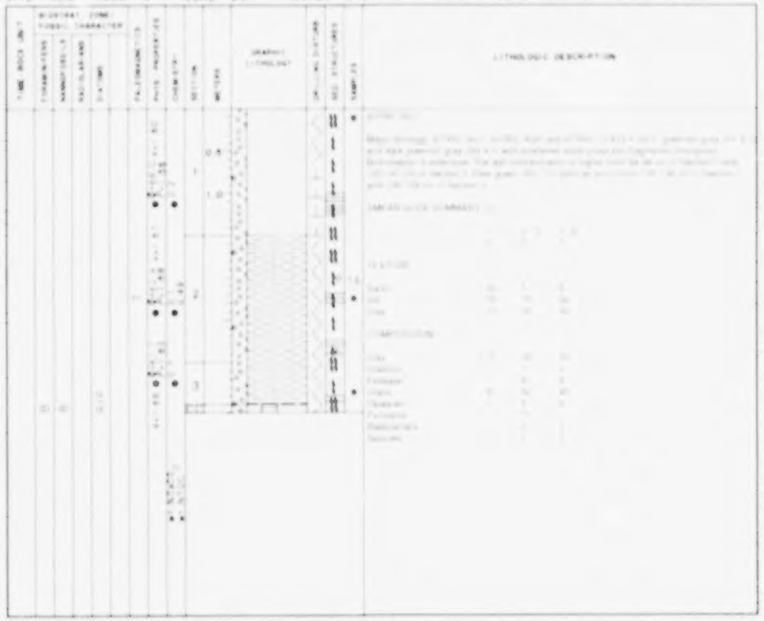
BIOSTRAT. ZONE/ FOSSIL CHARACTER
GRAPHIC LITHOLOGY
LITHOLOGIC DESCRIPTION
0.5
1.0
1
2
3
SMEAR SLIDE SUMMARY (%):
TEXTURE:
Sand
Silt
Clay
COMPOSITION:
Clay
Feldspar
Radiolarians

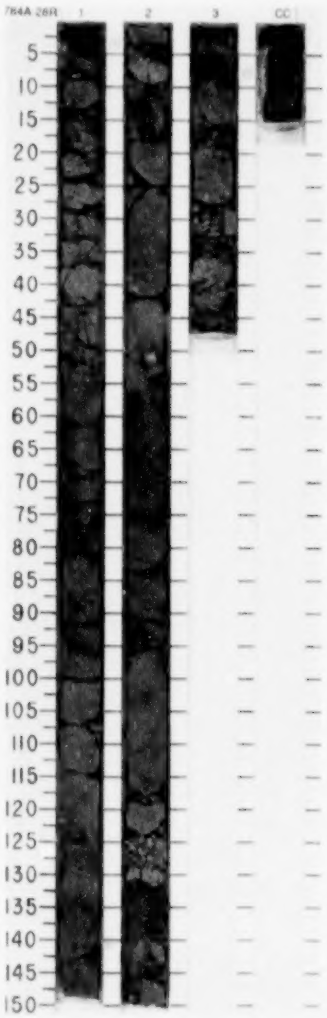
784A 28R
1
2
3
CC
5
10
15
20
25
30
35
40
45
50
55
60
65
70
75
80
85
90
95
100
105
110
115
120
125
130
135
140
145
150

SITE 784 HOLE A CORE 29R CORED INTERVAL 5162.2-5172.2 mbsl; 261.4-271.4 mbsf

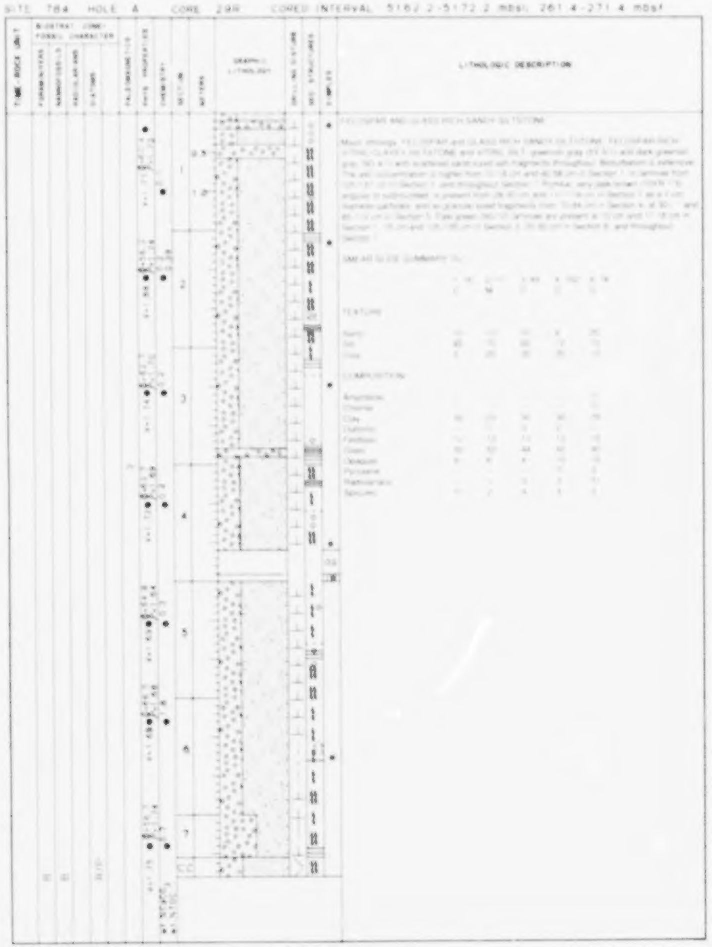
TIME-ROCK UNIT
BIOSTRAT. ZONE/ FOSSIL CHARACTER
FORAMINIFERS
NANNOFOSSILS
RADIOLARIANS
DIATOMS
PALEOMAGNETICS
PHYS. PROPERTIES
CHEMISTRY
SECTION
METERS
GRAPHIC LITHOLOGY
DRILLING DISTURB.
SED. STRUCTURES
SAMPLES
LITHOLOGIC DESCRIPTION
1
2
3
4
5
6
7
CC
0.5
1.0

FELDSPAR AND GLASS-RICH SANDY SILTSTONE

SMEAR SLIDE SUMMARY (%):

TEXTURE:

Sand
Silt
Clay

COMPOSITION:

Amphibole
Chlorite
Clay
Dolomite
Feldspar
Glass
Opaques
Pyroxene
Radiolarians
Spicules

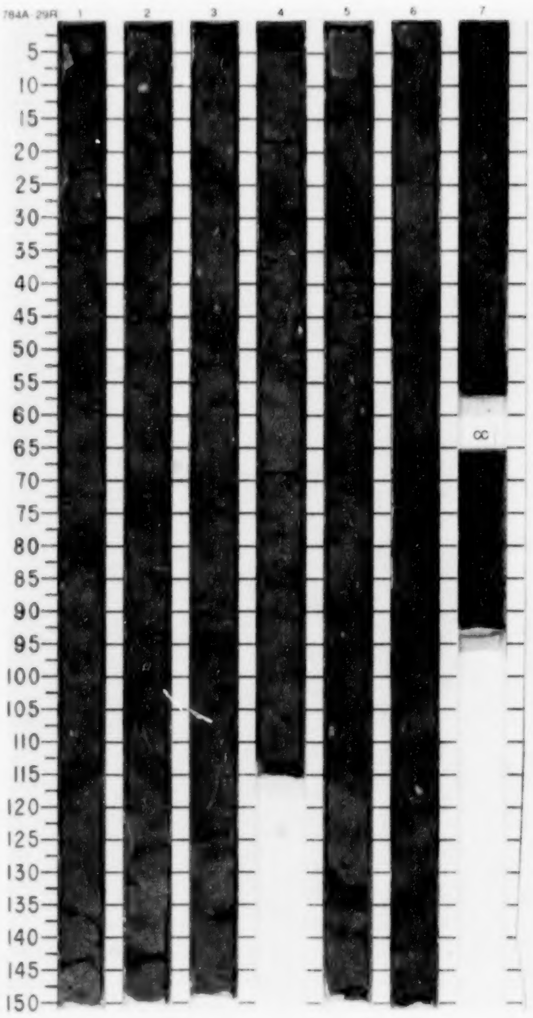
784A 29R
1
2
3
4
5
6
7
CC
5
10
15
20
25
30
35
40
45
50
55
60
65
70
75
80
85
90
95
100
105
110
115
120
125
130
135
140
145
150

SITE 784 HOLE A CORE 30R CORED INTERVAL 5200.8-5181.6 mbsl; 271.4-280.8 mbsf

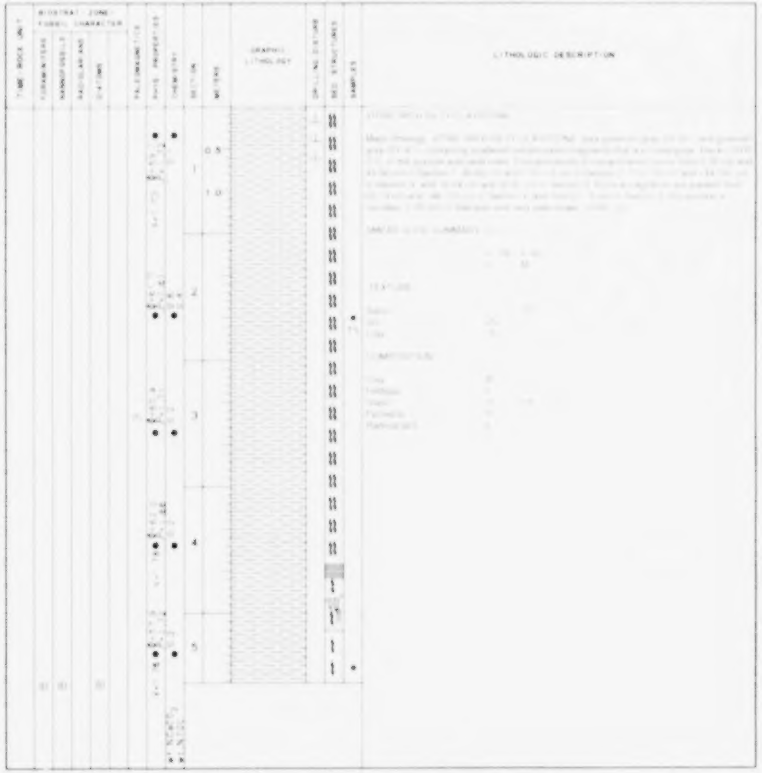
TIME-ROCK UNIT
BIOSTRAT. ZONE/ FOSSIL CHARACTER
FORAMINIFERS
NANNOFOSSILS
RADIOLARIANS
DIATOMS
PALEOMAGNETICS
PHYS. PROPERTIES
CHEMISTRY
SECTION
METERS
GRAPHIC LITHOLOGY
DRILLING DISTURB.
SED. STRUCTURES
SAMPLES
LITHOLOGIC DESCRIPTION
0.5
1.0
1
2
3
4
5
SMEAR SLIDE SUMMARY (%):
TEXTURE:
Sand
Silt
Clay
COMPOSITION:
Clay
Feldspar
Glass
Pyrite
Radiolarians

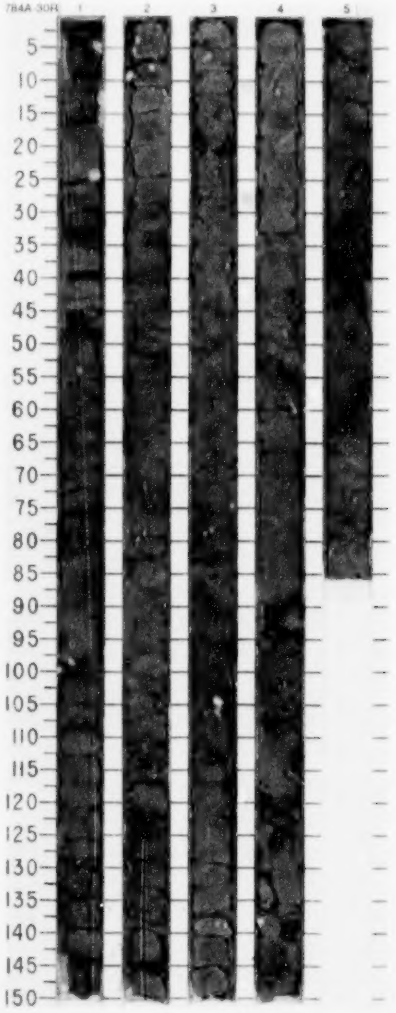
784A-30R
1
2
3
4
5
5
10
15
20
25
30
35
40
45
50
55
60
65
70
75
80
85
90
95
100
105
110
115
120
125
130
135
140
145
150

SITE 784 HOLE A CORE 31R CORED INTERVAL 5181.6-5191.2 mbsl; 280.8-290.4 mbsf

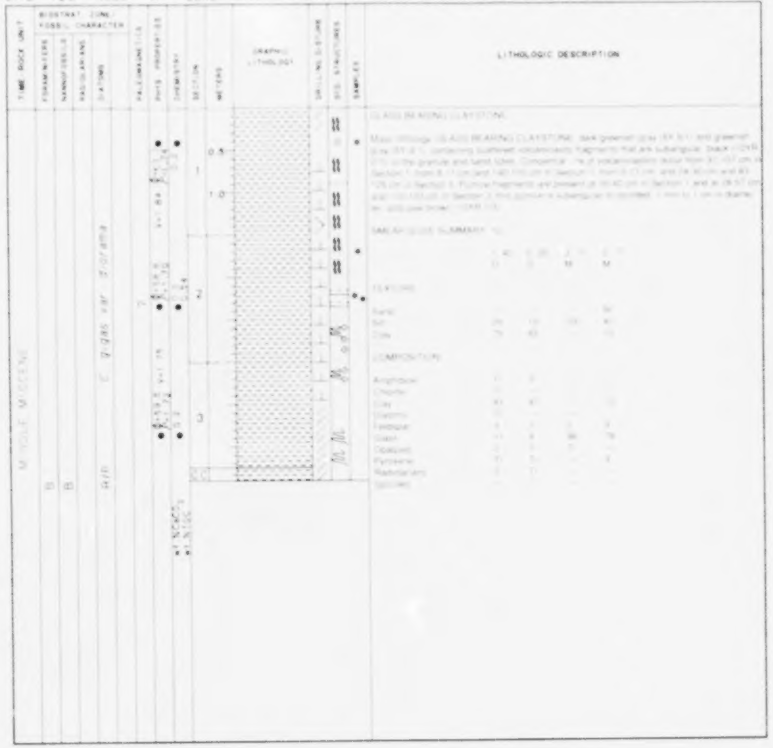

LITHOLOGIC DESCRIPTION

GLASS-BEARING CLAYSTONE

[illegible]

SMEAR SLIDE SUMMARY (%):

	1, 40	2, 20	2, [illegible]	3, [illegible]
	D	D	M	M
TEXTURE:				
Sand	—	—	—	[illegible]
Silt	25	15	[illegible]	40
Clay	75	85	—	[illegible]
COMPOSITION:				
Amphibole	[illegible]	[illegible]	—	—
Chlorite	[illegible]	—	—	—
Clay	[illegible]	[illegible]	—	[illegible]
Diatoms	[illegible]	—	—	—
Feldspar	[illegible]	[illegible]	[illegible]	[illegible]
Glass	[illegible]	[illegible]	[illegible]	[illegible]
Opaques	[illegible]	[illegible]	[illegible]	—
Pyroxene	[illegible]	[illegible]	—	[illegible]
Radiolarians	[illegible]	[illegible]	—	—
Spicules	—	—	—	—

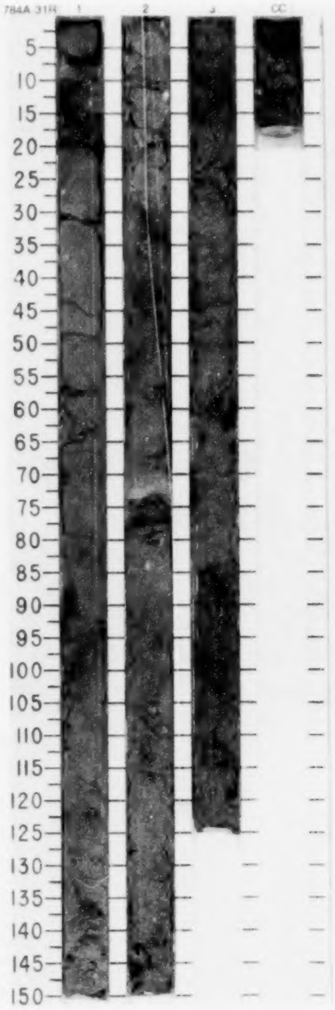
784A 31R
1
2
3
CC
5
10
15
20
25
30
35
40
45
50
55
60
65
70
75
80
85
90
95
100
105
110
115
120
125
130
135
140
145
150

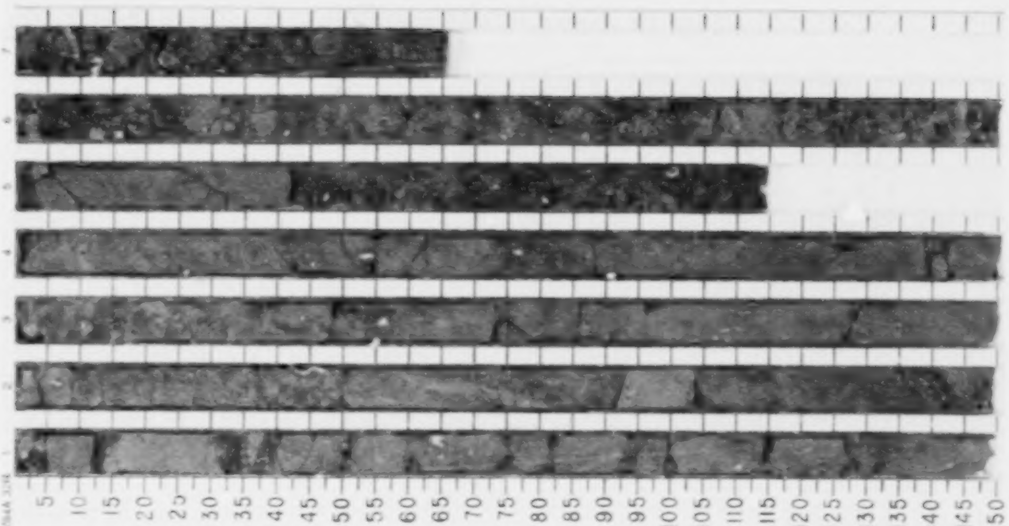
784A 32R
1
2
3
4
5
6
7
5
10
15
20
25
30
35
40
45
50
55
60
65
70
75
80
85
90
95
100
105
110
115
120
125
130
135
140
145
150

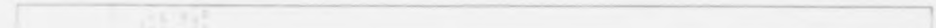

SITE 784 HOLE A CORE 33R CORED INTERVAL 5200.8-5210.5 mbsl; 300.0-309.7 mbsf

GRAPHIC LITHOLOGY
LITHOLOGIC DESCRIPTION

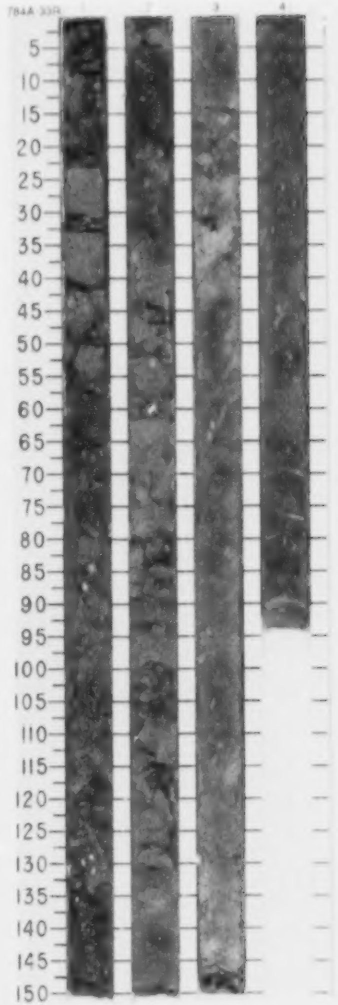
784A 33R
1
2
3
4
5
10
15
20
25
30
35
40
45
50
55
60
65
70
75
80
85
90
95
100
105
110
115
120
125
130
135
140
145
150

SITE 784 HOLE A CORE 34R CORED INTERVAL 5210.5-5220.1 mbsl; 309.7-319.3 mbsf

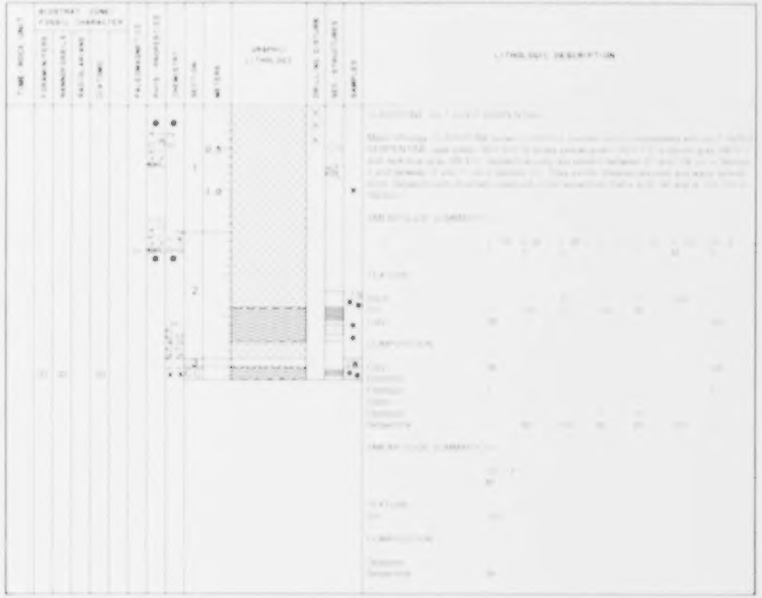
TIME-ROCK UNIT
BIOSTRAT. ZONE/ FOSSIL CHARACTER
FORAMINIFERS
NANNOFOSSILS
RADIOLARIANS
DIATOMS
PALEOMAGNETICS
PHYS. PROPERTIES
CHEMISTRY
SECTION
METERS
GRAPHIC LITHOLOGY
DRILLING DISTURB.
SED. STRUCTURES
SAMPLES
LITHOLOGIC DESCRIPTION
0.5
1.0
1
2

[illegible]

SMEAR SLIDE SUMMARY

TEXTURE:

COMPOSITION:

SMEAR SLIDE SUMMARY

TEXTURE:

COMPOSITION:

Serpentine

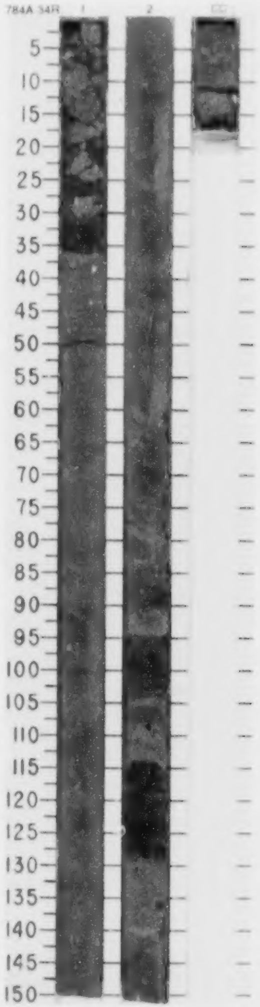
784A 34R
1
2
CC
5
10
15
20
25
30
35
40
45
50
55
60
65
70
75
80
85
90
95
100
105
110
115
120
125
130
135
140
145
150

SITE 784 HOLE A CORE 35R CORED INTERVAL 5220.1-5229.8 mbsl; 319.3-329.0 mbsf

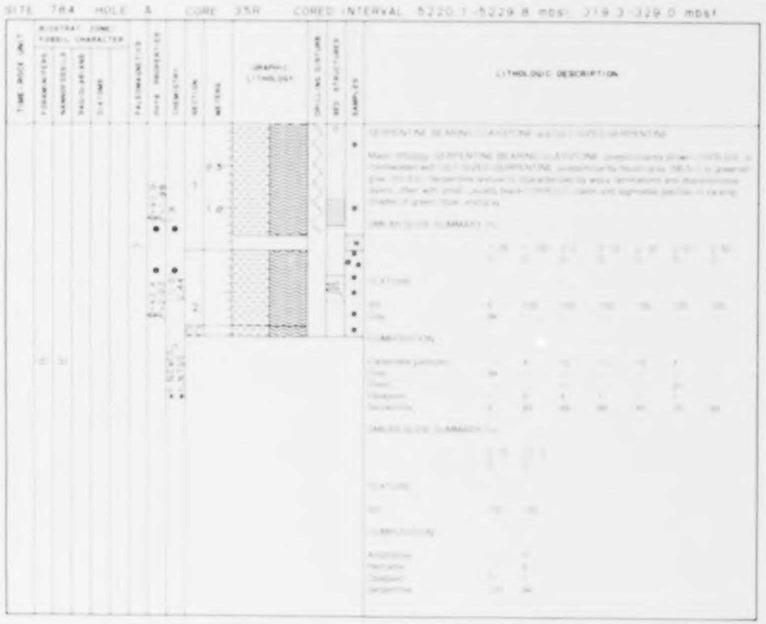
TIME-ROCK UNIT
BIOSTRAT. ZONE/FOSSIL CHARACTER
FORAMINIFERS
NANNOFOSSILS
RADIOLARIANS
DIATOMS
PALEOMAGNETICS
PHYS. PROPERTIES
CHEMISTRY
SECTION
METERS
GRAPHIC LITHOLOGY
DRILLING DISTURB.
SED. STRUCTURES
SAMPLES
LITHOLOGIC DESCRIPTION
0.5
1.0
1
2
CC

SERPENTINE BEARING CLAYSTONE and SILT SIZED SERPENTINE

Major lithology: SERPENTINE BEARING CLAYSTONE, predominantly brown [illegible] interbedded with SILT SIZED SERPENTINE, predominantly [illegible] gray [illegible] to greenish gray [illegible]. Serpentine texture is characterized by wispy laminations and discontinuous layers, often with small, usually black [illegible] clasts and aggregated patches in varying shades of green, blue and gray.

SMEAR SLIDE SUMMARY (%):

TEXTURE:

COMPOSITION:

SMEAR SLIDE SUMMARY (%):

TEXTURE:

COMPOSITION:

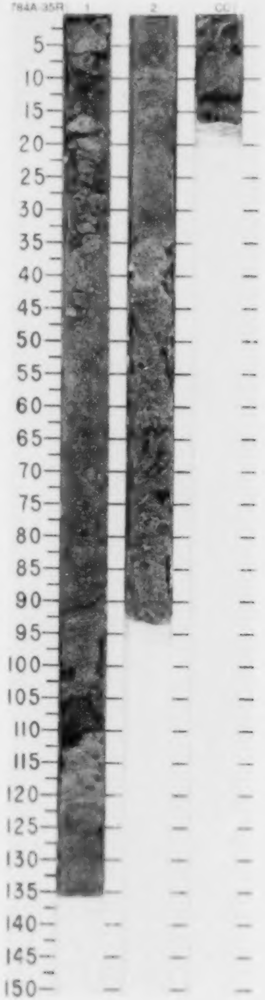
784A-35R
1
2
CC
5
10
15
20
25
30
35
40
45
50
55
60
65
70
75
80
85
90
95
100
105
110
115
120
125
130
135
140
145
150

SITE 784 HOLE A CORE 36R CORED INTERVAL 5229.8-5239.5 mbsl; 329.0-338.7 mbsf

TIME-ROCK UNIT	BIOSTRAT. ZONE/FOSSIL CHARACTER: FORAMINIFERS	NANNOFOSSILS	RADIOLARIANS	DIATOMS	PALEOMAGNETICS	PHYS. PROPERTIES	CHEMISTRY	SECTION	METERS	GRAPHIC LITHOLOGY	DRILLING DISTURB.	SED. STRUCTURES	SAMPLES	LITHOLOGIC DESCRIPTION
						●	●	1	0.5				●	[illegible]
						●		CC	1.0				●	SMEAR SLIDE SUMMARY (%):
													●	TEXTURE: [illegible]
														COMPOSITION: [illegible]

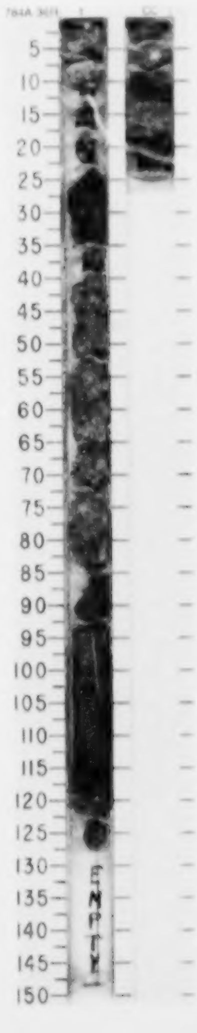
784A 36R
1
CC
5
10
15
20
25
30
35
40
45
50
55
60
65
70
75
80
85
90
95
100
105
110
115
120
125
130
135
140
145
150
EMPTY

SITE 784 HOLE A CORE 37R CORED INTERVAL 5239.5-5249.1 mbsl; 338.7-348.3 mbsf

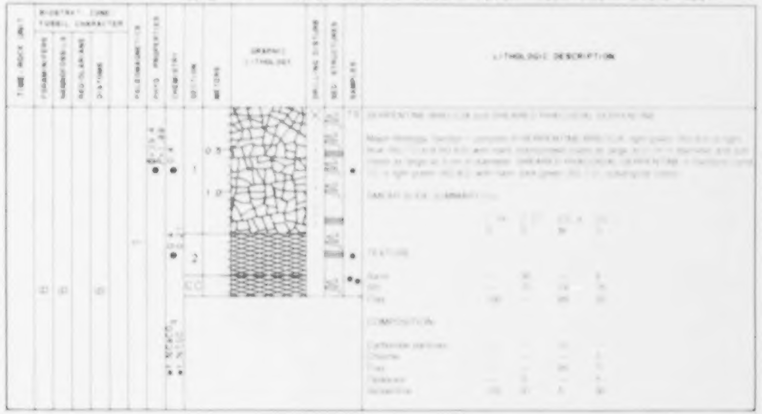
TIME-ROCK UNIT
BIOSTRAT. ZONE/FOSSIL CHARACTER
FORAMINIFERS
NANNOFOSSILS
RADIOLARIANS
DIATOMS
PALEOMAGNETICS
PHYS. PROPERTIES
CHEMISTRY
SECTION
METERS
GRAPHIC LITHOLOGY
DRILLING DISTURB.
SED. STRUCTURES
SAMPLES
0.5
1.0
1
2
CC
TS

LITHOLOGIC DESCRIPTION

SERPENTINE BRECCIA and SHEARED PHACOIDAL SERPENTINE

Major lithology: Section 1 consists of SERPENTINE BRECCIA, light green [illegible]

SMEAR SLIDE SUMMARY (%):

TEXTURE:

Sand
Silt
Clay

COMPOSITION:

Carbonate particles
Chlorite
Clay
Opaques
Serpentine

SITE 784 HOLE A CORE 38R CORED INTERVAL 5249.1-5258.7 mbsl; 348.3-357.9 mbsf

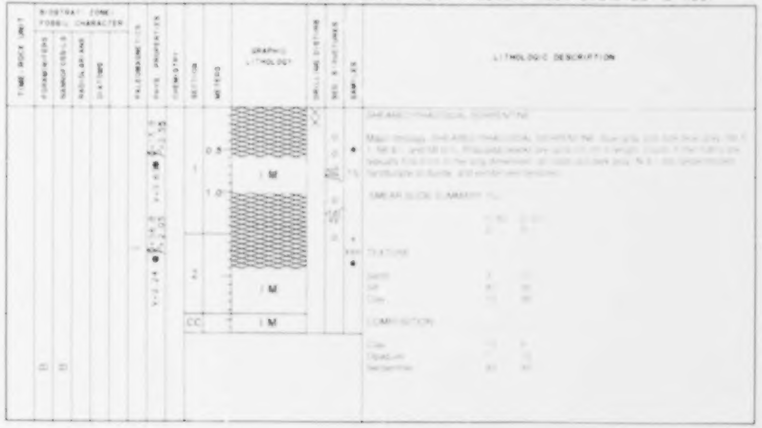
TIME-ROCK UNIT
BIOSTRAT. ZONE/FOSSIL CHARACTER
FORAMINIFERS
NANNOFOSSILS
RADIOLARIANS
DIATOMS
PALEOMAGNETICS
PHYS. PROPERTIES
CHEMISTRY
SECTION
METERS
GRAPHIC LITHOLOGY
DRILLING DISTURB.
SED. STRUCTURES
SAMPLES
0.5
1.0
1
2
CC
I M
I M
I M
TS

LITHOLOGIC DESCRIPTION

SHEARED PHACOIDAL SERPENTINE

Major lithology: SHEARED PHACOIDAL SERPENTINE, [illegible]

SMEAR SLIDE SUMMARY (%):

TEXTURE:

Sand
Silt
Clay

COMPOSITION:

Clay
Opaques
Serpentine

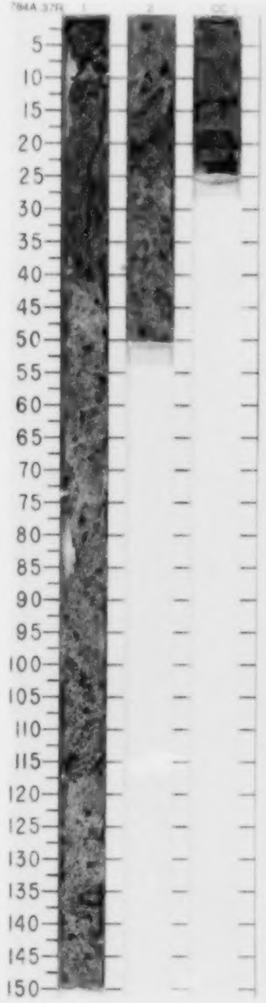
784A-37R
1
2
CC
5
10
15
20
25
30
35
40
45
50
55
60
65
70
75
80
85
90
95
100
105
110
115
120
125
130
135
140
145
150

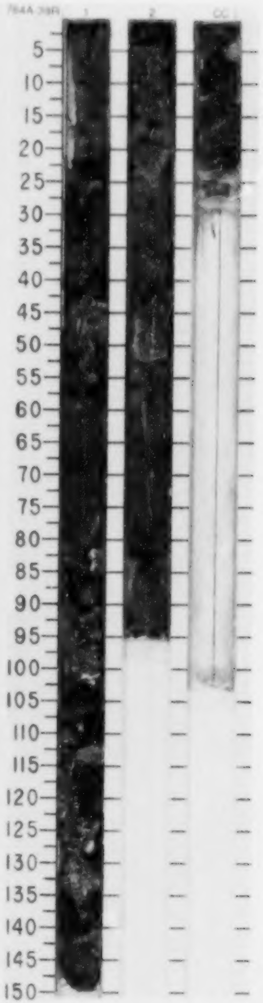
784A-38R
1
2
CC
5
10
15
20
25
30
35
40
45
50
55
60
65
70
75
80
85
90
95
100
105
110
115
120
125
130
135
140
145
150

SITE 784 HOLE A CORE 39R CORED INTERVAL 5258.7-5268.3 mbsl; 357.9-367.5 mbsf

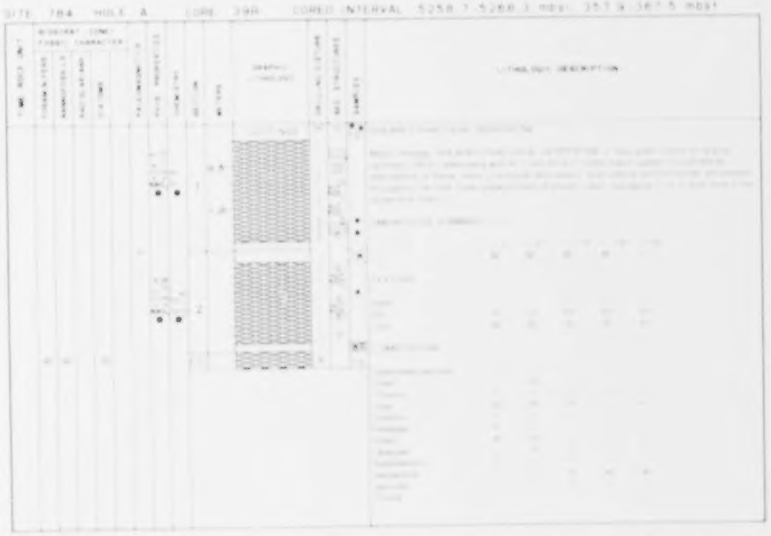
TIME-ROCK UNIT
BIOSTRAT. ZONE/FOSSIL CHARACTER
FORAMINIFERS
NANNOFOSSILS
RADIOLARIANS
DIATOMS
PALEOMAGNETICS
PHYS. PROPERTIES
CHEMISTRY
SECTION
METERS
GRAPHIC LITHOLOGY
DRILLING DISTURB.
SED. STRUCTURES
SAMPLES
LITHOLOGIC DESCRIPTION

SITE 784 HOLE A CORE 40R CORED INTERVAL 5268.3-5278.1 mbsl; 367.5-377.3 mbsf

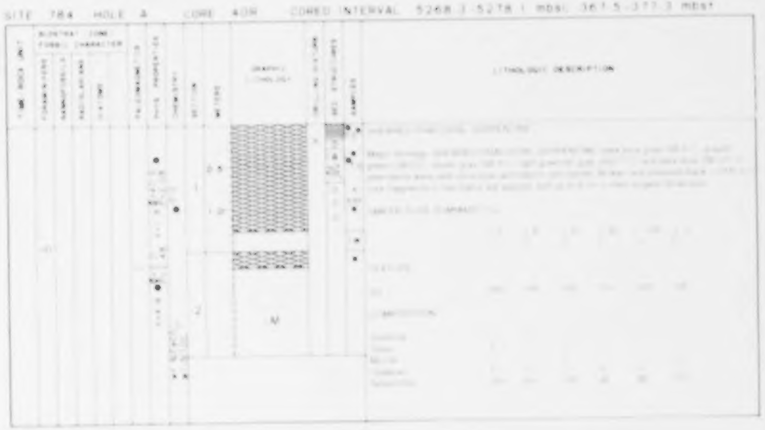
TIME-ROCK UNIT
BIOSTRAT. ZONE/FOSSIL CHARACTER
FORAMINIFERS
NANNOFOSSILS
RADIOLARIANS
DIATOMS
PALEOMAGNETICS
PHYS. PROPERTIES
CHEMISTRY
SECTION
METERS
GRAPHIC LITHOLOGY
DRILLING DISTURB.
SED. STRUCTURES
SAMPLES
LITHOLOGIC DESCRIPTION

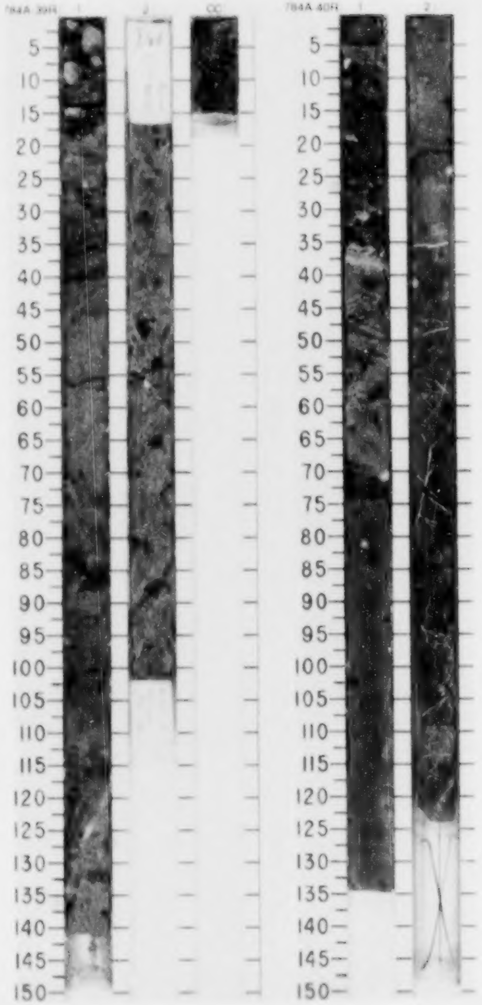
784A-39R
1
2
CC
784A-40R
1
2
5
10
15
20
25
30
35
40
45
50
55
60
65
70
75
80
85
90
95
100
105
110
115
120
125
130
135
140
145
150

SITE 784 HOLE A CORE 41R CORED INTERVAL 5278.1-5287.7 mbsl; 377.3-386.9 mbsf

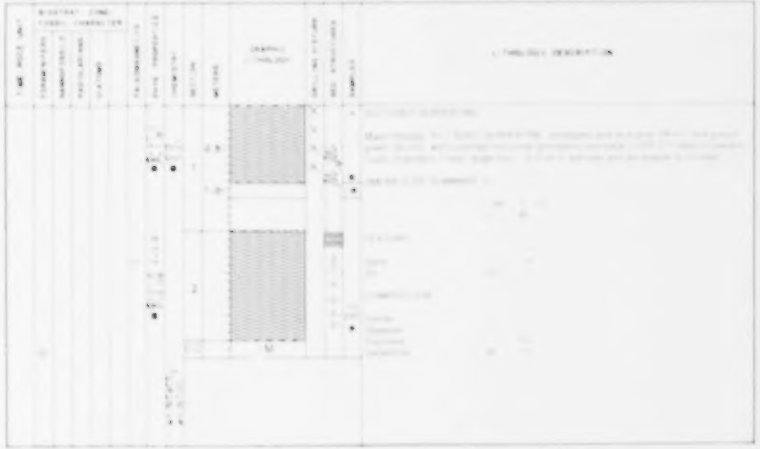
TIME-ROCK UNIT
BIOSTRAT. ZONE/ FOSSIL CHARACTER
FORAMINIFERS
NANNOFOSSILS
RADIOLARIANS
DIATOMS
PALEOMAGNETICS
PHYS. PROPERTIES
CHEMISTRY
SECTION
METERS
GRAPHIC LITHOLOGY
DRILLING DISTURB.
SED. STRUCTURES
SAMPLES
LITHOLOGIC DESCRIPTION
0.5
1.0
1
2
M

SITE 784 HOLE A CORE 42R CORED INTERVAL 5287.7-5297.4 mbsl; 386.9-396.6 mbsf

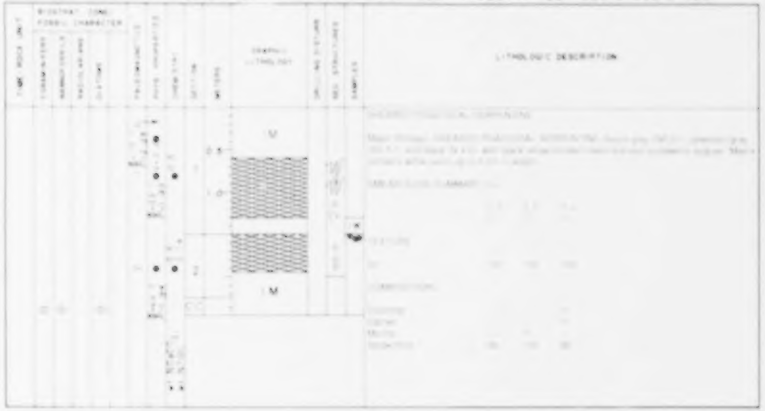
TIME-ROCK UNIT
BIOSTRAT. ZONE/ FOSSIL CHARACTER
FORAMINIFERS
NANNOFOSSILS
RADIOLARIANS
DIATOMS
PALEOMAGNETICS
PHYS. PROPERTIES
CHEMISTRY
SECTION
METERS
GRAPHIC LITHOLOGY
DRILLING DISTURB.
SED. STRUCTURES
SAMPLES
LITHOLOGIC DESCRIPTION
M
0.5
1.0
1
2
M

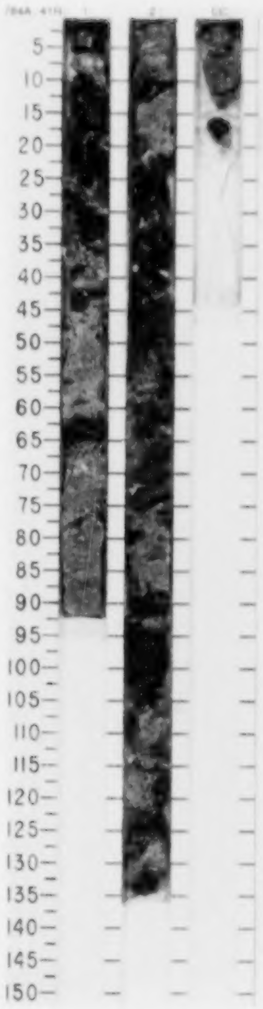
784A-41R
1
2
CC
5
10
15
20
25
30
35
40
45
50
55
60
65
70
75
80
85
90
95
100
105
110
115
120
125
130
135
140
145
150

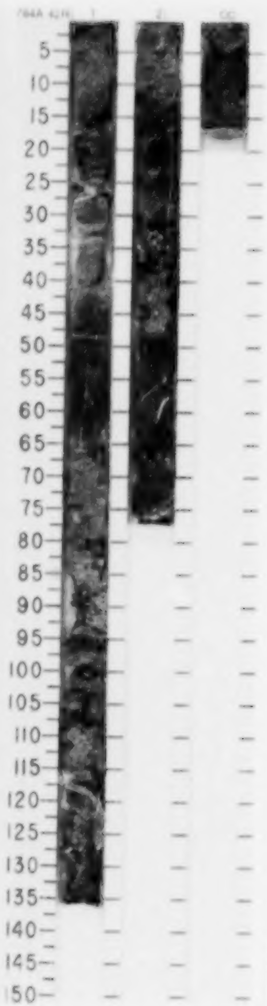
784A-42R
1
2
CC
5
10
15
20
25
30
35
40
45
50
55
60
65
70
75
80
85
90
95
100
105
110
115
120
125
130
135
140
145
150

SITE 784 HOLE A CORE 43R CORED INTERVAL 5297.4-5307.1 mbsl; 396.6-406.3 mbsf

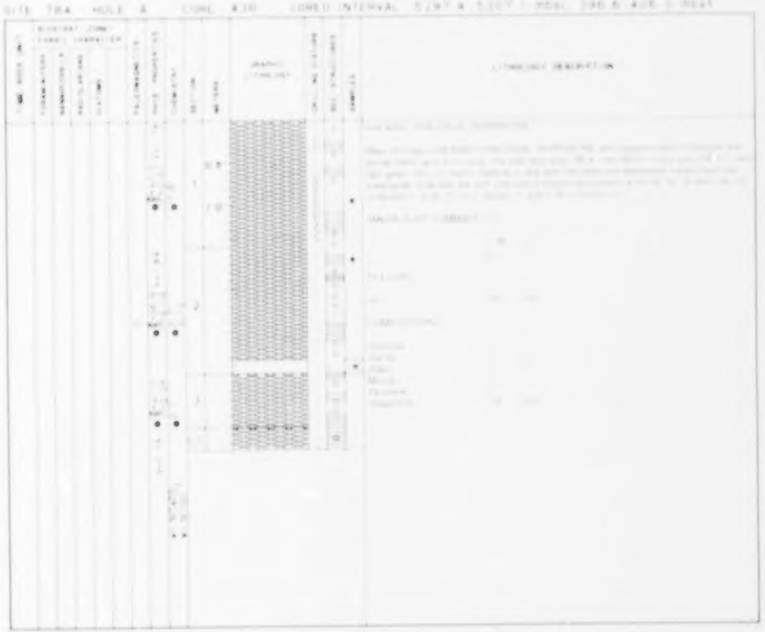
BIOSTRAT. ZONE/ FOSSIL CHARACTER
GRAPHIC LITHOLOGY
LITHOLOGIC DESCRIPTION
SECTION
METERS
SAMPLES

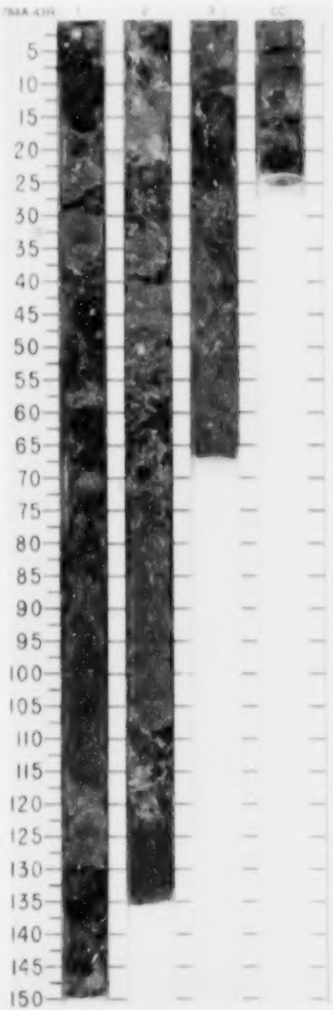
784A-43R
1
2
3
CC
5
10
15
20
25
30
35
40
45
50
55
60
65
70
75
80
85
90
95
100
105
110
115
120
125
130
135
140
145
150

SITE 784 HOLE A CORE 44R CORED INTERVAL 5307.1-5316.4 mbsl; 406.3-415.6 mbsf

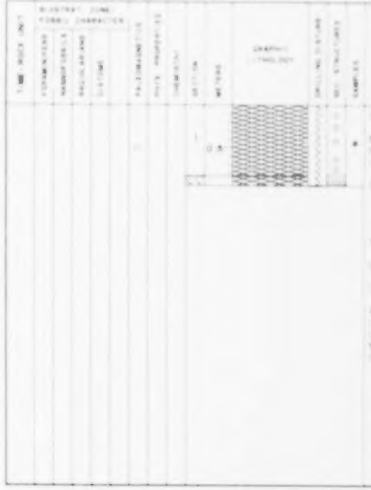
TIME-ROCK UNIT
BIOSTRAT. ZONE/ FOSSIL CHARACTER
FORAMINIFERS
NANNOFOSSILS
RADIOLARIANS
DIATOMS
PALEOMAGNETICS
PHYS. PROPERTIES
CHEMISTRY
SECTION
METERS
GRAPHIC LITHOLOGY
DRILLING DISTURB.
SED. STRUCTURES
SAMPLES
1
0.5
CC

LITHOLOGIC DESCRIPTION

SHEARED PHACOIDAL SERPENTINE

Major lithology: SHEARED PHACOIDAL SERPENTINE, light green (5G 6/2), bluish gray (5B 6/1), and dark bluish gray (5B 4/1 and 5B 5/1). The core contains serpentinized clasts up to [illegible] cm in length. [illegible] dolomite and aragonite are present in the matrix material.

SMEAR SLIDE SUMMARY (%):

	1, 46
	D
TEXTURE:	
Silt	100
COMPOSITION:	
Apatite	—
Dolomite	Tr
Glass	Tr
Micrite	Tr
Serpentine	100

SITE 784 HOLE A CORE 45R CORED INTERVAL 5316.4-5326.1 mbsl; 415.6-425.3 mbsf

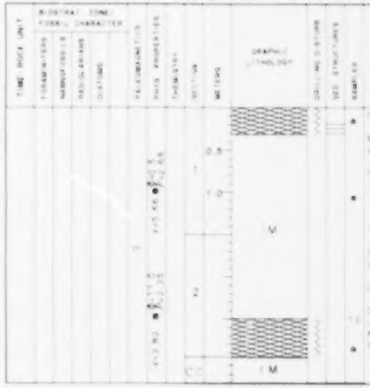
TIME-ROCK UNIT
BIOSTRAT. ZONE/ FOSSIL CHARACTER
FORAMINIFERS
NANNOFOSSILS
RADIOLARIANS
DIATOMS
PALEOMAGNETICS
PHYS. PROPERTIES
CHEMISTRY
SECTION
METERS
GRAPHIC LITHOLOGY
DRILLING DISTURB.
SED. STRUCTURES
SAMPLES
1
2
CC
0.5
1.0
IM
TS

LITHOLOGIC DESCRIPTION

PHACOIDAL SHEARED SERPENTINE

Major lithology: PHACOIDAL SHEARED SERPENTINE, dark blue gray (5B 4/1 and 5B 5/1) and light green (5G 7/2) interbedded with serpentinized ultramafic clasts.

SMEAR SLIDE SUMMARY (%):

	1, 111	2, 109	2, 134
	D	M	D
TEXTURE:			
Sand	—	30	—
Silt	100	70	100
COMPOSITION:			
Dolomite	Tr	Tr	Tr
Garnet	Tr	Tr	—
Micrite	Tr	Tr	—
Serpentine	100	100	99

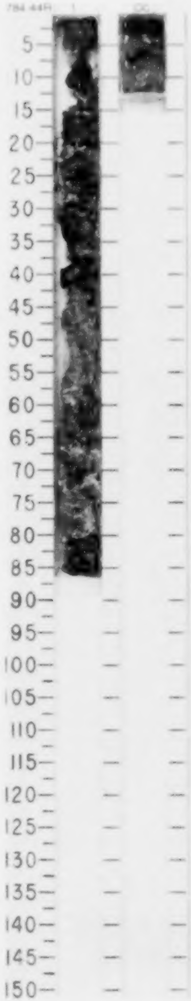
784-44R
1
CC
5
10
15
20
25
30
35
40
45
50
55
60
65
70
75
80
85
90
95
100
105
110
115
120
125
130
135
140
145
150

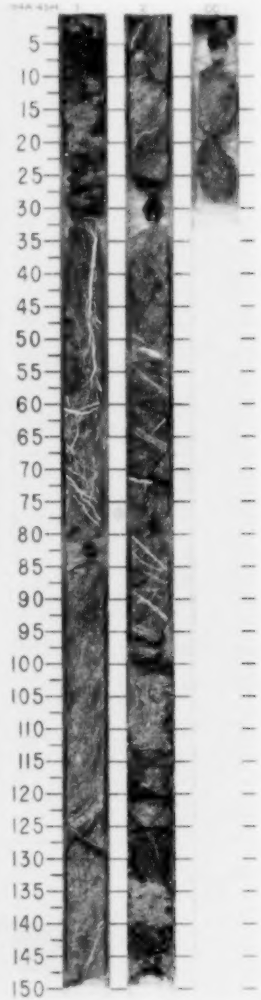
784-45R
1
2
CC
5
10
15
20
25
30
35
40
45
50
55
60
65
70
75
80
85
90
95
100
105
110
115
120
125
130
135
140
145
150

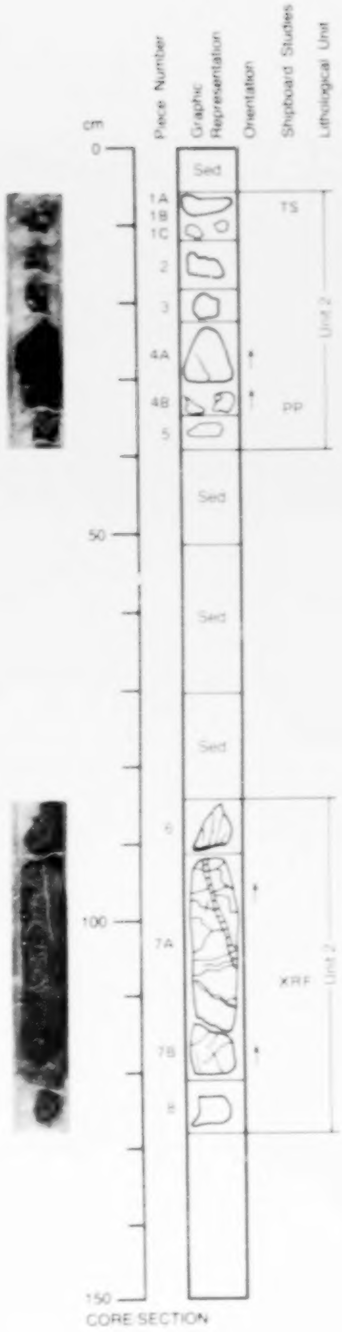
cm
0
50
100
150
CORE SECTION
Piece Number
Graphic Representation
Orientation
Shipboard Studies
Lithological Unit
Sed
1A
1B
1C
2
3
4A
4B
5
6
7A
7B
8
TS
PP
XRF
Unit 2
Unit 2

125-784A-36R-1

UNIT 2: CALCAREOUS SILTSTONE

Pieces 1A; 1B; 1C

COLOR: Light brownish gray (10YR 6/2).
LAYERING: Piece 1A shows 5-mm-wide lamination consisting of dark gray (10YR 4/1) material.
DEFORMATION: None visible.
PRIMARY MINERALOGY: No primary mineralogy is visible.
SECONDARY MINERALOGY:
Calcite (<1 mm) 40-60%; quartz (?) (<1 mm) 40-60%; opaque minerals (<2 mm) <2%.
Total percent: 100%.
Texture: Grain supported.
Vein material: None visible.
ADDITIONAL COMMENTS: This is a sedimentary rock whose mineralogy is difficult to see in hand sample. Piece 1A has lamination which probably represents bedding.

UNIT 2: SERPENTINIZED HARZBURGITE

Pieces 2, 3, 8

COLOR: Black (7.5YR 2/0).
LAYERING: None visible.
DEFORMATION: None visible.
PRIMARY MINERALOGY:
Primary silicates are variably serpentinized.
Olivine - Mode: 70-75%.
Crystal size: Not visible.
Crystal shape: Not visible.
Crystal orientation: None visible.
Percent replacement: 80-90.

Orthopyroxene - Mode: 20-25%.
Crystal size: 1-4 mm.
Crystal shape: Subhedral.
Crystal orientation: None visible.
Percent replacement: 50-70.

Clinopyroxene - Mode: 2-5%.
Crystal size: 1-2 mm.
Crystal shape: Subhedral.
Crystal orientation: None visible.
Percent replacement: 20-30.
Comments: Appears fresher than orthopyroxenes.

Spinel - Mode: Trace.
Crystal size: <1 mm.
Crystal shape: Ragged.
Crystal orientation: None visible.
Percent replacement: 0.
SECONDARY MINERALOGY:
Serpentine.
Total percent: 70-80%.
Texture: Bastite and mesh textures in areas.
Vein material: Piece 3 has <0.1-mm-wide white veins.

125-784A-36R-1 (continued)

UNIT 2: SERPENTINIZED HARZBURGITE

Pieces 4A; 4B; 6; 7A; 7B

COLOR: Dark greenish gray to dark gray (5BG 4/1 - N 4/).
LAYERING: None visible.
DEFORMATION: Abundant fracturing and veining throughout rock.
PRIMARY MINERALOGY:
Primary silicates are variably serpentinized.
Olivine - Mode: 75-85%.
Crystal size: 1-2 mm.
Crystal shape: Anhedral.
Crystal orientation: None visible.
Percent replacement: 80-90.

Orthopyroxene - Mode: 15-25%.
Crystal size: 1-4 mm.
Crystal shape: Subhedral.
Crystal orientation: None visible.
Percent replacement: 80-90.

Spinel - Mode: <1%.
Crystal size: <1 mm.
Crystal shape: Subhedral-ragged.
Crystal orientation: None visible.
Percent replacement: 0.
SECONDARY MINERALOGY:
Serpentine.
Total percent: 80-90%.
Texture: Mesh and bastite pseudomorphs after olivine and orthopyroxene.
Vein material: Abundant veins (0.5 mm-3 mm wide) throughout rocks. Piece 7A has large 3-m wide chrysotile (?) vein oriented 30 degrees from core barrel. Smaller serpentine veins cross it at a large angle (70-90 degrees).

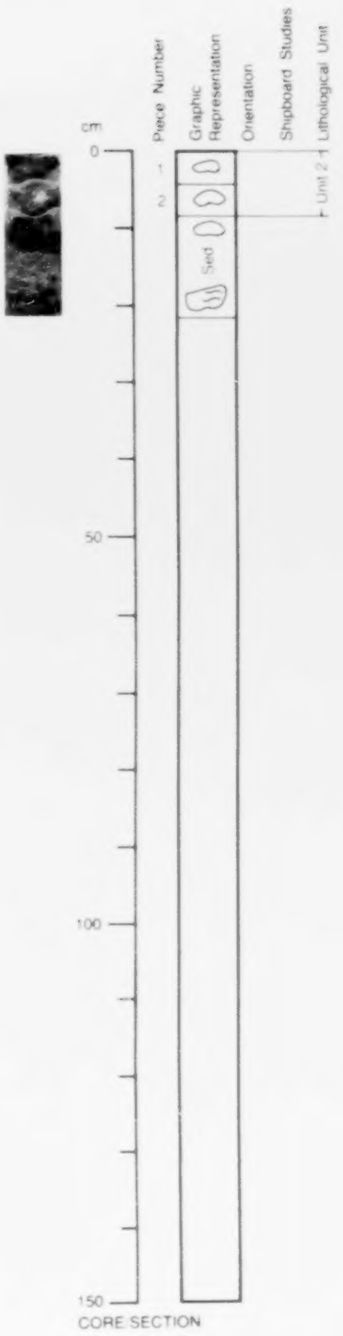
cm
Piece Number
Graphic Representation
Orientation
Shipboard Studies
Lithological Unit
0
1
2
Unit 2
Sed
50
100
150
CORE SECTION

125-784A-36R-CC

UNIT 2: SERPENTINIZED HARZBURGITE

Pieces 1 and 2

COLOR: Black (7.5YR 2/0)
LAYERING: None visible
DEFORMATION: None visible
PRIMARY MINERALOGY:
Primary silicates are variably serpentinized
Olivine : Mode: 70-75%
Crystal size: Not visible
Crystal shape: Not visible
Crystal orientation: None visible
Percent replacement: 80-90

Orthopyroxene : Mode: 25-30%
Crystal size: 1-4 mm
Crystal shape: Subhedral
Crystal orientation: None visible
Percent replacement: 50-70

Spinel : Mode: Trace
Crystal size: <1 mm
Crystal shape: Ragged
Crystal orientation: None visible
Percent replacement: 0
SECONDARY MINERALOGY:
Serpentine
Total percent: 70-80%
Texture: Mesh and bastite serpentine pseudomorphs after olivine and orthopyroxene
Vein material: None visible
ADDITIONAL COMMENTS: There are larger clasts (3-4 cm) of serpentinized harzburgites distributed in lower portion of core catcher within the phacodial serpentine.

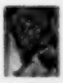

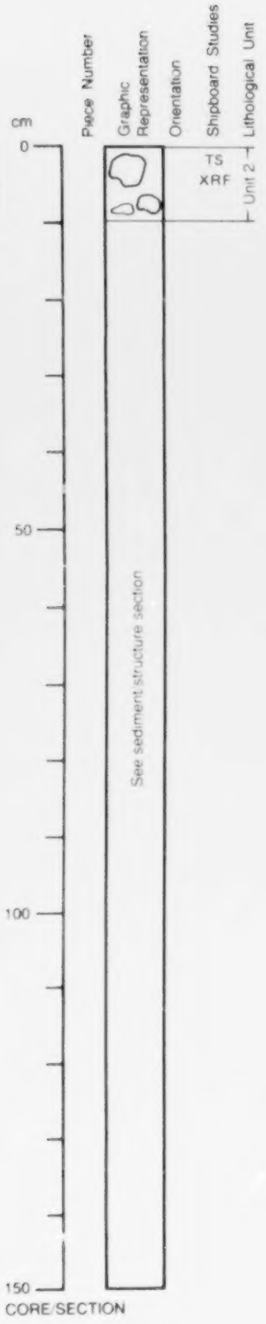
cm
Piece Number
Graphic Representation
Orientation
Shipboard Studies
Lithological Unit
0
50
100
150
CORE/SECTION
TS
XRF
Unit 2
See sediment structure section

125-784A-37R-1

UNIT 2: SERPENTINIZED HARZBURGITE

Pieces multiple fragments

COLOR: Black (7.5YR 2/0)
LAYERING: None visible
DEFORMATION: None visible
PRIMARY MINERALOGY:
Primary silicates are variably serpentinized
Olivine - Mode: 70-80%
Crystal size: Not visible
Crystal shape: Not visible
Crystal orientation: None visible
Percent replacement: 80-90

Orthopyroxene - Mode: 20-30%
Crystal size: 1-4 mm
Crystal shape: Subhedral
Crystal orientation: None visible
Percent replacement: 50-70

Clinopyroxene - Mode: Trace
Crystal size: 0.5-1 mm
Crystal shape: Subhedral
Crystal orientation: None visible
Percent replacement: 40-50

Spinel - Mode: Trace
Crystal size: <2 mm
Crystal shape: Ragged
Crystal orientation: None visible
Percent replacement: 0
SECONDARY MINERALOGY:
Serpentine
Total percent: 70-80%
Texture: Mesh and bastite serpentine pseudomorphs after olivine and orthopyroxene.
Vein material: Small (<0.5 mm wide) white green veins cutting rock at no particular orientation.

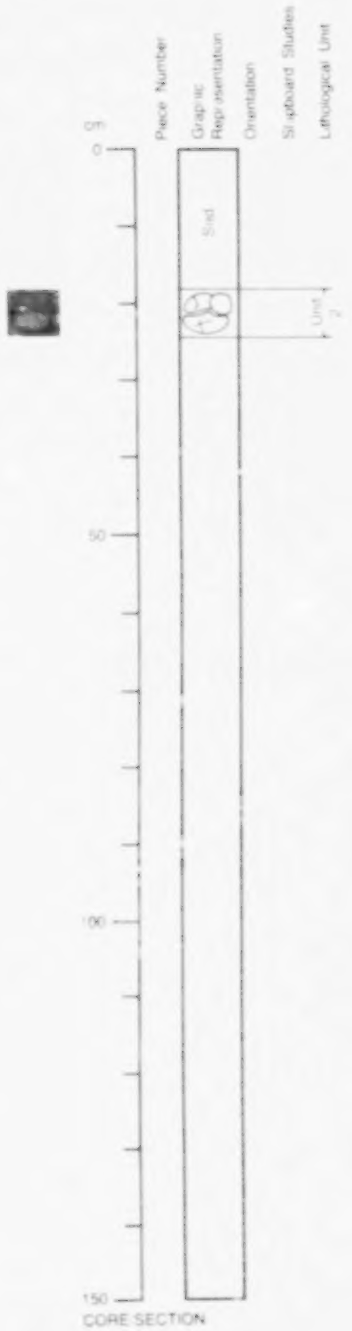
cm
Piece Number
Graphic Representation
Orientation
Shipboard Studies
Lithological Unit
0
50
100
150
Std
Unit 2
CORE SECTION

125-784A-37R-CC

UNIT 2: SERPENTINIZED HARZBURGITE

Pieces large clast

COLOR: Dark greenish gray to dark gray (5BG 4/1 - N 4)
LAYERING: None visible
DEFORMATION: Clast is severely fractured
PRIMARY MINERALOGY: Primary silicates are largely serpentinized
  Olivine - Mode: 85-90%
  Crystal size: Not visible
  Crystal shape: Not visible
  Crystal orientation: None visible
  Percent replacement: 90-95

  Orthopyroxene - Mode: 10-15%
  Crystal size: 1-3 mm
  Crystal shape: Equant
  Crystal orientation: None visible
  Percent replacement: 80-90

  Spinel - Mode: Trace
  Crystal size: <1 mm
  Crystal shape: Ragged
  Crystal orientation: None visible
  Percent replacement: 0
SECONDARY MINERALOGY
  Serpentine:
  Total percent: 80-90%
  Texture: Patches of serpentine bastite pseudomorphs
  Vein material: Small white veins (<1 mm wide) are oriented approximately 90 degrees to each other.

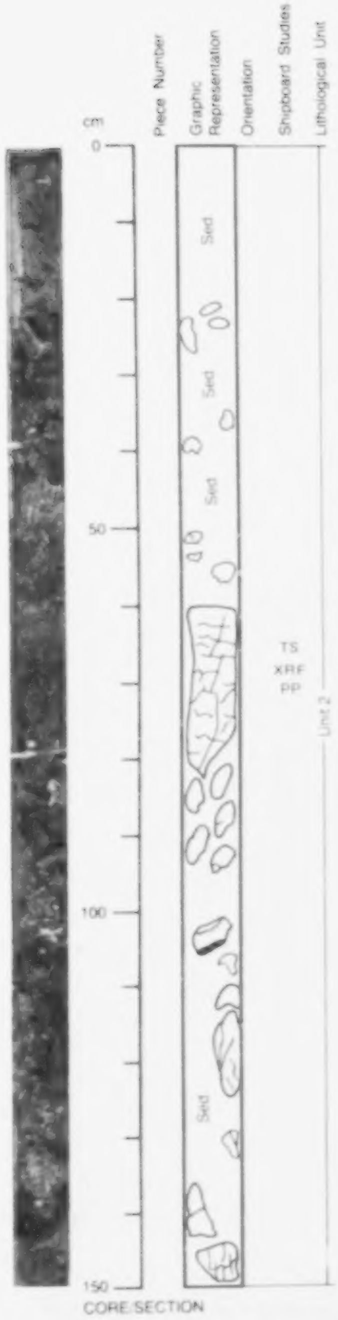
cm
Piece Number
Graphic Representation
Orientation
Shipboard Studies
Lithological Unit
0
50
100
150
Sed
Sed
Sed
Sed
TS
XRF
PP
Unit 2
CORE/SECTION

125-784A-38R-1

UNIT 2: SERPENTINIZED HARZBURGITE

Pieces multiple pieces

COLOR: Dark greenish gray to dark gray (5BG 4/1 - N 4)
LAYERING: None visible
DEFORMATION: Some clasts show abundant fracturing and veining
PRIMARY MINERALOGY:
Primary silicates are variably altered to serpentine
Olivine - Mode: 80-90%
Crystal size: Not visible
Crystal shape: Not visible
Crystal orientation: None visible
Percent replacement: 80-95

Orthopyroxene - Mode: 10-20%
Crystal size: 1-4 mm
Crystal shape: Equant to elongate
Crystal orientation: None visible
Percent replacement: 80-95

Spinel - Mode: Trace
Crystal size: <1 mm
Crystal shape: Equant to ragged
Crystal orientation: None visible
Percent replacement: 0
SECONDARY MINERALOGY:
Serpentine:
Total percent: 80-95%
Texture: Patches of serpentine bastite pseudomorphs.
Vein material: Large fragment has 2 mm wide black-green serpentine vein paralleling core barrel. This vein is crosscut perpendicularly by smaller white veins (<2 mm wide and 5 cm long). Other fragments also have small white veins (<2 mm wide) with random orientation.
ADDITIONAL COMMENTS: This section consists of multiple clasts of serpentinized harzburgite embedded in a phacoidal serpentine matrix.

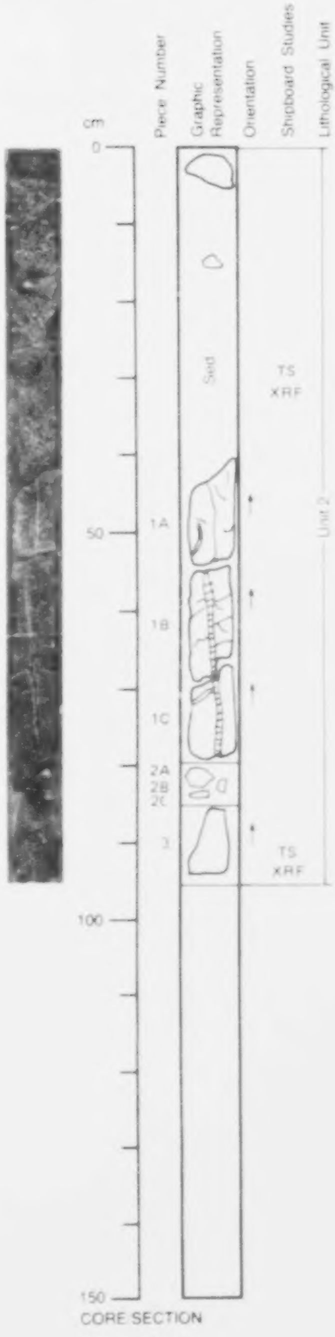

125-784A-38R-2

UNIT 2: SERPENTINIZED HARZBURGITE

Pieces 1A, 1B, 1C, 2A, 2B, 2C

COLOR: Dark greenish gray to dark gray (5BG 4/1 - N 4/)
LAYERING: None visible
DEFORMATION: Abundant fractures and veins.
PRIMARY MINERALOGY:
Primary silicates are variably serpentinized.
Olivine - Mode: 80%
Crystal size: Not visible
Crystal shape: Not visible
Crystal orientation: None visible
Percent replacement: 80-90

Orthopyroxene - Mode: 15-20%
Crystal size: 1-4 mm
Crystal shape: Subhedral
Crystal orientation: None visible
Percent replacement: 50-70

Spinel - Mode: 1%
Crystal size: <1 mm
Crystal shape: Equant-ragged
Crystal orientation: None visible
Percent replacement: 0
SECONDARY MINERALOGY:
Serpentine
Total percent: 70-80%
Texture: Serpentine bastite pseudomorphs after orthopyroxene.
Vein material: Abundant veins (0.5-3 mm wide) throughout pieces. Large 5 mm wide chrysotile vein oriented almost parallel to core barrel. This vein is fractured along its length and crosscut perpendicularly by small (1 mm wide and 6 mm long) green white serpentine veins.
ADDITIONAL COMMENTS: In upper portion of this section (0-2 cm) there is a serpentinized dunite clast (2 cm x 4 cm). This clast is >90% serpentinized and has no separate number on it.

UNIT 2: SERPENTINIZED HARZBURGITE

Piece 3

COLOR: Dark greenish gray to dark gray (5BG 4/1 - N 4/)
LAYERING: None visible
DEFORMATION: None visible
PRIMARY MINERALOGY:
Primary silicates are variably serpentinized.
Olivine - Mode: 57-67%
Crystal size: 1-3 mm
Crystal shape: Anhedral
Crystal orientation: None visible
Percent replacement: 50-70

Orthopyroxene - Mode: 30-40%
Crystal size: 1-6 mm
Crystal shape: Equant
Crystal orientation: None visible
Percent replacement: 50-70

Clinopyroxene - Mode: <3%
Crystal size: 1-2 mm
Crystal shape: Subhedral
Crystal orientation: None visible
Percent replacement: 50-70

Spinel - Mode: Trace
Crystal size: <2 mm
Crystal shape: Ragged
Crystal orientation: None visible
Percent replacement: 0
SECONDARY MINERALOGY:
Serpentine
Total percent: 50-70%
Texture: Patches of serpentine bastite pseudomorphs.
Vein material: None visible.
ADDITIONAL COMMENTS: Sample is rich in pyroxene and fairly fresh.

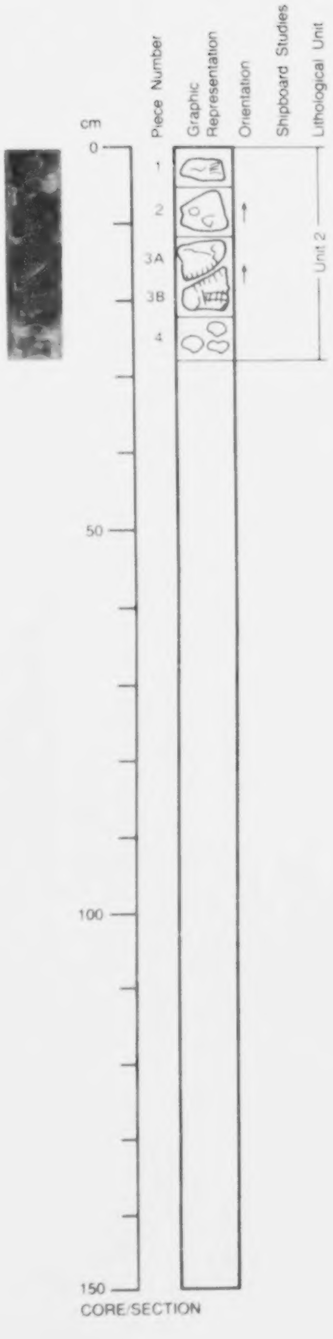
cm
Piece Number
Graphic Representation
Orientation
Shipboard Studies
Lithological Unit
0
50
100
150
1
2
3A
3B
4
Unit 2
CORE/SECTION

125-784A-38R-CC

UNIT 2: SERPENTINIZED HARZBURGITE

Pieces 1, 2, 3A, 3B, 4

COLOR: Dark greenish gray to dark gray (5BG 4/1 - N 4/)
LAYERING: None visible
DEFORMATION: Pieces 1, 3A and 3B show abundant fracturing and veining
PRIMARY MINERALOGY: Primary silicates are variably altered to serpentine
Olivine - Mode: 80-90%
Crystal size: 1-2 mm
Crystal shape: Anhedral
Crystal orientation: None visible
Percent replacement: 80-90

Orthopyroxene - Mode: 10-20%
Crystal size: 1-6 mm
Crystal shape: Subhedral
Crystal orientation: None visible
Percent replacement: 80-90

Spinel - Mode: Trace
Crystal size: <1 mm
Crystal shape: Equant to ragged
Crystal orientation: None visible
Percent replacement: 0
SECONDARY MINERALOGY:
Serpentine
Total percent: 80-90%
Texture: Serpentine bastite pseudomorphs after orthopyroxene.
Vein material: Piece 3 is fractured along a chrysotile "Frankenstein" vein. This vein is oriented 45 degrees to side of core barrel. It is perpendicularly cut by smaller (>2-mm wide) veins along its length. Other pieces have small (>1 mm wide) white green veins.

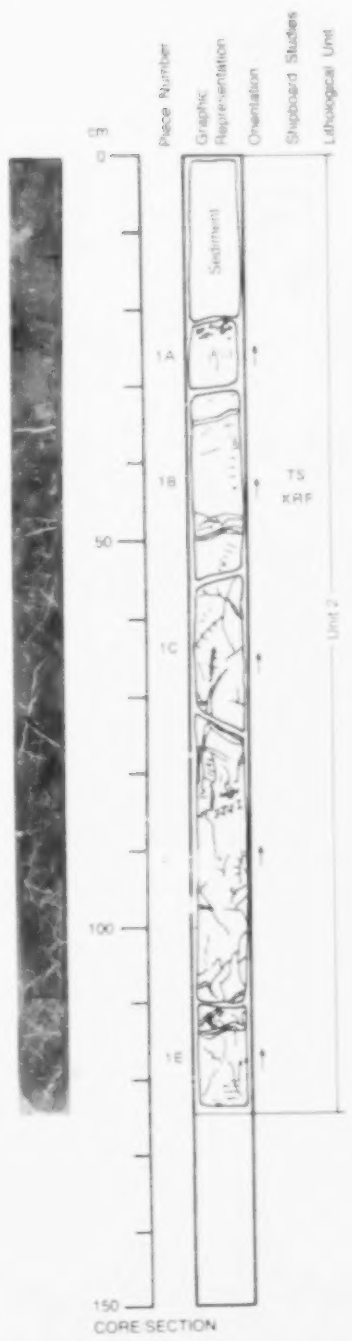
cm
Piece Number
Graphic Representation
Orientation
Shipboard Studies
Lithological Unit
0
50
100
150
Sediment
1A
1B
1C
1E
TS
XRF
Unit 2
CORE SECTION

125-784A-40R-2

UNIT 2: SERPENTINIZED DUNITE

Pieces 1A - 1E

COLOR: Black (N 4)
LAYERING: None visible
DEFORMATION: None visible
PRIMARY MINERALOGY:
Primary silicates are extensively and pervasively serpentinized
Olivine : Mode: 95-97%
Crystal size: None visible
Crystal shape: None visible
Crystal orientation: None visible
Percent replacement: 95-100

Orthopyroxene : Mode: 3-5%
Crystal size: 1-3 mm
Crystal shape: Subhedral
Crystal orientation: None visible
Percent replacement: Variable

Cr spinel : Mode: <1%
Crystal size: 0.1-0.5 mm
Crystal shape: Subhedral
Crystal orientation: Disseminated
Percent replacement: None visible
SECONDARY MINERALOGY:
Massive textured serpentine
Total percent: 99%
Texture: Mesh texture present in 4 cm of top of piece; otherwise massive, but
Vein material: White veins of chrysotile, mostly with shallow dip and often
anastomosing; some crosscutting dark greenish-black serpentine veins.
ADDITIONAL COMMENTS: All sub-pieces are part of one continuous cored pie

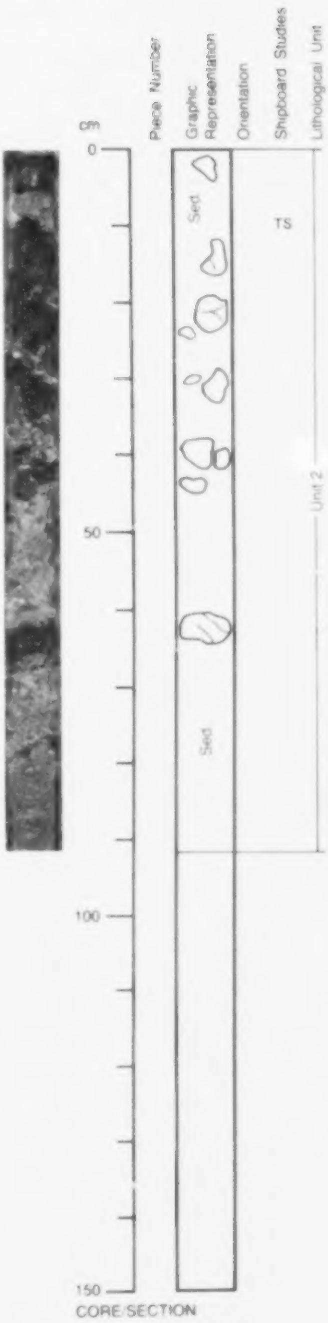
cm
Piece Number
Graphic Representation
Orientation
Shipboard Studies
Lithological Unit
0
50
100
150
Sed
TS
Unit 2
Sed
CORE/SECTION

125-784A-41R-1

UNIT 2: SERPENTINIZED HARZBURGITE AND DUNITE

Pieces assorted clasts in a matrix

COLOR: Black (N 4/)
LAYERING: None visible
DEFORMATION: None visible
PRIMARY MINERALOGY:
Extensively serpentinized rock
Olivine - Mode: 95-99%
Crystal size: None visible
Crystal shape: None
Crystal orientation: None visible
Percent replacement: 95-100

Orthopyroxene - Mode: 0-5%
Crystal size: 0.5-3 mm
Crystal shape: Subhedral
Crystal orientation: None visible
Percent replacement: Variable

Cr-spinel - Mode: Trace
Crystal size: 0.1-0.5 mm
Crystal shape: Anhedral
Crystal orientation: Disseminated
Percent replacement: None visible
SECONDARY MINERALOGY:
Massive serpentine
Total percent: 98-10%
Texture: Massive and bastite after orthopyroxene
Vein material: <0.2 mm wide, white fill of chrysotile, orientated sub-horizontal

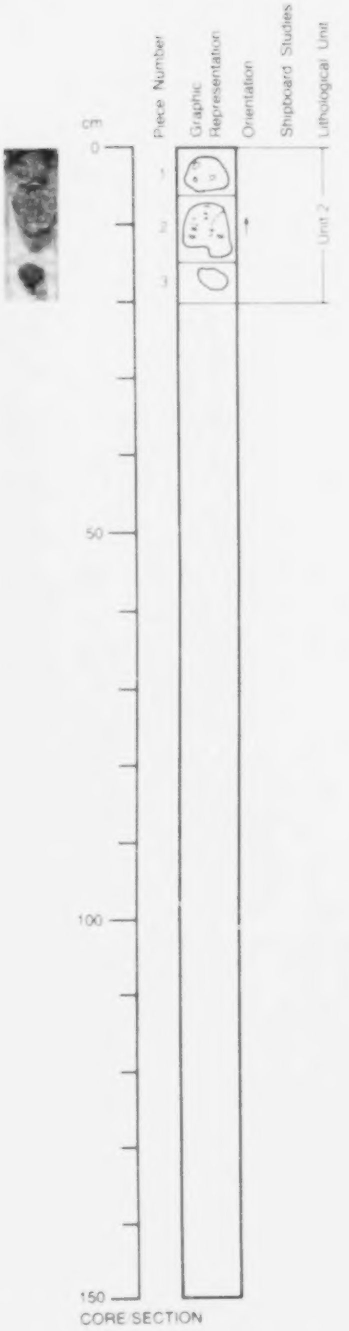

125-784A-41R-CC

UNIT 2: SERPENTINIZED HARZBURGITE

Pieces 1 and 2

COLOR: Dark greenish gray to dark gray (5BG 4/1 - N 4/)
LAYERING: None visible
DEFORMATION: None visible
PRIMARY MINERALOGY:
Primary silicates are variably serpentinized.
Olivine - Mode: 75-80%
Crystal size: Not visible
Crystal shape: Not visible
Crystal orientation: None visible
Percent replacement: 80-90

Orthopyroxene - Mode: 20-25%
Crystal size: 1-4 mm
Crystal shape: Subhedral equant
Crystal orientation: None visible
Percent replacement: 60-70

Spinel - Mode: Trace
Crystal size: <1 mm
Crystal shape: Equant
Crystal orientation: None visible
Percent replacement: 0
SECONDARY MINERALOGY:
Serpentine
Total percent: 70-80%
Texture: Patches of serpentine bastite pseudomorphs after orthopyroxene
Vein material: No veins are visible

UNIT 2: SERPENTINIZED DUNITE

Piece 3

COLOR: Dark bluish gray (5B 4/1)
LAYERING: None visible
DEFORMATION: None visible
PRIMARY MINERALOGY:
Olivine - Mode: 95-99%
Crystal size: Not visible
Crystal shape: Not visible
Crystal orientation: None visible
Percent replacement: 80-90

Spinel - Mode: Trace
Crystal size: <1 mm
Crystal shape: Equant
Crystal orientation: None visible
Percent replacement: 0
SECONDARY MINERALOGY:
Serpentine
Total percent: 80%
Texture: Serpentine mesh texture after olivine
Vein material: <2 mm wide white veins at no specific orientation

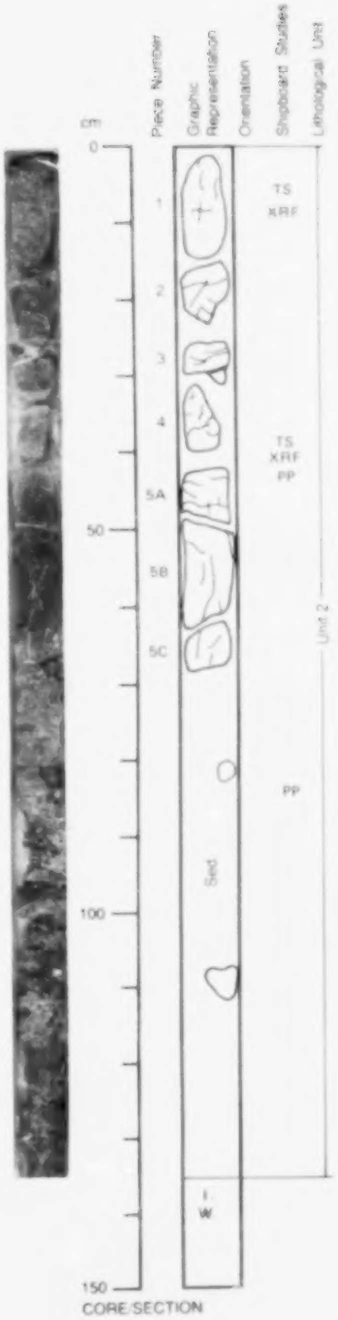
cm
Piece Number
Graphic Representation
Orientation
Shipboard Studies
Lithological Unit
0
50
100
150
1
2
3
4
5A
5B
5C
TS
XRF
TS
XRF
PP
PP
Sed
I-W
Unit 2
CORE/SECTION

125-784A-42R-1

UNIT 2: SERPENTINIZED HARZBURGITE AND DUNITE

Pieces 1-5

COLOR: Dark greenish gray to dark gray (5BG 4/1 - N 4/).
LAYERING: There appears to be a contact within Piece 2 (18-22 cm) between harzburgitic and dunitic rocks.
DEFORMATION: Locally abundant deformation, fractures and veins.
PRIMARY MINERALOGY:
Primary silicates are variably serpentinized.
Olivine - Mode: 70-95%
Crystal size: Not visible.
Crystal shape: Not visible.
Crystal orientation: None visible.
Percent replacement: 80-90.

Orthopyroxene - Mode: 5-30%
Crystal size: 1-4 mm.
Crystal shape: Equant.
Crystal orientation: None visible.
Percent replacement: 70-80.

Spinel - Mode: Trace.
Crystal size: <1 mm.
Crystal shape: Equant ragged.
Crystal orientation: None visible.
Percent replacement: 0.
SECONDARY MINERALOGY:
Serpentine.
Total percent: 75-90%.
Texture: Patches of serpentine mesh and bastite textures.
Vein material: Abundant white and pale green veins (0.5-3 mm wide) distributed throughout rocks at no specific orientation.
ADDITIONAL COMMENTS: There is a gradation between harzburgite and dunites within these fragments; fragments are clasts sitting in a serpentine matrix.

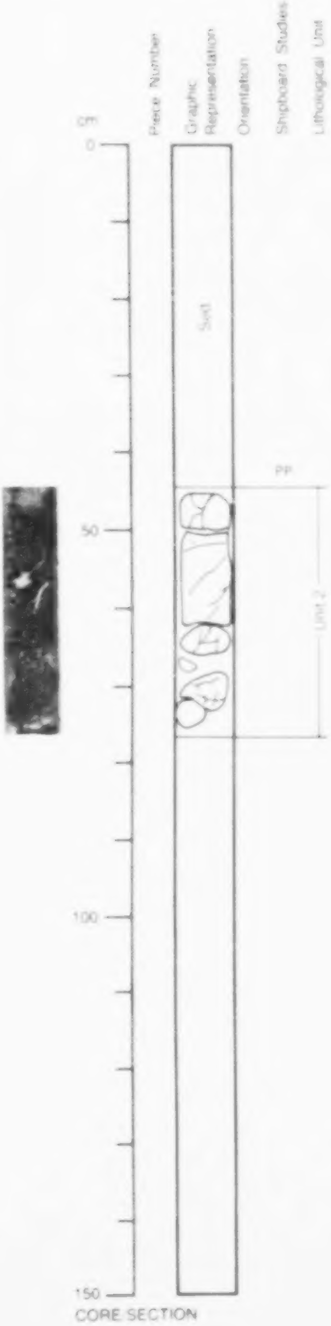
cm
Piece Number
Graphic Representation
Orientation
Shipboard Studies
Lithological Unit
0
50
100
150
Void
PP
Unit 2
CORE SECTION

125-784A-42R-2

UNIT 2: SERPENTINIZED DUNITE

Pieces multiple fragments

COLOR: Black (N 4)
LAYERING: None visible
DEFORMATION: None visible
PRIMARY MINERALOGY:
Primary silicates are variably serpentinized
Olivine : Mode: 95-99%
Crystal size: Not visible
Crystal shape: Not visible
Crystal orientation: None visible
Percent replacement: 80-90

Orthopyroxene : Mode: 1-2%
Crystal size: 1-2 mm
Crystal shape: Subhedral
Crystal orientation: None visible
Percent replacement: 70

Spinel : Mode: Trace
Crystal size: <1 mm
Crystal shape: Ragged
Crystal orientation: None visible
Percent replacement: 0
SECONDARY MINERALOGY:
Serpentine
Total percent: 80-90%
Texture: Minor serpentine bastite pseudomorphic texture in areas
Vein material: White veins (0.5-2 mm wide), and pale green (serpentine?)
fragments at no specific orientation

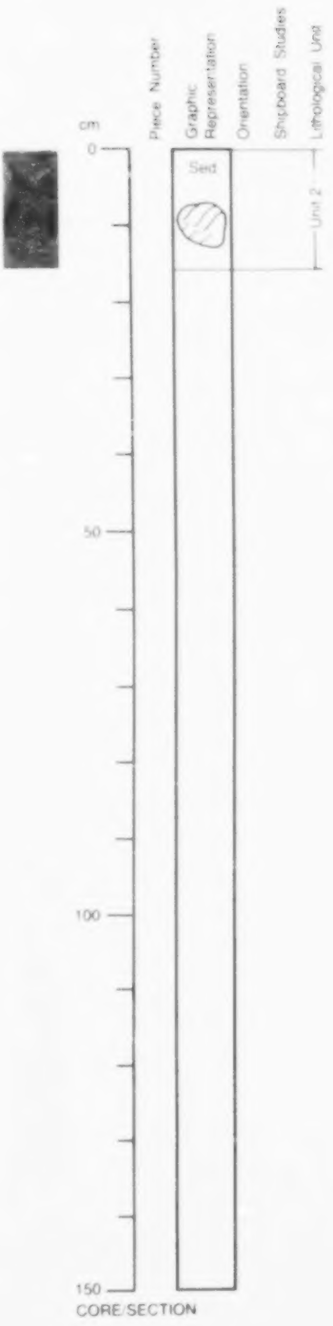
cm
Piece Number
Graphic Representation
Orientation
Shipboard Studies
Lithological Unit
0
Sed
Unit 2
50
100
150
CORE/SECTION

125-784A-42R-CC

UNIT 2: SERPENTINIZED DUNITE

Pieces one clast

COLOR: Black (N 4)
LAYERING: None visible
DEFORMATION: Abundant fractures and veining
PRIMARY MINERALOGY:
Primary silicates are variably serpentinized
Olivine - Mode: 90-99%
Crystal size: Not visible
Crystal shape: Not visible
Crystal orientation: None visible
Percent replacement: 80-90

Spinel - Mode: Trace
Crystal size: <1 mm
Crystal shape: Equant ragged
Crystal orientation: None visible
Percent replacement: 0
SECONDARY MINERALOGY:
Serpentine
Total percent: 80-90%
Texture: Serpentine mesh after olivine (?)
Vein material: Pale green serpentine veins (0.5-2 mm wide) oriented 45 degrees to core barrel

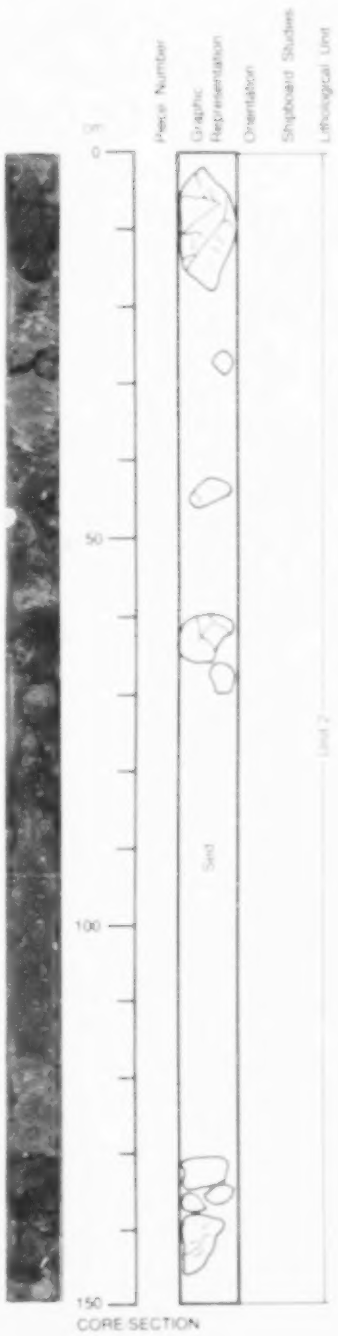
cm
0
50
100
150
Piece Number
Graphic Representation
Orientation
Shipboard Studies
Lithological Unit
Sed
Unit 2
CORE SECTION

125-784A-43R-1

UNIT 2: SERPENTINIZED HARZBURGITES AND DUNITES

Pieces multiple clasts in matrix

COLOR: Dark greenish gray to dark gray (5BG 4/1-N 4/).
LAYERING: None visible.
DEFORMATION: Abundant veining and fracturing.
PRIMARY MINERALOGY:
Primary silicates are variably serpentinized.
Olivine - Mode: 70-95%.
Crystal size: Not visible.
Crystal shape: Not visible.
Crystal orientation: None visible.
Percent replacement: 80-90.

Orthopyroxene - Mode: 5-30%.
Crystal size: 1-3 mm.
Crystal shape: Equant.
Crystal orientation: None visible.
Percent replacement: 70-80.

Spinel - Mode: Tr-1%.
Crystal size: <1 mm.
Crystal shape: Equant ragged.
Crystal orientation: None visible.
Percent replacement: 0.
SECONDARY MINERALOGY:
Serpentine.
Total percent: 70-90%.
Texture: Serpentine mesh and bastite pseudomorphs.
Vein material: Abundant veins (0.5-2 mm wide) of white and green (serpentine) minerals throughout rocks. The fractures in the clasts follow the general trend of the veins.

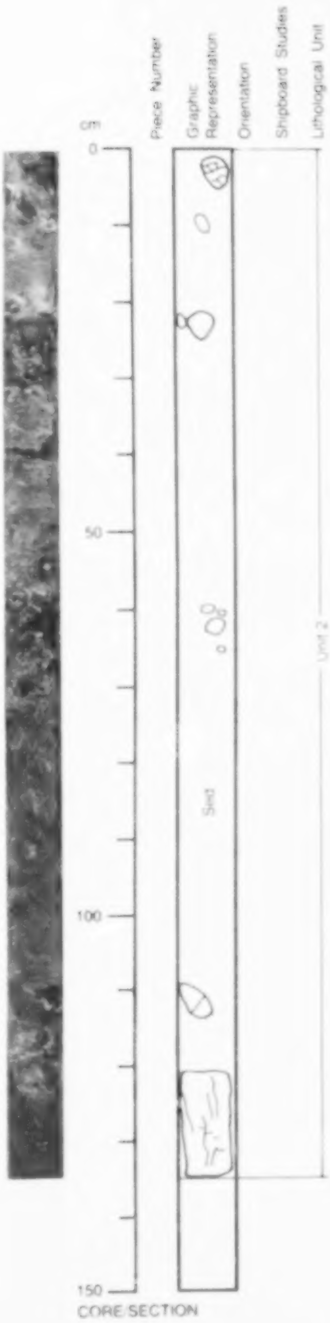
cm
Piece Number
Graphic Representation
Orientation
Shipboard Studies
Lithological Unit
0
50
100
150
Sed
Unit 2
CORE/SECTION

125-784A-43R-2

UNIT 2: SERPENTINIZED DUNITE AND HARZBURGITES

Pieces multiple clasts in matrix

COLOR: Dark greenish gray to dark gray (5BG 4/1-N 4/)
LAYERING: None visible
DEFORMATION: None visible
PRIMARY MINERALOGY:
Olivine - Mode: 70-95%
Crystal size: Not visible
Crystal shape: Not visible
Crystal orientation: None visible
Percent replacement: 80-90

Orthopyroxene - Mode: 5-30%
Crystal size: 1-2 mm
Crystal shape: Equant
Crystal orientation: None visible
Percent replacement: 70

Spinel - Mode: Tr-1%
Crystal size: <1 mm
Crystal shape: Ragged
Crystal orientation: None visible
Percent replacement: 0
SECONDARY MINERALOGY:
Serpentine
Total percent: 80-90%
Texture: Patches of serpentine mesh and bastite pseudomorphs.
Vein material: Some clasts have white veins (0.5-1 mm wide) at no specific orientation.

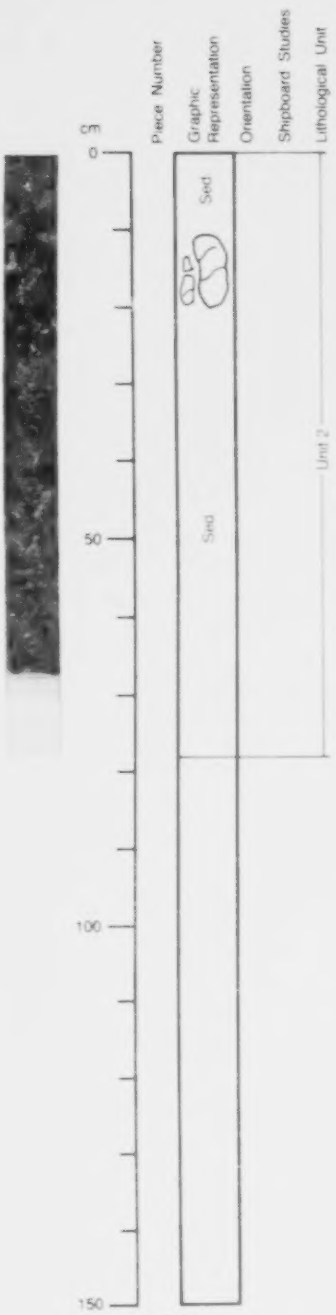
cm
Piece Number
Graphic Representation
Orientation
Shipboard Studies
Lithological Unit
0
50
100
150
Sed
Sed
Unit 2
CORE SECTION

125-784A-43R-3

UNIT 2: SERPENTINIZED HARZBURGITE

Pieces multiple clasts in matrix

COLOR: Dark gray (N 4).
LAYERING: None visible
DEFORMATION: None visible
PRIMARY MINERALOGY:
Primary silicates are variably serpentinized
Olivine - Mode: 75-85%
Crystal size: Not visible
Crystal shape: Not visible
Crystal orientation: None visible
Percent replacement: 80-90

Orthopyroxene - Mode: 15-25%
Crystal size: 1-2 mm
Crystal shape: Equant
Crystal orientation: None visible
Percent replacement: 70-80

Spinel - Mode: Tr?
Crystal size: <1 mm
Crystal shape: Ragged
Crystal orientation: None visible
Percent replacement: 0
SECONDARY MINERALOGY:
Serpentine
Total percent: 80-90%
Texture: Patches of serpentine bastite pseudomorphs
Vein material: Some clasts have white veins (1-2 mm wide) at no specific orientatio

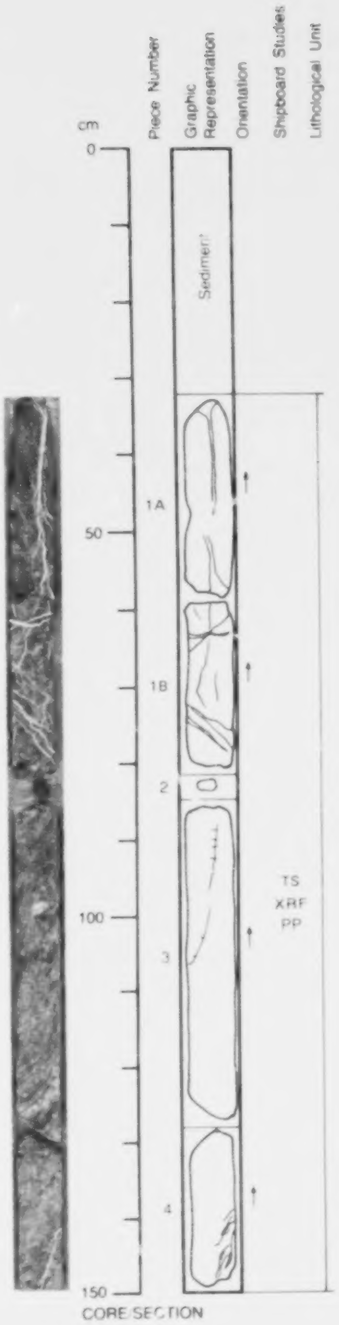
cm
Piece Number
Graphic Representation
Orientation
Shipboard Studies
Lithological Unit
0
50
100
150
Sediment
1A
1B
2
3
4
TS
XRF
PP
CORE/SECTION

125-784A-45R-1

UNIT 2: SERPENTINIZED TECTONIZFD HARZBURGITE

Pieces 1A, 1B, 2, 3, 4

COLOR: Dark gray to gray (N5/ to N4/)
LAYERING: None visible.
DEFORMATION: Aligned spinels, curved cleavage planes on orthopyroxene crystals.
PRIMARY MINERALOGY:
Primary silicates are variably serpentinized.
Olivine - Mode: 70-80%.
Crystal size: <8 mm.
Crystal shape: Not visible.
Crystal orientation: Not visible.
Percent replacement: Variable 50-100%.

Orthopyroxene - Mode: 20-30%.
Crystal size: <5 mm.
Crystal shape: Equant to elongate.
Crystal orientation: Not visible.
Percent replacement: Variable 50-80%.

Spinel - Mode: <1%.
Crystal size: <1 mm.
Crystal shape: Equant to elongate.
Crystal orientation: Short stringers at random orientations.
Percent replacement: Not visible.
Comments: Chlorite halos around crystals (<1 mm wide).
SECONDARY MINERALOGY:
Minor "Frankenstein" texture at bottom of heavily veined portion of the section.
Total percent: 80-99%.
Texture: Patches of serpentine bastite pseudomorphs.
Vein material: Piece 1 is highly veined. Three generations: first: subvertical, filled with amorphous green serpentine, <5 mm wide; second: also subvertical, follows tracks of first generation, white, probably chrysotile, 1-2 mm wide; third: subhorizontal to anastomosing, filled with chrysotile, <3 mm wide.

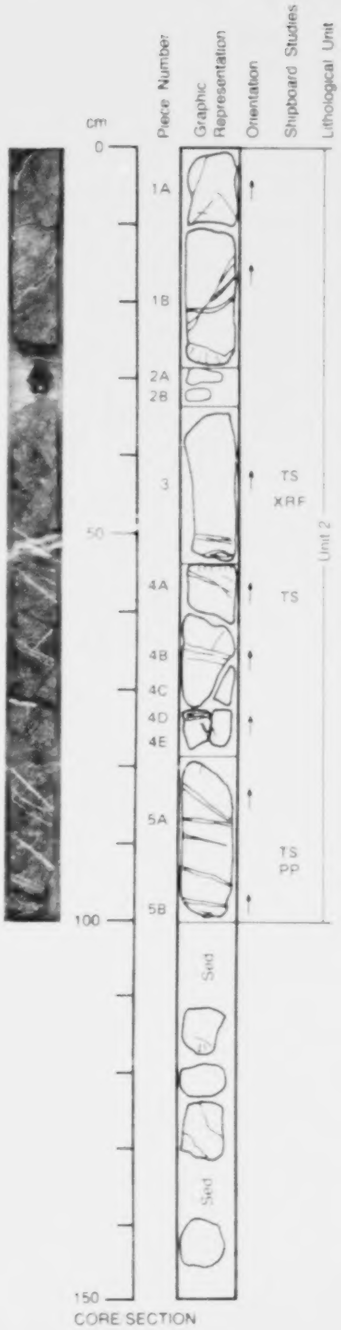
cm
Piece Number
Graphic Representation
Orientation
Shipboard Studies
Lithological Unit
0
50
100
150
1A
1B
2A
2B
3
4A
4B
4C
4D
4E
5A
5B
TS
XRF
TS
TS
PP
Unit 2
Sed
Sed
CORE SECTION

125-784A-45R-2

UNIT 2: SERPENTINIZED HARZBURGITE

Pieces 1A, B; 2A, B; 3; 4A-E; 5A, B;

COLOR: Dark gray-gray (N4-N5).
LAYERING: Some areas have alignment of orthopyroxene at 30 degrees to core axis.
DEFORMATION: Elongate spinels and trains of spinel; orthopyroxene cleavage has wavy extinction.
PRIMARY MINERALOGY:
Primary silicates are variably serpentinized 60-100%.
Olivine - Mode: 80-90%.
Crystal size: <6 mm.
Crystal shape: Not visible.
Crystal orientation: Not visible.
Percent replacement: 90-100.

Orthopyroxene - Mode: 10-20%.
Crystal size: <3-5 mm.
Crystal shape: Equant to elongate.
Crystal orientation: Some alignment.
Percent replacement: 40-60.

Spinel - Mode: <1%.
Crystal size: <1-1 mm.
Crystal shape: Equant to elongate.
Crystal orientation: Some stringers.
Percent replacement: None.
SECONDARY MINERALOGY:
The break between Pieces 3 and 4 appears to be along a major vein.
Total percent: 70-99%.
Texture: Serpentine mesh and bastite pseudomorphs.
Vein material: Two major generations: first, conjugate set, dipping at 45 degrees to core axis, dark to pale green and white chrysotile to dark amorphous serpentine, <4 mm wide, en echelon development especially in Piece 5; second, anastomosing, chrysotile filled, white, <2 mm wide.

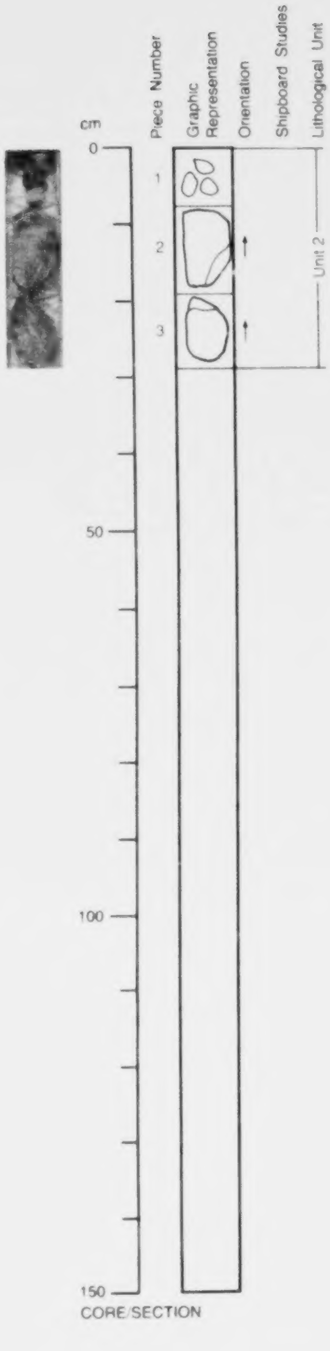
cm
Piece Number
Graphic Representation
Orientation
Shipboard Studies
Lithological Unit
0
1
2
3
Unit 2
50
100
150
CORE/SECTION

125-784A-45R-CC

UNIT 2: SERPENTINIZED TECTONIZED HARZBURGITE

Pieces 1 (3 fragments), 2, 3

COLOR: Dark gray to gray (N4/ to N5/)
LAYERING: None visible
DEFORMATION: Well developed spinel stringers, wavy cleavage on orthopyroxene
PRIMARY MINERALOGY:
Primary silicates are variable serpentinized
Olivine - Mode: 80-90%
Crystal size: <6 mm
Crystal shape: Not visible
Crystal orientation: Not visible
Percent replacement: 90-100

Orthopyroxene - Mode: 10-20%
Crystal size: <3-5 mm
Crystal shape: Equant to elongate
Crystal orientation: None visible
Percent replacement: 40-70

Spinel - Mode: <1%
Crystal size: <1-2 mm
Crystal shape: Equant to elongate
Crystal orientation: Stringers
Percent replacement: None visible
SECONDARY MINERALOGY:
Serpentine
Total percent: 80-99%
Texture: Patches of serpentine mesh and bastite pseudomorphs
Vein material: Minor chrysotile vein, white, <2 mm wide, dips 50 degrees to core axis

125-784A-[illegible], [illegible] cm   OBSERVER: [illegible]   WHERE SAMPLED: Torishima Forearc Seamount, west flank

ROCK NAME: Serpentinized dunite

GRAIN SIZE: [illegible] mm

TEXTURE: Mesh

PRIMARY MINERALOGY	PERCENT PRESENT	PERCENT ORIGINAL	SIZE (mm)	COMPO-SITION	MORPHOLOGY	COMMENTS
PHENOCRYSTS						
Olivine	[illegible]	[illegible]	Not visible		Not visible	Altered to serpentine and without mesh texture.
Spinel	1	2	[illegible]		Subhedral-anhedral	Reddish brown Cr-spinel.
Orthopyroxene	[illegible]	[illegible]	<2		Subhedral	Altered to bastite.
GROUNDMASS						
N/A	N/A	N/A	N/A		N/A	

SECONDARY MINERALOGY	PERCENT	REPLACING/FILLING	COMMENTS
Clays	[illegible]	Serpentine	Dusty clay is scattered throughout the thin section.
Serpentine	[illegible]	Olivine, orthopyroxene	Chrysotile and/or lizardite replaced olivine.
Brucite			Antigorite and brucite exist after olivine.
Opaques	1	Spinel; serpentine	Magnetite(?) is partly replacing spinel and serpentine.

VESICLES/CAVITIES	PERCENT	LOCATION	SIZE (mm)	FILLING	SHAPE
Vesicles	[illegible]				

COMMENTS: Mesh texture after olivine is not common, because serpentinization in this rock is associated with antigorite and brucite. Fine-grained opaque minerals are scattered throughout the thin section. No piece number given.

125-784A-[illegible] (Piece [illegible], [illegible] cm)   OBSERVER: [illegible]   WHERE SAMPLED: Torishima Forearc Seamount, west flank

ROCK NAME: Serpentinized harzburgite

GRAIN SIZE: [illegible] mm

TEXTURE: Mesh and bastite; [illegible]

PRIMARY MINERALOGY	PERCENT PRESENT	PERCENT ORIGINAL	SIZE (mm)	COMPO-SITION	MORPHOLOGY	COMMENTS
PHENOCRYSTS						
Olivine	[illegible]	[illegible]	[illegible]		Anhedral	[illegible], altered to serpentine mesh and magnetite.
Clinopyroxene	Trace	Trace	[illegible]		Anhedral	As exsolution lamellae in orthopyroxene.
Spinel	[illegible]	[illegible]	[illegible]	[illegible]	Subhedral-anhedral	Red-brown, irregular shape, minor inclusions.
Orthopyroxene	[illegible]	[illegible]	[illegible]		Subhedral-anhedral	[illegible] altered to serpentine (bastite); minor clinopyroxene exsolution lamellae; wavy extinction in some grains.
GROUNDMASS						
N/A	N/A	N/A	N/A		N/A	

SECONDARY MINERALOGY	PERCENT	REPLACING/FILLING	COMMENTS
Clays	[illegible]	Serpentine	Light brown-green clay intermixed with serpentine and magnetite and distributed throughout slide.
Serpentine	[illegible]	Olivine, orthopyroxene	Serpentine forming mesh texture and bastite texture. Antigorite and lizardite may both be present, but it is difficult to tell because of amount of magnetite. [illegible] with pronounced [illegible].
Magnetite	[illegible]	Olivine, spinel	Subhedral-anhedral crystals [illegible] mm surrounded by [illegible] serpentine. Magnetite is heavily concentrated in veins and in mesh centers and in mesh edges.

VESICLES/CAVITIES	PERCENT	LOCATION	SIZE (mm)	FILLING	SHAPE
Vesicles	[illegible]				

COMMENTS: [illegible] orthopyroxene [illegible]. Spinel crystals are rounded and appear to be out of equilibrium. This slide has abundant magnetite scattered throughout.

125-784A-34R-02 (87-89 cm) OBSERVER: TER WHERE SAMPLED: Torishima Forearc Seamount, west flank

ROCK NAME: Serpentinized dunite

GRAIN SIZE: 0.1 - <2 mm

TEXTURE: Mesh

PRIMARY MINERALOGY	PERCENT PRESENT	PERCENT ORIGINAL	SIZE (mm)	COMPO-SITION	MORPHOLOGY	COMMENTS
PHENOCRYSTS						
Olivine	0	97	Not visible		Not visible	Altered to serpentine and without mesh texture?
Spinel	1	2	0.1-1.5		Subhedral-euhedral	Reddish brown Cr-spinel.
Orthopyroxene	0	1	<2		Subhedral	Altered to bastite.
GROUNDMASS						
N/A	N/A	N/A	N/A		N/A	

SECONDARY MINERALOGY	PERCENT	REPLACING/ FILLING	COMMENTS
Clays	25	Serpentine	Dusty clay is scattered throughout the thin section.
Serpentine	65-70	Olivine, orthopyroxene	Chrysotile and/or lizardite replaced olivine.
Brucite			Antigorite and brucite exist after olivine.
Opaques	5	Spinel, serpentine	Magnetite(?) is partly replacing spinel and serpentine.

VESICLES/ CAVITIES	PERCENT	LOCATION	SIZE (mm)	FILLING	SHAPE
Vesicles	0				

COMMENTS: Mesh texture after olivine is not common, because serpentinization in this rock is associated with antigorite and brucite. Fine-grained opaque minerals are scattered throughout the thin section. No piece number given.

125-784A-36R-01 (Piece 7,133-135 cm) OBSERVER: SAB WHERE SAMPLED: Torishima Forearc Seamount, west flank

ROCK NAME: Serpentinized harzburgite

GRAIN SIZE: 0.5-7 mm

TEXTURE: Mesh and bastite; [illegible]

PRIMARY MINERALOGY	PERCENT PRESENT	PERCENT ORIGINAL	SIZE (mm)	COMPO-SITION	MORPHOLOGY	COMMENTS
PHENOCRYSTS						
Olivine	11	78-83	1-3		Anhedral	95-100%, altered to serpentine mesh and magnetite.
Clinopyroxene	Trace	Trace	N/A		Subhedral	As exsolution lamellae in orthopyroxenes.
Spinel	1.5	2	0.5-2	Cr	Subhedral-anhedral	Red-brown, irregular shape, minor inclusions.
Orthopyroxene	2	15-20	2-5		Subhedral-anhedral	95-100% altered to serpentine bastite; minor clinopyroxene exsolution lamellae, wavy extinction in some grains.
GROUNDMASS						
N/A	N/A	N/A	N/A		N/A	

SECONDARY MINERALOGY	PERCENT	REPLACING/ FILLING	COMMENTS
Clays	2	Serpentine	Dusty brown-black clay intermixed with serpentine and magnetite and distributed throughout slide.
Serpentine	78-84	Olivine, orthopyroxene	Serpentine forming mesh texture and bastite texture. Antigorite and lizardite may both be present, but it is difficult to tell because of amount of magnetite. Chrysotile forms 0.1- to 3-mm-wide veins throughout rock with no preferred orientation.
Magnetite	10-12	Olivine, spinel	Euhedral-subhedral crystals (0.05 to 0.3 mm) surrounded by mesh-textured serpentine. Magnetite is heavily concentrated in veins and in mesh centers and in mesh edges.

VESICLES/ CAVITIES	PERCENT	LOCATION	SIZE (mm)	FILLING	SHAPE
Vesicles	0				

COMMENTS: 98-100% altered ultramafic. Spinels have minor anhedral inclusions of orthopyroxene(?). Relic orthopyroxenes show wavy clinopyroxene exsolution lamellae; curved outlines of mesh texture are present. Spinel crystals are rounded and appear to be out of equilibrium(?). This slide has abundant magnetite scattered throughout.

125-784A-[illegible] cm) OBSERVER: SAR WHERE SAMPLED: Torishima Forearc Seamount, west flank

ROCK NAME: Serpentinized harzburgite

GRAIN SIZE: [illegible] mm

TEXTURE: Mesh and bastite

PRIMARY MINERALOGY	PERCENT PRESENT	PERCENT ORIGINAL	SIZE (mm)	COMPO-SITION	MORPHOLOGY	COMMENTS
PHENOCRYSTS						
Olivine	2	80	0.2-0.8		Anhedral	Altered to serpentine mesh; wavy extinction.
Clinopyroxene	2	3	0.05-1		Anhedral	As exsolution lamellae (100) and as individual grains.
Spinel	1	2	0.05-1	Cr	Euhedral-anhedral	Red-brown; altering to magnetite.
Orthopyroxene	5	15	0.1-3		Subhedral-anhedral	Altered to serpentine bastite; kink-banded, wavy extinction, bent exsolution lamellae.
GROUNDMASS						
N/A	N/A	N/A	N/A		N/A	

SECONDARY MINERALOGY	PERCENT	REPLACING / FILLING	COMMENTS
Clays	5	Serpentine	Dusty brown-black clay scattered throughout slide and intermixed with the serpentine.
Serpentine	[illegible]	Olivine, orthopyroxene	Mostly lizardite and/or chrysotile forming mesh and bastite textures.
Magnetite	[illegible]	Spinel, olivine, serpentine	Dusty 0.1-mm grains throughout slide and concentrated in veins (serpentine), mesh edges, and along cleavages.
Talc	[illegible]	Serpentine	Dusty; high birefringence; found associated with orthopyroxene and bastites in and along edges and cleavages.

VESICLES/CAVITIES	PERCENT	LOCATION	SIZE (mm)	FILLING	SHAPE
Vesicles	0				

COMMENTS: Relatively [illegible] porphyroclastic harzburgite. Spinels are fractured with silicates forming between fractures. Some spinels form ragged [illegible] shapes. Orthopyroxenes are wavy and kink-banded; have inclusions of clinopyroxene and [illegible]. One orthopyroxene grain is split by [illegible]-mm-wide serpentine veins. This slide has abundant magnetite mesh edges and in serpentine veins (which are almost all parallel throughout slide). This rock was further altered after serpentinization. No piece number given.

125-784A-[illegible] cm OBSERVER: SAR WHERE SAMPLED: Torishima Forearc Seamount, west flank

ROCK NAME: Serpentinized harzburgite

GRAIN SIZE: [illegible] mm

TEXTURE: Mesh and bastite

PRIMARY MINERALOGY	PERCENT PRESENT	PERCENT ORIGINAL	SIZE (mm)	COMPO-SITION	MORPHOLOGY	COMMENTS
PHENOCRYSTS						
Olivine	[illegible]	85-90	1-4		Anhedral	Altered to serpentine mesh texture.
Spinel	Trace	Trace	0.2-0.8		Subhedral-anhedral	Partly altered to magnetite.
Orthopyroxene	[illegible]	10-15	1-5		Anhedral	Altered to serpentine bastite.
GROUNDMASS						
N/A	N/A	N/A	N/A		N/A	

SECONDARY MINERALOGY	PERCENT	REPLACING / FILLING	COMMENTS
Clays	5	Serpentine	Dusty brownish-blackish clay distributed throughout rock and intermixed with serpentine.
Serpentine	[illegible]	Olivine, orthopyroxene	Lizardite and/or chrysotile forming mesh and bastite textures. Chrysotile is also abundant in veins (see below).
Magnetite	2	Spinel	Dusty, [illegible]-mm, fine-grained; scattered throughout slide and appears concentrated in serpentine veins and mesh centers.

VESICLES/CAVITIES	PERCENT	LOCATION	SIZE (mm)	FILLING	SHAPE
Vesicles	0				

COMMENTS: Veins of serpentine ([illegible] to 1 mm), magnetite and clays are abundant throughout slide and parallel one another. These smaller veins are then cut perpendicularly by a 1-mm-wide chrysotile vein (almost like "Frankenstein" texture). This larger chrysotile vein is also rimmed by a high birefringence, length [illegible] mineral. No piece number given.

125-784A-38R-02 (Piece 3, 92-95 cm) OBSERVER: SAB WHERE SAMPLED: Torishima Forearc Seamount, west flank

ROCK NAME: Serpentinized harzburgite

GRAIN SIZE: 0.2-5 mm

TEXTURE: Cumulate, mesh and bastite

PRIMARY MINERALOGY	PERCENT PRESENT	PERCENT ORIGINAL	SIZE (mm)	COMPO-SITION	MORPHOLOGY	COMMENTS
PHENOCRYSTS						
Olivine	3	70.5	1-3		Anhedral	Altering to serpentine mesh texture.
Clinopyroxene	2-4	2-4	0.5-2		Anhedral	As exsolution lamellae and as anhedral crystals.
Spinel	1.0	1.5	0.25-1.5		Anhedral	Reddish brown; fractured.
Orthopyroxene	17	25	2-5		N/A	Partly or fully altered to serpentine bastite texture, wavy extinction, kink-banded, exsolution lamellae.
GROUNDMASS						
N/A	N/A	N/A	N/A		N/A	

SECONDARY MINERALOGY	PERCENT	REPLACING/ FILLING	COMMENTS
Chlorite	Trace	Orthopyroxene, serpentine	Pale-green in color; rarely visible in orthopyroxene bastite.
Serpentine	74-76	Olivine, orthopyroxene	Lizardite and/or chrysotile forms mesh and bastite textures. Chrysotile veins are present.
Magnetite	<1	Spinel	Dusty 0.1-mm grains; occurs along the grain boundaries among olivine, orthopyroxene and clinopyroxene.

VESICLES/ CAVITIES	PERCENT	LOCATION	SIZE (mm)	FILLING	SHAPE
Vesicles	0				

COMMENTS: Spinels are fractured and have silicates forming within the fractures. Spinels are sometimes aligned in elongate trains. Orthopyroxenes are kink-banded, have wavy extinctions and have inclusions of clinopyroxene as well as serpentine pseudomorphic grains. Minor chrysotile veins (0.5 mm wide and 2 mm long) cross many orthopyroxene grains.

125-784A-39R-01 (8-9 cm) OBSERVER: BIR WHERE SAMPLED: Torishima Forearc Seamount, west flank

ROCK NAME: Meta-volcaniclastic rock

GRAIN SIZE: 0.1-2 mm

TEXTURE: Cataclastic

PRIMARY MINERALOGY	PERCENT PRESENT	PERCENT ORIGINAL	SIZE (mm)	COMPO-SITION	MORPHOLOGY	COMMENTS
Plagioclase	Trace	0.12	<0.1		Euhedral	Occurs in volcanic fragments.
Clinopyroxene	Trace	2.5	<0.2		Anhedral	Occurs in volcanic fragments and in matrix.

SECONDARY MINERALOGY	PERCENT	REPLACING/ FILLING	COMMENTS
Clays	70	Plagioclase	Matrix is occupied by brown dusty clay.
Chlorite	20-30	Clinopyroxene, hornblende	Showing abnormal interference color.
Sphene	Trace		Showing high refractive index, high birefringence and euhedral to subhedral shape; abundant in amphibolite clasts.
Hornblende	Trace		Occurring in amphibolite clasts; pale-green to colorless.

VESICLES/ CAVITIES	PERCENT	LOCATION	SIZE (mm)	FILLING	SHAPE
Vesicles	0				

COMMENTS: This rock contains subround to angular clasts of varying sizes (<2 mm) in a dusty clay matrix. Clasts consist of amphibolite and basalt. This rock underwent the low-grade metamorphism and associated cataclastic deformation. Amphibolite consists of pale-green hornblende, saussuritized plagioclase, chlorite and sphene. Basalt consists of chlorite, saussuritized plagioclase and relict clinopyroxene. No piece number given.

125-784A-[illegible]R-01 (4-6 cm) OBSERVER: [illegible] WHERE SAMPLED: Torishima Forearc Seamount, west flank

ROCK NAME: Metabasalt

GRAIN SIZE: Fine-grained

TEXTURE: Aphyric

PRIMARY MINERALOGY	PERCENT PRESENT	PERCENT ORIGINAL	SIZE (mm)	COMPOSITION	MORPHOLOGY	COMMENTS
Glass	0	60-75	N/A		N/A	100% altered to clays + limonite.
Plagioclase	[illegible]	15-25	0.05-0.08		Laths	Quench morphology, altered to clays.
Clinopyroxene	7-10	15-20	0.1-0.2		Anhedral, elongate	Small occasional radiation clusters.
Magnetite	<1	<1	0.01-0.02		Equant, euhedral	Randomly distributed throughout.

SECONDARY MINERALOGY	PERCENT	REPLACING/ FILLING	COMMENTS
Clays	65-70	Glass, plagioclase	Brown amorphous clays disseminated throughout slide obscuring original textures.
Carbonate	1-5	Veins	Calcite (0.02 to 0.04 mm wide), throughout.
Chlorite	5-10	Veins	Pale-green chlorite is scattered throughout the rock.
Limonite	10-15	Glass, matrix	Occurs as veins and patches. Veins are anastomosing and appear to converge to form patches. Veins are 0.5 to 1 mm wide, patches are up to 5 mm.

VESICLES/ CAVITIES	PERCENT	LOCATION	SIZE (mm)	FILLING	SHAPE
Vesicles	0				

COMMENTS: This sample is a small (1 cm diameter) altered clast of aphyric fine-grained basalt with limonite vein alteration. No piece number given.

125-784A-[illegible]R-0[illegible] (11-13 cm) OBSERVER: [illegible] WHERE SAMPLED: Torishima Forearc Seamount, west flank

ROCK NAME: Serpentinized harzburgite

GRAIN SIZE: [illegible] mm

TEXTURE: Mesh and bastite

PRIMARY MINERALOGY	PERCENT PRESENT	PERCENT ORIGINAL	SIZE (mm)	COMPOSITION	MORPHOLOGY	COMMENTS
PHENOCRYSTS:						
Olivine	[illegible]	[illegible]	[illegible]		Anhedral	Mostly altered to mesh textured serpentine.
Clinopyroxene	Trace	Trace	[illegible]		Anhedral	Forms exsolution lamellae in orthopyroxene and isolated anhedral crystals.
Spinel		[illegible]	[illegible]		Subhedral/anhedral	Dark red and translucent Cr-spinel is scattered throughout the rock.
Orthopyroxene	[illegible]	[illegible]	[illegible]		Anhedral	Mostly altered to bastite-textured serpentine.
GROUNDMASS:						
N/A	N/A	N/A	N/A		N/A	

SECONDARY MINERALOGY	PERCENT	REPLACING/ FILLING	COMMENTS
Chrysotile	[illegible]	Olivine, orthopyroxene	Forms mesh and bastite textures after olivine and orthopyroxene, respectively.
Lizardite			
Magnetite	<1		Occurs in serpentine veins.

VESICLES/ CAVITIES	PERCENT	LOCATION	SIZE (mm)	FILLING	SHAPE
Vesicles	0				

COMMENTS: Kink extinction and alteration are common in orthopyroxene crystals. Mesh texture is well developed in most of olivine and [illegible], thus there appears to be very little post-serpentinization deformation. Hourglass serpentine texture is also well developed in a portion of the slide. Clinopyroxene grains are usually near orthopyroxene edges. No piece number given.

125-784A-39R-CC (12-13 cm) OBSERVER: HIR WHERE SAMPLED: Torishima Forearc Seamount, west flank

ROCK NAME: Serpentinized dunite

GRAIN SIZE: 1-3 mm

TEXTURE: Mesh and bastite

PRIMARY MINERALOGY	PERCENT PRESENT	PERCENT ORIGINAL	SIZE (mm)	COMPO-SITION	MORPHOLOGY	COMMENTS
Olivine	0	91-94	1-3		Anhedral	Altered to mesh-textured serpentine.
Spinel	Trace	1	0.1-0.8		Anhedral	Altered to magnetite.
Orthopyroxene	0	5-8	0.5-1.5		Anhedral	Altered to bastite-textured serpentine.

SECONDARY MINERALOGY	PERCENT	REPLACING/ FILLING	COMMENTS
Clays	10	Serpentine	Dusty brown clay is scattered throughout the rock.
Chrysotile/ lizardite	88-89	Olivine, orthopyroxene	Form mesh and bastite textures.
Magnetite	1	Spinel	Fine-grained magnetite is scattered throughout the rock.

VESICLES/ CAVITIES	PERCENT	LOCATION	SIZE (mm)	FILLING	SHAPE
Vesicles	0				

COMMENTS: Fragmentation and veining are prevailed throughout the rock. Veins vary in width from 0.5 mm to 2 mm, and consist of chrysotile, magnetite and clays. Veins appear to have no preferred orientation. Veins also have bright purple color which probably results from impregnation when making the thin section. No piece number given.

125-784A-40R-01 (11-12 cm) OBSERVER: HIR WHERE SAMPLED: Torishima Forearc Seamount, west flank

ROCK NAME: Meta-volcaniclastic rock

GRAIN SIZE: 0.1-1 mm

TEXTURE: Clastic

PRIMARY MINERALOGY	PERCENT PRESENT	PERCENT ORIGINAL	SIZE (mm)	COMPO-SITION	MORPHOLOGY	COMMENTS
Clinopyroxene	25	25-30	0.5-1		Anhedral	Tectonically distorted and actinolitized.

SECONDARY MINERALOGY	PERCENT	REPLACING/ FILLING	COMMENTS
Clays	15-20	Matrix	Dusty brownish clays are scattered throughout the rock.
Carbonate	<5	Vein fill	Forms veins.
Chlorite	50	Matrix	Pale-green chlorite fills in matrix throughout the rock.
Actinolite	25	Clinopyroxene	Occurs as small acicular crystals along rim of clinopyroxene.
Prehnite	<2	Vein fill	Partly shows feather-like texture; colorless, high birefringence.

VESICLES/ CAVITIES	PERCENT	LOCATION	SIZE (mm)	FILLING	SHAPE
Vesicles	0				

COMMENTS: This rock contains abundant clinopyroxene fragments in highly sheared chlorite and clay matrix. Clinopyroxene is distorted to varying degrees and is partly or fully actinolitized. Veins of calcite and chlorite (0.01 to 0.1 mm wide) run throughout the rock. No piece number given.

125-784A-42R-02 (12-15 cm)   OBSERVER: [illegible]   WHERE SAMPLED: Torishima Forearc Seamount, west flank

ROCK NAME: Metabasalt

GRAIN SIZE: 0.05-0.2 mm

TEXTURE: Primary intersertal; secondary cataclastic

PRIMARY MINERALOGY	PERCENT PRESENT	PERCENT ORIGINAL	SIZE (mm)	COMPO-SITION	MORPHOLOGY	COMMENTS
Clinopyroxene	25-30	25-30	0.05-0.2		Anhedral	Mostly occurs as quench crystal.
Plagioclase	[illegible]	40-50	0.1		Euhedral-subhedral	Mostly occurs as quench crystal, replaced by chlorite.
Glass	[illegible]	20-30	N/A		N/A	Completely altered to clay and chlorite.
Opaques	[illegible]	[illegible]	[illegible]		Euhedral-anhedral	Scattered throughout the rock.

SECONDARY MINERALOGY	PERCENT	REPLACING/FILLING	COMMENTS
Clays	[illegible]	Glass, plagioclase	Brown dusty clay is locally oxidized; amorphous clays pervasive.
Carbonate	1		Occurs as vein minerals.
Chlorite	40-50	Glass	Pale-green in color; low refractive index; pervasive.
Actinolite	Trace		Pale-green in color.
Sphene	Trace		Fine-grained, high refractive index, distributed throughout the rock.

VESICLES/CAVITIES	PERCENT	LOCATION	SIZE (mm)	FILLING	SHAPE
Microveins	2				

COMMENTS: Fine-grained (0.01-0.05 mm) pale-green actinolite to actinolitic hornblende partly replaces primary clinopyroxene. Cataclastic deformation has prevailed throughout the rock. Fractured and pulverized fragments are predominant in the slide. No piece number given.

125-784A-40R-01 (12-14 cm)   OBSERVER: [illegible]   WHERE SAMPLED: Torishima Forearc Seamount, west flank

ROCK NAME: Serpentinized peridotite

GRAIN SIZE: Fine-grained

TEXTURE: Foliated, anastomosing foliation

PRIMARY MINERALOGY	PERCENT PRESENT	PERCENT ORIGINAL	SIZE (mm)	COMPO-SITION	MORPHOLOGY	COMMENTS
PHENOCRYSTS						
Olivine	[illegible]	[illegible]	N/A		N/A	Completely altered
Orthopyroxene	[illegible]	[illegible]	N/A		N/A	Completely altered
GROUNDMASS						
N/A	N/A	N/A	N/A		N/A	

SECONDARY MINERALOGY	PERCENT	REPLACING/FILLING	COMMENTS
Clays	[illegible]	Serpentine, olivine, orthopyroxene	
Serpentine	[illegible]	Olivine, orthopyroxene?	Fibrous. Fibers radial to create bundles and anastomosing in matrix.
Opaques	[illegible]	Olivine, orthopyroxene?	Concentrated along edges of fiber bundles in matrix.

VESICLES/CAVITIES	PERCENT	LOCATION	SIZE (mm)	FILLING	SHAPE
Vesicles	[illegible]				

COMMENTS: Slide almost [illegible] by polishing and grinding. Fine-grained fibrous serpentine anastomoses around serpentinite clasts. Probable serpentinite mud-flow. Original serpentine possibly foliated to yield the abundant fibers. No piece number given.

125-784A-40R-02 (Piece 1B,41-43 cm) OBSERVER: TER WHERE SAMPLED: Torishima Forearc Seamount, west flank

ROCK NAME: Serpentinized dunite

GRAIN SIZE: Not visible

TEXTURE: Mesh

PRIMARY MINERALOGY	PERCENT PRESENT	PERCENT ORIGINAL	SIZE (mm)	COMPO-SITION	MORPHOLOGY	COMMENTS
PHENOCRYSTS						
Olivine	0	99	Not visible		Not visible	Altered to mesh-textured serpentine.
Spinel	<1	1	0.2-0.5		Euhedral-subhedral	Dark brownish black Cr-spinel.
GROUNDMASS						
N/A	N/A	N/A	N/A		N/A	

SECONDARY MINERALOGY	PERCENT	REPLACING/ FILLING	COMMENTS
Clays	5	Serpentine	Dusty brownish clay is scattered throughout the rock, especially in veins.
Serpentine	90-95	Olivine	Chrysotile and/or lizardite replaced olivine.
Opaques	2	Spinel, serpentine	Magnetite(?) is replacing partly spinel, and observed in vein.

VESICLES/ CAVITIES	PERCENT	LOCATION	SIZE (mm)	FILLING	SHAPE
Vesicles	0				

COMMENTS: Mesh texture appears to define a crude foliation because mesh vein edges parallel one another to a great degree. Veins (0.3 to 0.5 mm wide) of serpentine and clays (after serpentine) run throughout the rock. Veins (0.01 to 0.02 mm wide) of opaque minerals also exist.

125-784A-41R-02 136-140 cm OBSERVER: AIR WHERE SAMPLED: Torishima Forearc Seamount, west flank

ROCK NAME: Serpentinized dunite

GRAIN SIZE: 1-3 mm

TEXTURE: Mesh

PRIMARY MINERALOGY	PERCENT PRESENT	PERCENT ORIGINAL	SIZE (mm)	COMPO-SITION	MORPHOLOGY	COMMENTS
PHENOCRYSTS						
Olivine	0	99	1-3		Anhedral	Completely altered to mesh-textured serpentine.
Spinel	<0.5	1	0.5-1.5		Euhedral to subhedral	Mostly altered to magnetite.
GROUNDMASS						
N/A	N/A	N/A	N/A		N/A	

SECONDARY MINERALOGY	PERCENT	REPLACING/ FILLING	COMMENTS
Clays	10	Serpentine	Dusty brownish clay is scattered throughout the rock and intermixed with serpentine.
Chrysotile/ lizardite	85	Olivine	Form mesh texture which is well developed.
Magnetite	5	Spinel	Replaced spinel and filled in vein with serpentine; dusty 0.1-mm grains.

VESICLES/ CAVITIES	PERCENT	LOCATION	SIZE (mm)	FILLING	SHAPE
Vesicles	0				

COMMENTS: This rock is highly altered, and contains abundant dusty brown clay fine-grained magnetite. Anastomosing veins of serpentine run throughout the rock. Some appear to form "Frankenstein-like" texture. Veins appear to be mostly chrysotile, clay and magnetite. No piece number given.

125-784A-42R-01 (Piece 1, 5-8 cm) OBSERVER: HIR WHERE SAMPLED: Torishima Forearc Seamount, west flank

ROCK NAME: Serpentinized harzburgite

GRAIN SIZE: 1-5 mm

TEXTURE: Mesh and bastite

PRIMARY MINERALOGY	PERCENT PRESENT	PERCENT ORIGINAL	SIZE (mm)	COMPO-SITION	MORPHOLOGY	COMMENTS
PHENOCRYST						
Olivine	0-1	80-85	1-3		Anhedral	Mostly altered to mesh-textured serpentine.
Clinopyroxene	[illegible]	[illegible]	1-2		Anhedral	Forms exsolution lamellae in orthopyroxene and isolate anhedral crystal.
Spinel	<0.5	<0.5	<1	Cr	Euhedral-anhedral	Reddish brown spinel scattered throughout the rock.
Orthopyroxene	10-15	15-20	2-5		Anhedral	Mostly altered to bastite textured serpentine.
GROUNDMASS						
N/A	N/A	N/A	N/A		N/A	

SECONDARY MINERALOGY	PERCENT	REPLACING/ FILLING	COMMENTS
Chlorite	Trace	Orthopyroxene	Pale-green chlorite occurs in pyroxene bastite.
Chrysotile/ lizardite	75-85	Olivine, orthopyroxene	Forms mesh and bastite textures after olivine and orthopyroxene, respectively.
Magnetite	Trace		Magnetite (0.01 to 0.02 mm) scattered throughout the rock.

VESICLES/ CAVITIES	PERCENT	LOCATION	SIZE (mm)	FILLING	SHAPE
Vesicles	0				

COMMENTS: Wavy extinction is common in orthopyroxene crystals. Small serpentine veins (0.05 to 0.1 mm in width) are visible. Clinopyroxene are usually at or near orthopyroxene margins. Spinels sometimes form crudely elongated trains. Veins have no regular orientation.

125-784A-42R-01 (Piece 4, 38-41 cm) OBSERVER: HIR WHERE SAMPLED: Torishima Forearc Seamount, west flank

ROCK NAME: Serpentinized dunite

GRAIN SIZE:

TEXTURE: Mesh

PRIMARY MINERALOGY	PERCENT PRESENT	PERCENT ORIGINAL	SIZE (mm)	COMPO-SITION	MORPHOLOGY	COMMENTS
Olivine	0	99	Not visible		Not visible	Altered to mesh-textured serpentine completely.
Spinel	Trace	1	0.2-0.4		Anhedral	Mostly altered to magnetite.

SECONDARY MINERALOGY	PERCENT	REPLACING/ FILLING	COMMENTS
Clays	5-10	Serpentine	Rusty brownish clay is scattered throughout the rock.
Chrysotile/ lizardite	88-93	Olivine	
Magnetite	<1	Spinel	Spinel is almost altered to magnetite.
Sulfides	1		Fine-grained sulfide minerals (pyrrhotite?) are scattered throughout the rock.

VESICLES/ CAVITIES	PERCENT	LOCATION	SIZE (mm)	FILLING	SHAPE
Vesicles	0				

COMMENTS: Anastomosing veins of serpentine run throughout the rock. Spinels form crudely elongated trails; mesh texture appears to define a crude foliation because mesh vein edges parallel one another to a great degree.

125-784A-45R-01 (Piece 3, 98-100 cm)   OBSERVER: SAB   WHERE SAMPLED: Torishima Forearc Seamount, west flank

ROCK NAME: Serpentinized harzburgite

GRAIN SIZE: 0.1-5 mm

TEXTURE: Mesh (minor bastite)

PRIMARY MINERALOGY	PERCENT PRESENT	PERCENT ORIGINAL	SIZE (mm)	COMPO-SITION	MORPHOLOGY	COMMENTS
PHENOCRYSTS						
Olivine	10	77	1-4		Anhedral	Altered to serpentine mesh texture, wavy extinction, kink-banded.
Clinopyroxene	1	2	0.1-0.5		Subhedral-anhedral	As exsolution lamellae and as individual crystals.
Spinel	0.5	1	0.01-0.5	Cr	Euhedral-subhedral	Dark brown to dark red brown, fractured.
Orthopyroxene	7	20	1-5		Anhedral	Altering to serpentine bastite texture, wavy extinction, (100) exsolution lamellae, kink-banded.
GROUNDMASS						
N/A	N/A	N/A	N/A		N/A	

SECONDARY MINERALOGY	PERCENT	REPLACING/ FILLING	COMMENTS
Serpentine	80	Olivine, orthopyroxene	Lizardite and/or chrysotile forming mesh and bastite texture from olivine and orthopyroxene, respectively.
Magnetite	0.5	Spinel	Dusty 0.01-mm grains disseminated throughout slide.

VESICLES/ CAVITIES	PERCENT	LOCATION	SIZE (mm)	FILLING	SHAPE
Vesicles	0				

COMMENTS: Relatively pyroxene-rich serpentinized harzburgite. Orthopyroxene and olivine show wavy extinctions and are kink-banded. Olivine appears to have been more altered than orthopyroxene. Orthopyroxenes have anhedral inclusions of clinopyroxene and of serpentine pseudomorphs. Most clinopyroxene grains are concentrated near orthopyroxene margins.

125-784A-45R-02 (Piece 3, 41-44 cm)   OBSERVER: HIR   WHERE SAMPLED: Torishima Forearc Seamount, west flank

ROCK NAME: Serpentinized harzburgite

GRAIN SIZE: 1-4 mm

TEXTURE: Mesh and bastite

PRIMARY MINERALOGY	PERCENT PRESENT	PERCENT ORIGINAL	SIZE (mm)	COMPO-SITION	MORPHOLOGY	COMMENTS
Olivine	5-10	62-68	1-4		Anhedral	Mostly altered to mesh serpentine.
Clinopyroxene	2-3	2-3	1-2.5		Anhedral	Occurs as anhedral crystal and as exsolution lamellae in orthopyroxene.
Spinel	Trace	Trace	<1		Euhedral-anhedral	Reddish brown in color.
Orthopyroxene	15-25	30-35	1-4		Anhedral	Partly altered to bastite textured serpentine wavy extinction, kink-banded.

SECONDARY MINERALOGY	PERCENT	REPLACING/ FILLING	COMMENTS
Chrysotile/ lizardite	65-70	Olivine, orthopyroxene	Forms mesh and bastite textures after olivine and orthopyroxene, respectively.
Magnetite	Trace	Serpentine, veins	Occurs in serpentine veins; very fine-grained, dusty grains.

VESICLES/ CAVITIES	PERCENT	LOCATION	SIZE (mm)	FILLING	SHAPE
Vesicles	0				

COMMENTS: Serpentine veins (0.02 to 0.1 mm wide) run throughout the slide at no preferred orientation. Wavy extinction and kink-bands are visible in orthopyroxene crystals. Clinopyroxene-exsolution lamellae appear bent in some orthopyroxene crystals. Olivines are more altered than orthopyroxene.

[illegible]

SITE 785 HOLE A CORE 1H CORED INTERVAL 2660.8-2670.3 mbsl; 0.0-9.5 mbsf

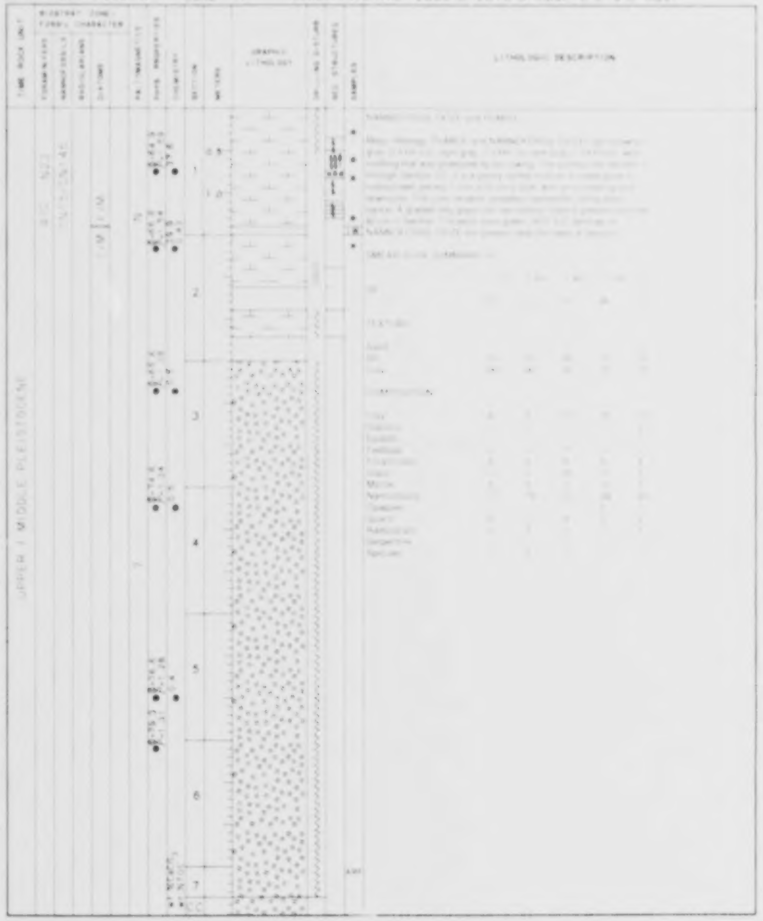
TIME-ROCK UNIT
BIOSTRAT. ZONE/FOSSIL CHARACTER
FORAMINIFERS
NANNOFOSSILS
RADIOLARIANS
DIATOMS
PALEOMAGNETICS
PHYS. PROPERTIES
CHEMISTRY
SECTION
METERS
GRAPHIC LITHOLOGY
DRILLING DISTURB.
SED. STRUCTURES
SAMPLES
LITHOLOGIC DESCRIPTION
UPPER / MIDDLE PLEISTOCENE
N
1
2
3
4
5
6
7
CC
0.5
1.0

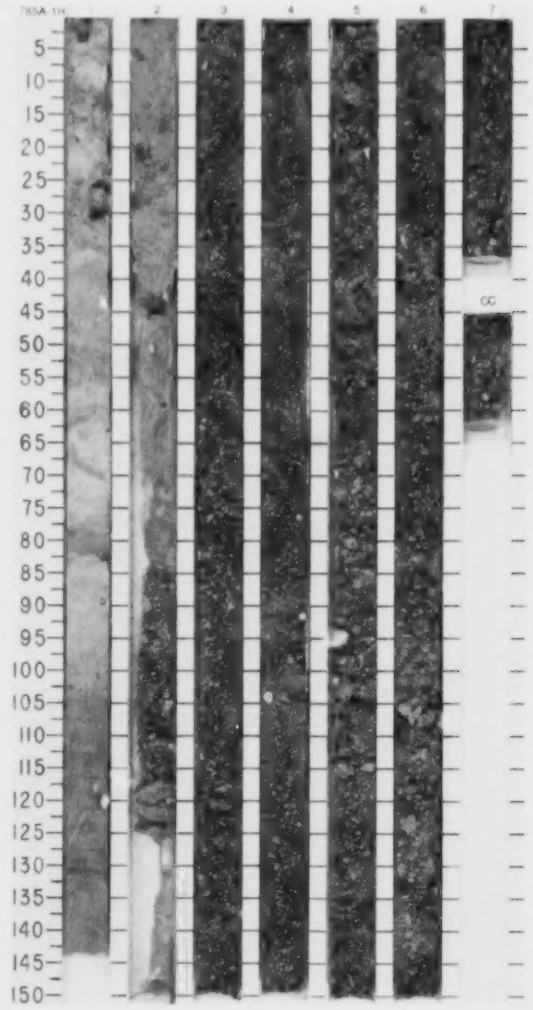
785A-1H
1
2
3
4
5
6
7
CC
5
10
15
20
25
30
35
40
45
50
55
60
65
70
75
80
85
90
95
100
105
110
115
120
125
130
135
140
145
150

SITE 785 HOLE A CORE 2H CORED INTERVAL 2670.1-2679.8 mbsl; 9.5-19.0 mbsf

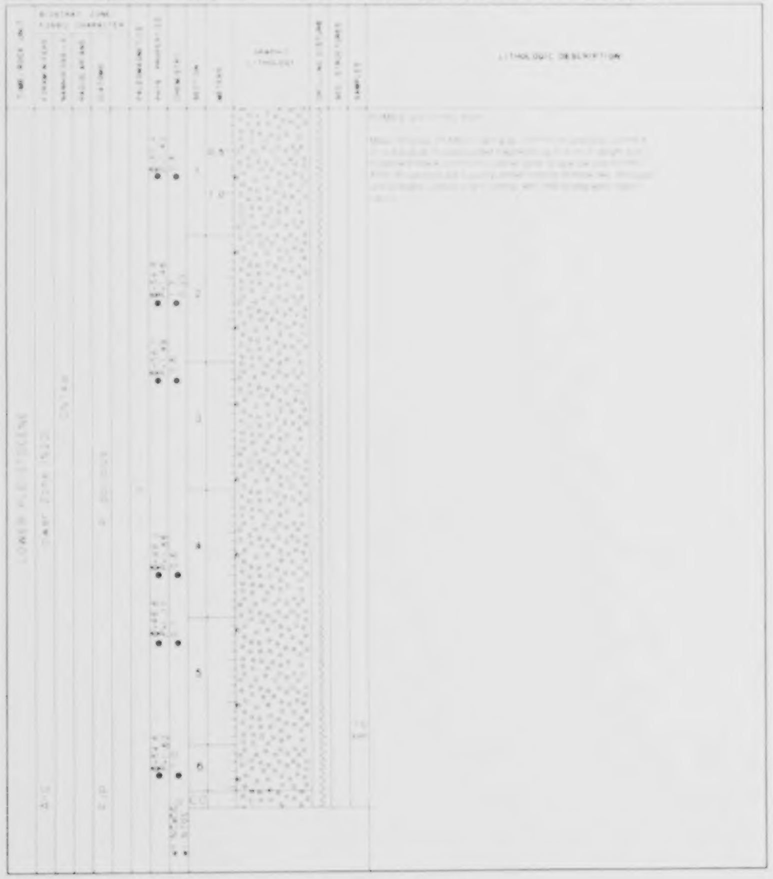
LITHOLOGIC DESCRIPTION
GRAPHIC LITHOLOGY
BIOSTRAT. ZONE/ FOSSIL CHARACTER
LOWER PLEISTOCENE
CC

785 A 3X NO RECOVERY

785 A 4X NO RECOVERY

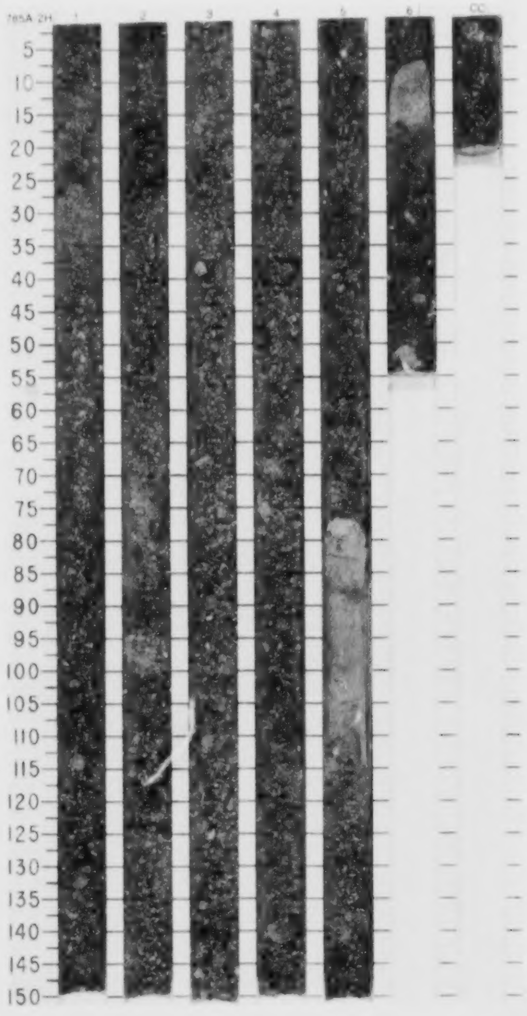
785A 2H
1
2
3
4
5
6
CC
5
10
15
20
25
30
35
40
45
50
55
60
65
70
75
80
85
90
95
100
105
110
115
120
125
130
135
140
145
150

SITE 785 HOLE A CORE 5X CORED INTERVAL 2699.1-2708.6 mbsl; 38.3-47.8 mbsf

TIME-ROCK UNIT	BIOSTRAT. ZONE/ FOSSIL CHARACTER: FORAMINIFERS	NANNOFOSSILS	RADIOLARIANS	DIATOMS	PALEOMAGNETICS	PHYS. PROPERTIES	CHEMISTRY	SECTION	METERS	GRAPHIC LITHOLOGY	DRILLING DISTURB.	SED. STRUCTURES	SAMPLES	LITHOLOGIC DESCRIPTION
LOWER PLEISTOCENE	lower Zone (N22) A/G	CN14a A/G		N. reinholdii F/M				CC						NANNOFOSSIL OOZE AND VITRIC ASH Major lithology: NANNOFOSSIL OOZE [illegible]

SITE 785 HOLE A CORE 6X CORED INTERVAL 2708.6-2718.1 mbsl; 47.8-57.3 mbsf

TIME-ROCK UNIT	BIOSTRAT. ZONE/ FOSSIL CHARACTER: FORAMINIFERS	NANNOFOSSILS	RADIOLARIANS	DIATOMS	PALEOMAGNETICS	PHYS. PROPERTIES	CHEMISTRY	SECTION	METERS	GRAPHIC LITHOLOGY	DRILLING DISTURB.	SED. STRUCTURES	SAMPLES	LITHOLOGIC DESCRIPTION
LOWER PLEISTOCENE	lower Zone N22 A/G	CN14a A/G		B				1 2	0.5 1.0					One cm of core recovered in the core catcher; all material given to paleontologists.

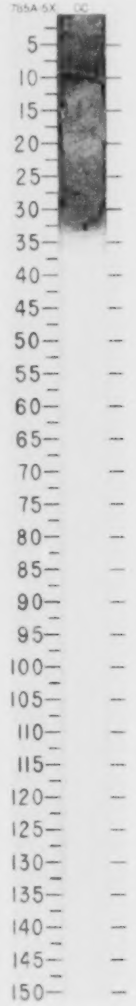

SITE 785 HOLE A CORE 7X CORED INTERVAL 2718.1-2727.8 mbsl; 57.3-66.8 mbsf

LITHOLOGIC DESCRIPTION
GRAPHIC LITHOLOGY
LOWER PLEISTOCENE

785 A 8X NO RECOVERY

785 A 9X NO RECOVERY

785 A 10X NO RECOVERY

785 A 11X NO RECOVERY

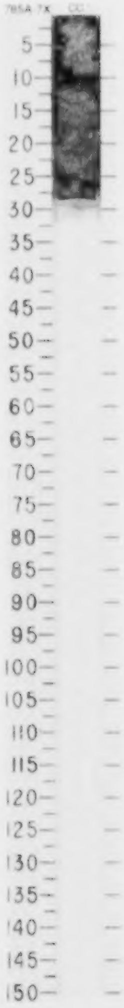
785A-7X
CC
5
10
15
20
25
30
35
40
45
50
55
60
65
70
75
80
85
90
95
100
105
110
115
120
125
130
135
140
145
150

[illegible]-785A-28-CC (132-134 cm)   OBSERVER: JOH   WHERE SAMPLED: Izu-Bonin forearc

ROCK NAME: Pumice

GRAIN SIZE: Glass

TEXTURE: Glassy vesicular

PRIMARY MINERALOGY	PERCENT PRESENT	PERCENT ORIGINAL	SIZE (mm)	COMPO-SITION	MORPHOLOGY	COMMENTS
PHENOCRYSTS						
Spinel	Trace	Trace	<0.01		Subhedral	Equant.
GROUNDMASS						
Glass	[illegible]	[illegible]	N/A		N/A	Glass, now brown and devitrified.

SECONDARY MINERALOGY	PERCENT	REPLACING/FILLING	COMMENTS
Clays	>95	Glass	Brown, amorphous, pervasive.
Chlorite	Trace	Glass	Slight yellow-green pleochroism.

VESICLES/CAVITIES	PERCENT	LOCATION	SIZE (mm)	FILLING	SHAPE	COMMENTS
Vesicles	[illegible]		<2			Stretched.

COMMENTS: Pumice fragment, stretched glass altered to clay. Pink tinge to section may result from thin section preparation or a Mn component in the clay. No piece number given.

[illegible]-785A-[illegible]-CC (21-24 cm)   OBSERVER: JOH   WHERE SAMPLED: Izu-Bonin forearc

ROCK NAME: Pumice

GRAIN SIZE: Glass

TEXTURE: Glassy vesicular

PRIMARY MINERALOGY	PERCENT PRESENT	PERCENT ORIGINAL	SIZE (mm)	COMPO-SITION	MORPHOLOGY	COMMENTS
PHENOCRYSTS						
Spinel	Trace	Trace	<0.01		Subhedral	Equant.
GROUNDMASS						
Glass	[illegible]	[illegible]	N/A		N/A	Brown, devitrified. Small portions of fresh, colorless glass.

SECONDARY MINERALOGY	PERCENT	REPLACING/FILLING	COMMENTS
Clays	[illegible]	Glass	Brown, amorphous, pervasive.

VESICLES/CAVITIES	PERCENT	LOCATION	SIZE (mm)	FILLING	SHAPE	COMMENTS
Vesicles	[illegible]		[illegible]			Elongate, irregular, stretched.

COMMENTS: Pink tint to section may result from clay or preparation of thin section. No piece number given.

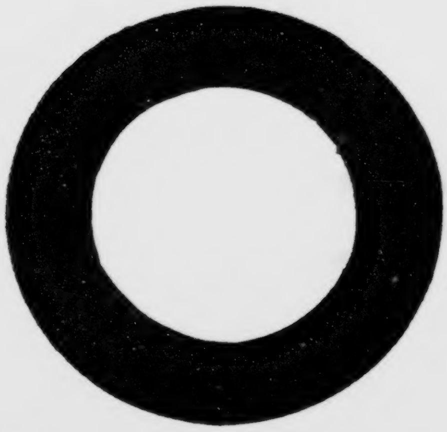

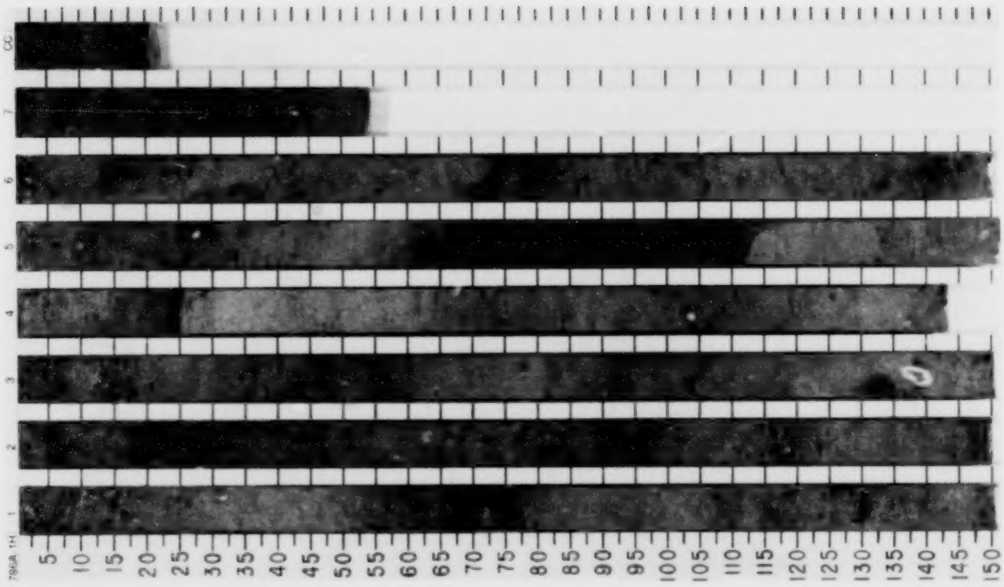
786A 1H
1
2
3
4
5
6
7
CC
5
10
15
20
25
30
35
40
45
50
55
60
65
70
75
80
85
90
95
100
105
110
115
120
125
130
135
140
145
150

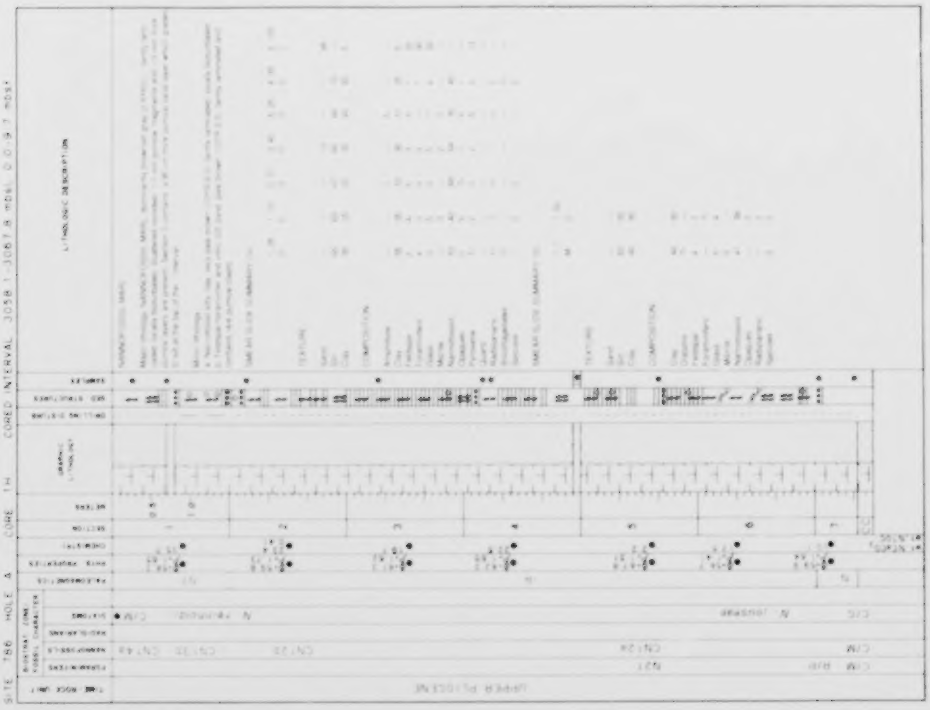
SITE 786 HOLE A CORE 1H CORED INTERVAL 3058.1-3067.8 mbsl; 0.0-9.7 mbsf
TIME-ROCK UNIT
BIOSTRAT. ZONE/ FOSSIL CHARACTER
FORAMINIFERS
NANNOFOSSILS
RADIOLARIANS
DIATOMS
PALEOMAGNETICS
PHYS. PROPERTIES
CHEMISTRY
SECTION
METERS
GRAPHIC LITHOLOGY
DRILLING DISTURB.
SED. STRUCTURES
SAMPLES
LITHOLOGIC DESCRIPTION
UPPER PLIOCENE
N21
CN12a
C/M
N
1
2
3
4
5
6
7
CC
0.5
1.0
NANNOFOSSIL MARL
SMEAR SLIDE SUMMARY (%):
TEXTURE:
Sand
Silt
Clay
COMPOSITION:

SITE 786 HOLE A CORE 2H CORED INTERVAL 3067.8-3077.3 mbsl; 9.7-19.2 mbsf

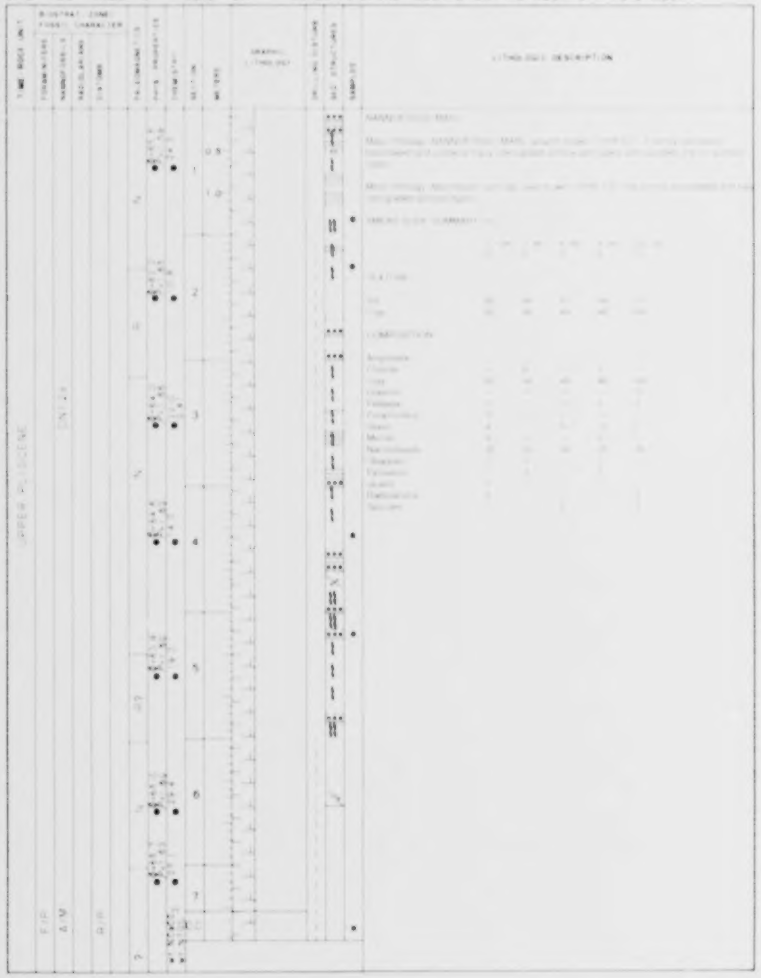
TIME-ROCK UNIT
BIOSTRAT. ZONE/FOSSIL CHARACTER
FORAMINIFERS
NANNOFOSSILS
RADIOLARIANS
DIATOMS
PALEOMAGNETICS
PHYS. PROPERTIES
CHEMISTRY
SECTION
METERS
GRAPHIC LITHOLOGY
DRILLING DISTURB.
SED. STRUCTURES
SAMPLES
LITHOLOGIC DESCRIPTION
UPPER PLIOCENE
F/P
A/V
R/P
0.5
1.0
1
2
3
4
5
6
7
CC

LITHOLOGIC DESCRIPTION

NANNOFOSSIL MARL

Major lithology: NANNOFOSSIL MARL [illegible]

Minor lithology: [illegible]

SMEAR SLIDE SUMMARY (%):

TEXTURE:

Silt

Clay

COMPOSITION:

[illegible]

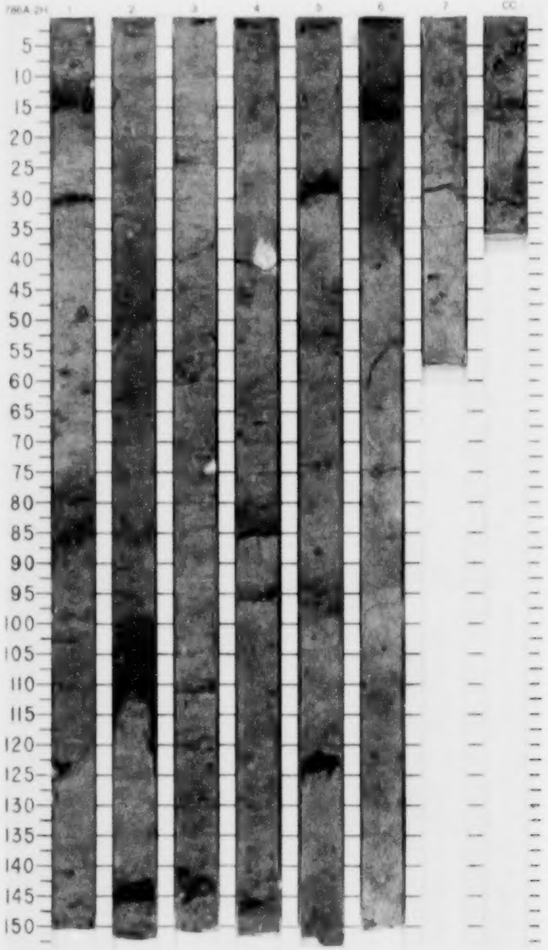
786A-2H
1
2
3
4
5
6
7
CC
5
10
15
20
25
30
35
40
45
50
55
60
65
70
75
80
85
90
95
100
105
110
115
120
125
130
135
140
145
150

SITE 786 HOLE A CORE 3H CORED INTERVAL 3077.3-3086.8 mbsl; 19.2-28.7 mbsf

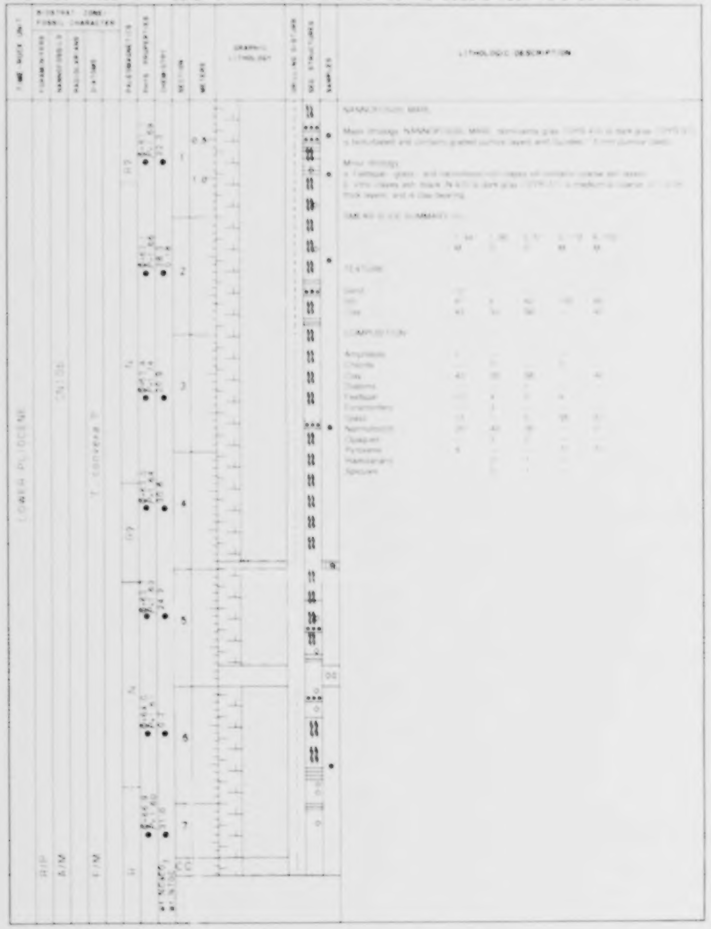
TIME-ROCK UNIT
BIOSTRAT. ZONE/FOSSIL CHARACTER
FORAMINIFERS
NANNOFOSSILS
RADIOLARIANS
DIATOMS
PALEOMAGNETICS
PHYS. PROPERTIES
CHEMISTRY
SECTION
METERS
GRAPHIC LITHOLOGY
DRILLING DISTURB.
SED. STRUCTURES
SAMPLES
LOWER PLIOCENE
CN10b
T. convexa ?
R/P
A/M
F/M
0.5
1.0
1
2
3
4
5
6
7
CC

LITHOLOGIC DESCRIPTION

NANNOFOSSIL MARL

Major lithology: NANNOFOSSIL MARL, [illegible]

Minor lithology:

[illegible]

SMEAR SLIDE SUMMARY (%):

TEXTURE:

Sand

Silt

Clay

COMPOSITION:

Amphibole

Chlorite

Clay

Diatoms

Feldspar

Foraminifers

Glass

Nannofossils

Opaques

Pyroxene

Radiolarians

Spicules

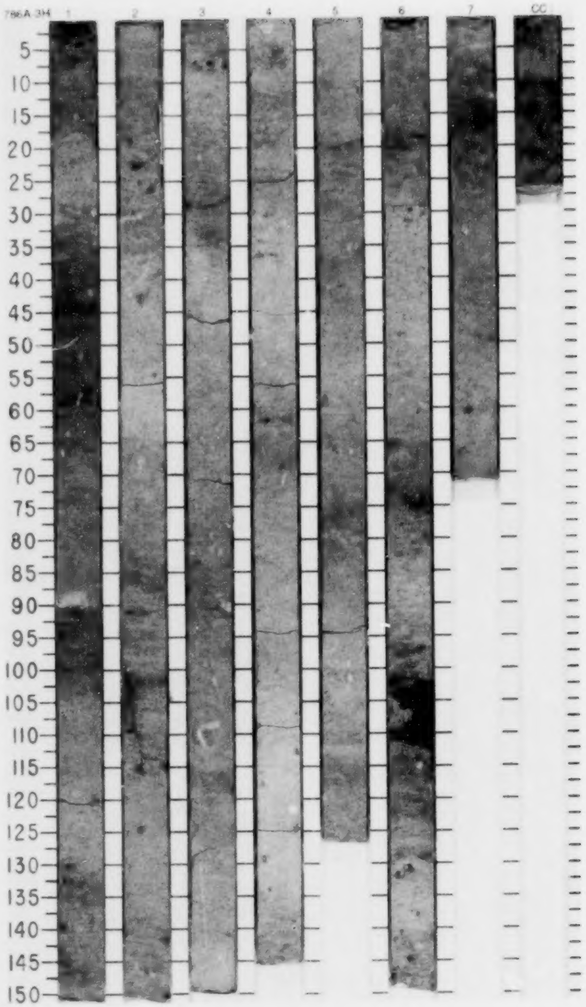
786A-3H
1
2
3
4
5
6
7
CC
5
10
15
20
25
30
35
40
45
50
55
60
65
70
75
80
85
90
95
100
105
110
115
120
125
130
135
140
145
150

SITE 786 HOLE A CORE 4X CORED INTERVAL 3086.8-3096.3 mbsl; 28.7-38.2 mbsf

TIME-ROCK UNIT	BIOSTRAT. ZONE/FOSSIL CHARACTER: FORAMINIFERS	NANNOFOSSILS	RADIOLARIANS	DIATOMS	PALEOMAGNETICS	PHYS. PROPERTIES	CHEMISTRY	SECTION	METERS	GRAPHIC LITHOLOGY	DRILLING DISTURB.	SED. STRUCTURES	SAMPLES	LITHOLOGIC DESCRIPTION
UPPER MIOCENE	B/M	CN9b C/P		N. miocenica C/M	N	● ●	● ● ●	1 2 CC	0.5 1.0				● ● ● ●	NANNOFOSSIL MARL

NANNOFOSSIL MARL

Major lithology: NANNOFOSSIL MARL, [illegible]

SMEAR SLIDE SUMMARY (%):

TEXTURE:

Silt

Clay

COMPOSITION:

Calcite

Clay

Diatoms

Feldspar

Glass

Nannofossils

Opaques

Pyroxene

Quartz

Radiolarians

Silicoflagellates

Spicules

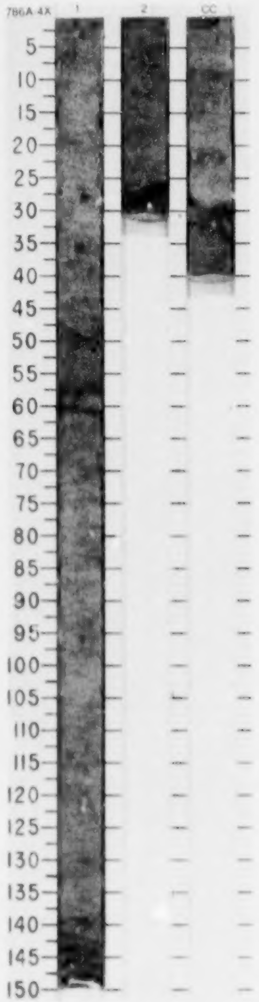
786A-4X
1
2
CC
5
10
15
20
25
30
35
40
45
50
55
60
65
70
75
80
85
90
95
100
105
110
115
120
125
130
135
140
145
150

SITE 786 HOLE A CORE 5X CORED INTERVAL 3096.3-3105.7 mbsl; 38.2-47.6 mbsf

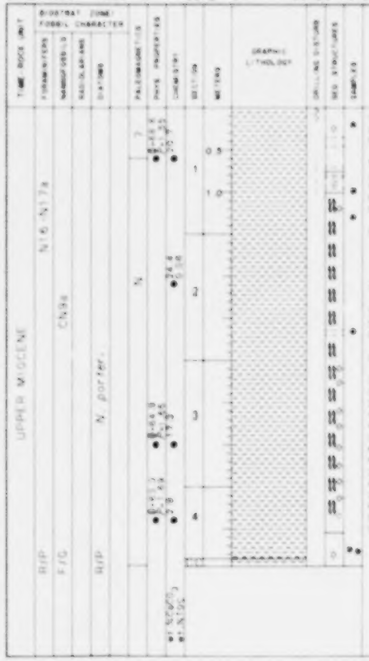
TIME-ROCK UNIT
BIOSTRAT. ZONE/ FOSSIL CHARACTER
FORAMINIFERS
NANNOFOSSILS
RADIOLARIANS
DIATOMS
PALEOMAGNETICS
PHYS. PROPERTIES
CHEMISTRY
SECTION
METERS
GRAPHIC LITHOLOGY
DRILLING DISTURB.
SED. STRUCTURES
SAMPLES
UPPER MIOCENE
N16-N17a
CN9a
N. porteri
R/P
F/G
R/P
?
N
1
2
3
4
0.5
1.0

LITHOLOGIC DESCRIPTION

GLASS-RICH CLAY. Major lithology: GLASS-RICH CLAY is grayish brown (2.5Y 5/2) to dark gray (5Y 4/1) and contains scattered pumice fragments. The core is burrowed and mottled throughout. Some burrows are filled with black (10YR 2/1) ash.

Minor lithologies:
a. Nannofossil marl, grayish brown (2.5Y 5/2), contains abundant, scattered, rounded pumice fragments up to 2 mm in diameter. The core is extensively bioturbated.
b. Vitric ash, black (N 4/0) and brownish gray (10YR 6/2) in 1-2 cm layers with both sharp basal contacts.

SMEAR SLIDE SUMMARY (%):

	1, 20	1, 106	1, 130	2, 110	4, 74	4, 76
	D	D	D	D	M	M
TEXTURE:						
Sand	—	50	10	—	—	—
Silt	65	50	60	49	21	37
Clay	35	—	30	51	79	63
COMPOSITION:						
Chlorite	—	1	—	—	1	—
Clay	35	10	30	51	72	60
Diatoms	1	—	2	1	—	—
Feldspar	2	8	—	6	5	10
Foraminifers	—	—	10	—	—	—
Glass	14	75	6	25	15	19
Mica	2	—	—	4	—	—
Nannofossils	40	4	50	10	—	1
Opaques	—	—	1	1	3	4
Pyroxene	1	1	—	1	1	3
Quartz	—	—	1	—	1	—
Radiolarians	2	1	1	1	—	—
Silicoflagellates	1	—	—	—	[illegible]	—
Sponges	1		2	1	1	

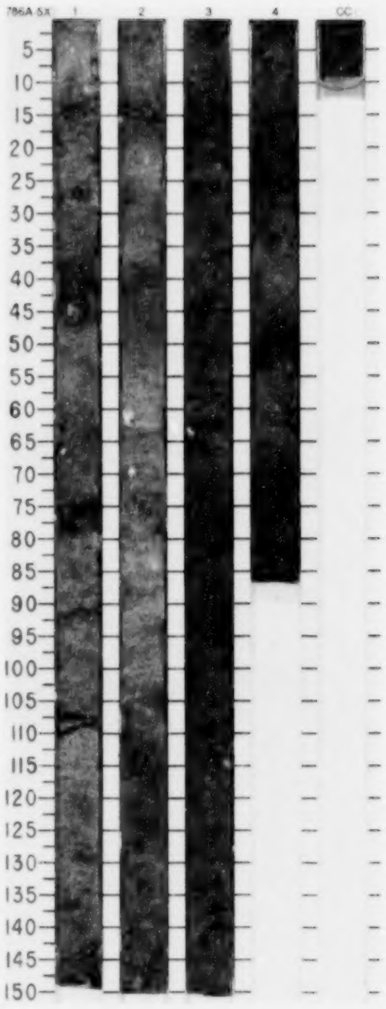
786A 5X
1
2
3
4
CC
5
10
15
20
25
30
35
40
45
50
55
60
65
70
75
80
85
90
95
100
105
110
115
120
125
130
135
140
145
150

SITE 786 HOLE A CORE 6X CORED INTERVAL 3105.7-3115.2 mbsl; 47.6-57.1 mbsf

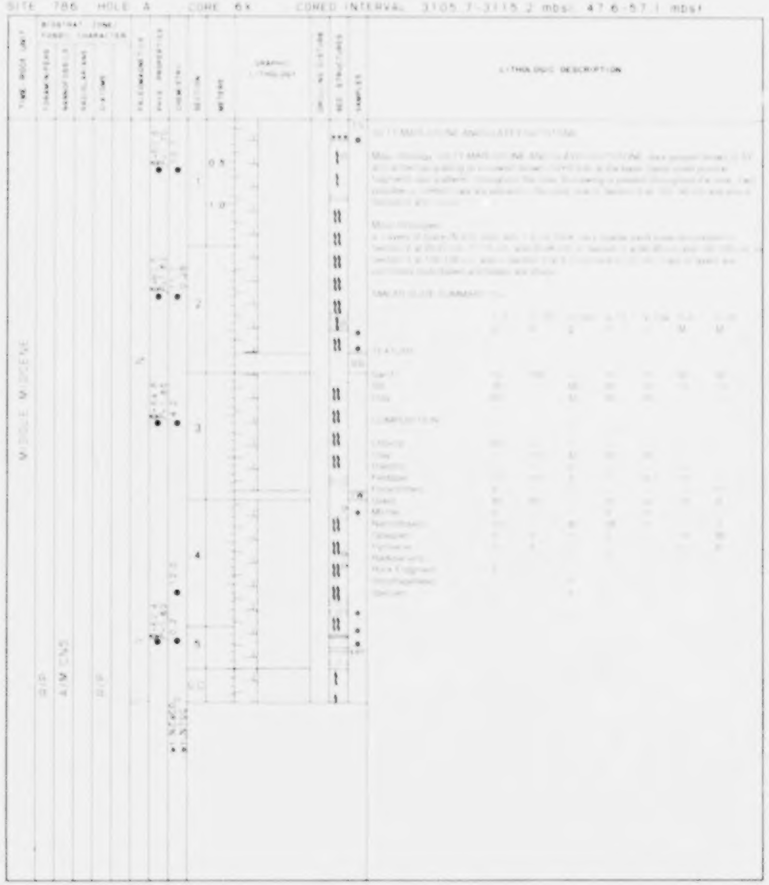
BIOSTRAT. ZONE/ FOSSIL CHARACTER
GRAPHIC LITHOLOGY
LITHOLOGIC DESCRIPTION
MIDDLE MIOCENE
0.5
1.0
1
2
3
4
5
CC
SMEAR SLIDE SUMMARY (%):
TEXTURE:
COMPOSITION:

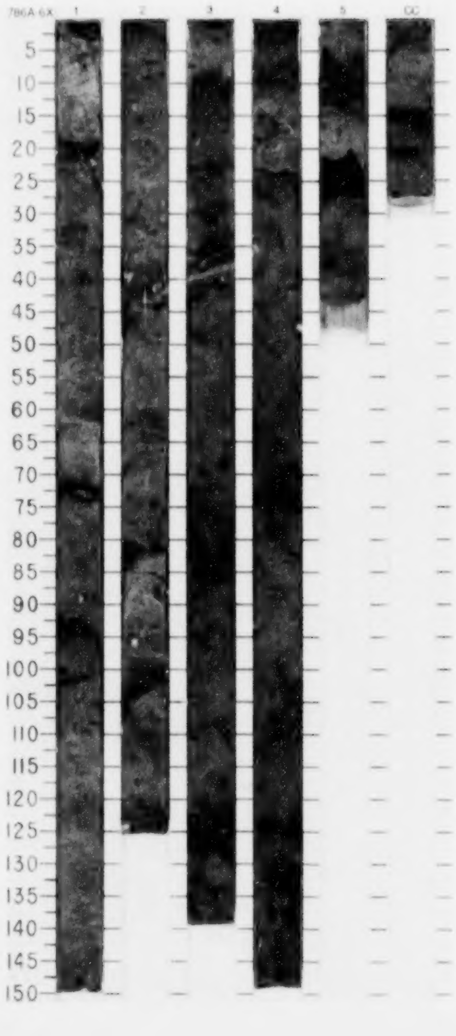
786A-6X
1
2
3
4
5
CC
5
10
15
20
25
30
35
40
45
50
55
60
65
70
75
80
85
90
95
100
105
110
115
120
125
130
135
140
145
150

SITE 786 HOLE A CORE 7X CORED INTERVAL 3115.2-3125.2 mbsl; 57.1-67.1 mbsf

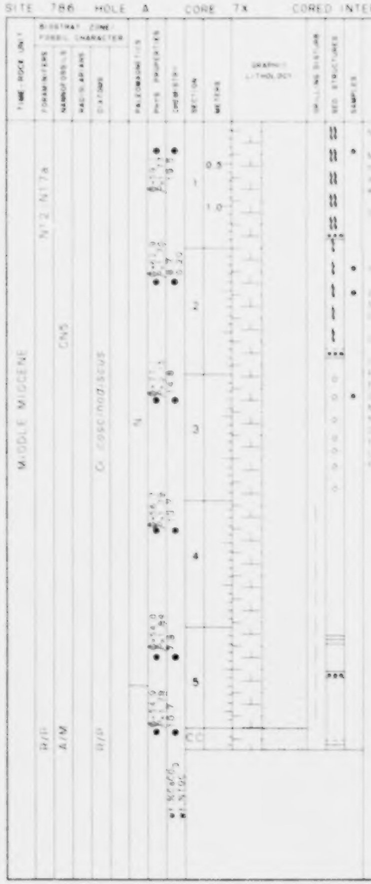
TIME-ROCK UNIT
BIOSTRAT. ZONE/ FOSSIL CHARACTER
FORAMINIFERS
NANNOFOSSILS
RADIOLARIANS
DIATOMS
PALEOMAGNETICS
PHYS. PROPERTIES
CHEMISTRY
SECTION
METERS
GRAPHIC LITHOLOGY
DRILLING DISTURB.
SED. STRUCTURES
SAMPLES
MIDDLE MIOCENE
N12-N17a
CN5
C. coscinodiscus
R/P
A/M
R/P
N
0.5
1.0
1
2
3
4
5
CC

LITHOLOGIC DESCRIPTION

NANNOFOSSIL MARL

Major lithology: NANNOFOSSIL MARL, varies from light brown [illegible] to gray [illegible] to reddish brown [illegible]. [illegible] pumice fragments are present. [illegible]

SMEAR SLIDE SUMMARY (%):

	1, 40	2, [illegible]	3, [illegible]	4, [illegible]
	D	M	[illegible]	[illegible]
TEXTURE:				
Sand	5	—	15	[illegible]
Silt	15	20	45	40
Clay	80	80	40	50
COMPOSITION:				
Clay	30	20	40	30
Feldspar	—	5	—	2
Foraminifers	10	1	5	2
Glass	—	—	5	5
Micrite	20	10	5	10
Nannofossils	30	50	40	35
Opaques	1	2		3
Pyroxene	2	5	—	2
Quartz	5	20	5	5
Radiolarians	—	—	5	—

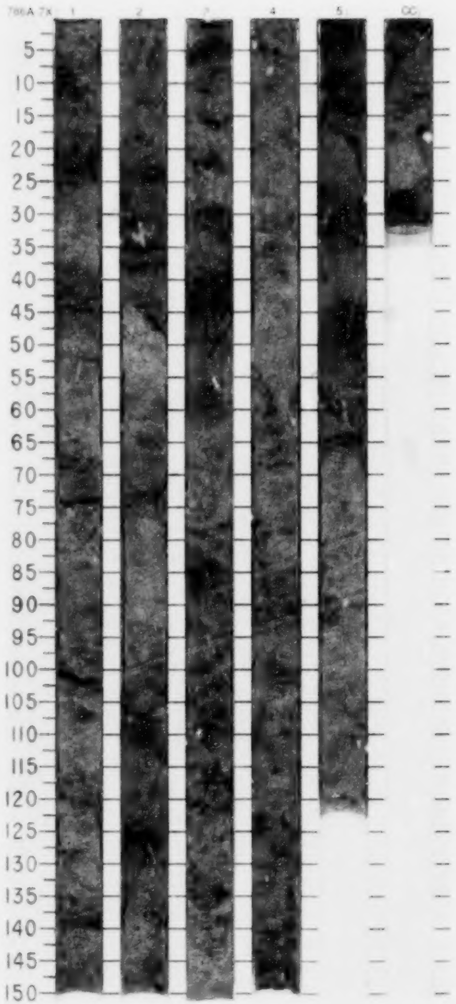
786A-7X
1
2
3
4
5
CC
5
10
15
20
25
30
35
40
45
50
55
60
65
70
75
80
85
90
95
100
105
110
115
120
125
130
135
140
145
150

SITE 786 HOLE A CORE 8X CORED INTERVAL 3125.2-3134.9 mbsl; 67.1-76.8 mbsf

LITHOLOGIC DESCRIPTION

NANNOFOSSIL MARL

[illegible]

SMEAR SLIDE SUMMARY (%):

TEXTURE:

COMPOSITION:

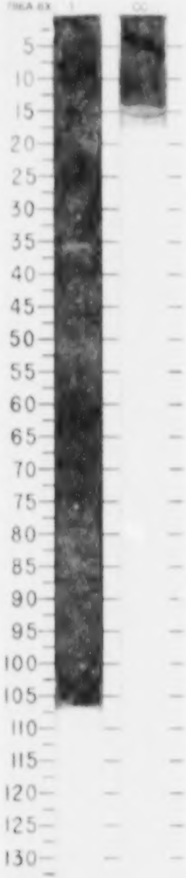
786A-8X
1
CC
5
10
15
20
25
30
35
40
45
50
55
60
65
70
75
80
85
90
95
100
105
110
115
120
125
130

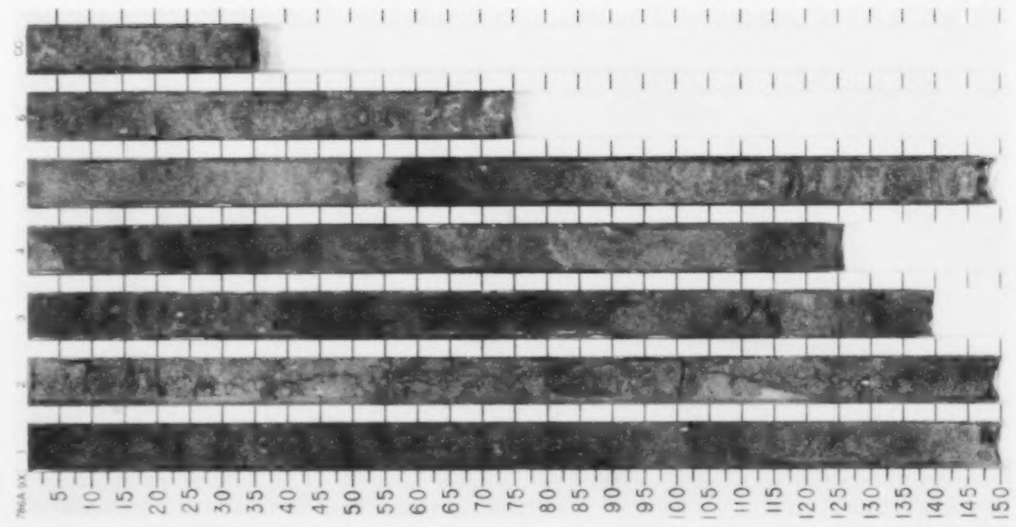
786A-9X
1
2
3
4
5
6
CC
5
10
15
20
25
30
35
40
45
50
55
60
65
70
75
80
85
90
95
100
105
110
115
120
125
130
135
140
145
150

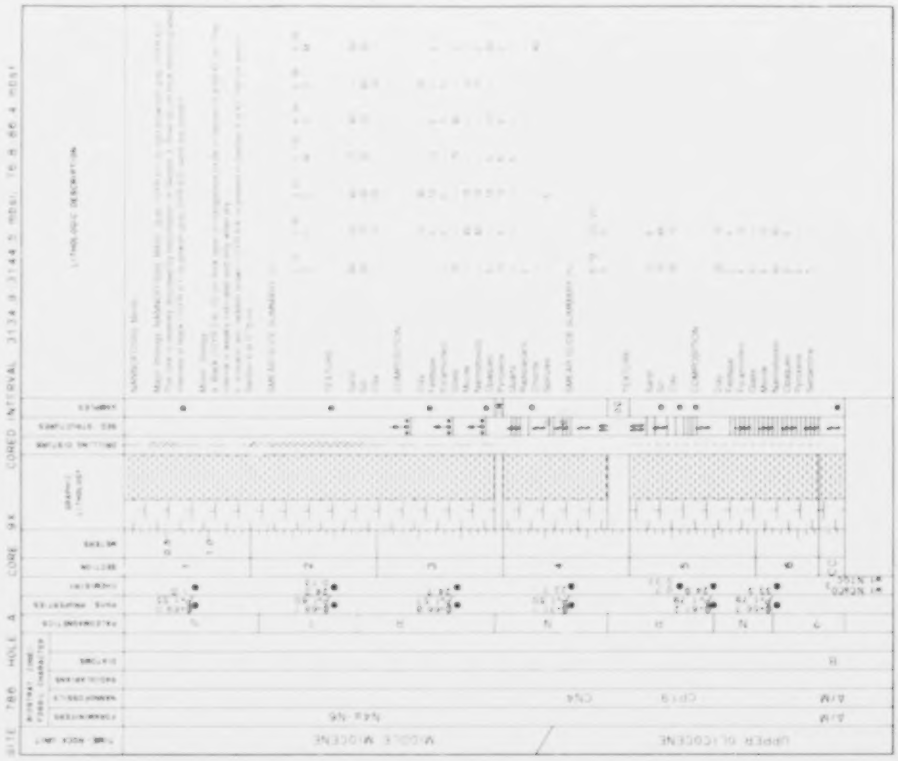

SITE 786 HOLE A CORE 9X CORED INTERVAL 3134.9-3144.5 mbsl; 76.8-86.4 mbsf

LITHOLOGIC DESCRIPTION
GRAPHIC LITHOLOGY
MIDDLE MIOCENE
UPPER OLIGOCENE

SITE 786 HOLE A CORE 10X CORED INTERVAL 3144.5-3154.1 mbsl; 86.4-96.0 mbsf

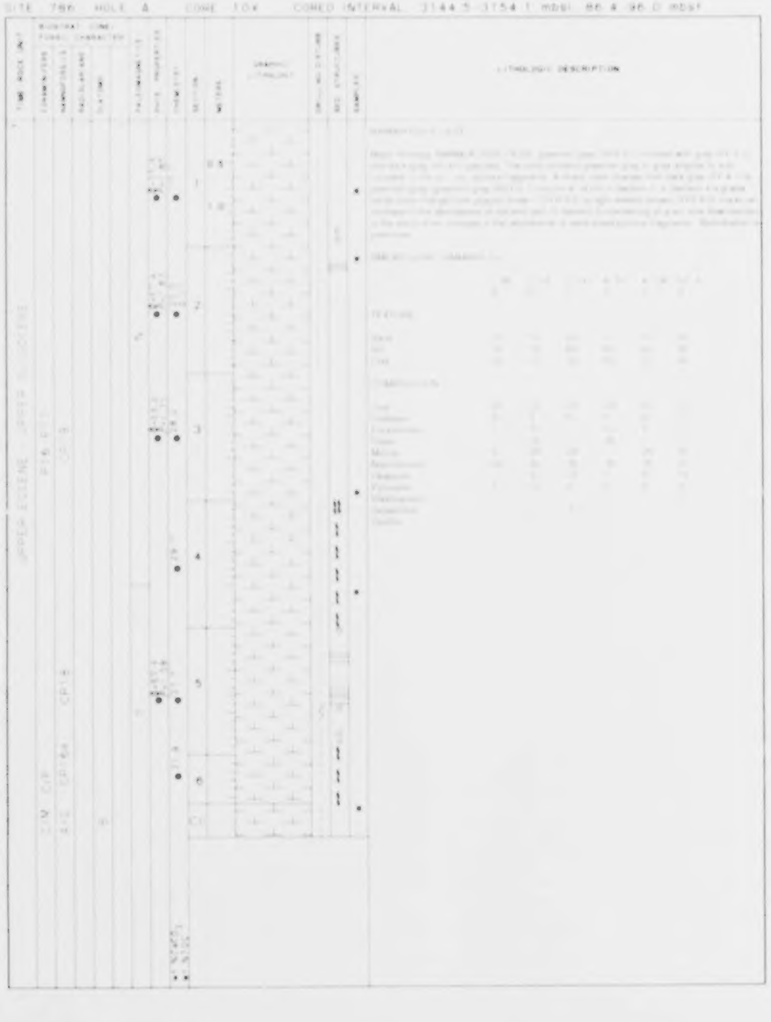
TIME-ROCK UNIT
BIOSTRAT. ZONE/FOSSIL CHARACTER
FORAMINIFERS
NANNOFOSSILS
RADIOLARIANS
DIATOMS
PALEOMAGNETICS
PHYS. PROPERTIES
CHEMISTRY
SECTION
METERS
GRAPHIC LITHOLOGY
DRILLING DISTURB.
SED. STRUCTURES
SAMPLES
LITHOLOGIC DESCRIPTION
UPPER EOCENE
CP18
CP16a
C/M
C/P
A/G
0.5
1.0
1
2
3
4
5
6
CC
TEXTURE:
COMPOSITION:

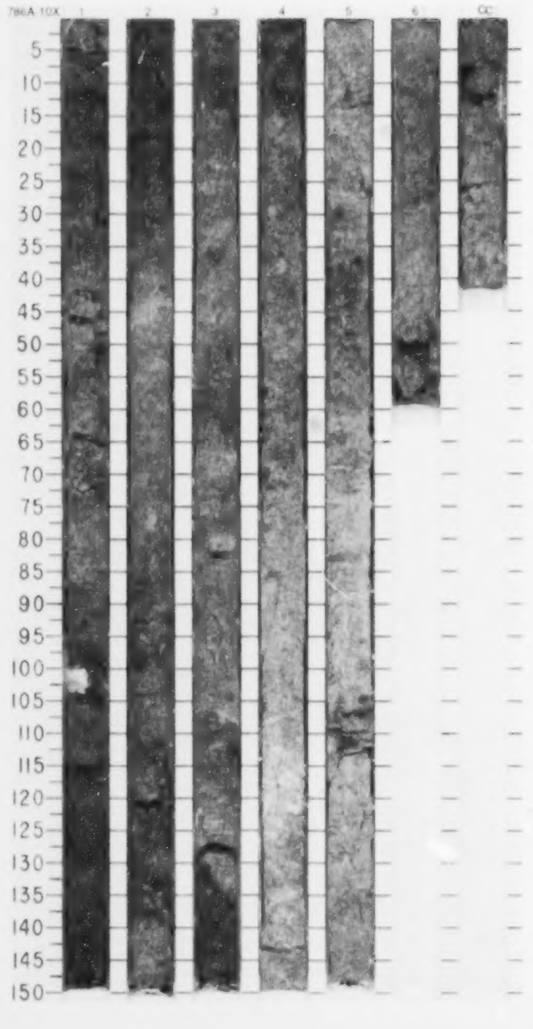
786A-10X
1
2
3
4
5
6
CC
5
10
15
20
25
30
35
40
45
50
55
60
65
70
75
80
85
90
95
100
105
110
115
120
125
130
135
140
145
150

SITE 786 HOLE A CORE 11X CORED INTERVAL 3154.1-3163.8 mbsl; 96.0-105.7 mbsf

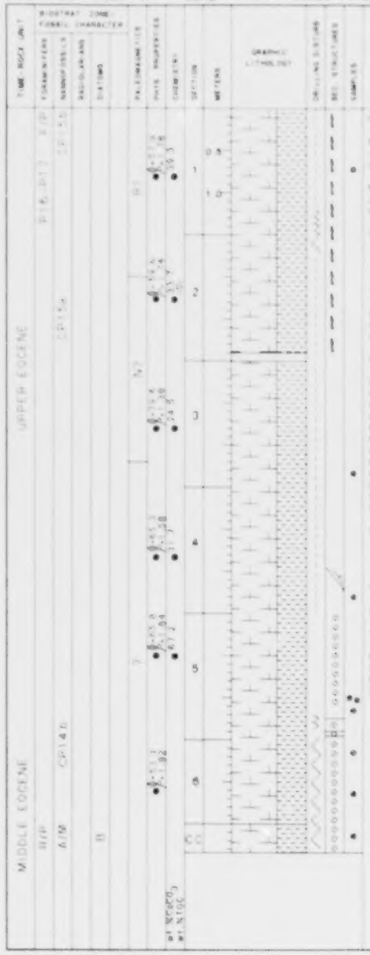
TIME-ROCK UNIT
BIOSTRAT. ZONE/ FOSSIL CHARACTER
FORAMINIFERS
NANNOFOSSILS
RADIOLARIANS
DIATOMS
PALEOMAGNETICS
PHYS. PROPERTIES
CHEMISTRY
SECTION
METERS
GRAPHIC LITHOLOGY
DRILLING DISTURB.
SED. STRUCTURES
SAMPLES
UPPER EOCENE
MIDDLE EOCENE
P16-P17
CP15b
CP15a
CP14b
R/P
A/M
B
N?
1
2
3
4
5
6
CC
0.5
1.0

LITHOLOGIC DESCRIPTION

NANNOFOSSIL MARL

Major lithology: NANNOFOSSIL MARL, [illegible]

Minor lithologies:
[illegible]

SMEAR SLIDE SUMMARY (%):

TEXTURE:

Sand [illegible]
Silt [illegible]
Clay [illegible]

COMPOSITION:

Clay [illegible]
Feldspar [illegible]
Foraminifers [illegible]
Glass [illegible]
Micrite [illegible]
Nannofossils [illegible]
Opaques [illegible]
Pyroxene [illegible]
Radiolarians [illegible]
Serpentine [illegible]
Siderite [illegible]
Spicules [illegible]

SMEAR SLIDE SUMMARY (%):

TEXTURE:

Silt [illegible]

COMPOSITION:

Feldspar [illegible]
Glass [illegible]
Pyroxene [illegible]
Zeolite [illegible]

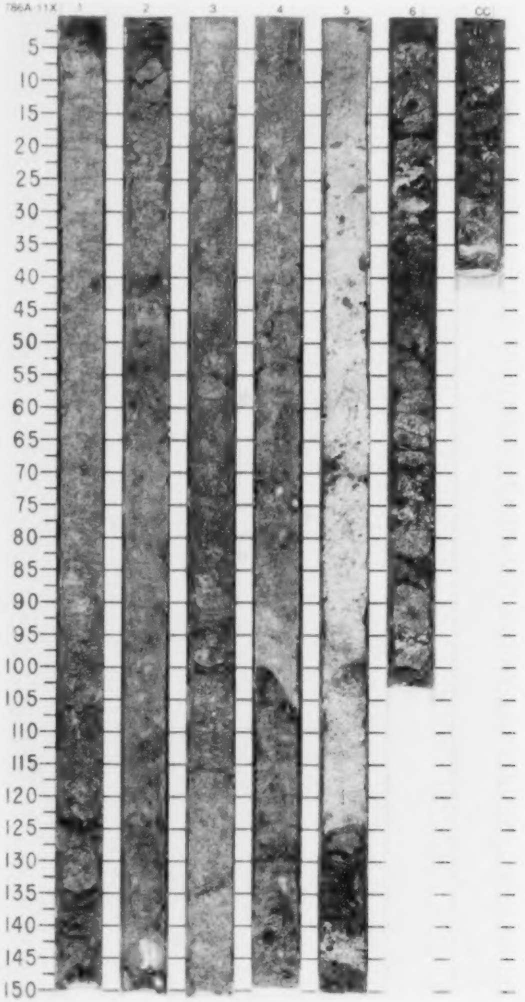
786A-11X
1
2
3
4
5
6
CC
5
10
15
20
25
30
35
40
45
50
55
60
65
70
75
80
85
90
95
100
105
110
115
120
125
130
135
140
145
150

SITE 786 HOLE A CORE 12X CORED INTERVAL 3163.8-3173.4 mbsl; 105.7-115.3 mbsf

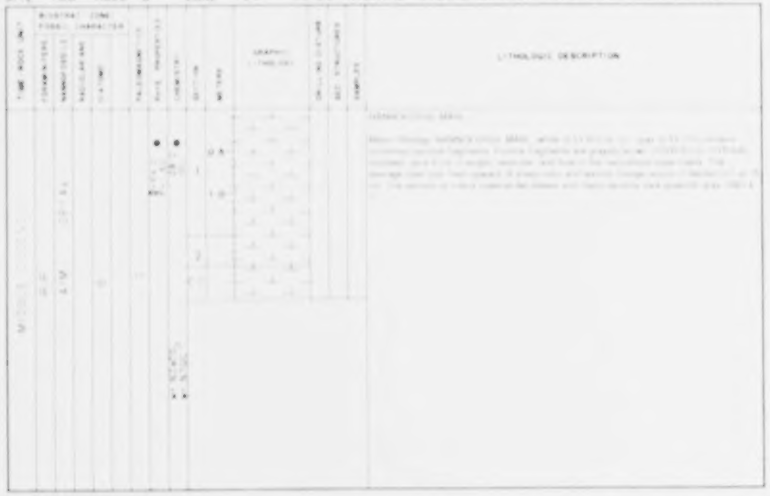
BIOSTRAT. ZONE/ FOSSIL CHARACTER
GRAPHIC LITHOLOGY
LITHOLOGIC DESCRIPTION
1
2
CC

[illegible]

SITE 786 HOLE A CORE 13X CORED INTERVAL 3173.4-3183.0 mbsl; 115.3-124.9 mbsf

BIOSTRAT. ZONE/ FOSSIL CHARACTER
GRAPHIC LITHOLOGY
LITHOLOGIC DESCRIPTION

[illegible]

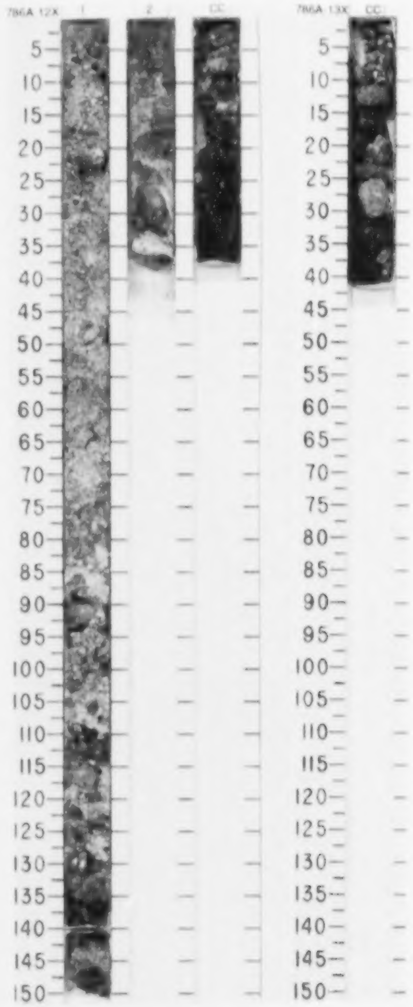
786A 12X
1
2
CC
786A 13X
CC
5
10
15
20
25
30
35
40
45
50
55
60
65
70
75
80
85
90
95
100
105
110
115
120
125
130
135
140
145
150

SITE 786 HOLE A CORE 14X CORED INTERVAL 3183.0-3192.7 mbsl; 124.9-134.6 mbsf

TIME-ROCK UNIT	BIOSTRAT. ZONE/ FOSSIL CHARACTER FORAMINIFERS	NANNOFOSSILS	RADIOLARIANS	DIATOMS	PALEOMAGNETICS	PHYS. PROPERTIES	CHEMISTRY	SECTION	METERS	GRAPHIC LITHOLOGY	DRILLING DISTURB.	SED. STRUCTURES	SAMPLES	LITHOLOGIC DESCRIPTION
					?	●		1		M	×		● ●	This core consists entirely of drill cuttings of igneous rocks and a few clasts from the overlying [illegible]
								CC		M	×			SMEAR SLIDE SUMMARY (%): TEXTURE: Silt Clay COMPOSITION: Chlorite Clay Feldspar Foraminifers Glass Nannofossils Pyroxene Serpentine

SITE 786 HOLE A CORE 15X CORED INTERVAL 3192.7-3202.4 mbsl; 134.6-144.3 mbsf

TIME-ROCK UNIT	BIOSTRAT. ZONE/ FOSSIL CHARACTER FORAMINIFERS	NANNOFOSSILS	RADIOLARIANS	DIATOMS	PALEOMAGNETICS	PHYS. PROPERTIES	CHEMISTRY	SECTION	METERS	GRAPHIC LITHOLOGY	DRILLING DISTURB.	SED. STRUCTURES	SAMPLES	LITHOLOGIC DESCRIPTION
						●		CC		M	×			This core consists of drill cuttings and chips primarily composed of igneous and [illegible] rocks.

SITE 786 HOLE A CORE 16X CORED INTERVAL 3202.4-3212.1 mbsl; 144.3-154.0 mbsf

TIME-ROCK UNIT	BIOSTRAT. ZONE/ FOSSIL CHARACTER FORAMINIFERS	NANNOFOSSILS	RADIOLARIANS	DIATOMS	PALEOMAGNETICS	PHYS. PROPERTIES	CHEMISTRY	SECTION	METERS	GRAPHIC LITHOLOGY	DRILLING DISTURB.	SED. STRUCTURES	SAMPLES	LITHOLOGIC DESCRIPTION
						●		1		CUTTINGS M	×			This core consists entirely of drill cuttings and igneous rock fragments.
						●		CC		CUTTINGS M	× ×		●	SMEAR SLIDE SUMMARY (%): TEXTURE: Silt COMPOSITION: Serpentine

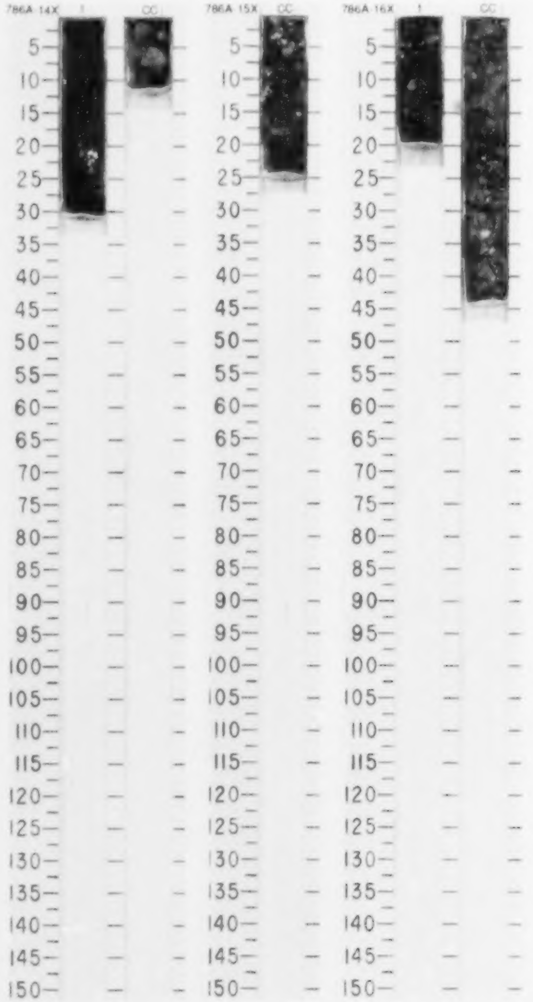

SITE 786 HOLE A CORE 17X CORED INTERVAL 3212.1-3213.1 mbsl; 154.0-155.0 mbsf

TIME-ROCK UNIT	BIOSTRAT. ZONE/ FOSSIL CHARACTER: FORAMINIFERS	NANNOFOSSILS	RADIOLARIANS	DIATOMS	PALEOMAGNETICS	PHYS. PROPERTIES	CHEMISTRY	SECTION	METERS	GRAPHIC LITHOLOGY	DRILLING DISTURB.	SED. STRUCTURES	SAMPLES	LITHOLOGIC DESCRIPTION
						●	●	CC		M	X X			This core contains [illegible]

SITE 786 HOLE A CORE 18X CORED INTERVAL 3213.1-3222.1 mbsl; 155.0-164.0 mbsf

TIME-ROCK UNIT	BIOSTRAT. ZONE/ FOSSIL CHARACTER: FORAMINIFERS	NANNOFOSSILS	RADIOLARIANS	DIATOMS	PALEOMAGNETICS	PHYS. PROPERTIES	CHEMISTRY	SECTION	METERS	GRAPHIC LITHOLOGY	DRILLING DISTURB.	SED. STRUCTURES	SAMPLES	LITHOLOGIC DESCRIPTION
								1	0.5 1.0	CUTTINGS M				This core contains [illegible] and [illegible]
								CC		M				

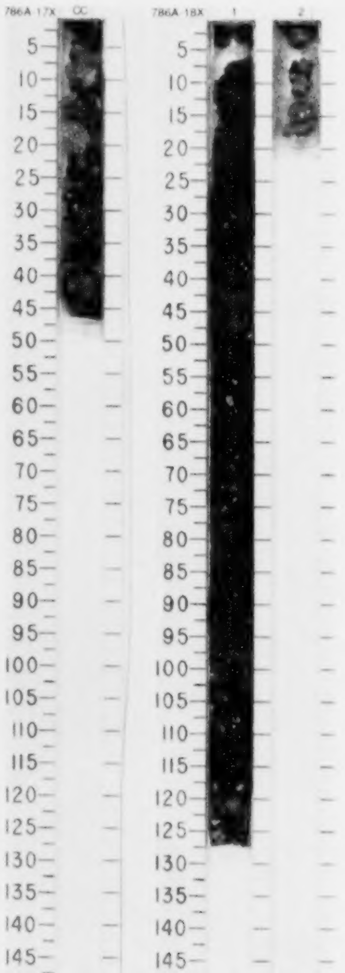
786A 17X
CC
786A 18X
1
2
5
10
15
20
25
30
35
40
45
50
55
60
65
70
75
80
85
90
95
100
105
110
115
120
125
130
135
140
145

SITE 786 HOLE A CORE 19X CORED INTERVAL 3222.1-3224.6 mbsl; 164.0-166.5 mbsf

TIME-ROCK UNIT	BIOSTRAT. ZONE/ FOSSIL CHARACTER: FORAMINIFERS	NANNOFOSSILS	RADIOLARIANS	DIATOMS		PALEOMAGNETICS	PHYS. PROPERTIES	CHEMISTRY	SECTION	METERS	GRAPHIC LITHOLOGY	DRILLING DISTURB.	SED. STRUCTURES	SAMPLES	LITHOLOGIC DESCRIPTION
									1		CUTTINGS	X			Section 1 and 0-8 cm in Section CC in this core consist entirely of drill cuttings. The remainder of the core (8-34 cm in Section CC) consists of igneous rock capped by a thin (1-1 cm) veneer of dark greenish gray (5G 4/1) to dark reddish brown (2.5YR 3/4) mixed coarse sand sized material.
									CC		IM	X		●●	

SMEAR SLIDE SUMMARY (%):

	CC, 1	CC, 17
	D	M
TEXTURE:		
Sand	75	—
Silt	25	10
Clay	—	90
COMPOSITION:		
Clay	—	8
Glass	85	—
Micrite	—	91
[illegible]	15	—

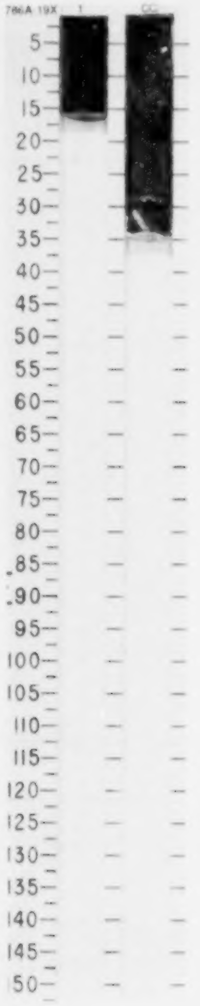
786A 19X
1
CC
5
10
15
20
25
30
35
40
45
50
55
60
65
70
75
80
85
90
95
100
105
110
115
120
125
130
135
140
145
150

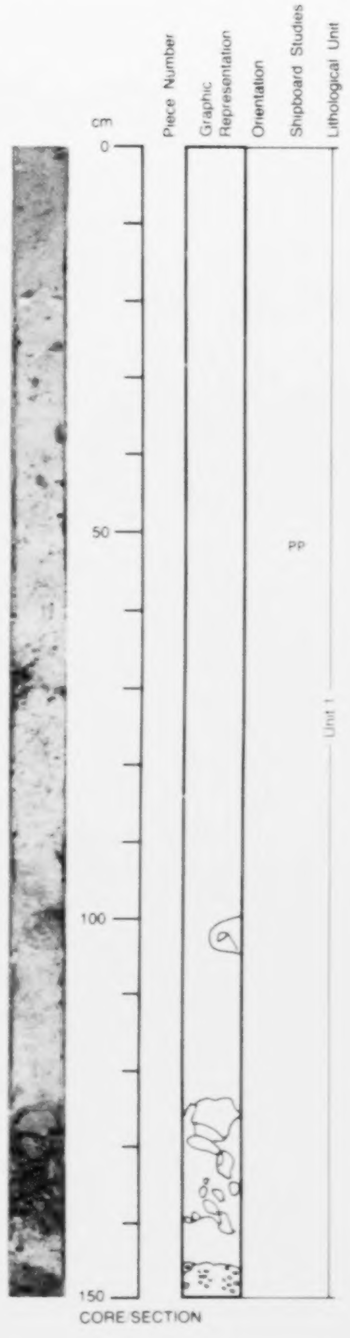
cm
Piece Number
Graphic Representation
Orientation
Shipboard Studies
Lithological Unit
0
50
100
150
PP
Unit 1
CORE SECTION

125-786A-11X-5

UNIT 1: VARIABLY ALTERED VOLCANICS

Pieces multiple fragments

CONTACTS: Clasts in mat.
PHENOCRYSTS:
Clinopyroxene - 1%, < 1 mm, euhedral, black.
GROUNDMASS: Glassy when green, maybe very finely crystalline when olive.
VESICLES: 10-30%, < 1 cm, sub-round, distributed throughout rock.
COLOR: Olive (5Y 4/3) ; tones of green (5GY 7/6 to 5GY 5/8).
STRUCTURE: None.
ALTERATION: Variably altered; locally white silky replacement.
VEINS/FRACTURES: Trace; 1 mm thick, randomly oriented, veins and zones of ochre-colored alteration.
ADDITIONAL COMMENTS: Reworked subrounded breccia clast at 100-105 cm; volcaniclastic horizon at 125-140 cm and at 146-150 cm.

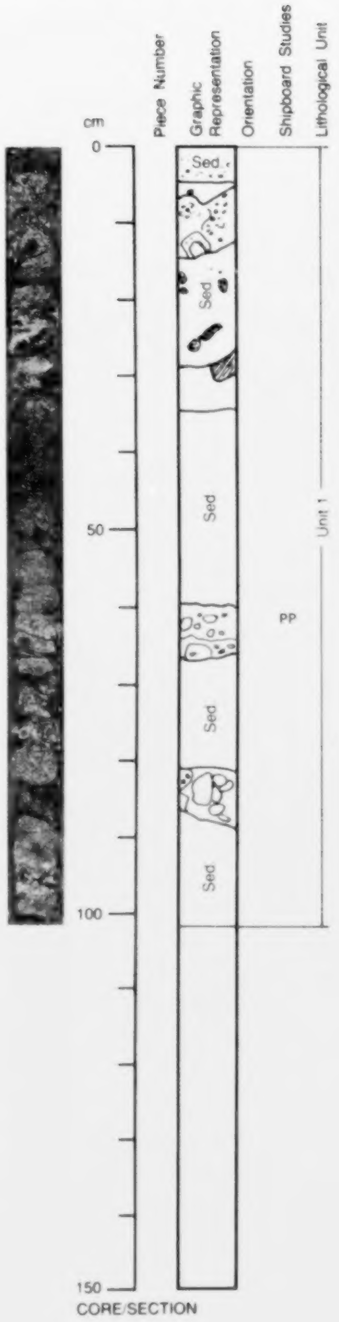
cm
Piece Number
Graphic Representation
Orientation
Shipboard Studies
Lithological Unit
0
50
100
150
Sed.
Sed.
Sed
Sed
Sed
PP
Unit 1
CORE/SECTION

125-786A-11X-6

UNIT 1: ALTERED VOLCANICLASTICS

Pieces multiple fragments

CONTACTS: Fragments in marl.
PHENOCRYSTS:
Clinopyroxene - trace, < 1 mm.
GROUNDMASS: Devitrified glass.
VESICLES: 10-30%, < 5 mm, sub-round, distributed throughout rock.
COLOR: Green (5GY 7/4 to 5 GY 4/8).
STRUCTURE: None.
ALTERATION: Variably altered.
VEINS/FRACTURES: Absent.
ADDITIONAL COMMENTS: Clasts in distinct beds, well sorted, variable bed thickness (0.25 - 15 cm).

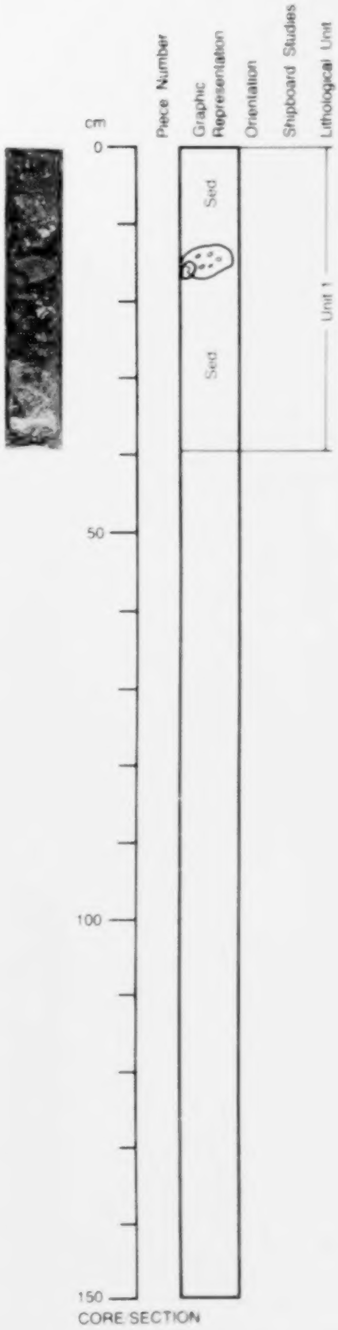
cm
0
50
100
150
Piece Number
Graphic Representation
Orientation
Shipboard Studies
Lithological Unit
Sed
Sed
Unit 1
CORE SECTION

125-786A-11X-CC

UNIT 1: ALTERED VOLCANICLASTICS

Pieces multiple fragments

CONTACTS: Fragments in marl
PHENOCRYSTS: Euhedral
Plagioclase - 1%, 1-2 mm, euhedral, altered
Clinopyroxene - trace, <1 mm, euhedral, black
Orthopyroxene - 1%, <2 mm, anhedral, light green
GROUNDMASS: Probably very finely crystalline and altered
VESICLES: 30%, < 4 mm, round to elongated, distributed throughout rock; some vesicle
may be filled with clear glassy material (or rock contains rounded quartz grains)
COLOR: Grayish brown (10YR 5/2 to 10YR 5/6)
STRUCTURE: None
ALTERATION: Around rim of clast and in core of largest cm-size green clasts
VEINS/FRACTURES: Trace, < 0.1 mm thickness, randomly distributed; black-appearing
veins, probably filled with white milky opal
ADDITIONAL COMMENTS: Bedding, sorting, description mainly relevant to large clast a
13-16 cm

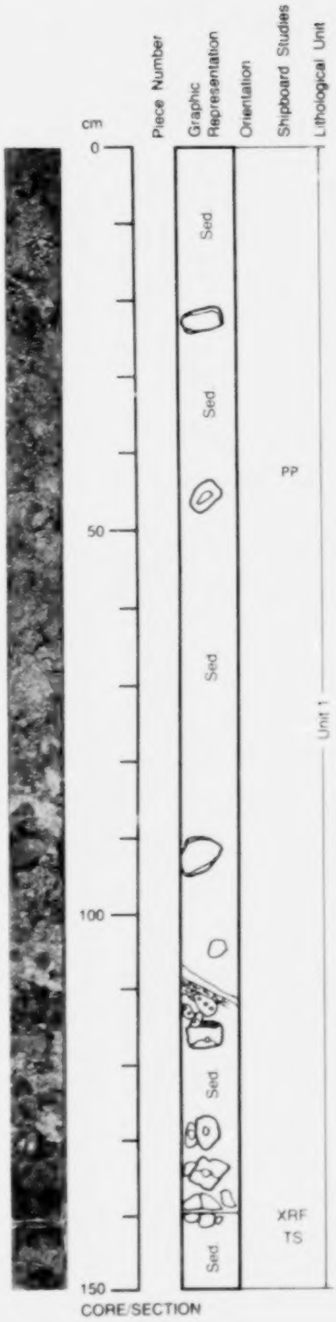
cm
Piece Number
Graphic Representation
Orientation
Shipboard Studies
Lithological Unit
0
50
100
150
Sed
Sed
PP
Sed
Unit 1
Sed
XRF
TS
Sed
CORE/SECTION

125-786A-12X-1

UNIT 1: ALTERED VOLCANICLASTICS

Pieces multiple clasts

CONTACTS: Clasts in marl

PHENOCRYSTS: Euhedral crystals, commonly surrounded by dark-green altered orthopyroxene in large grayish-brown clasts; small green fragments are phenocryst free.

Plagioclase - trace, <1 mm, euhedral, altered.
Clinopyroxene - trace, <1 mm, euhedral, black.
Orthopyroxene - 2%, <2 mm, anhedral, light green.

GROUNDMASS: Altered, very finely crystalline or glassy material in large clasts; small green clasts are altered glass.

VESICLES: 30%, < 4 mm, round to elongated, distributed throughout rock, some vesicle filling.

COLOR: Grayish brown (10YR 6/2 to 10YR 5/2); green (5GY 7/6 to 5GY 5/8).

STRUCTURE: None.

ALTERATION: Alteration at clast rim; green cm-size clasts altered in the center.

VEINS/FRACTURES: Trace, tiny <0.1 mm, randomly oriented; fractures postdating alteration are present; veinlets appear black but contain glassy opal.

ADDITIONAL COMMENTS: Large clasts at 90-95, 110-120, and 130-150 cm; well-sorted beds; green fragments are small (< 2 cm) and common in marl matrix.

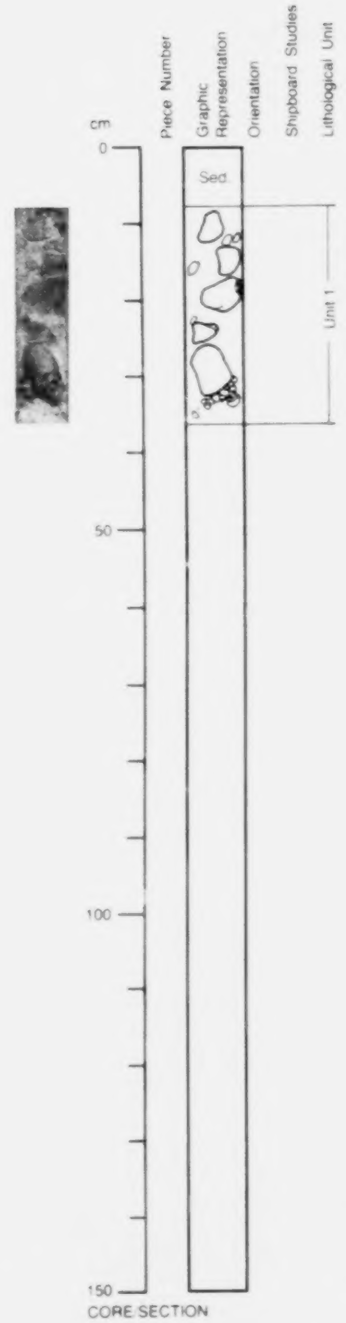
cm
Piece Number
Graphic Representation
Orientation
Shipboard Studies
Lithological Unit
0
50
100
150
Sed.
Unit 1
CORE/SECTION

125-786A-12X-2

UNIT 1: CONTINUED

Pieces multiple fragments

CONTACTS: N/A
PHENOCRYSTS: N/A
GROUNDMASS: N/A
VESICLES: N/A
Miaroles: N/A
COLOR: N/A
STRUCTURE: N/A
ALTERATION: N/A
VEINS/FRACTURES: N/A
ADDITIONAL COMMENTS: Interval 0-17 cm is continuation of 125-786A-12X-2

UNIT 1: ALTERED VOLCANICLASTICS

Pieces multiple fragments

CONTACTS: Clasts in marl
PHENOCRYSTS:
Plagioclase - trace, <2 mm, euhedral, altered
Orthopyroxene - 1%, 1-3 mm, anhedral to subhedral
GROUNDMASS: Very finely crystalline, altered
VESICLES: 30%, < 4 mm, round to elongated, distributed throughout sample, some a
filled with milky white opal(?)
COLOR: Grayish brown (7.5YR 6/2)
STRUCTURE: None
ALTERATION: Clast rims are ochre colored, strongly altered
VEINS/FRACTURES: Trace, white opal(?) veins, randomly oriented, veins and filled
vesicles contain same white material
ADDITIONAL COMMENTS: Large grayish brown and green clasts appear
consanguineous in this section

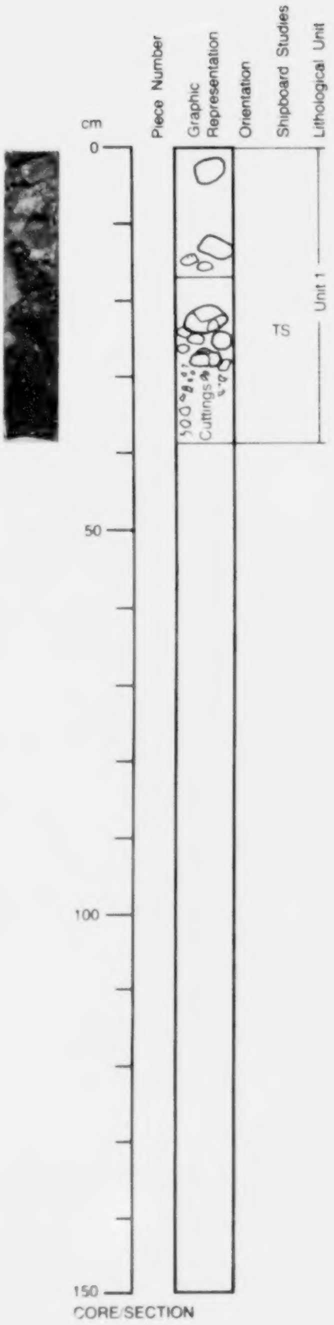
cm
Piece Number
Graphic Representation
Orientation
Shipboard Studies
Lithological Unit
0
50
100
150
Cuttings
TS
Unit 1
CORE/SECTION

125-786A-12X-CC

UNIT 1: ALTERED BASALTIC ANDESITE

Pieces multiple fragments

CONTACTS: Not visible
PHENOCRYSTS: Monomineralic glomerocrysts
Plagioclase 5%, <1 mm, euhedral, altered
Orthopyroxene 10%, <1 mm, anhedral, fresh
GROUNDMASS: Glassy, commonly altered
VESICLES: 20%, < 2 mm, sub round, randomly distributed
COLOR: Black when fresh and wet, grayish green (5G 4/2) when altered
STRUCTURE: None
ALTERATION: White opal along veins and alteration of glass
VEINS/FRACTURES: 5%, up to 2 mm thick veins, random orientation, white veins through black glass
ADDITIONAL COMMENTS: Brecciated clasts with white vein filling

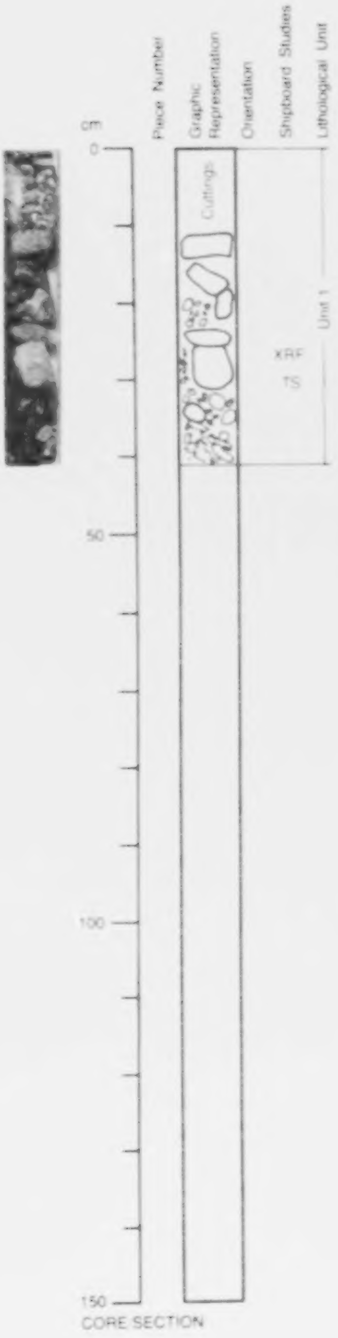
cm
0
50
100
150
CORE SECTION
Piece Number
Graphic Representation
Orientation
Shipboard Studies
Lithological Unit
Cuttings
XRF
TS
Unit 1

125-786A-13X-CC

UNIT 1: OLIVINE PHYRIC GLASS

Pieces multiple fragments

CONTACTS: Not visible.
PHENOCRYSTS:
Olivine - 20%, <1 mm, euhedral, yellow-colored, not very forsterite rich.
GROUNDMASS: Glassy, commonly pervasively altered.
VESICLES: 20%, < 3 mm, sub-round, distributed throughout rock.
COLOR: Fresh glass is gray to black (N 7 to 5B 4/1); altered glass is bluish gray (5BG 5/1).
STRUCTURE: None.
ALTERATION: Glass shows alteration.
VEINS/FRACTURES: Not visible.
ADDITIONAL COMMENTS: Probably holohyaline rock.

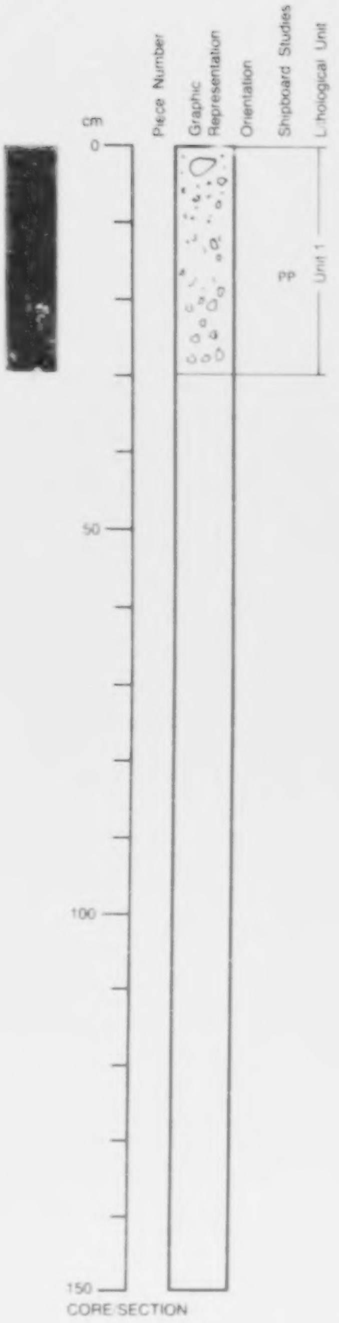
cm
0
50
100
150
Piece Number
Graphic Representation
Orientation
Shipboard Studies
Lithological Unit
PP
Unit 1
CORE/SECTION

125-786A-14X-1

UNIT 1: OLIVINE- AND BRONZITE-BEARING ANDESITE (BONINITE SERIES?)

Pieces drilling breccia

CONTACTS: None visible.
PHENOCRYSTS:
Orthopyroxene - ?; <0.5 mm; elongate; euhedral.
Olivine - ?; <0.3 mm; equant with spinel inclusions.
GROUNDMASS: Approximately 70-85% of rock; glassy with chilled plagioclase Microcrysts and spinel microcrysts (usually as inclusions within olivine).
VESICLES: 10-15%; <0.1 - 3 mm; irregular to rounded; n.a.; slight clay filling.
COLOR: Dark greenish gray (10Y 4/1); mottled.
STRUCTURE: None visible.
ALTERATION: Chlorite; clays.
VEINS/FRACTURES: <1%; <1.5 mm; no apparent orientation; dark green, amorphous material.
ADDITIONAL COMMENTS: Pieces vary in size from <1 mm to 4 cm; other rock types may be present but this appears to be the dominant lithology.

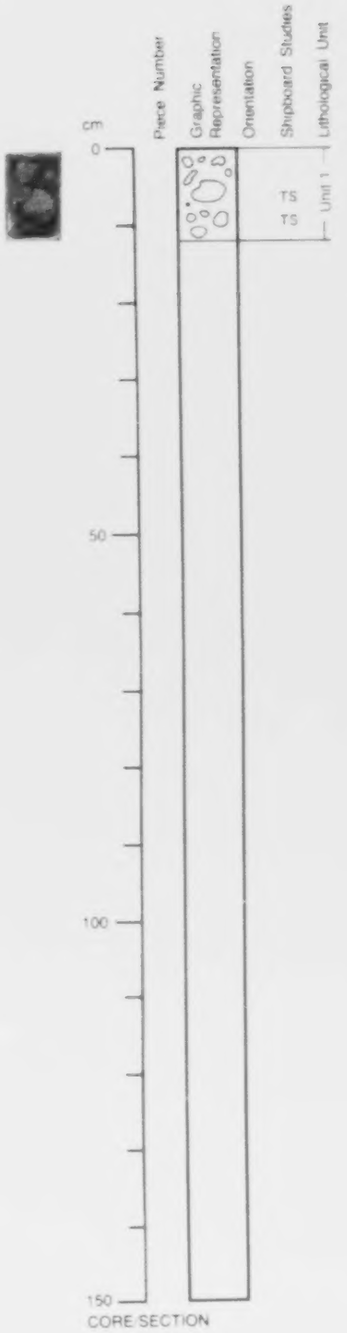
cm
Piece Number
Graphic Representation
Orientation
Shipboard Studies
Lithological Unit
0
50
100
150
TS
TS
Unit 1
CORE/SECTION

125-786A-14X-CC

UNIT 1: OLIVINE- AND BRONZITE-BEARING ANDESITE

Pieces: Clasts in sediment

CONTACTS: None visible.
PHENOCRYSTS:
Orthopyroxene - ?, <0.5 mm, elongate to euhedral.
Olivine - ?, <0.3 mm, equant with spinel inclusions.
GROUNDMASS: Glassy up to 70-80%, quench plagioclase and spinel microcrysts are present.
VESICLES: 10-15%, <0.1-3 mm, irregular to round, random.
COLOR: Dark greenish gray (10Y 4/1), mottled.
STRUCTURE: None visible.
ALTERATION: 30-80% altered to chlorite and clay minerals.
VEINS/FRACTURES: <1%, <1.5 mm, no apparent orientation.

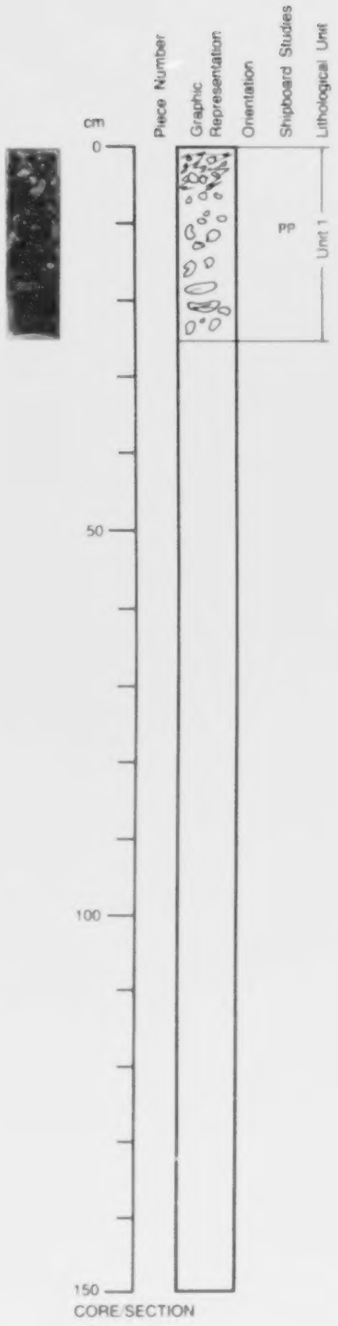
cm
Piece Number
Graphic Representation
Orientation
Shipboard Studies
Lithological Unit
0
50
100
150
PP
Unit 1
CORE/SECTION

125-786A-15X-CC

UNIT 1: OLIVINE- AND BRONZITE-BEARING ANDESITE (BONINITE SERIES?)

Pieces drilling breccia

CONTACTS: None visible

PHENOCRYSTS:

Orthopyroxene - ?, <0.5 mm, elongate to euhedral

Olivine - ?, <0.3 mm, equant with spinel inclusions

GROUNDMASS: Approximately 70-80%, glassy with quench crystals of plagioclase and spinel

VESICLES: 10-15%, <0.1-3 mm, round to irregular, random

COLOR: Dark greenish gray (10Y 4/1)

STRUCTURE: None visible

ALTERATION: Chlorite and clays

VEINS/FRACTURES: <<1%, <1-2 mm, no visible orientation, dark green amorphous material

ADDITIONAL COMMENTS: Pieces range from <1 mm to 3-4 mm in diameter. Other rock types may be present, but this appears to be the dominant lithology.

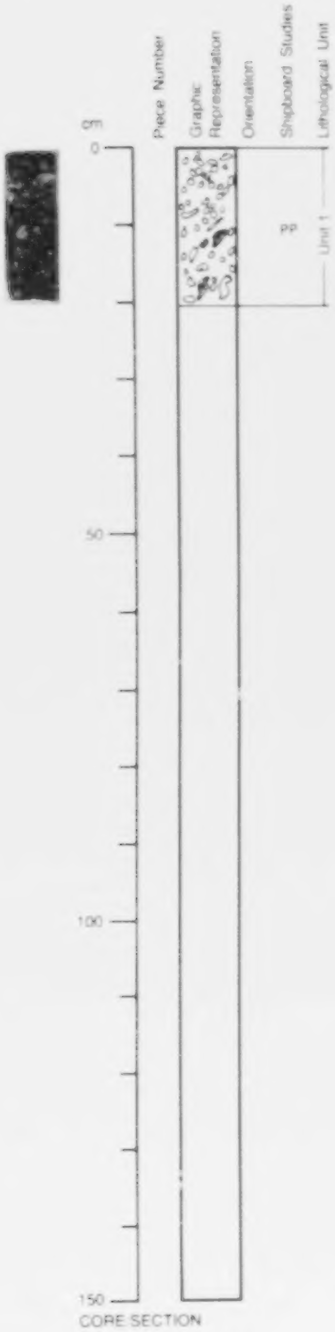
cm
Piece Number
Graphic Representation
Orientation
Shipboard Studies
Lithological Unit
0
50
100
150
PP
Unit 1
CORE/SECTION

125-786A-16X-1

UNIT 1: OLIVINE- AND BRONZITE-BEARING ANDESITE (BONINITE SERIES)

Pieces drilling breccia

CONTACTS: None visible.
PHENOCRYSTS:
Orthopyroxene - ?, <0.5 mm, elongate to euhedral.
Olivine - ?, <0.3 mm, equant with spinel inclusions.
GROUNDMASS: Approximately 80%, glassy with quench crystals of plagioclase and spinel (usually as inclusions within olivine).
VESICLES: 10-15%, <0.1-3 mm, round to irregular, random.
COLOR: Dark greenish gray (10Y 4/1).
STRUCTURE: None visible.
ALTERATION: Chlorite and clays.
VEINS/FRACTURES: <<1%, <1.5 mm, no apparent orientation, filled with dark green amorphous material.
ADDITIONAL COMMENTS: Pieces range from <1 mm to 3.4 cm in diameter; other rock types may be present but this appears to be the dominant lithology.

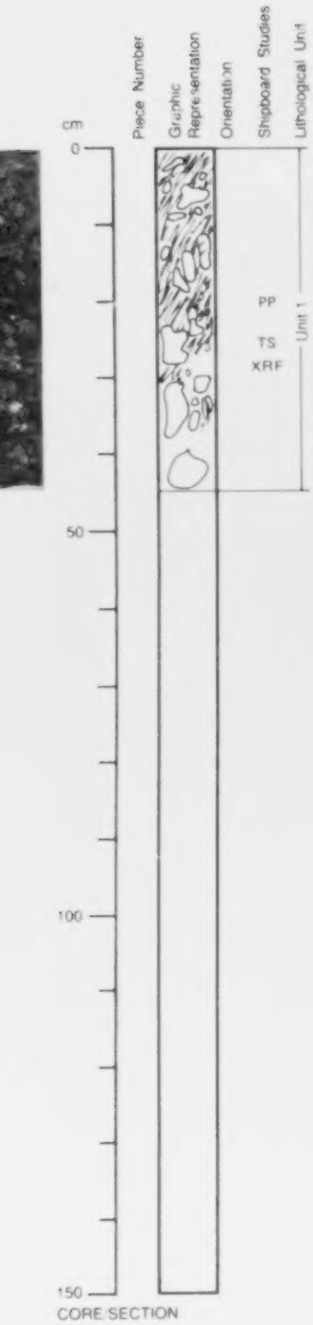
cm
Piece Number
Graphic Representation
Orientation
Shipboard Studies
Lithological Unit
0
50
100
150
PP
TS
XRF
Unit 1
CORE/SECTION

125-786A-16X-CC

UNIT 1: BASALT

Pieces multiple, set in sediment

CONTACTS: None visible.
PHENOCRYSTS:
  Olivine - 6-8%, <0.5-1 mm, equant, euhedral, green.
  Orthopyroxene - 4-6%, <0.3 mm, euhedral to elongate.
  Clinopyroxene - 3-5%, <0.3 mm, euhedral, equant.
  Plagioclase - 2%, <0.1 mm, laths.
GROUNDMASS: Approximately 80% of rock is glassy with quench crystals of plagioclase and clinopyroxene.
VESICLES: 7-10%, bimodal <0.5-1, 2-3 mm, round, random.
COLOR: Gray to dark gray (7.5YR 4/0-5/0).
STRUCTURE: None visible.
ALTERATION: Chlorite and celadonite staining on phenocrysts.
VEINS/FRACTURES: None visible.
ADDITIONAL COMMENTS: Rock pieces range from 3-6 cm in diameter.

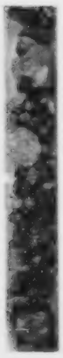

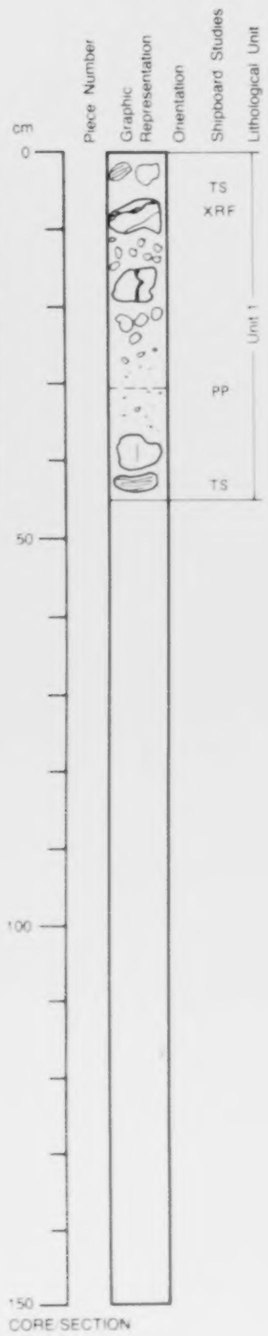
cm
Piece Number
Graphic Representation
Orientation
Shipboard Studies
Lithological Unit
0
50
100
150
TS
XRF
PP
TS
Unit 1
CORE SECTION

125-786A-17X-CC

UNIT 1: BASALT

Pieces multiple, set in sediment

CONTACTS: None visible.

PHENOCRYSTS:

Olivine - 6-8%, <0.5-1 mm, equant, euhedral; [illegible] contains fluid inclusions.

Orthopyroxene - 4-6%, <0.3 mm, euhedral; [illegible] with fluid inclusions.

Clinopyroxene - 3-5%, <0.3 mm, euhedral.

Plagioclase - 2%, 0.1 mm, laths.

GROUNDMASS: Approximately 70-80%, glassy with quench crystals of plagioclase and clinopyroxene.

VESICLES: 10-15%, bimodal: <0.5-1, 2-3 mm, usually round, [illegible] elongate, irregular, random.

COLOR: Gray to dark gray (7.5YR 4/0-5/0).

STRUCTURE: None visible.

ALTERATION: Chlorite, clays, with celadonite staining.

VEINS/FRACTURES: None present.

ADDITIONAL COMMENTS: Clasts are 2-6 cm in diameter.

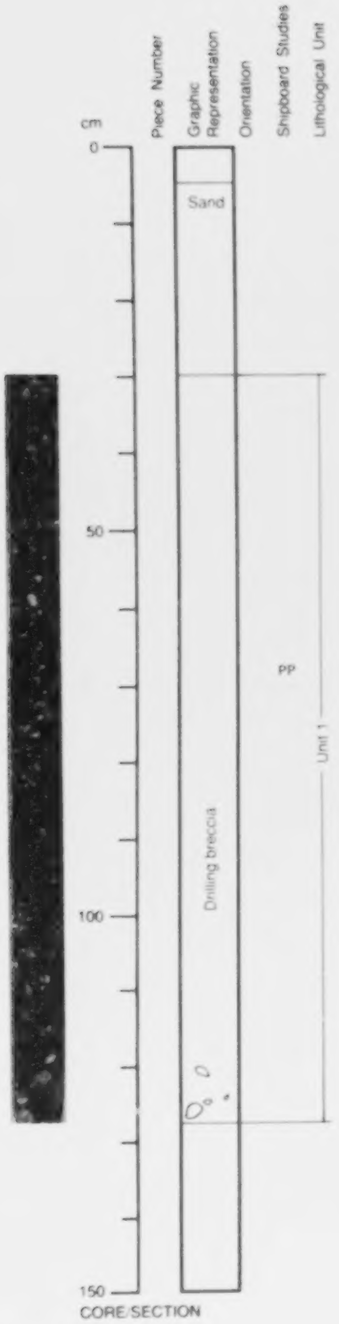
cm
0
50
100
150
Piece Number
Graphic Representation
Orientation
Shipboard Studies
Lithological Unit
Sand
Drilling breccia
PP
Unit 1
CORE/SECTION

125-786A-18X-1

UNIT 1: OLIVINE- AND BRONZITE-BEARING ANDESITE (BONINITE SERIES)

Pieces drilling breccia

CONTACTS: None visible.
PHENOCRYSTS:
Orthopyroxene - ?, <0.5 mm, elongate, euhedral.
Olivine - ?, <0.3 mm, equant with spinel inclusions.
GROUNDMASS: Approximately 70-80% glass, quench crystals of plagioclase and spinel are present.
VESICLES: 10-15%, <0.1-3 mm, irregular to rounded, random.
COLOR: Dark greenish gray (10Y 4/1).
STRUCTURE: None visible.
ALTERATION: Chlorite, clays.
VEINS/FRACTURES: <1%, <1.5 mm, no apparent preferred orientation, dark green, amorphous material.
ADDITIONAL COMMENTS: Pieces range from <1 mm to 2-3 cm in diameter; there may be other rock types present but this is the dominant lithology.

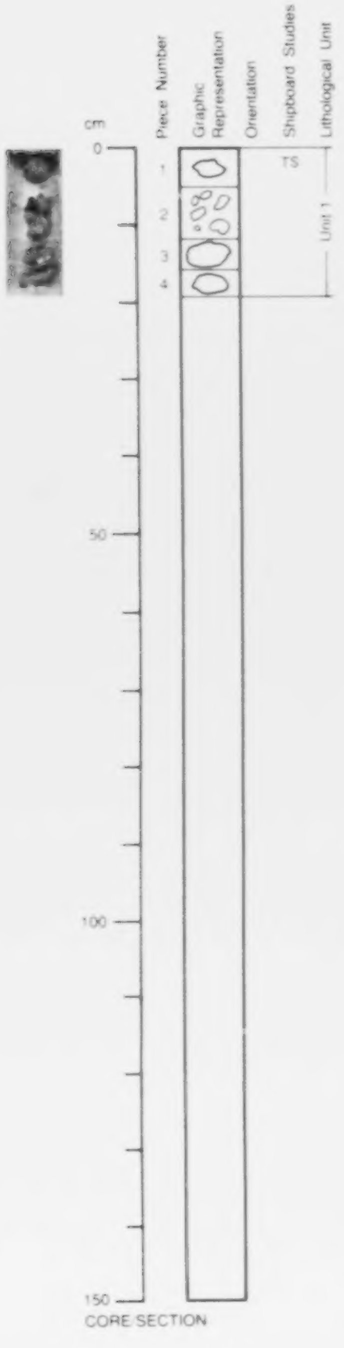
cm
0
50
100
150
CORE/SECTION
Piece Number
Graphic Representation
Orientation
Shipboard Studies
Lithological Unit
1
2
3
4
TS
Unit 1

125-786A-18X-2

UNIT 1: OLIVINE AND BRONZITE-BEARING ANDESITE (BONINITE SERIES) (CONTINUATION OF 18-1)

Pieces 1-4

CONTACTS: None visible.
PHENOCRYSTS: N/A.
GROUNDMASS: Same as 125-786A-18X-1.
VESICLES: None.
COLOR: Dark greenish gray (10Y 4/1).
STRUCTURE: None.
ALTERATION: Chlorite clays.
VEINS/FRACTURES: Dark green, amorphous material.
ADDITIONAL COMMENTS: Continuation of 125-786A-18X-1; same dominant lithology.

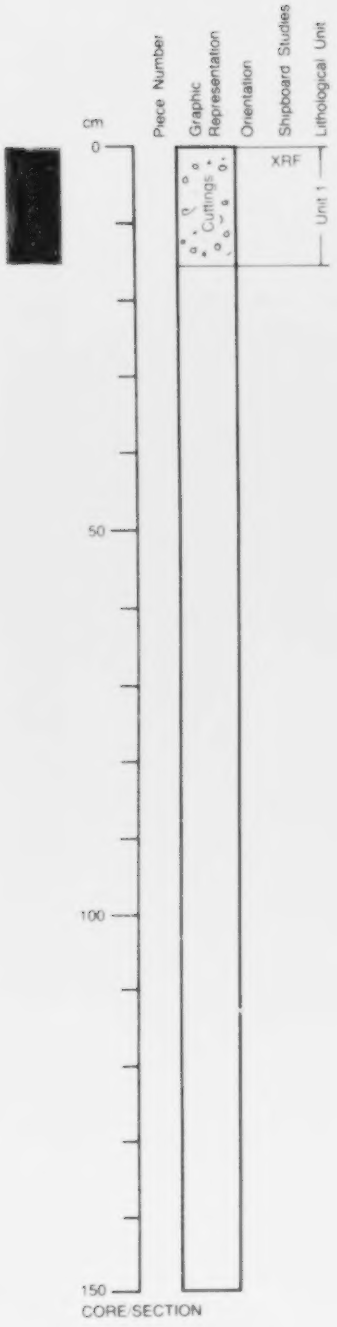
cm
0
50
100
150
Piece Number
Graphic Representation
Orientation
Shipboard Studies
Lithological Unit
Cuttings
XRF
Unit 1
CORE/SECTION

125-786A-19X-1

UNIT 1: OLIVINE PHYRIC GLASS/ROCK

Pieces drill cuttings

CONTACTS: Not visible.
PHENOCRYSTS: Olivine may be glomerocrystic.
Olivine - 10%, < 1 mm, subhedral, yellow-green.
GROUNDMASS: Black when glassy, gray when glass and fine crystals.
VESICLES: 10-25%, 2-3 mm, round, distributed throughout sample; some vesicles are filled with dark blue-green zeolite.
COLOR: Black (10YR 2/1) ; gray (10Y 5/1).
STRUCTURE: None.
ALTERATION: Glass alters to bluish green material.
VEINS/FRACTURES: Not present.
ADDITIONAL COMMENTS: Glass and partly crystalline material can be observed in gradational contact in some fragments indicating that they are the same composition.

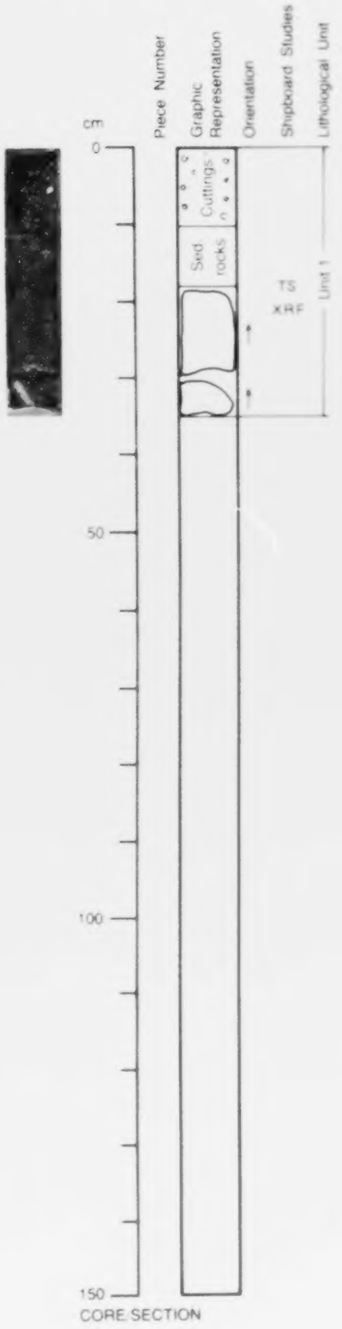
cm
Piece Number
Graphic Representation
Orientation
Shipboard Studies
Lithological Unit
0
50
100
150
Cuttings
Sed. rocks
TS
XRF
Unit 1
CORE/SECTION

125-786A-19X-CC

UNIT 1: 19X-1 CONTINUED

Pieces: drill cuttings

CONTACTS: N/A
PHENOCRYSTS: N/A
GROUNDMASS: N/A
VESICLES: N/A
COLOR: N/A
STRUCTURE: N/A
ALTERATION: N/A
VEINS/FRACTURES: N/A
ADDITIONAL COMMENTS: Interval 0-10 cm is continuation of 125-786A-19X-1.

UNIT 1: ALTERED PLAGIOCLASE MICRO-PHENOCRYSTIC BASALT

Piece 1

CONTACTS: Top in contact with chlorite/clay.
PHENOCRYSTS: Plagioclase is completely altered.
Plagioclase - 20%, [illegible] 1 mm, altered, white, lath shape.
GROUNDMASS: [illegible] altered.
VESICLES: 0.5%, [illegible] irregular to round, distributed throughout rock, some are filled with zeolites.
COLOR: Dark gray (N 4).
STRUCTURE: None.
ALTERATION: Basalt seems to alter to dark green chlorite (serpentine like) clay.
VEINS/FRACTURES: 10%, 1-2 cm wide, sub-horizontal with 60 degree dip; one vein is light gray with ochre-brown rims; other vein is chlorite-rich zone.

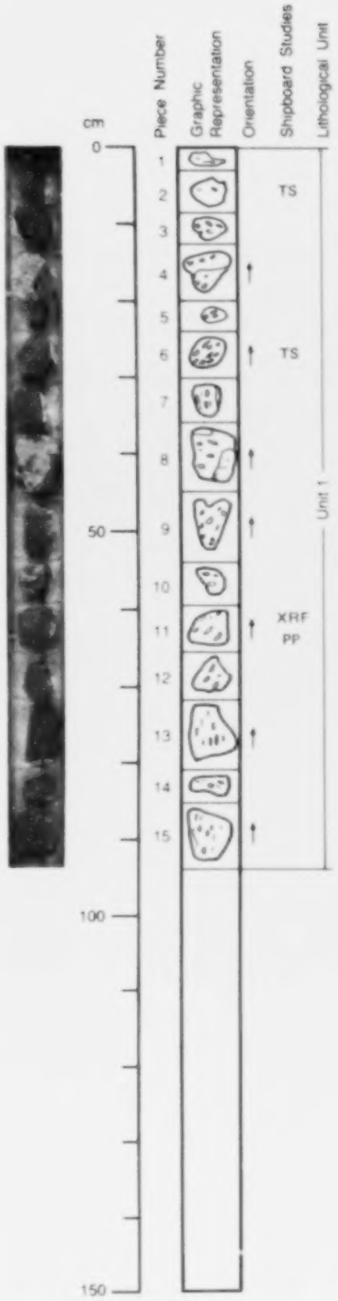
cm
Piece Number
Graphic Representation
Orientation
Shipboard Studies
Lithological Unit
0
50
100
150
1
2
3
4
5
6
7
8
9
10
11
12
13
14
15
TS
TS
XRF
PP
Unit 1
CORE/SECTION

125-786B-1R-1

UNIT 1: BONINITE

Pieces 1-15

CONTACTS: Not visible.

PHENOCRYSTS: Phenocrysts are fresh; glomerocrysts of olivine and of plagioclase are also present.
Plagioclase - 10-15%, <2 mm, euhedral to anhedral, fresh, clear, colorless.
Orthopyroxene - 5%, <3 mm, coke bottle green, euhedral.
Spinel - trace, <0.5 mm, glassy, black, as inclusions in olivine.
Olivine - 10%, <2 mm, anhedral, yellow to brown.

GROUNDMASS: Glassy to very fine grained.

VESICLES: 15-25%, <1 cm, round to elongated, distributed throughout rock, vesicles are always filled with bluish mineral.

COLOR: Gray (N 5).

STRUCTURE: Beige-colored streak (2 cm wide), in Piece 6 could be magma mixing.

ALTERATION: Clay minerals and/or zeolites in vesicles, orthopyroxene coloration might be caused by alteration. Pieces 4, 7, 8 are locally altered to bright green chlorite(?) rich material. Phenocrysts remain largely unaltered in these areas.

VEINS/FRACTURES: Not present.

ADDITIONAL COMMENTS: Slight variation in phenocryst content and proportion throughout rock.

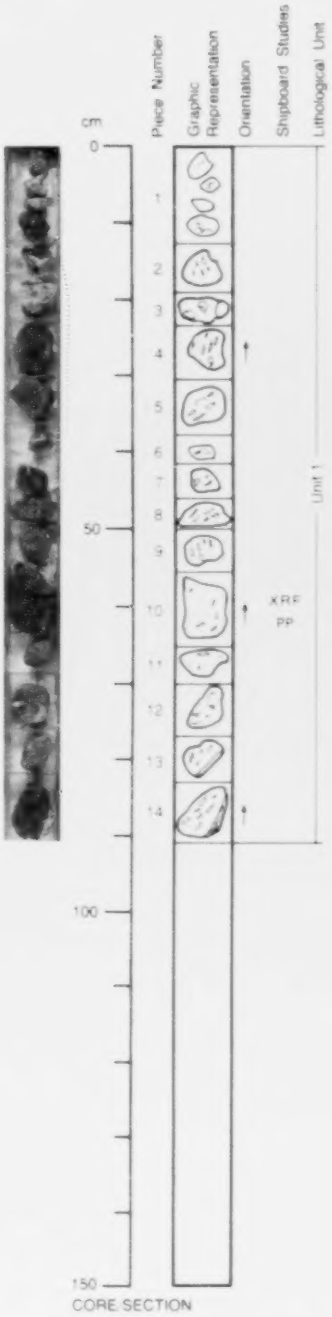
cm
0
50
100
150
Piece Number
Graphic Representation
Orientation
Shipboard Studies
Lithological Unit
1
2
3
4
5
6
7
8
9
10
11
12
13
14
XRF
PP
Unit 1
CORE SECTION

125-786B-2R-1

UNIT 1: BONINITE (786B-1R-1 CONTINUED)

Pieces 1-14

CONTACTS: None visible.
PHENOCRYSTS: Phenocrysts are fine.
Plagioclase - 10%, <2 mm, euhedral and anhedral, fresh, clear, colorless.
Orthopyroxene - 5%, <1 mm, coke bottle green, euhedral.
Clinopyroxene - trace, <0.5 mm, anhedral, black glassy.
Olivine - 10%, <2 mm, anhedral, yellow.
GROUNDMASS: Glassy to fine-grained.
VESICLES: 15-25%, <1 cm, round to elongated, distributed throughout rock, vesicles are filled with bluish mineral.
COLOR: Gray (N 5).
STRUCTURE: Absent.
ALTERATION: Clay minerals and/or zeolites in vesicles, sharp boundaries between green altered rock and gray fresh rock. Rock appears brecciated. Fracture-controlled alteration(?).
VEINS/FRACTURES: 0-90%, cm wide alteration zones, random orientation, very sharp contact going from altered to fresh rock. Locally highly altered, most pieces do not show green alteration zones.
ADDITIONAL COMMENTS: Section is continuation of 125-786B-1R-1.

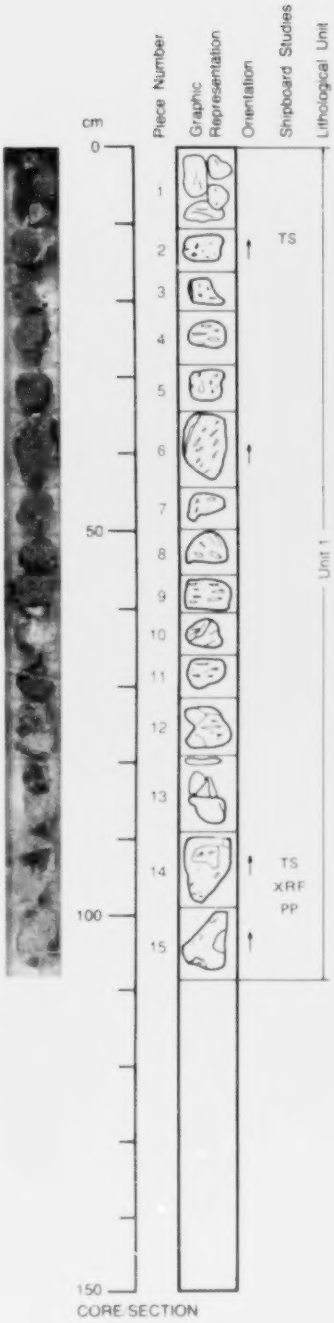
cm
0
50
100
150
CORE/SECTION
Piece Number
Graphic Representation
Orientation
Shipboard Studies
Lithological Unit
1
2
3
4
5
6
7
8
9
10
11
12
13
14
15
TS
TS
XRF
PP
Unit 1

125-786B-3R-1

UNIT 1: BONINITE (786B-2R-1 CONTINUED)

Pieces 1-15

CONTACTS: Not visible.
PHENOCRYSTS: Some variations in phenocryst mode from piece to piece.
Plagioclase - 2-15%, <2 mm, euhedral and anhedral, clear, colorless, fresh.
Orthopyroxene - 5-10%, <2 mm, euhedral, coke bottle green, fresh.
Olivine - 5-15%, <2 mm, anhedral, yellow, iddingsite.
Clinopyroxene - 1%, <0.5 mm, anhedral, black-glassy, only occurs with olivine in glomerocrysts.
GROUNDMASS: Glassy to finely crystalline.
VESICLES: 15-25%, <1 cm, round to flattened, parallel orientation, distributed throughout; vesicles are filled with bluish zeolite.
COLOR: Gray (N 5/).
STRUCTURE: Absent.
ALTERATION: Alteration zones with sharp transitions to fresh rock (e.g. in Piece 2). Towards bottom (Pieces 12-15) more strongly altered to light gray material.
VEINS/FRACTURES: 0-90%, alteration seems vein controlled, random orientation; alteration is not pervasive but occurs in varying proportions in adjacent pieces.
ADDITIONAL COMMENTS: Section is a continuation of 125-786B-1R-1 and 2R-1.

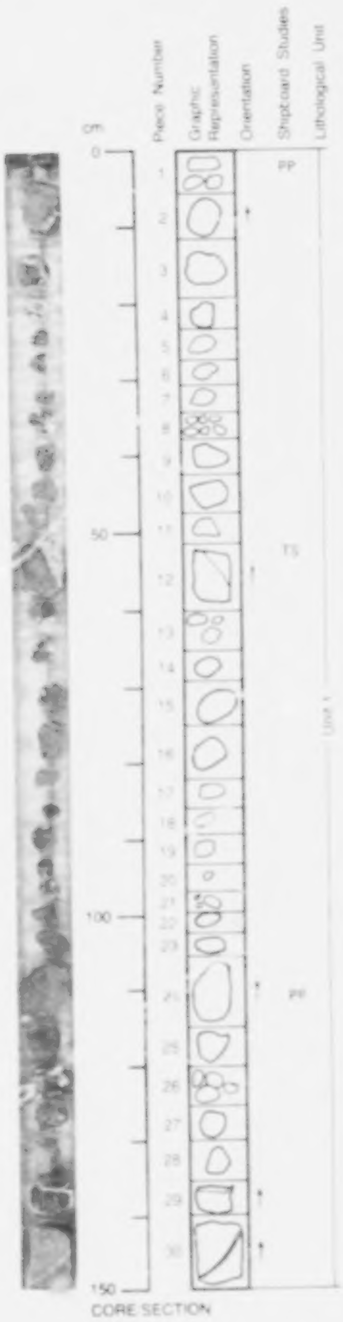
cm
Piece Number
Graphic Representation
Orientation
Shipboard Studies
Lithological Unit
0
50
100
150
1
2
3
4
5
6
7
8
9
10
11
12
13
14
15
16
17
18
19
20
21
22
23
24
25
26
27
28
29
30
PP
TS
PP
Unit 1
CORE SECTION

125-786B-4R-1

UNIT 1: BONINITE (3R-1 CONTINUED)

Pieces 1-30

CONTACTS: Not visible.
PHENOCRYSTS: Phenocrysts are fresh.
Plagioclase - 5-15%, <2 mm, euhedral, fresh, colorless.
Orthopyroxene - 5-10%, <2 mm, euhedral, coke bottle green.
Olivine - 5-15%, <1 mm, anhedral, yellow, in glomerocrysts.
Spinel - 1%, <1 mm, anhedral, included in olivine glomerocrysts.
GROUNDMASS: Glassy to partly crystalline.
VESICLES: 10-25%, <1 cm, elongated, parallel, distributed throughout, filled with bluish mineral.
COLOR: Gray (N 5).
STRUCTURE: Absent.
ALTERATION: Locally groundmass is altered and green in color.
VEINS/FRACTURES: Alteration may be fracture controlled.
ADDITIONAL COMMENTS: Continuation of Core 125-786B-3R-1 to 4R-1.

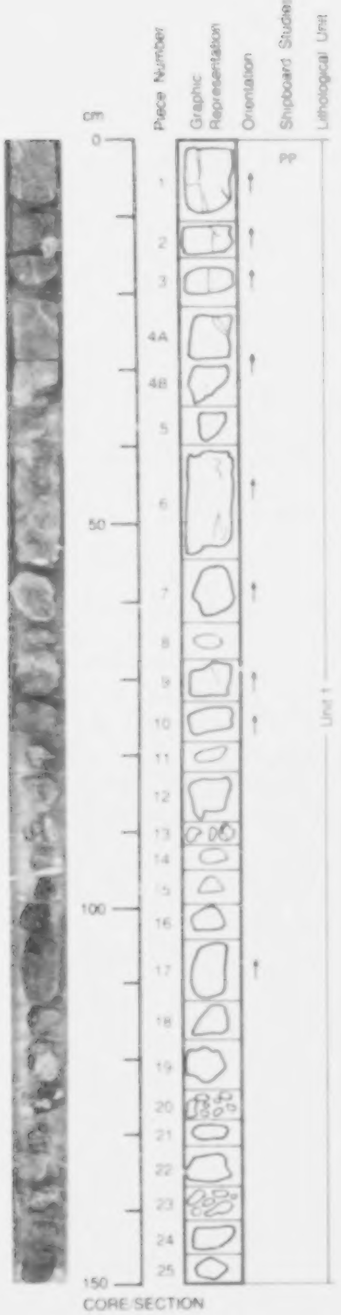
cm
Piece Number
Graphic Representation
Orientation
Shipboard Studies
Lithological Unit
0
50
100
150
1
2
3
4A
4B
5
6
7
8
9
10
11
12
13
14
15
16
17
18
19
20
21
22
23
24
25
PP
Unit 1
CORE/SECTION

125-786B-5R-1

UNIT 1: TWO-PYROXENE ANDESITE

Pieces 1-25

CONTACTS: None visible.
PHENOCRYSTS: Glomerocrysts of plagioclase and pyroxene are present.
Orthopyroxene - 5-10%; 0.2-1 mm; equant to elongate; bronze to black brown; euhedral.
Clinopyroxene - 2-5%; 0.2-0.5 mm; equant to elongate; coke bottle green.
Olivine - trace; 0.8-2 mm; highly altered to orange brown carbonate/Fe oxide assemblage.
Plagioclase - 5-10%; 0.3-4 mm; equant; euhedral.
GROUNDMASS: Glassy to fine-grained; variably altered from <10-90%.
VESICLES: 2-7%; <7 mm; elongate; throughout rock; some are filled with light blue amorphous material; often elongated and aligned.
COLOR: Olive gray to gray (5Y 4/2 - 5Y 5/1).
STRUCTURE: Massive with multiple alteration boundaries.
ALTERATION: Patchy with distinct boundaries between fresh glassy cores and highly altered, coke bottle green, material; cores are 2-5 cm in diameter; alteration minerals give a saussuritized appearance.
VEINS/FRACTURES: <1%; <1-2.5 mm wide; subvertical; calcite and chlorite; most common in Pieces 1-4.
ADDITIONAL COMMENTS: Sharp alteration fronts are unusual; matrix is highly altered and phenocrysts are quite fresh. Rock type is generally a continuation from Cores 1R-1 through 4R-1.

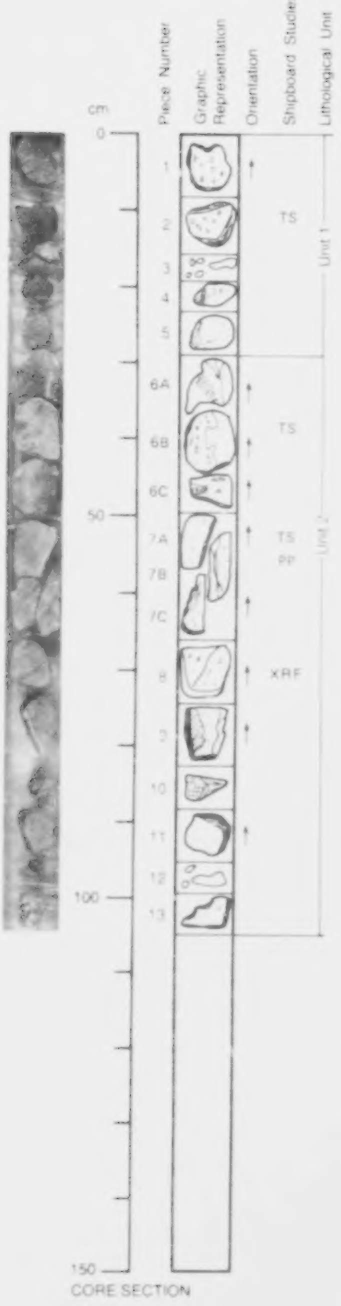

125-786B-5R-2

UNIT 1: TWO-PYROXENE ANDESITE

Pieces 1-5

CONTACTS: None visible.
PHENOCRYSTS: Glomerocrysts of plagioclase and pyroxene are present; most phenocrysts are quite fresh.
Orthopyroxene - 5-10%; 0.2-1 mm; equant to elongate; euhedral; bronze to black-brown.
Clinopyroxene - 2-5%; 0.2-0.5 mm; equant to elongate; coke-bottle green.
Plagioclase - 5-10%; 0.3-4 mm; equant; euhedral.
Olivine - trace; 0.8-2 mm; highly altered to orange-brown carbonate/Fe-oxide assemblage.
GROUNDMASS: 80-85%; glassy to fine grained; variably altered to a brown (hydrothermal?) appearance.
VESICLES: 10-15%; 1-5 mm; irregular and smooth; throughout; some vesicles are filled with amorphous light-blue material.
COLOR: Light yellowish brown to yellowish brown (10YR 6/4-5/4) for the altered portions; very dark gray to black (2.5Y 4/0-2/0) for the fresh portions.
STRUCTURE: Massive.
ALTERATION: Variable 5->50%; primarily brown clays.
VEINS/FRACTURES: <<1%; 3-4 mm by 7 mm; no orientation; only Piece 1 has an elongate patch of carbonate vein.
ADDITIONAL COMMENTS: Alteration in this part of the core is distinct from Core 5R-1; all alteration here is brown and amorphous; mineralogically this is a continuation from Core 1R-1 through 5R-1.

UNIT 2: TWO-PYROXENE ANDESITE/OLIVINE PHYRIC BASALT

Pieces 6A, B, C; 7A, B, C

CONTACTS: Contorted; appear to result from magma mixing between the two rock types.
PHENOCRYSTS: Assemblage varies between the two rock types.
Orthopyroxene - 5-10%; 0.1-1 mm; equant to elongate; euhedral; bronze to dark brown; similar in both rock types but smaller and less abundant (trace) in basalt segment.
Clinopyroxene - 2-5%; 0.2-0.5 mm; equant to elongate; coke-bottle green; similar but smaller (<0.2 mm) and less abundant (<1%) in basalt segment.
Plagioclase - 5-10%; 0.3-4 mm; equant; euhedral; microphenocrysts (<0.1 mm, <1%) in basalt segment.
Olivine - 5-7%; 0.5-2 mm; euhedral; altering to carbonate and Fe-oxides; none present in andesite; Cr-spinel inclusions; olivine only present in basalt.
GROUNDMASS: Basalt contains light brown glass with quench crystals of feldspar and pyroxene.
VESICLES: 5-10%; <0.5 - 4 mm; irregular; throughout; some are filled with a pale blue amorphous material.
COLOR: Alteration/compositional boundary is light yellow brown (2.5Y 5/4); bulk of rock is light yellowish brown to grayish brown (2.5Y 6/4 - 5/2).
STRUCTURE: Massive with the exception of the compositional/alteration boundary.
ALTERATION: Variable <10-65%; two patches (2-4 cm in diameter) of the andesite are fresh and black; the remainder is brown and altered to clays.
VEINS/FRACTURES: <1%; <1-2.5 mm; random to sub-parallel to core axis; mostly carbonate but some proportion of other white material.
ADDITIONAL COMMENTS: This is a boundary between Cores 1R-1 through 5R-1, Pieces 1-5, and below.

UNIT 2: OLIVINE PHYRIC BASALT

Pieces 8-13

CONTACTS: None visible.
PHENOCRYSTS:
Olivine - 5-7%; 0.2-2.5 mm; euhedral; slightly elongate; altering to carbonate/Fe-oxide assemblage; inclusions of Cr-spinel.
Clinopyroxene - 2-3%; 0.1-1 mm; equant; euhedral.
Orthopyroxene - trace; <1 mm; euhedral.
Plagioclase - 1%; <1 mm; euhedral laths.
GROUNDMASS: Glassy; light brown with quench crystals of feldspar and pyroxene.
VESICLES: 4-7%; 1-4 mm; irregular; elongate; throughout but locally concentrated; locally they trend in parallel strings.
COLOR: Light yellowish brown to grayish brown (2.5Y 6/4 - 5/2).
STRUCTURE: Massive.
ALTERATION: Alteration is relatively consistent throughout at 40-60%; altering to brown amorphous clays.
VEINS/FRACTURES: <1%; 0.5 - 4 mm; sub-parallel to core axis; random; vein filling is white carbonate material probably mixed with another white phase (zeolite?).
ADDITIONAL COMMENTS: This rock type is a continuation of the basaltic portion of 5R-2 Pieces 6 and 7.

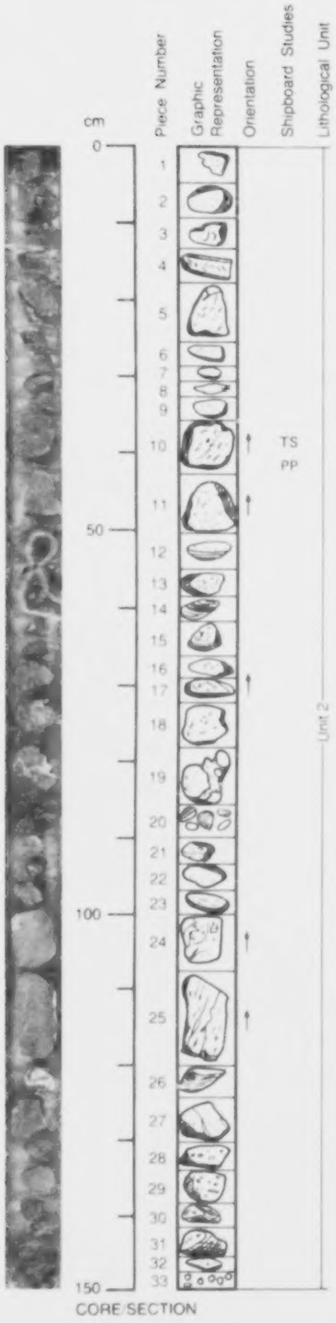
cm
Piece Number
Graphic Representation
Orientation
Shipboard Studies
Lithological Unit
0
50
100
150
1
2
3
4
5
6
7
8
9
10
11
12
13
14
15
16
17
18
19
20
21
22
23
24
25
26
27
28
29
30
31
32
33
TS
PP
Unit 2
CORE/SECTION

125-786B-6R-1

UNIT 2: OLIVINE PHYRIC BASALT (CONTINUATION OF 5R-2, PIECES 8-13)

Pieces 1-25, 27-33

CONTACTS: None visible
PHENOCRYSTS:
Olivine - 5-7%, 0.2-2.5 mm, euhedral, slightly elongate, altering to carbonate-Fe-oxide assemblage, inclusions of Cr-spinel.
Clinopyroxene - 2-3%, 0.1-1 mm, equant, euhedral.
Orthopyroxene - trace, <1 mm, euhedral.
Plagioclase - 1%, <1 mm, laths, euhedral.
GROUNDMASS: Glassy, light brown with quench crystals of feldspar and pyroxene.
VESICLES: 4-7%, 1-4 mm, irregular, elongate, throughout but locally concentrated, some alignment of elongate vesicles.
COLOR: Light yellowish brown to grayish brown (2.5Y 6/4 - 5/2).
STRUCTURE: Massive.
ALTERATION: Consistent throughout at 40-60%, consisting of brown amorphous clays; Piece 19 has red-orange (hematite?) alteration.
VEINS/FRACTURES: <1-1%, 0.5-3.5 mm, random, some preference for sub-parallel, white, amorphous predominantly carbonate with a second phase of an unknown white mineral (zeolite?).
ADDITIONAL COMMENTS: This rock type is continuous with Core 5R-2, Pieces 8-12.

UNIT 2: ZEOLITE (?)

Piece 26

CONTACTS: None.
PHENOCRYSTS: Not a volcanic sample.
GROUNDMASS: Not applicable.
VESICLES: None.
COLOR: White with streaks of olive green (5Y 5/3) along the edge.
STRUCTURE: Massive.
ALTERATION: Probably a piece of nearly pure (95%) zeolite.
VEINS/FRACTURES: May be a fragment of a large vein.
ADDITIONAL COMMENTS: Probably a zeolite, appears to be similar to the white vein filling phase in the surrounding volcanics, this piece is approximately 1x3x3 cm.

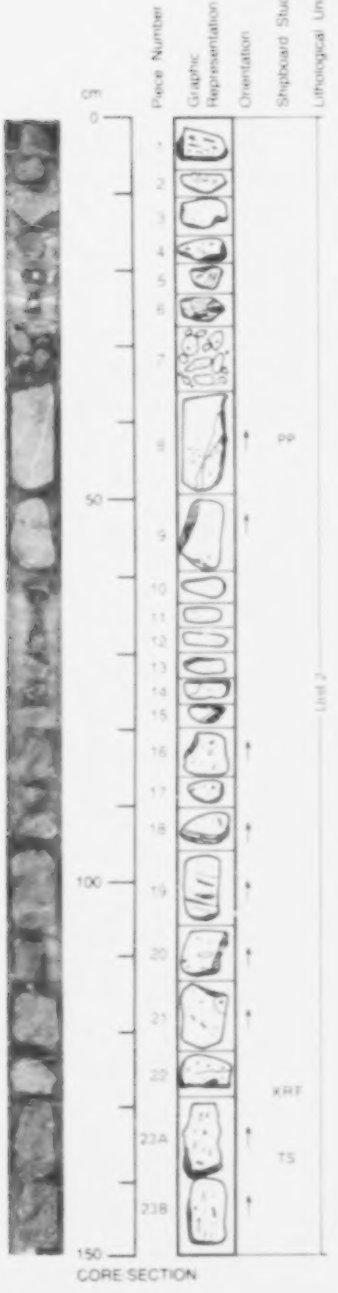
cm
Piece Number
Graphic Representation
Orientation
Shipboard Studies
Lithological Unit
0
50
100
150
1
2
3
4
5
6
7
8
9
10
11
12
13
14
15
16
17
18
19
20
21
22
23A
23B
PP
XRF
TS
Unit 2
CORE SECTION

125-786B-6R-2

UNIT 2: OLIVINE PHYRIC BASALT (CONTINUATION OF CORE 6R-1)

Pieces 1-23

CONTACTS: None.
PHENOCRYSTS:
Olivine - 5-7%, 0.2-2.5 mm, euhedral, slightly elongate altering to carbonate-Fe-oxide-zeolite assemblage; inclusions of Cr-spinel.
Clinopyroxene - 2-3%, 0.1-1 mm, euhedral.
Orthopyroxene - trace, <1 mm, equant, euhedral.
Plagioclase - 1%, <1 mm, euhedral laths.
GROUNDMASS: Glassy, light yellow brown, with quench crystals of feldspar and pyroxene.
VESICLES: <2-12%, 0.5 - 8 mm, irregular to elongate and oval, throughout but locally concentrated. Pieces 1-4, 20-23 have 10-15% vesicles of 2-8 mm diameters; some pieces have aligned vesicles. Pieces 19-20 and 23 have vesicles aligned perpendicular to core axis.
COLOR: Fresh portions are gray to dark gray (2.5Y 5/0 - 4/0); altered portions are yellowish brown to grayish brown (2.5Y 6/4 - 5/2).
STRUCTURE: Massive.
ALTERATION: Variable. Pieces 1-17 have 20-50% alteration to brown amorphous clay. Pieces 18-23 are much fresher with <10% alteration.
VEINS/FRACTURES: <1%, 1-3 mm, sub-parallel to core axis, filled with white amorphous carbonate and zeolite(?).
ADDITIONAL COMMENTS: This rock is a continuation of Cores 5R-2, Pieces 8-12 and 5R-1.

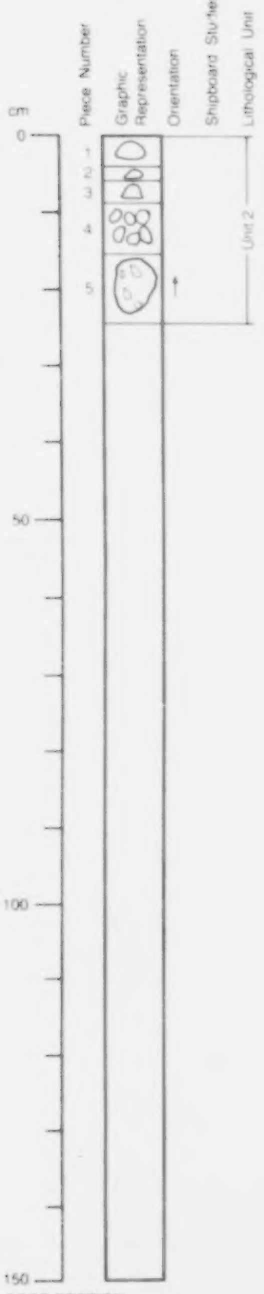
cm
0
50
100
150
Piece Number
Graphic Representation
Orientation
Shipboard Studies
Lithological Unit
1
2
3
4
5
Unit 2

CORE/SECTION

125-786B-6R-3

UNIT 2: OLIVINE PHRYIC BASALT (CONTINUATION OF CORE 6R-2)

Pieces 1-5

CONTACTS: None visible.
PHENOCRYSTS:
Olivine - 5-7%, 0.2-2.5 mm, euhedral, slightly elongate, altering to carbonate/Fe oxide/zeolite assemblage; inclusions of Cr spinel.
Clinopyroxene - 2-3%, 0.1-1 mm, equant, euhedral.
Orthopyroxene - trace, <1 mm, euhedral.
Plagioclase - 1%, <1 mm, euhedral.
GROUNDMASS: Glassy, light yellow brown, with quench crystals of feldspar and pyroxene.
VESICLES: 2-10%, 1-8 mm, irregular to elongate and oval, throughout, locally concentrated; alignment of large vesicles in Piece 5 at a 40 degree angle to core axis.
COLOR: Light yellowish brown to grayish brown (2.5Y 6/4 - 5/2).
STRUCTURE: Massive.
ALTERATION: Variable, but usually less than 20%, to brown amorphous clays.
VEINS/FRACTURES: None in these pieces.
ADDITIONAL COMMENTS: This rock type is continuous with Core 5R-2, Pieces 8-12, through 6R-2.

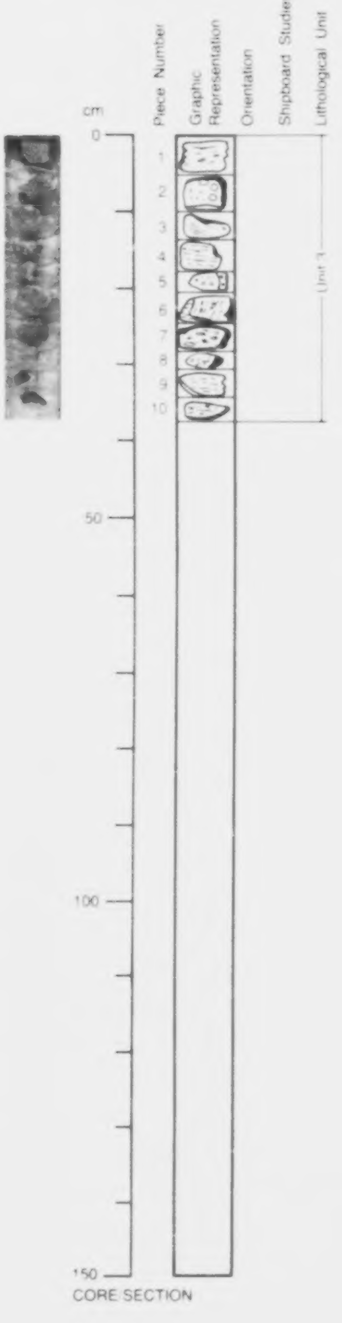
cm
Piece Number
Graphic Representation
Orientation
Shipboard Studies
Lithological Unit
0
50
100
150
1
2
3
4
5
6
7
8
9
10
Unit 3
CORE SECTION

125-786B-7R-1

UNIT 3: PYROXENE PHYRIC ANDESITE

Pieces 1-10

CONTACTS: None visible.
PHENOCRYSTS:
Clinopyroxene - 1-3%; 0.2-0.8 mm; euhedral; elongate to equant.
Orthopyroxene - 1-2%; 0.2-0.6 mm; euhedral to subhedral; elongate to equant.
Plagioclase - 1%; <0.1-0.4 mm; subhedral laths.
GROUNDMASS: Fine-grained with quench crystals of plagioclase.
VESICLES: 5-15%; 1-8 mm; round to irregular; throughout but locally concentrated; elongate vesicles are aligned especially in Piece 1.
COLOR: Fresh portions are gray (2.5Y 6/0-5/0); altered portions are dark grayish brown (2.5Y 5/2).
STRUCTURE: Massive.
ALTERATION: Variable <10-40% to brown amorphous clays; also rinds of green, coarse-grained sand(?) with small clasts (1-2 mm) of rock.
VEINS/FRACTURES: None present.
ADDITIONAL COMMENTS: Rock is relatively fresh.

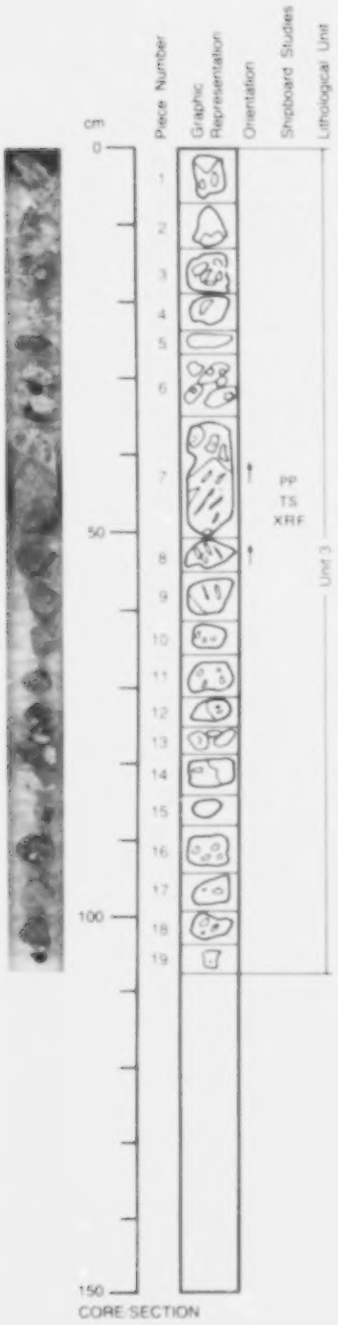
cm
0
50
100
150
Piece Number
Graphic Representation
Orientation
Shipboard Studies
Lithological Unit
1
2
3
4
5
6
7
8
9
10
11
12
13
14
15
16
17
18
19
PP
TS
XRF
Unit 3
CORE/SECTION

125-786B-8R-1

UNIT 3: PYROXENE PHYRIC ANDESITE (CONTINUATION OF CORE 7R-1) BRECCIA

Pieces 1-19

CONTACTS: None visible

PHENOCRYSTS: Glomerocrysts of clinopyroxene and orthopyroxene.

Clinopyroxene - 3-5%, 0.1-0.5 mm, equant, euhedral.

Orthopyroxene - 1-2%, 0.1-0.3 mm, equant, subhedral plagioclase - 4-5%, <0.2 mm, laths, euhedral.

GROUNDMASS: Very fine grained to glassy with quench crystals of plagioclase and pyroxene.

VESICLES: 2-15%, 1-22 mm, elongate, stretched, throughout, locally concentrated, most are aligned and stretched approximately sub-parallel to the core axis.

Miaroles: Green crystalline (sand, alteration?).

COLOR: Dark gray to light gray (2.5Y N7.0 - N4.0) in fresh rock to grayish green (5G 4/2) in breccia rinds.

STRUCTURE: "Brecciated" texture between black fresh rock and green alteration sand rinds and breccia matrix, brecciation in some pieces appears to be in situ.

ALTERATION: Green rinds containing pyroxene, olivine, and plagioclase fragments, 1-3 mm thick probably locally derived.

VEINS/FRACTURES: <<1%, ≤1 mm, 45 degrees to core axis, fracture in Piece 7 perpendicular to elongate vesicles.

ADDITIONAL COMMENTS: This rock appears to be a continuation of Core 7R-1 but the brecciated texture was not preserved in 7R-1.

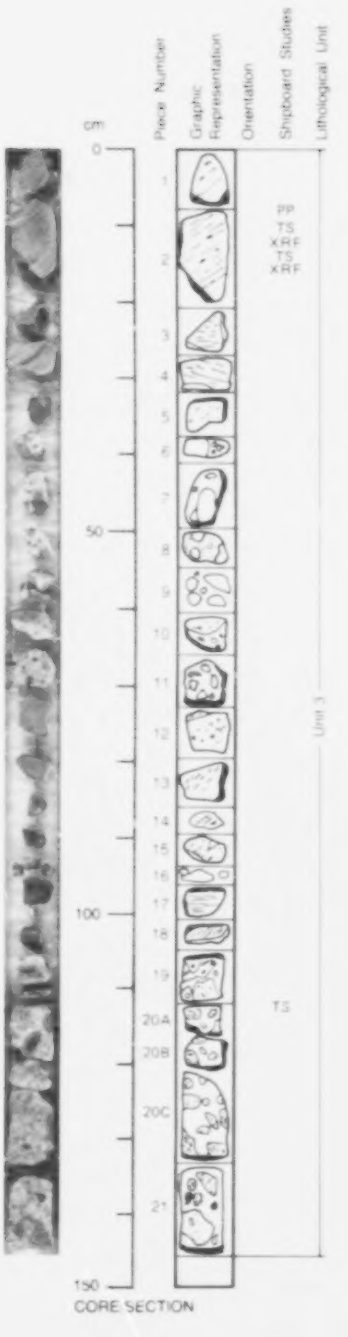
cm
Piece Number
Graphic Representation
Orientation
Shipboard Studies
Lithological Unit
0
50
100
150
CORE SECTION
1
2
3
4
5
6
7
8
9
10
11
12
13
14
15
16
17
18
19
20A
20B
20C
21
PP
TS
XRF
TS
XRF
TS
Unit 3

125-786B-9R-1

UNIT 3: PYROXENE PHYRIC ANDESITE BRECCIA (CONTINUATION OF 8R-1)

Pieces 1-21

CONTACTS: None visible.
PHENOCRYSTS:
Clinopyroxene: 3-5%, 0.1-0.5 mm, equant, euhedral.
Orthopyroxene: 1-2%, 0.1-0.3 mm, equant, subhedral.
Plagioclase: 4-5%, <0.2 mm, laths, euhedral.
GROUNDMASS: Very fine grained to glassy with quench crystals of plagioclase and pyroxene; green matrix material is coarse grained (1-3 mm) and appears to comprise pyroxene, olivine and plagioclase grains.
VESICLES: 1-8%, <1-3, round to elongate, throughout, locally dense; pieces 1-5 are nearly vesicle free (<1-1%, <1-1 mm); pieces lower in the section are rounder, larger and have a higher proportion of vesicles.
COLOR: From dark gray to light gray (2.5Y N7/0 - N4/0) in basalt to grayish green (5G 4/2) in breccia matrix.
STRUCTURE: "Brecciated" texture between black fresh rock and green sandy alteration matrix material; brecciation in some pieces appears to be in situ.
ALTERATION: Green rinds and matrix are composed of pyroxene, olivine, and plagioclase fragments (1-3 mm across) probably locally derived.
VEINS/FRACTURES: None.
ADDITIONAL COMMENTS: This rock appears to be a continuation of Cores 7R + 8R-1.

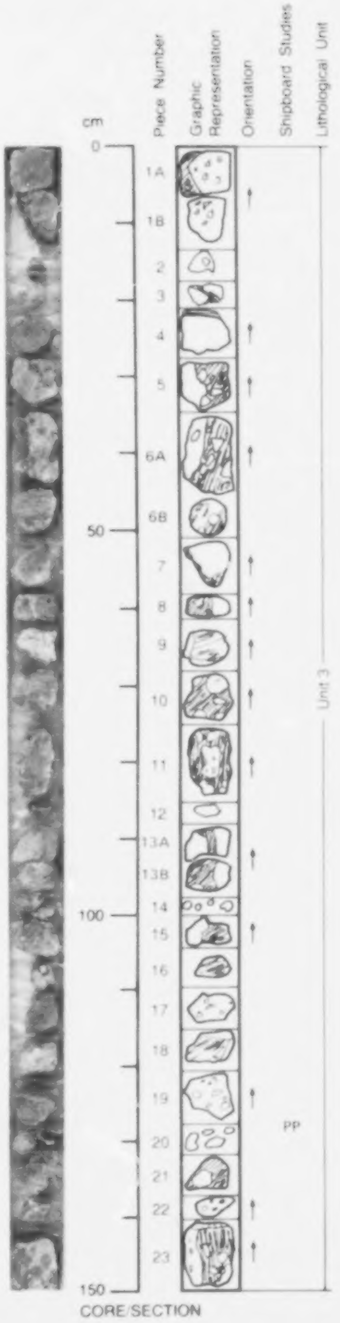
cm
Piece Number
Graphic Representation
Orientation
Shipboard Studies
Lithological Unit
0
50
100
150
1A
1B
2
3
4
5
6A
6B
7
8
9
10
11
12
13A
13B
14
15
16
17
18
19
20
21
22
23
PP
Unit 3
CORE/SECTION

125-786B-9R-2

UNIT 3: PYROXENE PHYRIC ANDESITE BRECCIA (CONTINUATION OF 9R-1)

Pieces 1-23

CONTACTS: None visible.

PHENOCRYSTS: Glomerocrystic patches with plagioclase, ortho - and clinopyroxene.
Clinopyroxene - 3-6%, 0.1-0.5 mm, equant, dark green, euhedral.
Orthopyroxene - 2-4%, 0.1-0.3 mm, equant yellow brown, euhedral.
Plagioclase - 3-5%, <0.2 mm, euhedral laths.

GROUNDMASS: Very fine grained to glassy with quench feldspar and pyroxene, green matrix material is coarse grained and appears to comprise pyroxene and feldspar grains cemented by green and white zeolites.

VESICLES: 1-10%, <0.2 - 3 mm, spherical - elongate, variable from clast to clast.

COLOR: Basalt is dark to light gray (2.5Y N7/0 - N4/0), breccia matrix is grayish green (5G 4/2).

STRUCTURE: Brecciated texture.

ALTERATION: Clasts have alteration rinds 0-1.5 mm thick. The matrix is composed of orthopyroxene, clinopyroxene, plagioclase and glass, these phases are angular, 1-3 mm in size. The glass is altered and the matrix as a whole is cemented by a green and white zeolite clay phase.

VEINS/FRACTURES: <1%, <0.5 - 1 mm wide, random, vein filling is white zeolite cutting both matrix and clasts.

ADDITIONAL COMMENTS: This lithology has different types of clasts ranging from pale gray pumice to dark basalt. The degree of pervasive alteration of the clasts is highly variable.

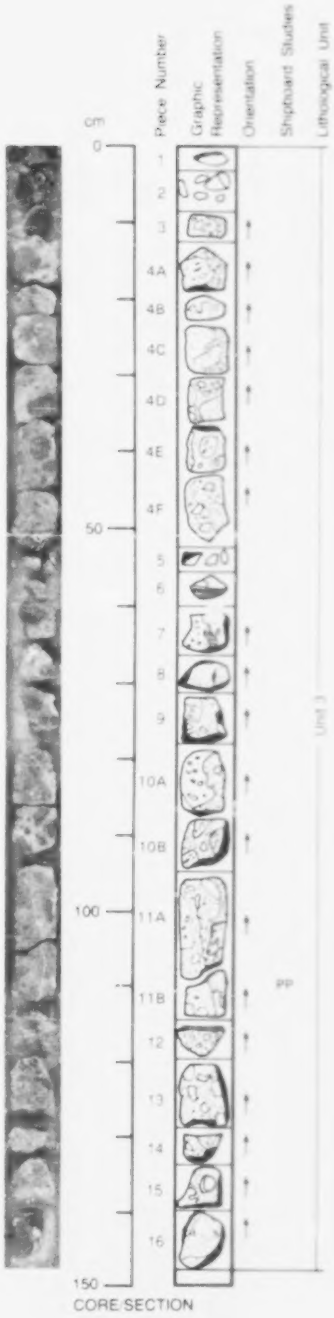

125-786B-10R-1

UNIT 3: ANDESITE BRECCIA

Pieces 1-16

CONTACTS: Not visible.
PHENOCRYSTS: Phenocrysts also occur in breccia matrix.
Orthopyroxene - 5-10%, <2 mm, glassy green (euhedral) and yellow, altering to orange-brown (anhedral). Probably two orthopyroxene varieties present.
Clinopyroxene - 2-5%, <2 mm, dark green to black, glassy. Often associated with yellow orthopyroxene in glomerocrysts.
Plagioclase - 0-5%, <1 mm, euhedral, clear, colorless, also in glomerocrysts with orthopyroxene.
Olivine - 0-1%, <2 mm, euhedral, but altered to red and white; also occurs in xenoliths and then contains nearly opaque Cr spinel.
GROUNDMASS: In breccia clasts, glassy to finely crystalline.
VESICLES: 10-20%, < 1 cm, round to parallel or elongated, randomly distributed throughout; breccia matrix does not contain vesicles; some have bluish coating.
COLOR: Beige to gray (10YR 6/2 to 7.5YR 5/0) for andesite; green for breccia matrix.
STRUCTURE: Matrix supported breccia.
ALTERATION: Andesite clasts alter to greenish matrix-like product but clast-matrix boundaries are distinct (e.g., in Piece 4C).
VEINS/FRACTURES: Trace, 1-5 mm, fractures in clasts only, random orientation; alteration of clasts seems to occur along fractures and clast surfaces.
ADDITIONAL COMMENTS: Evidence for brecciation: 1) clasts have different phenocryst modes than matrix, 2) vesicles in different clasts have different orientations but are parallel within a single clast, 3) sharp clast-matrix boundaries sometimes show reaction rim in clasts, 4) vesicles at clast rims are filled with matrix, 5) matrix is not vesicular. ADDITIONAL SPARSE CLASTS: Monolith of 1) olivine (with almost opaque Cr spinel inclusions + orthopyroxene + clinopyroxene), 2) Orthopyroxene + clinopyroxene (Piece 3), 3) Olivine (with spinel rim) + orthopyroxene (Piece 3), and 4) others, including pumice. Some large clasts are almost to completely plagioclase free and olivine is rare in all clasts and often absent.

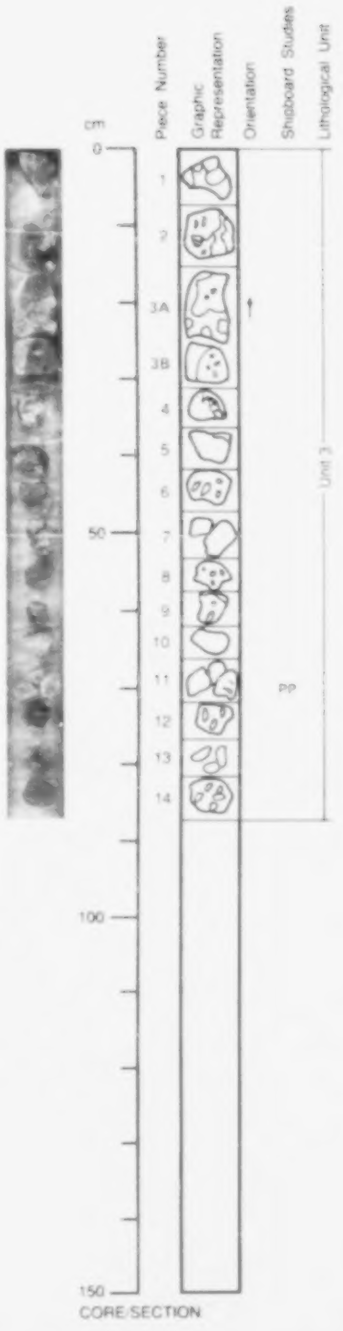
cm
0
50
100
150
Piece Number
Graphic Representation
Orientation
Shipboard Studies
Lithological Unit
1
2
3A
3B
4
5
6
7
8
9
10
11
12
13
14
PP
Unit 3
CORE/SECTION

125-786B-10R-2

UNIT 3: ANDESITE BRECCIA (10R-1 CONTINUED)

Pieces 1-14

CONTACTS: Not visible
PHENOCRYSTS: Microlith of orthopyroxene + clinopyroxene of 1 cm size in Piece 3B: phenocrysts also occur in breccia matrix where orthopyroxene is dominant.
Orthopyroxene - 8-15%; <2 mm; glass green (euhedral), yellow to brown (anhedral).
Clinopyroxene - 2-4%; <1 mm; black, glassy, with yellow.
Orthopyroxene: Anhedral.
Plagioclase - 0-5%; <2 mm; euhedral to anhedral.
Olivine - Trace; <1 mm; reddish alteration (olivine occurs in very few pieces only).
GROUNDMASS: Fine-grained to glassy in clasts, less glass than in 10R-1.
VESICLES: 5-15%; <1 cm; sub-round to parallel or elongated; randomly distributed.
COLOR: Gray (7.5 YR 5/0) for clasts, pale green (5G 6/2) for matrix.
STRUCTURE: Breccia.
ALTERATION: Clasts alter to green matrix-like product.
1%; 1-5 mm; along clast rim; white, soft, not carbonate (zeolite?).
ADDITIONAL COMMENTS: Altered olivine only in matrix; matrix is poorly packed; matrix grain size is larger (0.2 cm) than in 10R-1; voids along clast boundaries filled with sugary greenish colloform substance; light blue and gray material (zeolite?) in clasts.

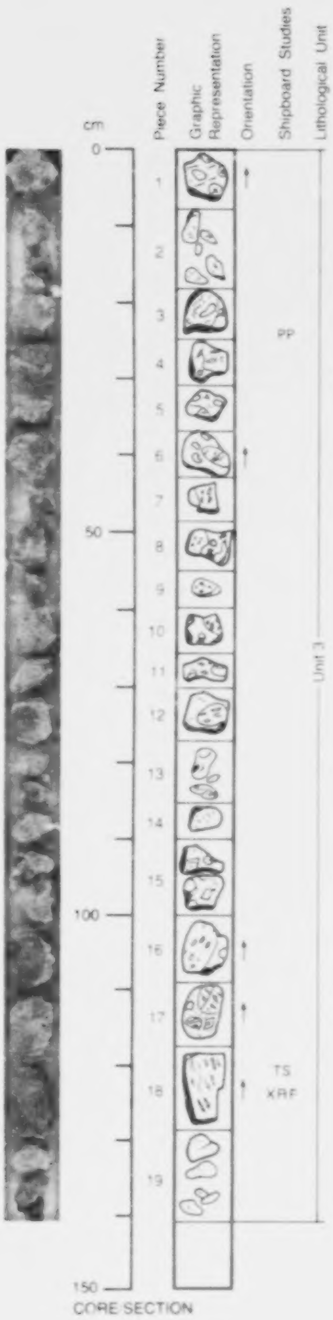

125-786B-11R-1

UNIT 3: ANDESITE BRECCIA (10R-2 CONTINUED)

Pieces 1-14

CONTACTS: Not visible
PHENOCRYSTS: Plagioclase and orthopyroxene microlith in Piece 7; orthopyroxene, clinopyroxene and plagioclase microlith in Piece 12.
Orthopyroxene - 8-15%, <2 mm, glass-green (euhedral), yellow to brown (anhedral)
Clinopyroxene - 2-4%, <1 mm, black, glassy, with yellow
Orthopyroxene - anhedral
Plagioclase - 0-5%, <2 mm, euhedral and anhedral
Olivine - trace, <1 mm, reddish alteration (olivine occurs in vary few pieces only)
GROUNDMASS: In clasts: fine-grained to glassy; less glass than in 10R-1.
VESICLES: 5-15%, <1 mm, sub-round to parallel, elongated, randomly distributed.
COLOR: Gray (7.5YR 5/0) for clasts; pale green (5G 6/2) for matrix.
STRUCTURE: Breccia.
ALTERATION: Clasts alter to green matrix like product.
VEINS/FRACTURES: 1%, 1-5 mm, along clast rim; vein filling is white, soft, not carbonate (zeolite?).
ADDITIONAL COMMENTS: Matrix grain size is 0-2 cm; section is a continuation of 125-786B-8R-1.

UNIT 3: BASALT BRECCIA

Pieces 15-19

CONTACTS: Not visible
PHENOCRYSTS:
Orthopyroxene - 2%, <2 mm, euhedral and anhedral, glass-green
Clinopyroxene - 3%, <1 mm, black as individual phenocryst and with orthopyroxene in glomerocrysts
Plagioclase - 5%, <2 mm, anhedral
Olivine - 1%, <1 mm, reddish, altered
GROUNDMASS: In clast: fine-grained to glassy; less glass than in 10R-1.
VESICLES: 5-15%, <1 cm, subround to parallel elongated, randomly distributed.
COLOR: Gray (7.5YR 5/0) for clasts; pale green (5G 6/2).
STRUCTURE: Breccia.
ALTERATION: Clasts alter to matrix like product.
VEINS/FRACTURES: 1%, 1-5 mm, along clast; vein filling is white, soft, not carbonate (zeolite?).
ADDITIONAL COMMENTS: Altered olivine only in matrix; matrix is poorly packed; matrix grain size is 0-2 cm; voids along clast boundaries; voids filled with sugary greenish colliform substance; light blue and gray zeolites/clay in clasts.

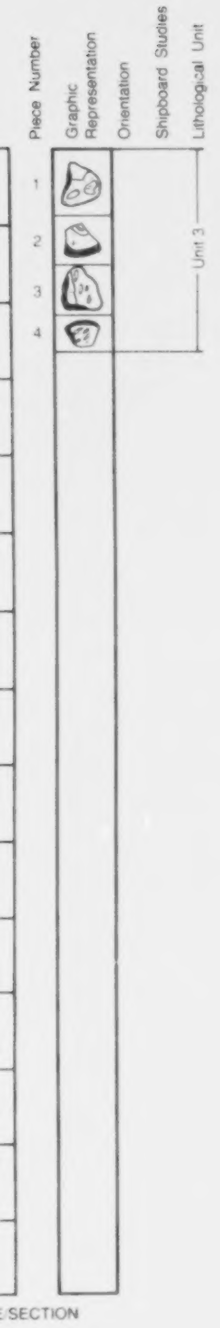

125-786B-11R-2

UNIT 3: BASALT BRECCIA (11R-1, PIECES 15-19 CONTINUED)

Pieces 1-4

CONTACTS: Not visible.
PHENOCRYSTS:
Orthopyroxene - 2%, <2 mm, euhedral and anhedral, glass-green.
Clinopyroxene - 3%, <1 mm, euhedral, black, as individual phenocrysts, with orthopyroxene in glomerocrysts.
Plagioclase - 5%, <2 mm, anhedral.
Olivine - 1%, <1 mm, reddish, altered.
GROUNDMASS: In clasts, fine-grained to glassy.
VESICLES: 5-15%, <1 cm, subrounded to parallel elongated, randomly distributed.
COLOR: Gray (7.5YR 5/0) for clasts, pale green (5G 6/2) for matrix.
STRUCTURE: Breccia.
ALTERATION: Clasts alter to green matrix-like product.
VEINS/FRACTURES: 1%, 1-5 mm, along clast rim, vein filling is white, soft, not carbonate (zeolite?).
ADDITIONAL COMMENTS: Groundmass of breccia matrix locally cellular structure within clasts, walls are green, filling is white, green tubules also present, amount of green material varies from 10-95%, at high % it looks like phenocrysts in green groundmass, coarse-grained breccia groundmass with voids caused by poor packing.

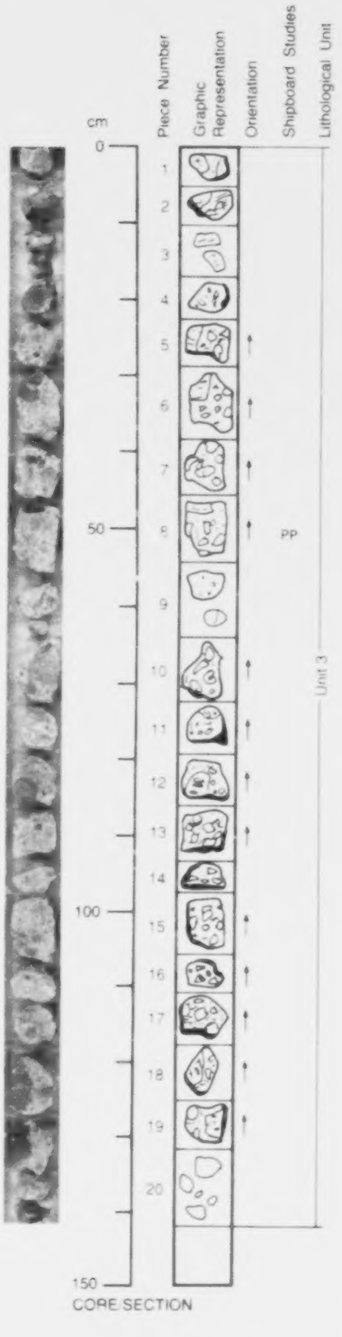
cm
Piece Number
Graphic Representation
Orientation
Shipboard Studies
Lithological Unit
0
50
100
150
1
2
3
4
5
6
7
8
9
10
11
12
13
14
15
16
17
18
19
20
PP
Unit 3
CORE/SECTION

125-786B-12R-1

UNIT 3: BASALT BRECCIA (11R-2 CONTINUED)

Pieces 1-20

CONTACTS: Not visible
PHENOCRYSTS:
Orthopyroxene - 2%, <2 mm, euhedral and anhedral, glass-green.
Clinopyroxene - 3%, <1 mm, euhedral, black, as individual phenocrysts and with orthopyroxene in glomerocrysts.
Plagioclase - 5%, <2 mm, anhedral.
Olivine - 1%, <1 mm, reddish, altered.
GROUNDMASS: In clasts, fine-grained to glassy.
VESICLES: 5-15%, <1 cm, subrounded to parallel elongated; randomly distributed.
COLOR: Gray (7.5YR 5/0) for clasts, pale green (5G 6/2) for matrix.
STRUCTURE: Breccia.
ALTERATION: Clasts alter to green matrix-like product.
VEINS/FRACTURES: 1%, 1-5 mm, along clast rim; vein filling is white, soft, not carbonate (zeolite?).
ADDITIONAL COMMENTS: Groundmass of breccia matrix has locally cellular structure within clasts; walls are green, filling is white; also green tubules present; amount of green material varies from 10-95%; at high % maybe phenocrysts in green groundmass; coarse-grained breccia groundmass with voids caused by poor packing. Pieces 18 and 19 contain very glassy clasts, consisting of plagioclase 5%, orthopyroxene 5%, and clinopyroxene trace; different clasts (very dark grayish-brown; 2.5Y 3/2) also occur in Pieces 6-17 and consist of plagioclase 10%, clinopyroxene 5%, and orthopyroxene trace %.

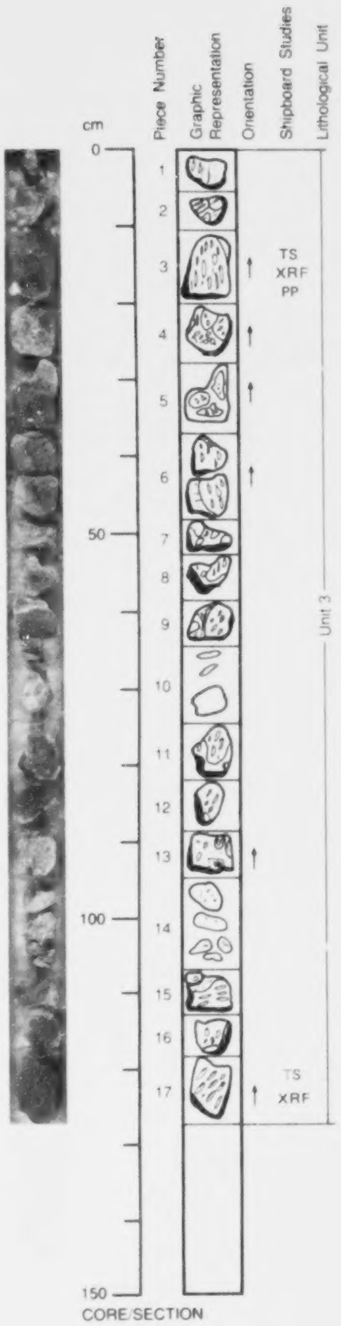
cm
Piece Number
Graphic Representation
Orientation
Shipboard Studies
Lithological Unit
0
50
100
150
1
2
3
4
5
6
7
8
9
10
11
12
13
14
15
16
17
TS
XRF
PP
TS
XRF
Unit 3
CORE/SECTION

125-786B-12R-2

UNIT 3: BASALT BRECCIA

Pieces 1-17

CONTACTS: Not visible

PHENOCRYSTS: Contains glomerocrysts of clinopyroxene + plagioclase; clinopyroxene + orthopyroxene; olivine + clinopyroxene.

Plagioclase - 5-8%, 1-4 mm, rounded, anhedral and euhedral; shows poikilitic texture with clinopyroxene.

Clinopyroxene - 2-8%, <2 mm, euhedral in individual crystals.

Orthopyroxene - tr-2%, <1 mm, yellow, anhedral, glomerocrystic.

GROUNDMASS: Glassy to finely crystalline in clasts; coarse-grained cellular altered clasts and fines with few voids in breccia.

VESICLES: 5-15%, <1 cm, subrounded to parallel elongated, randomly distributed.

COLOR: Gray (7.5YR 5/0) for clasts, pale green (5G 6/2) for matrix.

STRUCTURE: Breccia.

ALTERATION: Clasts alter to green matrix-like product.

VEINS/FRACTURES: 1%, 1-5 mm, random; vein filling is white, soft, not carbonate, zeolite (?).

ADDITIONAL COMMENTS: Pieces 8-17 have more phenocrysts (up to 30% with plagioclase 15%) and plagioclase microphenocrysts; some pieces (9, 12, 15, 16) consist almost entirely of greenish matrix.

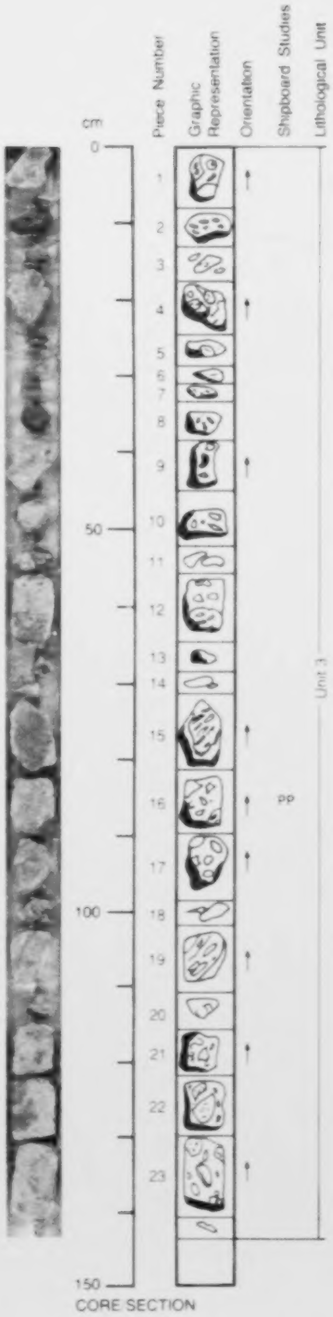
cm
Piece Number
Graphic Representation
Orientation
Shipboard Studies
Lithological Unit
0
50
100
150
1
2
3
4
5
6
7
8
9
10
11
12
13
14
15
16
17
18
19
20
21
22
23
PP
Unit 3
CORE SECTION

125-786B-13R-1

UNIT 3: BONINITE BRECCIA

Pieces 1-23

CONTACTS: Not visible
PHENOCRYSTS:
Plagioclase - 10-15%, 1-4 mm, rounded, euhedral
Orthopyroxene - 0-10%, <1 mm, yellow, anhedral
Clinopyroxene - trace, <2 mm, euhedral, individual crystal shows poikilitic texture with plagioclase
GROUNDMASS: Glassy in clasts; coarse-grained in breccia; cellular altered clasts and fines; few voids
VESICLES: 5-15%, <1 cm, subrounded to parallel elongated; randomly distributed, filled with bluish minerals
COLOR: Gray (7.5YR 5/0) for clasts; pale green (5G 6/2) for matrix
STRUCTURE: Breccia
ALTERATION: Clasts alter to green matrix like product
VEINS/FRACTURES: 1%, 1-5 mm, random, vein filling is white, soft, not carbonate, zeolite(?)
ADDITIONAL COMMENTS: In addition to common clasts, Pieces 12, 15, 22 and 23 contain plagioclase microphenocrysts in groundmass. Piece 21 (black clast) is glassy and contains phenocrysts of clinopyroxene 2%, plagioclase trace % and orthopyroxene trace %; some clasts have alteration rims with matrix occupying 70% of total rock.

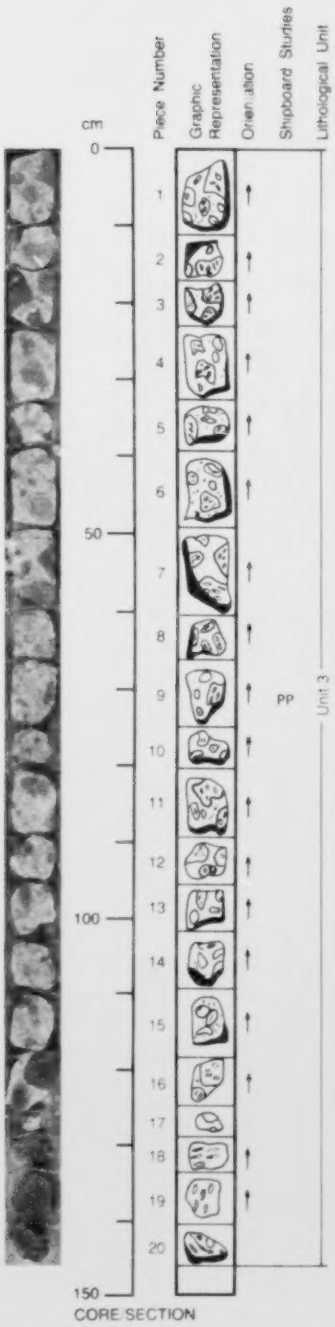
cm
0
50
100
150
Piece Number
Graphic Representation
Orientation
Shipboard Studies
Lithological Unit
1
2
3
4
5
6
7
8
9
10
11
12
13
14
15
16
17
18
19
20
PP
Unit 3
CORE/SECTION

125-786B-13R-2

UNIT 3: BONINITE BRECCIA

Pieces 1-20

CONTACTS: Not visible
PHENOCRYSTS:
Plagioclase - 5-10%; <4 mm; anhedral to euhedral
Orthopyroxene - 5-10%; <1 mm; yellow, anhedral
Clinopyroxene - trace; <2 mm; euhedral, usually associated with orthopyroxene
GROUNDMASS: Glassy to fine grained matrix with plagioclase microphenocrysts.
VESICLES: 5-15%; <1 mm; subrounded to parallel elongated; randomly distributed.
COLOR: Gray (7.5YR 5/0) for clasts; pale green (5G 6/2) for matrix.
STRUCTURE: Breccia.
ALTERATION: Clasts alter to green matrix like product.
VEINS/FRACTURES: 1%; 1-5 mm; random; vein filling is white, soft, not carbonate zeolite(?).

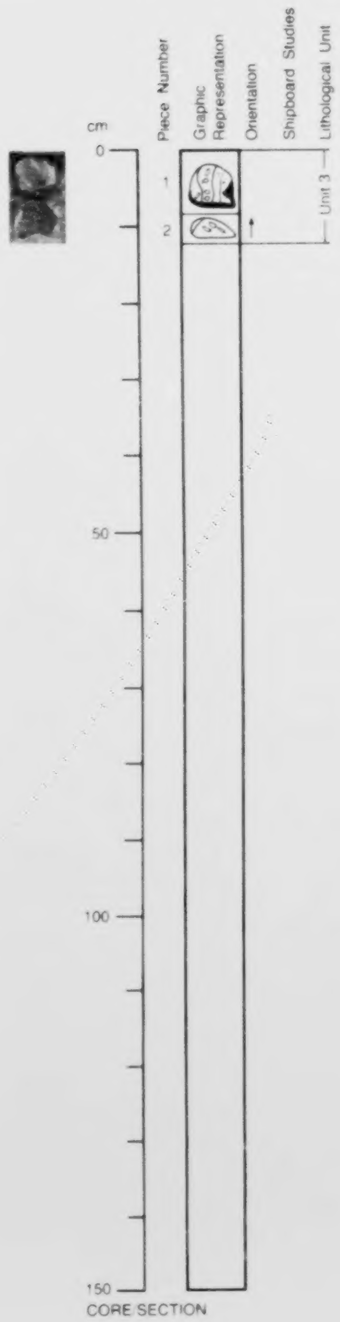
cm
Piece Number
Graphic Representation
Orientation
Shipboard Studies
Lithological Unit
0
50
100
150
1
2
Unit 3
CORE/SECTION

125-786B-13R-3

UNIT 3: BONINITE BRECCIA (13R-2 CONTINUED)

Pieces 1-2

CONTACTS: N/A
PHENOCRYSTS: N/A
GROUNDMASS: N/A
VESICLES: N/A
COLOR: N/A
STRUCTURE: N/A
ALTERATION: N/A
VEINS/FRACTURES: N/A
ADDITIONAL COMMENTS: Section is continuation of 125-786B-13R-2

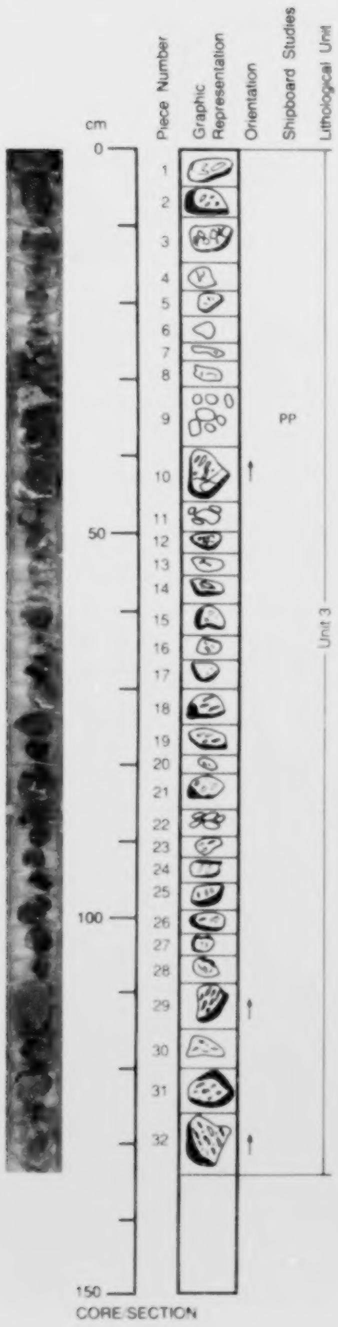
cm
Piece Number
Graphic Representation
Orientation
Shipboard Studies
Lithological Unit
0
50
100
150
1
2
3
4
5
6
7
8
9
10
11
12
13
14
15
16
17
18
19
20
21
22
23
24
25
26
27
28
29
30
31
32
PP
Unit 3
CORE/SECTION

125-786B-14R-1

UNIT 3: ANDESITE BRECCIA

Pieces 1-32

CONTACTS: Not visible

PHENOCRYSTS: Occur as glomerocrystic and poikilitic assemblages as well as isolated phases

Plagioclase - 5-8%; 0.5 - 1.5 mm; euhedral elongate

Orthopyroxene - 1-3%; <1 mm; euhedral equant - elongate

Clinopyroxene - 2-5%; <1.5 mm; equant euhedral

GROUNDMASS: Glassy to very fine-grained with quench feldspar

VESICLES: 1-15%; <10 mm long; elongate; locally aligned; blue coating to vesicle wall in Pieces 1 and 2

COLOR: Gray (7.5YR 5/0) clasts; pale green (5G 6/2) matrix

STRUCTURE: Breccia

ALTERATION: Variable alteration of clasts with reaction boundaries 2 - 10 mm in width. Pieces 3-8 are pervasively stained with possible manganiferous alteration having a brown color (10YR 5/3).

VEINS/FRACTURES: Trace; 1.5 mm wide; random; white non-carbonate filling

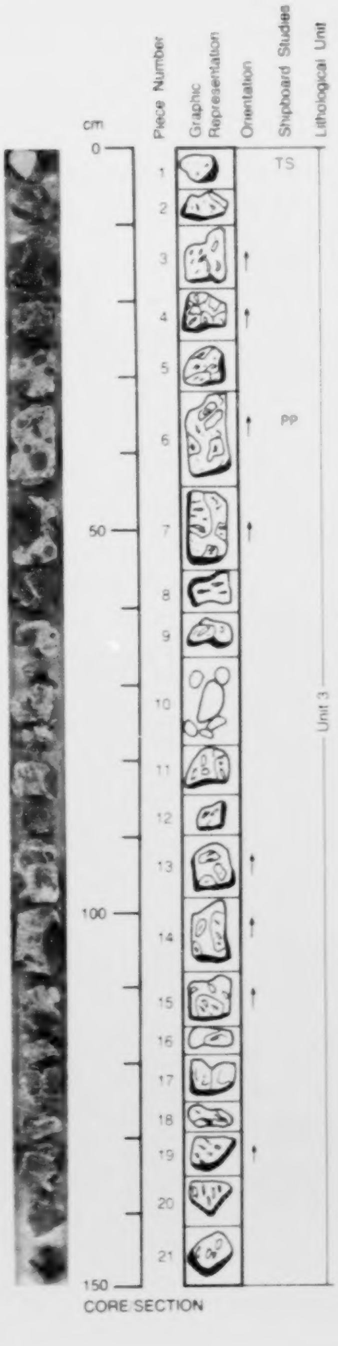

125-786B-15R-1

UNIT 3: MICRODIORITE

Piece 1

CONTACTS: Not visible
PHENOCRYSTS: Amphibole-pyroxene glomerocrysts as well as isolated phases.
Amphibole - 5-8%, 0.2-0.6 mm, equant, euhedral, elongate.
Orthopyroxene - 8-12%, 0.5-2 mm, elongate, subhedral.
Plagioclase - <80%, 0.1-1 mm, elongate, euhedral-subhedral.
Magnetite - <2%, <0.1 mm, euhedral, equant.
GROUNDMASS: Composed of same phases as phenocrysts; rock has hypabyssal texture.
VESICLES: None.
COLOR: Light gray (5Y 7/1).
STRUCTURE: Rock has isotropic fabric.
ALTERATION: Minor chlorotic alteration.
VEINS/FRACTURES: None visible.
ADDITIONAL COMMENTS: Texture of this piece is very different from under- and overlying core although phase assemblage is the same.

UNIT 3: ANDESITE BRECCIA

Pieces 2-21

CONTACTS: Not visible.
PHENOCRYSTS: Occur as glomerocrystic and poikilitic assemblages as well as isolated phases.
Plagioclase - 5-8%, 0.5-1.5 mm, euhedral, elongate.
Orthopyroxene - 1-3%, <1 mm, euhedral, equant, elongate.
Clinopyroxene - 2-5%, <1.5 mm, equant, euhedral.
GROUNDMASS: Glassy to very fine grained with quench feldspar.
VESICLES: 3-5%, 0.2-0.5 mm in diameter, <22 mm long, pipe shape, aligned; pale white(?) zeolites on walls of vesicles in Pieces 19-21.
COLOR: Gray (7.5YR 5/0) clasts, pale green (5G 6/2) breccia matrix.
STRUCTURE: Breccia.
ALTERATION: Variable alteration of clasts with reaction boundaries 2-10 mm in width.
VEINS/FRACTURES: Trace, 0.5 mm wide, subvertical, filled with white zeolite.
ADDITIONAL COMMENTS: Some of the clasts have a macroscopic orthorhombic fracture pattern; in situ brecciation of clasts; appears to be abundant altered glassy pillow rinds in Piece 15.

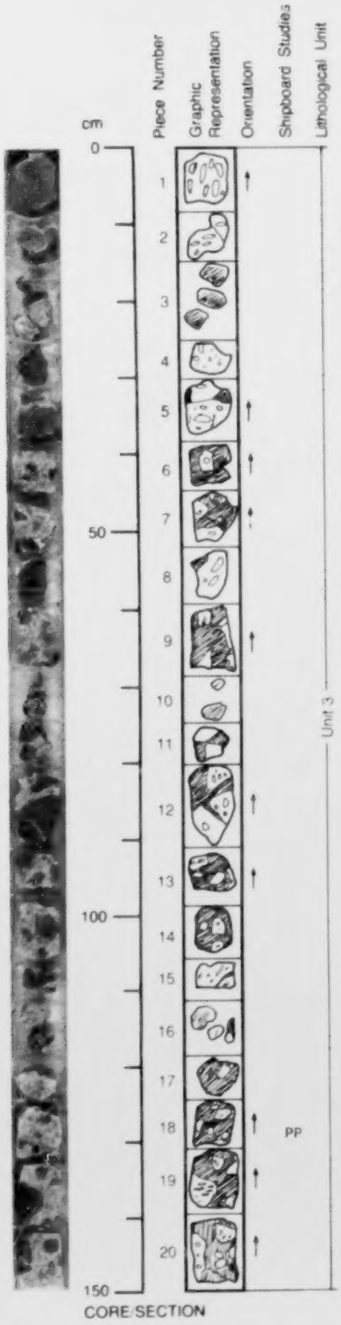
cm
Piece Number
Graphic Representation
Orientation
Shipboard Studies
Lithological Unit
0
50
100
150
1
2
3
4
5
6
7
8
9
10
11
12
13
14
15
16
17
18
19
20
PP
Unit 3
CORE/SECTION

125-786B-15R-2

UNIT 3: ANDESITE BRECCIA

Pieces 1-20

CONTACTS: Not visible.
PHENOCRYSTS: Occur as glomerocrystic and poikilitic assemblages as well as isolated phases.
Plagioclase - 3-5%; 0.5-1 mm; euhedral; lath.
Orthopyroxene - 1-3%; <1 mm; euhedral; equant.
Clinopyroxene - 2-5%; <1.5 mm; equant; euhedral; elongate.
GROUNDMASS: Glassy to very fine-grained with quench feldspar.
VESICLES: 1-15%; 0.2-3 mm; pipe shaped; aligned; mostly subvertical; pale white to transparent zeolites(?) on walls of vesicles.
COLOR: Gray (7.5YR 5/0) clasts; pale green (5G 6/2) matrix.
STRUCTURE: Breccia.
ALTERATION: Variable alteration of clasts with reaction boundaries 2-10 mm in width.
VEINS/FRACTURES: Trace; <0.3 mm wide; random; filled with white zeolite(?).
ADDITIONAL COMMENTS: Proportion of clasts to matrix is variable from piece to piece.

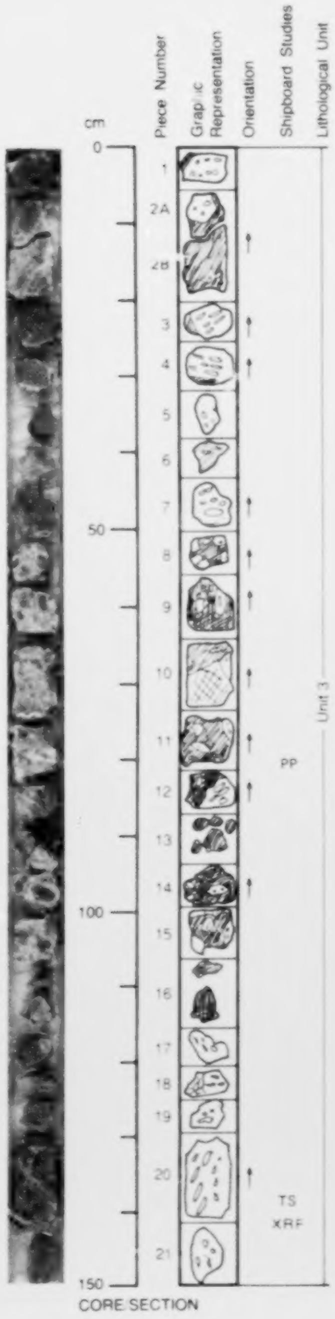
cm
Piece Number
Graphic Representation
Orientation
Shipboard Studies
Lithological Unit
0
50
100
150
1
2A
2B
3
4
5
6
7
8
9
10
11
12
13
14
15
16
17
18
19
20
21
PP
TS
XRF
Unit 3
CORE/SECTION

125-786B-16R-1

UNIT 3: ANDESITE BRECCIA

Pieces 1-21

CONTACTS: Not visible

PHENOCRYSTS: Occur as glomerocrystic and poikilitic assemblages as well as isolated phases.

Plagioclase - 3-6%, 0.5-1 mm, euhedral laths.
Orthopyroxene - 1-3%, <1.5 mm, euhedral, equant.
Clinopyroxene - 2-5%, <1.5 mm, equant, euhedral to elongate.

GROUNDMASS: Glassy to very fine-grained with quench feldspar.

VESICLES: 1-15%, 0.2-3 mm in diameter, pipe-shaped, oriented pieces horizontal-subvertical; pale white, transparent to pale blue zeolites(?) on walls of some vesicles.

COLOR: Gray (7.5YR 5/0) clasts; pale green (5G 6/2) matrix.

STRUCTURE: Breccia.

ALTERATION: Variable alteration of clasts with reaction boundaries 2 - 20 mm in width; some clasts totally altered.

VEINS/FRACTURES: Trace, <2 mm in width, random, filled with white zeolite.

ADDITIONAL COMMENTS: Matrix is cellular structured with green cell walls and white zeolites(?), feldspar, orthopyroxene and clinopyroxene filling the cells.

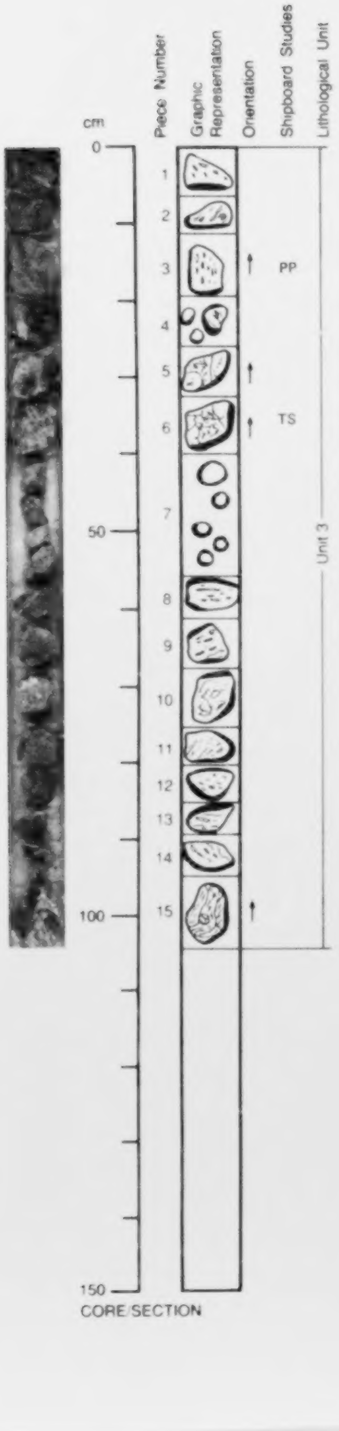
cm
Piece Number
Graphic Representation
Orientation
Shipboard Studies
Lithological Unit
0
50
100
150
1
2
3
4
5
6
7
8
9
10
11
12
13
14
15
PP
TS
Unit 3
CORE/SECTION

125-786B-16R-2

UNIT 3: ANDESITE BRECCIA

Pieces 1-15

CONTACTS: None visible.

PHENOCRYSTS: Occur as glomerocrystic and poikilitic assemblages as well as isolated phases.

Plagioclase - 3-6%; 0.5-1 mm; euhedral laths.
Orthopyroxene - 1-3%; <1.5 mm; euhedral, equant.
Clinopyroxene - 2-5%; <1.5 mm; equant, euhedral.

GROUNDMASS: Glassy to very fine-grained with quench feldspar.

VESICLES: 1-15%; 0.2-8 mm; irregular, elongate; throughout; some pieces have vertical orientation.

COLOR: Gray (7.5YR 5/0) clasts, pale green (5G 6/2) matrix.

STRUCTURE: Brecciated.

ALTERATION: Variable alteration of clasts with reaction boundaries 2-20 mm in width; some clasts are completely altered.

VEINS/FRACTURES: Trace; <1 mm wide; random orientation; white, zeolite(?)-filled.

ADDITIONAL COMMENTS: Matrix is cellular structured with green cell walls and white zeolites(?), feldspar, orthopyroxene and clinopyroxene filling the cells.

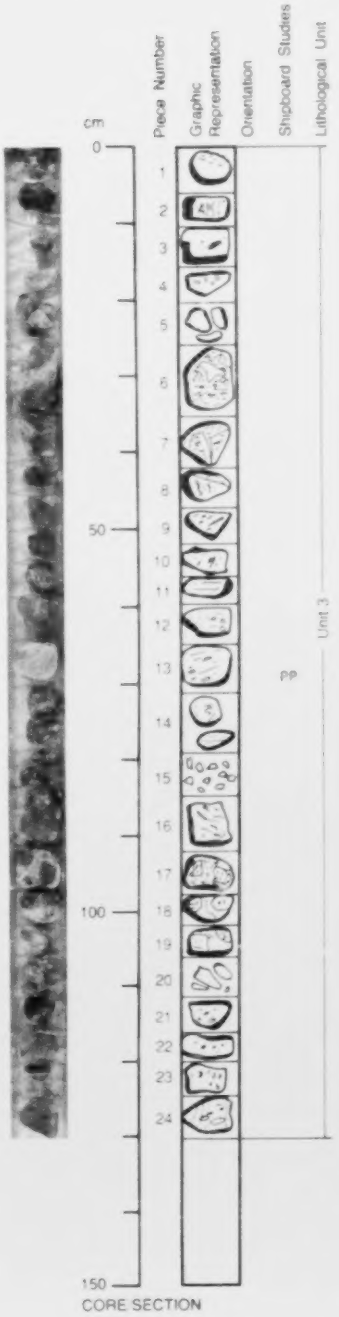

125-786B-17R-1

UNIT 3: ANDESITE BRECCIA

Pieces 1-2, 5-12, 14-24

CONTACTS: Not visible.
PHENOCRYSTS: Occur as glomerocrystic and poikilitic assemblages as well as isolated phases.
Plagioclase - 3-6%, 0.5-1 mm, euhedral laths.
Orthopyroxene - 1-3%, <1.5 mm, euhedral, equant.
Clinopyroxene - 2-5%, <1.5 mm, euhedral elongate.
GROUNDMASS: Glassy to very fine-grained with quench feldspar.
VESICLES: 1-15%, 0.2-3 mm in diameter, pipe, random; white to pale blue zeolites on the walls of some vesicles.
COLOR: Gray (7.5YR 5/) clasts, pale green (5G 6/2) matrix.
STRUCTURE: Breccia.
ALTERATION: Variable alteration of clasts with reaction boundaries 2-10 mm in width.
VEINS/FRACTURES: Trace, <1 mm in width, random, white zeolite(?) filled.
ADDITIONAL COMMENTS: Proportion of apparently relict hyaloclastic matrix is higher in Pieces 3-7 and 17 than in previous cores. Piece 7 has minor Fe-oxide staining in matrix.

UNIT 3: MICRODIORITE

Pieces 3, 4

CONTACTS: None visible.
PHENOCRYSTS: Amphibole-pyroxene-olivine glomerocrysts.
Amphibole - 5-8%, 0.2-0.6 mm, equant, euhedral, elongate.
Orthopyroxene - 8-12%, 0.5-2 mm, elongate, subhedral.
Plagioclase - <80%, 0.1-1 mm, elongate, euhedral-subhedral.
Magnetite - <2%, <0.1 mm, euhedral, equant.
Olivine - <1%, 0.5-1.5 mm, equant, altered with Fe-oxide staining.
GROUNDMASS: Composed of same phases that occur as phenocrysts; rock has hypabyssal textures.
VESICLES: None.
COLOR: Light gray (5Y 7/1).
STRUCTURE: Massive.
ALTERATION: Minor chlorite alteration.
VEINS/FRACTURES: None visible.
ADDITIONAL COMMENTS: Texture of this piece is very different from surrounding core; it is the same as 15R-1 Piece 1.

UNIT 3: SPARSELY PHYRIC ANDESITE

Piece 13

CONTACTS: None visible.
PHENOCRYSTS: Glomerocrysts of pyroxene, plagioclase and magnetite.
Clinopyroxene - <1-1%, <0.5 mm, equant, euhedral.
Orthopyroxene - <<1%, <0.25 mm, equant to elongate, euhedral.
Plagioclase - <2%, <0.5 mm, tabular laths, euhedral.
Magnetite - <<1%, <0.2-0.5 mm, equant, euhedral.
GROUNDMASS: Fine-grained and glassy with quench feldspar.
VESICLES: 2-5%, 1-3 mm, round to elongate, pipe shaped, throughout, filled with white zeolites(?).
COLOR: Gray to light gray (5Y 5/1 - 7/1).
STRUCTURE: Massive.
ALTERATION: None visible.
VEINS/FRACTURES: None.
ADDITIONAL COMMENTS: This sample is paler, less phyric and has less orthopyroxene than the other samples in this section.

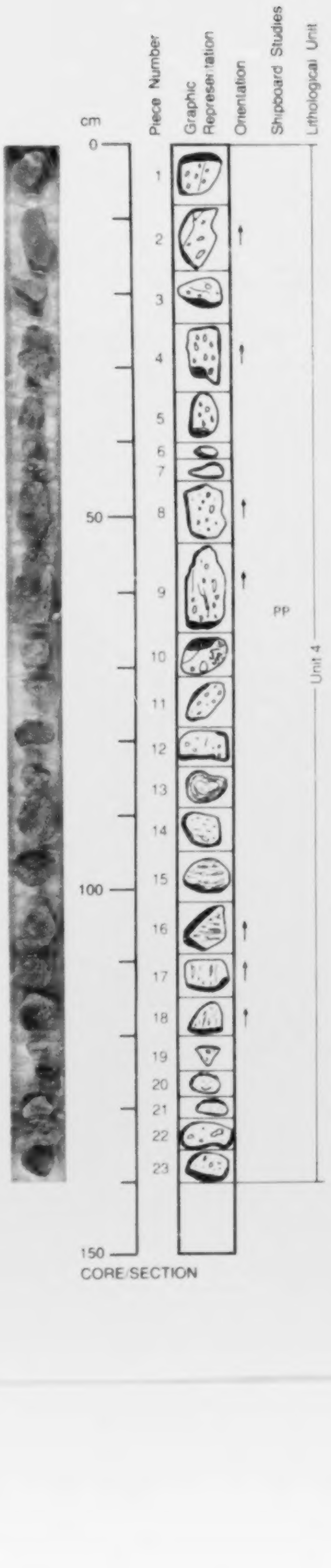
cm
Piece Number
Graphic Representation
Orientation
Shipboard Studies
Lithological Unit
0
50
100
150
1
2
3
4
5
6
7
8
9
10
11
12
13
14
15
16
17
18
19
20
21
22
23
PP
Unit 4
CORE/SECTION

125-786B-18R-1

UNIT 4: ANDESITE

Pieces 1-23

CONTACTS: None visible.

PHENOCRYSTS: Olivine phenocrysts occur sporadically throughout this section.

- Clinopyroxene - 5-7%, 0.4-1 mm, equant to elongate, euhedral.
- Orthopyroxene - 1-2%, 0.7-1.5 mm, elongate, subhedral.
- Plagioclase - 1-2%, 0.1-0.5 mm, elongate, euhedral-subhedral.
- Olivine - trace, 1-2 mm, elongate, euhedral, poikilitically enclosed in pyroxene glomerocrysts.

GROUNDMASS: Fine-grained plagioclase and pyroxene crystals and a small amount of brown glass; amount of glass is variable throughout.

VESICLES: 3-12%, 2-6 mm; oval to round; throughout; pipe morphology.

COLOR: Gray to light gray (5Y 6/1).

STRUCTURE: Massive.

ALTERATION: 10-40% chlorite and clays.

VEINS/FRACTURES: None.

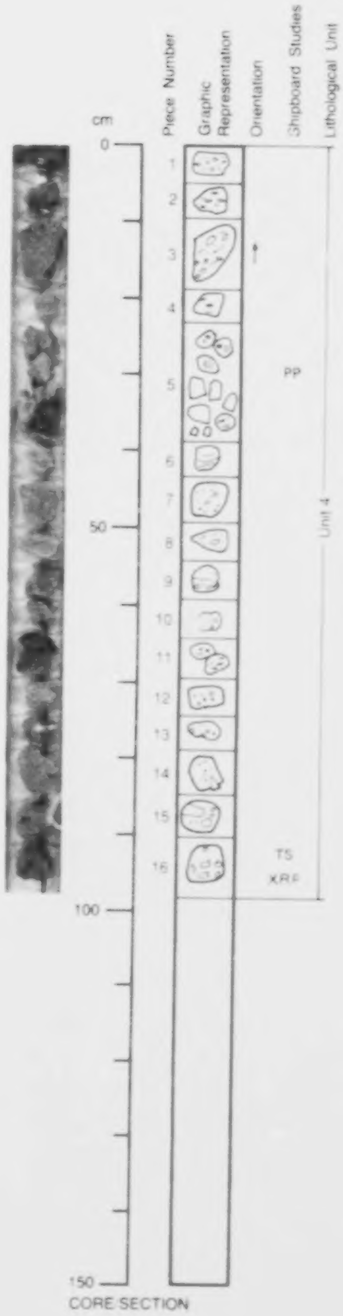
cm
Piece Number
Graphic Representation
Orientation
Shipboard Studies
Lithological Unit
0
50
100
150
1
2
3
4
5
6
7
8
9
10
11
12
13
14
15
16
PP
TS
XRF
Unit 4
CORE/SECTION

125-786B-19R-1

UNIT 4: ANDESITE

Pieces 1-16

CONTACTS: None visible.
PHENOCRYSTS: Pyroxene glomerocrysts enclose highly altered olivine crystals.
Clinopyroxene - 5-7%; 0.4-1 mm; equant to elongate; euhedral.
Orthopyroxene - 1-2%; 0.7-1.0 mm; elongate; subhedral.
Plagioclase - 1-2%; 0.1-0.5 mm; elongate; euhedral-subhedral.
Olivine - trace; 1-2 mm; elongate; euhedral; poikilitically enclosed in pyroxene glomerocrysts.
GROUNDMASS: Brown glass and quench crystals of plagioclase and pyroxene.
VESICLES: 3-10%; 2-6 mm; oval to round; pipe vesicles throughout.
COLOR: Gray to light gray (5Y 6/1).
STRUCTURE: Massive.
ALTERATION: Chlorite and clays 10-25%.
VEINS/FRACTURES: None visible.

[Blank page]

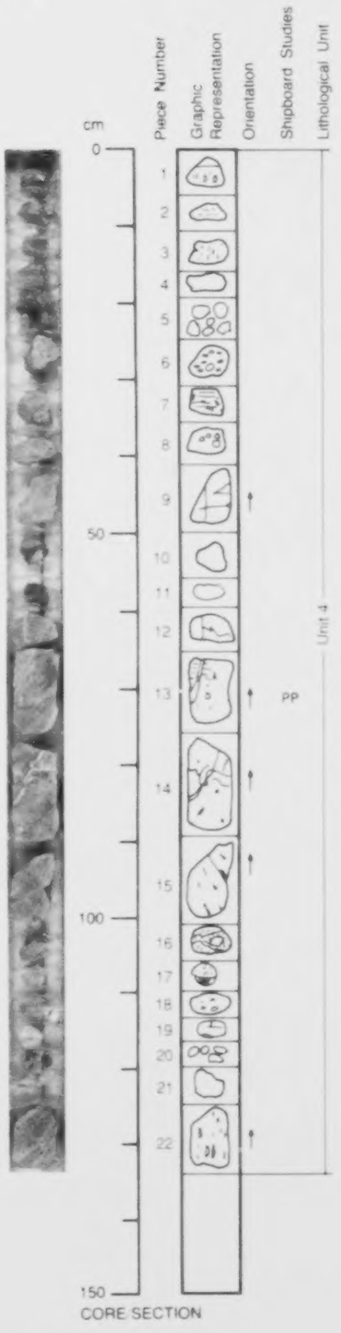
cm
Piece Number
Graphic Representation
Orientation
Shipboard Studies
Lithological Unit
0
50
100
150
1
2
3
4
5
6
7
8
9
10
11
12
13
14
15
16
17
18
19
20
21
22
PP
Unit 4
CORE SECTION

125-786B-20R-1

UNIT 4: TWO-PYROXENE ANDESITE

Pieces 1-22

CONTACTS: None visible.
PHENOCRYSTS:
Orthopyroxene - 2-3%, 0.5-2 mm, equant, euhedral.
Clinopyroxene - 1-2%, 0.2-0.4 mm, anhedral to subhedral.
Plagioclase - 2%, 0.2-0.8 mm, equant, euhedral.
Olivine - trace, <3 mm, equant, anhedral to subhedral, altered and appear to have orthopyroxene reaction rims.
GROUNDMASS: Fine- to medium-grained, plagioclase laths.
VESICLES: 1-12%, 2-4 mm, elongate, smooth outlines, througout, alignment parallel to core axis in Piece 22, lined with pale blue to gray zeolite or clay.
COLOR: Greenish gray (5GB 5/1 to 4/1).
STRUCTURE: Massive.
ALTERATION: Pervasive and patchy, chlorites and clays 10-30%.
VEINS/FRACTURES: 1-5%, <8 mm wide, steeply inclined, anastomosing, filled with white materials including carbonate, zeolite, and chlorite.
ADDITIONAL COMMENTS: Piece 4 has Fe-oxide staining as a pervasive alteration.

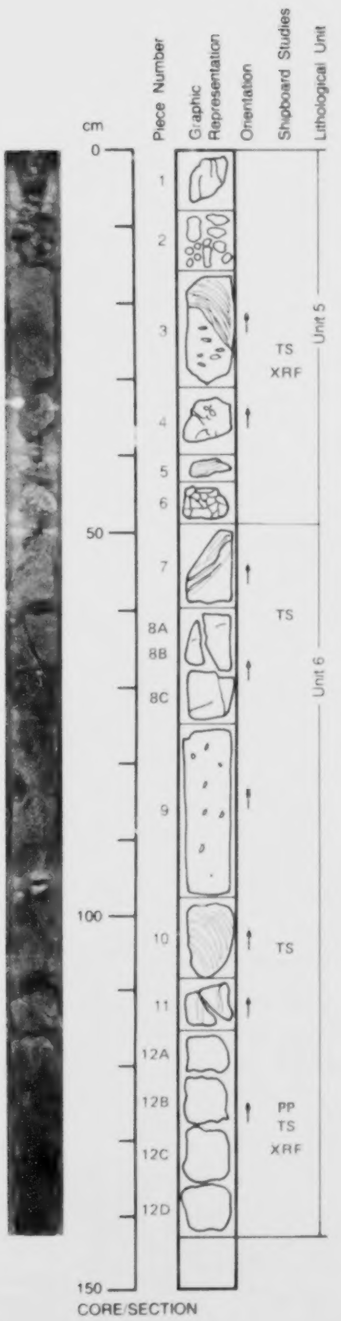

125-786B-21R-1

UNIT 5: TWO-PYROXENE ANDESITE BRECCIA

Pieces 1-4

CONTACTS: None visible.
PHENOCRYSTS: Glomerocrysts of clinopyroxene and orthopyroxene.
Orthopyroxene - <1%; <0.5 mm; euhedral; equant.
Clinopyroxene - <2%; <0.75 mm; euhedral; elongate.
Plagioclase - 1-2%; <1 mm; euhedral; tabular laths.
Olivine - trace; 0.5-1.5 mm; euhedral; elongate.
GROUNDMASS: Glassy to fine-grained with quench crystals of plagioclase.
VESICLES: 2-7%; <4 mm; elongate; random; locally concentrated; filled with transparent, white zeolite(?).
COLOR: Greenish gray (5BG 5/1 to 4/1).
STRUCTURE: Massive with alteration and possible shear boundaries.
ALTERATION: 10-40%; minor chlorite, zeolites and clays.
VEINS/FRACTURES: <1%; 1-3 mm wide; random; anastomosing; filled with white zeolite(?).
ADDITIONAL COMMENTS: Piece 3A is brecciated along a plane parallel to a vein that appears to be fault gouge. This rock is similar to the overlying Section 20R-1.

UNIT 5: HIGHLY BRECCIATED META-ANDESITE

Pieces 5-6

CONTACTS: None visible.
PHENOCRYSTS: None visible.
GROUNDMASS: Zeolite, clays and chlorite.
VESICLES: None present.
COLOR: Dark greenish gray to very light greenish gray (10Y 5/2 to 8/1).
STRUCTURE: Breccia.
ALTERATION: Pieces are altered andesitic breccia; minor iron oxide staining is present.
VEINS/FRACTURES: None present.
ADDITIONAL COMMENTS: Crystals of orthopyroxene, clinopyroxene, plagioclase and magnetite <0.2 mm in size are present in the matrix.

UNIT 6: FLOW-BANDED GLASSY DACITE

Pieces 7-12

CONTACTS: Piece 7: contact with overlying sediment (fine grained sand and silt with fragments of underlying rock).
PHENOCRYSTS:
Orthopyroxene - <2%; <0.5 mm; equant to elongate; euhedral.
Clinopyroxene - <1%; <0.5 mm; elongate; euhedral.
Plagioclase - <3%; <1.5 mm; equant to tabular; euhedral.
Magnetite - trace; <0.2 mm; equant; euhedral.
GROUNDMASS: Brown glass and minor quench crystals of plagioclase.
VESICLES: None.
COLOR: Black to dusky yellow to olive gray (5Y 6/4).
STRUCTURE: Flow banding at a high angle to the core axis.
ALTERATION: Pervasive Fe-oxide staining. Pieces 7 and 8 may contain palagonite.
VEINS/FRACTURES: <1%; <1 mm wide; subvertical; irregular; filled with white zeolite(?).
ADDITIONAL COMMENTS: These pieces appear to represent the top portion of a flow unit.

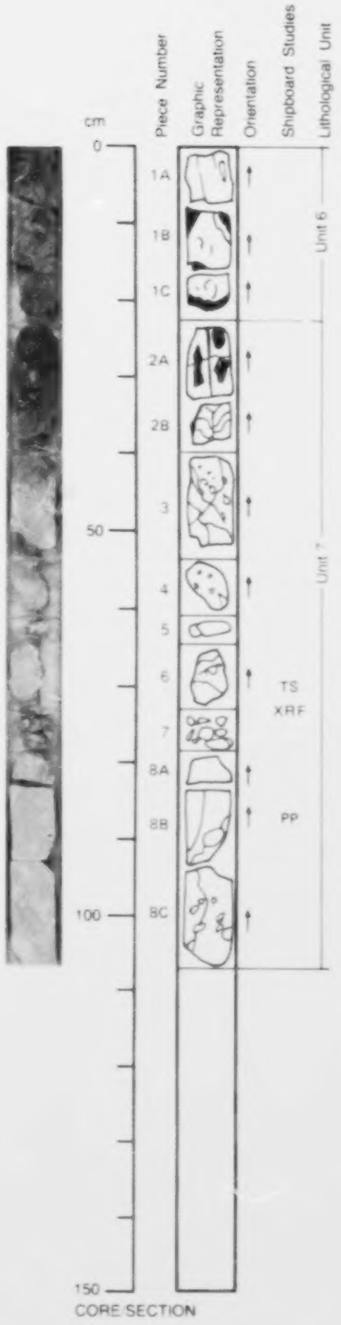

125-786B-21R-2

UNIT 6: GLASSY DACITE (CONTINUATION OF 21R-1, PIECES 7-12)

Piece 1

CONTACTS: None obvious.
PHENOCRYSTS:
Plagioclase - 7%; <1.5; equant to tabular; euhedral.
Olivine - 1%; 0.5; equant; subhedral.
Clinopyroxene - 1%; 0.5; equant; subhedral.
GROUNDMASS: Fine-grained to glassy with plagioclase microliths.
VESICLES: 10%; up to 1 cm; irregular to subrounded; none; mostly filled, but largest have vugs; possibly including zeolite.
COLOR: Pale gray to whitish brown (2.5Y 8/0 to 8/2) infilling.
STRUCTURE: N/A
ALTERATION: Pervasive brownish alteration (2.5Y 6/2) and olivine of groundmass; variable alteration of other phenocrysts.
VEINS/FRACTURES: <1%; <1mm; irregular; white infilling (carbonate(?) and zeolite).

UNIT 7: GLASSY BASALT

Pieces 2-6

CONTACTS: Between Pieces 1 and 2; two units (intrusion?).
PHENOCRYSTS:
Clinopyroxene - <1%; 0.5 mm; elongate; euhedral.
Orthopyroxene - 1-2%; <0.5 mm; equant to elongate; euhedral.
Plagioclase - <3%; <1.5 mm; equant to tabular; euhedral.
Olivine - trace; <0.2 mm; equant; subhedral.
Magnetite - trace; <0.2 mm; equant; euhedral.
GROUNDMASS: Clear, brown glass with quench crystals of plagioclase.
VESICLES: 0-12%; 0.2-2 mm; round; only in Pieces 3-7; in Piece 3 they are concentrated at the top (below the glassy margin) and in Piece 7 they are filled with a pale yellow clay.
COLOR: Black to dusky yellow to olive gray (5Y 6/4).
STRUCTURE: Pieces 2-7 appear to be the top of a cooling unit and Piece 1 the bottom of the overlying cooling unit. Piece 1 is mostly glass. Piece 1C is a glassy extrusion.
ALTERATION: Variable. Piece 1 has Fe-oxide staining. Piece 7 has clay filled vesicles.
VEINS/FRACTURES: <1%; 1-4 mm; subvertical; filled with carbonate and zeolite.
ADDITIONAL COMMENTS: Pieces 1 and 2 have a large amount of fresh glass and represent a contact between two volcanic units.

UNIT 7: BASALT

Pieces 7-8

CONTACTS: None obvious.
PHENOCRYSTS:
Plagioclase - 7%; <1.5 mm; equant to tabular; euhedral.
Clinopyroxene - 1%; 0.5 mm; equant; subhedral.
Olivine - 1%; 0.5 mm; equant; subhedral.
GROUNDMASS: Fine-grained to glassy with plagioclase microliths.
VESICLES: 10%; 1 cm; irregular to subrounded; n/a; mostly filled but largest have vugs; pale gray to whitish brown (2.5Y 8/0 to 8/2) infilling possibly including zeolite.
COLOR: N/A
STRUCTURE: N/A
ALTERATION: Pervasive brownish alteration (2.5Y 6/2) of groundmass and olivine; variable alteration of other phenocrysts.
VEINS/FRACTURES: < 1%; <1 mm wide; irregular; with white infilling (carbonate and zeolite).
ADDITIONAL COMMENTS: Pieces 7 and 8 appear distinct from 1-6, possibly suggesting a contact between 6 and 7.

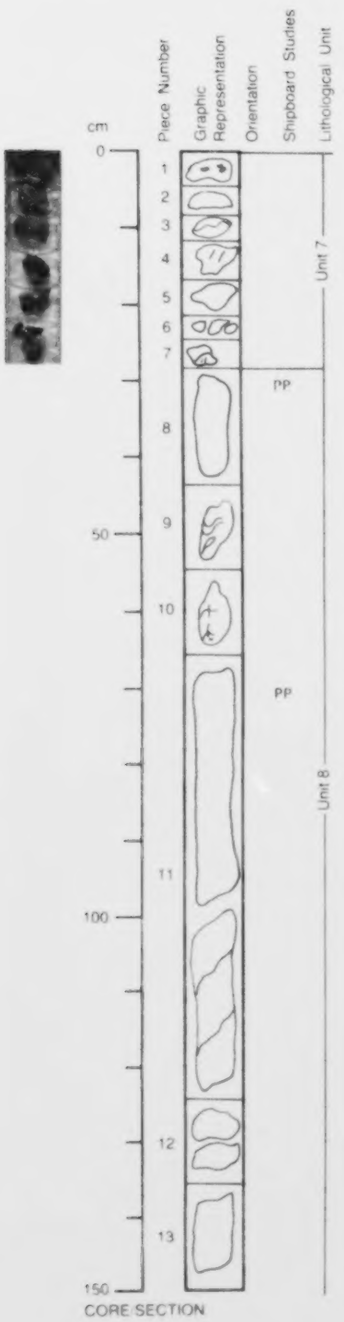

125-786B-22R-1

UNIT 7: BASALT PEBBLES

Pieces 1-7

CONTACTS: Piece 7 has sepiolite from underlying rock on lower surface.
PHENOCRYSTS: Clinopyroxene appears fresh; other phases are variably altered.
Clinopyroxene - <1%; 0.4-0.4 mm; equant; euhedral.
Orthopyroxene - trace; <0.5 mm; subhedral-elongate.
Plagioclase - <0.5%; <0.5 mm; euhedral laths.
GROUNDMASS: Glassy to fine-grained, variably altered.
VESICLES: 0-4%; 1-3 mm; round; Pieces 1, 2, and 7 only.
COLOR: Dark greenish gray (10Y 5/2).
STRUCTURE: Massive.
ALTERATION: To clays.
VEINS/FRACTURES: None.
ADDITIONAL COMMENTS: Pieces show a wide range of alteration. Piece 2 is freshest. Sepiolite appears on one side of Piece 5 and as a tiny vein (<0.5 mm) in working half, Piece 5.

UNIT 8: VITRIC SILTSTONE

Pieces 8-13

CONTACTS: N/A
PHENOCRYSTS: N/A
GROUNDMASS: N/A
VESICLES: N/A
COLOR: N/A
STRUCTURE: N/A
ALTERATION: N/A
VEINS/FRACTURES: N/A
ADDITIONAL COMMENTS: 28.5-41 cm: sepiolite foliated, massive and pink-red (5R 5/4-5R 7/4). 45-53 cm: vitric siltstone breccia with angular clasts in a silty matrix; gray (10YR 4/1). 55-65 cm: vitric clayey siltstone - breccia cut by a fault; gray (10YR 4/1-5/1). 66-99 cm: vitric clayey siltstone - slight brecciation with vertical streaks; small faults; slump feature; dark gray (2.5YR 5/10). 99-124 cm: vitric clayey siltstone - similar to above, but slumped and faulted; dip 50 degree; dark gray (2.5YR 3/0 to 10YR 5/1). 125-134 cm: breccia with one 2 cm basalt clast in a vitric siltstone matrix; dark gray (2.5YR 5/10). 135-148 cm: volcanic breccia; sheared and rounded basalt and pumice clasts in fine-grained matrix. Dark grayish brown (10YR 4/2).

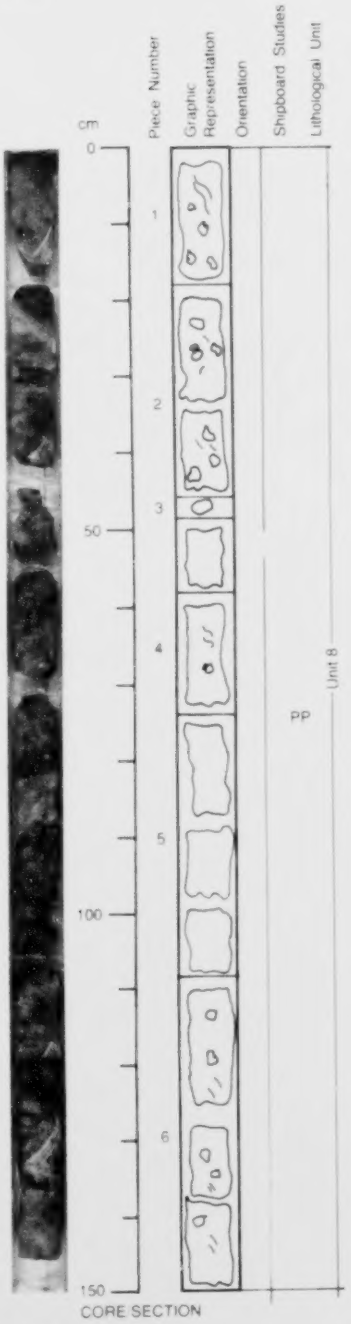
cm
Piece Number
Graphic Representation
Orientation
Shipboard Studies
Lithological Unit
0
50
100
150
1
2
3
4
5
6
PP
Unit 8
CORE SECTION

125-786B-22R-2

UNIT 8: VOLCANIC BRECCIA

Pieces 1-7

CONTACTS: None
PHENOCRYSTS: Clinopyroxene appears fresh; other phases are variably altered.
  Clinopyroxene - <1%; 0.4 mm; equant; euhedral.
  Orthopyroxene - trace; <0.5 mm; subhedral-elongate.
  Plagioclase - <0.5%; <0.5 mm; euhedral laths.
GROUNDMASS: Glassy to fine-grained; variably altered.
VESICLES: 0-4%; 1-3 mm; round; Pieces 1,2 and 7 only.
COLOR: Dark greenish gray (10Y 5/2).
STRUCTURE: Massive.
ALTERATION: To clays.
VEINS/FRACTURES: None.
ADDITIONAL COMMENTS: Clasts (0.5-3 cm in size) mainly of basalt (described above) but also pumice and vesicular basalt; matrix is sheared, palagonitic, with good stratification in upper portion; numerous small faults.

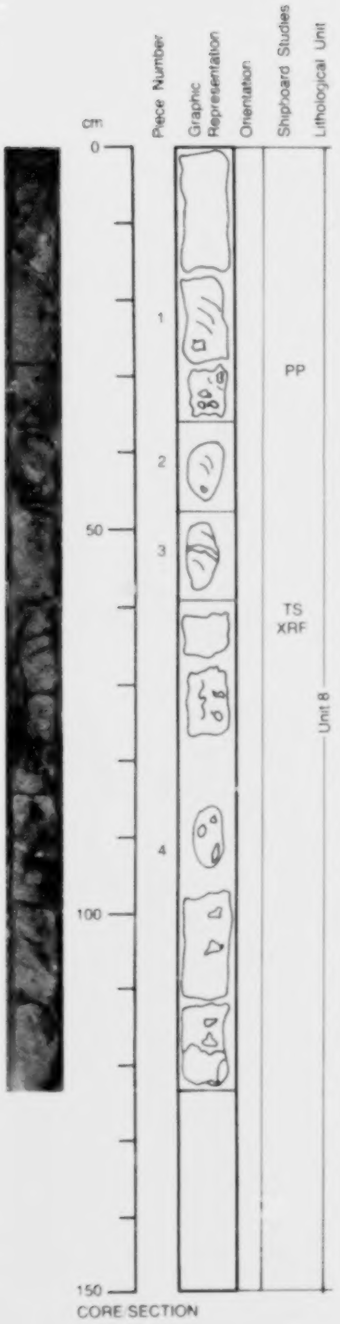
cm
Piece Number
Graphic Representation
Orientation
Shipboard Studies
Lithological Unit
0
50
100
150
1
2
3
4
PP
TS
XRF
Unit 8
CORE SECTION

125-786B-22R-3

UNIT 8: VOLCANIC BRECCIA

Pieces 1-3

CONTACTS: None obvious
PHENOCRYSTS: Clinopyroxene appears fresh; other phases are variably altered.
Clinopyroxene - <1%; 0.4 mm; equant, euhedral.
Orthopyroxene - trace; <0.5 mm; subhedral-elongate.
Plagioclase - <0.5%; <0.5 mm; euhedral laths.
GROUNDMASS: Glassy to fine-grained; variably altered.
VESICLES: 0-4%; 1-3 mm; round; Pieces 1, 2, and 7 only.
COLOR: Brown (10YR 4/3).
STRUCTURE: Massive.
ALTERATION: To clays.
VEINS/FRACTURES: None.

UNIT 8: VITRIC SILT-SANDSTONE

Piece 4

CONTACTS: None
PHENOCRYSTS: N/A
GROUNDMASS: N/A
VESICLES: N/A
COLOR: Dark grayish brown (10YR 4/2)
STRUCTURE: N/A
ALTERATION: N/A
VEINS/FRACTURES: N/A
ADDITIONAL COMMENTS: 80-80.5 cm: Silty layer with deformational structures perhaps the result of loading. 80.5-124 cm: graded breccia from 80.5 to 117 cm; lower portion finer grained but includes 5 cm basalt clast.

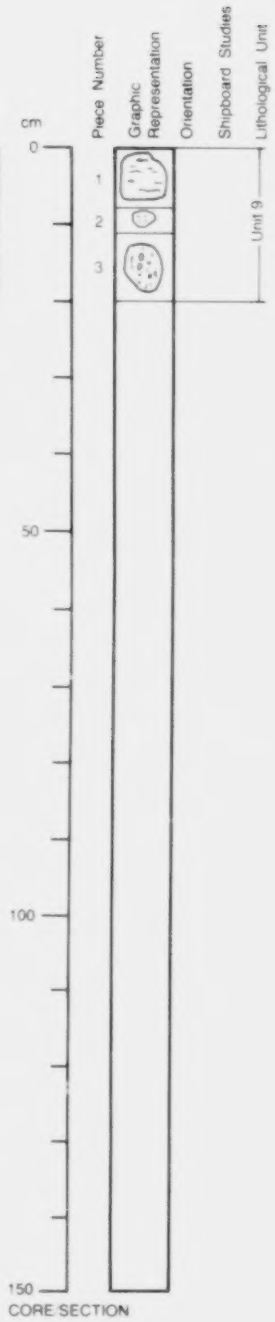
cm
Piece Number
Graphic Representation
Orientation
Shipboard Studies
Lithological Unit
0
50
100
150
1
2
3
Unit 9
CORE/SECTION

125-786B-23R-1

UNIT 9: TWO-PYROXENE DACITE

Pieces 1-3

CONTACTS: None visible.
PHENOCRYSTS: Sparse glomerocrysts of ortho- and clinopyroxene.
Orthopyroxene - <1%, 0.5-2 mm, elongate, subhedral.
Clinopyroxene - <1%, 0.2-0.5 mm, equant, euhedral.
Plagioclase - <1%, 0.5-1.0 mm, tabular laths, euhedral-subhedral.
Magnetite - trace, 0.2 mm, euhedral.
GROUNDMASS: Glassy to very fine-grained.
VESICLES: 7-15%, 0.5-6 mm, irregular-elongate, throughout, aligned, some lined with light blue mineral, also some translucent prisms with opalescent spherical cores.
COLOR: Dark greenish gray (10Y 5/1).
STRUCTURE: Massive.
ALTERATION: Plagioclase may be variably altered.
VEINS/FRACTURES: None.

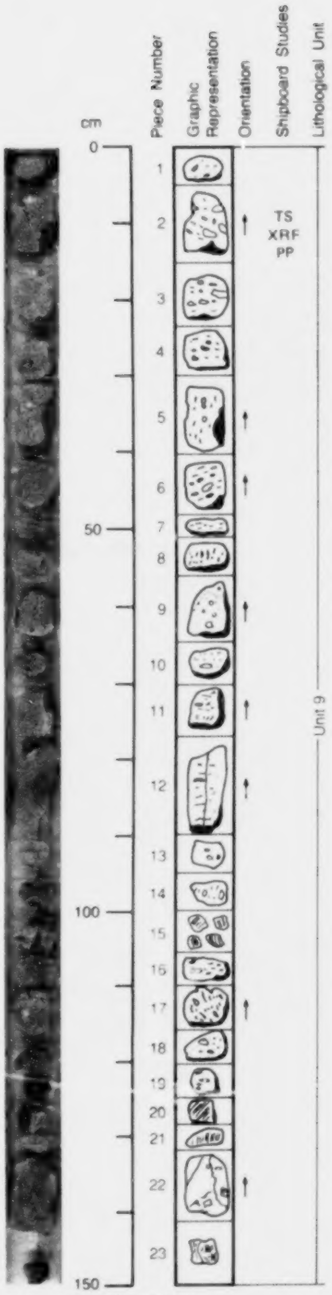
cm
Piece Number
Graphic Representation
Orientation
Shipboard Studies
Lithological Unit
0
50
100
150
1
2
3
4
5
6
7
8
9
10
11
12
13
14
15
16
17
18
19
20
21
22
23
TS
XRF
PP
Unit 9
CORE/SECTION

125-786B-24R-1

UNIT 9: TWO-PYROXENE DACITE

Pieces 1-23

CONTACTS: None visible.
PHENOCRYSTS: Glomerocrysts containing all phenocryst phases (clinopyroxene + orthopyroxene + plagioclase + magnetite).
Orthopyroxene - <1%; 0.5-1 mm; equant, euhedral.
Clinopyroxene - 1-2%; 0.2-2 mm; euhedral, tabular to lath-like.
Plagioclase - <1%; 0.5-0.8 mm; tabular, laths, euhedral-subhedral.
Magnetite - Trace; 0.2 mm; euhedral.
GROUNDMASS: Glassy to very fine grained.
VESICLES: 7-15%; 0.5-6 mm; irregular, **elongate**, throughout and aligned, some lined with light blue and translucent prisms with opalescent spherical cores of zeolite.
Miaroles: None.
COLOR: Dark greenish gray (10Y 5/1).
ALTERATION: Patches of variable alteration (5-35%) predominantly to clays.
VEINS/FRACTURES: Trace; <1 mm; random; filled with white zeolite(?).
ADDITIONAL COMMENTS: This unit is a continuation of the overlying core (23R-1).

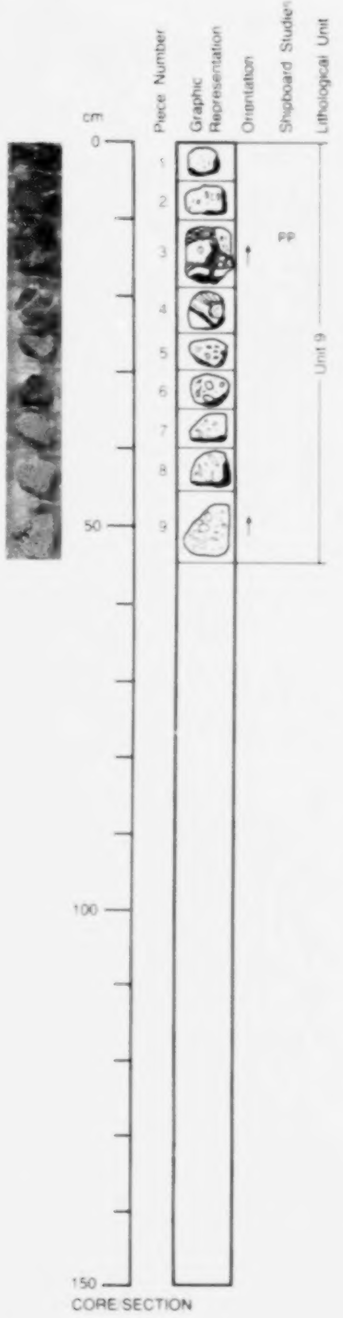
cm
Piece Number
Graphic Representation
Orientation
Shipboard Studies
Lithological Unit
0
50
100
150
1
2
3
4
5
6
7
8
9
PP
Unit 9
CORE/SECTION

125-786B-24R-2

UNIT 9: TWO-PYROXENE DACITE

Pieces 1-9

CONTACTS: None visible.
PHENOCRYSTS: Sparse glomerocrysts of ortho- and clinopyroxene, plagioclase and magnetite.
Clinopyroxene - <1%; 0.5-1 mm; equant elongate.
Orthopyroxene - <1%; 0.5-1 mm; equant euhedral.
Plagioclase - <1%; 0.5-1.5 mm; tabular laths.
Magnetite - trace; <0.2 mm; euhedral.
GROUNDMASS: Glassy to very fine-grained.
VESICLES: 5-20%; <15 mm; elongate; throughout; some empty, others are lined with light blue and prismatic pale green minerals.
COLOR: Dark greenish gray (10Y 5/1) to altered zones dark yellowish brown (10YR 4/4).
STRUCTURE: Massive.
ALTERATION: Variable. Pieces 5 to 9 are pervasively altered whereas Pieces 2 and 3 have alteration locally, concentrated in the vicinity of fractures and veins.
VEINS/FRACTURES: 2-5%, in Pieces 2 and 3; veins <3 mm wide; conjugate; steeply inclined; veins are filled with white, amorphous, zeolite with a subsequent fill of pale green microprismatic zeolite.

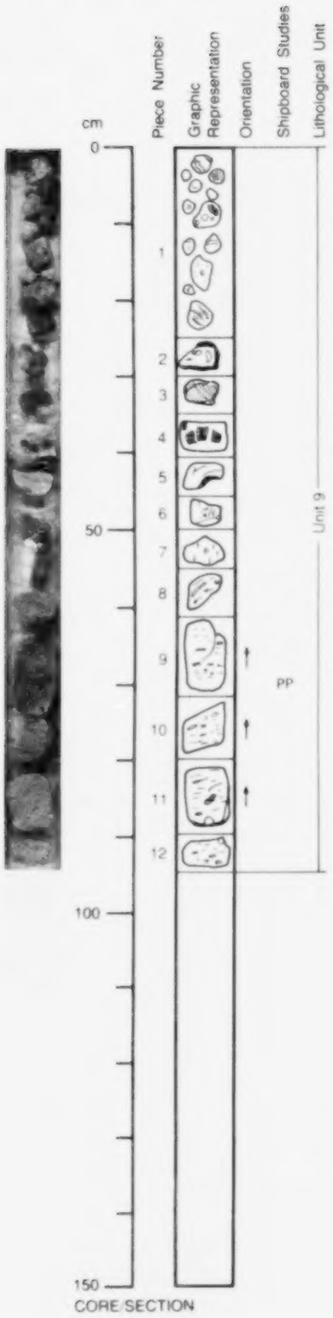
cm
Piece Number
Graphic Representation
Orientation
Shipboard Studies
Lithological Unit
0
50
100
150
1
2
3
4
5
6
7
8
9
10
11
12
PP
Unit 9
CORE/SECTION

125-786B-25R-1

UNIT 9: SPARSELY PHYRIC DACITE

Pieces 1-12

CONTACTS: None visible.
PHENOCRYSTS:
Clinopyroxene - 0-1%, <1 mm; euhedral, equant, black to dark green.
Plagioclase - 0-1%, <1 mm; euhedral, columnar.
Orthopyroxene - trace, <1 mm.
Magnetite - trace, <0.1 mm; euhedral, octahedral.
GROUNDMASS: Glassy to very fine-grained.
VESICLES: 15%, <2 cm; parallel elongated; randomly distributed; partially filled with hexagonal clear white flakes.
COLOR: Gray to grayish brown (10YR 5/1 - 5/2).
STRUCTURE: None.
ALTERATION: Pieces 1-5 are altered; some appear brecciated.
VEINS/FRACTURES: Not present.

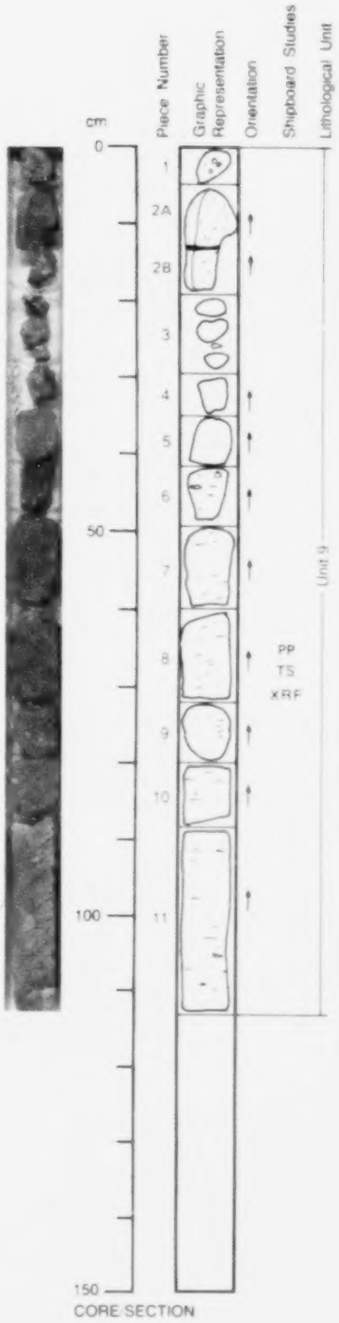
cm
Piece Number
Graphic Representation
Orientation
Shipboard Studies
Lithological Unit
0
50
100
150
1
2A
2B
3
4
5
6
7
8
9
10
11
PP
TS
XRF
Unit 9
CORE/SECTION

125-786B-26R-1

UNIT 9: SPARSELY PHYRIC DACITE

Pieces 1-11

CONTACTS: None visible
PHENOCRYSTS:
Plagioclase - trace; < 1mm; euhedral; also in glomerocrysts with clinopyroxene.
Clinopyroxene - trace; <1 mm; euhedral; commonly with plagioclase in glomerocrysts.
GROUNDMASS: Glassy to finely crystalline.
VESICLES: 10%; <1 cm; sub-round to elongate; random throughout; vesicles elongated in horizontal direction; hexagonal greenish flakes in vesicles.
COLOR: Dark greenish gray (10Y 4/1).
STRUCTURE: None.
ALTERATION: Piece 1 is altered to beige color; rim of Piece 2 is altered.
VEINS/FRACTURES: Not present.
ADDITIONAL COMMENTS: Piece 1 is continuation of 25R-1.

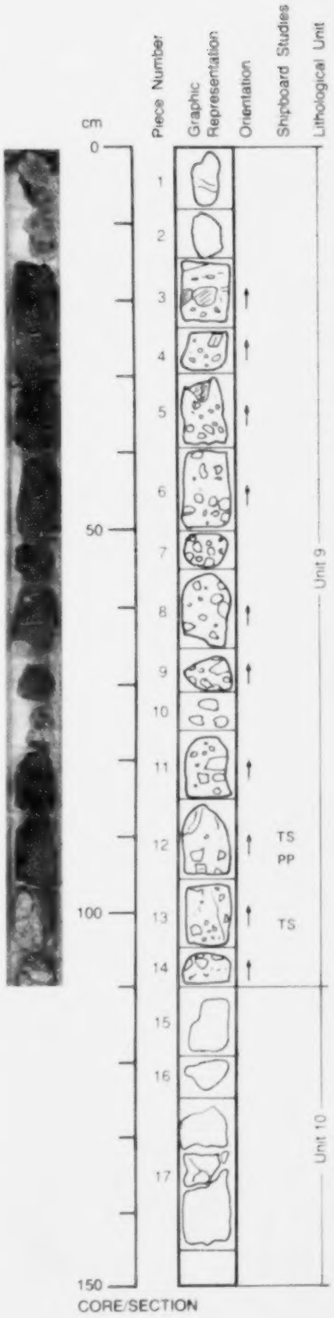

125-786B-27R-1

UNIT 9: DACITE BRECCIA

Pieces 1-14

CONTACTS: A sedimentary contact is present at 106 cm where coarse sand and breccia are in contact; at 96-103 cm, a steeply dipping contact between unaltered volcaniclastic breccia and sedimentary breccia occurs. Sediment to altered clinopyroxene-plagioclase-phyric andesite contact at 142 cm.
PHENOCRYSTS:
Plagioclase - 0-2%; <1 cm; euhedral.
Magnetite - trace; <0.1 mm; black specks in groundmass.
GROUNDMASS: Glassy; breccia matrix is also glassy.
VESICLES: 0-50%; 0-1 cm; round to elongated; some fragments are pumiceous; vesicles are differently oriented from clast to clast in breccia.
COLOR: Black to dark greenish-gray (10Y 3/1 - 4/2).
STRUCTURE: Breccia.
ALTERATION: In Piece 11 (98-103 cm), there is a sedimentary(?) or alteration boundary(?).
VEINS/FRACTURES: None present.
ADDITIONAL COMMENTS: Breccia is composed of a single kind of rhyolite clast. Beige-black color variation occurs also in single clasts (Piece 12).

UNIT 10: VITRIC SAND

Pieces 14-17

CONTACTS: Between volcanic breccia and sediment in Piece 14.
PHENOCRYSTS: N/A
GROUNDMASS: N/A
VESICLES: N/A
COLOR: Grayish green (5G 4/2) to pale green (5G 7/2) to light greenish gray (10Y 8/1) to white (N8/).
STRUCTURE: N/A
ALTERATION: Ubiquitous clay-chlorite alteration.
VEINS/FRACTURES: N/A
ADDITIONAL COMMENTS: Piece 15 is a sand that contains angular to subrounded mm to 0.25 cm-size clasts at top to 1 cm-size clasts at base, generally mottled with no primary sedimentary structures. Piece 17 ranges from very coarse sand to silt, is cross-bedded, and contains at least three depositional (flow or slump?) units defined by crossbed dips and erosive set bases. The basal unit is horizontal; the steepest unit is about 38 degrees.

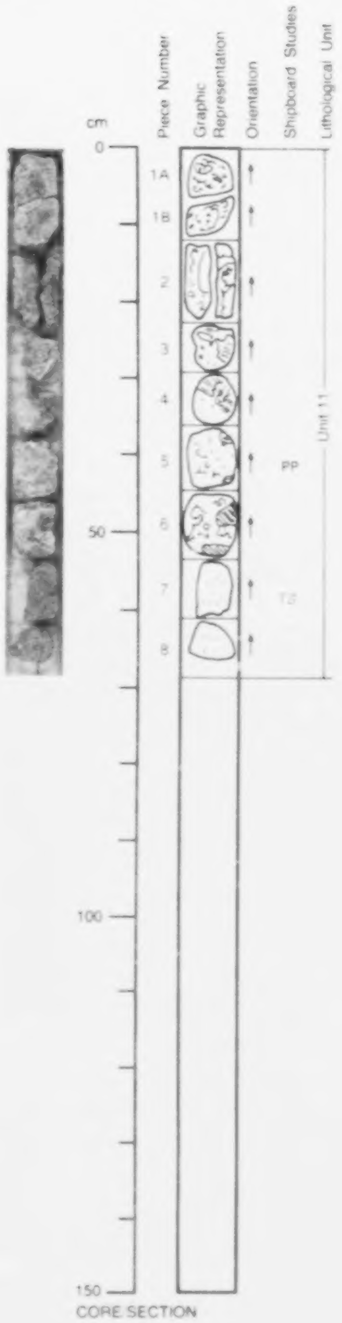
cm
0
50
100
150
CORE/SECTION
Piece Number
Graphic Representation
Orientation
Shipboard Studies
Lithological Unit
1A
1B
2
3
4
5
6
7
8
PP
TS
Unit 11

125-786B-27R-2

UNIT 11: TWO-PYROXENE, PLAGIOCLASE PHYRIC BONINITE

Pieces 1-8

CONTACTS: Not visible.

PHENOCRYSTS: Plagioclase is absent in weathered portions.

Orthopyroxene - 15%, 2-8 mm, euhedral, equant, black when unfractured, yellow-brown when fractured.

Plagioclase - 15-20%, 2-10 mm, euhedral, columnar.

Clinopyroxene - 1-2%, <1 mm, dark green when unfractured, pale green when fractured.

GROUNDMASS: Glassy to finely crystalline.

VESICLES: 10%, <3 mm, rounded to irregular shape, randomly distributed, no preferred orientation.

COLOR: Gray (2.5YR 4/0) to grayish yellow-green (5GY 7/4) in altered parts.

STRUCTURE: None.

ALTERATION: Progressively more altered up section. Pieces 7-8 are fresh.

VEINS/FRACTURES: Not present.

ADDITIONAL COMMENTS: This is not a breccia. In 27R-1 at 142-144 cm contact is exposed of this rock and overlying sediment.

125-786B-28R-1

UNIT 11: TWO-PYROXENE, PLAGIOCLASE PHYRIC BONINITE (27-2 CONTINUED)

Pieces 1-18

CONTACTS: None visible
PHENOCRYSTS:
Orthopyroxene - 10-15%, 1-4 mm, euhedral, black when unfractured, pale yellow when fractured.
Plagioclase - 10-15%, 1-5 mm, euhedral and round.
Clinopyroxene - 5%, not visible, dark green when unfractured, pale green when fractured.
GROUNDMASS: Glassy to partly crystalline.
VESICLES: 5-10%, <4 mm, irregular, randomly distributed, some have gray blue filling.
COLOR: Gray (5BG 5/1) when fresh to greenish gray (5G 6/1) when altered.
STRUCTURE: None.
ALTERATION: Pieces 1,4,7,12 and 16 are altered.
VEINS/FRACTURES: Trace, 1 mm, steeply dipping; in Piece 17 multiple calcite veins. Piece 15 crack with brown alteration zone.
ADDITIONAL COMMENTS: Continuation of Section 125-786B-27R-2.

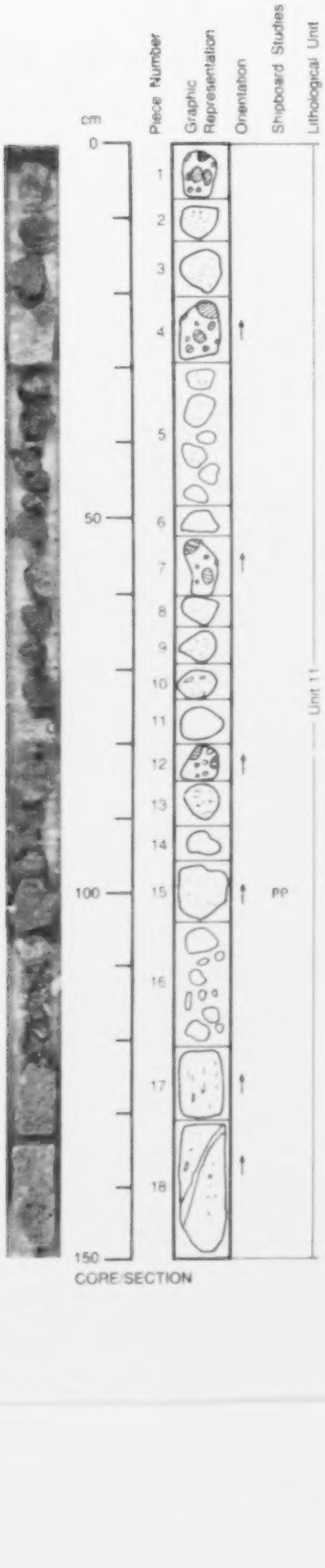
cm
Piece Number
Graphic Representation
Orientation
Shipboard Studies
Lithological Unit
0
50
100
150
1
2
3
4
5
6
7
8
9
10
11
12
13
14
15
16
17
18
PP
Unit 11
CORE/SECTION

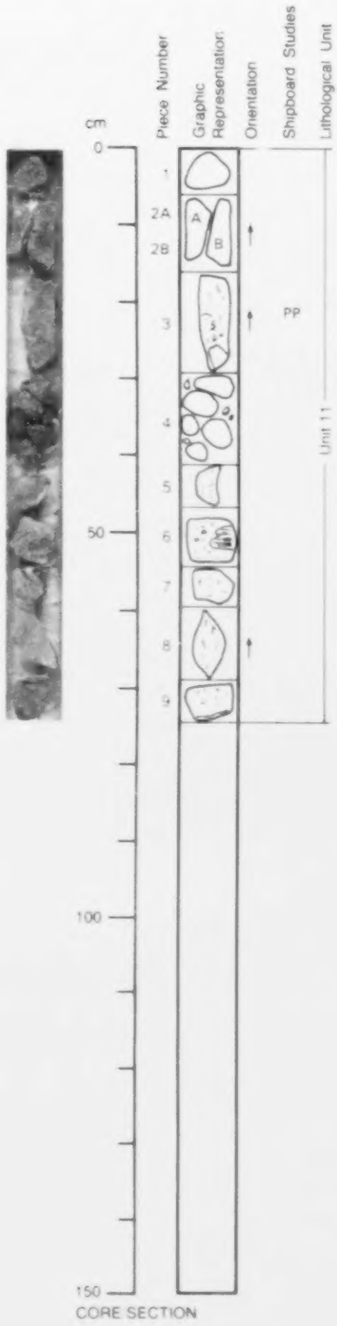
cm
Piece Number
Graphic Representation
Orientation
Shipboard Studies
Lithological Unit
0
1
2A
A
B
2B
3
PP
4
5
50
6
7
8
9
Unit 11
100
150
CORE SECTION

125-786B-29R-1

UNIT 11: TWO-PYROXENE, PLAGIOCLASE PHYRIC BONINITE (28-1 CONTINUED)

Pieces 1-9

CONTACTS: Not visible
PHENOCRYSTS:
Orthopyroxene - 8%, <4 mm, subhedral to euhedral, black when unfractured, yellow-brown when fractured.
Clinopyroxene - 6%, <2 mm, dark green when unfractured, pale greenish yellow when fractured, euhedral.
Plagioclase - 10%, <5 mm, euhedral and round.
GROUNDMASS: Partly glassy, partly finely crystalline.
VESICLES: 10%, <3 mm, irregular, randomly distributed, filled with pale gray blue mineral.
COLOR: Gray (10YR 4/1) to pale yellow brown (10YR 7/4) when altered.
STRUCTURE: None.
ALTERATION: Pieces 2, 3, 4, and 6 show brownish alteration.
VEINS/FRACTURES: Trace, <1 mm, sub-vertical; fractures are filled with white talc-like material and have alteration zones.
ADDITIONAL COMMENTS: Continuation of 125-786B-27R-2. Piece 8 is aphyric, sparsely vesicular and vesicles are filled with calcite.

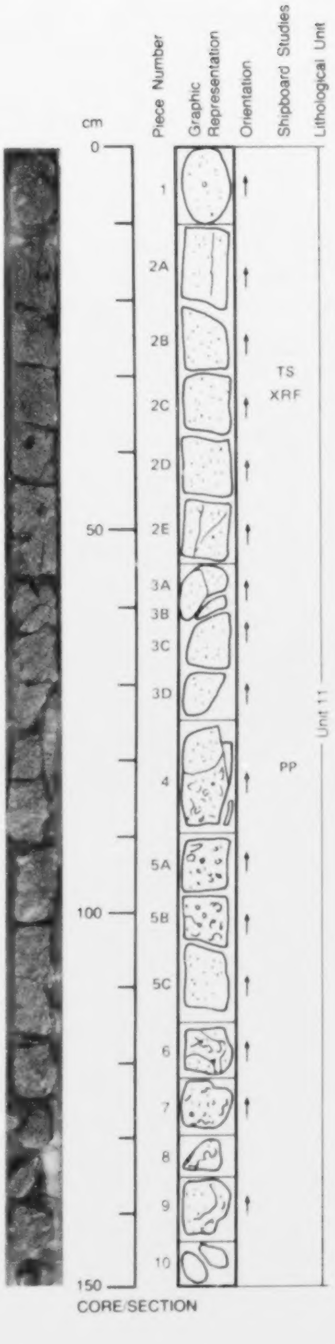
cm
Piece Number
Graphic Representation
Orientation
Shipboard Studies
Lithological Unit
0
50
100
150
1
2A
2B
2C
2D
2E
3A
3B
3C
3D
4
5A
5B
5C
6
7
8
9
10
TS
XRF
PP
Unit 11
CORE/SECTION

125-786B-30R-1

UNIT 11: TWO-PYROXENE, PLAGIOCLASE PHYRIC BONINITE (29-1 CONTINUED)

Pieces 1-10

CONTACTS: None visible
PHENOCRYSTS:
Orthopyroxene - 10-15%, 1-10 mm, yellow to brown, altering to serpentine
Plagioclase - 8-10%, <3 mm, euhedral and rounded.
Clinopyroxene - 2-5%, <2 mm, dark green, pale green when fractured, euhedral.
GROUNDMASS: Glassy with plagioclase microphenocrysts.
VESICLES: 5-10%, <4 mm, irregular shape, randomly distributed, filled with calcite or with greenish coating.
COLOR: Bluish gray (5B 5/1) where fresh, greenish gray (5G 5/1) and weak red (10R 4/3) where altered.
STRUCTURE: None.
ALTERATION: Along veins and cracks to reddish and greenish colors.
VEINS/FRACTURES: Trace, <0.2 mm, sub-vertical, veins filled with calcite, some fractures appear may be dark green serpentine(?).
ADDITIONAL COMMENTS: Section is a continuation of 125-786B-27R-2.

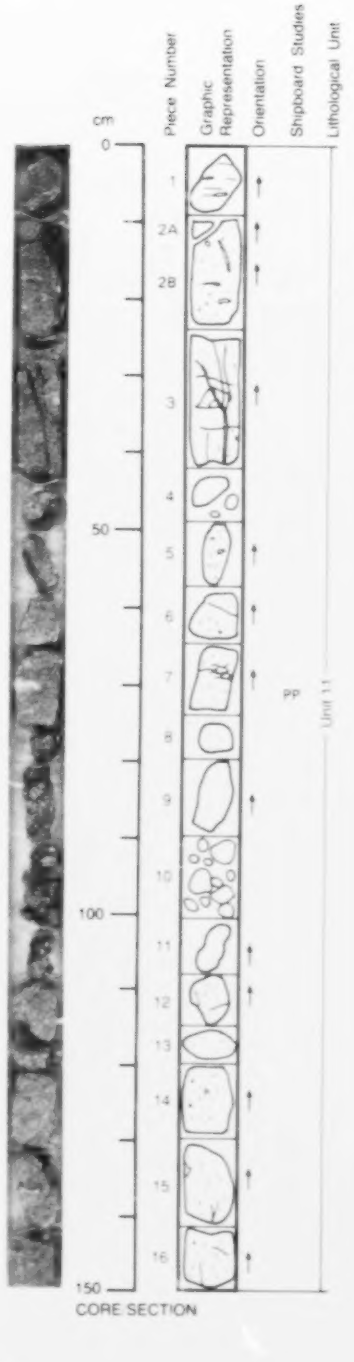
cm
Piece Number
Graphic Representation
Orientation
Shipboard Studies
Lithological Unit
0
50
100
150
1
2A
2B
3
4
5
6
7
8
9
10
11
12
13
14
15
16
PP
Unit 11
CORE SECTION

125-786B-30R-2

UNIT 11: TWO-PYROXENE, PLAGIOCLASE PHYRIC BONINITE (30R-1 CONTINUED)

Pieces 1-16

CONTACTS: None visible.
PHENOCRYSTS:
Orthopyroxene - 15-20%, 2-10 mm, yellow to brown, altering to serpentine.
Plagioclase - 8-10%, <3 mm, euhedral and rounded.
Clinopyroxene - 3-5%, <2 mm, dark green, pale green when fractured.
GROUNDMASS: Glassy with plagioclase microphenocrysts.
VESICLES: 5-10%, <4 mm, irregular shape, randomly distributed, filled with calcite or dark-green coating.
COLOR: Bluish gray (5B 5/1) where fresh, greenish gray (5G 5/1) and weak red (10R 4/3) when altered.
STRUCTURE: None.
ALTERATION: Along veins and cracks to reddish and greenish colors.
VEINS/FRACTURES: Trace, <0.2 mm, sub-vertical, some filled with calcite, some appear dark green (serpentine?).
ADDITIONAL COMMENTS: Section is a continuation of 125-786B-27R-2.

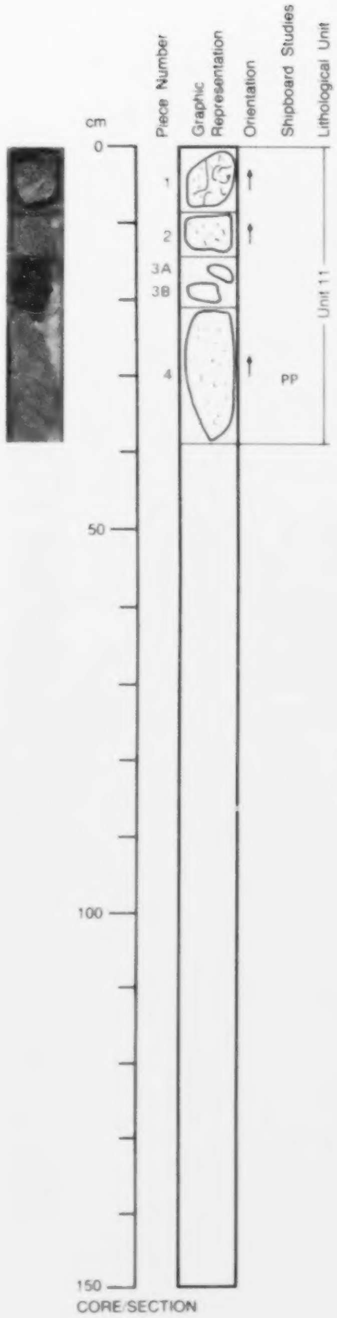
cm
0
50
100
150
CORE/SECTION
Piece Number
Graphic Representation
Orientation
Shipboard Studies
Lithological Unit
1
2
3A
3B
4
PP
Unit 11

125-786B-30R-3

UNIT 11: TWO-PYROXENE, PLAGIOCLASE PHYRIC BONINITE (30R-2 CONTINUED)

Pieces 1-4

CONTACTS: None visible.
PHENOCRYSTS:
Orthopyroxene - 15-20%, * 10 mm, yellow-brown, altering to serpentine, euhedral and anhedral.
Plagioclase - 8-10%, <3 mm, euhedral and rounded.
Clinopyroxene - 5-8%, <3 mm, dark green, euhedral.
GROUNDMASS: Glassy with plagioclase crystals.
VESICLES: 5-10%, <4 mm, irregular, n/a.
COLOR: Bluish gray (5B 5/1) where fresh, dark green (5G 4/2) when altered.
STRUCTURE: None.
ALTERATION: Dark green alteration veins and patches.
VEINS/FRACTURES: Trace, <0.2 mm, random orientation, dark green veins (serpentine?).
ADDITIONAL COMMENTS: Section is a continuation of 125-786B-27R-2. N.B. Piece 4 is like Section 31R-1.

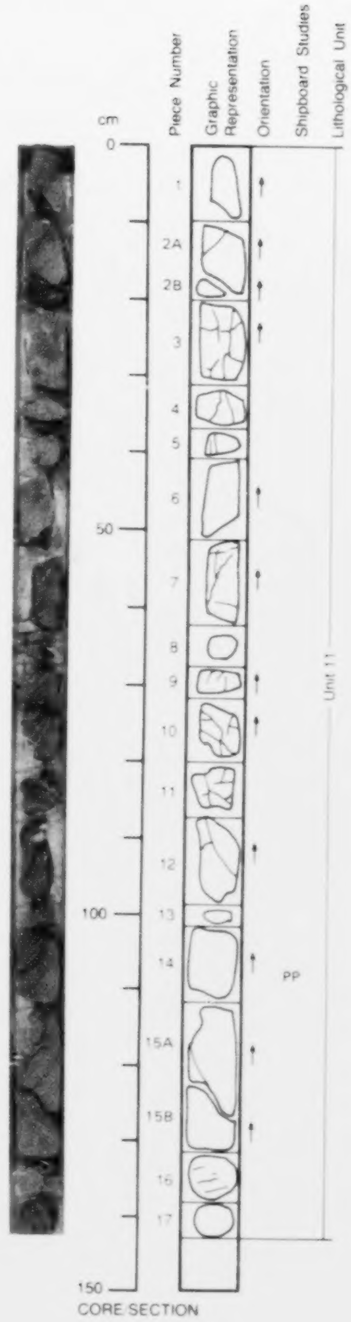
cm
Piece Number
Graphic Representation
Orientation
Shipboard Studies
Lithological Unit
0
50
100
150
1
2A
2B
3
4
5
6
7
8
9
10
11
12
13
14
15A
15B
16
17
PP
Unit 11
CORE/SECTION

125-786B-31R-1

UNIT 11: OLIVINE, PLAGIOCLASE, TWO-PYROXENE PHYRIC BONINITE

Pieces 1-17

CONTACTS: None visible.
PHENOCRYSTS: Glomerocrysts of orthopyroxene.
Orthopyroxene - 10-15%, < 5 mm, yellow, euhedral.
Plagioclase - 10-15%, <2 mm, subhedral to euhedral.
Clinopyroxene - 2-5%, <1 mm, dark green, euhedral.
Olivine? - 5%, <1 mm, alteration products are hematite and carbonate.
GROUNDMASS: Finely crystalline.
VESICLES: 0-1%, <2 mm, round, randomly distributed, filled with calcite and a green mineral.
COLOR: Gray (7.5RYR 5/0) to reddish gray (5R 5/1).
STRUCTURE: None.
ALTERATION: Olivine altered to hematite and carbonate.
VEINS/FRACTURES: 1%, <2 mm, random orientations, filled with calcite.

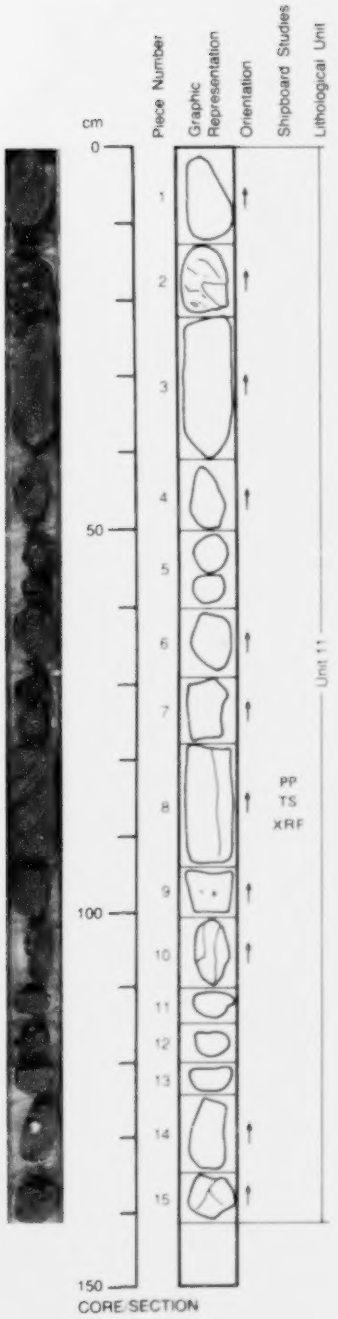
cm
Piece Number
Graphic Representation
Orientation
Shipboard Studies
Lithological Unit
0
50
100
150
1
2
3
4
5
6
7
8
9
10
11
12
13
14
15
PP
TS
XRF
Unit 11
CORE/SECTION

125-786B-31R-2

UNIT 11: OLIVINE, PLAGIOCLASE, TWO-PYROXENE BONINITE (31R-1 CONTINUED)

Pieces 1-15

CONTACTS: None visible.
PHENOCRYSTS: Orthopyroxene glomerocrysts.
Plagioclase - 10-15%; <2 mm; subhedral to euhedral.
Orthopyroxene - 10-15%; <5 mm; yellow, euhedral.
Clinopyroxene - 2-5%; <1 mm; dark green; euhedral.
Olivine - 5%; <1 mm; alteration products include hematite and carbonate.
GROUNDMASS: Finely crystalline.
VESICLES: 0-1%; <2 mm; round; randomly distributed; filled with calcite and green unidentified material (zeolite? clay?).
COLOR: Reddish gray (5R 5/1).
STRUCTURE: None.
ALTERATION: Olivine alters to hematite and carbonate.
VEINS/FRACTURES: 1%; 2 mm wide; randomly oriented; filled with calcite.
ADDITIONAL COMMENTS: Continuation of Section 125-786B-30R-1.

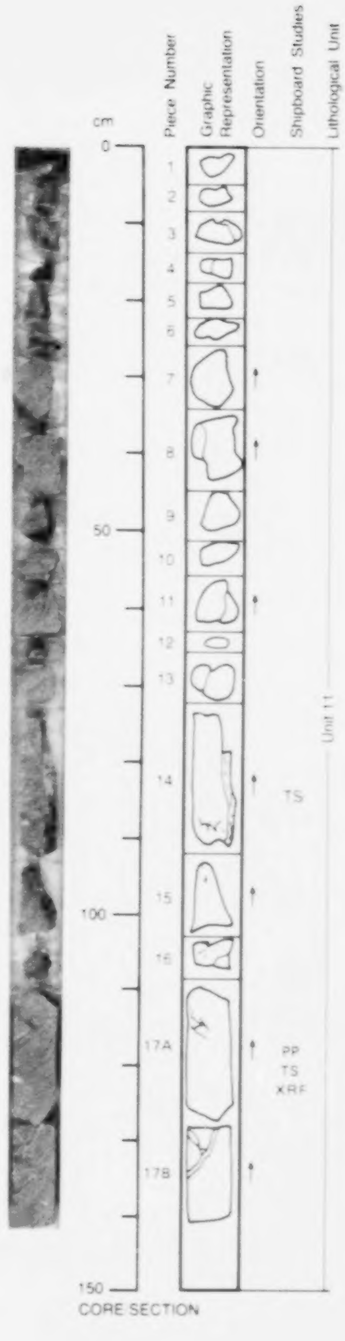
cm
0
50
100
150
Piece Number
Graphic Representation
Orientation
Shipboard Studies
Lithological Unit
1
2
3
4
5
6
7
8
9
10
11
12
13
14
15
16
17A
17B
TS
PP
TS
XRF
Unit 11
CORE SECTION

125-786B-32R-1

UNIT 11: OLIVINE-BEARING BONINITE

Pieces 1-17

CONTACTS: None visible.
PHENOCRYSTS: Two-pyroxene glomerocrysts, some with plagioclase, are common.
Orthopyroxene - 7-10%, 0.1-2.5 mm, elongate, subhedral.
Clinopyroxene - 5-8%, 0.2-2 mm, elongate, euhedral to subhedral.
Plagioclase - 5-7%, <0.5 mm, euhedral, lath-like.
Olivine - 3-5%, <2.5 mm, euhedral, elongate.
Magnetite - <1%, 0.25 mm, euhedral, equant.
GROUNDMASS: Fine-grained to glassy.
VESICLES: 1-3%, 0.5-1.5 mm, irregular, jagged, throughout, appear concentrated near glomerocrysts.
COLOR: Dark reddish gray (10R 4/1 to 3/1).
STRUCTURE: Massive.
ALTERATION: Hematitic staining along fractures; overall color of rock appears to result from minor alteration; chlorite is present in the matrix after glass. Olivine phenocrysts are pervasively altered to an Fe-oxide-carbonate assemblage.
VEINS/FRACTURES: <1%, 1-2 mm, subparallel, filled with carbonate and a pale green material (chlorite or zeolite?).
ADDITIONAL COMMENTS: Continuation of Section 125-786B-31R-02.

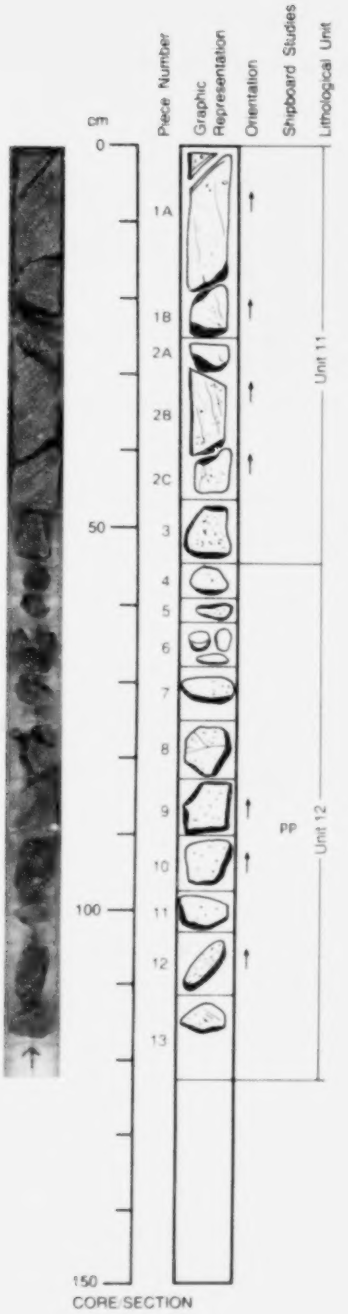

125-786B-32R-2

UNIT 11: OLIVINE-BEARING BONINITE (32R-1 CONTINUED)

Pieces 1-3, 12

CONTACTS: None visible
PHENOCRYSTS: Glomerocrysts of two pyroxenes with or without plagioclase
  Orthopyroxene - 7-10%, 0.7-2.5 mm, elongate, subhedral
  Clinopyroxene - 5-8%, 0.2-2 mm, elongate, euhedral to subhedral
  Plagioclase - 5-7%, <0.5 mm, tabular laths, elongate
  Olivine - 3-5%, <2.5 mm, equant, euhedral
  Magnetite - <1%, 0.25 mm, equant, euhedral
GROUNDMASS: Fine-grained to glassy with tiny magnetite crystals
VESICLES: 1-3%, 0.5-1.5 mm, irregular, jagged; throughout but random concentrations; tend to cluster near the glomerocrysts
COLOR: Dark reddish gray (10R 4/1 to 3/1)
STRUCTURE: Massive
ALTERATION: Hematitic staining along fractures, overall color of rock appears to result from minor alteration; glass is altered to chlorite, olivine phenocrysts are pervasively altered to an Fe-oxide-carbonate assemblage
VEINS/FRACTURES: <1%, 1-2 mm, subparallel, filled with carbonate and a pale green material (chlorite or zeolite?)
ADDITIONAL COMMENTS: Continuation of Section 32R-1

UNIT 12: RHYOLITE

Pieces 4-11, 13

CONTACTS: None
PHENOCRYSTS: Glomerocrysts of two pyroxenes with or without plagioclase
  Orthopyroxene - <2%, <0.5 mm, equant, euhedral
  Clinopyroxene - 1-2%, <0.5 mm, equant, euhedral
  Plagioclase - 4-5%, <2 mm, tabular laths, euhedral to subhedral
  Magnetite - trace, <0.25, equant, euhedral
GROUNDMASS: Fine-grained to glassy, altered
VESICLES: 1-2%, 0.5-1.5 mm, irregular, ragged, throughout, locally oriented
COLOR: Gray (5Y 5/1)
STRUCTURE: Massive
ALTERATION: Variably altered (5-35%) to clays and chlorite
VEINS/FRACTURES: None

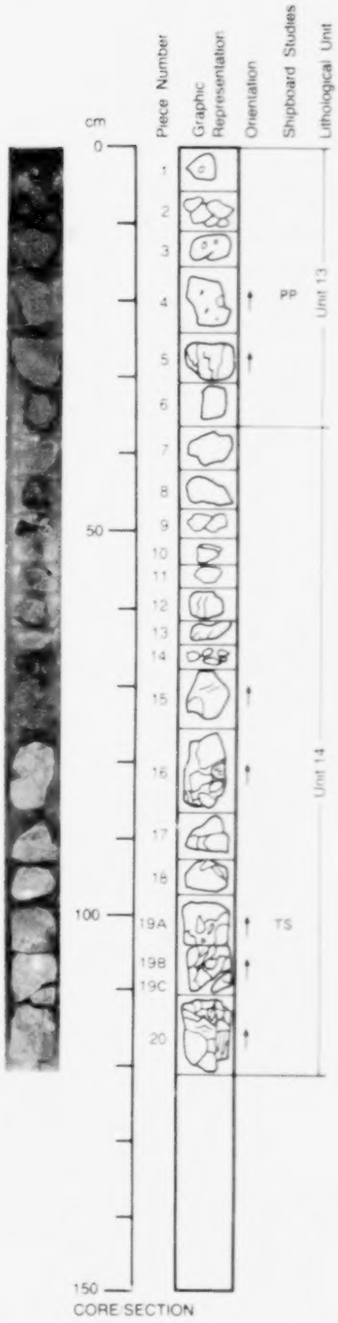

125-786B-33R-1

UNIT 13: OLIVINE-BEARING BASALTIC ANDESITE

Pieces 1-6

CONTACTS: None visible.
PHENOCRYSTS: Ortho- and clinopyroxene, plagioclase and magnetite occur as glomerocrysts as well as isolated phases.
Orthopyroxene - 7-10%, 0.1-4 mm, euhedral-subhedral, jacketed by clinopyroxene on some crystals.
Clinopyroxene - 3-6%, 0.2-2 mm, equant-elongate.
Plagioclase - 3-5%, 0.5-1.5 mm, equant, euhedral.
Olivine - 3-5%, 0.2-1.5 mm, euhedral-subhedral magnetite - trace, <0.2 mm, euhedral.
GROUNDMASS: Fine-grained, glassy and stained red.
VESICLES: None.
COLOR: Dark reddish gray (10R 4/1 to 3/1).
STRUCTURE: Massive.
ALTERATION: Redness appears to result from pervasive hematitic alteration, localized around olivine and disseminated in the matrix.
VEINS/FRACTURES: Trace, <0.1 mm, sub-vertical, carbonate-filled.

UNIT 14: MINERALIZED TWO-PYROXENE ANDESITE

Pieces 7-13

CONTACTS: None visible.
PHENOCRYSTS: Orthopyroxene, clinopyroxene and plagioclase form both glomerocrystic clusters and individual crystals.
Plagioclase - 3-5%, 0.5-2.5 mm, euhedral, equant.
Orthopyroxene - 1-2%, <0.5 mm, euhedral, tabular.
Clinopyroxene - <2%, <0.5 mm, euhedral, equant.
Magnetite - trace, <0.2 mm, equant, euhedral.
GROUNDMASS: Fine-grained, glassy, with chloritic alteration. Carbonate, zeolite and silica in vugs in the groundmass.
VESICLES: None visible.
COLOR: Gray (7.5YR 5/0).
STRUCTURE: Massive.
ALTERATION: Pervasive chloritization.
VEINS/FRACTURES: <1%, <1 mm wide, random, pyrite, silica and zeolite fill veins.
ADDITIONAL COMMENTS: The rock has a greenschist metamorphic alteration assemblage; disseminated pyrite (up to 1 mm in size) grains have euhedral habits when in open vugs, otherwise they form aggregates of ragged anhedral grains.

UNIT 14: ANDESITIC-GLASSY BRECCIA

Pieces 14-15

CONTACTS: None visible.
PHENOCRYSTS: Both pyroxenes are variably altered to chlorite.
Plagioclase - 5%, <1.5 mm, euhedral laths.
Orthopyroxene - 5-8%, <0.1 mm, euhedral, equant.
Clinopyroxene - 5%, <1.5 mm, equant, elongate.
Magnetite - trace, <0.5 mm, euhedral.
GROUNDMASS: Flow-banded glass comprises 70%-85%, now altered with trace amounts of pyrite (<0.2 mm grains).
VESICLES: 0-10%, <0.5 mm, elongate, variable, present in some clasts but not in others.
COLOR: Dark yellowish brown (10YR 4/6).
STRUCTURE: Breccia.
ALTERATION: Pervasive, Fe-oxide stained chloritization of pyroxenes.
VEINS/FRACTURES: <0.5%, <1 mm wide, sub-vertical, vein fill is predominately carbonate.

125-786B-33R-1 (continued)

UNIT 14: META-BRECCIATED ANDESITE

Pieces 16-20

CONTACTS: None visible.
PHENOCRYSTS: Two-pyroxene and plagioclase glomerocrysts.
  Plagioclase - <1%; 0.5-1 mm; subhedral laths.
  Clinopyroxene - 1-2%; 0.5-2 mm; elongate, equant.
  Orthopyroxene - 1-2%; 0.5-2 mm; elongate, equant and subhedral.
  Magnetite - trace; <0.2 mm; equant, euhedral.
GROUNDMASS: Fine-grained, chlorite and clay alteration products.
VESICLES: None.
COLOR: Light gray (10YR 7/2) to dark yellow-brown (10YR 3/6).
STRUCTURE: Breccia; includes in situ brecciation of individual clasts.
ALTERATION: Pervasive chloritization affecting both clasts and matrix; clasts have alteration rim 3-5 mm wide.
VEINS/FRACTURES: <1%; <3 mm wide; subvertical; filled with carbonate, chlorite and white zeolite. One vug in Piece 19A, is filled with 5-mm dog-tooth calcite crystals.
ADDITIONAL COMMENTS: Pyrite forms disseminated crystals, subhedral to euhedral, especially abundant in chloritized zones and veins (<0.1% of rock).

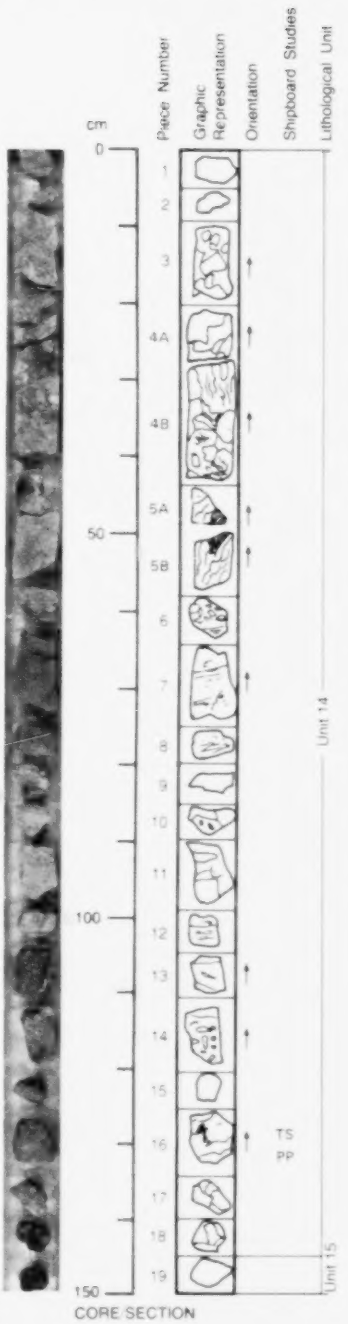

125-786B-34R-1

UNIT 14: TWO-PYROXENE ANDESITE

Pieces 1-2

CONTACTS: None visible
PHENOCRYSTS: Clino- and orthopyroxene and plagioclase form glomerocrysts as well as isolated phases.
Plagioclase - <2%, <0.5 mm, euhedral laths.
Orthopyroxene - <1%, <0.2 mm, equant, euhedral.
Clinopyroxene - <1%, <0.2 mm, equant elongate.
GROUNDMASS: Fine-grained, felted, feldspar-rich.
VESICLES: None
COLOR: Gray (7.5YR 6/0).
STRUCTURE: Massive
ALTERATION: Minor chlorotic alteration.
VEINS/FRACTURES: Trace, <0.2 mm, conjugate, appear to be filled with hematite and chlorite.

UNIT 14: BRECCIATED FLOW-BANDED ANDESITE

Pieces 3-6

CONTACTS: Bottom of Piece 6 with underlying sediment.
PHENOCRYSTS: Pyroxene and feldspar form as glomerocrysts and as individual crystals.
Plagioclase - 10-20%, 0.2-2.5 mm, equant, subhedral.
Clinopyroxene - 5-8%, 0.2-0.5 mm, equant, subhedral.
Orthopyroxene - 1%, <0.3 mm, equant, tabular.
Magnetite - trace, <0.2 mm, equant, euhedral.
GROUNDMASS: Very fine-grained to glassy, pervasively altered.
VESICLES: 2%, <0.2 mm, elongate, variable, partially filled with translucent zeolite.
COLOR: Gray (10YR 6/1) to yellowish brown (10YR 5/4).
STRUCTURE: Indurated, breccia, flow-banded at the base.
ALTERATION: Chlorite, minor epidote, some individual clasts show oxidation, others are greenschist facies.
VEINS/FRACTURES: <1%, <0.9 mm wide, sub-vertical, anastomosing, veins are filled with chlorite, epidote and some translucent zeolite.
ADDITIONAL COMMENTS: Disseminated pyrite, as aggregates of anhedral grains and individual cubes, is disseminated throughout. Contact with red sandstone below is glassy, flow banded and has rip-up clasts of the sediment. Contact with glassy chilled margin is 0.5 to 1 cm wide.

UNIT 14: VITRIC SILTY SANDSTONE

Pieces 7-9

CONTACTS: None.
PHENOCRYSTS: N/A
GROUNDMASS: N/A
VESICLES: N/A
COLOR: Dark reddish brown (2.5 YR 3/4).
STRUCTURE: N/A
ALTERATION: N/A
VEINS/FRACTURES: N/A
ADDITIONAL COMMENTS: Piece 7 is a redbed, homogeneous with suggestion of size-grading (normal), perhaps some burrowing (?) and vague laminae; upper edge of piece has slickensides. Piece 8 is lower portion of redbed, normal size-grading, may have slickensides. Piece 9 is a small piece of redbed attached to an andesite clast.

125-786B-34R-1 (continued)

UNIT 14: BRECCIATED FLOW-BANDED TWO-PYROXENE ANDESITE

Pieces 10-18

CONTACTS: Top contact (with red sediment) forms a 1 to 5 mm wide glassy chill; relationship with sediment is ambiguous; bottom contact defined by Pieces 18 & 19 forming a glassy chill at least 3 cm wide.
PHENOCRYSTS: Both pyroxenes and plagioclase form as glomerocrysts and as individual crystals.
Plagioclase - 10-20%; 0.2-2.5 mm; equant, subhedral.
Clinopyroxene - 5-8%; 0.2-0.6 mm; equant, subhedral.
Orthopyroxene - <1%; <0.3 mm; equant, euhedral.
Magnetite - <0.1%; <0.2 mm; equant, euhedral-subhedral.
GROUNDMASS: Very fine-grained to glassy, especially Pieces 18 & 19 which are >75% glass.
VESICLES: 1-2%; <0.2 mm; elongate; variable distribution; partially filled with translucent to pale green material.
COLOR: Gray (10YR 6/1) to olive (10YR 5/3).
STRUCTURE: Indurated breccia with flow-banded clasts and a matrix that is altered flow-banded glass.
ALTERATION: Patchy, chlorotic and Fe-oxidation, variable between clasts. Matrix is pale red (10R 6/2) in places.
VEINS/FRACTURES: <1%; vugs 0.2 to 2 mm wide; sub-vertical; veins are filled with a white stubby prismatic zeolite and green chlorite.
ADDITIONAL COMMENTS: Pyrite mineralization is disseminated throughout the rock especially concentrated in the chlorite-rich altered areas.
Sulfide forms <1% of the rock.

UNIT 15: BASALT

Piece 19

CONTACTS: None visible.
PHENOCRYSTS: Glomerocrysts of pyroxene and plagioclase are present.
Plagioclase - 3%; <1.5 mm; euhedral laths.
Clinopyroxene - 3%; <2 mm; equant to elongate.
Magnetite - trace; <0.2 mm; euhedral.
GROUNDMASS: Fine-grained to glassy; microlites of plagioclase.
VESICLES: 2-5%; <0.5 mm; spherical; localized in patches; some contain zeolite and carbonate.
COLOR: Black (7.5YR 7/0).
STRUCTURE: Massive.
ALTERATION: Minor chlorite alteration around vesicle patches.
VEINS/FRACTURES: 0%; none visible; none visible.
ADDITIONAL COMMENTS: The rock has disseminated sulfide (pyrite) as cubes and aggregates of anhedral blebs (<0.5 mm in size).

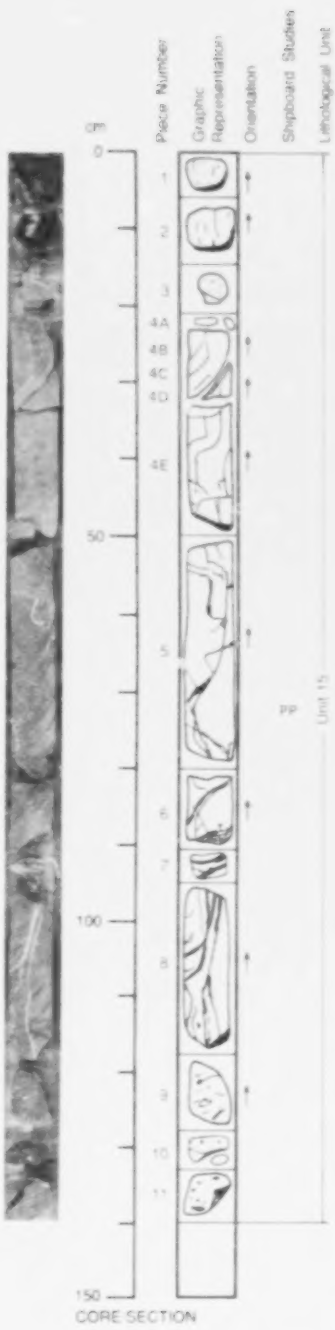
cm
0
50
100
150
CORE SECTION
Piece Number
Graphic Representation
Orientation
Shipboard Studies
Lithological Unit
1
2
3
4A
4B
4C
4D
4E
5
6
7
8
9
10
11
PP
Unit 15

125-786B-34R-2

UNIT 15: BASALT

Pieces 1-2

CONTACTS: None visible.
PHENOCRYSTS:
Plagioclase - 3-4%, <1.5 mm, euhedral laths.
Clinopyroxene - 3%, <2 mm, equant to elongate.
Magnetite - trace, <0.2 mm, euhedral.
GROUNDMASS: Glassy to very fine grained; micro laths of plagioclase are set in a matrix of glass.
VESICLES: 2-5%, <1 mm, spherical, in patches; some contain pale green to white zeolites(?) and minor carbonate linings.
COLOR: Black (7.5YR 2/0).
STRUCTURE: Massive.
ALTERATION: Minor chloritization about vesicles.
VEINS/FRACTURES: None.
ADDITIONAL COMMENTS: Disseminated sulfide (pyrite) is present, as both cubes and patches of anhedral grains, <0.5 mm in size.

UNIT 15: META-OLIVINE BEARING TWO-PYROXENE BASALTIC ANDESITE

Pieces 3-11

CONTACTS: None visible.
PHENOCRYSTS:
Plagioclase - 1-2%, <0.4 mm, elongate euhedral.
Orthopyroxene - <1%, <0.8 mm, equant subhedral to elongate and altered.
Clinopyroxene - 0.5-1%, 0.5-1 mm, equant euhedral to subhedral and fresh.
Magnetite - <1%, <0.1 mm, equant to subhedral.
Olivine - trace, <1 mm, elongate to equant, altered.
GROUNDMASS: Pervasively altered with quench crystals of plagioclase.
VESICLES: 5-10%, 1-2 mm, round, throughout, filled with pale green clay and carbonate.
COLOR: Greenish gray (5G 6/1).
STRUCTURE: Massive.
ALTERATION: Chlorite, clay and carbonate.
VEINS/FRACTURES: 1-2%, <3 mm, subvertical, filled with carbonate and hematite.
ADDITIONAL COMMENTS: Traces of pyrite disseminated throughout.

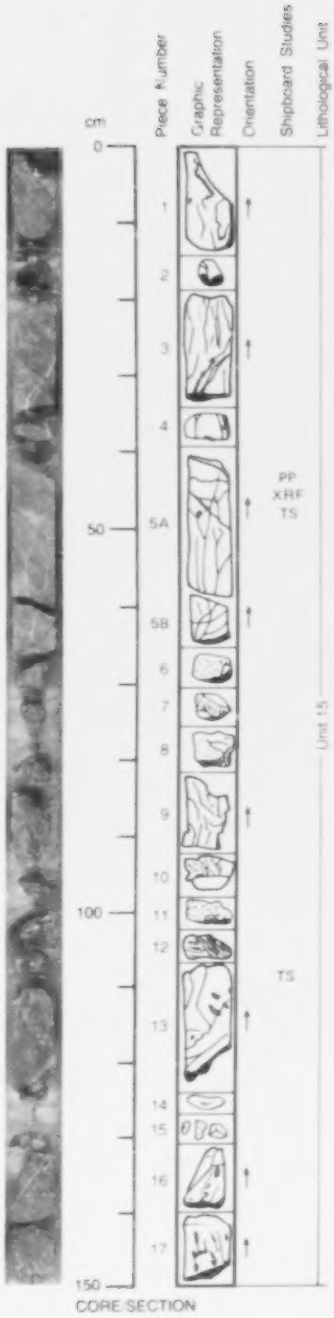
cm
0
50
100
150
Piece Number
Graphic Representation
Orientation
Shipboard Studies
Lithological Unit
1
2
3
4
5A
5B
6
7
8
9
10
11
12
13
14
15
16
17
PP
XRF
TS
TS
Unit 15
CORE/SECTION

125-786B-34R-3

UNIT 15: META-OLIVINE-BEARING TWO-PYROXENE BASALT

Pieces 1-17

CONTACTS: Vesicular meta two pyroxene andesite with glassy margin is in contact with host in pieces 11, 12 and 13, apparently as xenoliths.

PHENOCRYSTS:

Plagioclase - 1-2%, <0.4 mm, elongate euhedral.

Orthopyroxene - <1%, <0.8 mm, equant subhedral to elongate and altered.

Clinopyroxene - 0.5-1%, 0.5-1 mm, equant euhedral-subhedral, fresh.

Magnetite - <1%, <0.1 mm, equant to subhedral.

Olivine - trace <1 mm, elongate to equant.

GROUNDMASS: Pervasively altered with chlorite and clay minerals; originally glassy with feldspar quench crystals.

STRUCTURE: Massive.

ALTERATION: Chlorite, clay and carbonate.

VEINS/FRACTURES: 1-2%, <3 mm, subvertical, filled with carbonate and hematite.

ADDITIONAL COMMENTS: Traces of pyrite disseminated throughout; continuation of Section 125-786B-34R-02.

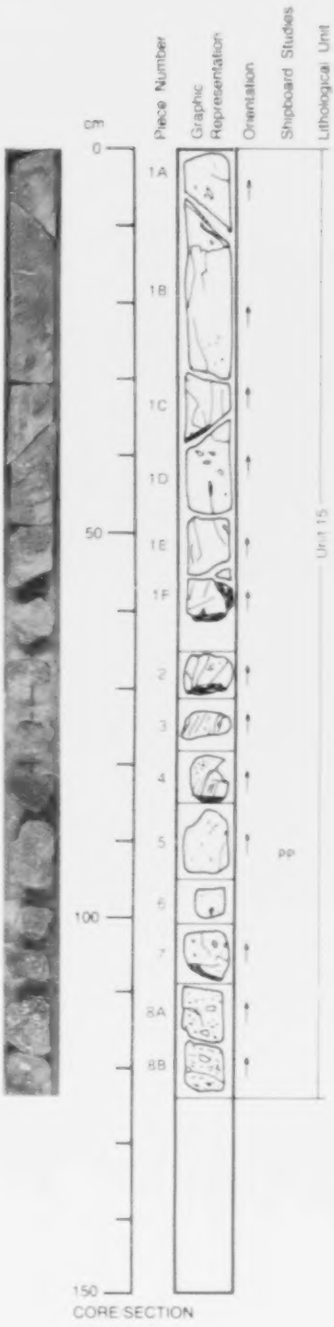

125-786B-34R-4

UNIT 15: META-BASALT

Pieces 1-6

CONTACTS: Chilled margin in Piece 4.
PHENOCRYSTS: Pervasively altered except for in Piece 4.
Orthopyroxene - <10%, <2 mm, euhedral, altered to serpentine.
Clinopyroxene - <5%, <1 mm, black to yellow, unaltered, lath shape, euhedral.
Plagioclase - <2%, <2 mm, only visible in Piece 4, altered?
GROUNDMASS: Fine-grained greenschist facies minerals (chlorite is visible).
VESICLES: Trace, <1 mm, round to elongate, in zones, filled with calcite.
COLOR: greenish gray (5G 5/1).
STRUCTURE: None.
ALTERATION: Groundmass and phenocrysts are altered to greenschist facies minerals.
VEINS/FRACTURES: Trace, <2 mm wide, dominantly steep dipping, filled with calcite, coarsely crystalline chlorite in veins.

UNIT 15: ORTHOPYROXENE, PLAGIOCLASE VESICULAR DACITE

Pieces 7-8B

CONTACTS: Not visible.
PHENOCRYSTS: Phenocrysts are fresh.
Plagioclase - 5%, <2 mm, rounded and as euhedral laths.
Orthopyroxene - 2%, <3 mm, euhedral, yellow.
GROUNDMASS: Glassy to partly crystalline.
VESICLES: 20%, <2 cm, round to elongated, parallel orientation, random distribution, filled with calcite and with dark green coating.
COLOR: Bluish gray (between 5B 5/1 and 6/1).
STRUCTURE: None.
ALTERATION: Little alteration.
VEINS/FRACTURES: Not present. Pyrite+chlorite zone at rim of stratigraphically highest clast. Related to contact with overlying flow?
ADDITIONAL COMMENTS: Lithology continues in 35R-1. Note contrasts in degree of alteration with overlying lithology.

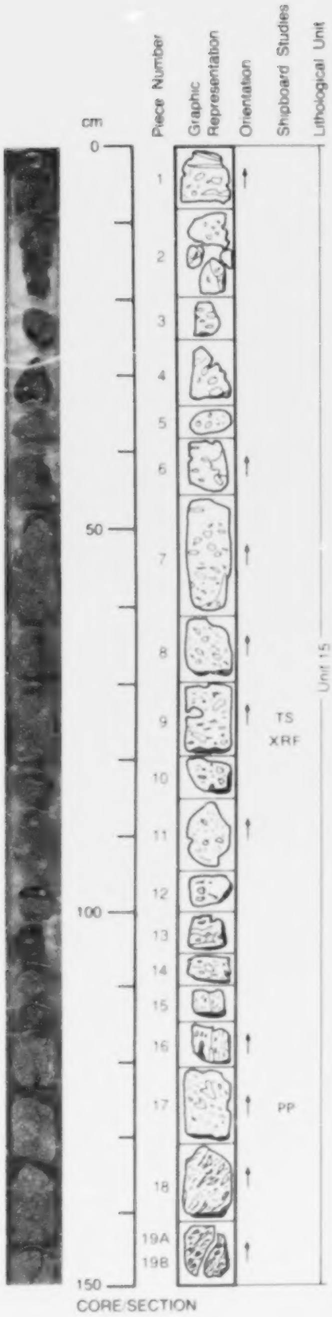
cm
Piece Number
Graphic Representation
Orientation
Shipboard Studies
Lithological Unit
0
50
100
150
1
2
3
4
5
6
7
8
9
10
11
12
13
14
15
16
17
18
19A
19B
TS
XRF
PP
Unit 15
CORE/SECTION

125-786B-35R-1

UNIT 15: ORTHOPYROXENE, PLAGIOCLASE VESICULAR DACITE (34R-4 CONTINUED)

Pieces 1-19B

CONTACTS: None visible
PHENOCRYSTS:
Plagioclase - 2-5%, <2 mm, euhedral lath and rounded zoned crystals
Orthopyroxene - 2-5%, <2 mm, some of 1 cm size, yellow to brown, euhedral
Clinopyroxene - <2%, <1 mm, dark green, euhedral
GROUNDMASS: Glassy to partly crystalline
VESICLES: 20-30%, < 2 cm, elongated, randomly distributed, locally filled with calcite in addition to green or gray coating
COLOR: Gray 2.5Y 4/0 to 5/0
STRUCTURE: None
ALTERATION: Very minor
VEINS/FRACTURES: Trace, 4 mm, 20 degree dip, vein in Piece 1 of light green to white coarse crystalline material containing pyrite and with margins and veins of silky dark-green material
ADDITIONAL COMMENTS: Continuation of Section 125-786B-34R-4. Finely vesicular clasts entrained.

[Blank page]

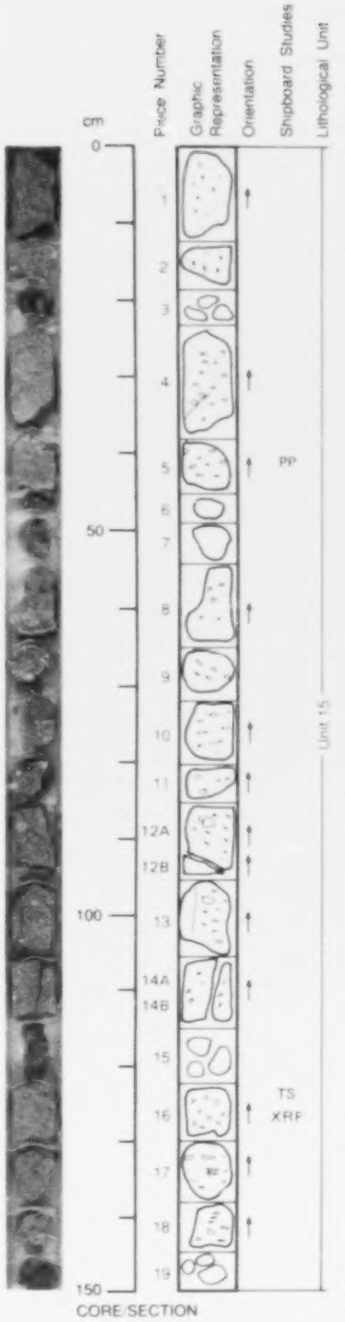
cm
Piece Number
Graphic Representation
Orientation
Shipboard Studies
Lithological Unit
0
50
100
150
1
2
3
4
5
6
7
8
9
10
11
12A
12B
13
14A
14B
15
16
17
18
19
PP
TS
XRF
Unit 15
CORE/SECTION

125-786B-35R-2

UNIT 15: ORTHOPYROXENE, PLAGIOCLASE VESICULAR DACITE (35R-1 CONTINUED)

Pieces 1-19

CONTACTS: None visible.
PHENOCRYSTS: Phenocrysts are fresh.
Plagioclase - 2-5%, <2 mm, euhedral laths and rounded, zoned crystals.
Orthopyroxene - 2-5%, < 2 mm, but some are 1 cm in size; euhedral; yellow.
Clinopyroxene - 0-2%, < 1 mm, euhedral; dark green.
GROUNDMASS: Glassy to partly crystalline.
VESICLES: 20-30%, < 1 cm, round to elongate; random distribution; rare pyrite and gray or green coating.
COLOR: Gray (2.5Y 4/0 - 5/0).
STRUCTURE: None.
ALTERATION: Very minor.
VEINS/FRACTURES: Trace, < 1 mm, mostly vertical; fractures are filled with gray (vesicle-coating) material; some have shiny fracture surfaces.
ADDITIONAL COMMENTS: Locally fine grained, vesicular clasts entrained. Section is a continuation of 125-786B-34R-4.

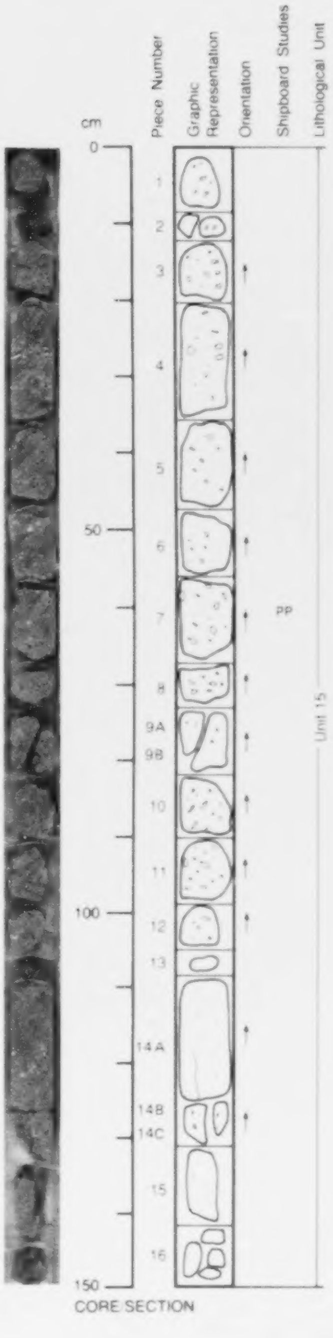
cm
Piece Number
Graphic Representation
Orientation
Shipboard Studies
Lithological Unit
0
50
100
150
1
2
3
4
5
6
7
8
9A
9B
10
11
12
13
14A
14B
14C
15
16
PP
Unit 15
CORE/SECTION

125-786B-35R-3

UNIT 15: PLAGIOCLASE, ORTHOPYROXENE VESICULAR DACITE (35R-2 CONTINUED)

Pieces 1-16

CONTACTS: None visible
PHENOCRYSTS: Fresh
Plagioclase - 2-5%, <2 mm, euhedral laths and rounded, zoned
Orthopyroxene - 2-5%, <2 mm, some 1 cm in size, yellow, euhedral
Clinopyroxene - 2%, <1 mm, dark green, euhedral
GROUNDMASS: Glassy to partly crystalline
VESICLES: 20-30%, < 1 cm, round to elongate, randomly distributed, filled with gray or green coating; zones with calcite filled vesicles occur locally
COLOR: Gray (2.5Y 4/0 - 5/0)
STRUCTURE: None
ALTERATION: Very minor
VEINS/FRACTURES: Absent
ADDITIONAL COMMENTS: Continuation of 125-786B-34R-4

125-786B-35R-4

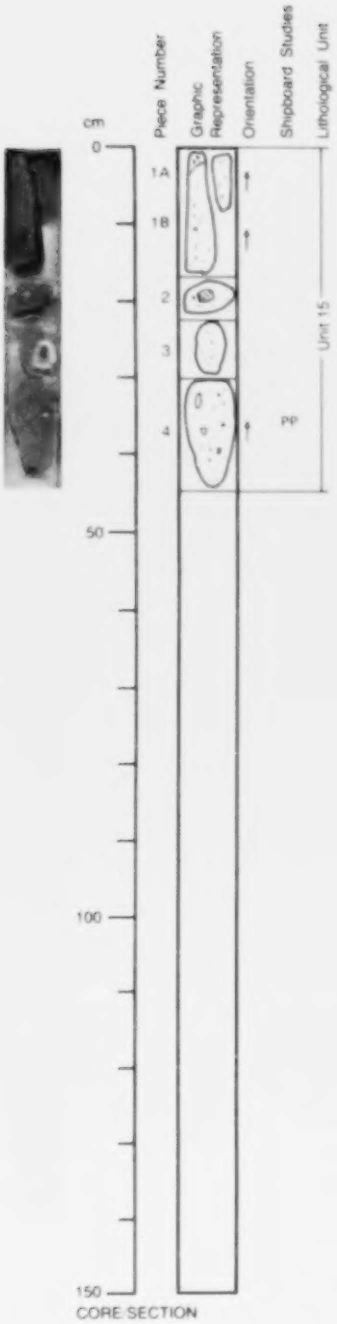
cm
0
50
100
150
Piece Number
Graphic Representation
Orientation
Shipboard Studies
Lithological Unit
1A
1B
2
3
4
PP
Unit 15
CORE/SECTION

UNIT 15: PLAGIOCLASE, ORTHOPYROXENE VESICULAR DACITE (35R-3 CONTINUED)

Pieces 1-4

CONTACTS: None visible
PHENOCRYSTS: Fresh
Plagioclase - 5-8%, < 3 mm, euhedral laths and rounded, zoned crystals
Orthopyroxene - 2-5%, < 2mm, subhedral, yellow
Clinopyroxene - 2%, < 1 mm, dark green
GROUNDMASS: Glassy to partly crystalline
VESICLES: 20%, < 5 mm, round to elongate, randomly distributed, gray coating
COLOR: Gray (2.5Y 4/0 - 5/0)
STRUCTURE: None
ALTERATION: Very minor
VEINS/FRACTURES: Trace, < 1 mm, sub-vertical, shiny fracture surface, possibly chlorite?
ADDITIONAL COMMENTS: Smaller vesicles towards bottom of section. Continuation of 125-786B-34R-4

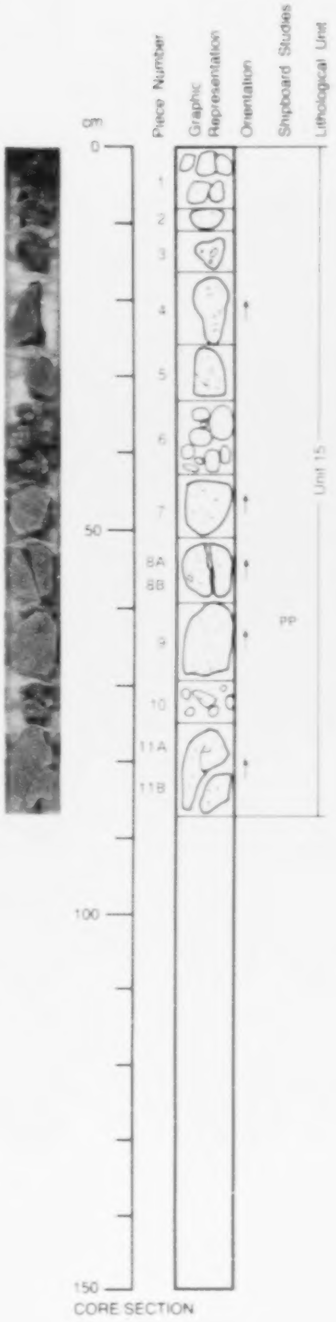
cm
Piece Number
Graphic Representation
Orientation
Shipboard Studies
Lithological Unit
0
50
100
150
1
2
3
4
5
6
7
8A
8B
9
10
11A
11B
PP
Unit 15
CORE SECTION

125-786B-36R-1

UNIT 15: PLAGIOCLASE-ORTHOPYROXENE DACITE (35R-4 CONTINUED)

Pieces 1-11B

CONTACTS: None visible.
PHENOCRYSTS: Plagioclase and clinopyroxene are fresh.
  Plagioclase - 5%, <2 mm, euhedral laths and rounded crystals.
  Orthopyroxene - 2%, <3 mm, euhedral, yellow, prismatic, altering to serpentine.
  Clinopyroxene - trace, <1 mm, dark green, equant.
GROUNDMASS: Fine crystalline, contains plagioclase.
VESICLES: 10%, < 3 mm, round to parallel, elongate, random distribution; light gray coating; some elongation directions dip at a shallow angle, possibly caused by flow.
COLOR: Greenish gray (5G 6/1).
STRUCTURE: None.
ALTERATION: Very little.
VEINS/FRACTURES: Trace, < 0.1 mm, vertical, chlorite on fracture surface.
ADDITIONAL COMMENTS: Continuation of 125-786B-34R-4.

125-786B-37R-1

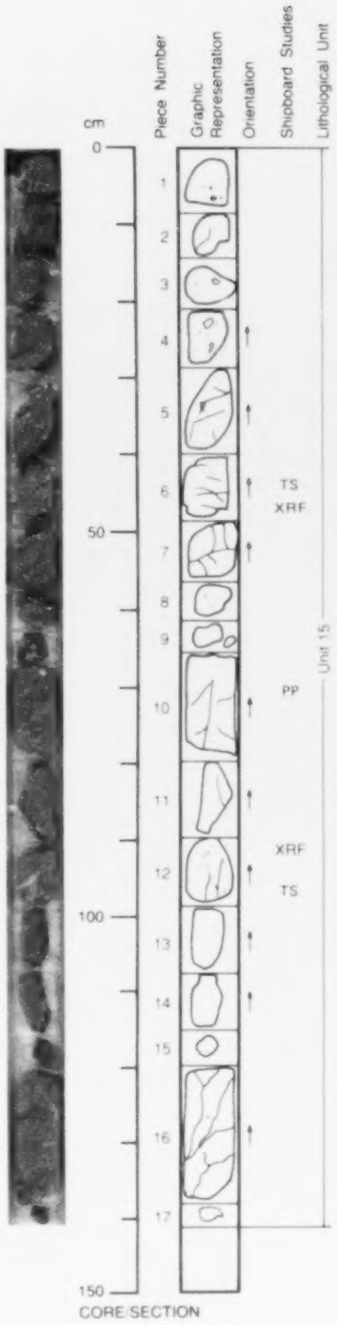
cm
0
50
100
150
CORE/SECTION
Piece Number
Graphic Representation
Orientation
Shipboard Studies
Lithological Unit
1
2
3
4
5
6
7
8
9
10
11
12
13
14
15
16
17
TS
XRF
PP
XRF
TS
Unit 15

UNIT 15: ORTHOPYROXENE, PLAGIOCLASE BONINITE (36R-1 CONTINUED)

Pieces 1-17

CONTACTS: None visible
PHENOCRYSTS: Orthopyroxene and olivine are altered; olivine is absent at top but becomes more abundant at below 80-cm level.
Plagioclase - 5-10%, < 3 mm, euhedral laths and prisms.
Orthopyroxene - 10-15%, <1 cm, yellow, prismatic; altering to serpentine.
Olivine - 0-3%, <1 mm, completely altered to red specks with white cellular structure.
GROUNDMASS: Glassy with abundant plagioclase, more crystalline below 80-cm level.
VESICLES: 10-15%, < 1 cm, round, large ones concentrated in zones, light green or gray coating, some filled with calcite.
COLOR: Greenish to bluish gray (5G 5/1 TO 5BG 4/1).
STRUCTURE: Fractured.
ALTERATION: Olivine and orthopyroxene are altered to serpentine and oxides.
VEINS/FRACTURES: 0-5%, up to 5 mm, random orientation; locally strongly fractured; fractures are filled with chlorite, some calcite and another white mineral, and contain pyrite cubes.
ADDITIONAL COMMENTS: The top of this section (1-80 cm) is a continuation of 786B-34R-4.

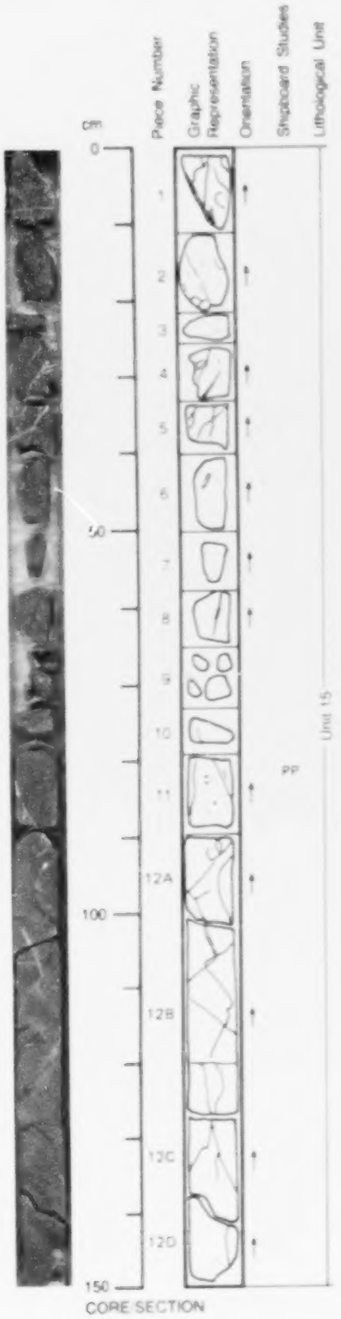
cm
Piece Number
Graphic Representation
Orientation
Shipboard Studies
Lithological Unit
0
1
2
3
4
5
6
50
7
8
9
10
11
PP
Unit 15
12A
100
12B
12C
12D
150
CORE SECTION

125-786B-37R-2

UNIT 15: PLAGIOCLASE, ORTHOPYROXENE, OLIVINE BONINITE (37R-1 CONTINUED)

Pieces 1-12D

CONTACTS: Differential alteration contact in Piece 2.
PHENOCRYSTS: Orthopyroxene and olivine are altered.
Plagioclase - 5-8%, <2 mm, euhedral laths and rounded crystals.
Orthopyroxene - 10-15%, <1 cm, yellow prisms, inclusions of equant, altered olivine.
Olivine - 3%, <1 mm, altered to red and white material.
Clinopyroxene - trace, <1 mm, dark green, euhedral.
GROUNDMASS: Fine crystalline, plagioclase-rich.
VESICLES: 3-5%, < 3mm, round to elongate, in zones, coated with greenish gray material, some filled with calcite.
COLOR: Dark greenish gray (5G 4/1) in Pieces 1 and 2, changing to dark reddish gray (5R 4/1 - 4/2) in Piece 2 and continuing through Piece 12D.
STRUCTURE: Fractures.
ALTERATION: Orthopyroxene and olivine are altered to serpentine and calcite.
VEINS/FRACTURES: 2%, < 5 mm, randomly oriented, filled with chlorite and/or white minerals, including calcite.
ADDITIONAL COMMENTS: Continuation from 125-786B-34R-4.

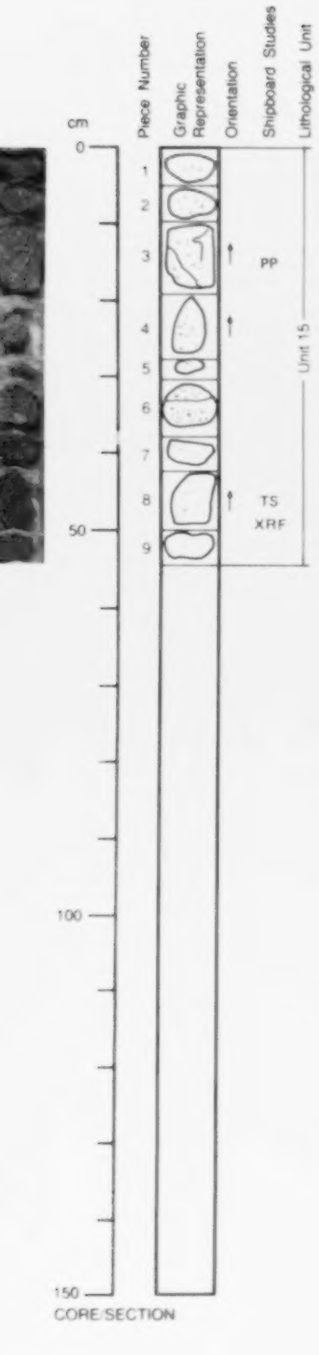
cm
0
50
100
150
CORE/SECTION
Piece Number
Graphic Representation
Orientation
Shipboard Studies
Lithological Unit
1
2
3
4
5
6
7
8
9
PP
TS
XRF
Unit 15

125-786B-37R-3

UNIT 15: PLAGIOCLASE, ORTHOPYROXENE, OLIVINE BONINITE (37R-2 CONTINUED)

Pieces 1-6

CONTACTS: Horizontally oriented contact with chilled margin in Piece 6.
PHENOCRYSTS:
Plagioclase - 5-8%, <2 mm; euhedral laths and rounded crystals.
Orthopyroxene - 10-15%, <1 cm; yellow prisms; inclusions of equant altered olivine.
Olivine - 3%, <1 mm; altered to red and white material.
Clinopyroxene - trace, <1 mm; dark green; euhedral.
GROUNDMASS: Fine-grained; plagioclase-rich.
VESICLES: 3-5%, <3 mm; rounded to elongate; in zones; coated with greenish gray material; some filled with calcite.
COLOR: Dark greenish gray (5G 4/1) to dark reddish gray (5R 4/1 - 4/2).
STRUCTURE: Fractures.
ALTERATION: Orthopyroxene and olivine are altered to serpentine and calcite.
VEINS/FRACTURES: 2%, <5 mm; randomly oriented; filled with chlorite and/or white minerals, including calcite.
ADDITIONAL COMMENTS: Continuation from 125-786B-34R-4.

UNIT 15: PLAGIOCLASE ANDESITE

Pieces 6-9

CONTACTS: Chilled margin in Piece 6.
PHENOCRYSTS:
Plagioclase - 5-10%, <1 mm; euhedral.
GROUNDMASS: Glassy.
VESICLES: Trace, < 1mm; collapsed; randomly distributed.
COLOR: Gray green (5G 4/1).
STRUCTURE: None.
ALTERATION: Glass is altered along fractures.
VEINS/FRACTURES: Microfractures in glass, probably from quench.

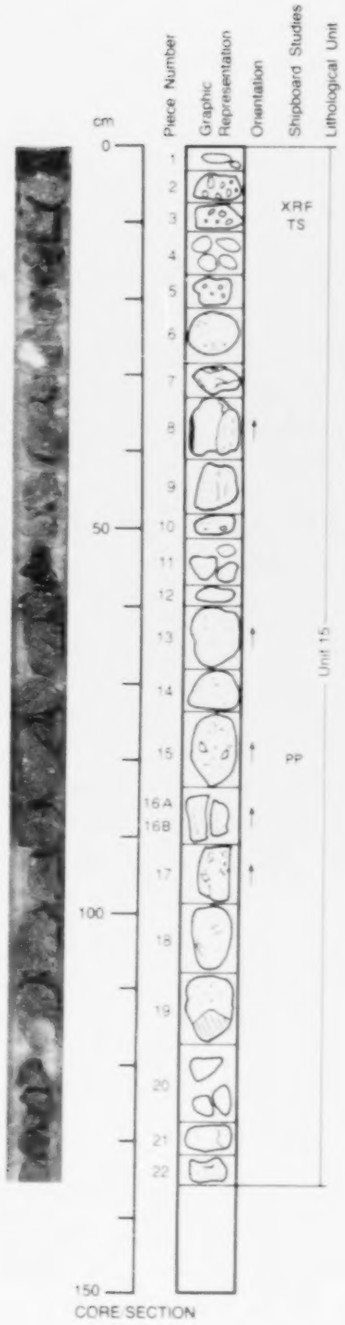
cm
Piece Number
Graphic Representation
Orientation
Shipboard Studies
Lithological Unit
0
50
100
150
1
2
3
4
5
6
7
8
9
10
11
12
13
14
15
16A
16B
17
18
19
20
21
22
XRF
TS
PP
Unit 15
CORE SECTION

125-786B-38R-1

UNIT 15: PLAGIOCLASE, ORTHOPYROXENE ANDESITE

Pieces 1-22

CONTACTS: Glass fragment of chilled margin in Piece 1.
PHENOCRYSTS:
Plagioclase: 5-10%, <1 mm, euhedral laths.
Orthopyroxene: 2%, <1 mm, euhedral, yellow to brown, prismatic.
GROUNDMASS: Glassy.
VESICLES: 15%, < 1 cm, round in Pieces 2-5, elongate otherwise, randomly distributed with bluish gray coating.
COLOR: Dark green (5G 4/1) in altered areas, blue gray (5B 6/1 to 5/1) when fresh.
STRUCTURE: Brecciation in Piece 6-22 with the exception of Piece 10.
ALTERATION: Altered in brecciated areas to chlorite-bearing mineralogy.
VEINS/FRACTURES: Absent.
ADDITIONAL COMMENTS: Clasts in breccia are very glassy, probably fragmented during flow; glass-rich portions are orthopyroxene free; breccia contains pyrite.

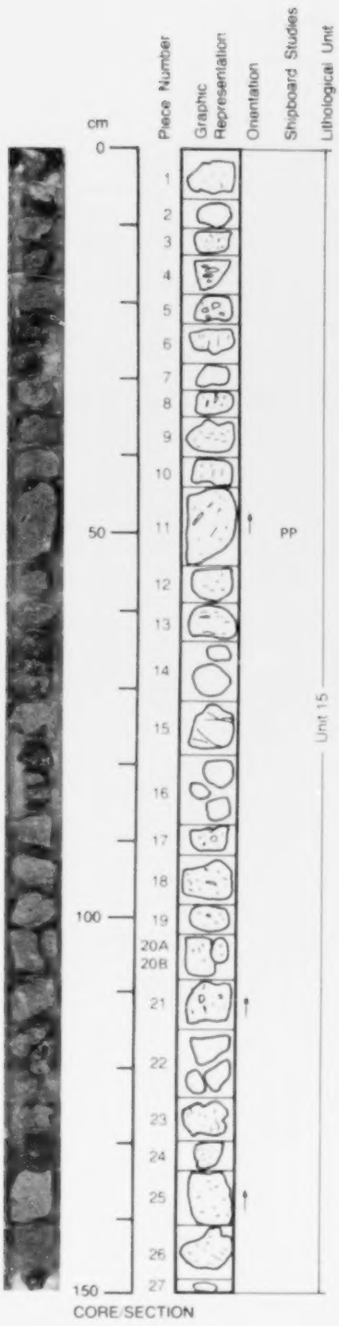
cm
Piece Number
Graphic Representation
Orientation
Shipboard Studies
Lithological Unit
0
50
100
150
1
2
3
4
5
6
7
8
9
10
11
12
13
14
15
16
17
18
19
20A
20B
21
22
23
24
25
26
27
PP
Unit 15
CORE/SECTION

125-786B-39R-1

UNIT 15: PLAGIOCLASE, ORTHOPYROXENE ANDESITE

Pieces 1-27

CONTACTS: None

PHENOCRYSTS:

Plagioclase - 5%, <1 mm, euhedral laths.

Orthopyroxene - 2%, <1 mm, euhedral, yellow.

GROUNDMASS: Glassy, locally plagioclase-rich.

VESICLES: 5-15%, < 1 cm, round to elongate, grouped by size and shape in zones, local bluish-gray coating.

COLOR: Blue gray (5B 6/1 to 5/1).

STRUCTURE: None

ALTERATION: Minor

VEINS/FRACTURES: n/a, < 0.2 mm; n/a; white material in fractures.

ADDITIONAL COMMENTS: Pyrite in vugs.

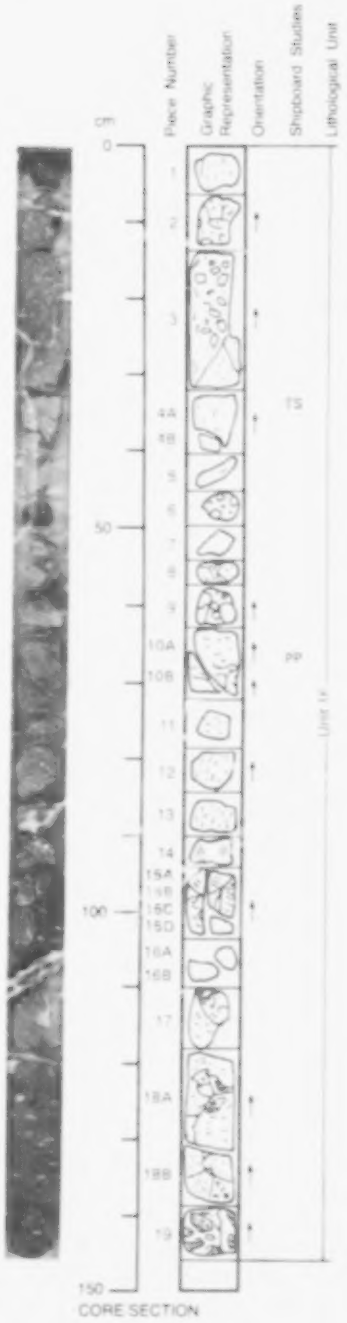
cm
0
50
100
150
CORE SECTION
Piece Number
Graphic Representation
Orientation
Shipboard Studies
Lithological Unit
1
2
3
4A
4B
5
6
7
8
9
10A
10B
11
12
13
14
15A
15B
15C
15D
16A
16B
17
18A
18B
19
TS
PP
Unit 16

125-786B-39R-2

UNIT 16: BRECCIATED TWO-PYROXENE ANDESITE

Pieces 1-19

CONTACTS: Piece 3 has a boundary between glassy material and crystalline ro
pieces have contacts between rock of differing vesicularity and grain size. P
have an oxidized matrix of mafic rock.

PHENOCRYSTS: Glomerocrysts of orthopyroxene, clinopyroxene and plagio
throughout.
Clinopyroxene - 3%, <0.5 mm, euhedral, elongate.
Orthopyroxene - 2%, <0.5 mm, euhedral, equant.
Plagioclase - 3.5%, <0.5 mm, euhedral, tabular.
Magnetite - trace, <0.2 mm, euhedral.

GROUNDMASS: Altered glass and fine grained crystalline matrix, predominantl
plagioclase.

VESICLES: 1.5%, <1 mm to 4 mm, oval to round, jagged, locally concentrated.
alignment is present especially in Pieces 4, 17, 18.

COLOR: Very dark gray to olive gray (5Y 3/1 to 5/2); oxidized matrix is dusky red
3/2).

STRUCTURE: Autobrecciated; clasts and matrix are of similar composition.

ALTERATION: Pyrite is present throughout this section as both disseminated
crystalline phases and occurs along veins associated with zeolites, glass and
moderately to strongly chloritized.

VEINS/FRACTURES: <1%, <1 mm wide, random, filled with white zeolite and
and, occasionally, sulfide.

ADDITIONAL COMMENTS: This rock type continues in 39R-3.

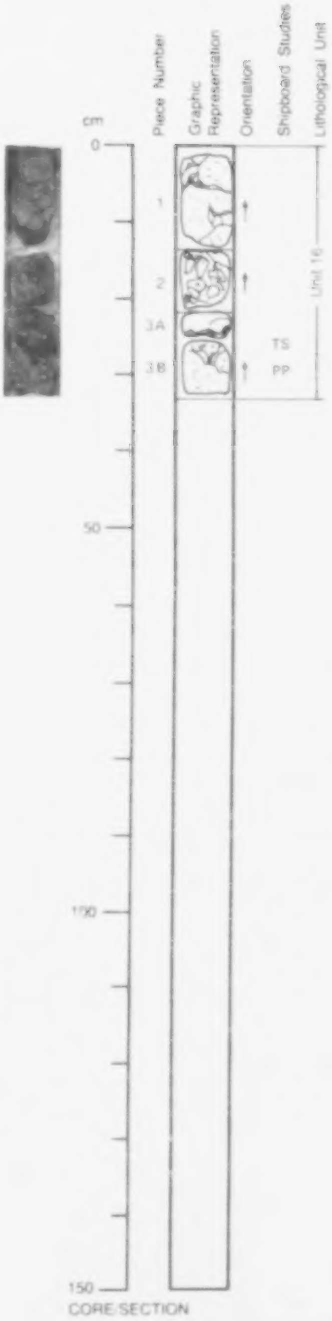
cm
Piece Number
Graphic Representation
Orientation
Shipboard Studies
Lithological Unit
0
50
100
150
1
2
3A
3B
TS
PP
Unit 16
CORE/SECTION

125-786B-39R-3

UNIT 16: BRECCIATED TWO-PYROXENE ANDESITE (39R-2 CONTINUED)

Pieces 1-3

CONTACTS: Sharp between matrix and clasts.
PHENOCRYSTS: Glomerocrysts of orthopyroxene, clinopyroxene and plagioclase in the clasts.
Clinopyroxene - 3%, <0.5 mm, euhedral, elongate.
Orthopyroxene - 2%, <0.5 mm, euhedral, equant.
Plagioclase - 3-5%, <0.5 mm, euhedral, tabular.
Magnetite - trace, <0.2 mm, euhedral.
GROUNDMASS: Clast matrix contains altered glass and fine-grained crystals predominantly of plagioclase.
VESICLES: 1-3%, <1 mm to 4 mm, oval/round, jagged; locally concentrated; some local alignment is present.
COLOR: Very dark gray to olive gray (5Y 3/1 to 5/2); oxidized breccia matrix is dusky red (2.5YR 3/2).
STRUCTURE: Autobrecciated; clasts and matrix are of similar composition.
ALTERATION: Pyrite is present throughout this section as both disseminated and crystalline phases and along veins associated with zeolites; glass and matrix are moderately to strongly chloritized.
VEINS/FRACTURES: <1%, <1 mm; random orientation; filled with white zeolite and/or quartz and some sulfide.
ADDITIONAL COMMENTS: This rock type is a continuation of the overlying Section 39R-2.

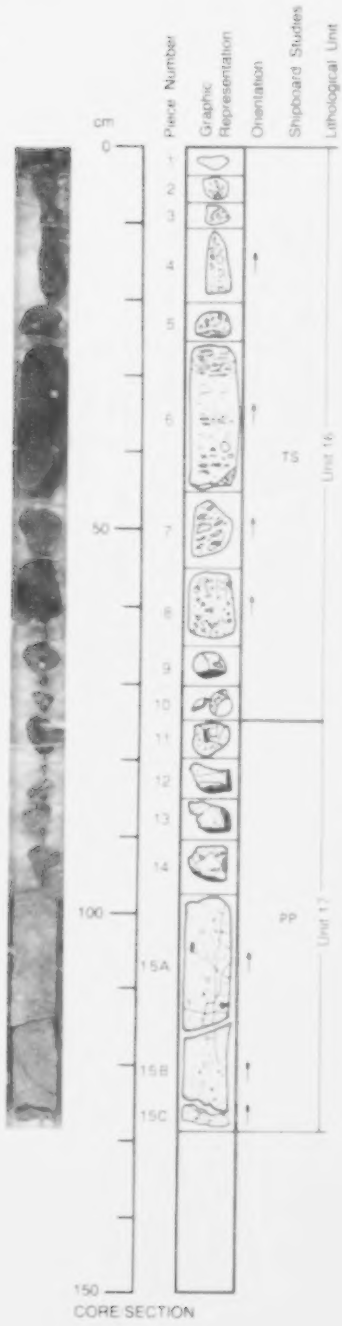

125-786B-40R-1

UNIT 16: BRECCIATED TWO-PYROXENE ANDESITE

Pieces 1-10

CONTACTS: Sharp between matrix and clasts.
PHENOCRYSTS: Glomerocrysts of orthopyroxene, clinopyroxene and plagioclase in the clasts.
Plagioclase - 3-5%, <0.5, euhedral, tabular.
Clinopyroxene - 3%, <0.5, euhedral, elongate.
Orthopyroxene - 2%, <0.5, euhedral, equant.
Magnetite - trace, <0.2, euhedral.
GROUNDMASS: Clast matrix contains altered glass and fine grained crystals predominantly of plagioclase.
VESICLES: 1-3%, <1 mm, oval-round, jagged, locally concentrated, some local alignment is present.
COLOR: Very dark gray to olive gray (5Y 3/1 to 5/2); oxidized breccia matrix is dusky red (2.5YR 3/2).
STRUCTURE: Autobrecciated; clasts and matrix are of similar composition.
ALTERATION: Pyrite is present throughout this section as both disseminated and crystalline phases and along veins associated with zeolites; glass and matrix are moderately to strongly chloritized.
VEINS/FRACTURES: <1%, <1 mm, random, filled with white zeolite and/or quartz and some sulfide.
ADDITIONAL COMMENTS: This rock type is a continuation of the overlying Section 39R-3; flow indicated by 1) shard orientation parallel to clast boundaries, 2) preferred shear orientation to clasts and 3) trails of smaller fragments behind clasts.

UNIT 17: GLASSY TWO-PYROXENE BASALT

Pieces 11 and 14

CONTACTS: Pieces are chilled margins.
PHENOCRYSTS:
Plagioclase - <1%, <0.3mm, laths.
Clinopyroxene - <1%, <0.5mm, euhedral, tabular.
Orthopyroxene - trace, <0.5 mm, euhedral, tabular.
GROUNDMASS: Predominately glassy with quenched plagioclase laths.
VESICLES: None visible.
COLOR: Dark gray (N 4/).
STRUCTURE: Massive.
ALTERATION: Minor chlorite; pyroxenes appear to be partially altered.
VEINS/FRACTURES: None visible.

UNIT 17: OLIVINE PHYRIC BASALT

Pieces 11-15

CONTACTS: None visible.
PHENOCRYSTS:
Olivine - 7-10%, <4 mm, euhedral, tabular, altered to iron oxides and carbonate, contain spinel inclusions.
Clinopyroxene - 3-5%, <0.5 mm, euhedral, tabular.
Plagioclase - 10%, <0.5 mm, euhedral, tabular.
GROUNDMASS: Very fine grained with plagioclase laths in glass, variably altered to chlorite, clay, zeolite and carbonate.
VESICLES: 1-2%, 2-6 mm, elongate, dip at 30 degrees; in Pieces 15D - 15G, vesicles are elongate <10 mm long; in Pieces 15A and 15B the vesicles are <4 mm in length, decreasing in size upwards.
COLOR: Bluish gray (5B 5/1).
STRUCTURE: Massive.
ALTERATION: Pervasive alteration to chlorite, carbonate.
VEINS/FRACTURES: <1%, <5 mm width, steeply to gently dipping, carbonate, chlorite and iron oxide filled.
ADDITIONAL COMMENTS: These pieces are continuous with 125-786B-40R-02, Pieces 15D to 15G, 0-40 cm.

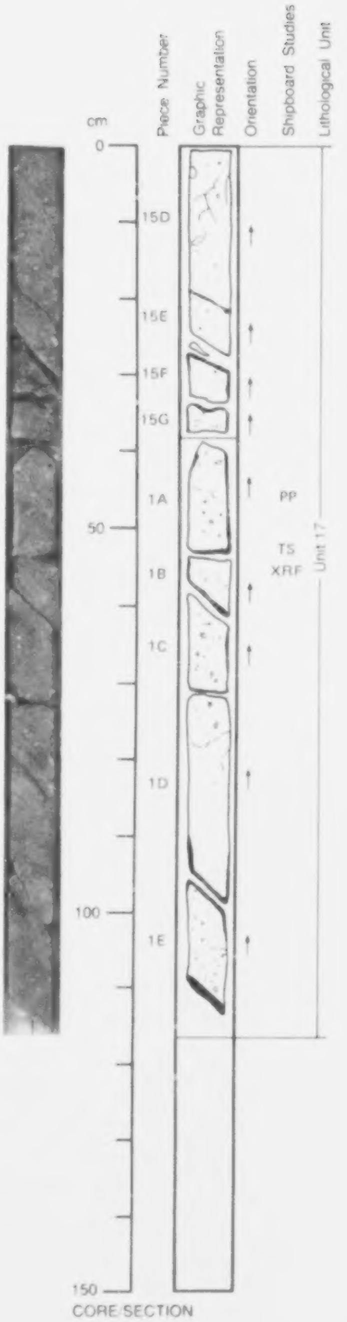
cm
Piece Number
Graphic Representation
Orientation
Shipboard Studies
Lithological Unit
0
50
100
150
15D
15E
15F
15G
1A
1B
1C
1D
1E
PP
TS
XRF
Unit 17
CORE/SECTION

125-786B-40R-2

UNIT 17: OLIVINE PHYRIC BASALT (CONTINUATION OF 40R-1)

Pieces 1A-1E

CONTACTS: None visible.
PHENOCRYSTS:
Plagioclase - 10%, <0.5 mm, euhedral, tabular.
Clinopyroxene - 3-5%, <0.5 mm, euhedral, tabular.
Olivine - 7-10%, <4 mm, euhedral, tabular, altered to carbonate/Fe-oxide assemblage.
GROUNDMASS: Very fine grained with plagioclase laths in glass, variably altered to chlorite, clay, zeolite and carbonate.
VESICLES: 1%, 2-3 mm, elongate, throughout, less common than in 40R-1.
COLOR: Bluish gray (5B 5/1).
STRUCTURE: Massive.
ALTERATION: Pervasive alteration to chlorite and carbonate.
VEINS/FRACTURES: <1%, <5 mm wide, steeply dipping, filled with carbonate, chlorite and Fe-oxide. Pieces 1F to 1O: same rock type as all of 40R-3 and 40R-4.

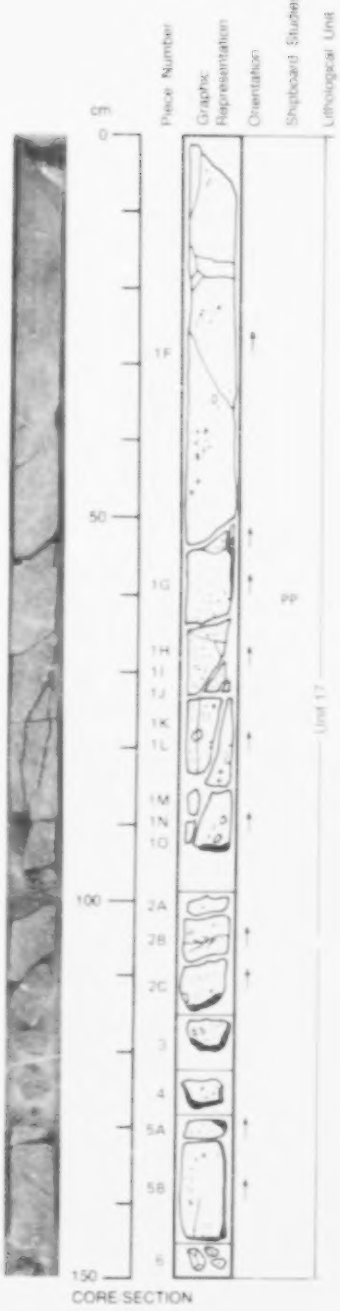
cm
Piece Number
Graphic Representation
Orientation
Shipboard Studies
Lithological Unit
0
50
100
150
1F
1G
1H
1I
1J
1K
1L
1M
1N
1O
2A
2B
2C
3
4
5A
5B
6
PP
Unit 17
CORE/SECTION

125-786B-40R-3

UNIT 17: OLIVINE PHYRIC BASALT (CONTINUATION OF 40R-2)

Pieces 1F-10, 2-6

CONTACTS: None visible.
PHENOCRYSTS:
Plagioclase: 10%, <0.5 mm, euhedral, tabular.
Clinopyroxene: 3.5%, <0.5 mm, euhedral, tabular.
Olivine: 7-10%, <4 mm, euhedral, tabular, altered to Fe oxide, carbonate assemblage; contains spinel inclusions.
GROUNDMASS: Very fine grained with plagioclase laths in glass, variably altered to chlorite, clay, zeolite and carbonate.
VESICLES: 1%, 2 mm, elongate to round, throughout, locally concentrated.
COLOR: Bluish gray (5B 5/1).
STRUCTURE: Massive.
ALTERATION: Pervasive chlorite and carbonate.
VEINS/FRACTURES: <1%, <5 mm wide, steeply dipping, filled with chlorite and Fe oxide.
ADDITIONAL COMMENTS: These pieces are continuous with those above (40R-2) and below (40R-4).

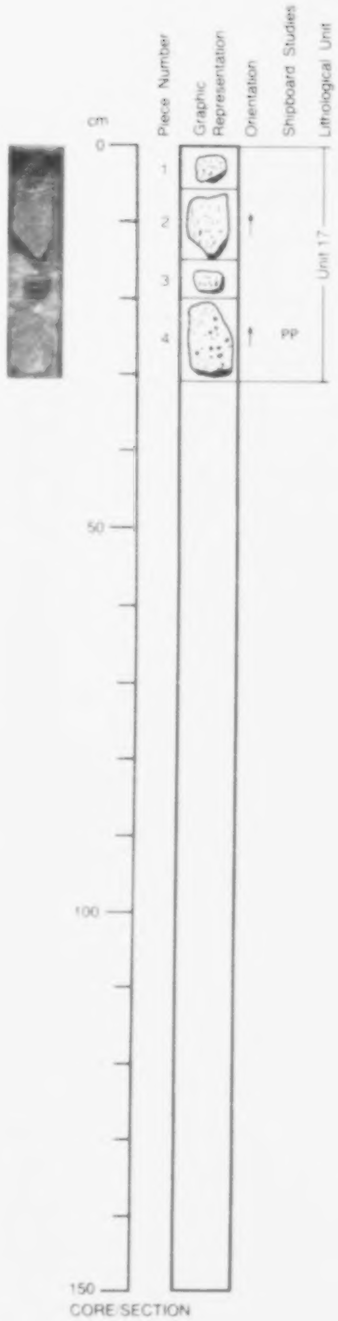
cm
Piece Number
Graphic Representation
Orientation
Shipboard Studies
Lithological Unit
0
1
2
3
4
PP
Unit 17
50
100
150
CORE/SECTION

125-786B-40R-4

UNIT 17: OLIVINE PHYRIC BASALT (40R-3 CONTINUED)

Pieces 1-4

CONTACTS: None visible

PHENOCRYSTS:

- Plagioclase - 10%, <0.5 mm, euhedral, tabular
- Clinopyroxene - 3-5%, <0.5 mm, euhedral, tabular
- Olivine - 7-10%, <4 mm, euhedral, tabular

GROUNDMASS: Very fine grained with plagioclase laths in glass, variably altered to chlorite, clay, zeolite, and carbonate.

VESICLES: 1-2%, <1-3, elongate to round, throughout, filled with carbonate.

COLOR: Bluish gray (5B 5/1).

STRUCTURE: Massive.

ALTERATION: Pervasive alteration by chlorite and carbonate; olivine phenocrysts altered to Fe oxide/carbonate assemblage.

VEINS/FRACTURES: <1%, <5 mm, steeply dipping, filled with chlorite and Fe oxide assemblage.

ADDITIONAL COMMENTS: These pieces are a continuation of 40R-3.

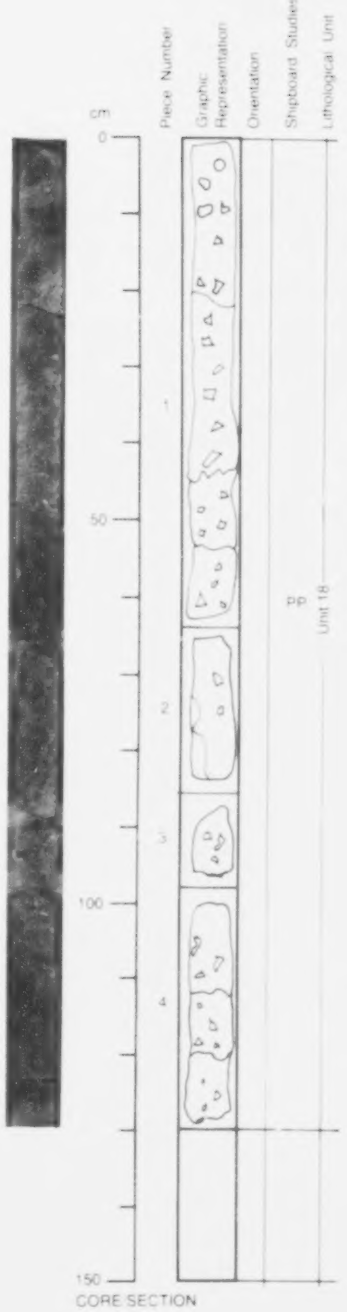
cm
0
50
100
150
Piece Number
Graphic Representation
Orientation
Shipboard Studies
Lithological Unit
1
2
3
4
PP
Unit 18
CORE SECTION

125-786B-41R-1

UNIT 18: ANDESITE BRECCIA

Pieces 1-4

CONTACTS: None visible.
PHENOCRYSTS:
Plagioclase - 10%, <2 mm, euhedral, tabular.
Clinopyroxene - 7%, <4 mm, euhedral, elongate.
Orthopyroxene - 5%, <1 mm, euhedral, equant.
GROUNDMASS: Fine-grained to glassy with pyroxene and feldspar laths.
VESICLES: 3-7%, 1-4 mm, elongate, ragged, throughout, locally concentrated. Miaroles. Coalesce locally into pipe-like structures.
COLOR: Dusky green matrix (10G 3/2) and dark gray clasts (2.5Y 4/0).
STRUCTURE: Brecciated.
ALTERATION: Matrix is pervasively altered to chlorite.
VEINS/FRACTURES: <1-2%, 1-3 mm, random, often sub-parallel to the core, filled with white, zeolitic material.
ADDITIONAL COMMENTS: Clasts are 1 mm to 6 cm (average 1 cm) maximum dimension and poorly sorted; matrix contains scattered vugs with a partial fill of fine-grained, white, non-carbonate mineral (zeolite?) and silt-sized vitrics rich in microlites.

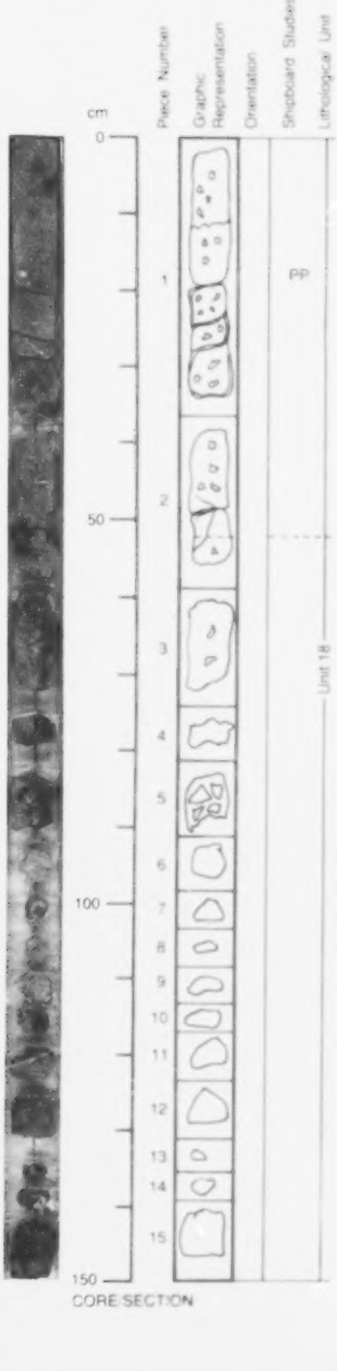
cm
Piece Number
Graphic Representation
Orientation
Shipboard Studies
Lithological Unit
0
50
100
150
1
2
3
4
5
6
7
8
9
10
11
12
13
14
15
PP
Unit 18
CORE/SECTION

125-786B-41R-2

UNIT 18: ANDESITE BRECCIA

Pieces 1-15

CONTACTS: None visible.
PHENOCRYSTS:
Plagioclase - 10%, ≤2 mm, euhedral, tabular.
Clinopyroxene - 7%, <4 mm, euhedral, elongate.
Orthopyroxene - 5%, <1 mm, euhedral, equant.
GRUNDMASS: Fine grained to glassy with pyroxene and feldspar laths.
VESICLES: 3-7%, 1-4 mm, elongate, ragged; throughout, locally concentrated; coalesce locally into pipe-like structures.
COLOR: Dusky green (10G 3/2) matrix and dark gray (2.5Y 4/0) clasts.
STRUCTURE: Brecciated.
ALTERATION: Matrix is pervasively altered to chlorite.
VEINS/FRACTURES: <1-2%, 1-3 mm wide, random, often sub-parallel to the core, filled with white, zeolitic material.
ADDITIONAL COMMENTS: Clasts are 1 mm to 6 mm in maximum dimension; a continuation of Section 41R-1.

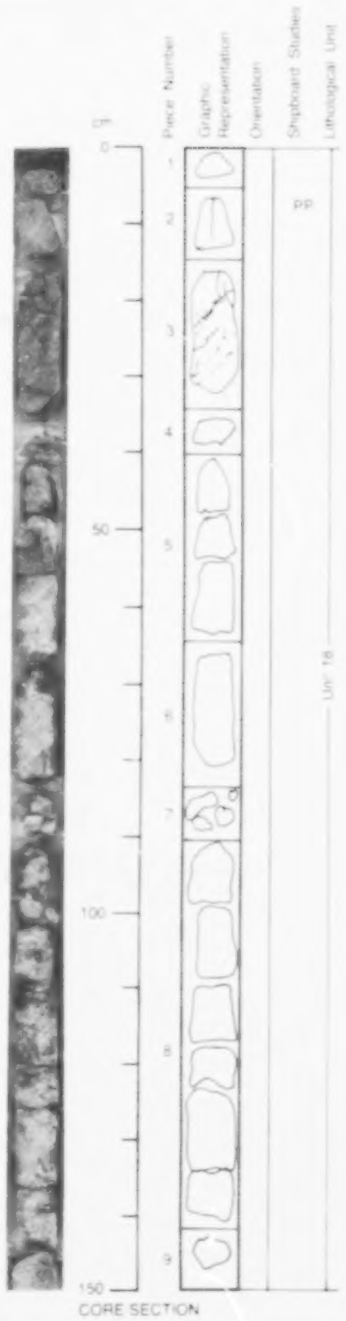

125-786B-41R-3

UNIT 18: ANDESITE BRECCIA

Pieces 1 and 5-9

CONTACTS: None visible.
PHENOCRYSTS:
Plagioclase - 10%, <2 mm, euhedral, tabular.
Clinopyroxene - 7%, <4 mm, euhedral, elongate.
Orthopyroxene - 5%, <1 mm, euhedral, equant.
GROUNDMASS: Fine-grained to glassy with pyroxene and feldspar laths.
VESICLES: 3-7%, 1-4 mm, elongate, jagged, throughout, locally concentrated, coalesce locally into pipe-like structures.
COLOR: Dusky green (10G 3/2) matrix and dark gray (2.5Y 4/0) clasts.
STRUCTURE: Brecciated at top, massive after Piece 5.
ALTERATION: Matrix is pervasively altered to chlorite.
VEINS/FRACTURES: <1-2%, 1-3 mm, random, often sub-parallel to the core, filled with white, zeolitic material.
ADDITIONAL COMMENTS: The clasts sizes 1 mm - 6 cm (average 0.5 cm), a continuation of Section 41R-2.

UNIT 18: VITRIC SAND

Pieces 2-4

CONTACTS: Between Pieces 1 and 2 and 4 and 5, nature not obvious.
PHENOCRYSTS: N/A
GROUNDMASS: N/A
VESICLES: N/A
COLOR: N/A
STRUCTURE: N/A
ALTERATION: N/A
VEINS/FRACTURES: N/A
ADDITIONAL COMMENTS: Piece 2 is a well-sorted vitric sand with water escape pipes. Piece 3 is made up of an upper sand (4 cm thick, fine-grained with water escape pipe along a micro fault), an upper middle sand (2.5 cm thick, coarser grained, also with water escape pipes), a lower middle sand (3 cm thick, medium-grained, massive with faint laminae), and a lower sand (3 cm thick, fine- to medium-grained, structureless). Piece 4 is a silty sand with a white pumice clast.

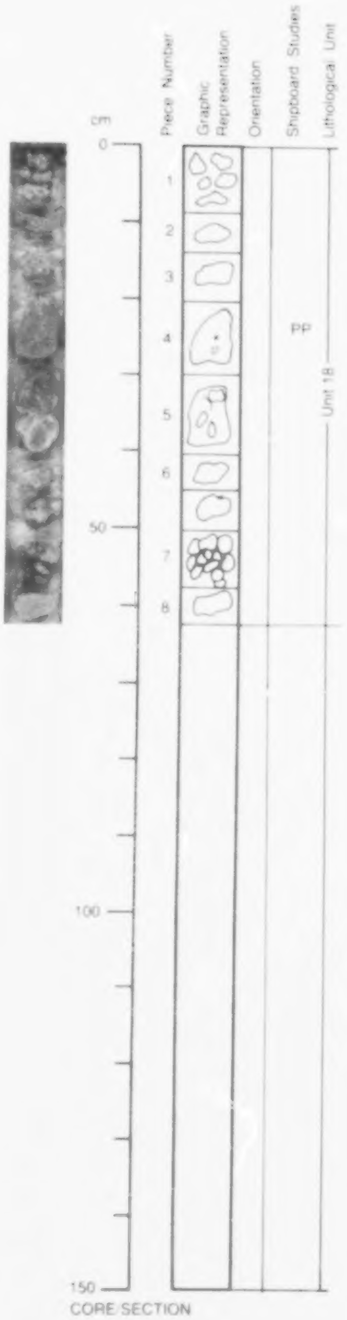
cm
Piece Number
Graphic Representation
Orientation
Shipboard Studies
Lithological Unit
0
50
100
150
1
2
3
4
5
6
7
8
PP
Unit 18
CORE/SECTION

125-786B-41R-4

UNIT 18: TWO-PYROXENE ANDESITE

Pieces 1-9

CONTACTS: None visible.
PHENOCRYSTS:
Plagioclase - 10%, <2 mm, euhedral, tabular.
Clinopyroxene - 7%, <4 mm, euhedral, elongate.
Orthopyroxene - 5%, <1 mm, euhedral, equant.
GROUNDMASS: Fine-grained to glassy with pyroxene and feldspar laths.
VESICLES: 3-7%, 1-4 mm, elongate, ragged; throughout, locally concentrated, coalesce locally into pipe-like structures.
COLOR: Dusky green (10G 3/2) matrix and dark gray (2.5Y 4/0) clasts.
STRUCTURE: Brecciated at top.
ALTERATION: Matrix is pervasively altered to chlorite.
VEINS/FRACTURES: <1-2%, 1-3 mm, random, often sub-parallel to the core; filled with white, zeolitic material.
ADDITIONAL COMMENTS: Continuation of Section 41R-3.

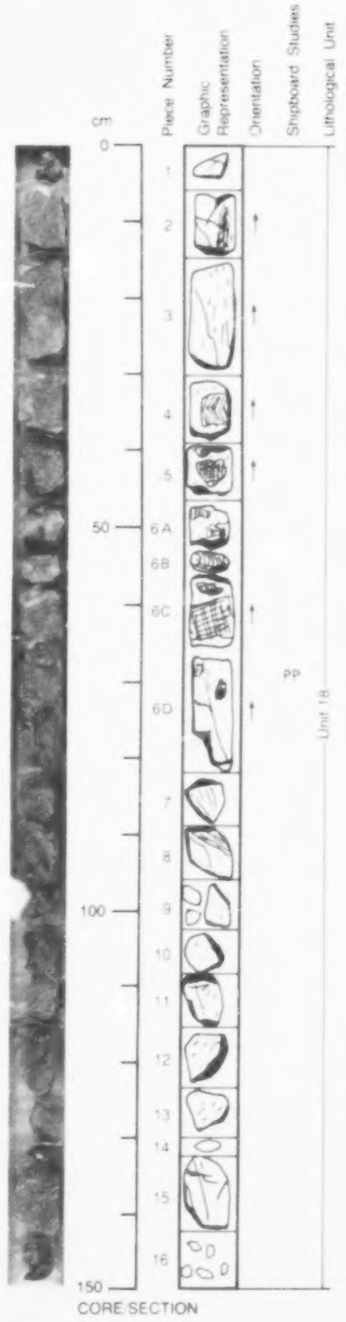
cm
0
50
100
150
CORE/SECTION
Piece Number
Graphic Representation
Orientation
Shipboard Studies
Lithological Unit
1
2
3
4
5
6A
6B
6C
6D
7
8
9
10
11
12
13
14
15
16
PP
Unit 18

125-786B-42R-1

UNIT 18: TWO-PYROXENE ANDESITE

Pieces 1-16

CONTACTS: None visible.
PHENOCRYSTS:
Plagioclase - 10%, <2 mm, euhedral, tabular.
Clinopyroxene - 7%, <4 mm, euhedral, elongate.
Orthopyroxene - 5%, <1 mm, euhedral, equant.
GROUNDMASS: Fine-grained to glassy, with pyroxene and feldspar laths.
VESICLES: 3-7%, 1-4 mm, elongate, ragged, throughout, locally concentrated; coalesce locally into pipe like structures.
COLOR: Greenish gray (5G 5/1).
STRUCTURE: Brecciated at top, massive after Piece 6.
ALTERATION: Matrix is pervasively altered to chlorite.
VEINS/FRACTURES: <1-2%, 1-3 mm wide, random, often sub parallel to the core, filled w/ white, zeolitic material.
ADDITIONAL COMMENTS: Pieces 1-6 are brecciated with clasts of the mafic rock described above and are a continuation of Section 41R-4.

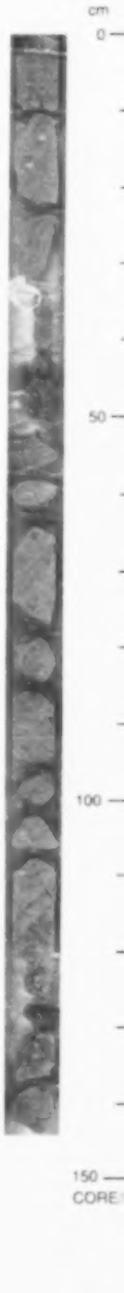
cm
0
50
100
150
CORE

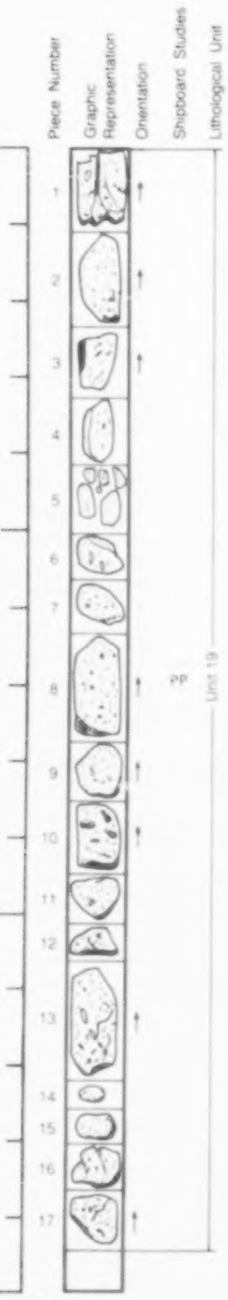
Piece Number
Graphic Representation
Orientation
Shipboard Studies
Lithological Unit
1
2
3
4
5
6
7
8
9
10
11
12
13
14
15
16
17
PP
Unit 19
E/SECTION

125-786B-42R-2

UNIT 19: TWO-PYROXENE, OLIVINE, BEARING ANDESITE

Pieces 1-17

CONTACTS: None visible.
PHENOCRYSTS: Glomerocrysts of pyroxene and plagioclase.
Plagioclase - 5%, <1.5 mm, equant laths.
Clinopyroxene - 8%, 1 mm, euhedral, tabular.
Orthopyroxene - 6%, 0.7 mm, euhedral, equant.
Olivine - trace, <1.5 mm, euhedral, elongate.
GROUNDMASS: Fine-grained to glassy with feldspar laths.
VESICLES: 2-5%, <1-3 mm, elongate, irregular, throughout.
COLOR: Greenish gray (5B 6/1).
STRUCTURE: Massive.
ALTERATION: Minor, pervasive chlorite and hematite alteration; hematite alteration of olivine and some orthopyroxene phenocrysts.
VEINS/FRACTURES: <1%, 1-2 mm wide, sub-parallel to core axis, only present in Piece 1, filled with green, amorphous material (chlorite?).

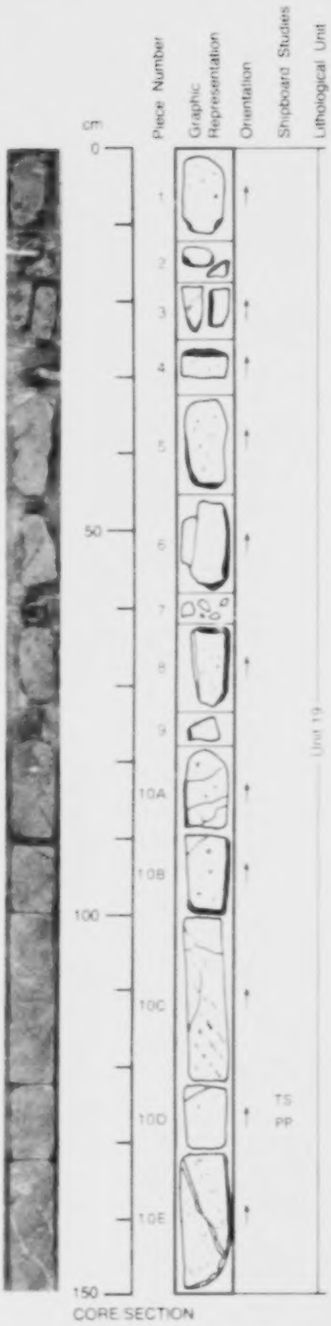
cm
Piece Number
Graphic Representation
Orientation
Shipboard Studies
Lithological Unit
0
50
100
150
1
2
3
4
5
6
7
8
9
10A
10B
10C
10D
10E
TS
PP
Unit 19
CORE SECTION

125-786B-42R-3

UNIT 19: TWO-PYROXENE, OLIVINE-BEARING ANDESITE (CONTINUATION OF 42R-2)

Pieces 1-10

CONTACTS: None visible.
PHENOCRYSTS: Glomerocrysts of pyroxene and plagioclase.
Plagioclase - 5%, <1.5 mm, equant laths.
Clinopyroxene - 4%, 1 mm, euhedral, tabular.
Orthopyroxene - 8%, 2-7 mm, euhedral, equant, minor alteration to hematite.
Olivine - trace, <1.5 mm, euhedral, elongate.
GROUNDMASS: Fine-grained to glassy with feldspar laths.
VESICLES: 1-5%, 1-3 mm, elongate, ragged, throughout; locally aligned similar to pipe vesicles and locally concentrated.
COLOR: Greenish gray (5BG 6/1).
STRUCTURE: Massive.
ALTERATION: Minor pervasive chlorite and hematite alteration; hematite alteration of olivine phenocrysts.
VEINS/FRACTURES: <1%, 1-3 mm, sub-parallel to core axis, only in Piece 10, especially Piece 10F.
ADDITIONAL COMMENTS: This section is a continuation of 42R-1 through 42R-2.

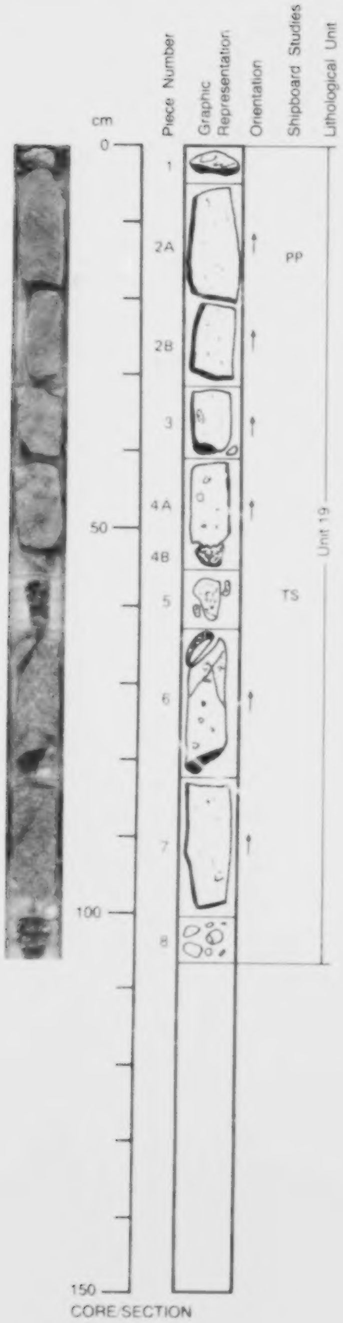

125-786B-42R-4

UNIT 19: TWO-PYROXENE, OLIVINE BEARING ANDESITE (CONTINUATION OF 42R-3)

Pieces 1-4

CONTACTS: None visible.
PHENOCRYSTS: Glomerocrysts of pyroxene and plagioclase.
Plagioclase - 5%, <1.5 mm, equant laths.
Clinopyroxene - 4%, 1 mm, euhedral, equant.
Orthopyroxene - 6%, 0.7 mm, euhedral, equant.
Olivine - trace, <1.5 mm, euhedral, elongate.
GROUNDMASS: Fine-grained to glassy with feldspar laths.
VESICLES: 2-4%, 1-5 mm, elongate, ragged; throughout, locally concentrated; some are filled with Fe-oxide and some with carbonate.
COLOR: Greenish gray (5BG 6/1).
STRUCTURE: Massive.
ALTERATION: Minor pervasive chlorite and hematite alteration; hematite alteration of olivine and some orthopyroxene phenocrysts.
VEINS/FRACTURES: Small, carbonate-filled vein on the edge of Piece 1.
ADDITIONAL COMMENTS: This section is a continuation of Section 42R-3.

UNIT 19: TWO-PYROXENE, OLIVINE BEARING ANDESITE

Pieces 5-8

CONTACTS: None visible.
PHENOCRYSTS: Glomerocrysts of pyroxene and plagioclase.
Plagioclase - 5%, <1.5 mm, euhedral to lath-shaped.
Orthopyroxene - 10%, <1.5 mm, euhedral, equant.
Clinopyroxene - 3-5%, <2.5 mm, euhedral, tabular.
Olivine - 1-2%, <3 mm, euhedral.
GROUNDMASS: Fine-grained to glassy with microliths of feldspar.
VESICLES: 3-5%, 1-5 mm, elongate, ragged; throughout, filled with carbonate.
COLOR: Weak red (2.5YR 5/2).
STRUCTURE: Massive.
ALTERATION: Pervasive chlorite and hematite alteration, olivine phenocrysts altering to hematite/carbonate assemblage.
VEINS/FRACTURES: <1%, <1 mm wide, subvertical, filled with carbonate.
ADDITIONAL COMMENTS: These pieces are more oxidized (redder) than overlying unit.

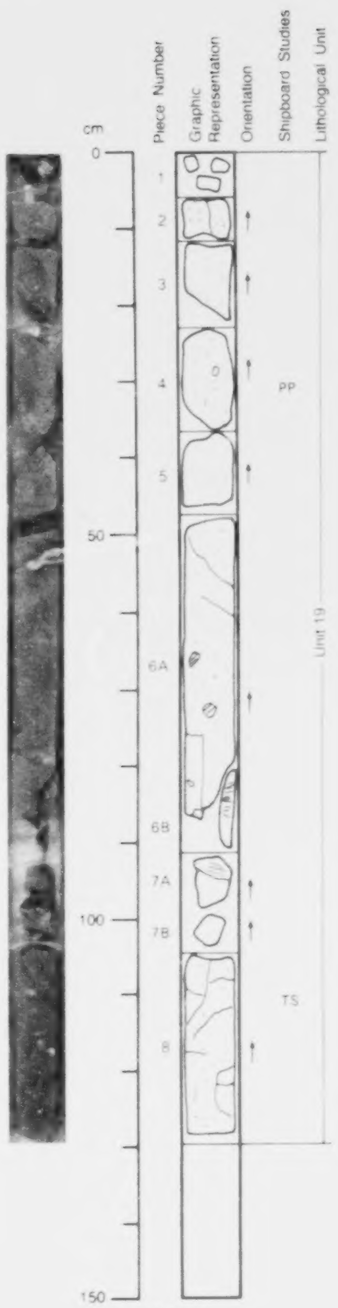
cm
Piece Number
Graphic Representation
Orientation
Shipboard Studies
Lithological Unit
0
50
100
150
1
2
3
4
5
6A
6B
7A
7B
8
PP
TS
Unit 19
CORE SECTION

125-786B-43R-1

UNIT 19: TWO-PYROXENE, OLIVINE, PLAGIOCLASE ANDESITE (42R-4 CONTINUED)

Pieces 1-8

CONTACTS: None visible
PHENOCRYSTS: Plagioclase with opaque inclusions
Plagioclase - 5-10%, <3 mm, euhedral prisms
Orthopyroxene - 5-8%, <3 mm, yellow, subhedral
Clinopyroxene - 5-8%, <3 mm, dark-green, subhedral
Olivine - 3%, <2 mm, altered to hematite and carbonate
GROUNDMASS: Glassy with abundant microcrystalline magnetite
VESICLES: 2-5%, <2 mm, round, random distribution
COLOR: Gray to weak red (N 5/0 - 2.5YR 5/2)
STRUCTURE: Massive
ALTERATION: Magnetite from groundmass gives red hematite stains; olivine is completely altered
VEINS/FRACTURES: Trace, <0.5 mm, random orientation; fractures have chlorite on surface; some calcite present
ADDITIONAL COMMENTS: Strike slip slickensides in chlorite on fracture surface in Pieces 6 and 7

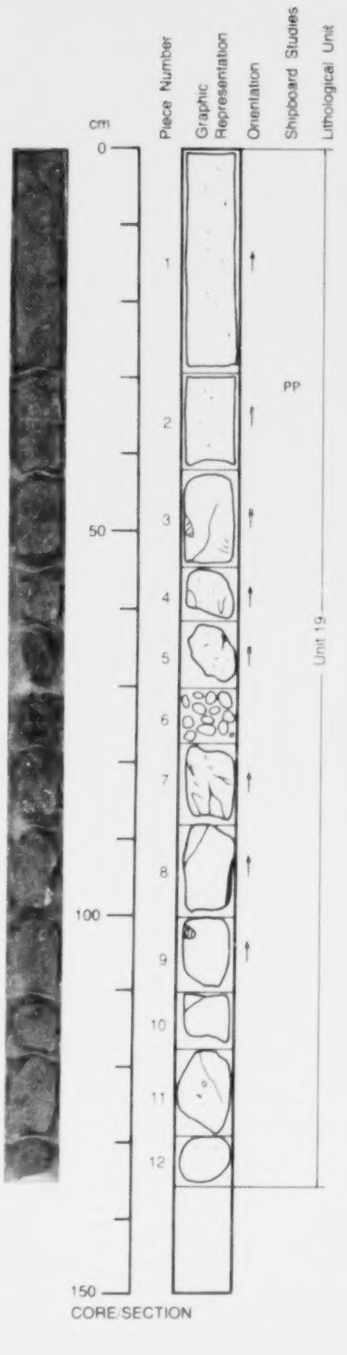
cm
Piece Number
Graphic Representation
Orientation
Shipboard Studies
Lithological Unit
0
50
100
150
1
2
3
4
5
6
7
8
9
10
11
12
PP
Unit 19
CORE/SECTION

125-786B-43R-2

UNIT 19: TWO-PYROXENE, PLAGIOCLASE ANDESITE

Pieces 1-12

CONTACTS: None visible
PHENOCRYSTS:
Plagioclase - 10-15%, <3 mm, euhedral.
Orthopyroxene - 10-15%, <3 mm, yellow, subhedral.
Clinopyroxene - 5-10%, <3 mm, dark green, subhedral.
Olivine - trace, <1 mm.
GROUNDMASS: Glassy with less magnetite than in 43R-1.
VESICLES: 5%, <2 mm, round to irregular, random distribution.
COLOR: Dark greenish gray (5GY 4/1 - 5G 4/1) locally reddish.
STRUCTURE: Massive.
ALTERATION: Orthopyroxene is altered to serpentine, olivine is altered to hematite and carbonate.
VEINS/FRACTURES: Trace, < 2 mm, random orientation, filled with calcite.
ADDITIONAL COMMENTS: Piece 1 is similar rock type to 43R-1.

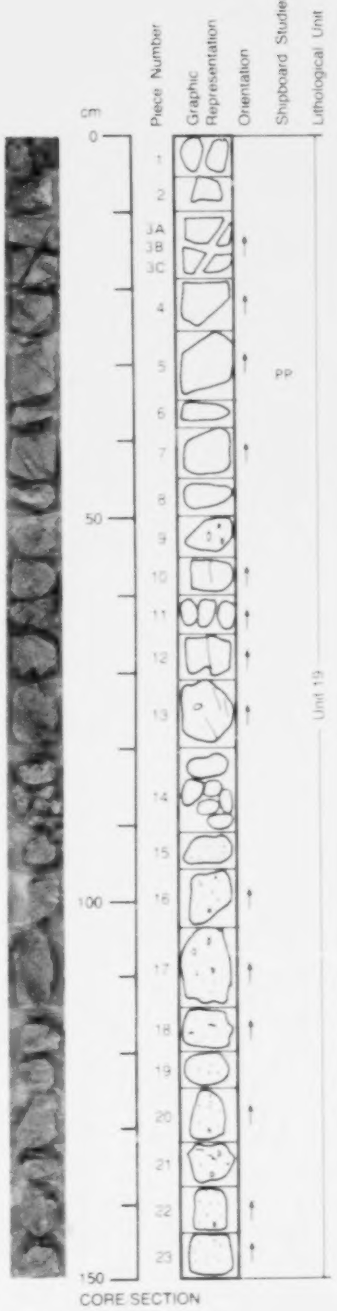
cm
0
50
100
150
CORE SECTION
Piece Number
Graphic Representation
Orientation
Shipboard Studies
Lithological Unit
1
2
3A
3B
3C
4
5
6
7
8
9
10
11
12
13
14
15
16
17
18
19
20
21
22
23
PP
Unit 19

125-786B-44R-1

UNIT 19: META-ANDESITE

Pieces 1-23

CONTACTS: None visible
PHENOCRYSTS:
Clinopyroxene - 5%, <2 mm, subhedral
GROUNDMASS: Altered glass and plagioclase
VESICLES: 0-1%, <4 mm, round; locally present
COLOR: Greenish gray (5GY 5/1)
STRUCTURE: Massive
ALTERATION: Rock is pervasively altered to very low grade mineralogy
VEINS/FRACTURES: Trace, < 0.3 mm, sub-vertical, filled with calcite
ADDITIONAL COMMENTS: Probably sparsely phyric, clinopyroxene andesite; more clinopyroxene below 90 cm (Pieces 15-23)

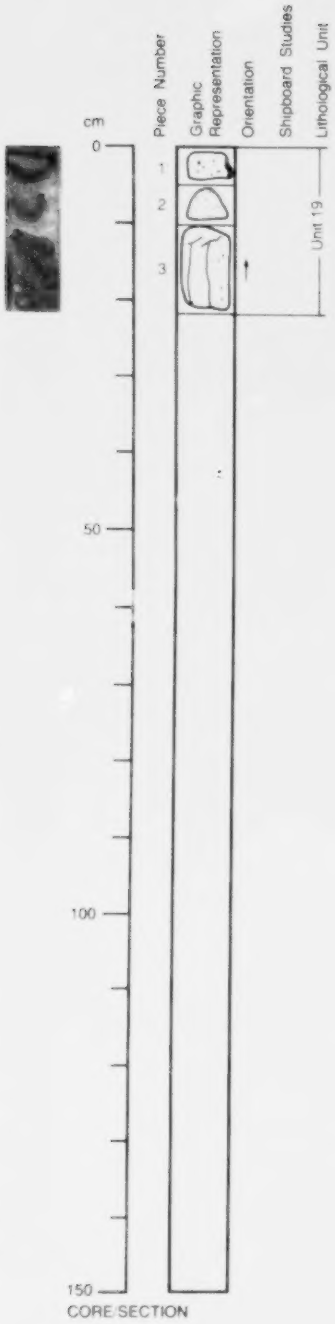
cm
Piece Number
Graphic Representation
Orientation
Shipboard Studies
Lithological Unit
0
50
100
150
1
2
3
Unit 19
CORE/SECTION

125-786B-44R-2

UNIT 19: META-ANDESITE

Pieces 1-2

CONTACTS: None visible
PHENOCRYSTS:
Clinopyroxene - 10-15%, <3 mm, euhedral, light green
GROUNDMASS: Altered glass and plagioclase
VESICLES: Trace, 1-2 mm, round, locally present
COLOR: Greenish gray (10Y 5/1)
STRUCTURE: Massive
ALTERATION: Pervasively altered to very low grade mineral assemblage
VEINS/FRACTURES: Absent
ADDITIONAL COMMENTS: Continuation of 125-786B-44R-1, 90-140 cm

UNIT 1: TWO-PYROXENE, PLAGIOCLASE, OLIVINE BRECCIATED ANDESITE

Piece 3

CONTACTS: Not visible
PHENOCRYSTS:
Plagioclase - 10-15%, < 3 mm, euhedral
Orthopyroxene - 3-5%, <3 mm, euhedral, yellow
Clinopyroxene - 5-10%, <3 mm, euhedral, dark green
Olivine - trace, <1 mm, altered to red spots
GROUNDMASS: Glassy with plagioclase crystals
VESICLES: 2%, <2 mm, flattened, randomly distributed
COLOR: Dark green (5BG 4/1) with light green (10Y 6/6) and red streaks from alteration
STRUCTURE: Massive
ALTERATION: Glass alters to green-colored product
VEINS/FRACTURES: Trace, < 0.2 mm, sub-vertical, probably filled with chlorite and zeolite

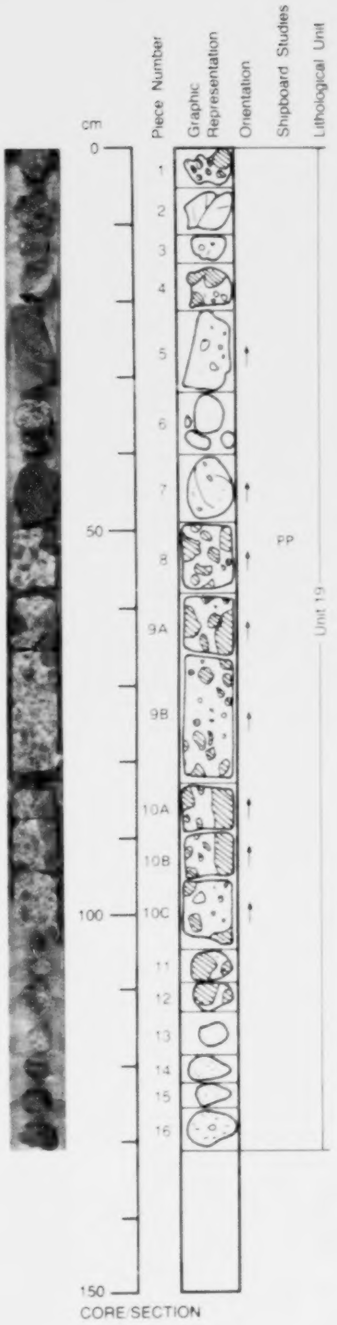
cm
Piece Number
Graphic Representation
Orientation
Shipboard Studies
Lithological Unit
0
50
100
150
1
2
3
4
5
6
7
8
9A
9B
10A
10B
10C
11
12
13
14
15
16
PP
Unit 19
CORE/SECTION

125-786B-45R-1

UNIT 19: TWO-PYROXENE, PLAGIOCLASE, OLIVINE ANDESITE-BRECCIA (44R-2 CONTINUED)

Pieces 1-16

CONTACTS: One visible
PHENOCRYSTS: Fresh
Plagioclase - 10-15%, <2 mm, euhedral
Orthopyroxene - 10%, <3 mm, yellow, euhedral, equant
Clinopyroxene - 5%, <2 mm, dark green, columnar
Olivine - trace, <2 mm, altered to red product
GROUNDMASS: Glassy with some plagioclase crystals
VESICLES: 5-8%, <4 mm, some 1 cm in size, round to elongate, randomly distributed, blue coating
COLOR: Dark bluish gray (5B 4/1) to greenish yellow (5Y 7/4) in brecciated zones
STRUCTURE: Brecciated
ALTERATION: Breccia matrix is altered to yellow green product
VEINS/FRACTURES: Absent
ADDITIONAL COMMENTS: Oligomictic breccia, continuation of 125-786B-44R-2, 10cm. Pieces 5-7 are single fragments without breccia matrix, matrix-dominated from Piece 8-12.

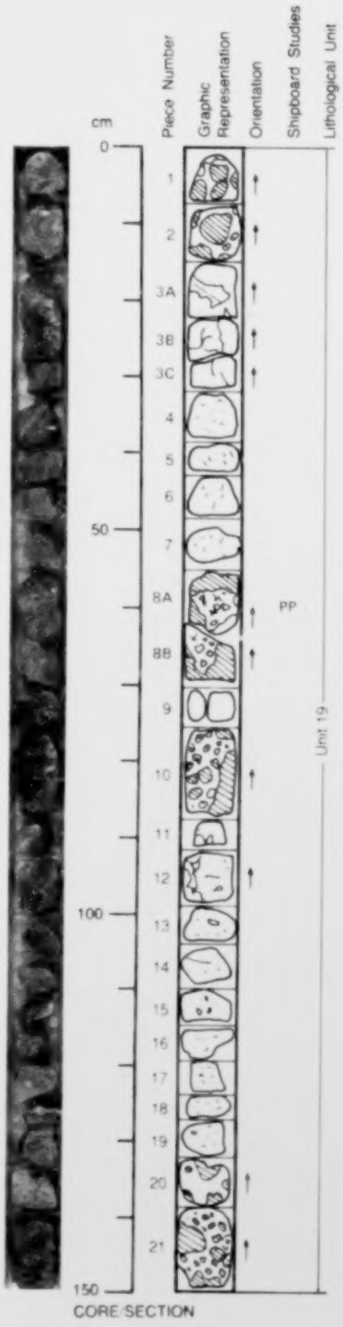
cm
0
50
100
150
Piece Number
Graphic Representation
Orientation
Shipboard Studies
Lithological Unit
1
2
3A
3B
3C
4
5
6
7
8A
8B
9
10
11
12
13
14
15
16
17
18
19
20
21
PP
Unit 19
CORE/SECTION

125-786B-46R-1

UNIT 19: TWO-PYROXENE, PLAGIOCLASE, OLIVINE ANDESITE BRECCIA

Pieces 1-21

CONTACTS: None visible.
PHENOCRYSTS: Fresh.
Plagioclase - 10%, <2 mm, euhedral.
Orthopyroxene - 5%, <3 mm, yellow, equant, euhedral.
Clinopyroxene - 10%, <2 mm, dark green, columnar.
Olivine - trace, <2 mm, altered to red product.
GROUNDMASS: Glassy with some plagioclase crystals.
VESICLES: 5-8%, <4 mm, some 1 cm in size, round to elongate, randomly distributed, blue coating.
COLOR: Dark bluish gray (5B 4/1) to greenish yellow (5Y 7/4) in brecciated zones.
STRUCTURE: Brecciated.
ALTERATION: Breccia matrix is altered yellow green product.
VEINS/FRACTURES: Absent.
ADDITIONAL COMMENTS: Oligomictic breccia; continuation of 125-786B-44-2, 10 cm. Piece 4-7 and 14-19 are single fragments without breccia matrix. Pieces 20 and 21 are vuggy.

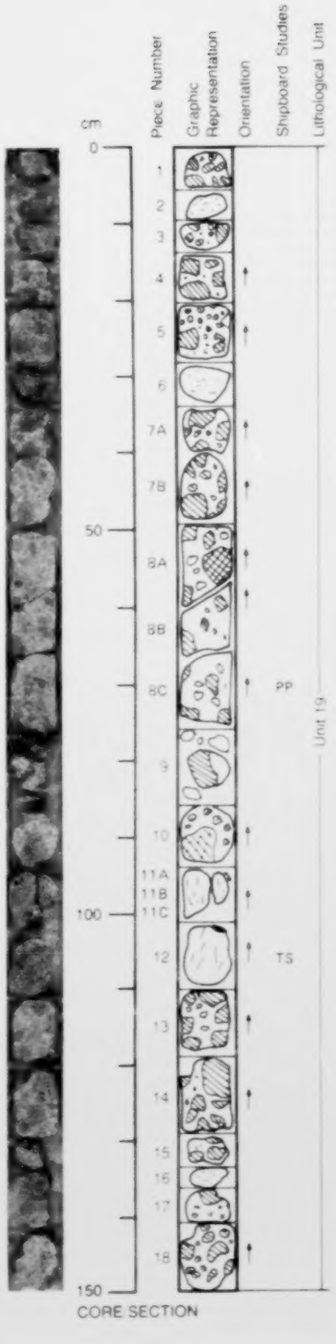
cm
Piece Number
Graphic Representation
Orientation
Shipboard Studies
Lithological Unit
0
50
100
150
1
2
3
4
5
6
7A
7B
8A
8B
8C
9
10
11A
11B
11C
12
13
14
15
16
17
18
PP
TS
Unit 19
CORE SECTION

125-786B-46R-2

UNIT 19: TWO-PYROXENE, PLAGIOCLASE, OLIVINE ANDESITE BRECCIA

Pieces 1-18

CONTACTS: None visible.
PHENOCRYSTS: Fresh.
Plagioclase - 10%, <2 mm, euhedral.
Orthopyroxene - 5%, <3 mm, yellow, equant.
Clinopyroxene - 10%, <2 mm, dark green, columnar.
Olivine - trace, <2 mm.
GROUNDMASS: Glassy with some plagioclase crystals.
VESICLES: 5-8%, <4 mm, some 1 cm in size, round and elongate, randomly distributed, blue coating.
COLOR: Dark bluish gray (5B 4/1) to greenish yellow (5Y 7/4) in brecciated zones.
STRUCTURE: Brecciated.
ALTERATION: Breccia matrix is altered yellow-green product, olivine phenocryst is altered to red product.
VEINS/FRACTURES: Absent.
ADDITIONAL COMMENTS: Oligomictic breccia, continuation of 125-786B-44-2, 10cm. Piece 6 a single fragment without breccia matrix.

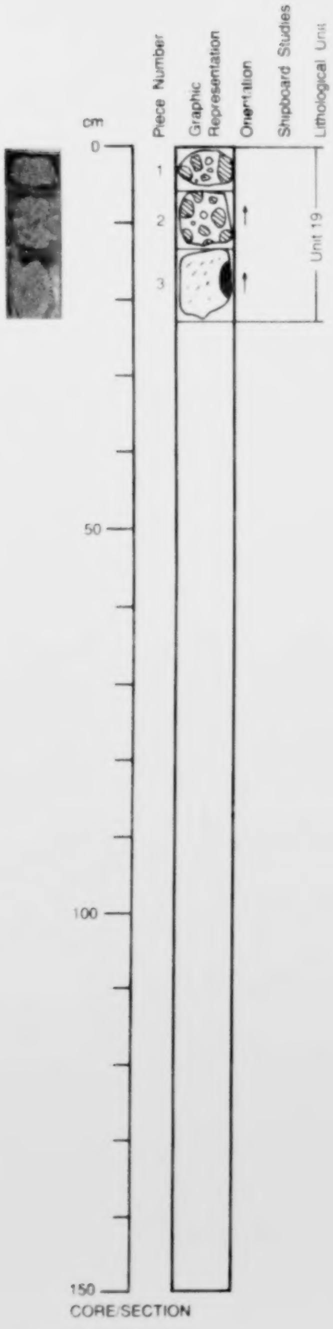
cm
Piece Number
Graphic Representation
Orientation
Shipboard Studies
Lithological Unit
0
1
2
3
Unit 19
50
100
150
CORE/SECTION

125-786B-46R-3

UNIT 19: TWO-PYROXENE, PLAGIOCLASE, OLIVINE ANDESITE BRECCIA

Pieces 1-3

CONTACTS: None visible.
PHENOCRYSTS: Fresh.
Plagioclase - 10%, <2 mm, euhedral.
Orthopyroxene - 5%, <3 mm, yellow, equant.
Clinopyroxene - 10%, <2 mm, dark green, columnar.
Olivine - trace, < 2 mm , altered to red product.
GROUNDMASS: Glassy with some plagioclase crystals.
VESICLES: 5-8%, <4 mm, some 1 cm in size, round and elongate; randomly distributed; blue coating.
COLOR: Dark bluish gray (5B 4/1) to greenish yellow (5Y 7/4) in brecciated zones.
STRUCTURE: Brecciated.
ALTERATION: Breccia matrix is altered yellow-green product.
VEINS/FRACTURES: Absent.
ADDITIONAL COMMENTS: Oligomictic breccia, continuation of 125-786B-44-2, 10cm. Piece 3 contains an orthopyroxene-rich pyroxenite xenolith.

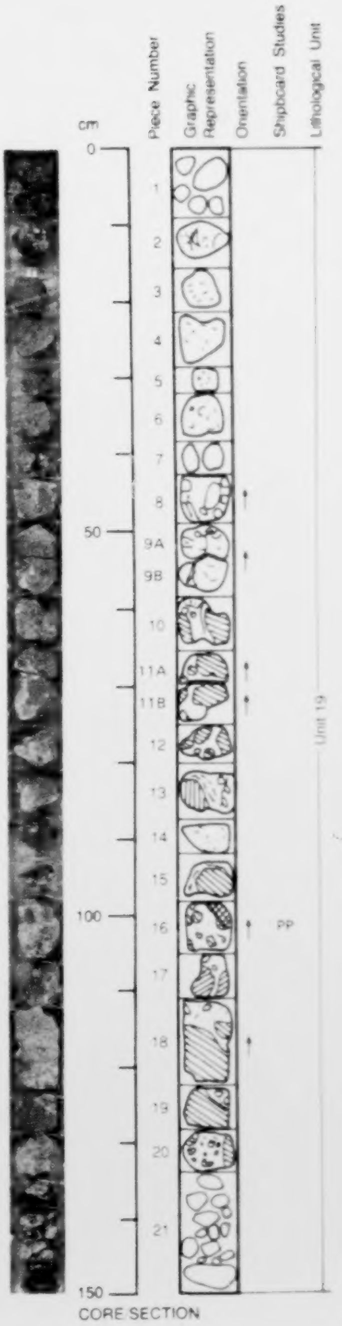
cm
Piece Number
Graphic Representation
Orientation
Shipboard Studies
Lithological Unit
0
50
100
150
1
2
3
4
5
6
7
8
9A
9B
10
11A
11B
12
13
14
15
16
17
18
19
20
21
PP
Unit 19
CORE SECTION

125-786B-47R-1

UNIT 19: TWO-PYROXENE, PLAGIOCLASE, OLIVINE ANDESITE BRECCIA (46R-3 CONTINUED).

Pieces 1-21

CONTACTS: None visible.
PHENOCRYSTS: Fresh in unaltered glassy rock portions.
Plagioclase - 10%, <2 mm, euhedral.
Orthopyroxene - 5-10%, <2 mm, subhedral.
Clinopyroxene - 5-10%, <2 mm, subhedral.
Olivine - trace, <1 mm.
GROUNDMASS: Glassy with plagioclase crystals; green, chlorite-rich in breccia matrix.
VESICLES: 5-20%, variable (1-10 mm), round to elongate, random within each fragment, bluish coating.
COLOR: Dark bluish gray (5B 4/1) to greenish yellow (5Y 7/4).
STRUCTURE: Brecciated.
ALTERATION: Breccia matrix is altered to chlorite-bearing product; clasts are fresh with locally altered rims; olivine phenocrysts altered to reddish product.
VEINS/FRACTURES: Absent.
ADDITIONAL COMMENTS: Continuation of 125-786B-45R-1 - oligomictic breccia.

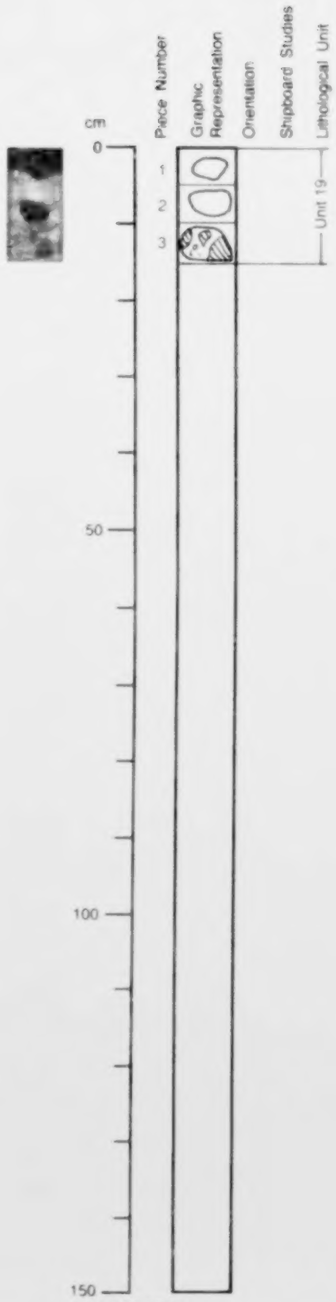
cm
Piece Number
Graphic Representation
Orientation
Shipboard Studies
Lithological Unit
0
1
2
3
Unit 19
50
100
150
CORE/SECTION

125-786B-47R-2

UNIT 19: TWO-PYROXENE, PLAGIOCLASE ANDESITE BRECCIA (47R-1 CONTINUED)

Pieces 1-3

CONTACTS: None visible.
PHENOCRYSTS: Fresh in unaltered glassy rock portions.
Plagioclase - 10%, <2 mm, euhedral.
Orthopyroxene - 5-10%, <2 mm, subhedral.
Clinopyroxene - 5-10%, <2 mm, subhedral.
Olivine - trace, <1 mm.
GROUNDMASS: Glassy with plagioclase crystals; green, chlorite-rich in breccia matrix.
VESICLES: 5-20%, variable (1-10 mm), round to elongate, random within each fragment, bluish coating.
COLOR: Dark bluish gray (5B 4/1) to greenish yellow (5Y 7/4).
STRUCTURE: Breccia matrix is altered to chlorite-bearing product, clasts are fresh with locally altered rims; olivine phenocrysts altered to reddish product.
ALTERATION: Brecciated.
VEINS/FRACTURES: Absent.
ADDITIONAL COMMENTS: Continuation of 125-786B-45R-1, oligomictic breccia.

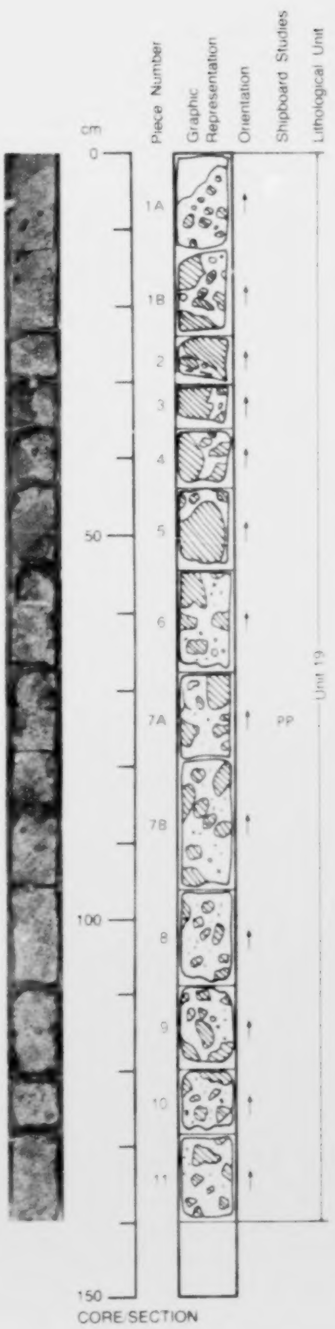
cm
Piece Number
Graphic Representation
Orientation
Shipboard Studies
Lithological Unit
0
50
100
150
1A
1B
2
3
4
5
6
7A
7B
8
9
10
11
PP
Unit 19
CORE/SECTION

125-786B-48R-1

UNIT 19: TWO-PYROXENE, PLAGIOCLASE ANDESITE BRECCIA

Pieces 1-11

CONTACTS: None visible.

PHENOCRYSTS: Fresh in unaltered glassy rock portions.
Plagioclase - 10%, <2 mm, subhedral.
Orthopyroxene - 5-10%, <2 mm, subhedral.
Clinopyroxene - 5-10%, <2 mm, subhedral.
Olivine - trace, <1 mm, altered to reddish product.

GROUNDMASS: Glassy with plagioclase crystals, green, chlorite-rich in breccia matrix.

VESICLES: 5-20%, variable (1-10 mm), round to elongate, randomly distributed, blue coating.

COLOR: Matrix is pale green (5G 6/2); clasts are gray (N 6/) to dark gray (N4/ to 5Y 4/1).

STRUCTURE: Brecciated.

ALTERATION: Breccia matrix is altered to chlorite-bearing product; clasts are fresh with locally altered rims.

VEINS/FRACTURES: Absent.

ADDITIONAL COMMENTS: Continuation of 125-786B-45R-1. The amount of matrix increases toward the bottom of the section and rare, different clast lithologies are present (probably welded tuffs).

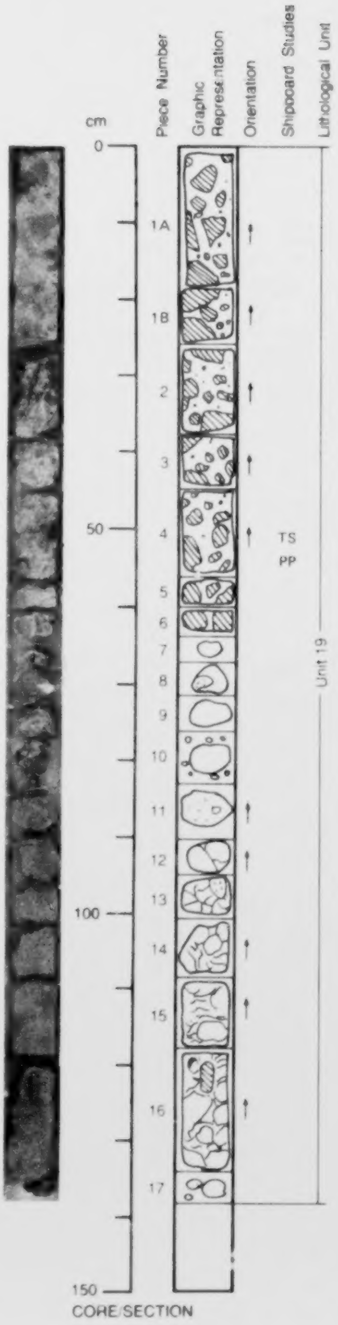
cm
0
50
100
150
CORE/SECTION
Piece Number
Graphic Representation
Orientation
Shipboard Studies
Lithological Unit
1A
1B
2
3
4
5
6
7
8
9
10
11
12
13
14
15
16
17
TS
PP
Unit 19

125-786B-48R-2

UNIT 19: TWO-PYROXENE, PLAGIOCLASE ANDESITE BRECCIA (47R-1 CONTINUED)

Pieces 1-17

CONTACTS: None visible
PHENOCRYSTS: Fresh in glassy unaltered rock portions.
Plagioclase - 10%, <2 mm, euhedral.
Orthopyroxene - 5-10%, <2 mm, subhedral.
Clinopyroxene - 5-10%, <2 mm, subhedral.
Olivine - trace, <1 mm.
GROUNDMASS: Glassy with plagioclase crystals; green, chlorite-rich in breccia matrix.
VESICLES: 5-20%; variable (1-10 mm); round to elongate; randomly distributed; bluish coating.
COLOR: Pale green (5G 6/2) matrix, clasts are gray (N 4/) to dark gray (5Y 4/1).
STRUCTURE: Brecciated.
ALTERATION: Breccia matrix is altered to chlorite-bearing product, clasts are fresh with locally altered rims; olivine phenocrysts altered to reddish product.
VEINS/FRACTURES: 0%; 0; 0.
ADDITIONAL COMMENTS: Continuation of 125-786B-45R-1. Below 83 cm (Piece 11) the section is pervasively fractured and oxidized along the fractures; identical mineralogy.

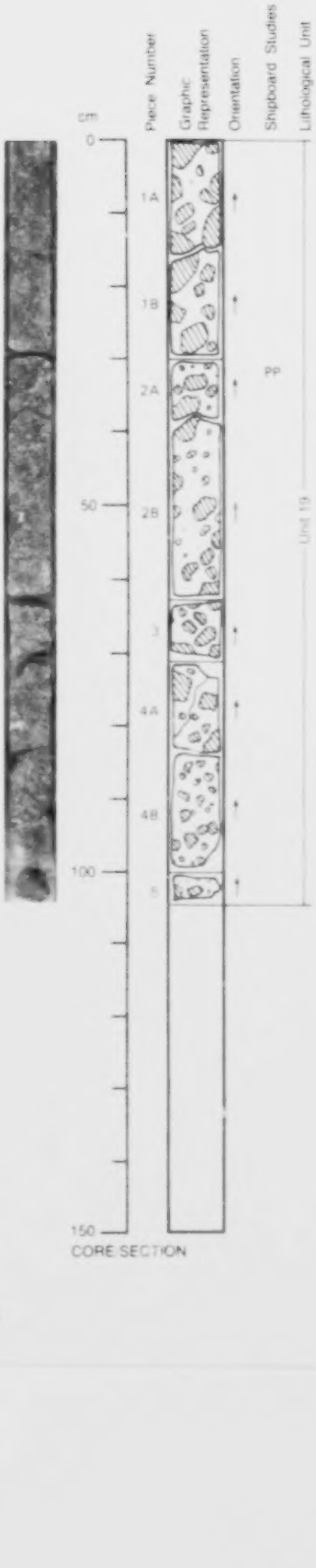
cm
0
50
100
150
CORE SECTION
Piece Number
Graphic Representation
Orientation
Shipboard Studies
Lithological Unit
1A
1B
2A
2B
3
4A
4B
5
PP
Unit 19

125-786B-49R-1

UNIT 19: TWO-PYROXENE ANDESITE BRECCIA

Pieces 1-5

CONTACTS: None visible.
PHENOCRYSTS: For most clasts:
Plagioclase - 5-10%; <2 mm; euhedral.
Orthopyroxene - 2-5%; <2 mm; subhedral.
Clinopyroxene - 2-5%; <2 mm; subhedral.
GROUNDMASS: Clasts have glassy to very fine-grained groundmass with
microliths and are pervasively altered; greenish alteration in matrix.
VESICLES: 1-15%; 0.1-10 mm; some flattened and aligned; variable dist
white coating to vesicles.
COLOR: Pale green (5G 6/2) matrix; clasts are mainly gray, 10YR 2.1 in fre
4/1 in most altered examples; a few clasts are reddish brown (5YR 6/4
STRUCTURE:
ALTERATION: Breccia matrix is altered to green and white minerals; glas
to clay minerals, and some, but not all, have alteration rims at their mar
VEINS/FRACTURES: Absent.
ADDITIONAL COMMENTS: Smaller clasts are less vesicular, finer graine
highly altered; clasts range in size from 2 mm to 6 cm in longest dimen
are subangular-rounded, and smaller clasts are rounded; vitric matrix.

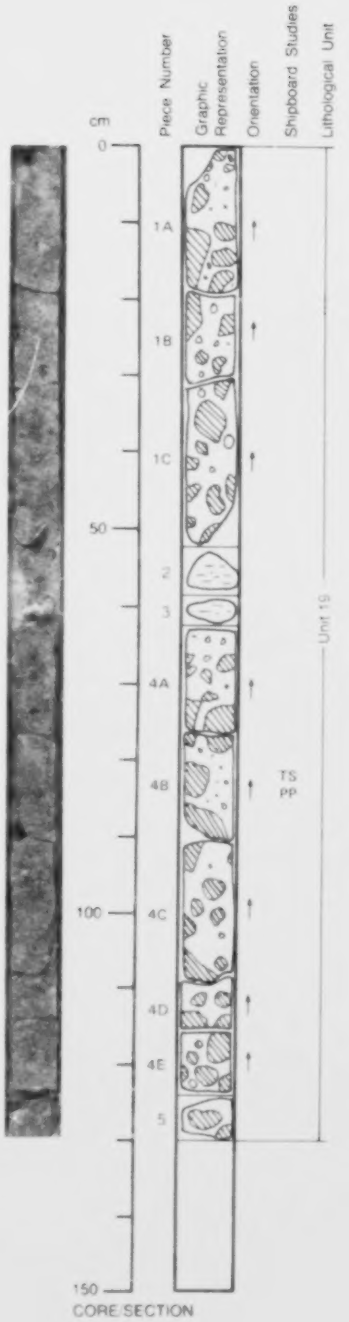
cm
0
50
100
150
Piece Number
Graphic Representation
Orientation
Shipboard Studies
Lithological Unit
1A
1B
1C
2
3
4A
4B
4C
4D
4E
5
TS
PP
Unit 19
CORE/SECTION

125-786B-49R-2

UNIT 19: TWO-PYROXENE ANDESITE BRECCIA

Pieces 1-5

CONTACTS: None visible.
PHENOCRYSTS: For most clasts
Plagioclase - 5-10%, <2 mm, euhedral.
Orthopyroxene - 3-5%, <2 mm, subhedral.
Clinopyroxene - 2-3%, <2 mm, subhedral.
GROUNDMASS: Clasts have glassy to very fine-grained groundmass with plagioclase microliths and are pervasively altered.
VESICLES: 1-15%, variable distribution - within and between clasts 1-10 mm, some flattened and aligned; bluish-white coating to vesicles.
COLOR: Pale green (5G 6/2) matrix, clasts are mainly gray, 10YR 2/1 in freshest and 10YR 4/1 in most altered; a few clasts are reddish brown (10R 4/8).
STRUCTURE: N/A
ALTERATION: Breccia matrix is altered to green and white minerals, glass in clasts altered to clay minerals, and some, but not all, have alteration rims.
VEINS/FRACTURES: Absent.
ADDITIONAL COMMENTS: Smaller clasts are less vesicular, finer-grained and more highly altered; clasts range in size from 2 mm to 6 cm in longest dimension; larger clasts are subangular-rounded, and smaller clasts are rounded; more red clasts towards the base of the section; vitric matrix.

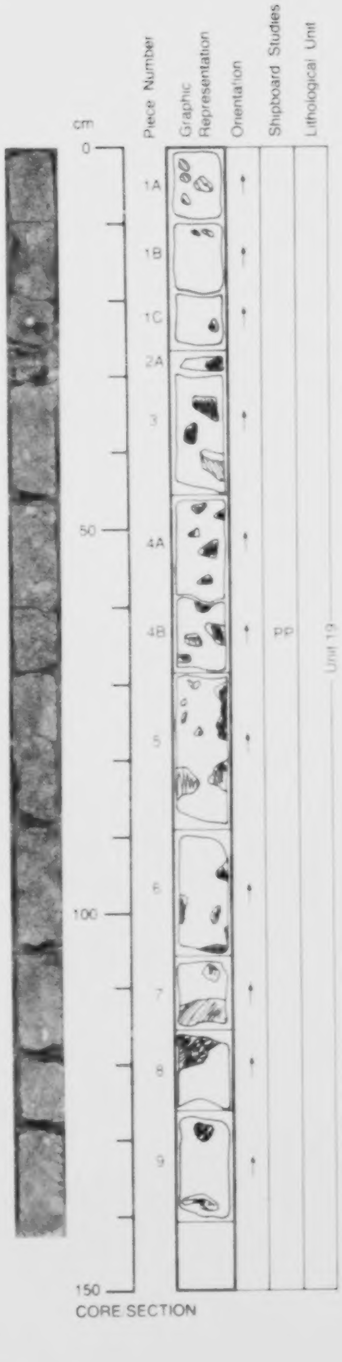
cm
Piece Number
Graphic Representation
Orientation
Shipboard Studies
Lithological Unit
0
50
100
150
1A
1B
1C
2A
3
4A
4B
5
6
7
8
9
PP
Unit 19
CORE SECTION

125-786B-49R-3

UNIT 19: TWO-PYROXENE ANDESITE BRECCIA

Pieces 1-9

CONTACTS: None visible.
PHENOCRYSTS: For most clasts.
Plagioclase - 5-10%, <2 mm, euhedral.
Orthopyroxene - 2-5%, <2 mm, subhedral.
Clinopyroxene - 2-5%, <2 mm, subhedral.
GROUNDMASS: Clasts have glassy to very fine-grained groundmass with plagioclase microliths and are pervasively altered.
VESICLES: 1-15%, 0.1-10 mm, flattened and aligned, variable distribution within clasts; bluish white coating to vesicles.
Miaroles: some.
COLOR: Red brown (10R 4/4) in matrix; clasts vary enormously in color to give most shades of gray to green; a few clasts are red brown.
STRUCTURE: N/A.
ALTERATION: Clasts are red brown; breccia matrix is altered to red brown oxides and clays; clasts show pervasively low-grade alteration.
VEINS/FRACTURES: Absent.
ADDITIONAL COMMENTS: Smaller clasts are less vesicular, finer grained and more highly altered; clasts range in size from 2 mm to 6 cm in longest dimension; larger clasts are subangular-rounded, and smaller clasts are rounded; vitric matrix.

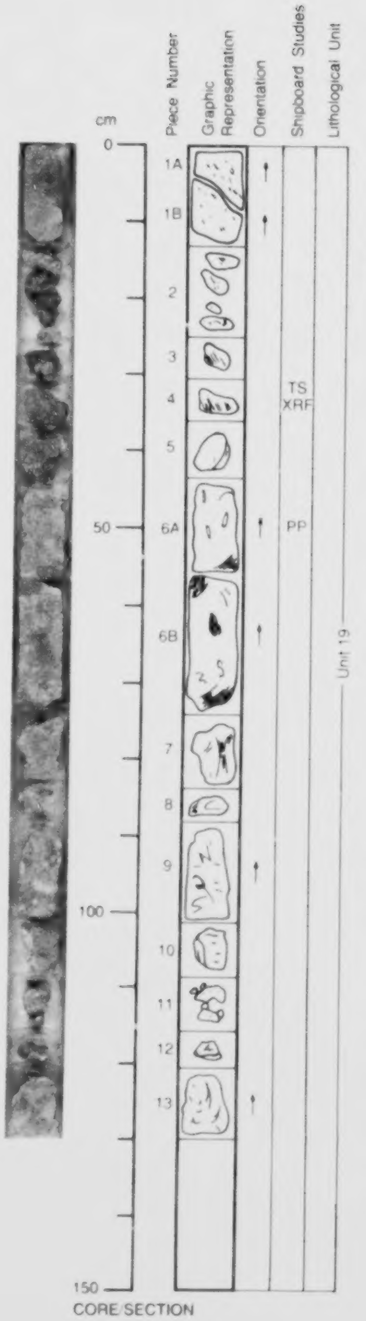
cm
Piece Number
Graphic Representation
Orientation
Shipboard Studies
Lithological Unit
0
50
100
150
1A
1B
2
3
4
5
6A
6B
7
8
9
10
11
12
13
TS
XRF
PP
Unit 19
CORE/SECTION

125-786B-49R-4

UNIT 19: TWO-PYROXENE ANDESITE BRECCIA

Pieces 1-13

CONTACTS: None visible
PHENOCRYSTS: For clasts
Plagioclase: 5-10%, <2 mm, euhedral
Orthopyroxene: 2-5%, <2 mm, subhedral
Clinopyroxene: 2-5%, <2 mm, subhedral
GROUNDMASS: Glassy clasts have very fine grained groundmass and are variably but pervasively altered.
VESICLES: 1-15%, 0.1-10 mm, flattened and aligned, variable distribution within clasts; bluish white coating to vesicles.
Miaroles: Some
COLOR: Grayish green (10G 4/2) to dusky yellowish green (10G 3/2) matrix; clasts are mainly gray, (10YR 2/1) in freshest and (10YR 4/1) in most altered examples; a few clasts are reddish brown (10R 4/8).
STRUCTURE: N/A
ALTERATION: Breccia matrix is altered to green and white minerals; clasts exhibit low-grade alteration and some have altered margins.
VEINS/FRACTURES: One irregular fracture with white mineral on fracture walls.
ADDITIONAL COMMENTS: Smaller clasts are less vesicular, finer grained and more highly altered; clasts range in size from 2 mm upwards; vitric matrix.

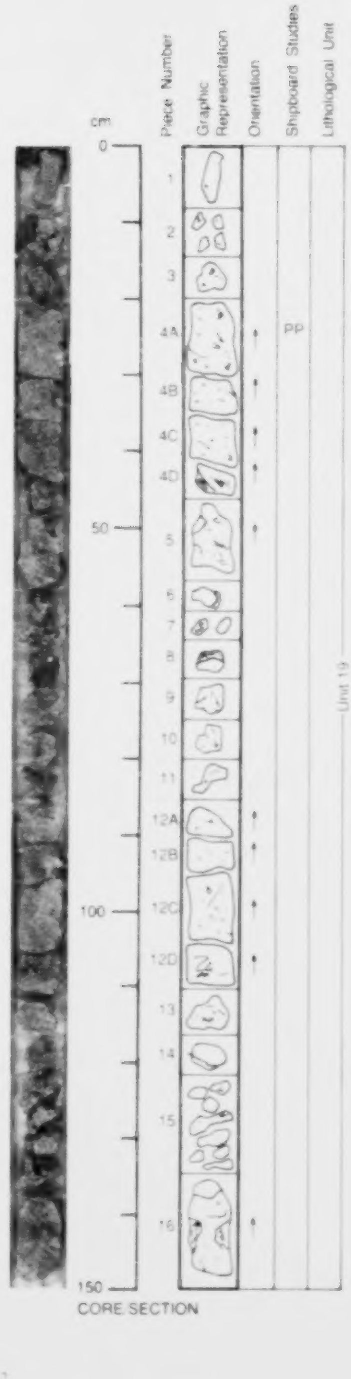
cm
Piece Number
Graphic Representation
Orientation
Shipboard Studies
Lithological Unit
0
50
100
150
1
2
3
4A
4B
4C
4D
5
6
7
8
9
10
11
12A
12B
12C
12D
13
14
15
16
PP
Unit 19
CORE SECTION

125-786B-50R-1

UNIT 19: TWO-PYROXENE ANDESITE BRECCIA

Pieces 1-16

CONTACTS: None visible.
PHENOCRYSTS: For clasts
Plagioclase - 5-10%, <2 mm, euhedral.
Orthopyroxene - 2-5%, <2 mm, subhedral.
Clinopyroxene - 2-5%, <2 mm, subhedral.
GROUNDMASS: Clasts are pervasively altered, and have a very fine grained to glassy groundmass with plagioclase microliths.
VESICLES: 1-15%, 0.1-10 mm, flattened and aligned, variable distribution within clasts, bluish white coating to vesicles.
Miaroles: Some.
COLOR: Grayish green (10G 4/2) to dusky yellowish-green matrix; clasts are mainly gray (10YR 2/1) in freshest and (10YR 4/1) in most altered examples; a few clasts are reddish (10R 4/6).
STRUCTURE: N/A.
ALTERATION: Breccia matrix is altered to green and white minerals which show a pervasive low-grade alteration; clasts have moderately fresh interiors, and some have alteration rims.
VEINS/FRACTURES: Absent.
ADDITIONAL COMMENTS: Smaller clasts are less vesicular, finer grained and more highly altered; clasts range in size from 2 mm to 6 cm in longest dimension; vitric matrix (no detrital component).

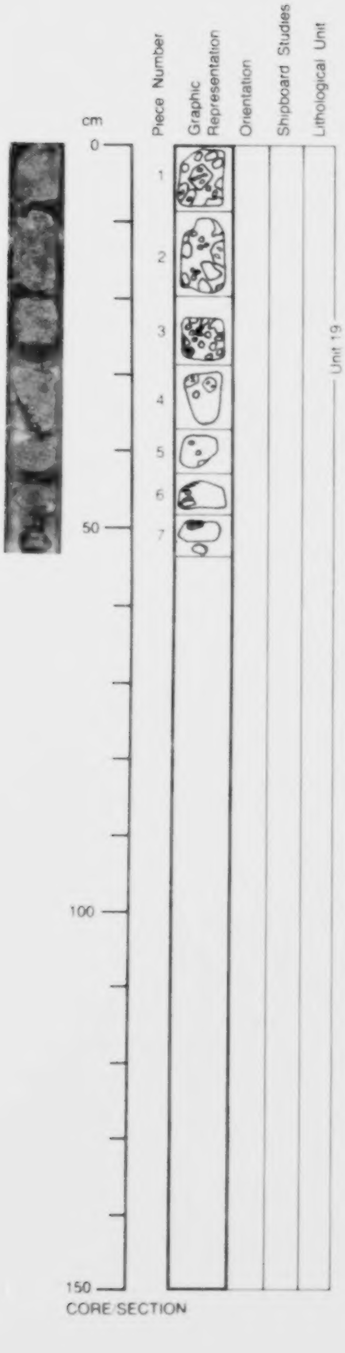
cm
Piece Number
Graphic Representation
Orientation
Shipboard Studies
Lithological Unit
0
50
100
150
1
2
3
4
5
6
7
Unit 19
CORE/SECTION

125-786B-50R-2

UNIT 19: TWO-PYROXENE ANDESITE

Pieces 1-7

CONTACTS: None visible.
PHENOCRYSTS: For clasts.
Plagioclase : 5-10%, <2 mm, euhedral.
Orthopyroxene : 2-5%, <2 mm, subhedral.
Clinopyroxene : 2-5%, <2 mm, subhedral.
GROUNDMASS: Clasts have a very fine-grained to glassy groundmass that shows pervasive alteration.
VESICLES: 1-15%, 1-10 mm; some flattened and aligned; variable distribution within clasts; bluish white lining.
COLOR: Grayish green (10G 4/2) to dusky yellowish green (10GY 3/2) matrix; clasts are mainly gray (10YR 4/1 to 6/1).
STRUCTURE: N/A.
ALTERATION: Breccia matrix altered to green and white alteration products; clasts show pervasive low grade alteration; some have alteration rims.
VEINS/FRACTURES: Absent.
ADDITIONAL COMMENTS: Smaller clasts are less vesicular, finer-grained and more highly altered; clasts range in size from 2 mm to 4 cm in largest dimension; larger clasts are subangular-rounded; matrix is vitric (no detrital component).

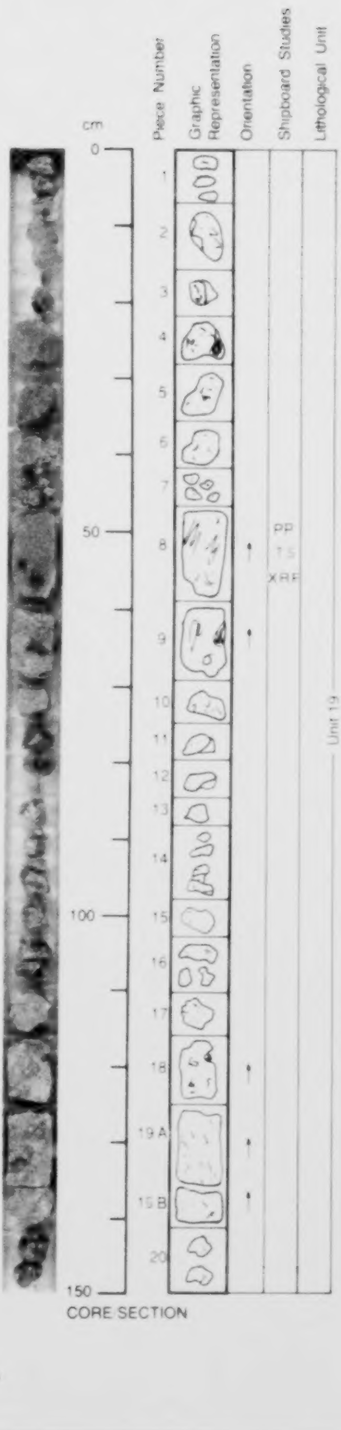
cm
0
50
100
150
CORE SECTION
Piece Number
Graphic Representation
Orientation
Shipboard Studies
Lithological Unit
1
2
3
4
5
6
7
8
9
10
11
12
13
14
15
16
17
18
19 A
15 B
20
PP
T S
XRF
Unit 19

125-786B-51R-1

UNIT 19: TWO-PYROXENE ANDESITE BRECCIA

Pieces 1-20

CONTACTS: None visible.
PHENOCRYSTS: For clasts.
Plagioclase : 20%; <2 mm; euhedral.
Orthopyroxene : 2-5%; <2 mm; subhedral.
Clinopyroxene : 2-5%; <2 mm; subhedral.
GROUNDMASS: Clasts have glassy to very fine-grained groundmass with plagioclase microliths and are pervasively altered.
VESICLES: 1-15%; 0.1-10 mm; some flattened and aligned; variable distribution within clasts; bluish white coating to vesicles.
COLOR: Grayish green (10G 4/2) to dusky yellowish green (10GY 3/2) matrix; clasts are mainly gray (10YR 2/1) in freshest and (10YR 4/1) in most altered examples.
STRUCTURE: N.A.
ALTERATION: Breccia matrix is altered to green and white minerals; clasts show pervasive low grade alteration and some have alteration rims.
VEINS/FRACTURES: Absent.
ADDITIONAL COMMENTS: Smaller clasts are less vesicular, finer grained and more highly altered; clasts range in size from 2 mm to 11 cm in longest dimension; larger clasts are subangular-rounded, and smaller clasts are rounded; vitric matrix (no detrital component).

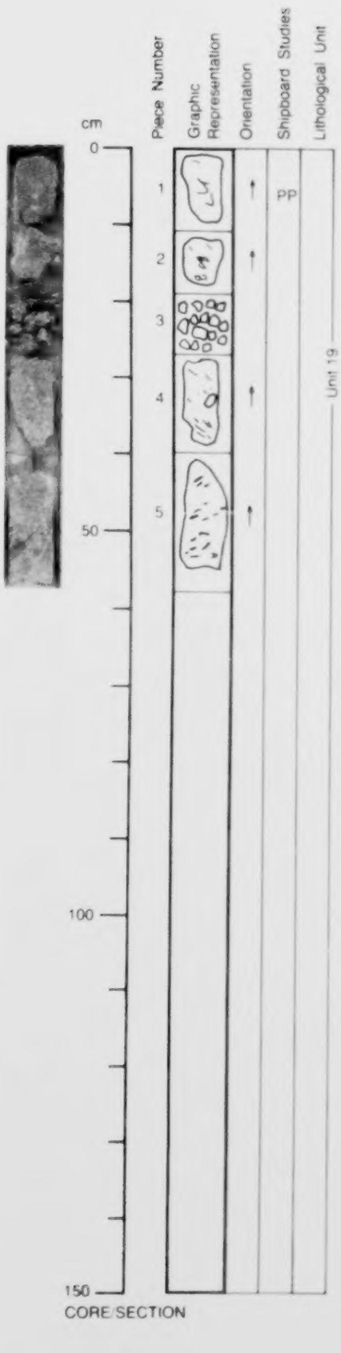
cm
0
50
100
150
CORE/SECTION
Piece Number
Graphic Representation
Orientation
Shipboard Studies
Lithological Unit
1
2
3
4
5
PP
Unit 19

125-786B-51R-2

UNIT 19: TWO-PYROXENE ANDESITE BRECCIA

Pieces 1-5

CONTACTS: None visible.
PHENOCRYSTS: For clasts:
Plagioclase - 5-10%, <2 mm, euhedral.
Orthopyroxene - 2-5%, <2 mm, subhedral.
Clinopyroxene - 2-5%, <2 mm, subhedral.
GROUNDMASS: Clasts have very fine grained to glassy groundmass and are pervasively altered.
VESICLES: 1-15%, 0.1-10 mm, some flattened and aligned, variable within clasts; bluish white lining.
COLOR: Grayish green (10G 4/2) to dusky yellowish green (10GY 3/2) matrix; clasts are mainly gray, (10YR 2/1), in least altered to (10YR 4/1) in most altered examples.
STRUCTURE: N/A.
ALTERATION: Breccia matrix altered to green and white minerals; clasts show pervasive low-grade alteration and some have alteration rims.
VEINS/FRACTURES: Absent.
ADDITIONAL COMMENTS: Smaller clasts are less vesicular, finer grained and more highly altered; clasts range in size from 2 mm to 6 cm in longest dimension; largest clasts are subangular-rounded; vitric matrix (no detrital component).

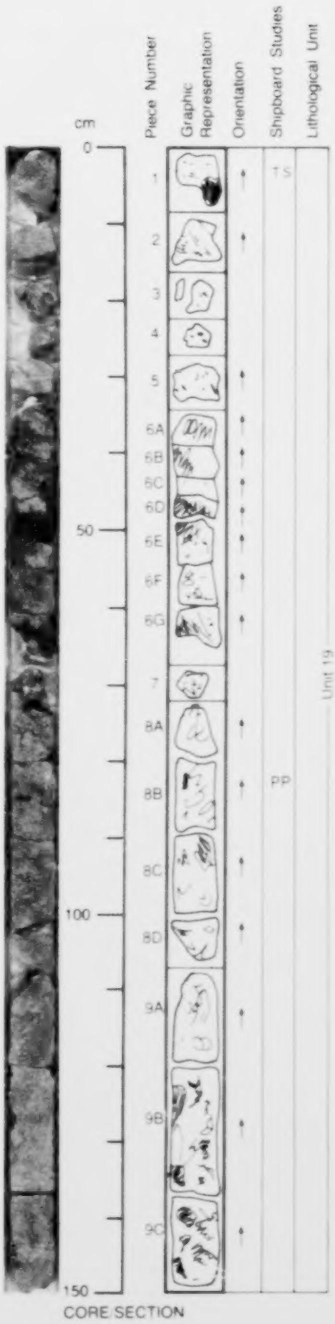
cm
Piece Number
Graphic Representation
Orientation
Shipboard Studies
Lithological Unit
0
50
100
150
1
2
3
4
5
6A
6B
6C
6D
6E
6F
6G
7
8A
8B
8C
8D
9A
9B
9C
TS
PP
Unit 19
CORE SECTION

125-786B-52R-1

UNIT 19: BONINITE BRECCIA

Pieces 1-9

CONTACTS: None visible
PHENOCRYSTS: For clasts
Plagioclase - 3-5%, <2 mm, euhedral
Orthopyroxene - 5-10%, <2 mm, euhedral
Clinopyroxene - 3-5%, <2 mm, subhedral
GROUNDMASS: Clasts have a very fine-grained to glassy groundmass that shows pervasive alteration.
VESICLES: 1-15%, 1-10 mm, some flattened and aligned; variable distribution within c bluish white lining.
COLOR: Grayish green (10G 4/2) to dusky yellowish green (10GY 3/2) matrix; clasts are mainly gray (10YR 4/1 to 6/1).
STRUCTURE: N/A
ALTERATION: Breccia matrix altered to green and white alteration products; clasts sh pervasive low-grade alteration and some have alteration rims.
VEINS/FRACTURES: Absent
ADDITIONAL COMMENTS: Smaller clasts are less vesicular, finer-grained and more highly altered; clasts range in size from 2 mm to 6 cm in largest dimension; larger cl are subangular/rounded; matrix is vitric (no detrital component).

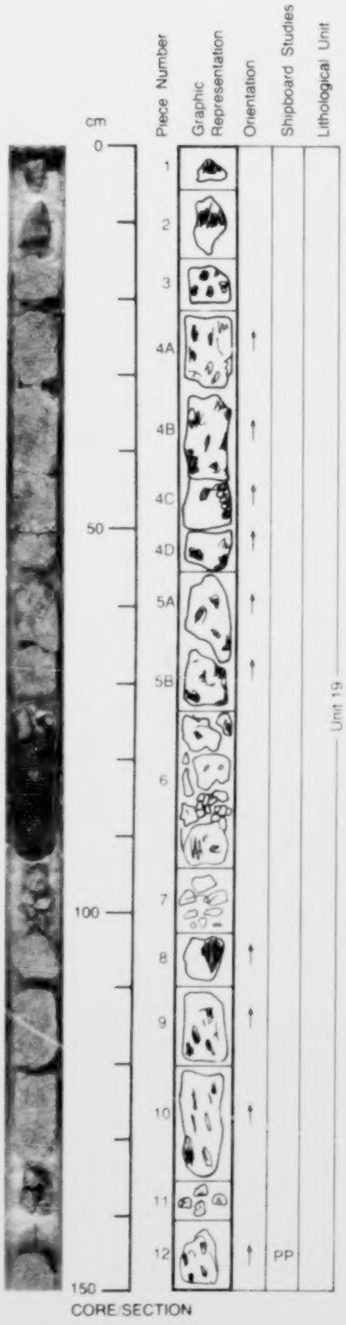
cm
Piece Number
Graphic Representation
Orientation
Shipboard Studies
Lithological Unit
0
50
100
150
1
2
3
4A
4B
4C
4D
5A
5B
6
7
8
9
10
11
12
PP
Unit 19
CORE/SECTION

125-786B-52R-2

UNIT 19: BONINITE BRECCIA

Pieces 1-12

CONTACTS: None visible
PHENOCRYSTS: For clasts
Plagioclase - 3-5%, <2 mm, euhedral
Orthopyroxene - 5-10%, <2 mm, subhedral
Clinopyroxene - 3-5%, <2 mm, subhedral
GROUNDMASS: Clasts have a very fine-grained to glassy groundmass that shows pervasive alteration
VESICLES: 1-15%, 1-10 mm, some flattened and aligned, variable distribution within clasts, some have bluish white lining, others are filled with greenish matrix material
COLOR: Grayish green (10G 4/2) to dusky yellowish green (10GY 3/2) matrix, clasts are mainly gray (10YR 4/1 to 6/1)
STRUCTURE: N/A
ALTERATION: Breccia matrix altered to green and white alteration products, clasts show pervasive low-grade alteration and some have alteration rims
VEINS/FRACTURES: Absent
ADDITIONAL COMMENTS: Smaller clasts are less vesicular, finer grained and more highly altered, clasts range in size from 5 mm to 6 cm in largest dimension, larger clasts are subangular-rounded, matrix is vitric (no detrital component)

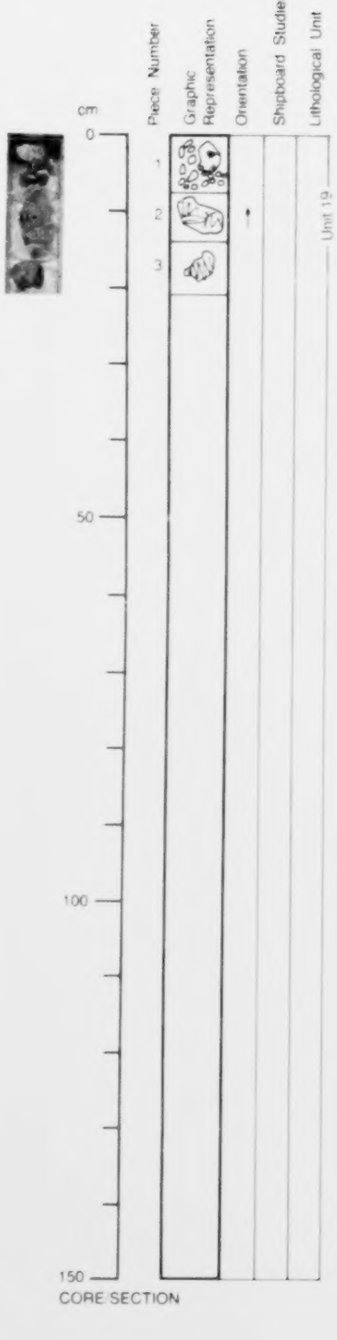
cm
Piece Number
Graphic Representation
Orientation
Shipboard Studies
Lithological Unit
0
1
2
3
Unit 19
50
100
150
CORE/SECTION

125-786B-52R-3

UNIT 19: BONINITE BRECCIA

Pieces 1-3

CONTACTS: None visible
PHENOCRYSTS: For clasts
  Plagioclase - 3-5%, <2 mm, euhedral
  Orthopyroxene - 5-10%, <2 mm, subhedral
  Clinopyroxene - 3-5%, <2 mm, subhedral
GROUNDMASS: Clasts have a very fine-grained to glassy groundmass that shows pervasive alteration.
VESICLES: 1-15%, 1-10 mm, some flattened and aligned, variable distribution within clasts, some have bluish white lining, others are filled with greenish matrix material.
COLOR: Grayish green (10G 4/2) to dusky yellowish green (10GY 3/2) matrix; clasts are mainly gray (10YR 4/1).
STRUCTURE: N/A
ALTERATION: Breccia matrix altered to green, and white alteration products; clasts show pervasive low-grade alteration and some have alteration rims.
VEINS/FRACTURES: Absent.
ADDITIONAL COMMENTS: Smaller clasts are very vesicular, finer grained and more highly altered; clasts range in size from 2 mm to 6 cm in largest dimension; larger clasts are subangular-rounded; matrix is vitric (no detrital component).

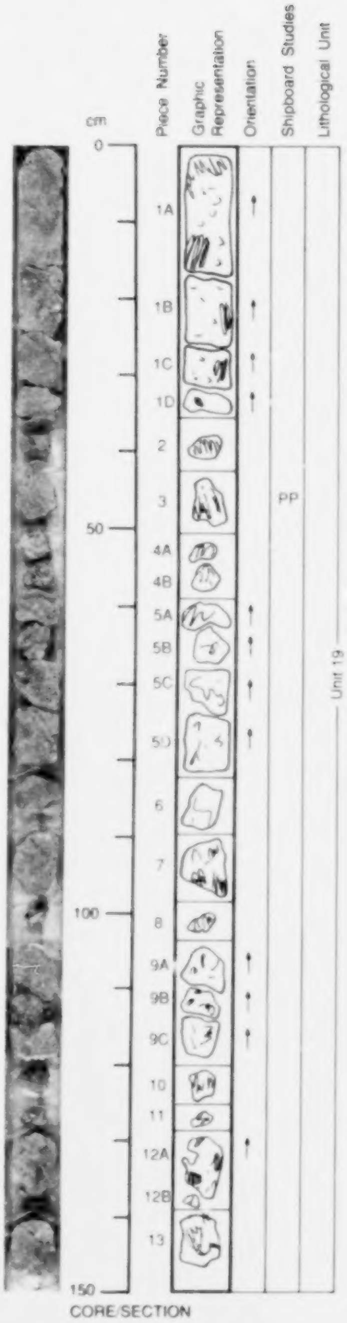
cm
Piece Number
Graphic Representation
Orientation
Shipboard Studies
Lithological Unit
0
50
100
150
1A
1B
1C
1D
2
3
4A
4B
5A
5B
5C
5D
6
7
8
9A
9B
9C
10
11
12A
12B
13
PP
Unit 19
CORE/SECTION

125-786B-53R-1

UNIT 19: BONINITE BRECCIA

Pieces 1-13

CONTACTS: None visible.
PHENOCRYSTS: For clasts.
Plagioclase - 3-5%, <2 mm, euhedral.
Orthopyroxene - 5-10%, <2 mm, subhedral.
Clinopyroxene - 3-5%, <2 mm, subhedral.
GROUNDMASS: Clasts have a very fine-grained to glassy groundmass that shows pervasive alteration.
VESICLES: 1-15%, 1-10 mm, some flattened and aligned; variable distribution within clasts, carbonate and white zeolite filling.
COLOR: Dark gray green (5G 3/4 - 5G 4/4) matrix; clasts are mainly dark gray to dark bluish gray (N 4/ to 5B 4/1).
STRUCTURE: N/A.
ALTERATION: Breccia matrix altered to green and white alteration products; clasts show pervasive low-grade alteration and some have alteration rims.
VEINS/FRACTURES: Absent.
ADDITIONAL COMMENTS: Clasts range in size from 2 mm to 6 cm in largest dimension; matrix is vitric and porous with 1-2% grain-interstitial pores from 0.5 mm to 5 mm; pores have a lining of pale-green and creamy white zeolite.

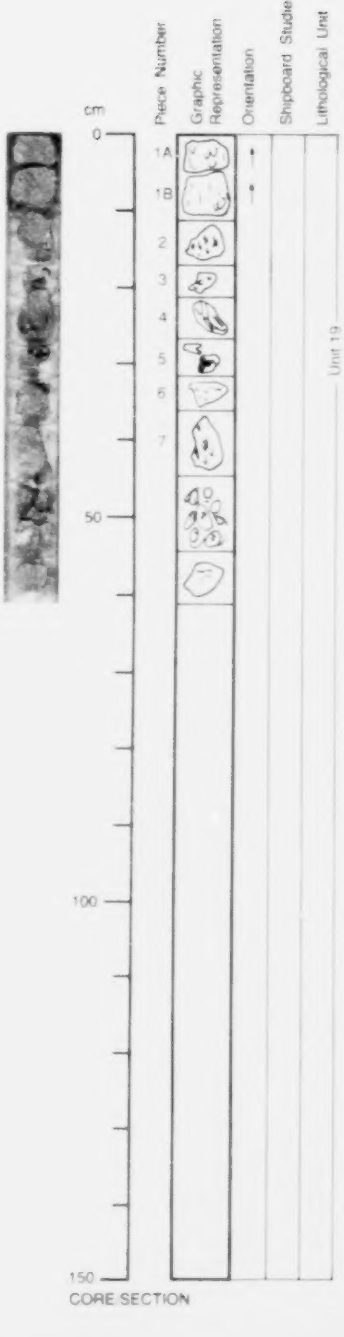
cm
0
50
100
150
Piece Number
Graphic Representation
Orientation
Shipboard Studies
Lithological Unit
1A
1B
2
3
4
5
6
7
Unit 19
CORE SECTION

125-786B-53R-2

UNIT 19: BONINITE BRECCIA

Pieces 1-9

CONTACTS: None visible.
PHENOCRYSTS: For clasts.
Plagioclase - 3-5%, <2 mm, euhedral.
Orthopyroxene - 5-10%, <2 mm, subhedral.
Clinopyroxene - 3-5%, <2 mm, subhedral.
GROUNDMASS: Clasts have a very fine-grained to glassy groundmass that shows pervasive alteration.
VESICLES: 1-15%, 1-10 mm, some flattened and aligned, variable distribution among clasts, filled with carbonate and white zeolite, parallel or concentric layers of zeolite (translucent white-eggshell blue) fill some vesicles.
COLOR: Dark gray green (5G 3/4 - 5G 4/4) matrix; clasts are mainly dark gray to dark bluish gray (N 4/ to 5B 4/1).
STRUCTURE: N/A.
ALTERATION: Breccia matrix altered to green and white alteration products; clasts show pervasive low grade alteration and some have alteration rims.
VEINS/FRACTURES: Absent.
ADDITIONAL COMMENTS: Smaller clasts are less vesicular, finer grained and more highly altered; clasts range in size from 2 mm to 6 cm in largest dimension; larger clasts are subangular-rounded; matrix is vitric (no detrital component).

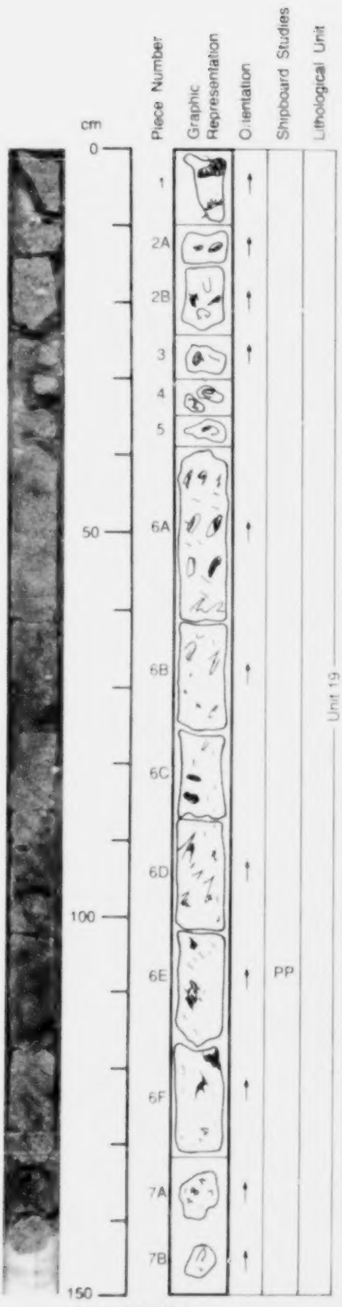
cm
Piece Number
Graphic Representation
Orientation
Shipboard Studies
Lithological Unit
0
50
100
150
1
2A
2B
3
4
5
6A
6B
6C
6D
6E
6F
7A
7B
PP
Unit 19
CORE/SECTION

125-786B-54R-1

UNIT 19: BONINITE BRECCIA

Pieces 1-7

CONTACTS: None visible

PHENOCRYSTS: For clasts

Plagioclase - 3-5%, <2 mm, euhedral
Orthopyroxene - 5-10%, <2 mm, subhedral
Clinopyroxene - 3-5%, <2 mm, subhedral

GROUNDMASS: Clasts have a very fine-grained to glassy groundmass that shows pervasive alteration

VESICLES: 1-15%, 1-10 mm, some flattened and aligned, variable distribution among clasts, bluish white lining

COLOR: Dark gray green (5G 3/4) matrix; clasts are dark bluish gray to black (10YR 5/1 to 10YR 2/1)

STRUCTURE: N/A

ALTERATION: Breccia matrix altered to green and white alteration products; clasts are pervasively altered and some have alteration rims

VEINS/FRACTURES: Absent

ADDITIONAL COMMENTS: Clasts range in size from 1 mm to 5 cm in largest dimension; matrix is vitric (no detrital component); the relative proportion of matrix to clasts is less than in previous cores and the distance between clasts is 1-3 mm; long axes of the clasts may be aligned with an apparent dip of 35 degrees; some clasts break up parallel to possible foliation

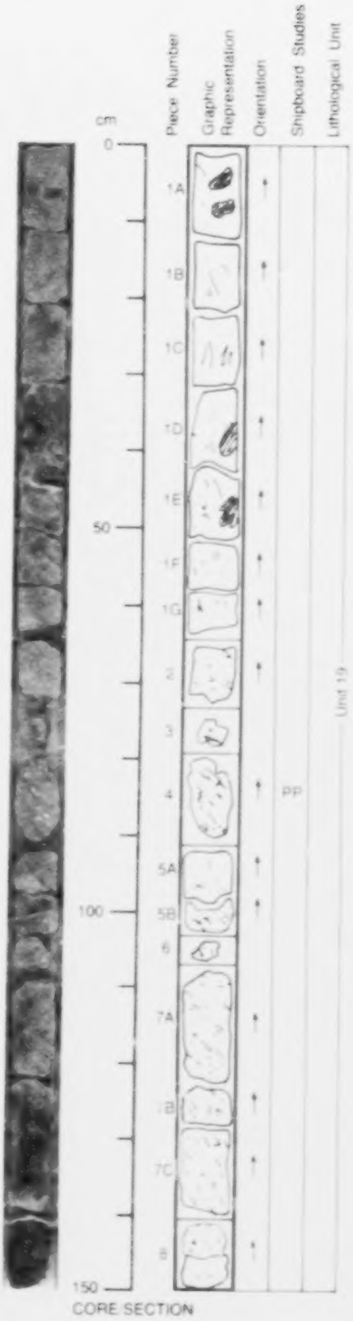
cm
Piece Number
Graphic Representation
Orientation
Shipboard Studies
Lithological Unit
0
50
100
150
1A
1B
1C
1D
1E
1F
1G
2
3
4
5A
5B
6
7A
7B
7C
8
PP
Unit 19
CORE/SECTION

125-786B-54R-2

UNIT 19: BONINITE BRECCIA

Pieces 1-8

CONTACTS: None visible.
PHENOCRYSTS: For clasts:
Plagioclase - 3-5%, <2 mm, euhedral.
Orthopyroxene - 5-10%, <2 mm, subhedral.
Clinopyroxene - 3-5%, <2 mm, subhedral.
GROUNDMASS: Clasts have a very fine grained to glassy groundmass that shows pervasive alteration.
VESICLES: 1-15%, 1-10 mm, some flattened and aligned; variable distribution among clasts; whitish carbonate and zeolite lining or filling.
COLOR: Dark gray green (5G 3/4) matrix; clasts are dark bluish gray to black (10YR 5/1 - 10YR 2/1).
STRUCTURE: N/A
ALTERATION: Breccia matrix altered to green and white alteration products; some have clasts show pervasive low grade alteration and some have alteration rims.
VEINS/FRACTURES: Absent.
ADDITIONAL COMMENTS: Smaller clasts are less vesicular, finer grained and more highly altered; clasts range in size from 1 mm to 11 cm in largest dimension; larger clasts are subangular - rounded; matrix is vitric, no detrital component.

125-786B-54R-3

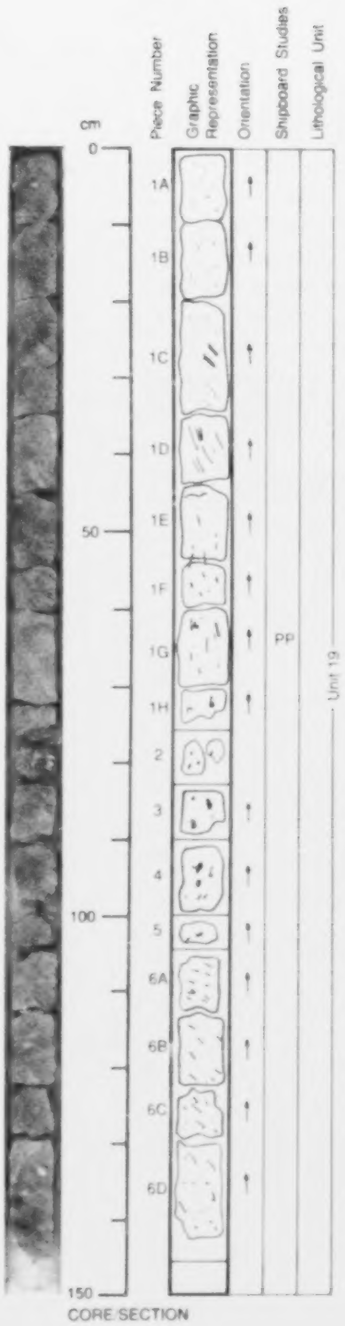
cm
0
50
100
150
CORE/SECTION
Piece Number
Graphic Representation
Orientation
Shipboard Studies
Lithological Unit
1A
1B
1C
1D
1E
1F
1G
1H
2
3
4
5
6A
6B
6C
6D
PP
Unit 19

UNIT 19: BONINITE BRECCIA

Pieces 1-6

CONTACTS: None visible.
PHENOCRYSTS: For clasts.
Plagioclase - 3-5%, <2 mm, euhedral.
Orthopyroxene - 5-10%, <2 mm, subhedral.
Clinopyroxene - 3-5%, <2 mm, subhedral.
GROUNDMASS: Clasts have a very fine grained to glassy groundmass that shows pervasive alteration.
VESICLES: 1-15%, 1-10 mm, some flattened and aligned; variable distribution within clasts; whitish lining and filling.
COLOR: Dark gray green (5G 3/4) matrix; clasts are dark gray to black (10YR 4/1 to 7.5YR 2/0).
STRUCTURE: N/A.
ALTERATION: Breccia matrix altered to green and white alteration products; clasts show pervasive low-grade alteration and some have alteration rims.
VEINS/FRACTURES: Absent.
ADDITIONAL COMMENTS: Smaller clasts are less vesicular, finer-grained and more highly altered; clasts range in size from 2 mm to 4.5 cm in largest dimension; larger clasts are subangular-rounded; matrix is vitric (no detrital component), but contains sand sized fragments; the relative proportion of matrix to clasts decreases down section.

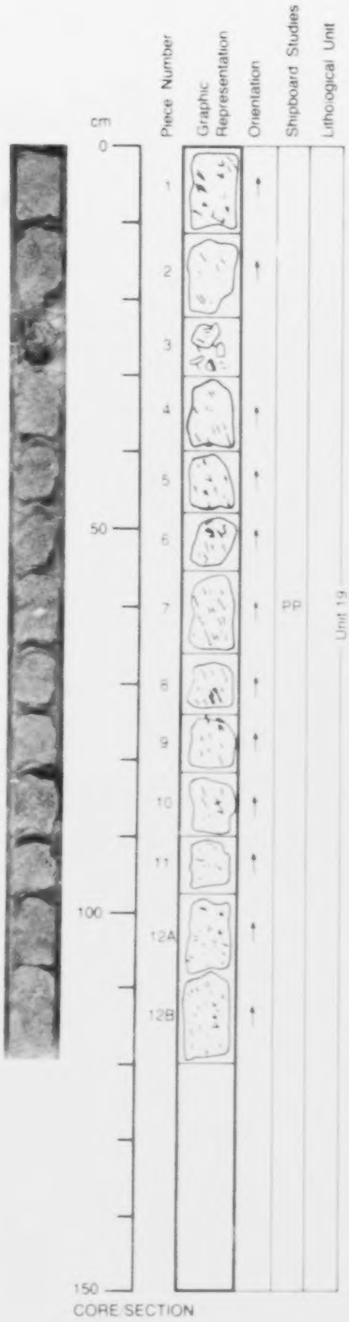
cm
Piece Number
Graphic Representation
Orientation
Shipboard Studies
Lithological Unit
0
50
100
150
1
2
3
4
5
6
7
8
9
10
11
12A
12B
PP
Unit 19
CORE SECTION

125-786B-54R-4

UNIT 19: BONINITE BRECCIA

Pieces 1-12

CONTACTS: None visible
PHENOCRYSTS: For clasts
Plagioclase - 3-5%, <2 mm, euhedral
Orthopyroxene - 5-10%, 2 mm, subhedral
Clinopyroxene - 3-5%, 2 mm, subhedral
GROUNDMASS: Clasts have a very fine-grained to glassy groundmass that show pervasive alteration.
VESICLES: 1-15%, 1-10 mm, some flattened and aligned, variable distribution within clasts, whitish lining and filling.
COLOR: Dark gray green (5G 3/4) matrix, clasts are mainly dark gray to black 10YR 4/1 to 7.5YR 2/0.
STRUCTURE: N/A
ALTERATION: Breccia matrix altered to green and white alteration products; clasts show pervasive low-grade alteration and some have alteration rims.
VEINS/FRACTURES: Absent.
ADDITIONAL COMMENTS: Smaller clasts are less vesicular, finer-grained and more highly altered; clasts range in size from 2 mm to 4.5 cm in largest dimension; larger clasts are subangular-rounded; matrix is vitric (no detrital component), but contains sand-sized fragments.

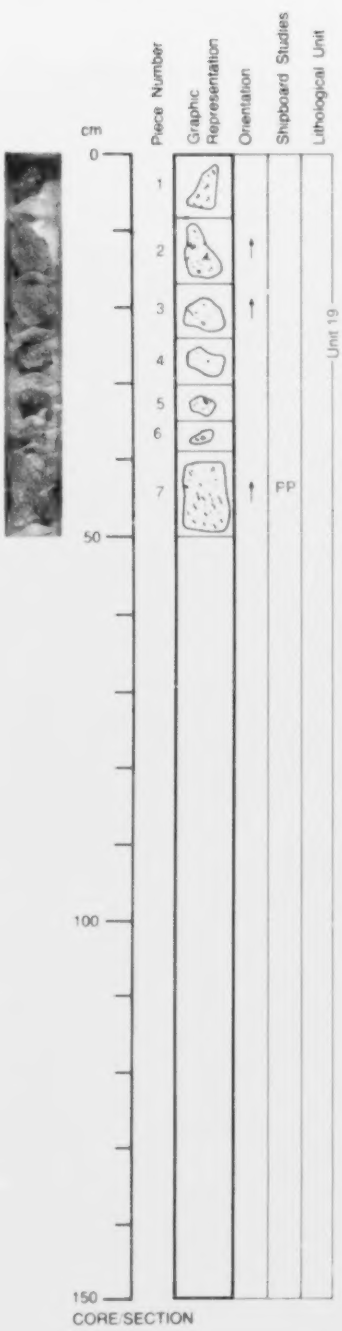
cm
0
50
100
150
CORE/SECTION
Piece Number
Graphic Representation
Orientation
Shipboard Studies
Lithological Unit
1
2
3
4
5
6
7
FP
Unit 19

125-786B-54R-5

UNIT 19: BONINITE BRECCIA

Pieces 1-7

CONTACTS: None visible.

PHENOCRYSTS: For clasts.
- Plagioclase - 3-5%, <2 mm, euhedral.
- Orthopyroxene - 5-10%, <2 mm, subhedral.
- Clinopyroxene - 3-5%, <2 mm, subhedral.

GROUNDMASS: Clasts have a very fine-grained to glassy groundmass that shows pervasive alteration.

VESICLES: 1-15%, 1-10 mm, some flattened and aligned; variable distribution within clasts; bluish white lining and filling.

COLOR: Dark gray green (10G 4/2) matrix, clasts are mainly dark gray to black (10YR 4/1 to 7.5YR 2/0).

STRUCTURE: N/A.

ALTERATION: Breccia matrix altered to green and white alteration products; clasts show pervasive low-grade alteration and some have alteration rims.

VEINS/FRACTURES: Absent.

ADDITIONAL COMMENTS: Smaller clasts are less vesicular, finer-grained and more highly altered; clasts range in size from 2 mm to 4.5 cm in largest dimension; larger clasts are subangular-rounded; matrix is vitric (no detrital component) and contains sand-sized fragments.

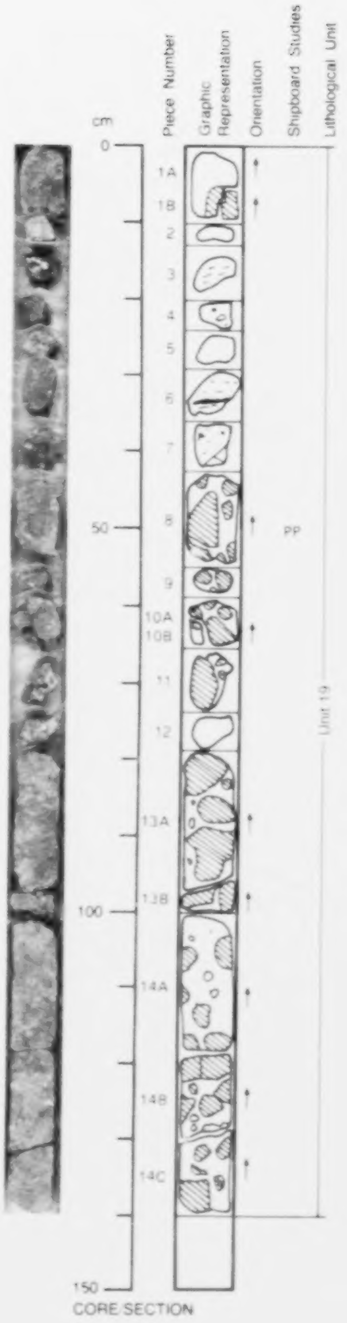
cm
0
50
100
150
CORE/SECTION
Piece Number
Graphic Representation
Orientation
Shipboard Studies
Lithological Unit
1A
1B
2
3
4
5
6
7
8
9
10A
10B
11
12
13A
13B
14A
14B
14C
PP
Unit 19

125-786B-55R-1

UNIT 19: TWO-PYROXENE, PLAGIOCLASE BONINITE BRECCIA

Pieces 1A-14C

CONTACTS: None visible.
PHENOCRYSTS:
Plagioclase - 2-5%, <2 mm, euhedral.
Orthopyroxene - 10%, <3 mm, yellow, subhedral.
Clinopyroxene - 5%, <2 mm, dark green, subhedral.
GROUNDMASS: Glassy to partly altered in clasts; chlorite-rich along cracks.
VESICLES: 5-20%, <3 mm, locally 1 cm diameter, round to elongate; sorted by size; blue coating.
COLOR: Gray (N 5) where fresh, greenish gray (5G 5/2 - 6/2) and white where altered.
STRUCTURE: Brecciated to intensely fractured.
ALTERATION: Along fractures to green and creamy white products.
VEINS/FRACTURES: Strongly fractured.
ADDITIONAL COMMENTS: Oligomictic breccia.

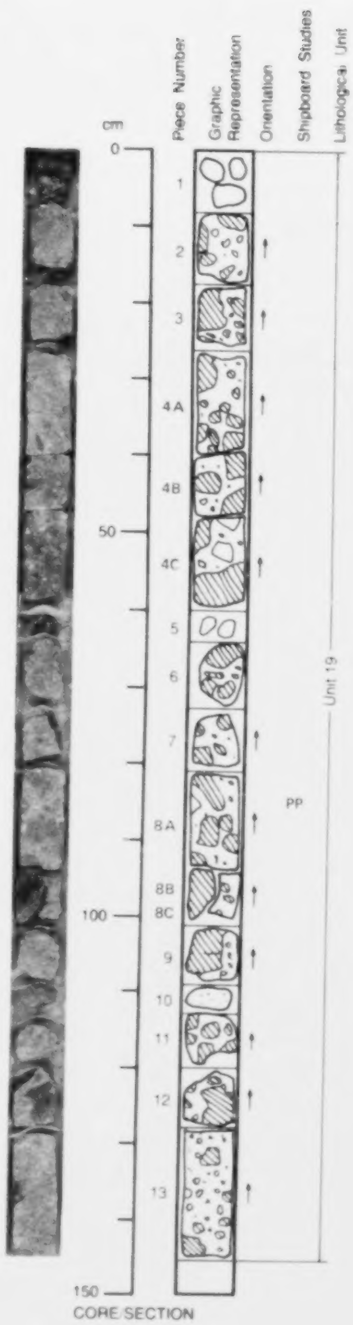
cm
0
50
100
150
CORE SECTION
Piece Number
Graphic Representation
Orientation
Shipboard Studies
Lithological Unit
1
2
3
4A
4B
4C
5
6
7
8A
8B
8C
9
10
11
12
13
PP
Unit 19

125-786B-55R-2

UNIT 19: TWO-PYROXENE, PLAGIOCLASE BONINITE BRECCIA

Pieces 1-13

CONTACTS: None visible.
PHENOCRYSTS:
Plagioclase - 2-5%, <2 mm, euhedral.
Orthopyroxene - 10%, <3 mm, yellow, subhedral.
Clinopyroxene - 5%, <2 mm, dark green, subhedral.
GROUNDMASS: Glassy to partly altered in clasts, chlorite-rich along cracks.
VESICLES: 5-20%, <3 mm, locally 1 cm, round to elongate, sorted by size, blue coating.
COLOR: Gray (N 5/) where fresh, greenish gray (5G 5/2 - 6/2) and white where altered.
STRUCTURE: Brecciated to intensely fractured.
ALTERATION: Along fractures to green and creamy white products.
VEINS/FRACTURES: Strongly fractured.
ADDITIONAL COMMENTS: Oligomictic breccia, the amount of altered matrix is increasing from Section 1. Pieces 8C and 10 are fresh clasts.

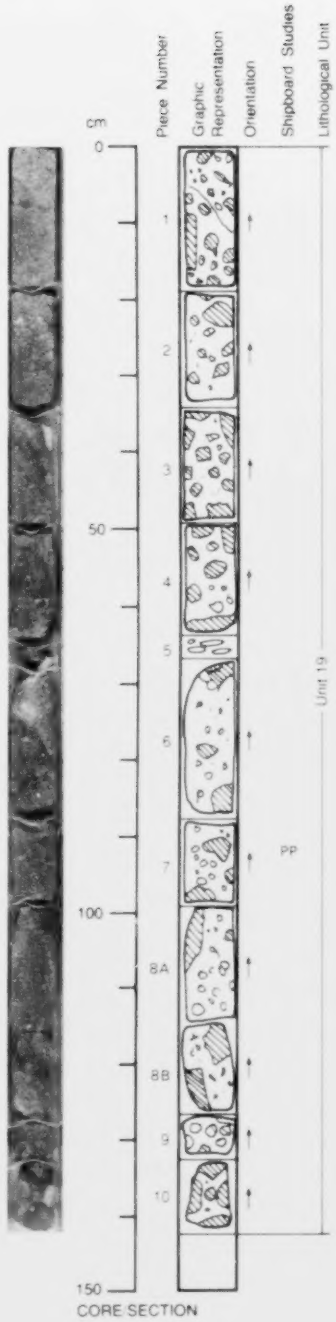
cm
Piece Number
Graphic Representation
Orientation
Shipboard Studies
Lithological Unit
0
50
100
150
1
2
3
4
5
6
7
8A
8B
9
10
PP
Unit 19
CORE/SECTION

125-786B-55R-3

UNIT 19: TWO-PYROXENE, PLAGIOCLASE BONINITE BRECCIA

Pieces 1-10

CONTACTS: None.
PHENOCRYSTS: Glomerocyrsts of plagioclase and orthopyroxene.
Plagioclase - trace, <2 mm, euhedral.
Orthopyroxene - 15-20%, <3 mm, yellow, subhedral.
Clinopyroxene - 5%, <2 mm, dark green, subhedral.
GROUNDMASS: Glassy to partly altered in clasts, chlorite-rich along cracks.
VESICLES: 5-20%, <3 mm, locally 1 cm, rounded to elongate, sorted by size, blue coating.
COLOR: Gray (N 5/) where fresh, greenish gray (5G 5/2 - 6/2) and white where altered.
STRUCTURE: Brecciated to intensely fractured.
ALTERATION: Along fractures to green and creamy-white product.
VEINS/FRACTURES: Strongly fractured.
ADDITIONAL COMMENTS: Oligomictic breccia, native copper is present in the fresh glass in Piece 4 and Piece 8B; glassy groundmass contains some plagioclase.

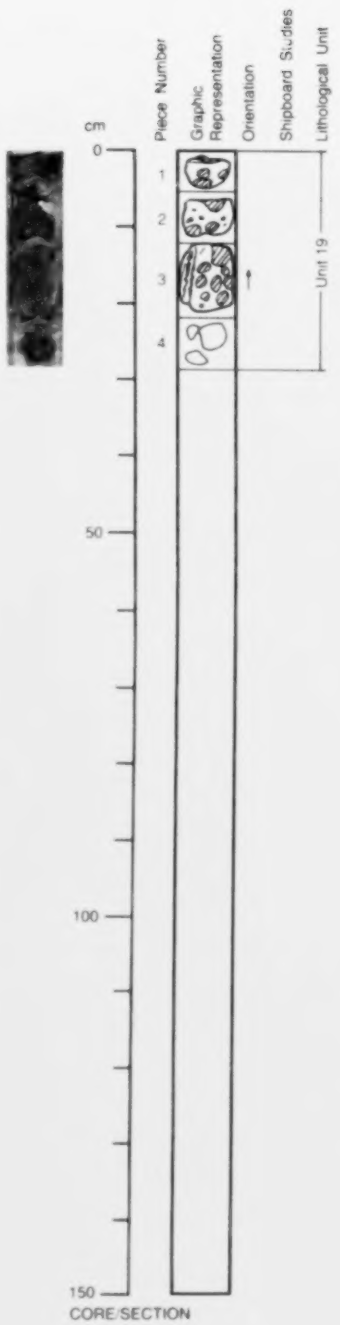
cm
Piece Number
Graphic Representation
Orientation
Shipboard Studies
Lithological Unit
0
50
100
150
1
2
3
4
Unit 19
CORE/SECTION

125-786B-55R-4

UNIT 19: TWO-PYROXENE, PLAGIOCLASE BONINITE BRECCIA

Pieces 1-4

CONTACTS: None.
PHENOCRYSTS: Glomerocyrsts of plagioclase and orthopyroxene.
Plagioclase - trace; <2; euhedral.
Orthopyroxene - 15-20%; <3; yellow; subhedral.
Clinopyroxene - 5%; <2; dark green; subhedral.
GROUNDMASS: Glassy to partly altered in clasts; chlorite-rich along cracks.
VESICLES: 5-20%; < 3mm, locally 1 cm; rounded to elongate; sorted by size; blue coating.
COLOR: Gray (N 5/) where fresh; greenish gray (5G 5/2 - 6/2) and white where altered.
STRUCTURE: Brecciated to intensely fractured.
ALTERATION: Along fractures to green and creamy-white product.
VEINS/FRACTURES: Strongly fractured.
ADDITIONAL COMMENTS: Continued from 125-786B-55R-3.

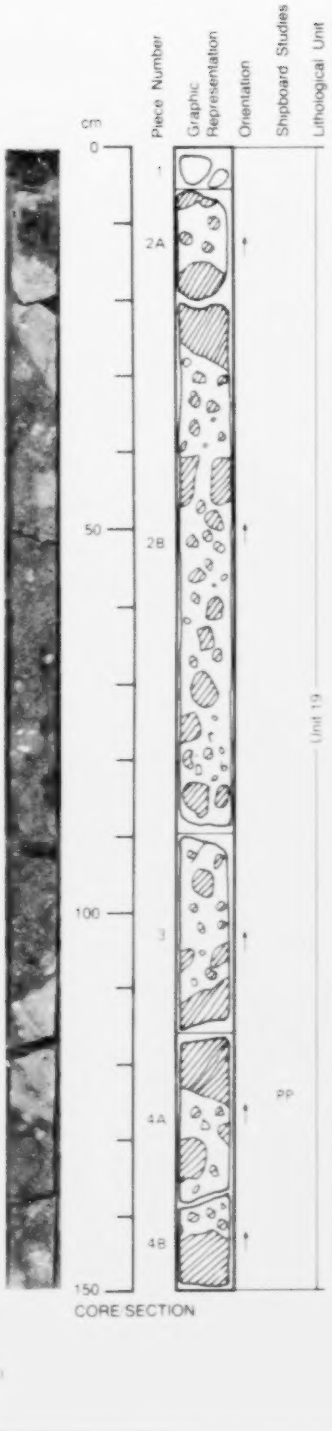
cm
0
50
100
150
Piece Number
Graphic Representation
Orientation
Shipboard Studies
Lithological Unit
1
2A
2B
3
4A
4B
PP
Unit 19
CORE/SECTION

125-786B-56R-1

UNIT 19: BONINITE BRECCIA

Pieces 1-4

CONTACTS: None

PHENOCRYSTS:

Orthopyroxene - 10-15%, <3 mm, yellow, euhedral

Cr-spinel - trace, <0.1 mm, black, euhedral

GROUNDMASS: Devitrified glass, contains plagioclase

VESICLES: 0-5%, <2 mm, locally 1 cm, round, sorted by size, filled with clay

COLOR: Dark gray (N 4/) to light greenish gray (5GY 7/1) and grayish green (5G 4/2); the fresh material is dark gray

STRUCTURE: Breccia, probably pillow fragments, some showing in situ fractures infilled with finer-grained debris

ALTERATION: Differentially altered

VEINS/FRACTURES: Trace, <1 mm wide, random, filled with zeolitic material

ADDITIONAL COMMENTS: A trace of copper is present

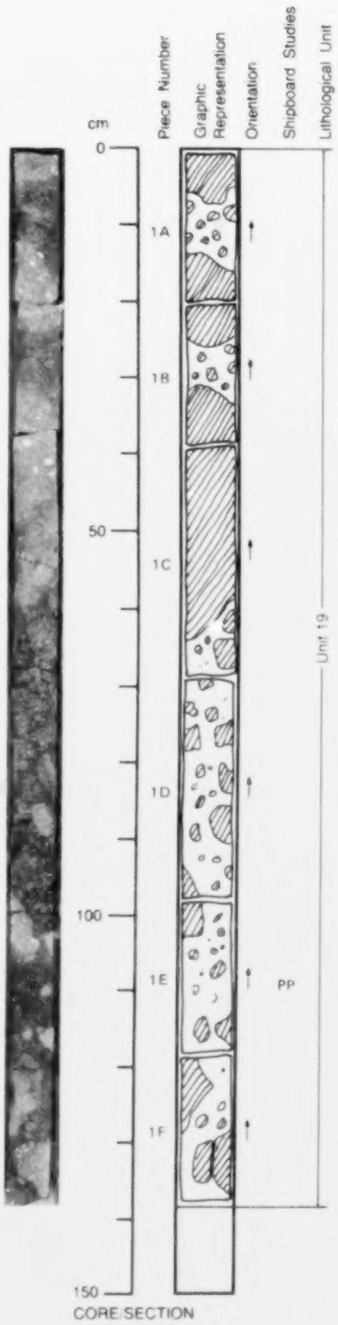
cm
Piece Number
Graphic Representation
Orientation
Shipboard Studies
Lithological Unit
0
50
100
150
1A
1B
1C
1D
1E
1F
PP
Unit 19
CORE/SECTION

125-786B-56R-2

UNIT 19: BONINITE BRECCIA

Pieces 1A-1F

CONTACTS: None visible
PHENOCRYSTS:
Orthopyroxene - 10-15%, < 3 mm, yellow, euhedral
Cr-spinel - trace, <0.1 mm, black, euhedral
GROUNDMASS: Devitrified glass, contains plagioclase.
VESICLES: 0-5%, < 2mm, locally 1 cm, round, sorted by size, filled with clay
COLOR: Dark gray (n 4/) when fresh; light greenish gray (5GY 7/1) and grayish green (5G 4/2) where altered
STRUCTURE: Breccia; individual fragments up to 30 cm in diameter
ALTERATION: Differentially altered
VEINS/FRACTURES: Trace, <1 mm, random, filled with zeolite and chlorite
ADDITIONAL COMMENTS: Continuation of 125-786B-56R-1

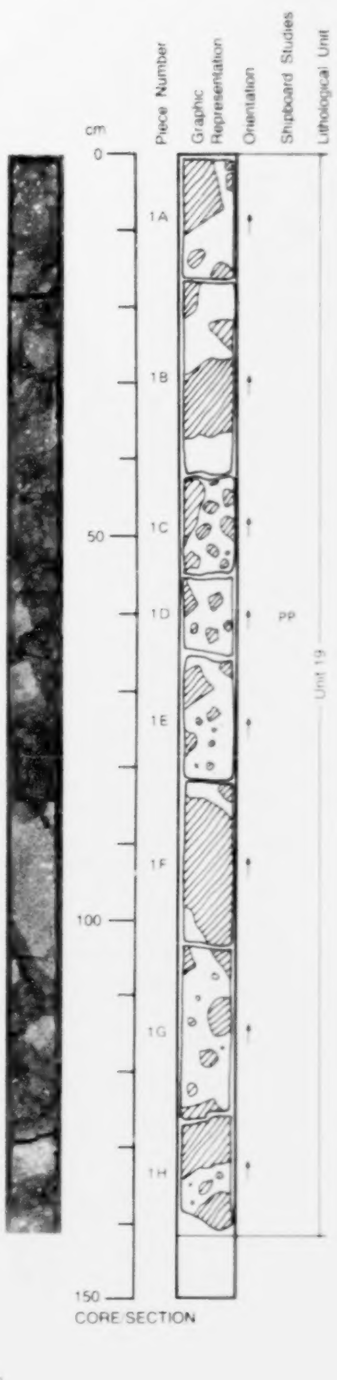
cm
Piece Number
Graphic Representation
Orientation
Shipboard Studies
Lithological Unit
0
50
100
150
1A
1B
1C
1D
1E
1F
1G
1H
PP
Unit 19
CORE/SECTION

125-786B-56R-3

UNIT 19: BONINITE BRECCIA

Pieces 1A-1H

CONTACTS: None
PHENOCRYSTS:
Orthopyroxene - 10-15%, <3 mm, yellow, euhedral
Cr spinel - trace, <0.1 mm, black, euhedral
GROUNDMASS: Devitrified glass, contains plagioclase
VESICLES: 0-5%, <2 mm, locally 1 cm, round, sorted by size, filled with clay
COLOR: Dark gray (N 4) when fresh, light greenish gray (5GY 7/1) and grayish green (5G 4/2) where altered
STRUCTURE: Breccia, individual fragments up to 15 cm in size
ALTERATION: Differentially altered
VEINS/FRACTURES: None
ADDITIONAL COMMENTS: Continuation of 125-786B-56R-1

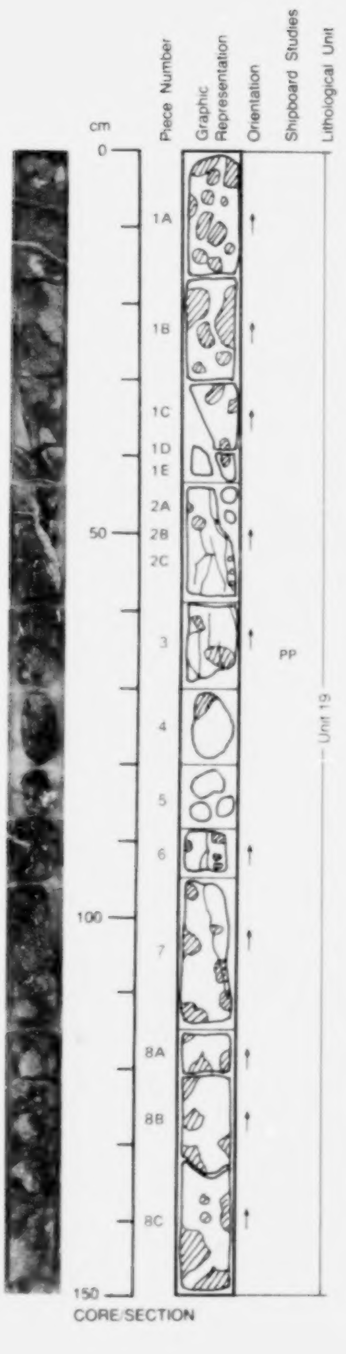
cm
Piece Number
Graphic Representation
Orientation
Shipboard Studies
Lithological Unit
0
50
100
150
1A
1B
1C
1D
1E
2A
2B
2C
3
4
5
6
7
8A
8B
8C
PP
Unit 19
CORE/SECTION

125-786B-56R-4

UNIT 19: BONINITE BRECCIA

Pieces 1-8

CONTACTS: None
PHENOCRYSTS:
Orthopyroxene - 10-15%, <3 mm, yellow, euhedral
Cr spinel - trace, <0.1 mm, black, euhedral
GROUNDMASS: Devitrified glass, contains plagioclase
VESICLES: 0-5%, <2 mm, locally 1 cm, rounded, sorted by size, filled with clay
COLOR: Dark gray (N 4/) where fresh; light greenish gray (5GY 7/1) and grayish green (5G 4/2)
STRUCTURE: Breccia, probably pillow fragments with individual fragments up to 20 cm in size
ALTERATION: Glass altered to clays
VEINS/FRACTURES: Absent
ADDITIONAL COMMENTS: Continuation of 125-786B-56R-1, slickensides indicating horizontal and vertical motion in fracture zone from Piece 2 to Piece 7

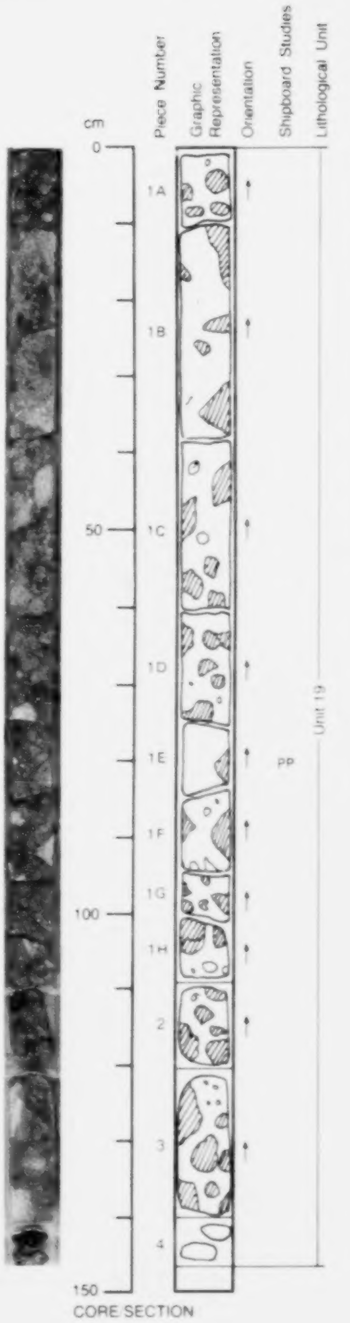
cm
Piece Number
Graphic Representation
Orientation
Shipboard Studies
Lithological Unit
0
50
100
150
1A
1B
1C
1D
1E
1F
1G
1H
2
3
4
PP
Unit 19
CORE SECTION

125-786B-56R-5

UNIT 19: BONINITE BRECCIA

Pieces 1-4

CONTACTS: None
PHENOCRYSTS:
  Orthopyroxene - 10-15%, <3 mm, yellow, euhedral
  Cr-spinel - trace, <0.1 mm, black, euhedral
GROUNDMASS: Devitrified glass, contains plagioclase
VESICLES: 0-5%, <2 mm, locally 1 cm, rounded, sorted by size, filled with clay
COLOR: Same as previous section
STRUCTURE: Breccia: individual fragments up to 15 cm in size
ALTERATION: Glass altered to clay
VEINS/FRACTURES: Absent
ADDITIONAL COMMENTS: Continuation of 125-786B-56R-1

125-786B-56R-6

UNIT 19: BONINITE BRECCIA

Pieces 1-5

COMMENTS: Continuation of 125-786B-56R-1

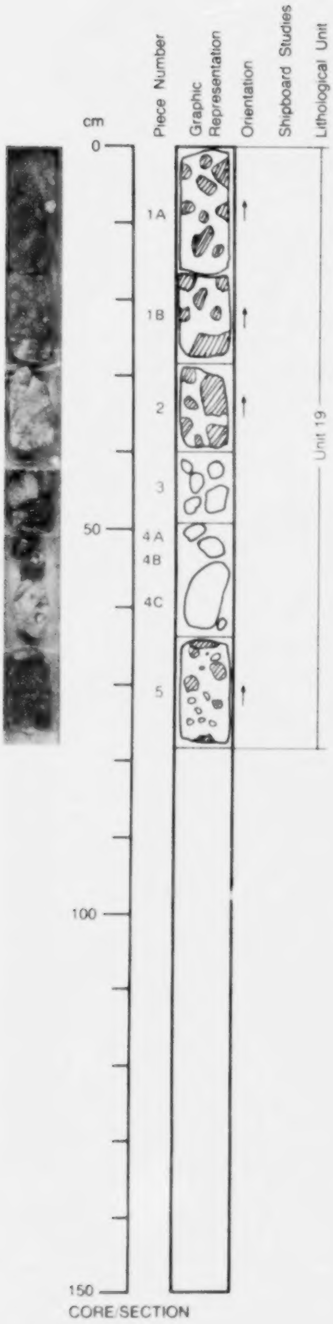
cm
0
50
100
150
Piece Number
Graphic Representation
Orientation
Shipboard Studies
Lithological Unit
1A
1B
2
3
4A
4B
4C
5
Unit 19
CORE/SECTION

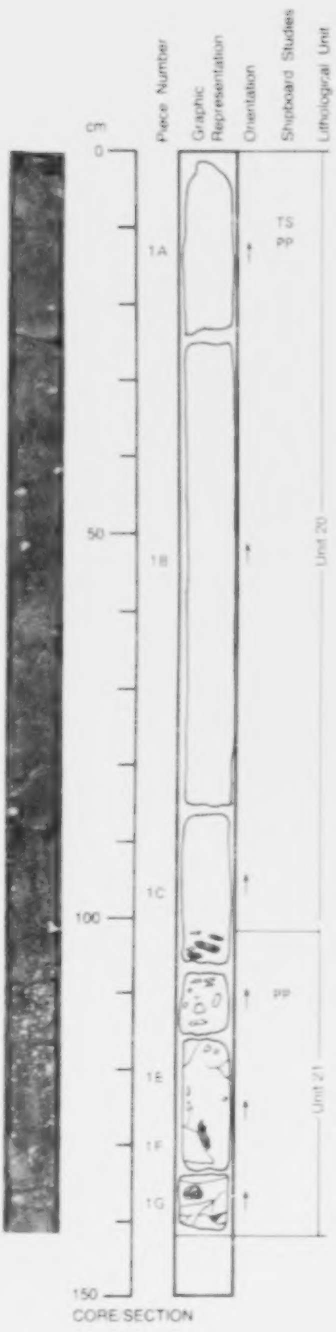
cm
0
50
100
150
CORE/SECTION
Piece Number
Graphic Representation
Orientation
Shipboard Studies
Lithological Unit
1A
1B
1C
1E
1F
1G
TS
PP
PP
Unit 20
Unit 21

125-786B-57R-1

UNIT 20: BONINITIC HYALOCLASTITE SAND

Pieces 1A-1C

CONTACTS: None.
ADDITIONAL COMMENTS: The unit is a fining-upward sandstone containi
cm-sized lithic and vitric fragments of glassy margins of boninite as well as s
of orthopyroxene. The unit exhibits basal graded bedding.

UNIT 21: BONINITE

Pieces 1C - 1G

CONTACTS: Between overlying boninite hyaloclastite sand and this flow.
PHENOCRYSTS: Orthopyroxene occurs as isolated crystals and glomerocrys
rarely with clinopyroxene.
Orthopyroxene: 3-10%, <1.5 mm, euhedral, tabular, with spinel inclusion
Clinopyroxene: trace, <0.3 mm, deep green, euhedral equant.
GROUNDMASS: Fine grained to glassy with microlites of feldspar.
VESICLES: 5-15%, <8 mm long, elongate ovoid to irregular; concentrated tow
fragment boundaries, filled with fibrous white zeolites.
COLOR: Dark greenish gray (5BG 4/1) to dark brown (7.5YR 3/4).
STRUCTURE: Partially fragmented pillow rims, interiors mostly massive.
ALTERATION: Variable, oxidized towards margins of fragments; possible chlo
Fe-oxide.
VEINS/FRACTURES: 2%, <4 mm wide, random; filled with zeolite and amorp
phase (zeolite?, altered glass?); also patches or cavities filled in the same m
ADDITIONAL COMMENTS: Appears to be pillow fragment at base of hyaloc
boninitic sand.

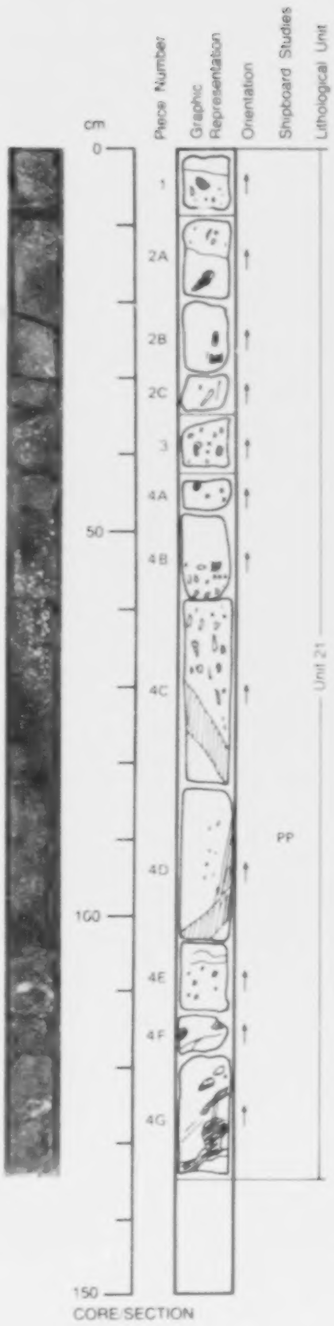
cm
Piece Number
Graphic Representation
Orientation
Shipboard Studies
Lithological Unit
0
50
100
150
1
2A
2B
2C
3
4A
4B
4C
4D
4E
4F
4G
PP
Unit 21
CORE/SECTION

125-786B-57R-2

UNIT 21: BONINITE PILLOWS AND BONINITIC HYALOCLASTITIC SAND (CONTINUED FROM 57R-1)

Pieces 1-4G

CONTACTS: Between hyaloclastite sand and pillows in Pieces 2 and 4.

PHENOCRYSTS: Glomerocrysts of orthopyroxene and sparse clinopyroxene, and isolated orthopyroxene.
Orthopyroxene - 3-10%, <1.5 mm, euhedral, with spinel inclusions.
Clinopyroxene - trace, <0.3 mm, euhedral, equant.

GROUNDMASS: Fine-grained to glassy with microlites of feldspar, variably altered.

VESICLES: 0-15%, <8 mm long, elongate-ovoid to irregular, concentrated at fragment boundaries; often filled with white zeolite and green amorphous altered glass (or zeolite?).

COLOR: Dark greenish gray (5BG 4/1) to dark brown (7.5YR 3/4).

STRUCTURE: Pillow lavas and brecciated hyaloclastite overlying pillow lavas.

ALTERATION: Zeolites and Fe-oxide filled (altered clays) veins and cavities.

VEINS/FRACTURES: 1-2%, 1-4 mm, random; some large (1 cm) diameter elongate cavities are present filled with Fe-oxide and zeolite.

ADDITIONAL COMMENTS: Continuation of 125-786B-57R-1.

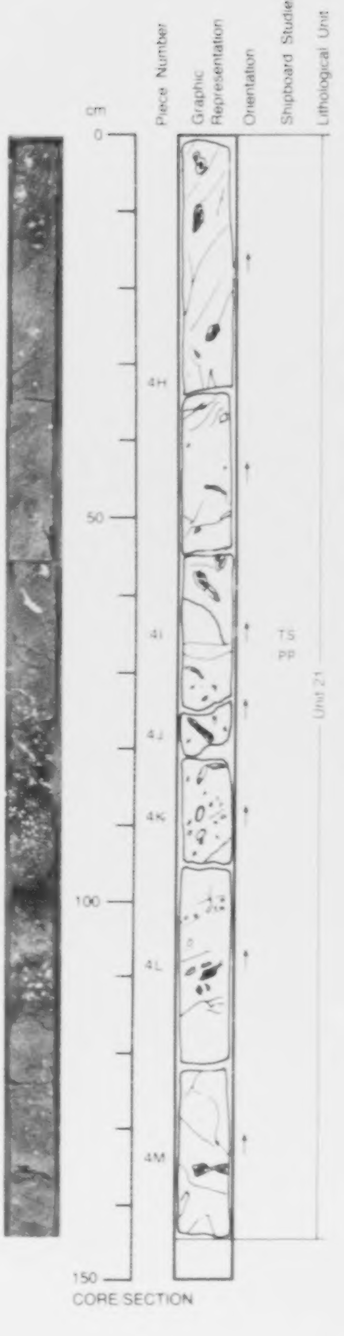
cm
Piece Number
Graphic Representation
Orientation
Shipboard Studies
Lithological Unit
0
50
100
150
4H
4I
4J
4K
4L
4M
TS
PP
Unit 21
CORE SECTION

125-786B-57R-3

UNIT 21: BONINITE PILLOWS AND HYALOCLASTITE (CONTINUED FROM 57R-2)

Pieces 4H-4M

CONTACTS: Between hyaloclastite sand and pillows in Pieces 4K and 4J.
PHENOCRYSTS: Orthopyroxene occurs as isolated crystals and glomerocrysts with sparse clinopyroxene.
Orthopyroxene - 3-10%, <1.5 mm, euhedral tabular, with spinel inclusions.
Clinopyroxene - trace, <0.3 mm, euhedral, equant, deep green.
GROUNDMASS: Fine grained to glassy with microliths of feldspar, variably altered.
VESICLES: 0-15%, 1-6 mm, round to elongate, irregular, concentrated in fracture boundary 4I-4L, filled with white and green zeolite, appear concentrated at pillow boundaries.
COLOR: Dark greenish gray (5BG 4/1) to dark brown (7.5YR 3/4).
STRUCTURE: Massive to pillow brecciated.
ALTERATION: Zeolite, Fe-oxide alteration of vein filling, chlorite in the groundmass.
VEINS/FRACTURES: 1-2%, 1-3 mm wide, random orientation, veins filled with zeolite and larger fractures (up to 1 cm) also zeolite filled.
ADDITIONAL COMMENTS: Continuation of 125-786B-57R-2.

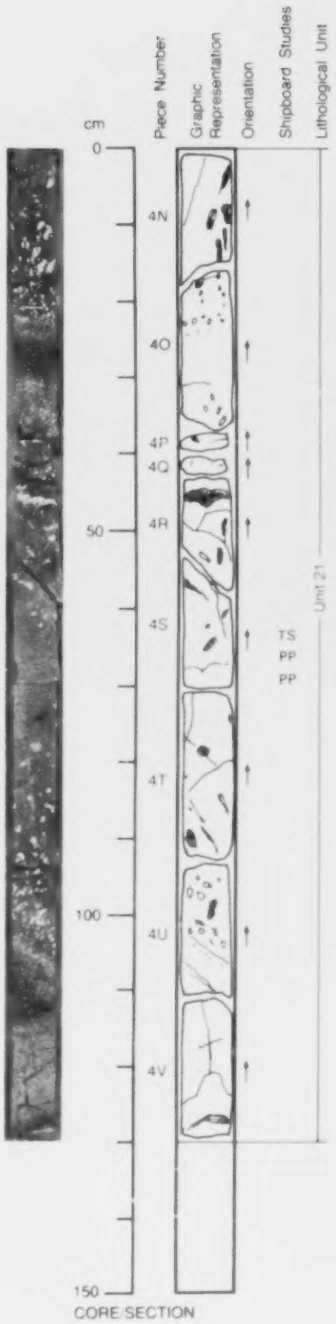
cm
0
50
100
150
CORE/SECTION
Piece Number
Graphic Representation
Orientation
Shipboard Studies
Lithological Unit
4N
4O
4P
4Q
4R
4S
4T
4U
4V
TS
PP
PP
Unit 21

125-786B-57R-4

UNIT 21: BONINITE PILLOWS AND HYALOCLASTITE (CONTINUED FROM 57R-3)

Pieces 4N-4V

CONTACTS: Between boninite pillows and hyaloclastite in Pieces 4O, 4U.
PHENOCRYSTS: Orthopyroxenes occur as glomerocrysts with and without clinopyroxenes, and as isolated crystals.
Orthopyroxene - 6-10%, <1.5 mm, euhedral, tabular, with occasional spinel inclusions.
Clinopyroxene - trace, <0.3 mm, euhedral, equant.
GROUNDMASS: Fine-grained to glassy with microlites of feldspar, variably altered.
VESICLES: 0-20%, 0-7 mm long, elongate to round, concentrated at fragment boundaries, filled with white and light-green zeolite.
COLOR: Dark greenish gray (5BG 4/1) to dark brown (7.5YR 3/4).
STRUCTURE: Massive to pillow lava and brecciated pillows.
ALTERATION: Zeolites alteration as vesicle and fracture filling.
VEINS/FRACTURES: 1-2%, 1-3 mm wide, random, filled with white and green zeolite.
ADDITIONAL COMMENTS: Continuation of 125-786B-57R-1.

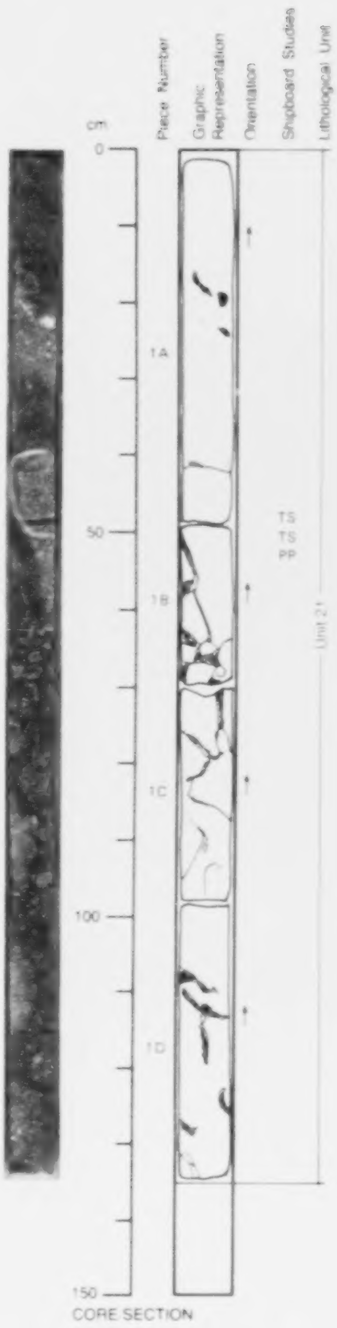
cm
0
50
100
150
CORE SECTION
Piece Number
Graphic Representation
Orientation
Shipboard Studies
Lithological Unit
1A
1B
1C
1D
TS
TS
PP
Unit 21

125-786B-57R-5

UNIT 21: BONINITIC PILLOWS AND HYALOCLASTITE (57R-4 CONTINUED)

Pieces 1A-1D

CONTACTS: No distinct contacts visible.
PHENOCRYSTS: Glomerocrysts of orthopyroxene with and without clinopyroxene.
Orthopyroxene - 5-10%, <1.5 mm, euhedral, tabular, some with spinel inclusions.
Clinopyroxene - trace, <0.3 mm, euhedral, equant.
GROUNDMASS: Fine grained to glassy with microlites of feldspar, variably altered.
VESICLES: 0-7%, 1-3 mm, round to elongate, concentrated at pillow rims, filled with white zeolite, vesicles concentrated just below glassy pillow rims.
COLOR: Dark greenish gray (5BG 4/1) to dark brown (7.5YR 3/4).
STRUCTURE: Pillow structure with minor brecciation.
ALTERATION: Zeolites and Fe-oxide alteration in vesicles, veins, fractures; minor chlorite in groundmass.
VEINS/FRACTURES: 1-4%, 1-4 mm wide, random, irregular, locally concentrated at fragment boundaries.
ADDITIONAL COMMENTS: Continuation of 125-786B-57R-4.

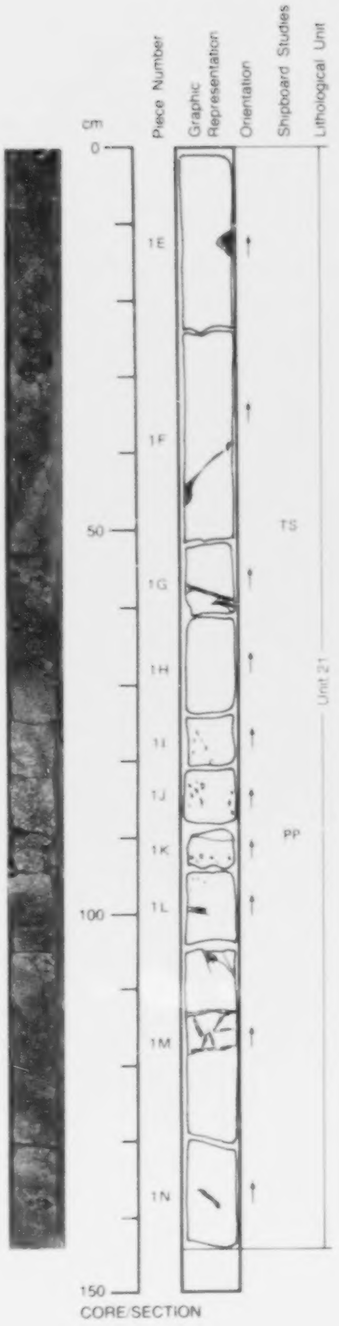
cm
Piece Number
Graphic Representation
Orientation
Shipboard Studies
Lithological Unit
0
50
100
150
1E
1F
1G
1H
1I
1J
1K
1L
1M
1N
TS
PP
Unit 21
CORE/SECTION

125-786B-57R-6

UNIT 21: BONINITIC PILLOWS AND HYALOCLASTITE (CONTINUED FROM 57R-5)

Pieces 1E-1N

CONTACTS: Between hyaloclastite and pillow in Pieces 1H to 1I.
PHENOCRYSTS: Glomerocrysts of orthopyroxene with and without clinopyroxene.
Orthopyroxene - 5-10%, <1.5 mm, euhedral, tabular.
Clinopyroxene - trace, <0.5 mm, euhedral.
GROUNDMASS: Very fine grained to glassy with microlites of feldspar, variably altered.
VESICLES: 0-25%, <6 mm, ovoid irregular, concentrated in pillow fragment, filled with fibrous white zeolite.
COLOR: Matrix hyaloclastite is dark gray green (5G 3/2), clasts are dark bluish gray (5B 4/1), interior of pillow fragment is reddish brown (5YR 4/4).
STRUCTURE: Hyaloclastite breccia.
ALTERATION: Extensive green alteration, possibly zeolitic and smectitic.
VEINS/FRACTURES: 2-3%, <8 mm, random, filled with altered glass; some filling by ferromanganese red fine-grained porcellanous sediment (yellowish red 5YR 4/6).
ADDITIONAL COMMENTS: Continuation of 125-786B-57R-5.

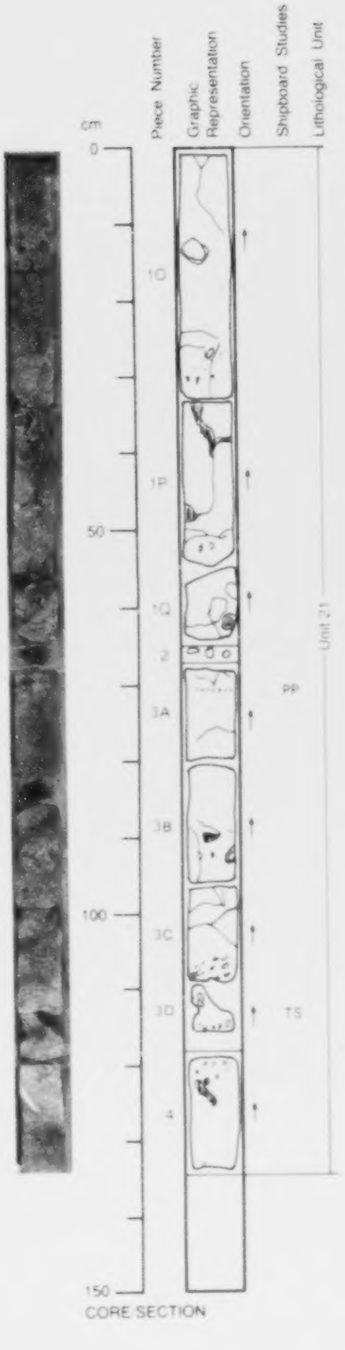
Piece Number
Graphic Representation
Orientation
Shipboard Studies
Lithological Unit
cm
0
50
100
150
CORE SECTION
1O
1P
1Q
2
3A
3B
3C
3D
4
PP
TS
Unit 21

125-786B-57R-7

UNIT 21: BONINITIC PILLOWS AND HYALOCLASTITE (CONTINUED FROM 57R-6)

Pieces 1O-4

CONTACTS: Between hyaloclastite and pillow in Pieces 3 and 4.
PHENOCRYSTS: Glomerocrysts of orthopyroxene with and without clinopyroxene.
Orthopyroxene - 5-10%, <1.5 mm, euhedral, tabular.
Clinopyroxene - trace, <0.5 mm, euhedral.
GROUNDMASS: Very fine grained to glassy with microlites of feldspar, variably altered.
VESICLES: 0-15%, <7 mm, avoid-irregular, concentrated at pillow rims; filled with fibrous white zeolite.
COLOR: Matrix: dark gray green (5G 1/2); clasts: dark bluish gray (5B 4/1); pillow interior: greenish gray (5G 5/1).
STRUCTURE: Hyaloclastite breccia.
ALTERATION: Extensive green alteration, possibly zeolitic and smectitic.
VEINS/FRACTURES: 2%, <2-4 mm, random, filled with altered glass and microfragments.
ADDITIONAL COMMENTS: Interstices between some clasts filled with ferromanganese red fine-grained porcellanous sediment (yellowish red 5YR 4/6); continuation of 125-786B-57R-6.

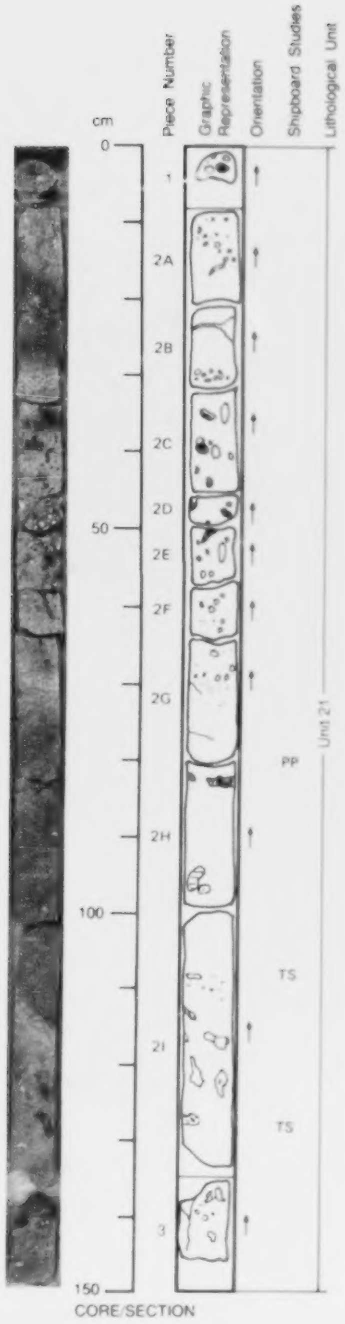
cm
0
50
100
150
Piece Number
Graphic Representation
Orientation
Shipboard Studies
Lithological Unit
1
2A
2B
2C
2D
2E
2F
2G
2H
2I
3
PP
TS
TS
Unit 21
CORE/SECTION

125-786B-58R-1

UNIT 21: BONINITIC PILLOW AND HYALOCLASTITE (CONTINUATION OF 57R-7)

Pieces 1-3

CONTACTS: Between pillows and hyaloclastite in Pieces 2A, B, G, I.
PHENOCRYSTS: Glomerocrysts of orthopyroxene and clinopyroxene.
Orthopyroxene - 3-7%; <1.5 mm; elongate, euhedral; inclusions of spinel.
Clinopyroxene - trace; <0.3 mm; equant to elongate.
GROUNDMASS: Fine grained to glassy with microlites of feldspar; variably altered.
VESICLES: 0-25%; 1-7 mm; round to elongate, ragged; locally concentrated; some are filled with white fibrous to fine grained zeolite, some are unfilled; Piece 1 and 2C-F are very vesicular, up to 25%, 6-7 mm wide.
COLOR: Light gray (5Y 7/1) to dark greenish gray (5G 4/1).
STRUCTURE: Massive to hyaloclastite.
ALTERATION: Zeolites, chlorite in the groundmass; minor hematite staining and veining especially in Piece 2I.
VEINS/FRACTURES: 0-2%; 0.5-3 mm wide; random orientation; filled with dark green amorphous and white crystalline zeolite.
ADDITIONAL COMMENTS: Continuation of 125-786B-57R-7.

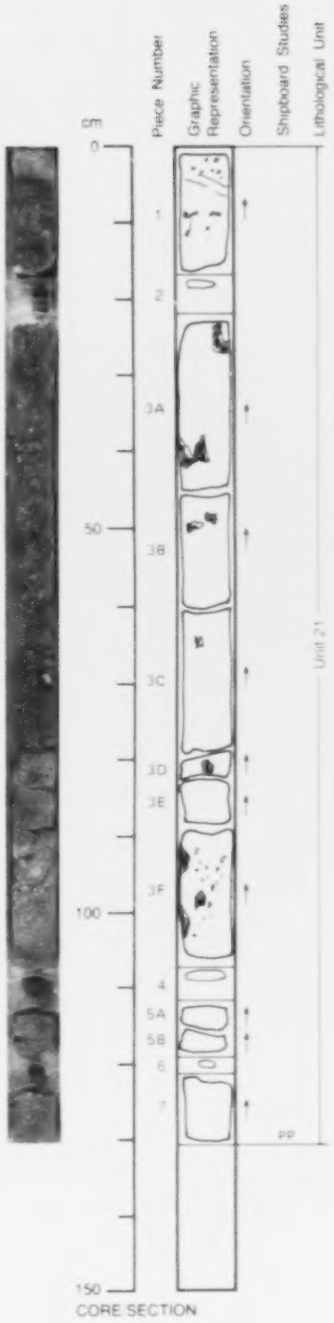
cm
0
50
100
150
CORE SECTION
Piece Number
Graphic Representation
Orientation
Shipboard Studies
Lithological Unit
1
2
3A
3B
3C
3D
3E
3F
4
5A
5B
6
7
PP
Unit 21

125-786B-58R-2

UNIT 21: BONINITIC HYALOCLASTITE, MINOR PILLOW LAVAS (CONTINUATION OF 58R-1)

Pieces 1-7

CONTACTS: Piece 1 only contact between pillow rind and hyaloclastite.
PHENOCRYSTS: Glomerocrysts of orthopyroxene with and without clinopyroxene.
Orthopyroxene - 3-5%, 0.5-1.5 mm, elongate, euhedral to subhedral.
Clinopyroxene - 1%, 0.5 mm, equant, euhedral.
GROUNDMASS: Hyaloclastite, fine- to medium-grained, variably altered.
VESICLES: 0-3%, 1-2 mm, round, Pieces 1 and 3F only, filled with white, fine-grained to fibrous zeolites; vesicles occur only at pillow-hyaloclastite interface.
COLOR: Grayish green (5G 6/2).
STRUCTURE: Hyaloclastite.
ALTERATION: Zeolites in vesicles and fractures, minor chlorite in groundmass.
VEINS/FRACTURES: 1-2%, fractures 2-15 mm, random, filled with amorphous green material and, rarely, white zeolite.
ADDITIONAL COMMENTS: Continuation of 125-786B-58R-1.

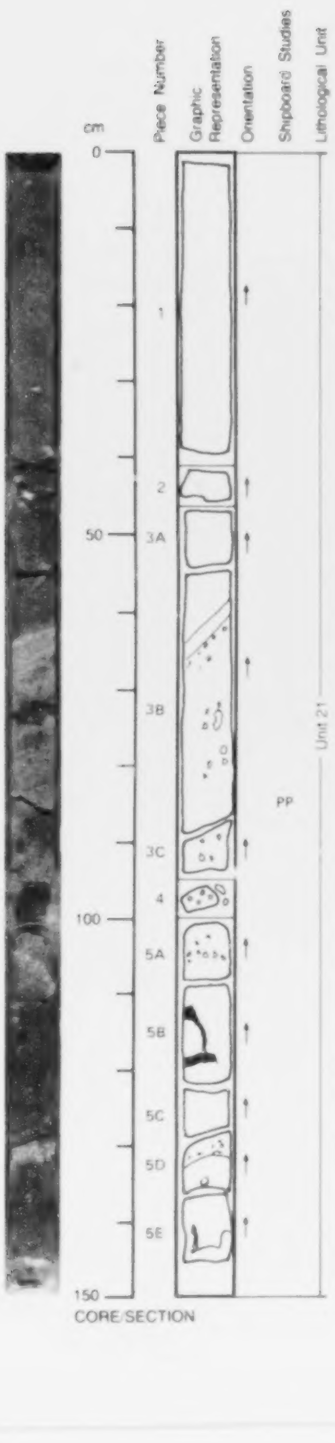
cm
Piece Number
Graphic Representation
Orientation
Shipboard Studies
Lithological Unit
0
50
100
150
1
2
3A
3B
3C
4
5A
5B
5C
5D
5E
PP
Unit 21
CORE/SECTION

125-786B-58R-3

UNIT 21: BONINITIC PILLOW AND HYALOCLASTITE

Pieces 1-5E

CONTACTS: In Pieces 3 - 5 between pillow and hyaloclastite.
PHENOCRYSTS: Glomerocrysts of orthopyroxene with and without clinopyroxene.
Orthopyroxene - 3-5%; 0.5-1.5 mm; elongate, euhedral.
Clinopyroxene - <1%; <0.5 mm; equant, euhedral.
GROUNDMASS: Fine grained to glassy with feldspar microlites, variably altered.
VESICLES: 0-15%; <4 mm; ovoid, concentrated at pillow rims; filled with fibrous white zeolite.
COLOR: Matrix: Dark gray green (5BG 4/1); pillow core dark gray (5Y 4/1) to dusky red (10R 3/4).
STRUCTURE: Fragmented pillow and hyaloclastite.
ALTERATION: Pervasive green alteration in matrix, possibly zeolitic and smectitic.
VEINS/FRACTURES: <2%; <3 mm; random; filled with altered glass, zeolite and ferromanganoan, extremely fine grained sediment (yellowish red 5YR 4/6).
ADDITIONAL COMMENTS: Continuation of 125-786B-58R-2.

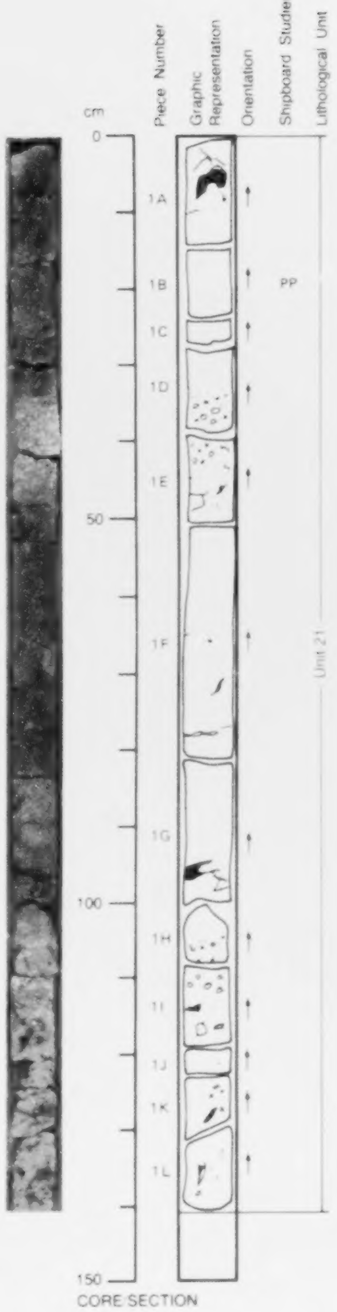
cm
Piece Number
Graphic Representation
Orientation
Shipboard Studies
Lithological Unit
0
50
100
150
1A
1B
1C
1D
1E
1F
1G
1H
1I
1J
1K
1L
PP
Unit 21
CORE/SECTION

125-786B-58R-4

UNIT 21: BONINITIC PILLOWS AND HYALOCLASTITE

Pieces 1A-1L

CONTACTS: In Pieces 1D-E and 1H between pillows and hyaloclastite.
PHENOCRYSTS: Glomerocrysts of orthopyroxene with and without clinopyroxene.
Orthopyroxene - 3-5%, 0.5-1.5 mm, elongate, euhedral.
Clinopyroxene - trace, <0.5 mm, equant, euhedral.
GROUNDMASS: Fine grained to glassy with feldspar microlites in pillow, variably altered.
VESICLES: 0-15%, <15 mm, ovoid-very irregular, concentrated near pillow rims; some filled with fibrous white zeolite.
COLOR: Matrix: Dark gray green (5BG 4/1); pillow interior: greenish gray (5GY 6/1).
STRUCTURE: Massive to fragmented pillow in hyaloclastite.
ALTERATION: Pervasive green alteration in matrix, possibly zeolitic and smectitic.
VEINS/FRACTURES: <3%, <10 mm, random, filled with altered glass, zeolite and some with very fine-grained ferromanganoan sediment (yellowish red 5YR 4/6).
ADDITIONAL COMMENTS: Continuation of 125-786B-58R-3.

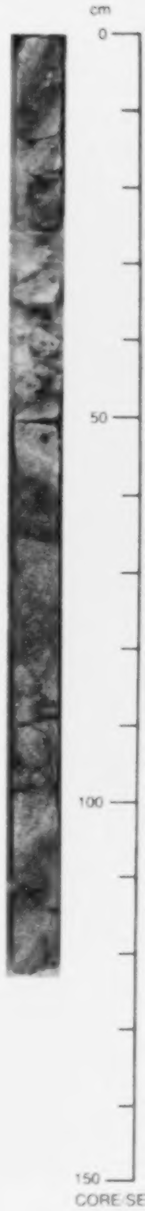
cm
0
50
100
150
CORE/SE

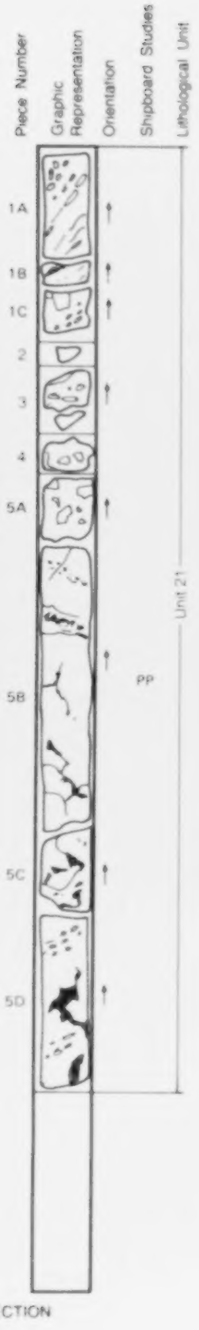
Piece Number
Graphic Representation
Orientation
Shipboard Studies
Lithological Unit
1A
1B
1C
2
3
4
5A
5B
5C
5D
PP
Unit 21
CTION

125-786B-59R-1

UNIT 21: BONINITIC PILLOW AND HYALOCLASTITE BRECCIA

Pieces 1-5D

CONTACTS: In 1B and 5B between pillows and hyaloclastite.
PHENOCRYSTS: Glomerocrysts of orthopyroxene as well as isolated phases.
  Orthopyroxene - 3-7%; 0.3-1.5 mm; elongate; euhedral.
  Clinopyroxene - trace; <0.3 mm; equant; euhedral.
GROUNDMASS: Fine grained to glassy with feldspar microlites in the pillows, variably altered.
VESICLES: 0-25%; <4 mm; ovoid; concentrated near pillow rims; filled with fibrous white zeolite.
COLOR: Matrix is dark gray (5GY 4/1) to dark greenish gray (5BG 4/1); pillow interior is greenish gray(5Y 6/1).
STRUCTURE: Massive to fragmented pillow in hyaloclastite.
ALTERATION: Pervasive green alteration in matrix; zeolitic and trace carbonate in pillow interiors.
VEINS/FRACTURES: Trace; <2 mm; random; filled with altered glass and possibly zeolite. <10 mm irregular pockets with angular boundaries filled with ferromanganoan, very fine grained sediment (dark reddish brown 2.5YR 3/4).
ADDITIONAL COMMENTS: Continuation of 125-786B-58R-4.

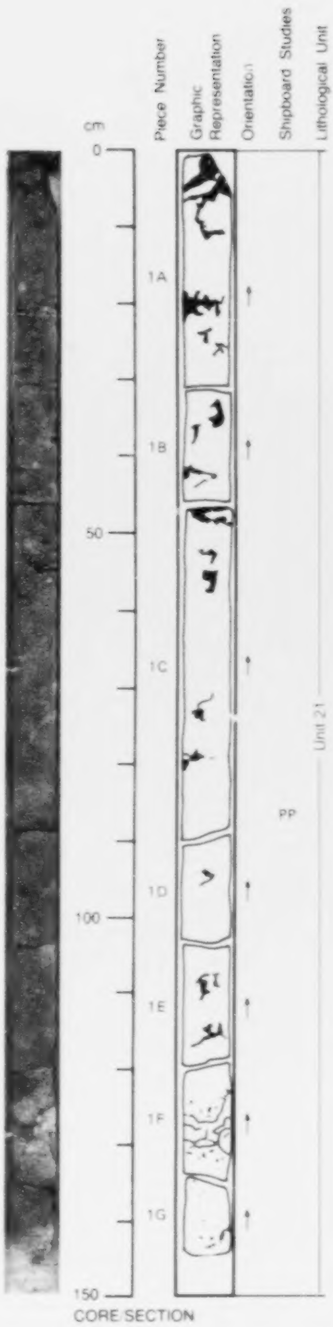
cm
Piece Number
Graphic Representation
Orientation
Shipboard Studies
Lithological Unit
0
50
100
150
1A
1B
1C
1D
1E
1F
1G
PP
Unit 21
CORE/SECTION

125-786B-59R-2

UNIT 21: BONINITIC HYALOCLASTITE AND PILLOW FRAGMENTS

Pieces 1A-1G

CONTACTS: In Pieces 1F and 1G between exterior of pillow fragment and hyaloclastite.
PHENOCRYSTS: Glomerocrystic orthopyroxene occurs with and without clinopyroxene.
Orthopyroxene - 3-8%, <3 mm, euhedral, elongate.
Clinopyroxene - trace, <0.3 mm, euhedral, equant.
GROUNDMASS: Fine grained to glassy with feldspar microlites in pillow fragments, variably altered.
VESICLES: 0-20%, <6 mm, ovoid, concentrated near pillow fragment rims, filled with white fibrous zeolite.
COLOR: Matrix is dark gray (5BG 4/1) to dark greenish gray (5G 4/1); pillow fragment interiors are dark grayish brown (10YR 4/2).
STRUCTURE: Hyaloclastite and fragmental.
ALTERATION: Pervasive green alteration in matrix; zeolitic and trace carbonate in pillow fragments.
VEINS/FRACTURES: <1%, <2 mm, random, filled with altered glass and white zeolite; large irregular fractures/pockets filled with ferromanganoan, very fine-grained sediment (dark reddish brown 10YR 4/2).
ADDITIONAL COMMENTS: Continuation of 125-786B-59R-01.

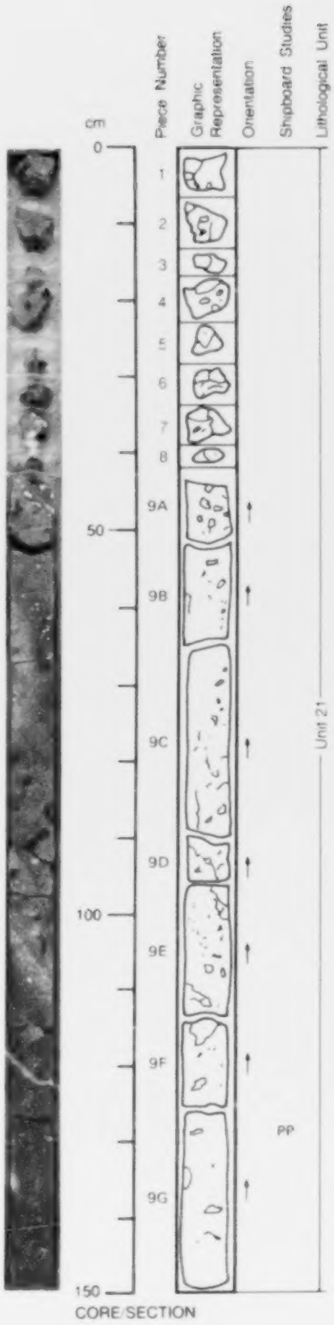
cm
Piece Number
Graphic Representation
Orientation
Shipboard Studies
Lithological Unit
0
50
100
150
1
2
3
4
5
6
7
8
9A
9B
9C
9D
9E
9F
9G
PP
Unit 21
CORE/SECTION

125-786B-59R-3

UNIT 21: BONINITIC PILLOW AND HYALOCLASTITE

Pieces 1-9G

CONTACTS: In Pieces 9A and 9E between pillow and hyaloclastite.
PHENOCRYSTS: Glomerocrystic orthopyroxene occurs with and without clinopyroxene.
Orthopyroxene - 3-10%, <3 mm, euhedral, elongate.
Clinopyroxene - trace, <0.2 mm, euhedral, equant.
GROUNDMASS: Fine-grained to glassy with feldspar microlites in pillow; variably altered.
VESICLES: 0-15%, <15 mm, ovoid, concentrated near pillow rims, filled with white fibrous zeolite.
COLOR: Matrix is dark gray (5B 4/1) to dark greenish gray (5G 4/1); pillow interior and fragments are greenish gray (5GY 6/1).
STRUCTURE: Hyaloclastite and massive pillow.
ALTERATION: Pervasive green alteration of matrix possibly zeolitic and smectitic.
VEINS/FRACTURES: Trace, <1 mm, random, filled with altered glass and zeolite.
ADDITIONAL COMMENTS: Pieces 1 - 8 are isolated pillow fragments; continuation of 125-786B-59R-02.

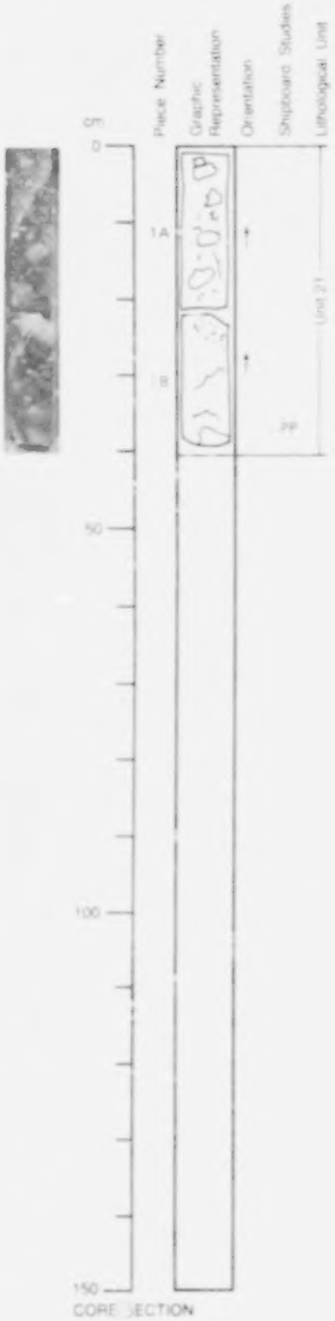
cm
0
50
100
150
Piece Number
Graphic Representation
Orientation
Shipboard Studies
Lithological Unit
1A
1B
PP
Unit 21
CORE SECTION

125-786B-59R-4

UNIT 21: BONINITIC HYALOCLASTITE

Pieces 1A-1B

CONTACTS: None visible.
PHENOCRYSTS: None.
GROUNDMASS: Altered glass with orthopyroxene (<3 mm) in clay and zeolite.
VESICLES: 0-15%, <2 mm, ovoid, concentrated in pillow fragments, filled with fibrous white zeolite.
COLOR: Dark greenish gray (5G 4/1).
STRUCTURE: Hyaloclastite breccia.
ALTERATION: Pervasive green alteration by zeolite and smectite.
VEINS/FRACTURES: Trace, <1 mm, irregular, filled with altered green glass.
ADDITIONAL COMMENTS: Continuation of 125-786B-59R-3 hyaloclastite matrix.

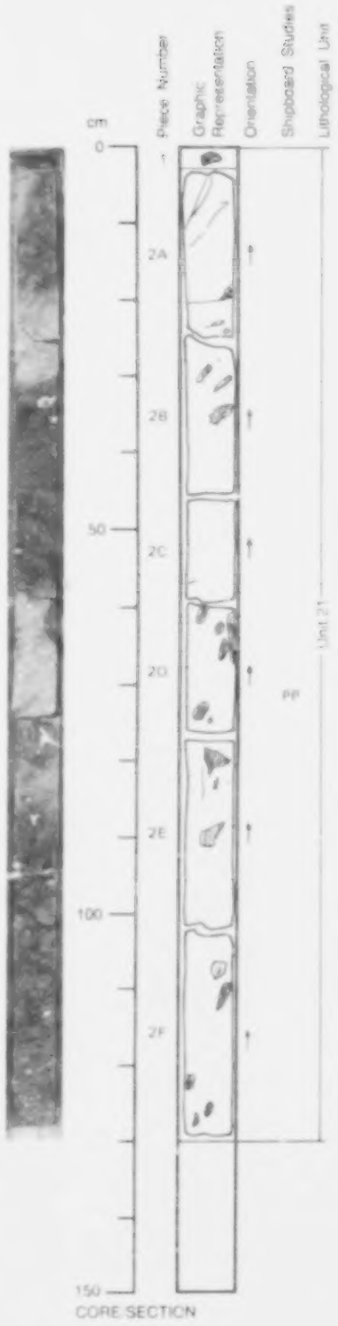

125-786B-60R-1

UNIT 21: TWO-PYROXENE BASALTIC ANDESITE

Piece 1

CONTACTS: None visible.
PHENOCRYSTS:
  Plagioclase - <8%, <0.5 mm, euhedral, tabular.
  Orthopyroxene - <5%, <0.4 mm, euhedral, equant.
  Clinopyroxene - <2%, <0.4 mm, euhedral, equant.
GROUNDMASS: Fine-grained to glassy with plagioclase microlites.
VESICLES: 2%, 0.3-1.5 mm, pipe-shaped, toward edge of piece, empty.
COLOR: Gray (5Y 6/1).
STRUCTURE: Massive.
ALTERATION: Pervasive slight chloritization.
VEINS/FRACTURES: None.
ADDITIONAL COMMENTS: First appearance of phenocryst plagioclase down-hole since 125-786B-55R-3; may be dike or sill.

UNIT 21: HYALOCLASTITE AND BONINITIC PILLOW AND HYALOCLASTITE

Pieces 2A-2F

CONTACTS: In Pieces 2A, 2B and 2E between pillow and hyaloclastite.
PHENOCRYSTS: Glomerocrystic orthopyroxene occurs with and without clinopyroxene.
  Orthopyroxene - 4-8%, <2 mm, euhedral to subhedral, equant.
  Clinopyroxene - <1%, <1 mm, euhedral, equant.
GROUNDMASS: Fine-grained to glassy with feldspar microlites in pillow, variably altered.
VESICLES: 5-15%, <1 cm, ovoid, random, filled with white fibrous zeolite and calcite.
COLOR: Matrix is dark gray (5B 4/1) to dark greenish gray (5G 4/1); pillow interior and fragments are greenish gray (5GY 6/1).
STRUCTURE: Hyaloclastite and massive pillow.
ALTERATION: Pervasive green alteration of matrix.
VEINS/FRACTURES: Trace, <1 mm, random, filled with calcite and zeolite.
ADDITIONAL COMMENTS: Continuation of 125-786B-59R-4.

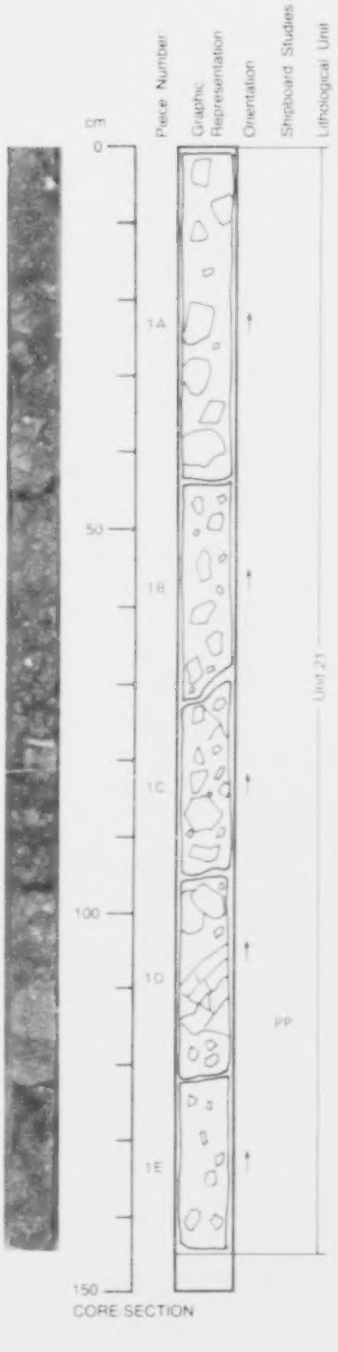
cm
Piece Number
Graphic Representation
Orientation
Shipboard Studies
Lithological Unit
0
50
100
150
1A
1B
1C
1D
1E
PP
Unit 21
CORE SECTION

125-786B-60R-2

UNIT 21: ORTHOPYROXENE ANDESITE BRECCIA

Pieces 1A-1E

CONTACTS: None visible.
PHENOCRYSTS: Pyroxenes are fresh in breccia matrix.
Orthopyroxene - 10%, <3 mm, pale yellow, euhedral, glomerocrystic.
Spinel - trace, <0.05 mm, included in orthopyroxene, black.
GROUNDMASS: Breccia matrix contains chlorite and clays; clasts contain devitrified and altered glass.
VESICLES: 0-5%, < 8 mm, elongate to round, in clasts only, filled with white material, which differs from the swelling clay.
COLOR: Matrix is dark grayish green (5G 4/1); clasts are bluish green gray (5B 4/1 - 5/1).
STRUCTURE: Hyaloclastite.
ALTERATION: Glass is pervasively altered; phenocrysts are often partially altered to serpentine in clasts.
VEINS/FRACTURES: Trace, < 1 mm, random orientation; clasts are fractured.
ADDITIONAL COMMENTS: Hyaloclastic pillow breccia of andesitic lava.

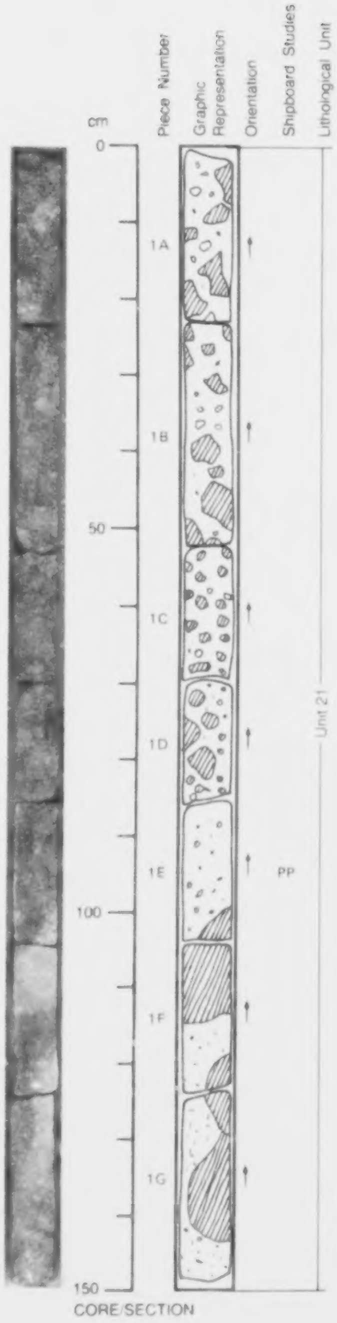
cm
Piece Number
Graphic Representation
Orientation
Shipboard Studies
Lithological Unit
0
50
100
150
1A
1B
1C
1D
1E
1F
1G
PP
Unit 21
CORE/SECTION

125-786B-60R-3

UNIT 21: ORTHOPYROXENE ANDESITE BRECCIA

Pieces 1A-1G

CONTACTS: None visible.
PHENOCRYSTS: Pyroxenes are fresh in breccia matrix, often altered to serpentine in clasts.
Orthopyroxene - 10%, <3 mm, pale yellow, euhedral, glomerocrystic.
Spinel - trace, <0.05 mm, included in orthopyroxene, black (not Cr- rich).
GROUNDMASS: Breccia matrix contains chlorite and clays, clasts contain devitrified and altered glass.
VESICLES: 0-5%, <8 mm, elongate to rounded, in clasts only, are filled with white material that differs from the swelling clay.
COLOR: Matrix is dark grayish green (5G 4/1), clasts are bluish green gray (5B 4/1 - 5/1).
STRUCTURE: Hyaloclastite.
ALTERATION: Glass is pervasively altered.
VEINS/FRACTURES: Trace, <0.1 mm, randomly oriented, clasts are fractured.
ADDITIONAL COMMENTS: Hyaloclastitic pillow breccia of andesitic lava.

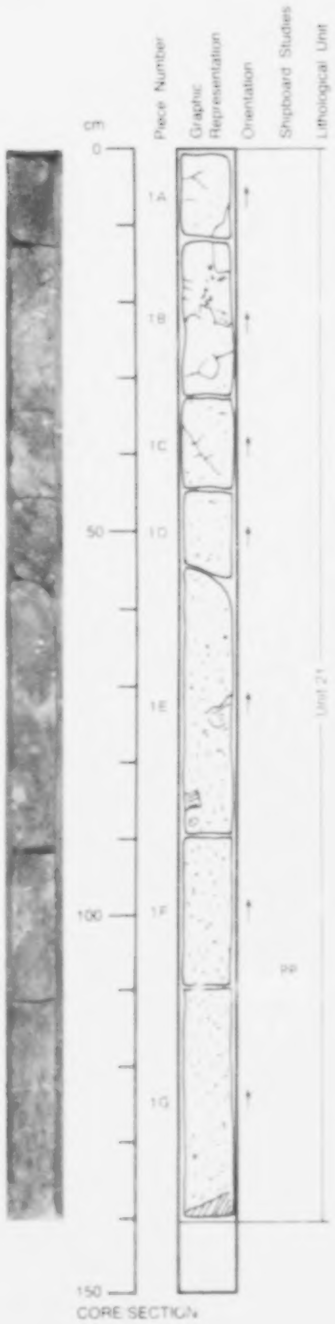
cm
Piece Number
Graphic Representation
Orientation
Shipboard Studies
Lithological Unit
0
50
100
150
1A
1B
1C
1D
1E
1F
1G
PP
Unit 21
CORE SECTION

125-786B-60R-4

UNIT 21: ORTHOPYROXENE ANDESITE BRECCIA

Pieces 1A-1G

CONTACTS: None visible.
PHENOCRYSTS: Pyroxene: are fresh in breccia matrix, often partially altered to serpentine in clasts.
Orthopyroxene: 10%, ≤3 mm, pale yellow, euhedral, glomerocrystic.
Spinel: trace, ≤0.05 mm, included in orthopyroxene, black (not Cr rich).
GROUNDMASS: Breccia matrix contains chlorite and clays; clasts contain devitrified and altered glass.
VESICLES: 0.5%, ≤8 mm, elongate to round, in clasts only, filled with white material that differs from the swelling clay.
COLOR: Matrix is dark grayish green (5G 4/1); clasts are bluish green gray (5B 4/1 - 5/1).
STRUCTURE: Hyaloclastite.
ALTERATION: Glass is pervasively altered.
VEINS/FRACTURES: Trace, ≤0.1 mm, randomly oriented; clasts are fractured.
ADDITIONAL COMMENTS: Hyaloclastic pillow breccia of andesitic lava.

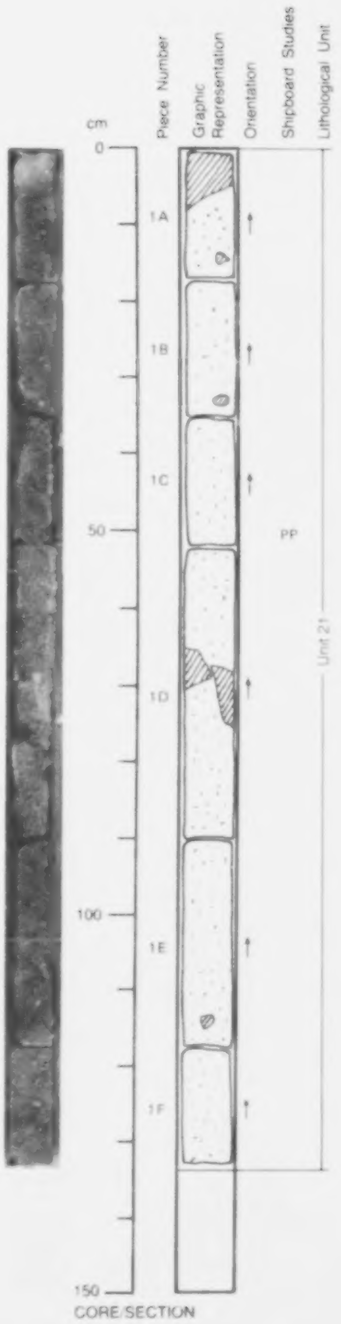
cm
Piece Number
Graphic Representation
Orientation
Shipboard Studies
Lithological Unit
0
50
100
150
1A
1B
1C
1D
1E
1F
PP
Unit 21
CORE/SECTION

125-786B-60R-5

UNIT 21: ORTHOPYROXENE ANDESITE BRECCIA

Pieces 1A-1F

CONTACTS: None visible.
PHENOCRYSTS: Pyroxenes are fresh in breccia matrix, often partially altered to serpentine in clasts.
Orthopyroxene - 10%, <3 mm, pale yellow, euhedral, glomerocrystic.
Spinel - trace, <0.05 mm, included in orthopyroxene, black (not Cr rich).
GROUNDMASS: Breccia matrix contains chlorite and clays; clasts contain divitrified and altered glass.
VESICLES: 0.5%, <8 mm, elongate to rounded, in clasts only are filled with white material that is different from the swelling clay.
COLOR: Matrix is dark grayish green (5G 4/1); clasts are bluish green gray (5B 4/1 - 5/1).
STRUCTURE: Hyaloclastite.
ALTERATION: Glass is pervasively altered.
VEINS/FRACTURES: Trace, <0.1 mm, randomly oriented; clasts are fractured.
ADDITIONAL COMMENTS: Hyaloclastitic pillow of andesitic lava; this section is more matrix rich than previous sections.

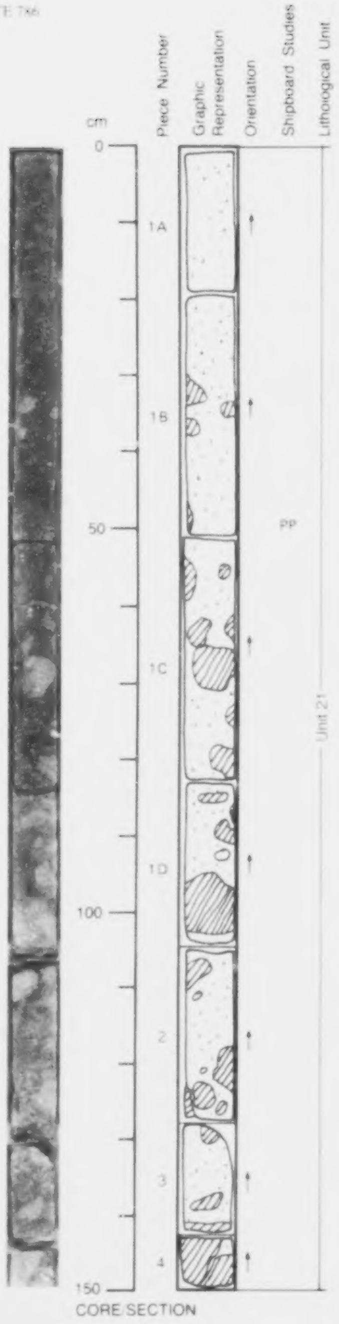
cm
Piece Number
Graphic Representation
Orientation
Shipboard Studies
Lithological Unit
0
50
100
150
1A
1B
1C
1D
2
3
4
PP
Unit 21
CORE/SECTION

125-786B-60R-6

UNIT 21: ORTHOPYROXENE ANDESITE BRECCIA

Pieces 1-4

CONTACTS: None visible.
PHENOCRYSTS: Pyroxenes are fresh in breccia matrix, often partially altered to serpentine clasts.
Orthopyroxene - 10%, <3 mm, pale yellow, euhedral, glomerocrystic.
Spinel - trace, <0.05 mm, included in orthopyroxene, black (not Cr rich).
GROUNDMASS: Breccia matrix contains chlorite and clays; clasts contain divitrified and altered glass.
VESICLES: 0-5%, <8 mm, elongate to rounded, in clasts only, filled with white material that is different from the swelling clay.
COLOR: Matrix is dark grayish green (5G 4/1); clasts are bluish green gray (5B 4/1 - 5/1) and rarely, red (2.5 YR 5/8).
STRUCTURE: Hyaloclastite.
ALTERATION: Glass is pervasively altered.
VEINS/FRACTURES: Trace, <0.1 mm, randomly oriented; clasts are fractured.
ADDITIONAL COMMENTS: Hyaloclastic pillow breccia, of andesitic lava; continuation of 125-786B-60R-05.

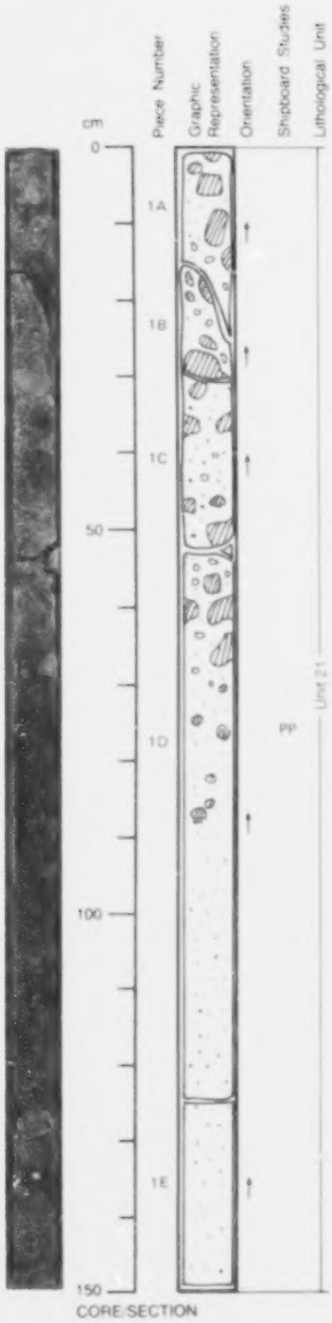
cm
0
50
100
150
CORE/SECTION
Piece Number
Graphic Representation
Orientation
Shipboard Studies
Lithological Unit
1A
1B
1C
1D
1E
PP
Unit 21

125-786B-61R-1

UNIT 21: ORTHOPYROXENE ANDESITE BRECCIA (60R-6 CONTINUED)

Pieces 1A-1E

CONTACTS: None visible.
PHENOCRYSTS: Pyroxenes are fresh in breccia matrix, often partially altered in serpentine clasts.
Orthopyroxene - 5%, <3 mm, pale yellow, euhedral.
Spinel - trace, <0.05 mm, included in orthopyroxene, black (not Cr rich).
GROUNDMASS: Breccia matrix contains strongly altered glass with orthopyroxene crystals; clasts contain altered glass.
VESICLES: 0-10%, < 4 mm, round to elongate, uniform size within clasts, filled with white material.
COLOR: Matrix is dark greenish gray (5G 4/1); clasts are gray (N 5/) and weak red to red (10R 5/3 - 5/6).
STRUCTURE: Brecciated.
ALTERATION: Pervasive alteration of glasses to chlorite.
VEINS/FRACTURES: Trace, <0.1 mm, random orientation; fracturing along clast rims.
ADDITIONAL COMMENTS: Continuation of 125-786B-60R-1; more reddish material; clasts are absent below 90 cm.

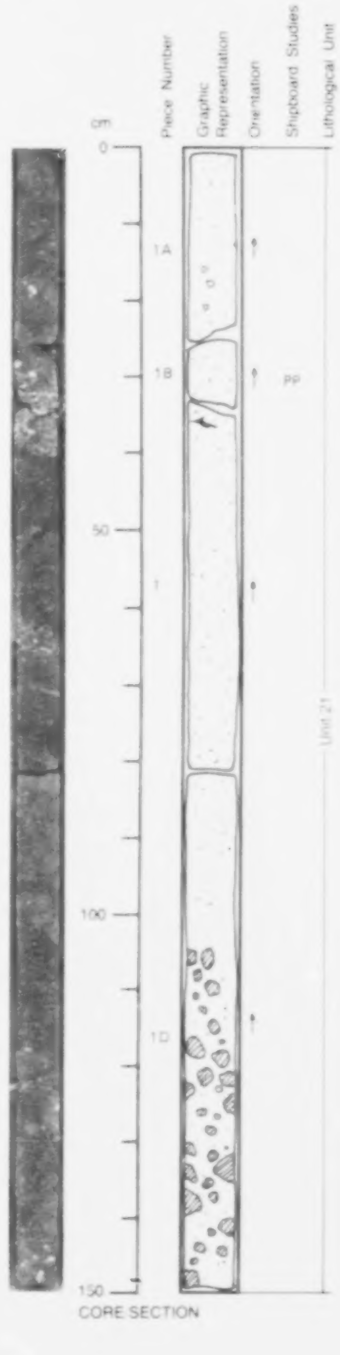
cm
0
50
100
150
CORE SECTION
Piece Number
Graphic Representation
Orientation
Shipboard Studies
Lithological Unit
1A
1B
1
1D
PP
Unit 21

125-786B-61R-2

UNIT 21: ORTHOPYROXENE ANDESITE SAND

Pieces 1A-1D

CONTACTS: None visible
PHENOCRYSTS:
Orthopyroxene - 3-5%, <2 mm, euhedral.
GROUNDMASS: N/A
VESICLES: N/A
COLOR: Dark greenish gray (5GY 4/1).
STRUCTURE: N/A
ALTERATION: Local oxidation to dark red material.
VEINS/FRACTURES: N/A
ADDITIONAL COMMENTS: Continuation of 61R-1.

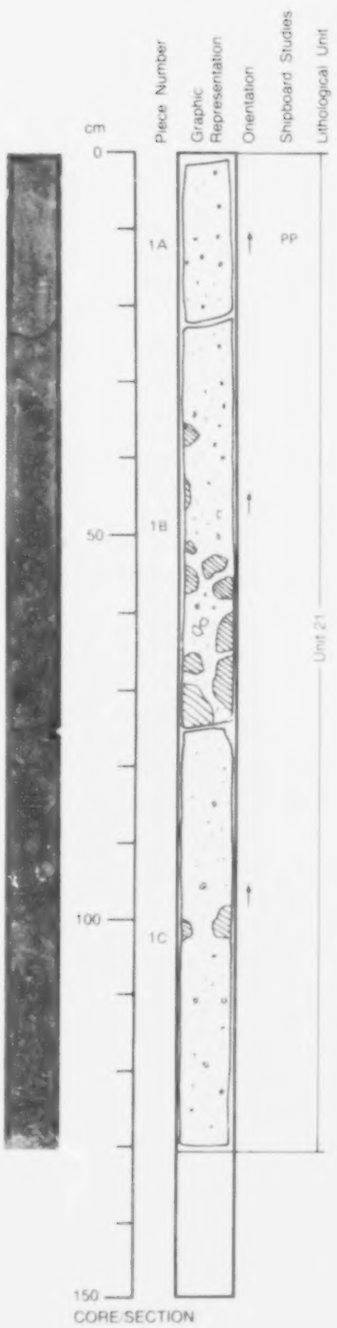
cm
0
50
100
150
Piece Number
Graphic Representation
Orientation
Shipboard Studies
Lithological Unit
1A
PP
1B
1C
Unit 21
CORE/SECTION

125-786B-61R-3

UNIT 21: ORTHOPYROXENE ANDESITE SANDSTONE

Pieces 1A-1C

CONTACTS: None visible.
PHENOCRYSTS:
Orthopyroxene - 3-5%; <2 mm; euhedral.
GROUNDMASS: N/A
VESICLES: Trace; <1 mm; round to elongate; in clasts.
COLOR: Dark greenish gray (5GY 4/1).
STRUCTURE: N/A
ALTERATION: Local oxidation to dark red material, alteration of glass to chlorite.
VEINS/FRACTURES: N/A
ADDITIONAL COMMENTS: Continuation of 61R-1.

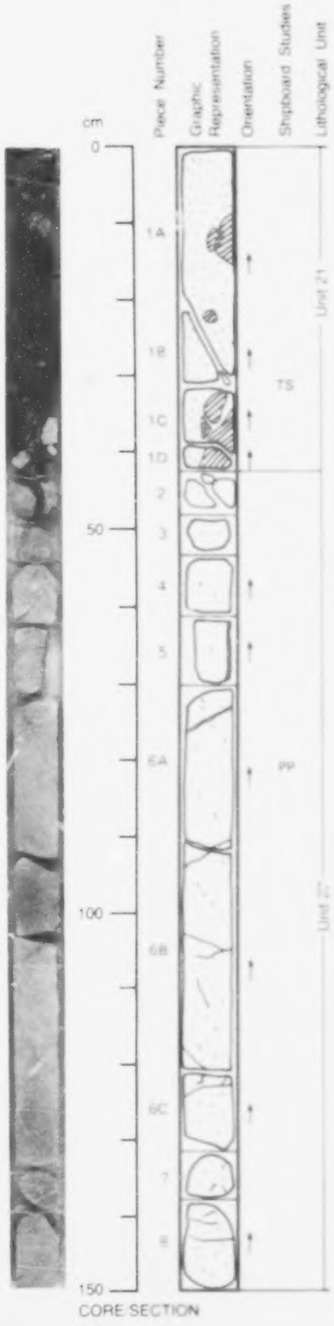
cm
Piece Number
Graphic Representation
Orientation
Shipboard Studies
Lithological Unit
0
50
100
150
1A
1B
1C
1D
2
3
4
5
6A
6B
6C
7
8
TS
PP
Unit 21
Unit 22
CORE/SECTION

125-786B-61R-4

UNIT 21: ORTHOPYROXENE ANDESITE SANDSTONE (61R-3 CONTINUED)

Piece 1

CONTACTS: None present.
PHENOCRYSTS:
Orthopyroxene - 3-5%, <2 mm, euhedral.
GROUNDMASS: N/A
VESICLES: N/A
COLOR: Dark greenish gray (5GY 4/1).
STRUCTURE: N/A
ALTERATION: N/A
VEINS/FRACTURES: Slickensides in bottom of Piece 1 have reddish coloration at the surface.

UNIT 22: RHYOLITE

Pieces 2-8

CONTACTS: None visible.
PHENOCRYSTS: Plagioclase is altered.
Plagioclase - 5%, <3 mm, euhedral laths.
Magnetite - trace, <0.1 mm, euhedral.
GROUNDMASS: Altered to serpentine and clay.
VESICLES: 5%, <2 mm, elongate, randomly distributed.
COLOR: Gray (2.5Y 5/0).
STRUCTURE: N/A
ALTERATION: Along fractures, ground mass is pervasively altered.
VEINS/FRACTURES: 1%, <2 mm, shallow dipping, but variable orientation; calcite in fractures; reddish oxide rims present.

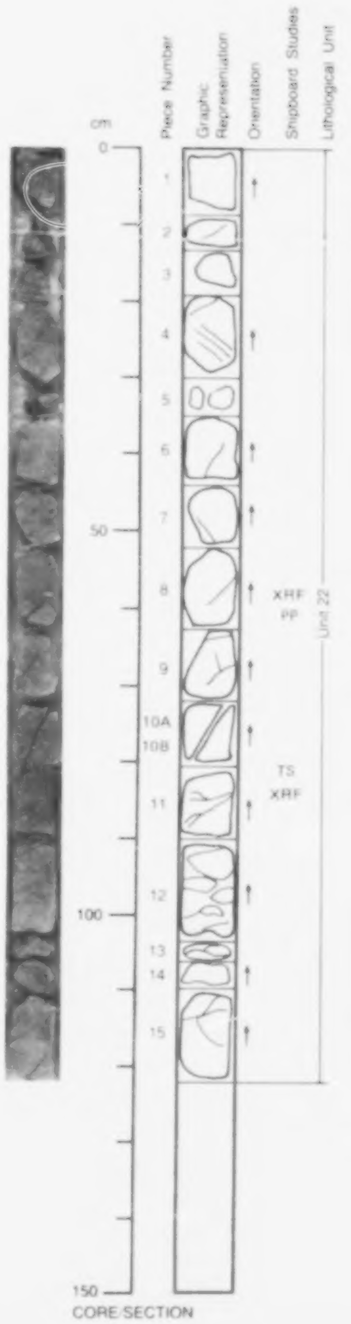
cm
Piece Number
Graphic Representation
Orientation
Shipboard Studies
Lithological Unit
0
50
100
150
1
2
3
4
5
6
7
8
9
10A
10B
11
12
13
14
15
XRF
PP
TS
XRF
Unit 22
CORE/SECTION

125-786B-61R-5

UNIT 22: RHYOLITE (CONTINUATION OF 61R-4)

Pieces 1-15

CONTACTS: None visible.
PHENOCRYSTS:
Plagioclase: 5%, <3 mm, euhedral laths.
Magnetite: trace, <0.1 mm, euhedral.
GROUNDMASS: Altered to serpentine and clay.
VESICLES: 1%, <2 mm, strongly elongate, randomly distributed, some filled with greenish serpentine.
COLOR: Gray (2.5Y 5/0).
STRUCTURE: N/A
ALTERATION: Pervasive alteration.
VEINS/FRACTURES: 1%, <2 mm, generally between 20-60 degree dips; calcite and some red staining along fractures.
ADDITIONAL COMMENTS: Continuation of 125-786B-61R-04.

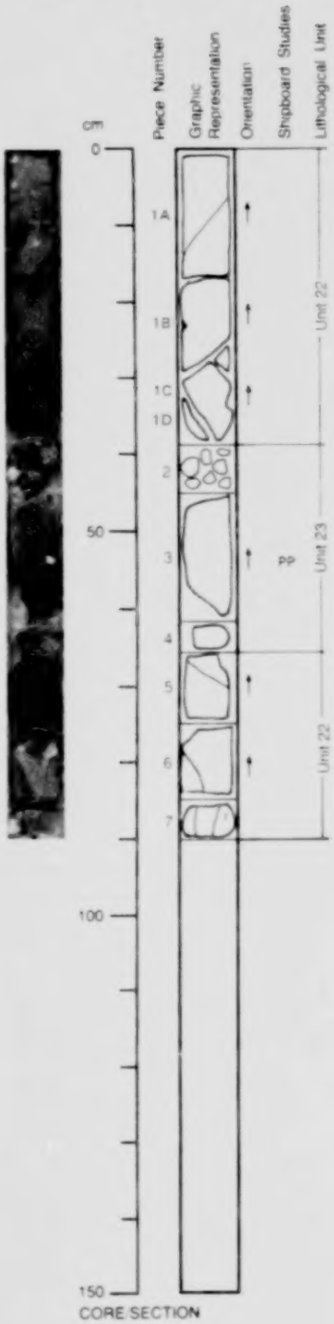
cm
Piece Number
Graphic Representation
Orientation
Shipboard Studies
Lithological Unit
0
50
100
150
1A
1B
1C
1D
2
3
4
5
6
7
PP
Unit 22
Unit 23
Unit 22
CORE SECTION

125-786B-61R-6

UNIT 22: RHYOLITE (61R-5 CONTINUED)

Pieces 1A-1D, 5-7

CONTACTS: Gradational contact from rhyolite to sediment at 10-30 cm; the rhyolite becomes fractured near the contact (brecciation); fracture surfaces are slickensided at 25-35 cm. Pieces 5, 6, and 7 are rhyolite again.
PHENOCRYSTS:
Plagioclase - 5%, <3 mm, euhedral laths.
Magnetite - trace, <0.1 mm, euhedral.
GROUNDMASS: Altered to serpentine and clay.
VESICLES: 1%, <2 mm, strongly elongate, randomly distributed, some filled with greenish serpentine.
COLOR: Gray (2.5Y 5/0).
STRUCTURE: N/A.
ALTERATION: Pervasively altered.
VEINS/FRACTURES: 1%, <2 mm, randomly oriented.

UNIT 23: SHEAR-ZONE BRECCIA AND SANDSTONE

Pieces 2-4

CONTACTS: N/A.
PHENOCRYSTS: N/A.
GROUNDMASS: N/A.
VESICLES: N/A.
COLOR: N/A.
STRUCTURE: N/A.
ALTERATION: N/A.
VEINS/FRACTURES: N/A.
ADDITIONAL COMMENTS: Fractured bluish gray clay that contains brecciated rhyolite clasts. The clay overlies a clay-rich vitric silt containing predominantly quartz and feldspar along with pyroxene.

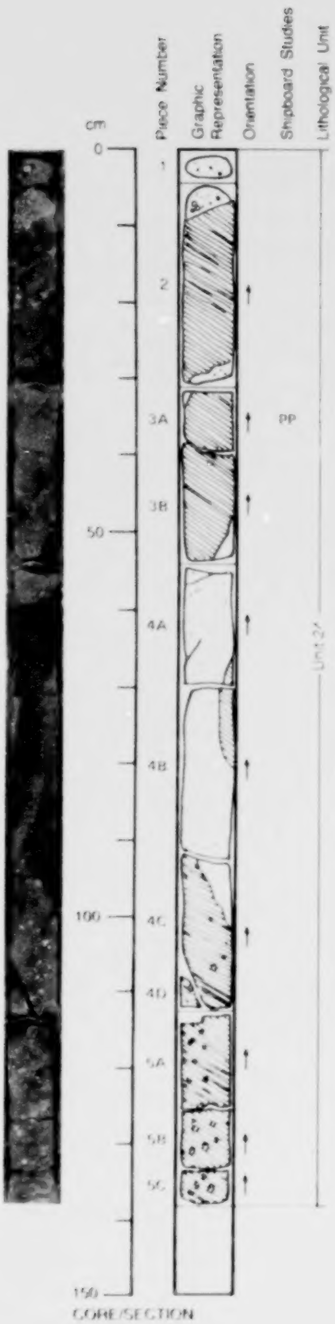
cm
Piece Number
Graphic Representation
Orientation
Shipboard Studies
Lithological Unit
0
50
100
150
1
2
3A
3B
4A
4B
4C
4D
5A
5B
5C
PP
Unit 24
CORE/SECTION

125-786B-62R-1

UNIT 24: BONINITE/TWO-PYROXENE ANDESITE

Pieces 1-5C

CONTACTS: Piece 2 contains contact between brecciated hyaloclastite and fine grained boninite. Piece 4B contains contact between fine grained, altered boninite pillow and very fine grained intrusive andesite vein 2-3 cm wide, which continues below Piece 4B.

PHENOCRYSTS: Two-pyroxene glomerocrysts, up to 5 mm long, are common.

Orthopyroxene - 4-10%, 0.75-2 mm, euhedral, elongate, inclusions of spinel.

Clinopyroxene - 2-4%, <0.75 mm, euhedral, equant, black.

GROUNDMASS: Fine grained, altered.

VESICLES: 0-5%, 2-6 mm, round to irregular, concentrated at Pieces 3B, 4C and 5A, filled with white, fibrous to fine-grained zeolite.

COLOR: Bluish gray to greenish gray (5B 5/1 to 5G 5/1).

STRUCTURE: Brecciated in Pieces 1 and 2A, massive but cut by veins and containing chilled margin.

ALTERATION: Zeolite filled vesicles and veins; groundmass is moderately chloritized and altered to amorphous clays.

VEINS/FRACTURES: <1%, 1-3 mm wide, random, filled with white zeolites, red oxidized sediments and, rarely, carbonate.

ADDITIONAL COMMENTS: Contact between boninite pillows and andesite intrusion. Andesitic dike in Piece 4B is sulfide bearing.

125-786B-62R-2

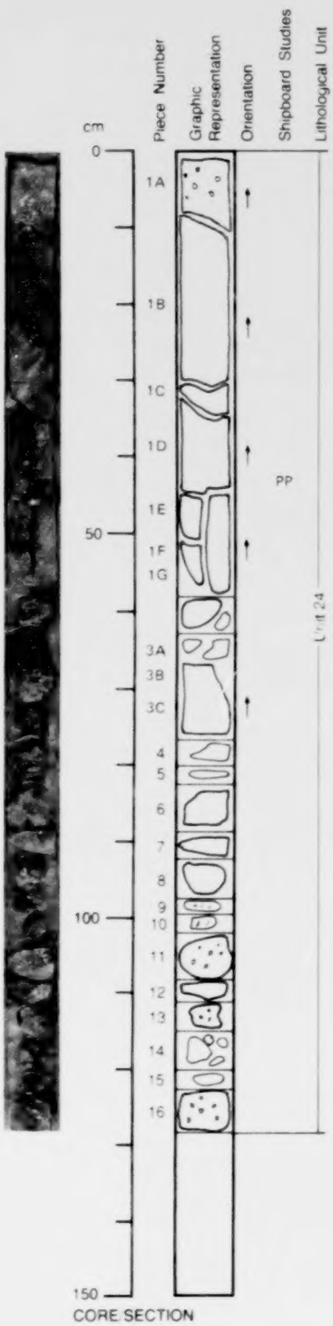
cm
Piece Number
Graphic Representation
Orientation
Shipboard Studies
Lithological Unit
0
50
100
150
1A
1B
1C
1D
1E
1F
1G
3A
3B
3C
4
5
6
7
8
9
10
11
12
13
14
15
16
PP
Unit 24
CORE/SECTION

UNIT 24: BONINITE/TWO-PYROXENE ANDESITE PILLOWS AND HYALOCLASTITE

Pieces 1 - 16

CONTACTS: In Piece 1B, between pillow rim and hyaloclastite breccia.

PHENOCRYSTS: Glomerocrysts of orthopyroxene and clinopyroxene with rare spinel inclusions.

Orthopyroxene - 5-9%; 0.8-1.5 mm; elongate, euhedral to subhedral.
Clinopyroxene - 4-7%; <0.8 mm; euhedral, equant.
Plagioclase - 2-5%; 0.3-0.5 mm; euhedral tabular.

GROUNDMASS: Fine-grained to glassy with sparse microliths of plagioclase; variably altered.

VESICLES: 0-17%; 2-6 mm; elongate to irregular; not present in Pieces 1B-3A; filled with white fibrous amorphous zeolite and, rarely, carbonate.

COLOR: Bluish gray to greenish gray (5B 5/1 to 5G 5/1).

STRUCTURE: Brecciated in Pieces 1-3C; massive but highly vesicular in remainder of core.

ALTERATION: Pervasive clay and chlorite alteration of glass and fine-grained matrix.

VEINS/FRACTURES: <<1%; 1-2 mm wide; random; filled with carbonate and zeolite and, rarely, hematite-altered sediment.

ADDITIONAL COMMENTS: Fine filaments of red ferromanganoan sediment, particularly in hyaloclastite breccia.

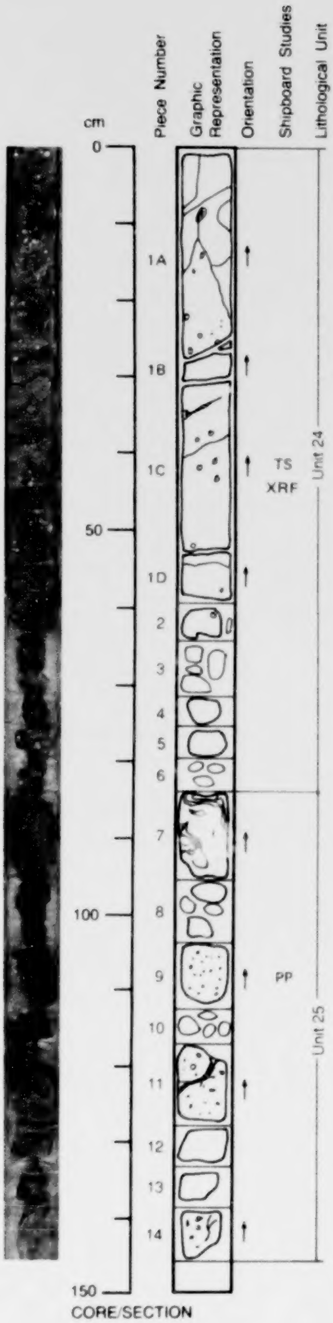

125-786B-62R-3

UNIT 24: BONINITE/TWO-PYROXENE ANDESITE PILLOWS AND HYALOCLASTITE

Pieces 1-6

CONTACTS: Normal to brecciated contact with sediment in Piece 7 (86 cm).
PHENOCRYSTS: Sparse glomerocrysts of orthopyroxene and clinopyroxene.
Orthopyroxene to clinopyroxene ratio decreases down section.
Orthopyroxene - 8-12%, 0.8-2.5 mm, elongate, euhedral to subhedral, some with spinel inclusions.
Clinopyroxene - 3-12%, <1 mm, equant to elongate, euhedral, mode increases down section.
GROUNDMASS: Fine- to medium-grained, with microliths of plagioclase and, possibly, orthopyoxene quench crystals.
VESICLES: 0-5%, 2-7 mm, round to elongate, concentrated in Piece 1, filled with white fibrous to finely crystalline zeolite and rare carbonate.
COLOR: Bluish gray to greenish gray (5B 5/1 to 5G 5/1).
STRUCTURE: Massive, sparsely to moderately phyric.
ALTERATION: Pervasive in groundmass to chlorite and some clay.
VEINS/FRACTURES: <1-2%, veins 1-3 mm, fractures up to 2 cm, random, filling is primarily hematite-altered sediment for the fractures and zeolite with sparse carbonate in the veins.
ADDITIONAL COMMENTS: This is a continuation of 125-786B-62-2.

UNIT 25: VITRIC SILT AND HYALOCLASTITE BRECCIA

Pieces 7-14

CONTACTS: N/A
PHENOCRYSTS: N/A
GROUNDMASS: N/A
VESICLES: N/A
COLOR: Red jasper and greenish gray (5G 5/1).
STRUCTURE: Breccia, cauliflower texture in jasper vitric sediment.
ALTERATION: Pervasive to chlorite/clay minerals.
VEINS/FRACTURES: N/A
ADDITIONAL COMMENTS: Piece 7 shows jasper with fine laminae in swirling and anastomosing pattern with irregular clasts of hyaloclastite breccia. Not certain whether Pieces 7-14 should have been assigned to Unit 24 or to Unit 25.

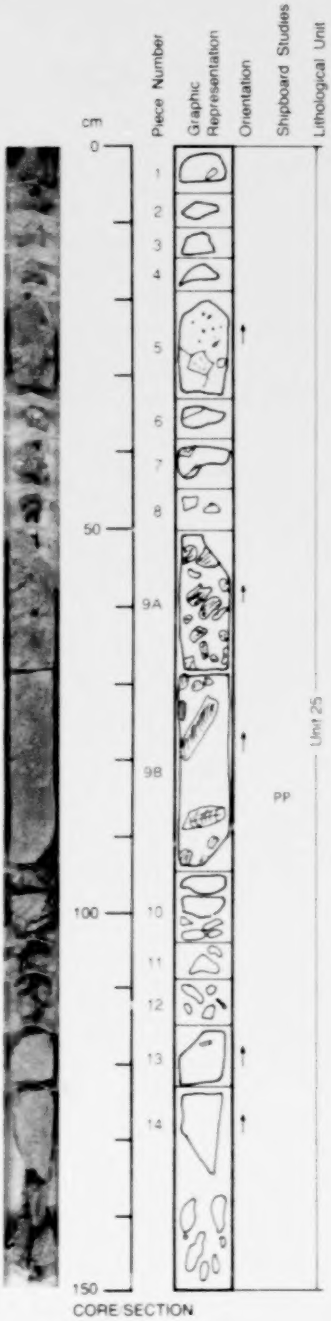

125-786B-63R-1

UNIT 25: META-TWO-PYROXENE ANDESITE

Piece 1

CONTACTS: None visible.
PHENOCRYSTS: Glomerocrysts of clinopyroxene and orthopyroxene.
Orthopyroxene - 2-4%, 0.5-1.5 mm, equant-elongate.
Clinopyroxene - 4-7%, 0.5-2.0 mm, equant euhedral.
Plagioclase - 2-4%, 0.3-0.5 mm, tabular, euhedral.
GROUNDMASS: Fine-grained, composed of 60% feldspar, 40% pyroxene.
VESICLES: None.
COLOR: Greenish gray (5G 5/2).
STRUCTURE: Massive.
ALTERATION: Pervasive chloritization, some fresh cores of pyroxenes remain.
VEINS/FRACTURES: 1%, 3-4 mm wide vugs, random, vugs filled with pale green and white stubby prismatic zeolite and chlorite.

UNIT 25: CATACLASTIC ANDESITE

Pieces 2-4

CONTACTS: None visible.
PHENOCRYSTS: Strings of ortho- and clinopyroxene together with plagioclase as fragmented crystals, proportions difficult to estimate.
GROUNDMASS: Very fine-grained.
VESICLES: None.
COLOR: Gray (5Y 6/1).
STRUCTURE: Strongly sheared.
ALTERATION: Chloritic.
VEINS/FRACTURES: Trace, <0.2 mm, indeterminable, filled with chlorite.
ADDITIONAL COMMENTS: These pieces are strongly sheared and brecciated forming an indurated cataclasite.

UNIT 25: META-TWO-PYROXENE XENOLITH-BEARING ANDESITE

Pieces 5-9

CONTACTS: None visible.
PHENOCRYSTS: Orthopyroxene is pervasively chloritized, clinopyroxene is variably altered. Pyroxenes occur in glomerocrystic patches.
Orthopyroxene - 5-8%, <1.5 mm, euhedral, equant.
Clinopyroxene - <3%, 1.5-0.5 mm, subhedral.
GROUNDMASS: Fine-grained, consisting of about 35% plagioclase and 65% pyroxene.
VESICLES: 15-20%, <5 mm, round ovoid, throughout, filled with zeolite and chlorite.
COLOR: Dark gray (N 4) to light greenish gray (5G 7/1).
STRUCTURE: Shearing prominent in Pieces 8 and 9A, dipping at 70 degrees, and showing normal faulting.
ALTERATION: Pervasive chloritic alteration.
VEINS/FRACTURES: Trace, <1 mm, random, filled with clay and zeolite.
ADDITIONAL COMMENTS: angular-subrounded xenoliths (1-10 cm long) of vesicular, two pyroxene andesite (pervasively chloritized, color is greenish gray, 5G 5/2); the xenoliths are of similar appearance to those in 125-786B-62R-3.

UNIT 25: CATACLASTIC ANDESITE

Pieces 10-14

CONTACTS: None visible.
PHENOCRYSTS: Orthopyroxene and clinopyroxene are present but proportions are difficult to determine.
GROUNDMASS: Very fine-grained.
VESICLES: None.
COLOR: Light greenish gray (10Y 6/1).
STRUCTURE: Tectonic lenses from fault gouge, pervasive shearing dips at 65 degrees and indicates normal brittle faulting.
ALTERATION: Chloritic.
VEINS/FRACTURES: None.

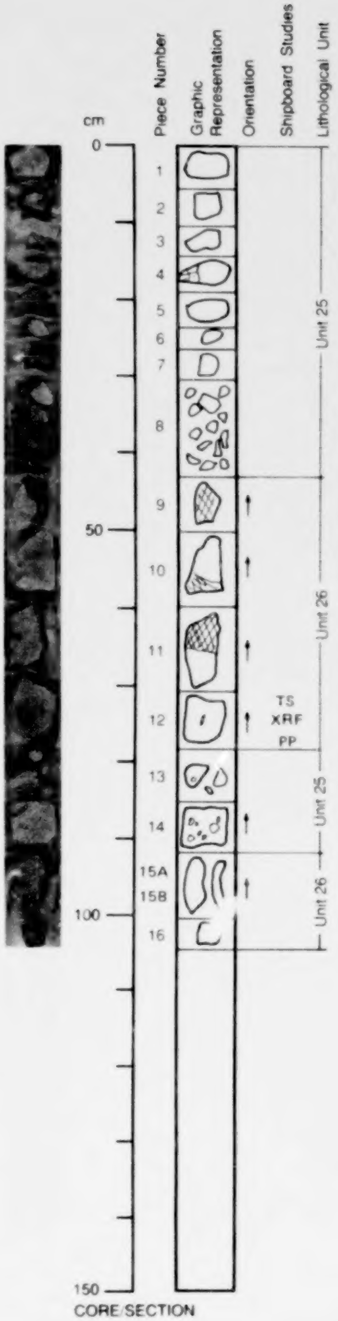

125-786B-63R-2

UNIT 25: CATACLASTIC ANDESITE

Pieces 1-8

CONTACTS: None visible
PHENOCRYSTS: Orthopyroxene and clinopyroxene are present but proportions are difficult to determine
GROUNDMASS: Very fine grained
VESICLES: None
COLOR: Greenish gray (10Y 6/1)
STRUCTURE: Strongly sheared fabric, subvertical
ALTERATION: Chloritic
VEINS/FRACTURES: None
ADDITIONAL COMMENTS: Continuation of Section 125-786B-063R-01

UNIT 26: META-TWO-PYROXENE ANDESITE

Pieces 9-11

CONTACTS: None visible
PHENOCRYSTS: Orthopyroxene is pervasively chloritized, clinopyroxene variably altered
Pyroxenes occur in glomerocystic patches and as isolated crystals
Orthopyroxene - 8-10%, 3-1.5 mm, equant euhedral
Clinopyroxene - 2-4%, 2.5-0.5 mm, subhedral
GROUNDMASS: Fine-grained, consisting of about 35% plagioclase and 65% pyroxene
VESICLES: 5-10%, <2 mm, round ovoid, throughout, filled with zeolite, carbonate and chlorite
COLOR: Dark gray (N 4/) to light greenish gray (5G 7/1)
STRUCTURE: Massive
ALTERATION: Variable chloritic alteration
VEINS/FRACTURES: Trace, <1 mm, random, filled with clay and zeolite
ADDITIONAL COMMENTS: Possible xenoliths of vesicular two pyroxene andesite or variable alteration defining color changes in pieces

UNIT 26: META-RHYOLITE

Piece 12

CONTACTS: None visible
PHENOCRYSTS: Orthopyroxene completely chloritized
Plagioclase - trace, <0.5 mm, euhedral lath
Clinopyroxene - 8-10%, <0.5 mm, euhedral
Orthopyroxene - <2%, <0.3 mm, equant elongate
GROUNDMASS: Very fine grained, altered
VESICLES: 2%, <3 mm, elongate, aligned, filled with zeolite
COLOR: Black (7.5YR 2/0)
STRUCTURE: Flow banded, dipping at 55 degrees
ALTERATION: Chloritic
VEINS/FRACTURES: None

UNIT 25: META-DACITE

Pieces 13 and 14

CONTACTS: None visible
PHENOCRYSTS: Orthopyroxene is completely replaced leaving a carbonate-chlorite-filled vug
Plagioclase - 5%, <1.5 mm, euhedral, tabular
Orthopyroxene - 1-2%, 1-2 mm, euhedral
GROUNDMASS: Fine grained, variably altered, disseminated pyrite
VESICLES: 5%, <5 mm, elongate-irregular, throughout, quartz and sulfide coating on some vesicle walls
COLOR: Gray (2.5YR 8/0)
STRUCTURE: Massive
ALTERATION: Chloritic
VEINS/FRACTURES: Trace, <0.1 mm, random, filled with zeolite

125-786B-63R-2 (continued)

UNIT 26: META-TWO-PYROXENE ANDESITE

Piece 15

CONTACTS: None visible.
PHENOCRYSTS: Mostly occur as isolated phases; pervasively altered.
Plagioclase - 2-3%, 0.5-1.5 mm; equant laths.
Orthopyroxene - 10-12%, 1.5-2.5 mm; euhedral, equant.
Clinopyroxene - 2-5%, 0.5-1.5 mm; euhedral, equant.
Magnetite - 0.5-1%, 0.1-0.3 mm; equant, cubic.
GROUNDMASS: Fine-grained, 40-50% feldspar, 40-50% pyroxene.
VESICLES: None.
COLOR: Greenish gray (5G 5/1).
STRUCTURE: Massive.
ALTERATION: Pervasive lower greenschist facies assemblage of albite after plagioclase, chlorite after orthopyroxene; includes disseminated pyrite and mesh texture of hematite veining.
VEINS/FRACTURES: Trace, <1 mm, sub-vertical, filled with carbonate.

UNIT 26: META-TWO-PYROXENE ANDESITE

Piece 16

CONTACTS: None visible.
PHENOCRYSTS: Orthopyroxene is pervasively chloritized, clinopyroxene variably altered; pyroxenes occur in glomerocrystic patches.
Orthopyroxene - 8-10%, 1.5-3 mm; equant, euhedral.
Clinopyroxene - 2-4%, 2.5-0.5 mm; subhedral.
GROUNDMASS: Fine-grained to very fine-grained, consisting of about 35% plagioclase and 65% pyroxene.
VESICLES: 2%, <1 mm, round to ovoid, throughout, filled with zeolite, carbonate and chlorite.
COLOR: Dark gray (N 4).
STRUCTURE: Massive.
ALTERATION: Pervasive chloritic.
VEINS/FRACTURES: None.
ADDITIONAL COMMENTS: Looks like host from Pieces 5 - 9 from 125-786B-63R-1.

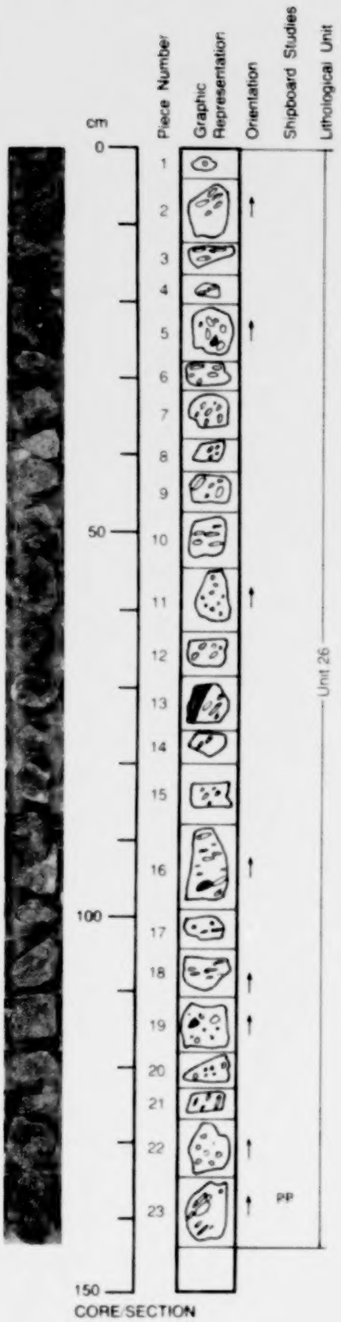
cm
0
50
100
150
Piece Number
Graphic Representation
Orientation
Shipboard Studies
Lithological Unit
1
2
3
4
5
6
7
8
9
10
11
12
13
14
15
16
17
18
19
20
21
22
23
PP
Unit 26
CORE/SECTION

125-786B-64R-1

UNIT 26: META-ORTHOPYROXENE ANDESITE

Pieces 1-23

CONTACTS: None visible.
PHENOCRYSTS: Primary mineralogy altered to lower greenschist facies assemblage (albite-chlorite).
Plagioclase - 3-5%; 0.2-0.8 mm; subhedral-euhedral.
Orthopyroxene - 1-2%; <3 mm; euhedral, elongate.
GROUNDMASS: Fine grained; <2% dusty euhedral magnetite disseminated throughout.
VESICLES: 10%, <15 mm, pipe-shaped; evenly distributed; some filled with carbonate, chlorite and white zeolite, strongly aligned, dipping at 60 degrees.
COLOR: Dark gray (2.5Y 4/0).
STRUCTURE: Massive.
ALTERATION: Variable chloritization of orthopyroxene and albitization of plagioclase.
VEINS/FRACTURES: None.

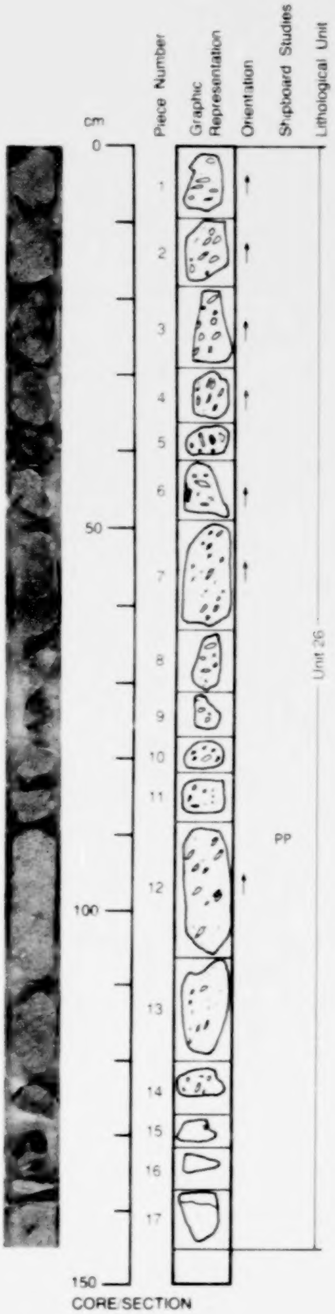
cm
Piece Number
Graphic Representation
Orientation
Shipboard Studies
Lithological Unit
0
50
100
150
1
2
3
4
5
6
7
8
9
10
11
12
13
14
15
16
17
PP
Unit 26
CORE/SECTION

125-786B-64R-2

UNIT 26: META-ORTHOPYROXENE ANDESITE

Pieces 1-17

CONTACTS: None visible
PHENOCRYSTS: Primary mineralogy altered to lower greenschist facies assemblage
Plagioclase - 3-5%, 0.2-0.8 mm, subhedral-euhedral
Orthopyroxene - 1-2%, <3 mm, euhedral, elongate
GROUNDMASS: Fine-grained, <2% dusty euhedral magnetite disseminated throughout
VESICLES: 0-15%, <20 mm, pipe-shaped, concentrated in Pieces 1-14, dipping at 30 - 60 degrees
COLOR: Dark gray (2.5Y 4/0)
STRUCTURE: Massive
ALTERATION: Variable chloritization of orthopyroxene and albitization of plagioclase
VEINS/FRACTURES: Trace, <0.5 mm, subhorizontal, filled with carbonate
ADDITIONAL COMMENTS: Continuation of 125-786B-64R-1

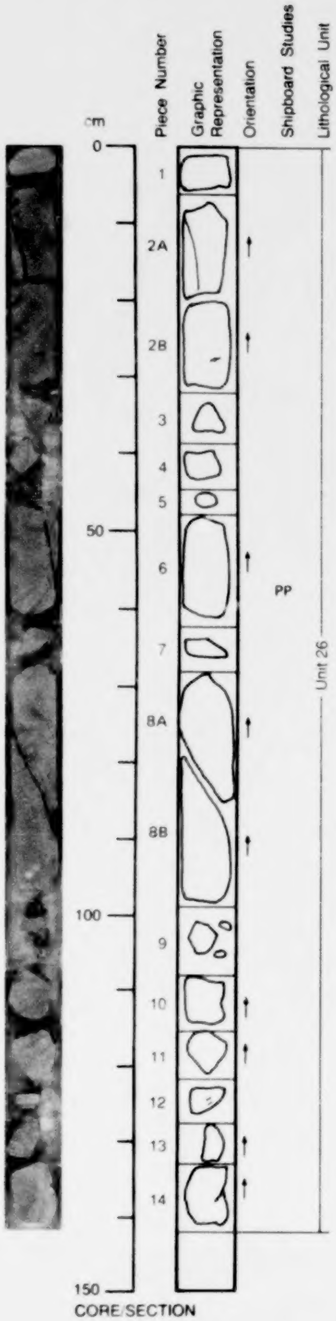
cm
Piece Number
Graphic Representation
Orientation
Shipboard Studies
Lithological Unit
0
50
100
150
1
2A
2B
3
4
5
6
7
8A
8B
9
10
11
12
13
14
PP
Unit 26
CORE/SECTION

125-786B-64R-3

UNIT 26: META-ORTHOPYROXENE ANDESITE

Pieces 1-14

CONTACTS: None visible

PHENOCRYSTS: Primary mineralogy altered to lower greenschist facies assemblage
Plagioclase - 3-5%, 0.2-0.5 mm, subhedral-euhedral
Orthopyroxene - 1-2%, <2 mm, euhedral, elongate

GROUNDMASS: Very fine-grained; <2% dusty euhedral magnetite disseminated throughout

VESICLES: Trace, <2 mm, elongate, concentrated in Pieces 8B-14, filled with carbonate

COLOR: Greenish gray (5G 6/1 to 5BG 5/1)

STRUCTURE: Massive

ALTERATION: Variable chloritization of orthopyroxene and albitization of plagioclase

VEINS/FRACTURES: Trace, <0.3 mm wide, subvertical, filled with carbonate

ADDITIONAL COMMENTS: Continuation of 125-786B-64R-2; on the basis of the absence of vesicles, this is probably a dike

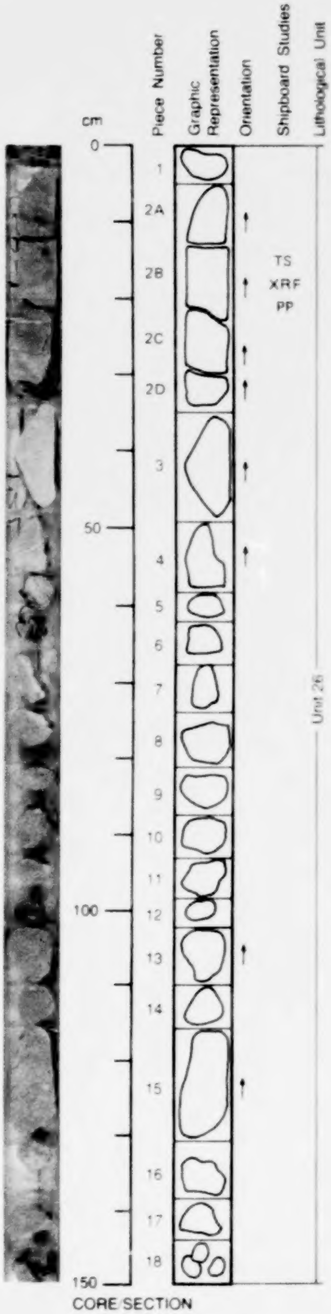
cm
0
50
100
150
Piece Number
Graphic Representation
Orientation
Shipboard Studies
Lithological Unit
1
2A
2B
2C
2D
3
4
5
6
7
8
9
10
11
12
13
14
15
16
17
18
TS
XRF
PP
Unit 26
CORE/SECTION

125-786B-65R-1

UNIT 26: CHLORITE-ALBITE ROCK

Pieces 1-7

CONTACTS: Contact with lower, metadacite dike is exposed in Piece 8; some black colored dacite seems to have intruded into overlying rock; no chilled margin or vesicle-free rock at contact.
PHENOCRYSTS: Absent.
GROUNDMASS: Fine-grained; albite-chlorite.
VESICLES: Absent.
COLOR: Greenish gray (5G 6/1).
STRUCTURE: Massive.
ALTERATION: Probably meta-andesite.
VEINS/FRACTURES: Absent.
ADDITIONAL COMMENTS: Continuation of 125-786B-64R-3.

UNIT 26: META-DACITE

Pieces 8-18

CONTACTS: Chlorite albite rock inclusion in Piece 18.
PHENOCRYSTS:
Plagioclase - 2%, <2 mm, euhedral.
Clinopyroxene - trace, <3 mm, euhedral, black, altering to chlorite.
Magnetite - trace, <0.1 mm, euhedral.
GROUNDMASS: Very fine-grained, albitic, chlorite.
VESICLES: 10%, <2 mm, irregular, randomly distributed; filled with hexagonal, colorless, transparent flakes and dark red flakes or pyrite.
COLOR: Gray (N 5).
STRUCTURE: Absent.
ALTERATION: Meta-dacite.
VEINS/FRACTURES: Absent.

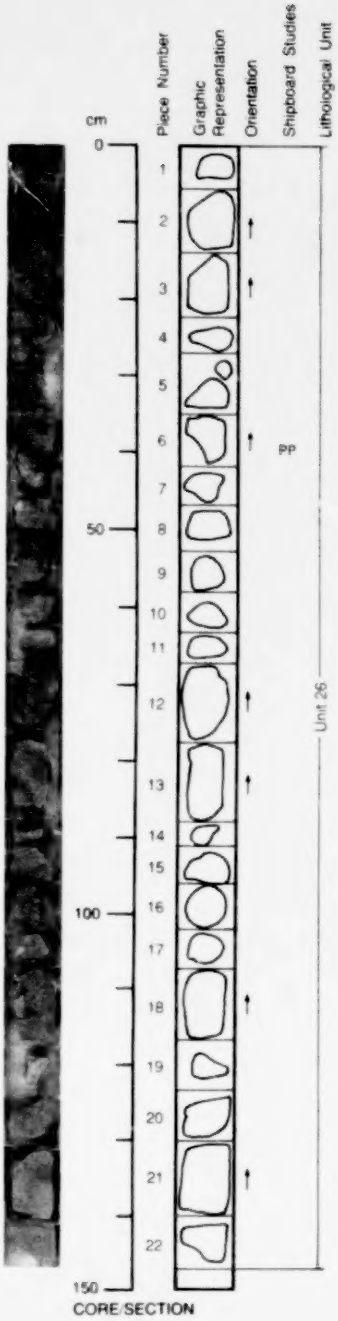
cm
Piece Number
Graphic Representation
Orientation
Shipboard Studies
Lithological Unit
0
50
100
150
1
2
3
4
5
6
7
8
9
10
11
12
13
14
15
16
17
18
19
20
21
22
PP
Unit 26
CORE/SECTION

125-786B-65R-2

UNIT 26: META-DACITE

Pieces 1-22

CONTACTS: None visible.
PHENOCRYSTS:
Plagioclase - 2%, <2 mm, euhedral.
Clinopyroxene - trace, <3 mm, euhedral, black, altering to chlorite.
Magnetite - trace, <0.1 mm, euhedral.
GROUNDMASS: Very fine grained, albite and chlorite.
VESICLES: 10%, <2 mm, irregular, randomly distributed, filled with hexagonal, colorless, transparent flakes and dark red flakes or pyrite.
COLOR: Gray (N 5/).
STRUCTURE: Absent.
ALTERATION: Meta-dacite.
VEINS/FRACTURES: Absent.

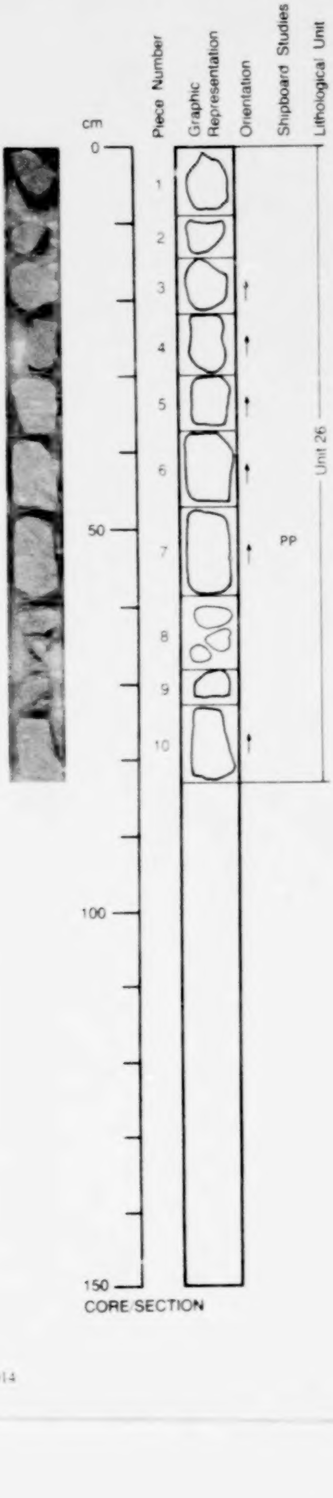
cm
Piece Number
Graphic Representation
Orientation
Shipboard Studies
Lithological Unit
0
50
100
150
1
2
3
4
5
6
7
8
9
10
PP
Unit 26
CORE/SECTION

125-786B-65R-3

UNIT 26: META-DACITE

Pieces 1-10

CONTACTS: None visible
PHENOCRYSTS:
Plagioclase - 2%, <2 mm, euhedral
Clinopyroxene - trace, <3 mm, euhedral, black, altering to chlorite
Magnetite - trace, <0.1 mm, euhedral
GROUNDMASS: Very fine-grained, albite and chlorite
VESICLES: 10%, <2 mm, irregular, randomly distributed, filled with hexagonal, transparent, colorless flakes and dark red flakes or pyrite
COLOR: Gray (N 5)
STRUCTURE: Absent
ALTERATION: Meta-dacite
VEINS/FRACTURES: Absent

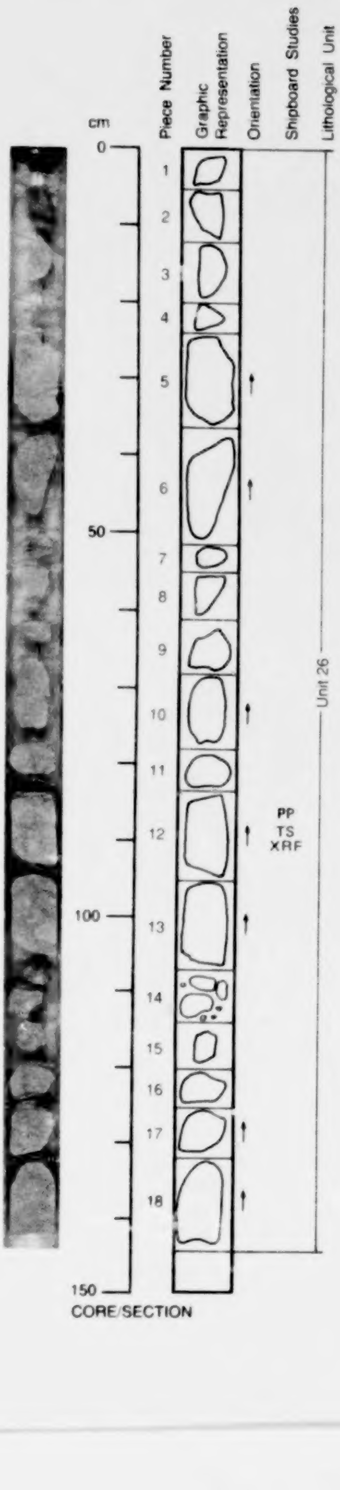
cm
0
50
100
150
CORE/SECTION
Piece Number
Graphic Representation
Orientation
Shipboard Studies
Lithological Unit
1
2
3
4
5
6
7
8
9
10
11
12
13
14
15
16
17
18
PP
TS
XRF
Unit 26

125-786B-66R-1

UNIT 26: META-ANDESITE TO DACITE

Pieces 1-18

CONTACTS: None.
PHENOCRYSTS:
Plagioclase - 5%, <2 mm, euhedral laths.
GROUNDMASS: Fine-grained, altered to chlorite.
VESICLES: 0-5%, <2 mm; elongate; appear locally in some pieces.
COLOR: Light gray (N 7/).
STRUCTURE: Massive.
ALTERATION: Altering to chlorite and albite.
VEINS/FRACTURES: None.
ADDITIONAL COMMENTS: Continuation of 125-786B-65R-3. Local round chlorite inclusions with complex white and green rims.

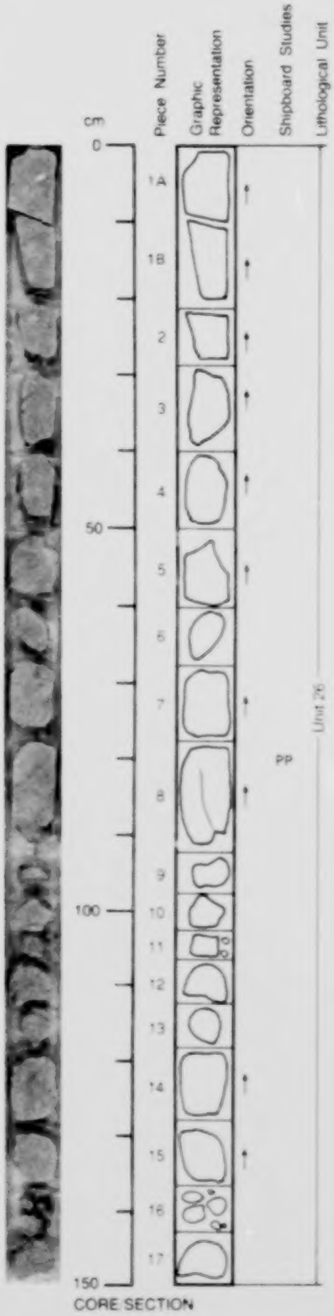
cm
Piece Number
Graphic Representation
Orientation
Shipboard Studies
Lithological Unit
0
50
100
150
1A
1B
2
3
4
5
6
7
8
9
10
11
12
13
14
15
16
17
PP
Unit 26
CORE SECTION

125-786B-66R-2

UNIT 26: META-ANDESITE TO DACITE

Pieces 1-17

CONTACTS: None visible
PHENOCRYSTS:
Plagioclase - 5%, <2 mm, euhedral laths.
GROUNDMASS: Fine grained, altering to chlorite and albite
VESICLES: 0-5%, <2 mm, elongate, in some pieces, rare
COLOR: Light gray (N 7)
STRUCTURE: Massive
ALTERATION: Altering to chlorite and albite
VEINS/FRACTURES: None
ADDITIONAL COMMENTS: Continuation of 125-786B-65R-3

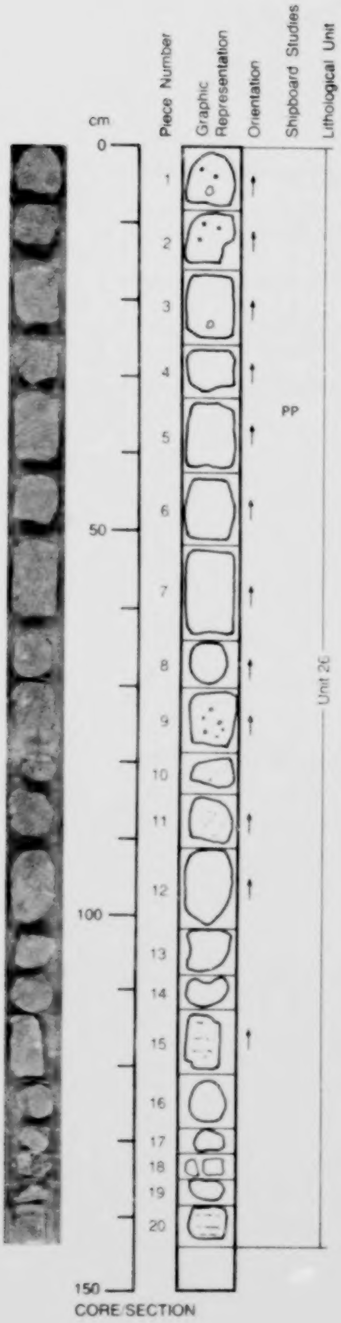
cm
0
50
100
150
CORE/SECTION
Piece Number
Graphic Representation
Orientation
Shipboard Studies
Lithological Unit
1
2
3
4
5
6
7
8
9
10
11
12
13
14
15
16
17
18
19
20
PP
Unit 26

125-786B-66R-3

UNIT 26: META-DACITE TO ANDESITE

Pieces 1-20

CONTACTS: None visible
PHENOCRYSTS:
Plagioclase: 5%, <2 mm, euhedral laths.
GROUNDMASS: Fine-grained, altering to chlorite and albite.
VESICLES: 0-5%, <2 mm, elongate, in some pieces; rare.
COLOR: Light gray (N/7).
STRUCTURE: Massive.
ALTERATION: Altering to chlorite and albite.
VEINS/FRACTURES: Absent.
ADDITIONAL COMMENTS: Continuation of 125-786B-66R-2.

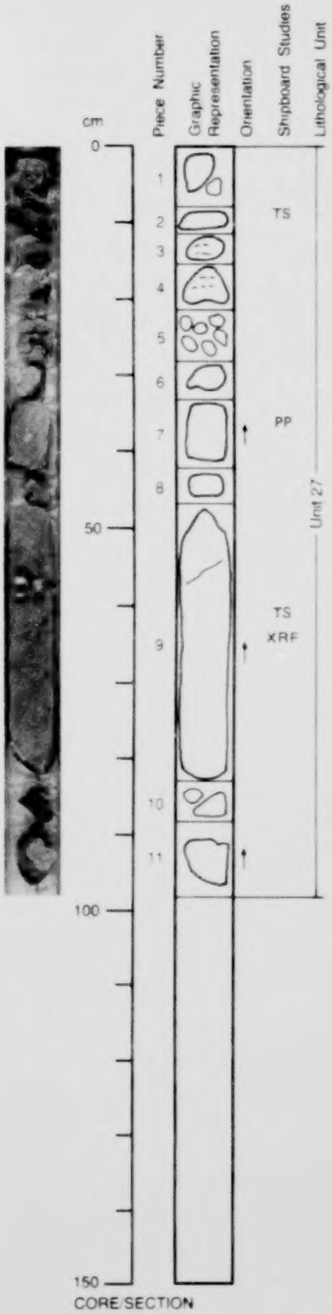

125-786B-67R-1

UNIT 27: META-PYROXENE ANDESITE

Pieces 1, 3 - 8

CONTACTS: None visible
PHENOCRYSTS: Pyroxene and feldspar occur as glomerocrysts and as isolated phases; orthopyroxene is pervasively chloritized.
Plagioclase - 5%, <1 mm, euhedral, tabular
Orthopyroxene - 3%, <3 mm, euhedral, equant
Clinopyroxene - trace, <0.5 mm, euhedral, tabular
Magnetite - trace, <0.2 mm, euhedral
GROUNDMASS: Fine-grained, feldspathic
VESICLES: 1-10%, n/a, elongate, variable, vesicle walls are coated with quartz
COLOR: Greenish gray (5BG 6/1)
STRUCTURE: Massive
ALTERATION: Chloritization of pyroxene and some albitization of feldspar
VEINS/FRACTURES: None

UNIT 27: OLIVINE-BEARING BONINITE

Piece 2

CONTACTS: None visible
PHENOCRYSTS: Pyroxene and plagioclase occur as isolated phases and as glomerocrystic patches; olivine is completely altered to a carbonate and Fe-oxide assemblage.
Orthopyroxene - 8-15%, <2 mm, euhedral, equant
Clinopyroxene - 5-10%, <1.5 mm, equant, tabular
Olivine - 3%, <2 mm, euhedral
Plagioclase - 5%, <1.5 mm, euhedral, tabular
GROUNDMASS: Fine-grained to glassy with variable alteration
VESICLES: None
COLOR: Weak red (5R 4/2)
STRUCTURE: Massive
ALTERATION: Some Fe-staining
VEINS/FRACTURES: None
ADDITIONAL COMMENTS: First reappearance of olivine downhole

UNIT 27: BONINITE

Pieces 9-11

CONTACTS: None visible
PHENOCRYSTS: Clinopyroxene is variably chloritized; olivine completely replaced by a chlorite-carbonate assemblage.
Orthopyroxene - 8-12%, <3 mm, euhedral, elongate
Clinopyroxene - trace, <0.5 mm, euhedral, equant
Olivine - 1%, <2 mm, euhedral, with spinel inclusions
GROUNDMASS: Fine-grained, rich in pyroxene and feldspar
VESICLES: None
COLOR: Dark greenish gray (5G 4/1)
STRUCTURE: Massive
ALTERATION: Some chloritic alteration of olivine, clinopyroxene and groundmass
VEINS/FRACTURES: Trace, <3 mm wide, dipping at 45 degrees, filled with carbonate
ADDITIONAL COMMENTS: Some slickensides on base of Piece 11, partly coated with carbonate

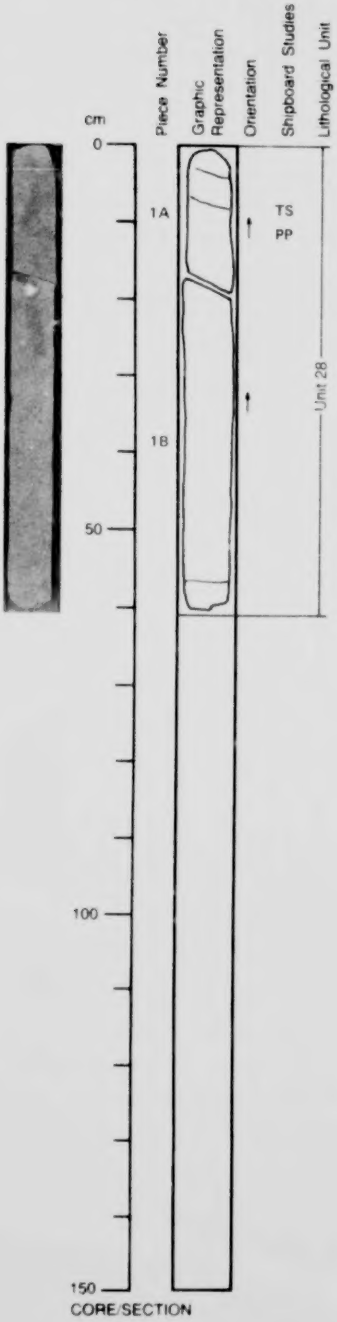
cm
0
50
100
150
Piece Number
Graphic Representation
Orientation
Shipboard Studies
Lithological Unit
1A
1B
TS
PP
Unit 28
CORE/SECTION

125-786B-68R-1

UNIT 28: META-TWO-PYROXENE ANDESITE

Pieces 1A-1B

CONTACTS: None visible.

PHENOCRYSTS: Highly altered to chlorite, carbonate and albite.

Clinopyroxene - 3-6%, <2 mm, equant, euhedral, altered to chlorite.

Orthopyroxene - 5-10%, <1.5 mm, equant to elongation, euhedral, altered to chlorite.

Feldspar - trace, <0.5 mm, euhedral tabular, altered to chlorite.

GROUNDMASS: Fine grained, altered to chlorite and carbonate.

VESICLES: None.

COLOR: Greenish gray (5G 5/1).

STRUCTURE: Massive.

ALTERATION: Highly altered to chlorite with subordinate amounts of carbonate and albite.

VEINS/FRACTURES: <1%, 1-2 mm, dip at 30 to 60 degrees to core axis, filled with carbonate and sulfide (pyrite, possibly chalcopyrite).

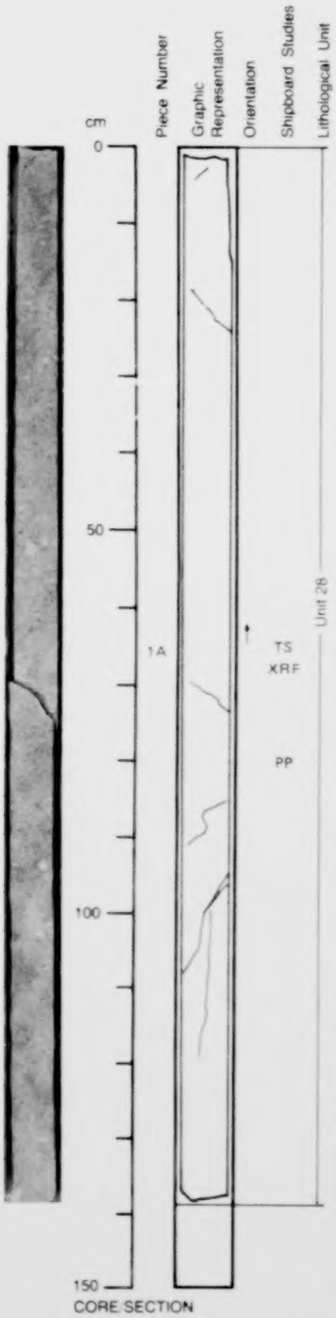
cm
Piece Number
Graphic Representation
Orientation
Shipboard Studies
Lithological Unit
0
50
100
150
1A
TS
XRF
PP
Unit 28
CORE SECTION

125-786B-69R-1

UNIT 28: META-TWO-PYROXENE ANDESITE (68R-1 CONTINUED)

Piece 1A

CONTACTS: None visible.
PHENOCRYSTS: Highly altered to chlorite, carbonate and albite.
  Clinopyroxene - 3-6%; <2 mm; equant to elongate; altered to chlorite.
  Orthopyroxene - 5-10%; <1.5 mm; equant to elongate; euhedral; altered to chlorite.
  Feldspar - trace; <0.5 mm; euhedral; tabular; altered to chlorite.
GROUNDMASS: Fine-grained; holocrystalline; variably altered to chlorite and carbonate.
VESICLES: None.
COLOR: Greenish gray (5G 5/1).
STRUCTURE: Massive.
ALTERATION: Highly altered to chlorite with subordinate amounts of carbonate and albite.
VEINS/FRACTURES: <1%; <1-2 mm wide; 30-60 degrees to core axis; filled with carbonate and sulfide.
ADDITIONAL COMMENTS: Continuation of 125-786B-68R-1.

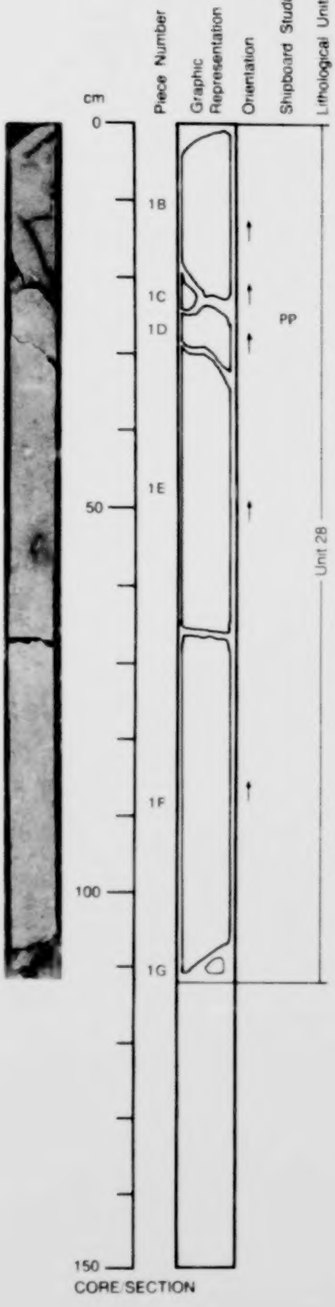
cm
0
50
100
150
CORE/SECTION
Piece Number
Graphic Representation
Orientation
Shipboard Studies
Lithological Unit
1B
1C
1D
1E
1F
1G
PP
Unit 28

125-786B-69R-2

UNIT 28: META-TWO-PYROXENE ANDESITE (69R-1 CONTINUED)

Pieces 1B-1G

CONTACTS: None visible

PHENOCRYSTS: Highly altered to chlorite, carbonate and albite
- Clinopyroxene - 3-6%, <2 mm, equant, euhedral, altered to chlorite.
- Orthopyroxene - 5-10%, <1.5 mm, equant to elongate, euhedral, altered to chlorite
- Feldspar - trace, <0.5 mm, euhedral, tabular, altered to chlorite/albite

GROUNDMASS: Fine-grained, holocrystalline, altered to chlorite and carbonate

VESICLES: None

COLOR: Greenish gray (5G 5/1)

STRUCTURE: Massive

ALTERATION: Extensive pervasive, to chlorite, carbonate and albite

VEINS/FRACTURES: <1%, 1-2 mm, 30-60 degrees to core axis

ADDITIONAL COMMENTS: Rock is a continuation of the Interval 125-786B-68R-1 to 125-786B-69R-1

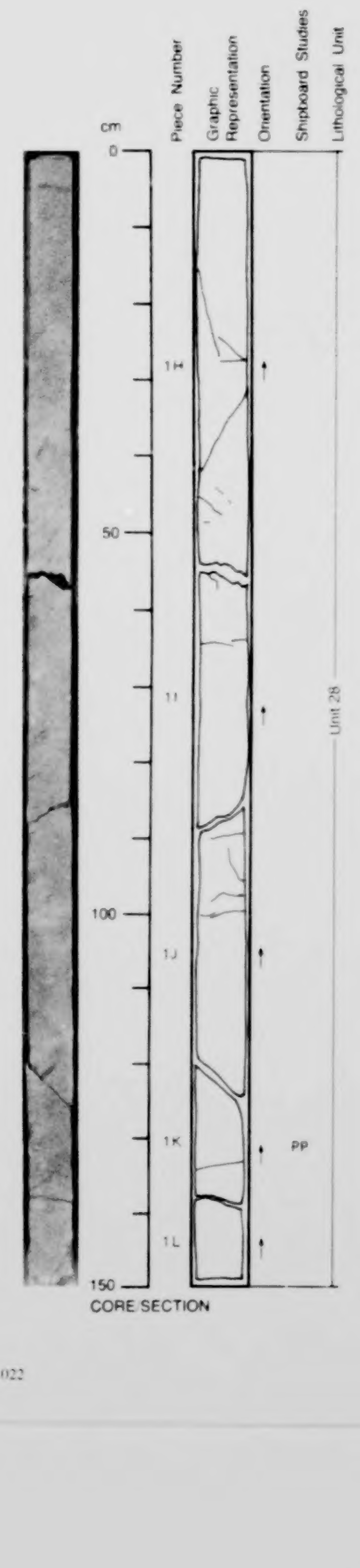
cm
0
50
100
150
CORE SECTION
Piece Number
Graphic Representation
Orientation
Shipboard Studies
Lithological Unit
1H
1I
1J
1K
1L
PP
Unit 28

125-786B-69R-3

UNIT 28: META-TWO-PYROXENE ANDESITE (69R-2 CONTINUED)

Pieces 1H-1L

CONTACTS: None.
PHENOCRYSTS: Highly altered to chlorite with subordinate amounts of carbonate and albite.
Clinopyroxene - 3-6%, <2 mm, equant, euhedral, altered.
Orthopyroxene - 5-10%, <1.5 mm, equant to elongate, euhedral, altered.
Feldspar - trace, <0.5 mm, euhedral, tabular, altered.
GROUNDMASS: Fine grained, holocrystalline, altered to chlorite and carbonate.
VESICLES: None.
COLOR: Greenish gray (5G 5/1).
STRUCTURE: Massive.
ALTERATION: Pervasive, extensive, to chlorite with subordinate amounts of carbonate and albite.
VEINS/FRACTURES: <1%, 1-2 mm wide, 30-60 degrees to core axis, filled with carbonate and sulfides.
ADDITIONAL COMMENTS: Rock is a continuation of 125-786B-68R-1 to 69R-2.

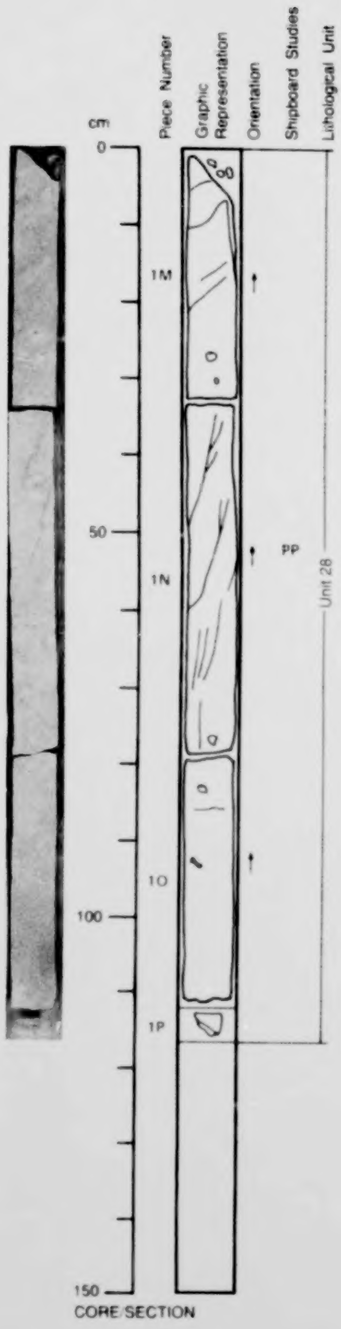
cm
0
50
100
150
Piece Number
Graphic Representation
Orientation
Shipboard Studies
Lithological Unit
1M
1N
1O
1P
PP
Unit 28
CORE/SECTION

125-786B-69R-4

UNIT 28: META-TWO PYROXENE ANDESITE (69R-3 CONTINUED)

Pieces 1M-1P

CONTACTS: None visible
PHENOCRYSTS: Highly altered to chlorite with carbonate and albite
Orthopyroxene - 3-6%, <2 mm, equant, euhedral, altered
Clinopyroxene - 5-10%, <1.5 mm, equant to elongate, euhedral, altered
Feldspar - trace, <0.5 mm, euhedral, tabular, altered
GROUNDMASS: Fine-grained, holocrystalline
VESICLES: None
COLOR: Greenish gray (5G 5/1)
STRUCTURE: Massive
ALTERATION: Extensive, pervasive, to an assemblage of chlorite with subordinate amounts of carbonate and albite
VEINS/FRACTURES: 1<, <1-2 mm wide, 30-60 degrees to core axis, filled with carbonate and sulfide
ADDITIONAL COMMENTS: Rock is a continuation of 125-786B-68R-1

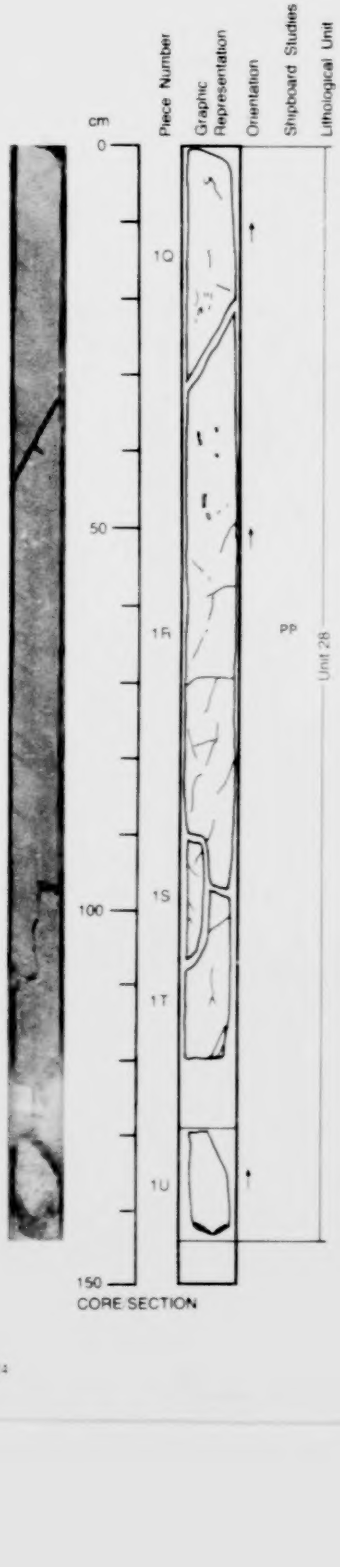
cm
Piece Number
Graphic Representation
Orientation
Shipboard Studies
Lithological Unit
0
50
100
150
1Q
1R
1S
1T
1U
PP
Unit 28
CORE/SECTION

125-786B-69R-5

UNIT 28: META-TWO-PYROXENE ANDESITE (69R-4 CONTINUED)

Pieces 1Q-1U

CONTACTS: None
PHENOCRYSTS: Variably altered; less altered, more plagioclase phyric zone at 12 cm.
Clinopyroxene - 3-6%, <1.5 mm, equant, euhedral.
Orthopyroxene - 5-7%, <1.8 mm, equant to elongate, euhedral.
Feldspar - 1-2%, <0.5 mm, 1-2 mm, elongate, equant.
Spinel - <1%, <0.1 mm, equant, usually as inclusions in pyroxene, also in groundmass.
GROUNDMASS: Fine grained, holocrystalline, altered to chlorite.
VESICLES: None.
COLOR: Greenish gray (5G 5/1) to grayish green (5G 6/2).
STRUCTURE: Massive; finer grained midway through section; less veining.
ALTERATION: Chlorite and minor carbonate, pervasive, variable.
VEINS/FRACTURES: <1%, 1-3 mm, random, filled with carbonate and minor sulfide; some fractures 1-2 cm long and 5-6 mm wide filled with carbonate.
ADDITIONAL COMMENTS: Rock is a continuation of 125-786B-68R-1 to 69R-4.

125-786B-69R-6

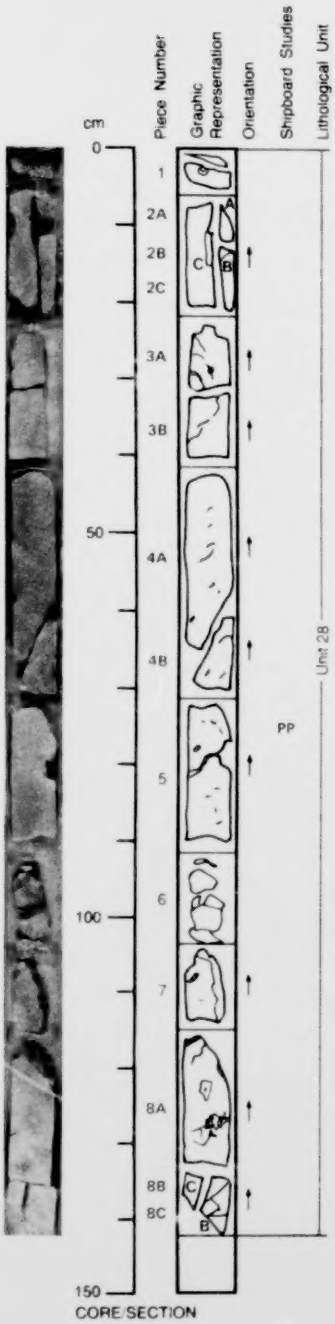
cm
Piece Number
Graphic Representation
Orientation
Shipboard Studies
Lithological Unit
0
50
100
150
1
2A
2B
2C
3A
3B
4A
4B
5
6
7
8A
8B
8C
A
B
C
C
B
PP
Unit 28
CORE/SECTION

UNIT 28: META-TWO-PYROXENE ANDESITE

Pieces 1-8C

CONTACTS: None visible
PHENOCRYSTS: Variably altered to chlorite and carbonate
Clinopyroxene - 3-6%, <2 mm, euhedral, altered
Orthopyroxene - 5-10%, <1.5 mm, equant to elongate, altered
Plagioclase - 1%, <1 mm, tabular, elongate
Magnetite - trace, <0.25 mm, equant
GROUNDMASS: Fine grained, holocrystalline, microcrysts of plagioclase and pyroxene
VESICLES: None
COLOR: Greenish gray (5G 5/1)
STRUCTURE: Massive. Piece 6 broken into multiple fragments, possibly caused by faulting
ALTERATION: Pervasive, to chlorite and carbonate
VEINS/FRACTURES: 1%, 1-2 mm wide in zone 1.5 cm wide; sub-perpendicular, filled with carbonate and sulfide; the wide zone contains anastomosing sulfide with subordinate amounts of carbonate; large vug 2 cm long in Piece 5, lined with euhedral quartz crystals and sulfide
ADDITIONAL COMMENTS: This is a continuation of 125-786B-68R-1 to 69R-5

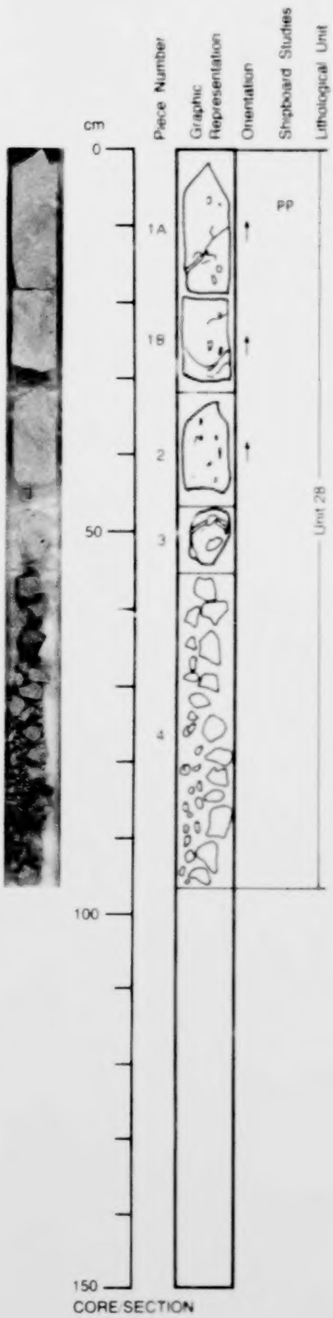
cm
Piece Number
Graphic Representation
Orientation
Shipboard Studies
Lithological Unit
0
1A
1B
2
3
4
50
100
150
PP
Unit 28
CORE/SECTION

125-786B-69R-7

UNIT 28: META-TWO-PYROXENE ANDESITE (69R-6 CONTINUED)

Pieces 1-4

CONTACTS: None visible.
PHENOCRYSTS: Variably altered to chlorite and carbonate.
  Clinopyroxene - 3-6%; <2 mm; euhedral; equant; altered.
  Orthopyroxene - 5-10%; <1.5 mm; equant to elongate; altered.
  Feldspar - 1%; <1 mm; tabular; elongate; altered.
  Magnetite - trace; <0.25 mm; equant.
GROUNDMASS: Fine-grained; holocrystalline; plagioclase and pyroxene microcrysts.
VESICLES: None.
COLOR: Greenish gray (5G 5/1).
STRUCTURE: Massive. Piece 4 multiple fragments, may be due to faulting; slickensides and pyrite veining are present.
ALTERATION: Chlorite and carbonate, pervasive.
VEINS/FRACTURES: <1%; 1-4 mm; 30-45 degrees to core axis; filled with carbonate and sulfide and a later episode of carbonate. Piece 4 has a vug 1 cm wide, filled with quartz and sulfide crystals with later stage carbonate.
ADDITIONAL COMMENTS: This rock is a continuation of 125-786B-68R-1 to 69R-6.

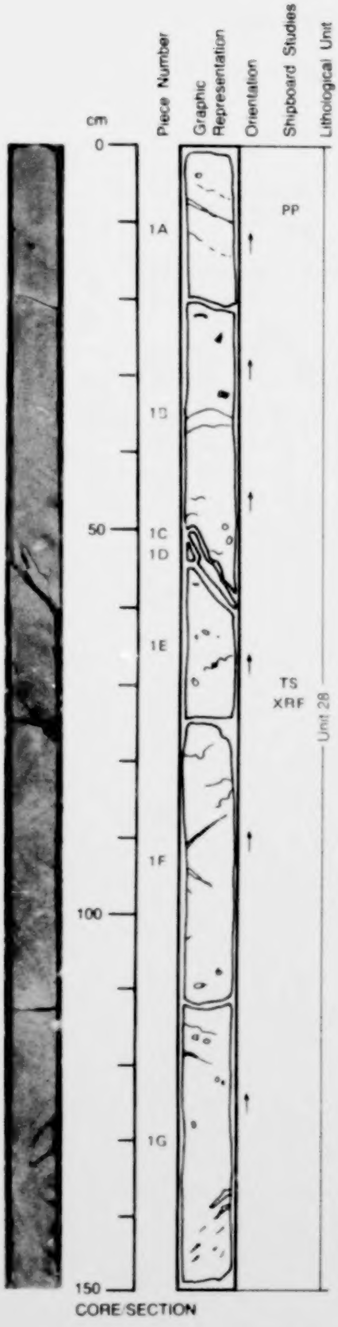
cm
Piece Number
Graphic Representation
Orientation
Shipboard Studies
Lithological Unit
0
50
100
150
1A
1B
1C
1D
1E
1F
1G
PP
TS
XRF
Unit 28
CORE/SECTION

125-786B-70R-1

UNIT 28: META-TWO-PYROXENE ANDESITE (69R-7 CONTINUED)

Pieces 1A-1G

CONTACTS: None visible

PHENOCRYSTS: Variably altered to carbonate and chlorite, glomerocrysts of pyroxene

Clinopyroxene - 5-7%, <2 mm, equant, euhedral

Orthopyroxene - 7-10%, <1.5 mm, equant to elongate, euhedral, variably altered

Feldspar - 1-2%, <1-2 mm, elongate, tabular, euhedral

GROUNDMASS: Fine-grained, holocrystalline, altered to chlorite and carbonate

VESICLES: None

COLOR: Greenish gray (5G 5/1)

STRUCTURE: Massive

ALTERATION: Variable intensity, pervasive, chlorite and carbonate

VEINS/FRACTURES: <1%, 1-2 mm wide, random, filled with sulfide and carbonate

ADDITIONAL COMMENTS: The rock type is a continuation of the 125-786B-67R-1 to 69-7.

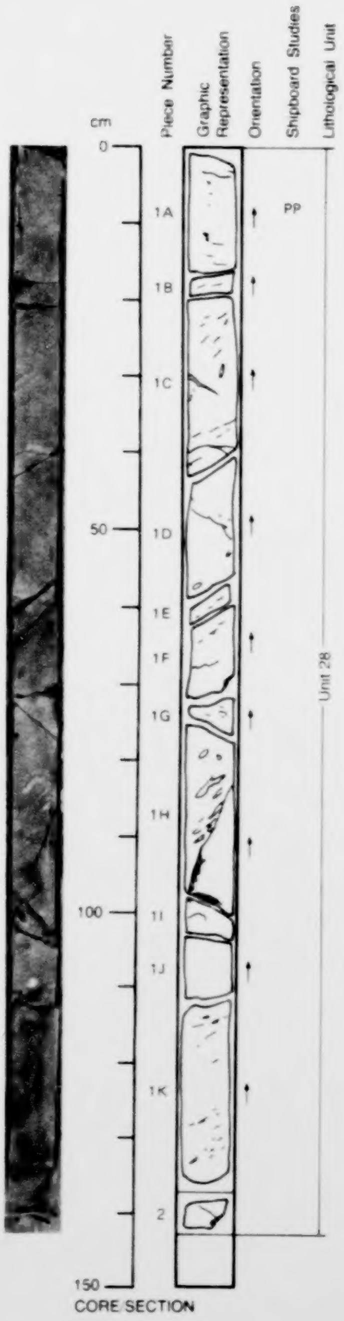
cm
Piece Number
Graphic Representation
Orientation
Shipboard Studies
Lithological Unit
0
50
100
150
1A
1B
1C
1D
1E
1F
1G
1H
1I
1J
1K
2
PP
Unit 28
CORE/SECTION

125-786B-70R-2

UNIT 28: META-TWO-PYROXENE ANDESITE (70R-1 CONTINUED)

Pieces 1A-1K, 2

CONTACTS: None visible.
PHENOCRYSTS: Variably altered to chlorite and carbonate; glomerocrysts of pyroxene.
Clinopyoxene - 5-8%, 1-2 mm, equant, euhedral, altered.
Orthopyroxene - 3-5%, <1.5 mm, elongate, euhedral.
Feldspar - 1%, <2 mm, tabular, euhedral.
Magnetite - trace, <0.25 mm, equant.
GROUNDMASS: Fine-grained, holocrystalline, microcrysts of plagioclase and pyroxene.
VESICLES: None.
COLOR: Greenish gray (95G 5/1).
STRUCTURE: Massive.
ALTERATION: Pervasive, variable, chlorite and carbonate.
VEINS/FRACTURES: 1-2%, 2 mm by 8-12 mm fractures, at 45 degrees to core axis, filled with chlorite, appear to be tension gashes.
ADDITIONAL COMMENTS: Rock is a continuation of 25-786B-67R-1 to 70R-1.

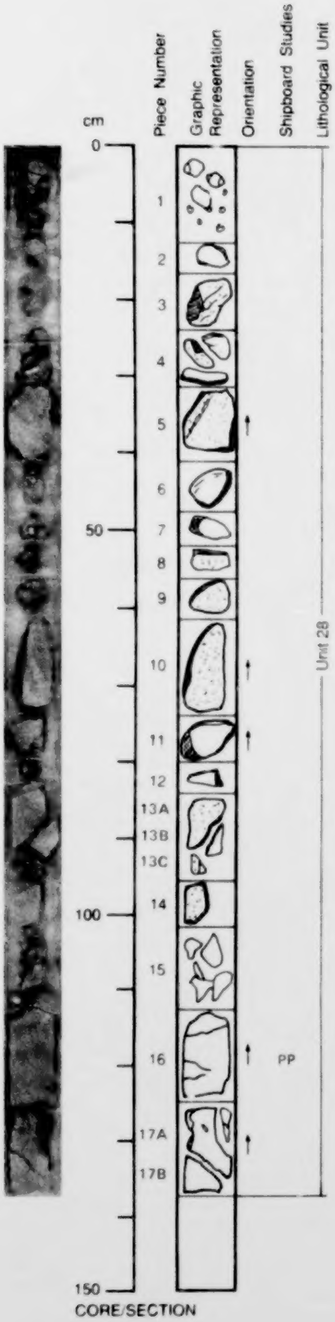
cm
Piece Number
Graphic Representation
Orientation
Shipboard Studies
Lithological Unit
0
50
100
150
1
2
3
4
5
6
7
8
9
10
11
12
13A
13B
13C
14
15
16
17A
17B
PP
Unit 28
CORE/SECTION

125-786B-70R-3

UNIT 28: META-TWO-PYROXENE ANDESITE (70R-2 CONTINUED)

Pieces 1-17

CONTACTS: None visible

PHENOCRYSTS: Variably altered with carbonate; glomerocrysts and intersertal texture.

Clinopyroxene - 7-10%; <2 mm; equant to elongate; euhedral; altered.

Orthopyroxene - 3-5%; <1.5 mm; elongate; euhedral; altered.

Feldspar - <1%; 1 mm; elongate; tabular; altered.

Magnetite - trace; <0.25 mm; equant.

GROUNDMASS: Fine-grained; holocrystalline; microcrysts of feldspar and pyroxene.

VESICLES: None

COLOR: Greenish gray (5G 5/1)

STRUCTURE: Massive. Pieces 1 and 4 are composed of many fragments. Piece 3 is very altered and appears brecciated.

ALTERATION: Pervasive; chlorite and carbonate.

VEINS/FRACTURES: 1%; 1-2 mm wide; random; filled with carbonate and sulfide, also unfilled fractures.

ADDITIONAL COMMENTS: Rock is a continuation of 125-786B-67R-1 to 70R-2.

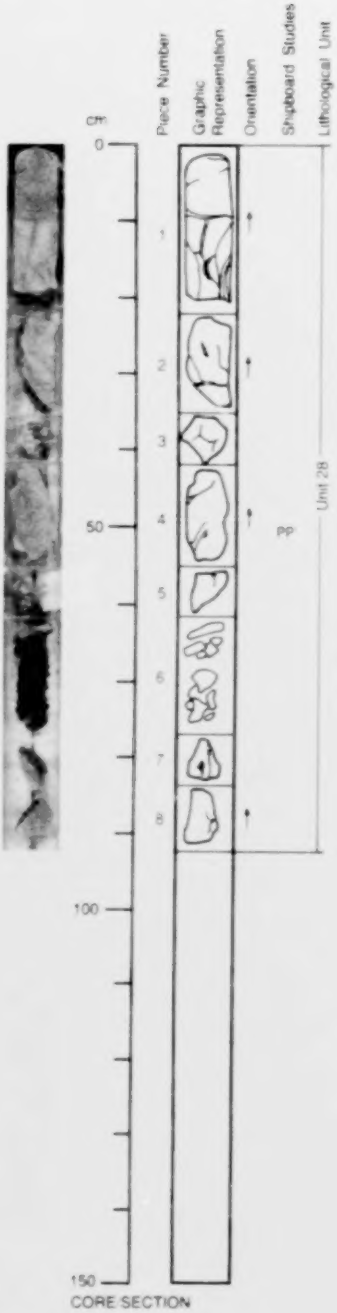
cm
Piece Number
Graphic Representation
Orientation
Shipboard Studies
Lithological Unit
0
50
100
150
1
2
3
4
5
6
7
8
PP
Unit 28
CORE SECTION

125-786B-70R-4

UNIT 28: META-TWO-PYROXENE ANDESITE (70R-3 CONTINUED)

Pieces 1-8

CONTACTS: None visible.
PHENOCRYSTS: Altered to chlorite and carbonate; glomerocrysts of pyroxene.
Clinopyroxene: 7-10%; 1-2 mm; equant to elongate; euhedral; altered; magnetite inclusions.
Orthopyroxene: 4-7%; <1.5 mm; elongate; euhedral; altered; magnetite inclusions.
Feldspar: <1%; <1-2 mm; tabular; altered.
Magnetite: <1%; 0.25 mm; equant.
GROUNDMASS: Fine-grained; holocrystalline; altered to chlorite and carbonate.
VESICLES: None.
COLOR: Greenish gray (5G 5/1).
STRUCTURE: Massive.
ALTERATION: Chlorite and carbonate; pervasive.
VEINS/FRACTURES: <1%; 1-2 mm; random; filled with carbonate and sulfide.
ADDITIONAL COMMENTS: Rock is a continuation of 125-786B-67R-1 to 70R-4.

125-786B-71R-1

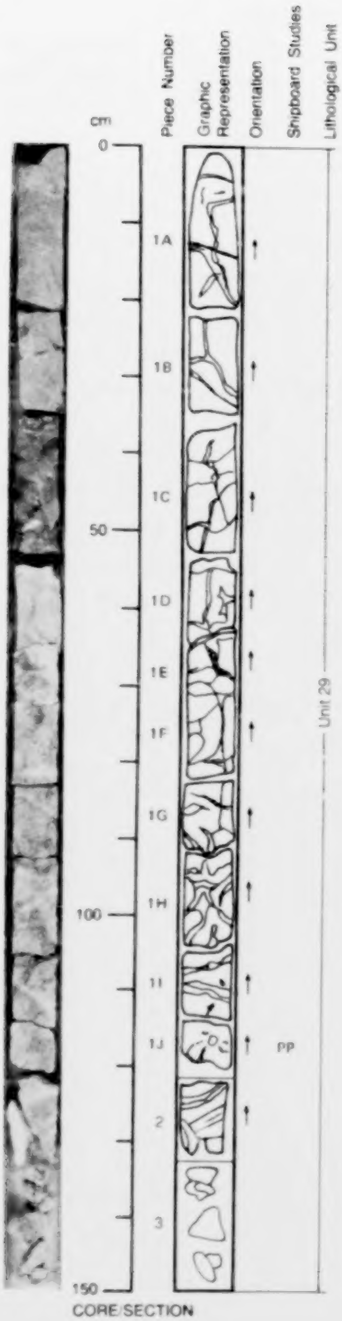
cm
Piece Number
Graphic Representation
Orientation
Shipboard Studies
Lithological Unit
0
50
100
150
1A
1B
1C
1D
1E
1F
1G
1H
1I
1J
2
3
PP
Unit 29
CORE/SECTION

UNIT 29: ANDESITE STOCK WORK ZONE

Pieces 1-2

CONTACTS: None visible
PHENOCRYSTS: Pyroxene and plagioclase are extensively altered
Plagioclase - 2-3%, <2 mm, euhedral laths
Pyroxene - 8-10%, <2 mm, subhedral
GROUNDMASS: Fine-grained, holocrystalline, granular, totally altered
VESICLES: None
COLOR: Host andesite, greenish gray (5BG 6/1) to dark greenish gray (10Y 5/2), more altered stock work is light gray (10YR 7/1)
STRUCTURE: Stockwork breccia with clasts <10 cm in size (autobrecciation)
ALTERATION: Pervasive chloritization, sulfidation, argillic alteration
VEINS/FRACTURES: 10-20%, <30 mm, predominantly sub-vertical & horizontal, multiple generations of fill, wall-rock reaction increases from 5 to 25 mm downhole, veins filled with sulfides, clays and epidote
ADDITIONAL COMMENTS: This section represents an argillaceous zone in a mineralized stockwork

UNIT 29: ALTERED-MINERALIZED CATACLASTITE

Piece 3

CONTACTS: None visible
PHENOCRYSTS: Rock is completely altered, no primary minerals remain
GROUNDMASS: Clay, epidote, sulfide
VESICLES: None
COLOR: Light greenish gray (5B 7/1)
STRUCTURE: Cataclasite
ALTERATION: Argillic
VEINS/FRACTURES: None
ADDITIONAL COMMENTS: Disseminated sulfides, <1.5%, in cubic morphology

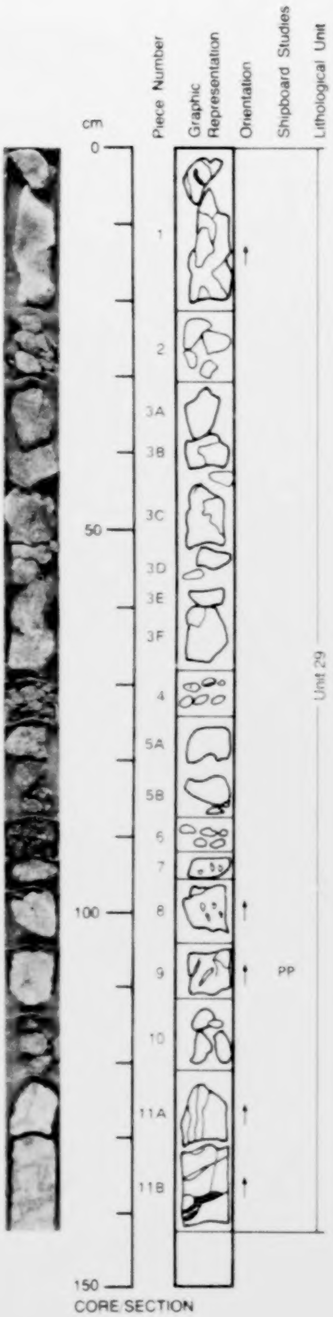
cm
Piece Number
Graphic Representation
Orientation
Shipboard Studies
Lithological Unit
0
50
100
150
1
2
3A
3B
3C
3D
3E
3F
4
5A
5B
6
7
8
9
10
11A
11B
PP
Unit 29
CORE/SECTION

125-786B-71R-2

UNIT 29: ANDESITE STOCKWORK

Pieces 1, 5, 7-11

CONTACTS: None visible
PHENOCRYSTS: Pyroxene and plagioclase extensively altered
Plagioclase - 2-4%, <1.5 mm, euhedral laths
Pyroxene - 5-10%, <2 mm, euhedral, tabular
GROUNDMASS: Fine-grained, holocrystalline, granular, totally altered
VESICLES: 0-5%, <<5 mm, elongate, irregular, coating of pyramidal quartz and sulfide in some vesicles
COLOR: Host andesite is greenish gray (5BG 6/1) to dark greenish gray (10Y 5/2), more altered stockwork is light gray (10YR 7/1)
STRUCTURE: Stockwork breccia with clasts <7 cm in size (autobrecciation)
ALTERATION: Pervasive argillic, chloritic, silicic and sulfidation (disseminated 0.5% pyrite cubes)
VEINS/FRACTURES: 10-40%, <20 mm, stockwork; in Pieces 7 - 11, wall-rock alteration decreases downhole, from 1 - 5 mm width
ADDITIONAL COMMENTS: Continuation of stockwork in 125-786B-71R-1

UNIT 29: ARGILLITIZED-MINERALIZED STOCKWORK

Pieces 2-4, 6

CONTACTS: None visible
PHENOCRYSTS: Pieces are completely altered; no primary minerals remain
GROUNDMASS: Clay, epidote, quartz and sulfide
VESICLES: None
COLOR: Greenish gray (5B 7/1)
STRUCTURE: Cataclasite
ALTERATION: Argillic
VEINS/FRACTURES: None
ADDITIONAL COMMENTS: Disseminated sulfides <1%, 0.1 mm, throughout

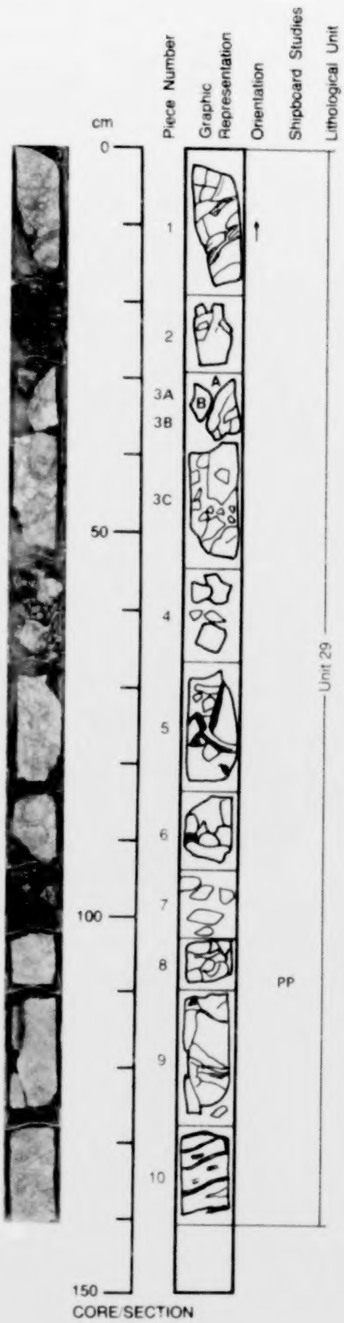
cm
0
50
100
150
CORE/SECTION
Piece Number
Graphic Representation
Orientation
Shipboard Studies
Lithological Unit
1
2
3A
3B
3C
4
5
6
7
8
9
10
A
B
↑
PP
Unit 29

125-786B-71R-3

UNIT 29: CLINOPYROXENE PLAGIOCLASE BASALT CATACLASTITE (CONTINUATION OF 71R-2)

Pieces 1-10

CONTACTS: None visible.
PHENOCRYSTS:
Plagioclase - 4%, <2 mm; completely altered to clays.
Clinopyroxene - 8%, <1.5 mm; completely altered to chlorite.
GROUNDMASS: Fine-grained; completely altered to albite/chlorite; contains disseminated pyrite.
VESICLES: Absent.
COLOR: Light gray to gray (7.5YR 7/0 - 6/0).
STRUCTURE: Cataclastic.
ALTERATION: Ground to clay in fracture zones; pyroxene and plagioclase phenocrysts and groundmass are extensively altered to clay and chlorite.
VEINS/FRACTURES: 15%; locally fractured; randomly oriented; some zones are entirely pulverized; interval from 0-110 cm is intensely fractured.
ADDITIONAL COMMENTS: Continuation of 125-786B-71R-1; clasts range from 0.5 to 8 cm.

125-786B-71R-4

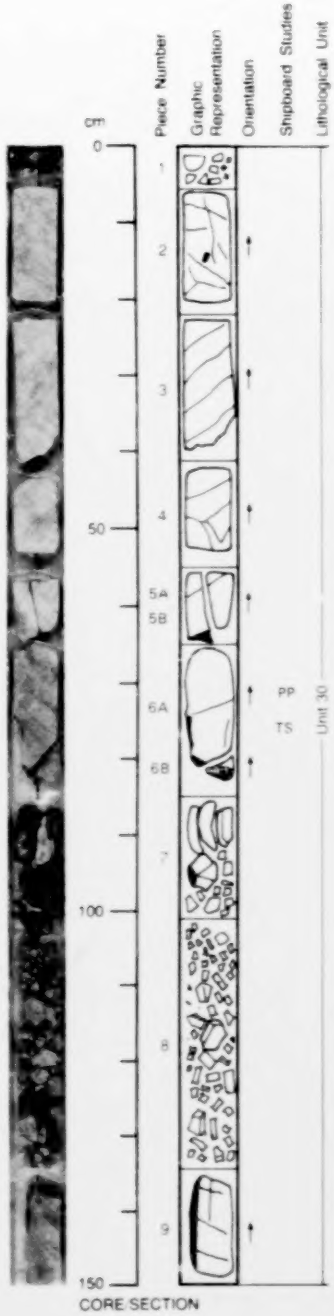
cm
0
50
100
150
CORE/SECTION
Piece Number
Graphic Representation
Orientation
Shipboard Studies
Lithological Unit
1
2
3
4
5A
5B
6A
6B
7
8
9
PP
TS
Unit 30

UNIT 30: CLINOPYROXENE PLAGIOCLASE BASALT CATACLASTITE (CONTINUATION OF 71R-2)

Pieces 1-9

CONTACTS: None visible
PHENOCRYSTS:
Plagioclase - 3-5%, <1.5 mm, completely altered to clays except in Pieces 6
Clinopyroxene - 8%, <1.5 mm, completely altered to chlorite except in Piec
9
GROUNDMASS: Fine-grained, completely altered to albite/chlorite, contains d
pyrite
VESICLES: Absent
COLOR: Light gray to gray (7.5YR 7/0 -6/0) and very dark gray (2.5YR 3/0) when
STRUCTURE: Cataclastic
ALTERATION: Extensively altered to clay, albite, and chlorite except for Pieces
VEINS/FRACTURES: n/a, <0.1 mm, randomly oriented, fractured in Pieces 2-5
Piece 8.
ADDITIONAL COMMENTS: Continuation of 125-786B-71R-3.

7 and 9
s 6, 7 and

sseminated

fresh

6, 7, and 9
and in

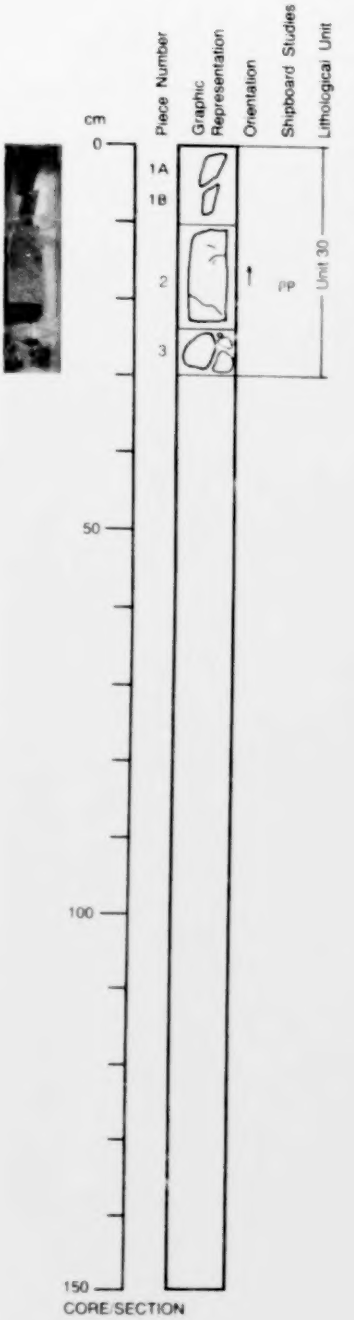
cm
0
50
100
150
CORE/SECTION
Piece Number
Graphic Representation
Orientation
Shipboard Studies
Lithological Unit
1A
1B
2
3
PP
Unit 30

125-786B-71R-5

UNIT 30: CLINOPYROXENE-OLIVINE BASALT (CONTINUATION OF 71R-4) CLINOPYROXENE-PLAGIOCLASE BASALT

Pieces 1-3

CONTACTS: None visible
PHENOCRYSTS: Extensively altered to albite/chlorite
Plagioclase - 2-3%, <1.5 mm; altered to clay
Clinopyroxene - 5-8%, <2 mm; altered to chlorite, some fresh
Olivine - 2%, <3 mm; altered to white calcite with a green chlorite/serpentine rim
GROUNDMASS: Fine grained, completely altered to chlorite
VESICLES: Absent
COLOR: Gray to dark greenish gray
STRUCTURE: Massive
ALTERATION: Extensively altered
VEINS/FRACTURES: Some pyrite and calcite in veins and fractures
ADDITIONAL COMMENTS: Continuation of 125-786B-71R-4

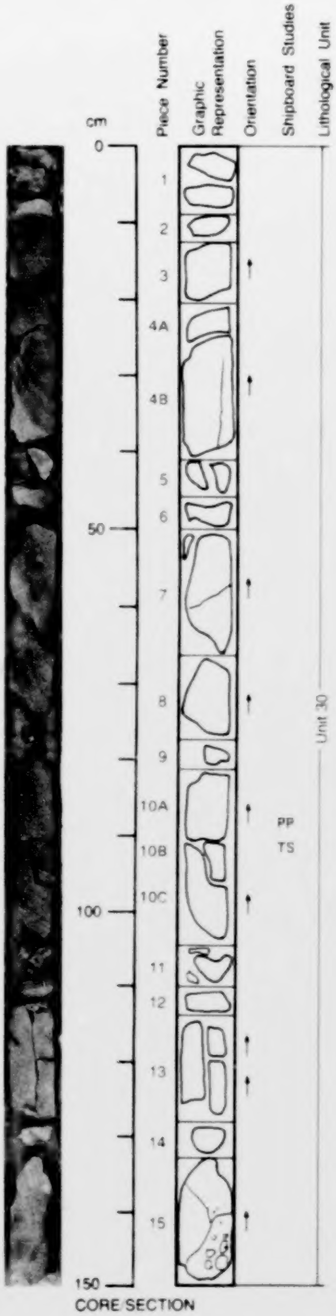
cm
Piece Number
Graphic Representation
Orientation
Shipboard Studies
Lithological Unit
0
50
100
150
1
2
3
4A
4B
5
6
7
8
9
10A
10B
10C
11
12
13
14
15
PP
TS
Unit 30
CORE/SECTION

125-786B-72R-1

UNIT 30: CLINOPYROXENE-OLIVINE BASALT

Pieces 1-15

CONTACTS: None visible.

PHENOCRYSTS: Extensively altered.
  Plagioclase - 1-2%, <1.5 mm, altered to clay.
  Clinopyroxene - 5-8%, <2 mm, altered to chlorite, locally fresh.
  Olivine - 2%, <2 mm, altered to white calcite with a green chlorite/serpentine rim.

GROUNDMASS: Fine-grained, completely altered to chlorite and albite.

VESICLES: Absent.

COLOR: Gray to dark greenish gray (5BG 4/1).

STRUCTURE: Massive.

ALTERATION: Extensively altered.

VEINS/FRACTURES: Pieces 1, 2, and 15 are fractured and altered; chlorite and calcite in fracture surfaces.

ADDITIONAL COMMENTS: Continuation of 125-786B-71R-5.

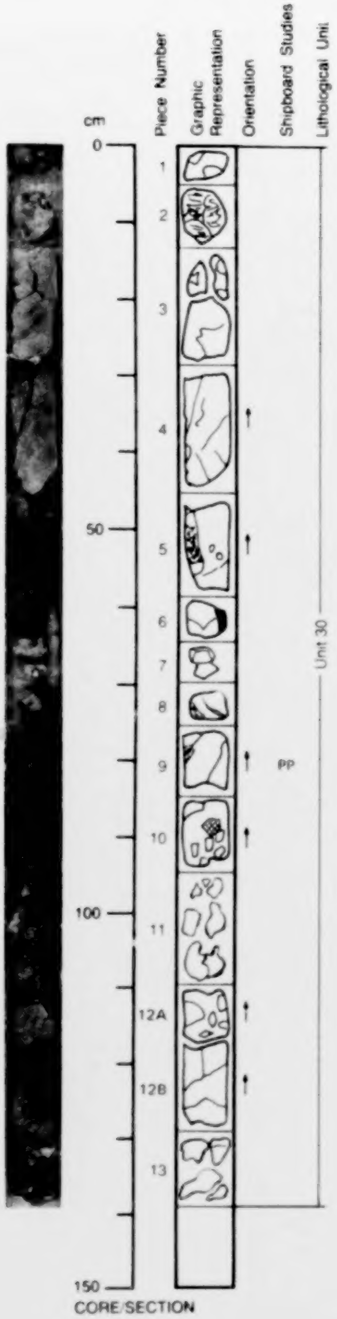
cm
Piece Number
Graphic Representation
Orientation
Shipboard Studies
Lithological Unit
0
50
100
150
1
2
3
4
5
6
7
8
9
10
11
12A
12B
13
PP
Unit 30
CORE/SECTION

125-786B-72R-2

UNIT 30: CLINOPYROXENE-PLAGIOCLASE BASALT (CONTINUATION OF 72R-1)

Pieces 1-13

CONTACTS: None visible

PHENOCRYSTS: Extensively altered

- Plagioclase - 5%, <1.5 mm; altered to clay
- Clinopyroxene - 5%, <2 mm; altered to chlorite, some fresh
- Olivine - 2%, <2 mm; altered to calcite and chlorite/serpentine

GROUNDMASS: Fine grained, completely altered to chlorite/calcite

VESICLES: Absent

COLOR: Gray to dark greenish gray

STRUCTURE: Massive

ALTERATION: Extensively altered to chlorite/albite

VEINS/FRACTURES: Strongly brecciated areas contain abundant disseminated pyrite locally pulverized to clays

ADDITIONAL COMMENTS: Continuation of 125-786B-72R-1

125-786A-12R-01 (140-142 cm) OBSERVER: [illegible] WHERE SAMPLED: Izu-Bonin outer-arc high

ROCK NAME: Basalt

GRAIN SIZE:

TEXTURE: Porphyritic

PRIMARY MINERALOGY	PERCENT PRESENT	PERCENT ORIGINAL	SIZE (mm)	COMPO-SITION	MORPHOLOGY	COMMENTS
PHENOCRYSTS						
Olivine	0	<1	1-1.4		Equant	99% altered to clays.
Plagioclase	2-3	5-10	0.2-1.4		Subhedral-anhedral	Laths, 50-100% altered.
Clinopyroxene	3-5	7-12	0.2-1.2		Euhedral-subhedral	Twinned.
Spinel	<1	<1	0.05-0.1		Subhedral	Rounded to equant and euhedral.
GROUNDMASS						
Glass	0	75-85	N/A		N/A	100% altered.
Plagioclase	<1	4-6	0.01-0.05		Lath, quench	

SECONDARY MINERALOGY	PERCENT	REPLACING/ FILLING	COMMENTS
Clays	80-90	Glass and quench plagioclase	Brown, amorphous, pervasive.
Hematite	[illegible]	Glass, veins	Red-brown, opaque, amorphous.
Zeolite	2-5	Vesicles	Isotropic to very low birefringence, fine-grained.

VESICLES/ CAVITIES	PERCENT	LOCATION	SIZE (mm)	FILLING	SHAPE
Vesicles	[illegible]	Throughout	[illegible]	[illegible] zeolite	Oval-jagged

COMMENTS: Glomerocrysts up to 3 mm of clinopyroxene and orthopyroxene plus plagioclase. No piece # given.

125-786A:12R-CC (16-18 cm) OBSERVER: [illegible] WHERE SAMPLED: Izu-Bonin outer-arc high

ROCK NAME: Monogenetic pyroclastic rock

GRAIN SIZE: 0.01-4 mm

TEXTURE: Hyalo-ophitic texture, glomeroporphyric

PRIMARY MINERALOGY	PERCENT PRESENT	PERCENT ORIGINAL	SIZE (mm)	COMPO-SITION	MORPHOLOGY	COMMENTS
PHENOCRYSTS						
Olivine	[illegible]	4	[illegible]		Euhedral-subhedral	Olivine partly replaced by carbonate.
Clinopyroxene	<1	2	[illegible]		Euhedral-subhedral	2V=+60 degrees.
Spinel	<1	<1	0.01-0.1		Euhedral-subhedral	Spinel is included in olivine.
Orthopyroxene	[illegible]	12	[illegible]	Bronzite	N/A	2V=-80 degrees, compositional zoning in some crystals, glomeroporphyric texture.
GROUNDMASS						
Glass	35-45	[illegible]	N/A		N/A	Partly fresh.
Clinopyroxene	Trace	Trace	[illegible]		Euhedral	Augite, showing prismatic shape (see comments).
Orthopyroxene	Trace	Trace	[illegible]		Euhedral	Showing prismatic shape.
Opaque	Trace	Trace	[illegible]		Euhedral	Existing in the glass.
Plagioclase	1	1	0.01-0.05		Euhedral	Showing prismatic shape under crossed polars. Clinoenstatite with lamellar twins.

SECONDARY MINERALOGY	PERCENT	REPLACING/ FILLING	COMMENTS
Clays	[illegible]	Olivine, glass	Dark brown clays are replacing olivine and glass.
Carbonate	[illegible]	Olivine, glass	In vesicles; carbonates are replacing olivine and glass.

VESICLES/ CAVITIES	PERCENT	LOCATION	SIZE (mm)	FILLING	SHAPE	COMMENTS
Vesicles	[illegible]	Random	[illegible]	Clay	Round	Vesicles are partly filled by clay and carbonate.

COMMENTS: Olivine crystals contain euhedral Cr-spinel and are surrounded by reaction rim of orthopyroxene. Clinopyroxene-olivine-orthopyroxene basaltic andesite magma was quenched and fragmented, then lithic fragments and matrix are made from the same rock. Matrix is more altered than lithic part, the glass of which is very fresh. Clinopyroxenes in groundmass are both Ca-rich and Ca-poor, or augite and "clinoenstatite", respectively. No piece # given. GROUNDMASS: Low-Ca-clinopyroxene; [illegible]; [illegible] mm; euhedral; equals clinoenstatite, showing lamellae twin.

125-786A-13X-CC (27-29 cm) OBSERVER: JOH WHERE SAMPLED: Izu-Bonin outer-arc high

ROCK NAME: Orthopyroxene-phyric high-magnesian basalt

GRAIN SIZE:

TEXTURE: Glomerophyric

PRIMARY MINERALOGY	PERCENT PRESENT	PERCENT ORIGINAL	SIZE (mm)	COMPOSITION	MORPHOLOGY	COMMENTS
PHENOCRYSTS						
Clinopyroxene	<1	<1	0.1-0.5		Subhedral	In glomerocryst with orthopyroxene.
Spinel	Trace	Trace	0.01		Euhedral-subhedral	
Orthopyroxene	12-17	15-20	0.1-1.5		Euhedral-subhedral	Frequently as glomerocrysts; spinel inclusions in rounded crystals.
GROUNDMASS						
Glass	35-40	40-45	N/A		N/A	Colorless, high relief.
Plagioclase	10-12	12-15	0.02-0.15		Quenched, needles	

SECONDARY MINERALOGY	PERCENT	REPLACING/ FILLING	COMMENTS
Clays	35-45	Glass matrix	Brown amorphous clay, pervasively replacing the matrix between fresh clasts of andesite.
Carbonate	7-10	Vesicles, veins	Lines vesicles (0.02 mm thick) and forms veins (0.01-0.1 mm thick).
Chlorite	2-5	Glass, pyroxene	Light green-yellow, pleochroic, amorphous to fibrous.

VESICLES/ CAVITIES	PERCENT	LOCATION	SIZE (mm)	FILLING	SHAPE
Vesicles	>10	Throughout	0.1-0.5	Carbonate	Oval

COMMENTS: Rock is a breccia of moderately phyric, orthopyroxene-rich glassy andesite fragments in a chloritized clay matrix. No piece # given.

125-786A-14X-CC (7-8 cm) OBSERVER: JOH WHERE SAMPLED: Izu-Bonin outer-arc high

ROCK NAME: Orthopyroxene-phyric boninite

GRAIN SIZE: 0.1-2 mm

TEXTURE: Moderately phyric

PRIMARY MINERALOGY	PERCENT PRESENT	PERCENT ORIGINAL	SIZE (mm)	COMPOSITION	MORPHOLOGY	COMMENTS
PHENOCRYSTS						
Spinel	<1	<1	0.05-0.1		Subhedral	Mostly low birefringence.
Orthopyroxene	5-7	7-10	0.1-2		Euhedral-subhedral	Random distribution, except for concentration in glomerocrysts.
GROUNDMASS						
Glass	0	70-85	N/A		N/A	No quench phases visible.

SECONDARY MINERALOGY	PERCENT	REPLACING/ FILLING	COMMENTS
Clays	65-75	Glass	Brown-gray, amorphous, pervasive throughout matrix and many phenocrysts.
Carbonate	10-12	Vesicles	White, radiating crystals.
Chlorite	15-20	Glass, pyroxenes	Light green, fine-grained, replacing matrix and especially trapped glass associated with glomerocrysts.

VESICLES/ CAVITIES	PERCENT	LOCATION	SIZE (mm)	FILLING	SHAPE
Vesicles	7-15	Throughout	0.5-3	40%	Round to irregular

COMMENTS: Glomerocrysts of orthopyroxene 1-4 mm in diameter. Pervasive clay and minor chlorite and zeolite(?) alteration obscure original textural and mineralogical features. Similar to 786A-18X-2, 0-2 cm, Piece 1. No piece # given.

125-786A-14X-CC (9-11 cm)   OBSERVER: JOH   WHERE SAMPLED: Izu-Bonin outer-arc high

ROCK NAME: Brecciated two-pyroxene boninite

GRAIN SIZE: Glassy, 0.2-3.5 mm

TEXTURE: Moderately phyric

PRIMARY MINERALOGY	PERCENT PRESENT	PERCENT ORIGINAL	SIZE (mm)	COMPO-SITION	MORPHOLOGY	COMMENTS
PHENOCRYSTS						
Olivine	<1	<1	0.5-1.5		Euhedral(relict)	90% altered; outline and small relict fragments (0.1 mm) remain.
Clinopyroxene	1-2	1-2	0.5-2		Euhedral-subhedral	Usually in glomerocrysts with orthopyroxene.
Orthopyroxene	7-10	8-12	0.2-1.5		Euhedral-subhedral	Glass inclusions, spinel inclusions, glomerocrysts.
GROUNDMASS						
Glass	40-60	75-85	N/A		N/A	
Plagioclase	3-7	5-10	0.02-0.12		Needles, quench texture	Locally aligned.

SECONDARY MINERALOGY	PERCENT	REPLACING/FILLING	COMMENTS
Clays	10-15	Glass	Light brown-yellow, amorphous, occurs with chlorite.
Carbonate	15-20	Vesicles, veins	Light yellow, white; lines vein walls.
Chlorite	20-30	Glass	Light brown-green, pleochroic, fine-grained or amorphous.

VESICLES/CAVITIES	PERCENT	LOCATION	SIZE (mm)	FILLING	SHAPE
Vesicles	15-17	Throughout	0.1-0.5	Carbonate	Round-elongate

COMMENTS: Rock may be autobrecciated-matrix material is chlorite and/or smectite-rich and appears to be crushed or altered glass such as that found in the clasts. Clasts of glassy andesite set in green, altered matrix. No piece number given.

125-786A-14X-CC (15-18 cm)   OBSERVER: TEN   WHERE SAMPLED: Izu-Bonin outer-arc high

ROCK NAME: Olivine-plagioclase-clinopyroxene basalt

GRAIN SIZE: 0.1-3 mm

TEXTURE: Hyalo-ophitic texture

PRIMARY MINERALOGY	PERCENT PRESENT	PERCENT ORIGINAL	SIZE (mm)	COMPO-SITION	MORPHOLOGY	COMMENTS
PHENOCRYSTS						
Olivine	0	1	1.5-2		Euhedral-subhedral	One olivine pseudomorph in section.
Plagioclase	3	3	1-1.5		Euhedral	Partly resorbed.
Clinopyroxene	5	5	0.1-0.5		Euhedral-subhedral	2V=+45 degrees.
Spinel	Trace	Trace	0.001-0.005		Euhedral	Inclusion in olivine pseudomorph.
Orthopyroxene	3	3	0.1-2		Euhedral-subhedral	Making glomerophyric aggregate with augite.
GROUNDMASS						
Glass	20-30	75-80	N/A		N/A	Partly devitrified to clays.
Plagioclase	10	10	0.05-0.15		Euhedral; laths	
Augite	2	2	0.05-0.20		Euhedral; prismatic	
Orthopyroxene	2	2	0.05-0.20		Euhedral; prismatic	

SECONDARY MINERALOGY	PERCENT	REPLACING/FILLING	COMMENTS
Clays	50-55	Glass and olivine	Replacing olivine and glass. Pale brown in color.

VESICLES/CAVITIES	PERCENT	LOCATION	SIZE (mm)	FILLING	SHAPE
Vesicles	20	Random	0.1-4	None	Round

COMMENTS: Glass-rich volcanic rocks. Glass is partly fresh, partly altered to clays. Olivine pseudomorph and orthopyroxene and augite make glomerophyric texture. Groundmass minerals are very fine grained, indicating quench texture. No piece # given.

125-786A-17X-CC (44-46 cm)   OBSERVER: JOH   WHERE SAMPLED: Izu-Bonin outer-arc high

ROCK NAME: Glassy basalt margin

GRAIN SIZE: Glassy; phenocrysts (0.2-1 mm)

TEXTURE: Glassy margin, sparsely phyric

PRIMARY MINERALOGY	PERCENT PRESENT	PERCENT ORIGINAL	SIZE (mm)	COMPO-SITION	MORPHOLOGY	COMMENTS
PHENOCRYSTS						
Plagioclase	<1	1-2	0.1-0.4		Euhedral-subhedral	
Clinopyroxene	1-2	3-7	0.2-1		Euhedral-subhedral	With magnetite/spinel inclusion.
Spinel	Trace	Trace	<0.02		Euhedral	Fresh, often as inclusions.
Orthopyroxene	<1	1-3	0.2-0.4		Subhedral	75% altered to chlorite + clays.
GROUNDMASS						
Glass	10-15	85	N/A		N/A	Clear with quench plagioclase.
Plagioclase	2-5	5-7	0.01-0.1		Laths, quench	Tiny needles within glass.

SECONDARY MINERALOGY	PERCENT	REPLACING/ FILLING	COMMENTS
Clays	65-75	Glass	Brown amorphous.
Chlorite	5-7	Glass	As veins. Slight yellow-green pleochroism.
Prehnite?	5?-7	Veins	Abnormal birefringence for clays and some development of bow-tie structure.

VESICLES/ CAVITIES	PERCENT	LOCATION	SIZE (mm)	FILLING	SHAPE
Vesicles	0				

COMMENTS: May be flow-banding or glassy layers interbedded in sediments. No piece # given.

125-786A-18X-02 (Piece 1,0-2 cm)   OBSERVER: JOH   WHERE SAMPLED: Izu-Bonin outer-arc high

ROCK NAME: Orthopyroxene-phyric boninite

GRAIN SIZE: 0.1-1.5 mm

TEXTURE: Sparsely phyric

PRIMARY MINERALOGY	PERCENT PRESENT	PERCENT ORIGINAL	SIZE (mm)	COMPO-SITION	MORPHOLOGY	COMMENTS
PHENOCRYSTS						
Orthopyroxene	<1-1	1-3	0.5-1.5		Equant-subhedral	90% altered to clays and chlorite.
Spinel	N/A	N/A	0.01-0.1	Cr-rich	Euhedral	Blood red-black, disseminated.
GROUNDMASS						
Clinopyroxene	5-7	15-20	0.1-0.2		Euhedral-laths	Quench texture "tails", altered to chlorite.
Glass	0	70-80	N/A		N/A	

SECONDARY MINERALOGY	PERCENT	REPLACING/ FILLING	COMMENTS
Clays	30-40	Glass, pyroxene	Brown, amorphous, occur as globular patches up to 0.2 mm in diameter and intimately mixed with chlorite.
Pyrite	Trace	Vesicle filling	Parallel extinction.
Chlorite	50-60	Glass, pyroxene	Yellow-green, birefringent, radiating habit, pleochroic.
Hematite	3-5	Matrix	Intimately mixed with chlorite and clays present throughout.
Carbonate	10-15	Vesicles	Lines vesicles, high birefringence, parallel extinction.

VESICLES/ CAVITIES	PERCENT	LOCATION	SIZE (mm)	FILLING	SHAPE	COMMENTS
Vesicles	10-15	Throughout	0.1-1.5	Carbonate	Irregular	Filled with white, radiating mineral with parallel extinction; carbonate?

COMMENTS: Clay patches appear in glass-rich (relict) areas while chlorite-rich alteration is concentrated in the microphyric matrix portions. Much of the texture and primary mineralogy is obscured by alteration. Similar to 786A-14X-CC (7-8 cm).

125-786A-19R-[illegible] (17-20 cm)   OBSERVER: JOH   WHERE SAMPLED: Izu-Bonin outer-arc high

ROCK NAME: Basalt

GRAIN SIZE: Fine-grained

TEXTURE: Glassy

PRIMARY MINERALOGY	PERCENT PRESENT	PERCENT ORIGINAL	SIZE (mm)	COMPO-SITION	MORPHOLOGY	COMMENTS
PHENOCRYSTS						
Clinopyroxene	<1	<1	<0.8		Euhedral	>95% altered to clay and chlorite.
Orthopyroxene	<1	<1	<0.5		Subhedral	>95% altered to clay and chlorite.
GROUNDMASS						
Clinopyroxene	10-15	15-20	<0.2		Subhedral	Equant and tabular; some have quench texture.
Orthopyroxene	<5	5-10	<0.2		Subhedral	Tabular; some have quench textures.
Spinel	1-2	1-2	<0.02		Subhedral	Equant.
Glass	<10	75-80	N/A		N/A	Pale yellow, devitrified.

SECONDARY MINERALOGY	PERCENT	REPLACING/ FILLING	COMMENTS
Clays	45-50	Glass	Brown, clustered around vesicles.
Carbonate	1-2	Pyroxene, vesicles	
Zeolites	1-3	Vesicles	Radiating, pale yellow, mixed with chlorite.
Chlorite	35-45	Glass	

VESICLES/ CAVITIES	PERCENT	LOCATION	SIZE (mm)	FILLING	SHAPE
Vesicles	5-10		<0.8	Chlorite, clay, zeolites	Round

COMMENTS: No piece # given.

125-786B-[illegible] (Piece 2, 3-6 cm)   OBSERVER: JOH   WHERE SAMPLED: Izu-Bonin outer-arc high

ROCK NAME: Two-pyroxene-plagioclase phyric boninite

GRAIN SIZE: 1.5-2 mm

TEXTURE: Moderately phyric

PRIMARY MINERALOGY	PERCENT PRESENT	PERCENT ORIGINAL	SIZE (mm)	COMPO-SITION	MORPHOLOGY	COMMENTS
PHENOCRYSTS						
Plagioclase	7-12	8-12	0.1-2		Euhedral-rounded	Glass inclusions, complex twinning, normal, reverse, and oscillatory zoning.
Clinopyroxene	5-7	4-7	0.3-1.5		Euhedral-anhedral	Complex twinning, glass inclusions
Spinel	Trace	Trace	<0.1		Subhedral	Appear randomly distributed, may be alteration.
Orthopyroxene	2-3	2-4	0.5-1.5		Euhedral	Glass inclusions
GROUNDMASS						
Glass	50-60	70-85	N/A		N/A	Minor pervasive chlorite alteration
Plagioclase	8-10	10-15	<0.1		Quench laths	Locally aligned and deflected around phenocrysts.

SECONDARY MINERALOGY	PERCENT	REPLACING/ FILLING	COMMENTS
Clays	1-5	Glass	Brown amorphous clay pervasively altering glass.
Chlorite	20-25	Glass	Fine-grained and pervasive lending a slight green pleochroism to the glassy matrix.

VESICLES/ CAVITIES	PERCENT	LOCATION	SIZE (mm)	FILLING	SHAPE
Vesicles	1-2	Throughout	0.5-1	No	Elongate

COMMENTS: Glomerocrysts of pyroxene and plagioclase up to 4 mm in diameter; also of plagioclase only.

125-786B-1R-01 (Piece 6,26-28 cm) OBSERVER: JOH WHERE SAMPLED: Izu-Bonin outer-arc high

ROCK NAME: Two-pyroxene-plagioclase phyric boninite

GRAIN SIZE: 0.3-1.2 mm, medium

TEXTURE: Moderately phyric

PRIMARY MINERALOGY	PERCENT PRESENT	PERCENT ORIGINAL	SIZE (mm)	COMPOSITION	MORPHOLOGY	COMMENTS
PHENOCRYSTS						
Plagioclase	6-8	7-9	0.15-1.2		Euhedral-subhedral	Spinel inclusions, Carlsbad twinning.
Clinopyroxene	9-11	10-12	0.7-1		Euhedral-subhedral	Frequently twinned, spinel inclusions, glass inclusions.
Spinel	Trace	Trace	0.01		Euhedral	
Orthopyroxene	2-4	3-5	0.3		Euhedral-subhedral	Spinel and glass inclusions.
GROUNDMASS						
Glass	<5	65-75	N/A		N/A	Devitrified.
Plagioclase	6-8	7-10	0.02-0.1		Laths	Usually twinned.
Clinopyroxene	3-5	4-5	0.02-0.08		Equant, euhedral	

SECONDARY MINERALOGY	PERCENT	REPLACING/ FILLING	COMMENTS
Clays	60-70	Glass	Dark brown, amorphous, pervasive.
Hematite	Trace	Clinopyroxene	In fine-grained glomerocrysts.

VESICLES/ CAVITIES	PERCENT	LOCATION	SIZE (mm)	FILLING	SHAPE
Vesicles	7-12	Throughout	0.1-2	No	Oval

COMMENTS: Glomerocrysts of orthopyroxene, clinopyroxene and plagioclase are abundant.

125-786B-3R-01 (Piece 2,12-15 cm) OBSERVER: JOH WHERE SAMPLED: Izu-Bonin outer-arc high

ROCK NAME: Two-pyroxene-plagioclase boninite

GRAIN SIZE: 0.2-1.5 mm

TEXTURE: Moderately phyric

PRIMARY MINERALOGY	PERCENT PRESENT	PERCENT ORIGINAL	SIZE (mm)	COMPOSITION	MORPHOLOGY	COMMENTS
PHENOCRYSTS						
Plagioclase	4-5	5-7	0.2-1.2		N/A	Abundant twins, glass and spinel inclusions.
Clinopyroxene	2-5	3-5	0.5-1		Euhedral-subhedral	Zoned with relict subrounded cores, glass and spinel inclusions.
Spinel	Trace	Trace	0.01-0.05		Euhedral	
Orthopyroxene	7-10	8-10	0.4-1.5		Euhedral-subhedral	Deep brown, fresh glass inclusions.
GROUNDMASS						
Glass	<5	75-85	N/A		N/A	
Plagioclase	4-5	5-7	0.2-0.3		Laths	Quench crystals and needles.

SECONDARY MINERALOGY	PERCENT	REPLACING/ FILLING	COMMENTS
Clays	65-75	Glass	Brown, amorphous, pervasive.
Chlorite	1-3	Veins	Green-light yellow-brown, <0.1 mm wide.
Hematite	<1	Orthopyroxene	Rust orange, irregular shaped patches associated with fine-grained glomerocrysts.

VESICLES/ CAVITIES	PERCENT	LOCATION	SIZE (mm)	FILLING	SHAPE
Vesicles	7-10	Throughout	0.1-3	No	Oval-round

COMMENTS: Glomerocrysts of orthopyroxene + or - clinopyroxene + or - plagioclase are frequent and have a bimodal grain size distribution (0.1-0.3; 0.7-1.5 mm). Clinopyroxenes are pale green in plane-polarized light (PPL) and slightly pleochroic.

125-786B-[illegible] (Piece 14, 94-97 cm) OBSERVER: [illegible] WHERE SAMPLED: Izu-Bonin outer-arc high

ROCK NAME: Two-pyroxene-plagioclase boninite breccia

GRAIN SIZE:

TEXTURE:

PRIMARY MINERALOGY	PERCENT PRESENT	PERCENT ORIGINAL	SIZE (mm)	COMPO-SITION	MORPHOLOGY	COMMENTS
PHENOCRYSTS						
Plagioclase	1-2	2-3	[illegible]		Euhedral, laths	
Clinopyroxene	6-8	7-9	[illegible]		Euhedral-subhedral	Glass inclusions.
Spinel	Trace	Trace	<0.1		Equant-subhedral	Mainly present in groundmass.
Orthopyroxene	4-6	5-7	[illegible]		Subhedral	
GROUNDMASS						
Glass	[illegible]	15-20	N/A		N/A	Light brown to light yellow, 1/2 devitrified.
Plagioclase	4-6	5-7	<0.1		Laths/needles/quench crystals	
Matrix (pyroxene)	[illegible]	[illegible]	[illegible]		Subhedral	Crystals of pyroxene set in clay.

SECONDARY MINERALOGY	PERCENT	REPLACING/FILLING	COMMENTS
Clays	60-70	Glass matrix	Brown, amorphous, pervasive and as matrix for breccia.

VESICLES/CAVITIES	PERCENT	LOCATION	SIZE (mm)	FILLING	SHAPE
Vesicles	<1				

COMMENTS: Finely brecciated; glassy, rounded boninite clasts [illegible] mm in diameter set in a clay-rich matrix.

125-786B-[illegible] (Piece 12, [illegible] cm) OBSERVER: [illegible] WHERE SAMPLED: Izu-Bonin outer-arc high

ROCK NAME: Two-pyroxene-plagioclase boninite

GRAIN SIZE: [illegible] mm

TEXTURE: [illegible] texture

PRIMARY MINERALOGY	PERCENT PRESENT	PERCENT ORIGINAL	SIZE (mm)	COMPO-SITION	MORPHOLOGY	COMMENTS
PHENOCRYSTS						
Olivine	0	8	[illegible]		Subhedral	Pseudomorphs.
Plagioclase	4	6	[illegible]		Anhedral-euhedral	Two generations.
Clinopyroxene	8	8	[illegible]	Augite	Euhedral-subhedral	Has compositional zoning; 2V=45 degrees.
Spinel	Trace	Trace	[illegible]	Cr-spinel	Euhedral	Included in olivine pseudomorph.
Orthopyroxene	10	10	[illegible]	Bronzite	Euhedral-subhedral	[illegible], Bushveld-type exsolution lamellae (augite (100) lamellae) in some crystals.
GROUNDMASS						
Glass	0	67	N/A		N/A	Devitrified to clays.
Plagioclase	5	5	[illegible]		Euhedral, laths	
Augite	5	5	[illegible]		Euhedral, prismatic	
Orthopyroxene	5	5	[illegible]		Euhedral, prismatic	

SECONDARY MINERALOGY	PERCENT	REPLACING/FILLING	COMMENTS
Clays	67-77	Glass, olivine	Replacing olivine and glass, brown to [illegible]
Carbonate	1	Plagioclase(?)	
Opaque	[illegible]	Glass	Glass was replaced partly by opaque minerals.

VESICLES/CAVITIES	PERCENT	LOCATION	SIZE (mm)	FILLING	SHAPE
Vesicles	[illegible]	Random	[illegible]	None	Round

COMMENTS: Some orthopyroxene grains have fine (100) augite lamellae which are common in basic plutonic rocks, and are surrounded by reaction rim of clinopyroxene (augite 2V=45 degrees). Olivine pseudomorph (now clays) contains euhedral Cr-spinel, and is surrounded by reaction rim of orthopyroxene ([illegible]) degrees).

125-786B-58R-02 (Piece 2,12-14 cm)   OBSERVER: SAB   WHERE SAMPLED: Izu-Bonin outer-arc high

ROCK NAME: Two-pyroxene phyric andesite

GRAIN SIZE: 0.2-4 mm

TEXTURE: Moderately phyric, glomerocrystic

PRIMARY MINERALOGY	PERCENT PRESENT	PERCENT ORIGINAL	SIZE (mm)	COMPO-SITION	MORPHOLOGY	COMMENTS
PHENOCRYSTS						
Plagioclase	6-12	7-13	0.5-4		Euhedral	Some with spinel inclusions. Complex zoning: normal, reverse, oscillatory.
Clinopyroxene	10-20	11-20	0.2-2		Euhedral-anhedral	Has glass inclusions; twinning and zoning.
Spinel	<1	<1	0.01-0.1		Subhedral-anhedral	Randomly distributed.
Orthopyroxene	1-3	2-4	0.5-1.5		Anhedral-subhedral	Has glass inclusions.
GROUNDMASS						
Glass	30-40	40-45	N/A		N/A	Altered to clay + chlorite.
Plagioclase	5-10	10-15	<0.1		Quench laths	Locally aligned and deflected around phenocrysts.
Clinopyroxene	1-3	3-6	0.05		Subhedral	

SECONDARY MINERALOGY	PERCENT	REPLACING/ FILLING	COMMENTS
Clays	25	Glass	Brown amorphous clays pervasively altering the glass and matrix material.
Chlorite	15	Glass	Fine-grained; slight green pleochroism.

VESICLES/ CAVITIES	PERCENT	LOCATION	SIZE (mm)	FILLING	SHAPE
Vesicles	1-4	Throughout	0.3-2	No	Mostly elongate

COMMENTS: There are glomerocrysts of plagioclase + pyroxenes up to 3 mm in diameter. There are also glomerocrysts consisting entirely of plagioclase phenocrysts. Glomerocrysts occur with and without spinels.

125-786B-58R-02 (Piece 4C, 38-41 cm)   OBSERVER: [illegible]   WHERE SAMPLED: Izu-Bonin outer-arc high

ROCK NAME: Two-pyroxene andesite

GRAIN SIZE: 0.1-4 mm

TEXTURE: Moderately to sparsely phyric

PRIMARY MINERALOGY	PERCENT PRESENT	PERCENT ORIGINAL	SIZE (mm)	COMPO-SITION	MORPHOLOGY	COMMENTS
PHENOCRYSTS						
Plagioclase	7-12	9-13	0.8-3.5		Euhedral	Some with spinel inclusions. Complex zoning, normal and reverse and oscillatory.
Clinopyroxene	15-20	17-20	0.3-2		Euhedral-anhedral	Spinel and glass inclusions, also relict rounded cores and complex zoning.
Spinel	<1	<1	0.01-0.2		Subhedral	Often as inclusions in plagioclase and clinopyroxene.
Orthopyroxene	1-3	2-4	0.4-1.5		Anhedral-subhedral	Crystals appear to have been broken from longer tabular crystals.
GROUNDMASS						
Glass	7-10	30-40	N/A		N/A	Patches of slightly fresh glass present in a brecciated texture.
Plagioclase	5-10	10-15	<0.1		Laths	Small tabular microphenocrysts and quench crystals.
Clinopyroxene	2-3	3-6	<0.05		Subhedral	

SECONDARY MINERALOGY	PERCENT	REPLACING/ FILLING	COMMENTS
Clays	35-45	Glass	Brown amorphous clays, chlorite and hematite intermix and pervasively alter the glass and matrix material. There is a second-order patchy fabric.
Chlorite	12-20	Glass	
Hematite	15-20	Glass	

VESICLES/ CAVITIES	PERCENT	LOCATION	SIZE (mm)	FILLING	SHAPE	COMMENTS
Vesicles	1-3	Throughout	0.2-1.5	Not usually	Random, jagged	More concentrated and smoother in glassy portion.

COMMENTS: Sharp boundary between fine-grained, glassy-textured zone and phyric coarser-grained zone. May be mixing boundary. Plagioclase and clinopyroxene in glassy zone are small (<0.8 mm), less abundant and more altered than in coarse part. Glass is altered to hematite, chlorite and clays in both sections but more clay is present in the finer-grained portion. Glomerocrysts of two pyroxenes and plagioclase with and without spinel are present.

125-786B-[illegible] (Piece [illegible]) OBSERVER: [illegible] WHERE SAMPLED: [illegible]

ROCK NAME: Pyroxene-plagioclase basalt

GRAIN SIZE: [illegible]

TEXTURE: Moderately phyric

PRIMARY MINERALOGY	PERCENT PRESENT	PERCENT ORIGINAL	SIZE (mm)	COMPOSITION	MORPHOLOGY	COMMENTS
PHENOCRYSTS						
Plagioclase	[illegible]	[illegible]	[illegible]		Euhedral	Glass inclusions; twinned, complex zoning.
Clinopyroxene	[illegible]	[illegible]	[illegible]		Euhedral-anhedral	Glass + spinel inclusions; complex twinning.
Spinel	[illegible]	[illegible]	[illegible]		Subhedral-euhedral	Randomly distributed.
Orthopyroxene	[illegible]	[illegible]	[illegible]		Subhedral-euhedral	Has glass + spinel inclusions.
GROUNDMASS						
Glass	[illegible]	[illegible]	N/A		Dendritic	Altered to clays.
Plagioclase	[illegible]	[illegible]	[illegible]		N/A	

SECONDARY MINERALOGY	PERCENT	REPLACING/FILLING	COMMENTS
Clays	[illegible]	Glass	Brown, finely disseminated, amorphous, pervasive (and yellow).
Chlorite	[illegible]	Glass, plagioclase	Light yellow to brownish green, slightly pleochroic.

VESICLES/CAVITIES	PERCENT	LOCATION	SIZE (mm)	FILLING	SHAPE	COMMENTS
Vesicles	[illegible]	Throughout	[illegible]	None	Random, irregular	Some may be voids caused during thin-section making.

COMMENTS: Glomerocrysts of pyroxene and plagioclase, of orthopyroxene and clinopyroxene, and of only plagioclase, from [illegible] mm in diameter. At least one example of clinopyroxene [illegible] orthopyroxene.

125-786B-[illegible] (Piece [illegible]) OBSERVER: [illegible] WHERE SAMPLED: [illegible]

ROCK NAME: Clinopyroxene-plagioclase-phyric andesite

GRAIN SIZE: Fine-grained

TEXTURE: Intersertal, moderately phyric

PRIMARY MINERALOGY	PERCENT PRESENT	PERCENT ORIGINAL	SIZE (mm)	COMPOSITION	MORPHOLOGY	COMMENTS
PHENOCRYSTS						
Plagioclase	[illegible]	[illegible]	[illegible]		Euhedral-subhedral	Tabular, sparse spinel inclusions, some radiating clusters.
Clinopyroxene	[illegible]	[illegible]	[illegible]		Subhedral-anhedral	Dusty pink to gray, spinel inclusions, twinning.
Spinel	[illegible]	[illegible]	[illegible]		Subhedral	Dispersed black, equant to irregular.
GROUNDMASS						
Glass	[illegible]	[illegible]	N/A		N/A	Brown to light green, altered to clays and zeolite.
Plagioclase	[illegible]	[illegible]	[illegible]		Laths	

SECONDARY MINERALOGY	PERCENT	REPLACING/FILLING	COMMENTS
Clays	[illegible]	Glass, plagioclase	Brown to dark yellow, amorphous, pervasive in glassy areas and dispersed throughout.
Chlorite	[illegible]	Glass, plagioclase, pyroxene	Pale green to yellow-brown, slightly pleochroic.
Hematite	[illegible]	Pyroxene	Completely alters and pseudomorphs pyroxene so that only outline and interior fractures are still present. This type of alteration is present in other thin sections associated with carbonate which may have been lost due to plucking in this section.

VESICLES/CAVITIES	PERCENT	LOCATION	SIZE (mm)	FILLING	SHAPE
Vesicles	[illegible]		[illegible]	No	Round-like polar

COMMENTS: There appear to be two generations of clinopyroxene: those still present and those now altered by hematite.

125-786B-8R-02 (Piece 23A,137-138 cm) OBSERVER: HIR WHERE SAMPLED: Izu-Bonin outer-arc high

ROCK NAME: Olivine-orthopyroxene-clinopyroxene basalt

GRAIN SIZE: 0.5-1.5 mm

TEXTURE: Glomerophyric and hyalo-ophitic texture

PRIMARY MINERALOGY	PERCENT PRESENT	PERCENT ORIGINAL	SIZE (mm)	COMPOSITION	MORPHOLOGY	COMMENTS
PHENOCRYSTS						
Olivine	0	8-9	1-1.5		Euhedral	Fully altered to brownish clay.
Plagioclase	<1	<1	[illegible]2-0.5		Euhedral-subhedral	Twinning is common.
Clinopyroxene	5	5	0.5-1		Subhedral	Shows glomerophyric texture with orthopyroxene.
Spinel	Trace	Trace	<0.01		Euhedral	Occurs as inclusion in olivine crystal.
Orthopyroxene	3	3	0.5-1		Euhedral-subhedral	Shows pale green to pale red pleochroism.
GROUNDMASS						
Clinopyroxene	5-10	5-15	0.05-0.1		Euhedral-subhedral	Twinned, prismatic shape.
Plagioclase	10-20	10-20	0.1-0.2		Euhedral	Occurs as quenched, elongate crystals.
Glass	0	30-40	N/A		N/A	Fully altered to dusty, brownish clay.

SECONDARY MINERALOGY	PERCENT	REPLACING/ FILLING	COMMENTS
Clays	10-15	Olivine, glass vesicle	Brownish dusty clay replaces glass and olivine and fills in vesicles.

VESICLES/ CAVITIES	PERCENT	LOCATION	SIZE (mm)	FILLING	SHAPE
Vesicles	7-10	Random	0.5-5	Brownish clay	Round

COMMENTS: This rock is relatively rich in olivine phenocrysts, that were fully altered to brownish clay. Clinopyroxene and orthopyroxene show glomerophyric texture.

125-786B-8R-01 (Piece 7,45-47 cm) OBSERVER: JON WHERE SAMPLED: Izu-Bonin outer-arc high

ROCK NAME: Clinopyroxene-plagioclase phyric andesite

GRAIN SIZE: Fine-grained

TEXTURE: Glomerophyric

PRIMARY MINERALOGY	PERCENT PRESENT	PERCENT ORIGINAL	SIZE (mm)	COMPOSITION	MORPHOLOGY	COMMENTS
PHENOCRYSTS						
Plagioclase	18-24	20-25	0.2-1		Euhedral-subhedral	Spinel inclusions, lath shaped.
Clinopyroxene	4-6	5-7	0.2-1.2		Subhedral anhedral	Dusty gray to gray green, spinel inclusions, glass inclusions.
GROUNDMASS						
Glass	8-12	35-40	N/A		N/A	
Plagioclase	10-15	15-20	<0.3		Needles	Preferred alignment throughout thin section.
Microlites	20	20-25	<0.02		Tabular	Higher relief than glass, no discernible optical properties.
Spinel	2-3	2-3	<0.01		Equant	

SECONDARY MINERALOGY	PERCENT	REPLACING/ FILLING	COMMENTS
Clays	25-30	Glass/matrix	Brown, amorphous, pervasive
Zeolites	<2	Vesicles	Radiating needles.
Chlorite	10-15	Glass/matrix	Slight green-yellow pleochroism.

VESICLES/ CAVITIES	PERCENT	LOCATION	SIZE (mm)	FILLING	SHAPE
Vesicles	10-12	Throughout	0.2-4	No	Elongate to equant

COMMENTS: Glomerocrysts of plagioclase and clinopyroxene up to 2 mm across.

125-786B-[illegible], Piece [illegible] cm   OBSERVER: [illegible]   WHERE SAMPLED: Izu-Bonin outer-arc high

ROCK NAME: Orthopyroxene-clinopyroxene andesite

GRAIN SIZE: <2 mm

TEXTURE: Glomeroporphyritic texture

PRIMARY MINERALOGY	PERCENT PRESENT	PERCENT ORIGINAL	SIZE (mm)	COMPOSITION	MORPHOLOGY	COMMENTS
PHENOCRYSTS						
Plagioclase	[illegible]	[illegible]	[illegible]		Euhedral	Compositional zoning and twinning are common.
Clinopyroxene	[illegible]	[illegible]	[illegible]		Euhedral-subhedral	Compositional zoning and twinning are common.
Orthopyroxene	[illegible]	[illegible]	[illegible]		Euhedral	Occurs as euhedral, elongate crystal, showing relatively low birefringence.
GROUNDMASS						
Plagioclase	[illegible]	[illegible]	[illegible]		Euhedral	Frequently showing quenched H-shaped crystals.
Clinopyroxene	Trace	Trace	[illegible]		Euhedral	Showing quenched acicular crystal.
Orthopyroxene	Trace	Trace	[illegible]		Euhedral	Showing quenched acicular crystal.
Glass	[illegible]	[illegible]	N/A		N/A	Fully altered to dusty brown clay.

SECONDARY MINERALOGY	PERCENT	REPLACING/ FILLING	COMMENTS
Clays	[illegible]	Glass	Replacing glass; dusty brown in color.

VESICLES/ CAVITIES	PERCENT	LOCATION	SIZE (mm)	FILLING	SHAPE
Vesicles	[illegible]				

COMMENTS: Phenocrysts and microphenocrysts define [illegible] flow lamination and the later fracturing (parallel to the lamination) is developed throughout the rock. Phenocrystic plagioclase is rarely fragmented and shows corroded rims. Clinopyroxene, orthopyroxene and plagioclase often form glomeroporphyritic texture.

125-786B-[illegible], Piece [illegible] cm   OBSERVER: [illegible]   WHERE SAMPLED: Izu-Bonin outer-arc high

ROCK NAME: Pyroxene-plagioclase phyric andesite [illegible]

GRAIN SIZE: [illegible] mm, [illegible]

TEXTURE: Moderately phyric

PRIMARY MINERALOGY	PERCENT PRESENT	PERCENT ORIGINAL	SIZE (mm)	COMPOSITION	MORPHOLOGY	COMMENTS
PHENOCRYSTS						
Plagioclase	[illegible]	[illegible]	[illegible]		Subhedral	Moth-eaten texture.
Clinopyroxene	[illegible]	[illegible]	[illegible]		Euhedral/subhedral	Complex and frequent twinning; [illegible] yellow-green pleochroism; spinel and glass inclusions.
Spinel	Trace	Trace	[illegible]		Euhedral	Black; primarily as inclusions.
Orthopyroxene	[illegible]	[illegible]	[illegible]		N/A	Spinel and glass inclusions.
GROUNDMASS						
Glass	[illegible]	[illegible]	N/A		N/A	Devitrified to very faintly green.
Plagioclase	[illegible]	[illegible]	[illegible]		Square and lath	Mostly elongate euhedral crystals.
Pyroxene	[illegible]	[illegible]	[illegible]		Needles and equant; [illegible]	High birefringence needles and small equant crystals.

SECONDARY MINERALOGY	PERCENT	REPLACING/ FILLING	COMMENTS
Clays	[illegible]	Groundmass	Brown, amorphous [illegible] replacing glass in part of thin section; also intimately mixed with chlorite in [illegible] matrix.
Chlorite	[illegible]	Matrix	Matrix; mixed with clays; filling between moderately altered glass shards.
Carbonate	[illegible]	Veins	[illegible] up to [illegible] mm thick.

VESICLES/ CAVITIES	PERCENT	LOCATION	SIZE (mm)	FILLING	SHAPE
Vesicles	[illegible]	Throughout	[illegible]	Some carbonate	Round

COMMENTS: Glomerocrysts of two pyroxenes with and without plagioclase. This brecciated section is difficult to describe using single mode estimates; [illegible] was originally derived primarily from glass.

125-786B-11R-01 (Piece 18,122-126 cm) OBSERVER: JON WHERE SAMPLED: Izu-Bonin outer-arc high

ROCK NAME: Two-pyroxene-plagioclase phyric basalt

GRAIN SIZE:

TEXTURE: Moderately phyric

PRIMARY MINERALOGY	PERCENT PRESENT	PERCENT ORIGINAL	SIZE (mm)	COMPO-SITION	MORPHOLOGY	COMMENTS
PHENOCRYSTS						
Plagioclase	10-12	11-13	0.5-2		Equant, altered	Glass and spinel inclusions, moth-eaten texture, zoning.
Clinopyroxene	9-11	10-12	0.5-1.2		Elongate, euhedral	Glass and spinel inclusions, complex and abundant twinning.
Spinel	Trace	Trace	<0.01		Euhedral	Primarily as inclusions.
Orthopyroxene	9-11	9-11	0.8-1.2		Elongate, euhedral	Glass and sparse spinel inclusions.
GROUNDMASS						
Glass	<1	45-55	N/A		N/A	Devitrified, locally fresh in glomerocrysts.
Plagioclase	2-3	2-3	0.1-0.2		Equant, lath-tabulars	
Pyroxene	3-5	3-5	0.1-0.2		Equant, subhedral	
Microlites	2-3	3-8	<0.01-0.02		Needles	Low birefringence, variable extinction

SECONDARY MINERALOGY	PERCENT	REPLACING/ FILLING	COMMENTS
Clays	50-60	Glass-matrix crystals	Brown amorphous clay, pervasively altering the glassy matrix.
Chlorite	<1	Glass in glomerocrysts	Weakly birefringent, locally fibrous; yellow to yellow-green.
Smectite	Trace	Pyroxene	Amorphous, intimately mixed with chlorite, present only in the middle of pyroxene glomerocrysts.

VESICLES/ CAVITIES	PERCENT	LOCATION	SIZE (mm)	FILLING	SHAPE
Vesicles	7-10	Throughout	0.1-3	No	Irregular

COMMENTS: Glass within glomerocrysts is slightly fresh, altering to minor chlorite but not brown clays. Glomerocrysts of one and two pyroxenes with and without plagioclase. Matrix phases are obscured by the intensive clay alteration of the glassy groundmass making a confident determination difficult.

[illegible] OBSERVER: [illegible] WHERE SAMPLED: Izu-Bonin outer-arc high

ROCK NAME: Pyroxene-plagioclase-phyric basalt

GRAIN SIZE: [illegible] mm

TEXTURE: Moderately phyric

PRIMARY MINERALOGY	PERCENT PRESENT	PERCENT ORIGINAL	SIZE mm	COMPOSITION	MORPHOLOGY	COMMENTS
PHENOCRYSTS						
Plagioclase	[illegible]	10-12	[illegible]		Elongate, subhedral	Oscillatory zoning, moth-eaten texture with altered glass inclusions, spinel inclusions.
Clinopyroxene	[illegible]	[illegible]	[illegible]		Euhedral-subhedral	Complex twinning, spinel and altered glass inclusions.
Spinel	[illegible]	[illegible]	[illegible]		Equant	In glassy matrix and as inclusions
Orthopyroxene	[illegible]	[illegible]	[illegible]		Equant, subhedral	Glass inclusions, two growth phases (relict cores).
GROUNDMASS						
Glass	[illegible]	[illegible]	[illegible]		N/A	Devitrified in patches. Some have a small amount of fresh glass.
Microlites	[illegible]	[illegible]	[illegible]		Needles	Probably plagioclase
Clinopyroxene	[illegible]	[illegible]	[illegible]		Subhedral-euhedral	Equant microphenocrysts
Plagioclase	[illegible]	[illegible]	[illegible]		Equant	

SECONDARY MINERALOGY	PERCENT	REPLACING/FILLING	COMMENTS
Clays	[illegible]	Groundmass	Brown to light yellow-brown, amorphous, pervasive after glassy matrix.
Chlorite	[illegible]	Clinopyroxene	Chlorite + hematite alteration at the center of a clinopyroxene (?) phenocryst.

VESICLES/CAVITIES	PERCENT	LOCATION	SIZE mm	FILLING	SHAPE
Vesicles	[illegible]	Throughout	[illegible]	[illegible]	Small round

COMMENTS: Glomerocrysts of clinopyroxene + [illegible] are common up to [illegible] mm in diameter. [illegible] are commonly rounded possibly indicating resorption or disequilibrium.

125-786B-12R-02 (Piece 17,120-124 cm) OBSERVER: [illegible] WHERE SAMPLED: Izu-Bonin outer-arc high

ROCK NAME: Two-pyroxene plagioclase boninite

GRAIN SIZE: [illegible]-4 mm

TEXTURE: Glomerophyric

PRIMARY MINERALOGY	PERCENT PRESENT	PERCENT ORIGINAL	SIZE (mm)	COMPO-SITION	MORPHOLOGY	COMMENTS
PHENOCRYSTS						
Plagioclase	5	5	1-4		Euhedral-subhedral-anhedral	
Clinopyroxene	8	8	0.1-2	Augite	Euhedral-subhedral	2V=+40-50 degrees.
Opaque	Trace	Trace	0.1-0.2	Magnetite(?)	Euhedral-subhedral-anhedral	Inclusions in pyroxenes.
Orthopyroxene	[illegible]	[illegible]	0.1-2	Bronzite	Euhedral-subhedral	2V=-80-85 degrees, (100) exsolution lamellae are rare, augite rim is common, compositional zoning is common.
GROUNDMASS						
Plagioclase	[illegible]	[illegible]	[illegible]		Euhedral-subhedral, prismatic	
Augite	[illegible]	[illegible]	[illegible]		Euhedral-subhedral, prismatic	
Orthopyroxene	[illegible]	[illegible]	[illegible]		Euhedral-subhedral, prismatic	
Glass	[illegible]	[illegible]	N/A		N/A	Brown glass.
Opaque	Trace	Trace	<0.05		Subhedral	Magnetite(?)

SECONDARY MINERALOGY	PERCENT	REPLACING/ FILLING	COMMENTS
Clays	[illegible]	Glass	Replacing glass.

VESICLES/ CAVITIES	PERCENT	LOCATION	SIZE (mm)	FILLING	SHAPE
Vesicles	[illegible]	Random	[illegible]	None	Round

COMMENTS: Orthopyroxene has (100) exsolution lamellae (rarely). In the groundmass glass, very fine needle-like crystals are observed. They may be pyroxene, but detail is not clear because the thin section is too thick [illegible]

125-786B-[illegible] (Piece [illegible] cm) OBSERVER: [illegible] WHERE SAMPLED: Izu-Bonin outer-arc high

ROCK NAME: Plagioclase [illegible]

GRAIN SIZE: [illegible] mm

TEXTURE: Subhedral equigranular

PRIMARY MINERALOGY	PERCENT PRESENT	PERCENT ORIGINAL	SIZE (mm)	COMPO-SITION	MORPHOLOGY	COMMENTS
PHENOCRYSTS						
Plagioclase	[illegible]	[illegible]	[illegible]		Euhedral	Relict cores, oscillatory zoning, glass and spinel inclusions, pyroxene inclusions.
Clinopyroxene	[illegible]	[illegible]	[illegible]		Subhedral	Uralitized, spinel inclusions.
Spinel	[illegible]	[illegible]	[illegible]		Subhedral-euhedral	
Orthopyroxene	[illegible]	[illegible]	[illegible]		Subhedral	Uralitized.
GROUNDMASS						
N/A	N/A	N/A	N/A		N/A	

SECONDARY MINERALOGY	PERCENT	REPLACING/ FILLING	COMMENTS
Clays	[illegible]	Plagioclase	Brown-gray clay, pervasive, replacing [illegible] of some plagioclase.
[illegible]	[illegible]	Orthopyroxene	Slight pleochroism, elongate crystals, parallel extinction.

VESICLES/ CAVITIES	PERCENT	LOCATION	SIZE (mm)	FILLING	SHAPE
Vesicles	0				

125-786B-16R-1 (Piece 2G,137-144 cm)　OBSERVER: [illegible]　WHERE SAMPLED: Izu-Bonin outer-arc high

ROCK NAME: Plagioclase-phyric andesite

GRAIN SIZE: 0.2-1 mm

TEXTURE: Glomerophyric, moderately phyric

PRIMARY MINERALOGY	PERCENT PRESENT	PERCENT ORIGINAL	SIZE (mm)	COMPO-SITION	MORPHOLOGY	COMMENTS
PHENOCRYSTS						
Plagioclase	10-12	10-12	0.2-1		Euhedral-subhedral	Pale brown glass inclusions, spinel inclusions.
Clinopyroxene	8-10	8-10	0.2-0.8		Euhedral-subhedral	Rare spinel and glass inclusions, light green in PPL.
Spinel	Trace	Trace	[illegible]		Euhedral-subhedral	Often associated with glomerocrysts.
Orthopyroxene	2-3	2-3	0.2-0.8		Euhedral	Rare spinel and glass inclusions.
GROUNDMASS						
Glass	35-45	35-45	N/A		N/A	Light brown glass (with microlites).
Microlites	35-45	35-45	[illegible]		Needles-laths	Probably half plagioclase and half pyroxene. Too small to identify accurately.
Spinel	1	1	[illegible]		Euhedral	

SECONDARY MINERALOGY	PERCENT	REPLACING/FILLING	COMMENTS
Clays	N/A	Glass	Brown amorphous clays following perlitic pattern.

VESICLES/CAVITIES	PERCENT	LOCATION	SIZE (mm)	FILLING	SHAPE
Vesicles	[illegible]	Throughout	[illegible]	None	Rounded-oval

COMMENTS: Glomerocrysts of plagioclase + cpx + pyroxene up to 3 mm diameter. This rock is very fresh although the matrix is microcrystalline with no patches of crystal-free glass. Same as rock in 786B-16R-1 (32-36 cm).

125-786B-16R-2 (Piece 4,32-36 cm)　OBSERVER: [illegible]　WHERE SAMPLED: Izu-Bonin outer-arc high

ROCK NAME: Brecciated andesite

GRAIN SIZE: 0.2-1 mm

TEXTURE: Brecciated glomerophyric

PRIMARY MINERALOGY	PERCENT PRESENT	PERCENT ORIGINAL	SIZE (mm)	COMPO-SITION	MORPHOLOGY	COMMENTS
PHENOCRYSTS						
Plagioclase	8-10	10-12	0.2-1		Euhedral-subhedral	Spinel and pale brown glass inclusions.
Clinopyroxene	[illegible]	8-10	0.2-0.8		Euhedral-subhedral	Glass and rare spinel inclusions, pale green in PPL.
Spinel	Trace	Trace	0.05-0.1		Euhedral-subhedral	Usually associated with glomerocrysts.
Orthopyroxene	1-3	2-3	0.2-0.8		Euhedral	Glass and rare spinel inclusions.
GROUNDMASS						
Glass	25-35	35-45	N/A		N/A	Light brown (interstitial to microlite mesh).
Microlites	35-45	35-45	[illegible]		Needles-laths	Probably plagioclase and pyroxene in equal proportions.
Spinel	1	1	[illegible]		Euhedral	

SECONDARY MINERALOGY	PERCENT	REPLACING/FILLING	COMMENTS
Clays	25-35	Glass	Brown-gray, amorphous clay filling perlitic fractures and replacing patches of glass/matrix.
Zeolites	8-10	Vesicles, fractures	Low birefringence, acicular needles.
Chlorite	5-10	Glass, veins	Pale green-yellow, slightly pleochroic. [illegible] 0.05-0.02 wide as veins.

VESICLES/CAVITIES	PERCENT	LOCATION	SIZE (mm)	FILLING	SHAPE
Vesicles	1-2	Throughout	[illegible]	Zeolite	Round-[illegible]

COMMENTS: Same as 786B-16R-1 (137-144 cm), but brecciated and more altered especially along breccia zones. Glomerocrysts of plagioclase + cpx + pyroxene up to 3 mm in diameter.

125-786B-19R-01 (Piece 14, 91-94 cm) OBSERVER: JON WHERE SAMPLED: Izu-Bonin outer-arc high

ROCK NAME: Andesite flow

GRAIN SIZE: Fine-grained

TEXTURE: Porphyritic

PRIMARY MINERALOGY	PERCENT PRESENT	PERCENT ORIGINAL	SIZE (mm)	COMPO-SITION	MORPHOLOGY	COMMENTS
PHENOCRYSTS						
Plagioclase	12-15	12-15	N/A		Euhedral	Spinel and glass inclusions.
Clinopyroxene	10-12	10-12	0.1-1.4		Euhedral	Spinel and glass inclusions, sparse twinning, pale green and slightly pleochroic.
Spinel	Trace	Trace	<0.1		Euhedral-subhedral	
Orthopyroxene	3-5	3-5	0.1-1.4		Euhedral-subhedral	Glass inclusions.
GROUNDMASS						
Glass	12-17	20-30	N/A		N/A	Pale to medium yellow-brown, 15-30% altered.
Matrix microlites	40-50	45-50	<0.01		Needles	Plagioclase and pyroxene needles (in glassy matrix).
Spinel	1	1	<0.01		Euhedral	

SECONDARY MINERALOGY	PERCENT	REPLACING/ FILLING	COMMENTS
Clays	10-25	Glass/matrix	Brown and gray amorphous clay altered in a patchy pattern, some patches 10-20% altered, some 30-40%.

VESICLES/ CAVITIES	PERCENT	LOCATION	SIZE (mm)	FILLING	SHAPE
Vesicles	3-7	Throughout	0.2-4	No	Round-oval

COMMENTS: Glomerocrysts of plagioclase + or - pyroxene up to 1.5 mm.

125-786B-21R-02 (Piece 3,26-29 cm) OBSERVER: JON WHERE SAMPLED: Izu-Bonin outer-arc high

ROCK NAME: Andesite

GRAIN SIZE: 0.2-1.2 mm

TEXTURE: Porphyritic

PRIMARY MINERALOGY	PERCENT PRESENT	PERCENT ORIGINAL	SIZE (mm)	COMPO-SITION	MORPHOLOGY	COMMENTS
PHENOCRYSTS						
Plagioclase	12-15	14-17	0.2-1.2		Subhedral	Spinel inclusions, altered, moth-eaten, oscillatory zoning.
Clinopyroxene	5-7	6-8	0.2-0.8		Euhedral-subhedral	Pale-yellow-green in plane light, altered, rare twinning.
Orthopyroxene	1-2	2-4	0.2-0.6		Subhedral	Altered.
GROUNDMASS						
Glass	0	55-65	N/A		N/A	
Plagioclase	15-20	20-25	<0.2		Laths	
Magnetite	1	1	<0.05		Euhedral-subhedral	Equant, mostly in matrix, same as inclusions.

SECONDARY MINERALOGY	PERCENT	REPLACING/ FILLING	COMMENTS
Clays	50-65		Dark brown; patchy; pervasive; variable.
Chlorite	5-15	Pyroxene, glass	Bright pale yellow-green pleochroism.

VESICLES/ CAVITIES	PERCENT	LOCATION	SIZE (mm)	FILLING	SHAPE	COMMENTS
Vesicles	3-5	Throughout	0.1-1	No	Irregular	Some may have been plucked during thin-section making.

COMMENTS: Alteration boundary between <50% clay alteration to >75%. Plagioclase is typically moth-eaten and appears to be making glomerocrysts of radiating plagioclase + or - pyroxene.

125-786B-21R-02 (Piece 7,59-63 cm)   OBSERVER: [illegible]   WHERE SAMPLED: [illegible]

ROCK NAME: Volcanic breccia

GRAIN SIZE: Glassy

TEXTURE: Brecciated

PRIMARY MINERALOGY	PERCENT PRESENT	PERCENT ORIGINAL	SIZE (mm)	COMPO-SITION	MORPHOLOGY	COMMENTS
PHENOCRYSTS						
Clinopyroxene	8-10	10-12	[illegible]		Anhedral	Fragmented. Do not have [illegible] texture.
[illegible]	<1	<1	[illegible]		Subhedral	Dark blood-red to black.
GROUNDMASS						
Glass	[illegible]	[illegible]	N/A		N/A	Glassy fragments 0.5-1 mm in diameter in a clay matrix. Fresh glass is yellow.

SECONDARY MINERALOGY	PERCENT	REPLACING/FILLING	COMMENTS
Clays	[illegible]	Glass	Yellow-brown to dark brown, amorphous, pervasive, [illegible] of glass fragments, 100% of breccia matrix.
[illegible]	<1%	Glass	[illegible] in glassy pieces in breccia.

VESICLES/CAVITIES	PERCENT	LOCATION	SIZE (mm)	FILLING	SHAPE
Vesicles	[illegible]				

COMMENTS: One end of this section is glass broken up in a clay matrix. The other is altered sediment with pyroxene fragments. The connecting portion is missing. The sediment is a hematite-stained clay matrix with 10% pyroxene ([illegible]) fragments. Faint layering is apparent.

125-786B-[illegible] (Piece [illegible], [illegible] cm)   OBSERVER: [illegible]   WHERE SAMPLED: [illegible]

ROCK NAME: Andesitic tuff

GRAIN SIZE: 0.1-2 mm

TEXTURE: Tuffaceous

PRIMARY MINERALOGY	PERCENT PRESENT	PERCENT ORIGINAL	SIZE (mm)	COMPO-SITION	MORPHOLOGY	COMMENTS
PHENOCRYSTS						
Plagioclase	5-7	4-6	0.4-2		Subhedral-euhedral	Twinning is common.
Clinopyroxene	1-2	2-4	[illegible]		Subhedral-euhedral	Pale green to colorless.
Opaque	2	2	<0.2		Anhedral	Black.
Orthopyroxene	[illegible]	3-5	[illegible]		Subhedral-euhedral	Pale green to colorless.
GROUNDMASS						
N/A	N/A	N/A	N/A		N/A	

SECONDARY MINERALOGY	PERCENT	REPLACING/FILLING	COMMENTS
Clays	80-85	Matrix	Brown, amorphous, pervasive.
Chlorite	5	Matrix	Pale green to colorless and intergrown with clays.

VESICLES/CAVITIES	PERCENT	LOCATION	SIZE (mm)	FILLING	SHAPE
Vesicles	[illegible]	Random	<1 mm	N/A	Round, elongate

COMMENTS: Glomerocrysts of plagioclase + pyroxene up to 3 mm in diameter in a tuff.

115-786B-21R-01 (Piece 12C,129-132 cm)   OBSERVER: JON   WHERE SAMPLED: Izu-Bonin outer-arc high

ROCK NAME: Dacite

GRAIN SIZE: 0.1-1.2

TEXTURE: Sparsely phyric

PRIMARY MINERALOGY	PERCENT PRESENT	PERCENT ORIGINAL	SIZE (mm)	COMPO-SITION	MORPHOLOGY	COMMENTS
PHENOCRYSTS						
Plagioclase	5-7	6-8	0.3-1.2		Euhedral	Fractured, sparse glass inclusions.
Clinopyroxene	1-2	<2	0.15-0.18		Anhedral	
Spinel	<1	<1	0.1-0.2		Euhedral, irregular	
Orthopyroxene	<1	<1	N/A		Anhedral	Pale green to gray, sparse spinel inclusions.
GROUNDMASS						
Glass	65-70	65-75	N/A		N/A	Yellow-gold, locally devitrified, perlitic fracture.
Microlites	18-25	18-20	<0.02		Needles	Locally aligned.

SECONDARY MINERALOGY	PERCENT	REPLACING/ FILLING	COMMENTS
Clays	???	Glass/veins	Brown to gray, amorphous.
Carbonate?	1-2	Veins	Very low birefringence, extinction perpendicular to vein.

VESICLES/ CAVITIES	PERCENT	LOCATION	SIZE (mm)	FILLING	SHAPE
Vesicles	5-6	Throughout	0.2-2	No	Irregular-round

115-786B-21R-02 (Piece 6,72-76 cm)   OBSERVER: JON   WHERE SAMPLED: Izu-Bonin outer-arc high

ROCK NAME: Two-pyroxene basalt

GRAIN SIZE: 0.1-1 mm

TEXTURE: Moderately phyric

PRIMARY MINERALOGY	PERCENT PRESENT	PERCENT ORIGINAL	SIZE (mm)	COMPO-SITION	MORPHOLOGY	COMMENTS
PHENOCRYSTS						
Clinopyroxene	5-8	15-25	0.1-0.8		Subhedral-anhedral	Some are completely replaced by carbonate +/- hematite, others have spinel inclusions.
Orthopyroxene	2-5	3-5	0.2-0.5		Euhedral-subhedral	Spinel inclusions.
GROUNDMASS						
Glass	0	50-60	N/A		N/A	100% pervasively altered to clays.
Plagioclase	18-20	25-30	<0.15		Laths	Plagioclase needles.
Magnetite	1-2	1-2	<0.05		Irregular	Mix of individual blebs and equant, euhedral crystals.

SECONDARY MINERALOGY	PERCENT	REPLACING/ FILLING	COMMENTS
Clays	35-40	Glass	Dark brown to gray, amorphous, pervasive.
Carbonate	18-22	Clinopyroxene, vesicles and veins	
Chlorite	10-12	Glass, clinopyroxene	Slightly yellow-green, pleochroic.
Hematite	5-10	Clinopyroxene	Intimately associated with carbonate, together pseudomorph clinopyroxene(?). May have been olivine - but shape and fracture patterns do not support this. These crystals are larger than other, fresher clinopyroxene and may be xenocrysts (0.2-0.8 mm).

VESICLES/ CAVITIES	PERCENT	LOCATION	SIZE (mm)	FILLING	SHAPE
Vesicles	5-8	Throughout	0.2-0.8	Carbonate	Round-irregular

COMMENTS: Glomerocrysts of pyroxene are common (both fresh and altered). Pervasive alteration similar to 786B-19R-01, 123-128 cm; 786B-21R-01, 84-87 cm.

125-786B-[illegible] (Piece 4A,41-44 cm) OBSERVER: JDB WHERE SAMPLED: Izu-Bonin outer-arc high

ROCK NAME: Plagioclase-phyric dacite

GRAIN SIZE: Fine-grained

TEXTURE: Sparsely phyric

PRIMARY MINERALOGY	PERCENT PRESENT	PERCENT ORIGINAL	SIZE (mm)	COMPO-SITION	MORPHOLOGY	COMMENTS
PHENOCRYSTS						
Plagioclase	7-8	7-8	0.2-1.2		N/A	Altered glass inclusions.
Clinopyroxene	1-2	1-2	<0.8		Subhedral-anhedral	Spinel inclusions, pale green; glass inclusions.
Spinel	<1	<1	<0.3	Cr?	Euhedral	Deep blood red.
Orthopyroxene	Trace	Trace	0.5		N/A	Pale gray to light brown.
GROUNDMASS						
Glass	<15	65-75	N/A		N/A	Yellow, locally devitrified, largely altered to clays.
Microlites	15-25	15-20	<0.05		Equant, needles	May be pyroxene, locally aligned.

SECONDARY MINERALOGY	PERCENT	REPLACING/FILLING	COMMENTS
Clays		Glass, plagioclase, microlites	Dark brown, amorphous, pervasive, especially concentrated along fracture in glass.

VESICLES/CAVITIES	PERCENT	LOCATION	SIZE (mm)	FILLING	SHAPE
Vesicles	<2		0.2-0.4	No	Rounded-irregular

COMMENTS: Sparse glomerocrysts of plagioclase and pyroxene up to 2 mm diameter. Some appear physically disaggregated. Clay alteration obscures much of the original texture of the groundmass.

125-786B-[illegible] (Piece 2,9-11 cm) OBSERVER: JDB WHERE SAMPLED: Izu-Bonin outer-arc high

ROCK NAME: Sparsely phyric dacite

GRAIN SIZE: 0.2-0.4 mm

TEXTURE: Glomeroporphyritic

PRIMARY MINERALOGY	PERCENT PRESENT	PERCENT ORIGINAL	SIZE (mm)	COMPO-SITION	MORPHOLOGY	COMMENTS
PHENOCRYSTS						
Plagioclase	4-6	5-7	0.2-0.4		Subhedral-euhedral	Well-zoned.
Clinopyroxene	<1	1-2	0.2-0.4		Subhedral-anhedral	Pale green, rarely twinned.
Spinel	Trace	Trace	<0.5		Irregular/rounded	
Orthopyroxene	<1	1	0.1-0.4		N/A	Pale-green to yellow pleochroism.
GROUNDMASS						
Glass	<5	15-45	N/A		N/A	Devitrified, altered.
Microlites	30-50	30-50	<0.1		Needles	Probably plagioclase, locally aligned.
Spinel/magnetite	1	1	<0.02		Equant-irregular	Tiny in groundmass; may be secondary.

SECONDARY MINERALOGY	PERCENT	REPLACING/FILLING	COMMENTS
Clays	48-75	Glass, matrix	Brown to dark gray, amorphous, pervasive, variable.
Hematite	1-2	Glass/matrix	Intimately mixed with clay.

VESICLES/CAVITIES	PERCENT	LOCATION	SIZE (mm)	FILLING	SHAPE
Vesicles	1-2	Throughout	0.1-0.3	None	Irregular

COMMENTS: Glomerocrysts of plagioclase + cx + pyroxene.

125-786B-26R-01 (Piece 8, 67-68 cm) OBSERVER: SAB WHERE SAMPLED: Izu-Bonin outer-arc high

ROCK NAME: Pumice

GRAIN SIZE: 0.5-2 mm

TEXTURE: Glassy, vesicular

PRIMARY MINERALOGY	PERCENT PRESENT	PERCENT ORIGINAL	SIZE (mm)	COMPO-SITION	MORPHOLOGY	COMMENTS
PHENOCRYSTS						
Plagioclase	2	2	0.5-2		Euhedral-subhedral	Twinning is present.
Clinopyroxene	1	1	0.5-1		Subhedral	
GROUNDMASS						
Glass	<5	97	N/A		N/A	Devitrified.

SECONDARY MINERALOGY	PERCENT	REPLACING/ FILLING	COMMENTS
Clays	>93	Glass	Brown, amorphous, pervasive.

VESICLES/ CAVITIES	PERCENT	LOCATION	SIZE (mm)	FILLING	SHAPE	COMMENTS
Vesicles	15-20	Random	<12			Stretched.

125-786B-27R-01 (Piece 12, 91-93 cm) OBSERVER: JDM WHERE SAMPLED: Izu-Bonin outer-arc high

ROCK NAME: Dacite

GRAIN SIZE:

TEXTURE: Sparsely phyric, brecciated

PRIMARY MINERALOGY	PERCENT PRESENT	PERCENT ORIGINAL	SIZE (mm)	COMPO-SITION	MORPHOLOGY	COMMENTS
PHENOCRYSTS						
Plagioclase	2-3	2-3	0.2-1.2		Tabular, Euhedral-subhedral	Altered. Moth-eaten texture.
Clinopyroxene	1-2	1-2	0.2-0.8		Euhedral-subhedral	Pale gray-green.
Spinel	Trace	Trace	<0.2		Equant	
Orthopyroxene	2-3	2-4	N/A		N/A	Very pale green, spinel and fluid inclusions(?).
GROUNDMASS						
Glass	<10	10-15	N/A		N/A	Brown-yellow, mostly altered.
Microcrysts	15-18	18-22	<0.02		Needles	May be plagioclase and/or pyroxene.

SECONDARY MINERALOGY	PERCENT	REPLACING/ FILLING	COMMENTS
Clays	35-45	Glass	Pale-brown to yellow pervasive but doesn't obscure original texture. Degree of alteration varies between individual breccia pieces.
Chlorite	<10	Glass	Yellow-green, weakly pleochroic, pervasive especially along breccia boundaries.

VESICLES/ CAVITIES	PERCENT	LOCATION	SIZE (mm)	FILLING	SHAPE
Vesicles	10-12	Throughout	0.1-2	None	Round-oval

COMMENTS: Crystallization sequence is clearly plagioclase-pyroxene. Individual breccia fragments have an alignment of matrix microcrysts, probably indicating flow direction.

[illegible]

[illegible]

[illegible] WHERE SAMPLED: [illegible]

ROCK NAME: [illegible] plagioclase [illegible]

GRAIN SIZE: [illegible] mm

TEXTURE: [illegible]

PRIMARY MINERALOGY	PERCENT PRESENT	PERCENT ORIGINAL	SIZE (mm)	COMPO-SITION	MORPHOLOGY	COMMENTS
PHENOCRYSTS:						
Olivine	[illegible]	[illegible]	[illegible]		Euhedral	100% altered to carbonate and hematite
Plagioclase	[illegible]	[illegible]	[illegible]		Subhedral-euhedral	Multi-zoned texture, glass and spinel inclusions
Clinopyroxene	[illegible]	[illegible]	[illegible]		Subhedral	Pale green to yellow, slightly [illegible] inclusions
Orthopyroxene	[illegible]	[illegible]	[illegible]		Subhedral-anhedral	
GROUNDMASS:						
Glass	[illegible]	[illegible]	N.A.		N.A.	Devitrified
Microcrysts	[illegible]	[illegible]	[illegible]		Anhedral	Probably plagioclase, [illegible] texture

SECONDARY MINERALOGY	PERCENT	REPLACING/FILLING	COMMENTS
Glass	[illegible]	[illegible]	Brown-gray, amorphous, pervasive
Carbonate	[illegible]	Olivine, [illegible]	[illegible]
Chlorite	[illegible]	Orthopyroxene, clinopyroxene, glass	Pale green, [illegible] pseudomorphing parts of pyroxenes
Hematite	[illegible]	Olivine	Intimate mixture of carbonate and hematite pseudomorphing euhedral olivine or clinopyroxene crystals. Crystal shape and fracture pattern is more like olivine than clinopyroxene.

VESICLES/ CAVITIES	PERCENT	LOCATION	SIZE (mm)	FILLING	SHAPE
[illegible]	[illegible]	[illegible]	[illegible]	[illegible]	Irregular

COMMENTS: Glomerocrysts of clinopyroxene, orthopyroxene and plagioclase. Some crystals [illegible] plucked during thin-section making. [illegible]

[illegible] WHERE SAMPLED: [illegible]

ROCK NAME: Plagioclase-[illegible]

GRAIN SIZE: [illegible]

TEXTURE: [illegible]

PRIMARY MINERALOGY	PERCENT PRESENT	PERCENT ORIGINAL	SIZE (mm)	COMPO-SITION	MORPHOLOGY	COMMENTS
PHENOCRYSTS:						
Plagioclase	[illegible]	[illegible]	[illegible]		Anhedral, subhedral	[illegible] glass inclusions
Clinopyroxene	[illegible]	[illegible]	[illegible]		Anhedral	[illegible] spinel and glass inclusions
[illegible]	[illegible]	[illegible]	[illegible]		[illegible]	Appear late in crystallization.
GROUNDMASS:						
Glass	[illegible]	[illegible]	N.A.		N.A.	
Plagioclase	[illegible]	[illegible]	[illegible]		Tabular, [illegible]	
Magnetite	[illegible]	[illegible]	[illegible]		[illegible]	

SECONDARY MINERALOGY	PERCENT	REPLACING/FILLING	COMMENTS
Clay	[illegible]	[illegible]	[illegible] pervasive, amorphous. [illegible]
Carbonate	[illegible]	[illegible]	Filling cracks, and some cavities, especially those associated with plagioclase
[illegible]	[illegible]	[illegible]	[illegible] mm in diameter

VESICLES/ CAVITIES	PERCENT	LOCATION	SIZE (mm)	FILLING	SHAPE	COMMENTS
[illegible]	[illegible]	[illegible]	[illegible]	None	Irregular	Some may have been plucked during thin-section making.

COMMENTS: Clay alteration of groundmass [illegible]

125-786B-[illegible] (Piece [illegible], 101-111 cm) OBSERVER: [illegible] WHERE SAMPLED: Izu-Bonin outer-arc high

ROCK NAME: Plagioclase-phyric andesite

GRAIN SIZE: Fine- to medium-grained

TEXTURE: Sparsely-phyric; glassy rind

PRIMARY MINERALOGY	PERCENT PRESENT	PERCENT ORIGINAL	SIZE (mm)	COMPO-SITION	MORPHOLOGY	COMMENTS
PHENOCRYSTS						
Plagioclase	[illegible]	[illegible]	[illegible]		Euhedral-subhedral	Spinel and glass inclusions, oscillatory zoning.
Clinopyroxene	<1	[illegible]	N/A		Subhedral	Pale brown-green, altered, rare spinel and glass inclusions.
Spinel	<1	<1	[illegible]		Subhedral	Deep red brown.
GROUNDMASS						
Glass	[illegible]	[illegible]	N/A		N/A	Not fresh in glassy rind, tan to yellow.
Microlites	[illegible]	[illegible]	<0.05		Needles	25% of glassy inclusions.

SECONDARY MINERALOGY	PERCENT	REPLACING/ FILLING	COMMENTS
Clays	[illegible]	Glass	Pale brown, amorphous, pervasive.
Carbonate	[illegible]	Veins	Fills large veins and vugs and vesicles.
Chlorite	[illegible]	Veins	Follows carbonate veins.
Sulfide	[illegible]	Veins	Secondary sulfide crystals-probably disseminated pyrite but mostly concentrated in veins with chlorite.

VESICLES/ CAVITIES	PERCENT	LOCATION	SIZE (mm)	FILLING	SHAPE
Vesicles	[illegible]		[illegible]	Carbonate	Irregular

COMMENTS: Rock has glassy yellow rind which is less altered than the rest of the sample. This rock is cut by carbonate veins and has secondary sulfide precipitation.

125-786B-[illegible] (Piece [illegible], 124-[illegible] cm) OBSERVER: [illegible] WHERE SAMPLED: Izu-Bonin outer-arc high

ROCK NAME: Plagioclase-phyric andesite

GRAIN SIZE: [illegible] mm

TEXTURE: Sparsely phyric, glassy

PRIMARY MINERALOGY	PERCENT PRESENT	PERCENT ORIGINAL	SIZE (mm)	COMPO-SITION	MORPHOLOGY	COMMENTS
PHENOCRYSTS						
Plagioclase	[illegible]	[illegible]	[illegible]		Subhedral-anhedral	Spinel and glass inclusions, oscillatory zoning, moth-eaten to relatively fresh, rounded.
Clinopyroxene	[illegible]	4-6	[illegible]		Euhedral-subhedral	Pale yellow-green, pleochroic, twinned, fractured.
Spinel	1-2	1-2	[illegible]		Irregular	Deep blood-red to black.
Orthopyroxene	1-2	1-2	[illegible]		Subhedral-anhedral	Pale yellow-green, pleochroic.
GROUNDMASS						
Glass	[illegible]	[illegible]	N/A		N/A	Mustard yellow-brown, devitrified, altered, fractured.
Microlites	1-2	10-12	<0.05		Needles	Probably plagioclase.

SECONDARY MINERALOGY	PERCENT	REPLACING/ FILLING	COMMENTS
Clays	[illegible]	Glass	Dark brown, amorphous, pervasive after glass, but concentrated along fractures; green clays rimming individual crystals and at boundaries in groundmass.
Smectite(?)	2-4	Vesicle lining	Vein filling, high variable birefringence, slightly fibrous, brown-green, only in coarser-grained groundmass associated with larger plagioclase.

VESICLES/ CAVITIES	PERCENT	LOCATION	SIZE (mm)	FILLING	SHAPE
Vesicles	2-3	Throughout	0.2-4	None	Irregular

COMMENTS: Phenocrysts tend to cluster but are not always in contact (glomerocrysts). Evidence of fracturing and dissociation of pieces is common. Sample may be brecciated or have large lithic, plagioclase-bearing xenoliths. Two matrix textures are present. This may also be a flow texture with variable alteration and recrystallization.

[illegible]

125-786B-16R-02 (Piece 11,100-104 cm) OBSERVER: JAP WHERE SAMPLED: Izu-Bonin outer-arc high

ROCK NAME: Basalt (with dacite inclusions)

GRAIN SIZE: Fine-grained to glassy

TEXTURE: Moderately to sparsely phyric

PRIMARY MINERALOGY	PERCENT PRESENT	PERCENT ORIGINAL	SIZE (mm)	COMPO-SITION	MORPHOLOGY	COMMENTS
PHENOCRYSTS						
Olivine?	0	1-2	0.3-1		Subhedral	Completely altered to carbonate and chlorite.
Clinopyroxene	1-3	2-3	0.3-3		Anhedral to subhedral	Usually tabular, rare spinel inclusions.
Spinel	<1	<1	<0.1		Subhedral	
Orthopyroxene	<1	0-1	1-3		Euhedral to subhedral	Jacketed by clinopyroxene, also [illegible] completely chloritized.
GROUNDMASS						
Glass	15-20	70-80	1-3		N/A	Light yellow to brown, devitrified.
Clinopyroxene	6-10	10-12	<0.3		Subhedral	Quench and microphenocrysts.

SECONDARY MINERALOGY	PERCENT	REPLACING/ FILLING	COMMENTS
Clays	35-45	Glass	Brown, amorphous, pervasive.
Clays	<3	Glass	Green, amorphous, patchy.
Carbonate	20-25	Veins, olivine, pyroxene	Mostly as veins and patches, 0.3-0.5 mm wide.
Chlorite	1-15	Pyroxenes, glass	Higher percentage in basalt than in dacite inclusions.

VESICLES/ CAVITIES	PERCENT	LOCATION	SIZE (mm)	FILLING	SHAPE
Vesicles	2-10		<0.5	Carbonate	Irregular

COMMENTS: Sample consists of two rock types in contact: a fresher glassy basalt (described here) containing inclusions of dacite (described on a separate form).

125-786B-15R-01 (Piece 9,73-76 cm) OBSERVER: MIR WHERE SAMPLED: Izu-Bonin outer-arc high

ROCK NAME: Clinopyroxene-plagioclase dacite

GRAIN SIZE: 0.3-1.5 mm

TEXTURE: Porphyritic, hyalopilitic

PRIMARY MINERALOGY	PERCENT PRESENT	PERCENT ORIGINAL	SIZE (mm)	COMPO-SITION	MORPHOLOGY	COMMENTS
PHENOCRYSTS						
Plagioclase	8-10	8-10	0.5-1.5		Euhedral	Shows compositional zoning and twinning.
Clinopyroxene	2-3	2-3	0.5-1		Euhedral-subhedral	Frequently twinned.
GROUNDMASS						
Plagioclase	11-15	11-16	<0.1		Euhedral	Typically quenched and slender prismatic crystals.
Glass	0	75-80	N/A		N/A	Completely altered to brown clay.
Opaque	Trace	Trace	<0.1		Euhedral-subhedral	Scattered in groundmass.

SECONDARY MINERALOGY	PERCENT	REPLACING/ FILLING	COMMENTS
Clays	75-80	Glass, vesicles	Pale green to pale brown in color.

VESICLES/ CAVITIES	PERCENT	LOCATION	SIZE (mm)	FILLING	SHAPE
Vesicles	15	Random	0.1-5	Clay	Round to elongate

COMMENTS: Some plagioclase phenocrysts show corroded form.

[illegible] OBSERVER: [illegible] WHERE SAMPLED: [illegible]

ROCK NAME: Plagioclase-pyroxene phyric [illegible]

GRAIN SIZE: [illegible] mm

TEXTURE: Moderately phyric

PRIMARY MINERALOGY	PERCENT PRESENT	PERCENT ORIGINAL	SIZE (mm)	COMPOSITION	MORPHOLOGY	COMMENTS
PHENOCRYSTS						
Plagioclase	[illegible]	[illegible]	0.2-2		Subhedral-rounded	Most large crystals are [illegible] with relict cores.
Clinopyroxene	[illegible]	[illegible]	0.2-1.5		Euhedral-subhedral	Pale green-yellow pleochroic, most have low (15-20 degrees) extinction angles, spinel inclusions.
Spinel	[illegible]	[illegible]	[illegible]		Rounded	
GROUNDMASS						
Glass	[illegible]	[illegible]	N/A		N/A	
Plagioclase	[illegible]	[illegible]	N/A		Needles, hollow squared	Very low birefringence, may not all be plagioclase.
Magnetite	[illegible]	[illegible]	[illegible]		Equant, irregular	

SECONDARY MINERALOGY	PERCENT	REPLACING/FILLING	COMMENTS
Clays	[illegible]	Glass	Brown amorphous clay, pervasive.
Chlorite	[illegible]	Glass, clinopyroxene, [illegible]	Green-yellow-brown birefringence pseudomorphing pyroxene and scattered intimately through glass.

VESICLES/CAVITIES	PERCENT	LOCATION	SIZE (mm)	FILLING	SHAPE
Vesicles	[illegible]	[illegible]	[illegible]	[illegible] clay	Elongate-oval

COMMENTS: Some plagioclase crystals have large (0.2 mm) pyroxene inclusions. Glomerocrysts of plagioclase + clinopyroxene up to 3 mm diameter.

[illegible] OBSERVER: [illegible] WHERE SAMPLED: [illegible]

ROCK NAME: Orthopyroxene-clinopyroxene-plagioclase [illegible]

GRAIN SIZE: [illegible] mm

TEXTURE: [illegible], locally glomerophyric.

PRIMARY MINERALOGY	PERCENT PRESENT	PERCENT ORIGINAL	SIZE (mm)	COMPOSITION	MORPHOLOGY	COMMENTS
PHENOCRYSTS						
Olivine	[illegible]	[illegible]	[illegible]		Euhedral	Completely altered to clay.
Plagioclase	[illegible]	[illegible]	[illegible]		Subhedral-anhedral	Compositional zoning and twinning are common.
Clinopyroxene	[illegible]	[illegible]	[illegible]		Subhedral-anhedral	Twinning is common.
Orthopyroxene	[illegible]	[illegible]	[illegible]		Euhedral	Partly altered to clay.
GROUNDMASS						
Plagioclase	[illegible]	[illegible]	[illegible]		Euhedral	Skeletal quenched crystals are predominant.
Clinopyroxene	[illegible]	[illegible]	[illegible]		Anhedral	Partly altered to clay, dusty.
Orthopyroxene	Trace	Trace	[illegible]		Euhedral-subhedral	Showing relatively low birefringence.
Glass	[illegible]	[illegible]	N/A		N/A	Completely altered to clay.
Opaque	[illegible]	[illegible]	[illegible]		Subhedral-anhedral	Scattered throughout groundmass.

SECONDARY MINERALOGY	PERCENT	REPLACING/FILLING	COMMENTS
Clays	[illegible]	Olivine, orthopyroxene, [illegible]	Pale green to pale brown in color, low birefringence.
Carbonate	[illegible]		Having characteristic high birefringence.

VESICLES/CAVITIES	PERCENT	LOCATION	SIZE (mm)	FILLING	SHAPE
Vesicles	[illegible]	Random	[illegible]	Clay	Round

COMMENTS: Calcite and clay veins ([illegible] mm wide) cut throughout the slide. Most of the plagioclase phenocrysts are dusty and show rounded form. Some plagioclase crystals occur as xenocrysts whose primary internal zonal structure was cut by their fragmented outlines.

125-786B-[illegible] (Piece [illegible] cm)   OBSERVER: [illegible]   WHERE SAMPLED: [illegible]

ROCK NAME: [illegible] plagioclase [illegible]

GRAIN SIZE: [illegible] mm

TEXTURE: [illegible] texture

PRIMARY MINERALOGY	PERCENT PRESENT	PERCENT ORIGINAL	SIZE (mm)	COMPO-SITION	MORPHOLOGY	COMMENTS
PHENOCRYSTS						
Olivine	0	[illegible]	[illegible]		Euhedral	Completely altered to clay.
Plagioclase	[illegible]	[illegible]	[illegible]		Euhedral-subhedral	Shows twinning and compositional zoning.
Clinopyroxene	[illegible]	[illegible]	[illegible]		Subhedral-euhedral	Shows twinning, locally forms glomerocrystic texture.
Orthopyroxene	[illegible]	[illegible]	[illegible]		Subhedral, sometimes elongated	Partly altered to clay.
GROUNDMASS						
Plagioclase	[illegible]	[illegible]	[illegible]		Euhedral	Slender prismatic plagioclase is predominant.
Clinopyroxene	[illegible]	[illegible]	[illegible]		Subhedral-anhedral	Scattered throughout groundmass.
Orthopyroxene	Trace	Trace	[illegible]		Euhedral	Relatively low birefringence.
Glass	0	[illegible]	N/A		N/A	Completely altered to brown clay.

SECONDARY MINERALOGY	PERCENT	REPLACING/FILLING	COMMENTS
Clays	[illegible]	Glass, vesicles	Pale brown to pale green in color.

VESICLES/CAVITIES	PERCENT	LOCATION	SIZE (mm)	FILLING	SHAPE
Vesicles	[illegible]	Random	[illegible]	Clay	[illegible]

COMMENTS: Two types of plagioclase phenocrysts are recognized: one is dusty and shows corroded rims, and another is clear and euhedral in shape.

125-786B-[illegible] (Piece [illegible] cm)   OBSERVER: [illegible]   WHERE SAMPLED: [illegible]

ROCK NAME: [illegible] basalt

GRAIN SIZE: [illegible] mm

TEXTURE: [illegible] texture

PRIMARY MINERALOGY	PERCENT PRESENT	PERCENT ORIGINAL	SIZE (mm)	COMPO-SITION	MORPHOLOGY	COMMENTS
PHENOCRYSTS						
Plagioclase	[illegible]	[illegible]	[illegible]		Euhedral	
Clinopyroxene	Trace	Trace	[illegible]		Euhedral	
GROUNDMASS						
Plagioclase	[illegible]	[illegible]	[illegible]		N/A	Fairly altered to clay.
Clinopyroxene	[illegible]	[illegible]	[illegible]		Elongate, prismatic	

SECONDARY MINERALOGY	PERCENT	REPLACING/FILLING	COMMENTS
Clays	[illegible]	Glass	Pale green clay is predominant.
[illegible]	[illegible]	[illegible]	Reddish, limonitic material is scattered throughout the rock.

VESICLES/CAVITIES	PERCENT	LOCATION	SIZE (mm)	FILLING	SHAPE
Vesicles	Trace	Random	[illegible]	Clay	Variable

COMMENTS: This rock is highly altered [illegible] basalt. Pale greenish clay present throughout the rock.

[illegible]

[illegible] (Piece [illegible], [illegible] cm) OBSERVER: [illegible] WHERE SAMPLED: [illegible]

ROCK NAME: Brecciated andesite

GRAIN SIZE: [illegible] mm

TEXTURE: Porphyritic

PRIMARY MINERALOGY	PERCENT PRESENT	PERCENT ORIGINAL	SIZE (mm)	COMPO-SITION	MORPHOLOGY	COMMENTS
PHENOCRYSTS						
Plagioclase	[illegible]	[illegible]	[illegible]		Subhedral	Compositional zoning is common.
Clinopyroxene	[illegible]	[illegible]	[illegible]		Subhedral	
GROUNDMASS						
Plagioclase	[illegible]	[illegible]	[illegible]		Subhedral; prismatic	
Clinopyroxene	[illegible]	[illegible]	[illegible]		Subhedral; prismatic	
Glass	[illegible]	[illegible]	N/A		N/A	Completely altered to clay.

SECONDARY MINERALOGY	PERCENT	REPLACING/FILLING	COMMENTS
Clays	[illegible]	Glass, plagioclase	Pale green to pale brown clay is predominant.
Zeolite	[illegible]	Glass	

VESICLES/CAVITIES	PERCENT	LOCATION	SIZE (mm)	FILLING	SHAPE
Vesicles	[illegible]	Random	[illegible]	Clay	Round to elongate

COMMENTS: Clay-rich material is locally predominant, especially along the brecciated fragments.

[illegible] (Piece [illegible], [illegible] cm) OBSERVER: [illegible] WHERE SAMPLED: [illegible]

ROCK NAME: Andesitic [illegible] breccia

GRAIN SIZE: [illegible] mm

TEXTURE: Porphyritic (in andesitic fragments)

PRIMARY MINERALOGY	PERCENT PRESENT	PERCENT ORIGINAL	SIZE (mm)	COMPO-SITION	MORPHOLOGY	COMMENTS
PHENOCRYSTS						
Plagioclase	[illegible]	[illegible]	[illegible]		Subhedral	In andesitic fragments
Clinopyroxene	Trace	Trace	[illegible]		Subhedral	In andesitic fragments
GROUNDMASS						
Plagioclase	[illegible]	[illegible]	[illegible]		Subhedral, acicular	
Clinopyroxene	Trace	Trace	[illegible]		Subhedral, prismatic	

SECONDARY MINERALOGY	PERCENT	REPLACING/FILLING	COMMENTS
Clays	[illegible]	Glass	Pale greenish clay is predominant in andesitic fragments. Dusty brownish clay occupies matrix between fragments.

VESICLES/CAVITIES	PERCENT	LOCATION	SIZE (mm)	FILLING	SHAPE	COMMENTS
Vesicles	[illegible]	Random	[illegible]	Clay	Round	Occurs in andesitic fragments.

COMMENTS: Phenocrysts of plagioclase and clinopyroxene in andesitic fragments are highly altered to clay.

[illegible]

125-786B-[illegible] (Piece [illegible]) OBSERVER: [illegible] WHERE SAMPLED: [illegible]

ROCK NAME: [illegible] andesite.

GRAIN SIZE: [illegible] mm

TEXTURE: Hyalopilitic.

PRIMARY MINERALOGY	PERCENT PRESENT	PERCENT ORIGINAL	SIZE (mm)	COMPO-SITION	MORPHOLOGY	COMMENTS
PHENOCRYSTS						
Olivine	1	2-3	0.5-1		Euhedral	Altered to clay.
Plagioclase	10-15	10-15	0.4-2		Euhedral-subhedral	Compositional zoning and twinning are common.
Clinopyroxene	8-10	8-10	0.4-2		Euhedral-subhedral	Compositional zoning and twinning are common.
Orthopyroxene	2-4	4-6	0.2-1.5		Euhedral	Partly or fully altered to clay.
GROUNDMASS						
Glass	5	50-55	N/A		N/A	Altered to clay.
Plagioclase	5-10	5-10	<0.1		Euhedral laths	Quench texture.
Clinopyroxene	2-4	2-4	<0.2		Subhedral-anhedral; prismatic.	
Opaque	Trace	Trace	<0.1		Euhedral-anhedral	Scattered throughout the groundmass.

SECONDARY MINERALOGY	PERCENT	REPLACING/FILLING	COMMENTS
Clays	50-55	Glass, olivine, orthopyroxene, vesicles	[illegible]

VESICLES/CAVITIES	PERCENT	LOCATION	SIZE (mm)	FILLING	SHAPE
Vesicles	Trace	Random	<0.1	Clay	Round

COMMENTS: Some orthopyroxene grains have fine [illegible] rims [illegible] and are surrounded by reaction rim of clinopyroxene (augite). Some plagioclase phenocrysts show corroded rims.

125-786B-[illegible] (Piece [illegible]) OBSERVER: [illegible] WHERE SAMPLED: [illegible]

ROCK NAME: [illegible]-plagioclase phyric andesite.

GRAIN SIZE: [illegible] mm

TEXTURE: Moderately phyric.

PRIMARY MINERALOGY	PERCENT PRESENT	PERCENT ORIGINAL	SIZE (mm)	COMPO-SITION	MORPHOLOGY	COMMENTS
PHENOCRYSTS						
Plagioclase	[illegible]	[illegible]	[illegible]		Euhedral-subhedral	Opaque and glass inclusions, commonly twinned, [illegible] texture.
Clinopyroxene	[illegible]	[illegible]	[illegible]		Subhedral-anhedral	Inclusions of fluid, pale green to colorless.
Opaque	Trace	Trace	[illegible]		Equant	Dispersed, black.
GROUNDMASS						
Glass	[illegible]	[illegible]	N/A		N/A	Altered to clays.
Plagioclase	[illegible]	[illegible]	[illegible]		Laths	Microlites in groundmass.

SECONDARY MINERALOGY	PERCENT	REPLACING/FILLING	COMMENTS
Clays	[illegible]	Glass	Red to red-brown clays, pervasive.
Carbonate	[illegible]	Vein	[illegible] mm vein.
Zeolites	[illegible]	Vesicles	Lines vesicles.
Chlorite	[illegible]	Vesicles	Pale green to colorless; lines some vesicles.

VESICLES/CAVITIES	PERCENT	LOCATION	SIZE (mm)	FILLING	SHAPE
Vesicles	N/A	Random	[illegible]	[illegible], zeolites	Round, irregular

[illegible] OBSERVER: [illegible] WHERE SAMPLED: [illegible]

ROCK NAME: Two-pyroxene andesite

GRAIN SIZE: <2 mm

TEXTURE: Porphyritic

PRIMARY MINERALOGY	PERCENT PRESENT	PERCENT ORIGINAL	SIZE (mm)	COMPO-SITION	MORPHOLOGY	COMMENTS
PHENOCRYSTS						
Plagioclase	[illegible]	[illegible]	[illegible]		Subhedral	Compositional zoning and twinning are common.
Clinopyroxene	[illegible]	[illegible]	[illegible]		Subhedral	Compositional zoning and twinning are common.
Orthopyroxene	[illegible]	[illegible]	[illegible]		Subhedral	Compositional zoning is common.
GROUNDMASS						
Plagioclase	[illegible]	[illegible]	[illegible]		Euhedral	Quenched H-shaped crystal.
Clinopyroxene	[illegible]	[illegible]	[illegible]		Subhedral-subhedral, anhedral	Quench texture.
Glass	[illegible]	[illegible]	N/A		N/A	
Orthopyroxene	[illegible]	[illegible]	[illegible]		[illegible]	Quench texture.

SECONDARY MINERALOGY	PERCENT	REPLACING/FILLING	COMMENT
[illegible]	[illegible]	[illegible]	

VESICLES/CAVITIES	PERCENT	LOCATION	SIZE (mm)	FILLING	SHAPE
[illegible]	[illegible]	[illegible]	[illegible]	[illegible]	[illegible]

COMMENTS: [illegible]

[illegible] OBSERVER: [illegible] WHERE SAMPLED: [illegible]

ROCK NAME: [illegible]

GRAIN SIZE: [illegible]

TEXTURE: [illegible]

PRIMARY MINERALOGY	PERCENT PRESENT	PERCENT ORIGINAL	SIZE (mm)	COMPO-SITION	MORPHOLOGY	COMMENTS
PHENOCRYSTS						
Plagioclase	[illegible]	[illegible]	[illegible]		[illegible]	[illegible]
[illegible]	[illegible]	[illegible]	[illegible]		[illegible]	[illegible]
[illegible]			[illegible]		[illegible]	[illegible]
[illegible]	[illegible]	[illegible]	[illegible]		[illegible]	[illegible]
GROUNDMASS						
Glass	[illegible]	[illegible]	N/A		N/A	
Plagioclase	[illegible]	[illegible]	[illegible]		Lath	Microlites.

SECONDARY MINERALOGY	PERCENT	REPLACING/FILLING	COMMENT
[illegible]	[illegible]	[illegible]	[illegible]
[illegible]	[illegible]	[illegible]	[illegible]

VESICLES/CAVITIES	PERCENT	LOCATION	SIZE (mm)	FILLING	SHAPE
[illegible]	[illegible]	[illegible]	[illegible]		[illegible]

COMMENT: [illegible]

125-786B-49R-02 (Piece 4,83-84 cm) OBSERVER: HIR WHERE SAMPLED: Izu-Bonin outer-arc high

ROCK NAME: Andesitic breccia

GRAIN SIZE: 0.1-1 mm

TEXTURE: Clastic texture

PRIMARY MINERALOGY	PERCENT PRESENT	PERCENT ORIGINAL	SIZE (mm)	COMPO-SITION	MORPHOLOGY	COMMENTS
PHENOCRYSTS						
Plagioclase	5-10	5-10	0.5-1		Euhedral-anhedral	Twinning and compositional zoning are common.
Clinopyroxene	2-3	2-3	0.5-1		Euhedral-anhedral	Twinning is common.
Orthopyroxene	3-5	3-5	0.5-1		Euhedral-anhedral	Clinopyroxene exsolution lamellae.
GROUNDMASS						
Plagioclase	2-3	2-3	<0.1		Euhedral-anhedral, acicular	

SECONDARY MINERALOGY	PERCENT	REPLACING/FILLING	COMMENTS
Clays	80-85	Glass	Brownish dusty clay is predominant.

VESICLES/CAVITIES	PERCENT	LOCATION	SIZE (mm)	FILLING	SHAPE
Vesicles	Trace	Random	<0.2	Clay	Round

COMMENTS: This rock contains fragments of andesite and crystals in a fine-grained matrix. Matrix is highly altered to clay.

125-786B-49R-04 (Piece 4,32-37 cm) OBSERVER: HIR WHERE SAMPLED: Izu-Bonin outer-arc high

ROCK NAME: Orthopyroxene-clinopyroxene andesite

GRAIN SIZE: 0.1-2 mm

TEXTURE: Porphyritic texture

PRIMARY MINERALOGY	PERCENT PRESENT	PERCENT ORIGINAL	SIZE (mm)	COMPO-SITION	MORPHOLOGY	COMMENTS
PHENOCRYSTS						
Plagioclase	10-15	10-15	0.5-2		Euhedral-subhedral	Shows compositional zoning.
Clinopyroxene	5-10	5-10	0.5-2		Euhedral	
Orthopyroxene	5-8	5-10	0.5-2		Euhedral	Partly altered to clay; has clinopyroxene exsolution lamellae.
GROUNDMASS						
Plagioclase	10-15	15-20	0.1-0.5		Euhedral	Slender, quenched crystals.
Clinopyroxene	5-10	5-10	0.1-0.2		Euhedral-subhedral	Slender, quenched crystals.
Orthopyroxene	5-10	5-10	0.1-0.4		Euhedral-subhedral	Slender, quenched crystals.
Glass	15-30	35-60	N/A		N/A	Partly altered to clay.

SECONDARY MINERALOGY	PERCENT	REPLACING/FILLING	COMMENTS
Clays	10-30	Glass, vesicles	Pale green to pale brown in color.
Carbonate	Trace	Orthopyroxene	High birefringence.
Zeolites	<1	Vesicles	Radial, wavy extinction.

VESICLES/CAVITIES	PERCENT	LOCATION	SIZE (mm)	FILLING	SHAPE
Vesicles	10-15	Random	0.5-5	Zeolite, clay	Round, deformed

COMMENTS: Clinopyroxene occurs as exsolution lamellae of orthopyroxene and as reaction rim of orthopyroxene.

125-786B-51R-1 (Piece 8,63-66 cm) OBSERVER: HIR WHERE SAMPLED: Izu-Bonin outer-arc high

ROCK NAME: Two-pyroxene basalt

GRAIN SIZE: 0.1-1.5 mm

TEXTURE: Porphyritic texture

PRIMARY MINERALOGY	PERCENT PRESENT	PERCENT ORIGINAL	SIZE (mm)	COMPO-SITION	MORPHOLOGY	COMMENTS
PHENOCRYSTS						
Plagioclase	15-20	15-20	0.5-1.5		Euhedral-anhedral	Compositional zoning.
Clinopyroxene	5-10	5-10	0.5-1.5		Euhedral-anhedral	
Orthopyroxene	5-10	5-10	0.5-1.5		Euhedral	Partly altered to clay.
GROUNDMASS						
Plagioclase	[illegible]	5-10	<0.1		Euhedral	Partly altered to clay.
Clinopyroxene	5-10	5-10	<0.2		Euhedral, elongate, prismatic	
Orthopyroxene	5-10	5-10	<0.2		Euhedral, elongate, prismatic	
Glass	5-10	40-50	N/A		N/A	Altered to clay.

SECONDARY MINERALOGY	PERCENT	REPLACING/FILLING	COMMENTS
Clays	30-40	Glass	Brown dusty clay replacing glass.

VESICLES/CAVITIES	PERCENT	LOCATION	SIZE (mm)	FILLING	SHAPE
Vesicles	N/A	Random	0.5-1		Round

COMMENTS: Plagioclase phenocrysts show corroded form. Clinopyroxene occurs as euhedral phenocryst, as exsolution lamellae of orthopyroxene, and as reaction rim of orthopyroxene.

125-786B-52R-1 (Piece [illegible]) OBSERVER: HIR WHERE SAMPLED: Izu-Bonin outer-arc high

ROCK NAME: Andesite breccia

GRAIN SIZE: [illegible] mm

TEXTURE: Breccia with porphyritic andesite fragments

PRIMARY MINERALOGY	PERCENT PRESENT	PERCENT ORIGINAL	SIZE (mm)	COMPO-SITION	MORPHOLOGY	COMMENTS
PHENOCRYSTS						
Olivine	0	0-1	[illegible]		Euhedral-subhedral	Completely altered to clay.
Plagioclase	0-1	0-2	[illegible]		Euhedral	Shows twinning and compositional zoning.
Clinopyroxene	0-1	0-1	[illegible]		Subhedral	
Orthopyroxene	0-1	0-2	[illegible]		Euhedral	
GROUNDMASS						
Orthopyroxene	[illegible]	[illegible]	[illegible]		Euhedral, elongate, prismatic	
Clinopyroxene	[illegible]	[illegible]	[illegible]		Euhedral, elongate, prismatic	Occurs as crystal.
Plagioclase	Trace	Trace	<0.1		Euhedral, acicular	
Glass	0	40-60	N/A		N/A	Altered to clay.
Opaque	Trace	Trace	<0.05		Euhedral	Scattered throughout groundmass.

SECONDARY MINERALOGY	PERCENT	REPLACING/FILLING	COMMENTS
Clays	40-60	Glass	Replacing groundmass glass and matrix of hyaloclastite; pale green to pale brown in color.

VESICLES/CAVITIES	PERCENT	LOCATION	SIZE (mm)	FILLING	SHAPE
Vesicles	1-5	Random	<1	Clay	Round

COMMENT: Hyaloclastite consists of highly altered glass fragments.

125-786B-57R-01 (Piece 1A,8-11 cm)   OBSERVER: JDH   WHERE SAMPLED: Izu-Bonin outer-arc high

ROCK NAME: Altered andesite

GRAIN SIZE: Fine-grained

TEXTURE: Sparsely phyric

PRIMARY MINERALOGY	PERCENT PRESENT	PERCENT ORIGINAL	SIZE (mm)	COMPO-SITION	MORPHOLOGY	COMMENTS
PHENOCRYSTS						
Clinopyroxene	1-3	10-20	<0.7		Euhedral-anhedral	Some crystals are completely altered to clays making phase determination difficult.
GROUNDMASS						
Glass	0	65-70	N/A		N/A	
Microlites	<5	10-20	<0.02		Needles	No optical properties discernible.

SECONDARY MINERALOGY	PERCENT	REPLACING/ FILLING	COMMENTS
Clays	80-85	Glass/matrix, clinopyroxene	Brown amorphous clays.
Chlorite	<1	Glass, veins	Pale yellow to green brown, slightly pleochroic.

VESICLES/ CAVITIES	PERCENT	LOCATION	SIZE (mm)	FILLING	SHAPE
Vesicles	0				

COMMENTS: Much of material polished away during thin-section preparation.

125-786B-57R-03 (Piece 1A,65-67 cm)   OBSERVER: RIB   WHERE SAMPLED: Izu-Bonin outer-arc high

ROCK NAME: Two-pyroxene andesite

GRAIN SIZE: 0.1-1 mm

TEXTURE: Porphyritic

PRIMARY MINERALOGY	PERCENT PRESENT	PERCENT ORIGINAL	SIZE (mm)	COMPO-SITION	MORPHOLOGY	COMMENTS
PHENOCRYSTS						
Plagioclase	0	10-15	0.5-1		Euhedral	Altered to clay.
Clinopyroxene	1-2	10-15	0.5-1		Euhedral-subhedral	Altered to clay.
Orthopyroxene	<5	15-20	0.5-3		Euhedral	Altered to clay.
GROUNDMASS						
Plagioclase	2-3	10-15	<0.2		Euhedral, elongate, prismatic	Altered to clay.
Orthopyroxene	0	1-10	<0.2		Euhedral-subhedral	Altered to clay.
Clinopyroxene	Trace	1-10	<0.2		Euhedral-subhedral, prismatic	
Glass	0	40-50	N/A		N/A	Altered to clay.

SECONDARY MINERALOGY	PERCENT	REPLACING/ FILLING	COMMENTS
Clays	40-50	Glass, plagioclase, orthopyroxene	Mainly illite.

VESICLES/ CAVITIES	PERCENT	LOCATION	SIZE (mm)	FILLING	SHAPE
Vesicles	5				

COMMENTS: This rock is highly altered andesite. Most of phenocrysts are replaced by illite-rich clay.

125-786B-[illegible]-1A (Piece 8B,44-46 cm)   OBSERVER: KIR   WHERE SAMPLED: Izu-Bonin outer-arc high

ROCK NAME: Andesite breccia

GRAIN SIZE:

TEXTURE: Brecciated

PRIMARY MINERALOGY	PERCENT PRESENT	PERCENT ORIGINAL	SIZE (mm)	COMPO-SITION	MORPHOLOGY	COMMENTS
PHENOCRYSTS						
Plagioclase	Trace	Trace	0.[illegible]-1		Euhedral	Highly altered to clay
Clinopyroxene	Trace	Trace	0.[illegible]-1		Euhedral	Mostly torn off by polishing
GROUNDMASS						
N/A	N/A	N/A	N/A		N/A	

SECONDARY MINERALOGY	PERCENT	REPLACING/FILLING	COMMENTS
Clays	[illegible]	Groundmass, glass, vesicles	Groundmass is highly altered to clay

VESICLES/CAVITIES	PERCENT	LOCATION	SIZE (mm)	FILLING	SHAPE
Vesicles	[illegible]	Random	0.[illegible]-2	Clay	Round

COMMENTS: This rock is highly altered andesite and is locally brecciated.

125-786B-[illegible] (Piece 1B,49-51 cm)   OBSERVER: KIR   WHERE SAMPLED: Izu-Bonin outer-arc high

ROCK NAME: Orthopyroxene andesite

GRAIN SIZE: [illegible] mm

TEXTURE: Vesicular

PRIMARY MINERALOGY	PERCENT PRESENT	PERCENT ORIGINAL	SIZE (mm)	COMPO-SITION	MORPHOLOGY	COMMENTS
PHENOCRYSTS						
Orthopyroxene	[illegible]	[illegible]	[illegible]		Euhedral	Partly altered to clay
GROUNDMASS						
Orthopyroxene	[illegible]	[illegible]	[illegible]		Anhedral, acicular	

SECONDARY MINERALOGY	PERCENT	REPLACING/FILLING	COMMENTS
Clays	40-45	Glass	Pale green to pale brown
Zeolites	[illegible]	Vesicles	Occur as radial crystals
Chlorite	Trace	Vesicles	Pale green
Prehnite	Trace		Refraction index is slightly higher than zeolite minerals

VESICLES/CAVITIES	PERCENT	LOCATION	SIZE (mm)	FILLING	SHAPE
Vesicles	[illegible]	Random	[illegible]	Zeolites, clay, prehnite	Round

COMMENTS: Vesicles are abundant throughout the rock.

125-786B-57R-2 (Piece 1A,30-31 cm) OBSERVER: JCH WHERE SAMPLED: Izu-Bonin outer-arc high

ROCK NAME: — yroxene boninite

GRAIN SIZE: Fine-grained to glassy

TEXTURE: Vesicular, sparsely phyric

PRIMARY MINERALOGY	PERCENT PRESENT	PERCENT ORIGINAL	SIZE (mm)	COMPO-SITION	MORPHOLOGY	COMMENTS
PHENOCRYSTS						
Clinopyroxene	<2	2-5	<0.5		Subhedral	Too altered to determine accurate original mode, spinel inclusions.
Orthopyroxene	<2	2-5	<1		Subhedral	Too altered to determine accurate original mode, spinel inclusions.
GROUNDMASS						
Glass	0	85-90	N/A		N/A	
Microlites	<5	10-15	<0.07		Needles	Brown in PPL, probably alteration.

SECONDARY MINERALOGY	PERCENT	REPLACING/ FILLING	COMMENTS
Clays	75-85	Glass, vesicles	Yellow-brown amorphous clay; <5% pale green, pervasive.
Zeolites	5	Vesicles	3 types, radiating, parallel extinction; small crystals (<0.01 mm) and mixed with chlorite.
Chlorite	<10	Glass, vesicles	

VESICLES/ CAVITIES	PERCENT	LOCATION	SIZE (mm)	FILLING	SHAPE	COMMENTS
Vesicles	25-35		0.2-1.2	Zeolite, chlorite	Round	Nice examples of zeolite filling.

COMMENTS: This rock is quite altered; primary mineralogy and texture are obscured by alteration.

125-786B-57R-CC (Piece 1,48-49 cm) OBSERVER: RIR WHERE SAMPLED: Izu-Bonin outer-arc high

ROCK NAME: Orthopyroxene boninite

GRAIN SIZE: Fine-grained to glassy

TEXTURE: Vesicular, porphyritic

PRIMARY MINERALOGY	PERCENT PRESENT	PERCENT ORIGINAL	SIZE (mm)	COMPO-SITION	MORPHOLOGY	COMMENTS
PHENOCRYSTS						
Orthopyroxene	25-35	25-35	0.5-1.5		Euhedral	Shows clinopyroxene exsolution lamellae.
GROUNDMASS						
Plagioclase	Trace	1-2	<0.1		Acicular	
Orthopyroxene	Trace	1-2	<0.1		Prismatic	

SECONDARY MINERALOGY	PERCENT	REPLACING/ FILLING	COMMENTS
Clays	65-75	Glass, plagioclase	Pale-green to pale-brown dusty clay replaces groundmass glass and fills in vesicles.

VESICLES/ CAVITIES	PERCENT	LOCATION	SIZE (mm)	FILLING	SHAPE
Vesicles	15-20	Random	<0.5	Clay	Round

[illegible] (Piece [illegible], 48-49 cm) OBSERVER: [illegible] WHERE SAMPLED: Izu-Bonin outer-arc high

ROCK NAME: Andesite

GRAIN SIZE: Fine-grained to glassy

TEXTURE: Sparsely phyric

PRIMARY MINERALOGY	PERCENT PRESENT	PERCENT ORIGINAL	SIZE (mm)	COMPOSITION	MORPHOLOGY	COMMENTS
PHENOCRYSTS						
Plagioclase	[illegible]	[illegible]	[illegible]		Subhedral-anhedral	Spinel inclusions.
Orthopyroxene	1-2	1-2	[illegible]		Subhedral-anhedral	Spinel inclusions.
GROUNDMASS						
Glass	[illegible]	[illegible]	N/A		N/A	[illegible] to green.
Plagioclase	[illegible]	[illegible]	[illegible]		Needles	[illegible] and clay alteration.

SECONDARY MINERALOGY	PERCENT	REPLACING/FILLING	COMMENTS
Clays	[illegible]	Glass, matrix	Dark brown to yellow to green, amorphous, pervasive in glassy portions.
Zeolites	[illegible]	Vesicles	Radiating, [illegible]
[illegible]	[illegible]	Glass, matrix	Green to [illegible] yellow, slightly pleochroic. Intimately mixed with clays.

VESICLES/CAVITIES	PERCENT	LOCATION	SIZE (mm)	FILLING	SHAPE
Vesicles	[illegible]		[illegible]	Zeolites	Elongate

COMMENTS: [illegible] small portion [illegible] mm diameter) remains. This and the degree of alteration make the rock difficult to characterize.

[illegible] (Piece [illegible]) OBSERVER: [illegible] WHERE SAMPLED: Izu-Bonin outer-arc high

ROCK NAME: [illegible]

GRAIN SIZE: Fine-grained to glassy

TEXTURE: Sparsely phyric

PRIMARY MINERALOGY	PERCENT PRESENT	PERCENT ORIGINAL	SIZE (mm)	COMPOSITION	MORPHOLOGY	COMMENTS
PHENOCRYSTS						
Clinopyroxene	[illegible]	[illegible]	[illegible]		Subhedral	Very low extinction angles. Spinel inclusions.
Spinel	[illegible]	[illegible]	[illegible]		Euhedral	Very dark red.
Orthopyroxene	[illegible]	[illegible]	[illegible]		Subhedral	Spinel inclusions. Mostly altered and altered material plucked out.
GROUNDMASS						
Glass	[illegible]	[illegible]	N/A		N/A	Totally altered to brown clays.
[illegible]	[illegible]	[illegible]	[illegible]		Needles, equant	Low birefringence, [illegible] equant ones may be zeolite.

SECONDARY MINERALOGY	PERCENT	REPLACING/FILLING	COMMENTS
Clays	[illegible]	Glass, matrix	Brown, amorphous, [illegible] pervasive.
Zeolites	[illegible]	Vesicle lining	Lining vesicles. May also be the equant crystals [illegible]. They occur as [illegible] into vesicles.

VESICLES/CAVITIES	PERCENT	LOCATION	SIZE (mm)	FILLING	SHAPE	COMMENTS
Vesicles	[illegible]		[illegible]	Zeolite-filled	Irregular	Some may be plucking during thin section preparation.

COMMENTS: [illegible] of orthopyroxene up to [illegible] mm. Totally altered rock [illegible] so severely altered that much of the original mineralogy is obscured.

125-786B-58R-01 (Piece 21,107-116 cm)   OBSERVER: DAB   WHERE SAMPLED: Izu-Bonin outer-arc high

ROCK NAME: Andesite

GRAIN SIZE: Fine-grained to glassy

TEXTURE: Sparsely phyric

PRIMARY MINERALOGY	PERCENT PRESENT	PERCENT ORIGINAL	SIZE (mm)	COMPO-SITION	MORPHOLOGY	COMMENTS
PHENOCRYSTS						
Plagioclase	1-2	1-2	0.2-1		Subhedral	Twinning is rarely visible.
Orthopyroxene	2-4	3-5	0.3-2		Subhedral-euhedral	Mostly altered.
GROUNDMASS						
Glass	0	90	N/A		N/A	

SECONDARY MINERALOGY	PERCENT	REPLACING/FILLING	COMMENTS
Clays	92	Glass, vesicles	Green-brown, amorphous clay pervasive and in vesicles.
Zeolites	2	Vesicles	Occurs as crystals pointing into vesicles.

VESICLES/CAVITIES	PERCENT	LOCATION	SIZE (mm)	FILLING	SHAPE	COMMENTS
Vesicles	15-20	Random	0.5-1	Clays	Round	Some filled with clays + zeolites.

COMMENTS: Very poorly made thin section. It is extremely difficult to tell what type of rock it is. Rock appears almost totally altered so primary mineralogy is obscured.

125-786B-58R-01 (Piece 21,127-128 cm)   OBSERVER: TRB   WHERE SAMPLED: Izu-Bonin outer-arc high

ROCK NAME: Andesite

GRAIN SIZE: Fine-grained to glassy

TEXTURE: Intersertal texture, sparsely phyric

PRIMARY MINERALOGY	PERCENT PRESENT	PERCENT ORIGINAL	SIZE (mm)	COMPO-SITION	MORPHOLOGY	COMMENTS
PHENOCRYSTS						
Plagioclase	0	3	1		Euhedral-subhedral	Replaced by clays.
Clinopyroxene	Trace	Trace	0.5		Subhedral	Dusty appearance.
Orthopyroxene	0	4	0.5-1	Bronzite	Subhedral	2V=85 degrees, replaced by clays.
GROUNDMASS						
Plagioclase	0	10	0.05-0.2		Euhedral-subhedral, prismatic, elongate	Altered to clay.
Clinopyroxene	1	1	0.05-0.1		Euhedral, prismatic	
Orthopyroxene	0	1	0.05-0.1		Euhedral, prismatic	
Glass	0	75-80	N/A		N/A	
Opaque	1	1	0.01-0.05		Subhedral	Magnetite?

SECONDARY MINERALOGY	PERCENT	REPLACING/FILLING	COMMENTS
Clays	85-90	Glass, plagioclase	Pale-brown clay replacing minerals and glass.
Opaque	1-2	Glass, vein	Replacing glass, vein.

VESICLES/CAVITIES	PERCENT	LOCATION	SIZE (mm)	FILLING	SHAPE
Vesicles	10	Random	0.1-5	None	

COMMENTS: Relatively altered andesite.

125-786B-[illegible] (Piece [illegible] cm) OBSERVER: [illegible] WHERE SAMPLED: Izu-Bonin outer-arc high

ROCK NAME: Andesite

GRAIN SIZE: Fine-grained to glassy

TEXTURE: Sparsely phyric; glassy margin

PRIMARY MINERALOGY	PERCENT PRESENT	PERCENT ORIGINAL	SIZE (mm)	COMPO-SITION	MORPHOLOGY	COMMENTS
PHENOCRYSTS						
Plagioclase	[illegible]	10-15	[illegible]		Subhedral	Sparse spinel inclusions
Clinopyroxene	[illegible]	[illegible]	[illegible]		Euhedral-subhedral	Some are pale green
Spinel	Trace	Trace	[illegible]		Subhedral	
Orthopyroxene	[illegible]	[illegible]	[illegible]		Subhedral	80-90% altered
GROUNDMASS						
Glass	[illegible]	25-40	N/A		N/A	Deep yellow to light brown, highly altered
Microlites	[illegible]	25-30	[illegible]		Needles	No discernible optical properties

SECONDARY MINERALOGY	PERCENT	REPLACING/ FILLING	COMMENTS
Clays	[illegible]		Brown to yellow-brown clays; pervasive
Chlorite	[illegible]	Glass/matrix	Bright yellow-green pleochroism; seems to be chlorite intimately mixed with brown clay.

VESICLES/ CAVITIES	PERCENT	LOCATION	SIZE (mm)	FILLING	SHAPE
Vesicles	0				

COMMENTS: Most of sample was ground away during thin-section preparation. The remaining portion appears to be the glassy margin attached to a piece of more crystal rock. The more crystalline rock is mostly missing. Therefore the above description is highly biased towards the glassy margins.

125-786B-[illegible] (Piece [illegible], 81-84 cm) OBSERVER: [illegible] WHERE SAMPLED: Izu-Bonin outer-arc high

ROCK NAME: Rhyolitic tuff

GRAIN SIZE: Variable

TEXTURE: Clastic texture

PRIMARY MINERALOGY	PERCENT PRESENT	PERCENT ORIGINAL	SIZE (mm)	COMPO-SITION	MORPHOLOGY	COMMENTS
PHENOCRYSTS						
Plagioclase	[illegible]	[illegible]	[illegible]		Euhedral	Mostly torn off by polishing
GROUNDMASS						
N/A	N/A	N/A	N/A		N/A	

SECONDARY MINERALOGY	PERCENT	REPLACING/ FILLING	COMMENTS
Clays	[illegible]	Matrix	Dusty gray patches in matrix.
Carbonate	[illegible]	Vesicles	Showing typical twinning and high birefringence.
Chlorite	[illegible]	Matrix, vesicles	Pale, green-colored chlorite is scattered throughout the rock.
[illegible]	[illegible]	Matrix	Showing euhedral shape, [illegible] mm

VESICLES/ CAVITIES	PERCENT	LOCATION	SIZE (mm)	FILLING	SHAPE
Vesicles	[illegible]	Random	[illegible]	Calcite, chlorite	Round-elongate

125-786B-62R-03 (Piece 1E, 40-42 cm) OBSERVER: JOH WHERE SAMPLED: Izu-Bonin outer-arc high

ROCK NAME: Orthopyroxene-phyric boninite

GRAIN SIZE: Fine-grained to glassy

TEXTURE: Porphyritic

PRIMARY MINERALOGY	PERCENT PRESENT	PERCENT ORIGINAL	SIZE (mm)	COMPO-SITION	MORPHOLOGY	COMMENTS
PHENOCRYSTS						
Spinel	<1	<1	<0.02		Euhedral-subhedral	
Orthopyroxene	2	2-10	0.5-2.5		Euhedral-subhedral	Most crystals plucked during preparation; those that remain have spinel inclusions. Some chlorite alteration.
GROUNDMASS						
Glass	<5	55-60	N/A		N/A	Slightly altered to clay.
Plagioclase	<10	30-35	<0.25		Needles	Random orientation.
Pyroxene	<5	10-15	<0.2		Tabular	Chloritic alteration.

SECONDARY MINERALOGY	PERCENT	REPLACING/ FILLING	COMMENTS
Clays	65-75	Glass/groundmass	Brown to yellow-brown clay, pervasive.
Carbonate	2-4	Veins, vesicles	Patchwork up to 0.8 mm blocks.
Zeolites	<2	Vesicle	Yellow and black in crossed polars with a radiating structure. Low-birefringence crystals mixed with carbonate.
Chlorite	5-10	Groundmass, pyroxene	Green to green-brown, slight pleochroism.

VESICLES/ CAVITIES	PERCENT	LOCATION	SIZE (mm)	FILLING	SHAPE
Vesicles	5-12	Rock	0.15-0.8	No	Irregular

COMMENTS: Plucking of pyroxene and plagioclase crystals was quite severe during thin-section preparation. This may indicate high alteration.

125-786B-63R-02 (Piece 13, 72-74 cm) OBSERVER: SAR WHERE SAMPLED: Izu-Bonin outer-arc high

ROCK NAME: Rhyolite tuff

GRAIN SIZE: Variable

TEXTURE: Clastic texture

PRIMARY MINERALOGY	PERCENT PRESENT	PERCENT ORIGINAL	SIZE (mm)	COMPO-SITION	MORPHOLOGY	COMMENTS
PHENOCRYSTS						
Plagioclase	5-10	5-10	0.5-1		Euhedral	Mostly plucked out by polishing.
GROUNDMASS						
Glass	0	70-85	N/A		N/A	
Plagioclase	10-20	10-20	<0.2		Anhedral	
Opaque	1-2	1-2	<0.2		Euhedral	Black, euhedral and as dusty grains distributed throughout matrix.

SECONDARY MINERALOGY	PERCENT	REPLACING/ FILLING	COMMENTS
Clays	70-85	Matrix	Dusty brown clay filling in matrix.

VESICLES/ CAVITIES	PERCENT	LOCATION	SIZE (mm)	FILLING	SHAPE
Vesicles	1-3	Random	<2		Round-elongate

[illegible] (Piece [illegible]) OBSERVER: [illegible] WHERE SAMPLED: [illegible]

ROCK NAME: Andesite

GRAIN SIZE: Fine-grained to glassy

TEXTURE: Aphyric

PRIMARY MINERALOGY	PERCENT PRESENT	PERCENT ORIGINAL	SIZE (mm)	COMPOSITION	MORPHOLOGY	COMMENTS
PHENOCRYSTS						
Clinopyroxene	Trace	Trace	[illegible]		Euhedral	
GROUNDMASS						
Glass	[illegible]	[illegible]	N/A		N/A	Highly altered to brown clays
Plagioclase	[illegible]	[illegible]	[illegible]		Subhedral	Occasional radiating clusters
Pyroxene	[illegible]	[illegible]	[illegible]		Anhedral	Equant
Opaques	2-4	2-4	[illegible]		Subhedral-Euhedral	Triangular-shaped, blades, evenly distributed.

SECONDARY MINERALOGY	PERCENT	REPLACING/ FILLING	COMMENTS
Clays	[illegible]	Glass matrix	Brown amorphous clay locally pervasive to patchy.
Carbonate	1-2	Vesicles, phenocrysts	May be completely altering phenocrysts, no relict crystal shapes remain.
Zeolite	[illegible]	Matrix	[illegible] fringe to glass and groundmass.

VESICLES/ CAVITIES	PERCENT	LOCATION	SIZE (mm)	FILLING	SHAPE
Vesicles	[illegible]		[illegible]	Carbonate	Round

[illegible] (Piece [illegible]) OBSERVER: [illegible] WHERE SAMPLED: [illegible]

ROCK NAME: [illegible]

GRAIN SIZE: Fine-grained to glassy

TEXTURE: [illegible]

PRIMARY MINERALOGY	PERCENT PRESENT	PERCENT ORIGINAL	SIZE (mm)	COMPOSITION	MORPHOLOGY	COMMENTS
PHENOCRYSTS						
Clinopyroxene	[illegible]	[illegible]	[illegible]		Anhedral	Ragged fragments of low birefringence mineral may be [illegible] of plagioclase
GROUNDMASS						
Matrix		[illegible]	N/A		N/A	May have been glassy or [illegible], no original texture preserved
Plagioclase	[illegible]	[illegible]	[illegible]		Laths	
[illegible]	[illegible]	[illegible]	[illegible]		Subhedral, equant	

SECONDARY MINERALOGY	PERCENT	REPLACING/ FILLING	COMMENTS
Carbonate	[illegible]	Vesicles, [illegible]	Small patches, equant, irregular shaped [illegible] mm across. May be replacing [illegible] in some cases.
[illegible]	[illegible]		Fragments of very low birefringence. Residual material may be primary minerals but no mineral forms or association preserved.
Clays	[illegible]	Groundmass	Brown, amorphous clay replacing groundmass/glass.

VESICLES/ CAVITIES	PERCENT	LOCATION	SIZE (mm)	FILLING	SHAPE
Vesicles	[illegible]	[illegible]	[illegible]	Carbonate	[illegible]

COMMENTS: [illegible]

```
125-786B-67R-01 (Piece 2,8-10 cm)        OBSERVER: JOH        WHERE SAMPLED: Izu-Bonin outer-arc high

ROCK NAME: Clinopyroxene-plagioclase-orthopyroxene andesite

GRAIN SIZE: Fine-grained to glassy

TEXTURE: Moderately glomerophyric
----------------------------------------------------------------------------------------------------------

PRIMARY          PERCENT PERCENT  SIZE       COMPO-
MINERALOGY       PRESENT ORIGINAL (mm)       SITION       MORPHOLOGY          COMMENTS

 PHENOCRYSTS
Plagioclase       <4      8-12   0.5-2.1                  Euhedral-subhedral  Spinel inclusions. Moth-eaten, highly
                                                                              altered to clays.
Clinopyroxene     <3      5-7    0.3-0.8                  Subhedral           Spinel inclusions, pale green.
Orthopyroxene      0      8-12   N/A                      Subhedral,          Crystals altered to Fe-oxide + carbonate
                                                          lath-shaped to      + chlorite.
                                                          equant

 GROUNDMASS
Glass             <5      50-60  N/A                      N/A                 Nearly completely altered to clays.
Plagioclase       <4      15-15  <0.15                    Needles
Clinopyroxene     <5      10-15  <0.3                     Tabular             Completely altered to clays and
                                                                              chlorite.

SECONDARY                  REPLACING/
MINERALOGY       PERCENT    FILLING                                            COMMENTS
Clays             45-50   Glass; plagioclase                       Brown, amorphous clay.
Carbonate          5-7    Orthopyroxene                            Pseudomorphs pyroxene; also in fractures and cleavages.
Chlorite          15-20   Glass, matrix, orthopyroxene             Altering glass and groundmass phases.
Hematite           3-5    Orthopyroxene                            Part of the Fe-oxide + carbonate + chlorite alteration
                                                                   assemblage.
----------------------------------------------------------------------------------------------------------
VESICLES/                          SIZE
CAVITIES        PERCENT  LOCATION  (mm)            FILLING                       SHAPE       COMMENTS
Vesicles         15-25   Rock      0.3-6           No                            Irregular   Some may be due to
                                                                                             plucking during
                                                                                             thin-section
                                                                                             preparation.
----------------------------------------------------------------------------------------------------------
COMMENTS: Glomerocrysts of plagioclase + clinopyroxene up to 3 mm across.

125-786B-27R-01 (Piece 9,62-65 cm)        OBSERVER: TPB        WHERE SAMPLED: Izu-Bonin outer-arc high

ROCK NAME: Plagioclase-clinopyroxene-orthopyroxene phyric basalt

GRAIN SIZE: Fine-grained to glassy (0.3 mm)

TEXTURE: Glomerophyric, hyalophitic texture
----------------------------------------------------------------------------------------------------------

PRIMARY          PERCENT PERCENT  SIZE       COMPO-
MINERALOGY       PRESENT ORIGINAL (mm)       SITION       MORPHOLOGY          COMMENTS

 PHENOCRYSTS
Olivine            0      Trace  Trace                    Subhedral           Olivine replaced by carbonate.
Plagioclase        1      1      0.1-0.4                  Subhedral-euhedral  Plagioclase is very sparse in this rock.
Clinopyroxene      4      5      0.2-1                    Subhedral-euhedral
Orthopyroxene      8      8      0.3-2                    Subhedral-euhedral  Orthopyroxene has reaction rim.

 GROUNDMASS
Plagioclase       15      30     0.05-0.1                 Euhedral            Showing lath shape.
Clinopyroxene      4      15     0.03-0.05                Subhedral-euhedral  Showing short prismatic shape.
Opaque             3      3      0.01-0.03                Subhedral-euhedral  Equant in shape.
Glass             15      40-45  N/A                      N/A                 Partly devitrified to clays.

SECONDARY                  REPLACING/
MINERALOGY       PERCENT    FILLING                                           COMMENTS
Clays             40-45   Glass, orthopyroxene, olivine(?)
Carbonate          3      Orthopyroxene, olivine(?)
----------------------------------------------------------------------------------------------------------
VESICLES/                          SIZE
CAVITIES        PERCENT  LOCATION  (mm)            FILLING                       SHAPE
Vesicles         <15
----------------------------------------------------------------------------------------------------------
COMMENTS: Orthopyroxenes are sometimes surrounded by clinopyroxene rim. Plagioclase poor, two-pyroxene basalt.
```

125-786B-[illegible] (Piece 1B, 7-9 cm) OBSERVER: [illegible] WHERE SAMPLED: Izu-Bonin outer-arc high

ROCK NAME: Meta-andesite

GRAIN SIZE: Fine-grained to glassy

TEXTURE: Moderately to highly phyric

PRIMARY MINERALOGY	PERCENT PRESENT	PERCENT ORIGINAL	SIZE (mm)	COMPO-SITION	MORPHOLOGY	COMMENTS
PHENOCRYSTS						
Plagioclase	<1	1-5	0.8-2		Subhedral	Highly altered; only "shells" remain
Clinopyroxene	[illegible]	4-6	0.8-1		Euhedral-subhedral	Spinel inclusions.
Spinel	[illegible]	<1	<0.15		Euhedral-subhedral	Black (opaque) to red.
Orthopyroxene	0	15-20	0.3-1.1		Euhedral-subhedral	100% altered to clay and chlorite; shape of crystals and direction of chlorite extinction used as mineral identification.
GROUNDMASS						
Groundmass	<15	70-80	N/A		N/A	Glass and possible microphenocrysts of plagioclase. Alteration has obscured the textural distinction.

SECONDARY MINERALOGY	PERCENT	REPLACING/ FILLING	COMMENTS
Clays	65-75	Glass, phenocrysts	Brown, amorphous pervasive.
Chlorite	15-20	Pyroxene, glass	Appears to have formed pseudomorphing orthopyroxene and later became overprinted by brown clays.
Magnetite	1-2	Veins	Black to deep blood-red, massive, forming veins up to 0.5 mm wide and rimming minerals.

VESICLES/ CAVITIES	PERCENT	LOCATION	SIZE (mm)	FILLING	SHAPE
Vesicles	0				

COMMENTS: Rock is highly altered to brown clays and minor chlorite which obscure the primary textural and crystallographic characteristics.

125-786B-[illegible] (Piece [illegible]) OBSERVER: [illegible] WHERE SAMPLED: Izu-Bonin outer-arc high

ROCK NAME: Meta-andesite

GRAIN SIZE: Fine-grained to glassy

TEXTURE: Moderately phyric

PRIMARY MINERALOGY	PERCENT PRESENT	PERCENT ORIGINAL	SIZE (mm)	COMPO-SITION	MORPHOLOGY	COMMENTS
PHENOCRYSTS						
Plagioclase	1-2	<1	<0.2		Tabular	Fresh microphenocrysts, twinned.
Pyroxene	[illegible]	15-20	[illegible]		Euhedral-subhedral	Highly altered to clays + chlorite, no original mineral fragments or optical character left. Morphologically these appear to be pyroxenes.
GROUNDMASS						
Groundmass	0	65-80	N/A		N/A	May have been glass or microcrystalline completely obscured by alteration.
Plagioclase	10	5-15	<0.1		Tabular	Low birefringence.
Spinel	1-2	1-2	<0.05		Equant	

SECONDARY MINERALOGY	PERCENT	REPLACING/ FILLING	COMMENTS
Clays		Glass, matrix	
Carbonate	1-5	Veins	
Chlorite	15-20	Pyroxene, glass	Orange-yellow to yellow-green pleochroism.
Magnetite	1-2	Veins	Intimately associated with albite or a low birefringence zeolite, and chlorite up to 0.15 mm equant euhedral-subhedral pieces.
Unknown	10-15	Matrix	Low birefringence, colorless, anhedral crystals approximately 0.05 mm across which interlock and may be albite, quartz or a zeolite.

VESICLES/ CAVITIES	PERCENT	LOCATION	SIZE (mm)	FILLING	SHAPE
Vesicles	0				

COMMENTS: Highly altered rock. Nearly all original mineralogy and texture have been obscured by alteration.

125-786B-70R-01 (68-72 cm) OBSERVER: JOH WHERE SAMPLED: Izu-Bonin outer-arc high

ROCK NAME: Meta-andesite

GRAIN SIZE: Fine-grained to glassy

TEXTURE: Sparsely phyric

PRIMARY MINERALOGY	PERCENT PRESENT	PERCENT ORIGINAL	SIZE (mm)	COMPO-SITION	MORPHOLOGY	COMMENTS
PHENOCRYSTS						
Pyroxene	Trace	20-25	<1		Subhedral	Crystals 100% replaced by clays and some carbonate. Tiny traces of relict mineral suggest orthopyroxene as does general morphology.
Spinel	1-2	1-2	<0.01		Equant	See pyroxene comments.
GROUNDMASS						
Glass	0	55-60	N/A		N/A	
Microlites	<10	20-25	<0.05		Needles	Probably plagioclase; alteration obscures optical character.

SECONDARY MINERALOGY	PERCENT	REPLACING/ FILLING	COMMENTS
Clays	75-80	Glass, matrix	Brown to light brown, amorphous, pervasive locally patchy.
Carbonate	5-10	Glass, vesicles	Locally intimately mixed with clays, fills vesicles and may completely replace minerals.
Chlorite	5-10	Glass, matrix	Slight yellow-green pleochroism.
Hematite?	Trace	Vesicle/glass	Maybe mixed with chlorite, slight radiating fabric.

VESICLES/ CAVITIES	PERCENT	LOCATION	SIZE (mm)	FILLING	SHAPE
Vesicles	0				

COMMENTS: This rock is highly altered and the original mineralogy and textural characteristics are obscured. No piece # given.

125-786B-71R-04 (Piece 69,71-74 cm) OBSERVER: JOH WHERE SAMPLED: Izu-Bonin outer-arc high

ROCK NAME: Clinopyroxene-phyric basalt

GRAIN SIZE: Fine-grained to glassy

TEXTURE: Sparsely phyric

PRIMARY MINERALOGY	PERCENT PRESENT	PERCENT ORIGINAL	SIZE (mm)	COMPO-SITION	MORPHOLOGY	COMMENTS
PHENOCRYSTS						
Plagioclase	7-9	10-14	0.3-1.5		Subhedral	Rare spinel inclusions, moth-eaten, oscillatory zoning.
Clinopyroxene	<4	5-7	0.15-0.4		Subhedral-anhedral	Pale green to yellow, slightly pleochroic, spinel inclusions.
Spinel	Trace	Trace	<0.02		Equant	As inclusions.
GROUNDMASS						
Glass	0	65-70	N/A		N/A	
Plagioclase	<10	10-15	<0.15		Laths	
Microlites	<10	10-15	<0.02		Needles	

SECONDARY MINERALOGY	PERCENT	REPLACING/ FILLING	COMMENTS
Clays	55-65	Glass	Brown amorphous clay, locally pervasive and patchy in appearance.
Chlorite	<10	Matrix	Green to yellow coloration in altered patches due to chlorite, small local patches of chloritic birefringence.
Magnetite	1-3	Veins, matrix	Strings and irregular pieces of black opaque material locally concentrated and in veins.

VESICLES/ CAVITIES	PERCENT	LOCATION	SIZE (mm)	FILLING	SHAPE
Vesicles	0				

COMMENTS: Glomerocrysts of plagioclase and of clinopyroxene, but not both. Some gaps in this section appear to be caused by plucking during thin-section preparation.

[illegible]

SECTION 5: POLICY

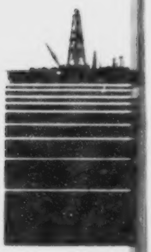

JOIDES ADVISORY GROUPS*

Executive Committee (EXCOM)

Charles E. Helsley
University of Hawaii

Roger N. Anderson (Wireline Logging Services liaison)
Columbia University

D. James Baker, Jr. (JOI liaison)
Joint Oceanographic Institutions, Inc.

Christopher R. Barnes
Geological Survey of Canada

Bernard Biju-Duval
IFREMER (France)

James C. Briden
Natural Environment Research Council (U.K.)

Douglas R. Caldwell
Oregon State University

Craig E. Dorman
Woods Hole Oceanographic Institution

Robert A. Duce
University of Rhode Island

Hans J. Dürbaum
Bundesanstalt für Geowissenschaften and Rohstoffe

Edward A. Frieman
University of California, San Diego

C.G.A. Harrison
University of Miami

G. Ross Heath
University of Washington

Donald F. Heinrichs (NSF liaison)
National Science Foundation (U.S.)

Arthur E. Maxwell
University of Texas at Austin

William J. Merrell
Texas A&M University at Galveston

Ralph Moberly (PCOM liaison)
University of Hawaii

Takahisa Nemoto
University of Tokyo

Philip D. Rabinowitz (Science Operator liaison)
Texas A&M University

C. Barry Raleigh
Columbia University

Jan H. Stel
Netherlands Council of Oceanic Research

Planning Committee (PCOM)

Ralph Moberly
University of Hawaii

Garrett W. Brass
University of Miami

Darrel S. Cowan
University of Washington

Olav Eldholm
University of Oslo

Louis E. Garrison (Science Operator liaison)
Texas A&M University

Richard D. Jarrard (Wireline Logging Services liaison)
Columbia University

Hugh C. Jenkyns
Oxford University

Miriam Kastner
University of California, San Diego

Yves P. Lancelot
Université Pierre et Marie Curie

Marcus G. Langseth
Columbia University

Margaret Leinen
University of Rhode Island

Bruce Malfait (NSF liaison)
National Science Foundation (U.S.)

John Malpas
Memorial University

Nicklas G. Pisias
Oregon State University

Thomas E. Pyle (JOI liaison)
Joint Oceanographic Institutions, Inc.

Thomas H. Shipley
University of Texas at Austin

Asahiko Taira
University of Tokyo

Brian E. Tucholke
Woods Hole Oceanographic Institution

Ulrich von Rad
Bundesanstalt für Geowissenschaften und Rohstoffe

Joel Watkins
Texas A&M University

Central and Eastern Pacific Detailed Planning Group (CEPDPG)

David K. Rea
University of Michigan

Helmut Beiersdorf
Bundesanstalt für Geowissenschaften und Rohstoffe

Earl E. Davis
Geological Survey of Canada

Martin F.J. Flower
University of Illinois, Chicago

Peter A. Floyd
University of Keele

Jean Francheteau
Université Pierre et Marie Curie

Loren W. Kroenke
University of Hawaii

Hakuyu Okada
Kyushu University

Constance A. Sancetta
Columbia University

Seymour O. Schlanger
Northwestern University

Hans Joachim Schrader
University of Bergen

William V. Sliter
U.S. Geological Survey

Downhole Measurements Panel (DMP)

Paul F. Worthington
British Petroleum Company, Ltd.

Keir Becker (LITHP liaison)
University of Miami

Sebastian Bell
Geological Survey of Canada

Bobb Carson
Lehigh University

Darrel S. Cowan (PCOM liaison)
University of Washington

Joris M. Gieskes
University of California, San Diego

Xenia Golovchenko (Wireline Logging Services liaison)
Columbia University

Eddie P. Howell
Arco Oil and Gas Company

---

*Membership at the time of the cruise.

Daniel E. Karig
Cornell University

Hajimu Kinoshita
Chiba University

Marcus G. Langseth (PCOM liaison)
Columbia University

Peter Lysne
Sandia National Laboratories

Roger H. Morin
U.S. Geological Survey

Suzanne O'Connell (Science Operator liaison)
Texas A&M University

J. P. Pozzi
Ecole Normale Superieure

Carl Sondergeld
Amoco Production Company

Ove Stephansson
University of Lulea

Heinrich Villinger
Alfred Wegener Institute for Polar and Marine Research

Roy H. Wilkens
University of Hawaii

Fluid Processes in Accretionary Prisms Working Group (FPAPWG)

Graham K. Westbrook
University of Birmingham

Keir Becker
University of Miami

Joris M. Gieskes
University of California, San Diego

Roy D. Hyndman
Pacific Geoscience Centre (Canada)

Daniel E. Karig
Cornell University

Xavier Le Pichon
Ecole Normale Superieure

J. Casey Moore
University of California, Santa Cruz

E. Nuti
Istituto Internationale de Geotermia

Thomas H. Shipley
University of Texas at Austin

Erwin Suess
GEOMAR (F.R.G.)

Roland von Huene
GEOMAR (F.R.G.)

Information Handling Panel (IHP)

Ted C. Moore, Jr.
Exxon Production Research Company

Cristina Broglia (Wireline Logging Services liaison)
Columbia University

Raymond V. Ingersoll
University of California, Los Angeles

Meirion T. Jones
Institute of Oceanographic Sciences (U.K.)

Yves P. Lancelot (PCOM liaison)
Université Pierre et Marie Curie

Alfred R. Loeblich, Jr.
University of California, Los Angeles

Michael S. Loughridge
National Geophysical Data Center (U.S.)

Russell B. Merrill (Science Operator liaison)
Texas A&M University

Judit Nowak
Bundesanstalt für Geowissenschaften und Rohstoffe

Niklas G. Pisias (PCOM liaison)
Oregon State University

John B. Saunders
Naturhistorisches Museum (Switzerland)

André Schaaf
Université Claude Bernard

Henry Spall
U.S. Geological Survey

Kensaku Tamaki
University of Tokyo

Lithospheric Panel (LITHP)

Rodey Batiza
University of Hawaii

Keir Becker
University of Miami

Garrett W. Brass (PCOM liaison)
University of Miami

Lawrence M. Cathles
Cornell University

Sierd Cloetingh
Vrije Universiteit

Henry Elderfield
Cambridge University

Jörg Erzinger
Universität Giessen

James M. Franklin
Geological Survey of Canada

Toshitsugu Fujii
University of Tokyo

Susan E. Humphris
Woods Hole Oceanographic Institution

John Malpas (PCOM liaison)
Memorial University

Catherine Mevel
Université Pierre et Marie Curie

Jason Phipps Morgan
Massachusetts Institute of Technology

John C. Mutter
Columbia University

John A. Orcutt
University of California, San Diego

Julian A. Pearce
University of Newcastle upon Tyne

Michael R. Perfit
University of Florida

Guy M. Smith
St. Louis University

Ocean History Panel (OHP)

Nicholas J. Shackleton
Cambridge University

Eric J. Barron
Pennsylvania State University

Wolfgang H. Berger
University of California, San Diego

William A. Berggren
Woods Hole Oceanographic Institution

Margaret L. Delaney
University of Southern California, Santa Cruz

Andre W. Droxler
Rice University

Robert E. Garrison
University of California, Santa Cruz

Eystein Jansen
Columbia University

Hugh C. Jenkyns (PCOM liaison)
Oxford University

Dennis V. Kent
Columbia University

Alan C. Mix
Oregon State University

Nicklas G. Pisias (PCOM liaison)
Oregon State University

Tsunemasa Saito
Yamagata University

Ruediger Stein
Universität Giessen

Edith Vincent
Université Pierre et Marie Curie

Pollution Prevention and Safety Panel (PPSP)

Mahlon M. Ball
U.S. Geological Survey

Yutaka Aoki
Japex Geoscience Institute, Inc

Carl Brenner (Databank liaison)
Columbia University

E. Cassani
AGIP S.p.A. (Italy)

George E. Claypool
Mobil Oil Company

Claude Delas
Total Compagnie Française des Pétroles

Mimi Frontier
Canadian Oil and Gas Lands Administration

Louis E. Garrison (Science Operator liaison)
Texas A&M University

Arthur R. Green
Exxon Production Research Company

Paul Haseldonckx
Deminex (F.R.G.)

Stephen Lewis (SSP liaison)
U.S. Geological Survey

David B. MacKenzie
Littleton, Colorado

Ralph Moberly (PCOM liaison)
University of Hawaii

David G. Roberts
British Petroleum Company, Ltd

Sedimentary and Geochemical Processes Panel (SGPP)

Erwin Suess
GEOMAR (F.R.G.)

Jacques Boulegue
Paris, France

Nicholas Christie-Blick
Columbia University

Shirley Dreiss
University of California, Santa Cruz

Henry Elderfield
Cambridge University

Philip N. Froelich
Columbia University

Martin B. Goldhaber
U.S. Geological Survey

Makato Ito
Chiba University

Noel P. James
Memorial University of Newfoundland

Miriam Kastner (PCOM liaison)
University of California, San Diego

Judith A. McKenzie
Eidgenossische Technische Hochschule

Larry Mayer
Université Pierre et Marie Curie

Jurgen Mienert
Woods Hole Oceanographic Institution

William R. Normark
U.S. Geological Survey

Frederick Prahl
Oregon State University

Dorrik Stow
University of Nottingham

Ulrich von Rad (PCOM liaison)
Bundesanstalt für Geowissenschaften und Rohstoffe

Sedimented Ridges Detailed Planning Group (SRDPG)

Robert S. Detrick
University of Rhode Island

Harald Bäcker
GEOMAR (F.R.G.)

Keir Becker
University of Miami

Wilfred B. Bryan
Woods Hole Oceanographic Institution

David Chapman
University of Utah

Earl E. Davis
Geological Survey of Canada

Craig B. Forster
Utah State University

James M. Franklin
Geological Survey of Canada

Hiromi Fujimoto
University of Tokyo

Steven P. Howard
Texas A&M University

Mitchell W. Lyle
Oregon State University

Catherine Mevel
Université Pierre et Marie Curie

Michael J. Mottl
University of Hawaii

Bernd Simoneit
Oregon State University

Robert Zierenberg
U.S. Geological Survey

Shipboard Measurements Panel (SMP)

Kate Moran
Bedford Institute of Oceanography

Ian L. Gibson
University of Waterloo

Joris M. Gieskes (DMP liaison)
University of California, San Diego

John W. King
University of Rhode Island

Margaret Leinen (PCOM liaison)
University of Rhode Island

Michael Mottl
University of Hawaii

J. Mike Rhodes
University of Massachusetts

Adrian Richards
Technische Hogeschool te Delft (Netherlands)

Asahiko Taira (PCOM liaison)
University of Tokyo

Ellen Thomas
Wesleyan University

Hidekazu Tokuyama
University of Tokyo

Site Survey Panel (SSP)

Gregory S. Mountain
Columbia University

Mahlon M. Ball (PPSP liaison)
U.S. Geological Survey

Carl Brenner (Databank liaison)
Columbia University

Frederick K. Duennebier
University of Hawaii

Robert B. Kidd
University College of Swansea

Yves P. Lancelot (PCOM liaison)
Université Pierre et Marie Curie

Birger Larsen
Technical University of Denmark

Stephen Lewis
U.S. Geological Survey

Alain Mauffret
Université Pierre et Marie Curie

Audrey W. Meyer (Science Operator liaison)
Texas A&M University

Heinrich Meyer
Bundesanstalt für Geowissenschaften und Rohstoffe

John W. Peirce
Petro-Canada

Thomas E. Pyle (JOI liaison)
Joint Oceanographic Institutions, Inc

Kiyoshi Suyehiro
University of Tokyo

Joel Watkins (PCOM liaison)
Texas A&M University

Technology and Engineering Development Committee (TEDCOM)

Charles Sparks
Institut Français du Pétrole

Jean Bonnasse-Gahot
Elf-Aquitaine

Garrett W. Brass (PCOM liaison)
University of Miami

Martin E. Chenevert
University of Texas at Austin

William R. Cotten
Chevron Services Company

Bert R. Dennis
Los Alamos National Laboratories

David D. Grassick
Enterprise Oil, plc

Barry W. Harding (Science Operator liaison)
Texas A&M University

Junzo Kasahara
University of Tokyo

Keith Manchester
Bedford Institute of Oceanography

Archie R. McLerran
Solana Beach, California

Keith Millheim
Amoco Production Company

Heinrich Rischmüller
Bundesanstalt für Geowissenschaften und Rohstoffe

Frank J. Schuh
Intertech Operations Technology, Inc

Paul N. Stanton
Exxon Production Research Company

Harald Strand
Norsk Hydro

Walter W. Svendsen
Longyear Company

Paul F. Worthington (DMP liaison)
British Petroleum Company, Ltd.

Tectonics Panel (TECP)

Ian W. D. Dalziel
University of Texas at Austin

Sebastian Bell (DMP liaison)
Geological Survey of Canada

Roger Buck
Columbia University

Dan M. Davis
State University of New York, Stony Brook

Olav Eldholm (PCOM liaison)
University of Oslo

David C. Engebretson
Western Washington University

Karl Hinz
Bundesanstalt für Geowissenschaften und Rohstoffe

David G. Howell
U.S. Geological Survey

Hans Christian Larsen
Greenland Geological Survey

Gregory F. Moore (WPAC liaison)
University of Hawaii

Yujiro Ogawa
Kyushu University

Robin P. Riddihough
Geological Survey of Canada

François Roure
Institut Français du Pétrole

Thomas H. Shipley (PCOM liaison)
University of Texas at Austin

Brian E. Tucholke (PCOM liaison)
Woods Hole Oceanographic Institution

Peter R. Vogt
U.S. Naval Research Laboratory

Anthony B. Watts
Columbia University

Graham K. Westbrook
University of Birmingham

Western Pacific Detailed Planning Group (WPDPG)

James B. Gill
University of California, Santa Cruz

Kent Brooks
University of Copenhagen

David S. Cronan
Imperial College

James V. Eade
CCOP/SOPAC (Fiji)

Roy D. Hyndman
Pacific Geoscience Centre (Canada)

H. R. Kudrass
Bundesanstalt für Geowissenschaften und Rohstoffe

Gregory F. Moore
University of Hawaii

James Natland
University of California, San Diego

Claude Rangin
Université Pierre et Marie Curie

Steven D. Scott
University of Toronto

Kensaku Tamaki
University of Tokyo

Brian Taylor
University of Hawaii

SAMPLE-DISTRIBUTION POLICY[1]

Distribution of Ocean Drilling Program (ODP) and Deep Sea Drilling Project (DSDP) samples is undertaken in order to (1) provide support to shipboard scientists in achieving the scientific objectives of their cruise and to support shore-based investigators who are preparing contributions to ODP reports, (2) provide individual investigators with materials to conduct detailed studies beyond the scope of ODP reports, (3) provide micropaleontological reference centers with samples for reference and comparison purposes, and (4) provide educators with samples for teaching purposes.

Funding for sample-related activities must be secured by the investigator independently of requesting the samples.

The Ocean Drilling Program Curator is responsible for distributing samples and for preserving and conserving core material. The Curator, who may accept advice from chairmen of the appropriate JOIDES advisory panels, is responsible for enforcing the provisions of this Sample-Distribution Policy. He is responsible for maintaining a record of all samples that have been distributed, both on board ship and subsequently from the repositories, indicating the recipients and the nature of investigations proposed. This information is available to interested investigators on request.

Every sample distributed from the ship or from a repository is labeled with a standard identifier, which includes leg number, hole number, core and section numbers, and interval within the section from which the sample was removed. It is imperative that this standard identifier be associated with all data reported in the literature, and that residues of the sample remain labeled throughout their lives, so that later workers can relate the data to the cores.

Distribution of sample materials is made directly from the repositories (Lamont-Doherty Geological Observatory, Scripps Institution of Oceanography, and Texas A&M University) by the Curator or his designated representative.

1. *Distribution of Samples for Research Leading to Contributions to ODP Reports*

Any investigator who wishes to contribute to the reports of a scheduled cruise may write to the Curator, Ocean Drilling Program, 1000 Discovery Drive, College Station, Texas 77845-9547, U.S.A., in order to request samples from that cruise. Requests for a specific cruise must be received by the Curator at least TWO MONTHS in advance of the departure of that cruise, in order to allow time for review of the request in conjunction with other requests, so that a suitable shipboard sampling program can be assembled. The request should include a statement of the nature of the proposed research, the size and approximate number of samples required to complete the study, and any particular sampling technique or equipment which may be required. Requests will be reviewed by the Staff Representative and co-chief scientists of the cruise and by the Curator. Approval/disapproval will be based on the scientific requirements of the cruise as determined by the appropriate JOIDES advisory panel(s). The scope of a request must be such that samples can be processed, that proposed research can be completed, and that the paper can be written in time for submission to the relevant ODP cruise report.

Except for rare, specific instances involving ephemeral properties, the total volume of samples removed during a cruise-related sampling program will not exceed one-quarter of the volume of core recovered, and no interval will be depleted. One-half of all recovered materials will be retained in the archives in as pristine a condition as is practicable. Investigators requesting shipboard samples of igneous materials may receive a maximum of 100 igneous samples per cruise.

Because many sample requests are received for shipboard work and because the time of the shipboard party is at a premium, co-chief scientists are strongly urged to limit shipboard sampling to the minimum necessary to accomplish the cruise objectives. Shore-based investigators whose requests for cruise-related samples are approved should expect that they will receive the samples after the cores are returned to the repository, and should schedule research activities accordingly.

Co-chief scientists may invite investigators who are not cruise participants to perform special studies of selected core samples in direct support of shipboard activities. If this occurs, the names and addresses of these investigators and details of all samples loaned or distributed to them must be forwarded to the Curator, via the ODP Staff Representative to that cruise, immediately after the cruise. These investigators are expected to contribute to the cruise reports as though they had been cruise participants. All requirements of the Sample-Distribution Policy apply.

Any publication of results other than in ODP reports within twelve (12) months of completion of the cruise must be approved and authored by the whole shipboard party and, where appropriate, shore-based investigators. After twelve (12) months, individual investigators may submit related papers for open publication, provided they have already submitted their contributions to ODP reports and had them accepted. Investigations which are not completed in time for inclusion in the ODP reports for a specific cruise may be published in a later edition of the ODP reports; however, they may not appear in another journal until the report for which they were intended has been published.

2. *Distribution of Samples for Research Leading to Publication Outside of the ODP Reports*

A. Researchers who wish to use samples for studies beyond the scope of the ODP reports should obtain sample-request forms from the Curator, Ocean Drilling Program, 1000 Discovery Drive, College Station, Texas 77845-9547, U.S.A. Requestors are required to specify the quantities and intervals of core required, to make a clear statement of the nature of the proposed research, to state the time which will be required to complete the work and to submit results for publication, and to specify funding status and the availability of equipment and space for the research.

Additionally, if the requestor has received samples from ODP or from DSDP previously, he/she will be required to account for the disposition of those samples by citing published works, four (4) copies of which must be sent to the Curator. If no report has been published, this requirement can be fulfilled by sending a brief (two- or three-page) report of the status of the research.

If the requestor has never before received samples from ODP or DSDP, he/she will be required to show that the samples will be used for responsible research. This requirement can be met by providing the Curator with a copy of the requestor's résumé and bibliography. If the requestor is a student working on a higher degree, he/she can meet this requirement by sending a copy of his/her dissertation or research proposal endorsed by the student's advisor.

Unused and residual samples should be returned and data should be sent to the Curator if the project has terminated. Paleontological materials may be returned either to the Curator at ODP or to one of the designated micropaleontological reference centers. If material is returned to a reference center, notify the Curator when it is sent.

Requests for samples from researchers in industrial laboratories will be honored in the same manner as those from academic organizations. Industrial investigators have the same obligations as other investigators to publish all results promptly in the open literature and to provide the Curator with copies of all reports published and of all data acquired in their research.

In order to ensure that all requests for highly desirable but limited samples can be considered together, approval of requests and distribution of samples will be delayed until twelve (12) months after completion of the cruise or two (2) months after official publication of the core descriptions, whichever occurs earlier. The only exceptions to this policy will be made for specific requests involving ephemeral properties. Requests for samples may be based on core descriptions published in ODP reports produced by the shipboard party, copies of which are on file at various institutions throughout the world. Copies of original core logs and data are kept on open file at ODP, and at the repositories at Lamont-Doherty Geological Observatory and Scripps Institution of Oceanography.

---

[1] Revised October 1988.

B. Most investigations can be accomplished handily with sample volumes of 10 mL or less. Investigators must provide explicit justification of requests for larger sample sizes or for frequent intervals within a core. Requests which exceed reasonable size or frequency limits will require more time to process and are unlikely to be granted in their entirety.

Requests for samples from thin layers, from stratigraphically important boundaries, or from sections which are badly depleted or in unusually high demand may be delayed in order to coordinate requests from several investigators or while the Curator seeks advice from the community. Investigators who submit such requests may expect to receive suggestions for alternative sampling programs or for joining with a research consortium which will share the samples. In any event, such exceptional requests will require more time for processing than will more routine requests.

Investigators who wish to study ephemeral properties may request a waiver of the twelve-month waiting period, however, such requests will be referred automatically to the relevant co-chiefs. If such a request is approved, the investigator will join the shore-based contributors to the shipboard science effort, and will incur the obligations thereof (see section 1).

C. Samples will not be provided until the requestor assures the Curator that funding for the proposed research is available or unnecessary. If a sample request is dependent in any way on proposed funding, the Curator is prepared to provide the proposed funding organization with information on the availability (or potential availability) of suitable samples.

D. Investigators who receive samples incur the following obligations:

(1) To publish significant results promptly; however, no contribution may be submitted for publication prior to twelve (12) months following the termination of the relevant leg unless it is approved and authored by the entire shipboard party.

(2) To acknowledge in all publications that the samples were supplied through the assistance of the international Ocean Drilling Program and others as appropriate.

(3) To submit four (4) copies of reprints of all published works to the Curator, Ocean Drilling Program, 1000 Discovery Drive, College Station, Texas 77845-9547, U.S.A. These reprints will be distributed to the repositories and to the ship. All reprints received will be logged in an on-line bibliographic data base.

(4) To submit all final analytical data obtained from the samples to the Data Librarian, Ocean Drilling Program, 1000 Discovery Drive, College Station, Texas 77845-9547, U.S.A. Please consult announcements in the *JOIDES Journal* or call (409-845-2673) for information on acceptable data formats. Investigators should be aware that they may have other data obligations under the National Science Foundation's Ocean Science Data Policy or under relevant policies of other funding agencies which require submission of data to national data centers.

(5) To return all unused or residual samples, in good condition and with a detailed explanation of any processing they may have undergone, upon termination of the proposed research. In particular, all thin sections and smear slides manufactured on board the vessel or in the repositories are to be returned to the Curator. Paleontological materials may be returned either to the Curator at ODP or to one of the designated micropaleontological reference centers.

Failure to honor these obligations will prejudice future applications for samples.

E. Cores are available for examination by interested parties at the repositories. Investigators are welcome to visit the repositories in order to inspect cores and to specify sample locations when that is required for their research; however, time and space in the workrooms are limited, so advance appointments are required. Occasionally, the space may be fully booked several weeks in advance, so investigators are urged to call for appointments well ahead in order to avoid disappointment. Only the Curator or his delegate may actually remove samples from the cores.

F. A reference library of thin sections, smear slides, and archive photographs is maintained in the repositories for the use of visiting investigators. All thin sections and smear slides produced on board the ship or in repositories belong to this library.

3. *Distribution of Samples to Micropaleontological Reference Centers*

As a separate and special category of repository activity, selected samples are distributed to micropaleontological reference centers, where the prepared material may be studied by visitors. Foraminifers, calcareous nannofossils, and diatoms can be viewed; radiolarians will be prepared in the future. The present centers are (1) U.S. East Coast: Lamont-Doherty Geological Observatory, Palisades, NY 10964 (Ms. Rusty Lotti; telephone, 914-359-2900; telex, 7105762653 LAMONTGEO); (2) U.S. National Museum: Smithsonian Institution, Washington, D.C. 20560 (Dr. Martin Buzas; telephone, 202-357-1390; telex, 264729); (3) U.S. Gulf Coast: Texas A&M University, Department of Oceanography, College Station, TX 77843 (Dr. Stefan Gartner; telephone, 409-845-8479; telex, 792779/ODP TAMU); (4) U.S. West Coast: Scripps Institution of Oceanography, La Jolla, CA 92093 (Dr. William Riedel; telephone, 619-534-4386); telex, 910337127 IUC WWD SIOSDG); (5) Western Europe: Natural History Museum, CH-4001 Basel, Switzerland (Mr. J. B. Saunders; telephone, 061-29-55-64); (6) U.S.S.R.: Institute of the Lithosphere, Staromonet 22, Moscow 109180, U.S.S.R. (Dr. Ivan Basov; telephone, 231-48-36); (7) Japan: National Science Museum, Department of Geology, 3-23-1 Hyakunin-cho, Shinjuku-ku, Tokyo 160, Japan (Dr. Y. Tanimura; telephone, 03-364-2311; telemail, 03-364-2316); (8) New Zealand: New Zealand Geological Survey, P.O Box 30368, Lower Hutt, New Zealand (Dr. Tony Edwards; telephone, (04) 699059).

Further details concerning the micropaleontological reference centers are reported periodically in the *JOIDES Journal*.

4. *Distribution of Samples for Educational Purposes*

Samples may be available in limited quantities to college-level educators for teaching purposes. Interested educators should request application forms from the Curator, Ocean Drilling Program, 1000 Discovery Drive, College Station, Texas 77845-9547, U.S.A. Requestors are required to specify preferred sample size and location, to make a very clear statement of the nature of the course work in which the samples will be used, to explain how the samples will be prepared and how they will be used in the classroom, to explain in detail why similar materials derived from outcrops or dredge hauls cannot be used (it is NOT acceptable to argue that it requires less effort for the requestor to obtain samples from ODP than to assemble them from other sources), and to certify that funds are available to prepare the materials for classroom use. In general, only samples of materials which are abundant in the collection and which are in little demand for research purposes should be requested for educational purposes. The Curator will not approve requests for materials which are limited in supply or for which demand (real or potential) is great, including most paleontological materials.

5. *Distribution of Data*

The Deep Sea Drilling Project and the Ocean Drilling Program have routinely captured much of the data generated on board ship and published in Program reports. Additionally, data supplied by investigators who have received samples are incorporated into the data bases, so data sets which are larger than can be published are available to investigators. Magnetic, downhole-logging, seismic-reflection, bathymetric, and other data collected by the drilling vessel become available for distribution to investigators at the same time as core samples.

Requests for ODP and DSDP data should be addressed to the Data Librarian, Ocean Drilling Program, 1000 Discovery Drive, College Station, Texas 77845-9547, U.S.A. Many varieties of DSDP data are included in ODP data bases. Information on sources of DSDP data is available from the ODP Data Librarian.

A charge will be made to recover material expenses greater than $25.00 incurred in filling individual requests. If required, estimates of charges can be furnished before the work is performed.

Drilling locations

Leg	Location	Sites
Phase 1 1968–1970		
1	North Atlantic	1–7
2	North Atlantic	8–12
3	South Atlantic	13–22
4	Central Atlantic	23–31
5	North Pacific	32–43
6	North Pacific	44–60
7	Central Pacific	61–67
8	Central Pacific	68–75
9	Central Pacific	76–84
Phase 2 1970–1972		
10	Gulf of Mexico	85–97
11	North Atlantic	98–108
Re-entry trials		109–110
12	North Atlantic	111–119
13	Mediterranean	120–134
14	Central Atlantic	135–144
15	Caribbean	146–154
16	Central Pacific	155–163
17	Central Pacific	164–171
18	North Pacific	172–182
19	North Pacific	183–193
20	North Pacific	194–202
21	Coral Sea	203–210
22	Indian Ocean	211–218
23	Arabian Sea	219–230
24	Indian Ocean	231–238
25	Indian Ocean	239–249
Phase 3 1972–1975		
26	Indian Ocean	250–258
27	Indian Ocean	259–263
28	Antarctic	264–274
29	Tasman Sea	275–284
30	South Pacific	285–289
31	North Pacific	290–302
32	North Pacific	303–313
33	North Pacific	314–318
34	South Pacific	319–321
35	South Pacific	322–325
36	South Atlantic	326–331
37	North Atlantic	332–335
38	Arctic	336–352
39	Atlantic	353–359
40	South Atlantic	360–365
41	South Atlantic	366–370
42A	Mediterranean	371–378
42B	Black Sea	379–381
43	North Atlantic	382–387
44	North Atlantic	388–392
44A	North Atlantic	393–394
IPOD 1 1975–1983		
45	North Atlantic	395–396
46	North Atlantic	396A–396B
47	North Atlantic	397–398
48	North Atlantic	399–406
49	North Atlantic	407–414
50	North Atlantic	415–416
51A	North Atlantic	417–417A
51B	North Atlantic	417B–417D
52	North Atlantic	417D–418A
53	North Atlantic	418A–418B
54	Central Pacific	419–429
55	North Pacific	430–433
56	North Pacific	434–437
57	North Pacific	438–441
58	North Pacific	442–446
59	North Pacific	447–451
60	North Pacific	452–461
61	Central Pacific	462
62	North Pacific	463–466
63	North Pacific	467–473
64	Gulf of California	474–481
65	Gulf of California	482–485
66	Central Pacific	486–493
67	Central Pacific	494–500
68	Central Pacific	502–503
69	Central Pacific	504–505, 501
70	Central Pacific	506–510, 504B
71	South Atlantic	511–514
72	South Atlantic	515–518
73	South Atlantic	519–524
74	South Atlantic	525–529
75	South Atlantic	530–532
76	North Atlantic	533–534
77	Caribbean	535–540
78	North Atlantic	541–543, 395A, B
79	North Atlantic	544–547
80	North Atlantic	548–551
81	North Atlantic	552–555
82	North Atlantic	556–564
83	Central Pacific	504B
84	Central Pacific	565–570
85	Central Pacific	571–575
86	North Pacific	576–581
87	North Pacific	582–584
88	North Pacific	581
89	Central Pacific	585–586, 462A
90	South Pacific	587–594
91	Central Pacific	595–596
92	Central Pacific	597–602, 504B
93	North Atlantic	603–605
94	North Atlantic	606–611
95	North Atlantic	612–613, 603
96	Gulf of Mexico	614–624

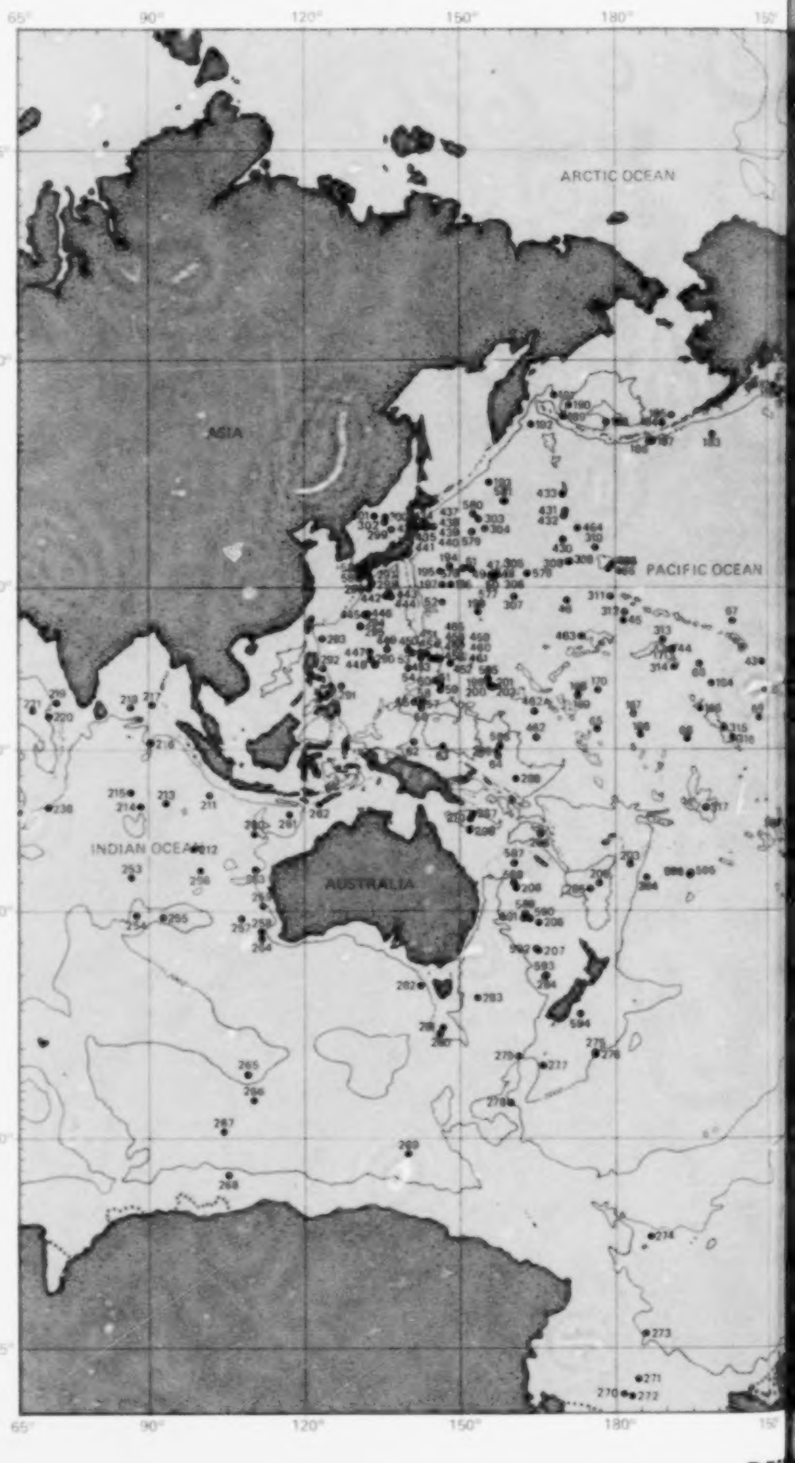

DEE

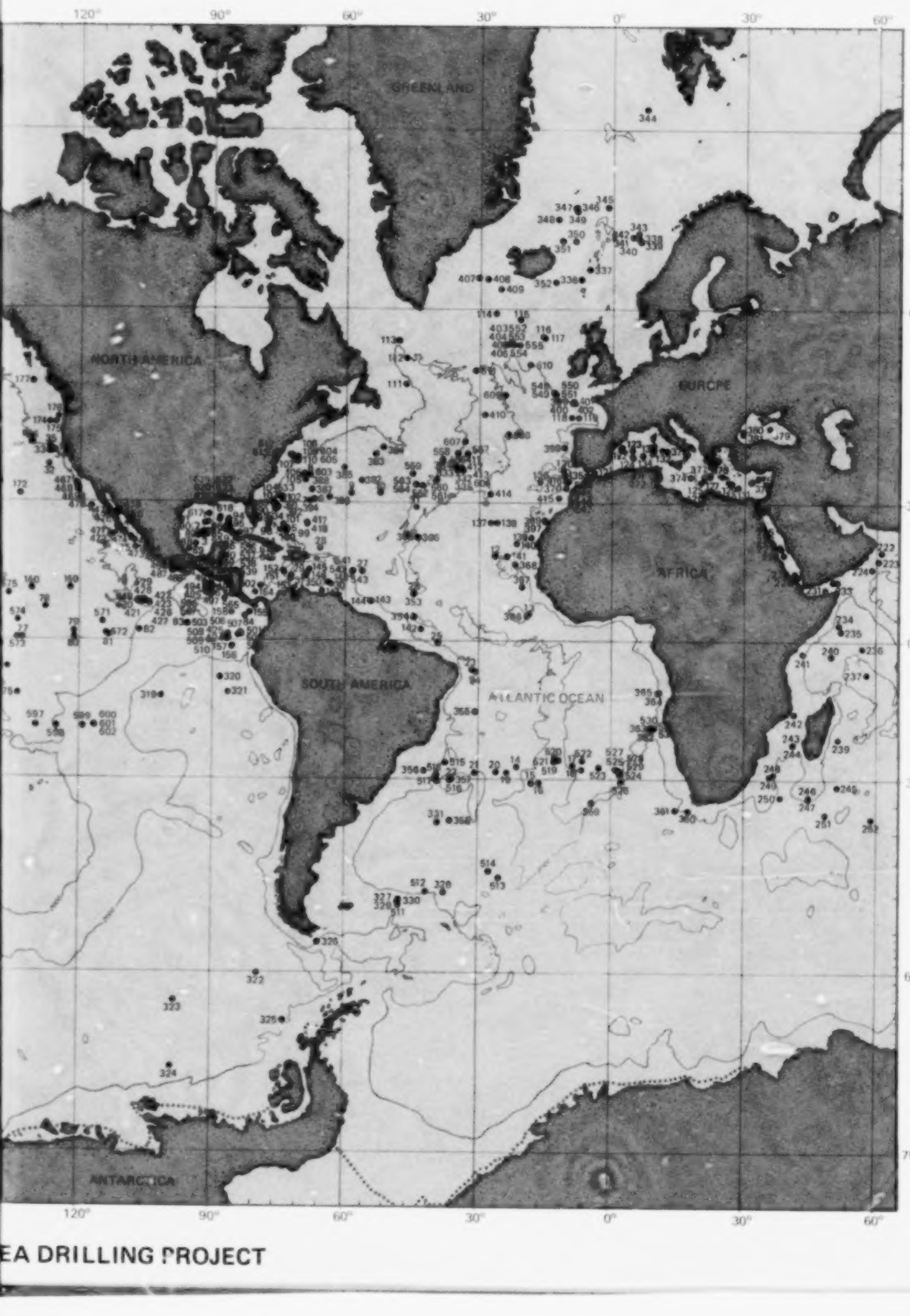
120°
90°
60°
30°
0°
30°
60°
75°
60°
30°
0°
30°
60°
75°
GREENLAND
NORTH AMERICA
EUROPE
AFRICA
SOUTH AMERICA
ATLANTIC OCEAN
ANTARCTICA
344
337
352
338
407
408
409
114
111
410
414
137
138
141
366
367
365
364
356
357
331
358
514
513
512
329
330
326
322
323
325
324
320
321
319
242
243
244
239
249
250
246
247
245
251
252
234
235
236
237
240
241
222
223
224
381
380
597
598
599
600
601
602
571
572
82
81

EA DRILLING PROJECT

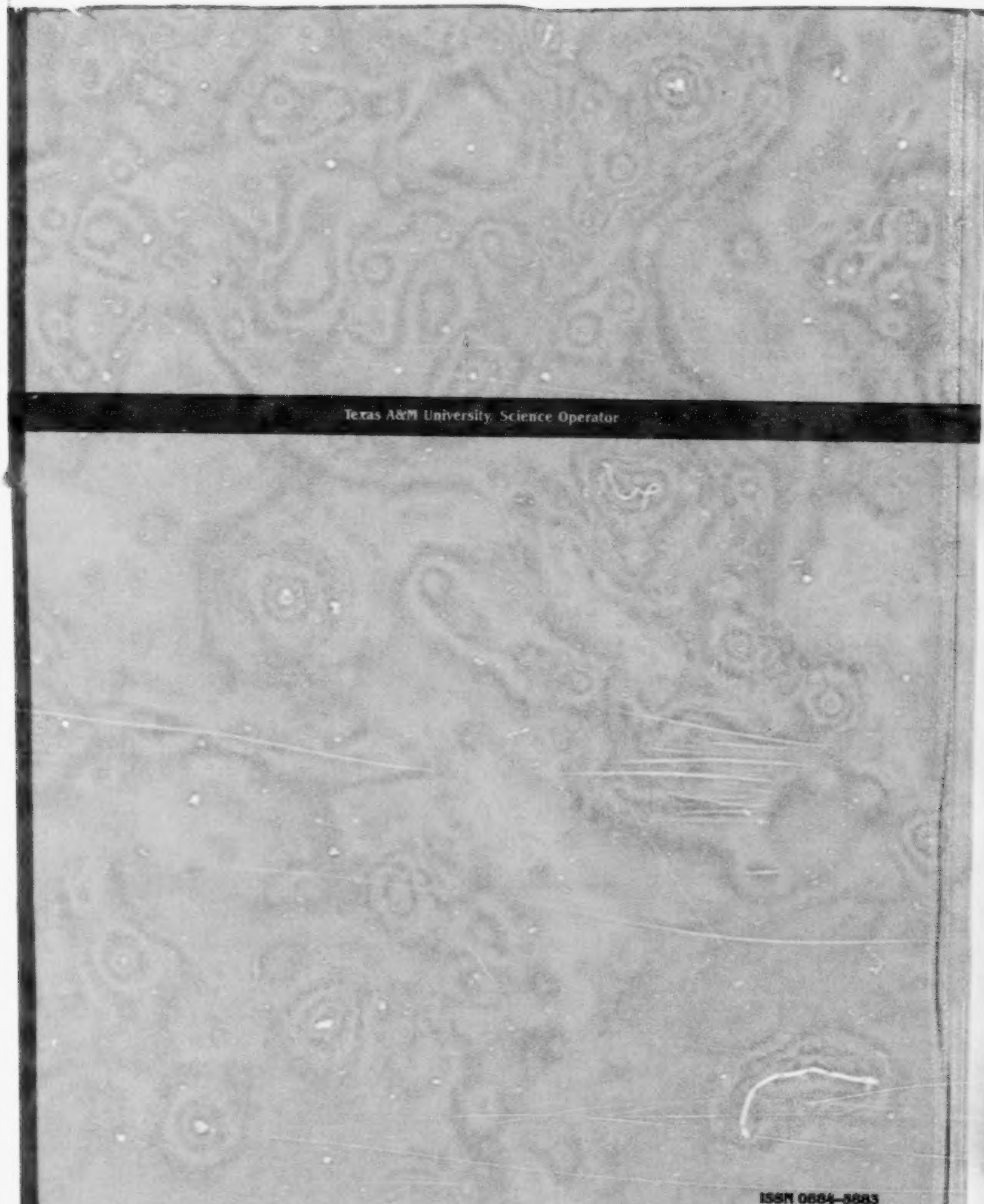

Texas A&M University, Science Operator

ISSN 0884-5883

Table 1. Satellite navigation and course- and speed-change data used to generate the Leg 125 trackline plots shown in Figures 1, 3, 4, 7, 10, 18, 19, 22, 25, and 28.

Date (1989)	Julian day	Time (UTC)	Latitude (N)		Longitude (E)		Distance (nmi)	Actual speed (kt)	Course (degrees)	Comment[a]
			(deg)	(min)	(deg)	(min)				
Feb. 20	51	0230	13	27.10	144	37.02	0.0	9.8	12	GPS
20	51	0330	13	36.70	144	39.05	9.8	11.0	17	GPS
20	51	0400	13	41.97	144	40.67	15.3	10.9	13	GPS
20	51	0430	13	47.28	144	41.96	20.8	11.0	13	GPS
20	51	0500	13	52.63	144	43.26	26.3	11.0	12	GPS
20	51	0512	13	54.80	144	43.70	28.5	11.0	12	c/cs
20	51	0538	13	59.40	144	44.80	33.2	11.0	12	c/cs
20	51	0558	14	3.00	144	45.60	36.9	10.9	12	c/cs
20	51	0600	14	3.40	144	45.66	37.3	10.8	13	GPS
20	51	0613	14	5.70	144	46.20	39.6	11.0	13	c/cs
20	51	0617	14	6.40	144	46.40	40.3	10.9	13	c/cs
20	51	0630	14	8.70	144	46.90	42.7	10.5	14	GPS
20	51	0639	14	10.23	144	47.30	44.3	10.9	15	SF
20	51	0644	14	11.10	144	47.50	45.2	10.9	15	c/cs
20	51	0657	14	13.40	144	48.20	47.6	10.7	16	c/cs
20	51	0700	14	13.90	144	48.34	48.1	10.8	14	GPS
20	51	0710	14	15.60	144	48.80	49.9	10.8	15	c/cs
20	51	0730	14	19.12	144	49.74	53.5	10.9	15	GPS
20	51	0736	14	20.20	144	50.00	54.6	10.9	15	c/cs
20	51	0749	14	22.40	144	50.70	56.9	10.7	15	c/cs
20	51	0759	14	24.20	144	51.10	58.7	11.1	15	c/cs
20	51	0800	14	24.35	144	51.20	58.9	11.0	16	GPS
20	51	0808	14	25.80	144	51.60	60.4	10.7	15	c/cs
20	51	0819	14	27.60	144	52.10	62.3	10.7	18	c/cs
20	51	0830	14	29.51	144	52.75	64.3	10.9	18	GPS
20	51	0849	14	32.80	144	53.90	67.7	11.0	18	c/cs
20	51	0858	14	34.40	144	54.40	69.4	10.9	17	c/cs
20	51	0911	14	36.60	144	55.10	71.7	10.9	18	c/cs
20	51	0917	14	37.70	144	55.50	72.8	11.0	19	c/cs
20	51	0947	14	42.80	144	57.40	78.3	11.0	20	c/cs
20	51	0950	14	43.33	144	57.57	78.9	10.9	24	SF
20	51	1009	14	46.50	144	59.00	82.3	10.1	24	c/cs
20	51	1011	14	46.60	144	59.10	82.7	10.8	23	c/cs
20	51	1041	14	51.80	145	1.30	88.1	10.8	24	c/cs
20	51	1105	14	55.80	145	3.10	92.4	10.9	24	c/cs
20	51	1112	14	56.90	145	3.60	93.7	10.9	23	c/cs
20	51	1113	14	57.10	145	3.70	93.9	10.6	18	SF
20	51	1142	15	1.90	145	5.40	99.0	10.6	20	c/cs
20	51	1210	15	6.60	145	7.10	103.9	10.6	20	c/cs
20	51	1219	15	8.11	145	7.65	105.5	10.3	21	SF
20	51	1230	15	9.90	145	8.30	107.4	10.4	20	c/cs
20	51	1243	15	12.00	145	9.10	109.6	10.1	19	c/cs
20	51	1245	15	12.30	145	9.20	110.0	10.3	19	c/cs
20	51	1301	15	14.92	145	10.16	112.7	10.6	22	SF
20	51	1311	15	16.60	145	10.90	114.5	10.8	22	c/cs
20	51	1323	15	18.60	145	11.70	116.7	10.6	22	c/cs
20	51	1353	15	23.40	145	13.80	122.0	10.6	22	c/cs
20	51	1407	15	25.74	145	14.78	124.4	10.7	17	SF
20	51	1409	15	26.10	145	14.90	124.8	10.6	16	c/cs
20	51	1425	15	28.80	145	15.70	127.6	10.5	17	c/cs
20	51	1431	15	29.80	145	16.00	128.7	10.4	17	c/cs
20	51	1443	15	31.80	145	16.70	130.7	10.6	17	c/cs
20	51	1449	15	32.80	145	17.00	131.8	10.7	17	c/cs
20	51	1459	15	34.50	145	17.60	133.6	10.5	17	c/cs
20	51	1503	15	35.15	145	17.77	134.3	10.5	19	SF
20	51	1510	15	36.30	145	18.20	135.5	10.5	18	c/cs
20	51	1604	15	45.32	145	21.15	145.0	10.8	20	SF
20	51	1629	15	49.50	145	22.80	149.5	10.9	21	c/cs
20	51	1644	15	52.10	145	23.80	152.2	10.9	21	c/cs
20	51	1650	15	53.10	145	24.20	153.3	11.0	21	c/cs
20	51	1718	15	57.90	145	26.10	158.4	11.0	21	c/cs
20	51	1721	15	58.40	145	26.40	158.9	11.0	20	c/cs
20	51	1732	16	0.30	145	27.10	161.0	10.9	20	c/cs
20	51	1744	16	2.30	145	27.90	163.1	10.8	21	c/cs
20	51	1750	16	3.33	145	28.28	164.2	10.7	19	SF
20	51	1750	16	3.30	145	28.30	164.2	10.9	19	c/cs
20	51	1807	16	6.20	145	29.30	167.3	10.8	19	c/cs
20	51	1818	16	8.11	145	30.02	169.3	11.1	17	SF
20	51	1822	16	8.80	145	30.20	170.0	11.0	17	c/cs
20	51	1828	16	9.90	145	30.60	171.1	11.1	17	c/cs
20	51	1841	16	12.20	145	31.30	173.6	11.3	17	c/cs
20	51	1858	16	15.25	145	32.25	176.7	11.0	20	SF
20	51	1907	16	16.80	145	32.80	178.4	11.1	20	c/cs
20	51	1911	16	17.50	145	33.10	179.1	10.9	20	c/cs
20	51	1915	16	18.20	145	33.40	179.9	11.0	20	c/cs

Table 1 (continued).

Date (1989)	Julian day	Time (UTC)	Latitude (N)		Longitude (E)		Distance (nmi)	Actual speed (kt)	Course (degrees)	Comment[a]
			(deg)	(min)	(deg)	(min)				
Feb. 20	51	1925	16	19.90	145	34.00	181.7	10.9	20	c/cs
20	51	1941	16	22.62	145	35.09	184.6	11.2	19	SF
20	51	1952	16	24.60	145	35.80	186.7	11.3	19	c/cs
20	51	1955	16	25.10	145	36.00	187.2	11.1	19	c/cs
20	51	2018	16	29.20	145	37.40	191.5	11.0	19	c/cs
20	51	2037	16	32.50	145	38.50	195.0	10.9	19	c/cs
20	51	2045	16	33.85	145	39.03	196.5	11.3	20	SF
20	51	2057	16	36.00	145	39.90	198.7	11.4	20	c/cs
20	51	2126	16	41.10	145	41.90	204.2	11.4	20	c/cs
20	51	2129	16	41.66	145	42.06	204.8	10.9	19	SF
20	51	2153	16	45.80	145	43.50	209.1	11.3	19	c/cs
20	51	2157	16	46.50	145	43.80	209.9	10.0	18	c/cs
20	51	2159	16	46.80	145	43.90	210.2	11.3	19	c/cs
20	51	2202	16	47.40	145	44.10	210.8	11.0	19	c/cs
20	51	2217	16	50.00	145	45.00	213.5	11.2	18	c/cs
20	51	2221	16	50.70	145	45.20	214.3	11.1	19	c/cs
20	51	2242	16	54.30	145	46.50	218.2	11.0	19	c/cs
20	51	2252	16	56.08	145	47.16	220.0	10.9	21	SF
20	51	2257	16	56.90	145	47.50	220.9	11.1	21	c/cs
20	51	2318	17	0.60	145	49.00	224.6	10.9	21	c/cs
20	51	2330	17	2.59	145	49.78	227.0	10.8	19	GPS
20	51	2336	17	3.60	145	50.10	228.1	10.9	19	c/cs
21	52	0000	17	7.71	145	51.64	232.4	11.1	20	GPS
21	52	0000	17	7.70	145	51.60	232.4	11.1	20	c/cs
21	52	0006	17	8.70	145	52.00	233.5	11.1	19	c/cs
21	52	0017	17	10.67	145	52.75	235.6	10.5	19	SF
21	52	0030	17	12.82	145	53.51	237.8	11.5	19	GPS
21	52	0033	17	13.40	145	53.70	238.4	11.4	20	c/cs
21	52	0035	17	13.72	145	53.84	238.8	10.7	19	SF
21	52	0049	17	16.10	145	54.70	241.3	10.6	19	c/cs
21	52	0100	17	17.91	145	55.39	243.2	10.8	20	GPS
21	52	0108	17	19.30	145	55.90	244.7	10.8	17	c/cs
21	52	0125	17	22.20	145	56.80	247.7	10.7	16	c/cs
21	52	0130	17	23.04	145	57.11	248.6	10.5	17	GPS
21	52	0138	17	24.40	145	57.50	250.0	10.0	18	c/cs
21	52	0148	17	26.00	145	58.10	251.7	10.5	17	c/cs
21	52	0157	17	27.50	145	58.50	253.2	10.3	17	c/cs
21	52	0200	17	27.97	145	58.68	253.8	10.8	20	GPS
21	52	0201	17	28.10	145	58.70	253.9	10.3	0	c/cs
21	52	0205	17	28.83	145	58.75	254.6	9.3	359	SF
21	52	0206	17	29.00	145	58.70	254.8	9.8	358	c/cs
21	52	0209	17	29.50	145	58.70	255.3	9.8	358	c/cs
21	52	0222	17	31.60	145	58.70	257.4	10.5	357	c/cs
21	52	0224	17	31.90	145	58.60	257.7	9.9	358	c/cs
21	52	0230	17	32.94	145	58.61	258.7	10.0	358	GPS
21	52	0230	17	32.90	145	58.60	258.7	10.2	358	c/cs
21	52	0235	17	33.80	145	58.60	259.6	9.6	357	c/cs
21	52	0243	17	35.10	145	58.50	260.9	9.9	357	c/cs
21	52	0252	17	36.50	145	58.40	262.3	9.5	358	c/cs
21	52	0258	17	37.50	145	58.40	263.3	9.4	358	c/cs
21	52	0300	17	37.80	145	58.35	263.6	9.6	2	GPS
21	52	0301	17	38.00	145	58.40	263.8	9.6	354	c/cs
21	52	0307	17	38.90	145	58.20	264.7	9.6	355	c/cs
21	52	0316	17	40.40	145	58.10	266.2	9.6	355	c/cs
21	52	0327	17	42.10	145	57.90	267.9	9.6	355	c/cs
21	52	0330	17	42.59	145	57.90	268.4	10.1	349	GPS
21	52	0335	17	43.40	145	57.70	269.3	10.1	349	c/cs
21	52	0339	17	44.10	145	57.60	269.9	10.1	349	c/cs
21	52	0348	17	45.60	145	57.30	271.5	11.1	348	c/cs
21	52	0400	17	47.73	145	56.80	273.7	10.6	352	GPS
21	52	0402	17	48.10	145	56.70	274.0	9.7	353	c/cs
21	52	0410	17	49.40	145	56.60	275.3	10.6	353	c/cs
21	52	0419	17	50.90	145	56.40	276.9	9.7	354	c/cs
21	52	0424	17	51.80	145	56.30	277.7	10.4	353	c/cs
21	52	0430	17	52.78	145	56.13	278.8	10.1	354	GPS
21	52	0432	17	53.10	145	56.10	279.1	9.8	354	c/cs
21	52	0450	17	56.00	145	55.80	282.0	9.7	353	c/cs
21	52	0500	17	57.65	145	55.54	283.7	9.9	348	GPS
21	52	0502	17	58.00	145	55.50	284.0	9.9	350	c/cs
21	52	0516	18	0.30	145	55.00	286.3	10.2	349	c/cs
21	52	0530	18	2.58	145	54.54	288.7	10.0	349	GPS
21	52	0530	18	2.60	145	54.50	288.7	9.7	350	c/cs
21	52	0538	18	3.90	145	54.30	290.0	9.8	350	c/cs
21	52	0600	18	7.40	145	53.62	293.6	10.5	348	GPS
21	52	0601	18	7.60	145	53.60	293.8	8.8	9	c/cs

Table 1 (continued).

Date (1989)	Julian day	Time (UTC)	Latitude (N)		Longitude (E)		Distance (nmi)	Actual speed (kt)	Course (degrees)	Comment[a]
			(deg)	(min)	(deg)	(min)				
Feb. 21	52	0603	18	7.90	145	53.60	294.0	8.8	33	c/cs
21	52	0616	18	9.50	145	54.70	296.0	8.4	33	c/cs
21	52	0627	18	10.80	145	55.60	297.5	8.6	33	c/cs
21	52	0630	18	11.13	145	55.84	297.9	8.4	31	GPS
21	52	0641	18	12.40	145	56.70	299.5	8.3	31	c/cs
21	52	0653	18	13.90	145	57.60	301.1	8.6	32	c/cs
21	52	0657	18	14.40	145	57.90	301.7	8.4	32	c/cs
21	52	0700	18	14.72	145	58.13	302.1	8.2	32	GPS
21	52	0701	18	14.80	145	58.20	302.3	8.5	30	~~c/cs~~
21	52	0713	18	16.30	145	59.10	304.0	8.4	30	c/cs
21	52	0728	18	18.10	146	0.20	306.1	8.6	31	c/cs
21	52	0730	18	18.35	146	0.38	306.3	8.8	29	GPS
21	52	0733	18	18.70	146	0.60	306.8	8.6	29	c/cs
21	52	0748	18	20.60	146	1.70	308.9	8.4	28	c/cs
21	52	0759	18	22.00	146	2.50	310.5	8.1	28	c/cs
21	52	0800	18	22.11	146	2.53	310.6	8.5	27	GPS
21	52	0806	18	22.90	146	2.90	311.5	8.8	27	c/cs
21	52	0812	18	23.70	146	3.30	312.4	7.8	25	c/cs
21	52	0814	18	23.90	146	3.50	312.6	8.3	26	c/cs
21	52	0817	18	24.30	146	3.70	313.0	8.1	27	c/cs
21	52	0822	18	24.90	146	4.00	313.7	8.4	26	c/cs
21	52	0830	18	25.87	146	4.51	314.8	9.2	26	GPS
21	52	0830	18	25.90	146	4.50	314.8	9.3	27	c/cs
21	52	0838	18	27.00	146	5.10	316.1	9.3	27	c/cs
21	52	0839	18	27.12	146	5.17	316.2	8.5	28	SF
21	52	0855	18	29.10	146	6.30	318.5	8.4	28	c/cs
21	52	0900	18	29.74	146	6.61	319.2	8.5	28	GPS
21	52	0906	18	30.50	146	7.00	320.0	8.1	31	c/cs
21	52	0914	18	31.40	146	7.60	321.1	8.4	31	c/cs
21	52	0929	18	33.21	146	8.77	323.2	8.3	34	SF
21	52	0930	18	33.30	146	8.90	323.3	8.1	33	c/cs
21	52	0940	18	34.50	146	9.60	324.7	7.5	34	c/cs
21	52	0948	18	35.30	146	10.20	325.7	8.3	33	c/cs
21	52	0958	18	36.40	146	11.00	327.1	7.9	34	c/cs
21	52	1005	18	37.20	146	11.60	328.0	8.0	37	c/cs
21	52	1017	18	38.50	146	12.60	329.6	8.0	37	c/cs
21	52	1024	18	39.20	146	13.20	330.5	8.4	37	c/cs
21	52	1046	18	41.70	146	15.10	333.6	8.4	37	c/cs
21	52	1051	18	42.28	146	15.57	334.3	8.3	35	SF
21	52	1057	18	43.00	146	16.10	335.2	0.9	255	c/cs
21	52	1058	18	43.00	146	16.10	335.2	7.4	37	c/cs
21	52	1100	18	43.20	145	16.20	335.4	8.1	35	c/cs
21	52	1120	18	45.40	146	17.90	338.1	8.3	35	c/cs
21	52	1124	18	45.80	146	18.20	338.7	8.0	35	c/cs
21	52	1135	18	47.00	146	19.10	340.2	8.0	36	c/cs
21	52	1140	18	47.60	146	19.50	340.8	7.4	37	c/cs
21	52	1142	18	47.80	146	19.70	341.1	8.2	35	c/cs
21	52	1151	18	48.76	146	20.42	342.3	8.2	37	SF
21	52	1155	18	49.20	146	20.80	342.8	8.0	39	c/cs
21	52	1212	18	51.00	146	22.30	345.1	8.5	37	c/cs
21	52	1229	18	52.90	146	23.80	347.5	8.3	37	c/cs
21	52	1239	18	53.98	146	24.70	348.9	8.1	36	SF
21	52	1249	18	55.10	146	25.50	350.3	7.6	38	c/cs
21	52	1252	18	55.40	146	25.80	350.6	7.5	35	c/cs
21	52	1303	18	56.50	146	26.60	352.0	8.1	36	c/cs
21	52	1308	18	57.00	146	27.00	352.7	8.1	37	c/cs
21	52	1321	18	58.50	146	28.20	354.5	8.5	37	c/cs
21	52	1326	18	59.00	146	28.60	355.2	8.3	37	c/cs
21	52	1337	19	0.20	146	29.60	356.7	8.5	36	c/cs
21	52	1339	19	0.47	146	29.76	357.0	8.9	39	SF
21	52	1342	19	0.80	146	30.10	357.4	8.6	39	c/cs
21	52	1349	19	1.60	146	30.70	358.4	9.2	39	c/cs
21	52	1355	19	2.32	146	31.32	359.3	9.5	34	SF
21	52	1358	19	2.70	146	31.60	359.8	8.7	33	c/cs
21	52	1404	19	3.40	146	32.10	360.7	8.5	37	c/cs
21	52	1416	19	4.80	146	33.20	362.4	8.4	39	c/cs
21	52	1423	19	5.60	146	33.80	363.4	8.1	39	c/cs
21	52	1430	19	6.30	146	34.50	364.3	8.4	39	c/cs
21	52	1440	19	7.40	146	35.40	365.7	8.2	39	c/cs
21	52	1448	19	8.30	146	36.10	366.8	7.3	38	c/cs
21	52	1457	19	9.10	146	36.80	367.9	7.6	38	c/cs
21	52	1518	19	11.22	146	38.57	370.6	6.7	51	SF
21	52	1518	19	11.20	146	38.60	370.6	6.2	41	c/cs
21	52	1519	19	11.30	146	38.60	370.7	5.9	38	c/cs
21	52	1520	19	11.40	146	38.70	270.8	4.0	347	c/cs

Table 1 (continued).

Date (1989)		Julian day	Time (UTC)	Latitude (N)		Longitude (E)		Distance (nmi)	Actual speed (kt)	Course (degrees)	Comment[a]
				(deg)	(min)	(deg)	(min)				
Feb.	21	52	1550	19	13.30	146	38.20	372.8	6.8	352	c/cs
	21	52	1600	19	14.40	146	38.10	373.9	6.9	352	c/cs
	21	52	1603	19	14.76	146	38.02	374.2	6.8	0	SF
	21	52	1630	19	17.80	146	38.00	377.3	6.8	16	c/cs
	21	52	1700	19	21.10	146	39.10	380.7	6.7	14	c/cs
	21	52	1705	19	21.62	146	39.21	381.2	6.5	357	SF
	21	52	1800	19	27.60	146	38.90	387.2	3.6	353	c/cs
	21	52	1822	19	28.85	146	38.75	388.5	4.8	4	SF
	21	52	1830	19	29.50	146	38.80	389.1	4.7	7	c/cs
	21	52	1842	19	30.40	146	38.90	390.1	5.4	2	c/cs
	21	52	1856	19	31.70	146	39.00	391.3	5.0	2	c/cs
	21	52	1900	19	32.02	146	38.98	391.7	4.7	360	SF
	21	52	1913	19	33.00	146	39.00	392.7	5.1	1	c/cs
	21	52	1928	19	34.30	146	39.00	394.0	4.6	5	c/cs
	21	52	1930	19	34.47	146	39.01	394.1	5.7	5	GPS
	21	52	1931	19	34.60	146	39.00	394.2	4.8	21	c/cs
	21	52	1933	19	34.70	146	39.10	394.4	5.5	346	c/cs
	21	52	1934	19	34.80	146	39.10	394.5	8.0	320	c/cs
	21	52	1935	19	34.90	146	39.00	394.6	9.1	300	c/cs
	21	52	1936	19	35.00	146	38.80	394.8	9.0	274	c/cs
	21	52	1937	19	35.00	146	38.70	394.9	9.3	256	c/cs
	21	52	1941	19	34.80	146	38.00	395.5	7.2	158	c/cs
	21	52	1946	19	34.30	146	38.30	396.1	6.7	156	c/cs
	21	52	1955	19	33.40	146	38.70	397.1	7.0	163	c/cs
	21	52	1956	19	33.30	146	38.70	397.2	6.2	150	c/cs
	21	52	2002	19	32.70	146	39.10	397.9	7.0	162	c/cs
	21	52	2009	19	31.95	146	39.32	398.7	5.9	160	SF
	21	52	2012	19	31.70	146	39.40	399.0	6.4	165	c/cs
	21	52	2029	19	29.93	146	39.93	400.8	3.3	157	778
	21	52	2029	19	29.90	146	39.90	400.8	3.1	155	c/cs
	21	52	2042	19	29.30	146	40.20	401.5	2.3	335	c/cs
	21	52	2100	19	29.93	146	39.93	402.1	2.0	155	778
	21	52	2100	19	29.90	146	39.90	402.1	0.0	90	c/cs
	24	55	0924	19	29.93	146	39.93	402.1	0.4	64	778
	24	55	1400	19	30.74	146	41.72	404.0	0.0	90	779A
	24	55	1700	19	30.74	146	41.72	404.0	0.0	90	779A
	27	58	2300	19	30.74	146	41.72	404.0	0.0	90	779B
March	03	62	1400	19	30.74	146	41.72	404.0	0.0	180	779B
	03	62	1715	19	30.72	146	41.72	404.0	0.7	338	779B
	03	62	1800	19	31.20	146	41.50	404.5	5.9	12	c/cs
	03	62	1830	19	34.10	146	42.20	407.5	7.3	249	c/cs
	03	62	1857	19	32.90	146	38.90	410.8	0.6	311	c/cs
	03	62	1902	19	32.90	146	38.90	410.8	5.6	235	c/cs
	03	62	1905	19	32.78	146	38.65	411.1	5.7	234	SF
	03	62	1925	19	31.70	146	37.00	413.0	5.5	237	c/cs
	03	62	1931	19	31.40	146	36.50	413.5	5.3	234	c/cs
	03	62	1936	19	31.10	146	36.20	414.0	5.4	238	c/cs
	03	62	1937	19	31.05	146	36.07	414.1	5.6	235	SF
	03	62	1946	19	30.60	146	35.30	414.9	5.5	232	c/cs
	03	62	1952	19	30.20	146	34.90	415.5	6.0	240	c/cs
	03	62	1959	19	29.90	146	34.20	416.2	5.9	242	c/cs
	03	62	2004	19	29.70	146	33.80	416.7	6.1	246	c/cs
	03	62	2015	19	29.20	146	32.70	417.8	5.9	243	c/cs
	03	62	2037	19	28.20	146	30.60	420.0	5.6	197	c/cs
	03	62	2038	19	28.10	146	30.60	420.0	5.7	159	c/cs
	03	62	2039	19	28.00	146	30.60	420.1	3.9	120	c/cs
	03	62	2041	19	28.00	146	30.80	420.3	3.3	63	c/cs
	03	62	2044	19	28.00	146	30.90	420.4	4.6	52	c/cs
	03	62	2053	19	28.46	146	31.50	421.1	3.9	47	SF
	03	62	2054	19	28.50	146	31.60	421.2	3.9	47	c/cs
	03	62	2102	19	28.90	146	32.00	421.7	3.5	47	c/cs
	03	62	2106	19	29.00	146	32.10	422.0	4.3	49	c/cs
	03	62	2112	19	29.30	146	32.50	422.4	4.9	60	c/cs
	03	62	2124	19	29.80	146	33.40	423.4	4.9	62	c/cs
	03	62	2139	19	30.40	146	34.50	424.6	4.7	61	c/cs
	03	62	2145	19	30.60	146	35.00	425.1	4.9	62	c/cs
	03	62	2200	19	31.18	146	36.11	426.3	5.6	63	GPS
	03	62	2204	19	31.35	146	36.46	426.7	5.3	61	GPS
	03	62	2204	19	31.30	146	36.50	426.7	4.6	62	c/cs
	03	62	2209	19	31.53	146	36.82	427.0	4.4	66	GPS
	03	62	2211	19	31.60	146	37.00	427.2	4.6	75	c/cs
	03	62	2214	19	31.65	146	37.20	427.4	5.2	75	GPS
	03	62	2218	19	31.70	146	37.60	427.8	5.0	74	c/cs
	03	62	2219	19	31.76	146	37.64	427.8	4.9	76	GPS
	03	62	2224	19	31.86	146	38.06	428.3	4.0	74	GPS

Table 1 (continued).

Date (1989)	Julian day	Time (UTC)	Latitude (N)		Longitude (E)		Distance (nmi)	Actual speed (kt)	Course (degrees)	Comment[a]
			(deg)	(min)	(deg)	(min)				
March 03	62	2227	19	31.90	146	38.30	428.5	4.2	61	c/cs
03	62	2230	19	32.02	146	38.46	428.7	4.3	56	GPS
03	62	2233	19	32.10	146	38.70	428.9	4.1	54	c/cs
03	62	2234	19	32.18	146	38.71	429.0	3.8	53	GPS
03	62	2239	19	32.37	146	38.98	429.3	4.1	53	GPS
03	62	2242	19	32.50	146	39.20	429.5	3.5	58	c/cs
03	62	2244	19	32.60	146	39.30	429.6	4.2	59	c/cs
03	62	2245	19	32.59	146	39.32	429.7	5.3	67	780A
03	62	2245	19	32.60	146	39.30	429.7	0.0	236	c/cs
04	63	0845	19	32.54	146	39.24	429.8	0.0	56	780A
04	63	1830	19	32.59	146	39.32	429.8	0.0	90	780A
05	64	0530	19	32.59	146	39.32	429.8	0.0	90	780B
05	64	1900	19	32.59	146	39.32	429.8	0.0	90	780B
05	64	1901	19	32.59	146	39.32	429.8	0.0	90	780C
08	67	1830	19	32.59	146	39.32	429.8	0.0	90	780C
09	68	0100	19	32.59	146	39.32	429.8	0.0	90	780D
10	69	1345	19	32.59	146	39.32	429.8	0.9	218	780D
10	69	1415	19	32.20	146	39.00	430.3	6.3	306	c/cs
10	69	1436	19	33.50	146	37.10	432.5	6.3	306	c/cs
10	69	1447	19	34.20	146	36.10	433.6	6.2	306	c/cs
10	69	1501	19	35.00	146	34.90	435.1	6.0	305	c/cs
10	69	1507	19	35.40	146	34.40	435.7	6.2	306	c/cs
10	69	1519	19	36.10	146	33.30	436.9	4.5	333	c/cs
10	69	1521	19	36.20	146	33.20	437.1	4.1	16	c/cs
10	69	1523	19	36.40	146	33.30	437.2	4.4	49	c/cs
10	69	1527	19	36.60	146	33.50	437.5	4.9	53	c/cs
10	69	1551	19	37.70	146	35.20	439.5	4.8	53	c/cs
10	69	1605	19	38.40	146	36.20	440.6	5.1	53	c/cs
10	69	1621	19	39.20	146	37.30	442.0	4.8	55	c/cs
10	69	1627	19	39.50	146	37.70	442.5	5.0	47	c/cs
10	69	1630	19	39.70	146	37.90	442.7	4.6	360	c/cs
10	69	1632	19	39.80	146	37.90	442.9	5.8	329	c/cs
10	69	1638	19	40.30	146	37.60	443.4	6.7	315	c/cs
10	69	1645	19	40.90	146	37.00	444.2	7.0	290	c/cs
10	69	1647	19	41.00	146	36.80	444.5	7.3	259	c/cs
10	69	1648	19	40.90	146	36.70	444.6	7.1	231	c/cs
10	69	1652	19	40.60	146	36.30	445.1	7.2	229	c/cs
10	69	1702	19	39.90	146	35.30	446.3	6.9	231	c/cs
10	69	1712	19	39.10	146	34.40	447.4	6.8	235	c/cs
10	69	1717	19	38.80	146	33.86	448.0	7.1	234	SF
10	69	1730	19	37.88	146	32.54	449.5	1.4	247	781
10	69	1731	19	37.90	146	32.50	449.5	1.4	235	c/cs
10	69	1738	19	37.80	146	32.40	449.7	1.6	223	c/cs
10	69	1805	19	37.30	146	31.90	450.4	3.9	327	c/cs
10	69	1810	19	37.50	146	31.70	450.7	2.8	284	c/cs
10	69	1811	19	37.50	146	31.60	450.8	2.2	200	c/cs
10	69	1812	19	37.50	146	31.60	450.8	3.2	151	c/cs
10	69	1814	19	37.40	146	31.70	450.9	8.9	73	c/cs
10	69	1816	19	37.50	146	32.00	451.2	10.0	54	c/cs
10	69	1820	19	37.88	146	32.54	451.9	5.4	53	781
10	69	1820	19	37.90	146	32.50	451.9	0.0	90	c/cs
13	72	0900	19	37.88	146	32.54	451.9	1.3	35	781
13	72	0940	19	38.60	146	33.10	452.8	5.0	171	c/cs
13	72	0957	19	37.20	146	33.30	454.2	6.6	333	c/cs
13	72	1000	19	37.51	146	33.15	454.5	5.3	337	GDRT
13	72	1007	19	38.10	146	32.90	455.1	4.0	311	c/cs
13	72	1009	19	38.20	146	32.80	455.3	3.9	273	c/cs
13	72	1014	19	38.20	146	32.40	455.6	4.2	263	c/cs
13	72	1029	19	38.10	146	31.30	456.7	4.2	266	c/cs
13	72	1044	19	38.00	146	30.20	457.7	4.3	266	c/cs
13	72	1055	19	37.90	146	29.40	458.5	4.4	289	c/cs
13	72	1100	19	38.05	146	29.03	458.9	5.5	282	GDRT
13	72	1101	19	38.10	146	28.90	458.9	5.4	342	c/cs
13	72	1111	19	38.90	146	28.60	459.8	7.7	339	c/cs
13	72	1115	19	39.40	146	28.50	460.3	9.5	338	c/cs
13	72	1130	19	41.60	146	27.50	462.7	10.2	338	c/cs
13	72	1140	19	43.20	146	26.80	464.4	10.5	338	c/cs
13	72	1200	19	46.40	146	25.39	467.9	11.2	329	GDRT
13	72	1200	19	46.40	146	25.40	467.9	11.2	330	c/cs
13	72	1211	19	48.20	146	24.30	470.0	10.7	331	c/cs
13	72	1214	19	48.70	146	24.00	470.5	11.2	330	c/cs
13	72	1244	19	53.50	146	21.10	476.1	11.5	330	c/cs
13	72	1314	19	58.50	146	18.00	481.9	11.8	331	c/cs
13	72	1316	19	58.80	146	17.80	482.3	11.5	331	c/cs
13	72	1340	20	2.80	146	15.40	486.8	11.5	331	c/cs

Table 1 (continued).

Date (1989)	Julian day	Time (UTC)	Latitude (N)		Longitude (E)		Distance (nmi)	Actual speed (kt)	Course (degrees)	Comment[a]
			(deg)	(min)	(deg)	(min)				
March 13	72	1343	20	3.32	146	15.08	487.4	11.8	329	SF
13	72	1349	20	4.30	146	14.40	488.6	11.4	329	c/cs
13	72	1407	20	7.30	146	12.60	492.0	11.5	329	c/cs
13	72	1411	20	7.90	146	12.10	492.8	11.9	327	c/cs
13	72	1422	20	9.80	146	10.90	495.0	11.9	327	c/cs
13	72	1434	20	11.80	146	9.50	497.4	11.9	327	c/cs
13	72	1445	20	13.59	146	8.24	499.5	11.2	331	SF
13	72	1455	20	15.20	146	7.30	501.4	11.2	332	c/cs
13	72	1508	20	17.40	146	6.10	503.8	11.3	333	c/cs
13	72	1525	20	20.20	146	4.50	507.0	11.1	332	c/cs
13	72	1537	20	22.20	146	3.40	509.2	11.4	332	c/cs
13	72	1540	20	22.66	146	3.10	509.8	11.7	334	SF
13	72	1542	20	23.00	146	2.90	510.2	11.4	334	c/cs
13	72	1556	20	25.40	146	1.70	512.9	11.6	335	c/cs
13	72	1603	20	26.60	146	1.10	514.2	11.6	335	c/cs
13	72	1610	20	27.90	146	0.50	515.6	11.7	335	c/cs
13	72	1617	20	29.10	145	59.90	516.9	11.5	335	c/cs
13	72	1631	20	31.56	145	58.70	519.6	12.1	338	SF
13	72	1631	20	31.60	145	58.70	519.6	12.2	338	c/cs
13	72	1659	20	36.80	145	56.40	525.3	12.3	339	c/cs
13	72	1728	20	42.36	145	54.06	531.3	12.3	335	SF
13	72	1729	20	42.50	145	54.00	531.5	12.2	336	c/cs
13	72	1744	20	45.30	145	52.60	534.5	12.4	336	c/cs
13	72	1757	20	47.80	145	51.50	537.2	12.4	337	c/cs
13	72	1817	20	51.60	145	49.80	541.3	12.2	338	c/cs
13	72	1833	20	54.60	145	48.50	544.6	12.4	338	c/cs
13	72	1852	20	58.27	145	46.89	548.5	11.1	338	SF
13	72	1903	21	0.10	145	46.10	550.6	11.1	338	c/cs
13	72	1905	21	0.49	145	45.91	550.9	11.8	337	SF
13	72	1933	21	5.60	145	43.60	556.4	11.9	336	c/cs
13	72	1950	21	8.70	145	42.10	559.8	12.0	335	c/cs
13	72	1955	21	9.60	145	41.70	560.8	11.9	335	c/cs
13	72	2021	21	14.20	145	39.40	566.0	11.9	335	c/cs
13	72	2038	21	17.30	145	37.90	569.3	12.0	335	c/cs
13	72	2040	21	17.66	145	37.67	569.7	12.0	338	SF
13	72	2048	21	19.10	145	37.00	571.3	10.9	338	c/cs
13	72	2050	21	19.50	145	36.90	571.7	12.0	338	c/cs
13	72	2056	21	20.60	145	36.40	572.9	11.1	338	c/cs
13	72	2059	21	21.10	145	36.20	573.4	12.0	338	c/cs
13	72	2105	21	22.20	145	35.70	574.6	11.8	338	c/cs
13	72	2113	21	23.70	145	35.10	576.2	11.8	338	c/cs
13	72	2137	21	28.10	145	33.20	581.0	11.9	338	c/cs
13	72	2156	21	31.60	145	31.70	584.7	11.8	337	c/cs
13	72	2200	21	32.28	145	31.34	585.5	12.1	338	GPS
13	72	2206	21	33.40	145	30.85	586.7	11.8	341	GPS
13	72	2207	21	33.60	145	30.80	586.9	11.8	341	c/cs
13	72	2211	21	34.33	145	30.50	587.7	11.9	338	GPS
13	72	2216	21	35.25	145	30.10	588.7	11.9	338	GPS
13	72	2218	21	35.60	145	29.90	589.1	11.9	338	c/cs
13	72	2221	21	36.17	145	29.70	589.7	12.1	337	GPS
13	72	2226	21	37.10	145	29.28	590.7	11.1	336	GPS
13	72	2229	21	37.60	145	29.00	591.2	11.2	336	c/cs
13	72	2230	21	37.78	145	28.96	591.4	12.6	335	GPS
13	72	2236	21	38.92	145	28.39	592.7	12.1	336	GPS
13	72	2241	21	39.84	145	27.95	593.7	12.2	336	GPS
13	72	2246	21	40.77	145	27.50	594.7	12.4	336	GPS
13	72	2248	21	41.10	145	27.30	595.1	12.3	336	c/cs
13	72	2251	21	41.71	145	27.05	595.7	12.0	337	GPS
13	72	2300	21	43.37	145	26.30	597.5	12.8	337	GPS
13	72	2306	21	44.55	145	25.77	598.8	12.4	337	GPS
13	72	2307	21	44.70	145	25.70	599.0	12.3	337	c/cs
13	72	2311	21	45.50	145	25.34	599.9	12.4	337	GPS
13	72	2316	21	46.45	145	24.91	600.9	12.3	337	GPS
13	72	2321	21	47.39	145	24.47	601.9	12.3	337	GPS
13	72	2326	21	48.33	145	24.04	602.9	11.3	337	GPS
13	72	2326	21	48.30	145	24.00	602.9	11.4	337	c/cs
13	72	2330	21	49.03	145	23.72	603.7	12.9	337	GPS
13	72	2336	21	50.22	145	23.18	605.0	11.8	338	GPS
13	72	2347	21	52.22	145	22.31	607.1	12.1	339	GPS
13	72	2352	21	53.20	145	21.90	608.1	12.0	339	c/cs
14	73	0000	21	54.65	145	21.31	609.7	11.8	339	GPS
14	73	0000	21	54.70	145	21.30	609.7	11.8	339	c/cs
14	73	0006	21	55.80	145	20.90	610.9	12.1	339	c/cs
14	73	0009	21	56.30	145	20.60	611.5	11.9	339	c/cs
14	73	0030	22	0.21	145	19.02	615.7	12.0	340	GPS

Table 1 (continued).

Date (1989)	Julian day	Time (UTC)	Latitude (N)		Longitude (E)		Distance (nmi)	Actual speed (kt)	Course (degrees)	Comment[a]
			(deg)	(min)	(deg)	(min)				
March 14	73	0034	22	1.00	145	18.70	616.5	11.9	340	c/cs
14	73	0054	22	4.70	145	17.30	620.5	12.0	340	c/cs
14	73	0100	22	5.83	145	16.81	621.7	11.8	340	GPS
14	73	0101	22	6.00	145	16.70	621.9	11.7	337	c/cs
14	73	0117	22	8.89	145	15.42	625.0	11.8	336	GPS
14	73	0117	22	8.90	145	15.40	625.0	11.7	337	c/cs
14	73	0130	22	11.23	145	14.34	627.5	11.9	337	GPS
14	73	0147	22	14.30	145	12.90	630.9	11.8	337	c/cs
14	73	0200	22	16.69	145	11.87	633.5	12.2	339	GPS
14	73	0207	22	18.00	145	11.30	634.9	1.1	355	c/cs
14	73	0208	22	18.00	145	11.30	634.9	12.1	339	c/cs
14	73	0213	22	19.00	145	10.90	635.9	12.1	338	c/cs
14	73	0230	22	22.14	145	9.50	639.3	11.7	338	GPS
14	73	0234	22	22.90	145	9.20	640.1	11.8	339	c/cs
14	73	0247	22	25.26	145	8.20	642.7	11.8	340	GPS
14	73	0300	22	27.67	145	7.25	645.2	11.6	340	GPS
14	73	0301	22	27.90	145	7.20	645.4	11.9	340	c/cs
14	73	0305	22	28.60	145	6.90	646.2	11.7	340	c/cs
14	73	0330	22	33.16	145	5.05	651.1	11.7	341	GPS
14	73	0334	22	33.90	145	4.80	651.9	11.4	341	c/cs
14	73	0337	22	34.40	145	4.60	652.4	11.7	340	c/cs
14	73	0347	22	36.27	145	3.85	654.4	11.7	341	GPS
14	73	0400	22	38.67	145	2.97	656.9	11.8	342	GPS
14	73	0405	22	39.60	145	2.60	657.9	11.8	341	c/cs
14	73	0430	22	44.26	145	0.88	662.8	12.1	341	GPS
14	73	0435	22	45.20	145	0.50	663.9	12.0	342	c/cs
14	73	0442	22	46.50	145	0.10	665.2	12.0	341	c/cs
14	73	0455	22	49.00	144	59.10	667.9	11.7	341	c/cs
14	73	0500	22	49.93	144	58.80	668.8	11.9	341	GPS
14	73	0509	22	51.60	144	58.20	670.6	12.2	339	c/cs
14	73	0517	22	53.13	144	57.51	672.2	11.8	338	GPS
14	73	0529	22	55.30	144	56.50	674.6	11.9	339	c/cs
14	73	0530	22	55.50	144	56.47	674.8	11.8	339	GPS
14	73	0534	22	56.20	144	56.20	675.6	11.7	339	c/cs
14	73	0547	22	58.59	144	55.16	678.1	11.5	339	GPS
14	73	0551	22	59.30	144	54.90	678.9	11.6	339	c/cs
14	73	0600	23	0.92	144	54.18	680.6	11.8	338	GPS
14	73	0602	23	1.30	144	54.00	681.0	11.7	334	c/cs
14	73	0621	23	4.60	144	52.30	684.7	11.6	334	c/cs
14	73	0630	23	6.18	144	51.44	686.4	11.6	332	GPS
14	73	0654	23	10.26	144	49.08	691.1	11.5	331	SF
14	73	0700	23	11.26	144	48.47	692.2	11.7	329	GPS
14	73	0717	23	14.08	144	46.59	695.5	11.8	328	GPS
14	73	0730	23	16.25	144	45.11	698.1	11.9	329	GPS
14	73	0800	23	21.36	144	41.78	704.0	12.2	327	GPS
14	73	0813	23	23.60	144	40.20	706.7	12.4	327	c/cs
14	73	0817	23	24.30	144	39.70	707.5	12.7	326	c/cs
14	73	0840	23	28.30	144	36.70	712.4	12.5	326	c/cs
14	73	0842	23	28.64	144	36.47	712.8	11.7	331	SF
14	73	0910	23	33.40	144	33.60	718.3	11.9	331	c/cs
14	73	0916	23	34.50	144	33.00	719.4	11.5	332	c/cs
14	73	0920	23	35.20	144	32.60	720.2	11.6	331	c/cs
14	73	0950	23	40.20	144	29.60	726.0	11.6	331	c/cs
14	73	0957	23	41.40	144	28.90	727.4	11.7	331	c/cs
14	73	1004	23	42.63	144	28.16	728.7	12.4	328	SF
14	73	1015	23	44.50	144	26.80	731.0	3.5	325	c/cs
14	73	1016	23	44.60	144	26.80	731.1	12.3	329	c/cs
14	73	1033	23	47.60	144	24.80	734.5	12.3	328	c/cs
14	73	1103	23	52.80	144	21.20	740.7	12.4	328	c/cs
14	73	1119	23	55.54	144	19.29	744.0	11.8	325	SF
14	73	1119	23	55.50	144	19.30	744.0	11.8	325	c/cs
14	73	1139	23	58.80	144	16.80	747.9	11.9	326	c/cs
14	73	1149	24	0.40	144	15.60	749.9	11.9	326	c/cs
14	73	1153	24	1.05	144	15.11	750.7	11.6	332	SF
14	73	1219	24	5.50	144	12.50	755.7	11.6	332	c/cs
14	73	1249	24	10.60	144	9.50	761.5	11.6	331	c/cs
14	73	1306	24	13.45	144	7.70	764.8	11.6	329	SF
14	73	1314	24	14.80	144	6.80	766.4	11.7	329	c/cs
14	73	1320	24	15.80	144	6.20	767.5	11.6	329	c/cs
14	73	1343	24	19.60	144	3.60	772.0	11.6	330	c/cs
14	73	1359	24	22.25	144	1.91	775.1	11.0	332	SF
14	73	1404	24	23.10	144	1.40	776.0	10.9	331	c/cs
14	73	1434	24	27.90	143	58.60	781.5	10.9	331	c/cs
14	73	1504	24	32.60	143	55.70	786.9	10.9	332	c/cs
14	73	1516	24	34.56	143	54.58	789.1	11.8	336	SF

Table 1 (continued).

Date (1989)	Julian day	Time (UTC)	Latitude (N)		Longitude (E)		Distance (nmi)	Actual speed (kt)	Course (degrees)	Comment[a]
			(deg)	(min)	(deg)	(min)				
March 14	73	1525	24	36.20	143	53.80	790.8	11.9	336	c/cs
14	73	1543	24	39.40	143	52.20	794.4	11.8	335	c/cs
14	73	1546	24	39.95	143	51.89	795.0	11.4	331	SF
14	73	1607	24	43.40	143	49.70	799.0	11.4	330	c/cs
14	73	1632	24	47.50	143	47.10	803.7	11.4	330	c/cs
14	73	1641	24	49.00	143	46.17	805.4	11.3	328	SF
14	73	1702	24	52.40	143	43.80	809.4	11.3	329	c/cs
14	73	1704	24	52.68	143	43.63	809.8	11.6	330	SF
14	73	1714	24	54.40	143	42.60	811.7	11.6	329	c/cs
14	73	1741	24	58.80	143	39.60	816.9	11.6	329	c/cs
14	73	1800	25	1.98	143	37.57	820.6	11.4	330	GPS
14	73	1811	25	3.80	143	36.40	822.7	11.4	330	c/cs
14	73	1825	25	6.10	143	34.90	825.3	11.5	330	c/cs
14	73	1828	25	6.60	143	34.62	825.9	12.0	331	SF
14	73	1847	25	9.90	143	32.60	829.7	11.9	331	c/cs
14	73	1858	25	11.80	143	31.40	831.9	11.8	331	c/cs
14	73	1920	25	15.60	143	29.00	836.2	11.8	332	c/cs
14	73	1931	25	17.50	143	27.90	838.4	11.9	331	c/cs
14	73	1942	25	19.40	143	26.70	840.6	11.8	331	c/cs
14	73	2000	25	22.47	143	24.76	844.1	11.3	330	GPS
14	73	2012	25	24.40	143	23.50	846.4	11.4	330	c/cs
14	73	2024	25	26.40	143	22.20	848.7	11.3	330	c/cs
14	73	2030	25	27.39	143	21.62	849.8	11.4	332	GPS
14	73	2053	25	31.20	143	19.30	854.1	11.1	332	c/cs
14	73	2100	25	32.36	143	18.64	855.4	11.4	329	GPS
14	73	2118	25	35.30	143	16.70	858.8	11.2	329	c/cs
14	73	2130	25	37.19	143	15.39	861.1	11.2	329	GPS
14	73	2148	25	40.10	143	13.50	864.4	11.1	330	c/cs
14	73	2200	25	41.98	143	12.26	866.6	10.9	329	GPS
14	73	2210	25	43.50	143	11.20	868.5	10.6	329	c/cs
14	73	2225	25	45.80	143	9.70	871.1	10.3	329	c/cs
14	73	2230	25	46.56	143	9.24	872.0	10.4	330	GPS
14	73	2240	25	48.10	143	8.30	873.7	10.3	331	c/cs
14	73	2253	25	50.00	143	7.10	875.9	10.6	331	c/cs
14	73	2300	25	51.09	143	6.39	877.2	10.5	330	GPS
14	73	2308	25	52.30	143	5.60	878.6	10.7	329	c/cs
14	73	2330	25	55.68	143	3.35	882.5	10.8	328	GPS
14	73	2333	25	56.10	143	3.00	883.1	11.0	329	c/cs
15	74	0000	26	0.40	143	0.24	888.0	11.2	330	GPS
15	74	0000	26	0.40	143	0.20	888.0	11.2	330	c/cs
15	74	0003	26	0.90	142	59.90	888.6	11.2	330	c/cs
15	74	0030	26	5.27	142	57.17	893.6	11.4	330	GPS
15	74	0030	26	5.30	142	57.20	893.6	11.2	330	c/cs
15	74	0038	26	6.60	142	56.30	895.1	11.3	330	c/cs
15	74	0052	26	8.80	142	54.90	897.7	11.1	330	c/cs
15	74	0100	26	10.12	142	54.05	899.2	11.0	329	GPS
15	74	0112	26	12.00	142	52.80	901.4	10.8	328	c/cs
15	74	0130	26	14.73	142	50.83	904.6	10.4	328	GPS
15	74	0140	26	16.20	142	49.80	906.4	10.5	328	c/cs
15	74	0200	26	19.17	142	47.72	909.9	9.9	329	GPS
15	74	0200	26	19.20	142	47.70	909.9	9.8	330	c/cs
15	74	0212	26	20.90	142	46.60	911.8	9.8	330	c/cs
15	74	0223	26	22.40	142	45.60	913.6	9.8	330	c/cs
15	74	0230	26	23.40	142	44.99	914.8	11.5	326	GPS
15	74	0240	26	25.00	142	43.80	916.7	11.4	326	c/cs
15	74	0245	26	25.80	142	43.20	917.6	10.8	326	c/cs
15	74	0247	26	26.10	142	43.00	918.0	11.6	326	c/cs
15	74	0258	26	27.80	142	41.70	920.1	11.8	327	c/cs
15	74	0300	26	28.17	142	41.41	920.5	11.4	328	GPS
15	74	0303	26	28.70	142	41.10	921.1	10.1	327	c/cs
15	74	0305	26	28.90	142	40.90	921.4	11.0	328	c/cs
15	74	0322	26	31.60	142	39.00	924.5	11.1	328	c/cs
15	74	0330	26	32.80	142	38.13	926.0	11.0	328	GPS
15	74	0350	26	35.90	142	36.00	929.7	10.8	328	c/cs
15	74	0400	26	37.42	142	34.90	931.5	10.6	329	GPS
15	74	0410	26	38.90	142	33.90	933.2	10.5	332	c/cs
15	74	0416	26	39.90	142	33.30	934.3	10.8	332	c/cs
15	74	0430	26	42.08	142	31.98	936.8	10.9	331	GPS
15	74	0431	26	42.20	142	31.90	937.0	11.0	331	c/cs
15	74	0445	26	44.50	142	30.50	939.5	10.6	331	c/cs
15	74	0500	26	46.82	142	29.09	942.2	10.9	332	GPS
15	74	0504	26	47.50	142	28.70	942.9	11.0	332	c/cs
15	74	0519	26	49.90	142	27.20	945.7	11.2	333	c/cs
15	74	0530	26	51.70	142	26.18	947.7	11.4	333	GPS
15	74	0531	26	51.90	142	26.10	947.9	11.3	334	c/cs

Table 1 (continued).

Date (1989)	Julian day	Time (UTC)	Latitude (N)		Longitude (E)		Distance (nmi)	Actual speed (kt)	Course (degrees)	Comment[a]
			(deg)	(min)	(deg)	(min)				
March 15	74	0540	26	53.40	142	25.30	949.6	11.5	334	c/cs
15	74	0551	26	55.30	142	24.20	951.7	11.4	334	c/cs
15	74	0605	26	57.70	142	22.90	954.4	11.5	334	c/cs
15	74	0622	27	0.62	142	21.34	957.6	10.3	336	GPS
15	74	0630	27	1.88	142	20.72	959.0	11.7	336	GPS
15	74	0635	27	2.80	142	20.30	960.0	11.7	337	c/cs
15	74	0639	27	3.50	142	19.90	960.8	11.6	336	c/cs
15	74	0700	27	7.21	142	18.08	964.8	11.2	337	GPS
15	74	0702	27	7.60	142	17.90	965.2	11.1	351	c/cs
15	74	0704	27	7.90	142	17.90	965.6	11.5	358	c/cs
15	74	0721	27	11.20	142	17.70	968.8	11.8	359	c/cs
15	74	0729	27	12.80	142	17.70	970.4	12.0	358	c/cs
15	74	0730	27	12.96	142	17.69	970.6	11.3	6	GPS
15	74	0736	27	14.10	142	17.80	971.7	11.0	6	c/cs
15	74	0754	27	17.40	142	18.20	975.1	10.9	6	c/cs
15	74	0802	27	18.80	142	18.40	976.5	10.8	6	c/cs
15	74	0808	27	19.90	142	18.50	977.6	11.0	6	c/cs
15	74	0821	27	22.26	142	18.81	980.0	10.8	2	SF
15	74	0828	27	23.50	142	18.80	981.2	10.8	2	c/cs
15	74	0852	27	27.80	142	19.00	985.6	10.9	2	c/cs
15	74	0906	27	30.40	142	19.10	988.1	10.0	348	c/cs
15	74	0907	27	30.60	142	19.00	988.3	10.5	350	c/cs
15	74	0943	27	36.78	142	17.77	994.6	10.0	347	SF
15	74	1002	27	39.90	142	17.00	997.8	10.0	346	c/cs
15	74	1028	27	44.10	142	15.80	1002.1	9.9	346	c/cs
15	74	1047	27	47.10	142	14.90	1005.2	9.9	346	c/cs
15	74	1050	27	47.58	142	14.80	1005.7	10.3	346	SF
15	74	1058	27	48.90	142	14.40	1007.1	10.1	346	c/cs
15	74	1151	27	57.60	142	12.10	1016.0	9.9	348	c/cs
15	74	1214	28	1.30	142	11.10	1019.8	9.8	348	c/cs
15	74	1228	28	3.50	142	10.60	1022.1	9.6	348	c/cs
15	74	1238	28	5.09	142	10.20	1023.7	8.2	344	SF
15	74	1238	28	5.10	142	10.20	1023.7	8.3	343	c/cs
15	74	1259	28	7.90	142	9.20	1026.6	8.3	341	c/cs
15	74	1316	28	10.10	142	8.40	1028.9	8.2	341	c/cs
15	74	1329	28	11.80	142	7.70	1030.7	8.5	342	c/cs
15	74	1355	28	15.30	142	6.40	1034.4	8.4	341	c/cs
15	74	1400	28	15.96	142	6.14	1035.1	10.1	344	DR
15	74	1412	28	17.90	142	5.50	1037.2	10.0	344	c/cs
15	74	1430	28	20.80	142	4.60	1040.2	9.9	344	DR
15	74	1435	28	21.60	142	4.30	1041.0	9.8	345	c/cs
15	74	1448	28	23.60	142	3.70	1043.1	10.2	346	c/cs
15	74	1457	28	25.10	142	3.30	1044.6	10.1	346	c/cs
15	74	1500	28	25.62	142	3.19	1045.1	11.6	352	DR
15	74	1506	28	26.80	142	3.00	1046.3	11.3	352	c/cs
15	74	1519	28	29.20	142	2.60	1048.8	11.4	351	c/cs
15	74	1538	28	32.80	142	1.90	1052.4	11.5	351	c/cs
15	74	1556	28	36.10	142	1.30	1055.8	11.2	351	c/cs
15	74	1614	28	39.50	142	0.70	1059.2	11.4	351	c/cs
15	74	1617	28	40.00	142	0.60	1059.7	11.3	351	c/cs
15	74	1647	28	45.60	141	59.60	1065.4	11.0	351	c/cs
15	74	1656	28	47.20	141	59.30	1067.0	11.3	351	c/cs
15	74	1700	28	47.98	141	59.12	1067.8	10.2	343	GPS
15	74	1709	28	49.40	141	58.60	1069.3	10.3	342	c/cs
15	74	1720	28	51.20	141	58.00	1071.2	9.8	342	c/cs
15	74	1722	28	51.60	141	57.80	1071.5	9.8	343	c/cs
15	74	1730	28	52.81	141	57.40	1072.8	10.0	343	GPS
15	74	1752	28	56.30	141	56.20	1076.5	10.2	343	c/cs
15	74	1800	28	57.64	141	55.76	1077.9	10.2	343	GPS
15	74	1826	29	1.87	141	54.27	1082.3	9.9	341	SF
15	74	1840	29	4.10	141	53.40	1084.6	9.9	341	c/cs
15	74	1851	29	5.80	141	52.70	1086.4	8.4	341	c/cs
15	74	1853	29	6.00	141	52.60	1086.7	10.1	341	c/cs
15	74	1859	29	7.00	141	52.27	1087.7	9.8	345	GPS
15	74	1905	29	8.00	141	52.00	1088.7	9.6	345	c/cs
15	74	1907	29	8.26	141	51.89	1089.0	9.6	347	GPS
15	74	1914	29	9.40	141	51.60	1090.2	9.9	347	c/cs
15	74	1921	29	10.50	141	51.30	1091.3	9.8	346	c/cs
15	74	1930	29	11.91	141	50.88	1092.8	10.3	345	GPS
15	74	1930	29	11.90	141	50.90	1092.8	4.4	349	c/cs
15	74	1931	29	12.00	141	50.90	1092.9	10.5	346	c/cs
15	74	1956	29	16.20	141	49.70	1097.3	10.4	346	c/cs
15	74	2000	29	16.92	141	49.48	1097.9	10.1	345	GPS
15	74	2008	29	18.20	141	49.10	1099.3	10.1	340	c/cs
15	74	2024	29	20.70	141	48.00	1102.0	10.6	339	c/cs

Table 1 (continued).

Date (1989)	Julian day	Time (UTC)	Latitude (N)		Longitude (E)		Distance (nmi)	Actual speed (kt)	Course (degrees)	Comment[a]
			(deg)	(min)	(deg)	(min)				
March 15	74	2030	29	21.73	141	47.57	1103.0	11.0	347	GPS
15	74	2049	29	25.10	141	46.70	1106.5	10.8	347	c/cs
15	74	2100	29	27.07	141	46.15	1108.5	10.6	338	GPS
15	74	2108	29	28.40	141	45.50	1109.9	10.6	339	c/cs
15	74	2130	29	32.00	141	43.89	1113.8	10.4	339	GPS
15	74	2138	29	33.30	141	43.30	1115.2	10.3	338	c/cs
15	74	2156	29	36.20	141	42.00	1118.3	10.3	339	c/cs
15	74	2200	29	36.80	141	41.72	1119.0	10.4	340	GPS
15	74	2212	29	38.70	141	40.90	1121.1	10.6	340	c/cs
15	74	2230	29	41.74	141	39.62	1124.3	10.9	344	GPS
15	74	2239	29	43.30	141	39.10	1125.9	10.5	344	c/cs
15	74	2255	29	46.00	141	38.20	1128.7	10.8	343	c/cs
15	74	2300	29	46.85	141	37.88	1129.6	10.9	339	GPS
15	74	2305	29	47.70	141	37.50	1130.5	10.8	337	c/cs
15	74	2318	29	49.90	141	36.50	1132.8	10.7	338	c/cs
15	74	2330	29	51.85	141	35.57	1135.0	10.6	335	GPS
15	74	2331	29	52.00	141	35.50	1135.1	11.0	335	c/cs
15	74	2349	29	55.00	141	33.90	1138.4	10.7	334	c/cs
15	74	2356	29	56.10	141	33.30	1139.7	10.9	335	c/cs
16	75	0000	29	56.80	141	32.90	1140.4	10.9	335	c/cs
16	75	0022	30	0.40	141	31.00	1144.4	11.1	335	c/cs
16	75	0023	30	0.60	141	30.90	1144.6	11.0	334	c/cs
16	75	0030	30	1.73	141	30.22	1145.9	11.7	335	GPS
16	75	0042	30	3.90	141	29.10	1148.2	11.2	336	c/cs
16	75	0043	30	4.03	141	28.99	1148.4	10.3	334	SF
16	75	0047	30	4.60	141	28.60	1149.1	10.1	335	c/cs
16	75	0100	30	6.62	141	27.56	1151.3	10.1	337	GPS
16	75	0109	30	8.00	141	26.90	1152.8	10.2	339	c/cs
16	75	0116	30	9.10	141	26.40	1154.0	10.4	339	c/cs
16	75	0126	30	10.70	141	25.60	1155.7	9.5	340	c/cs
16	75	0134	30	11.90	141	25.10	1157.0	10.3	340	c/cs
16	75	0141	30	13.10	141	24.60	1158.2	10.6	340	c/cs
16	75	0159	30	16.00	141	23.40	1161.4	10.4	340	c/cs
16	75	0200	30	16.20	141	23.30	1161.6	9.9	342	GPS
16	75	0217	30	18.90	141	22.30	1164.3	9.8	341	c/cs
16	75	0229	30	20.70	141	21.50	1166.3	9.5	342	c/cs
16	75	0239	30	22.20	141	20.90	1167.9	9.6	342	c/cs
16	75	0259	30	25.30	141	19.80	1171.1	9.3	341	c/cs
16	75	0300	30	25.40	141	19.70	1171.3	8.8	345	GPS
16	75	0306	30	26.30	141	19.40	1172.1	8.5	346	c/cs
16	75	0319	30	28.00	141	18.90	1174.0	8.3	346	c/cs
16	75	0400	30	33.50	141	17.30	1179.6	8.3	344	GPS
16	75	0415	30	35.50	141	16.60	1181.7	8.3	334	c/cs
16	75	0417	30	35.70	141	16.50	1182.0	8.2	334	c/cs
16	75	0423	30	36.50	141	16.10	1182.8	7.9	334	c/cs
16	75	0430	30	37.30	141	15.60	1183.7	7.8	336	GPS
16	75	0432	30	37.50	141	15.50	1184.0	7.8	350	c/cs
16	75	0437	30	38.20	141	15.30	1184.6	8.2	356	c/cs
16	75	0452	30	40.20	141	15.20	1186.7	8.2	356	c/cs
16	75	0500	30	41.30	141	15.10	1187.7	8.0	356	GPS
16	75	0502	30	41.60	141	15.10	1188.0	7.8	356	c/cs
16	75	0513	30	43.00	141	15.00	1189.4	8.0	356	c/cs
16	75	0517	30	43.50	141	14.90	1190.0	7.7	356	c/cs
16	75	0529	30	45.10	141	14.80	1191.5	7.9	356	c/cs
16	75	0530	30	45.20	141	14.80	1191.7	8.1	356	GPS
16	75	0539	30	46.40	141	14.70	1192.9	8.2	356	c/cs
16	75	0540	30	46.50	141	14.70	1193.0	5.1	2	c/cs
16	75	0541	30	46.60	141	14.70	1193.1	8.2	356	c/cs
16	75	0552	30	48.10	141	14.60	1194.6	6.4	358	c/cs
16	75	0554	30	48.30	141	14.60	1194.8	8.6	356	c/cs
16	75	0600	30	49.20	141	14.50	1195.7	9.2	358	GPS
16	75	0601	30	49.40	141	14.50	1195.8	5.8	5	c/cs
16	75	0602	30	49.50	141	14.50	1195.9	8.1	353	c/cs
16	75	0607	30	50.10	141	14.40	1196.6	8.9	352	c/cs
16	75	0611	30	50.70	141	14.30	1197.2	9.0	351	c/cs
16	75	0615	30	51.30	141	14.20	1197.8	9.0	346	GPS
16	75	0619	30	51.90	141	14.00	1198.4	8.3	341	c/cs
16	75	0630	30	53.30	141	13.50	1199.9	7.9	342	c/cs
16	75	0632	30	53.60	141	13.40	1200.2	7.8	14	c/cs
16	75	0633	30	53.70	141	13.40	1200.3	7.9	58	c/cs
16	75	0640	30	54.20	141	14.30	1201.2	8.1	105	c/cs
16	75	0657	30	53.60	141	16.90	1203.5	7.9	82	c/cs
16	75	0727	30	54.10	141	21.40	1207.4	9.6	84	c/cs
16	75	0728	30	54.20	141	21.60	1207.6	7.7	77	c/cs
16	75	0735	30	54.40	141	22.60	1208.5	6.5	175	c/cs

Table 1 (continued).

Date (1989)	Julian day	Time (UTC)	Latitude (N) (deg)	Latitude (N) (min)	Longitude (E) (deg)	Longitude (E) (min)	Distance (nmi)	Actual speed (kt)	Course (degrees)	Comment[a]
March 16	75	0742	30	53.60	141	22.70	1209.3	7.6	165	SF
16	75	0742	30	53.60	141	22.70	1209.3	4.0	266	c/cs
16	75	0759	30	53.50	141	21.40	1210.4	4.1	266	c/cs
16	75	0840	30	53.30	141	18.10	1213.2	6.6	163	c/cs
16	75	0846	30	52.70	141	18.30	1213.9	4.7	155	c/cs
16	75	0900	30	51.66	141	18.85	1215.0	5.2	189	782
16	75	0900	30	51.70	141	18.80	1215.0	3.5	112	c/cs
16	75	1000	30	50.40	141	22.60	1218.5	4.7	265	c/cs
16	75	1007	30	50.30	141	21.90	1219.0	3.9	300	c/cs
16	75	1028	30	51.00	141	20.60	1220.4	3.8	303	c/cs
16	75	1100	30	52.10	141	18.60	1222.4	5.5	82	c/cs
16	75	1130	30	52.50	141	21.80	1225.1	5.7	142	c/cs
16	75	1150	30	51.00	141	23.10	1227.0	5.8	286	c/cs
16	75	1158	30	51.20	141	22.30	1227.8	4.5	282	c/cs
16	75	1203	30	51.30	141	21.80	1228.2	2.6	265	c/cs
16	75	1207	30	51.20	141	21.60	1228.3	3.7	277	c/cs
16	75	1211	30	51.30	141	21.30	1228.6	3.3	275	c/cs
16	75	1221	30	51.30	141	20.70	1229.1	3.9	279	c/cs
16	75	1225	30	51.40	141	20.40	1229.4	4.3	286	c/cs
16	75	1228	30	51.40	141	20.20	1229.6	3.3	289	c/cs
16	75	1233	30	51.50	141	19.90	1229.9	2.8	294	c/cs
16	75	1247	30	51.80	141	19.10	1230.5	1.3	246	c/cs
16	75	1300	30	51.66	141	18.85	1230.8	0.7	330	782A
16	75	1300	30	51.70	141	18.80	1230.8	0.0	90	c/cs
20	79	2230	30	51.66	141	18.85	1230.8	0.0	90	782A
21	80	0700	30	51.66	141	18.85	1230.8	0.0	90	782B
23	82	1345	30	51.66	141	18.85	1230.8	1.3	155	782B
23	82	1352	30	51.50	141	18.90	1231.0	1.1	146	c/cs
23	82	1353	30	51.50	141	18.90	1231.0	7.9	91	c/cs
23	82	1401	30	51.50	141	20.20	1232.0	8.7	90	c/cs
23	82	1425	30	51.50	141	24.23	1235.5	9.5	94	SF
23	82	1431	30	51.40	141	25.30	1236.5	9.5	95	c/cs
23	82	1440	30	51.30	141	27.00	1237.9	9.5	94	c/cs
23	82	1457	30	51.10	141	30.10	1240.6	7.5	97	c/cs
23	82	1501	30	51.00	141	30.70	1241.1	6.4	101	c/cs
23	82	1506	30	50.90	141	31.30	1241.6	6.5	99	c/cs
23	82	1515	30	50.80	141	32.40	1242.6	6.9	88	c/cs
23	82	1524	30	50.81	141	33.62	1243.6	7.4	87	SF
23	82	1525	30	50.80	141	33.80	1243.8	6.0	83	c/cs
23	82	1530	30	50.90	141	34.30	1244.3	3.8	97	c/cs
23	82	1535	30	50.80	141	34.70	1244.6	5.2	86	c/cs
23	82	1540	30	50.90	141	35.20	1245.0	5.8	75	c/cs
23	82	1555	30	51.30	141	36.80	1246.5	7.5	69	c/cs
23	82	1605	30	51.71	141	38.20	1247.7	6.2	62	GPS
23	82	1608	30	51.90	141	38.50	1248.0	5.2	64	c/cs
23	82	1610	30	51.93	141	38.70	1248.2	6.1	60	GPS
23	82	1610	30	51.90	141	38.70	1248.2	5.7	61	c/cs
23	82	1615	30	52.16	141	39.18	1248.7	5.4	62	GPS
23	82	1620	30	52.37	141	39.64	1249.1	5.3	61	GPS
23	82	1625	30	52.58	141	40.09	1249.6	5.1	60	GPS
23	82	1630	30	52.79	141	40.52	1250.0	6.6	59	GPS
23	82	1635	30	53.07	141	41.07	1250.5	6.2	58	GPS
23	82	1640	30	53.34	141	41.58	1251.0	6.3	59	GPS
23	82	1645	30	53.61	141	42.10	1251.6	6.4	60	GPS
23	82	1650	30	53.88	141	42.64	1252.1	6.1	60	GPS
23	82	1700	30	54.39	141	43.67	1253.1	6.4	52	GPS
23	82	1700	30	54.40	141	43.70	1253.1	7.0	69	c/cs
23	82	1705	30	54.60	141	44.30	1253.7	6.8	82	GPS
23	82	1710	30	54.68	141	44.95	1254.3	6.8	82	GPS
23	82	1715	30	54.76	141	45.60	1254.8	7.1	78	GPS
23	82	1715	30	54.80	141	45.60	1254.8	6.8	85	c/cs
23	82	1720	30	54.81	141	46.26	1255.4	6.5	90	GPS
23	82	1724	30	54.80	141	46.80	1255.8	6.4	86	c/cs
23	82	1725	30	54.82	141	46.89	1255.9	5.6	89	GPS
23	82	1730	30	54.83	141	47.43	1256.4	7.0	86	GPS
23	82	1735	30	54.87	141	48.11	1257.0	7.0	85	GPS
23	82	1735	30	54.90	141	48.10	1257.0	6.5	85	c/cs
23	82	1740	30	54.92	141	48.74	1257.5	6.3	86	GPS
23	82	1742	30	54.90	141	49.00	1257.7	6.6	86	c/cs
23	82	1745	30	54.96	141	49.37	1258.1	6.2	82	GPS
23	82	1754	30	55.10	141	50.40	1259.0	6.3	82	c/cs
23	82	1806	30	55.30	141	51.90	1260.3	6.3	81	c/cs
23	82	1815	30	55.43	141	52.98	1261.2	5.8	78	GPS
23	82	1820	30	55.53	141	53.53	1261.7	5.6	72	GPS
23	82	1826	30	55.70	141	54.20	1262.2	4.8	37	c/cs

Table 1 (continued).

Date (1989)	Julian day	Time (UTC)	Latitude (N)		Longitude (E)		Distance (nmi)	Actual speed (kt)	Course (degrees)	Comment[a]
			(deg)	(min)	(deg)	(min)				
March 23	82	1829	30	55.90	141	54.30	1262.5	5.0	65	c/cs
23	82	1830	30	55.93	141	54.41	1262.6	5.3	73	GPS
23	82	1830	30	55.90	141	54.40	1262.6	6.2	108	c/cs
23	82	1832	30	55.90	141	54.60	1262.8	7.2	144	c/cs
23	82	1834	30	55.70	141	54.80	1263.0	7.3	186	c/cs
23	82	1835	30	55.55	141	54.79	1263.1	6.5	191	GPS
23	82	1835	30	55.50	141	54.80	1263.1	6.8	228	c/cs
23	82	1836	30	55.50	141	54.70	1263.3	7.6	253	c/cs
23	82	1840	30	55.33	141	54.13	1263.8	8.3	245	GPS
23	82	1842	30	55.20	141	53.80	1264.0	7.6	257	c/cs
23	82	1850	30	54.99	141	52.68	1265.1	6.9	263	GPS
23	82	1852	30	55.00	141	52.40	1265.3	6.1	267	c/cs
23	82	1855	30	54.95	141	52.06	1265.6	5.1	263	GPS
23	82	1900	30	54.90	141	51.57	1266.0	7.4	263	GPS
23	82	1900	30	54.90	141	51.60	1266.0	7.1	264	c/cs
23	82	1905	30	54.84	141	50.88	1266.6	6.0	263	GPS
23	82	1907	30	54.80	141	50.60	1266.8	6.2	265	c/cs
23	82	1910	30	54.79	141	50.29	1267.1	5.7	268	GPS
23	82	1915	30	54.77	141	49.74	1267.6	5.9	266	GPS
23	82	1916	30	54.80	141	49.60	1267.7	5.7	269	c/cs
23	82	1920	30	54.76	141	49.18	1268.1	5.9	268	GPS
23	82	1920	30	54.80	141	49.20	1268.1	4.4	274	c/cs
23	82	1921	30	54.80	141	49.10	1268.1	5.3	306	c/cs
23	82	1922	30	54.80	141	49.00	1268.2	5.5	337	c/cs
23	82	1929	30	55.40	141	48.70	1268.9	6.1	337	c/cs
23	82	1930	30	55.50	141	48.67	1269.0	7.2	334	GPS
23	82	1935	30	56.04	141	48.36	1269.6	6.2	333	GPS
23	82	1938	30	56.30	141	48.20	1269.9	5.1	334	c/cs
23	82	1940	30	56.50	141	48.10	1270.1	6.0	337	c/cs
23	82	1945	30	56.93	141	47.88	1270.6	5.1	332	GPS
23	82	1951	30	57.38	141	47.60	1271.1	6.1	333	GPS
23	82	1959	30	58.10	141	47.20	1271.9	6.1	334	c/cs
23	82	2000	30	58.20	141	47.12	1272.0	6.7	333	GPS
23	82	2001	30	58.30	141	47.06	1272.1	5.8	331	GPS
23	82	2006	30	58.72	141	46.79	1272.6	5.8	330	GPS
23	82	2009	30	59.00	141	46.60	1272.9	5.7	338	c/cs
23	82	2011	30	59.15	141	46.54	1273.1	6.5	333	GPS
23	82	2012	30	59.20	141	46.50	1273.2	7.0	291	c/cs
23	82	2014	30	59.30	141	46.20	1273.4	4.5	296	c/cs
23	82	2015	30	59.40	141	46.20	1273.5	5.0	335	c/cs
23	82	2016	30	59.44	141	46.11	1273.6	1.8	353	GPS
23	82	2016	30	59.40	141	46.10	1273.6	2.9	74	c/cs
23	82	2017	30	59.50	141	46.20	1273.6	4.8	104	c/cs
23	82	2018	30	59.40	141	46.30	1273.7	5.8	127	c/cs
23	82	2019	30	59.40	141	46.30	1273.8	8.8	141	c/cs
23	82	2021	30	59.10	141	46.60	1274.1	10.1	155	c/cs
23	82	2024	30	58.70	141	46.80	1274.6	9.2	154	c/cs
23	82	2030	30	57.87	141	47.28	1275.5	5.9	144	783
23	82	2030	30	57.90	141	47.30	1275.5	0.0	235	c/cs
24	83	0500	30	57.84	141	47.23	1275.5	0.0	55	783A
26	85	0215	30	57.87	141	47.28	1275.6	0.4	47	783
26	85	0230	30	57.90	141	47.40	1275.7	2.7	287	c/cs
26	85	0240	30	58.10	141	46.90	1276.1	2.5	205	c/cs
26	85	0250	30	57.70	141	46.70	1276.6	2.5	204	c/cs
26	85	0300	30	57.30	141	46.50	1277.0	0.7	184	c/cs
26	85	0330	30	57.00	141	46.40	1277.3	0.7	157	c/cs
26	85	0352	30	56.74	141	46.55	1277.6	1.0	180	GPS
26	85	0357	30	56.66	141	46.55	1277.6	0.8	180	GPS
26	85	0400	30	56.62	141	46.55	1277.7	0.4	162	GPS
26	85	0400	30	56.60	141	46.50	1277.7	0.7	162	c/cs
26	85	0407	30	56.54	141	46.58	1277.8	0.8	173	GPS
26	85	0412	30	56.47	141	46.59	1277.8	0.6	161	GPS
26	85	0417	30	56.42	141	46.61	1277.9	3.2	173	GPS
26	85	0430	30	55.74	141	46.71	1278.6	1.4	191	GPS
26	85	0430	30	55.70	141	46.70	1278.6	1.0	210	c/cs
26	85	0432	30	55.71	141	46.69	1278.6	1.4	217	GPS
26	85	0437	30	55.62	141	46.61	1278.7	1.1	213	GPS
26	85	0442	30	55.54	141	46.55	1278.8	1.0	234	GPS
26	85	0447	30	55.49	141	46.47	1278.9	0.9	263	GPS
26	85	0452	30	55.48	141	46.38	1279.0	0.8	262	GPS
26	85	0457	30	55.47	141	46.30	1279.1	0.6	249	GPS
26	85	0500	30	55.46	141	46.27	1279.1	1.0	194	GPS
26	85	0500	30	55.50	141	46.30	1279.1	1.1	242	c/cs
26	85	0507	30	55.40	141	46.14	1279.2	1.1	213	GPS
26	85	0512	30	55.32	141	46.08	1279.3	1.2	206	GPS

Table 1 (continued).

Date (1989)	Julian day	Time (UTC)	Latitude (N)		Longitude (E)		Distance (nmi)	Actual speed (kt)	Course (degrees)	Comment[a]
			(deg)	(min)	(deg)	(min)				
March 26	85	0517	30	55.23	141	46.03	1279.4	1.0	212	GPS
26	85	0522	30	55.16	141	45.98	1279.5	0.9	256	GPS
26	85	0530	30	55.13	141	45.84	1279.6	1.32	44	GPS
26	85	0530	30	55.10	141	45.80	1279.6	1.3	254	c/cs
26	85	0538	30	55.08	141	45.64	1279.8	1.1	245	GPS
26	85	0543	30	55.04	141	45.54	1279.9	1.2	247	GPS
26	85	0548	30	55.00	141	45.43	1280.0	1.1	251	GPS
26	85	0553	30	54.97	141	45.33	1280.1	1.2	252	GPS
26	85	0558	30	54.94	141	45.22	1280.2	1.1	254	GPS
26	85	0600	30	54.93	141	45.18	1280.2	0.9	260	GPS
26	85	0600	30	54.90	141	45.20	1280.2	1.2	252	c/cs
26	85	0608	30	54.88	141	45.00	1280.4	1.3	249	GPS
26	85	0613	30	54.84	141	44.88	1280.5	1.2	252	GPS
26	85	0618	30	54.81	141	44.77	1280.6	1.4	244	GPS
26	85	0623	30	54.76	141	44.65	1280.7	2.4	229	GPS
26	85	0634	30	54.47	141	44.26	1281.1	0.9	259	784
26	85	0700	30	54.40	141	43.80	1281.5	0.0	259	c/cs
26	85	0717	30	54.40	141	43.80	1281.6	0.4	79	c/cs
26	85	0830	30	54.47	141	44.26	1282.0	0.0	90	784
31	90	0100	30	54.47	141	44.26	1282.0	2.4	312	784
31	90	0112	30	54.80	141	43.90	1282.5	5.4	23	c/cs
31	90	0113	30	54.90	141	43.90	1282.5	3.8	339	c/cs
31	90	0115	30	55.00	141	43.80	1282.7	5.2	318	c/cs
31	90	0116	30	55.05	141	43.77	1282.8	4.1	305	GPS
31	90	0116	30	55.00	141	43.80	1282.8	6.6	273	c/cs
31	90	0118	30	55.10	141	43.50	1283.0	9.2	264	c/cs
31	90	0121	30	55.01	141	42.98	1283.4	9.3	262	GPS
31	90	0121	30	55.00	141	43.00	1283.4	11.4	263	c/cs
31	90	0126	30	54.89	141	41.88	1284.4	11.1	261	GPS
31	90	0130	30	54.77	141	41.03	1285.1	10.8	257	GPS
31	90	0134	30	54.60	141	40.20	1285.9	11.1	259	c/cs
31	90	0136	30	54.54	141	39.79	1286.2	12.6	266	GPS
31	90	0158	30	54.20	141	34.40	1290.8	12.6	265	c/cs
31	90	0219	30	53.80	141	29.30	1295.3	12.7	264	c/cs
31	90	0231	30	53.55	141	26.35	1297.8	11.5	260	SF
31	90	0247	30	53.00	141	22.80	1300.9	11.7	260	c/cs
31	90	0305	30	52.40	141	18.80	1304.4	11.6	260	c/cs
31	90	0332	30	51.50	141	12.90	1309.6	9.5	258	c/cs
31	90	0334	30	51.50	141	12.50	1309.9	6.9	258	c/cs
31	90	0341	30	51.30	141	11.60	1310.7	6.5	259	c/cs
31	90	0356	30	51.00	141	9.70	1312.3	6.9	260	c/cs
31	90	0412	30	50.68	141	7.61	1314.1	6.6	263	SF
31	90	0418	30	50.60	141	6.80	1314.8	6.7	266	c/cs
31	90	0431	30	50.51	141	5.17	1316.2	6.22	66	GPS
31	90	0436	30	50.47	141	4.57	1316.8	6.3	268	GPS
31	90	0441	30	50.45	141	3.96	1317.3	6.1	267	GPS
31	90	0445	30	50.40	141	3.50	1317.7	6.0	271	c/cs
31	90	0446	30	50.43	141	3.37	1317.8	6.3	270	GPS
31	90	0451	30	50.43	141	2.76	1318.3	6.1	275	GPS
31	90	0453	30	50.40	141	2.50	1318.5	6.3	279	c/cs
31	90	0456	30	50.50	141	2.16	1318.8	6.0	277	GPS
31	90	0500	30	50.55	141	1.70	1319.2	6.1	277	GPS
31	90	0506	30	50.62	141	0.99	1319.8	6.0	277	GPS
31	90	0511	30	50.68	141	0.41	1320.3	6.0	276	GPS
31	90	0516	30	50.73	140	59.83	1320.8	6.0	276	GPS
31	90	0521	30	50.78	140	59.25	1321.3	5.9	277	GPS
31	90	0523	30	50.80	140	59.00	1321.5	5.9	276	c/cs
31	90	0530	30	50.87	140	58.23	1322.2	5.9	275	GPS
31	90	0532	30	50.90	140	58.00	1322.4	5.9	262	c/cs
31	90	0536	30	50.83	140	57.55	1322.8	5.8	259	GPS
31	90	0540	30	50.80	140	57.10	1323.2	5.8	256	c/cs
31	90	0541	30	50.73	140	57.00	1323.3	5.9	258	GPS
31	90	0546	30	50.63	140	56.44	1323.8	5.9	258	GPS
31	90	0601	30	50.30	140	54.80	1325.3	5.9	260	c/cs
31	90	0617	30	50.07	140	52.97	1326.8	5.7	262	GPS
31	90	0619	30	50.00	140	52.70	1327.0	5.7	246	c/cs
31	90	0620	30	50.00	140	52.70	1327.1	4.4	204	c/cs
31	90	0622	30	49.87	140	52.58	1327.3	5.0	183	GPS
31	90	0622	30	49.90	140	52.60	1327.3	5.1	144	c/cs
31	90	0624	30	49.70	140	52.70	1327.4	6.0	118	c/cs
31	90	0626	30	49.60	140	52.90	1327.6	7.3	99	c/cs
31	90	0627	30	49.62	140	53.04	1327.7	5.8	92	GPS
31	90	0630	30	49.61	140	53.38	1328.0	6.6	85	GPS
31	90	0638	30	49.70	140	54.40	1328.9	6.4	84	c/cs
31	90	0645	30	49.77	140	55.27	1329.7	5.8	90	785

Table 1 (continued).

Date (1989)	Julian day	Time (UTC)	Latitude (N)		Longitude (E)		Distance (nmi)	Actual speed (kt)	Course (degrees)	Comment[a]
			(deg)	(min)	(deg)	(min)				
March 31	90	0645	30	49.80	140	55.30	1329.7	0.0	90	c/cs
31	90	1800	30	49.77	140	55.27	1329.7	0.0	90	785
April 01	91	1030	30	49.77	140	55.27	1329.7	1.5	24	785
01	91	1045	30	50.10	140	55.40	1330.0	8.4	7	c/cs
01	91	1050	30	50.80	140	55.50	1330.7	9.2	9	c/cs
01	91	1052	30	51.10	140	55.60	1331.0	10.2	9	c/cs
01	91	1105	30	53.30	140	56.00	1333.2	10.6	9	c/cs
01	91	1107	30	53.60	140	56.00	1333.6	3.5	13	c/cs
01	91	1108	30	53.70	140	56.10	1333.7	10.4	8	c/cs
01	91	1117	30	55.20	140	56.30	1335.2	10.6	8	c/cs
01	91	1127	30	57.00	140	56.60	1337.0	10.5	7	c/cs
01	91	1130	30	57.50	140	56.70	1337.5	10.5	6	GDRT
01	91	1136	30	58.50	140	56.80	1338.6	10.8	5	c/cs
01	91	1153	31	1.60	140	57.20	1341.6	10.7	3	c/cs
01	91	1214	31	5.30	140	57.40	1345.4	1.9	15	c/cs
01	91	1215	31	5.30	140	57.40	1345.4	10.7	3	c/cs
01	91	1230	31	8.01	140	57.51	1348.0	10.7	4	GDRT
01	91	1243	31	10.30	140	57.70	1350.4	10.8	6	c/cs
01	91	1313	31	15.70	140	58.30	1355.8	11.0	7	c/cs
01	91	1333	31	19.30	140	58.90	1359.4	10.9	6	c/cs
01	91	1356	31	23.50	140	59.40	1363.6	11.1	6	c/cs
01	91	1400	31	24.23	140	59.47	1364.4	11.4	0	GDRT
01	91	1425	31	29.00	140	59.50	1369.1	11.1	0	c/cs
01	91	1429	31	29.70	140	59.50	1369.9	11.4	0	c/cs
01	91	1449	31	33.60	140	59.50	1373.7	11.4	0	c/cs
01	91	1507	31	37.00	140	59.50	1377.1	11.3	2	c/cs
01	91	1537	31	42.60	140	59.70	1382.7	11.3	3	c/cs
01	91	1553	31	45.60	140	59.90	1385.8	11.3	3	c/cs
01	91	1600	31	46.96	140	59.99	1387.1	10.1	5	GDRT
01	91	1615	31	49.50	141	0.20	1389.6	7.7	2	c/cs
01	91	1617	31	49.70	141	0.20	1389.9	9.5	2	c/cs
01	91	1618	31	49.90	141	0.30	1390.0	6.2	4	c/cs
01	91	1628	31	50.90	141	0.30	1391.1	5.9	2	c/cs
01	91	1633	31	51.40	141	0.40	1391.6	6.0	4	c/cs
01	91	1640	31	52.10	141	0.40	1392.2	5.9	19	c/cs
01	91	1643	31	52.40	141	0.50	1392.5	5.3	54	c/cs
01	91	1645	31	52.50	141	0.70	1392.7	4.8	99	c/cs
01	91	1649	31	52.40	141	1.10	1393.0	4.4	90	c/cs
01	91	1651	31	52.40	141	1.30	1393.2	4.9	124	c/cs
01	91	1653	31	52.30	141	1.40	1393.3	4.7	90	c/cs
01	91	1655	31	52.30	141	1.60	1393.5	5.2	79	c/cs
01	91	1659	31	52.40	141	2.00	1393.9	5.5	80	c/cs
01	91	1700	31	52.42	141	2.10	1393.9	5.6	93	GPS
01	91	1706	31	52.40	141	2.80	1394.5	5.6	92	c/cs
01	91	1724	31	52.30	141	4.70	1396.2	5.6	89	c/cs
01	91	1740	31	52.40	141	6.50	1397.7	5.7	86	c/cs
01	91	1759	31	52.50	141	8.60	1399.5	5.5	88	c/cs
01	91	1800	31	52.50	141	8.70	1399.6	5.0	87	GPS
01	91	1806	31	52.50	141	9.30	1400.1	5.1	89	c/cs
01	91	1818	31	52.60	141	10.50	1401.1	5.2	93	c/cs
01	91	1830	31	52.50	141	11.70	1402.1	6.2	89	GPS
01	91	1848	31	52.50	141	13.90	1404.0	6.0	92	c/cs
01	91	1900	31	52.50	141	15.30	1405.2	4.6	89	GPS
01	91	1905	31	52.50	141	15.80	1405.5	4.7	91	c/cs
01	91	1924	31	52.50	141	17.50	1407.0	4.7	90	c/cs
01	91	1928	31	52.50	141	17.90	1407.3	4.7	115	c/cs
01	91	1929	31	52.40	141	18.00	1407.4	5.0	145	c/cs
01	91	1931	31	52.30	141	18.10	1407.6	4.5	110	c/cs
01	91	1932	31	52.30	141	18.20	1407.7	4.3	67	c/cs
01	91	1933	31	52.30	141	18.20	1407.7	4.0	5	c/cs
01	91	1935	31	52.40	141	18.20	1407.9	4.3	309	c/cs
01	91	1937	31	52.50	141	18.10	1408.0	5.0	267	c/cs
01	91	1940	31	52.50	141	17.80	1408.3	5.8	265	c/cs
01	91	1945	31	52.50	141	17.30	1408.8	6.2	271	c/cs
01	91	2000	31	52.50	141	15.40	1410.3	6.4	266	c/cs
01	91	2007	31	52.50	141	14.50	1411.1	6.1	272	c/cs
01	91	2015	31	52.48	141	13.58	1411.9	5.3	270	786A
01	91	2015	31	52.50	141	13.60	1411.9	0.0	90	c/cs
02	92	1715	31	52.48	141	13.58	1411.9	0.0	164	786A
04	94	0300	31	52.45	141	13.59	1411.9	0.0	90	786A
04	94	0845	31	52.45	141	13.59	1411.9	0.0	90	786B
16	106	1130	31	52.45	141	13.59	1411.9	1.7	189	786B
16	106	1226	31	50.90	141	13.30	1413.5	5.0	193	c/cs
16	106	1229	31	50.70	141	13.20	1413.7	4.3	225	c/cs
16	106	1230	31	50.61	141	13.16	1413.8	3.1	254	GDRT

Table 1 (continued).

Date (1989)		Julian day	Time (UTC)	Latitude (N)		Longitude (E)		Distance (nmi)	Actual speed (kt)	Course (degrees)	Comment[a]
				(deg)	(min)	(deg)	(min)				
April	16	106	1232	31	50.60	141	13.00	1413.9	3.7	308	c/cs
	16	106	1235	31	50.70	141	12.90	1414.1	4.3	351	c/cs
	16	106	1238	31	50.90	141	12.80	1414.3	5.1	351	c/cs
	16	106	1256	31	52.40	141	12.60	1415.8	5.3	354	c/cs
	16	106	1312	31	53.80	141	12.40	1417.2	5.1	356	c/cs
	16	106	1322	31	54.70	141	12.30	1418.1	4.7	356	c/cs
	16	106	1350	31	56.90	141	12.10	1420.3	4.3	317	c/cs
	16	106	1352	31	57.00	141	12.00	1420.5	3.5	276	c/cs
	16	106	1413	31	57.10	141	10.60	1421.7	3.5	269	c/cs
	16	106	1429	31	57.10	141	9.50	1422.6	4.0	268	c/cs
	16	106	1441	31	57.10	141	8.50	1423.4	3.8	258	c/cs
	16	106	1443	31	57.10	141	8.40	1423.6	3.2	206	c/cs
	16	106	1445	31	57.00	141	8.30	1423.7	4.0	174	c/cs
	16	106	1448	31	56.80	141	8.40	1423.9	4.1	140	c/cs
	16	106	1459	31	56.20	141	8.90	1424.6	3.7	130	c/cs
	16	106	1500	31	56.15	141	8.98	1424.7	5.3	129	GDRT
	16	106	1513	31	55.40	141	10.00	1425.8	5.5	121	c/cs
	16	106	1529	31	54.70	141	11.50	1427.3	5.3	117	c/cs
	16	106	1543	31	54.10	141	12.80	1428.5	5.3	133	c/cs
	16	106	1613	31	52.30	141	15.10	1431.2	5.4	134	c/cs
	16	106	1630	31	51.30	141	16.40	1432.7	4.4	137	c/cs
	16	106	1700	31	49.67	141	18.15	1434.9	4.4	137	GDRT

[a] GPS = Global Positioning System fix; SF = satellite navigation fix; c/cs = course/speed change; GDRT = dead reckoning position based in GPS fixes. Numbers (and letter) indicate site (hole) position.